ASB American Society of Biomechanics

FOUNDED IN 1977

ABSTRACT BOOK

ASB Annual Meeting

AUGUST 5 - 8 2024

Monona Terrace Community and Convention Center

Madison, WI

www.asbweb.org

#ASB2024

UNDERSTANDING PERCEIVED INSTITUTIONAL SUPPORT FOR UNDERGRADUATE RESEARCH IN BIOMECHANICS

Jacob W. Hinkel-Lipsker[1*], Craig M. Goehler[2], Allison R. Altman-Singles[3], David A. Phillips[4], Michael V. Potter[5], Mukul C. Talaty[6], Brooke M. Odle[7], and Kimberly E. Bigelow[8]

[1]California State University, Northridge; [2]University of Notre Dame; [3]Penn State Berks; [4]Oregon State University; [5]Francis Marion University; [6]Penn State Abington; [7]Hope College; [8]University of Dayton

*Corresponding author's email: jhlipsker@csun.edu

Introduction: Undergraduate research has been identified by the Academic Association of Colleges and Universities as a high impact practice to promote learning success as it provides high quality, equitable engagement opportunities to students [1]. Students benefit from working alongside a faculty member, increasing confidence, self-efficacy, sense of belonging, passion, enthusiasm for learning, academic success, and solidified identity as a scholar [2,3]. Thus, while undergraduate research in biomechanics has the potential to be a high impact practice, practices are highly varied across institution and program type and style [4].

In our previous study, biomechanics faculty principal investigators (PI) reported a variety of challenges to participating in undergraduate research. For example, funding challenges, recruitment, student preparedness, burdens on PI all tended to skew the cost-benefit analysis unfavorably for undergraduate research, especially in biomechanics [4]. To build on this previous work, the current study aimed to gauge institutional support for undergraduate research in biomechanics. These data can further help to inform university leadership and professional societies about how best to support both faculty and students to maximise opportunity and productivity of UG research.

Methods: A survey consisting of 34 required questions, and another 21 optional questions regarding undergraduate research experiences, perspectives and institutional support of undergraduate research was administered on-line to individuals who identified themselves as a principal investigator (PI) working with undergraduate students in a biomechanics lab. The survey was distributed at the 2023 American Society of Biomechanics meeting, as well as through word of mouth and various biomechanics newsletter and social media outlets.

Results presented here are for survey responses to four Likert scale questions regarding the PI's perspectives of the degree to which undergraduate research is valued, rewarded, resourced, and supported by their institution (1 "strongly disagree" to 5 "strongly agree"). Distributions of the responses were analyzed and a Chi Square test for association was performed to compare institutional rewards for the practice of undergraduate research, institutional resources for undergraduate research (funding, equipment, space, etc), and institutional mechanisms to participate in undergraduate research compared with perceived institutional value of undergraduate research. As such, we sought to assess whether a disconnect exists between institutional values and tangible support from institutions for undergraduate research.

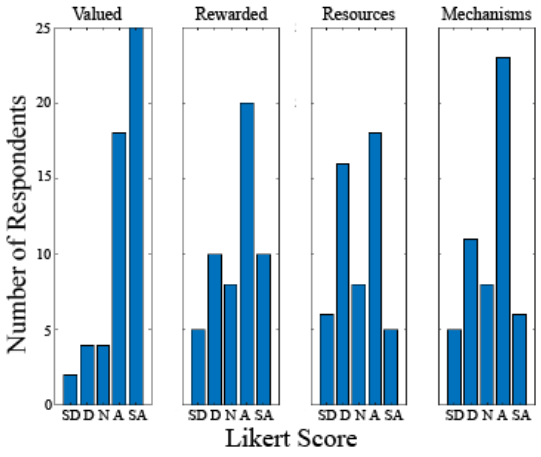

Figure 1: Comparison of survey responses to four Likert scale questions regarding PI perceptions of their institutions related to undergraduate research (SD = strongly disagree, D = disagree, N = neutral, A = agree, SA = strongly agree).

Results & Discussion: A total of 53 individuals completed the required questions for the survey and are included in the analysis presented here (R1/R2 = 39.3 % of respondents, Other academic institutions = 59.6%, other non-academic institutions = 1.1%; Biological Sciences = 7.4%, Engineering and Applied Science = 70.3%, Exercise and Sport Science = 46.3%, Health Sciences = 16.6%, Ergonomics and Human Factors = 5.5%).

Respondents indicate that undergraduate research is valued at their institution [M = 4.1, SD = 1.1]; however, they also indicate that institutional support (faculty rewards [M = 3.4, SD = 1.3], research resources [M = 3.0, SD = 1.2], and mechanisms [M = 3.3, SD = 1.2]) for undergraduate research is lower than their perceived institutional value of undergraduate research ($p < 0.001$). The distributions are shown in Figure 1.

These results indicate that while PI's perceive that undergraduate research is valued by their institutions, it is not perceived to be supported in kind through rewards, resources, or mechanisms. Future studies should further investigate the types of support that administrators could provide to have the highest impact on undergraduate research practices.

Significance: This study presents results that shed light on PI perceptions of gaps between institutional value and support for undergraduate research in biomechanics. These results may motivate institutional changes to bring institutional value and support (reward, resources, and mechanisms) for undergraduate research in better alignment.

Acknowledgements: Thanks to all survey participants for sharing their experiences and helping us to learn more about this topic.

References: [1] AACU https://www.aacu.org/trending-topics/high-impact; [2] Bauer & Bennett (2003), *J Higher Ed 74*(2); [3] Lopatto (2004), *Cell Bio Ed 3*(4); [4] Altman-Singles (2023), *J Biomech 159*.

SPEED MODULATES CENTER OF MASS SAMPLE ENTROPY DURING TREADMILL WALKING IN STROKE SURVIVORS WHO AMBULATE WITHOUT AN ASSISTIVE DEVICE, REGARDLESS OF HANDRAIL SUPPORT

Emily A. Steffensen,[1] Joel H. Sommerfeld,[1,2] Aaron D. Likens,[1,2] & Brian A. Knarr[1]
[1]Department of Biomechanics, University of Nebraska at Omaha, Omaha, NE;
[2]Nonlinear Analysis Core, Center for Human Movement Variability, Omaha, NE
email: easteffensen@unomaha.edu

Introduction: Stroke is a leading cause of adult long-term disability and survivors often have significant gait impairments [1]. Stroke survivors also often present with altered weight distributions and greater postural sway [2]. These presentations result in gait asymmetries that affect balance, and physical therapists often implement handrail use when conducting treadmill training paradigms [3]. Some evidence has demonstrated that stroke survivors have more normalized step parameters and reduced energy cost of walking on the treadmill while using the handrail with self-selected support rather than light-touch support [3,4]. One reason for this could be the role of stability in walking economy, which has been shown to have an inverse relationship in the context of walking speed [5]. However, the effects of handrail support on stability and variability of the center of mass (COM) during post-stroke treadmill walking have not been investigated. Therefore, the purpose of the study was to investigate the effects of handrail use during treadmill walking in individuals post-stroke on mediolateral COM stability using sample entropy. We hypothesized that COM entropy would decrease with increased handrail support during ambulation on a treadmill due to increased constraints imparted on the system. We also hypothesized that stroke survivors who are currently dependent on an assistive device (AD) would have greater reduction in entropy with increased handrail support.

Methods: 26 adults with chronic stroke walked at their self-selected walking speed on a steady state, instrumented treadmill for three minutes for each of the three conditions: walking without handrails (NoHR), walking with handrails at less than 5% body weight support (5%HR), and walking with handrails with self-selected support (SSHR). Handrails were used with the participants' less affected arm. During the 5%HR condition, visual biofeedback of force application on the handrail was utilized. If participants were unable to walk on the treadmill without handrails, the no-handrail condition was excluded. Two participants were excluded due to inability to complete the no-handrail and 5%HR conditions. Full kinematic data were collected, and full-body COM was calculated. Sample entropy for the COM was calculated to determine stability. AD dependence or independence in daily life was recorded.

Results & Discussion: Handrail support condition did not significantly affect the sample entropy of the mediolateral COM when looking at the total sample. However, our sample had a large range of walking speeds (0.1-1.35 m/s), which has been shown to have a relationship with entropy [5]. Interestingly, when controlling for speed, there was still no difference in sample entropy of the mediolateral COM between any of the three handrail support conditions (5%HR-NoHR $p = 0.198$; 5%HR-SSHR $p = 0.118$; NoHR-SSHR $p = 0.088$), which did not support our first hypothesis. There was also no significant difference in COM entropy between handrail support conditions when grouped by AD dependence (AD user $p = 0.209$; AD non-user $p = 0.804$), not supporting our second hypothesis. However, there was a significant difference in the effect of *speed* on COM entropy between AD non-users ($p = 0.044$) and those who are AD-dependent ($p = 0.100$). The correlation between speed and entropy was strong for all handrail support condition in the AD non-user group (NoHR $r = 0.67$, $p = 0.013$; 5%HR $r = 0.91$, $p < 0.001$; SSHR $r = 0.86$, $p < 0.001$), which is consistent with previous work that demonstrated a direct relationship between walking speed and COM entropy [5]. However, this was not true for the AD-dependent group, where there were negligible correlations between speed and entropy for all handrail conditions (NoHR $r = -0.35$, $p = 0.49$; 5%HR $r = 0.074$, $p = 0.83$; SSHR $r = -0.16$, $p = 0.64$). See Fig. 1. The negligible relationship of speed and sample entropy in the AD-dependent group could be due to their generally slower walking speed and/or their dependence on the AD for daily life ambulation.

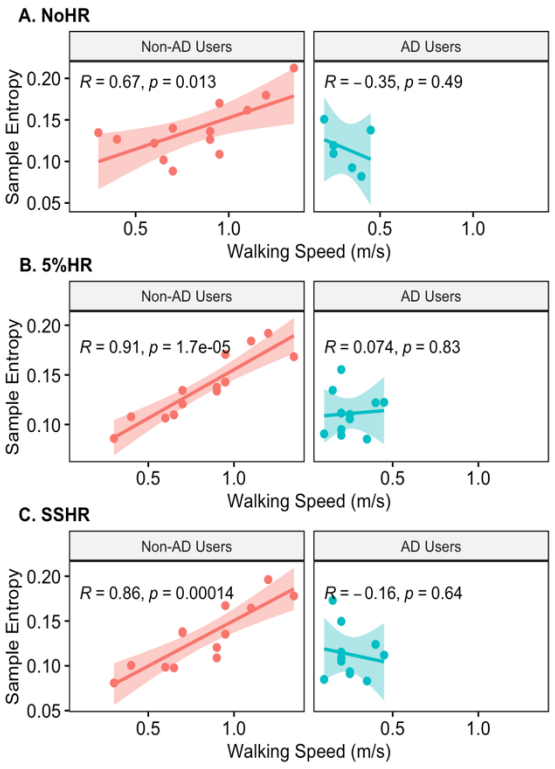

Fig.1: Sample entropy and speed for each AD use group by condition.

Significance: Our results here demonstrate that handrail support does not significantly affect mediolateral COM stability as measured by sample entropy. Speed, however, did have a strong relationship with mediolateral COM entropy, but only for individuals who are not dependent on assistive devices. Future research should explore the effects of speed and AD dependence on COM variability and its translation to rehabilitation outcomes.

References: [1] C.M. Cirstea, *Stroke*. (2020) 2892–2894. [2] S.F. Tyson, et. al, *Phys Ther.* **86** (2006) 30–38. [3] T. Ijmker, et. al, *J Neuroeng Rehabil*. **12** (2015). [4] T. Ijmker, et al., *Arch Phys Med Rehabil*. **94** (2013) 2255–2261. [5] L. Awad, et. al, *JNPT*. **47** (2023) 75–83.

ASSOCIATION BETWEEN HIP INTERNAL ROTATION DEFICIT AND GLENOHUMERAL INTERNAL ROTATION DEFICIT IN PROFESSIONAL TABLE TENNIS PLAYERS

Botao Zhang[1], Enming Zhang[2*], Xuedong Shang[3]
[1]Department of Physical Therapy, University of Florida. Gainesville, FL, USA
[2]Sports Medicine and Physical Therapy School, Beijing Sport University. Beijing, China
*Corresponding author's email: zhangenming@bsu.edu.cn

Introduction: Glenohumeral Internal Rotation Deficit (GIRD) is referred to the difference in internal rotation (IR) range of motion (ROM) between dominant shoulder and nondominant shoulders. [1] Recognized as a shoulder disorder, GIRD has been identified as a risk factor for shoulder injuries in various populations, including overhead players [2] and throwing players. [3] A recent study has even suggested the presence of GIRD in table tennis players, a group not traditionally associated with overhead or throwing activities and has found a correlation with shoulder pain. [4]

Hip ROM is believed to be related to shoulder ROM, and previous research indicates that a hip IR ROM deficit (the difference in hip IR ROM between two sides) would cause compensated excessive shoulder external rotation ROM in baseball players' pitching, [5] which might lead to altered shoulder ROM and even shoulder disorders. [6] Nevertheless, the direct association between hip IR ROM deficit (HIRD) and shoulder disorders are not clarified. Furthermore, the characteristics of HIRD and its association between GIRD are not well-defined in table tennis players, whose shoulder kinematics differ from baseball players. Therefore, the aim of this study is to investigate HIRD and its association with GIRD in professional table tennis players.

Methods: From January 2022 to February 2022, two assessors utilized an electronic goniometer to measure the shoulder and hip passive ROM of 46 Chinese professional table tennis players. The assessment took place in the therapy room of the Chinese table tennis training base in Zhengding, Hebei, China. A participant was determined to have exhibited GIRD if his or her mean value of the differences in IR ROM between the two shoulders in the supine position and the side-lying position was greater than 15.6 degrees. [7] The normality of data was checked by the Shapiro-Wilk test. The HIRD was compared between the players with and without GIRD. In addition, the association between HIRD and GIRD was analysed by binary logistics regression.

Results & Discussion: All the data was not normally distributed. The values of HIRD show a significant difference between players with Glenohumeral Internal Rotation Deficit (GIRD) and those without GIRD ($z= -2.062$, $p= 0.02$). The median of the value of HIRD in players with GIRD is considerably larger than in players without GIRD. Furthermore, HIRD is correlated with GIRD (OR= 1.09, 95% CI: 1.00-1.19, $p= 0.04$) in table tennis players. This implies that for each degree increase in HIRD, there is a 1.09 times higher risk of GIRD. To the authors' knowledge, this study is the first to compare the HIRD in table tennis players with and without GIRD, and its association to GIRD. The results of the current study suggest that table tennis players with and without GIRD exhibit distinct HIRD. Moreover, the results indicate that HIRD might serve as a risk factor for GIRD in table tennis players. This is in line with the previous studies on the relationship between hip ROM and shoulder ROM in baseball players. [7] However, beyond that, the present study innovatively established a direct association of hip ROM features to a specific shoulder disorder of GIRD.

Significance: Previous literature primarily focused on the local risk factors for GIRD, for instance the capsular and soft tissue alteration in shoulder. [3] Different from that, this study identified a potential risk factor located outside of shoulder girdle. This discovery probably offers a clue for future research on exploring additional potential risk factors for GIRD, particularly in the population of table tennis players, who requires further research. Additionally, the findings of this study have practical implications for athletic trainers and physical therapists. They highlight the importance of paying attention to HIRD in table tennis players with GIRD, which may play a crucial role in treatment or prevention of GIRD.

Acknowledgments: The authors are willing to thank the Chinese Table Tennis Team for the help and convenience the offered.

References: [1] Kibler WB, Sciascia A, Thomas SJ: Glenohumeral internal rotation deficit: pathogenesis and response to acute throwing. *Sports Med Arthrosc Rev* 2012;20:34–8; [2] Guney H, Harput G, Colakoglu F, Baltaci G. The Effect of Glenohumeral Internal-Rotation Deficit on Functional Rotator-Strength Ratio in Adolescent Overhead Athletes. *J Sport Rehabil*. 2016;25(1):52-57; [3] Hibberd EE, Shutt CE, Oyama S, et al: Physical contributors to glenohumeral internal rotation deficit in high school baseball players. *J Sport Health Sci* 2015;4:299–306; [4] Zhang B, Wang K, Zhang E, Shang X. Correlation of Glenohumeral Internal Rotation Deficit With Shoulder Pain in Elite Table Tennis Players. *Am J Phys Med Rehabil*. 2023;102(8):687-691; [5] Scher S, Anderson K, Weber N, Bajorek J, Rand K, Bey MJ. Associations among hip and shoulder range of motion and shoulder injury in professional baseball players. *J Athl Train*. 2010;45(2):191-197; [6] Vogelpohl RE, Kollock RO. Isokinetic rotator cuff functional ratios and development of shoulder injury in collegiate baseball pitchers. *Human Kinetics*. 2015; 20(3): 46 – 52; [7] Kamonseki DH, Cedin L, Habechian FAP, et al: Glenohumeral internal rotation deficit in table tennis players. *J Sports Sci* 2018;36:2632–6.

QUANTIFICATION OF THE THIGH/CALF CONTACT FORCE DURING HIGH KNEE-FLEXION TASKS

John Z. Wu[1]*, Kevin D. Moore[1], Liying Zheng[1], Robert E. Carey[1], Ting Xia[2], and Scott P. Breloff[1]
[1]National Institute for Occupational Safety and Health, Morgantown, WV and Cincinnati, OH, USA.
[2]Department of Mechanical Engineering, Northern Illinois University, DeKalb, Illinois, USA. *Email: jwu@cdc.gov

Introduction: In some occupational activities, such as floor installation, roofing, mining, gardening, and some construction repair, workers will need to perform tasks involving high knee flexion. High knee flexion tasks, such as deep squatting, could potentially increase the risk of the development of knee osteoarthritis [1,2]. Previous studies indicated that deep squatting tasks caused excessive joint loading [3]. The compressive force in the tibiofemoral joint may be 50% more than those during normal standing and walking [4]. The thigh-calf contact forces may reach approximately 34-43% of body weight during deep squatting [5,6]. For healthy, natural joints, the thigh/calf contact may help reduce the patellofemoral and tibiofemoral normal contact forces by as much as 42% and 57%, respectively, in a deep squatting posture [6]. Despite the importance of thigh/calf contact in joint loading during high-flexion tasks, the nature and character of the thigh-calf contact forces have not been analyzed.

Methods: If the time-histories of the knee flexion and the normal tissue contact force in the thigh/calf interface are measured experimentally, as illustrated in Fig. 1, the dependence of the normal tissue contact force on the knee flexion angle is modeled using a rotational spring: $F_n^{tis} = F_m - K_{tis}(\beta_m - \beta),\ \beta_0 < \beta < \beta_m;\ and\ F_n^{tis} = 0,\ \beta < \beta_0$, where β_m is the maximal knee flexion angle and β_0 is the minimal knee flexion angle, at which the calves come in contact with the thighs. F_m is the maximal tissue contact force between the thighs and calves, which occurs at $\beta = \beta_m$. F_0 represents the initial tissue contact forces between thighs and calves. The contact stiffness of the soft tissues (K_{tis}) is determined by: $K_{tis} = (F_m - F_0) / (\beta_m - \beta_0)$. Four model parameters ($i.e., F_m,\ F_0,\ \beta_m, and\ \beta_0$) need to be determined based on experimental data.

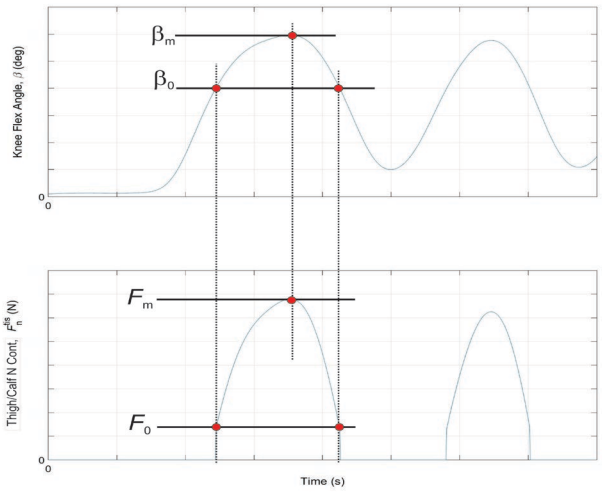

Figure 1: Determination of model parameters for the soft tissue contact

Results & Discussion: The time histories of the knee flexion angle and the normal contact forces between the thighs and calves were measured in our previous studies [6,7] (Fig. 2). The thigh/calf contact force calculated using the model is compared with the experimental data (Fig. 2B). The parameters used in the model were: β_m=120°, β_0=80°, F_0=75 N, F_m=350 N, and K_{tis} = 7.0 N/deg. The results show that the experimentally measured thigh/calf contact force profiles can be well characterized using the proposed model with a maximal error of 7% at the peaks. One of the challenges in the biomechanical modeling of the knee joint for high knee-flexion tasks is quantifying the contact force between the thighs and calves since the shear force component in the thigh/calf contact interface is difficult to measure reliably. In our previous study [6], this problem was resolved by assuming that contact forces applied on the legs and the thighs were aligned and in opposite directions.

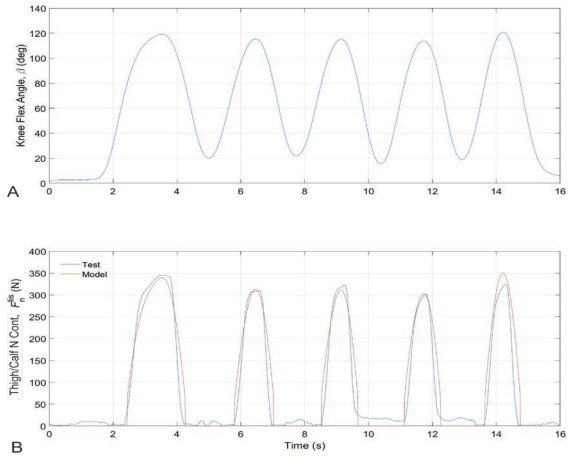

Figure 2: The comparison of the measured normal contact forces with the model. A: Knee flexion as a function of time. B: Thigh/calf normal tissue contact forces as a function of time.

Significance: Although the current method was derived for the knee joints, the proposed approach may also be used for other joints, such as elbows and fingers. In the existing biomechanical simulation software, such as OpenSim and AnyBody, the effects of the soft tissue contacts around the joint are not considered. The current approach may help biomechanical researchers improve their analysis to calculate the joint loading during deep flexion tasks more precisely.

Acknowledgments & Disclaimers: The findings and conclusions in this report are those of the authors and do not necessarily represent the official position of the National Institute for Occupational Safety and Health, Centers for Disease Control and Prevention. Mention of any company or product does not constitute an endorsement by the National Institute for Occupational Safety and Health, Centers for Disease Control and Prevention.

References: [1] Bernard et al. (2010) *J Occup Environ Med* 52, 33-8. [2] Reid et al. (2010) *J Occup Rehabil* 20. [3] Dahlkvist et al. (1982) *Eng Med* 11, 69-76. [4] Glitsch et al. (2013) *Proc. ISB-2013*. [5] Zelle et al. (2009) *J Biomech* 42. [6] Wu et al. (2019) *J Biomech* 96. [7] Breloff et al. (2019) *Int J Ind Ergon* 74.

INFLUENCE OF THREE DRILLS ON THE BIOMECHANICS OF THE BASEBALL SWING

Adam Thomas[1,2*], Sheng-Che Yen[1], Michael Nguyen[1], Robert Herron[2], Fred Cromartie[2]
[1]*Northeastern University (Department of Physical Therapy, Movement & Rehabilitation Sciences)*
[2]*United States Sports Academy*
*Corresponding author's email: ad.thomas@northeastern.edu

Introduction: The intersegmental coordination between the pelvis and hand is an important component of sound hitting mechanics in baseball. Several training methods have been used in the field to alter the hand-pelvis coordination during hitting, but the effectiveness of these methods has not been experimentally examined. The purpose of this study was to investigate immediate effects of selected hitting drills on the kinematics of hand and pelvis during baseball hitting.

Methods: Nine college baseball players were recruited, and a repeated measures design was used. Each participant underwent four hitting drills in a random order (Figure 1.): (1) no drill (BASELINE); (2) holding an 8.5-inch ball with the elbow of the front arm (FRONT); (3) holding the same ball with the elbow of the back arm (BACK); (4) stepping down from a 4-inch step (STEP) (see Fig. 1). The hand motion and pelvis motion were recorded with a camera-based motion capture system (Qualisys AB, Sweden). In each condition, the participant was asked to hit a ball attached to a standing hitting trainer. A cluster of four markers was attached to the hand segment and a cluster of three markers was attached to the pelvis segment, and the six degrees of freedom method was used to model these segments. The following kinematic variables were calculated at the time when the bat strikes the ball: (1) linear distance between the hand the pelvis; (2) range of pelvic rotation; (3) acceleration of pelvic rotation. Repeated measures ANOVAs were used to compare these variables across the four conditions, and post-hoc tests were conducted to determine which pairs of comparisons reached statistical significance.

Results and Discussion: There was a significant difference with the hand-pelvis linear distance at ball contact between BASELINE (47.8 ± 1.2 cm) and BACK (50.2 ± 1.3 cm), $p = 0.04$, Cohen's $d = 0.82$, a large effect. Originally, the BACK drill was designed to aid in keeping the hands more upright as the hitter progresses from the swing phase to ball contact, which prevents the hands from rotating posteriorly at ball contact. This was consistent with our results that in the BACK drill, participants tended to reach the hand further away from the pelvis at ball contact. The benefit of such change was discussed in previous research. Kim et al. (2009) found that increasing swing velocity can be achieved by increasing the distance between the hand and the axis of proximal joint rotation, which can be done by increasing trunk rotation[1]. The BACK drill is able to assist with increasing velocity as well. Effective and efficient hitting mechanics will cause the torso to rotate towards the front leg and progress into pelvis rotation towards the stride leg[2]. On the other hand, we did not find significant changes in other conditions. The participants were skilled baseball hitters, and their hitting patterns were stable, and the FRONT and STEP conditions were found to have minimal impact on changing their patterns. It would be interesting to examine if these drills have any impact on novice individuals who just started learning baseball hitting.

Significance: Among the three drills tested, the BACK drill was the only one that showed significant immediate effect on hand-pelvis coordination. The BACK drill is a technique that can be used to help baseball players who need to move their hand further away from the pelvis at ball strike.

References:

[1] Kim, Y.-K., Hinrichs, R. N., & Dounskaia, N. (2009). Multicomponent Control Strategy Underlying Production of Maximal Hand Velocity During Horizontal Arm Swing. *Journal of Neurophysiology, 102*(5), 2889–2899. https://doi.org/10.1152/jn.00579.2009
[2] Washington, J. K., & Oliver, G. D. (2020). Relationship of pelvis and torso angular jerk to hand velocity in female softball hitting. *Journal of Sports Sciences, 38*(1), 46–52. https://doi.org/10.1080/02640414.2019.1679584

Figure 1. Baseline condition and three drills

HOW FIGURE SKATERS SUCCEEDED IN THE QUADRUPLE AXEL JUMP : CASE STUDIES OF TWO MALE SKATERS' CHALLENGES

Seiji HIROSAWA[1,2*], Yoshimitsu AOKI[1]
[1]Graduate School of Science and Technology, Keio University
[2]Faculty of Sport and Health Sciences, Toin University of Yokohama
*Corresponding author's email: seiji.hirosawa.0226@keio.jp

Introduction: In the current scoring system, jumps account for a high weight of total competition points. Since the late 2010s, the number of skaters attempting quadruple jumps has increased. The quadruple axel jump (4A), the most difficult jump defined in the competition rules, was a significant challenge for the skaters, and there was much interest in who would be the first to succeed. Previous biomechanical studies have shown that jump heights do not change significantly even with more rotational jumps, indicating the importance of increasing rotational velocity in the air rather than increasing jump height [1]. However, these reports are based on the fact that there is no significant difference in jump height between triple, double, and single axel, which skaters have already mastered. In other words, it is unclear whether increasing height is a good strategy for skaters to acquire new jumps. At last, skater A succeeded in a 4A for the first time in the 2023 competition. In this study, we use kinematic data from a tracking system to examine the strategies of two skaters (A and B) who attempted 4A in competitions and compared them with triple axel (3A) of the world's top skaters.

Methods: For the analysis, kinematic parameters from a tracking system that can measure vertical height (m), horizontal distance (m), and speed after landing (m/s), based on a two-dimensional DLT method using two 4K cameras (30 fps), were used. For details of this system, please refer to [2]. Note that the data was broadcast as media content and was not used for judgment. We also calculated the distance-to-height ratio. We analyzed the following jumps: skater A's successful 4A (J1) in free skating (FS) at the World Championships in '23 and 3A (J2) in the short program (SP), skater B's downgraded 4A (J3) in FS at the National Championships in '21 and 3A (J4) in the SP, skater B's successful 3A in the SP at the World Championships in '19 (J5). In addition, a 3A group consisting of 24 jumps was created for comparison. 22 of these jumps (including J2) were from the men's 3A, which all 9 judges rated as having a grade of execution score of 0 or higher at the World Championships in '23. The other two were J4 and 5. The mean and standard deviation of each kinematic parameter of the 3A group were used to test for normality with the Shapiro-Wilk test. For parameters for which normality was ensured, we calculated 95% confidence intervals and examined whether the values of skater A's 4A(J1) and B's 4A(J3) were included in the confidence intervals. If not included in 95CI, we quantified the characteristics of the 4A relative to the 3A by calculating the probability of taking more extreme values than skaters A's 4A(J1) and B's 4A(J3) by obtaining a cumulative distribution function.

Table 1: Kinematic parameter of each jump from tracking system. LS: Landing Speed(speed after landing), H/D: Height / Distance, GOE: Grade of Execution (Theoretical range from 0-5, excluded negative values).<< :downgraded means lack of more than a half revolution. For 3A group, 95CI for each parameter is listed.

No.	Skater	Competition	SP/FS	Jump	Height[m]	Distance[m]	LS[m/s]	H/D[m]	GOE
J1	A	23W	FS	4A	**0.84**	2.96	3.36	0.28	0.29
J2	A	23W	SP	3A	0.71	2.37	0.94	0.30	2.71
J3	B	21N	FS	4A<<	**0.75**	3.10	2.50	0.24	-4.86
J4	B	21N	SP	3A	0.73	3.24	2.11	0.23	4.00
J5	B	19W	SP	3A	0.70	3.62	4.25	0.19	4.29
3A group (n=24)		23W21N19W	SP FS	3A	0.50-0.74	1.73-3.77	0.60-4.44	0.13-0.34	0.31-4.16

Results & Discussion: The distributions of the four parameters for the 3A group were non-significant and normal. Therefore, the sample mean and standard deviation for each parameter were used to estimate the 95% confidence interval; only the height was not included in the 95% confidence interval for the values of A's 4A(J1) and B's 4A(J3). We calculated a cumulative distribution function for the heights and found a 1.75% probability of a value greater than B's 4A(J3) and a 0.018% probability greater than A's 4A(J1). Therefore, their heights are the most significant difference between 4A and 3A. In the intra-individual comparison, the height values of 4A are greater than 3A for both skaters. The height of A's 4A(J1) is distinct from that of 3A(J2), and these data show that A's jumps have a greater height-to-distance ratio than average. B explained that he had changed the way of 3A to attempt 4A through the media. As we can see from the J5 data, initially, B's 3A had a large distance value compared to the height value, which may have contributed to the high GOE, like the results of the 2A study of ladies in [2]. However, the values of the height-to-distance ratio are larger in the J3 and J4 data, so he may have modified the jump to reduce the horizontal distance and increase the vertical height more. Although skater B failed 4A in the competition, the height-to-distance rate gradually changed to a height-dominant value, suggesting that B was aiming to jump in the same way as A. Conversely, skater A showed a larger height ratio even at 3A compared to skater B; suggesting that this difference may have been one of the factors that differentiated the success or failure of the 4A. Integrating the results of this study and [2], the strategies for executing jumps with higher GOE and jumps with more rotations may be different.

Significance: Unlike previous figure skating biomechanics research, this study showed a new perspective on the importance of jump height for the increase in revolutions, based on data from a 4A jump in which only one person in the world has succeeded. In addition, in scoring sports where judges evaluate athletes' performance, it is important to use real-world data, which includes expert judges' ratings, rather than laboratory environments. We offer the possibility of real-world data utilization methods in biomechanics research.

Acknowledgments: We thank Qoncept Inc. for providing the kinematic data from the tracking system.

References: [1] Sarah T.Ridge et al. (2022), *Sports Biomech* 40(4). Up in the air: the efficacy of weighted gloves in figure skating jumps. [2] Seiji HIROSAWA et al. (2022), *J. Sports Sci.* 40(1), Determinant analysis and developing evaluation indicators of grade of execution score of double axel jump in figure skating.

How Undergraduates are Engaged in Biomechanics Research

Michael V. Potter[1*], Jacob W. Hinkel-Lipsker[2], Craig M. Goehler[3], Allison R. Altman-Singles[4], David A. Phillips[5], Mukul C. Talaty[6], Brooke M. Odle[7], and Kimberly E. Bigelow[8]

[1]Francis Marion University; [2]California State University, Northridge; [3]University of Notre Dame; [4]Penn State Berks; [5]Oregon State University; [6]Penn State Abington; [7]Hope College; [8]University of Dayton

*Corresponding author's email: michael.potter@fmarion.edu

Introduction: Involving undergraduates (UGs) in research has established benefits for students, faculty and institutions [1]. Students benefit in many ways including increased confidence, improved overall academic performance and identifying career preferences [2]. Insufficient time for the research process and limited ability of students to contribute to the research process have been noted as barriers to involving UGs in the process, though many faculty do find varying benefits including personal satisfaction, creative inputs from students, and productivity [3]. As institutions continue to appreciate the value of UG research, it seems likely the push to involve more students will continue to increase. The purpose of this study is to explore what the roles of UG researchers were when they joined the lab and how their participation changes over their UG career. Determinations of how UGs are used, and their evolving roles may assist faculty to better craft high impact projects for students, and in turn, maximize their productivity in that research.

Methods: Data on UG recruitment methods and engagement practices were collected via a survey distributed through various biomechanics community channels and completed online by individuals identifying as a primary investigator (PI) with UGs participating in their lab. From this larger survey, Likert scale questions were used to assess PIs agreement with their overall use and recruitment of UG researchers. UG engagement for sixteen common research activities was studied by asking each respondent to indicate the year when students first become involved in that activity in their labs. Responses were classified as either 1st and 2nd year, 3rd and 4th+ year, or no undergraduate involvement.

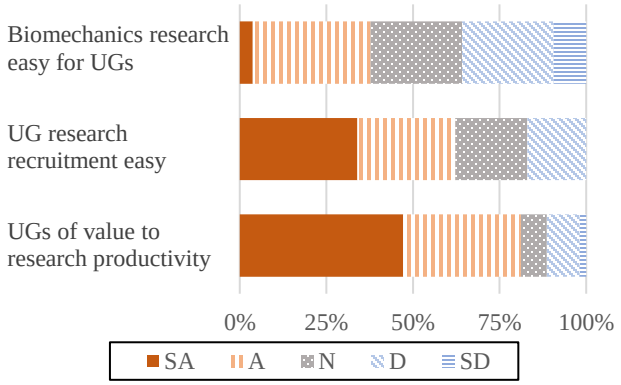

Figure 1. Comparison of survey responses to four Likert scale questions regarding PI perceptions of their institutions related to UG research (SD = strongly disagree, D = somewhat disagree, N = neither agree nor disagree, A = somewhat agree, SA = strongly agree).

Results & Discussion: 53 PIs responded to the survey from a variety of institution types (R1-2, M1-3, and baccalaureate). All respondents completed the Likert scale questions. A subset of 26 respondents detailed how they utilized UGs in their labs.

81% of respondents agreed (strongly or somewhat agreed) that UG research is of value to their research productivity, while 62% agreed that recruitment was easy, but only 38% of respondents agreed that biomechanics research was easy for UGs to perform (Figure 1). These data demonstrate the importance of meaningful engagement of UGs in biomechanics research.

Figure 2 shows each studied UG research activity, segregated by the most commonly identified level of first involvement. These data demonstrate that for most of the identified laboratory tasks a majority of respondents include UG researchers, with the exceptions of manuscript review and grant writing. Many tasks are introduced to 1st and 2nd years, while some more advanced tasks (presentations, manuscript preparation, coding, interpretation, and IRB preparation) are more commonly introduced to 3rd and 4th+ years.

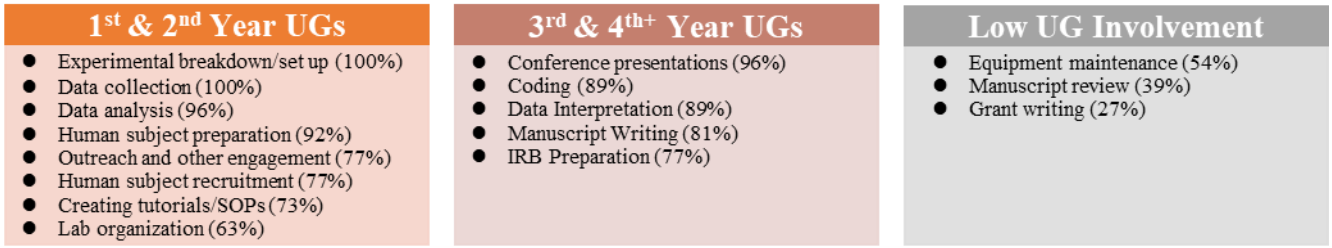

Figure 2. Most common level of first involvement of UGs for 16 research activities (% of respondents who indicated UG involvement in activity).

This breakdown may provide insight to PIs on how they can leverage the skills and abilities of undergraduates in their lab to contribute to scholarly research and lab productivity in a variety of meaningful ways. This list also identified opportunities to better foster professional development of students through earlier involvement in tasks such as conference presentations and manuscript writing.

Significance: This work demonstrates the potential for UGs to engage in biomechanics research in very intentional and purposeful ways. The nature of biomechanics, perhaps more than other fields, has a multitude of opportunities for UGs to engage in high caliber research, prior to the development of more advanced research skills.

Acknowledgements: Thanks to all survey participants for sharing their experiences and helping us to learn more about this topic.

References: [1] Malachowski (2019), *Scholarship and Practice of Undergraduate Research* 3; [2] Haeger (2020), *SPUR* 3; [3] Altman-Singles (2023), *J Biomech 159*.

Heaviness Perception of an Occluded Object in Older Adults

Alli Grunkemeyer[1], Aaron D. Likens[1]
[1]Department of Biomechanics, University of Nebraska at Omaha, Omaha, NE USA
*Corresponding author's email: agrunkemeyer@unomaha.edu

Introduction: Heaviness perception is the ability to use haptic feedback from effortful touch to determine the weight of a wielded object [1]. When wielding an object with your hand, you move it in all sorts of directions, with all sorts of speeds and forces, creating all sorts of patterns of deformation of the skin and muscles of the hand, forearm and shoulder. Many things are changing with respect to the perceiver and the object, except for the inertia tensor at a given grasp location. The inertia tensor is a 3 × 3 matrix that provides information about how mass is distributed in a rigid body in terms of its inertia. In this study, we sought to improve the perception of an object via wielding in young and older adults.
Somatosensory decline, as seen in healthy aging adults, is thought to decrease one's physiologic complexity, which is required to perceive everyday objects [2]. Many research efforts are aimed towards the augmentation of sensory function. We hypothesized (1) the age of the participant will influence accuracy in perceiving heaviness, (2) movement dynamics will influence perceptual accuracy, and (3) increasing time-to-wield will degrade perceptual accuracy.

Methods: Nineteen young adults (19-35 years of age) and thirteen older adults (> 56 years of age) were seated for the duration of the trial, as seen in **Figure 2**. Subjects wielded an occluded object with varying masses. There were five different mass stimuli being presented (in terms of added mass: 0, 125, 250, 375, and 500 g). Subjects rated the heaviness of the object in relation to a standard object by marking their perceived heaviness on a scale presented at the end of each trial. These responses were used to calculate perceptual accuracy. For statistical analysis, we fit a series of Tweedie-Generalized linear mixed effect (LME) models with percent error as the outcome variable and fixed effects of mass, age, time-to-wield, movement dynamics, and their interactions. Subsequent models were compared by likelihood ratio tests for model improvement.

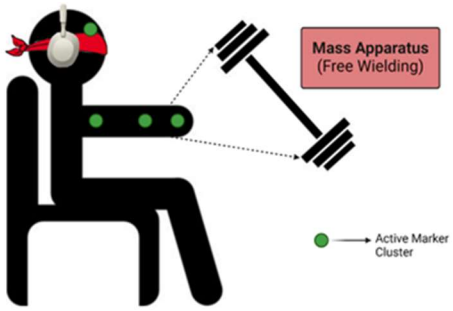

Figure 2. Experimental set up. Active markers (PhaseSpace Inc.) were applied to the participants' wielding hand, forearm, bicep, head, and the apparatus.

Results & Discussion: The best fitting model in support of our first hypothesis included all three terms, [$\chi^2(4) = 11.1455$, $p = 0.02498$]. A simple slope analysis was used to understand the interaction and revealed that the relationship between mass and percent error depended on age. For older adults, percent error decreased with increasing mass, and increased in younger adults (*Estimate = -0.039, p = .0004*). In support of our second hypothesis, our best fitting model included three terms, [$\chi^2(4) = 11.1455$, $p = 0.02498$]. A simple slope analysis revealed that in older adults, as the presence of long-range correlations in their movement patterns increased, so did their percent error. Percent error decreased in older adults with a stronger presence of long-range correlations (*Estimate = 0.0002, p = .0058*). In support of our third hypothesis, our best fitting model included three terms, [$\chi^2(4) = 8.0817$, $p = 0.0045$]. A simple slope analysis revealed that in older adults, as the time-to-wield increased, their percent error was relatively unchanged. In younger adults, an increase in time-to-wield increased their percent error (*Estimate = -0.649, p = .0045*).

Significance: As a general summary of the results, we found that percent error increased as a function of mass in younger adults. In contrast, older adults produced qualitatively different results such that decreasing the mass of the object appears to degrade their ability to perceive weight. In addition, while time-to-wield did not seem to influence percent error in older adults, the presence of long-range correlations in their movement patterns appeared to degrade perceptual accuracy. Hence, as we predicted, our results suggest that age influences one's ability to perceive the weight of an occluded object. Importantly, the direction of influence depends on mass of the object, and the movement patterns with which it is wielded. Contrary to our predictions, a stronger presence of long-range correlations in older adults' movement patterns decreased their perceptual accuracy. In the near future, we aim to replicate the finding concerning older adults while providing insight into the ineffectiveness of optimal movement dynamics during a wielding task. Other next steps involve including a larger range of masses added to the apparatus and introducing subthreshold stimulation to older adults during a wielding task.

Acknowledgments: This research was supported by an UNO GRACA to AG, and NASA Nebraska Space Grant FY23 and FY24 Fellowship to AG.

References:
[1] Pagano et al. Journal of Applied Biomechanics, 14: 331-359, 1998.
[2] Gerber et al. Journal of Human Movement Science, 90, 103119, 2023.

EFFECTS OF FATIGUE AND GROUND SLOPE ON THE BIOMECHANICS OF SNOWSHOE HIKING

Rebecca Zifchock[1*], Amy Silder[2], Josiah Steckenrider[1], Douglas Jones[2]
[1]Department of Civil and Mechanical Engineering, United States Military Academy; West Point, NY
[2]Naval Health Research Center, San Diego, CA
*Corresponding author's email: rebecca.zifchock@westpoint.edu

Introduction: Snowshoeing is a popular winter sport due to its low-cost and feasibility for people at all fitness levels. Over 3 million participate recreationally around the US [1], and it is also used for tactical travel such as for search-and-rescue and military dismounted missions. Despite this, there is very little known about the biomechanics of snowshoeing over long distances. Browning et al., showed that individuals walked more slowly and with more sagittal flexion at the hip, knee, and ankle during snowshoe walking, compared to overground during short, repeated trials [1]. Physiological effects of snowshoeing over moderate distances (500 yards) on varied terrain include increased heart rate and perceived exertion, compared to flat terrain [2]. While these findings suggest that snowshoeing is a physically-challenging sport, little information is available about how it affects musculoskeletal and cardiovascular loading over longer distances and on uphill and downhill terrain. The purposes of this study are to compare speed, tibial accelerometry, stride time, and heart rate while snowshoeing on: (1) uphill, downhill, and flat surfaces, and (2) throughout extended uphill and downhill segments.

Methods: Data were available from 12 male US Marines, aged 21±2 yrs, 80±14 kg, 1.74±0.05 m. Participants were generally novice snowshoers, but were fit, active-duty Marines and met all criteria to participate in cold-weather training. After donning their snowshoes, they traversed a standard hiking course, ~6.3 km in length on lightly packed snow (Fig 1). All participants carried a loaded ruck (~30 kg), generally stayed together and were allowed to rest as needed. Each participant wore a properly fitting GPS watch (Polar Grit) and an inertial measurement unit (IMU, Xsens DOT) strapped to each medial tibia just above their boots. IMU data were sampled at 60 Hz, calibrated to align with the tibial coordinate system, and used to calculate tri-axial tibial accelerations and stride time using custom algorithms in MATLAB. Synchronized data from the GPS watch were used to capture speed and heart rate. All variables of interest were averaged over the following timepoints to facilitate statistical comparisons: first 4 minutes of uphill walking >10%, first 4 minutes of downhill walking >10%, first 4 minutes of flat walking, each quartile of the total uphill section, each quartile of the total downhill section. Comparisons of the 4-minute sections were made using repeated-measured mixed model analysis. The relationships among distance travelled and slope were made using two-way repeated-measures ANOVA. All statistical analyses were conducted in SPSS.

Results & Discussion: Participants hiked for 177±14 min, of which they rested for 48±6 min. Most metrics showed expected differences between slope conditions, and findings were in line with similar research looking at the effects of running and walking on different slopes. Interestingly, stride times tended to be longer than typical walking gait and were closer in value to those measured during 60% of flat-ground preferred walking speed [3]. Results from the uphill and downhill sections of the hike showed increased acceleration in the 3rd and 4th quartiles of both sections ($p<.03$ for all comparisons), although speed showed corresponding increases ($p<.01$). While increased speed is contrary to the expected effects that might be attributed to fatigue, it is possible that the participants were motivated to complete each portion of the hike as they realized they were getting towards an endpoint. Decreased heart rate through the second half of the uphill section was also unexpected, given that speed increased, although this was inconsistent for the downhill section. These results suggest that the biomechanics of snowshoeing are very similar to changes in gait on other surfaces. The relative magnitudes of the measured metrics during uphill, downhill, and flat snowshoeing reflect similar research on grass, paved, and dirt surfaces [4, 5]. In this study, the cumulative distance travelled was expected to reflect increasing levels of fatigue, particularly for a more challenging task of snowshoeing on moderate sloping conditions. The results are not clearly in support of this hypothesis, as the participants moved faster and with lower heart rate in latter quartiles of the hike.

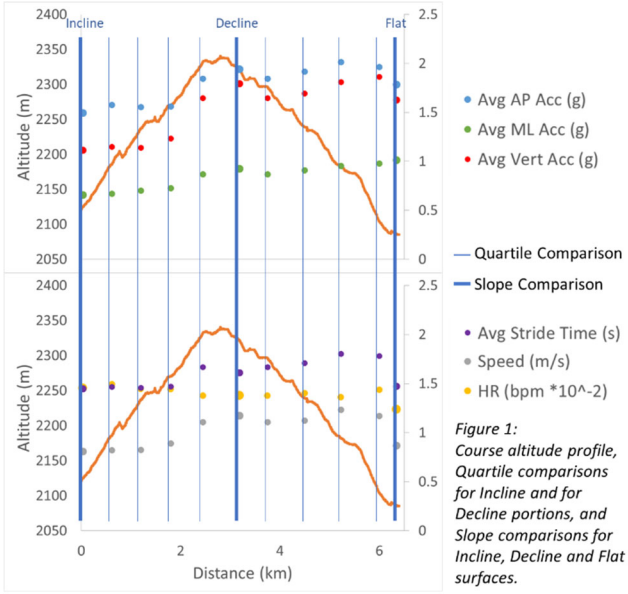

Figure 1: Course altitude profile, Quartile comparisons for Incline and for Decline portions, and Slope comparisons for Incline, Decline and Flat surfaces.

Significance: The results of this study suggest that moderate-distance snowshoeing has similar effects on musculoskeletal loading and physiology as walking, although the stride times tended to be similar to slow walking. Despite the load that was carried, the length and relatively steep grade of the hike, there was no clear indication of significant fatigue over time. These results suggest that snowshoeing is a viable alternative to hiking for both fitness, tactical travel, and bone health.

Acknowledgments: The authors appreciate the Office of Naval Research and the Marine Corps Mountain Warfare Training Center for their support of this research.

References: [1] Browning, (2012), *Sports Biomech* 11(1); [2] Schnieder (2001), *J Exerc Physiol* 4(3); [3] Beauchet (2009), *J Neuroeng Rehabil* 6(32); [4] Waite (2021), *J Appl Biomech* 37; [5] Lafortune (1991), *J Biomech* 24(10)

AGE AND ARM SUPPORT AFFECT BACK AND HIP MUSCLE EXCITATIONS IN SIT TO WALK TRANSITIONS

Michael F. Miller[1*], Eline van der Kruk[2], Anne K. Silverman[1]
[1]Department of Mechanical Engineering, Colorado School of Mines
[2]Department of Biomechanical Engineering, Delft University of Technology
email: *mfmiller@mines.edu

Introduction: Transitioning from standing up to walking is a critical and frequent movement for independent living, referred to as sit-to-walk (STW). STW requires regulating muscle activity to maintain dynamic balance and postural stability to avoid injurious falls [1]. Aging can introduce compensations such as using arm support for rising, but how age and arm support affects muscles responsible for torso movement during STW remains unclear. During sit-to-stand (STS) tasks, rising with arm support from the knees has been shown to reduce torso flexion and increase elbow and knee extension. Smaller torso flexion and mediolateral displacement of the body center of mass (COM) with arm supported push off may reduce the need for lumbar paraspinal (LP) and gluteus medius (GMED) activity [2], two muscles responsible for postural control of the trunk in the sagittal and frontal planes [3]. In addition, aging disproportionately reduces ankle plantarflexion strength, resulting in hip muscle compensations in tasks such as walking [4] and static postural stability [5], which may affect GMED muscle recruitment. The purpose of this study was to quantify the effect of arm supported rising and age on GMED and LP excitation during the STW task. We hypothesized that younger adults would have smaller GMED excitation compared to older adults, and LP and GMED excitation would be smaller when rising with arm supported push off from the knees.

Methods: As part of a larger study, thirty healthy younger (7M/8F, 24.26±4.41 yrs, 709±129.4 N, 1.73±0.10 m) and older (5M/10F, 62.24±6.62 yrs, 809.5±223.4 N, 1.69±0.11 m) adults completed self-paced STW trials. Each trial began with the individual without shoes, with socks, and seated on a backless stool, with both feet arranged in one of four initial positions: symmetric, offset, wide, and narrow. Each foot position was tested with two arm placements: arms folded across the chest and arms supported with hands on the knees. Participants rose from the chair and walked forward several steps at a comfortable speed. The STW task began (0%) when body center of mass (COM) exceeded 0.15 m/s and concluded at toe-off of the stepping limb stance phase (100%). Surface electromyography signals (EMG, Delsys, 2000 Hz) were collected bilaterally from LP and GMED. EMG data were digitally band-pass filtered with a 4th order Butterworth filter (20-500 Hz), full wave rectified, and low pass filtered (fc=6 Hz). Signals were normalized in magnitude by dividing each instant of the filtered signal by the mean peak value of a similarly processed signal on the stance limb of the posterolateral reach during a modified Star Excursion Balance test (SEBT) [6]. The normalized EMG signals were integrated for the time duration of the STW task to compute the integrated EMG (iEMG). iEMG values were averaged over three repeated trials for each arm and foot placement combination. For the purposes of this study, the initial foot position data was pooled to compare age and arm placement effects. A two-factor mixed model ANOVA was used to compare LP and GMED iEMG between age group and arm placement (α=0.05).

Results & Discussion: All participants were right limb dominant, which was also the stepping limb after rising. There was a significant age effect on both the stance limb ($p<0.001$) and stepping limb ($p<0.001$) GMED iEMG values, which supported our hypothesis (Figure). Older adults had 69.1% larger GMED iEMG values on the stance limb and 40.2% on the stepping limb compared to younger adults. These results are consistent with prior walking and rising studies that have shown higher muscle output in hip extension and abduction, like from the GMED, to compensate for postural instability during gait initiation [4]. In addition, there was a significant arm effect on stepping limb GMED ($p=0.04$), stance limb LP ($p=0.005$), and stepping limb LP ($p=0.036$) iEMG, which partially supported our hypothesis. For the GMED, rising with arm support from the knees reduced stepping limb iEMG values by 9.6%. For the LP, rising with arm support from the knees reduced stance limb iEMG values by 15.4% and stepping limb iEMG values by 15.9% compared o the arms folded condition. This smaller LP excitation when rising with arm support is likely due to reduced trunk flexion and the extension moment provided by the arms, resulting in smaller back extension moments. Rising with arm support may have reduced GMED excitation by lessening the demand for torso vertical and lateral stability from a hip abduction torque [3]. Our hypothesis was not supported for the stance limb GMED, which may be a result of that side of the body requiring greater body support during single limb stance [7].

Significance: Rising with arm supported push off reduced LP and GMED excitation during rising and may be recommended for older adults to effectively stabilize the torso.

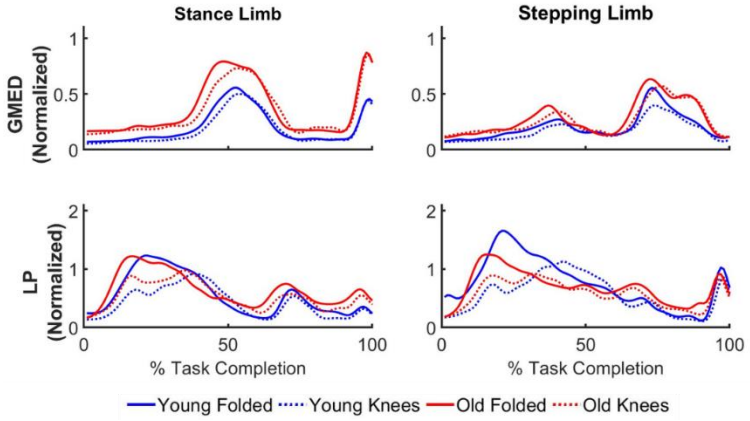

Figure: LP and GMED processed EMG for younger and older adults rising with arms folded and arm support from the knees during sit-to-walk.

References: [1] Alexander, et al., *J Am Geriatr Soc*., vol. 49, 2001. [2] Ansari, et al., *J Chiropr. Med.*, vol. 17, 2018. [3] Sadler S, et al., *BMC Musculoskelet. Disord.*, vol. 20, 2019. [4] McGibbon and Krebs, *J Rehabil. Res. Dev.*, vol. 36, 1999. [5] Amiridis, et al., *Neurosci. Lett.*, vol. 350, 2003. [6] Segal, et al., *J. Biomech.*, vol. 152, 2023. [7] Lee, et al., *J. Phys. Ther. Sci.*, vol. 26, 2014.

CORRELATION BETWEEN ON-BODY INERTIAL SENSORS AND LUMBAR SPINE LOADING DURING MILITARY PARATROOPER LANDINGS

Therese Parr[1,2], Jazmin Cruz[1,2], Hakan Celik[1,3], Ronald Richardson[1], Peter Le[1*]
[1]711th Human Performance Wing, Air Force Research Laboratory; [2]Oak Ridge Institute for Science and Education, Oak Ridge, TN, USA; [3]Innovative Element, Washington, D.C.
*Corresponding author's email: peter.le.3@us.af.mil

Introduction: Military paratroopers are at a high risk of injury, particularly to the lower extremities and lumbar spine/back, due to the high-impact nature of their duties [1]. During parachute landing, paratroopers can experience spinal loading up to 17G [2], which contributes to lumbar spine/back pain and injury risk. Most reports on paratrooper injury risk focus on acute injuries and there is a lack of understanding on how repetitive landing is associated with cumulative injury [1]. Repetitive loading increases muscle force requirements and spinal loading, and likely increases the risks of musculoskeletal injury for high-impact activities [3]. Although lumbar loading is important to assess injury risk for paratroopers, this metric has yet to be quantified in-field. It would be useful to monitor lumbar loading so that both acute and cumulative actions can be captured and guide p(re)habilitation. Recently, the use of wearable sensors, such as inertial measurement units (IMUs), and force measuring insoles, has allowed for the characterization of kinematics and vertical loading in remote/continuous in-field environments. However, typical sensor sets are cumbersome for the user to don and can interrupt paratrooper duties. The development of a sparse sensor set will allow for a more deployable in-field system. Therefore, the objective of this pilot study was to identify features of wearable sensors (i.e., IMUs and insoles) that are strongly correlated with lumbar loading during military paratrooper freefall landings for future feature extraction and loading algorithm development.

Methods: One participant (M, 104 kg, 193 cm) performed two military freefall jumps while wearing a full body IMU suit (MVN Link, Movella™, Inc., Henderson, NV) and bilateral pressure sensor insoles (F-Scan, Tekscan™, Inc., Norwood, MA). IMUs and insole sensors were filtered with a low-pass filter of 20 and 6 Hz, respectively. Using OpenSim (SimTK, Stanford, CA), inverse kinematics, inverse dynamics, and lumbar loading (L5/S1) were calculated. Resulting timeseries lumbar load was compared against timeseries foot, lower/upper leg, pelvis, and thoracic (T8) features (linear acceleration, orientation), as well as insole features (pressure) using Spearman's correlation (ρ).

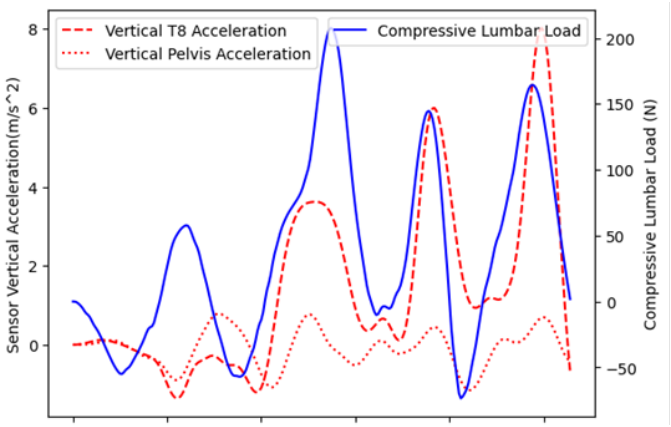

Figure 1: Thoracic and pelvis vertical accelerations vs lumbar load

Results & Discussion: The vertical acceleration from the T8 IMU had the highest correlation (ρ = 0.65; 0.42) with estimated lumbar load for both trials (Figure 1). The vertical acceleration from the pelvis IMU had a low/moderate correlation (ρ = 0.25; 0.30). Insole pressure and lower limb metrics were less correlated, likely because each foot/limb only captures half of the impacts affecting the lumbar spine. There was a weak correlation between lumbar loading and L5/S1 kinematics, likely because there was minimal motion exhibited (<2°). While the most promising sensor metric is the T8 acceleration, it is possible that the lower limb sensors are important in tracking some of the smaller loads that aren't translated to the T8 or pelvis accelerometers but still experienced by the lumbar spine, as seen in the first lumbar load peak in Figure 1. Therefore, because there was varied moderate correlations with individual sensors and a lack of correlations between sensors, freefall landings may require a larger subset of sensors to predict lumbar load. There is an additional need to explore static line landings because they exhibit much greater G forces than freefall and require a dynamic parachute landing fall that involves complex lumbar movements. Future work should include verification with loading calculations from ('gold standard') force platforms and motion capture as well as minimizing sensor metrics needed to predict loading in both landing scenarios.

Significance: In this pilot study of freefall landing, the T8 vertical acceleration had the most correlation to lumbar loads. This will help in the development of a sparse sensor set and algorithm that uses the most important sensor features to estimate lumbar loads in-field practically and accurately. With the quantification of joint loading forces and biomechanics, injury risk can be characterized for high-impact landing scenarios and appropriate interventions can be explored. The use of remote and continuous monitoring to aid in tracking cumulative loading (and capturing acute landing events) can provide individualized clinical insights into optimizing injury prediction, mitigation, and rehabilitation.

Acknowledgements: This work was supported, in part, by an appointment to the DoD Research Participation Program administered by Oak Ridge Institute for Science and Education. The views expressed herein do not reflect the official policy of U.S. Departments of the Army/Navy/Air Force, DoD, nor the U.S. Government. Study protocols were approved by the AFRL Institutional Review Board in compliance with all applicable federal regulations governing the protection of human subjects.

References:

[1]Knapik, et al. (2011) Aviation, Space, and Envt Med, 82(8):797-804. [2]Reid,et al. (1971) Aerospace Medicine, 42(11): 1207-1210.
[3]Orr, et al. (2021) Int J Environ Res Public Health, 18(8): 4010

PERSONALIZED MUSCLE STRENGTH SCALING IMPROVES ACCURACY OF SIMULATIONS OF MILITARY LOAD CARRIAGE

Anna C. Corman[1*], P. H. Sessoms[3], J. T. Sturdy[1], H. N. Rizeq[2,3], T. Whittier[2,3], A. Silder[3], C. Daquino[2,3], A. K. Silverman[1]
[1]Colorado School of Mines, Department of Mechanical Engineering
[2]Leidos, Inc., San Diego, CA, USA; [3]Naval Health Research Center, San Diego, CA, USA
email: * ancorman@mines.edu

Introduction: Musculoskeletal models are often based on median data from a small sample of adults, so strength adjustments may be needed to accurately represent the active duty military population. While strength scaled models are valuable in estimating joint forces [1] and muscle excitations [2, 3] in impaired populations, their effect on an athletic, military population is unknown. Due to many overuse load carriage injuries in the military [4], understanding effects of muscle strength in this population is important. Training that improves physical fitness can reduce injuries [5] and has been recommended to mitigate injuries from military load carriage [6]. The ability to modify muscle strength is a key target of interventions to prevent injury. The purpose of this study was to evaluate the effects of strength scaling on muscle excitation prediction accuracy from simulations of musculoskeletal models.

Methods: Muscle strength was measured with joint-level dynamometry from eight maximum voluntary isometric contractions (MVIC) of the lower limbs and back of 17 active duty participants. Full body motion (120 Hz), ground reaction forces (1200 Hz) and surface electromyography (min ~1200 Hz) were collected to develop and validate simulations of two walking (at 1.15 m/s) conditions: 1) unloaded, and 2) when carrying a 46-kg added load. Muscle group scaling was determined by placing models in the same muscle strength test poses and applying the measured MVIC joint torque. Muscle strengths were scaled so that at least one muscle was maximally activated to resist the applied torque in each joint-level strength test. Two versions of the musculoskeletal model [7] were applied after first adjusting the segment sizes and masses to match each participant: 1) generic, and 2) strength scaled. Muscle recruitment solutions reproducing walking kinematics were determined for both models under both walking conditions using Computed Muscle Control [8]. The generic and scaled simulated muscle excitations were then compared to bandpass filtered (35-400 Hz), full-wave rectified surface electromyography signals from 11 muscles. Simulated excitations and processed EMG signals were both lowpass filtered and the root mean square difference between the two linear envelope curves was computed. Differences between models and between loading conditions were compared using a two-factor, repeated measures ANOVA (α= 0.05).

Results & Discussion: Simulated muscle excitation accuracy improved in scaled models compared to generic models ($p=.003$) and was affected by loading condition ($p<.001$) (Table). Specifically, the longissimus ($p=.040$), iliocostalis ($p<.001$), external oblique ($p=.002$), rectus femoris ($p<.001$), and gluteus medius ($p=.008$) had improved accuracy with scaling. There was also significance between the unloaded and loaded conditions for multiple muscles, highlighting how muscle excitation agreement can change under different walking conditions. These results expand on previous studies that have shown improvements in simulation predictions from populations post-stroke [9] or with cerebral palsy [2, 3]. Impaired populations often are characterized by muscle weakness, whereas an active military population may be stronger than typical generic models. Future work will focus on continual improvement of the strength scaling framework and analysis of simulation outcome metrics associated with injury risk, such as joint contact forces.

Significance: Personalized strength scaling improved muscle excitation predictions in simulations of military service members. Specific muscles were affected, which highlights the importance of scaling task specific muscles to better match the individual. Personalized strength-scaled models will be useful for quantifying injury risks and evaluating training interventions.

References: [1]Knarr *et al.* (2015), *J Biomech* 48(11); [2]Hegarty *et al.* (2019), *J Biomech* 83; [3]Kainz *et al.* (2018), *Gait Posture* 65; [4]"2021 Health Of The Force Report," (2021); [5]Knapik *et al.* (2006), *Mil Med* 171; [6]Knapik *et al.* (2010) *Load Carriage in Military Operations*. Borden Institute; [7]Sturdy *et al.* (2024), *J Biomech* 163; [8]Thelen *et al.* (2003), *J Biomech* 36(3); [9]Knarr *et al.* (2014), *Stroke Res Treat* 2014

 This work was supported by the Military Operational Medicine Research Program (JPC-5) under work unit no. N1814. The views expressed in this article are those of the authors and do not necessarily reflect the official policy or position of the DoN, DoD, nor the U.S. Government. Research data were derived from Naval Health Research Center IRB protocol, number NHRC.2019.0015, which was approved in compliance with all applicable Federal regulations governing the protection of human subjects.

Table: Summary of root mean square differences between simulated and EMG excitation. Muscles with "S" superscript are significant for muscle strength scaling (generic/scaled). Muscles with "C" superscript are significant for condition (unloaded/loaded). Units are normalized excitation.

Condition & Scaling / Muscles	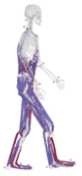 Unloaded		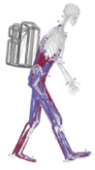 Loaded	
	Generic	Scaled	Generic	Scaled
Overall ^{SC}	.186	.175	.199	.168
Longissimus ^{S}	.076	.064	.082	.061
Iliocostalis ^{SC}	.061	.044	.087	.049
Rectus Abdominis ^{C}	.022	.020	.061	.035
External Oblique ^{SC}	.060	.042	.187	.102
Rectus Femoris ^{SC}	.181	.068	.366	.194
Vastus Lateralis ^{C}	.072	.071	.125	.124
Biceps Femoris	.083	.094	.080	.086
Gastrocnemius ^{C}	.192	.208	.279	.282
Soleus ^{C}	.192	.196	.293	.295
Tibialis Anterior ^{S}	.283	.340	.322	.366
Gluteus Medius ^{SC}	.824	.785	.305	.254

Investigation of hardware and instrumentation to measure hand grasp activity with the spacesuit gloves

Rachel L. Thompson[1*], Kyoung J. Kim[1], William Green[1], Linh Q. Vu[2], Nathaniel J. Newby[1]
[1]KBR, 2400 Nasa Parkway, Houston, TX
[2] Aegis Aerospace Inc., 18050 Saturn Ln, Houston, TX
*Corresponding author's email: rachel.l.thompson@nasa.gov

Introduction: During the 2022 suited injury summit, it was hypothesized that there will be concerns for hand and glove injuries for future exploration space missions, especially given the fact that the "total number of Extravehicular activity (EVA) hours and frequency" for lunar surface missions is expected to vastly increase [1]. It has been reported that the hands experienced the greatest "absolute number" of reported injuries and far exceeds other injuries during EVA [1, 2]. It was reported that the most fatiguing part of the surface EVA was the repetitive gripping tasks [3]. It was recommended that a "glove sub-team" be created to look at possible injury mechanism and mitigation strategies. Some of the recommendations that were suggested [1] are as follows: examine hand fatigue, utilize motion capture, examine the duration and frequency of hand movements, and identify frequent hand motions.

We started assessing hardware and instrumentation to measure hand grasp activity in the pressurized glove environment. The purpose of this test was to perform a hardware evaluation for motion capture (MoCap) gloves obtained from StretchSense (Auckland, New Zealand). The specific gloves used were the Pro Fidelity and SuperSplay to determine the repeatability, reliability, feasibility, and useability inside of a pressurized gloved environment.

Fig. 1: Customized MoCap glove used.

Methods: The MoCap gloves were customized (e.g., battery/Bluetooth pack relocated to upper arm) to better suit the pressurized testing environment and protect the subject from unintentional injury (Fig. 1). Fourteen total subjects from different demographics (i.e., gender and pressurized glove experience level) participated in this test series. Testing included one session each of a baseline data collection (NASA Johnson Space Center (JSC) building 21) and a spacesuit glove box (Fig. 2 at JSC building 7 room 2027) data collection (under vacuum down to 4.3 psid), where each session lasted 3-5 hours. Controlled and reproducible tasks to systematically evaluate the repeatability and reliability of the hardware were performed during baseline data collection. Additionally, subjects performed simulated EVA-like tasks in a pressurized gloved environment. For all sessions, MoCap gloves were placed on each of the subjects' hands and the signal from it, or the raw capacitance (Fig. 3), was analysed. The raw capacitance was used to estimate the open and closed hand states between the testing conditions and allow us to provide an offset caused by the pressurized environment.

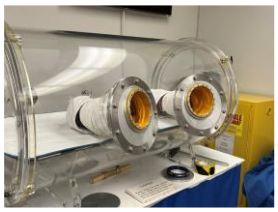

Fig. 2: Glove box used for testing.

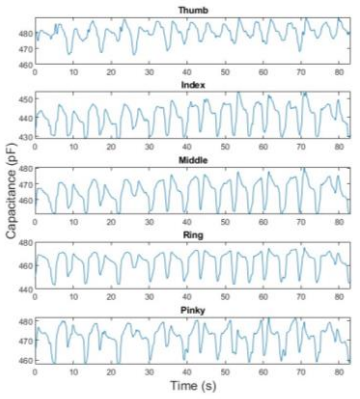

Fig. 3: Raw capacitance data for the object relocation task.

Results & Discussion: Initial observation with the bare hands (baseline) condition showed that the MoCap gloves appeared to track grasping and releasing of the fingers (opening and closing fist) with both high- and low-speed conditions, while adduction and abduction of the fingers were not relatively tracked. A hardware evaluation was done outside of the glove box to assess the reliability and repeatability of the MoCap glove. In one task, a point force was applied to various locations on the back of the hand. When the point force was applied to the space between the 1st digit and the pointer finger, there was a noticeable distortion to the MoCap data. Another task examining an increasing force from a 10 lb. sandbag applied to the back of the hand while lying flat on a table, showed a constant flat line with only a distortion when the weight was increased or added to the back of the hand. Fig. 3 shows an object relocation task where you can see when each individual finger "opened" and "closed" (changed position) when picking up and setting down the dumbbell. When the fingers were stationary, the signal remained relatively flat compared to the peaks and valleys that can be observed in Fig. 3.

This study showed promising results and imperative input into an attempt to discriminate between hand states across various functional tasks and should be evaluated with context to the repeatability and reliability outcomes. Depending on the task done inside of the pressurized glove box environment and outside, the results appear to be affected by many different factors (i.e., drift, pressure, hand size, etc.).

Significance: If this hardware proves to be reliable and repeatable in determining the open and closed hand states then this may provide critical insight into the characterization of the pressurized gloved environment and the effect on crew member exertion level. Ultimately, this tool will provide useful data for quantifying the repetitive nature of EVA training and tasks.

Acknowledgments: The authors would like to acknowledge the NASA Mars Campaign Office for providing funding for this research. Lastly, thanks to all the engineers and technicians at NASA JSC who helped with this data collection.

References: [1] Reiber, et al. (2022), *NASA/TM-20220007605*; [2] Scheuring, et al. (2009), *Av., Sp., and Envir. Med.* 80(2).
[3] Scheuring, et al. (2007), *NASA/TM–2007–214755.*

RIGID OR COMPLIENT: HOW UPPER PANEL STIFFNESS AFFECTS TRAIL RUNNING PERFORMANCE

Adam R. Luftglass[1*], Daniel F. Feeney[1], Eric C. Honert[1]
[1]BOA Technology
email: *adam.luftglass@boatechnology.com

Introduction: Understanding the impact of footwear design on biomechanical variables is essential for enhancing performance and improving athletes' trail running experience. The fit of footwear is critical as trail running shoes must be able to provide stability on uneven terrain [1]. Alterations of the fit in trail running footwear can have marked effects on trail running performance. For example, trail running footwear with a wrap upper (e.g. shoe in Figure 1) can increase running speed and improve footwear fit metrics such as decreased eversion velocity as compared with laced shoes [2]. Optimizing the material characteristics of the wrap structure to conform better to the foot could enhance performance further. For instance, the tensile stiffness of the panels comprising the wrap impacts performance in agility movements in a controlled laboratory setting [3]. The purpose of this study is to assess the impact of the material composition of wrap uppers during trail running. We hypothesize that 15 N/mm stiff panels will produce the best performance as similar material stiffness improved multidirectional performance and qualitative appeal during agility movements.

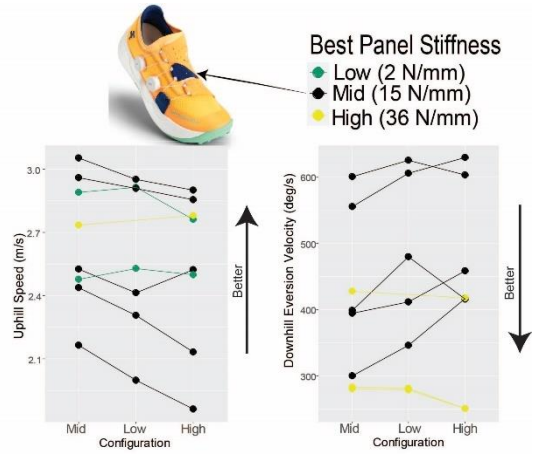

Figure 1: Running speed uphill and peak eversion velocity downhill. Dots indicate subject averages with lines connecting subject performances in each stiffness. Above graphs are a representative image of the shoe condition with the mid stiffness.

Methods: 10 male participants who run at least 24 km a week completed a trail loop in Morrison Colorado that had three sections (uphill: 580m, 4-degree average incline, technical top: 520 m, 2–degree average incline, downhill: 470 m, 6–degree average decline). The athletes wore three footwear conditions while biomechanics data was recorded with IMUs (1125 Hz, IMeasureU, USA) attached to the heel counter, a global positioning system (GPS) watch (1 Hz, Suunto, FIN), and an optical heart rate sensor (1 Hz, Polar Verity Sense, Polar Electro Inc., FIN) attached to the arm. The three footwear conditions only differed in upper panel tensile stiffness (Low: 2 N/mm, Mid: 15 N/mm, High: 36 N/mm). The materials stiffness was computed using a tensile cyclic loading test of 2.5 cm x 15.2 cm samples with a load amplitude of 30 N. The stiffness was determined as the slope of the ramp up of each cycle and averaged over 75 cycles. The primary outcome measures for this study were running speed, heart rate, and peak eversion velocity. IMU metrics were computed for each stride. The outcome metrics were segmented into trail sections for analysis as determined from GPS. After running, participants rated the fit shoes on a scale of 0 to 10 with 10 being the best.

Statistical analysis was performed in RStudio (RStudio Inc, Boston, MA, USA). Outcomes were converted into Z - Scores for each subject and entered into a random intercept, random slope probabilistic model with priors centered on 0. The percent of the posterior greater than zero (post > 0) indicates confidence in improvement. Average percent improvement and post > 0 is represented for all biomechanical outcome measures.

Results & Discussion: The mid stiffness condition increased running speed without increasing heart rate. For the uphill portion, the mid stiffness increased running speed on average by 3% compared to the high stiffness (98% post > 0) and 1% compared to the low stiffness (92% post > 0) with little change in heart rate (59% post > 0 and 34% post >0, respectively). For the top portion, the mid stiffness condition increased running speed on average by 4% compared to the high stiffness (93% post > 0) with little change in heart rate (64% post > 0). The mid stiffness also reduced peak eversion velocity. For the uphill portion, the mid stiffness reduced the eversion velocity on average by 3% compared to the high and low stiffness (87% post > 0, 84% post > 0, respectively). For the downhill portion, the mid stiffness reduced the eversion velocity on average by 6% compared to the low and high stiffness (96% post > 0, 80% post > 0, respectively). Qualitatively, the low stiffness condition received the highest average score (9/10), followed by mid (7.8/10), and then high (7/10).

The mid stiffness panel improved trail running performance along with improved quantitative fit. This aligns with previous findings in agility performance footwear [3]. This study further validates the importance of optimizing footwear upper material stiffness for improved multi-directional movement performance. However, it's essential to note that this study controlled specifically for the tensile stiffness of the wrap, not accounting for drape or conformability. The highest stiffness wrap was the least conformable (lowest drape) and corresponded to the lowest qualitative scores. The non-conformable nature may have also contributed to the decrement in trail running performance. Future studies should explore how drape can enhance affect quantitative and qualitative footwear fit and performance in multi-directional movements.

Significance: In footwear designed for multi-directional sports, there is an optimal level of stiffness (approximately: 15 N/mm for a 2.5 cm x 15.2 cm sample) of upper panels in footwear for peak, multi-directional, performance.

Acknowledgments: We would like to thank Milena Singletary, Bethany Kilpatrick, Kelsey Amoroso, and Kate Harrison for their help with data collections. We would like to thank the athletes as well for their hard work participating in this study.

References: [1] A. Warrick et al., 2019, [2] E. C. Honert et al., 2023, [3] A. R. Luftglass et al., 2023

HEAD IMPACT PROTECTION CAPABILITIES OF HARDWOOD SPORT/PERFORMANCE SURFACES

Paul W. Elliott, PhD, PE[1*], James F Elliott[1]
[1]ASET Services, Inc, Salem IN, USA
*Corresponding author's email: elliottp@asetservices.com

Introduction: Millions of square feet of hardwood sport/performance surfaces are installed annually throughout North America. Current standard specifications such as ASTM F2772[1] exclusively focus on lower extremity impacts. A more holistic approach to safety and testing that considers head impacts along with lower extremity impacts could provide users with a safer surface. Many industries are currently working to prevent, and reduce the severity of TBIs (traumatic brain injuries) during impacts. The sports industry is among those focused on TBIs, and standards have been developed for synthetic turf, playground surfacing, padding and other products. However, indoor surfaces used for sports, and dance, do not yet have a practical, non-destructive test that enables safer products to be selected, specified, or designed. This study selected the HIC (Head Impact Criteria) impact severity index as tested using ASTM F355 [2] as the base test method. The HIC value has known strong relationships to both injury probabilities and injury severity. This was based on the use of a similar test method used to evaluate similar surfaces in the United Kingdom (BS 7044-4 [3]) that was used until 2006.

The purpose of this study was to develop a non-destructive HIC test for hardwood, or area-elastic, sport/dance surfaces, and to determine if hardwood sport/dance system designs can offer meaningful differences in HIC values, or CHF (critical fall height). It included systems similar to legacy systems that are decades old but still in use, currently produced systems, and prototype systems.

Methods: The 10 lbs hemispherical 'E-missile' from ASTM F355 was selected as the basic test method. The missile is released from a given height and freefalls onto the test specimen, where the corresponding g-max (maximum deceleration) and HIC values, and Δt (duration used for HIC computation) were recorded. A ¼ in (6 mm) thick urethane sheet with a Shore A hardness exceeding 80 above the test surface produced no damage when testing Hard Maple surfaces. The CFH, or the theoretical height associated with an HIC=1000, for each system was computed using linear regression

A total of 6 systems were tested. Samples 1-5 all used the same wood system design over different elastic layers. Samples 1 and 2 represent elastic layers currently used in current systems. These elastic components are used in systems that meet various standard specifications. Sample 3 represented a possible future design and utilized a ¾ in thick prototype cushioning material. Sample 4 represents some of the harder, but still resilient systems, and utilized a continuous sheet of ¼ in thick closed cell foam. Sample 5 was unpadded system, and it represents numerous legacy systems without resilient components that are still being used in facilities throughout North America. Sample 6 is another current structural design and foam over current ½ in individual foam pads.

Results & Discussion: Figure 1 contains the computed CFH values for the 6 test samples. Table 1 contains the Δt values for all test samples. During the testing, all samples except #5 produced a Δt for the HIC calculation of 3.0 ms or greater. The HIC calculation was developed from the Wayne State Study, and because that study does not include impact pulses below 3.0 ms in the test data, the HIC value for sample 5 was not considered valid. Sample 5 was therefore excluded from consideration. The CFH values for the remaining 5 samples ranged from 2.5 ft to 5.1 ft. The same impact severity (HIC = 1000) is generated at each CFH. This means that the probability of a given injury from a fall of 4.3 ft on sample 2, is the same as the probability for that same injury from a fall of only 2.5 ft on sample 4. The HIC values generated on each sample from a fall of 3 ft are provided in Table 1. The relationship between injury probability for a given AIS injury severity and HIC values, known as the expanded Prasad Mertz (NHTSA [4]) equations, was used to estimate the probability of an AIS 3 injury at 3ft for 4 samples. The injury probability estimates are provided in Table 1. The results from the expanded Prasad-Mertz equations suggests that a fall from 3ft on Sample 3 would have a 9% chance of and AIS 3 head injury, while a 15-16% chance of the same injury occurs on the other 3 samples. HIC testing conducted using the 'E' missile, and a modified version of ASTM F355 was shown to be able to differentiate the fall protection afforded of existing sport/dance surfaces. HIC values also suggest that facilities can provide safer surfaces by replacing harder legacy systems with current more resilient systems.

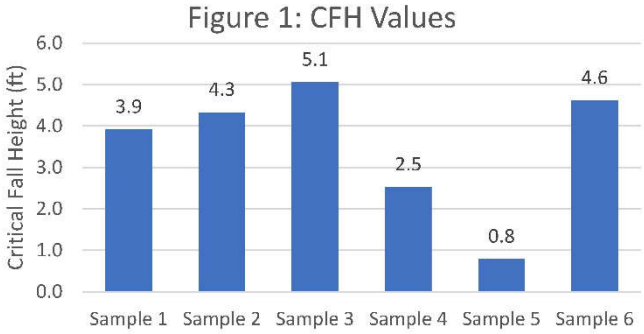

Table 1: Additional Statistics

Sample→	1	2	3	4	5	6
Δt (ms)	3.5	3.1	3.0	3.6	1.3	4.3
HIC @ 3ft	568	561	420	NA	NA	547
AIS3 Injury Probability @ 3ft	16%	15%	9%			15%

Significance: The results showed that a non-destructive HIC based standard method can be developed for hardwood sport/dance systems using existing ASTM standard test methods. HIC based testing provides a more holistic approach to impact attenuation that considers head impacts in addition to lower extremity tests. HIC based evaluations offer designers, and specifiers of hardwood sport/dance systems the ability to reduce the severity and risk of injury to participants through product development, selection and specification.

Acknowledgement: This project was funded in part by Action Floors, LLC of Mercer Wisconsin.

References: [1] ASTM F2772(2019), [2] ASTM F355(2016), [3] BS7044-4 (1991), [4] NHTSA, 6-1995 FMVSS No. 201

A UNIFORMITY INDEX, AND UNIFORMITY CLASS SYSTEM FOR SPORT/DANCE SURFACES USING FORCE REDUCITON

Paul W. Elliott, PhD, PE[1], James Elliott[1]
[1]ASET Services, Inc, Salem IN, USA
*Corresponding author's email: elliottp@asetservices.com

Introduction: Athlete's adjust the stiffness of their legs in response to the stiffness of the surface they are on (Ferris[1]). It makes sense that non-uniform stiffness levels result in constant adaptation by the athlete. Sport/Dance surfaces are tested and specified to a variety of specifications that include international standards, trade organizations, and governing bodies but none of these standards currently quantify uniformity. International standards (F2772[2], ANSIE1.26[3]), governing bodies (FIBA[4]), and trade associations(MFMA-PUR™[5]) have all recognized that uniformity is important, and adopted basic uniformity requirements. All current standards require all force reduction (ASTM F2569[6]) values fall within ±5% from the average, and all products that meet this basic requirement are considered equal. This system does not encourage the design of, or allow the specification of, more uniform performance.

The goals of this study were, i) to develop a meaningful Force Reduction Uniformity Index (FR-UI) of a sport/performance system, and ii) to determine if 'passing' systems have varying uniformity levels, iii) to propose a Force Reduction Uniformity Class (FR-UC) ranges that would allow systems with similar uniformity characteristics to be specified and selected.

Methods: The general method for Force Reduction testing can be found in ASTM F2569[6], but there are numerous harmonized versions published and used around the world. ASTM F2772 is just one of many specifications that require force reduction levels for all points to be within ±5% of the average. All samples within this study met this generic uniformity requirement. All tests for this study were conducted in a laboratory setting on hardwood systems measuring nominally 12ft x 12ft. The results from 15 wood, or area elastic, samples were used as the sample set for this study. Each sample was tested at 8 locations selecting a variety of structural conditions, in an attempt to capture the 'hardest' and 'softest' points within the design.

The FR-UI was computed by assuming a normal distribution of results and calculating the probability that a result would be within a given range around the average. Because all uniformity calculations would be performed using data from the same lab, on the same sample repeatability limits were used as a guide for selecting the initial uniformity range. ASET Services has participated in multiple round-robin test programs through the ISSS (Association for International Sport Surface Scientists), to determine the repeatability of the Force Reduction Test method. These studies routinely report repeatability for this method to be in the range of 0.5% to 1.7%. This study chose to use a range of ±2% to compute the FR-UI_2, in an attempt to minimize the effect of the uncertainty of the measurement method.

Computation of the FR-UI assumes a normal distribution of force reduction levels across the floor, and computes the probability, to the nearest whole percent, that a force reduction value lies within ±2% of the average, or P(avg-2.0 ≤ FR ≤ avg+2.0). The range of FR-UI_2 values produced by the systems in the sample study was then used to develop proposed Force Reduction Uniformity Classes, or FR-UC_2.

Results & Discussion: Table 1 contains the average, and standard deviation, of the force reduction measurements for each sample. study. All samples met basic uniformity requirements (all values within ±5% from the average). The uniformity index, or FR-UI_2, was then computed for each sample, and is also shown in Table 1. Uniformity index values range from a low of 45% to a high of 99% even when all samples met the basic requirement.

Uniformity classes (FR-UC_2) were developed from FR-UI_2 values, and are presented in Table 2. Considerations were given to the distribution of index values, as well as logical numeric breaks. Class 1 consists of FR-Ui_2 values ≥ 90; 4 samples (27%); Class 2 includes FR-UI_2 values from 80 to 89, 2 samples (13%); Class 3 includes FR-UI_2 values from 70 to 79, 7 samples (47%); Class 4 includes FR-UI_2 values from <70, 2 samples (7%).

Significance: This study found that the uniformity of sport/dance systems can vary widely within product groups that meet the same standard. The proposed Uniformity Index and Uniformity Class system allow for the development, selection, and specification of more uniform systems that may reduce the need for athletes to adapt to a variable surface stiffness.

Table 1: Average, Standard Deviation, and FR-UI_2 Values

Sample ID	1	2	3	4	5	6	7	8
Avg	61	57	57	60	63	62	61	62
StDev	0.74	0.99	1.51	3.38	0.99	1.89	0.74	1.98
FR-UI_2	99	96	81	45	96	71	99	69
Sample ID	**9**	**10**	**11**	**12**	**13**	**14**	**15**	
Avg	63	56	62	60	63	62	62	
StDev	1.69	1.36	1.91	1.85	1.69	1.89	1.89	
FR-UI_2	76	86	71	72	76	71	71	

Table 2: Proposed FR-UC_2 Uniformity Classes

FR-UC_2	FR-UI_2 Range	FR-$UI_{2.5}$ Distribution	
		Count	Percentile
Class 1	90 to 100	4	27%
Class 2	80 to 89	2	13%
Class 3	70 to 79	7	47%
Class 4	< 70	2	13%

Acknowledgement: This project was funded in part by Action Floors, LLC of Mercer Wisconsin.

References: [1] Ferris et al. (1999), J Biomech Aug 32(8); [2] ASTM F2772(2019); [3] ANSI E.16 (2022); [4] FIBA rules 2019, [5] MFMA-PUR standard, www.maplefloor.org/en/pur-standards/, (2024); [6] ASTM F2569, (2019)

A UNIFORMITY INDEX, AND UNIFORMITY CLASS SYSTEM FOR SPORT/DANCE SURFACES USING FORCE REDUCITON

Paul W. Elliott, PhD, PE[1], James Elliott[1]
[1]ASET Services, Inc, Salem IN, USA
*Corresponding author's email: elliottp@asetservices.com

Introduction: Athlete's adjust the stiffness of their legs in response to the stiffness of the surface they are on (Ferris[1]). It makes sense that non-uniform stiffness levels result in constant adaptation by the athlete. Sport/Dance surfaces are tested and specified to a variety of specifications that include international standards, trade organizations, and governing bodies but none of these standards currently quantify uniformity. International standards (F2772[2], ANSIE1.26[3]), governing bodies (FIBA[4]), and trade associations(MFMA-PUR™[5]) have all recognized that uniformity is important, and adopted basic uniformity requirements. All current standards require all force reduction (ASTM F2569[6]) values fall within ±5% from the average, and all products that meet this basic requirement are considered equal. This system does not encourage the design of, or allow the specification of, more uniform performance.

The goals of this study were, i) to develop a meaningful Force Reduction Uniformity Index (FR-UI) of a sport/performance system, and ii) to determine if 'passing' systems have varying uniformity levels, iii) to propose a Force Reduction Uniformity Class (FR-UC) ranges that would allow systems with similar uniformity characteristics to be specified and selected.

Methods: The general method for Force Reduction testing can be found in ASTM F2569[6], but there are numerous harmonized versions published and used around the world. ASTM F2772 is just one of many specifications that require force reduction levels for all points to be within ±5% of the average. All samples within this study met this generic uniformity requirement. All tests for this study were conducted in a laboratory setting on hardwood systems measuring nominally 12ft x 12ft. The results from 15 wood, or area elastic, samples were used as the sample set for this study. Each sample was tested at 8 locations selecting a variety of structural conditions, in an attempt to capture the 'hardest' and 'softest' points within the design.

The FR-UI was computed by assuming a normal distribution of results and calculating the probability that a result would be within a given range around the average. Because all uniformity calculations would be performed using data from the same lab, on the same sample repeatability limits were used as a guide for selecting the initial uniformity range. ASET Services has participated in multiple round-robin test programs through the ISSS (Association for International Sport Surface Scientists), to determine the repeatability of the Force Reduction Test method. These studies routinely report repeatability for this method to be in the range of 0.5% to 1.7%. This study chose to use a range of ±2% to compute the FR-UI_2, in an attempt to minimize the effect of the uncertainty of the measurement method.

Computation of the FR-UI assumes a normal distribution of force reduction levels across the floor, and computes the probability, to the nearest whole percent, that a force reduction value lies within ±2% of the average, or P(avg-2.0 ≤ FR ≤ avg+2.0). The range of FR-UI_2 values produced by the systems in the sample study was then used to develop proposed Force Reduction Uniformity Classes, or FR-UC_2.

Results & Discussion: Table 1 contains the average, and standard deviation, of the force reduction measurements for each sample. study. All samples met basic uniformity requirements (all values within ±5% from the average). The uniformity index, or FR-UI_2, was then computed for each sample, and is also shown in Table 1. Uniformity index values range from a low of 45% to a high of 99% even when all samples met the basic requirement.

Uniformity classes (FR-UC_2) were developed from FR-UI_2 values, and are presented in Table 2. Considerations were given to the distribution of index values, as well as logical numeric breaks. Class 1 consists of FR-Ui_2 values ≥ 90; 4 samples (27%); Class 2 includes FR-UI_2 values from 80 to 89, 2 samples (13%); Class 3 includes FR-UI_2 values from 70 to 79, 7 samples (47%); Class 4 includes FR-UI_2 values from <70, 2 samples (7%).

Significance: This study found that the uniformity of sport/dance systems can vary widely within product groups that meet the same standard. The proposed Uniformity Index and Uniformity Class system allow for the development, selection, and specification of more uniform systems that may reduce the need for athletes to adapt to a variable surface stiffness.

Table 1: Average, Standard Deviation, and FR-UI_2 Values

Sample ID	1	2	3	4	5	6	7	8
Avg	61	57	57	60	63	62	61	62
StDev	0.74	0.99	1.51	3.38	0.99	1.89	0.74	1.98
FR-UI_2	99	96	81	45	96	71	99	69
Sample ID	**9**	**10**	**11**	**12**	**13**	**14**	**15**	
Avg	63	56	62	60	63	62	62	
StDev	1.69	1.36	1.91	1.85	1.69	1.89	1.89	
FR-UI_2	76	86	71	72	76	71	71	

Table 2: Proposed FR-UC_2 Uniformity Classes

FR-UC_2	FR-UI_2 Range	FR-$UI_{2.5}$ Distribution	
		Count	Percentile
Class 1	90 to 100	4	27%
Class 2	80 to 89	2	13%
Class 3	70 to 79	7	47%
Class 4	< 70	2	13%

Acknowledgement: This project was funded in part by Action Floors, LLC of Mercer Wisconsin.

References: [1] Ferris et al. (1999), J Biomech Aug 32(8); [2] ASTM F2772(2019); [3] ANSI E.16 (2022); [4] FIBA rules 2019, [5] MFMA-PUR standard, www.maplefloor.org/en/pur-standards/, (2024); [6] ASTM F2569, (2019)

BODY SWAY BETWEEN MINIMAL AND EXPERIENCED WEIGHT TRAINING GROUPS DURING DUMBBELL FARMER'S WALK EXERCISE

Joyce Blandino[1*] and Mike Krackow[2]
[1]Department of Mechanical Engineering, [2]Department of Human Performance and Wellness Virginia Military Institute, Lexington, VA, USA
*Corresponding author's email: blandinojk10@vmi.edu

Introduction: The farmer's walk has become a normal exercise in training programs for individuals ranging from novice to elite athletes [1]. Studies showed that this exercise can increase core strength, as well as the strength in the upper and lower extremities, resulting in an improvement in trunk stability and overall balance during walking [2-3]. This exercise mimics common functional activities people perform daily by carrying loads on one side of the body (asymmetrical) or with two hands (symmetrical). An asymmetric load (15%-20% BW) resulted in an increase in hip abductor muscle activity and lateral trunk sway toward the non-loaded side to counteract load [4]. Previous studies demonstrated that subjects (novice and those with more weight training experience) can perform farmer's walk exercise (asymmetric and symmetrically) without affecting ankle and hip stresses and lateral trunk sway at 15% body weight [5-6]. It is unclear whether having weight training experience provides subjects with better trunk control when performing the farmer's walk exercise carrying a heavier weight. The objective of this study was to compare lateral sway during dumbbell farmer's walk at 20% BW symmetrically and asymmetrically between subjects with minimal weight training exercise and those with more years of strength training exercise.

Methods: Seventeen healthy subjects (7 Females, 10 Males, aged 32.8±16.0 years) participated in the study. The average body weight was 83.0±17.6 kg. Subjects were separated into two weight/resistance training experience groups: minimal (n=7, 0-2 years' experience) and experienced (n=10, >3-41 years' experience). Retro-reflective markers were placed on feet, shanks, thighs, chest, and lower back. Each subject performed three repetitions of the farmer's walk. Each subject walked on the force platform, with no load and carrying 20% body weight (BW) both symmetrically and asymmetrically (left and right) (Figure 1). Eight VICON Vero cameras were used to gather kinematic data at 200Hz. The Motion Monitor xGen software (TMMxGen) was used to collect data from both VICON cameras and the force platforms simultaneously. Subjects were given a one-minute rest period between tests. An independent Sample T-test was used to compare thorax position between minimal and experienced group for each load condition.

Figure 1: Symmetric load (*left*) Asymmetric load with left hand (*right*) for Farmer's walk exercise

Results & Discussion: When performing dumbbell farmer's walk exercise with a heavier load (20%BW), it is expected that subjects with more weight training experience would have better control of their body and less trunk sway during the single leg stance phase of the gait cycle as compared to those with minimal weight training experience. These preliminary findings demonstrated that there was no statistical difference in lateral trunk sway between subjects with minimal weight training experience and those had more experience. The result of this study showed that prior strength training experience is not necessary when performing the farmer's walk exercise while carrying 20% of the subjects' body weight.

Significance: Results of this study indicated that there was no significant difference in lateral trunk sway when performing the farmer's walk exercise between subjects with minimal weight training experience and those with more weight training experience with heavier loads. The preliminary findings suggest that it is safe for beginners to perform the farmer's walk exercise with 20% of their body weight as their base strength training routine.

Acknowledgements: The VMI Institutional Review Board approved testing protocol. This project was supported by funding from the VMI Center for Undergraduate Research.

References: [1] Winwood et al. (2014), *Int J Sports Sci Coach* 9(3): 1127-1143; [2] Stastny et al. (2015), *J Human Kinetics*, 45: 147-165; [3] Graber et al. (2021, *J Applied Biomech* 37(4): 351-358; [4] Fowler et al. (2006), *Gait and Posture* 23: 133-141. [5] Blandino et al. (2022), ASB2023 conference posters-part 1 page 37. [6] Krackow and Blandino (2022), ASB 2023 conference posters-part 1 page 45.

COMPARISON OF FOUR METHODS USED IN GAIT ANALYSIS: 6DOF, INVERSE KINEMATICS, AND TWO OPENSIM METHODS WITH TWO DIFFERENT CONSTRAINTS

Yinjie Zhou[1], Itay Coinfman[2], Raziel Riemer[2*]
[1]Mechanical Engineering, [2]Industrial Engineering and Management,
Ben-Gurion University of the Negev, Beer-Sheva, Israel
*Corresponding author's email: rriemer@bgu.ac.il

Introduction: Inverse dynamics, a key method in biomechanical analysis of human motion, relies on markers, ground force, and segment properties [1]. However, it is prone to errors in motion capture, segment property estimations, and skin movement [2]. Various inverse dynamics methods have been developed to mitigate these errors, with most labs opting for commercial (e.g., Visual3D, Vicon Nexus) or open-source (e.g., OpenSim) software. Some differences in joint angle, torque, and power calculations across methods have been found in walking and dancing [3]. Notably, these software programs, which have several algorithms that can be use Visual3D (6DOF and inverse kinematics [IK]) and OpenSim, have different weights for the markers. Additionally, running—another common activity—has not been tested. Thus, our study aimed to compare four inverse dynamics methods: Visual3D's 6DOF and IK, and two OpenSim methods. Visual3D's 6DOF method treats segments as independent entities connected to joints, while IK imposes constraints between segments. OpenSim uses global optimization, wherein each joint is constrained by anatomical linkage constraints according to the model of choice [3]. Our objective was to assess whether these methods yielded different kinetics and kinematics during walking and running.

Methods: To assess the differences in joint angles, moments, and power during walking and running, data from two experiments (each with 4 females and 4 male participants) were analyzed. Joint angles, moments, and power were calculated using four methods: 6DOF, IK, OpenSim with uniform weights (OSU), and OpenSim with different weights (OSW). For the Visual3D 6DOF and IK methods, a hybrid model was developed using anatomical landmarks to define the joint centers and rotation axes. Static trial data were utilized for calibration, with two algorithms employed for inverse dynamics calculation. OpenSim calibration involved aligning and fine-tuning biomechanical models using static trials. Data analysis employed linear mixed models to assess differences between methods, with significance set at $P < 0.05$. In addition, practical differences were defined as 10% error and absolute for angle (> 5º), moment (> 10 Nm), and power (> 45 W), ensuring real-life relevance.

Results and Discussion: The findings revealed that for all cases the study showed that the two methods used in Visual3D (6DOF and IK) were similar. This was also true for the two methods used in OpenSim. Differences between the two software's were found for -joint angle for the ankle and knee, there was no difference between the methods. At the hip, and differences between Visual3D and OpenSim method had a range of 5.7 º–9.4º. When analyzing joint moments and power, more significant differences were observed in ankle moments (19.5 Nm–33.15 Nm), hip adduction moments (41 Nm–49.4 Nm) during running, and knee moments (10.45 Nm–15.6 Nm) during walking. The power analysis showed significant differences across various joint angles in running and ankle power (Figure. 1) and in the knee and hip during walking and running (54 W–309 W). Overall, In the running data, there were more significant p-values compared to walking, indicating a stronger influence of methodological variations on the running movement analysis. When considering moment and power analysis, more differences were found between the Visual3D and OpenSim methods. We believe that these differences might stem from different calculations of accelerations and treatment of ground reactions.

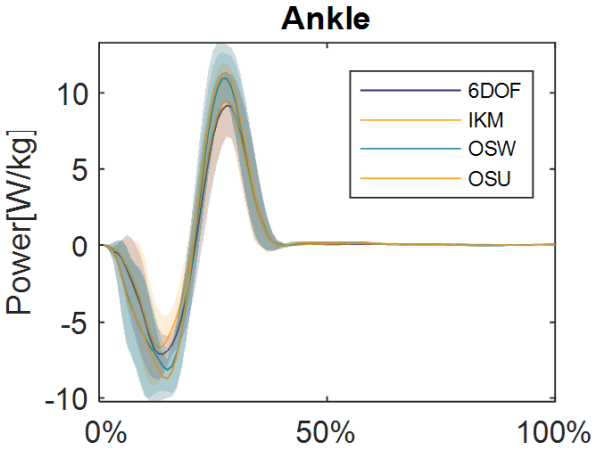

Figure 1: Example of differences in power during running the shaded area resemble 1 standard deviation of the subjects for each method. Average mass 61.4 Kg

Significance: The results of this study show that for sagittal joint angles, there are small or no differences between the methods used. Thus, the choice of method does not matter. However, in hip abdication, there was a greater difference. This aligns with previous findings for walking and dancing [3]. It should be noted that Visual3D and OpenSim have different methods for treating ground force. Although we used the same filtering and so on for both methods, it seems that there were still differences in ground force treatment in each of the methods.

Acknowledgments: This study was partially supported by Israel's Ministry of Science and Technology and the Helmsley Charitable Trust through the Agricultural, Biological, and Cognitive Robotics Initiative of Ben-Gurion University of the Negev.

References

[1] D. A. Winter. (2009). *Biomechanics and Motor Control of Human Movement*, (4th ed.). Hoboken, NJ: Wiley.
[2] R. Riemer et al. (2008). Uncertainties in inverse dynamics solutions: A comprehensive analysis and an application to gait. *Gait & Posture*, *27*(4), 578–588.
[3] A. Am et al. (2019). Effect of two different pose estimation approaches on lower extremity biomechanics in professional dancers. *Annual International Conference of the IEEE Engineering in Medicine and Biology Society.*

LIGAMANT KNEE BRACE DISTAL MIGRATION WHEN LOOSENED AT THE SHANK AND THIGH

Bethany Kilpatrick[1]*, Eric C. Honert[1], Milena Singletary[1], Adam Luftglass[1] Kathryn Harrison[1], Daniel Feeney[1]
[1]BOA Technology Inc.
*Corresponding author's email: bethany.kilpatrick@boatechnology.com

Introduction: It is commonplace to don a functional ligament knee brace post ACL surgery or in sports play as a preventative measure for stabilizing the knee and ACL. Apart from incorrect donning, ligament knee braces migrate distally due to repetitive flexing movements during physical activity [1]. This misalignment can negatively affect knee mechanics [2]. For proper alignment and migration mitigation, ligament knee braces have two tightening zonal components: the thigh straps and the shank straps. It is currently unknown which components of a ligament knee brace are most important for limiting distal migration. The purpose of this study was to examine the relative importance of the thigh and shank straps on ligament knee brace distal migration. We hypothesized that due to the curvature of the gastrocnemius, it would be a "catch-all" for the brace sliding downward and therefore, limit distal migration compared to a loose thigh strapped zone.

Methods: Ten(4F) subjects participated in this study. A Breg Fusion ligament knee brace (Carlsbad, CA, USA) was used for three brace conditions: Subject-Preferred brace strap tightness (PREF), Loose Thigh Straps (THI), Loose Shank Straps (SHK). For the loose zone conditions, the brace straps in the respective regions were loosened five millimeters from the marked PREF baseline. After the end of each brace condition, the brace was reset to the correct donning position. After the brace condition was donned, the subjects were instructed to walk around the space and do a series of five squats, adjusting the brace into place as needed before the data collection began. Subjects were not allowed to adjust the brace during data collection. The brace conditions were tested in a randomized order. Testing consisted of two agility drills: eight vertical counter-movement jumps and eight lateral skater jumps. After the agility drills, subjects walked at 1 m/s on an inclined treadmill, uphill and downhill, at 10 degrees. After the walking trial, the subjects performed another set of agility drills. To measure brace movement, standing static trials were taken before and after each activity for a total of four static trials (Fig. 1). Kinematic data were collected using 3D motion capture cameras (200Hz, Vicon, USA). Subjects were outfitted with reflective marker cluster sets on the pelvis, thigh, shank, and foot as well as a marker set on the brace. The vertical position of the brace was measured as the distance between the brace markers and the floor. Maximum and minimum knee joint angles were measured in the sagittal and frontal planes to calculate ROM. Data were analyzed from the counter-movement jump and processed in Python, with statistical analysis performed in R. Data were converted into Z-Scores for each subject and entered a random intercept, random slope probabilistic model with priors centered on 0. Data are presented as the percent of the posterior mass above or below 0 as well as a 95% credible interval (CI).

Table 1: Means and standard deviations for the in sagittal and frontal ROM degrees from the first and second counter-movement jumps.

Condition	Brace Migration	Knee Flex. ROM (deg)	Knee Frontal ROM (deg)
PREF	-7.46(3.7)mm	70.8(11.8)	9.28(3.4)
THI	-4.85(3.6)mm	68.5(12.9)	10.5(3.6)
SHK	-5.56(3.7)mm	68.8(11.6)	9.57(2.5)

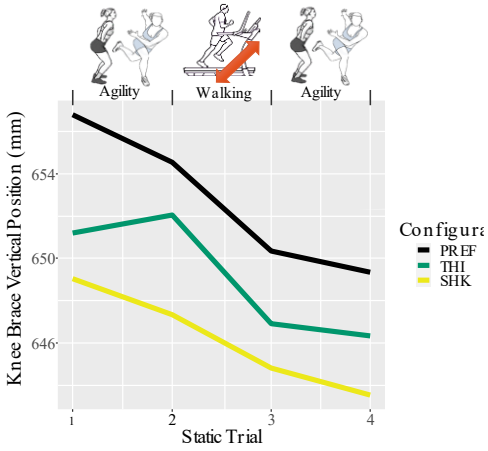

Figure 1: The brace conditions PREF, THI and SHK vertical positions on the leg at each standing static trial.

Results & Discussion: The THI (99% posterior < 0, CI: -0.8 to 0.3%) and SHK (100% posterior < 0, CI: -1.2 to 0.5 %) conditions started and ended physically further on the leg than the PREF condition (Fig.1). Due to the ill-fitting nature of the loose conditions, the brace likely fell before the first static trial, during pre-test physical activity, limiting the opportunity for them to migrate further. This would explain why PREF had a more migration during testing (Fig. 1). Both the THI (91% < 0, 95% CI:-4.6 to -0.1%) and SHK (78%< 0, 95% CI: -4.3 to 1%) conditions similarly reduced knee flexion ROM, compared to the PREF, due to being farther down on the leg, impeding joint movement. In the frontal plane ROM, however, the THI (86% < 0, 95% CI:-1.2 to 14.7%) had markedly higher ROM than the SHK (45% < 0, 95% CI: -5 to 5.8%) (Table 1). Due to the SHK condition being further distal on the leg, all ROM was reduced, although technically beneficial in the frontal plane. It is known that when the brace is donned in the correct position, knee joint function is less hazardously impeded [2]. However, it has not been previously tested which is more detrimental: to have a worse fit in the thigh or shank zones of the brace. Our hypothesis that the widest part of the gastrocnemius would be a key area to knee brace migration, was not supported. The THI condition fell nearly an equal amount to the SHK condition and had similar negative knee biomechanical outcomes.

Significance: This was the first study to investigate zonal components of a ligament knee brace. Both thigh and shank posterior straps similarly impact brace migration and knee joint kinematics demonstrating that both zones are equally important for injury prevention and should be considered in the design of future ligament braces.

References: [1]Miller et al., (1999) *Journal of Sport Rehabilitation*, *8*(2), 109–122.,[2] Singer, J. C., & Lamontagne, M. (2008). *Clinical Biomechanics*, *23*(1), 52–59.

USING KINEMATICS TO DEFINE POSTURES DURING PATIENT-HANDLING TASKS

Yeageon Song, Elsa Brillinger*, Regina Vicente, Taylor Novotny, Gabriel Wolthuis, Brooke Odle
Hope College, Hope College, Holland, MI, USA
*Corresponding author's email: elsa.brillinger@hope.edu

Introduction: Patient-handling tasks (PHT) involve lifting, lowering, pivoting, pushing, and pulling; and have been associated with incidences of musculoskeletal pain and injury (particularly at the low back) in nursing personnel [1]. Definitions for "good" and poor" posture vary in the literature. In the literature, PHT task performance is typically based on trunk flexion only. However, tasks like lifting a patient from a wheelchair or bed rely on knee flexion more than trunk flexion. Due to the multi-joint coordination required for PHT performance, we expected an approach based on trunk, hip, and knee flexion would provide consistent definitions for "good" and "poor" postures. Assuming that one may not instantaneously shift from "good" to "poor" posture, we also expected a window to emerge between these two thresholds. We have named this window the "neutral" posture.

Table 1: Thresholds for Tasks I – V (Treatment Table)

	Good (°)	Neutral Low (°)	Neutral High (°)	Poor (°)
Trunk	< 19.2 ± 3.6	26.3 ± 4.1	29.3 ± 3.8	>32.8 ± 4.4
R Hip	< 26.2 ± 7.2	33.1 ± 8.1	37.7 ± 9.0	>38.3 ± 8.0
L Hip	< 30.7 ± 8.9	38.4 ± 9.1	42.9 ± 9.8	>44.2 ± 9.6
R Knee	< 13.0 ± 4.4	15.8 ± 6.1	21.4 ± 5.7	>16.2 ± 4.5
L Knee	< 17.9 ± 4.6	19.9 ± 5.8	24.5 ± 6.7	>21.4 ± 6.2

Table 2: Thresholds for Task VI (Wheelchair)

	Good (°)	Neutral (°)	Poor (°)
Trunk	< 32.3 ± 7.5	32.3 - 34.5	>34.5 ± 7.9
R Hip	>66.9 ± 5.6	51.7 - 66.9	< 51.7 ± 7.9
L Hip	>67.9 ± 8.4	55.7 - 67.9	< 55.7 ± 8.4
R knee	>53.0 ± 9.9	29.0 - 53.0	< 29.0 ± 9.7
L Knee	>49.7 ± 1.6	29.1- 49.7	< 29.1 ± 8.5

Methods: Five subjects without nursing experience or PHT training were recruited (4 male, 1 female, ages 18-26). Four iPhone XRs and OpenCap [2] software were used to collect and analyze the data. Six tasks were collected: (i) rolling a patient on the side, (ii) sitting a patient up from supine position, (iii) lifting a patient's leg, (iv) adjusting a patient in bed using a slide sheet, (v) placing a sling under a patient, and (vi) lifting a patient from a wheelchair. Tasks i – v were performed on a treatment table, which was adjusted to hip height, mid-thigh height, and knee height to elicit "good", "neutral", and "poor" postures, respectively (based on [3]). For consistency across trials and subjects, patient-handling manikins (20 kg, 30 kg, 50 kg) served as "patients". Subjects elicited "good" posture during Task vi by using their legs more than their back to lift the manikins. Subjects elicited "poor" posture by using their trunk more than their legs to lift the manikin. Table height, manikin weight, task, and posture type were randomized. Each task and posture type were captured three times per trial. Two trials were captured for each task, posture type, and manikin weight. Subjects reported ratings for perceived stress at the low back [4] and effort [5] during task performance. Five-point Likert-type scales were used to report perceived safety and comfort during task performance. We assumed "good" posture would result in trunk flexion angles of 0° - 20° [3] and "poor" posture would exceed 45° [6]. The minimum and maximum trunk, hip, and knee flexion angles elicited for all tasks were averaged across subjects and used to determine thresholds. Ratings from the surveys were analysed using a Wilcoxon signed rank test in SPSS.

Results & Discussion: Data from one subject were excluded from analyses due to inconsistencies. Mean trunk flexion angles for Tasks i – v performed with "good" posture (Table 1) were consistent with the literature [3]. Since knee flexion did not change much across the posture types, it may not be a suitable metric for tasks performed on a treatment table. As expected, mean bilateral knee flexion was much greater than trunk flexion for Task vi (Table 2). Mean trunk flexion was similar across all three posture types, which suggests that it may not be a suitable metric for lifting tasks. Ratings for perceived comfort ($z = 3.836$, $p < .001$) and safety ($z = -2.588$, $p = .01$) were significantly higher for "good" posture compared to "poor" posture. This is consistent with recommendations that PHTs on treatment tables be performed with the table height as close as possible to the nurse's hip height [3]. No significant differences were found between the ratings for perceived stress at the low back and effort required to complete the tasks, when comparing "good" and "poor" postures. The subjects were not nursing students and did not have any prior experience performing PHT, so these findings may be attributed to their lack of familiarity with the tasks. Ongoing work is being conducted to repeat these experiments with nursing students.

Significance: The findings from this proof of concept study suggest that "good" and "poor" posture may be classified according to trunk, hip, and knee flexion angles. The findings also suggest that there may be "neutral" postures may exist as a window between "good" and "poor" postures. This work provides a foundation for future work to include wearables to provide postural feedback about PHT performance. This work also may also be applied to interventions to re-train nurses in the workforce and to train lay caregivers.

Acknowledgments: This work is supported by funding from the Hope College Engineering Department and the Restore Center, which is funded by the National Institutes of Health through grant P2CHD101913.

References: [1] Budhrani-Shani et al. (2013), *Nurs Res Prac*; [2] Uhlrich et al. (2022), biorxiv https://doi.org/10.1101/2022.07.07.499061; [3] Freitag et al. (2014), *Ann Occ Hy*. 317–325; [4] Borg, (1982), *Med Sci Sports Exerc*, 14:377–381; [5] Bieri et al. (2000), J Spinal Cord Med 23(3); [6] Ferrone et al. (2021), *Sensors* 21, 7158.

EFFECT OF HIP JOINT ROTATION ON THE TROCHANTERIC FORCE AND SOFT TISSUE DURING SIDEWAYS FALLS

Jongwon Choi[1], Junwoo Park[1], Seyoung Lee[1], Kitaek Lim[1], ChungHwi Yi[2], Stephen Robinovitch[3] and Woochol Joseph Choi[1*]
[1]Injury Prevention and Biomechanics Laboratory, Dept of Physical Therapy, Yonsei University, South Korea
[2]Dept of Physical Therapy, Yonsei University, South Korea
[3]Dept of Biomedical Physiology and Kinesiology, Simon Fraser University, Burnaby, BC, Canada
*Corresponding author's email: wcjchoi@yonsei.ac.kr

Introduction: The magnitude of impact force transmitted to the proximal femur ("trochanteric force") depends on the soft tissue thickness covering the proximal femur, which is influenced by hip rotation at impact [1, 2]. We determined the trochanteric force during sideways falls from standing to examine how it was affected by hip rotation at landing.

Methods: Twenty individuals (10 males and 10 females) participated in pelvis release experiments (Fig. 1a). The pelvis of a participant lying sideways on the right side was raised 5 cm above the pressure plate, and then released to cause a fall on the hip. Falling trials were acquired with three hip rotations: 15° external, 0° (neutral), and 15° internal, which controlled by a wooden wedge.

During trials, kinematics of falls was recorded via reflective markers placed on the participant's left greater trochanter (GT) and lateral epicondyle (LE) of the femur, right thigh and shin. And pressure distribution and impact force were also measured through a pressure measurement plate.

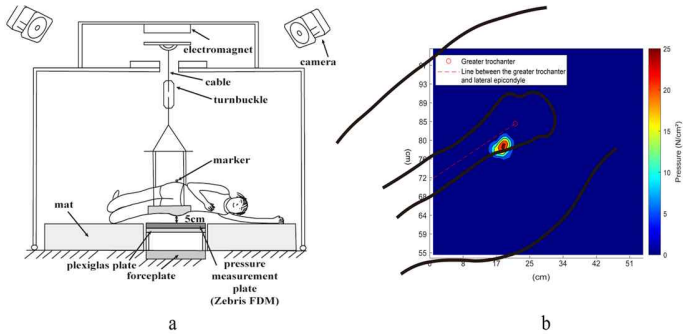

Figure 1: a. Plevis release experiment. b. Sample profile of pressure distribution with respect to the greater trochanter at maximum compression during a sideways fall.

To locate a point of peak impact force application, the coordinate system of motion capture system was first transformed to that of the pressure measurement system. Then, pressure distribution was plotted over time with respect to the GT and LE of the femur, which determined using a rigid body model with reflective marker data of body segments (Fig. 1b).

After identifying the location of peak impact force, participants lay sideways with the same position as in the pelvis release experiments. Then, the trochanteric soft tissue thickness was measured at right over the point of peak impact force application using ultrasound.

The force magnitude attenuated by the trochanteric soft tissue thickness ($F_{attenuation}$) was determined using a linear regression suggested in literature ($F_{attenuation}$ = 71*TSTT, where TSTT = trochanteric soft tissue thickness) [3]. The peak hip impact force was first determined using a one-link mathematical model of a human fall on the ground from standing height ("peak impact force" = 3.84*sqrt(mhk), where m = body mass, h = height of the center of mass, k = effective pelvis stiffness), where the effective pelvis stiffness (k) was defined as a tangent slope of a fitted force-deformation curve at an impact force of 300 N. Then, the trochanteric force ($F_{trochanteric}$) was determined as a difference between the peak hip impact force and the $F_{attenuation}$ ($F_{trochanteric}$ = 3.84*sqrt(mhk) - $F_{attenuation}$).

Results & Discussion: The $F_{trochanteric}$ was associated with hip rotation (F = 4.90, p = 0.013). On average, the $F_{trochanteric}$ was 21% smaller in external than internal rotation (3,849 versus 4,873 N) (Fig. 2). However, neither the trochanteric soft tissue thickness nor the $F_{attenuation}$ was associated with hip rotation (F = 2.92, p = 0.07; F = 2.30, p = 0.11, respectively).

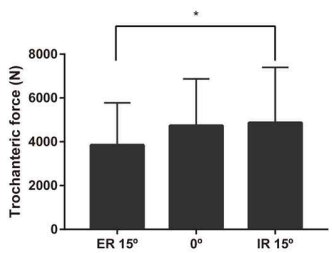

Figure 2: Effects of hip rotation on the trochanteric force during sideways falls from standing height.

The purpose of this study was to examine how the trochanteric force during a fall on the ground from standing height was affected by hip joint rotation at landing. We found that external rotation of the hip significantly reduced the trochanteric force, suggesting that hip fracture risk may decrease substantially with hip joint rotation at impact.

We also found that the trochanteric soft tissue thickness did not differ between external and internal hip rotation. This is interesting as it is against the previous finding that the trochanteric soft tissue thickness increases up to 12% depending on the femur rotation [2]. However, this discrepancy is maybe due, in part, to the site-specific variation of the trochanteric soft tissue. While Lafleur et al. compared the soft tissue thickness right over the GT, we measured and compared the thickness over a point of peak hip impact force application, which averaged 52 mm inferior to the GT along the shaft of the femur.

Significance: Our results provide insights on distribution of hip impact force, which may help improve fall-related hip fracture prevention strategies (i.e., exercise, safe landing strategies, padding devices).

Acknowledgements: This work was supported, in part, by the "Brain Korea 21 FOUR Project", and by the "Regional Innovation Strategy (RIS)" through the National Research Foundation of Korea (NRF) funded by the Ministry of Education (MOE) (2022RIS-005).

References: [1] Lafleur et al. (2021), *J Appl Biomech* 37(6); [2] Choi et al (2024), *J Biomech* 162(111885); [3] Robinovitch et al. (1995), *J Orthop Res* 13(6)

THE TWO-FREQUENCY RESONANCE MAP PREDICTS MULTIFREQUENCY COORDINATION IN DYADS

Marilena Kalaitzi Manifrenti[1*], Polemnia G. Amazeen[2], Jamie C. Gorman[3], Aaron D. Likens[1]
[1]Department of Biomechanics, University of Nebraska at Omaha, Omaha, NE, USA
[2]Department of Psychology, Arizona State University, Tempe, Arizona, USA
[3]Human Systems Engineering, Arizona State University, Mesa, Arizona, USA
*Corresponding author's email: mkalaitzimanifrent@unomaha.edu

Introduction: Each day, every individual engages in activities, whether alone or with others, that demand some degree of coordination. For example, driving necessitates intrapersonal hand-leg coordination, while smoothly merging onto the interstate demands interpersonal timing coordination among drivers. Any coordinated activity between two systems can occur at various frequency ratio combinations *p:q* (e.g. 3:1). These ratios are derived from the Farey Tree, which provides a hierarchical visualization for the two-frequency resonance map [1,2]. A major prediction of this map, verified from intra-personal multifrequency coordination (MC) work, is that the performance attempt of higher-level ratios results in the performance of lower-level ratios [3]. While intra-personal MC is biomechanically coupled, inter-personal MC (IMC) is informationally coupled. Concurrently, while spontaneous 1:1 coupling is known to emerge in visually coupled dyads [4], research on the breadth of intended ratios is limited. Given the broad applicability of the two-frequency resonance map across environmental systems [5], we hypothesize that this model will also offer predictions for IMC.

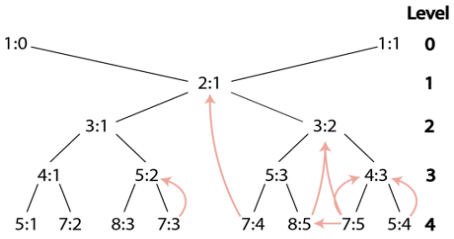

Figure 1. Farey Tree. The higher the level of a ratio, the lower the performed stability. Arrows indicate transitions to lower-level ratios from our experiment.

Methods: 21 dyads seated facing each other, holding an elevated horizontal bar with their dominant hand pronated, while extending their index finger. 16 multifrequency ratios were performed once (1:1, 2:1, 3:1, 3:2, 4:1, 4:3, 5:1, 5:2, 5:3, 5:4, 7:2, 7:3, 7:4, 7:5, 8:3, 8:5) through unique 1-minute trials. During each trial, one member of the dyad tapped to the 'p' frequency, while the other synchronized to the 'q' frequency, each using individual headphones. For the first 15 seconds, the participants tapped their fingers in synchrony to a metronome with their eyes closed. Then, the metronome ceased, and for the remaining 45 seconds they were told to maintain their prescribed tapping frequency while observing their partner's finger tapping. Kinematic data were captured with the Optotrak Data Acquisition Unit (100Hz). From each trial the first and last 5 seconds were trimmed. From each finger oscillation, phase angles and then instantaneous velocities were extracted in five 10-second windows. They were then plotted against each other, and a linear regression was fitted to obtain the instantaneous frequency ratio, per window, of the dyad. A multilevel model was then applied, with the regression coefficient as the dependent variable, and Window, Ratio, and their interaction as fixed effects.

Results & Discussion: The best fitting model included both Window and Ratio fixed effects ($\chi^2(15)$ =4208.82, p<0.0001, ICC=0.928, R^2=0.458). Because only the Ratio was significant in this model, we calculated the estimated marginal means (EMM) and their subsequent pairwise comparisons. All performed ratio distributions are reported in Figure 2. Ratio 5:4 was indistinguishable from 4:3 (Estimate: 0.0408, p=0.9999), with 5:4=1.25 (EMM=1.34, CL: [1.197, 1.48]) tending towards 4:3=1.33, marking a 1 level down transition (EMM=1.38, CL: [1.238, 1.52]). A 2 level down transition was prominent from ratios 7:5=1.4 (EMM=1.52, CL: [1.383, 1.66]) and 8:5=1.6 (EMM=1.65, CL: [1.508, 1.79]) towards ratio 3:2=1.5 (EMM=1.57, CL: [1.428, 1.71]), with the following pairwise comparisons respectively (Est: 0.0450, p=0.9997; Est: -0.0795, p=0.8901). A 3 level down transition was observed from 7:4=1.75 (EMM=1.97, CL: [1.827, 2.11]) towards 2:1 (EMM=2.02, CL: [1.882, 2.16]), indicating a statistically identical ratio performance (Est: 0.0551, p=9961).

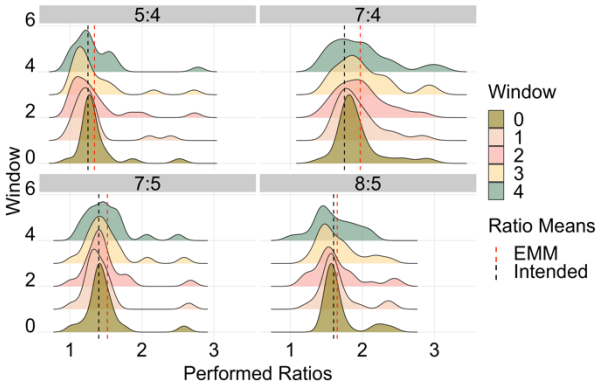

Figure 2. Performed ratio distributions (x-axis) per Window (y-axis) for each Ratio (each panel). Black dashed line indicates the intended ratio (e.g. 7:4=1.75), while the red dashed line indicates the EMM for that ratio (1.97).

As hypothesized, a consistent pattern is noticeable: higher-level ratios transition towards performing easier, lower-level ratios (Fig.1; orange arrows). Such observation indicates the tendency of informationally coupled dyads to lean towards performance of easier, simpler ratios, similar to the behaviour seen in intra-personal MC performances. While there are 16 ratios, due to space constraints we only report a subset of noteworthy cases; nevertheless, the remaining higher-level ratios likewise support our hypothesis.

Significance: This is the first study to explore such breadth of intended ratios in IMC, while investigating the differences between visually uncoupled and coupled tapping. The above findings hold significance for numerous joint-action tasks, including, but not limited to, team sports such as sailing, musical ensembles such as orchestras, and the coordination of household chores among family members.

Acknowledgments: NSF 1257112

References: [1] Bak. *Physics Today.* **39**, 38-45, 1986, [2] Hardy and Wright. *Oxford University Press*. 1960, [3] Peper et al. *J. Exp. Psychol*. **21**, 1117-1138, 1995, [4]Amazeen et al. *Biol. Cybern.* **72**, 511-518, 1995, [5]Maselko and Swinney. Phys. Scr. T9, 35-39, 1985.

VARIATION OF LUMBAR ROTATION DURING ASYMMETRIC PATIENT HANDLING TASKS

Elsa Brillinger[1*], Yeageon Song[1], Regina Vicente[1], Dr. Brooke Odle[1]
Hope College, Holland, MI, USA
*Corresponding author's email: elsa.brillinger@hope.edu

Introduction: Musculoskeletal injury to the lower lumbar vertebrae is among high prevalence in nursing personnel. Many patient handling tasks (PHT) require nurses and other caregivers to lift and reposition patients of a variety of weights in varying postures, causing low back pain in nurses to range from 50-80% globally [1]. Currently, lumbar rotation during PHT is not widely studied. This work specifically investigated lumbar rotation in asymmetric PHT tasks- tasks where the arms or shoulders are used to reach to different parts of a patient, causing the trunk to rotate. In addition, task performance was also analyzed with respect to patient weight. This work aims to analyze the effect of manikin weight and table height and how they impact lumbar rotation angles during PHT.

Methods: A pilot study was completed with 5 able-bodied volunteers, 4 males and 1 female, between the ages of 18 and 24. None of the volunteers had experience with performing PHT. Three tasks were analyzed: sliding a patient towards the head of the bed using a sling (2-slide), lifting a patient's leg up to vertical (leg-lift), and sitting a patient up in bed (situp). For consistency within and across participants, manikins were used as patients. To analyze how lumbar rotation changes during specific PHT, each task was completed at three different table heights (knee, mid-thigh, and hip height) and with three manikin weights (44lb, 66lb, 110lb). The table heights were kept standard for all participants. The table heights are as follows: 34.5in for hip height, 28in for mid-thigh height, and 24.5in for knee height. OpenCap [2], an open-source platform for capturing movement dynamics via video capture from at least two IOS supported devices, was used to record kinematic data and analyze lumbar rotation during these PHT at a frequency of 60 Hz. Four iPhones mounted onto tripods were used to record the movements. For a single trial, 3 repetitions were completed of the selected task. Each task was completed 2 times with each table height and manikin weight.

Kinematic data collected via OpenCap were filtered using a 4th order Butterworth filter with a cutoff frequency of 12 Hz. The peaks of each repetition were manually selected. When selecting peaks, both the positive most and negative most peaks were selected to indicate internal and external rotation. The absolute value of the negative values was computed and averaged with the positive values to determine the mean deviation from upright posture.

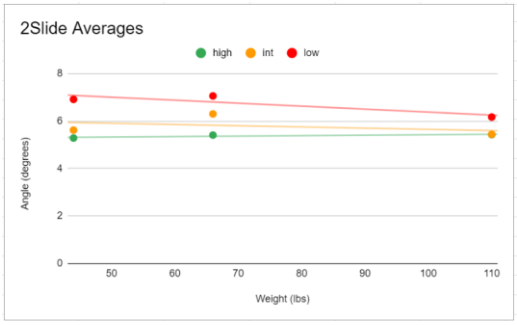

Figure 1: Lumbar rotation averages for the 2slide task.

Results & Discussion: Due to glitches within the data, some repetitions and trials had to be discarded. As seen in Figure 1, which refers to the averages of the 2-slide trials, as the table height decreased, lumbar rotation angles increased. This was expected because as the table lowers, the subject must reach further down. This same trend was observed for the leg-left trials as well. When analysing the effect of manikin weight on the 2-slide and leg-lift tasks, no correlation was observed.

Figure 2 shows the results for the averages of the situp task. These averages do not follow the same trend as the previous tasks. The averages for the high table height (hip height) and int or intermediate table height (mid-thigh height) are flipped. This is likely due to glitches in the data. Glitches made it difficult to select accurate peaks, and glitches were more prevalent at higher table heights. When looking at the low table trials (knee height), lumbar rotation angles increased as the weight of the manikin increased. Although this was not a trend for other tasks or table heights, it suggests that for specific PHT, lumbar rotation angles may increase with an increase in manikin weight. Future work entails repeating these experiments with nursing students. Future work may also include electromyography to understand low back muscle activation during PHT.

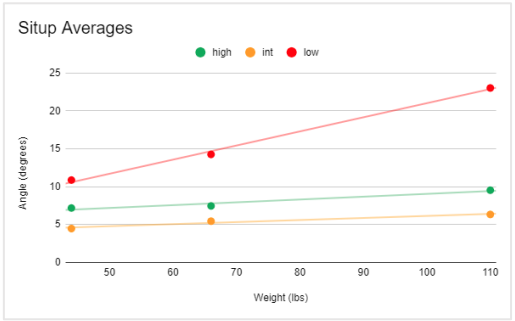

Figure 2: Lumbar rotation averages for the situp task.

Significance: Pilot experiments and data analyses demonstrate that trunk rotation is evident in asymmetric PHT and that it may increase or decrease depending on the table height or weight of the patient. As mentioned above, no literature at this time analyses lumbar rotation during PHT and how it may be affected by both patient weight and table height. Because this work shows potential relationships between manikin weight, table height, and lumbar rotation, future work includes extending this study to analyze nursing students. Thus, understanding the role of trunk rotation in asymmetric PHT may have implications for injury mitigation approaches to train nursing students and re-train nurses in the workforce.

Acknowledgments: This work was supported by funding from the RESTORE Center, which is funded by the National Institutes of Health through grant P2CHD101913, and Clare Boothe Luce Foundation. We would like to thank Nathan Ceja and Grant Seyller for their assistance during data collection sessions.

References:

[1] Budhrani-Shani, P, et al. National Library of Medicine. 2016. 38(3);
[2] Uhlrich, S. et al. 2022. biorxivhttps://doi.org/10.1101/2022.07.07.499061

INVESTIGATION OF FIREFIGHTER TURNOUT GEAR SHOULD CONSIDER THE FIREFIGHTING TASK DEMAND

Kuanting Chen[1*], Meredith McQuerry[2], Jennifer M. Yentes[1]
[1]Department of Kinesiology and Sport Management, Texas A&M University, College Station, TX
[2]Jim Moran College of Entrepreneurship, Florida State University, Tallahassee, FL
*Corresponding author's email: Kuanting.Chen@tamu.edu

Introduction: Proper fitting turnout gear is crucial for firefighter safety and effectiveness in combating heat, moisture, smoke and other hazardous elements in fireground. Previous studies have revealed that female firefighters experience turnout gear fit issues at a rate two to four times greater than their male counterparts, resulting in performance reduction and compromised safety for female firefighters [1, 2]. However, existing studies often focus on general perspectives of the gear or limitations during general movements, such as gait, lifting and reaching tasks, rather than firefighting-specific tasks. Therefore, this study aimed to investigate various aspects of turnout gear issues among male and female firefighters within the context of specific firefighting tasks. These preliminary data are necessary for future biomechanical investigations.

Methods: An online Qualtrics survey was disseminated through local firefighter training facilities, social media advertisements, and national firefighter organizations. The survey collected responses to the perceived fit and movement limitations imposed by turnout gear, as well as the level of satisfaction to the fit and the range of motion (ROM) of the gear in the context of firefighting tasks. Percentage of distribution was calculated for survey responses. Risk of experiencing turnout gear issues for female firefighters was quantified through relative risks (RR) and its 95% confidence interval (95% CI). A RR value greater than one indicates an elevated risk for gear issue among female firefighters compared to male firefighters, whereas a RR value less than one suggests a decreased risk.

Results & Discussion: The final analysis included 279 surveys from male firefighters (age: 38.24 ± 12.62 yrs) and 69 surveys from female firefighters (age: 37.54 ± 10.25 yrs). Nearly half of the female participants (47.83%) reported fit issues, a ratio two times greater than their male counterparts (21.58%; RR: 2.22, 95% CI: 1.59 – 3.09). Female participants also reported higher levels of mobility limitation (72.46% vs. 61.45% for male; RR: 1.18, 95%, 95% CI: 0.99 – 1.40) and range of motion restriction (70.59% vs. 62.55% for male; RR: 1.13, 95% CI: 0.97 – 1.31) while wearing turnout gear. In terms of specific firefighting tasks, greater percentages of female participants reported dissatisfaction with the fit and range of motion of their turnout gear to all the tasks (see Table 1). In comparison to male participants, female participants experienced a minimal of 2.73 times and 2.92 times higher risk for experiencing fit and ROM issues, respectively. RR for fit issues was more prominent for tasks involving ladders, and forced entry was the task with the highest RR for ROM.

Overall, female firefighters were more susceptible to fit issues and restrictions in mobility and range of motion when wearing turnout gear. These risks were magnified in the context of firefighting skill execution, which underscored the significance of task specificity in the evaluation of turnout gear issues.

Table 1. Percentage of dissatisfaction and RR for male and female firefighters with the Fit and ROM of their turnout gears.

Tasks	Fit			ROM		
	Dissatisfaction (%)			Dissatisfaction (%)		
	Male	Female	RR (95% CI)	Male	Female	RR (95% CI)
Mounting and dismounting fire apparatus	7.91	26.09	3.35 (1.92 – 5.85)	9.23	34.78	3.48 (2.15 – 5.63)
Force entry into a structure	6.20	17.65	3.10 (1.57 – 6.12)	5.17	20.59	4.29 (2.19 – 8.44)
Setting up a ground ladder	7.25	20.59	2.89 (1.56 –5.39)	8.89	26.09	2.92 (1.71 – 4.99)
Advancing an uncharged hose line on a flat surface	4.74	13.43	3.03 (1.36 – 6.73)	5.54	20.29	3.97 (2.04 – 7.70)
Advancing an uncharged hose line up stairs or a ladder	5.82	26.47	4.56 (2.48 – 8.38)	9.59	33.82	3.46 (2.14 – 5.59)
Operating a charged hose line from a ground ladder	7.66	17.65	2.73 (1.44 – 5.16)	8.55	26.09	3.06 (1.78 – 5.23)
Deploying a roof ladder	4.35	20.90	5.04 (2.48 – 10.26)	7.81	29.41	3.77 (2.21 – 6.60)
Carrying tools up and down a ladder	6.93	26.47	3.79 (1.44 – 5.16)	8.89	30.43	3.38 (2.03 – 5.60)
Deploying an attack hose line shoulder method	5.82	17.65	3.23 (1.62 – 6.43)	7.52	22.06	2.94 (1.62 – 5.36)
Hoisting tools or equipment	4.35	13.43	3.54 (1.58 – 7.93)	7.09	22.06	3.41 (1.87 – 6.23)

Significance: This study highlighted the importance of task specificity in the design of turnout gear. It is recommended that manufacturers prioritize task-specific functionality and comfort, particularly for female firefighters who are disproportionately affected by fit issues. Moreover, future research should explore biomechanical or physiological repercussion of ill-fitting gear in the context of firefighting task and develop targeted interventions to improve firefighter performance and safety. In conclusion, ongoing efforts are needed to ensure the safety and resilience of active-duty firefighters in the challenging fireground environment.

Acknowledgments: We would like to thank TEEX and Texas A&M Huffines Institute for assisting data collection.

References: [1] Hulett et al. (2008), A National Report Card on Women in Firefighting. [2] McQuerry et al. (2023), *Front Mater* 10:1175559.

THREE-DIMENSIONAL KINEMATICS IN PATIENTS WITH ANTERIOR SHOULDER INSTABILITY: A SYSTEMATIC REVIEW WITH META-ANALYSIS

Talissa Oliveira Generoso[1,2], Vitor La Banca, Felipe F. Gonzalez, João Artur Bonadiman, Lucas Valerio Pallone, Eliane C. Guadagnin, Grant E. Garrigues, Jonathan A. Gustafson, Leonardo Metsavaht, Gustavo Leporace[1]
1 Instituto Brasil de Tecnologias da Saúde, Brazil; 2 RUSH University Medical Center, USA
Correspondence to: Gustavo Leporace, gustavo@biocinetica.com.br

Introduction: Anterior Shoulder Instability (ASI) is a common orthopedic condition, often resulting in altered shoulder kinematics. Understanding biomechanics of the unstable shoulder is critical to determine the most appropriate treatment option. The aim of this study was to perform a systematic review and meta-analysis of the existing evidence regarding 3D shoulder kinematics in patients with ASI. We hypothesized that shoulder biomechanics, as measured by scapulohumeral rhythm and shoulder kinematics — including scapulothoracic, glenohumeral, and humerothoracic angles — would be significantly different from uninjured/stable shoulders.

Methods: A broad search was conducted within PubMed, Scopus, and Cochrane Library following PRISMA guidelines. All cross-sectional or longitudinal studies with 3D motion analysis describing shoulder kinematics in patients with ASI were included. Two researchers independently conducted rounds of data extraction. The quality of each study was assessed using MINORS criteria [1]. Qualitative and quantitative analyses were performed. For the qualitative analysis, data regarding the aims and type of each study, ASI characteristics, participant and group descriptions, as well as kinematic assessment methods and main findings, were extracted and analyzed. Quantitative meta-analysis used a random-effects model. Statistical analysis was performed with SPSS (v29).

Results & Discussion: Nine studies were included for data extraction and qualitative analysis [2-10], among which 2 studies were included for quantitative meta-analysis [2-3].

Meta-analysis Results:

- Glenohumeral peak angle in the coronal plane was higher for controls ($p = 0.01$), indicating that healthy shoulders have greater glenohumeral motion than unstable shoulders for abduction (Fig. 1).
- The instability group showed greater scapulohumeral rhythm in the coronal plane ($p = 0.02$) indicating greater contribution of the glenohumeral joint relative to the scapulothoracic joint (Fig. 2).

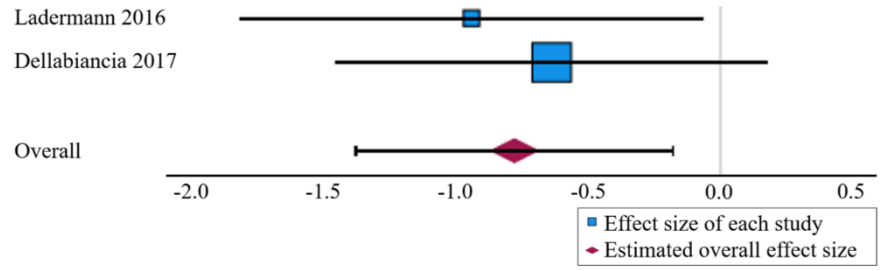

Fig 1. Glenohumeral peak angle on the coronal plane: standardized mean differences between shoulder instability and control group.

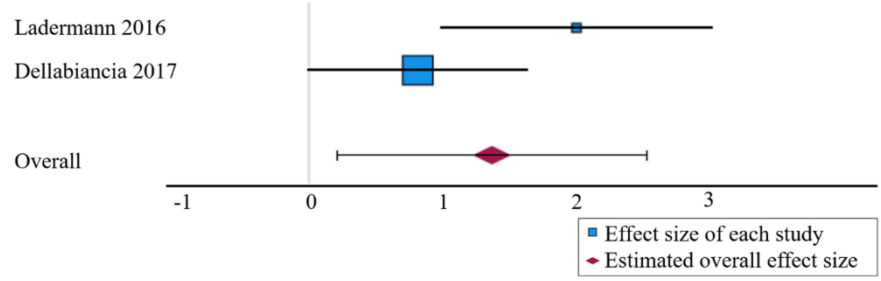

Fig 2. Scapulohumeral Rhythm: Standardized mean differences between shoulder instability and control group.

These motion alterations may be related to pain, apprehension, functional changes from capsule and ligament pathoanatomy, impaired neuromuscular control or a combination of each during shoulder tasks.

Contrasting these findings, the results of the studies included in the qualitative analysis present a more complex picture:

- The humeral head had greater anterior translation in unstable shoulders in three studies [3,7,8], while the difference was not significant in one [9] and another found higher variability for global humeral translation for instability patients [2]. The conflicting findings could be attributed to limited sensitivity of the motion analysis methods used.
- Two studies found that ASI shoulders exhibit a reduced ROM for active shoulder external rotation [2,8], while one study detected a lower ROM for flexion, abduction in the scapular plane and internal rotation [3]. These alterations in the active ROM could be related to pain or apprehension during the tasks.
- Among the nine studies evaluated, six analysed the scapulohumeral rhythm or scapular orientation [2,4-7,9] and reporting conflicting results, underscoring the importance of global shoulder positioning and the need for clear testing protocols.

Significance: This systematic review underscores the importance of assessing 3D shoulder kinematics in patients with anterior shoulder instability. The unique subject-specific motions at the scapulothoracic and glenohumeral joint present unique challenges for refining treatment interventions for ASI. The review underscores challenges in the current research, highlighting methodological inconsistencies in motion analysis studies of shoulder instability.

References: [1] Slim et al. (2003) ANZ J Surg; [2] Dellabiancia et al. (2017) MSK Surg; [3] Lädermann et al. (2016) Medicine; [4] Marchi, Blana & Chadwick (2014) Med Bioeng & Comp; [5] Hung & Darling (2014) Physiotherapy Research Intl; [6] Matias & Pascoal (2006) Clin Biomech; [7] Kim et al. (2017) J Ortho; [8] Peltz et al. (2015) AJSM; [9] Ernstbrunner et al. (2022) Clin Biomech; [10] Arzi et al. (2014) JSES.

QUANTIFYING BIOMECHANICAL DIFFERENCES: A PILOT STUDY COMPARING TENNIS STROKES IN PROFESSIONAL AND NON-PROFESSIONAL PLAYERS

Levi E. Harmon[1], Ashley N. Flores[1], Alec R. Walstra[1], Anton Petrenko[2], Yunju Lee[1,2*],
[1]Department of Physical Therapy and Athletic Training, Grand Valley State University, Grand Rapids, MI, USA
[2]School of Engineering, Grand Valley State University, Grand Rapids, MI, USA
*Corresponding author's email:leeyun@gvsu.edu

Introduction: Xsens MVN motion capture device (Movella Inc., Netherlands) is an inertial measurement unit (IMU) that uses inertial sensors, including accelerometers, gyroscopes, and magnetometers to provide objective, quantitative data on joint angles, acceleration, body posture, balance, and coordination to monitor athlete performance in a natural training environment [1]. Previous research has shown that there is a discrepancy in performance between tennis players of different skill levels; however there has been little exploration of the biomechanical positioning and efficiency of these players. Additionally, there is lack of biomechanical analysis of tennis forehand and backhand strokes is lacking in current literature. Further research is required to determine how skill level, age, and/or sex affect the understanding of serve and stroke mechanics for performance improvement [2].

The purpose of this study was to compare the joint angles of upper and lower extremities between professional and non-professional tennis players to determine the biomechanical differences in performance during various tennis strokes. We expected professional players to have refined technical ability and consistent joint angle optimization due to their increased skill level and playing experience.

Methods: Seven participants, aged 18-50 and categorized as professional (n=2) and non-professional (n=5), utilized Xsens MVN motion capture technology to perform six tasks: advantage side and deuce side serves, forehand cross court and down-the-line returns, and backhand cross-court and down-the-line returns while wearing Xsens Sensors. To ensure reliability, participants were instructed to stand in standard locations for each shot, and a ball machine was used to achieve consistent ball feed. Comparative analysis was utilized to assess the difference between joint angles of the dominant side at each extremity joint to identify differences between skill levels. To normalize the shot length, we used dominant shoulder abduction and adduction. For the serve and forehand, we used the lowest points before and after the highest point of abduction. Backhand strokes were normalized from the lowest point of adduction to the highest point of abduction.

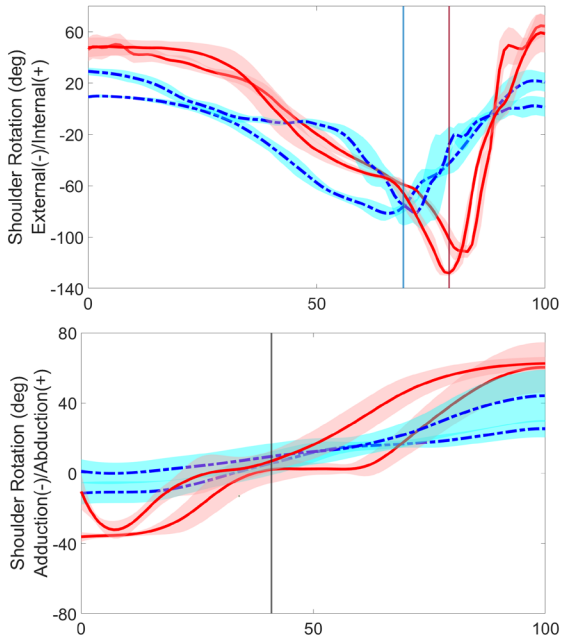

Figure 1: [Above] Shoulder rotation during a serve between professional (red) and non-professional (blue). Ball contact occurs just after the lowest point in the graph (external rotation). [Below] Shoulder abduction during backhand crosscourt groundstroke between professional (red) and non-professional (blue). Ball contact occurs at the point abduction briefly levels off (average ball contact demonstrated with vertical line).

Results & Discussion: In a tennis service, professional participants showed a larger average range of shoulder rotation. They had increased loading into external rotation (122.0°±8.4°) compared to non-professionals (105.1°±16.9°) and a larger follow-through into internal rotation (66.4°±6.6° vs 20.9°±18.3°) (Figure 1). This could be due to the professionals' increased flexibility, allowing them to load into a further range. Additionally, the increased external rotation would create a stretch-shortening cycle of their shoulder internal rotators, subsequently increasing internal rotation in the follow-through, resulting in more velocity in their swing [3]. Another difference between the groups was observed during backhand crosscourt groundstrokes. The participants who were professional achieved greater total range differences between shoulder adduction and abduction (96.1°±10.1° vs 51.8°±17.7°) during backhand crosscourt groundstrokes. Professionals may load into greater adduction and follow through into greater abduction range. This may indicate that professionals are more comfortable controlling their shot throughout their entire available range of motion while maintaining biomechanical effectiveness, resulting in greater racquet velocity [4].

Significance: The joint angle analysis between professional and non-professional tennis players within this study has influence on athlete training and could provide insight to mechanism of injury to guide therapeutic rehabilitation. Training and recovering athletes should focus on increasing flexibility of shoulder internal and external rotation, shoulder adduction, and wrist flexion and extension, as well as increased motor control and muscular strength within these ranges. This study can guide non-professional athletes to increase their biomechanical efficiency during play through optimizing joint angles in their training to improve performance. This study contributes to a small amount of research on tennis groundstrokes upon which future research can be built.

Acknowledgements: We thank to the participants, Grand Valley State University Tennis Teams, and Premier Athletic and Tennis Club for allowing us to use their facilities.

References: [1] Roetenberg et al. (2013) Online Published; [2] Genevois et al. (2015), *J Sport Sci Med* 14(1); [3] Roetert et al. (2009), *Strength Cond J* 31(4); [4] Pedro et al. (2022), *Sensors* 22(3).

THE EFFECTS OF ANTICIPATION ON DISTAL LEG MUSCLE EXCITATIONS IN RESPONSE TO SURFACE TRANSLATIONS DURING STANDING

Virginie Ruest*, Emily Eichenlaub, and Jason R. Franz
Joint Dept. of Biomedical Engineering, UNC Chapel Hill and NCSU, USA
*Corresponding author's email: virginie.ruest@unc.edu

Introduction: Control of standing posture is crucial for maintaining balance and minimizing the risk of falls. The timing and amplitude of local muscle excitations can provide insight into how the neuromechanical system governs standing balance. Postural control arises as a complex interplay between proactive adjustments in anticipation of instability and/or reactive adjustments to recover from that instability [1]. Balance perturbations, whether anticipated or unanticipated, allow us to quantify changes in local muscle neuromechanics that, in younger adults, can serve as a benchmark for detrimental changes due to aging and disease. Specifically, a posterior surface translation precipitates rapid tibialis anterior (TA) lengthening with medial gastrocnemius (MG) and soleus (SOL) shortening [2]. Conversely, an anterior surface translation precipitates rapid MG and SOL lengthening with TA shortening [2]. However, the interaction between anticipation and direction on the neuromechanical response to standing surface translations has not been previously studied. The purpose of this study was to investigate the interaction between anticipation and direction on distal length muscle excitations measured via surface electromyography (EMG). We first hypothesized that unanticipated balance challenges would elicit greater reactive EMG while anticipated balance challenges would elicit greater proactive EMG. We also hypothesized that the TA would show greater EMG following anterior surface translations while the MG/SOL would show greater EMG following posterior perturbations.

Methods: Twenty young adults (8M/12F; mean±standard deviation; age: 22.3±3.3 years) participated in this single-visit study. Participants responded to anterior and posterior 200 ms, 6 m/s^2 treadmill surface translations. Perturbations, delivered using a custom MATLAB interface, were delivered either unexpectedly (i.e., unanticipated) or at the end of a three-second verbal countdown (i.e., anticipated). Four combinations of perturbation direction (i.e., forward and backward) and anticipation (i.e., anticipated and unanticipated) were repeated three times in a randomized order for a total of 12 perturbations. Electromyographic (EMG) signals from the left MG, SOL, and TA were recorded using wireless electrodes at 1000 Hz (Delsys). We calculated integrated EMG (iEMG) over three distinct phases: pre-perturbation (i.e., 750 ms preceding the perturbation), early post-perturbation (0-750 ms following the perturbation), and late post-perturbation (750-1500 ms following the perturbation).

Results & Discussion: Pre-perturbation (Fig. 1A): Independent of direction, anticipation increased SOL (p=0.049) and TA (p=0.021) iEMG, supporting our first hypothesis. Early post-perturbation (Fig. 1B): We found a main effect of perturbation direction on MG (p=0.001), SOL (p=0.034), and TA (p<0.001) iEMG. Specially, as hypothesized, posterior perturbations elicited greater reactive MG and SOL iEMG, whereas anterior perturbations elicited greater reactive TA iEMG. We also found a significant main effect of anticipation (p=0.015) and an anticipation × direction interaction (p=0.019) for TA iEMG. Here, independent of direction, unanticipated perturbations elicited greater reactive TA iEMG than anticipated perturbations. Late post-perturbation (Fig. 1C): We found significant main effects of direction on MG (p=0.020) and SOL (p=0.009) iEMG wherein, independent of anticipation, anterior perturbations elicited greater reactive iEMG than posterior perturbations. Moreover, a significant main effect of anticipation for MG iEMG (p=0.038) and a significant anticipation × direction interaction (p=0.044) for SOL iEMG both supported that unanticipated perturbations elicited greater reactive EMG than anticipated perturbations. Finally, a significant anticipation × direction interaction for TA iEMG (p=0.002) revealed that, as hypothesized, unanticipated anterior perturbations elicited greater reactive EMG than other perturbations. Taken together, these data provide compelling support for of our two hypotheses.

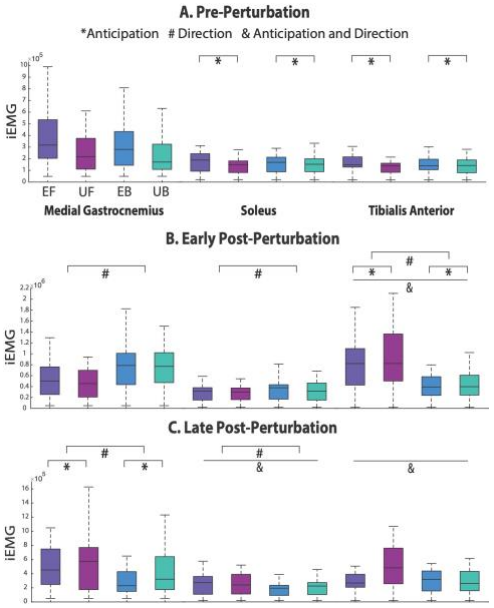

Figure 1: iEMG of the MG, SOL, and TA pre-perturbation, early post-perturbation, and late post-perturbation. EF: Expected Forward; UF: Unexpected Forward; EB: Expected Backward; UB: Unexpected Backward.

Significance: Our results in younger adults provide a significant first step toward understanding the role of anticipation and perturbation direction in governing the neuromechanical integrity of distal leg muscles. Our findings now serve as an important benchmark for identifying detrimental changes due to aging or disease and thereby risk factors or potentially-modifiable factors for intervention.

Acknowledgments: Supported in part by a grant from NIH (R21AG067388).

References: [1] Xie et al. (2019), *Exp Brain Res* 237; [2] Henry et al. (1998), *J Neurophysiol* 80(4).

MYOELECTRIC PERFORMANCE OF THE RECONSTRUCTED ELBOW FLEXOR IN PATIENTS WITH BRACHIAL PLEXUS INJURIES

Emily J. Miller[1*], Sandesh G. Bhat[1], Paul H. Kane[1], Alexander Y. Shin[2], Kenton R. Kaufman[1,2]
[1]Motion Analysis Lab, Department of Orthopedic Surgery, Mayo Clinic, Rochester, MN
[2]Department of Orthopedic Surgery, Mayo Clinic, Rochester, MN
*Corresponding author's email: miller.emily@mayo.edu

Introduction: Traumatic adult brachial plexus injury (BPI) is a debilitating injury and despite surgical reconstruction, some patients cannot perform elbow flexion in activities of daily living [1,2]. Myoelectric exoskeletons have been introduced as functional tools for elbow flexion. However, the commercially available myoelectric exoskeletons currently utilized in the BPI population are a cross-over application that do not specifically consider the needs of BPI patients [2]. Electromyography signals have been used to control many exoskeletons [3,4], but characterization of the EMG signal specific to the traumatic adult BPI population has yet to be performed. The purpose of this study was to determine if adult patients with traumatic BPI and a reconstructed elbow flexor can control a muscle-activated device.

Methods: Twenty-seven adult patients (3 female, age: 26±30 yr., BMI 28±5 kg/m^2, post-op (PO): 26±29 mo.) who underwent surgical intervention to restore elbow flexion with traumatic BPI participated in this cross-sectional study. These patients had surgical procedures to restore elbow flexion with a gracilis free functioning muscle transfer (gFFMT) innervated by the spinal accessory nerve (SPA) or the intercostal nerves (ICN), nerve grafting from the upper trunk, or nerve transfer (NT) (from the SPA, ICN or ulnar nerve fascicle to the musculocutaneous nerve or its biceps motor branch). Elbow flexor muscle activity was recorded while the patients performed a series of sequential tasks relevant to design criteria for exoskeleton control. These criteria included establishing a subject-specific activation threshold, the time between peak contraction and a stable, resting signal (i.e., 'settle-time'), and the ability to generate multiple, distinct signals in a supported flexed position necessary for bidirectional exoskeleton control. The myoelectric signal envelope and activation thresholds were used to evaluate the criteria for exoskeleton control algorithm development.

Results & Discussion: A single, subject-specific activation threshold (median (IQR): 7.8 (5) mV) can be utilized for exoskeleton control, but the calibration routine should consider the resting signal for both the extended and flexed elbow positions (Fig.1 A, B). The data indicated a 'settle-time' (median (IQR): 1.5 (2.0) s) following contraction that should be considered to prevent unintentional movement of the exoskeleton (Fig. 1 C, D). All the patients were able to activate their elbow flexor above the activation threshold in the supported, flexed position. However, there were different abilities to generate multiple, discrete signals (Fig, 1 E, F). These results were not specific to the surgery and the nerve implemented for reconstruction or the post-operative recovery time. A viable EMG signal pattern for BPI exoskeleton control can be achieved with a properly designed rehabilitation program and ample training time.

Significance: For patients with a BPI and a reconstructed elbow flexor a single subject-specific activation threshold can be established, a 'settle-time' is present following contraction, and the ability to generate discrete signals varies across patients. These criteria can guide algorithm development to control a BPI specific exoskeleton. Reconstructed elbow flexor signal control capabilities were patient specific and not limited to surgery type, nerve implanted and post-operative recovery time.

Acknowledgments: This study was funded by the Department of Defense Award Number W81XWH-20-1-0923 (Grant Number DM190721). Partial support was also provided by the W. Hall Wendel Jr. Musculoskeletal Research Professorship.

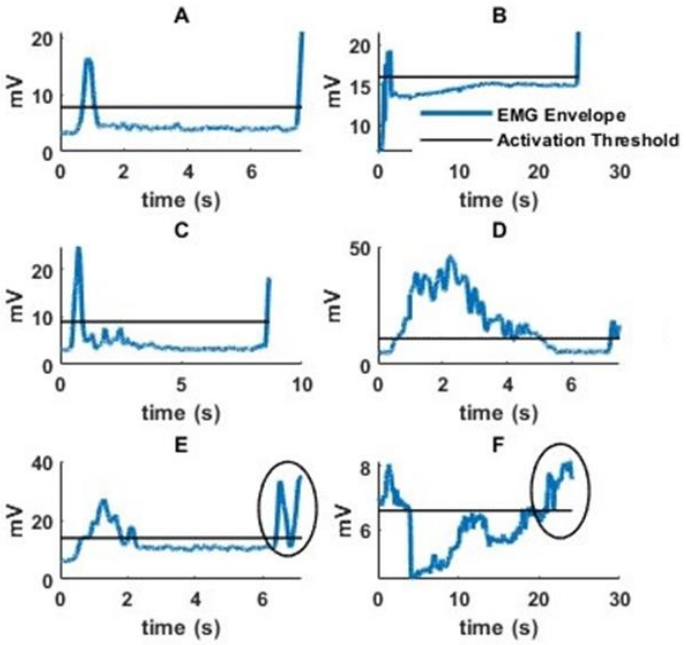

Figure 1: Representative elbow flexor signal during sequential tasks relevant to exoskeleton control. Trial starts with arm in full extension. Subject then flexes elbow flexor (denoted by first peak), and the forearm is then supported in the flexed position by a member of the research team. Subject then attempts two distinct rapid pulses in the supported, flexed position. (A) Similar resting signal flex/ext positions (NT: Ulnar Nerve, 12.4 mo. PO), (B) Different resting signal flex/ext positions, activation threshold accommodates flexed position (gFFMT: SPA, 34.1 mo. PO) (C) Short 'settle-time' (gFFMT: SPA, 34.1 mo. PO), (D) Long 'settle-time' (NT: Ulnar Nerve, 12.6 mo. PO), (E) Able to generate two distinct rapid pulses in the flexed position (circled in trial) (NT: Ulnar Nerve, 25.2 mo. PO), (F) Unable to elicit two distinct rapid pulses in the flexed position (circled in trial) (gFFMT: SPA, 8.2 mo. PO).

References: [1] Shin et al. (2022), *J Hand Surg Eur* 47(1); [2] Anderson et al. (2021), *J Pros Orth* 33(1); [3] Singh and Chatterji (2012), *Int J Sci&Eng Res* 3(8); [4] Lobo-Prat et al. (2017) *J Neuroeng Rehab* 14(1).

QUANTIFYING THE DYNAMIC POSTURAL STABILITY INDEX USING FULL-BODY KINEMATICS

Kevin D. Moore[1*], John Z. Wu[1], Robert E. Carey[1], Scott P. Breloff[1,2]
[1]HELD, National Institute for Occupational Safety and Health, Morgantown, WV, USA *email: qcp5@cdc.gov
[2]DFSE, National Institute for Occupational Safety and Health, Cincinnati, OH, USA

Introduction: Falls (i.e., loss of balance) account for over three million emergency room visits per year in the USA [1] and are one of the leading causes of death in occupations like roofing [2]. To better prevent falls and integrate interventions, it is necessary to evaluate the likelihood of a specific movement to cause a loss of balance — dynamic postural stability. Several approaches to assess dynamic postural stability exist, including the dynamic postural stability index (DPSI) [3] and time to stabilization [4]. While these approaches are valuable and reliable for assessing dynamic postural stability, they have some inherent limitations such as the requirement of a force-plate (FP). Another study modified the aforementioned FP-based DPSI approach, substituting FP data with center of gravity (COG) accelerations (A_{COG}) obtained using a single fixed inertial measurement unit (IMU) [5]. While the IMU-based DPSI approach is useful, it is a rough estimate of A_{COG} as the COG location varies relative to the body. Therefore, the purpose of this study is to develop a DPSI approach using A_{COG} obtained via full-body kinematics and to validate it using the FP-based DPSI approach [3].

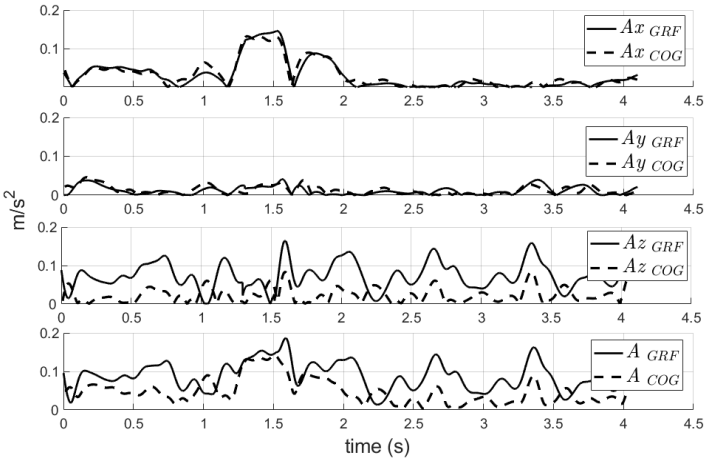

Figure 1: Acceleration magnitudes for both stability index approaches from a representative trail. From top to bottom: medial/lateral, anterior/posterior, vertical, and resultant.

Methods: We assessed dynamic postural stability for the same trials (trial details in next paragraph) using the FP-based DPSI approach and the proposed kinematic-based DPSI approach. Both DPSI approaches provide four stability indexes, three directional stability indexes — the medial/lateral stability index (MLSI), anterior/posterior stability index (APSI), and vertical stability index (VSI) — and an overall stability index called the DPSI, which is the resultant of the three directional indexes. The indexes for the FP-based DPSI approach were calculated using the three-dimensional (3D) (x- medial/lateral, y-anterior/posterior, z-vertical) ground reaction forces (GRF) as follows: for the MLSI $MLSI = \sqrt{\sum(GRF_x/mg)^2 \cdot 1/n}$, for the APSI $APSI = \sqrt{\sum(GRF_y/mg)^2 \cdot 1/n}$, for VSI $VSI = \sqrt{\sum(1 - GRF_z/mg)^2 \cdot 1/n}$, and for the DPSI $DPSI = \sqrt{MLSI^2 + APSI^2 + VSI^2}$. The indexes for the proposed kinematic-based DPSI approach using the 3D A_{COG} were computed as follows: $MLSI = \sqrt{\sum(Ax_{COG}/g)^2 \cdot 1/n}$, $APSI = \sqrt{\sum(Ay_{COG}/g)^2 \cdot 1/n}$, $VSI = \sqrt{\sum(Az_{COG}/g)^2 \cdot 1/n}$, and $DPSI = \sqrt{MLSI^2 + APSI^2 + VSI^2}$.

Three healthy males (age: 24 ± 4 yrs, height: 1.84 ± 0.1 m, mass (m): 86.3 ± 10.9 kg) participated in this study completing three trials of a shingle installation task on a level custom roofing simulator. Marker trajectories were captured using a 14-camera system (Vicon Inc.) at 100 Hz and were synchronized with three force-plates (Bertec Corp.) sampling at 1000 Hz. Using the marker trajectory data, motions of the anatomical body segments were modelled in Visual3D (C-motion Inc.) and then used to obtain COG trajectories [6]. The second derivative of the COG displacement with respect to time was then computed in MATLAB to obtain three-dimensional A_{COG}.

Results & Discussion: The time-histories of the acceleration magnitudes for both DPSI approaches are displayed in Fig. 1. The average (mean ± standard deviation) stability indexes for all trials/subjects for the FP-based DPSI approach were MLSI: 0.0206 ± 0.004, APSI: 0.0086 ± 0.0016, VSI: 0.0557 ± 0.0123, and DPSI: 0.0601 ± 0.0126. The average stability indexes for all trials/subjects for the proposed kinematic-based DPSI approach were MLSI: 0.0203 ± 0.0048, APSI:0.0080 ± 0.0020, VSI: 0.0128 ± 0.0047, and DPSI:0.0254 ± 0.0068. The mean differences between both DPSI approaches were MLSI: 0.0003 ± 0.001, APSI: 0.0005 ± 0.001, VSI: 0.0429 ± 0.009, DPSI: 0.0348 ± 0.0093.

Based on the results, minimal differences were observed for the MLSI and the APSI between the FP-based DPSI approach and the kinematics-based DPSI approach, suggesting acceptable comparability (Fig.1). There was a noticeable magnitude difference for the VSI and DPSI between the two approaches, but the trends of the curves were consistent (Fig. 1). Previous research has also suggested that the medial/lateral direction and anterior/posterior direction are the predominant factors in prediction of overall stability [5,7], making the comparability between the two approaches in these directions significant. Our future work aims to evaluate agreement between the two approaches in a more technical manner as well as between different tasks.

Significance: The proposed kinematic-based DPSI approach provides several advantages to previous approaches as it does not require the use of force-plates and is applicable to a larger range of activities since the task is not constrained to the force-plate location. Additionally, the A_{COG} used in the current study are theoretically more precise than those obtained using a single fixed IMU.

References: [1] Burns et al. (2018), *MMWR CDC* 67(18); [2] Moore et al. (2014), *Safety Sci* 70; [3] Wikstrom et al. (2005), *J Athl Train* 40 (4); [4] Ross et al. (2003), *Int J Athl Ther Train* 8(3); [5] Heebner et al. (2015) *Gait Posture* 41; [6] Hanavan. (1964), *W-P Air Force Base;* [7] Goldie et al. (1989), *Arch Phys Med Rehab* 70(7).

LUMBAR SPINE OPENSIM MODEL COMPARISON DURING MILITARY PARACHUTE JUMP LANDINGS

Jazmin Cruz[1,2] and Peter Le*[1]
[1]711th Human Performance Wing (711HPW), Air Force Research Laboratory (AFRL), WPAFB, OH 45433
[2]Oak Ridge Institute for Science and Education (ORISE)
*Corresponding author's email: peter.le.3@us.af.mil

Introduction: More than half of injuries during military training or operations occur during parachute landing due to high impact with the ground [1]. It is common for military test parachutists to perform up to six jumps within a day, across two to three consecutive days of testing. Test parachutists have reported low back pain which could be the result of the repetitive lumbar loading that occurs during jump days. Many musculoskeletal models have been developed to non-invasively estimate and evaluate lumbar loads during tasks like gait, running [2], or lifting [3] that often occur in controlled lab settings. To assess the effects of repetitive parachute jumps, there is a need for a model that can be driven by data obtained from in-field, high-impact jump landings. Therefore, the objective of this pilot study is to estimate lumbar loads using two validated OpenSim models and compare their performance for parachute landing scenarios.

Methods: An IMU-based motion tracking system (MVN Link, Movella™, Inc., Henderson, NV) was used to capture whole-body kinematics of a test parachutist (M, 104 kg, 193 cm) during three free-fall training jumps. Foot impact during landing was measured using plantar pressure in-soles (F-Scan, Tekscan™, Inc., Norwood, MA). Kinematics and kinetics from these wearables were used to drive two popularly used OpenSim models that contain detailed lumbar spines: the lifting full-body (LFB) model [3] and its predecessor, the full-body lumbar spine (FBLS) model [2]. Joint reaction forces (compressive lumbar load) at the L5/S1 disc level were estimated using identical OpenSim pipelines with both models.

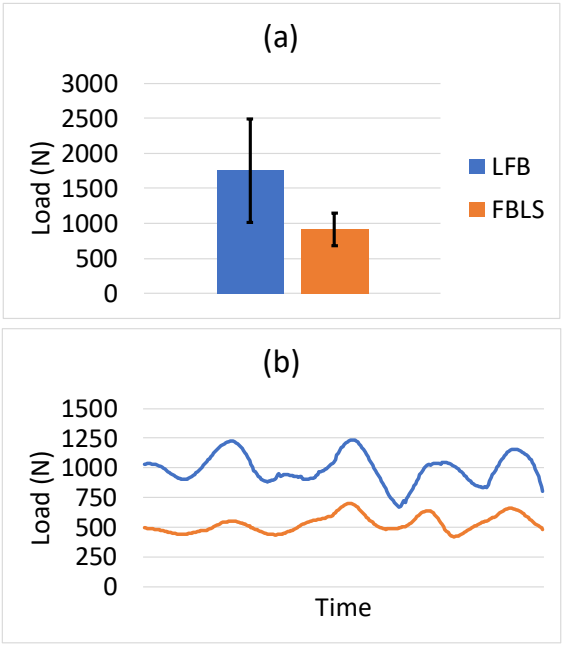

Figure 1a: Average maximum compressive lumbar load at L5/S1 disc level. **Figure 1b:** Compressive lumbar load at L5/S1 disc level across a single trial

Results & Discussion: The average compressive lumbar loads at the L5/S1 disc level for the LFB and FBLS models (Fig. 1a) were 1756.1 ± 919.4 N and 738.2 ± 231.3 N, respectively. Although there is a difference in magnitude between the models, both models predicted lumbar loads that were below the 3400 N limit that is widely adopted for lifting [4], suggesting that a properly performed single jump landing would not cause injury. However, there are no values in literature that would allow for the validation of either model under these jump landing conditions. Even so, the compressive lumbar load trends (Fig. 1b) between the two models are very similar, where the maximum lumbar loads occur at the same time point across all trials. Thus, both models seem to be capable of identifying lumbar load peaks during the jump landing task, which can help researchers identify which landing techniques produce relatively lower lumbar loads.

These preliminary results reflect a free-fall landing, which is likely the lowest impact jump profile that test parachutists perform. Data collection is ongoing and more intensive jump profiles, like static line jumps, will be incorporated into this analysis so that more model comparisons can be made. Additional considerations when choosing between the two models could include computational time and fidelity of body region of interest.

Significance: Currently, there is no musculoskeletal model that has been used to estimate lumbar loads during parachute jump landing. This work is the first to assess the performance of two currently available models using in-field parachute jumping data. Both models similarly capture lumbar loading trends, which can aid in identifying when peak lumbar loads occur. The analysis of jumper kinematics in combination with lumbar load during landing will help to improve landing strategies deployed during training and mitigate injury.

Acknowledgments: The views expressed in this abstract reflect the results of research conducted by the authors and do not necessarily reflect the official policy or position of the Department of the Air Force, Department of Defense, nor the U.S. Government. This work was supported, in part, by an appointment to the Oak Ridge Institute for Science and Education. The study protocol was approved by the Institutional Review Board (IRB) at the Air Force Research Laboratory (AFRL).

References: [1] Steele et al. (2016), *Stud Mechanobiol Tissue Eng Biomater* 19; [2] Raabe and Chaudhari (2016), *J Biomech* 49(7); [3] Beaucage-Gauvreau et al. (2019), *Comput. Methods Biomech. Biomed. Engin.* 22(5). [4] NIOSH (1981), *Tech Report* 81-122;

HOW TRANSTIBIAL LIMB LOSS INFLUENCES THE NEUROMOTOR AND MECHANICAL SIGNATURES OF DYNAMIC BALANCE IN OLDER INDIVIDUALS

Arianna S. Monteiro[1*], Matthew J. Major[2] and Nicholas P. Fey[3]
[1]Department of Mechanical Engineering, The University of Texas at Austin, Austin, TX 78712 USA
[2]Department of Physical Medicine & Rehabilitation, Jesse Brown VA Medical Center, Chicago, IL 60611 USA
*arianna.s.monteiro@utexas.edu

Introduction: Older individuals (≥65 years of age) constitute around two-thirds of lower limb amputations (LLAs) in large cities in Europe, North America and East Asia [1]. Unlike younger individuals, older individuals with LLA face unique mobility challenges due to expected neuromotor changes from aging as well as comorbidities such as diabetes and peripheral arterial disease [2, 3]. These conditions challenge the energy demands required for walking [4] and alter individuals' muscle activity and dynamic balance [5], which have been associated with orthopedic disorders such as lower back pain and osteoarthritis [6]. The purpose of this study was to identify how older LLAs alter the relationship between the neuromotor and mechanical signatures of dynamic balance. We hypothesized that older individuals with LLAs would express a different relationship between their neuromotor (i.e., muscle activity) and dynamic balance compared to able-bodied (AB) controls. We also hypothesized that these relationships would be walking speed dependent.

Methods: Participants included 13 individuals with unilateral transtibial amputation (10 males, 3 females; 10 trauma, 1 infection, 1 cancer, 1 vascular; 71 ± 4 years; 176 ± 9 cm; 86 ± 14 kg) and 10 AB controls (5 males, 5 females; 72 ± 4 years; 168 ± 6 cm; 77 ± 8 kg). Participants were fit with a modified Helen Hayes marker set and electromyographic (EMG) sensors attached bilaterally to the tibialis anterior (TA), medial gastrocnemius (GAS), rectus femoris (RF), medial hamstring (HAM), and the gluteus medius (GMED), as appropriate. Participants walked along a 10-m walkway at a comfortable normal (WN) and fast (WF) self-selected speed for at least five trials per condition. Kinematic and EMG data were measured at 120 and 1200 Hz, respectively. Laboratory-based measures of whole-body and segmental angular momentum (H_{COM} and $H_{Prosthetic}$ and H_{Intact}, respectively) were calculated for each participant and condition (normalized by body mass, height, and speed) of the non-dominant/prosthetic and dominant/intact leg sides. These data were averaged over strides and then an average positive and negative $\bar{H}$ ($\bar{H}_{pos}$ and $\bar{H}_{neg}$) was computed. Across participants, correlation coefficients were calculated between all whole-body and average segmental $\bar{H}$ values (computed over the stride) versus each muscle's integrated EMG value (iEMG) using the Pearson correlation method (α=0.05). EMG profiles for each participant and muscle were normalized to the peak value during the WN condition.

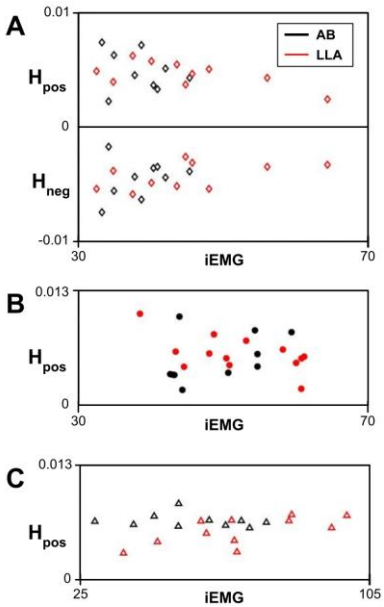

Figure 1: Whole-body and segmental transverse-plane $\bar{H}$ vs iEMG values, where $\bar{H}_{pos}$ is rotation toward the intact/ dominant leg and a $\bar{H}_{neg}$ is toward the prosthetic/non-dominant leg. (A) H_{COM} and non-dominant/prosthetic leg HAM during WN speed. (B) H_{COM} dominant/intact leg TA during WF speed. (C) $H_{Prosthetic}$ and non-dominant/prosthetic leg RF.

Results & Discussion: One of the most consistent findings supporting our hypotheses was related to the HAM within the amputated leg. The amputated leg HAM iEMG was negatively correlated with the positive H_{COM} (r=-0.71, p=0.01, Fig. 1A) in the transverse plane during WN walking, suggesting that an increase in muscle activity was related to a more balanced whole-body rotation towards the intact limb. This muscle was also positively correlated with negative transverse H_{COM} (r=0.62, p=0.04), suggesting that an increase in muscle activity was also related to a more balanced individual overall during gait. These relationships were not significant in the AB group (positive H_{COM}: r = -0.12, p=0.73; or negative H_{COM}: r = 0.02, p=0.97). Results from WF walking (Fig. 1B) differed from WN. The iEMG of the TA within the intact leg was negatively correlated with positive H_{COM} (r=-0.56, p=0.04), while the AB group did not demonstrate a significant correlation (r=0.44, p=0.21). Finally, the prosthetic leg RF (Fig. 1C) was positively correlated with the positive transverse plane H of the amputated leg ($H_{Prosthetic}$) during WF walking (r=0.67, p=0.03), suggesting that an increase in RF muscle activation of the prosthetic leg was related to worse balance (seen as a rotation of the prosthetic leg towards the intact leg). This trend was also not observed in the AB group (r=-0.21, p=0.56).

Significance: This study could inform rehabilitation strategies that enhance active regulation of dynamic balance in older individuals with LLAs. Our findings suggest that at *normal* walking speeds, the amputated leg HAM activity is negatively correlated with the whole-body transverse plane $\bar{H}$ (i.e., increased activity correlated with better dynamic balance). At *fast* walking speeds, this trend was observed within the intact leg TA. The amputated limb RF was the only muscle that produced the inverse relationship (i.e., increased activity correlated with worse balance), at *fast* speeds. The AB group did not express these same cross-sectional relationships, highlighting unique mechanisms used by LLAs.

Acknowledgment: This work was partially supported by the U.S. Department of Veterans Affairs (#1IK2RX001322, granted to MJ Major). Content does not reflect positions of the US Department of Veterans Affairs or US Government.

References: [1] Unwin (2000) *British J of Surgery* 87(3); [2] Fortington et al. (2012) *JAMDA* 13(4); [3] G. Carmona et al. (2005) *Diabetes Metab J* 31(5); [4] K.L. Andrews (1996) *Arch. Phys. M.* 77(3); [5] M.A. Price et al. (2019) *EMBS* 27(8); [6] L.Wade et al. (2022) *BMJ Open* 12(11)

DECREASED TRUNK CONTROL MECHANISMS DURING OBSTACLE AVOIDANCE IN OLDER ADULTS

Alyssa O. Vanderlinden[1*], Masood Nevisipour[2], Thomas Sugar[2], Hyunglae Lee[3]
[1]Department of Kinesiology, New Mexico State University, Las Cruces, NM, USA
*Corresponding author's email: avander@nmsu.edu

Introduction: Death rates due to falls have recently increased by over 4% annually among older adults aged 65 and older [1], with over 30% of adults in this age range experiencing a fall annually [2]. Trunk control is a crucial mechanism of stability, which leads to better control of an individual's center of mass to aid in preventing falls. Older adults have demonstrated a decreased ability to stabilize the trunk by reducing trunk flexion and velocity after a trip [3]. A potential scenario for a fall is during walking while avoiding an obstacle. There is limited research on the mechanisms of older adult trunk control during obstacle avoidance, specifically focusing on both kinematics and kinetics. A previous study examined lower body and trunk kinematics and kinetics in young healthy adults during an obstacle avoidance task, in which the trunk demonstrated the largest increase in flexion angle and extension torque during obstacle avoidance [4]. However, this type of analysis has not been done with an older population, and comparing the mechanisms behind trunk control between older and younger adults would support our understanding of how the older population maintains their trunk during this type of challenging task. Therefore, the purpose of the study is to compare lower-body and trunk kinematics and kinetics between young and older adults during an obstacle avoidance task. Due to past literature on young adults demonstrating the largest difference in trunk biomechanics during obstacle avoidance compared to walking [4], it is hypothesized that the trunk in older adults will be the main segment to reveal differences in kinematics and kinetics between groups during obstacle avoidance.

Methods: 10 healthy older adults (65+, 3 males, 7 females, 72.3±5.6 years, 166.6±7.3 cm, 75.8±15.2 kg), and 12 healthy young adults (18+, 7 males, 5 females, 23.2±2.7 yrs, 173.5±9.8 cm, 65.9±12.8 kg) participated in the study. Participants walked on an instrumented split-belt treadmill (2 kHz; Bertec, OH, USA) at 1 m/s while kinetic data was collected. After a 5-minute walking period, 5 obstacle avoidance trials were performed as a prism obstacle was manually released on the treadmill. Participants walked over the obstacle with their lead leg and the trail leg. During all trials, kinematic data was collected using an 8-camera three-dimensional motion capture system (200 Hz; Vicon Motion Systems, Oxford, UK). Kinematic and kinetic data were smoothed using a low-pass Butterworth filter at 6 Hz and 20 Hz, respectively. The filtered data were imported to OpenSim for analysis. Mean and standard deviation values were calculated for maximum hip, knee, ankle, and trunk flexion/dorsiflexion angle, and flexion/extension muscle torque during lead leg and trail leg obstacle avoidance. A linear mixed effects model (α=0.05) was used to determine significant differences between groups. Tukey's HSD was used for post-hoc comparisons.

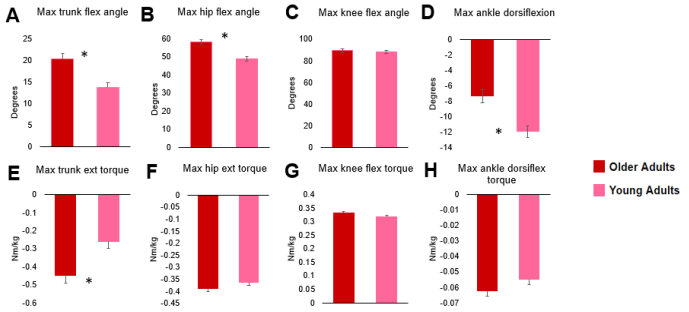

Figure 1: Lead leg kinematic and kinetic data comparisons between older and young adults. (*) denotes significance p<0.05

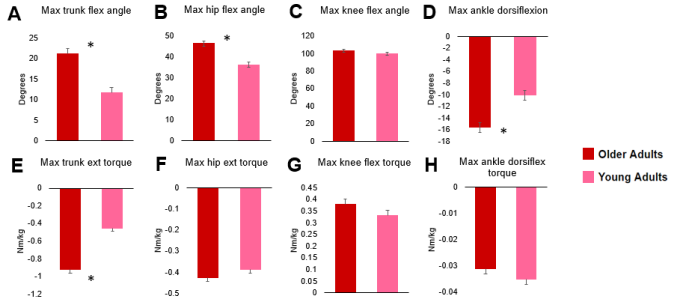

Figure 2: Trail leg kinematic and kinetic data comparisons between older and young adults. (*) denotes significance p<0.05

Results & Discussion: Analysis revealed that older adults had increased trunk flexion angles (lead leg: p=0.03; trail leg: p<0.001) and trunk extension torques (lead leg: p=0.03; trail leg: p<0.001) compared to young adults during obstacle avoidance. The trunk was the only segment/joint that demonstrated differences in both kinematic and kinetic data, when comparing older and younger adults, which was demonstrated in both the lead leg (Figure 1) and the trail leg (Figure 2). These findings suggest that older adults have limited trunk control mechanisms when crossing over an obstacle while walking, which supports the hypothesis. Increased trunk flexion is indicative of decreased stability [3], and the increased trunk muscular torque may have been used to assist in stabilizing the trunk to successfully avoid the obstacle. Since the trunk accounts for over half of an individual's body mass [3], older adults may be attempting to control their center of mass while crossing an obstacle which accounts for the observed differences in both trunk kinematics and kinetics [5].

Significance: Understanding limited trunk control during obstacle avoidance among older adults provides insightful information about the impacts of aging on stability. The amplified demands the trunk has to overcome to successfully avoid an obstacle may increase the risk of falling for adults who have decreased muscle strength or reduced mobility. The results from this study highlight that the trunk is important for clinicians and researchers to prioritize when considering therapies, interventions, and potential assistive devices.

Acknowledgments: This study was supported by a grant from "The Global KAITEKI Center" (TGKC) of the Global Futures Laboratory at Arizona State University.

References: [1] Kakara et al. (2024), *Pub Hlth Rprts* 139(1); [2] Appeadu et al. (2022), *StatsPrls Pub*; [3] Grabiner et al. (2008), *Jrl Elmyphy & Kin* 18(2); [4] Nevisipour, et al. (2023). *Hmn Mvmnt Sci*, 87; [5] Winter (1995), *Waterloo Bmch*

HIGHER COMPLEXITY IN MOVEMENTS INDICATES BETTER SENSORIMOTOR COORDINATION

Kolby J. Brink[1*], Aaron D. Likens[1]
[1]Department of Biomechanics, University of Nebraska at Omaha, Omaha, NE USA
*Corresponding author's email: kolbybrink@unomaha.edu

Introduction: Numerous studies spanning the last two decades have shown that healthy biological signals exhibit a complex time series structure portraying statistical long-range correlations such that the size of movements (e.g., steps, arm swings) tend to be related over time [1,2]. Those findings confer that movements exhibiting long-range correlations enhance coordination among physiological processes, leading to an optimal functional state [3]. Synchronizing movements to a variable metronome structured with long-range correlations restores complexity in pathological and older populations. Variable metronomes also promote resilience to mechanical disturbances, suggesting that an optimal state of complexity may also enhance sensorimotor efficacy. The purpose of this study was to investigate whether training movements to exhibit a complex variability during a generalized task will improve sensorimotor coordination.

Methods: 24 healthy adults performed a pre- and post- Sensorimotor Task (ST) as well as a training task. Subjects performed a pre-ST of tapping alternately between two rectangular target plates as quickly and accurately as possible. The amplitudes and widths of the targets were randomized with 16 different combinations, changing the index of difficulty of the task (Fig. 1A). Subjects were then randomly placed in one of three groups which dictated whether they received training and if so, what type of training they received. Subjects in Groups 1 and 2 underwent 4 sessions of training over 2 weeks following the pre-ST. During training, subjects were seated and performed wrist rotations in a chair with modified armrests that had attached manipulanda (Fig. 1B). Group 1 performed continuous wrist rotations synchronized to a variable metronome lasting 30 minutes. Group 2 performed wrist rotations at a self-selected pace with no metronome for 30 minutes. After the training sessions were completed, Groups 1 and 2 completed a post-ST. Group 3 only performed a pre- and post-ST with no training. Sample entropy was used as the dependent measure for assessing movement variability. Error percentage and index of performance were used as the dependent measures for the ST (Fitts' Law task).

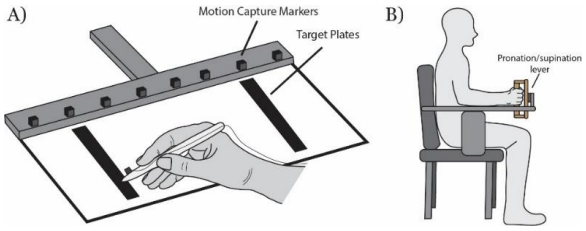

Figure 1: A) Illustration of motor task (Fitts' law task) used to determine pre and post changes in sensorimotor precision. B) Illustration of training task apparatus where subjects would be seated and perform pronated and supinated wrist oscillations.

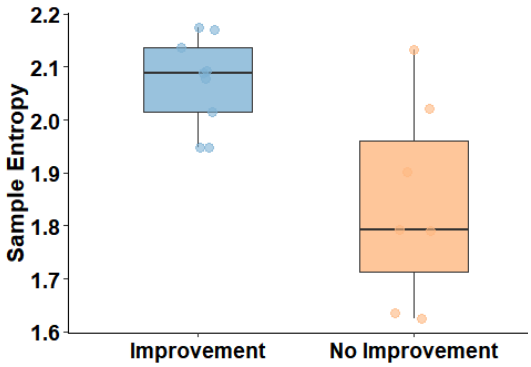

Figure 2: Box plots of sample entropy values for subjects who improved their index of performance for the ST compared to those who did not.

Results & Discussion: The error percentage in the ST was evaluated using a one-way Bayesian repeated measures ANOVA, employing default Cauchy priors. The model with session as a main effect (BF10 = 22.42) strongly favored the alternative over the Null model. The post hoc analysis indicated substantial evidence that error percentage did not vary between the Fractal training group and no training group. Similarly, there was substantial evidence that the Fractal training group did not differ from the SS group. Finally, substantial evidence suggested no difference between the no training group and SS group. We then compared the subjects who underwent training that improved and who did not improve on the ST (Fig. 2). A Bayesian paired samples t-test was used to compare the groups. The test indicated strong evidence of a difference in entropy during training between the improved and no-improvement groups ($BF_{10} = 4.373$).

Our study revealed that implementing a generalized fractal training program did not yield significant improvements in sensorimotor precision beyond participants' prior task experience. It may be that the lack of observed effects could be due to the inherent optimal variability in movement among young healthy adults, rendering additional training less impactful. However, when examining participants based on their performance improvement on the sensorimotor task (ST), we found that regardless of whether individuals received variability training or performed the task without intervention, those exhibiting higher movement complexity demonstrated greater enhancements in sensorimotor coordination post-training. Thus, individuals with more complex movement patterns appear to improve sensorimotor performance at a greater rate.

Significance: The current study's findings carry significant theoretical implications for the Optimal Movement Variability Hypothesis. Specifically, they suggest that simply modifying movements to achieve optimal variability might not directly apply from a broad task to a particular coordinated movement. In other words, young adults who already exhibit inherently optimal variability in their movement patterns might not derive additional benefits from targeted training aimed at enhancing such variability. However, individuals demonstrating greater complexity in their overall movements tend to exhibit improved performance on sensorimotor tasks.

Acknowledgments: KB is supported by the GRACA grant. AL is supported by awards from the NIH (P20GM109090) and the NSF (2124918). The authors declare no conflict of interest.

References: [1] Scafetta N et al. *Chaos Interdiscip J Nonlinear Sci.* 2009; 19:026108. [2] Goldberger AL. *Ann N Y Acad Sci.* 1990;591:402–9. [3] Stergiou N et al. *J Neurol Phys Ther.* 2006;30:120–9.

INFLUENCES OF PROSTHETIC FOOT TYPE ON TRUNK-PELVIS MECHANICS DURING GAIT

Julian C. Acasio[1,2], Pawel R. Golyski, Courtney M. Butowicz, Jason T. Maikos, Brad D. Hendershot
[1]Extremity Trauma and Amputation Center of Excellence, Falls Church, VA, USA [2]Walter Reed National Military Medical Center, Bethesda, MD, USA
*Corresponding author's email: julian.c.acasio.civ@health.mil

Introduction: Low back pain (LBP) is highly prevalent among individuals with lower limb loss [1]. While multifactorial, post-amputation LBP is often attributed to altered and exaggerated trunk motions during gait [2], suggested to be a compensatory mechanism to generate propulsive forces following the loss of lower limb musculature. Advanced prosthetic foot designs, such as powered ankle-foot prostheses (POW), may mitigate these compensatory motions. While prior work has extensively investigated trunk-pelvis mechanics with lower limb loss (e.g., amputation level, LBP status, walking speed [3-5]), the effect of prosthesis type has not been explicitly investigated. Thus, the purpose of this analysis was to characterize trunk-pelvis mechanics among persons with unilateral transtibial limb loss (UTLL) while walking with three different types of prosthetic feet – energy storing and returning (ESR), ESR with articulation (ART) and POW devices. We hypothesized that POW vs. ESR and ART devices would result in lesser trunk and pelvis angular ranges of motion (ROM) and smaller peak lumbar (i.e., L5-S1) moments.

Methods: Nine individuals with UTLL (7 male/2 female, mean±SD age: 40±8 yrs, stature: 179±5cm, body mass: 89.7±14.1kg, time since amputation: 63±96mo) wore three different prosthetic feet (ESR, ART, POW) for one week, each in a random order. After each acclimation period, overground gait evaluations tracking full-body kinematics (120Hz) and ground reaction forces (1200Hz) were completed at three targeted speeds (1.0, 1.3, 1.5 m/s). A full-body model with UTLL was scaled to each participant [6]; trunk and pelvis angles and lumbar moments were then estimated in OpenSim 4.4 [7]. Tri-planar trunk and pelvis ROM, peak lumbar moments, and walking speed (per stride) were determined. A linear mixed effects model with a fixed effect of prosthetic foot type and covariate of walking speed assessed main and interactive effects of prosthetic foot type and walking speed ($p<0.05$).

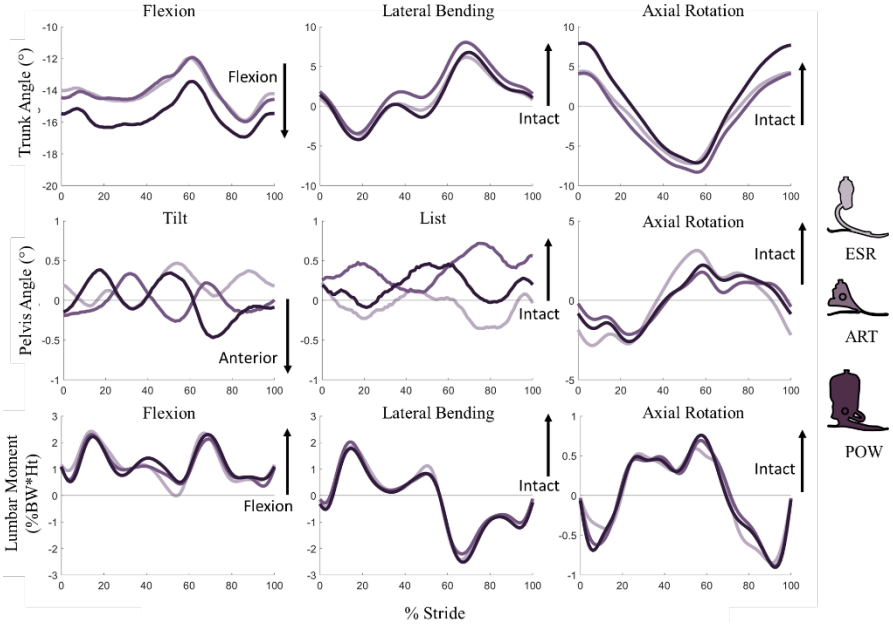

Figure 1. Trunk (top) and pelvis (middle) angles and lumbar moments (bottom) across intact-side stride using energy storing and return (ESR), articulating (ART), and powered (POW) devices.

Results & Discussion: A main effect of foot type was observed in tri-planar pelvis ROM ($p<0.033$). Additionally, foot-speed interaction effects were observed in pelvis axial rotation ROM ($p=0.001$), with POW vs. ESR and ART devices resulting in lesser increases in pelvis ROM with increasing walking speed. No other foot or foot-speed interaction effects were observed ($p>0.142$). In partial support of our hypothesis, lesser pelvis axial rotation ROM was observed in POW vs. ESR devices (Fig 1). However, contrary to our hypothesis, greater pelvis tilt and list ROM were observed in POW vs. ESR and ART feet (Fig 1). Moreover, no differences were observed in neither trunk ROM nor peak lumbar moments between devices (Fig 1). Together, our findings suggest POW devices may not mitigate aberrant trunk and pelvis motion following UTLL. However, observed foot-speed interactions suggest POW devices may offer benefits at higher task demands.

Significance: This analysis builds upon prior work characterizing trunk-pelvis mechanics following lower limb loss [3-5]. These results suggest that while POW devices may not affect trunk and pelvis mechanics at typical walking speeds, POW vs. ESR and ART devices may result in lesser demand on the trunk/pelvis at faster walking speeds. Future work should investigate more demanding tasks (e.g., ramp ascent) and/or other aspects of trunk-pelvis mechanics (e.g., segmental coordination), include trunk and pelvic musculature in musculoskeletal models [5], and incorporate data collected outside the lab to improve ecological validity and comprehensively characterize trunk-pelvis mechanics with different ankle-foot prostheses following UTLL.

Acknowledgments: Support was provided by the Congressionally Directed Medical Research Programs, Orthotics and Prosthetics Outcomes Research Program (Award #W81XWH-17-2-0014). The views expressed in this abstract are those of the authors, and do not reflect the official policies of the U.S. Departments of Defense, Veterans Affairs, nor the U.S. Government. The authors would like to thank Jonathan R. Gladish, John M. Chomack, and David V. Herlihy for their contributions to data collection and processing.

References: [1] Taghipour et al. (2009) *J Ortho Trauma* 23 [2] Coenen et al. (2012) *Clin Biomech* 27 [3] Hendershot et al. (2018) *J Biomech* 70 [4] Acasio et al. (2022) *J Biomech* 135 [5] Butowicz et al. 2024 *J Biomech* [6] Wilson et al. (2022) *Comput Methods Biomech Biomed Engin* 26 [7] Delp et al. (2007) IEEE Trans Biomed Eng 54

DESCENDING EXTENSION LADDER FOOT PLACEMENT AND ITS RELATIONSHIP TO SWING TRAJECTORY AND FOOT READJUSTMENTS

Violet M. Williams[1*], Mark S. Redfern[1], Kurt E. Beschorner[1]
[1]Department of Bioengineering, University of Pittsburgh, Pittsburgh, PA, USA.
*Corresponding author's email: violet.williams@pitt.edu

Introduction: Ladder falls accounted for over 169,000 trauma center visits in the US between 2007-2017 with 36% of these falls requiring hospital stays greater than 5 days, highlighting the health impact of these falls [1]. Although fall risk is present throughout all aspects of ladder use, descending the ladder is 4 times more likely to lead to an injury than during ascent [2]. While the events leading to ladder falls vary, missteps are common, accounting for 10% of ladder falls [3].

Accurate foot placement is necessary when descending ladders. Foot placements are preceded by swing phase, where the foot steps off a rung, moves around that rung, and then targets the placement on the next rung. On straight ladders, a farther anterior foot placement has been associated with decreased slip risk and maintained foot contact during slip recoveries [4]. The goal of this study was to examine the relationship between foot placement and the preceding swing trajectory and the succeeding misstep risk. This study hypothesized that greater swing trajectory adjustments and less movement efficiency would be associated with farther posterior foot placements. This study hypothesized that a farther posterior foot placement would be associated with an increased likelihood of misstep risk.

Methods: Two extension ladder configurations were used, each set to 75.5°. A traditional extension ladder with the fly section stacked on top of the base section, and the reversed design with the fly section stacked underneath the base section. The 3rd rung of each configuration was attached to a force plate (AMTI) while 12 motion tracking cameras (Vicon) were used to collected kinematic time-synced data. Participants were asked to descend from the 5th rung of the ladder at a comfortable but urgent pace for three trials of each configuration.

A metric of the swing trajectory was the peak heading curvature (i.e, a metric to capture a shift in trajectory direction) [5] quantifying the magnitude of swing adjustment. Another metric was the foot path ratio (the length of the foot path normalized by the optimal length), which is a metric of movement efficiency [6]. Peak heading curvature is the 2nd derivative of heading angle (angle between a marker's target and velocity vectors) [5] occurring during mid-swing. Mid-swing is when a trajectory adjustment will have the largest impact on foot placement with larger values indicating sharper, high intensity adjustments. Foot path ratio was calculated from the trajectory's posterior apex (the most posterior position reached by the foot during descent). Foot placement was found at initial foot contact with the 3rd rung, relative to the midpoint of the rung, normalized to foot length (0% = toe contact; 50% = midfoot contact). Foot readjustments were considered a metric of missteps since they indicated climber discomfort with their current foot placement. Foot readjustments were identified as a change in foot position to a new position after initial contact, identified based on a review rater of motion tracking videos conducted by 2 reviewers. The relationships between swing trajectory metrics and foot placement were investigated using Spearman correlations, while a logistic regression was performed with foot placement as the independent variable and foot readjustments as the dependent variable.

Results & Discussion: Foot placement was determined to be a significant predictor of foot readjustments ($\chi^2 = 15.33$; $p < 0.001$) yet no significant relationships were found between swing trajectory parameters (foot path ratio, $\rho_{87} = 0.15$; $p = 0.17$, or peak heading curvature, $\rho_{87} = 0.10$; $p = 0.36$) and foot placement. Farther anterior foot placements were associated with decreased foot readjustments (Figure 1). A 25% anterior shift in foot placement (approximately the distance between sections of an extension ladder) resulted in an Odds Ratio of 0.01, indicating that a climber would have 99% reduced odds of repositioning their foot given this anterior shift. These results indicate that foot placement may be independent of descending foot swing, with movement efficiency and intensity of movement adjustments having little impact on the final foot placement. Thus, foot placement is likely impacted by other factors such as ladder base/fly configuration. Farther anterior foot placements were again found to correspond with better outcomes that reflect lower fall risk, demonstrating the importance of maintaining anterior foot placements during ladder climbing.

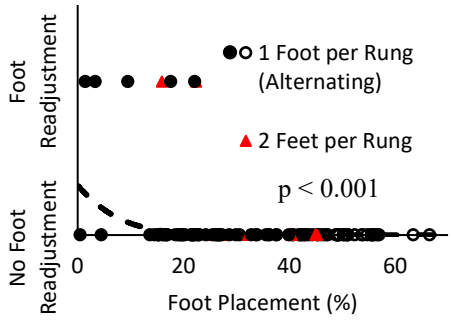

Figure 1: Logistic regression of foot readjustments against foot placement where lower foot placement values (farther posterior) predict higher odds of a foot readjustment. Filled circles = traditional, open circles = reversed, triangles = 2 feet per rung, and the dashed line represents the logistic equation.

Significance: The relationship between foot placement and foot readjustments further demonstrates the importance of foot placement in ladder climbing and expands our understanding of extension ladder use and misstep risk. This outcome provides strong support for changes in recommended climbing form and ladder designs that can shift foot placements anteriorly, particularly in extension ladders.

Acknowledgments: The authors would like to acknowledge Sarah Griffin, Julia Dunn, and Jenna Trout. This work was supported by NIOSH R01OH011799.

References: [1] Liasidis et al. (2022), *J. Trauma Acute Care Surg.* 93(3); [2] Rapp van Roden et al. (2021), *Appl. Ergon.* 96(103492).; [3] Cohen et al. (1991), *J. Saf. Res.* 22(1); [4] Martin et al. (2020), *J. Biomech.* 99(109507); [5] Reynolds et al. (2005), *J Physiol.* 569(2); [6] Lang et al. (2005), *Exp. Brain Res.* 166(1);

WEARABLE TENDON KINETICS ON SLOPES AND STAIRS

Elizabeth A. Schmida[1*], Yiteng Ma[1], Peter G. Adamczyk[1], Darryl G. Thelen[1], Alex J. Reiter[1,2]
[1]Department of Mechanical Engineering, University of Wisconsin-Madison
[2]Department of Biomedical Engineering, Saint Louis University
*schmida@wisc.edu

Introduction: Despite the increasing reliance on wearable sensors to monitor biomechanics in real-world environments, muscle loads reported in these activities are still based on indirect measures or derived from musculoskeletal models. Shear wave tendon tensiometry allows for the direct measure of muscle-tendon loading [1] and, with recent improvements in portability, allows for synchronous collection on up to four tendons and force calibration measurements outside of lab settings. The purpose of this study was to demonstrate the feasibility of the wearable tensiometry system to capture patellar tendon (PT) and Achilles tendon (AT) kinetics when walking on slopes and stairs.

Methods: Tensiometers [2] were placed bilaterally on a healthy participant's PTs and ATs. Shear wave excitation and data acquisition from skin-mounted accelerometers were controlled by two Raspberry Pi 4Bs and four Measurement Computing Corps MCC172 HATs [3] secured within a running-style backpack. The participant first performed calibration tasks [2] to determine the relationship between shear wave speed and tendon force [1]. The participant stood with the first metatarsophalangeal joint (for AT) or the ankle joint center (for PT) of each foot isolated on a portable force plate connected to the wearable system; the participant swayed right to left to vary foot load. The participant then walked at their self-selected pace up and downhill on an outdoor course. The wearable system simultaneously recorded tensiometer and GPS location data from a backpack-mounted receiver. GPS data was used to estimate slope of each step from a previously collected lookup table. The participant also walked up and down three continuous flights of stairs. A custom program calculated tendon forces and identified foot contacts. For up and downhill walking, strides were binned according to slope from -8° to +8° in two-degree increments for analysis (e.g. the 0° bin includes strides with –1° to +1°, and the 2° bin includes +1° to +3°).

Results & Discussion: Compared to the 0° bin, mean peak PT force increased for both up and downhill walking (26% and 56% respectively at the steepest slopes) (Fig. 1). This finding agrees with quadriceps force estimates from lab-based instrumented slope walking [4]. During uphill walking, greater peak PT forces can be attributed to increased knee flexion at foot contact [5-6]. Downhill walking may require increased PT loads to control the body's descent as the knee flexes late in stance [6]. Uphill walking also resulted in a 10% increase in peak AT force, and downhill a 28% decrease, for the ±8° bins relative to the 0° bin. In agreement with previous studies, the AT was also loaded earlier in stance to slow the body's advance during downhill walking [3][7]. Similar to joint moments collected during lab-based stair climbs [8-9], tensiometry-derived forces in both PT and AT featured a double peak pattern. The first peak reflects pull-up during stair ascent and weight acceptance during descent, while the second peak represents push-off in ascent and controlled lowering in descent. One study has reported similar quadriceps force trends during ascent [10]; further estimates of quadriceps and triceps surae forces could be derived from published stair data to fully compare lab-based and tensiometry measures for stairs. Future work will assess tendon kinetics across multiple subjects and incorporate kinematic data.

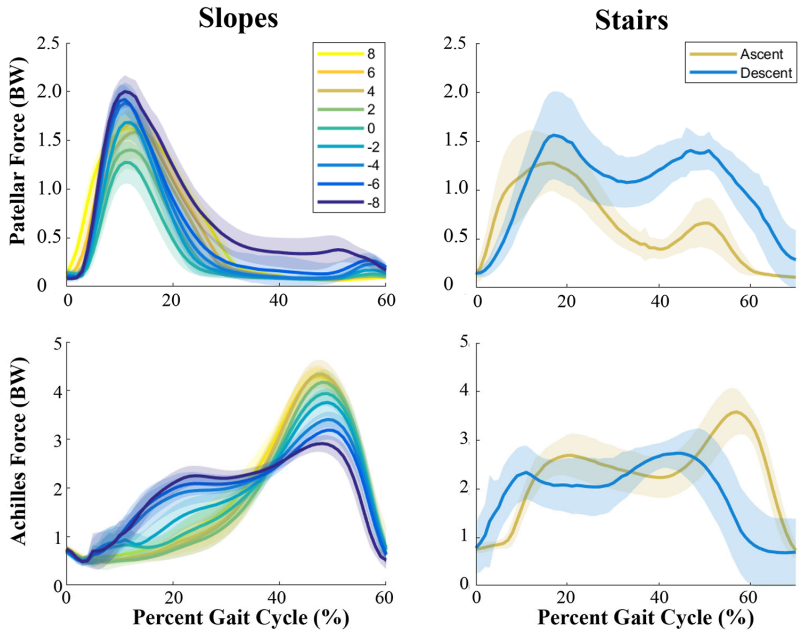

Figure 1: Representative walking patellar and Achilles tendon forces (body weight (BW)) during stance, collected using the wearable tensiometer system. Mean tendon forces (with shaded standard deviations overlaid) walking up/downhill binned by slope (left), and up/down three flights of stairs (right).

Significance: This methodology demonstrates the capabilities of wearable tensiometry to capture tendon kinetics during locomotion on slopes and stairs. This represents a significant advancement over lab-based studies that relied on complex, immobile equipment to obtain comparable results. The portability of the system may allow for objective assessments of performance, injury risk, and rehabilitation in real-world environments based on direct measures of muscle-tendon loading.

Acknowledgments: Funding from the DOD CDMRP (129866603), NSF DARE (2019621), and NIH STTR (R42AR074897).

References: [1] Martin+, *Nat Comm*, 9(1), 2018; [2] Reiter+, *MSSE*, 2024; [3] Harper+, *Sensors*, 22(4), 2022. [4] Alexander+, *Gait and Post*, 47, 2016; [5] McIntosh+, *J Biomech*, 39(13), 2006; [6] Lay+, *J Biomech*, 39(9), 2006; [7] Lichtwark+, *J Exp Biol*, 209, 2006; [8] Whitehead+, *J Biomech*, 49(13) 2016. [9] Protopapadaki+, *Clin Biomech*, 22(2), 2007; [10] Rasnik+, *PloS one*, 11(6), 2016.

MUSCLE FORCES DURING HIGH AND MODERATE INTENSITY HANDCYCLING EXERCISE

Kellie M. Halloran[1]*, Michael D.K. Focht[1], Joseph Peters[2], Ian Rice[2], Mariana E. Kersh[1,3,4]
[1]Department of Mechanical Science and Engineering, University of Illinois Urbana-Champaign
[2]Department of Kinesiology and Community Health, University of Illinois Urbana-Champaign
[3]Carle Illinois College of Medicine, University of Illinois Urbana-Champaign
[4]Beckman Institute for Advanced Science and Technology, University of Illinois Urbana-Champaign
*email: kellie2@illinois.edu

Introduction: People with spinal cord injuries face increased rates of cardiovascular disease (CVD) [1], which can be mitigated with exercise. However, exercise can be challenging to implement because of the risk of overuse injuries. Up to 63% of wheelchair users have rotator cuff tears [2], often in the supraspinatus and infraspinatus tendons [3]. While high intensity interval training (HIIT) improves cardiovascular health [4], the applied forces during handcycling—a crank-driven exercise mode—are 50% higher during HIIT compared to handcycling moderate intensity continuous training (MICT) [5]. We therefore hypothesized that muscles forces will be higher during HIIT compared to MICT, and aimed to quantify the degree to which muscles forces increase during HIIT compared to MICT.

Methods: Full-time wheelchair users (n=20) completed three exercise sessions using a recumbent handcycle (Top End, Invacare, USA) adjusted for each participant. Session 1: Incremental test to exhaustion, where power output increased by 10 W every minute. Session 1 was used to calculate each subject's peak power output (PPO). Session 2: HIIT- 10 intervals of 1 minute at 90% PPO and 1 minute at 10% PPO. Session 3: MICT - 45% PPO until reaching an equivalent workload to HIIT. During HIIT and MICT, 15 reflective markers were placed on the torso and arm to collect motion data with a 10-camera system (Vicon, Yarnton, UK). Applied forces and torques were measured using a custom handle instrumented with a six-axis load cell (ATI, Apex, USA). Kinetic and kinematic data were collected for 30 seconds at 6 workload-matched timepoints (TP1-TP6) during HIIT and MICT. Shoulder joint moments were calculated using inverse dynamics and decomposed into muscle forces using static optimization in a previously validated musculoskeletal model [6] (OpenSim [7]). Supraspinatus and infraspinatus muscle forces were compared during HIIT and MICT at TP1-TP6 (MATLAB, vR2021a). Data were tested for normality using the D'Agostino-Pearson K2 test. Most data were not normally distributed and were therefore compared using Statistical non-Parametric Mapping (SnPM, spm1d vM.0.4.10 [8]) with paired t-tests at $\alpha = 0.05$.

Results & Discussion: Both supraspinatus and infraspinatus muscle forces were largest during the beginning of the propulsion cycle (Fig. 1A, C, ~ 90°). During the first half (0-180°) of the propulsion cycle, supraspinatus forces were on average 1.4 times higher during HIIT compared to MICT during the beginning of exercise from TP1-TP3 (Fig 1B). Similarly, infraspinatus muscle forces were 1.3 times higher in HIIT compared to MICT both at the beginning of exercise (TP1 and TP2) and as exercise continued (TP4 and TP5). During the last quarter of propulsion (~270-360°), supraspinatus force was the same for both HIIT and MICT. However, there were higher forces in the infraspinatus during MICT throughout the entire exercise session (TP1-6, Fig. 1D). Thus, high intensity does not always result in increased muscle force when compared to moderate intensity exercise. Nonetheless, the largest supraspinatus and infraspinatus muscle forces occurred during HIIT.

Of note was the gradual but consistent increase in muscle force during MICT over the course of exercise. In contrast, the maximum muscle forces were more variable during HIIT with the highest forces occurring both early (TP1) and late in exercise (TP6). It is possible the lack of rest periods during MICT requires increased used of both supraspinatus and infraspinatus muscles forces to maintain the power required to complete the exercise session.

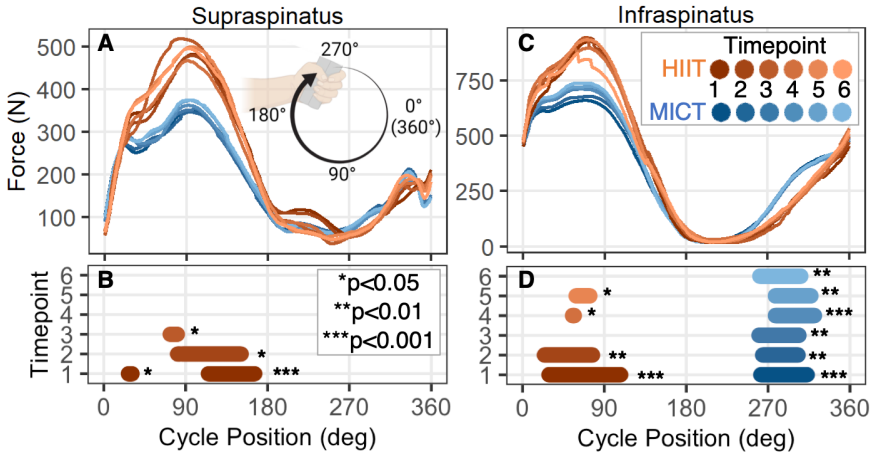

Figure 1: Supraspinatus (A) and infraspinatus (C) muscle forces during HIIT and MICT. (B,D) Significant differences in muscle forces between exercises, with orange indicating higher HIIT forces and blue indicating higher MICT forces.

Significance: Muscle forces are a direct indication of tendon loading and are an essential component of evaluating the potential risk of injury for an exercise intervention. While some tissue loading can lead to positive adaptations and strengthening, overloading can lead to tissue degradation and damage. Further work is needed to understand the long-term effects of HIIT vs MICT-based exercise and whether targeted strengthening regimens could be used to minimize the injury risk while still providing cardiovascular benefits.

Acknowledgments: Griffin Sipes, Ethan Park, and Danielle Siegel assisted with data collection and processing. Funding: NSF.

References:[1] Tanhoffer+ (2014), *J Phys Act Health*; [2] Akbar+ (2010), *J Bone Jt Surg*; [3] Lal (1998), *Spinal Cord*; [4] Koontz+ (2021) *Spinal Cord* [5] Halloran+ (2023), *J Biomech*; [6] Wu+, 2016, *J Biomech*; [7] Delp+ (2007), *IEEE T Biomed Engr*; [8] Nichols & Holmes (2008) *Hum Brain Mapp*.

IMPACT OF ARM ABDUCTION ACCELERATION ON CENTER OF MASS DYNAMICS DURING SLIPS: A COMPARATIVE STUDY OF OLDER AND YOUNGER ADULTS

Jonathan S. Lee-Confer[1*], Matthew K. Lo[2], Karen L. Troy[3]
[1]Department of Physical Therapy, University of Arizona, Tucson, AZ
[2]Department of Biomedical Engineering, University of California Irvine, Irvine, CA
3Department of Biomedical Engineering, Worcester Polytechnic Institute, Worcester, MA
*Corresponding author's email: leeconfer@arizona.edu

Introduction: Slips and falls are major health care concerns with injuries from falls ranking as a top 3 personal health care cost in the United States [1]. Prior research reported that arm abduction movements during a slip incident reduce falls by over 60% [2] by reducing center of mass excursions [3,4] in younger adults. Older adults have shown a 37.5% decrease in arm abduction acceleration compared to younger adults during a slip [5], and it is currently unknown how the decrease in arm abduction acceleration among older adults influences CoM dynamics during a slip incident. Given the established decrease in arm abduction acceleration with age, we expected that older adults would exhibit an increased CoM excursion compared to younger adults during a slip incident.

Methods: 11 older adults (average age: 72 years) and 11 younger adults (average age: 25 years) participated in this study. All walking trials were performed on a modified laboratory walkway imbedded with Plexiglas at University of Illinois Chicago. Participants were unaware of when the slip trial would occur, and during the slip trial, a thin film of dried water-soluble lubricant was activated with a spray bottle of water at a time unbeknownst to the older participants, whereas younger adults stepped onto a thin applied layer of mineral oil. The static coefficient of friction remained similar between younger and older adults with a COF of 0.19 ± 0.13. Motion analysis was modeled in three dimensions with an eight-camera motion capture system collecting data at 60 Hz. Peak abduction acceleration of the arm contralateral to the slipping foot and frontal plane CoM excursion was calculated. Independent one-tail t-tests compared CoM excursions between age groups in SPSS software.

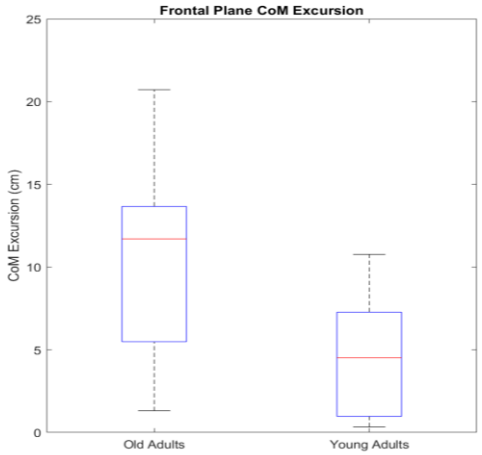

Figure 1: Frontal plane CoM excursion between older (n = 11) and young adults (n = 11). Young adults significantly reduced their frontal plane CoM excursion compared to old adults during a slip incident ($p < 0.01$).

Results & Discussion: *Our findings revealed that young adults significantly reduced their frontal plane CoM excursion compared to older adults* (4.6 ± 3.5 vs. 10.47 ± 6.6 cm, $p < 0.01$, Fig. 1). This finding is important as reducing CoM excursion is imperative to reduce the likelihood of losing balance. In the Margins of Stability (MoS) equation, one can reduce the likelihood of falling by increasing the base of support (BoS) or reducing the CoM excursion. As such, finding ways to increase arm abduction acceleration may potentially serve utility in reducing the CoM excursion and reducing the likelihood of falling. *A significant moderate correlation was found between peak lateral CoM excursion and peak arm abduction acceleration* ($r = -0.52$, $p < 0.02$, Fig. 2). This suggests that enhancing arm abduction could be a viable strategy for reducing falls during a slip incident. Particularly, this is important as older adults are reported to exhibit significantly decreased quantity and proportions of type IIb fibers in the deltoid muscle from the ages of 50 until 79 [6]. The older adults (average age: 72 years) in our prior study may have exhibited slower arm abduction acceleration due to decreases in fast twitch fiber types.

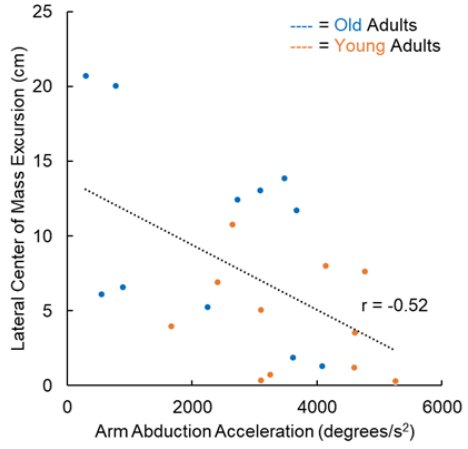

Figure 2: Correlation indicating a negative moderate correlation that increased arm abduction acceleration reduces lateral center of mass during a slip incident ($r = -0.52$, $p < 0.02$).

Significance: These findings provide a basis for incorporating arm strength and speed/power training into physical therapy fall prevention programs for older adults [7]. There is need for intervention studies exhibiting efficacy of this training and this study sets the stage for further research to explore the effect of targeted arm power training interventions across diverse populations.

References: [1] Dieleman (2016), *Jama*, 316(24); [2] Lee-Confer et al. (2022), *Human Mov Sci* 86,103016; [3] Marigold et al. (2003), *J Neurophysiol* 89(4); [4] Lee-Confer et al. (2023), *J Biomech* 157,111737; [5] Lee-Confer et al. (2023), *bioRxiv*, 2023-12; [6] Fayet et al. (2001), *Acta Neuropathologica* 101,358-366/ [7] Lee-Confer (2024), *Front Sports Act Living* 1371730

A NOVEL BIOMECHANICAL VARIABLE, THE FOOT-BODY COUPLING ANGLE, PREDICTS SLIP RISK WHILE DESCENDING A LADDER

Sarah C. Griffin[1*], Kurt E. Beschorner[1]
[1]Universtiy of Pittsburgh Department of Bioengineering *Corresponding author's email: scg57@pitt.edu

Introduction: Each year, 22,330 non-fatal injuries and 171 deaths cite ladders as the primary cause in the United States [1]. Slips are the cause for approximately 14% of these incidents, yet literature has not adequately investigated what factors influence a person's slip risk [2]. The required coefficient of friction (RCOF) quantifies the amount of friction needed to prevent a slip when an individual completes a task. In level walking, RCOF has been well characterized and is predictive of slips [3]. RCOF has been quantified for ladder ascent and a roof-to-ladder transition task [4,5]. In these tasks, RCOF is lower with level feet and with the body above the feet. The association between kinematic factors and RCOF has not yet been described for ladder descent. The kinetics of ladder climbing are unique because the friction plane is defined by the foot orientation on the rung. Further, the center of mass position influences the force vector orientation. Therefore, a reduced RCOF (lower slip risk) is likely to occur when the foot is oriented perpendicular to the body vector such that the force vector is normal to the friction plane (Fig. 1). We propose a new metric called the foot-body coupling angle to quantify the angle between these vectors. Understanding the relationship between the RCOF and climbing mechanics would allow for training of safer strategies. We hypothesized that a more plantarflexed foot and higher body angle will be associated with a higher RCOF in ladder descent consistent with trends observed during ladder ascent and roof-to-ladder transition (H1) [4,5]. Additionally, we hypothesized that the foot-body coupling angle would be positively associated with the RCOF (H2).

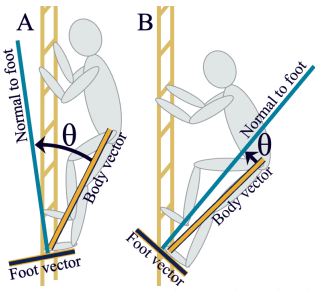

Figure 1: The foot-body coupling angle (θ) shown with a high (A) and low (B) value.

Methods: An instrumented ladder with interchangeable rungs and adjustable angle was constructed. 10 healthy participants (4 F, height = 1.70 ± 0.06 m, weight = 80.1 ± 16.3 kg, age = 42.9 ± 15.5 years) who regularly climb ladders completed 3 ladder descending trials on 6 different ladder conditions (three rung designs and two angles: 75° and 90°). Participants were fitted with 79 reflective markers which were tracked by 12 motion capture cameras (Vicon Motion Systems Ltd., Centennial, CO, USA) to collect kinematics. The third rung of this ladder was instrumented with a three-dimensional force plate (AMTI Inc., Watertown, MA, USA) to collect kinetics.

Time-series ratios of shear to normal forces in the plane of the shoe were calculated during foot contact. RCOF peak was chosen from the signal as the largest of the first three local maxima. Foot angle (the angle between the foot and horizontal in the sagittal plane with positive values indicating dorsiflexion/toe tilted up) and body angle (the angle between vertical and a vector connecting the toe center and trunk center of mass) were calculated at the time of the RCOF peak (Fig. 1). Finally, the foot-body coupling angle at the time of RCOF was calculated by subtracting the foot angle from the body angle. A multivariate regression model was generated which included the foot angle, body angle, and angle of the ladder as independent variables and RCOF as the dependent variable (H1). A linear bivariate model was also generated with the foot-body coupling angle as the independent variable and RCOF as the dependent variable (H2).

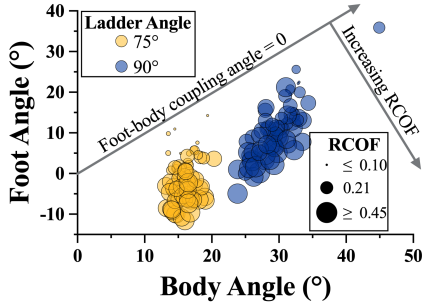

Figure 2: A visual representation of the relationship between foot angle, body angle, RCOF, and ladder angle.

Results & Discussion: The friction forces suggested a propensity for a forward slip. The multivariate analysis produced a significant model with strong predictions of RCOF ($F_{3,135}$= 90.63, $p < 0.001$, $R^2 = 0.668$, Fig. 2, H1 confirmed). Individually, the body angle ($t_{135} = 4.14$, $p < 0.001$), foot angle ($t_{135} = -14.55$, $p < 0.001$), and ladder angle ($t_{135} = -2.88$, $p = 0.005$) were significant predictors. A 10° increase in the foot angle was shown to decrease RCOF by 0.13 whereas a 10° increase in body angle increases RCOF by 0.09. These findings indicate that a lower RCOF is associated with a dorsiflexed foot and with the center of mass aligned above the foot.

As hypothesized, there was a strong, positive correlation between the foot-body coupling angle and RCOF ($F_{1,137} = 242.8$, $p < 0.001$, $R^2 = 0.639$, Fig. 3, H2 confirmed). These results indicate that rather than focusing on climbing with specific body or foot angles, one should attempt to synchronize the center of mass position with the foot orientation (e.g. F 1A). The correlation between RCOF and foot-body coupling angle showed a consistent relationship across ladder angles suggesting that this metric generalizes across ladder designs. Furthermore, a similar R^2 was achieved in H2 with one regressor as H1 with three regressors.

Significance: The foot-body coupling angle allows quantifying the foot and body coordination in a way that predicts RCOF. Thus, it has potential for ladder safety training or safety monitoring purposes to reduce the number of slips and falls during ladder use.

Acknowledgments: This research was funded by NIOSH R01OH011799 and NSF GRFP 2139321.

References: [1] U.S. BLS (Data from 2019). 2023, Dpt of Labor. [2] Cohen et al. (1991), *J Safety Res* **22**: 31-39. [3] Beschorner et al. (2016), *Gait Posture* **48**: 256-260. [4] Martin et al. (2020). *J Biomech* **99**: 19507. [5] Griffin et al. (2023), *J Biomech* **159**: 111780.

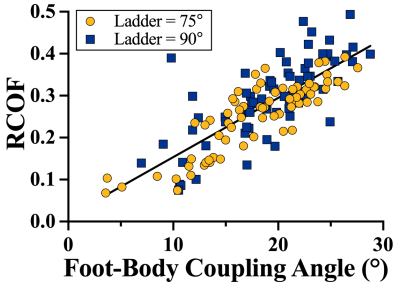

Figure 3: The relationship between the foot-body coupling angle and RCOF.

AN ELECTROMYOGRAPHIC COMPARISON OF NECK MUSCLE RESPONSE DURING OBLIQUE AND NON-OBLIQUE IMPACTS

John Adam Caraan[1]*, Jordan Ogbu Felix[1], Kevin Adanty[1], Sean D. Shimada[1]
[1]Biomechanical Consultants
*jadam.caraan@gmail.com

Introduction: Variables such as head and neck accelerations are often investigated to assess the severity of injury that may occur during motor vehicle collisions. Several studies have been conducted measuring electromyographic (EMG) activity to evaluate the kinematic responses of the neck during simulated lateral, oblique, and rear impacts [1-6]. The risk of injury to a specific muscle group is associated with a greater EMG signal from that muscle group as a result of stronger eccentric contractions in response to impacts [1].

Typical biomechanical analyses of an occupant's response to vehicle impacts are conducted at non-oblique impact directions of 0°, 90°, 180°, and 270°. However, occupant kinematics at oblique angles of 45°, 135°, 225°, and 315° may be different than at non-oblique angles (Fig. 1). It is unclear as to how these oblique impacts should be approached and which direction is to be used when analyzing human's biomechanical response in oblique impacts.

The purpose of this study was to compare the EMG activity of neck muscles during oblique and non-oblique impacts. The current study aims to provide a foundation for biomechanists and forensic experts to account for the human body response in oblique vehicle impacts.

Methods: A literature review was performed for studies that measured EMG activity of neck muscles in oblique and non-oblique impacts performed at different sled accelerations [2-6]. Kumar et al. (2005) suggested that the muscle groups most affected during impact were those contralateral to the side of impact [1], thus EMG responses for the muscle groups ipsilateral to impact were excluded. Right-sided muscles were analyzed in a comparison between the rear (180°), left rear (225°), and left lateral impacts (270°). Left-sided muscles were analyzed in a comparison between right lateral impacts (90°) and right frontal impacts (45°). A three-way ANOVA was conducted to determine the statistical effects of average sled acceleration, impact direction (Fig. 1), and occupant expectation to impact for peak neck EMG response. In the case that no significant interactions were found by the three-way ANOVA, a one-way ANOVA was subsequently conducted to determine if impact direction significantly affected peak neck EMG response. EMG data was reported in means and standard deviation.

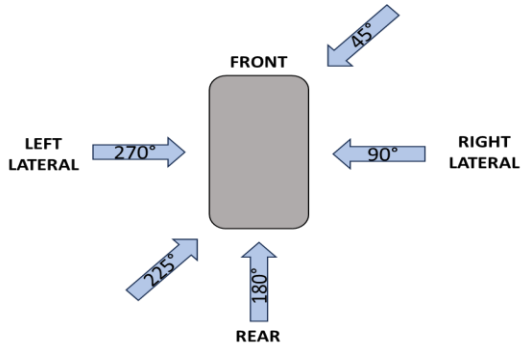

Figure 1: Selected oblique and non-oblique impact directions.

Results & Discussion: Data was included from five studies that measured EMG responses of the splenii capitis, sternocleidomastoid, and trapezii muscles at four different sled accelerations (0.5 to 1.44 g) [2-6]. No three-way interactions were found between average sled acceleration, impact direction, and occupant expectation to impact ($F = 0.81$, $p > 0.05$). A one-way ANOVA found no significant differences ($F = 0.70$, $p = 0.991$) between impact directions, therefore, the differences in neck EMG responses between oblique and non-oblique impacts was not significant. The means and standard deviations of EMG responses for the different impact directions are presented in Table 1.

Impact Direction (°)	Peak Normalized EMG (%MVC)	95% CI
45	31.54 ± 21.97%	[22.26% 40.81%]
90	30.95 ± 19.39%	[22.76% 39.14%]
180	29.83 ± 34.76%	[15.15% 44.51%]
225	32.04 ± 20.02%	[23.58% 40.49%]
270	33.37 ± 21.81%	[24.16% 42.58%]
225	32.04 ± 20.02%	[23.58% 40.49%]
All Directions	31.55 ± 23.88%	[27.23% 35.86%]

Table 1: Mean and standard deviations for peak normalized EMG in each impact direction.

Previous studies have observed that individual neck EMG responses are different for each impact direction [1-6]. In the present study, the EMG responses of individual neck muscles were not analyzed independently; rather, the mean EMG response on one side was analyzed. This may account for the lack of significant differences across impact directions. Based on our current findings, it is reasonable to suggest that for a given acceleration, the overall neck EMG response would be similar regardless of impact direction. Further analysis should investigate the individual muscle responses and compare across the different impact directions. This would allow experts to assess potential injury risks to specific regions of the neck when presented with oblique and non-oblique impact directions.

Significance: To our knowledge, there are no studies comparing the EMG responses of the neck during oblique and non-oblique impacts at various vehicle accelerations in one analysis. Overall, our findings established that neck EMG responses were relatively consistent at all impact directions, indicating that the potential risk of neck injury may be uniform across the two impact scenarios. It is of interest to expand the analysis to additional muscle groups, which may be susceptible to injury risk in oblique and non-oblique impacts.

References: [1] Kumar et al. (2005), *Clin Biomech 20*(2005); [2] Kumar et al. (2002), *Spine 27*(10); [3] Kumar et al. (2004), *Spine 29*(6); [4] Kumar et al. (2004), *Eur Spine J 13*(5); [5] Kumar et al. (2002), *Spine 29*(21) [6] Kumar et al. (2004) *The Spine Journal 4*(2004)

PITCHING BIOMECHANICS AND ABDOMINAL OBLIQUE STRENGTH IN ADOLESCENT BASEBALL PLAYERS

Henry T. Eilen[1]*, Wesley Kokott[2], Cody Dziuk[1], Janelle A. Cross[1]
[1]Department of Orthopaedic Surgery, Medical College of Wisconsin, Milwaukee, WI
[2]Freedom Physical Therapy, Mukwonago, WI
*Corresponding author's email: heilen@mcw.edu

Introduction: In baseball, the pitching cycle is a highly dynamic task that involves coordinated linear and rotational movement and kinetic energy transfer from the lower extremities through the pelvis and trunk, and eventually to the arm, forearm, and hand. This bottom-up kinematic sequence, known as the kinetic chain, allows a pitcher to throw at high velocities; however, it also creates a substantial amount of force on the upper extremities, which could lead to injury [1]. Having a more detailed understanding of the kinetic chain, including forces and relative timings, will help identify breaking points that could be leveraged to improve performance and minimize injuries. While substantial research has focused on upper extremity kinetics and kinematics, much less research has focused on the trunk, a key mediator in kinetic energy transfer. The purpose of this study is to determine the impact abdominal oblique strength has on pitching biomechanics in adolescent baseball pitchers.

Methods: Nineteen right-handed high school male baseball pitchers (age: 17.1 ± 1.1 years, height: 183.7 ± 6.5 cm, mass: 83.1 ± 10.1 kg) participated in the study. The throwing arm was defined as the right arm and glove arm as the left arm. Abdominal oblique strength was assessed via unilateral isometric contractions by a certified physical therapist in a random order between right and left using a hand-held dynamometer. The pitcher was supine on an incline bench set at 30° of trunk flexion [2]. The dynamometer was placed at the musculotendinous junction of their pectoral muscle and each subject was asked to lift their ipsilateral scapula off the bench [3]. Three trials of a 5-second maximal voluntary isometric contraction were performed for strength measurement, and the mean value was used for data analysis. Forty-seven markers were placed on the subjects and 8 Raptor-E cameras were placed around the mound to capture full body biomechanics during the pitching cycle. Kinematics and kinetics of each subject's six best fastballs (based on speed and location) were calculated using Visual 3D motion capture software (C-Motion, Inc). Pelvic rotation angle, torso rotation angle, trunk lateral flexion angle, body separation angle, pelvis rotation velocity, and torso rotation velocity were measured at foot contact (FC), maximum shoulder external rotation angle (MER), and ball release (BR). The two kinetic measurements analyzed were peak elbow varus torque and peak shoulder internal rotation torque. Torque was normalized by height (m) and body weight (N). Descriptive statistics including means and standard deviations were calculated. Shapiro-Wilk test confirmed the data were normally distributed. Scatterplots determined linear associations, so a 2-tailed Pearson correlation with Fisher option was used to examine associations between obliques strength measurements and biomechanical metrics. Correlation coefficients (r) were assessed as weak ($0.1 < r < 0.3$), moderate ($0.3 < r < 0.5$), or strong ($r > 0.5$). The p-value was set at .05.

Results and Discussion: The average fastball of the 19 subjects was 36.8 ± 2.2 m/s. Three kinematic measures were identified with $p < 0.05$ and $r > 0.5$, demonstrating strong correlations with abdominal oblique strength. Maximum pelvis rotation velocity was correlated with throwing arm oblique strength ($r = 0.52$, $p = 0.02$). Glove arm oblique strength was correlated with both maximum pelvis rotation velocity ($r = 0.69$, $p < 0.001$) and maximum torso rotation velocity ($r = 0.52$, $p = 0.02$). No correlations between abdominal oblique strength and peak elbow varus torque or peak shoulder rotation internal rotation torque were noted.

Glove arm abdominal oblique strength was found to have a strong effect on both maximum pelvis and trunk rotational velocity, which could be explained by the action of the internal abdominal oblique that is highly activated with trunk rotation toward the ipsilateral side.4 Additionally, throwing arm abdominal oblique strength was associated with maximum pelvic rotational velocity, but not trunk rotational velocity. This premise may be explained by external oblique strength providing constant EMG activation, 40-60% of maximum during the whole pitching cycle [4]. This may also be due to greater rotation at the pelvis compared to the trunk for the throwing side during wind up [5]. Stronger external obliques can allow for greater coiling during the wind-up phase during pitching, and as a result, greater rotational velocity. We found no correlations between oblique strength with ball velocity or elbow varus torque. Our study found the maximal pelvic rotational velocity occurred at 26.7% of the pitching cycle, which was defined as FC (0%) to maximal shoulder internal rotation (100%). Prior research has shown that those who achieve maximal trunk rotation later in the pitching cycle generate less internal shoulder and elbow torque, which could explain why abdominal oblique strength measurements in the present study were not correlated with increased shoulder and elbow forces [6,7].

Significance: These data highlight the importance glove arm and throwing arm abdominal oblique strength have on both pelvic and torso rotational velocity, as well as the effects timing of trunk and pelvic musculature activation has on shoulder and elbow forces. Training to improve strength of the abdominal obliques may increase both maximum pelvic and trunk rotational velocity while avoiding significant increase in elbow varus moment, which is important in optimizing performance and injury prevention.

References: [1] Seroyer ST et al. Sports Health 2010;2(2):135-146. [2] De Blaiser C et al. Phys Ther Sport 2021;47:165-172. [3] Karthikbabu S . JCDR 2017; doi:10.7860/JCDR/2017/28105.10672. [4] Ng JK -F. et al. J Orthop Res 2001;19(3):463-471. [5] Lin YC, et al. Int J Environ Res Public Health 2021;18(3):905. [6] Aguinaldo AL & Chambers H. Am J Sports Med 2009;37(10):2043-2048. [7] Aguinaldo AL et al. J Appl Biomech 2007;23(1):42-51.

RESTRICTED TOE MOVEMENT INCREASES ACHILLES TENDON LOAD IN HUMAN WALKING

Karen E Walker[1*], Darryl G Thelen[1], Lauren Welte[1, 2]
[1] University of Wisconsin – Madison, Department of Mechanical Engineering, USA
[2] University of Alberta – Edmonton, Department of Mechanical Engineering, CAN
*kewalker2@wisc.edu

Introduction: The human foot, comprised of 33 joints, 26 bones, and over a hundred muscles and ligaments, is exceptionally intricate. These structures offer stability, adapt to varied loading demands during locomotion tasks, and aid in forward propulsion during gait [1]. Characterizing structure-function relationships is imperative to gain a robust understanding of human locomotion and to design devices that mimic the human foot [2]. The metatarsal phalangeal joint (MTPJ) plays a critical role in human locomotion, as it can modify proximal joint motion, decrease the foot's effective length, and impact the gear ratio of the plantar flexor muscles [3]. The purported mechanism is a dynamic coupling between the toes and arch through toe flexor muscles and ligaments that span both the arch and the toe joints [4]. As a result, restricted MTPJ range of motion (ROM), which commonly occurs in pathologies, surgical interventions, and restrictive footwear [1], results in reduced arch mobility and increased ankle plantar flexor muscle activation, suggesting that plantar flexor muscles may produce additional force to compensate [5-6]. Recent evidence suggests that there is also a strong dynamic coupling between the arch and the ankle, with synchronous timing of peak dorsiflexion [7] and propulsion ROM [8]. However, the full chain of dynamic coupling between the toes, arch, and ankle, and the effect on ankle plantar flexor muscle force generation has never been empirically tested. Here, we tested the hypothesis that restricted toe movement would cause decreased ROM at each joint due to dynamic coupling among the toes, arch, and ankle. The decreased range of motion would also lead to reduced ankle velocity, resulting in increased plantar flexor muscle force generation to maintain push-off ankle power.

Methods: Participants (n=1 of 9) walked on an instrumented treadmill at 1.3 m/s at a self-selected cadence that was held consistent among trials using a metronome. Participants walked under two different conditions (toes braced/unbraced) with the goal of simulating a restrictive toe box. Motion capture kinematics from 54 markers were used together with a 4-segment foot model to track toe, arch, and ankle plantarflexion angles [9]. Shear wave tensiometry on the Achilles tendon was averaged across ~7 strides as a surrogate measure of triceps-surae load [10].

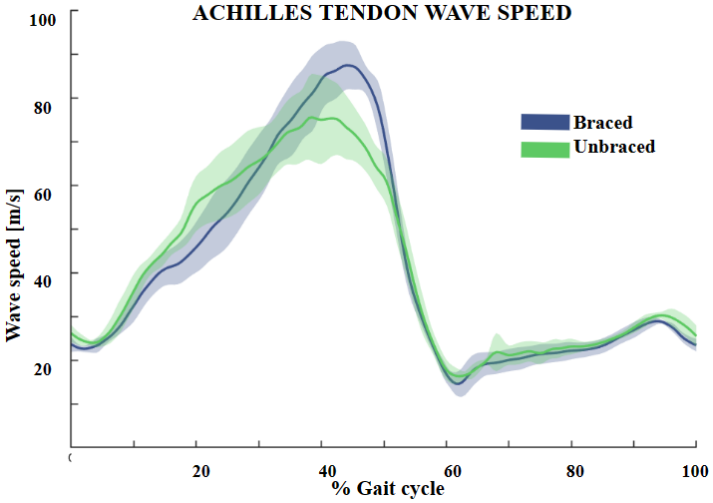

Figure 1: Average (± 1 s.d.) Achilles tendon wave speed patterns in toe braced and unbraced conditions.

Results & Discussion: With the toes braced, MTPJ, arch (midtarsal) and ankle joint ROM decreased. MTPJ and ankle dorsiflexion was reduced at push off (Table 1). There was a 16% increase in peak Achilles tendon wave speed when the toes were braced (Braced 86.6m/s ± 5.0; Unbraced 74.1m/s ± 3.6, Figure 1). During early stance, wave speed increased faster when the toes were braced compared to when toes were unbraced. The decreases in MTPJ, arch, and ankle dorsiflexion while wearing the brace suggest that there is dynamic coupling between the toes, arch, and ankle. When the toe, arch, and ankle ROM is reduced, the increase in peak Achilles tendon wave speed suggests that plantar flexor muscle demands are higher. This may reflect that more plantar flexor muscle force is necessary to generate sufficient positive push off power. Additionally, the faster increase in wave speed with the toe brace during early stance may demonstrate altered neuromuscular strategies to overcome reduced range of motion at the toes, arch and ankle. Our preliminary results suggests that the mobility of the MTPJ directly impacts Achilles tendon load, and likely increases the demand on the ankle plantar flexor muscles. Analysis of additional subjects is ongoing to further test this hypothesis.

Table 1: MTPJ, Midtarsal, Ankle Angles (mean ± S.D)

Joint	Range of Motion (degrees)	Peak Dorsiflexion (degrees)	Peak Plantarflexion (degrees)
MTPJ - Unbraced	21.5 (±0.9)	55.4 (±0.4)	34.0 (±0.9)
MTPJ - Braced	19.2 (±0.8)	51.7 (±0.6)	31.8 (±0.4)
Arch - Unbraced	21.2 (±0.7)	21.6 (±0.8)	-0.4 (±1.2)
Arch - Braced	19.2 (±0.5)	18.3 (±0.7)	-2.6 (±0.3)
Ankle - Unbraced	35.1 (±2.2)	32.7 (±1.7)	-2.4 (±1.0)
Ankle - Braced	31.8 (±1.2)	22.7 (±1.3)	-9.1 (±0.8)

Significance: This pilot study provides insight on dynamic coupling of the toes, arch, and ankle. It advances our understanding of healthy foot function and potential repercussions and compensations of restricting toe motion. Our preliminary findings suggest that the ankle is dynamically coupled with the toes and arch. The knowledge to be gleaned from this can lead to advancements in clinical treatments for ankle and foot pathologies and injuries, change how we prescribe and design footwear, and impact research design and development of ankle and foot prostheses.

Acknowledgments: Funded by NIH (R01HD092697) and NSERC (PDF 558140 – 2021).

References: [1] Manganaro+ (2023), *Statpearls*; [2] Zelik et al. (2018), *J Biomech*, 75(250; [3] McDonald+ (2021), *Sci Rep*, 1924(11); [4] Williams+ (2023), *J Foot & Ankle Research*, 12(44); [5] Farris+ (2020), *J.R. Soc. Interface*, 17; [6] Lichtwark+ (2006), *J Experi Bio*, 209(21); [7] Yetmen+, (2024). *BioRxiv*, preprint. [8] Welte+ (2023), *Frontiers*; [9] Maharaj+, (2022). *Computer Meth in Biomech*, 25(5); [10] Martin+, (2018). *Nat Comm*, 9(1).

EFFECTS OF PHYSICAL FATIGUE ON LOWER LIMB INTER-JOINT COORDINATION UNDER DIFFERENT WALKING CONDITIONS

Jinfeng Li[1], Hang Qu[1], Li-Shan Chou[1*]
[1]Department of Kinesiology, Iowa State University, Ames, IA, USA
*Corresponding author's email: chou@iastate.edu

Introduction: Movement coordination refers to the precise synchronization of multiple joints or segments required to carry out intended actions, such as walking. Achieving this coordination involves complex interactions within the central nervous system, integrating motor and sensory circuits. Physical fatigue can affect sensorimotor function and motor control during walking. Previous studies have indicated that exercise-induced physical fatigue may compromise gait stability by disrupting mechanoreceptor function [1] or impairing the capabilities of the vestibular system [2]. Nevertheless, the impact of physical fatigue on the inter-joint coordination of the lower extremities during diverse walking conditions remains insufficiently understood. Thus, the primary aim of this study was to investigate potential alterations in gait coordination resulting from physical fatigue.

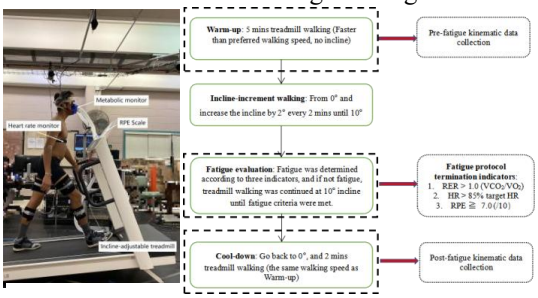

Figure 1: Experiment set-up and treadmill fatigue

Methods: Twelve healthy young adults (7M/5F, 22.3±3.2 yrs, 1.75±0.10 m, 68.62±11.69 kg) were recruited. A progressive inclined treadmill walking fatiguing protocol was applied, and respiratory exchange ratio (RER), heart rate (HR), and Borg rating of perceived exertion (RPE) were monitored to assess physical fatigue. (Fig.1). A twelve-camera motion analysis system (Qualisys AB, Sweden) was used to collect 3D-kinematic data of level and treadmill walking both before and after fatigue (sampling rate = 240 Hz). Sagittal plane joint angles and velocities of the hip, knee, and ankle of the right leg were calculated using Visual3D (C-Motion, Inc., MD), and all kinematic data were interpolated to 100% of a gait cycle. Continuous relative phase (CRP) was used to investigate the inter-joint coordination pattern and variability in this study. Joint angles (θ) and angular velocity (ω) data were normalized to [-1,1] to mitigate differences in amplitude and frequency. Phase angles (φ) of each joint were calculated as $\varphi = \tan^{-1}(\omega/\theta)$ for each data point ($\varphi \in (-\pi, \pi)$), and the CRP was then obtained by subtracting the phase angles of the distal joint from that of the proximal joint (e.g., $\varphi_{hip} - \varphi_{knee}$) [3,4]. Three metrics, mean absolute relative phase (MARP), deviation phase (DP) and cross-correlation [3], were employed to indicate the CRP variability. The two-way repeated measures ANOVA examined the effects of physical fatigue and walking conditions.

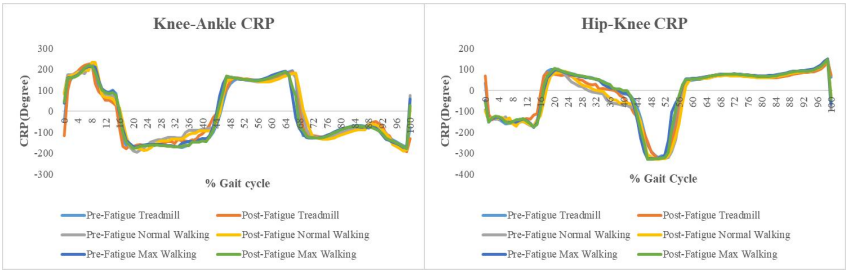

Figure 2: Ensemble mean hip–knee and knee-ankle CRP

Results & Discussion: Inter-joint coordination was examined in three walking conditions (normal walking (NW), maximum speed walking (MW), and treadmill walking (TW)) before and after the fatiguing protocol, and the RER, HR and RPE at the end of the fatiguing protocol were 1.0, 174 bpm and 9/10, respectively. For the hip-knee CRP pattern (Fig.2), the MARP and DP exhibited statistically significant differences across the three walking conditions (p_c = .01, p_c = .043), and the MARP between pre- and post-fatigue was statistically different only in the NW condition (Table 1). For the knee-ankle CRP pattern (Fig.2), the DP was significantly higher post-fatigue than pre-fatigue in the NW condition. Additionally, the MARP differed significantly across the three walking conditions (p_c = .005) (Table 1). Cross-correlation coefficients were all greater than 0.83 in both CRP patterns under diverse conditions (Table 1). No interaction effect was found.

Significance: This study provides an initial investigation into how inter-joint coordination adapts in response to physical fatigue. While we only observed partial changes in inter-joint coordination variabilities before and after physical fatigue under normal walking conditions, they might indicate that fast walking or constant-speed treadmill walking may somewhat regulate inter-joint coordination. This may be attributed to our physical fatigue protocol emphasizing cardiorespiratory stimulation, potentially not accurately reflecting the usual neuromuscular system's fatigue control mechanisms. Future research should consider collecting walking data before and after mental fatigue, allowing for more thorough analysis and insights.

Table 1. CRP variability results

	CRP Variabilities	Normal walking[Mean(SD)]		Max-speed walking[Mean(SD)]		Treadmill walking[Mean(SD)]		*P* values
		Pre-fatigue (1.3±0.16 m/s)	Post-fatigue (1.29±0.15 m/s)	Pre-fatigue (1.72±0.16 m/s)	Post-fatigue (1.67±0.15 m/s)	Pre-fatigue (1.56±0.06 m/s)	Post-fatigue (1.56±0.06 m/s)	
Hip-Knee	MARP(°)	127.3 (21.3)$^{*\#€}$	123.6 (18.9)*	114.9 (9.8)$^{\#}$	114.1 (7.2)	112.4 (13.1)$^{€}$	112.9 (17.2)	p_c = .010, p_t = .254, p_{c*t} = .393
	DP(°)	22.9 (6.7)	26.0 (16.6)	21.1 (4.1)	19.4 (3.9)	25.9 (15.1)	28.1 (16.5)	p_c = .043, p_t = .603, p_{c*t} = .706
	Cross-correlation	0.87 (0.04)	0.84 (0.09)	0.86 (0.04)	0.87 (0.04)	0.84 (0.08)	0.83(0.07)	p_c = .124, p_t = .535, p_{c*t} = .604
Knee-Ankle	MARP(°)	150.6 (7.4)	152.5 (6.8)	148.5 (7.1)	148.2 (5.0)	147.4 (5.1)	148.2 (10.5)	p_c = .005, p_t = .216, p_{c*t} = .616
	DP(°)	26.5 (9.3)$^{*€\#}$	30.6 (19.2)$^{*€}$	25.3 (7.0)$^{\#}$	23.4 (6.7)§	23.7 (8.3)$^{€}$	30.6 (19.2)$^{€§}$	p_c = .334, p_t = .283, p_{c*t} = .288
	Cross-correlation	0.87 (0.05)	0.85 (0.1)	0.87 (0.03)	0.88 (0.04)	0.88 (0.05)	0.84 (0.04)	p_c = .435, p_t = .864, p_{c*t} = .689

* p< .05, pre- vs post-fatigue under same walking condition; # p<0.05 NW vs. MW under same fatigue condition; € p<0.05 NW vs. TW under same fatigue condition; § p<0.05 TW vs. MW under same fatigue condition

References: [1] Donath, et al. (2014), *Gerontology* 61(1); [2] Charles, et al. (2003), *J Vestibular Res* 12(2-3); [3] Chiu & Chou (2012), *J Biomech* 45(2); [4] Chiu, et al. (2010), *Gait & Posture* 32(4).

THE RELATIONSHIP AMONG PREVIOUS SPORT PARTICIPATION, STANDING POWER THROW, AND BIOMECHANICS IN RESERVE OFFICERS TRAINING CORPS CADETS

Madison S. Mach[1]*, Hayley Ericksen[2], Jennifer E. Earl-Boehm[1]
[1]University of Wisconsin – Milwaukee, Milwaukee WI. [2]Illinois State University, Normal IL.
*Corresponding author's email: mmach@uwm.edu

Introduction: The Reserve Officers Training Corps (ROTC) is a collegiate program providing up to 60% of commissioned officers across all military branches. ROTC cadets must maintain physical military readiness (PMR) which is defined as the ability to meet all physical demands of any combat or duty position.[1] PMR is tested in the Army using the Army Combat Fitness Test (ACFT) which included 6 events including: Hex bar deadlift, standing power throw (SPT), hand release pushups, sprint drag carry, plank, and a 2-mile run. The SPT event in the ACFT is a highly technical task requiring a high level of coordination and biomechanical efficiency to throw a 10 lb medicine ball backwards overhead as far as possible. The SPT is typically a low scoring event which can negatively impact the overall ACFT score. It is essential for cadets to perform well on the ACFT because it will directly influence their duty placement after graduation. Understanding the biomechanics that relate to high performance on the SPT event would be beneficial. In addition, the extent to which cadets participated in sports prior to beginning ROTC may also relate to SPT performance. A current reliable method for assessing biomechanics in-field includes using 2-Dimentional (2D) video. 2D biomechanics have been used in traditional athlete populations to inform performance on various tasks. Currently, research within our lab has started investigating 2D biomechanics and performance on the ACFT. The motor skills that are developed throughout youth are required to perform the ACFT tasks safely and effectively. [2] Youth physical activity is drastically declining, and it is estimated that >70% of Americans between the ages of 17-24 may be ineligible for military service due to poor physical health [3]. Previous sport performance may provide cadets with a better background in the motor skills associated with high level physical performance. Due to the potential benefits from participating in sport prior to entering the ROTC, there is a need to identify how previous sport performance may be related to SPT performance. Therefore, the purposes of this study are: 1) to investigate the relationship between previous sport participation and 2D sagittal plane biomechanics during the SPT task, and 2) to identify if previous sport participation is predictive of SPT score.

Methods: 70 ROTC cadets ([M: n =52; 20.3±1.5yrs; 1.78±0.6m; 80.4±11.9kg][F: n=18; 20.5±2.0yrs; 1.66±0.9m; 64.8±.10kg]) from the Golden Eagle Battalion in Milwaukee WI with no duty or training restrictions participated in this study. The ACFT was conducted with standard Army protocol. 2D sagittal plane biomechanics were recorded using a high-speed camera placed approximately 10ft away from the participant on their right side. The videos were assessed, and biomechanics were extracted using Dartfish software by a researcher with extensive experience. Trunk (relative to vertical), hip (trunk relative to thigh), and knee flexion (thigh relative to shank) were measured at the lowest point of the countermovement phase of the SPT. Previous sport participation was self-reported using a questionnaire that inquired about how many years the cadet participated in sport since the age of five. A Hierarchical regression was used to investigate the relationship between previous sport participation and SPT performance (distance thrown). Sex and age were entered into the model first as controlling variables, followed by total years of sport participation. Three Pearsons bivariate correlations were performed comparing SPT biomechanics and previous sport participation: 1) Knee flexion angle and total years of sport; 2) Hip flexion and total years of sport; and 3) Trunk flexion and total years of sport. A priori p value was set at $p<.05$ and correlations were interpreted with the following scale: very strong (0.90-1.0), strong (0.70-0.90), moderate (0.50-0.70), weak (0.30-0.50), and negligible (0-0.30) [4].

Results and Discussion: Total years of sport was significantly, positively correlated to SPT performance ($R2 = .490$; $p=<.000$). After controlling for sex and age, total years of sport was a significant (<.000) predictor of SPT performance. Sex and age only accounted for 3.3% of the variance in SPT performance ($R2= .033$). When total years of sport was added into the model the R2 value increased to .261, indicating that total years of sport accounts for 22.8% of the variance in SPT performance. Interestingly, total years of sport had negligible relationships with all the biomechanical variables (trunk flexion: $R2=-.013$; hip flexion: $R2=.018$; knee flexion: $R2=.018$). These results suggest that previous sport participation plays a significant role in performance on the SPT task in the ACFT with greater total years of sport being more favorable for higher performance. However, 2D sagittal plane biomechanics did not share this relationship with previous sport performance as they had negligible relationships. There may be other variables that previous sport participation relates to outside of the biomechanics measured in this study such as coordination, power production, etc.

Significance: This is the first study to investigate the relationship between previous sport participation, SPT performance, and biomechanics. The ACFT directly influences the career path that a cadet is assigned and therefore high performance is essential. The results of this study are the first step in the direction of identifying potential screening methods for incoming ROTC cadets. Those who report less sport participation prior to entry into the ROTC could be provided with additional training to allow for greater exposure to skills that cadets need to perform well on the SPT.

Acknowledgements: We want to acknowledge the Golden Eagle Battalion Leadership and cadets for the enthusiasm and engagement they have provided throughout this study. Without their help we would not be able to conduct our research.

References: [1] Dot. A. 7-22 Army Physical Readiness Training. 2022. [2] Stodden, D. F., et al., (2008). *Quest, 60*(2), 290-306. [3] Spoehr, T., & Handy, B. (2018). *Backgrounder, 3282*, 1-16. [4] Mukaka, M. (2012). *Malawi Med J, 24*(3), 69-71.

IS ADAPTIVE FES BETTER THAN TRADITIONAL FES? THE RESULTS MAY SHOCK YOU.

Margo C. Donlin[1*], Jill S. Higginson[1,2]
[1]University of Delaware Departments of [1]Biomedical and [2]Mechanical Engineering
*Corresponding author's email: donlinm@udel.edu

Introduction: Stroke often causes limited mobility, which is frequently characterized by decreased walking speed. Functional electrical stimulation (FES) is a therapeutic intervention often used in post-stroke gait rehabilitation to augment impaired motor control and increase walking speed [1]. However, FES is not an effective rehabilitation protocol for all subjects [2], likely because the stimulation timing and amplitude are not able to respond to natural variations in gait. Several research groups have developed adaptive FES (AFES) systems that adjust stimulation timing or amplitude based on measured gait parameters, but these studies may only include dorsiflexor stimulation [3] or base plantarflexor stimulation on EMG signals that may not be directly correlated to propulsion [4]. Therefore, we developed a novel AFES system that adjusts stimulation timing and amplitude based on measured dorsiflexion angle and peak propulsive force. The purpose of this study was to evaluate the effects of the AFES system on post-stroke gait and compare to the effects of the existing FES system. Because some previous FES systems resulted in clinically meaningful improvements in functional gait outcomes, it was hypothesized that walking speed would increase with the AFES system compared to the existing FES system or no stimulation.

Methods: Twenty-four individuals with chronic post-stroke hemiparesis (9M | 15 F; 63 ± 10.2 years; 1.70 ± 0.08 m; 81.21 ± 18.09 kg; 102.21 ± 71.98 months post-stroke) completed six four-minute walking trials in a random order at their comfortable speed. Trials were on the adaptive or fixed-speed treadmill with no stimulation, stimulation from the existing FES system, or stimulation from the AFES system. Dynamic stimulation was applied to the paretic dorsiflexor muscles during swing phase to augment impaired dorsiflexion and to the paretic plantarflexor muscles during terminal stance to augment deceased forward propulsion. Stimulation timing was controlled by bilateral footswitches. Stimulation amplitude in the FES condition was constant and set to the amplitude that induced a strong motor response. Stimulation amplitude in the AFES condition was updated at every stride based on measured peak dorsiflexion angle and peak propulsive force asymmetry and was limited to within each subject's sensory and pain thresholds. For trials with stimulation, stimulation alternated on and off in one-minute intervals [5]. Walking speed (m/s) was calculated for each trial, averaged across all subjects, and compared between treadmill and stimulation conditions using a two-way ANOVA ($\alpha = 0.05$).

Results & Discussion: Walking speed was not statistically significantly different between stimulation conditions, although participants walked significantly faster on the adaptive treadmill than the fixed-speed treadmill ($p = 0.0157$, Figure 1). The increase in speed on the ATM is consistent with previous results in young healthy individuals [6] and individuals post-stroke [7], but the lack of difference between stimulation conditions contrasts previous research [1,2].

Because of the large variability between subjects, individual responses were categorized based on which stimulation condition resulted in the fastest ATM walking speed. Nine people walked the fastest with no stimulation, at an average of 0.79 ± 0.22 m/s. Because these individuals already walked fairly fast for individuals post-stroke, it is possible that they did not increase their speed with stimulation due to a ceiling effect where they were already walking as fast as was comfortable. One notable subject decreased walking speed substantially with stimulation (0.54 m/s with NONE, 0.21 m/s with FES, and 0.36 m/s with AFES), which is likely due to altered gait patterns because of discomfort and is reflected in increased stance time asymmetry (3.80 ± 1.69% with NONE, 5.75 ± 2.39% with FES, and 5.53 ± 2.19% with AFES).

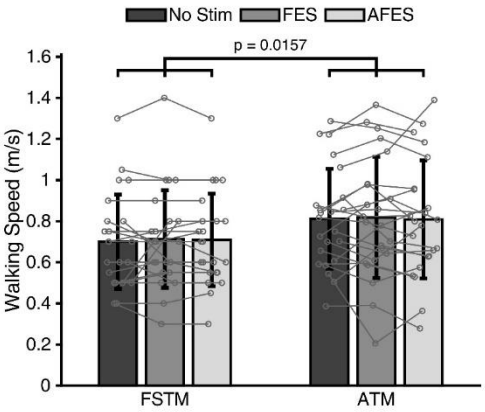

Figure 1: Walking speed on the FSTM and ATM with no stimulation (dark gray), stimulation from the existing FES system (medium gray) and the AFES system (light gray). Walking speed was significantly faster on the ATM than the FSTM ($p = 0.0157$) but not different between stimulation conditions.

Some subjects increased their walking speed on the ATM when walking with stimulation, suggesting that FES may be beneficial for some people. Specifically, 10 people walked the fastest in the FES condition and four people walked the fastest in the AFES condition, increasing their walking speed relative to no stimulation by 0.08 m/s on average. These 14 people may have achieved these increased speeds due to stimulation-driven increased in propulsion, which increased 1.29 ± 1.62% bodyweight in the FES group and 1.85 ± 1.55% bodyweight in the AFES group.

Significance: The results of this study demonstrate that adaptive rehabilitation technologies like AFES may be beneficial, but still may not be effective for all individuals post-stroke. Future research should determine which individuals will benefit from which therapeutic intervention to further optimize post-stroke gait rehabilitation.

Acknowledgments: NIH-NIGMS (P20 GM103446) and the State of Delaware; NIH GM 103333; University of Delaware Doctoral Fellowship. This content is solely the responsibility of the authors and does not necessarily represent the official views of NIH.

References: [1] Dickstein (2008) *Neurorehabil Neural Repair* 22(6). [2] Langhorne et al. (2009) *Lancet Neurol* 8. [3] Jiang et al. (2020) *IEEE Trans Neural Syst Rehabil Eng* 28(6). [4] Chen et al. (2010) *Disabil Rehabil* 32(1). [5] Awad et al. (2014), *Arch Phys Med Rehabil.* 95(5). [6] Ray et al. (2018) *J Biomech* 78. [7] Ray et al. (2020) *J Biomech* 101.

THE INFLUENCE OF HIP DYSPLASIA ON JOINT REACTION FORCES DURING MULTI-PLANAR CUTTING TASKS

Molly C. Shepherd[1*], Michael D. Harris[1]
[1]Washington University in St. Louis
*email: mollycshepherd@wustl.edu

Introduction: Developmental dysplasia of the hip (DDH) is a bony disease characterized by a shallow hip socket that reduces femoral head coverage and causes joint instability.[1] As a result, joint loads at the hip are often elevated due to the increased demand for stabilization, leading to chondrolabral damage and accelerated cartilage degeneration.[2,3] Many individuals with symptomatic DDH are young, active, and regularly participate in sports but become limited by pain that increases with activity.[4–6] Additionally, individuals with higher activity scores often present with symptoms at younger ages than those with lower activity scores.[6] It has been suggested that these symptoms may develop due to repeated high impact and rotational loading required by participation in sport activities.[7] However, most studies on DDH have been limited to sagittal plane movements,[8–10] and the effect of multi-planar or rotational activities on loading in dysplastic hips remains unknown. Therefore, the objective of this study was to compare hip joint reaction forces (JRFs) and joint angles between patients with DDH and controls during a multi-planar cutting activity.

Methods: Thirteen female patients with DDH (age = 26.5±8.0, BMI = 23.0±2.2) and nine controls with no history of hip disorders (age = 22.3±3.4, BMI = 22.7±1.9) were included with IRB approval and informed consent. Patients were diagnosed with DDH by an orthopaedic surgeon based on a lateral center edge angle <20° and unilateral hip/groin pain for 3+ months. Participants were asked to perform a series of 60° side-step hop cuts[11] while their kinematics were recorded at 100 Hz (Vicon) (**Fig. 1**). Ground reaction forces (2000 Hz) were collected from embedded force plates (Bertec), and surface electromyography (2000 Hz) was used to record muscle activity from 8 muscles of the lower limb and back (Motion Lab Systems). A baseline OpenSim musculoskeletal model was updated for each subject with three-dimensional reconstructions of the pelvis and femurs from MRI.[8] OpenSim Moco was used to calculate hip joint angles and JRFs (normalized to bodyweight (xBW)) while tracking experimental muscle electromyography.[12] A representative hop cut was chosen for each subject and analysed from the initial hop landing to when the trailing toe left the force plate (**Fig. 1**) with the trailing limb being either the symptomatic limb (DDH) or dominant limb (controls). Hip JRFs and joint angles from the hop cut were compared between the DDH and control groups. Inter-group differences were tested for significance across the hop cut motion using one-dimensional independent samples t-test statistical parametric mapping.[13]

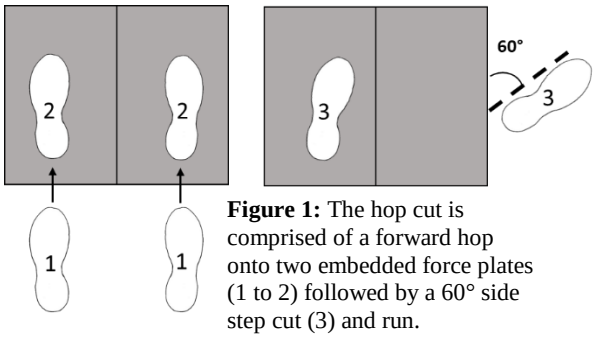

Figure 1: The hop cut is comprised of a forward hop onto two embedded force plates (1 to 2) followed by a 60° side step cut (3) and run.

Results & Discussion: There were no statistically significant differences in hip JRFs or joint angles between patients with DDH and controls during the hop cut activity (**Fig. 2**). However, patients were found to have larger medial joint forces than controls from 0-68% of the hop cut motion. Additionally, medial JRFs contributed a greater percentage to overall peak JRFs during hop cuts (40%) than previously found in gait (22%).[8]

Despite the lack of significance, the higher medial JRFs during the hop cut activity in DDH hips are of interest as medial femoral head cartilage damage is common in these patients.[3,8,9] The greater contribution of the medial forces may increase the risk for damage during hop cutting due to potential generation of large shear forces as the femur is pushed medially and simultaneously rotates axially. It is also important to note the small sample size and the possibility that group differences may increase with a larger sample.

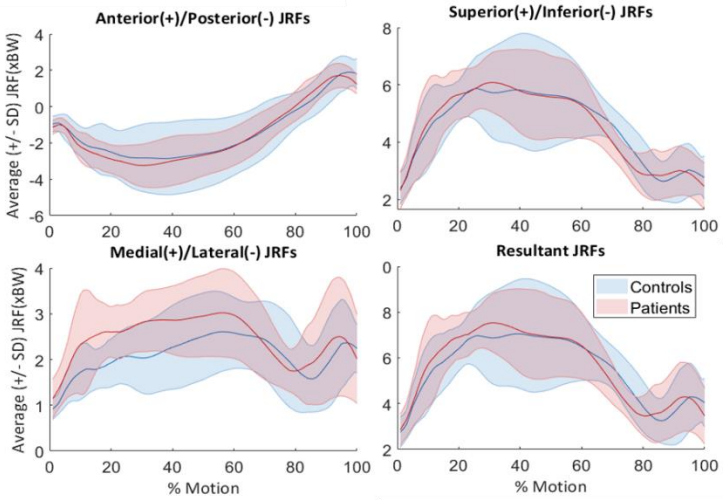

Figure 2: Average ± standard deviation hip joint reaction force (JRF) during the hop cut motion.

Significance: Due to the active nature of patients with DDH, identifying activities that elevate hip loading is important to understand mechanisms of damage and symptom onset. In doing so, clinicians may have earlier indicators of disease progression which can reduce time from presentation to diagnosis as well as inform activity modifications and optimal treatment techniques in patients with DDH.

Acknowledgements: Stanford Restore and Mobilize Center for assistance with OpenSim Moco. ReproRehab data science training program (NIH R25HD105583). Funding was provided through NIH grants R01AR081881, K01AR072072, and T32HD007434.

References:

[1] vanBosse *Clin. Orthop. Relat. Res.* 2015. [2] Murphy *J. Bone Jt. Surg.* 1995. [3] Harris *J. Orthop. Res.* 2022. [4] Petrie *J. Arthoplasty* 2020. [5] van Bergayk *J. Bone Jt. Surg.* 2002. [6] Matheney *J. Bone Jt. Surg.* 2016. [7] Kapron *J. Sports Med.* 2015. [8] Song *J. Biomech.* 2020. [9] Harris *J. Biomech.* 2017. [10] Song *J. Orthop. Res.* 2022. [11] Imwalle *J. Strength Cond. Res.* 2009. [12] Dembia *PLoS Comput. Biol.* 2020. [13] Pataky *Comput. Methods Biomech. Biomed. Engin.* 2012.

PREDICTING OCCUPANT PEAK LUMBAR ACCELERATION IN LOW-SPEED REAR-END IMPACTS

Clyde Westrom[1*], Keya Zambare[1], Rachel L. Tanczos[1], Kevin Adanty[1], Sean D. Shimada[1]
[1]Biomechanical Consultants
*cwwestrom@ucdavis.edu

Introduction: Rear-end impacts are frequently investigated in relation to whiplash-associated disorders affecting the head and neck [1]. Low back pain is a common consequence of this type of impact; yet, historically, there has been limited focus on assessing injury risk and kinematics for the lumbar spine in rear-end impacts [2]. Peak vehicle acceleration has previously been utilized as a predictor of injury potential [3], and in terms of occupant parameters, lumbar spine acceleration is a common metric for understanding and assessing injury risk. It is important for biomechanists and professionals in automotive safety and injury prevention to understand how vehicle kinematics influence occupant kinematics to progress the relationship between crash dynamics and injury tolerances.

The aim of this study was to develop a mathematical model to predict peak longitudinal lumbar acceleration from peak longitudinal vehicle acceleration during rear-end impacts. This work will aid engineers and safety experts in deriving lumbar kinematics from crash dynamics and contribute to the existing literature for lumbar injury risk analysis.

Methods: To minimize variability in crash test parameters and support model confidence, the current literature was reviewed for studies that specifically utilized human volunteers in vehicle-to-vehicle rear-end crash tests and reported peak longitudinal lumbar and peak longitudinal vehicle accelerations [3-5]. Volunteers were all positioned in the driver's seat in a normal seating position. Only target vehicle accelerations in rear-end impacts are presented in this analysis. Lumbar accelerometers were placed posteriorly at approximately L5-S1. Reported data was confounded by several experimental factors: occupant unexpecting vs. expecting impact, negligible vs. significant braking of the target vehicle, male vs. female test subject, and bumper-to-bumper vs. underride impact. For assessing the significance of these factors (i.e. impact expectation, braking, gender, and underride configuration) on the relationship between vehicle and lumbar acceleration, a ratio of peak longitudinal lumbar acceleration to peak longitudinal vehicle acceleration was calculated for each crash test. In support of data compilation involving these described experimental conditions, four independent t-tests were conducted for each experimental factor, using the Bonferroni correction (α=0.0125). A linear regression with a y-intercept set to 0 g was fit to the final dataset and assessed using the R^2 and the p-value of the coefficient (α=0.05).

Results & Discussion: Three studies satisfied crash test specifications of the present analysis (N = 31) [3-5]. Non-significant p-values were found for the impact expectation (p=0.928), braking (p=0.690), gender (p=0.597), and underride configuration (p=0.803) factors; therefore, these factors were not found to significantly affect the relationship between vehicle and lumbar acceleration. The linear regression (R^2=0.98, p<0.001) yielded a coefficient of 1.05 (Fig. 1), indicating peak lumbar acceleration was nearly consistent with vehicle acceleration. This result is suggestive of rigid coupling and/or low energy-absorbing characteristics of the seat relative to the L5-S1 level [1]. Although likely a suitable representation of overall lumbar kinematics, confident applicability of this result is currently limited to the lowest vertebrae of the lumbar spine within the range of 0.7g and 5.0g peak longitudinal vehicle acceleration.

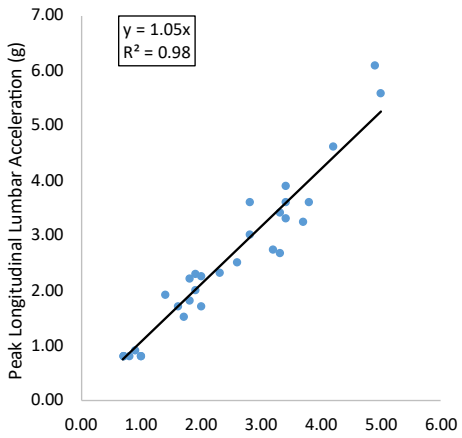

Figure 1: The resulting linear regression for peak longitudinal lumbar acceleration predicted by peak longitudinal vehicle acceleration.

McCleery et al. (2022) performed a similar analysis on anthropometric test device (ATD) kinematics in standardized sled tests, reporting a ratio of pelvic to sled acceleration of 1.24 ± 0.27, which indicated that the acceleration of the pelvis is likely higher than that of the vehicle. The variation between the ratio reported by McCleery et al. (2022) and the linear regression coefficient of the present study can likely be attributed to distinctions in testing parameters, such as the location of the accelerometer (center of gravity of the pelvis vs. L5-S1), occupant type (ATD vs. volunteer), and crash simulation type (sled vs. vehicle-to-vehicle). Pelvic accelerations are commonly considered representative of lumbar kinematics [6]; however, further investigation is needed to support compiling data from accelerometers at distinct anatomical locations. A collective analysis would be advantageous as ATDs instrumented with pelvic accelerometers allowed McCleery et al. (2022) to analyze kinematics at greater peak sled accelerations (i.e. 10 g).

Significance: A mathematical model predicting peak lumbar acceleration based on vehicle acceleration has been developed. The provided regression analysis serves as a tool for biomechanics and automotive safety experts to improve their comprehension of how lumbar kinematics correlate with the potential for low back injuries in rear-end collisions. To enhance this analysis, it would be advantageous to include additional accelerometer locations and conduct a parallel investigation into ATDs and cadavers.

References: [1] Atarod (2020), SAE Technical Paper 2020-01-0516. [2] Fewster et al. (2022), J Appl Biomech 38(3):155-163. [3] Welcher et al. (2001), SAE Technical Paper 2001-01-0899. [4] Anderson et al. (1998), SAE Technical Paper 980298. [5] Fugger et al. (2003), SAE Technical Paper 2003-01-0158. [6] McCleery et al. (2022), Accid Anal Prev 174:106761.

The effect of posterior strut stiffness on foot loading during gait with carbon fiber custom dynamic orthoses

Kirsten M. Anderson,[1] Wesley J. Gari,[1] Sara M. Magdziarz,[1] Molly S. Pacha,[1] Donald D. Anderson,[2] Jason M. Wilken[1]
Departments of [1]Physical Therapy & Rehabilitation Science and [2]Orthopedics and Rehabilitation, University of Iowa
kirsten-m-anderson@uiowa.edu

Introduction: Traumatic lower limb injuries often result in long term disability, poor outcomes, and persistent functional deficits including stiffness, weakness, and pain.[1,2] Carbon fiber custom dynamic orthoses (CDOs) are used to restore function, improve outcomes, and reduce pain for individuals following traumatic lower limb injury.[3] CDOs consist of a proximal cuff below the knee, a carbon fiber posterior strut that runs the length of the leg, and a full length footplate (Fig. 1). CDOs have previously been shown to alter forces on the plantar surface of the foot. [4,5] As the CDO is loaded, deformation of the strut transfers forces from under the foot to the lower limb within the proximal cuff.[5] Prior work investigating the effects of CDOs on foot loading have studied one type of CDO at a time and have not investigated the effects of different design characteristics, like posterior strut stiffness. In this study, three CDOs of differing stiffnesses (Posterior Spring Orthosis, Bio-Mechanical Composites, Inc.; Des Moines, IA) were tested to determine the effect of CDO posterior strut stiffness on foot loading during gait.

Figure 1. Carbon fiber custom dynamic orthoses consist of a proximal cuff, a carbon fiber posterior strut, and a full-length footplate.

Methods: Seven individuals (6 Male/ 1 Female, 35.9(10.1)yrs, 1.8(0.1)m, 92.2(19.4)kg) who had previously experienced a unilateral intra-articular ankle fracture provided written informed consent to participate in this study. Participants walked without a CDO (NoCDO) and with three CDOs of varying posterior strut stiffness: Stiff - 7.0(2.1)Nm/°, Moderate - 5.4(1.4)Nm/°, and Compliant - 3.9(1.2)Nm/°. Wireless Loadsol insoles (Novel Electronics; Pittsburgh, PA) were placed under the participant's foot as they walked at a controlled walking speed based on leg length.[6] Peak forces and force impulse were measured for the hindfoot (proximal 30% of insole), midfoot (middle 30% of insole), forefoot (distal 40% of insole), and total foot (100% of insole). Force impulse was calculated using the indefinite integral of forces acting on the plantar surface of the foot in the specified region over the stance phase of gait.

Results & Discussion: Compared to walking in the NoCDO condition, peak hindfoot force significantly decreased while walking in the Stiff (17.6%) and the Compliant (14.3%) CDOs (Fig. 2). Peak forefoot forces (Stiff – 20.4%, Moderate – 20.5%, Compliant – 20.8%) and forefoot force impulse (Stiff – 15.7%, Moderate – 17.9%, Compliant – 14.7%) also decreased in each of the CDOs compared to walking in the NoCDO condition. No significant differences were observed in peak forces or force impulse between stiffness conditions.

Prior work has shown up to 12% reductions in peak hindfoot loading[4], which was exceeded by the Stiff and Compliant CDOs included in this study. Previous work has reported reductions in peak forefoot greater than 60% and reductions in forefoot impulse by more than 50%, which exceed the reductions observed in this study.[4,5] Prior studies have investigated highly robust CDOs, which are generally very stiff in order to facilitate return to high energy activities, which may explain the differences observed in foot loading.[4,5,7] The lack of significant differences between the CDO stiffnesses suggest that, similar to its effect on gait mechanics[8], CDO stiffness has a limited impact on foot loading.

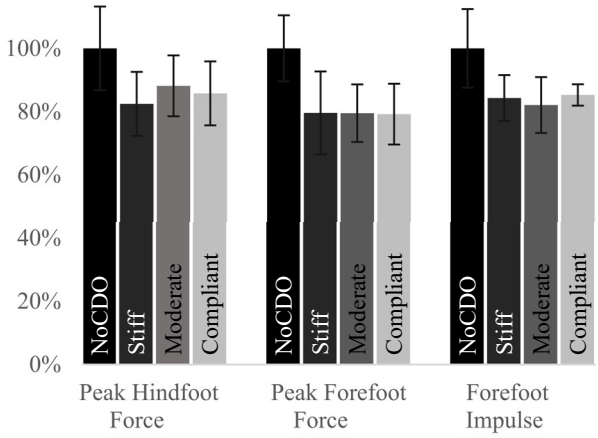

Figure 2. Peak hindfoot forces, peak forefoot forces, and forefoot force impulse for all study conditions (NoCDO, Stiff, Moderate, Compliant) presented as a percentage of NoCDO.

Significance: The results of this study demonstrate that CDOs can reduce peak hindfoot and forefoot forces, as well as forefoot force impulse during gait. These reductions in foot loading may benefit individuals who have experienced traumatic lower extremity injuries that result in residual pain with foot loading. The lack of significant differences in foot loading between CDO stiffnesses indicates that, similar to gait mechanics[8], CDO stiffness may not play a significant role in foot loading during gait.

Acknowledgments: This work was supported by grants from the Department of Defense, through the Peer Reviewed Medical Research Program (Award No. W81XWH-17) and the National Center for Advancing Translational Sciences of the National Institutes of Health (Award Number UM1TR004403). The view expressed in this abstract are those of the authors and do not necessarily reflect the official policy or position of the National Institutes of Health, the U.S. Department of Defense, or other federal agencies.

References: [1] McCarthy, et al. (2003), J Bone Joint Surg Am 85-A(9), [2] Pollak, et al. (2003), J Bone Joint Surg Am 85-A(10), [3] Ikeda, et al. (2019), Mil Med 184(11-12), [4] Stewart, et al. (2020), JPO 32(1), [5] Feng, et al. (2023), FAO 8(1), [6] Vaughan, et al. (2005), Gait Posture 21(1), [7] Harper, et al. (2014), J Biomech Eng. 136(9), [8] Harper, et al. (2014), Clin Biomech. 29(8)

The effects of carbon fiber custom dynamic orthosis proximal cuff design on foot loading during gait: A pilot study

Kirsten M. Anderson,[1] Wesley J. Gari,[1] Sara M. Magdziarz,[1] Molly S. Pacha,[1] Donald D. Anderson,[2] Jason M. Wilken[1]
Departments of [1]Physical Therapy & Rehabilitation Science and [2]Orthopedics & Rehabilitation, University of Iowa
kirsten-m-anderson@uiowa.edu

Introduction: Pain with foot loading during gait is common after lower limb trauma. Carbon fiber custom dynamic orthoses (CDOs) have been shown to enhance mobility and improve outcomes for those with lower limb pain[1]. CDOs consist of a semi-rigid carbon fiber foot plate, a carbon fiber strut, and a proximal cuff that sits just below the knee (Fig. 1). CDOs store energy in the strut during early-to-mid stance and return the energy in late stance to assist with push off. The cuff is the primary interface for loading the device and offloading the limb. The purpose of this pilot study is to examine the effect of cuff design on forces under the foot during gait. CDO use is expected to reduce foot loading, and a cuff with a ratcheting system designed achieve greater compression and foot offloading is expected to result in the greatest reductions in foot forces.

Figure 1. Chicago Screw (A), BOA Dial (B) and Anterior Shell (C) CDO cuff designs

Methods: Five healthy able-bodied individuals and one individual with a prior intra-articular ankle fracture (3 Female/3 Male, 47.8(15.7)yrs, 1.8(0.1)m, 74.4(4.2)kg) walked at a controlled speed based on leg length without a device (NoCDO), and with a CDO using three different cuff designs (Fabtech Systems; Everett, WA): Chicago Screw (CDOA), BOA dial (CDOB), and anterior shell (CDOC) (Fig. 1). CDO footplate and strut characteristics were maintained between each cuff design, and the three cuff designs were evaluated in randomized order. Loadsol insole sensors (Novel Electronics; Pittsburgh, PA) measured forces on the foot in three regions: hindfoot (proximal 30%), midfoot (middle 30%) and forefoot (distal 40%)[2]. Peak force and force impulse values were recorded for the total foot and for each region. Force impulse values were calculated as the indefinite integral of force during stance phase.

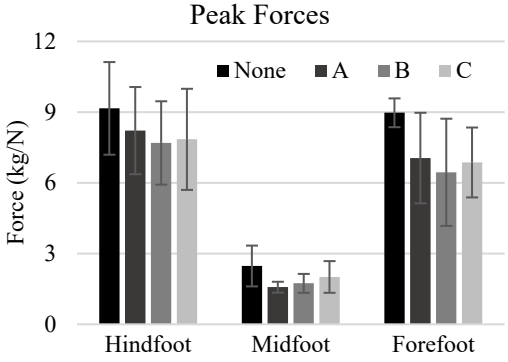

Figure 2. Mean hindfoot and forefoot peak forces.

Results & Discussion: No appreciable differences were observed between able-bodied individuals and the individual post-fracture, so their data were combined. No significant differences were observed via pairwise comparisons. Peak forefoot, midfoot, and hindfoot forces were lower in all three cuff designs compared to the NoCDO condition (Fig. 2), resulting in large effect sizes (Table 1). This is consistent with prior literature, further demonstrating the offloading capabilities of CDOs [1,3]. Peak forces varied between cuff designs, with medium-to-large effect sizes in the hindfoot, midfoot, and forefoot regions. The largest reductions in hindfoot and forefoot forces were observed with CDOB. This is likely due to the ratchet-dial system, as opposed to the hinge and Velcro strap of CDOA, or the dual Velcro strap of CDOC. CDOB also utilizes a more contoured patellar tendon bearing design, potentially aiding in offloading effects by transferring forces through the proximal tibia.

Significance: The results of this pilot study further demonstrate the offloading effect of CDO use during gait. Although cuff designs were not statistically significantly different in this small cohort of participants, effect sizes were large for multiple comparisons. The cuff with a ratcheting system decreased peak forces of the hindfoot and forefoot regions compared to other cuff designs, suggesting that loading interface and securement methods may impact the magnitude of regional foot loading. These data suggest a larger, fully powered, study evaluating the effect of CDO cuff design on foot loading is warranted in individuals who have experienced limb trauma.

Table 1. Cohen's d effect sizes for pairwise comparisons. Large > 0.8; Medium 0.8-0.2; Small < 0.2.[4]

Effect Sizes		None/A	None/B	None/C	A/B	A/C	B/C
Hindfoot	Peak Force	**1.5**	**1.9**	**1.8**	**3.0**	**1.7**	0.6
	Impulse	0.8	0.8	0.5	0.4	**1.9**	**0.9**
Midfoot	Peak Force	**1.0**	0.8	0.6	0.6	0.8	0.5
	Impulse	0.5	0.3	0.1	0.4	0.7	0.4
Forefoot	Peak Force	**1.0**	**1.2**	**1.4**	0.8	0.2	0.4
	Impulse	0.1	0.1	0.1	0.6	0.1	0.5
Total	Peak Force	0.8	**1.0**	**0.9**	**1.0**	0.3	0.8
	Impulse	0.8	0.5	**2.4**	0.2	0.4	0.4

Acknowledgments: This work was supported by grants from the Department of Defense, through the Peer Reviewed Medical Research Program (Award No. W81XWH-17) and the National Center for Advancing Translational Sciences of the National Institutes of Health (Award Number UM1TR004403). The view expressed in this abstract are those of the authors and do not necessarily reflect the official policy or position of the National Institutes of Health, the U.S. Department of Defense, or other federal agencies.

References: [1] Ikeda, et al. (2019), Mil Med. 184(11-12), [2] Renner, et al. (2019), Sensors 19(2), [3] Feng, et al. (2023), Foot Ankle Orthop 8(1), [4] Lakens (2013), Front. Psychol. 4(863)

The effects of proximal cuff tightness on foot loading with carbon fiber custom dynamic orthosis use

Kirsten M. Anderson[1], Wesley J. Gari,[1] Sara M. Magdziarz,[1] Molly S. Pacha,[1] Donald D. Anderson,[2] Jason M. Wilken[1]
Departments of [1]Physical Therapy & Rehabilitation Science and [2]Orthopedics & Rehabilitation, University of Iowa
kirsten-m-anderson@uiowa.edu

Introduction: Traumatic lower limb injuries often lead to limitations in physical activity and persistent pain.[1,2] Carbon fiber custom dynamic orthoses (CDOs) can restore function, improve patient outcomes, reduce pain, and alter foot loading during gait following traumatic lower extremity injury.[3-5] CDOs include a proximal cuff that wraps around the leg just below the knee, a posterior carbon fiber strut running the length of the limb, and a full-length footplate (Fig. 1). The cuff is a primary interface between the CDO and the individual wearing it. Tightening the cuff plays an important role in effectively securing the CDO to the limb. However, there is a distinct lack of information on how tightly the cuff is secured or what impact it may have on patient outcomes. In this study, participants walked without and with a CDO (Posterior Spring Orthosis, Bio-Mechanical Composites, Inc.; Des Moines, IA) fastened to three different tightness levels to determine the effects of cuff tightness on foot loading during gait.

Figure 1. CDOs consist of a proximal cuff wrapping around the limb just below the knee, a carbon fiber posterior strut, and a full-length footplate.

Methods: Eight healthy individuals and one individual with a prior intra-articular ankle fracture (4 Male/5 Female, 34.3(12.1)yrs, 1.7(0.1)m, 86.4(15.1)kg) participated in this study. Participants walked at a controlled speed based on leg length[6] without (NoCDO) and with a CDO fastened to three levels of tightness (30N, 50N, 70N) as wireless Loadsol insoles (Novel Electronics; Pittsburgh, PA) measured forces acting on the plantar surface of the foot. Peak force and force impulse data were measured for the hindfoot, midfoot, forefoot, and total foot (proximal 30%, middle 30%, distal 40%, and 100% of insole, respectively). Force impulse was calculated using the indefinite integral of force over the stance phase of gait.

Results & Discussion: No appreciable differences were found between data from the individual post fracture and the healthy individuals, so the data were combined. Compared to walking without a CDO, peak forefoot forces significantly decreased (30N – 24.4%, 50N – 22.1%, 70N – 22.8%) and midfoot force impulse significantly increased (30N – 37.0%, 50N – 40.3%, 70N – 35.3%) with each CDO cuff tightness (Fig. 2). Prior work has reported reductions in peak forefoot loading greater than 60%, exceeding the reductions observed in this study.[4,5] Because of design differences between the CDO included in this study and those studied previously, and a lack of details about how the cuff was fastened in prior work, the differences in foot loading cannot be attributed to cuff tightness rather than other design differences.[4,5] Additionally, non-significant reductions in peak hindfoot and total foot forces early in stance were observed. Increases in peak midfoot and total foot forces late in stance were observed, as were reductions in forefoot force impulse and increases in hindfoot and total foot force impulse. Medium to large effect sizes were generally observed when comparing between conditions (Table 1) and these changes align with previously reported changes in foot loading.[4,5]

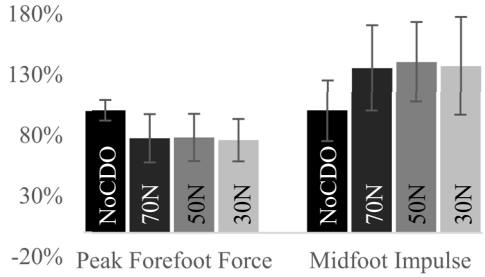

Figure 2. Peak forefoot forces and midfoot force impulse for all study conditions (NoCDO, 30N, 50N, 70N) are presented here as a percent of NoCDO.

Table 1: Effect sizes for all pairwise comparisons. Large >0.8; Medium 0.8-0.2; Small <0.2.[7]

	Hindfoot		Midfoot		Forefoot		Total Foot		
	Peak	Impulse	Peak	Impulse	Peak	Impulse	Peak (early)	Peak (late)	Impulse
NoCDO/30N	0.9	0.9	0.3	1.6	1.5	0.8	0.5	0.6	0.3
NoCDO/50N	0.7	0.8	0.4	1.6	1.2	0.8	0.3	0.8	0.4
NoCDO/70N	0.6	1.0	0.3	1.2	1.2	0.8	0.3	0.8	0.4
30N/50N	0.2	0.4	0.4	0.4	0.4	0.2	0.3	0.7	0.4
30N/70N	0.5	0.7	0.1	0.0	0.2	0.1	0.3	0.8	0.3
50N/70N	0.5	0.4	0.3	0.5	0.2	0.5	0.1	0.4	0.2

Significance: While different levels of cuff tightness were not shown to systematically influence foot loading, the impact of CDO use on peak forefoot forces and midfoot force impulse support the use of CDOs to alter foot loading during gait. Additionally, the medium to large effect sizes observed in this small cohort of individuals support continuing investigations with a larger group of individuals who have experienced traumatic lower limb injuries. Further information regarding the effects of cuff tightness on foot loading during gait would help to guide patient education upon delivery of the CDO.

Acknowledgments: This work was supported by grants from the Department of Defense, through the Peer Reviewed Medical Research Program (Award No. W81XWH-17) and the National Center for Advancing Translational Sciences of the National Institutes of Health (Award Number UM1TR004403). The views expressed in this abstract are those of the authors and do not reflect the official policy or position of the National Institutes of Health, the U.S. Department of Defense, or other federal agencies.

References: [1] McCarthy, et al. (2003), J Bone Joint Surg Am 85-A(9), [2] Pollak, et al. (2003), J Bone Joint Surg Am 85-A(10), [3] Ikeda, et al. (2019), Mil Med 184(11-12), [4] Stewart, et al. (2020), JPO 32(1), [5] Feng, et al. (2023), FAO 8(1), [6] Vaughan, et al. (2005), Gait Posture 21(1), [7] Lakens (2013), Front. Psychol. 4(863)

PREDICTING OCCUPANT HEAD ACCELERATION IN NEAR AND FAR-SIDE LATERAL IMPACTS WITH PIECEWISE REGRESSION MODELS

Clyde Westrom[1*], Jordan Ogbu Felix[1], Kevin Adanty[1], Sean D. Shimada[1]
[1]Biomechanical Consultants
*cwwestrom@ucdavis.edu

Introduction: The biomechanical response of an occupant's head in lateral impacts relies on many human-related factors (e.g., seat belt use and occupant positioning relative to the point of impact) and vehicle-related factors (e.g., the principal direction of force) [1]. In near-side lateral impacts, the occupant is seated adjacent to the impacted side of the vehicle. Common sources of impact between the occupant's head and vehicle interior include B-pillars, side curtains, and side-door windows. In far-side lateral impacts, the occupant is seated opposite the side of impact. Head contact with the vehicle's interior is less likely than in a near-side impact but may still occur with interior objects, such as adjacent seatbacks and occupants [2].

Biomechanical experts frequently rely on predictive models to extrapolate occupant head acceleration from vehicle kinematics [1,3]. Existing models function well to predict occupant head acceleration [4]; however, better accuracy is often desired for real-world crash scenarios that frequently occur at lower vehicle changes in velocity (ΔV). Occupant head acceleration in low ΔV impacts has a more predictable response, while impacts at higher ΔVs trend toward greater variability, likely due to differing types of test subjects (anthropometric test devices). Given low-speed impacts yield notable differences in variability of occupant response compared to high-speed impacts, a single linear model may not accurately predict head acceleration across all ranges of ΔV [3,5–7]. Therefore, since different linear trends may exist across discrete ranges of ΔV, this study aimed to develop piecewise linear regressions to predict peak lateral head acceleration accurately.

Methods: Simulated impacts were selected from peer-reviewed research and NHTSA crash tests that reported vehicle and occupant head kinematics in near- and far-side lateral impacts. Near and far-side lateral impacts were differentiated using impact principal direction of force (PDOF) and the occupant seat position. PDOF was restricted to the ranges of 90° ± 22.5° and 270° ± 22.5°. Anthropomorphic test devices (ATD), postmortem human subjects (PMHS), and volunteer occupants in the outboard seats of the first or second rows were included. Near-side lateral impacts involving head contact with the vehicle's interior remained included in the dataset. Piecewise regressions were performed to predict occupant peak lateral head acceleration in each ΔV range. Two near-side ΔV intervals were selected from 0 km/h to 9.8 km/h and 9.8 km/h to 40 km/h. One far-side ΔV interval was chosen from 0 km/h to 9.8 km/h, as there was insufficient data past 9.8 km/h. The cutoff at 9.8 km/h was selected as it was the maximum tested ΔV among all analyzed studies conducting low-speed tests, which contained only volunteer occupants.

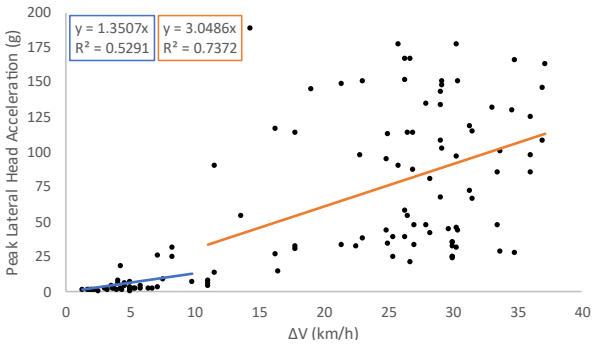

Figure 1: Piecewise regression for selected near-side impacts.

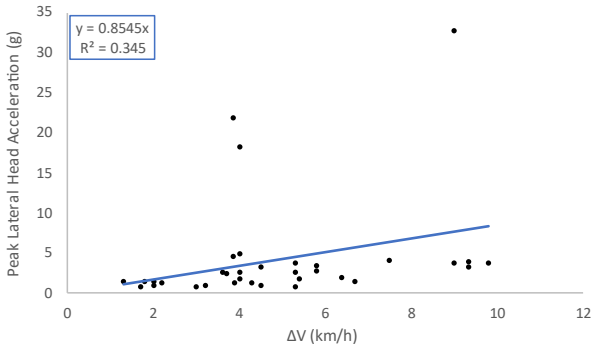

Figure 2: Regression for selected far-side impacts.

Results & Discussion: Near-side piecewise regressions indicated that the peak lateral acceleration of the head was greater than that of the vehicle (Fig. 1). Impacts below 9.8 km/h (N=36, R^2=0.53, p<0.001) yielded a good fit, with a distinct slope from the regression representative of ΔV greater than 9.8 km/h (N=82, R^2=0.74, p<0.001). The far-side regression (Fig. 2) conversely suggests that the peak lateral head acceleration of the head was lower than that of the vehicle (N=34, R^2=0.36, p<0.001). Regression coefficients indicated a greater peak lateral head acceleration in near-side than far-side lateral impacts. All regressions suggest that lateral ΔV is a significant predictor for peak lateral head acceleration.

Far-side lateral impact data at ΔV greater than 9.8 km/h was from one study that tested at two distinct ΔV values. At 11 km/h and 30 km/h, the average peak lumbar accelerations were 6.13 g and 21.92 g, respectively [8]. The authors did not regress between these points because of the uncertainty of whether the relationship was linear or otherwise.

Significance: An occupant's biomechanical response may not be uniform across low and high-speed impacts to apply a single linear regression to predict head acceleration from ΔV [4]. Therefore, piecewise regressions on near and far-side lateral impact tests were generated for distinct intervals of ΔV. Establishing the piecewise regressions can allow biomechanical engineers to accurately determine an occupant's peak lateral head acceleration in low-speed and high-speed impacts rather than relying on a single linear model to predict injury metrics.

References: [1] Schmitt et al. (2019), *Trauma Biomechanics*, 5th ed. [2] Perez-Rapela et al. (2019), Stapp Car Crash J. 63:83–126. [3] Fugger et al. (2002), SAE Technical Paper 2002-01–0020. [4] Westrom et al. (2023), Conference Abstract, BMES Annual Meeting [5] Furbish et al. (2019), SAE Technical Paper 2019-01–1027. [6] Toney-Bolger et al. (2020), SAE Technical Paper 2020-01–1218. [7] Shibata et al. (2019), SAE Technical Paper 2019-01–1030. [8] Pintar et al. (2007), SAE Technical Paper 2007-22–0014.

THE EFFECT OF WALKING SLOPE ON FEMORAL ARTERY DILATION

Jose Anguiano-Hernandez[1*], Kota Z Takahashi[1], Song-Young Park[2]
[1]Department of Health and Kinesiology, University of Utah, Salt Lake City, UT
[2]School of Health and Kinesiology, University of Nebraska Omaha, Omaha, NE
*Corresponding author's email: jose.anguianohernandez@utah.edu

Introduction: The common femoral artery is the major conduit artery delivering oxygenated blood to the lower limbs. Blood flow to the lower limbs increases during muscle activity, with greater muscle activity eliciting greater amounts of blood flow in the femoral artery, such as knee extensor voluntary isometric contraction tasks [1] and cycling [2]. Increased blood flow in an artery increases mechanical stress on the endothelium, which initiates vasodilation of the artery to accommodate increased blood flow [3]. However, it is unclear whether the magnitude of femoral artery vasodilation differs during walking at different intensities, such as on incline and decline slopes. Previous research has shown that activation of the large muscles proximal to the knee in the lower limb is highest during uphill walking and lowest during level walking [4]. Given these previous findings, it is likely that walking at different slopes may induce femoral artery dilation.

The purpose of this study is to measure femoral artery dilation after walking at different slopes in healthy young adults. We hypothesize that incline walking will cause the greatest percent increase in femoral artery diameter relative to baseline because of increased lower limb muscle activity [4]. We also hypothesize that level walking will elicit the lowest percent increase in femoral artery diameter relative to baseline because of reduced muscle activity compared to incline and decline walking [4].

Methods: Five healthy young adults (1 female, 23.4 ± 2.9 years old, 62.7 ± 18.7 kg, 16.9 ± 6.2 % body fat) have participated in this study so far. Participants walked on a treadmill for 10 minutes at 1.2 m/s at -5°, 0°, 5° slopes in random order. A 5° slope was chosen as it is comparable with slope requirements set by the Americans with Disabilities Act (4.8°). Participants rested seated for 20 minutes before each walking condition. The diameter of the right common femoral artery was measured using Doppler ultrasound (Terason uSmart 3300 NexGen, USA) by fastening the ultrasound probe using a 3D printed bracket. A 30-second recording of the right common femoral artery during quiet standing was taken immediately before and after walking. A similar technique has previously been used to investigate femoral artery blood flow during leg extension and cycling tasks [2-3]. An open-source software (FloWave.US, USA) was used to extract artery diameter from B-Mode videos of the right common femoral artery as a time series [5]. This software's diameter extraction feature has previously been validated using an ultrasound phantom and *in-vivo* anterior tibial artery imaging during a dorsiflexor maximum voluntary isometric contraction task [5]. MATLAB (R2023A, The MathWorks, USA) was used to calculate mean femoral artery diameter during the pre- and post-walking periods. SPSS (IBM, USA) was used to perform a One-Way Repeated Measures ANOVA to compare the percent change in artery diameter after each walking condition ($\alpha = 0.05$).

Results & Discussion: We observed femoral artery dilation in 11 of 15 walking trials across all conditions. On average, femoral artery diameter increased the most after the Level walking condition (10.31 ± 11.87%), followed by the Incline (10.13 ± 16.83%) and Decline (4.52 ± 12.83%) conditions relative to pre-walking diameter (Figure 1). We did not find a significant effect of walking slope on the percent change in femoral artery diameter ($p = .81$).

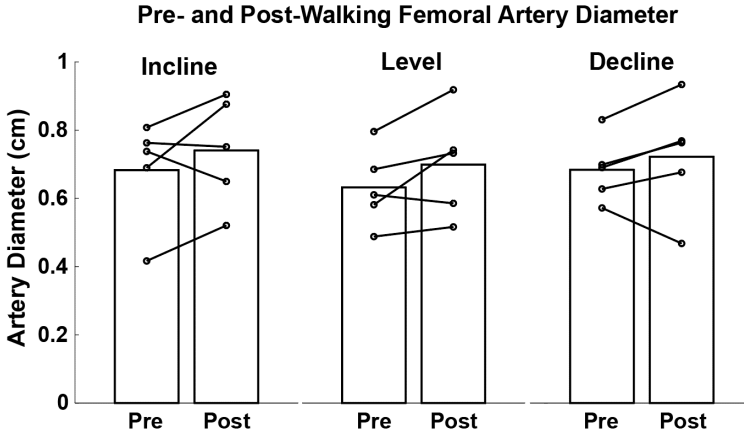

Figure 1: Femoral Artery diameter before and after walking in the Incline, Level, and Decline conditions. Connected dots represent one participant's pre- and post-walking artery diameter.

Significance: Understanding the femoral artery's response to walking could provide insights into the mechanisms by which oxygen is delivered to working muscles. In this study, we showed that the femoral artery dilated immediately after walking using a novel ultrasound technique. This novel technique could reveal the role of vascular physiology in accommodating the various intensities of walking. Individuals with cardiovascular diseases like Peripheral Artery disease and Diabetes can suffer from biomechanical dysfunctions [6-7], and this technique could reveal new insights about the consequences of impaired blood flow on muscle force production and energy dissipation during walking. Elucidating the link between vascular physiology and biomechanics could provide insight into therapeutics aiming to improve blood flow and walking function in patients with cardiovascular disease.

Acknowledgments: This work was supported by the NIH (R01HD106911) awarded to KZT and SP.

References: [1] Ratchford et al. (2019), *Am J Physiol Heart Circ Physiol* 317(6); [2] Rossman et al. (2015), *Am J Physiol Heart Circ Physiol* 309(5); [3] Gnasso et al. (2001), *Atherosclorosis* 156(1); [4] Franz et al. (2012), *Gait & Posture* 35(1); [5] Coolbaugh et al. (2016), *J Appl Physiol* 121(4); [6] Bapat et al. (2023), *Vasc Med* 28(1); [7] Rao et al. (2006), *Foot Ankle Int* 27(8)

INDEPENDENT ANALYSIS OF MOTION ANALYSIS CORP. VIRTUAL GRF CALCULATION

Pegah Jamali*, Robert D. Catena
Gait and Posture Biomechanics Lab, Washington State University
* pegah.jamali@wsu.edu

Introduction: Force plates are commonly used in biomechanics labs to measure ground reaction forces (GRFs). The GRFs measured by force plates form the gold standard but are not convenient because they tether the subject to walk a predefined path with a confined step length, and certain patient populations struggle to consistently hit force plates with their entire foot. Alternatively, a virtual ground reaction force (vGRF) can be calculated through inverse dynamics using measured kinematics of the whole body and assumed inertial parameters, ideally replicating the actual GRF. [1] Cortex is a Motion Analysis Corporation software and has a tool for computing triaxial vGRF during gait. [2] The purpose of this study is to quantitatively evaluate the accuracy of vGRFs compared to GRFs measured by force plates. The outcomes of this project will inform future use of this beneficial method to avoid prolonged lab testing waiting for clean natural foot strikes onto force plates or artificial gait patterns from instructing participants to make clean foot strikes onto force plates.

Methods: Twenty-three healthy young adult participants performed 5-10 minutes of natural self-selected pace over-ground walking with constant start location adjustments until a clean (one entire foot on each force plate) level-walking trial was performed. Participants walked across two in-series force plates that were adjusted in separation distance prior to testing based on an approximation of the participant's natural step length (another reason vGRF is preferable). Full body marker set data and de Leva [3] segment inertial parameters were used to derive inputs into vGRF calculations. Heel strikes and toe off events were determined by manual inspection. Besides triaxial magnitude of the vGRF, we also wanted to determine if the prescribed motion of the point of application (vCOP) accurately mimics true COP motion trajectories along the foot. To assess the validity of the triaxial vGRF and biaxial vCOP, the residual error between the calculated (virtual) and measured (real) data were determined using root mean square error (RMSE), mean absolute error (MAE), and coefficient of determination (R^2).

Results & Discussion: A sample of the calculated triaxial vGRF magnitude in comparison to the force plate GRF magnitude at each time point is shown in Figure 1a, showing good agreement between GRF and vGRF for both feet in X, Y, and Z directions. The vGRFs demonstrate the most accurate results in Anterio-Posterior (AP) direction (R^2=0.95, RMSE=18.27). The vertical vGRFs also illustrate excellent agreement with measured GRFs (R^2=0.88, RMSE=50.24). However, the small medio-lateral (ML) vGRF values with similar error to the AP direction result in reduced accuracy (R^2=0.59, RMSE=19.76) in the ML direction. We also found great agreement between actual COP and the vCOP (Figure 1b). The vCOP data closely matched the measured data in AP and ML directions (R^2=0.98, RMSE=37.36 and R^2=0.97, RMSE=10.38 respectively). Overall, results demonstrate the validity of whole-body inertial calculation of GRF (except in the ML direction) and COP without using a force platform.

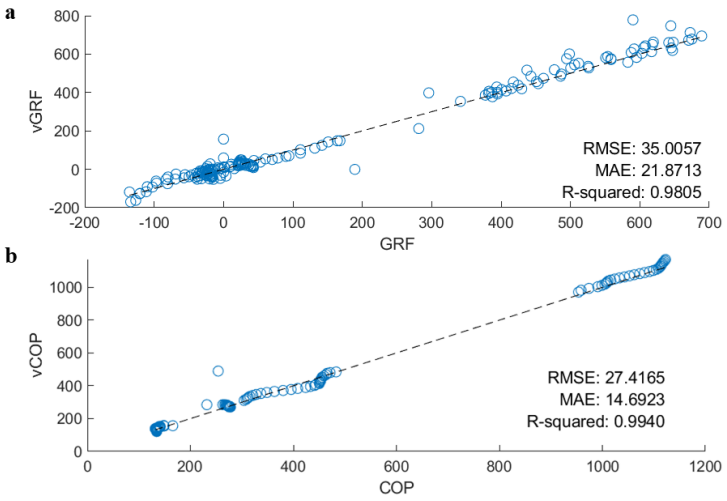

Figure 1: (a) Comparison of calculate triaxial vGRF against measured triaxial GRF. (b) Comparison of calculated vCOP against measured COP for both feet. The dotted line represents the identify line (y=x).

Here we discuss possible errors in the order (most to least) of what we believe could be contributing to errors in virtual calculations. First, how the foot is modeled, with changes in marker positions of the ankle and toe affecting calculations. Second, inaccurate inertial parameters. In our next analysis, we will be analyzing the sensitivity of vGRFs to errors in segment inertial parameters. Third, variations in gait patterns and sudden changes in movement may create non-smooth transitions between consecutive gait events. Fourth, the manual inspection of gait events and slight errors in event timing can also affect calculated force data. Fifth, this method means that skin motion artifact will affect the GRF calculation. Moreover, but not an error, down-sampling of the GRF to the frequency of motion capture data may lead to loss of information, especially when dealing with faster dynamic activities.

Significance: A virtual ground reaction force would allow researchers to study comprehensive human motion without using force plates with minimal error. The popularity of technologies like markerless motion capture demonstrates desire among biomechanists to untether research from controlled lab settings. This study sets the stage for conducting kinetic research outside laboratories in real environments without force plates. Even in the controlled environment of a lab, not having the rely on participants cleanly striking force plates will allow for more natural gait variations and eliminate significant time from setup and testing.

Acknowledgments: Funded by an ASB Junior Faculty Research Award. Motion Analysis Corp. had no input into this study.

References: [1] Ren (2008) *J Biomech.* 41, [2] Hatfield (2009) *Med Sci Sports Exerc.* 41, [3] de Leva (1996) *J Biomech* 29.

REDEFINING LONGITUDINAL FOOT ARCH STIFFNESS DURING GAIT

Zachary D. Katzman[1], Robert M. Yoho[1], Vassilios G. Vardaxis[2*]
[1]College of Podiatric Medicine and Surgery, Des Moines University, West Des Moines, IA, USA
[2]Department of Physical Therapy, Des Moines University, West Des Moines, IA, USA
*Corresponding author's email: vassilios.vardaxis@dmu.edu

Introduction: Lower extremity biomechanics during the stance phase of gait are impacted by foot arch stiffness [1]. These effects are of interest to clinicians, because they manifest as a variety of medical conditions and can be modified through either conservative [2] or surgical means [3]. Several static metrics have been introduced to measure arch stiffness, but while these may have clinical value, they exhibit a lack of association with dynamic arch stiffness [4]. On the other hand, past attempts to quantify dynamic arch stiffness have – in addition to relying on potentially unrepresentative surrogate variables – all been assessed at or before 50% of stance phase. However, peak arch deformation (PAD) and peak vertical ground reaction force both occur well after 50% of stance [5]. We argue that the PAD is a more clinically relevant timepoint, as it represents a greater stress experienced by the arch. Thus, we propose a new measure called medial longitudinal arch stiffness (MLAS). There is currently only indirect evidence that faster walking speeds are associated with increased arch stiffness [6], so the purposes of this study were to introduce MLAS and to determine: (1) its test-retest reliability and (2) how it is affected by walking speed.

Methods: Subjects (n=56) completed 3 walking trials each at a self-selected (typical) speed on a walkway equipped with force plates and a 10-camera motion-capture system. A subset of the subject pool (n=21) also completed walking trials at self-selected slow and fast speeds, and eight (*8*) of these subjects returned at a later date for an identical retest. Reflective markers were placed on the (1) calcaneus, (2) navicular, and (3) first and (4) fifth metatarsal heads. Using these markers and the method described by Eichelberger et al. [7], a dynamic sagittal plane was established through the midline of the foot, and markers 1-3 were then projected onto this plane to determine the medial longitudinal arch angle (MLAA). The percent of stance at which the MLAA was maximally deformed (Fig. 1) was defined as PAD. The changes in MLAA and resultant ground reaction force (rGRF) from initial contact (IC) to PAD, were then used in the following calculation of MLAS:

$$MLAS = \frac{MLAA_{PAD} - MLAA_{IC}}{rGRF_{PAD}}$$

Mean values, standard deviations, and 95% confidence intervals were calculated for PAD and MLAS at normal walking speeds. Test-retest reliability was determined for PAD and MLAS using a Pearson correlation ($\alpha < .05$). A one-way ANOVA elucidated the effects of walking speed on PAD and MLAS ($\alpha < .05$).

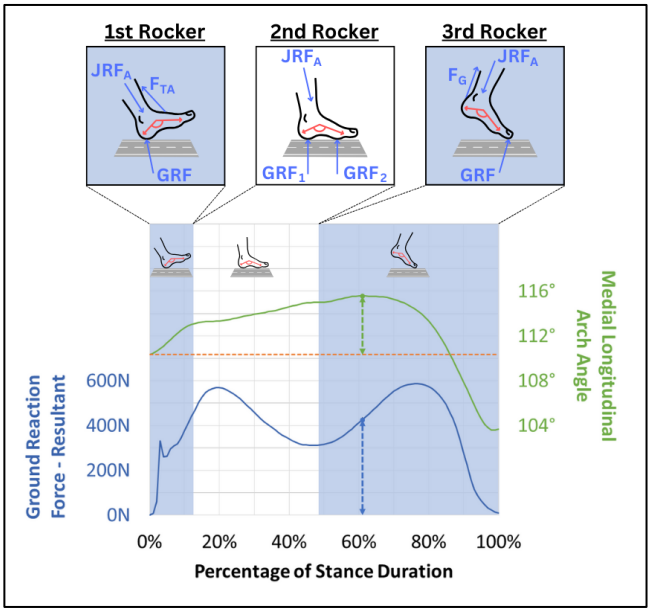

Figure 1: Example stance illustrating the ΔMLAA (*middle*) and rGRF (*bottom*) values that were used in the calculation of MLAS. Simplified free body diagrams of the three rocker phases of gait (*top*) with their approximate durations highlighted and the MLAA shown in red. Ankle joint reaction force (JRF_A), ground reaction force(s) (GRF / GRF_1 / GRF_2), and force of the tibialis anterior or gastrocnemius muscles (F_{TA} / F_G).

Results & Discussion: On average and at typical walking speeds, PAD occurred at 71.0 ±8.8% of the stance phase and MLAS was 8.93 ±4.47 deg/kN. Concerning test-retest reliability, the Pearson r was 0.792 (p=.019) for PAD and 0.768 (p=.026) for MLAS. One-way ANOVA with walking speed showed an earlier but non-significant PAD (F=1.915, p=.182) and a decrease in MLAS (F=10.686, p=.004) as speed increased. Measurements of both PAD and MLAS were found to be highly reliable. PAD occurred considerably later than 50% of stance, indicating that previous dynamic arch stiffness metrics measured at or before 50% are unlikely to adequately account for the longitudinal arch stiffness of the foot. With increasing walking speed, PAD occurred earlier, although this finding was not significant. Arch stiffness (inversely related to MLAS value) increased in conjunction with walking speed, corroborating evidence in the literature showing that with increasing speed, there is less MLAA deformation and greater ground reaction force [6]. This study shows that the body can dynamically adapt to a greater propulsive need by increasing medial longitudinal arch stiffness.

Significance: We introduced a dynamic metric of foot arch stiffness and showed that it: (1) represents a different and functional non-arbitrary timepoint during stance, (2) produced reliable results across separate days, and (3) confirmed existing evidence regarding how arch stiffness responds to changes in walking speed, information that clinicians can incorporate into patient management.

Acknowledgments: Des Moines University Mentored Student Research Program (MSRP 2023-24).

References: [1] Teyhen et al. (2009), *Clin Biomech*, 24(4); [2] García-Pinillos et al. (2020), *Int J Sports Physiol Perform*, 15(7); [3] Tweed et al. (2009), *J Am Podiatr Med Assoc*, 99(5); [4] Cashmere et al. (1999), *Foot Ankle Int*, 20(2); [5] Bencke et al. (2012), *Gait Posture*, 35(3); [6] Caravaggi et al. (2010), *J Anat*, 217(3); [7] Eichelberger et al. (2018), *J Foot Ankle Res* 11(1).

Influence Of Sport Specialization On Adolescent Baseball Pitchers' Timing Sequence And Kinetics

Alexandra L. Johnson[1*], BS, Meghan Caballero[1], MD, Shayne Fehr[1], MD, Cody Dziuk[1], BS, Janelle A. Cross[1], PhD
[1]Department of Orthopaedic Surgery, Medical College of Wisconsin, Milwaukee, WI, USA
*Corresponding author's email: alljohnson@mcw.edu

Introduction: Youth sports are moving away from multi-sport participation, emphasizing sport specialization for improved skill development and increased odds of making elite teams. Early sports specialization has been previously associated with increased overuse injury rates and literature lacks consensus regarding the overall benefits to performance metrics. Previous research has yet to reveal biomechanical differences among specialization level in adolescent baseball pitchers [1]. The purpose of this study was to examine pitching kinetics, peak velocities, and timing differences among low-, moderate-, and high-level specialized pitchers. It was hypothesized that kinetics would vary among specialization level, particularly observing biomechanical changes in highly specialized pitchers known to predispose to throwing arm injury.

Methods: Forty-six right-handed adolescent male baseball pitchers (age: 16.7 ± 1.2 years, height: 183 ± 7 cm, mass: 79.8 ± 9.9 kg) participated in the study. Each pitcher had at least three years of pitching experience, with no current throwing arm pain or surgical history. Sport specialization level was defined as low-, moderate-, or high-level specialization based upon answers to a questionnaire that determined baseball exposure history. Pitching biomechanics were measured using a 3D motion analysis system during a single pitching session. Biomechanical metrics were selected due to associations with pitching performance and injury (Table 1) [2, 3, 4]. Means and standard deviations were calculated for all metrics. A one-way ANOVA test was conducted for variables that were normally distributed. For non-normal distributions, a Kruskal-Wallis test was used to assess differences between high-, moderate-, and low-level specialization groups. Follow up pairwise comparisons were completed for significant variables. A significance level of $p<0.05$ was utilized.

Table 1. Pitching biomechanics and specialization level of high school baseball pitchers

	Low (n = 10)	Moderate (n = 19)	High (n = 17)
Pitch Speed (m/s)	32.9 (3.2)	34.2 (2.6)	35.5 (2.7)
Elbow Varus Torque (Nm, %BW)	0.04(0.01)	0.04(0.01)	0.05(0.01)
Shoulder Distraction Force (N, %BW)	0.81(0.13)	0.92(0.14)	0.96(0.12)
Max Pelvis Rotation Velocity (°/s)	646.2 (54.3)	671.8 (86.9)	696.8 (88.5)
Max Torso Rotation Velocity (°/s)	930.5 (68.4)	994.4 (90.4)	1020.00 (75.7)
Max Shoulder IR Velocity (°/s)	4284.2 (311.6)	4704.1 (579.20)	4827.7 (512.2)
Timing of Max Pelvis Rotation Velocity (%PC)	31.9 (14.8)	25.7 (8.5)	26.9 (8.1)
Timing of Max Torso Rotation Velocity (%PC)	42.3 (14.8)	37.0 (8.5)	39.0(8.1)
Timing of Max Shoulder IR Velocity (%PC)	82.3 (4.3)	79.7 (4.07)	81.6 (2.0)

Results & Discussion: Significant differences between low-, moderate-, and high-level specialization were observed in maximum shoulder internal rotation velocity ($p=0.032$), maximum torso rotation velocity ($p=0.028$), and shoulder distraction force ($p=0.028$), with each metric increasing with increased specialization level. Follow-up pairwise analyses found significant differences between low- and high-level specialization for maximum torso rotation velocity ($p=0.022$), maximum shoulder internal rotation velocity ($p=0.027$), and shoulder distraction force ($p=0.023$). There were no significant differences among age, height, weight, or average pitching speed across pitching specialization levels.

Significance: Differences in pitching biomechanics linked to enhanced performance and throwing arm injury risk were observed among specialization level of high school baseball pitchers. As youth sports continue to move toward sport specialization, it is crucial to consider the balance of pitching performance and injury risk.

Acknowledgements: We thank the Medical College of Wisconsin Department of Biostatistics for their assistance with the statistical analysis.

References [1] Hamer et al. (2022), *Int J Sports Phys Ther* 17(5):870-878; [2] Mercier et al. (2020), *BMJ Open Sport Exerc Med* 6(1): e000704; [3] Sgroi et al. (2015) *J Shoulder Elbow Surg* 24(9):1339-45; [4] Bullock et al., (2021), *J Sci Med Sport* 24(1): 13-20.

EFFECT OF RADIATION THERAPY FOR BREAST CANCER WITHOUT PRIOR AXILLARY SURGERY ON PECTORALIS MAJOR STIFFNESS

Sylvie G. Goudreau[1*], Susann Wolfram[1], David B. Lipps[1]
[1]School of Kinesiology, University of Michigan, Ann Arbor
*Corresponding author's email: sylvieg@umich.edu

Introduction: Women whose breast cancer diagnosis is managed with surgery and radiation therapy (RT) often experience shoulder morbidities following treatment, like reduced strength and range of motion [1]. These impairments may be due to changes to the mechanical properties of shoulder muscles like the pectoralis major [2]. The stiffness of the pectoralis major was greater in patients who received RT to the breast and axilla following axillary lymph node dissection but not in patients who received RT to the breast only following sentinel lymph node biopsy [3]. However, it is unclear if this greater stiffness of the pectoralis major is attributable to greater radiation exposure when managing the breast and axilla or instead is caused by the axillary lymph node dissection, where the pectoralis major is retracted to expose the axillary lymph nodes. This study aimed to investigate whether pectoralis major stiffness is greater in women who received RT to the breast and axilla compared to women who received RT to the breast only without prior axillary surgery.

Methods: We recruited 11 female breast cancer patients who received RT to breast + axilla (mean ± SD age 57.0 ± 7.9 years, height 164 ± 6.5 cm, weight 81 ± 12 kg) and 11 female breast cancer survivors who received RT to the breast only (age 60.3 ± 5.9 years, height 164 ± 8.0 cm, weight 70 ± 6.2 kg). All patients underwent breast-conserving surgery and sentinel lymph node biopsy before RT and completed their treatment 12-60 months prior. These women were compared to 11 female, age-matched cancer-free controls (age 60.8 ± 7.7 years, height 163 ± 6.8 cm, weight 60 ± 12 kg). We examined the pectoralis major of the affected side in breast cancer survivors and a randomly chosen side in controls. Participants were seated with their arm at 90° shoulder abduction and 90° elbow flexion placed in a plastic cast attached to a load cell. Ultrasound shear wave elastography (SWE) images (Hologic Mach 30) were obtained of the clavicular and sternocostal regions of the pectoralis major at rest, during adduction at 15% and 30% of maximum voluntary contraction (MVC), and during flexion at 15% and 30% of MVC. Mean shear wave velocities (SWV) were extracted from these SWE images, serving as a measure of muscle stiffness. A repeated-measures ANOVA tested if differences in SWV existed between groups (between-subject factor), conditions (within-subject factor), and pectoralis major regions (within-subject factor), as well as the interactions between them.

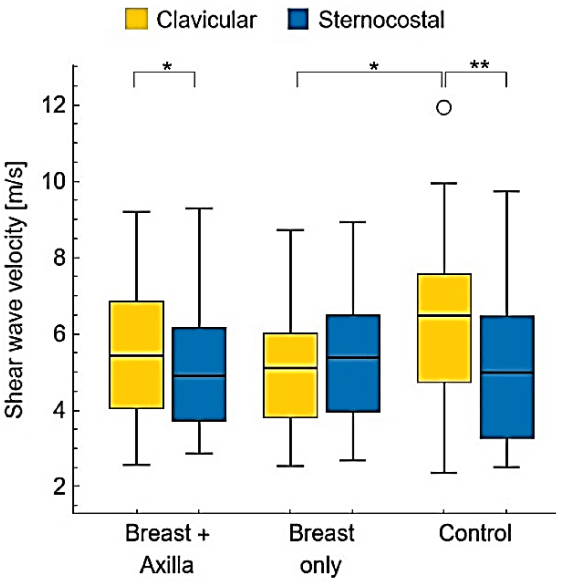

Figure 1: Shear wave velocities by muscle pooled across conditions in breast cancer patients who received radiation therapy to the breast and axilla, breast cancer patients who received radiation therapy to the breast only and in age-matched cancer-free controls. Boxes represent the first, median and third quartile, and whiskers show the variability as 1.5 times the interquartile range. Outliers are marked with empty circles.

Results & Discussion: Mean ± S.E. SWV pooled for the clavicular and sternocostal regions and all participants was 3.45±0.11 m/s at rest and increased significantly with an increase in contraction level (all $p < 0.001$). SWVs were similar between groups ($p = 0.41$), indicating that pectoralis major stiffness may not be affected by RT. SWV was significantly greater for the clavicular (5.81±0.16 m/s) than the sternocostal (4.94±0.18) region ($p < 0.001$) as reported previously [4]. However, this difference was dependent on group (Fig. 1). Greater SWV in the clavicular than the sternocostal region was only found in the breast + axilla group ($p = 0.037$) and the control group ($p < 0.001$) but not in the breast only group ($p = 0.23$). Furthermore, SWV of the clavicular region was greater in the control group compared to the breast only group ($p = 0.036$) and not compared to the breast + axilla group ($p = 0.134$) (Fig. 1). This greater stiffness of the clavicular region in the control group is surprising as muscle stiffness was found to increase as early as one month after RT [5]. However, this may indicate that the control group activated the clavicular region of their pectoralis major more than the breast cancer groups during the adduction and flexion tasks.

Significance: Expanding the radiation field to the axillary region during RT for breast cancer does not appear to affect pectoralis major stiffness, supporting the emerging clinical practice of omitting axillary lymph node dissection. However, RT may limit the extent to which the clavicular region of the pectoralis major can be volitionally activated. Thus, post-treatment rehabilitation could focus on restoring neuromuscular function to the clavicular region of the pectoralis major.

Acknowledgments: This study was funded by a University of Michigan Rogel Cancer Center Postdoctoral Small Grant and an American Cancer Society Research Scholar Grant (RSG2001601CCE).

References: [1] Johansen et al. 2014. *Acta Oncol*. 53(4); [2] Ebaugh et al. 2011. *Med Hypotheses.* 77(4); [3] Lipps et al. 2019. *Sci Rep.* 9(1); [4] Leonardis et al. 2017. *J Biomech.* 63; [5] Wolfram et al. 2023. *Radiother Oncol*. 179.

Effects Of Hip And Torso Muscular Fatigue On Pitching Biomechanics In Adolescent Baseball Pitchers

Alexandra L. Johnson[1*], BS, Wesley Kokott[2], DPT, Cody Dziuk[1], BS, Janelle A. Cross[1], PhD
[1]Department of Orthopaedic Surgery, Medical College of Wisconsin, Milwaukee, WI, USA
[2]Freedom Physical Therapy, Mukwonago, WI
*Corresponding author's email: alljohnson@mcw.edu

Introduction: Pitching is a dynamic motion where forces from the lower body are transferred to the torso and through the upper extremity, requiring extensive lumbopelvic control to divert upper extremity forces [1]. The importance of lower extremity biomechanics on the pitching cycle have been described in the literature, notably recognizing that muscular fatigue negatively contributes to worsening lower extremity kinematics in all phases of the pitching cycle [2]. Repetition of this motion also predisposes fatigued baseball pitchers to upper extremity injuries [3]. With muscular fatigue being an injury risk indicator, the effects of muscular fatigue on pitching biomechanics warrants further investigation [4]. This study evaluated hip and torso biomechanics to provide a quantifiable measurement demonstrating muscular fatigue after a single brief pitching session. We hypothesized that muscular fatigue would negatively impact pitching biomechanics, contributing to increased throwing arm kinetics.

Methods: Seventeen adolescent male baseball pitchers (age: 17.1±1.0 years, height: 183.9±7.1 cm, mass: 82.9±10.3 kg) threw an average of 35 pitches. Each participant had a minimum of three years pitching experience, no current arm pain or history of throwing-arm surgery. Hip and abdominal oblique strength were measured before and after a single pitching session. Pitching biomechanics were calculated from three pitches within the first five and last five of the throwing session. Means and standard deviations were calculated for all metrics. Paired T-tests were conducted to compare pitching and strength metrics from the start and end of the pitching session. A linear regression model examined the relationships between the total pitch number and the dependent variables. A significance level of $p<0.05$ was utilized.

Results & Discussion: Significant decreases were found for torso rotation angle and body separation angle at ball release, along with decreased timing of maximum shoulder internal rotation velocity. Strength significantly decreased in back hip extension, lead hip extension, back hip external rotation, lead hip external rotation, and lead hip internal rotation. The linear regression model showed three significant observations: body separation angle at foot contact, body separation angle at ball release, and peak pelvis rotation velocity. Scatter plots (Fig. 1) demonstrated a bimodal distribution between 35 and 40 pitches, with more variability at higher pitch counts.

Significance: Changes in pitching biomechanics were observed in pre- and post-pitching tests, highlighting the impact of muscular fatigue following a brief pitching session. Despite no significant changes in upper extremity kinetics, this study demonstrates areas for targeted strength training in baseball pitchers for proactive injury risk reduction.

Acknowledgements: We thank the Medical College of Wisconsin Department of Biostatistics for their assistance with the statistical analysis.

References: [1] Laudner et al. (2019) *J Shoulder Elbow Surg* 28(2): 330-334; [2] Erickson et al. (2016) *Arthroscopy* 32(5):762-771; [3] Yang et al. (2014) *Am J Sports Med* 42(6):1456-1463; [4] Kokott et al. (2023) *ISBS Proceedings Archive* 41(1): 66.

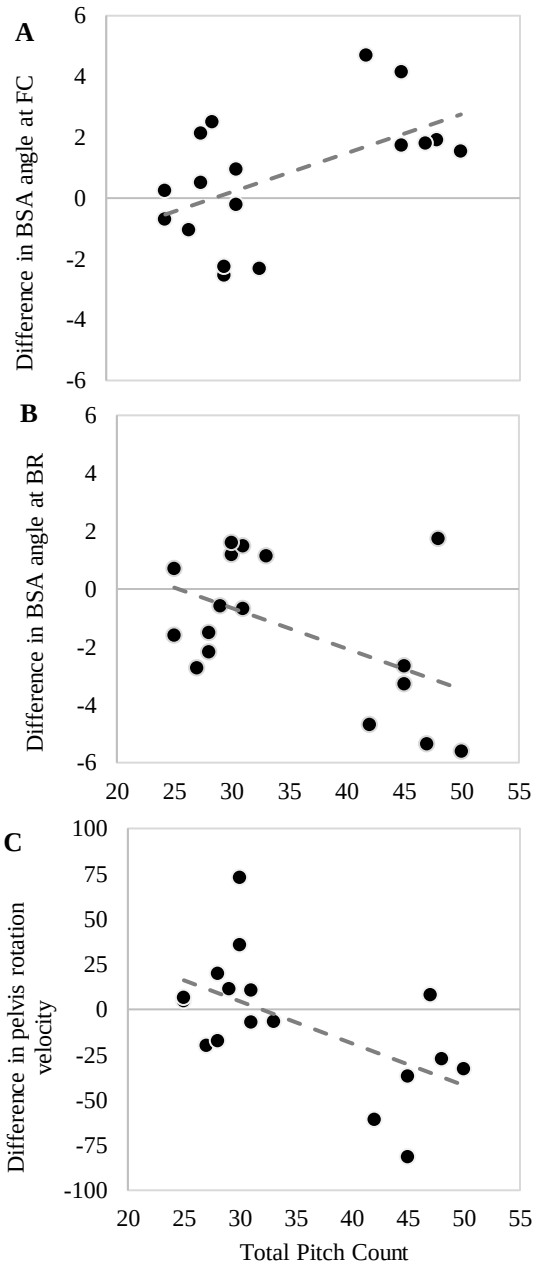

Figure 1. Scatter plots of differences pre- and post-pitching session of **(A)** body separation angle (BSA) at foot contact (FC) vs. total pitch count; **(B)** BSA at Ball Release (BR) vs. total pitch count; and **(C)** peak pelvis rotation velocity vs. total pitch count.

THE EFFECT OF MUSCULAR FATIGUE AND SEX ON SUPRASPINATUS OCCUPATION RATIO DURING THE BENCH PRESS EXERCISE IN COMPETITIVE POWERLIFTERS

Jodi G. Motlagh[1*], David B. Lipps[1]
[1]School of Kinesiology, University of Michigan
*Corresponding author's email: jmotlagh@umich.edu

Introduction: Powerlifting comprises three compound lifts: the squat, bench press, and deadlift [1]. As with any other sport, powerlifting carries an inherent risk of injury. Approximately 3.5% to 12% of all weight-training injuries, including tendinopathies, occurred due to overuse [2]. The past two decades have seen a 1,067% increase in male participation and a 2,529% increase in female participation in competitive powerlifting. With such expansive growth in powerlifting worldwide, overuse injuries have likely risen proportionally. While overall injury incidence appears similar between male and female powerlifters, females often reported higher injury rates in the neck and thoracic region [3]. Looking at the bench press specifically, current mechanisms of injury include using a wider grip width, high exercise dose, repetitive strain, and altered proprioception following an injury [2,4]. This study aimed to examine the impact of muscular fatigue during the bench press and biological sex on the supraspinatus tendon (SST), subacromial space (SAS – e.g., the acromiohumeral distance), and the supraspinatus occupation ratio (OR - the ratio of SST thickness to acromiohumeral distance [5]). Due to recurrent loading and increased mechanical stress on the shoulder joint during the bench press, we hypothesized supraspinatus OR would increase after a fatiguing bench press protocol and be enhanced in female lifters compared to male lifters.

Methods: Twelve competitive powerlifters (6 M, 6 F; mean (SD) age: 23.5(3.9); height: 168.1(9.3) cm; weight: 79.7(18.4) kg; Shoulder Pain and Disability Index (SPADI) score: 2.3(4.2)) enrolled in this study and provided written informed consent. To ensure participant safety and confidence, all participants completed an identical dynamic warmup and self-reported their bench press one-repetition maximum (1RM). Participants completed three sets of eight repetitions at a load equivalent to 74% of their 1RM.

Ultrasound imaging was used to visualize the SAS and SST (Supersonic Mach 30, Hologic). Images of the SST were taken with participants seated, hand in back pocket. SST thickness was measured in a single posture at three different points along the tendon and averaged. An identical imaging protocol was used to assess the SAS at three timepoints: pre-warmup, post-warmup, and post-exercise after completing the three sets of eight repetitions. Images of the SAS were taken in three positions: 'seated, relaxed,' 'seated, bench press,' and 'standard bench press, unracked barbell.' SAS was measured as the acromiohumeral distance between the inferior border of the acromion and the superior border of the humeral head and was also used to calculate the supraspinatus OR [5]. Repeated measures ANOVA was used for each position to test if OR differed by time, sex, and their interaction.

Results & Discussion: There were no significant main effects of sex or time on the mean supraspinatus OR in the seated, relaxed condition (all $p>0.217$). However, sex differences in OR became apparent as participants were instructed to assume their standard bench press position with an unracked barbell. Females had a significantly larger OR than males across all time points when examined in the standard bench press position ($p=0.021$) **(Figure 1)**. However, OR in the standard bench press position was not significantly impacted by time, and there were no significant interactions between time and sex (both $p>0.369$).

Our findings agreed in part with our hypotheses. A fatiguing bench press protocol did not result in OR increases throughout the experiment, regardless of imaging position. However, the OR values in female lifters were consistently greater than males when participants were imaged in a bench press position. This raises some concerns regarding injury incidence in female powerlifters during the bench press and highlights potential avenues of injury prevention in the rapidly rising number of female participants in powerlifting. Future research could expand upon whether sex differences in biomechanical form during bench press exercises (e.g., grip width, arch) exist and explore if the anatomical differences observed here result in higher rates of subacromial impingement syndrome in female powerlifters.

Significance: This study provides novel biomechanical insights into how muscular fatigue and biological sex influence SST and SAS during the bench press. Addressing changes in the OR between males and females during a fatiguing bench press protocol will help enhance performance and long-term injury prevention of powerlifters completing the bench press exercise.

Acknowledgments: University of Michigan Rackham Graduate Student Research Grant

References: [1] Bengtsson et al. (2018), *BMJ Open Sport Exerc Med.* 4(1); [2] Reeves et al. (1998), *Phys Sportsmed*. 26(3); [3] Strömbäck et al. (2018), *Orthop J Sports Med.* 6(5); [4] Fees et al. (1998), *Am J Sports Med.* 26(5). [5] Michener et al. (2015), *Knee Surg Sports Traumatol Arthrosc*. 23(2).

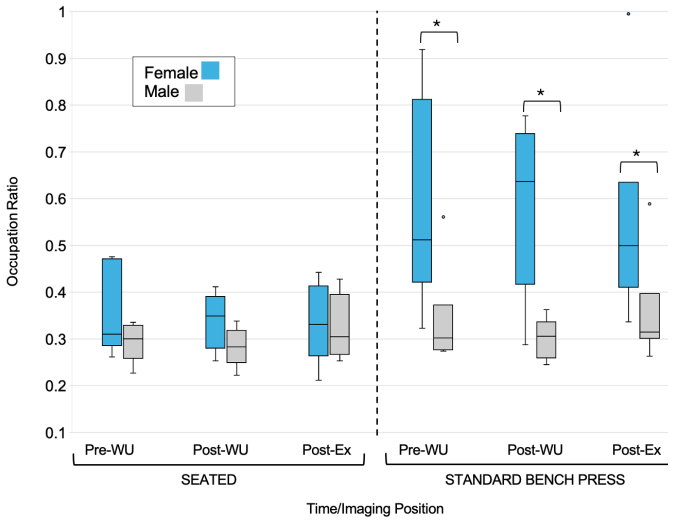

Figure 1: Box plots of occupation ratio, a ratio of supraspinatus tendon thickness to acromiohumeral distance, for females and males in the seated position and the bench press position with an unracked barbell. Differences between time (pre-warmup, post-warmup, and post-exercise), sex and the time*sex interaction were examined. A significant main effect of sex ($p=0.021$) is indicated using (*).

A MODELING APPROACH TO IDENTIFYING CONTRIBUTIONS OF STRATEGIES TO BALANCE RECOVERY

Michelle J. Karabin[1*], Mark S. Redfern[1], Hartmut Geyer[2]
[1]University of Pittsburgh, Dept. of Bioengineering [2]Carnegie Mellon University, Robotics Inst. *mjk160@pitt.edu

Introduction: Regulation of foot placement with respect to the center of mass (CoM) is the primary strategy used to maintain stability in walking, but it can be supplemented by other strategies, particularly when constrained [1,2]. Other strategies include 1) adjusting the center of pressure (CoP) location during single support through lateral ankle torques, 2) modifying push-off forces via ankle push-off during double support, and 3) generating angular momentum by movement of the trunk and upper body [1,2]. These strategies interact during walking, making their individual contributions difficult to identify [1]. Computer models can reveal the roles of individual subsystems. Thus, this work builds a model based on linear inverted pendulum model (LIPM) dynamics that includes four stabilization strategies and uses this model to investigate each strategy's importance in maintaining stability. The overall goal is to inform which strategies may be the best targets for training to improve stability.

Methods: The model consists of a 3D rigid body (i.e. head-arms-trunk segment) with massless legs. The model moves through 3D space via leg forces applied at the hips based on LIPM dynamics and maintains upright posture by proportional-derivative controllers applying torques in pitch, yaw, and roll. Foot placements are selected based on the mediolateral and anteroposterior position and velocity of the CoM. The lateral ankle strategy is implemented by adjusting the CoP location underfoot during single support. The ankle push-off strategy is implemented by adjusting the push-off force applied by the hind leg during double support. The trunk strategy is implemented by a frontal plane torque that modifies mediolateral ground reaction forces.

The controllers were optimized using the covariate matrix adaptation evolution strategy [3] with the objective to produce human-like walking in unperturbed conditions and in response to medial and lateral ground shift perturbations, as used in previous experimental work [4]. After tuning the model, an ablation study was performed where strategies supplemental to foot placement were removed from the model. Perturbations were applied in simulation to investigate the contribution of the removed strategy(ies) to the balance response. Balance recovery was quantified by the minimum margin of stability (MoS) and step width (SW) following the perturbation, specifically the deviations of these outcomes from unperturbed walking. Larger deviations of MoS or SW indicated worse stability, suggesting greater importance of the removed strategy(ies) to the balance response.

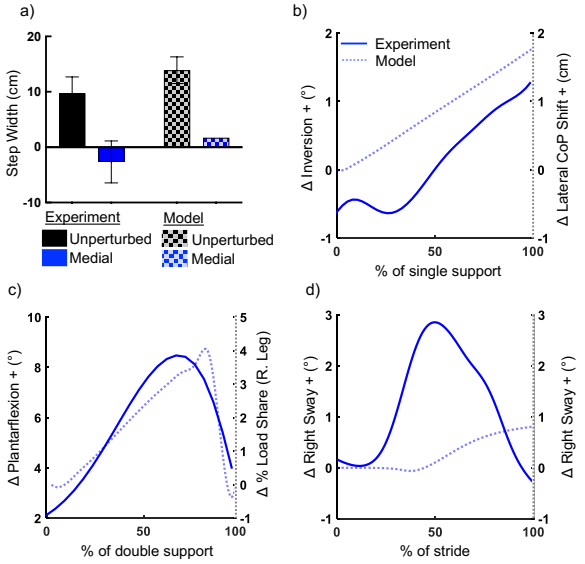

Figure 1: Responses to medial perturbations in experiment (solid) and model (dashed).

Results & Discussion: The model walked at 1.3m/s with an average step time (0.41 sec), step length (52 cm), step width (16 cm), and minimum MoS (8.3 cm cm) comparable to human walking. The model responded to medial perturbations similarly to humans [4], with a narrow recovery step (Fig. 1a), increased lateral CoP shift / increased ankle inversion (Fig. 1b), increased load share on hind leg / increased ankle push-off (Fig. 1c), and increased rightward trunk sway (Fig 1d.). The trunk sway magnitude and timing were smaller and later than reported experimental results [4]. Responses to lateral perturbations were also consistent with experiments (not pictured), altogether suggesting good correspondence between the model walking and human walking [4]. The ablation study showed that the model's balance recovery worsened when the lateral ankle or trunk strategies were removed, but not when the ankle push-off strategy was removed (Tab. 1, '1 removed'). The importance of the lateral ankle and trunk strategies was further emphasized by large deviations in both MoS and SW when both strategies were removed (Tab. 1, '2 removed'). When the ankle push-off strategy was also removed (Tab. 1, '3 removed'), there was negligible increase in MoS or SW deviation, suggesting its lesser importance in balance recovery.

Table 1: Results from ablation study following medial perturbations.

		MoS Absolute Deviation (%)	SW Absolute Deviation (%)
	Full Model	43.9	72.3
1 removed	Remove Ankle Push-Off	46.1	77.1
	Remove Trunk	63.5	93.6
	Remove Lateral Ankle	51.6	106.0
2 removed	Remove Ankle Push-Off + Trunk	60.1	88.7
	Remove Ankle Push-Off + Lateral Ankle	49.4	97.6
	Remove Lateral Ankle + Trunk	77.9	133.8
3 removed	Remove Ankle Push-Off + Lateral Ankle + Trunk	77.3	135.2

Significance: This analysis demonstrated that the lateral ankle and trunk strategies were more important supplemental strategies to foot placement compared to ankle push-off, suggesting potential benefit of training these strategies in people with poor balance. The findings from this study could provide insight for physical therapy practice and future studies with this model could test rehabilitation approaches for populations with specific sensory, neural, or motor deficits.

Acknowledgments: Funding: NIDCD/NIH: F311DC020110.

References: [1] Van Leeuwen et al. (2022). *SportRxiv*. [2] Bruijn et al. (2018). *J Roy Soc Interface*, 15(143). [3] Hansen (2006). Adv. in estimation of distribution algorithms, 75-102. [4] Karabin et al. (2024). *J Biomech* 162, 111898.

Vertebral Body Implant Biomechanical Assessments with a Novel Spine Simulator

Katherine F. Walters[1], Nathaniel A. Bates[2], Schuyler van den Nieuwenhuizen[1], Adolfo Viloria[1], Puya Alikhani[1], Nathan D. Schilaty[1*]
[1]University of South Florida, Department of Neurosurgery & Brain Repair
[2]The Ohio State University, Department of Orthopaedics
*Corresponding author's email: nschilaty@usf.edu

Introduction: Lower back pain is a leading cause of disability and musculoskeletal injury[1]. With both pediatric and adult patients, indications for vertebral body osteotomy (VBO) include severe and progressive sagittal plane deformity, resectable spinal tumors, and trauma, especially when nonsurgical treatments do not relieve symptoms of numbness, weakness, or pain from nerve compression[2]. The objective of this project was to characterize the Vertiwedge implant system (**Fig. 1A/B**) to restore native spinal stability after VBO.

Methods: Eight cadaveric specimens were acquired from Anatomy Gifts Registry (Hanover, MD) between the 45-75 years (Sex: 5M:3F; Age: 61.3 ± 12.4 years; Height: 173.5 ± 8.4 cm; BMI: 28.1 ± 6.5). Specimen exclusions were trauma to the spine, spinal tumor, Non-Hodgkins lymphoma, multiple myeloma, gout, rheumatoid arthritis, spinal metastasis, and severe osteoporosis. Specimens were thawed for 24 hours and then dissected to include all ligaments and multifidi musculature. Each lumbar spine was potted at T12/L1 and at S1 and then affixed to a novel spine simulator that was robotically controlled with Arcus stepper motors. Non-destructive spinal testing was then performed that included randomized compression loads (0, 100, 250, 400, 500 N) and planar motions in flexion/extension (20°/18°), lateral bending (19°), and axial rotation (9°). While the stepper motors moved the specimens (20°/sec), a 6-axis load cell (ATI Omega 160) measured forces and torques. From these data, stiffness (force vs displacement) was assessed as well as peak maximum and minimum moments. Each specimen was first evaluated in the native state. After native testing, a board-certified neurosurgeon performed a VBO and implanted the Vertiwedge system at L4. The specimen was then evaluated in a randomized order of compression and motions with the Vertiwedge in a full configuration (screws, staple). Thereafter, the staple was disengaged (screws only), and the randomized order of tests repeated.

Results & Discussion: A linear mixed model compared stiffness with covariates of condition, motion, compression, and their interactions. The model demonstrated no differences in maximum moments between testing conditions (Native, Full Configuration, Screws Only; $p>0.056$). The full interaction demonstrated no differences of biomechanical stiffness ($p>0.995$). Across the variables of motion, load, and condition the data demonstrated high consilience of two surgical conditions (Full Configuration and Screw Only) when compared to the Native condition with increasing compression load. Axial rotation had the highest variability of the three motions. The prediction intervals of the stiffness curves showed high overlay between the testing conditions. One potential limitation with this project is the use of cadaveric specimens which do not allow for tissue healing; however, healing should only provide more stability rather than affect stiffness.

Significance: The Vertiwedge system, when fully configured, maintained nearly native state biomechanics in all three planes of motion (**Fig. 1C**). Thus, the Vertiwedge system, when implanted in cadaveric specimens, demonstrated maintenance of spinal stability following VBO.

Acknowledgments: Foundation Surgical Group (Bradenton, FL) provided funding for this study. The authors declare no conflicts of interest.

References: [1] Ferreira et al. (2023), *Lancet Rheumatol* 5(6): e316-e329; [2] Kose et al. (2017), EFFORT Open Rev 2(3): 73-82

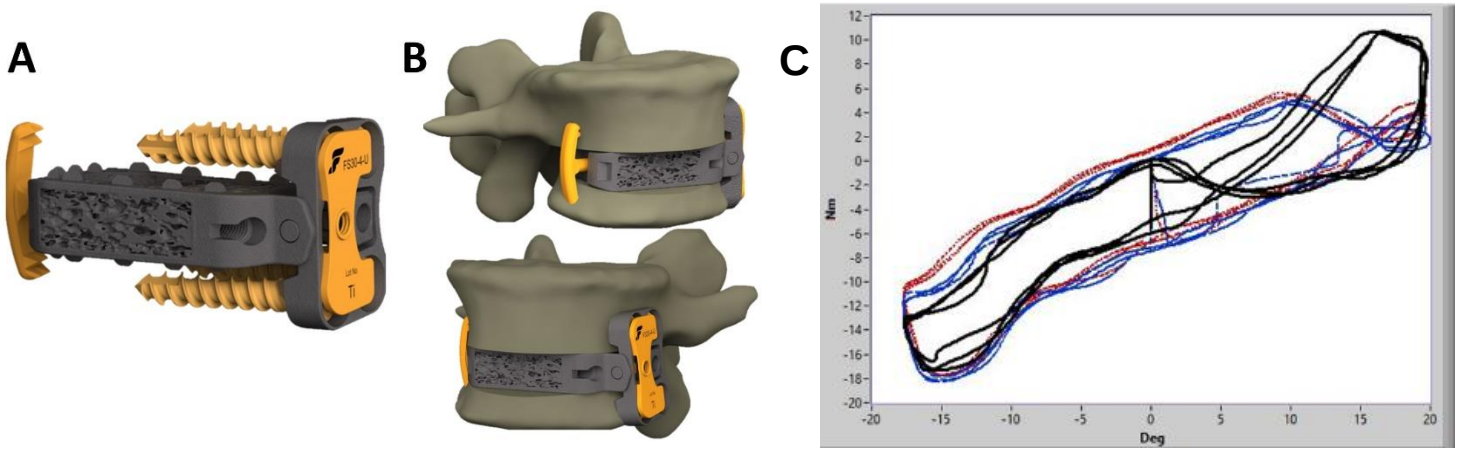

Figure 1: Vertiwedge Intraosseous System and Stiffness Data. A) 3D titanium printed structure allows for bone ingrowth. **B)** Sample placement of Vertiwedge within a lumbar vertebra. **C)** Sagittal plane stiffness of native (black), Vertiwedge (fully-configured; blue), and Vertiwedge (screws only; red).

SHOE FIT AND EFFECT ON GOLF BIOMECHANICS AND PERFORMANCE

Milena Singletary[1*], Daniel Feeney[1], Adam Luftglass[1], Bethany Kilpatrick[1], Eric C. Honert[1], Kathryn Harrison[1]
[1]Performance Fit Lab BOA Technology Inc. Denver, CO.
*Corresponding author's email: milena.singletary@boatechnology.com

Introduction: In golf it is advantageous to hit the ball farther. A key factor in ball displacement is club head speed. Faster club head speeds have been associated with greater vertical ground reaction forces [1], however there is debate around other biomechanical variables that impact club head speed. There is limited research on the fit of golf shoes and its impact on performance. Research has focused on traction or outsole design [2]. When considering the length of a golf round, a poor fitting shoe may cause discomfort, premature fatigue, and may decrease the benefits of other design features, thus shoe fit may be an important attribute. Metrics of fit such as heel contact area [3] and peak toe pressure may impact performance. The purpose of this test was to investigate the relationship between biomechanical metrics and club head speed, and to assess the effect of fit on biomechanics and performance.

Methods: Eighteen golfers (nine Female, handicap < 10) performed three golf-related tasks in three footwear conditions. The footwear conditions were performed in identical shoes (Adidas Motion Primegreen Mid BOA) differing only in closure: BOA, Lace, and Sock – the BOA shoe with the dial disengaged. First, participants walked on a 10° incline uphill and downhill on a treadmill at 1 m/s while wearing plantar pressure insoles (XSENSOR, CAN). Next, they performed eight swings with a driver and eight swings with an iron standing on a slope with 17.5-degree pitch with a full body marker set (Vicon, USA) while a radar unit (Trackman, Denmark) collected performance outcomes. Biomechanical metrics were only extracted for drives due to experimental limitations. Swings with the driver were segmented using the vertical ground reaction force of the target and trail limb. For each drive during the downswing, peaks of the vertical ground reaction force for both the lead and trail limb, knee extension velocity, torso and pelvis rotational velocity were extracted. For each iron shot during static stance, peak toe pressure and heel contact area were extracted. During walking, peak toe pressure and heel contact area was extracted from each step. For analysis, linear mixed effects models were used to assess the relationship between biomechanical variables on club head speed with random slopes for each subject. Bayesian models with random slopes and intercepts were used to assess the effect of footwear on biomechanics and club head speed. For simplicity, we present the differences between BOA and Lace for direct comparisons along with the percent of the posterior greater than zero and 95% credible intervals (CI).

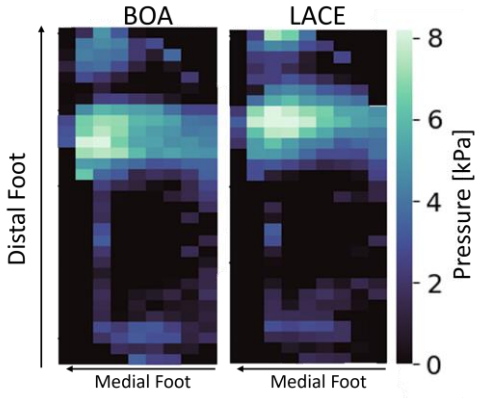

Figure 1: Pressure trace at toe-off of one athlete walking uphill. BOA on the left with lower toe pressure and greater heel pressure.

Results & Discussion: Significant relationships between club head speed and biomechanical metrics during the downswing of the drive including peak pelvis rotational velocity, peak vertical ground reaction force of the target limb, and peak frontal moment of the target ankle were observed ($p < 0.001$, $R^2 < 0.9$).

Club head speed was greater in BOA. For driving, on average BOA improved club head speed by 0.8 km/hr (97% > 0, CI: 0.2 to 2.9%). For sloped iron shots, on average BOA improved club head speed by 1.4 km/hr (100% > 0, CI:0.4 to 1.1%). In general, BOA improved quantitative fit with increased heel contact area by at least 5% and decreased peak toe pressure by at least 3%. BOA decreased toe pressure on slope at ball address (92% > 0, CI: -5.8 to -0.2%), walking uphill (80% > 0, CI: -3.8 to 0.8%), and walking downhill (97% > 0, CI: -6.8 to -1.5%). BOA also increased heel contact on slope at ball address (100% > 0, CI: 5.6 to 10.5%), walking uphill (100% > 0, CI: 2.2 to -6.2%), and walking downhill (99% > 0, CI: 2.1 to 7.1%). Finally, there was little difference between BOA and lace in biomechanical metrics correlated with performance.

Greater heel hold has been shown to improve endurance performance [3]. A better fitting shoe may allow golfers to maintain the level of performance over the course of a round ultimately enhancing outcome. Better fit may allow for full use of the mechanical design and proprioceptive functions of the shoe especially during a powerful movement like a drive [4]. Even though we found correlations between biomechanical metrics and golf performance, we did not see any differences between biomechanical metrics and BOA. We did however observe an improvement in fit in BOA (Fig. 1). We can reason that the performance improvements we observed were due to differences in fit specifically how the foot is connected with the shoe.

Significance: We found strong relationships between club head speed and peak pelvis rotational velocity, peak vertical ground reaction force of the target limb, and peak frontal moment of the target ankle. These biomechanical metrics can be used to evaluate golf performance. Improving quantitative fit of a golf shoe can also improve golf performance.

Acknowledgments: BOA Technology Inc.

References: [1] Hume, P. A., Keogh, J., & Reid, D. (2005). Sports Medicine (Auckland, N.Z.), 35(5), 429–449. [2] Worsfold, P., Smith, N. A., & Dyson, R. J. (2009). Journal of Sports Science & Medicine, 8(4), 607–615. [3] Honert, E. C., Harrison, K., & Feeney, D. (2023). Frontiers in Sports and Active Living, 4. [4] Isherwood, J., Kwak, M., Lee, J., Park, S., & Sterzing, T. (2023). Footwear Science, 15(sup1), S130–S131.

RELATIONSHIP BETWEEN GROUND REACTION FORCES AND PULLING VELOCITY DURING THE KUZUSHI PHASE OF A JUDO THROW

John Adam Caraan[1,2]*, Rodney Imamura[2], Daryl L. Parker[2]
[1]Biomechanical Consultants, [2]California State University, Sacramento
*jadam.caraan@gmail.com

Introduction: Force production is often suggested to be a determinant of overall improved sports performance [1-2]. In addition, it has been suggested that faster transmittance of forces through the body is associated with increased resultant peak body velocities [2]. The role of force and its subsequent velocities in other sports has been established, but its role within judo and throwing techniques remains unclear.

All judo throwing techniques are comprised of three phases, beginning with kuzushi, or unbalancing [3]. Kuzushi is an initiatory phase in which the thrower (tori) creates imbalance in the receiver (uke). This is typically done by moving the uke in such a way that they become unstable. In many throws, this is accomplished through manipulation of the uke's wrist. This is followed by the tsukuri phase involving positioning into the throw, and subsequently followed by kake, the execution of the throw itself. Prior investigations have suggested that large magnitudes of forces may be produced during the kuzushi phase to facilitate a better throw [4]. Creating sufficient kuzushi is necessary for successful throw execution [3], thus it may be necessary for throwers to generate large amounts of force to create high velocities onto the uke.

The aim of this study was to investigate the potential role of forces during the kuzushi phase of an ippon seoi-nage throw. This was achieved by comparing the relationship between peak ground reaction forces (GRF) and peak pulling wrist velocities during an ippon seoi-nage throw. In addition, timing characteristics between novice and advanced judo players were compared.

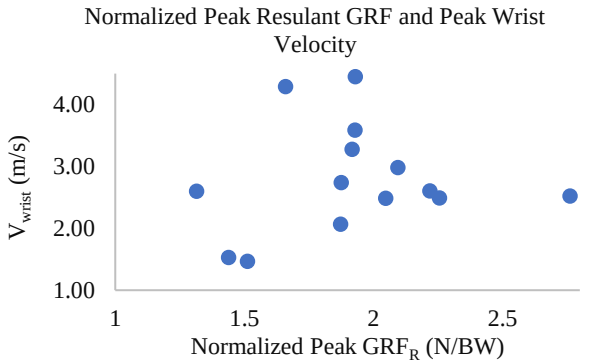

Figure 1: Normalized peak GRF_R and V_{wrist} during the kuzushi phase of an ippon seoi-nage throw.

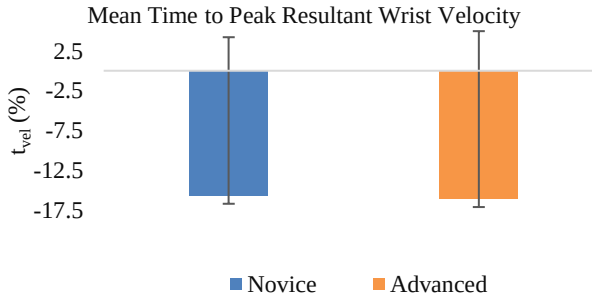

Figure 2: Mean time to peak resultant wrist velocity for advanced and novice judo players during the kuzushi phase of an ippon seoi-nage throw.

Methods: Eight advanced participants and seven novice participants were recruited for the current study. One advanced player served as uke for all trials. Given that participant populations were not matched for body mass, GRF data was normalized according to body weight. Kinematic data was measured using infrared cameras and reflective markers placed throughout the toris' bodies. Forces were measured using two force plates. Tori was instructed to perform an ippon seoi-nage throw on the uke with maximal effort. Peak resultant GRF (GRF_R) and peak resultant wrist velocity (V_{wrist}) were analyzed for correlation. Time to peak resultant wrist velocity (t_{vel}) was determined in percent time from the occurrence of GRF_R to the occurrence of V_{wrist}. Differences in peak resultant wrist velocity between the advanced and novice groups were determined using an independent t-test set at $p < 0.05$.

Results & Discussion: There was no significant correlation ($N = 15$, $r = -0.08$, $p = 0.77$) found between peak normalized GRF_R and V_{wrist} (Fig. 1). Time to peak resultant wrist velocity was not significantly different ($p = 0.97$) between the advanced and novice groups (Fig. 2).

Common findings in the literature indicate that large GRF are associated with greater resultant velocities in a target body region [2-3]. Similarly, previous literature has suggested that a shorter amount of time between GRF production and peak resultant wrist velocity indicates successful performance [3]. With these in mind, it was believed that within the present study, there would be an association between greater ground reaction forces and faster pulling velocities, as well an observation of shorter times to peak resultant wrist velocity in advanced players. However, the findings of this present study deviate from the previous literature. This may be explained by the complexity of this specific judo throw which involves performing a complete 180° turn and lowering the center of mass below the uke. Findings from a similar study reported that elite players had greater relative center of mass velocities than non-elite players during the same throw [5]. With respect to the present study, it is a possibility that advanced players are producing greater forces for the purposes of faster bodily positioning in lieu of greater pulling velocity.

Significance: This study provides further insight into judo from a biomechanical perspective. To date, there is a lack of research surrounding the sport with respect to biomechanical parameters throughout the course of a throw. The findings in the present study may provide a framework for future investigations into the determinants of a successful throw. In the case of the present study, it would appear that force production is not an important consideration for increasing wrist velocities, however, its effect on body positioning is yet to be understood.

References: [1] Vanezis et al. (2005) *Ergonomics* 48(11-14); [2] Masahiro et al. (2014), *J. Sports Sci. Med*. 13(4); [3] Kano (1994), ISBN 4770017995; [4] Imamura et al. (2006), *J. Sports Sci. Med.* 5(CSSI); [5] Ishii et al. (2018), *Sports Biomech. 17(2).*

AN OBJECTIVE AND SUBJECTIVE COMPARISON OF CUSTOM AND OFF-THE-SHELF FOOT ORTHOTICS: A CASE STUDY

Michael Krackow[1*] and Joyce Blandino[2]
[1]Department of Human Performance and Wellness, [2]Department of Mechanical Engineering, Virginia Military Institute, Lexington, VA, USA
*Corresponding author's email: krackowms@vmi.edu

Introduction: Every day, people use foot orthotics in their footwear to change the pressure distribution and mechanics within the foot and lower extremity to decrease pain and discomfort during gait by supporting the medial longitudinal arch, and stabilizing the subtalar and midtarsal joints [1,2,3]. The most common method is to use either custom-made or off-the shelf (prefabricated) inserts. It has been stated that while the prefabricated inserts cost considerably less than the custom orthotics, they do not provide the same support and are less comfortable to wear [1, 2]. The literature varies in which type of shoe insert provides the greatest discomfort relief for the user [1, 2, 4, 5, 6]. Research shows that foot orthotics help in controlling pain and discomfort associated with pes planes (flat feet) [7]. There are advantages and disadvantages to both custom-made and prefabricated shoe inserts. The users' particular needs and preferences, along with financial considerations can dictate which orthotic is preferred [7]. The purpose of this case study was to compare the custom made and prefabricated shoe orthotics in terms of comfort and trunk sway during walking.

Methods: A healthy 58-year-old, physically active male with a long history of pes planes volunteered to participate in the study. The subject also had an extensive history of using both custom-made and prefabricated foot orthotics to relieve lower extremity and low back discomfort resulting from pes planes. Retro-reflective markers were placed on feet, shanks, thighs, chest, and lower back. The subject performed three sets of four repetitions walking over 3 force platforms. The subject walked leading with the left leg first on the first force platform. Set one was performed with no foot orthotic, set two with the custom orthotic, and set three with the prefabricated insert. Eight VICON Vero cameras were used to gather kinematic data at 200Hz. Ground reaction force data were collected from the force platforms at 1000Hz. The Motion Monitor xGen software (TMMxGen) was used to collect data from both VICON cameras and the force platforms simultaneously. Results were reported as mean±std (average of 3 repetitions).

Results & Discussion: When walking over the force ~~p~~platforms with the custom orthotics, it is expected that lateral trunk sway and sacral movement would decrease during the single leg stance phase of the gait cycle as compared to that of with no orthotic and prefabricated shoe insert. Force platform data demonstrated that when walking with the custom orthotic, sacral and trunk movements were comparable to walking without a shoe insert. In contrast, the subject displayed less sacral and trunk sway when wearing the prefabricated orthotic. Subjectively, the subject~~ed~~ reported that he felt greater support within the foot, with less foot movement, specifically at the medial longitudinal arch area with the prefabricated orthotic.

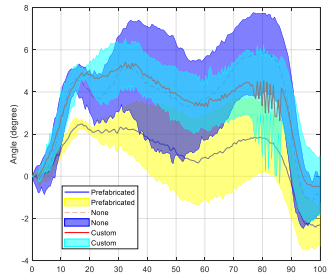

Figure 1: Sacrum Rt Side Bend for Left Leg

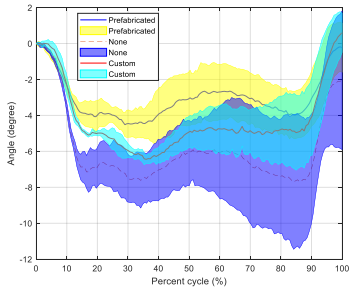

Figure 2: Sacrum Rt Side Bend for Right Leg

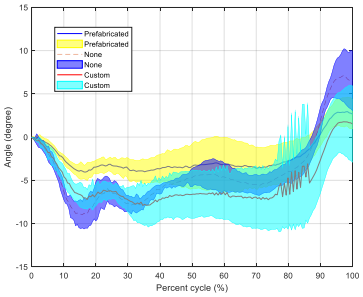

Figure 3: Thorax Right Lateral Flexion for Left Leg

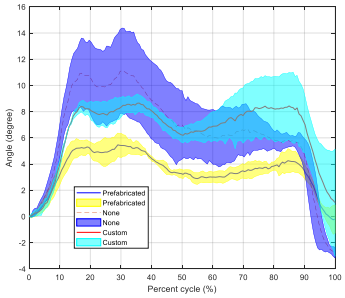

Figure 4: Thorax Right Lateral Flexion for Right Leg

Significance: Results of this case study indicated that sacral and trunk sway were similar when the subject walked wearing the custom orthotic and no shoe insert, as compared to the prefabricated orthotic treatment. Further research using a larger sample size is needed to validate the results of this study. However, the preliminary findings suggest that individuals who need foot orthotics to treat the symptoms resulting from pes planes may choose the cost-effective, off-the-shelf, prefabricated shoe insert as a first option before going directly to purchasing a more expensive, custom-made orthotic.

Acknowledgements: The VMI Institutional Review Board approved testing protocol. This project was supported by funding from the VMI Center for Undergraduate Research.

References: [1] Petrofsky, J. et al (2014), *Clinl Res on Foot and Ankle*, 3:1: 10000161. [2] Redman, et al (2009). *J of Foot and Ankle Res*. 2: 20 doi:10.1186/175701146-2-20. [3] Gallagher, K. et al. (2018*) J of Foot and Ankle Res*. 11:24 doi:.org/10.1186/s13047-018-0272-3. [4] Tran K, & Spry C. (2019). *Canadian Agency for Drugs and Technologies in Health*, PMID: 31714699. [5] Stark, S. et al (2023) *AOFA Annual Meeting*. http://www.creativecommons.org/licenses/by-nc/4.0/; [6] Angela, M., & Barbara, J. (2022). *Canadian J of Health Technologies*. 2(2) ISBN: 2564-6596.; [7] Bednarczyk, E. et al. (2024). *J of Ortho Reports*. 100250.

GAIT SYMMETRY ADAPATION TO COMBINED VISUAL DISTROTION AND SPLIT-BELT TREADMILL WALKING

Seung-Jae Kim[1], Omik Save[2], Arianna Marquez[3], Emily Tanner[3], Hyunglae Lee[2*]
[1]Biomedical Engineering, California Baptist University, Riverside, CA
[2]School for Engineering of Matter, Transport, and Energy, Arizona State University, Tempe, AZ
[3]School of Biological and Health Systems Engineering, Arizona State University, Tempe, AZ
*Corresponding author's email: Hyunglae.Lee@asu.edu

Introduction: Gait asymmetry is a prevalent symptom in populations with neurological disorders or injuries, leading to a significant reduction in gait efficiency. Seeking to develop an efficient training method to enhance gait symmetry, split-belt treadmill (SBT) walking has gained much interest. Although spatiotemporal gait adaptation can be readily achieved through SBT walking, the adapted gait pattern tends to diminish quickly. Another form of gait training involves visual feedback distortion (VFD) as a means to drive gait adaptation [1]. In VFD, visual vertical bar representing the right and left step length is displayed, and only one of the bars is distorted to appear smaller or taller than the actual step-length. The step-length symmetry is then altered to match the amount of distortion. A potential approach to maximize the adaptation and retention of the learned gait pattern can be to combine distinct strategies, especially a combination of SBT walking and VFD strategy. This study aimed to evaluate the effectiveness of this combined approach in improving gait symmetry adaptation and the retention of the adapted gait pattern.

Methods: A study was conducted with 33 healthy subjects under three 28-minute trials (SBT, VFD, and VFD+SBT conditions). The study was approved by Institutional Review Board of Arizona State University (STUDY 00012537). Each trial consisted of 3-min base, 10-min adaptation, and 15-min post-adaptation periods. During the adaptation period under SBT, the speed of only the right belt of the treadmill increased at a rate of 5% of the preferred walking speed per minute, reaching a total of 1.5 times of the preferred walking speed. In the VFD, a graphical representation of the subject's step-length (Fig. 1) was displayed on a computer screen in front of the treadmill in the form of two vertical bar graphs, with one representing each leg. The length of only the right visual bar decreased at a rate of 3% of the actual step length per minute until a total of 0.7 times the actual step-length was reached. Under the VFD+SBT, both split-belt and visual perturbations were implemented. Subjects were instructed to maintain their gaze on the visual feedback bars and match the height of the bars at every step. The VFD and SBT perturbations were removed during the post-adaptation period.

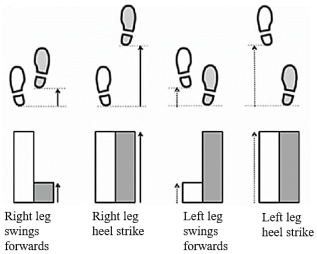

Figure 1: Visual representation of subject's right and left step-length during walking showing how the size of the bars is calculated.

Results & Discussion: In this study, we aimed to determine whether combined strategies (VFD+SBT) result in more effective changes in gait symmetry patterns with longer retention compared to the SBT or VFD strategy alone. We used the step-length symmetry ratio during a gait cycle as the primary measure. This ratio was averaged over a one-minute period for each subject's data, with a group mean computed across all subjects. Figure 2 illustrates the changes in step-length symmetry and retention under different conditions. Our results indicate an increase in the retention rate of the adapted asymmetric pattern with VFD+SBT compared to VFD or SBT alone. A two-way ANOVA analysis revealed a significant effect of the combined trial and elapsed time on step-length symmetry during the post-adaptation period. To explain the longer retention observed with combined training, we speculate on two factors: 1) the level of gait asymmetry produced during the adaptation period under VFD+SBT was larger than that produced under VFD or SBT alone, and 2) the sensory-prediction error induced by VFD engaged different motor learning processes than SBT, which involves recalibrating processes based on proprioceptive feedback, resulting in additive effects on gait adaptation. However, further studies are necessary to provide more clarity on these speculations.

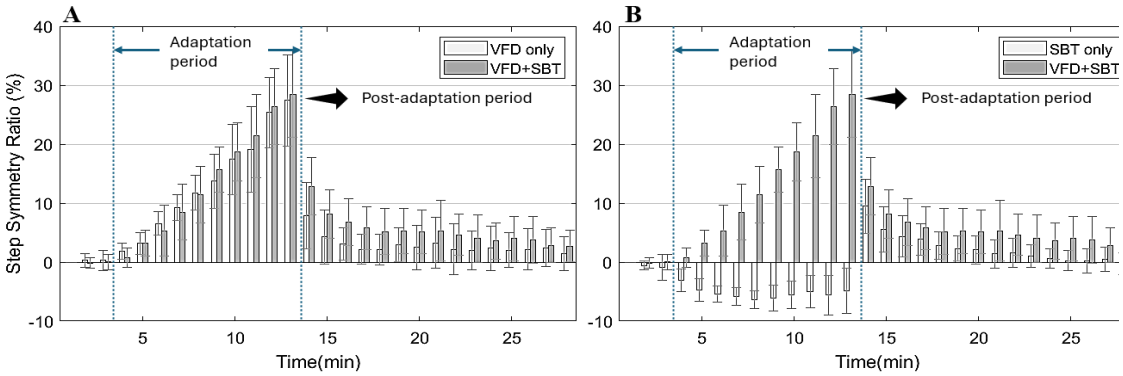

Figure 2: Comparison of changes in step length symmetry during adaptation and post-adaptation periods between VFD only and VFD+SBT (A) and between SBT only and VFD+SBT (B). The symmetry ratio (%) was measured by 2×(Right length - Left length)/(Right length + Left length)

Significance: This study highlights a potential advantage of incorporating VFD into SBT walking to enhance gait adaptation and improve retention effect. The results hold promise for contributing valuable insights to the development of a more efficient gait rehabilitation program.

References: [1] Kim et al. (2015), *TBME* 62(9); [2] Vasudevan et al. (2010), *J Neurophysiol.* 103(1).

CHARACTERIZATION OF HUMAN SHOULDER JOINT STIFFNESS ACROSS VARIOUS ARM POSTURES AND ITS SEX DIFFERENCES

Seunghoon Hwang[1], Dongjune Chang[1], Aditya Saxena[1], Ellory Oleen[2], Soe Lin Paing[1], John Atkins[1], and Hyunglae Lee[1,*]
[1]School for Engineering of Matter, Transport and Energy, Arizona State University, Tempe, USA
*Corresponding author's email: hyunglae.lee@asu.edu

Introduction: Stable control of the shoulder joint, as the basis of arm motion, allows for effective and natural control of distal joints and hand function. The stability of the shoulder joint is achieved through a complex interplay of bones, ligaments, tendons, and muscles, collectively providing resistance against external disturbances, a characteristic often described as stiffness[1]. Although substantial efforts have been made to characterize shoulder joint stiffness using system identification techniques, most studies focused on characterizations in a 2D horizontal plane or in a limited number of postures in 3D space. To address this limitation, this study aims to characterize shoulder joint stiffness across various arm postures in 3D space. Additionally, to enhance our understanding of sex-dependent shoulder joint stability and the risk related to shoulder injuries, this study investigates sex differences in shoulder joint stiffness.

Methods: Forty healthy young adults (20 males, 20 females; mean age: 24.8 years; mean height: 171.1 cm; mean mass 58.9 kg) were recruited for this study, which was approved by the Arizona State University Institutional Review Board approved this study (STUDY 00009059). The study utilized a custom-designed, parallel-actuated, shoulder exoskeleton robot[2], which applied rapid position perturbations directly to the subject's shoulder joint.

Shoulder stiffness was characterized across 15 arm postures, encompassing the following 4 boundary upper arm configurations: 0° and 90° shoulder horizontal extension, and 45° and 90° shoulder flexion. The exoskeleton robot applied filtered Gaussian noise perturbations (RMS: 2°, cut-off frequency: 3 Hz) to the shoulder joint in the horizontal flexion/extension (HFE) direction for 45 seconds per trial. Two trials were performed at each arm posture, resulting in a total of 30 trials for the entire study. Characterization took place while the subjects relaxed their shoulder muscles, a state monitored through surface electromyography signals from the anterior, medial, and posterior deltoid muscles. 3D shoulder kinematics and torque data were measured at 250 Hz using a motion capture system and force/torque sensor, respectively. Shoulder stiffness was characterized by estimating the impulse response function (IRF) between the input position perturbations of the shoulder joint and output torque measurements.

Prior to estimating IRF, both kinematic and torque data were high-pass filtered using a 2nd order Butterworth filter with a cut-off frequency of 0.25 Hz to minimize the impact of unintentional upper-body movements. Subsequently, the data were decimated to 125 Hz. The short data segment system identification algorithm was used to estimate the IRF[3], and shoulder joint stiffness was assessed by integrating the IRF. The quality of shoulder joint stiffness estimation was evaluated by calculating the variance accounted for (%VAF) between the measured torque output and the torque estimated from the IRF.

Results & Discussion: The quality of system identification was high, indicated by an average (SD) %VAF of 96.5 (0.5) %. The group results showed that shoulder joint stiffness decreased consistently with an increase in the shoulder flexion angle. For shoulder flexion of 45°, 67.5°, and 90°, the stiffness values were 17.4 (3.3), 12.7 (1.7), and 10.3 (1.9) Nm/rad, respectively (Fig. 1B). Specifically, the stiffness values at flexion angles of 45° and 67.5° were 68.6% and 23.6% greater than that at a flexion angle of 90°, respectively. Additionally, shoulder stiffness increased noticeably as arm positions approached the limits of shoulder range of motion (ROM), especially near 0° or 90° horizontal extensions. Comparative analysis showed stiffness increases of 54.5%, 18.7%, and 41.1% at the end of ROM compared to the midpoint for the three flexion angles (Fig 1C). The study observed changes in shoulder stiffness with arm posture without significant muscle activation (below 5 %MVC), suggesting these changes are likely due to the intrinsic mechanics of the shoulder joint rather than muscle activation.

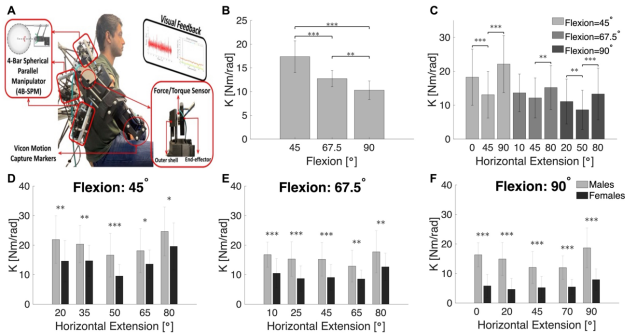

Figure 1: A) Experiment setup for characterization of shoulder stiffness. B) Comparison of shoulder stiffness at three distinct flexion angles. C) Comparison of shoulder stiffness in the middle vs. end of ROM in HFE. D-F) Comparison of shoulder joint stiffness between male (gray) and female (dark gray) across all 15 arm postures.

Furthermore, mixed ANOVA results indicated that male stiffness was higher than female stiffness ($p < 0.001$). Unpaired t-tests confirmed that sex had a significant impact on shoulder joint stiffness across all 15 postures (Fig. 1D-F). The sex difference remained pronounced even after normalizing for subject weight, suggesting that the observed sex differences could be attributed to factors such as greater laxity, increased flexibility, and smaller bone sizes in females compared to males.

Significance: The findings emphasize that both 3D arm posture and sex significantly influence shoulder joint stiffness, even when muscles are relaxed. This study lays a solid foundation for future research aimed at characterizing shoulder stiffness with active muscle engagement and during dynamic movement tasks. It also sets the stage for assessing changes in shoulder stiffness following neuromuscular injuries.

References: 1. Lugo, R et al. (2008), European Journal of Radiology. 2. D. Chang et al. (2021), *IEEE International Conference on Robotics and Automation (ICRA).* 3. Ludvig, D et al. (2012), *IEEE Transactions on Biomedical Engineering (TBME).*

MUSCLE CONTRIBUTIONS TO PROPELLING THE BODY UPWARD DIFFER BETWEEN SKIPPING AND RUNNING

Sarah A. Roelker[1*], Paul DeVita[2], John D. Willson[2], Richard R. Neptune[3]
[1]Department of Kinesiology, University of Massachusetts Amherst, Amherst, MA, USA
*Corresponding author's email: sroelker@umass.edu

Introduction: Skipping, a gait that combines a step and a hop on one limb followed by a step and a hop on the contralateral limb, is a common speed training activity [1] and a transitional rehabilitation activity between walking and running [2]. Skipping has a greater metabolic cost than running [3], yet lower peak vertical ground reaction forces (GRFs) [2] and muscle force impulses [4]. The increased metabolic cost of skipping is associated with a greater vertical center of mass (COM) displacement during the support and flight phases of the skipping hop compared to running [3,5]. The purpose of this study was to use modeling and simulation to identify differences in individual muscle contributions to body segment powers that enable greater vertical displacement in skipping despite lower muscle force impulses compared to running.

Methods: Five adults (22.4 ± 2.2 y) performed 10s running and skipping trials at 2.5 m/s on an instrumented dual-belt treadmill while motion capture and GRF data were simultaneously collected. In OpenSim 3.3 [6], a generic musculoskeletal model [7] was scaled for each participant and a representative running and skipping cycle was simulated using a traditional OpenSim pipeline (Inverse Kinematics, Residual Reduction Algorithm and Computed Muscle Control). A segmental power analysis [8] determined the mechanical power each muscle generated, absorbed, or transferred to or from each body segment over the gait cycle. The segments of interest were the trunk (contributions to the pelvis and torso were summed together) and left and right legs (contributions to the foot, shank and thigh of each leg were summed and analysed together). Muscle contributions to segmental power were integrated over the stance phase of running (Run) and the hop (Skip 1) and step (Skip 2) of skipping to calculate mechanical work. Separate one-way repeated measures ANOVA analyses compared muscle contributions to vertical and anteroposterior segmental work on the whole-body (net), trunk, ipsilateral leg, and contralateral leg between the stance phases of the Run, Skip 1, and Skip 2 steps. Post-hoc tests with Bonferroni corrections for multiple comparisons identified pairwise differences between steps. Statistical analyses were performed in MATLAB 2023a (MathWorks Inc., Natick, MA) with α=0.05 set *a priori*.

Results & Discussion: Muscle contributions to vertical segmental power differed between steps in both the magnitude and direction of the power flow (Fig. 1A), revealing differences in the mechanisms by which muscles contribute to propelling the trunk upward between Run, Skip 1, and Skip 2. The gluteus maximus, vasti, and soleus were three of the greatest contributors to vertical power and all contribute to positive net vertical work in Skip 1 and negative net vertical work in Run and Skip 2 (Fig 1B; $p \leq 0.01$). Gluteus maximus absorbs power from all segments in early stance of Run (decelerates downward COM motion), generates power to the trunk and contralateral leg in mid-to-late stance of Skip 1 (accelerates upward COM motion), and absorbs power from the ipsilateral leg and transfers that to the trunk in Skip 2 (decelerates downward COM motion). The vasti absorb power from the trunk in early stance and generate power to the trunk in late stance (accelerate upward COM motion) of Run, primarily generate power to the trunk in mid-to-late stance of Skip 1, and primarily absorb power from the trunk and ipsilateral leg in Skip 2. Soleus absorbs power from the trunk and ipsilateral leg during early stance and generates power to these segments in late stance of Run, generates power to the trunk and ipsilateral leg in Skip 1, and absorbs power from the trunk and ipsilateral leg in Skip 2. In contrast, muscle contributions to anteroposterior segmental power were consistent in the direction of power flow across gaits and differed only in magnitude, which suggests muscles contribute to forward propulsion using similar mechanisms across gaits.

Significance: Muscles contribute to propelling the body upward through different power flow mechanisms in skipping compared to running. In the hop step of skipping (Skip 1), greater vertical work is done by the gluteus maximus, vasti, and soleus, primarily through power generation to the trunk, compared to power absorption in Run and Skip 2. Thus, despite lower muscle forces in Skip 1 than in Run [4], those muscle forces are generating power through concentric contractions, leading to greater metabolic cost than in running [4]. These forces contribute to propelling the COM upward in Skip 1 (rather than decelerating downward COM motion in Run and Skip 2), which raises the COM and contributes to the greater COM displacement in skipping than in running.

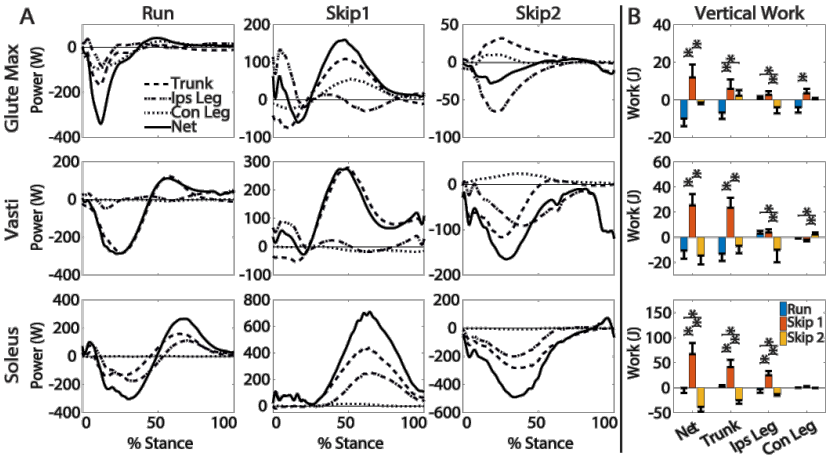

Figure 1: Muscle contributions to vertical A) segmental power and B) work during stance for whole-body (Net), Trunk, ipsilateral (Ips) leg, and contralateral (Con) leg. Positive (negative) power and work indicate a muscle generated (absorbed) power to that segment and accelerated (decelerated) the segment in the direction of motion. *indicates significant pairwise differences between steps.

References: [1] Cissik, Strength Cond J, 2004. [2] Johnson et al, J Sport Rehabil, 2005. [3] McDonnell et al, Gait Posture, 2019. [4] Roelker et al, J Appl Biomech, 2022. [5] McDonnell et al, J Biomech, 2017. [6] Delp et al, IEEE Trans Biomed Eng, 1990. [7] Hamner et al, J Biomech, 2010. [8] Fregly & Zajac, J Biomech, 1996.

DYNAMIC GAIT STABILITY IN PEOPLE WITH MILD TO MODERATE PARKINSON'S DISEASE

Rebecca Ban[1*], Jiyun Ahn[1], Caroline Simpkins[1], Feng Yang[1]
[1]Department of Kinesiology and Health, Georgia State University, Atlanta, GA 20202
email: rban1@gsu.edu

Introduction: Parkinson's disease (PD) is the fastest growing neurological disorder, which affects approximately 6 million people worldwide[1]. Motor dysfunction, postural instability, and gait impairments are common symptoms of PD and can contribute to an increased risk of falls[2]. Because falls often lead to a fear of falling in the future, people with PD (PwPD) may restrict activities to avoid potential falls. This restriction can reduce the quality of life for PwPD[3]. Dynamic gait stability, which describes the kinematic relationship between the body's center of mass (COM) and base of support (BOS) within the Feasible Stability Region (FSR) framework, has been identified as a key risk factor of falls[4,5,6]. Given that most falls occur during locomotion among PwPD, examining how PD impacts dynamic gait stability may uncover the mechanism by which PD increases fall risk. The purpose of this study was to compare dynamic gait stability between people with and without PD during level walking at a self-selected speed.

Methods: Twenty adults with mild to moderate PD (66.15 ± 5.69 years, 6 females, Hoehn and Yahr: 1.47 ± 0.39) and twenty age- and sex-matched healthy individuals (68.50 ± 5.57 years, 7 females) participated in this study. Each participant walked at their self-selected speed three times over a 10-m walkway. Full body kinematics from 26 reflective markers placed on body landmarks were collected using a 9-camera motion capture system (Vicon, UK). Marker paths were filtered and the average of the three trials was used for analysis. The body's COM kinematics were computed using sex-dependent segmental inertial parameters based on filtered marker paths. The two components of the COM motion state (position and velocity) were calculated relative to the BOS and normalized by foot length (l_{BOS}) and $\sqrt{g \times bh}$, respectively, where g is the acceleration due to gravity and bh is the body height. Two transitional instants: touchdown (TD) and liftoff (LO), were identified using foot kinematics. As the primary outcome measure, dynamic gait stability (a unitless variable) at TD and LO was calculated using the COM motion state according to the FSR. When the COM motion state is within the FSR limits (**A**, Fig. 1), balance can be maintained without changing the BOS. A COM motion state below/above the FSR indicates an unstable state against backward/forward falling (**B/C**, Fig. 1). The secondary outcome measures included several spatiotemporal variables. The temporal metric investigated in this study was the stance phase (from TD to the following ipsilateral LO). Cadence was determined as the average number of steps taken in one minute. Spatial measurements included step length and step width. Step length/width was measured as the anteroposterior/mediolateral distance between bilateral heels at their TDs and normalized to bh. Gait speed was determined as the average value of the instantaneous COM velocity over the middle 5-meter region of the walkway. The gait speed was also normalized by bh. Normality was checked using the Shapiro-Wilk test. Independent t-tests compared variables between groups. Statistical analyses were conducted using SPSS 28.0 (IBM, NY) with an α of 0.05.

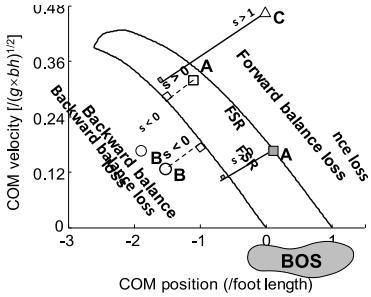

Fig. 1: Stability (s) defined by the FSR theory is calculated as the shortest distance from the COM motion state to FSR's lower limit. A larger stability indicates a more stable state resisting backward falling.

Results & Discussion: PwPD spent more time in the stance phase (p = 0.019, Fig. 2a) and showed a lower cadence ($p < 0.001$, Fig. 2b) than healthy adults. PwPD also walked more slowly ($p < 0.001$, Fig. 2c) and took shorter steps (p = 0.050, Fig. 2d). There were no significant group-related differences for step width (p = 0.176, Fig. 2e). Despite the differences in gait parameters, dynamic gait stability was similar between groups at TD (p = 0.525) and LO (p = 0.558, Fig. 2f). The results indicate that PwPD, relative to their healthy counterparts, took shorter steps, which causes an anterior shift in COM. The forward shifted COM could compensate for the potential negative effect of the reduced gait speed on dynamic gait stability in PwPD. Therefore, dynamic gait stability was comparable between groups. The results suggest that people with mild to moderate PD retain the ability to maintain dynamic gait stability. However, it remains unknown whether the findings of the present study can be generalized to people with more severe PD symptoms. Additional studies are needed to further inspect the control of dynamic balance in PwPD.

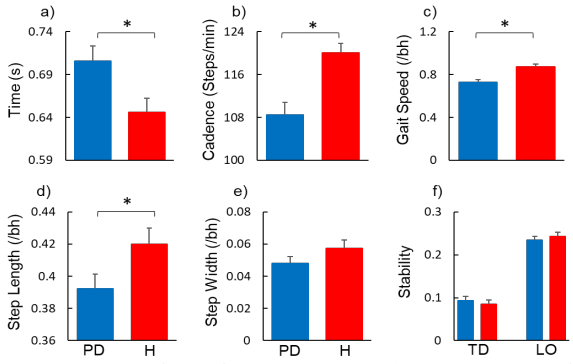

Fig. 2: Comparisons between PwPD (PD, n = 20) and healthy (H, n = 20) **adults** for a) stance phase, b) cadence, c) gait speed, d) step length, e) step width, and f) stability at touchdown (TD) and liftoff (LO). *Indicates $p \leq 0.05$.

Significance: Despite the different gait pattern parameters between groups, people with PD exhibited similar dynamic gait stability to their healthy counterparts while walking at their self-selected speed. To compensate for the potential dynamic gait stability deficit resulting from slow gait speed, individuals with PD adopted a short step length to shift the COM motion state closer to the feasible stability region.

References: [1] Dorsey et al. (2018). *JAMA Neurol*.75. [2] Fasano et al. (2017). *Mov Disord*. 32. [3] Adkin et al. (2003). *Mov Disord*. 2003. 18. [4] Pai et al. (1997). *J Biomech*. 30. [5] Yang et al. (2007). *J Biomech*. (2007). 40. [6] Yang et al.(2009). *J Biomech*. 42.

STUDYING THE KINEMATIC CONSISTENCY OF SWINGS IN NCAA SOFTBALL PLAYERS

Cassidy Grimm, Megan O'Connor, Delaney Burnett, Craig M. Goehler*
Department of Aerospace and Mechanical Engineering, University of Notre Dame
*Corresponding author's email: cgoehler@nd.edu

Introduction: Softball, unlike baseball [1, 2], lacks a comprehensive quantitative analysis of player swings, with most coaching methods relying on qualitative observations [3]. This study aims to address this gap by applying a scientific approach to analyze the kinematic consistency of swings in NCAA softball players. Our study seeks to answer the following research question: How does the kinetic chain of the swing affect game performance in NCAA softball players? We hypothesize that the efficiency and coordination of the kinetic chain in softball swings notably impact game performance. Specifically, due to the biomechanical principles underlying an efficient kinetic chain, we expected that a more efficient kinetic chain, characterized by better coordination and power transfer from lower to upper body segments, will lead to consistently improved performance outcomes such as bat speed and ball contact quality.

Methods: An XSens AWINDA System was used to collect various measurements such as segment velocity, acceleration, joint angles, and more from 6 NCAA softball players while performing swings at the main softball practice facility. The 16 inertial measurement unit sensors were placed on predefined anatomical landmarks. Prior to each session, the virtual avatar was scaled to the subject through a dynamic calibration procedure. Each session consisted of two parts: 10 swings off a stationary tee placed within the middle of the strike zone and 10 swings off a pitching machine. In addition to the kinematic data obtained from XSens, a Rapsodo Hitting 2.0 machine was also calibrated and implemented to obtain exit velocity, launch angle, distance hit, and the RPM of the ball. After each session, both the Rapsodo and XSens data were processed and coded to each unique subject. A custom MATLAB code was created to read in the desired data sets produced by the XSens MVN Analyze software for detailed analysis.

Results & Discussion: Two subjects hitting off of the pitching machine were selected for initial comparison in this abstract. For each swing, the maximum values for the pelvis angular velocity, sternum angular velocity, and left/right hand linear velocities were determined. The time that each maximum value occurred was determined and compared to a "reference" time (when the maximum pelvis angular velocity occurred). Table 1 reports the averages and standard deviations of the timing differences for each kinematic value of interest with positive values signifying that the respective maximum occurred after the "reference" time and negative values signifying that the respective maximum occurred before the "reference" time.

Subject A was selected due to having a very consistent swing as demonstrated by the small standard deviations in Table 1. Subject A's pelvis angular velocity was consistently roughly half the value of her sternum angular velocity (not shown here) with the average time difference for the sternum occurring 0.035s after the pelvis did. The lower angular velocity of Subject A's pelvis suggests a higher torque as these properties are inversely proportional. This reflects the kinetic chain of using power from the pelvis to drive the upper torso thus increasing the speed and power in the hands.

Conversely, Subject B was selected due to using a qualitatively less consistent swing which was confirmed by the larger standard deviations seen in Table 1. Subject B had consistently high values for both pelvis and sternum angular velocity. Interestingly, the sternum reached its maximum angular velocity 0.0416s *before* the pelvis. This does not reflect the kinetic chain philosophy as well as Subject A. This difference in results was reflected in the outcomes of the subjects' hits from the Rapsodo data (not shown here). The variability in swing kinematics suggests that Subject B was less adept at adjusting to pitches, particularly outside pitches, due to both the sternum moving before the pelvis and her left and right hand hitting their maximum velocities an average of 0.252s and 0.4s after the pelvis (trailing her upper body movement).

Table 1. Comparison of average (± standard deviation) timing differences (seconds) of the maximum value for each kinematic value of interest relative to the timing of the maximum pelvis angular velocity.

Subject A			Subject B		
Sternum	Left Hand	Right Hand	Sternum	Left Hand	Right Hand
0.035 (0.0309)	0.0167 (0.01757)	0.0267 (0.2383)	-0.0416 (0.12183)	0.25167 (1.1355)	0.4 (1.2715)

Significance: This exploration study represents an initial attempt to quantify various characteristics that have been traditionally assessed through qualitative methods. The observed differences in swing outcomes for the two subjects compared in this abstract was accurately reflected in the kinematic data. Of note, the average softball pitch only allows for 0.45s of reaction time. In order for Subject B's hands to cross the plate in time, she needs to start her swing before she can tell where the ball is going, inhibiting her ability to respond to the pitch. Subject A was able to wait on the pitch and adjust for it due to storing power in her pelvis. The ultimate goal of this study will be to use the recorded data to assist coaches in developing individualized training protocols to promote better hitting outcomes.

Acknowledgments: The authors would like to thank all of the study participants for volunteering their time and skills to the project.

References: [1] Welch et al.. (1995), *JOSPT* 22(5); [2] Inkster (2010), *OPUS*; [3] Bordelon et al. (2021), *Sports Biomech* (Dec).

NERUAL CORRELATES OF COGNITIVE-MOTOR FUNCTION: AN FNIRS PILOT STUDY

Scott M. Monfort[1*], Alexandra C. Lynch, Fatemeh Aflatounian, Keith A. Hutchison
Montana State University, Bozeman, MT, USA
*Corresponding author's email: scott.monfort@montana.edu

Introduction: Managing simultaneous cognitive and motor demands is a common challenge across widespread settings. For example, sports often require athletes to constantly monitor and respond to a rapidly changing environment while performing demanding, skilled movements. Added cognitive challenges during a motor task compete for attentional resources [1], with impairments reported in injury-relevant biomechanics during sport movements [2] and fundamental aspects of motor performance, such as postural control [3]. However, neuro-cognitive compensatory strategies may also exist to mitigate performance deficits in response to pathology (e.g. neuroplasticity following anterior cruciate ligament reconstruction) [4]. These complex interactions motivate the need to consider motor, cognitive, and neural contributions to cognitive-motor function, with a long-term goal being to more comprehensively identify individuals with strategies that may place them at high-risk for a negative outcome (e.g., (re-)injury). Therefore, the purpose of this study was to determine the extent that activation of the dorsolateral prefrontal cortex (DLPFC) during attention control tests relates to cognitive-motor function. Because effective engagement of attentional resources is integral to multitasking [5], we hypothesized that individuals with increased DLPFC activation would better mitigate dual-task induced deficits in cognitive and motor performance.

Methods: Twelve, physically-active, healthy adults (20.3±1.4 years, 6 females, 1.77±0.08 m, 77.8±13.8 kg, Tegner: 7.5±1.6) have participated in this ongoing study. Participants first performed a battery of computerized attention control tests (Stroop Squared, Flanker Squared, and Simon Squared) [6]. During the attention control tests, an 8-source, 8-detector functional near-infrared spectroscopy system (fNIRS; NIRSport2) was used to measure changes in oxygenated hemoglobin in several regions of interest on the left hemisphere, with left DLPFC being the primary region of interest for this study given its role in attention control. One fNIRS detector was used with a breakout cable to provide short-separation channels for each source to help regress out extracerebral signal. Thirty seconds of baseline (rest) data was collected prior to each 90 second attention control test in order to support block design analysis of the fNIRS data. fNIRS analysis largely followed previous methods [3], with the addition of temporal derivative distribution repair and a lowpass 0.5 Hz cutoff filter applied to the optical density time series. T-statistics from the subject-level general linear model with 8 short-separation channels as regressors were used to estimate subject-specific activation of the left DLPFC activation.

Cognitive and motor function were then assessed via a dual-task paradigm involving a separate attention control test (antisaccade [7]) and repeated single-leg squatting (0° ⇔ 45° knee flexion at 0.5 Hz). These tasks (5 blocks of 54 seconds each) were performed in isolation and combined, with the task order randomized. Cognitive performance was the accuracy on the antisaccade test and overall motor performance was the 95% ellipse area of the center of pressure during the squatting task. The primary interest in the dual-task paradigm was dual-task cost (DTC) for each outcome, which was the percent change from isolated to combined conditions for the respective task. Higher DTC was associated with worse accuracy and greater sway during the dual-task condition relative to the respective single-task condition. Pearson correlations were used to identify relationships between DLPFC T-statistics during the attention control tests and DTC (cognitive and motor).

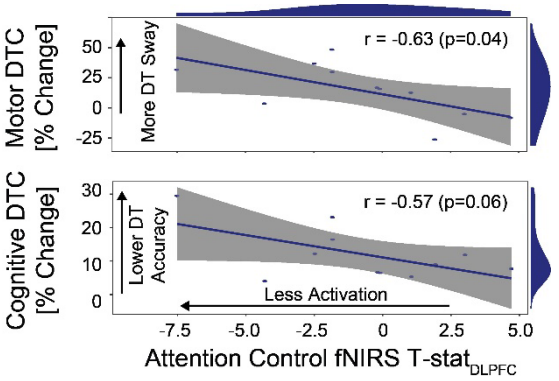

Figure 1. Relationships between dorsolateral prefrontal cortex activation (T-stat$_{DLPFC}$) and dual-task cost (% change) in cognitive or motor performance.

Results and Discussion: The preliminary data partially support our hypothesis, with higher DLPFC activation during attention control tasks associating with mitigated DTC in the motor task (r=-0.63, p=0.04, **Figure 1**). The data are consistent with decreased DLPFC activation during attention control tests indicating inefficient recruitment of attention control resources, which would exacerbate cognitive-motor interference because access to these resources may be more restricted. The relationship between individuals' DLPFC activation and motor DTC was present despite no significant groupwise motor DTC (**Figure 2**), which highlights the potential relevance of the observed relationship for identifying individuals who are prone to larger DTC versus those who are able to mitigate DTC.

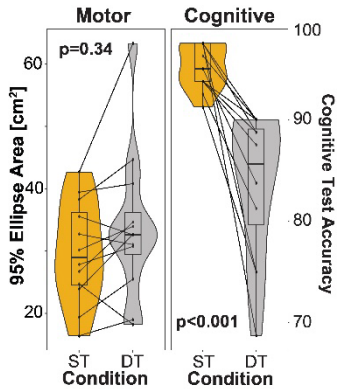

Figure 2. Motor and cognitive performance in single- (ST) and dual-task (DT) conditions with p-values for paired t-tests.

Significance: These preliminary results suggest that neural activation patterns during attention control tests may relate to individuals' ability to mitigate cognitive-motor deficits.

Acknowledgments: Funding via MSU VPREDGE Research Expansion Fund.

References: [1] Cinar et al. *Theor Erg Sci* (2021), [2] Monfort et al. *AJSM* (2019), [3] Reed et al. *Hum Mov Sci* (2022) , [4] Chaput et al. *J Orto Res* (2021) , [5] Draheim et al. *Psych Bull Rev* (2022) [6] Burgoyne et al. *J Exp Psych* (2023) , [7] Hutchison *J Exp Psych Mem Cog* (2007)

Functional Limitations in Scoliosis: A Gait and Over Head Deep Squat Analysis of Lower Extremity Dynamics

Prithwi Raj Das[1], Scott S. Russo[2], Yunju Lee[1,3*]
[1]School of Engineering, Grand Valley State University, Grand Rapids, MI, USA
[2]Orthopaedic Associates of Michigan, Grand Rapids, MI, USA
[3]Department of Physical Therapy and Athletic Training, Grand Valley State University, Grand Rapids, MI, USA
*Corresponding author's email: leeyun@gvsu.edu

Introduction: Scoliosis is a condition that causes abnormal changes in the shape of the spine, thorax, and trunk. In about 80% of cases, the origin of this deformity is idiopathic [1]. Overall mobility is significantly impacted by this condition [2]. The female-to-male ratio increases with age and can reach as high as 6:1 [3]. Decisions regarding the necessity of spinal fusion surgery are based on the severity of the deformity and the level of pain [4]. This study aims to discern variations in lower extremity joint angles and moments among female subjects undergoing surgical procedures for scoliosis, non-surgical scoliosis individuals, and those without scoliosis during the execution of overhead deep squats (OHDS) and gait. This study hypothesizes that both non-surgical and surgical groups will have limited functional movement compared to non-scoliosis subjects during gait and the performance of the OHDS due to spine deformation. High-resolution 3D motion data was collected and analyzed for each subject group while performing both gait and OHDS.

Methods: Utilizing the Vicon 3D motion capture system, comprehensive data were gathered from three distinct groups of female subjects: a surgical group (SG) with 11 subjects (age 31-72, height 146.1-170.2 cm, weight 56.2-99.8 kg), a non-surgical group (NSG) with 15 subjects (age 29-73, height 147.5-173 cm, weight 51.5-91.5 kg), and a group of normal individuals (NG) comprising 12 subjects (age 42-72, height 156.5-180 cm, weight 56.9-104.1 kg). The squat cycle is defined as the period when the pelvis moves downward and returns to its original position in the sagittal plane. Three optimal trials were selected from multiple sessions for each subject. Numerical data were extracted using Visual 3D software and an appropriate motion analysis model. This study analyzed the flexion and extension of lower extremity joints (ankle, knee, hip, and pelvic) to assess lower body movement abilities. The numeric data were processed and analyzed using MATLAB. Statistical analysis was conducted using SAS JMP Pro 17 software, a one-way ANOVA with post-hoc Tukey HSD, to determine significant differences in the mean range of joint angles and moments among the three groups.

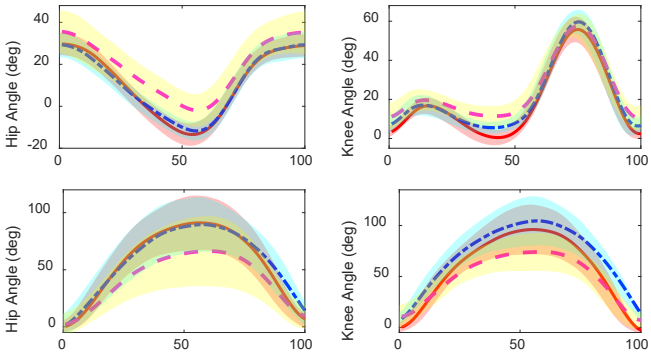

Figure 1: The joint angles of the left hip and left knee during gait (top row) and overhead deep squat (OHDS, bottom row) are presented. Mean values are represented by lines, and standard deviations (SD) are depicted by shading. The subject groups are differentiated by color: normal control (NG, red solid line/red shading), non-surgical scoliosis (NSG, blue dotted line/blue shading), and surgical scoliosis (SG, magenta dashed line/yellow shading). The x-axis represents the gait cycle (top row) and the squat cycle (bottom row).

Results & Discussion: Statistical analysis showed significant differences ($p<0.0001$) in temporal-spatial parameters, such as cadence, walking speed, and stride time, between the scoliosis (SG and NSG) and normal (NG) groups. This suggests that individuals with scoliosis may have gait limitations that could hinder their ability to navigate efficiently. Notably, the NSG group exhibited joint angle ranges (maximum and minimum angles within a cycle) similar to those of the NG group during both activities. The study suggests that non-surgical scoliosis does not significantly limit the range of motion in lower extremity joints during gait. However, the SG group showed significantly reduced joint angle ranges ($p<0.0001$) compared to both NSG and NG for both gait and OHDS, partially supporting the hypothesis of limited functional movement among individuals with scoliosis. Figure 1 visually illustrates these differences. These findings emphasize the possibility of distinct functional limitations in a surgical group with severe scoliosis scheduled for spinal fusion surgery with pelvic fixation. Although non-surgical individuals may maintain normal joint motion and exhibit gait patterns similar to healthy controls, surgical intervention seems to be linked to a decrease in functional movement capacity. This highlights the importance of developing customized rehabilitation strategies to address these limitations and enhance mobility and function in both moderate and severe scoliosis patients.

Significance: This study provides valuable insights into the functional limitations related to scoliosis, which have implications for both research and clinical practice. The differences observed in lower extremity joint kinematics highlight the importance of personalized interventions to address functional deficits and potentially improve surgical outcomes in scoliosis patients. Furthermore, the comparable movement patterns demonstrated by the non-surgical group in comparison to healthy controls suggest the potential effectiveness of conservative management approaches in preserving mobility for scoliosis patients. These findings emphasize the significance of comprehensive patient assessment and the development of tailored intervention strategies for scoliosis management. This has implications for both future research and clinical care.

Acknowledgments: We appreciate the study participants for their cooperation and B.H., G.A., M.P., and L.B. for contributions.

References: [1] Negrini et al. (2018), *Scoliosis Spinal Disord* 13(1); [2] Öhlén et al, (1988) *Spine*, 13(4), 413-416;
[3] Trobisch et al, (2010), *Dtsch Aerzteblatt Online*.107(49):875-884; [4] Jallob et al, (2023), *Pediatr Neurosurg* 58: 281-289.

EFFECTS OF THE MAGNITUDE OF MECHANICAL PERTURBATIONS USING SOFT ROBOTS ON HUMAN GAIT ENTRAINMENT

Omik Save[1], Sidhant Das[1], Evan Carlson[1], Anna Kruse[1], Jooeun Ahn[2], Hyunglae Lee[1*]
[1]School of Energy, Matter, and Transport Engineering, Arizona State University, Tempe, USA
[2] Department of Physical Education, Seoul National University, Seoul, South Korea
*Corresponding author's email: hyunglae.lee@asu.edu

Introduction: Gait entrainment refers to the synchronization of human gait to an external rhythmic perturbation of either the visual, auditory, electro-vibrational, or mechanical nature. Mechanical stimulus-based entrainment has recently received interest for its applications in gait modelling and exploiting neuroplasticity for rehabilitation purposes. Past studies that applied periodic perturbations to the lower extremities using robotic devices demonstrated successful gait entrainment within a finite range of human stride frequency, with the perturbations consistently supporting joint motion. This inspired a theory that the entrainment could be induced by optimizing mechanical assistance from external sources. However, a different paradigm of experiments observed that entrainment could also be synthesized by finite electrical stimulation (FES), haptic cues, or even mechanical perturbations that did not assist joint motion contradicting the mechanical assistance optimization theory. Although entrainment can be elicited by any combinations of the passive dynamics of the lower extremity, spinal neural networks, supraspinal networks, and afferent sensory feedback networks, the precise governing mechanism is still unknown. To address this issue, this study investigated whether low-magnitude rhythmic mechanical perturbations to the ankle and the hip could achieve gait entrainment. We hypothesized that sensory cues generated by low-magnitude perturbations could successfully entrain human gait suggesting the important role of afferent sensory feedback in gait entrainment.

Methods: Fifteen healthy adults (8 male, 7 female, mean age: 22 years, mean height: 1.8 m, mean weight: 76.6 kg) were recruited for this study which was approved by the Institutional Review Board of Arizona State University (STUDY00015183). The study utilized two distinct, lightweight, pneumatically activated devices to provide periodic hip flexion and ankle plantarflexion torques in 150 ms pulses (Fig. 1A) [2,3].

A calibration session was conducted prior to the experiment to calculate each participant's preferred walking speed (PWS) and natural gait frequency (*f*) during natural walking on an instrumented treadmill. Throughout the walking experiment, the treadmill speed was fixed to the participant's PWS, and the frequency of periodic perturbation was fixed to *f*. The walking experiment consisted of either the ankle or the hip perturbations conducted over two separate days. Each walking experiment included 15 trials in which the perturbation magnitude was randomly assigned to one of five pressure conditions: 25 kPa, 50 kPa, 75 kPa, 100 kPa, and 125 kPa, with three repetitions each. The joint torques for the ankle and hip both at a moment arm of 0.06 m in the pressure conditions examined were 1.2 Nm, 3.6 Nm, 5.2 Nm, 6.3 Nm, and 7.1 Nm, respectively. Each trial lasted 110 seconds, where the perturbations started at the first right step after the 20th second at either the 20%, 50%, or 80% of the gait cycle randomly to avoid potential learning effects. A trial was labelled successfully entrained if the perturbation timing in at least 80% of the last 30 strides were confined within ±10% gait phase of the mean perturbation timing of this timing window[4].

The parameter investigated in this study was the success rate of entrainment, defined as the percentage of entrained trials out of 3 in each perturbation magnitude condition for both the ankle and the hip study. A Friedman test was performed in both experiments to assess any differences in the success rates between different perturbation magnitudes. Further, Wilcoxon Signed Rank test was performed to compare pairwise success rates between different pressure conditions. Finally, the obtained *p*-values were adjusted using the Benjamin-Hochberg procedure considering a 5% false discovery rate.

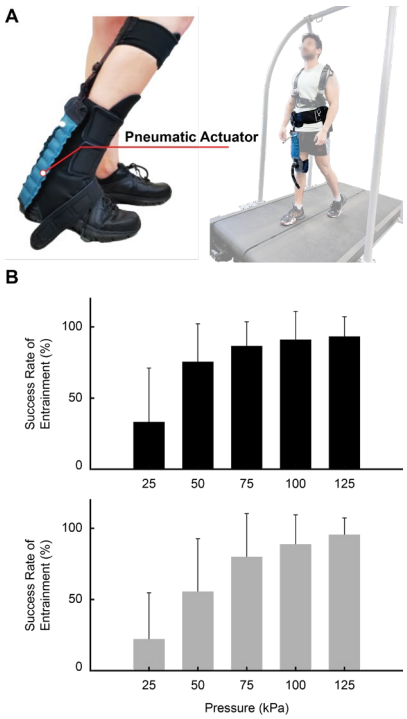

Figure 1. A: Subjects wearing pneumatically activated soft robotic devices at the ankle (left) and the hip (right) while walking on the treadmill. **B:** Group averaged results for entrainment success rate during the ankle experiment (top) and the hip experiment (bottom).

Results & Discussion: In the ankle study, a high success rate of entrainment (75.6%) was observed at 50 kPa magnitude condition which corresponds to only 3.1% of the peak ankle torque during walking (Fig. 1B Top). Similarly, in the hip experiment, a high success rate of entrainment was observed at 75 kPa magnitude condition which corresponds to only 7.8% of peak hip torque during walking (Fig. 1B Bottom). Furthermore, in both studies increasing the perturbation magnitude from the critical value to the maximum value of 125 kPa did not yield statistically significant improvements in the entrainment success rates.

Significance: Collectively, the results suggest that the sensory cues generated by the low-magnitude periodic perturbations at the ankle and the hip could have played a crucial role in modulating the human gait towards entrainment. Furthermore, it can be asserted that the afferent sensory feedback networks play an undeniable role in human gait modulation and entrainment.

References: 1. J. Ahn et al. (2011), *IEEE Eng. in Medicine and Biology Society (EMBC).* 2. C. Thalman et al. (2021), *IEEE Robotics and Automation Letters (RA-L)*. 3. L. Baye-Wallace et al. (2022), *IEEE Robotics and Automation Letters (RA-L)* 4. O. Save et al. (2024), *IEEE Transactions on Neural Systems and Rehabilitation Engineering (TNSRE).*

FALL RISK PREDICTION DURING VARIOUS ACTIVITIES USING KNOWLEDGE DISTILLATION

Seunghee Lee, Bummo Koo, Sumin Yang, Gayoung Yim, Jiwon Jang, Youngho Kim*
Department of Biomedical Engineering and Institute of Medical Engineering, Yonsei University, Wonju, Korea
*Corresponding author's email: younghokim@yonsei.ac.kr

Introduction: Fall is a significant threat to the elderly, often leading to fatal consequences [1]. Predicting the risk of falls is crucial for both rescue efforts and preventive measures. The peak acceleration value is a important factor that can represent the severity of risk [2]. Lee et al [3]. developed an algorithm for predicting dangerous movements in the high construction sites based on peak acceleration values. Lightweighting techniques such as knowledge distillation are necessary to implement deep learning models on edge devices like smartphones and wearable sensors. In this study, a deep learning regression model with knowledge distillation was developed to predict acceleration peak values, crucial for assessing the risk of falls and activities of daily living (ADLs).

Methods: 20 healthy adult subjects (24.8 ± 2.0 years old, 173.5 ± 6.1 cm, 76.6 ± 13.0 kg) were recruited from Yonsei University for the study and performed 14 ADLs and 11 falls (IRB No. 1041849-202204-BM-079-02) (Table1). An IMU sensor (Xsens Dot, Netherlands) was attached to S2 position of the subject. Data from the 6-axis IMU sensor were recorded at a sampling rate of 60 Hz. Data from 0.2 s to 0.7 s prior to the peak A_{SVM} value and eight features (Ax, Ay, Az, A_{SVM}, Gx, Gy, Gz, G_{SVM}) were extracted for the analysis. The data were divided into a 4:1 ratio for training and testing. Peak acceleration values were predicted by deep learning models. A large (teacher) model comprises 1D-CNN and LSTM layers, while a smaller (student) model consists of a 1D-CNN layer. Knowledge distillation (KD) is a technique in which information from a teacher model is transferred to a student model to enhance its performance. The Mean Absolute Error (MAE) was used as the loss function. Data augmentation techniques such as noise injection, scaling, and window slicing were applied to address data imbalance issue.

Table 1: Experimental movements

ADL	**D01**. Stand, **D02**. Sit and stand up from floor, **D03**. Squat, **D04**. Waist bending, **D05**. Walking, **D06**. Jogging, **D07**. Stumble while walking, **D08**. Jogging in place, **D09**. Jumping, **D10**. Walk upstairs and downstairs, **D11**.Sit and stand up from stool, **D12**. Collapse in a stool when trying to stand up, **D13**. Lying on the mattress, **D14**. Slowly sit and stand up from a low-height mattress
Fall	**F01**. Backward fall while walking caused by a slip, **F02**. Forward fall while walking caused by a trip, **F03**. Forward fall while jogging caused by a trip, **F04**. Backward fall when trying to sit down, **F05**. Forward fall while sitting, **F06**. Lateral fall while sitting, **F07**. Backward fall while sitting, **F08**. Forward fall when trying to get up, **F09**. Forward fall, **F10**. Lateral fall, **F11**. Backward fall

Results & Discussion: The teacher model showed the smallest error but had the biggest memory size. The KD model has been lightweighted to 18kB, suitable for deployment on edge devices. Figure 1 suggested that the teacher model showed smaller deviations in predicted values compared to the student model. Despite having the same number of parameters as the student model, the KD model demonstrated small deviations in predicted values, attributed to the information derived from the teacher model. In future studies, deep learning models will be deployed on edge devices such as smartphones and wearable sensors.

Table 2: Model performances

Model	MAE (g)	Memory (kB)	Number of parameters
Teacher	1.00	2,151	177,633
Student	1.33	33	385
KD	1.19	18	385

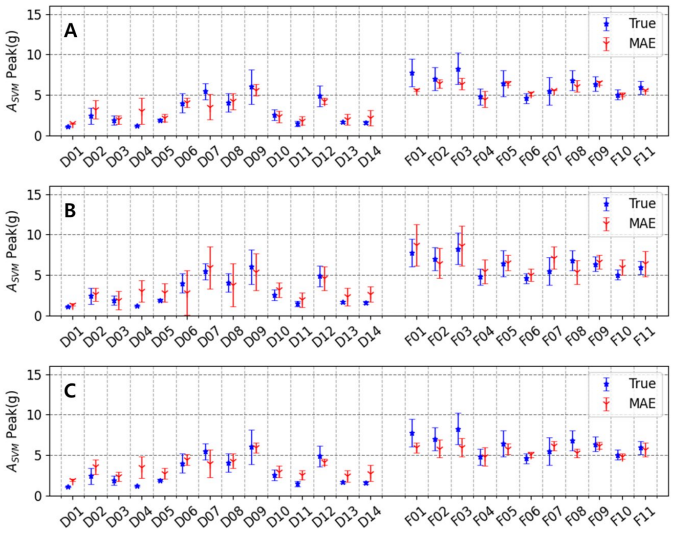

Figure 1: True and Predicted Values: A, B and C are teacher, student, and KD models, respectively.

Significance: The risk prediction algorithm could serve as a tool to alert individuals of potential risks and call emergency support when applied to mobile application. Our algorithm would employ to the edge device in the future. The algorithm is expected to prevent fatal injuries in fall accidents by providing proper feedback.

Acknowledgements: This research was partly supported by "Regional Innovation Strategy (RIS)" through the National Research Foundation of Korea (NRF) funded by the Ministry of Education (MOE) (Grant No.: 2022RIS-005) and "Rediscovery of the Past R&D Result" through the Ministry of Trade, Industry and Energy (MOTIE) and the Korea Institute for Advancement of Technology (KIAT) (Grant No.: P0026060).

References:

[1] Rubenstein L. Z. Age and ageing 35. suppl_2, 2006
[2] Hajiaghamemar M et al. Annals of biomedical engineering 43, 2015
[3] Lee S. H et al. Sensors 22.16, 2022

MEASUREMENTS OF ELECTRODERMAL ACTIVITY, TISSUE OXYGEN SATURATION, AND VISUAL ANALOG SCALE UNDER DIFFERENT CUFF PRESSURES AROUND THE THIGH

Seunghee Lee, Sunggun Pyo, Bummo Koo, Youngho Kim*
Department of Biomedical Engineering and Institute of Medical Engineering, Yonsei University, Wonju, Korea
*Corresponding author's email: younghokim@yonsei.ac.kr

Introduction: Assessing the comfort and wearability of these robots is crucial to prevent discomfort and potential injuries. In this study, a pneumatic cuff, a common component in rehabilitation robots, was used to analyse effects of cuff pressures on electrodermal activity (EDA) and tissue oxygen saturation (StO_2). Our aim is to explore the relationship between the cuff pressure and bio-signals, offering insights that could enhance the design and user interface of rehabilitation robots.

Methods: This study consisted of two experiments. In Experiment 1 for the measurement of EDA for different pressures in 1 minute, 13 adults (11 males, 2 females, 24.8 ± 0.7 years old, 174.5 ± 6.0 cm, 72.9 ± 14.2 kg) were tested. In Experiment 2 for the measurement of StO_2 and EDA for different pressures in 5 minutes, 10 adult males (23.2 ± 1.0 years old, 173.6 ± 6.0 cm, 72.3 ± 12.4 kg) were recruited. All participants wore pneumatic cuffs on both thighs, with pressure stimulation (10, 20, 30kPa) applied to the right thigh and EDA signals were measured on the hypothenar and thenar of the left palm [1]. The EDA signal was decomposed into tonic and phasic components using a high-pass filter with a cutoff frequency of 0.05 Hz [2]. For the phasic component, skin conductance response (SCR) was used to calculate SCR counts and the max amplitude, while for the tonic component, mean skin conductance level (SCL) was calculated. Tissue oxygen saturation (StO_2) was measured at the vastus lateralis muscle using the near-infrared spectroscopy (NIRS). ΔStO_2 was calculated as the difference between the minimum value of StO_2 during pressure application and the average StO_2 of the 30 second period before pressure application as the baseline (100%) [3]. Visual analogue scale (VAS) was normalized by the one of 60 kPa to the right thigh for 5 seconds and its correlation analysis with respect to EDA and ΔStO_2 were performed. Statistical methods such as Pearson correlation, RM ANOVA, post hoc paired t-test were used to determine significances as the stimulation pressure increased.

Results & Discussion: In Experiment 1, mean SCL increased to -0.12 ± 0.23, -0.06 ± 0.35, and -0.01 ± 0.67 for 10kPa, 20kPa, 30kPa respectively, while the max amplitude values were 1.08 ± 0.79, 1.40 ± 0.86, and 2.09 ± 1.27, and SCR counts were 5.3 ± 3.8, 10.2 ± 7.9, and 12.1 ± 1.4, respectively (Figure 1). RM ANOVA results indicated significant differences in mean SCL, the max amplitude, and SCR counts for different pressure conditions. Significant differences in mean SCL were observed for different pressure conditions from post-hoc tests. Significant differences in the max amplitude were also found between 10kPa and 30kPa pressure stimulations, but not between 10kPa and 20kPa. SCR counts showed significant differences between 10kPa and 20kPa, and 10kPa and 30kPa. Pearson correlation analysis indicated weak correlations between normalized VAS and mean SCL (r=0.21), the max amplitude (r=0.15), and SCR counts (r=0.18). In Experiment 2, mean SCL values increased to -0.10 ± 0.04, -0.07 ± 0.04, and -0.06 ± 0.05 for each pressure condition respectively, while the max amplitudes were 1.47 ± 1.21, 1.90 ± 1.53, and 2.27 ± 1.57, SCR counts were 27.8 ± 22.5, 34.7 ± 20.4, and 49.2 ± 35.2, and ΔStO_2 values were 11.46 ± 7.53, 55.56 ± 20.53, and 58.19 ± 21.82 respectively (Figure 2). RM ANOVA results showed statistical significance for pressure conditions on mean SCL, the max amplitude, SCR counts, and ΔStO_2. Post-hoc tests revealed significant differences in EDA for all pressure conditions except between 20kPa and 30kPa, while ΔStO_2 showed significant differences for all pressure conditions. Pearson correlation coefficients indicated A strong correlation existed between the normalized VAS and ΔStO_2 (r=0.74), a moderate correlation with mean SCL (r=0.37), and weak correlations with the max amplitude (r=0.032) and SCR counts (r=0.11).

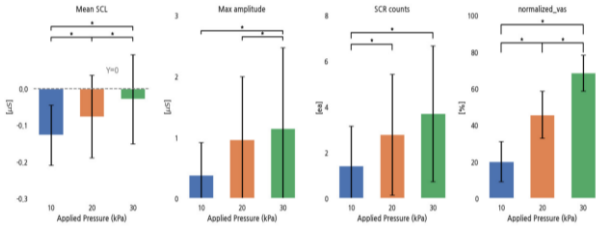

Figure 1: EDA parameters and normalized VAS according to different pressure conditions.

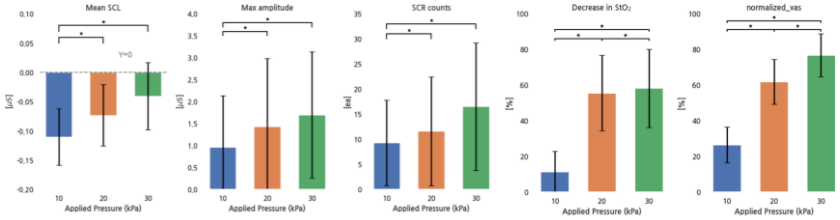

Figure 2: EDA parameters, Decrease in StO2 and normalized VAS according to different pressure conditions.

Significance: These findings suggested an increase in mean SCL, the max amplitude, SCR counts, and ΔStO_2 with increased stimulation pressure. ΔStO_2 showed a strong correlation with VAS, while mean SCL showed a moderate one.

Acknowledgments: This research was supported by a major project of the Korea Institute of Machinery and Materials (Project ID: NK238F) and 'Regional Innovation Strategy (RIS)' through the National Research Foundation of Korea (NRF) funded by the Ministry of Education (MOE) (2022RIS-005)

References:

[1] Kim JH et al. (2016). J. Sensor Sci. Technol., 25: 235-242
[2] Kong Y et al. (2021). IEEE Trans. Biomed. Eng., 68: 3122-3130
[3] Kermavnar T et al. (2020). Hum. Factors J. Hum. Factors Ergon. Soc., 62: 475-488

BILATERAL SHOULDER STRENGTH AND ROTATOR CUFF TENDON THICKNESS IN WHEELCHAIR USERS

Dustin Tran[1], Jungsun Moon[1], Matthew M. Hanks[1*]
[1]Department of Kinesiology and Community Health, University of Illinois at Urbana-Champaign, Urbana, IL, USA
*Corresponding author's email: hanksm@illinois.edu

Introduction: Strength deficits in the rotator cuff muscles are related to shoulder pain in manual wheelchair users (MWUs) [1]. Findings of within-individual, bilateral differences in shoulder biomechanics during propulsion [2] suggest within-individual, bilateral differences in shoulder strength may also exist in MWUs. Additionally, studies with healthy participants have examined bilateral differences in rotator cuff strength and the relationships among supraspinatus tendon thickness, acromiohumeral distance (AHD), and supraspinatus tendon occupation ratio (OR) [3, 4], yet these relationships remain understudied in MWUs. Thus, the purpose of this preliminary study was to explore bilateral shoulder strength and its relationship with clinical, quantitative measures of rotator cuff tendon health in MWUs.

Methods: Three MWUs (2 males and 1 female, age: 19.1 ± 1.0, years of manual wheelchair use: 15.0 ± 1.2) participated in this preliminary study. Musculoskeletal ultrasound images of AHD, and supraspinatus, infraspinatus, and subscapularis tendon cross-sectional thicknesses were obtained bilaterally with participants seated in their personal manual wheelchair and tested with their shoulders in standardized positions using standardized procedures [5-7]. Quantitative measures of rotator cuff tendon thicknesses and AHD were obtained using ImageJ software [8]. Supraspinatus tendon OR ratio was computed by dividing the average supraspinatus tendon thickness by the AHD. Abduction/adduction (Abd/Add), flexion/extension (Flx/Ext), and external rotation/internal rotation (ER/IR) concentric, isokinetic torques were measured using a HUMAC NORM isokinetic dynamometer. Average peak torques from three trials were computed for the six planar shoulder motions. Three planar torque ratios (Abd/Add, Flx/Ext, ER/IR) were computed bilaterally and used for within-individual analyses of strength symmetry. Torque ratios equal to 1.0 represented planar strength symmetry, whereas torque ratios greater or less than 1.0 represented planar strength asymmetries. Pearson correlation was used to describe associations between torque ratios and rotator cuff tendon thicknesses between shoulders.

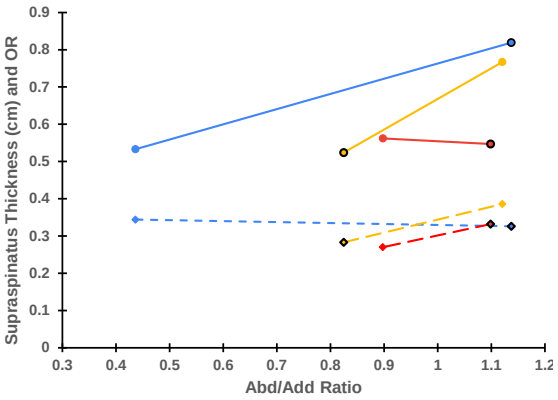

Figure 1: Associations between supraspinatus tendon thickness, occupation ratio, and Abd/Add ratio. Each color represents one participant and bolded and unbolded points represent each participant's right and left shoulders, respectively. Circles represent supraspinatus tendon thickness and diamonds represent occupation ratio.

Results & Discussion: All participants reported right-hand dominance. All participants demonstrated within-individual strength asymmetries for Abd/Add, with one shoulder favoring abduction (Abd/Add torque ratio >1.0) and the contralateral shoulder favoring adduction (Abd/Add torque ratio < 1.0) with bilateral torque ratio differences ranging from 0.2-0.7 across participants (Fig. 1). Supraspinatus tendon thickness was positively related to Abd/Add torque ratio (r_{right}=0.65, r_{left}=0.82), which suggests a positive adaptation (e.g., supraspinatus tendon hypertrophy) with greater abduction strength relative to adduction strength [9]. The shoulder with greater Abd/Add strength and greater supraspinatus tendon thickness exhibited a mild increase in OR (0.061cm ± 0.043) consistent with a mild increased risk of supraspinatus tendon impingement, though these observed ORs were less than previously reported values [10].

All participants demonstrated bilateral strength asymmetries for ER/IR (ER/IR < 1.0, range: 0.35-0.98 across participants) consistent with previous findings of greater shoulder IR strength in MWUs [11]. Infraspinatus tendon thickness was positively related to ER strength (r_{right}=0.95, r_{left}=0.69), whereas subscapularis tendon thickness was positively related to IR strength (r_{right}=0.71, r_{left}=0.90), which suggests positive tendon adaptations with strength. Greater infraspinatus tendon thickness and ER strength were observed in the nondominant shoulder (Right=0.43 ± 0.05 cm, Left=0.64 ± 0.20 cm) and greater subscapularis tendon thickness and IR strength were observed in the dominant shoulder (Right=0.83 ± 0.15 cm, Left=0.67 ± 0.08 cm) for all participants. These findings suggest that bilateral differences in infraspinatus and subscapularis tendon thicknesses and bilateral shoulder IR and ER strength exist in MWUs.

Significance: Findings from our preliminary analyses show within-individual, bilateral asymmetries in shoulder strength and rotator cuff tendon thicknesses in MWUs, as well as associations between shoulder strength and rotator cuff tendon thickness. These results further suggest that shoulder function is asymmetrical in MWUs. Increased supraspinatus tendon thickness was associated with only mild increases in OR, which suggests that tendon hypertrophy may not significantly increase the risk of developing shoulder impingement or pain. While currently limited in scope, these findings are part of ongoing research investigating shoulder health and function in MWUs across the lifespan, in which we will further explore associations between these measures and shoulder pain.

Acknowledgments: This work is supported by the University of Illinois College of Applied Health Sciences Center on Health, Aging, and Disability.

References: [1]: Mulroy et al. (2015), *Phys Ther.* (95)7; [2] Hurd et al. (2008) *Arch Phys Med*, 89(10) [3] Ueda et al. (2020), *Shoulder* 29(10); [4] Leong et al. (2012), *JSMS* (15)4; [5] Gil-Agudo et al. (2014), *Front. Bioeng. Biotechnol.*, 2; [6] Kim K et al., (2016), *JKMS*, 31(9); [7] Plomb-Holmes et al. (2018), *OTSR* 104(8); [8] Ohya et al., (2017) *J. Phys. Ther. Sci* 29(4) [9] Belley et al. (2017), *ACRM* 98(3); [10] Michener et al. (2015) *Shoulder* 23*;* [11] Ambrosio et al. (2005), *JSCM* 28(5).

DOES FEMORAL OSSEOINTEGRATION REDUCE HIP POWER DEMANDS DURING WALKING?

Pawel R. Golyski[1,2*], Benjamin K. Potter[2,3], Jonathan A. Forsberg[3], Christopher L. Dearth[1,3], Brad D. Hendershot[1-3]
[1]Extremity Trauma and Amputation Center of Excellence, Falls Church, VA, [2]Walter Reed National Military Medical Center, Bethesda, MD
[3]Uniformed Services University of the Health Sciences, Bethesda, MD
*Corresponding author's email: pawel.golyski.civ@health.mil

Introduction: Osseointegrated (OI), or bone-anchored, prostheses can serve as a valuable alternative to conventional socket-based prostheses, particularly for individuals with poor socket fit or residual limb health. [1] From a biomechanical perspective, a benefit of direct skeletal fixation of a prosthesis is the elimination of unactuated degrees of freedom (e.g., pistoning [2]) that dissipate energy between an individual and the environment. Assuming the overall mechanical energy demands on the prosthetic limb do not change after OI, removing a source of net energy loss over a stride should reduce the positive work demands on the other joints of that limb (i.e., the hip for individuals with transfemoral limb loss who use passive prostheses). Thus, here we first evaluated whether the mechanical work demands on the prosthetic limb are indeed similar pre- vs. post-OI and then tested the hypothesis that individuals with unilateral transfemoral limb loss would exhibit decreased positive hip work on their prosthetic limb while walking after OI.

Methods: Nine individuals with unilateral transfemoral limb loss (8 M/1F, mean±SD age: 39±12yr, stature: 175±12cm, pre-OI body mass: 86.3±18.6kg) completed biomechanical gait evaluations pre- and 24 months post-OI (two-stage implantation; time between pre-OI visit and initial amputation: 39±80mo). Full-body motions (120Hz) and bilateral GRFs (1200Hz) were collected as participants walked overground at three targeted speeds (0.7, 1.0, 1.4 m/s), when possible (307 strides total). Custom OpenSim models of both the conventional socket and OI interfaces were developed and scaled to each participant, informed by whole-body DEXA imaging. The socket model included a degree of freedom for socket-femur translation. Socket-femur displacements estimated by the model were 3.85 cm over stance, as compared to measured displacements of 1.6 cm over the gait cycle seen in literature [2]. Overall leg powers were calculated by summing the peripheral powers of leg segments with the dot product of GRF and center of mass velocity. [3] Hip joint power was calculated as the dot product of joint torque and angular velocity summed across all hip joint degrees of freedom. Mechanical work was calculated by integrating power with respect to time. A linear mixed model with a fixed effect of OI, a covariate of walking speed (measured as center of mass speed during each walking trial), and a random effect of participant assessed the main and interaction effects of OI and speed ($p<0.05$). All activities were approved by the local IRB, and participants provided informed consent.

Results & Discussion: Contrary to our baseline assumption, both positive and negative prosthetic side leg work were larger pre- vs. post-OI (Fig. 1A and 1B; $p<0.005$) and were exacerbated by speed ($p<0.001$). This difference suggests that individuals adopt altered prosthetic-side loading and movement strategies after OI, particularly during weight acceptance and push-off phases. Our hypothesis of decreased prosthetic side hip work post-OI was not supported (OI: $p=0.564$, OI and speed interaction: $p=0.125$; Fig. 1C). However, there was an interaction between OI and walking speed for negative hip work; at faster walking speeds, negative hip work was smaller post- vs. pre-OI (Fig. 1D). This indicates that while eliminating the "damping" action of the socket does not alter the positive work demands of the hip, there may be lower demands on residual limb hip flexors post- vs. pre-OI.

Significance: This multi-scale investigation provides insight into how direct skeletal attachment of a prosthesis alters the loading and flow of energy through the affected limb during walking. Future studies should expand on these findings to understand how such movement and loading strategies evolve after OI, particularly in the context of altered sensory input and the rehabilitation process.

Acknowledgments: This work was supported by Award #W81XWH-17-2-0060. The views expressed are those of the authors, and do not necessarily reflect the official policy or position of the U.S. Departments of the Army, Navy, Defense, nor the U.S. Government.

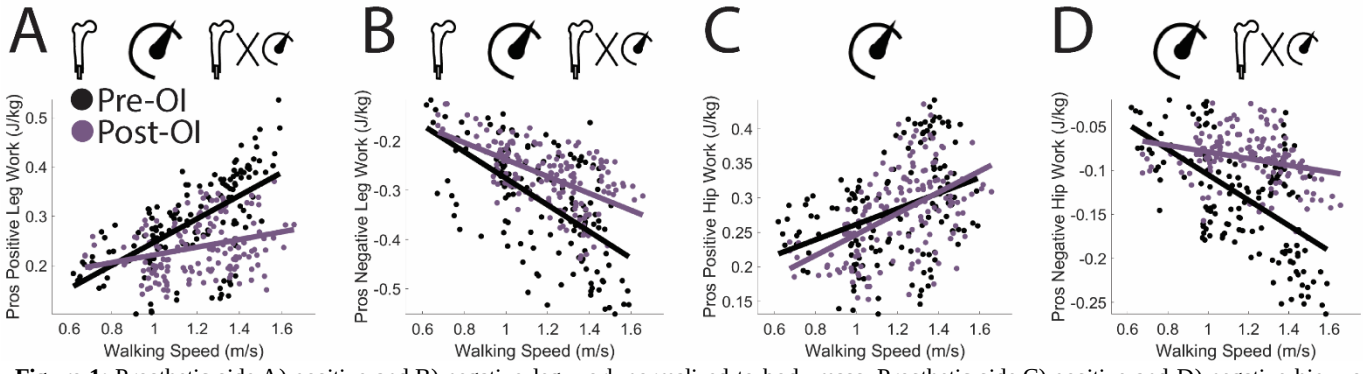

Figure 1: Prosthetic side A) positive and B) negative leg work normalized to body mass. Prosthetic side C) positive and D) negative hip work normalized to body mass. Symbols represent significant effects of OI, walking speed, or their interaction ($p<0.05$).

References: [1] Zaid et al. *JAAOS* 2022 [2] Maikos et al. *Front. Bioeng. Biotechnol* 2021 [3] Zelik et al. *JEB* 2015

PLANTAR SENSATION ASSOCIATES WITH GAIT INSTABILITY IN OLDER ADULTS

Andrew D. Shelton[1*], Kota Z. Takahashi[2], Jessica L. Allen[3], Howard E. Kashefsky[4], Jason R. Franz[1]
[1] Joint Department of Biomedical Engineering, UNC Chapel Hill & NC State University, Chapel Hill, NC, USA [2]Department of Health and Kinesiology, University of Utah, Salt Lake City, UT, USA [3]Department of Mechanical and Aerospace Engineering, University of Florida, Gainesville, FL, USA [4]School of Medicine, UNC Chapel Hill, Chapel Hill, NC, USA
*Corresponding author's email: adshelt@email.unc.edu

Introduction: Maintaining stability during walking requires a combination of vestibular, somatosensory, and visual feedback. Plantar sensation at the feet provides critical afferent feedback to the body necessary to regulate balance during walking. Advanced age brings a loss of plantar sensation [1], represented, for example, as higher sensation thresholds in standardized testing. This is intuitively thought to contribute to an increased risk of falls among older adults. Past research has hinted at this increased risk, using unperturbed standing or standing balance responses as proxies for increased fall risk or inducing loss of plantar sensation through anesthesia or hypothermia in younger adults [2,3]. However, no study to date has established an empirical relation between plantar sensation and vulnerability to perturbations applied during walking. This is important because walking is the task in which most falls occur among older adults. The purpose of this study was to address this gap and quantify the association between plantar sensation and the instability elicited by a suite of walking balance perturbations that differ in direction and context. We hypothesized that older adults with lesser plantar sensation, evidenced by higher average thresholds on a monofilament test, would also exhibit higher gait instability and vulnerability to walking balance perturbations.

Methods: 28 older adults (73.0±5.9 yrs, 15 F) had plantar sensation measured using the Semmes-Weinstein monofilament test with a rigorous 4-2-1 design. Plantar sensation thresholds were averaged between the heel and first metatarsal measures of their dominant foot. Participants also completed four treadmill walking trials at their preferred overground walking speed in randomized order, including: (i) unperturbed walking, (ii) treadmill-induced slip perturbations applied at heel strike, (iii) lateral waist-pull perturbations applied toward the swing leg at toe-off, and (iv) continuous mediolateral optical flow perturbations. Using 3D motion capture data, we calculated margins of stability in the anteroposterior (MoS_{AP}) and mediolateral (MoS_{ML}) directions at the instant of heel strike (that directly following perturbation onset for slip and waist-pull perturbations) and whole-body angular momentum (WBAM). We calculated vulnerability to perturbations as the change in WBAM or MoS from habitual walking to perturbation response.

Results & Discussion: Participants averaged monofilament thresholds of 4.43±0.48 and 4.49±0.90 on the plantar surface of the heel and base of the first metatarsal head, respectively. These values did not differ significantly ($p=0.73$), and thus we used their subject-specific average (i.e., 4.46±0.63) for further analysis. 5 participants surpassed the clinical cut-off for loss of protective sensation (i.e., ≥5.07), and an additional 7 participants were within 1 SD of this cut-off (i.e., ≥4.44) [5]. During habitual walking, we found that higher monofilament thresholds correlated with larger WBAM ($p=0.014$; Fig 1A) and larger MoS_{AP} and MoS_{ML} ($p\leq0.031$; Fig 1B&C). We found no correlations between monofilament thresholds and balance outcomes in response to optical flow or treadmill-induced slip perturbations. Conversely, we found that higher monofilament thresholds correlated with larger increases in WBAM ($p<0.001$; Fig 1D) and larger decreases in MoS_{AP} ($p=0.018$; Fig 1E) in response to lateral waist-pull perturbations. We have shown that perturbations elicit context-specific changes in gait instability [4]. Thus, we find it important to emphasize the disproportionate vulnerability of individuals with lesser plantar sensation to instability elicited by lateral force perturbations applied to their center of mass. This would be perhaps a less anticipated outcome than, for example, treadmill-induced slips applied more directly to the base of support.

Significance: This research study provides evidence for an important connection between plantar sensation and gait instability, impacting both habitual walking and vulnerability to lateral waist-pull perturbations. Ultimately, interventions to improve plantar sensation, possibly through insoles or footwear, could be critical to reducing falls in at-risk populations. Follow-up work in those with disease states that result in a loss of plantar sensation could provide important insight into their fall risk.

Acknowledgments: This work was supported by grants from the NIH (R21AG067388 to JRF, and F31AG079499 to ADS).

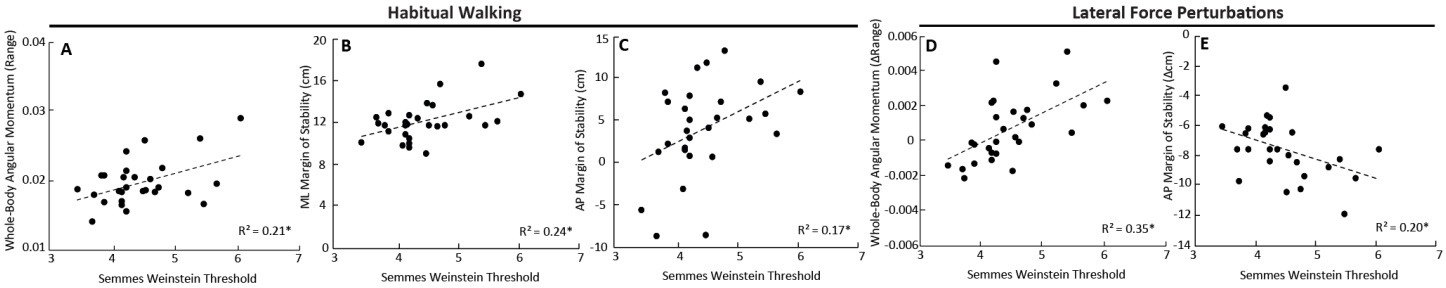

Figure 1: Evidence of instability during habitual walking through positive correlations of (A) WBAM, (B) ML MoS, and (C) AP MoS. Larger vulnerability to lateral force perturbations shown through Semmes-Weinstein Threshold positively correlating with (D) change in WBAM and (E) change in AP MoS.

References: 1. Perry et al. 2008, 2. Meyer et al. 2004, 3. Germano et al. 2016, 4. Shelton et al. 2024 5. Birke et al. 1986

Application of Virtual Obstacle Avoidance Program to assess the Effect of BMI on Postural Control

Chi-Whan Choi[1], Simone V. Gill[1]*
[1]Rehabilitation Sciences PhD Program, Boston University, 635 Commonwealth Avenue, Boston, MA, USA, 02215
*Corresponding author's email: simvgill@bu.edu

Introduction: Increased body mass index (BMI) is strongly correlated with postural instability [1]. A high BMI poses unique challenges for individuals' static and dynamic postural stability, which often leads to falls and injuries. Mounting evidence attributes their impaired postural control to the mechanical efforts needed to stabilize excess body mass against the force of gravity [2]. Another contributing factor may be mechanical restrictions imposed by increased adipose tissue, resulting in poor sensory-motor processing [3]. The physical environment including uneven terrain and/or obstacles in the real world could impact their postural stability, which may impair their balance [4]. Previous research reported that altered postural control linked with obesity is more evident when encountering physical constraints such as an obstacle [5]. However, we still know little about how BMI affects the ability to control posture to adapt to new situations. We propose the Virtual Obstacle Avoidance Program (VOAP), an exergame using inertial measurement units (IMUs), to assess postural control in a novel environment. This study aimed to (1) validate a VOAP framework by comparing it with a validated assessment tool, the Functional Gait Assessment (FGA), and (2) investigate the effects of BMI on strategies used to avoid virtual obstacles and amount of leg movement during obstacle clearance performance during the program. We tested participants in a seated position to reduce body mass-related mechanical constraints and to provide more stability to reveal underlying performance differences in postural adaptation. We hypothesized that BMI would contribute to performance differences when introducing a novel scenario.

Methods: Twenty-six participants took part in this study (n=26; Female=15; mean age=27.2 years old±7.7; BMI range=18.7—57.9 kg/m2) and performed VOAP (performance video resource). The Functional Gait Assessment (FGA) which consists of 10 tasks that assess walking, balance, and coordination was administered to investigate linear relations with the VOAP parameters including leg movement strategy (either hip adduction or abduction) to avoid virtual obstacles, Total Leg Movement from the home position to the target (TLM), and Maximal Distance from Midline (MDD) while avoiding the obstacles. The timing of the presentation of the obstacle were varied with 5 different timings of obstacle appearance including no obstacle (Condition 0), obstacle appears prior to cue (Condition 1), obstacle appears with cue (Condition 2), obstacle appears with movement onset (Condition 3), and obstacle appears at 20% of movement amplitude (Condition 4). Pearson's correlation coefficients, test-retest reliability between blocks, and random effects linear mixed models were conducted for statistical analysis. Condition 0 excluded for the linear mixed models.

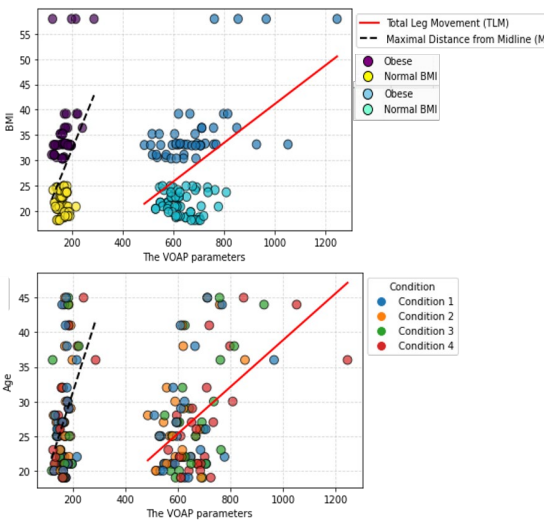

Figure 1: The effect of BMI on Total leg movement (TLM) and Maximal distance from midline (MDD). Red trend line indicates association between BMI and TLM while black trend line indicates association between BMI and MDD. Purple and skyblue dots indicate over 30 BMI, and yellow and aquamarine dots indicate Normal BMI (Left). The effect of Age and Condition on Total leg movement (TLM) and Maximal distance.

Results & Discussion: FGA scores were significantly correlated with TLM ($r(26)= -0.390$, $p<0.001$), MDD ($r(26)= -0.165$, $p<0.001$), and Strategy ($r(26)= 0.131$, $p<0.001$). Interclass correlation coefficients (ICCs) indicated a strong agreement in Strategy (ICCs = 0.989, p<0.001), TLM (ICCs = 0.882, p<0.001), and MDD (ICCs = 0.805, p<0.001). BMI (OR=0.767, p=0.038), significantly impacted increased use of hip adduction. BMI (β=3.632, p=0.022), age (β=4.099, p=0.023), and condition, the timing of obstacle appearance (β=25.554, p<0.001), had a significant main effect on the TLM, but not on the MDD (Fig. 1). Higher BMI influenced a preferential strategy to avoid the virtual obstacles during the VOAP, which is reflected by hip adduction strategy preference. Hip adduction may be an easier way to control center of mass with respect to base of support while avoiding obstacles while seated, and may be due to obesity-related reduced relative muscular strength or muscular fatigue. Moreover, a higher BMI was associated with greater ranges of total leg movement during the program, which can explain in part ineffective movement strategies associated with obesity. This may be why this population increases the rate of oxygen consumption and reduces participation in physical activity.

Significance: This study confirmed that the VOAP may be an effective tool to assess postural adaptation in a seated position, providing a more detailed account of the effects of BMI on postural control. The VOAP framework has the potential to be used to detect obesity-related postural adjustment deficits that are not detectable with standard clinical measures. In other words, VOAP can identify both within-subject and between-subject differences. Thus prospective studies are needed to clarify the nature of these relationships and identify underlying mechanisms, which is essential for the incorporating VOAP into clinical practice. These findings may present avenues for targeted rehabilitative evaluation and interventions to improve postural adaptation in this population in real-world.

Acknowledgments: This study was funded by ACL National Institute on Disability, Independent Living, and Rehabilitation Research.

References: [1] Hue et al. (2007), *Gait Posture* 26(1); [2] Wearing et al. (2006), *Obes Rev* 7(1); [3] Meng et al. (2017), *Gait Posture* 53; [4] LoJacono et al. (2018), *J Mot Learn Dev* 6(2); [5] Gill et al. (2016), *Surg Obes Relat Dis* 12(5).

The Virtual Obstacle Avoidance Program

The Virtual Obstacle Avoidance Program (VOAP) is the exercise game using Inertial Measurement Units (IMUs) system to investigate how participants are able to make adjustments to online movements of their lower limbs as task constraints change. Before participants perform the VOAP, IMUs will be attached to their trunk, thighs, and shins to measure leg motion (Fig. 1A). Once the computer program is operational, participants will be sitting down in front of the computer running the game. In the program, participants will be cued to move a cursor from a home position to a target by moving their leg (Fig. 1B). In some trials, an obstacle will appear, forcing participants to avoid it to reach the target using hip adduction or hip abduction (Fig. 1B). The timing of the presentation of the obstacle will vary to test how new information is integrated into the sensorimotor system. To be specific, participants will be required to cross obstacles in 5 different conditions The timing of the presentation of the obstacle were varied with different timings of obstacle appearance including no obstacle (Condition 0), obstacle appears prior to cue (Condition 1), obstacle appears with cue (Condition 2), obstacle appears with movement onset (Condition 3), and obstacle appears at 20% of movement amplitude (Condition 4). Participants will be given a "practice period" where they are given instructions about the task. to familiarize themselves with the system, and optimize comfortability. The main task will consist of 5 block with 40 trials. Total leg movement from Home to Target (TLM) and Maximal distance from midline (MDD) while each trial will be calculated with the 2D distance between starting position (Home) and final position (Target) of a Cursor (Fig. 1C).

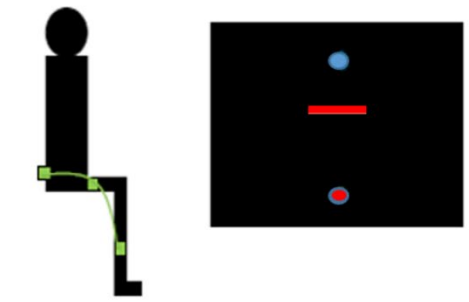

Figure 1A

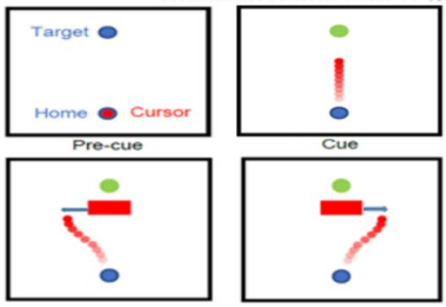

Figure 1B.

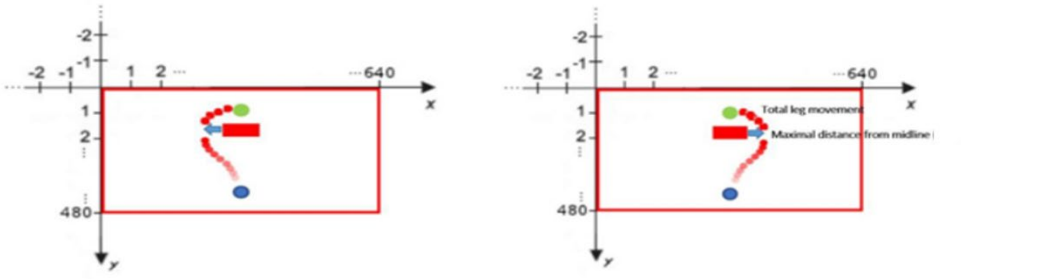

Figure 1C.

Fig. 1. —The Virtual Obstacle Avoidance Program: (A) The Virtual Obstacle Avoidance Program (B) The hip movement strategies (Left below: Hip Adduction, Right below: Hip Abduction) (C) Calculating Total leg movement (TLM) from Home to Target and Maximal distance from midline, blue arrow (MDD)

GAIT ADAPTATION IN YOUNG ADULTS AND CHILDREN AFTER UNILATERALLY LOADING AN ANKLE

Kaylan Johnson[1], Huaqing Liang[2*]
[1]East Tennessee State University, Johnson City, TN
[2*] Corresponding author: Marshall University, Huntington, WV, liangh@marshall.edu

Introduction: Walking, an everyday task, demands continual adaptations to varying environmental surroundings. Exposure to novel environments prompts gait pattern adaptations, with resulting aftereffects that persist for a short while upon return to familiar settings. Repetitive exposures to novel environments during gait training can reinforce such temporary learning and might help an individual to retain a new gait pattern.

For individuals with asymmetrical gaits such as people after a stroke, a split-belt treadmill has shown benefits in providing an asymmetrical disturbance to facilitate the recognition and correction of this asymmetry [1]. A unilateral ankle load could be a cost-effective and easy-to-obtain alternative to provide an asymmetrical disturbance to walking, thus has the potential to improve gait symmetry in clinical populations via error augmentation, recognition and correction. However, only a few studies examined the gait adaptation under this paradigm in young adults or children.

The purpose of this study was to assess the spatiotemporal gait adaptation to unilateral ankle loading in young adults (YA) and typically developing children (TD). Previous studies reported that some features of gait in children are still maturing beyond the age of 7 years [2]; still, children showed the capacity to adapt their gait to unilateral ankle loading [3]. Thus, we hypothesized that compared to YA, children might display similar gait adaptations in spatiotemporal gait parameters but have a larger gait variance in these variables.

Methods: This preliminary dataset includes 17 YA (8M/9F, 24.7±1.9 years) and 10 TD (5M/5F, 7-17 years, average 13.2±2.7 years). Participants walked on a treadmill at their preferred walking speeds under 3 conditions: 1) a Baseline 2-minute trial; 2) 3 bouts of 5-minute trials with a load (3-5% of bodyweight) attached to the dominant ankle (Loading); and 3) a 5-minute trial with the load removed (Unloading). We placed seven IMU sensors at the bilateral feet, shanks, thighs, and at the sacrum for data collection.

We extracted data from 5 periods to assess gait adaptations: the first 100 strides of the Baseline, Loading, and Unloading conditions to assess the baseline (T1), early adaptation (T2), and early post-adaptation (T4) periods; and the strides number 101-200 of the Loading and Unloading conditions to assess late adaptation (T3) and late post-adaptation (T5) periods. We calculated the step length, swing time percentage (Swing%), and double-limb support time percentage (DLS%) of these 100 strides, and further calculated the symmetry index (SI) using the equation $SI = 2 * (X_{NO} - X_L) / (X_{NO} + X_L) * 100\%$, where X_{NO} is the parameter's value of the no-load leg and X_L is the parameter's value of the loaded leg. We calculated the coefficient-of-variance (CV) of the abovementioned variables for the loaded leg to evaluate the variability of these gait parameters within each time period using the equation CV = standard deviation / mean * 100%. Two-way (2 groups by 5 time periods) repeated measures ANOVAs were conducted and post-hoc pairwise comparisons with Bonferroni adjustments were used when necessary.

Results & Discussion: Our results partially supported our hypothesis that the TD group displayed similar SI values as the YA group, and the TD group displayed a larger CV than the YA group only in the step length across different time periods examined.

The results of the spatial variable showed that there was no group or time differences for SI of step length (Figure 1A). However, the results of CV showed that there was a group main effect ($p=0.013$) and a time main effect ($p=0.014$) (Figure 1B). Specifically, in TD, the CV during early adaptation (T2) was larger than any other time periods.

The results of the temporal variables showed similar gait adaptation in both groups, where they displayed asymmetrical gait when walking with the unilateral load and returned to the symmetrical gait immediately after the removal of the load. The results of SI of swing% (Figure 1C) and SI of DLS% showed a time main effect (both $p<0.001$). Specifically, the values during early (T2) and late (T3) adaptation were significantly different than all the other time periods (all $p<0.05$). There were no group difference or time periods differences found in CV of these temporal parameters (Figure 1D).

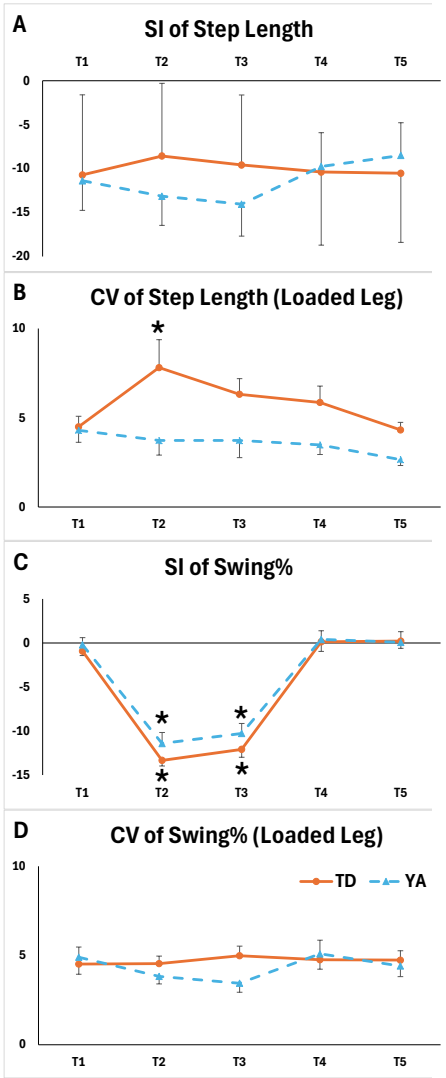

Figure 1: Mean and SD of A) SI of step length, B) CV of step length of the loaded leg, C) SI of swing%, and D) CV of swing% of the loaded leg. Values of the YA group are shown in dotted blue lines and values of the TD group are shown in solid orange lines. An asterisk (*) indicates a significant time period difference from the baseline value.

Significance: YA and TD might employ distinct motor control and adaptation mechanisms for spatial and temporal gait parameters, maturing at varying rates. When designing gait rehabilitation protocols for clinical population, we have to consider spatial and temporal parameters separately, particularly in pediatric populations.

References: [1] Regnaux et al. (2008), *Clin Biomech* 23(6); [2] Hillman et al. (2009) *Gait Posture* 29(1); [3] Damiano et al. (2017), *Front Hum Neurosci* Feb 8(11).

AGE AND INITIAL FOOT POSITION AFFECT ANKLE MUSCLE EXCITATIONS IN SIT TO WALK TRANSITIONS

Michael F. Miller[1*], Eline van der Kruk[2], Anne K. Silverman[1]
[1]Department of Mechanical Engineering, Colorado School of Mines
[2]Department of Biomechanical Engineering, Delft University of Technology
email: *mfmiller@mines.edu

Introduction: Muscle atrophy and joint degeneration are common in aging, reducing the ability to generate the forces and accelerations necessary to complete everyday movement tasks [1]. More than half of all injurious falls occur while performing transitional tasks such as walking, rising from a chair, or transferring between both [2], commonly referred to as sit-to-walk (STW). STW requires coordination and strength from plantarflexor muscles like the soleus (SOL) and gastrocnemius (GAS) to accelerate the body center of mass (COM) upward and forward [3] alongside the tibialis anterior (TA) to stabilize against posterior COM movement [4]. In addition, movement strategies, such as using different initial foot placements, can affect muscle excitations and biomechanics. For example, rising during sit-to-stand (STS) with one foot posterior to the other might offload one limb, but require greater ankle plantarflexor moments to propel the body forward [5]. Certain strategies may present challenges for older adults who have a lower musculoskeletal capacity and therefore often rely on proximal muscles to meet movement demands with ankle muscle weakness [6]. Older adults also often have greater co-contraction of ankle dorsiflexors and plantarflexors to anticipate perturbations and decrease body COM deviations [7]. Therefore, we quantified the effects of initial foot position and age on peak SOL, TA, and GAS excitation during STW. We expected greater muscle excitations from older adults, and when rising from a posteriorly offset foot position.

Methods: As part of a larger study, thirty healthy younger (7M/8F, 24.26±4.41 yrs, 709±129.4 N, 1.73±0.10 m) and older (5M/10F, 62.24±6.62 yrs, 809.5±223.4 N, 1.69±0.11 m) adults completed self-paced STW trials. Each trial began seated on a backless stool without shoes and with socks, with feet arranged in one of two initial positions: (1) a *symmetric* position with feet shoulder-width apart and knees and hips at 90°, (2) an *offset* position with the dominant limb offset backward 2/3 the dominant foot length. Participants rose from the stool and walked at a comfortable speed. STW events including the start, seat-off (SO), toe-off (TO) and the end were defined to isolate the phases of rising and stepping. The rising phase began when the body center of mass (COM) velocity exceeded 0.15 m/s and concluded when the stepping limb left its initial force plate (TO). The stepping phase began at TO and concluded at the following ipsilateral toe-off. Surface electromyography (EMG) signals (Delsys, 2000 Hz) were collected bilaterally from TA, GAS, and SOL. EMG data were digitally band-pass filtered with a 4th order Butterworth filter (20-500 Hz), full wave rectified, and low pass filtered (fc=6 Hz). Signals were normalized by functional toe-raise and heel-raise tasks [7]. A two-factor mixed model ANOVA compared peak TA, GAS, and SOL between age group and initial foot position (α=0.05) for both limbs for both the rising and stepping phases.

Results & Discussion: All participants were right limb dominant, which was also the stepping limb during the STW task. During the rising phase, there was a significant effect of foot position on peak stepping limb TA ($p<0.001$) and stance limb TA ($p<0.001$) excitation. The A/P offset position required 32.4% less stepping limb excitation and 40.8% stance limb excitation compared to the symmetric position (Figure). An A/P offset position may require less stabilizing TA excitation due to the larger base of support in the sagittal plane and the task goal of transitioning to gait. During the stepping phase, there was a significant foot position main effect on peak stance limb GAS excitation ($p=0.027$), where the A/P offset position generated 10.5% less excitation than the symmetric position. There was also a main age effect on peak stepping limb GAS ($p=0.022$) and stance limb GAS ($p<0.001$), which did not support our hypothesis. Older adults generated 10.2% smaller excitation and 19.1% smaller excitation on the stepping and stance limbs respectively compared to younger adults. There was a main effect of age during the stepping phase for the stance limb SOL ($p=0.013$), which also did not support our hypothesis. Older adults generated 14.3% less peak SOL compared to younger adults. Smaller SOL and GAS excitation may reflect altered movement strategy and muscle recruitment in older adults, consistent with previous observations of a proximal redistribution of muscle excitation associated with ankle muscle weakness [8]. Thus, future work will quantify ankle joint moments to help interpret our current EMG findings.

Significance: Rising with a limb posteriorly offset reduced ankle muscle excitation, suggesting the offset condition may facilitate the STW task. Older adults had less ankle plantarflexor muscle activity compared to younger adults, consistent with an altered movement strategy.

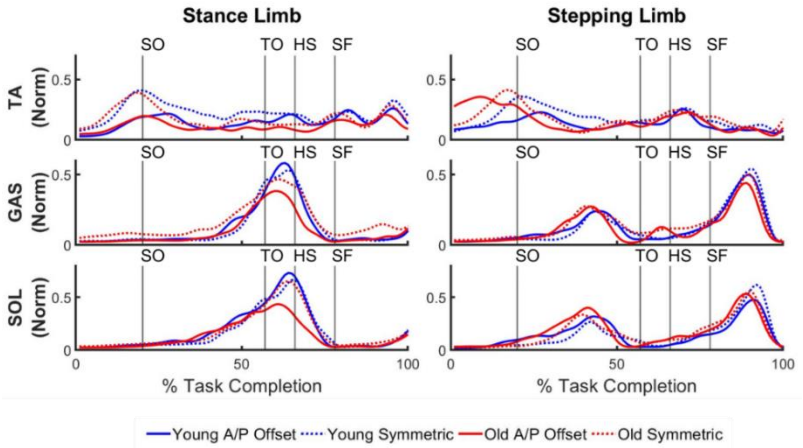

Figure: TA, GAS, and SOL processed EMG signals for younger and older adults completing sit-to-walk from a symmetric and offset position.

References: [1] E. van der Kruk, et al., *J Biomech.*, vol. 122, 2021. [2] Pengpid and Peltzer, *Curr Gerontol Geriatr Res.*, 2018. [3] Neptune, et al., *J. Biomech.*, vol. 34, 2001. [4] Afschrift, et al., *Gait Posture.*, vol. 68, 2019. [5] Kawagoe, et al., *J. Orthop. Sci.*, vol. 5, 2000. [6] Devita and Hortobagyi, *J Appl. Physiol.*, vol 88, 2000. [7] Segal, et al., *J. Biomech.*, vol. 152, 2023. [8] Dos Anjos, et al., *Front. Hum. Neurosci.*, vol. 11, 2017.

THREE DAYS OF RUNNING DOES NOT INFLUENCE DEVIATIONS FROM THE HABITUAL MOVEMENT PATH

Allison H. Gruber[1*], Jennifer Sumner[2], Edward Nyman[2], Kai-Wen Chien[1], Marni Wasserman[1], John S Raglin[1], Aaron Cohen[3], James J. McDonnell[1]
[1]H.H. Morris Human Performance Laboratories, Indiana University, Bloomington, IN, USA
[2] Brooks Sports Inc., Seattle, WA, USA
[3]Deptartment of Epidemiology and Biostatistics, Indiana University, Bloomington, IN, USA
*Corresponding author's email: ahgruber@indiana.edu

Introduction: Gait metrics acquired at the end of a prolonged run are hypothesized to be more predictive of running-related injury (RRI) risk than those performed in a rested state. The 'habitual movement path' paradigm suggests deviating from a runner's individual, natural movement pattern may cause abnormal loading that leads to RRI [1]. Previous research has demonstrated that prolonged running contributed to deviations from a runner's habitual movement path, which lends support to an exhausted gait mechanism for RRI [2]. Alternatively, prolonged running may simply cause temporary and typical deviations in the habitual movement path that are not injurious. For an exhausted gait mechanism for RRI to be supported, it is necessary to demonstrate that that changes in habitual movement path are exacerbated by multiple days of prolonged running. The purpose of this study was to investigate the effect of three days of running on habitual movement path deviations. We hypothesized that multiple days of running would result in progressively greater changes in habitual movement path with each run and that changes in habitual movement path across three days of running would be greater if these runs are performed on consecutive days compared with running bouts separated by a rest day.

Methods: Experienced runners completed two protocols of three runs each on an instrumented treadmill (TreadMetrix, LLC, Park City, UT, USA) at their lactate threshold speed and in their preferred footwear. The protocols were three consecutive runs ('consecutive') and three runs separated by a rest day between runs ('rest'). The order of these protocols was randomized across participants. For each run, three-dimensional motion capture of the right limb was recorded after 3-minutes ('start') and the last minute ('end', when Borg RPE = 17). Before each run, a series of movements (squat, lunge, step down, walk) while wearing minimal sock shoes were completed to establish participants' baseline habitual movement path of tibial internal rotation (TIR), knee abduction (ABD), and rearfoot eversion (EVE). Violin plots for baseline TIR, ABD, and EVE were generated using a kernel density estimation approach and summed across movements (Fig. 1). The baseline violin plot was then compared with the violin plots from recorded during the start and end of the run. The overlap between baseline and running violin plots represents the deviation that the stance phase of running deviates from the participants' habitual movement path. The absolute value of the change (|Δ|) in this deviation between the start and the end of the run was compared across runs within and between protocols using a repeated measures ANOVA (α=0.05).

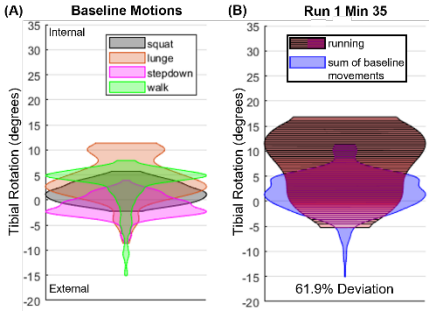

Figure 1: Violin plots for tibial internal rotation from one participant. The violin plots for the baseline movements (A) are summed (B, blue area) and compared with a violin plot for running (B, red/pink area). The overlap between baseline motions and running violin plots indicates the deviation from the habitual movement path occurring during running.

Results & Discussion: Twenty-two participants were included (males/females 12/10; age = 27.8 ± 6.5 yrs; BMI = 23.2 ± 4.9 kg/m^2; years running = 7.2 ± 4.9 yrs; volume = 19.7 ± 11.1 mi/wk); 16/22 completed both protocols and were assessed for the between-protocol interaction. Run duration was not significantly different between protocols (p=0.687). |Δ| deviation did not differ between runs within the consecutive protocol (TIR p=0.574; ABD p=0.512; EVE p=0.396) or the rest protocol (TIR p=0.313; ABD p=0.330; EVE p=0.946), possibly due to inter-participant variability (Table 1). No significant protocol by run interaction was evident (TIR p=0.116; ABD p=0.494; EVE p=0.373). Contrary to the hypotheses, this preliminary analysis indicates that three days of running did not influence TIR, ABD, or EVE deviation from the habitual movement path, and a day of rest between runs did not affect within-run change in deviation.

Table 1: Mean ± 1 standard deviation for run duration and the absolute value of the change (|Δ|) in tibial internal rotation (TIR), knee abduction (ABD), and rearfoot eversion (EVE) deviation between the start and end of each run for both protocols.

Protocol	**Consecutive Runs (N=22)**			**Rest Runs (N=16)**		
Run number	**Run 1**	**Run 2**	**Run 3**	**Run 1**	**Run 2**	**Run 3**
Run Duration (min)	27.11 ± 10.38	26.24 ± 11.83	27.34 ± 11.40	27.55 ± 10.37	27.61 ± 13.60	27.67 ± 10.56
TIR Deviation (%)	12.07 ± 12.97	9.07 ± 7.49	12.49 ± 13.64	8.93 ± 9.48	6.55 ± 5.07	10.35 ± 9.50
ABD Deviation (%)	10.71 ± 12.99	11.27 ± 10.36	8.53 ± 8.82	11.30 ± 11.12	7.30 ± 6.08	7.67 ± 6.22
EVE Deviation (%)	5.76 ± 6.14	6.04 ± 5.28	7.68 ± 7.76	6.13 ± 3.81	5.77 ± 6.37	6.40 ± 6.81

Significance: There does not appear to be a cumulative effect of multiple days of running on the change in habitual movement path deviation magnitude occurring between prolonged runs, and a day of rest between runs performed at a threshold pace may not be necessary to avoid compounding effects of exhaustion on gait in this group of experienced runners. Further analysis will explore differences in the deviation magnitude between days and the effects of potential covariates such as sleep, physical activity, and mood.

Acknowledgments: This study was funded by Brooks Sports, Inc. We thank Dr. Kiara Chan for her assistance initiating the study.

References: [1] Trudeau et al. (2019), *Footwear Sci* 11(3); [2] Willwacher et al. (2020), *Sci Reports* 10(1363).

ONLINE MUSCULAR WORK FEEDBACK TO MOTIVATE DURING HANDS-ON LOCOMOTOR REHABILITATION

Julia Manczurowsky[1*], Blake Karavas[1], Charles H. Hillman[1,2], Christopher J. Hasson[1]
Departments of [1]Physical Therapy, Movement and Rehabilitation Sciences, and [2]Psychology, Northeastern University
*Corresponding author's email: manczurowsky.j@northeastern.edu

Introduction: Providing patients with augmented biofeedback about their performance can have a powerful impact on their expenditure of effort and motor learning. However, all feedback is not created equal. For example, kinematic visual feedback during gait training has been shown to be no better than verbal instruction in changing patients' motor output and motivation [1]. But joint torque feedback, more directly related to effort, may promote patient activity and effort [2]. So, feedback of the mechanical work produced by muscles could motivate, connect effort with function, and counteract possible slacking from receiving physical assistance. Our purpose here is to present data supporting feasibility of stride-by-stride visual muscular work feedback during hands-on assisted locomotor training.

Methods: Healthy participants walked on a motorized treadmill at their preferred speed while a resistance band at the ankle pulled posteriorly with 3% of their bodyweight, measured by a load cell. For each participant, a target net muscular work was calculated as the force required to advance the right leg while wearing the resistance band and achieve their nominal, unresisted stride length. During training, their resisted locomotion was further challenged using a novel technique we call dysfunctional electrical stimulation (DFES) that disrupted muscular coordination by involuntarily activating the right hamstrings at the early swing phase. On a monitor, participants saw a horizontal line of their target work and a vertical bar that updated stride-by-stride with their last stride's actual work proportional to the target. Participants were instructed to oppose the resistance band and DFES so that the work bar reached the target. To simulate a clinical gait training scenario, a physical therapist assisted right leg advancement through an instrumented leg brace that measured applied forces. Participants rated their perceived exertion on each trial and completed a motivation questionnaire at the study's end.

Sagittal net muscular work calculations were made in MATLAB using the OpenSim (ver. 4.4) scripting API with right leg swing as our locomotor phase of interest; this was when the therapist assisted, the DFES was applied, and leg progression was opposed by the elastic band. During right leg stance, the inverse-dynamics problem was solved online using filtered, streamed marker and external force data to reconstruct skeletal motion via inverse kinematics with participant-specific anthropometric models [3]. Text files were written with inputs and outputs for commanding the native OpenSim API. Biofeedback was updated for the next right leg swing.

Results: We present results for three pilot participants to demonstrate the feasibility of our approach. The entire pipeline, including multiple file reading and writing operations, inverse kinematics, and inverse dynamics, for all time steps during swing was completed in less than 200ms. This was enough time to display sagittal muscular work biofeedback before the next stride was taken. The data showed that participant effort was maintained throughout practice based on consistent mechanical work values (see Fig. 1 for an example). Participants' perceived exertion increased when walking with the visual biofeedback. Questionnaire results showed participants were subjectively motivated during the task. The amount of force provided by the therapist was variable and did not always correspond to effort or work.

Figure 1: Exemplary data of one participant's right leg sagittal work during assisted swing for one trial (first 11 steps without DFES and assist excluded).

Discussion: During hands-on assisted locomotor treadmill training, it was feasible to give muscular work feedback stride-by-stride using online inverse dynamics for solving sagittal plane hip, knee and ankle torques with classical Newtonian physics. Since we were able to implement visual biofeedback that demonstrates muscular effort and is individually tailored to participants based on estimations from inverse dynamics, it provides a good motivation to use these mathematical tools for encouraging participants to achieve a movement goal not entirely based on kinematics. Additionally, though assistance forces did not greatly diminish in this preliminary sample, we observed participants maintaining a high level of muscular work during practice despite assistance. Thus, the feedback may counter the risk of "slacking off" from relying on help to move. Further investigation is necessary before testing in clinical populations.

Significance: We show the feasibility of providing online muscular work visual feedback during hands-on locomotor training without the use of a robotic device or machine learning. Our paradigm provides the opportunity to study the interaction between motor adaptation and motivation during training when providing human assistance. These early results suggest that control processes associated with adaptation to a neuromotor impairment may be influenced by feedback based on effort performance. It is possible that in improving patient motivation, motor learning will be enhanced, which could improve the generalizability of training outcomes to real world behavior. Quantifying physical therapist assistive strategies over practice is another promising avenue that could change the efficacy of delivering physical assistance on both the patient and clinician sides. Future analysis will begin to test study hypotheses when further data is collected to investigate if variations in online muscular work biofeedback changes motivation or the rate of motor learning.

Acknowledgments: NICHD support under Manczurowsky's Award F31HD110254. Content does not necessarily represent NIH views.
References: [1] Banz et al. (2008), *Phys. Therapy*; [2] Koenig et al. (2011), *JNER;* [3] Pizzolato et al. (2017), *IEEE (TNSRE)*

REAL-TIME BIOFEEDBACK DURING RUNNING IN A COLLEGIATE ATHLETE 4-MONTHS POST-ACLR

Keith A Knurr[1*], Elizabeth A Schmida[1,2], Daniel G Cobian[1], Bryan C Heiderscheit[1,2]
[1]Department of Orthopedics and Rehabilitation, University of Wisconsin-Madison
[2] Department of Mechanical Engineering, University of Wisconsin-Madison
*knurr@ortho.wisc.edu

Introduction: Altered running biomechanics following anterior cruciate ligament reconstruction (ACLR) are typically characterized by reduced peak knee flexion angles (PKF) and extensor moments (PKEM) of the surgical limb [1], with minimal changes appreciated in the non-surgical limb [2]. This asymmetrical gait pattern has been suggested to contribute to the development and progression of post-traumatic knee osteoarthritis (PTOA). As such, restoring symmetrical running biomechanics may reduce the risk for developing PTOA. Real-time biofeedback during walking has been previously implemented in individuals post-ACLR using a force instrumented treadmill [3] and an optical motion capture system [4]. Inertial measurement units (IMUs) offer a potentially more clinic-friendly alternative to provide real-time knee flexion biofeedback during running. Therefore, the purpose of this case study was to describe the application and initial efficacy of IMU derived real-time biofeedback of PKF symmetry during running in an athlete near the time of initiating running post-ACLR. We hypothesized that the athlete would partially improve between-limb symmetry in PKF, but would not fully resolve asymmetries due to the ongoing presence of quadriceps impairments [5].

Methods: The female Division I collegiate athlete in this case study underwent ACLR using a bone-patellar tendon-bone graft and had both menisci repaired. The biofeedback intervention was completed between 4- (pre) and 5-months (post) post-ACLR. Biofeedback was delivered 2-3 times per week for 4 weeks while the athlete wore a 7 sensor lower body IMU set (MTw Awinda, Xsens Technologies) and ran (session 1-5: 2.95 m/s; session 6-10: 3.35 m/s) on an instrumented treadmill (Bertec Corporation). For each session, the athlete ran for 30s without feedback, and then repeated a 2-minute run with feedback followed by a 2-minute walk five times. A final 30s run without feedback was then performed. For feedback, a custom MATLAB app displayed the average PKF of the 3 most recent strides for each limb as a bar chart. A dashed horizontal line depicted the PKF target (established from the within-session, pre-feedback, non-surgical PKF) on a screen in front of the treadmill. The athlete was instructed to attempt to bring the surgical PKF to the non-surgical limb target line while verbal cues were provided to promote this adaptation and between-limb symmetry in PKF. IMU data were simultaneously recorded throughout the duration of each session. Optical motion capture data were collected synchronously with ground reaction forces pre- and post-intervention to assess for changes in PKF between-limb difference (surgical PKF – non-surgical PKF) and PKEM limb symmetry index (LSI, (Surgical/Non-surgical)*100). In addition, the athlete performed isometric knee extensor strength and rate of torque development (RTD) assessments at 4-months post-ACLR.

Results: IMU derived PKF asymmetry improved within-session (1.6°±1.5°), but not between-sessions (Fig. 1). As the athlete explored the solution space and manipulated their gait, certain feedback trials resulted in greater reductions in asymmetry than others within and between sessions (Fig. 2). Optical motion capture revealed no improvement in PKF between-limb difference (Pre: -7.9°; Post: -9.6°) or PKEM LSI (Pre: 49.3%; Post: 47.4%) during running. Substantial deficits in surgical limb quadriceps strength (1.8 Nm/kg, 55.9% LSI) and RTD (3.75 Nm/kg/s, 30.9% LSI) were observed at 4-months post-ACLR.

Discussion: This is the first case, to our knowledge, where real-time biofeedback was implemented in attempt to improve stance phase knee flexion symmetry during running in an athlete post-ACLR. In 8 of the 10 biofeedback sessions, PKF difference improved from immediately before to immediately after the session, but no session-to-session carryover was observed. The lack of change from pre- to post-intervention may be a result of inadequate quadriceps torque production, improper dosage; and/or a lack of controlling activities (including running) outside of this intervention. This project is ongoing, and we are continuing to utilize biofeedback with this athlete and others within our institution to refine the intervention.

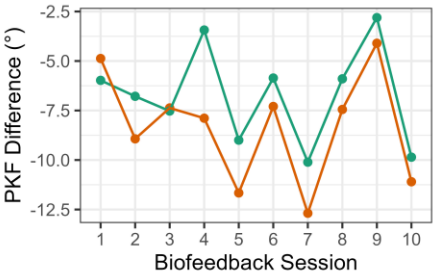

Figure 1: PKF difference immediately before (orange) and after (green) biofeedback training across all sessions (recorded by IMUs).

Significance: This case study describes an approach for delivering real-time biofeedback of knee kinematics during running for patients post-ACLR. As PTOA is a significant concern in this population, restoring symmetrical running mechanics may lead to improved long-term outcomes.

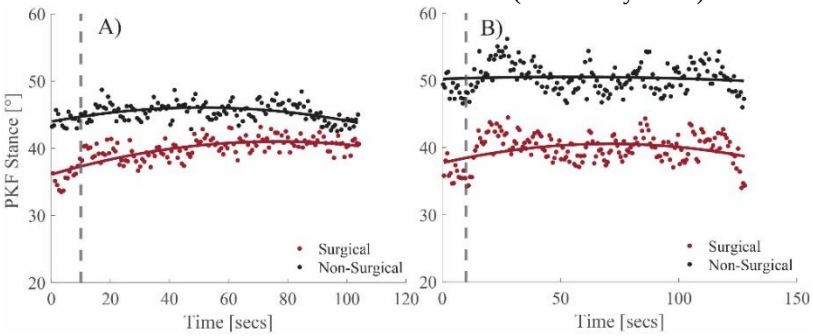

Figure 2: PKF of both limbs from IMU system for: A) positive/good adaptation to feedback; B) no/poor adaptation to feedback. Dashed line represents when the feedback was initiated.

Acknowledgments: NIH T32AG000213

References: [1] Pairot-de-Fontenay et al. (2019), *Sports Med* 49(9); [2] Knurr et al. (2021), *AJSM* 49(10); [3] Evans-Pickett et al. (2020), *Clin Biomech* 76(105014); [4] Munsch (2020), *PeerJ* 8(e9509); [5] Knurr et al. (2023), *AJSM* 51(12).

EFFECT OF CURVE RUNNING ON REARFOOT EVERSION AND TIBIAL ROTATION ANGLES

Holly Schmitz[1*], Timothy Derrick[1]
[1]Iowa State University, Ames, IA, Department of Kinesiology
*Corresponding author's email: schmitzh@iastate.edu

Introduction: Within the field of biomechanics, the kinematics of running has been widely studied to improve performance and prevent injury. One aspect of running less reported in research is submaximal running around a track or curve. When running around a curve, runners must counter a centripetal force to remain upright and follow the curve. Studies on sprinting a curve have found that this results in a larger mediolateral force, changing the lower extremity joint kinematics [1,2]. Specifically, these studies have found an increased rearfoot eversion angle on the inside leg during curved sprinting. Within biomechanical studies, the rearfoot angle is commonly used as an estimate for subtalar pronation, as it is easier to measure and a component of the three-dimensional movement. Increased ankle eversion in runners has also been associated with increased internal tibial rotation [3]. Both variables have been identified as risk factors for several running injuries, including patellofemoral pain, shin splints, and iliotibial band syndrome [3,4,5]. Long distance runners repeatedly circle a track, which could result in repetitive changes to their kinematics. If submaximal curved running increases kinematics that are known injury risk factors, distance runners may be more at risk of injury when running around a track. The purpose of this study is to identify the effect of running around a curve, equivalent to a standard 400m track on maximum rearfoot and tibial rotation angles. It is hypothesized that there will be a greater rearfoot eversion angle and increased tibial internal rotation with the curved conditions due to the increased mediolateral force generation and body lean.

Methods: Sixteen healthy runners (8M/8F; age: 20.7 ± 1.9 yrs.; height: 1.7 ± 0.1m; mass: 67.6 ± 11.0kg; weekly mileage: 37.6 ± 18.6 miles) completed this study. Kinematic data were collected using 12 Qualisys infrared cameras and ground reaction forces were captured using AMTI force platforms. Reflective markers were placed on the pelvis and lower extremity. Following a static trial, participants completed three dynamic conditions in a balanced order. The dynamic trials consisted of running in a straight line, running around a curve with the right leg on the inside, and the right leg on the outside. A 30-m curve with a 36.5-m radius was marked in white tape across the force platform on the ground and used for the two curve conditions. Participants were asked to run within ± 5% of their reported 10k training pace (4.0 ± 0.6m/s). The sacral marker was used to calculate the running velocity during the stance phase of the running cycle. Joint helical angles were calculated using singular value decomposition of segment clusters. The rearfoot angle was defined as the frontal plane angle between the tibial and calcaneus markers. The rearfoot angle and tibial rotation angles were both calculated across the stance phase, and the maximum values were averaged. A repeated measure ANOVA was used to analyze the maximum joint angles between the three conditions (straight, inside, and outside). Mauchly's test of sphericity was used to test for sphericity (α=0.05) and post hoc paired t-tests were used to compare the conditions ($p<.05$).

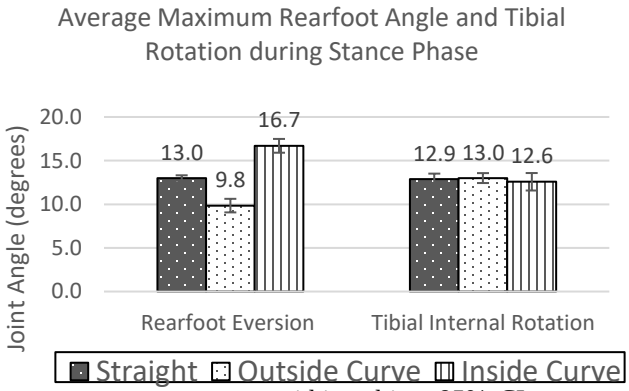

Figure 1: The average ± within-subject 95% CI maximal joint angles during running stance phase for rearfoot eversion and tibial internal rotation.

Results & Discussion: The maximum rearfoot and tibial rotation angles average and standard deviations from the stance phase are presented in Figure 1. The leg running around the inside of a curve resulted in the largest maximum rearfoot eversion angle (16.7 ± 5.4 degrees), followed by the leg on the outside of the curve (12.9 ± 5.0 degrees). Running in a straight line produced the least amount of rearfoot eversion (9.8 ± 3.8 degrees). The post hoc pairwise comparisons of the rearfoot angle showed all pairwise comparisons were significant and had large effect sizes with partial eta squared equal to 0.819. Running around a curve had no significant effects on tibial internal rotation and small effect sizes with partial eta squared equal to .014. The hypothesis that rearfoot eversion would increase around a curve was supported. While there isn't a specific increased risk threshold, previous studies have classified runners as excessive evertors when they display angles of 15-18 degrees or greater [6]. The average maximum value for the leg on the inside of the curve falls within this range. These greater ranges of eversion may subject the lower extremity tissues to more stresses and strain, increasing injury risk. The hypothesis about tibial internal rotation increasing around a curve was not supported. While ankle eversion is associated with increased tibial rotation, studies have found that the amount of eversion that transfers into tibial rotation may vary between individuals due to arch height or other coupling mechanisms [7,8].

Significance: This study provides insight into the kinematic changes in the lower extremity during curved running. It is important for athletes and coaches to understand injury risk factors to prevent injuries. Athletes developing or rehabbing from injuries associated with excessive rearfoot eversion may want to avoid track running until healthy. Further research should be done to understand the coupling mechanism between rearfoot eversion and tibial rotation, as both were not significantly increased around the curve.

References:[1] Hamill et al. (1987), *J Biomech* 38(3); [2] Alt et al. (2015), *J Sports Science* 33(6); [3]Messier & Pittala (1988), *Med and Sci in Sport &Exercise* 20(5) [4] Luz et al. (2018), *Gait and Posture* 61; [5] Mousavi et al. (2019), *Gait and Posture* 69; [6] McClay and Manal (1998), *Clinical Biomech* 13(3). [7] Nawoczenski et al. (1998), *Phys. Therapy* 78(4) [8] Hintermann et al. (1994), *Clinical Biomech* 9(6)

COMPARATIVE ANALYSIS OF COMMERCIAL ANKLE BRACES: EFFECTS ON ANKLE DEFLECTION DUE TO INDUCED ANKLE INVRESION PERTURBATIONS DURING WALKING

Soe Lin Paing[1] and Hyunglae Lee[1,*]
[1]School of Energy, Matter, and Transport Engineering, Arizona State University, Tempe, USA
*Corresponding author's email: hyunglae.lee@asu.edu

Introduction: Ankle sprain is one of the most prevalent musculoskeletal injuries, affecting over 2 million individuals in the United States annually[1]. Ankle braces are widely recommended as interventions to mitigate the risk of recurrent ankle sprains or the development of Chronic Ankle Instability (CAI)[2]. Various ankle braces, characterized by differences in material, types of restriction, support mechanisms, and design, are available in the market. Nevertheless, there remains a need to assess the efficacy of these braces in terms of mitigating excessive ankle deflection. This study aims to evaluate and compare the stabilizing effects of four commercially available ankle braces during a simulated foot-inversion movement induced on a robotic platform during walking.

Methods: Five healthy young adults (5 males, mean age: 24 years, mean height: 1.79 m, mean shoe size: US 10.2) participated in this study, which was approved by the Institutional Review Board of Arizona State University (STUDY00014244). The study utilized a dual-axis robotic platform recessed into the walkway to simulate ankle inversion during walking. An electro-goniometer was employed to measure ankle deflection during the experiment. Prior to entering the walkway and platform, subjects were equipped with safety harnesses. A metronome, set at 90 beats per minute (bpm), guided subjects to maintain a consistent cadence. Perturbations of 10 degrees in the inversion direction were applied within a time frame of 0.1 second. The onset of the perturbation is 0.2 seconds after heel strike which corresponds to roughly 50% of the entire stance phase duration assuming that the subject is walking to the rhythm of 90 bpm. There was a total of 20 perturbation trials and 20 rigid trials (without perturbation) for each brace condition. To ensure unpredictability, trials with and without perturbation were randomized. The trial order of brace conditions was also randomized for each subject.

The primary objective of this study was to assess differences in ankle deflection while wearing four different commercial braces: sleeve, strap, lace-up, and knob adjustable brace. The knob adjustable brace featured a BOA® Fit system allowing adjustable tightness, with three tightness conditions (loose, medium, and tight) were examined in this experiment. Additionally, the intrinsic condition without wearing any brace was included as a control condition for comparisons. To analyze the ankle deflection resulting from the perturbation, the maximum ankle deflection from heel strike to the end of the perturbation was calculated for each trial and averaged over 20 trials for each brace.

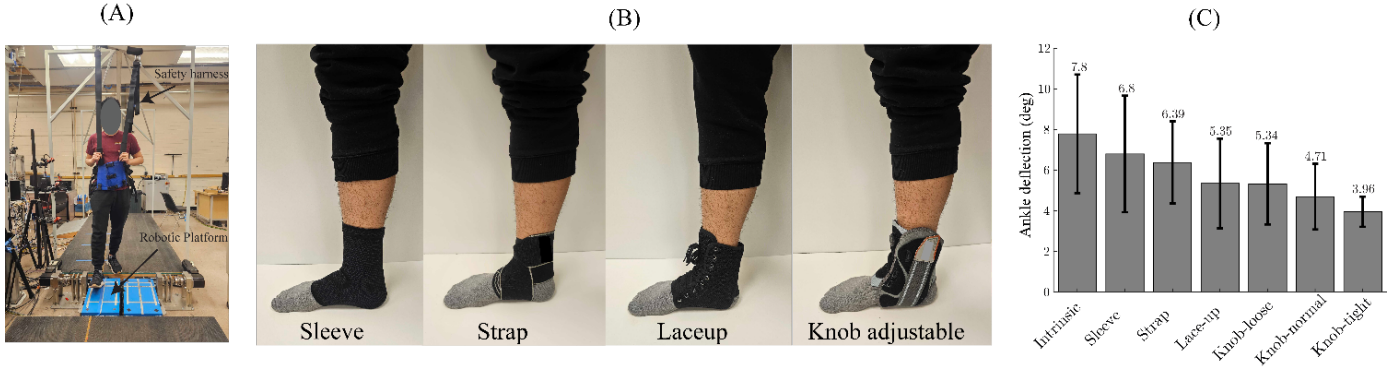

Figure 1: (A) A representative subject walking on the robotic platform. (B) Ankle brace conditions. (C) Group average results of ankle deflection using different brace conditions

Results & Discussion: Analysis of the average ankle deflection trends observed in five human subjects revealed varying degrees of support provided by all braces compared to the control condition without any brace (intrinsic). Specifically, the sleeve brace resulted in an average reduction of 13.1%, the strap brace showed a reduction of 16.4%, the lace-up brace exhibited a reduction of 29.7%, and the knob-loose, knob-normal, and knob-tight braces demonstrated reductions of 30.0%, 36.9%, and 45.2%, respectively, in ankle deflection compared to the intrinsic condition. Although statistical analysis was not feasible due to the limited number of subjects (N=5), the findings suggest that different types of ankle braces and levels of brace tightness can significantly affect the reduction of ankle deflection, thereby potentially reducing the risk of ankle sprains during physical activities.

Significance:
This study aimed to assess the effectiveness of various commercial ankle braces in providing support and reducing ankle deflection during walking, with a focus on ankle inversion simulated by external perturbations. Considering the fundamental role of walking in daily activities, the findings of this study are highly relevant to practical, real-life situations. By evaluating the impact of different ankle braces on walking, this research provides valuable insights that can guide clinicians and individuals in making informed decisions about selecting the most appropriate ankle brace, tailored to their specific needs and circumstances, ultimately aiming to prevent ankle sprains.

References: [1] Garrick JG, Requa RK. Role of external support in the prevention of ankle sprains. Med Sci Sports. 1973 Fall; 5(3):200-3. [2] Mickel TJ, Bottoni CR, Tsuji G, Chang K, Baum L, Tokushige KA. Prophylactic bracing versus taping for the prevention of ankle sprains in high school athletes: a prospective, randomized trial. J Foot Ankle Surg. 2006 Nov-Dec;45(6):360-5.

PLANTAR FLEXION STRENGTH IS RELATED TO FOOT AND ANKLE RUNNING BIOMECHANICS IN RUNNERS WITH ACHILLES TENDINOPATHY

Gustavo Leporace[1], Talissa Oliveira Generoso[1,2], Felipe F. Gonzalez, Lucas Valerio Pallone, João Emilio de Carvalho, Jonathan A. Gustafson, Eliane C. Guadagnin, Alexandre L. Godoy, Leonardo Metsavaht[1]
1 Instituto Brasil de Tecnologias da Saúde, Brazil; 2 RUSH University Medical Center, USA
Correspondence to: Gustavo Leporace, gustavo@biocinetica.com.br

Introduction: Achilles tendinopathy (AT) is a prevalent overuse injury in runners, with a multifactorial etiology. Biomechanical factors associated with AT include gastrocnemius-soleus weakness and greater rearfoot inversion at heel strike, followed by increased eversion, a shorter time to maximum eversion, and greater maximum eversion velocity through midstance [1-4]. Interestingly, others have reported increased lateral foot roll-over following heel strike in patients with AT, contradicting the often-described hyperpronation that occurs during midstance. Lastly, decreased ankle dorsiflexion range of motion (ROM) has been associated with AT [1,5,6]. Evidence suggests a complex relationship between ankle ROM, strength, and foot and ankle biomechanics [5,7,8], emphasizing the need for further comprehensive research, as identifying biomechanical factors associated with this condition may provide opportunities for injury prevention and rehabilitation strategies. This study aimed to identify the relationship between plantar flexion strength with ankle dorsiflexion ROM and other foot and ankle biomechanical parameters in individuals with AT. We hypothesized that triceps surae strength and ankle ROM would be related to the foot and ankle kinematic parameters during running.

Methods: This was a secondary analysis of a cross-sectional, prospective running study from 2020 to 2023 of patients with unilateral Achilles tendinopathy (n=18) evaluated in a motion analysis lab. Patients with rheumatological diseases, corticosteroid or quinolone antibiotic use, BMI over 35 kg/m², and conditions hindering test performance were excluded. Participants underwent treadmill running at a self-selected speed while foot and ankle kinematics were measured using a 4-camera motion analysis system (Vicon, UK). A handheld dynamometer (Lafayette, USA) was used for strength testing. Ankle dorsiflexion ROM was assessed with a digital inclinometer (Acumar, USA) in closed kinetic chain, and with the knee extended and flexed in open kinetic chain. Spearman's correlation was used to investigate the relationship between the foot and ankle kinematic parameters (Figure 1) with strength and flexibility parameters.

Results & Discussion: This study involved 18 AT patients with a mean age of 47.4 years (range 36-57), five females and 14 males. We observed that a stronger gastrocnemius led to lower ankle ($r = -0.53$; $p = 0.03$) and foot eversion ($r = -0.65$; $p = 0.00$) at initial contact for patients with AT, suggesting greater supination at initial contact. Just before heel strike and during the push-off phases of gait, the foot functions better when behaving as a rigid body, and foot supination, linked to the locking of the transverse tarsal joints, is directly associated with this motion [3].

At the same time, we found that a stronger triceps surae, more specifically the gastrocnemius, was associated with a faster eversion velocity of the foot ($r = 0.68$, $p = 0.00$), indicating accelerated foot pronation and a greater foot ROM in the coronal plane during stance ($r = 0.62$, $p = 0.01$).

Surprisingly, our study found no significant influence of ankle mobility on kinematic parameters during running. This could be attributed to the lower movement amplitude required during running compared to passive ankle ROM.

The main finding of this study is the link between relatively weaker gastrocnemius muscles and increased ankle and foot eversion at initial contact, coupled with faster foot eversion velocity. This leads to rapid pronation and a greater foot ROM in the coronal plane during stance, with a consequent whipping action and microtears in the Achilles tendon [1], potentially leading to Achilles tendon damage.

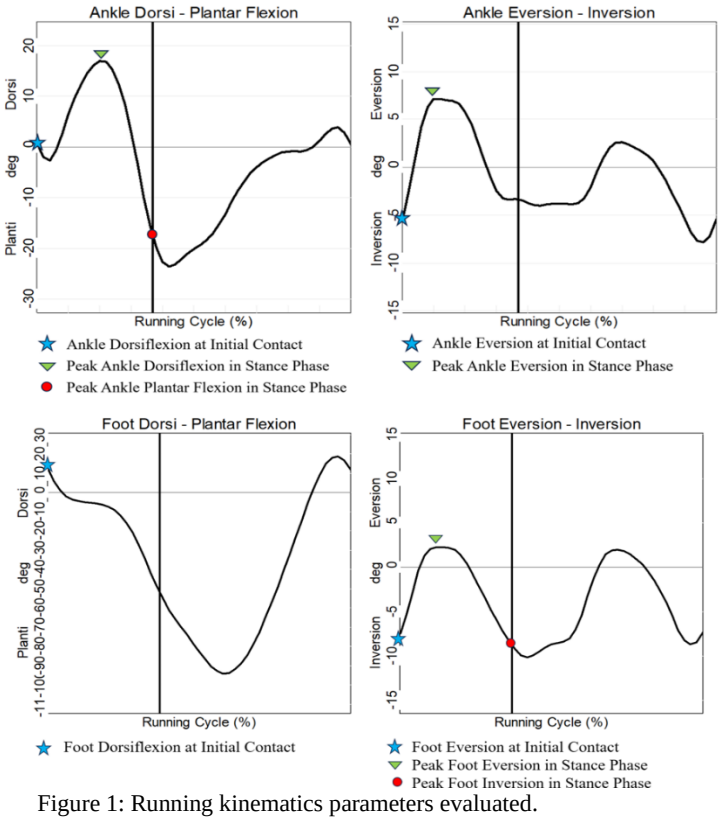

Figure 1: Running kinematics parameters evaluated.

Significance: This study showed the relationship between plantar flexor strength and range of motion with biomechanical characteristics of individuals suffering from Achilles tendinopathy during running. The identification of these biomechanical factors provides opportunities for injury prevention and rehabilitation strategies. Future studies with larger and more diverse samples could provide a more comprehensive understanding of these biomechanical factors in Achilles tendinopathy.

References: [1] Clement et al., Amer J Sports Med 1984. [2] McCRORY et al., Med&Sc in Sports & Exerc 1999. [3] James et al., Amer J Sports Med 1978. [4] Hasani et al., Sports Med 2021. [5] Mulder et al., J Sc and Med in Sport 2023. [6] Kaufman et al., Amer J Sports Med 1999. [7] Van Ginckel et al., Gait & Posture 2009. [8] Donoghue et al., Research in Sports Med 2008.

AGE INFLUENCES MUSCLE EXCITATION DURING THE FIVE TIMES SIT-TO-STAND CLINICAL TEST

Claire Beebe*, Anne K. Silverman, Michael F. Miller
Department of Mechanical Engineering, Colorado School of Mines
*Corresponding author's email: cbeebe@mines.edu

Introduction: Each year, 28-35% of people 65 and over have at least one injurious fall, which can limit mobility, reduce quality of life, decrease the ability to work, and cause loss of independence [1]. Clinical fall prediction assessments like the Five Times Sit-to-Stand (5xSTS) are accessible evaluations of gross muscle strength used to identify individuals who are at risk of an injurious fall. However, the main outcome of this assessment, time to completion, does not reveal muscle coordination or movement strategy. One stand-to-sit study showed that a shorter rectus femoris burst duration observed in older adults was linked to a reduction in time of the center of mass within the base of support, which can decrease stability during the task [2]. In a 5xSTS study of total knee arthroplasty, patients who underwent surgery had higher coactivation of the vastus lateralis and biceps femoris long head as well as a longer time to completion compared to a healthy control group [3]. These studies have shown that differences in muscle excitation between older and younger adults may explain how older populations adjust stability during sit-to-stand tasks. Thus, we evaluated lower limb muscle excitation and 5xSTS time to completion in healthy younger and older populations during 5xSTS.

Methods: Twenty-two participants were split into a younger (5F/6M, age 23.8±5.02 yrs, height 68.50±2.32 in, mass 151±27.8 lbs) and older (7F/4M, 62.1±7.82 yrs, 66.9±2.28 in, 178±47.4 lbs) group and completed 5xSTS movement trials. The participants started in a seated position with their hips and knees at 90°, feet spaced shoulder-width apart, and with arms folded across their chest. They rose from the seat to a standing position five consecutive times as quickly as possible and returned to the seat after the fifth rise. Ground reaction forces (GRFs) were collected from in-ground force plates (AMTI, 2000 Hz) synchronized with surface electromyography (EMG, Delsys, 2000 Hz) from lower limb muscles. The skin was shaved and cleaned, and then 14 wireless surface EMG sensors were placed bilaterally on the lumbar paraspinals, gluteus medius, rectus femoris, vastus lateralis, medial gastrocnemius, soleus, and tibialis anterior. Sensors were placed on each muscle belly halfway between origin and insertion and oriented parallel to the fiber direction [4]. GRFs were filtered with a 6 Hz Butterworth lowpass filter. The processed GRF underneath the stool was used to define a threshold (the weight of the stool) for first seat off and last seat on. Time to completion of 5xSTS was the duration from the first seat off to the final seat on. EMG signals were band pass filtered (4-50 Hz) and full wave rectified. For each participant, each EMG signal was normalized to its maximum linear envelope value during 5xSTS. Finally, the EMG signals were integrated over the 5xSTS time duration to calculate integrated electromyography (iEMG) values. Values for each muscle were averaged across both legs. We compared iEMG values for seven muscles and the time to complete the 5xSTS between younger and older participants with an unpaired t-test (α=0.05).

Results & Discussion: The younger group's mean (± SD) time to completion was 9.96 ± 2.47 s and the older group's mean was 10.58 ± 1.36 s. There was not a significant age effect for time to completion (p = 0.473). There was no significant difference in soleus (p = 0.783) or medial gastrocnemius (p = 0.514) iEMG between the groups. Muscle excitation for the gluteus medius (p = 0.025), lumbar paraspinals (p = 0.014), rectus femoris (p = 0.002), vastus lateralis (p = 0.011), and tibialis anterior (p = 0.038) was higher in older adults compared to younger adults (Fig 1). One older participant was removed from the lumbar paraspinals analysis due to movement artifact.

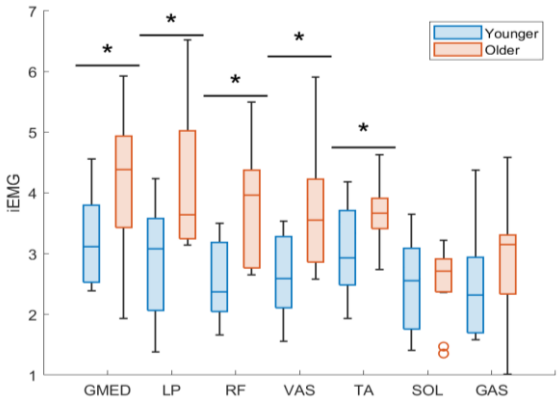

Figure 1: Mean (±SD) iEMG in younger and older adults for gluteus medius (GMED), lumbar paraspinals (LP), rectus femoris (RF), vastus lateralis (VAS), tibialis anterior (TA), soleus (SOL), and medial gastrocnemius (GAS). *Significant difference between groups (p<0.05).

Older adults required higher muscle excitation to complete the 5xSTS task in a similar amount of time as the younger participants. Higher tibialis anterior iEMG in older adults is consistent with previous studies that show the tibialis anterior is activated earlier in older adults during sit-to-stand [5]. Greater rectus femoris and vastus lateralis iEMG in the older group may be explained by coactivation as previous 5xSTS studies found higher coactivation in the vastus lateralis and biceps femoris long head in patients with total knee arthroplasty [3]. Hip abductors and back extensors contribute to postural control, which is important in 5xSTS. Greater excitation from the gluteus medius and lumbar paraspinals in older adults may indicate a compensation for potential muscle weakness [6,7], while still effectively controlling torso motion. No difference in soleus and medial gastrocnemius excitation between groups may be due to feet being planted during 5xSTS, and thus requiring low ankle plantarflexor demand. Future work will link body kinematics and net joint moments to the iEMG results.

Significance: Older adults complete 5xSTS in a similar amount of time as younger adults while using greater muscle excitation.

References: [1] "WHO global report on falls prevention in older age," World Health Organization, 2007; [2] J. Whitall, et al., Gait and Posture, vol. 86, 2021; [3] B. Davidson, et al., Journal of Electromyography and Kinesiology, vol. 23, 2013; [4] Konrad, 2005; Perotto, 2011; SENIAM, 1999; [5] P. Santos, et al., Frontiers, vol. 13, 2021, [6] M. Arvin, et al., Clinical Biomechanics, vol. 37, 2016, [7] R. Parreira, Eur J Appl Physiol, vol. 113, 2013.

THE IMPACT OF DATA AGGREGATION ON FEATURES OF A DECOMPOSITION-BASED GAIT ANALYSIS APPROACH IN HEALTHY SUBJECTS

Kübra Akbaş[1] and Jean-François Daneault[1*]
[1]Department of Rehabilitation and Movement Sciences, Rutgers University School of Health Professions, Newark, NJ 07107
*Corresponding author's email: jf.daneault@rutgers.edu

Introduction: Quantification of physical ability is a critical component in providing necessary care to patients with motor disorders. Core aspects of a person's motor capabilities can be gleaned from their walking patterns, which has driven great advancements in lower-limb gait analysis [1]. Common gait parameters in these analyses include linear metrics like walking speed or stride length however, nonlinear dynamics also need to be considered to fully study gait, due to the complexities of the underlying interconnected physiological systems. Considering the nonlinear dynamics of movement can address issues such as the nature of movement generation and investigate the time-dependent evolution of movement [2], a novel approach based on breaking down motion into sub-movements (called "movement elements") has been developed. This method has been successful in quantifying variations in motor function, such as ataxia severity [3] and upper-limb impairment in stroke survivors [4]. This decomposition-based approach draws from the central nervous system's (CNS) ability to integrate smaller processes for the execution of complex motor tasks [5]. Here, our aim is to apply this approach for the analysis of lower-limb kinematics in healthy subjects and investigate the impact of different data aggregation methods.

Methods: Kinematic data of variable speed treadmill walking was collected from 9 healthy adult subjects. Trials were then separated into swing and stance phases using the Coordinate-Based Treadmill Algorithm outlined in [6]; swing phases were used for this analysis. Left and right ankle marker velocities (w.r.t. the midpoint of the ASIS markers) in all three directions (x, y, and z) were first segmented into movement elements by identifying their zero-velocity crossing points (Figure 1). Movement elements were kept based on two criteria: 1) distance traveled during the element must be farther than 1 mm and 2) total time duration of the element must be longer than 80 ms. Each individual movement element was then time-normalized to contain 100 datapoints, and spatially normalized using the element's maximum velocity. For each normalized movement element, 184 statistical features were extracted in Python using the TSFEL package [7]. At the trial and subject levels, statistical aggregations—mean, median, interquartile range, and standard deviation—were obtained for each extracted feature across all movement elements corresponding to the group of interest (i.e., trial or subject), leading to a new total of 736 features. These trial- and subject-level aggregations were then compared to determine any significance in grouping level.

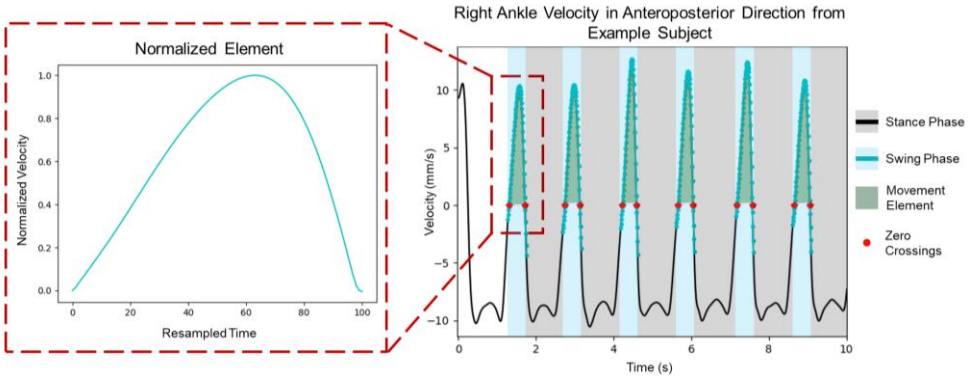

Figure 1: Right ankle velocity from the beginning 10-second portion of a subject's treadmill trial is presented on the right, where the swing and stance phases are separated, and zero-crossings are indicated in red. The first normalized movement element obtained from this trial is shown on the left.

Results: In total, there were 268 trials across all 9 subjects. There were 53,378 movement elements, which were then aggregated into 268 trials and 9 subjects. Each feature was then compared between the trial- and subject-level aggregations to determine differences between the two methods. Mann-Whitney U tests were used for most of the grouping comparisons, since 648 of the total 736 features were not normally distributed and did not meet the assumptions for a standard t-test. From these tests, 5.4% of the features presented a statistical significance ($p<0.05$) between trial- and subject-level groupings; some examples of significant features include entropy, median frequency, median difference, and standard deviations of FFT mean coefficients.

Discussion: Overall, we highlight the importance of comparing different levels of data aggregation in the evaluation of gait dynamics. Due to the small percentage of features with significant differences, this suggests that while the aggregation method used will not affect the outcome in most cases, feature dependent trial- and subject-level groupings could. This may provide important information when evaluating gait and functional impairments. This lays the foundation for future work involving movement elements, which can include determining the severity of a motor disorder or classifying disorders to aid in clinical diagnosis.

Significance: The presented approach can be used to advance current state-of-the-art gait analysis methods by addressing nonlinear dynamics. This approach is also generalizable to other movements outside of gait and can be extended to other areas of rehabilitation, such as postural balance and upper limb tasks—continuing to develop approaches that are accurate and precise will better help design personalized interventions for patients with mobility impairments. Additionally, better understanding how the CNS operates and how movements are integrated is translatable to related fields (e.g., neuroscience).

References:
[1] Cicirelli et al. (2021), *IEEE J. Biomed. Health Inform*. 26(1); [2] Stergiou and Decker (2011), *Hum. Mov. Sci.* 30(5); [3] Lee et al. (2022), *IEEE. Trans. Biomed. Eng.* 69(7); [4] Oubre et al. (2020), *IEEE Trans. Neural Syst. Rehabil. Eng*. 28(3); [5] de Lemos Fonseca et al. (2020), *Eur. J. Neurosci*. 51(10); [6] Zeni Jr et al. (2008), *Gait Posture* 27(4); [7] Barandas et al. (2020), *SoftwareX*. 11:100456.

JOINT COORDINATION PREDICTS STRIDE VARIABILITY IN HUMAN WALKING

Aaron D. Likens[1*], Mehrnoush Haghighatnejad[1], Tyler M. Wiles[1], Seung Kyeom Kim[1], Nick Stergiou[1,2]
[1]Department of Biomechanics, University of Nebraska at Omaha
[2]Department of Physical Education and Sport Science, Aristotle University, Thessaloniki, Greece
*Corresponding author's email: alikens@unomaha.edu

Introduction: Walking requires the coordination of the upper and lower limbs to maintain proper gait patterns, optimize stability, and minimize energy consumption [1]. The movement of these body segments, individually, are dynamical systems that exhibit variability changing over time [2]. This variability is not random, and it is characterized by long-range correlations, indicating the persistence or dependence of signals across a wide range of time scales, and reflect physiological well-being [3]. One approach to quantify the temporal structure of gait variability is the Hurst-Kolmogorov method, returning a Hurst exponent (H). H classifies statistically persistent behavior ($H > 0.5$), anti-persistent behavior ($H < 0.5$), or random, uncorrelated behavior ($H = 0.5$) [4]. Considering the interplay of different limbs in the human body, understanding how they coordinate in terms of variability is crucial. We constructed a structural equation model (SEM) to investigate the coordination of joints and its relationship to global gait patterns – stride interval variability. We hypothesized that during walking (1) the range of motion (ROM) time series of most joints (lumbar, thoracic, torso, shoulder, elbow, hip, knee, and ankle joints) would exhibit a persistent behavior ($H \sim 0.7$); (2) the persistence of each joint's ROM would load on body segment specific latent variables; (3) latent variables for given body segments (e.g., lower limbs, upper limbs, and trunk) would correlate with one another; and (4) joint ROM persistence would ultimately predict global stride interval variability.

Methods: We recruited 87 healthy adults divided into three groups: 31 young adults (ages 19-35), 29 middle-aged adults (ages 36-55), and 27 older adults (ages 56-82) as part of the NONAN GaitPrint project [5]. Each participant completed 18, 4-minute walking trials at a self-selected pace on a 200-meter indoor track wearing 16 Noraxon Ultium Motion inertial measurement units recording kinematics at 200Hz. For each trial we calculated the Hurst exponent from a time series created from the ROM of each stride. H correlations were computed across all joints and stratified by age group. Additionally, (SEM) was utilized to examine the interconnections between the Hurst exponents of various joints and their associated latent variables, which include the upper limb (shoulder, elbow), lower limb (hip, knee, and ankle), and trunk (lumbar, thoracic, torso). This analytical approach allowed for a comprehensive investigation into the changes in the range of motion (ROM). Lastly, the latent variables constructed with SEM were used to build a structural model to predict stride interval H from the variability contributions of body segment latent variables.

Results & Discussion: The structural equation modeling analysis investigated the dynamics of human gait by examining the Hurst exponents of joint range of motion (ROM) in upper limb, lower limb, and torso segments, as predictors of stride interval variability. The analysis utilized a robust maximum likelihood estimator to address the hierarchical nature of the data. The model showed a generally good fit, with a Comparative Fit Index (CFI) of 0.945 and a Tucker-Lewis Index (TLI) of 0.935, indicating the model's adequacy in capturing gait variability. The Root Mean Square Error of Approximation (RMSEA) was moderately good at 0.090, and the Standardized Root Mean Square Residual (SRMR) at 0.026 supported the model's effectiveness. Significant findings emerged from the parameter estimates, notably the strong factor loadings of latent variables for each body segment, demonstrating the Hurst exponent's validity in measuring gait variability. A notable relationship was between stride interval variability and lower limb ROM variability ($\beta = 0.545$, $p = 0.039$), highlighting the lower limbs' pivotal role in gait's temporal structure; upper limb and torso regressions were not statistically significant. This suggests a nuanced coordination among gait components rather than simple linear relationships. The analysis supports the hypothesis of persistent variability in joint ROM, reflecting the human gait system's adaptive capacity for stability and efficiency. The lack of significant covariances between segments implies complex inter-segment coordination mechanisms, allowing adaptability to varying walking conditions and tasks beyond straightforward regression models.

This study illuminates the complex interplay in human gait dynamics, emphasizing the lower limb variability's causal role in determining global patterns of gait while also suggesting that coordination among body segments may promote adaptability. The age-related aspects of gait variability, suggested by the stratification of participants, though not directly addressed in the results presented, remain an important area for further analysis. Understanding how the relationships among joint ROM variability change with age can offer insights into the biomechanical and neurological aspects of aging, potentially guiding interventions to preserve mobility and reduce the risk of falls in older adults. Future research should delve further into the causal relationships within gait dynamics and explore strategies for gait training and rehabilitation, with a keen focus on aging and mobility impairments.

Significance: We provided novel evidence that, during walking in healthy adults, statistical persistence is present in all joint angles. These findings advance understanding of human gait dynamics, revealing the causal role of lower limb variability in the regulation of walking patterns and highlighting the complex coordination among different body segments is responsible for optimal variability. By elucidating the adaptive mechanisms of gait variability, this research lays the groundwork for developing targeted interventions aimed at enhancing mobility and preventing falls in older adults, thereby improving their quality of life and independence.

Acknowledgments: NSF 212491, NIH P20GM109090, R01NS114282, University of Nebraska Collaboration Initiative, the Center for Research in Human Movement Variability at the University of Nebraska at Omaha, NASA EPSCoR, IARPA.

References: [1] Meyns et al. (2013), *Gait Posture* 38, 555–562; [2] Higgins et al. (2002), *J Biol Med* 75, 247–260; [3] Hausdorff, et al. (1995), J Appl Physiol. 78, 1349–358 ; [4] Likens et al. (2023), arXiv [Preprint]; [5] Wiles et al. (2023), *Sci Data* **10**, 867.

HOW TAKE-OFF TECHNIQUE AFFECTS MUSCLE DEMAND IN THE BACK HANDSPRING STEP OUT

Gabriella H. Small, Richard R. Neptune
Walker Department of Mechanical Engineering, The University of Texas at Austin, Austin, TX
*Corresponding author's email: gsmall@utexas.edu

Introduction: While gymnasts are judged in competition based on kinematic requirements [1], they can perform a given skill using different techniques while satisfying those requirements. Given the high biomechanical demands of gymnastics, a better understanding of the differences between techniques would be valuable for targeted muscle training routines. The back handspring step out (BHS) in particular is a foundational skill in balance beam routines [1]. Previous work identified three take-off techniques that gymnasts use in the BHS [2]: Simultaneous Flexion, Sequential Flexion and Double-Bounce. These techniques generate different ground reaction force (GRF) and kinematic profiles [2], which likely influence muscle demand. Muscle demand is an important consideration due to its influence on energy expenditure and fatigue as gymnastics routines can cause high heart rates and blood lactate levels [3]. Therefore, improved efficiency while performing specific skills could reduce fatigue as it can affect technical performance [3]. Determining the muscle demand required for each BHS technique could also help improve overall performance, especially in the take-off, where the majority of the power is produced. Therefore, the purpose of this study was to quantify the influence of BHS take-off technique on muscle demand using modeling and simulation. We hypothesized that the Simultaneous Flexion technique would have the lowest muscle demand among the take-off techniques due to its lower GRF peaks and impulses [2].

Methods: Simulations were generated using previously collected experimental BHS data [2] of twenty-one female gymnasts (age: 15.3±3.6 years, mass: 49.6±9.6kg, height: 154.0±7.2cm, gymnastics skill level (1-10): 8.3±1.2) performing a BHS on a balance beam. Gymnasts were grouped by technique based on their kinematics [2]. A 12-segment musculoskeletal model in OpenSim 4.4 [4,5] was used to simulate the BHS take-off. Static optimization estimated the muscle forces at each time step. Muscle power was then calculated as the product of the musculotendon force and velocity. The positive and negative muscle power were each integrated over the take-off phase and averaged across the legs to determine the work done, which was used as the measure of muscle demand. Muscles were combined into groups with similar biomechanical functions and work was summed within each group. Analyses of variance and Tukey follow up tests were used to assess differences in muscle demand across techniques.

Results & Discussion: Overall, differences in total muscle demand across techniques were small (Fig. 1a), which may partly explain why gymnasts self-select different take-off techniques [2]. However, there were slight differences for specific muscles (Fig. 1b), partially supporting our hypothesis. The vasti (VAS) generated both high positive and negative work across techniques due to its important role in controlling the body's forward rotation and extending the knees at the end of take-off. The Double-Bounce technique had higher VAS work than the other techniques (Fig. 1b) as the extra bounce required gymnasts to decelerate their downward motion twice. The Sequential Flexion technique had higher iliopsoas (IL) work than the other techniques (Fig. 1b), due to the large trunk flexion without knee flexion in this technique. Thus, IL required more muscle demand to maintain balance over the base of support, similar to its role in horizontal jumping [6]. Furthermore, the plantarflexor group (PF) had high positive and negative muscle work in all techniques, likely due to its role in propelling the body upward like in other tasks such as walking [7]. The hamstrings (HAM) and gluteus maximus (GMAX) groups together had moderately high work across the three techniques (Fig. 1), which is consistent with previous analyses of jumping that found GMAX and HAM were crucial in propelling the trunk upward [8].

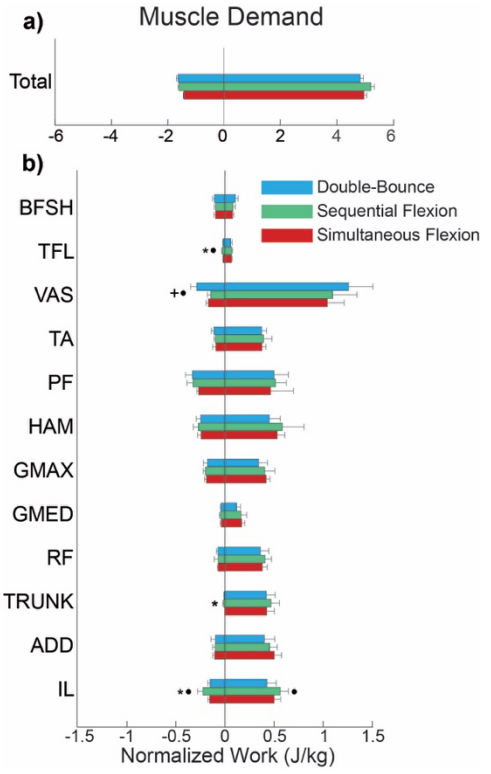

Figure 1: Muscle demand normalized by body mass for each gymnast. "*" = difference between Simultaneous and Sequential Flexion. "+" = difference between Simultaneous Flexion and Double-Bounce. "·" = difference between Sequential Flexion and Double-Bounce of $p < 0.05$.

Significance: Given the importance of the BHS as a foundational skill in balance beam routines, a better understanding of the underlying roles of the individual muscles in performing the BHS is crucial. While the differences in muscle demand were small across the take-off techniques, there were important individual muscle differences that gymnasts and coaches should consider when training. Regardless of the take-off technique used, VAS, PF, GMAX and HAM required the highest muscle demand. These results provide further insight into the muscle demand necessary to perform a BHS and guidelines for training regimens aimed at improving the BHS performance.

Acknowledgments: This work was supported in part by the NSF GRFP.

References: [1] FIG (2022). Fédération Internationale de Gymnastique Code of Points; [2] Small & Neptune (2024), *Sports Biomech* in review; [3] Marina & Rodríguez (2014), *Biol. Sport* 31; [4] Delp et al. (2007) *IEEE Trans. Biomed. Eng* 54; [5] Seth et al. (2018) *PLoS Comput. Biol.*14; [6] Nagano et al. (2007) *Biomed. Eng. Online* 6; [7] Neptune et al. (2001), *J. Biomech.* 34; [8] Pandy & Zajac (1991), *J. Biomech.* 24;

RELATIONSHIPS BETWEEN GYMNAST DEMOGRAPHICS AND CARTWHEEL BALANCE CONTROL

Emma S. Tyler[1*], Gabriella H. Small[2], Richard R. Neptune[2]
[1]Department of Biomedical Engineering, The University of North Carolina, Chapel Hill, NC
[2]Walker Department of Mechanical Engineering, The University of Texas at Austin, Austin, TX
*Corresponding author's email: etyler@unc.edu

Introduction: A cartwheel is a fundamental skill in women's gymnastics commonly featured in balance beam routines [1] and is often used to predict future skill development. Cartwheel performance is quantified by requirements in the Code of Points [1] and requires tightly maintained balance control. Whole-body angular momentum (*H*) has been used as a measure of balance control [2], where higher ranges of frontal plane *H* correlate with lower clinical balance scores, indicating poorer balance control [3,4]. Conversely, higher ranges of sagittal plane *H* have been correlated with higher skill levels in other gymnastics elements, representing increased confidence as gymnasts produce greater motions about their body center of mass [5]. Improving balance control is also crucial to reduce fall and injury risk. Furthermore, young gymnasts, especially female gymnasts ages ~12-15 years, have a higher risk of overuse and musculoskeletal injuries due to their developing bodies [6,7], which could affect their balance control. More skilled gymnasts usually have more training in performing cartwheels and may generate more sagittal plane *H* along the beam, while reducing frontal plane *H*. Therefore, there may be differences in the gymnasts' ability to control balance as they increase in height with age. The purpose of this study was to evaluate the relationship between gymnast level, height and age with cartwheel balance control. We hypothesized that gymnast level, height and age would have a positive correlation with sagittal plane *H* and a negative correlation with frontal plane *H*.

Methods: Twenty-seven female gymnasts (age: 16.2 ± 4 years; height: 154.7 ± 7.2 cm; mass: 50.6 ± 9.2 kg; skill level (1-10): 8.2 ± 1.3) performed six cartwheel trials on a 9'x4", high density foam beam mounted on the floor. Kinematic data were collected with 61 reflective markers recorded with 12 cameras at 120 Hz. Trials where the gymnast did not land on the beam were excluded, resulting in 98 total cartwheel trials, which were averaged across each gymnast. Linear regression analyses were used to determine the relationship between the gymnast's level, height and age and cartwheel balance. Cartwheel balance was quantified using the frontal and sagittal plane range of *H* normalized by gymnast mass and height.

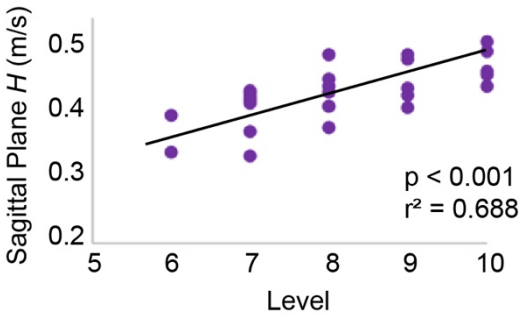

Figure 1: Sagittal plane whole body angular momentum (*H*, normalized by mass and height) is correlated with skill level (1-10).

Results & Discussion: In agreement with our hypothesis, increased skill level was correlated with larger sagittal plane *H* ($p < 0.001$, $r^2 = 0.688$, Fig. 1), highlighting that higher skilled gymnasts perform more dynamic cartwheels. This correlation is consistent with previous work that found a similar correlation in sagittal plane *H* and skill level for the more advanced back handspring on the balance beam [5]. Furthermore, increased gymnast height was also associated with larger sagittal plane *H* ($p = 0.003$, $r^2 = 0.557$, Fig. 2) due to the greater segmental moments of inertia and segmental velocities of the taller gymnasts. Unlike skill level or height, age was not correlated with sagittal plane *H* ($r^2 = 0.156$), likely due to gymnasts specializing at a young age, and thus expected motor learning differences across age were not seen [5]. Contrary to our hypothesis, gymnast level, height and age were not correlated with frontal plane *H* ($r^2 = 0.187$, $r^2 = 0.156$, $r^2 = 0.029$, respectively), likely because only successful cartwheels were included in these analyses, which highly constrain the frontal plane motion to remain on the narrow balance beam.

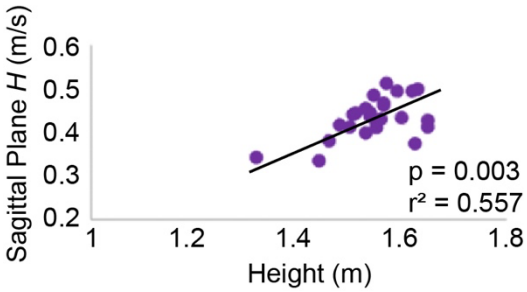

Figure 2: Sagittal plane whole body angular momentum (*H*, normalized by mass and height) during the cartwheel is correlated with gymnast height.

Significance: Considering the widespread interest and potential injury risk associated with gymnastics balance beam routines, these results give insight into the relationships between balance control and gymnast demographics. This analysis found no relationship between gymnast age and cartwheel balance control. However, taller and higher skilled gymnasts were able to perform more dynamic cartwheels along the beam. These differences in balance control can be used as an assessment of whether gymnasts are becoming more skilled on the balance beam, especially before more advanced skills are attempted.

Acknowledgements: This project was supported in part by the NSF GRFP.

References: [1] FIG, 2022. Fédération Internationale de Gymnastique Code of Points. [2] Neptune & Vistamehr. J. Biomech. Eng. 2019;141. [3] Nott et al. Gait & Posture 2014; 39. [4] Vistamehr et al. J. Biomech. 2016;49. [5] Small & Neptune. Sports Biomech. 2024 (in review). [6] Brüggemann. ISBS 2010; 28:108-111. [7] Bradshaw & Hume. Sports Biomech. 2012; 11(3):324-341.

THE EFFECT OF DYNAMIC TREADMILL WALKING ON CENTER OF MASS DISPLACEMENT: A FEASIBILITY STUDY FOR A NOVEL APPROACH

Stephanie N. Mace[1*] & David C. Kingston[1]
[1]Department of Biomechanics, University of Nebraska at Omaha, Omaha, NE, US
*Corresponding author's email: smace@unomaha.edu

Introduction: Cerebral palsy (CP) is the most common neuromuscular disability affecting a child's overall mobility and balance [1,2]. Roughly 80% of these children are diagnosed with spastic CP resulting in high muscular tone, overall weakness, and joint contractures that further impair motor control and development [3,4]. Treadmill gait training is a common therapeutic intervention allowing task-specific motor practice via repetitive movements for skill acquisition [5,1]. We speculate that this rehabilitation paradigm can be enhanced by integrating continuous multi-directional surface perturbations via roll and pitch that challenge balance in the anterior-posterior (AP) and medial-lateral (ML) directions. Therefore, this feasibility study aimed to develop a method of multi-directional surface perturbations, observe typically developing responses, learn from our assumptions, and iterate before implementing for pediatric clinical populations.

Methods: Two approaches were developed that consisted of treadmill walking on the Computer Assisted Rehabilitation Environment (CAREN; Motek, Amsterdam, Netherlands). Participants were instrumented with 54 retroreflective markers on their trunk and lower extremities to record estimated center of mass (CoM) displacement in the AP and ML directions. For the first approach, six healthy young adults (3M:3F, age: 26.5 ± 4.67 years; height: 1.68 ± 0.11 m; weight: 65.49 ± 16.45 kg) completed four 3-minute trials (U0, U1, U2, and U3) at their preferred walking speed (1.25 ± 0.08 m/s). Markers on the trunk and pelvis were used to determine the CoM position controlling a reactive walking surface perturbation. U0 consisted of none, but U1, U2, and U3 consisted of walking surface perturbations driven by CoM movement in which ML perturbations (roll) were driven by CoM sway and AP perturbations (pitch) were driven by the CoM fore-aft location on the treadmill. Furthermore, the sensitivity of the perturbations increased from 120% (U1), 160% (U2), and 200% (U3), with higher percentages creating more and faster walking surface movement. For the second approach, one healthy young adult (F; age: 20.91 years; height: 1.58 m; weight: 48.67 kg) completed seven trials at their preferred walking speed (1.25 m/s) on the CAREN with two 3-minute static walking trials and five 3-minute trials consisting of a progressive walking surface perturbation driven by two sinusoidal waves for pitch and roll (Pitch: 6*SIN(1.6*TIME); Roll: 6*SIN(0.8*TIME).

Results & Discussion: Participants in the first approach walked more anteriorly, which caused most participants to walk on a decline across all perturbation trials (Figure 1; U1: 15.05°; U2: 17.65°; U3: 18.97°). The second approach had the participant CoM slightly anterior to the treadmill origin and exhibit CoM displacement along both AP and ML directions while experiencing a maximum pitch and roll of 6°. As the participant gained repeated exposure to the fixed perturbation, they still exhibited CoM displacement in the ML and AP directions. Although the first approach uniquely implemented an individual's self-selected positioning on the walking surface, the declined walking surface and lack of ML and AP perturbations suggest we may not observe the desired effects that the second approach provided. Furthermore, the second approach allows for participant progression through modifications of the amplitude (degree of pitch and roll) to make the walking surface perturbation more challenging as their time to exposure and experience increases. The adaptability of the input parameters allows for subject-specific rehabilitation, which in turn could increase the benefits of this type of rehabilitation paradigm for pediatric clinical populations.

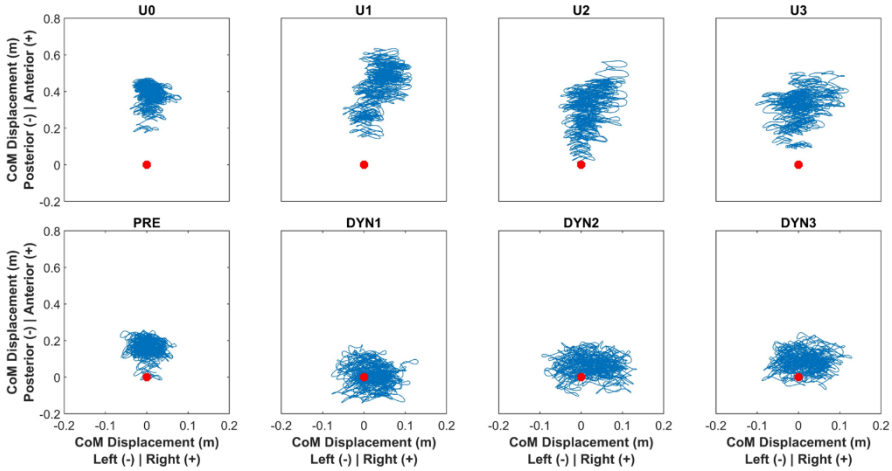

Figure 1: Visualization of CoM displacement (blue) during approach 1 (top row) and approach 2 (bottom row) of a single representative participant. Red dot indicates the treadmill origin (0,0) of walking surface. A static walking trial and three dynamic trials from both approaches are shown for comparisons.

Significance: Our results suggest that defining continual rolling and pitching of the walking surface based on a fixed path rather than self-driven movements would allow for assessing CoM displacement and challenges to walking mechanics, which may be used as a rehabilitation tool in pediatric clinical populations. To gain insight into how these fixed walking surface perturbations can be used to benefit gait and balance, additional data with typically developing children and children with CP will be collected.

References: [1] Novak et al. (2020), *Neuro Reports* 20(2); [2] Saxena et al. (2016), *Phys and Occu Ther in Peds* 20(3); [3] Campbell et al. (2012), *Phys Ther for Children*; [4] de Mello et al. (2014), *Research in Dev Disabilities* 35(10); [6] Booth et al. (2018), *Dev Med & Child Neuro* 60(9).

AUGMENTED REALITY FOR IMPROVING RESPONSE TIME WHILE NAVIGATING WATERCRAFT

Victoria Jolliff[1], Kevin Hernandez[2], Peter Crane[2], Stacie Ringleb[1*]
[1]Old Dominion University, Norfolk VA [2]Virtual Reality Rehab, Inc., Clermont FL
*Corresponding author's email: sringleb@odu.edu

Introduction: Marine and watercraft operators often face rapid decision-making in high-stress environments, which has driven the evolution of marine navigation instruments from basic tools like compasses to advanced technology [1]. Augmented reality (AR) can enhance situational awareness by overlaying geolocated synthetic vision onto a display [2], thus allowing for more information to be provided to an operator. For example, essential data for watercraft operators includes, but may not be limited to, speed, direction, GPS coordinates, hazard avoidance, and navigation path. Navigation performance and hazard identification are critical in maritime scenarios, where real-time feedback and efficient cognitive processing are necessary for mission success. Careful consideration must be given to understanding the trade-offs between enhancing performance, while avoiding cognitive overload.

This study focuses on assessing two AR navigation features to minimize steering a watercraft close to a hazard—minimaps and gaze guidance lines (GGLs) (Figure 1) [3]. Minimaps are condensed views of surroundings, while GGLs connect targets on the minimap to their physical locations, aiming to improve response time and accuracy as stated in the proximity compatibility principle [4]. We hypothesize that the integration of these AR features will improve situational awareness for target identification and reduce response time for marine operators.

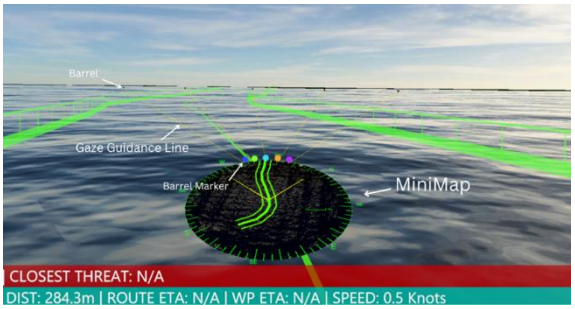

Figure 1: Augmented reality navigation system features including minimap, gaze guidance lines, and AI safe lanes. Gaze guidance lines connect the barrel markers on the minimap to the barrel location on the shore.

Methods: The study utilized HoloWarrior: Single Amphibious Integrated Precision Augmented Reality Navigation (SAIPAN), an augmented reality marine navigation system enabling users to simulate maritime missions by inputting coordinates. Fourteen participants (7 female, aged 18-26) completed three simulation trials driving a boat to shore while identifying five uniquely colored barrels placed on the shoreline. Each trial featured AR "safe lanes," which warn the navigator if the watercraft is traveling too close to a hazard and minefields. Data were collected during three conditions (minimap and gaze guidance lines (MM+GGL), minimap only (MM), or control). Barrel identification was evaluated by reaction time and distance from shore, standardized across scenarios.

Results & Discussion: The mean time it took to accurately observe a barrel were recorded. The average reaction time for participants who correctly identified targets under the MM+GGL condition was 1.50 seconds (SD = 0.72. In contrast, participants in the MM only condition and the control group exhibited mean reaction times of 2.29 seconds (SD = 1.26) and 2.57 seconds (SD = 1.68), respectively.

Additionally, the average number of correctly identified barrels were identified across the experimental conditions. Participants utilizing both the minimap and gaze guidance lines achieved an average of 4.85 correctly identified barrels out of 5 (SD = 0.36). With the minimap alone, participants identified an average of 4.43 barrels correctly (SD = 0.65), while those without the minimap identified only 3.21 barrels correctly (SD = 1.37).

The integration of gaze guidance lines with the minimap reduced reaction times and improved barrel identification accuracy. Participants benefited from MM+GGL by quicker response times and higher accuracy rates compared to MM only and control conditions. These findings highlight the efficacy of combining visual cues such as gaze guidance lines with minimap interfaces to optimize attentional focus and enhance task performance in dynamic environments.

Significance: The integration of gaze guidance lines with minimap interfaces carries significant implications for military applications, especially in dynamic and high-stakes environments where split-second decisions and precise target identification are critical. While minimaps are a common feature in many current navigation systems [5], gaze guidance lines are still novel to AR marine navigation and would benefit from additional validation [3]. By combining gaze guidance lines with minimaps, military personnel have the potential to enhance their operational effectiveness and success across various scenarios. Future studies will be able to compare the differences between the use of AR systems and traditional tools to help military personnel maintain their musculoskeletal health during mission in rough water.

Acknowledgments: This research was partially funded a by VRR's IR&D and a Small Business Innovation and Research (SBIR) Phase II contract with the Marine Corps Systems Command (MARCORSYSCOM), contract # M6785422C6504, topic N202-090 "Single Amphibious Integrated Precision AR Navigation (SAIPAN) System".

References: [1] Francesco et al. (2021), *J. Navigation* 74(5); [2] Wickens et al. (2023), *Hum Factors* 65(4); [3] Mifsud et al. (2022), *Proceedings of the Human Factors and Ergonomics Society Annual Meeting* 66(1); [4] Wickens, C. D., & Carswell, C. M. (1995), *Hum Factors* 37(3); [5] Schreiber et al. (1998), *Hum Factors* 40(2)

A BIOMECHANICS FRAMEWORK FOR ENCOURAGING CURIOUSITY IN ENGINEERING EDUCATION

Mikayla R. Hoyle[1*], Melany D. Opolz[2], Nikhil C. Admal[1], Wayne Chang[3], Shelby B. Hutchens[1], Blake E. Johnson[1], Gabriel Juarez[1], Brian S. Mercer[1], Matthew West[1], Mariana E. Kersh[1, 4]
[1] Dept. of Mechanical Science and Engineering, [2]Dept. of Chemical and Biomolecular Engineering, [3]Dept. of Aerospace Engineering, [4]Beckman Institute for Advanced Science and Technology; University of Illinois Urbana-Champaign, Urbana, IL
*Email: mrhoyle2@illinois.edu

Introduction: Teaching methods that emphasize theory without inclusion of practical applications can make the transition to industry challenging for both students and employers. Research and design engineering has moved to smaller, entrepreneurial companies where engineers may be asked to also take on business roles, and the transition to such roles is enabled by the development of an entrepreneurial mindset (EM) [1, 2]. The EM is a framework, focusing on the social and societal components of entrepreneurship, to stimulate curiosity, build connections, and demonstrate how courses create value (3Cs) for students [3]. Biomechanics-based examples are an ideal platform for the EM framework because they are intuitive and engaging applications of engineering principles. Therefore, the aims of this study were to (1) evaluate students' perceptions of the 3Cs and (2) use an EM framework for integrating real world problems.

Methods: We collected survey data from 264 students (female = 40, male = 222, neither/no answer = 4) enrolled in Statics at UIUC in the Fall of 2023. We asked 4 questions on a Likert Scale from 1 to 5 (strongly disagree to strongly agree):

Q1, create value: "I see how the content in this class helps engineers and scientists tackle major world challenges".
Q2, connection: "Outside of class, I understand how course concepts connect to the design and engineering of everyday objects".
Q3, curiosity: "The content in this class stimulates my curiosity about real-world problems".
Q4, create value: "The content in this class will be helpful for my future career as an engineer".

The Kolmogorov Smirnov (KS) test was used to compare the distributions of the survey responses ($p<0.05$, R v4.3.1). We used the grand challenges selected by the National Academy of Engineering (NAE) and the National Science Foundation (NSF) to identify a central theme that can be used to integrate across course concepts with a focus on biomechanics examples.

Results & Discussion: Students tended to agree/strongly agree (Fig. 1A) with the relevance of course content to world challenges (Q1, mean = 3.91), design/engineering of everyday objects (Q2, mean = 3.97), and students' future career (Q4, mean = 3.90). However, students agreed less that the course simulated curiosity about real-world problems (Q3, mean = 3.58, $p<0.05$). These results suggest that improvement can be made in this class to spark students' interest in real world applications. Therefore, from challenges identified by NAE, we selected the topic of exploring the universe. We next identified course content that was more theoretical in nature and revised the content to focus on fundamental engineering principals (forces in springs, rigid body equilibrium, and moments) with applications of running in space (Fig. 1B).

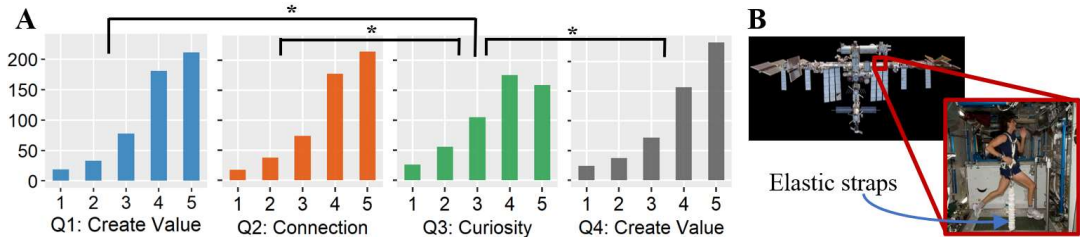

Figure 1: (A) Student impression of courses creating value, connection, and curiosity (1: strongly disagree, 5: strongly agree, *p<0.05, **p<0.001). **(B)** The international space station and running on the treadmill

Free-body diagrams (FBD): The FBD problem was initially a box held by springs and this was changed to an astronaut standing on the treadmill. To simulate gravity in space, runners wear a harness with elastic straps connected at their hips and the sides of the treadmill (Fig. 2A). We included calculating the minimum spring force to simulate gravity for Sally Ride, and a hands-on activity using springs and a pegboard to recreate the problem. Moments: Calculating the moment of a force was initially constructed using bent pipes. The problem was modified to instead calculate the knee moment during running, which included a FBD with the muscle forces, using both the scalar and vector formulation (Fig. 2B).

Significance: This work uses the EM framework of the 3Cs to incorporate more biomechanics problems into early engineering courses. By integrating this framework, it allows students to work on skills employer's value and often will pay more for [4]. For the university, it boosts 7 of the ABET learning outcomes by incorporating real world problems and altering how courses are ran [5]. Incorporating biomechanics can stimulate student interest within the field.

Acknowledgments: Funding: Kern Family Foundation, Department of Mechanical Science and Engineering

References: [1] Duval-Couetil+ *IJEE* 2012; [2] Bodnar+ *ASEE* 2018; [3] London+ *ASEE* 2018; [4] Carneval+ *Georgetown University CEW* 2020; [5] Bosman+ *Springer* 2018.

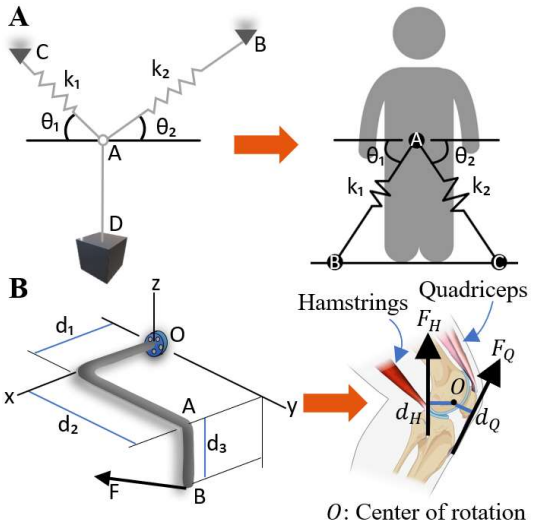

Figure 2: Transition of traditional theory (left) to application-driven examples (right). **(A)** The FBD and **(B)** moments problem.

ASSESSING THE IMPACT OF CONSECUTIVE RUNNING DAYS ON STRIDE-TO-STRIDE INTERVAL CORRELATIONS IN RECREATIONAL RUNNERS

James J. McDonnell[1*], Jennifer Sumner[2], Edward Nyman[2], Aaron Cohen[3], John, S., Raglin[1], Allison H. Gruber[1]
[1]H.H. Morris Human Performance Laboratories, Indiana University, Bloomington, IN, USA
[2]Brooks Sports Inc., Seattle, WA, USA
[3]Deptartment of Epidemiology and Biostatistics, Indiana University, Bloomington, IN, USA
*Corresponding author's email: jimcdon@iu.edu

Introduction: Training load errors are often cited as the cause of running injuries [1]. Given the multiple factors influencing mechanical stress accumulation during and between runs [2], it is challenging to identify the optimal progressive training load to enhance fitness without raising injury risk. One proposed method to identify appropriate training loads is to track changes in long-range correlations of a runner's stride-to-stride interval (α_{STRIDE}). Previous investigations have found α_{STRIDE} decreases during runs reaching a Borg rate of perceived exertion of 17 (RPE, 6-20 scale) [3]. Additionally, runners who experience maladaptation to chronic high training loads, such as decreased running performance, experience decreases in α_{STRIDE} [4]. Before α_{STRIDE} can be used to longitudinally monitor a runner's response to training, it is important to establish how α_{STRIDE} changes within and across multiple days of intense running. The purpose of this study was to examine the effect of multiple days of running and running load on α_{STRIDE}. We hypothesized that multiple runs in the lab would progressively decreases α_{STRIDE} within each run and between runs and this decrease would be larger with larger running loads.

Methods: Eighteen recreational runners ran on an instrumented treadmill (TreadMetrix, LLC, Park City, UT, USA) on three consecutive days at the speed corresponding to their first ventilatory threshold and in their preferred footwear. Runners reported RPE (6-20 scale) every five minutes during the run. The run continued until the runner: experienced an RPE of 17, ran for one hour, or reported they no longer wished to continue. Prior to each run, an inertial measurement unit (IMU, Blue Trident, Vicon) collecting at 1200 Hz was secured on the lateral aspect of the right shank. A MATLAB script was written to identify peaks in the axial acceleration recorded continuously throughout each run. Peaks were treated as the initial contact of the right foot [5,6]. Stride-to-stride interval was defined as the time between peaks. Stride-to-stride intervals were determined for the 601 strides occurring after the initial 6-minutes of the run ('start') and the last 601 strides of the run ('end'). Detrended fluctuation analysis (DFA) was then used to quantify the long-range correlations of the stride intervals (α_{STRIDE}) using 600 stride intervals and a window size from 16 to N/9 [7]. The α_{STRIDE} for the start and end of the run and the change in α_{STRIDE} between start and end was compared within and between each day of running with linear mixed effects models (α=0.05). Each model contained a random effect for subject, fixed effects for Run number (Run 1, 2, 3) and Load. Load was defined as the run's overall session RPE * run duration [8]. An interaction effect for Run*Load was included in the model to determine if the relationship between Run and α_{STRIDE} varied depending on Load.

Results & Discussion: Eighteen participants (males/females = 8/10; mean ± 1 SD: age = 28.22 ± 6.80 yrs; BMI = 23.5 ± 4.84 kg/m^2; years running = 7.94 ± 5.18 yrs; volume = 19.63 ± 8.98 mi/wk) completed three consecutive days of running. Contrary to the hypothesis, linear mixed models revealed no significant effect of Run ($p = 0.215$), Load ($p = 0.607$), or Run*Load ($p = 0.212$) on α_{STRIDE} at the start, at the end (Run $p = 0.212$, Load $p = 0.631$, Run*Load $p = 0.153$), or the change of α_{STRIDE} within each run (Run $p = 0.916$, Load $p = 0.713$, Run*Load $p = 0.887$) (Table 1). The inter-subject variability of the direction and magnitude of the change in α_{STRIDE} and the magnitudes of α_{STRIDE} at the start and the end are likely suppressing statistical significance.

Table 1: Mean ± 1 standard deviation for run duration and α_{STRIDE} values.

Run Number	Run 1	Run 2	Run 3
Load (Run Minutes * sRPE)	208.39 ± 70.67	181.59 ± 56.43	185.45 + 64.56
α First 600 Strides	0.77 ± 0.16	0.79 ± 0.15	0.78 ± 0.20
α Last 600 Strides	0.75 ± 0.18	0.76 ± 0.19	0.74 ± 0.22

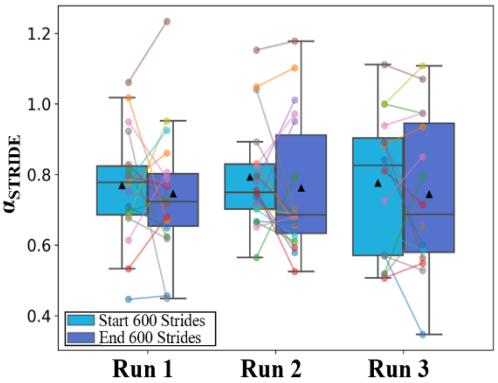

Figure 1: Box plots for the detrended fluctuation analysis results (α_{STRIDE}) for the start and end 600 stride intervals. Lines = subjects. Triangles = means across all subjects for each run.

Significance: While previous work linked decreases in stride-interval long-range correlations (α_{STRIDE}) to acute fatigue and performance decline, our results showed varied inter-individual responses within and between three consecutive days of running that detrimentally affected usability of α_{STRIDE} for tracking changes in runner's stride dynamics within and across multiple days of intense training loads. This variability may be linked with daily internal and external factors (e.g., sleep, mood states, and daily behaviors) and/or may indicate the necessity for an individualized approach when using α_{STRIDE} for training monitoring. Alternatively, α_{STRIDE} may lack the sensitivity to capture adaptations to this specific training protocol. These findings inform researchers considering α_{STRIDE} for training monitoring, and emphasize the need to consider its sensitivity across different training contexts and individual variation.

Acknowledgments: This study was funded by Brooks Sports, Inc. We thank Dr. Kiara Chan for her assistance initiating the study.

[1] Hreljac et al. (2005), *PM&R Clin* 16(3); [2] Kalkhoven et al. (2020), *J Sci Med Sport* 23(8); [3] Meardon et al. (2011), *Gait Posture* 33(1); [4] Fuller et al. (2017), *Int J Sports Physiol Perform* 12(3); [5] Kiernan et al. (2023), *Sensors* 23(11); [6] Mizrahi et al. (2000), *Hum Mov Sci* 19(2); [7] Damouras et al. (2010), *Gait Posture* 31(3); [8] Jordan et al. (2006), *Gait Posture* 24(1).

DYNAMICS OF EXOSKELETAL-ASSISTED WALKING IN FDA-APPROVED REHABILITATION ROBOTS AFTER SPINAL CORD INJURY

Gabriela B. De Carvalho[1*], Vishnu D. Chandran[2], Ann M. Spungen[3], William A. Bauman[4], Saikat Pal[1,3]
[1]New Jersey Institute of Technology, Newark, NJ, USA; [2]Hospital for Special Surgery, New York, NY, USA;
[3]James J. Peters Veterans Affairs Medical Center, Bronx, NY, USA; [4]Icahn School of Medicine at Mount Sinai, New York, NY, USA
*Corresponding author's email: gbd5@njit.edu

Introduction: Every 30 minutes someone suffers a spinal cord injury (SCI) in the United States. Currently, the only way to restore upright mobility in persons with SCI is by donning a wearable robotic exoskeleton. The growing popularity of these devices among persons with SCI necessitates quantification of the dynamics of exoskeletal-assisted walking (EAW) in FDA-approved devices. FDA approval is important because persons with SCI only have access to FDA-approved devices in clinics and for in-home use. Currently, knowledge of the dynamics of EAW from persons with SCI is non-existent. Accordingly, the **goal** of this study was to quantify the dynamics (joint kinematics and kinetics) of EAW from a person with SCI in three FDA-approved devices: ReWalk, Indego, and Ekso.

Methods: We recruited one participant with SCI (male, 49 years, 171 cm, 72.5 kg, American Spinal Injury Association impairment scale A, injury level T6, 24 years since injury) to train in EAW in the 3 FDA-approved exoskeletons. The participant provided written informed consent prior to participation in accordance with the IRB policies. Once the participant was able to walk independently in an exoskeleton, the participant's 3-D motion was recorded, including simultaneous measurements of marker trajectories, ground reaction forces, and exoskeleton encoder data. 3-D motion was collected in three separate sessions, one for each exoskeleton. A generic OpenSim musculoskeletal model [1] was scaled to match the anthropometry of the participant. Full-scale geometries of the ReWalk, Indego, and Ekso exoskeletons were integrated into the human model to create three subject-specific human-robot musculoskeletal models (Fig. 1A-C). Each human-robot model had 25 degrees of freedom to represent the human and 10 degrees of freedom to represent the exoskeleton (6 at the pelvic band to anchor the exoskeleton onto the human model, 2 at the hips, and 2 at the knees). We utilized OpenSim's Inverse Kinematics and Inverse Dynamics tools to compute joint angles and joint moments at the hips, knees, and ankles.

Results & Discussion: The subject-specific virtual simulators reproduced EAW within acceptable tolerances in all devices (average RMSE: 1.3 cm for the Rewalk, 1.6 cm for the Indego, and 1.4 cm for the Ekso). The participant experienced a lower range of motion at the knee while performing EAW in the ReWalk compared to EAW in the Indego and Ekso (Fig. 1D-F). Mean peak knee flexion angle during EAW in the ReWalk was 54.3°, compared to 65.0° and 66.1° in the Indego and Ekso devices, respectively (Fig. 1D-F). Mean peak knee extension moment during EAW in the ReWalk was 0.70 Nm/kg, compared to 0.62 Nm/kg and 0.50 Nm/kg in the Indego and Ekso devices, respectively (Fig. 1G-I). We obtained similar results at the hips and ankles during EAW (not shown here).

Significance: This study provides new insights into the dynamics of EAW from a person with SCI in commercially available robotic exoskeletons. This computational approach provides a low-risk and cost-effective technique to quantify loading in of the long bones during EAW and assess the risk of fracture in persons with SCI during EAW and other upright activities. The subject-specific virtual simulators will lay the foundation for future studies to characterize the human-robot system to improve user safety and accelerate design refinements.

Acknowledgments: VA RR&D #1 I01 RX003561; NSF GRFP 1000346414 (Fellow ID: 2022346414).

References: [1] Rajagopal et al. (2016), *IEEE Trans Biomed Eng* 63(10); [2] Chandran et al. (2023), *PLoS One* 18(2).

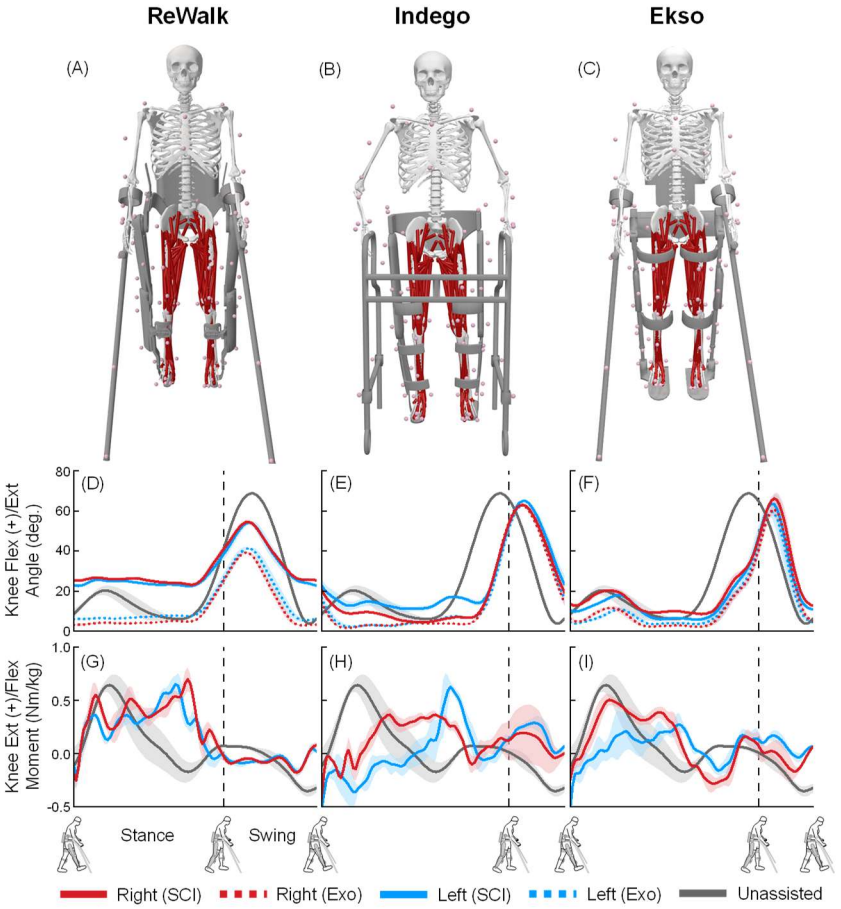

Figure 1: Subject-specific virtual simulators of EAW in the ReWalk (A), Indego (B), and Ekso (C) devices. Average (±1 SD) human and exoskeleton (Exo) knee flexion-extension angles (D-F) and moments (G-I) from EAW trials in each of the three exoskeletons. The knee flexion-extension moments were normalized to the combined mass of the user and the exoskeleton. These data were compared to unassisted walking dynamics [2]. Vertical lines represent toe-off.

EXPLORATORY FACTOR ANALYSIS OF POSTURAL SWAY MEASURES REVEAL POTENTIAL BIOMARKERS OF CHILDHOOD MENTAL HEALTH

Jenna G. Cohen[1*], Bryn C. Loftness, Ellen W. McGinnis, Ryan S. McGinnis
[1]Biomedical Engineering, University of Vermont
*jenna.g.cohen@uvm.edu

Introduction: Externalizing (e.g., ADHD) and internalizing (e.g., anxiety, depression) disorders are common in children [1], [2]. Current screening relies on parent-report surveys as children are unreliable reporters of their emotions [3], yet even the most attentive caregivers may underreport as many symptoms are unobservable [2], [3]. When presented with emotional stimuli, children with ADHD and internalizing disorders exhibit distinct bio-behavioral responses as compared to children without these disorders [4], [5]. In this analysis, we consider children's postural sway during an anxiety-inducing task. Overall, this study aims to enhance our ability to detect mental health disorders in children with ADHD, internalizing disorders, and controls by identifying objective biomarkers.

Methods: We present chest movement data from children ages 4-8 (N=94, 43% female, 19 with ADHD, 34 with internalizing disorders) during the three phases of the Speech Task, adapted from the Trier Social Stress Task. In this three-minute task, children are told they will be judged while telling an impromptu story. Two startling buzzers sounded halfway through the task (end of phase 1, start of phase 2) and with 30 seconds remaining (end of phase 2, start of phase 3). Child mental health diagnoses were established via a gold-standard semi-structured interview (KSADS-PL) with clinical consensus. Exploratory factor analysis (via principal component analysis) was used to reduce sixteen postural sway features derived from chest accelerometer data [6] into three factors, together explaining 78.2% of the variance. Repeated measures ANOVA were performed to compare children with ADHD, internalizing disorders, and controls across task phases.

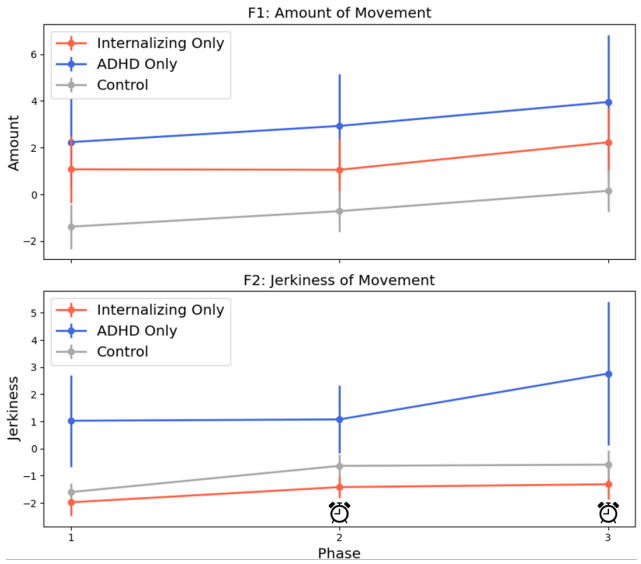

Figure 1: Mean and standard error of Amount (top) and Jerkiness (bottom) of Movement at each of the three Speech Task phases for children with only internalizing disorders, only ADHD, and controls.

Results & Discussion: The sixteen chest-based postural sway features reduced to the following three factors: Amount (F1), accounting for 42.5% of variance; Jerkiness (F2), accounting for 24.7%; and Complexity of Movement (F3), accounting for 11.0%. Amount of Movement describes intensity and size of movement as it was mainly determined by power, path, root mean square, and mean velocity. Jerkiness describes dynamic frequency characteristics of movement as it was mainly determined by frequency dispersion, range, centroidal frequency, and jerk. Complexity describes irregularity and unpredictability of the acceleration signal as it was primarily determined by sample entropy. Children with ADHD and/or an internalizing disorder had a significantly greater Amount of Movement than the control group ($p=0.02$, Fig. 1). Children with only ADHD (no comorbid internalizing disorder) had a significantly greater Jerkiness ($p=0.004$) and lower Complexity ($p=0.01$) than those with only an internalizing disorder. While children with only ADHD had a significantly greater Jerkiness than the control group ($p=0.01$), there were no other significant differences between ADHD or internalizing groups as compared to the control group for Jerkiness or Complexity of Movement. These results suggest that children with ADHD have more intense and dynamic movements as compared to children without disorders and those with only internalizing disorders. Children with only internalizing disorders have more varied, unpredictable movements as compared to those with only ADHD. There were no significant interactions between disorder groups and phases. Future work should leverage machine learning to develop models to predict the presence of ADHD and internalizing disorders from these factors, to support development of a more objective method for screening young children for mental health disorders. Future work could also consider movement features from other body segments to further explore how children respond to this anxiety-inducing task across diagnostic groups.

Significance: Applying exploratory factor analysis to chest-derived postural sway features created three factors that are significantly different by mental health disorder groups in a large sample of young children. The Amount factor identifies children with mental health impairment, and the Jerkiness and Complexity factors differentiate between types of mental health disorders.

Acknowledgments: Research supported by the US National Institutes of Health (MH123031) and the US National Science Foundation (2046440).

References: [1] B. C. Loftness et al. (2022), *EMBC*; [2] K. B. Madsen et al. (2018), *Eur Child Adolesc Psychiatry*; [3] B. C. Loftness et al. (2023), *IEEE journal of biomedical and health informatics* ; [4] M.G. Melegari et al. (2020), *J Atten Disord.*; [5] L. S. Wakschlag et al. (2005), *Clin Child Fam Psychol Rev* 8(3).; [6] B. M. Meyer et al. (2023), *IEEE Transactions on Neural Systems and Rehabilitation Engineering*.

LOADING RATE PREDICTION FROM SAGITTAL KINEMATIC METRICS IN RUNNERS

Cody Dziuk* and Janelle A. Cross
Department of Orthopaedic Surgery, Medical College of Wisconsin, Milwaukee, WI, USA
*Corresponding author's email: cdziuk@mcw.edu

Introduction: Excessive vertical loading rates have been identified as potential risk factors to the occurrence of running-related injuries [1, 2, 3]. In the laboratory, these metrics are measured via force plates or force treadmills. This is not always an option depending on the size and location of the lab, or budget constraints. Kinematic variables can be more accessible and less expensive to measure, with current technology providing measurements of sagittal kinematics using a phone or tablet [4, 5]. An application validated for smartphone use capable of providing accurate kinematic data could enable the prediction of loading rates based on limited kinematic input for runners. A key component of this method to reduce costs would be the development of a prediction model using data from a validated gold-standard data collection method.

Various methods have been used to predict loading rates. Neural network models trained on inertial measurement unit (IMU) data [6] have shown the ability to predict VGRFs and loading rate with high correlation. Sagittal plane kinematics combined with linear mixed-effects models have been used to predict vertical loading rate with moderate accuracy but involved pulling kinematics at multiple time points in addition to peak knee flexion, and horizontal distance between the center of mass and heel [7]. While promising, these methods require the use of expensive laboratory equipment. The goal of this study was to determine whether vertical loading rates during stance phase of running gait can be predicted based on discrete lower body sagittal kinematics at foot strike (FS) and foot off (FO), combined with subject metadata (mass, height, running speed).

Methods: A public dataset of running C3D files from the Laboratory of Biomechanics and Motor Control was analyzed for this study [8]. Eighteen healthy male runners were selected. Trials consisted of treadmill running recorded at three running speeds (2.5, 3.5, 4.5 m/s). Vertical instantaneous loading rate (VILR) and vertical average loading rate (VALR) were calculated. Two discrete time points were chosen, FS and FO. Each input vector consisted of nine metrics: hip, knee, and ankle sagittal plane angles at FS and FO; as well as subject mass, height, and running speed. Thirty strides per side were pulled at each speed for a total input dataset of 3240 steps.

An artificial neural network (ANN), random forest (RF), and support vector regression (SVR) were the chosen regression models. The training data was fed into regression models from the scikit-learn python library. Grid search cross-validation (cv = 10) was performed to determine optimal hyperparameters of each model. The set of hyperparameters that produced the highest mean cross-validation score was determined to be optimal set. Test data was then input into each optimal regression model and used for prediction.

Table 1: Results from VILR testing on the optimal regression models.

Regressor	R^2	RMSE	MAE	Loss	Bias	Variance
ANN	0.898	3.594	2.802	13.665	12.702	0.962
RF	0.907	3.483	2.691	13.055	12.329	0.726
SVR	0.890	3.671	2.836	15.300	13.268	2.033

Table 2: Results from VALR testing on the optimal regression models.

Regressor	R^2	RMSE	MAE	Loss	Bias	Variance
ANN	0.915	2.582	1.993	7.130	6.707	0.423
RF	0.923	2.503	1.942	6.661	6.281	0.380
SVR	0.906	2.665	2.052	8.140	6.964	1.176

Results & Discussion: All three regression models were able to predict loading rates with high accuracy (R^2) as shown in Tables 1 and 2. The RF had the best performance with the highest accuracy and lowest error values (root mean squared error (RMSE), mean absolute error (MAE)) for both VILR and VALR prediction. The RF also had the smallest bias and variance for both predicted loading rates.

The results showed that machine learning models can be used to predict VILR and VALR. All prediction models exhibited higher bias than variance, which could be in part due to the small magnitude of the dataset. With additional subjects and trials, bias could potentially be reduced. While the current study used data collected from a 3D optical motion capture system, only lower body sagittal plane variables were used for prediction. This deliberate choice aimed to assess model performance with limited input data. If a motion analysis application could provide validated sagittal plane kinematic data, our study suggests that optimal regression models could accurately predict VILR, and VALR with minimal hardware, thereby reducing both time and costs.

Significance: The study's findings contribute to the growing body of research on predictive models for running biomechanics, emphasizing the potential for streamlined equipment requirements and reduced costs. Recognizing the importance of understanding the association between loading rates and running injuries, the study suggests that further validation on an injured population is essential.

References: [1] Futrell et al., (2018), *Med and science in sports and ex 50*(9); [2] Johnson et al. (2020), *J Sports Med* 48(12); [3] Van der Worp et al. (2016), *J Sports Med* 50(8)**;** [4] Mousavi et al. (2020), *Phys Ther in Sport* 43; [5] Leporace et al. (2023), *J Biomech* 157; [6] Wouda et al. (2018), *Front in phys 9*(218); [7] Wille et al. (2014), *J Orth & Sport Phys Ther 44*(10); [8] Fukuchi et al. (2017), *PeerJ*(*5)*

COMPARISON OF BESS & M-CTSIB BALANCE TESTS IN UNIVERSITY STUDENTS

Ben W. Meyer[1*]
[1]Shippensburg University
*Corresponding author's email: bwmeyer@ship.edu

Introduction: The purpose of this project was to analyze the performance of university students in balance error scoring system (BESS) and modified clinical test of sensory integration of balance (m-CTSIB) tests. A recent meta-analysis indicated that balance training may enhance performance in the specific balance tasks that are trained, but may have limited effects on non-trained tasks [1]. Previous work has examined the BESS in collegiate athletes, finding a composite sway index for the BESS test of 2.43 [2]. A more recent study found a composite sway index of 1.43 for the BESS test in university athletes [3]. Other research has provided normative data (sway index = 1.0) for the m-CTSIB test [4]. In a more recent sample of university students, the composite sway index for the m-CTSIB test was 2.0 with a range from 1.3 to 3.1 [5].

This project aimed to add to the body of literature in the specificity of balance domain. Due to the most recent literature indicating that sway index values were 2.0 for the m-CTSIS and 1.4 for the BESS, it was hypothesized that participants in the present study would have composite sway index values that were larger in the m-CTSIB test than in the BESS test. In addition, due to the similar nature of the BESS and m-CTSIB tests, it was hypothesized that the relationship between the composite sway index scores on the tests would be moderate to strong.

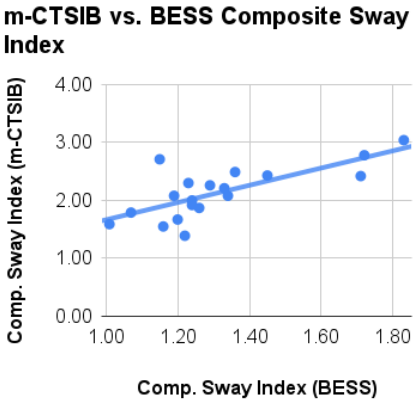

Figure 1: Relationship between composite sway index values for the BESS and m-CTSIB tests.

Methods: Eight males and eleven females (age = 21 ± 2 yrs; mass = 78 ± 16 kg; height = 1.73 ± 0.10 m) participated in the study. Participants came from a variety of backgrounds (e.g., softball, football, recreational athlete, etc.). Each participant completed the BESS and m-CTSIB tests using a Biodex Balance System SD. All participants wore athletic footwear, and the test order was randomized. The foot positioning recommendations provided by Biodex were used.

The BESS test consisted of single-leg, double-leg, and tandem stances, tested on both firm and foam surfaces for a total of six assessments. The m-CTSIB test required participants to stand in several configurations: eyes open firm, eyes open foam, eyes closed firm, and eyes closed foam for 30 seconds while maintaining upright balance on a static platform. Sway index (SI) data for each of the conditions was provided, as well as a composite measure that provided an overall indication of performance across all conditions. The composite sway index scores for the BESS and m-CTSIB tests were used for data analysis. The relationship between the BESS and m-CTSIB composite sway index values was assessed using correlation coefficients (r) and linear regression analyses. The differences between composite sway index values were assessed using paired-t tests. Statistical significance was set at $\alpha = 0.05$.

Results & Discussion: The mean composite sway index for the BESS was 1.32 ± 0.21, which is similar to the 1.43 obtained in a recent study [3]. Previous BESS testing in collegiate athletes found a larger composite sway index of 2.43 [2]. For the m-CTSIB test, mean composite sway index was 2.14 ± 0.43, which is similar to the 2.0 found in a recent study [5]. In a sample of collegiate athletes, a smaller sway index of 1.0 was obtained for the m-CTSIB [4]. Results of the paired-t test indicated that there is a significant difference between BESS (1.32) and m-CTSIB (2.14) tests, $p < 0.001$.

Results of the Pearson correlation (see Figure 1) indicated that there is a significant large positive relationship between the BESS and m-CTSIB tests ($r = 0.735$, $p < 0.001$). As the number of practitioners who utilize objective measures of balance continues to increase, it is important that the body of literature in this area grows in order to reflect the use of different tests and measures.

Significance: The results of this study add to the literature for Biodex balance tests. Balance assessments are used extensively in clinical, research, and sport settings. Both in and out of the field of biomechanics, significant time and attention is given to the improvement of balance. Prior to this study, it was unknown if there was a strong relationship between the BESS and m-CTSIB tests. Now that we have baseline sway index values for young healthy individuals, future research can examine other populations in the BESS and m-CTSIB tests.

Acknowledgements: The author would like to thank the College of Education and Human Services at Shippensburg University.

References: [1] Kummel et al. (2016), *Sports Med* 46(9); [2] Dabbs et al. (2017), *J Funct Morph Kines*; [3] Meyer (2022), *NACOB Proc*; [4] Moran et al. (2020), *Brain Inj* 34(1); [5] Meyer (2022), *J Sp Ex Psy* 44(Supp).

COGNITIVE DUAL-TASK COST DURING TREADMILL WALKING AND THE DYNAMIC GAIT INDEX: FIRST STEPS IN DEVELOPING A NOVEL WALKING ADAPTABILITY SCORE

Douglas Mitchell[1*], Francesca E. Wade[1]
[1]School of Exercise and Nutritional Sciences, San Diego State University, CA
*Corresponding author's email: dmitchell8281@sdsu.edu

Introduction: Walking adaptability is a crucial element in maintaining mobility and independence [1]. Walking adaptability allows us to adapt to the environment around us and any task demands that might be necessary, so plays a particularly important role in fall prevention and maintaining activity levels. Increased double support time variability is associated with greater fall risk [2] and reduced trailing limb angle is associated with less propulsion and slower walking speed [3], which in turn is indicative of higher fall risk. However, we do not have a comprehensive standardized method of measuring someone's capacity for walking adaptability. The Dynamic Gait Index (mDGI) is frequently used, yet this has a low ceiling effect and does not assess many domains of walking adaptability [1]. In this ongoing study, we aim to develop a comprehensive walking adaptability score through quantifying dual-task costs of different domains of walking adaptability. In this abstract, we present data on the dual-task cost of walking while talking on double support time variability and trailing limb angle and mDGI scores for our initial participants. Our working hypothesis is that greater dual-task cost will be associated with lower mDGI scores.

Methods: Participants provided written informed consent prior to data collections. Retroreflective markers were placed according to a modified Helen Hayes marker set and their motion was tracked by 9 cameras (Qualisys AB, Goteborg, Sweden). Each participant underwent the mDGI. A standardized protocol for determining preferred walking speed (PWS) was used on a single-belt treadmill (Treadmetrix, Park City, UT) and repeated for the dual-task condition. Participants walked on the treadmill for 3 minutes per task, and the first and last 30s were discarded from analysis. A visual-verbal Stroop test was performed to increase cognitive load while walking on the treadmill (WWT). Other dual-task walking conditions were collected, including walking while stepping over a foam obstacle and walking while carrying a weighted box. Performance on all 4 tasks will be assessed and summarized into a Walking Adaptability Score as the project proceeds. For this abstract, we assessed only PWS and WWT. Gait events were identified via kinematics using Visual3D, with custom MATLAB code computing double support time variability and trailing limb angle. Variability is presented as the coefficient of variation. Dual-task cost was calculated as $\frac{WWT-PWS}{PWS} \times 100$ for double support time variability and mean trailing limb angle. As more participants are collected, a simple linear regression will be run in R to investigate the relationship between the dual-task cost of double support time variability and trailing limb angle to mDGI score.

Results & Discussion: Here, we present data on our first two participants: one male (WASp01) aged 53, BMI=22.91kgm^2 , , mDGI=63 (out of 64); one male (WASp02) aged 21, BMI=25.74kgm^2 , mDGI = 57. Treadmill walking speed was 0.89 m/s and 0.67 m/s respectively, approximately 0.25 m/s slower than their overground speed. Walking speeds were slow due to lack of familiarity walking on an elevated treadmill in the lab environment. There appears to be a trend for reduced variability in both trailing limb angle and double support time during the WWT trial for WASp01 but not WASp02 (Fig 1). For trailing limb angle, the average dual-task cost was -7.60% (WASp01) and 6.23% (WASp02), while for double support time variability we found greater dual-task costs of -9.95% (WASp01) and 18.38% (WASp02). Our participant who scored lower on the mDGI (WASp02) had greater mean trailing limb angle and greater double support time variability during WWT than PWS and had a greater dual-task cost than our participant who scored higher on the mDGI (WASp01). Further, we see that double support time variability increased during WWT for one participant (WASp02), similar to that reported for stride time variability [4]. Interestingly, variability decreased during the same condition for our other participant (WASp01). If this trend continues, it may reflect differing prioritization of limited resources being allocated between gait and speech tasks between our older and younger participants. We caution overt discussion of these results due to the small sample size. Data collection is ongoing and we hope to have closer to 30 participants collected by summer.

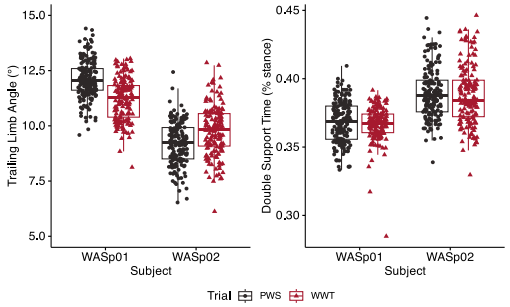

Figure 1: Box plots displaying trailing limb angle (left) and double support time (right) during the preferred walking speed (PWS, black circles) and walking while talking (WWT, red triangles) trials for two subjects. Data for individual steps are overlayed.

Significance: Our initial results indicate that dual-task cost may be related to mDGI score. If our ongoing data collections support this, it indicates that dual-task cost over multiple domains of gait may be an effective and sensitive measure of walking adaptability. This work furthers our understanding of how much capacity an individual has for responding to the world around them while walking, which is vital in fall prevention efforts.

Acknowledgments: This work is supported by the San Diego State Seed Grant (WADE242768).

References: [1] Balasubramanian et al. (2014), *Stroke Res Treat (*2014); [2] Callisaya et al. (2011), *Age aging* 4(40); [3] Hsiao et al (2015) *Hum Mov Sci* 39; [4] Al-Yahya et al (2011) *Neurosci Biobehav Rev 35*(5).

A MULTIFACETED EVALUATION OF A PASSIVE EXOSKELETON FOR LOAD HANDLING ASSISTANCE

Jangwhan Ahn[1], Hyeonhee Jung[1], Jeongin Moon[1], Jooeun Ahn[1, 2] *
[1]Department of Physical Education, Seoul National University, South Korea
[2]Institute of Sport Science, Seoul National University, South Korea
*Corresponding author's email: ahnjooeun@snu.ac.kr

Introduction: Although automation and mechanization have reduced the need for manual material handling, human labor still plays significant roles in industry owing to its adaptability and decision-making abilities. In particular, a substantial number of workers are still engaged in handling heavy loads, leading to a significant risk of work-related musculoskeletal disorders, notably low back pain (LBP). In response, passive or active back support exoskeletons (BSEs) have been developed to reduce spinal burden and prevent injuries. However, the evaluation of BSEs has mainly focused on objective measures such as muscle activation [1]. Considering the importance of the user perception, which may not be entirely reflected in the measured physiological outcomes, we aim to investigate the effect of a BSE in multifaceted aspects using both objective and subjective measures. Specifically, to take important but hitherto relatively neglected evaluation factors into account, we assessed whether a BSE may affect wearers' perceived exertion and local discomfort as well as the energy expenditure during repetitive lifting tasks.

Methods: We evaluated the assistive effect of a specific BSE, Angel Gear X (Angel Robotics, South Korea), on manual load handling. Fifteen young and healthy adult males (age: 24.5 ± 3.5 years; height: 177 ± 3.9 cm; weight: 74.4 ± 8.4 kg) participated. We measured the rate of oxygen consumption and carbon dioxide production using an indirect calorimetry equipment (COSMED K5, USA), and then estimated energy expenditure [2]. Before the first trial, participants took at least 10 minutes to adjust to the BSE. Six blocks of trials were included throughout the entire session, and each block included 40 repetitions of lifting a 10kg load from ankle height to a waist height table and then lowering it oppositely with or without the BSE. The six blocks alternated between with-device (W) and without-device (W/O) conditions with a start condition randomly chosen between the two. Participants subjectively assessed their rate of perceived exertion and local perceived discomfort during 6-minute intervals between trials.

Results & Discussion: A paired t-test reveals that the passive BSE reduced the energy expenditure by 13.6% ($p=1.5\times10^{-6}$) on average for 15 participants (Fig 1). The feature of Angel Gear X, which stores some portion of the energy using elasticity during the lowering phase, seems to contribute to this mechanical benefit. The results of subjective evaluation also support the benefits of the tested BSE; both the perceived exertion and local discomfort were reduced by the BSE (Figs 2 and 3).

Significance: A multifaceted practical evaluation of a passive BSE was carried out. In this study, the beneficial effect on metabolic power was verified by a well-controlled approach [3, 4], presumably enabling reasonable comparisons with the effects of other industrial exoskeletons. Considering the relation between the metabolic power consumption and the risk of LBP [5], our results from the controlled evaluation also support the potential efficacy of the tested BSE in reducing LBP. Beyond measuring physiological outcomes, we also collected subjective responses from the wearers and included the results to evaluate the BSE; this multifaceted evaluation process can provide more solid and practical grounds for accepting or rejecting BSEs designed to assist workers and prevent LBP.

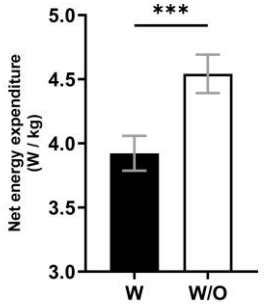

Figure 1: Averages and standard error intervals of energy expenditure of all participants (W: with-device, W/O: without-device). (***: p<0.001)

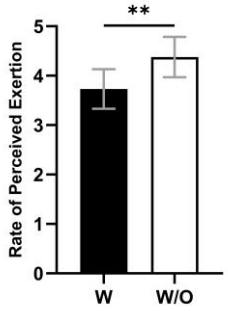

Figure 2: Averages and standard error intervals of perceived exertion of all participants (W: with-device, W/O: without-device). (**: p<0.01)

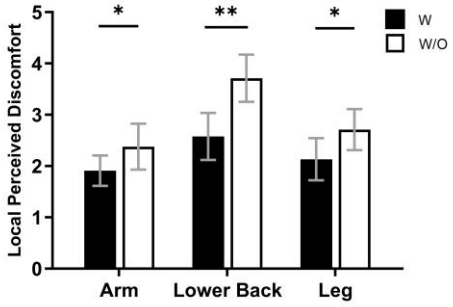

Figure 3: Averages and standard error intervals of local perceived discomfort in three body parts of all participants (W: with-device, W/O: without-device). (*: p<0.05, **: p<0.01)

Acknowledgments: This work was supported in part by the Korea Health Technology R&D Project through the Korea Health Industry Development Institute (KHIDI) funded by the Ministry of Health & Welfare (No. HK23C0071), Industrial Strategic Technology (No. 20018157) and Industrial Technology Innovation Program (No. 20007058, Development of safe and comfortable human augmentation hybrid robot suit) funded by the Ministry of Trade, Industry & Energy (MOTIE, Korea), and the National Research Foundation of Korea (NRF) grants funded by the Korean Government (MSIT) (No. RS-2023-00208052).

References: [1] Kermavnar et al. (2021), *Ergonomics*, 64(6); [2] Brockway et al. (1987), *Human nutrition. Clinical nutrition*, 41(6); [3] Robergs et al. (2010), *Sports medicine*, 40; [4] Fletcher et al. (2009), *J Applied physiology*, 107(6); [5] McGill et al. (1995), *Ergonomics*, 38(9).

THE EFFECT OF LOAD CARRIAGE ON ANKLE WORK SYMMETRY FOR TRANSTIBIAL PROSTHESIS USERS

Stephanie L. Molitor[1*], Krista M. Cyr[2], Glenn K. Klute[2], Richard R. Neptune[1]
[1]Walker Department of Mechanical Engineering, The University of Texas at Austin, Austin, TX
[2]Center for Limb Loss and MoBility, Department of Veterans Affairs, Seattle, WA
*Corresponding author's email: stephanie.molitor@utexas.edu

Introduction: Individuals with lower-limb amputations rely on prostheses to ambulate and perform activities of daily living. Clinicians typically prescribe passive prosthetic feet with a fixed ankle stiffness tuned to the user's body weight and activity level. However, when prosthesis users carry additional loads (e.g., wearing a backpack or carrying a child), their ankle stiffness may no longer be optimal for their new combined weight. Able-bodied individuals are able to modulate their ankle stiffness with added loads [1]. However, since standard passive prosthetic feet do not similarly modulate their stiffness, the intact limb must provide increased compensation in the presence of an added load. Previous studies have noted spatiotemporal changes and increased intact-limb power generation [2] during load carriage; however, few have evaluated the influence of load carriage on joint work symmetry. In addition, groups have developed powered prostheses that change stiffness in the presence of an added load to reduce metabolic cost [3]. However, the placement of the additional load is rarely considered. Therefore, the objective of this study was to determine how the presence and placement of an additional load affects ankle work symmetry while wearing either a passive or powered unilateral transtibial prosthesis. We hypothesized that the presence of an added load would result in increased ankle work asymmetry with more reliance on the intact limb. Furthermore, we hypothesized that the placement of the additional load would affect ankle-foot work symmetry. We also hypothesized that the powered foot would provide improved symmetry compared to the passive foot, as the onboard actuators can generate net positive work.

Methods: Kinematic and kinetic data were collected from 5 unilateral transtibial prosthesis users (3 male; body mass: 93.6 ± 23.3 kg; height: 1.7 ± 0.1 m) during overground walking trials while wearing their prescribed passive foot as well as a powered foot (Empower; Ottobock). Only two of the participants wore the powered foot due to residual limb length constraints. For each prosthesis, participants completed trials for the following load conditions: with a 13.6 kg (30lb) load worn on the back of their torso (BL), with the same load worn on the front (FL), and with no load (NL). Joint moments were normalized by participant body weight and height, and angles were recorded in radians. Moment-angle loops were then generated and integrated over the gait cycle to calculate net ankle work [4] for both the intact and prosthesis side. A work symmetry index (SI) was calculated to quantify the reliance on the intact limb, where SI=100% indicates perfect symmetry and SI >100% indicates more reliance on the intact limb [5].

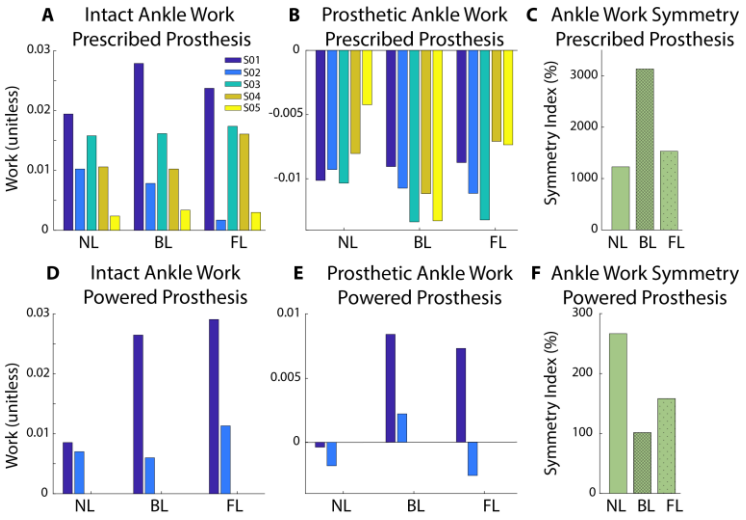

Figure 1: Net ankle work for the intact (left column) and prosthetic (middle column) limb, as well as work symmetry index (right column) while wearing a passive (top row) and powered (bottom row) prosthesis. Net work and work symmetry index were calculated for three loading conditions: no load (NL), back load (BL) and front load (FL).

Results & Discussion: Compared to the NL condition, SI increased with the added load in both positions while wearing a prescribed passive prosthesis (Fig. 1C), indicating greater reliance on the intact limb. Furthermore, placement of the additional load affected SI, as the BL condition demonstrated the greatest SI and most reliance on the intact limb (Fig. 1C). However, while wearing the powered prosthesis, the added load resulted in a notable decrease in SI and improved work symmetry (Fig. 1F), suggesting that individuals may utilize the benefit of added push-off from the powered prosthesis when carrying a load. Regardless of loading condition, SI was an order of magnitude smaller when wearing the powered prosthesis compared to the passive prosthesis, due to its ability to produce net positive work (Fig. 1E) in contrast to net negative work by the prescribed passive prosthesis (Fig. 1B). This finding is consistent with existing literature suggesting that powered prostheses reduce intact-limb compensations during normal walking [6].

Significance: Prosthesis users are at an increased risk for developing overuse injuries, such as knee osteoarthritis, due to prolonged asymmetry and intact-limb compensation [7]. This risk is increased in the presence of additional loads, in which the intact limb experiences increased joint contact forces [8]. Results from this study highlight the importance of developing prostheses that can adapt to changing load conditions to improve joint work symmetry and reduce the likelihood of developing overuse injuries. This work may also serve as a guide for recommending load carriage strategies for transtibial prosthesis users to maintain healthier gait patterns.

Acknowledgments: This work was funded in part by the NSF GRFP and VA Awards RX003138 and RX002974.

References: [1] Kern et al. (2019)., *PeerJ*, 7. [2] Doyle et al. (2014)., *Clin Biomech*, *29*(2). [3] Brandt et al. (2017)., *Sci Rep*, *7*(1). [4] Hansen et al. (2004)., *J Biomec*, *37*(10). [5] Nigg et al. (2013)., *Gait Posture*, *38*(1). [6] Herr and Grabowski (2011)., *Proc R Soc B: Biol Sci*, *279*(1728). [7] Gailey et al. (2008)., *J Rehabil Res Dev*, *45*(1). [8] Templin et al. (2021)., *J Prosthet Orthot*, *33*(2).

Pain-related beliefs in patients with chronic musculoskeletal pain

Vanitha N Shetty*, Y V Raghava Neelapala
Lecturer, Department of Physiotherapy, Manipal College of Health Professions, Manipal Academy of Higher Education, Manipal, India
Email: vanitha.shetty@manipal.edu

Introduction:

The prevalence of chronic pain in low- and middle-income countries is estimated to be 33% in the general population. According to the bio-psychosocial model, disability in individuals with chronic musculoskeletal pain can be influenced by biological, psychological, and socio-environmental factors and hence should be analyzed in detail. As pain-related beliefs have been found to influence recovery, it is essential to assess the beliefs of patients with chronic musculoskeletal pain. No studies have been found on pain-related beliefs among the Indian population; whose beliefs might differ from Western culture. Thus, knowing the pain-related beliefs will help us to analyze the extent of adaptive and maladaptive beliefs in patients of the Indian population with chronic musculoskeletal pain. The objective of the study was to determine pain-related beliefs using a preliminary questionnaire in patients with chronic musculoskeletal pain.

Methods:

A questionnaire-based survey was conducted on participants with chronic musculoskeletal pain. Inclusion criteria were pain intensity >3/10 on a numerical pain rating scale for more than three months in individuals between 20 to 50 years of age. Patients with non-musculoskeletal causes of chronic pain were excluded from the study. A preliminary questionnaire was developed and face-validated by two subject experts. Clearance was obtained from the institutional research committee and institutional ethics committee. Informed consent was obtained from the participants and a developed and validated questionnaire was administered to the selected participants.

Results & Discussion:

Results were analyzed using SPSS version 16 and stated in a descriptive format. A total of 83 participants with a mean age of 42.72 ±8.30 years (Females n= 52) responded to the survey. 59.03% of participants had moderate and high-severity fear-avoidance beliefs. 49.39% of participants had clinically significant pain catastrophizing and 2.4% of participants had poor self-efficacy. It is identified that the study population has moderate severity of fear-avoidance beliefs. The pain catastrophizing is identified as clinically significant. According to the reference scale, scores more than 8 fall in the good self-efficacy category. The results of our study are like the previous studies concerning fear avoidance and pain catastrophizing.

Significance:

An easy-to-administer, brief questionnaire to assess the pain-related beliefs was used to assess the levels of fear avoidance, pain catastrophizing, and self-efficacy in the Indian population with chronic musculoskeletal pain.

Future recommendations:

The psychometric properties of the translated questionnaire must be assessed on a larger sample. The influence of these beliefs on disability and functional status can be studied further.

References:

1. Morton L, de Bruin M, Krajewska M, Whibley D, Macfarlane GJ. Beliefs about back pain and pain management behaviours, and their associations in the general population: A systematic review. Eur J Pain. 2019 Jan;23(1):15-30. doi: 10.1002/ejp.1285. Epub 2018 Aug 7. PMID: 29984553; PMCID: PMC6492285.
2. Thomas EN, Pers YM, Mercier G, Cambiere JP, Frasson N, Ster F, Hérisson C, Blotman F. The importance of fear, beliefs, catastrophizing and kinesiophobia in chronic low back pain rehabilitation. Ann Phys Rehabil Med. 2010 Feb;53(1):3-14. doi: 10.1016/j.rehab.2009.11.002. Epub 2009 Dec 9. PMID: 20022577.
3. Orhan C, Van Looveren E, Cagnie B, Mukhtar NB, Lenoir D, Meeus M. Are Pain Beliefs, Cognitions, and Behaviors Influenced by Race, Ethnicity, and Culture in Patients with Chronic Musculoskeletal Pain: A Systematic Review. Pain Physician. 2018 Nov;21(6):541-558. PMID: 30508984.

PATIENT-ADAPTIVE ROBOTIC BALANCE TRAINING FOR CHRONIC STROKE PATIENTS

Soubhagya Nayak[1], Ellory Oleen[2], Connor Phillips[3], Megan C. Eikenberry[4], and Hyunglae Lee[1,*]
[1]School for Engineering of Matter, Transport and Energy, Arizona State University, Tempe, AZ USA
Corresponding author's email: Hyunglae.Lee@asu.edu

Introduction: Stroke survivors suffer from balance deficits that greatly reduce their quality of life. Repetitive rehabilitation exercise is known to help patients regain balance and movement control. Traditional rehabilitation predominantly involves one or two certified physical therapists who meticulously lead the patient through various lower extremity exercises, necessitating substantial human involvement. In recent years, robotic systems have been introduced into rehabilitation settings to automate some aspects of the physical therapist's duties [1]. To enhance the effectiveness of robotic balance training for chronic stroke patients, this study introduced perturbation-based balance training on compliant surfaces using robotic balance platforms and visual feedback and evaluated its effectiveness.

Methods: Five chronic stroke patients (age: 64.8 (3.8) years, height: 167.4 (6.8) cm, stroke type: ischemic & hemorrhagic) were recruited. The training occurred over the course of 10 sessions, with visits twice a week for 5 weeks. Participants maintained their balance on a twin dual-axis robotic platform that emulated different levels of ground compliance (Fig. 1A). Participants aimed to maintain the centre-of-pressure (CoP) of each foot and their weight distribution within designated areas displayed on a screen (Fig. 1B). If participants successfully remained within these visual boundaries for 2 consecutive seconds, the platform initiated random perturbations in either the sagittal or frontal plane to challenge their balance. During a training session, the platform's compliance for each trial was adjusted based on the participant's performance in the previous trial. The performance was quantified as the percentage of total trial time the participant maintained their CoP within the visual boundaries. This adaptive strategy of changing the ground compliance was maintained across subsequent training sessions, progressively aiding in balance improvement. Improvements were measured using two metrics: Time to Perturb and Time to Stabilize. Time to Perturb is defined as the amount of time the participant takes to stay within the visual boundaries for 2 seconds consecutively during the compliant ground condition to trigger the perturbation. Time to Stabilize is defined as the time the participant takes to stay within the visual boundaries for 0.5 seconds consecutively following the perturbation during the recovery period. A licensed physical therapist evaluated the participants' functional balance and walking capabilities using clinical assessments such as the Berg Balance Scale (BBS), 10-Meter Walk Test (10MWT), Five Times Sit-to-Stand (5XSTS), and Mini-BEST.

Results and Discussion: At the completion of training, all 5 chronic stroke patients showed improvements in metrics such as Time to Perturb and Time to Stabilize, compared to the initial phase (Fig. 1C & 1D). Notably, the stiffness level in the final phase was consistently lower than the initial phase, indicating that patients improved balance control despite more challenging ground conditions (Fig. 1E). Stiffness of the platform was adjusted according to each patient's balance performance throughout the training sessions (Fig. 1F). Clinical assessment results demonstrate all tested patients showed improvement in BBS, 10MWT and Mini-Best tests (Table 1). Only patients S3 and S4 showed improvement in 5XSTS test. Patients S1 and S2 showed no improvement in the 5XSTS test, possibly due to their level of impairment and the challenge presented by the test, which requires standing up from a chair without hand support.

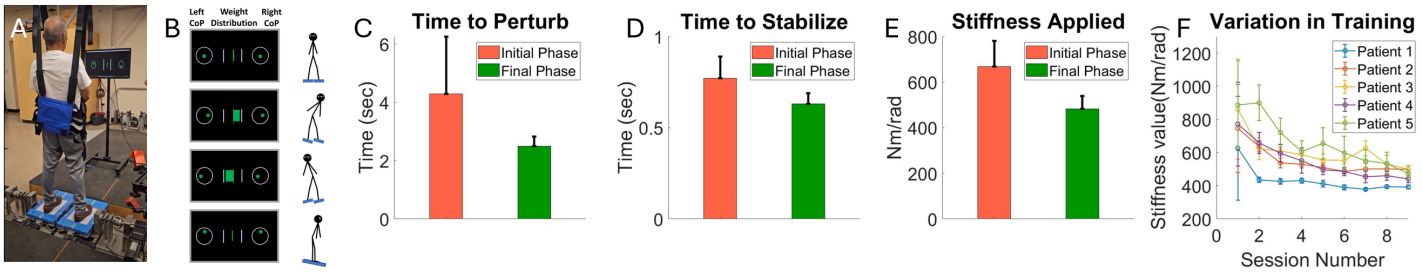

Figure 1: A) Patient balancing on the platform, B) Visual feedback for CoP and weight distribution, C) Time required to trigger perturbation, D) Time required to stabilize the posture post perturbation, E) Stiffness used in the robotic platform, and F) Variation of stiffness in training sessions.

Significance: We highlighted that the perturbation-based training on compliant surfaces could enhance postural balance control of chronic stroke patients. Our study aims to contribute to the advancement of robotic rehabilitation targeting the population with balance impairments.

Acknowledgments: This work was funded by Arizona Biomedical Research Centre (ABRC).

References: [1] E. M. Abd El-Kafy and H. M. El-Basatiny, "Effect of postural balance training on gait parameters in children with cerebral palsy," Amer. J. Phys. Med. Rehabil., vol. 93, no. 11, pp. 938–947, 2014.

Clinical Assessment								
S#	**BBS**		**10MWT (m/s)**		**5XSTS (s)**		**Mini-BEST**	
	Pre	**Post**	**Pre**	**Post**	**Pre**	**Post**	**Pre**	**Post**
S1	52	53↑	SS:1.41 Fast:1.64	SS: 1.41 Fast: 1.86↑	10.7	12.1↑	Not part of the protocol.	
S2	43	47↑	SS: 0.41 Fast: 0.55	SS: 0.45↑ Fast: 0.76↑	couldn't do.		6	19↑
S3	44	54↑	SS: 0.96 Fast: 1.42	SS: 1.08↑ Fast: 1.78↑	13.0	10.0↓	15	22↑
S4	52	53↑	SS: 1.02 Fast: 1.31	SS: 0.92↓ Fast: 1.32↑	15.8	11.5↓	18	20↑

Table 1: Clinical measures are shown where SS stands for self-selected walking. Patient S5 was unable to complete all aspects of clinical assessment due to an unfortunate accident, so their data is excluded from the table.

GAIT TRANSITION BETWEEN WALK AND RUN SECURES THE ORBITAL STABILITY OF LOCOMOTION

Taegyun Park[1,†], Ilseung Park[1,†], Jeongin Moon[1], Jooeun Ahn[1,2]*
[1]Department of Physical Education, Seoul National University, Seoul, Republic of Korea
[2]Institute of Sport Science, Seoul National University, Seoul, Republic of Korea; [†]Contributed equally
*Corresponding author's email: ahnjooeun@snu.ac.kr

Introduction: The mechanism of human gait transition between walking and running has not been clearly explained. One of the possible explanation for the gait transition relies on the attractor stability hypothesis [1], which proposes that humans select gait modes to maximize gait stability. Previous studies have discussed this hypothesis [1-2], but there is still a dearth of evidence that either supports or rejects the attractor stability hypothesis. We aim to address this research gap. We directly quantified the maximum Floquet multiplier (max FM), a stability metric indicating how rapidly the gait pattern converges to a limit cycle [3] at various speeds near the preferred transition speed (PTS). Then, we investigated whether the strength of stability benefits from the gait transition.

Methods: Nine young and healthy males participated in the study. First, preferred walking speed (PWS) and PTS were measured. PWS was identified by established protocol [4]. To measure PTS, we increased the speed of an instrumented treadmill (Bertec Inc., OH, USA) from 1.4 m/s; when five consecutive flying phases were detected, we recorded the speed as walk-to-run transition speed. Conversely, run-to-walk transition speed was measured at the speed where five consecutive double stance phases were observed when decreasing the treadmill speed from 2.4 m/s. PTS was obtained by averaging these two transition speeds.

We set seven speeds near the PTS. The speed interval, d, was 20% of the difference between PTS and PWS ($d = (PTS - PWS) \times 0.2$). Participants completed five walking and five running trials on the treadmill. Each trial was 3.5 minutes long. They walked at speeds ranging from PTS-3d to PTS+d and ran at speeds ranging from PTS-d to PTS+3d. The order of trials was randomized.

We placed reflective markers on bony landmarks of the participants, and recorded their kinematics by 9 infrared cameras (Arqus A5, Qualisys, Göteborg, Sweden). Lower limb kinematics including angles of 10 joints during 150 consecutive heel strikes were derived using the inverse kinematics tool in OpenSim [5]. To measure max FM, we constructed a Jacobian matrix that approximated the linear relation between the kinematics of 150 consecutive strides using the least square fit. Then, we calculated the eigenvalues of the Jacobian matrix to identify max FM. We plotted the curves of max FMs vs. speeds for both walking and running, and conducted two quadratic regressions on both curves to find the intersection point between the two curves.

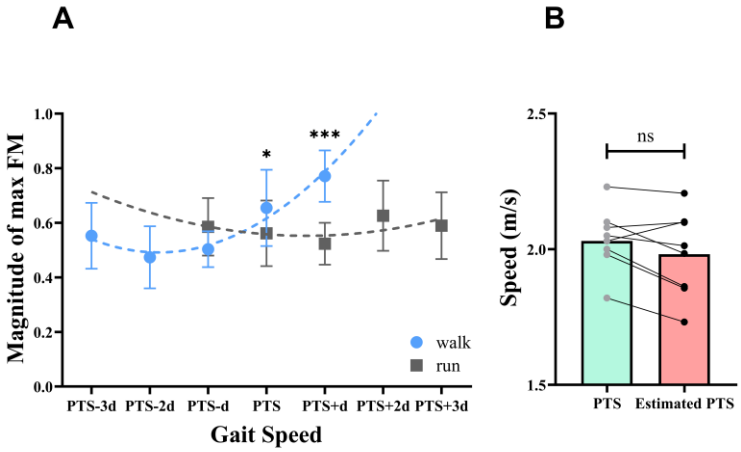

Figure 1: (A) max FM of walking (sky blue circles) and running (gray squares) at seven speeds ($\boldsymbol{d = (PTS - PWS) \times 0.2}$). Quadratic regressions were conducted to fit each participant's walking and running data (dashed lines). The speed corresponding to the intersection between the two was identified as the estimated PTS. (B) The distribution of the measured PTS (gray dots) and estimated PTS (black dots). There was no statistically significant difference between the measured PTS (mean: 2.03 m/s) and estimated PTS (mean: 1.98 m/s).

Results & Discussion: The magnitude of max FM close to unity and zero respectively indicate weak and strong stability [3]. At the speed of PTS+d, we observed that the maxFM of walking is 47.35% higher than that of running ($p<0.001$, Figure 1 A). The difference of the max FM between walking and running decreases at PTS, and there is no significant difference at PTS-d. Our finding indicates that high-speed walking can jeopardize the stability of locomotion; humans' preference for running over walking at high speed locomotion is beneficial for maintaining the gait stability. It is also noteworthy that PTS can be predicted from the max FM vs. speed curves of walking and running. The measured PTS and the speed of the intersection between the two max FM vs. speed regression curves are not significantly different (Figure 1 B). These findings support the attractor stability optimization hypothesis.

Significance: This study is the first attempt to investigate max FM near PTS. First, we observed clear dependence of stability on both gait speed and mode. Importantly, we further found that gait transition occurs near the speed at which the curves of stability vs. speed for walk and run cross each other. Our results support that the stability might be one of the possible objectives of human gait transition.

Acknowledgments: This work was supported in part by the Korea Health Technology R&D Project through the Korea Health Industry Development Institute (KHIDI) funded by the Ministry of Health & Welfare (No. HK23C0071), Industrial Strategic Technology (No. 20018157) and Industrial Technology Innovation Program (No. 20007058, Development of safe and comfortable human augmentation hybrid robot suit) funded by the Ministry of Trade, Industry & Energy (MOTIE, Korea), and the National Research Foundation of Korea (NRF) grants funded by the Korean Government (MSIT) (No. RS-2023-00208052).

References: [1] Diedrich et al. (1995), *J Exp Psychol Hum Percept Perform*; [2] Raffalt et al. (2020), *J Exp Biol*; [3] Hurmuzlu et al. (1994), J Biomech Eng; [4] Pathak et al. (2022), *PLoS One*; [5] Delp et al. (2007), *IEEE Trans Biomed Eng*

The Relationship between an Individual's Height and the Movement Strategies Implemented to Perform Manual Patient-Handling Tasks

Regina Vicente, Elsa Brillinger, Yea Geon Song, and Dr. Brooke Odle
Hope College, Holland, MI, USA
Email: regina.vicente@hope.edu

Introduction: Nurses are specifically at risk of low back pain and injury, which has been associated with the performance of daily tasks involving repositioning and handling patients in awkward postures [1]. We recently conducted a proof-of-concept study to understand multi-joint coordination of the trunk, hips, and knees during the performance of several patient-handling tasks. While interpreting that data, we noted a difference in performance of shorter subjects versus taller subjects. In this study, we present a secondary analysis of that data that explores the relationship of the movement strategies selected during tasks (based on trunk, hip, and knee joint coordination) and subject height. We hypothesized that the movement strategy elicited by shorter subjects would entail more trunk engagement, while the strategy of taller subjects would entail more engagement of the lower limbs The long-term goal of our work is to develop effective training interventions for nursing students and personnel. Thus, we expect the preliminary findings will provide additional insight on whether the height of the nurse needs to be considered when developing training interventions and recommendations.

Methods: In the proof-of-concept study, five volunteers (4 male, 1 female) that were between 18 and 24 years of age and had heights ranging between 1.6 and 1.86 m were recruited for participation. The subjects did not have patient-handling experience nor did they have a history of low back injury. All subjects signed informed consent forms approved by the Hope College Human Subjects Review Board.

Four iPhone XRs were synchronized and utilized OpenCap to collect and process kinematic data [2]. Subjects completed the following tasks: (1) repositioning a patient in bed using a sliding sheet, (2) turning a patient to one side, (3) sitting a patient up, (4) lifting patients's leg upwards, and (5) turning a patient on one side and placing a sling under the patient while another assistant holds the patient in that position. All tasks were performed on a height adjustable treatment table. In a given trial, each task was repeated twice at either hip height (good posture), mid-thigh height (neutral posture), or knee height (poor posture). The posture classifications are based on work by Freitag and colleagues [3], who investigated the relationship between bed height and tasks requiring forward bending. Manikins (Ruth Lee, Oxford, UK) served as patients and manikins of three different weights were used: 44 lb, 66 lb, 110 lb. One trial consisted of three repetitions of a task at a given table height. Two trials were collected for each task and table height. The order of tasks, table heights, and manikin weights were randomized to minimize fatigue.

Kinematic data were filtered using a second-order Butterworth filter with a 12 Hz cut-off. A custom MATLAB (The Mathworks, Natick, MA) script was used to select peaks in trunk, hip, and knee flexion angles during each repetition in each trial across each task and posture type. The average peak of each angle, across all tasks for each posture type, was computed for each subject.

Results & Discussion: Preliminary analyses suggest that shorter subjects performed tasks by flexing their knees more than their trunks (Figure 1). However, taller subjects typically performed tasks by flexing their trunks more than their knees (Figure 2). The subjects with heights between the shortest and tallest subjects typically performed tasks with similar trunk and knee flexion angles (Figure 3). In general, hip flexion angle increased as table height decreased, but there did not appear to be a relationship between this angle and subject height.

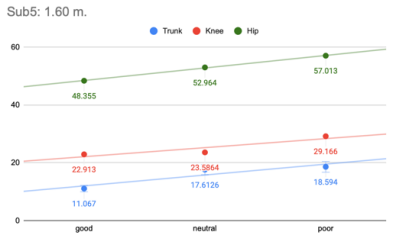

Figure 1: Representative plot of average trunk, hip, and knee flexion angles for each posture type of the shortest subject.

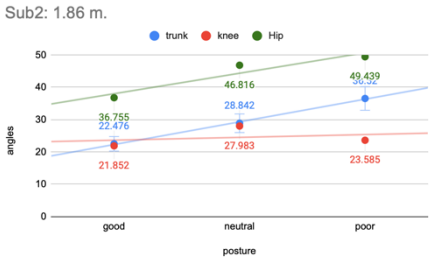

Figure 2: Representative plot of average trunk, hip, and knee flexion angles for each posture type of the tallest subject.

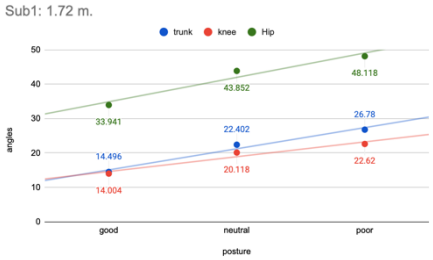

Figure 3: Representative plot of average trunk, hip, and knee flexion angles for each posture type of a subject with medium height.

In general, our findings for trunk flexion angle are consistent with those of Freitag et al [3], which suggests that trunk angle increases and bed height decreases. However, their work did not consider the height of participants or hip and knee flexion angles elicited during tasks. This work is the first to explore the effects of subject height and multi-joint coordination during tasks. Future work will further explore these relationships with a larger cohort.

Significance: These encouraging results suggest that the movement strategies implemented to perform patient-handling tasks may be influenced by the height of the individual performing the task. Recommendations or training may need to account for individual height.

References: [1] Hoy, D. et al. Ann. Rheum. Dis. 2014, 73, 968–974. [2] Uhlrich, S. et al. 2022. biorxiv https://doi.org/10.1101/2022.07.07.499061 [3] Freitag, S, et al. *The Annals of Occupational Hygiene.* 2013.. https://doi.org/10.1093/annhyg/met071

Acknowledgements: This work was funded by the Restore Center, which is funded by the National Institutes of Health through grant P2CHD101913 and the Provost's Office at Hope College.

PATELLOFEMORAL JOINT LOADING IN FEMALES WHO HAVE UNDERGONE ACL RECONSRUCTION

Thomas A. Demirjian[1], Olivia Tu[1], Gillian Northrup[1], Christopher M. Powers[1*]
[1]University of Southern California: Division of Biokinesiology and Physical Therapy
*Corresponding author's email: powers@pt.usc.edu

Introduction: Tears of the anterior cruciate ligament (ACL) are among the most common ligamentous knee injuries in the United States[1], with the gold standard treatment being ACL reconstruction (ACLr).[1,2] Persons who have undergone ACLr have been reported to have an increased prevalence of early onset patellofemoral joint (PFJ) osteoarthritis.[3,4] It has been proposed that elevated PFJ loading during the post-operative period may be contributory to early-onset cartilage changes in this population, however, evidence supporting this premise is mixed.[5-8] A limitation of previous research in this area is that the quantification of PFJ stress has not accounted for patient-specific contact area. This is important as persons post-ACLr have been reported to exhibit abnormalities in trochlear morphology and patellar alignment that may affect contact mechanics.[5] Using an individualized model of the PFJ that takes into consideration subject specific PFJ contact area, the purpose of this study was to compare measures of PFJ loading (peak stress and rate of stress development) during a single limb landing task between females who have undergone ACLr and healthy controls.

Methods: Thirty-four female athletes between the ages of 18 and 35 participated. Seventeen participants had previously undergone ACLr during the last 6-12 months. The remaining 17 participants were matched by age, sex, and sport to those in the ACLr group and served as a control group. All participants completed two phases of data collection. The first phase consisted of loaded MRI assessment of the PFJ (35% bwt) at 0º, 20º, 40º and 60º of knee flexion to quantify contact area. The second phase of data collection consisted of a biomechanical assessment of a single limb drop jump task from a 12-inch box (3D kinematics, kinematics, and electromyography). A previously described subject-specific model of the patellofemoral joint was used to calculate PFJ stress.[6] The dependent variables of interest were peak PFJ stress and average rate of PFJ stress development. Independent t-tests were used to compare differences in stress variables between groups.

Results: Females post-ACLr exhibited a trend towards higher peak PFJS compared to the control group however this difference was not statistically significant (11.50 ± 2.78 MPa vs. 9.88 ± 3.71 MPa; p=0.11; Figure). However, rate of stress development in was significantly higher in females post-ACLr compared to the control group (0.13 ± 0.04 MPa/ms vs. 0.09 ± 0.06 MPa/ms; p=0.02; Figure).

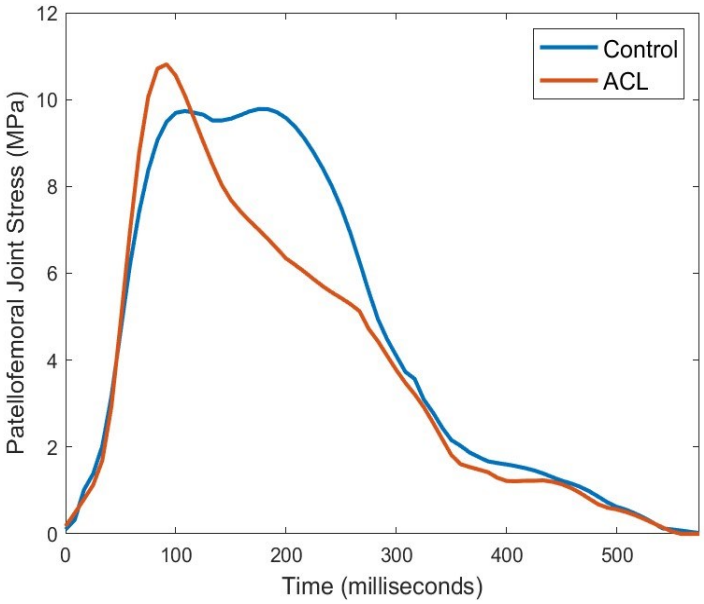

Figure. Comparison of ensemble averages for patellofemoral joint stress during a single limb drop-jump task.

Discussion: Our results indicate that females post ACLr exhibit elevated PFJ loading. Elevated High loading rates may underlie the observation of elevated risk of PFJOA in persons post-ACLr. This finding is consistent with previous basic science research and animal models of osteoarthritis that has shown articular cartilage health is more sensitive to loading rate as opposed to peak load.[7]

Significance: The current study provides insight into how joint loading may be associated with early cartilage changes in females who have undergone ACLr. Longitudinal studies are needed to determine how atypical PFJ loading contributes to cartilage changes in this population.

Acknowledgments: We would like to acknowledge RadNet inc. for providing access to MR scanner used in this study

References:

[1] Paterno et al., Clin. J. Sport Med. 22 (2012) 116. https://doi.org/10.1097/JSM.0b013e318246ef9e.
[2] Frank et al., J. Bone Joint Surg. Am. 79 (1997) 1556–1576. https://doi.org/10.2106/00004623-199710000-00014.
[3] Culvenor et al., Br. J. Sports Med. 47 (2013) 66–70. https://doi.org/10.1136/bjsports-2012-091490.
[4] Culvenor et al., Arthritis Rheumatol. 67 (2015) 946–955. https://doi.org/10.1002/art.39005.
[5] Macri et al., Knee Surg. Sports Traumatol. Arthrosc. 26 (2018) 2622–2629. https://doi.org/10.1007/s00167-017-4571-1.
[6] Teng & Powers J. Orthop. Sports Phys. Ther. 44 (2014) 785–792. https://doi.org/10.2519/jospt.2014.5249.
[7] Morel et al., J. Biomech. 39 (2006) 924–930. https://doi.org/10.1016/j.jbiomech.2005.01.026.

A TOOLBOX FOR GENERATING SUBJECT SPECIFIC FEMUR MODEL FROM COMPUTED TOMOGRAPHY SCAN

Zhiyuan Ren [1], Trung-Hieu Hoang[2], Minh N. Do[2]
[1] Department of Mechanical Science and Engineering, University of Illinois Urbana-Champaign, IL, USA
[2] Department of Electrical and Computer Engineering, University of Illinois Urbana-Champaign, IL, USA
*Corresponding author's email: zr11@illinois.edu

Introduction: Subject-specific musculoskeletal (SSMS) models provide an accurate way to evaluate human movements that are non-invasive and ethical [1]. In a study that investigates patients with a motor disability such as Cerebral Palsy, the gait analysis of the SSMS determined the patient's excessive internally rotated gait is mainly caused by his abnormally anteverted femur, not by the short hamstrings and adductors that the researchers previously assumed [1]. In such studies, the subject-specific musculoskeletal models are generated with geometric information from Computed Tomography (CT) scans and dynamic information from motion lab captures [2]. This process can be completed in 2-3 hours and requires the hospital to be equipped with a motion capture room and engineers with expertise in integrating data from different platforms and thus requires 2-3 hours to complete [2]. This resource and skill-intensive process makes patient-specific studies unfeasible for doctors to operate by themselves [3]. To streamline this process, the subject-specific models can be generated by modifying a few characteristic geometries, such as the tibia torsion, femoral neck-shaft angle (NSA), and anteversion angle (AVA), of generic OpenSim [1] models. As a result, no specific engineers are required, and generation time can be reduced to around 5 minutes. Though the subject-specific model sees a great reduction in time, it suffers some losses in accuracy. When comparing to the CT-based models, subject-specific models have different values for moment arms as they are prone to overestimation [4], but they have very similar directions of muscle acceleration, magnitude of muscle acceleration relative to the muscle, making subject-specific models a time-efficient and cost-effective option. However, there are few open-source tools with a free license available to generate such models [2].

Currently, OpenSim's default customization only allows pure rotation in the hip joint, which will not be able to recreate the patient's femur bone accurately due to its lacks in degrees of freedom. Our tool improves the accuracy by focusing on transforming two key geometric characteristics of the femur bone, which are NSA and AVA. These two femur geometries have the largest impact on human walking gait and the hip joint contact force (JCF) [5]. AVA has a larger impact on average JCF as both peaks of JCF values are affected within a gait cycle [5]. Modifying these parameters can have a direct effect on the patient's walking gait and joint health as 83.4% of the patients who have corrected their gait have surgically altered femoral anteversion angle and tibia [5].

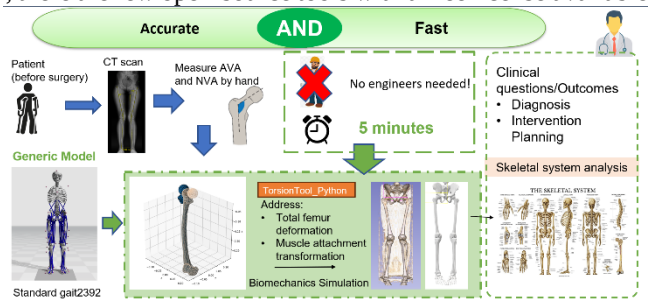

Figure 1: Our 3D model generation pipeline.

Methods: This program is written in Python(https://github.com/Jack-Zhiyuan-Ren/pySSMS_Builder) and generates personalized geometry of a generic OpenSim femur model [1] following the pipeline as demonstrated in Figure 1. Within the tool, the subject-specific femur is developed by following the method of *VeerKamp et al*.'s work. The program requires two inputs which are the AVA and the NSA. These data are measured by hand from the CT scan. Once these values are obtained, two rotation angles are calculated by finding the difference between the subject's AVA and NSA angles and the generic model's AVA and NSA angles. Then, the generic bone divided into three sections in the long axis and the transformation will be performed separately. The vertices in the upper box rotate first through an offset angle corresponding to the change in anteversion. Then the middlebox rotates through an angle that is decreased linearly as a function of distance along the axis. In the final step, the lower box is translated to restore the position of the femoral Head. After the program finished running, a new subject specific OpenSim model is generated with updated geometries.

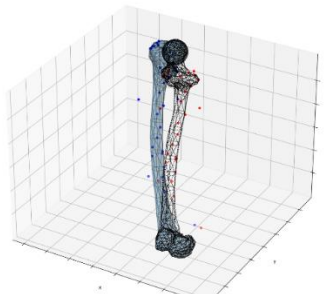

Figure 2: Modified Femur (white) and generic femur (blue)

Results & Discussion: Figure 2 visualizes a transformation with an NSA of 180 degrees and AVA of 16 degrees as the white bone being the transformed one. The red dots are the modified muscle attachment points again original blue ones. We evaluate the accuracy of the modified generic models by comparing them against the CT-based models. For our current samples, the AVA and NSA angles are identical on both models. Since there are only two patient's data available currently, to further investigate the accuracy of tool, the data from Veerkamp's 2021 work is used because their program in MATLAB share similar method. They compared the subject-specific models with AVA and NSA modified to adjusted generic models, meaning that the femur size is only modified parameter. Among 26 developing aged children patients, the subject-specific models have greater accuracy as they deviate less from the true angle with an average error of 2 degrees while adjusted generic models have an average error of 12 degrees.

Significance: Our tool has allowed people to generate subject-specific musculoskeletal models in a much shorter time of around 3 minutes and with less resources. This achievement could allow smaller hospitals or even individuals to access musculoskeletal models and improve the accuracy of mobility symptom diagnosis. Another potential application is that due to our program's small footprint in resources, it could be integrated into a mobile application where the camera could be utilized by an Artificial Intelligence tool for automatic angle measurement [6]. By doing this, the hand measurement process can be eliminated, and the model generation time will be further reduced.

Acknowledgments: This project has been funded by The Health Care Engineering Systems Center at University of Illinois Urbana Champaign.

References: [1] Allison S. Arnold, Journal of Biomechanics (2001); [2] Kirsten Veerkamp, Journal of Biomechanics (2021); [3] Modenese, Journal of Biomechanics (2018);[4] Correa, Journal of Biomechanics (2011); [5] Kainz, PLoS One (2020); [6] Tuck *et al.*

DEVELOPMENT OF TOOL FOR ANALYSIS OF SWIMMING USING POSE ESTIMATION ALGORITHM

Itay Coifman[1], May Hakim[1], Gera Weiss[2], Raziel Riemer[1*]
[1]Industrial Engineering and Management Department, Ben-Gurion University of the Negev, Beer-Sheva, Israel
[2]Computer Science Department, Ben-Gurion University of the Negev, Beer-Sheva, Israel,
*Corresponding author's email: rriemer@bgu.ac.il

Introduction: Swimming poses unique challenges in biomechanical research due to the complexity of analyzing human movement, including kinematics, kinetics, and neuromuscular aspects, in an aquatic environment [1,2]. Past studies have developed underwater computer vision models based on deep learning for human pose estimation [3,4] focusing on predicting joint positions. Yet, few studies have used such models for biomechanical feature extraction [5] or classification [6], and none has attempted to provide a comprehensive solution for general biomechanical analysis in swimming. This study introduces an end-to-end system for analyzing and tracking swimming biomechanics using a single uncalibrated underwater camera (e.g., GoPro®, iPhone). The aim was to evaluate the accuracy of features extracted by the system, including stroke rate [7], elbow angle at push time, and shoulder rotations [8], which are commonly used in swimming studies. The primary focus was not to replace motion capture systems but rather to explore how simple 2D data can deliver insights on swimming.

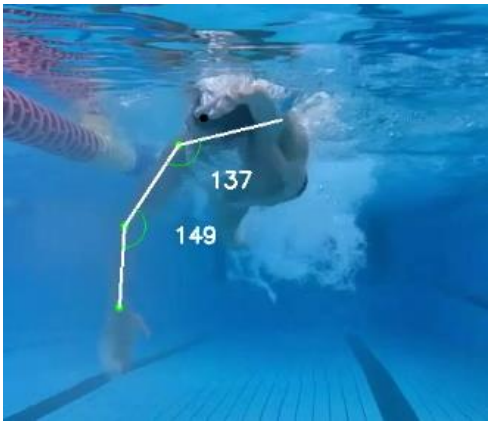

Figure 1: Example of underwater frame annotated by the human pose estimation model algorithm; annotated angles represent the joint angle at t_{push}, the point in the front crawl cycle when the hand starts moving backward (relative to the body).

Methods: We tested several human pose estimation algorithms, but none could identify the human joints underwater. Therefore, we trained the YOLO-V8 Pose by Ultralytics on transverse and sagittal videos of swimmers captured with various cameras and manually labeled (**Fig. 1)**. To evaluate the system's capabilities, we created a test set of spatial-temporal features typically used in swimming analyses. The data comprised 16 transverse and 12 sagittal front crawl videos not previously seen by the system. The kinematic data of this test set were manually labeled using Kinovea®. Keyframes for the start of the push phase (t_{push}) (**Fig. 1**) and hand entry (t_{entry}) were identified. Stroke rate was calculated as the average frequency between consecutive right-hand entries. Additionally, the 2D angles of the elbows in the transverse plane were measured from images at each t_{push} of the right hand. Shoulder rotation in the transverse plane was measured at t_{push} of both the right and left hands (i.e. two measurements for each cycle). We calculated the average error over all cycles for each video (average of two cycles per video). The reported errors correspond to the mean error, with each video considered as one sample.

Results & Discussion: As **Table 1** shows, the temporal features exhibit very low errors, which indicates that the system can predict the timing of specific events during the swim cycle with high accuracy. In cases where the angle errors are less precise, the accuracy of 2D angles was significantly influenced by minor errors introduced by the pose estimation model. One notable limitation is that angle comparisons were made against human annotations rather than a gold standard comparison method, such as a motion capture system. These annotations are prone to inaccuracies, particularly for small angle differences. We anticipate that more precise data will be available in the future to enable a more accurate comparison of our system.
The mean absolute percentage error (MAPE) of the shoulder rotation is relatively large (16%), whereas the root-mean-square error (RMSE) is relatively small (approximately 7 degrees), which is attributed to the relatively smaller body rotations measured during a swimming cycle. We believe that more training data will significantly improve the pose estimation accuracy driving the errors towards zero.

Feature name	Average GT	RMSE	MAPE
Stroke rate (Hz), transverse	0.47	0.11	1.74%
Stroke rate (Hz), sagittal	0.47	0.001	0.19%
Elbow angle (Deg)	122.84	8.93	7.17%
Shoulder rotation (Deg)	22.01	6.96	16.11%

Table 1: Average error metrics, with each video constituting a single sample; average Ground Truth (GT) represents the average actual value annotated in Kinovea®.

Significance: To our knowledge, this study represents the first application of monocular computer vision algorithms to analyze swimming biomechanics. Its significance lies in its demonstration that essential biomechanical features can be accurately extracted even in challenging video conditions (e.g., bubbles, color attenuation). To extract these features accurately, it is important to understand the limitations of the analysis and use features that are accurately represented in the 2D image projection. We believe that our approach can support studies with larger sample sizes.

Acknowledgments: This study was partially supported by the Israel Innovation Authority and the Helmsley Charitable Trust through the Agricultural, Biological and Cognitive Robotics Initiative of Ben-Gurion University of the Negev.

References: [1] Zecha et al. (2018), *CVPR Workshops*; [2] Fani et al. (2018), *ICIP*; [3] Giulietti et al. (2023), Sensors 23(4); [4] Zecha et al. (2019), *CVPR workshops*; [5] Zecha et al. (2012), *Multimedia on Mobile Devices (8304)*; [6] Einfalt et al. (2018), *IEEE WACV*; [7] Morais et al. (2022), *Front Physiol(13)*; [8] Vila Dieguez, Oscar, and John M. Barden (2022), *Sports Biomech 21(10);*

Explainability of machine learning models in the classification of patient-handling techniques of novice caregivers

Emanuel Sanchez[1], Giovanni Battaglia[1], Brooke Odle[1] (Ph.D.), Omofolakunmi Olagbemi[1]* (Ph.D.)
[1]Hope College, Holland, MI
*olagbemi@hope.edu

Introduction: Due to the "black box" nature of machine learning (ML) models, explainability is an important concept; it provides some understanding as to what features in a dataset contributed to a specific classification decision by the model, thus fostering trust in the models [1]. In 2021, an ML model called XCM [2], implemented using Gradient-weighted Class Activation Mapping (Grad-CAM) for explainability, was introduced. A related study being conducted by our group seeks to classify posture adopted while performing patient handling tasks as good, poor, or, in some cases, neutral. Our research uses explainability to identify the features (e.g. pelvic tilt, lumbar extension) of the data that are most critical in the classification process, and apply the knowledge gained in the formulation of metrics on task performance that can potentially help minimize the risk of musculoskeletal injuries sustained by caregivers.

Methods: For our preliminary data, we recruited five able-bodied subjects (18-24 years of age) to perform six patient-handling tasks while adopting good, poor and in some cases, neutral posture. With good posture, trunk flexion is minimized while bad posture is indicated by increased trunk flexion resulting in higher low back loading [3]; neutral posture lies between good and poor posture. The six tasks had the subjects (i) sit a patient up from a supine position (Sit Up), (ii) roll a patient from a supine position to their side (Roll), (iii) lift a patient's leg (Leg Lift), (iv) roll a patient first on to their left and then to their right side to place a sling under them (Two Roll), (v) slide a patient up and down a treatment table using a sheet placed under them (Slide), and (vi) lift a patient up out of a wheelchair (Wheelchair). Manikins served as the patients and tasks were completed using three manikins of different weights: 44 lbs, 66 lbs, and 110 lbs. Tasks (iv) and (v) were completed with a second person to assist. OpenCap [4] - a video-based data capture tool used during task performance - provided joint angles and positional data. We excluded Subject 5's data due to severe glitching in the data.

Subjects performed 18 trials per task. Data for the three repetitions of each trial file were separated into their individual files and each resampled to 100-time steps. The resulting data were further separated by task into training (80%) and testing (20%) sets for use by the ML models. The XCM model was trained on the datasets (separated by task), and the Grad-CAM implementation in XCM helped to identify the features most critical (in the data) to the classification of the different postures for each task.

Results & Discussion: Utilizing the OpenCap data, the XCM model generated a heatmap for each respective task, identifying the importance of each feature in the classification decision. The heatmap is color-coded: "the more intense the red, the more positively the feature contributed to the prediction." [2].When the subset of XCM-determined features was used to train three ML models (XCM, MiniRocket [5], and ResNet [6]), the results obtained from all the models were more accurate than when the full dataset of data obtained from OpenCap were used in training the models. Figure 1 displays the accuracy results for each model when using different combinations of features.

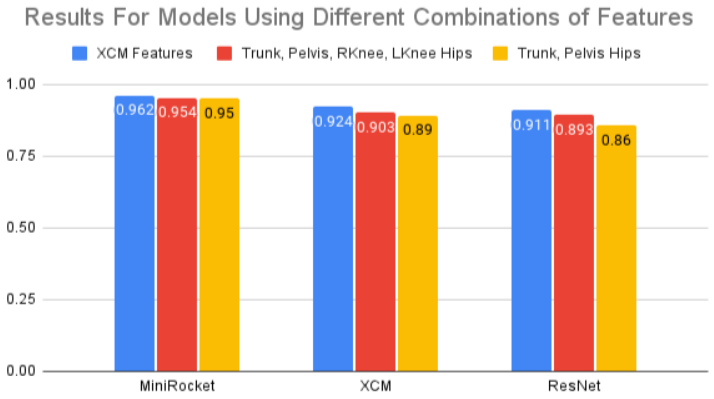

Figure 1: Accuracy using different feature combination for each of the models

Significance: The explainability function in XCM (Grad-CAM) provided insights into which features improved the accuracy of model classifications. Evaluating the XCM-identified features against the mechanics of movement from a biomechanical standpoint, the output from Grad-CAM was deemed reasonable. These findings have the potential to support the formulation of metrics that are indicative of good posture (beyond trunk flexion) which could in turn help to minimize the risk of musculoskeletal injuries in caregivers.

Acknowledgments: Research reported in this abstract was supported in part by funding provided by the National Aeronautics and Space Administration (NASA), under award number 80NSSC20M0124, Michigan Space Grant Consortium (MSGC). Other sources of funding and / or other support include the RESTORE Center of Stanford University, the Hope College Computer Science department, and the office of the Dean of Natural and Applied Sciences at Hope College. We also acknowledge Hope College students Haniah Kring, Ngoc Tran, Elsa Brillinger, Yea Geon Song, Regina Vicente, Grant Seyller, and Nathan Ceja for various valuable contributions to this study, and last but not least, our research participants.

References: [1] ACM Technology Policy Council. (2022, October 26), https://www.acm.org/binaries/content/assets/public-policy/final-joint-ai-statement-update.pdf; [2] Fauvel, K., Lin, T., Masson, V., Fromont, É., & Termier, A. (2021, December 5). *XCM: An explainable convolutional neural network for multivariate time series classification*. MDPI. https://www.mdpi.com/2227-7390/9/23/3137; [3] Uhlrich, S. et al. 2022. biorxiv https://doi.org/10.1101/2022.07.07.499061; [3] Freitag et al. (2014), Ann Occup Hyg. 2014; [4] Uhlrich, S. et. al. (2022), *https://doi.org/10.1101/2022.07.07.499061;* [5] Dempster, A. et. al. (2021), *27th ACM SIGKDD conference proceedings*; [6] He, K. et. al. (2016), *IEEE conference proceedings on computer vision and pattern recognition*

TOWARD PRECISION COACHING: QUANTITATIVE ANALYSIS OF FRONT CRAWL TECHNIQUE WITH ML

Itay Coifman[1], May Hakim[1], Gera Weiss[2], Raziel Riemer[1]
[1]Industrial Engineering and Management Department, Ben-Gurion University of the Negev, Beer-Sheva, Israel
[2]Computer Science Department, Ben-Gurion University of the Negev, Beer-Sheva, Israel
*Corresponding author's email: rriemer@bgu.ac.il

Introduction: Swimming coaches primarily rely on video-based qualitative methods to analyze their swimmers' techniques. Despite the importance of biomechanical analysis, practical constraints regarding time, cost, and resource availability limit the adoption of more quantitative approaches [1]. However, leveraging recent advancements in machine learning and underwater computer vision can potentially enable the extraction of meaningful information from videos without requiring human interaction [2]. Additionally, research has shown a strong correlation between an expert score of a swimmer's video and their actual technical performance (kinesthetic awareness), even when a coach is unable to quantitatively explain their evaluations (feel) [3,4]. More aspects are known to affect athlete performance, including anthropometric, physiological, and psychological factors [4]. This study conducted a pilot experiment to test the possibility of producing a quantitative explanation for an expert technique evaluation of front crawl swimming while relying on an ordinary camera video.

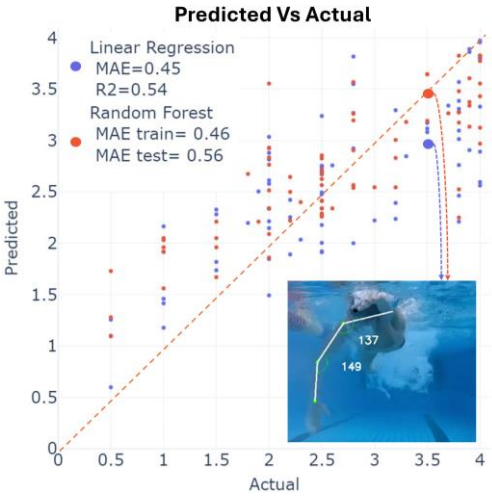

Figure 1: Actual and prediction scores of linear regression (purple) and random forest (red); example frame is taken from a video that represents a single sample in the dataset.

Methods: An experienced swimming coach scored the technique of 82 front crawl videos of 66 swimmers varying from beginners to Olympic medalists. Based on a short underwater transverse clip, each video was rated on a continuous scale from 0 to 4. Scores ranged from 0 to 1 for beginners and from 2 to 4 for competitive swimmers, with a score of 4 indicating world-class performance. Subsequently, we developed in-house swimming analysis software to analyze each video. The software backbone is a human pose estimation model (YOLO-V8 Pose by Ultralytics), a deep neural network tasked with predicting the joint locations in every frame. The model was trained on transverse videos captured with several camera types. After the processing by human pose estimation, our software tracked the main swimmer, removed unnecessary frames, and computed upper-body 2D angles, body orientation, and numerous spatial-temporal features. The extraction of various temporal features from the videos was followed by a flattening process that condensed the temporal information into a smaller set of features while preserving relevant information for subsequent analysis. The features were then filtered according to their univariate significance. This resulted in 30 features, which is in line with previous research [5]. Our primary objective was to determine which features were highly predictive of the coach's scores. Given our emphasis on interpretability, we employed the statistical method of linear regression (with up to three features) and a machine learning model, namely a random forest regressor, which is known for its explainable nature. The results of the machine learning model are based on a test set containing 30% (27 videos) of the dataset. The remaining videos were used for training.

Results & Discussion: For linear regression, the best features chosen were elbow angle at push start, elbow medial-lateral motion range, and head medial-lateral motion range. Range was calculated as the max-min distance from the body center. The model resulted in $R^2 = 0.54$ and a mean absolute error of 0.45. All features were significant ($Pv < 0.05$). The random forest with 10 trees, each with depth of 2, resulted in a mean absolute error of 0.56 **(Fig. 1)**, and the features with the most importance (i.e. highest significance to the forest decision) were elbow medial-lateral max distance, elbow medial-lateral range, elbow angle at push start, head medial-lateral range, and elbow vertical motion range. The mean absolute error of the models is approximately 0.5 which from the coach perspective is similar to his sensitivity when rating the different swimmers. The R^2 explains only 54% of the rating, possibly because there are several common front crawl techniques. Future research should include more swimmers to ensure accurate representation of the different techniques.

Significance: This study has significant implications for both the domain of swimming coaching and the broader field of sports biomechanics. With the goal of bridging the gap between qualitative assessments, towards algorithms that could quantify athlete's technique. The integration of machine learning and underwater computer vision technologies can not only facilitate the extraction of meaningful information from swimming videos but also increase its accessibility for coaches and swimmers. Furthermore, the identification of key features predictive of the front crawl technique could inform a more data-driven approach to swimming coaching that fosters advancements in athlete development and performance optimization.

Acknowledgments: This study was partially supported by the Israel Innovation Authority and the Helmsley Charitable Trust through the Agricultural, Biological and Cognitive Robotics Initiative of Ben-Gurion University of the Negev. We would like to thank the swimmers, coaches, and other individuals who were involved in this study.

References: [1] Mooney et al. (2016), *J Sports Sci* 34(11); [2] Einfalt, Zecha, and Lienhart (2018), *IEEE WACV;* [3] Zamparo, Carrara, and Cesari (2017), *PLoS One* 12(9); [4] Barbosa et al. (2023), *Sports Biomech* 22(12); [5] Reinbolt et al. (2009), *Gait Posture* 30(1).

WHERE IS THE DYSPLASTIC HIP JOINT CENTER?

Michael D. Harris[1*], Erin M. Mannen[2]
[1]Washington University School of Medicine in St Louis, [2]Boise State University
*Corresponding author's email: harrismi@wustl.edu

Introduction: Developmental dysplasia of the hip (DDH) often leads to early osteoarthritis due to acetabular and femoral head abnormalities altering joint loads and mechanically inducing joint damage. Accurately locating the hip joint center (HJC) is crucial for correctly quantifying joint loads, but is challenging because the hip is deep in the body and far from palpable landmarks. While HJCs can be located using image-based 3D reconstructions of the bony anatomy, obtaining high-quality image data is often impractical. Many studies have assessed functional or predictive HJC estimations using skin markers placed over bony landmarks [e.g. 1,2], but few have examined their accuracy in abnormally shaped hips [3,4]. The purpose of this study was to compare common functional and predictive HJC estimates to anatomic HJCs specifically in patients with DDH. We hypothesized that, as previously found in normal shaped hips, functional HJCs would be nearer than predictive HJCs to anatomic HJCs.

Methods: With IRB approval and informed consent, bilateral HJCs were determined for 19 female patients with DDH (age: 23.0±7.0 BMI: 22.4±2.6). For anatomic HJCs, patient-specific 3D pelvis and femur reconstructions were generated from T1-weighted MRI as reported previously [5]. The centers of best-fit spheres objectively fit to each femoral head were identified as the anatomic HJCs [5]. For functional and predictive HJCs, patients were instrumented with 70 14-mm reflective markers and performed lower-limb star-arc [6] and "hula" motions (**Fig 1**). Marker trajectories and patient anthropometrics were imported to Visual3d and functional star-arc and hula HJCs were calculated using a transformational technique from Schwartz and Rozumalski [7]. Two predictive HJCs were calculated using equations from Harrington et al [3] and Bell et al [8] based on skin markers (accounting for marker radius) over the right and left anterior and posterior superior iliac spines and virtual landmarks at midpoints between those markers. Functional (StarArc, Hula) and predictive (Harrington, Bell) HJCs along with pelvis marker coordinates during quiet standing were exported to Amira software. The MRI-based and marker-based pelvises' geometric centers and tilt were aligned. The mediolateral (Med-Lat), anteroposterior (Ant-Post), superoinferior (Sup-Inf), and resultant linear distances between anatomic HJCs and functional or predictive HJCs were calculated (**Fig 1**). We also calculated if an HJC's distance from anatomic was less than the radius of the best-fit femoral head sphere.

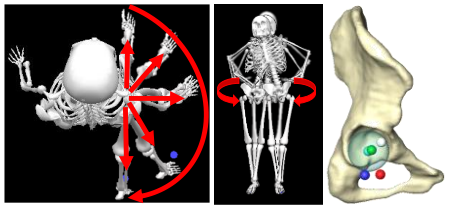

Figure 1. Star-Arc (left) and "hula" (center) motions used to calculate functional HJCs. MRI- and marker-based pelvises were aligned and Star-Arc (blue), hula (red), Harrington (green), and Bell (white) HJCs were measured relative to the anatomic HJC (cyan).

Results & Discussion: The Harrington method yielded HJCs closest to the anatomic standard (**Fig 2**). In most patients (13/19), Harrington HJCs were nearest to anatomic and fell within the radius of the best-fit femoral head sphere (15/19). Thus, in the absence of image-based anatomic HJCs, the Harrington predictive method may be the best approximation for dysplastic hips. Knowing the variability in HJC estimations is important when identifying mechanical differences among patient groups given that a 20-30 mm HJC difference can alter hip joint reaction forces by 50% [9] or hip moments by ~20% [10]. Interestingly, functional HJCs were not more accurate than predictive HJCs (Harrington only), contrary to our hypothesis and findings in normal hips [1,2]. It is unclear if this discrepancy is due to the unique DDH morphology or possible differences in how functional motions were completed in this versus prior studies. Despite Harrington HJCs being nearest to anatomic, errors were still around 2cm, suggesting a possible need for new predictive equations tailored to DDH and other pathology-specific populations. Of course, use of all these HJC methods assumes a rotation-only joint, which may not hold true for dysplastic hips during dynamic activities. Ultimately, we need definitive measurements of femoral head translation during a variety of activities. Until then, assuming a rotation-only joint will persist in practice. Another limitation is assuming a sphere as the best fit to the dysplastic hip; future work will explore alternatives such as the geometric center of elements comprising the femoral head or the appropriateness of the acetabulum to determine HJC location.

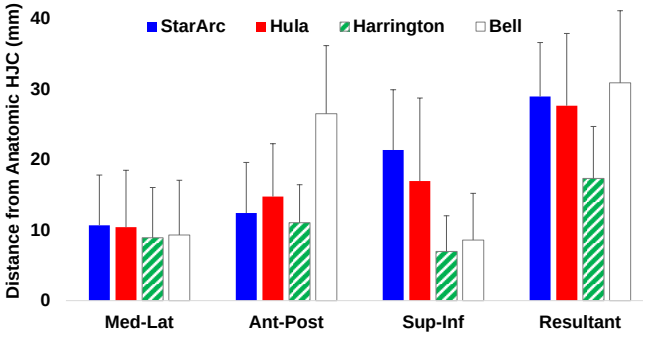

Figure 2. Average and 95% confidence interval distances from the anatomic HJCs.

Significance: This study demonstrates which HJC estimation methods may be most accurate for dysplastic hips. It is important that we identify HJCs with the highest possible accuracy in populations with known hip shape deformities, if we seek to characterize disease mechanisms and inform clinical interventions. HJC prediction may need to be customized for specific populations; such customizations can be facilitated by data sharing and collaboration, including sharing of medical imaging data.

Acknowledgments: Funding provided by NIH K01AR072072 and R01AR081881.

References: [1] Kainz (2015) *Clin Biomech* 30; [2] Fiorentino (2016) *Ann Biomed Eng* 44. [3] Harrington (2007) *J Biomech* 40. [4] Mantovani (2016) *Gait Post* 44. [5] Harris (2022) *J Orthop Res* 40. [6] Camomilla (2006) *J Biomech* 39. [7] Schwartz (2005) *J Biomech* 38. [8] Bell (1989) *Hum Move Sci* 8. [9] Lenaerts (2009) *J Biomech* 42. [10] Stagni (2000) *J Biomech* 33.

EFFECT OF QUADRICEP AVOIDANT GAIT PATTERN ON PATELLOFEMORAL JOINT STRESS IN INDIVIDUALS WITH PATELLAR INSTABILITY

Delaney M. McNeese[1*], Caitlin E. Conley[2], Austin V. Stone[2], Cale Jacobs[3], Brian Noehren[4], Meredith K. Owen[4]
[1]Department of Biomedical Engineering, University of Kentucky, Lexington, KY, [2]Department of Orthopaedic Surgery and Sports Medicine, University of Kentucky, Lexington, KY, [3]Mass General Brigham Sports Medicine, Harvard Medical School, Boston, MA, [4]Department of Physical Therapy, University of Kentucky, Lexington, KY
*Corresponding author's email: dmmc240@uky.edu

Introduction: Individuals with patellar instability often offload their knee to compensate for the injury, resulting in altered mechanics associated with a quadricep avoidant gait pattern [1]. However, the effect of a quadricep avoidant gait pattern on patellofemoral joint stress (PFJS) is still unknown. A quadricep avoidant gait pattern presents as a reduced internal extensor moment in early stance and an increased flexion moment in late stance, which may affect PFJS. Experiencing greater contact stress later in stance when the patellofemoral joint is not as congruent may contribute to instability and degeneration. Therefore, the study's purpose was to evaluate how compensatory patterns affect the timing and magnitude of PFJS throughout all of stance.

Methods: Fifteen individuals (age: 21.2 ± 6.9 years, height: 1.76 ± .08 m, mass: 74.8 ± 19.0 kg), each experiencing patellar instability (at least one clinically diagnosed dislocation within the previous 3 months), participated in an instrumented gait analysis while walking at 1.2 m/s. Knee extensor moment and knee flexion angle were calculated (Visual 3D, C-Motion) and served as inputs for a mathematical model designed to estimate PFJS throughout the stance phase for their injured limb. Quadricep force (N) was calculated by dividing knee moment (in N*m) by effective quadricep lever arm (in m) defined as a function of knee angle [2]. To estimate patellofemoral joint reaction force (PFJRF) (N), quadricep force (N) was multiplied by a constant k (a function of knee angle), which is a ratio of PFJRF and quadricep force [2]. PFJRF (N) divided by contact area (mm) defined as a function of knee angle [3] gave PFJS (MPa). PFJS was renormalized to mass and reported in KPa/kg. Participants were classified into two groups based on knee moment at peak PFJS. Peak PFJS during a knee extensor moment is representative of normal mechanics, while peak PFJS during a knee flexion moment is labelled as a quadricep avoidant gait strategy. Peak PFJS, knee angle at peak PFJS, and timing of peak PFJS during stance were compared between the two groups using Mann Whitney U Tests with significance set at $p < .05$.

Results & Discussion: Peak PFJS, knee angle at peak PFJS, and timing of PFJS during stance are reported in Table 1. Nine individuals demonstrated quadricep avoidant gait strategies. However, six individuals did not demonstrate a quadriceps avoidant gait pattern and experience peak PFJS earlier in stance. Figure 1 depicts peak PFJS occurring significantly later in stance ($U = 0$, $p < .01$) for the quad avoidant group but the magnitude of peak PFJS was not significantly different ($U = 24$, $p = .78$). Knee flexion angle at peak PFJS is significantly lower for the quad avoidant group ($U = 0$, $p < .01$). Consequently, the quadricep avoidant gait pattern results in the highest stress in the least congruent position of the patellofemoral joint and may contribute to a greater risk of recurrent dislocations [4]. In addition, the quadricep avoidant gait compensations lead to peak stresses being applied on the patellofemoral cartilage in regions that may not be accustomed to higher magnitude loading increasing the for patellofemoral osteoarthritis and subsequent injury [4].

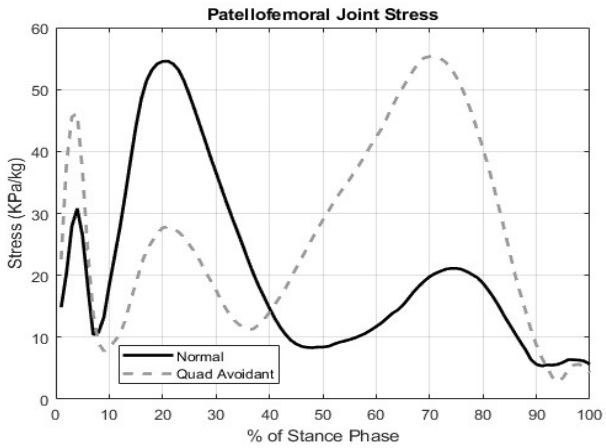

Figure 1: Patellofemoral Joint Stress as a function of stance phase for individuals with a normal and quadricep avoidant gait pattern

	Normal Mechanics	Quad Avoidant
Peak PFJS (KPa/kg)	56.0 ± 15.6	57.6 ± 12.4
Knee Angle	23.3° (range: 12.0°-27.2°)	6.8° (range: 4.3°-13.7°)*
% of Stance Phase	20.2	67.2*

Table 1: PFJS (Patellofemoral Joint Stress) (Mean ± SD), Knee Angle, and % of stance phase for individuals with a normal and quadricep avoidant gait pattern, *$p < .01$

Significance: This study furthers our understanding of how compensatory gait patterns can lead to alterations in timing of PFJS providing clinicians with further insight into how quadricep avoidant individuals have long-term risks for recurrent instability and patellofemoral osteoarthritis. Future work should relate location of peak PFJS during stance to patellar tracking in individuals with patellar instability leading to better preventative and treatment opportunities.

Acknowledgments: This research was funded by the Department of Defense Grant No. CDMRP- PR191214.

References: [1] Clark et al. (2023) *J Knee*; [2] Brechter et al. (2002) *Med. Sci. Sports Exerc.*; [3] Kernozek et al. (2015) *Gait Posture*; [4] Teng et al. (2015) *Clin Biomech*

AN INNOVATIVE APPROACH TO IDENTIFYING OPTIMAL SETTINGS FOR PHYSICAL ACTIVITY SENSORS.

Sydney M. Lundell[1], Kenton R. Kaufman[1]
[1]Mayo Clinic Motion Analysis Laboratory, Rochester, MN
Lundell.Sydney@mayo.edu, Kaufman.Kenton@mayo.edu

Introduction: As the push for personalized medicine has grown, researchers and clinicians alike have begun exploring the use of data from commercially available physical activity sensors (PAS) to track metrics of patient activity such as step count. However, the need for high repeatability and accuracy in research, especially at lower cadences, has highlighted the limitations of current commercially available sensors[1-3]. Presently, the accepted approach for validating step counts entails video recording participants walking with a PAS in a laboratory setting, manually counting each step recorded in the video, and subsequently comparing the observed count with the sensor's count[4-5]. While accurate, these human observations are limited by the range of walking speeds and setting combinations that can be tested in one session. Thus, a method for identifying a subset of sensor settings with minimal anticipated error is necessary to ensure that sensor validation is done accurately and efficiently. The goal of this project was to develop a reliable method for quantifying error of multiple sensor settings over a range of cadences prior to implementing the current gold standard of video validation.

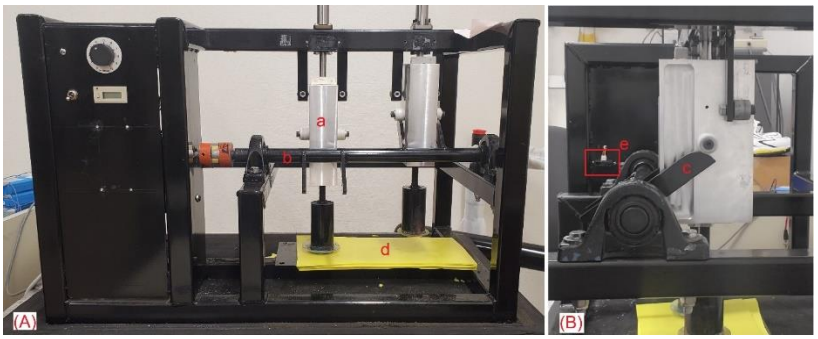

Figure 1: A front view of the continuous impactor is shown in (A). (B) is 90 degree rotation looking down the cam (b) towards the distance sensor (e). (a) is one of the two 2.5kg pistons. Each piston impacts 1 cm of poron foam (d) after being lifted a height of 8 cm by a pair of fins (c).

Methods: A mechanical system capable of continually emulating steps over a frequency range was designed and built. The system (Figure 1) consisted of a 1/8 hp motor connected to a cam which raised two alternating 2.5 kg pistons 13 cm and then drop them. The piston impacted a 1 cm thick poron foam slab with impacts were measured at 1.1g. An optical distance sensor (Sharp GP2Y0A21YK0F GP2Y0A21) detected each piston impact. Raw distance sensor data was collected at 100 Hz using a National Instruments DAQ USB X Series and used to determine total step count. The PAS consisted of a LSM6DSL Inertial Measurement Unit, which employed three key settings—threshold (0.032g – 1g), debounce time (80ms-2440ms), and minimum steps for collection (1-7)—via a black box algorithm to predict total steps. 2 PAS were attached to each piston and a total of 112 collections, each spanning 45 minutes at three cadence ranges (30-60, 30-90, 30-110 steps/min) were collected. In total 448 unique sensor settings equally spaced across the subspace of combinations were evaluated. Error for each sensor setting was calculated as the difference between the ground truth of the continuous stepper and the sensors divided by the ground truth.

A multivariate polynomial regression (MPR) was used to determine the relationship between the 4 independent variables (threshold, debounce time, minimum steps, and cadence) and sensor error. Two goodness of fit measures, R2 and the cross-validated mean absolute error (CVMAE), were calculated to determine which power produced the best fit. Training was conducted with 90% of the collected data and validated the 10% remaining data. Utilizing the MRP the anticipated error for each setting across three cadence ranges was calculated. To identify which setting combination had the lowest error, the standard deviation (STD) and absolute mean difference about zero (AMD) were computed. A composite score weighting 9/10 to AMD was then calculated to identify sensor setting combinations that were predicted to produce the least error (±10%). A subset of setting combinations was reported for each range of cadences.

Results & Discussion: The model with the lowest chance of overfitting was a 4th order polynomial with an R2 =0.8 and Cross-Validated Mean Absolute Error of 3.289 (Table 1). This model was used to calculate subsequent error profiles. A total of 7595 setting combinations were calculated. The proposed method identified 50 sensor setting combinations that fit within a STD ±10%. Of those combinations, a subset produced an average error within 1% of zero error.

Table 1: R-Squared, RMSE, and CVMAE of the multivariate polynomial from the 1st to 5th power.

Power	1st order	2nd order	3rd order	4th order	5th order
R-Square	0.271	0.524	0.722	0.800	0.847
RMSE	0.086	0.0813	0.075	0.044	0.185
CVMAE	5.085	5.295	3.383	3.589	4.171

Significance: As interest in wearable sensors for research increases a method to assure the optimized sensor setting is utilized is necessary to maintain research rigor and repeatability. This proposed method enables the reduction of the sensor setting matrix to a manageable subset that can be optimized before fine-tuning the settings through human subject validation. Notably, it allows researchers to identify settings with consistent error across a range of cadences, providing confidence in the observed changes during daily activities (e.g., for studying variable cadence).

Acknowledgments: Thank you to OPOS1 for providing the sensors for testing.

References: [1]L. S. Dhingra *et al. JAMA Netw Open*, 6(6) Jun. 2023. [2] A. Henriksen *et al.*, *J Med Internet Res*, 20(3),Mar. 2018. [3] F. A. Storm., *et al.*, *PLoS ONE*, 10(3) Mar. 2015.[4] H. M. Husted and T. L. Llewellyn, *Int. J. Exerc. Sci.*, 10(1), Jan 2017. [5] E. Fortune, V. Lugade, M. Morrow, and K. Kaufman, *Med. Eng. Phys.*, 36(6), Jun. 2014.

IMPACT OF FATIGUE PROTOCOL ON ANTERIOR KNEE LAXITY AND VERTICAL GROUND REACTION FORCES

Taliah J. Carlson[1*], Joshua T. Weinhandl[1]
[1]University of Tennessee Knoxville, TN, U.S.A
*Corresponding author's email: tcarlso3@vols.utk.edu

Introduction: Annually, estimates suggest over 120,000 anterior cruciate ligament (ACL) injuries occur [1], often due to rapid and sudden accelerations, decelerations, and changes in direction for non-contact injuries [2]. The stability of the knee joint is dependent on the ligaments and tendons surrounding the joint being sufficiently taught [3], so excessive anterior knee laxity (AKL), which is the anterior displacement of the tibia relative to the femur, is an ACL injury risk factor [4]. This emphasizes the importance of investigating AKL changes during athletic activities to aid in developing injury prevention strategies. Athletes frequently experience muscle fatigue, defined as a reduced force producing capability of the muscles involved [5]. Fatigue may increase ACL injury risk by temporarily decreasing muscle strength and adversely changing lower extremity kinematics and kinetics during high-risk tasks, such as landing and cutting. Thus, understanding individual risk factors and their potential interrelations could aid in injury prevention and rehabilitation approaches. This study aimed to examine the effects of a dynamic warmup and subsequent fatigue protocol on AKL and vertical ground reaction forces (vGRF). It was hypothesized the warmup would not influence AKL, but that AKL, peak vGRF, and average vGRF loading rate would increase as a result of fatigue.

Methods: Nine healthy, recreationally active females (age: 21.78 ± 2.73 years, height: 1.65 ± 0.08 m, mass: 61.92 ± 11.71 kg) engaged in a pre-warm laxity test then a dynamic warm-up followed by baseline measurements for the countermovement jump (CMJ), drop jump (DJ), and drop cut (DC). Subsequently, participants engaged in a fatigue protocol simulating a game or practice scenario using the Yo-Yo Intermittent Recovery Test. Participants engaged in three rounds of the Yo-Yo Test, with CMJ, AKL, DJ, and DC collected after each round. AKL was measured with a GNRB® arthrometer (Genourob, Lavel, France) and vGRF was measured with force plates (2000 Hz, AMTI, Inc., Watertown, MA, USA). The vGRF data was processed in MatLab and filtered with a 4th order low pass Butterworth filter with a cut-off frequency of 50 Hz. Examined variables were AKL of the preferred kicking leg, peak vGRF and average vGRF loading rate from initial contact to peak vGRF. Peak vGRF and loading rate were both normalized by body weight. Using SPSS, repeated measures ANOVA tests (1x6 for AKL and 1x4 for vGRF data) were performed with an alpha level of 0.05.

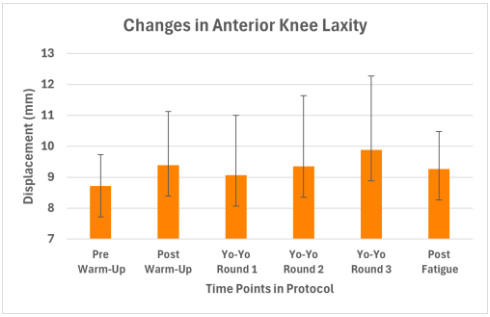

Figure 1: Changes in anterior knee laxity (AKL) throughout the data collection protocol.

Results & Discussion: For AKL, there was a medium to large effect size (η^2 =0.129), but there was no significant differences within-subjects. For the vGRF data, the peak loading and average loading rate was not significant for the DJ and DC, but there was a medium to large effect size (η^2 =0.128) for the DJ peak loading. There was a small to medium effect size for the average loading rate for both DJ and DC (respectively, η^2 =0.043 and η^2 =0.043) and for the DC peak loading a small effect size (η^2 =0.023). The hypothesis was partially supported because AKL did increase from baseline to completion of the fatigue protocol, but it did not increase across every timepoint as seen in the decrease from post warm-up to completion of Yo-Yo Round 1 (Fig. 1). The hypothesis for vGRF was partially supported: peak vGRF in the DJ consistently increased, while in the DC it increased until Yo-Yo Round 2, then decreased after Round 3. The average loading rate for DC followed a similar pattern, whereas for DJ, it increased to Round 1, then decreased in subsequent rounds.

This preliminary data from the ongoing study shows that there is a medium to large effect of fatigue on AKL. While not significant, from pre warm-up baseline measures: there was a 7.5% increase to post-warm up (Cohen's d_m=0.48), 3.5% increase to Yo-Yo Round 1 (Cohen's d_m=0.23), 7.4 increase to Yo-Yo Round 2 (Cohen's d_m=0.36), 12.6% increase to Yo-Yo Round 3 (Cohen's d_m=0.64), and a 6.5% increase to 30-minutes post fatigue (Cohen's d_m=0.49). Previous research has identified exercise-related increases in AKL, but varied in fatigue protocols, examined the stance limb rather than kicking leg, or studied a specific sport population [6]. This shows the importance of continued research on the potential link between muscle fatigue and its effect on AKL to aid in developing injury prevention and rehabilitation programs for ACL injuries.

Significance: This research was part of an ongoing study examining the effects of muscular fatigue on AKL as well as the vGRF supporting variables of peak loading at impact and average loading rate that are exploratory elements of the analysis. Thus far, the relationship between AKL and fatigue appears complex. The medium to large effect sizes, alongside the apparent increases in AKL and vGRF measures as a result of fatigue emphasize the necessity for continued research. As the study expands its sample size, the findings will deepen our understanding of muscular fatigue's role in ACL injury mechanisms. Once this relationship is established in a controlled, laboratory setting future studies can examine if it continues in an individual's natural environment or in developing clinical screening tools.

References: [1] Gornitzky et al. (2016), *Am J Sports Med*, 44(10); [2] De Ste Croix et al. (2015), *Scand J Med Sci Sports* 25(2); [3] Myer et al. (2008), *Am J Sports Med* 36(6); [4] Shultz et al. (2009), *Sports Health* 1(1); [5] Enoka & Duchateau (2008), *J Physiol* 586(1); [6] Shultz et al. (2013), *Med Sci Sports Exerc* 45(8)

EVALUATING ALTERNATIVE INERTIAL MEASUREMENT UNIT LOCATIONS ON THE BODY FOR SLIP RECOVERY MEASURES

Michelle A. Morris[1], Youngjae Lee[1], Neil B. Alexander[2], Christopher T. Franck[3], Michael L. Madigan[1*]
[1]Grado Department of Industrial and Systems Engineering, Virginia Tech, Blacksburg, VA, USA
[2]Department of Internal Medicine, University of Michigan, Ann Arbor, MI, USA
[3]Department of Statistics, Virginia Tech, Blacksburg, VA, USA
*Corresponding author's email: mlm@vt.edu

Introduction: Slip-induced falls are a leading cause of injuries in the United States [1-2]. Slips have traditionally been studied in a laboratory-controlled environment with optoelectronic motion capture (OMC) systems. Inertial measurement units (IMUs) are less expensive wearable devices that can also capture body kinematics for real-world data collection. The purpose of this study was to compare key slipping kinematic measures derived from IMUs on the foot and ankle with those derived from a gold standard OMC system. By placing IMUs on the foot and ankle, we aimed to provide more sensor wear options for participants in long-term studies, as ankle IMUs can be worn regardless of footwear. We hypothesized that any difference in key slipping kinematic measures between IMUs and OMC would be small enough to recognize clinically-important differences between falls and recoveries.

Methods: Thirty older adults (18 female, age = 71.8 ± 4.3 years, BMI = 27.3 ± 4.4 kg/m^2) were slipped while walking at a self-selected purposeful speed along a 10-meter walkway. Slips were induced by spreading vegetable oil over a 1.0 m^2 area on the walkway while participants were distracted. All participants had their dominant foot slipped at heel strike. Kinematic data were simultaneously collected from an IMU on the slipping foot and ankle, as well as markers on the ankles, heels, and toes using OMC (Qualisys North America, Inc., Buffalo Grove, IL). IMU local frames were aligned with anatomical planes [3], and a zero-velocity correction was used to account for IMU drift [4]. Slip distance and peak slip speed in the anterior-posterior (AP) direction were calculated from both systems. 90% confidence intervals of system differences were calculated and compared to equivalence intervals established using previous literature [5-7]. Equivalence intervals were determined as the minimum difference between falls and recoveries from slips reported across three studies (±11.4 cm for slip distance, and ±52.9 cm/s for peak slip speed) [5-7].

Results & Discussion: Of the 30 trials, three were excluded from the analysis due to a missed slip. 90% confidence intervals (CIs) of system differences for both foot and ankle IMUs were within equivalence margins (Table 1). A Bland-Altman analysis was also performed to determine 95% limits of agreement and mean biases (Figure 1). These results support our hypothesis.

Table 1. Equivalence test comparing the established equivalence interval to 90% CI of the difference between each IMU-derived measure and the corresponding OMC-derived measure

		Equivalence Interval	90% CI	*p*-value
AP Slip Distance (cm)	Foot IMU vs. OMC	[-11.4, 11.4]	[-5.86, -0.02]	<.001
	Ankle IMU vs. OMC	[-11.4, 11.4]	[-5.80, -2.09]	<.001
AP Peak Slip Speed (cm/s)	Foot IMU vs. OMC	[-52.9, 52.9]	[-24.72, -6.72]	<.001
	Ankle IMU vs. OMC	[-52.9, 52.9]	[-40.57, -24.41]	<.001

IMU = Inertial Measurement Unit; OMC = Optoelectronic Motion Capture

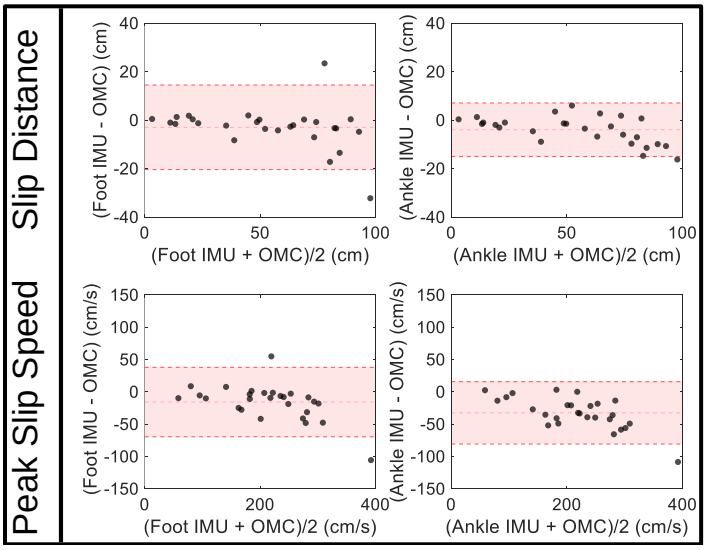

Figure 1. Bland-Altman analysis comparing foot and ankle inertial measurement units (IMUs) to gold-standard optoelectronic motion capture (OMC)-derived slip recovery measures. The shaded region indicates the 95% limits of agreement.

Significance: Our results provided evidence that IMUs can be a viable form of portable motion-capture for slip kinematics. Moreover, IMUs have potential for accurate slip measurement outside of the laboratory environment, potentially leading to a better understanding of real-world slip events. Using both ankle and foot IMUs for slip recovery measurement expands footwear flexibility for participants in long-term studies.

Acknowledgements: Research reported in this publication was supported by the National Institute On Aging of the National Institutes of Health under Award Number R21AG075430. The content is solely the responsibility of the authors and does not necessarily represent the official views of the National Institutes of Health.

References: 1. *WISQARS Leading Causes of Nonfatal Injury*, CDC (2020); 2. Courtney et al. *Ergonomics* (2001); 3. Cain et al. *Gait Posture* (2016); 4. Rebula et al. *Gait Posture* (2013); 5. Brady (2018). 7. Morris et al. *American Society of Biomechanics Conference 2023*

DO SHOE STRUCTURAL FEATURES MATTER FOR AGILITY AND STABILITY DURING WALKING?

Kavya Katugam-Dechene*, Ava Cook, Anh D. Nguyen, Ross E. Smith, Andrew D. Shelton, and Jason R. Franz
Joint Department of Biomedical Engineering, UNC Chapel Hill and NC State University, Chapel Hill, NC, USA
*Corresponding author's email: kkatugam@email.unc.edu

Introduction: Depending on design characteristics, shoes can serve to accommodate various foot pathologies, alleviate symptoms of musculoskeletal injury, and provide protection from the environment [1]. Intuitively, footwear geared towards an aging demographic and/or orthopedic consumers may opt to consider characteristics designed to enhance walking agility and/or stability to improve locomotor performance during activities of daily living [2-4]. Moreover, independent of the specific characteristics underlying footwear selection, shoes are often called upon to support the performance of many different types of activities, from steady-state walking to turns and reactive balance tasks in our communities. Thus, the purpose of this study was to investigate the extent to which shoe design features intended for stability versus agility affect walking tasks that would disproportionately depend on those features. We hypothesized that participants would experience task-specific benefits when wearing the corresponding feature-focused designs.

Methods: Fifteen adults (age: 43.1±20.2 yrs, 7M/8F, height: 1.70±0.10 m, mass: 68.9±11.0 kg, speed: 1.33±0.20 m/s) completed two walking tasks intended to disproportionately require greater agility (i.e., a figure-8 walking task involving continuous turning; Fig. 1A) or greater stability (i.e., walking while responding to treadmill-induced slip perturbations; Fig. 1B). In randomized order, participants completed those walking task while wearing each of two footwear designs produced by the same company: (1) a supportive hiking boot with a protective leather upper, stabilizing rubber outsole, and higher ankle collar, and (2) a flexible sneaker with lightweight construction, stretchable upper material, and lower ankle collar (Fig. 1C). As a benefit to our study design, both shoes use identical orthotic insole and midsole designs. These shoes were of course considerably different in their intended purposes and were thereby selected to inform follow-on studies designed to quantify the role of individualized shoe design features with better resolution. We recruited participants representative of the company's target population, including standing workers, older adults, and individuals prescribed orthopedic footwear. Primary outcome measures for the agility task included average figure-8 speed, overall major axis length and minor axis width, and step count. Primary outcome measures for the stability task included recovery step width and length as well as mediolateral and anterior-posterior margins of stability (i.e., MoS_{ML} and MoS_{AP}, respectively).

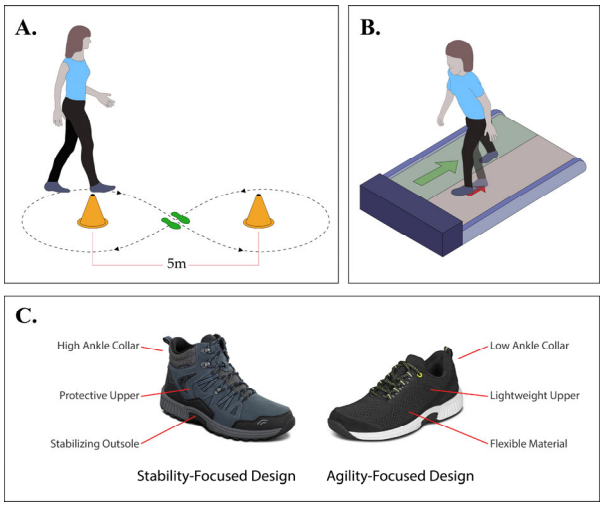

Figure 1: A. Agility-intensive walking task, consisting of figure-8 walking involving continuous turning. **B.** Stability-intensive walking task, consisting of walking while responding to treadmill-induced slip perturbations. **C.** Two footwear designs worn by participants: (1) stability-focused hiking boot and (2) agility-focused sneaker.

Results & Discussion: For the agility task, we found no significant differences between footwear designs in average figure-8 speed ($p = 0.27$, E.S. = 0.12), minor axis width ($p = 0.78$, E.S. = 0.03) or major axis length ($p = 0.51$, E.S. = 0.07). For the stability task, we found no significant differences between footwear designs for step width ($p = 0.43$, E.S. = 0.12), step length ($p = 0.33$, E.S. = 0.27), MoS_{AP} ($p = 0.51$, E.S. = 0.12), or MoS_{ML} ($p = 0.38$, E.S. = 0.20). Conversely, participant perceptions reflected differences in the design features of these two shoes. Perception of the hiking boot was mixed; some felt the shoe to be supportive and more stable, while others, like with any hiking boot, found it "large" and "bulky". For the sneaker, participants reflected positively on the lightweight design and flexibility, perceiving a greater ability to quickly react to and correct for perturbations. Despite differences in user perception, the results of this study suggest that shoe design features intended for stability versus agility minimally influence subject performance when faced with various walking challenges. More specifically, design features intended for agility or stability seemed to convey generalized performance characteristics on walking tasks we would presume to disproportionately depend on those features.

Significance: We suggest that our results may improve consumer confidence in footwear selection – often thereafter called upon to meet the needs of a variety of activities of daily living. That said, psychological factors such as balance confidence and self-efficacy – particularly in older consumers – have been shown to influence inclination towards and participation in physical activity [5,6]. Shoe design features that improve confidence and perceived ability may improve locomotor health by increasing engagement in physical activity.

Acknowledgments: This research was supported in part by a grant from Orthofeet, Inc. to the Applied Biomechanics Laboratory at UNC Chapel Hill. The views expressed in this abstract do not represent those of Orthofeet, Inc.

References: [1] Gerdhem et al. (2006), *Arch Phys Med Rehab* 87(7); [2] Koepsell et al. (2004), *J Am Geriatr Soc* 52(9); [3] Maki et al. (1997), *Phys Ther* 77(5); [4] McPoil. (1988), *Phys Ther* 68(12); [5] Cheval & Boisgontier (2021), *Ex & Sports Sc Rev* 49(3); [6] Talkowski et al. (2008), *Phys Ther* 88(2).

NONANR: AN R PACKAGE FOR NONLINEAR ANALYSIS

Joel H. Sommerfeld[1,2], Seung Kyeom Kim[1], Tyler M. Wiles[1], Aaron D. Likens[1,2*]
[1]Nonlinear Analysis Core, Center for Human Movement Variability, Omaha, NE
[2]Department of Biomechanics, University of Nebraska at Omaha, Omaha, NE
*Corresponding author's email: bmchnonan@unomaha.edu

Introduction: Quantifying variability can be challenging with many nonlinear analysis methods in existence, with many unvalidated versions of a single algorithm scattered across the web. The Nonlinear Analysis Core (NONAN) maintains a library of methods that can be used for time series analysis in MATLAB and Python[1]. These functions have been used in over 50 publications just in the past 4 years by faculty in our department alone.

NONAN works diligently to ensure that the collection of functions we maintain are accurate and reflect the changing landscape on nonlinear analysis. To that end, we are continually updating the existing functions and adding some new functionality. However, one of the main drawbacks of our existing functions was their execution time. With efficiency in mind, we have developed an R package that contains all the key nonlinear analysis methods written in C++ with Rcpp[2]. In this abstract, we highlight some of that work, demonstrating accuracy while showing impressive speed gains in many cases.

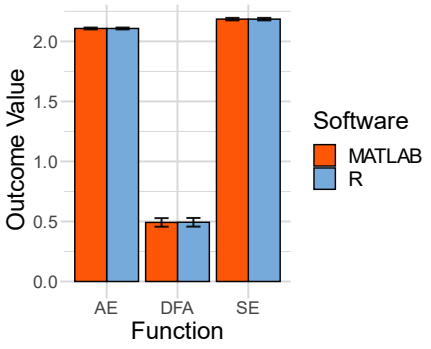

Figure 1: Bar chart depicting the average algorithm output as a function of software environment. Error bars depict standard deviations.

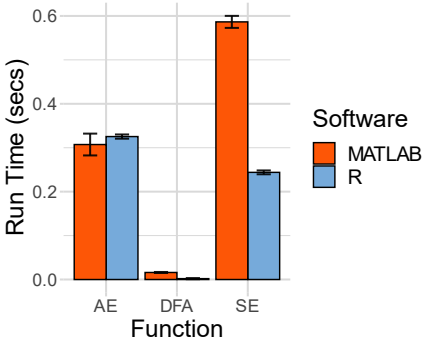

Figure 2: Bar chart depicting average run time as a function of algorithm and software environment. Error bars depict standard deviations.

Methods: 1000 random time series of 5000 data points in length were created and served as the data for all simulations of each function. To compare the speed of the old and new functions, we chose three nonlinear analysis methods to compare: Detrended Fluctuation Analysis (DFA), Sample Entropy (SE), and Approximate Entropy (AE) since they are some of the most common nonlinear analysis methods used in the literature.
We ran simulations on all 1000 time series, for each method in MATLAB (The Mathworks Inc., Natick, MA, USA) and in R (R Core Team, 2024, v4.3.2). Parameters measured were function run time and the result of the function. Once all the simulations were complete, the results were loaded into R for statistical analysis.

Results & Discussion: Figure 1 shows the average output value as a function of method and software (MATLAB vs R). The graph suggests that MATLAB and R function versions return essentially the same values. Paired t-tests were used to compare the output values and support that observation. In terms of output values, there were no significant differences observed for AE ($p = 0.072$, $d = 0.06$), DFA ($p = 0.139$, $d = -0.05$), or SE ($p = 0.205$, $d = -0.04$). Not only did t-tests not reach conventional levels of statistical significance, but the Cohen's d values also were close to zero.
Figure 2 depicts the average run time as a function of method and software (MATLAB vs R). That graph suggests that the R versions were dramatically faster for DFA and SE. Paired t-tests were again used to compare algorithms in in terms of speed. The R functions were significantly faster for DFA ($p < 0.001$, $d = 8.47$) and, SE ($p < 0.001$, $d = 23.93$). The only significant difference in run time where MATLAB was faster is in the case of AE ($p < 0.001$, $d = -0.71$), although the mean time difference was 0.01 seconds and the consistency was more varied than R (Fig. 3). Our results show that with nonanR, one can increase analytical efficiency while not sacrificing the accuracy of the nonlinear algorithms.

Significance: The results suggest the R package can greatly enhance efficiency by decreasing processing time. While speed and accuracy may be comparable for some functions, like AE, the R package has several advantages: speed, extensive documentation and outcome interpretation. The new package also brings with it a graphical user interface built on the Shiny platform for easy point and click nonlinear analysis – think SPSS but for nonlinear analysis.

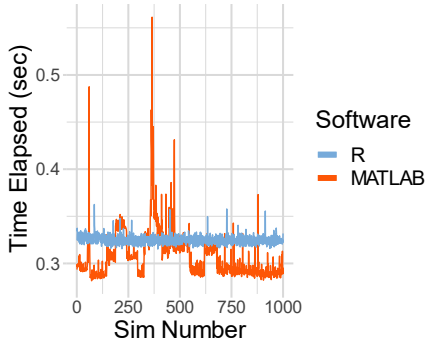

Figure 3: Time series of function run times for AE. MATLAB is more variable than R despite being significantly faster as per the t-test results.

Acknowledgments: This research was supported by NIH P20GM109090, the Center for Research in Human Movement Variability at the University of Nebraska at Omaha and NSF award 212451.

References:

[1] Nonlinear Analysis Core (2024). NONANLibrary. GitHub.
[2] Eddelbuettel D, et al. *Rcpp: Seamless R and C++*

SPRINT BIOMECHANICS IN COLLEGIATE AMERICAN FOOTBALL ATHLETES AFTER ACL RECONSTRUCTION

Naoaki Ito[1], Yi-Chung Lin[2], Jack A. Martin[1], Stephanie A. Kliethermes[1], Silvia S. Blemker[3], David A. Opar[2], Bryan C. Heiderscheit[1*]; HAMIR Consortium Investigators

[1]University of Wisconsin – Madison, Department of Orthopedics and Rehabilitation, Madison, WI, USA

[2]Australian Catholic University, School of Behavioural and Health Science, Fitzroy, VIC, Australia

[3]Springbok Analytics, Charlottesville, VA, USA

*Corresponding author's email: Heiderscheit@ortho.wisc.edu

Introduction: Aberrant walking and running biomechanics such as shorter stance times (antalgic gait) and lower knee flexion angles during weight acceptance are commonly seen in athletes after anterior cruciate ligament reconstruction (ACLR) surgery [1, 2]. Movement asymmetries during gait are associated with poor long-term knee joint health and worse clinical outcomes [3]. Sprinting is a crucial part of performance in many athletes involved in sports with high prevalences of ACL injuries. Biomechanics during overground sprinting (greater than 80% effort), however, has been seldom studied in this population due to challenges with movement artifact, spatial constraints using traditional 3D motion capture, and limitations with treadmill testing at high speeds. Inertial measurement unit (IMU) technology and accuracy in knee joint modeling continue to improve [4], allowing for overground sprint biomechanics analyses in athletes with lower limb orthopaedic injuries. The purpose of this study was to quantify stance time and knee joint kinematic asymmetries in Division-1 (D1) collegiate American football athletes with a history of ACLR. We hypothesized that shorter stance times and lower knee flexion angles would be observed in the involved compared to the uninvolved limb in athletes after ACLR.

Methods: This study is a secondary analysis from an ongoing multi-center prospective cohort study of D1 collegiate American football athletes (*ClinicalTrials.gov ID: NCT05343052*) [5]. Twenty male athletes (age = 21.6 ± 1.4 years, body-mass index = 29.2 ± 3.4 kgm^{-2}) with a history of unilateral ACLR (median [range] time from surgery = 20 [7 – 63] months) completed sprints between 20 to 60-yards (peak sprint speeds = 7.4 ± 0.6 ms^{-1}) while equipped with IMUs (Xsens MVN Awinda system, Movella, Enschede, The Netherlands) on their pelvis, thighs, shanks, and feet. N-pose calibrations were performed as recommended and knee flexion angles were obtained from the proprietary Xsens software (MVN Analyze 2022.0, Movella). Knee kinematics captured during sprinting using this method have demonstrated excellent agreement with 3D motion capture [4]. Initial contact and terminal stance events were also extracted from Xsens software and corrected with visual inspection of the model when indicated. Stance time (ms), knee flexion angle at initial contact (KFIC), peak knee flexion angle during stance (PFK), and knee flexion excursion (PKF – KFIC) were calculated during 2 (for athletes that sprinted less than 30-yards) or 5 strides near peak sprint speeds for each limb. Linear mixed effects models were used to evaluate the fixed effects of limb, time from surgery, and the interaction effects on both variables of interest. Time from surgery was included in the model to account for expected improvements in biomechanics over time after ACLR. Athletes were modelled as random intercepts.

Results & Discussion: No main effects of limb, time from surgery, or interaction effects were observed for all variables of interest (Figure 1, p = 0.15 – 0.97). In contrast to our hypothesis, the results showed no differences between limb in stance time (estimated marginal means [95% confidence interval]: Uninvolved = 143.2 [136.7, 149.6] ms, Involved = 145.6 [139.7, 152.0] ms), PKF (Uninvolved = 38.0 [34.4, 41.6] deg, Involved = 37.6 [34.0, 41.2] deg), KFIC (Uninvolved = 26.0 [22.0, 30.0] deg, Involved = 24.6 [20.5, 28.6] deg), and knee flexion excursion (Uninvolved = 12.0 [9.2, 14.8] deg, Involved = 13.1 [10.3, 15.8] deg). Asymmetrical knee kinematics may not present during sprinting in athletes after ACLR, unlike what has been observed in running gait at lower effort levels [2]. Time from surgery also did not influence our findings, however, many athletes in this cohort were more than 12 months post-surgery (80%). The greatest knee kinematic deficits and fastest improvements over time are expected during the initial months after ACLR [2]. A cohort more acutely after ACLR may present with greater deficits in knee kinematics, and may also demonstrate an effect of time as seen in the walking and running literature [1,2].

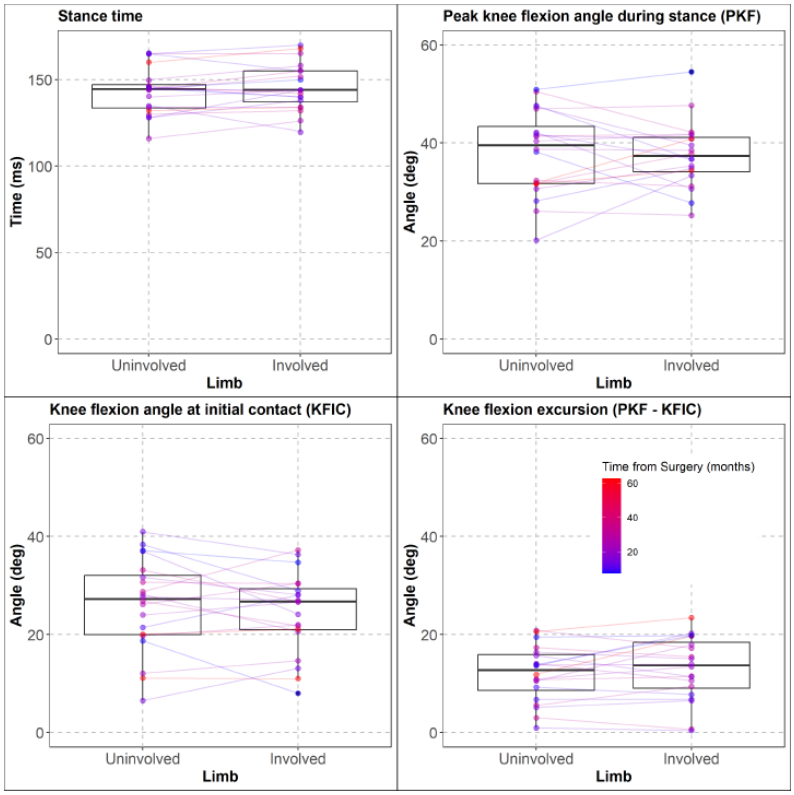

Figure 1: Box plots for stance time and knee flexion angles compared between limbs. Individual athlete data are also shown and connected between limbs with color gradient representing time from surgery in months.

Significance: This is the first study to our knowledge that quantified knee joint kinematics during on-field sprinting in athletes after ACLR. Similar approaches may be applied at earlier timepoints after ACLR and in larger cohorts to understand sprint biomechanics deficits after ACL injury.

Acknowledgments: Funding was provided by the National Football League (NFL).

References: [1] Ito et al. (2022), *MSSE*; [2] Knurr et al. (2021), *AJSM;* [3] Wellsandt et al. (2016), *AJSM*; [4] Lin et al. (2023), *Sensors*; [5] Heiderscheit et al. (2022), *BMC Sports Science*

BIOMECHANICS OF SUCCESSFUL AND UNSUCCESSFUL JERKS IN WEIGHTLIFTING COMPETITION

Wandasun Sihanath, Emma Patterson, and Kristof Kipp
Marquette University
*Corresponding author's email: wandasun.sihanath@marquette.edu

Introduction: The clean and jerk is a two-part lift that requires lower and upper body strength to first move the barbell from the floor to the front of the shoulders and then from the shoulders to overhead. The second part of the lift (i.e., jerk) is a technically complex movement that requires coordination and control because it involves a rapid downward countermovement followed by forceful leg extension to "drive" the barbell high enough for the lifter to rapidly reposition themselves underneath the barbell and to "catch" it in the overhead position with locked out arms.

Although the jerk is a crucial part of the clean and jerk lift, there exists very little research on the biomechanical and technical factors that contribute to its successful performance. When comparing lifters of different skill levels, laboratory work suggests that greater vertical force during the drive phase and a lower eccentric phase duration both positively correlate with better jerk performance [1]. Many lifters, however, fail to successfully complete the jerk during the competition. The purpose of this paper was to compare barbell kinematics and kinetics of successful and unsuccessful jerk attempts in competition.

Methods: Sagittal plane videos of clean and jerk attempts were recorded during the North American Open Finals competition with a digital camera (SONY) at 120 Hz. The position of the barbell for load-matched successful and unsuccessful attempts from six different lifters were automatically tracked (TEMPLO). Only jerks that were unsuccessful due to a forward drop were included. Vertical barbell velocity and force data were calculated. Time series were normalized to the start and end of the jerk. Force was normalized to 100% of bar load. Paired t-test statistical parametric mapping was used to compare the force and velocity time series of successful and unsuccessful lifts. Several discrete parameters were also extracted and compared with paired t-tests.

Results & Discussion: No significant differences in the barbell velocity or force time series of successful and unsuccessful jerks were found (Figures 1 and 2). However, discrete peak vertical velocity (1.76±0.08 and 1.67±0.08 m/s, $p = 0.002$), maximum barbell height (1.30±0.05 and 1.25±0.03 m, $p = 0.037$), and the estimated vertical velocity needed to achieve that height (2.35±0.19 and 2.19±0.08 m/s, $p = 0.037$) were greater for successful jerks. Lifters achieved similar ($p = 0.135$) peak vertical forces during successful and unsuccessful jerks (189±12% and 183±8%, respectively).

The total absolute time duration of successful jerks was shorter than that of unsuccessful lifts (1.26±0.16 vs. 1.41±0.22 s, $p = 0.035$). Time-normalized relative duration of the dip (32±1% vs 28±5%, $p = 0.128$), drive (24±2% vs 21±5%, $p = 0.135$), and catch phase (15±4% vs 25±11%, $p = 0.070$) did not significantly differ between successful and unsuccessful jerks. Only the relative duration of the reposition phase differed between successful and unsuccessful jerks (30±3% vs 27±3%, $p = 0.013$).

The presence of differences in relative duration of, and absence of differences in force during, the reposition phase suggests that lifters need to apply continuous upward force during the reposition phase. A greater applied impulse likely prevents the bar from freefalling and provides enough time for the lifter to move under the bar and reach greater peak heights needed for a successful jerk.

Significance: The results from the current study illustrate the role of barbell kinematics and kinetics of successful jerk performances, and therefore represent important information for coaches and athletes who aim to maximize clean and jerk performance in weightlifting competitions.

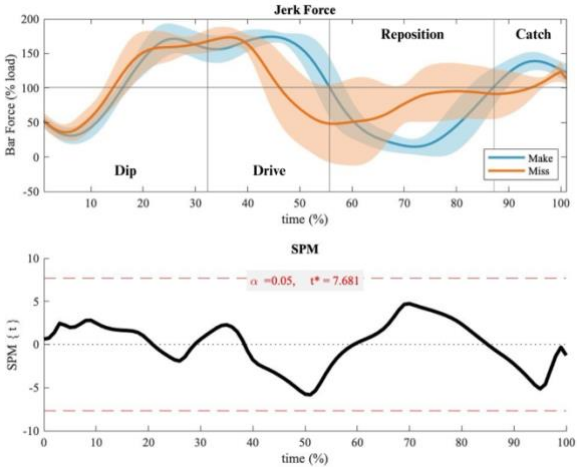

Figure 1: Bar force-time curve with corresponding SPM results. Data was normalized to 100% of the lift and load on the bar.

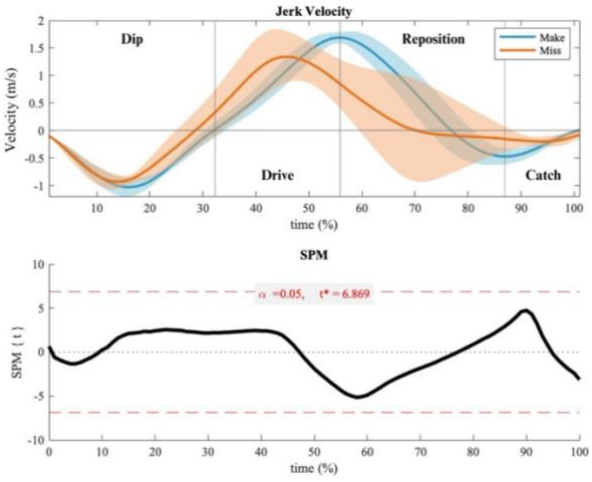

Figure 2: Bar velocity-time curve with corresponding SPM results. Data was normalized to 100% of the lift.

References:

[1] S. Grabe and C. Widule, "Comparative Biomechanics of the Jerk in Olympic Weightlifting," *Research Quarterly for Exercise and Sport*, vol. 59, pp. 1–8, Mar. 1988

SEX DIFFERENCES IN ACHILLES TENDON LOADING IN RECREATIONAL RUNNERS

Alex W. Olver[1], Haley A. Reierson[1], Amanda M. Thiers[1], Drew Rutherford[1], C. Nathan Vannatta[1,2], Thomas W. Kernozek[1,*]
[1]University of Wisconsin – La Crosse, Health Professions, La Crosse, United States
[2]Gundersen Health System – La Crosse, United States
*kernozek.thom@uwlax.edu

Introduction: Achilles tendon (AT) pathologies comprise 9-11% of all running-related musculoskeletal injuries.[1] Males have been reported to have a greater incidence of AT tendinopathy.[2] Vannatta et al.[3] reported greater gastrocnemius and soleus muscle force production in male runners in running which may result in AT loading differences. Greenhalgh & Sinclair[4] reported greater AT loading in male runners. Comparisons between males and females related to AT loading and cross-sectional area (CSA) in running have not been systematically evaluated. We aimed to compare sex differences in AT-related loading variables during running related to their implications in running-related injury risk.

Methods: Twenty-six female (age: 22.7 ± 1.26; mass: 66.9 ± 9.44; height: 169.2 ± 5.93) and twenty-three male (age: 23.6 ± 2.52; mass: 80.9 ± 10.2; height: 181.3 ± 8.13) recreational runners participated. After a warm-up, each ran at 3.35 meters per second on an instrumented treadmill (Treadmetrix, Park City, UT, USA) sampled at 1800 Hz. Kinematics were captured at 180 Hz using a 12-camera motion capture system (Motion Analysis Corp., Santa Rosa, CA, USA). Transverse ultrasound images of the AT were acquired using a GE LOGIQ Ultrasound (Waukesha, WI, USA) with an ML6-15 probe to measure AT cross-sectional area (CSA). Muscle forces were determined using static optimization from a 16-segment musculoskeletal model (Human Body Model, Motek Medical, Amsterdam, Netherlands). In the optimization, the sum of the squared muscle forces was minimized relative to their maximum strength. A 50 N vertical ground reaction force (vGRF) threshold was used to determine the right leg stance for ten steps. The mean across these steps was calculated for peak vGRF, AT-related loading variables (AT force, stress, and strain), peak medial and lateral gastrocnemius force, soleus force, foot strike angle, and stance time. Independent samples t-tests were used to examine sex differences in each variable in SPSS 29.0 (IBM Corporation, Armonk, NY, USA). Alpha was set to 0.05. Cohen's *d* was used to determine effect size.

Table 1
Mean, standard deviation (sd), statistical differences, and effect size for foot strike angle, stance time, vGRF, peak Achilles Tendon (AT) force, AT stress, AT strain, medial (med) and lateral (lat) gastrocnemius (gast) force, soleus force, and AT cross-sectional area (CSA).

Variable	Mean (sd) Female	Mean (sd) Male	Effect Size
Foot Strike Angle	25.52 (7.28)	22.43 (9.22)	0.38
vGRF (BW)	2.37 (0.24)	2.47 (0.23)	0.45
AT Force (BW)	6.75 (0.98)	7.66 (1.01)*	0.91
AT Stress (mPA)	10.37 (2.06)	10.78 (2.16)	0.20
AT Strain (%)	10.20 (2.02)	10.60 (2.12)	0.20
Med Gast (BW)	1.26 (0.23)	1.69 (0.54)*	1.10
Lat Gast (BW)	0.40 (0.08)	0.49 (0.11)*	0.91
Soleus (BW)	5.27 (0.70)	5.61 (0.76)	0.47
AT CSA (cm^2)	0.44 (0.10)	0.54 (0.09)*	1.04

*p < 0.05

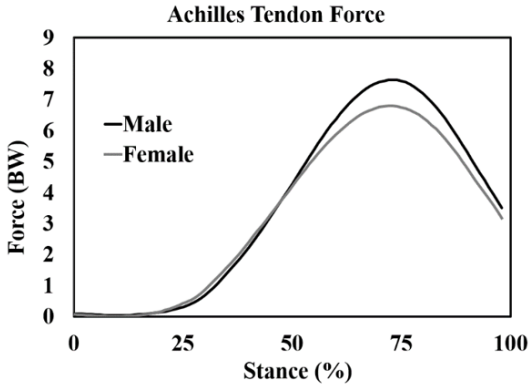

Fig. 1.
Ensemble averaged Achilles Tendon Forces during running stance between males and females.

Results & Discussion: Table 1 displays the findings of foot strike angle, stance time, ground reaction force (GRF), AT loading variables (force, stress, and strain), gastrocnemius and soleus forces, and AT CSA. All participants ran with a rearfoot strike pattern and no difference in foot strike angle or stance time was observed between males and females. Males displayed a higher AT force (13%), medial (34%), and lateral (23%) gastrocnemius peak force. Figure 1 depicts the mean AT force based on sex during the stance phase of running. Similar sex differences in gastrocnemius and soleus force in running were shown by Vannatta et al.[3] Higher AT loading was reported in male runners. Greater AT CSA in males has been previously reported.[5] Despite males exhibiting greater AT force, the concomitant 23% greater CSA compared to females contributed to small and statistically insignificant difference (4%) in AT peak stress.

Significance: While males appear to display a higher AT force, the absence of differences between males and females in AT stress suggests that the greater AT CSA in males may modulate this other loading variable. Males and females appear to demonstrate different loading patterns in the lower extremity, however, the relationship between Achilles tendon loading variables and the greater incidence of AT tendinopathies in males requires further investigation.

Acknowledgments: University of Wisconsin-La Crosse graduate studies and Gundersen Medical Foundation for funding.

References:
[1] Lopes et al. (2012), *Sports Med*, 42(10), [2] Chen et al. (2023) *J Sport Health Sci*. Mar 23. [3] Vannatta et al. (2020) *J Sports Sci*. Mar; 38(5), [4] Greenhalgh & Sinclair (2014), *J Hum Kinet, 44* [5] Intziegianni et al, (2017) *Sports Med Open*, *1*(4).

THE EFFECT OF SPEED AND TURN ANGLES ON SEGMENTAL COORDINATION DURING TURNING

Joseph A. Aderonmu* & Carolin Curtze
Department of Biomechanics, University of Nebraska at Omaha, NE, USA
*Corresponding author's email: jaderonmu@unomaha.edu

Introduction: Turning constitutes an essential aspect of daily activities and makes up about 45% of daily locomotion [1]. During turning, a craniocaudal sequence of head, trunk, and pelvis segmental coordination is often described [2]. However, aging and Parkinson's Disease can impair segmental coordination, resulting in delayed orientation timing between the head and the trunk – *en bloc* posture [3,4]. The role of head orientation in anticipating visual or vestibular information during turning is identified [5]. Yet, investigations of segmental coordination often explore temporal variables, and fewer studies have examined the angular separation that characterizes segmental coordination during turns. Here, we investigated the maximum angular divergence (separation) between body segments during pre-planned turns. Since the body must make higher segmental orientation with larger turns, we hypothesized an increase in the maximum angular divergence between body segments with larger turn angles and at fast walking speeds. Similarly, we hypothesize a higher maximum angular divergence between body segments during turns with horizontal head movements away from the pre-planned heading direction at fast walking speeds.

Methods: Healthy middle-aged and older adults performed turns through doorways at either 60°, 90°, or 120° at normal and fast walking speeds. Turn angles were randomized, and straight-ahead walks were performed between blocks of turn trials. To provide visual and vestibular perturbation during turns, participants performed a series of 90° turns with horizontal head turns away from the pre-planned heading direction by looking at a sign displayed opposite the direction of the turn at normal and fast walking speeds. Kinematic measurements during the trials were obtained using wearable sensors (Opal v2 APDM, Inc., Portland, OR, USA). We processed the data using a turn-detection algorithm validated by El-Gohary and colleagues [6]. Also, we integrated angular velocity differences in the vertical axis between the pelvis–head, sternum–head, and pelvis–sternum to obtain the angular divergence between segments during the trial. We defined a search window around the turn for every trial to obtain the maximum angular divergence between the segments. For the turns with horizontal head movements, maximum angular divergence was obtained when looking away from the pre-planned heading direction to the turn (first phase) and when executing the turn (second phase) (Fig. 1B). We will investigate differences in the maximum angular divergence between segments during turns using linear mixed effects model using turn angles (0°, 60°, 90°, 120°) and walking speeds (normal, fast) as fixed effects and participants as random effects. Differences in the maximum angular divergence will also be examined during 90° turns with and without horizontal head movements away from the pre-planned heading direction at normal and fast walking speeds.

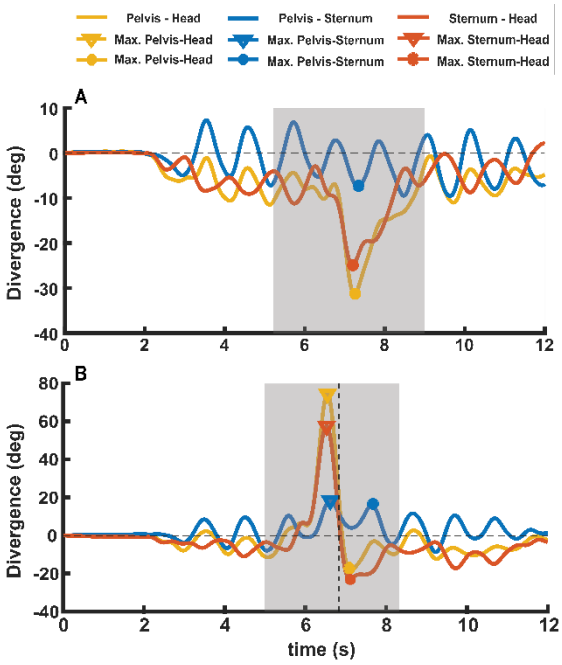

Figure 1. Maximum angular divergence during 90° turns A). without horizontal head movement away from the heading direction B). with horizontal head movement away from the turn direction. The dashed vertical line demarcates maximum divergence during horizontal head turns away from the pre-planned turns (first phase) and during the turn (second phase).

Results & Discussion: Our preliminary results (n = 13) show that larger turn angles and fast walking speeds increase the sternum–head maximum angular divergence. Also, larger turn angles increase the pelvis–head maximum angular divergence. However, the pelvis-sternum maximum angular divergence did not show a clear trend in its maximum angular divergence (Fig. 1A). 90° turns with horizontal head movements showed lower maximum angular divergence for the pelvis–head, sternum–head, and pelvis–lumbar without an apparent influence of speed compared to 90° turns without horizontal head movements (Fig. 1B). Taken together, these findings suggest the role of the head in anticipating new heading directions during turns.

Significance: Using the maximum angular divergence between body segments, we demonstrate segmental coordination and the role of body segments in sensory anticipation. Our results suggest that maximum angular divergence between body segments may serve as a measure of turning performance. We propose that future studies explore maximum angular divergence as a potential marker of functional decline.

Acknowledgments: This research is supported by the University of Nebraska at Omaha GRACA fund and the NIH P20 GM109090.

References: [1] Glaister *et al.* Gait Posture, 25, 289 – 294 [2] Akram *et al.* Can J Neurol Sci 40, 512 – 519, 2013 [3] Akram S, *et al.* Gait Posture 32, 211 – 214, 2010 [4] Huxham *et al.* Mov Disord 23, 1391 – 1397, 2008 [5] Grasso *et al.* Neuroreport 26, 1170 – 1174, 1996 [6] El-Gohary *et al.* Sensors 14, 356 -369, 2013.

ASSOCITATION BETWEEN GAIT ABILITY, FUNCTIONAL MOVEMNT AND METABOLIC SYNDROME SEVERITY IN YOUNG ADULTS

Tanner A. Thorsen[1*], Nuno Oliveira[1]
[1]School of Kinesiology and Nutrition, The University of Southern Mississippi
*Corresponding author's email: tanner.thorsen@usm.edu

Introduction: The association between metabolic syndrome (MetS) and poor gait and functional movement ability has been well established in older adults, and we recently demonstrated that a strong, negative association also exists among younger adults [1]. Recently, a continuous cardiometabolic risk score ($MetS_{index}$) was developed and may be equipped to identify individuals at risk for cardiometabolic disease who do not yet meet the stringent criteria for a formal MetS diagnosis [2]. This $MetS_{index}$ allows researchers and clinicians to evaluate cardiometabolic disease risk along a continuum, offering the potential to preemptively identify disease risk in individuals not yet meeting the defined criteria for MetS [2]. Utilizing $MetS_{index}$ in association with gait and functional movement ability may be crucial for the earlier detection of metabolic complications in younger adults. Thus, the purpose of this research was to compare gait and functional movement ability amongst young adults without a formal MetS diagnosis and a lower $MetS_{index}$, those without a formal diagnosis of MetS but with a positive $MetS_{index}$, and those with both a formal MetS diagnosis and positive $MetS_{index}$.

Methods: MetS diagnosis and $MetS_{index}$ was determined for 101 young adults using standard procedures [1]. Participants were categorized into three groups according to metabolic severity risk, $MetS_{index}$ below 0 and negative diagnosis of MetS (MetS--), $MetS_{index}$ above zero and negative diagnosis of MetS ($MetS_{index}$+-), and $MetS_{index}$ above zero and positive diagnosis of MetS ($MetS_{index}$++). Gait velocity was measured using photocell timing gates as participants completed a ten-meter walk test (10MWT, Blue, Dashr, Lincoln, USA). Distance travelled was recorded during 6-minute walk test (6MWT), and Time Up and Time Down one flight of stairs (11 steps) was recorded using photocell timing gates. A one-way ANOVA was used to assess differences in gait and functional movement variables amongst MetS groups. If a significant effect was observed, post-hoc pairwise comparisons with Bonferroni adjustments were performed to determine the significant comparison.

Results & Discussion: Of the 101 participants enrolled in this study, 65 were identified as MetS--, 25 were identified as MetS+-, and 11 were identified as MetS++. MetS++ walked significantly slower during 10MWT (p =.020) and significantly shorter distance during the 6MWT than MetS-- (p=.039, Table 1). Though a significant main effect was found for Time Down Stairs, post-hoc comparisons did not reveal any statistically significant differences in time (Table 1).

These results confirm our earlier results that declining gait velocity and functional movement ability exists in younger adults, both as $MetS_{index}$ progresses, and between the dichotomous MetS classifications. Interestingly, gait velocity was not different between MetS-- and MetS+- nor between MetS+- and MetS++. This suggests that the deleterious impact of MetS on gait velocity and functional ability may be more rooted in symptom presence, and not on arbitrary group classifications. For example, if a young adult is identified as MetS+- and presents with high blood pressure or low HDL cholesterol, they may not meet the criteria for formal MetS and also may not be as influenced in their gait performance. However, a participant classified as MetS+- and presenting with increased abdominal obesity may experience diminished gait velocity, largely influenced by the presence of obesity.

Significance: These results support the use of $MetS_{index}$ as a metric wherewith the metabolic risk of young adults may be determined. Furthermore, $MetS_{index}$ appears to be sensitive to changes in gait velocity and functional movement ability and was able to identify 25 young adults who otherwise would not have met the formal criteria for MetS. Thus, gait velocity may serve as a valid predictor of cardiometabolic risk in young adults. Future work may investigate the implications of MetS and $MetS_{index}$ on the gait and functional movement biomechanics in young adults to determine the specific effects of MetS and increasing MetSindex on movement parameters. This information may benefit younger adults by creating diagnostic standards in aimed at the earlier detection, treatment and prevention of MetS.

Table 1. Descriptive statistics (mean ± s.d.) and statistical results across MetS Groups. **Bold** indicates statistical significance.

	MetS (- -)	MetS (+-)	MetS (+ +)	p-value	Effect Size (η^2)
Gait Velocity (m/s)	1.25 ± 0.15	1.16 ± 0.20	1.1 ± 0.17[α]	**.006**	.210
6MWT (m)	479.97 ± 45.57	465.97 ± 68.03	437.09 ± 45.22[α]	**.037**	.164
Time Up Stair (s)	5.44 ± 0.55	5.65 ± 5.65	5.82 ± 0.54	.367	.089
Time Down Stair (s)	4.8 ± 0.74	4.96 ± 0.95	5.42 ± 1.18	**<.001**	.141

[α]Different than MetS (- -)
[β]Different than MetS (- +)

Acknowledgments: This work was supported by the National Institute of General Medical Sciences of the National Institutes of Health under grant number NOT-GM-23-034 (FAIN# U54GM115428).

References:

[1] Thorsen, T., et al., Exploring gait velocity as a predictor of cardiometabolic disease risk in young adults. *Front. Sports Act. Living*, 2024 (6).
[2] Gurka, M.J., et al., An examination of sex and racial/ethnic differences in the metabolic syndrome among adults: a confirmatory factor analysis and a resulting continuous severity score. *Metabolism*, 2014. 63(2): p. 218-25.

Comparing Leg Dominance In High School Basketball Players: Asymmetry In Force Generation During The Lateral Countermovement Jump

Alexandra L. Johnson[1*], BS, Jake Venes[2], CSCS, Cody Dziuk[1], BS, Janelle A. Cross[1], PhD
[1]Department of Orthopaedic Surgery, Medical College of Wisconsin, Milwaukee, WI, USA
[2]NX Level Sports Performance, Milwaukee, WI, USA
*Corresponding author's email: alljohnson@mcw.edu

Introduction: Jump assessments, such as the countermovement jump (CMJ), have been frequently used to assess lower body mechanics in athletes [1, 2, 3]. The traditional CMJ characterizes the quick downward movement (countermovement) that is immediately followed by a rapid upward jump [4]. As the CMJ focuses on a singular plane, this may limit assessment of multidirectional sports such as basketball [1]. A variation of the traditional CMJ is the lateral CMJ jump, where an explosive lateral jump follows the initial downward movement [1, 2]. Previous literature reports that basketball players spend 20-31% of the game shuffling laterally, thus studying the kinetics of the lateral CMJ can elucidate related in-game movements [1, 2]. The purpose of this study was to evaluate force generation of the lateral CMJ in high school basketball players, comparing dominant and nondominant legs using force-plates. We hypothesized observing increased biomechanical force generation in the dominant lateral CMJ compared to the nondominant extremity.

Methods: Twenty-eight high school male basketball players (age: 16.6 ±1.0 years, height: 186.2±7.9 cm, mass: 76.4±13.1 kg) performed three lateral CMJs as previously described [2] with each leg. Portable tri-axial force plates (model #4060-05-PT, Bertec Corporation, Ohio, USA) with Hawkins Dynamics software (Hawkin Dynamics, Inc., Westbrook, ME) were used to collect data at a 1000 Hz. Metrics were selected based on reliability assessments [2]. Averages of the three jumps were used for data analysis. Comparisons were made for each variable between dominant and nondominant jumping legs. Twenty-one players (75%) were left jumping leg dominant whereas seven players (25%) were right jumping leg dominant. A Shapiro-Wilk test was performed to check the normality assumption for each metric. With all variables normally distributed, paired sample t-tests were used. Statistical analysis was performed using R version 4.3.1. A significance level of $p < 0.05$ was utilized.

Table 1. Comparison of dominant and nondominant jumping leg for lateral CMJ metrics

Metric	Dominant			Nondominant			Mean Difference	p-value	
	Mean	±	SD	Mean	±	SD			
Peak Vertical Force (N)	1459.2	±	299.4	1392.4	±	283.5	66.8	<0.001	*
Peak Lateral Force (N)	633.7	±	113	625.8	±	114	7.9	0.410	
Relative Lateral Force (N/kg)	8.3	±	1.0	8.2	±	1.1	0.1	0.569	
Lateral Impulse (Ns)	188.6	±	34.9	191.1	±	31.6	-2.5	0.335	

* = significant $p < 0.05$

Results & Discussion: Only the peak vertical force demonstrated a statistically significant mean difference, with the dominant leg having a 66.8 N higher vertical force than the nondominant leg (Table 1). Significant differences in peak vertical force between the legs, a finding not observed in collegiate [1, 2] or professional [2] basketball athletes, may reveal functional strength imbalances and differences in movement strategy in youth players that are crucial to the shuffling movement. These findings provide opportunity for focused performance training and injury prevention strategies that target muscular asymmetry between dominant and nondominant jumping legs [3]. In contrast to professional athletes [2], the high school athletes in this study demonstrated reduced values in vertical and lateral forces, as well as lateral impulse.

Significance: As the studied metrics have been shown to demonstrate between-session reliability, incorporation of lateral CMJ testing may enhance performance assessments in high school basketball players [2]. Despite no significant changes in relative lateral force, findings in this study emphasize the need for future lateral CMJ studies in high school basketball athletes, as increased relative lateral force has been associated with higher shuffling speed at the collegiate and professional level [2].

Acknowledgments: We thank the Medical College of Wisconsin Department of Biostatistics for the statistical analysis.

References: [1] Reiter et al. (2023), *PLoS ONE* 18(4): e0284883; [2] Leisdorf et al. (2022), *Sports*. 10(11) 186; [3] Bishop et al. (2023), *Strength and Conditioning J*. 45(5): 545-55; [4] Van Hooren et al. (2017), *J Strength and Conditioning Research* 31(7): 2011-2020.

Analyzing The Impact Of Arm Swing On Countermovement Jump Performance In High School Basketball Players

Alexandra L. Johnson[1*], BS, Jake Venes[2], CSCS, Cody Dziuk[1], BS, Janelle A. Cross[1], PhD
[1]Department of Orthopaedic Surgery, Medical College of Wisconsin, Milwaukee, WI, USA
[2]NX Level Sports Performance, Milwaukee, WI, USA
*Corresponding author's email: alljohnson@mcw.edu

Introduction: Basketball is a multidirectional sport that requires acceleration, deceleration, change of direction, and shuffling [1]. Jump assessments, like the countermovement jump (CMJ), have been frequently utilized to assess lower body mechanics [2, 3]. The CMJ (Figure 1) involves a quick downward movement (countermovement) which is immediately followed by a rapid upward jump [4]. Popularity of force platforms in sports biomechanics and strength and conditioning have encouraged analysis of countermovement variables to assess performance (i.e. power and force generation), allowing means to assess effectiveness of training programs [2, 3]. The purpose of this study was to delineate differences in force-time variables and evaluate performance metrics of the CMJ in high school basketball players, with and without arm swing. We hypothesized that differences exist between the testing methods, with arm swing contributing to increasing jump height and propulsive metrics.

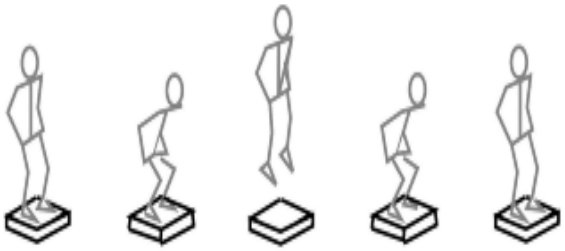

Fig 1. Diagram of the countermovement jump Kong et al. (2021) [4]

Methods: Twenty-eight high school male basketball players (age: 16.6 ±1.0 years, height: 186.2±7.9 cm, mass: 76.4±13.1 kg) completed 6 total CMJs, 3 with arms akimbo (hands on the hips during the entire movement) (CMJ no arm swing) and 3 with arms free to move (CMJ arm swing). Portable tri-axial force plates (model #4060-05-PT, Bertec Corporation, Ohio, USA) with Hawkins Dynamics software (Hawkin Dynamics, Inc., Westbrook, ME) were used to collect data at a 1000 Hz. The averages of the 3 jumps were used for data analysis. Key performance profiling metrics adapted from Bishop et al. (2023) were selected for comparison [2]. Comparisons were made for each variable between the CMJ no arm swing and CMJ arm swing tests. A Shapiro-Wilk test was performed to check the normality assumption for each metric. With all variables normally distributed, paired sample t-tests were used. Statistical analysis was performed using R version 4.3.1. A significance level of $p < 0.05$ was utilized.

Table 1. Comparison of CMJ no arm swing and CMJ arm swing metrics

	CMJ No Arm Swing			CMJ Arm Swing			Mean	p-value	
Metric	Mean	±	SD	Mean	±	SD	Difference		
Jump Height (m)	0.38	±	0.05	0.45	±	0.06	0.07	<.001	*
Peak Propulsive Force (N)	2063.2	±	449.4	2033.1	±	426.3	-30.2	0.396	
Peak Propulsive Power (W)	4355.8	±	874.7	5060.2	±	1044.3	704.3	<.001	*
Propulsive Impulse (Ns)	393.4	±	75.7	434.3	±	76.3	41.0	<.001	*
mRSI (m/s)	0.55	±	0.11	0.59	±	0.14	0.05	0.017	*

mRSI = Reactive Strength Index Modified (ratio of jump height to contraction time); * = significant $p < 0.05$.

Results & Discussion: Jump height, peak propulsive power, peak propulsive impulse, and mRSI were all significantly different between the CMJ tests (Table 1), with the mean values of all metrics increasing using arm swing compared to no arm swing. There was no statistically significant difference between tests for peak propulsive force. Our findings align with a previous study of professional basketball players that found significant increases in jump height, concentric peak power, and concentric impulse when using arm swing during a CMJ [5]. Relative to professional athletes [5], the high school athletes in this study typically exhibited lower measurements in jump height, force, and power. This discrepancy is reasonable given the variations in their competitive levels.

Significance: There is a current void in the literature for CMJ metrics in high school athletes. Biomechanical differences attributed to arm-swing may lend to improved assessment of basketball performance, whereas without arm swing may reveal important lower extremity forces crucial for multidirectional sports. These results highlight biomechanical differences between high school and professional basketball players, warranting further investigation of CMJ force-time metrics in younger populations.

Acknowledgments: We thank the Medical College of Wisconsin Department of Biostatistics for the statistical analysis.

References: [1] Leisdorf et al. (2022), *Sports*. 10(11) 186; [2] Bishop et al. (2023), *Strength and Conditioning J*. 45(5): 545-553; [3] Reiter et al. (2023), *PLoS ONE* 18(4): e0284883; [4] Kong et al. (2021), *J Men's Health* 18(5):1-7; [5] Caberkapa et al. (2023), *Int J of Strength and Conditioning* 3(1).

BILATERAL TORSO MUSCLE COORDINATION DURING ASYMMETRIC BOX TRANSFERS

Jordan T. Sturdy*, Ava Watson, Anna Corman, and Anne K. Silverman
Department of Mechanical Engineering, Colorado School of Mines, Golden CO
*Corresponding author's email: sturdy@mines.edu

Introduction: Low back pain is globally a leading cause of disability, and is projected to grow [1]. In addition, the prevalence of low back pain is higher in women than in men and varies with age [1]. Daily activities require maintaining balance while achieving movement objectives. Lifting a box, stepping up or down, bending to tie shoes, etc., all result in higher lumbar forces than walking [2], which may lead to injury resulting in low back pain [3,4]. Torso muscles generate the forces required to both stabilize and mobilize the spine [5,6], and produce coordinated activity to produce the required net torques [7,8]. However, many movement studies that include torso muscles are often limited to unilateral muscles [9], or a subset of back or abdomen muscles [10]. Thus, the purpose of this study was to improve comprehensive understanding of back and abdomen muscle coordination during asymmetric box lifting tasks in healthy men and women.

Methods: Three participants (1M/2F, age: 25±4.6 yrs, height: 1.71±0.03 m, weight: 62.1±7.6 kg) were instrumented with a full-body marker set and surface electromyography (EMG) bilaterally of the iliocostalis, longissimus, external oblique, and rectus abdominus. Marker positions (200 Hz, Qualisys), EMG (2000 Hz, Delsys), and ground reaction forces (2000 Hz, AMTI) were recorded synchronously. Participants transferred a 10lb box from a 30" shelf directly in front to a shelf on either the left or right for five repetitions in each direction. The task began with arms at sides at the moment participants began reaching forward and ended when the box was placed on the side shelf. EMG linear envelopes (bandpass: 30-400 Hz, rectify, lowpass: 5 Hz) for each muscle were magnitude normalized to the corresponding maximum amplitude during a prone back extension or supine abdominal crunch. The average of 5 repetitions was calculated for each muscle and were arranged into an 8x101 matrix for each participant. Using non-negative matrix factorization [11], three patterns (modes) of muscle activation and corresponding multipliers (weights) for each muscle were obtained in MATLAB. Muscle coactivations for each mode were classified as weak (weight <0.25), moderate (weight between 0.25 and 0.5), and strong (weight >0.5).

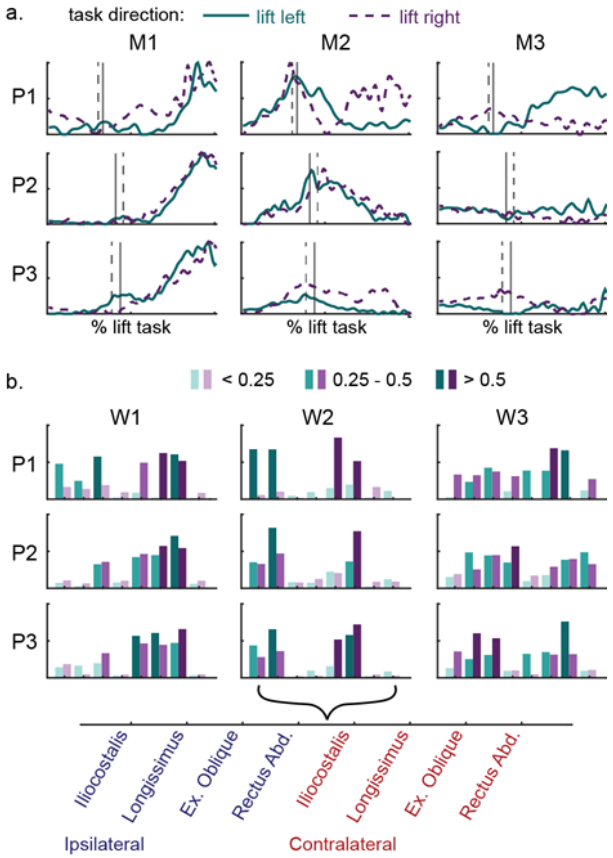

Figure 1: Muscle activation modes (a) for each participant when lifting to the left (solid teal lines) and to the right (dashed purple lines). Vertical lines show the start of box lift in solid for left and dashed for right lifts. Muscle weights corresponding to each activation mode (b) shown for left (teal bars) and right (purple bars) lifts. Weights for muscles on the lift direction side (ipsilateral) and on the opposite side (contralateral) are shown.

Results & Discussion: Muscle modes were similar between left and right lifts and across participants (Fig 1a). The first mode (M1) controlled the end of the lift task, when the torso rotation completes and the box is lowered to the shelf. The second mode (M2) is associated with picking up the box and subsequent rotation. Mode 3 (M3) comprises low amplitude muscle activity throughout the task. M1 represented moderate to strong coactivation from contralateral iliocostalis, longissimus, and bilateral external obliques for participants P2 and P3 (Fig 1b). P2 and P3 also had moderate to strong coactivation for M2 between ipsilateral iliocostalis and longissimus and contralateral longissimus. However, aside from a strong bilateral external oblique coactivation for M1, P1 had predominately left side muscle activations for both M1 and M2, regardless of lift direction. M1 suggests contralateral back extensors help lower the box while bilateral obliques maintain torso stability in axial rotation. M2 suggests bilateral longissimus generate extension torque for lifting while ipsilateral iliocostalis initiates torso rotation. The discrepancy in weights between participants may be due to EMG normalization, which is a limitation. Left side normalized activations had 2-3x greater magnitude than the right side for P1, resulting in lopsided weights. More robust signal normalization will be explored with additional participants.

Significance: These results characterize healthy bilateral back and abdomen muscle control of daily activities with 3D torso demands. Understanding this neural control is important for identifying and treating pathological movement.

References: [1] Hoy *et al.*, (2012) *Arthritis and Rheumatism*, 64(6);[2] Rohlmann *et al.*, (2014) *PLoS One*, 9(5);[3] Desmoulin, *et al.*, (2020) *Spine*, 45(8);[4] Stefanakis *et al.*, (2014) *Spine*, 39(17);[5] Granata and Orishimo, (2001) *J. Biomech.*, 34(9);[6] Lee *et al.*, (2006) *J. Electromyogr. Kinesiol.*, 16(1);[7] Ng *et al.*, (2001) *J. Orthop. Res.*, 19(3);[8] Thelen *et al.*, (1995) *J. Orthop. Res.*, 13(3);[9] Graham and Brown, (2014) *J. Biomech. Eng.*, 136(12);[10] Burnett *et al.*, (2011) *J. Electromyogr. Kinesiol.*, 21(4);[11] Rabbi *et al.*, (2020) *Sci. Rep.*, 10(1)

COMPARISON OF ACHILLES TENDON LOADING VARIABLES IN RUNNING BETWEEN DOMINANT AND NON-DOMINANT LEGS IN RECREATIONAL RUNNERS

Kaelyn C. Wagner[1], Maria K. Turco[1], Meghan S. Fraser[1], Drew Rutherford[1], C. Nathan Vannatta[1,2], Thomas W. Kernozek[1,*]
[1] University of Wisconsin-La Crosse, Health Professions Department, La Crosse, WI, United States
[2]Gundersen Health System, La Crosse, WI, United States
*kernozek.thom@uwlax.edu

Introduction: Tendons appear to adapt to mechanical stresses.[1] Running has been shown to have high Achilles Tendon (AT) loads.[2] This may explain why runners have a 36% larger AT cross-sectional area (CSA) than non-runners.[1] However, Bohm et al[3] reported the dominant AT had a greater Young's Modulus and length compared to the non-dominant side which may suggest different AT loading profiles between limbs. Differences in AT loading between limbs has yet to be fully characterized. Therefore, our purpose was to examine the AT loading differences between extremities in running. It is hypothesized that there may be differences in AT loading in running that may be relevant to AT tendinopathy.

Methods: 16 female (age: 23.2 ± 1.31, mass: 65.4 ± 8.32; height: 170.5 ± 6.03) recreational runners participated. Limb dominance was determined based on which leg the participant preferred to kick a ball. Each runner ran at 3.3 meters per second on an instrumented treadmill (Treadmetrix, Park City, UT, USA) after a running warm up. Kinetic data were sampled at 1800 Hz. A 12-camera motion capture system (Motion Analysis Corp., Santa Rosa, CA, USA) was used to sample kinematic data at 180 Hz. AT cross-sectional area (CSA) was measured for each limb from transverse ultrasound images from a GE LOGIQ Ultrasound (Waukesha, WI, USA) using an ML6-15 probe. Kinematic and kinetic data were used as input into a 16-segment musculoskeletal model (Human Body Model, Motek Medical, Amsterdam, Netherlands). Muscle forces were optimized from static optimization where the sum of the squared muscle forces was minimized relative to their maximum strength. Five steps from each leg were processed using a 50 N vertical ground reaction force (vGRF) threshold. The mean was calculated for these steps in peak vGRF, AT-related loading variables (AT force and stress), total gastrocnemius force, soleus force, foot strike angle, and stance time. Independent samples t-tests were used to examine limb differences in each variable in SPSS 29.0 (IBM Corporation, Armonk, NY, USA). Alpha was set to 0.05. Cohen's *d* was used to determine effect size. Percent asymmetry was calculated using the following equation: [|dominant leg -non-dominant leg| / (dominant leg + non-dominant leg) / 2] x 100%.[4]

Table 1
Mean, standard deviation (sd), statistical differences, effect size, and percent asymmetry for foot strike angle, stance time, peak ground reaction force (GRF), AT force and stress and gastrocnemius and soleus force, strain, gastrocnemius (gastroc) force, soleus force, and AT cross-sectional area (CSA).

Variable	Non-dominant Leg	Dominant Leg	Effect Size	Percent Asymmetry
Foot Strike Angle	26.4 (8.6)	25.6 (8.2)	0.26	3.1
Stance Time (s)	0.21 (0.1)	0.21 (0.1)	0.31	0
vGRF (BW)	2.41 (0.48)	2.38 (0.45)	0.41	1.3
Gastroc Force (BW)	2.06 (0.64)	1.87 (0.42)	0.54	9.7
Soleus Force (BW)	5.62 (1.44)	5.31 (1.18)	0.49	5.7
AT Force (BW)	7.49 (2.03)	7.11 (1.57)	0.41	5.2
AT CSA (cm^2)	0.50 (0.11)	0.49 (0.12)	0.21	2.0
AT Stress (MPa)	10.18 (1.86)	9.96 (1.63)	0.15	2.2

*p<0.05

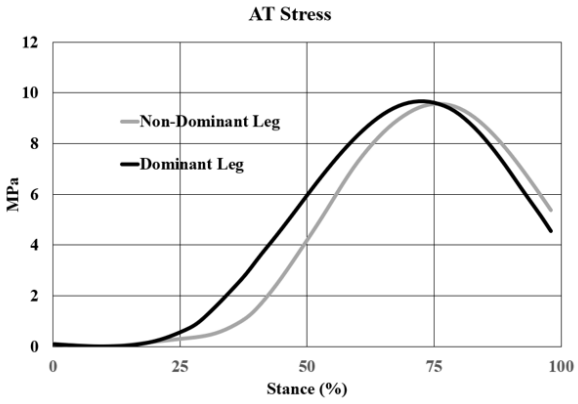

Fig 1.
Ensemble averaged AT stress from dominant and non-dominant leg during stance in running.

Results & Discussion: Table 1 displays foot strike angle, stance time, peak GRF, peak gastrocnemius force, peak soleus force, peak AT force, AT CSA, and peak AT stress. Foot strike angle indicated a rearfoot strike pattern.[5] There were no statistical differences between dominant and non-dominant limbs in any of these variables. AT loads were similar to those previously reported on rearfoot striker runners.[6,7] Effect sizes ranged from small to medium. Percentage asymmetry for the peak muscle forces of the gastrocnemius and soleus during stance (9.7 and 5.7, respectively) were similar to the muscle impulse asymmetries (10.1 and 2.26) reported by Vannatta et al.[8] in competitive runners. Our data appears to support that AT loading may be similar between dominant and non-dominant legs in healthy recreational runners.

Significance: Running appears to pose similar AT loading to the dominant and non-dominant limb during stance in female runners. While some asymmetry can be expected, these healthy runners displayed loading differences of less than 9.7%. Therefore, it may be that the task of running does not present enough mechanical asymmetry to explain previously reported asymmetries in the mechanical properties of the AT. Further research appears warranted to understand morphological asymmetries in the AT and how that may be related to running mechanics and the development of Achilles tendinopathies.

Acknowledgments: University of Wisconsin-La Crosse graduate studies and Gundersen Medical Foundation for funding.

References: [1] Bohm et al. (2015) *Sports Med Open, 1*(5), [2] Kernozek et al. (2018) *Gait & Posture*, *66*, [3] Magnusson & Kjaer (2003), *Eur J App Phys, 90.* [4] Stiffler-Joachim et al. (2021), *Med Sci Sports Exerc 53*(5), [5] Altman & Davis (2012), *Gait & Posture*, *35*(2), [6] Ertman et al. (2023), *J Sport Sciences,* 14 June, [7] Kernozek et al. (2018) *Gait & Posture*, *66*, [8] Vannatta et al. (2023), *Gait & Posture*, *103*.

NEUROMUSCULAR CHANGES TO REACTIVE BALANCE CONTROL MAY CONTRIBUTE TO INCREASED FALL RISK IN OLDER ADULTS WITH MILD COGNITIVE IMPAIRMENT

Jessica Pitts[1*], Shuaijie Wang[1], Tanvi Bhatt[1]
[1]Department of Physical Therapy, University of Illinois at Chicago, Chicago, IL, USA
*Corresponding author's email: jpitts5@uic.edu

Introduction: Mild cognitive impairment (MCI) is an intermediate state between healthy cognition and dementia which affects ~17% of older adults [1]. Older adults with MCI (OAwMCI) experience twice as many falls as cognitively intact older adults (CIOA), although the mechanisms underlying this predisposition remain unknown. When exposed to external perturbations, OAwMCI demonstrate lower reactive center of mass stability and delayed step initiation compared to CIOA [2,3], although these studies only examined kinematic outcomes. Neuromuscular factors (e.g., muscle onset latencies and patterns of activation) have also been identified as important fall determinants [4]. Thus, we compared lower limb muscle onset latencies and muscle synergies (i.e., activation patterns of multiple muscles) between young adults, CIOA, and OAwMCI when exposed to a perturbation. We hypothesized that OAwMCI would have delayed muscle onsets, along with differences in the number and spatial/temporal structure of recruited muscle synergies.

Methods: 20 young adults (YA) (ages 18-35) and 60 older adults (ages 55-90) were included. Older adults were classified as CIOA if they scored ≥25/30 on the Montreal Cognitive Assessment and OAwMCI if they scored 18-24 (n=30 each). Participants were exposed to an unexpected, forward support surface perturbation while standing on an instrumented treadmill (belt acc.=21.75 m/s^2). We calculated fall rate, reactive stability (center of mass position relative to the base of support at recovery step liftoff), and recovery step time (time from perturbation to recovery step touchdown). We also collected electromyography from bilateral lower limb muscles (biceps femoris (BF), vastus lateralis (VL), medial gastrocnemius (MG), tibialis anterior (TA)). We calculated onset latencies (time from perturbation to initiation of muscle activity) and extracted muscle synergies from perturbation onset to recovery step touchdown.

Results & Discussion: Reactive balance was impaired in older adults compared to YA (higher fall rate, lower reactive stability), and further impaired in OAwMCI than CIOA (Fall Rate-YA: 0%, CIOA: 40%, OAwMCI: 67%) (*p<0.05*). OAwMCI also had longer recovery step time than YA (*p=0.013*). These impairments may be partially attributed to delayed muscle onsets. Older adults had longer onset latencies than YA in almost all muscles, although some onsets were only delayed in OAwMCI (BF step, VL step, MG stand) (*p<0.05*). There were also group differences in the spatial structure (**Figure 1A**) and temporal activation (**Figure 1B**) of muscle synergies (W1-6). All groups first activated W1 (mainly TAs, BF step), although W1 activation was lower in OAwMCI<CIOA<YA, which could indicate dampening of the first stability-restoring response as perturbation detection occurs. Activation of W4 (mainly VL step) was also lower in OAwMCI<CIOA<YA, which could lead to a shorter backward recovery step. Older adults recruited a unique synergy (W6), which consisted mainly of later-stage MG step activity, possibly indicating delayed recovery step liftoff. There were also group differences in synergies related to limb support. Older adults (especially OAwMCI) had delayed activation of W3 (mainly stance VL and TA), and recruited this synergy less often than YA. Additionally, older adults did not recruit W2 (mainly BF stance activity), which could indicate failure to rapidly generate hip extensor torque. Lastly, in W5, older adults showed greater co-activation of stance limb muscles than YA, which could indicate a strategy to provide stability by 'stiffening' the stance limb. OAwMCI also recruited more muscle synergies than YA (3.75±0.11 vs. 3.15±0.14) (*p=0.005*), possibly because OAwMCI could not gauge which synergies would effectively regain balance (due to structural or functional CNS damage).

Significance: Aging in general impacted neuromuscular responses to perturbations (delayed muscle onsets and structural/temporal differences in muscle synergies), which were exacerbated when superimposed with cognitive impairment. MCI-related pathology may disrupt the transmission of perturbation-specific sensorimotor information to the CNS, thus delaying neuromuscular responses, reducing limb support generation, impairing recovery stepping (i.e., shorter step that does not re-stabilize the COM), and leading to ineffective recovery strategies (e.g., limb stiffening). Future fall prevention interventions for OAwMCI may consider targeting these neuromuscular deficits related to reactive balance control.

Acknowledgments: This work was supported by NIH R01AG073152 awarded to Dr. Tanvi Bhatt.

References: [1] Peterson (2008), *CNS Spectrums* 13(1); [2] Kannan & Bhatt (2021), *Phys Int* 108(3); [3] Kannan et al. (2024) *Frontiers in Rehab Sci (under review)*; [4] Sawers et al. (2017), *J of Neurophys* 117(2).

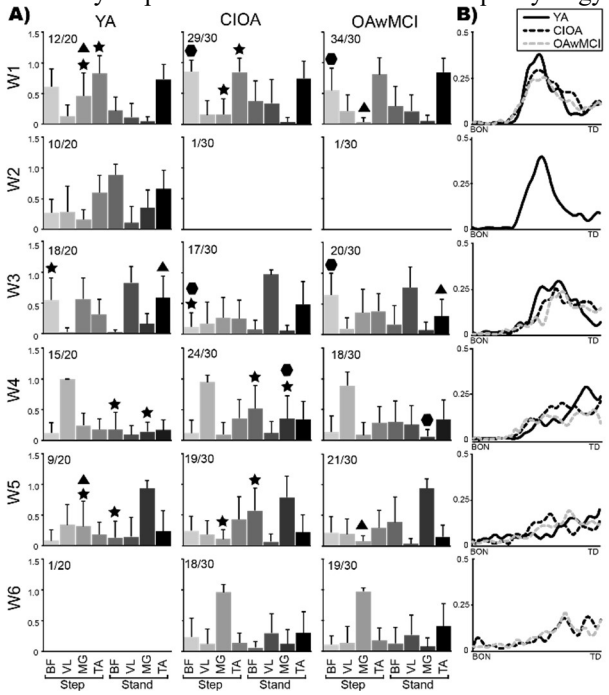

Figure 1: Muscle synergies (W1-6) recruited by young adults (YA), cognitively intact older adults (CIOA) and older adults with mild cognitive impairment (OAwMCI). **A)** Spatial structures of synergies. Significant group differences in muscle weights are indicated by a ★(YA vs. CIOA), ▲(YA vs. OAwMCI), or ⬢(CIOA vs. OAwMCI). # in the upper left indicate how many participants recruited each synergy. **B)** Average temporal activation of synergy.

SHOULD YOU OFFER A COURSE ON HOW TO BE A SCIENTIST AND A SUCCESSFUL GRADUATE STUDENT?

Samuel A. Acuña[1*]
[1]Department of Bioengineering, George Mason University, Fairfax, VA, USA
*Corresponding author's email: sacuna2@gmu.edu

Introduction: Graduate students in biomechanics are expected to conduct scientific research, including formulating hypotheses, conducting studies, and disseminating findings. However, new graduate students may not yet know how to conduct scientific research, which includes the practical and logistical realities of working in a research lab and within an academic institution. Complicating this further, new graduate students also need to learn how to navigate the competing priorities and expectations of graduate student life, balancing coursework, teaching, outreach, and research while not losing sight of their own professional development to meet their goals. So where might a new student learn fundamental research skills and how to be a successful graduate student? The process of teaching research and professional skills (and which ones) is not consistent across departments, research labs, or cohorts of students. Students may not know which skills they should even be pursuing or do not realize the importance of pursuing them [1]. Students might be taught these skills by direct mentorship with their research advisor, through university resources, or through formal courses, but the unspoken expectations for which party is responsible for teaching certain research and professional skills might also vary across departments, labs, and students. Some departments may be expecting their faculty to teach fundamental research skills to their mentored students, while some faculty may be expecting their department to prepare their students for conducting research. Some students might expect to learn these skills explicitly in their lab, but the lab does not have a system of mentorship in place or provide a trusted community of peers to teach best practices. Thus, there is a need for biomechanics education as a field to define consistent training opportunities that teach students how to be successful researchers and succeed in graduate school. We believe that graduate students will be more successful in their research activities if they are explicitly taught the fundamental research skills at the beginning of their graduate coursework. This presentation will describe a mandatory course at George Mason University that teaches new graduate students how to be successful researchers and how to be successful in graduate school. We advocate for the adoption and development of similar courses in the field of biomechanics.

Methods: We developed a graduate-level course to introduce students to the scientific research process and teach them the skills required for scientific research during their graduate studies (e.g., study design, writing papers). There is also a strong emphasis on the essential, transferrable skills they must develop in school (e.g., time management, communication, and interpersonal skills), as well as planning for their own professional development and living a fulfilling life (e.g., work-life balance, mental health, and finding a job after graduation). One of the major goals of the course is to help students optimize their time while in graduate school so that they take full advantage of the graduate experience and are prepared to reach their desired career goals. Unofficially, the course is referred to by students as "How to be a Scientist 101" and "How to be a graduate student in Biomechanics."

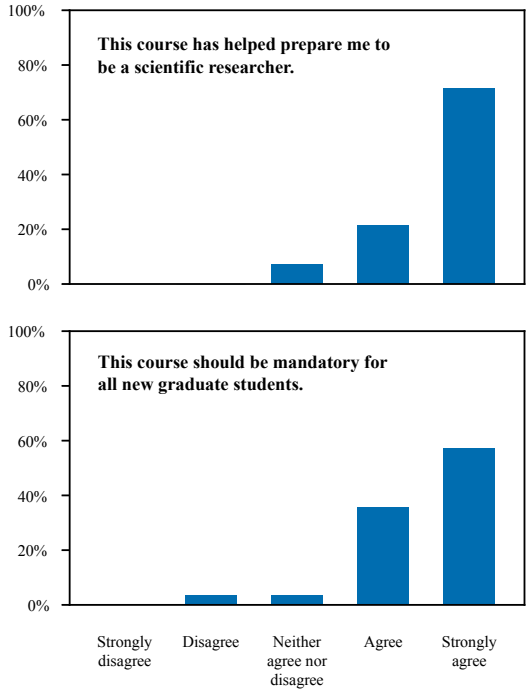

Figure 1: Post-course anonymous survey results show that the course helped prepare students for scientific research and should be mandatory for new graduate students. Data were collected from courses taught in 2022 and 2023. N = 28.

Results & Discussion: Students' perceptions of the course content and delivery were assessed through a post-course survey in 2022 and 2023 (**Fig. 1**). This course is well aligned with graduate student recommendations for improving graduate school to prepare them for research careers, including providing regular feedback, structured opportunities to work with peers, and strategic planning to meet professional goals [2]. Graduate students are eager for this type of in-person instruction [1, 2]. The reality is that stress is at the core of the modern graduate student experience, rooted in internal conflict (e.g., unrealized expectations, a sense of responsibility to others, compromised standards, and guilt) and made worse by conflicting demands. It is even harder for international graduate students who face additional personal and professional obstacles. We hope this course offers students a holistic and comprehensive roadmap of the skills they need to acquire in graduate school, how to acquire them, how to thrive during their graduate education, and how to prepare for their future after graduate school and a career in biomechanics.

Significance: Offering a course like this can help address disparities in access to previous research training and foster a more equitable learning environment [3]. This course may be especially relevant for first-generation college students, international students, as well as for students whose undergraduate degree was not related to biomechanics. By assessing the unique needs and motivations of students early in the course, the curriculum topics can be tailored to overcome limitations in prior training and address possible barriers. By offering a course like this, a department can help manage the often unspoken expectations of who is responsible for teaching students to be successful graduate students and help prevent promising students interested in biomechanics from being left behind.

References: [1] Fong et al. (2016), *J Acad Librariansh* 42(5); [2] Austin (2002), *J Higher Ed* 73(1); [3] Acuña (2024), *J BME Ed*

Effects of Brachial Plexus Birth Injury on the Evolution of Glenohumeral Macrostructure Changes

Jason Zhang[1*], Vivian Mota[1], Kyla Bosh[2], Jacqueline H. Cole[1,2], and Katherine R. Saul[1]
[1]North Carolina State University, [2]University of North Carolina at Chapel Hill
* Email: jzhan242@ncsu.edu

Introduction: Brachial plexus birth injury (BPBI) is a common neuromuscular injury that occurs during live birth, resulting in muscle paralysis, shoulder contracture, and scapular and humeral deformities [1–3]. Previous BPBI studies using rodent models establish that changes in the normal development of the glenoid are evident as early as 8 weeks of rat development. These deformities often result in recurring shoulder dislocations and significantly impact the function and mobility of the affected limb [4-5]. However, it is unclear how early changes begin postnatally, which is important to guiding timing of clinical intervention. Our goal is to better understand the development of glenohumeral deformities and characterize the early stages of bone deformity development following BPBI occurring proximal or distal to the dorsal root ganglion. We hypothesize that the postganglionic injury group will have the largest overall changes to macrostructure parameters and will be detectable as early as 4 weeks following surgery**.**

Methods: Sprague-Dawley rat pups (n = 99) underwent one of four distinct surgeries on one limb, 3-6 days post-birth: Postganglionic (post) or Preganglionic (pre) neurectomy, disarticulation (dis), and Sham. The postganglionic group underwent C5 & C6 nerve root excision distal to the dorsal root ganglion, mimicking nerve rupture. The preganglionic group underwent C5 & C6 nerve root excision proximal to the dorsal root ganglion, mimicking nerve avulsion. Forelimb disarticulation at the elbow was performed to simulate reduced limb usage similar to the neurectomy groups without any nerve injuries. The sham control group received sham surgery without any nerve injuries. The contralateral forelimb (unaffected) served as an additional control to the study. At various endpoints (2, 3, 4, 8, or 16 weeks) rats were sacrificed, torsos were harvested, and the uninjured and injured humeri and scapulae were fixed at 90 degrees prior to scanning. Macrostructural scans of the intact shoulder were obtained with micro-CT (SCANCO Medical μCT 80, 0.5-mm Al filter, 70 kVp, 114 μA, 800 ms integration time, 36 μm voxel size).

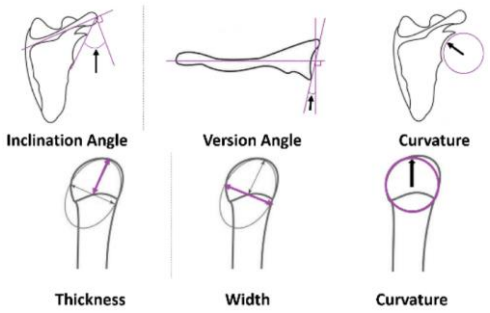

Figure 1: Macrostructural measurement on the scapula and humerus

CT scans of the scapula and humeral head were reconstructed, and macrostructural parameters were obtained using Materialise Mimics, 3D medical imaging software. Specific macrostructural parameters measured included glenoid version angle, glenoid inclination angle, glenoid radius of curvature, humeral head thickness, width, and curvature (**Fig. 1**). The percent difference between the injured and uninjured limb of each animal was calculated and mean percent difference for each group was compared using a non-parametric one-way ANOVA (GraphPad Prism, $\alpha = 0.05$). Image and statistical analysis are ongoing. The completed statistical analyses will assess the main effects of the nerve injury group (post, pre, dis, and sham), limb (injured vs uninjured), and time points (weeks).

Results & Discussion: Preliminary analysis has been completed on a subset of the data for the postganglionic (n = 7-12/endpoint) and sham groups (n = 2-7/endpoint) at the timepoints of 2, 3, and 4 weeks. Previously collected data for the 8-week endpoint are used for comparison [5]. Preliminary analysis (**Fig. 2**) indicates that at all endpoints the glenoid inclination angle is more declined for the injured limb vs the uninjured limb in all groups. At all endpoints, this difference was significantly larger for the postganglionic versus the sham group. Specifically, at 3 weeks the percent difference of the glenoid inclination angle for the postganglionic group (n =12) is 22.9% versus the sham group (n = 2) with -2.9%.

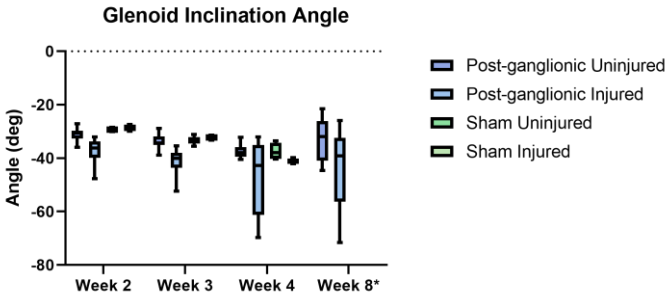

Figure 2: Glenoid inclination angle of injured (Inj) and uninjured (Un) limbs at 2, 3, 4, and 8 weeks.

Significance: This study provides insight into the effect of BPBI on the development of glenohumeral deformity at various endpoints post-injury. Our preliminary results indicate that altered macrostructure of the glenoid is detectable as early as 2 weeks after a postganglionic injury. Establishing the timeline of the deformity development and progression will lend insight into the most appropriate time for clinical intervention following BPBI. Ongoing analyses will expand the sample size for each injury group as well as provide more insight into the glenoid development at various endpoints post-surgery.

Acknowledgments: NIH R01HD101406. We thank Dr. Kerry Danelson and Dr. Roger Cornwall for their surgical support.

References: [1] Foad et al. (2008), *J Bone Joint Surg Am **90(6)***; [2] Hogendoom et al. (2010), *J Bone Joint Surg Am **92(4);*** [3] Pearl et al. (1998), *J Bone Joint Surg Am **80(5)***; [4] Dixit (2021), J Hand Surg Am 46:146; [5] Fawcett (2021), Doctoral Dissertation https://www.lib.ncsu.edu/resolver/1840.20/39052;

PREDICTING FATIGUE DURING TREADMILL RUNNING: A MACHINE LEARNING APPROACH

Paulo R. P. Santiago[1], Ligia Y. Mochida[2], Sérgio Baldo Junior[3], Kevin McDonald[2], Thiago Faria dos Santos[1], Renato Tinós[3], Guilherme M. Cesar [2*]
[1]School of Physical Education and Sport of Ribeirao Preto, University of São Paulo, Brazil
[2]Department of Physical Therapy, University of North Florida, FL, USA
[3]Department of Computing and Mathematics, University of Sao Paulo, Brazil
[*]Corresponding author's email: g.cesar@unf.edu

Introduction: The use of ground reaction forces (GRF) to correlate running performance with injury risks has been well-documented [1,2]. However, understanding the onset of fatigue during running remains a challenge due to the subtlety of its onset and impact [3]. The advent of computational models offers new approaches for analyzing running, especially in the context of fatigue. This study leverages Machine Learning and employs Multi-Layer Perceptron (MLP) with the goal of identifying patterns indicative of fatigue in *real-time* running using load cell signals from an open-source treadmill [4].

Methods: One participant (male, 20 y.o., 85 kg, 1.75 m) engaged in a sprinting high-intensity interval training (HIIT) protocol while running exertion was quantified with the adapted Subjective Rate of Perceived Exertion (RPE) scale. The initial step involved the extraction of 50 features reflecting foot movement patterns (Python 3.8). Fig. 1 outlines the procedural steps of our approach. GRF signals were filtered (4th-order digital Butterworth), normalized to participant's body weight, and data processed to extract features for MLP inputs. MLP outputs indicated instances of fatigue. To refine the feature sets provided to MLP, a Genetic Algorithm (GA) was employed ten times with various random seeds. This step optimized the classification process by focusing on the most relevant data for fatigue detection. Evaluation of MLP performance was based on *Accuracy* (ACC) for overall correctness, *True Positive Rate* (TRP) or Sensitivity for identifying 'tired' states, *Specificity* (SPC) for recognizing 'rested' states, and F1-score (relation between *true positive* and *false negative*). Additionally, MLP was evaluated when classifying fatigue state during running under two conditions: using of all available features with sliding window (SW) and without sliding window (NoSW).

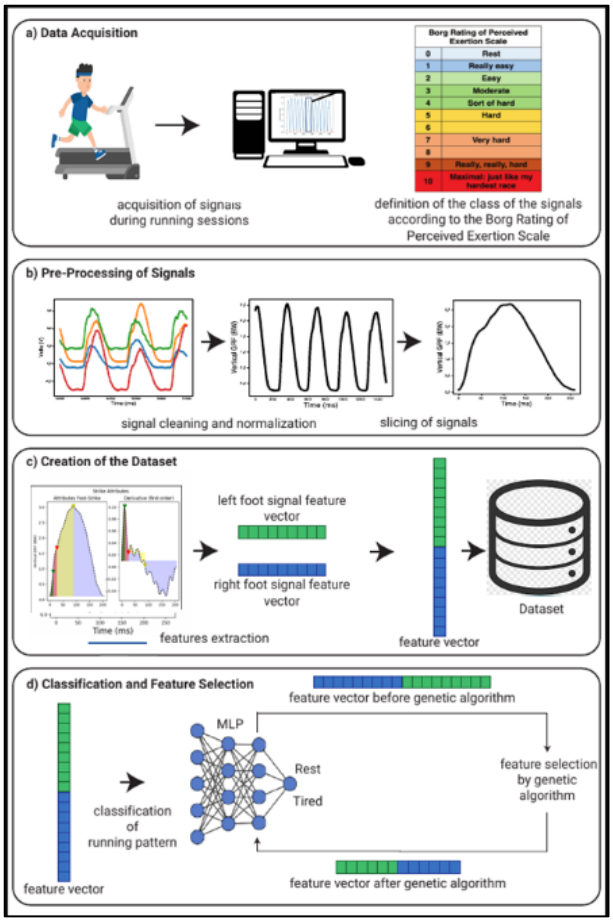

Fig. 1. a) Data collection via treadmill-attached load cells during sprinting HIIT protocol, including runner's RPE for MLP example labeling. **b)** Pre-processing digital filter, normalization, and segment signals. **c)** Feature extraction from consecutive force signals of right foot and left foot. **d)** Classification using MLP with GA-refined feature vectors for improved performance.

Results & Discussion: A total of 2,258 bouts of 60-sec 'not fatigued' and 1,312 bouts of 'fatigued' running were included in the analysis. NoSW MLP performance exhibited ACC of 0.68, a TRP of 0.52, SPC of 0.80, and an F1-score of 0.58. With the SW, performance improved to ACC of 0.76, a TRP of 0.61, specificity of 0.87, and F1-score of 0.68. The low TRP under NoSW highlights the challenges in accurately classifying instances marked as "tired" without a dedicated technique to enhance classification. Error analysis indicated an increase in classification errors for the "rested" class as RPE values arose, peaking at the rate of 7, the maximum threshold for the "rested" category. To refine the feature set for MLP, GA was employed to identify the most impactful features by evaluating the frequency of each feature's appearance in the top-performing vectors across all running bouts. Assessment of MLP performance with these optimized feature vectors at different frequency thresholds exhibited the most effective results at a 40% threshold, utilizing the following five specific features: impact value of right foot; 3rd Fourier amplitude of right foot; number of peaks of left foot; integral of left foot contact area; and 8th Fourier amplitude of left foot. These findings demonstrate GA's effectiveness in identifying the most informative features for fatigue classification.

Significance: MLP can classify fatigue during *real-time* treadmill running from GRF signals. This method can be adapted to diverse running patterns, enabling personalized fatigue detection and informing injury prevention strategies.

Acknowledgments: Grant #312597/2021-5, CNPq; USP Support Program for Projects that Make Use of Intelligent Digital Systems; Also financed in part by CAPES Brasil – Finance Code 001.

References: [1] Malisoux et al., *Scand J Med Sci Sports*, 2022. [2] Luo et al., *Appl Sci*, 2019. [3] Pereira et al., *Sci Rep*, 2015. [4] Baldo Junior et al., PREPRINT (Version 1) available at *Research Square*. 2021.

RELATIONSHIP BETWEEN ACTIVITY LEVELS AND PATIENT REPORTED OUTCOMES IN INDIVIDUALS WITH HIP DYSPLASIA

Christina A. Bourantas*, Molly C. Shepherd, Madison M. Wissman, John C. Clohisy, Michael D. Harris
Washington University School of Medicine in St. Louis, St. Louis, MO
*Corresponding author's email: bourantas@wustl.edu

Introduction: Developmental dysplasia of the hip (DDH) reduces hip stability and increases the risk for osteoarthritis [1,2]. Many individuals with DDH are young and highly active but may limit their activity and seek surgical intervention because of insidious pain [3]. While the focus in research about DDH is often on variables affecting joint loading or motion, it is important to consider both biomechanical measures and patients' perceptions of their physical function, pain, and mobility to fully understand the disease. Multiple studies have predicted surgical outcomes in other populations using wearable devices and patient-reported outcomes and have shown that pre-surgical measures predict post-surgical outcomes [4,5]. It is important to determine if any such relationships exist in individuals with DDH who receive corrective surgery. The objective of this study was to determine the relationships between objective measures of activity (i.e. step count and active minutes) and patient reported outcome measures (PROMs) in patients prior to corrective surgery for DDH. We hypothesized that higher activity would correlate with patient reports of better physical function (i.e. greater mobility and less pain) and better mental health.

Methods: PROMs and activity measures were collected from 10 pre-surgical patients with DDH with Institutional Review Board and informed consent. Average steps per day and active minutes per day were recorded for 7 consecutive days as patients wore wrist-worn devices (Fitbit Inspire 2) at home. Active minutes were classified as Sedentary, Lightly Active, Fairly Active, or Very Active using Fitbit proprietary algorithms (Table 1) and the minutes per day in each category were averaged across the 7 day period. Once during those 7 days, participants completed PROMs including the International Hip Outcome Tool-12 and the National Institutes of Health Patient-Reported Outcome Measure Information System (PROMIS) Pain Interference, Mobility, Anxiety, Mental Health, and Physical Health subscales (Table 1). Associations between PROMs and activity levels were tested using Spearman rank-order correlations of weak ($\rho<0.40$), moderate ($\rho=0.40$ to 0.59), or strong ($\rho\geq0.60$).

Results & Discussion: Higher activity levels had moderate to strong relationships with patient reports of physical function. Very Active minutes was strongly correlated with increased reports of physical health and mobility ($\rho=0.62$ and $\rho=0.61$, respectively) (Fig 1). A moderate negative correlation was found between Very Active minutes and pain ($\rho=-0.40$). Consistent with general populations, higher activity is related to better physical health and mobility, and less pain, even in patients with DDH who are symptomatic enough to be undergoing surgery [4,5]. Our results did not find strong correlations between mental health and activity, but it is important to note our small sample size and data from one time point. However, we did find a negative correlation just outside the moderate range between Sedentary minutes and mental health ($\rho=-0.35$). Thus, in a larger sample size, it may become true that worse mental health is related to being sedentary. It is important to understand the relationships between activity levels and PROMs to help interpret biomechanical assessments of patients with DDH. For instance, a prior study found moderate and strong relationships between biomechanical outcomes, such as joint reaction forces, and PROMs of physical function and pain [6]. Knowing how pre-operative activity levels relate to PROMs can help us more completely assess post-operative biomechanical outcomes, an area of ongoing study in our lab.

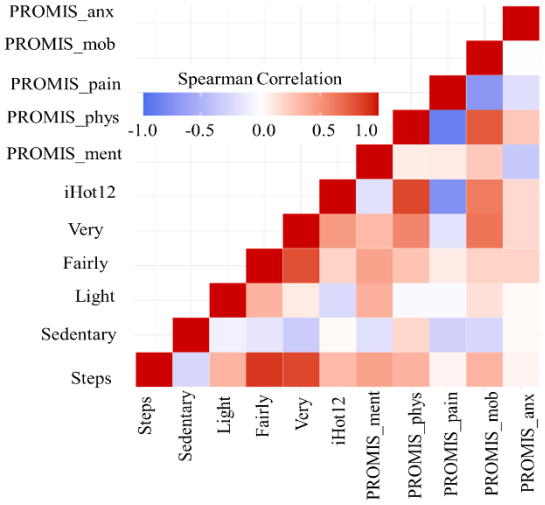

Figure 1: Heat map of Spearman correlation coefficients between PROMs and activity level

Significance: Understanding the relationships between self-reported pain, quality of life, and mobility and an objective measure of activity can help clinicians holistically treat individuals with DDH and help predict their potential for recovery.

Acknowledgments: Funding provided by the National Institute of Health T32HD007434 and R01AR081881.

References: [1]Wyles *Clin Orthop Relat Res* 2017. [2]Ganz *Clin Orthop Relat Res* 2008. [3]Schmitz *J Am Acad Orthop Surg* 2020. [4]Cos *J Med Internet Res* 2021. [5]Golinelli *J Patient-Rep Outcomes* 2022. [6]Wu *Clin Orthop Relat Res* 2023.

Table 1. Activity measures and patient reported outcomes

Steps	Average step count for 7 days	iHOT12	International Hip Outcome Tool (short)
Sedentary	Average Sedentary minutes for 7 days	PROMIS_ment	NIH PROMIS Global Mental Health
Lightly	Average Lightly Active minutes for 7 days	PROMIS_phys	NIH PROMIS Global Physical Health
Fairly	Average Fairly Active minutes for 7 days	PROMIS_pain	NIH PROMIS Pain Interference
Very	Average Very Active minutes for 7 days	PROMIS_mob	NIH PROMIS Mobility
		PROMIS_anx	NIH PROMIS Anxiety

IS WADDLING GAIT DURING PREGNANCY A SIGN OF POOR BALANCE OR MERELY A PROTECTIVE GAIT?

Zahra Abedzadehzavareh, Robert D. Catena*
Gait and Posture Biomechanics Laboratory, Washington State University, Pullman, WA, USA.
*Corresponding author's email: robert.catena@wsu.edu

Introduction: Pregnancy can cause many alternations to balance and gait patterns due to various biomechanical and physiological changes. One of these alterations is the waddling gait pattern. The defining features of waddling gait during pregnancy include amplified trunk lateral movement, expanded step width, increased thorax extension, and an increased anterior pelvic tilt [1]. Although waddling is typical during pregnancy, there is a lack of information regarding its exact purpose - its relationship to other spatiotemporal variables, balance, and energetics during walking in pregnant women. To what extent is waddling good as a protective mechanism for balance or bad as a sign of poor balance or because of increased energetic cost? This study addresses the current knowledge gap by examining how waddling (step width) during pregnancy correlates with balance and mechanical energy. Knowing the purpose of waddling and the link to balance control will provide a basis for clinical management of waddling gait in typical healthy pregnant women and women that use a prosthesis following limb amputation, the latter being a population where increased step width is common [5] until corrected through training and prosthetic adjustments.

Methods: Twenty-three pregnant women were assessed longitudinally in 4-week intervals between 18 and 34 weeks of gestation. Participants were asked to complete a 10s trial of quiet comfortable standing and walking at the preferred speed for 60s on a treadmill. Motion capture was used to measure spatiotemporal variables and body centre of mass (COM) motion, from which we derived measures of balance and gait energetics. Forward-step multiple linear regression analyses were used to explore the correlation between the variables.

Results & Discussion: We found no significant relationship between step width and BMI ($p=0.259$), step width and height ($p=0.549$), or step width and mass ($p=0.275$). Additionally, our analyses indicate no correlation of step width to other spatiotemporal measures ($p>0.059$). We hypothesized a natural inverse relationship between step width and length [2]. However, the results of the study rejected this hypothesis. Perhaps there is a local advantage at the hip and ankle to maintaining step length or a systems advantage through cost of transport. This should be explored further in future research.

We found a positive correlation between step width average and mediolateral center of mass velocity (ML-COMv) ($R^2=0.624$, $p<0.001$). This finding indicates that during pregnancy, wider steps correlate to increased lateral motion, as expected, but ML-COMv is also typically used as a measure of reduced balance control [3]. Additionally, we identified a positive correlation between step width variance and lateral margin of stability ($R^2=0.339$, $p=0.004$). Since there was a lack of correlation between margin of stability and step width average, we are led to believe that the wider steps are used to recapture balance control, but may not always be needed to do so, indicating either a lack of body awareness or a protective mechanism for unexpected perturbations. However, since we previously found no change in body awareness during pregnancy [4], we are led to believe our finding to indicate waddling as a protective mechanism. Interestingly, our analysis found no significant relationship between step width and recovery of energy during walking ($p=0.714$) or total mechanical work done in the sagittal plane ($p=0.530$). Combined, these findings indicate widening steps (characteristics of waddling gait) is not an inefficient movement pattern. Future research should examine this further through direct measure of metabolic energy consumption.

Our analysis between step width and standing balance measures indicates a moderate negative correlation between step width and anteroposterior center of mass motion ($R^2=0.315$, $p=0.005$), meaning as step width increases during pregnancy, standing balance actually improves. We conducted this analysis with standing balance hoping to verify a correlation between waddling and balance control independent of walking. Combined with walking findings, we are led to believe that waddling is not a sign of poor balance and is a positive gait pattern for pregnant women to increase safety with no apparent (as of yet) negative effect. This should be verified through a controlled waddling experimental design in future studies.

Significance: This study found that waddling is a protective mechanism for balance during pregnancy. This finding will be helpful for clinicians or prosthetists who work with pregnant women. Clinicians can use this information to train pregnant individuals to use waddling gait for safety. Since the goal of training waddling gait would be to only promote advantageous aspects, our future studies will expand from our definition of waddling (step width) to an all-encompassing definition mentioned in the introduction and focus on differentiating the beneficial aspects of waddling from the costly aspects through machine learning. Using that information can be helpful for both typical and lower-limb amputee pregnant women. Based on our current findings, prostheses for pregnant amputees should not be adjusted merely to eliminate waddling gait during pregnancy. This is the opposite of the typical goal of adjusting prosthetics to promote a more natural gait pattern for non-pregnant amputees. Perhaps instead, the prosthetics team can find methods to strategically enhance controlled waddling in a prosthesis during pregnancy.

Acknowledgments: We thank all are pregnant participants. This work was funded by WSU and Tidyware.

References: [1] McCrory et al. (2014) *J Biomech*, 47(12). [2] Kurz et al. (2007) *J Theoretical Biology*, 252(2). [3] Lee & Chou (2006) *APMR*, 87(4). [4] Jamali et al. (2024) *Exp Brain Research,* 242(2). [5] Su et al. (2007) *J Rehab Research and Development*, 44(4).

QUANTIFYING THE EFFECT OF TRUNK CONTROL ON REACHING COORDINATION IN HEMIPARETIC STROKE

Kathleen C. Suvada[1], Jasjit Deol[3], Julius P.A. Dewald [1,2], and Ana Maria Acosta[1]
[1]Department of Physical Therapy and Human Movement Sciences, Feinberg School of Medicine, [2]Biomedical Engineering, McCormick School of Engineering, Northwestern University, Chicago, IL, USA
[3]Neuroscience and Mental Health Institute, University of Alberta, Edmonton, AB, CA
Kathleen Suvada: kathleensuvada2022@u.northwestern.edu

Introduction: The trunk provides a stable base of support to facilitate upper limb interaction with the environment. Post hemiparetic stroke, damage to descending corticospinal pathways alters motor control and performance of activities of daily living. In the arm, impairments include weakness, hyperactive stretch reflexes, and involuntary coupling of shoulder abduction with elbow, wrist, and finger flexion, or flexion synergy[1].

The trunk also exhibits changes post stroke including increased movement during reaching, weakness compared to controls, improved elbow extension and integrity of reaching trajectories when restrained, and altered coordination compared to controls[2-4,5-7]. However, the impact of stroke on coordinated trunk and reaching function has been largely unexplored, particularly in the context of the flexion synergy. The goal of the present study is to examine reaching post stroke with the trunk unrestrained, more closely resembling reaching in daily life. We hypothesize that reaching deficits already present due to the flexion synergy will be further exacerbated when the trunk is unrestrained.

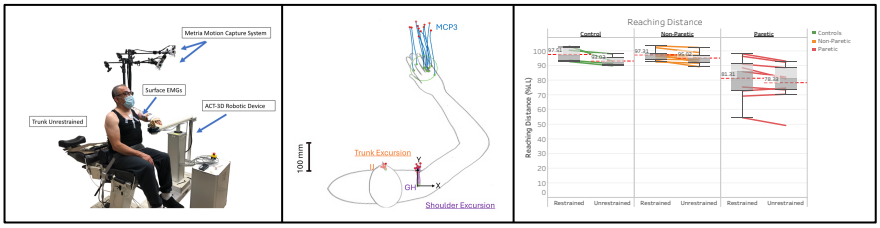

Figure 1A) Experimental setup with trunk unrestrained. B) Overhead trunk, shoulder, and hand trajectories. C) Effect of restraint on RD for paretic, non-paretic, and controls.

Methods: 9 individuals with hemiparetic stroke (64.11 ± 6.57 years old; Fugl-Meyer Assessment (FMA) 7-42/66; Reaching Performance Scale (RPS) 0-32/36; and Trunk Impairment Scale (TIS) 11-20/23); and 4 age-matched controls (66.25 ± .96 years old) participated in the study. As shown in Fig. 1A, the trunk, shoulder, and arm were instrumented with motion capture markers (Metria Innovation, Inc.) to record 3D position and orientation. Bone position and orientation was computed offline. Individuals sat in a Biodex chair with their forearm securely coupled to a robotic device used to apply vertical loads. Participants were asked to reach as far and fast as possible while on a frictionless table and generating 25% or 50% of their maximum shoulder abduction force, and with the trunk restrained or unrestrained. Hand position was displayed on a monitor with the reaching target set beyond limb length. Shown in Fig. 1B, the primary outcome measure was reaching distance and secondary measures were shoulder and trunk displacement. Reaching distance (RD) was defined as location of the 3rd metacarpophalangeal joint (MCP3) in the plane of the arm with the origin at the glenohumeral joint (GH[8]) at the end of the reach. The reach was identified by the velocity profile of the hand. RD was normalized as a percentage of participant limb length. A generalized linear mixed effects model was used to assess the effect of load and restraint on reaching distance. The relationship between RD and the clinical measures was evaluated using linear regression.

Results and Discussion: When reaching with the paretic limb, stroke participants had reduced reaching distance with limb loading, consistent with previous studies ($p<.05$) which did not occur in the non-paretic limb and controls. Consistent with our hypothesis, RD was reduced for the paretic limb in trunk restrained vs trunk unrestrained: (Table- 86.47±14.03 vs 84.67 ± 13.08 % LL), (25%- 79.03±15.03 vs 75.23 ± 14.47 % LL), (50%- 78.41±16.07 vs 75.54 ± 14.66 % LL) where $P<.05$. However, contrary to our hypothesis, RD was also reduced in the non-paretic limb and control participants ($P<.05$). In the paretic limb, RD was correlated with FMA and RPS when the trunk was both restrained and unrestrained ($p<.05$). In sum, all three participant groups had a significant effect of trunk restraint on decreasing reaching distance as shown in Figure 1C.

Significance: This study showed the detrimental effect of simultaneous trunk control on reaching ability, compounding the effects of the flexion synergy. Our study also found that there was an effect of trunk restraint on decreasing RD for the non-paretic limb and controls, suggesting that this decrease may not be due to the stroke itself. Previous studies have shown that trunk restraint alters the ability to reach to targets, even in controls. Future work will elucidate why there is decreased reaching distance and how there may be altered control strategies implemented depending on trunk restraint conditions. Despite the reduction in RD, the primary factor reducing RD was the flexion synergy. Since the reductions due to trunk restraint were minor in comparison, future work should consider un-restraining trunk as this is also more representative of reaching in daily life.

Acknowledgements: Research Training in Sensorimotor Neurorehabilitation - 5T32HD101395-02 and 1R01NS105759-01A1

References:

[1] McPherson et al. *J Physiol.* 2018;596(7):1211-1225.[2] Levin et al. *Exp Brain Res.* 2002;143(2):171-180.[3]Quintino et al. *Braz J Phys Ther.* 2018;22(3):231-237.[4]Perlmutter et al. 2013.ProQuest Dissertations Publishing.[5]Michaelsen et al. *Stroke.* 2001;32(8):1875-1883.[6]Michaelsen et al.*Stroke.* 2004;35(8):1914-1919.[7]Olczak et al.*Brain sciences.*2022;12(9):1234.[8]Mesker et al. *J Biomech.*1998;31(1):93-96.[9]Beer et al. *Experimental brain research.* 2000;131(3):305-319.

MINIMAL DETECTABLE CHANGE IN SPATIOTEMPORAL GAIT PARAMETERS DURING TREADMILL WALKING IN STROKE SURVIVORS

Alejandro Aguirre Ramirez[1], Andrian Kuch[2], Natalia Sanchez*[2,3]
[1]Schmid College of Science and Technology, Chapman University, Orange, CA. [2]Department of Physical Therapy, Chapman University, Irvine, CA. [3]Fowler School of Engineering, Chapman University, Orange, CA
*Corresponding author's email: sanchezaldana@chapman.edu

Introduction: Gait analysis is the standard method for evaluating walking behaviors [1]. Gait analysis is prone to inconsistencies due to differences in marker placement [2,3], variations in behaviors within and between participants post-stroke [4], and differences in experimental setups. A 2011 study established minimal detectable change (MDC) test-retest values for gait analysis in people post-stroke [5]. However, differences in technology used in our research laboratory might result in different MDC values. Therefore, we aim to determine the test-retest consistency of spatiotemporal gait measures over two consecutive days of treadmill walking in individuals post-stroke, and whether the MDC values in our laboratory are consistent with previous studies [5]. Our results will help identify the values above which changes in spatiotemporal gait characteristics after intervention studies in our laboratory are indicative of real changes in behavior beyond measurement error.

Methods: Six individuals post-stroke (age 45.5±16.7 years, stroke onset > 6 months, walking speed 0.80±0.34 m/s, Fugl Meyer Lower Extremity score 25±4) participated in our study. The self-selected speed was assessed through the six-minute walk test on the first day. We placed 26 reflective markers using a modified HBM2 marker set [6]. Participants performed a two-minute walk test on a GRAIL treadmill system (Motek Medical, Netherlands) at a self-selected speed for two consecutive days. Markers placed on the heel were used in the Gait Offline Analysis Tool (GOAT) for step detection. Spatiotemporal parameters, including stride length, stride time, step time, step length, stance time, and swing time for both paretic and non-paretic legs were calculated in GOAT. We used Pearson correlation coefficients to evaluate the relationship of the measures across days. We calculated the test-re-test intra-class correlation coefficient (ICC) using a 2,1 model [7] to obtain the standard error of the measurement and MDC. The significance level was set at 0.05.

Results & Discussion: We list correlations, ICCs, and MDCs between days of testing. Stride length: r=0.995, p<0.001, ICC 0.995 (Fig. 1A), and MDC 5.9 cm. Stride time: was r=0.994, p<0.001, ICC 0.970, and MDC 0.17 seconds (Fig. 1B). For the paretic limb, step length r=0.999, p<0.001, ICC 0.994, and MDC 2.9 cm (Fig. 1C), stance time r=0.983, p<0.001, ICC 0.933 and MDC 0.20 seconds (Fig. 1D) and swing time r=.999, p<0.001, ICC 0.990, and MDC 0.03 seconds (Fig. 1E). For the non-paretic limb, step length r=0.986, p<0.001, ICC 0.982, and MDC 6.6 cm (Fig. 1F). stance time r=0.995, p<.001, ICC 0.979, and MDC 0.14 seconds (Fig. 1G). swing time r=.816, p<0.05, ICC .765, and MDC .04 seconds (Fig. 1H). All variables had excellent consistency indicated by ICC>0.75. Paretic step lengths were more consistent between days than non-paretic step lengths. Non-paretic swing time had the highest variation between days.

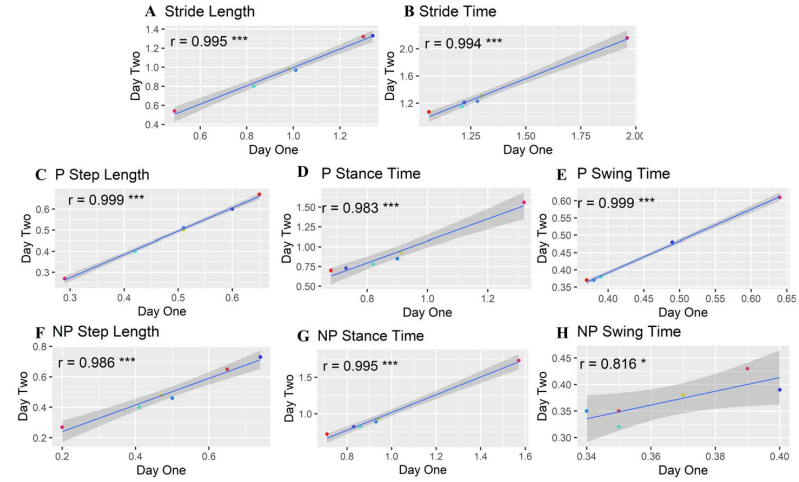

Figure 1: correlation plots for stride length (A), stride time (B), paretic step length (C), stance time (D), swing time (E), and non-paretic step length (F), stance time (G), and swing time (H). * represents p<0.05, ** p<0.01, ***p<0.001

Kesar et al. [5] observed MDC for the paretic step length of 6.75 cm and MDC for the non-paretic step length of 5.46 cm, which contrasts our findings as we observed a smaller MDC for the paretic step length. The ICC values for temporal parameters were similar in our study to those found by Kesar et al. [5], reported as percentage duration in the gait cycle. Differences between our study and Kesar et al. [5] can be explained by differences in participant impairment, as their sample average walking speed was 0.60 ± 0.30 m/s and Fugl-Meyer Lower Extremity score was 19±4. Future work will increase the sample size for our analysis and obtain temporal variables as a percentage of the gait cycle to allow comparison to previous literature.

Significance: Our findings have practical implications for the intervention studies being carried out in our lab with participants post-stroke. We have identified values that distinguish between intervention-induced changes in spatiotemporal parameters from measurement errors due to test-retest variability. Our results have broader implications for other labs that use the GRAIL system in post-stroke participants.

Acknowledgments: Funding: NIH NCMRR R03HD107630 and NIH NCATS R03TR004248 to N. Sanchez.

References: [1] Baker, JNER, 2006. [2] Capozzo et al., Clinical Biomechanics, 1995. [3] Davis et al, Human Movement Science, 1991. [4] Olney, Richards Gait and Posture 1996. [5] Kesar et al. Gait and Posture, 2011. [6] van den Bogert et al., Med Biol Eng Comput, 2013. [7] Shrout, Fleiss Physc Bull 1979.

PASSIVE EXOSKELETON REDUCES ANKLE MUSCLE DEMAND DURING WALKING IN PERIPHERAL ARTERY DISEASE

Farahnaz Fallahtafti[1*], Zahra Salamifar[1], Iraklis Pipinos[2], Sara A. Myers[1,2]
[1] Department of Biomechanics, University of Nebraska at Omaha, Omaha, NE USA
[2] Department of Surgery and Research Service, Omaha Veterans' Affairs Medical Center, Omaha, NE USA
*Corresponding author's email: ffallahtafti@unomaha.edu

Introduction: Peripheral artery disease (PAD) affecting the lower limbs is a cardiovascular condition caused by the narrowing or blockage of arteries supplying blood to the legs [1]. Claudication refers to the cramping pain experienced in the legs of individuals with PAD, triggered by physical exertion and alleviated by rest. Our research has highlighted a clear association between the functional limitations of claudicating patients and a deficit in the posterior calf muscles' ability to generate adequate ankle torque and power [2]. Previous work has also demonstrated the potential of wearable devices, such as ankle foot orthoses, to improve walking performance in patients with PAD [3]. We have developed a modified exoskeleton footwear (EF; **Figure 1**) that has similar characteristics to an AFO, but it is designed to increase push-off using a spring and clutch system that acts in parallel with ankle plantar flexor muscles. This study determined the effect of EF assistance on ankle joint biomechanics in patients with PAD. We hypothesized that wearing the EF would decrease the ankle joint workload and consequently reduce muscle workload during push-off.

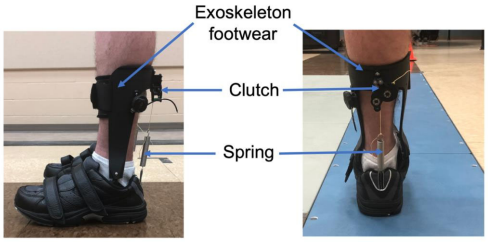

Figure 1: Exoskeleton footwear which was used in the proposed study. The EF includes 3D printed nylon, a spring that can be swapped with various stiffness values, and a clutch connected to a rigid posterior nylon frame.

Methods: Seven patients with PAD (Age: 69.7±6.3 years, height: 1.74±0.05 m, and body mass: 90.5±18.7 kg) were evaluated while walking at their preferred speed overground, across force plates embedded in the floor (AMTI, Watertown, MA, 1000 Hz). Participants wore a form-fitting suit, and 33 retro-reflective markers were placed on specific anatomical landmarks on the subject's pelvis, thighs, shanks, and feet. Kinetics and kinematics data were recorded and combined to quantify ankle torques and powers during the stance period of the gait cycle. Participants walked under three different conditions: 1) EF assistance (stiffness level of 7.9 kN/m), 2) EF zero assistance (disengaged spring), and 3) without the EF. Participants repeated each walking trial until five successful trials were obtained for each foot in which heel-strike and toe-off events were within the boundaries of the force plate. We used a one-way repeated measure ANOVA to capture the effect of the condition on ankle joint biomechanics.

Results & Discussion: The findings indicate a significant decrease in peak ankle dorsiflexor angle during EF assistance compared to walking without EF and EF zero assistance, $F(2,12) = 5.02$, $p = 0.02$ (Figure 2). This aligns with the previous study using a powered exoskeleton, showing that increasing assistance reduced the peak dorsiflexor angle compared to zero torque conditions [4]. A decrease in maximum dorsiflexion angle implies that the elongation of the Achilles tendon may have been minimized due to the ankle exoskeleton absorbing energy. The stretching and recoiling of the Achilles tendon enable the storage and release of elastic energy in the ankle joint. A decreased elongation suggests that the ankle joint absorbs less energy, with more being absorbed by the exoskeleton. This is in line with the comparison of ankle power absorption, indicating less power absorbed by the ankle during the EF assistance condition compared to two other conditions, $F(2,12) = 7.71$, $p = 0.007$. Additionally, the decrease in ankle power generation under EF assistance suggests that the EF is substituting power required for ankle movement during walking, resulting in reduced demand on ankle muscles, $F(2,12) = 15.14$, $p < 0.001$.

Significance: This redistribution of energy absorption from the ankle to the EF implies a shift in biomechanical dynamics, highlighting EF's role in assisting walking by providing power at the ankle joint.

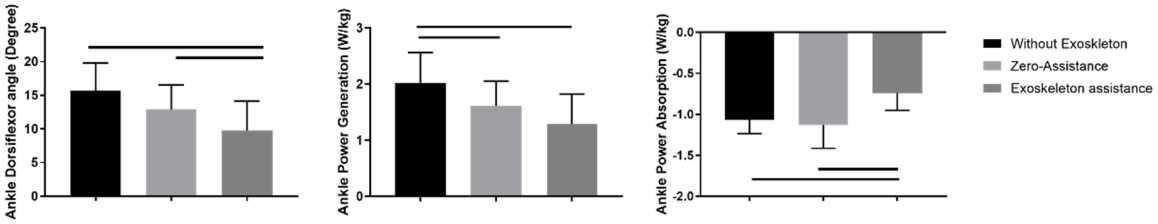

Figure 2: Comparison of ankle joint kinematic and kinetic data revealed significant differences among the three walking conditions: EF assistance, EF no assistance, and without EF. Horizontal bars in the figure indicate significant differences ($p < 0.05$).

References:
1. Criqui et al., 2021. AHA. CirC. 144(9)
2. Schieber et al., 2018. J Vasc Surg. 66(1), 178-186
3. Mays et al., 2019. J Vasc Med. 24(4), 324-331.
4. Wang et al., 2021. Front Neurorobotic. 10; 15:797147.

Acknowledgements: This research was funded by the National Institute of Health (R01AG034995, R01HD090333, R01AG049868), and United States Department of Veterans Affairs (I01RX000604, I01RX003266)

EMPLOYING PRINCIPAL COMPONENT ANALYSIS TO ASSESS VARAIABILITY IN HAMSTRING MORPHOLOGY

Jack A. Martin[1,2*], Christa M. Wille[3], Silvia S. Blemker[4], David A. Opar[5], and Bryan C. Heiderscheit[1,2,3]
University of Wisconsin-Madison [1]Badger Athletic Performance and Depts. of [2]Orthopedics & Rehabilitation and [3]Biomedical Engr.
[4]Springbok Analytics and University of Virginia Department of Biomedical Engineering
[5]Australian Catholic University SPRINT Research Center and School of Behavioral and Health Sciences
*Corresponding author's email: jamartin8@wisc.edu

Introduction: The risk for hamstring injury in athletes is multifactorial, and understanding risk factors is the first step towards implementing preventative strategies for at-risk individuals. The biceps femoris long head is at particularly high risk for injury during high-speed running, and it is likely that morphological factors play a role in determining injury risk. Variation in 3-dimensional muscle morphology can be studied using methods like statistical shape modeling. However, the supine or prone postures required by typical magnetic resonance imaging (MRI) scanners means that muscles can be quite deformed compared with how they are situated in an upright posture, and the fully extended hip is not representative of the flexed hip angle at which most injuries occur. Additionally, 3D shape variations can be difficult to interpret. Alternatively, variations in muscle cross-sectional area (CSA) vs. length are simpler to interpret and less affected by postural differences. Furthermore, while traditional shape analyses may focus on individual structures, it is likely useful to account for the interplay between the hamstring muscles given their similar functional roles. Thus, the purpose of this pilot analysis was to test the implementation of an approach employing principal component analysis (PCA) to examine concomitant variations in CSA vs. length profiles of the four hamstring muscles: semimembranosus (SM), semitendinosus (ST), and biceps femoris long head (BFL) and short head (BFS).

Methods: Data from 15 healthy active individuals (6 female) involved in University of Wisconsin-Madison club sports are included in this analysis. MRI examinations of the lumbo-pelvic region and bilateral lower extremities were performed on participants, and hamstring muscles were segmented using Springbok Analytics machine learning technology [1]. Muscle CSAs were determined for each axial slice, and mass-normalized CSA profiles were interpolated along the length of the femur. Hamstring CSA profiles were collated into one vector per limb, and PCA was performed on the collated vectors to assess patterns of variability in hamstring morphology. The first two principal components (PCs) are analyzed here, and PC scores are compared between sexes.

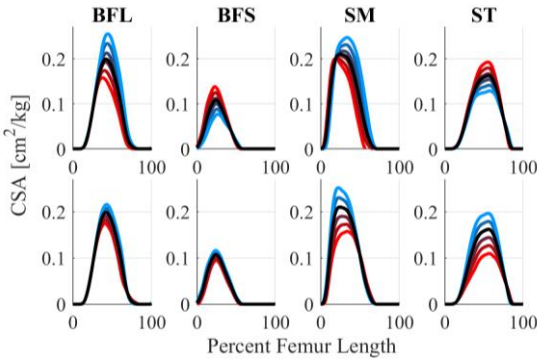

Figure 1: Hamstring cross-sectional area (CSA) profiles describing variation along the first 2 principal components (PCs; rows 1 and 2, respectively). Black indicates the mean CSA profile across participants. Greater blue and red intensity indicate higher and lower PC scores, respectively, and span the range of scores observed across participants.

Results & Discussion: The PCs describe variability in both relative muscle CSAs and lengths. For instance, PC1 primarily shows a trade-off between relatively greater BFL and SM size, and greater BFS and ST size (Fig. 1). The highest observed PC1 score corresponds with 28% greater peak BFL CSA, 29% lower peak BFS CSA, 18% greater peak SM CSA, and 21% lower peak ST CSA compared with mean values. PC1 also shows variation in the length of BFL and SM muscles relative to the femur. PC2 primarily shows tendencies towards smaller vs. larger SM and ST muscles (Fig. 1). The highest observed PC2 score corresponds with 20% greater peak SM CSA and 21% greater peak ST CSA compared with mean values. PC1 scores were generally greater in females (mean, range: 0.17, -0.08 to 0.52) than males (mean, range: -0.11, -0.46 to 0.21), and PC2 scores were generally lower in females (mean, range: -0.09, -0.48 to 0.16) than males (mean, range: 0.06, -0.28 to 0.31).

Variations in hamstring morphology observed here have potential relevance to injury risk. First, differences in relative size of the BFL may lead to differences in loading relative to its capacity. It is possible that relatively smaller BFL will not be as able to handle the high loads imposed on it during sprinting. Second, it is possible that relatively smaller SM and ST muscles may lead to greater demands on BFL, leading to greater injury risk, or alternatively that this may help explain the relatively less common injuries to SM and ST. Additionally, relative length of the muscles vs. tendons will affect strain patterns within the muscle, and thereby potentially affect injury risk. Further work will focus on combining this approach with cluster analyses [2] to identify hamstring morphology phenotypes which may place individuals at greater risk of future hamstring injury, and using this approach to examine morphological differences resulting from prior injury.

Significance: This work introduces a method for studying variations in hamstring morphology that avoids some limitations of traditional statistical shape modeling. The findings of a larger scale analysis of this type could provide insights into how hamstring morphology may relate to running kinematics, athletic performance, and injury risk, and could allow for tailored training approaches intended to make improvements in each of these areas.

Acknowledgments: The authors thank the NFL and GE Healthcare for their support of the work presented here. Neither had any role in this study or our decision to present the results. Drs. Blemker (Co-founder and Chief Science Officer) and Heiderscheit (advisory board member) declare potential competing interests related to this work due to their roles with Springbok Analytics.

References: [1] Ni et el. (2019), *J Med Imaging* 6; [2] Martin and Heiderscheit (2023), *J Biomech* 160.

CHANGES IN RUNNING GAIT BIOMECHANICS UNDER HEAT STRESS

Kai-Wen Chien[1*], Zachary J. Schlader[1], James J. McDonnell[1], Isaac D. Coker[1], Marni Wasserman[1], Jennifer Sumner[2], Edward Nyman[2], Allison H. Gruber[1]
[1]H.H. Morris Human Performance Laboratories, Indiana University, Bloomington, IN, USA
[2]Brooks Sports Inc., Seattle, WA, USA
*Corresponding author's email: kchien@iu.edu

Introduction: Running is one of the most common and popular exercises because of its accessibility and health benefits [1], it can be done nearly anywhere outdoors, and it is a significant component to many popular sports and unorganized physical activities. However, the hot and humid weather during the summer months increases the risk for heat stress injury, making outdoor physical activity challenging and potentially dangerous [2,3]. Exercising in hot and humid conditions results in physiological changes detrimental to physical performance and accelerates the effects of exhaustion [4]. Exhausted running is hypothesized to increase the risk of developing musculoskeletal injury [5]. It is unknown if running in the heat simply accelerates the onset of exhausted gait, or if the heat also exacerbates changes in gait patterns that could increase injury risk, thereby escalate the overall risks of exercising in the heat. Therefore, the purpose of this study was to explore changes in running biomechanics in the heat. It was hypothesized that running in the heat would increase the changes in joint angles typically observed following a prolonged run compared with a control environment.

Methods: Six recreational runners have been analyzed to date (males/females = 2/4; mean±1 standard deviation (SD): age = 25.0 ± 4.0 yrs; BMI = 23.02 ± 2.49 kg/m^2; years running = 5.0 ± 2.3 yrs). The order of the hot and control conditions was randomized across participants. The hot condition (35°C, 62% relative humidity) represents the 95th percentile of hottest days in the Bloomington, IN area. The control condition (16°C, 55% relative humidity) represents the environment that is optimal for marathon performance [6]. For each condition, participants ran at a comfortable, preferred speed (2.82 ± 0.36 m/s) on a treadmill in an environmental chamber as core temperature (Tc), Borg rate of perceived exertion (RPE, 6-20 scale), and two-dimensional high-speed video of the ankle and knee in the sagittal plane was measured at five-minute intervals. Participants ran until one of the following criteria was met: Tc exceeded 39.5°C, RPE exceeded 17, volitional exhaustion, or run duration exceeded one hour. Core temperature rate of change (ΔTc) was calculated as Tc at the end of the run divided by run duration. Foot strike angle at initial contact [7] and peak knee flexion angle during stance were measured with Kinovea (v 0.9.5). The means of 15 steps during the end of the first and last five-minute intervals of the run were used to calculate the change in joint angle between these intervals. Between-condition differences in Tc, ΔTc, and the change in joint angle were assessed with paired t-tests (α = 0.05). Due to the relatively low inter-day reliability of two-dimensional motion capture, differences in joint angles between the start and end of the run were assessed within-run only using paired t-tests (α = 0.05).

Results & Discussion: ΔTc was significantly greater in the hot condition (0.06 ± 0.02 °C/min) vs. the control (0.04 ± 0.02°C/min; p = 0.015) due to a significantly shorter run duration (hot: 26.0 ± 8.4 min; control: 40.3 ± 15 min; p = 0.028) as there was no difference in Tc at the end of the run (hot 38.82 ± 0.35°C; control 38.84 ± 0.58°C; p = 0.938). This result supports previous studies finding that exercising in hot conditions can affect exercise duration compared with cold or moderate temperatures [8]. The change in foot strike angle (p = 0.914) and the change in peak knee flexion angle (p = 0.893) were not significantly different between the control and hot conditions. The lack of significant differences in peak knee angle change may be due to individual participant responses (Fig. 1). For example, 3/6 participants had a larger change in peak knee flexion angle in the heat than the control condition, 2/6 had a smaller change in the heat, and the change was similar for one participant. This finding is consistent with previous observations that peak knee flexion angle tends to increase as a run progresses [9]. However, only the hot condition resulted in a significant difference in peak knee angle between the start and end of the run (p = 0.020) because all six participants increased peak knee flexion angle within the hot condition whereas 3/6 increased peak knee flexion within the control condition. Foot strike angle did not significantly change within either the control (p = 0.194) or hot (p = 0.685) condition.

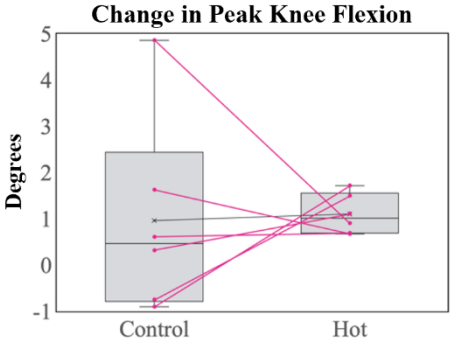

Figure 1: Box plots of the change in peak knee flexion angle within the control and hot conditions (negative = decrease). Red lines are individual participants; blank line is the mean.

Significance: Running in the heat may accelerate the onset of exhausted gait given that gait changed in a hot environment to an extent similar to running in an optimal temperature, but this change occurred over a shorter running duration. Thus, runners tended to stop before core temperature, and potentially gait loading patterns, reached dangerous levels. Additional participants and additional variables in this ongoing study may reveal statistical differences in joint angles between hot and control environments that offer insights into the biomechanical implications of running in a hot environment. This information will equip runners and coaches with a better understanding of how to monitor training for injury prevention when running in hot environments.

Acknowledgements: This study was funded by Brooks Sports, Inc.

References: [1] Nystoriak & Bhatnagar (2018), *Front Cardiovac Med*, 5; [2] Nichols (2014), *Curr Rev Musculoskelet Med*, 7(4); [3] World Meteorological Organization, https://public.wmo.int/en; [4] Galloway & Maughan (1995), *J PHYSIOLOGY-LONDON*, 489; [5] Fields et al., (2010), *Curr Sports Med Rep*, 9(3); [6] Scheer et al., (2021), *Front Physiol*,12; [7] Altman & Davis (2012), *Gait Posture*, 35(2); [8] Tatterson et al., (2000) *J Sci Med Sport*, 3(2); [9] Derrick et al., (2002), *Med Sci Sports Exerc*, 34(6).

SCAPULAR KINEMATICS AND SUPRASPINATUS TENDON OCCUPATION RATIO IN WHEELCHAIR USERS

Jungsun Moon[1], Dustin F. Tran[1], Matthew M. Hanks[1*]
[1]Department of Kinesiology and Community Health, University of Illinois at Urbana-Champaign, Urbana, IL, USA
*Corresponding author's email: hanksm@illinois.edu

Introduction: Shoulder pain and dysfunction are highly prevalent in manual wheelchair users (MWUs) [1], with subacromial impingement of the supraspinatus tendon being a commonly reported mechanism [2]. Scapular kinematics, such as increased anterior tilt, increased protraction, and decreased upward rotation, are shown to decrease the subacromial space, thereby increasing the risk of supraspinatus tendon impingement in MWUs [2]. Scapular kinematics and bilateral asymmetries have been primarily examined during dynamic tasks, such as manual wheelchair propulsion [3]; however, MWUs spend less than 10% of the day actively propelling [4]. Therefore, the relationship between scapular kinematics and quantitative shoulder rotator cuff tendon measures related to impingement should be examined under conditions other than propulsion, yet these investigations are lacking in the current literature. The purpose of this preliminary analysis was to examine the association between three-dimensional (3D) scapular kinematics and supraspinatus tendon occupation ratio (OR), a clinical predictor of subacromial impingement syndrome [5], in two static (i.e., non-propulsion) conditions.

Methods: Three MWUs (2 males and 1 female, age: 19.1 ± 1.0, years of manual wheelchair use: 15.0 ± 1.2) participated in this preliminary study. Musculoskeletal ultrasound images of supraspinatus tendon cross-sectional thickness and acromiohumeral distance were obtained bilaterally with participants seated in their personal manual wheelchair and tested with their shoulders in standardized positions using standardized procedures [6-8]. Quantitative measures of supraspinatus tendon thickness and acromiohumeral distance were measured using ImageJ software. Supraspinatus tendon OR was computed by dividing the supraspinatus tendon cross-sectional thickness by the acromiohumeral distance. Participants were outfitted bilaterally with passive markers on the scapulae and upper extremities, and the 3D marker trajectories were tracked using a Qualisys optical motion analysis system sampling at 100Hz during two static conditions: Resting (i.e., participant was relaxed through the shoulders with arms hanging comfortably by their sides) and Mock Push (i.e., participant positioned their hands atop the wheel aligned vertically with the wheel axle). Marker trajectory data were analyzed using a custom upper extremity biomechanical model in Visual 3D software to compute 3D scapular (i.e., acromioclavicular joint) kinematics: upward/downward rotation, protraction/retraction, and anterior/posterior tilt. Pearson correlation was used to describe the association between 3D scapular kinematics and supraspinatus tendon occupation ratio.

Results & Discussion: All participants reported right-hand dominance. During the Resting condition, increased downward rotation, increased anterior tilting of the left scapula, and greater protraction of the right scapula were associated with greater supraspinatus tendon occupation ratios (r=0.97, r=-0.83, and r=0.99, respectively, Fig. 1) consistent with the risk factors during wheelchair propulsion [3]. However, less downward rotation of the right scapula and less protraction of the left scapula were associated with greater supraspinatus tendon occupation ratio (r=-0.95 and r=-0.89, respectively), which is contradictory to the previously reported risk factors [3]. During the Mock Push condition, greater downward rotation of the left scapula and greater protraction and anterior tilting of the right scapula were associated with greater supraspinatus tendon occupation ratios (r=0.62, r=0.87, and r=-0.72, respectively), consistent with the risk factors during wheelchair propulsion [3]. However, less downward rotation of the right scapula was associated with greater supraspinatus tendon occupation ratio (r=-0.86), which is contradictory to the previously reported risk factors [3]. On a secondary basis, our preliminary findings also showed within-individual, bilateral asymmetries in scapular kinematics and supraspinatus tendon cross-sectional thicknesses during the static conditions.

Significance: Findings from our preliminary analyses show similarities between scapular kinematics during static conditions and those previously reported during wheelchair propulsion [2]. These scapular kinematics observed during the static conditions were also associated with greater supraspinatus tendon occupation ratio consistent with an increased risk of subacromial impingement [5]. This is clinically relevant as MWUs spend a significantly greater portion of their day in static conditions than propelling their manual wheelchair [4], and it is feasible that scapular orientation during static activities of daily living may be equally, if not more, culpable in the development of shoulder impingement as scapular orientation during wheelchair propulsion. Though interpretation of the current results is limited and should be viewed cautiously due to the small sample, these findings are part of ongoing research in which we will investigate the relationships between changes in scapular kinematics and rotator cuff tendon health in MWUs across the lifespan.

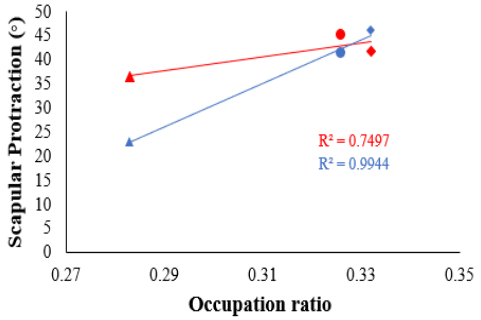

Figure 1: Relationship between occupation ratio and scapular protraction kinematics. Each symbol (●, ♦, ▲) denotes one participant tested in the two conditions: Mock Push (red) and Resting (blue).

Acknowledgments: This work is supported by the University of Illinois College of Applied Health Sciences Center on Health, Aging, and Disability.

References: [1] Liampas et al (2021). *Pain Ther* 10(2); [2] Morrow et al. (2011), *Clin Biomech* 26(4); [3] Hurd et al. (2008) *APMR* 89(10); [4] Sonenblum et al. (2012), *Rehabil Res Pract*; [5] Michener et al. (2015), *Knee Surg Sports Traum Arthro* 23; [6] Gil-Agudo et al. (2014), *Frontiers in Bioeng and Biotech* 2; [7] Kim K et al., (2016), *J Korean Med Sci* 31(9); [8] Plomb-Holmes et al. (2018) *Ortho Traum Surg Res* 104(8)

COMPARING UPPER EXTREMITY MUSCLE ACTIVITY MEANS ACROSS DIFFERENT COMPUTER MOUSE SENSITIVITIES IN VIDEO GAMING TASK

Kayla Russell-Bertucci[1*], Clark R. Dickerson[1],
[1]University of Waterloo, Department of Kinesiology, Faculty of Health
*Corresponding author's email: kl3russe@uwaterloo.ca

Introduction: Computer mouse sensitivity is the ratio between physical movement and cursor movement on a computer display, measured in dots per inch (DPI). Video game players optimize performance by selecting a preferred sensitivity to maximize cursor precision and accuracy in video gaming. While office ergonomics appears to be adjacent to video game ergonomics, previous research omitted modulation of mouse sensitivity as a modulating exposure factor. Currently, only a few studies quantified muscle activity of limited muscles while using different weighted computer mice [1][2] and inconsistent video gaming tasks. This study measured muscle activity on a robust set of muscles with a standardized video gaming task across multiple mouse sensitivities. Due to low sensitivity requiring more physical movement, it was expected that low mouse sensitivity would lead to higher muscle activity in shoulder and elbow muscles, while lowering that of the forearm muscles. Additionally, due to the increased mental and precision demands required to complete higher difficulty games, the high difficulty task was anticipated to result in higher muscle activity across all muscles.

Methods: Seventeen participants (15M, 2F), free of right upper extremity pain or injury in the past year and capable of completing the Hard level osu! beatmap participated. Surface electromyography (sEMG) was collected on 12 muscles Noraxon Ultium EMG system (Noraxon Inc., Arizona, USA): upper trapezius, supraspinatus, infraspinatus, anterior and middle deltoid, pectoralis major (clavicular, sternal), biceps brachii, triceps brachii, extensor digitorum, extensor carpi ulnaris, and extensor carpi radialis.

Participants adjusted the collection workspace and specified a preferred computer mouse DPI on a provided Logitech G Pro wireless mouse (80 g). Participants completed 42 1-minute-long trials of Easy and Hard level beatmaps. For each level, 7 trials were at their preferred sensitivity, and 7 trials each at low (400 DPI) and high (1600 DPI) sensitivity, with low and high randomized.

Participants performed maximal voluntary contractions (MVC) of the 12 listed muscle [3]. sEMG was sampled at 2000 Hz, with a digital high pass filter of 10 Hz and a low pass filter of 500 Hz applied. Both trial and MVC EMG were high pass filtered at 30 Hz to remove potential heart rate and motion artifacts [4], followed by full wave rectification to linearly envelope the signal. Three trials from each randomized block of difficulty and sensitivity were chosen based on in-game accuracy, and then the mean of the filtered trial was normalized to %MVC. A two-way repeated measures ANOVA was conducted to determine the effect of game difficulty and mouse sensitivity on mean muscle activity, using JMP (SAS, Cary, North Carolina, UA).

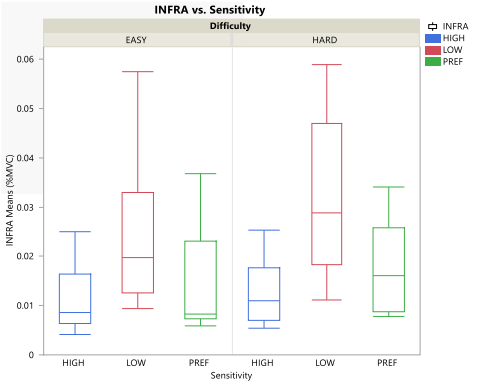

Figure 1: Infraspinatus muscle activity (%MVC) across Difficulty and Sensitivity. The figure is divided vertically by task difficulty. The box plots represent mouse sensitivity (blue: high sensitivity, red: low sensitivity, green: preferred sensitivity).

Results & Discussion The ANOVA revealed a significant Difficulty x Sensitivity interaction in supraspinatus ($F_{(2,17)}$=3.33, p = 0.0458), infraspinatus ($F_{(2,17)}$=9.61, p = 0.0004), biceps brachii ($F_{(2,17)}$=5.29, p = 0.004) and pectoralis major (clavicular) ($F_{(2,17)}$=3.33, p < 0.0001). Tukey's post-hoc tests revealed that muscle activity was significantly higher when participants used low sensitivity in both difficulties, leaving high sensitivity and preferred sensitivity significantly similar. The interaction effect between Difficulty and Sensitivity in the significant muscles reveal consistent trends. Specifically, low sensitivity trials consistently show the highest muscle activity mean, followed by preferred then high, and most cases results in higher muscle activity in the Hard difficulty factor (Fig. 1). This pattern aligns with previous office ergonomics research, in which increased mental and precision loads lead to higher muscle activity [5]. This interaction effect in our results expands on the idea that an increase in difficulty and varying precision demands can modify muscle activity. Main effects of Sensitivity in upper trapezius ($F_{(2,17)}$=21.94, p <0.0001), supraspinatus ($F_{(2,17)}$=22.35, p <0.0001), infraspinatus ($F_{(2,17)}$=30.22, p <0.0001), anterior deltoid ($F_{(2,17)}$=14.96, p <0.0001), extensor digitorum ($F_{(2,17)}$=3.4, p = 0.0457), and extensor carpi ulnaris ($F_{(2,17)}$=3.34, p = 0.0489). In all muscles except extensor digitorum, low sensitivity resulted in the highest means, whereas extensor digitorum saw the opposite effect. Lastly main effects of Difficulty in pectoralis major (clavicular) ($F_{(1,17)}$ = 8.93, p = 0.0433), and extensor carpi ulnaris ($F_{(1,17)}$ = 6.98, p = 0.013). Current results contrast with previous findings indicating higher muscle activity in professional players compared to high level players in upper trapezius, anterior deltoid, and middle deltoid [6].

Significance: Computer mouse sensitivity affected muscle activity and is relevant to video game and office ergonomics studies. Rotator cuff muscles should be added in future analyses for a more holistic evaluation. These results can assist clinicians in understanding which muscles are primarily active based on their patient's preferred mouse sensitivity. Despite variation in preferred mouse sensitivity in this sample (950 ± 450.62 DPI), players appear to choose a sensitivity that optimizes performance while decreasing muscular cost.

References: [1] Li et al. (2019) *Proceedings of the Human Factors and Ergonomics Society Annual Meeting* (63(1), 1969-1971); [2] Yan et al. (2022) *Proceedings of the Human Factors and Ergonomics Society Annual Meeting (*66(1), 868-870); [3] Perotto, Aldo O. *Anatomical guide for the electromyographer: the limbs and trunk*. Charles C Thomas Publisher, 2011; [4] Drake & Callaghan (2006), *J Electromyogr Kinesiol.* 16(2); [5] Visser et al. (2004), *Ergonomics* 47(2); [6] Li et al. (2022), *J Human-Computer Interaction* 38(8):691-706

BOLSTERING SCIENTIFIC IDENTITY VIA AN INTENTIONALLY-INCLUSIVE REAL-TIME JOURNAL CLUB

Laurel Kuxhaus[1], Melissa C. Richards[2*]
[1]Department of Mechanical and Aerospace Engineering, Clarkson University, Potsdam NY, USA
[2]Institute for STEM Education, Clarkson University, Potsdam NY, USA
* borealis@clarkson.edu

Introduction: Building students' scientific identity is key to fostering a sense of belonging [1, 2] and student persistence. Students from sociodemographically diverse backgrounds frequently face challenges integrating their scientific identity with their existing intersectional identities (e.g., racial, ethnic, family, and social backgrounds). This is additionally difficult for students who may rarely (at most) interact with faculty or other scientific role models who share their own demographical characteristics. To counter the "if you can't see it, you can't be it" mentality, as part of the BOREALIS (BiOengineering Research Education to AcceLerate Innovation in STEM) Scholars program at Clarkson U, we have curated a number of efforts to build scientific identity, including early coaching on introducing oneself as a scientist, early engagement in mentored research and scientific communication, and an intentionally-inclusive real-time Journal Club. We expect that, in the long term, our Journal Club will bolster students' scientific identities and lead to improved confidence. In this abstract, we share our practices in curating the Journal Club activity.

Methods: We held our Journal Club as part of credit-bearing courses (Introduction to Biomedical Engineering Research I and II) in the Fall and Spring semesters; these courses are exclusive to our BOREALIS Scholars cohort of first-year students. Each session (six times in the Fall semester, and three times in the Spring) included a virtual appearance by a featured guest author, and the article was chosen in advance by the course instructor. In the fall semester, we deliberately welcomed authors with a broad range of expertise, to expose students to the broad and encompassing field of biomedical engineering. In the Spring semester, articles and guest authors were chosen to align with the students' ongoing research project. To further align with the program's intent to advance the diversity of the bioengineering research workforce, instructors intentionally invited authors who had both relevant technical expertise and intersectionalities that resonated with students' sociodemographic identities. Students prepared for each session by reading the article and completing a worksheet that included identifying technical and career-related questions for the guest author. In rotation, one student was selected to prepare and deliver a presentation. Students' research mentors were invited to join the Journal Club.

Individual class discussions focused about 50% on scientific and technical aspects, and about 50% on the featured author's career journey. Each session began with a student's short (5-7 minute) presentation summarizing the article, followed by open-ended engagement with the author about how the presentation 'hit' the mark or 'missed' a few details. Students then engaged in Q&A with the author about the work. Then, the author informally described their career journey to date, and students engaged with additional Q&A about career/life questions. Students were required to send the guests a professional thank-you note after each session, and the BOREALIS Scholars program sent a formal thank-you letter to all guests at the end of each semester. As part of the BOREALIS Scholars program, we regularly assess the development of our students' scientific identity with a one-question survey. [3]

Results & Discussion: In our first year, we featured nine guest authors from eight institutions spanning the continental United States, many of whom disclosed aspects of their own intersectional identities within the context of their career path (e.g., national origin, ethnicity, and other sociodemographic factors) that overlapped with aspects of our students' identities. All students engaged in meaningful dialogue with each guest. Engagement was particularly high when the guest author described contributions that undergraduate researchers had made to the work. (We had not screened for this in our article selection process, as we were focused primarily on author representation, article topic, and readability.) We observed that the diverse backgrounds of our guest authors seemed to resonate with students – many of the students' thank-you emails included sharing a common aspects of their identity or life struggles.

As a direct result of these interactions, students also learned about summer research opportunities at other institutions, and have applied for summer 2024. (As of abstract submission time, it is too early to know about acceptances.) At the end of the first semester, when asked if the Journal Club format should be altered for the Spring semester, the resounding answer was "keep it the same!". We also acknowledge that while there is some coordination required to implement this (choosing articles, inviting guest authors and the correct virtual meeting link in advance), the instructor's effort is comparable to preparing for a typical class period.

Our students' scientific identity remained strong at the end of the fall semester, compared to its summer values. While we cannot necessarily attribute all of this to our Journal Club activity, we expect that the enthusiasm we see during these interactions contributes. We anticipate that the skills of introducing oneself as a researcher and engaging in meaningful technical and non-technical Q&A during discussions will translate to improved networking skills as these students grow their experience as researchers. We also recognize that this work is in its first year and building scientific identity is a lifelong process. That said, we wish to broadcast our approach and methods to encourage the community to embark on similar initiatives.

Significance: The work described represents a field-tested approach to catalyzing low-stakes interactions between emerging biomedical engineers and highly-respected established researchers. The interactions with nationally-renowned researchers give students tangible glimpses into what their future could be as researchers, and foster networking and professional development skills that are essential to thriving.

Acknowledgments: We thank our nationwide colleagues who engaged in rich dialogue with our students. This work was supported by NIH/NIBIB Award Number R25EB033080.

References: [1] Atkins+ (2020), IntJ STEM Ed; [2] McCartney+ (2022), J Microbiol Biol Ed; [3] McDonald+ (2019), Frontiers in Ed.

The effect of carbon fiber custom dynamic orthosis use and design on limb loading after lower extremity traumatic injury

Jason M. Wilken[1], Sapna Sharma*, Kirsten M. Anderson, Molly S. Pacha, Kierra J. Falbo, Clare Severe, Andrew H. Hansen, Brad D. Hendershot, CARBON (CARBon fiber Orthosis research Network)
[1]Department of Physical Therapy and Rehabilitation Science, Carver College of Medicine, University of Iowa, Iowa City, Iowa
*Corresponding author's email: sapna-sharma@uiowa.edu

Introduction: Use of carbon-fiber custom dynamic orthoses (CDOs) can significantly improve lower limb function following lower extremity trauma.[1] Previous studies have demonstrated that device design can influence limb loading,[2] however most studies are from a military setting and investigate a single type of device. Studies on other commercially available CDOs are limited,[3] and the extent to which CDOs now used in clinical practice alter limb loading is unknown. For example, stiff modular CDOs (MOD) with a rigid footplate (Figure 1. Reaktiv, FabTech Systems, Everett, WA) are thought to alter limb loading to a greater extent than more compliant, monolithic CDOs (MONO; Figure 1. PhatBrace, Biomechanical Composites, Des Moines, IA). The objective of this study was to compare limb loading and perceived smoothness of two CDOs commonly used in civilian clinical practice, relative to each other and no CDO, in individuals who have experienced lower limb trauma.

Figure 1: Modular (left) and Monolithic (right) CDOs.

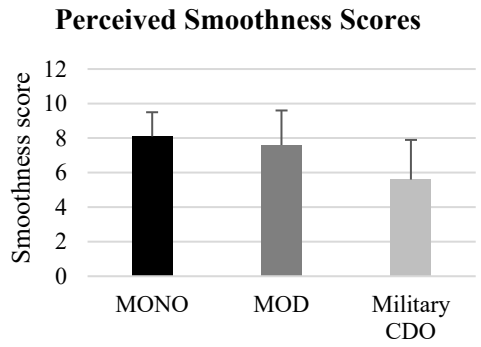

Figure 2. Mean perceived smoothness scores for the monolithic (MONO) and modular (MOD) CDOs in comparison to a military CDO used in a prior study [5].

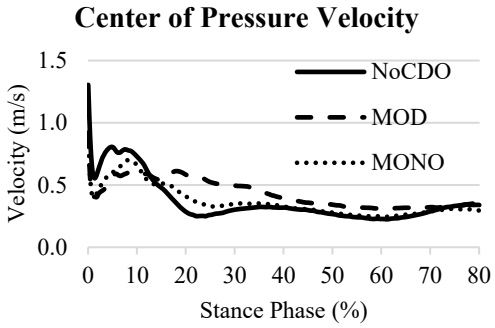

Figure 3. Plot of the velocity of the center of pressure (vCoP) for the three conditions; no device (NoCDO), modular CDO (MOD), and monolithic CDO (MONO)

Methods: Sixteen individuals (mean age = 42.9[11.0] years) who sustained a below-the-knee traumatic injury greater than two years prior and were still experiencing deficits including pain, weakness and/or impaired mobility were included in this study. Ground reaction force data (1200Hz, AMTI inc.) were collected as participants walked on an over ground walkway at a controlled speed based on participant's leg length.[4] Participants were assessed without a CDO (NoCDO), and with MOD and MONO CDOs in randomized order. Participants accommodated to each study CDO for three months prior to testing. Study measures included CDO alignment, CDO stiffness, participant rating of CDO smoothness, magnitude of the peak velocity of centre of pressure (vCoP), time to peak vCoP, and ankle zero-moment crossing (ZMC).

Results & Discussion: The MOD was significantly stiffer than MONO (stiffness: MOD=8.7[2.7] Nm/degree, MONO=4.6[2.4] Nm/degree), however, alignment, perceived smoothness, vCoP magnitude, and ZMC did not differ between the two CDOs. Perceived smoothness scores with the two study CDOs (Mean[SD] smoothness scores: MONO=8.1[1.4], MOD=7.6[2.0]) were approximately 40% greater (Figure 2), and vCoP magnitude values were 20% lower than prior studies with CDOs used in the military[5]. The time to peak vCoP occurred significantly later for the MOD as compared to MONO and NoCDO conditions, with large effect sizes observed for these differences (Figure 3).

Significance: Despite multiple design differences between the study CDOs, including apparent differences in the cuffs, struts, and footplates, only time to peak vCoP differed between the MONO and MOD CDOs. As compared to previous studies with military CDOs[2], MOD and MONO CDOs exhibited a more gradual center of pressure progression, as evident from the lower peak vCoP magnitudes, which may explain higher smoothness ratings with these CDOs.

Acknowledgements: Research reported in this publication was supported in part by a Department of Defense grant under award W81XWH-18-2-0073 and by the National Center for Advancing Translational Sciences of the National Institutes of Health under Award Number UM1TR004403. The content is solely the responsibility of the authors and does not necessarily represent the official views of the U.S. government, federal agencies, organizations, or foundations.

References: [1] Highsmith et al. 2016. J Rehabil Res Dev 53:157-184. [2] Russell Esposito et al. 2021. Prosthet Orthot Int 45:147-152. [3] Grunst et al 2023. Prosthet Orthot Int. [4] Gates et al. 2012. Gait Posture 36:33-39. [5] Ikeda et al. 2017. Prosthet Orthot Int 42:265-274.

ANALYSIS OF IMU SENSORS ON INDUCED ACL RUPTURES ON CADAVERIC LOWER LIMBS

Luana Niewelt[1], Victor Maldonado[2], Nathaniel A. Bates[3], Nathan D. Schilaty[1-2,*]
[1]Medical Engineering, University of South Florida, Tampa, FL
[2]Neurosurgery & Brain Repair, University of South Florida, Tampa, FL
[3]Orthopaedic Surgery, The Ohio State University, Columbus, OH
*Corresponding author's email: nschilaty@usf.edu

Introduction: Nearly 300K anterior cruciate ligament (ACL) ruptures occur each year costing over $2B. [1] Further, ACL injuries can have long-term detrimental sequelae. Therefore, it is important to understand the underlying mechanisms of ACL injuries as any progress in diminishing their occurrence would provide important long-term health and economic benefits. The objective of this study was to examine induced ACL ruptures on cadaveric specimens of drop landings by utilizing inertial motion unit (IMU) sensors to quantify leg acceleration leading up to, during, and following ground impact.

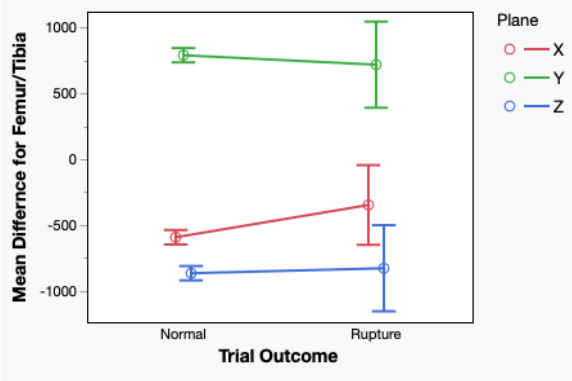

Figure 3: Mean acceleration difference according to trial outcome. When calculating mean acceleration difference across femur and tibia, lateral acceleration (X) shows an increase in the rupture trial, while superior acceleration (Y) decreases, and anterior acceleration (Z) remains approximately the same.

Methods: Nineteen cadaveric limbs (22-52 years) were acquired and prepped for testing. A mechanical impact device simulated ground reaction force impulse generated from landing in a physiologic and clinically relevant manner. [2-4] External knee abduction moment, anterior shear, and internal tibial rotation loads were applied to the specimen via pneumatic actuators as determined *in vivo* from a cohort of healthy athletes. Each limb had an IMU sensor placed on the tibia and femur that measured 3-axis acceleration. After randomized sub-injury thresholds, loads were increased until knee injury was induced.[1] Specimens were physically and arthroscopically examined at baseline and post-injury by a board-certified orthopedic surgeon. Following data collection, data was post-processed in LabVIEW to extract impacts and maximum/minimum accelerations. To align data across all axes (X, Y, Z), femur data was rotated 180° and tibia data was aligned by using each specimen's tibia angulation (calculated from a CT scan).

Results & Discussion: All specimens had confirmed ACL ruptures. The maximum and minimum acceleration ratios across specimens were observed. Mean acceleration ratio was 1.03 ± 0.24 across all specimens with an average difference of 0.38 between Normal and Rupture. These acceleration ratio ranges tended to be lowest on the trial where ACL rupture occurred. Maximum and minimum jerk ratios (derivative of acceleration) were observed across specimens. Mean jerk ratio across specimens was 0.85 ± 0.25 with an average difference of 0.46 between Normal and Rupture. Range of the jerk ratio across all specimens tended to be lower on observed rupture trials when compared to other trials of a particular specimen. After assessing the ranges of both the acceleration and jerk ratios across all specimens, a correlation can be observed. When evaluating the data further, the difference in anterior shear across all respective axes must be observed and analyzed.

Significance: A decrease in valgus lateral movement may be crucial when preventing ACL ruptures. Difference of mean acceleration in the lateral direction increases when ACL rupture occurs. It is likely that rapid valgus movement facilitates ACL ruptures. This IMU data may assist in the development of wearable devices that can correlate accelerations with ligament strain, the biomechanical property that causes rupture of viscoelastic materials.

Acknowledgments: The authors acknowledge support from NIAMS including R01AR056259 and L30AR070273 and the support of the Florida Department of State Center for Neuromusculoskeletal Research.

References: [1] Bates et al. (2016) *KSSTA* 24(9):2778-2786. [2] Bates et al. (2017) *Clin Biomech* 44:36–44. [3] Bates et al. (2018) *Am J Sports Med* 26(9):2113-2121. [4] Bates et al. (2018) *Am J Sports Med* 46(9):2113–2121.

WALKING ARM SWING ASYMMETRY DURING PREGNANCY

Hallie E. Music[1], Joshua P. Bailey[2], Robert D. Catena[1*]
[1]Gait and Posture Biomechanics Lab, Washington State University
[2]Integrated Sports Medicine Movement Analysis Lab, University of Idaho
*Corresponding author's email: robert.catena@wsu.edu

Introduction: Arm asymmetry is typically used to classify pathologic gaits. However, the general population has some degree of asymmetry in arm swing [1]. We previously showed there is an increase in arm swing over the course of pregnancy, thought to provide a counter rotation to leg momentum [2]. However, differences between the two arms have yet to be identified during pregnancy, which could have implications on balance control [3] and wrist-worn physical activity monitors (PAMs). The current research aimed to identify changes in arm swing symmetry in pregnant individuals and identify effects of this change. Since arm asymmetry is typical in most populations, we hypothesized that arm asymmetry will be present and consistent throughout gestation and correlate to balance control.

Methods: Twenty-three pregnant individuals (28 ±4 years, 70 ±2.1 kg) were tested in four-week intervals (±2 weeks) at 18-, 22-, 26-, 30-, and 34-weeks' gestation. Anthropometry and kinematic data were measured via motion capture as participants walked at a self-selected walking speed. Kinematics (projection angles), arm symmetry index (ASI), torso center of mass (COM) motion, dynamic balance control, gait velocity, and segment coordinations were calculated. Linear mixed model analyses were used to identify change over time and the interaction between body side and time. Forward-step multiple linear regression analyses were used to determine correlations between kinematics, asymmetry, torso COM motion, balance, gait velocity, and coordination couplings.

Results & Discussion: Arm range of motion (ROM) was asymmetric ($p<0.001$) (Fig 1) with a greater left arm ROM (M=36.4°, sd= 2.9°) than right (M=33.3°, sd=2.9°). However, the right arm (less motion to start on average) ROM had a greater rate of increase at 16.4% ($p=0.006$), while left arm ROM only increased by 12.2% ($p=0.046$). When dichotomizing arms based on dominance at first testing (most vs. least motion), dominant arm ROM did not significantly change through pregnancy ($p=0.101$), but non-dominant arm ROM significantly increased 19.7% ($p=0.002$). Directional ASI, based on side, decreased from an average of 10.14% to 5.7%. ASI based on dominant arm ROM also decreased, from an average of 16.8% to 9.2%, however, this was not statistically significant ($p=0.271$).

The ROM of both arms was positively correlated with gait velocity ($r>0.693$, $p<0.001$), as would be expected to create rotation with more leg momentum (similar motion, but more mass). After accounting for gait velocity, there was additional negative correlation to dynamic balance control, ($r>0.779$, $p<0.001$). After accounting for gait velocity and balance control, arm ROM also had a positive corelation to more arm dominant leg-arm coordinations ($r>0.9$, $p<0.001$). As directional ASI decreases through pregnancy, it was negatively correlated with Pelvis–Thorax In-phase coordination and gait velocity (both increased), but positively correlated with dynamic balance control (it degraded) ($r=0.500$, $p=0.006$). This negative relationship between directional ASI and Pelvis-Thorax coordination may have implications on trunk stiffness and low back pain [4]. Directional ASI was slightly correlated with lateral torso motion ($r=0.226$, $p=0.020$, ß=-1713.7) by itself, but it did not provide any unique contribution to the forward-step regression. Furthermore, neither torso COM position nor motion was correlated with right or left arm ROM. This shows that arm motion is not compensating for changes in the torso COM position associated with increased abdominal size during pregnancy.

Our hypothesis that arm asymmetry would be seen during pregnancy was supported; however; the large amount of variability seems to mask an ASI change over the course of gestation. The bilateral increases in arm swing seem to be tied to momentum generation, with a negative effect on balance control.

Significance: While falls significantly increase through gestation, pregnant individuals maintain slight asymmetric arm swing. Increased symmetry over time seems to affect walking speed and propulsion. This can have implications on energy expenditure, potentially at the expense of balance control. More research is needed to determine if asymmetric arm swing changes impact actual fall risk. Future studies should investigate potential benefits associated with asymmetry changes during pregnancy, including direct measure of metabolic energy, and determine if attachment side affects wrist-worn PAM measurements.

Acknowledgments: We would like to thank the participants for their time and funding through WSU and Tidyware.

References: [1] Killeen et al. (2018). *Sci Reports* 8(1); [2] Music et al. (2023). *Gait Posture* 104; [3] Siragy et al. (2020). *J Biomech* 99. [4] Prins et al. (2019). *Sci Reports* 9.

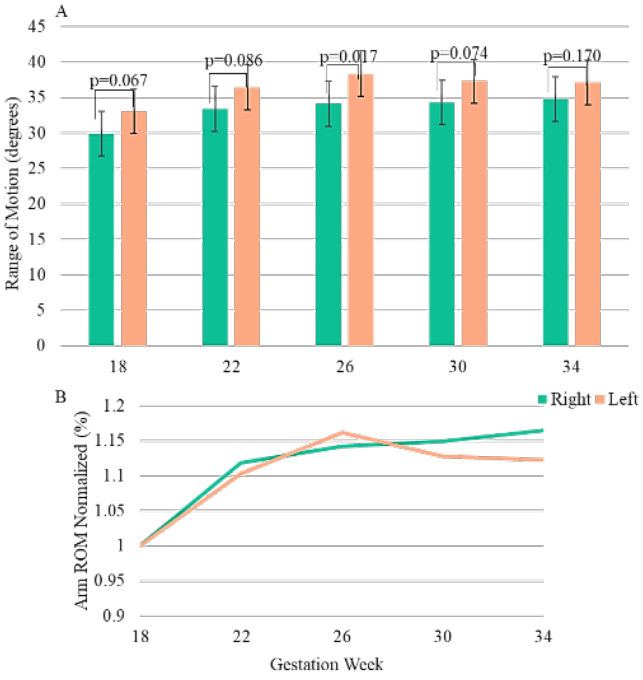

Figure 1 A: Arm ROM was significantly different by side throughout pregnancy. **B**: Percent increase in arm ROM over time, showing the right arm increased at a greater rate.

HUMANS CAN INDEPENDENTLY CHANGE FOOT PLACEMENT VARIANCE AND COVARIANCE WHILE CROSSING OBSTACLES

Ashwini Kulkarni[1*], Chuyi Cui[2], Shirley Rietdyk[3], Satyajit Ambike[3]
[1]Old Dominion University, Norfolk, VA; [2]Stanford University, CA; [3]Purdue University, IN, USA
*Corresponding author's email: a1kulkar@odu.edu

Introduction: While approaching the sandpit or the first hurdle, athletes progressively increase the precision of their foot placements, so that the long jumper lands her foot on the take-off board and the hurdler positions his foot appropriately to clear the hurdle [1, 2]. We call this behavior the '*variance reduction strategy*', and it also manifests during everyday locomotion when individuals approach and step over a visible obstacle [3]. Recently, we reported another pattern in the foot placements when approaching and crossing an obstacle: the covariance in consecutive foot placements also declined during approach, and it was smallest for the crossing step ($Step_0$; Fig. 1A) [4]. We call this the '*covariance reduction strategy*'.

Here, we explored the extent to which younger (YA) and older adults (OA) can change foot-placement variance and covariance independent of each other. Let '*f*' and '*b*' represent the distances of the front and the back foot from a stationary visible obstacle at heel strike. Then, the step length is: $s = b - f$, and $\mathrm{Var}(s) = \mathrm{Var}(b) + \mathrm{Var}(f) - 2\mathrm{Cov}(b,f)$. The variance reduction strategy requires $\mathrm{Var}(f) < \mathrm{Var}(b)$, and the covariance-reduction strategy indicates that $\mathrm{Cov}(b,f)$ reduces for consecutive steps. Furthermore, $\mathrm{Var}(s)$ would be bounded because consistent step length is important to maintain stable gait. Mathematically, it is possible for a system to demonstrate a range of positive and negative covariance even with these constraints on the variances in *f*, *b*, and *s*. Humans, however, have additional biomechanical and physiological constraints on their motions that change with age. Hence, mathematical independence of variance and covariance does not imply independence in human behavior, and any correlation between the variance and covariance could change with age. Therefore, we quantified to what extent variance reduction and covariance reduction are independent control strategies during obstacle crossing in YA and OA.

Methods: Fifteen younger (24±3 years) and fourteen older adults (64±5 years) walked on an 8 m walkway and crossed an obstacle placed midway in the walkway. They performed two tasks: control task with only the obstacle in the walkway, and a task with a visual target, located at their preferred foot placement, that they stepped on while approaching the obstacle (Fig. 1A). Each task was performed 20 times. The foot-placement variance was computed for five foot falls, and the covariance in the distances of the front and back heels from the obstacle was quantified using the inter-step covariation (ISC) index [4] for the corresponding five steps. To test whether the two strategies are independent, the across-task difference in the variances (ΔV) and the ISC index (ΔISC) were analysed using linear regression. A high association will suggest that the two strategies are not independent and vice-versa. Differences across age will suggest how this relation is altered by changes in body physiology and other aging-related factors.

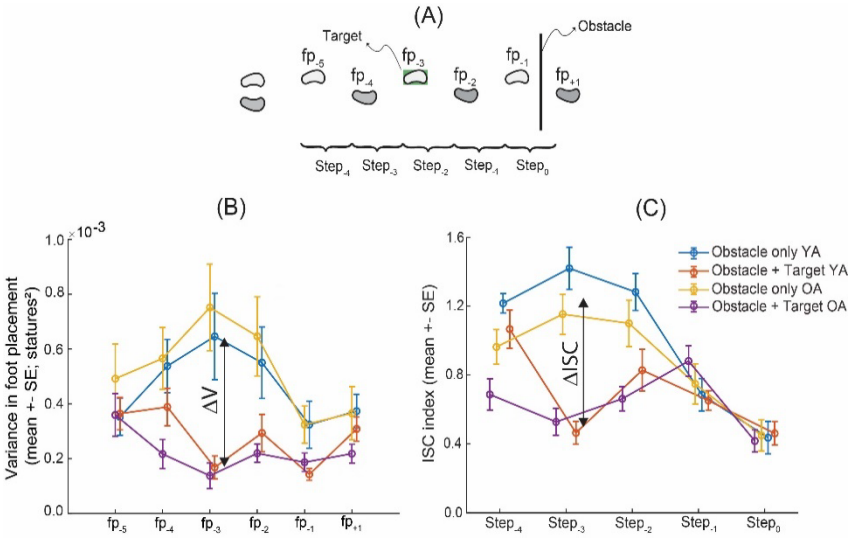

Figure 1. (A) Bird's eye view of walkway with target and obstacle. (B) Variance in foot placement. (C) Inter-step covariance (ISC). Difference variables (ΔV and ΔISC) illustrated in (B) and (C), respectively. ΔV for fp_{-4} to fp_{+1} was regressed against ΔISC for $Step_{-4}$ to $Step_0$.

Results & Discussion: Inclusion of the visual target changed the variance pattern (Fig. 1B) and the ISC index (Fig. 1C). When the regressions between ΔV and ΔISC were conducted separately for each participant, only two younger and two older participants had statistically significant slopes. When data were pooled across participants, the regression was significant for the younger adults ($p < 0.01$), but it was not significant for the older adults ($p = 0.09$). Thus, there is some degree of dependence between the strategies in younger individuals, although this is not very high ($R^2 = 0.27$). There was no evidence of dependence in the older adults. Overall, the variance- and covariance-reduction strategies are quite independent, and aging leads to greater independence.

Significance: Quantifying active anterior-posterior foot placement control is important as tripping, a significant cause of falls (17-59% of all falls) [5], primarily occurs in the sagittal plane. Our metrics quantify the kinematic outcomes of this active control and indicate that humans modulate foot placements in two ways to adapt to their environment. Furthermore, the variance- and covariance-reduction strategies are more independent in older compared to younger adults; but it is unclear if this difference is an adaptation, a deficit, or a spandrel. Therefore, the key next step is to study the relation between our metrics and trip rates in various populations. Our novel approach to analyzing spatial gait parameters could impact therapeutic practice aimed at minimizing fall risk.

References: [1] Lee et al., 1982, *J Exp Psych-Human Percep and Performance,* 8(3); [2] Smirniotou et al., 2022, *Motor Control,* 26(2). [3] Muir et al., 2019, *Gait & Pos*, 70; [4] Kulkarni et al., 2023, *Motor Control*, 27; [5] Berg et al., 1997, *Age Ageing*, 26(4).

EVALUATION OF A SOFT PASSIVE BACK EXOSKELETON FOR STRUCTURED AND UNSTRUCTURED EMERGENCY MEDICAL TASKS

Tiash Rana Mukherjee[1*], Tiago Gunter[1], Oshin Tyagi[2], Ranjana K. Mehta[3]
[1] Department of Mechanical Engineering. Texas A&M University – College Station
[3] Department of Industrial Engineering & Operations Research. University of Michigan – Ann Arbor
[2]Department of Industrial & Systems Engineering, University of Wisconsin - Madison
*Corresponding author's email: tiashrana@tamu.edu

Introduction: Back injuries account for ~40% of the reported non-fatal work-related musculoskeletal disorders across material handling occupations such as transportation, construction, and healthcare providers [1]. Tasks such as repetitive bending, frequent lifting, and twisting contribute to the prevalence of these disorders, affecting the well-being of these workers. Passive low back exoskeletons (LBEs) have emerged as an ergonomic solution to mitigate these injuries and aid workers while performing manual lifting tasks. Of these, hard LBEs present a hindrance to movement [2], while soft LBEs are lighter, easy to wear, and do not affect the natural movement of the wearer [3]. Soft LBEs have been known to reduce low back muscle loads during dynamic lifting and static tasks, but their use for highly dynamic, variable, and physically demanding work has not been studied. The objective of this study was to assess the effectiveness of soft LBEs on biomechanical and neuromuscular measures across structured and unstructured emergency medical tasks.

Methods: A within-subject study with 18 male and 2 female emergency medical technicians (EMTs) were conducted. The mean (SD) height, weight, and age of the EMTs were 1.76 (0.08) m, 97.3 (18.9) lb., and 33.1 (8.2) years. All EMTs performed a series of box lifting tasks and a series of circuital tasks with and without the assistance of the exoskeleton. The lifting tasks consisted of 6 distinct symmetrical and asymmetrical tasks performed with a 10 kg cardiac monitor from (i) ankle to hip, (ii) ankle to shoulder, (iii) ankle to overhead, (iv) left ankle to right hip, (v) right ankle to left hip, and (vi) left hip to right hip. The circuital task consisted of six tasks selected from the physical agility tests to mimic tasks commonly performed by EMT-Ps in the field. The tasks were: (i) squat lifting a backboard with a 150 lb dummy; (ii) carrying a cardiac monitor with the right hand across a staircase; (iii) carrying a barbell weighing 75 lbs at shoulder level across a staircase both facing front and without turning back; (iv) pulling out and holding the rear end of the stretcher from a parked ambulance until it automatically unloads and loads it back; (v) performing cardiopulmonary resuscitation (CPR) on a dummy for 120 s. To compare between conditions range of motion (ROM) and electromyography (mean:50th and peak:90th percentile amplitude probability density function; APDF) were evaluated using inertial measurement unit sensors and electromyography, respectively. Individual task-based Wilcoxon signed-rank tests were performed to analyze any significant differences between conditions due to exoskeleton use.

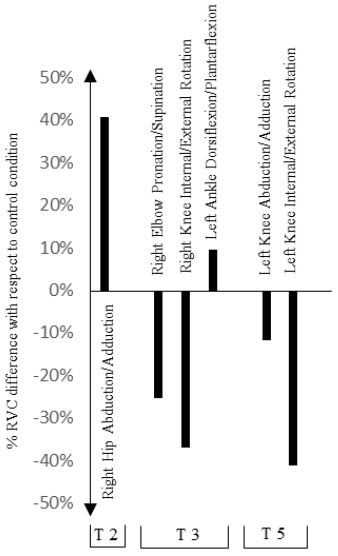

Fig 1. Significant ROM differences between conditions for T2: One-hand carry, T3: Barbell Carry and T5: CPR

Results & Discussion: APDF results for left erector spinae indicate that for symmetrical lifting tasks, mean (ankle to hip, $p = 0.004$) and peak (ankle to shoulder, $p = 0.027$) activity reduced with exoskeleton use by 17-22%. However, for the asymmetrical lifting task (left ankle – right hip, $p = 0.006$), there was a 55% increase in the peak right erector spinae activity with exoskeleton use and accompanied by a 37% decrease in the peak left upper trapezius activity ($p = 0.004$). Although no differences were observed in the ROM (all $p>0.064$), this may be due to the exoskeleton restricting asymmetrical bending, leading to compensatory mechanisms of lower back and contralateral shoulder activation. While no other significant differences for lifting tasks (all $p > 0.064$) were observed between conditions for APDF and ROM, results for the circuital tasks suggest that erector spinae and bicep femoris activity reduced with exoskeleton use for one-hand carry (23-29%), barbell carry (7-20%), stretcher push/pull (18%), and CPR (38-53%). Significant condition differences (all $p<0.049$) were also noted for the ROM of the right hip, right elbow, right knee, left knee, and left ankle (Fig 1). However, as these results vary with tasks, these cannot be generalized. For instance, ~40% increase in the hip ROM during one-hand carry suggests that the LBE might have engaged with the hip adductors [4], potentially helping EMT-Ps to improve their limb support. This might have helped with the redistribution of load, as seen by reduced activation in the left bicep femoris. Therefore, results from this study suggest human-exoskeleton interaction requires greater contextual evaluations as LBE use might not be equally beneficial or potentially detrimental for different tasks.

Significance: This evaluation provides valuable feedback on the implementation of soft LBEs that can be used in the future for improving exoskeletons and developing training modules for the intended user.

Acknowledgments: We thank the Cy-Fair EMS Department and the Neuroergonomic Laboratory for their significant help with this study. This research was partially supported by the National Science Foundation under award number 2033592.

References: [1] Occupational Injuries, Bureau of Labor Statistics, 2022 [2] Baltrusch, S.J., et. al. (2019) Ergonomics Pg. 903 - 916 [3] Lamers, E.P., et. al (2017) IEEE Transactions on Biomedical Engineering, 65(8): p. 1674-1680. [4] Lyons, K., et al. (1983), Physical therapy 63(10): p. 1597-1605

TRANSIENT SADNESS IS ASSOCIATED WITH ALTERED GAIT IN PEOPLE WITH GLAUCOMA

Natalie Bick[1*], Helmet T. Karim[2,1], Howard Aizenstein[2,1], Mark Redfern[1], and Rakié Cham[1]
[1]Department of Bioengineering, University of Pittsburgh, Pittsburgh, PA
[2]Department of Psychiatry, University of Pittsburgh, Pittsburgh, PA
*Corresponding author's email: nab173@pitt.edu

Introduction: Adults with glaucoma fall at a greater rate than similarly aged adults without glaucoma [1, 2]. Glaucoma is traditionally thought of as an ophthalmologic condition; however, recent evidence suggests glaucoma is a neurodegenerative condition with central nervous system implications, such as sensorimotor and psychological changes [3]. For example, depression occurs at a higher rate in people with glaucoma [4]. Though depression is a risk factor for falls in older adults, *the impact of depression on gait in glaucoma has not been studied.* The goal of this study was to understand how transient mood induction contributes to gait changes in people with glaucoma. We hypothesized that gait would be worse while participants reflected on sad memories compared to happy or neutral memories, and that individuals with glaucoma would be more impacted than those without.

Methods: Seventeen adults with glaucoma (G) between the ages of 65 and 85 years and nine similarly aged adults without (NG) were enrolled after screenings to exclude any vestibular, somatosensory, or neurological condition. Based on previous research on mood and gait [5] and worry-rumination [6], participants were asked to "Think of a time in your life when you felt extremely [happy or sad]," then rate how strongly they felt emotion during each memory on a scale of 1-5, where 1=no emotion and 5=extreme emotion. Each personalized memory, or induced transient mood (ITM) cue, was converted to an audio file (<10 s) using text-to-speech software, with 4 happy and 4 sad created for each participant, each with a rating ≥3. Participants were asked to walk back and forth at a comfortable pace along a straight 10-m walkway during 4 floor/lighting conditions: floor conditions were a hard, vinyl floor and a soft, carpeted floor; lighting conditions were well-lit (750-880 lux) and dim (15-20 lux). Participants were asked to focus on their feelings about a happy ITM and a sad ITM (order randomized), separated by a neutral fact (emotions rated ≤2) for each floor/lighting condition. Each gait condition lasted about 6 minutes, with the participant focusing on each ITM cue (happy, neutral, sad) for 2 minutes.

Gait data were collected using a motion capture system (Vicon Motion Systems, Oxford, UK) at a sampling frequency of 120 Hz. Gait speed was calculated from a maker placed on the C7 and step length standard deviations were calculated from toe and heel markers and averaged across both feet. Two mixed linear regression models were constructed, with fixed effects of floor/light, ITM, patient group, and the first order interactions, with subject as a random effect; dependent variables were gait speed and step length standard deviation, fit separately. Statistical significance was set at $\alpha=0.05$, and post-hoc student's t-tests were conducted at $\alpha=0.05$.

Results & Discussion: Gait Speed: During hard floor/well-lit, the G group walked significantly slower during the sad ITM than happy and neutral ($F_{(2,48)}=4.1$, *p=0.02*, Fig. 1a), but the NG group did not. During soft floor/dim and well-lit, G group had slower gait speed than NG (approaching significance $F_{(1,22)}=3.5$ and $F_{(1,24)}=3.4$ respectively, both p=0.08).
Step Length Standard Deviation: During soft floor/dim, sad ITMs resulted in greater step length standard deviation than happy or neutral ($F_{(2,46)}=3.2$, *p=0.05*, Fig. 1b) across all participants.

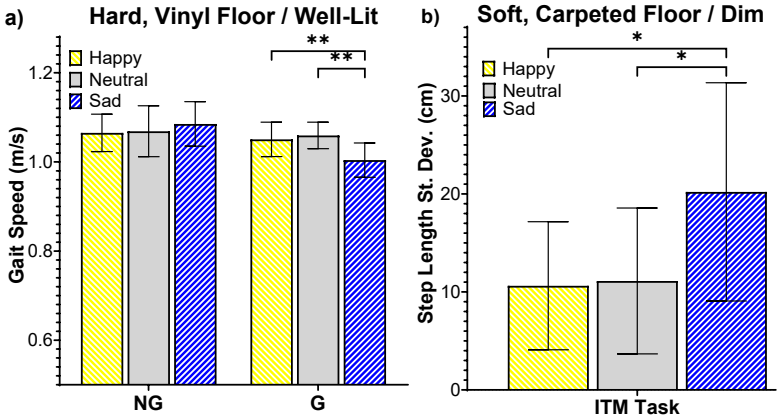

Fig. 1: (a) Participant x ITM interaction effect regarding gait speed on hard floor in well-lit condition and (b) ITM main effect on step length standard deviation in soft floor and dim lighting. Error bars are standard error of the mean. **p=0.02, *p=0.05

Individuals with glaucoma, but not those without glaucoma, had slower gait speeds during sad mood induction compared to happy and neutral. All participants had higher step length variability during sad compared to happy or neutral mood induction. Gait speed may be sensitive to glaucoma-specific gait changes, especially during sad emotional states. Step length standard deviation may be generally sensitive to the ITM task used in this study. Together, these results indicate that the relationship between emotions and sensory inputs may help us better understand fall risk in adults with glaucoma.

Significance: By further understanding the role of psychological factors in gait changes in people with glaucoma, we may ultimately find ways to reduce their fall risk related to mental health by developing alternate methods for gait rehabilitation, such as incorporating strategies from cognitive behavioral therapy.

Acknowledgements: Bioengineering in Psychiatry T32 Fellowship (5T32MH119168-02) & Lendvay-Newton Balance Disorder Research Philanthropic Gift

References: [1]Lamoureux et al., 2008. *Invest Ophthalmol Vis Sci*. 49(2). [2]Ramulu, 2009. *Curr Opin Ophthalmol*. 20(2). [3]O'Hare et al., 2012. *Clin Exp Ophthalmol*, 40(9). [4] Biderman et al., 2002. *Journal of Epidemiology and Community Health*. 56(8). [5] Kang and Gross, 2016. *J Biomech*. 49(16). [6] Andreescu et al., 2011. *Depress Anxiety.* 28(3).

TISSUE STIFFNESS CONSIDERATIONS FOR CONTROL OF ELECTROMAGNETIC PROSTHETIC LIMB SUSPENSION

Will Flanagan[1*], Alexandra I. Stavrakis[2], Nicholas M. Bernthal[2], Tyler R. Clites[1,2]
[1]Department of Mechanical and Aerospace Engineering, University of California, Los Angeles
[2]Department of Orthopaedic Surgery, University of California, Los Angeles
*Corresponding author's email: wflan@ucla.edu

Introduction: Prosthetic limb attachment is a main source of patient-reported problems [1], primarily due to suspension of the limb from soft tissues instead of bone. To address these issues, we are developing a novel prosthetic attachment system that transfers suspension loads directly to the bone across a closed skin envelope via magnetic attraction [2]. This system consists of a bone-anchored ferromagnetic implant within the limb, and an external electromagnet housed within a socket (**Fig. 1a**). In contrast to percutaneous osseointegration (OI), our system does not have a chronic wound which should greatly reduce the risk of infection compared to OI.

Our previous work studied feasibility of magnetic attachment under static conditions [2]. For this abstract, we investigate the system's dynamic behavior under feedback control of the electromagnet and the effects of varying tissue stiffness.

Methods: We modeled the system as a mass (2 kg for the socket and electromagnet) acted on by 3 forces: the tissue force (F_{tis}), the magnetic attraction force (F_{mag}), and the prosthesis force (F_p) as seen in **Fig. 1a**. A critical characteristic of this system is that F_{mag} can only attract the implant ($F_{mag} < 0$) and F_{tis} can only push the mass ($F_{tis} > 0$). The prosthesis force over the gait cycle was calculated using published biomechanics data [3] and accounts for gravity on the mass (**Fig. 2, top**). The magnetic force was obtained from the experimental relationship of force as a function of electromagnet current and the gap distance between the electromagnet and implant. The initial gap distance (at $x = 0$) was set to 17.5 mm [2]. The tissue force was based on an exponential fit ($F_{tis} = ae^{b\delta}$; a, b are fit coefficients) on measurements of a silicone model limb with the embedded implant (**Fig. 1b**). Three tissue stiffnesses were tested: low ($b_{low} = 0.5b$), nominal ($b_{nom} = b$), and high ($b_{high} = 2b$). The initial tissue deformation (δ) was set so F_{tis} balanced F_{mag} at the 17.5 mm gap distance.

We simulated the system over the gait cycle in Matlab. A proportional feedback controller set the magnet current based on the tissue force, $I = k(F_{tis} - F_0)$, where F_0 is the initial tissue force. The proportional gain, k, was 0.175 A/N from manual tuning. Currents were restricted to positive values since F_{mag} is limited to attraction. We control F_{tis} because it will be readily measurable in the physical system. We simulated the system for each tissue stiffness and evaluated performance based on pistoning (x displacement) of the mass, with lower pistoning being favored.

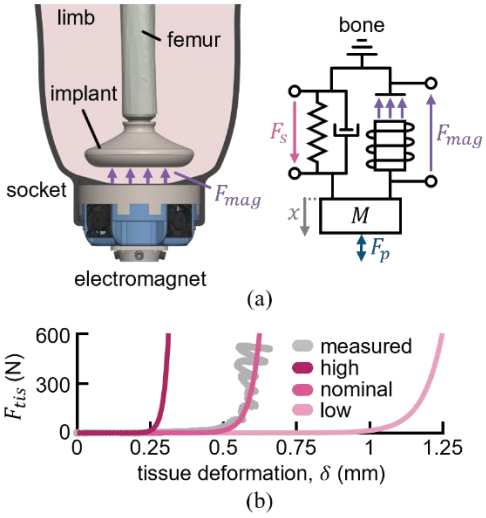

Figure 1. (a) Prosthetic limb suspension was modeled as a mass (M) acted on by a tissue force (F_{tis}), a magnetic force (F_{mag}), and a prosthesis force (F_p). (b) Three exponential tissue stiffnesses were tested: low, nominal, and high, based on measurements of a silicone model limb.

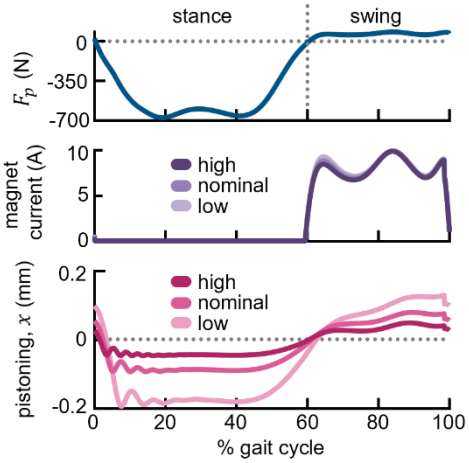

Figure 2. The system was driven by the prosthesis force derived from biomechanics of gait. Tissue stiffness had little affect on magnet current for this control scheme, however, pistoning decreased as stiffness increased.

Results & Discussion: As shown in **Fig. 2**, current was only applied during swing and varying stiffness had little affect on current. This was due to F_{tis} being relatively constant for the low tissue deformations present during swing such that the controller demands similar currents. Increased stiffness decreased the amount of pistoning, however. Since we rely on tissue forces for weightbearing, during stance the less stiff tissue deforms more. In the transition to swing, the increased travel from less stiff tissue allows the mass to gain more momentum as F_p changes from compression to tension. The electromagnet must counteract this increased momentum to keep the prosthesis attached, resulting in increased pistoning during swing. Pistoning could be reduced by increasing the control gain k at the cost of requiring more power, although it must be noted that our simulated pistoning is already sub-millimeter. This could be due to the relatively small gap distance that the tissue could compress into, such that the tissue quickly "bottoms out", along with our model limb tissue not exactly replicating biological tissue.

Significance: Controlling our proposed electromagnetic attachment system will be a technical challenge due to nonlinearities in the system. By understanding how tissue stiffness, which will change for each patient, in future work we can modify our controllers for each patient. As a result of better attachment, we can solve many patient-reported problems with prostheses.

Acknowledgments: This work was funded by DOD CDMRP (W81XWH2220046) and NSF GRFP (DGE-2034835).

References: [1] Dillingham et al. (2001), *AJPM&R*. [2] Flanagan et al. (2023), *IEEE TBME* [3] Hood et al. (2020), *Sci Data*

ARM SWING TRAINING TO IMPROVE GAIT IN OLDER ADULTS

Ines Khiyara[1*], Babak Hejrati[2]
[1]Department of Mechanical Engineering, The Biorobotics and Biomechanics Lab, University of Maine, Orono, 04469, United States of America
*Corresponding author's email: ines.khiyara@maine.edu

Introduction: Gait rehabilitation for older adults predominantly focuses on leg movements, often overlooking the critical role of arm movements despite the known neurological interconnectivity between upper and lower extremities. This study investigates the impact of a novel wearable haptic cueing system targeting arm swing to enhance gait parameters in older adults, addressing a significant gap in current rehabilitation practices. We hypothesized (1) that arm swing cycle time (CT) can be altered through haptic cueing and (2) that manipulation would change key gait parameters including their gait speed [1]. The implication of these hypotheses is that gait speed (and other gait parameters) can be improved through targeted arm swing training.

Methods: In this study, twenty older adults (73.4 ± 6.2 years) were recruited to evaluate the performance of the haptic cueing system aimed at enhancing their key gait parameters including speed. Inertial measurement units (IMUs) were placed on the participants' feet and arms to capture their gait. The experimental conditions included (1) self-selected Normal walking speed (N) without receiving any cues, (2) Cueing condition 1 (C1), the participants received cueing on both arms, maintaining a 20% reduced CT than normal walking, and (3) Cueing condition 2 (C2) which led to a CT that is 20% longer than their normal walking. The two cueing conditions show that changes in arm swing CT could both be increased and decreased. A smartphone app-driven system [2], equipped with vibrotactors attached to participants' arms, was created to provide rhythmic haptic cues tailored to adjust the arm swing CT (Fig. 1) which was assumed to be equivalent to the foot CT based on the 1:1 frequency ratio between arm and leg swings [1]. By comparing gait parameters during cued and non-cued walking trials, we assessed the immediate effects of such haptic cueing on gait speed, symmetry, and other spatiotemporal parameters.

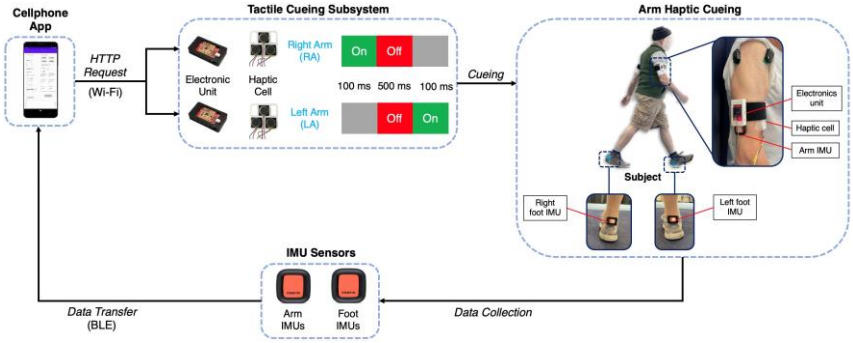

Figure 1: Haptic cueing system on a participant: illustration of components and one-cycle cueing mechanism. The system features rhythmic activation of three vibrotactors in each haptic cell on the anterior sides, alternating between the right and left anterior brachium with a delay between activations.

Results & Discussion: The presentation of the haptic cues significantly altered arm swing CT, resulting in a reduction of 8.3% in the C1 trial compared to the normal trial and an increase of 14.1% in the C2 trial compared to the N trial (Fig.2a). Significant differences were identified across the trials for arms CT ($F(3, 57) = 77.73$, $p < 0.001$, $\eta^2 = 0.577$). These significant changes in cycle times led to statistically significant changes in gait speed (Fig.2b) of 18.2% increase in C1 and 12.3% decrease in C2 compared to the N trial ($F(3, 57) = 44.52$, $p < 0.001$, $\eta^2 = 0.438$). The response to haptic cues was immediate, emphasizing the tight interlimb coupling of the arms and legs in the production of gait. In addition to changes and improvements in spatiotemporal parameters, better symmetry between the right and left arms were achieved, when using the tactile cues. A cross-correlation (r) analysis showed that arm swing symmetry improvement was present in both C1 (r = 0.930 ± 0.093) and C2 (r = 0.918 ± 0.085) conditions compared to N trial (r = 0.887 ± 0.123). Subjective evaluations further supported the system's potential for gait training. These results extend our knowledge of gait modulation through upper limb manipulation, offering a new perspective on integrating arm movement training in gait rehabilitation practices.

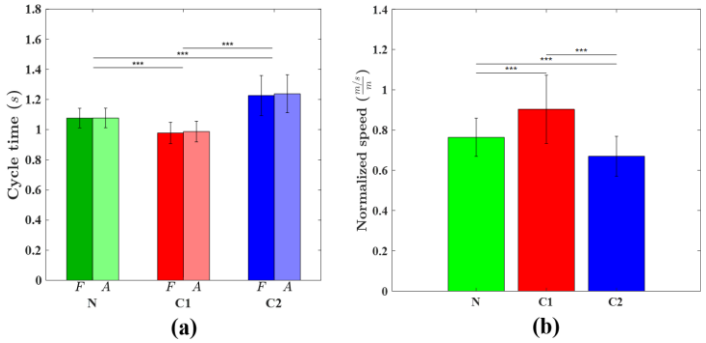

Figure 2: Results of: (a) foot (F) and arm (A) cycle time, and (b) height-normalized gait speed with asterisks representing the p value (one, two, and three asterisks represent $p < 0.05$, $p < 0.01$, and $p < 0.001$, respectively) and a line connecting the significant bar plots.

Significance: The study's results highlight the significant potential of the haptic cueing system to modulate gait via arm swing adjustments, exploiting interlimb neural coupling. This approach aligns with the growing need for home-based gait training solutions, particularly for the older population, and offers a new strategy that could be incorporated into existing gait rehabilitation practices.

Acknowledgments: This work was supported by the National Science Foundation under Grant 2145177.

References: [1] Noghani, M. A., Hossain, M. T., Hejrati, B., 2023, IEEE Trans. Neural Syst. Rehabil. Eng. 31.; [2] Noghani, M. A., Shahinpoor, M., Hejrati, B., 2021, IEEE Robot. Autom. Lett. 6(4).

CORRELATION BETWEEN MECHANICAL PROPERTIES AND PORE MORPHOLOGY IN REGIONS OF COMPRESSION IN THE FEMORAL DIAPHYSIS

Mikayla R. Hoyle[1*], Mariana E. Kersh[1, 2, 3]
[1] Dept. of Mechanical Science and Engineering, [2]Beckman Institute for Advanced Science and Technology, [3]Carle Illinois College of Medicine, University of Illinois Urbana-Champaign, Urbana, IL
*Corresponding author's email: mrhoyle2@illinois.edu

Introduction: Mechanical loading influences the remodeling processes in bone including the formation of the cortical pore network [1]. Pore morphology has been shown to vary in regions habitually loaded in tension and compression and of varying strain magnitude [2]. For example, we identified new measures of pore microstructure which were different in regions loaded in tension and compression during walking [3]. However, the relationship between pore morphology and mechanical properties remains unclear [4, 5, 6]. The aim of this study was to evaluate the compressive mechanical properties of bone and their correlation with morphological measures.

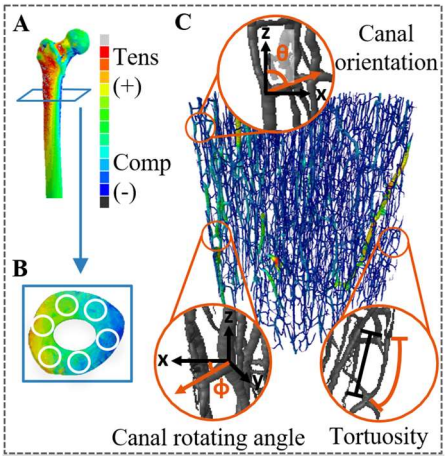

Figure 1: (A) Principal strains in the femur during walking. (B) Cross-section used as a map for sample extraction. (C) Skeletonized pore morphology from µCT with measures shown [3].

Methods: Six previously developed muscle-driven finite element (FE) models of the femur during walking were analysed using principal strains to identify regions of tension and compression (Abaqus 2020, Fig. 1A) [7]. The resulting strains within the diaphyseal cross-sections were to guide extraction of cadaveric cortical bone samples habitually exposed to compressive strains (n=6, Ø = 5.0 mm, length = 17 mm, Fig. 1B) from the femoral diaphysis (ages = 65,71; female). Micro-computed tomography (µCT) data (isotropic resolution = 5.3 µm, Rigaku CT Lab HX130) was acquired to measure 3D microstructural features within the sample (Matlab 2021a, Fiji, Amira 2022.2, BoneJ, Fig. 1C) [3]. Samples were potted in custom aluminium endcaps with PMMA (exposed length = 10.71±0.48 mm) and tested in compression to failure at a rate of 0.1 mm/min (Instron). Force data was normalized by cross-sectional area and displacement data was normalized by length to calculate stress and strain, respectively. Young's modulus was calculated as the slope of the linear region of the stress-strain curve. Yield stress and strain were calculated using the 0.2% offset rule. Ultimate stress and strain were the maximum values before failure. Normality was confirmed using a Shapiro-Wilk test ($p<0.05$).

Results & Discussion: Of the classical measures used when characterizing the cortical pore network, porosity, median canal length, and prevalence of large pores were significantly correlated for all mechanical properties (Fig 2). Others have reported significant correlations between mechanical properties and porosity in humans, canal length in mice/rats, and prevalence of large pores in FE stance models [5, 6, 8, 9]. Of the new measures, median haversian and median Volkmann canal length were significantly correlated with all mechanical properties (Fig. 2, orange). These results indicate that porosity, and more specifically haversian and Volkmann canal length, are strong predictors of mechanical properties. As canal length increases, mechanical properties decreased indicating that shorter canals result in stronger bone. The Volkmann: haversian canal diameter was greater than one, i.e. Volkmann canals tend to be wider than haversian canals, and positively correlated with mechanical properties. Increased Volkmann canal diameter compared to haversian canals are associated with stronger bone. The strongest bone sample would have short haversian and Volkmann canals with Volkmann canals having a greater diameter than haversian canals. Further work is ongoing to better understand whether these same characteristics of stronger bone hold for bone from regions typically exposed to tension.

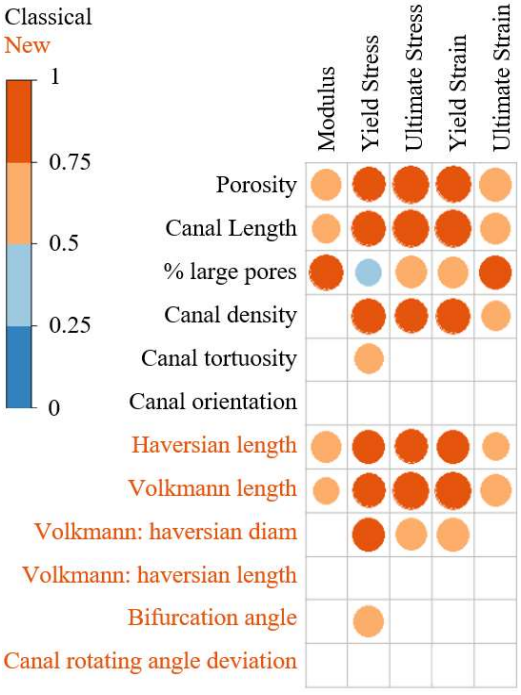

Figure 2: Correlation matrix of morphological measures and mechanical properties ($p < 0.05$).

Significance: This work is an important step towards developing a structure-function relationship for cortical bone. A robust relationship can be used to assess bone quality and help diagnose weaker bone before fracture to allow for intervention. By including new measures of pore morphology, we may expand our understanding of the connection between bone structure and mechanical function.

Acknowledgments: Assistance from Urvshi Thapar.

References: [1] Frost+ *The Anat. Record* 1990; [2] Skedros+ *The Anat. Record* 239(4), 1994; [3] Manandhar+ *J Biomech* 2023; [4] Uniyal+ *JMBBM* 2021; [5] Schneider+ *JBMR* 2007; [6] Hoyle+ *ORS* 2023; [7] Kersh+ *JBMR* 2018; [8] Wachter+ *Bone* 2002; [9] Iori+ *PLOS ONE* 2019.

EXOSKELETON RESISTANCE TRAINING IMPROVES GERIATRIC STRENGTH AND MOBILITY

Jack R. Williams[1*], Jenna C. Hylin[1], Ying Fang[2], Zachary F. Lerner[1]
[1]Northern Arizona University, [2]Rosalind Franklin University
*jack.williams@nau.edu

Introduction: Mobility deficits are prevalent among geriatric individuals and linked to reduced quality of life. These declines in mobility are thought to be a consequence of reduced ankle plantarflexor muscle strength and altered neuromuscular control, which, in turn, can create ankle propulsive power deficits [1]. While current interventions are successful at increasing plantarflexor muscle strength, they often fail to translate to improved mobility outcomes (i.e., walking speed) [2]. Wearable exoskeletons are an emerging technology that hold immense potential as therapeutic tools. Previous work from our group found that resistive gait training with an untethered ankle exoskeleton resulted in improvements in both strength and mobility in those with cerebral palsy [3]. It is unknown if a similar resistance training paradigm is also effective among a geriatric population. Therefore, the purpose of this study was to assess the efficacy of a wearable ankle exoskeleton resistance training paradigm to promote strength and mobility in elderly individuals. We hypothesized that, following four weeks of exoskeleton resistance gait training, participants would exhibit increased plantarflexor muscle strength, faster overground walking speeds, improvements in six-minute walk test (6MWT) distance, and lower metabolic cost of transport.

Methods: Eight participants (4 male, 4 female, age: 76 ± 5 years) completed four weeks of functional exoskeleton resistance training. This consisted of a pre-assessment visit, 12-training visits, and a post-assessment visit. The following measures were assessed pre- and post-training: plantarflexor muscle strength (via a handheld dynamometer), self-selected and fastest overground walking speed (during a 30-meter walk test), walking distance (during a 6MWT), and metabolic cost of transport (during the last two-minutes of a six-minute treadmill walk). Each training session consisted of 20 total minutes of treadmill walking while receiving resistance from an ankle exoskeleton device using a previously described protocol [3]. Briefly, the exoskeleton device applied a dorsiflexion-directed torque during stance phase that resisted the plantarflexion moment during forward propulsion. Users were provided plantar pressure audio-visual biofeedback to encourage them to increase recruitment of the plantarflexor muscles during push-off. Changes in variables of interest between pre- and post- training were compared using two-tailed paired t-tests (for parametric data) or Wilcoxon signed rank tests (for non-parametric data) as well as corresponding effect sizes and % changes. Statistical significance was defined as $\alpha = 0.05$.

Results & Discussion: Our hypotheses were partially supported. All functional measures of interest, except for the metabolic cost of transport, displayed beneficial improvements following exoskeleton resistance training (**Figure 1**). This included a large increase in plantarflexor muscle strength, increases in self-selected and fastest overground walking speeds, and further walking distances during a 6MWT. This could suggest that exoskeleton resistance training during a functional walking activity may not only promote improved muscle strength, but also beneficial changes in neuromuscular control that aid in the translation of strength that typical resistance training techniques fail to elicit. Future work should explore changes in neuromuscular control strategies to test this theory. While, on average, there was no difference in the metabolic cost of transport following training; on an individual level there were a mixture of metabolic responses post-training, with 50% having a reduced metabolic cost (average difference: -13%) and 50% having an increased metabolic cost (average difference: +14%). This could be a function of how metabolic cost was assessed as participants were forced to walk at the same self-selected speed between pre- and post-training. This fixed speed may have masked potential improvements in metabolics that an updated self-selected speed may have revealed. Future work should incorporate an updated treadmill walking speed during the post-assessment visit to explore this possibility. While no measure of propulsive ankle power generation during walking is incorporated into the current analyses, future work will assess collected gait data to assess the influence of training on this variable of interest.

Significance: Exoskeleton resistance training has the potential to promote strength and improve mobility among older adults.

References: [1] Franz JR. (2016), *Exerc. Sport Sci Rev*. (44). [2] Beijersbergen CMI et. al. (2013), *Aging Res. Rev.* (12). [3] Conner et al. (2020), *IEEE J Eng Med Biol.* (4).

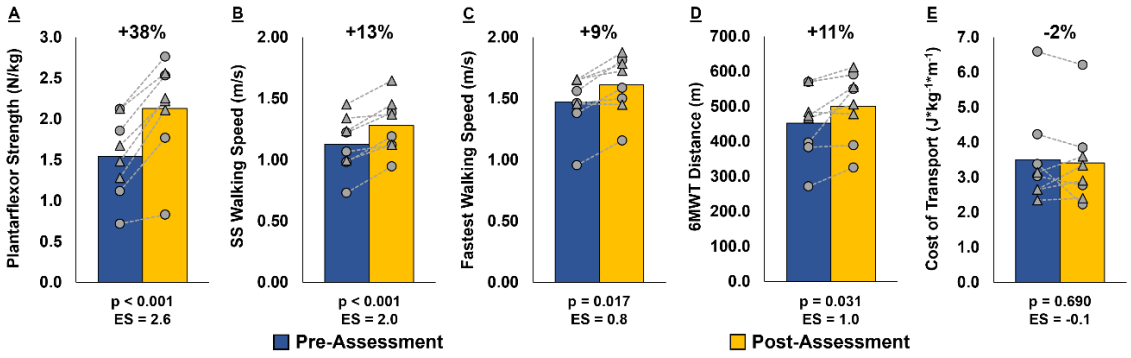

Figure 1: Average strength and mobility outcomes pre- (blue) and post- (yellow) exoskeleton resistance training. (A) plantarflexor strength, (B) self-selected walking speed, (C) fastest walking speed, (D) six-minute walk test distance, (E) metabolic cost of transport. Individual data points are represented by circles (men) or triangles (women) and connected by dashed lines to show changes. The percent change of the averages are shown above each figure and the results from the statistical tests and their corresponding effect size (ES) are displayed below each figure.

KINEMATIC SIMILARITY AND DIFFERENCE BETWEEN LABORATORY FALLS VERSUS REAL-LIFE FALLS IN OLDER ADULTS

Kitaek Lim[1], Seyoung Lee[1], Junwoo Park[1], Chunghwi Yi[2], Yijian Yang[3], Woochol Joseph Choi[1*]
[1]Injury Prevention and Biomechanics Laboratory, Dept of Physical Therapy, Yonsei University, South Korea
[2]Dept of Physical Therapy, Yonsei University, South Korea
[3]Dept of Sports Science and Physical Education, The Chinese University of Hong Kong, China
*Corresponding author's email: wcjchoi@yonsei.ac.kr

Introduction: It is common to reproduce falls with young adults in the laboratory (i.e., "self-initiated" falls by mimicking older adults' falls; "motor-induced" falls by perturbing the floor). While this has helped to provide insights to understand the mechanism of fall-related injuries (i.e., hip fracture, wrist fracture, head injury) in older adults, it has never been discussed how realistic the laboratory falls are when compared to real-life falls in older adults. We conducted falling experiments in the laboratory to discuss kinematic similarities and differences among the laboratory falls and real-life falls in older adults.

Methods: Eight healthy young adults (4 males, 4 females) participated in falling experiments (Fig 1a, 1b). *Self-initiated falls:* They watched video footage of typical older adults' falls [1] and mimicked the falls on a 40 cm thick mattress. *Motor-induced falls:* They stood on a carpet placed on the mattress, which connected to a linear motor (Linear motor, SL280, Sewoo Industrial Systems, Ansan, South Korea) that translated horizontally at 2.3 m/s, without a cue, to cause a fall. Falling trials were acquired with three fall directions: forward, sideways, and backward. During trials, kinematics of wrists, knees, and pelvis were recorded through 8 motion capture cameras (Vero v2.2, VICON, Oxford, UK) at a sampling rate of 200 Hz. *Real-life falls in older adults:* We have used data provided by Choi et al. (Fig 1c) [2].

During the experiments, participants stood barefoot on the centre of the carpet with their feet shoulder-width apart, while wearing a helmet, hip protector and wrist guards. Instructions were "fall as naturally as possible" for the self-initiated falls, and "try not to fall when the carpet translates" for the motor-induced falls. Three trials were acquired for each condition and averaged for data analysis. The order of testing conditions was randomized.

Outcome variables included body segments' peak vertical and horizontal velocities during descent, and descent duration.

One-way ANOVA was used to test whether these outcome variables were associated with fall type (self-, motor-, and real-). Two-way ANOVA was also used to examine whether these variables were associated with fall types (self- versus motor-) and fall directions.

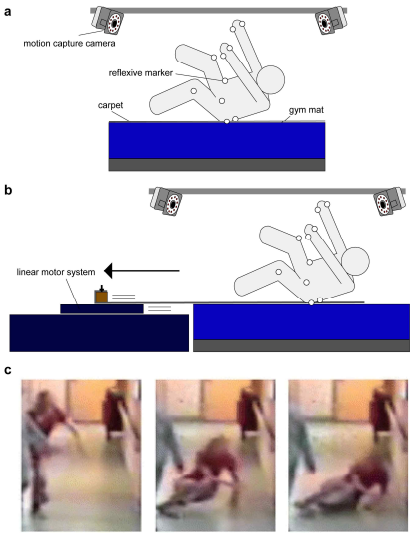

Figure 1: Schematic of laboratory falls (a, b), Snapshot images of real-life falls (c) [3]

Results & Discussion: One-way ANOVA suggested that all outcome variables were associated with fall type ($F = 8.34$, $p < 0.05$). When compared to real-life falls in older adults, the peak vertical velocity of the pelvis was 21.9% and 39.4% greater in self-initiated and motor-induced falls, respectively (2.61 versus 2.14 m/s; 2.98 versus 2.14 m/s, respectively). However, the horizontal velocity was 20% and 37.9% smaller (1.27 versus 1.59 m/s; 0.99 versus 1.59 m/s, respectively), and descent duration was 47.7% and 61.8% smaller (310 versus 593 ms; 226 versus 593 ms, respectively) (Fig. 2).

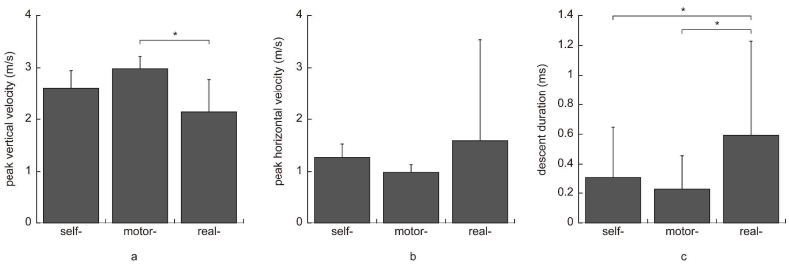

Figure 2: Effect of fall type on (a) peak vertical velocity, (b) peak horizontal velocity, and (c) descent duration of the pelvis

Two-way ANOVA suggested that the peak vertical velocity of the pelvis was associated with fall direction ($F = 35.6$, $p < 0.005$) but not with fall type ($F = 4.8$, $p = 0.07$). On average, the peak vertical velocity was 37.8 % greater in backward than forward falls (3.1 versus 2.25 m/s). The peak horizontal velocity of the pelvis was not associated with fall direction and fall type ($F = 5.3$, $p = 0.14$; $F = 5.3$, $p = 0.06$). Descent duration of the pelvis was associated with fall direction ($F = 6.9$, $p < 0.005$) and fall type ($F = 24.8$, $p < 0.005$). On average, the descent duration was 38.7% greater in self-initiated than in motor-induced falls (0.31 versus 0.22 ms) and 37.7% greater in sideways than in forward falls (309 versus 224 ms).

Significance: Our results suggest that kinematics of the laboratory falls differs from real-life falls in older adults. In particular, the laboratory falls, even the self-initiated falls, overestimate the impact severity (peak vertical velocity at impact) of real-life falls in older adults, which should be considered in data interpretation and application of the laboratory fall simulation.

Acknowledgments: This research was supported by Basic Science Research Program (RS-2023-00270689) and by the "Regional Innovation Strategy (RIS)" (2022RIS-005) through the National Research Foundation of Korea funded by the Ministry of Education.

References:

[1] Robinovitch et al. (2013), *Lancet* 381(9860); [2] Choi et al. (2015), *J biomech* 48(6); [3] Choi et al. (2015), *Osteoporos Int* 26.

BOUNDING BOX CAN STREAMLINE HUMAN GAIT RECOGNITION

Seung Kyeom Kim[1*], Benjamin Riggan[2], Nick Stergiou[1,3] & Aaron D. Likens[1]
[1]Division of Biomechanics and Research Development, Department of Biomechanics, and Center of Research in Human Movement Variability, University of Nebraska at Omaha, Omaha, Nebraska, USA
[2]Department of Electrical and Computer Engineering, University of Nebraska-Lincoln, Lincoln, Nebraska USA
[3]Department of Physical Education and Sport Science, Aristotle University of Thessaloniki, Greece
*Corresponding author's email: seungkyeomkim@unomaha.edu

Introduction: Gait signatures have emerged as a type of behavioral biometric for identifying persons in surveillance style videos. Most gait recognition methods require pre-processing of image/videos, including silhouette extraction and pose estimation. However, these approaches are easily affected by the image/video quality. Also, most existing algorithms do not effectively leverage discriminative information available in the temporal structure of human gait variability. Hence, we propose a novel approach that exploits the temporal properties of human gait variability with minimum reliance on the image/video quality.

Methods: A subset of the BGC1 database [1], the BRIAR Research Set 1.0 (BRS1.0), was used to assess our approach. Out of the dataset, we focused on performing gait recognition on the videos of indoor structured walking. 158 subjects were included from BRS1.0. The videos were taken from 10 different angles (0°, 15°, 45°, 55°, 70°, 90°, 115°, 135°, 165°, 180°) with each subject having varying numbers of angles recorded. We obtained the bounding boxes, rectangular regions that capture specific objects, of every video in the dataset via the MMDetection library [2]. Then, we generated a bounding box width time series for each video. To acquire the profiles of the stride-to-stride fluctuations in each walking trial, we performed fast Fourier transform (FFT) on the bounding box width time series. Then we used the power spectrum as our "feature set". Similar to common gait recognition algorithms, we considered each frequency on the power spectrum as each gait feature and the amplitudes at each frequency as the measured values of the gait features. Euclidean distance (ED), cosine similarity (CS), and dynamic time warping (DTW) were used to quantify similarities between pairs of videos. Based on the similarity measurements, we computed rank-1 and rank-5 accuracies to evaluate the performance of our approach. Cross-view recognition was done, meaning that each pair of different camera angles were taken as gallery and probe set to perform gait recognition.

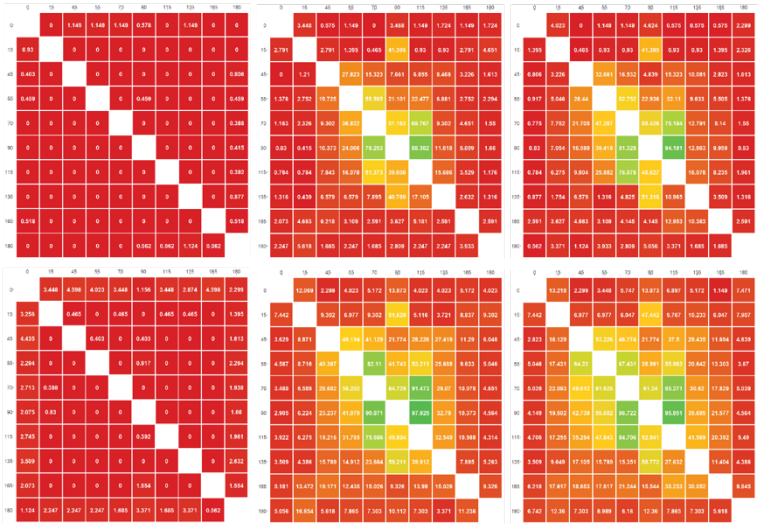

Figure 1. Cross-view Gait Recognition on BRS1.0. (Left Top) Rank-1 accuracy of algorithm with cosine similarity as the similarity metrics. (Middle Top) Rank-1 accuracy of algorithm with dynamic time warping as the similarity metrics. (Right Top) Rank-1 accuracy of algorithm with Euclidean distance as the similarity metrics. (Left Bottom) Rank-5 accuracy of algorithm with cosine similarity as the similarity metrics. (Middle Bottom) Rank-5 accuracy of algorithm with dynamic time warping as the similarity metrics. (Right Bottom) Rank-5 accuracy of algorithm with Euclidean distance as the similarity metrics.

Results & Discussion: The cross-view gait recognition between adjacent view angles were more accurate as the probe set approached 90° (Figure 1). In general, pedestrians captured by surveillance cameras move freely and unconstrained. Thus, improving the stability of our approach against camera view angle is a critical task. Distance-based metrics performed better than CS, especially on lateral view angles, likely because they provide richer information about the magnitude similarity between bounding box width time series. Among the distance-based metrics, DTW consistently outperformed ED for lateral view recognition, particularly at angles of 70°, 90°, and 115°. The accuracy range with dynamic time warping was also narrower, indicating its higher and more stable performance for lateral view gait recognition in our proposed method. However, further testing with other datasets should be done to verify its accuracy and stability.

Significance: In this study, we introduced a novel approach that was not presented previously. Conventionally in gait recognition, bounding box was considered merely as a step to accomplish silhouette extraction and pose estimation. However, in this study we adopted the dimension of bounding boxes as our discriminative metric of gait. This approach could be of great assistance to overcome the vulnerability of existing gait recognition algorithms to image/video quality. In addition, we introduced a new integration of data processing techniques to utilize the temporal structure of human gait variability, which has often been overlooked in gait recognition. Through this study we proposed an approach that not only captures the temporal properties of gait dynamics but also is computationally efficient, providing new insights to human gait recognition.

Acknowledgments: IARPA BRIAR, NSF 212491, NIH P20GM109090, R01NS114282, University of Nebraska Collaboration Initiative.

References:

[1] Cornett et al. (2023). *Proceedings of the IEEE/CVF Winter Conference on Applications of Computer Vision*
[2] Chen, K et al. (2019). *arXiv preprint* arXiv:1906.07155.

ARM SWING AND LEG SWING DURING GAIT MATCH TRENDS OF VARIABILITY OVER TIME

Seung Kyeom Kim[1*], Marilena Kalaitzi Manifrenti[1], Tyler M. Wiles[1], David Kingston[1], Nick Stergiou[1,2] & Aaron D. Likens[1]
[1] Department of Biomechanics and Center for Research in Human Movement Variability, University of Nebraska Omaha, US
[2] Department of Physical Education and Sport Science, Aristotle University of Thessaloniki, GR
*Corresponding author's email: seungkyeomkim@unomaha.edu

Introduction: Wearable smartwatches are increasingly used for health awareness and fitness tracking. Currently, most movement information provided by smartwatches are based on gait characteristics. However, this information relies mostly on linear measures (i.e., mean, standard deviation) that do not capture adequately temporal variations. In addition, smartwatches are attached to the upper limb, and thus they provide limited understanding about how the arm swing and leg swing variabilities relate. Long-range correlation (LRC), the temporal correlations among data points, characterizes the interaction among system components involved in a certain behavior, like walking. LRC can be quantified using a nonlinear metric known as the Hurst exponent (H) [1]. H has been used to evaluate temporal variations in gait for a variety of pathologies [2, 3, 4, 5]. While different systems exhibit unique LRC, when systems interact, they tend to match their LRC to enhance synchronization [6]. Thus, we hypothesized that arm swing and leg swing have matching temporal structure in their variabilities during walking. The study objective was to determine if the overall H of contralateral pairs of arms and legs during walking are similar. We also aimed to examine if windowed H time series of contralateral pairs of arms and legs during walking have similar temporal structures in healthy young adults.

Methods: 35 participants performed 18 overground walking trials, lasting 4 minutes each, while whole-body kinematics were collected via inertial measurement units (Ultium Motion, Noraxon Inc., Scottsdale, AZ) at 200Hz [7]. To compute swing intervals, the duration of a full swing cycle, segment angular velocities were low pass filtered with a cut-off frequency of 10 Hz. Zero crossings of both forearm and shank angular velocities following peak angular velocities of forward swings were identified as the starts of each swing interval. Time differences between consecutive heel strikes were calculated as swing intervals. We extracted the middle 180 swing intervals from each limb for each trial. Overall H [8] was calculated from the 180 swing intervals, which was then averaged across all 18 trials. A windowed H time series was computed in windows of 100 swing intervals, with 99 swing intervals overlapping as the window moves across all 180 strides. Consequently, for each limb, the windowed H time series consisted of 81 datapoints. To evaluate similarity, we calculated the cross-correlation between the windowed H time series of contralateral limbs. Cross-correlations were averaged across trials. We performed Bayesian paired t-tests on the overall H of arm and leg swing for each pair of limbs to assess if the overall H differed. We also performed Bayesian one-tailed, one-sample t-tests on the cross-correlations to examine if the windowed H time series of arm and leg were cross-correlated.

Results & Discussion: Summary statistics of the results are shown in Figure 1. Our results showed decisive evidence (left arm - right leg: BF_{10}: 7.17×10^{20}, right arm - left leg: BF_{10}: 1.54×10^{19}) supporting the difference between overall H of the arms and legs ($H_{right\ arm}$: 0.546±0.076, $H_{left\ arm}$: 0.537±0.076; $H_{right\ leg}$: 0.785±0.052, $H_{left\ leg}$: 0.783±0.049). Additionally, decisive evidence affirmed the similarity between trends of windowed H time series ($r_{left\_arm\text{-}right\_leg}$: 0.563±0.222, BF10: 8.55×10^{13}; $r_{right\_arm\text{-}left\_leg}$: 0.601±0.206, BF_{10}: 4.77×10^{15}). Differences between overall H may result from different constraints and/or behaviour of upper and lower limbs. During walking, lower limbs are biomechanically constrained to oscillate in a quasiperiodic fashion predominantly on the sagittal plane. Whereas the upper limbs are not, requiring less regularity and allowing higher degree of freedom. Despite the contrasting behaviour, the swings of contralateral limbs are coupled to conserve overall angular momentum, forcing the LRCs of the contralateral limbs on short time scale to fluctuate together. This would explain the similar trends of windowed H time series of contralateral limbs. Future work will incorporate gait variability measures into smart wearable devices, leading to more integrative daily health assessments.

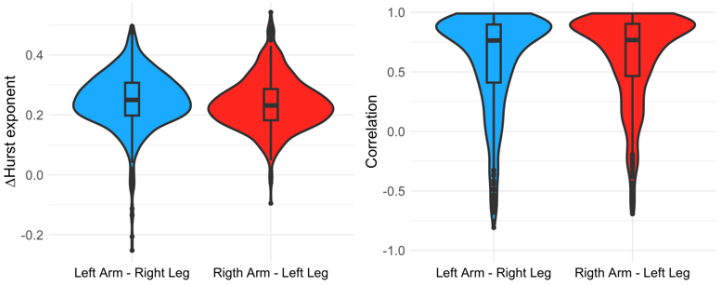

Figure 1. Differences between overall H of contralateral limbs (Left) and Correlations between windowed H time series of contralateral limbs (Right). Colored violins show the distribution of each variable. Boxes show interquartile range, bold horizontal lines show medians, vertical lines show the range of the data, and points specify outliers.

Significance: This study is significant because it provides an understanding of how upper and lower limb variability during gait differ on a longer time scale but synchronize on a shorter time scale. This finding can provide insights on how the complexities of upper and lower limb during gait interact as a whole system. In addition, as the interest in personal data for transitioning into a healthier lifestyle has increased, more precise and integrative information is needed. Our results laid the groundwork to include information on human gait variability, especially nonlinear metrics, into health tracking algorithms.

Acknowledgments: NSF 212491, NIH P20GM109090, R01NS114282, University of Nebraska Collaboration Initiative.

References: [1] Hurst, H. E. (1951). *Trans. Am. Soc. Civ. Eng.*, 116(1). [2] Hausdorff et al. (1995) *Physica A*, 302(1–4). [3] Hausdorff et al. (1997) *J. Appl. Physiol*, 82(1). [4] Hausdorff. (2001) *J. Appl. Physiol.*, 78(1). [5] Stergiou et al. (2006*) J Neurol Phys Ther*, 30(3). [6] West et al. (2008) *Phys. Rep.*, 468(1-3) [7] Wiles et al. (2023) *Sci. Data*, 10(1). [8] Tyralis, H., & Koutsoyiannis, D. (2014). *Clim. Dyn.*, 42(11).

DISTILLING LAWS OF HUMAN GAIT KINEMATICS

Seung Kyeom Kim[1*], Tyler M. Wiles[1], Nick Stergiou[2] & Aaron D. Likens[1]
[1] Department of Biomechanics and Center for Research in Human Movement Variability, University of Nebraska Omaha, US
[2] Department of Physical Education and Sport Science, Aristotle University of Thessaloniki, GR
*Corresponding author's email: seungkyeomkim@unomaha.edu

Introduction: When studying dynamical systems, understanding the long-term behavior of a system is pivotal. Models that depict systems are convenient tools to understand and even predict the long-term behaviors of diverse systems. In addition, mathematical models can give insights to how the systems' behavior alters as a function of its control parameters. For example, the Lorenz system has been extensively used to simulate how the atmospheric convection changes due to the tuning of control parameters such as fluid viscosity and thermal conductivity of the atmosphere [1]. Similarly, mathematical models of a passive dynamic walker can be tuned using the decline of the surface to help simulate human gait [2]. Despite the significance of each model, the passive dynamic walker and the inverted pendulum are still quantitatively and qualitatively dissimilar from human gait. The quantitative and qualitative "error" can lead to a less accurate evaluation and prediction of a system's behavior, especially gait. Therefore, a mathematical model that can accurately describe and predict gait dynamics under various sets of control parameters, is required. Our aim was to examine the performance of symbolic regression (SR) [3], a method that finds the underlying models of physical phenomena, by applying it to simulated data. Then, we applied SR to overground gait data to obtain a model of human gait kinematics and verified the validity of the obtained models.

Methods: SR was performed on two known dynamical systems, the logistic map and Lorenz system, using Turingbot (Turingbot software, São Paulo, Brazil). Turingbot returns a list of potential equations that may explain the provided data. Those equations, and their R^2 for the timeseries, were compared to known dynamical systems. Overground gait data of 26 young, 28 middle, and 27 older adults were extracted from the NONAN GaitPrint dataset [4]. Thigh, shank, and foot pitch angle, angular velocity, and angular acceleration time series from both limbs were ensemble averaged across the 18 trials, which were completed by every subject. Based on the averaged time series, SR was performed to predict the equations of motion for the thigh, shank, and foot, and were terminated once R-squared reached 0.99999. We took the most complex equation preceding marginal improvements in root mean square ($\Delta RMS < 0.001$) and eliminated constants and trivial terms with coefficients < 0.0001. To evaluate the fitness of SR models to the actual data of each walking trial, we generalized our equations by removing all coefficients, leaving only the predictors and operators between predictors on the right-hand side of the equation. Then, the cleaned SR models were fit to every trial using linear regression and the goodness of fit was verified using R^2.

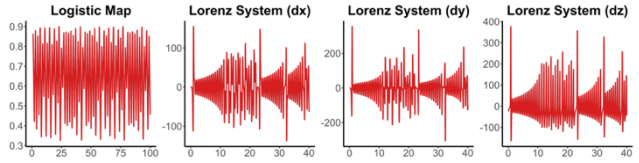

Figure 1. Time series of the predicted from SR models (Red) plotted over the original equations for the Lorenz system and logistic map (Black). Black lines are not seen because the equations had R-squared values close to 1.

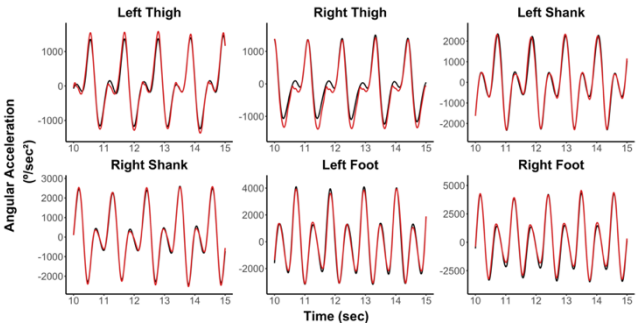

Figure 2. Time series of the predicted data from SR models (Red) plotted over actual gait data (Black).

Results & Discussion: Figure 1 shows the data simulated from the SR models plotted over the known dynamical systems. Figure 2 shows the data simulated from the obtained equations of motion plotted over the actual angular accelerations. SR models were indistinguishable from the logistic map and Lorenz system (R^2: 1.000). SR models were virtually indistinguishable from the left thigh (mean R^2: 0.985 ± 0.010), right thigh (mean R^2: 0.985 ± 0.010), left shank (mean R^2: 0.995 ± 0.005), right shank (mean R^2: 0.995 ± 0.005), left foot (mean R^2: 0.997 ± 0.007), and right foot (mean R^2: 0.997 ± 0.002). SR was able to derive equations that fit almost perfectly to dynamical systems, attesting the performance of SR. The equation of motions obtained from SR had some intriguing features. All models from each segment included the acceleration of their adjacent segments as a predictor. Based on Newton's second law, this may imply the influence of force exerted in the adjacent segments on the motion of each segment. Interestingly, SR models from left and right side had common predictors. This suggests that SR was able to capture identical components of motions and nonlinear interactions between components, regardless of the side, which should be case in normal symmetric gait. Future work will explore deeper into the application of SR on gait dynamics for simulation purposes and feasibility of the models derived from SR.

Significance: This study successfully deployed SR on human gait kinematics with the goal of finding equations that describe human gait kinematics from 1,458 gait trials across a large range of ages. The close-to-perfect fit on empirical data was supported with the perfect derivation of known dynamical systems that behave transiently, like gait. This study establishes the groundwork to use SR to create surrogate, human-like data, when an appropriate dataset is unavailable.

Acknowledgments: NSF 212491, NIH P20GM109090, R01NS114282, University of Nebraska Collaboration Initiative.

References: [1] Lorenz, E. N. (1963). *J Atmospheric Sciences*, 20(2). [2] Garcia et al. (1998). *J Biomedical Engineering*, 120(2). [3] Koza, J. R. (1994). *Statistics and computing*, 4. [4] Wiles et al. (2023). *Scientific Data*, 10(1).

STRIDE INTERVAL CORRELATIONS DEGRADE WITH AGE

Theodore A. Deligiannis[1*], Tyler M. Wiles[1], Seung Kyeom Kim[1], Nick Stergiou[1,2], Aaron D. Likens[1]
[1]Department of Biomechanics, University of Nebraska at Omaha, Omaha, Nebraska, USA
[2]Department of Physical Education, & Sport Science, Aristotle University, Thessaloniki, Greece
*Corresponding author's email: tdeligiannis@unomaha.edu

Introduction: As humans change over their lifetime from adolescence to adulthood, and then towards aging, so do their gait patterns [1]. Furthermore, traditional gait metrics like speed, cadence, coordination [2], and anthropometric measurements like muscle mass [3], as well as gait variability measures [4],[5] appear related to Timed Up and Go (TUG). TUG is a simple clinical measurement related to physical, socioeconomic, and psychological parameters, as well as overall health status [6]. In this study, we predicted that TUG would increase with age and degraded stride-to-stride variability. Specifically, we hypothesized that decreases in stride-to-stride variability would predict increases in TUG scores. This hypothesis was based on TUG being considered as a time-efficient way to assess functional mobility, which is shown to be reduced in older adults [6]. In addition, we explored the relationship between age and stride-to-stride variability, while investigating the role of individual differences.

Methods: Data were taken from 82 healthy adults (ages 19-85) from the NONAN GaitPrint database, each performing 18 (2 days, 9 sessions each day), 4-min indoor walking trials (200-m track). [7]. Participants wore 16 Noraxon Ultium Motion inertial measurement units (IMUS, 200 Hz). Anthropometrics and TUG results were obtained during a baseline session. Stride time intervals were obtained for both legs and used to calculate the Hurst exponent (H) to evaluate stride-to-stride variability in terms of the degree to which stride intervals are correlated over time [8]. Two linear mixed effect models were used to characterize how the H changes with age, and in a subset of older adults, the degree to which the H predicts TUG scores, after controlling for age. Both age and H were standardized to zero mean and unit variance to aid in interpretation of the model results.

Results & Discussion: The average TUG for the older adults was 10.62 ±1.69, consistent with the upper bound value (10.55) reported for ages 50-60[6]. 63% of our sample had TUG scores > 10, indicative of reduced physical capacity. The model relating TUG and H failed to reveal any reliable relationship. The model relating age and H (Figure 1) revealed a significant negative relationship between age and H (Estimate = -0.24, Std. Error = 0.09, df = 81.99, t = -2.78, p = 0.00669). This suggests that a 1 SD (17.35 years) change in age produces ~.24 SD (.13) reduction in H, indicating that the degree to which stride intervals are correlated decreases over time. The model included random intercepts for individuals (Variance = 0.57, Std.Dev. = 0.76) to account for repeated measurements. The random effects indicated substantial individual variability in the H independent of age. The model's R^2 values indicate that the fixed effect (age) explains approximately 5.6% of the variance in the H, while the total model, including random effects, explains 62.9% of the variance. This sizable difference between conditional and marginal R^2 values highlights the considerable impact of individual differences on the H.

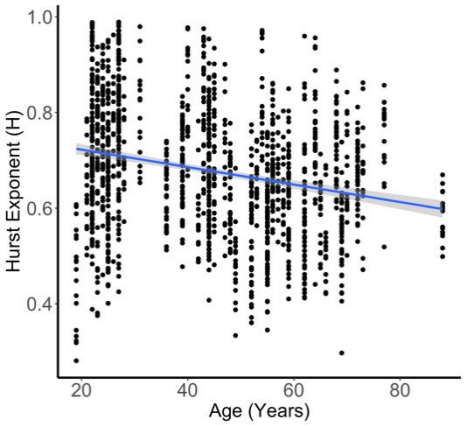

Figure 1. Scatter plot of the Hurst Exponent (H) as a function of Age.

The significant negative association between age and the H of stride intervals suggests that in the older individuals the degree to which stride intervals are correlated decreases over time. This could imply a decrease in gait predictability with aging, potentially decreasing stability and increasing the risk of mobility issues or falls. The relatively low marginal R^2 indicates that age alone does not account for a large portion of the variability in the H, underscoring the intricacy of the factors influencing gait dynamics. Conversely, the high conditional R^2 demonstrates the importance of individual differences in determining gait characteristics, suggesting that personalized assessments could be critical in understanding and addressing gait-related challenges in older adults. The latter result makes the lack of a relationship between TUG and H surprising, as one might have anticipated that TUG would reflect potential individual differences. It is possible that the discrete nature of the TUG score as a single quick evaluation, versus the continuous and more time involving measurement of stride-to-stride variability over a 4-min walk, is the reason for this result. Future work will need to address other possible sources of individual differences to further elucidate variability in H across the lifespan.

Significance: This study advances our understanding of how aging affects gait variability. By highlighting the role of individual differences in gait dynamics, it underscores the importance of personalized assessments in identifying and addressing age-related changes in gait. The findings have potential implications for developing targeted interventions aimed at enhancing mobility and reducing fall risk among older adults [9].

Acknowledgements: NSF 212491, NIH P20GM109090 & R01NS114282, University of Nebraska Collaboration Initiative, the Center for Research in Human Movement Variability at the University of Nebraska at Omaha, NASA EPSCoR, IARPA.

References: [1] Hamacher et al. (2015) *Med. Eng. and Ph.* 1152-1155(37), [2] Herssens et al. (2018) *Gait & Post.* 181-190(64), [3] Charlier et al. (2015) *Arch. of Ger. and Ger.* 161-167(61), [4] Bisi et al. (2016) *Gait & Post.* 37-421(47), [5] Vaz et al (2020) *Hum. Mov.Sc* 600-606(66), [6] Kear et al. (2017) *J. of Prim. Care* 8(1):9-13, [7] Wiles et al. (2023), *Sci. Data*, [8] Likens et al. (2023) arXiv:2301.11262v1, [9] Almurad et al (2018) *Front. In Phys.*1766(9)

Shape Analysis of Glenohumeral Bone Surface Deformity Due to Brachial Plexus Birth Injury

Reilly Stafford[1*], Morgan Dalman, M.S.[1], Katherine R. Saul, Ph.D.[1]
[1]Department of Mechanical and Aerospace Engineering, North Carolina State University, Raleigh, NC, USA
*Email: reillystafford05@gmail.com

Introduction: Brachial plexus birth injury (BPBI) is a nerve injury that occurs in up to 4 in 1000 live births [1]. Injury to the nerves can occur either proximal or distal to the dorsal root ganglion, which we refer to as pre- and post-ganglionic injury. BPBI is often associated with deformity and posterior dislocation of the glenohumeral joint [2], but prior work relies on simple measures of surface curvature and tilt. This research leverages a Generalized Procrustes Analysis (GPA), a statistical shape analysis used to analyze the distribution of two shapes [3], to better quantify the glenohumeral morphological differences following BPBI in a rat model.

Methods: Micro CT images (SCANCO Medical µCT 80, 70 kVp, 114 µA, voxel size = 36 µm) of intact glenohumeral joints from four groups of Sprague Dawley rat pups were obtained. The four groups included two surgical neurectomy procedures that represent BPBI. Neurectomies were performed to the C5-C6 nerve roots at two different injury locations relative to the dorsal root ganglion: postganglionic (POST) (distal, n=7) and preganglionic (PRE) (proximal, n=7). The third group, disarticulation (DIS) (n=5), underwent amputation of one forelimb at the elbow to induce altered and reduced limb usage consistent with the neurectomy groups but without nerve injury [4]. The last group, sham control (SHAM) (n=5), underwent similar incisions as the neurectomy groups, but the plexus was kept intact [4]. Each CT image was reconstructed and saved as a 3D point cloud in MIMICS (Materialize) then imported into MATLAB (R2022a) (The Mathworks, Natick, MA). Each of these cloud files contained a different number of data points, depending on factors such as bone length. Since the GPA compares shapes on a point-by-point basis, each bone file needs to have a uniform number of data points. A point redistribution method was constructed in MATLAB that redistributed a set number of data points (x=500,000) in a uniform orientation to each bone surface while maintaining the integrity of the original shape. This was also done on just the humeral head (x=240,000). The GPA performs scaling, rotation, and translation operations while returning a Procrsutes distance (PD) value (**Figure 1**). This returns an Euler 3D rotation matrix from the angles between the shapes, a translation value from the distance between centroids, and a scaling factor which is calculated from the root mean square distance between points and their centroid. A PD value is then obtained by taking the sum of squared differences of all landmark data points between the two shapes and standardizing that value by the reference scale. PD minimization was performed to superimpose landmarks between subjects and compute the deviations [5]. A larger PD indicates more morphological differences compared to the control, which allows injury severity to be analyzed. Scaling factors were also looked at between different groups.

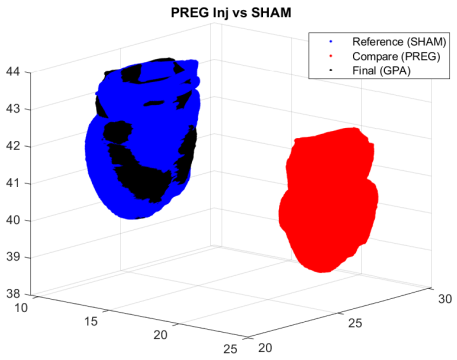

Figure 1: GPA example where the humeral head is scaled, translated, and rotated onto the reference bone.

Results & Discussion: GPA was performed initially on the humeral head from 19 different Sprague Dawley rats belonging to one of three different injury groups: PRE, POST, or DIS in reference to a SHAM humerus. The validity of the GPA was first confirmed by comparing one SHAM file to itself (with a PD of 0), and four other SHAMs (with low PDs). The mean PD value for the PRE group was 0.1473, 0.1317 for POST, and 0.1670 for DIS. A one way ANOVA was performed comparing mean PD of each injury group to the mean PD of the SHAM group with significance alpha set to 0.05 (**Figure 2**). No statistical difference was found between injury groups and injury groups to SHAM for the humerus. The majority of deformity at the glenohumeral joint is related to the scapula. The analyses will apply GPA to the scapulas of the same animals.

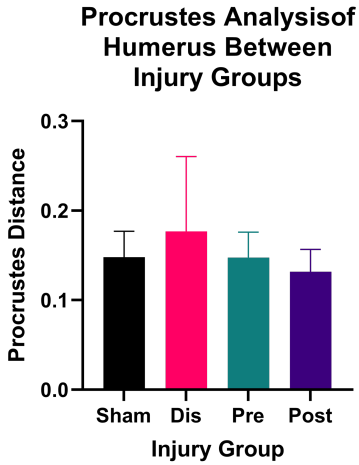

Figure 2: Procrustes distance for each injury group.

Significance: This research will help quantify morphological differences of the glenohumeral joint at a high level between different injury groups. Doing so will allow BPBI injuries to be determined based on the magnitude of humerus and scapula bone geometry changes. This could also be applied to other injuries/diseases such as rotator cuff tear injury or osteoarthritis.

Acknowledgements: NIH R01HD101406.

References: [1] Hale et al. (2010), *J Hand Surg Am*. **35**(2): 322-31. [2] Pearl et al. (1998), *J Bone Joint Surg Am.* **80**(5): 659-67. [3] Igual et al. (2014), *Patt Recog.* **47**(2): 659-71 [4] Fawcett (2021), Doctoral Dissertation https://www.lib.ncsu.edu/resolver/1840.20/39052. [5] Perez et al. (2006), *J Anat.* **208**(6): 769-84

CHANGES IN SPATIOTEMPORAL ASYMMETRY DUE TO WEAKNESS AND SPASTICITY IN PREDICTIVE WALKING SIMULATIONS

Nicholas L. Yaple[1*], Anne E. Martin[1]
[1]Mechanical Engineering, Penn State, University Park, PA, USA
*Corresponding author's email: nxy5047@psu.edu

Introduction: People post-stroke often have lasting walking impairments such as hemiparesis (weakness or reduced mobility in one half of the body) [1] and spasticity (abnormal muscle stiffness restricting movement) [2]. Consequently, they walk with slower preferred speeds, asymmetric gait, and increased metabolic cost [3]. However, it is not clear if hemiparesis and spasticity directly cause the observed asymmetries or if it is driven by other factors. Understanding how people with post-stroke hemiparesis self-select their gait is difficult to experimentally study, so simulations can be used although few predictive simulations have been employed. Since spasticity is complex, this work approximated spasticity via linear stiffness. Using a planar predictive walking model [4] at a constant speed, this abstract investigates how energetic cost and spatiotemporal asymmetry changes as joint-level unilateral weakness and stiffness vary.

Methods: Predictive walking simulations were generated with a 6-link planar biped with two legs, each consisting of a thigh, shank, and circular foot [4] (Fig. 1). Weakness was implemented by limiting the active joint torque in the paretic knee, ankle, and hip: $u_{j,lim} = (1-w)\max(|u_{j,act}|)$ where w is the percent weakness, $u_{j,lim}$ is the maximum allowable joint torque, and $u_{j,act}$ is the maximum active joint torque of healthy gait at the same speed. Stiffness was implemented by linearly increasing the passive torque on the paretic side during ankle dorsiflexion ($q_j > 90°$) and knee flexion ($q_j < -15°$): $u_{j,pass} = u^N_{j,pass} + k_j q_j$ where $u_{j,pass}$ is the passive torque, $u^N_{j,pass}$ is the normal passive torque [5], and k_j is the stiffness constant. Two-step optimal gaits, consisting of alternating single support and instantaneous double support phases, were found by minimizing the weighted sum of the squared active joint torques [4]. Using a model with a leg length of 0.9 m and a mass of 87 kg walking slowly at 0.8 m/s, twelve different gaits were generated using weaknesses of 0, 20, 40, and 60% and stiffnesses of 0, 0.5, and 1 N-m/°. Energetic cost was quantified using the objective function. Step length asymmetry (SLA) and step time asymmetry (STA) were quantified using $A = \frac{X_{NP}-X_P}{X_{NP}+X_P} \times 100\%$ where A is the asymmetry measure, X is the relevant metric, and P and NP indicate the paretic and nonparetic sides. When the nonparetic step was greater than the paretic step, asymmetry was positive.

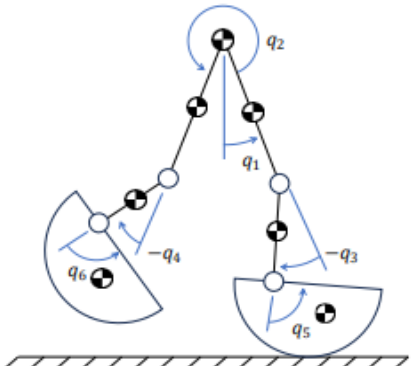

Figure 1: A diagram of the six-link planar biped. One hip joint (q_2) and both ankle and knee joints (q_3 through q_6) were actuated.

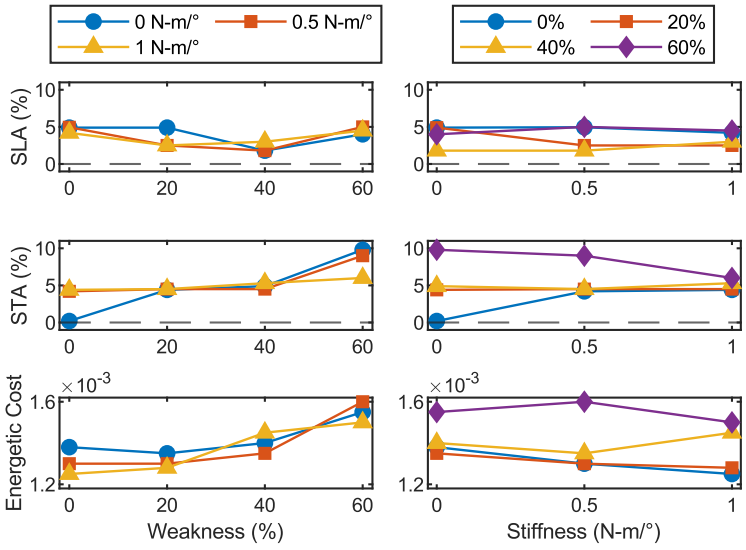

Figure 2: SLA (top), STA (middle), and the energetic cost (bottom) as weakness (left) and stiffness (right) vary. Changing stiffness had no effect, while weakness increased STA and the energetic cost.

Results & Discussion: When both weakness and stiffness were zero, the gait was slightly asymmetric (Fig. 2). This indicated that slight asymmetry in a gait can be energetically beneficial and supports previous observations of asymmetry in healthy gait [6]. Stiffness had no significant effect on energetic cost, SLA, or STA, indicating that it can be omitted in future work. With increasing weakness, only the energetic cost and STA showed a significant change. As expected, the energetic cost generally increased with increasing weakness. STA increased at 60% weakness but was relatively constant otherwise. This agrees with similar work showing that weakness can increase gait asymmetry [7], but weakness alone was not capable of reproducing experimentally observed asymmetry in hemiparetic gait [3]. However, it appears to be a contributing factor.

Significance: Additional factors beyond weakness appear to significantly contribute to gait asymmetry. This supports previous research showing that rehabilitation improving patient strength is not able to fully restore gait symmetry [8]. As implemented, stiffness had no significant effect on asymmetry or energetic cost, so this aspect of spasticity may be omitted or improved for future work.

Acknowledgments: This work was supported by NSF award 1943561.

References: [1] Bourbonnais & Noven (1989) *Am. J. Occup. Ther.* 43(5); [2] Pisano et al. (2000) *Clin. Neurophysiol.* 111(6); [3] Padmanabhan et al. (2020) *J. NeuroEngineering Rehabil.*17(105); [4] Martin & Schmiedeler (2014) *J. of Biomech.* 47(6); [5] Arnold et al. (2010) *Ann. Biomed. Eng.* 38(2); [6] Lathrop-Lambach et al. (2014) *Gait Posture* 20(4); [7] Nguyen et al. (2020) *J. NeuroEngineering Rehabil.*17(119); [8] Wist et al. (2016) *Physical Rehabil. Medicine* 114(124).

Comparison of plantar pressure distribution, spatiotemporal gait variables and postural sway following total knee arthroplasty in individuals with knee osteoarthritis: A pre-post design

Saidan Shetty[1*], Dr. Bincy M George[2], Dr. G Arun Maiya[3], Dr. Mohandas Rao KG[2], Dr. Sandeep Vijayan[4]
[1]Department of Anatomy, Melaka Manipal Medical College – Manipal Campus, Manipal Academy of Higher Education (MAHE), Manipal - 576104, Karnataka State, India

*Corresponding author's email: saidan.shetty2@learner.manipal.edu

Introduction: Knee osteoarthritis (OA) arises from abrasion of the articular surface and directly affects the functional ability of the individual [1]. Due to pain, movement dysfunction, and residual deformity, there are noticeable changes in gait patterns that affect daily activities [2]. Lower-limb involvement leads to sensorimotor changes that predispose individuals to postural instability, which increases the risk of falls [3]. Total knee arthroplasty (TKA) is frequently implemented as a treatment for knee OA when conservative treatment options fail to relieve disabling symptoms [4]. We hypothesize that there would be significant changes in the plantar pressure distribution, gait variables and postural control parameters following TKA. Therefore, the objective of the present study was to compare plantar pressure distribution, spatiotemporal gait variables, and postural sway using the Win-Track force platform in individuals with knee OA before and after TKA.

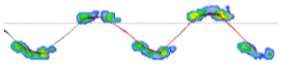

Fig. 1: Dynamic gait assessment

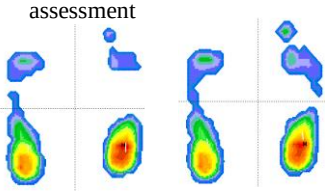

Fig. 2: Postural sway before TKA – EO & EC

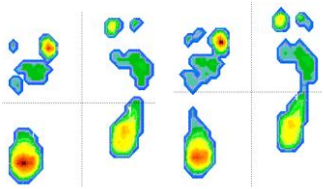

Fig. 3: Postural sway after TKA – EO & EC

Methods: This prospective observational study included individuals who were diagnosed with knee OA planned for TKA (n=20; 65.05±8.03 years; female:male-10:10; BMI: 27.26±4.31 kg/m2) via the medial-parapatellar retinacular approach. Plantar pressure, spatiotemporal gait variables, and postural sway were evaluated using the Win-Track Force Platform (Medicapteurs Technology France) at baseline and 6 months post-TKA. The spatiotemporal gait variables included step duration, stride duration, gait cycle duration, single stance duration, double stance duration, swing duration, step length, gait cycle length and angle of toe out (Fig. 1). Postural sway parameters included centre of pressure (COP) length, COP area, length/area, average Q speed, mediolateral speed, anteroposterior speed, mediolateral deviation, and anteroposterior deviation were noted in the eyes open (EO) and eyes closed (EC) conditions (Fig.2 and Fig.3). Statistical analysis was performed with the level of significance set at $p \leq 0.05$.

Results & Discussion: Individuals with knee OA put more weight on the less affected side especially the hindfoot area (>200 kPa/point) (Fig.2.red portion) and lack a normal heel toe gait pattern (Fig.1). The plantar pressure area, average pressure, stride, step, and gait cycle length, angle of toe out, step, stride and double stance duration, COP sway area and mediolateral control were significantly ($p<0.05$) altered in individuals with knee OA, possibly due to the compensation caused by pain and muscle imbalance. When pre-TKA data was compared with post-TKA data, plantar pressure area, average pressure (Table.1), stride length, gait cycle length, and gait speed significantly ($p<0.05$) improved post-TKA. Compared with the pre-TKA data, the plantar pressure loading improved by a balanced per-point distribution on both feet and through different regions of the operated foot with enhanced weight transfer over the forefoot (Fig.3). Double stance duration, stride duration and COP sway area decreased significantly ($p<0.05$) post-TKA. The angle of toe out and mediolateral deviation was lower post-TKA; however, the differences were not statistically significant (Table.2), possibly due to the altered neuromuscular control of the mediolateral muscles of the knee. The results suggest that altered biomechanics in patients with knee OA affect plantar pressure distribution, spatiotemporal gait variables and postural control. However, a significant change was noted in the plantar pressure area, average pressure, gait variables, and COP sway area post-TKA.

Table 1: Comparison of Plantar Pressure (PP)

PP distribution	Pre-TKA	Post-TKA	p-value
PP Area (cm2)	50.8±44.65	76.4±26.09	0.05
Average PP (kPa)	110.65±25.44	125.71±15.9	0.04
Maximal PP (kPa)	291.59±63.82	308.56±50.8	0.47

Table 2: Comparison of Postural sway

Variables (in mm)	Pre-TKA	Post-TKA	p-value
CoP sway area–EO	120.82±78.02	62.9±41.62	0.03
CoP sway area-EC	121.88±90.05	70.2±39.62	0.05
Mediolateral dev–EO	2.22±1.93	1.9±1.02	0.62
Mediolateral dev–EC	2.59±1.56	2.07±1.34	0.57

Significance: TKA significantly improved plantar pressure, spatiotemporal gait variables, and the COP sway area in individuals with knee OA. Redistribution of plantar pressure is essential after TKA because it reduces the load distribution on the knee, thereby facilitating postoperative recovery. Improved spatiotemporal gait variables denote better walking ability which can thereby enhance functional performance. A decreased COP sway area indicates better postural control post-TKA. This information is important for evaluating fall risk, monitoring patient prognosis, and targeting specific components during rehabilitation. Whether the changes are due to TKA or due to postoperative rehabilitation following TKA, could be a point for further research. This research is part of a larger ongoing study that aims to evaluate and find relationships between biomechanical, electromyographic and clinical data following TKA.

Acknowledgments: We acknowledge the participants for their time and voluntary participation in the study, and we thank Manipal Academy of Higher Education for providing the support and resources to conduct this research.

References: [1] Nelson (2017), *Osteoarthritis and Cartilage* 26(3); [2] Tan et al. (2021), *Journal of Orthopaedic & Sports Physical Therapy* 51(10), [3] Truszczyńska-Baszak et al. (2020), *The Knee* 27(5); [4] Martina et al. (2022), *Clinics in Geriatric Medicine* 38(2).

AUTONOMOUS ANKLE-BASED EXOSKELETON ASSISTANCE AT A RANGE OF WALKING SPEEDS

Joseph F. Seay[1*], Clifford L. Hancock[1], Isabella O'Keefe[1], John W. Ramsay[1], Brian S. Baum[2], Harvey Edwards[2], John Kuzmeski[2], Meghan P. O'Donovan[1]

[1] United States Army Combat Capabilities Development Command (DEVCOM) Soldier Center

[2] Massachusetts Institute of Technology (MIT LL) Lincoln Laboratories Sensorimotor Technology Realization in Immersive Virtual Environments (STRIVE) Center

*Corresponding author's email: joseph.f.seay.civ@army.mil

Introduction: Lower extremity gait assist exoskeletons (Exos) have successfully demonstrated reduction in the metabolic cost of walking when optimized at a single speed. Previous work on active autonomous exoskeletons have demonstrated an 8-11% reduction in metabolic cost at average walking speeds for healthy individuals [1]. While these results are promising, speed can vary during natural walking, so Exos should demonstrate similar benefits at a variety of walking speeds to effectively assist able-bodies individuals. Other studies have demonstrated that Exo emulators which individually optimize metabolic assistance at the ankle, knee and/or hip provide different levels of optimization over a range of walking speeds [2]. While these results are promising, ultimately, it is necessary for such augmentation to be provided by a fully autonomous system.

The purpose of our study was to evaluate changes in metabolic cost and gait biomechanics across three different speeds over four sessions with and without a powered, autonomous Exo. We used biomechanics measurements to gain insights into the mechanisms underlying any trends in metabolic rate.

Methods: Fourteen volunteers participated in our study (25±8 years old, 174±9 cm tall, 75±18 kg). Twelve were active-duty military (11 male, one female); the remaining two (one male, one female) were civilians. None had used exoskeleton technology prior to entering our study.

After 2 days of familiarization and baseline testing, all volunteers participated in four treadmill sessions on consecutive days, during which they walked with a powered ankle-based exoskeleton (EXOP) and without an exoskeleton (NOEX). Participants walked at 1.0, 1.3, and 1.5 m/s on a level treadmill for 5 minutes per bout for both conditions, and the footwear was matched in both conditions. The order of EXOP and NOEX condition presentation was randomized by participant and was preserved for all testing days.

Oxygen consumption normalized to body mass (VO_2, ml/kg/min) and parametric kinematic and temporal-spatial variables were analyzed using a 3-way repeated measures ANOVA (SESSION (4) x EXO condition (2) x SPEED (3)) to understand the effect of EXOP on speed and session, with significance levels set at $\alpha \leq 0.05$.

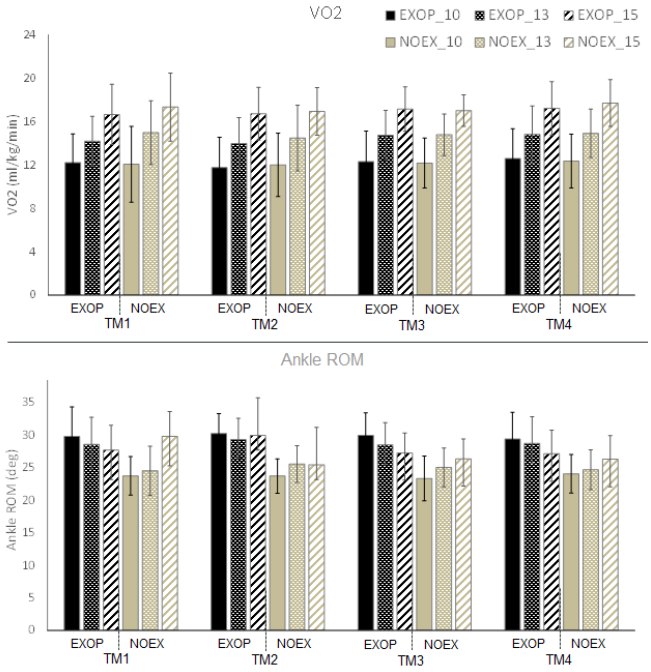

Figure 1. Average VO_2 (top) and Ankle ROM (bottom) values over all Exo conditions and speeds. EXOP and NOEX are defined in text; *_10, *_13, *_15 are data collected at treadmill speeds of 1.0, 1.3 and 1.5 m/s, respectively.

Results & Discussion: As expected, there was a main effect (ME) of speed for VO_2, during which VO_2 increased with speed ($p<0.001$). There were no additional MEs or interactions, suggesting no additional metabolic adaptation occurred during these bouts. (Figure 1, top panel). There was a ME for Exo condition (EXO.cond) for step width, in which individuals on average took wider steps in the EXOP v. NOEX conditions (Δ=1.2cm; $p=0.002$). For Hip Range of Motion (ROM), there was a ME for SPEED, ($p<0.001$), and post-hocs revealed that hip ROM increased with walking speed. For Ankle ROM, there was a SPEED x EXO.cond Interaction ($p=0.001$). Post-hocs revealed that Ankle ROM changed with speed, and that ROM *increased* with speed in EXOP, and *decreased* with speed in NOEX (Figure 1, bottom panel). Ankle ROM values in the NOEX condition were consistent with ankle responses to increases in walking speed. Average ankle ROM was significantly higher for the EXOP condition regardless of speed, suggesting that the augmentation, which occurred at toe-off, may have increased ankle ROM in the EXOP condition, and that the user may have allowed more increased ROM at the slow speed due to longer swing time.

Significance: Overall, significant differences were related to differences in speed and while wearing the Exo. VO_2 data suggest changes consistent with previous results related to increased walking speed, but no differences due to EXO condition were observed. There were no session-related differences, indicating that both metabolic and biomechanical variables did not adapt beyond the initial walking sessions. It is unknown if the Exo would have elicited greater metabolic benefit at faster walking speeds or if participants were fatigued. Also, further design changes, possibly combined with more active controllers that are tuned to the individual user may also be necessary to generate viable metabolic cost savings.

Acknowledgments: We thank study staff investigators across the DEVCOM Soldier Center and MIT-LL STRIVE Center for their efforts in data collection and processing. Many thanks also to our study participants for their participation in this research, especially to the Soldier human research volunteers from DEVCOM Soldier Center.

References: [1] Mooney et al (2016) *J NeuroEngineering Rehabil* 13(1); [2] Bryan et al (2021) *J NeuroEngineering Rehabil* 18(152).

KNEE EXTENSOR MUSCLE POWER RELATES TO TIMED UP AND GO PERFORMANCE IN OLDER ADULTS

Paige E. Rice[1*], Ryan Hill[1], Jason Fanning[1], Stephen Messier[1]
[1]JB Snow Biomechanics Laboratory, Department of Health and Exercise Science, Wake Forest University
*Corresponding author's email: ricep@wfu.edu

Introduction: As individuals age, the risk of falling steadily increases. Heightened fall risk is recognizably coupled with declines in muscle strength (maximum force output). While maximum force output is predictive of longevity, the temporal scale of catching oneself from falling may be more velocity-dependent, insinuating that preserving muscular force *and* velocity properties – power – are critical to prevent falls.[1] Simple clinical assessments such as the Timed Up and Go (TUG) test are used as a proxy to identify individuals that are at a higher risk of falling.[2] In efforts to elucidate what variables relate to and underpin estimated fall risk (TUG time), we implemented the TUG test on a force plate to capture sit-to-stand biomechanics and measured knee- and ankle-joint strength and power in older adults. Given that a distal-to-proximal shift in joint moments and powers during walking occurs with aging,[3] we posited that lower muscle power at the ankle-joint would be related to and predictive of fall risk. Additionally, we hypothesized that peak power during the sit-to-stand portion of the TUG test would also be related to and predictive of fall risk as evidence demonstrates that greater muscle power is essential for healthy aging.[4]

Methods: Participants were recruited from the parent randomized clinical trial, iGROOVE (NIA R01 AG076669) who were 65 years and older. After providing informed consent, body mass and height were obtained. Starting with the feet on a force plate (OR6-7-2000, Advanced Mechanical Technology, Inc., Watertown, MA), participants were familiarized with the TUG test prior to performing three trials each separated by one minute of rest. Forward dynamics were calculated from force plate data in a custom-designed LabVIEW program (Version 19.0, National Instruments, Austin, TX). TUG test outcome variables included time, sit-to-stand peak force, peak velocity, and peak power. The average of the three trials was used for further analysis. Next, participants randomly performed ankle- and knee-joint strength and power assessments on a HUMAC NORM isokinetic dynamometer (CSMi, Massachusetts, USA). Strength and power were assessed on the leg that participants chose to step forward with first during the TUG test. Participants warmed up and were familiarized with one maximal voluntary contraction (MVC) at 90˚ of knee extension (0˚ would be completely extended) prior to performing three trials separated by 90 seconds of rest to be used for further analysis. The highest peak torque obtained from the MVC was used to determine the 40% load for isotonic contractions. Participants were familiarized with one concentric-only 40% load isotonic knee extension contraction from 90˚ to 30˚ prior to performing three trials separated by 90 seconds to be used for further analysis. The ankle-joint strength and power assessments were identical with MVC's performed at 0˚ (neutral), and isotonic contractions performed from -10˚ of dorsiflexion to 10˚ of plantar flexion. Outcome variables included knee extension and ankle plantar flexion peak torque and rate of torque development from the MVC's and peak power and peak shortening velocity from isotonic contractions. All kinetic variables were divided by participants' body mass. In SPSS (Version 28.0, SPSS Inc., Chicago, IL, USA), we used a linear regression to understand what is the most predictive of TUG time. Additionally, we calculated partial correlations controlling for age and sex to determine the associations between TUG performance, sit-to-stand biomechanics during the TUG, and isolated ankle- and knee-joint strength and power.

Results & Discussion: Eleven older adults (n = 10 females, 1 male; age = 70.7 ± 3.4 yrs.; body mass = 73.5 ± 14.9 kg; height = 1.61 ± 0.08 m) were included in the analysis. From the linear regression, sit-to-stand peak velocity during the TUG test was significantly predictive of TUG time (β = -0.61, R^2 = 0.37, p = 0.048). Our results indicate that peak velocity during a simple sit-to-stand task explains the most variance of TUG performance. Such information might allow for clinicians to assess fall risk with little space by implementing a sit-to-stand task.[4] From partial correlations when controlling for age and sex, relative knee peak power and TUG time were significantly related to one another (r = -0.70, p = 0.03). Contrary to our hypotheses, all other statistical analyses were insignificant. These findings suggest that increasing muscle power about the knee-joint, and not the ankle-joint, should concomitantly reduce time to completion during the TUG test. As an index of fall risk, practitioners and researchers may consider implementing interventions that improve knee extensor muscle power to encourage healthy aging among older adults. We acknowledge that the small sample size is a limitation of our study, and further research is needed in this area.

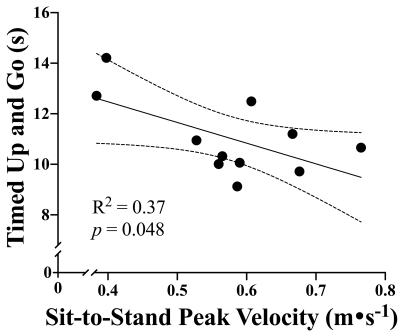

Figure 1. Relationship between Timed Up and Go (TUG) time and the sit-to-stand portion of the TUG test peak velocity among older adults.

Significance: Our results demonstrate in a small cohort of older adults that peak velocity during the sit-to-stand portion of the TUG test predicts TUG performance, and relative knee extensor peak power is related to TUG performance. These findings will help to direct future research endeavours and clinical practices to reduce fall risk and encourage healthy aging in older adults.

Acknowledgments: This study was funded by the Wake Forest University Provost's Pilot Research Grant (DM1087). We would like to thank Lauren Carter, Kaleigh Galinis, and Ava Johnson for their assistance with data collection and analysis and all the research participants for their time.

References: [1] Simpkins et al. (2022), *J Biomech* 134; [2] Barry et al. (2014), *BMC Geriatr* 14(1); [3] Boyer et al. (2017), *Exp Geron* 95; [4] Losa-Reyna et al. (2022) *J Geron* 77(4).

EXPLORING THE LINK BETWEEN KNEE EXTENSOR STRENGTH AND KINEMATICS IN ACL INJURY RISK: A STUDY OF COLLEGE ATHLETES

Colin W. Bond[1*], Benjamin C. Noonan[1]
[1]Sanford Health, Fargo, ND, USA
*Corresponding author's email: Colin.Bond@SanfordHealth.org

Introduction: Non-contact mechanisms are responsible for a significant portion of ACL injuries, with intrinsic factors such as inadequate lower extremity strength and risky kinematics during movements requiring high eccentric control likely contributing to injury risk. Strength, as evaluated by a dynamometer, is often considered a risk factor, as strength deficits are thought to contribute to risky kinematics during jumping and landing [1, 2]. Specifically, knee extension strength is critical to lower-extremity function, and resolving knee extension strength deficits after ACL reconstruction is often a critical objective. Although the relationship between strength and kinematics is considered important, the robustness of this association remains a point of contention, especially for knee extensors, and merits closer examination. Risky kinematics are characterized by increased knee and hip extension, elevated knee abduction, enhanced hip internal rotation, and increased hip adduction, often assessed during the eccentric phase of a double-legged drop vertical jump. Therefore, this study aims to investigate the relationship between knee extensor strength and knee and hip kinematics during a double-legged drop vertical jump. It was hypothesized that individuals with lower knee extensor strength would display higher-risk kinematics.

Methods: Twenty-two male and thirty-six female healthy college athletes (20.4 ± 1.5 y, 1.80 ± 0.11 m, 79.4 ± 16.6 kg) participated in this study. Athletes underwent concentric isokinetic knee extension testing at $60°\cdot s^{-1}$ on the right leg, and the instantaneous peak torque (Nm) normalized to the athlete's body mass ($Nm\cdot kg^{-1}$) was recorded as an indicator of knee extensor strength. Following this, athletes performed trials of a double-legged drop vertical jump from a 12-inch box, instructed to land on both feet simultaneously and quickly jump upwards, reaching as high as possible towards an overhead target. Three-dimensional markerless motion capture and side-by-side force plates were utilized to gather kinematic and ground reaction force data. This data was used to calculate one-dimensional right knee and hip angles from initial contact (0%) to the end of eccentric loading (100%). Statistical parametric mapping was used to conduct a series of general linear models to analyze the effect of knee extensor strength on knee and hip angles, controlling for sex effects. Significance was set at $p < 0.05$.

Results: There was no evidence of an effect of strength on sagittal plane knee angles ($p > .05$), frontal plane knee angles ($p > .05$), sagittal plane hip angles ($p > .05$), frontal plane hip angles ($p > .05$), nor transverse plane hip angles ($p > .05$) during the eccentric phase of a double-legged drop vertical-jump after controlling for the effect of sex.

Discussion: The hypothesis that knee extensor strength was associated with knee and hip kinematics during the eccentric phase of the double-legged drop vertical jump was not supported. Knee extensor strength may relate more to joint kinetics, as stronger muscles can better modulate joint kinetics during jumping and landing, without necessarily affecting kinematics [1]. Although knee extensor strength could be an indicator for overall strength, the strength of other muscle groups, like hip abductors and external rotators, might show associations with kinematics, particularly in the joints they control [2]. However, knee extensor strength and kinematics likely represent separate risk factors for ACL injury, without a direct connection. This indicates that an effective injury prevention strategy should focus on both enhancing strength and promoting safer kinematics. The study did not account for leg dominance. Considering most individuals are right-leg dominant, laterality could impact knee extensor strength and kinematics. Furthermore, younger athletes or those at lower competition levels might exhibit different relationships between knee extensor strength and kinematics. Despite a wide range of observed knee extension strengths and kinematics among these college athletes, their high level of sports participation might mean their knee extensor strength is above the threshold where riskier kinematics typically emerge. The double-legged drop vertical jump might not adequately challenge knee extensor strength. Movements like single-legged landings or tests including unanticipated, reactionary, or dual-cognition could reveal a relationship between knee extensor strength and kinematics.

Significance: This study enhances the understanding of the relation between knee extensor strength and kinematics during a double-legged drop vertical jump, revealing the intricate dynamics influencing ACL injury risk. The findings suggest that focusing solely on knee extensor strength to reduce injury risk may have limitations, as inadequate knee extensor strength may not be as closely linked to risky kinematics as often assumed. This insight holds significant value for individuals susceptible to primary ACL injuries and those recovering from such injuries. It highlights the vital role of combining strength training with specific interventions aimed at improving kinematics during jumping and landing movements. Thus, the study supports the development of ACL injury prevention, rehabilitation, and return-to-sport programs that embrace a comprehensive approach.

References: [1] Stearns et al. (2013), *Med Sci Sports Exerc* 45(5); [2] Rinaldi et al. (2022), *J Exp Orthop* 9(1)

Frontal Plane Knee Kinematics and Kinetics During Drop Landing

Katherine Perille[1*], Jake A. Melaro[1], and Joshua T. Weinhandl[1]
[1]Department of Kinesiology, Recreation, and Sports Studies, The University of Tennessee, Knoxville, TN
*kperille@vols.utk.edu

Introduction: ACL injuries typically occur because of non-contact mechanisms such as landing or quick deceleration [1]. It has been found that nearly 61% of ACL injuries are a result of those non-contact mechanisms [2]. The separation width of the feet has the potential to put greater forces on the knee and drive the knee into deep valgus, often considered a risk factor for ACL injuries [3,4,5]. Greater mediolateral displacement of the knees has shown increasing knee valgus angles [6]. Further, separating the feet or bringing the landing stance closer together can have an impact on knee abduction angles and internal knee adduction moments.

The purpose of this study is to examine the effects of stance width during bilateral drop landings in frontal plane knee kinematics and kinetics, specifically, initial contact knee abduction angle, peak knee abduction angle, peak knee adduction moment, and frontal plane knee angular impulse. Based on previous literature, it was hypothesized that increasing stance width would increase knee abduction angles at peak knee flexion. Additionally, the knee adduction moment and knee adduction angular impulse increase. These hypotheses are made because the GRF vector acts more laterally to the knee, forcing the knees into valgus loading.

Methods: The study involved 27 recreationally active participants: 13 females (63.05±8.81 kg, height 1.65±0.08 m) and 14 males (80.02±8.19 kg, height 1.78±0.07 m). Using 3D marker coordinates (200 Hz, Vicon) and ground reaction force data (GRF; 2000 Hz, AMTI), participants performed double leg drop landings from a trapeze bar. Drop landing height was set at 90% of each participant's average maximum height from three countermovement jumps. Stance width was adjusted to 50% (NARROW), 100% (PREF), and 150% (WIDE) of the average stance width from the countermovement jumps. Each participant completed a total of 15 drop landings, with five double leg drop landings in each stance width condition.

Frontal plane knee kinematics and kinetics of the right leg were calculated using the 3D marker positions and GRFs. Visual 3D was used to find the initial contact right knee abduction angle, peak knee abduction angle, peak knee adduction moment, and knee adduction moment impulse. Separate 2×3 ANOVAs (sex × stance width) were run on the drop landing stance width conditions (NARROW, PREF, and WIDE) for knee kinematics and kinetics between genders. Post hoc pairwise comparisons were conducted in the event of significant interactions or main effects. Significance for all tests was set as $p < 0.05$.

Results and Discussion: There were no significant sex × stance width interactions and no significant sex effects on any of the variables. However, the main effect of stance width was significant for peak knee abduction angle ($p=0.001$), peak knee adduction moment ($p<0.001$), and knee adduction angular impulse ($p<0.001$). Peak knee abduction angle was significantly greater during the wide ($p=0.002$) and preferred ($p=0.031$) stance width landings compared to narrow stance width landings. Increased stance width increases the lateral component of the GRF and pushes the knees into dynamic valgus, increasing stress on the ACL and compromising its ability to stabilize the knee.

Table 1. Mean ± STDV values for frontal plane initial contact (IC) and peak knee joint kinematics, as well as peak joint moments and angular impulse during the three-foot width conditions.

		Narrow	Preferred	Wide
IC Knee Adduction Angle (deg)	**men**	1.0 ± 3.1	0.6 ± 2.9	0.4 ± 3.4
	women	-0.8 ± 2.6	-0.8 ± 3.2	-1.2 ± 3.4
Peak Knee Abduction Angle (deg) [*a,b]	**men**	-0.9 ± 4.8	-2.1 ± 5.6	-2.4 ± 5.1
	women	-3.0 ± 3.4	-3.4 ± 4.3	-3.9 ± 4.1
Peak Knee Adduction Moment (Nm/kg) [*a,b,c]	**men**	0.09 ± 0.10	0.17 ± 0.15	0.31 ± 0.2
	women	0.12 ± 0.11	0.20 ± 0.17	0.30 ± 0.14
Knee Adduction Angular Impulse (Nms/kg) [*a,b,c]	**men**	-0.03 ± 0.04	-0.01 ± 0.03	0.04 ± 0.07
	women	-0.01 ± 0.03	0.01 ± 0.02	0.02 ± 0.02

* Significant foot width main effect ([a] Narrow significantly different from Preferred, [b] Narrow significantly different from Wide, [c] Preferred significantly different from Wide).

Peak knee adduction moment systematically increased from narrow to preferred to wide stance widths ($p<0.001$). Similarly, knee adduction angular impulse increased as stance width increased: narrow to preferred ($p<0.001$), narrow to wide ($p<0.001$), and wide to preferred ($p=0.004$). An increased adduction moment is indicative of valgus stress on the knees and can overload the ACL. Increased adduction angular impulse refers to the torque applied to the knee joint over the duration of a movement and can place greater stress on the ACL. Both of these kinetic factors can lead to an increase in ACL injury susceptibility, leaving it prone to injury.

It is important to note that foot progression angle was not controlled in this study. It is plausible that a more outward angle of the feet during landing would promote reduced knee abduction and therefore reduced frontal plane knee loading, even with increased stance widths.

Significance: The results of this study can be used in training and injury prevention programs across different clinical environments. Further studies should investigate the interaction between stance width and foot alignment during drop landings.

References: [1] Boden (2010), *J Am Acad Orthop. Surg.*, 18(9): 520-527; [2] Kaneko et al., (2017), *Asian J Sports Med.* 8(1): 1-6; [3] Fauno (2006). *Int J Sports Med*. 27: 75-79; [4] Hewett et al., (2005). *Am J Sports Med*. 33(4): 492-501; [5] Pauda et al., (2011) *J Sport Rehab*. 20: 145-156; [6] Lorenzetti et al., (2018). *BMC Sports Sci. Med Rehabil.* 10(1): 1-11

HOW DOES LUMBAR MUSCLE ASYMMETRY AFTER UNILATERAL LOWER LIMB LOSS INFLUENCE TRUNK POSTURAL CONTROL?

Pawel R. Golyski[1,2], Sujay Kestur[2,3], Brad D. Hendershot[1,2,4], Courtney M. Butowicz[1,2,4]*
[1]1Extremity Trauma and Amputation Center of Excellence, Defense Health Agency, Falls Church, VA [2]Walter Reed National Military Medical Center, Bethesda, MD; [3]Henry M. Jackson Foundation for the Advancement of Military Medicine, Inc., Bethesda, MD; [4]Uniformed Services University of the Health Sciences, Bethesda, MD
*Corresponding author's email: courtney.m.butowicz.civ@health.mil

Introduction: Low back pain (LBP) is remarkably common after lower limb loss and is the condition most often associated with perceived impairment and decreased quality of life [1]. Regardless of limb loss, LBP is associated with changes in lumbar muscle morphology such as increased intramuscular fat infiltration, though the functional significance (i.e., impact on postural control) of fat infiltration is unclear [2]. Recent work suggests that among persons with unilateral lower limb loss, intramuscular fat infiltration is greater within lumbar musculature on the intact versus prosthetic side [3]. While some asymmetry may be expected after unilateral limb loss, it is unclear how asymmetry in lumbar muscle morphology influences trunk postural control. Thus, the purpose of this study was to use a modeling and simulation approach to investigate how lumbar muscle asymmetry alters trunk postural control during an unstable sitting task. Based on previous experimental findings [4], we hypothesized that decreasing the strength of intact-side lumbar musculature (corresponding to greater fat infiltration) would increase impairments in trunk postural control during unstable sitting, evidenced by an increasing range in center of pressure (COP) trajectory with bias (mean COP) toward the prosthetic side.

Methods: We developed an *in-silico* model of an unstable sitting task commonly used to experimentally assess trunk postural control [4,5]. The model, consisting of a two-segment (trunk and pelvis/chair) inverted pendulum model in the frontal plane, was generated in Simulink (R2023b). The frontal plane was of interest given persons with unilateral lower limb loss demonstrate impaired frontal plane control [4]. The pelvis/chair segment was linked to the ground with a torsional stiffness equal to 60% of the product of bodyweight and trunk center of mass height. Bilateral lumbar muscles acting about the lumbar joint were implemented as idealized actuators with first-order activation dynamics representative of slow-twitch muscles [6]. Maximum isometric muscle forces, lumbar moment arms, and passive stiffness contributions about the lumbar joint were estimated from literature [7-9]. Stabilizing lumbar torque commands to muscles were implemented using LQR control. Motor noise was implemented as Gaussian noise superimposed on the stabilizing torque command, which produced a COP trajectory with the same range (3.23 cm) and mean frequency (0.22 Hz) as experimental data [4]. To introduce strength asymmetry representative of increased intramuscular fat infiltration, maximum isometric forces were incrementally decreased on the "intact" (vs. "prosthetic") side of the model. Trunk postural control was quantified as the range (max - min) and mean of the mediolateral COP trajectory during the middle 50 seconds of 60-second trials.

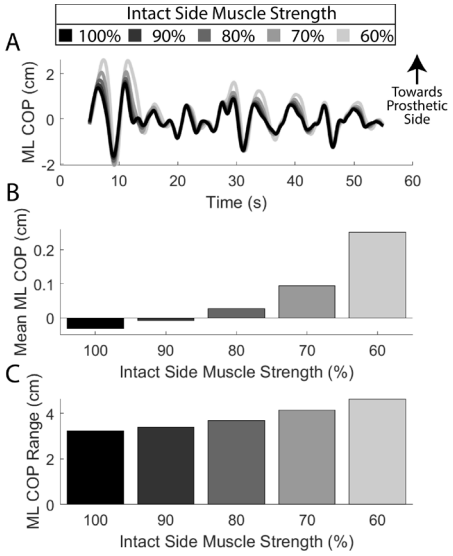

Figure 1: Mediolateral (ML) center of pressure (COP) A) timeseries traces, B) means and c) ranges across intact-side strength levels

Results & Discussion: In support of our hypothesis, as maximum isometric strength of trunk musculature on the intact side decreased, there was a bias in COP toward the prosthetic side and an increased COP range (Fig. 1). This behavior resulted from the model's controller not compensating for the decreases in strength on the intact side. While LQR control is likely a gross simplification of the human brain and somatosensory system's postural controller, our results did capture salient features of experimental findings [4], which leads us to hypothesize that structural differences in lumbar musculature following lower limb loss are not fully compensated by the nervous system.

Significance: This work presents a simple, interpretable model to generate and test hypotheses of how structural and functional alterations following lower limb loss influence trunk postural control. Subsequent iterations of this model will be improved by incorporating patient-specific characteristics of lumbar muscle morphology, along with measured strength and endurance from persons with lower limb loss and LBP. Additionally, future work should specifically evaluate whether differences among persons with lower limb loss with and without LBP can be captured using this model, and if not, what aspects of LBP aside from muscle asymmetry may explain alterations in trunk postural control.

Acknowledgments: The views expressed herein are those of the authors and do not necessarily reflect the official policy of the Uniformed Services University of the Health Sciences, Department of Defense, nor the US Government.

References: [1] Highsmith et al. (2019) *Spine J* [2] Kjaer et al. (2007) *J Physiol* [3] Sions et al. (2021) *Arch. Phys. M.* [4] Butowicz et al. (2019) *Gait & Posture* [5] Hendershot et al. (2013) *Gait & Posture* [6] Dick et al. (2017) *JEB* [7] Parnianpour et al. (1988) *Spine* [8] Anderson et al. (2012) *J Biomech* [9] McGill et al. (1994) *Spine*.

Accuracy of low dose CT scanning for shoulder morphology and motion analysis

Stacey Chen[1], Erin C.S. Lee[2], Michael J. Rainbow[2], Rebekah L. Lawrence[1]
[1]Washington University School of Medicine, St. Louis, Missouri, USA
[2]Queen's University, Kingston, Ontario, Canada
email: r.lawrence@wustl.edu

Introduction: Computed tomography (CT) imaging is frequently used in many biomechanical research applications including 3D shape analysis [1] and kinematic tracking using biplane videoradiography [2, 3]. Careful planning is warranted when employing this technology in human subjects given the associated radiation exposure. When bony anatomy is the primary structure of interest, there is an opportunity to substantially reduce CT dose compared to clinical scanning protocols due to the contrast between bone and surrounding tissues. However, unclear the extent to which low-dose CT protocols impact the accuracy of geometric and kinematic data. Thus, the purpose of this study was to describe the dose-accuracy trade-off between incrementally lower-dose CT scans and the geometric and kinematic tracking accuracy of the humerus, clavicle, and scapula. We hypothesize that accuracy will decrease as CT dose decreases, but the low dose CT protocols will achieve acceptable accuracies (≤1°, ≤1 mm).

Methods: Three fresh-frozen cadavers consisting of the torso and bilateral shoulders (n=6 shoulders) were acquired. Tantalum beads (1.6mm diameter) were implanted into the humerus, scapula, and clavicle using sharp dissection in preparation for radiostereometric analysis (RSA). Specimens were scanned on a Siemens CT scanner using five helical CT protocols that varied in tube current (mAs) and voltage (kVp) to influence dose: 1) 120 kVp, 450 mAs, 2) 120 kVp, 120 mAs, 3) 120 kVp, 100 mAs, 4) 100 kVp, 100 mAs, 5) 80 kVp, 80 mAs. Protocol 1 corresponds to a standard clinical CT shoulder scan and protocols 2-5 represent the experimental low dose protocols, which correspond to a 70.6%, 78.0%, 87.0%, and 92.8% dose reduction, respectively. All scans had a pitch of 1.0, voxel size of 0.664 mm × 0.664 mm × 0.6 mm, and a field of view of 34 cm.

For kinematic testing, cadavers were secured to a chair, and a rope and pulley system was used to actuate scapular plane abduction and internal/external rotation at 90° abduction. Biplane videoradiographic images were acquired using a baseline protocol of 60 kVp, 80 mA, 1.5 ms pulse duration, and 60 Hz. From the CT scans, the humerus, scapula, and clavicle were segmented and reconstructed into 3D surface models. To describe geometric accuracy, we compared the distance between each point on the low-dose mesh and the nearest surface of the full-dose mesh. To describe kinematic tracking accuracy, we compared model-based tracking to RSA by calculating 1) the finite helical displacement between solutions, and 2) differences in glenohumeral (GH) and acromioclavicular (AC) joint orientation and position. Errors for geometric and kinematic tracking accuracy were pooled across all shoulder motions and described using mean absolute error (MAE).

Results & Discussion: Geometric data has been processed on 100% of specimens; kinematic tracking is complete for 83.3% (n=5) and remains ongoing. For the geometric analysis, lower dose scans resulted in higher geometric errors but were generally <0.5 mm across all bones (Figure 1). Errors for segmental tracking appeared less sensitive to CT dose than 3D geometric reconstructions, which is evidenced by an apparent lack of dose-accuracy trade-off (Figure 2). In general, the average MAE of total bone displacement was <1 degree across all bones and CT scanning protocols. For relative kinematics, the average MAE ranged from 0.33°-67° and 0.39-0.72 mm for the GH joint (Figure 2b), and 0.33°-0.68° and 0.51-1.07 mm for the AC joint (Figure 2c).

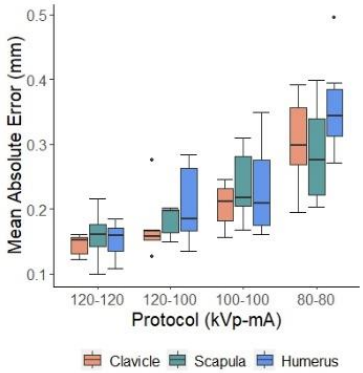

Figure 1: Boxplots displaying the geometric mean absolute error of the low dose protocols compared to the full dose protocol for each bone.

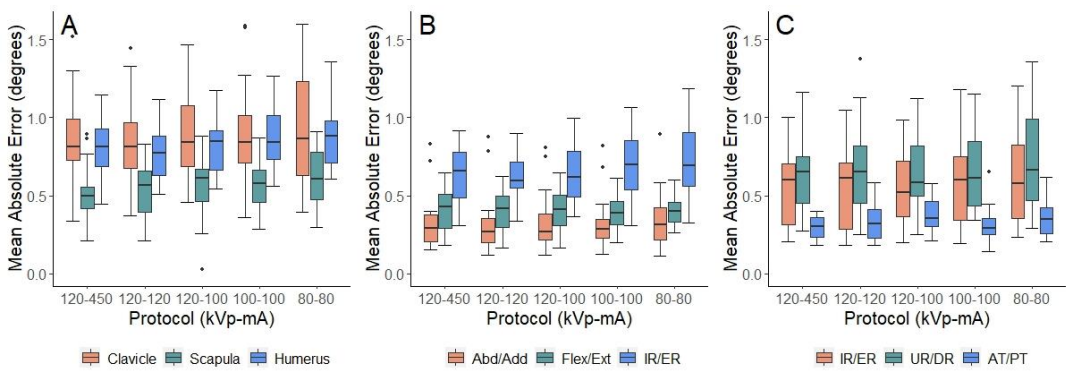

Figure 2: Boxplots displaying the (A) total bone displacement, (B) GH orientation, and (C) AC orientation mean absolute error of the low dose protocols compared to the full dose protocol. Abbreviations: Abd, abduction; Add, adduction; Flex, flexion; Ext, extension; IR, internal rotation; ER, external rotation; UR, upward rotation; DR, downward rotation; AT, anterior tilt; PT, posterior tilt.

Significance Lowering the CT dose decreased geometric and kinematic accuracy; however, errors remained generally within ≤1°, ≤1 mm. These data suggest low dose CT scans may be appropriate for biomechanical applications such as kinematic tracking and modelling.

Acknowledgments: This project was funded by the NIH (R00AR075876).

References: [1] Lee et al., *Clin Biomech*, 2020. [2] Lawrence et al., *Orthop Res*, 2023. [3] Lawrence et al., *J Orthop Res*, 2024.

DISTAL RESIDUAL LIMB SKIN SHEAR STRAIN AND SHEAR RATE ARE ASSOCIATED WITH PATIENT REPORTED COMFORT OF PROSTHETIC SOCKETS

Tom Gale[1*], Paige Paulus[1A], Drew Buffat[2], Goeran Fiedler[1B], and William Anderst[1A]
[1]University of Pittsburgh, [A] Department of Orthopaedic Surgery, [B] School of Health and Rehabilitation Science
[2]Union Orthotics & Prosthetics
*Corresponding author's email: tom.gale@pitt.edu

Introduction: There are approximately 29,000 cases of above knee amputations recorded in the United States every year [1]. Artificial limbs are generally connected to the residual limb with a socket prosthesis that facilitates weight bearing, suspension, and force coupling. Surface contact pressure and friction between the socket and the residual limb induce skin problems such as ulcers, calluses, or blisters [2]. Although a previous study that measured skin movement within the socket prosthesis demonstrated that increased skin strain was associated with decreased prosthetic use [3], it is not known how well individuals with transfemoral amputation can perceive changes in skin shear strain during gait. This is important because socket fitting is an iterative process wherein the prosthetist relies on patient feedback to inform socket design. This ongoing study aims to determine if skin shear strain within the socket correlates to the prosthetic user's perception of socket comfort and function. It was hypothesized that increased skin shear strain and shear rate during gait would be associated with a decrease in patient-reported socket comfort and function.

Methods: Following institutional review board approval and informed consent, 7 people with transfemoral amputations were enrolled in the study [4]. A key inclusion criterion was the ability to ambulate without the use of assistive devices. Participants were casted and fitted for 4 custom check sockets by a licensed prosthetist. One check socket was modified to create two additional sockets, yielding a total of 6 socket fits (standard of care, 6% decreased volume, lowered brim, ischial containment, quad, and pliable material). Approximately 40-60 stainless steel beads (1.6-2.0mm diameter) were glued to the participants' residual limb, then usual donning of the liner and socket was performed. The beads were imaged using a biplane radiography system (100 images/sec, 80kV, 125mA maximum, 1ms pulse width, 2s trial duration) while participants walked at a self-selected gait speed (0.77±0.20 m/s) on a treadmill. Images were collected for three steps per socket, including the 6 check sockets and the participant's definitive socket. The participants were blinded to the socket modification and asked at the end of each socket testing to rate the comfort and function of the socket using the 15-point Global Rate of Change (GROC) scale, where -7 is considered greatly worse and +7 is considered greatly better and 0 is no change compared to their definitive socket. Additionally, the residuum and beads were imaged as the participant stood within the system without wearing the socket or liner. For each socket tested, one trial of bead locations was semi-autonomously tracked in each pair of synchronized radiographs with an accuracy of 0.02mm using radiostereometric analysis (RSA) [4]. The bead locations in the no-liner condition were used to create a skin mesh model, and the change in position of the beads during walking was used to drive the deformation of the skin mesh. The skin mesh model deformation was fed into FEBio [5] to calculate the skin shear strain, and the strain rate was calculated from the strain waveform. The maximum shear strains and shear strain rates were calculated in 24 regions for each socket (Figure 1). Association between the GROC comfort and function scores and the maximum regional skin shear and rates were tested using linear regression with a forward stepwise method with a criterion of F>0.05 for variable inclusion.

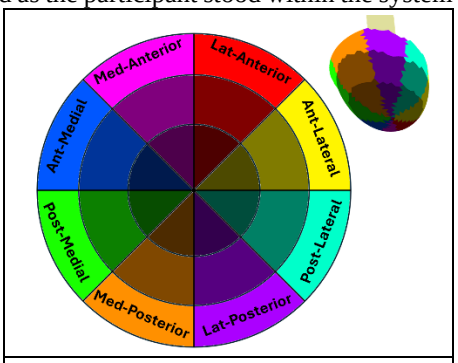

Figure 1: Subregion representation of the distal residuum, with a corresponding 3D model shown at the top right corner. The limb is divided into 8 sections along the circumference, which is then further divided into 3 subsections approximately 30 mm in height. The darker colors represent sections closer to the distal end.

Results & Discussion: Data from 27 sockets across 5 subjects were included in this interim analysis. An increase in shear strain and rate in the lateral half of the anterior region in the center of the residuum (Figure 1, dark red region) was associated with an increase in comfort scores (β=0.449, p=0.019 and β=0.486, p=0.010, respectively). No associations with patient-reported function were observed. This interim analysis suggests that patient-reported comfort of the socket may be related to skin shear and rate in the distal end of the residuum during gait, but the direction of association found was contrary to our hypothesis. A possible explanation is that this area is tolerant of higher deformation characteristics, and higher deformation in this area is related to better kinematics. This may lead to higher perceived comfort. The sockets were not worn for an extended period, which may also affect the perception of comfort. The lateral-anterior area where the association was found typically corresponds to the area where the distal end of the residual femur migrates to with load during gait, which warrants further analysis with consideration to distal residual femur motion.

Significance: Design decisions may be made for sockets to allow for more skin movement in the antero-lateral region of the distal end of the residuum to increase comfort of a socket, but other quantitative measures are needed to improve the function of the socket.

Acknowledgments: This work was supported by the Department of Defense Office of the Congressionally Directed Medical Research Programs (CDMRP) through the Restoring Warfighters with Neuromusculoskeletal Injuries Research Award (RESTORE).

References: [1] U.S. Department of Health & Human Services (2021); [2] Dudek et al. (2005), *Arch of Phys Med and Rehab*; [3] Gale et al. (2021), *J Biomech*; [4] Andert et al. (2022), *Trials*; [5] Anderst et al. (2003), *J Biomech Eng*; [6] Mass et al. (2012), *J Biomech Eng*.

ALTERING PASSIVE-DYNAMIC ANKLE FOOT ORTHOSIS STIFFNESS AFFECTS COST OF TRANSPORT IN INDIVIUDALS POST-STROKE

Shay R. Pinhey[*1,2], Darcy S. Reisman[1,3], Elisa S. Arch[1,2]
[1]Biomechanics and Movement Science Interdisciplinary Program, [2]Department of Kinesiology and Applied Physiology, [3]Department of Physical Therapy, University of Delaware, Newark, DE
*Corresponding author's email: spinhey@udel.edu

Introduction: Stroke is one of the primary causes of long-term disability in the United States and results in mobility reductions in more than half of stroke survivors [1]. One cause for this reduced mobility is muscle paresis on one side of the body. The plantar flexor muscles are commonly affected by this hemiparesis making walking difficult. Individuals post-stroke are often prescribed an ankle-foot orthosis (AFO) to address such plantar flexor impairments. A specific class of AFO, called a passive-dynamic AFO (PD-AFO), can mimic some plantar flexor function to help control rotation of the tibia over the ankle joint in midstance and store and return energy to assist with push-off in terminal stance [2], [3]. We previously found that PD-AFOs improve walking mechanics for some individuals post-stroke [3], [4]. This previous work customized PD-AFO stiffness to each individual's level of plantar flexor weakness and found improvements in walking mechanics for some, but results were variable across subjects [3]. However, we do not know if this is the best stiffness prescription model as we do not know how altering PD-AFO stiffness affects post-stroke walking function. Mechanical cost of transport (COT) can be used as an indicator of walking function as it describes how much work the lower limbs expend to progress the body forward. A reduction in COT would indicate improved walking function as it indicates that less mechanical energy is required to walk the same distance. The purpose of this study was to explore the affect of altering PD-AFO stiffness on COT in individuals with chronic stroke. Due to the mixed improvements to walking function previously seen with the use of a PD-AFO, we hypothesized varying PD-AFO stiffness would cause changes in COT.

Methods: 8 participants (Age: 62.4 ± 6.1 yrs, Time since stroke: 8.1 ± 8.3 yrs, Height: 1.74 ± 0.08 m, Mass: 84.3 ± 19.8 kg) with chronic stroke were enrolled in this study. First, participants performed a 10-meter walk test at both their self-selected and fast walking speeds wearing just shoes. This study used a modular PD-AFO consisting of a footplate and a cuff attached together with a posterior strut. Each participant was fit with the appropriately-sized footplate and cuff. To alter the PD-AFO stiffness, 5 struts of varying thicknesses were interchanged. Participants underwent an acclimation session with a physical therapist while wearing the middle stiffness PD-AFO. Participants then walked at both walking speeds for one minute on an instrumented treadmill (Bertec, USA) while full body motion capture data was collected (Qualysis, USA) for each of the 5 stiffness conditions. The order of PD-AFO stiffness conditions was randomized and rest was provided as necessary. All data was processed in Visual 3D (C-Motion Inc., USA). COT was calculated as the sum of the work (positive + absolute value of negative, normalized by body mass) from all lower limb joints during the gait cycle, plus the distal feet during stance, all scaled by stride length.

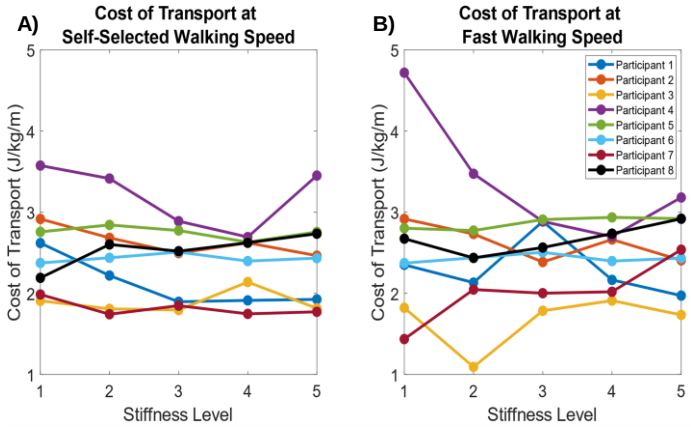

Figure 1: Cost of transport for all participants across all 5 PD-AFO stiffnesses at (A) self-selected and (B) fast walking speeds.

Results & Discussion: Figure 1 shows the COT for each of the 5 PD-AFO stiffnesses for each participant at both walking speeds. Three participants showed large differences in COT (>0.5 J/kg/m) across stiffnesses at self-selected walking speed and five showed large differences in COT across stiffnesses at fast walking speed while others showed minimal differences in COT across stiffnesses. These results partially support our hypothesis that altering stiffness affects COT, at least for some. Notably, no single stiffness produced the lowest COT for all participants. This indicates that PD-AFO stiffness needs to be individually customized. Additionally, the stiffness that had the lowest COT for each participant was not the same at both walking speeds, which can be expected as walking speed affects ankle stiffness.

Significance: These results show that PD-AFO stiffness influences COT, at least for some. While more participants still need to be collected to strengthen the conclusions that can be drawn, these initial findings suggest that PD-AFO stiffness likely needs to be customized in order to optimize walking efficiency, as measured by COT, for post-stroke PD-AFO users. Ultimately, developing a method to individually optimize PD-AFO stiffness may greatly improve walking efficiency and community ambulation capacity for individuals with chronic stroke.

Acknowledgments: This work was supported by the USAMRAA Orthotics & Prosthetics Outcomes Research Program (Award No. HT94252310106). Opinion, interpretations, conclusions, and recommendations are those of the author and not necessarily endorsed by USAMRAA.

References: [1] Tsao CW et al. *Heart Disease and Stroke Statistics—2023 Update*; [2] Arch et al. *Prosthet Orthot Int*. 2016;40(5); [3] Arch and Reisman (2016), *J Prosthetics and Orthotics* 28(2); [4] Koller et al. *Prosthet Orthot Int*. 2021;45(4)

A HOME DEVICE FOR IMPROVED ANKLE DORSIFLEXION REHABILITATION

Brayden White[1], Esther Smith[2], Corey A. Pew[1*]
[1]Montana State University Mechanical and Industrial Engineering, Bozeman, MT, [2]Grassroots Physical Therapy, Bozeman, MT
*Corresponding author's email: Corey.Pew@montana.edu

Introduction: Ankle range of motion is an important degree of freedom for performing activities of daily living such as negotiating stairs, ramps, and squatting. Limited ankle dorsiflexion has been defined as an ankle dorsiflexion range limited to 4.2-11.2˚ and has been related to Achilles tendonitis, lower limb injury, and abnormal gait leading to overuse injury [1, 2]. In addition, individuals with limited ankle dorsiflexion have a reduced minimum foot clearance which is one of the leading causes of falling [3-5]. While stretching and massage of the affected area can help increase ankle range of motion, the amount and frequency of manual manipulation needed to affect this range of motion is not accessible to an individual in their home. A novel device called the "Grassroots Ankle Flex" device, has been developed to allow deep stretching of the ankle and surrounding muscles to help increase ankle dorsiflexion (Fig. 1). This device can be used in an individual's home, without assistance, allowing more frequent stretching without increased visits to physical therapy. The Ankle Flex device is used to stretch patients into a dorsiflexion position by securing the foot to the base of the device and the shin to the leg strap attached to the pulley system. The patients can then pull the handle of the pulley system, giving them the mechanical advantage to gently mobilize their ankle into dorsiflexion with their foot firmly secured to the base of the device. This can allow for a deeper and more controlled stretch than previous stretching methods done during at home care. This study aims to determine the effect of using this device as a treatment to improve ankle dorsiflexion in individuals with decreased ankle range of motion. Due to the ease of use and more controlled nature of stretching this device offers, we expected to see improved ankle range of motion and dorsiflexion following use of the Ankle Flex device.

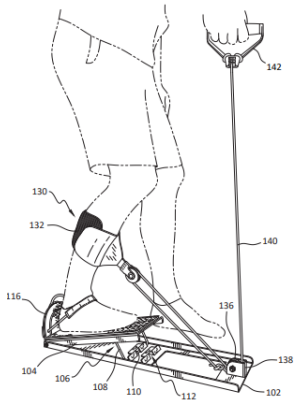

Figure 1: Figure of the Grassroot device showcasing the foot securement system, pulley system and foot dorsiflexion platform.

Methods: Two participants (both women, aged 54 and 55) were identified as individuals with limited ankle dorsiflexion through the physical therapy practice of the device inventor, Esther Smith, DPT. Qualified participants were then referred to volunteer for the IRB approved protocol in the Montana State University Neuromuscular Biomechanics Laboratory (NMBL).The testing protocol consisted of two visits to the lab with three weeks in between visits to use the Ankle Flex device in their home. During each visit clinical ankle range of motion was evaluated by a certified DPT via goniometer while both actively dorsiflexing and being passively pushed into dorsiflexion with the knee at 90° and straight. A knee-to-wall test was also performed due to the consistent reliability of its measurements [6]. Following the clinical assessment, participants performed straight walking, squat, stair, and ramp activities while measuring lower limb kinematics and kinetics using marker-based motion capture and in-ground force plates, with 5 repetitions of each activity. Between lab visits, participants used the Ankle Flex device for 20 second durations with 10 seconds of rest for fifteen repetitions every day for a duration of 3 weeks. Successful completion of the protocol consisted of not missing two consecutive days and no more than 5 days total missed in the three-week period. The participants then returned to the MSU NMBL and repeated all measurements. Assessment of the outcomes utilized a linear mixed effects model with the dependent variable (ankle range of motion, toe clearance, and squat depth) with fixed effects for visit (initial or post) and random effects for participant.

Results and Discussion: Clinical measures of ankle dorsiflexion indicated an increase in Dorsiflexion ability for the affected limb from 4-10° between visits with a 2.5 cm increase in knee-to-wall ability (Table 1). Biomechanical measures indicated increased range of motion up to 1.26° while walking straight, 15.5 mm deeper squat depth, and increased toe clearance, possibly reducing future fall risk (Table 2). Following intervention, both participants achieved dorsiflexion ability in their affected limb similar to the healthy limb, indicating restored use of their ankle joints. These initial results are promising for the use of the Grassroots Ankle Flex device to help restore ankle function following injury. The study is currently recruiting more individuals, with a goal of 5 total participants for this pilot. Future work will incorporate analysis of kinetic measures and ramp and stair activities.

Table 1: Clinical Measures, diff between days

Ankle Dorsiflexion Measure		Healthy Ankle (mean +/- SE)	Affected Ankle (mean +/- SE)
Knee at 90°	Active	1.0 +/- 4.0°	8.0 +/- 2.0°
	Passive	-1.5 +/- 3.5°	4.0 +/- 1.0°
Knee Straight	Active	0 +/- 0°	10.5 +/- 0.5°
	Passive	1.5 +/- 3.5°	5.5 +/- 4.5°
Knee-To-Wall		-0.4 +/- 0.4 cm	2.5 +/- 1.0 cm

Table 2: Biomechanical Measures, diff between days

	Diff btw visits (mean+/- SE)	p-val
Healthy Ankle ROM Straight Walking	-0.62 +/- 0.71°	0.385
Affected Ankle ROM Straight Walking	**+1.26 +/- 0.60°**	**0.039**
Squat Depth	**+15.5 +/- 5mm**	**0.009**
Healthy Toe Clearance	**+4.2 +/- 1.3 mm**	**0.002**
Affected Toe Clearance	+2.9 +/- 1.4 mm	0.052

Significance: This work describes a stretching based intervention device for the improvement of ankle dorsiflexion range of motion following injury. The device allows for manual therapy in the patient's home, reducing dependency on a physical therapist for treatment. Use of the device could help individuals regain functional motion in their ankle as well as reduce future risk of falling through increased toe clearance.

Acknowledgments: Thank you to Mojtaba Mohasel for help with data collections.

References: [1] Dill, K. E. (2014). *Journal of Athletic Training*, *49*(6), 723–732; [2] Moseley, A. M. (2003). *Gait & Posture*, *18*(2), 73–80. [3] Sato, K. (2015). *Open Journal of Therapy and Rehabilitation*, *03*(04), 109–115; [4] Elble, R. J. (1991). *Journal of Neurology*, *238*(1), 1–5; [5] Maki, B. E. (1997). *Journal of the American Geriatrics Society*, *45*(3), 313–320; [6] Konor, M. M. (2012). *International journal of sports physical therapy, 7*(3), 279–287.

A KIRIGAMI-INSPIRED SHOULDER PATCH TO IDENTIFY SHOULDER HUMERAL ROTATION

Amani A. Alkayyali[1*], Susann Wolfram[2], Max Shtein[1], David B. Lipps[1,2]
[1]College of Engineering and [2]School of Kinesiology, University of Michigan, Ann Arbor, MI 48109, USA
*Corresponding author's email: aaalkay@umich.edu

Introduction: The complexity of the shoulder, with the humerus capable of movement in six degrees of freedom, makes it a challenge to measure the movement of the glenohumeral joint. Monitoring shoulder kinematics is important for injury prevention and rehabilitation, along with optimizing physical performance. Restoration of internal and external rotation is particularly important for athletes participating in overhand throwing motions [1] or patients recovering from total shoulder arthroplasty [2]. However, quantifying internal and external rotation of the shoulder is often a challenge in the clinic, as motion capture requires large, expensive experimental setups, and inertial measurement units require careful placement and reporting between sensors. The current study evaluates a novel, engineered, wearable sensor system (**Figure 1A**) for improved monitoring of internal and external shoulder rotation. Using the design principles of the Japanese art of kirigami (cutting of paper to design 3D shapes), the sensor platform conforms to the shape of the shoulder with on-board strain gauges to measure movement. Our objective was to examine how well this kirigami-inspired shoulder patch could identify differences in shoulder kinematics between internal and external rotation as healthy individuals moved their humerus through specified movement patterns.

Methods: A custom-developed kirigami-inspired shoulder patch (**Figure 1A**) measured local changes in strain as an individual moves their shoulder [3]. Seventeen participants (11 males, 25.5 years, 177cm, 75.6kg) were recruited to wear the device and move their right arm in internal and external rotation, as specified in Codman's paradox [4]. As the participants moved their arms in internal and external rotation, a trigger was used to identify three stages of the movement (e.g. when a participant moved their forearm from above to resting on their head (0-33%), moving to internal or external rotation (34-66%), and moving their arm back to their side (67-100%)). The strain gauge data was low-pass filtered (0.001 passband frequency), and time was normalized to % of activity movement. Differences in the change of strain voltage between the internal and external rotation movement patterns were evaluated using one-dimensional statistical parametric mapping (SPM).

Results & Discussion: The movement patterns for each strain gauge of the kirigami shoulder patch were consistent within each participant, suggesting participants performed the movements similarly without hardware discrepancies between trials. Intra-subject SPM models showed that 14/17 individuals had at least one significant difference between internal and external rotation in at least one of the three stages of movement. The most common movement phase with a significant difference was between 33-66% of the movement, when the arm is lowered into internal or external rotation. This suggests wearable conformal sensors overlaying the shoulder can detect differences in skin deformation as the underlying humerus rotates into internal or external rotation. Three of four strain gauges detected significant temporal differences between internal and external rotation (all $p < 0.047$, **Figure 1B**).

The strain gauges most beneficial in detecting differences in rotation were placed distal (over the humeral head) or posterior (over fascial tissues of posterior shoulder muscles) to the acromion. The posterior strain gauge exhibited a more significant voltage change as the shoulder moved into internal than external rotation (between 67-100 percent of the movement). This would correspond with the tightening of the posterior capsule in response to internal rotation. The least beneficial strain gauge for detecting humeral rotation may be the one placed proximal to the acromion, the skin sensor farthest from the humeral head. While intra-subject differences for the proximal strain gauge were detected, the averaged group data did not differ. While a kirigami-inspired shoulder patch can delineate between internal and external rotation, further work is needed to determine its effectiveness at detecting other shoulder movements and to develop different-sized patches to accommodate a wide range of users.

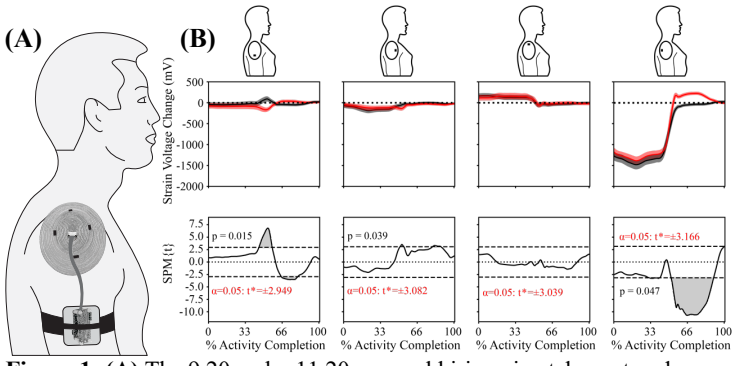

Figure 1: (A) The 9.20cm by 11.20 cm oval kirigami patch, centered on the acromion, measured skin deformation using four strain gauges placed distal, anterior, proximal, and posterior to the acromion. The patch was connected to an armband containing a Bluetooth board and Wheatstone bridge. **(B)** (top) The mean times-series group data (N=17) for each strain gauge normalized to 100% of activity movement. External rotation is the bold black line, internal rotation is the bold red line, and shaded areas indicate standard error. (bottom) Results from SPM models for the four strain gauges. 3 of 4 strain gauges exhibited statistical differences between internal and external rotation movements, as indicated by the shaded areas.

Significance: A new class of kirigami-inspired wearable sensors conforming to the shoulder can detect differences in skin deformation corresponding to the underlying humeral rotation. Given their lower cost and enhanced portability, expanded use of this sensor platform may better inform clinical decision making for shoulder pathologies than traditional approaches for measuring shoulder kinematics (e.g., marker-based motion capture).

Acknowledgments: National Science Foundation Graduate Research Fellowship Program - Grant No. 1841052

References: [1] Fleisig et al. (1996) *Sports Med* 21; [2] Oh et al. (2020) *JSES* 29(4); [3] Evke et al. (2019) *Adv Matter Tech* 4(12); [4] Cheng (2006) *J Biomech* 39(7).

IS GAIT CONSISTENT FROM THE BEGINNING TO THE END OF A BOUT OF OUT-OF-LAB WALKING?

Fany Alvarado*, Julien A. Mihy, Mayumi Wagatsuma, Millissia Murro, Jocelyn F. Hafer
Graduate Program in Biomechanics and Movement Science; Kinesiology & Applied Physiology, University of Delaware
*Corresponding author's email: fany@udel.edu

Introduction: Traditionally gait is collected in the lab in a highly controlled manner. This highly controlled gait may not represent how people walk in the real world, out of the lab. There are currently no standardized procedures on how to analyze gait data that is collected outside the lab. In-lab data is analyzed by identifying a bout of data, calculating variables within that bout, and then taking an average of those variables with the assumption that gait is consistent within that bout. Out-of-lab gait data can be analyzed similarly by averaging all strides within each bout. However, we don't know if gait outside of the lab is consistent from the beginning to the end of longer bouts. This out-of-lab analysis could be influenced by or mask some of the gait variations within a longer bout of data. Therefore, the purpose of this study was to determine whether gait mechanics are comparable between the beginning and end of an out-of-lab walk. Because gait out of the lab can vary due to factors such as environment and walking bout duration [1], we compared data that were captured in the same location at the beginning and end of a standard out-of-lab walking route. We hypothesized that hip, knee, and ankle range of motion (ROM), stride velocity and length would be consistent from the beginning to the end of a bout of out-of-lab walking.

Methods: Eight adults, four without (60.0±2.8years) and four with knee osteoarthritis (64.9±3.1years) walked outside the lab at a self-selected speed. Five inertial measurement units (IMUs) (Opal v2, APDM) were placed on the pelvis, lateral thigh, and shank (right side for healthy, symptomatic for knee osteoarthritis), and bilateral feet. All participants walked ~10 minutes out-of-lab in a campus building in a designated walking route. Walking data that occurred in the same hallway at the beginning and the end of the walk were selected for analysis. Foot trajectories were computed using a zero-velocity update algorithm [2]. A continuous wavelet transform was used to identify gait events. Stride velocity and stride length were calculated from foot trajectory data based on consecutive heel strikes. IMU data medial-lateral axes were defined using a functional sensor-to-segment alignment [3]. Functionally oriented angular velocity data were integrated stride-by-stride to obtain segment excursions. Hip, knee, and ankle ranges of motion (ROM) were calculated based on the difference in the excursions of adjacent segments [4].

Thresholds were used to select only steady-state strides (<0.1m/s difference from surrounding strides) that occurred in a straight line (<45° difference in direction from surrounding strides). Stride length, stride velocity, and hip, knee, and ankle knee ROM were calculated for each identified stride and averaged within the beginning and end bouts for each subject. A two one-sided tests (TOST) procedure was used to test for equivalence of gait variables (hip, knee, and ankle ROM, stride velocity and length) between the beginning and end of the walk. Equivalence was defined a priori as an effect size (Cohen's d) within the bounds of +/-0.5. To meet the criteria for equivalence, the TOST 90% confidence interval (CI) for each variable had to fall fully within its upper and lower equivalence bounds [5].

Results & Discussion: No variables met the criteria for equivalence between the beginning and end of the walk (Fig 1). However, no variables met the criteria for being significantly different, as indicated by all 90% CIs crossing 0 (Fig 1). The differences in mean magnitude were small (<2° for ROMs, <0.1 m or m/s for stride length and stride velocity), suggesting that the lack of equivalence may not be meaningful in this context. In the real world, these differences may increase due to changes in the environment and not being able to process data at the same location between bouts.

Significance: Gait was not equivalent from the beginning to the end of an out-of-lab walk but showed only small, non-significant differences over time. Special consideration should be taken when selecting data in the real world, as differences in environment and behavior would be expected to be larger than in the current out-of-lab demonstration.

Acknowledgments: F Alvarado is supported by a University of Delaware Graduate Scholar Award

References: [1] Wagatsuma et al., 2023. *ISB23*; [2] Rebula et al., *Gait Posture* 2013, 38, 974-980; [3] Mihy et al., *medRxiv* 2022.11.29.22282894; [4] Hafer et al., *J.Biomech*, 2020;99 109567; [5] Lakens et al., *AMPPS*, 2018,2,259-269

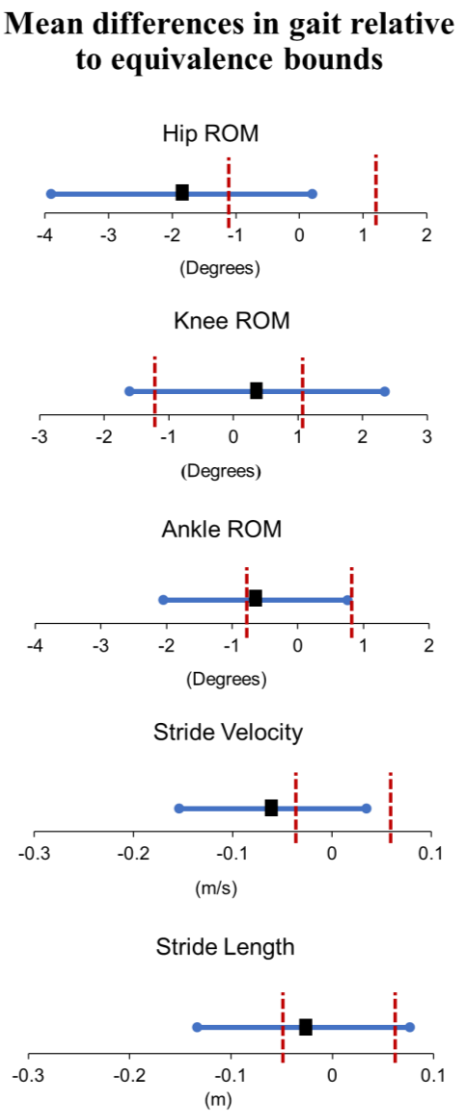

Figure 1: Equivalence TOST test between the beginning and end of the out-of-lab walk for gait kinematics. The black boxes indicate mean differences and the blue lines indicate the 90% CI for each variable.

RELATIONSHIPS BETWEEN QUADRICEPS STRENGTH AND DIFFUSION TENSOR IMAGING PARAMETERS

Meredith K. Owen[1*], Peter A. Hardy[2], Thorsten Feiweier[3], Brian Noehren[1]
[1]Department of Physical Therapy, University of Kentucky, Lexington, KY, [2]Department of Radiology, University of Kentucky, Lexington, KY, [3]Siemens Healthineers AG, Erlangen, Germany
*Corresponding author's email: mow229@uky.edu

Introduction: Quadriceps **s**trength loss is highly prevalent and leads to overall poorer outcomes following an anterior cruciate ligament (ACL) tear. The cause of strength loss is multifactorial, but microstructural changes within the muscle may be a large contributing factor. As a potential alternative to biopsies which have been used historically to determine muscle microstructure, diffusion tensor magnetic resonance imaging (DTI) may be a non-invasive method to investigate tissue microstructure and can be leveraged to determine muscle microstructural properties [1]. DTI in skeletal muscle relies on the basic principle that diffusivity of water will be greatest in the direction parallel to the primary muscle fiber [1]. From DTI, the three principle diffusion directions (e1, e2 and e3) and their magnitudes (λ1, λ2, and λ3) can be used to calculate fractional anisotropy (FA) of the imaged tissue. The purpose of this study was to determine the relationships between quadriceps strength and skeletal muscle microstructure determined from DTI after an ACL tear.

Methods: Following Institutional Review Board approval, and after providing informed consent, 44 individuals with recent ACL tear (20 female, 21.4 ± 5.6 years, 1.7 ± 0.1 meters, 75.4 ± 16.1 kg, 21 ± 15 days from injury) completed isometric quadriceps strength testing and DTI of both thighs prior to ACL reconstruction surgery.

Maximum quadricep strength was determined through a 5-second maximum voluntary isometric knee extension. Participants completed four maximum effort kicks. The maximum value from each kick was normalized to body mass and then all trials were averaged.

Imaging was performed on a 3T scanner (MAGNETOM Prisma^{fit}, Siemens Healthineers AG, Erlangen, Germany). Participants were positioned supine and feet first into the scanner. A flexible, 18-element body array was secured closely around the thigh. Twenty-one slices centered at the largest portion of the vastus lateralis muscle belly were acquired using a research sequence which combined a stimulated echo diffusion preparation with an echoplanar readout module [2]. Specific sequence parameters included a repetition time/echo time of 7500/36.4 ms, a mixing time of 173 ms, gradient separation of 185.5 ms, gradient duration of 5.4 ms, and 3 excitations. Image field-of-view was 192 mm by 192 mm with an acquisition matrix of 96 by 96 and slice thickness of 6 mm resulting in a voxel size of 2 x 2 x 6 mm^3. Eigenvalues and eigenvectors were calculated from the raw diffusion weighted images (b = 50, b = 500 s/mm^2) using a custom developed code (MATLAB, MathWorks, Natick, MA). Mean diffusivity (MD, average of λ1, λ2, & λ3), radial diffusivity (RD, average of λ2 & λ3), axial diffusivity (λ1), and fractional anisotropy (FA) were determined. Associations between each DTI parameter and peak quadriceps strength were determined using Pearson's product moment correlations. Statistical analyses were performed using SPSS (IBM) with a significance level of .05.

Results & Discussion: Average peak quadriceps strength was lower on the ACL-injured side (1.96 ± 0.68 Nm/kg) than the contralateral side (2.57 ± 0.53 Nm/kg). Table 1 lists the correlation coefficients between strength and DTI parameters.

Associations between DTI parameters and isometric quadriceps strength follow expected trends. As FA increases, quadriceps strength decreases likely due to decreases in fiber cross-sectional area. The opposite relationship is true for RD, which may reflect muscle fiber cross-sectional area. Larger fiber cross-sectional area has previously been related to greater strength [3].

Significance: Regardless of injury status, associations between DTI parameters, FA and RD, and strength were maintained, potentially indicating that the relationships between DTI and strength are robust and not affected by other changes in muscle due to injury. DTI, and specifically FA and RD measures, demonstrated potential utility for determining underlying changes in skeletal muscle microstructure that may influence overall quadriceps strength.

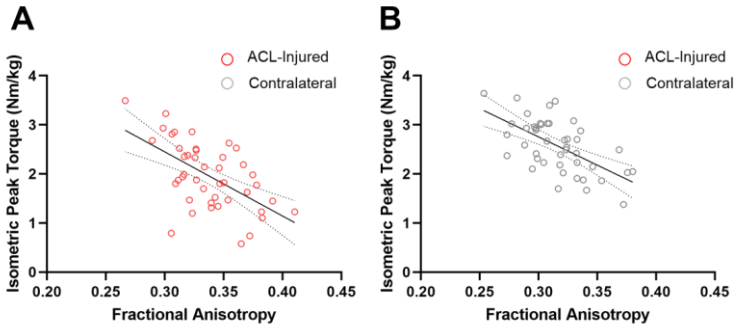

Figure 1. Scatterplots for fractional anisotropy vs. peak torque for the (A) ACL-injured and (B) contralateral limbs

Table 1. Correlation coefficients for DTI parameters vs. isometric strength for both the ACL-injured limb and the contralateral limb. *p < .01, **p < .001

		FA	MD	RD	λ1
Strength	ACL-injured	-.582**	.129	.390**	-.284
	Contralateral	-.607**	.107	.383*	-.372*

Acknowledgments: This work was supported through funding from the NIH under grant numbers R01AR071398 and 1S10OD023573.

References: [1] Oudeman et al. (2016), *J Magn Reson Imaging* 43(4). [2] Noehren et al. (2016), *J Bone Joint Surg Am*, 98(18). [3] Herman et al. (2010), *J Strength Cond Res*, 24(1).

THUMB METACARPAL INTERNAL ROTATION IN CONTROL AND SURGICAL PARTICIPANTS

Adam J. Chrzan[1], Nicole D. Arnold[1], Kevin Chan[2], Tamara Reid Bush[1*]
[1]Mechanical Engineering, Michigan State University, East Lansing, MI, USA
[2]Orthopedic Hand and Upper Extremity Surgery, University of Michigan, Ann Arbor, MI, USA
*Corresponding author's email: reidtama@egr.msu.edu

Introduction: Internal rotation of the thumb carpometacarpal (CMC) joint, at the base of the thumb, is essential for completion of daily tasks. This rotation turns the thumbnail towards/away from the palm, and is thought to arise from the joint's unique saddle morphology [1]. However, the CMC joint commonly develops osteoarthritis (OA) along with pain, stiffness, and difficulty completing tasks [2]. Surgery has effectively reduced pain in those with severe CMC OA, but research has not shown any one of the surgical techniques to be superior in post-operative motion ability [3]. Specifically, there is limited discussion of internal rotation in the literature, particularly how it is impacted by OA and surgery. The goals of this work were to determine internal rotation ranges of motion and motion patterns in 1) healthy control males and females, and 2) participants with CMC OA before and after receiving the most common CMC OA surgery: ligament reconstruction with tendon interposition (LRTI) [4].

Table 1: Internal rotation range for control and OA participants. 3- and 6-month ranges were significantly less than pre-surgery and controls.

	Range
Younger males	49.7 ± 11.2
Younger females	50.0 ± 11.5
Older males	51.1 ± 12.0
Older females	52.8 ± 12.0
Pre-surgery	47.2 ± 9.8
3-months	35.2 ± 8.4
6-months	40.4 ± 8.3

Methods: Control participants included younger (18-39 years) male (YM) and female (YF), and older (40+ years) male (OM) and female (OF). Control participants did not have thumb CMC OA, were not pregnant, had no prior surgery or injury to the thumb, and were tested once. OA participants had doctor diagnosed CMC OA, consented to LRTI surgery, and were tested pre-surgery, 3-, and 6-months post-surgery. Only female OA participants were reported, as 84% of the sample was female, which matches the literature indicating CMC OA was more prevalent in females than males [2].

A six-camera motion capture system was used to obtain motion data (Qualysis, Gothenburg, Sweden) at 100 Hz. Individual retroreflective markers were placed on the ulnar styloid, distal radial tubercle, and the distal end of the 2nd metacarpal, and a rigid marker cluster was placed on the thumb metacarpal. A maximum circumduction motion was performed by all participants to explore their thumb movement boundaries. Flexion, abduction, and internal rotation angles of the thumb metacarpal were calculated throughout motion using the Grood and Suntay method and local coordinate systems [5]. Zero-degree angles occurred when coordinate systems were coaxial. Internal rotation angle ranges and range midpoints were recorded. Range midpoints were used to identify a shift in region of motion (e.g. a 40° range could be 0-40° or 20-60°). Plots of internal rotation (x-coordinate) and flexion (y-coordinate), and internal rotation (x-coordinate) and abduction (y-coordinate) were established, averaged across each group and examined for changes in motion patterns. Statistical analysis of sex and age in controls, and the effect of study group (control females, pre-surgery, 3-, and 6-months post-surgery) in control and OA females was conducted.

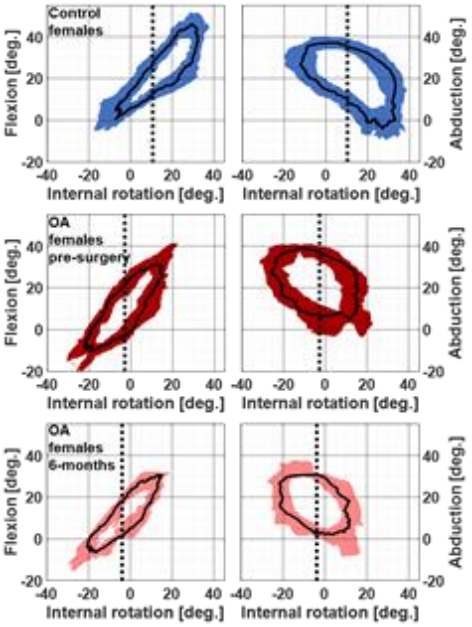

Figure 1: Average (solid black line) and ±1 standard deviation (shaded region) metacarpal angles for control females (blue), and OA females pre-surgery (dark red) and 6-month post-surgery (light red). Internal rotation range midpoints (dashed line) were shifted towards negative values in OA participants compared to controls.

Results & Discussion: 13 YM (28.8 ± 5.6 years), 13 YF (25.8 ± 5.1 years), 13 OM (60.2 ± 11.4 years), 13 OF (58.0 ± 9.3 years). 16 OA females (64.0 ± 8.5 years) were tested before surgery (36.4 ± 66.9 days before), 3-months (92.5 ± 9.6 days after) and 6-months post-surgery (186.0 ± 15.9 days after). Sex and age were not significant for internal rotation ranges or range midpoint (sex $p>0.092$, age $p>0.311$) for controls (Table 1). Pre-surgery internal rotation ranges were not significantly different than control ($p=0.576$), but decreased significantly 3- and 6-months post-surgery compared to pre-surgery and controls ($p<0.009$). Range midpoints did not significantly change post-surgery compared to pre-surgery ($p>0.510$), but all OA timepoints were significantly less than control ($p<0.005$). All control subcohorts showed similar motion patterns in both angle plots, but pre and post-surgery abduction vs internal rotation plots did not demonstrate the kidney shape motion pattern seen in controls (Fig. 1). Pre and post-surgery internal rotation shifted toward negative values compared to controls (shown by smaller range midpoint), and the surgery was not normalizing. Pre-surgery internal rotation ranges were similar to controls, motion patterns did not visually change after surgery (Fig. 1), and substantial internal rotation ability (~40°) persisted after surgical removal of the saddle joint.

Significance: This investigation of CMC internal rotations identified a shift in range midpoint as a potential indicator of OA onset. The surprising lack of change in internal motion pattern pre-to-post-surgery and substantial range of motion post-surgery suggested the trapezium was not solely responsible for CMC internal rotation ability. These findings could be leveraged to preserve key CMC motion abilities and inform surgical practice and future implant design.

Acknowledgments: Funding was received from the Corewell Health – Michigan State University Alliance Grant.

References: [1] Fontaine et al. (2021), *Hand Surg Rehab* 40; [2] Haugen et al. (2011), *Ann Rheum Dis* 70; [3] Vermeulen et al. (2011), *J. Hand Surg* 36(1); [4] Deutch et al. (2018), *Hand* 13(4); [5] Grood & Suntay (1983), *J. Biomech Eng* 105

SEX/GENDER BALANCE OF STUDY POPULATIONS IN AMERICAN SOCIETY OF BIOMECHANICS (ASB) ABSTRACTS: 2023 UPDATE

Richard E. Hughes[1*], Ross H. Miller[2], Melissa M. B. Morrow[3]
[1]University of Michigan, Ann Arbor, MI
[2]University of Maryland, College Park, MD
[3]University of Texas Medical Branch, Galveston, TX
*Corresponding author's email: rehughes@umich.edu

Introduction: Sex and gender equity is important in science and is relevant to research questions, research investigators, students, and also study participants. Bach *et al*. [1] reported on the sex balance of study subjects in American Society of Biomechanics (ASB) annual meeting abstracts at ten-year intervals: 1983, 1993, 2003, and 2013. Random samples of abstracts were assessed in each of these years to quantify the proportion of abstracts that (i) reported sex of study subjects, (ii) included both males and females, and (iii) had a between 30% and 70% female subjects ("approximately balanced"). Abstracts that investigated inanimate objects or were computer simulation studies that did not collect human/animal data were excluded. The study showed increasing trends in representation of females in study samples over time, but the "approximately balanced" proportion was still well below 100% in 2013. The purpose of this project was, therefore, to quantify the sex/gender balance of study samples in ASB annual meeting abstracts ten years following the report of Bach *et al*.[1]

Methods: The methods used in Bach *et al*. [1] were applied to abstracts from the 2023 ASB annual meeting abstracts. Forty-three abstracts were randomly selected. The methodology was slightly modified to include sex and gender instead of just sex. Each abstract was scored for three criteria: (i) was sex/gender reported, (ii) was a more than one sex/gender included, and (iii) was the study population "approximately balanced" (split between 30% and 70%). Additionally, each abstract was scored for whether humans or animals were used and whether subjects were described in terms of sex or gender. Statistical differences in proportions between 2013 and 2023 were assessed using Chi-squared tests in R and 95% confidence intervals for proportions were computed. The sample size of 43 was determined to provide a statistical power of detecting an effect size of 0.25 when controlling the Type I error at the 0.05 level.[1] Proportions were converted to percentages for reporting.

Results & Discussion: 44% [95% CI, 28%-58%] of the abstract sample reported sex/gender of study participants. 33% [95% CI, 17%-45%] of the abstracts included both males and females. Only 30% [95% CI, 15%-43%] of the abstracts reported using an "approximately balanced" study population. None of these percentages were statistically different from the values in the sample of abstracts studied in 2013 by Bach *et al*. [1] (Figure 1). Forty-two (98%) of the abstracts used human subjects and one was an animal study (2%). No abstract explicitly differentiated sex from gender, although a mix of "female" and "woman" terms were used; "male" was used without any mention of "man." Abbreviations M/F were also used. There was no reporting of nonbinary participants.

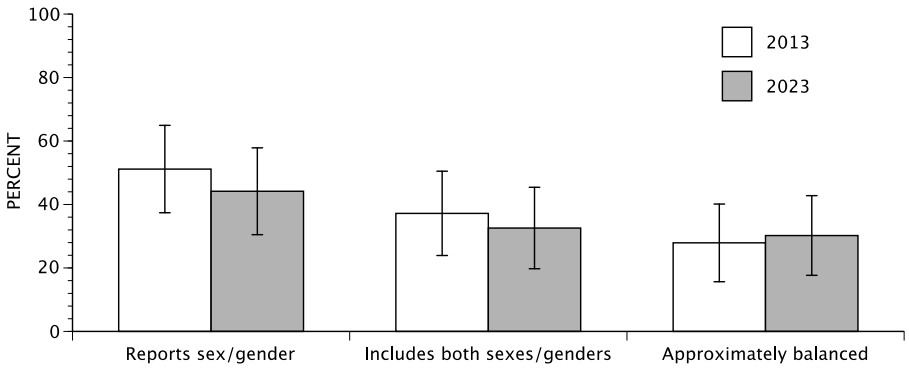

Figure 1: Proportions of 2023 ASB annual meeting abstracts that (a) report sex/gender of study participants, (b) include both male and female participants, and (c) study population is "approximately balanced" (30% - 70%) along with 95% confidence intervals.

The most significant limitation of this study was that it utilized a random sample of abstracts rather than a complete enumeration of 2023 ASB abstracts or full-length archival publications. A random sampling approach is scientifically valid, although it does not provide direct evidence about all abstracts presented at the annual meeting. Lamia *et al*. [2] has shown similar results of unbalanced sex distribution of study populations in biomechanical studies based on review of full-length biomechanical papers.

Significance: No statistically significant differences were found compared to 2013. Moreover, the percent of approximately balanced abstracts was very similar (27% vs. 30%) and the upper limit on the 95% confidence interval was only 43%. This suggests there has not been an improvement in sex/gender balance in the last ten years and the percent of approximaly balanced abstracts was far from 100%. Education is needed to ensure that the biomechanics community is following best practices in rigor and reproducibility and incompliance with NIH policy. ASB could consider adding study population demographic reporting as a criteria for reviewers to use.

References: [1] Bach *et al*. Plos ONE. *DOI:10.1371/journal.pone.0118797;* [2] Lamia, S.N. *et al*., Evidence of sex bias in finite element modeling of hip arthroplasty. SB[3]C2021.

JOINT TENSIONING AND ACROMIAL FRACTURE RISK AFTER REVERSE SHOULDER ARTHROPLASTY

Joshua E. Johnson[1*], Maria F. Bozoghlian[1], Brendan M. Patterson[1], Donald D. Anderson[1]
[1]Department of Orthopedics & Rehabilitation, University of Iowa, Iowa City, IA
*joshua-e-johnson@uiowa.edu

Introduction: Reverse shoulder arthroplasty (RSA) was originally indicated for patients with a deficient rotator cuff to improve shoulder function. RSA indications now also include patients with advanced glenohumeral arthritis with intact rotator cuff integrity. Acromial stress fractures are a concerning complication after RSA that occurs more often in patients with a deficient cuff. The intact cuff helps stabilize the healthy glenohumeral joint, and in patients with a deficient cuff, surgeons select appropriate implant combinations to adequately tension the joint for stability while maximizing range of motion and functional outcome. However, the mechanical trade-offs between joint tensioning and acromial fracture risk are not well understood. The purpose of this study was to evaluate changes in acromial fracture risk with changes in joint tension in RSA.

Methods: A finite element (FE) model of RSA [1] was used to simulate the scenario of cuff tear arthropathy (CTA). The model incorporated deltoid, subscapularis, infraspinatus, and teres minor tendon and muscle geometries, augmented with Stryker Perform inlay humeral stem and 36 mm glenosphere RSA implants (Figure 1). Deformable soft tissues were assigned isotropic, hyperelastic properties. The acromion was assigned representative scapula-specific cortical and trabecular bone properties [2]. Rotator cuff muscles were tensioned and wrapped around the glenohumeral joint prior to motion simulation by pulling their proximal ends back to pre-RSA origins, while their distal/lateral insertions were tied to humeral attachment sites. The deltoid muscle was tied at its bony origin/insertion sites. Implant joint tensioning was evaluated by comparing joint contact normal force after virtual implantation of the RSA components and subsequent simulation of internal rotation from neutral to 50°. Joint tensions were evaluated throughout rotation for a baseline RSA configuration with intact cuff, then after progressive removal of cuff elements. For each cuff configuration, acromial fracture risk was evaluated by quantifying the percentage of the total cortical bone region experiencing stresses above yield strength (corresponding to 0.62% yield strain of bone in tension [3]) throughout rotation. RSA simulations were also performed with 3 mm of glenoid lateralization. To evaluate the mechanical trade-off of implant joint tensioning, contact normal force and acromial fracture risk for each cuff configuration with 3 mm glenoid lateralization were compared with the intact cuff baseline RSA configuration.

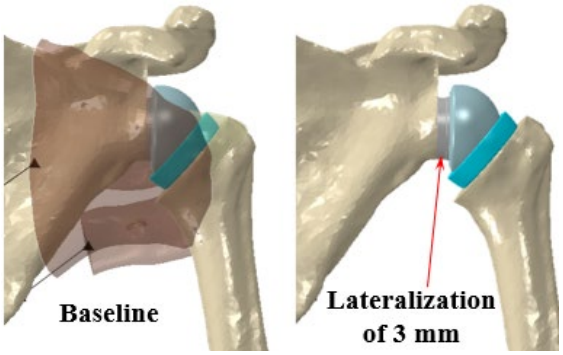

Figure 1. FE models of the baseline RSA configuration with intact cuff (left), and 3 mm glenoid lateralization with cuff absent (right). Deltoid not shown.

Results & Discussion: For the baseline RSA configuration, joint tension decreased as expected with progressive removal of cuff muscles compared to the intact cuff (18%, 29%, 41%, 60% average decreases throughout rotation with infra, subscap, infra-subscap, all cuff absent, respectively). Bone regions above yield strength were similar across cuff configurations (8%, 8.3%, 7.8%, 8.4%, 8.5% average throughout rotation with intact cuff, and infra, subscap, infra-subscap, all cuff absent, respectively), since acromial stresses depend solely on passive deltoid stretching, which is a direct function of glenoid lateralization in our model. With 3 mm glenoid lateralization, joint tension increased (39% overall average) for all cuff configurations compared to baseline, as expected. Additional stretching of the deltoid with the 3 mm lateralization resulted in a 0.6% (overall average) larger bone region above yield strength. CTA patients undergoing RSA demonstrate varying subscapularis and infraspinatus muscle integrity. For the teres-only cuff configuration, the modest 3 mm glenoid lateralization did not restore joint tension of the intact cuff baseline configuration (normalized contact force <1; Figure 2). For the subscap-teres/infra-teres 3 mm glenoid lateralization configurations, joint tension was similar to the intact cuff baseline but with the trade-off of larger acromial regions experiencing stresses above yield strength.

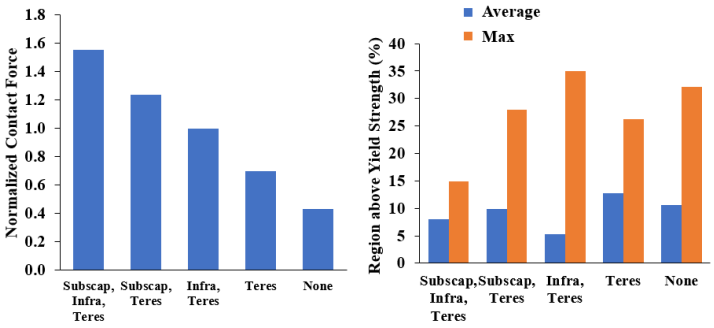

Figure 2. Results from cuff configurations with 3 mm glenoid lateralization compared to the baseline RSA configuration with intact cuff.

Significance: In the healthy shoulder, the rotator cuff provides a compressive force to help stabilize the joint during motion. In patients with a deficient cuff, an over-tensioned RSA implant configuration intended to improve stability may increase acromial fracture risk. Conversely, lack of appropriate tension can lead to joint dislocation. We were able to parametrically evaluate joint tension changes with implant lateralization and corresponding changes in acromial stresses. FE models may help surgeons select the appropriate implant configuration based on patient clinical presentation to optimize joint tension while limiting dislocation and acromial fracture risk.

Acknowledgements: This research was funded by a grant from Stryker Orthopaedics.
References: [1] Johnson et al. (2021), *Semin Arthroplasty: JSES* 31(1):36-44; [2] Chae et al. (2016), *J Orthop Res* 34(6):1061-8; [3] Bayraktar et al. (2004), *J Biomech* 37(1):27-35

MODELING SHANK TISSUE PROPERTIES AND QUANTIFYING BODY COMPOSITION WITH A WEARABLE ACTUATOR-ACCELEROMETER SET

Nataliya Rokhmanova[1,2*], Julian Martus[1], Robert Faulkner[1], Jonathan Fiene[1], Katherine J. Kuchenbecker[1]
[1]Max Planck Institute for Intelligent Systems, Stuttgart, Germany
[2]Department of Mechanical Engineering, Carnegie Mellon University, Pittsburgh, USA
*Corresponding author's email: rokhmanova@is.mpg.de

Introduction: Soft-tissue artifacts impact the accuracy of kinematic estimation from skin-mounted reflective markers or wearable inertial measurement units [1]. The extent of skin deformation and motion of the skin relative to the bone can depend on subject-specific factors [2] such as body composition and skin elasticity. Here, we take a system-identification approach to capture differences in tissue composition across anatomical sites and across subjects as a step toward individualized characterization of tissue properties that contribute to soft-tissue artifacts. Using an accelerometer, we measured the skin's response to transient vibrations applied at four locations around the shank (Fig. 1A) and created a fourth-order linear dynamic model (Fig. 1B) that captures tissue properties via optimized stiffness and damping parameters. As rigid tissues attenuate vibration more than soft tissues [3], we hypothesized that 1) vibration amplitudes will be lower at bony sites and that 2) tissue properties will depend on body composition: higher body fat will correlate with lower stiffness and damping.

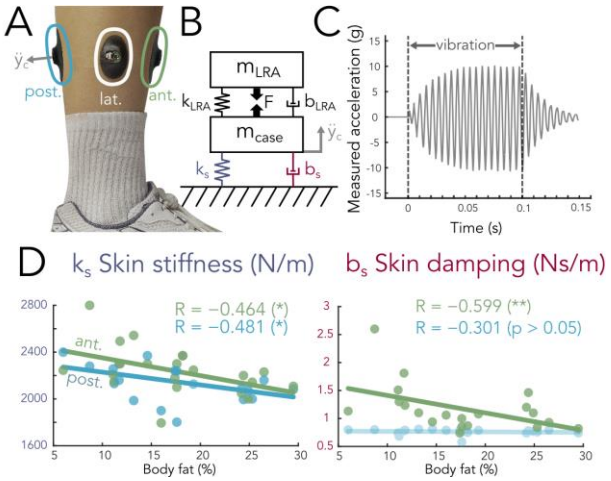

Figure 1: (A) The device was placed on four locations spaced around the shank. (B) The lumped-parameter model represents the tissue properties as stiffness (k_s) and damping (b_s) parameters. (C) Sample vibration measured by the on-board accelerometer. (D) Per-subject correlations between body-fat percentage and optimized stiffness (left) and damping (right) parameters at the anterior (green) and posterior (gray) sites. Each subject is represented as a single dot. * $p < 0.05$ and ** $p < 0.01$.

Methods: We designed and built an adhesive skin-mounted device that provides transient vibration pulses (177 Hz sinusoid, 0.1 s long, five voltage levels ranging from 20% to 100%) with a linear resonant actuator (LRA) and measures the physical vibration of the device on the skin with an on-board accelerometer (±16 g range, 6 kHz bandwidth, 26.7 kHz data rate) (Fig. 1C). We measured the skin acceleration response from 20 subjects (10M/10F) at four locations around the shank (anterior, lateral, medial, and posterior) at 30% of the distance from the lateral malleolus to the lateral condyle. Each subject's body-fat percentage was assessed using an electrical-impedance scale (Beurer, Ulm, Germany). The device mounted on the skin was represented as a one-dimensional lumped-parameter model, where skin stiffness and damping were optimized for each subject and each location by minimizing the root-mean-squared error between the model response and measured acceleration data using the Nelder-Mead Simplex search method [4]. Model constants (case mass; LRA mass, stiffness, and damping; gain from voltage to force) were derived experimentally.

Results & Discussion: We found that peak-to-peak vibration amplitudes in the normal direction were significantly smaller at the anterior site, where the device was placed directly over the tibia; the difference in amplitudes (mean ± SD) at 100% voltage between the anterior (5.46 ± 1.12 g) and posterior (7.12 ± 0.44 g) sites is similar to the difference in acceleration magnitudes when comparing skin- and bone-mounted accelerometers used to estimate tibial shock (2.1 g) [5], suggesting that mounting location plays a significant role in tissue displacement. The reduction in amplitude at this site can be explained by the higher optimized stiffness (2238 ± 212 N/m) and damping (1.18 ± 0.42 Ns/m) values at the anterior site compared to the lateral, medial, and posterior sites, confirming our first hypothesis. Furthermore, body composition measurements were predictive of stiffness and damping coefficients at the anterior site, and predictive of stiffness at the posterior site (Fig. 1D), partially confirming our second hypothesis. The absence of correlation between skin damping and body fat percentage at the posterior site could be attributed to standardizing device placement at a fixed distance from the ankle: muscle activation tunes the damping of applied vibration [3], but differences in gastrocnemius insertion sites and Achilles tendon lengths may have impacted our ability to detect a relationship between subcutaneous fat and damping near the calf muscle. Also, the electrical-impedance scale used here provides only a rough estimate of body-fat percentage; a DEXA scan would enable more accurate and precise values for tissue composition at specific anatomical sites. It is critical to note that although these findings provide a means to capture and characterize tissue composition non-invasively, the relationship between tissue vibration amplitude and soft-tissue artifacts remains to be quantitatively linked. Validating these findings against biplane fluoroscopy, for instance, would help to determine if regions where skin stiffness and damping are higher, and vibration amplitude is smaller, are less susceptible to soft-tissue artifacts.

Significance: We developed an inexpensive, portable, and non-invasive method to characterize differences in tissue composition across individuals with varying levels of subcutaneous fat, as well as across different anatomical sites. The relationship between tissue displacement and stiffness and damping properties can contribute to mechanistic explanations for soft-tissue artifacts. Future kinematic estimation algorithms could one day be precisely tailored to the individual and the mounting location to account for tissue deformations.

References: [1] Hoglund et al. (2021) *Med Eng & Phys*; [2] Schallig et al. (2021) *J Biomech*; [3] Wakeling and Nigg (2002) *J Appl Phys;* [4] Lagarias et al. (1998) *SIAM J of Opt;* [5] Lafortune (1995) *J Biomech.*

REAL-WORLD VARIABILITY IN GAIT MECHANICS IN RESPONSE TO PAIN

Julien A. Mihy[1*], Mayumi Wagatsuma[1], Spencer N. Miller[2], Stephen M. Cain[2], Jocelyn F. Hafer[1]
[1]Kinesiology & Applied Physiology, University of Delaware, [2] Chemical and Biomedical Engineering, West Virginia University
Corresponding author's email: mihyj@udel.edu

Introduction: Knee osteoarthritis (OA) is an irreversible degenerative joint disease and one of the leading causes of musculoskeletal pain in older adults [1]. Pain affects gait and, because of the effect of gait on joint loading, responses to pain may affect knee OA progression [2]. The foundational understanding of the effect of pain on gait mechanics was established in controlled lab settings that do not replicate daily life. Lab-based measurements represent a small percentage of daily strides and may not account for the inter and intraday fluctuations in pain and function in individuals with knee OA. Additionally, lab-based measurements are inherently less variable than real-world gait mechanics. To better understand how gait mechanics change in response to pain in real-world settings we must understand: 1) the variability in gait mechanics in real-world settings throughout and between days and 2) how that variability changes in response to pain. Therefore, the purpose of this project was to determine if there is greater variability in gait mechanics within and between three days of real-world typical activities in adults with knee osteoarthritis who had within-day changes in pain compared to those who did not.

Methods: Six adults with knee osteoarthritis (3 with changes in pain: 65±3 years; 3 with no changes in pain: 64±2 years) wore three inertial measurement units (IMUs) for three days as they went about their typical daily activity. IMUs were placed on the lateral thigh, lateral shank, and dorsum of the foot of their symptomatic limb. Walking bouts were identified as ranges of walking of greater than five consecutive strides and an inter-stride time less than five seconds. Raw IMU data were oriented to segment functional axes based on the primary axis of rotation during each identified walking bout [3]. A zero-velocity update algorithm was used to calculate drift-corrected foot trajectory. Gait events were identified using a continuous wavelet transform and these gait events were used to integrate segment angular velocity data to obtain stride-by stride joint ranges of motion [4]. Pain was collected via text messages delivered to participants 5 times each day. Text messages asked what participant's current pain level was in their legs from 0-10 with 0 being no pain and 10 being the worst imaginable pain.

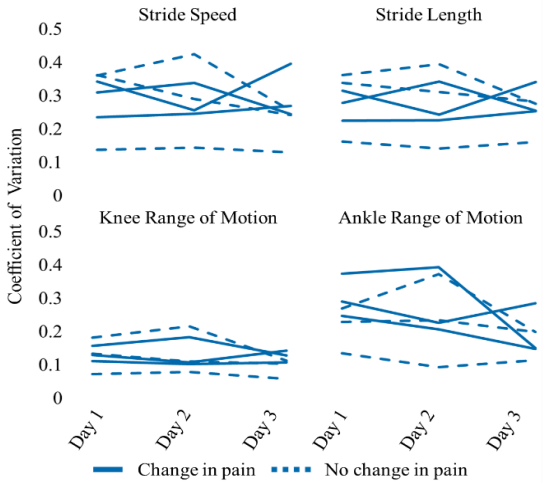

Figure 1. Coefficient of variance for stride speed, stride length, and knee and ankle range of motion calculated for 3 days of typical daily activity. Solid lines represent individuals who had a change in pain throughout the day and dashed represent those who did not.

Outcome variables of interest were the variability in stride speed, stride length, and knee and ankle ranges of motion (ROM) during steady state strides. Stride length during walking was calculated as the net horizontal displacement between consecutive heel strikes. Stride speed was calculated as the stride length divided by the time between heel strikes. Knee and ankle ROM were defined as the peak joint excursion minus the minimum joint excursion over the entire gait cycle.

Coefficients of variation for stride length, stride speed, and joint ranges of motion were calculated for all strides within each day. Variables of interest were compared between groups (change in pain vs. no change in pain) and days (day 1 vs. 2 vs. 3) using a 2-way repeated measures ANOVA (α=0.05).

Results and Discussion: Coefficients of variation for all variables of interest were not significantly different between groups (all $p>0.05$) or between days (all $p>0.05$) (Fig. 1). Participants reported pain levels between 0-4 with a change of 2 over three hours being the greatest change within a day. Although not significant, the individual with the highest reported pain across the three days had the lowest coefficient of variance for the change in pain group. Additionally, the only individual in the no change in pain group that reported pain had the lowest coefficient of variance. These findings demonstrate that variation in gait mechanics may be independent of variation in pain in adults with knee OA.

Significance: This project provides new knowledge about the fluctuations in gait mechanics throughout and between days in adults with knee OA. These findings reveal individuals with knee OA may compensate for fluctuations in pain via changes in stride speed or length and not by altering knee range of motion. Understanding inter and intra-day variability in gait mechanics and identifying the variables that fluctuate most in real-world settings may better inform how gait should be assessed in controlled lab settings to improve the ecological validity of lab-based studies.

Acknowledgments: This work was supported by a grant from the National Institute on Aging (R21AG076989) from NIH.

References: [1] Kaufman et al., J Biomech, 2001; 34 907-915; [2] Mundermann et al. Arthritis Rheum. 2005 52(9):2835-2844; [3] Mihy et al., medRxiv 2022.11.29.222828; [4] Hafer et al, Journal of Biomechanics, 2020; 99 109567;

DO REAL-WORLD GAIT KINEMATICS VARY BY TIME OF DAY OR WALKING BOUT DURATION?

Mayumi Wagatsuma[1*], Julien A. Mihy[1], Spencer N. Miller[2], Stephen M. Cain[2], and Jocelyn F. Hafer[1]
[1]Kinesiology & Applied Physiology, University of Delaware, [2] Chemical and Biomedical Engineering, West Virginia University
*Corresponding author's email: mayumiw@udel.edu

Introduction: Older adults have altered gait mechanics and lower mobility compared to young adults. Our understanding of gait kinematics in older adults is primarily from data collected in single sessions of standard walking distances and durations inside the lab. However, in daily life, bouts of walking occur throughout the day and for varying durations. Time of day may influence gait because self-reported fatigue increases throughout the day in older adults [1], but a recent review found no consensus on whether the time of the day affects gait [2]. Longer walking bouts tend to produce faster walking speeds and longer stride lengths compared to shorter bouts [3]. It is important to understand the influence of time of day and bout duration on gait, which would provide insight into which factors influence mobility during daily life. The purpose of this study was to determine whether time of day or walking bout duration affects gait mechanics during daily life in older adults.

Methods: Five healthy older adults (59.4±3.0yrs) wore three inertial measurement units (IMUs) [Opal v2, APDM] on the right thigh, shank, and foot during three days of typical activity. The shank sensor's raw angular velocity signal was used to identify walking bouts. A bout was defined as at least five strides with inter-stride times of less than five seconds. We defined walking bout duration as the time between the first and last heel strikes in each bout. Gait events were identified using a continuous wavelet procedure. A zero-velocity update algorithm was used to calculate drift-corrected foot trajectories [4]. Foot trajectories and heel strike times were used to calculate stride length and walking speed. Medial-lateral axes for the thigh, shank, and foot were defined using a functional sensor-to-segment orientation method [5]. The stride-by-stride integral of angular velocity about each segment was used to calculate segment excursion, and the segment excursions of adjacent segments were subtracted to estimate joint excursion. Joint ROMs were defined as maximum minus minimum joint excursion [6]. Strides included in this analysis had height <0.19m, direction <45° relative to neighboring strides, time 0.2-3 sec, and length 0.2-3 m. Three days of data per participant were compiled for the analysis. Walking speed, stride length, and knee and ankle angular ROM were averaged within each bout. The relationships between gait and bout duration and gait and time of day were modeled with a random coefficient model (α=0.05).

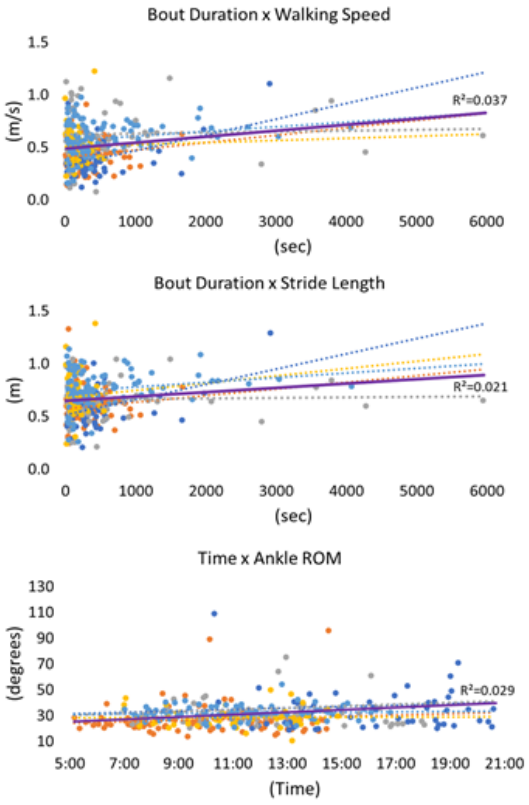

Figure 1. Scatterplots for significant relationships between gait kinematics and bout duration or time of day. Purple solid lines represent best-fit linear regression lines for the whole group. Colored dotted lines represent regressions for each participant.

Results & Discussion: The average bout duration was 440.6±672.5 s (range 3.6-5944.8 s). Walking speed (p<0.001, R^2=0.037) and stride length (p=0.007, R^2=0.021) had significant but weak positive correlations with walking bout duration, while knee and ankle ROM did not (p>0.05). On average, we captured 7.7±0.7 hours of activity per day (range 6.6-8.5 hours). Ankle ROM (p=0.001, R^2=0.029) showed a significant weak positive relationship with time of day (Figure 1). Our finding that longer walking bout durations were associated with faster walking speeds and longer stride lengths agrees with our previous study in a semi-controlled environment, where people walked faster with long bout duration compared to short bout duration [3]. Most participants showed similar weak correlations between bout duration and gait (walking speed R^2 range 0.0002-0.036, stride length R^2 range 0.001-0.031), however, one participant had a notably higher R^2 (Walking speed: R^2=0.17, stride length: R^2=0.15). In an attempt to explain these findings, we further examined their data. The participant's average bout duration (440.9±520.4 s) was in the middle range of the rest of the group (average 429.1±450.4 s, range 160.1-677.4 s). The cause of their higher R^2 is still unknown. Our ability to detect relationships between time of day and gait may have been limited by IMU battery life. We captured 6.6-8.5 hours of data per day, on average, but this may not have been sufficient to see how gait patterns change from morning to evening, especially if fatigue increases substantially towards the end of the day.

Significance: Bout duration appeared to have a larger influence on gait mechanics than time of day. Our findings suggest a need to consider behavioral factors such as bout duration and time of day when analyzing real-world gait data.

Acknowledgments: This work was supported by a grant from the National Institute on Aging (R21AG076989) from NIH.

References: [1] Murphy et al. (2008) *Arthritis Rheum* 59 (6); [2] Halpern et al. (2022), *Gait Posture* 92 153-166; [3] Wagatsuma et al. (2023), *ISB*; [4] Rebula et al. (2013) *Gait Posture* 38 974-980; [5] Mihy et al. (2022), *medRxiv* 11.29.22282894; [6] Hafer et al, *J Biomech*, 2020; 99 109567.

EFFECTS OF SIMULATED BODY FAT MASS DISTRIBUTION ON POSTURAL STABILITY

Jiyun Ahn[1*], Rebecca Ban[1], Caroline Simpkins[1], Feng Yang[1]
[1]Department of Kinesiology and Health, Georgia State University, Atlanta, GA, 30303, USA
e-mail: jahn12@student.gsu.edu

Introduction: Obesity is characterized by excessive body fat accumulation. Based on the distribution of body adipose tissue, obesity can be classified into two main categories: android and gynoid. In android obesity, the body fat is mainly accumulated around the abdomen region while the extra body fat is concentrated in the thigh and hip areas for gynoid obesity [1]. Extensive efforts have been dedicated to examining how these two obesity phenotypes affect the human body differently from the physiological and metabolic perspectives. However, limited studies inspected how obesity types affect the body biomechanically. The android fat moves the body's center of mass (COM) to a higher position compared to gynoid fat. According to the physics law, a higher COM would biomechanically make the human body less stable [2]. Our recent study indicated that a simulated body fat mass could alter the fall risk after an unexpected standing-slip on a treadmill [3]. In detail, a simulated android fat mass is associated with a greater fall risk than the simulated gynoid fat mass after a slip in young adults. However, it remains unknown if the fat mass distribution also affects postural stability during quiet standing. The purpose of this study was to assess the impact of the simulated fat mass distribution on postural stability during standing among young adults. Two fat mass distributions (android and gynoid) were simulated by applying external weights on different body sites in healthy lean adults to avoid potential physiological, neurological, and metabolic interferences by actual obesity. It was hypothesized that people with simulated android obesity would display greater postural instability during standing than those with simulated gynoid obesity.

Methods: Twenty healthy and lean young adults (6 males/14 females, age: 23.8 ± 5.22 years, height: 1.69 ± 0.08 m, mass: 63.70 ± 8.91 kg, body mass index: 22.28 ± 2.09 kg/m^2) were evenly randomized into two groups: android (Group A) and gynoid (Group G). To simulate android obesity, weight belts with the desired load were attached over the frontal and lateral abdomen. Gynoid obesity was simulated by placing weight belts around the upper thighs. Both obesity simulations targeted a body mass index of 32 kg/m^2 [4]. After undergoing warm-up and familiarization sessions, participants walked onto two side-by-side force plates (AMTI, one leg per force plate) and performed standing balance tests under two different conditions: eyes open (EO) and eyes closed (EC). During the standing, participants were instructed to stand "as still as possible" with their hands resting on their abdomen. Each condition lasted 30 seconds. The ground reaction force data collected from the force plates were used to calculate the time trace of the center of pressure (COP). The outcome measures included the COP excursion and mean speed in the anteroposterior (AP) direction. The COP excursion was the difference between the maximum and minimum values of the COP trace in the AP direction. The COP mean speed was calculated as the average value of the instantaneous COP speed across the entire trial. Independent *t*-tests were used to compare both variables between groups (A vs. G) under the two conditions (EO and EC). To quantify the magnitude of the between-group differences, Cohen's *d* was calculated as the effect size. SPSS 29.0 (IBM) was used for statistical analyses with a significance level of 0.05.

Results & Discussion: The results supported our hypothesis. The demographic and anthropometric information was comparable between groups ($p > 0.118$ for all). Group A showed a significantly greater COP excursion ($p = 0.025$, Fig. 1a) and faster COP speed ($p = 0.004$, Fig. 1b) in the AP direction compared to Group G in the EO condition. During standing with EC, significant group differences were also found in the COP excursion and speed in the AP direction, where Group A displayed a greater COP excursion ($p = 0.024$ Fig. 1c) and faster speed ($p < 0.001$, Fig. 1d) than Group G. The findings suggested that simulated android obesity could impair the body's postural stability in the AP direction more than simulated gynoid obesity during standing. Given that the weight was applied on the front of the upper body in Group A, the extra load might produce a greater forward momentum of the body on the sagittal plane, making the stability control more challenging for individuals in Group A than Group G. In addition, the applied weight in Group A relocated the COM to a higher and more anterior position than Group G. This superiorly and anteriorly shifted COM is related to higher postural instability and fall risk [2], as evidenced by the greater and faster COP in the AP direction. In sum, simulated android obesity could disturb the body's balance and increase the risk of falls more than simulated gynoid obesity. More studies involving adults with android and gynoid obesity are needed to further investigate the effects of fat mass distribution on balance control.

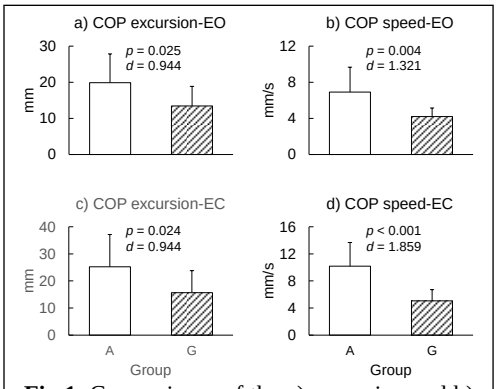

Fig 1. Comparisons of the a) excursion and b) mean speed of the center of pressure (COP) in the anteroposterior (AP) direction during standing with eyes open (EO), and the COP c) excursion and d) mean speed in the AP direction during standing with eyes closed (EC) between Groups A (android) and G (gynoid). Cohen's *d* is provided.

Significance: This study could advance our understanding of the influence of fat mass distribution on postural stability during standing. Considering that healthy and lean adults were recruited, the findings of this study would provide meaningful observation on how different fat mass distributions biomechanically alter the body's balance without obesity-related physiological, metabolic, and neurological influences. This study could suggest fat mass distribution as an additional fall risk factor for fall risk screening.

References: [1] World Health Organization. (2000); [2] Almeida., C. W. (2011), *Gait Posture* 32(2); [3] Ahn, J. (2024), *J Biomech* 164(111962); [4] Wang, L. Y. & Cerny, F. J. (2004), *Med Sci Sports Exerc* 36(5).

IN-SOCKET PRESSURE CHARACTERISTICS FOR POWERED TRANSTIBIAL PROSTHESES

A.B. Jigida[1*], M.M. Dickens[1], J. Denune[2], S.C. Gnyawali[3], P.M. Wensing[1], S. Roy[3], & J.P. Schmiedeler[1]
[1]University of Notre Dame, [2]NuTech Institute, & [3] McGowan Institute for Regenerative Medicine, University of Pittsburgh
*Corresponding author's email: ajigida2@nd.edu

Introduction: Socket fit is crucial for individuals who use lower limb prostheses [1] because poor fit can elevate pressure, causing sores and abrasions [2]. Active and powered transtibial prostheses, such as the microprocessor-controlled PROPRIO FOOT® by Ossur (Proprio) and powered Empower ankle by Ottobock (Empower), provide controlled plantar/dorsiflexion during swing/late stance, respectively, and are known to improve mobility compared to alternative ankle-foot mechanisms [3]. While previous literature has examined in-socket pressure at various locations on the residual limb when using Proprio [4], the authors know of no study either measuring in-socket pressure when using Empower or comparing in-socket pressure across devices for the same subjects using Proprio, Empower, and a passive prosthesis. This study seeks to quantify the effects of these prosthetic devices on in-socket pressure.

Methods: Six subjects with unilateral transtibial amputation, all K3 level or higher ambulators utilizing passive standard-of-care (SOC) prostheses, participated in this study approved by Indiana University (IRB#12143). At each of 3 visits, each separated by at least 4 weeks, the residual limb was 3D scanned, and thin, flexible pressure sensors (Tekscan F-Socket System, 80 Hz) were wrapped around the residual limb before the subjects donned their SOC socket (Fig. 1). Wearing an IMU-based motion capture suit (XSENS MVN Awinda, 80 Hz), subjects first completed 6 repetitions of level-ground, stair ascent/descent, and ramp ascent/descent walking tasks with their passive SOC prosthesis during Visit A. A prosthetist then fit and aligned either Proprio or Empower (order randomized) to the SOC socket, provided 30 minutes of acclimation, and recorded data for 6 repetitions of each of the walking tasks. With the pressure sensors removed, subjects left with the new-to-them Proprio/Empower for exclusive use for at least 4 weeks, returned for Visit B, repeated the instrumented walking tasks with same device, and then were fit with the other device. After 30 minutes of acclimation, 6 repetitions of each of the walking tasks, and removal of the pressure sensors, the subjects left to exclusively use the second new-to-them device for at least 4 weeks. At Visit C, the instrumented walking tasks were repeated with the second device, the prosthetist refit the SOC prosthesis, provided 30 minutes of re-acclimation, and recorded data for 6 more repetitions of each walking task. Pressure data were normalized by body weight and analyzed in 4x4 cell groupings to identify peak pressure and pressure-time integral (PTI) within eight residual limb areas (Fig. 1(a)): Anterior-Proximal (AP), Anterior-Medial (A/M), Medial-Anterior (M/A), Medial-Distal (MD), Lateral-Proximal (LP), Lateral-Posterior (L/P), Posterior-Lateral (P/L) and Posterior-Distal (PD). Two-way ANOVAs quantified the effects of prosthesis and visit on each subject's peak socket pressures and PTIs.

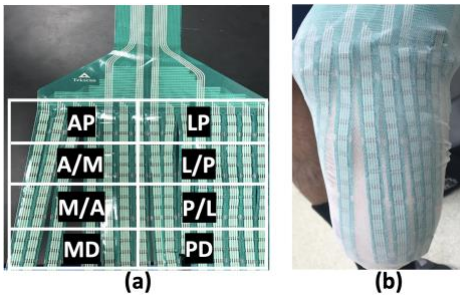

Fig 1: Tekscan F-Socket pressure sensor locations (a) before and (b) after installation on residual limb.

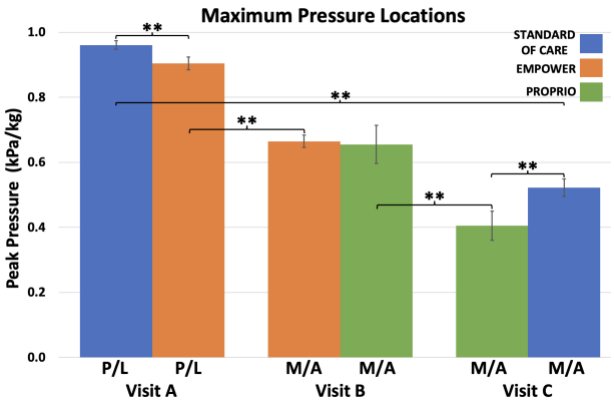

*Fig. 2: Locations of maximum peak pressures for all prosthesis-visit combinations. (** indicates $p<0.01$)*

Results & Discussion: Representative results from a single subject's level-ground walking are reported here. ANOVA results indicated that device and visit had significant main effects across almost all sensor locations. 3D scan analysis indicated no significant change in limb volume across visits (0.0024 m^3, 0.0024 m^3, and 0.0023 m^3), so differences in pressure should not be attributed to differences in limb volume. **Figure 2** shows that the maximum peak pressure occurred at the P/L sensor location for both devices during Visit A, but the location shifted to M/A during Visits B and C and was again the same across devices. These peaks occurred at approximately 40% of the gait cycle, which is mid-to-late single support on the prosthetic side. Socket pressure was higher with both SOC and Empower than with Proprio. Pressure decreases were observed across successive visit days with both Empower and Proprio, showing that the acclimation period was important for both devices. Note that the peaks from follow-up testing with Empower and initial testing with Proprio at Visit B were not significantly different. Results for PTI were similar to those for peak pressure. While recorded maximum peak pressures and PTI were marginally lower than reported in a prior study [4], that work grouped subjects together, while this work examines subjects individually. Results indicate that device, time, and their interactions significantly influence pressure distribution on the residual limb.

Significance: The study's findings suggest that microprocessor-controlled prostheses like Proprio and powered prostheses like Empower do not necessarily cause increased in-socket pressure compared to passive devices, and acclimation periods longer than 30 minutes, such as up to 4 weeks, are required to achieve the reduction in in-socket pressure associated with greater familiarity with a new transtibial prosthesis. Moreover, these results could inform the design of prosthetic sockets to account for the regions with peak pressure on the residual limb to mitigate risk of sores and abrasions that can be linked to prosthesis abandonment.

References: [1] M. W. Legro et al. (1999) *J Rehabil Res Dev* 36(3):155-63; [2] M. J. Highsmith et al. (2016) *Technol Innov* 18(2-3): 115–23; [3] S. R.Wurdeman et al. (2019) *J Rehabil Ass Tech Eng.*;[4] S. I. Wolf et al. (2009) *Clin Biomech* 24(10):860–65.

MODELING ANKLE EXOSKELETON USER COMFORT: GAUSSIAN PROCESS REGRESSION WITH VS. WITHOUT PHYSIOLOGICAL SIGNALS

Axl Maberry[1*], Bo Cheng[1], Anne E. Martin[1]
[1]Mechanical Engineering, Penn State, University Park, PA, USA
*Corresponding author's email: akm6700@psu.edu

Introduction: While comfort is an important factor for exoskeletons, it is largely subjective and not easily quantified [1]. It is known that biomechanical and metabolic factors are correlated both with each other and comfort [2]. However, it is unknown the relative importance of exoskeleton control parameters vs. physiological signals for predicting user comfort. A model would allow for a user's comfort to be predicted and used in exoskeleton controller optimization without needing feedback from the subject [3]. Gaussian process regression (GPR) is a model that estimates the underlying nonlinear mapping, updates with additional data, and can be used with a relatively small number of data points [4], making it appropriate for exoskeleton studies. This abstract tests the hypothesis that the accuracy of a GPR model of self-reported user comfort can be improved by the inclusion of physiological signals.

Methods: 13 young adult subjects walked at a slow speed on a treadmill while wearing a pneumatically powered ankle exoskeleton on each leg [5]. A motion capture system and indirect calorimetry mask were used to collect physiological data from the subjects. 10 sets of exoskeleton parameters were tested twice each for a total of 20 trials. Each trial lasted 3 minutes, enough time to predict steady-state metabolic cost [6]. After each trial, the subjects electronically reported their comfort via a modified 100mm visual analog scale [7].

The recorded signals were processed into 39 features by splitting the data into steps and finding the mean and standard deviations of the relevant value over all steps in a trial. The features were steady-state metabolic cost amplitude (1), spatiotemporal factors (6), joint angle extrema (14), and maximum absolute angular velocities (6), moments (6), and powers (6). Using all of a subject's trials, the features, exoskeleton parameters, and self-reported comfort scores were normalized from 0-1. The dimensionality of the features was reduced via PCA and the first *n* principle components that explained 95% of the variance in the data were used.

Two GPR models were created for each subject; Model 1 was trained with just the exoskeleton control parameters and Model 2 included the reduced physiological features as well. Due to the small size of the data, Leave-One-Out Cross-Validation was used. The models were sampled 50 times to create a distribution of predictions for each sample point. Using this distribution, the percentage of trials whose reported comfort was captured within 3 standard deviations was calculated. The errors between the mean model prediction and the reported comfort were used to calculate a root mean squared error (RMSE). Additionally, the Akaike information criterion (AIC) was calculated for each model to show how well each model was able to balance accuracy and complexity where lower values are better.

Results & Discussion: Subject-specific models were created due to the large variance between subjects in their reported comfort for the same control parameters. Qualitatively, Model 1 tends to have a narrower distribution but its mean value does not vary much across the trials (Fig. 1). Therefore, it is not as likely to capture the reported comfort value in its distribution. On the other hand, the mean sample values of Model 2 tend to shift with the reported comfort and more often than not captures the reported comfort within its sample distribution. Quantitatively, Model 1 captured 73.54 ± 9.23% of the reported values and Model 2 captured 95.14 ± 5.84%. This indicates that the inclusion of physiological signals did substantially improve the accuracy of the model. Model 1 had an RMSE of 0.2744 ± 0.0694 and Model 2 had a slightly better RMSE of 0.2660 ± 0.0584. Model 1 had an AIC of -11.7458 ± 3.9121 and Model 2 had an AIC of 9.4993 ± 3.0483. Given the similar RMSE values and the increased number of inputs for Model 2, this was expected.

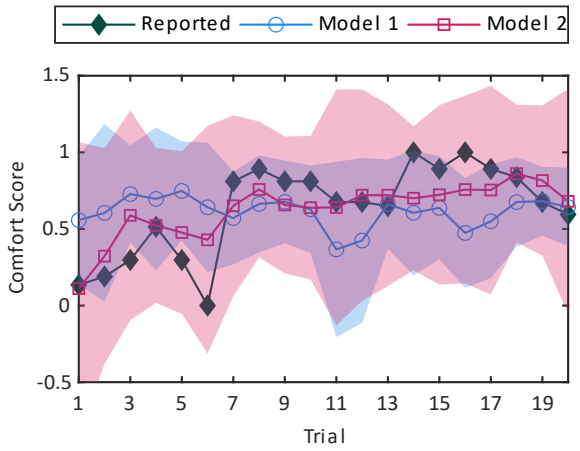

Figure 1: Reported comfort, model mean and 3 standard deviations for a representative subject. Model 1, without physiological signals, tends to center on the mean reported comfort. Model 2, with physiological signals, changes with the reported comfort and consistently captures the reported comfort. in its distribution.

Significance: Exoskeletons can enhance user ability or help in rehabilitation although they will likely need to be comfortable. While the user's physiological state likely affects their comfort, the strength of the correlation is unknown. Our results indicate that physiological signals improve the prediction of comfort. However, in the context of human in the loop experiments, collection of physiological signals greatly increases experimental complexity. Given that our results also indicate that a model without physiological signals may be preferred, experimental studies looking to optimize user comfort may be better off excluding these signals. Future researchers can assess their need for model accuracy vs. experimental complexity to determine which model type best suits their application.

Acknowledgments: This work was supported by NSF awards 1943561 and 1930430.

References: [1] Mündermann et al. (2002), *Gait Posture* 16; [2] Mündermann et al. (2003), *Med Sci Sports Exerc*, 35(10); [3] Cao et al. (2018), *IEEE-RAS Humanoids*; [4] Frigola et al. (2014), *Adv Neur In* 27; [5] Mohammed et al. (2023), *Sci Rep* 13(1); [6] Selinger & Donelan, (2014), *J Appl Physiol* 117(11); [7] Sung & Wu (2018), *Behav Res Methods* 50(4).

PREDICTING GROUND REACTION FORCES FROM FROUDE NUMBER IN GROWING FOALS

Melany D. Opolz[1*], Sara G. Moshage[2,6], Annette M. McCoy[3], Mariana E. Kersh[2,4,5]
[1]Department of Chemical and Biomolecular Engineering, [2]Department of Mechanical Science and Engineering, [3]Department of Veterinary Clinical Medicine, [4]Carle Illinois College of Medicine, [5]Beckman Institute for Advanced Science and Technology, University of Illinois Urbana-Champaign, Urbana, IL; [6]Exponent, Inc, Philadelphia, PA
*Email: mopolz2@illinois.edu

Introduction: The horse is an ideal model system for understanding the biomechanics of exercise during post-natal (ontogenetic) growth because they reach skeletal maturity within a few years of age and are naturally engaged in physical activity. To that end, ground reaction forces (GRFs) are crucial for estimating joint kinetics but the use of force plates in natural ground conditions remains impr actical. Moreover, ontogenetic studies of gait require normalization for size, age, and speed. To our knowledge, most equine research has focused on adult horses [1, 2] with less data available on GRF patterns in foals [3]. Therefore, the aims of this study were to (1) analyse GRFs in growing foals ranging from 2 to 14 months of age in relation to foal size, gait type, and speed and (2) develop an analytical model for predicting GRF data in foals for future use in equine biomechanical analysis.

Methods: GRF, motion capture, and subject mass data during walking and trotting gaits were collected longitudinally from foals (n=3, age: 2-14 months). The vertical (z) and anterior-posterior (y) GRFs were filtered and normalized to body mass (MATLAB, vR2021a). Gait velocity (v) and foal forelimb length (l) were obtained from motion capture videos (Qualisys). For each trial, the Froude number (Fr), which accounts for size differences between foals, was calculated as $Fr = v^2/g*l$ (g=9.81 m/s^2). Changes in Fr with respect to age and gait was analysed (R, v4.3.1). We evaluated two analytical models for predicting GRF data using R: a non-linear logistic regression ($y=a/[1+b*exp(-c*x)]$ [4]) and a linear regression ($y=m*x+b$).

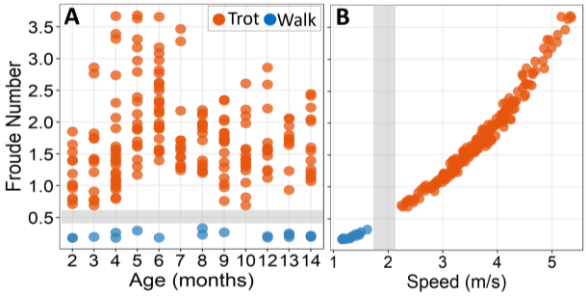

Figure 1: (A) Distribution of Fr related to age in months. (B) Relation between Fr and speed in meters/second.

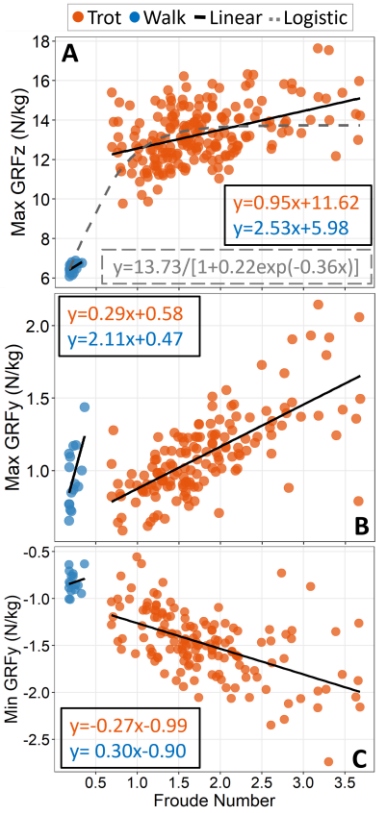

Figure 2: (A) Logistic regression describing overall max GRF_z and Fr relation. (A, B, C) Linear regressions used to predict this relation by gait.

Results & Discussion: The walk-trot transition was centered around a Fr = 0.5 and was consistent for all ages evaluated (Fig. 1A) and corresponds to a velocity range of 1.75-2.15 m/s (Fig. 1B). Therefore, Fr and thus implied, speed, in which the walk-trot transition occurs is independent of age. Interestingly, the gait transition in foals occurs at a similar Fr as adult horses (0.35 [2]) suggesting that the gait transition is also independent of developmental stage.

The maximum GRF_z during trot was nearly twice (13.29 ± 1.43 N/kg) that of walking (6.53 ± 0.22 N/kg), which correlated to increased Fr and thus, velocity. The maximum and minimum GRF_y represent the propulsion and braking forces, respectively. At walk, the maximum absolute propulsive and braking forces were 14.40% and 12.71% of the vertical force peak value, respectively, while at the trot, they were 8.35% and 11.14%.

The linear regression-based prediction of GRF_z from Fr was more accurate (avg. abs. % error for trot: 7.97%, walk: 2.39%) than the logistic expression (avg. abs. % error for trot: 39.88%, walk: 3.91%) (Fig. 2A) and we therefore used the linear regressions for all GRF predictions (Figs. 2A,B,C). Errors could be attributed to within subject variation or gait variation which could influence our calculation of gait speed and therefore Fr.

The maximum GRF_z increased at a higher rate during walking (2.53 N/kg/Fr) than trot (0.95 N/kg/Fr) (Fig. 2A). Propulsion forces increased at a higher rate with increasing Fr during walk (2.11 N/kg/Fr) compared to trot (0.29 N/kg/Fr) (Fig. 2B). Interestingly, braking forces decreased with walking (0.30 N/kg/Fr) but increased with trotting (-0.27 N/kg/Fr) (Fig. 2C).

Significance: To our knowledge, this is the first study to develop a predictive model of GRFs in foals that includes a comprehensive assessment of foals younger than 12 months of age. Unlike other mammals, horses begin standing and walking within hours of birth and it may be that their musculoskeletal system is genetically primed to transition from walking-trotting without requiring an adaptation period to locomotion.

Our development of an analytical model for predicting GRFs based on limb length and velocity now enables GRF predictions in real world settings. This data can be paired with in-field markerless motion capture or treadmill exercise to calculate internal joint moments and muscle forces. The capacity to collect such data will enable further studies of natural locomotion in horses with implications for studies of exercise and other musculoskeletal diseases.

Acknowledgments: Griffin Sipes and Kellie Halloran assisted with data collection and software implementation.

References: [1] Merkens+(1986), *Equine Vet J* 18(3); [2] Griffin+(2004), *J Exp Bio* 207(24); [3] Gorissen+(2017), *Equine Vet J* 49(4); [4] Valette+(2008), *Animal* 2(4).

DATA-DRIVEN APPRAOCH TO PREDICT PHYSICAL PERFORMANCE: APPLICATIONS IN MILITARY MARCHING TASKS

Darius Sattari[1*], Rebecca Zifchock[1], J. Josiah Steckenrider[1], Seth Elkin-Frankston[2,3], Wade Elmore[2], Victoria G. Bode[2]
[1]United States Military Academy, West Point, [2]US Army DEVCOM Soldier Center, [3] Tufts University of Engineering, Center for Applied Brain and Cognitive Sciences
*Corresponding author's email: sattaridarius@gmail.com

Introduction: The emerging applications of Artificial Intelligence and Machine Learning technologies in the civilian and military sectors are topics gaining rapid attraction in terms of performance optimization. A loaded foot march is one of the most critical tactical tasks in the military, and while the Army Combat Fitness Test (ACFT) is assessed at least twice per year to gauge physical combat readiness, it does not include a loaded foot march. Thus, this study presents a novel methodology to predict a soldier's loaded foot march performance based on their ACFT scores. While the methods in this abstract are applied specifically to the ACFT and a loaded foot march, the framework presents an opportunity to make any testing in a stable environment predictive of performance in an unknown, unstable, or tactical environment.

Methods: 143 male U.S. Army Infantry soldiers consented to participate in the Army's Measuring and Advancing Soldier Tactical Readiness and Effectiveness (MASTR-E) 72-Hour Field study in 2021 and 2022. These soldiers participated in an 8.25-mile ruck march as the start of a 72-hour training exercise. Baseline ACFT data were also recorded on these soldiers within 90 days. Written informed consent was collected from all subjects. The pool of participants was then split into 80% training and 20% validation data sets.

Soldier physical exertion levels were characterized by seven biometrics: training impulse, heart rate variability (HRV) (Polar Team Pro), leg strength, Rating of Perceived Exertion (RPE), testosterone levels, stride width, and stride length [1,2,3,4,5,6]. The percent change in these metrics from the beginning to the end of the ruck march is assumed to determine characterize their physical exertion. As depicted in Figure 1, the percent change in these biometrics are inputted into a Cumulative Distribution Function (CDF) to rank performance among all soldier participants. The CDF yields a performance score ranging from 0 to 1 for each biometric. As these performance scores quantified loaded foot march performance, they acted as the trained output to predictive Neural Network algorithms where an individual's baseline ACFT scores, as well as the ratio of their body weight to load they carried during the ruck march were inputted as training inputs. As a result, 7 distinct Neural Networks (NN) were created, called *sub-models* in Figure 1, to predict the performance score for each biometric. To evaluate the accuracy of these models on the testing data, root mean squared error (RMSE) was calculated for each NN. Further, a total RMSE is calculated by calculating the average the RMSEs of each model.

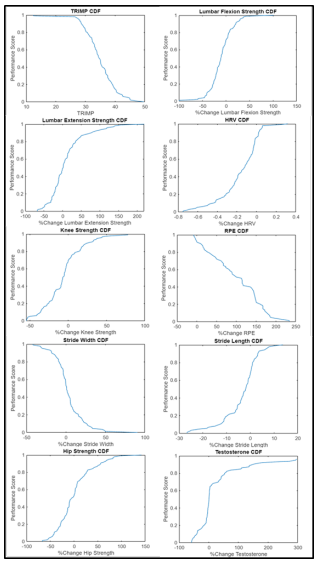

Figure 1: Cumulative Distribution Function Scoring of Training Group

While all Machine Learning modeling techniques leveraged NN, advanced methods in extracting features and interpolation were explored. Features were extracted from ACFT data creating score buckets for Upper Body, Lower Body, Cardio, Power, and Endurance based events. Interpolation increased the sample size by a factor of six where all training inputs and outputs were interpolated linearly. Further, each modeling technique (NN, NN w/Extracted Features, NN w/Interpolation) were all compared to the performance of a standard linear regression model to justify the use of a computationally powerful modeling technique. All models were generated from the 80% training set and compared against the 20% validation set.

Results & Discussion: The RMSEs generated when applying the NN to the testing dataset all yielded high levels of error yet indicate that the base NN performed more accurately than Linear Regression and the two advanced ANN techniques, showing higher-level analysis is necessary to describe such a complex relationship between variables. Across all the models, training impulse and hip extension strength had consistently low errors when the models were evaluated on the testing set. This is likely because these performance biometrics are most directly related to ACFT events. Training impulse is based upon an individual's cardiovascular strength, while the ACFT is heavily weighted towards endurance fitness, primarily exemplified by the 2 Mile Run. Further, hip extension strength is most significantly prevalent in performing the 3 Repetition Maximum Deadlift. Meanwhile HRV and lumbar extension/flexion strength performed least accurately across the different modelling techniques, on average. Lumbar-based metrics may not necessarily be a strong predictor of performance on a ruck march, nor would it correlate strongly to ACFT events, both of which are aerobic and lower-body centric tasks. Also, it is possible that there was significant noise in HRV data as the soldiers were not provided a dedicated recovery time before collecting HRV values.

Significance: The proposed models are not currently useful for predicting readiness following a ruck march, however this study has proposed a framework for using machine learning strategies to utilize available biometric data to measure soldier performance on longer, operational tasks based on examining exertion levels and relating them to performance on baseline tasks.

References: [1] De Meersman, *Am. Heart J*, 1993. [2] Daanen et. al, *Int. J. Sports*, 2012 [3] Martin et. al, *J. Sports Med. Phys. Fitness*, 1997. [4] Aguilar et. al, *Physiol. Behav.*, 2013. [5] Gatti, *Scand J. Med. Sci. Sports*, 2011. [6] Bloch et. al, *Mil. Med.,* 2023.

PRESS-FIT TIBIAL TRAY MICROMOTION IS SIMILAR DURING LOADING IN HIGH FLEXION BETWEEN MANUAL AND ROBOTIC-ASSISTED TOTAL KNEE ARTHROPLASTY

Ana V. Figueroa[1*], Ayobami Ogunsola[1,2], Michael Marinier[1], Marc Brouillette[1], Jessica Goetz[1], Jacob Elkins[1]
[1]University of Iowa, Iowa City, IA, [2]Wake Forest University, Winston-Salem, NC
*anavictoria-figueroa@uiowa.edu

Introduction: Robot assisted TKAs (rTKA) are becoming more prevalent when compared to manual TKAs (mTKA) [1]. Most studies comparing the two focus on revision rates [2], implant positioning [3], and patient satisfaction [4]. However, another key factor in the success of a TKA is overall stability of the tibial implant, and initial implant stability is perhaps even more critical in the setting of modern press-fit components. The objective of this study was to determine differences in the motion of the posterior edge of the press-fit tibial component relative to the tibia when the surgery was performed with and without the use of a surgical robot.

Methods: 10 fresh-frozen lower-body (pelvis to toe-tips) cadaveric specimens were implanted with Attune press-fit Cruciate Retaining Knee Systems (DePuy Synthes, Warsaw, IN). One side of each specimen was randomized to undergo a mTKA with a traditional gap-balancing technique, and the contralateral underwent rTKA with a VELYs Robotic-Assisted Solution (DePuy Synthes, Warsaw, IN). All implanted tibias were harvested, soft tissues and the fibula were removed, and the bones embedded in polymethylmethacrylate bone cement for mechanical testing. A custom Delrin® insert was manufactured, which permitted loading scenarios on the tibial tray similar to those seen during weight-bearing deep flexion. The custom insert was loaded with a ball-end, two-pronged, simulated femoral component mounted on an MTS actuator (MTS Inc. Eden Prairie, MN). Specimens were axially loaded with 250 N to seat the implants into the tibia, replicating initial post-operative, protected weightbearing standing. Specimens were then rotated to a 60° angle from vertical and cyclically loaded for 10 cycles from 10 N to 600 N to represent stair climbing. Displacement of the posterior edge of the implant relative to the tibia was measured using a digital image correlation system (ARAMIS, GOM, Braunschweig, Germany) and expressed in a local coordinate system orthogonal to the plane of the proximal surface of the tibial component (Figure 1). Average displacement within each loading cycle and maximum displacement of the implant under load were calculated independently for the medial and lateral sides of the implant. Within-cycle displacement differences were compared using Students' t-tests, and repeated-measures (medial/lateral), two-way ANOVA with Fisher's LSD pairwise comparisons were used to determine the statistical significance of differences in maximum displacement during cyclic testing ($p<0.05$).

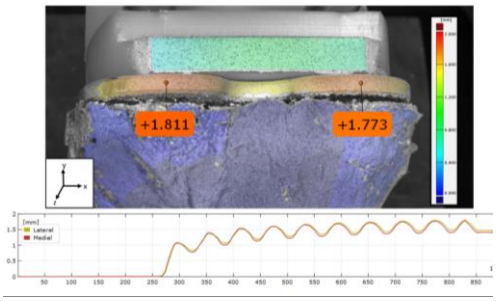

Figure 1. Digital image correlation analysis was conducted for each specimen to track the displacement (mm) of the posterior-most edge of the tibial implant relative to the tibia which was set to be a rigid reference frame (blue). Implant displacements are shown in both heat map and graph form.

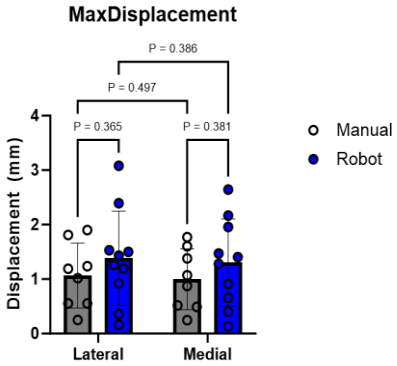

Figure 2. Maximum displacement of the posterior tibial implant edge relative to the tibia.

Results & Discussion: Data from n=2 mTKA specimens was not available due to a software failure during data capture (n=1) and to a tibia fracture during testing (n=1). Within-cycle (between 10 N and 600 N) implant displacement for rTKAs averaged 0.32 ± 0.18 mm, and mTKAs had an average of 0.20 ± 0.11 mm of displacement, which was significantly different ($p = 0.018$), but of a negligible magnitude. Maximum displacement on the lateral side of the implant averaged 1.07 ± 0.60 mm for mTKA and 1.38 ± 0.86 mm for rTKA. Similarly, maximum implant displacement on the medial side averaged 1.00 ± 0.56 mm for mTKA and 1.30 ± 0.80 mm for rTKA. There were no significant differences between surgery types nor laterality (Figure 2): between lateral manual and robot ($p = 0.365$), between medial robot and manual ($p = 0.381$), manual surgery type between laterality ($p = 0.497$) and robotic surgery type between laterality ($p = 0.386$). This study determined that there was no significant difference in press-fit tibial implant motion between rTKAs and mTKAs when loaded in high flexion. The wide variation in implant displacement for both rTKA and mTKA and could be the result of large variation in bone density among cadaveric specimens. Slight variation in displacement between the medial and lateral sides of the implant may be the result of the orientation of the tibial implant relative to the digital image correlation cameras, as well as slight overhang of the implant relative to the posterolateral tibial cortex.

Significance: Both manual and robotic-assisted press-fit TKAs performed similarly regarding tibial implant motion during the extreme weight-bearing conditions of deep flexion loading. The degree of tibial tray unsupported by cortical bone should be minimized to reduce incidence of early implant motion and possible loosening.

Acknowledgments: The authors would like to acknowledge DePuy Synthes and the Roy and Linda Crowninshield Fund for Biomechanics Research for supporting this work.

References: [1] Siebert, W., et al. *The Knee.* 2002. [2] Sione AO., et al., *Arthroplasty Today*, 6(4), 2020. [3] Song EK., et al., *Clin Orthop Relat Res.*, 471(1), 2013. [4] Khlopas A, et al., *J Knee Surg*, 33(07), 2020.

THE EFFECT OF MOTOR SOLUTION EXPLORATION ON THE ADAPTABILITY OF AN ACQUIRED MOTOR SKILL

Matthew Beerse[1*], Kimberly E. Bigelow[2], Joaquin A. Barrios[3]
[1]Department of Health and Sport Science, University of Dayton
[2]Department of Mechanical and Aerospace Engineering, University of Dayton
[3]Department of Physical Therapy, University of Dayton
*Corresponding author's email: mbeerse1@udayton.edu

Introduction: Motor variability is increasingly viewed as functional within the context of motor learning rather than noise that must be minimized. However, there is mixed evidence for this role where higher variability has been associated with better rates of learning [1-2], but also worse ability to adopt new motor solutions [3]. Likely, the structure of the studied motor tasks, as well as the presence and type of feedback contributed to these conflicting results. When considering the task structure, an important consideration is whether it translates to real-life contexts. One such real-life context is the learning of a complex, whole-body motor skill with access to intrinsic feedback only. In this context, our previous study demonstrated that young adults followed an exploration-exploitation pattern when learning the kettlebell swing motor skill [4]. However, it is unclear whether the acquired motor skill was adaptable and whether exploration early in learning would facilitate adaptability. Therefore, we aimed to assess the adaptability of the kettlebell swing motor skill following a week of practice by challenging subjects to perform repetitions with a kettlebell filled with water, shifting the load from static to dynamic. In addition, we sought to determine whether the maintenance of high exploration of motor solution exploration in practice predicted adaptability. Due to prior evidence of the benefits of variability on learning rate, we hypothesized that subjects with higher motor solution variability on the first day of practice would better adapt to the dynamic load evidenced by a better ability to reduce task related deviations.

Methods: Twelve young adults aged 18-25 years old (9F/3M, 20.53 ± 1.27 years) participated. Subjects practiced the kettlebell swing over seven days with data collections occurring on the first and seventh days. Between the first and seventh days, subjects practiced on three separate days by performing five sets of 20 repetitions. On the first day, subjects watched a video of a skilled performer complete the kettlebell swing while being read instructional cues. Subjects then completed three sets of 20 repetitions (*no practice*) followed by five practice sets of 20 repetitions, then finishing with three more sets of 20 repetitions (*immediate practice* condition). On the seventh day, subjects completed three sets of 20 repetitions (*short-term practice* condition) and then completed three sets of 20 repetitions with the water-filled kettlebell (*adaptation* condition). The water-filled kettlebell was filled to be the same mass as the kettlebell used during practice. Subjects received at least three minutes of rest between every set. Subjects were allowed to rewatch the video and hear the instructional cues over the course of the study (range: 3-9 views). During data collection, a full-body PSIS marker set was attached to the subject and kinematic data was captured at a sampling frequency of 150 Hz.

An uncontrolled manifold (UCM) analysis was implemented to partition segment angle solution variability (GEV) from error variability (NGEV) based on the effect on the center of mass position [5]. To quantify adaptation, we implemented a single cycle variation of the UCM analysis [6] which quantified deviations for each repetition from the reference posture (mean segment angles of the last 10 repetitions). The task related deviations for the *adaptation* condition were converted to a percentage change from the average of the last 10 repetitions of the *short-term practice* condition. Therefore, a value of zero would indicate the same amount of deviation while a positive value would indicate elevated deviation. Subjects were separated into groups based on whether their *immediate practice* GEV was greater or less than the median GEV. The average task related deviations for each group were compared qualitatively. In addition, a correlation analysis of GEV and NGEV for the *no practice* and *immediate practice* conditions were conducted.

Results & Discussion: The high motor solution variability group did not demonstrate a better ability to adapt to the water-filled kettlebell condition (Fig. 1). Contrarily, the group with lower GEV during the *immediate practice* condition appeared to be more proficient adapters. Not only did they begin the condition with less task-relevant deviations, but by the end, had corrected deviations to be lower than the average of the most recent ten repetitions with their practiced kettlebell, i.e., *short-term practice*. Similar to prior research [3], subjects with greater motor solution variability (GEV) also had greater error related variability (NGEV) during the first day of practice (r=0.867).

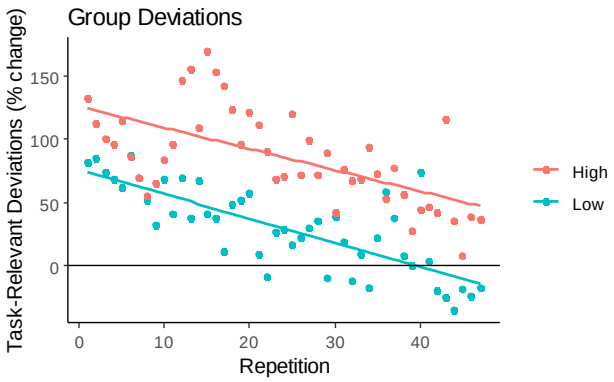

Figure 1: Average deviations during the *adaptation* condition for low and high motor solution variability groups.

Significance: Contrary to our hypothesis, our findings did not support the proposal that greater inherent motor solution variability during early practice facilitates the acquisition of a more adaptable motor skill. Our task structure, i.e., no augmented feedback and imprecise knowledge of results, required subjects to intrinsically perceive their solution variability as such, i.e., solutions, in order to operationalize them when adapting the motor skill. Likely, subjects with higher variability, regardless of type, had difficulty in making these perceptual-motor connections.

References: [1] Dhawale et al. (2019), *Current Biology* 29(21); [2] Wu et al. (2014), *Nat Neurosci* 17(2); Ranganathan et al. (2021), *Neuroscience* 479; Beerse et al. 2020, *Exp Brain Res* 238(9); Selgrade & Chang (2015), *J Neurophys* 113(5)

THE STRAIN OF SAFETY: CHARACTERIZING BIOMECHANICS OF INFANT CAR SEAT CARRYING IN MOTHERS

Kathryn L. Havens[1*], Yunsheng Zou[1], Kornelia Kulig[1]
[1]Division of Biokinesiology and Physical Therapy, University of Southern California
Corresponding author's email: khavens@usc.edu

Introduction: Every day, millions of parents across the globe rely on infant car seats as a vital safeguard for their babies during travel, shielding them from the potential dangers of vehicular accidents. Yet, in the mundane routines of mother-infant pairs, a remarkable aspect often goes unnoticed: the physical strain and awkwardness of carrying both baby and car seat during transitions. While the seamless transfer from home to vehicle may seem routine, the reality is far from effortless. The burden of lugging a cumbersome car seat, coupled with the weight of precious cargo, presents a significant challenge for mothers. Surprisingly, despite its ubiquity, little attention has been paid to the biomechanical implications of this everyday task.

Existing studies have demonstrated that other methods of infant carrying (in arms or babywearing) impact gait biomechanics, including altering ground reaction forces, trunk mechanics, and lower extremity joint loading compared to walking without a load [1-6]. Clamann et al. examined infant car seat grip and lifting strategies when placing an infant mannequin plus car seat into a simulated car [7], but comprehensive research in this area is scarce.

This study aimed to investigate the spatiotemporal, ground reaction force (GRF) and kinetic differences during gait between mothers carrying their infants in an infant car seat and carrying nothing (unloaded condition). We hypothesized that when compared to walking without a load, mothers would walk slower with shorter steps, and increased loading of the lower extremity.

Methods: Nine healthy postpartum women (34.5±2.7 years; 68.5±15.0 kg; 1.7±0.1 m) walked overground for 20 m at self-selected speed under two conditions: unloaded and carrying their own infant (6.2±0.6 kg, 16.0±3.2 weeks old) in an infant car seat (4.6±0.6 kg). Participants self-selected the car seat carrying method.

Lower extremity movements were identified using 3D marker-based motion capture (100 Hz; Vicon & Qualisys systems). GRFs were collected using force plates embedded into the lab floor (900Hz; AMTI & Bertec plates). Spatiotemporal variables were normalized to body anthropometrics [8]. Spatiotemporal variables, peak anteroposterior, mediolateral, and vertical GRF, and peak ankle, knee, and hip sagittal plane kinetics were compared using paired t-tests ($\alpha <= 0.05$; SPSS, Version 27, Chicago IL).

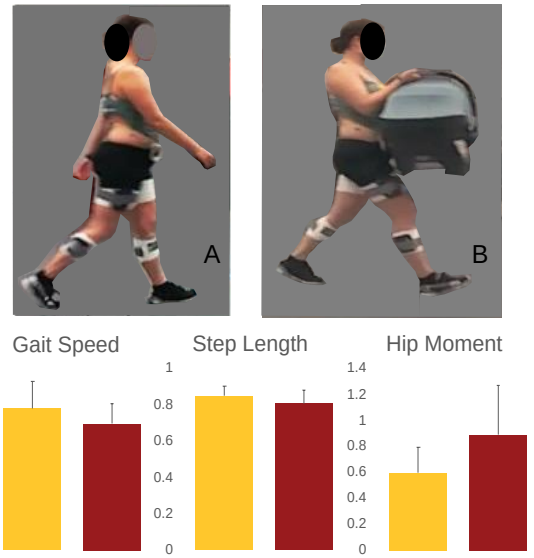

Figure 1: Top images show a mother participant (A) walking in unloaded condition, (B) carrying her baby in an infant car seat; Bottom row of plots demonstrate differences between carrying conditions with gold bars representing unloaded and red bars representing car seat condition. Compared to unloaded, individuals walked with their baby in the car seat slower (left figure, unit: m/s), with shorter step lengths (middle figure, unitless: step length/participant leg length) and greater hip extensor moment (right figure, unit: Nm/kg)

Results & Discussion: Infants in car seats represented up to 18% of participant weight, and mothers anecdotally complained about how arduous this daily task is for them. Mothers varied in the method of carrying the car seat, but most held it with one or two arms in front of the body. This appeared to constrain their upper body, trunk and pelvis motion.

When compared to the unloaded condition, mothers carried their infants in the car seat at slower speeds, with shorter step lengths and wider stride widths ($p<0.05$). Slower speed and shorter step lengths is consistent with other infant-carrying research [2,6] and military load carriage [9]. This may be related to difficulty flexing the hip with a large object in front of the body and to the limited pelvic rotation available.

Mothers also exhibited greater vertical ground reaction forces ($p<0.05$) when carrying the car seat, which increased approximately proportionally to the increased load. This makes sense mechanically and is consistent with other infant carrying research [1,5,6]. Interestingly, statistically significant differences were found in GRFs in the anteroposterior or mediolateral direction.

In the lower extremity, mothers exhibit mechanics to increase propulsion, including greater hip extensor and ankle plantarflexor moments ($p<0.05$) when carrying. Considering the spatiotemporal differences described above, these differences likely facilitated the forward progression of a larger mass rather than increasing speed or lengthening strides.

Significance: These preliminary results demonstrate interesting gait patterns, including alterations in spatiotemporal, force and lower extremity loading. By describing the biomechanics of this routine yet physically demanding task, our research aims to inform the design of safer and more ergonomic infant car seat systems, ultimately reducing the risk of musculoskeletal discomfort and injury for mothers and infants.

Acknowledgements: We thank the mothers and infants who participated in this study.

References: [1] Havens et al., *J Applied Biomech*, 2024, [2] Junqueira et al., *Gait & Posture*, 2015, [3] Schmid et al., *Gait & Posture*, 2019, [4] Williams et al., *Gait & Posture*, 2019, [5] Brown et al., *Human Factors*, 2015, [6] Havens et al., *Gait & Posture*, 2020 [7] Clamann et al., *Applied Erconomics*, 2012 [8] Hof, *Gait Posture*, 1996, [9] Birrell et al., *Ergonomics* 2009

MEASUREMENT OF GROUND REACTION FORCE VARIABLES USING LOADSOLS DURING OVERGROUND WALKING

Dylan J. Mulligan[1], Clare E. Milner[2*]
[1]School of Biomedical Engineering, Sciences, and Health Systems, Drexel University
[2]Department of Physical Therapy and Rehabilitation Sciences, Drexel University
*Corresponding author's email: milner@drexel.edu

Introduction:

Force sensing insoles can measure and record vertical ground reaction force (VGRF) data over time and transmit it wirelessly. An advantage of these insoles is that they enable collection of VGRF data in non-laboratory environments, such as outdoors.

Loadsol force sensing insoles have been validated against the gold standard of force platforms for walking on an instrumented treadmill [1]. However, their validity during overground walking has not been evaluated.

The purpose of this study was to assess the within session test-retest reliability and criterion-related validity of Loadsols for determining VGRF variables during overground walking. We hypothesized that when compared to force plates, the peak vertical ground reaction forces, loading rates, impulse, and stance time from Loadsol data would have excellent criterion-related validity and that within-session test-retest reliability would be similar to that of the force plates.

Methods:

As part of an ongoing study, 18 healthy young adults were recruited to participate (10F, 8M; age 22.1 (1.9) y; height 1.67 (0.07) m; weight 65.6 (7.3) kg). All participants provided written informed consent. Participants completed two blocks of five overground walking trials at a self-selected pace. Trials with right foot contact on force plates were included. VGRF data were collected using both force plates (1000 Hz) and the Loadsols (100Hz.)

Impact and active peak, and average and instantaneous loading rates from 20-80% of time to impact peak [2] were calculated. Impulse was the trapezoidal integration of force over stance. Stance time was foot contact to toe off. A VGRF threshold of 20N identified foot contact and toe off. Variables were averaged over five steps per block for each participant and group means and standard deviations calculated.

Two-way mixed model intraclass correlation coefficients (ICCs) for average measures with absolute agreement were used to determine the reliability of each variable. Additionally, these ICCs were used to determine the validity of Loadsol variables in comparison to the gold standard of force plate variables. Minimum detectable difference (MDD) and the standard error of measurement (SEM) were also calculated for each variable.

Results & Discussion:

The test-retest reliability of variables from Loadsol data during overground walking ranged from good (r=0.785) to excellent (r=0.969) (Table 1). The reliability of force plate variables also ranged from good (r=0.881) to excellent (r=0.991). However, only two Loadsol variables had excellent reliability compared to five force plate variables. Relatedly, the Loadsol MDDs were generally larger than for force plate variables. The validity of variables from Loadsol data ranged from moderate (r=0.697) to excellent (r=0.992). Notably stance time had excellent validity. Therefore, our hypotheses were partially supported.

Peak VGRF variables were consistently lower with the Loadsol, likely due to its sampling rate being lower by a factor of 10. Fewer samples per second increases the likelihood that the true peak will not be captured as a data point. This limitation should be considered when designing studies using the Loadsol. In particular, this effect may be more pronounced with faster activities with higher impacts, such as running.

The MDDs provided here can be used to help the researcher match their research question to the most appropriate device. If data collection in novel outdoor or in-home environments is desired, and expected changes are greater than the Loadsol MDD, then the Loadsols will be appropriate.

Significance:

This study demonstrated the ability of Loadsols to provide reliable and valid overground walking data, noting that some variables have larger MDDs than with force plates. These findings provide a means for researchers to evaluate whether Loadsols will meet the needs of their study.

References:

[1] Renner et al., 2019, *Sensors* 19.
[2] Milner et al., 2006, *Med Sci Sports Exerc* 38.

Table 1. Vertical ground reaction force (VGRF) variables during overground walking measured using force plates and Loadsols, Means, standard deviations (SD), reliability ICCs, standard errors of measurement (SEMs), minimum detectable difference MDDs, and validity ICCs.

Variable	Device	Mean 1 (SD)	Mean 2 (SD)	ICC (95% CI)	SEM	MDD	Validity ICC (95% CI)
vGRF peak 1	FP	722±83	723±91	0.987 (0.9650.995)	10	28	0.800 (0.465-0.925)
	Loadsol	665±97	646±85	0.785 (0.427-0.920)	42	117	
vGRF peak 2	FP	724±94	720±91	0.991 (0.975-0.997)	9	24	0.752 (0.337-0.907)
	Loadsol	687±105	655±112	0.844 (0.611-0.946)	41	114	
Average loading rate	FP	5252±1489	5446±1631	0.957 (0.886-0.984)	324	897	0.861 (0.628-0.948)
	Loadsol	6282±1868	6289±2002	0.969 (0.918-0.989)	341	945	
Instantaneous loading rate	FP	10036±2007	10129±2048	0.881 (0.681-0.955)	700	1939	0.913 (0.768-0.968)
	Loadsol	9484±2218	9664±2050	0.966 (0.909-0.987)	393	1091	
Impulse	FP	334.39±40.522	335.00±39.319	0.989 (0.970-0.996)	4.19	11.61	0.697 (0.189-0.887)
	Loadsol	296.44±64.499	278.22±66.395	0.797 (0.458-0.924)	29.49	81.74	
Stance time	FP	0.65±0.05	0.65±0.049	0.975 (0.933-0.991)	0.01	0.02	0.992 (0.978-0.997)
	Loadsol	0.67±0.043	0.68±0.044	0.966 (0.910-0.987)	0.01	0.02	

ASSOCIATION BETWEEN FINE MOTOR FUNCTION AND FUNDAMENTAL COOKING SKILLS IN CHILDREN AGED 3-5 YEARS OLD

Rachael Harmon[1], Diana Cuy Castellanos[1], Nicole Atkins[2], Matthew Beerse[1*]
[1]Department of Health and Sport Science, University of Dayton
[2]Occupational Therapy, Northern Kentucky University
*Corresponding author's email: mbeerse1@udayton.edu

Introduction: Cooking skills are uniquely situated to improve children's long-term nutrition behavior [1-2] while advancing fine motor function. However, realizing this potential is currently limited due to the paucity of empirical evidence aligning cooking skills with fine motor domains and an inability to assess performance. Age-appropriate cooking skills have been recommended for practice as early as 2 years old with a repertoire of skills suggested by 3-5 years [3]. While recommended, the capacity for children to effectively perform these cooking skills has yet to be determined. In addition, having a measurement tool to assess performance would enable tracking over time, as well as an ability to identify motor delays. No such tool currently exists. Therefore, we evaluated a piloted criterion-based cooking skills test to establish preliminary associations with fine motor function. In addition, shoulder and elbow joint kinematics were measured during cooking skill performance to better characterize potential associations. We hypothesized that the recommended 3-5 year old age-appropriate cooking skills of mashing, spooning, spreading, and stirring would be associated with better fine motor function across multiple domains including manual dexterity and fine motor precision.

Methods: Thirty-eight children aged 3-5 years old (20F, 3.89 ± 0.70 years old) participated. Mashing, spooning, spreading, and stirring were evaluated using standardized utensils and food products. Briefly, subjects mashed a half cup of canned black beans with a metal fork, stirred 3 drops of green food coloring in a half cup of plain yogurt with a plastic spoon, completed three spooning transfers of applesauce from a 4 oz container to a bowl using a plastic spoon, and spread 1 tbsp of strawberry jam across a slice of white bread using a plastic knife. Performance was scored on the following criteria: ability to pick up and maintain a grip on the utensil, the hand grip used, the outcome, and the time to complete. Scoring ranged from 0 (unable to complete) to 3 (developed performance). During performance, shoulder and elbow kinematic data were captured using an inertial measurement unit motion capture system (Noraxon, AZ, USA). Average joint angle position, excursion, and velocity were calculated.

To assess manual dexterity and fine motor precision, subjects completed the Nine Hole Peg Test (NHPT) and Circle Drawing Test (CDT), respectively. The standardized procedures were followed. A composite score for each cooking skill was determined as a sum of the criteria scores. A total cooking skill score was calculated as a sum of composites. Kendall's tau-b correlations were conducted between the fine motor skill tests (NHPT and CDT) and the total cooking skill score, as well as the composites. An association with NHPT was identified, so we separated subjects into groups based on whether they were above (n=16, 3.75 ± 0.72 years) or below (n=21, 4.07 ± 0.68 years) the average NHPT time. Wilcoxon rank tests compared the shoulder and elbow joint kinematics between these groups.

Results & Discussion: The total cooking skill score was significantly correlated with NHPT performance, but not CDT performance (Fig. 1), partially supporting our hypothesis. These results are the first to empirically associate the performance of cooking skills with fine motor function. Of the individual composite score for each cooking skill, only mashing (τb=-0.319, p=0.009) and spreading (τb=-0.294, p=0.014) were significantly associated with NHPT. Mashing and spreading were the most difficult for this age group, evidenced by a larger spread of scores, compared to spooning and stirring where most subjects received a maximum score. The group with faster than average NHPT times demonstrated a more anatomically neutral shoulder posture during spooning and stirring, as well as higher elbow and shoulder velocities during spreading and stirring. These differences suggest that cooking skills provide the opportunity to practice rapid upper limb movements while maintaining proximal stability.

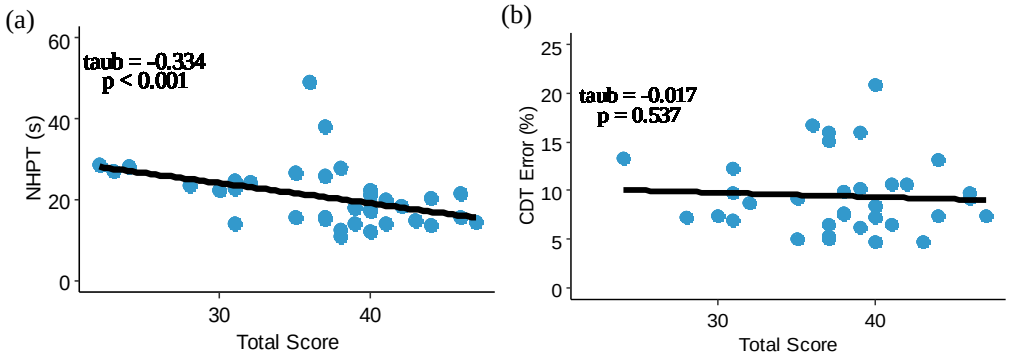

Figure 1: Correlation of total cooking skill score and Nine Hole Peg Test performance (a) and total cooking skill score and Circle Drawing Test performance (b).

Significance: This study provides empirical evidence that cooking skills are associated with fine motor function, supporting their implementation along with more traditional approaches to advancing fine motor development in children. Moreover, we presented preliminary results for the creation of a criterion-based cooking skill test to be used to assess performance and underlying movement qualities. Such a test would be invaluable to practitioners such as early childhood educators and occupational therapists. Further work is necessary to establish validity and reliability metrics.

References: [1] Bennett et al. (2021), *Children* 8(12); [2] Lavelle et al. (2016), *Int J of Beh Nutr & Phys Act* 13(1); Dean et al. (2021), *Appetite* 161

A COMPUTATIONAL MODELING APPROACH TO COMPARE STOOP AND SQUAT LIFTING POSTURES

Elias Rush[1], Michael Bennett[2], Alexander T. Peebles[2]*
[1]Biomedical Engineering, University of the District of Columbia
[2]Department of Mechanical Engineering, University of the District of Columbia
*Corresponding author's email: alexander.peebles@udc.edu

Introduction: Low back pain (LBP) is a leading cause of disability in middle- and older-aged adults, which disrupts activities of daily living and poses a significant financial burden [1]. Prior research suggests that frequent exposure to manual lifting tasks can contribute to the incidence and progression of LBP [2]. Along with limiting the magnitude and frequency of lifting activity in workplace environments, lifting with good posture is recommended to reduce the risk of injury [3]. Lifting is a kinematically redundant task, where there are an infinite number of joint configurations which allow our hands to grasp and lift a box lying on the ground. Ergonomic guidelines, suggest that lifting postures with large amounts trunk flexion and limited knee flexion places excessive stress in the lumbar spine which can cause LBP. Instead of this 'stoop posture', it is recommended to lift with a 'squat posture' where trunk flexion is minimal and knee flexion is increased. While this recommendation does have scientific support, there are many contradicting findings throughout literature as to whether or not stoop posture increases or decreases lumbar joint compression, shear force, and extension moment [3-7]. Differences in experimental protocols, differences in data analysis procedures, and errors in measuring motion of difficult to track segments (i.e. the pelvis and spine) could all contribute to contradicting literature. The purpose of this study was to use a simple static musculoskeletal model to compare lumbar mechanics between stoop and squat lifting postures. Based on prior literature [3], we hypothesized that a squat posture would decrease lumbar extension moment and shear force relative to a stoop posture.

Methods: A rigid-link musculoskeletal model was implemented and analyzed using a custom MATLAB program (The MathWorks Inc.). The model was used to determine the effect of lifting posture on joint mechanics during the lowest point of the lift with negligible inertial forces (i.e., static posture). This was done because joint moments are known to be highest at the lowest point of the lift, where lifting speeds are their lowest point [4]. The model consisted of seven segments, connected with frictionless pin joints, and constricted to the sagittal plane. The length, mass, and center of mass location of each segment were estimated based on existing regression equations with anthropometrics representing an average adult with a height of 1.75 meters and weight of 90 kg. It was assumed that the feet would remain flat on the floor and head to have the same segment angle as the trunk, reducing the model to five degrees of freedom. The distal end of the arm segment was fixed to be 20 cm anterior and 8 cm vertical from the foot segment, similar to the lifting procedure of previous experimental studies [3], which restricted an additional two degrees of freedom. These last three degrees of freedom (shank, thigh, and pelvis) were prescribed to produce both a stoop and semi-squat posture (Figure 1), while ensuring that the bodies center of mass (including the applied load) remained within the base of support. The applied load was set to 23 kg, which represents the maximum amount of weight considered safe by the Revised NIOSH Lifting Equation Guidelines [8]. A top-down inverse dynamics approach was used to estimate joint reaction forces and moments.

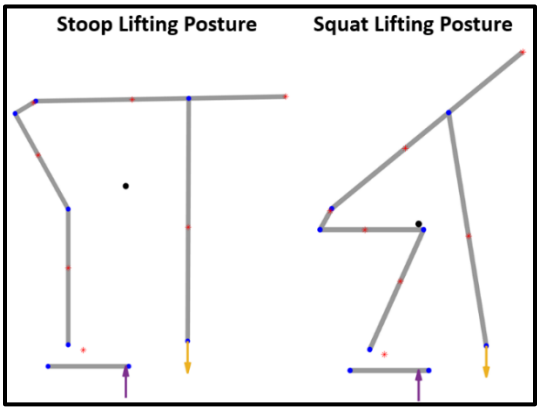

Figure 1: Stoop and squat lifting postures.

Results & Discussion: We found that stoop lifting resulted in slightly larger extension moments of the lumbar (Stoop: 473 Nm; Squat: 442 Nm) and hip joints (Stoop: 275 Nm; Squat: 243 Nm), as well as larger knee flexion moments (Stoop: 158 Nm; Squat: 9 Nm) relative to squat lifting. Previous work has found that lumbar extension moment was increased [7], decreased [5], or similar [4] during stoop lifting relative to squat lifting all using inverse dynamics with experimental kinematic and kinetic data.

We also found that the stoop lifting posture had reduced lumbar compression (Stoop: 506 N; Squat: 877 N) and increased shear force (Stoop: 877 N; Squat: 506 N) relative to squat lifting. These findings partially agree with von Arx et al. [3] who found decreased lumbar compression during stoop relative to squat using a detailed musculoskeletal model (OpenSim) and experimental kinematic and kinetic data. However, the authors found that shear force was increased at the L4/L5 and decreased at the L5/S1 levels during stoop relative to squat lifting [3]. Our findings also partially agree with Bazrgari et al. [7] who found increased compression and increased shear force at the lumbar spine during stoop lifting relative to squat lifting using a finite-element modelling approach with experimental kinematic data. Dreischarf et al. [6] found 4% larger resultant loads during squat relative to stoop lifting using an instrumented vertebrae implant.

Significance: A better understanding of how lifting posture effects lumbar mechanics could help develop ergonomic recommendations and interventions aimed at reducing the incidence and impact of low back pain. This study supports the theory that stoop lifting poses a threat to the lumbar spine, as stoop lifting resulted in larger lumbar extension moments and shear forces.

Acknowledgments: Financial support was received from NSF (Award Number 1914751) and NIH (Award Number R25AG067896).

References: [1] Kent et al. (2005), *Chiropractic and Osteopathy* 12(1); [2] van Nieuwenhuyse et al. (2004), *Occupational Medicine* 45(8); [3] von Arx et al. (2021), *Front. Bioeng. Biotechnol.* 9; [4] van der Have et al. (2019), *Appl. Sci.* 9; [5] Hwang et al. (2009), *BMC Musc. Dis.* 10(15); [6] Dreischarf et al. (2015) *J. Biomech.* 49; [7] Bazrgari et al. (2007) *Eur. Spine J.* 16. [8] Walter et al. (2021), *Revised NIOSH Lifting Equation*;

Ultrasound Measures of Achilles Tendon Thickness: Intra-Rater and Inter-Rater Reliability

Kendall Mulvaney[1], BS, MS, PA-C, Julio Serrano Samayoa[2], BS, Michelle Sabick[3], PhD
Center for Orthopaedic Biomechanics; University of Denver, Email: Kendall.mulvaney@du.edu

Introduction: Musculoskeletal ultrasonography (MSUS) is an accessible and minimally invasive method of evaluating Achilles tendon size to correlate with symptoms and pathology as a screening/diagnostic tool. Little training is required, allowing for use in clinical practice and research. This study aims to: (1) assess the reliability of Achilles tendon thickness made by two examiners with different experience using handheld ultrasound, and (2) validate the accuracy of Achilles tendon thickness measurements made using MSUS on cadaveric tissue. Studies have demonstrated good to excellent intra- and inter-rater reliability can be achieved using different MSUS techniques [1,2,3]. However, there is no consensus on optimal location (distal or mid-tendon) or probe orientation (longitudinal or transverse) for Achilles tendon thickness measurement.

Methods: A test-retest design was implemented bilaterally on 14 healthy subjects (mean age 28.7) in 4 distinct US location-orientation combinations: Distal Long-Axis, Distal Short-Axis, Mid Short-Axis, Mid Long-Axis. This protocol was repeated by two examiners (A and B) twice on each leg for a total of 32 US images per subject. Images were collected using a portable handheld Butterfly IQ+ ultrasound probe (Butterfly Network Inc., Guilford, CT) connected to a tablet (Apple iPad Pro). Subjects lay in prone position, with the ankle stabilized in neutral flexion using a stabilization device with 1cm markings to standardize US image locations (0 cm, 3 cm from calcaneal insertion). Achilles tendon thickness values were extracted from images using an electronic caliper tool in ImageJ software (National Institutes of Health, USA) on all images by both examiners, who were blinded to all previous results.

Data analysis was completed using SPSS (IBM, USA) and Excel (Microsoft, USA). Relative intra- and inter-rater reliability were calculated using intra-class correlation coefficients (ICC). Absolute reliability was calculated using standard error of measurement (SEM, %) and minimal detectable change (MDC). Normality of the data was confirmed using Kolmogorov-Smirnov tests.

The accuracy of the MSUS technique was quantified using a protocol identical to that above, but on a cadaveric lower extremity. Achilles measurements from US (ImageJ and Butterfly built-in caliper) were compared to physical caliper measurements of anterior-posterior thickness on the same cadaveric tendon after dissection.

Results & Discussion: All but two of the inter-rater ICCs were good (0.75-0.9) [4] (Figure 1), suggesting that deep experience is not required to accurately quantify Achilles thickness using MSUS. However, Examiner A had clinical MSUS experience and generally had higher ICC values.

The highest inter-rater ICC values occurred in the Distal Long (0.896), Mid Short (0.852), and Mid Long (0.851) location-orientation combinations. The worst inter-rater ICCs occurred in Distal Short combination (0.734), likely due to difficulty in visualizing the tendon edges in the transverse orientation distally. ICC values for 1st and 2nd measurements for each examiner, (AB1, AB2) showed there was no appreciable learning bias. Higher AB1 ICC values may be due to experimental design as Distal Long was measured first. The lowest inter-rater SEM (and SEM%) values were Distal Long (0.111 (2.9%)) and Mid Short (0.146 (3.5%)); the lowest MDC values were Distal Long (0.308) and Mid Long (0.380).

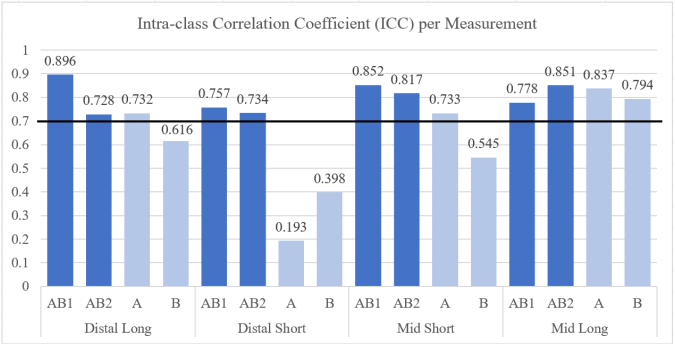

Figure 1: ICC Values for Each Measurement Site.

Table 1: Validation Thickness of Cadaveric Achilles Tendon (mm).

Location	Orientation	Caliper Mean (SD)	ImageJ		Butterfly	
			Mean (SD)	Error (%)	Mean (SD)	Error (%)
Distal	Long	6.02 (0.2)	4.14 (0.17)	1.88 (31.2)	4.1 (0)	1.92 (31.9)
	Short		5.13 (1.06)	0.90 (14.9)	5.6 (0)	0.42 (6.98)
Mid	Short	5.86 (0.17)	5.58 (0.34)	0.29 (4.86)	5.8 (0)	0.06 (1.07)
	Long		5.85 (0.59)	0.02 (0.26)	6.5 (0)	0.64 (10.9)

The highest intra-rater ICC values were Mid Long for both examiners (A 0.837, B 0.794). The lowest intra-rater SEM (and SEM%) values were Mid Long (0.160) for A and (0.201) for B, both under 5%. The lowest MDC values were Mid Long for both examiners (0.442 and 0.557). Both examiners had good reliability at this combination. In cadaveric tissue, the most accurate measurements were collected using ImageJ at Mid Long combination (0.26% error) and at the mid-tendon location (Table 1). Butterfly's built-in caliper measurements were reported in two significant figures which limited the accuracy compared to ImageJ.

Significance: This study adds evidence that portable ultrasound is a reliable technique for quantifying Achilles tendon thickness even with minimal user experience, as validated by both ICCs and cadaveric measures. The data also suggest an optimal methodology for future studies of Achilles tendinopathy. The most reproducible measurements were collected at the mid-tendon location (3 cm proximal to calcaneal edge near insertion) using the longitudinal probe orientation (Long-Axis) and quantified with ImageJ. This study also provides baseline Achilles tendon thickness data obtained in a relatively young healthy population. By reporting results for two locations and two probe orientations we hope to improve clinical measurement of Achilles tendon thickness with ultrasound including screening for tendinopathy, as increased thickness has been associated with tendon injury [2,3]. Thus, validating a reliable measuring protocol is essential.

Acknowledgements: Special thanks to DU's Center for Orthopaedic Biomechanics.

References: [1] Thoirs et al., 2018. *Ultrasound in Med.&Biol*. 44(12); [2] del Bano-Aledo et al., 2017. *Muscles Ligaments Tendons J.* 7(192); [3] Kharate et al., 2012. *Int J Physiother Rehabil.* 2(1); [4] Koo et al., 2016. J Chiropr Med. 15(155)

CHARACTERIZING LANDING STRATEGIES DURING A DROP JUMP: APPLICATION OF K-MEANS CLUSTERING TO ESTABLISH ACL INJURY RISK

Stanley Smith[1*], Christopher Powers[1], Nicholas Schweighofer[1], Susan Sigward[1]
[1] The Jacquelin Perry Musculoskeletal Biomechanics Research Laboratory, University of Southern California
Corresponding author's email: stanleye@usc.edu

Introduction: Tears of the anterior cruciate ligament (ACL) are common among athletes who participate in sports that require frequent deceleration and changes in the direction. [1] Females have a higher incidence of injury compared to males participating in the same sport[2]. Prospective studies have identified several variables as being predictive of future non-contact ACL injury including limited hip and knee flexion,[3, 4] elevated knee valgus moments and angles,[5, 6] high ground reaction forces,[3] and high knee extensor moments.[7] There is evidence to suggest that identified risk factors for ACL injury as quantified during the drop-jump task may co-exist as part of a generalized movement strategy used to decelerate the body's center of mass.[8] The purpose of this study was to use K-means clustering to ascertain whether a high-risk landing strategy could be identified during a drop-jump task as determined by the presence of multiple, coexisting risk factors. It was hypothesized that a high-risk landing strategy could be identified in male and female athletes. We also hypothesized that a greater proportion of females would be assigned to the high-risk cluster.

Methods Kinematic and kinetic data were obtained from 74 healthy athletes (31 males and 43 females) while performing a drop-jump task from a height of 30 cm. Selection of biomechanical variables for this investigation was based on the findings of prospective studies for ACL injury that identified specific risk factors as quantified during a drop-jump task. In total, 8 variables were chosen: peak vertical ground reaction force (N/kg), peak knee flexion angle (deg), peak hip flexion angle (deg), peak knee extensor moment (Nm/kg), knee abduction angle at peak knee flexion (deg), knee valgus moment at peak knee flexion (Nm/kg), peak hip extensor moment (Nm/kg), and the average knee-to-hip extensor moment ratio. Prior to clustering, the 8 biomechanical variables underwent a standardization process. Each variable was scaled to achieve a zero mean and a unit standard deviation, ensuring uniformity in the variable scale for unbiased comparative analysis. Given that the purpose of the study was to identify two specific drop-jump landing strategies (ie. high and low risk clusters), the number of clusters was set at two. Following the clustering procedure, independent T-tests (2-tailed) were used to assess between-cluster differences for each biomechanical variable of interest. A chi-square test was utilized to explore the distribution of males and females across the two clusters.

Results & Discussion: we used K-means clustering to categorized the 74 participants into two groups (Cluster 1: N=36, Cluster 2: N=38). T-tests revealed statistically significant differences in 7 of the 8 variables used in the clustering analysis (Table 1). On average, participants assigned to Cluster 1 exhibited significantly lower peak hip and knee flexion and lower peak hip extensor moments compared to participants assigned to Cluster 2 (Table 1). Participants assigned to Cluster 1, also demonstrated greater knee valgus moments and angles at peak knee flexion, a greater knee/hip extensor moment ratio, and higher peak vertical ground reaction force (Table 1). There was no significant difference in the peak knee extensor moment between clusters. The Chi-square analysis revealed a significant association between sex and cluster assignment (χ^2 3.70, p=0.05); The proportion of females assigned to Cluster 1 was 69.4% (N= 25), compared to 30.6% males (N=11). Cluster 2, had a more balanced sex representation (47.4% female, N=18 vs. 52.6% male, N=20).

Table 1. 3D Cluster Differences

Variables	Cluster 1 Mean (SD)	Cluster 2 Mean (SD)	P-Value
Hip Flexion Angle (deg)	75.0 (12.8)	102.4 (13.4)	< 0.001
Knee Flexion Angle (deg)	87.9 (10.6)	104.8 (13.6)	< 0.001
Knee Abduction Angle (deg)	0.9 (4.3)	-8.6 (4.8)	< 0.001
Knee Valgus Moment (N*m/Kg)	0.1 (0.2)	-0.3 (0.3)	< 0.001
Hip Extensor Moment (N*m/Kg)	1.6 (0.4)	2.4 (0.7)	< 0.001
Knee Extensor Moment (N*m/Kg)	2.2 (0.5)	2.2 (0.4)	0.703
Knee to Hip Moment Ratio	1.9 (1.0)	1.2 (0.4)	< 0.001
Normalized Vertical GRF (N/Kg)	18.1 (3.2)	16.4 (3.0)	0.022

Two distinct landing strategies were identified as evident by the finding of statistically significant between cluster differences in 7 of the 8 biomechanical variables evaluated. Participants assigned to cluster 1 exhibited differences in variables that would be considered high risk compared to those assigned to cluster 2. Of these differences, 6 are known risk factors for non-contact ACL injury based on prospective studies.

Significance: The results of this study revealed that the drop-jump task may be used to identify a high-risk landing strategy for ACL injury. The fact that a greater proportion of females demonstrated the high-risk strategy supports the premise that the strategy exhibited by those assigned to cluster 1 may be considered higher risk for ACL injury. Prospective studies are needed to validate this assumption.

References: [1] Weiss et al. (2015), *Sports Med* 45(9); [2] Renstrom et al. (2008), *Br J Sports Med* 42(6); [3] Leppanen et al. (2017), *Am J Sports Med* 45(2); [4] Bakker et al. (2016), *J Orthop Res* 34(9); [5] Myer et al. (2015), *Br J Sports Med* 49(2); [6] Hewett et al. (2005), A*m J Sports Med* 33(4); [7] Leppanen et al. (2017) *Orthop J Sports Med* 5(12); [8] Pollard et al. (2010), *Clin Biomech* 25(2).

THE IMPACT OF DOG LEASH TENSION ON LUMBAR AND KNEE MECHANICS

Michael K. Bennett[2], Nicole Arnold[1], Lara Thompson[1,2], and Alex Peebles[2]
[1]Biomedical Engineering Program, University of the District of Columbia
[2]Department of Mechanical Engineering, University of the District of Columbia
*Corresponding author's email: alexander.peebles@udc.edu

Introduction: Chronic pain conditions such as low back pain (LBP) and knee osteoarthritis place an extreme burden on our society [1]. While chronic pain can develop after a traumatic injury, it often develops progressively through routine submaximal loading of musculoskeletal structures. Some activities of daily living which contribute to the development of LBP have been identified, such as jobs which require frequent forward flexion of the trunk of lifting heavy objects repetitively [2]. Dog walking is another activity of daily life, common to many, in which a considerable amount of load is applied to the human musculoskeletal system. A recent study investigated the nature of 9244 dog-walking related injuries and found that 44.8% of injuries were the result of the dog pulling on the leash without causing a fall [3]. While the upper extremities were the most common injury location, 15% of the dog-walking related injuries were to the torso [3]. There has been limited biomechanics research evaluating the impact that leash tension has on the human musculoskeletal system. Therefore, the purpose of this study is to compare lumbar and knee mechanics expected while restraining a dog on leash with mechanics expected during lifting and reaching, two tasks known to cause or exacerbate LBP. We hypothesize that leash tension will result in greater shear forces and joint moments within the lumbar and knee joints relative to lifting and reaching conditions.

Methods: A rigid-link musculoskeletal model was implemented and analyzed using a custom MATLAB program (The MathWorks, Inc.). The model consisted of seven segments (feet, shank, thigh, pelvis, trunk, head, and arms), connected with frictionless pin joints, and constricted to the sagittal plane. The length, mass, and center of mass location of each segment were estimated based on existing regression equations with anthropometrics representing an average adult with a height of 1.75 meters and weight of 90 kg. Three different postures were developed to compare across conditions, as shown in Figure 1. The posture and applied load location (20 cm anterior and 8 cm vertically off the ground) for the lifting condition were based on prior literature [4]. The load magnitude for the lifting condition was set to 23 kg, representing the maximum amount of weight considered safe by Revised NIOSH Lifting Equation Guidelines [5]. The posture and hand location for the reach condition were also based on prior literature [6], with no additional load applied to the model. A neutral upright posture with slight knee and hip flexion was set for the leash condition, with the body's center of mass projecting close to the ankle joint. Pilot data from a related study suggests that a medium-sized dog (50 lbs) can generate pulling forces of about 90 lbs (40 kg). Therefore, leash simulations were run twice, first with an applied load of 23 kg (for direct comparison with lift) and second with an applied load of 40 kg. A static top-down inverse dynamics approach was used to estimate joint reaction forces and moments, which were represented in the distal coordinate system.

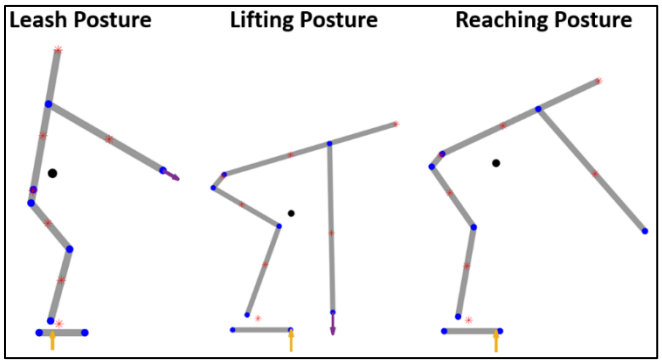

Figure 1: Postures and loading developed for each condition.

Results & Discussion: Study outcomes for each condition are shown in Table 1. At matched loads of 23 kg, lifting did result in greater lumbar extension moments, compressive forces, and shear forces. However, a leash load of 40 kg resulted in lumbar extension moments, compressive and shear forces which exceeded lifting 23 kg. Knee flexion moments and shear forces were greater for the leash-tension conditions at 23 kg relative to lifting. All loading outcomes were greater for leash-tension relative to reaching. These results demonstrate that the forces applied to the human body while restraining a dog on leash can cause a greater mechanical response in the lumbar spine and knee joints relative to reaching and lifting. Future work should explore how dog-walking impacts joint mechanics experimentally and the impact that dog-walking has on chronic joint pain.

	Leash (23 kg)	Leash (40 kg)	Reaching (0 kg)	Lifting (23 kg)
Lumbar Ext. Mom. (Nm)	319	477	272	464
Lumbar Comp. (N)	707	821	430	776
Lumbar Shear (N)	522	835	361	651
Knee Ext. Mom. (Nm)	-108	-219	-64	-58
Knee Comp. (N)	561	604	512	701
Knee Shear (N)	353	514	90	255

Table 2: Study outcomes compared across conditions.

Significance: Prior work has demonstrated that dog-walking can result in serious acute musculoskeletal injuries that cause patients to visit an emergency room [3]. This study suggests that dog-walking could also contribute to the high prevalence of chronic joint pain at the knee and lumbar spine. A better understanding of the impact that leash loads have on human health and wellness can help us develop novel strategies to reduce injury risk.

Acknowledgments: Funding support was received from NIH (Award Number R25AG067896).

References: [1] Kent et al. (2005), *Chiropractic and Osteopathy* 12(1); [2] van Nieuwenhuyse et al. (2004), *Occupational Med.* 45(8); [3] Maxson et al. (2023), *MSSE*; [4] von Arx et al. (2021), *Front. Bioeng. Biotechnol.* 9; [5] Walter et al. (2021), *Revised NIOSH Lifting Equation*; [6] Thomas & France (2007), *Spine* 32(16).

REAL-TIME ESTIMATION OF MOVEMENT INTENTION OF STROKE SURVIVORS WITH MACHINE LEARNING TO CONTROL A SOFT WEARABLE ROBOT

James Arnold[1], Prabhat Pathak[1], Carolin Lehmacher[1], Connor McCann[1], Yichu Jin[1], Tanguy Lewko[1], John Paul Bonadonna[1], Sarah Cavanagh[1], David Pont-Esteban[1], Kelly Rishe[2], David Lin[2], Conor Walsh[1*]

[1]John A. Paulson School of Engineering and Applied Sciences, Harvard University, Cambridge, MA, USA

[2]Department of Neurology, Massachusetts General Hospital, Harvard Medical School, Boston, MA, USA

*Corresponding author's email: walsh@seas.harvard.edu

Introduction: Stroke affects nearly one million people in the US annually, with 75% of stroke survivors having long-term challenges using at least one of their arms in their daily lives [1]. Recently, portable, wearable robots have shown promise for assisting the upper extremity which could be used to improve the capacity of stroke survivors to use their affected arm during daily life tasks and/or at-home rehabilitation. Inferring users' intended movements from residual function is an intuitive way to control wearable robots. However, variability in arm motor impairments after stroke makes it challenging to infer users' intended movements from motion sensors [2]. For example, common post-stroke symptoms such as spasticity and flexor synergies can lead to involuntary movements that a robot should not augment.

In this work, we explore the use of a machine learning model based on motion and pressure sensors to predict a user's intended direction of movement in real-time to control a soft wearable shoulder robot. A personalized intention detection model was trained during a set of guided, specific motions and evaluated during a set of shoulder-elevated, joint individuation activities.

Methods: Three individuals with chronic post-stroke upper extremity motor impairments (age = 56.0±19.5 years, years since stroke = 4.7±2.1 years, FMA scores = 45±9.2) participated in the study. The participants wore a soft inflatable shoulder robot which our group recently introduced and evaluated for people living with amyotrophic lateral sclerosis [3]. In the previous study, the device was controlled with the users' arm elevation angles estimated using inertial measurement units (IMUs). Building on this work, we integrated soft deformation sensors into the robot to capture the interaction forces between the user and the pneumatic actuator and devised a machine-learning based control method that combines data from the interaction sensors and IMUs to, in real-time, classify a user's intended movement into three classes: UP (lifting), HOLD (maintaining shoulder elevation), and DOWN (lowering).

We trained intention detection models (fully connected neural networks) for each participant from data collected during a 15–20-minute guided session where we provided commands to the user on how to attempt to move their limb while we recorded sensor data. After the model was trained, we evaluated the effectiveness of the model for real-time robot control. To collect the evaluation data, we instructed the participants to lift their arm to 90° shoulder elevation, then maintain this shoulder elevation while simultaneously performing three repetitions of different joint individuation movements (shoulder horizontal abduction/adduction, shoulder internal/external rotation, elbow flexion/extension, forearm supination/pronation, and wrist flexion/extension), and then lower their arm back to the side. This procedure was repeated with and without the robot controller enabled while collecting optical motion capture and video data.

Results & Discussion: The accuracy of the intention detection model compared to post-processed, ground truth video labels was 79.6±14.3% for UP, 92.4±14.1% for HOLD, and 82.9±10.8% for DOWN (Fig 1, top). Despite an average 6.3±8.0° change in elevation angle within each movement labelled as HOLD, the model predicted, on average, the user's intention to move up within 103±141ms after lifting 3.1±3.5° and to move down within 133±135ms after lowering 1.12±1.69° (Fig 1, bottom). Misclassifications in UP and DOWN were typically at the beginning and end of the segments when initiating and terminating movement. The most misclassified movement in the HOLD state was internal shoulder rotation, which was sometimes misclassified as DOWN. However, the robot still helped to minimize involuntary changes in shoulder elevation: the maximum downward shoulder elevation speed during internal rotation was reduced from a mean of 24.6±13.0°/s when the controller was off to 11.2±7.0°/s when the controller was on.

While using the robot, all three stroke survivors were able to elevate their shoulders closer to the instructed 90° (on: 84.1±10.6°, off: 76.4±8.3°). With this proximal support provided by the robot, modest increases in distal joint range of motion (unassisted) were observed, with the elbow and wrist flexion/extension range of motion increased on average by 3.1° and 2.7°, respectively.

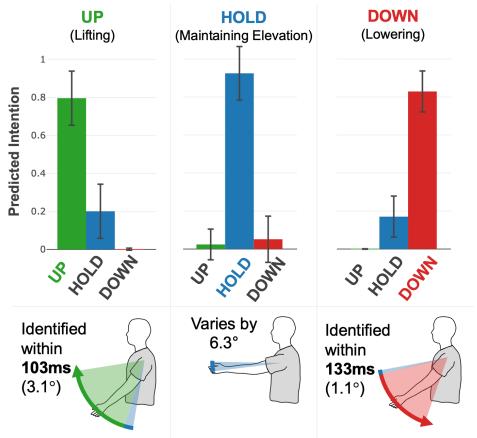

Figure 1: Intention detection model performance. In the top, a confusion bar plot of the model predictions, with the height of each bar corresponding to the mean (across movement segments) ratio of predicted intention states. In the bottom, visual representations of the movement segments and typical model responses.

Significance: In this study, we demonstrate the benefits of personalizing the control of a wearable shoulder robot for chronic stroke patients. As wearable robots continue to become more portable and suitable for integration into unstructured environments, intuitive and reliable control will be critical for enabling functional use.

Acknowledgments: This study was supported by the National Science Foundation under Awards No. 2236157 and 2345107.

References: [1] Smith, et al. (2023), *Journal of NeuroEng.* and Rehab. 20(1). [2] Parnandi, et al. (2023), *Bioeng.* 10(648). [3] Proietti, et al. (2023), *Sci. Trans. Med.* 15(681).

THE IMPACT OF LOWER EXTREMITY MOTOR IMPAIRMENT ON POST-STROKE COACTIVATION IN GAIT

Andrian Kuch, PhD[1*], Kristan Leech, PhD, DPT[2], Nicolas Schweighofer, PhD[2], Carolee Winstein, PhD, PT[2], Natalia Sánchez, PhD[1,3]
[1]Department of Physical Therapy, Chapman University, Irvine, CA. [2]Division of Biokinesiology and Physical Therapy, University of Southern California, Los Angeles, CA. [3]Fowler School of Engineering, Chapman University, Orange, CA
*Corresponding author's email: kuch@chapman.edu

Introduction: Stroke survivors generate abnormal coactivation of agonist and antagonist muscles in the paretic and non-paretic extremities during walking [1]. This coactivation can be quantified using non-negative matrix factorization (NMF) [2,3], to obtain modules of muscles that are coactivated [4]. Researchers typically extract modules to account for 90% of the muscle activity variance, indicative of neural control complexity [5]. In neurotypical individuals, 4-6 modules account for muscle activity during gait [4,6], while only 2-4 modules account for muscle activity during gait after stroke [6,7]. However, the identified modules cannot always accurately reconstruct the task from which they were extracted [8], suggesting that the modular representation of the neuromuscular control is not fully representative of the motor task. An alternative approach that was developed is to use the variance explained by one module (VAF1), i.e. a single synergy representing all coactivated muscles during a gait cycle [5]. During walking, VAF1 increases with age in neurotypical adults [9-11] and with impairment in children with cerebral palsy [5], while it decreases with self-selected speed (SSS) in the acute phase of stroke [7]. Here, we aim to investigate if VAF1 during gait is related to impairment and function post-stroke. We hypothesize that coactivation in the paretic extremity will be higher in older, more impaired, and slower post-stroke individuals.

Methods: 11 participants post-stroke (age 52±16 years, stroke onset>6 months) participated in this study. Participants walked on a treadmill at their SSS. We collected surface electromyography of 7 lower extremity muscles for the paretic and non-paretic extremities (Vastus Medialis, Rectus Femoris, Biceps Femoris, Semitendinosus, Gastrocnemius Lateralis, Soleus, Tibialis Anterior). We segmented data into gait cycles, and the activation of each muscle was averaged to obtain one time-normalized gait cycle. We performed NMF of the normalized data using one synergy for each lower extremity to compute VAF1. The degree of motor impairment was assessed using the lower extremity portion of the Fugl-Meyer scale (FM-LE). The association between VAF1 and clinical measures (FM-LE, SSS, and age) for both extremities was done using the Pearson correlation coefficient. VAF1 between both extremities was compared using a Mann-Whitney U-test. The significance level was set at 0.05.

Results & Discussion: The average FM score was 24±4, SSS was 0.80±0.38 m/s, non-paretic VAF1 was 0.79±0.10, and paretic VAF1 was 0.80±0.09. VAF1 did not differ between limbs (p=0.90). We observed a significant negative correlation between FM score and paretic VAF1 (r=-0.76, p=0.006, Fig.1A). No significant relationship was found between VAF1 and SSS for the paretic (r=-0.34, p=0.30, Fig.1B) or non-paretic limb (r=-0.48, p=0.14, Fig. 1C). Participant's age was not correlated with paretic VAF1 (r=0.43, p=0.19, Fig.1D), but was positively correlated with non-paretic VAF1 (r= 0.77, p =0.005, Fig.1E)

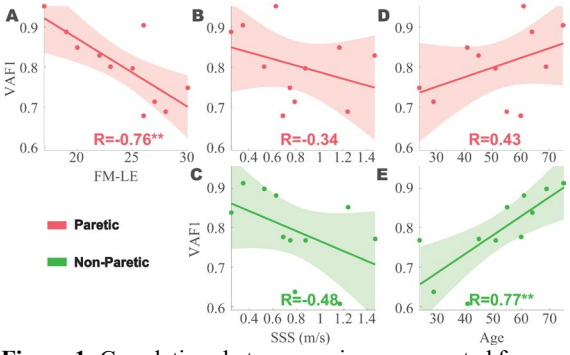

Figure 1: Correlations between variance accounted for one module (VAF1) and clinical measures for the non-paretic (green) and paretic (red) limbs. A: Fugl-Meyer Lower Extremities, B-C: Self-Selected Speed, D-E: age. **p<0.01

The same level of coactivation was detected in both extremities, contrary to another study [6], that found the paretic VAF1 was higher. This could be explained by faster walkers in our study compared to SSS 0.58±14 in previous studies [6], despite having the same level of impairment (FM score 22±8 in [6]). As hypothesized, more impaired participants exhibited higher levels of paretic extremity coactivation, showing that VAF1 could be used as a measure of stroke impairment during gait. VAF1 was not related to walking speed, suggesting that coactivation does not limit walking function during the chronic phase, which contrasts findings in the acute phase of stroke, where higher coactivation was correlated with slower gait speeds [7]. The non-paretic VAF1 increased with age, while the paretic VAF1 was not associated with age, probably caused by a larger effect of stroke impairment, and the need for a simpler neuromuscular organization in the affected extremity [6]. Future work will explore the Dynamic Motor Control Index, which expresses muscle coactivation relative to that observed in neurotypical controls [5,10]. Further studies could investigate the sensitivity of overall coactivation to different types of gait retraining to provide more specific exercises with better restitution of more complex modular muscular activation patterns to each individual.

Significance: Our results show that the overall paretic extremity coactivation level is related to motor impairment and could be used in future studies as 1) a marker of motor control impairment during gait retraining interventions and 2) as an assessment of changes in neuromuscular control after walking intervention.

Acknowledgments: NIH NCMRR R03HD104217(K. Leech), NIH NCMRR R03HD107630, NIH NCATS R03TR004248(N. Sanchez)

References:

[1] Rosa et al. (2014), *J. E. Kinesiol.*, 24(1) [2] Lee et al., (2000), *Adv. Neu. Inf. Process. Syst.,* 13 [3] Rabbi et al. (2020), *Sci. Rep.,* 10 [4] Ivanenko et al. (2004), *J. Physiol.*, 556(1) [5] Steele et al., (2015), *Dev. Med. Child. Neurol.,* 57(12) [6] Clark et al., (2010), *J. Neurophy.,* 103(2) [7] Mizuta et al., (2022), *PLoS One.,* 17(2) [8] Barradas et al. (2020), *J. Neurophy*. 123(6) [9] Lo et al., (2017), *G. Posture,* 53 [10] Collimore et al. (2021), *Front. Aging. Neurosci.,* 13 [11] da Silva Costa et al. (2020), *Exp. Gerontol.,* 140

DIFFERENCES IN SPATIOTEMPORAL GAIT MEASURES BETWEEN OUTDOOR WALKING SURFACES

Ashlyn M. Jendro[1*] & Abigail C. Schmitt[1]
[1]University of Arkansas
*Corresponding author's email: amjendro@uark.edu

Introduction: Walking gait has been studied extensively within laboratory and clinical settings and can provide clinicians with benchmarks of disease progression or mobility assessments. The ability to maintain gait velocity has been recommended as a possible "vital sign" for healthy aging as it is correlated with functional status, adverse events, and survival [1]. Yet, older adults often exhibit decreased gait velocity and increased variability with age [2]. In particular, variability may better predict gait pattern disturbances, where increased stride-to-stride variability is correlated with an increased risk of falls and may even be a useful measure to identify high fall-risk individuals [3]. Although walking gait has been extensively studied in the laboratory, evidence shows that gait patterns differ from indoor to outdoor environments, especially among older adults [4]. Fortunately, with recent technological advancements, researchers can assess walking outside, in real-world settings. This study aims to compare spatiotemporal gait measures and their variability in older adults while walking on three different surfaces: a paved walkway, manicured grass, and a hiking trail.

Methods: Fifteen older adults (8 men, 69 ± 4 yrs, 1.72 ± 0.11 m, 75.9 ± 14.8 kg) completed three walking trials at a local outdoor park. Participants reported no history of neurological or orthopedic problems that impaired walking or general mobility. Participants wore 8 inertial measurement unit (IMU) sensors (Ultium Motion System, Noraxon) on the dorsal side of each foot, the anterior tibias, the lateral thighs, over the sacrum, and over L1/T12. Following IMU placement, participants walked 400m on three outdoor surfaces (a paved walkway, a multi-use hiking trail, and a manicured grass field; Fig 1). For each trial, participants walked at their *"comfortable, preferred speed"* while research staff followed at a distance to ensure safety and that participants stayed on the correct path.

Figure 1: Walking conditions (A) paved walkway, (B) hiking trail, and (C) manicured grass.

Spatiotemporal variables (gait velocity, step and stride length, step width, double support percent) were used to assess walking strategies. Raw step data was analyzed using a custom MATLAB code. Data from steps outside three median absolute deviations on any variable were removed. Standard deviations of each spatiotemporal measure were computed from the entire gait trial to quantify gait variability. Separate repeated measures ANOVAs compared means and variability between outdoor surfaces with alpha set to .05.

Results & Discussion: For analysis, Greenhouse-Geisser adjustments for the repeated measures ANOVAs were used between outdoor surface conditions. Gait velocity ($F(1.878)= 7.840$, $p=.003$; $F(1.566)= 39.279$, $p <.001$), and double support ($F(1.905)=17.986$, $p<.001$; $F(1.736)=15.489$, $p<.001$) showed significant differences for means and variability, respectively. Step length ($F(1.638)=43.750$, $p<.001$), step width ($F(1.584)=42.484$, $p<.001$), and stride length ($F(1.525)=36.175$, $p<.001$) showed significant differences only in variability measures (Table 1).

Table 1: Spatiotemporal gait measures across conditions.

	Means			Standard Deviations		
	Paved Walkway	**Hiking Trail**	**Manicured Grass**	**Paved Walkway**	**Hiking Trail**	**Manicured Grass**
Gait Velocity (m/s)	1.46 ± 0.16	1.37 ± 0.19	1.39 ± 0.20	0.05 ± 0.02	0.08 ± 0.03	0.06 ± 0.02
Step Length (cm)	77.7 ± 8.8	75.4 ± 10.0	76.7 ± 10.4	2.2 ± 0.7	4.0 ± 1.1	2.7 ± 0.7
Stride Length (cm)	155.4 ± 17.7	150.9 ± 20.1	153.5 ± 20.8	3.4 ± 0.8	6.5 ± 2.1	4.3 ± 1.1
Step Width (cm)	11.8 ± 3.8	10.7 ± 4.4	9.8 ± 3.6	2.6 ± 0.5	4.2 ± 0.9	3.0 ± 0.4
% Double Support	22.9 ± 4.1	21.9 ± 3.8	24.3 ± 4.6	1.7 ± 0.7	2.3 ± 0.4	1.7 ± 0.7

Major findings include gait velocity being significantly faster on the paved walkway compared to both the hiking trail ($p<.001$) and manicured grass ($p=.011$). However, the percentage of double support was shortest in the hiking trail condition compared to the paved walkway ($p=.039$) and the manicured grass ($p<.001$). All variability measures showed significant differences between the hiking trail and the paved walkway and manicured grass with the hiking trail exhibiting the most variability (all $p<.05$).

Significance: These results suggest that healthy older adults adopt different walking strategies to adjust to the demands of various outdoor surfaces. Participants exhibited greater variability while walking on the hiking trail. As it presents both complex visual and surface textures, this likely necessitated an altered walking strategy to meet the task demands. These data underscore how important ambulating surface is to spatiotemporal mean and variability gait measures. Caution should be used when extrapolating laboratory gait measures and variability to real-world ambulation.

Acknowledgments: Equipment used for this project was provided by University of Arkansas for Medical Sciences.

References: [1] Middleton et al. (2015), *J Aging Phys Act* 23; [2] Winter et al. (1990), *Physical Therapy* 70; [3] Maki. (1997), *J Amer Geriat Soc.* 45. [4] Schmitt et al. (2021), *Gait & Posture* 90.

WITHIN-SUBJECT COMPARISON OF GAIT KINEMATICS USING PASSIVE, MICROPROCESSOR-CONTROLLED, AND POWERED TRANSTIBIAL PROSTHESES

M.M. Dickens[1*], A.B. Jigida[1], J. Denune[2], S.C. Gnyawali[3], P.M. Wensing[1], S. Roy[3], & J.P. Schmiedeler[1]
[1]University of Notre Dame, [2]NuTech Institute, [3] McGowan Institute for Regenerative Medicine, University of Pittsburgh
[*]Corresponding author's email: mdicken2@nd.edu

Introduction: Of the over 2 million people living with an amputation in the United States, many more are likely to have a lower limb amputation than an upper limb amputation [1]. While passive devices are the most commonly used prostheses for individuals with transtibial amputation, both microprocessor-controlled and powered prostheses offer benefits for K3- and K4-level ambulators [2]. These more advanced prostheses, however, are generally heavier, and the acclimation periods required to achieve their benefits are unclear from existing literature [3]. This study examines within-subject changes in gait kinematics associated with both 30-minute and 4-week acclimations to microprocessor-controlled and powered prostheses and compares them to kinematics when using a passive prosthesis.

Methods: Six subjects with unilateral transtibial amputation participated in 3 study visits, each separated by at least 4 weeks, as approved by the Indiana University IRB#12143. At each visit, pressure sensors (Tekscan F-socket System, 80Hz) were placed on the residual limb before donning the standard-of-care (SOC) socket. Inertial measurement units (Xsens Awinda IMU, 80Hz) were then attached to the lower extremities, pelvis, and sternum. First using their passive SOC prosthesis at Visit A, subjects completed at least 6 repetitions of stair ascent/descent, ramp ascent/descent, and level walking. Then, a prosthetist fit and aligned either (order randomized) the microprocessor-controlled PROPRIO FOOT® by Ossur (PRO) or the Empower ankle by Ottobock (EMP) to the SOC socket, provided 30 minutes of acclimation, and recorded data for 6 repetitions of each of the walking tasks. Subjects left with the new-to-them device and used it exclusively for at least 4 weeks. At Visit B, the walking tasks were repeated with this device (PRO/EMP) before a prosthetist fit and aligned the other device (EMP/PRO), provided 30 minutes of acclimation to it, and recorded data for at least 6 repetitions of the walking tasks with it. Subjects left with this second new-to-them device to use for at least 4 weeks. At Visit C, 6 repetitions of the same walking tasks were completed with this device, a prosthetist refit the SOC prosthesis, and a final 6 repetitions of the walking tasks were recorded with it. Kinematic analysis of the motion capture data employed methods from [4] for gait event detection. To calculate symmetry, the ratio between the right and left leg variables was used (unity indicating symmetry). A two-way, type-II ANOVA with no interaction for device and visit and a one-way, type-II ANOVA for the combinations of device and visit were conducted. Comparisons among the main effects and their combinations were completed post hoc using the Tukey and Games Howell tests.

Results & Discussion: Representative results for one subject during level ground walking are reported here using variables of gait duration (GD), stance duration (ST), swing duration (SW), ratio index of gait duration, and maximum knee flexion (MKF) in swing for both the prosthetic and intact sides. This subject received EMP at Visit A and PRO at Visit B, as noted on the x-axis of Fig. 1. For the prosthetic side, the combination of device and visit was a main effect for all variables except ST, where only device was a main effect. After 4 weeks of acclimation, there was a significant increase in SW for EMP, MKF for PRO, and GD for both compared to wearing the same device for just 30 minutes. ST with EMP after both acclimation periods was less than it was in any other condition except the initial PRO testing. For the intact side, the combination of device and visit were a main effect for GD, and device was a main effect for the other variables. After 4 weeks wearing EMP, there was a significant increase in MKF and SW compared to just 30 minutes of acclimation. During Visit A, ST decreased from initial SOC to initial EMP, and then after 4 weeks at Visit B, it decreased again both with follow-up EMP and with initial PRO. At Visit C, however, ST for follow-up PRO returned to a value not significantly different from initial SOC at Visit A. The results of GD for the intact side are similar to those for the prosthetic side. The similarities between the prosthetic and intact sides resulted in improvement in GD symmetry with additional acclimation to EMP (from 30 minutes to 4 weeks), but not PRO (Fig. 1). With large variations in GD symmetry for EMP@A and SOC@C (Fig. 1), the subject's gait was clearly affected by both the transition from passive to non-passive devices, and vice versa, but seemingly less so by the transition from EMP to PRO at Visit B. The changes in both SW and MKF from 30-minutes to 4-weeks of acclimation reinforce that the subject was still adapting to each new prosthesis after 30 minutes.

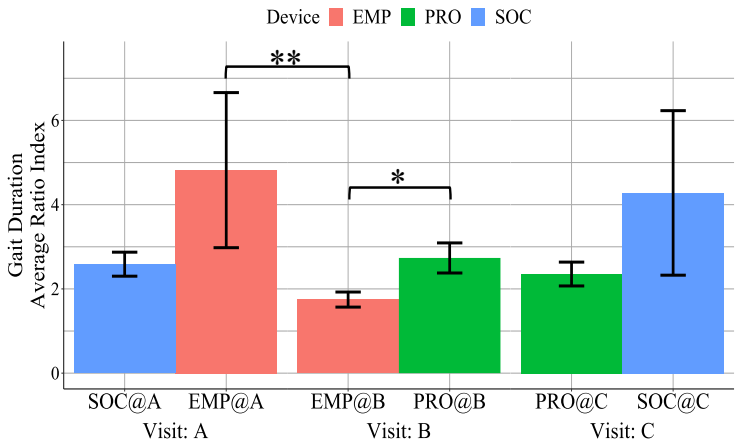

Figure 1: 4-week acclimation yielded most symmetrical gait duration (nearest 1.0) with EMP@B, but not significantly different from SOC@A, SOC@C, and PRO@C. (* indicates $p<0.05$; ** indicates $p<0.01$.)

Significance: The results suggest that 30 minutes is an inadequate acclimation period to realize the changes in gait kinematics associated with using a microprocessor-controlled or powered transtibial prosthesis. With an extended acclimation period, powered devices, like EMP, offer the potential for gait duration symmetry benefits in level-ground walking, and despite their greater weight, do not compromise ground clearance as measured by maximum knee flexion in swing.

References: [1] Esquenazi (2004), Disabil. Rehabil. 26(14–15); [2] Rábago et al. (2016), PLoS One 11(12); [3] Wanamaker et al. (2017), Prosthet Orthot Int 41(5); [4] Jasiewicz et al. (2006), Gait Posture 24(4).

ANALYSIS OF COMPRESSION ON POSTURAL ORTHOSTATIC TACHYCARDIA SYNDROME – A PILOT STUDY

S. Marston[2], Kurt M. DeGoede[1*]
[1]School of Engineering and Computer Science, Elizabethtown College
[2]School of Sciences, Elizabethtown College
*Corresponding author's email: degoedek@etown.edu

Introduction: Postural Orthostatic Tachycardia Syndrome (POTS) is an expanding condition classified as a form of autonomic dysfunction. Defining symptoms of POTS are orthostatic intolerance, increased heart rate upon standing, dizziness, and pre-syncope. This condition also manifests in a variety of other symptoms including brain fog, fatigue, and nausea. Due to the unique and variable etiology of POTS, treatment approaches focus on management of symptoms. Patients living with POTS may utilize pharmacological and non-pharmacological treatments to manage symptoms [1]. Non-pharmacological treatments include increased salt and water intake, physical therapy, cognitive behavior therapy, exercise programs, and compression garments [2 3]. A recent article suggests benefits in minimizing increased heart rate and maintaining blood pressure by wearing 20-40 mmHg compression stockings. [4]. While more research on the effects of traditional compression garments on orthostatic symptoms is in progress, evidence on the efficacy of compression is sparse. A large portion of earlier literature recommends the use of compression stockings to reduce and manage POTS symptoms but does not adequately address benefits. Several past analyses on POTS encourage the use of compression stockings from the ankle to abdomen to treat venous pooling in the extremities [2 5]. However, these articles did not utilize any testing to evaluate the effects on POTS symptoms. Furthermore, the effects of other compressive modalities on POTS symptoms, such as standing in water, have not been evaluated. Standing in waist-deep water produces pressures comparable to or more than those achieved by compression stockings. This pilot study will investigate the potential benefits of in-water standing compared to traditional compression garments. It will also evaluate the potential benefits of compression garments compared to no interventions. It is hypothesized that compression stockings and in-water standing will reduce pulse rate and increase systolic blood pressure.

Methods: Three participants (n=3) were recruited from the Lancaster County area. Participants completed three trials of different compression strengths. A randomized, three-trial design supplemented with surveys was used. Three trials of no compression, traditional 30-40 mmHg graduated compression leggings, and in-water standing were applied. Each trial contained a 10-minute supine period, 10-minute active stand, and at least a 15-minute recovery period. Baseline blood pressure and pulse rate were recorded at the end of the supine period. Additional blood pressure and pulse rate measurements were collected regularly over the active stand. Subjective symptom evaluations were collected after each trial using surveys and a final survey on intervention perception after all trials. The maximum pulse rate and blood pressure during standing were normalized to baseline values for each subject. Students t-tests were performed for no compression and compression stocking data and the no compression and in-water standing data.

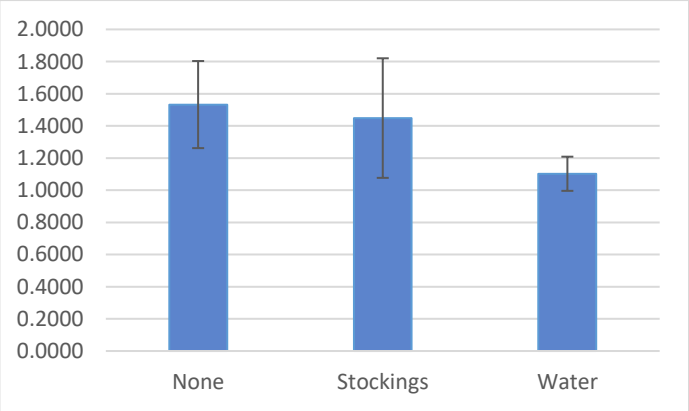

Figure 1: Pusle rate response to different compression interventions.

Results & Discussion: Recruitment and data collection for this study is ongoing. Preliminary results suggest a reduction in pulse rate for both traditional compression and in-water compression compared to no compression (Fig. 1). The difference between no compression and standing in water is approaching significance ($p<0.06$) and may be reached with the inclusion of our next scheduled subject. Excessive tachycardia upon standing is used as a diagnostic criterion for POTS. Interventions to address tachycardia are a key focus of symptom management. Reduced pulse rate seen in the traditional compression stockings and in-water standing trials suggest both interventions may be effective for POTS management. Systolic and diastolic blood pressures were stable across all interventions. While systolic blood pressure was predicted to increase, it was found to have minimal change. Self-reported symptoms and subject perceptions also showed early results for decreasing symptoms for both compression legging and in-water standing interventions. Overall, favorable reports of symptoms reduction and observation of lower pulse rates were seen in the compression trials compared to no compression.

Significance: Compression garments may be an effective intervention for POTS symptom management. However, compression must be of an adequate medical grade strength to derive benefits. Additionally, compression garments may be difficult to put on or remove, limiting applicability to patients with reduced mobility. Standing in water provides consistent compression and may be an option for patients with access to a pool. Aquatic therapy should be considered as a step in treating POTS patients with severe symptoms who cannot perform upright exercise.

Acknowledgments: Elizabethtown College SCARP program

References: [1] Vernino et al. (2021), *Aut neuro* 235; [2] Bryarly et al. (2019), *JACC* 73(10); [3] Bruce et al. (2016), *Cln Ped* 55(14); [4] Bourne et al. (2021), *JACC* 77(3); [5] Fedorowski (2018), *J Int Med*, 285(4).

Comparing Gait Strategies of Young and Older Adults While Transitioning From Even to Uneven Surfaces

Mitchell L. Talton, Ilana Levin, Peter C. Fino, Katherine L. Hsieh, Lisa A. Zukowski
[1]Department of Health and Human Performance, High Point University, High Point, NC
Email: mtalton@highpoint.edu

Introduction: Older adults often fall while walking in complex environments [1]. Compared to young adults, older adults tend to exhibit a more cautious gait strategy while walking on even ground, spending more time in double limb support and taking shorter steps [1], and while walking on uneven surfaces, taking shorter steps and lowering their center of mass [2]. However, to date, no research has examined how much time older adults spend in single versus double limb support while walking on an uneven surface or analyzed gait strategies while transitioning from an even surface to an uneven surface. Therefore, this study will compare gait strategies, in terms of gait speed (GS) and percentage of gait cycle spent in single limb support (SLS), double limb support (DLS), and stance phase (Stance), of young adults (YA) and older adults (OA) while transitioning from an even to an uneven surface. Based on previous research, we hypothesized that OA would exhibit a more cautious gait strategy, demonstrating slower GS, spending a greater percentage of the gait cycle in DLS and Stance, and spending a smaller percentage in SLS, compared to YA.

Methods: Fifty-four OA [age=78.3(4.6), 24 females] and 29 YA [age=30.7(3.4), 11 females] completed 2 sets of walking trials on a custom-built walkway that consisted of even and uneven surface sections. The 2 sets of walking trials utilized a different uneven surface: an uneven grass surface and an uneven rock surface.

Gait data were recorded using six Opal sensors (128 Hz, APDM Inc.) and post-processed in Mobility Lab (APDM Inc.) software and a custom Matlab (MathWorks) program that calculated gait metrics for five stride locations that occurred around the transition from the even to the uneven surfaces. The gait metrics were GS (m/s), SLS (% of gait cycle), DLS (% of gait cycle), and Stance (% of gait cycle). The 5 stride locations were the Approach stride (i.e., 2 strides before the transition); the Pre-Transition stride (i.e., 1 stride before the transition); the Transition stride; the Post-Transition stride (i.e., 1 stride after the transition); and the Uneven stride (i.e., 2 strides after the transition). A linear mixed effects model assessed the effects of age group on GS, SLS, DLS, and Stance at each stride location.

Results: In both the rocks and grass conditions, compared to their GS at the Approach stride, OA and YA slowed down during the Transition (Grass: -0.02 m/s, $p=0.04$; Rocks: -0.6 m/s, $p<0.001$), Post-Transition (Grass: -0.03 m/s, $p=0.004$; Rocks: -0.03 m/s, $p=0.01$), and Uneven (Grass: -0.03 m/s, $p=0.001$; Rocks: -0.03 m/s, $p=0.02$) strides. Additionally, in both conditions, OA slowed down more than YA on the Post-Transition (Grass: -0.07 m/s, $p<0.001$; Rocks: -0.04 m/s, $p=0.01$) and Uneven (Grass: -0.07 m/s, $p<0.001$; Rocks: -0.05 m/s, $p<0.001$) strides.

In both the grass and rocks conditions, OA and YA reduced their SLS during the Transition (Grass: -0.56%, $p=0.005$; Rocks: -1.07%, $p<0.001$) and Post-Transition (Grass: -0.40%, $p=0.05$; Rocks: -1.11%, $p<0.001$) strides, relative to the Approach stride. Relative to YA, OA exhibited a smaller SLS on the Approach stride (Grass: -0.095%, $p=0.02$; Rocks: -0.87%, $p=0.05$), in both conditions.

OA exhibited a larger DLS, relative to YA, during the Approach (Grass: 2.00%, $p=0.01$; Rocks: 1.88%, $p=0.03$) and Post-Transition (Grass: 1.31%, $p<0.001$; Rocks: 1.17%, $p=0.004$) strides, in the grass and rocks conditions.

Similar to the changes in DLS, in the grass and rocks conditions, OA exhibited a larger Stance than YA during the Approach (Grass: 1.04%, $p=0.01$; Rocks: 1.05%, $p=0.02$) and Post-Transition (Grass: 0.88%, $p<0.001$; Rocks: 0.82%, $p=0.001$) strides.

Discussion: These results provide evidence that both groups exhibited a more cautious gait strategy, slowing down and spending a smaller percentage of time in SLS, while transitioning onto and walking on the uneven surfaces. These results are consistent with previous findings that OA exhibit a more cautious gait strategy, reducing GS and step length, while walking on an irregular surface, relative to a level surface [3]. In partial support of our hypothesis, OA exhibited a more cautious gait strategy than YA, slowing down more, spending a smaller percentage of time in SLS, and spending a larger percentage of time in DLS and Stance, during the Post-Transition stride, but exhibiting less consistent differences from YA across the other strides. The Post-Transition stride may have posed the greatest challenge to dynamic balance, relative to the other stride locations, because it was the first stride in which both feet were planted on the uneven surface. Spending a larger percentage of time in DLS and Stance during the Post-Transition stride may have helped OA to stabilize before continuing to walk on the uneven surface. This interpretation is supported by previous research that observed older adults to exhibit a more cautious gait strategy, reducing GS and stride length and increasing gait smoothness, while transitioning from an even to an uneven surface [4].

Significance: This study provides a novel comparison of gait strategies exhibited by YA and OA while performing an ecologically valid and complex gait task. These results provide the first evidence that OA exhibit a more cautious gait strategy while transitioning onto an uneven surface, relative to while walking on an uneven surface. Transitioning onto uneven surfaces should potentially be included in gait training and fall prevention programs for OA.

Acknowledgement: This project was supported by the National Institutes of Health, through an Administrative Supplement funded through B-NET (R01-AG052419), the Wake Forest University Claude D. Pepper Older Americans Independence Center (P30-AG21332), and the Wake Forest Clinical and Translational Science Institute (UL1-TR001420).

References: [1] Woollacott and Tang (1997), *Phys Ther* 77(6): 646-60; [2] Dixon et al. (2018), *Gait & Posture* 61: 257-262; [3] Hylton et al. (2003), *Age Ageing* 32:137-42; [4] Zukowski et al. (2024), *Hum Mov Sci* 93: 103175.

COMPARING THEIA3D ANALYSIS SETTINGS TO MARKER-BASED OUTCOMES IN LOWER LIMB KINEMATICS OF CHILDREN WITH CEREBRAL PALSY(CP)

Jutharat Poomulna[1*], David C Kingston[1]
[1]1Department of Biomechanics, University of Nebraska at Omaha, Omaha, NE, USA
email: jpoomulna@unpomaha.edu

Introduction: Accurate assessment of lower limb joint kinematics is vital in clinical and research contexts with marker-based (MB) systems being ubiquitous. However, MB approaches require time-consuming calibration and post-processing data and subject preparation procedures due to manual marker placement. In contrast, Theia3D uses multiple color videos for a markerless (ML) approach, leveraging deep learning algorithms for human pose estimation [1]. The ML approach has reduced data collection time and consistent joint kinematics across multiple sessions in healthy young adult subjects [2]. By default, the Theia3D model uses varying degrees of freedom (DOF) for each joint in the lower limb kinematic chain: six at the pelvis, three at the hip, two at the knee, and three at the ankle. We are unaware of a direct comparison between Theia3D's default settings and available options to assess their impact on kinematic outcomes compared to a MB approach. This study aimed to explore available settings options by adjusting DOF and cutoff frequency settings during Theia3D's analysis. Test parameters in Theia3D's analysis settings were assessed in children with CP during overground walking, comparing outcomes to MB approaches. We hypothesized that variations in kinematic model, DOF, and cutoff frequency settings in Theia3D analysis will lead to significant differences in hip, knee, and ankle joint kinematics compared to MB approaches in this clinical population.

Methods: Five children with CP (GMFCS 1-3), M: F (3:2), age (12.79±4.99 yrs.), height (1.41±0.2 m), weight (34.87±11.76 kg) were recruited to this study. A 10 camera MB system (Oqus, Qualisys AB, Gothenburg, Sweden) and 10 camera ML system (Miqus Hybrid) were used to record motion data from 54 markers on the pelvis and lower limbs. The two camera systems were synchronized and recorded motion data at 70 Hz. Video data were processed using Theia3D software (v2023.1.0.3161[patch 11], Theia Markerless Inc., Kingston, ON) at five different cutoff frequencies (5 Hz, 10 Hz, 15 Hz, 20 Hz, and 25 Hz) for both default settings (2 DOF knee, 3 DOF feet) and settings with a 3 DOF knee and a 6 DOF feet. Kinematic outcomes from ML were analyzed in Visual3D software (C-Motion, USA) alongside marker trajectories from the MB to compute 3D hip, knee, and ankle joint angles. Root means square difference (RMSDs) between each Theia3D settings and the MB approach were computed using MATLAB (version R2021a, Natick, MA). Descriptive statistics, three-way ANOVA with a within-subjects design (3x2x5 levels), were conducted using R software (RStudio version 2022.12.0) to determine how combination of main effects (kinematic model, DOF, and cutoff frequency in Theia3D settings) influence on the sagittal plane lower limb joint angles. A p-value < 0.05 was considered statistically significant.

Results & Discussion: The knee joint with default DOF at 10 Hz showed the highest RMSD (12.30° ± 3.20°), while the hip joint with enabled DOF at 25 Hz exhibited the lowest RMSD (10.36° ± 4.37°). ANOVA results indicated a non-significant main effect of joint ($F(2,120) = 2.393$, $p = 0.096$), DOF ($F(1,120) = 0.173$, $p = 0.678$), and frequency ($F(4,120) = 0.017$, $p = 0.999$). Additionally, there was no significant two-way interaction between kinematic model and frequency ($F(8,120) = 0.001$, $p = 1.00$), DOF and frequency ($F(4,120) = 0.011$, $p = 0.100$), or kinematic model and DOF ($F(2,120) = 0.017$, $p = 0.983$). Similarly, the three-way interaction was non-significant ($F(8,120) = 0.009$, $p = 1.00$). These findings suggest that there is no significant influence of kinematic model, DOF and cutoff frequency on joint kinematics. The DOF modification at knee and feet appears to have greater impact on knee and ankle joints compared to hip joint, as indicated by lower RMSD at the hip joint. Enabling DOF might have a potential to reduce RMSD between systems, however, further study with larger samples, and multiple movement planes is needed to confirm these findings and improve understanding of factors impacting joint kinematics estimation.

Significance: The study provides insights into optimizing Theia3D, a markerless motion capture system, by analyzing the effects of kinematic model, DOF configuration and cutoff frequency on joint angles compared to MB approaches. Results emphasize the advantages of specific DOF configurations and highlight the significance of larger sample sizes and varied frequencies to improve reliability, especially for users in paediatric or clinical settings.

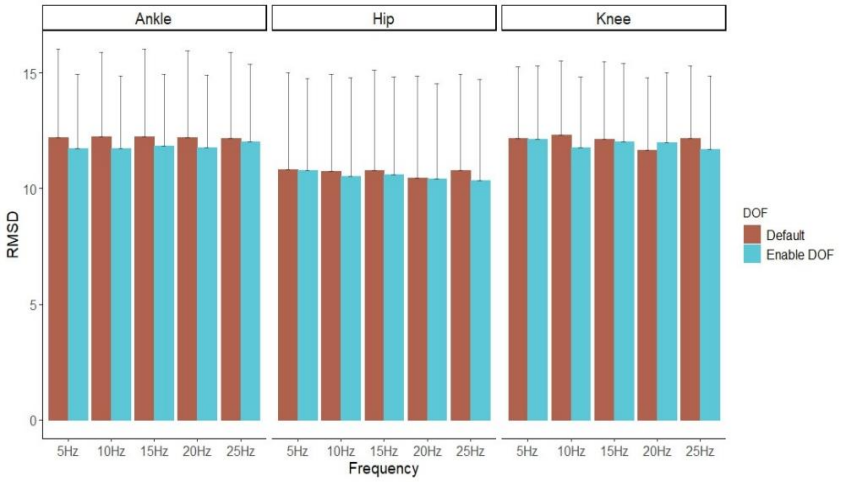

Figure 1: Bar charts depict RMSD values for hip, knee, and ankle joint angles, comparing Theia3D settings: default and with enabled degrees of freedom (DOF) at five different frequencies to MB approach.

References: [1] Mathis et al.,2020, Nat Neurosci 21(1281-1289); [2] Kanko et al.,2020, BioRxiv; [3] Steffensen et al.,2023, Research Square; [4] Riazati et al.,2022, Front. Hum. Neurosci (16);[5] Wren et al.,2023, Gait &Posture (104)

AGE AND GENDER DIFFERENCES IN TRUNK-PELVIS COORDINATION WHEN USING BACK-SUPPORT EXOSKELETONS TO PERFORM REPETITVE LIFTING

Rahul N. Raghuraman[1], Divya Srinivasan[1*]
[1]Department of Industrial Engineering, Clemson University, Clemson, SC 29631
*Corresponding author's email: sriniv5@clemson.edu

Introduction: Repetitive lifting, often prevalent in manual material handling (MMH) tasks found in manufacturing, construction, and logistics industries, is known to be a leading cause of low back pain. Back-support exoskeletons (EXO) have emerged as a promising ergonomic intervention, due to their ability to alleviate the biomechanical load in the back. Contemporary lab studies have evaluated a multitude of EXOs with different designs and mechanisms. They have reported positive benefits mostly in terms of reduced EMG in the primary trunk extensor muscles associated with exoskeleton use. However, while changes in primary agonist muscle activity may be indicative of lower physical loading, external assistance applied through either torque generators or elastic elements surrounding the hips/lumbar region may cause redistribution of loads among the low-back musculature and may also lead to different kinematic compensation strategies among users of EXOs. Accordingly, a few recent studies have reported altered trunk dynamics (i.e., reduced trunk stability) and trunk-pelvic coordination when using EXOs [1]. However, there is insufficient understanding of the effects of different EXO designs (e.g., soft vs. rigid), as well as whether such differences in kinematic strategies are different among users of diverse age and gender groups. This is important to understand, given that there is currently limited understanding of the long-term consequences of using EXOs, and given that there is correlation between altered trunk neuromuscular dynamics and low-back disorder risk [2]. In this context, the aim of this study was to quantify the changes in trunk-pelvis coordination when users of different age and gender groups (young and old males and females) used two different EXOs to complete a repetitive lifting/lowering task in the sagittal plane. The two different EXOs included a rigid EXO with passive torque generators at the hips and a soft textile-based exosuit with elastic bands running parallel to the trunk extensors. Since users of these devices, especially women, have reported low-moderate levels of perceived movement restrictions in other studies, we expected that trunk-pelvis coordination would be affected using the EXOs, and that the extent to which coordination was affected would be further differentiated by device type and gender.

Methods: Thirty-two females and males from two age groups (young: 18-35 years old and old: 45-60 years old) were recruited from Clemson, SC area to voluntarily participate in the study. The study was approved by the Institutional Review Board of Clemson University. Two different passive EXOs – HeroWear Apex (Soft design - weighs 1.6 kg and supports using elastic bands) and Ottobock Paexo Back (Rigid design - weighs 4 kg and supports using springs) – were used. Participants tried on each device, and chose their preferred level of support, after an initial familiarization session. Participants repeatedly lifted and lowered a load of 16 lbs (7.3 kg) between waist and ankle level in the sagittal plane at the rate of 10 cycles/minute, for 3 minutes (totalling to 15 lifts and 15 lowers), in each of three EXO conditions – Control (i.e., without EXO), Apex, and Paexo Back. Participants were instrumented with Inertial Measurement Unit sensors from Xsens (MTw Awinda). Data were recorded at 60 Hz and subsequently low pass filtered at 5 Hz using a 4^{th} order bidirectional Butterworth filter. The standard ZXY rotation sequence recommended by ISB was used, to compute trunk and pelvis joint angles and angular velocities. Continuous relative phase (CRP) was used to compute trunk-pelvic coordination, and the mean-absolute relative phase (MARP), as well as the variability in coordination (i.e., deviation phase, DP) were computed for lifting and lowering [3]. Three-way repeated measures ANOVA models were used to test the effect of EXO conditions (3 levels), Age (2 levels), and Gender (2 levels) on MARP and DP for lifting and lowering separately. Statistical significance was concluded when $p<0.05$.

Results & Discussion: Analysis of CRP measures (MARP and DP) for lifting and lowering indicated several significant main and interaction effects. During lifting, on average, MARP was 9.3 degrees and DP was 8.5 degrees, while during lowering, MARP was 9.3 degrees and DP was 8.4 degrees, in the control condition. Use of both EXOs increased MARP and DP significantly, when compared to the baseline Control (i.e., no EXO condition), for both lifting and lowering ($p < 0.0001$, 59% increase with Paexo back and 29% increase with Apex during lifting and 63% increase for Paexo back and 33% increase for Apex during lowering). Furthermore, three-way interactions between EXO, Gender (GEN), and Age (AGE) were also significant. The rigid EXO increased MARP and DP significantly for both males and females of the young and old groups, while the soft EXO significantly affected only males, during lifting tasks, as compared to the control condition. Furthermore, males in the older group were affected more (i.e., showed further increase in MARP and DP) as compared to males in the young group. These interactions were similar for lifting and lowering.

Significance: Our results show that trunk-pelvic coordination was more out of phase when using back-support exoskeletons, and that the cycle-to-cycle variation in trunk-pelvic coordination was also increased, when using the exoskeletons. Whether this was because users were adopting a more "optimal" kinematic strategy or were still "searching" for a new optimum is unclear, although the increase in DP suggests that it may be the latter case. Furthermore, the influence of EXO design (i.e., soft vs. rigid) was fairly evident from the results, and the designs affected users from all groups. The difference with age and gender in the Apex (and not in the Paexo back) may be because females, and older individuals, generally preferred lower levels of support from the elastic bands, while assistance levels were standardized according to manufacturer recommendations for the Paexo back. Whether altered trunk-pelvic coordination may have detrimental effects to spinal stability and biomechanical loading in the longer-term need to be better understood.

References

[1] Madinei et al. (2021), *J Biomech* 123, 110501; [2] Panjabi (2003), *J Electromyogr. Kinesiol.* 13 (4), 371-379; [3] Zehr et al. (2018), *J Electromyogr. Kinesiol.* 39, 104-113.

STRIDE-TO-STRIDE VARIABILITY IN TRANSTIBIAL AMPUTEES' HIP MUSCLE RECRUITMENT PATTERNS

Julie Ferrell-Olson, MSc[1*], Moaz Tobaigy, MPO[1], Andrew Sawers, PhD, CPO[1]
[1]University of Illinois Chicago, Department of Kinesiology and Nutrition
*Corresponding author's email: jferre26@uic.edu

Introduction: Hip muscle recruitment patterns in transtibial (TT) amputees show greater magnitude and duration of activity in the residual limb compared to intact and non-amputees during gait [1]. No studies have characterized how variable hip muscle recruitment is in TT prosthesis users. Greater variability in hip muscle recruitment may indicate altered neuromuscular control [2]. Changes in recruitment variability over time may offer insight into motor learning [3]. The objective of this study was to quantify and compare stride-to-stride EMG variability between TT prosthesis users' residual and intact limb hip muscles and to reference values for unimpaired adults. Due to the loss of degrees of freedom and key biomechanical functions at the ipsilateral ankle, we hypothesized that residual limb hip muscle recruitment patterns would exhibit greater stride-to-stride variability compared to intact limb hip muscles and reference values for unimpaired adults. We also hypothesized that lower stride-to-stride variability in residual limb hip muscle recruitment patterns would be associated with longer times since amputation, reflecting a shift away from exploration and learning.

Methods: Surface EMG activity was recorded at 1200Hz from the adductor magnus (ADMG), gluteus maximus (GMAX), gluteus medius (GMED), and rectus femoris (RFEM) on the residual and intact hips of 10 traumatic transtibial prosthesis users walking on a treadmill at their preferred speed (1.18 ± 0.21 m/s). Participants' mean age was 53.3 years, time since amputation ranged from 4 to 57 years, and 8 were male. EMG signals were bandpass and notch filtered at 20 to 500Hz and 59.5 to 60.5Hz, respectively, full-wave rectified then low-pass filtered (10Hz) to create linear envelopes, amplitude normalized to the peak during gait, and time normalized to the gait cycle. Stride-to-stride EMG variability was quantified using the variance ratio (VR) [4]. The VR, defined as the sum of the variance at each time point within a gait cycle relative to the total variance in the data, provides a measure of the relative similarity of EMG waveform shape over a number of gait cycles [4,5]. VR values can fall between 0 and 1, with lower numbers (closer to 0) indicating more similar waveform shape across gait cycles (i.e., lower variability), and higher numbers (closer to 1) indicating more dissimilar waveforms (i.e., greater stride-to-stride variability) [4]. Here, VR was calculated over 40 consecutive strides. Independent sample t-tests were run, and Cohen's d effect sizes calculated to compare VR between residual and intact limb hip muscles. Pearson correlation coefficients were calculated to assess the relationship between VR in residual limb hip muscles and time since amputation.

Results & Discussion: Mean variance ratios (VR) ranged from 0.25-0.45 (Table 1). Except for the RFEM, and therefore in partial support of our primary hypothesis, VR in residual limb hip muscles were greater than intact limb VR, but this difference did not reach statistical significance ($p>0.05$). Greater stride-to-stride variability in residual than intact limb hip muscles may be the result of residual limb hip muscles compensating for the loss of stride-to-stride variability in the amputated/prosthetic ankle by increasing variability at the hip to maintain a desired level of "whole limb" variability [4,6]. VR for residual and intact limb hip muscles were both greater than published reference values for unimpaired adults (i.e., VR=.21 at ~ 1.5m/s) [6]. Higher VR (i.e., greater variability) in the residual and intact limb compared to unimpaired adults may arise from efforts by hip muscles to replace biomechanical functions of the amputated ankle muscles (e.g., propulsion,), or transtibial prosthesis users' slower walking speeds [4,7]. Apart from GMAX, residual limb VR negatively correlated with time since amputation (r_p= -.41 to -.49); there was no correlation between time since amputation and intact limb VR. Lower stride-to-stride EMG variability with increasing time since amputation is consistent with reductions in VR reported during motor development of typically developing children [3]. The time-VR relationship may reflect a shift away from motor exploration while learning to walk with a prosthesis, towards a more consistent and proficient control strategy.

Significance: Pending further research, residual limb hip muscle VR may help monitor adaptation to amputation, progress through rehabilitation, and/or changes in prosthetic componentry. While increased residual limb hip variability may occur in response to the loss of the ankle in TT amputees, further work is needed to assess how individual joints compensate for deficits elsewhere. Future research is also needed to determine amputation-related increases in VR are associated with the loss of sensory and/or motor function(s), whether differences in VR post-amputation and post-rehabilitation represent adaptive or maladaptive compensations, and if VR is sensitive to changes in prosthetic fit or function.

Table 1. Variance ratios for four residual and intact limb hip muscles in unilateral transtibial prosthesis users.

	Residual limb	Intact limb	
	mean [95% CI lower limit, upper limit]	mean [95% CI lower limit, upper limit]	Cohen's d
Adductor Magnus	0.45 [0.31, 0.58]	0.38 [0.26, 0.50]	.18
Rectus Femoris	0.33 [0.25, 0.42]	0.36 [0.27, 0.45]	.12
Gluteus Maximus	0.30 [0.18, 0.43]	0.26 [0.20, 0.32]	.14
Gluteus Medius	0.26 [0.14, 0.37]	0.25 [0.18, 0.32]	.13

References: [1] Fey et al. (2010), *J. of Electromyo. Kinesio* 20(1) [2] Richards et al. (2014), *Gait & Posture* 39 [3] Granata et al. (2005), *Gait & Posture* 22(4) [4] Hershler & Milner (1978), *IEEE Trans. Biomed. Eng* 25(5) [5] Steele et al. (2019), *Gait & Posture* 67 [6] Kadaba et al. (1985) *J. Orthop. Res* 3(3) [7] Wentink et a. (2013), *J. NeuroEngineering Rehab*

Patient-Reported Surveys Are Not Sensitive to Post-Stroke Changes in Biomechanics or Walking Function With Ankle Foot Orthoses

Zahra McKee[1,2], Jacob Skigen[3], Darcy Reisman[1,4], Elisa Arch[1,2]
[1]Biomechanics and Movement Science, University of Delaware, [2]Kinesiology and Applied Physiology, University of Delaware,
[3]Biomedical Engineering, University of Delaware, [4]Physical Therapy, University of Delaware
*Corresponding author's email: mckeezn@udel.edu

Introduction: Weakness of the plantar flexor muscles is commonly experienced post-stroke and can lead to limited motor function in gait [1]. To combat this, ankle-foot orthoses (AFOs) are often prescribed to align and support the ankle joint. Passive dynamic ankle-foot orthoses (PD-AFOs) are a subtype of AFO that provide rotational spring-like assistance about the ankle joint during gait [2]. PD-AFOs have shown promising results in the post-stroke population [3]. However, many measures to evaluate AFO effectiveness like cost of transport (COT) and paretic plantarflexion moment (PFM) require expensive equipment that cannot be widely implemented in a clinical setting. Instead, clinicians often use a combination of subjective observations and standardized patient-reported surveys on preference and experience. It is unknown whether these patient-reported measures are actually indicative of AFO effectiveness. The purpose of this study was to determine whether a relationship exists between these surveys and the key biomechanical measures of interest for a post-stroke population when comparing two different AFO conditions.

Methods: 18 individuals with chronic stroke participated in a study that investigated the efficacy of customizing PD-AFO stiffness customized based on an individual's level of plantar flexor weakness. Participants came in for 3 visits where they walked with No AFO (baseline), their previously prescribed standard of care (SOC) AFO, and the stiffness customized PD-AFO respectively. Participants performed a 10 Meter Walk Test overground to determine their self-selected walking speed (SSWS) for each AFO condition. They then underwent an instrumented gait analysis, walking on a treadmill at their baseline speed (determined as their SSWS in the No AFO condition). The Activity-specific Balance Confidence Scale (ABC), Orthotics and Prosthetics User Survey Satisfaction With Device and Services (OPUS), and Quebec User Evaluation of Satisfaction with assistive Technology (QUEST) 2.0 surveys were also conducted at each visit focusing on the relevant AFO condition. Data was processed through Qualysis Track Manager, followed by analysis in Visual 3D to extract mechanical COT and peak PFM. For each measure, group means, standard deviations, and the differences between the SOC and PD-AFO results were calculated. Correlations between the SOC and PD-AFO differences for the 3 surveys and 3 biomechanical outcome measures of interest were performed in RStudio using a Spearman rank-order test for non-parametric data (9 total regressions).

Results & Discussion: Group means and standard deviations for the survey and biomechanical outcomes are presented in Table 1. On a group level, there were improvements in all outcomes except for PFM for the PD-AFO condition compared to SOC AFO. However, there was also large variance in all outcomes, as is to be expected in a heterogeneous post-stroke population. Additionally, no significant relationship was found between changes in any of the surveys and changes in any of the biomechanical outcome measures (Table 2), indicating that changes in self-selected walking speed, cost of transport, or peak paretic plantarflexion moment were not reflected in any of the survey scores. While these surveys and biomechanical measures target different aspects of an individual's device use experience and thus may seem unrelated, the lack of relationship between these surveys and biomechanical measures reveals important information about how patient-reported outcome measures miss underlying biomechanical changes with different AFO conditions. Previous research has found correlations between patient-reported outcome measures, including surveys, and biomechanics in other clinical orthopedic populations [4-6]. Some potential explanations for why this may not have been seen in this study include more tangential surveys, possible sensory or neurological deficits caused by stroke, or a disconnect between the walking biomechanics we associate with better gait performance and the experiences, demands, or preferences of participants post-stroke. More functional clinical measures or targeted surveys may be more appropriate predictors of biomechanical improvements than patient-reported clinical measures like the surveys used in this study.

	SOC AFO	PD-AFO	Difference
SSWS (m/s)	0.64 ± 0.29	0.69 ± 0.31	0.05 ± 0.09
COT (J/kg/m)	2.51 ± 0.69	2.29 ± 0.45	-0.22 ± 0.37
PFM (Nm)	-0.90 ± 0.25	-0.89 ± 0.24	0.01 ± 0.11
ABC	71.90 ± 13.38	72.48 ± 17.02	0.59 ± 13.79
OPUS	28.22 ± 4.60	30.50 ± 3.19	2.28 ± 4.44
QUEST	32.94 ± 7.67	36.78 ± 3.26	3.83 ± 7.12

Table 1. Group means and standard deviations for AFO conditions and differences between SOC and PD-AFOs

	SSWS	COT	PFM
ABC	0.62	0.33	0.45
OPUS	0.65	0.49	0.63
QUEST	0.50	0.63	0.16

Table 2. P values for linear regression of difference in SOC and PD-AFO values between three surveys (ABC, OPUS, QUEST), and three biomechanical outcome measures (SSWS, COT, PFM)

Significance: Clinicians using ABC, OPUS, or QUEST to evaluate a patient's preference or experience with a mobility device like a PD-AFO should not assume an improvement in scores on these surveys represents improvements in walking function, biomechanics, or AFO effectiveness. Future research should explore other methods to assess biomechanical AFO effectiveness in a clinical setting.

Acknowledgments: This work was supported in part by USAMRAA (Award No. W81XWH-18-1-0502)

References: [1] Nadeau (1999), Clin Biomech 14(2) [2] Faustini (2008), IEEE Biomed Eng 55(2) [3] Koller (2021), Prosthet Orthot Int 45(4) [4] Fischer (2019), Gait Posture 69 [5] Wu (2023), Clin Orthop Relat R 481(12). [6] Moyer (2016), Osteoarthr Cart 24(1)

DEVELOPMENT AND VALIDATION OF A MULTI-DIMENSIONAL PSEUDORANDOM BALANCE ASSESSMENT

Sophia G. Chirumbole[1], Andrew R. Wagner[2], Jaclyn Caccese[1], Daniel M. Merfeld[1], Ajit MW Chaudhari*[1]

[1]Ohio State University, [2]Creighton University

*Corresponding author's email: chaudhari.2@osu.edu

Introduction: Pseudorandom balance perturbation assessments use disturbances of the support surface that cannot be predicted by the participant to quantify reactive postural control. Yet, up until this point, only one-dimensional perturbations (e.g., roll or pitch tilts) have been studied. These one-dimensional (1-DoF) perturbations provide a robust paradigm for modeling closed loop postural control [1]. However, the nature of these perturbations — requiring unidimensional roll or pitch responses in isolation — conflicts with the multidimensional perturbations experienced during naturalistic motion. The aim of this study was to bridge this gap by developing and validating a paradigm that utilizes two spectrally independent sum of sinusoids signals (SoS_1 and SoS_2), one for each orthogonal dimension of tilt (roll and pitch), to deliver a two-dimensional (2-DoF) pseudorandom balance perturbation. Our hypotheses were (1) that during 2-DoF perturbations, the mediolateral (ML) and anteroposterior (AP) center of pressure postural response (CoP) would increase primarily at the roll and pitch platform perturbation frequencies, respectively and (2) that the postural response during a 1-DoF perturbation trial would be similar to the postural response to an identical 1-DoF stimulus delivered as part of a 2-DoF perturbation.

Methods: Signals SoS_1 and SoS_2 were developed by selecting two groups of interleaved prime numbers ([1, 3, 7, 13, 19, 29] and [2, 5, 11, 17, 23, 31]) and multiplying them by a fundamental frequency of 0.044 Hz. This yielded frequency components f_{SoS1} and f_{SoS2}. Displacement trajectories were then created by the summation of sinusoidal signals, resulting in two SoS time trajectories (SoS_1 and SoS_2) that have interleaved, spectrally separated perturbation frequencies. Postural responses of ten healthy participants (37 ± 13 years of age, 3 F) were collected using embedded force plates during both 1-DoF and 2-DoF test conditions. A metric representing total ML and AP CoP magnitude was calculated by summing the CoP spectral magnitudes separately at the f_{SoS1} and f_{SoS2} perturbation frequencies. Center of mass (CoM) height was estimated at the waist. This estimate of CoM height was combined with CoM horizontal displacement, estimated by low pass filtering the ML and AP CoP data at 0.47 Hz, to calculate roll and pitch sway angles in units of degrees [2]. The normalized response magnitude (R_{Norm}) was quantified using the absolute value of the complex numbers, calculated through the ratio between the discrete Fourier transform of the estimated CoM angles and the platform tilt angles at the perturbation frequencies [3]. CoM phase values, describing the timing of CoM sway relative to the platform perturbation, were calculated using the *unwrap* function in MATLAB (v2020b, Natick, MA).

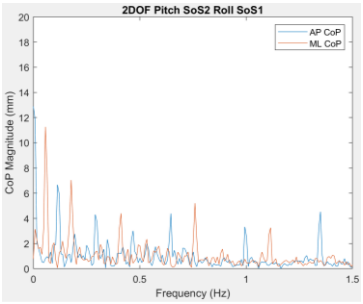

Figure 1: The spectral magnitudes of the mediolateral (ML, orange) and anteroposterior (AP, blue) center of pressure (CoP) responses for a single subject during a 2-DoF test condition.

Results & Discussion: We found that during 2-DoF perturbation conditions, spectral peaks in the sway response were larger at the perturbed frequencies when compared to (1) the adjacent non-perturbed frequencies and (2) the frequencies contained within the orthogonal, spectrally independent perturbation signal (Figure 1). We also found that for each of the two spectra studied (SoS_1 and SoS_2), the magnitude and timing of the sway response relative to the platform disturbance was similar when measured during 1-DoF (i.e., roll or pitch tilt in isolation) and 2-DoF (i.e., roll and pitch tilts delivered simultaneously) conditions (Figure 2). Collectively, these data support that our novel 2-DoF SoS perturbation paradigm was able to provoke ML and AP postural responses that were (1) specific to the roll and pitch perturbations, respectively, and (2) similar to the responses provoked by individual 1-DoF perturbations.

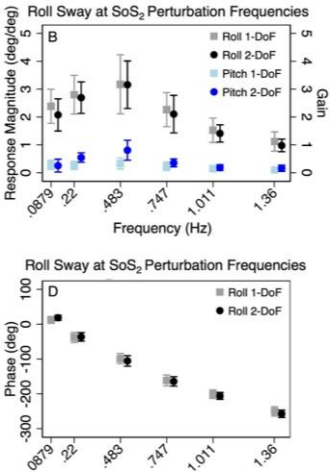

Figure 2: The mean (across subjects) normalized response magnitudes (B) and phases (D) of the center of mass (CoM) in the roll plane are shown for the 2-DoF (black) and 1-DoF (grey) roll perturbation conditions, at each of the individual f_{SoS2} frequencies.

Significance: These results show that 2-DoF pseudorandom perturbation responses are directionally independent, and, further, that responses in each direction due to 1-DoF and 2-DoF perturbation signals are comparable. This suggests that the human balance system senses multi-dimensional perturbations, that can be combined by the central nervous system to generate appropriate multi-dimensional responses, leading to the directionally independent biomechanical response metrics detailed above. This assessment could screen for balance impairment more efficiently, as it cuts test time in half by testing two perturbation directions during a single test trial. Also, this may be a more ecologically valid test paradigm, as our sensory systems simultaneously sense multi-directional stimuli, and many natural activities of daily living are multi-directional in nature.

Acknowledgments: This work was supported by the National Institutes of Health [5R01AG073113-02].

References: [1] Peterka RJ. (2002), *J Neurophysiology*. 88(3):1097–1118. [2] Campbell KR. (2022), *Front Neurol*. 13:897454. [3] Peterka RJ. (2018), *Front Neurol*. 9:1045.

EVALUATING THE EFFECT OF AGING ON THE SPEED-ACCURACY TRADE-OFF DURING PRECISION WALKING

Isaiah J. Lachica* and James M. Finley
Division of Biokinesiology and Physical Therapy, University of Southern California, Los Angeles, CA
*Corresponding author's email: ilachica@usc.edu

Introduction: In motor tasks where precision is paramount, we often slow our movements to improve accuracy. This trade-off between speed and accuracy [1] is thought to be driven by two factors. First, fast movements often require large forces, and these forces are more variable [2]. Second, there may be insufficient time to use visual feedback to perform error corrections when moving fast [1]. Thus, moving more slowly could improve precision by reducing speed-dependent variability and providing more time for feedback-mediated corrections. While the contributions of these factors have been evaluated in upper extremity tasks, it remains unclear whether they would similarly contribute to the speed-accuracy trade-off observed in precision walking [3].

There is evidence that the relationship between speed and accuracy during upper extremity movements is modified with aging as older adults move more slowly than young adults as accuracy demands increase [4]. This effect is believed to be due to older adults generating slower feedback corrections [5] and compensating for greater speed-dependent variability [6]. However, the effect of aging on the speed-accuracy trade-off during precision walking remains unclear.

Here, we seek to determine the factors contributing to the speed-accuracy trade-off during precision walking and how the roles of these factors change with aging. We hypothesize that the inability to perform feedback corrections but not speed-dependent variability will contribute to the speed-accuracy trade-off. We also hypothesize that speed will have a greater effect on error in older adults as they will have greater difficulty performing feedback corrections at fast speeds.

Methods: Five healthy young and three healthy older adults completed a treadmill-based precision walking task at 60%, 80%, 100%, 120%, and 140% of their self-selected walking speed while viewing a screen with online feedback of a set of actual and target step lengths. The target step lengths were randomly sampled from the self-selected step lengths observed at each speed. Foot placement error was calculated as the distance between the actual and target step length. Step length variability was calculated as the interquartile range of the actual step lengths in a trial. Feedback corrections were estimated by calculating the number of velocity peaks of the heel marker during the swing phase. Group data are reported as means and standard deviations. Linear mixed-effects models were used to test for the effect of speed on foot placement error in young adults and the effects of speed and age group on step length variability and number of velocity peaks.

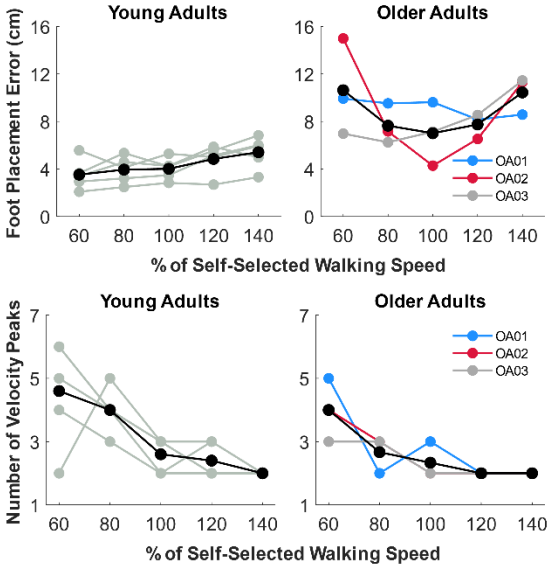

Figure 1: Preliminary data from young and older adults for (A) foot placement error and (B) number of velocity peaks for the heel marker during swing phase. Data in black represent group means.

Results & Discussion: Foot placement error increased with gait speed in young adults ($\beta = 1.8 \pm 0.4$, $p = 8.5e\text{-}05$), consistent with the classic speed-accuracy trade-off (Fig. 1A). While the older adults had greater errors than young adults across speeds (on average 8.7 ± 2.6 cm and 4.4 ± 1.3 cm, respectively), they exhibited different speed-accuracy trends (Fig. 1A). OA03 increased their errors with gait speed (60%: 7.0 cm, 140%: 11.5 cm) while OA01 did not (60%: 9.9 cm, 140%: 8.6 cm). The minimum error for OA02 was observed at self-selected walking speed (100%: 4.3 cm), and error increased as they deviated from it (60%: 15.0 cm, 140%: 11.3 cm).

Step length variability did not change with gait speed in young or older adults ($\beta = -0.8 \pm 1.2$, $p = 0.5$). Additionally, step length variability was lower in older adults (7.0 ± 2.9 cm) than in young adults (11.4 ± 3.8 cm). As such, speed-dependent variability does not explain the speed-accuracy trade-off during precision walking or the heightened error observed in older versus young adults.

The number of velocity peaks decreased as gait speed increased similarly in young and older adults ($\beta = -2.6 \pm 0.4$, $p = 0.7.4e\text{-}07$; Fig. 1B). Thus, movements become more ballistic when moving at faster speeds, which may increase errors during precision walking. However, the lack of difference between groups suggests that this factor does not explain the greater error exhibited by older adults.

Significance: Our result suggests that speed-dependent variability does not drive the speed-accuracy trade-off during precision walking in young or older adults. Since the number of velocity peaks did not differ between groups, future work is needed to identify factors contributing to the greater errors demonstrated by older adults than young adults across all speeds during precision walking. Future work is also needed to determine factors that may explain the different speed-accuracy trends observed in older adults. Understanding this relationship in older adults is important as impairments in adapting gait to various demands may increase fall risk.

Acknowledgments: This work is supported by NSF Award 2043637.

References: [1] Woodworth (1899), *Psychol Rev Monogr Suppl* 3(3); [2] Schmidt et al. (1979), *Psychol Rev* 86(5); [3] Roerdink et al. (2021), *Gait Posture* 85; [4] Ketcham et al. (2002), *J Gerontol Ser B* 57(1); [5] Sarlegna (2006), *Neurosci Lett* 403(3); [6] Galganski et al. (1993), *J Neurophysiol* 69(6).

ARE PASSIVE-DYNAMIC ANKLE-FOOT ORTHOSES MORE BENEFICIAL TO PARETIC OR NON-PARETIC LIMB ENERGETICS FOR INDIVIDUALS POST STROKE?

Jacob T. Skigen[1*], Corey A, Koller[2,3], Zahra N. McKee[2,3], Shay R. Pinhey[2,3], Elisa S. Arch[2,3]
[1]Department of Biomedical Engineering, [2]Biomechanics & Movement Science Program, Department of Kinesiology & Applied Physiology, University of Delaware, Newark, DE
*Corresponding author's email: jtskigen@udel.edu

Introduction: Passive-dynamic ankle-foot orthoses (PD-AFOs) are commonly prescribed to individuals post-stroke to supplement weakened plantar-flexor muscles in their paretic limb. Our previous research demonstrated stiffness-customized PD-AFOs can reduce the net mechanical cost of transport (COT) for individuals post-stroke when walking compared to walking with No AFO or with their standard-of-care (SOC) AFO [1]. The purpose of this study was to further investigate the source of this COT reduction. We hypothesized that net COT reductions would be driven primarily by reductions in the COT of the paretic limb.

Methods: Twenty individuals (mean (SD) age 63.5 (10.1) years; height 1.74 (1.1) m; mass 88.2 (17.7) kg; 14 male, 6 female) with hemiparetic chronic stroke took part in this study. Instrumented gait analysis was conducted using an instrumented treadmill and motion capture cameras as participants walked with No AFO, their SOC AFO, and a stiffness-customized PD-AFO, all at their self-selected walking speed determined via a 10-Meter Walk Test with No AFO. Biomechanical data were processed and analysed in Visual 3D. Mechanical COT was calculated per limb for each condition by summing the absolute value of both the positive and negative work performed by the hip, knee, and ankle throughout the gait cycle, and distal foot during stance, normalized by body mass, and then normalized again by stride length [2]. Net COT was then calculated by summing the COT of the two limbs together. Skillings Mack tests were used to compare average COT values across the three conditions for the paretic and non-paretic limbs. When significant main effects were found, Wilcoxon signed-rank tests were used to perform post-hoc pairwise comparisons, with a Holm-Bonferroni correction to account for multiple comparisons.

Table 1: Group means and standard deviation of mechanical cost of transport for paretic and non-paretic limb in each brace condition (J/kg/m). * Denotes significant difference.

	Paretic	**Non-paretic**
No AFO	1.08 ± 0.33 (n = 19)	1.58 ± 0.40 (n = 18)
SOC AFO	0.98 ± 0.34 (n = 18)	1.53 ± 0.53 (n = 18)
PD-AFO	0.90 ± 0.22 (n = 20)	1.38 ± 0.40 (n = 20)
p-value	*0.340*	*0.003**

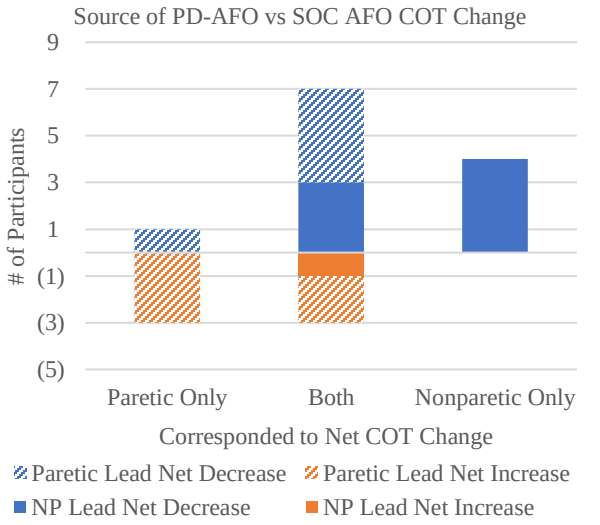

Figure 1: Source of COT change by limb while walking with the PD-AFO compared to SOC AFO (n=18).

Results & Discussion: One participant could not walk without a hinged orthosis and therefore no data were collected for the No AFO condition. Due to a technical issue, mechanical COT could not be calculated for one participant's non-paretic limb for the No AFO condition. While there was a significant difference in non-paretic COT between No AFO and PD-AFO ($p < 0.01$) and between SOC AFO and PD-AFO ($p < 0.01$), there was no significant change in paretic COT between conditions (Table 1).

After observing reduced COT in the non-paretic limb across brace conditions but not in the paretic limb, additional analysis was performed to compare whether the direction of mechanical COT change (increase or decrease) in the paretic and non-paretic limbs aligned with the direction of change in net COT for each participant. Figure 1 only shows the comparison between SOC AFO and PD-AFO due to space constraints but results from both comparisons are summarized here. Of the 15 participants who reduced net COT with the PD-AFO compared to No AFO, 12 had a larger magnitude change in their non-paretic limb than paretic. Of the 12 participants who reduced COT with the PD-AFO compared to SOC AFO, seven had a larger magnitude change in the non-paretic limb. In instances where the paretic and non-paretic limb COT changes were in the opposite direction with the PD-AFO compared to walking with their SOC AFO, a decrease in net COT was more likely to be driven by a decrease in the COT of the non-paretic limb than the paretic; and net increases were only caused by an increase in the paretic limb's COT. Previous research has shown that for individuals post-stroke, weakness of their paretic limb necessitates non-paretic limb compensation to maintain walking speed [3]. This can be observed in how much higher non-paretic COT is than paretic COT across all brace conditions. In that context, our results suggest that the PD-AFO reduced the need for participants to compensate with their non-paretic limb, which indirectly produced reductions in net COT, even if paretic COT increased.

Significance: Results from this study suggest that while stiffness-customized PD-AFOs can enhance the paretic limb of individuals post-stroke, as evidenced by reduced paretic COT for several participants, a larger benefit for most participants is lessening the burden on their non-paretic limb. This study highlights the importance of considering the effect on the entire lower limb system - notably the non-paretic limb - when designing and customizing AFOs, and likely other rehabilitation interventions, for individuals post-stroke.

Acknowledgments: This work was supported in part by USAMRAA (Award No. W81XWH-18-1-0502)

References: [1] Skigen, J. et al. Preprint, in review; [2] Ebrahimi, A. et al. Gait & Posture, 56, 49-53, 2017; [3] Roelkar, S. et al. Gait & Posture, 68, 6-14, 2019

AQUATIC TREADMILL WALKING LOWERS MUSCLE CO-CONTRACTION IN CHILDREN WITH CEREBRAL PALSY

Joseph W. Harrington[1*], Colina Matthews[1], Brian A. Knarr[1], Vivek Dutt[2], David C. Kingston[1]
[1]Department of Biomechanics, University of Nebraska at Omaha, Omaha, NE, US
[2]Department of Orthopaedic Surgery, University of Nebraska Medical Center, Omaha, NE, US
*Corresponding author's email: josephharrington@unomaha.edu

Introduction: Children with cerebral palsy (CP) have movements characterized by lower-extremity muscle weakness, increased muscle co-contraction, and spasticity [1,2]. There is a need for innovative rehabilitation approaches to develop motor skills and endurance in this clinical population. Aquatic treadmill walking offers a unique environment to facilitate repetitive gait cycles while capitalizing on the benefits of altered body weight support, increased hydrodynamic resistance on limbs, and postural stability. We investigated muscle co-contraction indices (CCI) during aquatic treadmill walking compared to conventional treadmill walking. By exploring the dynamics of CCI in this aquatic setting, we aimed to contribute valuable insights into the effectiveness of aquatic treadmill training in addressing muscle co-contraction and spasticity management, thus potentially advancing rehabilitation strategies for children with cerebral palsy.

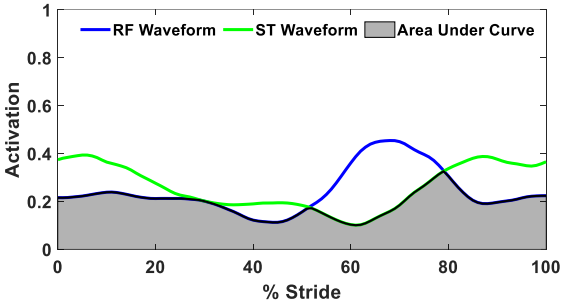

Figure 1: Visual representation of mean muscle activation waveforms of the rectus femoris (RF) and semitendinosus (ST) for one child with CP. In this example co-contraction is equal to the shaded region (the area under the curve).

Methods: Fifteen typically developing (TD) children (30 limbs, 7M | 8F, 11.3 ± 4.1 yrs., 1.46 ± 0.18 m, 44.2 ± 16.8 kg) [3] and ten children with CP (20 limbs, 6M | 4F, 13.1 ± 3.5 yrs., 1.54 ± 0.18 m, 53.2 ± 26.2 kg, 7 GMFCS I and 3 II) completed three 3-minute walking trials on a conventional (Dry) and aquatic (Wet) treadmill based on varying self-selected walking speed (Slow or 75%, Normal or 100%, and Fast or 125%) determined using a previously described protocol [3]. Children were instrumented with wireless waterproof surface electromyographic (EMG) sensors and inertial measurement units (Cometa srl., Milan, IT) to detect contact events for data truncation. Specific muscle sites include the rectus femoris (RF), semitendinosus (ST), tibialis anterior (TA), and medial gastrocnemius (MG). Raw EMG data were full wave rectified, filtered using a dual pass 2nd order Butterworth filter with a cut-off frequency of 6 Hz, and normalized using the greatest magnitude found in the Dry Fast walking trial. The primary outcome was mean co-contraction of all strides for RF/ST and TA/MG muscle pairings. Co-contraction was calculated in three ways: 1) ∫ area of overlap (Figure 1) [4], 2) (EMG_s / EMG_l)*(EMG_s + EMG_l) [5], and 3) (2*EMG_ant /EMG_total)*100% [6], where EMG_s, EMG_l, and EMG_ant represent activity of the smaller, larger, and antagonist muscles, respectively. Separate linear mixed-effects models examined the influence of population (TD vs CP), walking speed (Slow, Normal, Fast), and treadmill environment (Dry vs Wet) on co-contractions for each equation. Individual differences were accounted for with a random effect of participant. Statistical analysis was performed in R (RStudio 2023, Boston, MA, US) with an *a priori* $\alpha = 0.05$.

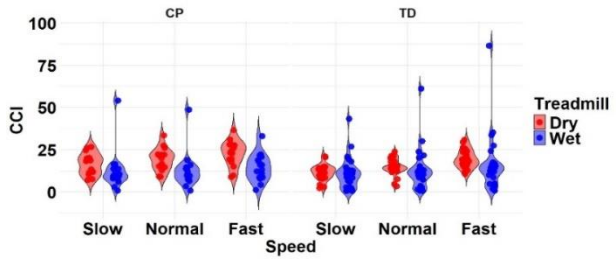

Figure 2: Violin plot of mean stride-normalized co-contraction (∫area of overlap) for the RF/ST muscle pairing of children with CP and TD children during Dry (red) and Wet (blue) treadmill walking trials. Speeds are defined in-text. Each data points represents one subject.

Results & Discussion: Linear mixed-effects models were performed with increasing complexity until the model with the lowest akaike information criterion (AIC) and bayesian information criterion (BIC) with statistical significance was found [fixed effects for Environment, Population, Speed, and their two-way interactions, along with random intercepts for each subject (AIC = 1457.7, BIC = 1501.2, $p = 0.046$) for the RF/ST muscle pairing]. Further ANOVA testing of the model revealed significant main effects of Environment ($p < 0.001$), Population ($p < 0.001$), and Speed ($p < 0.001$), as well as a significant interaction effect of Environment x Population ($p < 0.001$). Pairwise comparisons revealed there were significant differences within CP ($p < 0.001$) and TD ($p = 0.003$) when comparing the co-contraction of Wet and Dry (Figure 2). These results demonstrate that co-contraction is reduced by 4.90 for CP and 1.48 for TD when walking on an aquatic treadmill. This may be explained by the increased RF activation and reduced ST activation observed in TD children during aquatic trials [3] and similar trends in children with CP. This reduction in co-contraction may suggest that children have increased selectivity (reduced spasticity) during aquatic trials, potentially improving gait efficiency.

Significance: Aquatic treadmill walking reduced muscle co-contraction in both TD and CP populations, highlighting the importance of treadmill type in rehabilitation. Tailored interventions using an aquatic treadmill environment may help optimize gait outcomes in clinical populations that have challenges with lower-extremity muscle weakness, increased muscle co-contraction, and spasticity.

Acknowledgments: This work was supported by the National Institutes of Health (1R15HD109666).

References: [1] Dallmeijer et al. (2010), *Gait Posture*, (31), [2] Ikeda et al. (1998), *Electromyogr Clin Neurophysiol* (38), [3] Harrington et al. (2023), *J Electromyogr Kinesiol* (68), [4] Unnithan et al. (1996), *Electromyogr Clin Neurophysiol* (36), [5] Rudolph (2000), *Knee Surg Sports Traumatol Art* (8), [6] Falconer and Winter (1985), *Electromyogr Clin Neurophysiol* (25)

STRIDE TO STRIDE VARIABILITY IN TRANSFEMORAL AMPUTEES' HIP MUSCLE RECRUITMENT PATTERNS

Andrew Sawers[1*], Julie Ferrell-Olson[1], Stefania Fatone[2]
[1]University of Illinois Chicago, Department of Kinesiology and Nutrition
[2]University of Washington, Department of Rehabilitation Medicine
*Corresponding author's email: asawers@uic.edu

Introduction: Hip muscles play a vital role in adaptations made by transfemoral (TF) prosthesis users to walk with a prosthesis. Residual limb hip muscles in particular perform critical biomechanical tasks typically accomplished by ipsilateral ankle and knee muscles. Residual limb hip muscles also assume responsibility for prosthetic-specific functions including stabilization of the residual limb in the socket. Compared to kinematic and kinetic compensations [1], little is known regarding the stride-to-stride variability with which TF prosthesis users recruit their residual limb hip muscles [2,3]. Understanding stride-to-stride variability in TF prosthesis users' residual limb hip muscle recruitment may provide insight into neuromuscular control strategies that serve to motivate novel targets for locomotor rehabilitation and identify solutions to challenges associated with myoelectric control of transfemoral prostheses. The objective of this pilot study was to quantify and compare stride-to-stride electromyographic (EMG) variability in TF prosthesis users' residual limb hip muscles relative to reference values for unimpaired adults. Due to the loss of degrees of freedom at the ipsilateral ankle and knee, we expected stride-to-stride variability in the recruitment of TF prosthesis users' residual limb hip muscles to exceed that of unimpaired adults. We also hypothesized that stride-to-stride EMG variability would decrease with increasing time since amputation.

Methods: Surface EMG activity was recorded at 1200Hz from the gluteus maximus (GMAX), biceps femoris (BFLH), adductor magnus (ADMG), rectus femoris (RFEM), gluteus medius (GMED), and tensor fascia latae (TFL) on the residual limb of six TF prosthesis users while walking on a treadmill at self-selected speeds (~0.8 m/s) and wearing ischial containment sockets. Participants' mean age was 53 yrs, time since amputation ranged from 3 to 33 yrs, 3 were male, and 4 had traumatic while 2 had dysvascular amputations. EMG signals were bandpass (20Hz to 500Hz) and notch filtered (59.5Hz to 60.5Hz), full-wave rectified, and low-pass filtered (10Hz) to create linear envelopes that were time normalized to the gait cycle. Stride-to-stride EMG variability was quantified using the variance ratio (VR) [4]. The VR, defined as the sum of the variance at each time point within a gait cycle relative to the total variance in the data, measures the relative similarity of EMG waveform shape over a given number of strides [4,5]. A VR of 0 represents no variability (identical waveforms), and a VR of 1 represents fully stochastic behavior (dissimilar waveforms) (Fig. 1). Here, VR for each muscle was calculated over 30 strides. This method has been used extensively in the literature [4-7], enabling a comparison of our results with published data from unimpaired adults using identical analyses [7].

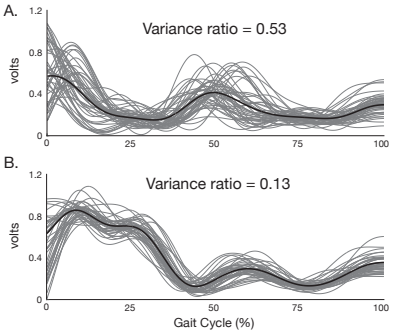

Figure 1. Residual limb gluteus medius EMG activity from two transfemoral prosthesis users. (A) high variance ratio (i.e., greater stride to stride variability) and (B) low variance ratio. Black line: mean; grey lines: individual strides.

Results & Discussion: Mean variance ratios (VR) ranged from 0.232 to 0.383 (Table 1). In support of our hypothesis, mean VR exceeded published reference values for unimpaired adults (i.e., VR=0.21 at ~ 1.5m/s). Higher VR (i.e., greater stride-to-stride variability in EMG waveform shape) may arise from efforts by residual limb hip muscles to replace the degrees of freedom and biomechanical functions of amputated knee and ankle muscles, stabilize the residual limb in the socket, or TF prosthesis users' slower walking speeds [7,8]. Residual limb VR were also found to negatively correlate with time since amputation (r_p = -0.22 to -0.69). Lower stride-to-stride EMG variability (i.e., smaller VR) with longer time since amputation is consistent with reductions in VR observed during motor development of typically developing children [6], as well as substantially higher VR in TF prosthesis users who were only 5-8 months post amputation (i.e., VR=0.55 to 0.64) [2]. The time-VR relationship may reflect a transition from motor exploration and learning to a more consistent, mature neuromuscular control strategy.

Significance: Pending further research, residual limb hip muscle VR may serve as a marker of adaptation to amputation, rehabilitation, and/or prosthetic design. VR may also improve myoelectric control of transfemoral prostheses by identifying more consistent control signals (i.e., muscles with lower VR). Next steps include determining if factors such as gait speed and stride number influence VR, and whether amputation-related changes in VR reflect adaptive or maladaptive compensations.

Table 1. Variance ratios for six residual limb hip muscles in unilateral transfemoral prosthesis users (n=6).

	Variance Ratio mean [95% CI lower limb, upper limit]
Gluteus Maximus	0.23 [0.06, 0.40]
Adductor Magnus	0.26 [0.22, 0.32]
Gluteus Medius	0.29 [0.17, 0.39]
Biceps Femoris	0.31 [0.21, 0.47]
Rectus Femoris	0.31 [0.10, 0.55]
Tensor Fascia Latae	0.38 [0.28, 0.48]

Acknowledgements: This work was supported by the Department of Defense under award number W81XWH-19-1-0547.

References: [1] Sagawa et al. (2011), *Gait Posture* 33(4); [2] Wentink (2013), *JNER* 10(87); [3] Jaegers et al. (1996), *Clin Orthop Relat Res* (328); [4] Hershler et al. (1978), *IEEE Trans Biomed Eng* 25(5); [5] Steele et al. (2019), *Gait Posture* (67); [6] Granata et al. (2005), *Gait Posture* 22(4); [7] Kadaba (1985), *J Orthop Res* 3(3); [8] Pierotti et al. (1991), *J Orthop Res* 9(5).

HAND LOADING AND LOWER LIMB KINEMATICS DURING SIMULATED ASSISTED GAIT TRAINING: PROOF OF CONCEPT

Holton C. Gwaltney[1*], Brian A. Knarr[1], Danae Dinkel[2], David C. Kingston[1]
[1] Department of Biomechanics, University of Nebraska at Omaha, Omaha, NE USA
[2] Department of Health and Kinesiology, University of Nebraska at Omaha, Omaha, NE USA
*Corresponding author's email: hgwaltney@unomaha.edu

Introduction: Cerebral Palsy (CP) is the most common cause of motor disability in children, occurring in 3.3/1000 live births[1]. Children with CP commonly have mobility limitations, but there are several clinical rehabilitative options used to improve walking. Partial Body Weight Supported Treadmill Training (PBWSTT) is one of the widest used interventions and typically requires a harness around the pelvis and trunk. Many children with CP receive orthopedic surgery, and progressive weight bearing rehabilitation using PBWSTT is an option to progress bone and muscular loading. Previous research has investigated walking speed, balance, and endurance, but few studies have investigated changes in lower limb kinematics resulting from different amounts of body weight offloaded to the hands. Obtaining kinematic data could show compensation patterns and allow clinicians to make treatment decisions to help children use or change movement patterns. The first aim of the full study, based on this pilot, aims to quantify how sagittal kinematics of the lower limb change when children with CP use varying amounts of body weight offloaded to a custom handrail that more closely resembles assistive devices used in non-laboratory settings. A second aim is to determine hand loading, speed effects, and quartile ranges during offloading in response to visual feedback.

Methods: One healthy adult subject (34 yrs, F, 1.57 m, 44 kg) took part in this pilot. Following informed consent procedures, height, weight, and anatomical measurements needed for Plug-in Gait model predictions were completed. The subject had 38 reflective markers attached according to the Plug-in Gait full body model plus medial knee and ankle markers. A 16-camera motion capture system (Vero, Vicon, Denver, CO) recorded marker trajectories at 100 Hz. A measurement from the trochanter to the floor was taken for matching the custom handrail to a comfortable height for the volunteer, with the goal of having ~30° of elbow flexion. The subject walked on a split belt treadmill (Bertec Fit5, Bertec, Colombus, OH) with force sensing handrails. A custom apparatus made of tubular steel and 3D printed clamps connected the instrumented handrails to provide handholds for the volunteer (Figure 1). The test protocol consisted of walking at a self-selected speed for 2-minutes during four hand loading (i.e., body weight offloading) conditions (self-selected, minimal, 30%, and 50% body weight) for a total of 8 minutes of walking. Visual feedback was displayed as a moving bar showing real-time force at the hands, and a stationary bar with target body weight offloaded. Handrail forces were collected at 1000 Hz. Visual3D (C-Motion, Germantown, MD) was used to calculate sagittal plane kinematics of the hip and knee. Right and left peak hip flexion (RHPF, LHPF)/extension (RHPE, LHPE) and right/left peak knee flexion (RKPF, LKPF)/extension (RKPE, LKPE) were analysed unilaterally. Forces from the handrails were filtered with a low pass dual pass Butterworth filter with a 6 Hz cutoff in MATLAB (R2023b, The MathWorks Inc. ,Natic, MA). Then, hand loading and quartile ranges were reported.

Figure 1 Instrumented subject walking with the force-sensing assistive device.

Results & Discussion: For the first aim, peak hip extension, knee flexion, and knee extension decreased as BWO increased, and peak hip flexion increased (Table 1). We speculate that, from this limited sample, leaning onto the assistive device would cause the hip flexion to increase and limit the amount of extension. The decrease in knee flexion and extension could be due to the decrease in full hip ROM which caused a shortening in stride length. For the second aim, the volunteer spent 100% of the trial within ± one inter-quartile range of the set loading target during the 30% and 50% BWO conditions. The mean force at the hands for 30% and 50 % BWO conditions was 28.8% and 45.5%, respectively. Speed effects could not be determined due to sample size.

Table 1: Average peak joint measurements for hip and knee flexion/extension.

	Condition		
Peak Joint Angle	**Minimal**	**30%**	**50%**
Left Hip Flexion	43.6°	48.6°	50.7°
Left Hip Extension	-6.3°	5.5°	9.2°
Left Knee Flexion	-79.9°	-72.8°	-69.1°
Left Knee Extension	-9.8°	-13.3°	-14.7°
Right Hip Flexion	42.0°	47.7°	50.6°
Right Hip Extension	-7.3°	6.8°	12.5°
Right Knee Flexion	-80.2°	-71.0°	-68.2°
Right Knee Extension	-6.9°	-10.5°	-12.8°

Significance: Collecting kinematics and kinetics from children with CP during treadmill walking with an assistive device that mimics a real-world prescription could help clinicians design more effective training programs for post-op rehabilitation. This training paradigm could help pediatric children learn to use an assistive device more efficiently and potentially offer a novel training platform.

Acknowledgments: NIH grant P20GM109090 and GRACA number 46649

References: [1] Kirby et al. (2011), *Re in Dev Dis*, 32(2); [2] Zhou et al. (2017), *Front in Hum Neuro*, 11.

THE MEDIATING EFFECT OF BRAIN CONNECTIVITY ON DUAL-TASK PERFORMANCE: A PILOT STUDY

Jack Manning[1*], Jessica Bernard[2], Joseph Orr[2], Jennifer Yentes[1]
[1] Human Movement Complexity Laboratory; Department of Kinesiology and Sport Management, Texas A&M University
[2]Department of Psychological & Brain Sciences, Texas A&M University
*Corresponding author's email: jackpmanning@tamu.edu

Introduction: Dual tasking is an experimental paradigm where a motor task and a cognitive task are completed simultaneously, which is useful in determining whether the tasks share neural processing [1]. Set shifting is a cognitive task where participants switch their behavior based on predefined rules [2]. Neural connections between the prefrontal cortex and the striatum, known as cortico-striatal connections (CStr), are important in both set shifting and gait [2,3]. The motivation for this study is to determine if CStr connectivity plays a pivotal role in both gait and set shifting in healthy older adults. Therefore, we posit that it may serve as a mediator in the relationship between dual-tasking and gait performance (**Figure 1**). Thus, the purpose of the current study was to investigate the mediating role of cortico-striatal resting-state functional connectivity in the relationship between dual-tasking and gait in older adults. We made two primary hypotheses: 1) set shifting dual-task would exert a significant direct effect on gait measures and 2) task would exert a significant indirect effect on gait through CStr functional connectivity.

Methods: Two older adult participants (mean age 70 years) were asked to walk on a treadmill at a self-selected speed during four randomized trials: 1.) single-task, 2.) set-shifting, 3.) number naming, and 4.) letter naming. During single-task participants walked with no concurrent cognitive task. During all cognitive tasks, a letter-number combination (e.g. V7) appeared on the screen with either a blue or orange background. If the background was blue, they were asked to verbalize the number; if it was orange, the letter. During set-shifting the background changed randomly, while during number and letter naming the background stayed the same. Each trial was two-minutes in duration, with each prompt appearing for two-seconds, a total of 60 prompts. Average stride length during gait was calculated using foot position relative to pelvic position.

During a second visit, structural and functional magnetic resonance images of subject's brains were collected. fMRI data were preprocessed using fmriprep [4] and were post-processed in CONN Toolbox. During post processing data were spatially smoothed, and a 3.5 mm^3 seed was placed in the dorsal caudate on the right side of the brain [5]. Resting-state functional connectivity was assessed by computing the correlation coefficient between the dorsal caudate and the medial prefrontal cortex, which was then Fisher-transformed into a Z-score. To test the hypotheses: 1) simple linear regression was used to determine the direct effect of dual-task on gait and 2) a mediation analysis was used to determine the indirect effect of dual-task on gait while considering CStr functional connectivity as a mediator.

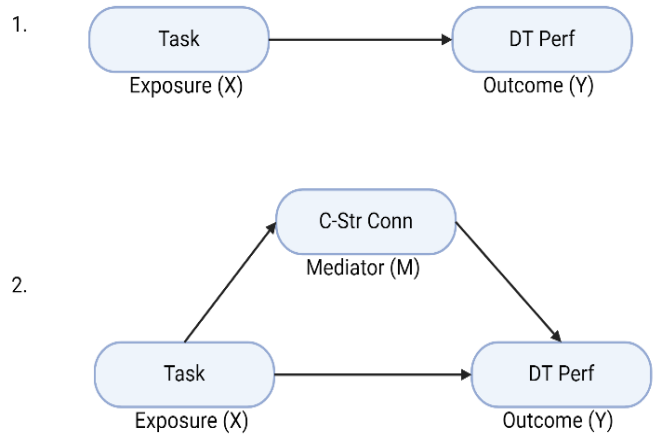

Figure 1. Schematic of mediation analysis. **1.** The total effect of Task on dual-task performance (DT perf) and **2.** The indirect effect of Task on DT perf through cortico-striatal connectivity (C-Str Conn)

Results and Discussion: Results of the simple linear regression indicate no relationship between dual-task and gait (β=-0.03, p=0.62). Results of the mediation analysis indicate there is not a significant indirect effect of dual-task on gait through CStr connectivity (ie=-0.024, p=0.77). These preliminary data do not provide evidence to support the hypotheses: 1) there was not a significant direct effect of dual-task on gait measures and 2) there was not a significant indirect effect of dual-task on gait through functional connectivity. However, these pilot data must be interpreted with caution. Low sample sizes cause regression coefficients to become inflated, thus artificially lowering the calculated p-values. Similarly, low sample size also reduces the statistical power of mediation analyses. This pilot work provides a proof-of-principle in determining the effect of CStr functional connectivity on dual-task gait metrics. The current analysis is limited in the sense that previous work has established the importance of six different striatal seeds in CStr connectivity, while here we are only considering one seed. This study is ongoing, and additional data with healthy older adults are still being collected, prepared, and incorporated into the full presentation.

Significance: The present pilot work aims to fill in a gap in the literature with regards to how CStr connectivity is causally involved in dual-task gait in healthy older adults. The long-term goal of the study is to characterize the effects of normal aging on CStr connectivity and dual-task performance, so that future research can investigate the effects of pathological aging in a similar paradigm.

Acknowledgments: This work was support by a SEED grant provided by the Texas A&M Department of Kinesiology and Sport Management, and a Graduate Research Grant provided by the Texas A&M School of Education and Human Development.

References: [1] Leone, C. *et al. Neuroscience & Biobehavioral Reviews* **75**, 348–360 (2017). [2] Bissonette, G. B., Powell, E. M. & Roesch, M. R. *Behavioural Brain Research* **250**, 91–101 (2013). [3] Bell, P. T., Gilat, M. & Shine, J. M. *Brain* **140**, 1174–1177 (2017). [4] Esteban, O. *Nature Protocols* **15**, (2020). [5] Bo, J. *et al. Brain Connectivity* **4**, 166–180 (2014).

QUADRICEPS STRENGTH AND STEADINESS IN INDIVIDUALS WITH KNEE INJURY AND DISEASE

Nicholas L. Hunt[1*], Matthew V. Robinett[1], Tyler N. Brown[1]
[1]Boise State University, Boise, ID, USA
*Corresponding author's email: nichunt@u.boisestate.edu

Introduction: Following knee musculoskeletal injury, such as ACL reconstruction (ACL-R), quadriceps strength decrements and altered neuromuscular activation may accelerate knee osteoarthritis (OA) development [1]. Previous literature primarily focuses on strength decrements following ACL-R and OA development; despite the fact both quadriceps contraction strength and steadiness may prevent knee instability and provide valuable insight to the underlying neuromuscular function to mitigate injury and disease development [2]. We hypothesize that ACL-R and OA individuals will exhibit less knee extensor strength and steadiness compared to controls, and a positive, linear relationship will exist between extensor strength and steadiness regardless of knee injury or disease.

Methods: Four adult cohorts (1: 12 ACL-R, 2: 8 radiographic knee OA, 3: 13 young adult controls, and 4: 8 older adult controls) performed three 5 second knee extensor MVICs on an isokinetic dynamometer with the knee fixed to 60 degrees. The MVIC trial with the highest maximal voluntary torque was selected for analysis.

From the raw torque-time curve, peak knee extensor torque and rate of torque development (RTD) were calculated as the largest value and maximum slope of the torque-time curve, respectively. Then, the raw torque-time curve was bandpass filtered (2 to 15 Hz), linearly detrended, and submitted to a fast-Fourier transform to obtain the power spectral density (PSD) of the signal which provides the signal frequency content for fluctuation analysis. Torque fluctuation magnitude was calculated as the coefficient of variance (CV), or the standard deviation of the filtered torque-time curve divided by the mean of the raw torque time curve expressed as a percentage. From the PSD, peak power, mean, and median frequency as well as total power were calculated. Specifically, peak power frequency (PPF) was calculated as the frequency with the highest power, mean frequency is the weighted average frequency of the signal, median frequency splits the area under the PSD curve in two equal parts, and total power is the area under the PSD curve.

Knee extensor strength (peak torque and RTD) and steadiness (PPF, mean and median frequency, and total power) measures were submitted to a Kruskal-Wallis H test to assess cohort (ACL-R, OA, and age-matched controls) differences. Spearman's rho correlation analysis tested the association between muscle strength and steadiness variables.

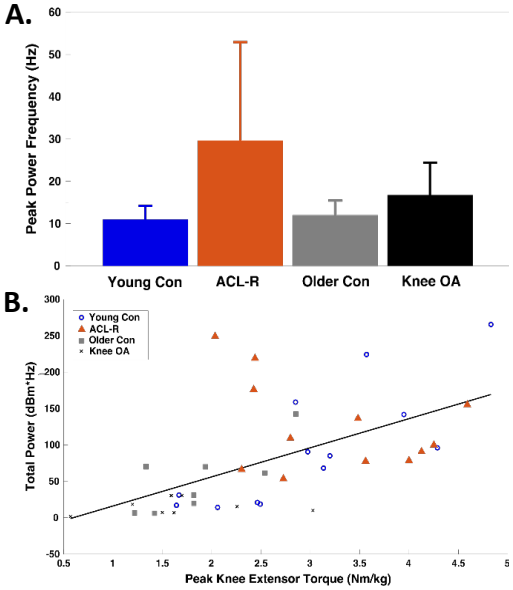

Figure 1: (**A**) Mean (SD) for peak power frequency by cohort and (**B**) relation between total power and peak knee extensor torque.

Results & Discussion: In partial agreeance with our hypothesis, the ACL-R and young control cohorts were 47% to 63% stronger (p=0.016; p=0.006) and developed torque 45% to 99% faster (p=0.016; p<0.001) than the OA cohort. Yet, neither peak extensor torque or RTD differed between ACL-R and young controls or OA and older controls. The ACL-R cohort, however, exhibited altered quadriceps neuromuscular function that may predispose them to knee OA development. Specifically, ACL-R were as strong, but less steady (92% increase in PPF, p=0.050) than their healthy counterparts (**Fig. 1A**). Further, the OA cohort also exhibited poor knee extensor strength and neuromuscular function, which may contribute to the progression of their OA. The OA cohort had 157% less total power than the ACL-R and young control cohorts (p<0.001; p=0.019), indicating lower signal energy and less fluctuation content throughout the knee extensor contraction that signifies weaker muscle contraction.

Knee extensor strength and function were not entirely independent and individual strength may affect joint neuromuscular control, regardless of knee injury or disease. As expected, we observed a significant, positive relationship between knee extensor strength and steadiness. Specifically, peak extensor torque exhibited moderate, positive relation with RTD (ρ=0.668; p<0.001), while mean and median frequency exhibited strong, positive correlation with PPF (ρ=0.656-0.746; both: p<0.001). Total power showed moderate, positive correlation with peak torque (ρ=0.683) (**Fig. 1B**), RTD (ρ=0.656), and CV (ρ=0.342) (all: p<0.028). More specifically, an increase in strength, the ability to produce strength quickly, and magnitude of torque fluctuations relates to greater signal energy. Therefore, an individual's strength may affect overall neuromuscular control of the joint, regardless of knee injury or disease.

Significance: These results provide valuable insight on quadriceps strength and the related underlying neuromuscular function in individuals with knee injury and disease. Individuals with ACL-R and OA may exhibit harmful biomechanics that affect the quality of knee extensor muscle contractions. Thus, clinicians may need to include rehabilitation that targets restoration of contraction steadiness to facilitate improved knee neuromuscular control and help prevent the development and progression of knee OA.

Acknowledgments: NIH NIA (R15AG059655) and NIGMS (2U54GM104944) supported this work.

References: [1] Tayfur et al. (2021), *Sports Medicine* 51; [2] Satam et al. (2022), *Clin. Biomech* 99.

IS ULNAR COLLATERAL LIGAMENT STRENGTH PROPORTIONAL TO HEIGHT AND WEIGHT?

Jonathan S. Slowik*, David P. Beason, Ricardo E. Colberg, Brandon K. Kimbrel, Marcus A. Rothermich, Glenn S. Fleisig
American Sports Medicine Institute, Birmingham, AL, USA
*jons@asmi.org

Introduction: The ulnar collateral ligament (UCL) provides roughly one-third of the elbow varus torque in throwing [1] and is one of the most commonly-injured soft tissue structures in baseball [2]. To provide insight on UCL injury risk and prevention, numerous biomechanical studies have reported elbow varus torque during pitching, but controversy exists regarding whether this torque should be normalized by pitcher height and weight [3]. While it is generally accepted that the pitching torque on the elbow increases with body size, it is unknown whether UCL strength also increases. Therefore, the purpose of this study was to quantify the relationships between body size and mechanical properties of the UCL, measured directly from cadaveric specimens. Previous research has suggested that tendon diameter has a positive linear relationship with both body weight and height [4], so we hypothesized that body size parameters (height, weight, height*weight, and body mass index) would also have positive correlations with our UCL parameters (cross-sectional area, stiffness, and strength).

Methods: Twenty fresh-frozen cadaveric right upper extremities from adult male donors (age: 33.3±5.6yrs; height: 1.80±0.06m; weight: 817±174N) were used in this study. Prior to dissection, and with each specimen stabilized at 90° of elbow flexion and neutral forearm pronation/supination, UCL thickness at three locations (origin on the medial epicondyle, midsubstance, and insertion on the sublime tubercle) was assessed using a Samsung HS60 ultrasound machine with an LA4-18BD linear probe (Samsung/Neuro Logica Corp., Danvers, MA). After dissection, a single overall cross-sectional area value was calculated by measuring UCL width at the same three locations with a digital caliper, multiplying by the corresponding thickness ultrasound measurements, and averaging the three values. Each specimen was then prepared for biomechanical testing as previously described [5] and mounted into an MTS 858 MiniBionix II servohydraulic mechanical test frame (MTS Systems, Eden Prairie, MN). Biomechanical testing was conducted by internally rotating the humerus while holding the forearm stationary, creating a valgus torque on the medial elbow. After ten preconditioning cycles between 2 and 10 Nm, the specimen was tested to failure at a rate of 1 deg/s. Stiffness was calculated as the slope of the linear region of the torque-rotation curve leading up to the point of ultimate failure. Correlation analyses were performed to quantify the relationships between UCL parameters and body size parameters.

Results & Discussion: Of the twenty specimens, eighteen failed at the UCL and two specimens failed via humeral fracture. Failure strength data were not used for the latter; however, their cross-sectional area and stiffness were included. Of the eighteen UCL failures, seven (39%) failed near the medial epicondyle, six (33%) failed near the sublime tubercle, and five (28%) failed in the midsubstance. A summary of the UCL parameter values and their relationships with the body size parameters is provided in Table 1. Cross-sectional area had a moderately-strong and statistically significant relationship with height (p=0.032, R=0.48, Fig. 1), had trends toward significance with height*weight (p=0.052, R=0.44) and weight (p=0.085, R=0.40), but had no correlation with body mass index (BMI) (p=0.23, R=0.28). There were no significant correlations between stiffness or strength and any of the body size parameters. This suggests that UCL stiffness and strength do not scale with body size. It should be noted that the donors in this study were restricted to males between the ages of 19 and 40 (to approximate adult baseball players), and therefore, it is unknown whether these results would hold across a more diverse study population (e.g., youth athletes, females).

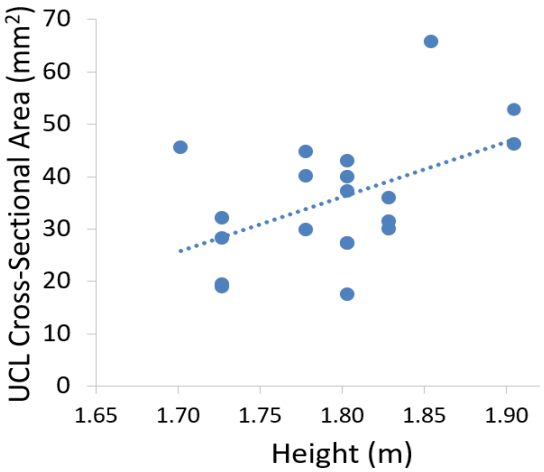

Figure 1: UCL cross-sectional area showed a positive correlation (p=0.032, R=0.48) with donor height.

Table 1: Mean and standard deviation values for UCL parameters, and the p- and R-values from their correlations to body size parameters. Relationships reaching statistical significance (p<0.05) are in bold, while relationships approaching significance (p<0.1) are in italics.

	Mean ± SD	vs. Height		vs. Weight		vs. Height*Weight		vs. BMI	
		p	R	p	R	p	R	p	R
Cross-sectional area	35.7 ± 12.0 mm²	**0.032**	**0.48**	*0.085*	*0.40*	*0.052*	*0.44*	0.23	0.28
Stiffness	2.72 ± 0.48 Nm/deg	0.24	0.28	0.21	0.29	0.18	0.31	0.35	0.22
Failure torque / strength	45.0 ± 10.5 Nm	0.25	0.28	0.85	0.05	0.72	0.09	0.85	-0.04

Significance: This study addressed a long-standing question in the biomechanical analyses of baseball and other athletic activities. UCL strength did not scale with body size, and thus when analyzing collegiate and professional pitchers, elbow varus torque should not be normalized by height and weight.

Acknowledgments: The authors would like to thank Major League Baseball for funding the acquisition of the cadaver arms.

References: [1] Buffi et al. (2015), *Ann Biomed Eng* 43:404-415; [2] Conte et al (2016), *Am J Orthop* 45(3):116-123; [3] Giordano et al. (2024), *Sports Biomech*: 1-12. [4] Atbaşi et al. (2017), *Joints* 4(4):198-201; [5] Shahien et al. (2024), *Am J Sports Med*: 03635465231220382.

INVESTIGATING THE IMPACT OF VIRTUAL-REALITY BALANCE TRAINING IN OLDER ADULTS

Nicole D. Arnold[1*], Oshin Wilson[1], Younes El Hakour[1], Aliya Newby[1], Brian Douglas[1], J'niya Butler[1], Roni Romero Melendez[1], Frank Borris III[1], Bridget Thorpe[2], Alexander Peebles[1], Lara A. Thompson[1]
[1]Center for Biomechanical & Rehabilitation Engineering, University of the District of Columbia,
George Washington University[2]
*Corresponding author's email: Nicole.arnold@udc.edu

Introduction: The purpose of this study was to investigate the effects of virtual reality (VR) training on balance control in older adults, over the course of multiweek exercise training. Falls are the leading cause of fatal and nonfatal injuries among persons over 65 years old [1,2]. As the population ages, falls in older adults are a major concern leading to decreased quality of life and thus the inability to care for oneself. Postural instability during quiet stance, measured using center of pressure (COP), was identified as a risk factor for falls in older adults [2]. Additionally, some studies have reported lack of exercise increased fall risk for older adults [3,4]. Several types of programs have been used to increase mobility and balance to reduce falls in older adults such as resistance training and balance exercises. Recently, researchers investigated virtual reality (VR) toward improving balance and falls in older adults [5]. Here, we hypothesized that several weeks of VR training could impact balance and falls observable by the COP.

Methods: This study was approved by the IRB and all eight participants (four participants with the VR headset and four without (or control)) consented to the research study (aged 73 ± 7). Participants completed a pre-assessment, 6-week exercise training, and a post-assessment. Exercise training included: two, 30-minute sessions per week for six weeks with specific exercises targeting static and dynamic balance with motor coordination by both groups. The VR group viewed a non-moving tropical scene, while control participants viewed the laboratory environment during exercise training. For the assessments, participants were instructed to perform five, 20 s trials of double, tandem and single leg standing on a force plate (Tekscan, Norwood, MA) with eyes closed to acquire COP data at 50Hz. From the COP, Root Mean Square (RMS) was calculated for both the anteroposterior (AP) and mediolateral (ML) directions pre- and post-assessment. These data are only a subset of the total data collected and due to the small sample size, statistical analysis was not conducted.

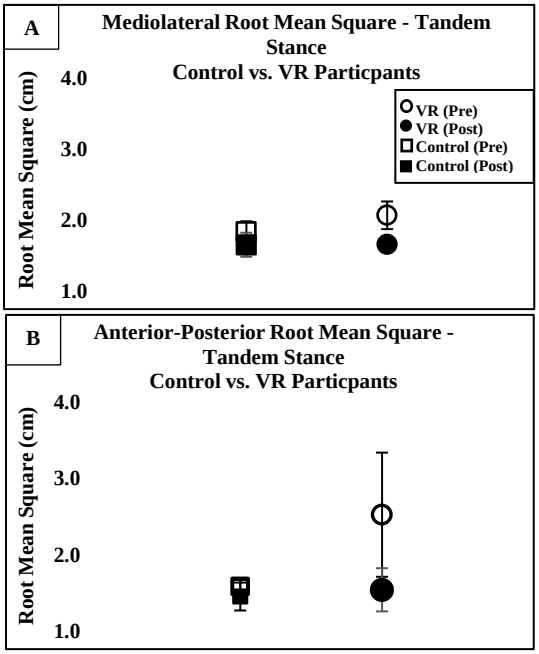

Figure 1: Tandem stance A) Mediolateral root mean square B) Anterior-Posterior root mean square for control (square) and VR (circle) participants both pre (open) and post (filled) assessment. Pooled results with standard errors of the mean (SEM) are shown.

Results & Discussion: Figure 1 shows RMS and standard errors of the mean (SEM) of COP measures, both in ML and AP directions, for the tandem stance test condition. Data reported in this abstract presents the variance in COP movement between control and VR participants before and after exercise training. Both the control and VR groups post training had reduction in the RMS for both ML and AP COP. Post-assessment results of these data showed the control group reduced ML RMS in the tandem stance by 9.8%, however the VR group demonstrated a larger reduction, at 19.5%, after exercise training compared to pre-assessment. Additionally, the AP RMS tandem stance resulted in an 8.5% and 38.8% reduction after exercise training by control and VR participants post-assessment, respectively. VR based training resulted in greater reduction of RMS COP measures in both directions for VR participants compared to control. VR-based training provides insight to an alternative exercise treatment in the older population with poor balance aimed at reducing falls. Furthermore, falls are a complex and multifaceted event that occurs in the older population. This study showed preliminary results of a small cohort of older individuals that benefited from VR-based exercise training.

Significance: The results of this study determined implications for the expansion of VR-based training programs as preemptive measures to reduce falls in older adults. Other common training methods have their merit to improve balance, however observance and incentive may contribute to the compliance and effectiveness of training based on individual preferences. Home-based VR training in older adults may provide an alternative or an addition to standard exercise training to reduce the occurrence of falls and holds potential for evolving interventions aimed at enhancing physical well-being in aging individuals prone to falls.

Acknowledgments: We acknowledge the National Institutes of Health grant (1R25AG067896) and National Science Foundation grant (Award Abstract #2229575). We would like to acknowledge Ms. Tiana McFarlane for participant coordination and the UDC Center for Advancement of Learning (CAL) for the VR headsets.

References: [1] Casey et al. (2017), *Gerontologist* 57(4); [2] Liu et al. (2015), *Am J Emerg Med* 33(8); [3] Stel et al. (2003), *J Clin Epidemiol* 56(7); [4] Barnett et al. (2003), *Age Ageing* 32(4); [5] Kamińska et al. (2018), *Clin Interv Aging* 13

Effects of Increasing Step-Rate on Vertical Ground Reaction Forces per Step and per Meter in Young Adults

Dante D. Goss[1*], Jay Hertel[1]

[1]University of Virginia, Department of Kinesiology, Charlottesville, VA

*Corresponding author's email: nxq9uz@virginia.edu

Introduction: Walking step rate is correlated with gait speed but can be changed independently using auditory devices like metronomes. An increase in walking step-rate has been shown to decrease knee joint loading and vertical ground reaction forces (vGRFs) per step and per kilometer during walking in knee osteoarthritis patients [1]. However, it is unknown if this relationship is specific to that population. Thus, the primary aim of this analysis was to investigate the effects of increasing step-rate on the vGRFs per step and per meter in a healthy adult population. Due to previous work finding decreased joint loading both per step and per meter in individuals with knee osteoarthritis [1], we hypothesized that the same pattern would hold true in our sample of healthy adults.

Methods:

Nine healthy young participants (Age = 20.56 ± 2.13; Females n=5; Mass = 74.84 ± 12.27 kg; Height = 174.61 ± 8.99 cm) underwent gait analysis. Walking trials were conducted at a fixed gait self-selected speed under three step-rate conditions: preferred step-rate, 5% increased step-rate, and 10% increased step-rate. Increased step-rate conditions were enforced using a metronome and gait speed was held constant for all conditions using an instrumented treadmill (Bertec FIT4). vGRF data was recorded for the last thirty seconds and normalized to bodyweight. Additionally, oxygen consumption and rating of perceived exertion were recorded as measures of exertion. Separate repeated measures analyses of variance (RMANOVAs) were used to assess the influence of step-rate on vGRF per step, vGRF per meter, and measures of exertion. Variables found to be significant via RMANOVA were tested between step-rate conditions using paired samples t-tests.

Results & Discussion: The only significant variables from the repeated measures ANOVA were vGRF per step ($p<0.001$) and vGRF ($p<0.001$) per meter. This suggests that both physical and perceived measures of exertion were not significantly influenced by increases in step-rate. As seen in the Figure, vGRF per step decreased as step-rate increased. Notably, vGRF per meter increased as step-rate increased. This result was contrary to our original hypothesis and suggests that the magnitude of offloading taking place with increased step-rate is not large enough to offset the extra steps required to walk a meter.

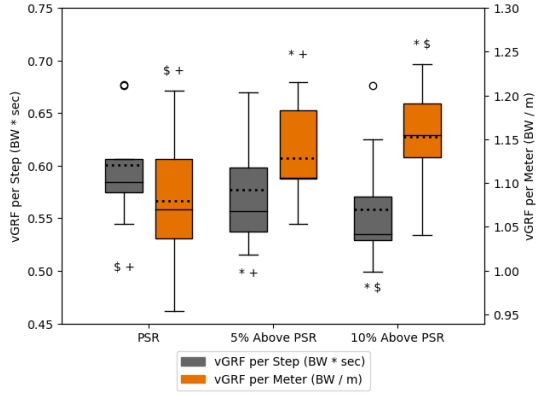

Figure: Boxplots of Normalized vGRF Impulse and vGRF per Meter. Dashed black line denotes mean. * Denotes significant difference from preferred step-rate ($p<0.05$), $ denotes significance significant difference from 5% above preferred step-rate ($p<0.05$), and + denotes significant difference from 10% above preferred step-rate ($p<0.05$). ° denotes outliers.

Significance: Current findings demonstrated that increasing step-rate caused a decrease in vGRF per step, but increased vGRF per meter. This finding is surprising as it is contrary to previous research [1], though the population differences should be considered. We also found no difference in exertion with step rate increases, which is notable as increasing step-rate has been previously shown to increase energy expenditure [2]. Further study is needed to understand if these relationships are consistent across other factors like increasing age or gait speed. Additionally, further study should be done to test cumulative loading of individual joints, as those may be more insightful for certain pathologies where step-rate based gait retraining would be an intervention.

Acknowledgements: This project was supported by a grant from the Innovative, Developmental, Exploratory Awards (IDEAs) program at the University of Virginia School of Education and Human Development.

References: [1] Hart (2023), *Med Sci Sports Exer*. 55, 633; [2] Zarrugh, M. Y. & Radcliffe, C. W. (1978), *Eur J Appl Physiol Occup Physiol* 38, 215–223

COMPLETE UPPER BODY BAR ENHANCES UPPER BODY STRENGTH TRAINING DURING BENCH PRESS

Henry Wang[1*], Hannah Bradshaw[1], Ben VonGunten[1], John Andamasaris[1], Emma Burns[1], Caroline Ashton[1], Clark Dickin[1]
[1]School of Kinesiology, Ball State University
*Corresponding author's email: hwang2@bsu.edu

Introduction: ACSM advocates resistance training for health and encourages people of all ages to regularly participate in resistance exercise for physiological benefits [1]. The bench press is a popular resistance modality for developing major musculature of the chest, shoulders, and upper arms [2,3]. The barbell (BB) and dumbbell (DB) devices are commonly used by individuals during bench press. Recently, the Complete Upper Body Bar (CUBB) (Resistance in Rotation LLC) was developed to train the muscles of the forearm by allowing for pronation and supination, while simultaneously providing traditional training for the rest of the upper body [4]. Specifically, there is adjustable resistance introduced to the forearm pronators and supinators during lifting[4]. To date, the effectiveness of using the CUBB during bench press has yet to be determined. It is necessarily to examine the biomechanics of the CUBB along with the traditional devices (BB and DB) during the bench press. It was hypothesized that the three bench press conditions would promote similar activation level in shoulder muscles (anterior deltoid), chest muscle (pectoralis major), and upper arm muscles (triceps brachii). It was also hypothesized that the forearm muscles (pronator teres and supinator) would be more active in the CUBB condition than the other two conditions.

Methods: 21 healthy college-aged males (age: 21 ± 2 yr; body mass: 88 ± 15 kg; body height: 181 ± 5 cm) volunteered for the study. Wireless Electromyography (EMG) sensors were placed on the right anterior deltoid (AD), pectoralis major (PEC), triceps brachii (TRI), pronator teres (PRO), and supinator (SUP). The participants went through a bench press test in a series of three different randomized conditions: the DB, the BB, and the CUBB. Each set was done at 30% body weight guided by a 60-bpm metronome. EMG data were collected through a Delsys Trigno wireless system at 2000 Hz. A maximal voluntary contraction (MVC) was recorded for each muscle to normalize muscular contraction levels for each participant. Root mean square (RMS) procedure was used to process raw EMG. A repeated measures MANOVA was used to analyse the normalized RMS EMG data expressed in %MVC (alpha=0.05).

Table 1 Means and standard deviations of peak RMS EMG (%MVC) of AD, PEC, TRI, PRO, and SUP during the concentric phase of a bench press

Muscles\Conditions	CUBB	BB	DB
AD	98 ± 76	101 ± 80	104 ± 66
PEC	101 ± 87	117 ± 114	102 ± 52
TRI	100 ± 81$^{\#}$	97 ± 71	81 ± 65$^{\#}$
PRO	100 ± 83$^{\#}$	73 ± 67	71 ± 65$^{\#}$
SUP	87 ± 70* $^{\#}$	52 ± 47*	67 ± 68$^{\#}$

Note. * significantly different between CUBB and BB ($p<0.05$), $^{\#}$ significantly different between CUBB and DB ($p<0.05$)

Results & Discussion: Table 1 shows that there were significant differences in muscle activations among the three bench press conditions. Our hypotheses were largely supported by the results. For the forearm muscles, the CUBB exhibited 41% higher PRO activation than that of the DB. The CUBB also showed a trend of higher PRO activation than that of the BB (37% higher, $p=0.063$). Furthermore, the CUBB exhibited 67% and 30% more SUP activation than those of the BB and DB, respectively. For the upper arm muscle, the CUBB showed a higher TRI activation than that of the DB (23% more). For the shoulder and chest muscles (AD and PEC), all three conditions engaged high muscle activations and no significant differences were found among them.

Traditional bench press protocols such as using a barbell and dumb bells are effective to train and build shoulder, chest, and upper arm muscles. However, other upper body muscles such as the forearm muscles represented by pronators and supinators are less involved during these traditional exercises. The current study determined that bench press with a CUBB can engage more upper body muscles and offer individuals with additional training benefits. The feature of providing elevated resistance to forearm muscles during bench press with a CUBB appears to be valuable. For individuals who have a need and want to address their forearm muscles along with their shoulder and chest muscles simultaneously, using a CUBB appeals to be a viable option.

Significance: This study examined a new form of bench press with a novel device and confirmed the effectiveness and efficiency of the application. Personal trainers and exercise practitioners will be benefited from adopting this new training tool.

Acknowledgments: Supported in part by Resistance in Rotation LLC.

References: [1] Singh et al. ACSM Resistance Training for Health (2019); [2] Lehman (2005), *J Strength Cond Res* 19(3). [3] Lauver et al (2016), *Eur J Sport Sci* 16(3); [4] https://resistanceinrotation.com

A MODEL TO PREDICT KINEMATICS THAT RESULT IN SHOULDER INSTABILITY IN PATIENTS WITH DEFECTS OF THE HUMERAL HEAD AND GLENOID

Clarissa LeVasseur1,2, Zhaoyi Fang1, Devon Scott1, Jill Brockhoff1, Jonathan Hughes1, Albert Lin1,2, William Anderst1
[1]University of Pittsburgh, Pittsburgh, PA, US [2]Bethel Musculoskeletal Research Center, Pittsburgh, PA, US
Corresponding author's email: cll100@pitt.edu

Introduction: Anterior shoulder instability accounts for approximately 80% of all shoulder instability [1,2], and occurs at a rate of 3% per year in specific at-risk young athletes and military personnel [2,3]. Simultaneous defects of the humeral head (Hill-Sachs lesion) and glenoid occur with anterior shoulder instability [4], therefore understanding the dynamic articulation between the bones is vital for clinical and surgical decision-making. Determining when the Hill-Sachs lesion engages the anterior rim of the glenoid is challenging because it requires an understanding of how bone morphology, Hill-Sachs lesion and glenoid bone loss size and location, and glenohumeral (GH) kinematics interact and lead to anterior shoulder instability. The aim of this ongoing study is to create and evaluate an in vivo model that can predict GH kinematics that will result in anterior shoulder instability based upon patient-specific humeral and glenoid bone loss.

Methods: Healthy individuals with no history of shoulder pathology provided written informed consent prior to participating in this IRB-approved study. Participants received bilateral CT (0.44x0.44x0.625mm) and bilateral MRI scans (DESS sequence, 0.3x0.3x0.3mm). Participants performed 2 trials with each arm of continuous internal/external rotation in four different humerothoraic abduction angles (approximately 30°, 60°, 90°, and 120°) while synchronized biplane radiographs of the shoulder were collected at 50 images/s (90 kV, 50mA, 2ms pulse width) to capture external rotation (ER). One of the two trials on each side at each abduction angle was performed with the participant holding a 5lb weight. Digitally reconstructed radiographs, created from CT-based bone models, were matched to the biplane radiographs with sub-millimeter accuracy using a validated model-based tracking technique [5] to determine six degree-of-freedom GH kinematics. Bone and cartilage were segmented from the MRIs and co-registered to the CT-based bone models. The glenoid to humeral cartilage overlap was determined for every frame of data and the boundary of that region was expressed in spherical coordinates normalized to the subject's humeral head. Data from corresponding trials (same side, weight condition) at all four abduction angles were then used to interpolate the cartilage contact region (i.e., the dynamic glenoid track) at 5° increments of GH abduction and ER. Cartilage contact regions were normalized across subjects by a cube-to-sphere morphing algorithm comprising 1200 regions [6]. The hemisphere was aligned with the humeral head, and each region was evaluated for whether it overlapped with the cartilage contact area at that abduction angle, ER angle, and load condition. The total number of shoulders in contact within each region was then summed (Figure 1). The likelihood of each region being in contact was then calculated by dividing the number of shoulders in contact by the total number of shoulders.

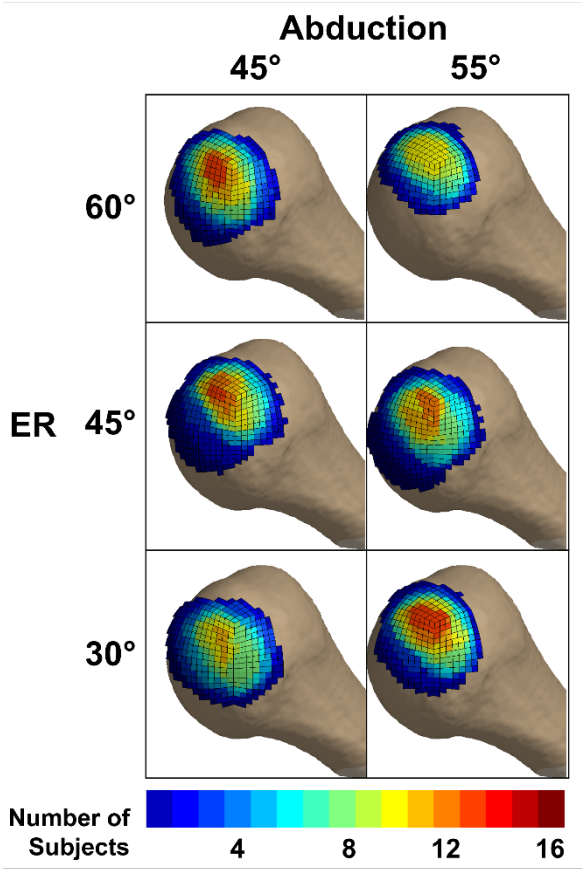

Figure 1: Humeral head color-coded according to the number of shoulders with cartilage contact in each region at 30°, 45°, and 60° of ER and 45° and 55° of GH abduction.

Results & Discussion: Data processing is complete for 16 male shoulders of 30 participants who completed the study (30.3±11.9years, BMI: 25.5±4.1kg/m^2), resulting in 128 movement trials included in the analysis. On average, the center of the contact regions moved 0.4±0.1mm posterior and 0.9±0.3mm superior with each 5° increase in external rotation while the regions moved 0.0±0.7mm in the anterior/posterior direction and 2.1±0.4mm superior with each 5° increase in abduction. These results can help guide surgeons in their choice for surgical approach by providing a comparison between the location and size of the contact region to the location and size of the Hill Sachs lesion of their patients. Future work will incorporate subject specific measurements of the bony morphology to potentially help increase the patient-specific accuracy of the model in determining the region of contact.

Significance: This predictive model of GH cartilage contact will allow surgeons to optimize their surgical plan for patients with anterior shoulder instability and bone loss based on the patient's anatomy and bony defect morphology.

Acknowledgments: This work was funded by NIH Grant R01-AR080425.

References: [1] Dodson et al. Orthop Clin North Am. 2008. [2] Owens et al. AJSM. 2007. [3] Waterman et al. Sports Health. 2016. [4] Lemme et al. JBJS Rev. 2019. [5] Bey et al. J Biomech. 2006. [6] Dimitrijević et al. Facta Universitas, Series: Mathematic and Informatics. 2016.

CAN SACRAL OR SHANK ACCELERATION PREDICT PROSTHETIC LEG PROPULSIVE FORCE?

Thomas Madden*, Corey Pew
Department of Mechanical Engineering, Montana State University, Bozeman, MT
*Corresponding author's email: thomasmadden4@montana.edu

Introduction: Prostheses aim to restore walking ability after lower limb amputation (LLA), yet individuals walking with passive prostheses show deficits in propulsive force (F_P; anterior ground reaction force) and walking speed relative to nonamputees [1,2]. F_P is directly related to walking speed [3], a significant predictor of function [4] and mortality [5], and therefore, represents an important target for rehabilitative outcomes and interventions. Wearable accelerometers may provide a more accessible alternative to force plate measurements of F_P. Because F_P contributes center of mass and trailing limb acceleration during late stance, acceleration at the sacrum or shank may be able to predict F_P. However, these relationships have not been investigated for individuals with LLA. The purpose of this study was to evaluate the associations between peak sacral and shank accelerations near toe-off and peak F_P while walking in healthy adults and individuals with LLA. Based on correlations between shank acceleration and F_P in healthy young adults [6], we hypothesized that peak resultant accelerations at the sacrum and shank near toe-off would correlate with peak F_P in healthy adults and individuals with LLA.

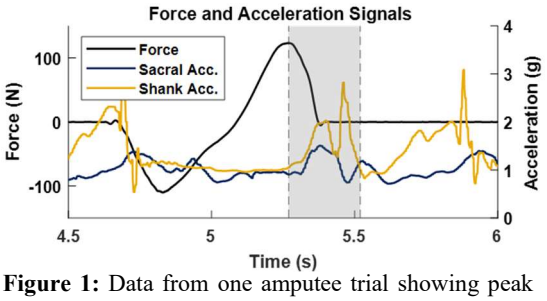

Figure 1: Data from one amputee trial showing peak sacral and shank accelerations near toe-off captured within 0-250ms from the time of peak F_P (shaded area).

Methods: Lower limb amputee participants included two females (19-26y, 164-180cm, 56.3-86.6kg), one transtibial amputee and one nonamputee prosthesis user. Four healthy nonamputee adult females (21 ± 1y, 174 ± 9cm, 60.0 ± 5.7kg) served as controls. Participants walked overground at three speeds (self-selected, 15% slower, 15% faster) while inertial measurement units placed on the sacrum and distal shank (prosthetic leg or bilaterally for controls) recorded acceleration (148Hz) with synchronous force plate data (1000Hz). Correlations between peak F_P and resultant accelerations at 0-250ms from the time of peak F_P (Fig. 1) were tested using Spearman correlation coefficients with a 0.05 overall significance level, adjusted for multiple tests (0.0125 for controls and 0.025 for amputee participants).

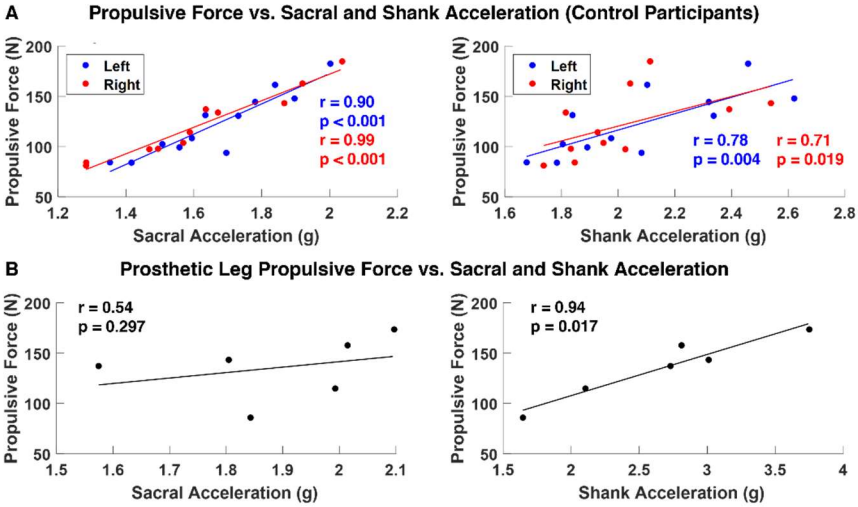

Figure 2: (A) Peak F_P correlated with left and right peak sacral acceleration and left peak shank acceleration in control participants. Three speeds yielded 12 points per side except for one participant's right side (11 points). **(B)** Peak prosthetic leg F_P correlated with peak shank but not sacral acceleration in lower limb amputee participants.

Results & Discussion: In control participants, peak F_P correlated significantly with peak resultant sacral ($p < 0.001$ both legs) and left shank acceleration ($p = 0.004$), while right shank acceleration showed a similar albeit nonsignificant ($p = 0.019$) correlation with F_P (Fig. 2A). These results are overall consistent with our hypothesis and previous work showing a significant association between F_P and shank acceleration [6]. Our results suggest sacral acceleration may be a better predictor of F_P than shank acceleration in healthy young adults.

Peak prosthetic leg F_P correlated significantly with peak resultant shank ($p = 0.017$) but not sacral ($p = 0.297$) acceleration (Fig. 2B). In partial support of our hypothesis, these results identify shank acceleration as a potential predictor of peak prosthetic leg F_P. The lack of a significant correlation between sacral acceleration and prosthetic leg F_P was inconsistent with our hypothesis, potentially due to the small sample size or sensor placement relative to the sacrum and greater frontal plane trunk motion in individuals with LLA [7]. We plan to recruit 10 control and amputee participants for a full analysis. Interestingly, shank acceleration showed a stronger correlation with F_P than sacral acceleration – opposite our results in healthy young adults – underscoring the need to investigate amputee-specific relationships.

Significance: These preliminary results suggest peak shank acceleration near toe-off can predict peak prosthetic leg F_P during walking. This will allow clinicians to assess changes in F_P using small inexpensive sensors, enhancing their abilities to implement and evaluate rehabilitative interventions for individuals with LLA. Future work is needed to examine the clinical utility of this approach.

Acknowledgments: Supported from the NIGMS of the NIH under Award Number P20GM103474. The content is solely the responsibility of the authors and does not necessarily represent the official views of the NIH. Mojtaba Mohasel helped collect the data.

References: [1] Carse et al. (2020), *Gait Posture* 75(1); [2] Silverman et al. (2008), *Gait Posture* 28(4); [3] Campanini et al. (2009), *Gait Posture* 30(2); [4] Batten et al. (2019), *Prosthet Orthot Int* 43(2); [5] Studenski et al. (2011), *JAMA* 305(1); [6] Pieper et al. (2020), *J Biomech* 98(1); [7] Rueda et al. (2013), *Gait Posture* 37(3).

REACTIONS TO SPLIT-BELT TREADMILL PERTURBATIONS IN CHIARI MALFORMATION

Brittany N. Sommers[1*], Brian L. Davis[1]
[1]Cleveland State University, Cleveland, Ohio, Center for Human Machine Systems
*b.n.sommers@vikes.csuohio.edu

Introduction: Perturbation training during gait is a way of testing reactions and adaptations to disturbances in a person's natural moving environment [1]. Perturbation training is common in fall risk studies, and in movement disorder research for case-control scenarios [1]. The types of perturbation trainings used in research are vast, but many revolve around treadmill training. This study utilized a MOTEK M-Gait split-belt treadmill, where the belt speeds are controlled independently.

Chiari Malformation (CM) is a congenital condition of the cerebellum in which the cerebellar tonsils herniate through the foramen magnum and enter the spinal canal. This leads to severe headache, instability, muscular weakness, and poor joint coordination. Feedback control, or reactions, can occur without intervention form the cerebellum [2]. Thus, it was hypothesized that for reactive movements specifically, the CM group would (1) display similar reaction patterns to a non-impaired control group, and (2) show improved reactions to perturbations over time. There is no cure for CM, and no standard therapeutic procedures for enhancing gait and stability performance. If the above hypotheses are true, this work could lay the groundwork for a non-invasive, non-surgical form of gait rehabilitation for individuals with CM.

Methods: Data were collected on 12 adult CM individuals, and 12 age and weight matched control subjects in accordance with approved IRB protocols at Cleveland State University in the Center for Human Machine Systems. There were no restrictions on gender, however CM is known to effect women twice as often as men. All participants completed three sessions of perturbation training. Each session lasted seven minutes total, with 12 perturbations in each session. There were six perturbations per left and right limb in each session. In total, each participant received 36 perturbations. For all participants, perturbations were delivered in the mid-foot position of stance, with a magnitude of 0.4 m/s. This occurred by a rapid transient acceleration of the left or right belt speed. To the authors knowledge, this is the first perturbation study to date on the CM population. Thus, to minimize the effects of variables influencing gait reactions, the perturbation magnitudes were kept the same (0.4 m/s) for all participants, regardless of walking speed, age, weight, or condition. Stride length immediately before and after the perturbation occurred were taken as the reactive variables. These were measured on the "response" limb i.e., the one *not* receiving the perturbation. Stride length was calculated as the horizontal heel to heel marker distance from consecutive response limb heel strikes.

Results & Discussion: Stride length variability is represented by the standard deviation, in centimeters. For both before and after (Table 1), the Chiari group displayed significantly higher variability in stride length than the control group ($p < 0.0001$, $\alpha = 0.05$). To assess the equality of variances for stride length for the Chiari and control groups, Levene's test [4] was the inferential statistic that was used. Both the Chiari and control group displayed reduced stride length variability for stride length after, supporting the hypothesis. However, both for stride length before and after, the Chiari group exhibited significantly higher variability than controls. Higher stride length variability has been suggested to be an indicator of poor locomotor performance and control [3]. Chiari did reduce their response variability, suggesting improved reactions to the perturbations.

Table 1: *Stride length variability immediately before and after the perturbation occurred.*

Stride Length Before			
Group	*N*	*Variability (cm)*	*95% CI*
Chiari	231	25.07	(20.90,30.37)
Control	231	7.74	(6.14,9.85)
Stride Length After			
Group	*N*	*Variability (cm)*	*95% CI*
Chiari	231	18.95	(16.99,21.32)
Control	231	7.34	(6.27,8.75)

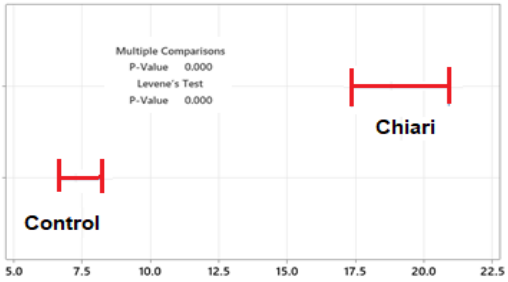

Figure 1: *Stride length variance data after perturbation were 250% higher for the Chiari group.*

Significance: This is the first study to examine how individuals with Chiari respond to gait disturbances. Reactive responses occur without cerebellar intervention; thus, Chiari were hypothesized to react similarly to controls. The results support this; however, there is a clear deficit in Chiari variability compared to controls. Improvement in Chiari variability after a perturbation is promising, as it suggests that with exposure to disturbance training, individuals with Chiari may improve their motor performance and reduce movement variability. This emphasizes the need for physiotherapy techniques to be developed and practiced in Chiari to improve commonly associated gait impairments.

Acknowledgments: Acknowledgements are made to the Conquer Chiari Research Center for participant recruitment.

References: [1] McCrum, C, et al. *Eur Rev Aging Phys Act.* 14(3). 2017, [2] Bastian, A. *Curr Opin Neurobiol.* 16:645-9. 2006., [3] Hausdorff, J. *Chaos*. 19(2). 2009, [4] Gaßner H et al. J Neural Transm. 129(9):1189-1200. 2022.

The Reliability of a New Instrumented Device to Measure Ankle Laxity and Strength

Choi JY[1], Mingo MJ[2], Knarr BA[2], Vogel CM[3], Rosen AB[1]
[1]School of Health and Kinesiology, University of Nebraska at Omaha, Omaha, NE, USA
[2]Department of Biomechanics, University of Nebraska at Omaha, Omaha, NE, USA
[3]College of Applied Health Sciences, University of Illinois Urbana-Champaign, Urbana, IL, USA
Email: jiyeonchoi@unomaha.edu

Introduction: One of the most common musculoskeletal injuries is a lateral ankle sprain [1]. Up to 40% of individuals who have previously injured their ankle report symptoms consistent with chronic ankle instability (CAI), a common consequence of an initial ankle sprain [2]. Clinical characteristics of ankle sprains and CAI include increased laxity and reduced strength in the ankle [3,4]. However, reliable and accurate point-of-care devices to assess laxity and strength are often unavailable due to high cost, accessibility, and convenience. Creating a portable, simple, and reliable device to assess laxity and strength will enhance rehabilitation paradigms, long-term results, and prevention of repetitive injury in individuals with ankle injuries. To address these issues, we have developed a lower-cost, portable, multi-component diagnostic device to assess ankle strength and laxity known as the Ankle-Portable Laxity and Strength Tester (Ankle-PLAST) (Figure 1). The purpose of the present study was to examine the test-retest reliability of the Ankle-PLAST for measuring ankle laxity and strength. We hypothesize that the Ankle-PLAST will have good-excellent reliability.

Methods: Forty physically active, healthy participants (age=25.44±5.29, height=170.23±9.39, mass=72.01±14.60) participated in this study and were tested bilaterally. For the strength measurements, participants placed their ankles in the heel cup. They were instructed to press against the load cells as hard as possible in the dorsiflexion, inversion, or eversion directions for five seconds each. Participants had their inversion laxity assessed utilizing the rotary encoder of the device. With the ankle in the heel cup, a 150N force was placed on the ankle while rotating the ankle into inversion. Participants were asked to return one week later to perform laxity and strength measurements again on the Ankle-PLAST to assess test-retest reliability. Test-retest reliability was assessed via Intraclass correlation coefficients (ICC2,1) using a two-way mixed effects analysis of variance (ANOVA) model combining data from both ankles. Statistical significance was set at $p \leq .05$ for all statistical analyses, and the ICCs were interpreted as considered poor if they were <0.5, moderate between 0.5 and 0.75, good between 0.75 and 0.90, and excellent >0.90 [5].

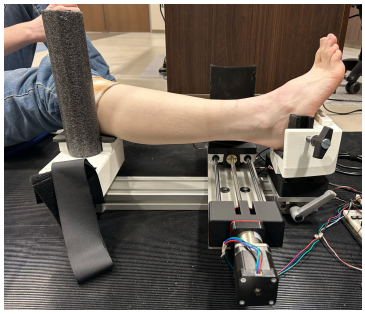

Figure 1: Ankle-Portable Laxity and Strength Tester (Ankle-PLAST)

Results & Discussion: The test-retest reliability between testing sessions was considered good in both strength and laxity (Table 1). These data suggest that the Ankle-PLAST can be considered as a reliable and portable tool for measuring ankle laxity and strength.

Table 1. Ankle-PLAST reliability between Day 1 and Day 2 for measuring ankle laxity and strength

	Mean ±SD	95% CI	SEM	MDC	ICC (95% CI)
Talar tilt, degree					
D1	8.75±6.97	7.19, 10.30	0.78	2.16	.794 (0.68, 0.87)
D2	8.61±6.87	7.08, 10.14	0.77	2.13	
Displacement, mm					
D1	75.47±12.23	72.75, 78.19	1.37	3.79	.791 (0.67, 0.87)
D2	75.08±12.87	72.22, 77.94	1.44	3.99	
Dorsiflexion, N					
D1	153.52±40.44	144.52, 162.52	4.52	12.53	.838 (0.75, 0.90)
D2	155.68±50.04	144.55, 166.82	5.59	15.51	
Inversion, N					
D1	76.52±28.41	70.19, 82.84	3.18	8.80	.862 (0.78, 0.90)
D2	83.32±32.92	75.99, 90.64	3.68	10.20	
Eversion, N					
D1	74.90 ±29.43	68.35, 81.45	3.29	9.12	.860 (0.78, 0.91)
D2	75.93±29.28	69.41, 82.45	3.27	9.07	

Significance: Due to their relatively high cost, complexity, and limited accessibility, ligamentous laxity and strength devices are not often used even though they provide clinicians with vital insights into ankle injuries. Providing objective, reliable data to clinicians may improve patient outcomes with ankle injuries and potentially the prevention of secondary injury.

Acknowledgments: The project described is supported by the National Institute of General Medical Sciences, U54 GM115458, which funds the Great Plains IDeA-CTR Network. The content is solely the responsibility of the authors and does not necessarily represent the official views of the NIH.

References: [1] Gribble et al. (2016), *BJSM* 50(24); [2] Doherty et al. (2016), *AJSM* 44(4); [3] Hertel & Corbett (2019) *JAT* 56(6); [4] Rosen et al. (2015), *Scand J Med Sci Sports* 25 (2); [5] Koo & Li (2016), *J Chiropr Med* 15(2).

VALIDATION STUDY DEMONSTRATES THAT USE OF SUBJECT-SPECIFIC PARAMETERS REDUCES PREDICTION ERROR OF HUMAN ISOMETRIC MUSCLE FORCE

Zheng Wang[1], Benjamin I. Binder-Markey[2], Lomas Persad[1], Alexander Shin[1], Richard L. Lieber[3], *Kenton R. Kaufman[1]

1 Department of Orthopedic Surgery, Mayo Clinic, Rochester, MN, USA.

2 Departments of Physical Therapy and Biomedical Engineering, Drexel University, Philadelphia, PA, USA

3 Shirley Ryan Ability Lab, Chicago, IL, USA.

*Correspondence Kenton R. Kaufman: kaufman.kenton@mayo.edu

Introduction: Most human skeletal muscle models were developed based on muscle data from cadaveric specimens or animals. Use of these data was recently shown to lead to sizeable inaccuracy in predicting muscle-tendon unit length (MTU) [1] and passive muscle force [2]. Since active muscle force is a strong function of length and covaries with passive tension, we suspected that current models would also suffer low accuracy in predicting maximal isometric active force (F_{max}). Thus, the purpose of this study was to validate F_{max}, measured intraoperatively, against that predicted from commonly used musculoskeletal modeling software.

Methods: Gracilis isometric active force and morphological data were collected intraoperatively during gracilis muscle transfer surgery in patients with brachial plexus injury. Muscle force was measured at 4 different joint configurations (JC) using electrical stimulation [3]. F_{max} was defined as the peak of the fitted quadratic curve to *in-vivo* data [4]. Optimal fiber length (L_f) was calculated from the full width at half maximal [5]. Tendon length (TL) was calculated as (MTU – L_f) to substitute the tendon slack length in the model where MTU was directly measured intraoperatively. The normalized length tension curve (F_L) was fit to each subject's data by minimizing the sum of squared error (SSE). Initially, the default gracilis muscle model used was that published by Hamner *et al.* [6]. Two further modifications of the default model were calculated by adding our measured subject-specific parameters (**Table 1**). Error was defined as (predicted force - measured force)/F_{max}*100%.

Table 1: Model variations.

	Subject specific parameters	Default Parameters
Variation 1	None	F_{max}, L_f, TL, F_L curve
Variation 2	F_{max},	L_f, TL, F_L curve
Variation 3	F_{max}, L_f, TL, F_L curve	None

Results & Discussion: Measured F_{max} (176± 83 N) was close to the predicted F_{max} (162 N), but with almost 50% coefficient of variation. The default model overestimated gracilis active force under full activation with 54% error across JCs (**Figure 1.a.** Variation 1). The error was greatest when gracilis length was furthest from optimal fiber length. As expected, including each subject's F_{max} decreased the average error to 37% (Variation 2). After incorporating subject specific L_f, TL and F_L curve (**Figure 1.a.** variation 3), the error decreased to 26%.

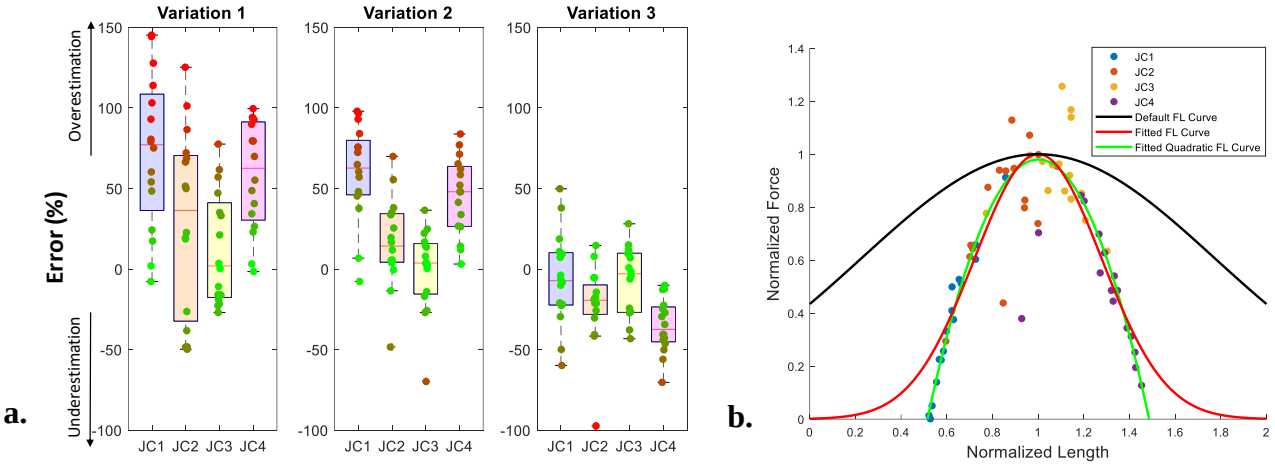

***Figure 1*: a.** Gracilis active force error predicted under 3 variations as a boxplot at each JC. **b.** Length-tension curves. The black curve represents the default F_L curve in the model [6] (SSE: 6.46) while the red curve is best fit curve to subject data (SSE: 1.93). The quadratic fit curve provided the best fit (SSE: 1.65).

Significance: The are large errors predicting gracilis muscle maximal isometric active force, especially near the extremes of joint range of motion. The default F_L curve was wider than the fitted F_L curve (**Figure 1.b.**) which explains the model overestimated muscle active force when fiber length was further away from L_f. We have shown that such errors are reduced by incorporating subject-specific parameters. However, subject specific data require considerable amount of effort, and, in this case, are highly invasive and rare. Thus, generic models are commonly used. Active force simulation error will lead to further inaccurate estimations, such as joint load, and could mislead clinical judgement. Therefore, caution should be exercised when interpreting active force data from the computational model.

Acknowledgments: This work was supported by VA funding 1 I01 RX002462 and Research Career Scientist Award Number IK6 RX003351 from the United States (U.S.) Department of Veterans Affairs Rehabilitation R&D (Rehab RD) Service.

References:

[1] Persad et al. (2021), *J Biomech* 125:110592; [2] Persad et al. (2023), *J Biomech* 111798; [3] Persad et al. (2022), *Sci Report* 12(1):1-16; [4] Binder-Markey et al. (2023), *J Physiol* 601(10):1817-30; [5] Winters et al. (2011), *J Biomech* 44(1):109-15; [6] Hamner SR et al. (2010), *J Biomech* 43(14), 2709-2716.

THE FORCE PRODUCT AND ITS RELATIONSHIP TO PERFORMANCE IN SOFTBALL PITCHING

Takato Ogasawara[1*], Laura McDonald[2], Brian A. Knarr[1]
[1]Department of Biomechanics, University of Nebraska at Omaha, Omaha, NE, USA
[2]OGX Softball LLC., Romeoville, IL, USA
*Corresponding author's email: togasawara@unomaha.edu

Introduction: Ground reaction forces (GRFs) are important in pitching because muscles of the lower extremity and trunk are larger than those in the upper extremity and provide the only external contact a pitcher has between the feet and the ground. While the interaction between the body and the ground is fundamental to softball pitching by generating forces at the trunk and legs, little research has focused on how the drive leg GRFs are generated and related to softball pitching biomechanics. A previous study regarding drive leg GRFs in baseball pitching reported that ball speed was only weakly correlated with peak resultant and vertical GRF and resultant GRF at the time of peak anterior force [1]. For softball research, only peak vertical GRF of the drive leg was positively correlated to ball velocity. Most studies, however, have only examined peak GRFs as independent variables; although useful, peak GRFs give a limited view of the interaction between the feet and the ground. In contrast, GRF impulse (integral of force over time) provides information about the overall profile of the force-time curve which may be more valuable. GRF impulse is a better performance indicator for dynamic motion than peak GRFs which suggests that looking solely at the peak GRFs does not provide adequate information about the performance profile of either leg [2]. While a goal of softball pitching is to generate maximum horizontal ball velocity towards a hitter, the GRFs created by the pitcher to advance the body requires a certain amount of vertical force to the ground to resist gravity. However, the trade-off of vertical to horizontal has not yet been investigated.
Therefore, this research aimed to describe the force product at the drive leg GRFs and investigate relationships to key performance indicators later in the pitching motion. We hypothesized that 1) a higher forward force product positively correlates with model kinetic energy and ball velocity 2) impulse ratio positively correlates with model kinetic energy and ball velocity.

Methods: Seven collegiate female softball pitchers (Age: 20.9 ± 1.6y, Height: 1.72 ± 0.1m, Weight: 78.0 ± 4.6kg) were recruited. Subjects consistently played at a collegiate level and had no injury history within six months. Subjects were fitted with 41 retroreflective makers for a 21-camera motion capture system, capturing at 250 Hz. After a warm-up, the subjects pitched with maximum effort. Ground reaction forces were recorded at 1000 Hz while pitching from a custom-built softball pitching surface with four force plates. One plate was placed under pitching rubber and three under the landing area. Ball velocity was measured with a radar gun with the two fastest pitches chosen for analysis.
The impulse at the drive leg was calculated as the integral of GRF over time from the leg from the moment that the center of mass starts to move forward to the drive leg toe-off. The impulse ratio was determined as vertical force impulse divided by horizontal force impulse. Model kinetic energy was calculated using $\frac{1}{2}mv^2$. The center of mass horizontal velocity at toe-off was used as velocity. Pearson's correlation metrics were calculated to test the relationship between force product, model kinetic energy, and ball velocity.

Results & Discussion: The average ball velocity was 60 ± 5.0 mph and peak vertical and horizontal GRF was 160 ± 34.9% BW and 18.2 ± 3.9%BW respectively. The impulse ratio showed the positive relationship with forward model kinetic energy (r=.92, p<.01; Figure 1) and ball velocity (r=.78, p<.01). Also, the forward model kinetic energy had positive relationship with ball velocity (r=.71, p<.01). The peak GRF in this research had similar result with previous study [3]. The results imply that a higher anterior to vertical impulse ratio, meaning more forward force impulse is generated relative to vertical force impulse, leads to higher model forward energy and is related to higher ball velocity.

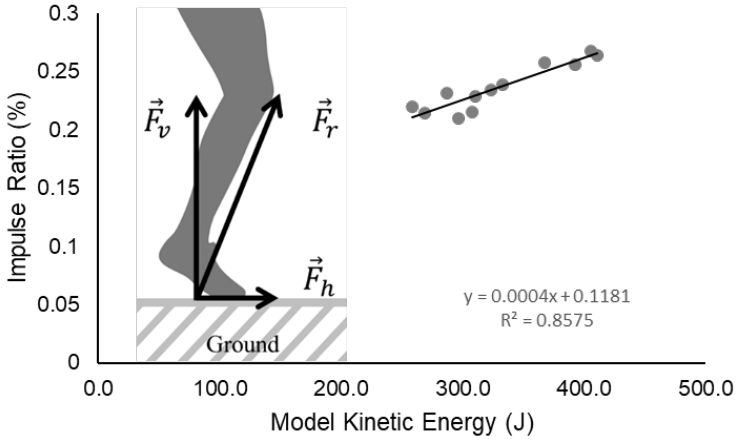

Figure 1: The correlation between the impulse ratio (horizontal/vertical force impulse) and model kinetic energy. The force impulse was calculated as the integration of the force from set-up to toe-off and the model kinetic energy at toe-off was used for analysis.

Significance: The anterior/vertical GRF impulse ratio can explain the relative contributions of each force component in the pursuit of maximizing ball velocity. In addition to training methods that increase the overall force product for pitchers, coaches should also support pitchers in improving the angle at which they generate drive leg GRFs. Kinetic energy is potentially used to assess the overall performance during drive phase. Further research will be conducted about the kinematic characteristic to give more insight into an optimal drive phase during softball pitching. Additionally, this impulse ratio may be applicable to other sports and movements to assess performance.

References: [1] Oyama and Myers (2018), *J Strength Cond Res,* 32(5); [2] Morin et al. (2011), *Med Sci in Sports Exe*, 43(9); [3] Nimphius et al. (2016), *Human Movement Science* 47, 151-158

MEASURING MUSCLE FORCES IN THE NECK DURING HELMET WEAR WITH ULTRASOUND SHEAR WAVE ELASTOGRAPHY

Constantin Heinemann[1*],Mackenzie Hoey[1], Zachary J Domire[1]
[1]East Carolina University, College of Health and Human Performance, Performance Optimization Lab
*heinemannc22@students.ecu.edu

Introduction

Due to muscle redundancy, even single-joint motor tasks can theoretically be produced by an infinite number of muscle force combinations. Accurate quantification of the force produced by individual muscles is necessary for biomechanical analysis. Currently, we rely on simulated models or electromyography to estimate how a muscle moment is split between each component. However, optimization has shown inaccuracies, and electromyography lacks the ability to differentiate between overlapping muscles [1][2]. Shear modulus, measured by Shear wave elastography (SWE), has shown a linear relationship with both active and passive force production in muscles [3][4]. Using SWE, we can directly measure the shear wave speed and shear modulus of a muscle, and with conventional ultrasound imaging, we can determine the muscle's cross-sectional area, thus enabling us to solve for muscle force from shear wave speed and shear elastic modulus measured with ultrasound. In the cervical spine muscles, conventional muscle activity measures fall short due to the diminutive size and overlapping architecture of the individual muscles. The origin and insertion of these muscles, and therefore their function, differ. There are likely muscle-specific effects of posture and head weight.

Methods: Healthy participants (n=9) with no history or current neck pain. Shear wave velocity and shear modulus are related by the equation $c^2 = \frac{\mu k' + \sigma}{\rho}$where c is shear Where c is the shear wave speed, μ is the shear elastic modulus, σ is muscle stress, k is a correction factor and ρ is tissue density. If the shear modulus is measured at rest and muscle length is accounted for then with isometric muscle contraction at that length any increase in shear wave speed can be attributed to muscle stress. Stress (σ) $= Force \times Cross\ Sectional\ Area.$ Using SWE, we can directly measure the shear wave speed and shear modulus of a muscle, and with conventional ultrasound imaging, we can determine the muscle's cross-sectional area, enabling us to solve for muscle force from shear wave speed and shear elastic modulus measured with ultrasound. Shear modulus and shear wave speed of the individual cervical muscles were measured with elastography ultrasound. Measurements were taken in several positions to tease out muscle force. First, in a prone lying position at rest to minimize the load experienced by the cervical muscles. Second, in a prone lying position extending the head into a dynamometer isometrically at 50% of maximum effort. These measurements were taken to establish the force/activation relationship in these muscles without passive force produced by stretch. In the second set of images, participants were seated. Measurements of shear wave speed and shear modulus were taken of the cervical muscles while participants sat with neutral, forward, and low left and right rotation (>60°). These measurements mirror the head positions taken by a pilot during flight and allow us to include passive force production by stretch to the active force production by activation. Electromyography (EMG) measurements were taken contralaterally simultaneously during SWE imaging. Motion markers were placed on the participant, and the same postures were recorded in motion capture. Marker movement was used to simulate the movement in an OpenSim static optimization. The OpenSim model was based on the HYOID model and edited to fit our needs [5].

Results & Discussion: The measured and simulated force results are shown in Table 1. From Table 2, the OpenSim model showed generally higher muscle force in the cervical extensors. From shear wave elastography measurements, the least force production is in the neutral posture where the flexion moment of the head is the least, and muscles are near a resting length. There was a general increase in cervical extensor force in a forward posture when the flexion moment of the head is increased, and cervical extensors are stretched, increasing both passive and active force. During rotation, the greatest force production is made by SCM and multifidus. Conversely, rotation produced the greatest force in the upper trapezius in the OpenSim simulation. In each muscle, in each posture, in both the SWE measurement of force and the OpenSim model, muscle forces of the cervical extensors and SCM were increased with the introduction of the weighted helmet. This is due to the anterior weight of the helmet creating a greater flexion moment about the neck

Shear Wave Elastography					OpenSim				
No Helmet									
Muscle	Neutral	Forward	Turn Right	Turn Left	Muscle	Neutral	Forward	Turn Right	Turn Left
Right									
Trap	0.5	5.5		1.3	Trap	3.6	1.1	0.8	47.6
SP CAP	0.8	10.3		5.4	SP CAP	0.7	3.3	0.6	0.6
SS CAP	0.8	16.2		3.6	SS CAP	0.9	1.8	0.8	0.7
SS Cerv	0.7	20.5		4.3	SS Cerv	3.3	13.7	40.7	4.4
Multifidus	2.0	25.1		16.4	Multifidus	0.4	0.4	23.1	1.6
SCM				37.4	SCM	1.6	1.4	6.9	5.1
Left									
Trap	0.5	5.7	1.8		Trap	1.1	5.9	57.5	0.9
SP CAP	0.6	7.9	5.4		SP CAP	1.6	4.3	0.6	0.6
SS CAP	0.9	18.7	3.3		SS CAP	0.9	5.0	0.7	0.8
SS Cerv	0.9	21.2	5.1		SS Cerv	4.0	2.2	62.5	10.7
Multifidus	1.9	27.3	20.6		Multifidus	0.4	0.4	23.1	1.6
SCM			20.8		SCM	1.3	1.4	1.6	1.2
Helmet									
Muscle	Neutral	Forward	Turn Right	Turn Left	Muscle	Neutral	Forward	Turn Right	Turn Left
Right									
Trap	0.9	7.1		1.5	Trap	2.9	2.1	48.0	1.7
SP CAP	1.4	17.8		7.3	SP CAP	2.2	1.9	9.0	1.8
SS CAP	2.9	35.8		5.7	SS CAP	2.1	2.4	0.6	1.3
SS Cerv	2.9	32.6		7.1	SS Cerv	36.7	75.5	74.2	36.9
Multifidus	5.2	32.2		24.6	Multifidus	17.5	23.8	25.7	16.8
SCM				27.3	SCM	36.6	98.1	28.7	16.3
Left									
Trap	0.9	8.4	2.0		Trap	2.5	2.4	1.7	30.4
SP CAP	2.7	16.9	7.0		SP CAP	2.5	1.7	0.8	1.3
SS CAP	4.9	30.4	4.8		SS CAP	2.1	2.1	1.7	1.1
SS Cerv	3.6	32.5	7.1		SS Cerv	30.9	75.4	71.5	41.0
Multifidus	4.1	33.5	28.7		Multifidus	17.5	23.8	25.7	16.8
SCM			29.3		SCM	31.5	96.3	38.6	15.2

Table 1. Force values (N) measured with SWE and simulated with OpenSim static optimization

SWE					
		Neutral	Forward	Turn Right	Turn Left
No Helmet	Right	4.8	77.6		31.1
	Left	4.8	80.8	36.3	
Helmet	Right	13.3	125.5		46.2
	Left	16.2	121.7	49.6	
OpenSim					
		Neutral	Forward	Turn Right	Turn Left
No Helmet	Right	9.0	20.4		54.9
	Left	8.0	17.9	144.4	
Helmet	Right	61.5	105.7		58.5
	Left	55.4	105.3	101.4	

Table 2. Summed force values of the cervical extensors. SCM not included

Significance: Accurately measuring individual muscle forces is pivotal in biomechanics and rehabilitation. It enables tailored interventions for musculoskeletal disorders, informs sports training and equipment design, and advances our understanding of human movement mechanics. This precision enhances clinical practice and drives innovations in multiple disciplines.

Acknowledgments: Thank you to Taylor Job who assisted with data collection.

References: [1] Prilutsky & Zatsiorsky 2002, [2]Farina et al 2004, [3]Maïsetti et al. 2012, [4] Bouillard et al. 2011, [5] Mortensen, Vasavada & Merryweather 2018

USING DIGITAL IMAGE CORRELATION TO VALIDATE STRAIN ESTIMATIONS FROM A FINITE ELEMENT MODEL OF A TRANSTIBIAL RESIDUAL LIMB

Mohammadreza Freidouny[1], Carson Squibb[1], Masaki Hada[1], Abbie Bailey[1], Brian Kaluf[2], Trevor Johnson[3], Michael K. Philen[1], Michael L. Madigan[1*]
[1]Virginia Tech, Blacksburg, Virginia, USA. [2]Ottobock, USA [3]Virginia Prosthetics & Orthotics, Christiansburg, VA, USA
* Corresponding author email: mlm@vt.edu

Introduction: Socket discomfort and skin problems are prevalent issues among amputees [1]. Excessive strain on the residual limb surface can be an important contributor to these problems, and measuring this strain may help to improve prosthetic socket design and fit [2]. Finite element analysis (FEA) is one potential approach to estimating this strain, but would greatly benefit from validation against empirical data. Digital image correlation (DIC) is an optical technique that can measure surface strains, making it a viable measurement for validating FEA results. Therefore, the goal of this study was to use DIC to validate strain estimations on a prosthetic liner surface of a transtibial amputee during walking.

Methods: One male amputee (67 years, 105 Kg) with a right transtibial amputation was recruited. Upon arrival, the participant was asked to remove their prosthesis for 20 minutes to allow their limb volume to equilibrate. The limb was then scanned [3] to obtain its 3D geometry for the FEA model. The participant subsequently donned a speckled liner for DIC and clear diagnostic socket and completed several walking trials. A FEA model was developed and used to estimate the liner surface strain. A two-camera DIC system was used to measure strain on the liner's anterior surface at mid-stance for comparison with FEA (Figure 1).

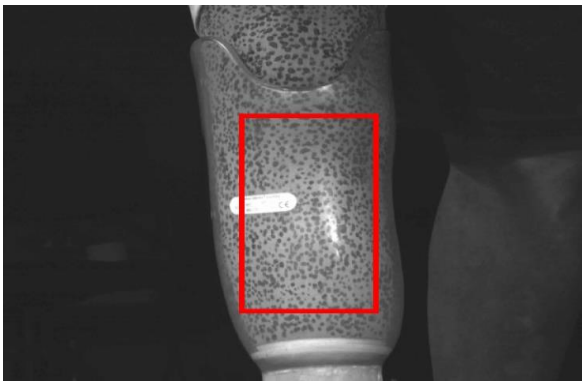

Figure 1 :Approximate Scan region of the DIC.

Results & Discussion: Maximum principal strain (ε_1) on the liner surface during the stance phase is illustrated in Figure 2. Proximal within our scan region, FEA estimated the highest value of ε_1 to be 5.2% while DIC measured this value to be 5.0%. Distal within our scan region, FEA estimated the highest value of ε_1 to be 6.9% while DIC measured this value to be 5.7%. Minimum principal strain (ε_2) on the liner surface during the stance phase is illustrated in Figure 3. Proximal within our scan region, FEA estimated the lowest value of ε_2 to be -6.8% while DIC measured this value to be -4.9%. Distal within our scan region, FEA estimated the lowest value of ε_2 to be -7.3% while DIC measured this value to be -6.8%. It is also worth noting that the strain color increment in Figures 2 and 3 was made more coarse (approximately 0.7%) to enhance reliability and avoid smaller differences in strain that are not clinically important.

The FEA model results show qualitative similarities with the DIC measurements. Furthermore, the regions exhibited the highest strain by FEA strains agreed with the regions reported by the participant to have the greatest discomfort.

Limitations: First, only the anterior region on the liner surface was investigated due to a limited number of DIC cameras available. Second, the approach used here quantifies liner strain rather than skin strain. Future research should study more participants with different socket shaping strategies to enhance the generalizability of this approach.

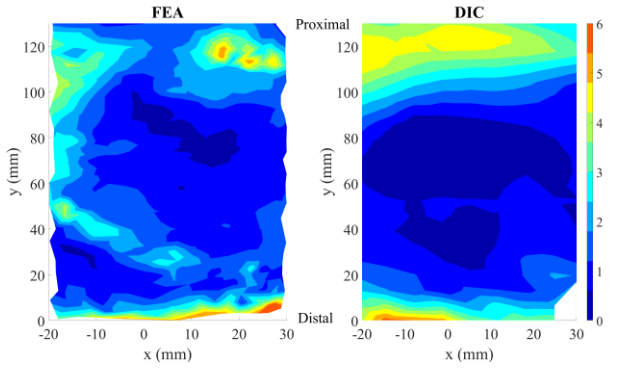

Figure 2: Maximum principal strain (ε_1) percentage estimated by FEA (left) and DIC (right) on the liner anterior surface (Regions with brighter colors represent higher values of tension)

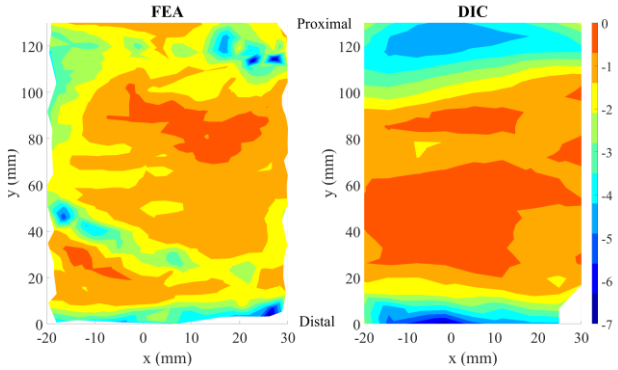

Figure 3: Minimum principal strain (ε_2) percentage estimated by FEA (left) and DIC (right) on the liner anterior surface (Regions with darker colors represent higher values of compression)

Significance: This study demonstrates an approach for validating strain measurements using FEA. This approach has the potential to improve FEA models of residual limbs and may contribute to efforts for improving prosthetic socket design and fit.

Acknowledgements: This work was supported by U.S. Army Medical Research and Development Command under award number: W81XWH-21-1-0220

References: [1] Gupta et al. (2019) Biomed Eng Lett; [2] Al-Fakih et. Al (2016) Sensors; [3] Squibb et al. (2024) Measurements: Sensors (In review);

CONCURRENT ASSESSMENT AND INTER-SESSION REPEATABILITY OF MARKERLESS MOTION CAPTURE

Hector A. Carbajal-Mendez[1,2], Eric Hammond[2], Joshua Johnson[2], Brooke Schultz[3], Anthony Luke[3], Richard B. Souza[1,4]
[1]UCB-UCSF Joint Graduate Program in Bioengineering, San Francisco, CA, United States
[2]UCSF Department of Radiology and Biomedical Imaging, San Francisco, CA, United States
[3]UCSF Department of Orthopaedic Surgery, San Francisco, CA, United States
[4]UCSF Department of Physical Therapy and Rehabilitation Science, San Francisco, CA, United States
Hector.carbajalmendez@ucsf.edu

Introduction: Advancements in computer vision and deep learning have ushered in an era of marker-less motion capture, which claims similar performance [1] and improved repeatability [2] over their markered counterparts, avoiding skin motion artifacts and marker placement variability. These systems continually improve, but lack sufficient validation with many factors still unexplored. Our goal was to perform an independent analysis of the latest advances in markerless systems via concurrent assessment against the gold standard, and inter-session repeatability.

Methods: All testing was performed at the UCSF Human Performance Center. Ten healthy volunteers (5M, 5F) with varying attire participated in sit-to-stand and overground walking trials. Markerless (video) and markered (optoelectric) systems simultaneously acquired data at a sampling rate of 250 Hz. To assess repeatability, five participants returned one week later to repeat tasks. Data was processed using Theia3D (v2023.1) software and Qualysis Track Manager software and exported to Visual 3D and MATLAB. Theia3D software uses multiple video inputs and computer vision and deep learning algorithms to identify features and landmarks to estimate pose. Ground reaction forces (GRFs) were captured at 1000 Hz from two AMTI force plates mounted flush with the floor. Marker trajectories and GRF data were filtered at 6Hz and 50 Hz, respectively. Trajectory data and GRFs were used to determine gait events. The root-mean-square of the differences (RMSD) of joint angles was used to characterize agreement between systems. Intraclass correlation coefficients (ICCs) of joint angles and joint moments were also calculated between marker and markerless systems. Repeatability was analyzed across sessions for walking trials by quantifying inter-trial variability, inter-session variability, and the variability ratio with their root-mean-square (rms) values as in [2]. Markerless video-based sampling rate is inversely proportional to video-based spatial resolution. At 250Hz, the corresponding spatial resolution is 540p. We compared the effect of resolution on RMSD for one pair of matched subjects (1080p/85Hz vs. 540p/250Hz). Clothing effects on RMSD values were also investigated.

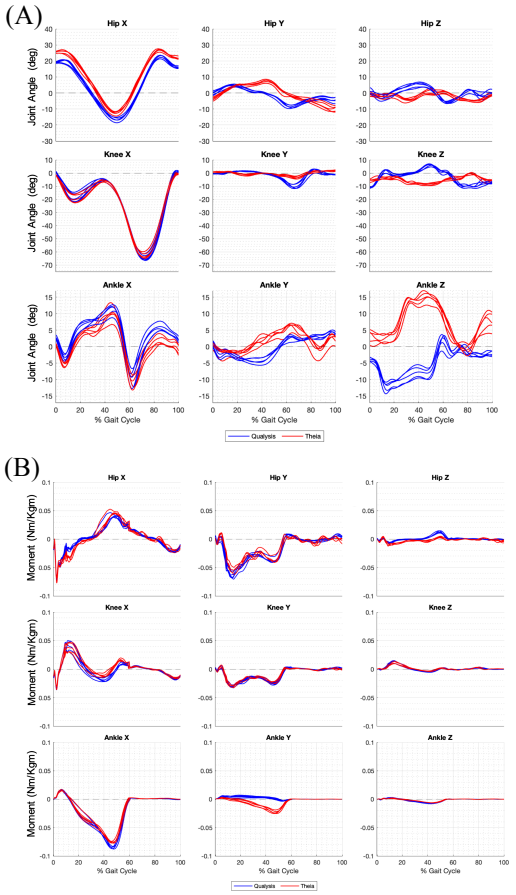

Figure 1. Left lower limb joint angles for 5 gait cycles from one subject (A) and corresponding joint moments in (B) in the sagittal (X), frontal (Y), and transverse (Z) planes.

Table 1. Joint angle root-mean-square-difference (RMSD) in degrees, and joint angle and joint moment intraclass correlation coefficients (ICC) for sit-to-stand (S2S) and freewalk (FW) in the X,Y,Z planes.

		Angle RMSD (deg)			Angle ICC			Moment ICC		
		X	Y	Z	X	Y	Z	X	Y	Z
S2S	Hip	5.51	3.70	8.29	0.98	0.56	0.35	0.98	0.85	0.79
	Knee	2.88	5.07	9.22	0.99	0.04	0.11	0.99	0.52	0.81
	Ankle	4.37	5.22	11.34	0.80	0.19	-0.02	0.89	0.52	0.92
FW	Hip	6.70	3.69	6.43	0.90	0.61	-0.01	0.93	0.97	0.65
	Knee	2.98	3.26	7.00	0.99	0.07	-0.03	0.93	0.96	0.96
	Ankle	2.75	3.65	13.83	0.92	0.29	0.07	0.99	0.14	0.98

Results & Discussion: Markerless data showed RMSDs under 7° in sagittal and frontal plane motions with greater differences in the transverse plane for both tasks (Figure 1, Table 1). ICCs between systems were good to excellent in the sagittal plane across joints, but poor in the other planes. For net joint moment reliability data, ICCs were good to excellent for most planes and joints. Markered data had similar inter-trial variability across joints compared to markerless data (0.80° vs 0.86° respectively), but markerless data had lower inter-session variability (1.25° vs 1.07°). Markerless data also had a lower rms of the variability ratio across joints (1.59 vs 1.27). Wearing shorts improved frontal plane and sagittal plane knee angle agreement within a few degrees across subjects. Similarly, fitted shirts improved hip angle estimation. Finally, higher resolution video acquisition improved agreement by 0.27°-3.34° across joints and tasks. Estimated joint angles from Theia3D software appear comparable to marker-based methods for activities of daily living (faster activities were not studied), particularly in the sagittal and frontal planes. Theia3D performs better with fitted clothing.

Significance: Marker-less motion capture can make it easier to perform biomechanical analysis in a more natural form. The validation of this technology's accuracy to the state of the art and the development of best practices gives confidence in its use for different tasks.

Acknowledgments: Research reported in this abstract was supported by NIAMS of the National Institutes of Health under award number K24 AR072133.

References: [1] Kanko et al. (2021), J Biomechanics 121; [2] Kanko et al. (2021), J Biomechanics 127

HIGH INTENSITY GAIT TRAINING IMPROVES WALKING SPEED AND BALANCE IN PEOPLE WITH INCOMPLETE SPINAL CORD INJURY BUT COMMUNITY WALKING IS ELUSIVE

Anna Shafer[1*], Shamali Dusane[2], Heather Henderson[2], Jennifer H. Kahn[2], Colleen Johnson[3], Jane Gyarmaty[2], Gabrielle Brazg[3], Kwang-Youn Kim[2], Keith E. Gordon[1, 2]
[1]Edward Hines Jr. VA Hospital, Hines, IL; [2]Northwestern University, Chicago, IL; [3]Shirley Ryan AbilityLab, Chicago, IL
*Corresponding author's email: anna.shafer@northwestern.edu

Introduction: Among ambulatory people with incomplete spinal cord injury (iSCI) impaired control of lateral balance during walking is common [1, 2] and correlated with clinical gait and balance measures [3]. Further, balance is a primary determinant of participation in walking activities in this population which averages only 2,600 step/day [4], well below the sedentary threshold. Thus, we sought to understand if gait training to improve lateral walking balance in people with iSCI would increase participation in walking activities. Specifically, we created a movement amplification (MA) environment to magnify mediolateral whole-body center of mass (COM) motion during treadmill walking using a cable-driven robot to apply continuous forces to the pelvis proportional in magnitude and direction to real-time lateral velocity [5]. The MA environment may accelerate learning control of lateral COM motion by augmenting sensory motor feedback. Current clinical practice guidelines recommend high intensity gait training (HIGT) (repetitive stepping practice at a target heart rate) to improve walking distance and speed for people with iSCI [6]. Here, we tested if HIGT performed in a MA environment can further improve outcomes. We hypothesized that ambulatory people with iSCI would make greater improvements in their ability to control their lateral COM excursion during walking, clinical measures of walking speed and balance, and participation in walking activities following HIGT performed in a MA environment than HIGT performed in a traditional treadmill environment.

Methods: 36 ambulatory people with chronic iSCI (American Spinal Injury Association Impairment Scale C or D) were recruited to participate in 20, 45-min HIGT sessions. Half of the participants received the HIGT in a traditional treadmill environment and the other half in a MA environment. We conducted assessments Pre- and Post-training (n=30 due to drop out). Clinical outcomes measured included a 10-meter walk test (10MWT) at participants' fastest speed to determine walking speed and a Functional Gait Assessment (FGA), a ten-item test to evaluate dynamic balance during gait. We quantified participants' average lateral COM excursion per stride for data collected during treadmill walking at the participant's self-selected speed. Participants wore a StepWatch (Modus Health, Inc.) to record walking activity in their home and community for a 1-week period Pre- and Post-training.

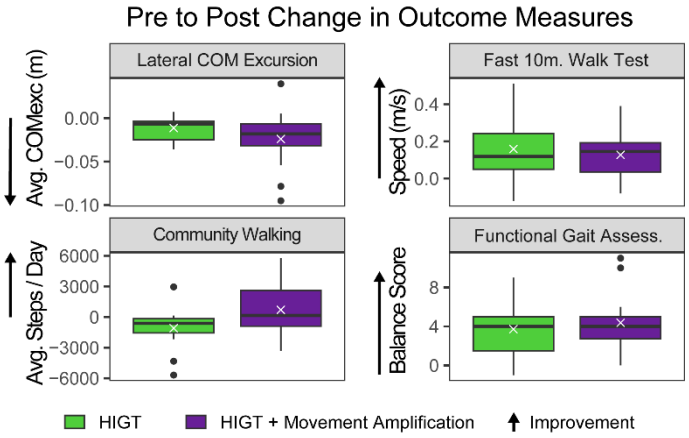

Figure 1: Participants received High Intensity Gait Training (HIGT) in a traditional treadmill environment or in a Movement Amplification environment (HIGT + Movement Amplification). Changes in outcome measures show improvement Post training for lateral balance (COM excursion), walking speed (10 m walk test), and walking balance (Functional Gait Assessment) for both groups. No changes were observed in walking participation in the community (average steps/day).

Results & Discussion: Average lateral COM excursion decreased, indicating greater ability to control mediolateral motion during walking by 0.011m for the HIGT group and by 0.024m for the HIGT+MA group (Fig. 1). Clinical measures of speed and balance also improved Post training when compared to baseline. For the 10MWT, speed increased by 0.16±0.17 m/s for the HIGT group and by 0.13±0.12 m/s for the HIGT+MA group (minimally clinically important difference is 0.06 m/s). For the FGA, scores improved for both groups by 3±3 points for HIGT and by 4±3 points for HIGT+MA. Avg Steps did not significantly change from baseline for either group (HIGT: -1092±2120, HIGT+MA: 704±2582 steps). No significant differences were found between groups for any of the measures. These findings partially supported our hypotheses by demonstrating that HIGT helped all participants with iSCI to improve their speed and walking balance. However, there was no significant difference found in ability to control lateral COM movement following HIGT+MA. Finally, even with improved walking capacity, there was no noticeable difference in walking activity in the community.

Significance: Our findings suggest that HIGT is an effective intervention to improve both gait speed and balance in persons with iSCI; however, further interventions may be necessary to address barriers to increasing community walking.

Acknowledgements: This study was funded by the U.S. Department of Veteran Affairs #1 I01 RX003371. The authors thank Katherine Martinez, Kyle Bostedt, Christina Lui, Shay Pinhey, Jordan Dembsky, Mackenzie Mattone, Yuchan Choi, Keri Han.

References: [1] Zwijgers et al. (2022), *J of Neuroengineering and Rehabilitation* 19(1); [2] Ochs et al. (2021), *J of Neuroengineering and Rehabilitation*, 18(1); [3] Dusane et al. (2023), *Frontiers in Neurology*; [4] Saraf et al. (2010) *Phys Ther*; [5] Brown et al. (2017) *IEEE EMBC*; [6] Hornby et al. (2020), *J of Neurologic Physical Therapy.*

A Telehealth tool to Automate Mobility Testing for Lower Limb Amputees

Mojtaba Mohasel, Corey A. Pew*
Montana State University, Mechanical and Industrial Engineering, Bozeman, Montana
***Corey.Pew@montana.edu**

Introduction: Clinical mobility testing critically evaluates health, functionality, and prosthesis fit in individuals with lower limb amputation (LLA). The 2-Minute Walk Test (2MWT) [1] and Timed Up and Go (TUG) [2] tests are simple assessments used to measure mobility [3]. Currently, mobility testing is performed in-clinic, during regular visits; however, in many states, the closest clinic is hours away from the patient's location. Lack of access to medical care can result in poor prosthesis fit limiting mobility and damaging long-term health outcomes. Remote healthcare options, such as mobile assessment devices can surmount some of these challenges. Yet, current mobile assessment devices (StepWatch and MoveMonitor) are prohibitively expensive and must be returned to the clinician with a time delay between measurement and assessment. Therefore, no live telehealth tool enables individuals with LLA to conduct mobility testing at home with low-cost, real-time assessment. Our purpose is to create this telehealth tool.

Methods: Hardware/software development utilized data from 16 non-amputee participants and 2 individuals with LLA. Hardware development selected Inertial Measurements Unit (IMU) [4] sensors for data collection. Eleven IMUs were placed on the lower limb segments with 2 on each thigh and shank, one on each foot, and one on the lower back of participants. Each participant performed 5 trials of the 2MWT and TUG tests in a randomized order. Two experimenters measured the distance for 2MWT jointly and had individual measurements for the TUG times. The resultant IMU acceleration was mean corrected to zero [5] and used as the primary signal for calculation. We developed 3 methods for 2MWT and 1 for TUG assessment. 2MWT methods: *1) Integration:* Employs double integration to derive velocity from acceleration and displacement from velocity on non-zero intervals [5]. *2) Step Count:* Determines steps taken by identifying peaks in the signal, then multiplying by average step length obtained by integration. *3) Machine Learning (ML):* Divides the 2-minute duration into 120 one-second windows. Each window is labeled with the overall distance divided by 120. *ML* extracts features [6] for windows and uses a Random Forest regressor [7] to estimate the distance for each window. *ML* model training employs hold-out method, utilizing data from all participants except the test participant. TUG method: *1) Threshold:* Identifies a specific value (e.g., 10 $\frac{m}{s^2}$) as an indicator for the start and stop of the TUG task through manual observation of signals from several participants. Acceptable error for 2MWT methods was set at +/- 6 m to the human measurement [5]. Success for TUG calculation should be within the two experimenters' 95% confidence intervals. We randomly selected three participants for an initial evaluation of the 2MWT to demonstrate the effectiveness of each developed method. However, for the TUG test, we only reported results for one randomly selected participant, as the code is still in the early stages of development.

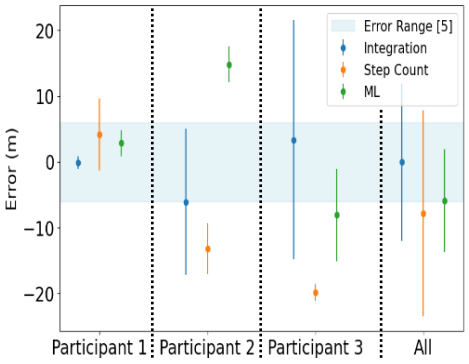

Figure 1: 2MWT Error (Mean+/-SD)

Results and Discussion: For the 2MWT, *Integration* outperformed other methods (Fig. 1), closely predicting participant 1 within a meter in all trials. *Step Count* was the weakest distance estimator due to averaging step lengths and missing peaks. The *ML* model overestimated participant two and underestimated participant three. The utilization of uniform approximations for one-second windows by the *ML* limited exposure to diverse data, hindering effective regression fitting. *Integration* was positioned at the center of the shaded area for all test participants. This demonstrates that our *Integration* method closely resembles the previous automated distance estimator, achieving a similar error rate (15 meters in the worst case) [5]. *ML* exhibits the lowest standard deviation error across all participants, indicating its potential for further development as our final distance estimator. Our current results fall within the minimal detectable change range for LLAs (34.3 meters) [8], indicating clinical relevance.

For the TUG test (Fig. 2), *Threshold* was successful in 3 out of 5 trials for Experimenter 1 and in 2 out of 5 trials for Experimenter 2. However, it inaccurately predicted trial 2 due to signal quality issues, resulting in a time difference of 3.3 seconds from the average of experimenters. To address this issue, we plan to implement a signal quality validation stage before start and stop identification. Our current results fall within the minimal detectable change range for LLAs (3.6 seconds) [8]. Future work will move in two directions: 1) Improving *Integration* and *ML* by incorporating a validation stage for selected intervals and including deep learning. 2) Evaluating varying sensor placement.

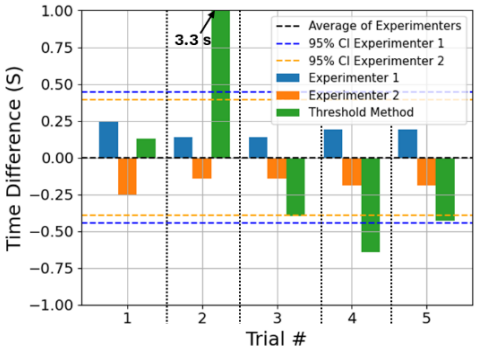

Figure 2: Threshold TUG Compare

Significance: A potentially low-cost software and hardware system that can improve access to healthcare for LLA is in development. It is built with open-source code that utilizes a single sensor. It reliably calculates clinical mobility measures automatically. The availability of our open-source code will facilitate researchers in developing their own methods or enhancing our approach. This endeavor aims to provide clinicians with a reliable assessment tool, highlighting the potential of IMU sensors in telehealth solutions.

Acknowledgment: Thank you to Thomas Madden for helping with data collection. Research reported in this publication was supported by the National Institute of General Medical Sciences of the National Institutes of Health under Award Number **P20GM103474**. The content is solely the responsibility of the authors and does not necessarily represent the official views of the National Institutes of Health.

References: 1) N. A. Capela et al, IEEE EMBS 36 2014; 2) E. Barry et al, BMC Geriatr, 14 (1), 2014; 3) S. C. White, ASHA, 32, 1990; 4) N. Ahmad et al, Int. J. Signal Process. Syst, 1(2), 2013; 5) K. Trentzsch et al, Brain Sci, 11(11), 2021; 6) M. Christ et al, Neurocomputing, 307, 2018; 7) S. M. Moghadam et al, IEEE Sens J, 2023. 8) Resnik et al, Physical therapy, 91(4), 2011

DESPITE IMPAIRED GAIT KINEMATICS AND KINETICS, LOWER EXTREMITY MUSCLE SYNERGIES REMAIN INTACT IN PEOPLE WITH DIABETES WITHOUT NEUROPATHY

Roya Hoveizavi[1]*, Simon J. Fisher[2], Fan Gao[3]
[1] Department of Kinesiology, California State University- Sacramento, Sacramento, CA
[2] Division of Endocrinology, Diabetes and Metabolism, Dept. of Internal Medicine, University of Kentucky, Lexington, KY
[3] Department of Kinesiology and Health Promotion, University of Kentucky, Lexington, KY, USA
*Corresponding author's email: roya.hoveizavi@csus.edu

Introduction: Individuals with diabetes often experience compromised neuromuscular function, increasing the risk for plantar ulcers and amputations. Historically, alterations in gait kinematics, kinetics, and electromyography (EMG) observed in people with diabetes were attributed to diabetic neuropathy. However, our previous studies identified the development of these pathologic changes prior to the development of neuropathy. The current study aims to investigate whether, in the absence of diabetic neuropathy, these diabetes-related gait changes are accompanied by altered muscle synergies.

Methods: Participants included eleven individuals with type II diabetes mellitus without diabetic neuropathy (DM; age 53±11, 87±16 kg, HbA1C 7.37±1.80, duration of disease 75±79 months) and ten non-diabetic controls (CON; age 52±14 y; 76±15 kg). Monofilament testing confirmed the absence of diabetic neuropathy. Surface EMG data were collected from seven lower extremity muscles (vastus lateralis (VL), rectus femoris (RF), biceps femoris (BF), semitendinosus (ST), lateral gastrocnemius (LGS), soleus (SOL), and tibialis anterior (TA)) during twenty barefoot walking trials. Synergy complexity was evaluated by the number of synergies accounted for >90% of the total variance in the EMG data (Nsyn), total variance accounted for by one synergy (tVAF1), and total variance accounted for by four synergies (tVAF). The average synergy weights and activations for a four-synergy solution were compared between DM and CON using cosine similarity (CS). Additionally, an EMG co-contraction index (CCI) was obtained for agonist and antagonist muscle pairs.

Results & Discussion: Nsyn, tVAF1, or tVAF did not significantly differ between DM and CON. Synergy composition including synergy weights and activations demonstrated considerable similarity across DM and CON, though some minor differences were present. Furthermore, a slight increase in muscle co-contraction was noted in DM, especially in VL-BF pair. Our findings demonstrate that individuals with diabetes without neuropathy employ comparable muscle synergies to their non-diabetic counterparts during walking. Despite previously documented impairments in gait kinematics, kinetics, and EMG in people with diabetes, it is possible that such impairments may be attributed to other diabetes-related processes, which seem to be independent of the muscle synergies and central mechanisms underlying movement control. To better understand the complex relationship between diabetes and neuromuscular function, future investigations should explore whether individuals with neuropathic diabetes demonstrate analogous synergies with their non-diabetic counterparts. This is crucial since no prior studies have examined muscle synergies in people with established diabetic neuropathy. Such investigation holds promise for developing targeted therapeutic interventions and monitoring tools that could lead to enhanced treatment strategies for individuals with diabetic neuropathy.

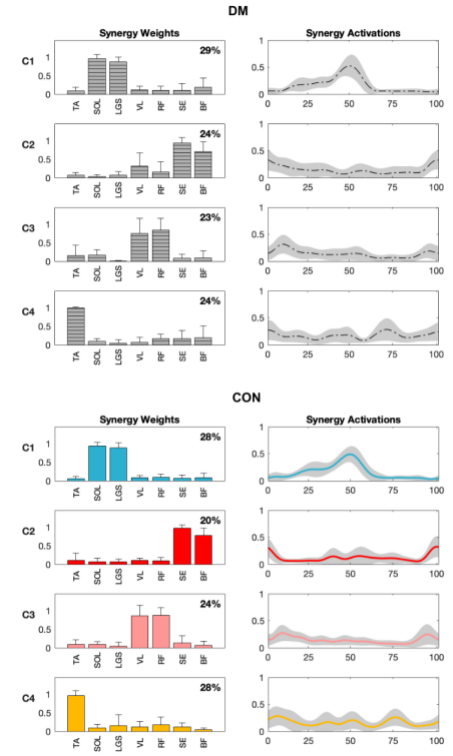

Figure 1: Average synergy weights and activations for a four-synergy solution in DM (top) and CON (bottom). The percentage contribution of each synergy to the overall variability of reconstructed data (W*C) is displayed at the top right corner of each synergy weight graph.

Significance: The present study provides novel insights into the impact of diabetes on the central mechanisms of movement control. To the best of our knowledge, this is the first study investigating muscle synergies during gait in individuals with non-neuropathic diabetes. Our findings identify that, despite previously reported gait abnormalities in this population, muscle synergies are preserved. These finding suggest that central mechanisms controlling movement may remain largely unaltered at the non-neuropathic stage of diabetes. The aforementioned results have crucial implications for guiding future research directions to better understand the complex relationship between diabetes, neuropathy, and neuromuscular function.

Acknowledgments: This work was supported by the teaching assistantship provided by the department of Kinesiology and Health Promotion at the University of Kentucky (to RH), in part by the National Institute of Diabetes and Digestive and Kidney Disease (R01DK118082 to S.J.F.), and the Barnstable Brown Diabetes Center and University of Kentucky Diabetes and Obesity Research Priority Area (to S.J.F).

References: [1] Akashi, P.M., et al., *The effect of diabetic neuropathy and previous foot ulceration in EMG and ground reaction forces during gait.* Clinical Biomechanics, 2008. **23**(5): p. 584-592. [2] Sacco, I. and A. Amadio, *Influence of the diabetic neuropathy on the behavior of electromyographic and sensorial responses in treadmill gait.* Clinical Biomechanics, 2003. **18**(5): p. 426-434. [3] Bernstein, N., *The co-ordination and regulation of movements Oxford Pergamon.* 1967.

A methodology for the design and fabrication of an artificial gravid uterus

Jairo A. Mantilla[1*], Diego F. Villegas[2],
[1]Grupo de investigación en energía y medio ambiente, Industrial University of Santander, Colombia.
*Corresponding author's email: jairo2218051@correo.uis.edu.co

Introduction: An estimated 13 million preterm infants are born each year, with preterm birth being the leading cause of death in children under 5 years old [1]. This population occupies more than 50% of neonatal intensive care units with long hospital stays [2] and high costs to the health care service. In addition, psychological disorders have been documented in families with preterm infants [3], interfering with maternal responsiveness. In the last decade, several postpartum strategies have been developed in preterm infants, such as exposure to maternal voice [4], massage therapies [5], positioning [6] and the kangaroo care program [7], achieving significant improvements in their prognosis by strengthening the mother-infant bond. These investigations are the basis of the project hypothesis: "If the preterm infant is stimulated by means of a cradle-type device whose movement emulates the kinematic conditions experienced by the fetus inside the maternal uterus, an improvement in recovery will be obtained", however, it is first necessary to find the fetal kinematics, a movement that has not been documented to date and that is needed to be emulated by the clinical device. This work presents the detailed development for an experimental setup of an artificial gravid uterus for the third trimester of gestation, where the fetus is in an advanced stage of development, surrounded by amniotic fluid that allows its movement and protects it from possible mechanical trauma. The setup considers the structures of the pelvis, the uterus, the amniotic fluid and the fetus, allowing the measurement of fetal kinematics characterized by three rotation angles from the pelvic movement of pregnant woman during gentle walking.

Methods: The gait analysis presented by Branco [8] was used to obtain the pelvic motion of an average pregnant woman in the third trimester. This movement was emulated with a rotating platform with two degrees of freedom, making the simplification that the pregnant uterus has the same pelvic movement. The experimental model assembled on the platform "Figure 1" was defined for the 34th week of gestation, when the highest volume amniotic fluid volume is present [9] and the greatest range of fetal movement is expected to be obtained. The pelvic model was developed through segmentation by computed axial tomography. Subsequent steps involved refining the geometry and ensuring the appropriate configurations for the attachments of the uterus and the platform, it was printed through fused deposition modeling using poly lactic acid (PLA +) to enhance the model's rigidity. A three-dimensional, parametric modeling of the uterus was conducted in accordance with the methodology outlined by Louwagie [10], utilizing ultrasound measurements as the basis. This complex model was simplified into two distinct structures: one internal and one external. The outer uterus structure is rigid to achieve the attachment between the uterus and the pelvic structure and to avoid its collapse due to the internal elements; on the other hand, the internal structure has the detailed geometry of the uterus and was manufactured using molding silicone with shore hardness 30A. The silicone was tested in traction at different strain rates to validate its mechanical response with experimental references in uterine tissue [11]. The external structure of the uterus was generated by 3D printing in PLA+ whereas the internal structure was cast using the external structure and a negative mold. For the fetal model, the average measurements of head circumference, abdominal circumference and femur length were defined [12], to scale a generic fetal model. The fetal model was fractionated to distribute its weight using small lead spheres, located at the centers of mass of the limbs, head and trunk. An inertial measurement unit (IMU) was implanted inside the fetal model to determine its kinematics. Finally, water was used as amniotic fluid on the basis that amniotic fluid is composed of 98% water and its viscosity is similar for the recreated gestational age [13].

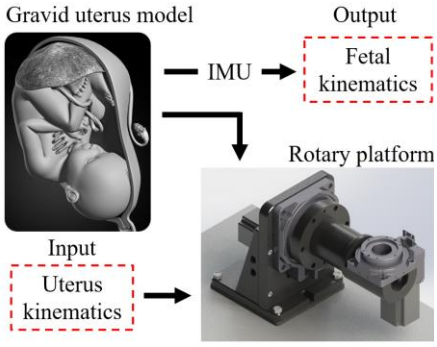

Figure 1: Experimental dynamic setup.

Results & Discussion: An experimental model has been developed consisting of a rotating platform fitted with an artificial uterus containing a fetal model suspended in water. The standard fetal position implies a flexed posture with shoulder and elbow adduction and hip and knee flexion, but the model can be oriented either occipital-anterior or occipital-posterior. Mechanical tests performed on the molded silicone show a strain rate-dependent hyper elastic behavior, in agreement with what has been reported in the literature [11]. The model developed reproduces the kinematic conditions of the fetus and is not limited to a specific application; it can be scaled for different gestational ages and used in experimental studies such as trauma and intrauterine pressure variations.

Significance: Fetal kinematics is a movement that has not yet been reported and is of great importance to be reproduced in the clinical device. It is expected that treatment with the device will have an impact on neonatal health by reducing mortality, stress and anxiety indices in families, minimizing the risk of infection due to prolonged hospitalization and consequently reducing costs. On the other hand, the experimental model allows various studies on the mechanical behavior of a pregnant uterus.

References: [1] Ohuma, et al. (2023), *Lancet* 402(10409); [2] Seaton, et al. (2021), *J Pediatrics* 233, 23-32; [3] Villamizar, et al. (2018), *Enfermería intensiva* 29(3); [4] Picciolini, et al. (2014), *Early Hum Dev* 90(6); [5] Wang, et al. (2013), *Am J Perinatol* 30(9); [6] Madlinger, et al. (2014), *Res Dev Disabil* 35(2); [7] Kucukoglu, et al. (2021), *J Pediatr Nurs* 60; [8] Branco, et al. (2016), *Acta Bioeng Biomech* 18(2); [9] Beall, et al. (2007), *Placenta* 28(8-9); [10] Louwagie, et al. (2021), *Plos One* 16(1); [11] Manoogian, et al. (2012), *J Biomech* 45(9); [12] Loughna, et al. (2009), *Ultrasound* 17(3); [13] Rosati, et al. (1991), *Int J Gynaecol Obstet* 35(4).

BALANCE DISRUPTION TIMING WITHIN THE GAIT CYCLE IMPACTS STEP WIDTH BALANCE ADAPTATIONS

Madison L. Lang[1*], Francis M. Grover[2], Anna Shafer[3], Xenia Schmitz[1], Keith E. Gordon[2, 3]
[1]Department of Biomedical Engineering, Northwestern University, McCormick School of Engineering, Evanston IL 60208
[2]Physical Therapy and Human Movement Sciences, Northwestern University, Feinberg School of Medicine, Chicago, IL 60611
[3]Research Service, Edward Hines Jr. VA Hospital, Hines, IL 60141
*Corresponding author's email: madisonlang2024@u.northwestern.edu

Introduction: Creating a gait training environment for improving reactive balance (ability to detect and recover from unexpected balance disruptions) is challenging due to dual objectives to maximize task-specific practice responding to unexpected balance disruptions while avoiding adoption of general protective strategies [1]. Protective strategies (e.g., slow walking, short/wide steps) help position a person to resist all forms of external disturbances but can be detrimental to the quality of reactive balance practice, as they decrease the intensity of balance disruptions [2]. We have a limited understanding of how balance disruption characteristics (e.g., magnitude, timing, direction) affect balance strategies adopted during an intervention [3]. Our objective is to understand the effect of modulating balance disruption timing within the gait cycle on step width (SW). We believe that when balance disruptions occur within the gait cycle will influence which balance strategies people adopt [4]. When balance disruptions occur during single limb support (SLS), people can make within-step changes to SW by adjusting their swing limb trajectory, encouraging use of reactive balance strategies. In contrast, when balance disruptions occur during double limb support (DLS), people cannot immediately modulate SW, encouraging use of protective strategies (i.e., systemic changes in SW occurring every step). *We hypothesized people will adopt general protective strategies in response to balance disruptions occurring during DLS but not in response to disruptions occurring during SLS.*

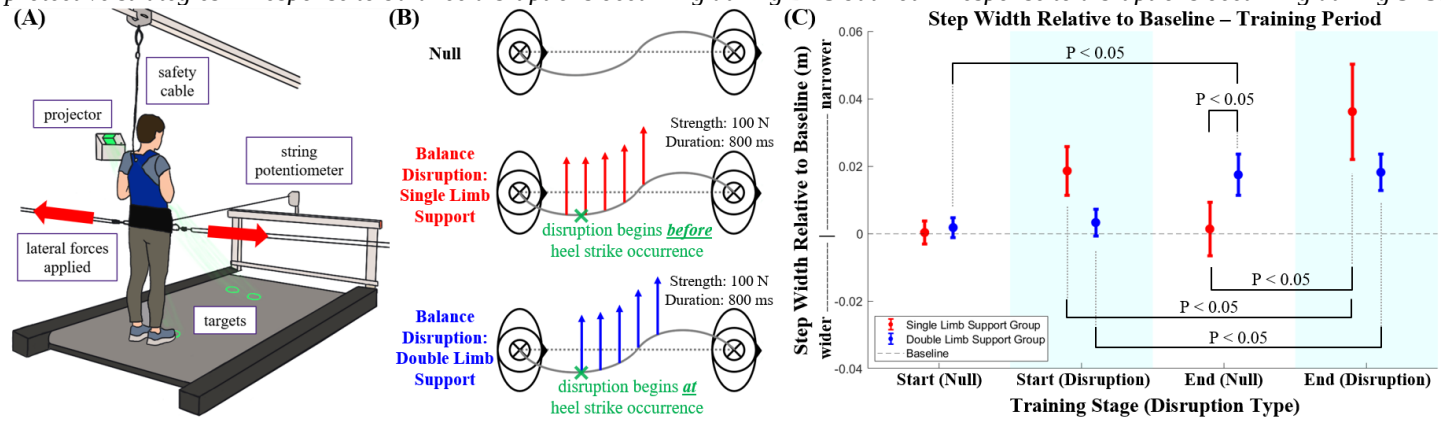

Figure 1: (A) Experimental Set-Up. (B) Forces applied by the cable-driven robot. The green X indicates the first right heel strike occurrence. (C) Step width results. The data represents the average and standard error values for all participants. Statistically significant differences are indicated.

Methods: 20 healthy adults (20 females, 24.4 ± 2.7 years) performed a series of discrete walking trials moving from start targets to end targets and always stepping with their right foot first (Fig. 1A). Each trial, participants experienced either a null field (no net lateral forces applied) or a leftward balance disruption (a cable-driven robot applied lateral forces to the pelvis) (Fig. 1B). Participants performed 10 **baseline** trials (null field) followed by a 180-trial **training** period with balance disruptions occurring randomly once every 4-6 trials (144 null trials, 36 balance disruption trials). Participants were randomly assigned to either a SLS or DLS group, which received balance disruption during late swing phase, or at first right heel strike, respectively (Fig. 1B). We quantified SW at the first right heel strike each trial. We used paired-sample t-tests to analyze within-group differences in SW between the start of training (first four null and first four disruption trials) and the end of training (last four null and last four disruption trials). We used two-sample t-tests to analyze differences between the SLS and DLS groups. SW results were normalized by the average of the last four baseline trials.

Results & Discussion: SW significantly narrowed for only the DLS group when comparing null trials from the start and end of training (Fig. 1C), suggesting the DLS group developed a protective strategy—systemically adopting their SW in the direction of the balance disruption. This strategy may aid in generating ground reaction forces and modulating moments about the ankle joint. For the balance disruption trials, SW significantly narrowed for both groups when comparing the start and end of training. However, only the SLS group showed a significant difference between the null end of training and disruption end of training. This suggests the SLS group adopted reactive balance strategies, where the DLS group's change in SW for the disruption trials at end of training was likely due to protective strategies as observed during the null end of training trials. Our results support our hypothesis—the DLS group adopted general protective strategies while the SLS group did not.

Significance: Our results suggest that modulating the timing of balance disruptions within the gait cycle influences the types of balance strategies adopted. Balance disruptions during DLS led to adoption of general protective strategies (systemic changes in SW during null trials), whereas balance disruptions during SLS led to adoption of reactive balance strategies during disruption trials only. This information may help guide future gait training protocols to improve reactive balance following neurological injury.

Acknowledgments: Supported in part by the U.S. Department of Veterans Affairs, RR&D Service #I01RX003371.

References: [1] Horak et al. (1997), *Phys Ther.* 77(5):517-33; [2] Bone et al. (2021), *Nat Hum Behav.* 749. [3] Vlutters et al. (2016), *J Exp Biol.* 219(Pt 10):1514-23. [4] Zwijgers et al. (2022), *J Neuroengineering and Rehabilitation*. 19(1).

IMMEDIATE EFFECTS OF STANDARD OF CARE AND 3D-PRINTED CUSTOM ACCOMMODATIVE INSOLES ON STATIC BALANCE IN INDIVIDUALS WITH DIABETES MELLITUS

Mathew Sunil Varre[1,2*], Kimberly A. Nickerson[1,2], Brittney C. Muir[1,2]
[1]Center for Limb Loss and Mobility, Veterans Affairs Health Care System, Puget Sound, [2]Department of Mechanical Engineering, University of Washington, Seattle.
*email: msvarre@uw.edu

Introduction: Therapeutic footwear and custom accommodative insoles (CAI) are commonly prescribed in the clinical management of diabetes mellitus (DM) to mitigate the risk of foot ulcers by reducing plantar pressure [1]. The standard of care accommodative insoles (SoC) are designed using multiple layers of foam with an ethylene-vinyl acetate base that are molded to conform to the foot [2]. The SoC stiffen over time leading to inadequate offloading of the foot necessitating a replacement device every few months [2,3]. To potentially address the issues of longevity and efficacy, our team has leveraged advances in 3D printing, materials, and software to develop a 3D-printed pressure-based CAI (3DPI) [3,4]. While these interventions have been shown to be effective in offloading the high-pressure regions of the diabetic foot, their impact on postural balance is unclear. Furthermore, variations in the design of the CAI and the materials used can alter the plantar cutaneous sensation [2] and exacerbate the balance deficits already seen in older adults with DM and diabetic peripheral neuropathy (DPN) [5]. Static balance, using center of pressure (COP) measures, has been reported to be both negatively impacted [6] and improved [7] by CAI with arch support in patients with DM and DPN. Since balance is especially critical in older adults with DM [8], the effect of CAI on balance must be determined. Therefore, in this study, we investigated the immediate effects of 3DPI and SoC compared to a no-insole (NI) condition on static balance in individuals with DM. We hypothesized that the SoC and 3DPI would improve the postural balance of patients with DM during quiet standing compared to the NI condition.

Methods: Five participants (4 male, 1 female diagnosed with DM [73(2) years; 1.7 (0.1) m; 82 (13) Kg]) were recruited for this study. Foot impressions and in-shoe PP measurements (Novel, DE) while walking in a standardized research shoe (Dr. Comfort, USA) were collected during a baseline visit and were used to design SoC and 3DPI [3]. During a follow-up visit, in-shoe PP measurements during quiet standing were recorded during three 30 second trials in the NI, SoC, and 3DPI conditions. The data were processed to compute center of pressure (COP) measures (mean, range, velocity, path length along medial-lateral (ML) and anterior-posterior (AP) directions, and 95% confidence ellipse area) [9; Table 1].

Results & Discussion: Mean COP amplitudes in the ML direction were slightly greater in SoC (4%) and 3DPI (3%) conditions over NI condition, however, in the AP direction there was a decrease of 11% and 6%, respectively. When compared to the NI condition, COP range, path length, and velocity decreased in ML and AP directions for both SoC (19-26%) and 3DPI (17-23%; Table 1) conditions. 95% confidence ellipse area measure showed a decrease of 49% and 21% respectively for the SoC and 3DPI conditions. Overall, a trend toward smaller deviations in COP measures was found in the two insole conditions over the NI condition. The decreased COP oscillations suggests reduced center of mass sway in order to maintain balance, thereby indicating improved postural stability during quiet standing with the use of CAI [10].

Significance: The preliminary findings of our study suggest that SoC and 3DPI have the potential to improve postural balance in individuals with DM during quiet standing. Future studies with larger sample sizes are needed to definitively establish and generalize the immediate and long-term effects of custom accommodative insoles on both static and dynamic balance in individuals with DM. Such evaluations would be useful in refining the design of custom accommodative insoles to effectively reduce the risk of foot ulcers in individuals with DM without compromising their balance.

Acknowledgments: Funding for this study was provided by VA RR&D Merit Award (A3539R).

References: [1] Bus et al. (2020), *Diabetes Metab Res Rev* 32(1); [2] Shi et al (2022), *Sci. Rep*, 12; [3] Hudak et al. (2022), *Med Eng Phys* 104; [4] Muir et al. (2022), *Clin Biomech* 98; [5] Bhatt et al., *J Clin Diagnostic Res*., 2022; [6] Paton et al. (2016), *J Foot Ankle Res* 9(40); [7] Hemmati et al..(2023), *J Am Podiatr Assoc*., 113(3); [8] Hijmans et al. (2007), *Gait Posture* 25(2); [9] Quijoux et al. (2021), *Physiol Rep* 9(22); [10] Palmieri et al. (2002), *J Sport Rehabil* 11.

Table 1. Average (SD) and percentage (%) differences in the COP measures of the SoC and 3DPI compared to the NI condition.

	Mean (mm)		Range (mm)		Path Length (mm)		Velocity (mm/s)		95% Ellipse Area (mm^2)
	ML	AP	ML	AP	ML	AP	ML	AP	
NI	64.7 (5.1)	117.7 (32.4)	4.2 (3)	32.5 (15.4)	38 (17)	241.3 (83)	1.9 (0.9)	12.1 (4.1)	90.4 (85.9)
SoC	67.3 (3.9)	104.2 (23)	3.2 (2.2)	26.2 (9.7)	29 (10)	179.1 (42.7)	1.5 (0.5)	9.2 (2.1)	46.4 (55.1)
	4%	- 11%	- 23%	-19%	- 24%	- 26%	- 24%	- 26%	- 49%
3DPI	66.5 (4.6)	110.6 (27.3)	3.2 (2.6)	26.4 (11.9)	31.4 (12.6)	185 (51.7)	1.6 (0.6)	9.2 (2.6)	71.1(114.6)
	3%	-6%	- 23%	-19%	-17%	-23%	-17%	- 23%	-21%

MOTOR LEARNING FROM REPEATED STANDING-TRIPS IN YOUNG ADULTS

Sara Mahmoudzadeh Khalili[1], Caroline Simpkins[1], Feng Yang[1*]
Department of Kinesiology and Health, Georgia State University, Atlanta, GA, USA
*Corresponding author's email: fyang@gsu.edu

Introduction: Falls are a major public health concern with devastating consequences, emphasizing the critical importance of fall prevention measures [2]. While treadmill-based perturbation training has shown efficacy in reducing falls and developing balance recovery strategies among various populations, existing research predominantly focuses on slip-related perturbations. Studies examining the effects of trip-based perturbation training on a treadmill are scarce [3-5]. Given that trips are one of the most common causes of falls among older adults in daily living conditions, it is imperative to examine how trip-based perturbation training can reduce fall risk. The main objective of perturbation training is to help the trainees develop effective recovery step strategies to battle external perturbations. To our knowledge, no studies have investigated the effects of repeated trips on how fast the recovery step is implemented after a trip perturbation. Therefore, this pilot study aimed to identify whether repeated trips could alter the duration of the recovery step following the standing-trip perturbation among healthy young adults. We hypothesized that repeated trips would shorten the duration of the recovery step in response to the external perturbation in young adults.

Methods: Eight healthy young adults (mean ± standard deviation age: 25.37 ± 4.17 years, body mass: 78.66 ± 20.47 kg, and body height: 1.78 ± 0.04 m; 7 males and 1 female) were recruited. To be eligible, participants should not have had acute or chronic neurological or musculoskeletal conditions, recent major injuries to the lower limbs, or trip-based training experience. After providing written consent approved by the Institutional Review Board, participants underwent a 3-minute warmup walk. Then, they were outfitted with 26 reflective markers at anatomical landmarks. Next, participants stepped onto the ActiveStep treadmill (Simbex, NH) and donned a safety harness. The harness was connected to an overhead arc through ropes. Participants were instructed that they would first stand on the treadmill while experiencing "trip-like" belt movements later. They were also told to try their best to recover their balance and not to grab onto the ropes if a trip occurred. After about 6 standing trials without a trip, they experienced the first trip with no knowledge about when the trip was triggered. The trip was induced by rapidly moving the treadmill belt backward at an acceleration of 4 m/s^2 over 0.3 seconds to a belt speed of 1.2 m/s. Then, the belt decelerated (-4 m/s^2) for 0.3 seconds to return its speed to zero. The total belt displacement during the trip was 0.36 m. The same trip was repeated four more times following the first trip. The full-body kinematics data during all trips were collected using a 9-camera motion capture system (Vicon, UK) at 100 Hz. The initial step taken to recover the balance after the trip was identified as the recovery step. Two characteristic events were determined for this recovery step: liftoff (LO) and touchdown (TD). The LO was defined as the instant when the recovery foot took off from the belt, and the TD was when the recovery foot re-established contact with the belt. Both events were recognized based on foot kinematics and verified by the recorded videos. The step duration was calculated as the interval from LO to TD. A two-tailed paired *t*-test was used to compare the step duration between the first and fifth trips. The effect size was also calculated using Cohen's *d*. SPSS (v 29.0, IBM) was used with a significance level of 0.05.

Results & Discussion: All participants lost their balance forward as they took a forward recovery step after each trip. The paired *t*-test results showed a significant difference in the recovery step duration between the first trip and the fifth trip ($p = 0.033$, Cohen's $d = 1.05$) (Fig. 1). Specifically, participants completed the recovery step much faster on the last trip in comparison to the first trip. Such a reduction implied that healthy young adults could quickly adapt to repeated and unexpected standing trips. Given that falls could happen within a fraction of a second after a balance loss is initiated, the recovery step must be promptly and successfully implemented to restore balance and avoid falls. Our findings suggested that the treadmill-based trip training program could enhance the execution of the recovery step after a trip, which would lower the risk of falls after a trip. A few limitations were associated with this study. First, this study enrolled a small and sex-imbalanced sample size. Second, although the preset standing-trip profile provided a standardized tool to induce trip-like perturbation, it differs from the trips encountered during real-life conditions, where trips usually happen during gait. Both limitations may reduce the generalizability of the findings. More studies are needed to address these limitations.

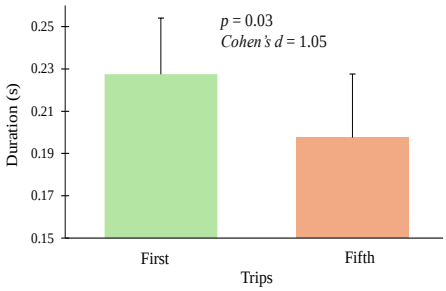

Fig. 1: Comparison of the recovery step duration between the first and last trips among 8 young adults. Also shown is the effect size quantified by the Cohen's *d*.

Significance: The results could enrich our understanding of how young adults adapt to repeated trips induced while standing on a treadmill. Additionally, our findings could provide preliminary results for us to design future studies with multiple groups and larger samples to further investigate the possibility of motor learning from treadmill-based trip training for reducing falls among various populations with elevated fall risk.

Acknowledgments: The authors thank Diane' Brown for her assistance with the data collection.

References: [1] Chen, T.-Y., et al. (2020), *The Journals of Gerontology: Series A* **75**(5). [2] Peel, N.M. (2011), *Canadian Journal on Aging/La Revue canadienne du vieillissement* **30**(1). [3] Wang, T.-Y., et al. (2019), *Journal of Biomechanics* **84**. [4] Simpkins, C., et al. (2022), *Journal of Biomechanics* **145**. [5] Namayeshi, T., et al. (2023), *Frontiers in Sports and Active Living* **5**.

ACCURATE ESTIMATION OF REAL-WORLD ENERGY EXPENDITURE USING A SMARTPHONE

Haedo Cho[1], Patrick Slade[1*]
[1]JohnA.Paulson School of Engineering and Applied Sciences, Harvard University, Boston, MA, USA.
*Corresponding author's email: slade@seas.harvard.edu

Introduction: Physical inactivity is a major global epidemic, the fourth leading cause of global mortality [1]. To understand how physical activity relates to health outcome, health policy committees have requested an accurate, scalable tool to monitor physical activity using an objective metric like energy expenditure [2]. Effective physical activity monitoring should consider four components: frequency, intensity, time and the type of activity involved [2]. A number of tools for monitoring physical activity are available; however, there are trade-offs between these methods. Self-report surveys are commonly used for large-scale physical activity monitoring, but they lack accuracy and objectivity as they rely on individuals' own perceptions [3]. Pedometers are portable devices used to monitor physical activity, but step counts alone are not able to capture the intensity and type of various workouts [4]. Smartwatches are practical for daily use but their accuracy is unreliable as they rely on heart rate and wrist kinematics [5]. We developed OpenMetabolics, a data-driven method for estimating energy expenditure using only a smartphone worn in a pocket. We hypothesized that a data-driven model could accurately estimate energy expenditure from thigh kinematics that capture underlying leg muscle activity throughout the gait cycle. OpenMetabolics has the lowest error compared to existing methods under naturalistic walking conditions (Fig. 1d).

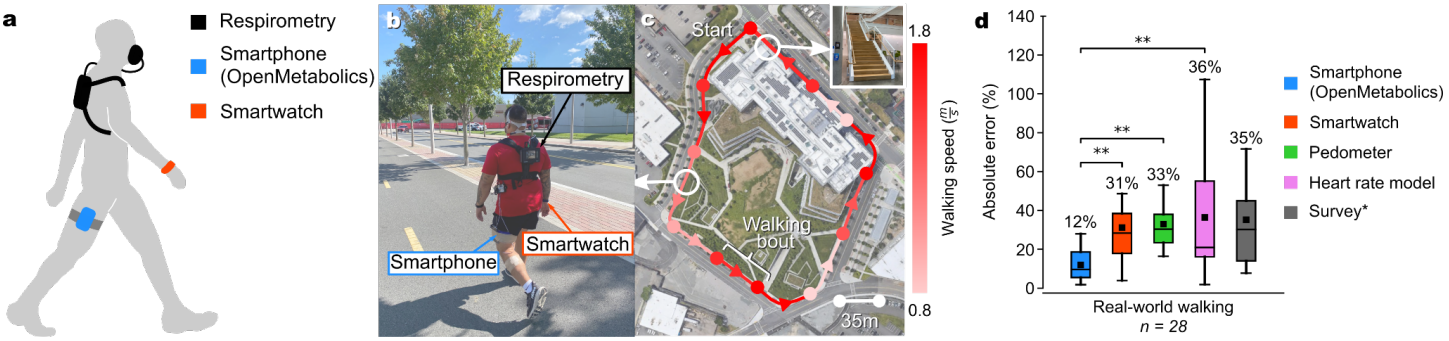

Figure 1: a, OpenMetabolics was compared with a commercial smartwatch and portable respirometry. **b,** Participant walking on the public sidewalk. **c,** Map of the 650-meter course used for real-world evaluation. Participants walked the course repeatedly, including climbing stairs each time they passed the starting point. **d,** OpenMetabolics significantly reduced the absolute error of the cumulative energy expenditure compared to a commercial smartwatch, pedometer, heart rate model, and self-report survey during real world walking (paired *t*-test, $n = 28$, **P<0.005).

Methods: We developed a machine learning model to estimate energy expenditure once per gait cycle using a previously collected dataset that includes lower-limb kinematics data and steady-state metabolic rate [6]. OpenMetabolics was compared with a commercial smartwatch (Fitbit Charge 4, USA) and portable respirometry (K5, COSMED) (Fig. 1a). We performed a real-world walking experiment ($n = 28$) where participants walked on the public sidewalk (Fig. 1b). Real-world walking was emulated by providing ecologically relevant audio prompts that caused participants to self-select a naturalistic walking bout duration and speed [7]. Participants walked the 650-meter course repeatedly, climbing stairs each time they passed the starting point (Fig. 1c).

Results & Discussion: OpenMetabolics showed a cumulative error of 12% during real-world walking experiments with new subjects, the lowest error among all methods. This result highlights that thigh kinematics are a strong predictor to effectively capture the rapid change of energy expenditure. A smartwatch and other methods showed nearly three-times higher error compared to OpenMetabolics, indicating that wrist kinematics and heart rate are weak predictors for estimating energy expenditure at various walking bouts. Future research on energy expenditure estimation could benefit from these results by monitoring these informative biomechanical signals from lower-limb motion.

Significance: OpenMetabolics is an accurate and objective tool that could be used for large-scale epidemiological study to relate physical activity to health outcomes. OpenMetabolics can be deployed as an open-source smartphone app to reach the majority of the global population, especially for low-income countries with high rates of physical inactivity.

References: [1] Global health risks: mortality and burden of disease attributable to selected major risks (2010). [2] Physical Activity Guidelines Report (US Department of Health and Human Services, 2018). [3] Prince, Stéphanie A., et al. International journal of behavioral nutrition and physical activity 5.1 (2008): 1-24. [4] Melanson, Edward L., et al. Preventive medicine 39.2 (2004): 361-368. [5] Shcherbina, Anna, et al. Journal of personalized medicine 7.2 (2017): 3. [6] Slade, Patrick, et al.Nature Communications 12.1 (2021): 4312. [7] Slade, Patrick, et al. Nature 610.7931 (2022): 277-282.

THE COST OF TRANSITION: A COMPARISON BETWEEN ACTIVE AND STEADY STATE COST OF TRANSPORT DURING BOTTLENOSE DOLPHIN SWIMMING

Ningshan Wang[1], Gabriel Antoniak[1], Kira Barton[1], Nicole West[2] and K. Alex Shorter[1*]
1 University of Michigan, Ann Arbor, MI, USA, 2 Dolphin Quest Oahu, Honolulu, HI, USA
*Corresponding author's email: kshorter@umich.edu

Introduction: Efficient movement through water is important for biological and engineered systems alike. Dolphins use lift-based propulsion to locomote in the marine environment by oscillating their fluke through the water. To date most research has focused on swimming biomechanics during steady state swimming where animals use a continuous fluking gait. These results have shown that animals modulate steady state swimming speed by increasing fluking frequency but not amplitude [1]. Further, animals select average swimming speeds that minimize steady state cost of transport (COT) [2]. However, these studies have not included costs associated with transient behavior required to reach steady state. Here we investigate additional costs required to reach steady state swimming speeds.

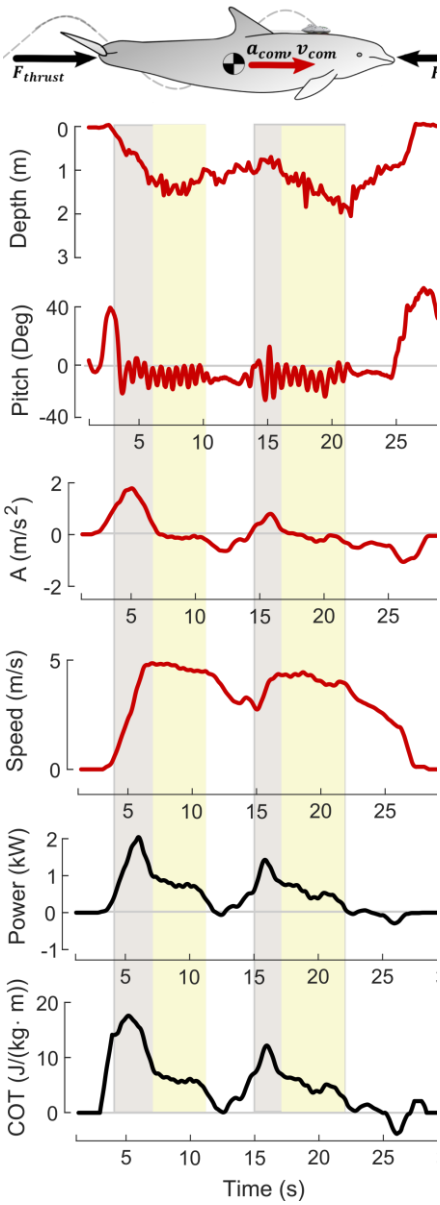

Figure 1: ***(Top)*** Illustration of the dolphin wearing a tag. ***(Middle)*** Measurements (red) of depth, torso pitching angle and speed during point to point swimming**. (Bottom)** Estimates (black) of power and cost of transport during. Two Periods of active swimming (grey and yellow) and steady state swimming (yellow) are highlighted.

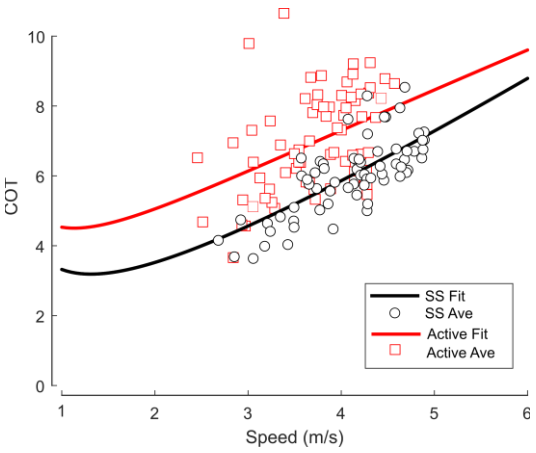

Figure 2: Average Cost of Transport during steady state (black) and active swimming (red).

Methods: Experiments were conducted at Dolphin Quest Oahu, Oahu, HI, with several bottlenose dolphins. The experiments involved biologging tags using sensors (e.g., accelerometers, magnetometers, gyroscopes, water-pressure, and water-speed turbine) to record data about animal movement, behaviour, and the environment. The dolphins were trained by the animal care specialists to wear biologging tags and were asked to start at a floating dock (denoted "at station"), swim away typically 35 m from the dock, and then return to station to complete the lap, all underwater.

We post-processed the collected biologging data, the outputs are depth, pitch angle, forward acceleration and speed in body-fixed coordinate, mechanical thrust power and energetic cost of transportation (COT) [2], as presented in Figure 1. Given the segmented time-series of speed, power and COT, we conducted nonlinear curve fitting with given data.

Different from the existing research [2], which segmented the swimming period into consistent-speed (CS) segment and non-CS segment by the speed, we added active-fluking segment in this process, which is determined by the pitch angle dynamics of the dataset. When the recorded data is judged to be in active-fluking (AF) segment, it has fluctuating pitch angle, which indicates the animal is fluking, and acceleration larger than -0.5m/s2. We expect the time-averaged COT from AF segments will be relatively larger than CS segments for the same lap trial dataset, because the higher thrust power during the transient period when the animal accelerated will boost the local COT in low-speed period.

Results & Discussion: We conducted power-speed curve fitting and then used the fitting result to curve the relationship between speed and COT. The result is presented in Figure 2. It is obvious that the COT curve from AF segmentation is larger than the one from CS segmentation for the same dataset.

Significance: Understanding costs associated with accelerating the animal through the water provides important context for understanding the potential energetic benefits of fluke an glide gait patterns that have been observed during self-selected swimming [3].

Acknowledgments: This work was supported by a Contribution Agreement with the Department of Fisheries and Oceans Canada (DFO), and the National Science Foundation under Grant No. 2238432.

References: [1] Fish, Frank E., et al. JEB 217.2 (2014): 252-260. [2] Gabaldon, J. T., et. al. (2022). JEB, 225(22), jeb244599. [3] Zhang, Ding, et al. JEB 226.15 (2023).

EFFECT OF VISUAL TRACKING ON LANDING ROUND REACTION FORCE FOLLOWING A SOCCER HEADER

Rachel Hicks, Hannah Parsley, Ciarra Valdez, Sarah Conlon, Mostafa Hegazy*
Science Department, Southwest Minnesota State University
*Corresponding author's email: mostafa.hegazy@smsu.edu

Introduction: Soccer is the most popular sport in the world and continues to grow. There number of female participants has experienced tremendous growth over the last few decades. This stems from FIFA's (Fédération internationale de football association) prioritization of women's soccer growth within its development strategy. However, this growth is also associated with an increase in injuries in female players. A common injury mechanism in soccer involves players landing after jumping for a header.

Several researchers recognized that landing from a soccer header is different from landing from a vertical jump, considering there is a heading motion during the jump [1, 2]. Thus, studied soccer players jumping and performing a header on a hanging ball. More recently, researchers recognized that although a hanging ball includes the heading motion, it does not include visually tracking a moving ball, which adds to the cognitive load, potentially impacting landing mechanics [3, 4]. These researchers compared landing mechanics following a jump header when a ball following a throw-in to those following a vertical jump and a jump header of a hanging ball. They reported that landing mechanics following a game like soccer header was different from those following a vertical jump and heading a hanging ball. Although using a throw-in is closer to a game situation than a hanging ball, it does not account for throw consistency. They presented no methods to control ball speed, height, or angle. Controlling these variables would be ideal to properly study landing mechanics following a header. Using a soccer ball launcher may be a solution to controlling these different ball variables.

Thus, the purpose of this study was to compare landing vertical ground reaction force when heading a hanging ball, a swinging ball, and a launcher projected ball.

Methods: Fifteen female soccer players from an NCAA Division II soccer team (age: 19.73 ± 1.03 years, mass 63.91± 8.33 kg, height 165.47± 6.37cm) participated in this study. Loadsol force insoles (Novel, Munich, Germany) were inserted into participants' shoes to measure ground reaction forces. Participants performed three maximal vertical jumps, from which their highest jump was used to determine target height for all other conditions. Participants then performed three jump header types, three times each. These included: 1) A hanging ball (HB), during which participants jumped and headed a ball hanging at 75% of their maximum jump height; 2) A swinging ball (SB), during which the same hanging ball was allowed to swing, participants then jumped and headed the ball. This condition was added to allow full control and at the same time have participants track a moving ball; 3) A ball launcher (BL), during which a ball was projected using a ball launcher set up to target 75% of the participants' maximum height. All trials were performed in a counterbalanced order.

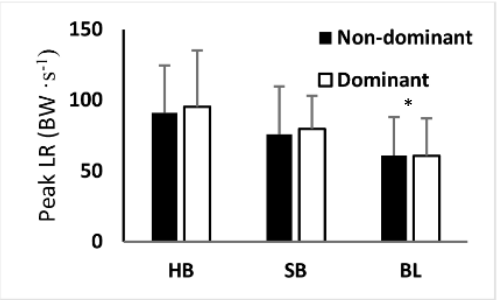

Figure 1. Peak loading rate normalized to body weight for the hanging ball (HB), swing ball (SB), and ball launcher (BL). * indicates significantly lower than HB & SB.

Two-way 3x2 ANOVAs with repeated measures with header condition (HB, SB, BL) and foot (dominant, non-dominant) as independent variables were to performed to compare peak ground reaction force normalized to body weight (nGRF) and peak leading rate normalized to body weight (LR). A Bonferroni correction was used for all post-hoc analyses.

Results & Discussion: Our analysis showed no significant difference in nGRF between header conditions ($F(2,28) = 1.99$, $p>0.05$) as well as foot ($F(1,14) = 0.5$, $p>0.05$). However, there was a significant difference in peak LR with for header conditions ($F(2,28) = 9.13$, $p<0.01$) but not foot (($F(1,14) = 0.08$, $p>0.05$). Post-hoc analysis showed significantly lower peak LR in the BL condition compared to both HB and SB ($p<0.05$). Previous studies have shown that jump headers in response to a throw-in result in greater nGRF and peak LR [3,4] on the dominant side, which was not the case in our study. A likely reason was that participants did not jump as high in the BL condition. Qualitative video analysis showed participants naturally took a step or two to reduce the need to jump as high to head the ball. In agreement with previous studies, visually tracking a ball resulted in different ground reaction forces compared to not visually tracking a ball. Furthermore, the SB was similar to a hanging ball, suggesting it is no substitute to a projected ball. Thus, it is crucial for investigators to have participants experience a true jump header with a projected ball, rather than a simulation with a hanging ball.

Contrary to our expectations, the ball launcher was not consistent. In some ball launcher trials, the ball did not go as high or drifted right or left. When target height was not met, the trial was repeated until target height was achieved. Thus, projecting a ball through a throw-in or kick may be a better option as it would give participants visual cues that are available in real game situations.

Significance: Current research related to jump headers involves participants performing a heading motion but not visually track a projected ball. Although more recent studies involved a manually thrown projected ball, however, manual throwing can be inconsistent. In this study we compared landing after heading a ball projected by a ball launcher to those when the ball is hanging or swinging. Our results showed that projecting a ball involves different mechanics and thus, should be used in future studies. Using a ball launcher yielded inconsistencies, thus, it projecting a ball using a throw-in or kick may be a better option.

Acknowledgments: We would like to thank the Southwest Minnesota State Soccer team for participating in our study.

References: [1] Butler et al. (2013), *Clin J Sport Med* 23(1); [2] Alfayyadh (2018), Master's Thesis; [3] Nascak et al. (2023), *IJSPE* 9(3); [4] Cycenas, et al. (2023), *ASB*, Knoxville, TN, Aug 8-11.

SEX DIFFERENCES IN PERIARTICULAR SCAPULAR MORPHOLOGY

Colleen M. Vogel[1*], Denali M. Hutzelmann[1], Heath B. Henninger[2], Joshua M. Leonardis[1,3]
[1]College of Applied Health Sciences, [2]Department of Orthopaedics, University of Utah, Salt Lake City, UT, [3]Beckman Institute for Advanced Science and Technology, University of Illinois Urbana-Champaign, Urbana, IL
*Email: cv29@illinois.edu

Introduction: Periarticular scapula morphology may contribute to shoulder pain through its mechanistic role in subacromial impingement, glenohumeral instability, and osteoarthritis. Acromion shape can increase the risk of subacromial impingement and the likelihood of rotator cuff overuse by increasing deltoid shear forces [1]. Glenoid and coracoid shape are influential factors in glenohumeral stability. Glenoid shape can increase the likelihood of anterior or posterior glenohumeral instability by promoting humeral head migration [2]. Coracoid length and orientation relative may contribute to instability through its impact on the coracohumeral distance [3]. Females are more likely to report shoulder pain and multidirectional glenohumeral instability than males [4]. We suspect that these sex-specific health disparities may be driven in part by sex-related differences in periarticular scapular morphology. Preliminary evidence suggests females have narrower glenoids [5]. However, measurements of glenoid morphology alone lack the nuance to appropriately determine sex-differences in scapular shape. Therefore, the purpose of this pilot study was to expand on prior knowledge by comprehensively quantifying sex differences in acromion, coracoid, and glenoid morphology.

Methods: Twelve pain and pathology-free individuals (6F, 6M, mean (SD) age: 22 (2) years) underwent bilateral magnetic resonance imaging (3T MAGNETOM Prisma-Fit, Siemens) of the upper extremities using body and large flex coils and a two-point Dixon sequence (TE_1: 1.34ms, TE_2: 2.57ms, TR: 4.21ms, flip angle: 9°, field of view: 380mm, 1.2mm isotropic voxel size). Humeri and scapulae were segmented from water-only images and left bones were mirrored to the right.

Two coordinate systems were defined: a scapula-based coordinate system using the spinoglenoid notch, root of the scapular spine, and the inferior angle, and a glenoid-based coordinate system with its origin at the center of the inferior glenoid. Then, strategic landmarks were digitized on the scapula and humerus and best-fit planes were placed through the center of the scapular spine and coracoid pillar. Together, these allowed us to quantify acromion (acromial index (AI, ratio of glenoid-acromion to glenoid-humeral distances); critical shoulder angle (CSA); scapular spine angle), coracoid (pillar angle; deviation angle) and glenoid shape (inclination, version, glenoid index (GI; ratio of glenoid height to its width)) (Figure 1A). Morphometrics were chosen for their established relationships with common shoulder pathologies. Separate general linear models determined the impact of arm dominance and sex on each outcome (α=0.05).

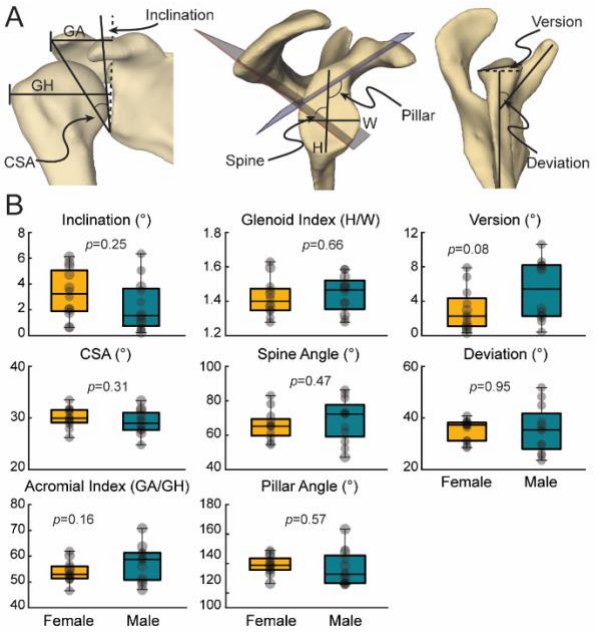

Figure 1: (A) Representative scapular and humeral models with the included morphometrics. Measurements represent examples chosen to aid in visualization. (**B**) Sex differences in each morphometric. Box plots represent median ± IQR. Individual participant data are presented as opaque dots.

Results & Discussion: Arm dominance did not impact any measurement. Similarly, males and females did not differ in any measure of acromion (AI: females (0.54±0.04), males (0.57±0.07); p=0.16); CSA: females (30±2.0°), males (29±2.4°); p=0.30); spine angle: females (66±8.6°), males (69±12°) (p=0.47)) or coracoid shape (pillar angle: females (133±6.0°), males (131±12°); p=0.57); deviation angle: females (35±4.2°), males (36±9.2°); p=0.95). These values generally align with those reported in previous work [3]. However, sex has never been considered when evaluating these metrics, making it challenging for us to position our findings in the field. While glenoid shape did not differ significantly between the sexes (inclination: females (3.3±1.9°), males (2.3±2.0°); p=0.25); GI: females (1.4±0.11), males (1.4±0.11) p=0.66), glenoid version did trend in a manner that may suggest an impact of sex with a larger sample size (females (3.0±2.4°), males (5.3±3.5°); p=0.08). In this case, male glenoids were more retroverted than female glenoids. Inclination, GI, and version values obtained from both sexes fell within what is considered a normal range. Because glenoid version may contribute to anterior-posterior migration of the humeral head, the functional impact of sex differences in this measure warrants further inquiry. Our results indicate that there is no sex-related difference in periarticular scapular morphology in a small sample of healthy adults between 18 and 30. However, it is possible our participants were not skeletally mature. Musculoskeletal development follows sex-specific timelines. Scapular and humeral growth terminates as many as 4 years earlier in females, typically around 16 years of age [6]. In contrast, male growth will continue into the early twenties [7]. True sex-differences in periarticular scapular morphology may exist in skeletally mature individuals. Differences related to arm dominance may prevail in populations in which high demand is placed on the shoulders, such as manual wheelchair users.

Significance: While our results failed to detect arm dominance or sex-related differences in morphology in healthy adults, our ongoing research is evaluating sex-specific scapular morphology as a potential contributor to shoulder pain and pathologies with the hope of uncovering easy to monitor morphological biomarkers.

References: [1] Nyffeler, *J Bone Joint Surg*, 2006; [2] Cohn, *J Shoulder Elb Surg*, 2022; [3] Jacxsens, *J Shoulder Elb Surg*, 2019; [4] Lucas, BMC *Musculoskelet Disord*, 2022; [5] Merrill, *Surg Radiol Anat*, 2009; [6] Sidharthan, *Arthroscopy*, 2020; [7] Carme, *Int J Legal Med*, 2013

JOINT COORDINATION PREDICTS STRIDE TO STRIDE VARIABILITY DURING WALKING

Aaron D. Likens[1*], Mehrnoush Haghighatnejad[1], Tyler M. Wiles[1], Seung Kyeom Kim[1], Nick Stergiou[1,2]
[1]Department of Biomechanics, University of Nebraska at Omaha, USA
[2]Department of Physical Education and Sport Science, Aristotle University, Thessaloniki, Greece
*Corresponding author's email: alikens@unomaha.edu

Introduction: Walking requires the coordination of the upper and lower limbs to maintain proper gait patterns, optimize stability, and minimize energy consumption [1]. The movement of these body segments, individually, are dynamical systems that exhibit variability changing over time [2]. This variability is not random, and it is characterized by long-range correlations, indicating the persistence or dependence of signals across a wide range of time scales, and reflecting physiological well-being [3]. One approach to quantify this temporal structure of gait variability is the Hurst-Kolmogorov method, returning a Hurst exponent (H). H classifies statistically persistent behavior ($H > 0.5$), anti-persistent behavior ($H < 0.5$), or random, uncorrelated behavior ($H = 0.5$) [4]. Considering the interplay of different limbs in the human body, understanding how they coordinate in terms of variability is crucial. We constructed a structural equation model (SEM) to investigate the coordination of joints and its relationship to global gait patterns – stride interval variability. We hypothesized that during walking (1) the range of motion (ROM) time series of most joints (lumbar, thoracic, torso, shoulder, elbow, hip, knee, and ankle joints) would exhibit a persistent behavior ($H \sim 0.7$); (2) the persistence of each joint's ROM would load on body segment specific latent variables; (3) latent variables for given body segments (e.g., lower limbs, upper limbs, and trunk) would correlate with one another; and (4) joint ROM persistence would ultimately predict global stride time variability.

Methods: We recruited 87 healthy adults divided into three groups: 31 young adults (ages 19-35), 29 middle-aged adults (ages 36-55), and 27 older adults (ages 56-82) as part of the NONAN GaitPrint project [5]. Each participant completed 18, 4-minute walking trials at a self-selected pace on a 200-meter indoor track wearing 16 Noraxon Ultium Motion inertial measurement units recording kinematics at 200Hz. For each trial we calculated the Hurst exponent from a time series created from the ROM of each stride. H correlations were computed across all joints and stratified by age group. Additionally, SEM was utilized to examine the interconnections between the Hurst exponents of various joints and their associated latent variables, which include the upper limb (shoulder, elbow), lower limb (hip, knee, and ankle), and trunk (lumbar, thoracic, torso). Lastly, the latent variables constructed with SEM were used to build a structural model to predict stride interval H from the variability contributions of body segment latent variables.

Results & Discussion: The structural equation modeling analysis investigated the dynamics of human gait by examining the Hurst exponents of joint range of motion (ROM) in upper limb, lower limb, and torso segments, as predictors of stride interval variability. The analysis utilized a robust maximum likelihood estimator to address the hierarchical nature of the data. The model showed a generally good fit, with a Comparative Fit Index (CFI) of 0.945 and a Tucker-Lewis Index (TLI) of 0.935, indicating the model's adequacy in capturing gait variability. The Root Mean Square Error of Approximation (RMSEA) was moderately good at 0.090, and the Standardized Root Mean Square Residual (SRMR) at 0.026 supported the model's effectiveness. Significant findings emerged from the parameter estimates, notably the strong factor loadings of latent variables for each body segment, demonstrating the Hurst exponent's validity in measuring gait variability. A notable relationship was between stride time variability and lower limb ROM variability ($\beta = 0.545$, $p = 0.039$), highlighting the lower limbs' pivotal role in the temporal structure of gait variability; upper limb and torso regressions were not statistically significant. This suggests a nuanced coordination among gait components rather than simple linear relationships. The analysis supports the hypothesis of persistent variability in joint ROM, reflecting the gait system's adaptive capacity for stability and efficiency. The lack of significant covariances between segments implies complex inter-segment coordination mechanisms, allowing adaptability to varying walking conditions and tasks beyond straightforward regression models.

This study illuminates the complex interplay in human gait dynamics, emphasizing lower limb variability's causal role in determining global patterns of gait while also suggesting that coordination among body segments may promote adaptability. The age-related aspects of gait variability, suggested by the stratification of participants, though not directly addressed in the results presented, remain an important area for further analysis. Understanding how the relationships among joint ROM variability change with age can offer insights into the biomechanical and neurological aspects of aging, potentially guiding interventions to preserve mobility and reduce the risk of falls in older adults. Future research should delve further into the causal relationships within gait dynamics and explore strategies for gait training and rehabilitation, with a keen focus on aging and mobility impairments.

Significance: We provided novel evidence that, during walking in healthy adults, statistical persistence is present in all joint angles. These findings advance understanding of human gait dynamics, revealing the causal role of lower limb variability in the regulation of walking patterns and highlighting the complex coordination among different body segments is responsible for optimal variability. By elucidating the adaptive mechanisms of gait variability, this research lays the groundwork for developing targeted interventions aimed at enhancing mobility and preventing falls in older adults, thereby improving their quality of life and independence.

Acknowledgments: NSF 212491, NIH P20GM109090, R01NS114282, University of Nebraska Collaboration Initiative, the Center for Research in Human Movement Variability at the University of Nebraska at Omaha, NASA EPSCoR, IARPA.

References: [1] Meyns et al. (2013), *Gait Posture* 38, 555–562; [2] Higgins et al. (2002), *J Biol Med* 75, 247–260; [3] Hausdorff, et al . (1995), J Appl Physiol. 78, 1349–358 ; [4] Likens et al. (2023), arXiv [Preprint]; [5] Wiles et al. (2023), *Sci Data* **10**, 867.

CONVERGENT VALIDITY OF KNEE KINEMATICS ASSESSED WITH MARKER-LESS AND MARKER-BASED MOTION CAPTURE DURING SPORT-SPECIFIC TASKS

Dannyelle Long[1*], Jessica Peters[3], Mark Vorensky[2], Smita Rao[1,3]
[1]Department of Physical Therapy, NYU Steinhardt School of Culture, Education and Human Development
[2]Department of Physical Therapy, School of Health Sciences, Touro University
[3]Department of Biomedical Engineering, NYU Tandon School of Engineering
*Corresponding author's email: dpl8745@nyu.edu

Introduction: Advances in computer vision technology and machine learning algorithms have made marker-less (ML) motion capture a feasible alternative to traditional marker-based (MB) approaches. ML motion capture offers the potential for more efficient movement analysis, requiring less time for data collection and processing compared to MB[1], potentially allowing for the analysis of a greater number of athletes and tasks within a shorter timeframe. While existing studies indicate promising validity of ML analysis in quantifying knee kinematics during walking,[2,3] few studies have assessed the validity of ML in higher velocity tasks, such as a diverse set of sports-specific activities. The purpose of this study is to examine the convergent validity of ML versus MB approaches to assessing knee kinematics during 4 basketball-specific tasks.

Methods: All procedures were approved by the institutional review board. Ten individuals without musculoskeletal pain (7 males, 3 females, mean age: 21.1±2.8 years; 23.0 ±2.0 years, mean BMI: 23.1±1.5 kg/m^2; 22.7±2.7 kg/m^2) who engaged in a minimum of 50 hours of basketball per year, participated in the study. Following written informed consent, a trained physical therapist affixed 41 retro-reflective skin markers to the pelvis, thigh, shank, and foot. A 16-camera system (Qualisys, Sweden), 8 MB cameras (120Hz) and 8 ML video cameras (60 Hz), concurrently recorded data while each participant performed four activities with their shoes on: walking at self-selected speed(Walk),[2,3,5] shuttle run (SRun),[6] 180-degree pivot turn (Turn),[7] and single leg drop landing (SLD).[8] Two force plates (Kistler, Amherst, NY) recorded ground reaction forces at 1000 Hz. Stance phase for each activity was defined using ground reaction force data. Kinematic data were processed using custom software (ML Theia3D v2023.1.0.3161, Theia Markerless Inc., Kingston, ON, Canada), and ML and MB data were exported to Visual3D (HAS Motion, Canada). Subject-specific co-ordinate systems were set up per ISB guidelines.[9] Sagittal and frontal knee kinematics were calculated using Euler angles[10] over each stance phase. Peak knee flexion and knee abduction was identified from time normalized knee kinematics were primary outcomes of interest. Descriptive statistics, root mean square difference (RMSD) and intra-class correlation coefficient (ICC) (Model (3,*k*) were used to compare knee kinematics obtained using ML and MB approaches.

		ML	MB	RMSD	ICC		ML	MB	RMSD	ICC
Walk	**FL**	-19.4	-19.3	3.8	0.84	**AB**	-0.8	-0.6	1.4	0.77
	EX	-0.2	-3.1	3.8	0.53	**AD**	2.3	4.0	2.4	0.56
Turn	**FL**	-72.3	-68.3	5.6	0.77	**AB**	-16.0	-8.2	8.8	-0.07
	EX	-19.0	-20.5	3.8	0.89	**AD**	-0.3	2.7	5.3	0.35
SRun	**FL**	-77.9	-76.0	3.7	0.96	**AB**	-12.5	-5.5	8.9	-0.06
	EX	-23.2	-24.7	3.7	0.89	**AD**	-1.9	3.0	6.7	-0.81
SLD	**FL**	-55.2	-57.4	3.8	0.96	**AB**	-2.7	-1.9	3.6	0.30
	EX	-9.3	-16.25	6.9	0.40	**AD**	2.6	4.2	4.5	0.30

Table 1: Mean knee flexion (FL), extension (EX), abduction (AB) and adduction (AD, RMSD in degrees, ICC (3,*k*), walking (Walk), shuttle run (SRun), 180-degree pivot turn (Turn), single leg drop landing (SLD),

Results & Discussion: Descriptive statistics of mean knee kinematics, RMSD and ICC (3, *k*) during 4 sport-specific tasks quantified using ML and MB are in Table 1. Mean RMSD in the sagittal and frontal plane knee kinematics during walking are comparable to RMSD reported in prior literature.[1,2] However, for sport-specific tasks, the mean RMSD ranges from 3.7 to 5.6 degrees for sagittal plane and 3.6 to 8.9 degrees for frontal plane knee kinematics, greater than RSMD noted during to walking. Our findings indicate that ML estimates of knee kinematics during walking demonstrated fair to good agreement in both the sagittal and frontal planes. Stronger agreement was observed in the sagittal plane compared to the frontal plane across sport-specific activities with ICC values ranging from 0.40 – 0.96 and 0.06 – 0.81 respectively.

Significance: Our outcomes align with previous evidence of the accuracy of ML motion capture evaluating knee kinematics during walking.[2,5] To our knowledge, this is the first study to assess the validity of ML motion capture for the assessment of knee kinematics during these high-velocity, basketball-specific activities.

ML motion capture had overall good agreement in the sagittal plane for sports specific activities. The observed stronger agreement in the sagittal plane compared to the frontal plane during sport-specific tasks suggests a potential limitation of ML motion capture in capturing lateral movements accurately. Researchers should consider the potential limitations of ML motion capture when analyzing frontal plane knee kinematics during higher velocity sport-specific tasks.

Acknowledgement: SR was supported by NIDDK R01DK114428, NIAMS R01AR079182, NIH NCATS UL1TR001445, Georgeny High Priority Award from the Foundation for Physical Therapy Research.

References: 1. Wade L, et. al. (2022) DOI:10.7717/peerj.12995. 2. Kanko RM, et. al. (2021) DOI:10.1016/j.jbiomech.2021.110665.
3. Wren TAL, et. al. (2023) DOI:10.1016/j.gaitpost.2023.05.029 4. Stojanović E, et. al. (2023) DOI:10.1111/sms.14328.
5. Song K, et. al. (2023) DOI:10.1016/j.jbiomech.2023.111751. 6. Jang SH, et. al. (2014) DOI:10.1016/j.knee.2013.08.017
7. Leppänen M, et. al. (2021) DOI:10.1177/03635465211026944 8.Vorensky M, et. al. (2023) DOI:10.1123/ijatt.2021-0108.
9. Wu G, et. al. (2002) DOI:10.1016/S0021-9290(01)00222-6. 10.Yu B, Lin CF. et. al. DOI:10.1016/j.clinbiomech.2005.11.003

EFFECTS OF CARBON FIBER PLATED SHOES ON LOWER BODY MUSCLE ACTIVITY DURING GRADED RUNNING IN FEMALE LONG DISTANCE RUNNERS

Jessy Capua*, Jacob Goodin, PhD, CSCS, Ryan Nokes, PhD, ATC, Arnel Aguinaldo, PhD, ATC
Department of Kinesiology, Point Loma Nazarene University, San Diego, CA, United States
*Corresponding author's email: jcapua0022@pointloma.edu

Introduction: World record marathon times for both women's and men's have been broken since athletes started using carbon fiber plated (CFP) shoes. Prior research on carbon fiber plated shoes investigated the metabolic costs of running level [1], at an incline of 5% [2], and an incline of 15% [3]. Studies that investigated changes in muscle activity in CFP shoes are limited, with some using ultrasound to detect changes in fascicle length [4] and even fewer using EMG [5]. With the World Marathon Major races having an average grade of 3%-5%, the purpose of this study was to investigate changes in lower body muscle activity during graded running in CFP shoes for female runners. It was hypothesized that the gastrocnemius lateralis, gastrocnemius medialis, and tibialis anterior activities will contract earlier in the CFP condition than the TRN condition. It was also hypothesized that the rectus femoris and biceps femoris will not undergo any changes between the two shoe conditions.

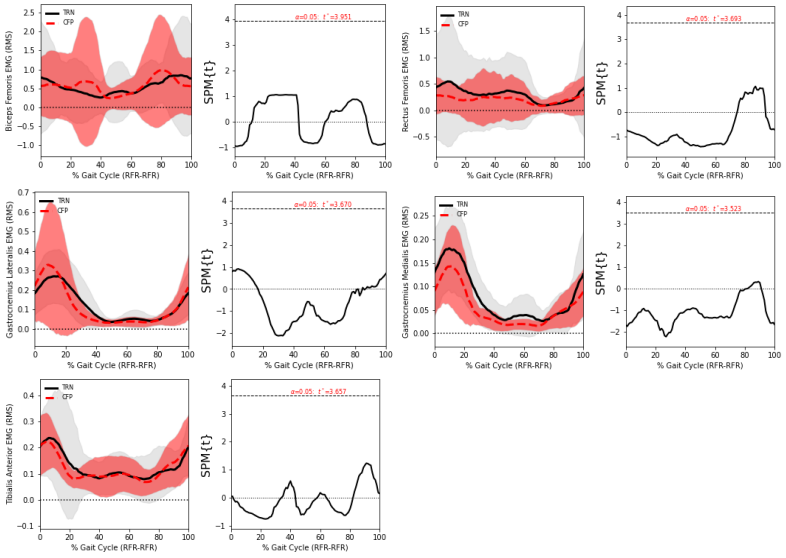

Figure 1: SPM of lower limb muscle activity between CFP and TRN conditions. EMG signals were normalized based on maximal muscle activity while running.

Methods: Ten female runners who have completed a long-distance race participated in the study after providing written informed consent. Race times must be comparable to a 4:30:53 marathon according to the 2022 World Athletics Scoring Table. The Nike *Vaporfly* 3 was the carbon fiber plated shoe (CFP) compared against the subjects' normal training shoes (TRN). For testing, subjects ran at a constant speed of 12 km/h at an incline of 3% for 5-minutes. Surface electrodes (Delsys) were placed on the biceps femoris, rectus femoris, gastrocnemius lateralis, gastrocnemius medialis, and tibialis anterior. Fifteen strides were markerlessly captured (Theia3D) at 300 Hz during the final minute of the test. Statistical Parametric Mapping (SPM) analysis was performed in Python using the *spm1d* package at an *a priori* level of significance of α=0.05.

Results & Discussion: The timing of activity in the biceps femoris and rectus femoris were different between the CFP and TRN conditions (Figure 1). The amplitude of muscle activity in the gastrocnemius lateralis and medialis was different between the CFP and TRN conditions, but the timing of activity remained the same. The tibialis anterior exhibited little change between the two conditions. All changes in muscle activity were not statistically significant, however footwear research using SPM is scarce. To the author's knowledge, this is the first study to investigate CFPs using markerless motion capture and with SPM analysis. Through SPM, novel shoe geometry does have significant effects on lower body kinetics, kinematics, and EMG [6]. An increasing amount of published footwear research explores different methods of analysis [7], and it may be beneficial to update previous findings using these new methodologies and analyses.

Significance: The presence of a carbon fiber plate did not significantly change muscle activity due to the runners' maintaining their efficient movement path based on their own technical idiosyncrasies. Future research should consider using new forms of data analyses such as SPM or Bayesian statistics to account for individual differences and previous biases on carbon fiber plated shoes, especially due to the popularity of using them as racing shoes.

Acknowledgments: CFP shoes were provided by Road Runner Sports.

References: [1] Healy et al. (2022), *Journal of Sport and Health Science,*11(3); [2] Whiting et al. (2022), *Journal of Sport and Health Science* 11(3); [3] Perrin et al. (2023), *International Journal of Sports Physiology and Performance*, 18(2); Cigoja et al. (2021), *Journal of Science and Medicine in Sport*, 22(11); [5] Beck et al. (2020), *Scientific Reports* 10(1); [6] Nüesch et al. (2019). *Gait & Posture,* 69(March 2019); [7] Sinclair et al. (2021)

AN IMPROVED METHOD TO MODEL MUSCLE MOMENT ARMS OF THE GLENOHUMERAL JOINT FOLLOWING REVERSE TOTAL SHOULDER ARTHROPLASTY

Breydon J Hardy[1,2*], Brittany Percin, B.S.[1], Peter N. Chalmers, M.D. [1], Robert Z. Tashjian, M.D. [1], Heath B. Henninger, Ph.D.[1,2,3]
Departments of Orthopaedics[1], Biomedical Engineering[2], and Mechanical Engineering[3], University of Utah, Salt Lake City, UT
*Corresponding author's email: breydon.hardy@utah.edu

Introduction: Reverse total shoulder arthroplasty (rTSA) replaces the humeral ball with a cup and the glenoid socket with a hemisphere in patients who experience degenerative changes, acute injuries, and shoulder instability. The rTSA was developed for patients with irreparable rotator cuff tears to create a biomechanical advantage to overcome the deficient cuff. The constrained non-anatomic joint configuration is now steadily replacing anatomic total shoulder arthroplasty for many surgical indications [1]. The rTSA shifts the joint center of rotation from the humeral head center to the center of the glenosphere, changing the moment arms, lines of action, and length excursion of the muscles. This dramatic alteration in muscle function could be responsible for the highly variable range of motion and inconsistent clinical outcomes after rTSA [2]. The aim of this study was to pilot the modeling of static poses for analyzing patient specific shoulder anatomy and implant placement, comparing muscle moment arms between healthy controls and post-operative rTSA patients. Analyzing changes in post-operative muscle moment arms and length change will provide insights into the origins of post-operative functional advantages and limitations.

Methods: Three-dimensional (3D) models of the humerus and scapula were aligned with calibrated biplane fluoroscopy images of healthy controls (N=3) and rTSA patients (N=2). Subjects posed with their forearm flexed forward at a 90-degree angle. The aligned 3D models quantified the relative position and orientation of the bones using model-based markerless tracking. These 3D models were then imported into the finite element and visualization software FEBio [3]. Infraspinatus, teres minor, subscapularis, and deltoid muscles were modeled as muscle lines (Fig. 1). The anterior deltoid was not modeled because of issues with wrapping around the coracoid. Muscle wrapping issues are currently being worked on using a finite element approach that constrains the muscle path. Muscle lines were created using anatomic insertions and origins to calculate their in vivo lengths and moment arms relative to the joint center of rotation. Three lines were modeled for each muscle to approximate the entirety of the muscle footprint, where different subregions may contribute different functions during motion. However, one muscle line was used for the teres minor due to its small size and homogeneous line of action. A MATLAB script converted all the points into the scapular coordinate system and calculated the magnitude and direction of each muscle moment arm relative to the joint center of rotation. Each moment arm was decomposed to calculate the muscle's contribution to the typical glenohumeral joint angles (e.g., elevation, plane of elevation, axial humerus rotation). Muscle moment arms were normalized based on the glenoid height of each subject to control for anthropometric scaling. Statistical significance was determined using a two-sided unpaired t-test with $P \leq 0.05$.

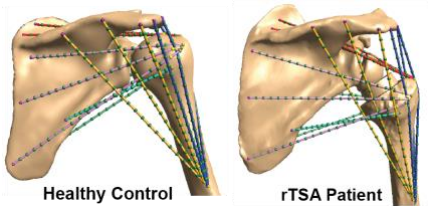

Figure 1: Models of a healthy control and rTSA patient are shown with muscle lines for the infraspinatus (pink), teres minor (cyan), subscapularis (green), posterior deltoid (orange), and middle deltoid (blue). Both subjects are shown with their arm at rest.

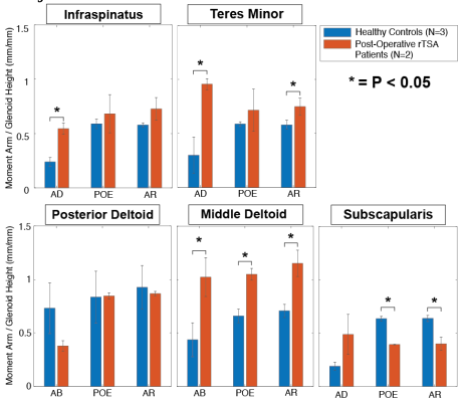

Figure 2: Muscle moment arm comparison for the infraspinatus, teres minor, subscapularis, posterior deltoid, and middle deltoid between normal controls and post-operative rTSA patients with their arm at rest. Where AD is adduction, AB is abduction, POE is plane of elevation, and AR is axial rotation.

Results & Discussion: The abduction moment arm of the middle deltoid increased dramatically when comparing healthy controls to post-operative rTSA patients at rest (Fig. 2). Since rTSA is designed to increase the efficiency of the deltoid in elevation by increasing its moment arm, this result was expected. However, this was counteracted by the increased adduction moment arm of the infraspinatus and teres minor (128% and 221% respectively, Fig. 2). The axial rotation moment arm of the subscapularis decreased 37% (Fig. 2), which could contribute to some rTSA patients not recovering internal rotation range of motion. No changes in muscle length were statistically significant.

Significance: The preliminary analysis from this study will be used to develop a more robust muscle moment arm analysis pipeline for use with a variety of highly variable subject specific motions derived from prior and ongoing studies. A previous study from our lab examined the relationship between high and low performing subjects with weighted scaption and internal rotation but did not analyze muscle moment arms [2]. Data resulting from this study will be used to identify why subjects were stratified this way using muscle moment arms. Ongoing work will analyze muscle moment arms additional healthy controls, and other static poses and dynamic motions, relating them to range of motion limitations and advantages. The muscle moment arm and muscle length/excursion analysis pipeline could be used by surgeons and device manufacturers to determine what surgical and implant parameters best optimize post-operative shoulder function for each patient based on their unique anatomy and available muscle architecture.

Acknowledgments: Funding provided by the National Institute of Arthritis and Musculoskeletal and Skin Disease (R01 AR067196).

References: [1] Drake et al. (2010), *Clin Orthop Relat Res.* 468(6); [2] Sulkar et al. (2023), *J Shoulder Elbow Surg* 32(4); [3] Maas et al. (2012), *J Biomech Eng* 134(1);

AGE-DIFFERENCE IN NECK CONTROL TO PREVENT HEAD IMPACT DURINF FALL

James R Fang[1], Seyed A. Tabatabaei[1], Elleann Kohl[1], Lingjun Chen[1], Neil B Alexander[3], Jacob J Sosnoff[1*,]
[1] Department of Physical Therapy, Rehabilitation Sciences and Athletic Training, University of Kansas Medical Center
[3] Department of Internal Medicine, Division of Geriatric and Palliative Medicine, University of Michigan
*Corresponding author's email: jsosnoff@kumc.edu

Introduction: Falls are the leading causes of accidental injury and injury-related death among the elderly [1]. During fall, head impact is common and associated with morbidity and mortality [2]. Nonetheless, little effort has been made on preventing head impact during fall. Age has been established as an important risk factor for fall-related head injuries [3,4]. Older adults have elevated risk for head impact during a fall [5]. It is postulated that this elevated risk stems in part from age-related deterioration in neck muscle [6], however, there is a lack of direct evidence on this hypothesis. The current study aims to fill this knowledge gap by investigating age-related differences in neck muscle function during falls and the roles of neck muscle in preventing head impact during fall.

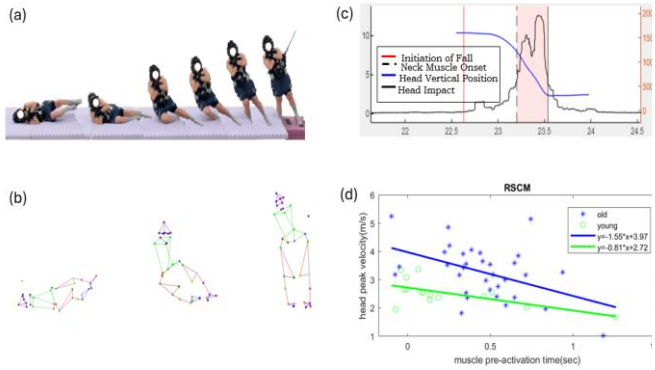

Figure 1:(a) Experimental Fall Paradigm detail described in [7]. (b) Full-body marker set, detail described in [7]. (c) Neuromuscular and movement events definition and the EMG outcome were calculated accordingly. (d) The regression analysis between RSCM pre-activation time and head peak velocity during fall. The result shows RSCM pre-activation time has significant association with head peak

Methods: Twenty one older adults at risk for fall related injury (age 77±7 yr; 1/3 female) and eight healthy young adults (age: 29±4 yr; 1/3 female) participated in the study. All participants underwent experimentally induced falls (**Figure 1**(a)) in three directions (backwards, left, and right falls) for two falls in each direction (total of six falls). The falling movement was captured using video recording and 8 cameras marker base motion capture system sample at 100Hz (MotionAnalysis, Inc) with full-body marker set described in [7] and displayed as in **Figure 1**(b). Muscle activities of bilateral sternocleidomastoid (SCM) and upper trapezius (UT) were collected using surface electromyograms (EMG; Delsys, Inc) sample at 2148Hz. Head impact rate was derived from video analysis using a standardized questionnaire. Peak vertical head velocity was calculated as an estimator of the head impact risk. Reaction time, peak EMG value, and pre-activation time of the four neck muscle were calculated to as estimators for neck muscle function during fall, where reaction time is the time difference between the fall initiation and the muscles onset time, peak EMG value is the peak amplitude after the muscle onset, and pre-activation time is the time difference between the muscles onset time and head impacted the floor or stopped(**Figure 1**(c)). Chi-square test was used to assess the effect of age on rate of head impact. Independent t-test was used to test the age-difference in head velocity and neck muscles function during fall. Linear regressions were used to test the association between neck muscle function and head velocity during fall and the effect of age on this association.

Results & Discussion: Older adults had significantly higher occurrence of head impact (13/37 falls = 35.41% vs. 1/16 falls = 6.25%, p = 0.02), and higher head peak velocity (3.16±0.93 vs. 2.49±0.48 m/s, p = 0.009) during backward fall compared to young adults. Results of neck muscle function between old and young adults in backward fall are listed in **Table 1**, where differences are seen in the right SCM(RSCM) reaction time and pre-activation time. The regression result also shows RSCM pre-activation time is a better predictor of head velocity in older adults. Our results contrast with Choi et al. [8] who reported that peak EMG values was negatively associated with head velocity in self-initiated falls in young adults (**Figure 1**(d)). This association is not observed in our data. Our result suggested older adults were pre-activating their neck muscle earlier to reduce head velocity. However, this strategy is not observed in young adults, yet the young were able to reduce the head velocity during fall.

Table 1.	Old	Young	pvalue
LSCM Reaction time(sec)	0.73(0.28)	0.72(0.33)	0.91
RSCM Reaction time(sec)	0.64(0.25)	0.86(0.36)	**0.01***
RUT Reaction time(sec)	0.69(0.39)	0.79(0.25)	0.33
LUT Reaction time(sec)	0.65(0.45)	0.66(0.29)	0.94
LSCM Pre-act time(sec)	0.36(0.21)	0.42(0.34)	0.49
RSCM Pre-act time(sec)	0.45(0.27)	0.23(0.36)	**0.02***
RUT Pre-act time(sec)	0.41(0.40)	0.29(0.24)	0.31
LUT Pre-act time(sec)	0.46(0.43)	0.45(0.29)	0.92
LSCM peak %MVC	53(35)	53(30)	0.97
RSCM peak %MVC	57(37)	45(36)	0.28
RUT peak %MVC	61(35)	51(34)	0.37
LUT peak %MVC	53(39)	62(29)	0.37

Significance: The current study shows consistence results with previous studies that older adults has elevated head impact risk than young adults. Contrast with previous studies, we found that there's no association between peak EMG value and head velocity. We found young adults utilized different strategies than older adults in neck control during fall. Future study should focus on how young adults reduce head velocity during fall.

Acknowledgements: This project is supported by Grant T32HD057850-13 and R21AG073892.

References:

[1] CDC (2017) weblink; [2] Heidel, M. M. et al. (2023), *JAMDA* 24; [3] Gardner, R. C. et al. (2018), *J Neurotrauma* 35; [4] V. Komisar et al. (2022), *BMC Geriatrics* 22; [5] Wood T. A. et. al. (2019), *BioMed R. Inter* s2; [6] Wood T. A. et. al. (2020), *J emg & kinesiology* 51; [7] Zanotto, T. et. al. (2023), *Contemporary clin. trials comm* 33; [8] Choi W. J. et al. (2017), *J Clin Biomech* 49.

THE EFFECTS OF CALF MUSCLE LENGTH ON LOCAL MUSCLE FATIGABILITY

Anh D. Nguyen[1*], Aubrey Gray[1], Gregory Sawicki[2], Jason R. Franz[1]
[1]Joint Dept. of Biomedical Engineering, UNC Chapel Hill and NC State University, Chapel Hill, NC, USA
[2]George W. Woodruff School of Mechanical Engineering, Georgia Tech, Atlanta, GA, USA
*Corresponding author's email: anguyen4@unc.edu

Introduction: Preventing walking disability among our rapidly aging population presents a significant public health challenge. A key factor is that older adults consume metabolic energy more rapidly than younger adults during walking [1], making them more prone to fatigue and exhaustion. We and others have shown that, compared to younger adults, older adults operate their calf muscles at shorter lengths which associates with a diminished capacity to enhance push-off intensity during walking [e.g., 2]. According to principles of muscle physiology, shorter muscle lengths require higher activation levels to produce a requisite force. Conceptually, those higher activations should precipitate an earlier onset of local muscle fatigue. However, the specific role of muscle length in governing the onset of local muscle fatigue has yet to be empirically established, even in healthy young adults. The goal of this study was to empirically examine the effect of muscle length on the onset of local calf muscle fatigue in a cohort of young adult participants. We focused on the calf muscles due to their relevance to walking performance and age-related mobility decline. We hypothesized that, compared to those when operating at longer fascicle lengths, calf muscle activity would increase and time to onset of fatigue would decrease when performing fixed-end calf muscle contractions to failure at shorter calf muscle lengths.

Methods: We used a repeated measures design to investigate the effect of muscle length on the onset of local muscle fatigue in a cohort of 16 young adults (age: 22.7±4.5 yrs). All testing was completed on the right leg in a computerized robotic dynamometer (System 4 Pro, Biodex) with knee flexed to 110° to isolate force production to uniarticular ankle muscles. We collected resting *in vivo* B-mode ultrasound images of the medial gastrocnemius at 15° of dorsiflexion (DF15) and 15° of plantarflexion (PF15) to assess fascicle length, the relative change in which we assumed would be indistinguishable from that of the soleus. Throughout testing, we recorded posterolateral soleus surface EMG. Prior to fatiguing trials, participants performed 3 maximal voluntary isometric contractions (MVIC) at a neutral ankle position to determine their maximum ankle moment. Thereafter, participants performed repeated fixed-end calf muscle contractions at DF15 and PF15, in randomized order, while a real-time biofeedback system implemented in Matlab monitored instantaneous net ankle moment. We instructed participants to push against the dynamometer pedal to replicate a continuous stream of target square waves displayed on a screen (0.5 Hz, 35% duty cycle, 75% MVIC ankle moment amplitude). We defined the onset of fatigue as an inability to produce an average of at least 75% of that target ankle moment over 5 consecutive pushes. Participants were provided a 25-minute rest between the two ankle postures to allow recovery. As a neuromuscular surrogate of fatigue, we also quantified median frequency and rms amplitude of soleus EMG, which we averaged over the first 5 ("early") and last 5 ("late") pushes.

Results & Discussion: Changes in ankle joint posture elicited anticipated changes in muscle fascicle lengths, which were 21% (8.9±4.4 mm; $p<0.001$) shorter for PF15 than for DF15 (Fig. 1A). Consistent with principles of muscle physiology, these shorter lengths were accompanied by roughly 2-fold higher EMG rms amplitudes ($p<0.01$) (Fig. 1B). This supports our theoretical motivation to interrogate the effects of shorter muscle lengths, and the higher requisite activation they require, on local muscle fatigability. Indeed, as one of the primary contributions of this study and consistent with our hypothesis, we found that the shorter fascicle lengths at PF15 precipitated, on average, a 60% reduction in time to fatigue onset compared to the longer lengths at DF15 (Fig. 1C). As another validation of our study protocol, soleus fatigue was also associated with hallmark changes in EMG independent of ankle joint posture and thus fascicle length; compared to earlier contractions, later contractions exhibited higher EMG median frequency (DF15, $p=0.046$; PF15, $p<0.01$) – a neuromuscular marker of fatigue. An unanticipated modest but significant negative correlation between decreases in fascicle length (i.e., from DF15 to PF15) and change in time to onset of fatigue ($r=-0.540$, $p=0.046$) requires further investigation.

Significance: Our results point to an ecological impact of the increased physiological demand placed on calf muscles when operating at shorter lengths – namely accelerated fatigue. We contend that these findings have clinical relevance for mechanisms associated with mobility impairment among older adults, who often operate their calf muscles at shorter lengths. These insights have practical implications for personalized rehabilitation and training protocols and may help refine ways – such as assistive devices – to mitigate fatigue in older adults.

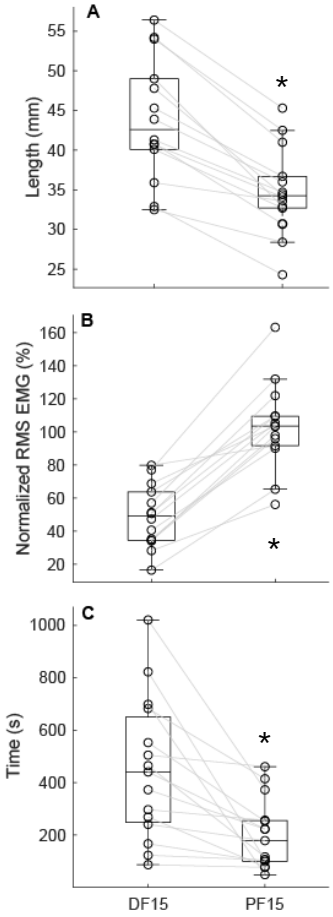

Figure 1. Fascicle length (**A**), EMG amplitude (**B**), and time to onset of fatigue (**C**) at 15° dorsiflexion (DF15) and 15° plantarflexion (PF15).

Acknowledgments: We thank Andrew Shelton for assistance with EMG processing. Supported in part by NIH (R01AG058615).

References: [1] Ortega and Farley (2007), *J Appl Physiol 102(6)*. [2] Conway & Franz (2020), *Gait & Posture* 77.

HOW MOMENTUM CONTROL LEADS TO LOWER JUMP HEIGHTS DURING TWO-FOOT RUNNING JUMPS WITH VS. WITHOUT A BALL IN MALE BASKETBALL PLAYERS

Jun Ming Liu[1*], Antonia Zaferiou[1]
[1]Stevens Institute of Technology
*Corresponding author's email: jliu130@stevens.edu

Introduction: Jump heights have direct performance implications in basketball [1], and two-foot running jumps (TFRJs) are performed either with or without a ball during games. Jump height is directly controlled by the initial center of mass (COM) downward velocity prior to final ground contact and net upward impulse generated during final ground contact prior to takeoff. When compared to TFRJs without a ball, we found that TFRJs with a ball had significantly lower jump heights and net upward impulses, and no significant difference in initial downward COM velocities at a *group-level* [2]. However, some participants did not exhibit significant differences in upward impulse, i.e., their lower jump heights with a ball could not be explained by the *group-level* findings. This prompted us to investigate these variables at the *participant-level*. We hypothesized that TFRJs with a ball would have more initial downward COM velocity and/or lower net upward impulse than TFRJ without a ball.

Methods: Recreation to college-level basketball players (n=13, male, M(SD) of 22 (3.5) years of age; 1.84 (0.1) m height; 84.1 (9.6) kg weight) volunteered for the study. They self-reported to be comfortable performing TFRJs with and without a ball and jump at least 0.5 m. They performed self-selected warm up after markers on rigid clusters were attached to 15 body segments. Anatomic landmarks for the body segments were digitized with a micron-calibrated markered probe, which allowed for calculation of the body's COM position [3] and velocity. 3D motion capture and force platforms (250 fps, Optitrack and 1000 Hz, Bertec) were used. Participants performed TFRJs with and without a ball from NBA combine test distance (4.57 m) for 5-10 repetitions each with at least 1 minute rest time and used the same approach direction, run up trajectory, and take-off sequence for all jumps. They were instructed to jump as high as they can and either tap their preferred limb on the hoop as high as they can or dunk the basketball into the hoop. To elicit intent to jump as high as possible, the height for the hoop (2.70-3.05m) was found per-participant during warm up trials. Jump height was calculated from final COM velocity which is the sum of initial downward COM velocity and mass-normalized net upward impulse. Initial downward COM velocity was calculated at the frame before initial first leg ground contact. Net upward impulse is calculated as the sum of the time-integral of first and second leg ground reaction forces (GRFs) and body weight through the ground contact. These variables of interest were expressed in the global upward axes and computed from start of final ground contact until take-off. Linear mixed models with jump condition as fixed effect and trial as random effect were used for participant-level analysis (α<0.05).

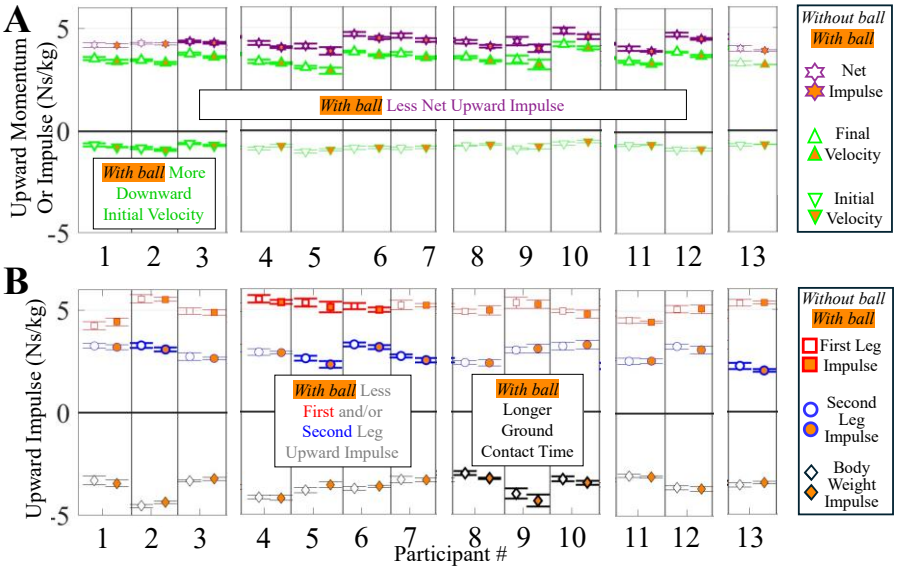

Figure 1: Mean (S.D.) of each participant's (A) initial downward and final upward COM velocities, and net upward impulse, and (B) first and second leg upward impulses and body weight impulse. Participants are manually grouped by mechanisms. Thicker lines indicate significantly lower values in jumps with ball (p<0.05).

Results & Discussion: Participants were re-numbered by participant-specific mechanisms in **Figure 1**. The lower jump heights in TFRJs with a ball were explained by significantly more initial downward COM velocities (**Fig. 1A** #1-3) and/or significantly less net upward impulses (**Fig. 1A** #3-12). For participants with more initial downward COM velocity but similar net upward impulse with a ball (**Fig. 1A** #1-2), more upward impulse from GRF was used to counteract the initial downward COM velocity, resulting in less net upward impulse to generate upward COM velocity. On the other hand, those with similar initial downward COM velocity but less net upward impulse generation with a ball (**Fig. 1A,** #4-12) also had lower final upward COM velocity with a ball. These participants did so with combinations of less first leg upward impulse (**Fig. 1B** #4-6) and/or second leg upward impulse (**Fig. 1B** #5-7), and/or more downward impulse due to body weight from longer ground contact time (**Fig. 1B** #8-10). For the participant with similar jump heights between conditions (**Fig. 1**, #13), the first leg generated similar upward impulse with greater average GRF and shorter ground contact time, and the significantly lower second leg upward impulse generated by the second leg was offset by the smaller (non-significant) downward impulse due to bodyweight because of the shorter ground contact time.

Significance: A novel approach leveraging participant-level statistics allowed us to understand which momenta control mechanisms explained lower jump heights during TFRJs with a ball in this cohort of basketball players. The various mechanisms behind each participant's lower jump heights may guide future research that examine and training intervention that address each mechanism.

References: [1] Ziv & Lidor (2009) *Sports Med. 39(7).* [2] Liu & Antonia (2023) *ISBS Proceedings. 41(1)* [3] de Leva (1996) *J. Biomech.* 29(9)

TASK-SPACE CONTROL FOR A KNEE-ANKLE PROSTHESIS

David J. Kelly[1*], Patrick M. Wensing[1]
[1]Department of Aerospace and Mechanical Engineering, University of Notre Dame
*Corresponding author's email: dkelly7@nd.edu

Introduction: Everyday tasks like level-ground walking can pose challenges for individuals with amputation, who have heightened fall risk [1]. While passive prostheses are the standard-of-care approach, recent research has demonstrated the benefits of powered devices to generate normative kinematic/kinetic joint profiles using sensors isolated to the lower limbs [2]. By expanding the sensing suite beyond the lower limbs, the prosthesis could better consider its role in balance, with its actions coordinated at a goal- or task-level to promote synergy between user and device. This work focuses, in particular, on control of the Center of Mass (CoM), which is vital for balance and locomotion [3]. The task-level approach taken aligns with previous work showing that CoM kinematic feedback can lead to more accurately reconstructing muscle activity during balance recovery than joint-level feedback [4].

Previous research on Task-space Control (TSC) for an ankle prosthesis [5] investigated the joint-level response from commanding the device based on task-space information. Specifically, this previous framework used desired CoM kinematics and ground reaction forces (GRFs) to determine the desired ankle torque. As a key result, the framework retained normative ankle kinematics/kinetics without ever commanding those joint-level characteristics. This abstract pursues an extension of TSC for knee-ankle prostheses.

Methods: The control framework in this study consisted of two components, offline reference trajectory generation and online joint torque calculations. A data set of CoM kinematics for healthy individuals at comfortable walking speed [6] was non-dimensionalized across an average gait cycle based on subject height and leg length. Desired CoM kinematics were determined for a user by rescaling the non-dimensionalized trajectories based on those same characteristics. Reference GRF profiles were then generated by fitting the Bipedal Spring-Loaded Inverted Pendulum (B-SLIP) model to the CoM kinematics, as outlined in [7].

The reference trajectories were then used online while taking feedback from an XSENS motion capture suit to collect whole-body kinematics. Since GRFs were one of the reference trajectories, TSC was only active during the stance phase, while a phase-based impedance controller was used in swing [5]. A thigh-based phase variable tracked progression through the gait cycle [8]. GRF profiles $\mathbf{F}$ were converted into a feedforward torque $\boldsymbol{\tau}_{\mathrm{FF}}$ via the configuration Jacobian $\mathbf{J}$: $\boldsymbol{\tau}_{\mathrm{FF}} = \mathbf{J}^{\mathsf{T}}\mathbf{F}$. The error between the reference CoM and estimated CoM position $\mathbf{e}_{\mathrm{com}}$ was converted into a feedback torque $\boldsymbol{\tau}_{\mathrm{FB}}$ with joint velocity damping $\dot{\boldsymbol{\theta}}$ to prevent sudden joint changes: $\boldsymbol{\tau}_{\mathrm{FB}} = \mathbf{J}^{\mathsf{T}}\mathbf{K}_{\mathrm{F}}\mathbf{e}_{\mathrm{com}} - \boldsymbol{D}_{\mathrm{F}}\dot{\boldsymbol{\theta}}$, where $\mathbf{K}_{\mathrm{F}}$ is based on the user's height and weight, and $\mathbf{D}$ is based on the joint gear ratio. Knee and ankle torques were then commanded as $\boldsymbol{\tau} = \boldsymbol{\tau}_{\mathrm{FB}} + \boldsymbol{\tau}_{\mathrm{FF}}$.

Results & Discussion: Initial tests were conducted with an able-bodied individual (male, 27) using the Open Source Leg (OSL) [9] via a bypass adapter at a comfortable walking speed (0.7 m/s). The user walked on a passive controller and TSC for 45 seconds each. The resulting average joint displacements and torques for the knee and ankle from each trial are presented in Fig. 1.

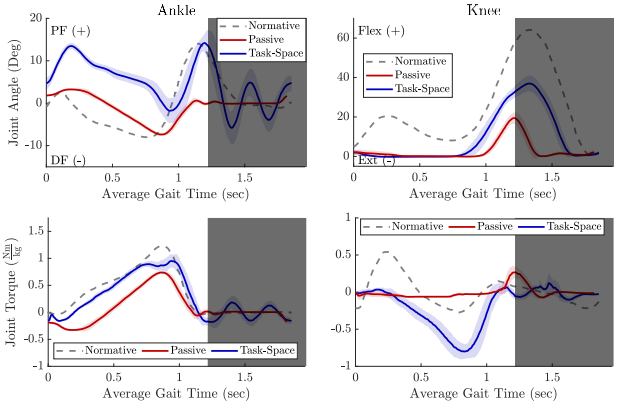

Figure 1:Mean and standard deviation for ankle (left) and knee (right) angle and normalized torque of the prosthesis with respect to average gait cycle time. The red and blue lines correspond to passive and TSC, respectively. Normative trajectories are adapted from [10]. Shaded regions denote the swing phase.

For joint angles, TSC generated ankle push-off that the passive controller did not. This joint-level push-off was emergent from task-level coordination. Likewise, TSC achieved almost double maximum knee flexion (36.9°) compared to passive control (19.8°), which is critical to avoid foot scuffs during swing. TSC generated slight plantarflexion in midstance where dorsiflexion is desired, which did lead to knee lock-out during stance. The ankle oscillations in swing for TSC were most likely due to low damping in the impedance controller.

For joint torques, both TSC and the passive controller qualitatively match normative ankle kinetics, although peak TSC torque (0.95 Nm/kg) is 28% higher than peak passive torque (0.74 Nm/kg). For the knee joint, TSC showed general trends of normative knee kinetics during stance, however, the positive peak torques were minimal compared to normative data, while the negative peak torque was more pronounced. This trend may be due to the consistent ankle plantarflexion during stance.

Significance: While only task-space information was used to generate desired joint torques, resulting joint-level characteristics show promising characteristics similar to normative walking kinematics/kinetics. These results highlight that joint-level characteristics may be the by-products of mechanisms related to whole-body coordination, rather than an end goal themselves. This novel task-level perspective for prosthesis control may help promote synergy between user and device, while also considering balance in the control.

Acknowledgments: This work was funded by the National Science Foundation award CMMI-1943703.

References: [1] Miller et al. (2001), *Phys. Med.* 82(8); [2] Best et al. (2023), *TRO* 39(3); [3] Lugade et al. (2011), *Gait&Posture* 33(3); [4] Safavynia and Ting (2013), *J. NeuroPhys.* 110(6); [5] Kelly et al. (2024), *ICRA* (To Appear); [6] Fukuchi et al. (2018), *PeerJ* (6); [7] Kelly et al. (2022), *ICORR*; [8] Best et al. (2021), *IROS* (p 6182-6189); [9] Azocar et al. (2018), *BioRob*; [10] Winter et al. (1983), *J. Motor Behav.* 15(4).

COMPARISION OF AZURE KINECT AND ORBBEC FEMTO BOLT SPATIAL SENSING CAMERAS FOR BODY MOTION TRACKING

Trent M. Guess*, Jamie Hall, Grace Purcell
University of Missouri, Columbia, MO
*Corresponding author's email: guesstr@health.missouri.edu

Introduction: The Microsoft Azure Kinect DK (developer kit) was introduced in 2019 as a spatial computing platform that included sensors for computer vision and speech recognition. An SDK (software development kit) for tracking human body movement was also introduced for use with the Azure Kinect computer vision outputs. The body tracking SDK combines an infrared 2D image, a time-of-flight 3D depth image, and machine learning to fit a 3D skeleton to the body. Outputs of the body tracking SDK include the location of 32 joint centers and body segment orientations relative to the Azure Kinect sensor. The Azure Kinect, and its predecessor the Kinect V2, provide body tracking data for many commercial rehabilitation and sport applications and 67 journal articles have been recently published on Azure Kinect DK body tracking (Pubmed, March 9th, 2024). In August of 2023, Microsoft announced discontinuation of the Azure Kinect and the sensor is no longer available for purchase. However, Microsoft has licensed their Azure Kinect technologies to other companies. The Orbbec Femto Bolt, introduced in October 2023, uses the same depth camera module as the Azure Kinect and is intended to be a direct replacement for the Azure Kinect DK for body tracking. The purpose of this study is to compare body tracking measures from the Azure Kinect DK to the Orbbec Femto Bolt during simultaneous data collection of functional movement tasks.

Methods: With IRB approval and informed consent, 5 persons (Age: 22.2 ± 0.4 yrs, Height: 179 ± 13 cm, 1 = F) performed walking, lateral-step-down and sit-to-stand tasks while body motion was simultaneously tracked with a Microsoft Azure Kinect DK and Orbbec Femto Bolt spatial sensor. Each sensor used a separate laptop computer and custom software recorded body tracking data during each task. The Azure Kinect was mounted 95 cm above the floor and the Orbbec Femto Bolt was mounted parallel to the Kinect but 8 cm above and 3 cm to the side. The software used by both spatial sensors was identical with the exception that a SDK wrapper was used to extend the custom code for use with the Orbbec spatial sensor. Each task was performed 5 times. The lateral-step-down task included both the right and left limb, for a total of 10 trials for each participant. Joint center location and segment orientation data from each task was converted to osteokinematic and spatiotemporal parameters using previously described methods [1-3]. For this study, the primary discrete parameters for each task were compared. This included stride length and stride time for walking, maximum knee extension velocity and task completion time for sit-to-stand, and peak knee flexion, hip flexion at peak knee flexion, and hip adduction/abduction at peak knee flexion for lateral step down. Walking spatiotemporal parameters for the right and left limb were extracted from joint center locations and combined. For the sit-to-stand, body segment orientations were used to find the maximum knee extension velocity during standing. Time to complete is derived from joint center locations and the final four cycles were used. Body segment orientations were used to find three-dimensional joint angles at the hip and knee during lateral step down. A Bland-Altman analysis was used to analyse agreement between instruments as well as the Pearson correlation coefficient. Ensemble averages of each task were used in the analyses.

Results & Discussion: Measurements derived from joint center locations produced small differences between spatial sensors (Table 1). Walking stride time and time to complete four sit-to-stand cycles were calculated from events detected in the joint center waveforms [1,3]. Walking stride time had essentially no difference between spatial sensors. The time to complete four continuous sit-to-stand cycles had an average difference of 0.05 seconds with Bland-Altman limits of agreement within 1% of the mean. Stride length distance during walking was derived from joint center motion during the walk cycle [1]. The average difference between sensors and the Bland-Altman limits of agreement were all under 1% of the mean stride length. Relative three-dimensional joint angles at the hip and knee were determined from body segment orientation data provided by the body tracking SDK. The average difference in knee flexion between sensors during the lateral step down was 0.4 deg which is less than 1% of mean knee flexion. However, 95% confidence Bland-Altman limits of agreement were relatively high compared to joint center derived measures. This may indicate increased variability in the orientation measures rather than sensor differences. Good agreement for time rate of change of knee flexion was found.

Significance: The Orbbec Femto Bolt spatial sensor provides body motion measures equivalent to the Microsoft Azure Kinect DK. The Femto Bolt sensor can be used interchangeably with the discontinued Azure Kinect for measurement of human body movement.

Movement Task	Measurement	Kinect Avg	Orbbec Avg	Average Difference	Lower Limit	Upper Limit	R
Walking	Stride Length (mm)	1407	1400	6	-5	6	1.00
	Stride Time (s)	1.18	1.17	0.02	-0.06	0.02	1.00
Sit-to-Stand	Knee Velocity (deg/s)	163.7	160.4	3.3	-2.0	3.3	1.00
	Time to Complete (s)	11.78	11.83	-0.05	-0.12	-0.05	1.00
Lateral Step Down	Hip Flexion (deg)	44.3	45.5	1.3	-6.7	4.1	0.98
	Hip Ad/Ab (deg)	4.4	5.1	-0.7	-3.1	1.6	0.98
	Knee Flexion (deg)	69.6	70.0	-0.4	-5.4	4.6	0.94

Table 1: Comparison of body motion measures during simultaneous data collection with the Microsoft Azure Kinect and the Orbbec Femto Bolt.

Acknowledgments: Funding for portions of this work was provided by the University of Missouri Coulter Biomedical Accelerator.

References: [1] Guess et al. (2022), *Gait & Posture,* 96:130-6, [2] Guess et al. (2017), *J Appl Biomech,* 33(2):176-8, [3] Thomas et al., *Gait & Posture*, 94:153-91.

A RE-EXAMINATION OF THE RELATIONSHIP BETWEEN FOOT STRIKE ANGLE AND EARLY STANCE LOADING VARIABLES DURING RUNNING

Caleb D. Johnson[1], Lauren K. Sara[2], Torstein E. Dæhlin[3], Molly M. Bradach[2], David J. Zeppetelli[1], Katelyn I. Guerriere[1], Leila A. Walker[1], Ian M. Hussian[1], Stephen A. Foulis[1], Julie M. Hughes[1], Irene S. Davis[3],
[1] Military Performance Division, U.S. Army Research Institute of Environmental Medicine, Natick, MA
[2]Spaulding National Running Center, Spaulding Rehabilitation Network, Cambridge, MA
[3]School of Physical Therapy and Rehabilitation Sciences, University of South Florida, Tampa, FL
*Corresponding author's email: caleb.d.johnson24.civ@health.mil

Introduction: A forefoot strike pattern during running, compared to rearfoot, has been associated with lower vertical ground reaction force loading rates (VLRs) and thereby potentially lower injury risk [1]. However, recent work has shown a more complex relationship, with VLRs varying significantly within foot strike patterns, depending on an individual's foot strike angle (FSA), or the sagittal plane angle of the foot at initial contact [2]. Their study, which utilized Division I athletes, showed a curvilinear relationship between FSA and VLRs, with angles in the middle of the distribution associated with the highest VLRs. However, this work has yet to be replicated in a large sample and one that is more representative of the general population. Second, no research has examined the relationship between FSA and peak vertical tibial accelerations (VTAs), which have been proposed as a more accessible surrogate of loading during running. Our purpose was to examine the relationship between FSA and VLRs and VTAs during running, while also controlling for competitive running experience. We hypothesized that there would be a curvilinear relationship between FSA and VLRs/VTAs, based on the previous study demonstrating this in athletes. We also hypothesized that the relationship would be affected by competitive running experience.

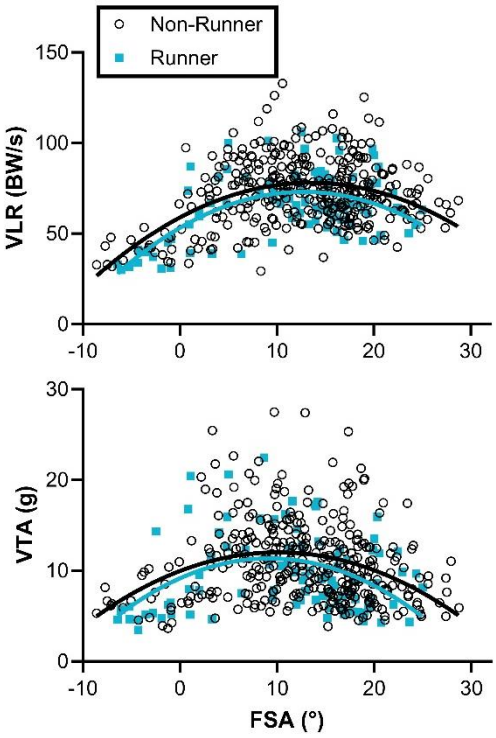

Figure 1: Results of regression models for FSA x VLR and VTA. BW= body weights, g= gravitational equivalent

Methods: Data was available for the current study from 475 U.S. Army trainees (156 females, age= 21±4 yrs, height= 1.71±0.097 m, weight= 73.5±14.6 kg). Participants completed surveys on their participation in sports and a running gait assessment on an instrumented treadmill (sampling rate= 1000Hz). For the gait assessment, peak TAs were measured using an inertial measurement unit attached to the distal-medial tibia (1600Hz) and sagittal plane videos were captured using high-speed cameras (240Hz). A 3-minute warm-up was given at a self-selected pace. The speed was then increased to 2.68-2.9 m/s, one minute was given for acclimation, and then at least 14 strides of data were collected. Average VLRs and peak VTAs were calculated for each stride [1,3]. Foot strike angles were calculated using deep learning-based, feature detection (DeepLabCut v2.2, Mackenzie Mathis, Alexander Mathis, Jessie Lauer) [4]. Variables were averaged over 7 strides and the right leg was used for analysis. Participants were grouped based on self-reported history of competitive running experience at the high-school level or higher (104 Runners, 371 Non-runners). Multiple regression was used to assess the relationship between FSA x VLR and FSA x VTA, including the quadratic and cubic terms. Models were adjusted for competitive running experience.

Results & Discussion: The model for FSA x VLR showed significantly better fit with the inclusion of the quadratic term (R^2 change= 0.15, F= 89.3, p< 0.01), but not the cubic term (R^2 change< 0.001, F= 0.1, p= 0.74). Running experience was a significant predictor in the full model (t= 2.73, p< 0.01). Separate models (Figure 1) showed similar shapes, but a better fit for those with running experience (R^2= 0.38, F= 26.5, p< 0.01) versus those without (R^2= 0.21, F= 45.4, p< 0.01). These results corroborate previous work [2], finding a curvilinear relationship between FSA and VLR in a larger sample. Although the relationship was slightly weaker in those without running experience, we found that it was comparable to those with experience. We also found that VLRs peaked at similar FSAs as in the previous study (≈10-15°), despite using two-dimensional angles vs three-dimensional angles in the previous study.

The model for FSA x VTA was also found to be characterized best by a quadratic curve (quadratic R^2 change= 0.12, F= 60.1 p< 0.01; cubic R^2 change< 0.001, F= 1.4, p< 0.01), and significantly affected by running experience (t= 2.49, p=0.01). Like VLRs, the model fit was better for those with running experience (R^2= 0.16, F= 8.5, p< 0.01) versus those without (R^2= 0.11, F= 20.9, p< 0.01). The shape of curves appeared to be slightly different from those for VLRs, with a more marked drop in VTAs at higher FSAs (more rearfoot strike).

Significance: Our results indicate that it is important to consider continuous rather than categorical measures of foot strike patterns (i.e., FSA) for practitioners attempting to reduce or assess the causes of higher lower-extremity loading in runners.

Acknowledgments: Supported by US DoD award W81XWH-20-C-0123 P0001. Opinions in this manuscript are the private views of the authors and are not to be construed as official policy or reflecting the views of the US Army

References: [1] Futrell (2020), *J Sport Health Sci*, 9(3); [2] Stiffler-Joachim (2019), *Med Sci Sports Exerc*, 51(10); [3] Johnson (2020), *J Biomech*, 113; [4] Johnson (2022), *J Applied Biomech*, 38(2)

DEVELOPING NOVEL COHERENCE MEASURES TO ESTIMATE WHICH MUSCLES ARE MOST RESPONSIBLE FOR TREMOR

Nolan H. Howes[1*], Matthew S. Allen[1], Dario Farina[2], Steven K. Charles[1]
[1]Brigham Young University, Provo, UT; [2]Imperial College London, London, UK
*email: nohowes@gmail.com

Introduction: Peripheral methods for suppressing hand tremor, such as injections of botulinum toxin, filtering orthoses, and electrical stimulation, have shown potential [1-3], but their effectiveness is currently limited because we do not know which muscles contribute most to a patient's tremor, and therefore where best to intervene. Tremor propagation through the upper limb can be described as a neuromechanical system, with tremorogenic muscle activity as inputs and hand tremor as the output. These inputs are filtered and mixed in complex ways as they pass through the system [4, 5], making it difficult to determine how much any given input contributes to the output using existing methods. This research aims to tease apart the complex relationships between tremorogenic muscle activity and hand tremor using novel coherence measures to identify which muscles are most responsible for a patient's tremor.

Methods: Coherence can be understood as a frequency-dependent correlation that, for a system with uncorrelated inputs, describes the portion of measured output power that can be attributed to each input. However, in a system with correlated inputs (as is the case with tremor propagation) the relationships between inputs become more complicated, and existing coherence measures are no longer able to adequately distinguish between the contributions of each input. To bridge this gap, we leveraged the theory and assumptions behind multiple coherence [6] to derive a novel coherence measure, referred to as component coherence, that optimally (least-squared error) decomposes output power into distinct components, each of which can be interpreted physically in terms of either power from a given input or cross power due to interference between a pair of inputs.

Using component coherence, we next defined a second novel coherence measure, referred to as adjusted coherence, that describes the portion of the output power that would be removed if the given input (or group of inputs) were removed (i.e., set to zero). Adjusted coherence is calculated as the sum of all component coherence terms associated with the specified input (or group of inputs). This measure represents the optimal linear estimate of the portion of output power contributed by a given input or group of inputs.

For application to tremor, we recorded surface sEMG in the four major wrist muscles (inputs) and translation of the hand in three degrees of freedom (outputs) from 14 subjects with Essential Tremor (ET) as they attempted to maintain neutral wrist posture. Three 2-minute trials were recorded for each subject, and each trial was divided into 30-second segments for subsequent analysis. In segments that exhibited definitive tremor and high multiple coherence (>0.5) between the set of inputs and each output, we calculated component coherence at the tremor frequency for the system. Using these values, we calculated adjusted coherence for each muscle and each pair of muscles in that trial.

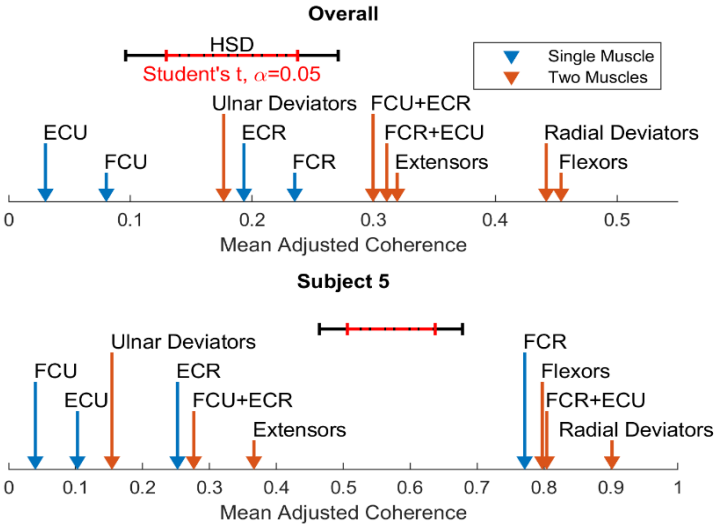

Figure 1: Predicted contributions to tremor by each muscle or pair of muscles, averaged across all subjects (top) and within a particular subject (bottom). Black intervals represent the 95% confidence honest-significant-difference width and red intervals represent the standard t-test-significance width with no correction for multiple comparisons. Two means are considered significantly different under the corresponding test assumptions if their difference is greater than these widths.

Results and Discussion: To predict which muscles contribute most to tremor, we compared the mean adjusted coherence values for each muscle and each pair of muscles (Figure 1). As might be expected, we observed that muscle pairs generally contribute more to tremor than single muscles. However, the results from Subject 5 show an important exception to this trend, where the adjusted coherence of the flexor carpi radialis alone is greater than or comparable to that of any pair of muscles. In such a case, optimal treatment could be performed by targeting only a single muscle, maximizing suppression while minimizing undesirable side effects (e.g., muscle weakness, discomfort, etc.).

In patients with ET generally, preliminary results suggest that it is best to suppress tremor by targeting either the pair of wrist flexors or the pair of radial deviators. Further research will extend this method to tremor in the full upper limb, including the 15 major superficial muscles of the upper limb as inputs.

Significance: This research offers a promising method to predict which muscles are most responsible for tremor using only experimentally measured data. Such a method is ideal for subject-specific tremor decomposition because it requires no assumptions regarding the system through which tremor propagates. With further refinement, this method could potentially be implemented clinically to predict which muscles are most responsible for a specific patient's tremor and help guide peripheral tremor suppression techniques.

Acknowledgments: Research supported by NIH NINDS grant R15NS087447-02.

References: [1] Samotus et al., 2018, *Can J Neurol Sci*, Vol 45. [2] Belda-Lois et al., 2007, *Technol Disabil*, Vol 19. [3] Dosen et al., 2015, *IEEE Trans Neural Syst Rehabil Eng*, Vol. 23. [4] Corie & Charles, 2019, *J Biomech Eng*, Vol. 141. [5] Davidson & Charles, 2017, *Ann Biomed Eng*, Vol. 45. [6] Bendat & Piersol, 2010. *Random Data: Analysis and Measurement Procedures*. 4E.

USING VOICE RECORDERS TO DOCUMENT LOSSES OF BALANCE AND THEIR CONTEXT DURING THE DAILY LIVES OF COMMUNITY-DWELLING OLDER ADULTS

Youngjae Lee[1], Linda Nyquist[2], Neil B. Alexander[2], Michael L. Madigan[1]*
[1]Virginia Tech, Blacksburg, VA, United States; [2]University of Michigan, Ann Arbor, MI, United States
*Corresponding author's email: mlm@vt.edu

Introduction: Falls are the leading cause of injury-related deaths among older adults in the USA. An estimated 60% of falls, or 84% of extrinsically-induced falls, among independent-living older adults are due to losses of balance (LOBs) [1,2]. Obtaining detailed information on the prevalence, mechanisms, and context of real-world LOBs is challenging given the limitations of recall and few eye-witness reports [3]. Video recordings have been used to overcome these limitations [4], but have their own limitations regarding where such recordings can be obtained. The goal of this study was to evaluate the usage of wrist-worn voice recorders for collecting information on the prevalence, mechanisms, and context of LOBs during the daily lives of community-dwelling older adults. This study builds upon our prior work using voice recorders and wearable inertial measurement units to obtain details and context of real-world falls [5].

Methods: Thirty community-dwelling older adults (18F and 12M; mean ± SD age = 71.8 ± 4.4 years; height = 1.68 ± 0.10 m; mass = 77.1 ± 16.8 kg; unipedal stance time = 17.6 ± 12.3 sec) who satisfied exclusion criteria based on a medical history and DEXA were asked to wear a wrist-worn voice recorder (BestRec Digital Voice Recorder) daily for three weeks and record the answer to the questions noted below whenever they experienced an LOB. For participants, an LOB was defined as "a sudden, unexpected, and unintended change in body position that requires you to do something to regain your balance or else you will fall." Voice recordings that did not meet this definition were excluded. Participants' responses were then categorized and tabulated.

Results & Discussion: 123 LOBs were reported across all participants with a three-week median of 1.5 LOBs per participant, an IQR of 1-4 LOBs, and a range of 0-23 LOBs. In response to the question *"Did you recover your balance or fall after the LOB?"* no participants reported falling. To reduce bias in our summary toward participants reporting the highest number of LOBs, participants were grouped based upon their number of LOBs reported and what appeared to be gaps in the distribution (groups: 15 participants reported 0-1 LOBs; eight participants reported 2-6 LOBs; and seven participants reported >=7 LOBs). Out of the 30 participants, 22 used the voice recorder for all 21 days, seven used it for 20 days (due to researcher scheduling constraints), and one used it for 19 days (due to sickness and minimal activity on the other two days). 54 LOBs were reported during the first week, 36 during the second week, and 33 during the third week. The most common response indicated most LOBs 1) occurred while participants were walking (not on stairs), 2) resulted from a trip or trip-like perturbation, and 3) elicited stepping responses to recover balance (Tables 1-3). These responses were generally similar across groups, with the only exception being the group who reported 0-1 LOBs per participant most commonly grasped/leaned on something to recover balance rather than stepping.

Table 1. Percentage of responses within each participant group to the question *"WHAT were you doing when the LOB occurred?"*

Top five responses	Group reporting >=7 LOBs each	Group reporting 2-6 LOBs each	Group reporting 0-1 LOBs each
Walking (Non-Stairs)	31%	28%	55%
Walking (Stairs)	17%	12%	18%
Turning or Changing Directions	6%	4%	9%
Standing up after sitting	7%	0%	0%
Picking up / putting down something	5%	0%	0%
Number of LOBs in group	87	25	11

Table 2. Percentage of responses within each participant group to the question *"WHY do you think you lost your balance?"*

Top five responses	Group reporting >=7 LOBs each	Group reporting 2-6 LOBs each	Group reporting 0-1 LOBs each
Trip or trip-like perturbation	48%	64%	82%
Slip or slip-like perturbation	11%	12%	9%
Lost control	11%	4%	0%
Bent / leaned over too much	10%	4%	0%
External interference	3%	0%	0%
Number of LOBs in each group	87	25	11

Table 3. Percentage of responses within each participant group to the question *"How did you try to regain your balance?"*

Top five responses	Group reporting >=7 LOBs each	Group reporting 2-6 LOBs each	Group reporting 0-1 LOBs each
Took step(s)	49%	44%	27%
Grasped / leaned on something	17%	12%	36%
Sat down on something	3%	4%	0%
Unspecified	30%	40%	36%
Number of LOBs in each group	87	25	11

Limitations: First, inter-participant variability in activity level may be a confound and is currently under investigation. Second, voice recorders were worn for approximately 12 hours/day with starting times ranging from 6am to 10am based on participant preference. LOB recordings outside of these hours were not obtained. Third, 68 of 492 total responses (123 LOBs × 4 questions) were unspecified and may indicate additional training on recorder usage may be needed.

Significance: Voice recorders hold great promise in providing informative data on the context underlying LOBs, leading to a better understanding of the mechanisms underlying real-world LOBs.

Acknowledgments: Funding was provided by R21AG075430. The content is solely the responsibility of the authors and does not necessarily represent the official views of the NIH.

References: [1] Luukinen et al. (2000), *Osteoporos Int* 11(7); [2] Berg et al. (1997), *Age Ageing* 26(4); [3] Wagner et al. (2005), *The Gerontologist* 45; [4] Robinovitch et al. (2013), *Lancet* 381; [5] Handelzalts et al. (2020), *Front Med* 7:514.

ASSESSING THE IMPACT OF MUSCLE FATIGUE ON LOWER EXTREMITY BIOMECHANICS DURING LAY–UP AND LANDING IN RECREATIONAL BASKETBALL PLAYERS

Brandon Yang and Li Jin*
Departments of Kinesiology, San José State University, San José, CA USA
*Corresponding author's email: li.jin@sjsu.edu

Introduction: It is crucial to understand how muscle fatigue can lead to musculoskeletal injuries in sports. Dynamic physical activities frequently lead to muscle fatigue. It was reported that muscle fatigue could put athletes at risk of injuries [1]. Muscle fatigue, which is associated with the risk of sustaining a musculoskeletal injury, often impacts maximum force production, reaction time, and exercise capacity [2]. Additionally, fatigue was associated with a reduced knee–abduction angle at initial contact, increased maximum knee–flexion moment, and delayed muscle activation times in the semitendinosus, multifidus, and gluteus maximus [3].

Sufficient studies are being conducted on the knee joint movements under fatigued conditions, however, there is a lack of research focusing on the ankle and hip joint movement under similar conditions. Therefore, the purpose of this study was to investigate the effects of fatigue on ankle, knee and hip joint biomechanics patterns during lay–up and landing activities. We hypothesized that fatigue would increase peak vertical ground reaction force (GRF) and peak joint moment in landing, while decrease peak vertical GRF and joint moment in lay–up activity.

Methods: Eight healthy participants (age: 25.63 ± 4.31 years; height: 1.76 ± 0.07 m; mass: 74.94 ± 13.52 kg) participated in this study. Initially, participants executed 3–step approach lay–up using their dominant leg, taking off from the force plate. Subsequently, participants performed drop–jumps from a 0.3 m box, landing on the force plate with the dominant leg. Following this, participants underwent the fatigue protocol [4]. After that, they repeated the same lay–up and landing tasks.

36 retro reflective markers were affixed bilaterally to anatomical landmarks on the lower body [5]. An 8–camera motion capture system (Vicon, Oxford, UK) was used to collect kinematic data at 100 Hz. Two force plates (AMTI, Watertown, MA USA) were used to collect GRF data at 1000 Hz. The outcome measurements include peak vertical GRF, peak ankle plantar flexion moment, peak knee and hip extension moment, all variables were processed via inverse dynamics model in Visual 3D software (C–Motion, Germantown, MD, USA). Paired t–test was used to determine the biomechanical differences (α = 0.05) between pre– and post–fatigue outcome measures using SPSS software (V26.0, IBM, Armonk, NY, USA).

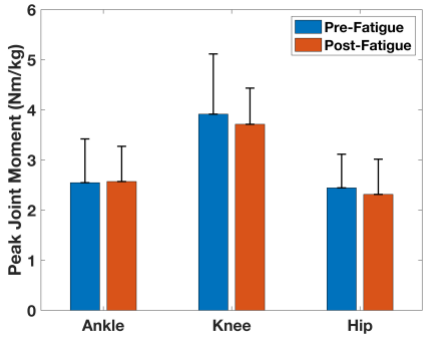

Figure 1: Group average (n = 8) peak joint moment in lay–up between two conditions.

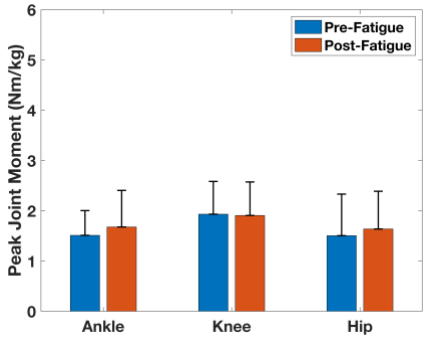

Figure 2: Group average (n = 8) peak joint moment in landing between two conditions.

Results & Discussion: A statistically significant difference was observed in the peak vertical GRF between pre–fatigue (3.35 ± 0.21 BW) and post–fatigue: (3.15 ± 0.23 BW) during the lay–up phase (p = 0.007). Due to the small sample size, no other statistically significant differences were found for the outcome measures between pre–fatigue and post–fatigue conditions. While participants exhibited a 5.39% decrease in peak knee extension moment and a 5.46% decrease in peak hip extension moment after the fatigued protocol during the lay–up (Figure 1). Additionally, there was a 10.51% increase in the peak ankle plantar flexion moment after fatigue during the landing phase (Figure 2). Moreover, in landing phase, peak hip extension moment increased by 8.52% after fatigue (Figure 2).

Significance: During lay–up, peak vertical GRF was significantly decreased when participants experienced muscle fatigue. This might be due to the fatigue related diminished neuromuscular control of the lower extremity system during ground contact. Additionally, fatigue tended to elevate peak hip extension moment during landing. This suggests that fatigue modifies lower extremity landing mechanics, leading to increased reliance on hip extensors for stabilizing whole–body motion. It also implied that fatigue leads to increased dependence on larger muscle groups, such as the hip extensors, to sustain consistent movement performance. Moreover, fatigue simultaneously decreased hip and knee extension moment during lay–up. This indicates muscle fatigue tended to reduce knee and hip extensor muscles force generation during the lay–up propulsive phase, this may compromise the movement performance. These findings suggest that acute muscle fatigue alters lower extremity joint biomechanics in both landing and lay–up activities. Such insights could inform injury prevention programs for athletic trainers and clinical professionals. Future study should investigate the effect of fatigue protocol on joint and limb mechanical work and power patterns in lay–up and landing activities.

Acknowledgments: The authors would like to acknowledge Dr. Matthew Leineweber and Dr. Masaaki Tsuruike for their suggestions on the project.

References: [1] Pappas et al. *J of Sport Sci & Med*, 6(1): 77–84, 2007; [2] Kim et al. *The Knee*, 24(6), 1342–1349, 2017; [3] Haddas et al. *J of Athlete Training*, 50(4), 378–384, 2015; [4] Liederbach et al. *Am J Sport Med*, 42(5), 1089-95, 2014; [5] Horst et al. *Plos One*, 12(6), 2017.

DOES SPM ANALYSIS SHOW DIFFERENT RESULTS THAN TRADITIONAL LOCOMOTOR LEARNING ANALYSES?

Elanna Arhos[1*], Jennifer Perry[1], Karin Grävare Silbernagel[2], Susanne M. Morton[2]
[1]Ohio State University, Columbus, OH , [2]University of Delaware, Newark, DE
*Corresponding author's email: elanna.arhos@osumc.edu

Introduction: Biomechanical analyses typically use discrete variables (e.g., peaks) or summary metrics (e.g., means of strides) to assess changes in movement. While these discrete analyses help in understanding movement at key points in time, they fail to take into consideration potentially relevant differences in movement occurring around the peaks and across time. Statistical parametric mapping (SPM) is a type of continuous waveform analysis that calculates data for every point of a continuous series [1]. Locomotor learning paradigms assess sensorimotor adaptation, and analyses are traditionally based on summary metrics, for example the first 5 strides for a perturbation [2]. An analysis using SPM is based on random field theory and applies temporal smoothing to reduce noise and enhance sensitivity. A critical threshold is calculated such that only 5% of the smooth random trajectory is expected to cross the threshold. The clusters of data that cross the threshold correspond to points in the time series data that are statistically significant. Individuals after ACL reconstruction (ACLR) is a relevant clinical group to assess sensorimotor adaptation in, given the reduction in afferent feedback that may contribute to a limited capacity for motor learning. After ACLR, reduced peak knee flexion (PKFA) and peak knee extension (PKEA) joint angles are common and persist for years [3]. A previous analysis in individuals after ACLR showed no differences in the learning of a new gait pattern for PKFA and PKEA compared to uninjured controls during a split-belt treadmill adaptation paradigm [4]. This analysis used the means of specific strides throughout the paradigm to assess learning. The purpose of this study was to compare the traditional discrete analysis results with SPM analysis to further understand motor learning capacity by taking advantage of the entire time-series data available for each learning period. Due to the sensory impairments after ligament injury [5], we expected that individuals after ACLR would adapt knee joint kinematics differently compared to uninjured controls during the SPM analysis when assessing the time series data, but not in the traditional discrete analysis.

Methods: 15 individuals 6.2 ± 1.8 months after ACLR (9 females, 20.8 ± 3.5 years) and 15 age, sex, and activity level matched controls were included in the study. Participants underwent a split-belt treadmill adaptation paradigm consisting of treadmill walking during baseline (3 min), learning I (12 min), washout (12 min) and learning II (12 min) periods. During baseline and washout, the belts were moving the same sped (tied). During learning, the belts moved in a 2:1 ratio to induce adaptation. Kinematic data were collected using an 8-camera motion analysis system (Vicon MX) and a sampling rate of 100 Hz and calculated using commercial software (MATLAB, TheMathWorks). For the discrete analysis, we characterized learning as the magnitude of the initial perturbation or aftereffect (average of first 5 strides during learning and washout) and the asymmetry remaining at the end of the learning and washout periods (average of the last 50 strides). Primary variables of interest were PKFA and PKEA interlimb differences (involved minus uninvolved limb) during the stance phase of gait. We used a 2x5 ANOVA with repeated measures on the factor time period to compare differences between groups across time periods. For SPM, we performed separate SPM *t*-test (alpha set to 0.05) to compare differences between groups continuously across each study time period (i.e., learning I, baseline, learning II).

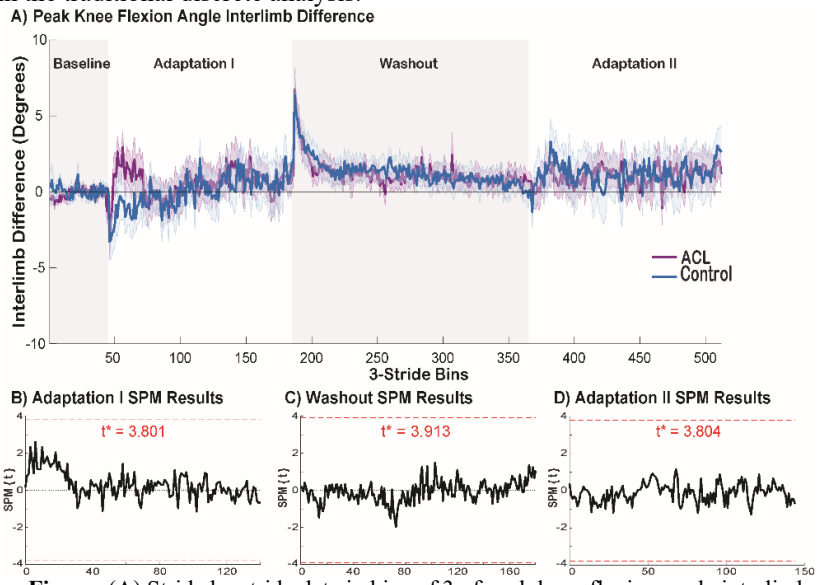

Figure. (A) Stride by stride data in bins of 3 of peak knee flexion angle interlimb difference. Shading around the lines represents ± 1 SEM. (B) Statistical parametric mapping results of the adaptation I, washout, and adaptation II periods.

Results & Discussion: Using traditional discrete analysis, individuals after ACLR demonstrated no differences in learning of PKFA and PKEA during the learning and washout phases compared with the uninjured control individuals (main effect of group: $p>0.67$; interaction effect: $p>0.091$). Using SPM, we also found no significant difference between groups across each study period (Fig). These results suggest that SPM confirms the discrete analysis and adds to previous results suggesting that throughout each 12-minute study period, and not just at the beginning and end of each period, individuals after ACLR did not differ in their adaptation strategy.

Significance: These continuous analysis results suggest that PKFA and PKEA are malleable and respond similarly across time in individuals after ACLR compared to uninjured controls.

Acknowledgements: This study is supported by the National Institutes of Health (F31-AR078580, S10-RR028114).

References: [1] Pataky et al. (2016), *PeerJ* e2652; [2] Helm et al. (2015), *Phys Med Rehabil* 26(4); [3] Hart et al. (2016) *Br J Sports Med* 50(10); [4] Arhos et al. (2024), *Clin Biomech* (in revision); [5] Needle et al. (2017), *Sports Med* 47(7).

FOOT TEMPERATURE RESPONSES DURING A 30-MINUTE WALK SUGGESTS A COMPLEX INTERACTION OF THERMOREGULATION PROCESSES

Jenna K. Burnett[1*], Jose Anguiano-Hernandez[1], Kota Z. Takahashi[1]
[1]Department of Health and Kinesiology, University of Utah, Salt Lake City, UT
*Corresponding author's email: Jenna.Burnett@hsc.utah.edu

Introduction: Foot temperature is commonly monitored in pathological populations such as those with diabetes to identify risk factors for tissue breakdown and ulcer development [1]. External mechanical factors (e.g., shear stress) on the foot from ground contact has been suggested to contribute to temporal temperature changes [2]. However, there may be other internal thermoregulation processes such as physiological and autonomic factors that contribute to the temperature changes, with the interaction of the mechanical, physiological, and autonomic factors on the temperature response not well understood. One potential way to discern which factors drive the thermal response is to study temperature profiles during a walk. If the mechanical factors are the *only* contributor, then a linear temperature response would be expected during a constant speed walk, as mechanical stress is constant from step to step. However, if the physiological and autonomic factors contribute to temperature changes, then a non-linear temperature response would be expected, as the physiological and autonomic factors are expected to vary throughout activity.

During running, the skin temperature across the whole body appears to follow a non-linear, sigmoidal or S-shaped trend [3], with the temperature initially decreasing, and then increasing before plateauing [3]. The sigmoidal relationship was attributed to physiological and autonomic factors, with the initial temperature decrease believed to be due to increased muscle blood flow and decreased skin blood flow [3]. However, as the run continued, it was postulated that, due to an internal temperature increase, the physiological and autonomic factors respond by increasing the sweating and skin blood flow to facilitate thermoregulation and cooling [3]. While the whole body's temperature appears to be driven by physiological and autonomic factors, the foot tissue is likely exposed to greater mechanical stress during ground contact, perhaps increasing the mechanical factors' influence on foot temperature. In addition, when compared to running, a lower intensity activity like walking may result in reduced thermoregulation and cooling demands, reducing the physiological and autonomic factors' contribution to the foot temperature. Therefore, the purpose of this study was to investigate the temporal temperature response of the foot during a long walk. We hypothesized that the temperature would change linearly with time. If supported, this suggests that external mechanical factors are the main contributor to the foot's temporal temperature response during walking.

Methods: Eight healthy adults (ages 18 to 35) walked shod for 30 minutes overground at 1.25 m/s. Thermal photos of the plantar foot were taken at baseline and every 5 minutes of walking with shoes and socks off. Regional temperature at the hallux, metatarsophalangeal joint, midfoot, medial arch, and heel were extracted using FLIR Research Studios. Two models using linear regression (Fig. 1, Eq. 1) and non-linear sigmoidal (Fig. 2, Eq. 2) equations were used to fit temporal temperature changes during walking. Model fit was assessed using the residual standard deviation (S_{res}) and mean square error (MSE), with lower values associated with better model fit.

Results & Discussion: Across foot regions, the linear model resulted in a S_{res} between 0.231 and 0.579, and MSE between 0.053 and 0.335, while the non-linear model had an S_{res} between 0.016 and 0.208, and MSE between 0.001 and 0.108 (Fig. 1). The non-linear model had better fit when compared to the linear model, as the S_{res} and MSE were lower in all regions. Based on these results, our hypothesis of a linear temporal temperature response was not supported. However, these results do not necessarily imply that mechanical factors (e.g., stress) do not contribute to temperature changes. There may be a more complex interaction between walking and temperature, with physiological and autonomic factors driving the temperature response simultaneously with mechanical factors. For example, as postulated by Tanda (2015), the initially constant temperature may be due to increased muscular blood flow with concurrent reductions in skin blood flow [3]. The temperature increase and plateau may be due to increased skin blood flow, sweating, and other cooling mechanisms which protect the body from high temperatures [3]. Research which disentangles the mechanical, physiological, and autonomic factors' contributions to temperature is required to understand the thermal response during walking.

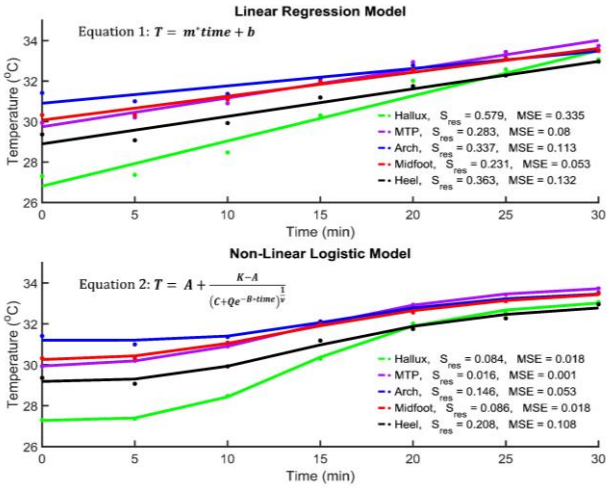

Figure 1: Right foot regional temperature during walking modeled with a linear regression equation (Eq.1, top) and a non-linear sigmoidal equation (Eq.2 bottom). Lower residual standard deviation (S_{res}) and mean square error (MSE) for all regions indicate the non-linear model fits better than the linear model.

Significance: The foot's temperature response to walking appears to be a complex balance of the physiological, autonomic, and mechanical factors in healthy adults. However, pathological populations with impaired vascular physiology (e.g., those with diabetes) may also have impaired thermoregulation, potentially resulting in altered temperature responses to activity. These populations may provide a unique opportunity to study how mechanical, physiological, and autonomic factors interact to influence foot temperature.

Acknowledgments: This work was supported by the NIH: R01HD106911 awarded to KZT, and 1T32DK11096601 awarded to JKB.

References: [1] J. Ena *et al, Int. J. Low. Extrem. Wounds*, vol. 20, 2021. [2] M. Yavuz *et al, J. Biomech.*, vol. 47, 2014. [3] G. Tanda, *J. Phys. Conf. Ser.*, vol. 655, 2015.

SEX IMPACTS LEG, BUT NOT KNEE STIFFNESS DURING LOADED WALK, JOG, AND RUN

Abigail C. Aultz[1*], Eric B. Francis, Tyler N. Brown
[1]Department of Kinesiology, Boise State University, Boise ID USA
email: abbyaultz@u.boisestate.edu

Introduction: Adequate lower limb stiffness is necessary for locomotor performance; yet, excessive leg and torsional knee joint stiffness reportedly increases musculoskeletal injury risk. Limb stiffness is reported to increase with faster locomotor speeds and addition of body-borne load, which may contribute to the sex dimorphism in lower limb injury [1,2]. However, it is unknown if females exhibit larger increases in lower limb stiffness with faster locomotor speeds during load carriage. We hypothesized that females would exhibit a stiffer leg and knee joint as well as larger stiffness increases than males with each incremental addition of load and locomotor speed.

Methods: 9 male and 9 female recreational runners had lower limb biomechanics quantified during a walk (1.3 m/s), jog (3.0 m/s), and run (4.5 m/s) with (15 kg) and without (0 kg) body-borne load. During each task, synchronous 3D marker trajectories and GRF data were collected using ten high-speed optical cameras (240 Hz, Vantage, Vicon Motion Systems LTD, Oxford, UK) and a single force platform (2400 Hz, OR6, AMTI, Watertown, MA). Marker and GRF data were lowpass filtered (12 Hz, 4th order Butterworth), and processed in Visual3D (C-Motion, Rockville, MD) to obtain knee joint biomechanics.

Custom MATLAB (Mathworks, Natick, MA) code quantified each dependent variable. From filtered GRF data, peak vertical GRF and loading rate, defined as the slope of the vertical GRF between 20% and 80% of the period between heel strike and impact peak, were quantified. Leg stiffness was calculated as GRF component directed from COP to the hip joint center divided by the change in leg length during stance. Knee joint stiffness was calculated as the change in joint flexion moment divided by the corresponding change in joint flexion angle from initial contact to peak knee flexion.

Vertical GRF metrics and stiffness measures were submitted to a linear mixed model with load, speed, and sex as fixed effects and subject identity as the random effect. A Bonferroni correction was used for post-hoc comparisons. Alpha level was $p < 0.05$.

Results & Discussion: Contrary to our hypothesis, the females did not exhibit larger increases in leg and knee stiffness than males with increased locomotor speed or body borne load. Sex only impacted leg stiffness ($p=0.033$), and unexpectedly the males exhibited a 12% stiffer leg than females (Fig. 1). The male's stiffer leg may be attributed to smaller changes in leg length during stance [2], which may help them perform locomotor tasks, but may also increase GRF transmission to the musculoskeletal system, elevating their injury risk.

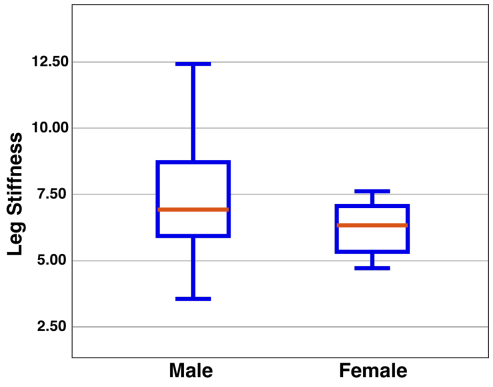

Figure 1: Depicts mean (SD) leg stiffness for male and female participants,

Faster locomotion speeds increased leg and knee joint stiffness, and peak vertical GRF (all: $p<0.001$). Specifically, with each incremental increase in locomotor speed (walk to jog, and jog to run) participants exhibited a significant increase in peak vertical GRF and knee joint stiffness (all: $p<0.001$). Leg stiffness, however, was only greater for jog and run compared to walk ($p<0.001$), as participants exhibited an insignificant, negligible 2% decrease in leg stiffness during the run compared to jog. Further study is needed to determine whether the slight reduction in leg stiffness is necessary during running to aid with elastic energy storage and forward propulsion.

In agreement with previous literature, adding body-borne load may elevate musculoskeletal injury risk by producing a stiffer leg and knee, and larger, faster vertical GRFs (all: $p<0.038$). Specifically, peak and loading rate of the vertical GRF increased 12% and 21% with load, which may elevate injury risk by coinciding with the subsequent 5% and 18% increases in leg and knee joint stiffness currently observed with body borne load. Considering recreational runners with a stiffer knee are 18% more likely to suffer an overuse injury [3], the large knee stiffness increases with load may pose a great musculoskeletal injury risk. Interestingly, however, there was significant load-by-speed interaction for leg stiffness ($p=0.021$), as participants increased leg stiffness with the addition of load during the walk ($p<0.001$), but not jog or run tasks ($p>0.05$). Further study is needed to determine why participants needed a stiffer leg to walk, but not jog or run with load.

Significance: These results provide valuable insight into the sex dimorphism of lower limb stiffness during load carriage, and whether the differences are magnified by locomotor speed. Although males exhibited a stiffer leg, sex difference were not magnified by locomotor speed. Highlighting these sex differences, or lack thereof, may inform targeted training and injury prevention programs need to tailor to participant size, rather sex to facilitate a meaningful reduction in musculoskeletal injury during load carriage.

Acknowledgments: NIH NIGMS (2U54GM104944, P20GM109095, P20GM148321) supported this work.

References: [1] Brown et al. (2020) *JAB* 37(2); [2] Silder et al. (2015) *J Biomech* 48(6); [3] Messier et al. (2018) *AJSM* 46(9)

BIOMECHANICAL ANALYSIS OF FDM PRINTED ANKLE-FOOT-ORTHOSES

Jacquelyn Brokamp[1*], Michael Zabala[1,2]
[1]Department of Mechanical Engineering, Auburn University, Auburn, AL, USA, [2]XO Armor Technologies, Inc., Auburn, AL, USA
* jrb0209@auburn.edu

Introduction: Ankle-foot orthoses (AFOs) are one of the most common orthotics used to treat patients with musculoskeletal and neurological disorders resulting in impaired gait. AFOs help normalize gait patterns by providing an external support to the lower limb, reducing neurological spasticity, and correcting muscle contractures [1, 2]. AFOs are commonly used for patients who have equinus deformity (i.e., foot drop), prevalent among cerebral palsy, muscular dystrophy, and post-stroke populations. An increase in gastrocnemius and soleus muscle tone causes a hyper-resistance to dorsiflexion, opposing the passive stretching of the muscle [3]. Consequently, the calf muscle shortens due to the increased muscle tone, prompting excessive plantarflexion of the ankle-joint throughout the gait cycle. AFOs are used to correct excessive plantarflexion throughout the gait cycle and to provide increased stability about the ankle-joint [4]. Patients with equinus can obtain an AFO that is standard off-the-shelf or custom-fit. Although the traditional fabrication methods yield successful results, the manufacturing process is laborious, and it can take up to 4 weeks for the patient to receive the device [5]. Additive manufacturing (AM) has recently been explored as a possible means of decreasing the manufacturing time while also improving user comfort and cost efficiency. AFOs are intended to be worn daily, but the mechanical strength and fatigue properties of 3D-printed AFOs are not yet fully understood. Accordingly, a pilot study was conducted on the gait analysis of a single subject wearing a custom-fit, 3D-printed AFO to capture the kinematics of the user and the resulting deflection of the AFO for eventual use during benchtop fatigue testing.

Methods: A 23-year-old healthy male subject was recruited to participate in the study. The participant provided informed consent, and the study protocol was approved by the Auburn University IRB (no. 23-476). The participant was scanned using XO Armor 3D-scanning technology to create a custom-fit model of an AFO. The AFO was fabricated using a fused deposition modeling (FDM) 3D-printer, retrofitted by XO Armor for this purpose, and proprietary material filament. The subject was asked to perform three trials of walking, jogging, single-step up, single-step down, and squatting. Each action was performed while wearing an AFO on the left lower limb (side randomly selected) and while not wearing an AFO for a total of 30 trials. A Vicon motion capture system and two AMTI force plates (2000 lb capacity) were used to capture the kinematic and kinetic data during the trials. The sagittal plane ankle kinematics were used to evaluate the effects of the AFO throughout gait. Ankle kinematics were normalized to stance phase by using the corresponding kinetic data, and the average of all three trials was calculated and reported. AFO deflection was also measured and reported. The AFO deflection was assessed by comparing the ankle-joint angle at anatomical neutral to the ankle-joint angle measured throughout the gait cycle.

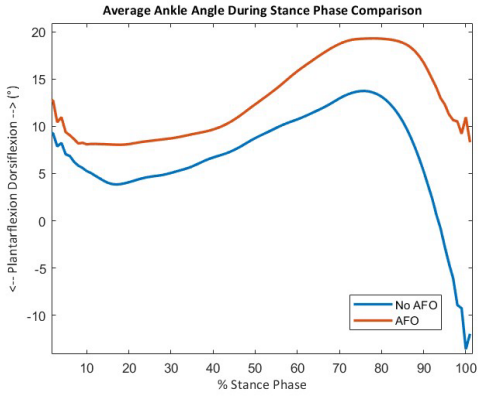

Figure 1: Comparison of the average ankle-joint angle during gait while the user is wearing an AFO (orange) and not wearing an AFO (blue).

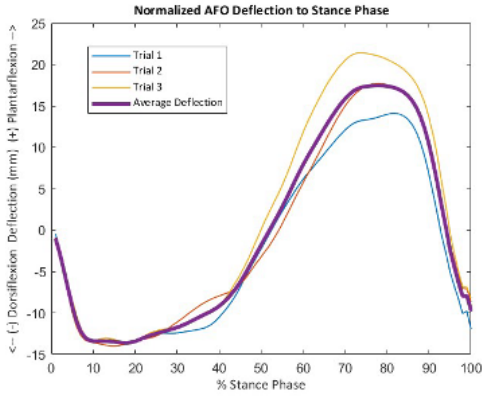

Figure 2: The deflection of the AFO in all 3 trials normalized to percent stance phase.

Results & Discussion: The results of this study found that the ankle-joint angle of the AFO-fit limb deviated from normal gait patterns, as demonstrated by comparing it to the ankle-joint angle of the user without the AFO (Fig. 1). While the AFO constrained the ankle to only dorsiflexion, the change of the ankle-joint angle during the trials established that the AFO did experience some deflection from heel strike to toe-off (Fig. 2). The measured ankle moment, unreported here, revealed that the AFO underwent compressive loading from heel-strike to midstance and tensile loading from midstance to toe-off. As seen in Fig. 2, the AFO experiences compression and tension during stance phase, with an average deflection of 13.64 mm in dorsiflexion and 17.46 mm in plantarflexion. The study aims to establish an understanding of the AFO gait kinematics and the resulting deflection experienced by the AFO. The data collected from this study will be used to conduct benchtop fatigue testing on these custom AFOs to simulate the deflection the device would experience during daily living. In turn, this data will provide an understanding of the strength and fatigue resistance of an AM custom-fit AFO and will ultimately provide insights into suggested durations of use by the patient.

Significance: The results of this study will help establish the anticipated use of life for an FDM-printed AFO. AM has the potential to significantly reduce manufacturing time and cost while enhancing the comfort of the user.

Acknowledgments: We would like to thank the Advanced Medical Technology Initiative (AMTI) (Contract No. W81K0222P-113) for funding this study.

Declared Conflict of Interest: Dr. Michael Zabala is the founder and a shareholder of XO Armor Technologies, Inc.

References: [1] Aboutorabi et al. (2017) Ann Phys Rehabil Med 60(3); [2] Wingstrand et al. (2014) BMC Musc Dis 14(1); [3] Boulard et al. (2019) Eur J Appl physiol 119(1); [4] Goldstein et al. (2007) Dev Med Child Neurol 43(8); [5] Silva et al. (2022) J Bioeng 9(6).

Wearable ultrasound can track quadricep symmetry after ACL injury

Erica L. King[1,2,3], M. Lamarre[1], G. Gibson[1], A. Bashatah[1], T. Croy[5], M.T. Jones[3,4], Q. Wei[1], S. Sikdar[1,2], P.V. Chitnis[1,2]
[1] Department of Bioengineering, George Mason University, Fairfax, VA, USA
[2] Center for Adaptive Systems of Brain-Body Interactions, George Mason University, Fairfax, VA, USA
[3] Frank Pettrone Center for Sports Performance, George Mason University, Fairfax, VA, USA
[4] School of Sports, Recreation, and Tourism Management, George Mason University, Fairfax, VA, USA
[5]School of Health Sciences, Liberty University, Lynchburg VA
*Corresponding author's email: eking20@gmu.edu

Introduction: Only 65% of patients return to preinjury activity levels following injury to the anterior cruciate ligament (ACL) [1]. There is no one protocol for ACL rehabilitation; only consensus on prolonging the timeline for returning to sport to allow for adequate healing [1]. Symmetrical quadricep activity, defined as the strength between the injured and non-injured limbs, should be stressed in rehabilitation. Quadricep activity deficits after ACL injuries have been shown to negatively influence knee movement symmetry and functional performance tests, such as the single leg hop [2]. Therefore, it is important for sports medicine teams to implement optimal rehabilitation approaches that focus on attaining symmetrical quadricep activity before patients return to sport activity [1,2].

A wearable Simultaneous Musculoskeletal Assessment with Real Time Ultrasound (SMART-US) system deploying multiple wearable imaging sensors strategically placed over muscles of interest can rapidly obtain quantitative muscle-level information to monitor quadricep function during ACL rehabilitation. The purpose of this study was to determine if SMART-US is feasible to measure bilateral symmetry in quadricep muscle activity after ACL injury.

Methods: Subjects (2 control, 1 with a left ACL-III deficiency) performed 3 trials of 3 bilateral, bodyweight squats with SMART-US imaging sensors placed on the right (Fig. 1A) and left rectus femoris (Fig. 1B) on two separate days. Controls' sessions were 48 hours apart, and ACL-III was four weeks apart. ACL-III submitted a modified clinical qualitative functional assessment survey (scores: 17 to 85 = best to worst) on each visit. Image data were collected simultaneously and analyzed with a custom MATLAB (MathWorks, Natick, MA, USA) script. SMART-US images were processed to automatically identify rectus femoris fascia. The sine function was fitted to the periodic displacement of rectus femoris fascia observed during the squats to calculate the maximum rectus femoris contraction and bilateral symmetry index (BSI) of rectus femoris activation (BSI=1 -> perfectly symmetric). The coefficient of variation (COV) was used to confirm the stability of BSI over multiple days in controls. In shoe force sensors, loadsol® (Novel, Pittsburgh, PA, USA), was used for additional BSI validation.

Results & Discussion: SMART-US showed stability over testing days in multiple subjects during a rehabilitation task and changes that correspond to clinical outcomes over a rehabilitation period. BSI for control subjects was 0.95±0.02 and 0.98±0.01 indicative of bilateral symmetry and healthy function. The corresponding COV was 2.6% indicating good measurement stability. BSI from the ACL-III subject improved from 0.5±0.06 to 0.89±0.03 over 4 weeks of rehabilitation, which correlated with a change in their functional assessment score from 70 to 45 (Fig. 1C). Results from loadsol® for healthy controls were similar to SMART-US with a BSI of 0.91±0.03 and a COV of 5.0%. Results from loadsol® for ACL-III improved over the four weeks from 0.56±0.07 to 0.76±0.03. These findings provide support that SMART-US can be used during squat tasks reliably and establish the potential to track rehabilitation longitudinally.

Significance: SMART-US offers the potential for assessing ACL recovery and facilitating assessment during treatment and rehabilitation periods by yielding new quantitative information on healing progression. SMART-US system can provide an objective method to monitor muscle performance during functional activity and exercises to inform return to sport decisions in new ways.

Acknowledgments: Efforts are sponsored by the Government under Other Transactions Number MTEC-MPAI W81XWH-15-9-0001 and MOMRP RESTORE W81XWH-21-1-0190.

References: [1] Waldron, et al. (2022) *Arthrosc. Sports Med. Rehabil.* [2] Palmieri-Smith et al. (2015) *Am. J. Sports Med.*

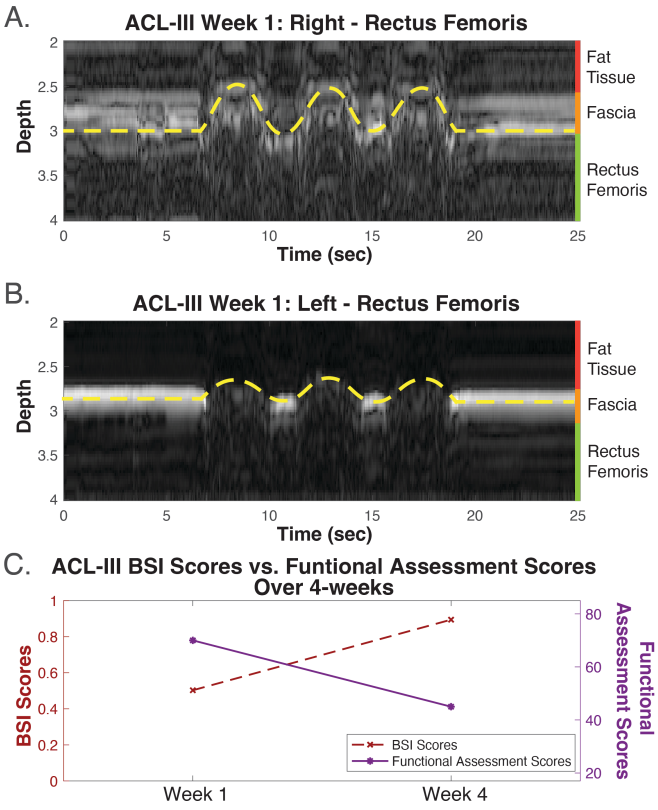

Figure 1: A) Zoomed in SMART-US image of ACL-III's right rectus femoris at week 1 during squats. Sine wave overlayed in a yellow-dashed line shows amplitude of muscle displacement during movement. B) Zoomed in SMART-US image of the ACL-III's left rectus femoris at week 1 during squats. Sine wave overlayed in a yellow-dashed line shows difference in amplitude compared to right. C) Comparison of ACL-III functional assessment scores vs. BSI Scores from week 1 to week 4.

Developing a visual-cognitive single-leg vertical jump test

Fatemeh Aflatounian[1], Kaylan Wait[1], Brendan Silvia[1], Alexandra C. Lynch[1], James N. Becker[1], Keith A. Hutchison[1], Janet E. Simon[2], Dustin R. Grooms[2], and Scott M. Monfort[1]
[1]Montana State University, Bozeman, Montana, USA, [2]Ohio University, Athens, Ohio, USA
Email : fatemehaflatounian@montana.edu

Introduction: High re-injury rates following anterior cruciate ligament reconstruction (ACLR) motivate the need for improved methods to determine readiness for safe return to sport (RTS). The single leg vertical jump (SLVJ) test, assessing upward jumping ability, has shown promise in detecting altered function post-ACLR even after common hop tests normalize [1]. However, like many RTS tests, SLVJ focuses solely on motor performance, neglecting the visual-cognitive demands experienced during sport competition, which are associated with higher-risk biomechanics and injury [2]. Dual-task screening, evaluating function with simultaneous cognitive and motor tasks, offers an opportunity to identify impairments under these demands [3]. Incorporating visual-cognitive demands into the SLVJ may further enhance its clinical utility post-ACLR. As an initial step, this study aimed to evaluate the impact of a visual-cognitive challenge on previously-established outcomes of the SLVJ in a healthy population. We hypothesized that adding cognitive tasks would cause performance deficits during SLVJ compared to the standard single-task version.

Methods: 28 healthy individuals (18F/10M, 20.5±2.1 yrs; 1.68±0.12 m; 68.0±8.7 kg; Tegner: 6.5±1.7; Marx: 10.6±4.1) participated in this study. Participants performed the SLVJ as high as possible, while keeping their hands on their hips [1] and looking at an overhead target. The SLVJ was done in single task (ST) and dual task (DT) conditions on each limb (3 trials per limb-condition). The DT condition added a visual-cognitive challenge using FITLIGHT cues. Participants initiated the jump upon a predetermined 'Go' color displayed on one of two peripheral lights, while also recalling three colors displayed by a light above them during the jump for a visually-demanding memory task (remember a series of colors). The approach is an adaptation of a previously developed visual-cognitive triple hop [4]. Kinematics and ground reaction force data were collected using a maker-based motion capture system. We used an inverse kinematics model in Visual 3D to calculate kinematic outcomes that were previously found to distinguish ACLR versus healthy controls during the SLVJ [5]. Dependent variables included jump height and peak knee flexion angle (pKFA), peak hip and trunk flexion angle, peak pelvic tilt angle during SLVJ in both propulsion (0.4 sec before leaving the force plate until toe off) and landing (initial contact until pKFA after the jump) [1] in both single- (ST) and dual-tasks (DT). Mixed effect statistical models tested for Limb*Condition interactions as well as Condition (ST and DT), and Limb (dominant, nondominant) main effects. Jump height was also considered as a covariate to isolate what effects may be largely due to task changes in jump height.

Results & Discussion: The results showed significant differences for conditions between DT and ST during SLVJ for all variables (all p <0.004, **Figure 1**), but not for Limb*Condition interactions and limb differences. Specifically, participants exhibited reduced jump height (d = 0.75) and decreased pKFA during both propulsion (d = 1.54) and landing (d = 0.47) phases, resembling ACLR patients' performance in previous study [1]. Additionally, DT elicited a decrease in hip flexion, pelvic tilt and trunk flexion during both propulsion (d = 1.5, 1.47, and 1.5 respectively) and landing (d = 0.6, 0.57, and 0.45 respectively) phases, less similar to the ACLR group (compared to health controls) in previous work [1]. The introduction of an overhead goal that altered visual gaze likely influenced the specific kinematic adaptations observed, although the visual gaze was restricted to the same target for both ST and DT in our study. Despite jump height being a significant covariate for many of the outcomes, the significant condition effects persisted even after controlling for jump height except for knee flexion angle during landing. Collectively, these results demonstrate that the performance of healthy participants during SLVJ is influenced by the introduction of a visual-cognitive challenge, a clinically-feasible method to augment RTS assessment to better reflect cognitive-motor demands athletes experience during competition. Future efforts are needed to benchmark the test-retest reliability and clinical relevance of the visual-cognitive SLVJ.

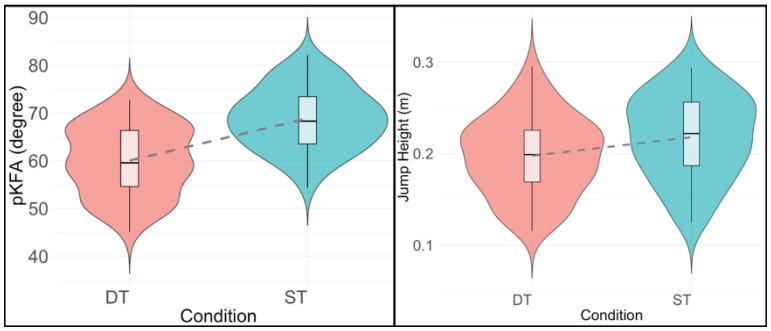

Figure 1: Violin plots of jump height and peak knee flexion angle (pKFA) in single leg vertical hop during propulsion for single task (ST) and dual task (DT)

Significance: An additional visual-cognitive challenge resulted in widespread alterations to kinematic outcomes of the SLVJ. This dual-task extension of an already promising clinical assessment for ACLR RTS may further enhance its ability to identify performance deficits in scenarios that better reflect the cognitive-motor challenges athletes experience during competition. Future studies are needed to understand the reliability of this task and how performance on it relate to clinical outcomes following ACLR.

Acknowledgements: This research was supported by the NIH award R03HD101093.

References: [1] Kotsifaki et. al. (2022) *Br J Sports Med* 56(9): 490-498, [2] Vargas et. al. (2023) *IJSPT* 18(1): 122-131, [3] Bertozzi et. al. (2023) *Sports Health*, [4] Farraye et. al. (2023) *J Sport Rehabil* 32(7): 802-809, [5] Fischer et al. (2021) *J Applied Biomech* 37(4)

Knee Kinematics during Yoga poses using Marker-based vs Marker-less motion capture systems

Soniya Kadam, Riva Karia, Smita Rao
[1]Department of Physical Therapy, NYU Steinhardt School of Culture, Education, and Human Development
*Corresponding author's email: sk9984@nyu.edu

Introduction: Yoga, a mind-body practice, demonstrates substantial benefits in improving musculoskeletal and cardiovascular health outcomes.[1] While yoga is believed to enhance joint mobility, research predominantly employs marker-based (MB) motion capture for biomechanical assessment.[2,3] Recent studies suggest that markerless motion capture (ML) shows promise in recognizing human movements by using deep learning algorithms.[4,5] There is little existing literature comparing lower extremity three-dimensional kinematics from concurrent ML and MB motion capture systems.[6,7] However, the convergent validity of ML motion capture in quantifying knee joint kinematics has not been assessed against standard MB motion capture systems during yoga. Understanding the biomechanical effects of yoga, which often involves a wide joint range of motion, is essential when compared to ADLs.[8] This study aims to explore knee joint kinematics during various yoga poses and ADLs using MB and ML motion capture systems. We hypothesized that estimates from ML motion capture would closely align with the MB system at the knee joints during yoga poses commonly prescribed for lower extremity musculoskeletal conditions.

Methods: Twelve asymptomatic adults, between 18-50 years and BMI 18.5-35 kg/m^2 years were enrolled in the study. Participants performed four ADLs such as Walk, Sit-to-stand (STS), Step Up (SU), and Step Down (SD)[8] and five yoga poses including Chair, One-Leg Balance, Warrior-I, Warrior-II, and Prayer Squat.[3,9] All yoga poses were performed using standard instructions and included a static 3-second hold. Kinematic data were captured using a 16-camera system (Qualysis), synchronized with two embedded force plates. Eight cameras each were used for MB and ML data acquisition. MB and ML data were processed using Visual 3D (HAS Motion, Canada) software and Theia 3D (Theia, Canada), respectively. Raw marker trajectories were interpolated and filtered with a low-pass, 4th-order Butterworth filter with cut-off frequencies of 6 and 12 Hz.[10] Raw marker-less video data were pre-processed by Theia3D, and default inverse kinematics solutions were calculated. Stance phase kinematics were assessed for ADLs, and knee kinematics during yoga poses were assessed for dominant leg during a 3-sec hold.[3,10] Standing offsets were subtracted from all ADLs and yoga trials, peak knee flexion and adduction were primary dependent variables of interest. Descriptive statistics, root mean square difference (RMSD), and intraclass correlation coefficient [ICC (Model (3, *k*)], were used for statistical analysis.

	Peak Knee Flexion				Peak Knee Adduction			
	MB	**ML**	**RMSD**	**ICC**	**MB**	**ML**	**RMSD**	**ICC**
Walk	-15.0	-14.6	3.3	0.92	-1.7	-0.6	3.7	0.33
Sit to Stand	-95.8	-91.8	6.1	0.96	-6.9	-2.5	9.9	-0.45
Step Up	-88.2	-82.9	6.9	0.86	-88.2	-82.9	9.8	-0.09
Step Down	-80.0	-73.8	7.2	0.98	-6.8	-2.5	9.4	-0.06
Chair	-99.1	-91.8	9.6	0.81	-0.7	5.6	14.4	-0.12
OLB	-0.1	-1.2	2.7	0.95	0.9	-0.5	3.4	-0.15
Warrior1	-84.7	-77.5	8.4	0.86	5.1	10.6	13.6	0.34
Warrior2	-82.5	-72.5	10.5	0.64	11	20.3	14.8	0.44
Prayer	-137.0	-128.5	9.8	0.78	2.7	-1.0	8.8	0.76

Table 1: Mean knee kinematics and RMSD in degrees using MB and ML and ICC for ADLs and Yoga

Results: Mean knee kinematics and RMSD in degrees and ICC (Model (3,*k*) are summarized in Table 1. We found moderate to excellent agreement in peak knee flexion angles in the sagittal plane between MB and ML motion capture systems across various yoga poses and ADLs. Higher RMSD was noted in yoga poses compared to RMSDs noted during ADLs in both planes. Peak knee adduction showed poor agreement and high RMSD between MB and ML systems. Our results support the findings of Song et al. (2023) that the knee kinematics estimated using the ML approach closely correspond to MB approaches during walking, particularly in the sagittal plane.[7] ML offers practical benefits such as minimal subject preparation time and interference during performance.

Significance: We evaluated the concurrent validity of knee kinematics calculated using ML versus MB approaches during ADL and yoga poses relevant to the lower extremity. We found that ML motion capture estimates of knee joint kinematics demonstrated moderate to excellent convergent validity when compared to MB motion capture, particularly in the sagittal plane, for yoga poses and ADLs, with RMSD ranging from 5-10 degrees. Knee adduction RMSDs were higher indicating that there may be opportunities for continued algorithm development in this area. These findings contribute to our understanding of the convergent validity of ML versus MB approaches in quantifying knee kinematics. Future studies are indicated to extend these findings in larger samples.

Acknowledgment: SR was supported by NIDDK R01DK114428, NIAMS R01AR079182, NIH NCATS UL1TR001445, Georgeny High Priority Award from the Foundation for Physical Therapy Research.

References:[1] McCaffrey R.et al. *J Yoga Phys Ther*.2012;02(05),[2] Kuntz AB, et al. *PLOS ONE*. 2018;13(4), [3] Salem GJ,et al.2013:165763,[4] Drazan JF et al. *J Biomech*.2021;125:110547,[5] Kanko RM et al. *J Biomech*. 2021;122:110414, [6] Kanko *J Biomech*. 2021;127:110665,[7] Song K et al. *J Biomech*.2023;157:111751,[8] Whissell E. 2015.http://hdl.handle.net/10393/33174 [9] Brenneman EC et al. *PLoS ONE*. 2015;10(9),[10] Wang MY, *BMC Complement Altern Med*. 2013;13(1):8.

EVALUATION OF DROP VERTICAL JUMP KINEMATICS AND KINETICS USING 3D MARKERLESS MOTION CAPTURE IN A LARGE COHORT

Ty Templin[1]*, Christopher D. Riehm[2] , Travis Eliason[1], Tessa C. Hulburt[2], Samuel T. Kwak[2], Omar Medjaouri[1], David Chambers[1], Kase Saylor[1], Manish Anand, Gregory D. Myer[2], Daniel P. Nicolella1[1]
[1]Southwest Research Institute, San Antonio, TX
[2] Emory Sports Performance And Research Center (SPARC), Flowery Branch, GA, USA
*Corresponding author's email: ty.templin@swri.org

Introduction: Analysis of complex human movements provides critical insight across a broad range of health, disease, and performance-related applications. To generate meaningful insights, scientists and clinicians frequently aim to associate both quantified patterns of movement (kinematics) and dynamic forces and torques applied to the joints (kinetics) with specific health-related conditions. Traditionally, the accurate and reliable measurement of kinematics, through three-dimensional (3D) marker-based motion capture, requires a dedicated laboratory space with advanced instrumentation operated by highly trained individuals. This process is exceedingly time-consuming, especially to develop musculoskeletal models from the marker data, and can significantly limit its use in routine clinical and functional athletic assessments. Markerless motion capture technology addresses several limitations of marker-based motion capture, though it remains unclear if similar accuracy and fidelity is produced in all three planes of motion to reliably compute the metrics necessary to assess dynamic movements. One of the most investigated movement tasks employed to assess movement quality, ACL injury risk, and rehabilitation progress through 3D kinematic and 3D kinetic analysis is the drop vertical jump (DVJ) [1,2]. From the widespread utilization of DVJ in the biomechanics literature, the resultant 3D kinematic and kinetic profiles during movement have been extensively characterized, making the DVJ task an ideal movement for comparison of different motion capture methods. Therefore, the purpose of this study was to evaluate 3D kinematics and kinetics calculated from a markerless motion capture system relative to kinematics and kinetics derived from a marker-based system for the DVJ.

Methods: Data were collected from 127 female athletes (age: 15.57 ± 1.36 years, height: 1.66 ± 0.07m, weight: 64.42 ± 12.16kg) at Emory University's Sports Performance And Research Center (SPARC). Each participant performed three repetitions of the DVJ. The DVJ consisted of the subjects dropping directly down off a 31cm box and immediately performing a maximum vertical jump towards an overhead target. Concurrent Qualisys marker-based motion capture system and video-based cameras for markerless motion capture (Qualisys AB, Göteborg, Sweden) were used to capture time synchronized movement data. The markerless system used 12 Qualisys Miqus cameras which recorded video at 120 Hz, while optical marker-based motion capture was collected at 240 Hz using 16 Qualisys cameras. Two AMTI force plates collected ground reaction forces (GRF) and center of pressure at 1200 Hz. The video data was processed using the ENABLE™ markerless system to derive a scaled OpenSim [3] model and the full body kinematics for each participant. Marker data was gap filled and processed through the OpenSim inverse kinematics tool. The scaled model and kinematics from both markerless and marker-based systems were used in combination with the force plate data to calculate joint moments using the OpenSim inverse dynamics tool. Joint moments were normalized by bodyweight.

Results & Discussion: Markerless kinematics demonstrated good agreement with the marker-derived data evidenced by average RMSE values of between 2.52– and 9.21° for hip, knee, and ankle angles (Table 1). Sagittal plane hip, knee, and ankle values had consistently low RMSE (≤ 6.93°) and very strong correlations (≥ 0.97). Frontal and transverse plane knee and hip kinematics also demonstrated reasonable RMSE values (≤5.68°) and moderate correlations (0.45–0.69). The ankle subtalar angle had the highest RMSE (9.61°) and the poorest correlation (0.06). Similar to the kinematic results, good agreement was observed for hip, knee, and ankle sagittal plane moments. Strong correlations (≥0.90) were observed for the sagittal plane hip, knee, and ankle moments. Strong correlations (0.71 - 0.78) were also observed in the transverse and frontal plane hip, transverse plane knee, and subtalar ankle joint moments. While the frontal plane knee moment exhibited a moderate correlation (0.61). The largest difference with respect to RMSE was in hip extension moment (0.23 N*m/kg). All other degrees of freedom had RMSE values of 0.08–0.17 N*m/kg. All RMSE values were smaller than the range of corresponding joint moment data, demonstrating reasonable agreement between the two systems.

Table 1: RMSE and Pearson correlation of markerless systems relative to marker-based system for lower limb kinematics and kinetics for drop vertical jumps.

Joint		Kinematics		Kinetics	
		RMSE(std) deg.	Pearson (std)	RMSE (std) Nm/kg	Pearson (std)
Hip	Flex/Ext	6.93 (0.27)	0.98 (0.02)	0.23 (0.07)	0.90 (0.07)
	Ad/Ab	2.52 (1.2)	0.69 (0.34)	0.17 (0.11)	0.73 (0.22)
	Int/Ext	5.82 (2.45)	0.67 (0.29)	0.08 (0.07)	0.78 (0.21)
Knee	Flex/Ext	5.55 (1.55)	0.99 (0.01)	0.14 (0.05)	0.95 (0.02)
	Ad/Ab	4.75 (2.15)	0.45 (0.43)	0.16 (0.13)	0.61 (0.32)
	Int/Ext	5.86 (1.90)	0.59 (0.37)	0.11 (0.09)	0.71 (0.33)
Ankle	Flex/Ext	5.77 (1.79)	0.97 (0.01)	0. 14 (0.08)	0.95 (0.04)
	Subtalar	9.61 (4.72)	0.06 (0.48)	0.15 (0.14)	0.74 (0.28)

Significance: Reliable and valid markerless motion capture has the potential to vastly expand the impact of 3D motion analysis across many patient and athlete populations. The cohort analysed in this investigation represents one of the largest efforts to date aiming to estimate the performance of a commercially available markerless system compared to a marker-based system. The results highlight the promising potential of markerless motion capture, particularly for measures of hip, knee and ankle across rotations.

References: [1] Hewett et al. (2015), *Braz J Phys Ther* 19:398-409; [2] Myer et al. (2014), *IJSPT*. 9:289-301; [3] Delp et al. (2007), *IEEE Biom. Eng.* 54(11)

SEX DIFFERENCES IN BARBELL FORCES DURING THE SNATCH IN WEIGHTLIFTERS IN THE 81 KG WEIGHT CATEGORY

Emma Patterson[1], Wandasun Sihanath[1], Kristof Kipp[1]
[1]Marquette University, Milwaukee, WI
*Corresponding author's email: emma.patterson@marquette.edu

Introduction: Men have competed in the sport of weightlifting since the first Olympic games was held 1896, but it wasn't until 1987 that women started to participate. The goal in weightlifting competitions is to successfully lift the most weight per kilogram of body mass in two separate lifts: the snatch and the clean and jerk. The snatch consists of one continuous movement of the barbell from the floor to an overhead catch position [1] and can be further broken down into five different phases: first pull, transition, second pull, turnover, and the catch phase. Biomechanical research indicated that women generally tend to spend more time in the transition and second pull phase of the snatch, and reached higher maximal vertical velocities, than men [3]. While some research examined sex differences in weightlifting biomechanics and performance, there is a current lack of comparative analyses between men and women within the same weight category. Although both men and women compete in weight categories, only two of the categories are identical (i.e., 55kg and 81kg). Previous research identified sex differences in the snatch technique of elite level weightlifters who participated in the 69kg weight category, which used to be the only weight category for which a match existed before the introduction of the new weight categories in 2018. Given that kinematic variables differ across weight categories (e.g., lighter lifters display less vertical velocity and acceleration, and exhibit an overall shorter time for the barbell to reach maximum height) [2], it would be valuable to reexamine sex differences in weightlifting biomechanics in a heavier weight category. Matching weight categories between males and females can be beneficial to account for possible differences in body dimensions, such as limb length or torso length. Therefore, the purpose of the current study was to compare barbell forces between males and females in the 81-kg weight category during the snatch lift.

Methods: Sagittal plane videos of snatch lifts were recorded during 81kg sessions **(Table 1)** at the 2023 North American Open Finals competition with a digital camera (SONY) at 120 Hz. The position of the barbell from all three snatch attempts from each lifters were automatically tracked (TEMPLO). The vertical position data were used to calculate vertical velocities and accelerations. The vertical acceleration data were used to calculate the net force applied to the barbell, which in turn was normalized by the barbell load to obtain a dimensionless technical indicator of weightlifting performance because it accounts for the strength of the lifter. All data were trimmed from the instant of barbell lift-off (vertical velocity > 0.03 m/s) to the instant of overhead stabilization (second zero-crossing of vertical velocity). The time series of the normalized net barbell forces from the male and female lifters were compared with two sample statistical parametric mapping. The criterion for statistical significance was set at an alpha level of 0.05.

Table 1:

Subject	Age (y)		Body Mass (kg)		Barbell Load (kg)*	
Rank	Men	Women	Men	Women	Men	Women
1	26	25	81	80.2	141	96
2	27	32	80.8	80.7	135	96
3	19	26	79.8	79.9	131	92
4	27	20	81	80.6	130	88
5	26	29	80.4	78	128	85
6	20	30	80.5	80.7	127	80
7	20	21	80.4	81	123	-
8	35		81		120	
9	25		81		120	
Mean (+/-SD)	25 ± 4.9	26 ± 4.5	80.6 ± .4	80 ± 1	128 ± 7.5	91.6 ± 7.6

*heaviest snatch attempt successfully lifted

Figure 1:

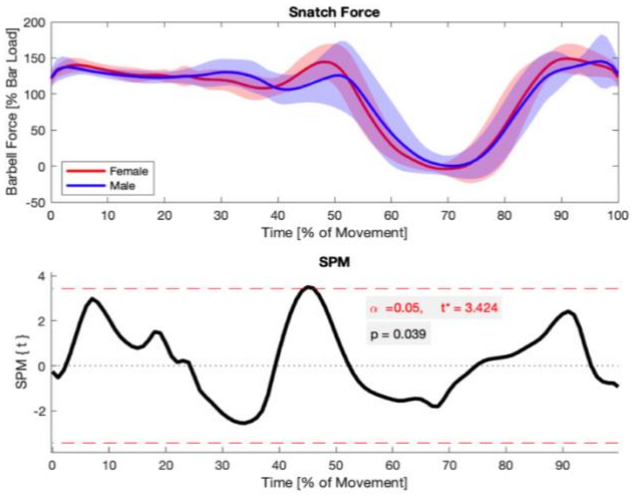

Results and Discussion: Barbell force application differed between males and females from 40%-50% of the movement phase of the snatch lift (**Figure 1).** This portion of the movement phase aligns with the second pull of the snatch, when most lifters apply the largest forces to the barbell. Therefore, female lifters in the 81kg weight category apply greater relative force with respect to the barbell load during the second pull than male lifters in the same weight category. This finding aligns with previous literature that showed that women within the 69kg weight category perform more mechanical work (relative to body mass) during the second pull than men within the 69kg weight category [4].

Significance: Sex differences in force application during the second pull phase of the snatch lift are present when comparing between males and females in the 81kg weight category. Coaches should be aware of these differences as they partially represent different technical characteristics or reflect a different approach to performing the snatch. Similarly, this information should also be taken into consideration by coaches when choosing different exercises and intensities when designing training programming for their athletes.

References:

[1] Mastalerz et al., (2019), *Journal of human kinetics*, *68*, 69–79; [2] Granell et al., (2006), *Journal of strength and conditioning* 20. 843-50; [3] Gourgoulis et al., . *Journal of strength and conditioning research*, *16*(3), 359–366; [4] Harbili, E. (2012), *Journal of sports science & medicine*, *11*(1), 162–169.

EYE DROP INSTILLATION SUCCESS IS RELATED TO INDIVIDUAL AND POSTURAL FACTORS

Daniel Duque Urrego[1*], Maddy Weber[2], Gül Kabil[2], Cameron Haire[2], Alanson P. Sample[2], David T. Burke[2], Susan H. Brown[2], Paula Anne Newman-Casey[2], and Stephen M. Cain[1]
[1]West Virginia University, Morgantown, WV and [2]University of Michigan, Ann Arbor, MI
*Corresponding author's email: dd00055@mix.wvu.edu

Introduction: Glaucoma is the primary cause of blindness among Black Americans and the second most common cause of irreversible blindness in the United States. The American population over 65 years of age is expected to grow in the next four decades [1], which will increase the number of Americans with glaucoma as well. To prevent vision loss, patients with glaucoma must take their daily eye drop medications. Unfortunately, at least 40% of patients do not take their medications regularly, and 20% are unable to apply the drops to their eyes correctly [2]. Understanding why people struggle to apply drops correctly is necessary to develop better interventions. This study aimed to evaluate the relationships between instillation success, individual factors (age, hand used, left or right eye), and postural factors (head angle and bottle inclination) during eye drop instillation, where bottle and head motion was captured by bottle-mounted and head-mounted inertial measurement units (IMUs). We hypothesized that individual and postural factors would have a significant relationship to instillation success.

Methods: Twenty older adults (8M/12F, age: 72.6 ± 4.7 years) who do not use eye drops daily participated in this University of Michigan IRB-approved study. Participants applied eye drops from an instrumented bottle with their dominant hand into both eyes during three different body postures: standing, sitting, and supine, performing at least three attempts in each eye in each position (18 total instillation attempts). Subjects wore an IMU on the head while performing the tasks. We defined the orientation of the IMU on the head (sensor to segment alignment) using a functional calibration. The velocity and displacement of the bottle were calculated from the measured linear acceleration and angular velocity from the bottle IMU using a Zero Velocity Update (ZUPT) algorithm [3]. The instillation period, or the time during which a participant was attempting to instill eye drops, was defined using the bottle velocity where the start/end time was the point at which the bottle's velocity was less/greater than 5% of the peak bottle's velocity during the movement toward/away from the face. We calculated the bottle tilt and mean head pitch and roll using IMU data measured during the instillation period. We defined instillation success as $Success = Drop\ on\ Eye\ [0\ or\ 1]/\#\ of\ drops\ used$. We used Generalized Regression within JMP software (R&D, Cary, NC) for our statistical analysis, employing the Adaptive Lasso method. The model included the main effects for all variables (success, bottle tilt, head pitch and roll, age group, hand used, eye, and position) and considered all possible interactions to explore their collective influence on the response variable. The model's explanatory power was assessed using the R-squared statistic, and the significance of predictors was evaluated using Wald Chi-Square tests with associated p-values.

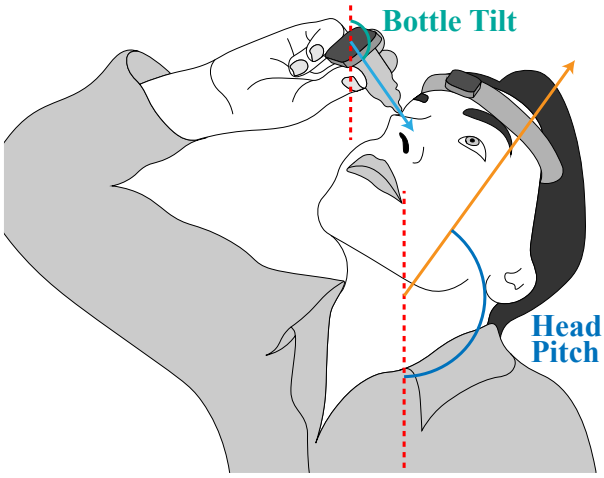

Figure 1: Eye drop instillation using the instrumented bottle and inertial measurement unit (IMU) on the head.

Results & Discussion: The model exhibited a moderate explanatory power, with an R-squared value of approximately 41.7%, indicating that it explains a significant portion of the variance in instillation success. Notably, the Adaptive Lasso method efficiently reduced the model complexity, reducing an initial 154 parameters to 70, optimizing the model based on the minimum AICc of 185.6. We observed that age group had a significant relationship with instillation success ($p < 0.0001$), with older age groups having less success than younger groups. Older adults may encounter more challenges during eye drop application, possibly due to diminished motor function. Additionally, the interaction between age group, eye, and bottle tilt emerged as significant ($p = 0.002$), indicating that the success rate varies with the eye (right or left) and the angle at which the bottle is tilted. The interaction involving hand, head pitch, and bottle tilt ($p = 0.0053$) was significant, underscoring the importance of head positioning for instillation success. Increasing the head pitch angle brings the frontal plane of the eye closer to horizontal, effectively increasing the area in which a drop can fall and enter the eye. Our findings underscore the importance of individual factors, such as age, as well as postural and biomechanical factors, including head pitch and bottle tilt, in influencing the success of eye drop instillation.

Significance: With 20% of glaucoma patients unable to instill eye drop medication correctly, it is critical to understand the biomechanics of eye drop instillation to develop better interventions. Our results demonstrate that head orientation and the tilt of the bottle significantly impact instillation success, suggesting that simple changes in the instillation technique can improve eye drop medication adherence.

Acknowledgments: Supported by the NIH National Institute of Biomedical Imaging and Bioengineering (R01EB032328).

References: [1] Vajaranant et al. (2012), Investigative Ophthalmology & Visual Science 53, 2464-2466; [2] GRF. National Survey Reveals Glaucoma Has Significant Impact on Patients' and Caregivers' Daily Lives and Well-Being (2019); [3] Rebula et al. (2013), Gait & posture, 38(4), 974-980.

THE FACET JOINTS UNDERGO SEVERE BONY DEGENERATION PRIOR TO THE VERTEBRAL ENDPLATES IN INDIVIDUALS WITH CHRONIC LOW BACK PAIN

Patrick Smith[1*], Cortez Brown[1], Clarissa LeVasseur[1], Tom Gale[1], Sabreen Megherhi[1], Cate Gray[1], Joseph Shoemaker[1], Caroline Pellegrini[1], Gina McKernan[2], William Anderst[1]
[1]Department of Orthopaedic Surgery, [2]Department of Health Information Management, University of Pittsburgh, Pittsburgh, PA
*Presenting author's email: pss42@pitt.edu

Introduction: Chronic low back pain (cLBP) has been associated with intervertebral disc degeneration, lumbar segmental instability, facet joint osteoarthritis, spondylosis, and osteophyte formation[1]. The process of spinal aging has been documented to progress through a degenerative cascade as outlined by Kirkaldy-Willis[2], however, the sequence of osteophyte development in the lumbar spine of individuals with cLBP remains unclear. Some studies suggest facet degeneration is a precursor to disc degeneration[3], while others contend that degeneration initiates in the anterior structures[4]. The purpose of this study was to determine the sequence of severe bony degeneration in the lumbar spine, represented by osteophyte formation in the facet joints and the vertebral body. Based upon prior studies that provide conflicting evidence, we hypothesized that severe degeneration would occur with equal frequency on the vertebral endplates and on the corresponding facet joints in individuals with cLBP.

Methods: Written informed consent was acquired from individuals with cLBP (defined as low back pain for at least 3 months that persists >50% of the time in the last 6 months[5]), with BMI <35kg/m^2, who were not pregnant, and were able to perform lumbar flexion/extension and lateral bending exercises. Lumbar spine CT scans (resolution: 0.5 x 0.5 x 0.625mm) were obtained in the supine position. Bone tissue from L1 through S1 was segmented from the CT scans using a combination of automated and manual segmentation (Mimics 24, Materialise). Lumbar vertebral body 3D models were then created from the segmented bone tissue. Osteophytes on the endplates were assessed by viewing each 3D bone model; osteophytes on the facets were assessed by viewing the segmented CT scan of each facet joint. Endplates and facets were assessed in a randomized order by two reviewers using customized Matlab code to blind reviewers to the subject and vertebral level. Lumbar endplates were evaluated using a previously reported 0-4 scale[6] by viewing only the vertebral body of the 3D bone model. Facets were evaluated on slices of the segmented CT scan using a previously reported 0-3 scale[7] by viewing only the facet joint. Following grading of individual endplates, the 0 to 4 endplate score was re-categorized such that grades 0 through 2 were category 1 (no to moderate osteophyte growth), while endplate grades 3 and 4 were assigned category 2 (severe to extensive bridging osteophytes). Facet grades were re-categorized in a similar manner such that grades 0 and 1 were category 1 (none to joint space narrowing) and grades 2 and 3 were category 2 (facet hypertrophy to severe osteophyte growth). The frequency distribution of more severe endplate osteophytes (endplate is category 2, facet is category 1) or more severe facet osteophytes (endplate is category 1, facet is category 2) was evaluated using a chi-squared goodness of fit test with an expected frequency of 50% for each condition, with significance set at $p < 0.05$.

Results & Discussion: Data processing is complete for 110 out of 300 participants who have completed testing (64F, 46M; average age 50.6 ± 16.3 yrs.; BMI: 26.4 ± 3.8kg/m^2). The observed frequency of more severe facet osteophytes was greater than the observed frequency of more severe endplate osteophytes for all combinations of endplates and their corresponding facets for both graders (χ^2 from 0.29 to 1.0; all $p<=0.006$)(Figure 1). These interim results suggest that severe bony degeneration in the lumbar spine occurs in the facets prior to the endplates.

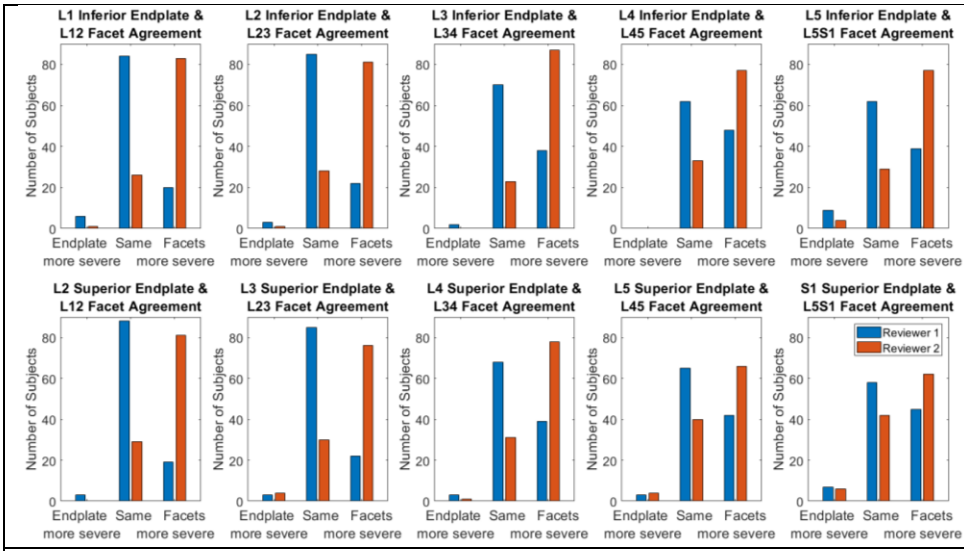

Figure 1. Frequency distribution of more severe endplate osteophytes, same severity of endplate and facet osteophytes, and more severe facet osteophytes at corresponding lumbar levels.

Significance: These findings provide insight into the sequence of bony degeneration in the lumbar spine in individuals with cLBP. Improved understanding of the sequence of bony degeneration may help identify patients for early intervention or targeted treatments.

Acknowledgments: This research is supported by the National Institutes of Health (NIH) through the NIH HEAL Initiative under award number U19AR076725. The content is solely the responsibility of the authors and does not represent the official views of the NIH or its NIH HEAL Initiative.

References: [1] Goode et al. (2013), *Curr Rheumatol Rep* 15(2); [2] Kirkaldy-Willis et al. (1978), *Spine* 3(4); [3] Kong et al. (2009), *Spine* 34(23); [4] Suri et al. (2011), *BMC Musculoskeletal Disorders* 12(202); [5] Deyo et al. (2014). *J. of Pain.* [6] Snodgrass (2004), *J Forensic Sci* 49(3); [7] Pathria et al. (1987) *Radiology* 164(1)

THE FACET JOINTS UNDERGO SEVERE BONY DEGENERATION PRIOR TO THE VERTEBRAL ENDPLATES IN INDIVIDUALS WITH CHRONIC LOW BACK PAIN

Patrick Smith[1*], Cortez L. Brown[1], Clarissa LeVasseur[1], Tom Gale[1], Sabreen Megherhi[1], Emily C. Gray[1], Joseph Shoemaker[1], Caroline Pellegrini[1], Gina McKernan[2], William Anderst[1]
[1]Department of Orthopaedic Surgery, [2]Department of Health Information Management, University of Pittsburgh, Pittsburgh, PA
*Presenting author's email: pss42@pitt.edu

Introduction: Chronic low back pain (cLBP) has been associated with intervertebral disc degeneration, lumbar segmental instability, facet joint osteoarthritis, spondylosis, and osteophyte formation[1]. The process of spinal aging has been documented to progress through a degenerative cascade as outlined by Kirkaldy-Willis[2], however, the sequence of osteophyte development in the lumbar spine of individuals with cLBP remains unclear. Some studies suggest facet degeneration is a precursor to disc degeneration[3], while others contend that degeneration initiates in the anterior structures[4]. The purpose of this study was to determine the sequence of severe bony degeneration in the lumbar spine, represented by osteophyte formation in the facet joints and the vertebral body. Based upon prior studies that provide conflicting evidence, we hypothesized that severe degeneration would occur with equal frequency on the vertebral endplates and on the corresponding facet joints in individuals with cLBP.

Methods: Written informed consent was acquired from individuals with cLBP (defined as low back pain for at least 3 months that persists >50% of the time in the last 6 months[5]), with BMI <35kg/m^2, who were not pregnant, and were able to perform lumbar flexion/extension and lateral bending exercises. Lumbar spine CT scans (resolution: 0.5 x 0.5 x 0.625mm) were obtained in the supine position. Bone tissue from L1 through S1 was segmented from the CT scans using a combination of automated and manual segmentation (Mimics 24, Materialise). Lumbar vertebral body 3D models were then created from the segmented bone tissue. Osteophytes on the endplates were assessed by viewing each 3D bone model; osteophytes on the facets were assessed by viewing the segmented CT scan of each facet joint. Endplates and facets were assessed in a randomized order by two reviewers using customized Matlab code to blind reviewers to the subject and vertebral level. Lumbar endplates were evaluated using a previously reported 0-4 scale[6] by viewing only the vertebral body of the 3D bone model. Facets were evaluated on slices of the segmented CT scan using a previously reported 0-3 scale[7] by viewing only the facet joint. Following grading of individual endplates, the 0 to 4 endplate score was re-categorized such that grades 0 through 2 were category 1 (no to moderate osteophyte growth), while endplate grades 3 and 4 were assigned category 2 (severe to extensive bridging osteophytes). Facet grades were re-categorized in a similar manner such that grades 0 and 1 were category 1 (none to joint space narrowing) and grades 2 and 3 were category 2 (facet hypertrophy to severe osteophyte growth). The frequency distribution of more severe endplate osteophytes (endplate is category 2, facet is category 1) or more severe facet osteophytes (endplate is category 1, facet is category 2) was evaluated using a chi-squared goodness of fit test with an expected frequency of 50% for each condition, with significance set at $p < 0.05$.

Results & Discussion: Data processing is complete for 110 out of 300 participants who have completed testing (64F, 46M; average age 50.6 ± 16.3 yrs.; BMI: 26.4 ± 3.8kg/m^2). The observed frequency of more severe facet osteophytes was greater than the observed frequency of more severe endplate osteophytes for all combinations of endplates and their corresponding facets for both graders (χ^2 from 0.29 to 1.0; all $p<=0.006$)(Figure 1). These interim results suggest that severe bony degeneration in the lumbar spine occurs in the facets prior to the endplates.

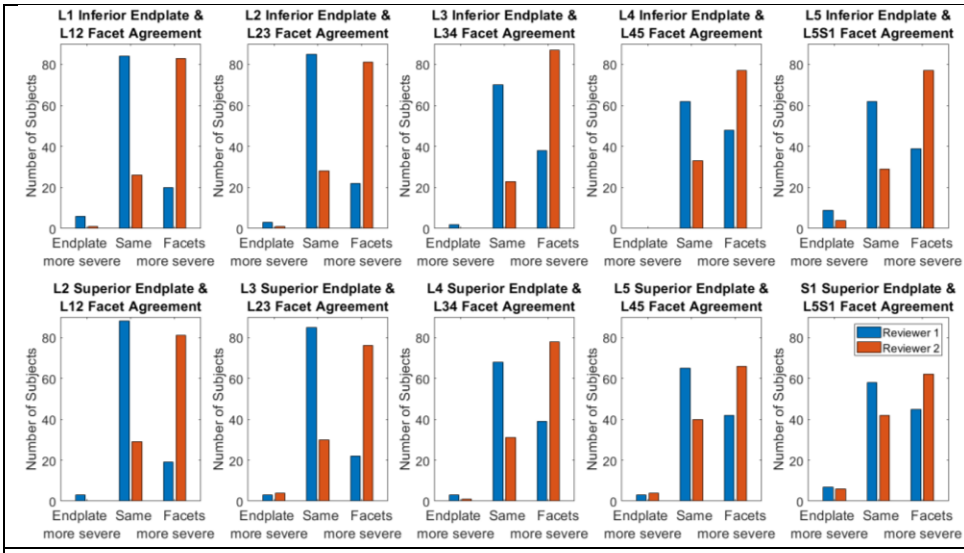

Figure 1. Frequency distribution of more severe endplate osteophytes, same severity of endplate and facet osteophytes, and more severe facet osteophytes at corresponding lumbar levels.

Significance: These findings provide insight into the sequence of bony degeneration in the lumbar spine in individuals with cLBP. Improved understanding of the sequence of bony degeneration may help identify patients for early intervention or targeted treatments.

Acknowledgments: This research is supported by the National Institutes of Health (NIH) through the NIH HEAL Initiative under award number U19AR076725. The content is solely the responsibility of the authors and does not represent the official views of the NIH or its NIH HEAL Initiative.

References: [1] Goode et al. (2013), *Curr Rheumatol Rep* 15(2); [2] Kirkaldy-Willis et al. (1978), *Spine* 3(4); [3] Kong et al. (2009), *Spine* 34(23); [4] Suri et al. (2011), *BMC Musculoskeletal Disorders* 12(202); [5] Deyo et al. (2014). *J. of Pain.* [6] Snodgrass (2004), *J Forensic Sci* 49(3); [7] Pathria et al. (1987) *Radiology* 164(1)

THE SHEAR MODULUS OF THE VASTUS LATERALIS MUSCLE DOES NOT FOLLOW THE RESIDUAL TORQUE ENHANCEMENT IN THE KNEE EXTENSORS

Gustavo H. Halmenschlager[1], Maria C. A. Brandão[2], José C. S. Albarello[2], Thiago T. da Matta[1], Liliam F. de Oliveira[2]
[1]Escola de Educação Física e Desportos, Universidade Federal do Rio de Janeiro, Rio de Janeiro, Brazil.
[2]Programa de Engenharia Biomédica, Universidade Federal do Rio de Janeiro, Rio de Janeiro, Brazil
*Corresponding author's email: liliam@peb.ufrj.br

Introduction: Passive residual torque enhancement (RTEpass) is the increase in the passive steady-state torque capacity of a muscle group after an isometric contraction preceded by an eccentric contraction in comparison to a reference (i.e., purely isometric contraction) at the same joint angle/muscle-tendon unit length [1]. Although the mechanisms underlying this physiological phenomenon are not entirely clear in the literature, the newest scientific studies indicate that the contractile aspects of the musculotendinous unit are the main origin of the increase in the passive force of the skeletal muscle, with this muscle force increase potentially associated with the increase in the stiffness of the titin protein [2]. The shear wave elastography technique by Supersonic Imaging (SSI) is capable of estimating the mechanical properties (stiffness) of biological tissue in real-time in a non-invasive assessment [3]. Stiffness is estimated through the shear modulus (μ), calculated by the measurement of shear wave propagation speed in the medium (c_s), considering tissue density (ρ) as a constant ($\mu = c_s^2 * \rho$). For the vastus lateralis (VL) muscle, the technique is valid and reliable (ICC: 0.95) [3,4]. In this work, we applied SSI elastography to estimate the stiffness of the VL muscle concomitant with the acquisition of passive torque from the knee extensors. The objective of the study was to correlate the Δμ of the VL muscle and the RTEpass of the knee extensors under the RTEpass protocol.

Methods: The passive torque of 20 healthy young participants was evaluated at a joint angle of 100° of knee flexion (0° = extended knee) for pure isometric contractions (control protocol) and during the isometric contractions preceded by an eccentric contraction (from 70° to 100°). Elastographic videos of the VL were acquired immediately before and after both protocols and at the same joint angle, with the muscle relaxed, confirmed by EMG. Passive torque and μ variables were considered as the mean values during a time period of 10s for the pre-test and 20s for the post-test moments. The RTEpass of the knee extensors was calculated as the absolute mean difference between the protocols. The Δμ of the VL muscle was considered the normalized mean difference between the protocols. The Student T test and Wilcoxon test were applied to assess whether RTEpass and Δμ were observed between protocols. Spearman's correlation coefficient (*r*s) was applied between RTEpass and Δμ.

Results & Discussion: In agreement with some previous studies, the RTEpass of the knee extensors was identified in the present study, indicating an increase in passive forces. The comparison between protocols showed a mean RTEpass of 1.03 ±0.3 Nm ($P < 0.001$). However, no differences were observed in μ ($P = 0.148$), although a mean increase in μ was observed after the control (6.3%) and experimental (4.7%) protocols. Spearman's analysis indicated that there was a weak correlation and non-significant between RTEpass and Δμ (Fig. 1; *r*s = 0.248; $P = 0.332$). These results imply that differences in VL stiffness, as assessed by the SSI technique, alone cannot account for the RTEpass phenomenon observed in the knee extensors. Although it is known that the SSI technique is reliable to estimate changes in mechanical properties during a submaximal isometric contraction [5,6], it may not have the same sensitivity to detect the difference in passive torque between the protocols tested in this study. The μ measure showed excellent reliability and CV lower than the TorqPass variable (μ - CV: 0.27%; ICC: 0.999; CI: 0.997–1.000; TorqPass - CV: 1.14%; ICC: 0.999; CI: 0.996–1.000). *In vitro*, passive torque enhancement is addressed to titin stiffness configuration, within the muscle fibre. In our *in vivo* study, however, SSI elastography, solely from VL, showed not to be sufficient to characterize the RTEpass.

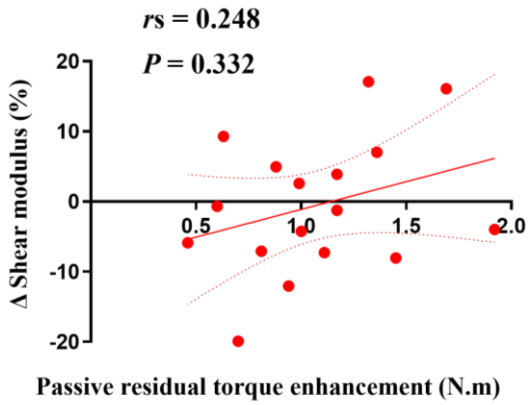

Figure 1: Individual participants data (three outliers), linear regression line (solid line) and 95% confidence interval (dashed lines) for the variables passive residual torque enhancement and shear modulus delta.

Significance: The variation in passive knee extensor torque between the control and experimental protocols is not related to the changes in the mechanical properties of the vastus lateralis muscle, as measured by shear wave elastography of SSI type. Future studies that address the SSI technique in the context of RTE should analyse all quadriceps muscles as well as the patellar tendon, which may reveal a relation between RTEpass and different tissue stiffness changes.

Acknowledgments: Fundação de Amparo à Pesquisa do Estado do Rio de Janeiro FAPERJ; Conselho Nacional de Desenvolvimento Científico e Tecnológico CNPq; Fundação Coordenação de Aperfeiçoamento de Pessoal de Nível Superior CAPES; and Financiadora de Estudos e Projetos FINEP.

References: [1] Hahn et al. (2007) Eur J Appl Physiol 100(6); [2] Leonard & Herzog (2010) Am J Physiol Cell Physiol 299(1); [3] Genisson et al. (2013) Diag Intervent Imag 94(5) [4] Coombes et al. (2018) Eur J Appl Physiol 118(1); [5] Ateş et al. (2015) J Electromyogr Kinesiol 25(4); [6] Otsuka et al. (2019) J Electromyogr Kinesiol 45.

INCREASED FOOTWEAR STIFFNESS REDUCES ESTIMATED SOLEUS METABOLIC COST IN WALKING

Daniel J. Davis[1*], Samuel F. Ray[2], Jason R. Franz[3], and Kota Z. Takahashi[1]
[1]Department of Health & Kinesiology, University of Utah, Salt Lake City, UT
[2]Northwestern University Prosthetics-Orthotics Center, Northwestern University, Evanston, IL
[3]Biomedical Engineering, UNC Chapel Hill and NC State University, Chapel Hill, NC, USA
*Corresponding author's email: Daniel.J.Davis@utah.edu

Introduction: Advances in footwear technology have successfully improved the metabolic cost of human gait [1]. A recent study [2] indicated that the metabolic energy consumption benefits of increased footwear longitudinal bending stiffness via carbon fiber shoe insoles are walking speed specific (10% increase at 1.25 m/s, 7% reduction at 2.0 m/s). Previous studies on carbon fiber enhanced footwear have reported changes in ankle, knee, and hip joint mechanics, but these changes have not provided definitive explanations for the observed speed-specific changes in whole-body metabolic energy consumption. The mismatch between measured joint mechanics and whole-body metabolic energy consumption likely arises due to complexities in regulating lower-limb muscle-tendon-unit (MTU) behavior. While it is not yet feasible to directly measure the metabolic energy consumed by individual muscles *in vivo*, bioenergetic modeling can provide key insights [3,4]. The purpose of the present study was thus to estimate the effects of increased footwear longitudinal bending stiffness and gait speed on the metabolic energy consumed by the largest ankle plantarflexor muscle (i.e., the soleus), and to compare these model-based estimates with measured whole-body metabolic cost.

Methods: Motion capture, cine B-mode ultrasound, whole-body metabolic cost, and electromyography data from 14 participants (12M/2F, 23 ± 2.1 yrs, 177.7 ± 7.1 cm, 76.5 ± 13.0 kg) were reanalyzed to estimate soleus metabolic cost of transport (MCoT [W/kg/m]) [2]. Participants walked on an instrumented treadmill at 1.25, 1.75, and 2.0 m/s wearing standardized shoes. At each speed, participant's shoes had either no carbon fiber insole (low stiffness), a 1.6 mm thick insole (medium stiffness), or a 3.2 mm thick insole (high stiffness).

Soleus MCoT was estimated using experimentally derived fascicle length, velocity, force, and muscle activation input into two commonly used bioenergetics models [3,4]. Fascicle force was derived from estimated Achilles tendon force partitioned based on muscle cross section [2]. The longest fascicle length in the 1.25 m/s, low stiffness condition was considered the optimal fascicle length, given that the soleus operates on the ascending region of the force-length curve [5]. A sensitivity analysis for assumed participant optimal fascicle lengths verified that the present analysis results were not specific to the parameter selected. Statistical differences in soleus MCoT were examined using a two-way (stiffness, speed) repeated measures analysis of variance ($\alpha = 0.05$).

Results & Discussion: The two metabolic energy models produced the same stiffness and speed×stiffness trends; therefore, the results from [4] are presented, with each MCoT expressed as a proportion of the MCoT in the low stiffness, 1.25 m/s condition for visualization (i.e., Fig. 1). Significant main effects ($p < 0.001$) of speed and stiffness were found on estimated soleus MCoT. Estimated soleus MCoT increased with faster gait speed and decreased with stiffer footwear (Fig. 1B). For example, carbon fiber insoles reduced the estimated soleus MCoT by 17.6% on average across stiffness and speed conditions. The reduction in soleus MCoT with increasing footwear stiffness was primarily due to slower fascicle shortening velocities and occurred despite increased peak fascicle forces [2]. The match between measured whole-body and estimated soleus metabolic cost at only the fastest speed (i.e., a metabolic benefit of added stiffness) may be explained by a speed-dependent contribution of individual muscle groups to whole-body metabolic cost. Indeed, Sawicki & Ferris [6] argued that the ankle plantarflexor muscles consume a higher proportion of the total metabolic cost at faster walking speeds. This is in line with *in vivo* and modeling studies that indicate that muscle (compared with in-series tendons) performs a larger proportion of MTU work with increasing walking speed [7,8]. Future analyses should extend this bioenergetic modeling approach to other major muscles to identify the joint- and muscle-specific loci of MCoT benefits/penalties with increased footwear stiffness.

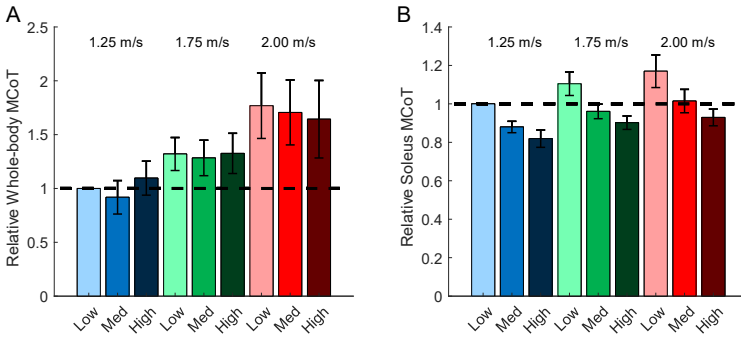

Figure 1: Influence of footwear stiffness (Low, Med, and High) and walking speed on whole-body (A) and soleus (B) metabolic cost of transport (MCoT) as a proportion of the cost in the low stiffness, 1.25 m/s condition. Data in panel A are reproduced from [2].

Significance: The large decrease in soleus metabolic energy consumption with stiffer footwear indicates that other muscles (e.g., crossing the hip and/or knee) are likely shouldering a higher metabolic burden with increased footwear stiffness at typical walking speeds. However, large reductions in estimated soleus energy consumption and increased peak soleus force suggest a mechanism by which those with disproportionate plantarflexor muscle deficits stand to benefit from increased footwear bending stiffness. These insights are crucial for the future design of joint- and task-specific assistive devices aimed at improving human mobility.

Acknowledgments: This work was supported by NIH award R01AR081287 awarded to KZT and JRF.

References: [1] Hoogkamer et al., 2018. *Sports Med* 48(4). [2] Ray & Takahashi, 2020. *Sci Reports* 10(1). [3] Bhargava et al., 2004. *J Biomech* 37(1). [4] Umberger, 2010. *J Roc Soc Interface* 7(50). [5] Rubenson et al., 2012. *J Exp Biol* 215(20). [6] Sawicki & Ferris, 2009. *J Exp Biol* 212(1). [7] Sasaki & Neptune, 2006. *Gait Posture* 23(3). [8] Lai et al., 2015. *J Appl Physiol* 118(10).

ERROR INDUCTION TO IMPROVE MOTOR PERFORMANCE AND INCREASE EEG THETA BAND POWER DURING A REHABILITATIVE TRAINING TASK

Sophie Dewil[1*], Yu Shi[1], Raviraj Nataraj[1]
[1] Department of Biomedical Engineering, Stevens Institute of Technology, Hoboken, NJ, USA
*Corresponding author's email: sdewil@stevens.edu

Introduction: After a neurological trauma, such as a spinal cord injury (SCI) or a stroke, affected individuals undergo energy-consuming and time-intensive physical rehabilitation [1]. However, functional outcomes are often marginal, prompting the need for research to optimize therapy processes further [2]. Previous research has highlighted the beneficial role of errors in learning cognitively-intensive tasks, whereby a person will positively re-evaluate their approach to a problem based on experiencing the error. As such, a person assumes brain states primed for improved performance compared to when no information about errors is presented [3]. In this study, participants completed a series of reaching tasks in a virtual reality (VR) environment and received visuomotor rotation manipulations to induce experiences of error during training. We then assess subsequent motor performance and verify changes in neurological patterns (theta band power) associated with error detection [4]. As such, we hypothesized that systematic and purposeful presentation of movement errors during training would further improve subsequent performance of a motor task.

Methods: Neurotypical participants (n = 3) wore a 64-channel scalp-surface cap for EEG recording (USBamp g.tec). Marker-based motion capture (Prime17W, Optitrack) tracked the position and orientation of the participant's reaching hand (Fig. 1, left). The marker data drove the motion of a virtual arm in a custom digital environment (Unity) displayed to the participant on a large (40 in) flat-screen (Roku Select Series HDTV) placed directly in front of them. During training, participants reached toward target spheres (designated by color cues) positioned in one of 8 directions (Fig. 1, right) and received positive feedback upon successful reaches. Participants were randomly assigned to one of two training groups: 1) control (no error movements presented) and 2) error (error movements presented in 30% of trials). Participants experienced an error when they observed the virtual hand moving at a visuomotor distortion (rotation) relative to their actual hand motion, leading to a failed reach. Before and after training, participants completed testing trials involving various directional reaches, including curves to the right and left. The primary motor measure of interest (i.e., reaching pathlength) was assessed and compared between trials before and after training to infer the impact of training.

Figure 1 Experimental setup showing performance of reaching task (left) and VR training environment (right)

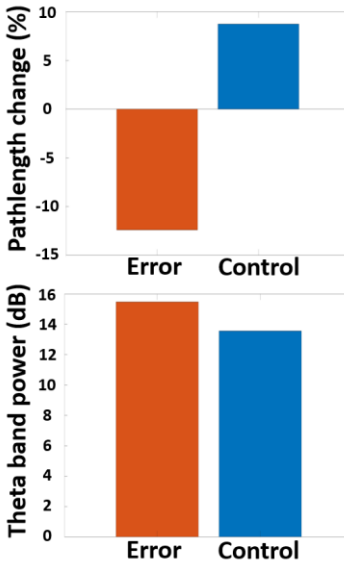

Figure 2: Percentage change in pathlength after training for error and control groups (top); theta band power in error vs. control trials

Results: Motor performance after training improved (i.e., mean pathlength was reduced) with the error group but worsened with the control group (Fig. 2, top). Theta band power was significantly higher during training among participants in the error group than the control group ($p = 0.0012$) (Fig. 2, bottom).

Discussion: Pathlength has been previously used as a reliable performance marker for efficient movement control [5]. This study suggests that systematically introducing errors during training can support better motor performance outcomes [3]. We verified the neurological impact of introducing errors during training by observing significantly higher theta band power with error trials as expected [4]. In this study, we postulate that imposing errors encouraged participants to assume a heightened neural awareness of movement strategies that persisted even after training. While error-based training constructs have been well-validated in cognitive learning tasks [6], our preliminary results encourage expanding their use with motor training.

Significance: Findings from this study motivate further consideration of inducing error-related neurological responses for supporting greater gains in motor function with rehabilitative training. This research aims to support the development of novel rehabilitation techniques that are broadly applicable to clinical populations with motor dysfunction. Although making errors is natural to learning processes, purposefully inducing them to accelerate learning is inherently counterintuitive. However, leveraging the notion that the brain is primed to enter phases of enhanced performance primarily due to the experience of errors deserves further exploration, for rehabilitation applications and beyond.

Acknowledgments: The authors acknowledge support from the Schaefer School of Engineering and Science at Stevens Institute of Technology, NSF CAREER award 2238880, and the Stevens Provost Doctoral Fellowship.

References: [1] Maclean N. et al., Soc. Sci. Med. 1982; 50 [2] Spooren et al., JRM. 2009;41(7) [3] Steib S. et al., Neurorehab. Neur. Repr. 2017; 31(8) [4] Dias C. et al, PeerJ. 2022; 10 [5] Sanford S. et al., Front. Virtual Real. 2022; 3 [6] Falkenstein M.et al., Electroencephalogr. clin. neuro-physiol. 1991; 78(6)

IDENTIFYING RIGHT AND LEFT IMPACT DURING LEVEL AND GRADED RUNNING USING A SACRUM-MOUNTED IMU

Aida Chebbi [1*], Rachel Robinson [1], Seth Donahue [2], and Mike Hahn [1]
[1]University of Oregon, Eugene OR 97403, USA
[2]Northwestern University, Chicago IL 60611, USA
*Corresponding author's email: achebbi@uoregon.edu

Introduction: Gait analysis is crucial in various fields such as sports science, rehabilitation, and clinical diagnostics [1]. Traditional methods often involve complex setups with multiple sensors, cameras, force plates, and instrumented treadmills, which can influence natural movement patterns. However, the advent of wearable sensors, particularly inertial measurement units (IMUs) [2], has revolutionized gait analysis by offering an affordable and practical alternative to traditional three-dimensional motion capture systems while maintaining comparable accuracy in monitoring running kinetics and kinematics. Wada et al. [3] demonstrated that pelvic orientation can vary significantly between the right and left leg support phases during running. To account for this, three sacrum/low-back placed IMU methods have been previously proposed to identify the side of impact (right or left) with the ground. A recent study by Kiernan et al. [4] reproduced these three methods and evaluated their accuracy in identifying the side of ground contact. The study found that the Lee [5] method was the most accurate, correctly identifying the impact side 81.9% of the time. However, these methods were only tested on level ground track and treadmill conditions. There remains a need for a more accurate method, especially for outdoor running scenarios, where the grade can differ from level ground and the rhythm can be disrupted by unexpected events such as tripping, falling, or slowing down due to obstacles, changes in terrain, or fatigue. In response to this need, as part of a broader effort to identify right and left gait events using a single wearable device (IMU) placed on the sacrum, this study was performed not only on level ground but also in incline and decline conditions. The purpose of this work is to detect the side-specific impact of the right and left legs, reducing the number of sensors traditionally needed for running assessment, thus enhancing user comfort and convenience especially in competitive events such as the marathon. Furthermore, this study will compare the presented method with previously documented methods [4], as well as with previous method developed our research team [2].
In this work, we hypothesized that the new method will be more accurate in identifying right and left side impacts. This could lead to the development of targeted training programs to improve performance and reduce the risk of injury. This work is a substantial step towards a more comprehensive and accurate method for running gait analysis.

Methods: Ten healthy recreational runners (7 F, 25.5±8.2 yrs) were equipped with an IMU (Casio, JPN) on the dorsal aspect of each foot and at the sacrum. The foot-mounted IMUs were used only as a ground truth, to confirm the impact side. Participants ran thirteen trials on a force instrumented treadmill (Bertec, Columbus, OH), at three different grades: level ground (LG; 0 degrees), incline (IN), and decline (DE) at ±7.5 degrees. . The range of speeds run by participants was 3.16-4.88 m s^{-1} based upon each participant's most recent 5k race pace The new approach uses the peaks of the third derivative of the sacral IMU resultant acceleration (a_{mag}), referred to as 'crackle,' to find the first peak in a_{mag} within a 10 ms window during each impact, then, the corresponding sacral angular velocity ω_y peak was found. If ω_y was a maxima, then the a_{mag} peak was deemed a right side impact. If ω_y was a minima, then the a_{mag} peak was deemed a left side impact. The peak selection can be observed in Figure 1.

Results & Discussion: In comparison to other methods, this study demonstrated better accuracy in identifying the side of ground impact during running on level ground (LG). The mean accuracy was 99.2%. This result is a large improvement over the methods reproduced by Kiernan et al. [4], who reported accuracies ranging from 54.6 to 81.9%. The method also performed well in decline and incline conditions with mean accuracy of 99.8% and 90.8% respectively.

Significance: The novel algorithm developed in this study enhances the capabilities of the single IMU by employing the 'crackle' function, the third derivative of linear acceleration. This function effectively captures the initial peak in acceleration data, a critical aspect of the running cycle often overlooked by other methods. Furthermore, the algorithm incorporates angular velocity data to confirm whether the identified peak in resultant acceleration corresponds to a right or left foot impact. Future work aims to improve the ability to accurately identify gait events using sacral IMU data, enhancing our understanding of running mechanics and the general utility of this method. This will allow for a more in-depth study of running biomechanics across various terrains, ultimately helping to prevent and manage running-related injuries.

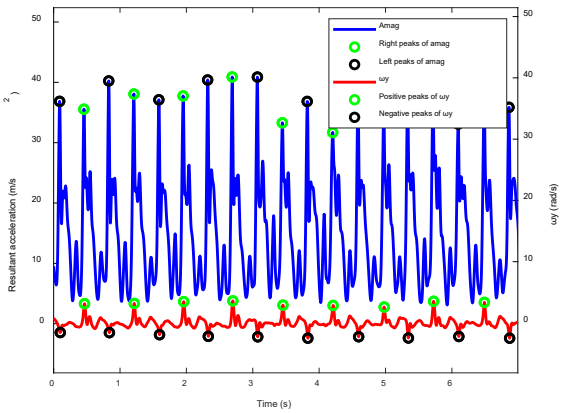

Figure 1: Right and Left impact identification during level running from resultant linear acceleration a_{mag}, confirmed using the maximum and minimum sacral angular velocity ω_y.

Acknowledgments: This work was partially supported by Casio. Additional support was provided by the Wu Tsai Human Performance Alliance and the Joe and Clara Tsai Foundation.

References: [1] Smith et al. (2018), *J Biomech* 25(4); [2] Chebbi et al. (2023), *ISB JSB*; [3] Wada et al. (2020), *In Proceedings* 2020 49(1) ; [4] Kiernan et al. (2023), *Sensors* 23.; [5] Lee et al (2012) J. Sci. Med. Sport 13, 270–273.

EVALUATION OF PROPULSION BIOMECHANICS DURING EXERCISE WITH A SUSPENDED-WHEEL EVERYDAY WHEELCHAIR

Griffin C. Sipes[1], Ian Rice[2], Mariana E. Kersh[1,3,]
[1]Department of Mechanical Science and Engineering, University of Illinois Urbana-Champaign, Urbana IL
[2]Department of Kinesiology and Community Health, University of Illinois Urbana-Champaign, Urbana, IL
[3]Beckman Institute for Advanced Science and Technology, University of Illinois Urbana-Champaign, Urbana, IL
gsipes2@illinois.edu

Introduction: The risk for developing cardiovascular disease and metabolic syndrome is increased by 50% in persons with spinal cord injuries (PwSCIs), compared to age-matched, able-bodied counterparts, due to a lack of physical activity [2]. PwSCIs are also at increased risk of upper limb pain and injury, which impacts quality of life. Rotator cuff injuries have an incidence rate of up to 98% for tendinopathy and 68% for tears [2]. It is critical to identify exercise options for improving cardiovascular health that do not contribute to or exacerbate upper limb strain. Moreover, accessibility continues to be a challenge for manual wheelchair users with specialized equipment often being costly and most gyms having limited choices for wheelchair users. One underexplored option is the conversion of an everyday wheelchair to a three-wheeled system via the use of a cost-effective, commercially available attachment (FreeWheel) that is designed to enable more options for manual wheelchair-based exercise. The device is a large, inflated wheel that attaches to the footrest of a standard wheelchair, raising the front caster wheels off the ground, and lengthening the wheelbase. Due to the increased wheelbase [3], we hypothesized that a suspended-wheel wheelchair (S-EW) would lower the musculoskeletal loading on the shoulder during physical activity. While not a direct measure of shoulder loads, the hand reaction forces are a useful proxy measure of arm loading. Therefore, the aim of this study was to compare the propulsive forces during exercise in an everyday wheelchair (EW) to the forces when using an S-EW.

Methods: Four able-bodied participants completed an intensity-matched, MWP-based exercise protocol on an overground level surface using both an EW and an S-EW. An instrumented wheel (SmartWheel) was mounted on the right wheel to measure six-degree-of-freedom loads applied to the handrim. An inactive SmartWheel was used on the left wheel to balance weight. The exercise protocol consisted of 5 minutes of moderate-intensity manual wheelchair propulsion (50% heart rate reserve (HRR) target). The 50% HRR target was calculated by measuring resting heart rate on the day of the protocol and estimating maximum heart rate ($HR_{max} = 216.6 - 0.84 \times age$) [4]. Percent HRR was calculated as: $\%HRR = \%Intensity \times (HR_{max} - HR_{rest}) + HR_{rest}$ [5]. Propulsion statistics of each push cycle were extracted and included: average and peak total and tangential force, peak negative tangential force, cadence, mechanical effectiveness, and speed. Metrics were averaged over every push cycle in the exercise protocol and analyzed using paired t-tests in Python.

Results & Discussion: Of the propulsion metrics, there was a moderate decrease in both peak tangential and total forces applied to the handrim (Fig 1). Tangential forces, which are the only forces that contribute to forward motion, during S-EW propulsion were 16.7% lower than EW. Similarly, the peak total applied force was 12.5% lower with an S-EW. While there was not sufficient statistical power to yield significant differences, the decreases in tangential and total force between activities at the same speed suggest that an S-EW may enable participants to achieve similar speeds with lower applied forces compared to a manual wheelchair alone. There were no notable trends or differences between exercise modes for the remaining propulsion metrics (Table 1). Further study with more participants, including wheelchair users, is needed to confirm these results.

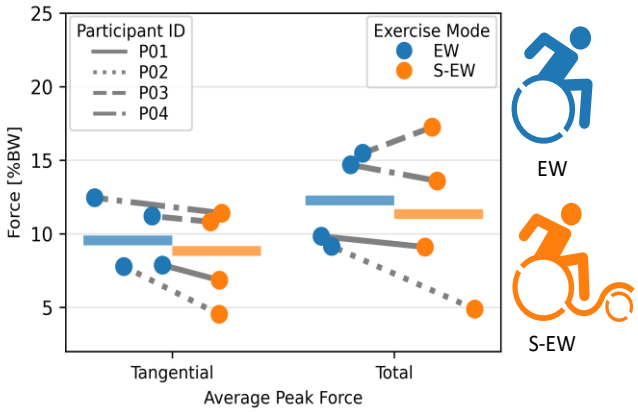

Figure 1: Mean peak handrim forces during exercise. EW and S-EW exercise modes shown in blue and orange, respectively, with median bars. Participants shown in different line styles.

Significance: This is the first study to demonstrate the potential biomechanical benefits of using a suspended wheelchair attachment and provides promising options for the use of an S-EW for engaging in physical activity. Identifying optimal modes of exercise for persons with spinal cord injuries remains a priority to improve cardiovascular health.

Acknowledgments: We would like to thank the National Science Foundation and the De Luca Foundation for supporting this project.

References: [1] Myers+ *Am J Phys Med Rehabil* 2007; [2] Jahanian+ *J Spinal Cord Med* 2022; [3] Dennison+ RESNA Conference Proceedings (2011). [4] Fox+ *Ann Clin Res* (1971); [5] Nobel+, ACSM (2018).

Table 1: Metrics for EW and S-EW exercise modes. Values shown are Mean (SD).

	Peak Tangential Force [%BW]	Peak Total Force [%BW]	Avg. Speed [m/s]	Cadence [pushes/min]	Mechanical Effectiveness [%]	Avg. Heart Rate Reserve [%]
EW	9.8 (2.0)	12.3 (2.8)	1.3 (0.5)	56.9 (16.2)	78.3 (5.9)	48.3 (5.3)
S-EW	8.4 (2.8)	11.2 (4.7)	1.2 (0.3)	45.7 (14.1)	76.2 (9.3)	50.0 (2.0)

RELATION OF BMI TO POSTURAL CONTROL AND GAIT AMONG SPECIAL OLYMPICS ATHLETES

Kaitlin Briggs[†], Isabel Munoz Orozco[†], Katelyn Warkentien, Haylie L. Miller[*]
School of Kinesiology, University of Michigan
[†] Co-first authors
* Corresponding author's email: MillerHL@mich.edu

Introduction: Postural control and gait support independence and safety during daily living activities. Atypical or inefficient postural control or gait can increase the risk of falls or injury, particularly for people with sensorimotor processing differences. People with neurodevelopmental conditions (NDCs) and intellectual disability (ID) show delayed motor development and high heterogeneity in cognitive and motor ability throughout their lifespan [1, 2]. In addition, there are higher rates of both overweight and obesity in people with NDCs or ID [3]. However, there is limited literature on confounding factors such as age and BMI on motor proficiency within these populations. Special Olympics' Healthy Athlete Screening program provides a unique opportunity to assess physical and health-related characteristics of people with NDCs and ID outside of the lab, increasing accessibility of participation. In this study, we assessed differences in the postural control and gait of Special Olympics athletes by BMI classifications (normal, overweight, obese).

Methods: We tested 47 Special Olympics of Michigan athletes (M_{age} = 34.15±14.89 yrs) diagnosed with an NDC or ID. Participants performed a series of motor assessments in a capture volume instrumented with an array of 8 Sony RX0-II cameras with a frame rate of 120 Hz. Here, we focus on performance of a single-leg stance task and over-ground walking along a 4 m path at a self-selected pace. Data were analyzed using Theia3D markerless motion capture software [4]. Outcome measures for single-leg stance included trial duration, lower-limb joint angles, and postural sway. Outcome measures for over-ground walking included step length, stride length, and step width. We used participants' height (M = 164±10.24 cm) and weight (M =198.97±52.84 lbs) to calculate BMI. BMI was classified into four groups: underweight (<18.5), healthy weight (18.5-24.9), overweight (25-29.9), and obese (>30).

Results & Discussion: Preliminary results suggest differences in postural control and gait between BMI classification groups. During single-leg stance, obese participants had a higher rate of loss of balance prior to the end of the trial and more often opted out of attempting a second trial due to discomfort, fatigue, or fear of falling. Hip-hinging compensatory behaviors and use of external supports (e.g., grabbing a nearby chair or the administrator's arm) were more frequent in obese and overweight participants compared to those classified as healthy weight. Planned analysis of torso angle in reference to the pelvis will quantify the degree of hip-hinging behavior for each participant. Overall, results suggest variable postural control strategies and performance among obese individuals within NDC and IDD (Fig. 1). During over-ground walking, we observed similar variability in gait patterns between BMI classification groups. Obese individuals more frequently exhibited a wider gait pattern characterized by increased step width and shorter step length, and observed stiffening at the knee joint. Planned analysis will quantify the degree of knee-stiffening behavior for each participant (i.e., joint angle of the shank in reference to the thigh) to determine if variability exists between BMI classification groups. Wider steps and knee stiffening may reflect an effort to relieve stress on the knee joint for individuals carrying greater body mass [5].

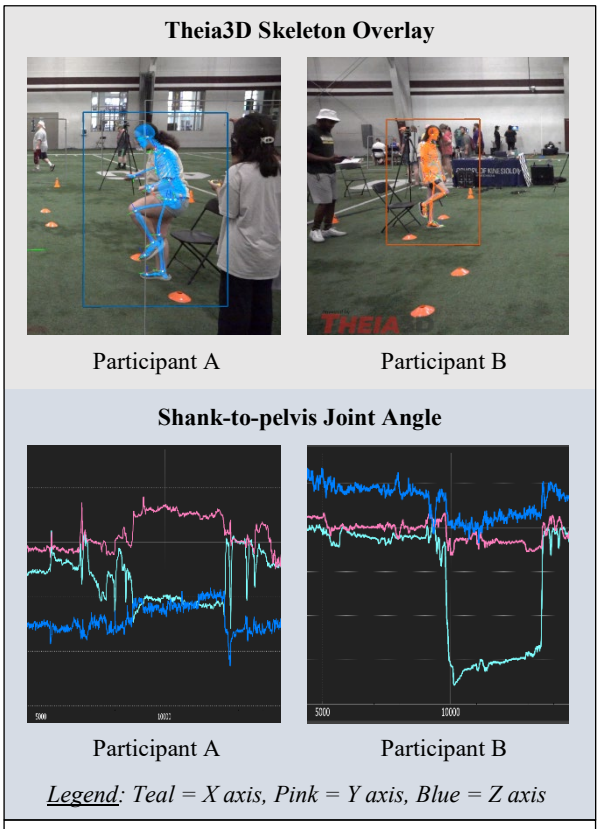

Figure 1. Single-leg stance for two sample participants.

Significance: Atypical postural control and gait can lead to barriers in social participation and healthy levels of physical activity, in turn placing individuals at higher risk of obesity. Motion analysis can inform personalized interventions designed to increase physical activity and reduce risk of negative health outcomes associated with NDCs/ID and obesity [3]. Community-based, non-invasive assessment of postural control and gait can increase access to clinically- and functionally-relevant information, particularly when conducted in high-participation settings like Special Olympics. However, questions regarding the relation between postural control and obesity in NCDs and ID must be resolved. Future research is needed to determine whether general fitness, body composition, or condition-specific atypicality in motor control drives observed behavioral differences in postural control and gait.

Acknowledgments: We thank Special Olympics of Michigan leadership, coaches, and athletes for their time, energy, and enthusiasm. We thank Dr. Leah Ketcheson and Wayne State University students for assisting with event access and logistics. We thank Theia 3D staff for technical support. This research was supported in part by the National Institutes of Health (K01-MH107774).

References: [1] Lum et al. (2020), *Autism Res* 14(4); [2] Almuhtaseb et al. (2014), *Res Dev Disabil* 35(11); [3] Hsieh et al. (2013), *J Intell Disabil Res* 58(9); [4] Moro et al. (2022), *Sensors* 22(5); [5] Powell et al. (2005), *Am J Sport Med* 39(1)

QUANTIFYING STATIC BALANCE FOLLOWING ANKLE SPRAINS USING METRICS OF POSTURAL CONTROL

Caroline Althouse[1], Isaiah McNeilly[1], Paige McHenry, MS, ATC[2], Jamie Morris, PT, DPT, DSc[2], Erin Florkiewicz PhD, ATC[2], Eliot Thomasma PT, DPT, DSc[2], Will Pitt PT, DPT, PhD[3], Michael Crowell DPT, DSc[4], Gregory Freisinger, PhD[1]*
[1] United States Military Academy West Point, [2] Baylor University – Keller Army Community Hospital Division I Sports Physical Therapy Fellowship, [3] Army-Baylor DPT Program, [4] University of Scranton DPT Program
*Corresponding author's email: gregory.freisinger@westpoint.edu

Introduction: Ankle sprains are the most common injury in young athletes and active-duty service members, with an estimated 2 million ankle sprains occurring each year. This results in an annual aggregate healthcare cost of approximately 2 billion dollars [1]. At the United States Military Academy (USMA), from 2005 to 2007, the incident rate of ankle sprains was 58.4 per 1000 person-years [1]. Sprains have the potential to result in Chronic Ankle Instability (CAI) that can impact performance, increase the risk of a subsequent sprain, and result in long-term pain [2]. USMA cadets who had previously sustained an acute ankle sprain were three times more likely to sustain one during Cadet Basic Training compared to cadets with no history of ankle sprains [3]. Quantifying postural stability using center of pressure (COP) is one way to assess performance degradation following lower extremity injury. Linear metrics of COP, such as range in the mediolateral (ML) and anteroposterior (AP) directions, average excursion velocity (VEL), and 95% Ellipse Area (95%EA), have been shown to reliably assess postural control following injury [4]. Identifying quantifiable metrics for detecting ankle sprains is necessary to help physical therapists make informed clinical decisions and prevent patients from being cleared to return to duty before adequate recovery. We hypothesized that linear metrics of postural control would be significantly different pre- and post-rehabilitation and when comparing pre-rehabilitation metrics to a control group. Additionally, we anticipated no difference between participants' post-rehabilitation metrics compared to a control group, which indicates adequate postural control to return-to-duty.

Methods: The population used for the study included 42 participants from the United States Military Academy. 22 participants had a lateral ankle sprain (5f:17m, 20.6 ± 1.9 years, 1.72 ± 0.07 m, 80.6 ± 14.9 kg), and 20 were healthy controls (5f:15m, 20.8 ± 1.3 years, 1.73 ± 0.8 m, 81.4 ± 15.9 kg). Participants with ankle sprains underwent data collection before (PRE) and after 4 weeks of rehabilitation (POST), while controls (CONT) conducted a single session. Participants executed three single-leg static balancing assessments on a force plate as part of a modified Balance Error Scoring System evaluation (mBESS). Participants attempted to maintain static balance for 10 seconds on their involved and uninvolved legs with their eyes closed. 39 out of 374 trials were discarded as participants were unable to maintain static balance for greater than 5 seconds. The data was filtered using a 4th-order lowpass Butterworth filter with a cutoff frequency of 5 Hz. The range of each trial is calculated by finding the difference of the extrema in the mediolateral (ML) and anteroposterior (AP) directions. The velocity (VEL) was calculated by finding the ratio of the path length to the trial's recording time. The 95% confidence ellipse area (95%EA) was calculated using the Least Squares Criterion to estimate the best fit of an ellipse for each participant's COP [5]. A paired t-test was used to determine the differences between the PRE and POST sessions, while PRE and POST were compared to the control group using unpaired t-tests. The significance level was set at $\alpha < 0.05$.

Results & Discussion: Significant differences were found between PRE and POST for ML ($p = 0.03$), AP ($p = 0.02$), VEL ($p = 0.01$), and 95%EA ($p = 0.01$) as hypothesized. Significant differences were also observed between the PRE and CONT groups in ML ($p < 0.01$), AP ($p < 0.001$), and 95%EA ($p = 0.02$). Significant differences were found between the POST and CONT for AP ($p = 0.02$) and a trend towards significance in 95%EA ($p = 0.06$). There is no significant difference in VEL between PRE and CONT ($p = 0.53$) or POST and CONT ($p = 0.11$).

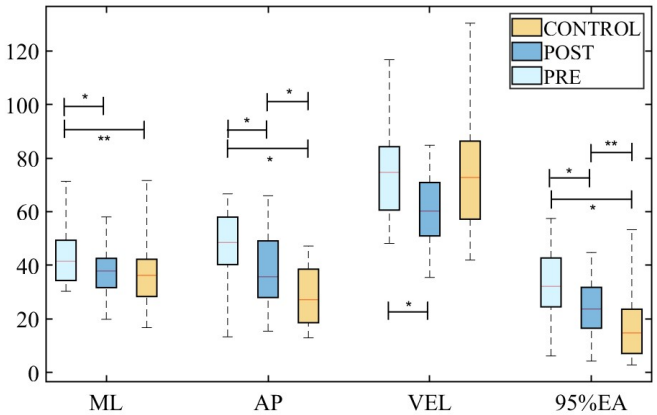

Figure 1: Means and Standard Deviation for Injured Leg Pre- and Post-rehabilitation and Controls. * Indicates $p < 0.05$, ** Indicates $p < 0.10$. Y-axis units: mm, mm/s, 10^{-2}*mm^3

Significance: Measuring linear metrics of COP is a valid metric for detecting the presence of an ankle sprain and monitoring return-to-duty (RTD) status. The average time between sessions 1 and 2 was 32 days, and the average RTD time was 39 days. After 4 weeks of rehabilitation, there was still a significant difference between in AP and EA metrics between those recovering from a lateral ankle sprain and healthy controls. These results demonstrate that individuals being considered for RTD may still have certain deficits in function. More research is required to understand changes in postural control following lateral ankle sprain injury and identify quantitative metrics related to risk of future injury.

Acknowledgments: This work was funded by the Telemedicine and Advanced Technology Research Center at the U.S. Army Medical Research and Development Command through the Advanced Medical Technology Initiative (Award Number W911QY-16-A-0014)

References:[1] Waterman, AJSM, 2010. [2] Waterman, JBJS, 2010. [3] Kucera, NLM, 2016. [4] Prieto, TBME, 1997 [5] Gander, Stanford, 1994.

EFFECTS OF INSTRUMENTED HOSPITAL BED ON PHYSICAL LOADS AT A DISC BETWEEN L5 AND S1 VERTEBRAE DURING PATIENT REPOSITIONING

Seyoung Lee[1], Kitaek Lim[1], Jongwon Choi[1], Junwoo Park[1], Woochol Joseph Choi[1*]
[1]Injury Prevention and Biomechanics Laboratory, Dept of Physical Therapy, Yonsei University, South Korea
*Corresponding author's email: wcjchoi@yonsei.ac.kr

Introduction: Lower back pain/injury are common in healthcare providers, and patient care involving repetitive movements (flexion, extension, bending and rotation of the trunk) is considered a primary risk factor of the lower back injuries [1]. In particular, physical loads at the lower back during patient repositioning on bed may be large enough to cause such injuries. In this study, we have characterized physical loads at a disc between L5 and S1 to assess biomechanical benefits of an instrumented hospital bed, which designed to help alleviate the physical stress during patient repositioning on bed.

Methods: Fourteen individuals (6 males, 8 females) repositioned a patient lying on an instrumented hospital bed, which featured with automated tilting functions to help decrease caregivers' physical stress during patient repositioning (JINB-1000, Jeongin Ens, Gyeonggi-do, Koera) (Figure 1). Trials were acquired for three common types of repositioning (boosting superiorly, pulling laterally, and rolling from supine to sidelying). Trials were also acquired with two bed heights (10 cm and 30 cm below individual's ASIS), and with and without the help of the bed feature (manual versus tilt-assisted). During trials, kinematics of an upper body and hand pulling forces were recorded through motion capture cameras (Vero v2.2, VICON, Oxford, UK) and a load cell (SB-100L, CAS Scale Korea, Seoul, Korea) attached to the linen underneath the patient, respectively.

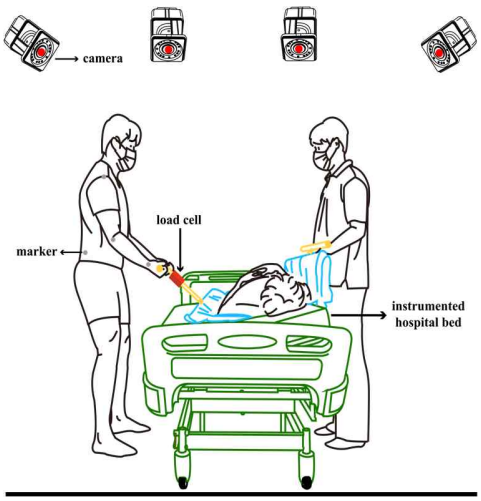

Figure 1: Patient repositioning.

The centre of gravity of body segments and joint centres were acquired from anthropometric data [2] and calculated based on a 6-segment model [3], respectively. Furthermore, a disc centre was determined at about 95.9 mm and 92.6 mm anterior to the L5 marker for males and females, respectively, considering the thickness of soft tissue and diameter of a disc and spinal canal [4,5,6].

Outcome variables included the peak compressive and shear force. Repeated measures ANOVA was used to test if the outcome variables were associated with repositioning type (3 levels), bed height (2 levels), and repositioning method (2 levels) with a significance level of alpha = 0.05.

Results & Discussion: The peak compressive force ranged from 951 N to 3,264 N, and was associated with type ($F = 11.4$, $p < 0.005$) and height ($F = 41.4$, $p < 0.005$), but not with method ($F = 0.8$, $p = 0.37$) (Table 1). Similarly, the peak shear force ranged from 46 N to 389 N, and was associated with type ($F = 3.9$, $p = 0.03$) and height ($F = 29.5$, $p < 0.005$), but not with method ($F = 0.009$, $p = 0.92$).

Significance: Our results suggest that the instrumented hospital bed we tested in this study does not provide biomechanical benefits to reduce physical loads at L5/S1 during patient repositioning on bed.

Acknowledgments: This research was supported, in part, by the Transitional Research Program for Care Robots funded by the Ministry of Health & Welfare, Republic of Korea (HK21C0008) and by "Regional Innovation Strategy (RIS)" through the National Research Foundation of Korea (NRF) funded by the Ministry of Education (MOE) (2022RIS-005).

References: [1] Yassi & Lockhart (2013), *Int J Occup Environ Heath*. [2] Winter (2009), *Biomechanics and Motor Control of Human Movement*. [3] Vaughan (1992), *Dynamics Of Human Gait*. [4] Griffith et al. (2016), *Quant imaging Med Surg*. [5] Mahmoudi et al. (2020), *J Neuroimaging*. [6] Tunset et al. (2013) *Chiropractic & manual therapies*.

Table 1: Average values of outcome variables.

		Peak compressive force (N)		Peak shear force (N)	
		mean	se	mean	se
Repositioning method	Manual	1890.9	92.3	192.1	13.1
	Tilt-assisted	1864.9	97.2	191.5	13.3
Repositioning type	Boosting superiorly	2055.7	107.8	205.8	13.8
	Pulling laterally	1731.8	87.9	188.1	13.8
	Rolling from supine to sidelying	1844.7	108.5	181.3	14.1
Bed height	High	1806.1	87.7	166.2	10.7
	Low	1948.7	100.8	217.3	16.1

MAXIMIZING PRACTICE WHILE AVOIDING PROTECTIVE STRATEGIES: ARE MORE FREQUENT BALANCE DISRUPTIONS BETTER FOR LEARNING REACTIVE BALANCE?

Xenia Schmitz[1*], Francis M. Grover[2], Anna Shafer[3], Madison Lang[1], Keith E. Gordon[2, 3]
[1]Department of Biomedical Engineering, Northwestern University, McCormick School of Engineering, Evanston IL 60208
[2]Physical therapy and Human Movement Sciences, Northwestern University, Feinberg School of Medicine, Chicago, IL 60611
[3]Research Service, Edward Hines Jr. VA Hospital, Hines, IL 60141
*Corresponding author's email: xeniaschmitz2024@u.northwestern.edu

Introduction: Reactive balance (the ability to detect and respond to specific unexpected disruptions) can be improved through training that enhances the ability to rapidly detect a balance disruption and then generate an effective motor response [1]. Motor learning literature suggests that improvements in performance are proportional to practice [2]. Therefore, to maximize training experience within a fixed intervention time, unexpected balance disruptions should be frequent. However, research also finds that frequent unexpected disruptions promote reliance on general protective strategies (preplanned movements anticipating disruptions such as systemic modulations in step width) that can inhibit learning reactive balance [3]. If protective strategies are adopted, continued exposure to unexpected balance disruptions will not have the desired training effect because protective strategies will reduce the intensity of any balance disruption and thus, reduce the quality of practice. *We hypothesized improvement in reactive balance would be greatest when unexpected balance disruptions are less frequent.* We anticipated this improvement would be because infrequent unexpected balance disruptions would allow reactive balance practice without inducing general protective strategies during training.

Methods: Twenty healthy adults (25 +/- 4.9 years, 20 females) each performed 230 discrete stepping trials, stepping from a standing position to a projected end target 1.5 leg lengths ahead. Participants always stepped with their right leg first. A cable-driven robot (Fig. 1A) was used to apply a left lateral force to the pelvis on select trials. Participants were not informed if forces would be applied. All participants first performed 10 **baseline** trials (null field, Fig. 1B). Participants were randomly assigned to one of two groups. An Infrequent group then completed a 180-trial **training intervention** with 18 perturbations interspersed randomly every 8-10 trials (Fig. 1C). A Frequent group completed a 180-trial **training intervention** with 36 perturbations interspersed randomly every 4-6 trials (Fig. 1C). After their respective training interventions, both groups completed a **retention task** consisting of 2 rounds of 19 null trials followed by 1 perturbation trial. The retention task was used to quantify the learning of reactive balance. Changes in reactive balance were assessed by comparing target accuracy between the initial perturbations during training and the perturbations during the retention task. Changes in step width during the training intervention was used to assess the adaptation of general protective strategies.

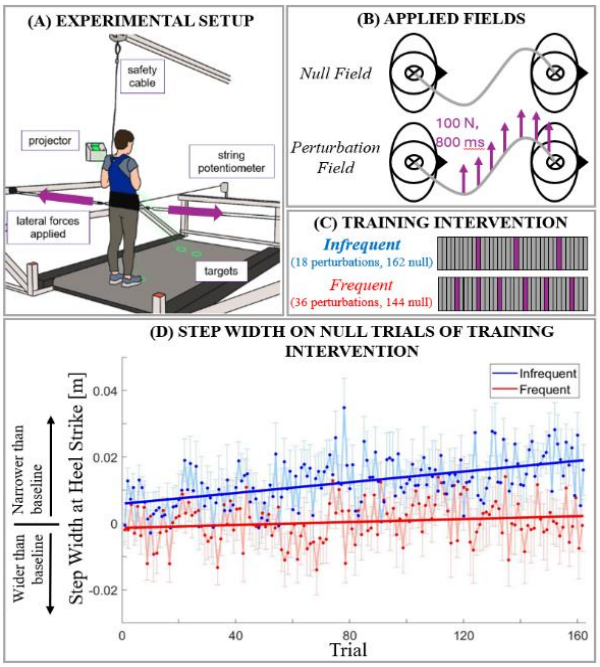

Fig 1. (A) Experimental setup. (B) Types of forces fields. (C) Example training intervention protocols. (D) Step width at 1st right heel strike results for training intervention.

Results & Discussion: A significant improvement ($p=0.0249$) in target accuracy for the Frequent group was found when comparing the initial two perturbation trials to the two retention task perturbation trials. There was no improvement in the Infrequent group. These results are contrary to our hypothesis that the learning of reactive balance would be greatest when unexpected balance disruptions were less frequent. A mixed-effects linear model examined the fixed effects of Group and Trial on step width while considering a random effect of Participant. A significant interaction between Group and Trial ($p=6.7988e-05$) indicated that step width with respect to baseline gradually became narrower during the null trials of the training intervention for both groups (both $p<0.05$), but these systemic changes were greater for the Infrequent group than the Frequent group (Fig 1D). There was no main effect of Group. The decrease in step width in the Infrequent group was again contrary to our hypothesis that the adoption of general protective strategies would be less when perturbations were less frequent. A possible explanation is that it was easier for the Frequent group to remain focused during the protocol, thereby making it easier to use a reactive rather than protective strategy. With very infrequent perturbations, a general strategy positioning a person favourably to resist any perturbation may have been beneficial because less focus was required on any given trial.

Significance: Our results clearly show that modulating frequency impacts the underlying strategies people use to respond to balance disruptions. It may be possible to leverage the frequency at which perturbations are experienced to improve learning of reactive balance without the development of general protective strategies. This may help with balance training following neuromuscular injury.

Acknowledgements: Supported in part by the U.S. Department of Veterans Affairs, RR&D Service #I01RX003371.

References: [1] McCrum et al. (2022), *Frontiers in Sports and Active Living* 4; [2] Moore et al. (2010), *Stroke* 41(1); [3] Okubo et al. (2018), *Plos One* 13(3).

PORCINE CARPAL BIOMECHANICS: FEASIBILITY AS A PRECLINICAL ANIMAL MODEL FOR THE HUMAN WRIST JOINT

Madison K. Altieri, M.Sc.[2], Rohit Badida, M.Sc.[1], Quianna M. Vaughan, B.S.[2],
Edward Akelman, M.D.[1], Joseph J. Crisco, Ph.D.[1,2]
[1] Dept. of Orthopedics, The Warren Alpert Medical School of Brown University and Rhode Island Hospital, Providence, RI 02903
[2] Center for Biomedical Engineering and School of Engineering, Brown University, Providence, RI 02912
*Corresponding author's email: joseph_crisco@brown.edu

Introduction: Large animal models have been useful for the evaluation of novel treatments of end stage joint diseases and their translation into clinical settings. Arthroplasties that involve the hip, knee, or shoulder provide higher success rates than wrist due to years of in vitro, preclinical animal models and in vivo research. Previous studies evaluating ACL repair, bone fracture, and cartilage damage, have used porcine models because of the resemblance of the porcine knee in bony anatomy, bone mineral density, morphology, and healing to humans. In comparison, the wrist joint has poor success rates compared to the larger joints in terms of successful surgeries and clinical outcomes, partly due to the lack of a characterized preclinical animal model. Advancing successful treatments for carpal instabilities are hindered due in part to limited preclinical animal models. The purpose of this study is to evaluate the Yucatan minipig (YP) as an animal model for the human wrist by quantifying carpal biomechanics in vitro during intact and ligament transection conditions.

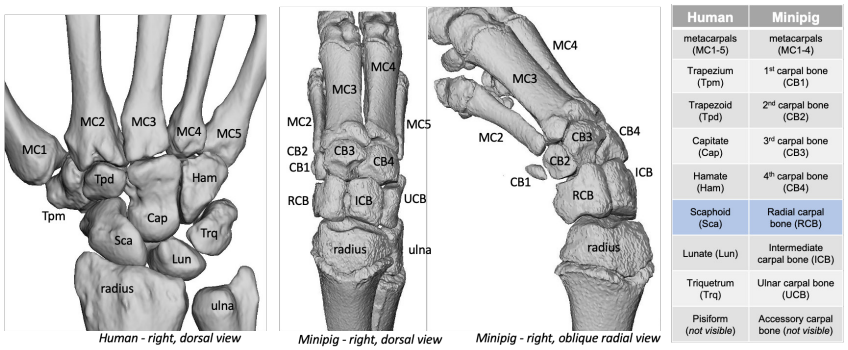

Human	Minipig
metacarpals (MC1-5)	metacarpals (MC1-4)
Trapezium (Tpm)	1st carpal bone (CB1)
Trapezoid (Tpd)	2nd carpal bone (CB2)
Capitate (Cap)	3rd carpal bone (CB3)
Hamate (Ham)	4th carpal bone (CB4)
Scaphoid (Sca)	Radial carpal bone (RCB)
Lunate (Lun)	Intermediate carpal bone (ICB)
Triquetrum (Trq)	Ulnar carpal bone (UCB)
Pisiform (*not visible*)	Accessory carpal bone (*not visible*)

Figure 1. Renderings from CT studies of the human and Yucatan minipig wrist, comparing the skeletal anatomy. The minipig carpus has bone homologues for all of the human carpal bones but lacks a thumb metacarpal (MC1). The pisiform and accessory carpal bone are both sesamoid bones, not true carpals, on the ulnar side and are not visible in these renderings.

Methods: Gross anatomical review of the YP revealed that the carpus includes 8 individual carpal bones, each with a unique size and geometry (Fig. 1). The carpal bones are assembled in two distinct rows bound together by a system of connective tissues with four metacarpals distally. Of the ligaments identified in the YP carpus, two were postulated to be homologous to the critical stabilizers of the human carpus; the radial intermediate ligament (RIL- homologous to the scapholunate interosseous ligament) and dorsal intercarpal ligament (DIC). Range of motion and stiffness were determined in twelve YP forelimb specimens tested using a six-axis robot in 28 directions about the carpus, pronation-supination, and volar-dorsal translation. The testing was implemented in three conditions – intact, and after sequential transection of the RIL and the DIC. Mixed models were utilized to evaluate the differences in kinematics as a function of testing direction, ligament condition, and sex. The difference in ROM between male and female specimens were consistently less than 1°, thus reported results were not stratified by sex.

Results & Discussion: The intact ROM envelope was elliptical in shape and oriented toward ulnar flexion with highest ROM about 15° from flexion-extension axis (Fig. 2). The carpus was most stiff in radial deviation and least stiff in ulnar flexion. Transection of RIL and DIC did not alter the ROM envelope orientation, however, significant ROM increase ($p<0.05$) was observed in flexion, extension and radial deviation following transection of both RIL and DIC. Supination of the YP carpus was significantly lower than pronation ($p<0.05$) in all three conditions. Volar translation was significantly higher ($p<0.05$) than dorsal translation in all three conditions.

Significance: This study provided insight into the influence of the carpal anatomy and biomechanics that maintains the stability of the porcine wrist and assesses the feasibility of whether it can be used as a preclinical animal model for the treatment of the degenerative wrist.

Acknowledgments: Supported in part by the National Institute of Arthritis and Musculoskeletal and Skin Diseases of the National Institutes of Health under Award Number R21AR08213. The content is solely the responsibility of the authors and does not necessarily represent the official views of the National Institutes of Health.

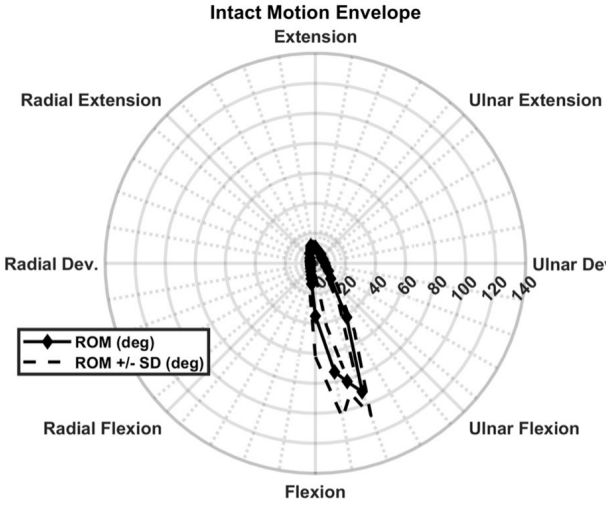

Figure 2. Envelope of the average (solid line) Intact ROM (±SD (dashed line) (deg)) across the 28 directions of forelimb motion.

MODELING FEMORAL ANTEVERSION AND FOOT ORTHOSIS INTERVENTIONS TO REDUCE JOINT LOADS

Benjamin B. Wheatley[1*], Allyson K. Clarke[1], Marianne J. Voigt[1], Mark A. Seeley[2]
[1]Bucknell University, Lewisburg, PA [2]Geisinger Medical Center, Danville, PA
*Corresponding Author b.wheatley@bucknell.edu

Introduction: Excessive lower limb torsion can cause gait impairment and joint pain and is treated by surgical intervention in many cases [1]. Femoral anteversion (inward torsion of the femur bone) varies throughout growth but is typically ~15° in adults, however excessive anteversion (30°+) often present clinically and can be associated with confounding conditions such as cerebral palsy or hip dysplasia. Unfortunately, it is not always clear which patients would benefit from physical therapy, which therapy plans would best suit individual patients, or which patients need invasive surgery. Therefore, improved methods to treat joint pain due to torsional malalignments is needed. We propose to use video-based motion capture and musculoskeletal modeling as a tool to aid in the implementation of patient-specific orthoses to reduce knee and hip join pain for patients with excessive lower limb torsion. Specifically, we aim to use motion analysis and modeling to explore how potential orthosis and gait pattern interventions affect hip and knee joint loads. The specific goal of this work was to use optimal control to study the interactions between femoral anteversion and ground contact (simulated orthosis interventions) in a musculoskeletal model of gait using data generated by video-based motion capture.

Methods: This work uses the open-source video-based motion capture tool OpenCap [2] and the open-source musculoskeletal modeling tool OpenSim Moco [3]. Three-dimensional gait kinematics from a healthy adult male measured from OpenCap were used as inputs into musculoskeletal modeling simulation. The LaiArnold2017 musculoskeletal model was used for this study, which modifies of the commonly used Rajagopal model to include ground contact via Hunt-Crossley contact spheres and improved passive muscle force accuracy [4]. To incorporate excessive femoral anteversion, we used an open-source bone deformation tool [5] to increase femoral anteversion from a baseline of 12° to a value of 32° (Figure 1A). To simulate an orthosis intervention, we modified all contact sphere locations in the transverse plane by one cm in each direction (anterior, posterior, medial, and lateral, Figure 1B) and one that combined both a lateral and posterior shift (due to the prevalence of lateral and posterior wedges as interventions for joint pain). We ran a muscle-driven Moco control problem for each model that tracked the above input kinematics, minimized muscle excitations ("effort"), and upon convergence calculated joint reaction forces for the hip (hip joint force) and knee (knee adduction moment, knee torsion moment, patellofemoral joint force, and lateral:total patellofemoral load ratio).

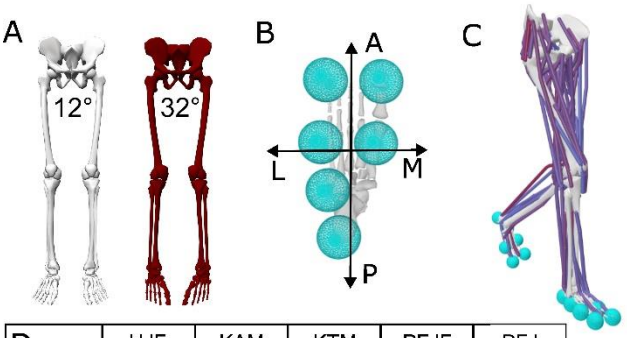

D	HJF (BW)	KAM (BW*HT)	KTM (BW*HT)	PFJF (BW)	PFJ Ratio (-)
TD	3.8	0.011	0.0064	0.45	0.14
+20° FA	3%	-6%	21%	12%	102%
Lat	0%	-18%	14%	7%	91%
Post	-2%	-9%	10%	0%	91%
LapPost	-2%	-10%	16%	1%	118%
Med	10%	11%	28%	15%	106%
Ant	13%	3%	-2%	25%	125%

Figure 1: A) Typically developing and femoral anteversion lower extremity geometries. B) Contact spheres with labeled anterior (A), posterior (P), medial (M) and lateral (L) direction. C) Lower extremity of model with muscles (colored for activation) and contact spheres during stance. D) Relative percent changes of joint loads for each model: hip joint contact force (HJF), knee adduction moment (KAM), knee torsion moment (KTM), total patellofemoral joint load (PFJF) and lateral:total patellofemoral joint load (PFJ Ratio).

Results & Discussion: All muscle-driven tracking problems converged to tracked gait kinematics, with ranging simulation times between 5-12 hours (Figure 1C). Compared to the typically developing (TD) model, the femoral anteversion (FA) model predicted increased hip joint loads, knee torsion moment, patellofemoral joint load, and patellofemoral joint ratio (Figure 1D), suggesting that femoral anteversion produces a general worsening joint mechanics with gait, though unlike the other joint loads the internal knee adduction moment decreased by 6%. Regarding contact sphere shifts, a 18% reduction in knee adduction was observed from the TD to the FA-lateral shift model and there were negligible differences between the TD model and FA-posterior shift model, suggesting that lateral and posterior shifts may be best suited to improve joint loading. Our slightly increased hip joint loads and considerable worsening of patellofemoral joint load alignment with increasing femoral anteversion also agrees with our prior modeling works [6,7]. These results suggest subject-specific interventions such as custom orthoses that modify ground reaction force vectors could be further enhanced by musculoskeletal modeling. Along with increasing healthy control and patient sample sizes, future implementation of patient-specific muscle activity patterns informed by electromyography and more robust methods to measure foot-ground or foot-shoe contact would benefit this work. Additionally, robust model validation is needed before implementation into clinical practice.

Significance: This work is significant for two reasons: I) we have presented here a modeling framework for simulating foot orthosis interventions to alter joint loads in individuals with lower limb torsional malalignments and II) we have used open-source tools and low-cost video-based motion capture for easier and cheaper implementation into research or clinical practice. Modeling-informed, patient specific interventions could be developed for patients with lower extremity torsional malalignments, for example for patellofemoral pain a posterior wedge or for medial tibiofemoral pain a lateral wedge.

References: [1] Bruce et al. (2004) *J Pediatr Ortho* 24. [2] Uhlrich et al. (2023) *PLOS Comput Biol* [3] Dembia et al. (2020) *PLOS Comput Biol* 16. [4] Lai et al. (2017) *Ann Biomed Eng* 45. [5] Modenese et al. (2021) *Gait Posture* 88. [6] Wheatley et al. (2023) *J Orthop Res* 41. [7] Voigt et al. (2023) *Biomed Eng Soc* San Antonio, TX.

ENERGY GENERATION AND ABOSRPTION ACROSS JOINTS IN THE DRIVER SWINGS OF FEMALE GOLFERS

Cameron Jensen[1*], Sam Wilkins[2], Adam Rosen[2], Brian Knarr[1]
[1]Department of Biomechanics, University of Nebraska at Omaha, Omaha, Nebraska, USA
[2]School of Health and Kinesiology, University of Nebraska at Omaha, Omaha, Nebraska, USA
*Corresponding author's email: cameronjensen@unomaha.edu

Introduction: The golf swing is a complex biomechanical motion that requires the coordination of body segments to successfully hit a long and well-positioned ball. One of the keys of being an excellent golfer is generating energy and transferring as much of that energy to the club, which will launch the ball upon impact [1,2]. Thus, a detailed understanding of the energy flow through the golfer would be beneficial to identify deficiencies and improve performance related to their swing [1]. Additionally, women have distinct golf swings from men [3] yet represent only 11% of subjects in golf biomechanics research [4], so understanding the energy flow through female golfers specifically, is also informative.

The purpose of this study is to develop a method of analyzing the energy flow of female golfers and to understand which joints produce the most energy for their golf swing. We investigated the work (the time integral of power) taking place at the joints throughout the body that are relevant to the golf downswing motion [1]. We hypothesized the trunk and hips would be responsible for producing the highest percentage of work, as power in the golf swing is primarily generated through a torso twisting motion [1,2].

Methods: Motion capture (Qualisys, Gothenburg, Sweden) and force plates (AMTI, Watertown, MA, USA) collected the kinematic and kinetic data of 7 right-handed female collegiate golfers (age: 20 ± 0.9 yrs.; height: 167.6 ± 4.6 cm.; weight: 64.1 ± 5.4 kg.; handicap: 8.2 ± 2.3) performing golf swings with their driver. Visual3D (C-Motion, Germantown, MD, USA) and MATLAB (MathWorks, Natick, MA, USA) were used to process and analyse the data. Variables were collected for the downswing portion of the swing. The three-dimensional vectors of the segment moments and angular velocities were extracted to calculate the segment torque power of the proximal (STP_p) and distal segments (STP_d), and summed to calculate joint torque power (JTP) [5]: $JTP = STP_p + STP_d = M_p \cdot w_p + M_d \cdot w_d$

All JTP values were normalized by body weight. A joint was created for the trunk by expressing the pelvis coordinate system with respect to abdomen/thorax coordinate system. An integral of the JTPs were taken, with respect to time, from the top of the backswing to impact to calculate the work done at each joint. The percentage each joint contributes to the total work done was determined. Positive work refers to energy being generated, and negative work indicates eccentric contraction and thus energy absorption.

.

Results & Discussion: The generation of work during the golf swing primarily comes from the right and left hips at 38.86 ± 21.9% and 31.4 ± 9.9%, respectively (Fig. 1). These results support our hypotheses and are similar to previous research in males who also had their hip joints produce the greatest percentage of work [1]. The left ankle was the secondary source of energy generation at 28.85 ± 8.1%. We suspect this is due to the left ankle, being the lead ankle, provides a grounded point that the body rotates over contributing to the rotational energy. The left ankle likely also experiences a greater amount of linear energy from the weight shift that occurs from the right to the left leg during the downswing. The trunk was the tertiary source of energy generation at 7.49 ± 12.3%, this was surprisingly low and likely due to our model for the trunk oversimplifying this region of the body. The region of the body from the pelvis through the spine to the shoulders is a series of many small joints, and we are representing it as one joint. Minimal work (< 5%) is generated or absorbed through the joints of the arms. The left knee produces negative energy, indicating energy absorption. Meaning the left knee provides static support as the body rotates.

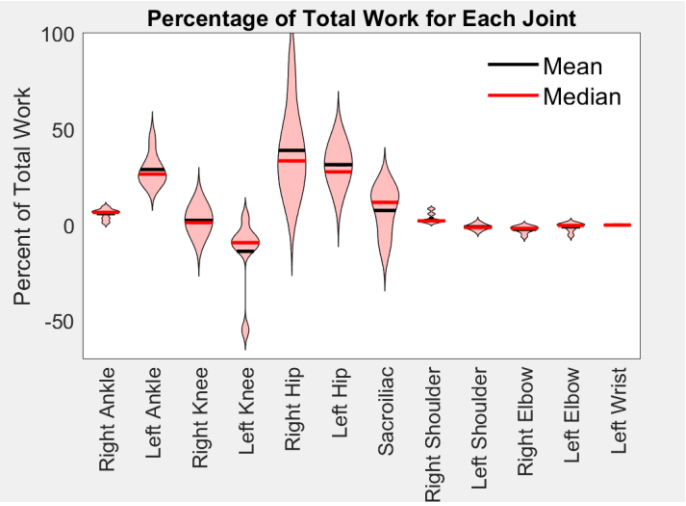

Figure 1: The average percentage of total work each joint contributes during the driver downswing.

Significance: This study applies a method for analysing energy generation and absorption through the body in female golfers. With this analysis golfers, coaches, trainers, and healthcare providers can make more educated decisions to improve performance and reduce injury. For example, supposed Golfer 1 produces a high percentage of energy through their hips, at 80.5% for the right hip (mean: 38.9%) and 42.8% for the left hip (mean: 31.4%), but also absorbs the most amount of energy through the left knee at -54.8% (mean: -13.8%). This is a potential injury concern due to the amount of energy experienced by the left knee. Additionally, this study provides further insight into the energy trends of golfers of different skill levels and demographics, than previously studied, and helps to better inform golfer development and injury risk.

References: [1] Nesbit SM and Serrano M (2005). *J Sports Sci Med*, 4: 520-533.; [2] Takagi T (2018). *ISBS Proceedings*, 36.; [3] Egret et al. (2006). *Int J Sports Med*, 27:463-467.; [4] Bourgain M et al. (2022). *Sports*, 10: 91.;[5] Pryhoda MK and Sabick MB (2022). *Front Sports Act Living*, 4: 975107.

ANALYSIS OF GROUND REACTION FORCES AND THEIR EFFECT IN BASEBALL PITCH VELOCITY

Zyanya Burgos Resendiz[1*], Moira K. Pryhoda[2], Jacob Howenstein[3], Kristof Kipp[4], Michelle Sabick[1]
[1]Department of Mechanical and Materials Engineering, University of Denver, Denver, CO
Email: z.burgosresendiz@du.edu

Introduction: Overhead throwing is a complex skill that requires careful coordination of the entire body [1]. During the foot contact phase of the pitching motion, the front and back legs of the pitcher both generate forces that contribute to the overall ball velocity the pitcher produces. Vertical ground reaction forces (GRF) are the largest force components affecting the overall velocity of the pitch [2]. Energy generated by the legs flows upward through the body segments to the arm when stride foot contact normally occurs between 56-66% of the pitch duration [2,3]. The aim of this study is to investigate the timing of the weight transfer from the drive leg to the stride leg determine how it relates to pitch velocity in a group of youth pitchers. A deeper understanding of this transition may help us provide critical information to players and coaches to increase pitch velocity while protecting developing athletes from injury.

Methods: Motion capture data from the three fastest pitches for strikes was collected from 23 male baseball players ranging from 9-13 years of age. Data was collected using a 14-camera motion capture system operating at 250 Hz (Vicon Motion Systems, Oxford, UK) [3]. GRF were collected using two portable force platforms operating at 1000 Hz (Kistler, Winterthur, Switzerland). The force platforms were embedded in a custom pitching mound that allowed the location of the forward force platform to be adjusted depending on the pitcher's stride length [3]. The duration of the pitching motion was normalized from 0% (ball leaves glove) to 100% (maximum internal rotation of the shoulder after ball release). The maximum vertical GRF generated by the stride (front) leg after the instant of stride foot contact (SFC) was recorded for the three fastest strikes for each subject, as was the mean vertical GRF for the stride leg after SFC. The timing of weight transfer from the drive leg to the stride leg was also recorded. Subjects were divided into groups based on the timing of the weight transfer from the drive leg to the stride leg relative to the optimal time (Table 1). Two-tailed Students t-test were performed to compare mean GRF, peak GRF, and pitch velocity between the groups. The Pearson correlation coefficient between timing of SFC and pitch velocity was also computed.

Table 1: Group GRF data for groups based on timing of SFC, reported as Mean (SD).

Groups Based on SFC Timing	Number of Subjects in Group	Mean Force During Foot Contact (N/BW)	Max Force During Foot Contact (N/BW)	Mean Pitch Velocity (mph)
From 30-55 %	3	0.943 (0.29)	1.307 (0.25)	26.37 (4.38)
From 56-66%	13	0.806 (0.18)	1.342 (0.19)	28.52 (3.82)
From 67-85%	5	0.819 (0.17)	1.436 (0.44)	29.08 (3.38)

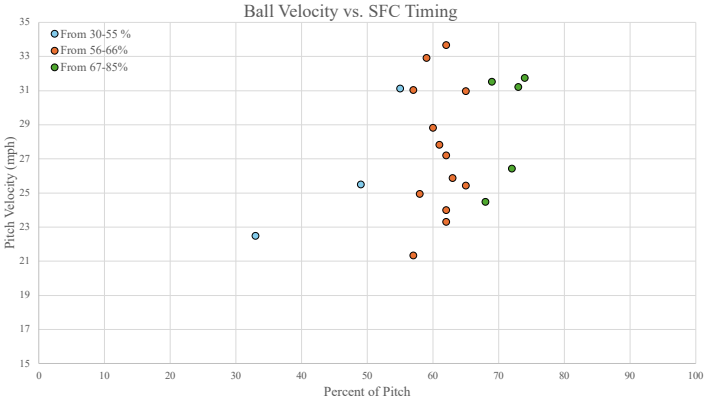

Figure 1: Pitch velocity generated across subject groups with respect to pitch percentage. Subject pitch velocity values range from 0-35 mph.

Results & Discussion: No significant differences in vertical GRF or pitch velocity existed between the groups based on the timing of SFC in this group of youth subjects (Table 1). Pitch velocity was only moderately correlated with timing of SFC (r=.37). Negative correlations between SFC and ball release have indicated that a potential relationship between longer time to peak vertical GRF during SFC could be associated with a higher pitch velocity [4]. Subjects who initiated stride foot contact in what is considered by coaches to be the optimal range (between 56-66% of the pitch) generated mean velocities of 28.52 ± 3.82 mph, which was not greater than the "early" or "late" groups. In fact, subjects who initiated stride foot contact between 67-85% of the pitch generated maximum forces of 1.436 ± 0.44 N/BW and had pitch velocities of 29.08 ± 3.38mph. Stride leg vertical GRF are considered to be more effective when they are generated prior to maximum external rotation of the throwing arm happening at about 61% of the pitch [2,5]. When evaluating timing of stride foot contact versus pitch velocity, subjects exhibited wide variation in pitch velocities even when their timing was optimal. The highest pitch velocity was produced when SFC was at 62% of the pitch while the lowest velocity was produced when SFC was 57% of the pitch (Figure 1).

Significance: This study analysed the magnitude and timing of the vertical GRF generated by the stride leg during the baseball pitch and their impact on the overall velocity of the pitch. Subjects who initiated stride foot contact between 56-66% of the pitch did not consistently generate higher pitch velocities than subjects who initiated stride foot contact earlier or later. In fact, the subjects with the highest and lowest mean pitch velocities were both in this group. This observation may be due to the large range of subject ages and abilities in this study. We will continue to investigate coordination and timing during the pitching motion to help coaches and pitchers to understand the optimal timings for stride foot to help athletes achieve their greatest performance.

Acknowledgments: The authors would like to thank Moira Pryhoda, Jacob Howenstein, Andrew Bryan, and Kristof Kipp for their contributions to project conceptualization and data collection.

References: [1] MacWilliams, B. A., et al. (1998). *AJSM*, *26*(1), 66–71, [2] Pryhoda, M. K., & Sabick, M. B. (2022). *Frontiers in Sports and Active Living*, *4*, [3] Howenstein, J., Kipp, K., & Sabick, M. (2020). *J Biomech*, *108*, 109909. [4] Guido, J. A., & Werner, S. L. (2012). *J Strength Cond Res*, *26*(7), 1782–1785. [5] Elliott, B., Grove, J. R., & Gibson, B. (1988). *Int J Sport Biomech*, *4*(1), 59–67.

IMPACTS OF ADDED TORSO MASS ON REACTIVE BALANCE CONTROL: IMPLICATIONS FOR STABILITY IN PREGNANCY

Autumn M. Routt[1*], Kristen L. Jakubowski[2], Gregory S. Sawicki[1], Lena H. Ting[1,2]
[1]George W. Woodruff School of Mechanical Engineering, Georgia Institute of Technology
[2]Walter H. Coulter Department of Biomedical Engineering, Emory University & Georgia Institute of Technology
*Corresponding author's email: aroutt3@gatech.edu

Introduction: Pregnant women fall at a similar rate as women over the age of 65 [1, 2]. Despite their prevalence, the cause of falls during pregnancy remains poorly understood, in part due to the vast array of contributing factors such as the influence of hormones on tissue properties [3, 4, 5], the exacerbation of previously minor gait asymmetries [6] and the change of center of mass (COM) location due to added mass [7, 8, 9].

Isolating the effects of added mass on instability in pregnancy is an essential step to teasing apart the influence of each of these variables on falls and balance in pregnant women. While other changes are difficult to separate, the use of a weight vest on non-pregnant women allows for a straightforward investigation of the short-term effects of added mass on balance control.

Here, we preliminarily tested the effect of altering mass and mass distribution during standing balance perturbations in a non-pregnant female participant. We predict that front-loaded mass would result in less COM movement during forward support-surface perturbations that send the COM backward, as it acts as a counterweight; and greater COM movement in backward support-surface perturbations (Fig 1A). We predicted the opposite results for back-loaded mass.

Methods: One healthy young adult (25 year-old female) stood with arms crossed during forward and backward support-surface perturbations of 12.6 cm over 500 ms (Fig. 1A) while wearing a weight vest in four conditions: no added mass (black/gray), 24 lbs- evenly-distributed (purple), front-loaded (red), or back-loaded (blue). The participant was outfitted with a full-body motion capture marker set (Vicon). We quantified the peak change in COM displacement relative to the feet, after each ramp perturbation ("peak COM excursion") and at 2.5 s (just before the platform returned to its home position) ("COM return") (Fig. 1B).

Results & Discussion: Adding mass increased COM excursion in both forward and backward perturbations when mass was added evenly (Fig 1C, purple). However, back- and front-loaded mass reduced COM excursion in forward perturbations, but increased COM excursion in backward perturbations (Fig. 1C, red, blue). Future analysis will investigate whether participant posture at the time of perturbation onset explains the unexpected reduced COM excursion in forward perturbations. COM return was greater than 0 cm in all conditions for both perturbation directions and did not correspond with that of peak COM excursion. This suggests that longer pauses before resetting the platform to its home position will provide further information about the effect of added mass on the ability to regain stability following a perturbation.

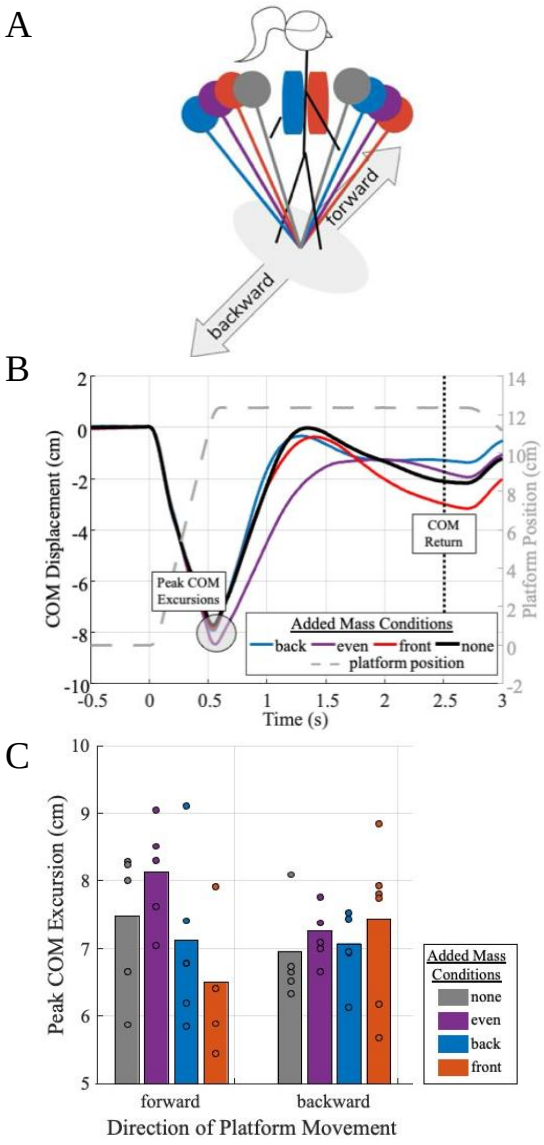

Figure 1: (A) Experimental set-up with added mass worn on perturbation platform. Colorful projections indicate hypothesized response to perturbations by condition. (B) Example of COM displacement during one forward perturbation. (C) Peak COM excursions for all four conditions after forward and backward perturbations.

Significance: The unexpected results in response to forward perturbations indicate a need to repeat this experiment with the starting COM position and joint angles more carefully controlled. If maintaining consistent COM starting positions and joint angles across weighted conditions impacts the response to perturbations significantly, this information could be valuable to understanding what postures reduce fall risk in unevenly added mass conditions. Our data suggests that some of the impacts of added mass may not be in the initial CoM excursion but rather changes in the return to a stable, upright stance. Understanding this is crucial to effectively recreating fall conditions in a laboratory environment.

Acknowledgments: Funding provided by Georgia Tech Interdisciplinary Research Fellowship and NSF: ASEE #2127509

References: [1] Dunning et al. (2003) *Am. J. Ind. Med.* 44(6); [2] O'Loughlin et al. (1993) *Am. J. Epidemiol.* 137(3); [3] Bey et al. (2019) *Front. Physiol.* 10; [4] Danos et al. (2023) *J. Anat.*; [5] Chidi-Ogbolu et al. (2019) *Front. Physiol.* 9; [6] Lefranc et al. (2023) *J. Appl. Biomech.* 1; [7] Catena et al. (2018) *J. Biomech.* 71; [8] McCrory et al. (2010) *J. Biomech.* 43(12); [9] Aguiar et al. (2015) *Gait Posture* 42(4)

RESISTANCE TRAINING ALONE DOES NOT COUNTERACT GAIT CHANGES AFTER IMMOBILIZATION: A CASE STUDY

Keven Santamaría-Guzmán[1], Brandon M. Peoples[1], Kenneth D. Harrison[1], Valeria. Robles-Cerdas[1], J Max. Michel[2], Michael D. Roberts[2], Jaimie A. Roper[1]
[1]Locomotor and Movement Control Lab, School of Kinesiology, Auburn University, Auburn, AL, U.S.A.
[2]Nutrabolt Applied and Molecular Physiology Laboratory, School of Kinesiology, Auburn University, Auburn, AL, U.S.A.
*Corresponding author's email: kgs0071@auburn.edu

Introduction: Immobilization, a standard orthopedic treatment, can reduce neuromuscular and motor control, affecting stability, balance, and injury prevention[1,2,3]. This impairment results from joint stiffness, muscle loss, and altered gait biomechanics[4,5,6]. Even short periods of immobilization can lead to reduced knee range of motion and strength, with irreversible joint deficits after longer periods[7,8]. This study explores the impact of 2-week knee immobilization followed by 8 weeks of resistance training (RT) on gait parameters in a healthy individual. The goal is to understand how immobilization affects gait and whether specific training can restore normal function.

Methods: A single 29-year-old male participant underwent 14 days of leg immobilization using a knee brace locked at 90 degrees and crutches. Gait analysis was conducted at four-time points: baseline (Pre), after 14 days of immobilization (Post 1), after 8 weeks of resistance training (RT) (Post 2), and 14 weeks after completing RT (Post 3). Gait data were collected during 2-minute walk tests at comfortable (*COM*) and maximum (*MAX*) speeds using a wireless APDM Movement Monitoring inertial sensor placed on the sternum, lumbar area below L5, bilateral wrists, upper legs, lower legs, and feet. Parameters analyzed included cadence, stride length, gait speed, cycle duration, step duration, stance, swing, and foot strike angle. The 8-week RT program involved 3 weekly sessions targeting all major muscle groups, with intensity progressing from 65% to 70% and back to 65% of 1-rep max over the 8 weeks. Volume increased solely for knee extensors, reaching 8 sets per exercise by week 8. Repeated measures ANOVA examined the effects of immobilization and RT across time points.

Results & Discussion: Short-term, 2-week unilateral knee immobilization significantly impaired multiple spatiotemporal gait parameters compared to baselines. Cadence changed at both speeds (COM: $F=188.449$, $p<.001$; MAX: $F=28.278$, $p<.001$), increasing after Post 1 (COM: $p<.001$; MAX: $p=0.534$) but partially recovered after RT (COM/MAX: $p<.001$) and fully recovered after 14 weeks. Stride length was affected at both speeds (COM: $F=118.171$, $p<.001$; MAX: $F=46.055$, $p<.001$), increasing after Post 1 (COM: $p<.001$; MAX: $p=0.855$) but partially recovered after RT (COM/MAX: $p<.001$). Gait speed was impacted at both speeds (COM: $F=193.336$, $p<.001$; MAX: $F=45.402$, $p<.001$), increasing after Post 1 (COM: $p<.001$; MAX: $p=0.915$) but partially recovered after RT (COM: $p<.001$). Gait cycle and step duration also showed similar trends. Stance and swing periods had significant asymmetries at baseline ($p<.001$), eliminated by immobilization and RT. Foot strike angle decreased after immobilization and RT (COM: $F=257.180$, $p<.001$; MAX: $F=193.263$, $p<.001$), recovering after 14 weeks. Major metrics remained impaired post-training, suggesting limitations in addressing biomechanical deficits induced locally by immobilization (Fig. 1). These findings align with literature noting immobilization-induced neuromuscular deficits, proprioceptive impairment, and altered motor control due to muscle atrophy and joint stiffness. RT coupled with rehabilitation focusing on proprioception, joint mobility, neural function, and inter-limb coordination may improve comprehensive gait biomechanics restoration following temporary immobilization.

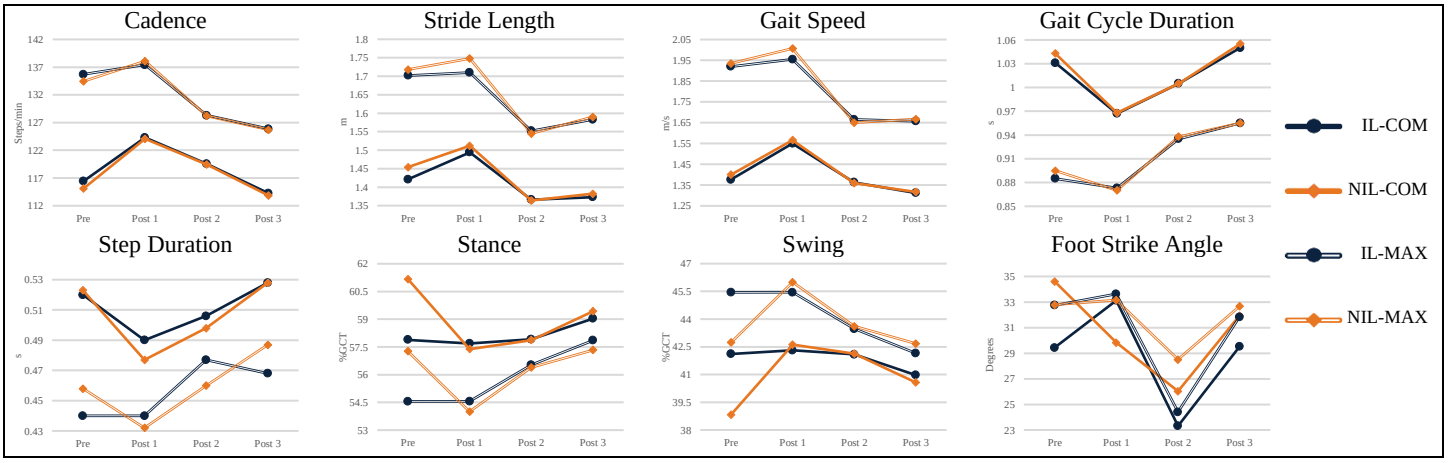

Figure 1. Gait parameters. Notes: IL: Immobilized leg, NIL: Non-Immobilized Leg.

Significance: Short-term knee immobilization causes acute impairments in gait parameters, and RT provides partial recovery, highlighting current rehabilitation strategy limitations. These insights can inform future protocols, enhancing outcomes and restoring gait biomechanics post-limb immobilization.

Acknowledgments: We thank the Nutrabolt Applied and Molecular Physiology Laboratory, School of Kinesiology, Auburn University, for their vital support and collaboration in this study case.

References: [1] Kaneguchi et al. (2020). *Clin Biomech*, 75, 104992.; [2] Curtze et al. (2016). *Phys Ther*, 96(11); [3] Zhou et al. (2022). *Sensors*, 22(17); [4] Clark et al. (2008). *J. Appl. Physiol*, 105(3); [5] Trudel et al. (2014). *J. Appl. Physiol*, 117(7); [6] Guan et al. (2019). *J. Healthc. Eng*, 2019; [7] Kaneguchi et al. (2017). *J. Orthop. Res*, 35(7); [8] Trudel et al. (2000). *Arch. Phys. M.*, 81(1).

REDO-TRANSCATHETER AORTIC VALVE REPLACEMENT PROCEDURE: A PATIENT-SPECIFIC *IN-SILICO* FEASIBILITY ANALYSIS

Symon Reza[1*], Brandon Kovarovic[1], Danny Bluestein[1]
[1]Stony Brook University
*Corresponding author's email: symon.reza@stonybrook.edu

Introduction: Transcatheter aortic valve replacement (TAVR), a minimally invasive procedure, has demonstrated comparable hemodynamic performance to surgical aortic valve replacement (SAVR) and has become the standard procedure for high and intermediate-risk aortic stenosis patients. However, prosthetic TAVR leaflets are inherently subjected to degeneration, along with calcification and thrombosis [1]. Hence, durability remains one of the major concerns for TAVR technology. This evidence of thrombosis and rapid degeneration of prosthetic valves poses a significant risk to the increasing number of young and low-risk TAVR recipients, necessitating repeat intervention. Transcatheter aortic valve-in-transcatheter aortic valve (TAV-in-TAV) or redo-TAVR is being considered as a potential treatment of choice for transcatheter heart valve (THV) degeneration which has shown success in addressing suboptimal outcomes. However, the current lack of data is preventing redo-TAVR from being established as a safe and viable procedure. A comprehensive structural and hemodynamic performance analysis of different redo-TAVR combinations in a patient-specific scenario may provide vital insights into the feasibility of redo-TAVR procedures and help identify the optimal combination.

Methods: A patient with a 23.5mm CT-derived annular diameter was selected for this study. The patient model was reconstructed (Fig. 1a) following the procedures described in our previous study [3]. The most widely used self-expandable (SE) and balloon-expandable (BE) TAVR systems were considered for this study. TAVR implantation simulations were then performed following our previous studies (Fig. 1b) [4] using Abaqus Explicit 2019. The selected TAVR devices result in four redo-TAVR combinations (Fig. 1c) including - i) SE-in-BE, ii) BE-in-BE, iii) BE-in-SE, and iv) SE-in-SE. A 2-way coupled fluid-structure interaction (FSI) using a body-fitted sub-grid geometry resolution (SGGR) method was then performed following our previous study [5] to analyze the hemodynamic performance of the redo-TAVR combinations (Fig. 1d). FSI simulations were performed by coupling the fluid solver, FlowVision 3.12, and Abaqus Explicit 2019.

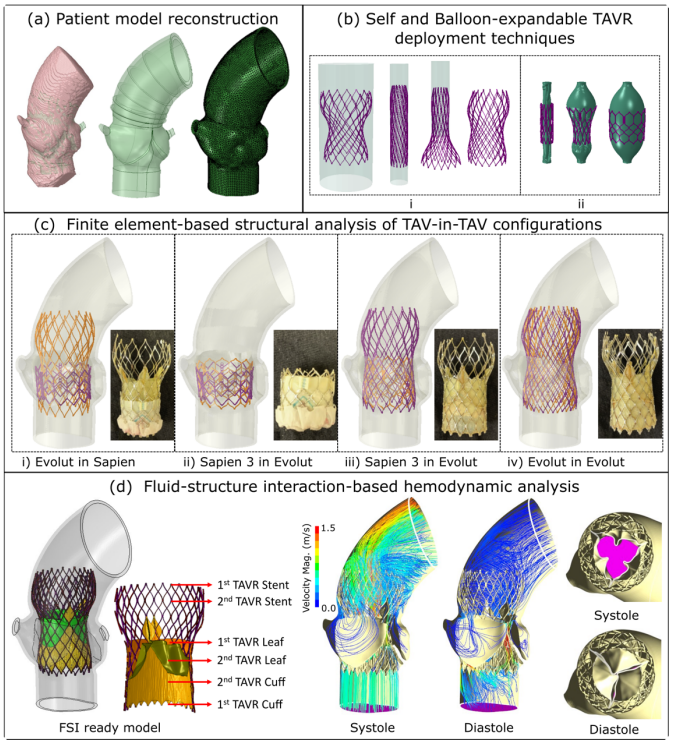

Figure 1: Schematic of the (a) model reconstruction, (b) implantation of i) self-expandable, ii) balloon-expandable TAVR devices, (c) four combinations of redo-TAVR deployed inside the aortic root of the selected patient model with in-vitro representation of the corresponding redo-TAVR combinations [2], (d) FSI ready fluid domain of the SE-in-SE combination (left) followed by the velocity streamline, and leaflet opening during systole, and diastole.

Results & Discussion: Structural and hemodynamic analyses were performed following redo-TAVR simulations. The SE-in-SE combination demonstrated the highest eccentricity and the narrowest coronary access. The combinations involving SE devices (BE-in-SE, and SE-in-BE) demonstrated limited coronary access. SE-in-BE demonstrated the narrowest opening at the annular plane. BE-in-BE demonstrated superior performance from the structural perspective with the widest coronary access and opening at the annular plane. However, BE-in-SE demonstrated 40% leaflet overhang which may impact the hemodynamic performance. Successful implantation and optimal hemodynamic performance of redo-TAVR requires careful assessment of specific device characteristics due to the technical and structural differences in TAVR prostheses including mode of deployment (BE and SE), valve function, and valve design. Patient-specific features and the interaction between the second THV with the patient's anatomy also play crucial roles in the performance of redo-TAVR procedures. Therefore, patient-specific preprocedural planning is critical in minimizing peri-procedural and post-procedural risk [6]. In this study, we addressed the aforementioned clinical concerns by performing a set of computational analyses starting from finite element-based TAVR deployment in patient-specific models to FSI-based hemodynamic analysis revealing insights into redo-TAVR combinations. Initial findings from structural and hemodynamic analyses suggest BE-in-BE as the optimal combination, although further analysis on the hemodynamic effect of leaflet overhang associated with BE-in-BE is required.

Significance: In summary, this study introduced a comprehensive computational framework to assess the patient-specific structural and hemodynamic performance of redo-TAVR combinations, addressing clinical concerns regarding THV degeneration and potential solutions with redo-TAVR. These techniques can potentially be used to aid the clinicians in lifetime management of aortic stenosis patients through optimal first and second THV selection.

Acknowledgments: Funding provided by NIH-NIBIB 1U01EB026414-01 (DB). Industry Partners: Dassault Systems, and Capvidia,

References: [1] Sellers, SL et al. JACC Cardiovasc Imaging. 2019; [2] Hatoum, H et al. JTCS 161.2 (2021): 565-576; [3] Reza, S et al. Artificial Organs 46.7 (2022): 1305-1317; [4] Bianchi, M et al. BMMB 18.2 (2019): 435-451; [5] Ghosh, R et al. BMMB 19 (2020): 1725-1740; [6] Tarantini, G, et al. The American journal of cardiology 192 (2023): 228-244.

COMPARISON OF UNSTABLE & STABLE LOAD DEADLIFT EXERCISES MOVEMENT COORDINATION USING MODIFIED VECTOR CODING IN THE SAGITTAL PLANE

Seung-Jun Ko [1], HunMin Kim [2], Joohyun Lee[3], Eunwook Chang[4*]
[1-4] Department of Sports Science, Inha University, Michuhol-gu, Incheon, Republic of Korea
*Corresponding author's email: change@inha.ac.kr

Introduction: The deadlift is a widely utilized exercise among athletes from various sports to enhance power and strength[1]. It is generally believed that unstable loading during multi-joint exercises increases muscle activation and strengthens muscles more effectively[2]. Comparison of minimum or maximum kinematics does not consider simultaneous segment motion or potential differences in various parts of the movement. A modified vector coding technique can be used to determine if the motion between segments is in the same direction (in-phase), opposite (anti-phase), or which direction is dominant. Therefore, the purpose of the current study was to compare lower extremity and trunk sagittal plane coordination patterns during unstable load deadlift and conventional deadlift. We hypothesized that the unstable load deadlift would have more variability and therefore would be different from the conventional deadlift in the coordination of thigh/shank, torso/thigh, and torso/shank.

Methods: Twenty young males (age:22.5±2.3, BMI: 27.4±5.2) performed a conventional deadlift (CD) and an unstable load deadlift (ULD) at 80% of 1RM. The unstable load deadlift was performed with a 12kg kettlebell hanging from both sleeves of a barbell. Each deadlift was divided into an ascending phase, a descending phase, and an upright phase. Participants were attached with retroreflective markers for a full-body motion capture system (OptiTrack, NaturalPoint, Corvallis, OR). Three-dimensional kinematic angles of the femur, tibia, and trunk segments relative to the global coordinative system were processed in Visual3D software (C-Motion, Inc., Rockville. MD). Custom MATLAB (R2023a; MathWorks, Natick, MA, USA) code was used for vector coding calculations.

Results: In the ascending phase, the torso-shank coupling angle illustrated slightly different conditions for CD and ULD. The torso-shank coupling angle frequency, IPPD (0°-45°) tended to be more dominant ULD than CD. In the upright phase, the thigh-shank coupling angle illustrated slightly different conditions in CD and ULD. APDD (270°-315°) tended to be more dominant in CD than in ULD, and IPPD (0°-45°) tended to be more dominant in ULD than in CD. The torso-shank coupling angle illustrated slightly different conditions in CD and ULD. APDD (90°-135°) tended to be more dominant in CD than in ULD, and APPD (315°-360°) tended to be more dominant in ULD than in CD (Fig 1).

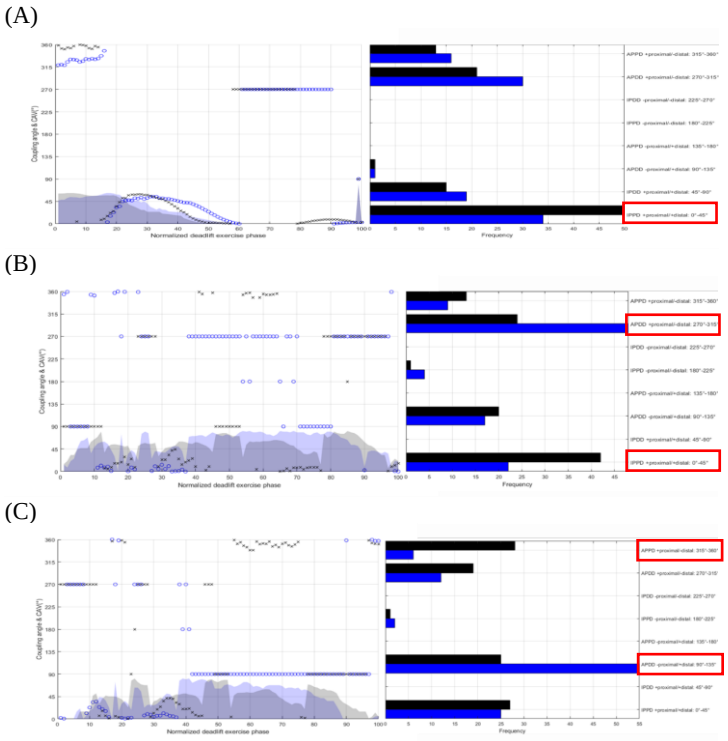

Figure 1: (A) Ascending phase, torso_shank, (B) Upright phase, thigh_shank, (C) Upright phase, torso_shank, mean coupling angle and coupling angle variability in left axis (blue dots/shade:CD, black x/shande:ULD), the frequency of each coordination pattern in right axis (blue:CD, black:ULD),In-phase distal dominancy(IPDD), In-phase proximal dominancy(IPPD), Anti-phase proximal dominancy(APPD), Anti-phase distal dominancy(APDD)

Discussion: Our primary findings partially supported our hypotheses. In the ascending phase, the torso-shank coordination suggested that trunk extension was more dominant in ULD. In the upright phase, thigh-shank coordination suggested that shank extension was more dominant in CD and thigh extension was more dominant in ULD, while torso-shank coordination suggested that shank extension was more dominant in CD and trunk extension was more dominant in ULD. The increased movement of the thigh and trunk during the upright phase of the ULD can be interpreted as control of the center of the body, which is required to control the movement. Previous study shown that the core must be strong and capable of control to perform at peak performance[3]. We could speculate that the core would have been used in ULD to maintain balance, and therefore thigh and trunk movements near the hip joint would have been dominant in movement coordination.

Significance: The current study showed increased thigh and trunk movement during the upright phase of ULD. This could be shown to indicate the need to control the center of the body to control the movement. Pelvic control is an important part of high-speed, multi-directional sports, and it has also been suggested that a strong and controlled core is necessary for high performance. Based on this, it was expected that ULD may have a positive effect on cutting, horizontal transitions, and performance.

References: [1] Zatsiorsky et al. (2020), *Human Kinetics*, [2] Haff et al. (2015), *Human kinetics,* [3] McGill et al. (2010), *Strength & Conditioning Journal.*

COMPARATIVE ANALYSIS OF THE EFFECTS ON MUSCLE ACTIVATION: CONVENTIONAL DEADLIFT VS CONVENTIONAL DEADLIFT WITH UNSTABLE LOAD

HunMin Kim[1], Seung-Jun Ko[2], Joohyun Lee[3], Eunwook Chang[4*]
[1-4] Department of Sports Science, Inha University, Michuhol-gu, Incheon, Republic of Korea
*Corresponding author's email: change@inha.ac.kr

Introduction: The conventional deadlift is a fundamental exercise in strength and conditioning programs [1]. It is known for its ability to enhance muscle strength, power, and muscle hypertrophy [2]. Despite the popularity of conventional deadlift, little is known about the effects of unstable load on deadlift exercises on muscle activation patterns. This study investigated the effects of unstable loading with kettlebells on muscle activation. The current study hypothesized that using a kettlebell to provide an unstable load during a deadlift exercise would result in higher muscle activation.

Methods: 20 young males (age: 22.5±2.3) participated based on their regular weight training experience and without specific injuries or disorders. The deadlift was performed at 80% of one repetition maximum (1RM) and the conventional deadlift with kettlebell was performed with a 12kg kettlebell hanging from elastic bands at each end of the barbell. The weight was the same for conventional deadlift (CD) and conventional deadlift with kettlebells (CDKB). Each deadlift was divided into an ascending phase, a descending phase, and an upright phase. To measure muscle activation, surface electromyography (EMG) (Trigno Sensor System, Delsys Inc., Natick, MA) was attached to the Vastus Medialis (VM), Vastus Lateralis (VL), Biceps Femoris (BF), Semitendinosus (ST), Gluteus Maximus (GM), Erector Spine (ES), and Latissimus Dorsi (LD). The EMG electrodes were placed on the right side of the body. The EMG signals were band-pass filtered at fourth-order zero-lag Butterworth at 10–500Hz and the amplitudes of the signals were expressed as root mean square (RMS) values (MATLAB, The MathWorks Inc, MA).

Results & Discussion: This study identified significant differences between CD and CDKB. During various phases, EMG analyses revealed distinct muscle activation patterns. In the upright phase, only the ST muscle (t=-2.606, p=0.017) showed significantly higher activation for CDKB than CD. This study provided valuable insight into how the ST muscle is activated to manage the instability caused by the unstable loading that occurs when combining kettlebell and deadlift. Due to the anatomical position of the ST muscle, it could play an important role in utilizing internal rotation of the hip joint and stabilizing the hip joint. It could be speculated that the higher activation of the ST muscles in the CDKB was more attributable in engaging these muscles for stabilization and balance during unstable load deadlifts than in the CD. These adaptations were not only a response to the immediate need to maintain balance but also indicated the potential for targeted muscle strengthening and injury prevention strategies.

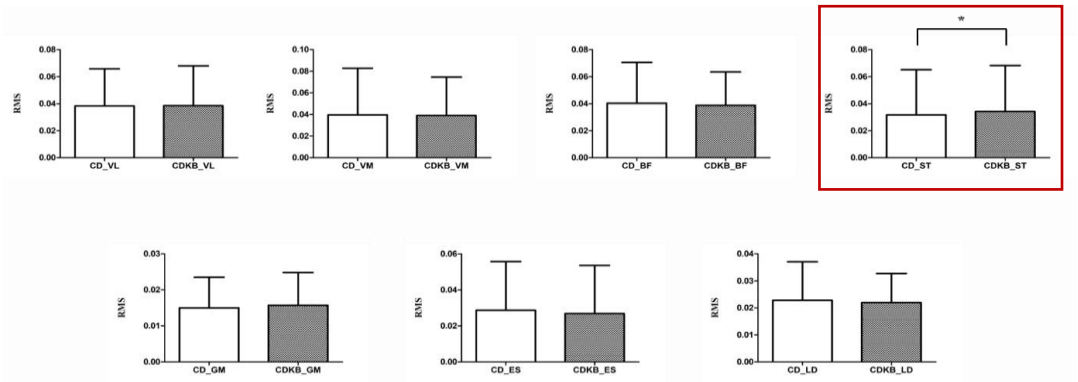

Figure 1: Mean and SD values of muscle activation among upright phase of each deadlift exercise.
RMS: Root Mean Square, CD: Conventional Deadlift, CDKB: Conventional Deadlift with Kettlebell, VL: Vastus Lateralis, VM: Vastus Medialis, BF: Biceps Femoris, ST: Semitendinosus, GM: Gluteus Maximus, ES: Erector Spine, LD: Latissimus Dorsi.
White: CD, Black: CDKB, Red Box: ST muscle activation (* p=0.017).

Significance: According to this result, the ST muscle might act as a stabilizer in the standing position, representing an advancement in the understanding of muscle function. Previous studies showed that hamstring injuries were different between BF and ST and that the tone of the ST muscles worsened as the competition season progressed [3]. ST is significant for injury prevention and performance enhancement and requires attention [4]. Based on these previous studies, the results of this research suggested that hamstring injury prevention and performance enhancement may be possible, especially during competition season. Consequently, combining kettlebells and conventional deadlift showed the potential for strategic integration into an athlete's training program. These findings could lead to further research efforts, such as developing protocols to increase functional strength and prevent injury in both athletic and non-athletic populations.

References:
[1]Zatsiorsky, V.M., W.J. Kraemer, and A.C. Fry, *Human Kinetics*(2020); [2]Haff, G.G. and N.T. Triplett, *Human kinetics*(2015); [3]Mense, S. and A.T. Masi, *Muscle pain: understanding the mechanisms*(2010); [4]Schuermans, J., et al., *British journal of sports medicine*(2014).

CONTINUOUS INTER-LIMB GAIT COORDINATION AND STABILITY IN VETERANS AND SERVICE MEMBERS WITH TRANSTIBIAL LIMB LOSS: INFLUENCES OF PROSTHETIC ANKLE-FOOT DEVICES

Alexis Sidiropoulos, PhD[1], Brad D. Hendershot, PhD[2], Jonathan Gladish, MS[2], David Herlihy, BS[1,3], Jason Maikos, PhD[1]
[1]Department of Veteran Affairs New York Harbor Healthcare System, New York, NY, USA
[*]Corresponding author's email: alexis.sidiropoulos@va.gov

Introduction: Most research available to clinicians for proper prosthetic prescription is noncommittal and lacks guidance for clinical practice [1]. The primary outcomes traditionally used to determine effectiveness of prosthetic devices indicate mixed results, limiting evidentiary support for optimal prescription guidelines [2]. Conversely, continuous measures of coordination and stability, evaluated using Relative Phase (RP) analysis, provide superior sensitivity over traditional spatiotemporal measures and detect changes at a greater resolution [3]. The primary aim of this study was to quantify levels of continuous inter-limb gait coordination and stability among Veterans and SMs with transtibial limb loss (TLL). We hypothesized that individuals with vs. without TLL will indicate less coordination and stability. The secondary aim was to determine the extent to which gait coordination and stability of Veterans and SMs with TLL are influenced by different Energy Storing and Returning (ESR) ankle-foot devices (i.e., ESR, articulating ESR (ART), and powered ESR (PWR)). It was hypothesized that the PWR device will indicate greater levels of coordination and stability compared to the other devices.

Methods: Thirty individuals with unilateral TLL were fit and evaluated with ESR, ART, and PWR devices. Participants separately utilized each device for 1 week at home, followed by biomechanical gait analysis. Ten individuals without TLL (control group) performed 1 gait analysis session. All participants walked at 1.3 m/s across a 10-meter instrumented walkway until at least 15 steps per foot were recorded. RP analysis calculated continuous measures of coordination, Mean Absolute Relative Phase (MARP), and stability, Deviation Phase (DP), between limbs. A low MARP value (closer to 0°) indicates a more in-phase relationship, while a high MARP value (closer to 180°) indicates a more anti-phase relationship. A low DP value (closer to 0°) indicates a more stable organization of the neuromuscular system and a high DP value (closer to 180°) indicates less stability. Two sample T-tests determined differences between the control group and each device for MARP and DP separately. Linear mixed effect models compared MARP and DP between devices, while accounting for repeated observations. Pairwise comparisons were conducted using estimated marginal means. Significance was set at $p<0.05$.

Results and Discussion: *Primary Aim*: Veterans and SMs with vs. without TLL experience deficits in coordination and stability (Table 1). *Secondary Aim*: The PWR device indicates a less coordinated gait pattern than the ART device between the prosthetic-side arm and leg, and lesser coordination than both the ESR and ART devices between the prosthetic-side arm and intact-side leg. However, the PWR device indicates a more stable gait pattern than the ESR device between the intact-side arm and leg and is more stable than the ART and ESR devices between the intact-side arm and prosthetic-side leg.

Table 1. Deficits in coordination (MARP) and stability (DP) in Veterans and SMs with TTL compared with intact individuals.

	MARP	t-value	p-value
Arm to Arm			
Control	157.66	-3.06	0.004
ART	162.65		
Prosthetic-side Arm to Intact-Side Ankle			
Control	17.32	-2.19	0.036
ART	22.87		
	DP	**t-value**	**p-value**
Leg to Leg			
Control	2.98	-2.27	0.037
PWR	3.64		
Control	2.98	-2.32	0.032
ART	3.58		
Prosthetic-Side Wrist to Intact-Side Ankle			
Control	5.58	-2.04	0.049
PWR	7.86		
Control	5.58	-2.09	0.045
ART	7.44		

RP analysis is sensitive enough to identify differences between individuals with vs. without TLL and between the prosthetic devices. As expected, individuals with vs. without TLL experience deficits in both measures. Interestingly, the PWR device indicated greater levels of stability and lower levels of coordination compared to the other devices, which may be due to the novelty of the device for some individuals. It is possible that the active push-off of the PWR device disrupts the accustomed coordinative pattern of a non-powered device, while the new pattern of the PWR device allows for greater motor pattern consistency compared to the other devices. This device is also associated with large outliers in the coordination measure. When removed, the coordination deficits of the PWR device may be eliminated. If so, a clear advantage of the PWR device would be evident, as it provides the greatest stability advantage to individuals with TLL.

Significance: The deficits in gait coordination and stability among Veteran and SMs with TLL across different types of prosthetic ankle-foot devices can help support development of rehabilitation programs focused on improving these parameters. Importantly, findings can directly influence prescription guidelines to optimize healthcare for all Veterans and SMs with TLL, helping them to live high quality, active lives.

Acknowledgments: We thank Dr. Timothy Moore, the Narrows Institute, the VISN 2 BRAVO lab, and Walter Reed National Military Medical Center for their support and contributions. The views expressed herein are those of the authors and do not necessarily reflect the official policies of the U.S. Departments of the Army, Navy, or Air Force, nor the US Government. The identification of specific products or instrumentation is considered an integral part of the scientific endeavor and does not constitute endorsement or implied endorsement on the part of the authors nor by the US Government. This study is funded by the DoD Orthotics and Prosthetics Outcomes Research Program (OPORP) (W81XWH2-1-0409) and expands upon an ongoing study (DoD OPORP, W81XWH-17-2-0014).

References: [1] Highsmith et al. (2016), *J Rehab Res Dev*, 53; [2] Healy et al. (2018), *PLoS ONE*, 13(3); [3] Haddad et al. (2010), *J App Biomech*, 26(1).

COMPARISON OF RELIABILITY BETWEEN BAREFOOT AND SHOD CONDITIONS FOR A NOVEL FORCE CONTROL TASK

Madison J. Mingo[1*], Amelia S. Lanier[1], Adam B. Rosen[2], Elizabeth A. Wellsandt[3], Brian A. Knarr[1]
[1]Department of Biomechanics, University of Nebraska at Omaha, Omaha, NE USA
[2]School of Health and Kinesiology, University of Nebraska at Omaha, Omaha, NE USA
[3]Department of Health and Rehabilitation Sciences, University of Nebraska Medical Center, Omaha, NE USA
*Corresponding author's email: mmingo@unomaha.edu

Introduction: Returning to cutting and pivoting sports following anterior cruciate ligament reconstruction (ACLR) increases the odds of a graft rupture by a factor of 3.9 and a contralateral rupture by a factor of 5.0 [1]. Neuromuscular assessments during rehabilitation can identify deficits in individuals after ACLR and may be useful as screening tools for anterior cruciate ligament (ACL) re-injury risk. Recently, a neuromuscular force control task has been developed that differentiates control strategies between high-performance athletes, recreational athletes, individuals with ACL deficiency, and individuals following ACLR [2]. Those with an ACL injury exhibited diminished motor control compared to uninjured individuals. The task was previously completed barefoot, which allowed for fine control of movement through increased sensory input to the foot [3]. However, when participating in sports, individuals often wear shoes that provide surface traction and lateral support [4, 5]. Thus, the purpose of this study was to identify the reliability of performing the novel force control task barefoot and shod.

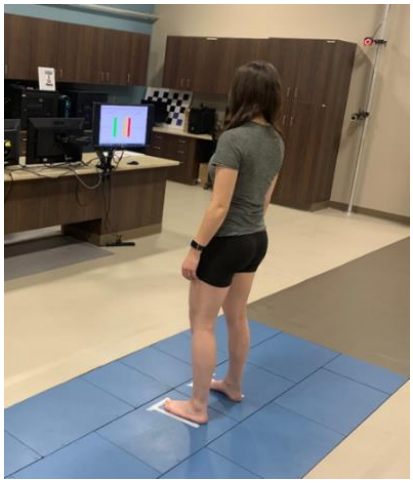

Figure 1: Experimental setup of the novel force control task.

Methods: Thirteen individuals (7 M, 24.9±4.6 years, BMI: 23.4±3.8 kg/m^2) completed the force control task for the barefoot condition. Twenty-two individuals completed the force control task for the shod condition (12 M, 23.3±4.6 years, BMI: 23.1±4.5 kg/m^2). For the task, participants stood on force plates and generated shear forces bi-directionally to the beat of a metronome set at 60 beats per minute (bpm). Participants were asked to align a slider on the screen in front of them with stationary indicators set at 50% of their maximal force (measured initially during the testing session) in each direction (Figure 1). The task was completed for medial/lateral (ML) and anterior/posterior (AP) directions for both legs. Force control variability was measured using the largest Lyapunov exponent (LyE), which was calculated using the algorithm from Wolf et al. [6]. Participants completed the testing protocol during two sessions that occurred exactly one week apart. Intraclass correlation coefficient (ICC) for a two-way mixed effects model, single rating, and absolute agreement with 95% confidence intervals, standard error of measurement (SEM), and minimum detectable change (MDC) were calculated. ICC values were interpreted as follows: less than 0.5 (poor reliability), 0.5 to 0.75 (moderate reliability), 0.75 to 0.9 (good reliability), and greater than 0.9 (excellent reliability) [7].

Results & Discussion: For the barefoot condition, ICC values across all measures were considered good to excellent, and the Right ML direction was statistically significant (Table 1). For the shod condition, ICC values across most measures were considered good, with the Left AP direction considered moderate (Table 2). The confidence intervals between the barefoot and shod conditions overlap across all measures, suggesting that the reliability between the two conditions is not significantly different.

Table 2: P-value, ICC, SEM, and MDC for the barefoot condition

Test Direction	P (H_0=0.75)	ICC (95% CI)	SEM	MDC
Right ML	*0.025	0.92 (0.75-0.98)	0.39	0.91
Right AP	0.172	0.82 (0.50-0.94)	0.62	1.45
Left ML	0.265	0.82 (0.51-0.94)	0.63	1.48
Left AP	0.401	0.78 (0.39-0.93)	0.58	1.35

*Statistical significance

Table 1: P-value, ICC, SEM, and MDC for the shod condition

Test Direction	P (H_0=0.75)	ICC (95% CI)	SEM	MDC
Right ML	0.456	0.76 (0.50-0.90)	0.72	1.69
Right AP	0.210	0.78 (0.54-0.91)	0.81	1.89
Left ML	0.435	0.77 (0.51-0.90)	0.74	1.74
Left AP	0.529	0.74 (0.48-0.89)	0.98	2.29

Significance: These results suggest that the novel force control task can reliably measure force control variability for both barefoot and shod conditions. Furthermore, the reliability is not altered by footwear condition. Future studies are required to determine if force control variability is related to patient outcomes following ACL injury.

Acknowledgments: This project was funded through the University of Nebraska Omaha's Office of Creative Activity and Research.

References: [1] Webster et al. (2014), *Am. J. Sports Med.* 42(3); [2] Lanier A et al. (2020), *J Orthop Res.* 38(8); [3] Francis & Schofield (2020), *Sens. Switz.* 18(8); [4] Worobets & Wannop (2015), *BMJ Open Sport Exerc. Med.* 6(1); [5] Stacoff et al. (1996), *Med. Sci. Sports Exerc.* 28(3); [6] Wolf et al. (1985), *Phys. Nonlinear Phenom.* 16(3); [7] Koo & Li (2016), *J. Chiropr. Med.* 15(2).

LIMITATIONS IN SHOULDER RANGE OF MOTION AFTER RADIATION THERAPY FOR BREAST CANCER ARE DEPENDENT ON RADIATION TREATMENT REGIMEN

Blaire Park, Parasar Athmakuri, Susann Wolfram, David B. Lipps
School of Kinesiology, University of Michigan, Ann Arbor
*Corresponding author's email: siyeonp@umich.edu

Introduction: Limitations in shoulder range of motion (ROM) are a common side effect of radiation therapy (RT) for breast cancer, especially when the radiation field is extended to include the axillary lymph nodes after prior axillary lymph node dissection (ALND) [1]. It is unclear if these ROM limitations are attributable to the increased radiation dose or axillary surgery. Shoulder ROM limitations may result from RT treatment regimen, as shoulder ROM was not different in women receiving RT to breast and axilla with or without prior ALND [2]. These limitations in shoulder ROM may be caused by greater pectoralis major stiffness after RT [3], but this is currently unknown. The present study aimed to investigate if shoulder ROM differs between breast cancer patients who received RT to the breast only and breast cancer patients who received RT to the breast and axilla without ALND, and to establish if shoulder ROM is associated with pectoralis major stiffness. We hypothesize that shoulder ROM will be more limited in patients receiving RT to the breast and axilla than in patients receiving RT to the breast only and that smaller ROM is related to greater pectoralis major stiffness.

Methods: We recruited 16 patients with a unilateral breast cancer diagnosis who underwent breast-conserving surgery with sentinel lymph node biopsy followed by RT 12-60 months prior. Eight patients (mean ± S.D. age 57.4 ± 8.9 yrs, height 164.4 ± 6.0 cm, weight 79.2 ± 11.9 kg) received RT to breast and axilla, and eight patients (age 58.4 ± 7.6 yrs, height 163.9 ± 6.4 cm, weight 69.8 ± 6.4 kg) received RT to the breast only. These patients were compared to a control group of eight age-matched, cancer-free women (age 57.6 ± 7.7 yrs, height 162.8 ± 5.4 cm, weight 61.3 ± 5.6 kg). Active ROM of both shoulders was assessed for abduction, flexion and extension in random order using inertial measurement units (IMU) (Opal, APDM Inc.) worn on the upper arms. Shoulder ROM was calculated from the IMU elevation angle estimated from acceleration and angular velocity. Shear wave velocities (SWV) were extracted from shear wave elastography images (Hologic Mach 30) of the sternocostal region of the pectoralis major on the affected side at rest with the shoulder 90° abducted, serving as a measure of muscle stiffness. Differences in ROM between groups, shoulders and their interactions were examined with a repeated-measures ANOVA. Group (RT to breast + axilla, RT to breast only, control) was a between-subjects factor, and shoulder (affected side, unaffected side) a within-subjects factor. In the control group, shoulders were randomly assigned to be the affected and unaffected side. Pearson's correlation was used to identify associations between ROM on the affected side and SWV.

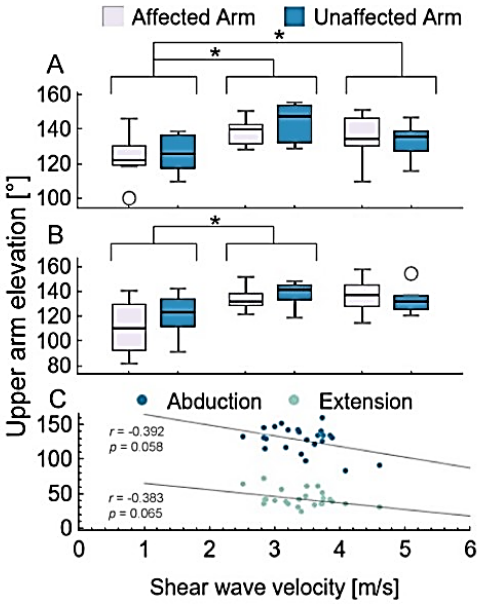

Figure 1: Shoulder ROM in abduction (A) and flexion (B) expressed as the elevation angle of an IMU worn on the upper arm. (C) Association of pectoralis major stiffness with abduction or extension ROM on the affected side. *$p < 0.05$

Results & Discussion: A significant main effect of group existed for abduction ROM ($p = 0.003$) and flexion ROM ($p = 0.011$) and trended towards significance for extension ROM ($p = 0.051$). Tukey's post-hoc comparison showed that abduction and flexion ROM were significantly lower in the breast + axilla group than in the breast only group ($p \leq 0.008$), indicating that breast cancer patients receiving RT to the breast and axilla experience ROM limitations in support of our first hypothesis (Fig. 1A+B). There was no significant main effect of shoulder (all $p \geq 0.17$), indicating that the observed ROM limitations exist in both shoulders. Patients receiving RT to the breast only had similar ROM to the control group (all $p \geq 0.15$) and did not seem to experience ROM limitations. We found no group*shoulder interaction effect (all $p \geq 0.249$) for any ROM. Reduced ROM may be associated with increased pectoralis major stiffness. There was a trend towards a significant negative correlation of SWV with abduction ROM ($r = -0.392$, $p = 0.058$) and extension ROM ($r = -0.383$, $p = 0.065$) (Fig. 1C).

Significance: The findings of the present study indicate that expanding the radiation field to a larger region of the chest may negatively affect shoulder ROM, even when ALND is omitted. Omitting ALND has positive outcomes for lymphedema management [2], but patients receiving RT to breast and axilla still appear to be at risk of developing shoulder ROM deficits in both their affected and unaffected shoulders. These patients would likely benefit from screening for post-treatment rehabilitation, which should include both shoulders, even in patients with a unilateral breast cancer diagnosis. Limitations in shoulder ROM on the affected side may be related to a stiffer pectoralis major after RT, and post-treatment rehabilitation should likely also focus on decreasing pectoralis major stiffness.

Acknowledgments: This study was funded by a University of Michigan Rogel Cancer Center Postdoctoral Small Grant and an American Cancer Society Research Scholar Grant (RSG2001601CCE).

References: [1] Johansen et al. 2014. *Acta Oncol*. 53(4); [2] Donker et al. 2015. *Lancet Oncol.* 15(12); [3] Lipps et al. 2019. *Sci Rep.* 9(1).

ROLES OF ANGULAR MOMENTA FOR BALL SPEED IN HIGH SCHOOL BASEBALL PITCHERS

Jun Ming Liu[1*], Christopher Knowlton, Mathew Gauthier, Zach Tropp, Nikhil Verma, Gregory Nicholson, Anthony Romeo, Antonia Zaferiou[1]
[1]Stevens Institute of Technology
*Corresponding author's email: jliu130@stevens.edu

Introduction: Baseball pitching involves sequential rotations of body segments from the ground up to produce high ball velocity at release [1]. Angular momentum (H) about the body's center of mass (COM) measures rotational behavior. It can provide insight into the contribution of each body segment towards rotation generation and achieving ball velocity. H for each body segment is the sum of (1) the 'local term': the segment's angular velocity multiplied by its moment of inertia, and (2) the 'remote term': the cross product of (a) the vector from the body's COM to the segment's COM and (b) the segment's COM linear momentum relative to the body's COM [2]. Prior research of angular momentum in pitching only focused on the 'local term' [3-4] and did not include the 'remote term' that accounts for the segment's linear momentum relative to the body's COM. Also, prior work did not investigate how angular momentum relates to ball speeds [3-5]. We aimed to examine segmental and whole-body H in high school baseball pitchers. We hypothesized that maxima whole-body, trunk, and pitch-side upper- and forearm H would positively associate with ball velocity.

Methods: High school male pitchers (n=19; mean (S.D.) age of 15.3 (1.0) years) volunteered for this study in accordance with the IRB. Pitchers self-reported an ability to throw 75-mph fastballs. They pitched at least 5 fastballs on a regulation practice mound at regulation distance (18.44 m) with optical motion capture. Markers and rigid-body clusters were attached to body segments.

All variables are expressed in a global coordinate system with a horizontal forward axis from mound to home plate, an upward axis as global vertical, and a leftward axis as a cross product of upward and forward axes. Whole-body H was calculated as the sum of all segments H. Segment and whole-body COM position, and H were calculated using prior methods [2, 6]. H_{max} was computed for whole-body and each segment's H about each global axis. Ball speed was measured using a radar gun. Linear mixed models were used with ball speed as the outcome measure, each H_{max} as the fixed effect, and pitchers as the random effect (α<0.05).

Results & Discussion: Ball speed is significantly associated with whole-body H_{max} about the leftward axis ($p<0.001$), trunk H_{max} about leftward and upward axes ($p<0.01$ in each), and pitch-side forearm about all three axes ($p<0.05$ in each) (**Figure 1A-C**). Whole-body and trunk H_{max} about leftward axis was larger than the other two directions. Trunk H_{max} was also a large contributor to whole-body H_{max} about leftward axis. The association of ball speed with the trunk H_{max} about upward axis was consistent with the prior findings of a correlation between ball speed and peak trunk rotation velocity [7]. The associations of ball speed with the pitch-side forearm H_{max} were expected as it was the closest body segment to the ball. The pitch-side forearm H_{max} was dominated by the 'remote term' due to the forearm segment's high linear momentum relative to the body's COM.

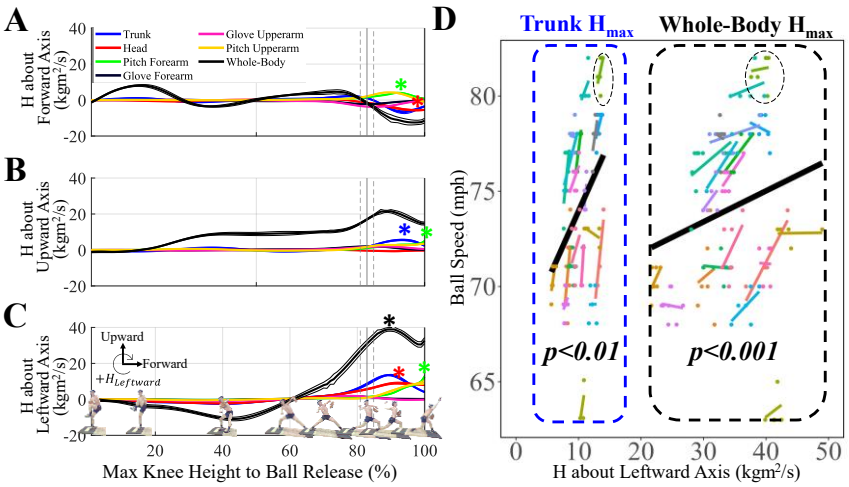

Figure 1: Whole-body and select segment angular momentum (H) about (**A**) forward, (**B**) upward, and (**C**) leftward axes from an example pitcher (circled in **D**). *Indicates significant association between H_{max} and ball speed at the group-level. Group association plots (**D**) between ball speed and trunk (blue) and whole-body (black) H_{max} about leftward axis with dots representing trials, color lines for each pitcher and the black line as the group trend line.

The significant positive association between ball speed and H_{max} about the leftward axis and the observation that H about the leftward axis was the largest component of the resultant H both highlight the importance of generating rotation in this plane. Trunk H_{max} was a major contributor to whole-body H_{max} about the forward and upward axes. Trunk H peaked before ball release before decreasing, coinciding with an increase in the pitch-side upper arm and forearm H, indicating a transfer of angular momentum distally. Notably, some pitchers exhibited trends that did not follow the group trends, prompting future research into individual strategies to increase ball speed.

Significance: The significant positive associations between ball speed and whole-body and segmental H_{max} in specific axes highlighted the importance of momentum generation and transfer in pitching. H may be a more appropriate measure to fully describe the rotational behaviours of the body during baseball pitching by accounting for more than just the segment's angular velocity.

Acknowledgments: We thank the pitchers for volunteering and financial support from a Major League Baseball research grant.

References: [1] Pappas A.M. et al (1985) *Am J Sports Med*. (13)4 [2] Herr H., Popovic M. (2008) *J of Exp. Bio*. 211(4) [3] Lin HT. et al (2003) *J Chinese Inst. of Eng.* 26(6) [4] Ramsey D., Crotin R. (2016) *Human Move. Sci.* 46 [5] Betzel R.F. (2010) *Thesis Indiana. U*. [6] de Leva (1996) *J. Biomech.* 29(9) [7] Orishimo K.F. et al (2023) *J. Strength Cond. Res.* 37(3)

UNILATERAL MUSCLES COMPENSATE AFTER ROTATOR CUFF TEAR DURING A STATIC BIMANUAL TASK: A BILATERAL MODEL ANALYSIS

Zoe M. Moore[1*], Joshua Pataky[1], Meghan E. Vidt[1,2]
[1]Biomedical Engineering, The Pennsylvania State University, University Park, PA, USA
[2]Physical Medicine and Rehabilitation, Penn State College of Medicine, Hershey, PA, USA
email: *zmm5238@psu.edu

Introduction: Rotator cuff tears (RCT) are common among the adult population [1]. Tears are characterized by partial or full thickness tearing of the supraspinatus tendon, often accompanied by tears in infraspinatus and subscapularis tendons. RCT are associated with pain and decreased function [2]. Loss of function is particularly detrimental in an occupational setting for workers that are required to regularly lift and move weighted objects. Previous work by our group showed that with a RCT uninjured muscles, including deltoid and teres minor, increase their force production during unimanual functional tasks as a form of compensation [3]; other unpublished work showed that the same uninjured muscles increase their force contribution with increased RCT severity to perform a loaded forward reach task. However, daily routines rely on completion of bimanual tasks, such as lifting and holding weighted objects, and little work has been performed to determine how muscles compensate bilaterally in the context of a RCT. Therefore, the objective of this study was to develop and use a bilateral model to study muscle compensation strategies for a RCT during a loaded static task.

Methods: A bilateral model representing 50th percentile young adult males was developed using the unilateral MoBL-ARMS model in OpenSim software (v.3.3) [4,5]. Briefly, the joint definitions and muscle paths from the sternoclavicular joint through the hand on the right side were mirrored to the left side to produce a bilateral model. The baseline model represented no RCT and 3 additional models were developed to represent unilateral (right side) RCT severities: partial thickness supraspinatus tear; full thickness supraspinatus tear with infraspinatus involvement; and massive 3-tendon tear involving supraspinatus, infraspinatus, and subscapularis. To represent each RCT severity, peak isometric force of the corresponding muscle actuator was reduced to a percentage (e.g. 50% of peak force for partial thickness tear) of the force in the no RCT model. For all models, a 13.3N (3lb) and a 44.5N (10lb) box was separately applied to the model via a weld joint on the left hand and a weld constraint on the right hand to represent the weighted box as a shared load. A static posture in which the arms were fully extended in front of the model (shoulder elevation: 80°; elevation angle: 80°; shoulder rotation: 0°, elbow flexion: 0°) 2s in duration was used as the input to the Computed Muscle Control [6] algorithm. Average muscle force for the task was calculated for each of the 13 muscle paths crossing the shoulder for left and right sides (26 muscle paths total), then normalized to each muscle actuator's peak isometric force. The small sample size precluded formal data analysis, thus normalized average muscle force between the left and the right sides for each loading condition and RCT severity model permutation were assessed qualitatively.

Results & Discussion: There were no large force increases in the left side to compensate for the injury in the right shoulder for either the 13.3N or the 44.5N load for any RCT severity models studied (Fig. 1). However, muscles in the right shoulder increased force contribution. The clavicular compartment of pectoralis major muscle had the greatest normalized muscle force, indicating it was activated closest to its maximal capacity; this muscle actuator decreased from 90% (no RCT) to 85% (massive tear) of maximum capacity for the 13.3N load, and from 80% (no RCT) to 100% (massive tear) of maximum capacity for the 44.5N load (Fig. 1). Other muscles, including middle deltoid and teres minor, also increased force contribution, achieving 48% and 28% of maximum capacity, respectively, for the massive RCT model with the 44.5N load. Increased force contribution from deltoid and teres minor is consistent with our prior work, suggesting that these muscles may be primary compensators for upper extremity tasks. There was no major change in muscle force on the uninjured side (left), which may be due to the static nature of the task, in which holding a box anteriorly requires approximately equal force between left and right sides to maintain stability. This work shows that the side with a RCT compensates for muscle force lost due to injury without additional changes in muscle force from the uninjured (left) side during a bimanual task. Ongoing work continues to examine these trends in other static and dynamic bimanual tasks and loading conditions to better understand bilateral muscle compensation.

Significance: With a unilateral RCT, muscle compensation occurs within the injured side but not on the unaffected side, for a static loaded task. The model developed and used here will enable ongoing studies to better understand bilateral muscle compensation in the context of RCT and help to inform rehabilitation protocols.

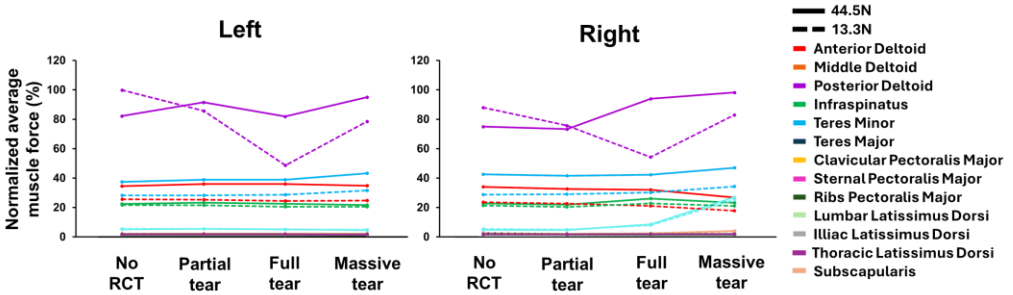

Figure 1: Normalized average muscle force for the 13 muscles crossing the shoulder on left and right sides for 13.3N and 44.5N loads.

Acknowledgments: Pennsylvania State University start-up funds (Vidt)

References: [1] Yamamoto et al. J Shoulder Elbow Surg. 2010;19(1). [2] Vidt et al. J Biomech. 2016;49(4). [3] Pataky et al. Clin Biomech. 2021. [4] Delp et al. IEEE Trans Biomed. Eng. 2007;54(11). [5] Saul et al. Comput Methods Biomech Biomed Eng. 2015; 18. [6] Thelen et al. J Biomech. 2003;36(3).

COMPARISON OF A SINGLE-VIEW IMAGE-BASED SYSTEM TO A MULTI-CAMERA MARKER-BASED SYSTEM FOR HUMAN STATIC POSE ESTIMATION

Jonathan S. Slowik*, Thomas W. McCutcheon, Benjamin G. Lerch, Glenn S. Fleisig
American Sports Medicine Institute, Birmingham, AL, USA
*jons@asmi.org

Introduction: Postural assessment can be critical to the prevention and treatment of injuries. Traditional assessment methods typically depend on the subjective opinion of an experienced clinician, while more recent attempts at objective quantification usually involve complicated setups of multiple cameras or inertial measurement devices, each with their own specific drawbacks [1]. With the continued improvement of cameras in ubiquitous technologies such as mobile phones and video game systems, an assessment tool utilizing these devices would have great potential for more widespread usage [2]. However, it is important to understand the capabilities and limitations of any emerging technology before utilizing it for research or medical applications and advocating for its extensive use. Therefore, the purpose of this study was to compare human static pose estimation from an innovative single-view image-based system to standard multi-camera marker-based capture. We expected that the single-view system would be able to produce similar measurements to the multi-camera system for some participant orientations, but that occlusion would cause much larger errors at other orientations.

Methods: Thirty participants (20 male / 10 female, mean ± standard deviation 29.1 ± 10.0 years old, 1.75 ± 0.10 m tall, 79.1 ± 18.0 kg) performed six repetitions each of static holds during arm-raises (T-pose) and squats, rotating their orientation by 60° between repetitions. These trials were captured simultaneously with a 120-Hz 12-camera marker-based system (Motion Analysis Corporation, Rohnert Park, CA) and a variable-frequency (24–30 Hz) single-view image-based system (Phyxd, Inc., New York City, NY). The marker-based system directly estimated the marker 3D positions, while the image-based system utilized a Kinect Azure DK camera (Microsoft Corp., Redmond, WA) and a patented volumetric computer-vision approach (Aemass, Inc., San Francisco, CA) to generate marker position estimates. In simplified terms, a 3D surface model of each participant (including the markers) was generated from a series of three simple calibration movements, fitted to the arm-raise and squat data, and used to predict the 3D positions of each marker. Discrete estimates of bilateral shoulder angles during arm-raises and bilateral knee angles during squats were then calculated and compared between the systems using repeated measures Bland-Altman analyses [3] and descriptive statistics. Pearson correlation coefficients were calculated, comparing the participant trial mean values across systems. Finally, a two-way repeated measures ANOVA was used to examine whether participant orientation in the capture volume significantly affected either system.

Results & Discussion: Biases for discrete measurements ranged in magnitude from 1.3 to 1.9 degrees (e.g., Fig. 1), standard deviations of the differences between systems ranged from 2.4 to 4.7 degrees, and Pearson correlation coefficients were all above 0.97. Thus, the marker-based and image-based systems produced similar measurements of static shoulder and knee angles. Surprisingly, the ANOVA was unable to find any statistically significant orientation effects for either system, suggesting that the volumetric computer-vision approach of the image-based system was able to overcome any systematic occlusion effect from its dependence on a single view. Future work should examine more complex measurements from the volumetric scan-based models and also investigate the ability of single-view image-based systems to measure dynamic movements.

Significance: This study demonstrated that a single-view image-based system can provide remarkably similar estimates of human static pose data to a "gold standard" 12-camera marker-based system. By utilizing commonplace technologies such as the cameras included in mobile phones and/or video game systems, such systems may overcome many of the hurdles to widespread adoption in remote clinics or even individual residences [1,2].

Acknowledgments: The authors thank Travis Dias for help with initial study conceptualization and methodology development.
Funding: This work was funded by Phyxd, Inc. (New York City, NY). The funding organization had no role in the study design; in the collection, analysis, and interpretation of data; in the writing of the manuscript / conference abstract; or in the decision to submit for publication / presentation.

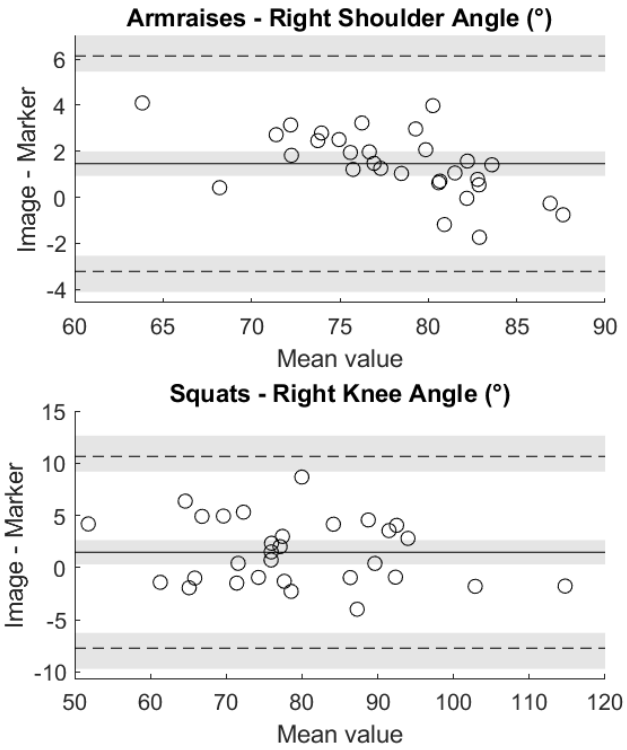

Figure 1: Bland-Altman plots for right shoulder angles (during arm-raises) and right knee angles (during squats). Each data point represents the average values for a single participant. The solid line denotes the bias between measurement systems, the dashed lines are the upper and lower limits of agreement, and the three shaded regions are their respective 95% confidence intervals.

References: [1] Wade et al. (2022), *PeerJ* 10: e12995; [2] Stenum et al. (2021), *Sensors* 21: 7315; [3] Olofsen et al. (2015), *J Clin Monit Comput* 29: 127-139.

EFFECT OF ROTATOR CUFF TEAR AND SURGICAL REPAIR ON SUPRASPINATUS MUSCLE MECHANICS

Kathryn T. Rex[1*], Lilla Caton[1], Zoe M. Moore[1], April D. Armstrong[2], Meghan E. Vidt[1,3]
[1]Department of Biomedical Engineering, Pennsylvania State University, University Park, PA, USA
[2]Department of Orthopaedics & Rehabilitation, Penn State College of Medicine, Hershey, PA, USA
[3]Department of Physical Medicine & Rehabilitation, Penn State College of Medicine, Hershey, PA, USA
*Corresponding author's email: ktr5133@psu.edu

Introduction: Rotator cuff tears (RCT) are common in the older adult population [1] and can cause pain and limit range of motion during functional tasks [2, 3]. Muscle degradation and fatty infiltration are known to occur post-injury in the supraspinatus muscle [4]. The rate at which muscle composition changes over time and how these changes affect muscle mechanical properties are unknown. This study's objective is to quantity how supraspinatus muscle mechanical properties change over time following RCT and surgical repair.

Methods: Eight New Zealand White rabbits (3M/5F) were studied. Animals were randomly assigned to either 2-, 4-week after injury,16-week repair, or 16-week sham groups (n=1; n=4; n=2; n=1, respectively). All groups received rotator cuff injury surgery, where the supraspinatus tenson was severed with sharp dissection [5]. The sham group received a sham injury surgery. At 8-weeks after injury, the 16-week repair group received a rotator cuff repair, and the 16-week sham group received a sham repair surgery. Animals were euthanized at their assigned timepoints and the supraspinatus muscle from both the injured and contralateral limbs were harvested. For mechanical testing, muscles were dyed with methylene blue, followed by application of 3 Verhoff stain lines evenly spaced along the long axis of the muscle using water based white paint. An MTS 858 Bionix System (MTS Systems Corp., Eden Prairie, MN) was used to perform mechanical testing with an adapted protocol previously used by our group [6]. Briefly, muscles were loaded to 1% of original measured muscle length. The muscle then underwent 10 preconditioning cycles from 1% to 5% of original measured length, followed by a 300 second rest period. Stress-relaxation was then performed by holding the muscle at 5% of original length at a rate of 5% of original length per second, followed by a 600 second hold. Load to failure in axial tension was performed at a constant rate of 0.1mm/second [6, 7]. Digital image correlation and Harris corner detection was used to calculate strain [8]. Elastic modulus (E) and yield strength were calculated as the slope and end point of the elastic region of the stress-strain curve, respectively. Percent relaxation was calculated as the percent change between maximum stress experienced and equilibrium stress achieved during stress-relaxation. Due to the small sample size, formal statistical analysis could not be conducted, thus, qualitative assessments were performed.

Results & Discussion: There is a trend toward injured muscle having lower elastic moduli (Fig.1A) at the longer (4-week injury, 16-week repair, 16-week sham) timepoints compared to the elastic modulus at the shortest (2-week injury) timepoint, which may be caused by changes in muscle quality over time [9]. There is also a trend toward a lower elastic modulus of the injured muscle than the elastic modulus of the contralateral muscle, which presents for the longer timepoints. Yield strength (Fig.1B) for the injured muscle shows a trend toward being reduced compared to the contralateral muscle for all timepoints. These findings are consistent with literature [6, 10], and may be driven by compensation in the contralateral limb during movement post-surgery. There is a trend toward the percent relaxation (Fig.1C) of the injured limb being lower than the percent relaxation of the uninjured limb for the 16-week repair group, which could suggest that RCT repair surgery has an influence on muscle elasticity and strength, which is consistent with our results for elastic modulus and yield strength, respectively. Ongoing work continues to study these trends in a larger sample and at additional time points.

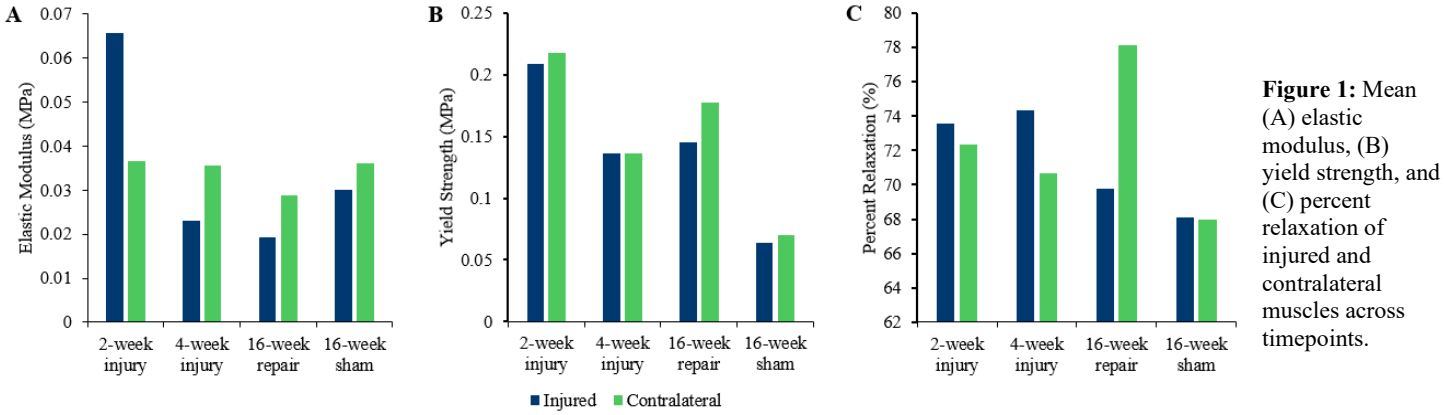

Figure 1: Mean (A) elastic modulus, (B) yield strength, and (C) percent relaxation of injured and contralateral muscles across timepoints.

Significance: Understanding the impact of RCT and repair on muscle mechanics will improve our understanding of the mechanical behavior of muscle after injury. The temporal effects of RCT on muscle mechanics will also be compared with ongoing work to quantify 3-dimensional measures of muscle composition to describe the structure-function relationship of muscle after RCT injury.

Acknowledgments: NIH-NIAMS R01AR079999; Penn State Animal Resource Program; Mitch Vanden Heuvel.

References: [1] Yamamoto et al. (2010), *J Shoulder Elbow Surg* 19(1); [2] Lin et al. (2008). *J Am Med Dir Assoc* 9(9); [3] Van Schaardenburg et al. (1994); [4] Barry et al. (2013), *J Shoulder Elbow Surg* 22(1); [5] Rubino et al., 2008. *Arthroscopy* 24(8); [6] Khandare et al. (2022), *J Biomech,* 132; [7] Luyckx et al. (2014), *J Exp Orthop* 1(7); [8] Elliott et al. (2022), *Ann Biomed Eng* 50(5); [9] Isogai et al. (2022), *J Phys Ther Sci* 34(12); [10] Peltz et al. (2009), *J Orthop Res* 27(3).

GLENOHUMERAL JOINT DYNAMICS VARIABILITY IN MANUAL WHEELCHAIR USERS WITH PEDIATRIC-ONSET SPINAL CORD INJURY

Caleb M.A. Cordes[1*], Joshua M. Leonardis, Alyssa J. Schnorenberg, Anthony Nguyen, Shubhra Mukherjee, Brooke A. Slavens
[1]Department of Rehabilitation Sciences & Technology, University of Wisconsin-Milwaukee, Milwaukee, WI
*Corresponding author's email: cmcordes@uwm.edu

Introduction: Decreased glenohumeral joint dynamics variability during manual wheelchair propulsion has been shown to increase risk for shoulder pain and pathology in manual wheelchair users with spinal cord injury (SCI) [1-4]. Manual wheelchair users with pediatric-onset SCI will be exposed to that risk far longer than users with adult-onset SCI [5]. By determining the relationship of glenohumeral joint dynamics variability with duration of manual wheelchair use in wheelchair users with pediatric-onset SCI, we hope to inform the development of personalized strategies for reducing the incidence of shoulder pathology [5]. Therefore, the purpose of this study was to explore the association of glenohumeral joint dynamics variability during propulsion with age and time since injury in children and young adults with pediatric-onset SCI.

Methods: Nine manual wheelchair users with pediatric-onset SCI (3 males, 6 females; age: 15.2 ± 5.9 years; time since injury: 6.3 ± 5.7 years; SCI levels: C6-T10) participated. A SmartWheel instrumented handrim sampled kinetics at 240 Hz while a Vicon motion capture system sampled marker trajectories at 120 Hz during propulsion at a self-selected speed [6]. A validated model computed 3D joint motions, forces, and moments [6]. Joint dynamics variability was quantified using the coefficient of variation (CV; standard deviation divided by mean). The hypothesis that joint dynamics variability would decrease with increasing age and increasing time since injury was assessed using simple linear regression.

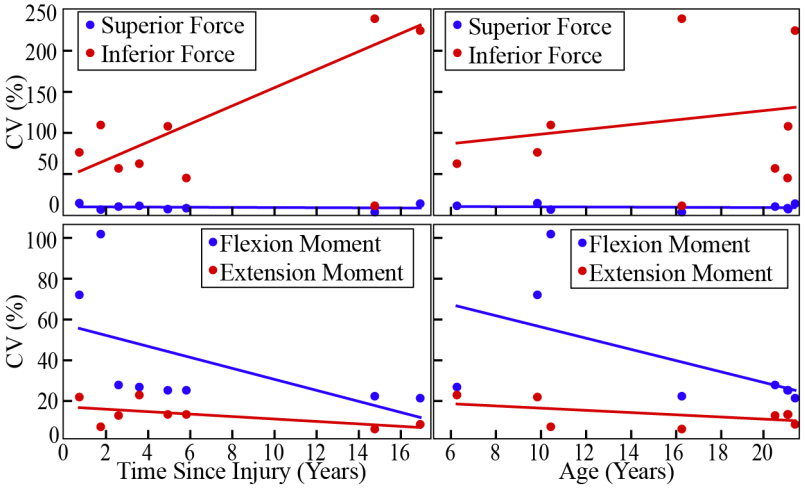

Figure 1: The relationship of sagittal plane glenohumeral joint dynamics variabilities with time since injury and age. Superior force and flexion moment: blue; inferior force and extension moment: red.

Results & Discussion: Peak inferior force variability (CV) was strongly associated with time since injury (Fig. 1; Table 1). Interestingly, no such relationship was identified with age. Peak inferior force variability may change more with duration of wheelchair use than age, which is consistent with prior work identifying relationships between glenohumeral joint dynamics magnitude and years of wheelchair use [7]. Peak anterior force and peak flexion and extension moment variabilities were weakly associated with time since injury and age, and these relationships should be examined further (Fig 1; Table 1). Decreasing joint dynamics variability with increasing years of wheelchair use could potentially contribute to the known concurrent increase in shoulder injury prevalence. Peak superior force variability was not associated with time since injury or age (Table 1).

*Table 1: Relationships between glenohumeral joint dynamics variability, time since injury, and age. * denotes significance (p<0.05).*

Variable	Superior Force CV	Inferior Force CV	Anterior Force CV	Posterior Force CV	Flexion Moment CV	Extension Moment CV
R^2: Time Since Injury	0.02	0.79	0.16	0.22	0.3	0.34
p-value: Time Since Injury	0.74	*0.003	0.32	0.24	0.16	0.13
R^2: Age	0.02	0.05	0.16	0.09	0.31	0.28
p-value: Age	0.72	0.58	0.33	0.47	0.15	0.18

Significance: This is the first exploration of glenohumeral joint dynamics variability in manual wheelchair users with pediatric-onset SCI. These data indicate that time since injury may influence glenohumeral joint dynamics variability, and therefore risk for shoulder injury. The young ages of these individuals may also influence the joint dynamics variability identified. Other potential contributing factors are being examined, including additional planes of motion, pain, function, sex, age at onset of SCI, and level of injury [3,5,7,8,9]. This will help define shoulder injury risk profiles for manual wheelchair users. Lower glenohumeral joint dynamics variability is related to increased shoulder injury risk in adult-onset SCI [3,4]. Determining the relationship of glenohumeral joint dynamics variability to time since injury is an important step toward developing approaches for preventing shoulder pathology in manual wheelchair users.

Acknowledgments: This research is supported by the NICHD of the NIH, award number: R01HD098698.

References: [1] Briley et al. (2021), *J Biomech* 126; [2] Braaksma et al. (2023) *Am J Phys Med Rehabil* 102(10); [3] Walford et al. (2019), *Clin Biomech* 65; [4] Moon et al. (2013), *Clin Biomech* 28(9-10); [5] Slavens et al. (2015) *Biomed Res Int* 2015; [6] Schnorenberg et al. (2014), *J Biomech* 47(1); [7] Leonardis et al. (2022) *Arch Rehabil Res Clin Transl* 4(4); [8] Leonardis et al. (2023) *J Appl Biomech* Nov 20:1-10; [9] Mulroy et al. (2004) *Arch Phys Med Rehabil* 85(6)

OPTIMAL CONTROL SIMULATIONS OF WALKING ON ASYMMETRIC SURFACE IMPEDANCE

Banu Abdikadirova[1*], Mark Price[1,2*], Wouter Hoogkamer[2], and Meghan E. Huber[1]
[1]Department of Mechanical and Industrial Engineering, University of Massachusetts Amherst
[2] Department of Kinesiology, University of Massachusetts Amherst

*Corresponding author's email: babdikadirov@umass.edu

Introduction: Impaired gait often arises from neurological disorders, negatively affecting one's quality of life and restricting their mobility. A promising approach to addressing loading asymmetries caused by gait impairments is to asymmetrically perturb the dynamic loading response, or the mechanical impedance, of the foot-ground interface. Changes in the magnitude of ground reaction forces have been demonstrated to affect both ankle range of motion and the forces exerted by the ankle dorsiflexor muscles [1]. While one might expect such a perturbation to result in neuromotor adaptation, there is limited understanding of the way in which the biomechanics of gait can be expected to adjust under asymmetric foot-ground mechanical impedance.

Along with behavioral experiments with variable surface impedance perturbations, model-based simulations can be a complementary source of insight and provide predictions for later experiments. Chambers and Artemiadis [2] employed a model-based analysis of a single step asymmetric stiffness perturbation, using a three-dimensional muscle-reflex model with both supraspinal and spinal control layers. This method is useful for predicting the transient response to a perturbation but tends to result in a failure to produce walking strides for perturbations of larger magnitude than the preconfigured model is tuned to handle.

An alternative for simulating stable, periodic gait under severe ground stiffness asymmetry is through an optimal control simulation methodology. As opposed to a muscle-reflex approach, this method estimates "steady-state", or the optimal biomechanics for a given condition to maximize performance according to the measure being optimized. In this study, we developed an optimal control gait model optimizing for minimal muscle effort during walking on a variable impedance surface under a range of asymmetric stiffness and damping conditions. We hypothesized that increasing damping would result in higher muscle effort as more energy is dissipated by the compliant surface, and that decreasing stiffness would also result in higher muscle effort as asymmetric compensations to maintain upright walking are required.

Methods: We generated periodic strides with a 2D musculoskeletal model minimizing muscle effort with a direct collocation approach in OpenSim Moco [3]. The musculoskeletal model contained 8 body segments, 10 anatomical degrees-of-freedom, and was actuated by 18 Hill-type muscles. The model included two platforms of negligible mass (0.1 kg), each located under one of the model's feet, constrained to move vertically, and connected to a global ground reference frame with linear spring-damper coordinate actuators. Foot-ground contact was calculated via smoothed Hunt-Crossley viscoelastic contact spheres and half-surfaces, with contact spheres for each foot paired with the half-surface representing the corresponding platform. The optimization minimized the sum of cubed muscle excitations, and was constrained to generate periodic strides at 1.2 m/s walking speed. The simulation was performed with 16 spring constants (5–1000 kN/m) and 7 damping coefficients (5–2000 Ns/m) for one of the platforms while the other was locked at its maximum height for a total of 112 unique combinations.

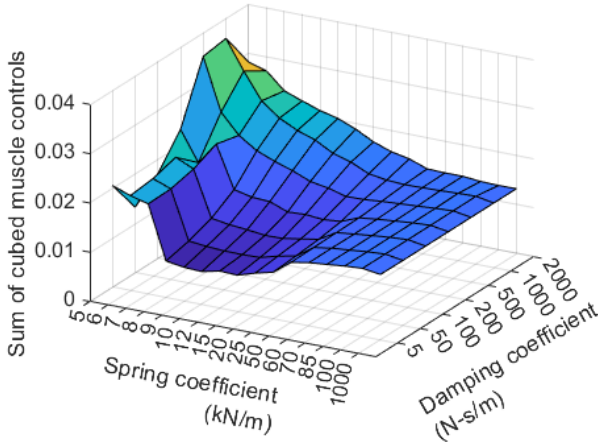

Figure 1: The optimal control muscle effort cost function value for the asymmetrical stiffness-damping landscape ranging from 5–1000 kN/m and 5–2000 Ns/m. Note that impedance parameter axes are not linearly spaced.

Results & Discussion: Figure 1 demonstrates the muscle effort cost function as a function of both asymmetric stiffness and damping. Damping exhibited a minimal impact on the muscle effort for high stiffness values, while it showed a major effect for stiffness values below 25kN/m. As predicted, for high damping, overall muscle activity increased as stiffness decreased. However, for low damping, simulations found an optimal stiffness around 10kN/m, which decreased overall muscle effort relative to more symmetrical ground stiffness. Contrary to our hypothesis, the model was able to take advantage of elastic energy stored by the lower stiffness surface to reduce the effort of walking, despite that this stiffness change only occurred on one side. As stiffness continued to decrease, however, the muscle effort measure increased, likely due to the asymmetry required to walk outweighing energetic benefits of the compliant surface. Overall, these results indicated that not only ground stiffness significantly affects muscle effort, but also damping plays a crucial role in shaping the relationship between muscle effort and asymmetric ground stiffness.

Significance: The findings of this study highlight the importance of the relationship between stiffness and damping when considering asymmetric surface impedance perturbations for human experiments. They also provide a framework for experimental hypotheses regarding the energetics of asymmetric human walking – do humans reduce their energy expenditure when walking on asymmetric stiffnesses with low damping given time to adapt? The answer to this question will impact intervention design using stiffness perturbations targeting neuromotor adaptation.

References: [1] Gefen (2001), *IEEE Trans Neural Systems & Rehab Eng* 9(4); [2] Chambers and Artemiadis (2021), *IEEE Trans Neural Systems & Rehab Eng* 29; [3] Dembia et al. (2020), *PLOS Comp Bio* 16(12).

TRAIL RUNNING SHOE FIT AND PERFORMANCE: A MULTI-STUDY EXPLORATION

Eric C. Honert*, Adam R. Luftglass, Milena Singletary, Kathryn Harrison, Bethany Kilpatrick, Daniel Feeney
Performance Fit Laboratory, BOA Technology Inc., Denver, CO, USA
*Corresponding author's email: eric.honert@boatechology.com

Introduction: Footwear fit is important for trail running shoes [1], especially as these shoes are worn for long periods of time over varying terrain. Quantitative metrics of footwear fit, such as peak toe pressure and heel contact area can be obtained outside of the lab during trail running with wearable plantar pressure sensors [2,3]. These metrics are also associated with improved qualitative fit [2,3]. Yet, the connection between these fit metrics and trail running performance has not been directly evaluated. Furthermore, many studies lack the statistical power to evaluate gross changes in metrics and thus cannot provide broader running insights, rather only providing insights for certain shoes and conditions. The purpose of this abstract was to understand how metrics of footwear fit affect trail running speed across several studies.

Methods: Data were combined across three different studies that combines previously published data [2] and internal investigations. All studies had multiple conditions that only varied the shoe upper. In two of the studies, runners wore La Sportiva Cyklon shoes. In the third study, runners wore the Speedland GS:Tam. The number of runners in each study were: 30 (15 female), 10 males, and 10 males, respectively with 39 unique individuals in total. All runners ran the same trail loop near Morrison, CO. This loop has three distinct portions: an uphill (avg. slope: 4°), technical (avg. slope: 2°), and downhill (avg. slope: 6°). All runners were experienced with trail running. Runners wore a GPS watch (Suunto, FIN) for trail segmentation, inertial measurement units (IMUs, Vicon, GBR) attached to the heel counter, and plantar pressure under their feet (XSENSOR, CAN). From each stride, running speed was computed from the IMU and peak toe pressure from the plantar pressure sensors. Heel contact area was the average contact area in the rear 20% of the sensor during each step.

We used two linear models (RStudio) to understand how peak toe pressure and heel contact area affect trail running speed. Average pressure metrics and running speed from each different footwear condition and trail section were used as model inputs. We encoded the linear models to have independent intercepts for the trail section and the three different studies: Speed ~ Metric + (1|Section) + (1|Study). T-values for plantar pressure metrics were converted to p-values using the infinite degrees of freedom approximation in their respective models. Model performance was evaluated using R^2.

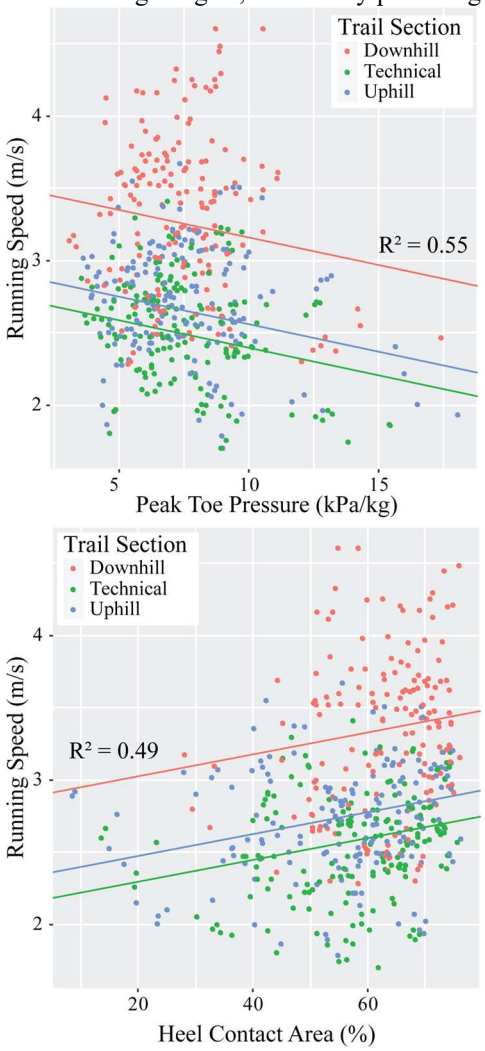

Figure 1: Relationship between trail running speed and plantar pressure metrics of footwear fit. Lines indicate the linear fit for the different trail sections. The linear models fit 509 observations across 39 runners.

Results & Discussion: Both peak toe pressure and heel contact area impact running speed (Fig. 1). Running speed increased with decreased toe pressure ($R^2 = 0.55$, $p < 0.001$) and increased with increasing heel contact area ($R^2 = 0.49$, $p < 0.001$).

Peak toe pressure decreasing with increasing running speed is a seemingly counter-intuitive finding. It has been well established that peak forces (and thus pressure) increase with speed. However, this one portion of the foot has a reduced role in the overall ground reaction force in comparison to other portions of the foot [4]. In footwear studies, increases in toe peak pressure have been interpreted as toe clawing – the act to keep the shoe in contact with the foot [3]. In trail running, this is costing speed. This detriment to speed could be due to the increased amount of work the athletes perform with increased toe clawing, as we have observed a positive relationship between peak toe pressure and centre-of-mass work during treadmill running [5].

Contrary to the peak toe pressure, the trail running speed increased with higher heel contact area. Previously, we have seen that this metric indicates better heel fit [2] and we hypothesize that this metric indicates better heel hold. For instance, a shoe with poor heel hold (e.g. flip-flop) will cause the heel contact area to decrease, particularly in the push-off phase of running. Enhanced heel hold improves the connection between the foot and shoe to improve trail running performance.

This study provides a glimpse of the power of combining multiple studies together that utilize the same protocol and measurements to understand broader heuristics of trail running biomechanics. While our current research combined studies with two different footwear models, further research is needed to ensure that these trends are consistent across a variety of different trail running shoes.

Significance: Footwear fit affects trail running performance. Harnessing multiple studies across different footwear allows researchers to understand broader trends in biomechanics. Combining multiple studies, we observe that increasing heel contact area and decreasing peak toe pressures improves trail running speed – thus performance.

References: [1] Warrick et al. (2019), *Curr Phys Med Rehabil Rep* 7**;**[2] Honert et al. (2023), *Front Sports Act Living* 4; [3] Dobson et al. (2018), *Footwear Sci* 10; [4] Matijevich et al. (2022), *J Biomech* 141; [5] Honert et al. (2024), *ISBS, accepted*.

VARIABLE GEARING IMPROVES EFFICIENCY IN AGILITY TASKS

Alexander Gioia[1*], Adam Luftglass[2], Daniel Schmitt[3], Robin M. Queen[1]
[1]Virginia Tech, Blacksburg, VA, USA
[2]BOA Technology, Denver, CO, USA
[3]Duke University, Durham, NC, USA
*Corresponding author's email: agioia@vt.edu

Introduction: The human foot is a remarkable mechanism whose length and complexity allows variability in gear ratios between moments generated by ground reaction force (GRF) and that of the calf muscles. Modelling the foot and ankle system as two gears provides deep insight into the contribution of the plantar flexors during force attenuation and production during steady-state and accelerating movements. The gearing system is defined as the GRF gear (*R*) divided by the triceps surae gear (*r*) (Fig 1). Variable gearing may allow for optimal stretch of the triceps surae during the landing phase and force production during the propulsive phase of a movement. Lower gear ratios during the landing phase result in increased stretch of the triceps surae. Higher gear ratios during the propulsive phase result in lower Achilles muscle tendon velocity (AMTV). Carrier et al. has demonstrated variable gearing to be advantageous during human running, however, such investigation has not been conducted in agility tasks involving a change of direction such as the anterior-posterior (AP) drill in which participants sprint forward and plant one foot to change direction and backpedal. [1] The AP drill is important for athletic performance in sports requiring agility movements such as basketball and soccer. [2,3]

Methods: 40 active young adults participated in this study (20 M (21.7 ± 2.2 yrs) and 20 F (23.2 ± 4.3 yrs)). 3D motion capture and force plates recorded foot and ankle motion and GRFs during eight AP drills. During the AP drill participants sprinted forward 4.3 meters as fast as possible, planted their dominant foot on a force plate, and backpedalled to the starting position. The gear ratios were determined as the GRF gear (*R*) divided by the triceps surae gear (*r*) (Fig 1); where *R* is the perpendicular distance between the GRF vector and the ankle joint center and *r* is the perpendicular distance between the Achilles tendon and the ankle joint center. The variable gear ratio was calculated continuously throughout the task and a constant gear ratio was taken at the midpoint of each landing. AMTV was defined as the triceps surae gear multiplied by the ankle angular velocity. A one-way repeated measures ANOVA ($\alpha = 0.05$) was conducted through statistical parametric mapping to assess differences in AMTV throughout ground contact between variable and constant gearing.

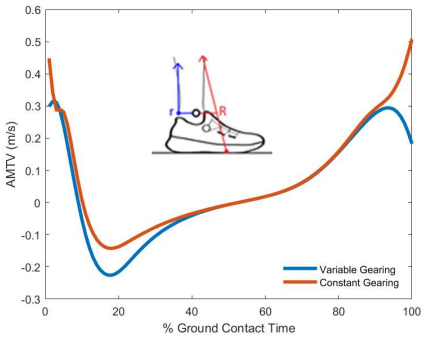

Figure 1: AMTV for variable and constant gearing during the entire ground contact of the AP drill. The foot depicts the lever arms where the GRF gear (*R*) is in red and the triceps surae gear (*r*) is in blue.

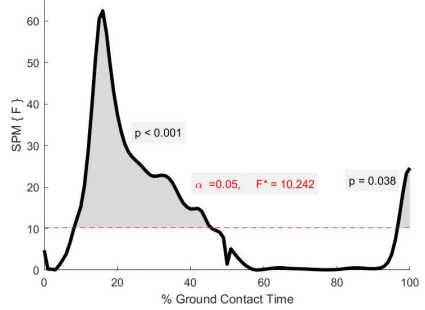

Figure 2: SPM comparison between variable and constant gearing on AMTV during ground contact of the anterior-posterior drill

Results & Discussion: The ankle gear ratio was near one at initial ground contact, and quickly dipped to 0.4 during the eccentric phase of the movement. The gear ratio then rose to near 0.7 at 60% of ground contact before dropping again to 0.6 at 80% of ground contact and rapidly rose to near 1.1 at the end of ground contact. Compared to constant gearing, variable gearing resulted in average 0.041 m/s higher AMTV values (max 0.084 m/s higher at 16%) during the first 8-45% of ground contact, and an average 0.282 m/s lower AMTV values (max 0.376 m/s lower at 100%) during 97% and later of the movement. The higher AMTV observed with variable gearing during nearly the entire eccentric portion of the movement results in increased stretch of the triceps surae. The triceps surae may be able to produce more work during the succeeding concentric portion of the movement as a result of the increased stretch during the eccentric phase. [4] The higher gear ratios and lower AMTV observed with variable gearing during the concentric portion of the movement may keep the triceps surae in an optimal portion of the force-velocity curve, thus allowing for higher force production. These findings can provide insight on methods to improve footwear designed for agility movements. Higher gear ratios during the concentric phase of the movement are largely driven by the increase of GRF gear and thus the forward progression of the GRF vector. Forward progression of the GRF vector is namely caused by higher stiffness of the foot. Prior literature has shown that increasing foot stiffness, through footwear and insoles, have led to higher gear ratios and lower triceps surae shortening velocity in the concentric phase of walking [5]. Therefore, footwear design that increases longitudinal foot stiffness may also increase gear ratios and lower AMTV during the concentric portion of an agility movement, in addition to what is observed with variable gearing.

Significance: The findings illustrate that variable gearing may allow for more optimal and efficient movement, through greater force attenuation and production, in humans during an agility task such as the anterior-posterior drill.

Acknowledgments: We would like to thank the participants for their time and hard work completing the agility task.

References: [1] Carrier et al. (1994), *Science*; [2] McLellan et al. (2011), *Journal of Strength & Conditioning Research*; [3] Mathisen et al. (2015), *Journal of Sports Science*; [4] Cavagna et al. (1986), *American Physiological Society*; [5] Takahashi et al. (2016), *Nature*

PERFORMANCE ANALYSIS OF JOINT ANGLE ESTIMATION ALGORITHMS TO CONTROL A LOWER-LIMB ANKLE EXOSKELETON EMULATOR

Sarah M. Bass[1*], Ryan S. Pollard[1], Michael E. Zabala[1]
[1]Department of Mechanical Engineering, Auburn University, Auburn, AL, USA
*smb0186@auburn.edu

Introduction: Assistive devices, such as exoskeletons, have become a prominent subject of research due to their wide-ranging applications and potentially large impacts. Exoskeletons are being utilized in rehabilitation for cases such as regaining mobility [1], occupational settings to reduce the likelihood of injuries during repetitive or strenuous tasks [2] and performance enhancement to allow healthy operators to perform tasks at an elevated level [3]. However, a primary challenge for active exoskeletons is discerning intent to seamlessly actuate the exoskeleton with the user. The objective of this study, therefore, was to evaluate the detached ankle exoskeleton emulator realization performance of two joint angle estimation algorithms: a kinematic extrapolation algorithm and a Random Forest machine learning algorithm. We hypothesized that the trained Random Forest algorithm would have a lower emulator realization accuracy error, but the kinematic extrapolation algorithm would have a shorter emulator realization delay.

Methods: The sagittal ankle angles from 25 subjects (12 males, 13 females; age: 22.9 ± 4.7 years; height: 1.7 ± 0.1 m; weight: 69.0 ± 11.9 kg) walking on a single belt treadmill were obtained through inverse kinematics (79 marker set, Point Cluster Technique [4], Visual 3D) and served as the provided operator angles for algorithm creation and performance analysis testing (IRB no. 17-096 MR 1705). To test the algorithms, a detached ankle exoskeleton emulator was built based on Witte and Collins' open-source design [5]. A metal cable attached between a continuous servo motor and the ankle cuff provided actuation while a rotary potentiometer at the ankle joint provided joint angle measurements. An elastic band on the front of the emulator assisted with dorsiflexion. Both algorithms estimated joint angles 100 ms into the future and relied on the current provided operator joint angle along with the previous two joint angles to make a future estimation. The kinematic extrapolation model used a kinematic equation based on current provided operator angle, angular velocity, and angular acceleration to estimate future joint angle. The Random Forest machine learning model was trained on ankle angles from 10 randomly selected subjects and validated on angle ankles from 5 subjects. For performance testing, the provided operator angles were fed into the algorithms, and the resulting joint angle estimations were compared to the current emulator joint angle to calculate motor control instructions to actuate the emulator accordingly. The current provided operator angles were also directly compared to the emulator angles to serve as a control test condition (streaming). Walking data from the remaining 10 subjects were tested three times on the emulator for each of the three methods for a total of 90 trials. The emulator realization RMSE value was calculated by locally shifting the emulator angles time series and the provided operator angles time series in time to minimize RMSE. The emulator realization delay was defined as the associated time shift to minimize RMSE. An ANOVA and two-sample t-tests were used to determine significance.

Results & Discussion: The average emulator realization RMSE values for kinematic extrapolation, Random Forest, and streaming were 6.3 ± 0.9°, 5.4 ± 0.9°, and 4.5 ± 0.7°, respectively. The emulator realization delays for kinematic extrapolation, Random Forest, and streaming were 44 ± 25 ms, 37 ± 31 ms, and 109 ± 13 ms, respectively. ANOVA results indicated significant comparisons within emulator realization RMSE ($p < 0.001$) and emulator realization delay ($p < 0.001$). Figure 1 shows these results and the statistical analysis results of the two-sample t-tests. These results supported our hypothesis that the Random Forest algorithm would have a lower emulator realization accuracy error. However, our hypothesis that the kinematic extrapolation algorithm would have a shorter emulator realization delay was rejected by these results since there was no significant difference in the realization delays of these algorithms, though the emulator realization delays of both algorithms were still significantly lower compared to streaming. The average RMSE value for both algorithms fell within one standard deviation above the average proprioception detection threshold of 5.31 ± 2.12° during dynamic movement [6]. Temporally, the Random Forest emulator realization delay is on the cusp of one standard deviation above the average just noticeable difference of actuation delay of 30.1 ± 6.5 ms [7-8]. The emulator realization delay of the kinematic extrapolation algorithm was over two standard deviations over this threshold.

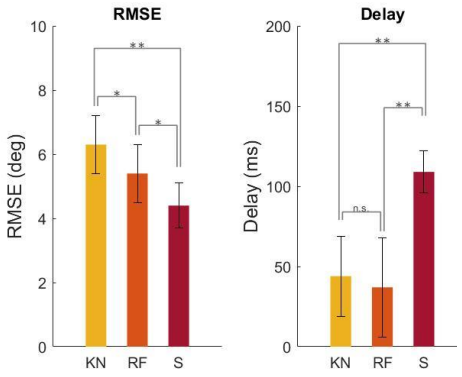

Figure 1: Statistcal analysis results of two-sample t-tests of the emulator realization RMSE values and realization delays between kinematic extrapolation (KN), Random Forest (RF), and streaming (S). n.s. – no significance, * ($p<0.05$), ** ($p<0.01$).

Significance: Using a single sensor, these algorithms operated within a standard deviation of proprioception thresholds and within two or three standard deviations of timing perception thresholds. With mechanical improvements and computational optimization, the emulator realization accuracies and emulator realization delays of these algorithms could fall below these perception thresholds and could demonstrate utility as control methods for ankle exoskeletons.

References: [1] Singh et al. (2021), *J NeuroEngineering Rehabil,* 18(1); [2] Rashedi et al. (2014), *Ergonomics,* 57(12); [3] Zoss et al. (2006), *IEEE/ASME Trans. Mechatron,* 11(2); [4] Andriacchi et al. (1998), *J Biomech,* 120(6); [5] Witte and Collins. (2020), *Wearable Robotics,* 13; [6] Belley et al. (2016), *Gait & Posture,* 49; [7] Peng et al. (2022), *IEEE Trans. Neural Syst Rehabil Eng,* 30; [8] Kadaba et al. (1989), *J Orthopaedic Research,* 7(6)

HEEL-STRIKE DETECTION ALGORITHM FOR EXOSKELETON WALKING AFTER SPINAL CORD INJURY

Annika Pfister[1*], Rich Henderson[2], Chet Moritz[1,2], and Kimberly A. Ingraham[1]
[1]Department of Electrical and Computer Engineering, University of Washington, Seattle, WA USA
[2] Department of Rehabilitation Medicine, University of Washington, Seattle, WA USA
*Corresponding author's email: apfist8@uw.edu

Introduction: Exoskeletons are increasingly used for gait rehabilitation following spinal cord injury (SCI) in research and clinical settings. Gait biomechanics are a key indicator of whether a rehabilitative technique is successful. To evaluate the effects of using exoskeletons for rehabilitation settings, muscle activity (EMG), inertial measurement units (IMUs), and other gait data must be segmented by stride for analysis, often using heel-strike as a marker for segmentation. Without automation, heel-strike detection must be done manually, relying on visual evaluation of considerable amounts of data. This requires a deep understanding of gait patterns in adults with SCI, is incredibly time-consuming, and can introduce inherent bias in stride segmentation. Previous methods for automated heel-strike detection have been proposed using data from both nondisabled and SCI participants [1], [2], [3]. However, these works do not account for the added influence of wearing a robotic exoskeleton, particularly with high levels of swing assistance, which may influence the characteristics of heel strike during the gait cycle. This study demonstrates the utility and accuracy of automated heel-strike detection for gait analysis of exoskeleton walking in adults with SCI.

Methods: We collected 3-D acceleration and shank angular velocity, as well as force-sensitive resistor (FSR) data (Delsys Trigno Avanti, sampled at 148 Hz) from a representative participant with SCI (male, age 49, injury level C6, AIS C). The participant walked overground in an Ekso Bionics exoskeleton using the ProStep+ mode. The algorithm defined a heel-strike as the first "zero-crossing" following a mid-swing peak in the sagittal plane gyroscope data (filtered using a 5 Hz-lowpass 5th order Butterworth). Peaks were detected using the SciPy 'findpeaks' function, with a minimum peak height defined as 80% of the mean of all data points greater than the average (a user-adaptive threshold [1]), and a prominence of 50. We defined mid-swing peaks as being separated by at least a 200-sample window length. Between each mid-swing peak, heel-strike was detected as the first index where the angular velocity was less than or equal to zero. We validated the algorithm by comparing detected heel-strike time indices to the ground truth, determined via FSR data collected from the center of the heel. FSR heel-strike was determined as a local minimum prior to the characteristic peak during stance phase.

Results & Discussion: We compared the performance of our IMU-based heel-strike detection algorithm to the FSR-defined ground truth for the representative participant (Fig. 1A). Over 2 minutes of continuous overground walking data, we found that our IMU-based method had an overall mean error of 10-150 milliseconds (ms). Compared to the participant's average step duration of 5.5 seconds, this is a relatively small error – less than 2.7% of the gait cycle. Similar work has reported errors on the order of 10 ms for automated heel-strike detection, validated by force plate data [1]. We applied the same algorithm to data from three different participants with SCI. The algorithm yielded consistent stride segmentation of sagittal-plane gyroscope data (Fig. 1B), indicating that this method is robust to individual variation in gaits in adults with SCI using an exoskeleton.

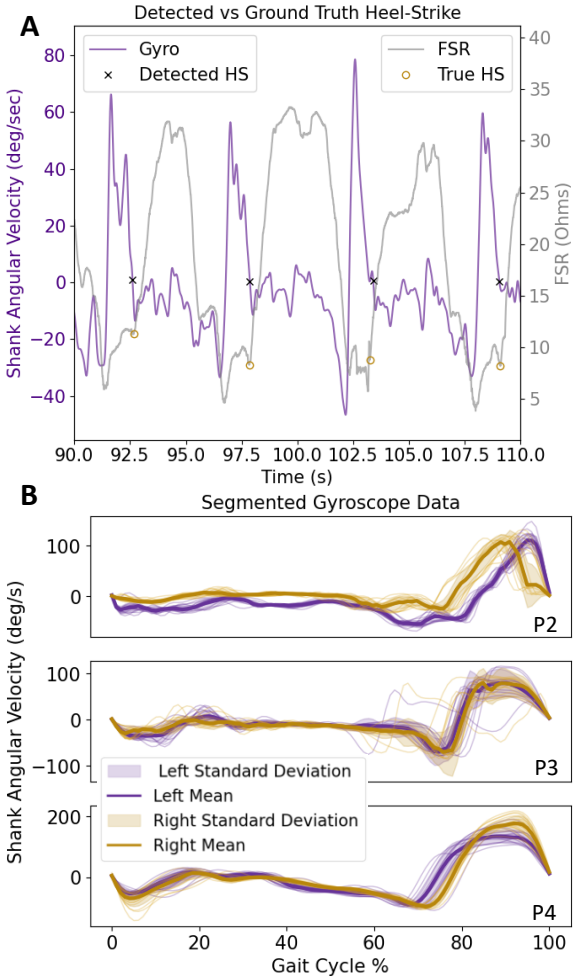

Figure 1: A) Validation of IMU-based heel-strike detection algorithm using FSR data for the representative participant (P1). **B)** Stride-segmented angular velocity data for novel participants (P2-P4) when our heel-strike detection algorithm is applied.

Significance: Accurate heel-strike detection is crucial for biomechanical analysis of data including EMG signals and gait kinematics, especially in participants with SCI who have variable gait speed and kinematics. Our algorithm for automating heel-strike detection demonstrated relatively low error while successfully implementing a consistent and objective method for determining heel-strike time indices. Future work will address algorithm robustness to periods of standing or pivoting in an exoskeleton, as well as detecting toe-off for more refined gait segmentation. Ultimately, this work holds promise for creating streamlined data processing pipelines to analyze exoskeleton gait training in the field of SCI rehabilitation.

Acknowledgements: We would like to thank our research participants, and funding from Mission Yogurt that supported this work.

References: [1] Greene et al. (2010), *Med. Biol. Eng. Comput.* 48(12); [2] Han et al. (2019), *IEEE Sens. J.* 19(9); [3] Jasiwicz et al. (2006), *Gait Post.* 24(4).

LATE PREGNANCY AND EARLY POSTPARTUM MAY IMPACT DYNAMIC BALANCE DURING GAIT: A CASE STUDY

Kaitlyn Kleeman, Abigail Salvadore, Sarah A. Roelker
Department of Kinesiology, University of Massachusetts Amherst, Amherst MA

Introduction: Throughout pregnancy and early postpartum, changes in weight and weight distribution may impact dynamic balance in pregnant individuals during gait [1]. Roughly 25% of employed pregnant women sustained a fall during pregnancy at work [2]. This number is similar to that of individuals 65 years or older [2]. Whole body angular momentum (WBAM) about the body's center of mass can be used to evaluate dynamic balance [3] and provides a good assessment of stability during gait [4]. The control of WBAM, is proposed to be important in maintaining dynamic balance and preventing falls during walking [5]. This control can be quantified by the peak-to-peak range in WBAM, with larger ranges indicative of poorer balance control [6]. Pregnant women often walk with wider step widths [7], which are associated with greater range of frontal plane WBAM and decreased balance control [8]. This case study evaluated the impact of pregnancy and early postpartum on dynamic balance during gait. Due to changes in weight distribution, primarily in the sagittal plane, and increased step width during pregnancy, we hypothesized that the range of WBAM would 1) increase in the sagittal and frontal planes during late pregnancy relative to early pregnancy and decrease postpartum relative to late pregnancy, and 2) remain unchanged in the transverse plane across timepoints.

Methods: One active pregnant female (31.9 y) participated in this study. At 8, 14, 20, 26, 32, and 38 weeks of pregnancy and 6 weeks postpartum (PP), the participant performed 5 walking trials at her preferred speed while motion capture data was collected at 200 Hz from 77 reflective markers. Ground reaction forces were collected at 1000 Hz from force plates embedded in the floor. From the marker data, a full body model of the participant was developed in Visual 3D based on the Plug-in-Gait model. For each time point, the participant's WBAM was normalized to height, mass, and gait speed. The peak-to-peak range in WBAM was calculated in the sagittal, frontal, and transverse planes. The range of WBAM in each plane was averaged across trials at each time point. Mass, gait speed, and step width were also compared across time points. To date, data has been analyzed from 14 (early) and 38 (late) weeks of pregnancy and 6 weeks postpartum.

Results & Discussion: Contrary to our hypothesis, the range of WBAM decreased by 31.0% in the sagittal plane and 42.6% in the frontal plane in late pregnancy compared to early pregnancy (Fig. 1A). The reduced range in WBAM suggests that the individual controlled their balance more in the frontal and sagittal planes during late pregnancy, perhaps as an adaptive response to the greater challenge to balance in late pregnancy. Some studies report reduced trunk range of motion in pregnancy [7], which may have contributed to the decreased range of WBAM in the frontal and sagittal planes, despite the increased body mass (early: 65.20 kg; late: 80.84 kg; Fig. 1B), walking speed (early: 1.34±0.00 m/s; late: 1.43±0.01 m/s; Fig. 1C), and step width (early: 0.08±0.02 m; late: 0.16±0.03 m; Fig. 1D) in late pregnancy. In the transverse plane, the range of WBAM increased by 37.7% from early to late pregnancy, which indicates reduced control of dynamic balance in the transverse plane during late pregnancy. Postpartum frontal and sagittal plane ranges of WBAM increased compared to both early and late pregnancy, while the transverse plane range of WBAM decreased, returning to near early pregnancy values. These postpartum ranges of WBAM may reflect a decrease in the need to carefully regulate WBAM in the sagittal and frontal planes as mass and step width return to near early pregnancy values. As we continue to process and analyze the data from this case study, we will investigate potential kinematic and kinetic changes during pregnancy that may have contributed to the observed changes in WBAM.

Significance: This case study suggests that pregnant women can increase dynamic balance control in late pregnancy in both the sagittal and frontal planes. However, it is unclear which factors (e.g., physical activity, presence of pain) may promote or impair an individual's ability to regulate dynamic balance during pregnancy. In addition, fall risk was not explicitly evaluated in this study. Future work is needed to identify the factors that promote WBAM regulation and their relationship to fall risk in pregnancy.

Acknowledgements: The authors thank Dr. Katherine Boyer Kali Shamaly and Aidan Gross for their assistance with data collection.

References: [1] Catena et al, Gait Posture, 2020. [2] Dunning et al, Am J Ind Med, 2003. [3] Hisano et al, IEEE Trans Neural Syst Rehabil Eng, 2023. [4] Liu et al, Med Eng Phys, 2023. [5] Simoneau & Krebs, J Appl Biomech, 2000. [6] Nott et al, Gait Posture, 2014. [7] Conder et al, J Funct Morphol Kinesiol, 2019. [8] Molina et al, J Biomech, 2023.

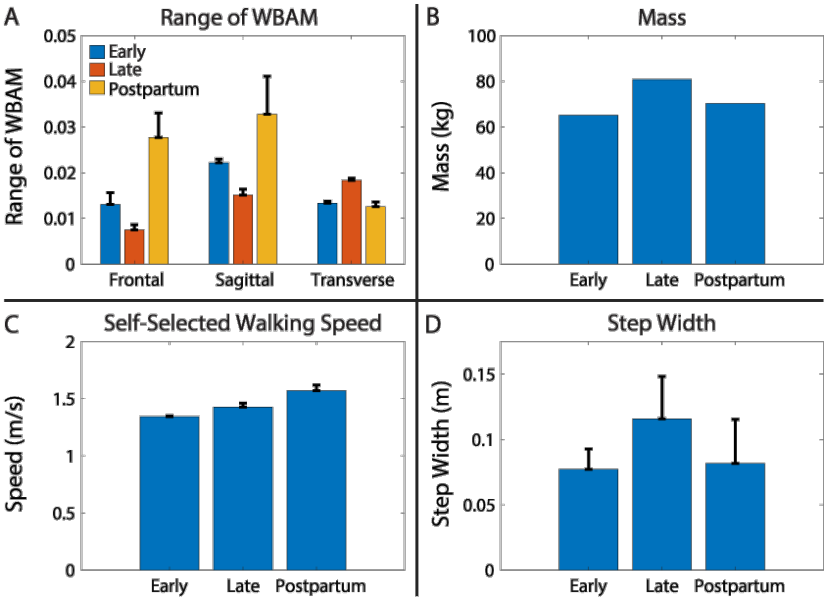

Figure 1: Comparison of the A) range of WBAM, B) mass, C) self-selected walking speed, and D) step width in a pregnant individual during early and late pregnancy and early postpartum. The normalized range of WBAM is unitless.

COMPARISON OF GROUND REACTION FORCES, JOINT MOMENTS AND KINEMATICS BETWEEN INCREASED HIP FLEXION GAIT, RUNNING AND CYCLING

Nuno Oliveira[1*], Hunter Haynes[1], Chuang-Yuan Chiu[2], Tanner Thorsen[1]
[1]School of Kinesiology and Nutrition, The University of Southern Mississippi, MS, USA
[2]School Sports Engineering Research Group, Sheffield Hallam University, Sheffield, UK
*Corresponding author's email: nuno.oliveira@usm.edu

Introduction: Exercise is a critical element in the treatment and improvement of function and quality of life. The American Heart Association, and the American College of Sports Medicine recommend regular exercise of moderate intensity for the prevention and complementary treatment of several diseases. Additionally, a positive relationship has been established between the health benefits resulting from exercise and the intensity of that exercise.
Running and cycling are two of the most commonly used exercise modalities to meet these guidelines. However, these exercise modalities might limit improvements in some populations (e.g. obesity, osteoarthritis, older adults). Running has been associated with high tibial peak positive acceleration at ground impact and high average and instantaneous vertical ground reaction force loading rates that might present increased risk of injury in some clinical populations. On the other hand, stationary cycling has biomechanical and neuromuscular characteristics that might limit the potential benefits of exercise in specific populations (e.g. lack of collaborative whole-body work or restricted movement variability that limits the improvement of balance and coordination effectively). Increased hip flexion angle gait (HFgait) is an exercise modality that has been shown to result in similar energy expenditures (< 1 MET difference) to treadmill running for the same heart rate, and to provide a more accurate alternative to control exercise intensity [1, 2]. During HFgait, participants walk on a treadmill at a comfortable speed and try to flex their hips during the swing phase as much as possible. Although the metabolic cost of this activity has been investigated, how this exercise modality compares biomechanically to treadmill running or stationary cycling is unknown. The purpose of the current study is to investigate the ground reaction forces, and lower limb joint moments and kinematic between increased hip flexion gait and running and cycling.

Methods: Ten healthy individuals (5M, 5F; age 30.1 ± 9.8 years; height 169.9 ± 0.09 cm; body mass 67.9 ± 14.3 kg) participated in the study. Participants completed three sessions. Each session involved performing a different exercise modality (running, cycling, and HFgait) at four different intensities (S1, S2, S3, S4). The intensities used for each modality aimed to cover the range of intensities typically used for each modality. For cycling, intensity was increased by increasing the cycling resistance (1.6 W/Kg, 2.4 W/Kg, 3.2 W/Kg, 4.0 W/Kg) while keeping cadence at 80 rpm. For running and HFgait, intensity was increased by increasing the treadmill speed (running: 4 mph, 6 mph, 8 mph, 10 mph; HFgait: 1.2 mph, 1.8 mph, 2.4 mph, 3.0 mph). During HFgait, participants used a biofeedback system (hip flexion feedback system) that uses markerless motion tracking for hip flexion angle calculation [1]. This system displays the real-time hip flexion angle and the target peak hip flexion angle while participants walk on the treadmill. This ensured that participants maintained a consistent peak hip flexion angle during the trial. Spatiotemporal parameters for each modality were determined using a standard bilateral lower extremity marker set to record lower extremity kinematics (240 Hz, Qualisys, Göteborg, Sweden). All Spatiotemporal parameters were calculated using Visual 3D (version 6.0, C-Motion, Germantown, MD, USA). A two-way repeated measures ANOVA was used to test the effects of exercise modality and exercise intensity on ground reaction forces (GRF), and lower limb joint moments, and kinematics in the sagittal plane.

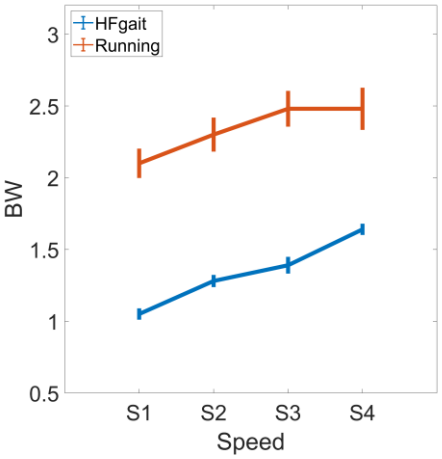

Figure 1: Peak vertical GRF (BW) at heel contact for the HFgait and running exercise modalities across four different speeds.

Results & Discussion: HFgait resulted in lower loading rates during heel contact than running across all speeds ($p < 0.001$, $\eta^2 = 0.907$) (Fig. 1). This finding supports the idea that the HFgait might be a suitable exercise modality for populations that suffer or might be at higher risk of knee pain. Additionally, HFgait resulted in larger peak hip flexion than running ($p < 0.001$, $\eta^2 = 0.876$) and larger peak hip extension than cycling ($p < 0.001$, $\eta^2 = 0.883$) during the movement. Except for hip extension moment, HFgait resulted in larger ($p < 0.001$) ankle, knee, and hip joint sagittal moments than cycling. This overall trend indicates that HFgait is an exercise modality with an open-chain component that requires balance and involves the whole body, which might elicit greater biomechanical and neuromuscular responses than cycling.

Significance: Regular exercise of moderate-high intensity is a well-established guideline for the prevention and complementary treatment of several diseases. The present study investigates a new exercise modality that might optimize the benefits of exercise in specific clinical populations.

Acknowledgments: The current study has been supported by the American Heart Association (grant 23AIREA1055000).

References:[1] Oliveira et al. (2023), *Eur J App Phy*, 123(10). [2] Oliveira et al. (2022), *J Sports Eng Tech.*

BETWEEN LIMB DIFFERENCES IN GAIT COMLEXITY AND ASSOCIATIONS WITH CARTILAGE DEFORMATION IN INDIVIDUALS WITH ACL RECONSTRUCTION

Steven A. Garcia*, McKenzie White, Riann M. Palmieri-Smith
[1] Department of Kinesiology and Nutrition, University of Illinois Chicago; Chicago, IL, USA,
[2] Department of Physical Therapy, University of Kentucky; Lexington, KY, USA
[3] School of Kinesiology, University of Michigan; Ann Arbor, MI, USA
*Corresponding author's email: stevenag@uic.edu

Introduction: Those with anterior cruciate ligament reconstruction (ACLR) are at high risk for post-traumatic osteoarthritis (OA). Rapid alterations in the cartilage matrix, particularly in the patellofemoral joint (PFJ), have been reported 6-12 months following ACLR and have been associated with impaired walking mechanics [1]. Typically, gait after ACLR is evaluated using peak metrics, which only provide a discrete snapshot of the peak load or motion applied about cartilage. However, a significant amount of step-to-step variation in gait mechanics are present in normal walking. Capturing such variability may provide unique insight into how consistent (or inconsistent) knee cartilage may be loaded during gait. Some evidence exists showing ACLR patients exhibit reduced knee flexion and adduction variability during gait where lesser variability is linked with poorer tibiofemoral cartilage composition (T1ρ) [2]. Nonetheless, only kinematic variability has been evaluated to date and it is unclear if ACLR individuals also employ altered variability in joint- and limb level loading metrics. Further, whether step-to-step variability is associated with PFJ cartilage health is unclear. Ultrasound (US) is able to evaluate trochlear regions in the PFJ and is a low-cost alternative to magnetic resonance imaging. US has previously been used following ACLR to evaluate cartilage strain and composition changes (via echo-intensity [EI]) following acute exercise as a surrogate of cartilage health and function [3]. Thus, we evaluated associations between gait variability and US measures of cartilage strain and EI following walking in individuals between 18-36 months after ACLR. We hypothesized lesser movement and loading variability (i.e., increased consistency) would be associated with greater cartilage strains and increased echo-intensity (EI) following acute exercise.

Methods: We recruited sixty-four participants with ACLR (Age:24.8±6.9 yrs., Body Mass Index: 26.5±4.4 kg/m^2, Time Post-Op: 27.6±7.5 mo.) to undergo walking and cartilage imaging. Treadmill biomechanics (camera sampling: 200 Hz, force sampling: 2000 Hz) were collected at a self-selected speed. US images of the trochlea were collected in the involved limb before and after a 30-minute incline walk (1.3m/s, 5° slope) using standard imaging parameters (12MHz, depth=3.5cm). Briefly, participants rested for 45 minutes to minimize effects of preceding activity and images were collected at 140° of knee flexion. Gait variables included sagittal plane knee angles and moments. Step-to-step variation in vertical ground reaction forces (GRF), knee flexion angles (KFA), sagittal and frontal plane knee moment waveforms (KFM, KAM) were evaluated across 3-minutes of walking or about 150 steps of continuous data per participant. The regularity (or consistency) of gait data was assessed using sample entropy analyses via MATLAB where smaller entropy values indicate a predictable and consistent waveform and larger values indicate greater irregularity or inconsistency [4]. For US analyses, cartilage thickness pre- and post-walking were assessed in medial and lateral regions using an open-source MATLAB program. Briefly, thickness was assessed as the Euclidean distance between superficial and deep cartilage interfaces at each pixel across the entire contour while EI was assessed as the average pixel density within each ROI. Linear regressions controlling for sex and BMI were utilized to evaluate associations between gait and cartilage outcomes in medial and lateral trochlear regions ($\alpha<0.05$). Paired t-tests were used to compare gait metrics between limbs and Cohen's *d* effects sizes were also calculated.

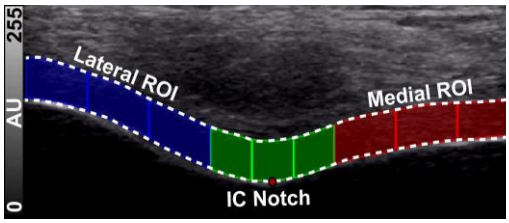

Figure 1: Medial and lateral trochlear regions of interest. Red dot is center of the intercondylar notch (IC) to aid in region segmentation. Dashed white lines depict the superficial and deep contours. AU (Arbitrary Units) refers to units for echo-intensity which are the gray scale pixel intensity in the image with 0 indicating black and 255 indicating white.

Results & Discussion: After controlling for sex and BMI, lesser involved limb KFM sample entropy (i.e., greater regularity) was associated with greater lateral cartilage strain (t=-2.05, Δ0.07 R^2 , p=0.04) and trended for medial strain (t= -2.0, p=0.051). However, KFA, KAM, and GRF sample entropy were not associated with cartilage strain (p>0.05). The involved limbs exhibited greater regularity than the uninvolved limb in the GRF (t=-3.70, *d* = 0.46, p<0.01), KFA (t=-2.64, *d* = 0.33, p=0.01) and KAM (t=-12.99, *d* = 1.6, p<0.01), but KFM trended towards significance (p = 0.07). Individuals who exhibited greater peak KFM consistency between strides exhibited greater lateral cartilage strain after exercise which may reflect a more localized level of joint loading applied about the tissue leading to increased stresses applied about the trochlea and subsequently, greater acute fluid loss. Further, findings of greater knee angle consistency between limbs may represent a movement pattern that consistently loads similar regions of the joint. Overall, stride-to-stride movement and loading variability appears to be altered in ACLR limbs and is associated with surrogate markers of cartilage integrity.

Significance: Articular cartilage is a viscoelastic tissue sensitive to the magnitude, rate, and frequency of loading. While load magnitude and rates have been typically assessed when evaluating gait alterations and their associations with tissue, entropy analyses may provide additional insight into how these loads may be consistently (or inconsistently) applied during gait. Future studies using more advanced imaging methods to evaluate the entire joint may be beneficial to comprehensively understand if nonlinear entropy analyses provide unique insight into the biomechanical influences on post-traumatic OA development after ACLR.

Acknowledgments: These data were funded through a National Institutes of Health F31 pre-doctoral award (# F31 AR078592).

References: [1] Liao, T.C., et al. Osteoarthritis Cartilage, 2023 31(9); [2] Armitano-Lago, C., et al. Med Sci Sports Exerc, 2023 55(8); [3] Pamukoff, D.N., et al. J Orthop Res, 2024. **42**(2); [4] Yentes, J.M. and P.C. Raffal. Ann Biomed Eng, 2021. **49**(3).

RUNNING SPEED AFFECTS JOINT KINEMATIC HABITUAL MOTION PATH DEVIATIONS

Megan Saftich[1*], Emily Eichenlaub[1], Evan M. Day[1], Ed Nyman[1], Jennifer Sumner[1]
[1]Brooks Sports, Seattle, WA, USA
*Corresponding author's email: megan.saftich@brooksrunning.com

Introduction: Deviation from one's habitual motion path (HMP) when running is associated with greater soft tissue loading [1]. Deviations, the quantification of the difference in kinematics when running versus performing daily habitual movements (squat, lunge, walk, stair step-down), are theorized to be the result of larger external forces that uniquely push the body to move differently or require production of greater muscle force when running [2]. Changes in running speed are associated with changes in external force magnitude [3] that require internal muscle forces to counteract, potentially causing speed dependent HMP deviations. The purpose of this study was to investigate how changes in running speed affect joint kinematic HMP deviations.

Methods: Data from human-participant product testing rounds were aggregated (n=96). Participants ran on an instrumented treadmill (Bertec, Columbus, OH, USA) at two speeds: (1) 3.35 m/s, and (2) self-selected preferred running speed. This self-selection in running speed resulted in 17 participants speeding up and 79 participants slowing down. Footwear was controlled across all participants (Brooks Launch 4). Three-dimensional kinematics of the rearfoot, shank, and thigh segments were acquired using an optical motion capture system (Motion Analysis Corporation, Rohnert Park, CA, USA) and ground reaction forces from the instrumented treadmill were used for analysis. Joint angles were calculated using a Cardan-Euler approach. Each participant's habitual motion path and deviation when running were quantified [4]. Deviations were calculated for ankle eversion and knee internal rotation (TIR) at both running speeds. Due to the nature of self-selected preferred running speed, participants were binned into groups based on change in speed by 1-10% or 10-20% from the standard test speed of 3.35 m/s. As most participants slowed down (79/96), this analysis focused the comparison on how deviations changed when slowing down from 3.35m/s to 10% slower (speed range: 3.04-3.25 m/s, average speed 3.14 m/s, n=32) and 10-20% slower (speed range: 2.68-3.00 m/s, average speed 2.90 m/s, n=45). Dependent t-tests ($p < .05$) were used to determine statistical significance between the preferred speed bins and 3.35 m/s.

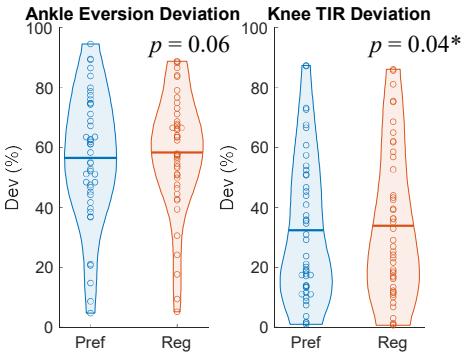

Figure 1: Population distribution for deviations at the ankle and knee (TIR = knee internal rotation) for Pref (10-20% slower) and Reg (3.35 m/s) running speeds. Dev = deviation.

Results & Discussion: Deviations changed with running speed at the knee, but not the ankle. At the ankle, the 1-10% bin did not reflect statistical significance ($p = .64$), nor did the 10-20% bin ($p = .06$) (Fig.1). At the knee, the 1-10% bin changed significantly ($p < .01$), as did the 10-20% bin ($p = .04$) (Fig 1), with the deviation magnitude lower at one's preferred speed as compared to running at 3.35 m/s. These results suggest that the knee is more sensitive to deviation than the ankle when slightly increasing speed (~0.5 m/s) from one's preferred running speed within the analysed speed range of 2.68-3.35 m/s. Cadaveric studies suggest that the minimal resistance path of the knee is sensitive to changes in force [5], which may explain the observance of deviations changing at the knee but not the ankle as a result of running speed. The knee being more susceptible to deviation may partially explain why it is the most common running-related injury location [6], as soft tissue loading is greater when deviation occurs [1]. Although the analysed speed ranges did not show statistically significant changes at the ankle, the ankle plantar flexors are the primary muscle group that increase joint work (muscle force) when running at speeds beyond those tested here [7], which may influence kinematic deviation. Thus, further research across a broader range of running speeds is required before concluding that ankle joint deviations do not change with running speed.

Significance: The observed change in joint kinematic deviation suggests that the ability to stay near one's habitual motion when running is speed dependent. Footwear has been shown to increase or decrease one's HMP deviation [1]. These results suggest that optimal footwear support to reduce one's HMP deviation may be running speed dependent. It may be advantageous for runners to consider footwear with different support systems when running at different speeds.

Acknowledgments: Thank you to all Brooks' Run Research Team members who assisted with data collection and processing.

References: [1] Willwacher et al. (2020), *Sci Reports* 10(1363); [2] Fischer et al. (2013), *Footwear Sci* 5(sup1) S135-136; [3] Clark & Weyand (2014), *JAP* (117)604-615; [4] Sumner et al. (2023), *Footwear Sci* 3(sup1) S161-163; [5] Wilson et al. (2000), *J Biomech*, 33(465-473). [6] Kakouris et al. (2021) *J. Sport. Health Sci*. 10(5), 513-522; [7] Scache et al. (2011), *MSSE*, 43(7) 1260-1271

EXPERT SPLIT BELT WALKERS? GAIT BIOMECHANICS AND ENERGETICS IN TWO INDIVIDUALS OVER TEN DAYS OF ADAPTATION

Samantha N. Jeffcoat[1*], Andrian Kuch[1], Russell T. Johnson[2], Natalia Sanchez[1]
[1]Department of Physical Therapy, Crean College of Health and Behavioral Sciences, Chapman University
[2]Department of Physical Medicine and Rehabilitation, Feinberg School of Medicine, Northwestern University
*Corresponding author's email: jeffcoat@chapman.edu

Introduction: People continuously adapt their walking behavior in a changing environment. In the lab, gait adaptation can be induced with a split-belt treadmill [1], where the belt under each leg moves at a different speed, leading to an asymmetric walking pattern. Over time, the neuromotor system adapts to this novel environment by transitioning from a negative to a more positive step length asymmetry [1,2]. This adaptation occurs in parallel with a reduction in energetic cost [2,3] and in positive work by the legs [2,4], indicating that people learn to use external assistance to improve economy [2,4]. Research has shown that adaptation of walking patterns can be retained from one day to the next, allowing faster relearning with retraining [5]. What remains to be determined is, given the novelty of the split-belt treadmill, if individuals continuously adapt their gait over multiple sessions to reduce energetic cost. We hypothesized: 1) participants will adapt walking patterns during 10 sessions, exemplified by a stable, positive step length asymmetry by day 10, 2) participants will continue to adapt metabolic cost during the 10 sessions, with ongoing reductions in metabolic cost and work done by the legs after 10 sessions [6], 3) gait patterns and energetic cost adapted over the 10 days will be retained in a follow-up session one month after the 10th session.

Methods: We tested two participants in a 10-day split-belt training protocol over the course of 3 weeks, and again at one month follow-up. **P1:** age 30, male, 1.7 m, 72 kg, exercise: cardio 4 hours a week. **P2:** age 30, female, 1.52 m, 50 kg, exercise: 2 hours a week low intensity. Participants walked on a split-belt for 10 minutes with the left belt at 1.5 m/s and the right belt at 0.5 m/s. We measured net metabolic power, step length asymmetry (SLA), and positive work by the fast leg (W+). We obtained average values of metabolic power, SLA, and W+ during early (EA) and late adaptation (LA), which were roughly the first and last 30 seconds of split-belt walking. We calculated correlations between outcome variables and session number.

Results & Discussion: We observed distinct participant responses (Fig. 1). **P1:** Metabolic power did not decrease with repeated exposure during EA ($r = -0.23$, $p = 0.517$) or LA ($r = -0.62$, $p = 0.095$). SLA was positively associated with session number during EA ($r = 0.79$, $p < 0.005$) such that the participant had a less negative SLA with each session. SLA did not change consistently over the 10 sessions during LA ($r = -0.35$, $p = 0.317$). SLA was sustained in the one-month follow-up during EA (day 10 = -0.07, day 11 = -0.06). W+ was significantly associated with session number during EA ($r = -0.77$, $p = .009$) but not LA ($r = -0.60$, $p = 0.069$). **P2:** Metabolic power did not decrease with repeated exposure during EA ($r = -0.10$, $p = 0.780$) or LA ($r = 0.16$, $p = 0.527$). SLA was not associated with session number during EA ($r = 0.59$, $p = 0.072$) or LA ($r = -0.14$, $p = 0.696$). SLA was sustained in the one-month follow-up during EA (day 10 = -0.093, day 11 = -0.098). W+ was not associated with session number during EA ($r = -0.57$, $p = 0.084$) or LA ($r = 0.08$, $p = 0.830$).

We observed distinct responses in repeated split-belt treadmill adaptation. In agreement with our hypotheses, P1 retained changes in SLA and W+ during EA and adapted toward positive asymmetries during LA with repeated exposure. However, P1 did not continuously reduce W+ or metabolic power between sessions during LA. P2 only reduced EA SLA from day 1 to day 2 and plateaued after day 2. P2 also did not consistently adapt metabolic power or W+ during EA or LA across days. Both participants retained EA SLA at follow-up but Metabolic Power and W+ were not retained. Our findings contrast those observed over a long 45-minute bout of adaptation where individuals continuously adapted SLA toward positive values while reducing W+ and metabolic power [2]. Our results suggest that short bouts of repeated adaptation do not lead individuals to maximize external assistance from the environment.

Significance: External assistance is used in clinical settings to retrain walking patterns in individuals with gait impairment. Our findings indicate that adaptation during short bouts of multi-day training cannot be equated to long bouts in a single session [2]. We also show that there is variability between individual responses to split-belt adaptation, which points at the need to tailored training for each individual.

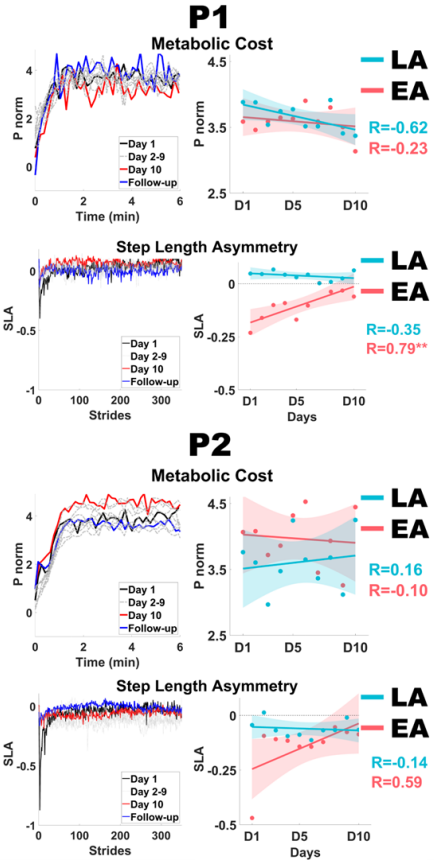

Figure 1: P1 and P2 timeseries for metabolic power (Pnorm) and SLA across sessions and correlation with session number during early and late adaptation.

Acknowledgments: Funding: NIH NCMRR R03HD107630 and NIH NCATS R03TR004248 to N. Sanchez.

References: [1] Reisman DS et al. (2005) *J Neurophysiol* 94(4); [2] Sánchez N et al. (2021) *Journal of Neurophysiology* 125(2); [3] Finley JM et al. (2013) *J Physiol* 591(4); [4] Sánchez N et al.(2019) *J Physiol* 597(15); [5] Leech KA et al. (2018) *Journal of Neurophysiology* 120(4); [6] Poggensee KL et al. (2021) *Sci. Robot* 6(58)

AN ULTRASOUND-BASED METHOD TO MEASURE KNEE KINEMATICS ENABLED BY DEEP LEARNING

Matthew B. Blomquist[1*], Christopher M. Endemann[1], Joshua D. Roth[1]
[1]University of Wisconsin-Madison, Madison, WI
*mbblomquist@wisc.edu

Introduction: Medical imaging can enhance the accuracy of tracking knee kinematics in small excursion degrees of freedom (e.g., varus-valgus (V-V) rotation) by enabling direct visualization of the bones, which avoids errors introduced by soft tissue motion. However, common imaging-based methods such as fluoroscopy and stress radiography are limited in their broad applicability because they require expensive equipment and data processing expertise, expose the participant to ionizing radiation, and/or are quasi-static. Prior studies indicate that an ultrasound-based (US-based) method may overcome these limitations [1–3]. However, these US-based methods are also quasi-static and/or require manual post-processing, which limits their ability to measure kinematics real-time and/or in large cohorts. Accordingly, *our objective for this study* was to develop and validate an US-based method to measure knee kinematics using deep learning. We used varus and valgus laxity exams as an example use case.

Methods: *Robotic testing:* In five fresh-frozen human cadaveric knees (1F/4M, 66.2 ± 3.4 years), we performed varus and valgus laxity assessments at 0°, 20°, and 45° flexion using a six degree-of-freedom robotic testing system (KR300 2700-2, KUKA; **Figure 1a**). The robot loaded each knee to ±15 Nm at 0.75 Nm/s and measured the resulting V-V kinematics. During each assessment, we placed an US transducer (LF11-5H60-A3, ArtUS, TELEMED) over the lateral or medial aspects of the knee during varus or valgus loading, respectively, that recorded 40 B-mode frames per second.

US-based measure of kinematics: We trained a custom, convolutional neural network (CNN) to predict V-V kinematics from pairs of every 40 B-mode frames to simulate loading rates that would be present during a 1-second load-unload laxity exam (**Figure 1b**). Our CNN had a standard architecture of convolutional layers, rectified linear units, and pooling layers [4]. Our CNN took in pairs of US frames as a two-channel image and output the relative V-V motion between the frames. Additionally, we augmented our dataset by adding random rotation, blur, and noise (probabilities of 50%, 25%, and 25%, respectively) to the B-mode frames. Finally, because our B-mode frames involve a temporal process, we tested adding a recurrent long short-term memory (LSTM) layer on top of the CNN [5], allowing us to train on *sequences* of B-mode frame pairs rather than *individual* B-mode frame pairs.

Analysis: We implemented a five-fold cross validation to test both networks. For each fold, we used one specimen as our test data and trained a CNN with the other four. For each laxity assessment in our test data, we computed the errors between the US-measured kinematics and the time-synched robot-measured kinematics at each US frame (**Figure 1c**). We pooled errors across specimens and flexion angles and computed the root-mean-square errors (RMSEs) for each clinical assessment.

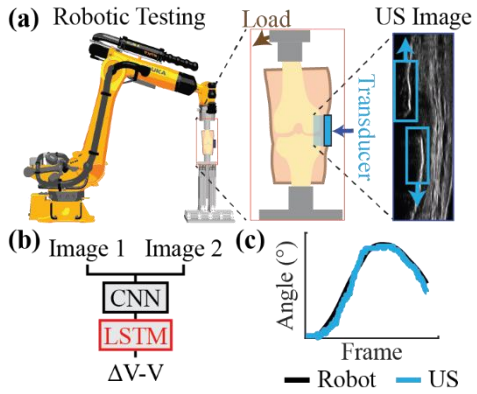

Figure 1: (a) We performed clinical laxity exams and measured knee kinematics with a KUKA robot while using ultrasound (US) to image bone motion. **(b)** We measured the change in varus-valgus (ΔV-V) kinematics using a convolutional neural network (CNN) with and without a long short-term memory (LSTM) layer **(c)** Representative plot of US vs robot kinematics.

Table 1: Root-mean-square errors (RMSE) for estimating varus-valgus kinematics. The average maximum varus-valgus rotations measured by the robot were 2.60°.

		RMSE (°)
Varus	CNN	1.98
	CNN+LSTM	1.14
Valgus	CNN	1.34
	CNN+LSTM	0.86

Results & Discussion: Using the standard CNN, the RMSEs in measuring varus and valgus rotation were 1.98° and 1.34°, respectively (**Table 1**). Adding in the LSTM layer, errors decreased by as much as 42% to RMSEs of 1.14° and 0.86° for varus and valgus, respectively (**Table 1**). This improvement is expected because LSTMs are effective at capturing temporal patterns in data. Thus, when paired with CNNs that are effective at capturing spatial patterns in data, the CNN+LSTM model worked best for measuring kinematics during a laxity exam.

The reported errors are slightly larger than previous errors on the same dataset using a cross-correlation approach in place of the current deep-learning approach to estimate V-V kinematics (range of RMSEs: 0.4° to 1.3° [3]). However, while the cross-correlation approach currently has lower errors, our deep-learning approach has the potential to improve because deep learning models are most accurate and robust when trained on a large, diverse dataset. Thus, our ongoing work is to expand our dataset to not only include more specimens from a diverse population, but also to include additional activities (e.g., walking) to make our model more robust. Additionally, we are currently investigating inputting additional measures (e.g., knee flexion angle, optical flow [6]) and testing other network architectures (e.g., transformer models) to improve the accuracy of our US-based method to measure joint kinematics.

Significance: Our US-based method should enhance measurements of joint kinematics in studies requiring real-time feedback and/or requiring a large cohort, especially in vulnerable populations (e.g., adolescents), because ultrasound is a safe, non-radiating imaging modality that is familiar to both clinicians and researchers. This study showed that our US-based method is a promising approach to assess kinematics for a range of applications, such as diagnosing disorders, monitoring healing, and informing rehabilitation.

References: [1] Slane et al. (2017), *Arch Orthop Trauma Surg* 137(8); [2] Saengsin et al. (2022), *J Orthop Res* 40(10); [3] Blomquist et al. (2023), *engrXiv*; [4] Prevost et al. (2018), *Medical Image Analysis* 48; [5] Sainath et al. (2015), *ICASSP*; [6] Farnebäck (2003), *Lecture Notes in Computer Science* 2749.

ROCKY SURFACE DECREASES TIBIAL STRESS WHILE RUNNING

Thomas A. Wenzel[1*], Eric B. Francis, Tyler N. Brown[1]
[1]Department of Kinesiology, Boise State University, Boise, ID
*Corresponding author's email: thomaswenzel@u.boisestate.edu

Introduction: Tibial stress fracture is a common, destructive overuse injury commonly suffered by runners. Large tibial stress magnitudes during running may result in bone microdamage accumulation and injury. Tibial stress results from both axial and bending forces but is primarily attributed to the tibial bending moment that reportedly increases with changes in gait biomechanics, speed, and external factors, such as load and grade. Irregular surfaces, such as rocky, are purported to produce alterations in biomechanics and muscular forces at the ankle that may increase bending and stress at the tibia [1]. Therefore, we hypothesize that running over a rocky surface will increase tibial stress and bending moment amplitudes compared to a flat surface, resulting in an amplified risk of stress fractures.

Methods: 15 recreational runners had lower limb biomechanics quantified during a run (4.5 m/s) over a flat and rocky surface. During the run, synchronous 3D marker trajectories and GRF data were collected using ten high-speed optical cameras (240 Hz) and a single force platform (2400 Hz), and then, lowpass filtered (12 Hz, 4th order Butterworth) and processed in Visual3D obtain lower limb biomechanics.

Custom Matlab code was used to estimate tibial stress. Specifically, axial stress at the distal third of the tibia and bending moments along with their AP and ML components were calculated according to the methods described by [2], using internal muscle forces and their moment arms according to [3]. The resultant magnitude of the previously calculated AP and ML moments and stress was calculated to represent off-axis bending at the distal third of the tibia.

Total axial stress and bending moment, the AP and ML components of both stress and bending, and the resultant bending moments and stresses were submitted to paired *t-tests* to determine the effect of surface of off-axis tibial bending. The alpha level was 0.05.

Results & Discussion: Contrary to our hypothesis, running over the rocky surface did not increase tibial stress and bending. Participants, in fact, exhibited ~6 % less tibial stress and bending moments on the rocky surface. Specifically, total tibial axial stress, AP, ML, and resultant bending moments decreased on the rocky compared to the flat surface (all: $P < 0.025$) (Fig. 1). However, the surface did not alter either AP and ML bending stresses. Running over similar irregular surfaces purportedly shifts lower limb muscular work production away from the ankle, towards the hip [1]. The increase in hip work production, or conversely, the reduction in ankle work stems from decreases in force produced by the associated musculature when traversing irregular surfaces. Considering internal, i.e., muscular, forces at the ankle are the largest contributor to tibia bending stresses and moments the irregular, rocky surface may shift work production up the distal chain, decreasing tibial stress [1]. It appears the irregularity of the rocky surface did not alter the magnitude of external forces placed on the tibia to increase bone stress during running, but future work should determine the specific external factors that lead to hazardous increases in tibial stress and bending during gait.

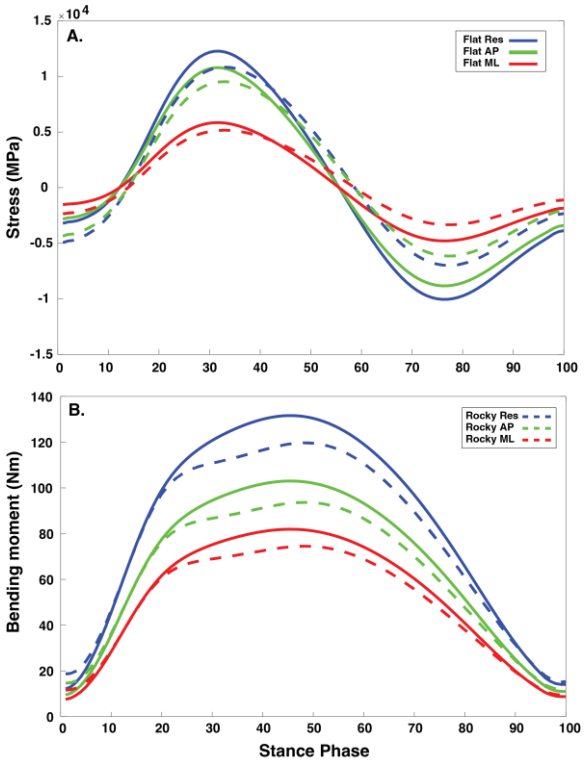

Figure 1: Depicts bending stress (A) and moment (B) for the resultant, AP and ML axis for the flat and rocky surfaces.

Significance: Running over a rocky surface did not increase tibial stress fracture risk. With these bone stress injuries being a large issue for recreational and professional runners, demonstrating that irregular rocky surfaces do not increase tibial stress and bending may be a critical step towards designing safe running and/or injury prevention programs. Yet, identifying the specific biomechanical and external factors that increase bending stress may be necessary for a beneficial reduction in the occurrence of these common running injuries.

Acknowledgments: NIH NIGMS (2U54GM104944, P20GM109095, P20GM148321) supported this work.

References: [1] Schrøder et al. (2022), *J Biomech* 141; [2] Rice et al. (2019), *MSSE* 51(11); [3] Hamner et al. (2010), *J Biomech* 43(14);

SYSTEMATICALLY DETERMINING ROBOTIC SUPERNUMERARY LIMB ASSISTANCE FOR SIT-TO-STAND

Patrick Slade[1*], Xabier Irizar[2], Zoe Kutulakos[3]
[1]John A. Paulson School of Engineering and Applied Sciences, Harvard University, Boston, MA, USA
[2]Professorship of Healthcare and Rehabilitation Robotics, Technical University of Munich (TUM), Germany
[3] Division of Engineering Science, University of Toronto, Toronto, ON, Canada
*Corresponding author's email: slade@seas.harvard.edu

Introduction: Robotic assistive devices aim to improve human mobility, but determining what assistance will achieve objective mobility benefits is challenging. Predicting a human's response to robotic assistance is difficult due to the complexity of the person's central nervous system, musculoskeletal system, and motor control. Biomechanical simulation encapsulates information about a human's musculoskeletal system and the dynamics of movement [1], but modeling assumptions and errors in this multi-scale model result in differences between experimental and simulation results for assistive devices [2]. Device designers often rely on hand-tuning, intuition, or biologically-inspired models to develop assistance controllers, resulting in slow but steady improvement in device benefits over years of research [3]. Human-in-the-loop optimization provides a different approach by systematically searching for effective assistance through experimental testing to maximize the specified mobility metrics, quickly determining the best device assistance [4]. Human-in-the-loop optimization can be challenging to apply to new devices or activities because it requires carefully defining many settings, like the assistance parameterization, that are typically informed by prior experimental results [5]. There is a need for a more general and systematic approach to determine effective robotic assistance. We propose a systematic method for finding effective robotic assistance using biomechanical musculoskeletal modeling and experimental assistance tuning. We validate this systematic method by identifying the assistance provided by a supernumerary robotic limb during sit-to-stand (Fig. 1A).

Methods: Our systematic process of determining effective assistance involved three steps: collect participant motion during a task, perform a biomechanics simulation to determine an initial assistance profile optimized for a movement objective, and experimentally tune assistance parameters informed by the biomechanical simulation (Fig. 1B). The person's motion was measured with smartphone motion capture (OpenCap) and merged with kinetics measured from force plates (Bertec) in the ground beneath the person's feet and the chair. The scaled model and kinematic data was used to perform a static optimization problem in OpenSim to minimize muscle activity during the sit-to-stand motion. OpenSim was allowed to optimize an OpenSim force vector placed at the person's center of mass, emulating an ideal assistive device support. The resulting simulated assistance profile was a simple shape, similar to a single node on a spline. Timing and magnitude of simulated assistance is often different from experimentally optimal [2], so we compared a set of simple splines, with the same magnitude of assistance and different timing of the peak assistive force (Fig. 1C). A robotic supernumerary limb was designed to provide the idealized simulation assistance (Fig. 1A). Our assistance objective was to reduce muscle activation, which we measured using surface electromyography sensors (DELSYS Trigno) on the vastus medialis and rectus femoris, placed on both legs. Participants performed maximum voluntary contractions to calibrate the muscle activation signals. Participants performed five repetitions of sit-to-stand to evaluate each assistance condition, which were presented in a randomized order. The reported reductions in average muscle activity were averaged across the repetitions and the two measured muscles on both legs to provide one comprehensive measurement of the change in knee extensor activity.

Results & Discussion: Biomechanical simulation identified an assistance profile that provided reductions in muscle activity without any prior knowledge of the assistive device or mobility task. The OpenSim simulated assistance profile provided experimental reductions in muscle activity for both participants (Fig. 1D), indicating OpenSim captures meaningful information about the musculoskeletal system and dynamics of the movement and can select beneficial assistance profiles. Biomechanics simulation encapsulates useful information relevant to designing assistive devices and assistance controllers.

The experimentally-tuned assistance reduced muscle activity by twice as much as the OpenSim simulated assistance, highlighting the effectiveness of the proposed systematic assistance development approach (Fig. 1D). Although the OpenSim assistance provided benefits, the complex interaction between the human and robot required experimental tuning to determine some parameter settings, in this case, the best timing to provide the peak assistive force. Systematic tuning may be necessary to overcome the human-robot modeling complexities and improve device benefits without any hardware changes.

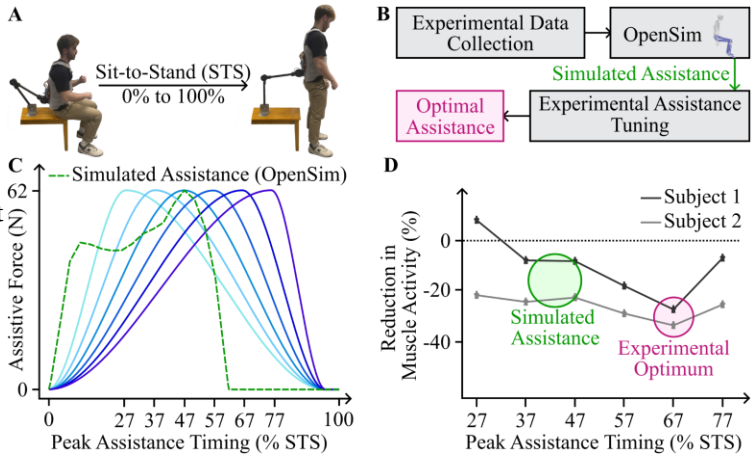

Fig. 1. Systematically identifying robotic assistance during sit-to-stand.

Significance: This assistance tuning framework may generalize to objectively select effective assistive controllers for a wide range of tasks and devices without extensive prior experimentation or intuition from the device designer.

References: [1] Seth et al. *PLoS Computational Biology* (2018). [2] Franks et al. IEEE BioRob. (2020). [3] Sawicki et al. *Journal of Neuroeng. And Rehab.* (2020). [4] Slade et al. *Nature* (2022). [5] Welker et al. *Royal Society of Open Science* (2020).

THE EFFECT OF MRI-BASED FULL-FIELD FIBER ORIENTATIONS ON TENDON MECHANICS

Michael D. K. Focht[1*], Roberto Pineda Guzman[2], Mariana E. Kersh[1,3,4]
[1]Department of Mechanical Science and Engineering, University of Illinois Urbana-Champaign, Urbana, IL
[2]Carle Clinical Imaging Research Program, Stephens Family Clinical Research Institute, Carle Health, Urbana, IL
[3]Beckman Institute for Advanced Science and Technology, University of Illinois Urbana-Champaign, Urbana, IL
[4]Carle Illinois College of Medicine, University of Illinois Urbana-Champaign, Urbana, IL
*Corresponding author's email: mfocht2@illinois.edu

Introduction: Variation in local fiber orientation and dispersion are important contributors to tendon mechanical behavior [1, 2]. Until recently, characterizing local fiber morphology has required invasive techniques and typically been limited to sub-sections of tissue. In contrast, diffusion tensor imaging (DTI), a magnetic resonance imaging (MRI) technique, enables the non-invasive inference of full-field microstructural properties by measuring the diffusion of water within the tissue [3]. Changes in DTI metrics, such as diffusivity and principal diffusion orientation, have been linked to microstructural rearrangement and fatigue-induced damage in tissue-mimicking helical fiber constructs [4]. However, the sensitivity of the mechanical response of tendon to the inclusion of DTI-based local fiber orientations, in contrast to assuming parallel fibers, remains unclear. Therefore, the objective of this study was to evaluate the in silico mechanical response of tendon with DTI-based local fiber orientations compared to tendon with a uniform fiber orientation.

Methods: Porcine digital flexor tendons (n = 6) were harvested and DTI scans of the central region (length = 20 mm) were obtained using a diffusion-weighted spin-echo sequence (9.4T, details in [5]). The raw data was filtered, and the diffusion tensor was computed for each voxel using a weighted linear least squares method [6]. The first eigenvector was calculated (MATLAB) as the metric for local fiber orientation. Structural scans of the tendon were used to create three-dimensional tetrahedral-based finite element (FE) models (Amira, Geomagic, Abaqus). The local fiber orientations were mapped to each element and used as input to the Holzapfel-Gasser-Ogden (HGO) strain energy function [7]. Tensile stress-strain data of porcine digital flexor tendons [8] were converted to sample-specific force-displacement data and used to optimize the material parameters (k1, k2) in the fiber term of the HGO model using the inverse-FE approach. Material parameters for the ground matrix and fiber dispersion were assumed from previous work [9]. A second set of FE models were created using the same material parameters but with the fiber orientation assumed to be uniform along the main tendon axis. All models were subjected to 4% strain, which corresponds to the toe and initial heel region of the J-shaped curve characteristic of tendon. The maximum stress and maximum principal strain distributions between models were compared using paired t-tests in R.

Results & Discussion: The median DTI-based fiber angle relative to the long axis of the tendon was 17.16° with a median absolute deviation of 7.03° (Fig. 1A). The mean root-mean-square error of the DTI-based stress-strain curves was 0.22 MPa (Fig. 1B). The mean maximum stress of the uniform fiber models was greater ($p < 0.0001$) than the DTI-based models (31.3 MPa and 4.32 MPa, respectively). The total stiffness of the uniform fiber models was more than seven times that of the DTI-based models up to 4% strain. The length of the toe region in the uniform fiber models was more variable than the DTI-based models, which is likely a result of inter-sample variation in the DTI-based fiber distributions that were used for optimizing the fiber terms of the material model (Fig. 1B). While more compliant at the bulk scale, the peak strains in the DTI-based models were larger in all samples, though not significantly different ($p = 0.095$) (Fig. 1C).

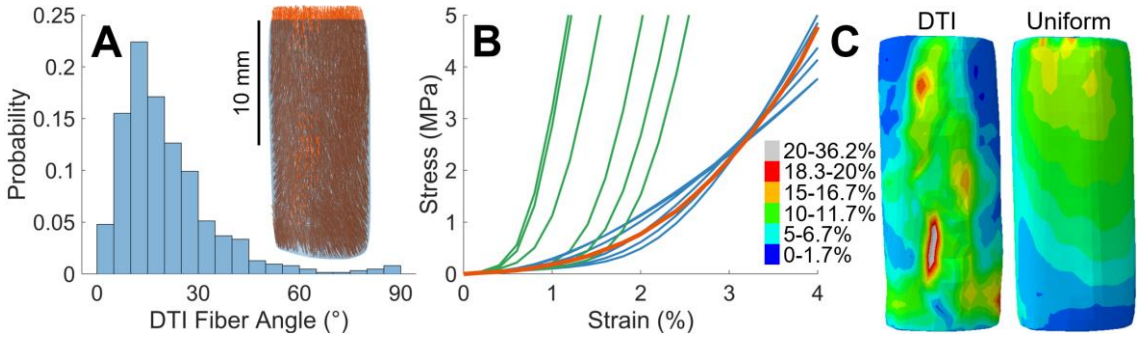

Figure 1: A) Distribution of DTI-based fiber angles relative to the long axis of the tendon for all samples and a representative DTI-based fiber distribution. B) Engineering stress-strain curve from the literature [8] (orange), for the DTI-based models (blue), and for the uniform fiber models (green). C) Maximum principle logarithmic strain distributions for a representative DTI-based model (left) and uniform fiber model (right).

Significance: Full-field fiber orientations are important determinants of both the local and bulk mechanics of tendons and ligaments. DTI enables the non-invasive acquisition of full-field fiber orientations of tendons, which can be incorporated into FE models for predicting the mechanics of these tissues more accurately. Such models may provide insights into the origins of tissue failure, and when translated to clinical level MRI, could be useful for early detection of damage.

Acknowledgments: Thanks to Dr. Bruce Damon and Dr. Shreyan Majumdar for their help with MRI sequence optimization and the Beckman Institute Biomedical Imaging Center seed grant for supporting this research.

References: [1] Lake+ *Journal of Biomechanics* 2009; [2] Thomopoulos+ *Journal of Biomechanics* 2006; [3] Zellers+ *Journal of Orthopaedic Research* 2023; [4] Pineda Guzman+ *Annals of Biomedical Engineering* 2023; [5] Pineda Guzman+ *Orthopaedic Research Society* 2024; [6] Damon+ *Journal of Biomechanics* 2021; [7] Gasser+ *Journal of The Royal Society Interface* 2006; [8] Duenwald-Kuehl+ *Annals of Biomedical Engineering* 2012; [9] Kersh *University of Wisconsin* 2010.

HOW HARD CAN IT BE TO SLIP PARTICIPANTS?

Gaspard Diotalevi[1,2], Denis Rancourt[2,3], Chantal Gauvin[4], Cécile Smeesters[1,2]*
[1]Research Centre on Aging, Sherbrooke, QC, Canada
[2]Department of Mechanical Engineering, Université de Sherbrooke, Sherbrooke, QC, Canada
[3]Centre for Research in Acoustics-Signal-Human of the Université de Sherbrooke (CRASH-UdeS), Sherbrooke, QC, Canada
[4]Institut de recherche Robert-Sauvé en santé et en sécurité du travail (IRSST), Montreal, QC, Canada
*Corresponding author's email: Cecile.Smeesters@USherbrooke.ca

Introduction: Human slips have been the subject of experimentation for decades in an effort to reduce their societal toll [1]. To that end, several researchers have slipped participants overground on a vast array of lubricants and surfaces. However, one would be surprised at how hard it actually can be to slip participants, and to collect usable data in doing so. Based on 49 experimental papers on true overground slips (i.e., no surface translations considered [2]) published between 1981 and 2024, we assessed the slipping and falling yields of such experiments, to highlight the need for improved equipment and protocols when one wants participants to slip.

Methods: The 49 papers identified in the context of our own research on slips shared 53 analyses of 45 unique experiments. Local slipping yield was computed as the fraction of trials where participants actually slipped across trials in which a slip could have occurred (lubricant or slippery surface encountered), while global slipping yield considered all trials (including training, dummy, and failed trials). Local falling yield was computed as the fraction of trials where participants fell across trials in which a slip could have occurred, while global falling yield considered all trials. We kept the authors' own definitions of what was a "slip" and a "fall" to classify trial outcomes, however permissive these definitions could be. Finally, as the exact number of training, dummy or failed trials and slip or fall outcomes were not always provided, we considered the best-case scenario to maximize yields. We thus considered the minimal number of training, dummy or failed trials possible and the maximal number of slips and falls possible, when such trials and outcomes were reported.

Results & Discussion: From the 53 analyses, only 75% of local and global slipping yields and 42% of local and global falling yields could be estimated (Figure 1). Indeed, the number of trials in which a slip could have occurred was incoherent or not reported in several analyses. For example, the number of "no slip" and "slip" steps were often not reported in maximal ramp angle tests, since a slip could occur at every step but only actually occurred on the last step in these incremental protocols. Moreover, all yields are overestimated by our best-case scenario assumption and certain yields are further overestimated by the permissive "slip" and "fall" definitions used in certain analyses.

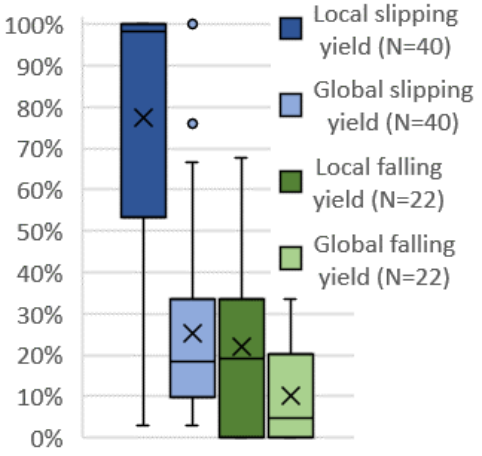

Figure 1: Best-case scenario experimental yields from reviewed analyses

The local slipping yields showed a very high variability in the percentage of slips that were successful, which could be explained by key differences in experimental methods. Indeed, of the ten analyses in which local slipping yields were equal to or under 53%, two had equipment or protocol adherence issues, and eight took little to no care to minimize participants' anticipation of the upcoming slip. On the other hand, of the 30 analyses in which local slipping yields exceeded 53%, 15 took adequate steps to minimize participants' anticipation, while 15 reached an unreasonable local slipping yield of 100%. Of the latter, one used volitional slipping, while the other 14 classified slips based on their severity, considering trials with no lubricant or slippery surface as a particular case of a slip with minimal heel velocity or slip distance after heel strike.

The global slipping yields showed that for 75% of analyses, less than a third of all trials actually provided usable slipping data. More than two thirds of trials thus consisted of training trials to ensure that heel strike occurred on sensors, dummy trials to prevent adverse anticipatory effects or failed trials due to equipment problems. Interestingly, the revised WASP device by Rasmussen and Hunt [3] showed much better global slipping yields than other analyses (2 outliers, Figure 1).

Falls proved even rarer with 8/22=36% of analyses reporting no fall at all (local and global falling yields = 0%). For 75% of analyses, less than a third of slipping trials lead to a fall, and only 20% of all trials lead to a fall.

Significance: Son [4] stated back in 1990 that experiments on human slips and falls on short walkways used since the late seventies were expected to yield very low fall rates. Yet even though sensors have come a long way since, one has to acknowledge that our experimental equipment and protocols have not changed much in the past 50 years. Future slipping analyses should start by doing a better job of reporting slipping and falling yields, using reasonable "slip" and a "fall" definitions. Future slipping experiments should also minimize participants' anticipation, thus allowing for repeated slipping trials to boost the statistical power of reported results. Finally, future slipping equipment and protocol designs should strive to improve slipping and falling yields by reducing the number of training, dummy and failed trials, as it would mean collecting more data in the same time frame with fewer participants.

Acknowledgments: The Fonds de recherche du Québec – Nature et Technologies (FRQNT) and the Natural Sciences and Engineering Research Council of Canada (NSERC) for their financial support. Elliot Durocher for his assistance with the literature review.

References: [1] Parachute (2021), *The Cost of Injury in Canada*; [2] Diotalevi and Smeesters (2023), *ASB2023*; [3] Rasmussen and Hunt (2021), *J Biomech* 125; [4] Son (1990), PhD Dissertation, Texas Tech University.

Exploring the Feasibility of Measuring Walking Symmetry at Home from Thigh Angular Acceleration

Sangwon Shin[1]MS, Mukul Mukherjee[1] Ph.D., Philippe Malcolm[1] Ph.D.
[1]Department of Biomechanics, University of Nebraska at Omaha, Omaha, NE, USA
Email: sangwonshin@unomaha.edu

Introduction: Step symmetry, a significant indicator of movement efficiency and rehabilitation outcomes, traditionally requires elaborate motion capture systems for detailed analysis [1]. These systems are confined to laboratory settings, limiting their applicability to home-based monitoring. This research addresses the critical need for accessible and practical gait analysis tools, particularly for use outside specialized laboratory environments. Inertial Measurement Units (IMUs) have been used to estimate spatiotemporal parameters for step symmetry indices [2]. The accuracy of IMU data depends on the number of errors per unit time and the application of appropriate processes to reduce errors due to noise. Despite this limitation of IMUs, it still is very useful for tracking continuing gait data in environments outside the lab. In this study, our aim is to estimate step symmetry from hip angular acceleration data obtained from IMUs. We aim to evaluate how well step symmetry from thigh angular acceleration correlated with the step length symmetry, which could be obtained from lab-based motion capture data. We hypothesized a moderate to strong correlation between candidate step symmetry metrics and motion-capture based step symmetry metrics. We did not expect perfect correlation since step length is defined at end-effector region (foot instead of thighs), and it only considers one instant (i.e., heel strike) rather than the full stride.

Methods: This is secondary analysis of data from three healthy young adults (two females and one male, 1.66 ± 0.18 m, 78.44 ± 15.72 kg) [3]. Participants walked on a split-belt treadmill with varying levels of step symmetry. We used symmetry data from 5 phases of the protocol: Baseline, Early-Adapt, Late-Adapt, Early-Post, and Late-Post. We calculated the step length on the split belt following guidelines from Hoogkamer et al. [4], and used the symmetry index (SI) following Robinson et al. [5]. A value of zero indicated complete symmetry, while larger negative or positive values denoted greater asymmetries between legs. We investigated the thigh angular acceleration derived from motion-capture data as an approximation of measurements that could be obtained from IMUs. Two different candidate metrics (Mean relative phase (MRP) and Pearson correlation) based on thigh angular acceleration were used. MRP was calculated based on the root mean square of the difference between the left and right hip angular accelerations [6]. Mean Pearson correlation coefficients between right and left hip angular accelerations were calculated. We analyzed the changes of both candidate metrics and step length SI at each phase of the protocol. We evaluated how well both metrics correlate with the standard method of step length SI using repeated measures correlation.

Results & Discussion: Our findings supported this hypothesis, revealing significant correlations between step length SI and MRP (r = 0.74, p = 0.0036, Fig. 1A) and Pearson correlation (r= 0.71, p = 0.0062, Fig. 1B). These results suggest that thigh-based angular acceleration metrics, which could be obtained from IMUs, could serve as reliable estimators of step symmetry. This finding suggests that IMU-based thigh angular acceleration could be used to evaluate the effectiveness of home-based interventions. One limitation of the study is that this is a secondary data analysis based on motion capture data. It will be necessary to evaluate this question with actual IMUs instead of motion-capture based thigh acceleration. Furthermore, step length SI has some limitations: step-length SI only characterizes symmetry at a fixed point in the gait cycle and it is possible that marker errors could affect step-length SI results. It is unclear to what extent the submaximal correlations were a result of limitations of our angular acceleration metrics or the limitations of step-length SI calculation.

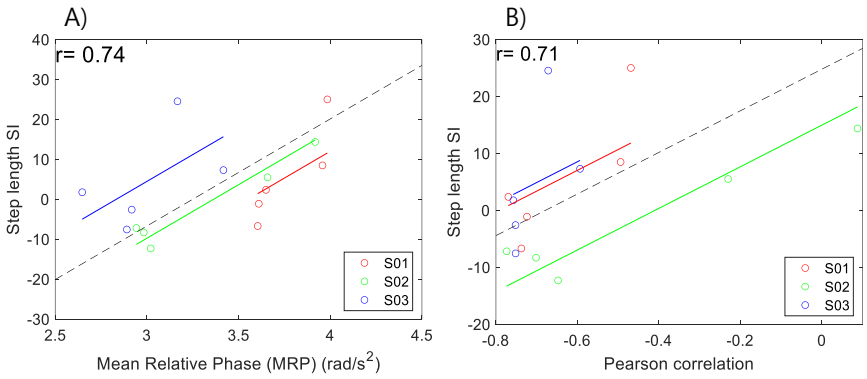

Figure 1 Repeated measures correlation versus step length symmetry index. A) Mean relative phase (MRP) B) Pearson correlation.

Significance: This research exhibited the calculation of hip angular acceleration from motion capture data for at-home gait analysis in individuals with gait asymmetry, representing substantial progress in achieving step symmetry outside the traditional laboratory environment when compared to other symmetry metrics. By identifying correlations between the step length SI derived from motion capture data and different symmetry metrics (MRP and Pearson correlation), our findings could suggest a novel perspective to calculate step symmetry and mobility within daily life settings. Furthermore, the results indicate the feasibility of monitoring step symmetry throughout interventions, such as with exosuit applications, in people with gait asymmetry, offering a valuable approach to improve rehabilitation efforts.

Acknowledgements: P20-GM109090, NSF2203143, and AHA (18AIREA33960251, #959486) and NU GRACA award.

References: 1. Viteckova et al. (2018). *Biomed. Signal Process. Control.*, *42*, 89–100.; 2. Crecan & Peștean (2023). *Sensors*, *23*(14); 3. Kowalczyk et al. (2023). *J. NeuroEng. Rehabil.*, *20*(1), 88.; 4. Hoogkamer et al. (2014). *Gait & Posture*, *39*(1), 652–654.; 5. Robinson et al. (1987). *J. Manipulative. Physio. Ther.*, *10*, 172–176.; 6. Hejrati et al. (2016). *Hum. Mov. Sci.* 49, 104–115.

EFFECTS OF 12-WEEK STRETCHING PROGRAM ON TRICEPS SURAE: STIFFNESS AND TORQUE-ANGLE CURVE ANALYSIS

Maria Clara A. Brandão[1*], Liliam F. de Oliveira[1]
[1]Engineering Biomedical Program (PEB), Federal University of Rio de Janeiro, Brazil.
*Corresponding author's email: mclara@peb.ufrj.br

Introduction: Stretching programs are commonly applied to improve or restore joint range of motion (ROM). However, there is still a gap in understanding the mechanical and structural adaptations of muscles after static stretching programs. Potential mechanisms for an increase in ROM include neural properties [1] and mechanical properties of the muscle and/or tendon [2], as well as passive joint structures [3].

To analyze tissue mechanical properties non-invasively, the technique of dynamic elastography, particularly Supersonic Imaging (SSI) elastography, has been applied as it provides a real-time method for assessing muscle stiffness before and after interventions [4]. The SSI technique functions in two main modes: the pushing mode applies high-intensity acoustic radiation forces at different tissue depths, generating transverse waves. These shear wave propagation speed (c_s) is promptly captured via imaging mode. Assuming tissue isotropy and pure elasticity, the shear modulus (μ) can be estimated as $\mu = \rho * c_s^2$ (where $\rho = 1010$ kg/m³, biological medium density) [5].

Consequently, SSI elastography has been used to investigate alterations in tissue mechanical properties after static stretching programs on the triceps surae. These studies revealed significant decreases in the stiffness of the gastrocnemius lateral (LG) and medial (MG) muscles after 5 (inclined platform) [6] and 12-week (heel drop exercise) [7]. Nonetheless, neither study examined the structure of the Achilles Tendon (AT) nor conducted a torque-angle curve (TxA) assessment. Analysis of altered passive torque-angle curves can provide insights into neural and/or structural changes induced by stretching interventions.

Hence, this study aimed to analyze the stiffness of the LG, MG and AT and the TxA curve during the ROM test, after a 12-week of wall-static stretching (WSP).

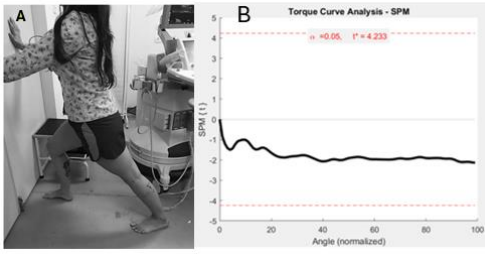

Figure 1: a) Wall-static stretching exercise. b) Plot showing the statistical test SPM results, with no significant difference found.

Methods: After approval by the ethics committee (number 3.672.989), 11 healthy women underwent testing before and immediately after the WSP. Tests included measurements of ROM, Maximum Voluntary Isometric Contraction (MVIC), peak passive torque (PPT), and TxA curve using an isokinetic dynamometer (Biodex Medical System Inc, New York, USA). Elastography images were obtained using an Aixplorer (version 11, Supersonic Image, Aix-en-Provence, France) for the MG, LG and AT, following the protocol by Lima et al. (2017) [8]. A 1D Statistical Parametric Mapping (SPM) analysis was conducted to compare the shapes of the TxA curves after the stretching program. The WSP (Fig. 1a) involved standing with both hands on the wall, one foot maximally dorsiflexed behind with the knee extended, performing 5 sets of 1 minute, 5 times a week, for 12 weeks.

Results: After the program, there was a significant increase in ROM ($p<0.001$) and PPT ($p=0.001$). However, the stiffness of the AT ($p=0.19$), LG ($p=0.18$), and MG ($p=0.25$) muscles did not change significantly, as well as the MVIC ($p=0.32$). Analysis using SPM found no statistically significant changes between the TxA curves before and after WSP (Fig. 1b).

Discussion: Only two studies utilizing SSI elastography examined changes in mechanical properties of the gastrocnemius muscle, both reporting significant decreases post-stretching program (after a 5-week program [6] and 12 weeks [7]), despite different stretching exercises. Considering the findings of Taniguchi et al. (2015) [8], who observed a significant reduction immediately after a stretching session using the same exercise against the wall, with μ values returning to baseline levels after 20 minutes, our initial hypothesis of significant reductions was not confirmed. This suggests that the transient stiffness alterations observed in a previous study were not consolidated in the long term. Despite this, our protocol effectively improved ROM (33% increase) and PPT (55% increase), possibly due to a tolerance response to stretch. Torque-angle curve analysis showed no statistical differences, implying neural adaptations.

Significance: Our study emphasizes the significance of examining the impact of WSP on triceps surae stiffness. Although the 12-week program notably increased ROM, it did not affect muscle and tendon stiffness, suggesting not enough to induce tissue remodeling. The observed stretch tolerance response in the torque-angle curve implies neural adaptations. Integrating SSI technique with neurophysiological assessments could offer a comprehensive understanding of mechanical and neural factors in the stretch response. Future comparative studies on diverse stretching modalities may optimize clinical and sports protocols.

Acknowledgments: The funding agencies FINEP, FAPERJ, CAPES and CNPq for their financial support.

References: [1] Behm et al. (2021), *J Clin Exerc Physiol* 10(4). [2] Shan et al. (2023), *Appl Sci* 13(21). [3] Bryant et al. (2023), *J Funct Morphol Kinesiol*, 8(2). [4] Lima et al. (2018), *Ultrasonography*, 37(1). [5] Gennisson et al. (2013), *Diagn Interv Imaging* 94(50). [6] Akagi & Takahashi (2014), *Scand J Med Sci* 24(6). [7] Andrade et al (2020), *J Appl Physiol* 129(5). [8] Lima et al. (2017), *Muscles Ligaments Tendons J* 7(2). [8] Taniguchi et al. (2015), *J Med Sci Sports* 25(1).

CHILDREN WITH HEEL PAIN AND ADULTS WITH ACHILLES TENDINOPATHY PRESENT WITH SIMILAR SYMPTOMATIC AND STRUCTURAL TENDON DEFICITS

Kayla D. Seymore[1,2*], Shawn L. Hanlon[3], Morgan N. Potter[1,2], Bradley Bley[4], Karin Grävare Silbernagel[1,2]
[1]Biomechanics and Movement Science Program, University of Delaware, Newark, DE, USA
[2]Department of Physical Therapy, University of Delaware, Newark, DE, USA
[3]Department of Physical Medicine and Rehabilitation, University of Colorado, Aurora, CO, USA
[4]Delaware Sports Medicine, Wilmington, DE, USA
*Corresponding author's email: seymorek@udel.edu

Introduction: In adults, pain with loading and loss of function are clinical symptoms of Achilles tendinopathy [1]. In children and adolescents, the same clinical symptoms are instead considered typical of a growth plate injury (calcaneal apophysitis) [2]. The structural alterations associated with Achilles tendinopathy are undetermined in the pediatric population, as imaging techniques are rarely used for diagnosis when evaluating children with heel pain. With no clear difference in the clinical diagnosis of calcaneal apophysitis and Achilles tendinopathy for patients under 18 years old with heel pain, Achilles tendon pathology may be overlooked in children. Misdiagnosis and subsequent misaligned treatment of Achilles tendon injury in children may cause long-term health detriments [3] and impede the development of a physically active lifestyle in adulthood. Before new approaches to treatment can be developed for children with heel pain, research is needed to fill the gap in knowledge between the impact of Achilles tendon pathology in children and adults. The purpose of this study was to compare Achilles tendon symptoms, structure, and lower limb impairments between children (7-17 years) with heel pain and young adults (18-25 years) with Achilles tendinopathy.

Methods: Eighteen children (8 F, 11.5 ± 2.4 years) with heel pain and 24 young adults (14 F, 21.5 ± 2.3 years) with Achilles tendinopathy were included in the study. Clinical diagnosis was confirmed by a licenced physical therapist. Symptom severity was evaluated via pain on palpation (scale of 0-10) of Achilles tendon midportion and insertion, and the Victorian Institute of Sport Assessment-Achilles (VISA-A) questionnaire. Achilles tendon size (cross-sectional area [CSA] and thickness) were measured using B-mode ultrasound, according to previously validated protocol [4]. Mechanical properties of shear modulus and viscosity were measured using continuous shear wave elastography (cSWE) [5]. A test battery was used to assess lower limb functional performance [6]. Total repetitions and work for a maximum endurance single-leg heel-rise test were measured using a linear encoder affixed to the heel. Maximum height and average plyometric quotient (PQ=flight time/contact time) were calculated during a single-leg hopping test using a light-mat. The maximum counter-movement jump (CMJ) and drop CMJ height from 3 single-leg jumps were also measured with the light-mat. Achilles tendon symptoms in the most symptomatic limb (self-reported) and limb symmetry index (LSI=most symptomatic/least symptomatic limb*100) structural and functional measures were compared between children and young adults using MANOVAs, controlling for sex, limb, weight, and physical activity level. Alpha was $p<0.05$.

Results & Discussion: Children with heel pain and young adults with Achilles tendinopathy both reported moderate Achilles tendon midportion and insertion symptom severity and displayed mild structural differences between limbs, with no difference between groups ($p>0.05$). CMJ height LSI was 45% higher in children compared to young adults after controlling for covariates ($p=0.002$) (Fig. 1). Averaged across all tests, young adults had an 8% deficit in function on the most symptomatic side, whereas children had 5% greater function on the most symptomatic side.

Significance: Children with heel pain have similar symptoms and structural pathology as young adults with Achilles tendinopathy yet have greater function on their most symptomatic side. Thus, treatment for children with heel pain may be better aimed at symptom and load management rather than improvement in function. This novel comparison of Achilles tendon symptoms, structure, and lower limb impairments between the clinical pediatric and adult population provides necessary evidence for future research to establish the pathoetiology of heel pain in children and improve clinical diagnoses.

Acknowledgments: Research reported in this abstract was supported by the National Institute of Arthritis and Musculoskeletal and Skin Diseases of the National Institutes of Health under award number F31AR081663.

References: [1] Scott et al. (2020), *Br J Sports Med* 54:260-262; [2] Ramponi & Baker. (2019), *Adv Emerg Nurs J* 41:10-14; [3] Fares et al. (2021), *Clin Med Res* 14:95; [4] Smitheman et al. (2023), *J Vis Exp* 200:10.3791/65798; [5] Cortes et al. (2015), *Ultrasound Med Biol* 41:1518-29; [6] Silbernagel et al. (2006), *Knee Surg Sports Traumatol Arthrosc* 14:1207-17.

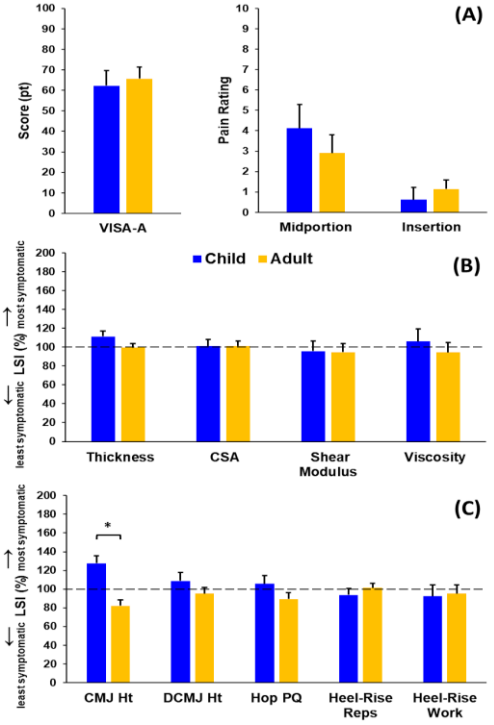

Figure 1: Mean (SE) Achilles tendon symptomatic (A), structural (B), and lower limb functional (C) outcomes for children with heel pain and young adults with Achilles tendinopathy. Dashed line (- -) indicates 100% limb symmetry.
**significant group difference ($p<0.05$)*

Ankle Stiffness During Drop Jumps: A Case Study on Its Role in Achilles Rupture Risk

Jackson Dickey[1*], Brandon Peoples[1], Hillary Holmes[2], Jaimie Roper[1]
[1]Auburn University, Auburn, AL, U.S.A.
[2]High Point University, High Point, NC, USA
*Corresponding author's email: jld0090@auburn.edu

Introduction: Although the Achilles tendon is the thickest and strongest in the human body, it is also the most ruptured due to the demand placed on it [1]. In February and July of 2020, a professional basketball player was brought into our lab to have his walking and jumping biomechanics assessed. Though the athlete reported pain around his Achilles tendon periodically, he never received any treatment or imaging for Achilles Tendinopathy. Three weeks after having the biomechanics of his walking gait and his jumps analyzed in July, the athlete suffered their first full rupture of the Achilles tendon 8.5cm proximal to the calcaneus insertion. The injury occurred during an organized basketball competition as the athlete attempted to dunk the ball. Jumping off his left leg, the athlete recalls feeling a "kick" in his left heel during the jump's takeoff, or push-off, phase. Therefore, this case study explores changes in ankle stiffness before the Achilles rupture.

Methods: This athlete was a 24-year-old male professional basketball player with a mass of 115.39kg and a height of 2.06m. Vicon's lower-body plug-in gait functional AI model was used for jump testing. The data was collected using a 16-camera motion capture system (VICON, Oxford, UK) at 100 Hertz and two bilateral embedded force platforms (AMTI Inc., Natick, MA, USA). During the jump testing, the individual completed drop-jumps and drop-lands onto the two force plates from a 1-foot-tall box placed half the individual's height away from the force plates [2]. The athlete completed these drop jumps and landed under four conditions: standard, choice, auditory, and visual. Joint stiffness was calculated as the change in joint angle over the change in joint moment. The loading rate was calculated as the peak vertical ground reaction force (vGRF) over the time to reach peak vGRF.

Results and Discussion: Significant asymmetries were observed in joint angles, moments, and stiffness at the ankle, knee, and hip in both the frontal and transverse planes. On the affected side, decreased stiffness in the ankle (Fig. 1) was observed during drop jumps. (Auditory: *M = 47.03, SD = 10.4,* Visual*: M =37.3, SD=8.6,* Choice: *M = 56.6, SD = 9.7* Standard: M = *54.8, SD = 13.8)*. Ankle stiffness is measured in Newton millimeters per kilogram (Nmm/kg). The individual had 36.7% less stiffness in the affected ankle when compared to the unaffected ankle across all drop-jump conditions. The *s*tandard condition showed a 43.2% decrease in stiffness in the affected side. Reduced ankle stiffness could decrease joint stability, making the ankle more susceptible to injuries such as an Achilles tendon rupture [3][4]. An increase in vertical ground reaction forces and decreased power absorption at the knee and hip possibly led to increased power absorption at the ankle. Further, the rate of loading was also higher on the affected side. The loading rate was, on average, 8% greater in the affected side across all conditions compared to the non-affected side (Fig. 2). (Auditory: *M = 44.9, SD = 2.8,* Visual*: M =44.6, SD=0.3,* Standard: M = *44.7, SD = 1.5,* Choice: *M = 38.4, SD = 5.3)*. Loading rate was measured in Newtons per second (N/s). During fast movements, such as sprinting and jumping, higher loading rates are placed on the Achilles tendon over shorter periods [5]. This fast-loading rate may not give the tendon enough time to adapt to and dissipate these forces, possibly increasing the risk of injury. Also, the Achilles tendon does not store as much energy during high loading rates as slow [6]. The findings of this case study align with previous findings in other studies [3, 4, 7] that suggest low ankle stiffness may contribute to an Achilles tendon injury, indicating that low ankle stiffness compounded with a high loading rate may be a significant determinant of an Achilles tendon injury.

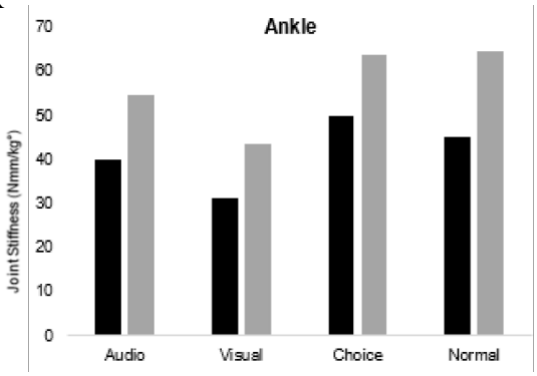

Figure 1: Ankle stiffness in affected ankle vs. unaffected ankle. The dark bar represents the affected ankle, and the grey bar represents the unaffected ankle.

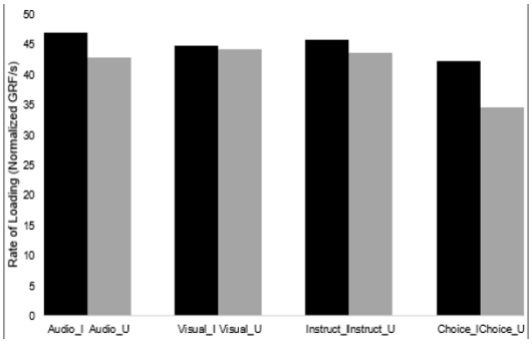

Figure 2: Rate of loading in the affected limb vs. the unaffected limb. The dark bar represents the affected ankle, and the grey bar represents the unaffected ankle.

Significance: The findings of this study indicate that it may be important to analyze an individual's kinematics and kinetics as a potential tool to reduce the risk of injury. By doing such analysis, researchers can proactively identify biomechanical factors that lead to increased risk of injury. This would allow professionals to develop injury prevention strategies to help athletes better control their bodies to reduce the risk of injury. Understanding an individual's movement patterns can also allow coaches and/or trainers to develop personalized training programs that will reduce the risk of injury in the athlete and optimize their performance.

References: [1] Doran et al. (2010), [2] Pauda et al. (2009), [3] Sakanaka et al. (2018), [4] Ugsu et al. 2023, [5] Starbuck et al. (2021), [6] Rosario and Roberts (2020), [7] Maquirriain (2011)

EFFECTS OF ASSISTIVE DEVICE USE AND EXPERIENCE IN POST-STROKE WALKING WITH CANES

Martins E. Amaechi[1*], Emily Steffensen[1], Oluwaseye Odanye[1], Brian Knarr[1]
[1]Department of Biomechanics, University of Nebraska at Omaha, Omaha, NE USA
*Email: mamaechi@unomaha.edu

Introduction: Impairments following a stroke significantly decrease walking ability and community engagement [1]. The severity of hemiparesis correlates with functional impairment [2], emphasizing the importance of enhancing paretic propulsion post-stroke [3] to improve walking velocity. Assistive devices (AD) like canes, are often used to enhance balance, alleviate pressure on hemiplegic joints, and enhance walking velocity, promoting community reintegration [4]. While the introduction of a cane can notably enhance walking within a month of its prescription following a stroke, these benefits are not transferred to walking without the cane [5]. Evaluating how canes affect post-stroke recovery is crucial for interventions aiming to restore independent mobility and reduce reliance on assistive devices, this may guide targeted rehabilitation programs, ultimately enhancing long-term outcomes and the quality of life for stroke survivors. Therefore, the purpose of this study is to investigate the biomechanical disparities in lower limb function post-stroke while walking with a cane, specifically how propulsion is influenced. We hypothesize that current AD users will exhibit lower paretic propulsive force and slower walking velocity without the cane, whereas previous AD users will demonstrate greater propulsive force and faster walking speed. This is based on research showing that the percentage of body weight applied on the cane correlates with the severity of hemiplegia, decreasing as rehabilitation progresses [6].

Methods: Twenty-three post-stroke participants (10 males, 13 females, age 59 ±12.6 yrs., ≥6 months post-stroke) were recruited. Only 19 subjects: no history of assistive device use (N=7), history of assistive device use (N=6), and current dependence on an assistive device (N=6), completed all walking tasks. Participants were included if they were 19-80 years old, had a single-chronic stroke, and were ambulatory. Kinetic and kinematic analysis using a motion capture system was performed and an instrumented cane. subjects were asked to walk in three walking conditions with a cane using 5% of their body weight (5%BW), walking with a cane comfortably (SSBW), and walking without a cane. Propulsion impulse (PI), braking impulse (BI), and walking speed (WS) were derived for the paretic limb, non-paretic limb, and the cane. linear mixed-effect regression model was used to quantify the change in PI, BI, and WS.

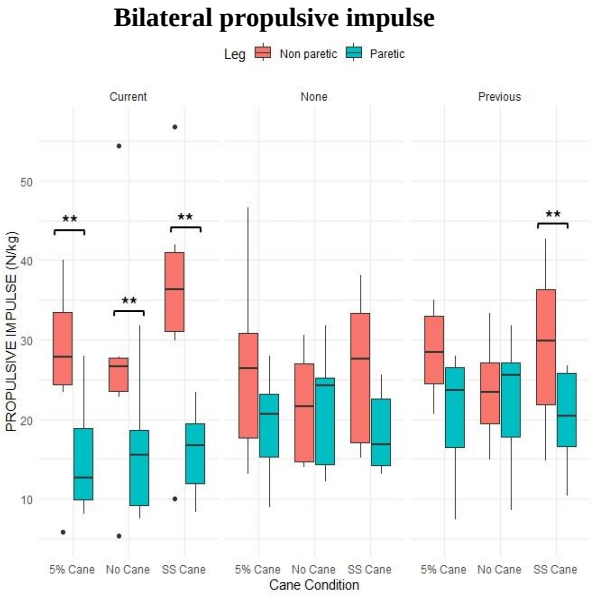

Figure 1: Paretic (blue), and non-paretic (orange) propulsive impulse for 5%, self-selected and no cane use conditions during overground walking.

Results & Discussion: No significant differences were observed in the braking impulse across all AD experience groups. Current AD users exhibited significantly greater propulsion on the less affected limb regardless of cane use ($p<0.01$), indicating no effect on propulsion for either limb. No significant difference was seen in the cane propulsion across AD use groups ($p>0.05$). Interestingly, post-stroke AD users walked faster without the cane compared to when using it lightly ($p<0.05$), suggesting that our participants may have employed other strategies resulting in a greater walking speed without the cane unlike previous work [5]. The difference in walking velocity could result from factors such as the additional weight of our instrumented cane (4 lb) compared to the average cane (1 lb) or the dual-task nature of cane-assisted walking, which has been associated with increased energy cost [7]. For stroke patients, tasks like distributing a percentage of their body weight onto the cane while maintaining proper positioning on a force platform could pose cognitive challenges, potentially influencing outcomes [8], [9].
Previous AD users walked faster without a cane than current AD users walking with self-selected body weight on a cane ($p<0.05$). It may be due to the severity of stroke of current AD users [2]. It may also be because previous AD users don't need it for mobility or the cognitive load of the dual task associated with cane-assisted walking on dependent AD users [8], [9].

Significance: These results suggest that assistive device use and prior experience with assistive devices did not influence propulsion but affected the participants walking speed. How this difference may change through rehabilitation process may be a quantitative way to progress and guide clinical decision-making regarding transitions to independent walking.

Acknowledgements: This research was funded by the NIH(R15HD094194), and UNO GRACA (46684).

References: [1] Olney et al. (1996), *Gait & Posture* 4(2); [2] Bowden et al. (2006), *Stroke* 37(3); [3] Alingh et al. (2020), *Clinical Biomechanics* 71(176-188); [4] Gosman-Hedstrom et al. (2002), *IJTAHC* 18(520-527); [5] Avelino et al. (2021), *Clin Rehabil* 35(11); [6] Laufer et al. (2004), *Clin Gerontl* 14(2); [7] Ijmker et al. (2013), *Archives of physical medicine and rehabilitation* 94(11); [8] Woollacott and A. Shumway-Cook,. (2002), *Gait & Posture* 16(1); [9] Wright and Kemp. (2004), *Phys Ther* 72(4).

INFLUENCING HUMAN GAIT DYNAMICS WITH AN ADAPTIVE SPLIT-BELT TREADMILL

Zijie Jin[1], Jason T. Isa[1], Samuel A. Burden[1] and Kimberly A. Ingraham[1 *]
[1]Department of Electrical and Computer Engineering, University of Washington, Seattle, WA, USA
*Corresponding author's email: zijiejin@uw.edu

Introduction: Walking on a split-belt treadmill, in which one belt moves faster and one belt moves slower, is a task that has commonly been used to study human locomotor adaptation and learning [1,2]. Recent studies have shown that walking on a split-belt treadmill can reduce the energy cost of walking—but only if the human learns to exploit this assistance by changing their gait pattern. The treadmill can produce net positive work to a human if they adopt a positive step length asymmetry (SLA), which is defined as the difference in step length between steps taken on the faster belt and those on the slower belt [3,4]. Previous studies have shown that humans require external guidance [3] and/or very long exposure times (> 30 minutes) to learn to adopt a positive SLA, but once they have learned this strategy, they can quickly converge to energetically efficient gaits. Previous studies have investigated how varying the split-belt ratio of the treadmill (the ratio of speeds between the faster and slower belts) might affect the SLA humans naturally choose [5], but so far these investigations have been limited to using a constant split-belt ratio. The overall goal of our work is to understand how humans adapt to walking on a split-belt treadmill with a continuously time-varying split-belt ratio. In this study, we designed an adaptive algorithm that dynamically adjusts the split-belt ratio as a function of the human's SLA, and we seek to understand how systematically varying the learning rate of the adaptive algorithm influences the human's gait.

Methods: We completed a pilot study with three participants who had previous experience with this task. Participants walked on a split-belt treadmill at a fixed total belt speed (the sum of the belt speeds) of 2 m/s. We calculated the human's SLA in real time using the center of pressure measured from the force plates under each belt. The split-belt ratio time-varied according to the following update rule: $m_{i+1} = m_{i-1} - a * (m_i - h_i - 2)$, where m_i and h_i are the ith split-belt ratio (treadmill) and SLA (human), respectively, with a learning rate a that is empirically varied. When $a = 0$, the split-belt ratio is constant and fixed at 2 (the faster and slower belt speeds are 1.32 m/s and 0.67 m/s, respectively), which we consider the baseline condition for this experiment. Each participant performed five walking trials that lasted 200 seconds, each with a different learning rate (0, 0.1, 0.5, 0.7, and 1.0). The split-belt ratio was updated every three seconds, using the average SLA of the previous 3 steps. For each condition, we calculated the human's steady-state SLA as the average over the last 10 updates (30 seconds).

Results & Discussion: Our initial observations indicate that the human's steady-state gait pattern may be changed as a result of the way the machine adapts. At the baseline fixed split-belt ratio of 2 ($a = 0$), across-participant mean (SD) steady-state SLA was 0.03 (0.08). During conditions with adaptive split-belt ratios ($a > 0$), mean steady-state SLA increased with learning rate, with a maximum of 0.09 (0.15) at $a = 0.7$. Despite overall increasing trends, participants' individual responses varied (Figure 1a). Different learning rates also resulted in differences in the steady-state split-belt ratio (Figure 1b). As an example, across participants, the aforementioned $a = 0.7$ case led to a mean (SD) split-belt ratio of 2.09 (0.15) at steady state. All participants were able to adopt a positive SLA at some learning rates, which means they were able to take advantage of the assistance from the treadmill. It is important to note that all participants had previous experience walking on a split-belt treadmill, which likely contributed to their ability to spontaneously adopt a positive SLA. As a next step, we will extend this pilot study to include more participants with a longer protocol, as well as include users without prior experience walking on split-belt treadmill.

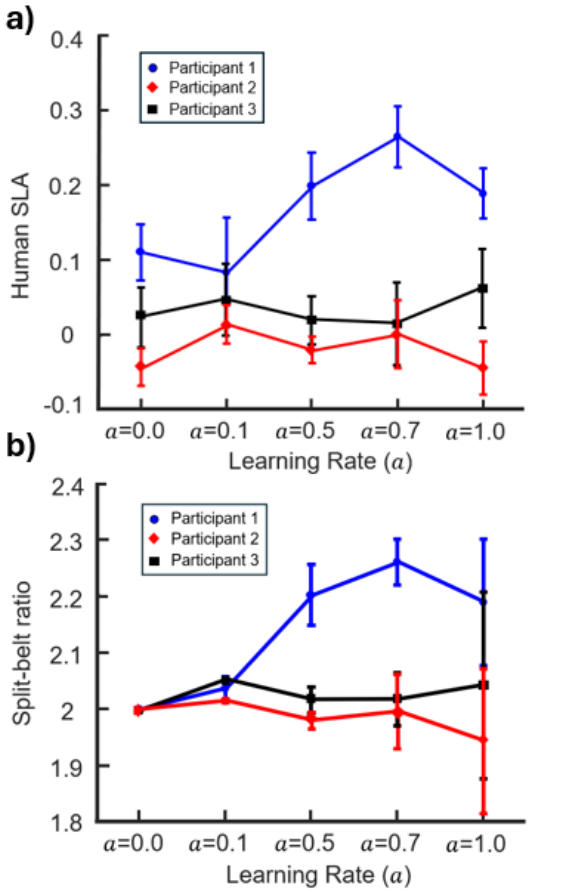

Figure 1: Average steady-state **(a)** Human step length asymmetry (SLA) and **(b)** Split-belt ratio for three participants at different learning rates. Colored markers and error bars show mean and standard deviation over the last 10 updates (30 seconds) of each trial.

Significance: These pilot results demonstrate the potential of steering human SLA choices within a split-belt walking task using an adaptive split-belt ratio. These results provide further insight into human motor learning and how humans adapt to novel energy cost landscapes. This knowledge may guide the future development of control strategies and training protocols for assistive robots.

Acknowledgements: We thank the participants for their time and effort in these experiments.

References: [1] Malone et al. (2010), *J. Neurophysiol*. 103(4); [2] Leech et al. (2018), *Sci. Rep*. 8 (94); [3] Sánchez at al. (2019), *J. Physiol*. 597 (15); [4] Sánchez at al. (2021), *J. Neurophysiol*. 125(2); [5] Stenum et al. (2020), *J. Physiol*. 598(18).

Determining the Effect of Gluteal Muscle Bias on Lower Extremity Biomechanics in Baseball Pitching

Dimitri Haan, BS[1], Adam B. Rosen, PhD, ATC[2], Samuel J. Wilkins, PhD, ATC[2], & Brian A. Knarr, PhD[1]
[1]Department of Biomechanics, University of Nebraska Omaha, Omaha, NE USA
[2]School of Health & Kinesiology, University of Nebraska Omaha, NE USA
Email: dhaan@unomaha.edu

INTRODUCTION

For baseball pitchers, the most used determinant of skill is the velocity of their fastball pitch, as high fastball velocity gives batters less time to react to the pitch and gives baserunners less time to get to the next base. Thus, improving velocity has potential to help the pitcher improve and advance to higher levels of play. Previous research on the lower body has investigated the biomechanical factors that may correlate with increased velocity[1,2] but did not consider the control strategies that may affect the primary muscles involved in generating distal forces that help generate energy to increase forward velocity. Insight from postural control strategies allow for assumptions to be made using the location of the center of pressure, with a center of pressure behind the midfoot creating increased gluteal activation and center of pressure in front of the midfoot creating higher quad activation[3]. Therefore, the purpose of this study is to define pitchers by their lower body muscle group biases and investigate variables that may correlate with increased velocity. It was hypothesized that pitchers that throw with a gluteal bias will throw faster, generate more ground reaction force impulse and more pelvic acceleration than quadriceps bias.

METHODS

Previously collected motion capture data from 40 college-aged pitchers was sampled for this study. Motion capture data (Qualisys, Gothenburg SWE) provided data on the location of the pitcher's foot and 6-degree of freedom force plates provided data on the location of the COP (Bertec, Columbus, OH, USA). Motion capture data was exported to Visual3D (Germantown, MD, USA) to calculate model-based data the location of the midfoot. The calculated model-based data was pelvic angular acceleration about the Z-axis with respect to the pelvis, and ground reaction force (GRF) in the anterior direction. Foot model data from the timeframe of setup to 200ms before stride foot contact (SFC) was normalized to 101 points and exported to a custom MATLAB (MathWorks, Natick, MA, USA) script. Setup was automatically defined as the moment when the front heel marker exceeded 0.02m/s, offset by -1 frame. SFC was manually defined as the instant that the pitcher's lead foot made full contact with the mound. The MATLAB script used the location of the COP to differentiate pitchers into gluteal bias and quadriceps bias. Pitchers whose COP was behind their midfoot during < 50% of the timeframe were defined as gluteal biased and pitchers with ≥5 0% were quadriceps biased. The MATLAB function *cumtrapz* was used integrate GRF values to calculate the propulsive impulse between setup and SFC. Pelvis acceleration was calculated from setup to ball release. Data was tested for normality by a Shapiro-Wilk Test. Normally distributed data was tested for significance by an independent t-tests at α=0.05. Data that was not normally distributed was tested for significance with a Mann-Whitney U test and α=0.05.

RESULTS

The mean values and results of significance tests are displayed in Table1.

*Table 1 displays the mean values of each measurement for both glute and quad bias groups. The results of the significance tests are displayed on the bottom row with * indicating significance. **data for pelvic acceleration was not normally distributed.*

	Velocity (mph/kg)		Impulse (Ns/kg)		Pelvis Acceleration (m/s^2)**	
Bias	Glute	Quad	Glute	Quad	Glute	Quad
Mean	0.992 ± 0.107	0.927 ± 0.091	8.883 ± 4.07	9.591 ± 3.69	9546.5 ± 4521	8203.0 ± 1962
p value	0.03*		0.30		0.842	

DISCUSSION

The measurement that displayed a significant difference between muscular bias groups was normalized velocity (p=0.03). Two of the collected measurements, pelvic acceleration, and propulsive impulse, produced no significant results (p=0.842 and p=0.30 respectively). The hypothesis that players generating force through gluteal muscle biases would throw with greater velocity, higher impulse and higher pelvic acceleration was partially supported, with velocity being the hypothesis that was supported. These results would indicate that players who bias generate force generation with their glutes are more likely to throw faster, but the mechanisms behind this difference remain unknown. The lack of significance in propulsive impulse and pelvic acceleration leads to the conclusion that these measurements do not add additional information about the biomechanical differences between pitchers in glute and quad muscle bias groups.

CONCLUSION

The results of this study were that players who pitched with a gluteal bias threw with a significantly higher velocity compared to quad biased pitchers. No significant results were found between groups for pelvic acceleration and propulsive impulse. These results indicate that pitchers who throw with a gluteal bias are more likely to throw harder, but the biomechanical variables that contribute this have yet to be found. Players that are interested in increasing their pitching velocity are encouraged to complete exercises that improve gluteal muscle strength and activation. Further research is required to understand biomechanical factors that may contribute to increased pitching velocity.

SIGNIFICANCE

Injuries are unfortunately very prevalent in baseball pitchers of all ages. This research offers insights into the mechanisms behind improving velocity and how it interacts with safe pitching biomechanics.

REFERENCES

[1] Kageyama, M., Sugiyama, T., Takai, Y., Kanehisa, H. & Maeda, A. *J. Sports Sci. Med.* **13**, 742–750 (2014).
[2] Oyama, S. & Myers, J. B. *J. Strength Cond. Res.* **32**, 1324 (2018).

[3] Guihard, M. & Gorce, P. *IEEE/RSJ International Conference on Intelligent Robots and System* vol. 3 2587–2592 (IEEE, Lausanne, Switzerland, 2002).

REAL-TIME UPPER LIMB JOINT ANGLES ESTIMATION IN THE PRESENCE OF WIRELESS DATA DROP USING LSTM

Kezhe Zhu[1*], Dongxuan Li[1], Jinxuan Li[1], Peter B. Shull[1]
[1] Department of Mechanical Engineering, Shanghai Jiao Tong University, Shanghai, China
*Corresponding author's email: kezhe_zhu@sjtu.edu.cn

Introduction: Wireless inertial motion capture holds significant promise for facilitating portable, home-based rehabilitation with real-time feedback. However, wireless data drop can lead to substantial estimation errors, rendering the system inoperable. Therefore, this study developed an LSTM-based model for real-time estimation of upper limb joint angles based on IMU measurements in the presence of wireless data drop.

Methods: The proposed model (Fig 1(a)), comprising a two-layer MLP encoder (128-128 neurons), a two-layer unidirectional LSTM (128 neurons), and a three-layer MLP decoder (128-64-18 neurons), is designed to estimate segment orientations from the three IMU data stream with randomly dropped intervals. Subsequently, these estimated segment orientations are used to calculate the joint angles. The data from three IMUs, comprising 3D accelerometer, 3D gyroscope, and estimated 6D orientation readings, undergo gap filling with zeros, concatenation, and subsequent input into the LSTM-based model. The model's output (dim = 18) corresponds to the orientations of three segments: thorax, upper arm, and forearm, each represented as a 6D rotation vector [1]. The neural network's loss function is defined as the mean segment orientation error across the three segments. For comparison, the No Prediction approach serves as a baseline, wherein it retains the most recent available segment orientation estimation from the respective IMU until the data sample becomes available again. The data drop intervals are assumed to follow a uniform distribution, both in terms of interval duration and occurrence throughout the trial. Additionally, the joint angle estimation error is assessed using the RMSE of joint orientation error [2] to avoid gimbal lock.

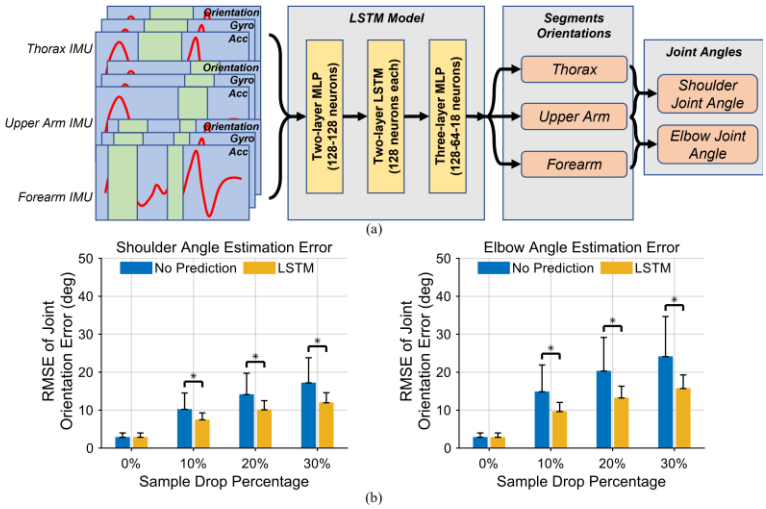

Figure 1: (a) The proposed architecture for real-time estimation of upper limb joint angles in the presence of data dropout, and (b) the RMSEs of joint orientation error for estimated shoulder and elbow angles across varying levels of data drop. Green blocks denote intervals of data drop.

The proposed model undergoes training and testing using a dataset comprising twenty-four subjects (age: 22.92±0.86; height: 1.73±0.07 m; weight: 60.92±9.38 kg; gender:16 males and 8 females), each performing five 2-minute trials of sports activities, including yoga, golf, swimming, dancing and badminton. Carbon fiber plates equipped with three retro-reflective markers are aligned with the IMUs (Fig 2) positioned on the thorax, upper arms, and forearms. During the initial 5-second static N-pose period, both sensor and marker plates coordinates are aligned with the same upright body segment coordinate [3]. A thirteen-camera stereophotogrammetric system (Vicon, Oxford, UK) and Visual3D software (C-Motion, MD, USA) were utilized to track segment movements using triple marker sets and to calculate reference segment orientations and upper limb joint angles.

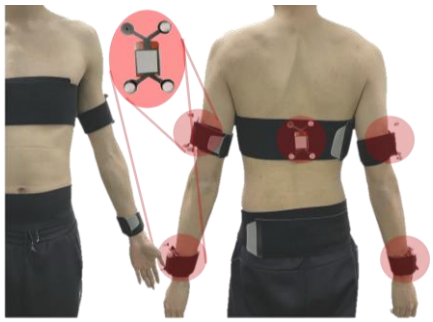

Figure 2: Experimental setup. Five IMUs are affixed to the thorax, right/left upper arms, and right/left forearms of the subjects, respectively.

Results & Discussion: The proposed model achieved RMSEs of 12.0±2.6°and 15.7±3.6° for shoulder and elbow angle estimation, respectively, with a 30% data drop percentage (Fig 1(b)). This reflects a reduction of 30% and 35% in error compared to the No Prediction strategy. The effectiveness of LSTM in estimating upper limb kinematics with discontinuous data is attributed to its capacity to capture temporal and internal vector dependencies within the IMU signals.

Significance: The proposed model could enable wearable IMU dynamic motion analysis in the presence of data drop. This could further facilitate home-based wearable rehabilitation applications by enhancing their robustness in various transmission environments and expanding their effective application scope.

Acknowledgments: This work is supported by the National Natural Science Foundation of China under grant 52250610217.

References:

[1] Zhou et al. (2019). Proceedings of the IEEE/CVF conference on computer vision and pattern recognition, 5745-5753;
[2] Van Wouwe et al. (2023). arXiv preprint arXiv:2308.16682; [3] Fan et al. (2021). Journal of Biomechanics, 124: 110549.

DEVELOPMENT OF A REHABILITATIVE MEDICINE BASED BIOMECHANICS CONCEPT INVENTORY

Brian Wallace[1*], Duane Knudson[2], ChengTu Hsieh[3]
[1]Department of Kinesiology, University of Wisconsin Oshkosh, USA,[2]Department of Health and Human Performance, Texas State University, USA, [3]Department of Kinesiology, California State University Chico, USA
Email: wallaceb@uwosh.edu

Introduction: The Biomechanics Concept Inventory (BCI) is a nationally normed 24-question standardized test based on 4 prerequisite and 8 course competencies from guidelines [1] for introductory biomechanics courses in kinesiology in the United States [2]. The first version was published in 2003, with two additional versions published by 2006. The purpose of the different BCI versions were to give instructors a greater pool of questions from which to create custom assessments for determining their student's learning [3]. However, there are no norms for instructors to compare their custom assessments to, other than the validated norms of the original BCI (BCI1). Additionally, the content in many undergraduate biomechanics courses has changed since the latest BCI version was created nearly 20 years ago. Many instructors now focus less on application to sport and more on application to allied health professions due to the significant proportion of students who desire to enter these fields. Therefore, the purpose of this project was to develop and assess a new BCI (BCI_Rehab) that focuses questions on rehabilitative medicine and compare to previously reported data related to BCI1.

Methods: Students (n=28) enrolled in a three credit-hour introductory biomechanics class at a comprehensive university in the USA participated. Ethics approval was obtained prior to any testing and students provided written Informed Consent.

Students completed BCI_Rehab on the first day of class (pre-test), and again on the last day of class (post-test). The new assessment's questions aligned with the same competency areas as prior BCI versions. Gain scores (g), a measure of student learning that incorporates the increase in correct responses between pre and post-tests, were calculated [4]. The post-test was used for all analyses, except for the pre-test being required to calculate g scores. Discrimination analyses (ID) measuring the effectiveness of each question on its ability to separate students who vary in content knowledge were calculated [ID = (upper group percent correct) – (lower group percent correct)]. Descriptive statistics for pre-test, post-test, and g were calculated. One-sample t-tests compared BCI_Rehab values for pre-test, post-test, g, correct responses per competency, and ID to previously reported results for BCI1 [5]. Alpha was set at 0.05.

Table 1: Correct responses on post-tests by competency category. BCI1 scores are from [5]. Correct responses are out of a maximum score of 2. Values are mean (SD), Means between tests not different.

	Correct Responses	
Competency	BCI1	BCI_Rehab
Anatomical terms and landmarks	1.73 (.49)	1.68 (.55)
Muscles and joint movements	1.02 (.72)	1.07 (.66)
Interpretation of graphs	1.1 (.68)	1.57 (.63)
Algebra	1.55 (.65)	1.46 (.64)
Muscle mechanical characteristics	0.63 (.57)	0.46 (.58)
Motor unit recruitment and EMG	0.57 (.61)	1.11 (.63)
Linear kinematics	0.61 (.61)	1.21 (.57)
Angular kinematics	1.22 (.65)	0.79 (.63)
Linear kinetics	0.65 (.56)	0.29 (.46)
Angular kinetics	0.55 (.74)	0.46 (.74)
Fluid mechanics	0.53 (.58)	0.36 (.49)
Application in qualitative analysis	0.92 (.70)	0.39 (.50)
Mean (SD)	0.92 (0.41)	0.90 (0.51)

Results & Discussion: Pre and post scores were not significantly different between previously reported findings [5] for BCI1 and BCI_Rehab (9.34±2.46 vs 9.64±2.47 and 11.50±2.74 vs 11.76±2.68, respectively). The g score of BCI_Rehab was significantly higher ($p=0.001$), although the absolute difference was small (0.14±0.17 vs 0.15±0.12). The number of correct post-test responses by students for each competency category were on average similar (Table 1). The most notable differences were with the linear kinetics, angular kinematics, and application sections scoring notably higher with BCI1, and interpretation of graphs and linear kinematics higher for BCI_Rehab. With only two questions per competency, one question can greatly increase or decrease the competency mean. One linear kinetics question, for example, had no students answer correctly, while three other questions had three or fewer correct responses.

BCI1 significantly better discerned high from low performers based on ID (0.41±0.07 vs 0.28±0.14, $p=0.001$), although BCI_Rehab was qualitatively better in this regard than the third BCI version [5]. Most ID values could be classified as "excellent" (≥0.40) or "good" (0.25-0.39). However, one linear kinetics, one fluid mechanics, and one application question had an ID value of 0.06 or lower and should be reassessed.

Significance: We created a new BCI version that may more closely align with many contemporary introductory biomechanics courses. Select questions require further assessment and validation before the new assessment can be widely used.

References:

[1] Abraham et al. (2018). *Guidelines for Undergraduate Biomechanics* 4th ed. [Guidance Document] Retrieved from SHAPE America website: https://www.shapeamerica.org/uploads/pdfs/2018/guidelines/Guidelines-for-UG-Biomechanics.pdf
[2] Knudson et al. (2003). Development and evaluation of a biomechanics concept inventory. *Sports Biomechanics*, *2*, 267-277.
[3] Knudson. (2006). Biomechanics concept inventory. *Perceptual and Motor Skills*, *103*, 81-82. doi:10.2466/PMS.103.1.81-82.
[4] Hake. (1998). Interactive-engagement versus traditional methods. *American Journal of Physics*, 66, 64-74.
[5] Wallace et al. (2019). A quantitative comparison of two biomech concept inventory versions, *ISBS Proceed Archive*: 37(1), https://commons.nmu.edu/isbs/vol37/iss1/50

THE EFFECTIVENESS OF NECK, SHOULDER, AND BACK EXOSKELETONS ON THE RISK FOR MUSCULOSKELETAL DISORDERS IN THE DENTAL INDUSTRY

Josh Riesenberg[1*], Madeline Jenkins[1], and Jason Gillette[1]
[1]Iowa State University, Ames, IA
*Corresponding author's email: josh.riesenberg@gmail.com

Introduction: In 2019, over 1.7 billion musculoskeletal disorders (MSDs) were reported [1]. The dental industry, for example, suffers from high levels of MSDs in the shoulder, back, and neck. When surveyed, nearly 80% of dental professionals reported MSD pain within a 6-month period, with the neck, low back, and shoulders indicated as frequently affected areas [2]. In another study, dentists and dental hygienists were found to spend more than 50% of the time with trunk flexion and shoulder abduction at or above 30°, and more than 85% of the time with neck flexion at or above 30° [3]. Exoskeletons (exos) are assistive devices that are designed to reduce loading on the body during certain postures and movements. Promising results for exos are reported both in lab and worksite settings. When holding static postures, a neck exo provided significant reductions in splenius capitis activity between flexion angles of 30-55°, a shoulder exo provided significant reductions in medial deltoid activity between abduction angles of 10-70°, and a back exo provided significant reductions in lumbar extensor activity between flexion angles of 15-65° [4]. In a workplace study, anterior deltoid muscle activity was significantly reduced in assembly line workers at Toyota when wearing a shoulder exo as compared to without [5]. However, there is a gap in research regarding the effects of exos during tasks performed by dental professionals. The goal of this study was to evaluate how three different exos (neck, back, and shoulder) impacted muscle activity during a simulated teeth cleaning task commonly performed by dental professionals. Due to their provided support, it was hypothesized that each exo would significantly reduce muscle activity in its intended muscle region as compared to the control condition without increasing muscle activity in surrounding muscles.

Methods: Twenty-one young, healthy adults participated (11F/10M). Electromyography (EMG) sensors were placed over the dominant anterior deltoid, medial deltoid, upper trapezius, and latissimus dorsi, as well as bilaterally on the lumbar erector spinae and splenius capitis. Maximum voluntary isometric contractions were completed for each muscle group. Participants performed a simulated teeth scaling task using handheld dental tools on a model of the human mouth. The task was completed during the following conditions: without an exo (control), with a shoulder exo (Levitate Airframe Flex), with a back exo (HeroWear Apex 2), and with a neck exo (Levitate prototype). Muscle activity was analyzed by calculating the 50th percentile (median) and 95th percentile (peak) EMG amplitudes. Results for the right and left lumber erector spinae and splenius capitis were averaged. Values were averaged across participants for each condition. Paired t-tests were performed for each exo condition compared to the control condition with statistical significance set at $p < 0.05$.

Results & Discussion: The shoulder exo significantly reduced median and peak muscle activity in the upper trapezius and splenius capitis and peak muscle activity in the medial deltoid compared to without an exo during the simulated teeth cleaning task (Table 1). In addition, the neck exo significantly reduced median and peak muscle activity in the splenius capitis and peak muscle activity in the upper trapezius compared to without an exo. Surprisingly, the back exo significantly increased peak activity in the anterior deltoid. However, it should be noted that the anterior and medial deltoid median and peak muscle activity were quite small (< 5 %MVC) for this simulated dental task. The shoulder anchoring of the back exo for trunk support might explain the small increase in anterior deltoid activity. No significant differences were found for the latissimus dorsi or erector spinae. The most promising findings may be the reduction in upper trapezius and splenius capitis activity with shoulder exo and neck exo usage as a potential intervention to reduce shoulder and neck muscle fatigue in dental professionals. Analysis of the motion capture data collected during this study may provide insight into whether adjustments in posture with the shoulder exo explain the reduction in neck extensor activity.

*Table 1: Median and peak EMG amplitudes (%MVC) during a simulated dental teeth cleaning task. * indicates significant difference ($p<0.05$) between with and without exoskeleton conditions.*

	Anterior Deltoid		Medial Deltoid		Upper Trapezius		Lat. Dorsi		Erector Spinae		Splenius Capitis	
	50th	95th	50th	95th	50th	95th	50th	95th	50th	95th	50th	95th
Control	1.14	2.67	1.11	2.48	4.72	8.26	4.97	9.33	7.52	16.61	10.00	15.42
Shoulder exo	1.05	2.51	1.10	**1.82***	**3.02***	**5.37***	5.24	9.61	6.84	13.35	**8.80***	**13.36***
Back exo	1.54	**4.04***	1.04	2.23	4.26	7.54	4.30	7.97	7.46	13.91	9.79	15.43
Neck exo	1.18	2.88	1.12	2.33	4.12	**6.98***	4.90	9.07	7.98	15.47	**8.45***	**13.32***

Significance: This study provides insight into the muscle requirements for dental professionals during the common task of teeth cleaning. The highest levels of muscle activity were in the erector spinae and splenius capitis, which are consistent with reports of prevalent back and neck pain and MSDs for dentists. Results of this study indicate that shoulder and neck exos may be a promising intervention to reduce shoulder and neck muscle fatigue. Further analysis of the motion capture, perceived exertion, and usability data collected during this study may provide further insights. The back exo may require additional systematic testing in order to optimize the support level and activation angle. Future studies with dental professionals is suggested as the next level in assessing realistic movements and the feasibility of exos in terms of longer-term usage, comfort, and productivity in the workplace.

References: [1] Cieza et al. (2021), *Lancet*, 396(10267), 2006–2017; [2] Harutunian et al. (2011), *Medicina Oral Patología Oral y Cirugia Bucal*, 1(16), 425–429; [3] Marklin & Cherney (2005), *J California Dental Association*, 33(2), 133–136; [4] Tetteh et al. (2022), *Applied Ergonomics* 100, 103646; [5] Gillette et al. (2022), *Wearable Technologies*, 3, E23;

Relationships between propulsive force, specific torque, and redistribution ratio in younger and older adults

Ryan M. Gladfelter[1*], Jane A. Kent[1], Athulya Simon[1], Katherine A. Boyer[1]
[1]Department of Kinesiology, University of Massachusetts-Amherst, Amherst, MA, USA
*Corresponding author's email: rgladfelter@umass.edu

Introduction: Older adults exhibit hallmark declines in ankle kinematics and kinetics for reasons that are poorly understood. When walking at the same speed, older adults generate ~20% less propulsive force [1], and commonly display a redistribution of joint work to a more hip-dominant pattern compared to young adults [2]. It has been suggested that this redistribution may be driven by limitations in peak ankle moment generation during gait [3]. With older age, there is typically a loss of lean muscle mass, an increase in intramuscular fat, and a reduction in muscle specific torque, which is the maximal torque produced per unit of fat-free maximum cross-sectional area [4, 5]. The role of muscle weakness or reduced plantar flexor specific torque in the redistribution of joint work or the reduction in propulsive force production remains unclear. Thus, the first aim of this study was to compare the ratio of hip to ankle joint work, termed the redistribution ratio, at matched walking speeds in younger and older adults. It was hypothesized that older adults would have a larger redistribution ratio, indicating a distal-to-proximal shift in joint work, and smaller propulsive ground reaction force. The second aim was to determine whether the redistribution of joint work was related to plantar flexor specific torque or maximum isometric torque (MVIC). It was hypothesized that an inverse relationship exists between plantar flexor specific torque and joint work redistribution.

Methods: Seven young (2F, 35 ± 2.8 y, 88.4 ± 13.7 kg, 341 ± 180.3 min moderate-to-vigorous physical activity (MVPA) per week) and eight older (5F, 72 ± 1.9 y, 69.8 ± 12.6 kg, 281 ± 117.6 MVPA/wk) adults participated in the study after completing an informed consent process approved by the University's IRB. Participants completed three maximum plantar flexion MVIC trials on an isokinetic dynamometer (Biodex System 4 Pro, NY). Participants were also fit with a 73 bi-lateral marker set consistent with the point cluster technique and completed 5 overground walking trials at a fixed speed of 1.2 m/s. Marker trajectories and external forces were recorded by a 9-camera system (Qualisys, Sweden) and in-ground force plate setup (AMTI, USA) at 200 and 2000 Hz respectively. An inverse dynamics approach was used to calculate external joint work for the hip and ankle joints. Participants also completed MR imaging of the shank musculature with a 6-point Dixon sequence (2 stacks, 12-mm slice thickness, 40 slices, 1.25 x 1.25 x 12 voxel volume). The borders of the soleus and medial and lateral gastrocnemii were segmented along the length of the shank, and maximum fat-free cross-sectional area (CSA, cm^2) and fat fraction (FF%) were quantified. The primary outcomes were: peak propulsive force; plantar flexor MVIC, muscle specific torque (MVIC divided by triceps surae maximum CSA); and joint work redistribution ratio [6].

Results & Discussion: Contrary to our first hypothesis, neither the redistribution ratio (Y: 0.57 ± 0.16; O: 0.67 ± 0.21; p = 0.157), nor propulsive force (Y: 0.20 ± 0.01; O: 0.19 ± 0.02; p = 0.122) differed between older and younger groups. This redistribution is thought to occur due to a disproportionate decline in ankle plantar flexor strength and function [2, 7]; however, neither MVIC (Y: -118.11 ± 39.78; O: -93.47 ± 38.28; p = 0.122), nor specific torque (Y: 2.48 ± 0.88; O: 2.69 ± 0.72; p = 0.312), differed between groups. For the second aim, no correlation between redistribution ratio and specific torque was found in younger, older, or combined groups (Fig 1, p > 0.241, all). While prior work has reported a redistribution of lower limb joint powers or work in older adults at walking speeds matched to young [2, 8], here we found no difference in redistribution ratio, propulsive force, plantar flexor MVIC or specific torque production between younger and older adults. Likewise, preferred gait speed was not slower for the older adult group. Collectively, these results suggest that the older adults studied here may have more youthful ankle function compared to prior work; the lack of baseline characteristics is consistent with a lack of differences during gait.

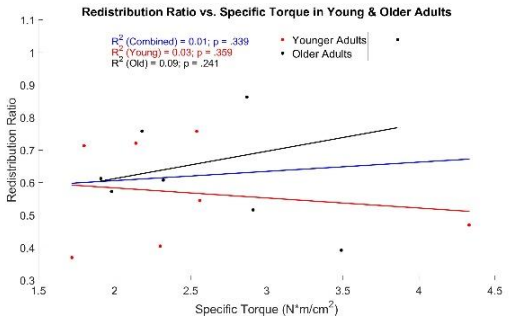

Figure 1: *Redistribution Ratio is not associated with plantarflexor specific torque in younger or older adults.*

Significance: In well-functioning older adults, who far exceed the recommended physical activity level of 150 min MVPA per week and who have preserved plantar flexor function, we found no evidence of a redistribution of joint work or reduction in propulsive force during gait. While an increase in the metabolic cost of walking is a proposed consequence of a larger redistribution ratio, it is not yet known if older adults with preserved plantar flexor function and gait mechanics also retain a youthful metabolic cost of walking.

Acknowledgements: This work was funded by NIH grant 5R01AG068102

References: [1] Browne & Franz (2017), *J Biomech* 55; [2] DeVita & Hortobagyi (2000), *J Appl Phys* 88; [3] Conway & Franz (2020), *J Aging & Phys Act*, 28; [4] Hasson et al. (2011), *J Biomech* 44; [5] Morse et al. (2005) *J Appl Phys* 99; [6] Browne & Franz (2018), *PLoS ONE* 13(8); [7] Naruse et al. (2023), *J Appl Phys* 134; [8] Boyer et al. (2017), *Exper Ger* 95

DISTINGUISHING INDIVIDUALS WITH MILD COGNITIVE IMPAIRMENT FROM CONTROLS USING MOTOR FUNCTION DATA AND MACHINE LEARNING

Jamie B. Hall[1*], Sonia Akter[1], Praveen Rao[1], Andrew Kiselica[1], Rylea Ranum[1], Jacob M. Thomas[1], Trent M. Guess[1]
[1]University of Missouri
*Corresponding author's email: halljami@umsystem.edu

Introduction: Alzheimer's Disease (AD) represents a public health crisis with 6.7 million Americans over 65 years old estimated to have AD-related dementia, at a total cost of $345 billion. Mild cognitive impairment (MCI) is a pre-dementia condition; identification at this early stage is vital to addressing the crisis of AD. [1] Neuropathologies associated with MCI affect not only cognition but balance and gait performance as well. The addition of a cognitive task to a motor task in a dual task paradigm magnifies these deficits. [2] Understanding the motor function deficits associated with MCI can be leveraged to improve access to screening for dementia risk. Recent studies have explored the use of machine learning (ML) to build models that aid in the prediction of MCI, AD, and falls in older adults based on motor function data. [3,4] The technologies used for motor assessment in these studies are relatively expensive, unidimensional, and not readily available for use in widespread screening in healthcare and community settings. To increase accessibility, portable, inexpensive technologies capable of assessing multiple constructs related to motor function are needed. The purpose of this study was to determine the feasibility of using a portable, multidimensional motor function assessment platform to build a model using ML which accurately discriminates individuals with MCI from controls.

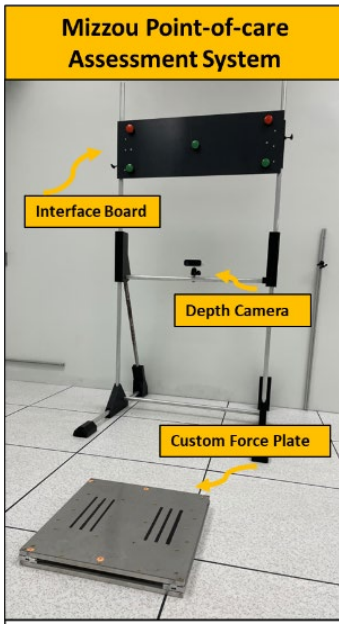

Figure 1: MPASS integrates a custom force plate, depth camera, and interface board.

Methods: We enrolled adults over 60 years old with and without MCI. Exclusion criteria included neuromuscular disease, recent injury or surgery impacting functional mobility, and use of assistive devices or above ankle orthoses. Participants were placed in the MCI group if they already had a diagnosis of MCI or their Montreal Cognitive Assessment score was less than 25. [5] 20 healthy older adults (70.5 ± 5.4 years old, 13 females, 168.9 ± 9.5 cm, 81.35 ± 24.07 kg, MOCA score 27.8 ± 1.3) and 12 older adults with MCI (75.3 ± 6.4 years old, 8 females, 167.44 ± 13.14 cm, 76.85 ± 23.0 kg, MOCA score 24.6±2.7) participated. We collected data using the Mizzou Point-of-care Assessment System (MPASS), which integrates a spatial sensor (Azure Kinect) with body tracking, custom force plate, and interface board. For balance trials, participants stood on the force plate with feet shoulder width apart and arms crossed in both eyes open and closed conditions. For gait trials, participants walked at their preferred speed. For sit to stand trials, participants performed 5 repetitions of sit to stand as fast as possible from a 17" bench with arms crossed. We collected 2 trials in both single and DT conditions for all tests. For DT trials, participants subtracted 7 serially from a randomly generated number. We calculated discrete spatiotemporal gait, balance sway center of mass (CoM) and center of pressure (CoP), and temporal and kinematic sit to stand parameters for each test.

The Support Vector Machine (SVM) model was trained to classify participants into 2 groups, MCI and controls. A total of 72 features, including participant demographics and data from motor function tests, were included as predictors. The training dataset included 41 participants and the testing data set included 6 participants (3 MCI and 3 control). Feature importance was determined using the permutation importance method, which evaluates the impact of each feature on the model's predictive accuracy.

Table 1: Top 10 Features in the SVM Model

Feature (condition)	Importance
95% Ellipse Area CoM (Eyes open, firm, dual task)	0.300
95% Ellipse Area CoM (Eyes closed, firm, dual task)	0.250
95% Ellipse Area CoP (Eyes closed, firm, single task)	0.188
Sit to stand avg max knee velocity (dual task)	0.138
95% Ellipse Area CoP (Eyes open, firm, dual task)	0.105
95% Ellipse Area COM (eyes closed, firm, single task)	0.083
Sit to stand avg sit knee velocity (single task)	0.061
95% Ellipse Area CoP (Eyes open, firm, single task)	0.061
Sit to stand avg sit hip velocity (dual task)	0.038
95% Ellipse Area CoP (Eyes closed, firm, dual task)	0.033

Abbreviations: CoM=center of mass, CoP=center of pressure, avg=average, max=maximum

Results & Discussion: The SVM classifier achieved an accuracy of 84% with a sensitivity of 0.83, specificity of 1.00, and a F1 score of 0.83. The top 10 most significant features were extracted and ranked according to their importance scores (Table 1).

Significance: Preliminary data based on this small sample size suggest ML models built on multidimensional motor function data obtained from an inexpensive, portable assessment platform identifies individuals with MCI with an accuracy of 84%. A device of this type could easily be used in primary care and community settings, thereby increasing access to screening and diagnosis. Future work will include larger sample sizes and use of other machine learning classifiers, such as Random Forest and XGBoost.

References: [1] Alzheimers Dement (2023); 19(4):1598-1895; [2] Bahureksa et al. (2017), *Gerontol* 63(1); [3] Ghorani et al. (2021), *Biomed Signal Process Control* 10/1016/j.bspc.2020.102249; [4] Noh et al. (2021), *Scientific Reports* 11:12183; [5] MOCA website at https://www.mocatest.org/faq/

THE USER-LEVEL EFFECTS OF VARYING AUGMENTED SENSORY FEEDBACK DURING TRAINING OF A MOTOR REHABILITATION TASK

Yu Shi[1], Mingxiao Liu[1,2], Sophie Dewil[1], Noam Harel[2], Raviraj Nataraj[1,*]
[1]Stevens Institute of Technology, [2]James J. Peters VA Medical Center
*Corresponding author's email: rnataraj@stevens.edu

Introduction: Physical therapy remains a primary solution for recovering motor function after spinal cord injury (SCI) [1]. Emerging approaches leverage advanced technologies like virtual reality (VR) and wearable devices to motivate patient participation. Still, the functional benefits of VR motor rehabilitation are notably reduced when controlling for therapeutic dosage. Thus, new ways are sought to optimize customizable computerized interfaces towards better outcomes. Augmented sensory feedback (ASF) during rehabilitative training, which entails providing sensory-driven cues about performance, is proven to enhance motor learning [2] and is readily incorporated with immersive computerized interfaces. This study examines the effects of varying ASF training (i.e., cueing through different sensory modalities) on user performance and physiological responses while engaging in a motor task requiring force modulation and real-time spatial orientation.

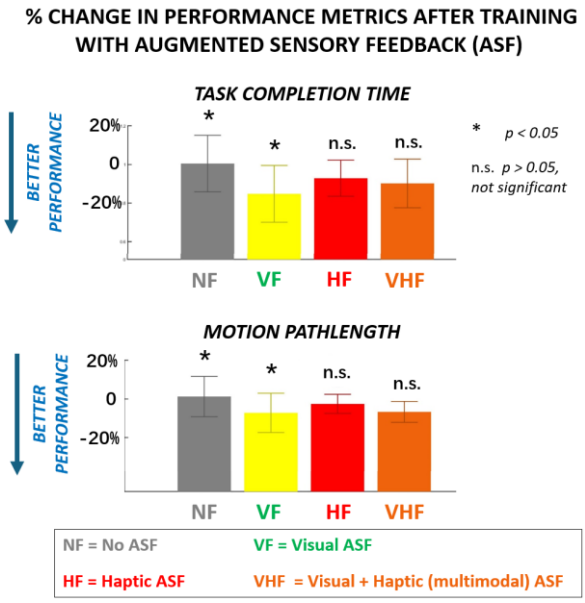

Figure 1: Performance after ASF training.

Methods: Fifteen neurotypical participants were recruited for this study, whose protocols are approved by the Stevens Institutional Review Board. We developed a myoelectric control task in a VR environment (Unity) where participants maneuver a robot arm toward designated targets. Participants exerted semi-isometric muscular efforts using their dominant upper extremity, supported in a position-adjustable brace. Skin-surface sensors *(Delsys Trigno)* recorded electromyography (EMG) signals from fourteen muscle groups, serving as inputs to a regression support vector machine *(Matlab)* that detected command intentions (i.e., direction and speed in moving robot end-effector in two dimensions). Furthermore, a 64-channel electroencephalography (EEG) cap (*g.tec USBamp*) and finger-sensors (*Shimmer3 GSR+)* were used to measure brain and electrodermal activity (EDA) responses to ASF training. During ASF training, participants could receive visual or audio that guided them to move the robot arm more directly toward intended targets. Participants underwent three blocks of trials (pre-training, ASF training, and post-training) for each of three modes of ASF training: no ASF, visual, haptic (vibration), or multimodal (visual and haptic). Performance responses to ASF were assessed as the relative change in completion time and end-effector pathlength undertaken in post-training trials compared to pre-training.

Results & Discussion: In assessing the impact of ASF on rehabilitation task performance, our study found notable improvements across all ASF modes compared to the control group, which received no feedback. Specifically, visual ASF significant ($p<0.05$) enhancements in both motor performance metrics, thereby demonstrating its superiority in facilitating task execution (Figure 1). At the participant level, we also noted specific preferences for certain ASF modes (based on surveys) and several significant differences between specific ASF modes. Across all participants, ASF led to increased EEG activity as expected due to heightened sensory stimulation, with multimodal feedback eliciting the highest EEG responses. Interestingly, visual ASF also resulted in the greatest increase in EDA, suggesting enhanced emotional arousal and engagement concurrent with improved performance. These findings indicate that while ASF may facilitate motor learning by expediting the crossing of neural thresholds [3], optimizing the delivery of ASF during training may depend on person- and task-specific considerations. Visual ASF may have been best aligned with the visually-driven nature of this task [4], and additional (haptic) cueing may have only served as a sensory-level distractor (i.e., increased cognitive load not serving improved performance). Such findings that provide a deeper understanding of ASF's impact on optimizing sensory-driven interfaces are essential to personalize computerized methods for motor rehabilitation.

Significance: This research underscores the significant potential of integrating ASF into rehabilitative practices with computerized interfaces, such as VR, for enhancing gains in function. By demonstrating clear benefits in motor performance after ASF training, our study suggests a promising avenue for optimizing engagement and training trajectories with computerized rehabilitation methods. These findings hold broader implications beyond motor rehabilitation through physical therapy, potentially improving the deployment of assistive technologies through better design of interactive systems for persons with a disability.

Acknowledgments: NSF career award 2238880 and Charles V. Schaefer, Jr. School of Engineering and Science, Stevens Institute of Technology, provided funds to support the fundamental development of this research.

References: [1]R. M. Hakim, et al. *Disability and Rehabilitation: Assistive Technology*, vol. 12, no. 8, Nov. 2017.
[2] S. Prasad, et al. *Asian Spine J*, vol. 12, no. 5, Oct. 2018.
[3] A. R. Seitz and H. R. Dinse, *Current Opinion in Neurobiology*, vol. 17, no. 2, Apr. 2007.
[4] Sanford, Sean, et al. Frontiers in Virtual Reality 3 (2022): 943693.

Age Moderates the Relationship between Body Mass Index and Gait Variability

Narges Shakerian[1], Tyler M. Wiles[1], Seung Kyeom Kim[1], Nick Stergiou[1, 2], Aaron D. Likens[1*]
[1] Division of Biomechanics and Research Development, Department of Biomechanics and Center for Research in Human Movement Variability, University of Nebraska at Omaha, Omaha, Nebraska, USA
[2]Department of Physical Education & Sports Science, Aristotle University, Thessaloniki, Greece
*Corresponding author's email: alikens@unomaha.edu

Introduction: Human gait is a motor activity affected by physiological, environmental, and psychological factors [1]. Gait undergoes significant transformations with aging, affecting the variability of stride intervals, the time elapsed between successive footfalls of the same leg [2]. Similarly, body mass index (BMI) impacts gait characteristics, where deviations from normative anthropometrics are associated with altered gait patterns [3]. However, the interaction between age and BMI and its effect on stride interval complexity has yet to be thoroughly investigated. Nonlinear metrics like the Hurst exponent (H) – a measure of autocorrelation in stride intervals – provide insight into gait variability and how it is influenced by factors such as age, BMI, or other characteristics. Therefore, we aimed to explore how aging, and BMI might collectively influence gait variability. We hypothesized that advancing age and increasing BMI would decrease the H of gait variability, reflecting changes in gait patterns [2,5].

Method: Ninety-six participants in three groups of individuals, young adults, middle-aged adults, and older adults, were recruited (Table 1)[6]. Gait kinematics were collected using 16 Noraxon Ultium Motion™ inertial measurement units (IMU) attached to the head, upper limbs, lower limbs, pelvis, and trunk to record gait. This study was conducted in two separate sessions, with a one-week interval between sessions. The participants engaged in 18 (9 trials over two days), 4-minute walking trials at a self-selected pace on a 200-meter indoor track. This study calculated the H as the dependent variable [1]. In analyzing the data, we used a linear mixed-effects model to evaluate how BMI, age, and the interaction between BMI and age influence the H stride intervals. All variables were z-scored prior to modeling to facilitate interpretation. Model significance was obtained via an ANOVA-like Wald test with Satterthwaite correction for degrees of freedom, ensuring a robust approach to analyzing the linear mixed-effects model. The α level was set at 0.05.

Age Group	Age	BMI	Height (cm)	Weight (kg)
Young	24.6 (2.63)	23.7 (4.49)	174 (7.87)	71.6 (14.6)
Middle	46.7 (5.92)	28.3 (5.36)	171 (7.22)	82.4 (16.4)
Old	65.2 (8.06)	27.4 (5.63)	170 (9.19)	79.4 (16.0)

Table 1. All values are Mean (Standard Deviation).

Results & Discussion: The Wald test failed to reveal a main effect of BMI, $F(1, 91.32) = 0.14$, $p = 0.70$, but did reveal a main effect of age, $F(2, 91.28) = 4.52$, $p = 0.01$; however, that main effect was modified by an interaction with BMI, $F(2, 91.52) = 5.62$, $p = 0.05$. This finding suggests a differential impact of BMI on gait variability that varies by age group. A simple slope analysis was conducted to understand that interaction further. That analysis entailed investigating the H-BMI relationship within each age group and revealed three key findings (Fig.1): a one standard deviation (SD) increase in BMI predicted a one SD increase in H. Conversely, for middle-aged adults, a one SD increase in BMI predicted a .28 SD decrease in H, suggesting a reversal in the relationship. No detectable relationship between BMI and H was observed for older adults. The conditional R^2 of .602 for the final model indicates that both fixed and random effects account for a considerable portion of the variability in gait dynamics. In contrast, the marginal R^2 of .080 highlights the substantial role of individual differences. These results suggest that the influence of BMI on gait dynamics is nuanced, likely reflecting physiological changes across the lifespan. The positive association between BMI and gait variability in young adults may point to the beneficial aspects of a higher BMI, such as increased muscle mass, contributing to better gait stability.

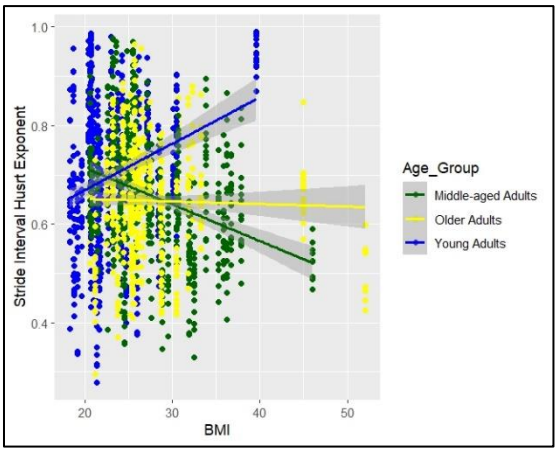

Figure 1. BMI's Impact on Stride Hurst by Age Group

Significance: The findings of this research highlight the nuanced influence of BMI and age on gait variability, emphasizing the need to consider individual differences and the specific interactions between these factors. Future research should further explore the mechanisms underlying these relationships and investigate targeted interventions to enhance mobility and reduce the risk of falls, particularly focusing on age-specific strategies to address the variable impact of BMI on gait stability.

Acknowledgments: This work was supported by the Center for Research in Human Movement Variability at the University of Nebraska at Omaha, the University of Nebraska Collaboration Initiative, the NSF award 212491, the NIH awards P20GM109090 and R01NS114282, the NASA EPSCoR mechanism, and the IARPA BRIAR WatchID award.

References: [1] N. Stergiou (2020). *Academic press*. [2] M. L. Callisaya et al, (2010). *Age and Ageing* 39 (2).[3] V. Rosso et al (2019). *Sensors* 19(19). [4] U. H. Buzzi et al. (2003). *Clinical Biomechanics* 18(5). [5] M. Gonzalez et al (2020*). Journal of Biomechanics100.* [6] T. M. Wiles et al., (2023). *Sci. Data*, 10(1).

EXPLORING THE ROLE OF PROPRIOCEPTION IN SPLITTING INTRAMUSCULAR REDUNDANCIES

Michael J. Rose[1*], Will Flanagan[1], Brian K. Zukotynski[1], Tyler R. Clites[1]
[1]Mechanical and Aerospace Engineering, UCLA, Los Angeles, CA;
*Corresponding author's email: michaeljrose@g.ucla.edu

Introduction: There are many examples throughout the body of discretely-innervated muscle compartments that activate synergistically to control a single joint. The two heads of the biceps brachii, for instance, are discrete muscle bodies that typically activate together to drive elbow flexion, and are difficult to isolate or command independently [1]. This "tying together" of neural inputs leads to redundancy in the human control system: there are more independently-innervated muscle bodies than independently-controllable degrees of freedom (DOFs). Thus far, we have been unable to leverage these redundancies to create supernumerary control DOFs [2]. However, we know from the near-universal success of tendon transfers, a medical procedure where a (sometimes redundant) tendon is disinserted from its native insertion and inserted elsewhere, that these redundancies can feasibly be separated and repurposed to control a new joint [3]. It is our position that the ability to learn independent control of the transferred muscle compartment depends on the intact, natural proprioception that muscle feels while *moving* its new joint. In this work, we explore whether the proprioceptive information that comes from linking activation of two typically-synergistic muscle compartments to distinct motions is useful in learning to activate these muscle compartments differentially.

Methods: We enrolled six participants without paralysis to participate in a preliminary EMG-based evaluation of muscle control. In half of these subjects, electromyography (EMG) signals were measured using fine-wire electrodes implanted in both the long and short heads of the biceps brachii. Gains on the EMG system were then tuned such that each subject was below 5% activation at rest, and above 95% activation when fully contracting in free space. Participants in this group were instructed to activate either one head of the biceps independently, or both heads at once and hold the contraction for five seconds. Targets for "activated" and "not activated" were defined as above 50% and less than 30% activation respectively. A separability factor was calculated using the middle four seconds of the trial, defined as the activation level of the "activated" compartment minus the "not activated" compartment, all divided by the "activated" level. Given our targets of above 50% and below 30%, a separability factor of 0.4 or above would correspond with successful differential activation. This was carried out under two different testing conditions: a "free space" condition where participants were allowed to move, brace, resist and co-contract however they wanted to achieve the activation goal, and a "restricted" condition where participants had to hold a beaker of water upright in the palm of their hand without spilling. The remaining participants completed the same test, but with surface EMG rather than fire-wire electrodes. This second group also performed a round of "free space" tests with electrodes on their middle and lower trapezius. In this group, EMG activation was normalized to a maximum voluntary contraction collected before the trials and activation was defined as above 16% of MVC and inactive below 10% of MVC (differential activation for separability factor greater than 0.375). All participants for all trials were provided visual feedback showing target activation levels and real-time activation levels from each muscle compartment.

Results & Discussion: In both groups, participants showed some ability to differentially activate the two heads of the biceps in the free space condition (fig 1). This is of interest as it had previously been reported that grouped individuals did not show separability in the same muscles [2]. Additionally, participants were more successful in completing the task in the free space condition as opposed to when their hand and arm position was restricted through a secondary task. This supports our idea that associated motion can aid in splitting intramuscular synergies. Finally, individuals were more consistently able to split the middle/lower trapezius synergy compared to the biceps heads synergy. Again, we believe this is due to there being more distinguishable motions that separately fire parts of the trapezius compared to the biceps.

Significance: Volitional differential activation of typically-synergistic muscle compartments could enable myoelectric assistive devices with more controllable DOFs than the natural human body.

References: [1] Lendaro (2018), IEEE, 10.1109/EMBC.2018.8513103; [2] Eden et al. (2022), *Nat. Commun.* 13:1345; [3] Pirela-Cruz et al. (2005), *BJBMS* 5(3).

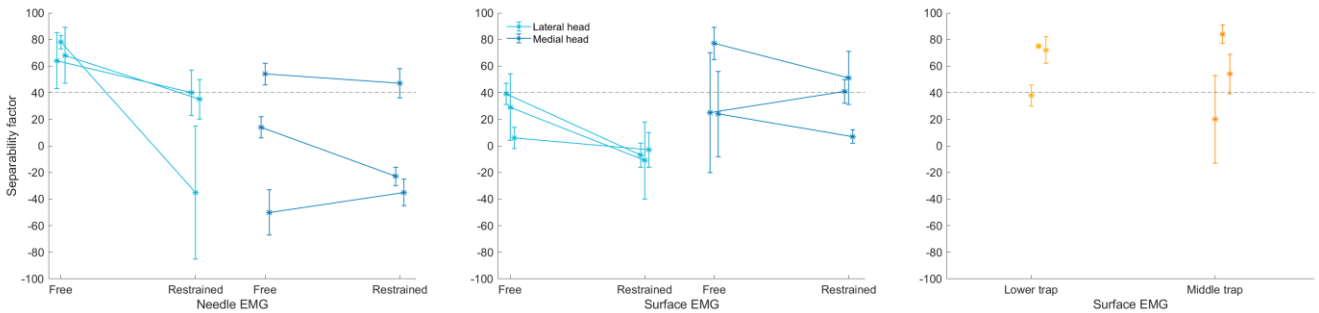

Figure 1: Separability factor of two heads of biceps brachii using needle electrodes with tuned gains (left), surface electrodes normalized to MVC (center), and of the middle and lower trapezius using surface electrodes normalized to MVC (right). Differential trapezius activation was the most consistent but biceps heads also showed varying differential activation.

A PILOT STUDY TO EXPLORE THE USE OF PERCUTANEOUS SPINAL STIMULATION FOR IMPROVING GAIT IN A PARTICIPANT WITH MULTIPLE SCLEROSIS

Omid Jahanian*, Megan L. Gill, Anders J. Asp, Sarah M. Hildreth, Daniel D. Veith, K. A. Fernandez, Candee J. Mills, Andrew R. Thoreson, Peter J. Grahn, William O. Tobin, and Kristin D. Zhao
Mayo Clinic, Rochester, MN, USA
*email: jahanian.omid@mayo.edu

Introduction: Multiple Sclerosis (MS) is a chronic and degenerative neurological condition that affects over 200 per 100,000 individuals in the US [1], resulting in significant functional impairments. Gait dysfunction, characterized by spasticity, weakness, and impaired balance, has been cited by individuals with MS as one of the most debilitating symptoms [2]. Current treatment options for progressive MS are limited to addressing the inflammatory component of the disease; they do not halt or reverse the neuronal death and axonal loss that often leads to a decline in motor function and walking ability. This pilot study aims to investigate the feasibility and potential efficacy of percutaneous epidural electrical spinal stimulation (ES) in enhancing volitional motor function and improving gait in an individual with MS.

Methods: Following FDA IDE and Mayo Clinic IRB approval, one individual with progressive MS (male, age: 56 years, BMI: 24.7 kg/m², no clinical or radiologic MS relapses for > 5 years) was recruited for this pilot study. Baseline assessments, including gait analysis and spasticity assessment, were obtained prior to implantation. Two percutaneous epidural spinal cord stimulator electrode leads (Abbott, Plano, TX) were temporarily placed parallel to one another along the dorsal epidural surface of the lumbosacral enlargement and connected to a neurostimulation system for delivering electrical pulse waveforms. Subsequently, the participant completed one month of rehabilitation including ES and task-specific training (12 sessions). Finally, prior to explantation, the participant underwent post-rehabilitation assessments, including gait analysis and spasticity assessment, with stimulation off (ES-Off) and on (ES-On). ES parameters during the ES-On condition for both leads were as follow: current amplitude of 4.4 mA, pulse frequency of 150 Hz, utilizing an asymmetric charge-balanced waveform with 250 µs pulse width. For the gait analysis, the participant was outfitted with retro-reflective markers on his extremities, pelvis, trunk, and head, and surface electromyography (EMG) electrodes on lower extremity (LE) muscles. The participant walked at a self-selected preferred walking speed using a front-wheeled walker. LE spasticity was assessed using the Modified Ashworth Scale [3]. Additionally, the pendulum test [4] was conducted to quantify spasticity utilizing inertial measurement unit sensors on the shank and thigh, while surface EMG electrodes were employed to collect LE muscle activity.

Results & Discussion: Gait analysis data during the baseline assessment indicated a reduced gait speed (0.25 m/s) and decreased range of motion in the LE joints, compared to normative data, with right knee hyperextension and no ankle dorsiflexion. Analysis of gait data during the post-rehabilitation assessment (ES-Off) revealed notable enhancements in gait including increased hip extension, knee flexion, and ankle dorsiflexion compared to baseline visit. These findings imply a synergistic effect of one month of ES combined with task-specific training on walking ability. The post-rehabilitation comparison between ES-Off and ES-On conditions (Table 1 and Figure 1) demonstrated that ES led to marked increase in right knee maximum flexion during swing phase (39%) and in hamstring peak muscle activity (30%), and decreased rectus femoris peak muscle activity (14%). These findings suggest ES may enhance volitional motor function during walking in this participant. Spasticity assessments indicate that the Modified Ashworth Scale score for the right side decreased from 2 during ES-Off to 1^+ during ES-On. Data from the pendulum test indicate that the first swing angle increased by 6%, and rectus femoris muscle activity decreased by 58% during passive swing of the lower limb with ES-On compared to ES-Off, suggesting a decrease in knee extensor muscle spasticity with ES.

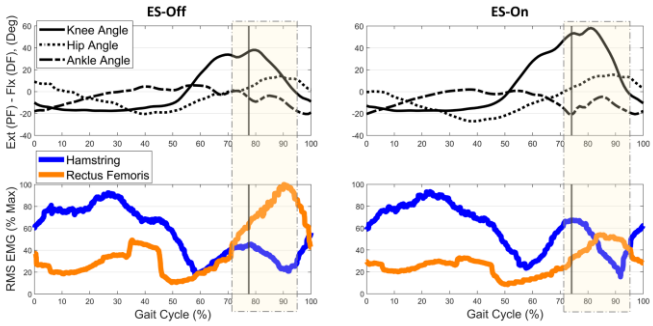

Figure 1: LE joint kinematics and RMS (time averaging, period of 0.25 sec) EMG (normalized to the max value during all gait cycles) of hamstring and rectus femoris for a representative gait cycle during post-rehabilitation assessments with ES-Off and ES-On (right limb). Vertical lines represent transition from stance to swing. Highlighted boxes represent the time that kinematic and EMG data were processed.

Significance: The preliminary findings from this pilot study suggest that ES, when combined with task-specific training, may have a positive impact on facilitating volitional motor function and enhancing gait in patients with MS. These promising results highlight the need for further research with larger sample sizes to confirm and refine these outcomes, as well as to optimize the application of ES for individuals with MS.

Acknowledgments: This research was supported by Mayo Clinic Center for Multiple Sclerosis and Autoimmune Neurology.

References: [1] Walton et al. (2020), *Mult. Scler. J. 26*(14); [2] Alonso et al. (2008), *Neurology*, *71*(2); [3] Bohannon et al. (1987), *Phys Ther 67*(2); [4] Whelan et al. (2018), J Neuroeng Rehabil 15(1).

Table 1. Average speed and mean (SD) of maximum knee flexion and peak RMS EMG of hamstring (HS) and rectus femoris (RF) during swing phase of gait for stimulation off (ES-Off) and stimulation on (ES-On) conditions (right limb) at end of study.

Gait Spead (m/s)		Max Knee Flexion (Deg)		Peak HS EMG (% Max)		Peak RF EMG (% Max)	
ES-Off	ES-On	ES-Off	ES-On	ES-Off	ES-On	ES-Off	ES-On
0.171	0.184	34 (4)	47 (12)	41 (5)	53 (26)	69 (13)	60 (33)

A COMPARATIVE STUDY OF GAIT PARAMETERS BETWEEN BAREFOOT WALKING AND SHOD WALKING

Yunbeom Nam*, Yujin Kwon, Gwanseob Shin
Department of Biomedical Engineering, Ulsan National Institute of Science and Technology, Ulsan, South Korea
*Corresponding author's email: bbbeommm@unist.ac.kr

Introduction: Walking is one of the most fundamental activities in daily life, and gait parameters such as walking speed are used to assess an individual's mobility and health status. Previous research has primarily focused on kinetic and kinematic differences under various conditions by varying walking environment (i.e., indoor versus outdoor [1]) or types of footwear [2]. However, comprehensive comparisons of gait parameters between shod and barefoot walking are yet limited [3], and the effect of wearing shoes on gait parameters has not been fully explored. This study aims to analyze how key gait parameters, including walking speed and other parameters that have been reported to associate with walking speed, differ with and without footwear, with an intention to use the analyzed data as normative data for future gait research. This study's findings would enhance our understanding of the biomechanical effects of footwear on walking, offer valuable insights for the design of footwear and rehabilitation programs, and lay the groundwork for future research in gait disorders and physical rehabilitation by offering normative gait data.

Methods: The study involved 129 healthy young adults in their 20s and 30s (66F/63M, age: 26.3 ± 5.5 yrs, height: 168.9 ± 8.0 cm, mass: 66.0 ± 14.1 kg). All participants walked on a 10m walkway in which a pressure mat (Zebris FDM, Zebris Medical GmbH, Germany) was installed in the middle. They were asked to walk at their self-selected speeds under two conditions: barefoot and shod walking, for 3 minutes each. For the shod walking condition, participants wore their own shoes that they brought to the study. Walking speed, stride time, stride length, maximum force, maximum pressure, cadence, lateral symmetry, and stance phase of the dominant side were collected from the pressure mat and compared between the two walking conditions using t-test ($p<.05$). Cohen's d values, the effect size, are calculated to interpret as follows: values from 0 to 0.2 represent a negligible effect, 0.2 to 0.5 a small effect, 0.5 to 0.8 a moderate effect, and above 0.8 a large effect. The sign of the d value (+ or -) indicates the direction of the effect where positive values mean that the shod condition has a greater impact on the gait parameter, and negative values indicate a greater impact of the barefoot condition.

	Barefoot		Shod		Paired Cohen's d	P-value
	M	SD	M	SD		
Walking velocity, km/h	4.15	0.47	4.48	0.54	1.5	<0.0001
Stride Length, cm	124.02	10.96	135.41	12.89	2.3	<0.0001
Stride Time, s	1.08	0.07	1.09	0.06	0.4	<0.0001
Stance Phase, %	62.43	1.35	64.09	1.71	1.2	<0.0001
Loading Response, %	12.55	1.34	14.13	1.61	1.3	<0.0001
Single Limb Support, %	37.38	1.46	35.79	1.68	-1.2	<0.0001
Pre-Swing, %	12.50	1.35	14.17	1.67	1.3	<0.0001
Maximum Force, N	641.04	129.20	667.03	136.42	1.1	<0.0001
Maximum Pressure, N/cm^2	40.93	9.70	23.67	5.69	-1.9	<0.0001
Cadence, steps/min	111.43	7.02	110.13	6.54	-0.5	<0.0001
Lateral Symmetry, mm	2.48	2.23	2.43	2.12	-0.03	0.77

Table 1: Comparison of mean (M) and standard deviation (SD) values for gait parameters under both shod and barefoot conditions.

Results & Discussion: The results showed significant differences in all gait parameters except lateral symmetry between barefoot and shod walking conditions ($p<.05$) (Table 1). Shod walking resulted in faster walking velocities and longer strides compared to barefoot walking, with a large effect size. Shod walking significantly increased stride time, demonstrating a moderate effect size. Maximum force during the push-off phase was higher in the shod condition, while maximum pressure during push-off decreased, both with large effect sizes. Barefoot walking showed a slightly higher cadence with a moderate effect size, with no notable difference in lateral symmetry between conditions. The stance phase lasted longer in shod walking, with extended loading response and pre-swing phase, but a shorter single limb support phase, with large effect sizes. These findings underscore footwear's nuanced impact on walking dynamics, essential for gait analysis and footwear design.

Significance: The results of this study offer information on the characteristics of walking with wearing shoes. These findings can be utilized in research related to gait disorders, physical rehabilitation, gait analysis, or development of footwear designs. By understanding the impact of footwear on walking dynamics, this research can help correct or accommodate gait issues, improving rehabilitation outcomes and encouraging proper walking patterns.

Acknowledgments: This work was supported by the Ulsan Metropolitan City, Korea.

References: [1] Hollander et al. (2022), *Gait & Posture* 95, 284-291; [2] Demura et al. (2012), *The Foot* 22, 18-23; [3] Samson et al. (2001), *Aging Clin Exp Res* 13, 16–21

IDENTIFYING FREQUENCY BASED FEATURES TO CHARACTERIZE DYNAMIC STABILITY

Darius B. Sattari[1*], Rebecca Zifchock[1], J. Josiah Steckenrider[1]
[1]United States Military Academy at West Point, Department of Civil and Mechanical Engineering
*Corresponding author's email: sattaridarius@gmail.com

Introduction: Characterization of postural stability, one's ability to control their body in space, can provide insight to an individual's physical exertion levels, possible brain injuries, or vestibular conditions [1]. Dynamic stability is an emerging metric that analyzes equivalent human skills and abilities as postural stability but is measured based on dynamic trials such as walking and running. Characterizing this metric can aid in evaluating fall risks and physical fatigue in subjects [2]. Previous literature focuses on metrics derived from an individual's Center of Pressure (COP) measured on a force plate. As this process requires at least quasi-static poses, it would be unfeasible to similarly measure dynamic stability. Small body-mounted accelerometers are well-suited for dynamic trials as they can travel with the test subject as they move. Previous work has employed accelerometer data to estimate COP during static trials with limited success, often applying a necessary machine learning based or mathematical transformation on the dataset to align with force plate outputs more accurately [3]. Parameters extracted from accelerometer data demonstrate stochasticity in the time domain [4]. Therefore, this study investigates how metrics extracted from the frequency domain of accelerometer data may be useful for characterizing dynamic stability in varying conditions intended to elicit instability. It was expected that walking in unstable conditions would elicit different frequency components within the medial-lateral acceleration signal, as compared to walking in stable conditions.

Methods: Pilot data were collected on three young and healthy individuals at the United States Military Academy. IMU sensors were mounted to the ankle, lower back, sternum, and forehead, and the accelerometer data were recorded as the participants walked approximately 10 feet. Two trials each of two conditions were analysed for this study: (1) STABLE: where the participant walked normally on a stable surface, and (2) UNSTABLE: where the participant walked across a soft mat with a 10 lb weight in one hand [5]. Accelerometer data in the medial-lateral direction were processed in MATLAB. A Fast Fourier Transform (FFT) was calculated on the data to complete frequency-based feature analysis for each trial, for each body-mounted sensor (see Fig. 1). From each FFT plot, three frequency peaks were identified: Low, Cadence, and High. Low frequencies were identified from 0 – 0.8 Hz, Cadence from 0.8 – 2 Hz, and High frequencies from 2 - 50 Hz (Figure 1). The ratio between the Low:Cadence and High:Cadence frequencies were then calculated and compared between the STABLE and UNSTABLE trials. Effect Sizes (ES) were calculated due to the small sample size, and an ES > 0.8 was considered large.

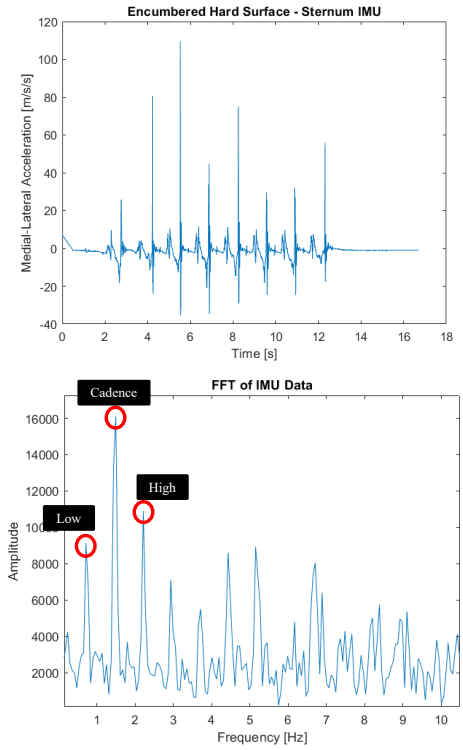

Figure 1: Methodology Overview of Deriving FFT and Low, Cadence, and High Frequencies (bottom) from time-domain data (top).

Results & Discussion: The trends in the Low:Cadence Frequency Ratios indicate that a higher ratio corresponds to the test subject exhibiting higher levels of dynamic stability. This is supported by three out of four IMU locations showing a large ES for comparisons between STABLE and UNSTABLE conditions (Figure 2). Considering all frequency ranges, preliminary data suggests that the forehead IMU may classify stability well when walking at lower frequencies, the ankle and lowerback IMUs are best employed at higher frequencies, and the sternum IMU performed strong across all frequencies. Physically, this can be explained by the body acting as a low-pass filter such that higher frequencies are indistinguishable from each other at the forehead sensor and are read with the highest resolution at the ankle.

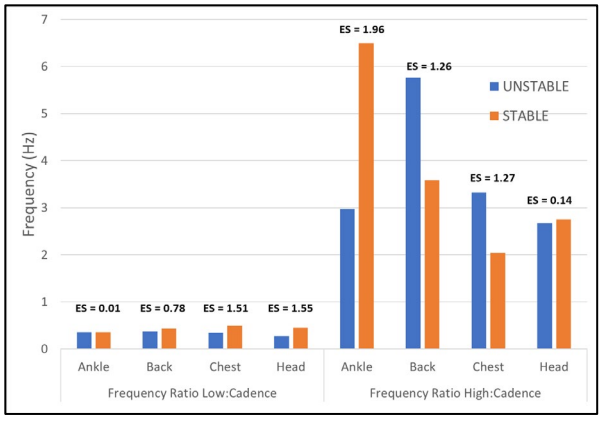

Figure 2: Effect Size of Stable/Unstable Conditions on Each Frequency Ratio Metric at Each IMU Location

Significance: Although these results are preliminary in nature, they present promising trends to guide further exploration of frequency-based accelerometer features, where most of the current research has been examined features from the time domain to characterize dynamic stability. Future work will include comparing ratios of FFT amplitude values at different frequency domains, centroids of FFTs, variance of FFT distribution, and a large-scale data collection of 30 participants to begin to draw statistical significance of findings.

References: [1] T. Paillard (2012), *Neurosci Biobehav Rev*; [2] L. Bizovska et. al (2017), *Gait Posture*; [3] A. Giachin et. al (2021), *Biomed. Biotechnol.*; [4] O. Dehzangi et. al (2017), *Sensors 17(12);* [5] M. Patel et.al (2008), *Gait & Posture 28*.

Cognitive and motor predictors of dual-task performance

Alexandra C. Lynch, Fatemeh Aflatounian, Keith A. Hutchison, Scott M. Monfort
Montana State University, Bozeman, MT, USA
Email: alexandralynch@montana.edu

Introduction: In sport, athletes are subject to scenarios that challenge both motor and cognitive function. Concurrent cognitive and motor demands (i.e., a dual-task (DT) scenario) require that the athlete distributes finite amounts of cognitive resources between these two tasks, often resulting in detriments to one or both facets of the DT. Identifying correlates of DT (dys)function may enhance risk assessment efforts for preventative and rehabilitation efforts. Previous research suggests that baseline cognitive function influences lower extremity injury risk[1] and DT function[2]; however, prior literature has not systematically assessed the relevance of attention control (AC) to physically-demanding cognitive-motor function. The prominent role that AC has in relation to other cognitive processes and cognitive multitasking motivates the need to evaluate its potential as a correlate for cognitive-motor function[3]. Baseline testing of cognitive and motor correlates of DT performance provides a potential pathway to predict individuals who may have deficits in DT performance which could be present in sport scenarios. The purpose of this study was to determine the extent that isolated cognitive and motor tasks could predict performance during a cognitively challenging single-leg squatting task. We hypothesized that increased performance on cognitive and motor single-tasks (ST) would result in less DT deficits.

Methods: Twelve healthy controls (20.3±1.4 years, 6 females, 1.77±0.08 m, 77.8±13.8 kg, Tegner: 7.5±1.6, Marx: 13.3±2.0) participated in the study, which included assessments of attentional control and motor tasks both as single- and DTs. The cognitive assessment consisted of a battery of computerized tests (Stroop Squared, Flanker Squared, Simon Squared) that assessed baseline AC [4]. The scores [# correct - # incorrect] of each test in the AC battery was then weighted into a composite score based on previous weightings to define an AC latent variable from these tests (0.58*Stroop, 0.64*Flanker, 0.82*Simon)[4].

Isolated and combined cognitive and motor tasks were used to evaluate DT deficits. Motor performance was evaluated with repeated single-leg squats (45° knee flexion at 0.5 Hz, auditory metronome to maintain frequency). 95% confidence ellipse area of the center of pressure (10 Hz lowpass filtered) was the metric used to assess gross motor performance during the task, with increased ellipse area corresponding to more sway[5]. The isolated cognitive task was the Antisaccade test of attention control[6], with the performance metric being participants' accuracy in identifying briefly-presented stimuli on the opposite side of a screen from a distractor cue. The DT condition consisted of the repeated squatting and Antisaccade tests performed concurrently. Each condition was repeated for 5 blocks of 54 seconds and the average over the five blocks was used in analyses. The order of the conditions was randomized. Cognitive (DTC_c) and motor DT (DTC_m) deficits were characterized as percent change relative to ST conditions, with positive values indicating worse DT performance, and lower magnitude DTC indicating less change between ST and DT. Pearson correlations (Spearman if data were not normally distributed) were used to assess correlations between ST and DTC measures.

Results: A significant negative correlation was found between AC and DTC_m ($r = -0.783$, $p = 0.002$) with a similar, albeit nonsignificant, negative correlation between AC and DTC_c ($r = -0.542$, $p = 0.069$) **(Figure 1)**. Other correlations were also negative but did not reach statistical significance.

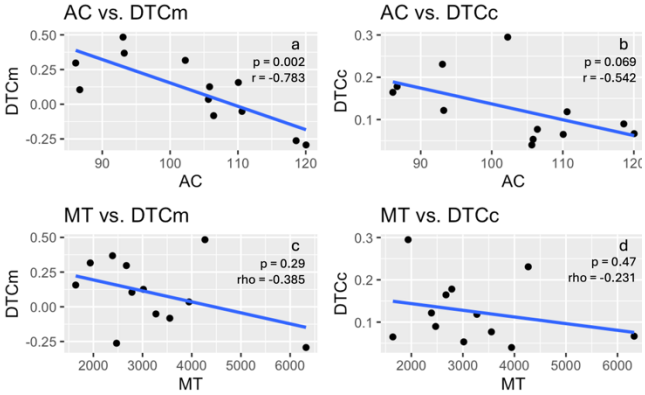

Figure 1: Correlations between cognitive ST (AC) and motor ST (MT) variables and DT change measured with motor (DTC_m) or cognitive (DTCc) variables.

Discussion: The purpose of this study was to determine how well ST cognitive or motor performance could predict DT deficits. Our hypothesis was partially supported, as the results show negative correlations between AC and DTC_m. Low magnitude DTC scores reflect little difference between the ST and DT conditions. The significant negative relationship between AC and DTC_m suggests that high performers in AC tasks mitigated differences in postural sway between ST and DT conditions. These findings illustrate how AC may provide a protective role in DT scenarios. Although not all significant, these correlations show trends indicating that this healthy control group was likely to have less DT change either from a cognitive or motor variable when they performed better on a cognitive ST. This study is ongoing and additional data are currently being collected, which will help further elucidate the relationships that are present.

Significance: These preliminary results show that AC may be a salient correlate of DT performance deficits. This has the potential to augment efforts to identify those who are likely to be most adversely affected by real-world DT demands, which has injury risk assessment applications. Future work is needed to clarify the clinical relevance of AC for musculoskeletal injury risk applications.

Acknowledgments: This work was supported by a MSU VPREDGE Research Expansion Fund grant.

References: [1] Swanik et al. (2007); [2] Monfort et al (2019); [3] Draheim et al (2019); [4] Burgoyne et al [2023]; [5] Prieto et al [1996]; [6] Hutchison (2007)

AGING PREDICTS TURN VELOCITY DURING SINGLE AND DUAL TASK CONDITIONS

Brandon M. Peoples[1], Kenneth D. Harrison[1], Keven G. Santamaria-Guzman[1], Valeria Robles-Cerdas[1], Jaimie A. Roper[1]
[1]Auburn University, Auburn, AL, U.S.A
*Corresponding author's email: bmp0049@auburn.edu

Introduction: Turning is a critical component of balance confidence and mobility that requires complex coordination of multiple body segments and sensory systems[1]. Turn velocity, measured using wearable inertial sensors, is a more sensitive marker of age-related mobility decline compared to gait speed [2]. Yet, the influence of task complexity and fall history on the relationship between age and turn velocity remains unclear. Dual-tasking during transitions between walking, turning, and sitting may reveal mobility deficits, particularly in aging individuals. Therefore, this study aims to investigate whether age predicts turn velocity in adults when factoring in fall status (faller vs non-faller) during single and dual-task conditions.

Methods: 136 adults aged 19-87 (58yr ± 17) performed the instrumented Timed Up and Go (iTUG) during single (Normal & Fast) and motoric dual-task (iTUG while carrying a tray with a cup of water) conditions using APDM Opals inertial measurement units. A total of 273 assessments were used for the analysis -118 Normal (23 Fallers), 66 Fast (11 Fallers), and 89 Dual-Task (17 Fallers). Mean turn velocity (deg/s) was calculated using the walk-to-turn and sit-to-turn phases of the iTUG. Participants were stratified as fallers based on self-reported retrospective fall history. Multiple linear regression analyses were conducted in JASP 0.18.

Results & Discussion: The multiple linear regression model results indicate turn velocity decreases as we age across all conditions when factoring condition (single-task vs. dual-task) and fall history (R = 0.67). The variance in turn velocity can be explained by predictors added in the model (R^2_{adj}=.448, p <.001). In the full model (H_1), the intercept is 294.44 degrees per second when all predictors are at their reference levels (age = 0, condition = Normal iTUG, and non-faller). Age negatively affects turn velocity (β = -1.289, p < .001), indicating a 1.3 degrees per second decrease per year after age 19. Compared to the normal iTUG, the turn velocity in our sample increased by 39.52 degrees per second during the Fast iTUG (β = 39.52 p < .001), while the iTUG + Tray trial decreased turn velocity by 50.15 degrees per second (β = -50.15, p < .001) when holding other predictors constant (Figure 1). Fall status (0 for non-fallers and 1 for fallers) did not significantly affect turn velocity (β = -13.044, p = 0.072).

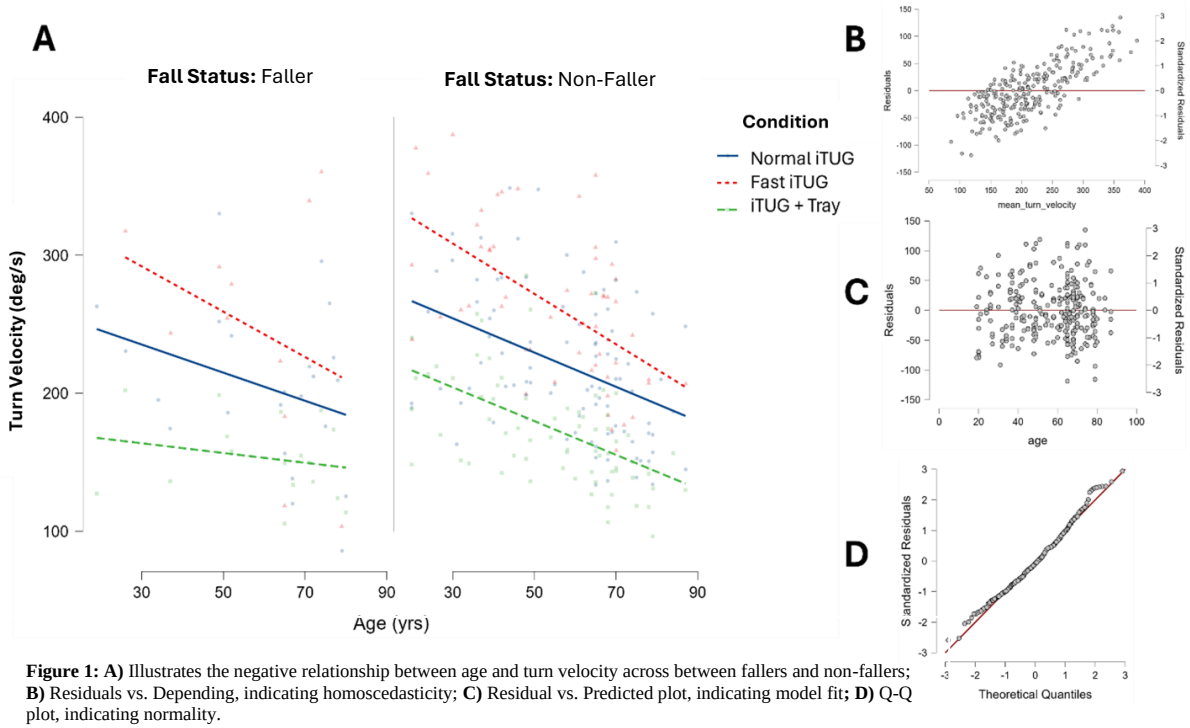

Figure 1: A) Illustrates the negative relationship between age and turn velocity across between fallers and non-fallers; **B)** Residuals vs. Depending, indicating homoscedasticity; **C)** Residual vs. Predicted plot, indicating model fit**; D)** Q-Q plot, indicating normality.

Significance: The findings of our study suggest turning velocity is a sensitive marker of mobility decline in aging during simple and complex turning tasks but did not discriminate fallers from non-fallers. Further, these findings have clinical implications as turning velocity may be a prognosticator of sensorimotor dysfunction, making it necessary to assess turning velocity across the lifespan proactively. Incorporating turn velocity into single and dual-task clinical assessments may identify individuals with functional decline, allowing for earlier intervention. Future studies should investigate if dual tasking with a cognitive task yields similar findings.

References:

1. Adusumilli, G., et al., *Turning is an important marker of balance confidence and walking limitation in persons with multiple sclerosis.* PLoS One, 2018. **13**(6): p. e0198178.
2. Weston, A.R., et al., *Turning speed as a more responsive metric of age-related decline in mobility: A comparative study with gait speed.* Clin Biomech (Bristol, Avon), 2024. **113**: p. 106196.

DEVELOPMENT OF MUSCULOSKELETAL LOWER EXTREMITY SIMULATOR FOR THE KNEE PROSTHESIS

Yoshimori Kiriyama[1*], Kosuke Tsukazaki[1], Kanta Takasu[1], Katsumasa Tanaka[2], Yasuhito Takahasi[3], Kengo Yamamoto[3]
[1]Department of Mechanical Systems Engineering, Kogakuin University
[2]Department of Mechanical Engineering, Kogakuin University
[3]Department of Orthpaedic Surgery, Tokyo Medical University
*Corresponding author's email: kiriyama@cc.kogakuin.ac.jp

Introduction: Knee and hip prosthesis are used widely, and the fundamental mechanical functions are quite important to evaluate the kinematics and kinetics. Especially, the knee prosthesis is required to move three-dimensionally such as the roll-back or axial rotation. These movements change contact places between the femoral component and the tibial insert, and then the contact pressure can change due to the kinematics of the knee. To understand well the kinematics of the knee prosthesis, the elucidation of the relationship between the combinations among muscle forces during motion and the detail movements of the prosthesis is required. One of the useful methods is a usage of a musculoskeletal simulator. The simulator is a kind of robotic system, and the joints are driven by wire forces as muscle forces. In this simulator, the knee joint is bared and the kinematics is measured directly. Also, the muscle forces as inputs are controlled and obtained quantitatively. Such as the simulator, it is possible to embed some sensors as load sensor or tactile sensor to evaluate the kinetics as outputs. Therefore, we have developed the musculoskeletal lower extremity simulator for the knee prosthesis. In this study, we had the simulator perform a normal gait, and showed the reproduction of the human gait evaluating the kinematic of the prosthesis on the stance phase.

Methods: Fig.1 shows the musculoskeletal lower extremity simulator. This simulator consists of the pelvis, femur, tibia and the foot. The knee and hip joints have prosthesises. Especially, in this study, Persona (component size EF/3-11, insert height 10 mm, ZIMMER-BIOMET) was embedded into the knee joint. The simulator has the major nine muscles around the lower extremity. The stainless wires are imitated as the muscles, and they are attached at the insertion of the muscles. The wire length and tension are controlled with stepper motors (AR98AA-N10-3, Oriental motor) via elastic springs. At the proximal to the joints, 6-component force sensors (LFX-A-3KN, Kyowa) are embedded to measure the joint loads including three forces and three moments. In this study, the muscle forces during gait were calculated using OpenSim[1]. To measure the joint kinematics, reflective markers were placed on the anatomical characteristics on the simulator. The knee movements were expressed as ISB recommendation [2]. The gait motion was captured with Coretex (Kestrel2200 camera, 120 Hz, MotionAnalysis) on a force platform (FP4060-07, Bertec).

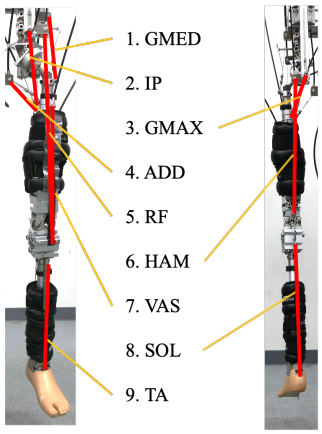

Figure 1: Musculoskeletal lower extremity simulator, (Left) front view, (Right) back view
Note: GMED(Gluteus medius), IP(Iliopsoas), GMAX(Gluteus maximus) ADD(Adductor muscles), RF(Rectus femoris), HAM(Hamstrings), VAS(Vastus), SOL(Soleus), TA(Tibialis anterior)

Results & Discussion: Fig.2 shows the changes of the contact point on the tibial surface during gait from the simulator. At the heel-contact, the lateral and medial contact points move to the anterior, and the area could be more congruous to resist large ground reaction force (Fig.2 (Top)). Toward the mid-stance phase, the contact points move to the middle and then to the posterior (Fig.2 (Middle)). In the mid-stance phase, the knee joint is extended and then the contact points could move to the middle area. Moreover, the knee joint flexes toward the late-stance phase and toe-off and then the contact points move to the posterior (Fig.2 (Bottom)). The movements of the contact points accompanied by the knee flexion could be due to the rollback movement. This knee kinematics is quite similar to the human knee, and the simulator could reproduce the gait as human movement. The joints of the simulator are driven by the combinations of the muscle forces, and the geometrical structure of the muscle could be adequate and the patterns of the muscle forces should be calculated based on an appropriate assumption using OpenSim model.

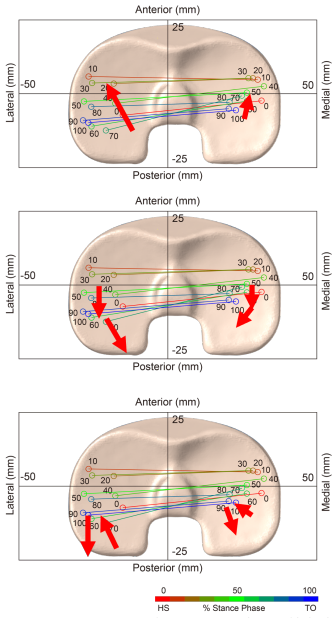

Figure 2: Contact points on the tibial surface during gait, (Top) Heel-contact, (Middle) Mid-stance phase, (Bottom) Toe-off. The number expresses % stance phase.

Significance: A musculoskeletal lower extremity simulator was developed. This simulator has an imitated anatomical structure and muscle force-driven robot system, and allows us to evaluate quantitatively kinematics and kinetics of prosthesis such as the knee joint. Using the simulator, the relationship between the joint movements and load condition could be elucidated.

Acknowledgments: A part of this research was supported by The Uehara Memorial Foundation and JKA and its promotion funds from KEIRIN RACE.

References: [1] Delp et al. (2007), *IEEE Trans. on Biomed. Eng.* 54; [2] Grood & Suntay (1983), *J Biomech Eng* 105.

CHARACTERIZING POSTURAL STABILITY DURING STATIC TASKS

CDT James Peterson[1*], Dr. Rebecca Zifchock[2], Dr. Josiah Steckenrider[3]
[1]United States Military Academy; West Point, NY 10996
*Corresponding author's email: james.peterson@westpoint.edu

Introduction: Postural stability is defined as "the ability to control the body position in space for the purpose of balance and movement" [1]. Proper sensory input from cognitive, motor, and sensory neural networks is imperative in maintaining proper stability [2]. A disruption in any one of these systems can result in an individual becoming unstable. Postural stability is typically measured using force plate data to calculate metrics derived from center of pressure (COP) data: total excursion, mean velocity, 95% confidence circle area, and 95% confidence ellipse area [3]. Recent literature has examined the use of inertial measurement units (IMUs) to calculate similar COP metrics. While the force plate is the gold standard for COP calculations, data collections are typically limited to controlled laboratory-based environments, which can limit expediency and generalizability. To date there is limited agreement between the force plate and IMU-derived metrics, where the latter tend to be larger. This has previously been attributed to the increased sensitivity of the measurement [4]. Additionally, previous studies have placed the IMU on the lower back to represent the body center of mass. Given that the body is not a rigid system, but rather a collection of linked segments, it is unclear whether a single IMU placed near the center of mass is sufficient to characterize stability using COP metrics. Therefore, the goal of this research is to determine the most effective locations for placing IMU sensors to generate COP-derived metrics that most closely match those from a force plate. The IMU placed on the lower back was expected to produce the most similar COP metrics when compared with the force plate considering its proximity to the center of mass.

Methods: Force plate and IMU data sets from three male participants were included in this pilot study. Prior to conducting the trials, IMUs were placed on each subject's right ankle, lower back, sternum, and forehead. Participants were asked to stand on a force plate and place their hands by their side while staring straight ahead at wall in front of them while balancing in three stances that were intended to elicit a range of stability. The types of stances used in the trials included feet apart, feet together, and balanced on one foot, each on a hard and a soft (foam) surface. For each of the six trials, data sets were collected from the force plate and the four IMUs and were filtered using a fourth-order zero phase Butterworth low-pass digital filter with a 5-Hz cut-off frequency [3]. The filtered data was then synchronized in post-processing and COP-derived metrics were derived from the IMU data and the force plate data using the same techniques: total excursion, mean velocity, and 95% confidence circle area. For each metric, linear regression models of each IMU sensor location against the force plate data was conducted along the spectrum of stable to increasingly unstable stance conditions as shown in Figure 1.

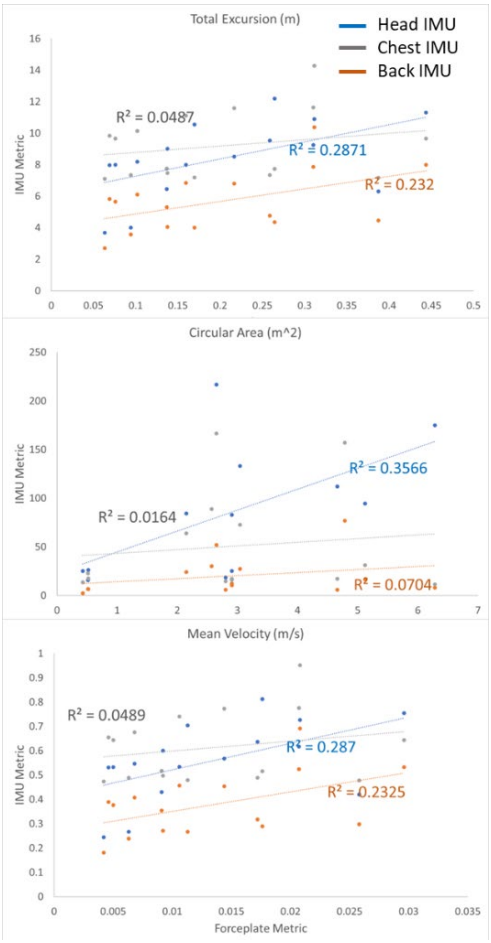

Figure 1: Correlational Statistics for IMU Sensor COP Metrics Compared with Force Plate COP Metrics

Results & Discussion: As expected the COP spread tended to be much larger for the IMU than the force plate. IMU COP metrics for the chest and back showed moderate correlation when compared with force plate COP metrics using a linear regression model, where the head consistently showed the highest correlation, and the chest consistently showed the weakest (Figure 1). Contrary to the original hypothesis, the metrics derived from the head IMU sensor appears to match most closely those from the force plate. Furthermore, the 95% confidence circle area calculations for the IMUs showed weak correlation to the corresponding force plate calculations. One limitation of the research thus far is the relatively small sample size as well as the similarity of the participants in age and gender. The data collected from participants of varying age and gender could slightly alter the results of the data. Nonetheless, additional trials will have to be conducted with a larger and more diverse demographic to confirm these findings and improve the correlation statistics.

Significance: Validation of an acceptable level of agreement between IMU-derived and force plate-derived metrics to characterize postural stability could potentially allow for additional expedient measurements in more realistic environments than a laboratory setting. This research is pertinent to the civilian and military communities for potentially providing better methods in assessing individuals who experience traumatic brain or lower extremity injury.

References: [1] Nusseck and Spahn (2020), *Front. Psychol.* 11, 1253; [2] Appeadu and Gupta (2024), *StatPearls Publishing*; [3] Prieto et al. (1996), *IEE Transactions On Biomedical Engineering* 43(9); [4] Mayagoitia et al. (2002), *Gait and Posture* 16(1).

TOWARDS A UNIFYING FRAMEWORK FOR COGNITIVE-MOTOR SYSTEMS SHARING GRAVITY INFORMATION

Chase G. Rock and Young-Hui Chang
Comparative Neuromechanics Lab, School of Biological Sciences, Georgia Institute of Technology, Atlanta, GA, USA
*Corresponding author's email: crock@gatech.edu

Introduction: Predicting the outcomes of movement is essential for successfully interacting with the world. As an action is repeated, its result becomes predictable, a process that can involve estimating certain aspects of the action that are important for motor control, such as the underlying physics. The underlying physics of movement are often constant between tasks, including the effects of gravity, which is learned during motor development [1]. Multiple tasks rely on anticipating the effects of gravity, meaning that it would be beneficial if gravity information was shared between tasks to ensure accurate motor control. As such, investigating gravity adaptation can help us elucidate how information is shared between different motor and cognitive systems. Information-sharing between systems has previously been shown in the bilateral transfer of force-field adaptation [2] and adaptation of imagined movements to altered gravity [3], leading to our hypothesis that gravity information is shared between motor and cognitive systems.

Methods: All participants provided informed consent according to the protocol approved by the Georgia Tech IRB (H19325). *Experiment 1*: Participants (n = 20) performed targeted vertical jumps before (PRE), during, and after (POST) exposure to simulated hypogravity. Hypogravity was simulated using a combination of constant-force springs mounted above the participant and attached to a customized rock-climbing harness. Aftereffects were investigated in the ability of the participants to achieve the vertical target and in the preactivation of the plantarflexor muscles in preparation for landing [4].

Experiments 2 and 3: Two new sets of participants (n = 10 for each) performed the Experiment 1 protocol, but in between each set of jumps they performed sets of vertically targeted arm movements (Exp. 2) or a cognitive decision task (Exp. 3). For Experiment 2, they started with their arm at their side and were instructed to point towards a physical target directly in front of them using only flexion of the shoulder. Aftereffects were investigated by comparing the velocity profiles of the arm movements that occurred prior to (PRE) and immediately after (POST) jumping in simulated hypogravity. For Experiment 3, Participants were given a keyboard and faced a monitor that displayed a virtual scene of a ball suspended in the air. When they pressed the spacebar, the ball fell with one of 11 accelerations, ranging from 50-150% Earth's gravity. After the ball fell to the ground, participants indicated whether it fell faster or slower than 'normal'. Each gravity level was seen multiple times in random order, enabling us to construct psychometric curves for each participant and estimate the gravity level that they perceived as 'normal'. Cognitive aftereffects were investigated by comparing the perceived 'normal' gravity prior to (PRE) and after (POST) jumping in simulated hypogravity.

Results & Discussion: We first showed that adaptation to simulated hypogravity could be achieved using targeted vertical jumping (Exp. 1). Hypogravity adaptation led to an expectation of lower forces and longer aerial times. In POST, this expectation resulted in shorter jumps and diminished muscle preactivation (Fig. 1, left panel) prior to landing. We next aimed to test the transfer of the jumping-induced adaptation to arm movements (Exp. 2) and a cognitive decision task (Exp. 3). In PRE, the velocity profiles of targeted arm movements were slightly asymmetric, with peak velocity occurring between 40 and 50% of the total movement duration, similar to previous findings [5]. In POST, peak velocity shifted to even earlier in the reach (Fig. 1, middle panel), which surprisingly matched previous data on *hypergravity* reaching [5]. Similarly, in Experiment 3, the participants in PRE perceived 'normal' gravity to be close to 1 g (mean: 1.04 g; Fig. 1, right panel). In POST, their perceived 'normal' gravity level *increased* to a mean of 1.12 g. Both the arm movement and cognitive decision results can be explained by an updated expectation of hypogravity going into the task, despite the hypogravity adaptation being performed in a totally separate task. The recent adaptation to hypogravity jumping led the nervous system to expect hypogravity such that, when faced with normal gravity movement (Exp. 2) or the assessment of observed accelerations (Exp. 3), the mismatch between the expected and actual experience caused the emergence of hypergravity movement and the perception of hypergravity acceleration as more normal. Therefore, it appears clear that gravity-information is shared between the motor and cognitive systems assessed in these experiments although their relationship is not always an obvious one.

Significance: This research provides evidence for gravity information being shared between motor and cognitive tasks. By continuing to reveal how cognitive-motor predictions are informed by experience, we can advance our understanding of how motor and cognitive systems interact to generate successful movement. In doing so, we can bolster efforts to treat those who are affected by cognitive-motor disorders and develop countermeasures for the effects of spaceflight.

Acknowledgments: This material is based upon work supported by the NSF GRFP (DGE-1650044). Any opinions, findings, and conclusions or recommendations expressed in this material are those of the authors and do not necessarily reflect the views of the NSF.

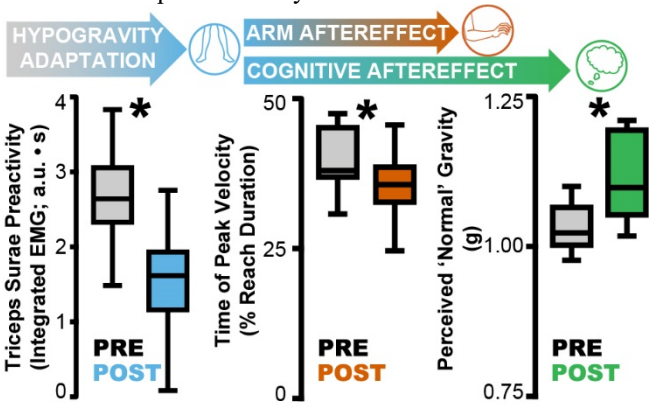

Figure 1. Gravity adaptation during jumping (blue) affects arm movement (orange) and the perception of 'normal' gravity (green). *p < .05

References: **[1]** Kim et al. 1999 *Dev Sci* **2**(3) **[2]** Wang et al. 2004 *J Neurophysiol* **92**(1) **[3]** Rannaud Monany et al. 2022 *J Neurophysiol* **127**(2) **[4]** Santello et al. 1998 *Exp Physiol* **83**(6) **[5]** Crevecoeur et al. 2009 *J Neurophysiol* **102**(2)

THE RELATIONSHIP BETWEEN PATELLAR TENDON STRUCTURE AND QUADRICEPS STRENGTH LIMB SYMMETRY IN PATIENTS WITH CHRONIC PATELLAR TENDINOPATHY

Dan O'Brien[1*], Naoaki Ito[1], Kenneth Lee[2], Bryan C. Heiderscheit[1]
[1]Department of Orthopedics and Rehabilitation, University of Wisconsin, Madison, WI
[2]Department of Radiology, University of Wisconsin, Madison, WI
Author's email: Heiderscheit@ortho.wisc.edu

Introduction: Patients with patellar tendinopathy often present with weak quadriceps and altered patellar tendon structure such as focal thickening[1,2]. Tendon morphology (thickness) and mechanical properties (shear wave speeds) can be quantified on B-mode ultrasound (US) and shear wave elastography. Quadriceps strength plays an important role in knee joint function and outcomes in patients with patellar tendinopathy, hence, understanding the relationship between tendon structure and quadriceps strength may inform clinical practice. This study aimed to explore the associations between symmetry in peak quadriceps strength and patellar tendon structure (thickness and shear wave speed) in patients with chronic patellar tendinopathy.

Methods: IRB and informed consent were obtained. 24 subjects (Age = 26.1 ± 5.3 years; 19 male, 5 female, Victorian Institute of Sport Assessment Questionnaire, Patellar Tendon [VISA-P] = 53.3 [17.6]) with chronic patellar tendinopathy, presenting with symptom duration longer than 3 months and failure of conservative management including physical therapy and at least two alternative non-operative treatment options (NSAIDs, relative rest, ice, and bracing) were included. B-mode ultrasound and shear wave elastography (Supersonic Imagine, Aix-en-Provence, France) were collected with a 6-15MHz linear array high-frequency transducer by a single experienced musculoskeletal radiologist. Images of the patellar tendon were obtained with the participant in supine with the knee in 30° flexion. Thickness was measured anterior to posterior from the thickest portion of the tendon identified by the radiologist. Shear wave speeds were captured in the region of greatest pathology (i.e., thickening or low echogenicity) using the average shear wave speeds from three 10 mm diameter pre-set boundaries placed within the region of interest (Figure 1). Maximum voluntary isometric quadriceps strength was assessed using an in-line dynamometer (Kiio, Madison, WI) with the participant seated in 90º of hip flexion and 90º of knee flexion. Limb symmetry indexes [LSI = (most symptomatic limb / least symptomatic limb × 100)] were calculated for all three variables. Simple linear regressions were used to determine the relationship between quadriceps strength LSI and both patellar tendon thickness and shear wave speed LSIs.

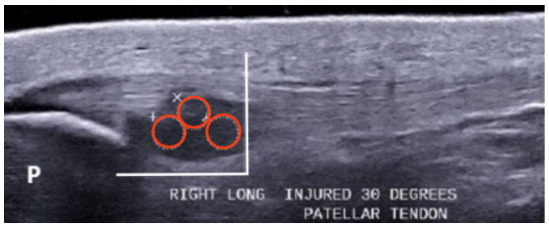

Figure 1: Example B-mode ultrasound with regions of interest identifying the boundaries (red circles) for capturing shear wave speeds.

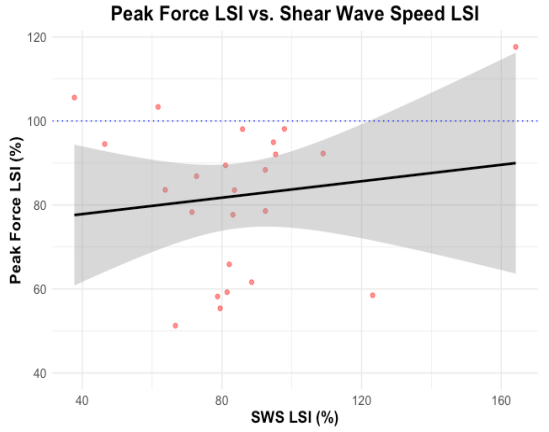

Figure 2: Shear wave speed limb symmetry index (LSI) was not related to peak force LSI ($p = 0.528$, $R^2 = .018$). The shaded region indicates the 95% confidence interval.

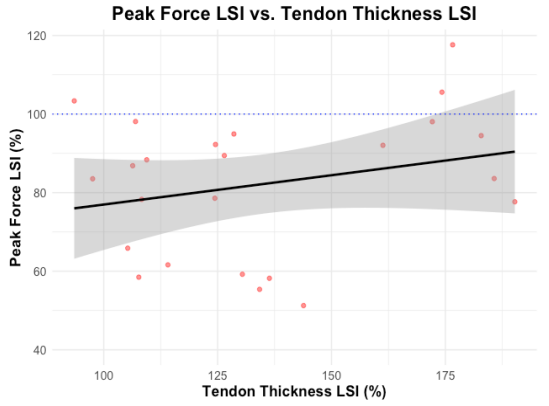

Figure 3: Patellar tendon thickness limb symmetry index (LSI) was not related to quadriceps peak force LSI ($p = 0.228$, $R^2 = .065$). The shaded region indicates the 95% confidence interval.

Results & Discussion: LSI for patellar tendon thickness (mean [SD]: involved = 7.2 [1.7] mm, uninvolved = 5.5 [1.6] mm) and shear wave speeds (involved = 6.6 [1.6] m/s, uninvolved = 8.1 [1.7] m/s) did not relate to quadriceps strength LSI (involved = 28.3 [12.8] kg, uninvolved = 35.4 [16.1] kg). These findings align with previous studies showing no relationship between tendon morphology, mechanical properties, and maximum isometric voluntary contraction strength in a typical cohort of patients with patellar tendinopathy[3]. Our results demonstrate that this lack of relationship may also hold true in a cohort of patients with further progressed tendinopathy, given our stringent inclusion criteria.

Significance: Assessment of patellar tendon morphology and mechanical properties on ultrasound does not reflect quadriceps strength symmetry in patients with chronic patellar tendinopathy.It may be necessary for future research to explore tendon microstructure and its relationship to quadriceps function.

Acknowledgments: This work was funded by the NBA & GE Healthcare Orthopedics and Sports Medicine Research Collaboration.

References: [1]Rosen et. al. (2022) J Athl Train. 57(7):621-631, [2] Helland et. al. (2013) Br J Sports Med. 47(13):862-868, [3] Sprague et. al. (2022) J Orthop Res Off Publ Orthop Res Soc. 40(10):2320-232

RETHINKING MoS: RE-EXAMINING, *Richards et al 2019* WITH PROBABILITY OF INSTABILITY (PoI)

Sarah E. Overby[1], Jonathan B. Dingwell[1]
[1] Department of Kinesiology, Pennsylvania State University, University Park, PA, USA
*Corresponding author's email: seo5285@psu.edu

Introduction: The lateral Margin of Stability (MoS_L) is one measure of how stable a person is [1] since it is defined as a distance from the stability threshold at any given instant [1,2]. However, calculating the mean (μ) of MoS_L across several steps often leads to counterintuitive results when compared across conditions [2]. Under less stable conditions, $\mu(MoS_L)$ has been shown to increase, suggesting that people are more stable in less stable circumstances. Taking an unstable step is more unlikely than taking a step at or near the mean distance away from the stability threshold. When calculating the average of MoS_L, we are only looking at the most likely MoS_L value for a person. Therefore, the mean does not capture the possibility of them falling or take into account step to step variability. To resolve this problem, Kazanski et al. proposed calculating the lateral Probability of Instability (PoI_L) using both the μ and the standard deviation, (σ) of MoS_L in the equation:

$$PoI_L = \mathrm{P}\left(MoS_{Ln} < 0\right) = \frac{1}{2}\left[1 - erf\left(\frac{\mu\left(MoS_{Ln}\right)}{\sigma\left(MoS_{Ln}\right)} \cdot \frac{1}{\sqrt{2}}\right)\right] \times 100\% \quad (1)$$

PoI_L is a measure indicating how likely someone is to be unstable on any given step. Here, we demonstrate how PoI_L can be used to resolve these paradoxical findings with publicly available data [4]. Here, we hypothesized that PoI_L can help explain counterintuitive results mentioned in [2] and predict that PoI_L will capture that particpants in [4] are more likely to be unstable in less stable circumstances.

Methods: We used publicly available data from [4] where 13 older adults (9F/4M, 78.7±6.6 years) were subjected to modulated visual perturbations while walking. Richards et. al calculated $\mu(MoS_L)$ and $\sigma(MoS_L)$ from each of four perturbation phases: baseline, early, late, and post. Baseline represents no perturbations, early represents initial three minutes of perturbation, late represents last three minutes of pertrubations, and post is after all perturbations have stopped. We then calculated PoI_L (Eq.1) using these $\mu(MoS_L)$ and $\sigma(MoS_L)$ [4]. We used a one-factor ANOVA to evaluate the differences between visual perturbation phases for $\mu(MoS_L)$, $\sigma(MoS_L)$, and (PoI_L).

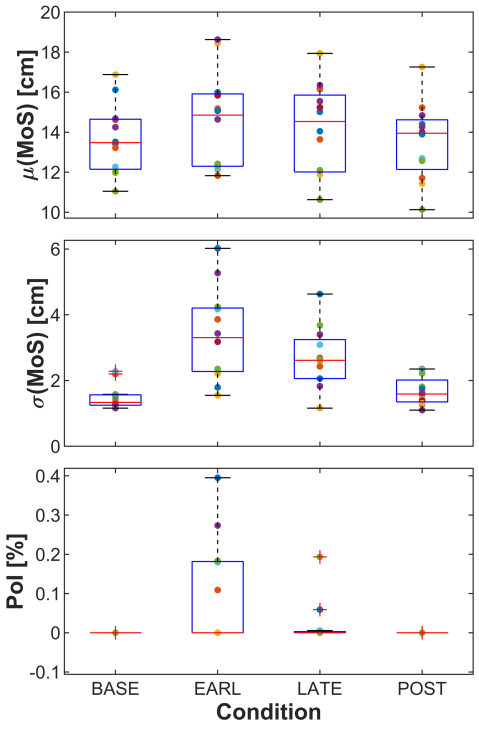

Figure 1: A) Mean MoS across phases of perturbations. Baseline represents no perturbations, early represents initial three minutes of perturbations, late represents last three minutes of perturbations, and post is after all perturbations have stopped. **B)** Standard Deviation of MoS across phases of perturbations as described above. **C)** PoI represented as a percentage across phases of perturbations as described above.

Results & Discussion: Despite destabilizing perturbations, $\mu(MoS_L)$ did not change ($p = 0.601$; Fig. 1A). Thus, the $\mu(MoS_L)$ does not capture the destabilizing effects of the intervention. The $\sigma(MoS_L)$ was greater for both the early and late phases compared to the baseline ($p < 0.001$; Fig. 1B). Perturbations do induce substantial deviations from the mean but suggest participants did not adapt to the perturbations and remained more variable throughout the entire duration of the perturbations. The PoI_L was only significantly greater for the early phase when compared to the baseline ($p = 0.007$; Fig. 1C). PoI_L captures effects of perturbations, given that we see the PoI_L increase, meaning instability increases, in the early phase of perturbations. However, it also captures the effects of adaptation given that we see no difference in the late phase of walking, so participants were able to return their likelihood of being unstable back to baseline. Alone, the mean and standard deviation do not give enough information about the instability of a person. When used to compute PoI_L, we no longer see paradoxical results.

Significance: Taking the mean of MoS_L alone can yield paradoxical findings regarding a person's stability, and variability alone does not give enough information. However, PoI_L, a measure of instability, can resolve this problem by taking both metrics into account to give results that make more sense intuitively.

References: : [1] Hof et al. (2005) *J Biomech* 38(1); [2] Watson et al. (2021) *BMC Musc Disord* 22(1); [3] Kazanski et al. (2022) *J Biomech* 144; [4] Richards et al. (2019) *JNER* 16(81).

A PORTABLE, MULTIDIMENSIONAL MOTOR FUNCTION ASSESSMENT SYSTEM CAN IDENTIFY DIFFERENCES IN HEALTHY OLDER AND YOUNGER ADULTS

Jamie B. Hall[1*], Jacob Thomas[1], Trent M. Guess[1]
[1]University of Missouri
*Corresponding author's email: halljami@umsystem.edu

Introduction: Emerging evidence suggests motor function assessment can identify devastating conditions in aging populations such as cognitive decline, fall risk, and frailty [1,2]. In developing models and protocols for this purpose, it is important to understand normal age-related changes in constructs of interest. Age-related differences in balance and gait are well documented. [3,4] However, many studies of motor function have used expensive, unidimensional technologies that may not be suited to widespread use in clinical and community settings. [1-4] The purpose of this study was to evaluate the feasibility of using a portable, inexpensive, easy to use, multidimensional motor function assessment platform in identifying age-related changes in balance, gait, and reaction time with the ultimate goal of improving our ability to distinguish differences related to normal aging from those related to neuropathologies.

Methods: We collected data on over 100 healthy young (HYA, 18-49 years) and older adults (HOA, 50+ years old) in a variety of settings including the ASB 2023 Annual Meeting, healthcare clinics, a local senior center, and our research laboratory. We used the novel Mizzou Point-of-care Assessment System (MPASS), which integrates depth camera (Kinect Azure) body tracking, a custom force plate, and interface board (Arduino microcontroller, push buttons, LEDs, and microphone) (Figure 1). Dual task (DT) conditions during walking and balance trials consisted of serial subtraction of 7. [5] 2-3 trials of walking, eyes closed balance on a firm surface, and reaction time tests were completed, and ensemble averages were calculated. Discrete balance center of pressure (CoP) sway and gait spatiotemporal parameters were calculated from continuous data. Reaction test parameters consisted of reaction time from LED activation to pushing a button and number of correct button pushes during a 30 sec trial. Data were analysed using Mann Whitney U tests, followed by Benjamini Hochberg correction and effect size (Cohen's d) calculation. [6]

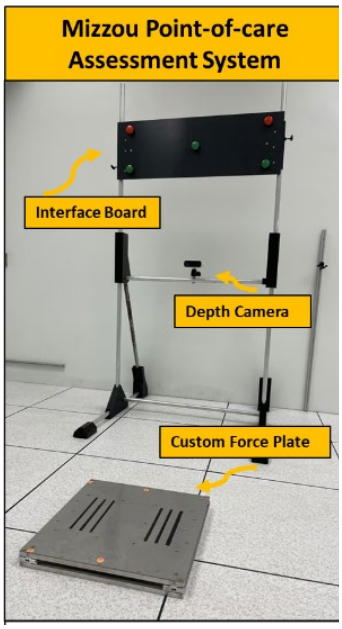

Figure 1: MPASS integrates a custom force plate, depth camera, and interface board.

Results & Discussion: Significant differences were found between groups for reaction and balance tests with large effect sizes. Differences were noted in stride length between groups in both single and dual task conditions with small to medium effect sizes (Tables 1-3). Stride time between groups was not different. The data were from several data collection sessions during which different tests were administered, thus the number and sample are not consistent between analyses.

Table 1: Sway Balance Parameters

Variable	HOA Median (n=30)	HYA Median (n=50)	Unadjusted p-value	p-value	Cohen's d
Age (years)	70	25			
Area 95 CoP ST	259.68	147.83	.001	.001	.723
Area 95 CoP DT	286.98	128.24	< .001	< .001	.793
Mean total velocity CoP ST	20.56	12.29	< .001	< .001	1.732
Mean total velocity CoP DT	21.38	13.43	< .001	< .001	1.274

Table 2: Gait Spatiotemporal Parameters

Variable	HOA Median (n=50)	HYA Median (n=50)	Unadjusted p-value	p-value	Cohen's d
Age (years)	70	25			
Stride Length ST	1.69	1.77	.037	.074	.39
Stride Length DT	1.56	1.64	.013	.052	.46
Stride Time ST (s)	1.06	1.10	.145	.193	.27
Stride Time DT (s)	1.15	1.16	.700	.700	.07

Table 3: Reaction Time

Variable	HOA Median (n=20)	HYA Median (n=101)	Unadjusted p-value	p-value	Cohen's d
Age	67	25			
Reaction Time (ms)	873.2	688.7	<0.001	0.001	1.06
Number Completed	14.33	16.5	<0.001	0.001	1.05

Significance: These preliminary results demonstrate the ability of a portable, multidimensional motor function assessment platform to discriminate expected age-related differences between groups. In addition, it highlights the usefulness of assessing multiple constructs when the goal is to discriminate between populations. Gait is often the construct most tested; however, in our study balance and reaction tests were more discriminative. Future work will include building models for assessment of risk for cognitive decline, falls, and frailty in older adults based on multidimensional motor function assessment data and machine learning.

Acknowledgments: Funding for portions of this work was provided by the University of Missouri Coulter Biomedical Accelerator.

References: [1] Ghorani et al. (2021), *Biomed Signal Process Control* 10/1016/j.bspc.2020.102249; [2] Noh et al. (2021), *Scientific Reports* 11:12183; [3] Herssens et al. (2018) *Gait Posture 64;* [4] van Humbeeck et al. (2023) *Sci Rep* 13; [5] Bahureksa 25 al. (2017) *Gerontology* 63(1); [6]Lenhard et al. (2022) *Psychometrica.*

EFFECTS OF FATIGUE ON LIMB COORDINATION WITHIN THE FRAMEWORK OF THE UNCONTROLLED MANIFOLD ANALYSIS

Joelle F. Dick [1*], Melody S. Modarressi [1], Gregory S. Sawicki [1,2], Young-Hui Chang[1]
[1] School of Biological Sciences, [2] School of Mechanical Engineering, Georgia Institute of Technology, Atlanta, GA, USA
*Corresponding author's email: jdick7@gatech.edu

Introduction: Motor redundancy is a fundamental characteristic of human movement that facilitates compensatory adjustment [1] particularly to internal factors such as fatigue. Previous investigations on motor control of bouncing gaits, running, and hopping, during fatigue have revealed that humans strategically manipulate the variability of joint-level kinematics (joint segment angles) to minimize variations in performance-level variables, notably the center of mass trajectory [2]-[4]. These findings suggest that the central nervous system (CNS) exploits motor redundancy as a compensatory strategy, enabling the maintenance of task performance even under conditions of heightened fatigue.

Existing literature has explored motor control during fatigue in the context of dynamic activities like running and hopping. However, an analysis of how lower limb joint coordination changes to stabilize leg dynamics following fatigue is notably absent. This study aims to pursue two objectives: 1) investigate how humans employ interjoint coordination to stabilize leg length throughout squat cycles, and 2) examine the impact of fatigue on the synergy structure responsible for stabilizing leg length during repetitive squatting. We posited two hypotheses: 1) subjects will coordinate segment angles to stabilize leg length throughout the entire squat cycle, with a specific emphasis on the target squat depth, and 2) the stabilization of leg length would remain unaffected despite increasing fatigue levels.

Methods: 8 healthy participants (5F/3M) gave informed consent prior to participating in this Georgia Tech IRB approved protocol.

Experimental Data Collection: Participants underwent an exercise protocol designed to induce targeted fatigue in major leg extensor muscle groups. They performed repetitive squats to a target knee flexion angle of 90° at a 50-bpm pace. The protocol continued with blocks of continuous exercise until either the participant squatted for 4 consecutive minutes or failed 3 successive squat cycles to the target on beat. Following this, 3 maximal single-leg jumps (SLJs) were attempted. If the target height was achieved in any of these jumps, the fatigue protocol was repeated until all three SLJs failed to reach the target height, or 5 4-minute blocks of squats were accomplished.

Locomotor EMG Analysis: The first and last 30 seconds of the 1st and 5th block band-pass EMG signals of major muscles [5] were transformed to measure the mean power frequency (MPF) as an indicator of fatigue [6].

UCM Kinematic Model: A 4 segment kinematic MATLAB model was created to determine whether joint segments coordinate to stabilize leg length within key phases of a squat cycle [7]. A Jacobian relating segment angles to leg length was derived using segment angles averaged over the first block's first 30 squats. IMA (Index of Motor abundance) values were calculated for the 1st and 5th block of squats. The changes in MPF and IMA within each block were averaged across subjects. MPF was compared using a 1-tailed, paired t-tests with an alpha level of 0.05.

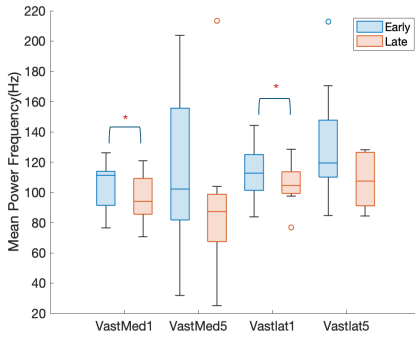

Figure 1: MPF (n=8) for Vastus Lateralis and Vastus medialis in early and late stages of Block 1 and 5. (* = p<0.05)

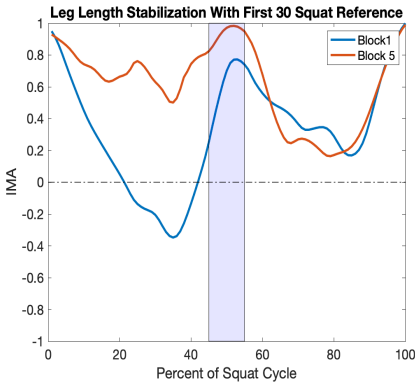

Figure 2: IMA of leg length control. Data represents mean IMA values across subjects (n=3). The shaded region represents target squat depth.

Results & Discussion: There was a general trend of lower MPF for major muscle groups with exercise indicating fatigue (Fig. 1). MPF significantly declined within Block 1 for both muscles. A preliminary UCM analysis shows that leg length is generally stabilized throughout the entire squat cycle for both Block 1 and 5. IMA reached a peak at the target squat depth (45-55% of squat cycle) in Block5 (Fig. 2). As MPF decreased, IMA increased within the descent phase (0-45% of squat cycle) and at the target depth (45-55% of squat cycle). The increase of IMA with fatigue suggests that the subjects increasingly selected a consistent joint coordination strategy favoring the stabilization of leg length.

Significance: These preliminary results provide additional insights on how the human locomotor system can maintain limb-level performance through a compensation strategy that exploits joint-level motor abundance in the presence of fatigue.

Acknowledgements: The authors would like to thank the Comparative Neuromechanics Lab group at Georgia Tech for their assistance during data collection. This project was funded by the DOE GAANN fellowship program: DSP200A210046.

References: [1] Preatoni et al. (2013) *Sports Biomech* 12(2); [2] Muide et al. (2016), *Hum Mov Sci* 48; [3] Möhler et al. (2019), *Hum Mov Sci* 66:133-141; [4] Möhler et al. (2022), *Biology (Basel)11(6);[5]* Signorile et al. (1994), *J Strength Cond Res* 8(3):178-183. [6] Chaffin. (1973), *J Occup Med.*(4):346-54; [7] Auyang et al. (2009), *Exp Brain Res.*192(2):253-64

EVALUATION OF A ROTATING SWIM BENCH AS A SURROGATE FOR FREESTYLE SWIMMING

Kathryn F. Webster[1*], Carla McCabe[2], Clark R. Dickerson[1]
[1]University of Waterloo, Department of Kinesiology and Health Sciences, Ontario, Canada
[2]Ulster University, School of Sport, Belfast, Northern Ireland
*k4webste@uwaterloo.ca

Introduction: The swim bench is an isokinetic ergometer designed for competitive swimming training and is used in research as an accessible alternative to in-water data collection. However, limited literature addresses the biomechanical fidelity of the swim bench relative to in-water swimming. The lack of body roll on a conventional fixed swim bench may limit realistic simulation of the freestyle stroke pull. Accordingly, the KayakPro SwimFast swim bench includes a rotating bench setting; yet specific changes to a competitive swimmer's kinematics and muscle activity on a rotating bench compared to a fixed bench or in-water swimming are unknown.

The purpose of this study was to assess the effect of swim bench setting on freestyle stroke 3D kinematics and muscle activity and evaluate the similarities between the swim bench and pre-existing in-water kinematic data [1]. The rotating bench setting was expected to produce greater shoulder angles and shoulder roll, narrower elbow angles, and less torso flexion than the fixed. Further, the rotating bench setting was expected to generate greater muscle activation of the shoulder prime movers, rotator cuff and scapular stabilizers. In comparison to the in-water data, the stroke length, elbow flexion, total shoulder roll, and length of entry phase were expected to differ on the swim bench.

Methods: Fifteen, male, right-handed, collegiate and national level competitive swimmers [20.4±1.18 yrs., 1.81±5.11 m, 78.5±6.01 kg] recruited from local varsity swim teams participated. Upper limb and torso kinematics were collected bilaterally, and surface electromyography (sEMG) collected on 12, right, upper limb muscles. Participants performed 8 sets (4 rotating & 4 fixed) of 30 seconds freestyle stroke pulling on a KayakPro SwimFast swim bench (KayakPro USA LLC, Florida, USA) at 55 stroke cycles/minute.

Kinematic data was filtered with a low-pass Butterworth filter at a 4 Hz cut off, and time normalized to percent stroke cycle (%SC). sEMG data was filtered with a band-pass Butterworth filter between 30 to 500 Hz, amplitude normalized to maximum voluntary isometric contraction and time normalized to %SC. Swim bench setting continuous joint angles and muscle activations were compared using statistical non-parametric mapping, one-tailed, paired t-tests. In-water measures were compared to the swim bench using mixed one-way ANOVAs via JMP 17 software (SAS Institute, North Carolina, USA).

Results & Discussion: Contrary to the hypotheses, few kinematic and sEMG differences existed between the rotating and fixed swim bench settings. Significant differences were found in the right shoulder elevation ($p = 0.021$) (Fig. 1), posterior deltoid activation ($p = 0.015$) (Fig. 2), and infraspinatus activation ($p = 0.026$). However, the fixed bench produced greater activations and angles rather than the hypothesized rotating setting. Regardless of bench setting, participants laterally flexed the torso, potentially as compensation for the lack of roll allowance on the swim bench overall. The similarities between the settings indicate that the rotating swim bench may not substantially augment the realistic simulation of the underwater freestyle pull. Thus, swimmers can choose the more comfortable setting for training.

Compared to in-water swimming, both swim bench settings produced similar elbow flexion ranges; however, the stroke length decreased ($p<0.0001$), total shoulder roll decreased ($p<0.0001$), and entry phase duration decreased ($p<0.0001$) significantly. Despite the difference in shoulder roll magnitude, the movement pattern aligns with current literature, indicating at least partial replication of in-water swimming [2]. The reduction in stroke length may relate to the lack of entry phase on the swim bench because swimmer's commonly glide further forward during entry and elevate the shoulder to facilitate a longer moment arm for the catch [3]. The reduction in stroke length, total shoulder roll, and entry phase duration with the addition of the lateral torso flexion are notable considerations for long term use. Swimmers could develop associated habits that reduce swimming economy and increase drag when translated to in-water training.

Significance: This study provides novel findings for coaches and researchers to consider for the use of the swim bench for training and research purposes.

References: [1] McCabe et al. (2011), *J Sport Sci* 29(2); [2] Andersen et al., 2019. J Strength Cond Res. 34(1); [3] Yanai & Hay (2000), *Med Sci Sports Exerc* 32(1)

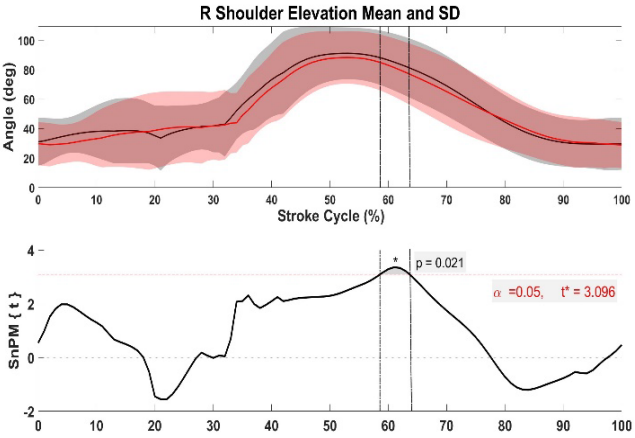

Figure 1: Right shoulder elevation ($p = 0.021$, 58 – 63%). Mean and standard deviation above, SnPM {t} result below. Rotating setting denoted by the red, fixed: black, significance with*

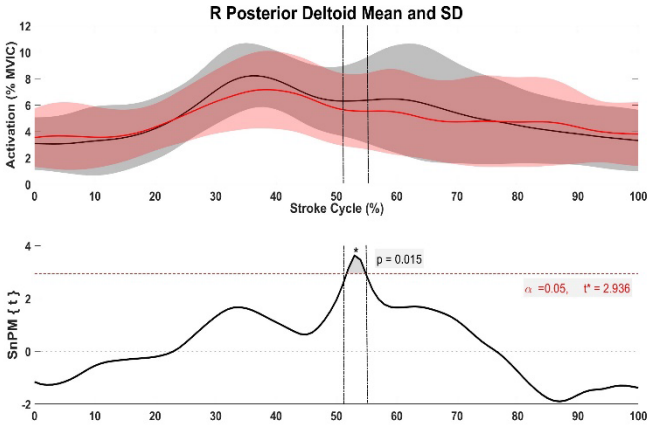

Figure 2: Right posterior deltoid activation ($p = 0.015$, 51 – 54 %). Mean and standard deviation above, SnPM {t} result below. Rotating setting denoted by the red, fixed: black, significance with*

THE IMPACTS OF ALTERED GRAVITY AND MENTAL FATIGUE ON SENSORIMOTOR ASSESSMENTS

Kieran M. Nichols[1*], Jeevan Jayasuriya[1], John Hayes[2], Blake Fairchild[2], Ranjana K. Mehta[1]
Industrial and Systems Engineering, [1]University of Wisconsin-Madison and [2]Texas A&M University
*Corresponding author's email: knichols4@wisc.edu

Introduction: Alterations in vestibular function during and immediately following gravitational transitions can impact critical spaceflight tasks, which can exacerbate under fatigue (e.g., work overload). However, existing sensorimotor assessments do not capture interactions of these multiple spaceflight hazards. For example, sensorimotor tests such as tandem walking (TW) with eyes open and closed, where individuals walk in a heel-to-toe manner at their preferred pace [1], is a standard measure of locomotor capability in astronauts and have shown impairments with vestibular challenges. Postlanding assessments of this test include completion time and percent correct steps. However, by utilizing body-based IMUs, more granular metrics such as torso acceleration can be captured that offer insights into potential compromised or compensatory biomechanical pathways of postural stability. For example, the tandem walk parameter (TWP) [2], which combines the percentage of correct steps, total completion time, and torso RMS acceleration, has shown sensitivity to vestibular impairments. However, this metric has not been assessed to capture interactions of multiple spaceflight hazards, such as mental fatigue and altered gravity. The present study aims to address this gap by examining the impacts of mental fatigue (induced via a 2-hour working memory test) and altered gravity (acute exposure to pseudorandom bilateral bipolar galvanic vestibular stimulation; GVS) on granular sensorimotor metrics during tandem walk tasks of eyes open, eyes closed, and dual-task. We hypothesized that reweighting of sensory inputs during GVS-based vestibular impairments will impose increased mental demands, and therefore, under states of mental fatigue, a person with a short-term vestibular impairment will demonstrate lower TWP values (stat. sig. of $p<0.05$).

Methods: Thirteen participants (4F/9M) were instrumented with the GVS system and Xsens motion tracking, and a video camera recorded their movements. Participants completed a mental-fatigue protocol of twelve 10-minute blocks of 2-back visuospatial working memory tests [3]. Before and after the fatigue tests, they were tested with a sensorimotor test battery (STB; two trials each of eyes open (EO), eyes closed (EC), and dual-task (DT) tandem walk) with and without GVS. Performance data from the STB was calculated from the video and Xsens recordings. TWP was used to assess walking performance and was calculated by $TWP = \ln\left(1 + \frac{Percentage\ of\ CorrectSteps}{TotalTime\ x\ RMS(Torso\ Acceleration)}\right)$. Separate linear mixed model analyses were performed on TWP, completion time, and % correct steps for each task, with fixed effects of altered gravity (GVS vs. no-GVS) and mental fatigue (pre-fatigue vs. post-fatigue), and participants as a random effect. The data presented in this abstract is part of a preliminary analysis that includes 5 participants.

Results & Discussion: Mental fatigue did not significantly impact any variable for any task (all $p>.28$). In general, GVS adversely impacted all variables, however its effect varied based on task type and sensorimotor assessment. EO and DT tandem walk showed greater impairments in % correct steps with GVS (both $p<0.016$). The TWP and RMS of the Torso Acceleration were sensitive to GVS in the EC tasks (all $p<0.056$). In particular, a GVS x fatigue interaction effect was observed ($p=0.043$) on RMS torso acc. in the EC task, where higher variability in acceleration in the GVS condition was observed pre-fatigue when compared to post-fatigue, indicating slower and more kinematically variable gait post fatigue. This result can be explained as a more conservative walking strategy that relies less on vestibular and visual inputs and more on the hip proprioceptors to regulate mediolateral walking balance [4]. Statistical analysis of more participants is necessary to test the significance of this potentially interactive effect, and other trends (e.g., EC TWP trends observed in Fig 1). However, the lack of support for our hypothesis also highlights the potential need for new evaluative metrics that can be sensitive to mental fatigue and altered gravity. For instance, the composite TW metrics derived using principal component analysis from six kinematic features of a single lower-back IMU [5] may be applicable to evaluate altered gravity and mental fatigue-related sensorimotor impairments.

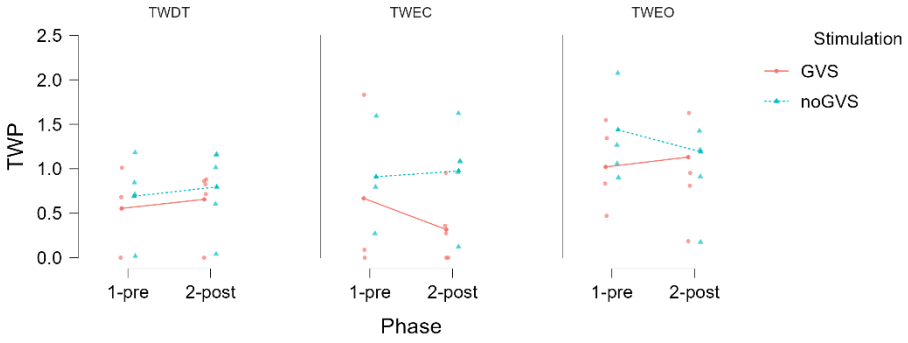

Figure 1: Separate Linear Mixed Models for TWP with each task: Tandem Walk (TW) for Dual-Task (DT), Eyes-Closed (EC), and Eyes-Open (EO).

Significance: This preliminary analysis presented evidence on TWP trends that may show potential sensitivity to altered gravity or mental fatigue and across different sensorimotor tasks. Nonetheless, the interactions captured by RMS torso acc. hint at changes in postural gait strategies that may be captured with newer evaluative metrics for cognitive and motor performance. This study is important in assessing the influence of short-term vestibular impairment and mental fatigue on tandem walk balance and could contribute to more granular sensorimotor metrics for evaluating the effect of spaceflight stressors after gravitational transitions.

Acknowledgments: This study was funded by a Student Research Grant from Huffines for Sports Med. and Human Perf.

References: [1] Rosenberg et. al.(2022), *Brain Sciences* 12(10); [2] Miller et al. (2018), *A.M.H.P.* 89(805).; [3] Karthikeyan et al. (2021), *Pro. HFES.* 65(1).; [4] Honegger et al. (2013), *Neurosc.* 254(285).; [5] Ganz et al. (2021), *J Gerontol Med Sci,.*, 76(1)

AUTOMATING GENERIC BONE MODEL REGISTRATION FOR X-RAY BASED BIOMECHANICS RESEARCH

Seyed Mohammadali Rahmati[1*], Liang-Ching Tsai[2], Jarred Kaiser[3], Young-Hui Chang[1]
[1] Comparative Neuromechanics Lab, School of Biological Sciences, Georgia Institute of Technology, Atlanta, GA, USA
[2]Department of Physical Therapy, Georgia State University, Atlanta, GA, USA
[3]School of Medicine, Emory University, Atlanta, GA, USA
*Corresponding author's email: srahmati3@gatech.edu

Introduction: Radiography systems have revolutionized biomechanics research by enabling precise *in vivo* tracking of skeletal movements where optical methods are intractable, such as in rodent models. Biplanar X-ray videography allows for the detailed analysis of bone positions and orientations during motion. Historically, methods like rotoscoping required labor-intensive manual adjustments of bone models to align with X-ray images, proving to be both time-consuming and subjective [1]. Burton et al. introduced a breakthrough fully automatic approach using high-speed stereo-radiography, employing convolutional neural networks (CNNs) for image annotation and a multi-stage optimization for refining pose estimates of the femur, patella, and tibia-fibula based on subject-specific models [2]. This method utilizes singular value decomposition (SVD) for direct transformation of three-dimensional (3D) key points from bone models to biplanar image reconstructions. However, it necessitates subject-specific geometries, limiting its use in high-throughput applications with generic bone models. Our study advances this methodology by extending closed-form solutions for translation, rotation, and scaling across all axes, enabling precise registration of generic bone models with X-ray data, thus enhancing analysis versatility. Applied to rat hind limb models from Johnson et al. [3], we defined joint axes and calculated 3D angles, significantly augmenting precision, adaptability, and efficiency in biomechanical movement analysis.

Methods: This study employed a custom trained DeepLabCut (DLC) model, an open-source machine learning-based tracking tool, for annotating 17 bone landmarks on the hind limbs of rats. DLC outputs were then processed through XMALab for 3D reconstruction of biplanar X-ray videos, capturing the spatial positions of these landmarks [4]. Initial key points were manually identified on the corresponding locations of the 3D bone surface mesh models ($A \in R^{3\times n}$) to align with the identified bone landmarks ($B \in R^{3\times n}$). The goal was to align matrix A with matrix B for each bone segment via transformation, covering translation, rotation, and scaling within the 3D virtual capture volume. This was achieved by centering matrices on their centroids and applying SVD-based closed-form solutions for precise mapping. A one-time optimization process then refined manual key point selection on 3D models to reduce errors. Bone axes were established from these landmarks, allowing the calculation of relative Euler angles and, subsequently, the 3D joint angles—internal-external rotation (I-E Rot), abduction-adduction (Abd-Add), and flexion-extension (Flex-Ext), respectively—during rat locomotion.

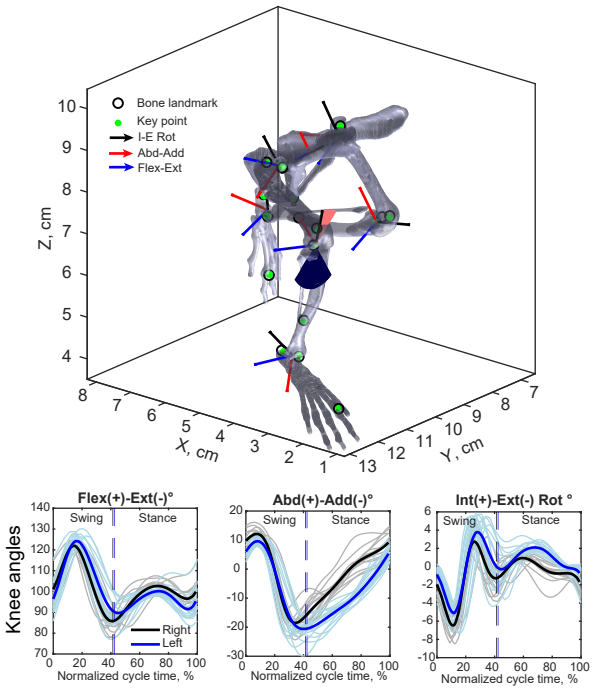

Figure 1. Rat hind limb skeletal model and gait kinematics. The top panel shows the skeletal model at the onset of right stance phase, with 3D bone STL key points as solid green circles and tracked landmarks as hollow black circles. Anatomical bone axes are marked by arrows, and knee angles are color-coded: blue for Flex-Ext, red for Abd-Add, and black for I-E Rot. The bottom panel illustrates kinematic angles for both knees over 16 gait cycles, offering a comparison of locomotion dynamics.

Results and Discussion: The new closed-form method significantly improves the registration of generic models with 3D bone landmarks, enhancing versatility, speed, and precision. On a system with a 13th Gen Intel® Core™ i9-13900K CPU and 64 GB DDR4 RAM, it processed 17 bony landmarks in 500 frames in 0.9 seconds. The implementation of SVD facilitated a robust computation of the transformation matrices, resulting in precise registration of bone surface mesh models with 3D data points. The average deviation between the manually identified key points and bony landmarks was found to be 0.8±0.2 mm. This method showed strong correlation with X-ray images in rotoscoping, and captured knee flexion patterns expected in rat locomotion, with primary and secondary maxima during mid-swing and mid-stance, respectively (Fig. 1). Observed asymmetries in joint angles suggest potential influences of limb dominance or motor skill development associated with treadmill exercise.

Significance: The proposed method addresses the limitations of previous bone model registration techniques, which were time-consuming and subjective. Our approach enables more accurate in vivo movement analysis, promising advancements in orthopedic diagnosis, personalized rehabilitation, and insights into locomotion across species.

Acknowledgments: NIH R01AR080154. Special thanks to Dr. Reza Sameni for his assistance with the SVD computation development.

References: [1] Gatesy, Stephen M., et al. (2010), *J Exp Zool Part A Ecol Genet Physiol* 313(5); [2] Burton, William S., et al. (2021), *Comput Biol Med* 139; [3] Johnson, Will L., et al. (2008), *J Biomech* 41(3); [4] Kirkpatrick, Nathan J., et al. (2022), *J Exp Biol* 225(16); [5] Winter, David A. (1991), Biomech Motor Control Hum Gait: Normal, Elderly and Pathological.

VISUAL IMPAIRMENTS AND RISK FACTORS RELATED TO NECK MUSCULOSKETAL DISORDERS

Galen Holland[1*], Anna Bailes[2], Mark S Redfern[2], William Smith[1], Emily Grattan[3], Brenna M Baker[2], Rakié Cham[2,1]
[1]Department of Ophthalmology, University of Pittsburgh
[2]Department of Bioengineering, University of Pittsburgh
[3]Department of Occupational Therapy, University of Pittsburgh
*Corresponding author's email: galen.holland@pitt.edu

Introduction: Visual impairments (VIs) are associated with an increased risk of occupational injuries, particularly among older workers [1-3]. For example, Lam et al. (2008) reported the average risk of occupational injuries increases by nearly 60% for those with self-reports of "untreated or uncorrected vision problems." More specifically, for workers affected by macular degeneration, the adjusted odds ratio of occupational injury is ~3.5 times the risk in healthy workers [1]. The mechanism of occupational injuries in older workers with VIs is unknown. One potential mechanism is that VIs impact risk factors known to be associated with musculoskeletal disorders (MSDs)-related injuries (e.g. awkward postures, movement speed, etc.) [4]. The link between VIs and MSDs risk factors has not been investigated. The most prevalent ocular conditions in older adults that cause irreversible vision loss [5] are age-related macular degeneration (AMD), diabetic retinopathy (DR) and glaucoma [6, 7]. These conditions deteriorate visual function in different ways. For example, performance of hand coordination tasks is differentially affected by simulated central and peripheral vision loss [8]. As the labor force ages, there will be an expected increase in the that rate of VIs in the workplace. Therefore, the goal of this preliminary study is two-fold: (1) to determine whether well-established risk factors for MSDs (e.g. awkward neck postures during the performance of work-related manual tasks) are affected by the type of ocular diagnosis, and (2) to determine if an easily-implementable intervention, i.e. adjustment of ambient lighting [9], reduces neck MSDs risk factors in adults with VIs.

Methods: Seven (N=8, 4 males) individuals between the ages of 58 and 70 years (mean±s.d. 63.9±4.5 years) and with a VI diagnosis (3 AMD, 3 glaucoma and 2 DR) participated. Subjects performed a multi-level sorting task, specifically the Valpar Component Work Sample #7 (VCWS7, Bases of Virginia, LLC, Yorktown, VA) task under various lighting conditions presented in a random order. The analysis here is focused on the dimmest (50 lux) and brightest (1000 lux) settings. The VCWS7 task is used as an assessment of rapid sorting skills, requiring participants to discriminate tiles of different colors, numbers and/or letters and to place these tiles into matching slots. Participants were asked to sort as many tiles as possible in a time limit of 5 minutes. To capture neck postures (defined as the relative orientation of the head with respect to the torso), kinematics of the torso and head segments were tracked at 120 Hz using an electromagnetic system (G4™ system (Polhemus, Burlington, VT)). Full 6 Degree-Of-Freedom (DOF) movements from the head and torso segments were then used to compute "neck" angles, specifically flexion/extension angle (i.e. chin down/up), lateral flexion angle (i.e. touch shoulder with ear), and lateral rotation angle (i.e. turn head to right/left). Percent time spent in extreme postures (defined by Shall et al. [4]), movement speed and rest/recovery periods were computed based on existing measures in the literature [4]. For brevity purposes in this abstract, only the percent time spent in extreme posture in the sagittal plane is considered. Additional outcome measures and statistical analyses will be presented at the national meeting.

Results & Discussion: Ocular diagnosis affected sorting performance, with AMD, DR and glaucoma groups completing on average 101, 87 and 82 tiles, respectively. The brightest lighting setting was associated with better performance in AMD and DR. For example, participants with DR and AMD sorted 20 and 7 more tiles in the brightest lighting setting compared to the dimmest setting, respectively. In contrast, lighting had a minimal effect on the number of sorted tiles in glaucoma (80 vs. 83 sorted tiles). The percent of time in extreme neck postures during sorting was impacted by the lighting condition for AMD and DR. (Figure 1). Greater light levels reduced time in extreme postures in these groups, but not in glaucoma.

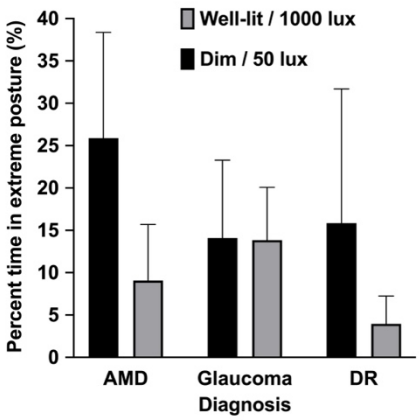

Figure 1: Percent time neck is in extreme postures in the sagittal plane. Error bars are standard errors.

Significance: Certain ocular conditions appear to put individuals at increased risk for MSDs based on extreme neck postures. Simple changes in ambient lighting may reduce such risk factors and should be considered as simple accommodations that can be implemented in the workplace.

Acknowledgments: National Institute of Occupational Safety and Health (NIOSH R21 OH012204, PI Cham),

References: [1] LT Lam et al. Inj Prev, 14:396-400, 2008. [2] KT Palmer et al. Occup Environ Med, 72:195-9, 2015. [3] L Peng et al. Human Aspects of IT for the Aged Population. Healthy and Active Aging, 2020, pp. 365-80. [4] MC Schall, Jr. et al. Appl Ergon, 93:103356, 2021. [5] D Laliberte Rudman et al. The Gerontologist, 56:e32-e45, 2016. [6] AL Pelletier et al. "Vision loss in older adults," Am Fam Physician, 94:219-26, 2016. [7] Statistics and data. (Accessed: January 25, 2017). National Institutes of Health. National Eye Institute. Available: https://nei.nih.gov/eyedata. [8] NA Baker et al. IISE Transactions on Occupational Ergonomics and Human Factors, 5:148-57, 2017. [9] HT Juslen et. a. Ergonomics, 50:615-24, 2007.

High-Density Surface Electromyographic Signal Composites for Lower Limb Prosthetic Control

Joseph R. Redmond, Fred W. Christensen, Corey A. Pew*
Department of Mechanical and Industrial Engineering, Montana State University, Bozeman, MT
*corey.pew@montana.edu

Introduction: Surface electromyography (sEMG) is utilized as a control interface for active, robotic protheses, resulting in higher quality of life for individuals with lower limb amputation [1]. sEMG reads myoelectric signals from a residual limb, providing a natural control interface for the user. However, signal noise from skin impedance, motion of the skin relative to the muscle, and sensor displacement are common for sEMG, reducing robustness [1]. Lower limb prostheses (LLP) require reliable control signals, as errors risk falls and subsequent injury to the user [2]. High-Density surface electromyography (HDsEMG) shows potential in improving signal quality, allowing for more reliable and integrated control. We hypothesize that **(1)** signal-to-noise ratio (SNR), a quantification of signal quality [3], is better with HDsEMG relative to Standard sEMG (SsEMG), **(2)** individual HDsEMG signals have a lower root-mean-square (RMS) power due to smaller electrodes, **(3)** composite signals can compensate for the decrease in individual signal power.

Figure 1: Delsys SsEMG and HDsEMG sensors

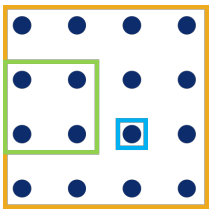

Figure 2: 16 Ch. Sensor composites Best-1 (blue), Comp-16 (gold), Comp4 (green).

Methods: 11 Participants (3 individuals with lower limb amputation and 9 non-amputees) were recruited for the Montana State IRB approved protocol. Data was collected using bipolar SsEMG sensors and 16 channel HDsEMG sensors (Fig. 1). Four superficial muscles, two knee flexors, the Semitendinosus (ST) and Bicep Femoris (BF), and two extensors, the Vastus Laterallus (VL) and Rectus Femoris (RF) were measured. Sensors were placed optimally and displaced distally 1 cm to simulate sensor displacement during prosthesis pistoning. Participants performed activities of daily living, walking straight, turning left/right, stair and ramp ascent and descent, sit to stand, and squats. An analysis using straight walking data of 1 participant was conducted to initially evaluate signal compositing methods. SNR was calculated for the SsEMG signals, and the individual channels of HDsEMG sensors. RMS values were computed in a previous study of this data [4]. The single HDsEMG channel with the best SNR was selected (Best-1). Composite HDsEMG signals were computed, including a combination of all 16 channels (Comp-16) and a cluster of 4 channels (Comp-4) (Fig. 2). Comp-4 was created by evaluating the mean SNR in the 9 possible 2x2 square clusters. The 4-node cluster with the highest mean SNR was then combined.

Results & Discussion: SNR was found to be over 200% better for Best-1 compared to the Standard signal (Fig. 3). Previous work indicated sEMG data to be clean from noise artifacts with an SNR over 10dB [5]. This 10dB SNR threshold provides an initial benchmark for signal viability prior to control system implementation. The standard signals fail to meet this threshold for both optimal and displaced positions with an SNR under 5dB. In optimal placement, Best-1 exceeded this mark at over 18dB, a product of selectivity based on signal quality. Standard signals had a higher RMS compared to Best-1 by a factor of 150-300%, depending on the muscle evaluated (Fig. 4). The smaller size of the HDsEMG nodes reduces voltage pickup by a function of unit area, driving the need for composite analysis. Comp-16 has an SNR near the 10dB threshold, while Comp-4 is slightly better around 15dB. A higher SNR is indicative of a cleaner and more reliable signal, which can be trusted more when integrated into the control of LLP. Composites are of lower quality than Best-1, as signal combination will combine the best signal with lower quality signals. Within the size of the HDsEMG sensor field, some signals had lower SNR, lowering the overall SNR of Comp-16. Comp-4 maintained selectivity in the combination method, improving SNR. The standard signal saw minimal change in SNR with displacement, which has been attributed to low overall signal quality. In displacement, HDsEMG signals have the highest SNR along a single row/column, and the geometry of the composite configurations evaluated incorporate nodes of poor signal quality. Composite schemes that do not include fixed geometric configurations and are adaptive to sensor behavior over time need to be explored to maintain signal quality over a greater range of operating conditions. Future data analysis will evaluate signal composites for both SNR and RMS in all participants and activities.

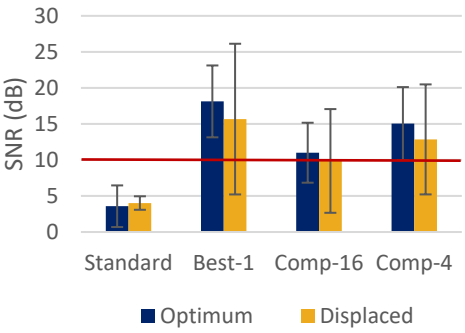

Figure 3: Average SNR +/- Standard Deviation computed of VL, SL, and BF, 8 straight walking trials of 1 participant for SsEMG and 3 HDsEMG configurations

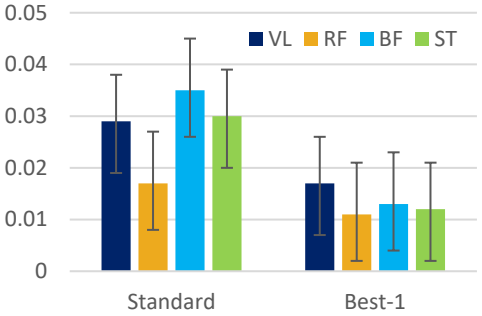

Figure 4: Previous analysis of normalized RMS in all participant trials for Standard and Best-1 Configurations, with standard error [4]

Significance: HDsEMG showed improvements in SNR over SsEMG. Improved signal quality from sEMG sensors can enable more integrated and robust control of lower limb prostheses through a natural human-machine interface.

Acknowledgements: Support from the NIGMS, NIH under grant number U54 GM104944.

References: [1] Gehlhar et al. (2023) Annual Reviews in Control (55); [2] Ahkami et al. (2022) IEEE TMRB (5-3); [3] Sinderby et al. (1995) J Applied Physiology (79-3); [4] Christensen (2022) Theses at Montana State; [5] Fraser et al. (2014) IEEE TIM (63-12)

A LOW-COST MOVEMENT ASSESSMENT SYSTEM CAN DETECT DUAL TASK DIFFERENCES IN COUNTERMOVEMENT JUMP PERFORMANCE

Jacob M. Thomas[1*], Jamie B. Hall, Trent M. Guess
[1]School of Health Professions, University of Missouri
*Corresponding author's email: jmt2mb@missouri.edu

Introduction: Recent findings in ACL injury literature indicate cognitive load during dynamic movement tasks may contribute to ACL injury mechanisms [1,2]. This presents a need for tools which mimic the simultaneous cognitive and physical demands of sport and can measure their effects on performance. Therefore, the purpose of this study was to use a low-cost movement assessment system to measure the effects of both visual and auditory cognitive dual tasking on countermovement jump performance.

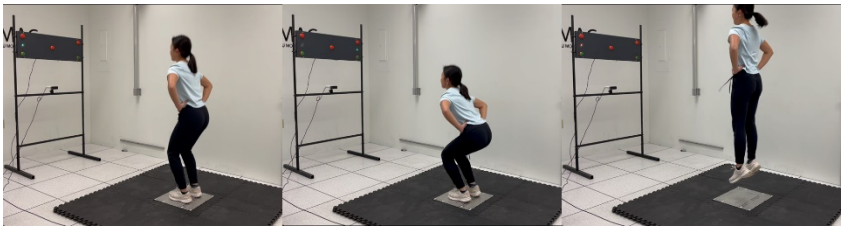

Figure 1. Participant Completing VDT CMJ Condition While Being Recorded by MPASS.

Methods: 31 recreationally active young adults (21.1 ± 1.9 yrs, 168.9 ± 11.8 cm, 69.1 ± 13.6 kg) participated in this study. Participants performed 3 trials of a countermovement jump (CMJ) under 3 different testing conditions: control (C), audio dual tasking (ADT), and visual dual tasking (VDT). All tasks were assessed using a low-cost system comprised of a custom force plate, depth camera with body tracking, and custom interface board (Figure 1). For the C condition, participants stood still with hands on hips until they saw lights on the interface board and then jumped as high as they could. For ADT, the interface board emitted high and low frequency tones during CMJ; participants reported the number of high tones. For VDT, green and red lights were emitted; participants reported the number of green flashes. Condition order was randomized with 3 trials collected in each condition. Data (Table 1) were normally distributed. CMJ test conditions were compared using one-way repeated measures ANOVAs. Post-hoc paired-samples t-tests were used to assess condition-based differences in outcome measures with significant ANOVA p-values. CMJ test conditions were compared using one-way repeated measures ANOVAs. Post-hoc paired-samples t-tests were used to assess condition-based differences in outcome measures with significant ANOVA p-values.

Table 1. ANOVA Results

Parameter	Avg ± Std 95% CI [ ]				Paired Samples t-test Cohen's *d* Effect Size		
	C	ADT	VDT	ANOVA	C vs. ADT	C vs. VDT	ADT vs. VDT
Time in Concentric Phase (s)	0.24 ± 0.05 [0.22, 0.25]	0.22 ± 0.05 [0.21, 0.24]	0.22 ± 0.05 [0.20, 0.24]	<.01*	<0.01* 0.29	<0.01* 0.33	0.51 0.05
Jump Height (m)	0.23 ± 0.06 [0.20, 0.25]	0.21 ± 0.05 [0.19, 0.23]	0.21 ± 0.06 [0.19, 0.23]	<.01*	<0.01* 0.29	<0.01* 0.26	0.57 -0.02
Eccentric Impulse (N-s/kg)	2.46 ± 0.42 [2.31, 2.62]	2.37 ± 0.46 [2.20, 2.53]	2.34 ± 0.46 [2.17, 2.51]	0.02*	0.04* 0.21	0.01* 0.27	0.49 0.06
Concentric Impulse (N-s/kg)	4.32 ± 0.52 [4.13, 4.51]	4.12 ± 0.53 [3.93, 4.32]	4.09 ± 0.54 [3.90, 4.29]	<.01*	<0.01* 0.39	<0.01* 0.43	0.52 0.05
Jump MKF (deg)	79.82 ± 10.80 [75.86, 83.78]	75.61 ± 11.53 [71.38, 79.84]	75.78 ± 11.33 [71.62, 79.94]	<.01*	<0.01 * 0.38	<0.01* 0.36	0.84 -0.01
Hip Flexion at Jump MKF (deg)	71.54 ± 14.42 [66.26, 76.83]	66.88 ± 14.06 [61.73, 72.04]	65.72 ± 13.87 [60.63, 70.80]	<.01*	<0.01* 0.33	<0.01* 0.41	0.31 0.08

*All p-values were adjusted using Benjamini-Hochberg to control for false discovery rate.

Results & Discussion: Results (Table 1) indicate a significant decrease in jump height, concentric phase time, concentric and eccentric impulse, and peak knee flexion at jump between both ADT and VDT conditions and C. Both ADT and VDT negatively impact CMJ performance, and these effects can be measured using a low-cost assessment tool. Findings provide support for future work to develop tools for risk assessment, rehabilitation monitoring, and ACL return-to-play decision-making in athletics.

Significance: These findings demonstrate the effects of auditory and visual cognitive tasks on dynamic motor task performance while also indicating promise for addressing the clinical need for multidimensional objective tools to inform precision rehabilitation.

References: [1] Avedesian et al. (2022), *Am J Sports Med* 50(2); [2] Bertozzi et al. (2023), *Sports Health 15*(6)

KNEE MUSCULATURE CO-ACTIVATION IS ALTERED BY PROLONGED LOAD CARRIAGE

Matthew V. Robinett[1*], Samantha M. Krammer[1], Micah D. Drew[1], Tyler N. Brown[1]
[1]Boise State University, Boise, ID, USA
*Corresponding author's email: matthewrobinett@u.boisestate.edu

Introduction: Prolonged (> 60 minutes) walking with heavy load (> 15 kg) is common military task that contributes to a high rate of musculoskeletal injury by increasing lower limb joint moments and muscular activity, and stiffening the knee and ankle joints [1]. Yet, it is unknown if knee and ankle joint stiffness, and activity of the joint's musculature continually increase throughout prolonged load carriage. We hypothesize that knee and ankle joint stiffness, and muscle co-activation will increase with heavy load, and throughout the prolonged load carriage task.

Methods: 11 participants had lower limb neuromechanics quantified during an over-ground walk task with three body borne loads (0 kg, 15 kg, 30 kg). For the walk task, participants walked 1.3 m/s continuously for 60 minutes, and neuromechanics data (joint biomechanics and muscle activation) was recorded at minutes: 0, 15, 30, 45, and 60. At each time point, participants walked 1.3 ± 5% m/s through capture volume three times and contacted force platform with their dominant limb.

During each trial, synchronous 3D marker and force plate data were collected with 10 high-speed optical cameras (240 Hz) and single force platform (2400 Hz), while 4 surface electromyography electrodes (2400 Hz) recorded knee and ankle muscle activity. The marker and force plate data were low pass filtered (12 Hz, 4th order Butterworth) and processed in Visual 3D to calculate knee and ankle sagittal plane biomechanics. Then, knee and ankle torsional joint stiffness were calculated according to [3]. Dominant limb vastus lateralis (VL), tibialis anterior (TA), lateral hamstring (LH), and gastrocnemii (GAS) muscle activity were high-pass filtered (20 Hz; 4th order Butterworth) to remove motion artifact, and then, rectified and low pass filtered (10 Hz; 4th order Butterworth) to create a linear envelope. Filtered signal was normalized to corresponding MVICs, and then, VL:LH and TA:GAS co-activation were quantified according to [3] during pre-activity (100 ms prior to heel strike) and weight acceptance.

Knee and ankle joint stiffness, and VL:LH and TA:GAS co-activation were submitted to a repeated measures ANOVA to test the main effects and interactions between load (0, 15, and 30 kg) and time (0, 15, 30, 45, and 60 minutes). Alpha level was 0.05.

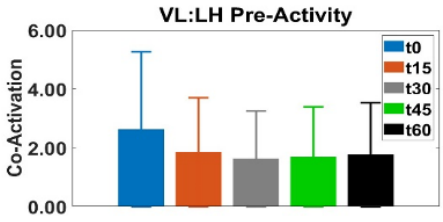

Figure 1: Depicts average VL:LH co-activation during the pre-activity phase at each time point.

Results & Discussion: Although knee and ankle joint stiffness reportedly increase up to 38% with body borne load [2], the current participants did not exhibit similar increases with load (both: $p>0.05$). Considering participants exhibited an insignificant 19% and 81% increase in knee and ankle joint stiffness with the addition of the heavy, 30 kg load, further work is needed to determine if the lack of statistical significance can be attributed to insufficient sample size. Load, however, did impact VL:LH co-activation during weight acceptance ($p=0.008$), which increased 38% with the 30 kg compared to the 0 kg load. Interestingly, participants increased knee co-activation without a corresponding increase in knee joint stiffness during the loaded walking. Additional study is needed to determine whether participants can increase co-activation without constraining the joint flexion that would stiffen the joint.

Contrary to our hypothesis, time impacted VL:LH co-activation, but not joint stiffness. Both pre-activity and weight acceptance phase VL:LH co-activation decreased 41% and 55% at minute 60 compared to minute 0 ($p=0.017$; $p=0.04$, respectively; Fig. 1). The decrease in VL:LH co-activation may be attributed to reduced LH activation or shift to a quadricep-dominant strategy after prolonged walking with load. As such, the participants may be increasingly reliant on quadriceps activation throughout the task, which may elevate their injury susceptibility.

Significance: Individuals who perform physical activity with heavy body borne load may rely on their knee extensors to attenuate the increased impact forces and prevent limb collapse. But, prolonged physical activity with load may increase this reliance, and military practitioners may need to incorporate hamstrings training into injury prevention or training programs to reduce fatigue-related injury exacerbated by a body borne load.

Acknowledgements: NIH NIGMS (2U54GM104944, P20GM109095, P20GM148321) supported this work.

References: [1] Santos et al., (2021), *JAB* [2] Brown et al., (2021), *JAB* [3] Don et al., (2007), *Clin Biomech*

Metabolic cost of transport is influenced by both walking speed and gait variability in people with Parkinson Disease

Dheepak Arumukhom Revi[1,2], Jenna A. Zajac[2], Franchino Porciuncula[2], Terry Ellis[2], and Louis Awad[1,2*]
[1]Department of Mechanical Engineering, Boston University, Boston, MA
[2]College of Health and Rehabilitation Sciences: Sargent College, Boston University, Boston, MA
*Corresponding author's email: louawad@bu.edu

Introduction: Humans naturally walk at speeds that minimize the energy cost of walking [1]. Walking speed is significantly affected by neurological diseases, such as Parkinson Disease (PD)—a progressive neurodegenerative disease characterized by substantial movement impairment [2,3]. Beyond slow walking speeds, gait deficits such as increased stide time varaiblity, are evident even in the early stages of PD [2,3] and contribute to reduced mobility and an increased fall risk [4]. The objective of this study is to examine the interplay between walking speed, stride time variability, and the metabolic cost of transport in people with PD. We hypothesize that both speed and stride time variability will influence the metabolic cost of transport. Specifically, we expect that gait variability will moderate the relationship between walking speed and the cost of transport, such that individuals with lower speeds and higher variability will have a higher cost of transport compared to those with higher speeds and lower variability.

Methods: Thirty-one individuals with mild to moderate PD (Age: 66 ± 9 year, Sex: 14F/17M, Onset: 6 ± 5 year, Hoehn-Yahr: 2-2.5) completed a 6-minute walk test (6MWT), with instructions to cover as much distance as possible. Subjects were instrumented with inertial sensors (Xsens) and an indirect calorimetry system (COSMED-K5) during the 6MWT, from which gait variability and the metabolic cost of transport were, respectively, computed. Gait variability was computed as the coefficient of variation of the stride times collected during the test [5]. The metabolic cost of transport was computed by dividing steady-state metabolic data by each subject's average 6MWT speed. A moderated regression model was used to predict the metabolic cost of transport as a function of walking speed, stride time variability, and their interaction. The interaction was further examined using a subgroup analysis, where individuals with lower walking speeds and higher gait variability (N=8) and individuals with higher walking speeds and lower gait variability (N=7) were grouped. Medians were used for the per-variable cutoffs. Between-group differences were tested using Kruskal Wallis tests.

Results & Discussion: As hypothesized, we observed a significant interaction between walking speed and stride time variability when predicting the metabolic cost of transport of individuals with PD. More specifically, the log of walking speed (β = -3.0, p=0.006), stride time variability (β = -2.0, p=0.06), and their interaction (β = 2.1, p=0.04) were associated with the metabolic cost of transport (R^2 = 0.45, F = 7.2, p=0.001). Across walking speeds, higher stride time variability was predictive of a higher metabolic cost of walking, especially among slower individuals (Figure 1, left). Our subgroup analysis quantified this interaction as a 41% higher metabolic cost of transport among individuals with slow speeds and high gait variability compared to individuals with fast speeds and low gait variability (Figure 1, right).

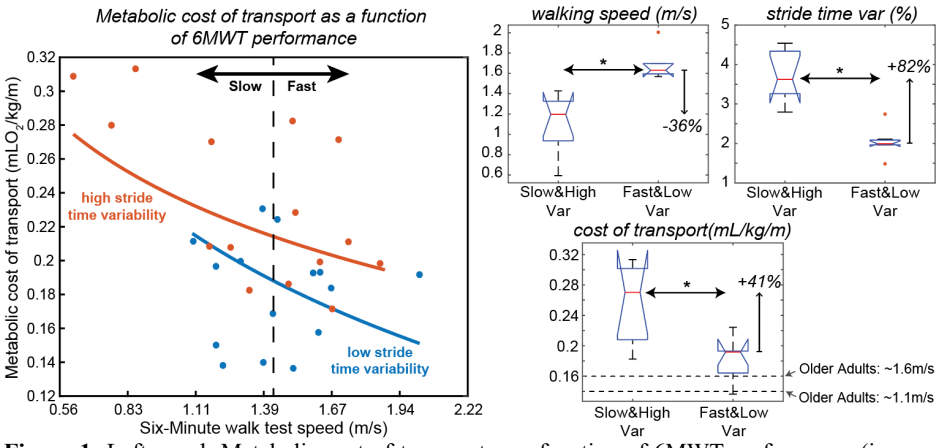

Figure 1: Left panel: Metabolic cost-of-transport as a function of 6MWT performance (i.e. avg speed and stride time variability). Right panel: Difference in walking speed, stride time variability, and metabolic cost of transport between slow individuals with high stride time variability vs. fast individuals with low stride time variability. Normative costs of transport for older adults, from [6].

It is especially notable that, when comparing those with high vs. low gait variability, we observed an upward and left shift of the expected U-shaped relationship between walking speed and the metabolic cost of transport. This finding is likely explained by PD-specific deficits that are not present in healthy aging. Indeed, when comparing the fast-speed and low-variability subgroup to older adults with similar walking speeds (i.e., 1.61 vs. 1.56 m/s), we observed comparable metabolic costs of transport (i.e., 0.19 vs. 0.16 mL/kg/m) [6]; In contrast, when comparing the slow-speed and high-variability subgroup to older adults with a comparable speed (i.e., 1.17 vs. 1.11 m/s), we observed a much higher metabolic cost of transport (0.27 vs. 0.14 mL/kg/m) [6]. Though, in older adults, slower walking closer to self-selected walking speed (from 1.56 m/s to 1.11 m/s) is associated with a 14% *improvement* in walking economy [6], we observed a 41% *worsening* in walking economy when comparing individuals with PD across these same speed levels.

Significance: This study highlights the metabolic consequences of increased gait variability in people with PD. Interventions designed to reduce gait variability have potential to markedly improve the walking economy of people with PD, especially for slower individuals.

Acknowledgments: The authors would like to thank all our study participants. Study data were collected as part of NCT05733819.

References: [1] Ralston (1958), Int. Z. Angew Physiol (17: 277-283); [2] Shulman et al. (2008), Mov Disorders (23(6)); [3] Nonnekes et al. (2018), Nat Rev Neurol (14:183-189); [4] Canning et al. (2014), Neurodegener Dis Manag (4: 203-221); [5] Arumukhom Revi et al. (2021), Sensors (21:6976); [6] Berryman et al. (2012), Eur J Appl Physiol (112: 1613-1620)

ELECTRICAL STIMULATION OF THE SOLEUS DURING WALKING MAY NOT AFFECT METABOLIC RATE

Ningzhen Zhao*, Lisa Griffin, Owen N. Beck
Department of Kinesiology and Health Education, University of Texas at Austin, TX
*Corresponding author's email: lareina@utexas.edu

Introduction: Neuromuscular electrical stimulation (NMES) is often used during rehabilitation and in clinical settings to improve walking neuromechanics [1]. But NMES is rarely used throughout daily life and in young neurotypical populations, perhaps due to its detrimental effects, including early onset of fatigue & increased metabolic rate vs. not using NMES [2].

We posit that the strategic use of soleus NMES may not increase metabolic rate during walking in young neurotypical adults. Soleus NMES can increase ankle extensor mechanical power output and local metabolic rate. Yet, this local increase in metabolic rate may be balanced by decreased proximal muscle metabolic rate. That is because increasing ankle extensor mechanical power is often balanced by reduced hip extensor mechanical power [3]. Moreover, the metabolic rate of operating the ankle is less than that at the hip [4]. Thus, NMES of the soleus may increase ankle mechanical power, thereby decreasing hip extensors mechanical power output, without increasing whole-body metabolic rate during walking.

Here, we investigated how NMES applied to the soleus during late-stance affects walking biomechanics and metabolism. We hypothesized that NMES of the soleus would modify walking biomechanics, but not metabolic rate, compared to walking without NMES.

Methods: Five young females (Avg ± SD; age: 25 ± 4 yrs; height: 175 ± 4 cm; mass: 74 ± 22 kg) performed 5 walking trials at 1.25 m/s on a split-belt force-instrumented treadmill. After a 5-min treadmill familiarization trial, participants walked without NMES for 5 min before and after two 5 min trials with bilateral soleus NMES. There was 5-min rest between the first 4 trials, and 20-min rest before the last trial. During the NMES trials, we provided square-wave 200 µs pulses at 30 Hz NMES to the participants' soleus when the horizontal ground reaction force (GRF) was ≥0.1 of body weight (Fig. 1). The average duration of NMES was 0.29 s for each leg per stride. NMES intensity was individually tuned to the highest tolerable intensity for each participant. We measured how NMES affected GRFs, kinematics, and metabolic rate using open circuit spirometry and standard equations.

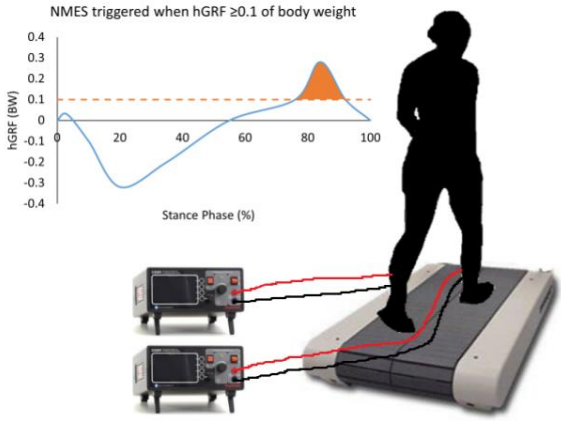

Figure 1: We applied bilateral soleus NMES during walking when horizontal GRF was ≥0.1 body weight.

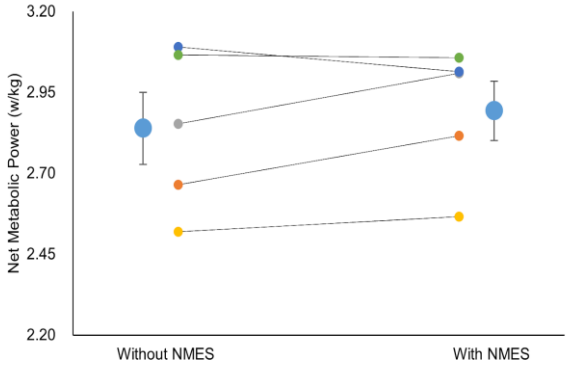

Figure 1: Average (±SE) (large symbols) and individual (small symbols) net metabolic power with and without NMES.

Results & Discussion: Walking with NMES applied to the soleus during 78-92% of stance did not change net metabolic power (with NMES: 2.89 ± 0.09 W/kg; without NMES: 2.84 ± 0.11 W/kg, p = 0.30) (Fig. 2). There was a small but significant decrease in duty factor when walking with NMES compared to without NMES (p = 0.02). There were no significant differences in peak GRFs, or step time with vs. without NMES (Table 1). Our future joint-level analyses will reveal whether NMES can modify ankle and hip neuromechanics without detectible changes in whole-body metabolism.

Table 1: Average (±SD) kinematics and GRFs data with and without NMES. * denotes statistical significance (p<0.05).

	Step time (s)	Duty factor*	Peak vertical GRF (BW)	Peak Propulsive GRF (BW)
Without NMES	1.093 ± 0.05	0.614 ± 0.02	1.071 ± 0.03	0.190 ± 0.00
With NMES	1.088 ± 0.04	0.612 ± 0.02	1.085 ± 0.04	0.199 ± 0.01

Significance: NMES is typically used to improve walking biomechanics during rehabilitation and in clinical populations [1]. Perhaps NMES can be used more broadly without increasing user metabolic rate during walking by stimulating the soleus during the late-stance phase of walking. Depending on our future findings, NMES may prove to be a useful technique that increases ankle mechanical power output, without causing undesired increases in metabolic rate.

References: [1] Kesar et al., (2009), Stroke. 40(12); [2] Muthalib et al., (2016), Eur. J. Transl. Myol. 26(2); [3] Fickey et al., (2018), J. Exp. Biol. 221(Pt 22); [4] Huang et al., (2015), J. Exp. Biol. 218.

GRIP STRENGTH DECREASES BRIEFLY AFTER BACKPACK CARRIAGE EXERCISE

Malea N. Lopez[1], Jennifer L. Hein[1], Nina B. Tong [1], Alan Aguirre [1], Katherine Saul[2], and Deanna J. Schmidt[1*]
[1]Department of Kinesiology, California State University San Marcos, San Marcos, CA
[2]Department of Mechanical and Aerospace Engineering, North Carolina State University, Raleigh, NC
*Corresponding author's email: djschmidt@csusm.edu

Introduction: Heavy backpack load carriage can place forces on the shoulder area that compress the nerves of the brachial plexus and blood vessels. Potential effects on the upper limbs from backpack straps can include changes in blood flow [1], nerve conduction [2] and consequently grip strength. Previous research investigated whether grip strength and pinch strength were impacted by walking for 45 min with a 40% bodyweight (BW) backpack load in male participants [1]. Grip strength showed no significant change when measured immediately after load carriage, however, after a seated recovery time, pinch strength for the non-dominant hand was decreased compared to a no backpack condition [1]. This study suggests that the timing of strength measurements after load carriage may be important. In another study it was demonstrated in lower limb muscles that there is muscle force depression in the first 30 min following several different regimens of metabolically and mechanically demanding exercise [3]. Due to the compression of the backpack straps, we expect that backpack carriage at 15% BW and 30% BW will lead to decreases in grip strength as compared to a no-load condition. Further, based on previous research [3], we hypothesize that the metabolically demanding exercise of backpack carriage will lead to decreases in grip strength within 30 min after exercise.

Methods: We measured 15 female (24.3±3.3 yrs, 152.9±37.3 kg, 166.3±7.1 cm) and 15 male (26.6±7.3 yrs, 196±31.6 kg, 181.6±11 cm) participants. Five participants (3 female) were left-hand dominant. Participants completed 3 load conditions: 1) no backpack, 2) 15% BW backpack, and 3) 30% BW backpack. Load conditions were completed in randomized order on separate days. Maximum grip strength was measured bilaterally using a dynamometer before and after participants walked on a treadmill at 1.1 m/s for 30 min per load condition. Maximum grip strength measurements were taken while participants were standing with their elbow at a 90° angle. We took 2 measurements for each hand alternating between hands. We used the maximum of the two trials for statistical comparisons. Grip strength was measured before they put the backpack on (PRE), after walking with the backpack still on (BP), and immediately after they doffed the backpack (DOFF). After DOFF, nerve conduction measurements were taken lasting 5 min and then grip strength was measured every 5 min for 30 min to investigate the possible timing of force depression after exercise (0 min to 30 min). Two-way RMANOVA with Bonferroni post-hoc testing was used to compare load conditions and timepoints. Level of significance was $p<0.05$.

Results & Discussion: For female participants, for the dominant hand there was a significant main effect of timepoint on grip strength ($F=2.858$, $p=0.034$, Table 1). Specifically, there was significant decrease in grip strength between PRE and DOFF timepoints. The decrease in grip strength between PRE and DOFF for females was on average .9 to 1.7 kg depending on load condition. In male participants, there was no difference among timepoints of grip strength measurements ($F=1.282$, $p=0.260$). However, grip strength for males was on average 0.4 to 1.5 kg lower at DOFF then PRE. Contrary to our hypothesis, there was no significant difference in grip strength among load conditions for male or female participants. This indicates that the decrease in grip strength may be due to the exercise and not the compression of the backpack straps on the nerves and blood vessels of the upper limbs. The results for the female participants also demonstrate that the timing of the grip strength measurements is important. Grip strength significantly decreased, supporting our second hypothesis, but then recovered to levels not significantly different from the PRE timepoint. However, our results differed from previous research [3] as the force depression did not last for 30 min after exercise.

Significance: The results reveal that the same physical activity caused a brief statistically significant decrease in grip strength for females, but not males. Grip strength remained on average within 1.5 kg of PRE measurements for males and recovered in females during the time measured. However, the data demonstrate that the timing at which grip strength is measured after exercise could affect results. For those who may use their hands after physical activity, such as first responders and military personnel, it is important that the decrease in grip strength was not prolonged.

Table 1: Mean ± SD grip strength in kg for the dominant hand of female (n=15) and male participants (n=15) measured before walking (PRE), after walking with backpack still on (BP), immediately after doffing the backpack (DOFF) and every 5 min after. *significant decrease from PRE timepoint

	Load %	PRE	BP	DOFF	0 min	5 min	10 min	15 min	20 min	25 min	30 min
Females	30%BW	28.6±4.5	28.1±4.7	26.9±4.8*	27.5±4.3	27.3±4.7	28.1±4.7	28.3±4.7	28.5±4.4	27.7±4.8	27.7±4.7
	15%BW	27.9±4.6	28±4.1	27.0±4.2*	28.8±4.6	28.0±5.0	28.4±5.0	28.5±4.3	28.6±4.7	28.7±4.2	29.0±3.8
	0%	28.8±5.7		27.8±5.0*	28.0±5.0	28.7±4.6	29.1±4.6	28.7±4.6	28.7±4.7	28.4±4.7	29.2±4.6
Males	30%BW	46.5±12.5	46.7±11.5	45.5±12.0	46.8±12.8	47.9±12.2	46.2±14.1	47.1±13.3	47.6±13.4	47.5±14	46.9±13.6
	15%BW	47.4±12.3	45.7±12.7	45.9±11.8	47.1±11.5	47.5±13.8	47.2±13.5	46.1±13	46.9±12.4	46.9±13.7	47.1±13.5
	0%	46.9±13.5		46.5±13.2	47.5±13.2	46.6±12.2	47.5±12.5	47.5±11.8	47.1±10.9	47.5±10.9	46.8±11.7

Acknowledgments: Research was supported by the NIGMS of the National Institutes of Health, Award Number SC3GM139683.

References:[1] Hein et al. (2021) *Appl Ergo* 97; [2] Schmidt et al. (2022) *IJES* 14(2); [3] Skurvydas et al. (2016) *EurJ Appl Phys* 116.

EFFECTS OF POSITIVE AND NEGATIVE SELF-TALK ON BALANCE AND POSTURAL SWAY IN COLLEGE STUDENTS

Fabricio Saucedo[1]*, Irene Muir[1], Venkata Naga Pradeep Ambati[2], Takehiro Iwatsuki[3]
[1]Department of Kinesiology, Penn State Altoona, Altoona, PA, USA
[2]Department of Kinesiology, California State University at San Bernardino, San Bernardino, CA, USA
[3]Department of Kinesiology and Exercise Science, The University of Hawaii at Hilo, Hilo, HI, USA
*Corresponding author's email: fns5045@psu.edu

Introduction: Self-talk is a frequently used psychological skill that involves reciting phrases aloud or internally [1]. Self-talk can enhance sport performance [2], based on the principle that what people say to themselves and how they say it affects performance-related outcomes [3]. These outcomes include enhancing confidence, reducing performance anxiety [4], and regulating effort [5]. Self-talk can also direct or redirect attentional to focus cues relevant for task success [6]. Despite the benefits of self-talk, few studies have examined its potential to improve activities of daily living, such as balance [7]. Self-talk has been found to improve static and dynamic balance in individuals with knee injuries [8] and intellectual disabilities [9]. Development of a low-impact training paradigm (i.e., self-talk) is essential for the growing aging population as the rate of accidental falls continues to increase, resulting in declining health or death. Therefore, the purpose of this study was to examine the effects of two different self-talk strategies on static balance and body stability during a single-leg balance task. Given negative self-talk hinders performance, and positive self-talk can enhance performance [1], it was hypothesized that use of the positive and negative self-talk would impact single-leg balance task performance accordingly.

Methods: Twenty-nine participants were randomly assigned to three groups: control group (n= 9), positive self-talk group (n= 10), negative self-talk group (n= 10). All participants performed a single-leg balance task on the right and left leg while reciting either a positive ("I am great at keeping my balance"), negative ("I am terrible at keeping my balance"), or no self-talk strategy (i.e., control). Spontaneous body sway (cm) was recorded with a force plate during three 30 second trials for each condition. Each leg and was used to calculate center of pressure and average body sway velocity in both anteroposterior and mediolateral direction. Motion data during these trials were used to compute the body center of mass displacement-velocity trajectory using known segmental parameter information. A 2 X 3 ANOVA was used to detect the effect of self-talk and corrected pairwise comparisons were used on any significant effects.

Results & Discussion: No significant differences (p >0.05) were detected in anterior-posterior center of pressure displacement and velocity, and anterior-posterior center of mass displacement and velocity of the right and left legs (Table 1). The results showed no performance effects associated with negative or positive self-talk; no benefits or decrements were observed between or within groups. These results do not support the hypothesis and oppose extant findings, which indicate a directional performance effect corresponding to the type of self-talk (i.e., negative or positive). Therefore, future studies are required to assess the impact of self-talk as a low-impact strategy for balance improvements.

Table 1 Performance changes (pre vs post) during the single-leg balance task for each experimental group.

	CON (n=9)	POS (n=10)	NEG (n=10)	p-value
AP COP Disp. (R)	2.78±1.53 vs. 3.63±1.43	2.45±1.39 vs 2.45±1.60	2.25±1.87 vs. 2.67±1.88	0.27
AP COP Disp. (L)	2.95±1.96 vs. 3.66±1.44	2.89±1.69 vs. 2.95±1.31	2.58±1.00 vs. 2.74±1.83	0.42
AP COP Vel (R)	4.01±0.69 vs. 3.44±0.63	3.76±0.56 vs. 3.36±0.60	3.95±0.94 vs. 4.09±1.38	0.19
AP COP Vel (L)	3.17±1.74 vs. 2.53±0.85	3.81±0.83 vs. 3.81±1.25	3.51±0.97 vs. 3.92±1.15	0.73
AP COM Disp. (R)	0.25±0.19 vs. 0.24±0.36	0.01±0.01 vs. 0.01±0.003	0.01±0.003 vs. 0.01±0.01	0.99
AP COM Disp. (L)	0.20±0.25 vs. 0.24±0.38	0.17±0.27 vs. 0.21±0.39	0.28±0.21 vs. 0.26±0.32	0.57

Values are n, mean ± standard deviation, or as otherwise indicated and acquired with a 2 X 3 ANOVA. Center of pressure displacement (cm), center of pressure velocity (cm/s), center of mass displacement (cm).

Significance: Future studies will aim to refine current methods, as single leg balance represents a vital component of activities of everyday living. This is particularly true for future applications of the self-talk strategy among older adults and other populations with gait and balance deficits. If successful, self-talk can offer an alternative to other training paradigms to decrease the risk of falling and improve balance and overall quality of life in at-risk groups.

References: [1] Monroe-Chandler & Hall, (2016). *Imagery*. Routledge International Handbook of Sport Psychology.
[2] Hardy et al. (2009). *The Sport Psychologist*, *23*(4), 435–450
[3] Ellis, (1976). *Reason and Emotion in Psychotherapy*. Lyle Stewart.
[4] Hardy et al., (1996). *Understanding Psychological Performance Preparation for Sport*. John Wiley e Sons Ltd.
[5] Williams et al., (2015). *Applied sport Psychology: Personal Growth to Peak Performance.* 274–303.
[6] Nideffer & Sagal, (1993). *Applied Sport Psychology: Personal Growth to Peak Performance*, *2*, 243–261.
[7] Araki et al. (2006). J*ournal of Sport Psychology,* 8(4).
[8] Beneka et al. (2013). *European Journal of Physiotherapy*, 15(2).
[9] Rai et al. (2015). *Applied Sciences,* 4(6).

THE IMPACT OF REMOVABLE CAST WALKER DESIGN ON METABOLIC COSTS OF WALKING AND PERCEIVED EXERTION

Emily Standage[1], Dylan Tooky[1], Uchechukw Ukachukwu[2], Marco Avalos[2], Ryan Crews2, Noah J. Rosenblatt[2*]
[1]Chicago Medical School, Rosalind Franklin University of Medicine and Science
[2]Center for Lower Extremity Ambulatory Research (CLEAR) , Rosalind Franklin University of Medicine and Science
*Corresponding author's email: noah.rosenblatt@rosalindfranklin.edu

Introduction: Up to 34% of persons with diabetes will experience a diabetic foot ulcer (DFU) within their lifetime [1], with 25% of nonhealing ulcers leading to amputation [2]. Clinicians commonly prescribe removable cast walkers (RCWs) to offload DFUs due to ease of fitting and use [3] However, healing outcomes tend to be worse with RCWs compared to irremovable options[4], which may reflect low adherence [5] resulting from the negative impact of RCW on the user's experience. For example, RCWs add mass to the foot and promote offloading through ankle immobilization which limits push-off and increases the work requirements of the other joints [6]. Collectively this may contribute to greater metabolic demands of walking with the device, which is critical for patients with DFUs given that they have a lower tolerance for increased metabolic demands [7]. Moreover, RCWs typically include a thick rocker bottom sole, which induces a limb length discrepancy that can further contribute to greater oxygen consumption and higher ratings of perceived exertion when walking [8]. The purpose of this study was to evaluate the effects of different commercially available RCW options on the metabolic costs and perceived exertion of walking in healthy participants as an initial step to understanding factors that may impact RCW adherence in patients with DFUs. Specifically, we sought to evaluate the effects of reducing the height of the RCW encasements (i.e. reducing mass and extent of ankle immobilization) and of providing a contralateral shoe lift to limit induced limb-length discrepancies.

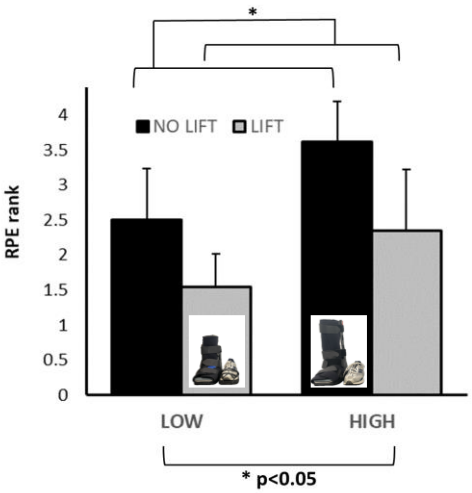

Figure 1: Rating of perceived effort (RPE) for each of the four RCW conditions relative to each individual. Data for each participant's RPE data was rank-transformed and then entered into the analysis. A rank of 1 is used for the lowest RPE and a 4 for the highest RPE. RCW strut height and contralateral lift had a main effect on RPE

Methods: A sample of fourteen young adults (age: 25.71±2.87 years) were recruited under the Institutional Review Board-approved study. Participants walked on a treadmill at a standardized speed (Froude number of 0.20) for six minutes under five footwear conditions: 1) athletic shoes only (control); 2) ankle-high RCW on the dominant limb (LOW in Figure 1) with athletic shoe on contralateral limb; 3) condition two with an external lift on the athletic shoe; 4 and 5) conditions two and three with a knee-high RCW (HIGH in Figure 1). During all conditions a portable calorimeter recorded gas exchange on a breath-by-breath basis. The metabolic costs of transport (MCoT) was quantified as the mean oxygen consumed per meter walked per kilogram body mass, after accounting for oxygen consumed during two minutes of quiet standing. After walking, participants reported perceived exertion using the Borg Rating of Perceived Exertion scale (RPE). For each outcome, statistical tests compared each RCW conditions with the control, and tested for main effects of RCW height (ankle-high (HIGH) vs knee high (LOW)) and of the lift.

Results & Discussion: MCoT and RPE were significantly higher for all RCW conditions compared to the control. There was no effect of RCW height or of lift on MCoT. In contrast, RPE was significantly lower using the ankle- vs. knee-high RCW and when using a lift (Figure 1). Although we anticipated certain aspects of the RCWs would contribute to changes in MCoT, ultimately, there are a number of interacting factors (e.g., level and timing of muscle activity, degree of stability, and asymmetries in spatiotemporal gait kinematics) that can contribute to metabolic costs; changes in one factor that would be expected to reduce costs could be offset by changes in another that raises costs. Moreover, the change in mass between the high and low boot, which was concentrated proximally, may have been insufficient to observe significant effects on MCoT. Nonetheless, assessments of perceived mass are important to consider regarding adherence to diabetic footwear [9]. Perceived effort need not be causally linked to physiological indicators of intensity. For patients with diabetes, consideration of perceived effort may be particularly important with regard to dictating behavior, given that these patients perceive harder effort for the same amount of work [10].

Significance: Although the cost of transport was unaffected by changes in the design of the RCW, perceived exertion was reduced through design changes. Future work should seek to directly evaluate the impact of RCW design changes on perceived exertion in patients with active DFU and the relationship to RCW adherence and wound healing Reductions in offloading due to reduced strut height, which could negatively impact healing, may be compensated for by improved user experiences that promote RCW use.

Acknowledgments: The work was partially supported by NIDDK under award numbers T35DK074390 and R01DK131303.

References: [1] Armstrong et al (2017) *NJEM*, 376(24); [2] Hoffstad et al (2015) *Diab Care* 28(10); [3] Raspovic et al (2014) *J Foot Ankle Res* 7(1); [4] Gutekunst et al (2011) *Clinic Biomech* 26(6); [5] Crews et al (2016) *Diab Care* 39(8); [6] Vanderpool et al (2008) *Gait & Pos* 28(3); [7] Regensteiner et al (1998) *J App Phys* 85(1); [8] Gurney at el (2001) *JBJS* 83(6); [9] Ababneh et al (2022) BMJ Open Daib Res Care 10(1); [10] Huebschmann et al (2009) *App Phys Nut Met* 34(5).

USING DYNAMIC JOINT SPACE DURING PHYSIOLOGICAL LOADING TO OBJECTIVELY MEASURE HIP STABILITY

Edward Godbold*, Connor Luck, Camille Johnson, Ashley Disantis, Craig Mauro, Michael McClincy, William Anderst
Department of Orthopaedic Surgery, University of Pittsburgh, Pittsburgh, PA, USA
*Corresponding author's email: edg54@pitt.edu

Introduction: There are currently no objective measures of dynamic hip stability that can reliably classify patients according to their functional instability. For example, there is no gold standard for differentiating normal joint motion from instability associated with femoroacetabular impingement (FAI) or from instability caused by acetabular dysplasia (AD)[1]. Finding an accurate method for characterizing hip instability might therefore help guide treatment decisions as well as evaluate the success of treatments aimed at restoring stability. The change in distance between the femur and acetabulum subchondral bone surfaces during physiological loading[2] could serve as an objective measure of functional joint stability. However, there remains a lack of evidence indicating which hip regions and activities are most appropriate for this novel, objective measure of hip instability. The aims of this analysis were to quantify dynamic hip joint space in radial and sagittal regions of the acetabulum and to determine side-to-side differences (SSD) and sex differences in dynamic hip joint space of healthy controls in order to provide a reference for stable hip motion.

Methods: 24 healthy adults (13F, 11M; age 21.9±2.2 years; BMI 21.5±5.0 kg*m^2/s) consented to be included in this IRB-approved study. Synchronized biplane radiographs were collected at 50 images/sec for 1 second (80 kV, 320mA, 4 ms exposure, 3 trials per hip) during treadmill walking at a self-selected speed and squatting. Subject-specific bone models were created by segmenting computed tomography (CT) scans of each participant's femur and pelvis. Bone motion was determined by a validated volumetric model-based tracking technique that matched digitally reconstructed radiographs created from the bones to the radiographs with submillimeter accuracy during each trial (bias: 0.2˚, 0.2 mm; precision: 0.8˚, 0.3 mm)[3]. Anatomic coordinate systems were established in each femur and hemi-pelvis[4], mirrored to the contralateral side, and co-registered to produce identical coordinate systems for each hip. The acetabulum was split into fifteen regions comprising five radial regions[2] and three sagittal segments (medial, middle, lateral). For each motion frame, the minimum subchondral bone distance in each of the radial and sagittal acetabular regions was identified and normalized to gait cycle (walking trials) or hip flexion (squat trials). The change in minimum gap within each respective acetabular region was determined for each trial as the difference between the smallest and largest minimum gaps. Differences between acetabular regions, SSD, and sex differences were identified through a repeated measures linear model with one within-subject factor (acetabular region) using IBM SPSS statistics (α=0.05, Version 28) and Benjamini-Hochberg correction for comparisons across multiple acetabular regions.

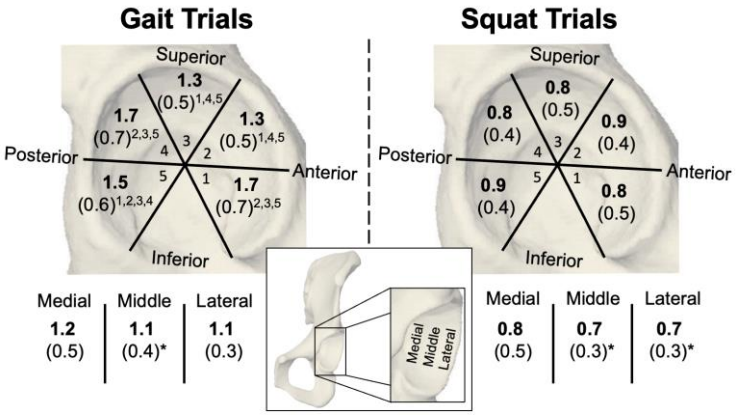

Figure 1: Average dynamic change in minimum joint space (bold font, standard deviation in parentheses; unit: mm) during gait and squat trials, separated into five evenly-spaced radial acetabular regions (1=anterior inferior, 2=anterior superior, 3=superior, 4=posterior superior, 5=posterior inferior) and three evenly-spaced sagittal acetabular regions that progress from in to out of the page. Superscript numbering indicates significant difference from the corresponding radial region. An asterisk (*) indicates significant difference of a sagittal region from the medial region.

Results & Discussion: 118 trials of walking and 97 trials of squatting were included in the analysis. The change in minimum gap during gait was larger in the anterior-inferior and posterior-superior regions than in the anterior-superior and superior regions (Fig. 1, p≤0.001). No differences in minimum gap were identified during squat. During both gait and squat, the average change in minimum gap varied no more than 0.1 mm between medial, middle, and lateral regions (Fig. 1). No significant SSD or sex differences were identified during gait (all SSD under 0.2±0.2mm with all p≥0.099; all sex differences under 0.2±0.2mm with all p≥0.206) or squat (all SSD under 0.1±0.2mm with all p≥0.161; all sex differences under 0.2±0.1mm with all p≥0.485). This data indicates that, for healthy hips, there is variability in dynamic stability between radial regions of the acetabulum during gait, with higher stability in the superior and anterior-superior regions but less stability in the anterior-inferior and posterior-superior regions. In contrast, dynamic stability in healthy hips is consistent during squat across radial regions of the acetabulum.

Significance: An objective method for characterizing hip stability under physiologic load is important for identifying, properly treating, and evaluating outcomes for patients with symptomatic hip pathology. Our results provide baseline values for dynamic hip stability in healthy hips and suggest stability is more variable during gait than during squatting. Future investigation will use similar methods to evaluate hip stability in surgical patients and to identify common clinical exams or imaging techniques that correspond to dynamic hip stability during physiological loading as measured using biplane radiography.

References: [1] Freiman et al. (2022), *Orthop J Sports Med* 10(2). [2] Lewis et al. (2023), *J Orthop Res* 41(1).
[3] Martin et al. (2011), *J Arthroplasty* 26(1). [4] Wu et al. (2002), *J Biomech* 35(4).

WOMEN WITH PATELLOFEMORAL PAIN SYNDROME EXHIBIT DIFFERENT MOVEMENT PATTERNS IN COMPARISON TO MEN: A SYSTEMATIC REVIEW AND META-ANALYSIS

Lucas Pallone[1, 2]; Felipe F. Gonzalez[1, 2]; Talissa Generoso[1, 2]; Rodrigo Saad Berreta[1]; Kaitlyn Joyce[1]; Eliane C. Guadagnin[2]; Jorge Chahla[1]; Jonathan A. Gustafson[1], Leonardo Metsavaht[2], Gustavo Leporace[2]
[1]Rush University, Chicago, IL, [2]Instituto Brasil de Tecnologias da Saúde, Rio de Janeiro, RJ, Brazil
Corresponding author: gustavo@biocinetica.com.br

Introduction: Patellofemoral pain (PFP) is a prevalent musculoskeletal condition with significant social and economic impact. Biomechanical factors, including abnormal lower limb mechanics, are implicated in PFP [1]. While there is a higher incidence of PFP among women [2], it is uncertain whether differences in movement patterns are observed between men and women with PFP during functional activities. Therefore, the aim of this systematic review is to identify the current evidence regarding biomechanical differences between men and women with PFP during functional activities.

Methods: A systematic review was conducted following PRISMA guidelines. PubMed/MEDLINE, Embase, Scopus, CINAHL, Cochrane CENTRAL Register of Controlled Trials, Cochrane Database of Systematic Reviews, and Google Scholar databases were searched from inception to January 10th, 2024. Studies comparing the biomechanics of men and women with PFP in functional tasks were included. Studies with mixed-gender cohorts or solely focusing on a single gender were excluded. A meta-analysis and a qualitative descriptive analysis were conducted with kinetic and kinematic outcomes.

Results & Discussion: Four studies [3-6] (Level of Evidence: IV) consisting of 146 patients met the inclusion criteria and reported gender differences in kinematics across single-leg squats, step-down, and mini-squats. Meta-analysis identified that women with PFP exhibited greater peak hip adduction and peak knee abduction in comparison to men. Qualitative analysis showed that these differences may extend to hip internal rotation, femoral adduction, and tibial abduction. Limited kinetic data showed non-significant differences between the two genders. Methodological quality ranged from moderate to high quality for the included studies.

Table 1 – Meta-analysis of gender differences in hip kinematics during single-leg squats.

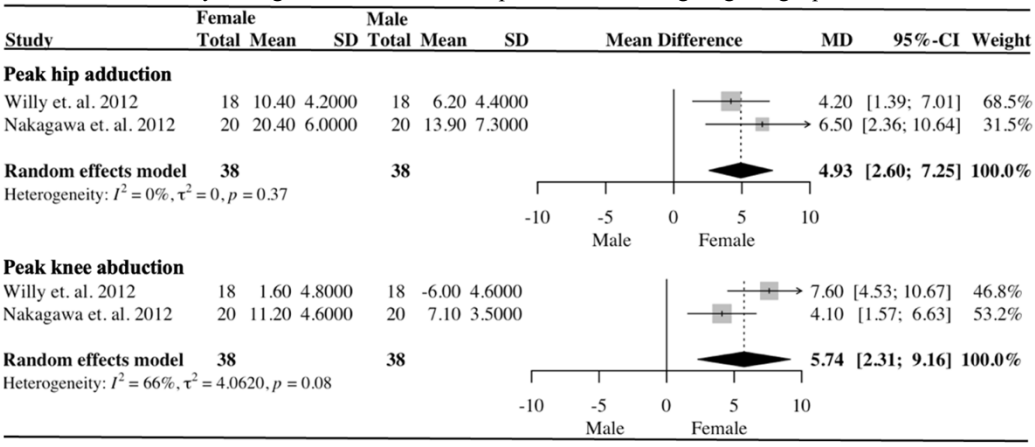

SD = standard deviation; MD = mean difference; CI =. confidence interval

The most significant finding of this systematic review was the consistent observation of gender-related differences in kinematics among individuals with PFP, across diverse functional activities. Females presented increased knee valgus (knee abduction) and hip adduction during a step-down task and single-leg squat. Despite most studies reporting biomechanical gender differences being published over a decade ago, a substantial portion of the identified studies still rely on mixed-gender cohorts (27). This review also identified that 83 out of 84 (98%) single-gender studies were based solely on female cohorts. While this is justified, given the higher prevalence of PFP in females, neglecting the distinct biomechanical characteristics of males risks misinterpreting the factors contributing to PFP in this population.

Significance: This systematic review and meta-analysis reveal that current evidence suggests distinct movement patterns between men and women with PFP during the execution of functional tasks. However, biomechanical research exploring these gender differences remains scarce. Most of the knowledge in the field is based on studies focused on female cohorts only. Consequently, therapeutic interventions and injury prevention programs derived from these studies may fail to address the specific needs of male patients. Future studies with robust methodologies are crucial to understanding the distinct biomechanical characteristics of PFP in each gender.

References: [1] Powers et al. (2017), *Br J Sports Med*. 51(24), [2] Smith et al. (2018), Screen HR, ed. *PLoS ONE*. 13(1), [3] Willy et al. (2012), *Med Sci Sports Exerc*.44(11), [4] Nakagawa et al. (2012), *J Orthop Sports Phys Ther*.42(6), [5] Nakagawa et al. (2013), *Int J Sports Med*. 34(11). [6] Hassan et al. (2023), *Hong Kong Physiother J*.43(2).

Pitching Biomechanical Changes During Long Innings Of A Division-I Collegiate Baseball Game

Matthew P. Valencia[1,2*], Bryson H. Nakamura[1,2], Nicole S. Pham[1], Michael T. Freehill[1,2]
[1]Department of Orthopaedic Surgery, Stanford University School of Medicine, Stanford, CA
[2]Stanford Baseball Science Core, Stanford University, Stanford, CA
*mpvalenc@stanford.edu

Introduction: During a baseball game, maintaining pitching performance is essential for in-game success. Pitchers must sustain pitch velocity levels and command in order to execute during the course of the game. Previous research done by Whiteside et al. (2016), showed that pitch velocity changes and becomes more variable across the game. Concerning these changes in pitch velocity, it is hypothesized that pitching biomechanics may change. Escamilla et al. (2007) conducted a study during a lab-based simulated game with results demonstrating that pitch velocity and forward trunk tilt differed in the final inning compared to the first two innings. It remains unknown how pitching mechanics change during live play of a long inning. This atypical spike in workload within an inning may lead to changes in pitching mechanics or pitch velocity. Therefore, the aim of this study was to determine if there are in-game biomechanical and pitch velocity changes during the course of a longer inning. Our hypothesis was pitch velocity would decrease and baseline biomechanics would change.

Methods: Ninety-one (91) male NCAA Division-I pitchers were included this study. Data was collected during the 2022-2023 NCAA Season then filtered using the following inclusion criteria: 1) recorded at least one (1) appearance in a collegiate, regular season game and 2) pitched a minimum of greater than 15 pitches in an inning. If a pitcher logged more than one (1) inning with greater than 15 pitches, only the longest inning was included. Ball tracking data was collected via TrackMan In-Stadium V3 (Vedbæk, Denmark). Videos of pitching events were collected during each game using an in-stadium, eight (8) camera Markerless Motion Capture System and processed using KinaTrax computer vision software (Boca Raton, FL) to derive joint-center tracking data (Pitching Model v6.3.9). Kinematics were calculated from C-Motion Visual 3D software (Boyds, MD). Ball tracking data and Markerless Motion Capture data were time-synchronized for each pitch to conduct analysis. Kinematics assessed were: Max Center of Mass Anterior/Posterior Velocity (CoM A/P Vel Max), Center of Mass Anterior/Posterior Velocity at Foot Contact (CoM A/P Vel FC; positive: toward home plate), Stride Length as a percentage of Body Height, Step Width (positive: lead leg closed with respect to the rear foot), Max Elbow Extension Velocity (MEEV), Max Shoulder Rotational Velocity (MSRV), Max Pelvis Rotational Velocity (MPRV), Max Trunk Rotational Velocity (MTRV), Lead Knee Angle Velocity Max, Lead Knee Flexion Velocity at Ball Release, and Trunk Flexion at Ball Release. A mixed-effects linear regression model ($\alpha<0.05$) was used to determine the effect of pitching greater than 15 pitches in an inning in comparison to the first 10 pitches thrown on various biomechanical variables related to pitch velocity.

Results: Pitch velocity showed a significant positive curvilinear trend in the pitches thrown after a count of 15 in comparison to the baseline first 10 pitches thrown in the inning (8.13 km/h (5.05 mph), = 0.004). Max CoM A/P Vel Max was observed to significantly increase in pitches thrown after 15 (16.69 cm/s, = 0.021). Table 1 highlights the results from both linear and quadratic regression models across pitch velocity and biomechanical kinematic variables of interest.

	CoM A/P Vel Max (cm/s)		**CoM A/P Vel FC (cm/s)**		**Stride Length (%BH)**		**Step Width (cm)**		**MEEV (deg/sec)**	
	Estimate	*p*	*Estimate*	*p*	*Estimate*	*p*	*Estimate*	*p*	*Estimate*	*p*
Pitch Count[1]	16.69*	0.021	-4.17	0.693	1.21	0.502	-4.50	0.223	-132.42	0.385
Pitch Count[2]	1.65	0.805	-1.12	0.909	-0.80	0.628	-5.94	0.079	-184.47	0.186
	MSRV (deg/sec)		**MPRV (deg/sec)**		**MTRV (deg/sec)**		**Lead Knee Angle Vel Max (deg/sec)**		**Trunk Flexion BR (deg)**	
	Estimate	*p*	*Estimate*	*p*	*Estimate*	*p*	*Estimate*	*p*	*Estimate*	*p*
Pitch Count[1]	-64.86	0.849	74.26	0.234	79.28	0.35	72.10	0.246	0.60	0.822
Pitch Count[2]	27.17	0.932	-8.36	0.883	59.12	0.456	64.79	0.257	-4.48	0.067
	Pitch Velocity (km/h)		**Lead Knee Flexion Vel BR (deg/s)**							
	Estimate	*p*	*Estimate*	*p*						
Pitch Count[1]	4.02	0.207	112.33	0.095						
Pitch Count[2]	8.13*	0.004	-3.89	0.949						

*1Linear regression model; 2Quadratic regression model; *p < 0.05*

Table 1: Regression Results of Biomechanical Variables and Pitch Velocity

Discussion: During a long inning, pitch velocity demonstrated a significant curvilinear trend where velocity decreased after pitch 15 then trended towards an increase back to baseline at the end of the inning. This finding thus could be caused by multiple factors such as psychological internal motivation, coaches employing different in-game strategy, or the effect of a potential mound visit during a long inning. Further studies are recommended to evaluate these possible factors. As previously hypothesized, results demonstrated that CoM A/P Vel Max significantly increased. Given that there are no other significant differences among the other kinematic variables of interest, future research may look to identify if other kinematics are related to fluctuations in pitch velocity (e.g. lead leg block). Limitations of this study includes defining a long inning as pitching a minimum of greater than 15 pitches. It may be appropriate to increase the minimum pitch count to greater than 20. Another limitation of the current study was including all pitch types in the analysis. Pitch velocity variability may affect these results and future work should look at the effect of pitch type.

Significance: The results from this study may have implications for coaches, clinicians, and trainers who aim to understand the impact of long innings on health and performance. Understanding biomechanical changes during a long outing of an inning may affect performance and injury risk. Further studies based on these biomechanical changes are warranted.

References: Escamilla, R. F. et al (2007), AMERICAN JOURNAL OF SPORTS MEDICINE, 35(1), 23–33
Whiteside, D. (2016), International Journal of Sports Physiology and Performance, 11(2).

PHASE-SPECIFIC PLYOMETRIC PERFORMANCE ASYMMETRY IN ACTIVE ACL RECONSTRUCTED ATHLETES DURING SINGLE-LEG HOP TESTS

Kinyata J. Cooper[1*], C. Roger James[2] Larry Munger[2,] Phillip S. Sizer Jr. [2] John Harry[3], Troy L. Hooper[2]
[1]University of Florida, [2]Texas Tech University, [3]Texas Tech University Health Sciences Center
*Corresponding author's email: kinyata.cooper@ufl.edu

Introduction: Rate of force development (RFD) and ground reaction force (GRF) impulse are plyometric skills that reflect the neuromuscular system's capacity to react quickly[1]. Following anterior cruciate ligament injury and subsequent reconstruction (ACLR), reinjury risk increases as biomechanical deficits in movement control and joint load asymmetry increase[2]. Phase-specific movements should be considered to distinguish where deficits in movement control occur following ACLR[3]. Studies report deficits in eccentric and concentric impulse, suggesting compensatory strategies in load absorption and force production after ACLR[3,4]. However, these deficits may be influenced by the activity status of the ACLR population and the constraints of the specific task. It is important to evaluate movement control in multidirectional hops not only during later rehabilitation stages but also after full sport return[5,6]. Clinically, an interlimb asymmetry index is used to score hop test performance[7]; thus, this study used the same approach to investigate 1) eccentric and concentric phase differences in GRF impulse and RFD asymmetry indexes and 2) phase-specific differences between individuals who returned to full sports participation after ACLR and healthy controls during vertical and lateral single-leg hop tests.

Methods: Nineteen ACLR athletes participating in their sport (6-18 months post-surgery, 20.7 ± 3.7 years) and 19 active, healthy controls (21.4 ± 4.0 years) performed a single-leg drop vertical jump (SLDVJ) and single-leg standardized rebound side hop (SRSH) as part of a hop test battery. Hop test order and testing limb order were randomized. Three hop trials were captured with one minute recovery between trials to minimize fatigue. For the SLDVJ, participants stood on a 24-cm box on one leg, dropped down onto a force plate, jumped for maximum height, and landed on the same limb. The SRSH involved standing on one leg, then hopping 40 cm medially, and immediately back to the starting position. Here the rebound portion (the medial hop and return to start) was the movement of interest.

Eccentric phase was defined from the maximum negative to point of zero velocity. The concentric phase began at upward center of mass movement until take-off. RFD and GRF impulse are the slope of the line and area under the force-time curve, respectively. Asymmetry indexes were calculated using the following formula[4,8]: *ACLR = [(non injured limb – injured limb) / non injured limb + injured limb* 100]*. A positive value indicated non-injured limb dominance. *Control = [(dominant limb – non dominant limb) / non dominant limb + dominant limb* 100*]. A positive value indicated dominant limb dominance.

Mixed 2 (group: ACLR vs. Healthy) X 2 (phase: concentric vs. eccentric) ANOVAs compared asymmetry index differences during the SLDVJ and SRSH hops. A family wise correction adjusted the alpha: SLDVJ, $\alpha = .01$; SRSH, $\alpha = .025$.

Results & Discussion: During the SLDVJ, concentric **GRF impulse** asymmetry index was greater than the eccentric phase ($p = .01$, $\eta_p^2 = 0.09$). This highlights deficits in propulsion dominated by the injured limb (Figure 1A). There was no difference in GRF asymmetry indexes between groups ($p = .016$, $\eta_p^2 = 0.08$) following the alpha adjustment nor a phase by group interaction effect ($p = .10$, $\eta_p^2 = 0.04$). The ACLR and healthy group presented similar **RFD** asymmetry indexes across phase ($p = .19$, $\eta_p^2 = 0.02$) and across group ($p = .58$, $\eta_p^2 = 0.02$). There was no interaction effect ($p = .27$, $\eta_p^2 = 0.02$ Figure 1B).

During the SRSH, the ACLR and healthy groups presented similar **GRF impulse** asymmetry indexes across phase ($p = 0.84$, $\eta_p^2 < 0.01$) and across group ($p = .77$, $\eta_p^2 < 0.01$, Figure 1C). There were similar **RFD** asymmetry indexes across phase ($p = .76$, $\eta_p^2 < 0.01$) and across group ($p = .58$, $\eta_p^2 < 0.01$) (Figure 1D). There were no interaction effects for GRF impulse ($p = .93$, $\eta_p^2 < 0.01$) nor RFD ($p = .41$, $\eta_p^2 < 0.01$).

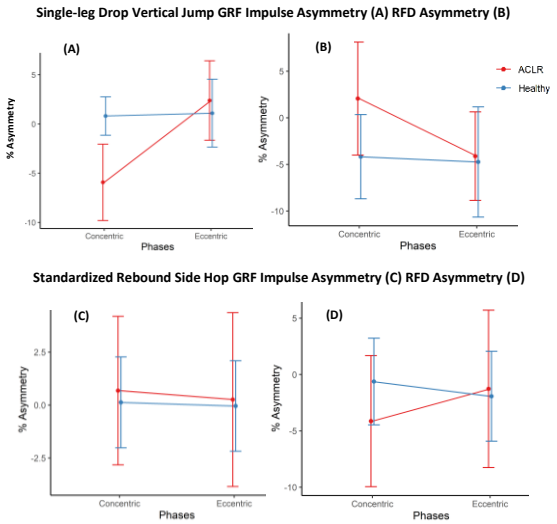

Figure 1: Anterior cruciate ligament reconstruction (ACLR) and healthy control group phase-specific asymmetry indexes during the Single-leg Drop Vertical Jump (top row) and Standardized Rebound Side Hop (bottom row) for ground reaction force impulse (A, C) and rate of force development (B, D). Values are means and error bars show 95% confidence intervals.

Significance: Phase-specific deficits in plyometric ability are present during a single-leg drop vertical jump but not a rebound side hop. This finding indicates plyometric deficits are task dependent and may persist longer in vertical tasks than side hops even after sports participation return. Interventions may target the concentric GRF impulse in the injured limb during a SLDVJ to improve movement control. This was the first study to evaluate phase-specific movements in a standardized side hop. The RFD and GRF impulse may not be useful variables during the SRSH at this performance stage. Further research is needed determine phase-specific implications on reinjury risk.

Acknowledgments: CH Foundation; NIH/NIAMS R21 AR077231

References: [1] Aagaard et al. (2002) *J Appl Physiol*. 93(4); [2] Gokeler et al. (2019) *Sports Med* 49(6); [3] Baumgart et al. (2017) *Orthop J Sports Med* 5(6); [4] Jordan et al. (2020) *Aspetar Sports Med* 4; [5] Buckthorpe, (2021) *Sports Med* 49(7); [6] Read et al. (2020) *J Athl Train;* [7] Reid et al. (2007) *Phys Ther* 87(9); [8] Bishop et al. (2016) *Strength Cond J* 38(6).

THE BROKEN WINDLASS: LOWER-LIMB BIOMECHANICS IN PATIENTS WITH PLANTAR FASCIITIS

Lucas Pallone[1,2], Pedro Benevides[1,2], Talissa Generoso[1,2], Felipe Gonzalez[1,2], Gláucia Bourdignon[1,2], Dov Rosemberg[1,2], Gustavo Leporace[2], Leonardo Metsavaht[2], Daniel Bohl[1], Jonathan A. Gustafson[1]
[1] Rush University, Chicago, IL. [2]Instituto Brasil de Tecnologia em Saúde, Rio de Janeiro, RJ. Email: Jonathan_A_Gustafson@rush.edu

Introduction: Plantar fasciitis (PF) is one of the most common causes of foot pain. It is estimated that one million Americans seek medical care every year to treat symptoms of PF [1]. Despite the high incidence, the pathophysiological mechanism is not completely understood. Recently, importance has been placed on the metatarsal-phalangeal joints and tension of the plantar fascia—the Windlass mechanism [2]. The goal of this study was to evaluate differences in gait measurements in patients with plantar fasciitis as compared to healthy subjects using a multi-segment foot model [3] to focus on the motion of the first metatarsal-phalangeal joint. Considering the plantar fascia anatomy, with its insertion on the base of the proximal phalanx of lesser toes as well into both sesamoids and consequently, to the hallux [4], we hypothesized that patients with plantar fasciitis present greater dorsiflexion of the hallux.

Methods: Data from an ongoing, prospective, IRB-approved study were analyzed from twelve individuals (5 with PF and 7 healthy subjects). Individuals underwent gait analysis using a 20-camera OptiTrack motion capture system (NaturalPoint, Inc., Corvallis, OR) and an embedded force plate system within a 12ft walkway. All subjects underwent repeated (n=5) walking trials at self-selected speeds and fast speeds (30% increase). All motion data was labeled and tracked in Motive and further processed using Visual 3D. A multi-segment foot model [3] was used to calculate maximum and minimum joint angles, as well as the range of motion (ROM) for the hallux and the medial forefoot (1st metatarsal-proximal phalanx) during the stance phase of gait. Lower limb range of motion and strength were also measured manually (using a handheld dynamometer and standard goniometer.

Results & Discussion: Kinematic results can be found in **Table 1.** Regarding the manual measurements, the angle of hallux dorsiflexion during standing was 79.06º for the PF group (SD=23.75), while the control group showed 93.34º (SD=19.06). The ROM of the first metatarsophalangeal joint for the PF group was 100.15º (SD=23.55) (the maximum 120.2º and minimum 59.93º). For the control group, the ROM was 115.92º (SD=27.50º) (the maximum 124.6º and minimum 72.6º).
Considering the force for plantarflexion of the hallux, the PF group showed a force of 63.33N (SD=31,74) while the control group was 69.50N (SD=28.30).
Contradictory to our hypothesis, the ROM of the hallux during gait was greater in the control group in comparison to the PF group. This finding was also present in previous studies [5]. One possible explanation for this finding is the possible mechanism of adaptation that the patient develops to avoid pain in the late stance phase [5]. The hallux ROM during standing also contributed to this finding, where the PF group showed lower ROM compared to the control group. Our findings should be taken in the context of our limitations. The multi-segment foot model used also showed several technical limitations including collinearity between segments which influenced the data quality and its analysis. Addressing the foot motion during gait using multi-segment foot models is of high importance for better understanding PF, its pathophysiological mechanism, and also for the development of treatment strategies. Future studies with more patients, which can overcome the challenges faced in the present study are required for improved conclusions.

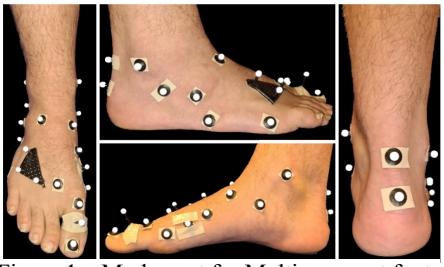
Figure 1 – Marker set for Multi-segment foot model (Ghent)

Significance: The present study contributes to a better understanding of the biomechanics of the foot during normal gait for patients with PF. Especially for analyzing the foot in six different segments and considering the relation between each of them. The main hypothesis could be questioned bringing focus to the pathologic mechanism of the disease. Another important achievement was to find technical barriers that can limit the research using the multi-segment foot models. Bringing those limitations into discussion is of main importance for future studies.

Table 1. Joint kinematics during normal and fast walking. PF=plantar fasciitis group

	Subject Groups	**Minimum angle, ° (Mean±SD)**		**Maximum angle, ° (Mean±SD)**		**ROM, ° (Mean±SD)**	
		Normal	Fast	Normal	Fast	Normal	Fast
Hallux vs Medial Forefoot (dorsiflexion)	PF (n=5)	23.82±6.89	22.67±7.09	62.16±14.74	61.91±13.49	38.33±16.50	39.23±15.90
	Controls (n=7)	20.18±9.73	20.57±9.83	74.22±10.94	76.25±11.81	54.03±8.75	55.68±9.49

References: [1] Riddle et al., FAI, 2004. [2] Hicks et al., J. of Anatomy, 1954. [3] de Mits et al., J. of Orthopaedic Research, 2010. [4] Wearing et al. Sports Med, 2006 [5] Pazhooman et al,. Gait Posture, 2023.

THE INFLUENCE OF SEX AND CENTER OF MASS VARIABILITY ON WALKING SPEEDS IN INDIVIDUALS BEFORE AND AFTER TOTAL HIP ARTHROPLASTY

Ogundoyin J. Ogundiran[1*], Steven A. Garcia[1], Rrita Zejnullahi[1], Kharma C. Foucher[1]
[1]The University of Illinois Chicago, Chicago, IL
*Corresponding author's email: oogund4@uic.edu

Introduction: Walking speed (WS) is highly associated with motor functioning, quality of life, and overall health [1]. Individuals with hip osteoarthritis (OA) walk slower than their healthy counterparts, and women often display slower WS than men. Following total hip arthroplasty (THA), patients often display increases in WS, but do not return to average healthy speeds [2]. Further, many patients face physical limitations after THA such as fatigue, insufficient physical activity, [3] and increased fall risk [4]. Women appear to be disproportionally affected compared to men. Center of mass (COM) displacement, trajectory, and variability may be linked to WS [5], metabolic cost [5], and postural stability [6]. Individuals with THA exhibit altered gait mechanics and slower WS, however the role in which THA impacts COM control, and the association with improvements in gait mechanics post THA is unclear. Thus, a better understanding of the relationships among WS, sex, and COM trajectory variability in individuals with hip OA undergoing THA could lead to targeted intervention plans to improve functional outcomes within these patients. We aimed to characterize the influence of sex and COM variability on WS before and after THA. We hypothesized sex and COM variability are associated with WS before and after THA. Specifically, 1.) COM variability is associated with WS, and faster WS will be associated with greater variability. 2.) Men will have faster WS and greater COM variability compared to women pre to post THA.

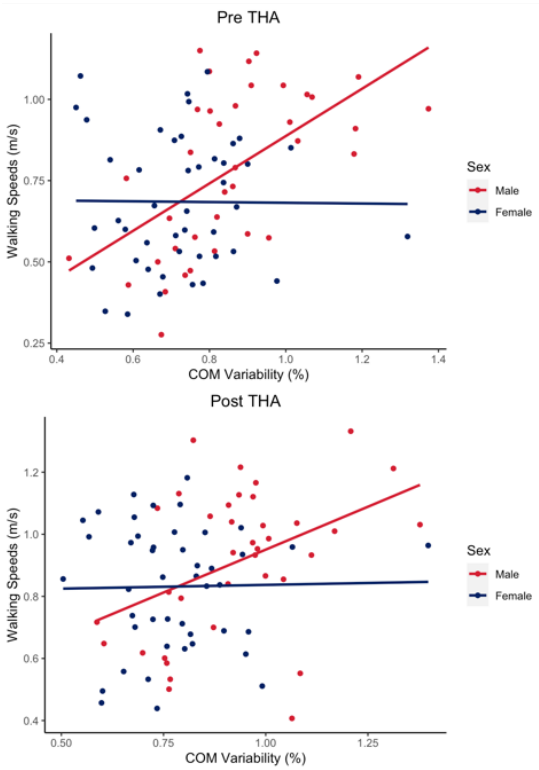

***Figure 1**: Scatterplots depicting associations between COM variability and Walking speed stratified by sex across Pre- and Post THA.*

Methods: Data was sourced from an open dataset [7]. 45 women (age 69 ± 9 years, height 1.59 ± 0.065 m, mass 69.5 ± 16.0 kg pre THA) and 37 men (age 66 ± 9 years, height 1.70 ± 0.072 m, mass 86.3 ± 16.2 kg pre THA) with hip OA underwent an overground gait assessment at self-selected comfortable speed before and 6 months after THA, using standard 3D motion capture methods. Each participant walked for at least 10 trials. The vertical trajectory of the COM and the WS for each trial were obtained from the dataset. The average speed among the walking trials for each participant was utilized to determine participant WS. The coefficient of variation (CV) of the COM vertical trajectory was calculated as 100 x (COM vertical trajectory Standard Deviation / COM vertical trajectory Mean) for each participant. The average COM CV and WS from all trials were utilized in the analysis (Table 1). Statistical analyses were completed using R (Version 4.3.3). A linear mixed-effect model was used to determine the association of sex and COM variability on WS before and after THA to account for the individual differences within a participant, at varying timepoints (pre and post THA) within one model.

	Pre THA		Post THA	
Sex	Females	Males	Females	Males
Walking Speeds (m/s)	0.69 ± 0.20	0.78 ± 0.25	0.83 ± 0.20	0.91 ± 0.24
COM Variability (%)	0.72 ± 0.16	0.86 ± 0.19	0.78 ± 0.16	0.93 ± 0.18

***Table 1**: Average Walking Speeds and COM Variability.*

Results & Discussion: WS in men and women pre to post THA was observed to be different pre to post THA ($p<0.001$), as well as in COM variability (Table 1). Both WS pre THA, and COM Variability pre THA were associated with WS post THA ($p=0.042$). There was no significance observed in the association specifically between sex and COM variability pre or post THA to WS post THA ($p=0.192$, $p=0.123$). These results partially supported our hypothesis that COM variability is associated with WS pre and post THA. This study however raises the question regarding how COM variability changes post THA, and how specifically this influences WS. We observed that COM variability and speed increased after THA. However, COM variability was not predictive of WS post-THA which suggests additional gait factors may be impacting associations between these variables which may be sex-specific. Additional research can investigate other aspects of gait variability integral to balance and function, such as trunk kinematics or step length. Lastly, future research can additionally consider alternative methods to characterize COM variability, specifically looking into non-linear analysis methods to quantify variability.

Significance: This study indicates that there is a relationship between COM variability and WS among participants, though these only existed pre THA. Our findings suggest that there may be unique mechanisms at play pre THA that may be impacted post THA recovery in individuals with hip OA. Future research can further explore the role COM variability has on WS, to determine the mechanisms that can further explain our findings.

References: [1] Middleton, A., et al. J of aging and physical activity. 23,2 (2015); [2] Bahl, J. S., et al. Osteoarthritis Cartilage.26,7 (2018); [3] Wallis J.A., et al. Osteoarthritis Cartilage (2013); [4] Smith, T. O., et al. J of Rheumatic Diseases 21 (2018); [5] Ortega, J., et al. JAP. 99,6 (2005); [6] Devetak, G. F., et al. Gait & Posture vol. 72 (2019); [7] Bertaux, A., et al. Scientific data vol. 9,1 (2022).

LOWER EXTREMITY STIFFNESS DURING RUNNING IN AN ADVANCED FOOTWEAR AND A MINIMAL SHOE

Li Jin[1*], Luisa Westley[1], JJ Hannigan[2]
[1]Department of Kinesiology, San José State University, San José, CA, USA
[2]Program in Physical Therapy, College of Health, Oregon State University – Cascades, Bend, OR, USA
[*]Corresponding author's email: li.jin@sjsu.edu

Introduction: The incorporation of carbon fiber plate technology into racing shoe design has been reported to enhance running performance. Specifically, this Advanced Footwear Technology (AFT) promotes the improvement of mechanical energy storage and return efficiency of the muscle tendon complex in the foot–ankle system [1]. Conversely, minimalist footwear advocates for a return to natural running mechanics, emphasizing proprioception during running.

The lower extremity stiffness reflects musculoskeletal system dynamic loading and response to the external loading during running. The joint stiffness reflects each joint movement coordination and neuromuscular control of movement [2,3]. Stiffness can serve as the indicator of the running performance and injury risk [3,4]. Despite the profound disparities in between the advanced footwear and the minimalist shoe, the comparative effects of the distinct footwear paradigms on lower body stiffness remain largely unknown. The purpose of the study was to compare joint and vertical stiffness between Nike NEXT% and a common minimal shoe. We hypothesized that the NEXT% would increase joint and vertical stiffness.

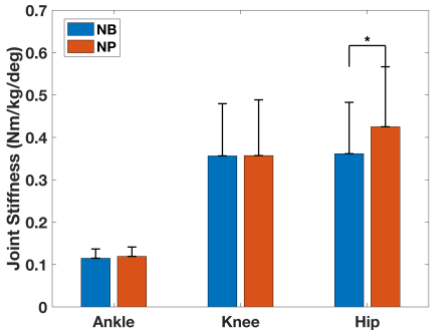

Figure 1: Group average (n = 12) joint stiffness between two shoes (NB and NP).

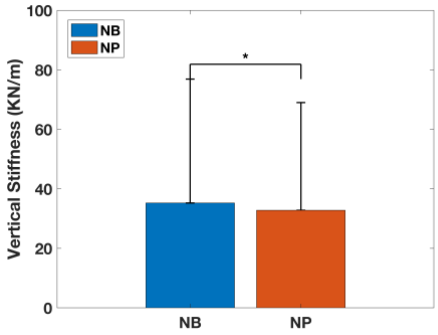

Figure 2: Group average (n = 12) vertical stiffness between two shoes (NB and NP).

Methods: Twelve healthy runners (10M, 2F; age = 21.0 $\pm$ 2.5 yrs; height: 174.8 $\pm$ 10.9 cm; mass: 62.2 $\pm$ 7.4 kg) participated in this study. Subjects ran overground in the lab at their marathon pace by wearing 1) the Nike Vaporfly NEXT% (NP), and 2) the New Balance Minimus (NB) shoes in random order. Twenty–one reflective markers and six marker clusters were placed on the pelvis and lower extremities. Five successful running trials were conducted per shoe while kinematic data were recorded at 100 Hz using a 16–camera motion capture system (Vicon Motion Systems, Oxford, UK). Ground reaction force data was collected by two force plates at 1000 Hz (Kistler Instrument Corp., Novi, MI, USA).

The kinematic and kinetic data were further processed via an inverse dynamics model in Visual3D software (C–Motion, Germantown, MD, USA). Joint stiffness (K_{joint}) was calculated as the sagittal plane change in joint moment (ΔM_{joint}) divided by the change in joint angular displacement ($\Delta\theta_{joint}$) during the first half of stance phase, based on the anterior–posterior ground reaction force [4]. Vertical stiffness (K_{vert}) was calculated as the peak vertical ground reaction force ($vGRF_{peak}$) divided by the whole–body center of mass (COM) vertical displacement (Δy) during the first half of stance phase [4]. All outcome measures were compared using paired *t*–tests (α = 0.05) in SPSS (V29.0, IBM, Armonk, NY, USA).

Results & Discussion: Hip joint stiffness (K_{hip}) was significantly higher in the NP shoe condition (p = 0.041, Figure 1). No statistically significant differences were observed for ankle (K_{ankle}) or knee joint stiffness (K_{knee}) between the NP and NB shoe condition. We further compared the change of joint moment (ΔM_{joint}) and angular displacement ($\Delta\theta_{joint}$) between the NP and NB shoes. We found both the ΔM_{ankle} (p < 0.001) and $\Delta\theta_{ankle}$ (p < 0.001) were significantly lower in the NP compared to the NB. Additionally, ΔM_{knee} was significantly higher in the NP (p = 0.003), while $\Delta\theta_{hip}$ was significantly lower in the NP compared to NB condition (p = 0.007).

For the vertical stiffness (K_{vert}) comparison, we found wearing the NP shoe significantly decreased K_{vert} compared to wearing NB shoe (p = 0.019, Figure 2). Moreover, wearing the NP shoe significantly increased whole body COM vertical displacement (p = 0.029).

Significance: Although there were no significant differences in K_{ankle} and K_{knee} between NP and NB shoes, NP shoes significantly reduced loading phase sagittal plane ankle range of motion (ROM) and the variation of ankle joint moment. This indicates NP shoes reduced the ankle joint dynamic loading and response during the first half of stance phase. This reduction could lessen the foot–ankle system muscle tendon complex mechanical work absorption and generation, which may be beneficial to reduce metabolic cost during running. Additionally, the higher K_{hip} in the NP shoe condition is primarily due to the decreased sagittal plane hip joint ROM. This indicates the advanced footwear may alter hip joint kinematics during the loading phase. Lastly, lower K_{vert} in NP shoe condition was due to the increased whole–body COM vertical displacement, which might be related to a larger NP shoe surface compression during loading [3]. Future studies should include leg stiffness and metatarsophalangeal (MTP) joint stiffness in comparisons between shoes.

Acknowledgments: The authors would like to acknowledge Junko Griffith for her assistance in data collection.

References: [1] Cigoja et al. (2021), *Sci Rep* 11(1), 749; [2] Hamill et al. (2014), *Eur J Sport Sci* 14(2), 130-136; [3] Borgia et al. (2019), *Footwear Sci* 11:1, 45-54; [4] Butler et al. (2003), *Clin Biomech* 18(6), 511-517; [4] Jin et al. (2022), *Biomech* 2, 441-452.

ADVANCING FITNESS MONITORING: ALGORITHMS FOR IMPROVED EXERCISE INTENSITY EVALUATION WITH ACCELEROMETERS

Wen-Wen Yang[1], Chun-Chen Lin[1], Yi-Chih Lin[2], Hsu-Fang Chang Chien[3], Tzyy-Yuang Shiang[3], Madelyn McCullen[4], and Vincent Chen[4*]
[1]Department of Sports Medicine, China Medical University, Taichung, Taiwan
[2]Office of Physical Education, Tunghai University, Taichung, Taiwan
[3]Department of Athletic Performance, National Taiwan Normal University, Taipei, Taiwan
[4]Department of Engineering, Loyola University Chicago, Chicago, IL, USA
*Corresponding author's email: cchen17@luc.edu

Introduction: Accurately estimating exercise intensity is pivotal for effective health management and physical rehabilitation [1]. Heart rate has been a primary indicator, yet concerns arise regarding skin irritation and allergies due to the physical contact required for measurement [2]. Moreover, as exercise intensity approaches maximum capacity, heart rate becomes limited by the maximum heart rate [3]. Seeking alternatives to address these issues, accelerometers offer a promising alternative [4]. However, our research hypothesis suggests that the accuracy of this estimation hinges on various factors including the type of activity (walking or running), the specific placement of the accelerometer [5], and the efficacy of the data processing algorithm employed. By comprehensively examining these variables, we aim to refine the estimation of exercise intensity, thus enhancing its utility in health monitoring programs.

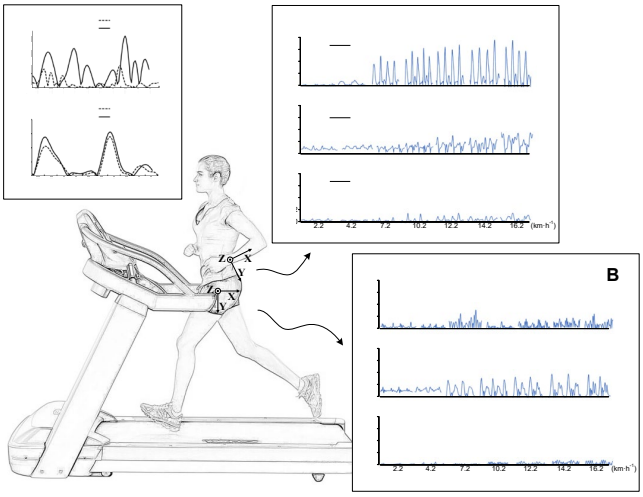

Figure 1: Anterior-Posterior, Vertical, and Medial-Lateral acceleration data acquired from A. wrist-worn and B. hip-worn accelerometers.

Methods: Seventeen healthy male participants, with an average age of 22.8 ± 3.0 years, height of 1.76 ± 6.2 m, weight of 67.7 ± 5.9 kg, and resting heart rate of 66.5 ± 7.0 bpm, were enlisted for the study. Heart rate was monitored for one minute in both lying and standing positions on a treadmill. Each participant underwent a preferred transition speed (PTS) assessment, a natural transition between walking and running [6]. Subsequently, they engaged in a discontinuous treadmill exercise test comprising three walking conditions (PTS−5 km·h-1, PTS−3 km·h-1, and PTS) and five running conditions (PTS+3, PTS+5, PTS+7, PTS+9, and PTS+11 km·h-1). Participants were required to wait until their heart rate returned to resting levels before proceeding to the next speed test. Tri-axial accelerometers were affixed to the volunteer's left hip and non-dominant wrist to capture acceleration data (Fig. 1), which was processed using algorithms such as integral acceleration, peak acceleration, and mean amplitude deviation (MAD) to compare with heart rate reserve (HRR).

Results & Discussion: Specifically, the integral algorithm effectively summed the accelerations of entire gaits, providing a comprehensive reflection of acceleration changes during running conditions. Regardless of the algorithm used, the wrist-worn approach consistently outperformed the hip-worn approach in estimating exercise intensity during running. These differences in performance can be attributed to distinct muscle activation and contraction dynamics associated with walking and running, characterized respectively by an inverted pendulum model and a spring-mass model [7]. Our findings align with previous studies, showing that heart rate response (HRR) reaches a plateau during higher speed running. Conversely, the wrist-worn accelerometer recorded accelerating speeds that continued to rise with running speed without any apparent constraint. These results underscore the importance of considering both algorithm and accelerometer placement when assessing physical activity levels, providing valuable insights into the nuanced dynamics of human locomotion across various intensities and modalities.

Significance: The findings can be integrated into smartphone applications or through the development of wearable inertial measurement unit (IMU) devices by utilizing a range of customizable algorithms. Such devices will offer innovative and highly precise solutions for assessing exercise intensity, thereby fostering improved fitness results and overall well-being among individuals from diverse backgrounds and fitness levels.

Acknowledgments: We acknowledge support from the National Science and Technology Council, Taiwan (NSTC 111-2410-H-039-013-MY2), the National Science Foundation, USA (NSF CAREER CBET-2144472), and the Higher Education Sprout Project of National Taiwan Normal University, sponsored by the Ministry of Education, Taiwan.

References: [1] Hansen et al. (2022), *EJPC* 29(1); [2] Hawkins et al. (2017), *J Dermatol Dermatol Surg* 21(2); [3] Karvonen et al. (1988), *Sports Med* 5; [4] Kurihara et al. (2011), *IEEE TSMC Part C* 42(4); [5] Chen et al. (2018), *Clin Biomech* 60; [6] Thorstensson et al. (1987), *Acta Physiol Scand* 131(2); [7] Shih et al. (2016), *Gait Posture* 46

EFFECTS OF EXTERNAL HAND FORCE MODELING ON VALIDITY OF INVERSE ANALYSIS OF LIFTING

Eunsik Choi[1], Ilseung Park[1], Jooeun Ahn[1,2] *
[1]Department of Physical Education, Seoul National University, Seoul, Republic of Korea
[2]Institute of Sport Science, Seoul National University, Seoul, Republic of Korea
*Corresponding author's email: ahnjooeun@snu.ac.kr

Introduction: The knowledge of internal loads during lifting is essential for preventing occupational injuries [1]. Such internal loads can be estimated by musculoskeletal simulation models, which rely on the input data of external forces and moments [2]. However, measuring external hand contact forces and moments (EHF&M) is challenging, and therefore, simplified EHF&M models are commonly used. Although previous studies tried to validate a simple model of EHF&M [3] or conducted comparative studies among simple models [4], there has been a lack of systematic comparison between the results from true EHF&M and those from models. To address this research gap, we measured EHF&M using load cells and conduct inverse analysis with the measured data. The results were compared with the results from the common approaches with EHF&M models.

Methods: One participant performed 20 repetitions of two-handed lifting and lowering of a box (15.02 kg). The participant moved the box from a shelf (height: 33 cm) in front of feet to a table (height: 78 cm) for lifting, and vice versa for lowering. Auditory triggers set at 10 bpm regulated the execution. Fifty seven markers were attached to the skeletal landmarks of the participant and eight corners of the box. Seventeen infrared cameras (OptiTrack Prime13, NaturalPoint Inc., USA) tracked marker motion. Two force plates and load cells (BMS400600 and MC3A6-1000, AMTI, MA, USA) recorded external forces and moments on the feet and hands, respectively. We applied a scaled lifting full-body model with unlocked wrist degrees of freedom in OpenSim 4.4, using static posture marker data [5]. We used three approaches for inverse analyses:

APP 1. Apply measured EHF&M data to each hand in the global coordinate system.
APP 2. Add the mass of the half-box to each hand.
APP 3. Design two half-box bodies with specified material properties and geometries, join one to each hand as a weld joint, and affix them with a weld constraint solely for inverse kinematics analysis.

We sequentially processed inverse kinematics, static optimization, and the joint reaction analysis tools in OpenSim 4.4 [6]. The magnitude and time of peak, and root mean square (RMS) were calculated from the L_5S_1 joint reaction forces and vertical residual forces normalized to lowering time. One-way repeated measures analysis of variance and Bonferroni post hoc test were performed.

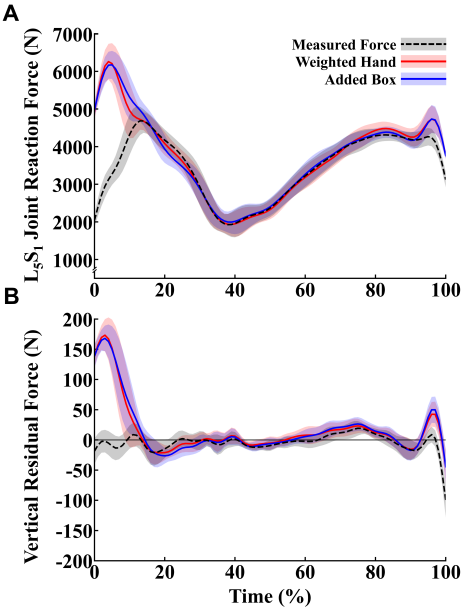

Figure 1: (A) Normalized L_5S_1 joint reaction force and (B) vertical residual force profiles over a normalized time for 20 lifting repetitions. APP 1 (dotted black), APP 2 (blue), and APP 3 (red).

	L_5S_1 Joint Reaction Force			Vertical Residual Force		
	Peak time (%)	Peak Mag. (N)	RMS (N)	Peak time (%)	Peak Mag. (N)	RMS (N)
APP 1	**12.7±2.27**	**4869±241**	**3567±77.7**	**95.5±20.1**	**100±28.4**	**20.3±2.34**
APP 2	**4.55±1.79**	**6474±446**	**3927±83.5**	**3.50±1.70**	**181±30.3**	**49.4±10.5**
APP 3	**4.95±1.88**	**6366±335**	**3938±73.3**	**3.60±1.67**	**175±25.3**	**49.8±9.61**

Table 1: Statistical comparison of peak times, magnitudes, and RMS for L_5S_1 joint reaction forces and vertical residual forces across three approaches, showing significant variations in force characterization across the approaches ($p < 0.001$).

Results & Discussion: Significant differences in L_5S_1 joint reaction forces and vertical residual forces were observed across the three EHF&M modeling approaches ($p < 0.001$), with APP 1 generating lower peak magnitude and RMS than APP 2 and APP 3 (all $p < 0.001$) (Figure 1 and Table 1). This result indicates that model simplification can impact the accuracy of simulated internal forces, which could affect risk assessment of injuries [1]. Conversely, no significant differences were observed in the RMS of L_5S_1 joint reaction forces and vertical residual forces between APP 2 and APP 3 ($p = 0.018$ and $p = 0.628$, respectively). Given that APP3 needs more material information to build the model than APP2, this result demonstrates that APP2 can be a more efficient choice than APP3.

Significance: This study quantified the effects of simplified EHF&M models on the validity of the inverse analysis. Our findings suggest that the frequently used EHF&M simplification models might lead to miscalculation of internal loads. Our experimental setup will also contribute to devising a more valid and/or efficient modelling of EHF&M in more general situations.

Acknowledgments: This work was supported in part by the Korea Health Technology R&D Project through the Korea Health Industry Development Institute (KHIDI) funded by the Ministry of Health & Welfare (No. HK23C0071), Industrial Strategic Technology (No. 20018157) and Industrial Technology Innovation Program (No. 20007058, Development of safe and comfortable human augmentation hybrid robot suit) funded by the Ministry of Trade, Industry & Energy (MOTIE, Korea), and the National Research Foundation of Korea (NRF) grants funded by the Korean Government (MSIT) (No. RS-2023-00208052).

References: [1] R. Norman et al. (1998), *Clin. Biomech.*; [2] L. Ren et al. (2014), *J. Bionic Eng.*; [3] A. Muller et al. (2020), *IEEE Trans. Biomed. Eng.*; [4] M. Akhavanfar et al. (2022), *Multibody Syst. Dyn.*; [5] E. Beaucage-Gauvreau *et al.* (2019), *Comput. Methods Biomech. Biomed. Engin.*; [6] S. L. Delp et al. (2007) *Trans. Biomed. Eng.*

RELATIONSHIP BETWEEN THE INERTIA TENSOR OF WHOLE BODY AND DIVING PERFORMANCE INCLUDING FORWARD PIKE AND TWIST ROTATIONS

Mamoru Fukui[1*], Katsumasa Tanaka[2], Yoshimori Kiriyama[3]
[1]Graduate School of Mechanical Engineering, Kogakuin University, Tokyo, Japan
[2]Department of Mechanical Engineering, Kogakuin University, Tokyo, Japan
[3]Department of Mechanical Systems Engineering, Kogakuin University, Tokyo, Japan
*Corresponding author's email:am23055@ns.kogakuin.ac.jp

Introduction: In springboard diving competition, athlete competitors have to bend and twist their whole bodies in quite short time, competing of the proper amounts of rotation and revolution upon completion of the dive and entry into the water. To increase the numbers of rotation and revolution, they change the postures decreasing the moment of inertia of the body. Hence, competitive divers adequately have to change their joint angles and the whole posture in three-dimension to control their moment of the inertia tensor. To understand the mechanism to control the body posture, it is required to clarify the posture changes of divers. Therefore, in this study we investigated the relationship between the aerial movements and the moment of the inertia tensor of the whole body during somersaults and twists. Especially, we analyzed the competition footage of the performance by a world medalist that shows forwards 2 and 1/2 somersaults with 2 twists in the pike position.

Methods: In this study, we used the competition footages from 3 m springboard diving in the 2016 Olympics and obtained the whole postures of during performance. Based on the body segments on the movie, we calculated the moment of inertia tensor of the whole body. The movies of the performance by the Olympic gold medallist were taken in the sagittal and frontal planes [1]. The frame rate was 59.77 /fps, and the 15 joint positions of the divers for each frame were acquired using an image analysis software Image J (National Institutes of Health, USA). We estimated the mass, the position of center of mass, and the moment of inertia around each axis of each segment based on the proportional data of Asian [2]. The position of the center of mass of the whole body ${}^0\mathbf{p}_{\mathrm{CoM}}$ was calculated by using each center of mass of the body segment ${}^0\mathbf{p}_i$ (i is the number of the body segments) during the performance. The position $\mathbf{p}_i$ from ${}^0\mathbf{p}_{\mathrm{CoM}}$ were used to calculate the moment of the inertia tensor of whole body $\mathbf{J}_{\mathrm{CoM}}$ as shown in eq. (1).

$$\mathbf{J}_{\mathrm{CoM}} = \sum m_i \widehat{\mathbf{P}}_i \widehat{\mathbf{P}}_i + {}^0\mathbf{R}_i \mathbf{J}_i \left({}^0\mathbf{R}_i\right)^T, \tag{1}$$

where, m_i is the mass of body segment, $\widehat{\mathbf{P}}_i$ is the skew symmetric matrix of $\mathbf{p}_i$, ${}^0\mathbf{R}_i$ is rotation matrix expressing the posture of each segment, and $\mathbf{J}_i$ is a diagonal matrix expressing the moment of inertia of each segment ($\mathbf{J}_i$ = diag[J_{ix} J_{iy} J_{iz}]). In the equation, $\widehat{\mathbf{P}}_i$ and ${}^0\mathbf{R}_i$ varies along the time. The obtained moment of the inertia tensor $\mathbf{J}_{\mathrm{CoM}}$ can be uniquely decomposed, as shown in equation (2)

$$\mathbf{J}_{\mathrm{CoM}} = \mathbf{R}_{\mathrm{CoM}} \mathbf{J}_{\mathrm{body}} \left(\mathbf{R}_{\mathrm{CoM}}\right)^T, \tag{2}$$

where $\mathbf{R}_{\mathrm{body}}$ is a rotation matrix and $\mathbf{J}_{\mathrm{body}}$ is a diagonal matrix including each value of the principal moment of inertia ($\mathbf{J}_{\mathrm{body}}$ = diag[J_{bx} J_{by} J_{bz}]). The axes of $\mathbf{J}_{\mathrm{body}}$ correspond to $\mathbf{R}_{\mathrm{CoM}}$ and the values of the obtained principal moment of inertia mean the ease of rotational movement in the whole body. In addition, we calculated the somersault and twist angles during performance. We evaluated the changes of the $\mathbf{J}_{\mathrm{body}}$ compared to the somersault and twist angles.

Results & Discussion: Figure 1 shows the somersault and twist rotation angles (Fig.1 (a)), and the three principal moments of inertia of the whole body (Fig.1 (b)). Diving motion is divided into three phases; 1 somersault phase from the start to 13 frame (red background), 2 twists and ½ somersault phase from 14 to 23 (white background), and 1 somersault phase from 24 to the end (blue background). The somersault and twist angles increase rapidly at each rotation phase. The moments of inertia around the somersault and tilt axis show large values. These moments of inertia are around axis vertical to the longitudinal direction of the body, and show the similar change of the values. On the other hand, the moment of inertia around the twist axis is around the longitudinal direction, and show small value. After the take-off, the diver has a bending posture and then takes pike position. At this time, the moments of inertia around somersault and tilt axis decreased to the minimum values through the performance. Then the moments of inertia around the axes increased. As the results, the somersault angle turned from rapid to gradual change. Moreover, the moments of inertia around the somersault and tilt axes increased. However, the one around the twist axis decreased. Thus, the twist axis angle could increase rapidly. In the second somersault phase, the moment of inertia around the twist axis increased, and the ones around somersault and tilt axes rapidly dropped again. The relationship between the changes of moments of inertia. And the rotation angles means that the competitive diver could control of the rotations adjusting efficiently the inertia tensor of the whole body.

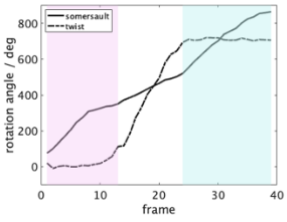

(a): Rotation angles

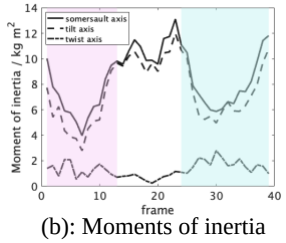

(b): Moments of inertia

Figure 1: Somersault & twist rotation angles and the three principal values of inertia

Significance: This research revealed that the relationship between the inertia tensor and the angle of somersault and twist. This report provides insights into posture adjustments required to execute challenging techniques.

Acknowledgments: A part of this research was supported by The Uehara Memorial Foundation and JKA and its promotion funds from KEIRIN RACE.

References: [1] Cao Yuan ALL dives from Rio 2016!: https://www.youtube.com/watch?v=xqSJXcsI4jA&t=602s; [2] Tang et al. (1994), *Japan J. Phys. Educ* 38

ASSESSING RISK FACTORS FOR ANKLE AND KNEE INJURY: COMPARISON OF BASKETBALL COURT SLIP RESISTANCE MEASUREMENTS FROM COMMON SLIP METERS

Rachel L. Hybart[1*], Brian Grieser[1], Rosemarie Figueroa Jacinto[1], Jessica Zendler[1]
[1]Rimkus
*Corresponding author's email: rachel.hybart@rimkus.com

Introduction: The ankle and knee are two of the most commonly injured joints in sports, including basketball, and can lead to time away from sport and long-term disability [1-2]. The available friction of the surface, or slip resistance, is one factor that may contribute to injury, with too high friction potentially leading to ankle sprain and ACL injury and too low friction leading to slipping [3-4]. Several methods exist for assessing slip resistance of a surface. ASTM International and the International Basketball Federation (FIBA) provide standards for testing sports surfaces using a Pendulum Tester (PT). However, the English XL Variable Incidence Tribometer (XL VIT) is more commonly used in the US for testing, given its portability and versatility. This study aims to compare slip resistance assessments in basketball courts using the PT and the XL VIT to identify suitable methods for future injury research.

Methods: Testing with the PT (Munro Portable Skid Tester) was generally conducted according to the ASTM E303-22 standard, and testing with the EXL VIT was generally conducted according to the EXL VIT User Guide (March 21, 2016). Seven different hardwood basketball courts were tested over 4 months by the same individual. The courts were cleaned before testing by the court facility staff per their standard procedures. Courts were tested in dry and wet (sprayed with water) conditions, except for one where only the dry condition was tested. Measurements were taken at three standardized locations on the court and averaged. Linear correlation between the EXL VIT and PT measurements were calculated and are presented as R^2 values.

Results & Discussion: Figure 1 shows the results of dry and wet testing of the courts. Dry testing resulted in an average value across courts of 85 ± 7.3 PTV for the PT and 0.62 ± 0.04 ACOF for EXL VIT. The R^2 for dry testing between the PT and EXL VIT was 0.274. Wet testing resulted in an average value across courts of 10 ± 1.2 PTV for the PT and 0.28±0.04 ACOF for the EXL VIT. The R^2 value for wet testing between the PT and the EXL VIT was 0.0637. Additionally, per the standards, three calibration surfaces (glass, tile, pink lapping film) were tested under wet conditions, and the R^2 value of the calibration surfaces was 0.9349. All courts were considered slip-resistant (ACOF>0.5 and PTV>36) in the dry condition and not slip-resistant in the wet condition. Both devices varied in their readings across courts when testing in the dry condition and were positively correlated, albeit weakly. In contrast, PT wet results were similar across courts, whereas EXL VIT findings were more variable, resulting in a minimal correlation between PT and EXL VIT for wet testing. Interestingly, the PT and XL had a high correlation in their results on the clean, homogeneous calibration surfaces. One reason for these disparate findings may be the cleanliness of the court before testing. Although exact instructions were given to each facility, there were noticeable differences in the amount of contaminant on each court. The presence of contaminant may change the relationship between the PT and EXL VIT for both dry and especially wet conditions, compared to the pristine calibration surfaces. Additionally, the PT measures the dynamic coefficient of friction, while the XL VIT measures the static coefficient of friction. While these values are expected to be well correlated, they may be affected differently by contaminants and water, resulting in different relationships under different conditions.

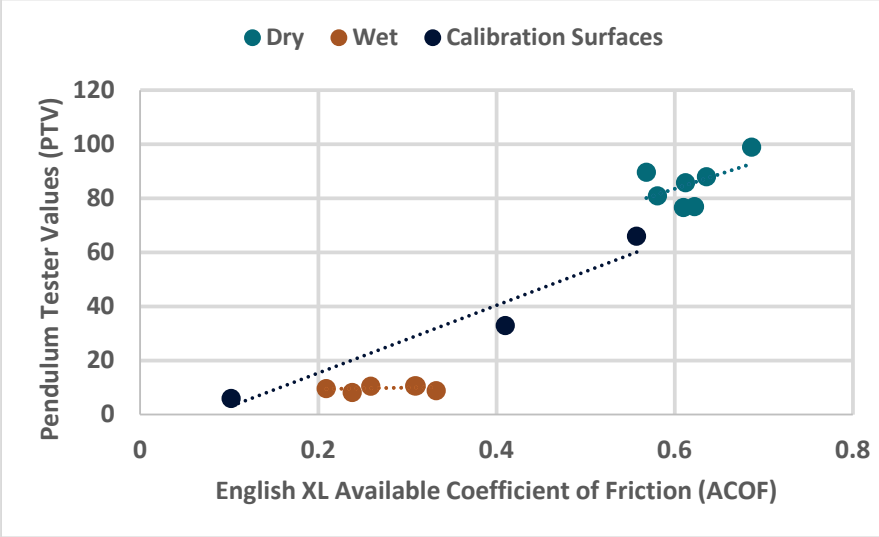

Figure 1: Average slip resistance data collected by the PT and EXL VIT at identical locations across different basketball courts under dry (blue) and wet conditions (orange) as well as on three standardized wet calibration surfaces.

Significance: Most studies on slip meters are focused on pedestrians. Though, slip meters are also part of test procedures found in standards for sports flooring, including hardwood basketball courts. Our findings suggest that the homogeneity and cleanliness of the basketball court may affect the consistency of readings between the PT and EXL VIT such that results cannot be readily correlated or interchanged unless the surface is consistently clean. Follow-up work could include a human subject study to determine which slip meter better reflects human-court interaction.

References: [1] Herzog, M, et al. (2019). "Ankle Sprains in the National Basketball Association, 2013-2014 Through 2016-2017."
[2] McKay, G, et al. (2001). "A prospective study of injuries in basketball: A total profile and comparison by gender and standard of competition."
[3] Wannop, J, et al. (2015). "The Effect of Translational and Rotational Traction on Lower Extremity Joint Loading."
[4] Olsen, O, et al. (2003). "Relationship between floor type and risk of ACL injury in team handball."

ASYMPTOMATIC CAM FAI OR DDH IMPACTS DYNAMIC HIP JOINT COVERAGE DURING BOTH LOW AND HIGH-FLEXION ACITIVITIES

Camille C. Johnson[1], Ethan Ruh[1], Naomi Frankston[1], Shaquille Charles[1], Craig Mauro[1], Michael McClincy[1], William Anderst[1]
[1]Department of Orthopaedic Surgery, University of Pittsburgh, Pittsburgh, PA, USA
*Corresponding author's email: ccj17@pitt.edu

Introduction: Pathomorphologies such as femoroacetabular impingement (FAI) and developmental dysplasia of the hip (DDH) have been shown to impact the stability of the hip joint and are major sources of hip pain and osteoarthritis progression [1]. *In vivo* coverage of the femoral head by the acetabulum has been described during low-flexion activities [2], but dynamic *in vivo* coverage during higher-flexion activities, where morphologies may have a greater impact on maintaining dynamic hip stability, have not been fully described. The goal of the study was to determine *in vivo* dynamic acetabular coverage of the femoral head during activities of daily living in an asymptomatic cohort and explore the relationship between coverage and hip morphology. We hypothesized that alpha angle would be correlated with acetabular coverage of the anterior superior region of the femoral head and lateral center edge angle (LCEA) would correlate with coverage in the superior region of the femoral head for both low and high-flexion activities.

Methods: Twenty-three healthy young adults (12 F, 11 M; 22.0±2.2 years; BMI: 21.4±5.1kg/m^2) consented to participate in this IRB-approved study. Participants stood, walked on a treadmill, squatted, and ascended a step from a position of deep hip flexion while synchronized biplane radiographs were collected (50 images/s for 1s, 80kV, 320mA, 3 trials per hip, per dynamic activity [static stand: 0.1s, 1 trial per hip]). Subject-specific bone models of the pelvis and proximal femur were created from computed tomography (CT) scans. A board-certified orthopaedic surgeon measured each hips' alpha angle and LCEA from the scout CT scans. Coordinate systems were established [3] and regions of interest were identified on the femoral head and acetabulum articulating surfaces. *In vivo* bone motion during each activity was determined by matching digitally reconstructed radiographs, created from the CT-based bone models, to each frame of the biplane radiographs [4]. The femoral head was sub-divided into anterior superior, anterior inferior, posterior superior, and posterior inferior regions; the area in each region was calculated. Covered area was determined for each frame by the creating a vector from the femoral head center to each point on the femoral head surface and testing if the vector intersected the acetabulum. Dynamic coverage was calculated within each region for each activity as a percentage of each regional femoral head area and averaged to obtain an average coverage in each region for each activity. Data were assessed for normality using a Shapiro-Wilk test and the relationship between average acetabular coverage in each region and morphology was assessed for each activity, independently, using Spearman's correlation. Significance was set at $p<0.05$ for all tests.

Results: Data from 321 trials (104 walk, 92 squat, 79 step ascent, and 46 static stand) of 46 hips from 23 individuals were analyzed. Alpha angles ranged from 31-80° and LCEA ranged from 20-39°; two hips had asymptomatic borderline DDH (LCEA between 20-25°) and seven hips had asymptomatic cam FAI (alpha angle>60°). Average walking velocity was 1.0±0.2m/s, average maximum hip flexion during squatting and step ascent was 98.0±16.9° and 90.5±9.3°, respectively. During standing, greater alpha angle correlated with more anterior inferior coverage and greater LCEA correlated with more posterior superior coverage (Table 1). Greater LCEA correlated with more anterior superior and posterior superior coverage during walking and squatting (Table 1). Greater alpha angle correlated with more anterior inferior coverage during squatting (Table 1).

Table 1: Regional acetabular coverage of the femoral head during each activity [mean (SD)] and morphology correlations (ρ_a=alpha angle, ρ_l=LCEA). "*" indicates significant correlation.

	Anterior Superior	**Anterior Inferior**	**Posterior Superior**	**Posterior Inferior**
Stand	54.0% (8.8%) ρ_a=0.21, p=0.16 ρ_l=0.16, p=0.07	16.6% (6.7%) ρ_a=0.32, ***p=0.03** ρ_l=0.06, p=0.68	76.6% (9.2%) ρ_a=-0.12, p=0.41 ρ_l=0.40, ***p=0.007**	64.5% (13.8%) ρ_a=-0.02, p=0.89 ρ_l=0.23, p=0.13
Walk	55.9% (6.9%) ρ_a=0.17, p=0.28 ρ_l=0.34, ***p=0.03**	19.9%, 6.3% ρ_a=0.22, p=0.16 ρ_l=0.02, p=0.92	75.1% (7.4%) ρ_a=-0.03, p=0.87 ρ_l=0.33, ***p=0.03**	60.8% (10.9%) ρ_a=-0.11, p=0.48 ρ_l=0.17, p=0.29
Squat	78.2% (7.7%) ρ_a=0.23, p=0.16 ρ_l=0.33, ***p=0.04**	75.3% (17.5%) ρ_a=0.39, ***p=0.01** ρ_l=0.14, p=0.39	76.3% (16.0%) ρ_a=0.20, p=0.21 ρ_l=0.38, ***p=0.02**	54.7% (21.6%) ρ_a=0.24, p=0.13 ρ_l=0.15, p=0.36
Step Ascent	57.8% (7.7%) ρ_a=0.27, p=0.15 ρ_l=0.23, p=0.22	76.8% (13.8%) ρ_a=0.22, p=0.24 ρ_l=0.24, p=0.20	46.7% (11.7%) ρ_a=0.09, p=0.64 ρ_l=0.15, p=0.43	41.2% (13.2%) ρ_a=-0.19, p=0.31 ρ_l=0.28, p=0.13

Discussion: The main finding of this study was that a more dysplastic hip (lower LCEA) results in undercoverage in the superior regions and a more aspherical femoral head (higher alpha angle) results in greater coverage of the anterior inferior region of the femoral head during both low and high-hip flexion activities. This suggests, even among an asymptomatic population, that alpha angle and LCEA may affect the regional loading of the femoral head. Shifts in contact to areas of the acetabulum where the femoral cartilage is thinner (i.e. the more lateral, inferior region [5]) may contribute to pain and the eventual development of osteoarthritis in individuals with abnormal hip morphologies.

Significance: Morphology impacts dynamic hip joint coverage during both low and high-flexion activities, providing insight into dynamic healthy hip stability, and has implications for restoring coverage following surgical correction in pathological populations.

References: [1] Bedi, et al. (2011) *Arthroscopy.* [2] Uemura, et al. (2018) *Clinical Anatomy.* [3] Wu, et al. (2002) *J Biomech.* [4] Martin, et al. (2011) *J Arthroplasty.* [5] Nakanishi, et al. (2001) *Eur. Radiology.*

HOW DOES USE OF AN ADJUSTABLE SOCKET AFFECT LOWER LIMB POWER IN PEOPLE WITH TRANSTIBIAL AMPUTATION DURING WALKING?

Luis Morata[1], Gabriela B. Diaz[1], & Alena M. Grabowski[1,2]
[1]Applied Biomechanics Lab, University of Colorado Boulder, Boulder CO USA
[2]Department of Veterans Affairs Eastern Colorado Healthcare System, Denver CO USA
Corresponding author's email: Luis.MorataMoreno@colorado.edu

Introduction: To walk, people with unilateral transtibial amputation (TTA) typically use a rigid carbon-fiber prosthetic socket attached to components such as passive-elastic prosthetic feet. The socket provides a critical interface between the residual limb and the prosthesis [1] and the most important reported factor associated with using a prosthesis [2]. However, the use of a rigid socket can contribute to functional impairment and secondary injury in people with TTA such as osteoarthritis, osteoporosis, and chronic leg and back pain [3]. These secondary conditions likely result from asymmetry between the affected leg (AL) and unaffected leg (UL). It is likely that because a rigid prosthetic socket cannot adapt to residual limb volume fluctuations, it may affect fit and asymmetry. Thus, a prosthetic socket that adjusts to residual limb volume fluctuations may provide a more secure attachment, improve force and energy transfer, and reduce asymmetric biomechanics in people with TTA, which could reduce comorbidities and improve quality of life. A prosthetic socket has been developed that includes adjustable panels (Quatro, Quorum Prosthetics, Windsor, CO) and can accommodate residual limb volume changes up to 12%. We determined the underlying biomechanics and asymmetry of people with unilateral TTA using a rigid socket (RS) and an adjustable socket (QS) by quantifying unified deformable (UD) power [4, 5] and calculating lower limb work of the AL and UL during walking. We predicted that for people with TTA, the work performed by the UL would be greater than that of the AL in both socket conditions. We hypothesized that people with TTA would have: 1. reduced work asymmetry between the UL and AL for the QS compared to the RS, and 2. a lower magnitude of net negative work in their AL for the QS compared to the RS.

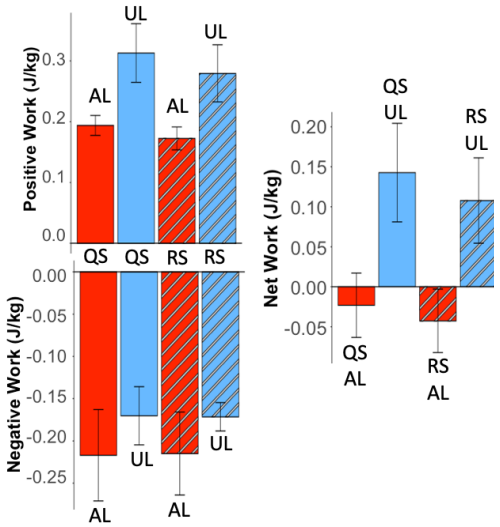

Figure 1: Mechanical power and work production of below-knee structures during stance phase for the affected leg (AL), and unaffected leg (UL), when 4 people with a transtibial amputation used an Adjustable socket (QS), and Rigid socket (RS). Error bars represent SE.

Methods: Four subjects (3 M, 1 F) with unilateral TTA participated. Each subject completed two randomized 40 sec walking trials at 1 m/s on a level dual-belt force-instrumented treadmill (Bertec, Columbus, OH) wearing an RS and QS. The QS was fabricated by a certified prosthetist who replicated each subject's RS. Each subject utilized their own passive-elastic prosthetic foot and components so that the only difference between trials was the prosthetic socket. We measured ground reaction forces at 1000 Hz and lower body 3D kinematics at 100 Hz (Vicon, Centennial, CO) throughout each trial. The last 10 steps were analyzed for each leg and each subject per condition. We filtered ground reaction forces and kinematics with a 4th-order Butterworth lowpass filter with a 38 Hz cut-off frequency. Stance phase was identified with a vertical ground reaction threshold of 32 N. We calculated UD power performed by below-knee structures of the UL and AL in both socket conditions using V3D software (C-Motion, Germantown, MD) and calculated work as the integral of UD power with respect to time. Symmetry Index (SI) [6] between the AL and UL for the positive and negative work performed during stance phase was calculated for each socket condition. Paired t-tests were employed to assess the differences in work performed between the AL and UL for both socket conditions, SI between socket conditions, and work performed by the AL between socket conditions. For all statistical analyses, we used a significance level of $p < 0.05$. All statistical analyses were performed in RStudio (Boston, MA, USA).

Results & Discussion: The positive work performed during stance phase was on average 0.119 J/kg greater for the UL compared to the AL ($p = 0.045$) for the QS, and 0.107 J/kg greater for the UL compared to the AL ($p = 0.046$) for the RS (Fig. 1). However, we detected no significant difference in negative work performed by the UL versus AL in either socket condition. Thus, our prediction was supported. Our results do not support our first and second hypotheses. We found no significant difference in SI for positive work for the QS and RS, where SI was 44.19 ± 17.99% and 44.42 ± 19.05%, respectively (Fig. 1) and no significant difference in SI for negative work for the QS and RS, where SI for QS and RS was 58.50 ± 35.50% and 41.97 ± 27.26%, respectively (Fig. 1). In addition, the net work performed by the AL was not statistically different between socket conditions, where the net work for the QS and RS was -0.023 ± 0.04 J/kg and -0.042 ± 0.03 J/kg, respectively. Our findings suggest that the UL performs more positive work than the AL in people with a TTA, which results in asymmetric mechanical work between legs, and this asymmetry is not affected by use of an adjustable versus rigid socket. Future research is needed to determine if and how use of different prosthetic sockets affect asymmetry in people with TTA.

Significance: We implemented a UD analysis to determine the mechanical power and work due to the use of different prosthetic sockets and the effects on asymmetry. Our results can be used to inform the design and development of prosthetic sockets that could optimize walking performance through decreases in asymmetry.

Acknowledgments: Funding from the VA RR&D Service RX003643
References: [1] Paterno, L., et al., *Trans. on Biomed. Eng.*, 2018, [2] Aydin, A. and S.C. Okur, *Med. Sci. Mont.*, 2018, [3] Gailey, R., et al., *JRRD*, 2008, [4] Takahashi, K. Z., Kepple, T. M., & Stanhope, S. J., *J. of Biomech.*, 2012, [5] Takahashi, K. Z., Horne, J. R., & Stanhope, S. J., *Prost. and Ort. Int.*, 2015, [6] Cabral, S. et al., *J. of App. Biomech.,* 2016.

Step time asymmetry increases both metabolic cost of transport and tibiofemoral joint contact forces via predictive simulation.

Ryan D. Wedge[1*] and Russell T. Johnson[2]
[1]Department of Physical Therapy, East Carolina University
[2]Department of Physical Medicine and Rehabilitation, Northwestern University
*Corresponding author's email: wedger19@ecu.edu

Introduction: Gait asymmetry is observed across many clinical populations, such as people with a unilateral lower limb amputation [1], people post-stroke [2], and people with incomplete spinal cord injury [3]. These populations also walk with a greater metabolic cost compared to age matched controls [2,4] and often have musculoskeletal pain and an increased incidence of knee osteoarthritis [5,6]. Rehabilitation interventions frequently target restoring symmetric gait for these individuals, with the goal of reducing metabolic cost and joint loads. However, both *in vivo* and *in silico* data suggests that improving gait symmetry for both lower limb prosthesis users and people post-stroke does not result in a reduction of metabolic cost [7,8,9]. Additionally, inducing gait asymmetries in healthy young adults was not associated with increases in knee joint reaction force or loading rates [10]. A comprehensive understanding of the relationships across gait asymmetry, metabolic cost, and joint loading is crucial to developing rehabilitation programs that improve mobility. Therefore, the purpose of our study was to determine if bilateral tibiofemoral joint loading is greater when walking with asymmetric step times compared to symmetric step time via predictive simulations using a sagittal-plane musculoskeletal model.

Methods: We used a musculoskeletal model with 12 degrees-of-freedom and 28 (14 per limb) Hill-type muscles based on the *DeGrooteFregley2016Muscle*. We used OpenSim Moco [11] to generate optimal control simulations of walking across five different walking speeds (0.5 – 1.5 m/s) and across a range of step time asymmetries between 0 and 25%. We used a weighted objective function that minimized the following two terms: 1) the sum of the integrated muscle excitations cubed and 2) the difference between the target and the achieved step time asymmetry [9]. Target step time asymmetries were 0% (symmetric), 5%, 10%, 15%, 20%, and 25%.

Our outcome measures were 1) metabolic cost of transport and 2) right and 3) left limb peak tibiofemoral joint contact forces. We computed the metabolic energy expenditure of the model using functions based on the muscle activations and muscle fiber velocities with an assumed basal metabolic rate of 1 W/kg [12] and divided by the constrained gait speed to get the metabolic cost of transport. We computed local vertical joint reaction forces using the OpenSim Joint Reaction Analysis.

Results & Discussion: First, faster gait speed resulted in a decrease in the metabolic cost of transport (Figure 1A), which is expected when metabolic energy expenditure is normalized to distance travelled. Faster gait speeds also resulted in greater peak tibiofemoral contact forces for both limbs (Figure 1B [right limb] and 1C [left limb]). Second, as step time asymmetry increased, the peak tibiofemoral contact forces on the left limb (fast step) increased consistently across all speeds (r-range = 0.150 – 0.870). The right limb (slow step) peak tibiofemoral contact forces increased at speeds of 0.5 and 1.5 m/s as asymmetry increased, but these values did not change for the intermediate speeds (r-range = -0.325 – 0.892).

Our results show that the peak tibiofemoral contact forces may increase bilaterally when walking with step time asymmetries, as opposed to increasing just on the limb performing the faster step. Therefore, these results suggest that asymmetric gait patterns could help explain the increased prevalence of bilateral joint pain and osteoarthritis in prosthesis users, people post-stroke, and people with incomplete spinal cord injury. While it was not a primary target for this project, step time asymmetries also induced step length asymmetries in our gait simulations. Future work should investigate whether step time or step length asymmetry has a greater impact on tibiofemoral contact forces by manipulating one domain while holding the other constant across conditions.

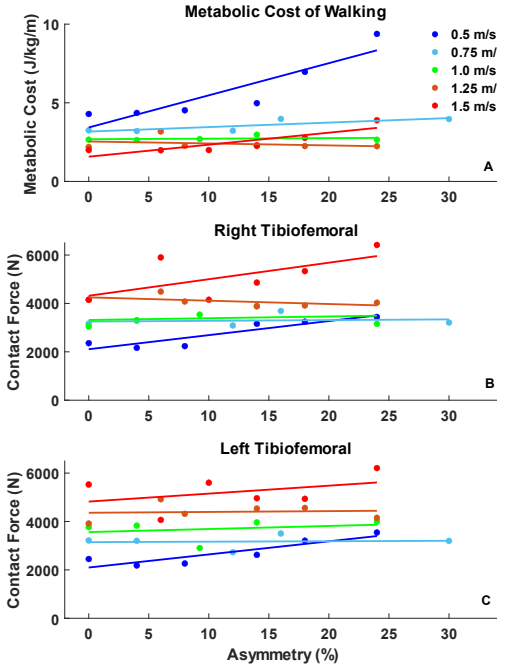

Figure 1: Metabolic cost of walking (A), right (B) and left (C) peak knee joint contact forces across (a)symmetry levels with linear trends. Generally, metabolic cost decreased with increasing speed, and contract forces increased with both speeds and asymmetry.

Significance: Greater peak knee joint contact forces have been linked to osteoarthritis risk due to increased risk for cartilage degeneration. Therefore, people who walk asymmetrically may be more likely to develop knee osteoarthritis due to greater peak tibiofemoral joint contact forces.

Acknowledgements: This research was supported in part through the computational resources and staff contributions provided for the Quest high performance computing facility at Northwestern University.

References: [1] Sanderson & Martin (1997) *Gait & Posture* 6(2); [2] Finley & Bastian (2017) *NNR* 31(2); [3] Thibaudier et al (2020) *Gait & Posture* (75); [4] Struyf et al. (2009) *Arch Phys Med Rehabil.* 90(3); [5] Waters et al., (1976) *J Bone Jt Surg* (58); [6] Fournier et al., (2021) *Stroke* 52(10); [7] Wedge et al. (2022) *C Biomech* (94); [8] Padmanabhan et al. (2020) *JNER* 17(1); [9] McCain et al. (2023) *J Biomech* (153); [10] Johnson et al. (2022) *PLOS CB* 18(9); [11] Dembia et al. (2020) *PLOS CB* 16(12); [12] Umberger et al. (2003) *Comput. Methods Biomech. Biomed. Engin.* 6(2)

COGNITIVE FLEXIBILITY SHOWS STRONGER CORRELATION WITH MOTOR DUAL TASK EFFECT IN THOSE WITH ESSENTIAL TREMOR COMPARED TO CONTROLS

Kenneth Harrison[1], Patrick Monaghan[1], Brandon Peoples[1],
Keven Santamaria Guzman[1], Harrison C. Walker[2], Jaimie Roper[1]
[1]Auburn University, Auburn AL, [2]University of Alabama in Birmingham Heersink School of Medicine, Birmingham AL
Kdh0077@auburn.edu

Introduction: Cognitive flexibility and task-set inhibition are important skills that are known to be affected in several Movement Disorders such as Parkinson's Disease (PD) and Essential Tremor (ET) leading to an increased incidence of falls and mobility disability. One of the clinical measures used to assess cognitive flexibility is known as the Trail Making Test (TMT) and has been shown to be associated with motor dual task performance in those with PD [1], but little work has looked at this relationship in those with ET. This study aimed at investigating the relationship between cognitive flexibility and motor dual task effect in those with ET. Due to previous associations shown between ET and cerebellar disruptions [2], we expected those with ET to have a stronger correlation between cognitive flexibility and motor dual task effect compared to those without.

Methods: 15 adults (66 ± 16) diagnosed with ET were matched based on age, sex, and mass with adults who did not have ET (66 ± 15). Motor dual task performance (Figure 1) was assessed using an instrumented Timed Up and Go (TUG) with verbal fluency and serial subtraction. Cognitive flexibility was measured using the difference in time taken to complete A and B portions of the TMT (Trails Δ), with a higher score indicating worse performance. Correlations were analyzed between these two variables and compared across groups.

Results & Discussion: Pearson's r showed a moderate negative correlation between mental flexibility and motor dual task effect (r = -.41, p = .039). When separated by group (ET vs. Control) there was a strong negative correlation for those with ET (r = -.67, p = .019) meaning slower walking speeds during dual task related to higher Trails Δ or worse cognitive flexibility. There was no significance found for controls (r = -.11, p = .685). In our sample having ET differentially impacted the relationship between Trails Δ and motor dual task effect. These findings confirm our hypothesis and indicate a unique reliance on cognitive flexibility for those with ET to multitask effectively.

Significance: This study helps illuminate the critical role that cognitive flexibility plays in the dual-task motor performance of ET patients. From a clinical perspective, these results indicate that cognitive flexibility could be an important consideration and potential treatment target when addressing the functional motor limitations experienced by ET patients. More broadly, the observed relationship illuminates the cognitive contributions to dual-tasking abilities and has implications for understanding their neural underpinnings. Overall, this work establishes cognitive flexibility as a factor that has a disproportionate impact on dual-task motor capacity in the context of a common movement disorder.

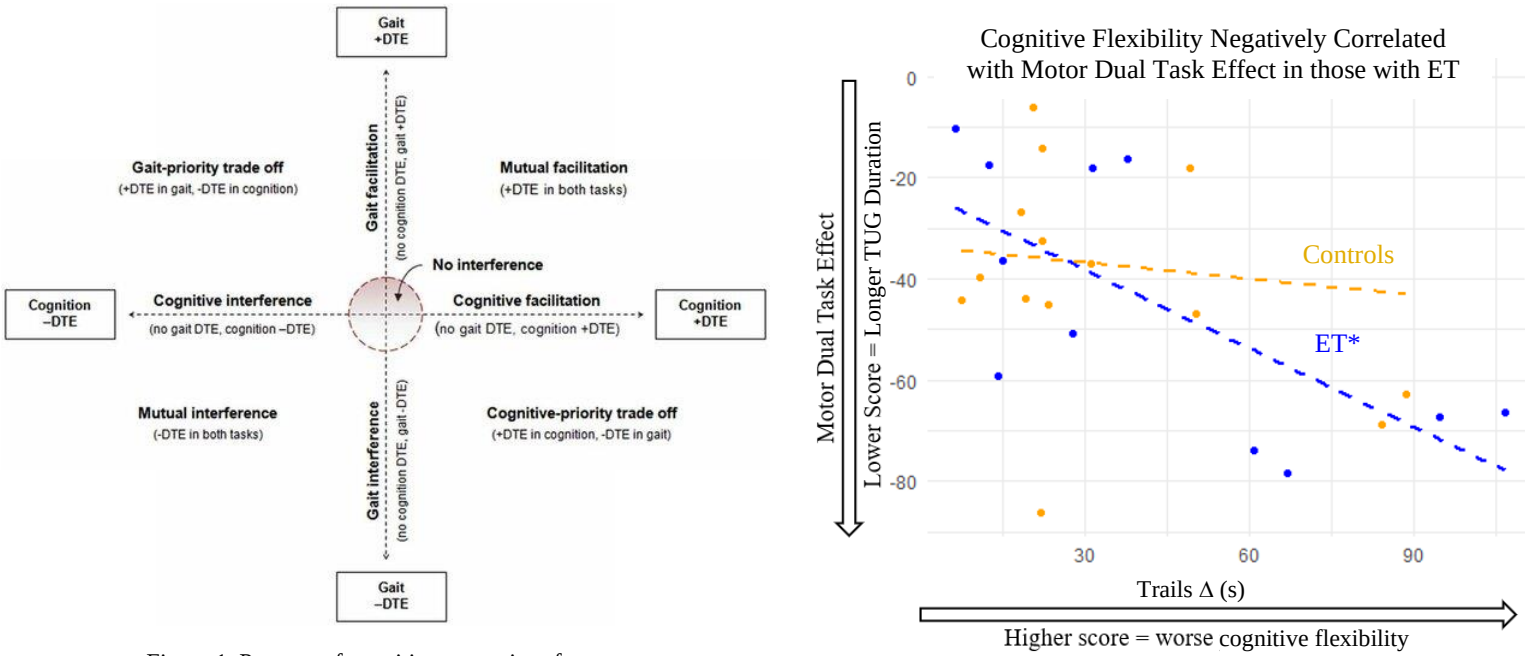

Figure 1. Patterns of cognitive-motor interference.

References:

[1] Plotnik, M., Dagan, Y., Gurevich, T., Giladi, N., & Hausdorff, J. M. (2011) Experimental Brain Research, 208
[2] Louis, E. (2016) Cerebellum 15, 235–242

ALTERATIONS IN CORTICAL CROSS-SECTIONAL AREA RESULTING FROM GROWTH-PERIOD LOWER LIMB LOADING IN GUINEA FOWL

Valeria Ortiz[1*], Derek Jurestovsky[1], Kavya Katugam-Dechene[1], Timothy Ryan[2], Stephen J. Piazza[1], Jonas Rubenson[1]

[1]Dept. of Kinesiology, The Pennsylvania State University, University Park, PA, USA
[2]Dept. of Anthropology, The Pennsylvania State University, University Park, PA, USA
*Email: vio5036@psu.edu

Introduction:

Sedentary time among both adults and adolescents has increased dramatically in the United States population over the last decades [1]. A lack of regular exercise has been tied to increased rates of heart disease, obesity, and other potential health risks [2]. In this study, we used a guinea fowl animal model to investigate the effects of limb loading on a single limb. We predict that chronic growth-period loading will produce greater cortical cross-sectional areas in the loaded limb, because a stronger bone is needed to withstand a higher load. Changes in bone structure in response to stimuli during the growth period also allow us to make conclusions about developmental plasticity throughout childhood.

Methods:

Using a sample group of 10 guinea fowl birds, we placed a mass unilaterally onto the right lower limb of each bird. The mass was increased proportionally as the birds grew over a 16-week period. The mass was equivalent to 2.5% of the bird's body weight for the first week, then increased to 3.5% for weeks 2-4, and set to 4.5% for the remainder of the 14-week loading period. Beginning at 2 weeks old, birds were exercised 3 times per week by herding them around their circular pen for 30 minutes in 5-minute intervals in alternating directions [3].

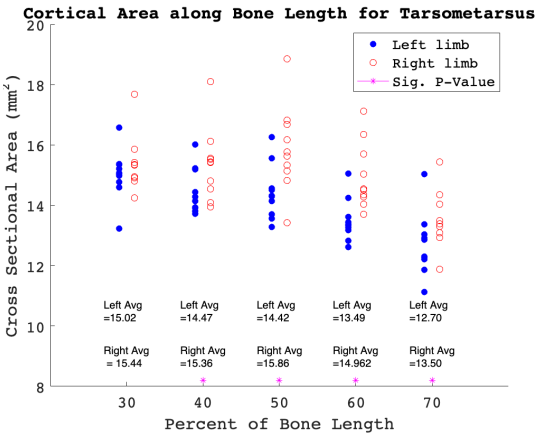

Fig. 1: Bilateral cortical area comparison along Tarsometatarsus bone cross-sections. Asterisk indicates p<0.004.

After 16 weeks the birds were euthanized, and the lower limbs were imaged using micro-CT. The scans included the right (weighted) and left (unweighted) tibiotarsus and the tarsometatarsus. The bones were then separated and aligned vertically along their respective axes via FIJI using the BoneJ plug-in, before being segmented using a regularized deep network approach [4]. Cross-sections were extracted along the diaphysis of each bone at increments of 10% of the total length. Proximal and distal sections in each bone were excluded from the analysis, so only sections between 30-70% of length in the tarsometatarsus and 20-80% in the tibiotarsus were used. Differences in cortical bone area were compared using paired t-tests with Bonferroni correction (p<0.0416).

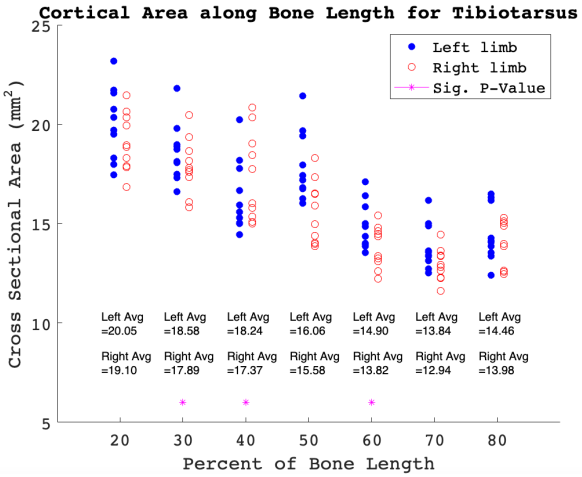

Fig. 2: Bilateral cortical area comparison along Tibiotarsus bone cross-sections. Asterisk indicates p<0.004.

Results & Discussion:

The tarsometatarsus displayed significantly greater cortical area in the loaded limb (right) compared to the unloaded limb (left) in all sections except 30% (Fig. 1). These results supported our hypothesis and showed that a plastic response occurred in the bone, even within a 16-week growth period.

Conversely, cortical bone area in the tibiotarsus was significantly higher in the unloaded limb than in the loaded limb (Fig. 2), contradicting our predictions.

The precise lengths of the respective bones will be analyzed next for differences correlated with limb loading, as well as other cross-sectional geometric properties that may explain the inverse cortical area findings across the bones. We will also determine how the loaded and unloaded limbs compare to a control group (no load during growth).

Significance:

Our study emphasizes how different levels of activity can trigger a rapid plastic response in bone development of animals, even bilaterally within the same individual. The different response in the tarsometarsus and tibiotarsus of the loaded limb, nevertheless, underscores the complexity of bone interactions in response to external loading stimuli.

Acknowledgments:

We would like to thank America Campillo, and the Pennsylvania State University Center for Quantitative Imaging. This research was supported by NIH grants R21AR071588 and R01AR080711.

References:

[1] Yang et al. (2019), *JAMA* 321(16).
[2] Penedo et al. (2005), *Current Opinion in Psychiatry* 18(2).
[3] Katugam-Dechene (2023), *Pennsylvania State University.*
[4] Yazdani et al. (2020), 54th Asilomar Conference on Signals, Systems, and Computers. *IEEE.* (pp. 1553-1557).

UNDERSTANDING THE DYNAMICS OF MOTOR LEARNING ON THE LOWER LIMBS IN A NOVEL TASK

Stephanie B. Hernández Hernández[1*], Kristan Leech[2], Peter G. Adamczyk[1]
[1]Department of Mechanical Engineering, University of Wisconsin – Madison
[2] Division of Biokinesiology and Physical Therapy, University of Southern California
*Corresponding author's email: hernandezher@wisc.edu

Introduction: Understanding principles of motor control can aid the development of targeted rehabilitation therapy to improve essential daily activities. To date, most motor control research has focused on the control of the upper limb[1-2]. Determining how motor control is similar or different in the lower limbs may help with rehabilitation strategies for walking, standing, balance, and other leg and foot movements for persons recovering from neural injury. For this reason, our aim is to understand the dynamics of motor learning on the lower limbs.

NOTTABIKE, a custom haptic leg robot, was designed to train and test new motor control tasks through novel haptic environments [3]. Preliminary experiments of leg-reaching tasks against a virtual spring of different stiffness levels have found that the motor system plans movement based on the stiffness experienced in the preceding trial, with unexpected changes causing characteristic errors, and that individuals have distinct preferences in balancing speed vs. accuracy [3]. In this pilot study, we examine how individuals learn a new motor skill with their legs – repositioning an unfamiliar virtual dynamic system – and how effectively they can retain and transfer it from the dominant leg leading to the opposite leg leading. We hypothesize that as the skill is learned, performance will improve (reduced settling time and path length). We also anticipate that performance will worsen when the dynamic system is removed (catch trials).

Methods: Five healthy right-dominant subjects (27-30 years, 2F/3M) performed leg-reaching tasks on NOTTABIKE. The goal was to move a virtual rotational inertia disk to reach 4 different targets (-75, -45, 45 and 75 degrees – **Fig.1A**) as quickly as possible. The disk interacted with the pedals through a virtual spring, forming a sprung-mass system that the user had to control. Leg reaching trials included *test* trials with the environment on and *catch* trials with the environment turned off. The study spanned two days. On day 1, subjects reached with their right leg leading, in a Baseline Phase (BP) of 39 trials with no environment and an Acquisition phase (AP) of 83 test trials and 36 randomized catch trials. On day 2 they completed a Retention Phase (RP) identical to AP; a Transfer Phase (TP) consisting of the same trial sequence as AP but with the left leg leading; and a Washout Phase (WP) with the right leg leading, of 16 test trials followed by 40 no-environment trials. An auditory motivational system gave feedback on the time taken to settle at the target (excellent, good, poor = coin clink, beep, buzz sound).

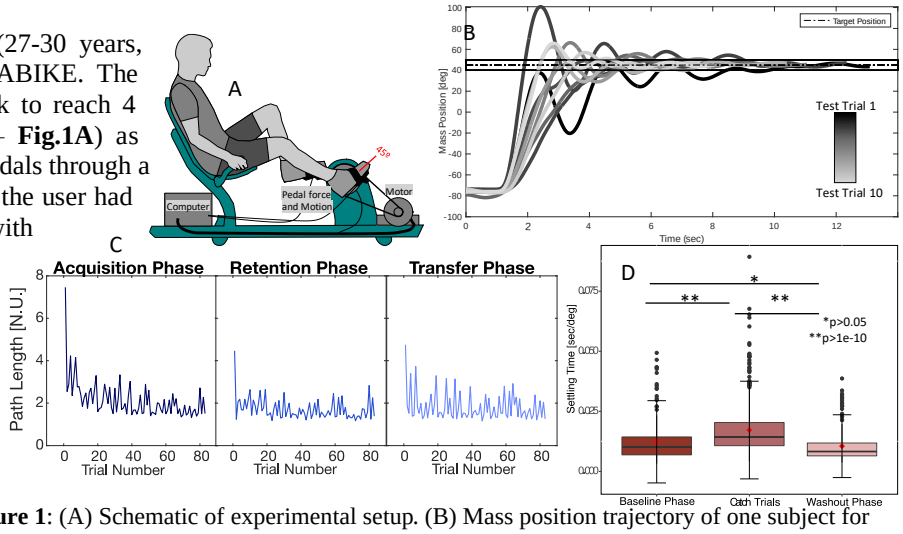

Figure 1: (A) Schematic of experimental setup. (B) Mass position trajectory of one subject for reaches throughout AP. (C) Normalized path length, mean for all subjects, for all learning phases. (D) Mean normalized settling time averages for all subjects for BP, catch trials within all learning phases, and WP.

Table 1: First 5 reaches for the different learning blocks (test trials).

Metrics	AP_{first}	RP_{first}	TP_{first}
Path length(SD) [N.U]	19.5(10.6)	11.6(6.3)	12.9(7.3)
Settling Time(SD) $[\frac{sec}{deg}]$	58.4(40.6)	38.1(26.8)	39.9(29.2)

Results & Discussion: Fig. 1B shows learning occurring over the AP for one of the reaching conditions. As the block progressed, the subject was able to learn the task resulting in a reduced path length. **Fig.1C** shows the path length (normalized to total reaching angle) throughout the experiment; a declining trend indicates learning, and retention and transfer are shown by reduced initial path length in both the RP and TP compared to the beginning of AP. **Table 1** compares the first 5 reaches of each block, indicating 40.5% and 33.9% initial path length reductions in RP and TP, respectively. The same pattern is seen for Settling Time (Table 1). The reaction time was also calculated but no significant difference was found between phases. **Fig1 D** shows the effect of the learned environment when performing catch trials. Settling time increased in catch trials from AP, RP, and TP, in comparison to BP and WP, indicating that the subject's motor planning adapted to perform well on the test trials with the environment "on", at the expense of catch trials with the environment "off". Additionally, settling time for the WP was smaller than BP, suggesting ongoing motor learning in WP. Further analysis of crank angle and pedal force will help clarify the contribution of each leg to learning and achieving the task. In addition, a larger cohort of subjects may enable grouping behaviors based on the different strategies used to "master" the task.

Significance: The aim of this study is to investigate and describe motor learning in the lower limbs of young adults, with the goal of informing assessment and rehabilitation protocols for stroke survivors in the future. Examining motor control and learning processes can deepen our understanding of movement coordination, skill acquisition, and the complexity of motor tasks. Foundational understanding young adults can be tailored to develop rehabilitation tasks targeting lower limb function in impaired populations.

Acknowledgments: NSF grants (CMMI-1830516, HRD-1612530), and UW-Madison OVCRGE with funding from WARF.

References: [1] Latash+ 1996 *Dis & Reh*; [2] Leech+ 2022 *PT*; [3] Dawson-Elli 2022 *PhD Diss., UW-Madison*.

THE TOTAL HIP JOINT MOMENT IS HIGHER DURING WALKING IN PEOPLE WITH MARFAN SYNDROME

Amara G. Sharp*, Mariana V. Jacobs, Christopher McLouth, Brian Noehren, Jody L. Clasey, Mary B. Sheppard, Michael A. Samaan
University of Kentucky
*Corresponding author's email: amara.sharp@uky.edu

Introduction: Marfan syndrome (MFS) is a connective tissue disorder that is associated with ligamentous laxity, musculoskeletal weakness, and lower extremity joint pain. Despite well documented rates of hip pain in the MFS population (46%) [1], few studies have attempted to assess the altered musculoskeletal function of this population during walking tasks. Evaluation of the hip joint loading patterns exhibited by individuals with MFS during walking may provide insight into potential biomechanical factors associated with the development of hip pain in the MFS population. Assessment of peak planar joint moments may not provide a suitable measure of total hip joint loading. The total joint moment (TJM) [2] can be used to estimate total hip joint loading during walking in the MFS population. Therefore, the purposes of this study were to compare hip joint loading patterns during walking between individuals with MFS and healthy, asymptomatic individuals as well as to determine the relationship between hip joint loading patterns with hip-related patient reported outcomes within individuals with MFS. We hypothesized that individuals with MFS would ambulate with higher hip joint loading compared to healthy controls and that higher hip joint loading would be associated with worse hip-related outcomes within the MFS cohort.

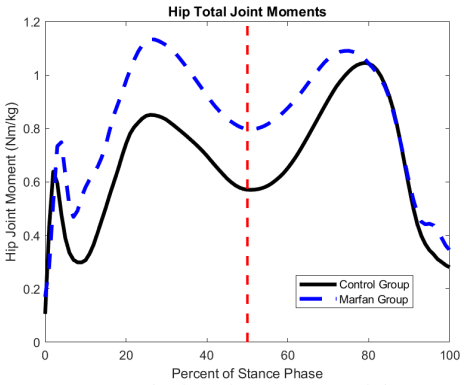

Figure 1: Total Hip Joint Moment of the control and MFS groups

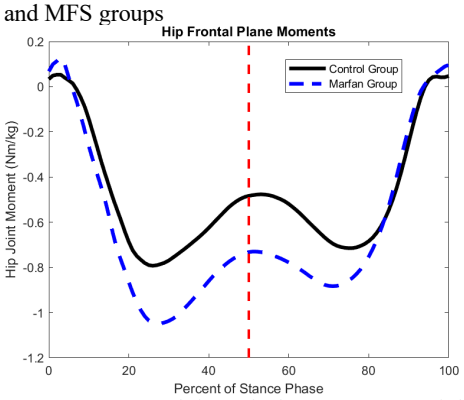

Figure 2: Internal frontal plane moments of the control and MFS groups

Methods: Eighteen participants with MFS and eighteen sex and body mass index (BMI) matched, asymptomatic controls underwent 3D gait analysis. All study participants walked at a fixed speed of 1.35±0.7m·s^{-1}, the average level ground walking speed for adult females and males. The total joint moment (TJM) was calculated as the square root of the sum of the squared planar internal sagittal, frontal, and transverse plane hip moments (Nm·kg^{-1}) at each frame of the stance phase (initial contact to toe-off). The corresponding sagittal, frontal, and transverse planar moments at the peak TJM in the first and second half of the stance phase were extracted. Prior to testing, all study participants completed the Hip Disability and Osteoarthritis Outcome Score (HOOS) [3] in order to obtain self-reported hip pain, symptoms, function during activities of daily living (ADL) and quality of life (QOL). A HOOS sub-score of 0 represents severe hip pain, symptoms, ADL and QOL and a sub-score of 100 indicates no hip pain, symptoms, disability and excellent QOL. As the MFS group was significantly older, an analysis of covariance (adjusting for age) was used to assess for between-group differences in TJM-related parameters. An independent t-test was used to assess between group differences in demographics and HOOS sub-scores. Spearman's rho correlation was used to determine the relationship between the statistically significant TJM-related parameters and HOOS sub-scores. Statistical significance was set at an alpha level of 0.05.

Results & Discussion: The MFS group was significantly older than the control group ($p < 0.01$). Compared to the control group, the MFS group displayed a 1.29x greater first peak TJM ($p=0.01$) and a 1.43x greater internal abduction moment ($p=0.04$) at the first peak TJM (Fig. 1, Fig. 2). Despite no significant differences observed at the second peak TJM, the internal abduction moment occurring at the second peak TJM was 1.23x greater ($p=0.001$) in the MFS group. Individuals with MFS displayed significantly lower HOOS pain sub-scores ($p=0.003$), lower HOOS Symptom sub-scores ($p=0.003$), lower HOOS ADL sub-scores ($p=0.02$), and lower HOOS QOL sub-scores ($p=0.02$). No significant relationships ($p>0.05$) were observed between TJM-related parameters with HOOS sub scores. These study results indicate that the MFS group ambulated with a significantly larger amount of hip joint loading particularly during the first half of stance. A higher internal hip abduction moment may be the contributing factor to the higher hip joint loading present in the MFS cohort. Despite reporting significantly worse hip-related pain, symptoms, ADL and QOL, there was no relationship between the TJM-related parameters with hip-related patient reported outcomes.

Significance: Individuals with MFS ambulate with higher hip joint loading and self-report worse hip-related outcomes compared to healthy controls. The hip abduction moment may serve as a biomechanical target for gait interventions to reduce hip joint loading in the MFS population. Also, future work should assess the ability of the TJM to predict hip-related outcomes during other activities of daily living, such as the sit-to-stand, that place a larger mechanical demand on the hip joint.

Acknowledgments: The Marfan Foundation, NIH (KL2-TR001996, K01-AG073698, & K01-HL149984).

References: [1] Nelson et al. (2015), *Clin j Pain* 31(12); [2] Asay et al. (2018), *Journal of Orthopaedic Research*; [3] Nilsdotter et al. (2003), BMC Musculoskelet Disord 4(10)

CHANGE IN GROUND REACTION FORCE DURING MEASUREMENT OF FOOT STRENGTH IN SITTING AND STANDING POSITIONS

Karen Stevens[1*], Laya Adams[1], Julian De La Rosa[1], Alexis Fletcher[1], Catherine Li[1], Noah Payant[1], Irmina Shareef[1], Hannah Siebert[1], Maxine Olson[1]
[1]Rosalind Franklin University of Medicine and Science, Department of Physical Therapy
*Corresponding author's email: karen.stevens@rosalindfranklin.edu

Introduction: Measures and application of ground reaction force (GRF) for gait analysis are well established. GRF has also been used during tasks such as stair climbing and resistance exercises, providing insight into changes associated with muscle strength post total hip arthroplasty [1], and loading between different resistance exercises [2]. Furthermore, the analysis of GRF may help explain observed differences in peak force during a foot strength test when performed in sitting versus standing positions.

Different methods have been used to measure foot strength, including a paper grip test [3], plantar pressures [4] [5], ultrasonography [6], and dynamometers [5] [7] [8]. Differences in foot strength have been reported when measured by pressing toes into a pressure mat in standing and pulling on a bar with the toes in sitting [5]. Differences in foot strength between sitting and standing positions were also reported during a foot strength test involving pulling on a towel by curling the toes [8]. Why these differences exist between strength testing measures in seated and standing positions is not known. Measuring GRF during a foot strength test in different positions may help explain why differences exist and help to identify a preferred test position.

The purpose of this study was to investigate differences in the change in GRF (cGRF) from rest to peak muscle force during a foot strength test in sitting and standing positions. Because we expected that cGRF in the anterior direction ($cGRF_X$) would be related to the primary direction of pull during the foot strength test, and because more peak force has been reported in the standing position, we expected that the $cGRF_X$ would be greater in the standing versus sitting position. Also, because plantar pressures during a toe strength test have been shown to be greater in standing, and GRF in the vertical direction (GRF_Z) has been related to plantar pressure, we expected that $cGRF_Z$ during a foot strength test would be greater in standing versus sitting.

Figure 1: GRF Coordinate System

Methods: 20 adults ($\bar{x}$ = 24.7 years; 9 males, 11 females) without recent injury or surgery consented and completed the study. After completing a demographic questionnaire, participants were randomly assigned to the first testing position, sitting or standing. A force plate (Kistler Instrument Corp.; Amherst, NY) was calibrated prior to each testing session. Participants placed their right foot on the force plate with their forefoot resting on a 4-inch x 6-inch towel which was connected to a dynamometer (Figure 2). After completing 3 practice trials participants pulled the towel with their toes until peak force was achieved for 3 recorded trials. The procedure was then repeated in the second testing position. A video recording of the dynamometer identified peak force and time to peak force. Custom MATLAB code was used to extract resting GRF and GRF at peak force to determine cGRF.

Results & Discussion: Peak force (kg) was significantly greater ($p<0.001$) in standing ($\bar{x}$ = 4.13 kg +/- 1.75) than in sitting ($\bar{x}$ = 2.83 kg +/- 1.98). This was expected, and is consistent with previous findings using similar strength testing methods [8]. As expected, $cGRF_x$ in standing ($\bar{x}$ = 25.56N +/- 17.02) was significantly greater ($p<0.001$) than sitting (6.33N +/- 15.11). Additionally, some participants (36.67%) had negative cGRFx in the sitting position. This might suggest that the rearfoot pressed or slid in the anterior direction, opposite the posteriorly-directed toe curl. This could impact the ability of muscles to translate their effort into the pull on the towel. For example, if the muscle origin (e.g. the calcaneus) is pressed or slid in the anterior direction it might reduce the tension that the muscles are able to develop. An unstable rearfoot may also require additional muscular effort aimed at rearfoot stabilization and therefore reduce muscular effort into pulling the towel. $cGRF_Z$ was not different ($p=0.183$) between sitting (8.08N +/-19.54) and standing (2.56N +/-16.85). This may be due to the different methods used in studies which examined plantar pressures and simply had subjects press down into a mat [5]. In this study, participants were required to both press down and pull back with their toes.


Figure 1: Position of Foot, Towel, and Dynamometer for Strength Test

Significance: The standing foot strength test position demonstrated more consistent $cGRF_X$ and may better measure the effort of the foot musculature. Therefore, the standing position may be the preferred position for measuring foot strength. Future studies, though, are needed to examine foot strength testing in the seated position to reduce $cGRF_X$ variability and further understand differences with standing measures as some patients will likely be unable to perform the test in standing.

Acknowledgments: We would like to thank Tyler Arl SPT, Frank DiLiberto PT, PhD and Mary Rahlin PT, DHS, PCS, for their contributions to this study.

References: [1] Arima et al. *Clin Biomech (Bristol, Avon)*. 2020;78; [2] Jönsson et al. *J Biomech*. 2019;87;[3] Menz et al. *Foot Ankle Int.* 2006;27(12); [4] Mickle et al. *Clin Biomech*. 2009;24;; [5] Bruening, DA et al. *BMC Musculoskelet Disord*. 2019;20:608; [6] García- García et al. *Biomedicines*. 2023;11,2115; [7] Uritani D et al. *J Foot Ankle Res*. 2014;7:28; [8] Stevens et al. *J Orthop Sports Phys Ther*.2014;44(1).

ALTERED HIP MECHANICS ARE ASSOCIATED WITH POOR HIP-RELATED OUTCOMES IN PEOPLE WITH MARFAN SYNDROME

Mariana V. Jacobs[1*], Justin M. Pol[1,2], Jody L. Clasey[1], Christopher J. McLouth[1], Mary B. Sheppard[1], Michael A. Samaan[1]
[1]University of Kentucky, Lexington, KY
[2]Southern Illinois University-Carbondale, Carbondale, IL
*Corresponding author's email: mariana.jacobs@uky.edu

Introduction: Marfan Syndrome (MFS) is an autosomal dominant connective tissue disorder caused by mutations in the fibrillin-1 (*FBN1*) gene. [1,2] These genetic mutations lead to alterations in muscle tissue composition and muscle function. Individuals with MFS exhibit higher instances of osteoarthritis (OA) compared to individuals without MFS. In addition, approximately 46% of individuals with MFS self-report hip pain.[4] which may be caused by altered hip joint mechanics. Despite these detrimental clinical outcomes, there have been no prior assessments to determine if altered hip joint mechanics during gait are associated with hip-related patient reported outcomes (PRO). Therefore, the purposes of this study were to: 1) assess if individuals with MFS ambulate with altered hip joint mechanics compared to healthy, asymptomatic individuals and 2) determine the relationship between hip joint mechanics with hip-related PRO within the MFS population. We hypothesized that individuals with MFS would ambulate with altered hip joint mechanics and that hip joint mechanics would be associated with hip-related PRO within the MFS group.

Methods: Eighteen participants (16F; 39.3±4.6 yrs; BMI 25.8±5.7 $kg \cdot m^{-2}$) with clinically confirmed MFS (according to the Revised Ghent Nosology of 2010 [2]) and 18 healthy, asymptomatic controls (16F; 26.4±7.5 yrs; BMI 23.7±3.9 $kg \cdot m^{-2}$) participated in this study. Each participant completed 5 successful level ground walking trials at a fixed speed of 1.35±0.7$m \cdot s^{-1}$ (the average level ground walking speed for healthy adults). The most symptomatic limb and dominant limb was selected as the test limb for the MFS and control groups, respectively. Sagittal plane hip joint kinematics, internal joint moments and internal joint moment impulses were compared between the MFS and control groups. The MFS group completed the Hip disability and Osteoarthritis Outcome Survey (HOOS) [5] in order to obtain self-reported hip pain, symptoms, function during activities of daily living (ADL) and quality of life (QOL) for the test limb. A HOOS sub-score of 0 and 100 represents severe outcomes and positive outcomes, respectively. Between group differences in demographics were assessed using an independent t-test. Between-group differences in hip mechanics were assessed using an analysis of covariance with age as a covariate. The statistically significant hip-related biomechanical parameters were used in a multi-variate, stepwise linear regression model to determine if hip mechanics were able to predict HOOS outcomes within the MFS cohort. Statistical significance was set at an alpha level of 0.05.

Results & Discussion: The MFS group was significantly older than the control group ($p<0.01$). Individuals with MFS ambulated with significantly higher peak hip flexion ($p=0.02$) and higher hip extensor moment impulse ($p=0.02$). Peak hip flexion angle was able to predict 25% of the variance in HOOS pain sub-scores within the MFS group ($p=0.04$, $R^2=0.25$). Within the MFS cohort, higher peak hip flexion was associated with lower HOOS pain sub-scores (i.e. worse hip pain). Prior work demonstrated that individuals with hip osteoarthritis (OA) ambulate with higher peak hip flexion angles compared to those without hip OA.[6] In addition, individuals with femoroacetabular impingement syndrome (FAIS), a form of pre-arthritic hip disease, ambulate with a higher internal hip extensor moment impulse compared to asymptomatic controls.[7] The MFS cohort in this study exhibited similar hip joint mechanics as individuals with hip OA and FAIS.

Figure 1. Stance phase kinematic group profiles

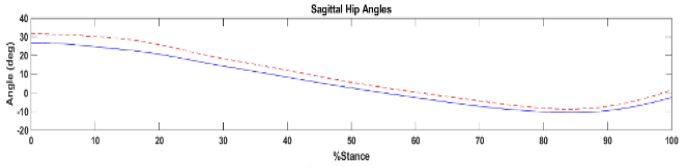

Figure 2. Stance phase kinetic group profiles

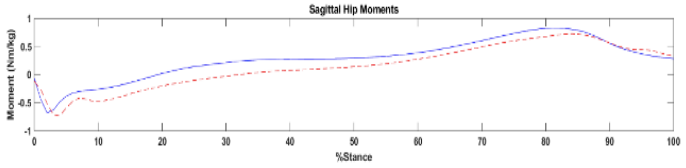

Significance: Our study results support our hypothesis that hip joint mechanics were altered in the MFS cohort and that hip joint mechanics would predict HOOS outcome scores in individuals with MFS. In addition, our results indicate that individuals with MFS demonstrate similar hip joint mechanics during walking as individuals with pre-arthritic hip disease and hip OA. Gait interventions that optimize sagittal plane hip joint kinematics and the hip extensor moment impulse may prove beneficial in reducing hip pain and mitigating the development of hip OA in individuals with MFS.

Acknowledgements: The Marfan Foundation, NIH (KL2-TR001996, K01-AG073698, & K01-HL149984)

References: [1] Giske et al, J Rehabil Med 35(5), 2003. [2] Loeys et al, J Med Genet, 47(7), 2010. [3] Hasan et al, Int J Clin Pract, 61(8), 2007. [4] Nelson et al, , Clin J Pain 31(12), 2015. [5] Nilsdotter et al, BMC Musculoskelet Disord, 4(10), 2003. [6] Kumar et al, J Orthop Res, 33(4), 2015. [7] Samaan et al, AJSM, 45(4), 2017.

DEEP BRAIN STIMULATION IMPROVES DYNAMIC BALANCE CONTROL IN INDIVIDUALS WITH PARKINSON'S DISEASE

Moll AN, Kuhman DJ, Walker HC, Green A, and Hurt CP[1]
[1]University of Alabama at Birmingham, 1705 S. University Blvd, Birmingham, AL 35205
email: *amoll@uab.edu

Introduction: As Parkinson's Disease (PD) progresses individuals are at a greater risk for developing postural instability and falls. In fact, for individuals with PD, falls are the leading cause of injuries, hospitalization and even death [1,2]. Deep brain stimulation (DBS) is a second line therapeutic modality in which an electrode is implanted in the basal ganglia to alleviate worsening symptoms of PD. It is equivocal whether DBS reduces fall risk in this population despite positively affecting other cardinal symptoms of PD [3]. We tested how DBS impacts postural control and dynamic stability in participants with PD. Maintenance of balance requires that the nervous system is able to effectively respond to external postural disturbances that are encountered in everyday life. Responding to postural disturbances is a multifactorial problem the nervous system must solve to maintain stability. Additionally, individuals with PD have difficulties in scaling their postural responses due to abnormal sensorimotor integration [4]. We performed a study to test the effect of DBS on the reducing the amount of postural sway during increasingly more challenging balance tests and to avoid taking a step in response to scaled external postural disturbances to measure dynamic balance control [5]. We collected both static balance data as well as dynamic balance on a group of individuals who were part of a larger study. We hypothesize that individuals on DBS would be more stable to complete higher step thresholds reflecting in an increase in dynamic balance response.

Methods: Twenty-eight individuals with PD (mean age: 61 years, UPDRS off medication: 49) participated in this study. The data collected here is part of a larger clinical trial (NCT03353688). For this analysis, participants visited the lab at baseline, prior to surgery and 2 and 4 months after a DBS electrode was surgically implanted. For all conditions, Participants stood quietly on a force platform for 60 seconds with feet shoulder width apart, feet together, semi-tandem, and tandem postures while we quantified their sway area as the task of balance became more challenging. Additionally, we assessed individuals step threshold [5]. Participants stood on a treadmill while experiencing progressive balance disturbances by increasing treadmill belt acceleration incrementally by 0.5 m/s,^{2} while we instructed participants to avoid taking a step unless they must. The magnitude of the disturbance was increased until individuals were unable to avoid stepping 4 times in a row resulting in their step threshold [5]. We also clinically assessed the motor effects of PD using the MDS-UPDRS, which allows us to assess the postural instability and gait disorder (PIGD). A two-way ANOVA repeated measures was performed to determine if treatment state (Baseline vs. DBS) and task (quiet standing, feet together, semi-tandem) had a significant effect on sway area (mm^2). Paired samples t-tests were used to compare step threshold magnitude and balance capability between all static posturography positions. Paired samples t-tests were used to compare step threshold magnitude and balance capability between "Baseline" and "DBS" states. Based on previous work in our lab, we were also interested in assessing the extent that being able to complete a tandem stance task would differentiate our participants into distinct groups for the step threshold tasks [6]. Based on previous findings from our lab, we wanted to assess whether clinical markers of PD progression will negatively correlate to the magnitude of postural disturbances that create a stepping response. Statistical significance was achieved if $p<0.05$.

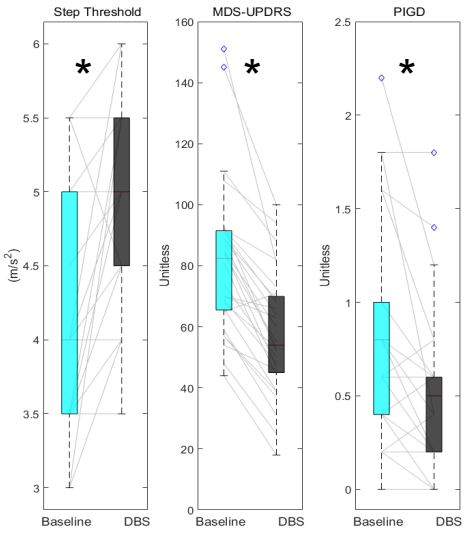

Figure 1: Step threshold magnitude, MDS-UPDRS, and PIGD results comparing "Baseline" and "DBS" states. * $p < 0.001$

Results & Discussion: For participants with Baseline or "off" medication state and "DBS" states, step threshold magnitude was significantly higher for "DBS" ($p < 0.001$; Figure 1). The effect size for the "DBS" state in comparison to the Baseline or "off" medication state was medium to large ($\eta^2 = 0.72$). Step thresholds for participants off medication were negatively correlated to MDS-UPDRS part III total ($p = 0.021$; $r = -0.433$) and PIGD ($p = 0.027$; $r = -0.418$) scores. A two-way ANOVA revealed that treatment ($p < 0.001$) had a statistically significant effect on the sway balance test. The data showed a medium effect size from tasks ($\eta^2 = 0.454$). The participant performing the more challenging balance test demonstrated significantly higher sway area than participants performing the less demanding task. Further, a Bonferoni post hoc analysis's test for multiple comparisons found that semi-tandem and feet together sway area was significantly higher than the quiet stance task ($p < 0.001$ for both). However, there was no significant difference in sway area between participants that performed the feet together and semi-tandem tasks.

Significance: Although it is equivocal if DBS can benefit fall risk symptoms for participants with PD, these results support our hypothesis that individuals reach higher step thresholds with DBS during dynamic balance testing. This is important for clinical purposes, especially to inform evidence-based perturbation-based training intervention programs for individuals with Parkinson's Disease.

References: [1]Horak FB, et al. Physical Therapy. 1997; 517-33.; [2]Allen NE, et al. Parkinsons Dis. 2013; doi.org/10.1155/2013/906274; [3] Fasano et al. Nat Rev Neurol. 2015; [4]Jacobs JV, et al. Neuroscience. 2006; 141:999–1009; [5]Kuhman D, et al. Gait & Posture. 2020; 68-74.; [6] Hurt C. et al., *International Society of Biomechanics*. 2019: Calgary CA.

AUTO-SEGMENTATION OF SHOULDER CT SCANS IS MORE ACCURATE IN YOUNG HEALTHY CONTROLS COMPARED TO OLDER SURGICAL PATIENTS

Emily C. Gray[1*], Clarissa LeVasseur[1,2], Tom Gale[1], Sabreen Megherhi[1], Zhaoyi Fang[1], Gillian Kane[1], Nathan Hyre[1], Albert Lin[1,2], William Anderst[1]
[1]University of Pittsburgh, Pittsburgh, PA [2]Bethel Musculoskeletal Research Center, Pittsburgh, PA
*Corresponding author's email: cate.gray@pitt.edu

Introduction: Medical image segmentation allows for 2D-3D image registration, subject-specific modeling, and morphology analysis in research settings and pre-surgical planning for clinical settings. While artificial intelligence (AI) and deep-learning algorithms are used to advance segmentation efforts, manual segmentation is still considered the gold standard for detailed structures. The process of manually segmenting bones is tedious due to noise, varying tissue and bone density, and low contrast in images [1], whereas AI-assisted segmentation programs can substantially reduce segmentation time. However, the varying quality and anatomic heterogeneity of patient scans can lead to variable success of automated segmentation. Previous studies have evaluated auto-segmentation compared to manual segmentation [2], but the accuracy of auto-segmentation across patient populations remains unclear. The primary objective of this study was to compare commercially available AI-based auto-segmentation (ScanIP, Simpleware) to manual segmentation of humerus and scapula bones for young healthy individuals and older patients with irreparable rotator cuff tears. Based upon previous research that found a negative correlation between age and complete auto-segmentation [3], we hypothesized that (1) auto-segmentation would be more successful for the young asymptomatic group for both the humerus and scapula and (2) that auto-segmentation of the humerus would be better than the scapula due to the more complex bony morphology of the scapula.

Methods: Patients scheduled to undergo superior capsular reconstruction and healthy, asymptomatic individuals with no history of shoulder pathology provided written informed consent prior to participating in IRB-approved studies. Asymptomatic individuals received bilateral shoulder CT scans (resolution: 0.44x0.44x0.625mm), while patients received a CT scan of their affected shoulder (resolution: 0.47x0.47x1.25mm). Each CT scan was resliced to create isometric voxels (average: 0.45x0.45x0.45mm). From the resliced CT scans, bone tissue was manually segmented (Mimics, Materialise) to construct masks and 3D surface models of the humerus and scapula. The ScanIP Shoulder CT Auto Segmentation was run on a computer with 32 GB RAM, Intel Core i9-7900X CPU @ 3.30 GHz, and NVIDIA GeForce GTX 1080 GPU. The manual and auto-segmented masks were compared using Dice similarity coefficient (DSC) on both the entire mask and the 1-pixel edge of each mask [4]. The average differences between the surface models were determined in GeoMagic Design X. A two-way repeated measures ANOVA assessed differences in the overall DSC, 1-pixel edge DSC, and surface deviation between bones (scapula vs humerus), groups (surgical vs asymptomatic), and their interaction, with significance set at $p < 0.05$.

Results & Discussion: Sixty shoulders of 30 asymptomatic volunteers (15M, 15F) and nine shoulders of nine patients with massive rotator cuff tears (7M, 2F) were included in this analysis. The patients were older (62±8 years, $p<0.001$) and had a higher BMI (29±4.25 kg/m², $p<0.007$) compared to the asymptomatic group (25±7 years; 25±4.25 kg/m²). Auto segmentation of the asymptomatic and affected shoulders took 1.2±0.4 minutes, while manual segmentation of a shoulder took approximately 60 minutes. DSC scores were better for the humerus (0.98±0.01) compared to the scapula (0.96±0.02; $p = 0.003$) and better for asymptomatic controls (0.97±0.02) compared to patients (0.96±0.03; $p = 0.001$; Figure 1A). There was also an interaction between the group and bone such that the difference between the DSC in the surgical group between bones was larger than the difference in the asymptomatic group ($p = 0.007$; Figure 1A). We failed to find a difference between bones or groups for the 1-pixel edge DSC (all $p > 0.05$; Figure 1B). 3D surface deviations were lower for the humerus (-0.06±0.3 mm) compared to the scapula (-0.13±0.2 mm; $p = 0.047$) and lower for the asymptomatic group (-0.08±0.2 mm) compared to surgical patients (-0.20±0.3 mm; $p =0.045$; Figure 1C), but there was no interaction between bones and groups for the surface deviations ($p = 0.409$). Our results confirm both of our hypotheses that the humerus auto-segmentation was better than scapula and the auto-segmentation from older pre-surgical patients was worse than for the young asymptomatic controls. The average 3D surface deviation was below one voxel for almost all scapulas and humeri, and the 1-pixel edge DSC average was over 0.5 for both bones, suggesting the auto-segmentation accuracy is within the 1-pixel range. Additional young surgical subjects are needed to clarify if the differences between groups are due to age or pathology.

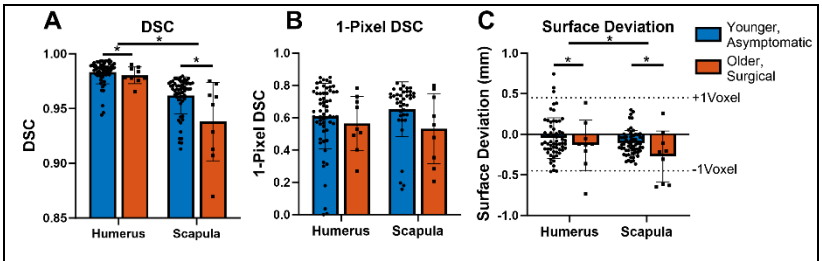

Figure 1: Average, standard deviation, and distribution of (A) DSC, (B) 1-pixel DSC, and (C) surface deviation for both the scapula and humerus in surgical (red) and asymptomatic (blue) groups.

Significance: Auto-segmentation is much faster than manual segmentation and nearly as good in young asymptomatic shoulders, but auto-segmented shoulders of older patients may need more refinement to accurately replicate bone morphology.

Acknowledgments: This work was funded by NIH Grant: R01-AR080425.

References: [1] Alahmadi, Mohammad D. (2022), *Diagnostics (Basel)* 12(7); [2] Gao et al. (2023), *Pract Radiat Oncol* 13(5); [3] Wasserthal et al. (2023), *Radiol Artif Intell* 5(5); [4] Dice, Lee R. (1945), *Ecol* 26(3).

EFFECTS OF COGNITIVE LOAD ON POSTURAL SWAY AND PUPILLARY RESPONSE

Chandler Brock[1], Joseph A. Aderonmu[1], Arun Karumattu Manattu[1], Carolin Curtze[1*]
[1]University of Nebraska at Omaha, Omaha, NE
*Corresponding author's email: ccurtze@unomaha.edu

Introduction: Postural control allows the body to maintain balance and orientation in space [1,2]. Traditionally, it has been viewed as an automatic function governed by reflexes. However, contemporary research indicates that cognition, particularly attention, also significantly influences this process [3]. Simultaneous performance of both a cognitive and postural task results in dual-task interference [4] and leads to performance deficits due to capacity limits. Thus, dual-task interference will allow us to study how cognitive load impacts postural sway parameters such as jerk and root-mean-square (RMS) sway. Further, pupillary response can provide insights into cognitive load with pupil diameter changes reflecting cognitive demand [5]. However, the association between postural sway and pupillary response while conducting a cognitive task with increasing levels of difficulty is incompletely understood. The overall goals of this study are 1) to determine the relationship between pupillary response and task difficulty, 2) to determine the relationship between postural sway and cognitive load, and 3) to describe the relationship between pupillary response and postural sway with increasing cognitive load. We hypothesize that 1) the pupils will dilate to a greater extent as cognitive load is increased via increasing cognitive task difficulty, 2) postural sway will increase as cognitive load is increased, and 3) a positive relationship between pupil dilation and postural sway as cognitive load is increased.

Methods: Healthy subjects aged 45-90 years old who are free of neurological disorders and orthopaedic problems were recruited for this study. Participants completed questionnaires prior to engaging in testing. These included demographic, Montreal Cognitive Assessment, History of Falls, and Activities-specific Balance Confidence (ABC) Scale questionnaires. Seated and standing trials were performed both with and without a cognitive task. Subjects fixated on a 2-inch diameter black dot placed 2 meters in front of them at eye level for all trials. The cognitive task that we used was an N-back test. This test is a letter sequencing test in which the participant must determine if the current letter matches the letter "N" items ago. N-back tests with increasing difficulty levels (1-back and 2-back, respectively) were performed. A wearable sensor (Opal V2, APDM) attached to the lumbar region was used to measure postural sway during the standing postural sway trials. Further, measurement of the pupillary response via eye-tracking glasses (Tobii Pro Glasses 2, Tobii) were used to gain insight into cognitive load as the pupil diameter increased with cognitive demand.

Results & Discussion: Preliminary analysis of thirteen (n=13) individuals reveals increases in pupil diameter with increasing cognitive task difficulty, confirming our first hypothesis. Notably, postural sway parameters did not consistently increase with increasing cognitive load and task difficulty in all subjects, contrary to our second hypothesis. As can be seen in Figure 1, the changes in both RMS and jerk in the mediolateral (ML) direction are small across the 3 conditions. Finally, we observed a positive correlation between pupil diameter and RMS sway in the ML direction, which confirms our primary hypothesis. However, the correlation between pupil diameter and jerk in the ML direction showed varying trends.

Significance: Our preliminary results show how increasing cognitive load affects both postural sway and pupillary response. By implementing cognitive dual tasks with increasing difficulty levels, this study will further enhance our understanding of the automaticity of postural sway and the role of cognitive load.

Acknowledgments: We would like to thank the University of Nebraska at Omaha GRACA fund and the NIH P20 GM109090.

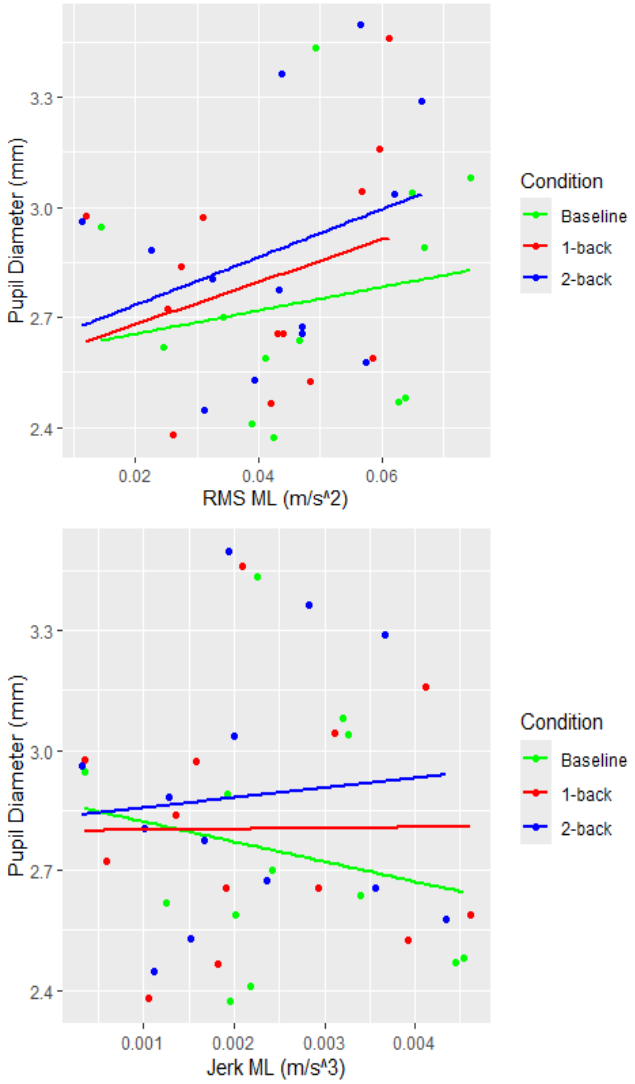

Figure 1: Correlation of pupil diameter and RMS sway and jerk in the ML direction across single- (baseline) and dual-task conditions for all subjects.

References: [1] Shumway-Cook & Woollacott (2000), *J Gerontology* 55(1); [2] Shumway-Cook & Woollacott (2000), *Motor Control: Theory and Practical Applications*; [3] Woollacott & Shumway-Cook (2002), *Gait & Posture* 16(1); [4] Huxhold et al. (2006), *Brain Research Bulletin* 69(3); [5] Kahya et al. (2018), *Frontiers in Aging Neuroscience* 10.

ALTERATIONS IN FORELIMB GAIT DURING DEVELOPMENT FOLLOWING BRACHIAL PLEXUS BIRTH INJURY

Vivian M. Mota[1*], Kyla B. Bosh[1,2], Katie B. Taran[1,2], Jennifer R. Potts[1,2], Jacqueline H. Cole[1,2], Katherine R. Saul[1]
[1]North Carolina State University, Raleigh, NC, [2]University of Chapel Hill, Chapel Hill, NC
*Email: vmmota@ncsu.edu

Introduction: Brachial plexus birth injury (BPBI) is a pediatric nerve injury that is prevalent in 1 of 1,000 live births [1]. BPBI results in limb paralysis, shoulder contracture, deformed scapular and humeral growth [2–4], and lifelong impairment. Previous BPBI murine studies have shown that animals with more declined glenoids use their injured limb for less weight-bearing time (stance time) relative to a healthy control group [5-6]. However, earlier studies focused on a single timepoint of 8 weeks of development when bone deformities are already well established, and it is not clear when initial gait alterations appear nor if they resolve over time. Our objective was to determine how metrics in forelimb gait (stride length, stride time, stance time, duty factor, and gait symmetry) are affected by BPBI across developmental time points in a murine model. The time course of clinical intervention for BPBI is not well defined; thus this study will shed light to help clinicians create well-informed decisions for initiating treatment.

Methods: Three groups of Sprague Dawley rat pups (n=145; preganglionic or postganglionic neurectomy, or disarticulation) underwent surgery 3-6 days post-birth on one forelimb to model BPBI. Neurectomy procedures were applied to the C5-C6 nerve roots relative to the dorsal root ganglion: postganglionic (distal) and preganglionic (proximal). The disarticulation group underwent amputation at the elbow to induce altered and reduced limb usage [7]. A fourth group with no intervention acted as the control group (n=20). Animal walking (5 m/min) and running (10 m/min) gaits were recorded using an Exer 3/6 Treadmill (Columbus Instruments) and two GoPro cameras at 3, 4, 6, 8, 12, and 16 weeks post-surgery. Kinovea was used for video analysis of the forelimbs at each speed for metrics including stride length (**Figure 1**), stride time, stance time, duty factor (stance time/stride time), and stance factor (limb ratio of stance duration, left/right and injured/uninjured) [5]. Metrics for the injured limb (control: left) were compared using a two-way ANOVA (main factors: group, time) (GraphPad Prism, α=0.05).

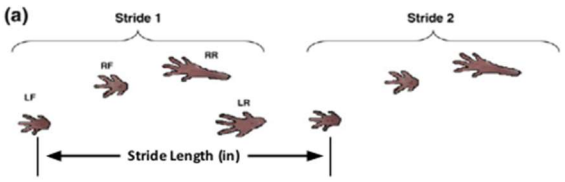

Figure 1: Stride Length, (Image adapted [10])

Results & Discussion: Stride length during walking (**Figure 2**) of the injured limb exhibited a significant main effect for surgical groups ($p<0.0001$) and timepoint ($p<0.0001$). Surgical groups had an increase in injured limb stride length compared to control. All groups had an increase in stride length over time, consistent with previously collected data [8]. Stride time and stance time of the injured limb also increased over time ($p=0.0005$ and $p=0.0009$, respectively). Main effects for surgical group were also significant for stride time ($p=0.0002$), stance time ($p=0.0029$), stance factor ($p<0.0001$), and duty factor ($p<0.0001$). The control group exhibited symmetric gait (indicated by stance factor within 20% of a value of 1), whereas the surgical groups had a lower stance factor. These data are consistent with previously collected 8-week data compared to a sham group [5]. Preliminary results suggest alterations in functional weight-bearing activity are detectable throughout growth, as early as 3 weeks in our murine model. Translating this to early human musculoskeletal development [9], we would observe alterations as early as 6 months. Analyses for running gait (10 m/min) are ongoing.

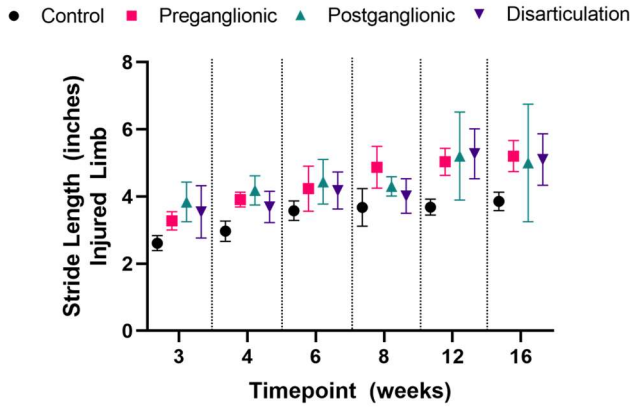

Figure 2: Stride Length - Over Time

Significance: Clinicians need a better understanding of the timeline for deformity development following BPBI to enhance treatment options when navigating patient rehabilitation. These quadrupedal animal models provides insight into functional limb gait, in which we showed early postnatal changes following injury. Understanding the alterations to forelimb gait following BPBI is crucial when comparing to human limb function, specifically at a young age when babies are considered quadrupedal during a period of rapid musculoskeletal growth and development.

Acknowledgments: NIH R01HD101406. We thank Dr. Kerry Danelson and Dr. Roger Cornwall for their surgical support.

References: [1] Defranesco *et al*. (2019) *J Pediatr Orthop* 39(2); [2] Hogendoom *et al*. (2010), *J Bone Joint Surg Am 92(4);* [3] Pearl *et al*. (1998), *J Bone Joint Surg Am 80(5)*; [4] Poyhia *et al*. (2005) *J Pediatr Radiol 35(4)*; [5] Hennen *et al*. (2018), *J Orthop Res 36(7)*; [6] Doshi *et al*. (2022) *J Orthop Res* 40(6); [7] Merritt *et al*. (2021) *Manuscript in Prep.;* [8] Taran *et al*. (2023), *NCUR Eau Claire, WI*; [9] Sengupta et al. (2013) *Int J Prev Med 4(6):624-30.*; [10] Vincelette *et al*. (2007) *Arthritis Res Ther* 9(6).

MACHINE LEARNING BASED RUNNING GRADE CLASSIFICATION USING IMU DATA

Abdelbadiâ Chaker[1], Hanin Atiga[1], Seth Donahue[3], Rachel Robinson[2], Aida Chebbi[2], Sami Bennour[1], Michael Hahn[2]
[1] Mechanical Laboratory of Sousse, National School of Engineers of Sousse, University of Sousse, Tunisia
[2] University of Oregon, Eugene OR, USA
[3]Northwestern University, Chicago, IL, USA
abdelbadia.chaker@eniso.u-sousse.tn

Introduction: Various research has investigated categorizing ground inclination in running using IMU data, employing both machine learning and non-machine learning methods [1]. Non-machine learning studies have primarily analyzed biomechanical parameters, including stride length, step frequency, joint angles, and ground reaction forces, using technologies such as accelerometers, gyroscopes, force plates, and load soles [2]. However, these studies encounter challenges with subject variability and replicating real-world conditions, resulting in limited accuracy and time-consuming manual analysis. Hence, advanced machine learning methods are needed for improved ground grade classification. Nguyen et al. [3] proposed a method using smart shoes with plantar pressure sensors to classify ambulatory activities. Ahamed et al. [4] investigated subject-specific vs. group-based models in identifying changes in running gait biomechanics. Previous studies are limited by small or homogeneous datasets and sensitivity to treadmill speed changes. Therefore, this paper introduces a machine learning classification method tailored for determining running grades using IMU-acquired data. A set of features associated with IMU data were discerned and extracted to suit the intended application.

Methods: Ten healthy runners (7 females, 3 males), averaging 25.5 years old, 168.6 cm tall, and weighing 59.6 kg, participated in the study. Each wore three Casio IMUs on their feet and sacrum while running on a treadmill at speeds from 3.16 to 4.88 m/s across various grades (level ground, incline, and decline). The IMUs recorded 3D accelerations and angular velocities at 200 Hz during thirteen 30-second trials, where participants varied their paces and ran on surfaces with different inclinations. IMU data underwent Kalman filter post-processing for synchronization and alignment of angular velocities and accelerations, creating a comprehensive dataset. Features were then extracted via windowing, segmenting acceleration and angular velocity time series into complete running cycles. Using a 600 ms window and 20 ms overlap, 6450 samples were generated across all conditions (Fig.1). Extracted features of nine parameters from both time and frequency domains enabled thorough biomechanical analysis, comprising 432 features capturing various dynamics conveyed by IMU measurements. The dataset was divided into training and test sets, with 90% for training and 10% for testing.

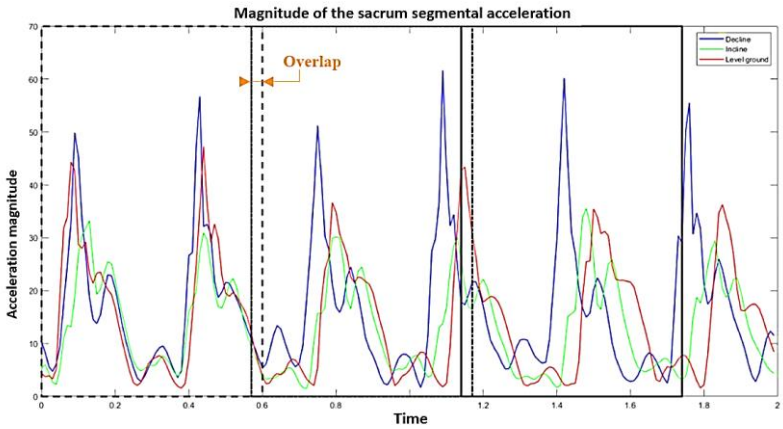

Figure 1: Windowed Data of the magnitude of sacrum segmental acceleration.

Results & Discussion: Following an analysis of results for the three tested machine learning models: Kernel Naive Bayes, Support Vector Machine Kernel, and Quadratic Support Vector Machine (QSVM) algorithms, each of the algorithm demonstrates relatively high accuracy in classifying instances across the three classes: Decline, Incline, and Level Ground, with an overall accuracy exceeding 90%. A closer examination of algorithm performance using predefined metrics: precision, recall, and F1 score (presented in Table 2), reveals that the QSVM algorithm performs better compared to the two others, with higher accuracy rates, recall, precision, and F1 score, exceeding 99%. This algorithm appears to be the preferable choice for ground grade classification within the given dataset, demonstrating more reliable performance in classification tasks.

Table1: Performance metrics of the studied Machine learning algorithms

Model Type	Accuracy	Recall (%)			Precision (%)			F1 score (%)		
	(%)	Dec	Inc	LG	Dec	Inc	LG	Dec	Inc	LG
SVM Kernel	99,5	99,7	98,7	99,4	99,4	99,8	99	99,5	99,2	99,2
Kernel Naive Bayes	92,4	93,4	93,5	93,5	93,1	97,5	93,4	93,2	95,5	92,4
Quadratic SVM	99,7	99,7	99,5	99,5	99,7	99,7	99,5	99,7	99,6	99,5

Significance: The study introduced a precise machine learning classifier for ground levels in running, using data from three IMUs easily collected outdoors. This offers improved insights into runner performance and valuable inputs for injury risk detection studies. Future work aims to reduce the number of IMUs used with a larger dataset and incorporate additional levels of classification, particularly focusing on different speed levels.

Acknowledgments: This work was partially supported by Casio. Additional support was provided by the Wu Tsai Human Performance Alliance and the Joe and Clara Tsai Foundation.

References: [1] Chandra et al. (2005), *Artificial Intelligence Review 49*; [2] Kim et al. (2019), *Sensors 19(18)*; [3] Nguyen et al (2018). *IEEE Sensors Journal 18. (13)*; Ahamed et al.(2019), *Journal of Biomechanics 84.*

FUNCTIONAL DEMAND DURING WALKING DOES NOT DIFFER BETWEEN LIMBS AFTER ANTERIOR CRUCIATE LIGAMENT RECONSTRUCTION

Alexa K. Johnson[1*], Ryan Mahoney[1], Beyza Tayfur[1], Riann M. Palmieri-Smith[1,2]
[1]School of Kinesiology, University of Michigan, Ann Arbor, MI
*Corresponding author's email: akjohns@umich.edu

Introduction: Following anterior cruciate ligament (ACL) reconstruction quadriceps weakness has been well documented [1,2]. Restoring quadriceps strength following ACL reconstruction is important for joint stability and lower extremity load attenuation during walking and other types of physical activity. However, it remains unclear the extent to which quadriceps strength is impacting load attenuation during walking. Quadriceps muscle functional demand can be used to provide insights into the influence of quadriceps muscle weakness on knee loading during gait, after ACL reconstruction. Functional demand is the ratio between joint kinetics and muscle strength and has been explained as the muscle capacity used during a functional task [3]. An assessment of quadriceps muscle capacity during gait has yet to be explored in an ACL reconstructed population throughout rehabilitation, though is warranted due to the known muscle deficits following surgery. Therefore, the purpose of this study was to examine the changes in functional demand between the ACL and NonACL limbs following ACL reconstruction. We hypothesized that while quadriceps strength and knee loading would be less in the ACL limb compared to the NonACL limb, that functional demand would be higher in the ACL limb compared to the NonACL limb indicating that the quadriceps would be required to work at a higher capacity in the ACL limb.

Methods: A total of thirty-four individuals (18 F, 16M; Age 23.8 ± 8.7 yrs; Height 1.73 ± 0.07m; Mass 77.4 ± 14.3kgs) completed two testing sessions following a primary unilateral ACL reconstruction, the first happening 4.43 ± 0.46 months (T4M) after surgery and the second happening 9.08 ± 0.45 months after surgery (T9M). At both testing sessions, individuals completed bilateral isometric strength testing and gait biomechanics. Individuals first sat in an isokinetic dynamometer according to manufacturer guidelines with their knees locked at 60 degrees of flexion. They completed a standardized warm up protocol and three maximal effort isometric strength trials. The average of the three trials were recorded as the maximal voluntary isometric contraction (MVIC). Individuals then completed gait analysis utilizing 3D motion capture while walking overground at their self-selected pace. Internal knee moments were calculated using inverse dynamics, and peak knee extension moments during the first half of stance were extracted. Functional demand was calculated as the peak knee moment divided by the MVIC, reported as a percentage, for each limb (ACL vs NonACL). Repeated measures analyses of variance with two repeated factors (limb and time) were used to compare functional demand, knee moments, and MVIC between limbs and over time. Bonferonni multiple comparison procedures were used post hoc in the case of time by limb interactions.

Results & Discussion: There was no significant interaction or significant main effects for functional demand ($p > 0.05$) (Table 1). There were, however, significant limb x time interactions for the peak knee moment ($p=0.020$) and MVIC ($p<0.001$). Post-hoc testing indicated that peak knee moment and MVIC were significantly lower in the ACL limb compared to the NonACL limb at both T4M (MVIC: $p<0.001$; Knee Moment: $p<0.001$) and T9M (MVIC: $p<0.001$; Knee Moment: $p=0.002$). Additionally, post-hoc testing indicated a significant decrease in the NonACL limb MVIC from T4M to T9M ($p=0.004$). The differences in ACL limb quadriceps strength and knee loading are expected and similar to previous research showing weaker quadriceps muscles [1,2] and underloading during gait [4] in the ACL limb compared to the NonACL limb. Alternatively, the lack of differences in functional demand are surprising given the deficits in quadriceps strength, though it is likely that the underloading happening on the ACL limb keeps the ratio consistent to indicate similar muscle capacity.

	T4M		T9M	
	ACL	**NonACL**	**ACL**	**NonACL**
Functional Demand (%)	30.7 ± 13.3	29.1 ± 10.8	31.2 ± 13.3	30.4 ± 10.2
Peak Knee Moment (Nm)	46.5 ± 19.7*	60.6 ± 23.6	49.7 ± 20.7*	57.8 ± 18.1
MVIC (Nm)	160.2 ± 55.6*	214.2 ±55.8$^{\alpha}$	167.8 ± 57.0*	199.9 ± 61.1

Table 1: Mean ± Standard deviation of functional demand, peak knee moments, and MVICs in both ACL and NonACL limbs 4 and 9 months after surgery. * indicates differences between ACL and NonACL limb. α indicates difference between time.

Significance: Our results reveal that functional demand is equivalent between limbs at 4 and 9 months after ACL reconstruction. This is significant because it suggests that there is not improvement in muscle capacity usage during walking throughout rehabilitation. However, it is possible that functional demand is also affected in both limbs after ACL reconstruction given there are no differences between the ACL and NonACL limbs at either stage in rehabilitation. Previous research has identified a functional demand of 24% in younger healthy adults [4], 6% lower than our findings. Thus, future research should include a healthy control group to better understand if functional demand is elevated in individuals following ACL reconstruction. Overall, knee joint underloading and MVIC deficits still persist following rehabilitation and require targeted interventions to improve muscle capacity during walking.

Acknowledgments: Research reported in this abstract was supported by the Eunice Kennedy Shriver National Institute of Child Health & Human Development of the NIH under Award Number R01HD093626. The content is solely the responsibility of the authors and does not necessarily represent the official views of the NIH.

References: [1] Lisee, C., et al., (2019). *Sports Health*, 11(2), 163-179. [2] Brown, C., et al., (2021). *Ortho J of Sports Med*, 9(4), 2325967121991534. [3] Hafer, J. F., & Boyer, K. A. (2020). J Appl Biomech, 36(3), 163-170. [4] Krishnan, C., et al., (2022). *MSSE*, 54(12), 2208.

Biomechanical Analysis of NCAA D1 Gymnasts: A neuromuscular performance prediction model

Julio Serrano Samayoa, Kendall Mulvaney, Zyanya Burgos Resendiz, Jessica Hutchinson, Malia McGadden, Michelle Sabick, Ph.D.
University of Denver
Julio.serranosamayoa@du.edu

Introduction

This study focuses on analyzing the neuromuscular performance in NCAA DI Gymnasts. The primary goal is to construct a predictive model to help develop training strategies and injury prevention protocols specific to each athlete. Drop jumps onto force plates have been used to research biomechanical and neuromuscular characteristics of athletes [1]. To build a predictive model, a force plate dataset (with parameters such as power, strength, reaction time, and more) was used. Principal component analysis (PCA), a multivariate statistical technique which when applied to entire curves or time-series in biomechanics has been referred to as PCA of waveforms [2], was used to reduce the dimensionality of the data set. The model aims to categorize gymnasts into classes based on their performance level and will be applied to predict the performance of gymnasts and identify key variables that distinguish them from one another.

Methods

15 female NCAA DI Gymnasts (18-23 y.o., 60.14 ± 3.52 kg, 1.61 ± 0.06 m), completed drop jump (DJ) tests weekly on two force plates (FP) (VALD Performance, Newstead, Australia) with a sampling rate of 1,000 Hz over the course of the 2022-23 and 2023-24 seasons. This produced datasets with 43 variables quantifying the athlete's performance on both jumps and landing from each data collection session. All data analysis was performed using MATLAB (Mathworks, Natick, MA). PCA was used to reduce the dimensionality of the dataset, enabling the identification of key modes of variability in PCA space. Distinct clusters were identified within the dataset such as athletes who had received the most performance accolades (Figure 1) [3]. A quadratic discriminant function was used to create a decision boundary between the clusters using linear discriminant analysis. To test the model, one third of the data was kept for testing while two thirds was used for training. Training and testing data was not selected randomly. Special care was taken to ensure that the distribution of data represented all athletes evenly. This way the decision boundary would not be influenced by the performance of one athlete. The training sample for class 1 (high performers) consisted of 80 datapoints, testing sample for class 2 (rest of team) consisted of 117 datapoints, while the testing samples for class 1 and 2 were 40 and 58, respectively. The significance of each variable's contribution to the three principal component scores was assessed, and variables with the most contribution were extracted. Studying the feature space (Figure 1) provided insight into which variables from the force plates produced the most variance that separated the classes (Figure 2).

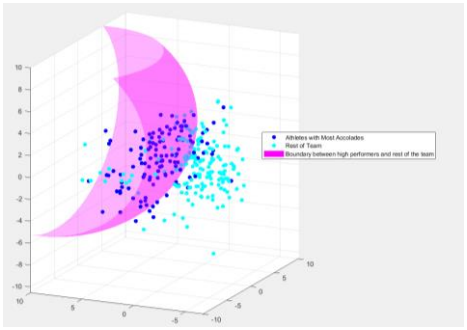

Figure 1. Quadratic discriminant function separating clusters in the PCA space based in athletes' accolades.

Results and Discussion

The PCA analysis revealed distinct clusters among NCAA Division I gymnasts based on their neuromuscular performance characteristics. The prediction accuracy of the model was 76.5%, with precision of 0.71, and a sensitivity of 0.7. Analysis of the PCA space provided insights into biomechanical variables that significantly contributed to the variability among these clusters: active stiffness index, coefficient of restitution, contact time, displacement at takeoff, drop height, drop landing RFD, eccentric mean force, and peak takeoff acceleration (Figure 2). These findings underscore the importance of considering multiple parameters when evaluating neuromuscular performance and its potential implications for athletic training and injury prevention protocols.

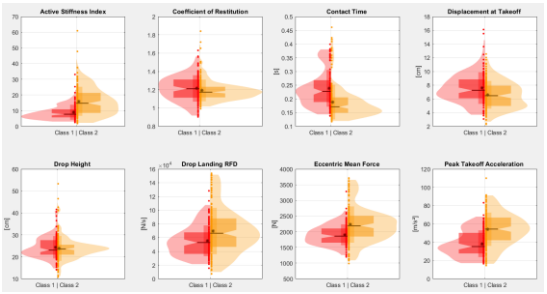

Figure 2. Violin plots displaying the variables that contribute most to the principal component directions of the dataset. Class 1: red, Class 2: orange.

Significance

This study is a step toward the future for athletic performance optimization and injury prevention protocols in the of collegiate gymnastics. By analyzing neuromuscular performance and identifying distinct clusters based on performance characteristics, these findings may offer valuable insights into the relationships between neuromuscular function, athletic performance, and injury occurrence, especially regarding muscle resistance, energy transfer efficiency, power generation, coordination, force production, and absorption. These relationships could provide guidance for developing tailored training methods that target specific performance attributes and mitigate injury risks. Furthermore, this model can be applied with parameters other than accolades, such as asymmetries, previous reported pain, or Achilles tendon thicknesses, which would allow for a potential biomechanical system of performance prediction using FP datasets.

Acknowledgments

Thank you to Julie Campbell, the Deputy Athletic Director for Pioneer Health and Performance, Melissa Kutcher-Rinehart, Head Women's Gymnastics Coach as well as all the gymnasts and gymnastic staff for participating in this research project.

References

[1] Ambegaonkar JP et al. Sports Health. 2011 Jan;3(1):89-96.
[2] Warmenhoven, J Biomech, Volume 16, 2021, 110106
[3] Road to nationals - NCAA gymnastics rankings. http://roadtonationals.com/

Biomechanical Analysis of NCAA D1 Gymnasts: Trend study of Achilles Tendon Loading for Injury Exploration

Julio Serrano Samayoa, Kendall Mulvaney, Zyanya Burgos Resendiz, Jessica Hutchinson, Malia McGadden, Michelle Sabick, Ph.D.
University of Denver

Introduction

This study aims to determine the biomechanical factors that precede Achilles tendon pain in collegiate gymnastics athletes. Achilles tendon ruptures, an increasingly prevalent injury in collegiate gymnastics [1][2], are believed to result from the intense strain placed on the tendon due to sudden stops or repetitive jumping motions [3]. To quantify training effects, it is essential to consider external load factors, such as exercise intensity and frequency, alongside performance metrics like strength and endurance. Additionally, subject pain perception offers valuable subjective insights into athletes' physiological responses and potential injury risks during training sessions [4]. In this project, inertial measurement units (IMUs), force plates (FP), weekly pain surveys and ultrasound were used to determine whether we can predict when athletes will report pain. Ultrasound measures of thickness changes (objective measure) and pain surveys (subjective measures) of tendon pathology need to be compared against a baseline for this population, which this project is establishing. By integrating data from several sources, we ultimately aim to identify the relationships between pain perception, biomechanical metrics, and Achilles tendon thickness, to provide insights into injury mechanisms and prevention strategies in gymnastics.

Methods

Baseline values were collected from 15 female NCAA DI gymnasts (18-23 y.o., 60.14 ± 3.52 kg, 1.61 ± 0.06 m), during pre-season, the 16 weeks of practice before intercollegiate meets begin, for two seasons (2022-23 and 2023-2024). The gymnasts wore tri-axial IMUs on their left shanks during two, 3-hour practices per week. The number of vertical and resultant impacts per minute at both moderate (>5Gs) and substantial (>7Gs) levels were extracted from the IMU data for each practice session. The gymnasts also performed drop jumps (DJ) onto two force plates (VALD Performance, Newstead, Australia) with a sampling rate of 1,000 Hz once a week using a standardized protocol. DJ were performed from a drop height of 20 cm. Peak power per kg of body mass, and reactive strength index (RSI) values were extracted from DJ trials. Athletes were grouped by their specialization (all-around or specialized) and the FP and IMU data between season and specialization were compared. Paired T-tests were performed on FP variables (jump height, peak power normalized by body mass, and RSI) to compare means and maxima values between seasons and unpaired T-tests were used to compare FP data from the all-around and specialized groups.

Results and Discussion

For jump height and peak power there were no significant differences observed between seasons. The mean jump heights were 33-35 cm. Team mean and team maximum RSI values were higher in the 2023-24 season ($p<<0.05$) (Figure 1). This could suggest improvements in athletic performance and physical conditioning and technique refinement or might be indicative of the different athletes participating each season.

Less variation occurred in the IMU metrics as compared to FP. When comparing 2022-23 and 2023-24 seasons, most variables showed no significant differences ($p > 0.1$). However, moderate vertical impacts/min and substantial vertical impacts/min exhibited significant differences, particularly in all-around and specialized athletes ($p << 0.02$). These findings emphasize specific variations in high-impact events between seasons, with potential implications for performance and injury risk assessment. Furthermore, in the 2023-24 season all-around and specialized athletes showed significant differences in moderate vertical impacts/min ($p<<0.01$). Similarly, resultant moderate impacts /min had a p-value of 0.007 for both groups. Moreover, impacts exceeding 7 Gs exhibited p-values around 0.004 (Figure 2).

2022-23 Season

		Team Mean (SD)	All-Around Mean (SD)	Specialized Mean (SD)	All-Around Max (SD)	Specialized Max (SD)
IMU	Y-Axis Impacts/min >5g	2.52 (0.72)	2.71 (0.73)	2.12 (0.83)	4.48 (0.14)	3.22 (1.17)
	Resultant Impacts/min >5g	3.53 (0.97)	3.81 (0.98)	3.04 (1.14)	6.1 (1.45)	4.44 (1.67)
	Y-Axis Impacts/min >7g	1.37 (0.37)	1.5 (0.39)	1.09 (0.38)	2.59 (0.59)	1.69 (0.57)
	Resultant Impacts/min >7g	1.9 (0.49)	1.96 (0.49)	1.48 (0.50)	3.24 (0.71)	2.2 (0.73)
FP	Jump Height (cm)	33.34 (9.50)	33.19 (10.06)	34.08 (9.08)	40.2 (10.58)	39.94 (10.71)
	Peak Power / BM (W/kg)	177.20 (44.66)	173.34 (58.01)	186.33 (40.30)	224.5 (84.50)	223.92 (46014)
	RSI (Flight/Contact Time ms)	2.59 (0.22)	2.43 (0.32)	2.94 (0.26)	3.33 (37)	3.62 (0.29)

2023-24 Season

		Team Mean (SD)	All-Around Mean (SD)	Specialized Mean (SD)	All-Around Max (SD)	Specialized Max (SD)
IMU	Y-Axis Impacts/min >5g	1.7 (0.70)	1.9 (0.77)	1.18 (0.67)	4.05 (1.32)	2.59 (1.41)
	Resultant Impacts/min >5g	3.18 (1.18)	3.51 (1.20)	2.31 (0.96)	6.12 (1.62)	4.25 (1.65)
	Y-Axis Impacts/min >7g	0.86 (0.37)	0.98 (0.39)	0.54 (0.33)	2.18 (0.61)	1.3 (0.72)
	Resultant Impacts/min >7g	1.61 (0.53)	1.81 (0.58)	1.27 (0.6)	2.99 (1.00)	2.15 (0.82)
FP	Jump Height (cm)	35.49 (0.71)	35.53 (0.70)	35.08 (1.64)	43.66 (1.85)	38.52 (1.85)
	Peak Power / BM (W/kg)	182.32 (8.38)	173.79 (7.54)	212.42 (13.42)	216.22 (13.26)	252.56 (13.93)
	RSI (Flight/Contact Time ms)	2.99 (0.17)	2.83 (0.14)	3.64 (0.27)	3.64 (0.15)	4.138 (0.69)

Figure 1. IMUs and FP values for 2022-23 and 2023-24 in all-around and specialized gymnasts.

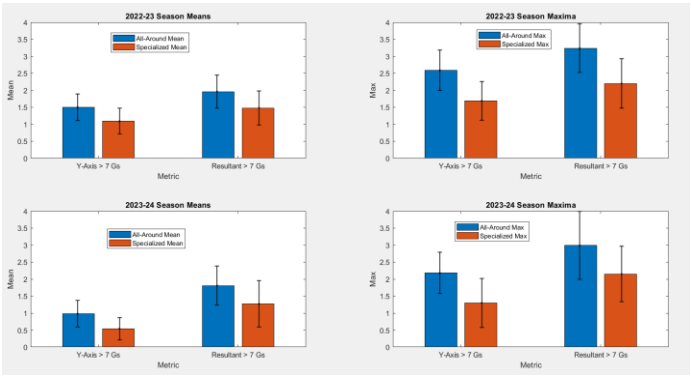

Figure 2. Team mean (left) and maximum (right) values of impacts/min over 7 Gs resultant and in Y-axis between 2022-23(top) and 2023-24 (bottom)

Significance

This study aims to develop a reproducible, accessible methodology for monitoring external training loads and neuromuscular performance in collegiate gymnasts. Establishing normative values for load and FP values during preseason provides comparison data and will facilitate future studies of both Achilles tendon and other injuries in gymnastics and other sports with high impact loads.

Acknowledgments

We want to thank the Deputy Athletic Director for Pioneer Health and Performance Julie Campbell, the Head Women's Gymnastics Coach Melissa Kutcher-Rinehart and the gymnasts and gymnastic staff for participating in this research project.

References

[1]. Bonanno J, et al. Sports Health. 2022 May-Jun;14(3):358-368
[2]. Chan JJ, et al. Int Orthop. 2020 Mar;44(3):585-594
[3]. Kvist M. Sports Med. 1994 Sep;18(3):173-201
[4]. Halson SL. Sports Med. 2014 Nov;44 (Suppl 2): S139-47.

MUSCLE FASCICLE BEHAVIOR OF THE VASTUS LATERALIS DURING LEVEL AND DOWNHILL RUNNING

Montgomery Bertschy[1*], Adam Grimmitt[1], Amanda E. Munsch[2], Brian Pietrosimone[3], Jason R. Franz[2], Wouter Hoogkamer[1]
[1]Department of Kinesiology, University of Massachusetts, Amherst, MA, USA
[2]Joint Department of Biomedical Engineering, UNC Chapel Hill and NC State University, Chapel Hill, NC, USA
[3]Department of Exercise and Sport Science, UNC Chapel Hill, Chapel Hill, NC, USA
*Corresponding author's email: mbertschy@umass.edu

Introduction: Muscle fascicle operating lengths and contraction velocities are important determinants of the efficiency of muscular action. Downhill running has long been assumed to elicit eccentric muscle actions in the quadriceps muscles based on indirect observations: metabolic cost, joint mechanics, and muscle damage. Muscle fascicle behavior in the vastus lateralis (VL) in level-ground running has been observed to be near isometric during stance, despite significant lengthening and shortening of the muscle-tendon unit (MTU) due to knee flexion. Those results implicate considerable contribution of the series elastic elements (SEE) [1]. However, direct evidence of quadriceps muscle actions during downhill running is lacking. Our understanding of the energetics of, performance during, and recovery from downhill running will benefit from empirical *in vivo* measurements of muscle fascicle behavior during level and downhill running. Compared to that during level-ground running, we hypothesized that VL fascicle lengthening during early stance would increase during downhill running.

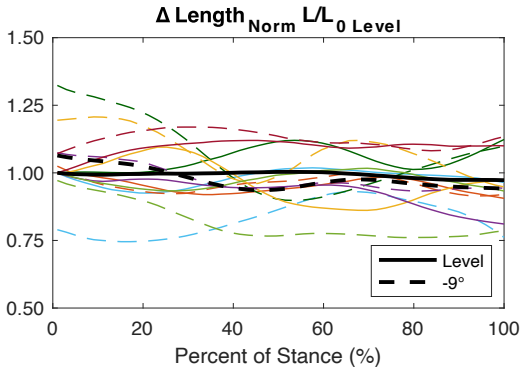

Figure 1: Group average (black) and individual (colored) change in fascicle length between level and -9° during stance. Change >1 indicates a longer fascicle length than heelstrike in level-ground running ($L_{0\ Level}$).

Table 1: Average ± SD for key parameters

Parameters	Treadmill Slope	
	Level	-9°
Δ $Length_{50\%}$ ($L/L_{0\ Level}$)	0.00 ± 0.08	-0.13 ± 0.17
Δ $Length_{100\%}$ ($L/L_{0\ Level}$)	-0.03 ± 0.11	-0.12 ± 0.11
Velocity ($L_{0\ Level}$/s)	0.02 ± 0.30	-0.36 ± 0.65
Stance time (s)	0.24 ± 0.02	0.23 ± 0.02

Methods: Recreational runners (n = 7, 1F/6M, age: 26.1 ± 4.4, height: 177.9 ± 9.8 cm, mass: 74.5 ± 10.5 kg) capable of running a 20-minute 5k or equivalent participated in this study. Participants ran on an instrumented treadmill at 3 m/s on level and 3°, 6°, and 9° downhill slopes. A 60-mm linear array ultrasound transducer was placed midway between the greater trochanter and the superior patella insertion to image a longitudinal cross-section of the right VL. Cine B-mode ultrasound was recorded at 60 frames/s through a depth of 50 mm. A MATLAB-based program (TimTrack) was used for automatic tracking of fascicle lengths over 4-11 strides (6.4 ± 1.7) [2]. Fascicle lengths were extrapolated when outside the view of the 60 mm ultrasound window, filtered using a second-order Butterworth filter with a cut-off frequency of 6 Hz, normalized to stride time, and averaged across strides for each participant [1]. Fascicle velocity was calculated as the first derivative of length with respect to time. Statistical parametric mapping (SPM) was used to compare fascicle length and velocity throughout the stride (right heelstrike to right heelstrike). Pairwise t-tests were conducted for stance-average velocity and change in fascicle length at 50% and 100% of stance. Results are presented for level and steepest downhill grade (9°) only.

Results & Discussion: SPM analysis did not reveal any significant differences between the level and downhill grades in fascicle length (Figure 1) or velocity. There were also no statistical differences for stance-average velocity or changes in fascicle length at 50% and 100% of stance (Table 1). Lack of statistical significance could reflect a relatively small sample size, high variability between participants (i.e., different kinematic response to downhill running), and/or errors accumulated from extrapolation during fascicle tracking. Despite previous reports of larger knee flexion compared to level-ground running [3], participants, on average, had larger *shortening* in fascicle length (-0.13 of $L_{0\ Level}$) at 50% of stance with a larger average shortening velocity (-0.37 $L_{0\ Level}$/s) during downhill running (Table 1). The resulting excursion of the MTU with greater knee flexion must then be accommodated by the SEE. The movement frequency of running may be finely tuned to the natural frequency of the SEE, optimizing loading in the passive elements [4]. Still, these cumulative differences may be too small to elicit meaningful changes in muscular efficiency or injury and recovery mechanisms. Further analyses are needed to fully understand the interaction between MTU dynamics and speed, grade, and joint loading.

Significance: Our early findings do not support the intuitive assumption that downhill running elicits eccentric muscle actions. We find that downhill may elicit muscle fascicle shortening during stance. While downhill running has been shown to increase load and range of motion at the knee joint, the SEE may contribute more to energy absorption than in level-ground running.

Acknowledgments: We thank Ricky Pimentel, Andrew D. Shelton, and the rest of the teams at UNC for welcoming us into their facilities and assisting with data collection, Rodger Kram for helping conceptualize this study, and the Company of Biologists for supporting our trip to collect the presented data.

References: [1] Bohm et al. (2018), *Sci Rep* 8(1); [2] van der Zee TJ, Kuo AD (2022), *PLOS ONE* 17(3); [3] Park et al. (2019), *Gait & Posture* 68; [4] Robertson et al. (2015), *PNAS* 122(43).

RELATIONSHIP BETWEEN THE PERCEIVED BENEFIT OF CARBON FIBER INSOLES AND 6-MINUTE WALK TEST DISTANCE IN OLDER ADULTS

Christopher L. Long[1*], Logan T. White[2], Philippe Malcolm[2], Jason R. Franz[3], Kota Z. Takahashi[1]
[1]Department of Health & Kinesiology, University of Utah, Salt Lake City, UT
[2]Department of Biomechanics, University of Nebraska Omaha, Omaha, NB
[3]Biomedical Engineering, University of North Carolina at Chapel Hill and North Carolina State University, Chapel Hill, NC
*Corresponding author's email: christopher.long@utah.edu

Introduction: Older adults walk slower [1] and with greater metabolic energy costs [2] than younger adults. One prevailing hypothesis is that older adults consume more energy due to diminished ankle push-off mechanics (moment and power) and compensatory reliance on less efficient hip musculature [3]. A solution that may enhance older adult ankle mechanics is walking with carbon fiber insoles (CFI). Shoes fitted with CFIs can increase plantar flexor force output with no change in muscle activation, improving walking economy in young adults during fast walking [4]. Older adults may also benefit from CFIs, but their adoption of a footwear intervention is likely influenced by subjective footwear perceptions such as comfort or perceived benefit [5,6]. The present study aimed to assess whether older adults benefit from shoes fitted with CFIs, either objectively or subjectively, and to evaluate the relationship between perceived speed benefit and actual change in 6-Minute Walk Test (6MWT) distance in older adults. We hypothesized that individuals who felt they could walk faster with CFIs would also improve their 6MWT distance when walking with CFIs.

Methods: Twenty healthy older adults (10M/10F, 75.9 ± 6.0 yrs, 166.4 ± 10.3 cm, 79.6 ± 24.7 kg) were recruited. Participants completed a 6MWT for each of the following footwear conditions in a randomized order, split across two days: 1) Participant's own shoe 2) Control Shoe alone 3) Control shoe with 1.6-mm CFI 4) Control shoe with 3.2-mm CFI. The 6MWT was performed following guidelines established by the American Thoracic Society. Participants were instructed to walk as far as possible in 6 minutes while walking around two cones spaced 30 meters apart in a long hallway. After each 6MWT, participants responded to the following survey question: "Compared to my everyday walking, I feel like I can walk faster in these shoes." Responses followed a 5-point Likert scale, ranging from "strongly disagree" to "strongly agree". 6MWT performance outcomes (Improved, No Change, Got Worse) were determined using a "meaningful change" threshold of ±20 m compared with the participant's own shoe [7,8]. The relationship between survey response and 6MWT performance outcome for each CFI shoe condition was examined using Fisher's Exact Test ($\alpha = 0.05$).

Table 1: Participant count by survey response and 6MWT performance outcome for both insole conditions: 1.6-mm / 3.2-mm

	6MWT Performance Outcome			
Survey Response	Improved	No Change	Got Worse	Total
Strongly Agree	1 / 1	5 / 0	1 / 0	7 / 1
Agree	1 / 1	2 / 0	0 / 0	3 / 1
Neutral	2 / 2	4 / 1	0 / 2	6 / 5
Disagree	0 / 0	3 / 4	1 / 2	4 / 6
Strongly Disagree	0 / 0	0 / 5	0 / 2	0 / 7
Total	4 / 4	14 / 10	2 / 6	20 / 20

Results & Discussion: For the 1.6-mm insole condition, 4 participants improved walk distance, 14 saw no change, and 2 got worse. For perceived benefit, 7 strongly agreed, 3 agreed, 6 were neutral, and 4 disagreed that they felt they could walk faster (Table 1). For the 3.2-mm insole condition, 4 participants improved walk distance, 10 saw no change, and 6 got worse (Table 1). Regarding perceived benefit, 1 participant strongly agreed, 1 agreed, 5 were neutral, 6 disagreed, and 7 strongly disagreed that they felt they could walk faster. However, there was no statistically significant relationship between survey response and 6MWT distance for either CFI condition (3.2-mm: $p = 0.083$; 1.6-mm, $p = 0.901$). Independent of insole condition, the data did not support our hypothesis that older adults who perceived a speed benefit would objectively walk further. However, it should be noted that the 6MWT measures walking endurance/capacity and is not a measure of maximal walk speed, per se. Our results leave open the possibility that participants who perceived a speed benefit from CFIs have the capacity to walk faster, but, those gains may have diminished over time due to cardiorespiratory limitations. It remains to be seen if there are other psychophysiological factors that better relate with changes in walking endurance. Therefore, a comprehensive analysis of footwear perception factors (e.g., comfort, ease of walking, etc.) and their relation to CFI-assisted walking outcomes is warranted.

Significance: The current study highlights essential considerations in evaluating the efficacy of CFI footwear interventions for improving older adult walking performance. While subjective perceptions of footwear may not directly relate with walking outcomes – at least for 6MWT distance – they are likely to influence the adoption of such interventions. These insights will inform the design of future wearable device research and advance our understanding of effective interventions for older adult mobility.

Acknowledgments: This work was supported by the NIH (R01AR081287) awarded to KZT and JRF.

References: [1] Himann et al. (1988), *Med & Sci Sport & Exer* 20(2); [2] Das Gupta et al. (2019), *Sci Rep* 9; [3] Boyer et al. (2017), *Exp Geront* 95; [4] Ray & Takahashi (2020), *Sci Rep* 10(1); [5] Hatton & Rome (2019), *Clin Geriatr Med* 35(2); [6] Menz et al. (2016), *Gerontology* 63(2) ; [7] Bohannon & Crouch (2017), *J Eval Clin Pract* 23(2); [8] Perera et al. (2006) *J Amer Geriatric Soc* 54(5)

UTILIZING WEIGHT BEARING CT TO EVALUATE PTOA RISK AFTER ACL RECONSTRUCITON

Tyce C. Marquez[1*], Shelby Hulsebus[1], Shannon Ortiz[1], Brian R. Wolf[1], Donald D. Andseron[1]
[1]University of Iowa, Iowa City, IA
tyce-marquez@uiowa.edu

Introduction: The risk of post-traumatic osteoarthritis (PTOA) and associated joint space narrowing after ACL injury is high, with roughly 50% of individuals experiencing symptoms 10 to 20 years after injury [1]. Efforts to mitigate PTOA risk after ACL injury have been stalled by the lack of sensitive, specific, and affordable early imaging markers. However, recent reports have linked the load-bearing pose of the knee following ACLR to early compositional MRI changes in articular cartilage consistent with PTOA [2]. We have developed a fully automated method to measure tibiofemoral 3D pose and joint space width (JSW) from weight bearing CT (WBCT) [3] that shows promise for early detection of PTOA [4]. The objective of this study is to explore the potential for WBCT to provide affordable, objective, and predictive longitudinal knee pose and 3D JSW measures following ACLR to identify early signs of PTOA.

Methods: Twenty individuals (7M/13F, age: 22.0±8.6 years) with a unilateral isolated partial or complete ACL tear reconstructed by one of four surgeons were recruited to participate in this IRB-approved study. Bilateral WBCT scans of the knee in a semi-flexed (~20°) pose [4] were acquired 3.2±0.5 months and again 12.4±0.7 months after ACLR. 3D JSW distributions were successfully measured at both scan timepoints for 17 intact contralateral and 18 ACLR knees using fully automated methods [3]. Areas where the JSW was less than 5 mm were considered regions of particular interest to longitudinally monitor in each compartment (Fig. 1).

Results & Discussion: The areas with JSW < 5 mm for the intact knees increased modestly over the roughly 9-month period between WBCT scans 1.05±5.63% and 1.13±4.08% for the medial and lateral compartments, respectively. For ACLR knees, the lateral compartment demonstrated roughly equal areas with JSW < 5 mm at both timepoints (increase of 0.02±5.22%). The medial compartment for ACLR knees, however, demonstrated substantially larger changes, with a decrease in areas with JSW < 5 mm (i.e., joint space widening) at the 1-year timepoint of 6.45±7.30%. The lateral compartment showed approximately equal distributions of changes in areas with JSW < 5 mm for both ACLR and intact knees. The medial compartment indicated different results, with the ACLR knees showing more subjects with widening JSW at the 1-year follow up (Fig. 2). On the ACLR side, roughly 60% of subjects had joint space widening at 1-year follow up. This relationship has previously been demonstrated with radiographic JSW in ACLR knees. At a 46-month follow up, it has been reported that 8% of ACLR subjects had increased JSW compared to baseline [5], and another reported at 2-year follow up 74% of ACLR subjects had larger JSW compared to the intact contralateral [6]. The widening of JSW observed may be related to articular cartilage thickening or swelling, a possible early indicator of PTOA [7].

Significance: The establishment of new WBCT-based 3D imaging markers that reliably and affordably assess PTOA risk and detect degenerative joint changes earlier can facilitate more efficient interventions.

Acknowledgments: This research was supported by a grant from the Arthritis Foundation (Award #851789).

References: [1] Lohmander LS, et al. *Am J Sports Med*. (2007), 35(10):1756-69. [2] Lansdown DA, et al. *J Orthop Res*. (2020), 38(6):1289-95. [3] McFadden EJ, et al. *Osteo Cart.* (2022), 30(S1):S284-5. [4] Segal NA, et al. *Osteo Cart*. (2023), 31(3):406-13. [5] Tourville TW, et al. *Am J Sports Med*. (2013), 41(4):769-778. [6] Jones MH, et al. *Osteo Cart*. (2015), 23(4):581-588. [7] Li X and Majumdar S. *J Magn Reson Imaging*. (2013), 38(5).

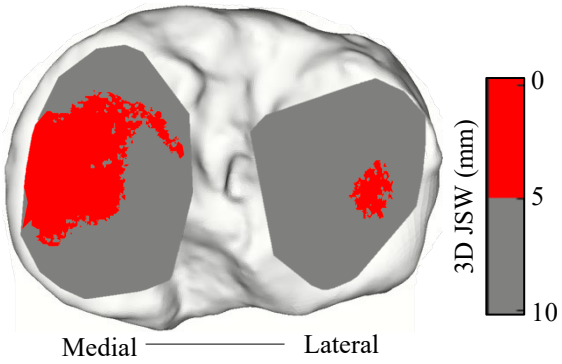

Figure 1. Regions of the tibial plateau with 3D JSW above/below 5mm are here indicated.

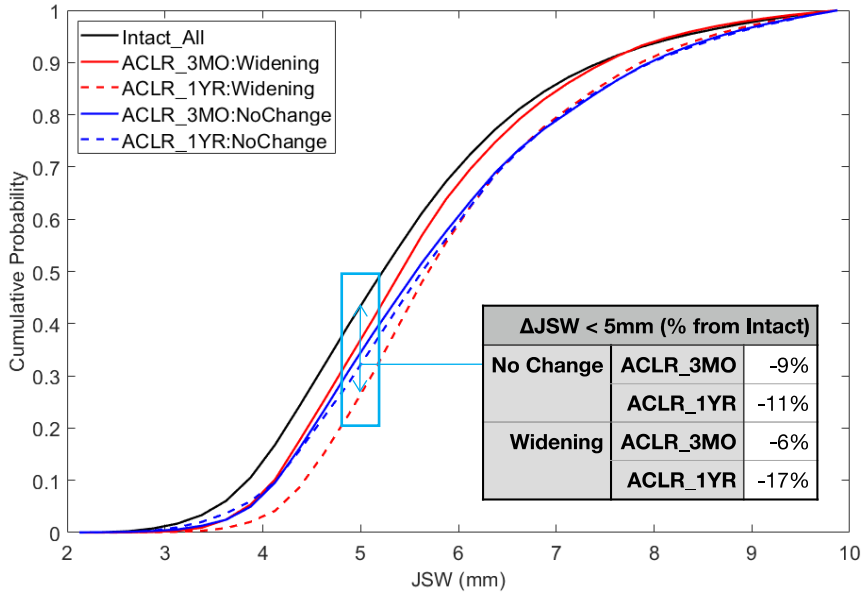

Figure 2. Medial JSW distribution comparison between widening and minimal change groups at follow up.

KNEE ADDUCTION MOMENT DURING GAIT IS CORRELATED WITH PATIENT REPORTED PHYSICAL FUNCTION AFTER TOTAL KNEE ARTHROPLASTY

Raghav Ramraj*, Tom Gale, Yuuka Tanabe, Kenneth L. Urish, William J. Anderst
[1]Department of Orthopaedic Surgery, University of Pittsburgh, Pittsburgh, PA
*rar186@pitt.edu

Introduction: External knee adduction moment (KAM) is a common indirect measure of medial to lateral tibiofemoral load distribution that has been correlated to the progression of medial compartment OA [1, 2]. Knee arthroplasty is performed in over 700,000 patients with end-stage osteoarthritis each year in the United States, yet 20% report limited function, persistent disability, and reduced quality of life [3]. The importance of restoring bilateral symmetry in knees post-operatively has been established, but the association between post-op KAM and clinical outcomes has not. Given that KAM has been used to quantify the load reducing effect of total knee arthroplasty (TKA), relating reductions in KAM and restoration of KAM symmetry to patient reported outcomes (PROs) may help guide surgical decision making and provide insight into patient satisfaction [4, 5]. Thus, the objective of this study was to evaluate the relationship between KAM symmetry and patient satisfaction after cruciate retaining (CR) or posterior stabilized (PS) TKA. We hypothesized that implant type would not affect the post-TKA KAM symmetry and that lower peak KAM would correlate with better PROs.

Methods: Participants were imaged one year after surgery using biplane radiography (100 images/s, 80 kV, 125 mA, 1 ms exposure) during treadmill walking at self-selected speed for 6 trials per knee. Ground reaction forces (GRF) were collected from the instrumented treadmill at 1000Hz. CT scans of the knee were obtained bilaterally, and bone tissue was segmented using Mimics (Materialise). The segmented bones were used to create digitally reconstructed radiographs that were matched to biplane radiographs using a previously validated method [6]. Tibiofemoral kinematics were calculated [7] and normalized to gait cycle. The GRF vector was transformed into the tibia anatomical coordinate system each frame, and the KAM was calculated as the cross product of the GRF and the moment arm vector (perpendicular between the GRF and the tibia origin at the knee joint center) perpendicular to the coronal plane and normalized to weight and height. The average peak KAMs during the impact and push off phases were calculated for analysis. Peak KAM side-to-side differences (SSDs) were calculated and asymmetry was tested using a paired t-test. Peak KAM SSDs were compared across implant types using unpaired t-tests. Correlation between peak KAM and post-operative Knee Injury and Osteoarthritis Outcome Knee Score (KOOS) and RAND 36-Item Health (RAND36) scores were tested using a Pearson's correlation.

Results: A total of 15 patients (6F, 9M, average age 65.5 ± 5.6 years), seven that received CR (Journey II CR, Smith & Nephew) and eight that received PS (Journey II BCS, Smith & Nephew) TKAs, completed post-operative testing. A total of 180 trials were included in this analysis. No differences between post-op and contralateral KAM were found in either implant type. CR knees were more asymmetric in peak KAM than PS knees during the impact phase of gait (Table 1). Less peak KAM was correlated with better patient reported RAND36 physical function (r=-0.636) (Fig 1) during the impact phase and the push-off phase.

Table 1. *Average SSD between peak KAM during impact and push-off phases of stance. The SSD in peak KAM during the impact phase was greater in CR knees (p=0.046).*

Implant Type	Peak KAM SSD (Nm/kgm)	
	Impact	Push-off
PS-TKA	-0.15 ± 0.3*	-0.13 ± 0.9
CR-TKA	0.59 ± 0.4*	0.31 ± 0.6

Discussion: The results suggest that bilateral symmetry with regards to KAM was maintained post-op, contradicting much of the previous literature that showed significant reduction in KAM post-op [8]. The greater asymmetry observed in CR compared to PS TKAs in the impact phase of stance suggest may be due to the central stabilizing post in PS implants. The negative correlation observed between KAM and pain limited physical function score indicates that a reduction in KAM is associated with improved patient-reported physical function. This lends support to the idea that reductions in KAM can be used as a proxy for the efficacy of surgical interventions on knee OA.

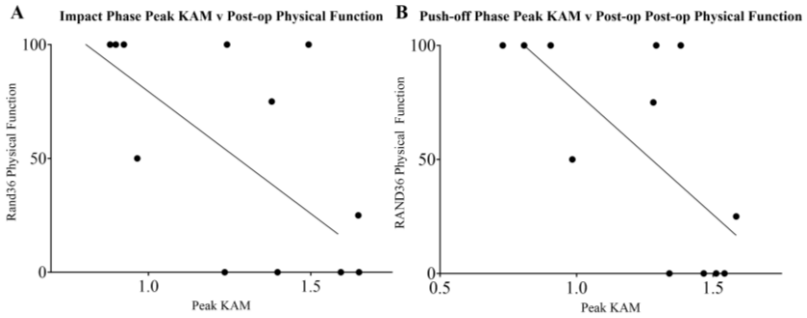

Figure 1. *Peak KAM values during the impact phase* ***(A)*** *or push-off phase* ***(B)*** *and post-operative physical function scores. 0 indicates limitation; 100 indicates no limitation (p=0.0353 and 0.0119, respectively)*

Significance: Although implant type may not affect the size of the KAM, it may affect post-operative symmetry in KAM during the impact phase of gait. KAM may be an objective measure of patient function after TKA.

Acknowledgments: Smith and Nephew provided funding and the implant CAD models used to recreate the TKA plus bone models.

References: [1] Jackson et al. (2004) *J Sci Med Sport* 7(3); [2] Foroughi et al. (2010) *Knee* 16(5); [3] Fingar et al. (2012) *Agency for Health Res and Qual*. [4] Nagura et al. (2017) *Knee* 24(2). [5] Lee et al. (2021) *Gait Posture* 90. [6] Anderst et al. (2009) *Med Eng Phys* 31(1). [7] Grood et al. (1983) *J Biomech Eng*. 105(2). [8] Mandeville et al. (2008), *Gait Posture* 27(1).

MYOCARDIAL WALL THICKNESS DYNAMICS: A CROSS-SECTIONAL STUDY USING FINITE ELEMENT SIMULATIONS AND MRI DATA ACROSS CARDIAC PHASES

Mohsen Darayi[1], Mary E. Robakowski[1], Daniel H. Pak[2], Yiling Fan[3], Danielle Kara[1], Ojas Potdar[1], Christopher T. Nguyen[1], Debkalpa Goswami[1]

[1]Cleveland Clinic; [2]Yale University; [3]Massachusetts Institute of Technology

Corresponding author's email: goswamd@ccf.org

Introduction: Computational models are essential for elucidating the mechanics and function of the heart, leveraging advancements in 3D imaging for patient-specific simulations [1,2,3]. We can validate these models against imaging data, e.g., focusing on the behavior of the left ventricle (LV) across cardiac phases to examine pressure-volume dynamics and wall thickness [4,5]. This comparison seeks to enhance model accuracy in describing physiological processes, thus aiding in the diagnosis and management of disease conditions [6]. Here, we compare myocardial thickness across the AHA segments [7] of the LV in a pericarditis case, emphasizing the importance of accurately modeling LV wall characteristics [8] and highlighting the utility of segment-based analysis in cardiac assessment.

Methods: We used finite element (FE) simulations of the LV derived from 4D MRI scans of a patient (76 year old male) with constrictive pericarditis, captured using a 3T MR system (MAGNETOM Cima.X, Siemens Healthineers) at a resolution of 1.6 mm³ and 30 fps [1]. Segmentation was performed manually with 3D Slicer and meshed in ABAQUS using 65,186 tetrahedral elements (**Fig. 1a**). We generated detailed fiber architecture applying the Laplace–Dirichlet Rule-Based algorithm [9], with orientations between -60° and 60°. Myocardial material behavior was modeled as transversely isotropic hyperelastic, using the Fung formulation [3], and active contraction was simulated in ABAQUS Explicit, integrating systemic and pulmonary circulation (**Fig. 1b**) [2,3]. We analyzed LV deformation over 10 cardiac cycle frames using deformable image registration and mesh correspondence [10], focusing on 17 AHA segments. This method enabled tracking of LV and segment-specific deformations, quantifying myocardial thickness variations throughout the cycle, and provided a detailed view of cardiac mechanics.

Results & Discussion: Our study integrates FE simulations with ten segmented 4D MRI frames to analyze myocardial wall thickness variations across the cardiac cycle within the 17 AHA segments. We used subject-specific LV models to examine systolic and diastolic phases, incorporating fiber orientation and myocardial biomechanics for detailed cardiac function insights. Initial findings include LV pressure-volume relationship analysis, comparing simulation outcomes with MRI-derived volumes (**Fig. 1c**). We observed a consistent increase in LV wall thickness from end-diastole to peak systole, aligning with expected cardiac muscle behavior. Notably, a minor thickness variation (1-3 mm) between simulations and MRI confirms the fidelity of our model in capturing myocardial dynamics (**Fig. 1d-g**). In our study, LV myocardial segment thickness from simulations varied from 7.02 mm in the Apex (AHA-17) to 18.20 mm in the Mid Inferior (AHA-10), closely mirroring the MRI data range of 6.65 mm to 15.20 mm (**Fig. 1d**). This similarity underscores the effectiveness of our simulations in depicting dynamic myocardial geometry. Both datasets showed significant systolic thickening: 2.04 mm to 5.46 mm in simulations and 1.66 mm to 7.12 mm in MRI (**Fig. 1e**), highlighting the potential for segment-specific analysis in diagnosing disease conditions. Note that MRI measurements are heavily reliant on the accuracy of manual segmentation, which can influence the measured thickness. Though simulations slightly overestimate thickness, the close averages affirm its utility in modeling myocardial dynamics (**Fig. 1f**). A correlation coefficient of r = 0.857 between simulation and MRI data further confirms the accuracy of simulations in reflecting myocardial dynamics, highlighting its potential for non-invasive, *in silico* patient-specific cardiac assessment (**Fig. 1g**).

Significance: Our study bridges computational modeling with real-world cardiac MRI data, offering a validated approach for subject-specific myocardial thickness analysis. This research lays the foundation for precise and non-invasive cardiac diagnostics and personalized treatment strategies by closely replicating myocardial thickness variations and dynamic cardiac behavior. The high correlation coefficient (r = 0.857) between simulation and MRI measurements indicates the potential for simulations to improve patient-specific diagnostics, offer insights into disease conditions, and advance cardiac care.

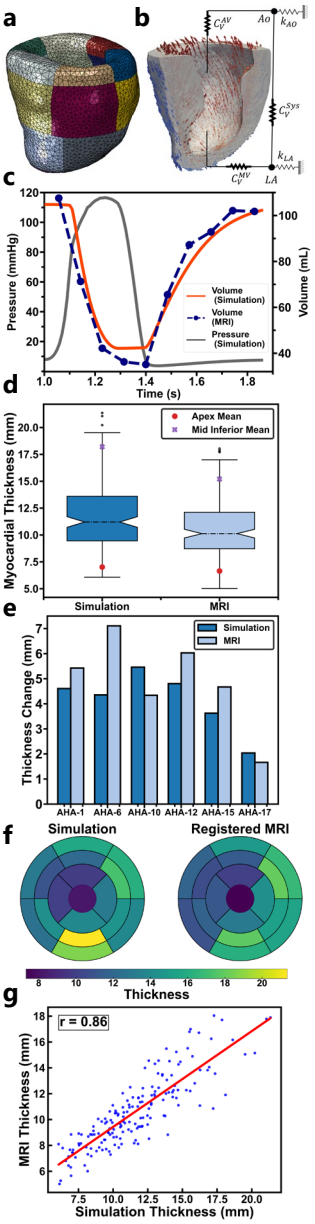

Figure 1: a) FE mesh. b) Fiber orientation and circulation system. c) Simulated pressure and volume, and actual volume obtained from MRI. d) LV thickness distribution across cardiac cycle and segments. e) LV thickness change from diastole to systole. f) Myocardial thickness in different segments during systole. g) Correlation between simulation and MRI-derived LV thickness.

References: [1] Lopez-Perez et al. (2015) *Biomed Eng* 14(1);[2] Guan et al. (2022) *Comput Biol Med* 145; [3] Fan et al. (2019) *Int J Numer Meth Biomed Eng* 35(9); [4] Huelnhagen et al. (2018) *Sci Rep* 8(1); [5] Dabiri et al. *Front Phys* 7(117); [6] Aung et al. (2023) *Circ Genom Precis Med* 16(1); [7] Cerqueira et al. (2002) *Circulation* 105(4); [8] Campos et al. (2019) *Biomech Model Mechanobiol* 18(15); [9] Bayer et al. *Ann Biomed Eng* 40(10). [10] Pak et al. (2023) *IEEE Trans Med Imaging* 43(1)

JOINT COORDINATION DURING GAIT DIFFERS BY RACE AND SEX

Cherice Hill[1*], Lex Gidley[2], Daniel Schmitt[3], Robin M. Queen[4]
[1]University of Rochester, Biomedical Engineering
[2]The United States Olympic and Paralympic Committee, Sports Medicine
[3]Duke University, Department of Evolutionary Anthropology
[4]Virginia Tech, Biomedical Engineering and Mechanics
*Corresponding author's email: chill4@ur.rochester.edu

Introduction: Biomechanical coordination describes the optimization strategy used to organize segments and joints to accomplish a motor task while kinematics describe the resultant motion based on the coordination strategy [1]. Previously, we observed kinematic differences in gait at regular and fast set gait speeds between racial groups; observed differences were also affected by sex [2]. From the kinematic data alone, it is not possible to determine whether the groups utilized different optimization strategies to accomplish the same task (walking at set speeds), resulting in different joint kinematics, or if the groups utilized the same optimization strategy but had different resultant kinematics, for example, due to anthropometric differences. Evaluation of joint coordination and kinematic data together could clarify this point. The objective of this study was to determine whether, in addition to previously identified kinematic differences, joint coordination patterns also differed between racial groups and by sex. We hypothesized that the kinematic differences between racial groups that we saw previously were due to coordination differences and that sex would continue to act as a moderator. To describe any potential energetic effect of coordination differences we also calculated the percent energy recovery.

Methods: In an institutional review board approved study, 3D motion capture and force plate data were recorded during walking trials at regular (RW, 1.35m/s) and fast (FW, 1.6m/s) walking speeds [2]; data from 88 participants, evenly divided by self-identified race (African American, white American) and sex (male, female), was analysed. Sagittal and frontal plane hip, knee, and ankle angles and angular velocities were used to compute continuous relative phase (CRP), a measure of coordination, between each set of joints in both planes. Based on prior results, CRP data was stratified by sex. Statistical Parametric Mapping was used to compare CRP curves for each set of joints between racial groups throughout the stance phase, identifying regions of significant difference between racial groups (α=0.05). Percent energy recovery was calculated from force plate data [3] and compared between racial groups using T-tests (α=0.05).

Results & Discussion: Sagittal and frontal plane joint coordination differed between racial groups, suggesting a varied optimization strategy to accomplish the same motor task (walking at set speeds); as expected, results also varied by sex. In the sagittal plane, Hip-Ankle and Knee-Ankle coordination differed between racial groups during RW and FW (Figure 1). The largest region of difference was in female Hip-Ankle coordination during early midstance (~20-50% of stance, $p<0.001$). Since all sagittal joint coordination differences involved the ankle, smaller peak ankle plantarflexion angles previously observed in this African American group [2] may have been the result of an altered coordination strategy involving the ankle. In the frontal plane, coordination differences were only observed during RW in males. Hip-Knee and Hip-Ankle coordination differed between racial groups at heel strike while Hip-Knee coordination differed in late stance. During RW, energy recovery was higher in African Americans in both males (AA: 61.1±3.4%, WA: 58.7±4%.1, $p=0.036$) and females (AA: 62.4±4.0%, WA: 59.6±3.8%, $p=0.019$). Fewer coordination differences were observed during FW compared to RW, and energy recovery did not differ between groups during FW; the differing coordination strategy observed may have weakened when optimizing another parameter, in this case speed. Based on prior [2] and current findings, African Americans seemed to implement a different optimization/coordination strategy to maintain limb proximity to the center of mass, resulting in smaller peak joint angles and improved energetic efficiency; decreased plantar flexion and hip extension in AA could lead to more incongruous kinetic and potential energy curves and enhance recovery. The RW set speed being almost equivalent to the preferred speed for WA (1.34m/s) but faster than that of AA (1.23m/s) may also have affected the optimization strategy and energy recovery. Future work will examine how utilized strategies may be driven by a combination of physical and socio-cultural influences along with energetics of step-to-step redirection.

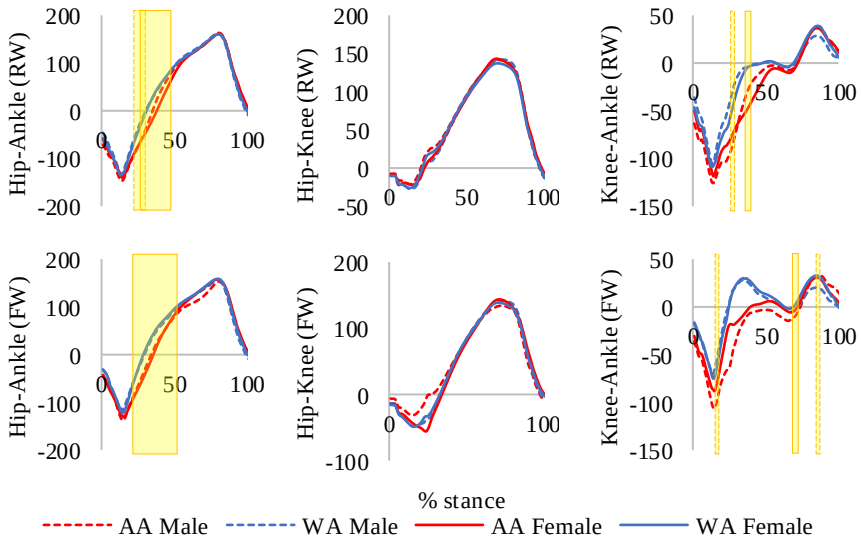

Figure 1: Sagittal plane joint coordination in regular & fast walking. Regions of significant racial difference ($p<0.05$) shown with yellow shading (male/female: dashed/solid border).

Significance: These findings emphasize the importance of sample diversity in establishing normative biomechanical gait and motor control data. This work also justifies further evaluation of how we define optimal gait, which informs references for rehabilitation and gait retraining. Collection of large, diverse datasets from which we can interpret with greater intersectionality to maximize translational applicability is essential.

Acknowledgments: Gilliam Fellowship (HHMI) and VT ISCE supported dataset collection.

References: [1] Lamb, et al. (2014), *Clin Biomech* 29(5); [2] Hughes-Oliver et al. (2020), *J Biomech* 112; [3] Starling et al. (2014), *OA & C* 22(6).

EFFECT OF RHYTHMIC AUDITORY STIMULATION ON JOINT KINEMATICS DURING TREADMILL WALKING IN CHILDREN AND YOUNG ADULTS

Haneol Kim[1*], Matt Beerse[2], Jianhua Wu[3]
[1]University of Wisconsin-La Crosse
[2]University of Dayton, [3]Georgia State University
*Corresponding author's email: hkim2@uwlax.edu

Introduction: Human locomotion is a rhythmic yet complex movement [1], characterized by neuromuscular coordination involving complex muscle activation and joint coordination, adapting to the environment and task constraints [2, 3]. Joint coordination during walking is essential to accomplish a smooth gait pattern in response to external perturbations. Rhythmic auditory stimulation (RAS), acting as an external timekeeper, has been shown to affect gait parameters and improve pathological gait in clinical populations such as patients with Parkinson's disease whose dysfunction of temporal processing impairs motor performance [4]. Despite its clinical efficacy in certain populations, limited research has been conducted with healthy children and young adults. Children are affected, to a greater degree, by external disturbances such as treadmill speeds and RAS frequencies due to their underdeveloped gait patterns. Therefore, this study aimed to investigate the effect of RAS with different frequencies on joint kinematics in children and young adults.

Methods: Twenty healthy young adults aged 18 to 35 years (10M/10F) and twenty typically developing children aged 7 to 11 years (9M/11F) participated in the study. Participants walked at their preferred speed on a 10-meter walkway three times. The average walking speed was used to set the preferred treadmill speed. A 9-camera Vicon motion capture system and a lower-body model of marker placement were used to collect the kinematic data. A 5-min walking trial was collected first at the preferred treadmill speed with the RAS frequency corresponding to 100% of the preferred cadence (100RAS), followed by manipulations of RAS frequency: 75% and 125% of the preferred RAS (75RAS and 125RAS, respectively). Joint kinematic variables included peak hip extension/flexion, peak knee extension/flexion, and peak ankle plantarflexion/dorsiflexion angles. Two-way (2 Group × 3 Condition) mixed ANOVA was conducted at a significant level of $\alpha = 0.05$. Post-hoc pairwise comparisons with a Bonferroni adjustment were completed if necessary.

Results & Discussion: Peak hip extension decreased with increasing RAS frequency for both children and adults, showing a condition effect ($p < 0.001$, Fig. a). Post-hoc analysis revealed significant differences between every condition ($p < 0.05$). Children exhibited the least hip flexion at 75RAS and the greatest hip flexion at 100RAS, while adults showed the least hip flexion at 100RAS and the greatest hip flexion at 75RAS (Fig. b). A group by condition interaction effect was found for peak hip flexion ($p = 0.027$).

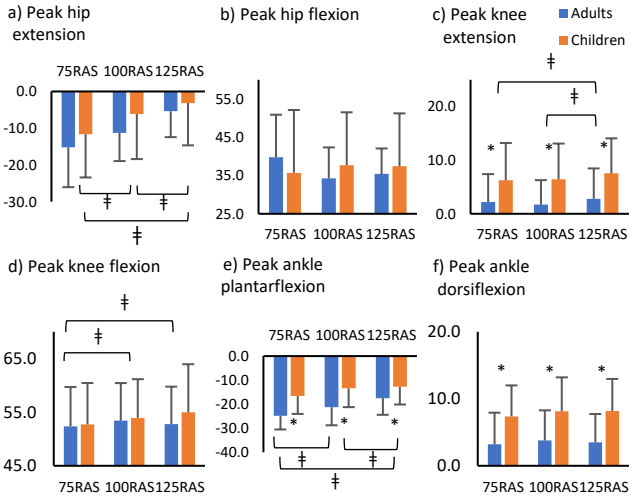

Figure 1: Mean and standard deviation of kinematic joint angles for peak hip extension and flexion, knee extension and flexion, ankle plantarflexion and dorsiflexion. The symbol * indicates a group difference between typically developing children and healthy young adults; ǂ indicates a condition difference between 75RAS, 100RAS, and 125RAS.

Children showed a greater peak knee extension across RAS conditions, with a group main effect ($p = 0.018$, Fig. c). Peak knee extension increased with increasing RAS frequency for both groups, with a condition effect ($p = 0.039$). Post-hoc analysis revealed significant differences between 75RAS and 125RAS ($p = 0.041$) and between 100RAS and 125RAS ($p = 0.018$). For peak knee flexion, children increase peak knee flexion with increasing RAS frequency ($p = 0.016$, Fig. d). Post-hoc analysis revealed there were significant differences between 75RAS and 100RAS ($p = 0.046$) and between 75RAS and 125RAS ($p = 0.032$). Children showed a smaller decrease with increasing RAS frequency in peak ankle plantarflexion than adults, showing a group by condition interaction ($p = 0.040$, Fig. e). Post-hoc analysis with a Bonferroni adjustment on speed conditions revealed that there were significant differences between every condition ($p < 0.05$). Children had greater peak ankle dorsiflexion than adults across RAS conditions ($p = 0.004$, Fig. f).

Significance: Under RAS frequencies different from their preferred cadence, both children and young adults exhibited modifications in their lower limb joints by adjusting peak hip and knee extension, knee flexion, and ankle plantarflexion angles. The knowledge gained from this study provides the baseline data of gait adaptation to external auditory cues in children and young adults. It has potential clinical implications in designing and implementing therapeutic interventions and rehabilitation strategies for individuals with disabilities, particularly for children with gait disorders.

Acknowledgments: We are grateful to all the participants for volunteering their participants. This study was partially supported by the Georgia State University Provost's Dissertation Fellowship program.

References: [1] Comstrock et. (2018), *Front. Comput. Neurosci.* 12; [2] Desrochers & Gill. (2021), *Hum. Mov. Sci.* 77; [3] Yokoyama et al. (2018), *PLos One*, 13(4); [4] Harrington et al. (1998), *J Neurosci*, 18(3).

EFFECT OF KNEE VELOCITY FEEDBACK ON GROUND REACTION FORCES, KINETICS, AND KINEMATICS DURING INCREASED HIP FLEXION GAIT

Jade Sharretts[1], Meagan Bubeck[1], Hunter Haynes[1], Chuang-Yuan Chiu[2], Tanner Thorsen[1], Nuno Oliveira[1*]
[1]School of Kinesiology and Nutrition, The University of Southern Mississippi, MS, USA
[2]School Sports Engineering Research Group, Sheffield Hallam University, Sheffield, UK
*Corresponding author's email: nuno.oliveira@usc.edu

Introduction: With the increasing prevalence of conditions such as osteoarthritis and lower extremity injuries, the ability to maintain a well-structured and high-intensity exercise routine is dwindling. Changes need to be made to common exercise techniques to accommodate the needs of these various populations. Increased hip flexion gait is a new exercise modality that involves walking on a treadmill at a comfortable speed while flexing the hip as much as possible during the swing phase [1, 2]. During the exercise, participants use a hip flexion feedback system (HFFS) that uses markerless motion tracking for hip flexion angle calculations and displays on a screen the peak hip flexion target that participants need to meet while walking. Due to the elevation of the foot resulting from the increased hip flexion during swing, strategies that might assist the participant in decelerating the foot before heel contact might be needed. Therefore, the HFFS system includes an added feature that allows the participant to receive feedback on their knee vertical velociy. We hypothesize that this feature might help the participant to create a gentler impact with the treadmill, which causes less stress on the joints and lower extremities.

To test this hypothesis, we investigated the effect of the knee velocity feedback on ground reaction forces (GRF), kinematics, and kinetics. By viewing these variables, we will be able to determine if this is an effective substitute for running and other high-intensity exercises while avoiding large loading rates at heel contact and in turn avoiding possible low extremity injuries.

Methods: Ten healthy individuals (5M, 5F; age 30.1 ± 9.8 years; height 169.9 ± 0.09 cm; body mass 67.9 ± 14.3 kg) participated in the study. All participants underwent two testing sessions using the HFFS: one with and one without the knee velocity feedback. For each session, participants performed increased hip flexion gait on a treadmill at four different speeds (1.2 mph, 1.8 mph, 2.4 mph, 3 mph). These speeds represent the range of speed at which the execution of this exercise modality is possible. The knee velocity feedback involved a color coded indicator that would flash red if the participant recorded a knee velocity above a specific threshold, and flash green if it was lower than the set threshold.
The variables analyzed included ground reaction forces, and lower limb kinematics and kinetics. Spatiotemporal parameters for each modality were determined using a standard bilateral lower extremity marker set to record lower extremity kinematics (240 Hz, Qualisys, Göteborg, Sweden). All Spatiotemporal parameters were calculated using Visual 3D (version 6.0, C-Motion, Germantown, MD, USA). A two-way repeated measures ANOVA was used to test the effects of the knee velocity feedback on ground reaction forces (GRF), and lower limb joint moments, and kinematics in the sagittal plane.

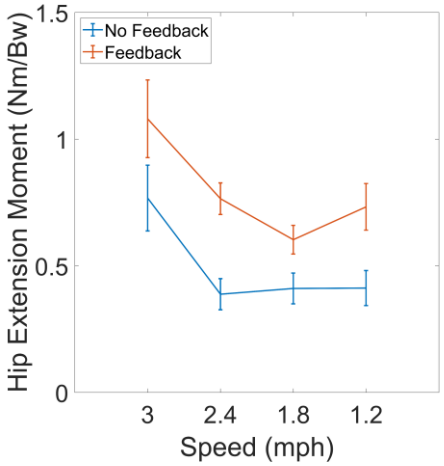

Figure 1: Hip Extension Moment (mean ± SE) during increased hip flexion gait exercise with and without knee velocity feedback across four different speeds.

Results & Discussion: Hip extension moment was larger for the feedback condition than the no feedback condition ($p = 0.012$, $\eta^2 = 0.521$). Post-hoc tests identified differences at 2.4 mph ($p = 0.003$) and 1.2 mph ($p = 0.032$) speeds. Additionally, hip peak hip flexion during the swing phase was larger for the feedback condition than the no feedback condition ($p = 0.038$, $\eta^2 = 0.395$). Post-hoc tests identified differences at 2.4 mph ($p = 0.023$), 1.8 mph ($p = 0.036$) and 1.2 mph ($p = 0.044$) speeds. No differences were observed for GRF and other kinematic and kinetic variables. Differences in hip extension moment are attributed to the need to increase the stability of their pelvis which helps the participant achieve the required hip flexion target and also create a gentler and more structured stride to then help them receive positive (green) feedback rather than negative (red). On the other hand, differences in the peak hip flexion during swing might have been associated with a strategy to allow more time to decelerate the foot before heel contact.

Significance: Increased hip flexion gait is a novel exercise modality that might address limitations in exercise participation in certain clinical populations. When performing this exercise participants use a HFFS to assist them at maintain a target exercise intensity. The HFFS system has various features that can be modified and utilized within the exercise science field, to both prevent the risk of some injuries and allow pain relief, while also helping in the recovery process of some individuals. While the knee velocity feedback feature did not result in differences in GRF, it led to changes in the movement pattern. The current results further inform the development and application of the HFFS.

Acknowledgments: The current study has been supported by the American Heart Association (grant 23AIREA1055000).

References:
[1] Oliveira et al. (2023), *Eur J App Phy*, 123(10); [2] Oliveira et al. (2022), Feasibility of a hip flexion feedback system for controlling exercise intensity and tibia axial peak accelerations during treadmill walking, *J Sports Eng Tech 0(0).*

Hip Joint Mechanics During a Bilateral Squat in Individuals with Femoroacetabular Impingement Syndrome (FAIS)

Holly M. Stanze[1*], Kate N. Jochimsen[2,3], Stephen T. Duncan[4], Michael A. Samaan[1,4]
[1] Dept. of Kinesiology & Health Promotion, University of Kentucky
[2] Center for Health Outcomes and Interdisciplinary Research (CHOIR), Massachusetts General Hospital
[3] Dept. of Psychiatry, Harvard Medical School
[4] Dept. of Orthopaedic Surgery, University of Kentucky
*Corresponding author's email: hmst263@uky.edu

Introduction: Femoroacetabular Impingement Syndrome (FAIS) is a pre-arthritic hip joint condition associated with hip pain, stiffness, and dysfunction in young individuals. FAIS is characterized by bony morphology resulting in premature contact between the femoral head and acetabulum. Previous studies have investigated lower-limb biomechanics in individuals with FAIS during gait and found inconsistent results, which may be due to the fact that walking does not result in deep hip flexion where hip impingement occurs. Therefore, recent studies have examined the biomechanics of deep squat tasks in individuals with FAIS in order to assess hip joint mechanics during a task that places the hip at a larger risk of impingement. However, studies related to deep squatting in the FAIS population are limited and lack consistency in findings. One study found that individuals with FAIS perform a deep squat with lower peak internal hip rotation angles and hip extensor moments and higher anterior pelvic tilt at the instance of peak hip flexion [1]. Another study found decreased squat depth and sagittal pelvic range of motion and no differences in hip kinematics [2]. These prior squat-related studies did not separately analyze the eccentric (descent) and concentric (ascent) phases of the squat, which may provide for a more sensitive method in detecting alterations in hip mechanics in FAIS. As individuals with FAIS exhibit hip muscle weakness, assessing hip joint mechanics during the eccentric and concentric phases of the deep squat may prove to be beneficial in understanding hip muscle dysfunction during dynamic activity. Additionally, assessment of peak hip joint moments may not be sensitive enough in detecting altered hip joint mechanics during a deep squat in individuals with FAIS, whereas examining total joint moment (TJM) may provide a more comprehensive evaluation of hip joint loading during a squatting task. The goal of this study was to compare hip joint biomechanics during the eccentric and concentric phases of a bilateral squat between individuals with FAIS and asymptomatic controls. We hypothesized that the FAIS group would exhibit altered pelvic- and hip-related mechanics in comparison to the control group.

Methods: 3D kinematics and kinetics were evaluated during a bilateral squat task (self-selected speed) in 7 pre-operative patients with FAIS and 7 age, sex, and body mass index matched, asymptomatic controls as part of a previous study. For the current analysis, a custom MATLAB algorithm was developed to calculate the average center of gravity (COG) velocity in the vertical direction, average sagittal plane pelvis position, average sagittal, frontal, and transverse plane hip position, and the time to completion during the eccentric and concentric phases of the squat task. The peak TJM during the eccentric and concentric phases as well as the sagittal, frontal, and transverse plane internal moments at the first and second peak TJM were calculated. The eccentric phase was defined as the timepoint of the start of the squat to the minimum COG position, and the concentric phase was defined as the timepoint of the minimum COG position to the end of the squat. The start and end points of the squat were defined using a modified version of a previously described methodology [3]. Group differences in squat-related outcomes were assessed using an independent t-test or Mann Whitney U-test, as needed, with statistical significance set at the 0.05 level.

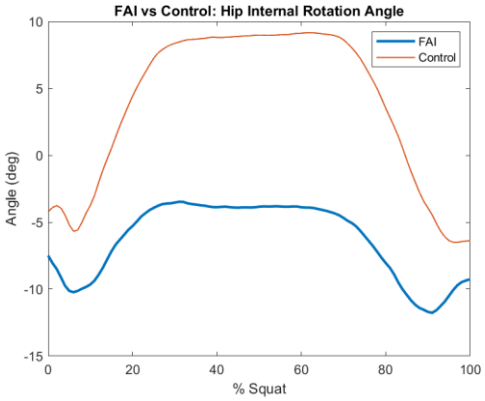

Figure 1. Transverse plane hip angle in the FAIS and Control groups.

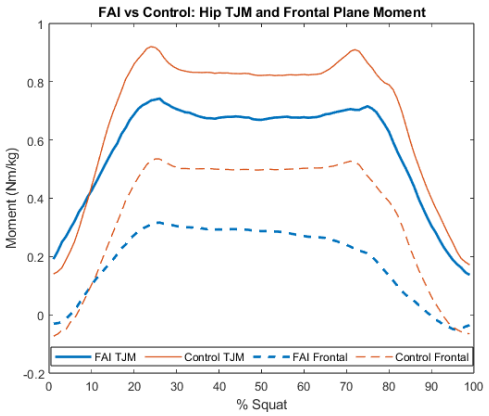

Figure 2. Hip TJM (solid lines) & frontal plane moments (dashed lines) for the FAIS & Control groups.

Results & Discussion: The FAIS group exhibited lower average hip internal rotation angles during both the eccentric ($p=0.01$) and concentric ($p=0.02$) phases of the squat (Fig. 1). Additionally, the FAIS group exhibited a lower hip adduction moment at the peak TJM during the concentric phase ($p=0.045$) as well as a lower peak TJM during the concentric phase, though this difference did not reach statistical significance ($p=0.06$; Fig. 2). In summary, this study identified that individuals with FAIS squatted with greater external hip rotation during both the eccentric and concentric phase and squatted with lower overall hip joint loading by using a lower hip adduction moment during the concentric phase.

Significance: Our results indicate that the FAIS group utilized different biomechanical strategies, potentially to avoid a painful hip impingement position during the eccentric and concentric phases of the deep squat. Analyzing the eccentric and concentric phases separately may be more sensitive in detecting alterations in hip mechanics during the deep squat in FAIS.

Acknowledgements: National Institutes of Health (K01-AG073698, K23-AT011922 and KL2-TR001996)

References: [1] Bagwell et al. (2016), *Clin Biomech*, 31, 87-92. [2] Lamontagne et al. (2019), *Clin Orthop Relat Res*, 467(3), 645-650. [3] Malloy et al. (2019), *J Orthop Sports Phys Ther,* 49(12), 908-916.

SPATIOTEMPORAL PATTERNS AND MUSCLE ACTIVITY FOLLOWING TOTAL HIP ARTHROPLASTY USING DIRECT ANTERIOR APPROACH

Maeve McDonald[1], Austin Middleton[1], Thomas Geissler[1], Cody Dziuk[1], Karl Canseco[1], Adam Edelstein[2], Jessica M Fritz[1]
[1] Medical College of Wisconsin, Wauwatosa, WI, USA
[2] Northwestern University Feinberg School of Medicine, Chicago, IL, USA
E-mail: mmmcdonald@mcw.edu

Introduction: Osteoarthritis (OA) is a disease affecting the joints, contributing to the functional impairment of about 10% of people over the age of 60, and OA of the hip is one of the most common causes for disability and pain in adults [1]. Total hip arthroplasty (THA) is a procedure commonly performed in OA patients to relieve pain, restore functional movement, and improve quality of life [2]. It has been shown that the approach to THA can influence recovery, post-surgery dislocation, intraoperative fractures, nerve injury, and invasiveness of surgery [3]. The direct anterior approach (DAA) is a minimally invasive approach to THA that negates the need for sectioning and detachment of muscles surrounding the hip, instead utilizing an intramuscular plane. This results in faster surgery time and lower complication rates [4]. However, there is limited research regarding muscle activation and spatiotemporal gait parameters following DAA. The goal of this study was to determine if there are differences in spatiotemporal gait parameters and muscle activation and timing patterns when comparing affected and unaffected sides after performing DAA THA. Due to reported outcomes in DAA THA, we hypothesized that there will be no significant differences regarding timing and duration in single limb support and stance phase and muscle activity when comparing the affected and unaffected sides during gait.

Methods: Subjects who underwent unilateral DAA for THA at least one year prior to data collection were recruited for this IRB approved study. Subjects were consented and instrumented for data collection at the Center for Motion Analysis. Muscle activity was synchronously collected with gait dynamics using 10 surface electromyogram (EMG) electrodes on the left and right gastrocnemius, vastus lateralis, rectus femoris, and gluteus medius. Six fine wire EMG electrodes were used to record activity of the left and right gluteus maximus, piriformis, and the tensor fasciae latae (TFL) muscles. EMG data was analyzed from 11 subjects across 10 dynamic walking trials at a comfortable, self-selected speed. EMG data was band pass filtered (surface: 20-500Hz, fine wire: 20-1500Hz), rectified, and then low pass filtered at 10 Hz to create a linear envelope. Signal was normalized from 0-100% gait cycle. The activation threshold was determined from the average signal of the inactive muscle plus three standard deviations. Timing of single-limb support, overall stance phase, and muscle activation onset, as well as duration of muscle activation were compared between affected and unaffected sides using a paired t-test with a significance set at $p < 0.05$. Effect size was tested using Hedge's correction to determine clinical significance.

Results & Discussion: Muscle activation onset was significantly earlier ($p<0.05$) in the piriformis muscle on the affected side (Figure 1). This finding was also clinically significant based on effect size. No other significant differences were found. Our results indicate that symmetry was maintained between the affected and unaffected sides for duration of stance phase and single limb support. Symmetry was also maintained for duration of muscle activation for all muscles and for onset of muscle activation for all muscles except the piriformis. Previously assessed kinematics showed no differences between limbs during hip flexion and extension [5]. Symmetric kinematic and muscle activation patterns following surgery is essential to prevent occurrence of OA symptoms in other joints and reduce implant wear. Early activation of the piriformis muscle could suggest perceived instability or a protective mechanism resulting from surgery. Future work will involve assessment of isometric strength data as well as muscle activation onset at different walking speeds and stair ascension and descension.

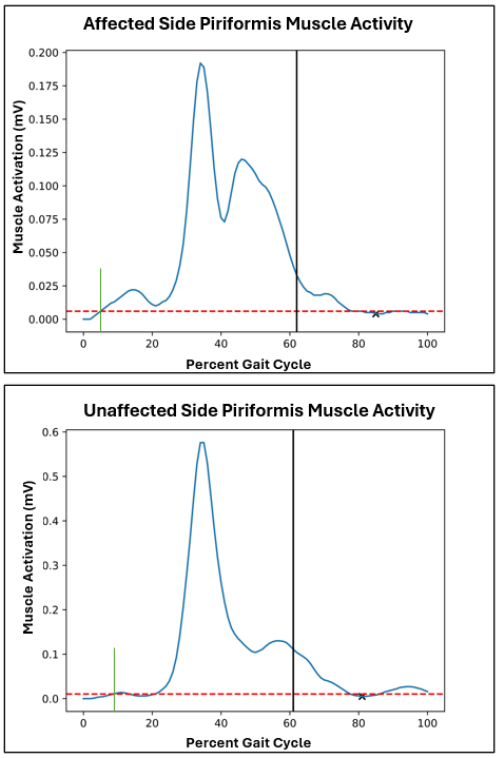

Figure 1: EMG data of the piriformis muscle from a representative participant's affected side (top) and unaffected side (bottom). The red horizontal line indicates the threshold that must be passed to consider muscles activated or "on". The short vertical line indicates percent of gait cycle when muscle was activated. The long vertical line indicates the end of the stance phase.

Significance: This study provides a novel insight into the postoperative effects of DAA for THA on gait and muscle activation patterns to better inform surgeons and patients as they consider surgical approaches.

References: [1] Buckwalter, J. A. et. al. (2004) Clinical Orthopaedics and Related Research, (427 Suppl), S6–S15; [2] Varacallo M et. al. (2018) Journal of Orthopaedics, 15(2):495-499; [3] Moretti VM (2017) Indian Journal of Orthopaedics, 51(4):368-376; [4] Connolly KP (2016) World Journal of Orthopaedics, 7(2):94-101; [5] Mueller, E. Sagittal Plane Kinematics Following Total Hip Arthroplasty Using Direct Anterior Approach Poster presented at: Orthopaedic Research Society Annual Meeting 2024

EFFECTS OF FATIGUE ON GROUND REACTION FORCE, KINETICS AND KINEMATICS DURING INCREASED HIP FLEXION GAIT

Meagan Bubeck [1], Jade Sharretts[1], Hunter Haynes[1], Chuang-Yuan Chiu[2], Tanner Thorsen[1], Nuno Oliveira[1*]
[1]School of Kinesiology and Nutrition, The University of Southern Mississippi, MS, USA
[2]School Sports Engineering Research Group, Sheffield Hallam University, Sheffield, UK
*Corresponding author's email: nuno.oliveira@usc.edu

Introduction: Effectively exercising is a pertinent aspect of health, fitness, and quality of life. Although there are many forms of exercise, the factors that most greatly influence the type chosen are safety, accessibility and needed equipment, and the general level of difficulty. Due to these factors, walking, jogging or stationary cycling are some of the most popular forms of aerobic exercise. However, these types of exercise might not be optimal for some clinical populations. Increased hip flexion gait (HFgait) is an alternative exercise modality that involves increasing exercise intensity (metabolic cost) by increasing peak hip flexion above normal levels during treadmill walking [1]. To assist participants in maintaining a specific exercise intensity a hip flexion feedback system was developed. This system used a markerless motion tracking system for hip flexion angle calculations and displays on a screen positioned in front of the treadmill a specific peak hip flexion threshold that participants should meet while walking on the treadmill [2].
Fatigue during exercise has been associated with overuse injuries. Additionally, it is important to understand the biomechanical responses to acute fatigue for exercise prescription, and measurement pre/post training interventions and understand its impact in functional tests. Because biomechanical changes with fatigue are activity and context specific, the selection of appropriate exercise modalities is critical. However, the effects of acute fatigue on HFgait have not yet been investigated.
The purpose of this study was to test how fatigue impacted ground reaction force, and lower limb kinetics and kinematics during HFgait. It was predicted that fatigue would lead to changes in the biomechanics of the movement due to the participant's decreasing ability to control their movements as they fatigue.

Methods: Ten healthy individuals (5M, 5F; age 30.1 ± 9.8 years; height 169.9 ± 0.09 cm; body mass 67.9 ± 14.3 kg) participated in the study. Participants performed HFgait in two trials: one before (pre) and one after (post) a fatigue protocol. Participants performed the increased hip flexion gait at speeds 1.2 mph, 1.8mph, 2.4 mph, and 3 mph. These speeds represent the range of speed at which the execution of this exercise modality is possible. The fatigue protocol consisted of a HFgait high intensity interval training session of ten repetitions of 1 minute of exercise alternated with 1 minute of rest. This occurred for a total of 20 minutes with 10 minutes spent resting and 10 minutes spent performing the exercise. The HFgait for this portion was performed at a challenging but safe speed. The participant's goal was to reach and maintain an exercise intensity of 90% of their heart rate reserve. The variables analyzed included ground reaction forces, and lower limb kinematics and kinetics. Spatiotemporal parameters for each modality were determined using a standard bilateral lower extremity marker set to record lower extremity kinematics (240 Hz, Qualisys, Gothenburg, Sweden). All Spatiotemporal parameters were calculated using Visual 3D (version 6.0, C-Motion, Germantown, MD, USA). A two-way repeated measures ANOVA was used to test the effects of fatigue on ground reaction forces (GRF), and lower limb joint moments, and kinematics in the sagittal plane.

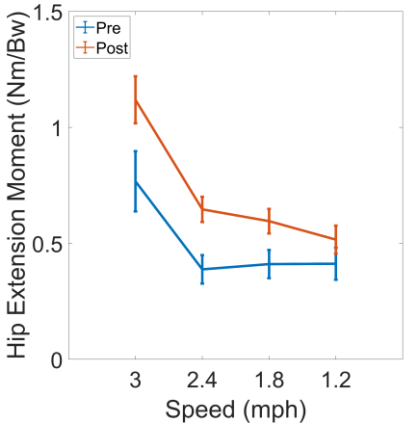

Figure 1: Hip Extension Moment (mean ± SE) during increased hip flexion gait exercise pre and post fatigue across four different speeds.

Results & Discussion: Hip extension moment was larger for the post fatigue condition compared to the pre fatigue condition ($p = 0.005$, $\eta^2 = 0.602$). Post-hoc tests identified differences at 3 mph ($p = 0.020$), 2.4 mph ($p = 0.003$), and 1.8 mph ($p = 0.043$) speeds. No differences were found for other GRF, kinetic or kinematic variables. The increase in hip extension moment with fatigue might represent a modification in the neuromuscular control of the HFgait with fatigue. Contrary to other activities, this might not have resulted in differences in movement kinematics because this exercise relies on participants meeting a specific kinematic target (target peak hip flexion). Additionally, the fact that differences were not found at the lowest speed (1.2 mph) might indicate that performing the exercise at this speed might not be challenging enough and does not require an adaptation to fatigue status. Finally, joint motions in the frontal and transverse plane and electromyography should be investigated to provide a more comprehensive understanding of the modifications that took place due to fatigue.

Significance: The effect of fatigue on HFgait biomechanics is unknown. This study suggests that hip extension moment is an important parameter during this activity. Additionally, these findings can be used to better inform: 1) the functional tests involving the lower extremity neuromuscular response used during exercise interventions using this exercise modality, and 2) training load prescriptions and injury risk management during increased flexion gait exercise programs.

Acknowledgments: The current study has been supported by the American Heart Association (grant 23AIREA1055000).

References:
[1] Oliveira et al. (2023), *Eur J App Phy*, 123(10); [2] Oliveira et al. (2022), Feasibility of a hip flexion feedback system for controlling exercise intensity and tibia axial peak accelerations during treadmill walking, *J Sports Eng Tech 0(0).*

Dexterous manipulation capabilities are associated with change in discharge rate properties of motor neurons.

Mukta N Joshi[1]*, Francesco Negro[3], Kristian M O'Connor[2], Scott J Strath[2], Brooke Slavens[4], Allison Hyngstrom[5], Kevin G Keenan[2]
[1]Department of Health and Kinesiology, University of Utah, Salt Lake City, UT
*Corresponding author's email: mukta.joshi@utah.edu

Introduction: Aging is associated with a decreased ability to hold a steady force and manipulate objects with the hand [1]. Tasks requiring the use of smaller forces and precise force control are often most challenging for older adults [2]. These changes are in dexterous control are associated with changes in discharge rate properties of motor neurons and changes in the common oscillatory drive of motor units involved in muscle force regulation [3]. The development of high-density surface EMG arrays enables recording activity over a larger muscle area and using algorithms to extract motor unit data from surface EMGs [4]. While a number of studies have examined motor unit properties using this technology, fewer studies have examined age-associated changes in dexterity using this technology [5]. The objective of this research was to examine age-associated differences in dexterous performance and examine associations between the force steadiness and measures of dexterity and motor unit parameters such as discharge rate, discharge rate variability and low-frequency common oscillatory drive using the multichannel HD EMG arrays

Methods: 26 older adults (66-86 years) and 28 young adults (19-38 years) participated in the study. Research participants performed force matching tasks during index finger abduction and precision pinch tasks. They also performed tests of manual dexterity such as the coin rotation, box and block test and grooved pegboard test. The standard deviation (SD) and coefficient of variation (CV) during the force-matching task was computed. Multichannel high-density EMG was measured from the First Dorsal Interosseus (FDI) and extensor Digitorum Communis (EDC). The EMG signals were decomposed to obtain motor unit discharge rate parameters such as discharge rate and discharge rate variability of the motor neurons was computed. The first principal component referred to as the First Common Component (FCC) of the Principal Component Analysis (PCA) of the smoothed motor unit discharge rates explained the largest variations in the motor unit discharges and was used as a measure of low-frequency common oscillatory drive to the motor neurons [6]. Associations between the force variability, dexterity scores and motor unit parameters were analyzed for group differences and associations.

Results & Discussion: Force steadiness, measured as SD of force on the index finger abduction task was greater in older adults (8.09 ± 5.414 N) vs younger adults (6.33 ± 3.86 N), f (1, 98) = 5.418; p = 0.022). Our data did not show any age-associated changes in pinch force variability. On the abduction task, the discharge rate (p = 0.002), as well as the first principal component of motor unit discharges (p = 0.001), which represents the strength of the common oscillatory drive to the muscle were greater in in FDI muscle of the young adults as compared to the older adults. Correlation analysis showed a positive association between force variability and discharge rate variability (r = 0.261, p = 0.033), and a negative correlation between force variability and measures of neural drive as represented by the average discharge rate and FCC of the motor units (r = -0.295, p = 0.014). Our data showed a differential activation patterns of the EDC and FDI motor units. While the FDI is the prime mover for the index finger abduction task, data from older adults showed a higher discharge rate of EDC motor units as compared to the FDI motor units (p < 0.001). Also, the FCC for the EDC motor units was greater (p < 0.001). Conversely, the discharge rate variability (p = 0.013) and the variability of the first principal component (p = .045) were higher for the FDI motor units. Furthermore, pinch data in older adults showed greater variability in the FCC of the FDI motor units as compared to the EDC motor units (p = 0.04). This difference between the motor unit activation of the 2 muscles was not observed in the younger adults. Previous research has pointed to a decrease in coordination patterns in older adults [7]. The differential activation of FDI and EDC motor units in our data likely point to a diminished coordination pattern present with age. For the tests of manual dexterity, age associated changes were seen in the grooved pegboard test (p < 0.001), but not other measures of dexterity. There were significant association between force variability on the pinch task and box and block task score for young (r = -0.601; p <0.001) and older adults (r = -0.606; p < 0.001). Our results showed that older adults' data on the box and block test was significantly associated with several motor unit parameters across the abduction and pinch. Higher discharge rate variability of the motor units, and lower motor unit discharge rates, were associated with fewer blocks being transferred on the box and block test.

Significance: Our results showed a change in motor unit properties with age. However, only the index finger abduction and the grooved pegboard test showed an age-associated change in dexterous performance. This could have a likely association with differences in dexterous experience between the two groups. While majority of the older in the study engaged in dexterous activities such as writing, knitting, quilting, playing an instrument, bowling etc., a large number of the younger adults listed texting or playing video games as their dexterous activity. Although all these activities use hands the former activities require precise force and position control using fingers, which is not the demand of a typing task used in texting. Thus, the key to preserving dexterous control with increasing age may lie in including more dexterous activities involving individual fingers and small forces such as writing, cutting vegetables, knitting, etc. in everyday life.

Acknowledgments: College of Health Sciences Graduate Student Research Grant at the University of Wisconsin – Milwaukee.

References: [1] Marmon et al. (2001), Med Sci Sports Exerc, 43; [2] Kern et al. (2001), J Appl Physiol 91; [3] Enoka et al. (2003), J Electromyogr Kinesiol, 13; [4] Merletti et. al. (2008), J Electromyogr Kinesiol 18(6); [5] Feeney et. al (2018), J Physiol, 596; [6] Negro et al. (2009), J Physiol, 587; [7] Shinohara et al. (2004), Exp Brain Res, 156(3)

MECHANICAL-INDUCED FACTORS OF RESTENOSIS: A REVIEW

Luci Duncan[1*], Josiah Owusu-Danquah, PhD[2]
[1]Cleveland State University, Cleveland, Ohio, Center for Human-Machine Systems
l.r.duncan@vikes.csuohio.edu*

Introduction: In the field of biomechanics, computational modeling offers the benefit of simulating interactions within the body at different levels without the need for biological experiments. A major challenge to this is accurately portraying such complex systems as the human body under appropriate computational cost and time conditions. An essential concept for computational models is striking a balance between simplifying models and prediction accuracy. Oversimplification may lead to less accuracy in model simulations, while more complex models introduce computational challenges. With a focus on coronary stents, in silico modeling offers an insight into the interactions between device and tissue. This review focuses on the different approaches used to model the behavior of stent-tissue interactions and assesses the limitations of these existing models that alter accurate biological and material responses. The prevention of restenosis is a paramount concern, and computational models offer a promising avenue for understanding and optimizing these interactions. It is essential to recognize that restenosis, characterized by at least a fifty percent decrease in diameter within a stent, serves as a critical metric in assessing the effectiveness of stent designs [1]. Understanding these interactions from a bottom-up perspective would allow for optimized stent design, including patient-specific suggestions.

Methods: In the pursuit of a comprehensive understanding of cardiovascular stent interactions, an extensive literature review was conducted through Google Scholar. The search focused on articles using keywords such as "(In-Stent) Restenosis," "Computational Modeling," "Coronary Arteries," and "Cardiovascular Stent." Inclusion criteria involved papers written in English, subjected to peer review, and encompassing information related to restenosis, mechanical properties of arterial wall tissues and coronary stents, and modeling using finite element methods or other applicable practices. Consideration extended to general biomechanics of coronary vessels and review papers to provide a holistic view beyond specific modeling studies.

Results & Discussion: In-depth exploration of existing computational models reveals pivotal factors influencing in-stent restenosis and highlights challenges hindering their biological accuracy. The optimization of stent design emerges as a focal point, where geometry, material properties, and embedding direction within the arterial wall play critical roles. Balancing factors such as surface roughness, material flexibility, and overall design becomes paramount in influencing mechanical forces on the arterial wall. Forces applied by stents to the surrounding tissue are critical determinants in restenosis rates. High radial stresses induced by specific stent deployment techniques contribute to neointimal hyperplasia, a key factor in vessel renarrowing [2]. The technique itself, whether balloon-expanded or self-expanding, introduces variations in force interactions, affecting the risk of endothelial damage and subsequent restenosis [3, 4]. Existing models, while informative, grapple with inherent limitations. Simplifications in arterial wall properties, such as assuming isotropic and homogeneous material behavior, diverge from the inherently anisotropic and heterogeneous nature of real arterial tissues. The geometric representations often fall short of capturing the natural curvature, impacting the understanding of stent-artery interactions. Neglecting the complexities of plaque and lesions further limits the models' ability to mirror real-world scenarios accurately. The challenge of achieving computational models that emulate in vivo interactions lies in the intricate nature of biological systems. Tissue properties, plaque characteristics, and patient-specific variations pose formidable obstacles. The diverse types of stents, ranging from balloon-expandable to self-expanding, necessitate a meticulous approach to account for individual differences in force-based interactions. The continued evolution of computational models for cardiovascular stent interactions stands as a beacon of progress in addressing the challenges of in-stent restenosis. By navigating the complexities and limitations inherent in current models, the field can pave the way for more accurate simulations. These simulations, reflective of real-world biological responses, hold the potential to revolutionize stent design, intervention protocols, and pharmaceutical strategies, ultimately benefiting a vast population grappling with cardiovascular diseases.

Significance: The significance of advancing computational models lies in their potential to inform stent design, pharmaceutical research, and interventions for cardiovascular diseases. Improved models, with fewer limiting conditions, hold the promise of revolutionizing stent insertion procedures, pharmaceutical advancements, and addressing the needs of the population afflicted by cardiovascular diseases. By understanding and mitigating in-stent restenosis, these advancements contribute to better patient outcomes and a reduced need for reintervention, marking a substantial step forward in cardiovascular healthcare.

Acknowledgments: This work is funded by NSF award 2152135.

References: [1] Kibos, A., A. Campeanu, and I. Tintoiu. "Pathophysiology of coronary artery in-stent restenosis." *Acute cardiac care* 9.2 (2007): 111-119; [2] Freeman, Joseph W., Patrick B. Snowhill, and John L. Nosher. "A link between stent radial forces and vascular wall remodeling: the discovery of an optimal stent radial force for minimal vessel restenosis." *Connective tissue research* 51.4 (2010): 314-326; [3] Harnek, Jan, et al. "Differences in endothelial injury after balloon angioplasty, insertion of balloon-expanded stents or release of self-expanding stents: an electron microscopic experimental study." *Cardiovascular and interventional radiology* 22 (1999): 56-61; [4] Okamoto, Y., et al. "In-vitro evaluation method to measure the radial force of various stents." *13th International Conference on Biomedical Engineering: ICBME 2008 3–6 December 2008 Singapore*. Springer Berlin Heidelberg, 2009.

BREAST RECONSTRUCTION-SPECIFIC COMPUTATIONAL MODEL DEVELOPMENT TO IDENTIFY MECHANISMS OF SHOULDER DYSFUNCTION FOLLOWING BREAST CANCER SURGERY

Joshua Pataky[1*], Camille L. Graves[1], Jared Heitzenrater[2], Meghan E. Vidt[1,3]
[1]Biomedical Engineering, The Pennsylvania State University, University Park, PA, USA
[2]Public Health Sciences, Penn State College of Medicine, Hershey, PA, USA
[3]Physical Medicine and Rehabilitation, Penn State College of Medicine, Hershey, PA, USA
*Corresponding author's email: jjp6192@psu.edu

Introduction: Many breast cancer patients undergo mastectomy as part of treatment, followed by reconstruction surgery [1], but these common surgical interventions result in persistent shoulder dysfunction long after treatment concludes [2]. However, the underlying biomechanical mechanisms driving dysfunction are unknown. Computational models specific to the breast cancer population would enable study of these mechanisms, but no model currently exists for this population. Thus, our objectives were: 1) develop breast cancer surgery-specific models representing lumpectomy, implant-based, and autologous flap-based breast reconstruction; and 2) use these models to determine how muscle contribution to hand acceleration during movements representing daily tasks differs across groups.

Methods: Using the MoBL-ARMS upper extremity model [3] in OpenSim (v.4.1) [4] as a baseline, a breast cancer surgery model was developed by scaling muscle force-generating properties to those of middle-aged adult females [5] and anthropometry of 50th percentile adult females [6]. The 3 paths of the pectoralis major muscle were altered to more closely match moment arms in literature [7]. To develop models specific to lumpectomy, implant-based, and flap-based reconstruction, mass properties of the model were adjusted to account for differences in density between native breast tissue [8], silicone breast implants [9], and autologous flap tissue [10], respectively. For the implant model, a cylindrical wrapping surface matching manufacturer's specifications of a 405cc implant [11] was added beneath the pectoralis major muscle path, consistent with subpectoral implant placement (Fig. 1A). No additional changes were made to the muscle paths to represent lumpectomy or flap-based reconstruction. To validate the models, the inverse dynamics tool in OpenSim was used to predict shoulder moment in 5 postures (external rotation; internal rotation; scapular plane elevation; horizontal abduction; horizontal adduction), with an external load applied equal to mean force (strength) previously measured from a cohort of breast cancer patients [12]. Induced acceleration analysis (IAA) was used to identify the 5 muscles with the largest contribution to hand acceleration during functional movements (external-internal rotation; scapular plane elevation; horizontal abduction-adduction).

Results & Discussion: The pectoralis major moment arm for all breast cancer surgery models more closely matched literature compared to the MoBL-ARMS model, although moment arm was reduced in the implant model compared to lumpectomy and flap models (Fig. 1B). Shoulder moments predicted with inverse dynamics fell within 1 standard deviation of the mean experimentally-measured moment for all models and tasks, except horizontal abduction for all models and elevation for the lumpectomy model, providing model validation. Results of IAA revealed no differences in muscle contribution to hand acceleration between breast cancer models. Large shoulder muscles, including deltoid, infraspinatus, and subscapularis, were found to be among the largest contributors to hand acceleration (Fig. 1C). Sternal and ribs compartments of pectoralis major were also found, possibly relating to reported functional deficits post-surgery.

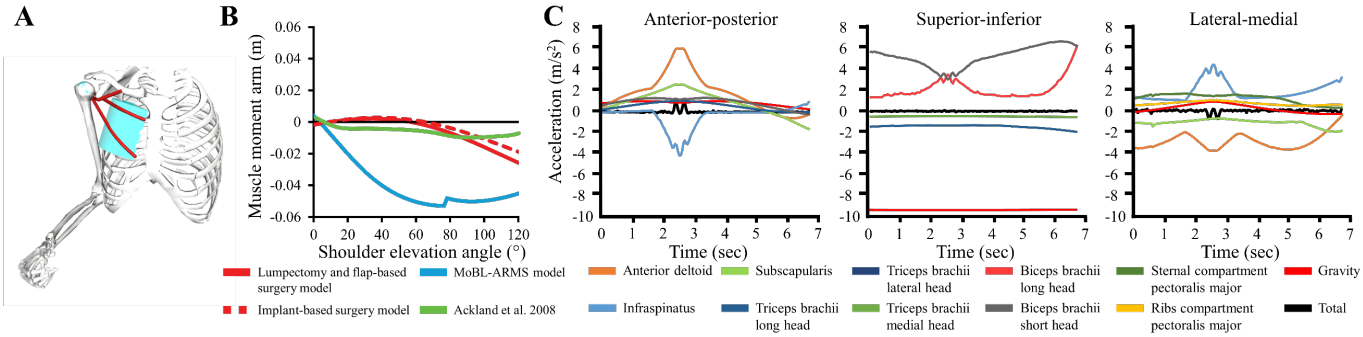

Figure 1: A) Implant-based breast reconstruction model, with cylindrical wrapping surface beneath sternal and ribs compartments of the pectoralis major muscle paths. B) Pectoralis major ribs compartment moment arm more closely matches literature [7] compared to the MoBL-ARMS model, while the implant surgery model moment arm is reduced compared to lumpectomy and flap models. C) Muscles with the largest contribution to hand acceleration, evaluated along thorax coordinate system axes. No differences were seen between breast cancer surgery models.

Significance: This model-based work showed that implant reconstruction alters pectoralis major moment arm. Surgical alterations to primary contributors to shoulder movement may account for functional deficits reported by survivors. These models can be used in the future to further study the mechanisms driving shoulder dysfunction in breast cancer survivors and identify rehabilitation targets.

Acknowledgments: Penn State College of Medicine, Junior Faculty Development Program Seed Grant (Vidt).

References: [1] Kummerow et al. (2015), *JAMA Surg* 150(1):9-16; [2] Nesvold et al. (2011) *J Cancer Surviv* 5:62-72; [3] Holzbaur et al. (2005) *Ann Biomed Eng* 33:829-40; [4] Delp et al. (2007) *IEEE Trans Biomed Eng* 54:1940-50; [5] Saul et al. (2015) *J Appl Biomech* 31:484-91; [6] Gordon et al. (2014); [7] Ackland et al. (2008) *J Anat* 213:383-90; [8] Martin et al. (1994) *Int J Obes Relat Metab Disord* 18:79-83; [9] Hsieh et al. (2013) *Plas Reconstr Surg Glob open* 1:e43; [10] Razzano et al. (2018) *J Plast Reconstr Aesthetic Surg* 71:1410-16; [11] Natrelle (2016); [12] Pataky (2024) *Doctoral Dissertation, Pennsylvania State University*.

Restoration And Maintenance of Physical and Neurosensory Performance in Naval Aviation

Ty Cardinale[1*], Julia Lytle[1], Andrew Plows[1], Patrick Desrosiers[1], Victoria Medved[1], Eric Infante[1], Andy Kittleson[2], Brian Loyd[2], Joshua Winters[3], Trevor Kingsbury[1]
[1]Naval Medical Center San Diego, San Diego, CA, USA
[2]University of Montana, Missoula, MT, USA
[3]University of Kentucky, Lexington, KY, USA
Corresponding author's email: tycardinale@gmail.com

Introduction: The rigorous demands of Naval Aviation necessitate peak human performance and musculoskeletal (MSK) health, yet comprehensive assessments in this population have historically been elusive despite high incidence of injury[1]. Leveraging a multi-domain clinical assessment framework designed to swiftly pinpoint areas of intervention support the high-performance standards required in Naval Aviation. By evaluating and contrasting performance across multiple domains of naval aviators and aircrew/maintainers (AWR/AT), specific performance and MSK health needs can be distinguished and addressed. Specifically, incorporating patient-reported outcomes with biomechanical and neurosensory performance measurements offers a comprehensive evaluation framework. This approach allows for an in-depth understanding of the servicemember that is aligned with the occupational demands unique to pilots and naval aviators. Such a nuanced perspective is critical for devising interventions that are both effective and occupation-specific. This multi domain clinical assessment can quickly identify functional deficits, training opportunities, and provide an avenue for direct clinical treatment strategies. Therefore, the purpose of this study was to evaluate differences in performance across multiple domains between naval aviators (1310) and aircrew/maintainers (AWR/AT) to assess the specific performance needs within squadrons.

Methods: Data were collected retrospectively under an approved IRB protocol (NMCSD.2021.005). 62 Servicemembers (SM) were assessed: 37 helicopter pilots (23 male, 14 female; average age = 30 yrs old, average flight hours = 1155) and 25 aircrew/maintainers (24 male, 1 female, average age = 28 years old). Each SM underwent a human performance battery consisting of physical performance tasks (countermovement jump (CMJ), isometric mid-thigh pull (IMTP), hop test, 300-yard shuttle run, 5-10-5 agility test), MSK/biomechanical health (dynamic strength index (DSI), a ratio of strength and power), neurosensory performance (dynamic visual acuity (DVA)), and psychosocial health (demographics, sleep quality). Independent samples T-Test's were used to compare groups. Significance set at alpha = 0.05

Variable	Pilot	AWR/AT
CMJ Jump Peak Power (W)*	3432	3900
DSI*	0.72	0.78
DVA*	0.26	0.30
PSQI*	5.6	6.8
CMJ Height (in)	11.5	12.2
IMTP Peak Vertical Force (N)	2382	2514
RSI	1.66	1.60
5-10-5 Agility Time (s)	5.44	5.45
300 Yard Shuttle Time (s)	69	70

Figure 1: Pilot and AWR/AT mean values for all variables of interest. * indicating statistically significant differences seen in the corresponding variable.

Results & Discussion: Pilots displayed a significantly lower counter-movement jump peak power and demonstrated better vestibular health and sleep quality, as evidenced by their DVA (0.26 vs 0.30) and PSQI scores (5.6 vs 6.8) compared to AWR/AT. These findings highlight the operational demands and the differentiated physical and health profiles between the two groups. The pilots superior DVA reflects the taxing vestibular demands of flying. Although there were no statistically significant differences in CMJ height (11.5 vs 12.2in), IMTP peak vertical force (2382 vs 2514 N), RSI (1.66 vs 1.60), 5-10-5 agility time (5.44 vs 5.45 s), both groups mean scores indicates a broadly high level of physical conditioning across Naval Aviation. Additionally, AWR/AT had a significantly higher mean DSI (0.78), closer to the top range of the accepted scale. This trend reinforces the necessity for role-specific training and MSK health.

Significance: Pilots and AWR/AT exhibit significantly varied performance across several domains, underscoring the importance of offering resources and care to the entire squadron while addressing the distinct needs of each Navy Enlisted Classification (NEC). DVA is clinically trainable, and though the pilots excelled at DVA, understanding how DVA responds to physically demanding flight training would significantly improve strategies to optimize performance within pilots. Because AWR/AT had greater power along with a DSI closer to .80, a training programs with a strength focus may be beneficial. Overall, by evaluating performance across multiple domains between naval aviators and aircrew/maintainers to assess their specific performance needs, we can systematically assess current performance and identify areas for corrective improvement or clinical referral.

Acknowledgments: The views expressed in this work are those of the author(s) and do not reflect the official policy or position of the Department of the Navy, Department of Defense, nor the US Government.

References:

1. Hiebert R, Brennan T, Campello M, et al. Incidence and Mechanisms of Musculoskeletal Injuries in Deployed Navy Active Duty Service Members Aboard Two U.S. Navy Air Craft Carriers. *Mil Med*. 2020;185(9-10):e1397-e1400. doi:10.1093/milmed/usaa004

THE ROLE OF EXTRINSIC FOOT MUSCLES IN VERTICAL JUMP PERFORMANCE

Ben K Perrin*, John H Challis
Biomechanics Laboratory, The Pennsylvania State University, University Park, PA 16802, USA
*Corresponding author's email: bkp5431@psu.edu

Introduction: Many muscles cross more than one joint; for bi-articular muscles the implications of their bi-articularity has been examined [1]. For jumping in particular, the role of the bi-articular gastrocnemius has received considerable attention [e.g., 2, 3]. A recent study has highlighted the role of the intrinsic foot muscles in jump performance [4], but this raises the question of the role of extrinsic foot muscles. The extrinsic toe flexor muscles (flexor hallucis longus, FHL; flexor digitorum longus, FDL) span both the ankle and metatarsophalangeal joints, and therefore could contribute to jump performance due to their actions at both of these joints.

The plantarflexion moment arm of the triceps surae is approximately twice that of the FHL [5], while the physiological cross-sectional area of the triceps surae is approximately seven times greater than that of the combined physiological cross-sectional areas of the FHL and FDL [6, 7]. To magnify the potential role of these muscles, a model was formulated, and maximum height jumps were simulated with all joints above the ankle joint locked [8]. Jumps were simulated with varying potential contributions from the FHL and FDL to elucidate their role in jumping.

Methods: A direct dynamics, muscle-driven, optimal control model was developed of jumping with joints above the ankle locked. The task was to maximize jump height. The model was actuated by Hill-type muscle models of the plantar-flexors, FHL, and FDL, where their muscle properties were based on cadaver data [6, 7]. The joints of the model were the ankle, tarsometatarsal, and metatarsophalangeal joints, where the plantar-flexors crossed only the ankle joint, but the FHL and FDL spanned all modelled joints. Coordinate limiting forces were enforced to represent the effects of ligaments at each joint.

Optimization simulations were performed using SCONE [9]. A piecewise, feedforward controller was used to determine default excitation level (0 to 1), final excitation level (0 to 1), and time of excitation (0.001 to 1s) for each muscle in the model. Simulations ran until new generations provided no increase to calculated maximum jump height. Multiple simulations were performed where the physiological cross-sectional area (PCSA) of the toe flexors was systematically varied from their nominal value of about one seventh of the PCSA of the triceps surae [6, 7].

Results & Discussion: The nominal model produced a jump height similar to experimental data [10]. Increasing and decreasing toe flexor contributions resulted in increased and decreased maximum jump heights respectively (Fig 1). The results followed distinct patterns for increased vs decreased toe flexor contributions. To clarify the cause of these differences, another simulation was run where FHL and FDL contributions were set to 0%, while triceps surae contribution was increased so that moment generated about the ankle was approximately the same as the nominal model. This produced a maximum jump height (red circle in Fig 1) that was much lower than that achieved by the original model, suggesting that changes in results are due to more than just the changes in moment produced about the ankle.

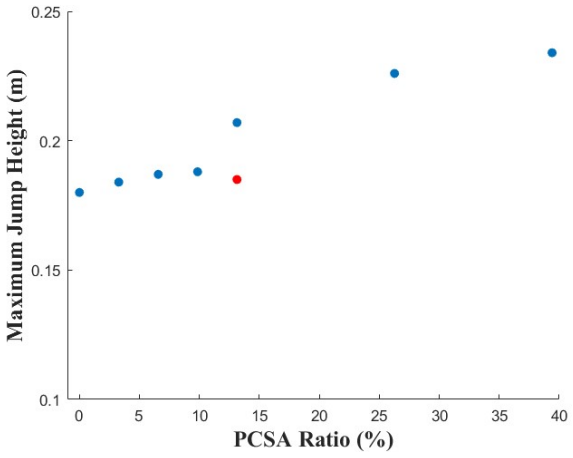

Figure 1: Jump height plotted against PCSA of toe flexors as a percentage of PCSA of plantar-flexors. The red circle is the result from the trial with triceps surae PCSA increased to compensate for no toe flexors.

Significance: The results of this study highlight that foot strength and structure have a large role in our ability to move efficiently. It is possible that the bi-articular nature of the FHL and FDL allow them to transfer energy to the toes, in a similar manner to the gastrocnemius [3]. While this study looked at the effects of toe flexors in jumping, these findings likely translate to walking and running due to their similar proximal to distal activation sequences.

References:

[1] Van Ingen Schenau (1989) *Human Movement Science*, 8(4), 301-337.
[2] Pandy & Zajac (1991) *Journal of Biomechanics*, 24(1), 1-10.
[3] Van Soest et al. (1993) *Journal of Biomechanics*, 26(1), 1-8.
[4] Smith et al. (2023) *Journal of Sport and Health Science*, 12(5), 639-647.
[5] Klein et al. (1996) *Journal of Biomechanics*, 29(1), 21-30.
[6] Wickiewicz et al. (1983) *Clinical Orthopaedics and Related Research*, 179, 275-283.
[7] Klein Horsman et al. (2007) *Clinical Biomechanics*, 22(2), 239-247.
[8] Levine et al. (1983) *IEEE Transactions on Automatic Control*, 28(11), 1008-1016.
[9] Geijtenbeek (2019) *Journal of Open Source Software,* 4(38), 1421.
[10] van Werkhoven & Piazza (2017) *Journal of Biomechanics,* 57, 27-31.

AN INVESTIGATION INTO THE RELATIONSHIP BETWEEN SOCKET FIT AND BALANCE CHARACTERISTICS IN INDIVIDUALS WITH TRANSFEMORAL AMPUTATIONS

Paige Paulus[1*], Tom Gale[1], Yulia Yatsenko[1], Kelly Mroz[1], Justin Elder[1], Drew Buffat[2], Goeran Fiedler[3], and William Anderst[1]
[1]University of Pittsburgh, Department of Orthopaedic Surgery, Pittsburgh, PA
[2]Union Orthotics and Prosthetics, Pittsburgh, PA
[3]University of Pittsburgh, School of Health and Rehab Science, Pittsburgh, PA
*Corresponding author's email: pap82@pitt.edu

Introduction: More than 50% of individuals with lower extremity amputations report falling within the past 12 months due to factors such as poor balance and prosthetic fit [1,2]. Of those who have fallen, up to 75% of individuals with lower extremity amputations reported falling more than once [2] and up to 57% reported sustaining a fall related injury [1]. Current methods for evaluating prosthetic fit are relatively iterative and dependent upon clinician expertise. Previous studies have shown that individuals with lower extremity amputations tend to have more asymmetrical and variable lateral center of pressure (COP) and ground reaction forces (GRF) compared with healthy controls [3,4]. However, the link between perturbations to prosthetic socket fit and balance characteristics has not been established. The aim of this interim analysis of an ongoing study is to explore the relationship between socket fit and balance characteristics of individuals with transfemoral amputations.

Methods: Individuals with unilateral traumatic transfemoral amputations who had been ambulating for more than a year with their prosthesis provided written informed consent to participate in this IRB approved study [5]. Participants were casted and fitted by a licensed prosthetist with 3 custom check sockets which varied in stiffness, brim height, and shape (quad socket) and a standard of care (SoC) check socket which matched their definitive socket geometry. Participants were tracked using a 12-camera Vicon motion capture system (100 Hz) while they walked across a 10m lab walkway at a self-selected pace for 4 trials per socket (0.7±0.2 m/s) Ground reaction forces (GRF) were collected for 1-2 steps per trial over the 4 trials per socket using a Bertec instrumented treadmill centred in the walkway (1000 Hz). Medial-lateral (ML) COP was calculated from Vicon and GRF data in Visual3D. Full waveform ML GRF and COP values were interpolated to percent stance. Symmetry in ML COP and GRF was calculated by the side-to-side differences (SSD) between limbs over stance. Step to step variability in ML COP and GRF was defined as the standard deviation between steps per socket type and participant. Full waveform ML COP and GRF symmetry and step-to-step variability were plotted, and peak values were extracted for qualitative analysis.

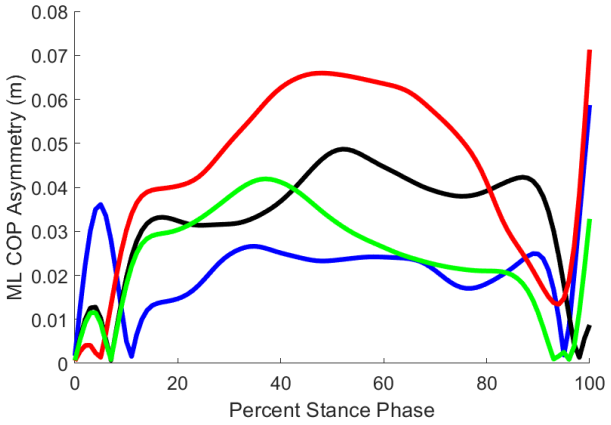

Figure 1: *An example of one participant's average ML COP asymmetry over stance phase of gait. The red line indicates the more pliable socket, black the quad socket, blue the low brim socket, and green the SoC socket.*

Results & Discussion: Six individuals (1F, age: 56±15 years, height: 180.5±7.1 cm, weight with prosthesis: 81.0±16.6 kg) were included in this interim analysis. Some participants did not walk in all socket designs due to safety concerns. ML COP asymmetry tended to be greatest in the more pliable socket from foot flat through midstance of gait for 4 out of the 6 participants (Figure 1) and lowest in the low brim socket during midstance of gait for all participants (Figure 2). No notable trends were found in ML GRF asymmetry or step to step variability during stance phase of gait. The results from this preliminary analysis indicate that socket characteristics have a small but notable influence on the balance characteristics of individuals with transfemoral amputations, most notably with variations in brim height and socket pliability. Additional testing is ongoing to confirm these findings. Further investigation into the long-term effects of socket fit on balance are required to fully understand this relationship and to determine how individuals can adapt to altered socket fit over time.

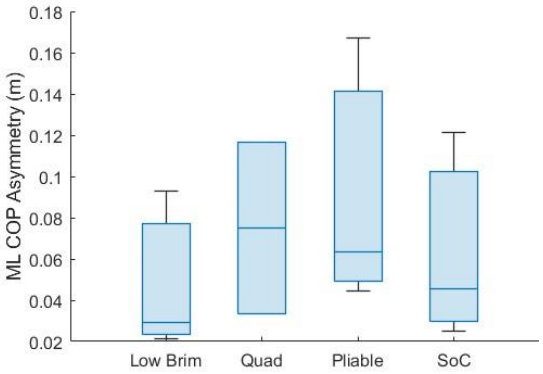

Figure 2: *Average ML COP asymmetry for all participants with full datasets over stance phase. Boxes indicate the upper and lower quartiles and median values. The lines extending from the boxes indicate the highest and lowest values within the group.*

Significance: The findings from this study provide context on socket characteristics which most profoundly influence balance characteristics of individuals with lower extremity amputations.

Acknowledgments: The research was supported by the DoD Office of the Congressionally Directed Medical Research Programs (CDMRP) through the Restoring Warfighters with Neuromusculoskeletal Injuries Research Award (RESTORE).

References: [1] Kilkarni et al. (1996), *Physiotherapy* 82(2); [2] Miller et al. (2001), *Arch PMR* 82(8); [3] Ichimura et al. (2022), *Sci. Rep.* 12(1); [4] Soares et al. (2016), *POI* 40(6); [5] Anderst et al. (2022), *Trials* 23(1)

MARKERLESS MOTION TRACKING IN NATURAL ENVIRONMENTS WITH A SINGLE MOVING CAMERA

Soyong Shin[1*], Zhixiong Li[1], Vu Phan[1], Evy Meinders[1], Michael J. Black[2], Eni Halilaj[1]
[1]Carnegie Mellon University, Pittsburgh, PA, USA [2]Max Planck Institute for Intelligent System, Tübingen, Germany
*Corresponding author's email: soyongs@andrew.cmu.edu

Introduction: Computer vision has emerged as one of the most promising tools in the recent history of biomechanics, offering an alternative to expensive and time-consuming marker-based motion capture systems. Although multi-view methods (e.g., Theia3D [1], OpenCap [2]) can capture accurate three-dimensional (3D) kinematics without the need for markers, they are spatially constrained and require camera calibration. However, sports analysis, where the cameras are moving, or the ability to gain insight about human movement from corpuses of unstandardized historical videos of unprecedented size is not currently possible with these techniques. To address these demands, we have built bioWHAM—a new motion-tracking approach designed to capture 3D movement from a single, static or moving, RGB camera. We hypothesized that bioWHAM would yield consistent performance, regardless of whether the camera was static or in motion. We also hypothesized that by integrating biomechanical modelling, bioWHAM would outperform computer-vision-only solutions and approximate multi-camera systems like OpenCap. A demo video can be viewed through Google Drive.

Methods: We recently developed, WHAM, an open-source model designed to capture 3D human motion in a world coordinate system using a single moving camera [3] (Fig. 1). Given an in-the-wild video, WHAM estimates 3D kinematics by integrating the sequence of 2D joint centers and the video's pixel-level information. Importantly, it reconstructs the global translation and orientation of the body in the world coordinate system by building camera-agnostic motion features learned from a large-scale synthetic dataset of virtual cameras and human motion. Here we build on WHAM, leveraging height and weight information to improve body shape and motion prediction, extract virtual anatomical markers that can be used to reconcile this vision-based solution with a biomechanical model, and run OpenSim's Inverse Kinematics solver to compute biomechanically constrained kinematics. To test the first hypothesis, we used data from 4 subjects (2M, 2F; age = 27.0 ± 2.7), who walked with a range of velocities while tracked with a set of static and hand-held moving cameras (Apple, Cupertino, CA). Twenty infrared cameras (Optitrack, Corvallis, OR) were used to compute ground-truth kinematics from a modified Rizzoli markerset. To test the second hypothesis, we used data from 10 subjects (5M, 5F; age = 32.8 ± 7.7) who performed 8 different physical therapy exercises, while recorded with 10 RGB and 20 infrared cameras (Optitrack, Corvallis OR).

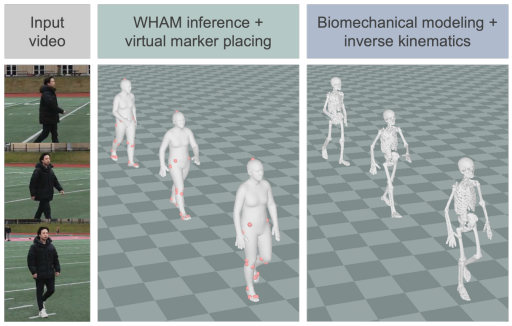

Figure 1: Overview. The proposed method uses a single RGB camera, static or moving, to extract a meshed model of the human in motion, which can then be reconciled with any biomechanical model through the use of virtual markers (shown in orange).

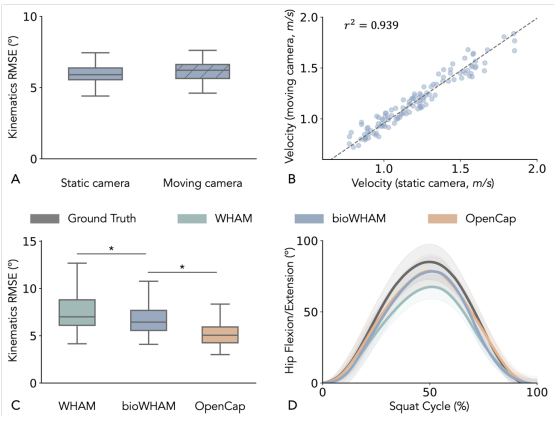

Figure 2: Results. (A-B) bioWHAM performs equally well whether the camera is static or moving. (C-D) In addition, it approximates the accuracy of Multiview systems that require spatial calibration.

Results & Discussion: bioWHAM showed consistent performance under static or moving camera scenarios (p=0.1448; Fig. 2A), across gait cycles and degrees of freedom. Further, velocity estimates from the two cameras were in strong agreement (r^2 =0.939; Fig. 2B), with the root mean squared difference being 0.06 m/s during walking. This difference is below the clinically significant threshold and below the agreement between clinical tools like GaitRite and marker-based motion capture. Although bioWHAM was less accurate than OpenCap (6.8±1.8° vs. 5.2±1.3°, p<0.0001), it outperformed its baseline (7.7±2.3°, p<0.0001; Fig. 2C). It is worth noting that OpenCap uses two calibrated and synchronized cameras, which increases set-up time and constrains capture volume, in return for an accuracy gain of approximately 1.6°. bioWHAM demonstrated the highest accuracy improvement over WHAM in hip kinematics (6.5±2.3° vs. 7.6±2.8, p<0.0001), while maintaining similar performance at the knee (5.5±2.1° vs. 5.7±2.3°, p=0.1625; Fig. 2D). This indicates that biomechanical modelling improves hip kinematics the most over computer-vision-only models. bioWHAM was the least accurate at the ankle compared to OpenCap (9.0±3.9° vs. 5.9±1.9°, p<0.0001), primarily because the ankle was excluded during the training of our baseline model—a shortcoming that can be easily addressed.

Significance: While existing multi-view algorithms show good performance in estimation of kinematics, they keep the field of biomechanics spatially constrained and require time-consuming calibration procedures. The proposed method overcomes these challenges by enabling 3D gait analysis from a single hand-held RGB camera with nearly comparable accuracy to multi-camera approaches. In addition to enhancing the realism of future biomechanics studies, this work will enable the mining of historical video data, giving biomechanists the opportunity to answer questions using research-grade internet-scale datasets of unprecedented size.

Acknowledgments: We thank Caitlynn Owens and the funding sources: the Chan Zuckerberg Initiative and NSF (CBET 2145473).

References: [1] Kanko *et al.*, *J. Biomech*, 2020; [2] Uhlrich *et al.*, *PLOS Com Bio*, 2023; [3] Shin *et al.*, *CVPR*, 2024

EXPERIMENTAL TRACKING SIMULATIONS TO ASSESS NEURAL CONTROL STRATEGIES FOR GAIT

Kaitlyn E. Downer[1*], Mohammad Rahimi Goloujeh[1], Jessica L. Allen[1]
[1]Department of Mechanical & Aerospace Engineering, University of Florida, Gainesville, FL, USA
*email: k.downer@ufl.edu

Introduction: Motor modules are groups of co-activated muscles hypothesized to be a neural strategy for controlling complex movements [1]. While motor module analysis is becoming an increasingly popular method to quantify muscle recruitment, one criticism is that modules might simply be representative of task constraints and not a neural control strategy. A previous study using a musculoskeletal simulation framework found that experimentally collected motor modules could be explained through task constraints and the minimization of muscle effort, providing evidence for the role of neural control in motor module structure (i.e., minimizing effort) [2]. However, this study used static optimization to determine muscle activity, which is a time-independent method that lacks activation dynamics and models tendons as rigid. Moreover, they only simulated a single gait cycle per subject, yet how the nervous system controls step-to-step variability is important to understand. To address these gaps, the study objective was to develop a pipeline for generating simulations of multiple gait cycles within a subject. We developed tracking simulations of gait using OpenSim Moco [3], which allows for slight variation between experimental and simulated data to account for dynamic inconsistencies. We hypothesized that we would identify the same result as [1], in which similar motor modules would be discovered in both the simulations and the experimental data by only minimizing muscle effort. Future work will explore modifications to the cost function to explore the effect of different neural control strategies, such as minimizing joint reaction forces, balance, etc.

Methods: Electromyography (EMG) and kinetic data were collected for a single subject walking at their self-selected walking speed (Female, 67 years old). Simulations were performed using a 3D musculoskeletal model with 23 degrees of freedom and 92 musculotendon actuators (gait2392). Model scaling was performed using OpenSim, followed by residual reduction. Custom OpenSim Moco [3] code was created to perform tracking simulations of 10 separate gait cycles. The cost function included tracking of joint coordinates and ground reaction forces (GRF) and minimizing control effort. An initial guess was generated from iterative simulations of a torque and muscle driven model in which the contributions from joint torques were slowly reduced until the model was completely muscle driven. This initial guess was used across all simulated gait cycles. The relative cost of each term for each simulated gait cycle was weighted so that at 0 iterations both the kinematic and GRF tracking were equal, with control effort weighted one magnitude smaller. Root mean square error (RMSE) was computed between the experimental and simulated data to assess simulation accuracy. Motor modules were then extracted separately from the muscle activity of the simulated and experimental data, focusing on the 12 muscles in which EMG was recorded (Fig 1). The number of motor modules for each dataset was chosen to reach 90% variance in the EMG accounted for (VAF). Experimental and simulation module structures were then compared via Pearson's correlations.

Results & Discussion: Simulations successfully tracked the experimental kinematics and GRF with less than 3.5° RMSE (Table 1). In contrast to our hypothesis, the motor modules identified from the simulations did not match those identified from the experimental data. Only 2 motor modules were needed to achieve 90% VAF from the simulated data, whereas 3 were required for the experimental data. Qualitatively, the simulated muscle activity was less variable from step-to-step than the experimental data, perhaps explaining the smaller number of modules in the simulated dataset. To enable better comparison of motor module structure, we extracted 3 motor modules from each. Of these, only two were similar between simulated and experimental data (Fig. 1). The first consisted primarily of the ankle dorsiflexors and knee extensors and was recruited during late swing into early stance. The second was primarily composed of the ankle plantarflexors and was recruited in late stance. The remaining module in each dataset was composed of different hip and knee muscle recruitment. Similar to [2], our results provide additional evidence that motor modules are not entirely defined by task constraints. Moreover, the finding that minimizing effort did not produce identical modules from the simulations as compared to the experimental data highlights the importance of including stride-to-stride variability and, in the future, additional cost function terms.

Table 1: Tracking Error

Joint	RMSE [°]
Lumbar Ext	1.59±0.24
Lumbar Bend	0.81±0.34
Lumbar Rot	0.22±0.08
Hip Flex	3.38±0.72
Hip Add	1.11±0.44
Hip Rot	0.85±0.52
Knee	2.58±0.46
Ankle	1.69±0.38

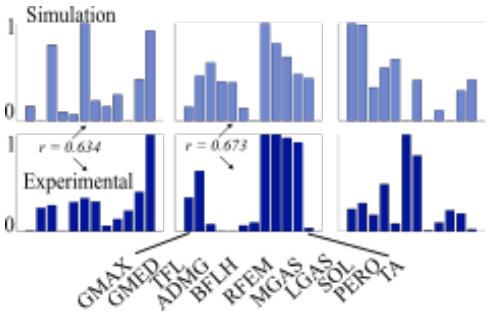

Figure 1: Comparison of motor modules between simulated muscle activity (top) and experimental EMG (bottom). Only two of the motor modules were similar, with r>0.6.

Significance: This study aimed to investigate to what extent motor modules are representative of task constraints or of an underlying neural control strategy. The mismatch between experimental and simulated motor modules in this subject provide evidence that neural strategies affect motor module structure. Moreover, the pipeline developed in this study allows for modifications to the cost function to further investigate the role of different neural control strategies for muscle coordination during gait.

Acknowledgments: Funding was provided by an NSF GRFP (to K.E.D) and NSF 2245260.

References: [1] Ting and McKay (2007), *Curr Opin Neurobiol* 17(6); [2] De Groote et al. (2014), *Front Comput Neurosci* 8(115); [3] Dembia et al. (2020), PLoS Comput Biol 16(12)

DUAL-LAYER EEG MOTION ARTIFACTS: ROBUST PREDICTORS FOR GAIT EVENTS

Rushikesh Kankar[1*], Helen J. Huang[2,3,4]
[1] Dept of Computer Science, [2]Mechanical and Aerospace Engin. Dept, [3]Biionix TM Cluster, [4]Disability, Aging, and Technology Cluster, University of Central Florida, Orlando, FL, USA
*Corresponding author's email: kankarrushikesh@ucf.edu

Introduction: Electroencephalography (EEG) is crucial for monitoring brain activity and utilized in dynamic tasks like walking. However, motion artifacts during walking can obscure true brain signals, limiting EEG's applicability [1]. We propose an approach using a dual-layer EEG system capturing scalp electrical activity and motion-induced noise. Our study focuses on predicting gait events through machine learning, leveraging motion artifacts as a valuable data source, particularly their resilience and robustness. Our hypothesis is that since these motion artifacts are resultant from movements, they inherently contain valuable information about the gait movements. Contrary to conventional views, we find that motion artifacts significantly enhance gait event prediction and withstand methodological variations and maintain high predictions, challenging the notion of EEG noise as purely disruptive.

Methods: In this study, we utilized EEG and motion artifact data from a prior experiment involving 14 participants walking on a treadmill, captured through a 128-channel dual-layer EEG system over four-minute trials [2]. The dataset underwent a 3 Hz high-pass filter, leading to five refined subsets for analysis: Artifact (128), retaining all outer layer channels with motion artifacts; Artifact Cleaned zscore (78) and EEG Cleaned zscore (78), where channels with excessive noise were removed; EEG (128), the raw inner layer EEG signals; Source Signals (78), isolating neural signals via ICA; and EEG Good channels (78), selecting the most reliable channels post-ICA. Each dataset was epoched around gait events within a 100ms window and normalized to ensure uniformity. We analyzed Event-Related Potentials (ERPs) for insights into the patterns of gait. A Support Vector Machine (SVM) with an RBF kernel motivated by its effectiveness in handling non-linear data relationships in EEG and artifact signals [3], trained on both processed signal data and TSFEL-extracted features, was employed to predict gait events, employing individualized and aggregated cross-validation to test the model's performance across different contexts. Furthermore, we explored the resilience of the artifact layer through epoch size variations.

Results & Discussion: The artifact dataset has consistently showed highest accuracies, Artifact (128) dataset, which achieved accuracies from 73% to 84%, challenging the conventional perception of motion artifacts as merely disruptive noise. This dataset's mean accuracy was 83.9%, higher than both the EEG (128) and Source Signals (78) datasets, which had accuracies in the ranges of 52-75% and 46-77% respectively. The Artifact (128) dataset outperformed others, including the EEG Cleaned zscore (78) and EEG Good channels (78) datasets, which had average accuracies of 47.9% and 50.6%. Statistical analysis using Welch's ANOVA confirmed differences among datasets (p-value ~ 1.264424e-12), emphasizing the role of dataset choice on prediction accuracy. The Games-Howell post-hoc tests further highlighted the contrasts between the Artifact datasets and traditional EEG-focused datasets, pointing to the potential of artifacts in enhancing prediction accuracy, as depicted in Fig 1.The Artifact (128) dataset and the Artifact Cleaned zscore dataset demonstrated better performance, with the former reaching the highest accuracy (~83%) and F1 score (83.81%), indicating efficient event classification with less error. In contrast, EEG-based datasets, especially the EEG Cleaned zscore and EEG good channel datasets, struggled with lower precision and recall (<50%), underlining their classification difficulties. Interestingly, we noted minimal impact of epoch size changes on classification accuracies within artifact layers, suggesting their resilience to methodological shifts. Specifically, artifact dataset accuracies exceeded 90% for an epoch length of 400ms, showing better performance compared to EEG 128 and Source Signals datasets, which showed declines in aggregated dataset scenarios. This resilience underscores the consistency and robustness of Artifact datasets against epoch size variations and dataset combinations, as accuracy remained within the 80-90% range, emphasizing the potential for further refining model sensitivity in future research, particularly for distinguishing left/right heel strikes/toe offs events which are often confused, evident from the confusion matrix.

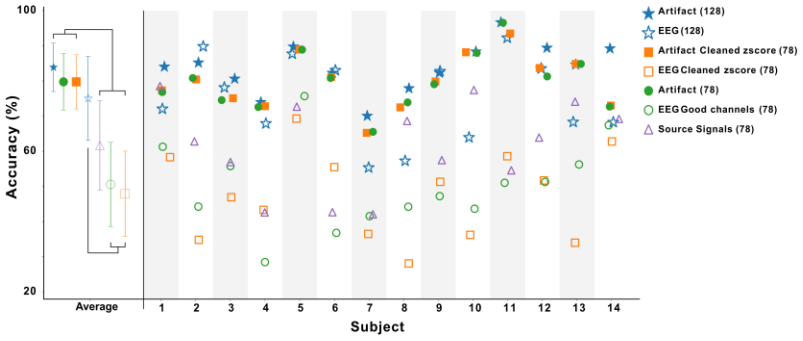

Fig.1: Gait event classification accuracies averaged across subjects and for individual subjects. The artifact layer (filled symbols) consistently had higher accuracies for the averaged data and for most individual subjects.

Significance: The study underscores the potential of artifact layer and artifacts in EEG analysis for gait event prediction, establishing alternative way of EEG-based gait research. It demonstrates an alternative approach of utilizing what was previously considered noise as not only a valuable but also a robust data source, which might help in providing better methods for gait analysis using EEG.

Acknowledgments: We thank the National Science Foundation (NSF) for partially funding this research with grant number 19427121.

References:

[1] Schmoigl-Tonis et al., Front. Hum. Neurosci. 17:1251690, 2023; [2] Li, J., UCF Electronic Theses and Dissertations. 2022.
[3] Hasan et al., J Neuroeng Rehabil. 17:50, 2020.

STATISTICAL PARAMETRIC MAPPING REVEALS POSITIONAL DIFFERENCES IN FOUR-DIMENSIONAL COMPUTED TOMOGRAPHY-DERIVED WRIST INTEROSSEOUS PROXIMITY DISTRIBUTIONS

Taylor Trentadue [1*], Cesar Lopez [1], Andrew Thoreson [1], Thor Andreassen [1], Shuai Leng [1], Sanjeev Kakar [1], Kristin Zhao [1]
[1] Mayo Clinic, Rochester, Minnesota | *Corresponding author's email: trentadue.taylor@mayo.edu

Introduction: The distal radioulnar joint (DRUJ), defined as the articulation between the sigmoid notch of the radius and the head of the ulna, transmits load through the wrist and permits forearm pronosupination. The limited osseous congruency of the radius and ulna contribute to intrinsic DRUJ instability, with volar-dorsal translation of the radius occurring during pronosupination [1]. Previous studies have suggested that DRUJ joint spacing is closer in supination versus pronation [2] and that the sigmoid notch contact area is more volarly-translated in supination and dorsally-translated in pronation [3, 4]. Clinically, ulnar-sided wrist pain has a myriad of causes and can be difficult to diagnose [5]. MRI has moderate sensitivity and specificity in detecting DRUJ soft tissue or ligamentous injury, which may be attributed to the static nature of the exam [6]. Finding imaging-derived biomarkers may improve diagnosis of DRUJ instability. Four-dimensional computed tomography (4DCT = 3DCT over time) allows assessment of wrist biomechanics during functional tasks. We seek to relate CT-derived DRUJ interosseous proximities to forearm pronation using statistical parametric mapping (SPM) [7, 8], a technique that quantifies variability in spatiotemporal data (1) across participants and (2) over one dynamic motion arc. We hypothesize that forearm pronation angle influences DRUJ proximity, particularly along the volar-dorsal axis of the sigmoid notch.

Methods: Data were collected from 30 healthy wrists (50% female, 96.7% right-hand dominant, median (25^{th}–75^{th} percentile) age: 27.0 (23.0–33.0) years) in a study of normative wrist anatomy and biomechanics. Participants were positioned in a head-first prone position with palms oriented downward. Additionally, 4DCT data were collected from one unique uninjured wrist (21F) during unresisted pronosupination. The participant moved in a CT-compatible motion-guiding device [9] at a cadence of 35 bpm while 4DCT volumes were captured at a temporal resolution of 66 ms, resulting in 15 dynamic volumes over a two-second data collection. CT images were acquired using dual-source photon-counting detector CT hardware (NAEOTOM Alpha, Siemens, DE) [10]. The right-sided radius and ulna were segmented from static CT images using a semi-automated pipeline; three-dimensional meshes were generated. Static-to-dynamic bone registration was performed for 4DCT data using custom algorithms [11, 12]. A multi-domain statistical shape model was used to generate a canonical mean DRUJ and high-resolution sigmoid notch (edge length=0.2 mm) [13]. All participant meshes were morphed to the canonical DRUJ and sigmoid notch using a generalized regression neural network [14]. Forearm pronation in static CT data was estimated using the second principal component score, which reflected forearm position, or calculated as the finite helical axis in 4DCT data. A statistical parametric mapping (SPM) regression analysis was used to assess the relationship between relative pronation and DRUJ interosseous proximities across participants from static imaging (α_{static}=0.01) and across a 4DCT pronosupination arc ($\alpha_{dynamic}$=0.05) [7]. The test statistic, SPM{t}, was calculated at each vertex on the sigmoid notch. The critical threshold (t*), which α% of smooth random proximity maps would traverse, was used for hypothesis testing [15].

Results & Discussion: As hypothesized, there was a significant relationship between wrist pronation and DRUJ interosseous proximities at the sigmoid notch, particularly toward the volar margin of the joint. This pattern was consistent across 30 static CTs (**Fig. 1**) and within one participant's 4DCT-derived pronosupination arc (**Fig. 2**). For each vertex in the significant region, a 10% increase in relative pronation (**Fig. 1**) or pronation angle (**Fig. 2**) is associated with a corresponding **β** mm change in DRUJ interosseous proximity.

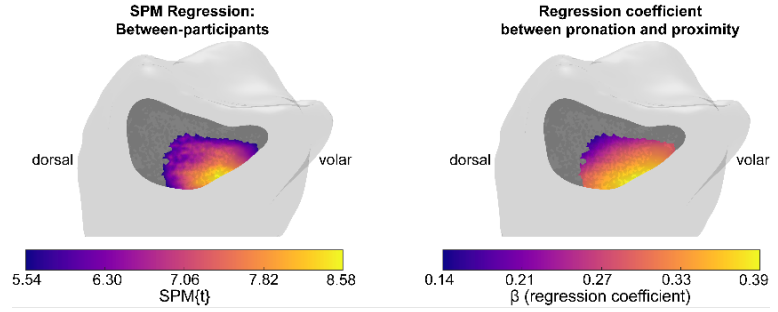

Figure 1: Statistical parametric mapping regression analysis considering the relationship between forearm pronation and interosseous proximity distribution at the sigmoid notch (patch) on the radius (transparent mesh) from the static-neutral CT image volumes of thirty healthy wrists. The ***left*** panel, SPM{t}, represents the effect magnitude. The ***right*** panel, β, represents the vertex-wise regression coefficient.

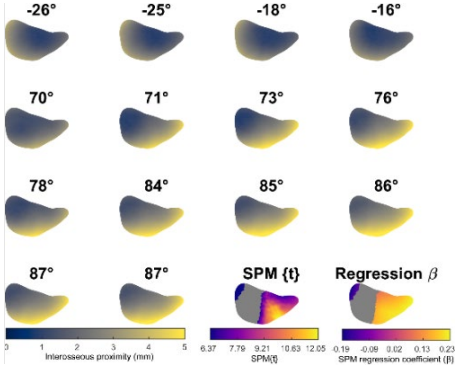

Figure 2: DRUJ interosseous proximities projected onto the canonical sigmoid notch over one participant's 4DCT-acquired pronation (+) – supination (-) arc. SPM{t} represents the effect magnitude. β represents the vertex-wise regression coefficient.

Significance: Forearm pronosupination is related to interosseous proximities at the DRUJ, with more pronation associated with increased space at the volar margin of the joint. This demonstrates a novel application of SPM regression to dynamic 4DCT data, allowing quantitative and spatial analysis of how joint surfaces interact during motion. This technique can be applied both across and within participants. Future studies will compare bilateral extremities to determine if specific regions demonstrate injury-related change.

Acknowledgments: This work was supported by R01 AR071338, T32 AR056950, F31 AR082227, T32 GM065841, T32 GM145408, the Mayo Clinic CT Clinical Innovation Center, Department of Orthopedic Surgery, and W. Hall Wendel, Jr., Musculoskeletal Center.

References: [1] Flores D (2023) Radiographics 43(1). [2] Crowe M (2020) JHS 45(11). [3] Olerud C (1988) Acta Orthop Scand 59(2). [4] Chen Y (2013) JHS 38(8). [5] Kakar S (2016) JHS 41(4). [6] Daunt N (2021) Skeletal Rad 50(8). [7] Pataky T (2012) CMBBE 15(3). [8] Turmezei T (2021) Radiology 299(3). [9] Amrami K (2010) Hand Clin 26(4). [10] Foley R (2023) Skeletal Rad. [11] Trentadue T (2023) J Wrist Surg 12(3). [12] Trentadue T (under rev.). [13] Cates J (2017) ShapeWorks. [14] Andreassen T (2024) Med Phys Eng. [15] Friston K (1994) Hum Brain Mapp 2(4).

BIOMECHANCIAL EVALUATION OF A KNEE EXOSKELETON FOR PEOPLE WITH KNEE OSTEOARTHRITIS

Minori Iizuka[1*], Maddi Viteri[1], Alicia Koontz[1,2], Cheng-Shiu Chang[1], Sara Peterson[1], Dan Ding[1,2]
[1]Human Engineering Research Laboratories, Pittsburgh, PA
[2]University of Pittsburgh, School of Health and Rehabilitation Sciences
*Corresponding author's email: mii36@pitt.edu

Introduction: Approximately, 14 million people in the United States have symptomatic knee osteoarthritis (KOA), with military populations aged ≥ 40 having twice the unadjusted incidence rate as the general population within the same age group [1,2]. Biomechanical measures including knee range of motion (ROM), knee flexion moments (KFM), and knee adduction moments (KAM) are shown to be related to internal joint loading, disease progression, and pain. Increases in KFM and KAM have been associated with increased medial contact forces, leading to pain and medial compartment KOA disease progression [3,4]. Conservative interventions (e.g. cortico-steroid injections, viscosupplementation, pain medications, physical therapy, and lifestyle changes) and assistive devices (e.g. braces, orthoses) are used to initially treat KOA [5]. However, these intervention improvements are small to moderate [6]. Additionally, a survey study reports as low as 25% brace compliance after two years since prescription [7]. After all other treatments fail, total knee arthroscopy (TKA) surgery is seen as a last resort, but there are risks associated with TKA surgery. Thus, the Keeogo exoskeleton is being investigated as an alternative KOA treatment. The objective of this study was to evaluate the biomechanical responses of veterans with KOA when using an active assistance knee exoskeleton compared to their typical walking conditions, which may include walking with or without braces.

Methods: Four male veterans (age: 63.75+/-17.5years, height: 1.81+/-0.08m, weight: 111.1+/-24.5kg) with KOA (two bi-lateral and two uni-lateral KOA) participated in the study. Participants walked with (KON) and without (NON) the Keeogo (B-temia, Canada) on the Computer-Assisted Rehabilitation Environment (CAREN; Motek, Netherlands) equipped with a split-belt instrumented treadmill and 10 Vicon camera set-up. They walked on 0% grade, 15% grade uphill, and 15% grade downhill surfaces at their preferred walking speed for 2 one-minute trials. A custom marker set was placed on the body in order to calculate swing phase knee ROM, peak KFM, and peak KAM. Marker and force data were filtered with a fourth-order, low-pass Butterworth filter at 6Hz and 25Hz, respectively. Moments were transformed into the local shank coordinate system, time normalized to the stance phase, and normalized by the product of body weight (BW) and height (Ht). For participants with bi-lateral KOA, the study analyzed the more severe leg. The mean and standard deviation for each measure were calculated. A Wilcoxon-signed rank test was conducted with an alpha-level of 0.05.

Results & Discussion: Table 1 highlights the kinematic and kinetic measures in each condition. No significant differences were found for any of the measures or conditions likely due to the small sample size. The KON condition had smaller mean peak KAM for the neutral and downhill grades. The peak KFM and ROM are higher while wearing the Keeogo except in the downhill condition.

Comparatively, this study with KOA subjects shows similarities with McGibbon et al. who found decreased KAM and increased early stance KFM while wearing the Keeogo for healthy subjects [8]. Additionally, greater knee ROM exhibited under the KON condition may suggest improved gait mechanics and joint function as prior studies found an inverse relationship between KOA severity and knee ROM [9]. Thus, the Keeogo may help restore proper walking mechanics and reduce antalgic gait characteristics.

Further analysis with more subjects that incorporates covariates such as uni-lateral versus bi-lateral, history of traumatic knee injuries, and severity level need to be done to elucidate who may benefit from the Keeogo.

Table 1: Comparison between NON and KON conditions for ROM, KFM, and KAM.

	KON (mean±SD)	**NON** (mean±SD)	**KON-NON** (mean±SD)	**p-value**
ROM (°)				
Neutral	52.5 ± 14.6	43.3± 10.1	9.20 ± 4.42	0.125
Uphill	38.8 ± 16.0	26.8 ± 7.61	12.04 ± 8.64	0.125
Downhill	49.1 ± 10.8	57.1 ± 16.7	-8.06 ± 18.6	0.625
KFM (%BW*Ht)				
Neutral	2.63 ± 1.31	2.46 ± 1.23	0.17 ± 0.40	0.625
Uphill	2.73 ± 1.71	2.19 ± 1.46	0.55 ± 0.39	0.125
Downhill	2.43 ± 0.69	2.56 ± 0.47	-0.13 ± 0.78	0.875
KAM (%BW*Ht)				
Neutral	2.26 ± 0.98	2.34 ± 1.15	-0.08 ± 0.52	1
Uphill	2.82 ± 1.24	2.52 ± 1.21	0.31 ± 0.43	0.375
Downhill	1.93 ± 0.66	2.22 ± 1.08	-0.28 ± 0.88	1

Significance: The potential reductions in KAM and increased ROM in the KON condition show a promising KOA treatment alternative. This may be especially relevant for the treatment gap that exists for individuals with KOA who are not radiographically severe enough to be eligible for TKA. Additionally, those who are overweight and therefore surgically ineligible may benefit from the improved biomechanical environment, promoting physical fitness and better weight management.

Acknowledgments: This research was funded by the United States Veterans Affairs (VA)'s Rehabilitation Research and Development Services under the grant number #I01RX003228. The content is solely the responsibility of the authors and does not represent the official views of the VA.

References: [1] Deshpande et al. (2016) *Arthritis Care & Research* 68(12):1743-1750 [2] Cameron et al. (2011) *Arthritis & Rheumatism* 63(10): 2974-2982; [3] Manal et al. (2015) *Osteoarthritis Cartilage* 23(7) [4] Thorp et al. (2007) *Arthritis care &research* 57(7) [5] DOD V. CLINICAL PRACTICE GUIDELINE FOR THE NON-SURGICAL MANAGEMENT OF HIP & KNEE OSTEOARTHRITIS [6] Cudejko et al. (2018) *Arch Phys Med Rehabil.* 99(1): 153-163 [7] Squyer et al. (2013) *Clinical Orthopaedics and Related Research* 471: 1982-1991 [8] McGibbon et al. (2017) *The Knee* 24(5): 977-993 [9] Steultjens et al. (2000) *Rheumatology* 39(9): 955-961

BONY DISPLACEMENT OF COMPLETE TIBIA-FIBULA FRACTURES WITH FOAM AND SAM SPLINTING

Nathaniel A. Bates,[1] John Heyniger,[1] Kenan Alzouhayli,[1] Grace P. Hobayan,[1] Franco Piscitani,[1] Adam T. Groth,[1] Kevin D. Martin[1]
[1]The Ohio State University Wexner Medical Center, Department of Orthopaedics, Columbus, OH, USA
*Corresponding author's email: Nathaniel.Bates@osumc.edu

Introduction: Rigid fracture stabilization is essential during transports following a traumatic fracture event, as improper splinting can cause loss of fracture reduction, neurovascular compromise, increased pain, and compartment syndrome.[1,2] FastCast foam splinting has been presented as an alternative solution that reduces rotations, accelerations, and overall segment motion across a fracture line as compared to standard of care SAM splints.[3] The current study assessed splint material integrity relative to bony displacement and angular alignment for tibia/fibula fractures during dynamic tasks.

Methods: Transverse, full tibia/fibula osteotomies were performed on eight cadaver shanks. State-licensed, practicing EMS professionals splinted and tested each specimen in a SAM and FastCast foam splint in a randomized order. Splinted specimens were subjected to Transport (soft stretcher carry for ~50 m and 3 flights of stairs, ~100 m of gurney transport, ambulance loading) and Impact (~1 m fall with gravity). Before and after each Event, mini C-Arm radiographs were taken of the fracture site in the anterior and lateral views. Custom MATLAB image digitization quantified distances and angular alignment between critical points (**Figure 1**). A repeated-measures ANOVA with factor of Material (FastCast, SAM) repeated over Events (Splint, Transport, Impact) assessed significance ($\alpha < 0.05$).

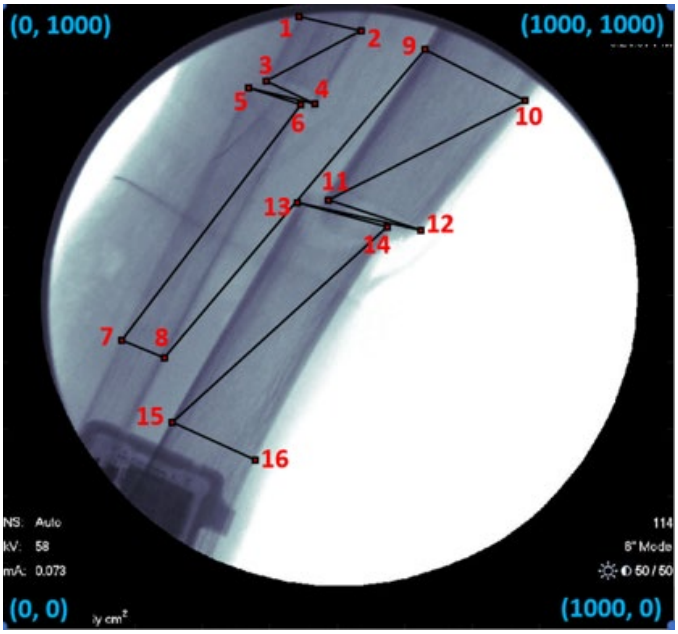

Figure 1: Sample digitization of a tibia-fibula fracture specimen within MATLAB. 16 points (8 on each bone) were selected. Points 3,4,5,6 defined the fibula fracture line, while points 11,12,13,14 defined the tibia fracture line. Points 1,2; 7,8; 9,10; and 15,16 were used to identify midpoints and the long axis of each bone segment shaft relative to the fracture line. Displacements were calculated based on mm of movement between points 3,5; 4,6; 11,13; and 12,14. Means were then calculated for the tibia and fibula. Angular displacements were calculated based on change in the intersection angle between the long axis lines defined for the superior and inferior segments of each bone.

Results & Discussion: Material was not a significant factor for tibia or fibula point-to-point displacement or angular alignment for any Event ($P \geq 0.10$). During Splinting, the mean FastCast and SAM split displacements were, respectively, 1.3 (0.9) mm & 1.2 (1.4) mm for the tibia and 0.9 (0.7) mm & 1.0 (0.7) mm for the fibula, while the mean angular displacements ranged, respectively, from 7.6-16.16.6° for the tibia and 8.0-17.4° for the fibula. The mean translational and angular displacements for SAM and FastCast splints during Transport and Impact activities are displayed in Table 1. During Transport the fibula translated 0.7 mm more in the anterior view with FastCast ($P = 0.05$). During Impact, the tibia rotated 1.8° more with SAM ($P = 0.03$). No other significant differences were noted between Materials.

Significance: The lack of significance between splint Materials indicated equivalent bony stabilization was present between SAM and FastCast splints across both anterior and lateral radiographic views. Further, all displacements were under 2.0 mm, which is the threshold for a fracture to be considered displaced. Thus, both splints maintained rigid stabilization throughout each Event. The present data indicate that FastCast splints are equivalently robust to SAM splints in stabilizing bony displacement in complete tibia-fibula fractures. Further, the FastCast splint was able to maintain distraction of the tibia-fibula fracture line.

Acknowledgments: The authors would like to acknowledge the Surgical Skills Laboratory at The Ohio State University Wexner Medical Center for the donation of the facilities to perform these experiments.

References: The format of the reference list can be brief and does not have strict requirements but must include the minimum information needed for readers to unambiguously determine the reference. For example: [1] Kilian et al. (2003), *Mil Med* 168(4); [2] Wojcik et al. (2008), *Mil Med* 173(9); [3] Hobayan et al. (2024) *Mil Med* Online ahead of print.

Table 1: Observed changes in displacement from each splint Material based on pre- and post-Event radiology images.

	ANTERIOR VIEW			LATERAL VIEW		
	Tibia (mm)	**Fibula (mm)**	**Tib. Angle (°)**	**Tibia (mm)**	**Fibula (mm)**	**Tib. Angle (°)**
TRANSPORT						
SAM	0.5 (0.3)	0.4 (0.4)	2.5 (1.6)	0.5 (0.5)	0.3 (0.3)	1.5 (1.5)
FastCast	1.2 (1.0)	0.8 (0.8)	2.0 (2.4)	0.9 (0.6)	0.4 (0.3)	1.2 (1.3)
IMPACT						
SAM	0.7 (0.3)	0.5 (0.4)	3.4 (5.4)	0.8 (0.4)	0.5 (0.2)	2.6 (2.0)
FastCast	0.7 (0.7)	0.4 (0.6)	1.7 (2.6)	0.8 (0.6)	0.4 (0.4)	0.8 (0.8)

INFLUENCE OF SUBJECT ORIENTATION ON ISOMETRIC HIP ABDUCTION STRENGTH IN ACLR ATHLETES

Nathaniel A. Bates,[1] Gregory D. Myer,[2] Kim Barber Foss,[2] Nathan D. Schilaty,[3] Alexander Fischbach,[1] Alexandra Sheldon,[1] Christopher V. Nagelli,[4] April McPherson,[1,2] Aaron J. Krych[4]
[1]The Ohio State University Wexner Medical Center, Columbus, OH, USA; [2]Emory University, Flowery Branch, GA, USA; [3]University of South Florida, Tampa, FL, USA; [4]Mayo Clinic, Rochester, MN, USA
*Corresponding author's email: Nathaniel.Bates@osumc.edu

Introduction: Moments around the hip and knee are significant factors that contribute to both primary and secondary ACL injury risk, that can be readily modified via targeted neuromuscular training.[1] As lower extremity strength contributes to joint control, rapidly assessable metrics of strength offer utility in both clinical and research capacities. This study aimed to examine whether patient orientation influences maximal potential force generation for isometric hip abduction strength.

Methods: 16 subjects (age = 17.9 (3.4) years; mass = 87.3 (22.8) kg; height = 171 (11) cm) who suffered primary ACL injury and underwent ACLR were recruited to perform maximum effort isometric hip abduction tests at a single academic medical center. Surgical selection and clinical rehabilitation were left to discretion of each patient and their medical team. Following clinical clearance for return to sport, subjects were recruited into the study. Subjects were asked to perform isometric hip abduction using a custom clamshell device that has been published previously.[2,3] Briefly, subjects would lay down on their side with ankles aligned with the spine and knees flexed at ~20°. Subjects would then be asked to open their hips in a 'clamshell' style while maintaining contact between both feet (Figure 1). Subjects received verbal encouragement to abduct as hard a possible in the clamshell position while the custom device recorded resistance in N. After three repeated trials with rest in between, subjects switched sides and repeated the protocol for the opposite side. In addition to the side-lying orientation, subjects were asked to perform maximum effort hip abduction in a standing orientation with feet approximately shoulder width apart and knees flexed to ~20°. Again, three trials were recorded, verbal encouragement was provided, and the custom device recorded force output. For each orientation peak values from all 3 trials were averaged for analysis. Four Groups were designated for analysis: side-lying orientation with the uninvolved limb superior (Uninvolved), side-lying orientation with the involved limb superior (Involved), summation of side-lying orientation values (Summation), and standing orientation (Standing). Intra-session reliability was assessed with interclass correlation coefficients (ICC, 2-k). Significance of Group was assessed via a 4x1 ANOVA with Group as the factor. Post-hoc all-pairs differences were performed with Tukey HSD tests. Significance was determined by $\alpha < 0.05$.

Figure 1: Orientation of a subject in the side-lying position with the custom device secured around the thighs and the superior limb opened into the 'clamshell' position.

Results & Discussion: Group was a significant factor ($P<0.01$). Standing strength was significantly greater than either Involved or Uninvolved side-lying strength (334 (110) N vs. 174 (52) N vs. 183 (73) N; $P<0.01$). There were no differences between mean Standing and Summation strength (334 (110) N vs. 357 (119) N; $P=0.49$). There were no differences between Involved and Uninvolved side-lying strength ($P=0.77$). The lack of difference between Standing and Summation Groups indicate that subject orientation lacks relevance to hip abduction strength so long as each limb is able to apply force to the custom restraint. Whether this is accomplished independently (and summated) or simultaneously lacks relevance.

Intra-session reliability within the Uninvolved Group was excellent (ICC = 0.981), within the Involved Group was excellent (ICC = 0.964), within the Summation Group was excellent (ICC = 0.982), and within the Standing Group was excellent (ICC = 0.989). Excellent reliability echoes previous literature regarding this custom device and its comparison to isometric hip abduction on a dynamometer.[2,3]

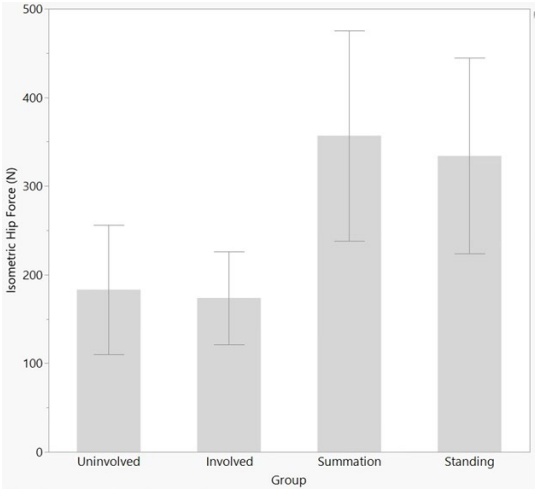

Figure 2: Mean and standard deviation of hip abduction strength (N) for each orientation Group.

Significance: Whether summated from a side-lying position or taken from a standing position, orientation does not have a significant impact on the peak abduction strength that can be generated by an ACLR patient. Results from both orientations can be generalized and compared. Side-lying orientation does offer the advantage of assessing limb symmetry where standing orientation cannot. The custom clamshell device remains excellently reliable for assessment of isometric hip abduction assessment.

Acknowledgments: NIH R01-AR055563; Florida Department of State Center for Neuromusculoskeletal Research

References: [1] Myer et al. (2017), *Am J Sports Med* 45(9):2142-7; [2] Nagai et al. (2023), *J Int Acad Neuromusc Med* 20(2):9-18; [3] Roewer et al. (2013), *Med Sci Sports Exer* 45(5):690.

TRANRADIAL PROSTHESIS USE REQUIRES DIFFERENT MUSCLE COORDINATION THAN CONTROLS FOR SOME ACTIVITIES OF DAILY LIVING

Amanda Kemper[1*], Michael Consentino[1,2], Wendy Murray[1,2,3], Russell T. Johnson[1,3], Matthew J. Major[1,3]
[1]Northwestern University, [2]Shirley Ryan AbilityLab, [3]Jesse Brown Veterans Affairs Medical Center
*Corresponding author's email: amanda.kemper@northwestern.edu

Introduction: Transradial prostheses are prescribed to help support the performance of activities of daily living (ADLs) for individuals with upper limb differences. However, these devices have limited ability to replicate biological wrist motion and, while not universal to every prosthetic arm, typically offer only a single degree of freedom: pronation and supination. Therefore, many upper limb prosthesis users need to recruit compensatory movements to adjust to the device or refrain from using their affected limb to complete ADLs [1]. Common compensatory movements for individuals with transradial level amputations include increased shoulder abduction angles and increased tri-planar trunk range of motion [1,2]. Although compensatory movements allow upper limb prosthesis users to exploit kinematic redundancy for completing ADLs, there is an association between these compensations and musculoskeletal complaints, including shoulder, neck, and elbow pain [2,3]. The increased incidence of musculoskeletal complaints in upper limb prosthesis users may be driven by increased muscle forces and joint contact forces on the impaired side while performing ADLs.

Therefore, the purpose of this study was to quantify the effect of transradial prosthesis use on muscle forces for major muscle groups in the upper limb. We hypothesized that prosthesis users would have greater peak muscle forces compared to able-bodied controls.

Methods: The current study is a secondary analysis from a previously published study [1]. We collected kinematic data with six able-bodied controls (3m/3f; 35±11yrs; 75±17kg) and six unilateral transradial level myoelectric prosthesis users (4m/2f; 48±19yrs; 76.7±14.7kg) who were fitted with a custom upper extremity marker set. Participants completed five trials of five ADL tasks: 1) cutting vegetables, 2) pouring from a cup, 3) page turning, 4) lifting and transferring a weighted object, and 5) lifting and transferring a tray. We then created a custom bimanual upper body musculoskeletal model (OpenSim v3.3) [4,5] to estimate muscle forces for the triceps brachii, biceps brachii, and deltoid via static optimization. We assessed the main and interaction effects of group (control, prosthesis user) and ADL task on peak muscle force (averaged across the five trials per task) using a two-way mixed ANOVA with a Sidak correction for post-hoc multiple comparisons and critical α of 0.05. If the interaction effect was significant, we followed up with a simple main effects analysis to assess group differences for each task separately.

Results & Discussion: Overall, we found that peak muscle forces differed for two tasks between prosthesis users and able-bodied individuals but that the direction of differences were dependent upon the task performed. Specifically, peak muscle forces were different between the controls and prosthesis users for only two of the tasks: cutting vegetables and lifting and transferring a tray (Figure 1). For vegetable cutting, triceps and deltoid peak muscle forces were greater in the prosthesis user group than controls ($p \leq 0.041$). Surprisingly, for tray transfer, the triceps and deltoid peak muscle forces were greater for controls than the prosthesis user group ($p \leq 0.027$). Therefore, our hypothesis that prosthesis users would produce greater peak muscle forces was not supported across all tasks. However, a commonality in these results is that the muscles responsible for arm elevation and extension were significant for both tasks, albeit in different directions.

Differences in peak muscle forces could be driven by several factors. First, prosthesis users completed tasks two to three times slower than the controls, which also means that the duration of each trial was longer. Slower velocities may have contributed to decreased peak muscle forces throughout the trial. Second, prosthesis users displayed pelvis and trunk compensations to alter their body posture while executing tasks, which may have altered the muscle requirements in the shoulder and elbow to perform the tasks. For example, during tray transfer, the prosthesis users tended to hold the tray closer to their body than controls. Decreasing the distance of the object to the trunk can reduce the amount of muscle forces required to support the weight of the tray, which may help explain why prosthesis users had lesser peak muscle forces during tray transfer than controls.

Significance: Upper arm muscle forces will affect shoulder and elbow joint reaction forces. Our results suggest that prosthesis users do not consistently have greater joint reaction forces across many ADLs. This indicates these types of tasks may not drive the elevated prevalence of musculoskeletal complaints in this population. Future research investigating muscle forces and joint contact forces at different joint positions and for different tasks will be crucial for determining the impact of prosthesis use on musculoskeletal injury.

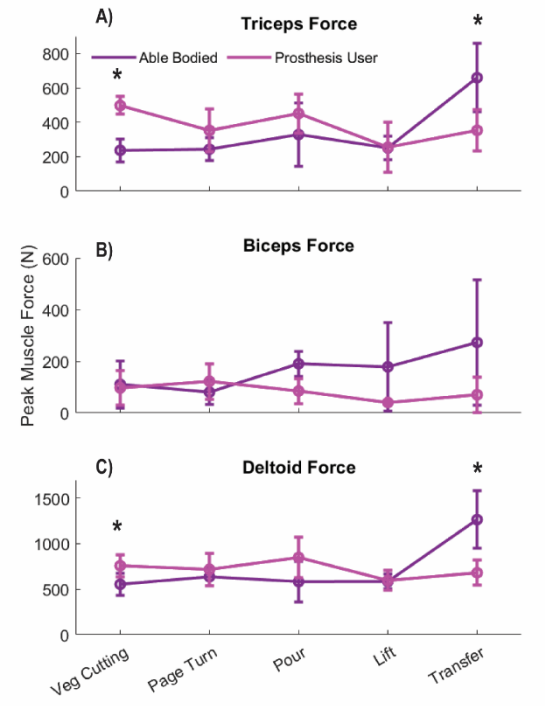

Figure 1: Estimated peak muscle forces for the A) triceps, B) biceps, and C) deltoid for prosthesis users (pink) and able-bodied participants (purple); asterisks denote significance.

References: [1] Major MJ. J Neuroeng Rehabil. 11, 132, 2014. [2] Bouswema H. Clin Bimech. 25, 523-9, 2010. [3] Burger H. Prosthet Orthot Int. 40, 497-502, 2016. [4] Seth A. Procedia IUTAM. 2, 212-232, 2011. [5] Saul KR. Comput Methods Biomech Biomed Engin. 18, 1445-58, 2015.

ASSOCIATION OF LAXITY MEASURES ACROSS ARTHROMETERS IN ACLR PATIENTS RETURNING TO SPORT

Nathaniel A. Bates,[1] Gregory D. Myer,[2] Kim Barber-Foss,[2] Nathan D. Schilaty,[3] Alexander Fischbach,[1] Alexandra Sheldon,[1] Christopher V. Nagelli,[4] April McPherson,[1,2] Aaron J. Krych[4]
[1]The Ohio State University Wexner Medical Center, Columbus, OH, USA; [2]Emory University, Flowery Brach, GA, USA; [3]University of South Florida, Tampa, FL, USA; [4]Mayo Clinic, Rochester, MN, USA
*Corresponding author's email: Nathaniel.Bates@osumc.edu

Introduction: Anterior knee laxity is a known risk factor for ACL injury risk and is often included as an evaluation metric in assessing whether ACL reconstruction (ACLR) has successfully restored knee stability.[1,2] Multiple mechanisms exist to assess this factor including manual clinical exams, manual KT-1000 style arthrometers, and automated mechanical arthrometers.[3,4] Despite the clinical utility of anterior knee laxity measurements, a dearth of literature exists that attempts to draw consilience between mechanical and manual arthrometer results. The current study used a manual and mechanical arthrometer on common ACLR subjects to identify associations between the devices in both the involved and uninvolved limbs.

Methods: 44 limbs from 22 unique subjects (19.3±3.2 years; 173±9 cm; 81.1±21.1 kg) underwent two forms of knee arthrometer (Genurob GNRB; BlueBay) assessments of anterior knee laxity in the same visit. Each subject had previously suffered primary ACLR and was clinically cleared for return to full sport participation. Both involved and uninvolved limbs were assessed. Mechanical GNRB assessment was performed according to the manufacturer's instructions.[3] Manual BlueBay assessment was performed according to published CompuKT/KT-1000 protocol specifications.[4] Both arthrometers documented anterior tibial displacement to a maximum of 134 N of applied anterior shear force. To assess differences in magnitude of raw laxity scores between arthrometers, two-way repeated-measures ANOVA was applied with groups of Device (GNRB, BlueBay) and Side (Involved, Uninvolved). Inter-device associations were assessed via best-fit linear regression with Pearson's Correlation Coefficients and R-squared values.

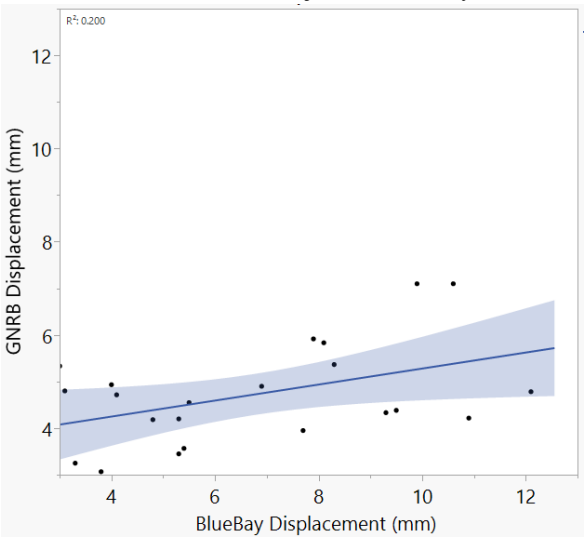

Figure 1: Association between manual and mechanical arthrometer values for the uninvolved limbs. This case was the strongest observed association and only produced an $r^2 = 0.20$.

Results & Discussion: For GNRB vs. BlueBay laxity, both Device ($P < 0.01$) and Side ($P = 0.02$; Table 1) were significant factors, but there was no interaction between factors ($P = 0.25$). By Device, BlueBay measures of laxity displacement (7.0±2.9 mm) exceeded GNRB measures (5.6±1.5 mm) in both magnitude and standard deviation. This was side specific as post-hoc analysis demonstrated no differences between Devices on the Involved side ($P = 0.19$; Table 1), but that BlueBay exceeded GNRB for the Uninvolved side ($P < 0.01$). Pearson correlations between Devices were not significantly associated ($P = 0.36$, $r^2 = 0.02$). There were Side-specific differences in these associations as the involved side lacked significance ($P = 0.45$, $r^2 = 0.03$) while the uninvolved side did exhibit a significant association ($P = 0.03$, $r^2 = 0.20$, Figure 1), but only accounted for 19.7% of the variance. Association between devices was only significant for the uninvolved limb, and even in that case the association only accounted for 20% of the variance which is the minimum threshold for inclusion in a clinically predictive model.

In general, involved limbs had greater laxity than uninvolved limbs (6.8 (2.3) vs. 5.7 (2.3) mm; $P = 0.03$). However, this was device specific as side differences were significant for the GNRB ($P < 0.01$), but not the BlueBay arthrometer ($P \geq 0.13$). While the manual arthrometer estimated greater displacements in anterior knee laxity, the mechanical arthrometer expressed less variability. This reduced variability may be what allowed for identification of side-specific differences with the GNRB device whereas the BlueBay did not.

Significance: Association of anterior knee laxity measurements between manual and mechanical arthrometers in ACLR patients was limited. The mechanical arthrometer was superior at identifying asymmetry likely due to its reduced measurement variability. Neither device expressed mean measurements >10 mm, so both were able to identify restoration of anterior stability in most reconstructed limbs, but individual manual device measurements did exceed 10 mm of displacement. Consilience of raw measurements between devices was limited; thus, direct generalization of results between devices should be limited to deltas observed across repeated measurements.

Acknowledgments: NIH R01-AR055563; Florida Department of State Center for Neuromusculoskeletal Research

References: [1] Pugh et al. (2009), *Am J Sports Med* 37(1):199-210; [2] Lindanger et al. (2021) *Am J Sports Med* 49(5):12227-35; [3] Robert et al. (2009), *Orthop Traumatol Surg Res* 95(3); [4] Wordeman et al. (2012) *Clin Biomech* 27(8):830-6.

Table 1: Observed anterior knee laxity values.

	BlueBay Manual Arthrometer	GNRB Mechanical Arthrometer	Cumulative Average
Involved Limb	7.3 (3.3) mm	6.4 (1.3) mm	6.9 (2.3) mm
Uninvolved Limb	6.8 (2.8) mm	4.7 (1.1) mm	5.7 (2.3) mm
Cumulative	7.0 (2.9) mm	5.5 (1.5) mm	6.3 (2.4) mm

KINEMATIC COMPARISON OF THE LOWER EXTREMITIES IN SPORT-SPECIFIC AND LABORATORY ENVIRONMENTS FROM VARSITY COLLEGIATE ATHLETES

Pratham Singh[1*] and Timothy Burkhart[1]
[1]Faculty of Kinesiology, University of Toronto, Toronto, ON
*Corresponding author's email: pratham.singh@mail.utoronto.ca

Introduction: There is an inherent risk of injury in every sport [1] and many biomechanical screening assessments have been developed to identify these risks. However, the majority of these risk assessments have been developed and are performed, in a laboratory setting which may not be representative of the environment the athlete performs in. Therefore, obtaining measurements in a laboratory setting may not be comprehensive enough to identify the true risk of injury or to determine when an athlete is ready to return to sport following an injury. Therefore, the purpose of this study was to compare lower extremity kinematics in collegiate level lacrosse, basketball and volleyball athletes between their sport environment and the laboratory. We hypothesized that athletes would have a greater range of motion (RoM) when completing similar multiplanar tasks in the sport environment compared to the laboratory environment.

Table 1: The left knee RoM was greater in the sport specific environment than the laboratory for lacrosse, volleyball and basketball athletes.

	Flexion/ Extension (°)	Abduction/ Adduction (°)	Internal/ External Rotation (°)
Lacrosse			
Cut	31.06 [8.26]	9.66 [2.68]	15.56 [2.27]
Three Cone Drill	36.77 [8.20]	20.56* [9.97]	33.24* [10.86]
Volleyball			
Stop Jump	47.65 [8.24]	6.50 [2.62]	7.45 [1.92]
Approach Jump	37.65 [9.17]	7.29 [4.19]	12.14* [4.77]
Basketball			
Cut	32.06 [8.11]	9.04 [3.59]	10.93 [2.01]
Lane Agility Drill	30.59 [7.37]	20.53* [7.23]	31.50* [4.29]

*denotes significantly greater knee RoM

Methods: Eight lacrosse athletes (M: 5, F: 3; Age: 21.4 [3.67]), nine volleyball athletes (M: 6, F: 3; Age: 20.0 [0.94]) and seven basketball athletes (M: 3, F: 4; Age: 21.0 [1.51]) participated in this study. On the field, lacrosse athletes performed a three-cone drill and in the laboratory, they performed a sidestep cut (run for 5 meters, decelerate, and perform a 90˚ cutting manoeuvre with the contralateral limb). On the court, basketball athletes performed a lane agility drill while volleyball athletes performed an approach jump. In the laboratory, basketball athletes performed a sidestep cut while volleyball athletes performed a stop jump (run for 5 meters, decelerate, and perform a two footed jump immediately followed by a maximal countermovement vertical jump). Motion capture data was collected for each kinematic evaluation using a markerless motion capture system (Theia Markerless, Kingston, ON). Motion data was recorded using eight motion capture cameras sampling at 120 Hz (Sony, Tokyo, Japan). Kinematic data was processed from initial contact to 200 ms after using Visual 3D (C-Motion Inc., Boyds, MD). The range of motion (RoM) was calculated as the difference between the minimum and maximum angles for the cutting phase of each task. A one-way repeated measures ANOVA was used (IBM SPSS, V29; Armonk, NY, USA) to determine if statistical differences existed between each set of athletes' environment and laboratory settings (α=0.05).

Results: In lacrosse and basketball athletes, the left knee RoM for knee abduction/adduction (Lacrosse: $F(1,5) = 7.92$, $p < 0.05$; Basketball: $F(1,5) = 13.19$, $p < 0.05$) and internal/external rotation (Lacrosse: $F(1,5) = 12.30$, $p < 0.05$; Basketball: $F(1,5) = 14.88$, $p < 0.05$) were significantly greater during the cutting phase of the task performed in the sport environment compared to the sidestep cut to the right in a laboratory environment (Table 1). In volleyball athletes, the left knee RoM for knee internal/external rotation ($F(1,8) = 12.96$, $p < 0.05$) was significantly greater during the landing phase of the approach jump performed on court in comparison to a stop jump in a laboratory environment (Table 1).

Discussion: Data from the study quantified increased knee range RoM on the field and on the court when compared to the laboratory tasks. Athletes in different sports exhibited varying degrees of knee RoM depending on the environmental context. Results suggest primary injury risk identification and return to sport assessments following rehabilitation from injuries such as ACL injuries should be comprehensive and take into consideration differences that may be dependent on the environment.

Significance: Given that clinicians and coaches are interested in minimizing the risk of injury in sports such as basketball, lacrosse and volleyball [2-3], performing injury risk or return-to-sport assessments directly on the field may reduce the amount of practice or competition time the athlete misses due to injury. Incorporating sport-specific tasks, in an athlete's actual sport environment could enhance the accuracy of kinematic assessments by identifying athletes at higher injury risk and determining those who show greater readiness to return-to-sport.

Acknowledgments: The research is funded by an NSERC Discovery Grant.

References: [1] Pfeifer et al. (2018), *IJSPT* 15; [2] Huang et al. (2014), *J Athl Train* 49 [3] Agel et al. (2016), *CJSM* 26

PHYSIOLOGY & BIOMECHANICS OF A FENCER'S LUNGE

Supriya Nair[1*], Dr Scott Telfer[2]
[1]Sophomore, Stanford Online High School, Founder - Neurofencing www.neurofencing.com
[2]Department of Orthopaedics and Sports Medicine, University of Washington, Seattle
*Supriya Nair: supriya@neurofencing.com

Introduction: Fencing is one of five sports which have been permanent fixtures at the Olympics. USA Fencing has over 40,000 members and the sport has become popular in the recent years as US athletes have been earning medals at the Olympics and World Cups. Based on sword fighting, fencing demands speed, anticipation, and good reflexes, it requires agile footwork and bladework. Competitive fencing is demanding and injuries of the lower extremities is common. One of the main fencing attack techniques involves the lunge – an explosive extension of the fencer's body propelled by the non-dominant (ND) leg in which the dominant (D) leg is kicked forward. This can be a standard lunge (SL), which involves a single forward step, or an advanced lunge (AL), where 3 rapid steps are taken, ending in the lunge. These lunge techniques provide both power and range to the fencer and helps accelerate the weapon (foil, epee, and saber) for a rapid strike. In this study we analyze the kinematic and kinetic differences between the standard and advanced lunge.

Methods: 30 USA Fencing members from Northwest fencing clubs participated in this IRB approved study (STUDY00019084). These individuals represented all three fencing weapons (Epee, Foil and Saber). A full-body retroreflective motion capture marker set was attached to the fencer to allow 3D kinematics to be captured (Figure 1), and the lunges were performed with the target positioned such that the lead leg during the lunge landed on a floor embedded force plate. After warming up, the fencer performed five SLs and five ALs towards a dummy target. Data were processed and ground reaction forces and joint kinematics were compared between the SL and AL techniques.

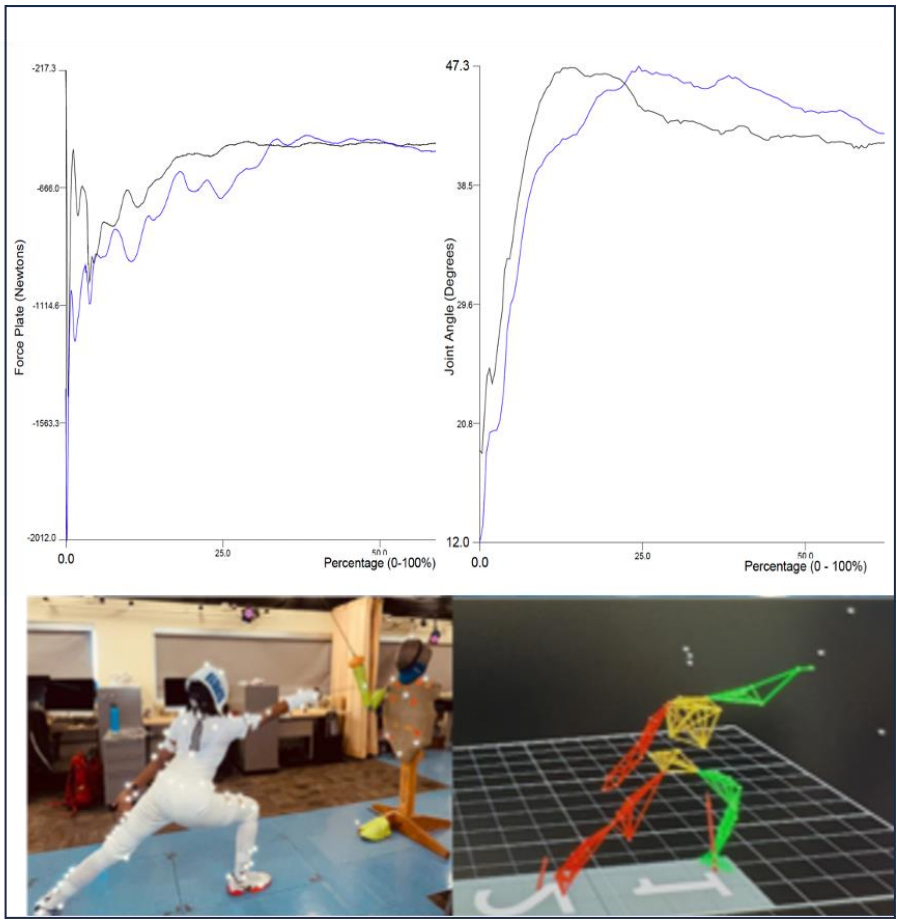

Figure 1: Top left: example vertical ground reaction force data for standard lunge (black) and advanced lunge (blue) from initial contact with the force plate. Top right: sagittal plane knee kinematics for standard and advanced lunges (flexion: positive; extension: negative). Bottom row: fencing lunge and motion capture model.

Results & Discussion: Significant differences were seen between the vertical and anteroposterior components of the ground reaction force for the leading leg, as well as for sagittal plane knee kinematics. During the extended lunge motion, the dominant (leading) foot lands with more force than the standard lunge, and the peak force is reached in a shorter period of time (Figure 1). Fencers who have a style that involves the use of many extended lunges during a bout could potentially risk injuring or stressing the knee, hip, and ankle joints. The dominant knee was also found to be more extended when the foot is landing during an extended lunge versus the standard lunge. This is because the fencer is trying to kick the front leg in order to propel them forward to hit the target. Both the hamstring and rectus femoris play critical roles in regulating the knee's flexion and extension, as the rectus femoris gets the dominant leg moving forward and the hamstring slows it down preventing over flexion of the knee. Fencers who do many extended lunges risk putting additional stress on the knee joint because they are landing with greater force with the knee extended.

Significance: Understanding the biomechanics of the fencing lunge and extended lunge may help fencers to optimize their movements, enhance performance and prevent injuries. The rapid and repetitive fencing lunges (as characterized by take-offs and landing) along with rapid extension and flexion of the dominant leg would produce strenuous impact loading on the lower extremities of fencers particularly the knee, hip, and ankle joints. These can be contributing factors for chronic knee injuries and ankle sprains.

Acknowledgments: USA Fencing, Dr Kat Steele & Dr Eric Chudler from UW, Seattle, Dr Paul DeVita from NBD.

References: Engstrom, Ian et al. "The effect of foot-stretcher position and stroke rate on ergometer rowing kinematics." PloS one vol. 18,5 e0285676. 11 May. 2023, doi:10.1371/journal.pone.0285676

IMU-DERIVED KNEE EXCURSION FOR OUTDOOR RUNNING

Matthew B. Rhudy[1], Joseph M. Mahoney[1,2,3], Allison R. Altman-Singles[1,3,*]
[1] Mechanical Engineering, The Pennsylvania State University, Berks College, Reading, PA, USA
[2] Mechanical Engineering, Alvernia University, Reading, PA, USA
[3] Kinesiology, The Pennsylvania State University, Berks College, Reading, PA, USA
*Corresponding author's email: ara5093@psu.edu

Introduction: Running is a popular form of physical activity which is associated with a high risk of injury. Knee injuries have been associated with knee kinematics in previous research studies [1]. While optical motion capture results in high accuracy joint angle calculations, the application of these systems is limited to laboratory environments. To investigate outdoor running, which represents a significant portion of running activities in the general population, Inertial Measurement Units (IMUs) offer an affordable and portable tool for analyzing knee kinematics in various environments, including outdoors. A method for joint angle estimation originally proposed by Seel et al. [2] was further refined and adapted for the purpose of knee angle estimation during running [3]. The methods in [3], which were validated using optical motion capture data, are applied to outdoor running data in the present study. The purpose of this work is to calculate knee excursion angle while running using only IMU's in an outdoor setting. This method was applied to compare running with and without a stroller.

Methods: This study utilized two Blue Trident (Vicon, Centennial, CO, USA) IMUs fixed to the anterior distal aspect of the thigh, and the anteromedial distal aspect of the tibia of the dominant leg. The first was considered a warm-up and accommodation to stroller running, and the second and third were randomized to running with or without the stroller (*i.e.*, stroller vs. control). Participants were asked to run at a comfortable "talking" speed and to run both stroller and control trials at the same speed.

For each participant and condition, the knee angle was calculated using the methods presented in [3]. One of the limitations of this method as reported in [3] is the difficulty in accurately identifying the initial knee angle for the filter purely from the IMU data. While an approximate initial condition is obtained by assuming the knee angle is zero during a static standing pose prior to the start of running, there are still possible bias errors in the estimated knee angle due to initialization error or alignment error in the sensor data. Due to these limitations, knee excursion was selected as the metric to analyze kinematic differences due to the removal of any bias errors for this calculation. Knee excursion was extracted during stance phases of running for each gait event, which was detected using a peak detection algorithm on the unfiltered shank accelerometer signals (Fig. 1).

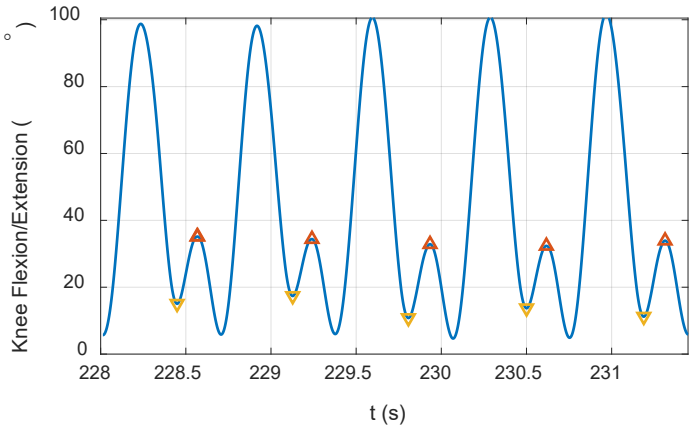

Figure 1: Knee excursion detection example on five strides for one subject. Min and max values at stance phase are found for each stride.

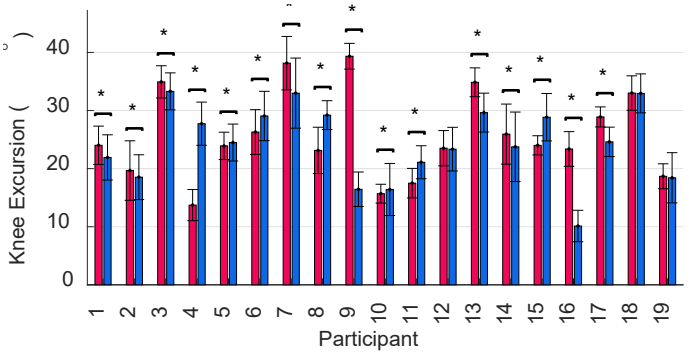

Figure 2: Knee excursion per stride per subject and condition (Control and Stroller). A "*" indicates a significant difference in means.

Results & Discussion: 6 male, 13 female runners participated in this study). The participants were (μ±σ): age (31.1±9.07 yrs), height (167±7.25 cm), body mass (63.6±8.87 kg). The knee excursion is shown during stance phase in Fig. 2, for each of the participants. When comparing within each participant, a two-sample t-test revealed that 7 participants had significant increases in excursion, 9 had significant decreases, and 3 had no detectable change. Overall, there was no *group* difference between stroller and control conditions. This effect is consistent with what was observed using optical motion capture, where no difference in knee excursion was observed between stroller and control conditions [4].

Significance: The differences in knee excursion vary significantly based on the individual runner. However, some individuals experienced large changes in knee excursion, which could be a possible concern for injury risk. Therefore, individual stroller running behaviors merit additional research in outdoor conditions. It is important to note that this is the first study to successfully apply methods from [3] to an IMU data set in the real world.

Acknowledgements: This work received funding from the Franco, Cohen-Hammel, MC REU, and RDG Awards from PSU.

References: [1] Duffey et al. (2000), *MSSE* 32(1); [2] Seel et al. (2014), *Sensors* 14(4); [3] Rhudy et al. (2024), *Sensors* 24(2). [4] Lista et al., (2023) *ASB* Knoxville, TN.

Mechanical somatosensory function is not related to obstacle crossing performance in older adults

Romina Torchia[1*], Ania Lipat, Yenisel Cruz-Almeida, Chris Hass
[1] Department of Applied Physiology & Kinesiology, University of Florida, Gainesville, FL
*Corresponding author's email: rominatorchia@ufl.edu

Introduction: Approximately 30–53% of community-dwelling adults 65 years or older experience at least one fall each year [1]. Epidemiological reports have shown that falls commonly occur during complex mobility tasks, such as obstacle crossing [2] Moreover, older adults at low- and high-risk of falling differ in obstacle crossing biomechanical strategies [1]. Taken together, these studies suggest that proper movement mechanics while avoiding obstacles are crucial to fall prevention. As such, it is essential to gain a better understanding of factors that contribute to obstacle crossing performance to reduce falls. An understudied factor that may contribute to obstacle crossing performance is mechanical somatosensory function. Declines in mechanical somatosensory function occur with aging and have been shown to contribute to deficits in balance and normal gait in older adults [3-5]. Current literature, however, has failed to fully characterize the relationship between mechanical somatosensory function and obstacle crossing performance in older adults. To our knowledge, only one study has investigated this relationship, and found that impaired somatosensory function was associated with failing an obstacle crossing task [6]. Therefore, the aim of this study was to determine if mechanical somatosensory function was associated with obstacle crossing performance in older adults. Based on previous findings, we hypothesized that worse mechanical somatosensory function would be associated with worse obstacle crossing performance.

Methods: This study was a secondary analysis of older adult participants (N = 44, average age = 74 years) enrolled in the Mind in Motion study. Mechanical somatosensory function was characterized as mechanical detection thresholds (MDT). Five Semmes-Weinstein monofilaments, ranging from 0.007 to 10 grams of force, were applied to the sole of the foot. MDTs were defined as the lowest force accurately detected in at least two of three trials [7]. Participants also completed five trials of obstacle crossing. For these trials, a 10 cm obstacle (wooden dowel) placed in the middle of an 8-meter walkway. Motion capture technology (Vicon, version 2.14.0) was used to obtain specific obstacle crossing performance parameters, including toe clearance, approach distance, and recovery distance. 39 reflective markers were placed on the participant's body in accordance with Vicon's Plug-in-Gait model and two reflective markers were placed on each side of the obstacle. Toe clearance was calculated as the vertical distance between the toe marker and obstacle markers during the step over the obstacle. Approach distance was calculated as the horizontal distance between the toe marker and obstacle markers at the beginning of the step over the obstacle. Recovery distance was calculated as the horizontal distance between the heel marker and obstacle markers at the end of the step over the obstacle. The lead limb was defined as the first limb to cross the obstacle, whereas the trail limb was defined as the second limb to cross the obstacle. Multiple linear regressions were run to assess associations between MDTs and obstacle crossing parameters, controlling for age, gender, body mass index, and grip strength.

Results & Discussion: MDTs were not significantly associated with any obstacle crossing parameter ($p > 0.05$) (Table 1). These findings suggest that age-related declines in mechanical somatosensory function do not contribute to obstacle crossing performance in older adults. These results contradict our hypothesis and prior work that has shown somatosensory function was associated with balance, normal walking, and failing an obstacle crossing task in older adults [3-6]. This discrepancy may be due to the differences in measures between studies. Prior reports that found a relationship between mechanical somatosensory function and normal walking and balance did not examine obstacle crossing performance, and studies that found a relationship between obstacle crossing performance and somatosensory function included a combined measure of vibratory, pressure, proprioception, and mechanical somatosensory function.

Table 1. Average Participant Obstacle Crossing Parameters and Multiple Linear Regression Results

Obstacle Crossing Parameter		Participant Average	Overall Regression Model		MDT Regression Coefficients	
Limb	Parameter	Mean ± SD (mm)	R^2	*p*	β	*p*
Lead	Toe Clearance	211.21 ± 41.51	0.084	0.626	-0.105	0.515
	Approach Distance	743.89 ± 165.09	0.070	0.720	-0.212	0.196
	Recovery Distance	184.38 ± 63.97	0.181	0.162	0.116	0.447
Trail	Toe Clearance	207.05 ± 56.47	0.157	0.241	-0.008	0.960
	Approach Distance	205.81 ± 65.98	0.091	0.583	-0.189	0.243
	Recovery Distance	753.17 ± 158.42	0.162	0.223	-0.043	0.778

Significance: As mechanical somatosensory function was not associated with obstacle crossing performance in the present study, other factors should be investigated to improve our understanding of complex walking performance in older adults. Ultimately, a greater understanding of complex walking performance in older adults can inform interventions to reduce falls in this population.

Acknowledgments: This work was funded by the National Institute of Aging (U01AG061389).

References: [1] Pan, H. F., et al. (2016). *J. Phys. Ther. Sc.*, *28*(5), 1614-1620; [2] Robinovitch, S. N., et al. (2013). *Lancet*, *381*(9860), 47-54; [3] Shaffer, S. W., & Harrison, A. L. (2007). *Phys. Ther.*, *87*(2), 193-207; [4] Cruz-Almeida, Y., et al. (2014). *Front. Aging Neurosci.*, *6*, 68; [5] Frigon, A., Akay, T., & Prilutsky, B. I. (2021). *Compr. Physiol.*, *12*(1), 2877; [6] Deshpande, N., Metter, E. J., & Ferrucci, L. (2011). *Arch. Phys. M.*, *92*(7), 1074-1079; [7] Perry, S. D. (2006). *Neurosci. Lett.*, *392*(1-2), 62-67.

TASK-ORIENTED IDENTIFICATION OF MOTOR MODULES USING NON-NEGATIVE AUTOENCODERS

Ryan E. Novotny[1*], Nicolas Schweighofer[1,2], James M. Finley[1,2]
[1]Neuroscience Graduate Program, University of Southern California, Los Angeles
[2]Division of Biokinesiology and Physical Therapy, University of Southern California, Los Angeles
*Corresponding Author's Email: rnovotny@usc.edu

Introduction: Determining how the central nervous system (CNS) coordinates muscles during a task is a fundamental focus in the study of motor control [1]. One of the most common methods for studying muscle coordination is to use dimensionality reduction techniques such as Principal Component Analysis and Non-Negative Matrix Factorization (NNMF) to extract activation patterns (i.e., motor modules) from EMG [2,3,4]. However, when extracted modules are used to estimate forces generated during a task, these estimations are generally inaccurate until the number of modules approaches the number of muscles, leading to approximately independent muscle control [5,6]. Our work addresses limitations in motor module-based force estimations by using autoencoders that extract motor modules while reconstructing both EMG and forces [7]. We extend prior methods by enforcing non-negativity in the module weights and implementing a direct mapping from EMG to force. We hypothesized that the autoencoder would 1) reconstruct input EMG comparably to NNMF, and 2) outperform NNMF and independent muscle control when estimating forces.

Methods: Twelve healthy young adults (8M, 25 ± 6yr) produced isometric forces in eight directions with their dominant arm with their wrist secured to a force transducer. EMG was recorded from Posterior Deltoid, Pectoralis, Triceps Long and Lateral Head, Biceps Long Head, Brachioradialis, and Pronator Teres.

An undercomplete autoencoder was used to extract task-oriented motor modules. This network encodes EMG into lower-dimensional motor modules while constraining the module weights and activations to be non-negative. The reconstructed EMG is then used to linearly estimate endpoint forces. For each participant, we trained 10 sets of networks where each set had a fixed number of motor modules ranging from one to the number of muscles recorded. We then selected the first network to estimate both EMG reconstruction and force estimation to ≥ 80% variance accounted for (VAF). Similarly, for NNMF, we extracted motor modules ranging from one to the number of recorded muscles and evaluated the goodness of fit between the reconstructed and actual EMG, with the final number of modules determined when VAF ≥ 80%.

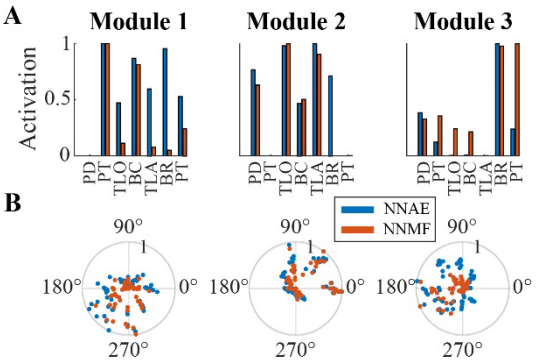

Figure 1: Extracted motor modules for a representative participant. *A*: Motor module spatial structures. *B*: Motor modules preferred activation directions.

We compared the ability of three approaches for estimating endpoint forces from EMG: 1) the NNAE, 2) independent muscle control, and 3) module-based control derived from NNMF. Independent muscle control (IC) was computed by regressing recorded EMG m to endpoint forces f such that $f = H * m$. To estimate forces based on motor modules derived from NNMF, we first extracted participant-specific modules via NNMF. We then estimated endpoint forces such that $f = H * W * W^{+} * m$, where W is the spatial motor module structure identified by NNMF, and W^{+} is the pseudo-inverse of this spatial structure.

Results & Discussion: The structure and preferred directions of the extracted modules varied for the NNAE and NNMF (Fig. 1). We found no significant difference in the number of modules extracted via NNMF (range 3-4) and the NNAE (range 3-5; p = 0.275). We also found no difference between both models' ability to reconstruct input EMG (p = 0.99; Fig. 2A). However, when endpoint forces were estimated using modules derived from NNMF, the estimates were significantly worse than those estimated from independent muscle control ($p < 0.001$) and the NNAE ($p < 0.01$; Fig. 2B). This suggests that integrating task-related information during module extraction produces modules capable of reconstructing both EMG and forces.

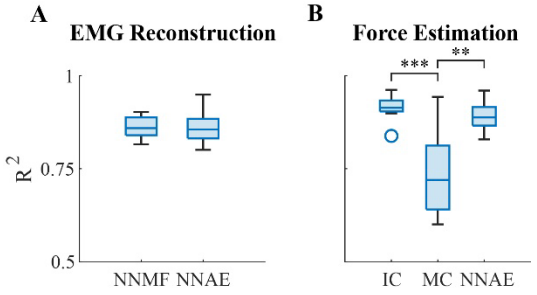

Figure 2: R^2 values for EMG reconstruction and force estimation methods across all participants.

Significance: Current methods for identifying motor modules primarily consider only EMG reconstruction, and consequently, the extracted modules may not accurately explain variance in task-related kinetics. By including force information during motor module extraction, we restrict modules to the task space, allowing for simultaneous, participant-specific insight into control patterns employed by the CNS and how they influence task performance.

References: [1] Ting et al. (2015), *Neuron* 86(1); [2] Cheung & Seki (2021), *J Neurophys* 125(5); [3] Tresch et al. (2006), *J Neurophys* 95(4); [4] Allen et al. (2019) *J Neurophys* 122(1); [5] Barradas et al. (2020), *J Neurophys* 123(6); [6] DeRugy et al. (2013) *Front Comput Neurosci* 7; [7] Buongiorno et al. (2020) *Information* 11(4)

KINEMATIC AND KINETIC COMPARISON OF FEMALE GYMNASTIC AND CHEERLEADING ROUNDOFFS

Avery Takata, John Collins, Emma Caringella, Henry G Chambers, Eric Edmonds, Patrick Curran
Rady Children's Hospital, San Diego, CA, USA
Motion Analysis Laboratory, Southern Family Center for Cerebral Palsy, Rady Children's Hospital, San Diego, CA, USA

Introduction: Gymnasts and cheerleaders perform repetitive tumbling exercises where the upper extremities withstand high impact loads during weight-bearing [1-4]. In gymnastics, young female athletes most frequently injure their wrist during these basic tumbling exercises (e.g. round off, back handspring) [2]. Previous studies have identified compression joint reaction forces and moments occurring at the wrist and elbow to be related to injury risk [1-4]. However, in cheer, ankles are the most injured joint [5]. Although each sport requires its own skills (e.g. uneven bars in gymnastics and stunting in cheer), both groups of athletes undergo high volume loads on upper extremities when tumbling However, young female gymnastic injuries are dominated by upper extremity injuries, whereas cheerleading injuries are not as isolated to the upper extremities [5]. This study sought to compare previously identified upper extremity kinematic and kinetic risk factors in a roundoff between female gymnasts and cheerleaders to further understand this injury difference.

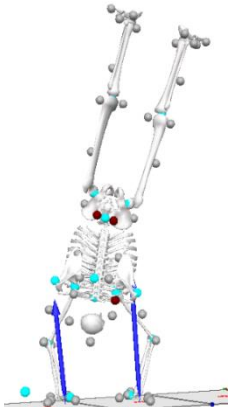

Figure 1: Gymnast in double support phase of roundoff

Methods: Seven female competition level gymnasts and five female cheer and tumbling athletes were included in this analysis (Age = 11.8 ± 1.6, mass = 45.1 ± 10.1 kgs). 51 reflective markers were placed using the PitchTrak marker set. 3D motion data were collected with a 10-camera Arqus system (Qualisys, Inc, Gothenburg, Sweden) at 120 Hz. Participants were instructed to perform three roundoffs as they were trained to perform them where cheerleaders begun with a hurdle step and placed hands parallel over force plates while the gymnasts begun from a standing position and placed hands in the T-position over two force plates (AMTI, Watertown, MA) sampled at 1200 Hz. Trials were included if the athlete landed with one hand on each force plate. Time-series data was extracted for both hands from initial contact to hand off. Visual 3D (HAS-Motion, Inc, Ontario, Canada) was used to calculate wrist and elbow joint angles, joint reaction forces, and joint moments during each hand's contact phase. Statistical parametric mapping (SPM) was used for paired t-testing.

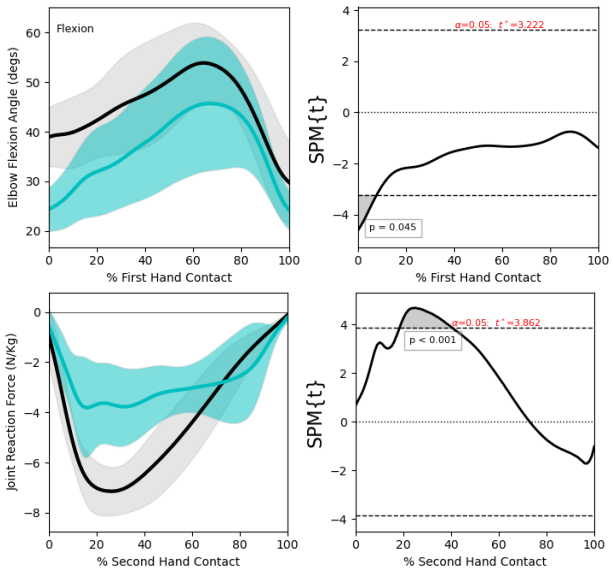

Figure 2: Time series mean and ± 1 SD bands (left) of gymnasts (black) and cheerleaders (blue) and SPM analyses (right) with critical threshold (t and dotted lines) for paired t testing at an alpha level (α) of 0.05.*

Results & Discussion: The closed chain kinetic movement pattern of the roundoff requires the athlete to propel themselves into and out of an inverted position in preparation for more advanced skills, but gymnasts and cheerleaders employ different strategies that could result in different injury patterns. Significant differences were found between cohorts in elbow flexion at the first-hand initial contact ($p = 0.045$) and in the vertical wrist reaction force at 20-40% of the second-hand contact phase ($p>0.001$) (Fig. 2). The gymnasts display increased elbow flexion at initial contact and move through less range of motion potentially creating a stable base for their center of mass to rotate over, whilst the cheerleaders land with a more extended elbow and move through a greater range of motion possibly to dampen impact forces and propel into and out of the inverted position. Further, the second-contact hand is reportedly exposed to higher loads than the first and the T-hand position reduces kinematic risk factors and vertical ground reaction forces [2]. However, the current findings suggest that gymnasts experience increased wrist joint reaction forces in the second-contact limb when compared to cheerleaders even though they were using the T-hand position. This disparity could be due to differing tumbling surfaces where gymnasts tumble over soft mats that increase wrist hyperextension and cheerleaders tumble over hard surfaces (e.g. gym floors, etc.) [5]. Increased wrist hyperextension during impact has been reported to be associated with wrist pain [4]. Although they performed on the same hard surface in the present study, gymnasts had more force through their second-hand when compared to cheerleaders, pushing out of the inverted position as may be required in the gymnastics setting with increased wrist extension resulting on the softer mats.

Significance: Gymnasts and cheerleaders perform similar high impact movement patterns while weightbearing on their upper extremities but display different strategies for entering and exiting an inverted position as well as different injury prevalence. Gymnasts not only perform on soft mats but are also judged according to aesthetic components that may place their joints at higher risk of injury.

References: [1] Webb, B.G., et al. (2008). Current Sports Med. Reports. 7(5), 289-295.
[2] Farana, R., et al. (2017). Journal of Sports Sciences. 35(2), 124-129.
[3] DiFiori, J. P., et al. (2006). The American Journal of Sports Medicine. 34(5), 840–849.
[4] Heck, K. et al. (2021). Orthop J Sports Med. 9(1).
[5] Xu. A.L, et al. (2021). Orthop J Sports Med. 9(10).

Cervical forced-based manipulation increases jugular vein flow velocity

Jacob A. Connolly[1], Theresa S. Brown[2,3], Shannon Schueren[2,3], Katherine F. Walters[1-3], Nathan D. Schilaty[1-3*]
[1]Morsani College of Medicine, University of South Florida, Tampa, FL
[2]Department of Neurosurgery & Brain Repair, University of South Florida, Tampa, FL
[3]Center for Neuromusculoskeletal Research, University of South Florida, Tampa, FL
*Corresponding author's email: nschilaty@usf.edu

Introduction: Force-based manipulation (FBM) is a technique performed by a licensed chiropractic physician who assesses the biomechanics of a subject's cervical region for areas of hypomobility [1] via spinal motion palpation [2] before mobilizing these areas through Maitland Grase III, IV [3], and V [4] techniques. Grades III and IV are large and small amplitude movements and grade V is a high velocity, low amplitude thrust. Previous work has demonstrated that FBM influences lymphatic flow [5] and may have a role in glymphatic clearance of the CNS, thereby reducing the potential buildup of toxic metabolites that contribute to neurodegenerative changes. Glymphatic dysfunction has been implicated in neurodegenerative disorders [6]. The glymphatic system is a specialized waste system that promotes elimination of neurotoxic compounds [7]. Neurotoxic compounds identified in neurogenerative conditions are excreted into the cerebrospinal fluid and transported into the venous system [8]. Ultrasound can be used to measure vessel flow velocity through of B-mode and pulse wave (PW) Doppler imaging of the vascular structures of the neck. The purpose of this study was to determine if FBM had an immediate effect upon neck vasculature.

Methods: With subjects laying supine, B-mode and PW ultrasound were used (*GE VScan;* Wauwatosa, WI) to visualize the neck vasculature bilaterally (internal carotid artery and jugular vein). While the ultrasound probe was stabilized on the neck and the anatomical site of interest was visualized (**Fig. 1**), the PW window was positioned within the blood vessel of interest and a 4 second measure was taken. The images were then processed within *Weasis* software to extract vessel diameter, vessel cross-sectional area (CSA), peak systolic volume (PSV) and end diastolic volume (EDV). With *JMP Pro 17* software, a Matched Pairs T-test was used to determine the difference between pre- and post-intervention measurements.

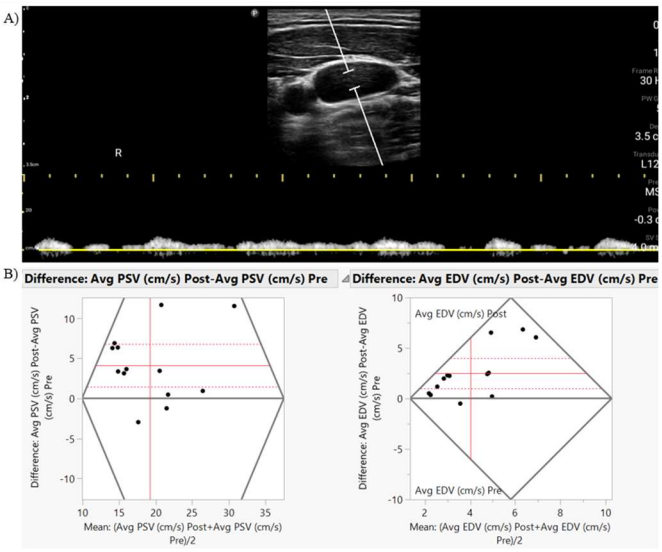

Figure 1: A) Pulse wave Doppler measurement of jugular vein. **B)** After FBM, the average peak systolic velocity of the jugular vein increased by 4.1 cm/s and average end diastolic velocity increased by 2.5 cm/s.

Results & Discussion: After a cervical FBM (n=3), the average PSV of the jugular vein increased by 4.1 cm/s [95% CI (1.5, 6.8) cm/s, p=0.006] and the average EDV increased by 2.5 cm/s [95% CI (1.0, 4.0) cm/s, p=0.0032]. Furthermore, the average vessel diameter decreased by 0.1 cm [95% CI (-0.2, 0.01) p=0.083] and the average cross-sectional area decreased by 0.2 cm^2 [95% CI (-0.5, 0.0), p=0.0582]. These results show that after a cervical FBM, there is an increased venous flow exiting the brain.

Significance: The bilateral increase in jugular vein flow velocity immediately following a FBM (<1 hour) to the cervical spine has important implications for potential therapeutic applications. Once the longevity of the effect is determined, as well as the optimal parameters of application, FBM could be used as a potential preventative or treatment of neurodegenerative disorders to decrease toxic accumulation of CNS waste products. The long-term effect of FBM on venous flow dynamics still needs to be elucidated and further research must be conducted to validate the results and determine the optimal parameters for FBM in this setting.

Acknowledgments: The authors acknowledge the support of the Florida Department of State Center for Neuromusculoskeletal Research and the Florida Chiropractic Association.

References:

[1] Flynn et. al. *Spine (Phila Pa 1976)*. 2002;27(24):2835-2843
[2] Cooperstein R et al. *J Can Chiropr Assoc*. 2013;57(2):156-164
[3] Cleland JA et al. *Phys Ther*. 2007;87(4):431-440
[4] Galindez-Ibarbengoetxea X et al. *Journal of Alternative and Complementary Medicine*. 2017;23(9):667-675
[5] Dayan JH et al. *Annu Rev Med*. 2018;69(1):263-276
[6] Mestre H et al. *Nat Commun*. 2022;13(1):3897
[7] Iliff JJ et al. *Journal of Neuroscience*. 2013;33(46):18190-18199
[8] Benveniste H et al. *Gerontology*. 2019;65(2):106-119

REDUCING SOLEUS ACTIVITY USING A PASSIVE HIP EXOSUIT WITH FLEXION AND EXTENSION SPRINGS IN PATIENTS WITH PERIPHERAL ARTERY DISEASE AND HEALTHY

Hiva Razavi[1], Sara A. Myers[1,2], Iraklis I. Pipinos[2,3], Philippe Malcolm[1]
[1]Department of Biomechanics, University of Nebraska at Omaha, Omaha, NE, USA
[2]Department of Surgery and Research Service, Nebraska-Western Iowa Veterans Affairs Medical Center, Omaha, NE USA
[3]Department of Surgery, University of Nebraska Medical Center, Omaha, NE, USA
email: pmalcolm@unomaha.edu

Introduction: Impaired gait and excessive muscle fatigue are common challenges for individuals with nervous and musculoskeletal system impairments, leading to inefficient walking patterns [1]. Despite the body's ability to optimize walking rapidly [2], those with conditions such as Peripheral Artery Disease (PAD) or stroke often exhibit decreased step length, cadence, and increased stance time, which can lead to increased muscle activation and higher energy costs during walking [3]. Assisting hip motion has been identified as a potentially energy-effective strategy to alleviate these issues, with simulations showing that assisting the hip flexion motion could be more energy-effective than assisting other joints [4]. Recent advancements have shifted focus from rigid exoskeletons to more adaptable soft exosuits and from powered to passive devices to support joint movements more naturally and comfortably [5], [6]. While passive hip flexion exosuits have shown promise in reducing the metabolic cost of walking, it is possible that using passive exosuits to assist hip extension or even combining assistance for both hip flexion and extension could yield even greater reductions in the activation of the muscles of the leg and improved walking outcomes.

Our research aims to fill this void by exploring the effects of a passive exosuit that assists both hip flexion and extension, with adjustable force application, on gait parameters in individuals with PAD. We hypothesized that an optimal combination of frontal and dorsal elastic bands would reduce activity in the soleus muscle and that the effects of the exosuit on patients with PAD would differ from those observed in healthy populations, given that PAD substantially impacts posterior calf muscles and resulting gait biomechanics measures during push-off.

Methods: We employed a within-subjects design to investigate the effects of a bilateral passive exosuit on gait parameters in six healthy adults and four patients with PAD. Each participant walked on a treadmill at 0.8 m/s for one minute under nine different exosuit conditions, with rest allowed between trials. The exosuit, featuring garment-like texture and elastic bands, provided adjustable assistance to hip flexion and extension by altering the length of the bands (Fig. 1). EMG and motion data were collected to measure muscle activity and gait dynamics, while the force exerted by the exosuit was measured using load cells. Data were processed using inverse dynamics and mixed-effects model analyses to assess the impact of the exosuit on walking efficiency.

Figure 1. Passive hip exosuit from the front and back view.

Results & Discussion: In healthy participants, there was an interaction effect between flexion and extension torques on soleus activity ($p = 0.016$), whereby maximum hip extension torque reduced Soleus activity by 22.7% (Fig. 2). In participants with PAD, peak hip flexion torque and the square of peak hip flexion torque were significantly affected ($p = 0.001$ and 0.0006). Intermediate flexion torque minimized soleus activity independent of the exosuit extension torque. The highest reduction was 15.6%.

These findings suggest that targeted assistance at the hip can influence distal muscle activation patterns, consistent with our hypothesis and the soleus-hip-trade-off [7]. The decrease in soleus activity in response to the exosuit's assistance aligns with the hypothesis that enhanced ankle push-off can reduce hip muscle torques, suggesting a shift in the biomechanical burden from the hip to the ankle and vice versa. It is remarkable that roughly the same amount of reduction is achieved via a different mechanism in healthy participants compared to patients with PAD. This may be due to differences in the relative strength of the hip and ankle muscles.

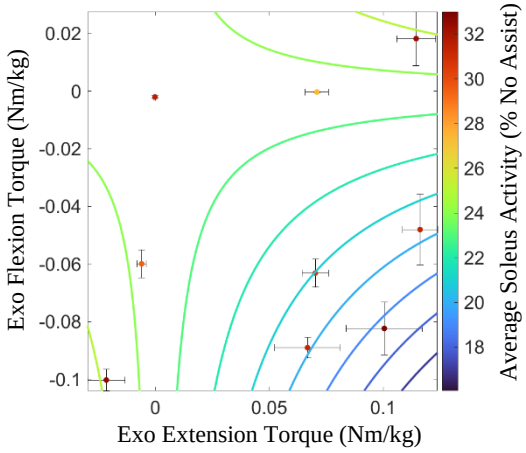

Figure 2. Combined effects of exosuit's flexion and extension torques on soleus activity in healthy group.

Significance: This study shows that adjustable elastic band assistance via passive hip exosuit can significantly impact the activation of important leg muscles. These findings offer new avenues to address the energy demands of lower extremities affected by common diseases such as PAD. The interaction between the soleus muscle and hip torques deepens our biomechanical understanding and paves the way for personalized gait support. This progress promises to improve mobility and independence for those with gait challenges.

Acknowledgments: This work was supported by the National Institutes of Health under grant number P20GM109090.

References: [1] Penke K et al. (2019), Arch Phys Med Rehabil. 100(6); [2] Selinger JC et al. (2015), Curr. Biol. 25(18); [3] Szymczak M et al. (2018), BMC Geriatr. 18; [4] Chen W et al. (2018), Bioinspir Biomim. 14(1); [5] Malcolm P et al. (2013), PloS One. 8(2); [6] Shin SY et al. (2022), J NeuroEngineering Rehabil. 19(1); [7] Lewis CL, Ferris DP. (2008), J Biomech. 41(10).

TOWARD A BETTER UNDERSTANDING OF HOW FOOTWEAR INFLUENCES HABITUAL MOTION PATH DEVIATIONS WHEN RUNNING

Rebekah Pallone[1], Evan M. Day[1*], Katherine Wagner[1], Ed Nyman[1], Jennifer Sumner[1]
[1]Brooks Sports, Seattle, WA, USA
*Corresponding author's email: evan.day@brooksrunning.com

Introduction: The extent to which an individual deviates from their habitual motion path (HMP) has been used to inform whether that individual benefits from a shoe to keep them close to or guide them back to their HMP, as decreasing deviation from one's HMP decreases soft tissue loading [1]. Trudeau et al. (2019) detailed a method to quantify HMP deviation when running [2], with Sumner et al. (2024) further evolving this method to use the entire stance phase when running [3]. Using the entire stance phase enables analysis of the sub-phases of stance. Deviations during sub-phases of stance may be of interest for understanding footwear effects, where parameters such as heel geometry [4], midsole thickness [5], or torsional stiffness [6] affect gait parameters during specific phases.

Methods: Three-dimensional kinematic data of lower limb segments (foot, rearfoot, shank, thigh) collected via optical motion capture (Motion Analysis Corporation, Rohnert Park, CA, USA) and vertical ground reaction forces collected from an instrumented treadmill (Bertec, Columbus, OH, USA) during a product testing round were used for method development. Utilised data were 10 stance phases from each runner (n=9) in five different footwear conditions. Kinematic variables calculated were ankle eversion-inversion, knee internal-external rotation (TIR), and knee ab-adduction; using a Cardan-Euler approach. Total stance phase deviations for each joint angle were quantified [3]. This process time-normalizes joint angle stance phase data to 101 data points which are used to create kernel density plots that are further divided into 51 segments of equal size [3]. To advance this method, time-normalized kinematics were further divided into 5 equal phases, representing 20% increments of stance. The proportion of kinematic data points for each phase within each of the 51 segments for each variable was found, and each sub-phase deviation was calculated by multiplying the HMP deviation for that segment by the proportion; and then the segments within each sub-phase were summed. As this method was developed for product testing purposes, deviation magnitudes were contextualized to a shoe of interest by subtracting the absolute deviation of a comparison shoe (shoes B-E) from the primary test shoe (shoe A). Relative deviations were plotted to showcase each unique individual, as opposed to a group-average statistical approach. Shaded grey regions represent the standard error of measurement. If a data point for a shoe lies outside the grey region, that point is flagged as a 'meaningful' difference for that individual. Deviations for TIR have been used for exemplar purposes (Fig 1 & 2).

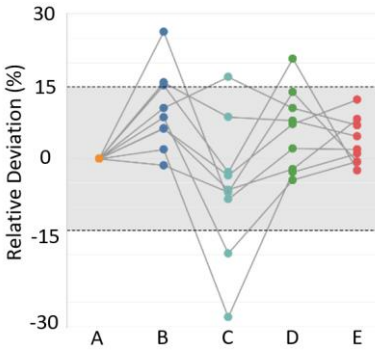

Figure 1: Full stance relative deviations of four comparison shoes (B-E) with respect to the primary test shoe (A) for internal knee rotation. Each dot is an individual (n=9).

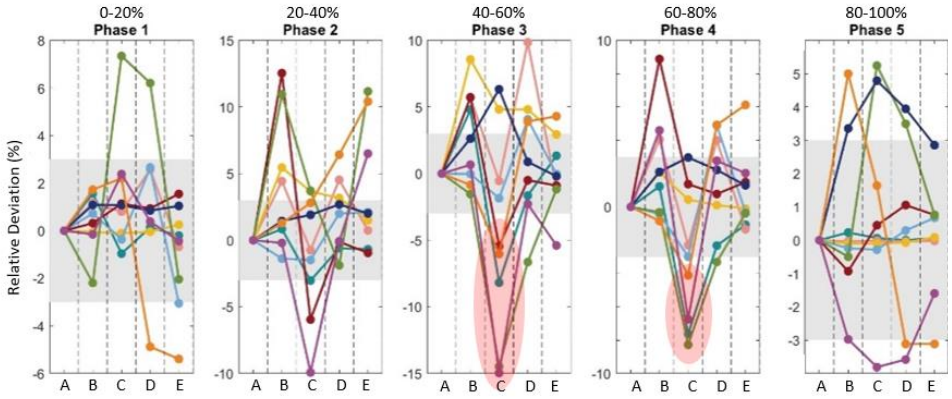

Figure 2: Relative deviations for each sub-phase of stance from Figure 1. Sub-phases reveal footwear effects that may be missed by analyzing whole stance only. Transparent red ovals highlight performance differences for Shoe C relative to Shoe A for half of the study population.

Results & Discussion: Sub-phase deviation values revealed performance differences between shoes that were not apparent when evaluating full-stance deviations. Full-stance TIR deviations were similar across all comparison shoes (B-E) with respect to the primary test shoe (A) (Fig 1), whereas sub-phase deviations revealed a performance difference between Shoe A and Shoe C in Phases 3 and 4 (Fig 2). Phases 3 and 4 represent 40% to 80% of stance phase, during which, on average, the foot moves from initially flat on the ground to beginning push off, with heel off occurring around 60% of stance. These results reveal functional shortcomings in Shoe A compared to Shoe C in the midfoot and forefoot regions relative to minimization of HMP deviation otherwise not detected via full stance phase deviations.

Significance: Sub-phase HMP deviations provide a more intricate understanding of how footwear affects HMP deviations throughout stance phase, unlocking more intentionality with respect to recommended footwear construction parameters. This work may also provide future insight for categorizing functional groups of runners based on deviation timing and further elucidate construction of footwear solutions based on *when* during stance an individual exhibits deviation.

References: [1] Willwacher et al. (2020), *Sci Reports* 10(1363); [2] Trudeau et al. (2019), *Footwear Sci* (3)135-145; [3] Sumner et al. (2024), *Footwear Sci* DOI:10.1080/19424280.2024.2329250; [4] Willwacher et al. (2013), *J Appl Bmech* 29(740-748); [5] Zhang & Lake (2022), *Frontiers* 4(824183); [6] Graf & Stefanyshyn (2012), *Footwear Sci* 4(199-206).

THE QUADRICEPS MUSCLES MAY NOT CONTRIBUTE TO KNEE UNDERLOADING IN INDIVIDUALS THREE MONTHS AFTER ACL RECONSTRUCTION

Evy Meinders[1*], Zhixiong Li[1], Andrew Sprague[2], James J Irrgang[2,3], Volker Musahl[3], Eni Halilaj[1,3]

[1]Department of Mechanical Engineering, Carnegie Mellon University, Pittsburgh, PA USA
[2]Department of Physical Therapy, School of Health and Rehabilitation Sciences, University of Pittsburgh, Pittsburgh, PA USA
[3]Department of Orthopaedic Surgery, University of Pittsburgh, Pittsburgh, PA USA
Corresponding author's email: emeinder@andrew.cmu.edu

Introduction: Over half of individuals undergoing anterior cruciate ligament reconstruction (ACLR) develop post-traumatic osteoarthritis (PTOA) 20 years after surgery [1]. Knee underloading is commonly experienced after ACLR and has been associated with the development of radiographic osteoarthritis [2]. Restoring knee loading early in rehabilitation may effectively prevent or slow future onset of PTOA. While current rehabilitation programs prioritize quadriceps strengthening, gait asymmetries, such as knee underloading, persist even after quadriceps-strength symmetry is reached [3]. Rehabilitation may, therefore, need to focus on factors other than quadriceps strength to restore knee loading. Muscle coordination retraining programs have been shown to alter knee loading in healthy individuals [4] and may be effective in restoring knee loading in individuals after ACLR. However, it remains unknown which muscles contribute to knee underloading. We therefore investigated muscle contributions to knee loading in individuals three months after ACLR, hypothesizing that it is not the quadriceps but other muscles spanning the knee that contribute to underloading.

Methods: After obtaining approval from the Institutional Review Board at the University of Pittsburgh and informed consent, ten participants (9F; height: 1.7±0.1m, weight: 68±10kg) at three months after ACLR walked at a comfortable speed on an instrumented treadmill (speed: 1.3±0.1m/s). Participants were equipped with a lower-body marker set and 16 electromyography (EMG) sensors (eight on each leg; vastus medialis and lateralis, rectus femoris, gastrocnemius medialis and lateralis, semitendinosus, biceps femoris, and gluteus maximus). A calibrated neuromusculoskeletal model was used in CEINMS [5] to calculate muscle and knee contact forces using an EMG-assisted approach for the injured and contralateral limb. Muscle contributions to total knee contact force were calculated over the stance phase for five muscle groups: hamstrings, quadriceps, gastrocnemii, other knee- and hip-spanning muscles (tensor fascia latae, sartorius, and gracilis), and non-knee spanning muscles. A paired t-test was performed using statistical non-parametric mapping [6] to identify significant differences between injured and contralateral limbs in total knee contact force and muscle group contributions.

Results & Discussion: Total knee contact force was lower at the second loading peak in the ACL reconstructed compared to the contralateral knee at three months post ACLR (Fig 1; median difference [Q1-Q3]: 0.7 [0.6-1.1] BW, p=0.001). This lower knee contact force at late stance coincided with lower intersegmental force (0.1 [0.1-0.2] BW, p=0.001) and lower contributions from the gastrocnemii (0.3 [0.2-0.4] BW, p=0.018), hamstrings (0.3 [0.2-0.4] BW, p=0.008), and other hip and knee spanning muscles (0.2 [0.1-0.4] BW, p=0.012) in the injured limb compared to the contralateral limb. No differences between limbs were found for the contributions of the quadriceps and non-knee spanning muscles to knee contact force.

The similar contribution of quadriceps in the injured and contralateral limb suggests that it is not the quadriceps but rather other knee-spanning muscles that are contributing to knee underloading. These results may help explain why previous research failed to find a correlation between quadriceps strength asymmetry and persistent knee underloading in individuals after ACLR [3]. Restoring knee loading early in rehabilitation may require focusing on the gastrocnemii, hamstrings, and other knee and hip spanning muscles. Future research should aim to investigate whether these differences in muscle contribution to knee loading persist for longer than three months, understand the mechanism underlying the asymmetries, and seek to develop programs that rebalance muscle contributions and increase loading to pre-injury levels.

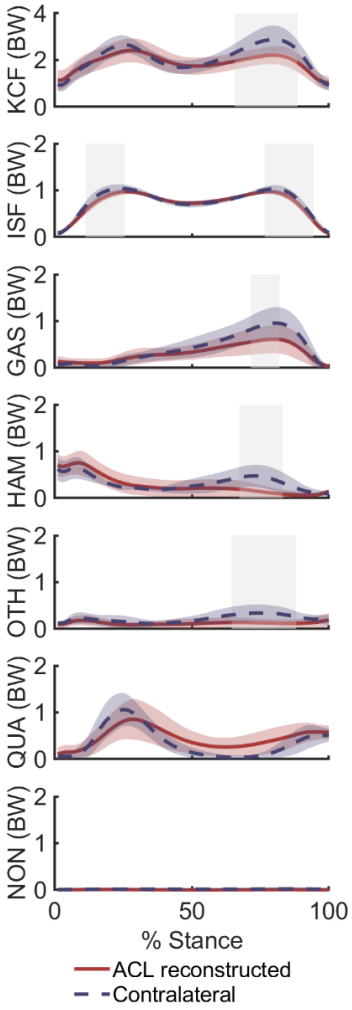

Figure 1. Muscle Contributions. Total knee contact force and the contribution of intersegmental force (ISF), gastrocnemius (GAS), hamstrings (HAM), other knee and hip spanning muscles (OTH), quadriceps (QUA), and non-knee spanning muscles (NON) for the ACL reconstructed (red) and contralateral (dashed blue) limb over stance phase. Grey areas show significant differences between limbs. BW – Body weight.

Significance: Increasing the contribution of the gastrocnemii, hamstrings, and other hip- and knee-spanning muscles, possibly through strengthening and/or muscle coordination training programs, may be needed to restore knee loading early in ACLR rehabilitation. Our work supports the premise that continued focus on the quadriceps alone may be ineffective to improving gait asymmetry, such as knee underloading.

Acknowledgments: This work was funded by the National Institutes of Health, under Award # R01AR080310.

References: [1] Cinque *et al.*, 2018, *AJSM;* [2] Wellsandt *et al.,* 2015, *AJSM;* [3] Arkhos *et al.,* 2022, *AJSM*; [4] Uhlrich *et al.,* 2022, *Scientific Reports*; [5] Pizzolato *et al.,* 2015, *J. Biomech*; [6] Pataky *et al.* 2015, *J. Biomech*.

ONE STEP AT A TIME: VISUAL AND AUDITORY GAIT CUEING THROUGH AUGMENTED REALITY

Alique A. Malakian[1], Gwendolyn R. Retzinger[1], Jacob W. Hinkel-Lipsker[1]
[1]Kinesiology, California State University, Northridge, California, USA.
Corresponding author's email: alique.malakian.559@my.csun.edu

Introduction: People with Parkinson's disease (PD) often encounter challenges with walking, including shorter and more variable step lengths, a slower and more variable cadence, and freezing [1]. While there is no cure for this disease, evidence indicates that visual and auditory cueing can induce gait adaptations that improve the aforementioned spatial and temporal aspects of gait [2]. Traditionally, visual cues have been presented as transverse lines on the ground, while auditory cues typically are implemented through a metronome. However, these interventions are typically confined to clinical or laboratory settings. Thus, there is a need to introduce more portable cueing systems that populations such as those with PD can use on-demand in daily life. Augmented reality (AR) technology, which overlays holograms on a person's field of view, has the potential to provide such cues [2-4]. However, given the novelty of the technology it is unknown how cues delivered through AR drive gait adaptations, and recent work has described how people with PD found an AR cueing system to not be user-friendly. Therefore, the purpose of this study was to determine how feasible implementation of an AR cueing system is, beginning with a young, healthy population and, in the future, a sample of people with PD and healthy age- and sex-matched controls. Because of AR's potential to provide a cueing system, we hypothesized that visual and auditory cues would individually impact gait parameters for all participants, and when combined, would improve both spatial and temporal parameters. We also hypothesized that those with PD would exhibit the greatest change in gait parameters compared to a baseline (no cueing) condition and would report the system to be less usable compared to the young, healthy population.

Methods: 20 young, healthy participants (7 F/13 M; 25.5 + 4 yrs) were recruited to walk for 10 steps in four different cueing conditions using a Magic Leap AR headset: No Cues (NC) (i.e., natural gait), Visual (V), Auditory (A), and Auditory + Visual + Auditory (AV). Each condition was completed three times in a random order for a total of 12 trials. An inertial measurement unit (IMU) system with integrated footswitches was used to collect spatiotemporal gait data (step length and cadence) at 200 Hz. A System Usability Survey (SUS) was administered afterward to determine the usability of our novel application. A repeated-measures multivariate analysis of variance (MANOVA) was used to test for the main effect of condition on all dependent variables, and linear regressions were performed to determine the relationship between reported usability and gait variability (coefficients of variation (CV) for step length and cadence). The second phase of this study is currently underway; we are recruiting a sample of 10 people with PD, and control participants matched to the PD group based on age and sex. These groups will complete the same experimental procedure as the healthy, young population.

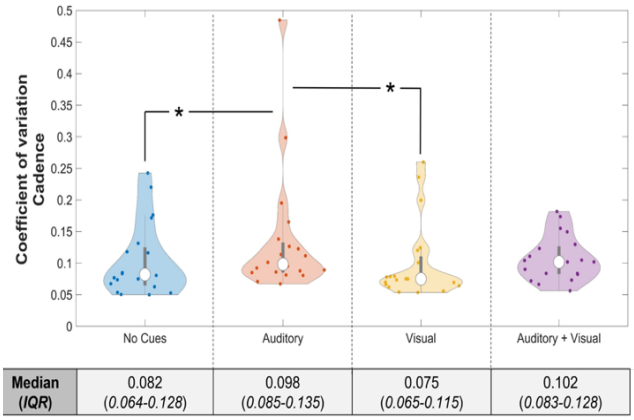

	No Cues	Auditory	Visual	Auditory + Visual
Median (*IQR*)	0.082 (*0.064-0.128*)	0.098 (*0.085-0.135*)	0.075 (*0.065-0.115*)	0.102 (*0.083-0.128*)

Figure 1: Violin plots demonstrating the mean and distribution of individual data points in each cueing condition for cadence variability.

Results and Discussion: All cueing conditions induced a significantly faster cadence compared to NC trials ($p < 0.05$). In addition, cadence variability was significantly higher for the A condition compared to the V condition ($p < 0.05$; Figure 1). This result does not support our hypothesis. One possible explanation for this result is that participants were not easily able to adapt their cadence to a novel one, or that the auditory cues induced a level of cognitive interference that shifted their attention more towards their cadence–causing more variability. In addition, V trials exhibited significantly decreased stride lengths compared to NC ($p < 0.05$), but did not affect stride length variability, indicating that participants were able to consistently match their stride length to the cued distance. There was no noted effect of combining cues (AV) compared to any other conditions across all dependent variables. Increased reported system usability was significantly correlated with decreased stance time across A trials (adj $R2 = 0.262$, $\beta = -0.549$, $p = 0.012$), highlighting the importance of implementing cueing technology that is user-friendly.

Significance: Our findings reinforced that certain visual and auditory cues affect gait parameters, albeit at times in a direction opposite of what was hypothesized (e.g., greater cadence variability with auditory cues). Healthy, young participants were able to match their stride length to the cued distance without an increase in variability. As we are currently implementing this paradigm in people with PD, it will be important to compare these outcomes across populations to determine how different groups of people respond to these cues. As AR technology is advancing rapidly, it is of great importance for researchers to examine how users respond to the technology. In doing so, implementation of AR for applications in clinical settings will be well-grounded in research that examines AR-user interactions.

Acknowledgements: Thanks to Joshua Vicente, Wendy Pham, Borna Golbarg, Kyle Dang, Isaiah Lachica, and other members of the Move-Learn Lab and Positive Augmented Research and Development (PAR-D) Lab for assistance with app development and data collection. This work was supported by the Department of Defense (Contract # W911NF2110273).

References: [1] Ginis P et al. Ann. Phys. Rehabil. Med. 61:407-413, 2018; [2] Vaz J.R. et al. Physiol. 11:1-10, 2020; [3] Dibble L.E. et al. Gait Posture 19:215-225, 2004; [4] Wittwer J.E. et al. Gait Posture 37:219-222, 2013.

EFFECTS OF AGE AND FATIGUE ON SIMULATED MUSCLE FORCES IN FEMALE YOUTH RUNNERS

Susan Basile[1*]
[1]California State University - Fresno
*Corresponding author's email: basile@mail.fresnostate.edu

Introduction: There is currently no definitive guidance as to how much running volume is appropriate for younger distance runners, and whether too much too soon can produce negative long-term outcomes. To investigate the effects of fatigue on young female distance runner muscle activation strategies, the motion and ground reaction forces of 10 girls between the ages of 8 and 17 were recorded before and after an all-out 5-kilometer run. The inverse kinematics and static optimization tools in the OpenSim modeling software were used to simulate the muscle forces, and how they changed as a function of fatigue and age. Fatigue affected the age groups differently at the hip abductors and the ankle joint, with the younger runners typically exhibiting higher muscle forces as a percentage of their body weight, with steeper decreases post-run. These results have implications and suggest that age-based volume limits may be beneficial for young runners.

Methods: Eleven female children and young adults between the ages of eight and seventeen were recruited for this study. All had been running for at least a year and had experience running a distance of at least five kilometers. Based on average developmental ages, subjects were separated into 2 age groups to determine if there was a difference in how fatigue affected younger, potentially pre or mid-pubertal runners (14 and under) compared with those aged 15-17. After warm up, subjects ran down the gait lab walkway in order to obtain at least 3 acceptable foot contacts with the force plate. After collection, subjects performed a 5K within 30 seconds of their personal best pace on a treadmill in the biomechanics lab. Post-run data was then collected in the same manner as the pre-run data, with all subjects running within 0.5 meters per second of their pre-run collection speed. The marker trajectories and force data collected were employed to estimate joint reaction and muscle forces, and muscle forces in the OpenSim software.

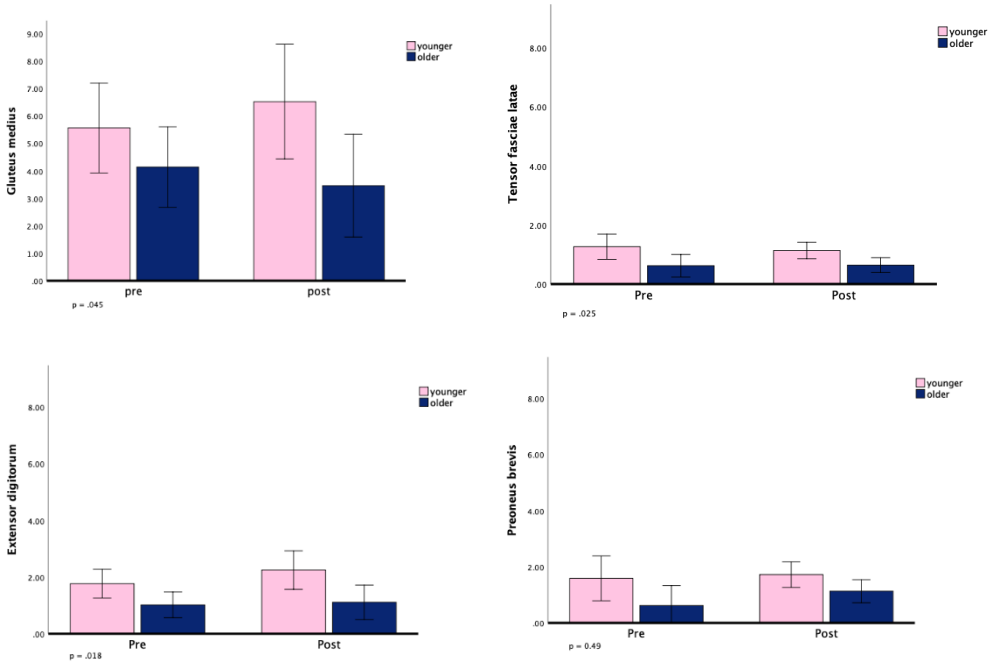

Figure 1. Estimated muscle forces with significant age differences (in times bodyweight).

Results & Discussion: Fatigue affected the two age levels quite differently pre and post run. Muscles most affected include the gluteus medius and minimus, the sartorius, tensor fasciae latae, gracilis, flexor digitorum, peroneus brevis and longus, and extensor digitorum and hallucis longus (Figure 1). The decrease in tensor fascia latae force and apparent compensation by the gluteus medius and minimus muscles both occurred just prior to foot contact. These changes may place the younger group at higher risk for iliotibial band syndrome, which is the most common running injury of the lateral knee [1] and the cause of 7% of female high school running injuries [2]. Prevention strategies in this group could include stretching and/or hip strengthening exercises.

Similarly, there is a shift towards the balance at the ankle towards the dorsiflexors and away from the plantarflexors. This can lead to repeated bending of the tibia, aggravated over longer periods with higher running volume. In addition, if development of the tendons happens to lag behind growth of the tibia, the relevant musculotendon units are now acting from a stretched resting position, which has been documented at the quadriceps femoris in late adolescent males [3]. These factors would further increase tensile forces that can contribute to mid and distal tibial stress fractures. In addition, this ankle imbalance has been associated with increased shank acceleration and impact, adding to the potential accumulation of stress in the area [4].

Significance: Overall, evidence from this study points to the idea that younger runners may especially benefit from hip and ankle strengthening exercises to avoid imbalances that may predispose them to injury. Based on the simulation results which are currently the first estimates of how different age runners handle fatigue differently on a muscular level, they may also benefit from more careful monitoring of their running load.

References: [1] R. Lavine et al. *Curr Rev Musculoskelet Med*, vol. 3, no. 1–4, pp. 18–22, Oct. 2010; [2] A. S. Tenforde et al. *PM&R*, vol. 3, no. 2, pp. 125–131, 2011; [3] G. Charcharis et al. *Front. Physiol.*, vol. 10, 2019; [4] J. Mizrahi et al. *Annals of Biomedical Engineering*, vol. 28, no. 4, pp. 463–469, Apr. 2000.

VERTEBRAL BENDING MOMENTS DURING LOW-LOAD, LOW-ANGLE, HIGH-REPETITION LOADING

Kimberly Collins[1*], Laurel Kuxhaus[1]
[1]Department of Mechanical and Aerospace Engineering, Clarkson University, Potsdam, NY
*collinskim1998@gmail.com

Introduction: Currently 16 million adults – 8% of all adults – suffer from some degree of back pain [1]. Adolescent back pain may be as common as that of the adult populations and has been attributed to several factors including sports [2]. One of the causes of chronic back pain in healthy adolescents are ring apophysis fractures (RAFs) [3]. Though rare, RAFs are avulsion type fractures [4] and are likely underdiagnosed due to poor visibility on an x-ray [5] and the costs and risks of CT imaging [6]. The objective for this research was to use existing data to calculate bending moment of the spine over time, with the hypotheses that bending moment is altered as loading increases and fractures develop.

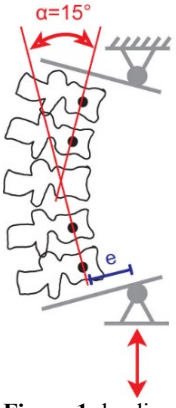

Figure 1: loading schematic [8]

Methods: The analysis was done on an existing data set; this data set captured movement from nine ex-vivo five-vertebra L1-L5 cervine motion segments, of which five have been analyzed to date (2 male and 3 female, 2.4 +/- 0.22 years) during loading conditions designed to induce ring apophysis fractures via low-load, low-angle, high-repetition cyclic loading applied in a load frame. Cervine motion segments are of a similar degree of skeletal maturity to adolescent humans, the population in which these fractures are most frequently diagnosed [7]. These data were collected using a 4-camera Qualisys motion capture system and an eccentric loading fixture (Fig. 1), which enforced planar flexion-extension and ensured that the L1 vertebra pivoted about an axis orthogonal to the plane of motion and loading direction. The motion segments were cyclically loaded from a neutral position to 15° of flexion. Each specimen was cyclically loaded to 20,000 cycles with interspersed "witness tests" (slower cycles at 0.1 or 0.01 Hz), which occurred at 1, 1,000, 3,000, 6,000, 10,000, and 19,995 cycles. Custom MATLAB code was used. First, 3D motion capture coordinates were transformed to a 2D plane (as enforced by the physical boundary conditions of our load frame fixtures); the plane was fitted to the motion of the L1 vertebra, and the loading direction of the actuator was estimated by fitting a circle to the motion of L1. Then the bending moment of each vertebra during all witness cycles was calculated by taking the cross product of the distance between centroid of each vertebra's markers to the applied force.

Results & Discussion: Four out of the five specimens show roughly a 30 % percent drop of bending moment across all vertebrae from the first set to the second set of witness cycles. Then the rest of the witness cycles continue to decrease but at a slower rate. Figure 2 shows the bending moment on each vertebra during the middle (3rd of 5th) cycle from each group of witness cycles from a representative specimen. As anticipated, bending moment increases from L1 to L5, consistent with our load frame's displacement actuation (from the bottom). We also note that the peak bending moment for all vertebra decreases as cycle increases for all vertebrae, but the decrease is more marked for the lower vertebrae than the upper. That is, L5 specifically experiences the greatest bending moment. This agrees with our previous work that laxity of the motion segment increases with our loading protocol, and suggests that the laxity increase may be more prominent in the lower lumbar spine. Toward our goal of predicting ring apophysis fracture initiation, this suggests that the lower vertebrae may fail first.

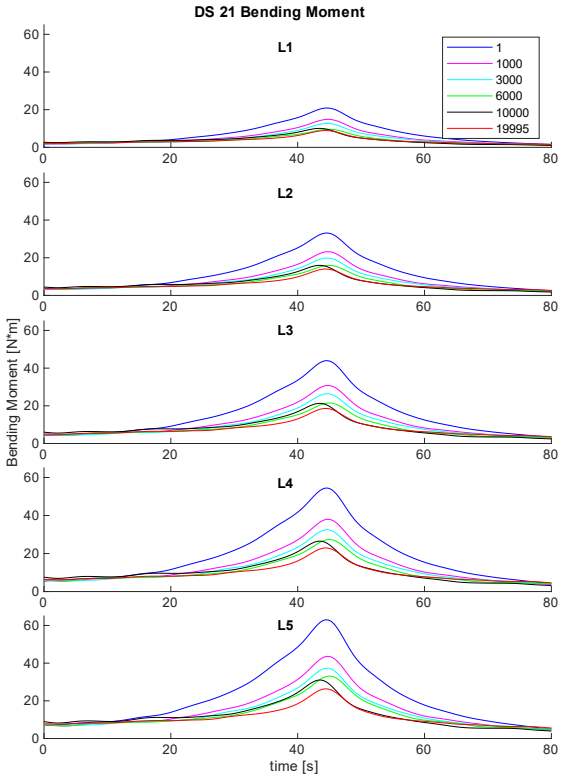

Figure 2: Bending moment over time of for all lumbar vertebrae from a representative specimen.

Significance: These results add specificity to our group's prior work by suggesting that L4 and L5 experienced the highest bending moment during our low-load low-angle high-repetition loading. Future work and imaging can confirm the presence of fractures. Clinically, this confirms that the lower lumbar vertebrae are the most vulnerable to ring apophysis fracture.

Acknowledgments: The authors thank Nicole Gale for prior work, and the MAE Department at for student support.

References: [1] *Health Policy Institute*,2019; [2] "Adolescent Back Pain," *Physiopedia*; [3] Alvarenga+, *NCBI*, 2014; [4] Takata+, *J. Bone*, 1988; [5] Akhaddar+, *J. Neurosurg. Spine*, 2011; [6] "American College of Radiology." *Accreditation*; [7] Corbiere+., *J Biomech*, 2016.

INVESTIGATING THE ROLE OF HIP JOINT MOMENTS IN MODULATING MEDIOLATERAL STEP PLACEMENT DURING PERTURBED WALKING

Vibha R. Iyer[1*], Jennifer K. Leestma[2,3], Aaron J. Young[2,3], Gregory S. Sawicki[2,3,4]
[1]Wallace H. Coulter Department of Biomedical Engineering, [2]George W. Woodruff School of Mechanical Engineering, [3]Institute for Robotics and Intelligent Machines, [4]School of Biological Sciences, Georgia Institute of Technology
*Corresponding author's email: viyer72@gatech.edu

Introduction: During normal walking, humans are excellent at maintaining biomechanical stability. However, environmental disturbances, or perturbations, can cause varying degrees of imbalance during gait. For larger magnitude perturbations, common balance recovery strategies include large changes in step placement, primarily driven by hip musculotendons [1]. Understanding the role of the swing and stance limb hip moments during step placement could provide insight into how humans achieve such robustness to external perturbations and how sensorimotor deficits in the hip joint may influence balance recovery. Moreover, investigating hip moments across a variety of perturbations could illuminate if and when humans alter stance and swing limb contributions to balance. In this work, we aimed to determine the relationship between stance and swing limb hip moments and step placement during perturbed walking.

Methods: This study was approved by the Georgia Institute of Technology Institutional Review Board. Using a 6 degree-of-freedom perturbation platform containing a treadmill, we had participants (N = 11) walk at 1.25 m/s while suddenly moving the walking platform with various magnitudes (5, 10, 15 cm) and directions (eight at 45-degree increments), with perturbation onset during double stance (Fig. 1A). We identified gait events using a kinematic method and collected data from full-body motion capture [2]. Analysis was limited to frontal-plane step placement, as imbalance in the mediolateral direction tends to induce greater step placement modulation [3]. We calculated hip joint moments using OpenSim and filtered moment data with a 6 Hz lowpass filter. We calculated integrated hip moment over the single stance following the perturbation onset and normalized by participant mass (Fig. 1B). We calculated step width (SW) using the mediolateral distance between heel markers at the end of the same single stance and normalized by participant height. We evaluated the correlation between integrated hip moment in the stance and swing limbs and step placement during the perturbed step.

Results & Discussion: We found a significant relationship ($p < 0.01$) between both swing and stance integrated hip moments and step width (Fig. 1C). However, there was a much stronger correlation between the swing hip moment and step width ($R = 0.682$) compared to the stance hip ($R = 0.054$). This indicates that the swing limb is the primary driver of step placement when perturbed. Conversely, there is very little correlation between the stance limb hip moments and step width. The stance limb's integrated moment during steady state walking was negative (widening-abduction); even during perturbations requiring a narrowing step (green) in which some hip adduction would be required. This suggests that any stance hip moment modulation during balance recovery may be constrained by the stance hip's typical role in supporting and directing the center of mass during walking. Indeed, the swing limb is more manoeuvrable because it can move in all degrees of freedom, subject only to inertial constraints.

Significance: Understanding the links between stance and swing limb hip moments and step placement could inform biomechanical stabilization strategies, and also help diagnose contributors to balance deficits in clinical populations. Future work will include investigating how different perturbation conditions cause varied hip moment contributions and analysing the role of the ankle joint in step placement to better understand balance recovery. We will also mine this data for balance augmenting exoskeleton assistance strategies - focusing on benefits of targeting swing leg step placement modulation versus stance leg stability assistance. Long term, we expect this data to inform studies on 'best-practices' in the effective control of dynamic balance using our 2DOF hip exoskeleton [4].

Acknowledgments: Supported by Georgia Tech President's Undergrad Research Award (PURA) and NSF GRFP Award #1324585.

References: [1] Hof et al. (2010) *J. Exp. Biol*. [2] Zeni et al. (2008) *Gait Posture.* [3] Leestma et al. (2023) *J Exp Biol*. [4] Leestma et al. (2024) *RAL*.

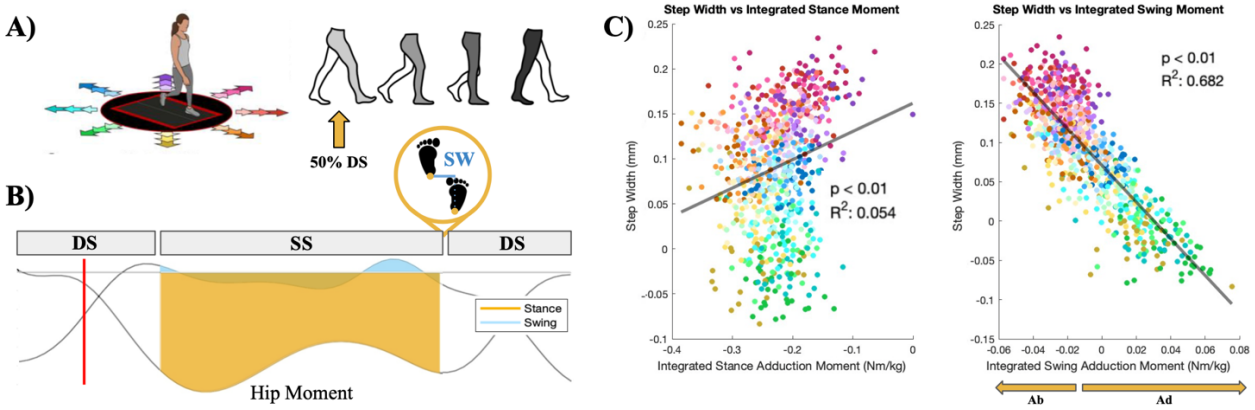

Figure 1: A) Perturbation conditions with varying magnitudes (hue) and direction (color) at 50% double stance. B) Integrated hip moment for stance and swing limbs calculated using the single stance (SS) following the double stance (DS) containing the perturbation onset (red line). Step Width (SW) calculated at the end of SS. C) Correlation between normalized SW vs. integrated hip moment. Trend lines and statistical values are displayed.

RECONSTRUCTED JOINT KINEMATICS DURING ONE NORMAL GAIT CYCLE IN STROKE PATIENTS USING PRINCIPAL COMPONENT ANALYSIS REVEALED BILATERAL DIFFERENCES

Hogene Kim[1*], Jieun Cho[2], Sunghe Ha[3], Jooyoung Lee[4], Minseok Kim[4], Jung Hwan Kim[2]
[1] Department of Mechanical Engineering, University of Michigan, Ann Arbor, MI, [2]National Rehabilitation Center, Seoul, Korea, [3]Department of Physical Education, Yonsei University, Seoul, Korea, [4]Department of Applied Statistics, Chung-Ang University, Seoul, South Korea,
*Corresponding author's email: hogenekim@gmail.com

Introduction: Stroke survivors has asymmetric and distinguished characteristics of joint kinematics during gait compared to normal age-matched controls. Recent studies on biomechanics have frequently used principal component analysis (PCA) to measure the joint coordination of body segments. This study aimed to examine the differences between reconstructed kinematic characteristics using a PCA method among stroke patients.

Methods: participants were asked to walk at a comfortable, self-selected speed in a room with a straight 10-meter. During gait, three-dimensional(3D) kinematics were measured during walking, using 3D motion capture system (VICON, Saint Helens, UK) sampled at 100 Hz. PCA was applied to the correlation matrix of the 4,848 variables calculated from the 132 data points (44 participants in three trials). The specific PCA procedure was as follows.

1) Each participant's intra-participant average and SDs.
2) Paretic and non-paretic averages and SDs for 101-time points using the z transform.
3) Input matrices of 44 participants by 2,424 variables (both paretic and nonparetic sides).
4) PC vectors were extracted.
5) Joint kinematics during a gait cycle were reconstructed.
6) Magnitude of PC1 and PC2 loading values were determined.

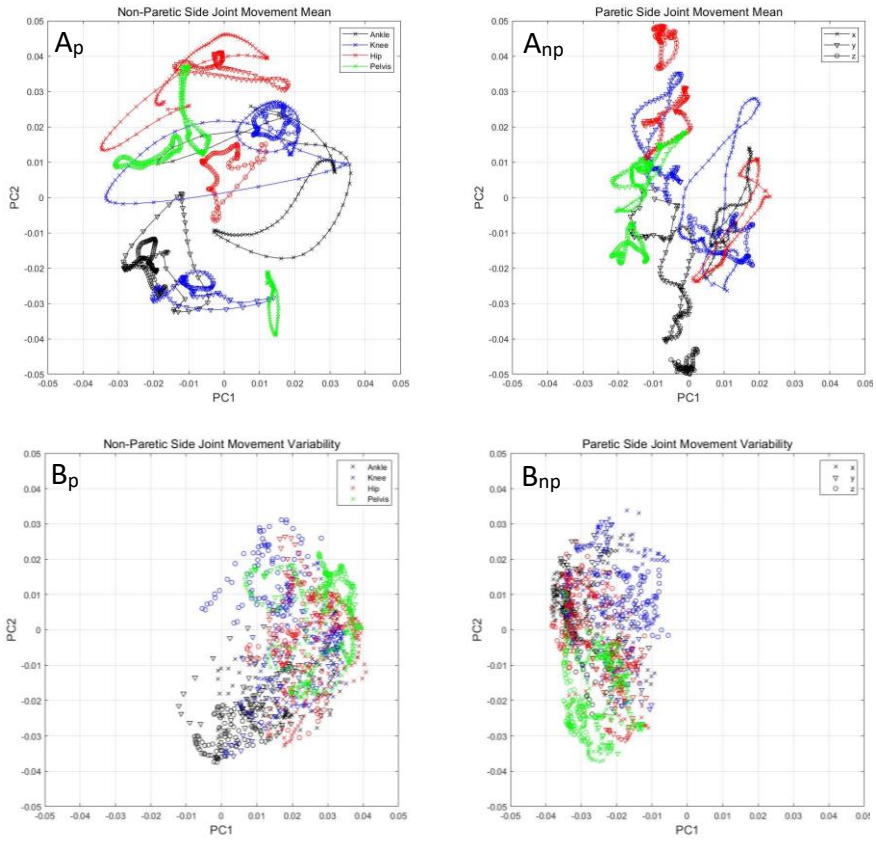

Figure 1: Loading values representing contributions to PC1 and PC2. Mean trajectory (A) , distribution of variability (B) of paretic (p) and nonparetic (np) PC1 and PC2 during a gait cycle, respectively.

Results & Discussion: A total of 44 individuals with chronic strokes voluntarily participated in the study. Joint kinematics during a gait cycle (mean and SD) of the pelvis, hip, knee, and ankle joint angles on the sagittal, frontal, and horizontal planes were reconstructed using the PCs that showed significant between-group differences. In this study, both paretic PC1 and nonparetic PC1, which accounted for 56.7% and 59.3% of the total variance, respectively Figure 1 presents the loading values, which describe the contribution of principal component (PC)1 and PC2 with 63.8% of the total variance. The distribution of joint kinematics indicated that the PC1 loadings were greater in the nonparetic than in the paretic side, while the distribution of PC2 loadings was similar in both sides (Figure $1A_{p/np}$). The joint kinematics variability of PC1 and PC2 loadings on the nonparetic side was generally positively distributed, while the joint variability of loadings on the paretic side was generally negatively distributed (Figure $1B_{p/np}$).
This study presented PCA to create stroke-specific gait trajectories. Patients with strokes, both paretic and nonparetic, exhibited differences in the reconstructed kinematic characteristics during gait. The PC1 and PC2 loading results in this study may have been more heavily weighted towards the nonparetic limb because of this altered gait.

Significance: This study presents its usefulness of PCA to reveal the kinematic characteristics of the paretic and nonparetic sides in stroke survivors. The differences in reconstructed joint kinematics are both paretic and nonparetic changes in joint kinematics of ankle, knee, and hip and increased joint variability in the sagittal plane during the swing phase.

Acknowledgments: This work was supported by Translational Research Centre for Rehabilitation Robots, Korea National Rehabilitation Centre, Ministry of Health and Welfare, Korea. Award Number: #NRCTR-IN18003.

References: [1] Hendrickson et al. (2014), *Gait & Posture*, 39(1), 177-181

FOOT COUPLING KINEMATICS IN RUNNERS WITH PLANTAR HEEL PAIN DURING RUNNING GAIT

Hanieh Pazhooman[1*], Mohammed S. Alamri[1], Zahra Mollaei[1], Stephen C. Cobb[1]
[1] Foot & Ankle Biomechanics Laboratory, Milwaukee, WI, USA
*Corresponding author's email: pazhoom2@uwm.edu

Introduction: Plantar heel pain (PHP), which has been associated with an overall decline in health-related quality of life, is one of the most common injuries in runners [1,2]. The general cause of PHP is believed to be mechanical overload of plantar aponeurosis during gait that leads to microtrauma and subsequent degeneration [3]. In addition to kinematics at a single joint, the coupling between adjacent joints may influence the loading of the plantar aponeurosis during gait. In a study exploring foot joint coupling during walking, Chang et al. [4] revealed that individuals with PHP had fewer frontal plane anti-phase movements between the rearfoot and medial forefoot compared to healthy individuals. Although the study improves the understanding of the effect of PHP on walking gait, the results may not be generalizable to running. The investigation of foot kinematics in patients with PHP during running has been limited [5]. Moreover, all the previous studies have evaluated differences in discrete variables during gait. Statistical parametric mapping (SPM) on-the-other hand allows investigation of joint angle differences over an entire time series [6]. Finally, most previous studies have combined males and females into a single group. Results of our previous investigation, however, suggested that PHP may affect the foot kinematics differently in males and females [5]. Therefore, the purpose of this study was to use SPM to investigate running gait foot joint coupling in male runners with and without PHP, and in female runners with and without PHP. We hypothesized that the degenerative changes in the plantar aponeurosis that occur with PHP would change the foot joint coupling angles of individuals with PHP during the stance phase of running gait.

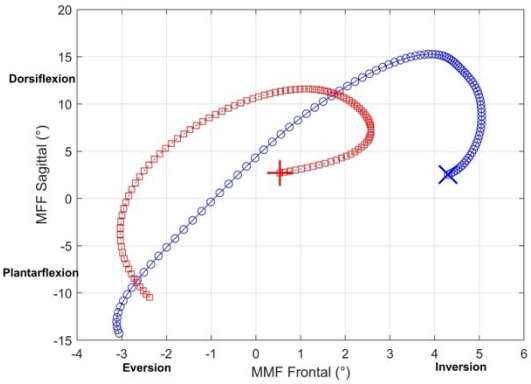

Figure 1: Frontal plane MMF and sagittal plane MFF angle - angle plots. Red + and blue + indicate initial contact in uninjured and PHP groups respectively.

Methods: 13 uninjured (6 f, 7 m, age: 31 ± 5.7 y, mass: 69 ± 10.1 kg) and 13 runners with PHP (7 f, 6 m, age: 29 ± 8 y, mass: 67 ± 7.9 kg) participated in the study. A seven-segment foot model that defines six functional articulations (rearfoot complex [RC], medial midfoot [MMF], lateral midfoot [LMF], medial forefoot [MFF], lateral forefoot [LFF], first metatarsophalangeal [1MTP]) was used to quantify foot motion [7]. Participants completed 5 shod running trials at 4.0 m/s (± 10%) along a runway. A 10-camera system captured marker positions, and a force plate identified initial contact and toe-off events. A MATLAB program was used to low-pass filter (12 Hz) the data, perform rigid body transformation procedures, and calculate stance phase coupling angles [8] of interest (Table 1). Next, the spm1d package for one-dimensional SPM was used to perform independent t-tests of the joint coupling time series. Separate analyses were performed for male and female runners.

Results & Discussion: Inconsistent with our hypotheses, the independent t-test results revealed no significant differences in coupling angles between uninjured and PHP runners. The lack of significant RC_{Fron} - MMF_{Fron} and/or MMF_{Fron} – MFF_{Fron} differences are also inconsistent with Chang et al. [4] that reported significantly fewer rearfoot frontal plane – medial forefoot frontal plane anti-phase coupling movements in participants with PHP during walking gait. The inconsistency may be due to differences in the gait investigated, foot model utilized, and the statistical analysis. With respect to the gait investigated, it is possible that PHP affects joint coupling during walking gait differently than running gait. With respect to the foot model utilized, the Chang et al. [4] model did not include a midfoot segment. Thus, the coupling between the rearfoot and forefoot may be different than the coupling between the rearfoot and medial midfoot and between the medial midfoot and medial forefoot. Finally, with respect to the statistical analyses, Chang et al. [4] performed a discrete analysis (number of anti-phase coupling movements) and included males and females in the same group. The current study, however, used SPM to investigate coupling time-series differences, and performed separate analyses for the male and female runners.

Significance: The lack of significant coupling differences between the PHP and uninjured runners is also inconsistent with the discrete analysis of stance phase ROM of this same group of runners. Among the significant differences reported were significantly increased MMF eversion ROM and MFF dorsiflexion ROM during the propulsion phase in male runners with PHP compared to uninjured male runners [5]. The lack of significant MMF_{Fron} – MFF_{Sag} coupling differences during the propulsion phase in the current study (Fig. 1) may suggest that while PHP affects the ROM of individual foot joints, it may not affect the coupling between the joints.

Table 1: Joint couples investigated.

RC	RC - MMF	RC - LMF	MMF - MFF	LMF - LFF	MFF - MTP
C_{Fron} - RC_{Tran}	RC_{Sag} - MMF_{Sag}	RC_{Sag} - LMF_{Sag}	MMF_{Fron} - MFF_{Sag}	LMF_{Fron} - LFF_{Sag}	MFF_{Sag} - MTP_{Sag}
	RC_{Fron} - MMF_{Fron}	RC_{Fron} - LMF_{Fron}	MMF_{Fron} - MFF_{Fron}	LMF_{Fron} - LFF_{Fron}	
	RC_{Tran} - MMF_{Tran}	RC_{Tran} - LMF_{Tran}			

Acknowledgments: UW-Milwaukee, CHS, Student Research Grant Award; ASB Graduate Student Grant-in-Aid.

References: [1] Di Caprio et al. (2010), *J Sports Sci Med* 9; [2] Irving et al. (2008), *J Am Podiatr Med Assoc* 98; [3] Tountas et al. (1996), *Clin Orthop Relat Res* 170; [4] Chang et al. (2021), *Clin Biomech* 88; [5] Pazhooman et al. (2023), *Gait Posture 104*; [6] Pataky et al. (2010), *J Biomech* 43; [7] Cobb et al. (2016), *J App. Biomech* 32; [8] Heiderscheit et al. (2002), *J Appl Biomech* 18.

DUAL TASK COST DURING BACKWARD WALKING WHILE USING PROSTHETICS FOR AMBULATION

Srikant Vallabhajosula*, Alys Giordano
Department of Physical Therapy Education, Elon University, Elon, NC
*Corresponding author's email: svallabhajosula@elon.edu

Introduction: Prosthetic users are at a higher risk of experiencing an unexpected fall during gait. It is critical to design and use assessment methods that can quantify fall-risk level in individuals who use prosthetics for ambulation. Recent evidence on backwards walking indicates that it could be a viable option to assess and treat balance impairments in high fall-risk populations as it provides a greater challenge particularly to those individuals who may show a ceiling effect with currently used assessments of fall-risk [1]. Currently, there is a paucity of evidence on utility of backward walking as an assessment tool for prosthetic users. Increase in fall-risk during walking could further be heightened while performing a concurrent cognitive task as is commonly seen in other populations. Previous evidence has shown that dual tasking interference is prominent in individuals with lower extremity amputation [2,3] and that dual tasking while walking resulted in slower gait, lesser cadence and longer stride time in individuals with transtibial lower extremity amputation [4]. Whether these results hold for a novel assessment task like backwards walking in this population is still unknown. Hence the purpose of the current study was to examine how walking backwards and dual tasking affects prosthetic users.

Methods: Six individuals (mean age, 62.7 (7.8) years) with unilateral (n=5) or bilateral (n=1) lower extremity amputation, at least six months experience using prosthetic(s), well-fitting prosthetic(s), and ability to walk and navigate curbs or stairs with or without using an assistive device walked the length of an instrumented walkway in forward and backward directions five times, under single task and dual task conditions. For dual task, participants counted backwards in increments, recited months in reverse order, or spelled a 5-lettered word backwards. Gait parameters were analysed under 4 domains – Pace (velocity and stride length), Rhythm (stride time and cadence), Base of Support (stride width) and Variability (coefficient of variation of stride length and stride time) [4]. Dual task cost of a gait parameter was defined as 100 times the difference between single task and dual task over single task. A 2-way repeated measures ANOVA were used estimate effects of direction and task. A paired-samples t-test was used to compare dual task costs associated with forward and backward walking.

Results & Discussion: Data are reported in Table 1 below. Significant main effects of direction suggested that participants walked significantly slower ($p=0.007$), with shorter stride length ($p<0.001$), and with greater spatial ($p=0.006$) and temporal ($p=0.03$) variability while walking backwards compared to forwards. Significant main effects of task suggested that participants walked significantly slower ($p=0.015$), with shorter ($p=0.001$) but wider ($p=0.01$) stride while walking in dual task condition compared to single task condition. There were no significant interactions ($p>0.05$). Comparison of dual task cost between forwards and backwards walking did not yield any significant differences ($p>0.05$). Overall, backwards walking seems to affect pace and variability of gait more than rhythm and base of support. In addition to being a novel task, backwards walking also challenges balance during walking as it forces the participants to rely more on somatosensory and vestibular input than on the unreliable visual system. Only findings like reduced gait speed during forward walking agreed with those from previous literature [4] thereby suggesting the need for more studies on dual tasking during gait in this population. Even though pace and variability were affected by direction of walking, the dual task cost associated with those variables was not significantly different, possibly indicating that the burden of doing a cognitive task concurrently while walking forwards or backwards was similar. A greater sample size is required to strengthen these findings. Further research will also need to examine whether these results differ for those with unilateral and bilateral amputations.

Significance: Fall prevention is emphasized in rehabilitation for individuals learning to use prosthetics for ambulation. As rehabilitation strategies and newer prosthetics are developed, knowledge of appropriate assessments to estimate and improve the fall-risk level are needed. The current study adds to the body of knowledge on the utility of using backwards walking and dual tasking paradigms as part of assessments for individuals who use prosthetics for ambulation.

References: [1] Taulbee et al. (2021) *J Geriatr Phys Ther.* 44(4); [2] Morgan et al. (2018), *Prosthet Orthot Int.* 42(6); [3] Frengopoulos et al. (2018), *PM&R* 10 (10); [4] Hunter et al. 2018, *Gait Posture* 61 (March)

Table 1. Means (SE) of gait parameters during forward and backwards walking under single task and dual task conditions

		Forward Walking			Backward Walking		
Domain	**Gait parameter**	**Single Task**	**Dual Task**	**Dual Task Cost**	**Single Task**	**Dual Task**	**Dual Task Cost**
Pace	Velocity (cm/s) *#	118.5 (6.1)	109.5 (7.7)	8.0 (2.9)	83.9 (6.6)	67.6 (8.6)	19.4 (7.6)
	Stride Length (cm) *#	139.4 (8.3)	131.3 (8.5)	5.9 (1.9)	96.3 (7.7)	82.4 (8.3)	14.6 (4.0)
Rhythm	Stride Time (s)	1.2 (0.1)	1.2 (0.1)	-2.4 (1.4)	1.2 (0.0)	1.3 (0.1)	-8.9 (6.2)
	Cadence (steps/min)	102.5 (4.6)	100.3 (4.8)	2.2 (1.3)	105 (5.1)	97 (5.1)	7.1 (5.1)
Base of Support	Stride Width (cm) #	19.8 (1.8)	21.8 (1.9)	-10.2 (2.5)	15.3 (1.7)	16.9 (1.1)	-13.5 (7.5)
Variability	CV Stride Length (%) *	3.1 (0.3)	3.9 (0.5)	-25.2 (5.5)	9.1 (0.8)	13.6 (2.9)	-52.7 (36.5)
	CV Stride Time (%) *	2.2 (0.2)	2.6 (0.4)	-14.0 (11.1)	4.4 (0.8)	6.2 (1.4)	-66.6 (46.9)

* Significant main effect of Direction ($p<=0.03$); # Significant main effect of Task ($p<=0.015$)

EFFECTS OF EXERCISE INTERVENTION ON DYNAMIC STABILITY IN CANCER SURVIVORS DURING CURB NEGOTIATION

Francis O. Fasuyi*, Reid Hayward, Gary D. Heise, Jeremy D. Smith, Abbie E. Ferris
Department of Kinesiology, Nutrition, and Dietetics, University of Northern Colorado, Greeley, CO
Biomechanics Education and Research Laboratory, BEaR Lab
*francis.fasuyi@unco.edu www.unco.edu/nhs/sport-exercise-science/biomechanics

Introduction: Cancer and its treatment can have detrimental effects on the physical function and quality of life of survivors. To counteract these effects, survivors are often encouraged to engage in regular exercise and physical activity [1]. However, exercise and physical activity also pose challenges and risks for survivors, especially when they involve complex and dynamic tasks such as curb negotiation; that requires a higher level of physical coordination, balance, and strength [2]. Curb negotiation is a common activity of daily living and is a singular disturbing event while walking – unlike stair negotiation. Successful negotiation requires the adjustment of spatiotemporal parameters, joint kinematics and kinetics, and muscle activation patterns to maintain dynamic stability and avoid falls over the obstacle [3]. This task offers a unique opportunity to evaluate a singular destabilizing event and how exercise intervention may help cancer survivors improve their dynamic stability and reduce their fall risk. Therefore, the aim of this study was to investigate the effects of a 12-week individualized exercise intervention on the dynamic stability of cancer survivors during curb negotiation. Biomechanical metrics (margin of stability (MOS), and whole-body angular momentum (WBAM)) that have been shown to reflect the dynamic stability and fall risk of individuals during locomotion were chosen to evaluate how pre- and post-intervention time and leg positions impact measures of balance and stability during curb negotiation performance [2], [4]. We hypothesized that the exercise intervention would improve the dynamic stability of the survivors, as indicated by lower values of these metrics.

Methods: 15 (9 female) cancer survivors (61.9 ± 10.3 years, 77.7 ± 22.9 kg, 1.72 ± 0.07 m) participated in a 12-week individualized exercise training intervention at the University of Northern Colorado Cancer Rehabilitation Institute (UNCCRI). The exercise intervention was comprised of aerobics, strength/resistance, balance, and flexibility training sessions conducted three times weekly [5]. Pre and post intervention training, participants walked at a self-selected pace (pre - 1.27 ± 0. 15 m/s and post – 1.32 ± 0. 16 m/s) across a curb positioned midway along a 5-m walkway. 3 force plates (AMTI, Waterford, MA) (Fig. 1) were configured to simulate a 16 cm curb, along with a raised wooden walkway after the curb. Full-body kinematics were recorded at 100 Hz and kinetic data at 1000 Hz. The data were low-pass filtered using a fourth-order Butterworth filter with a cut-off frequency of 10 Hz for ground reaction force (GRF) data and 6 Hz for kinematic data. Measures of stability were calculated in mediolateral and anteroposterior directions. A repeated measure MANOVA was conducted in R to examine the effects of the 12-week individualized exercise intervention on balance metrics in cancer survivors. Factors including intervention, leg position (curb or ground), and sex, as well as covariates like step width, stance time, and walking speed were explored.

Results: The MANOVA revealed significant main effects for sex (Pillai's trace = 0.410, F (4,46) = 8.00, $p < 0.001$), step width (Pillai's trace = 0.475, F (4,46) = 10.42, $p < 0.001$), stance time (Pillai's trace = 0.501, F (4,46) = 11.56, $p < 0.001$), and walking speed (Pillai's trace = 0.239, F (4,46) = 3.61, p = 0.012). However, the main effect of intervention was not significant (Pillai's trace = 0.109, F (4,46) = 1.41, p = 0.246). Furthermore, significant interaction effects were observed between leg position and sex (Pillai's trace = 0.289, F (4,46) = 4.67, p = 0.003), indicating that the influence of leg position on balance metrics varies depending on the participant's sex. No other interaction effects reached significance ($p > 0.05$).

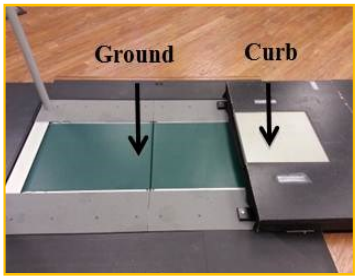

Fig. 1. Image of the curb design.

Table 1: ***Results of Repeated Measures ANOVA for the Effects of Pre-Post Time, Leg, and their Interaction on Dependent Variables***

Dependent Variable	ground		curb	
	pre	*post*	*pre*	*post*
MOS min ML (m), †**	*.008 ± .009*	*.006 ± .006*	*.006 ± .004*	*.006 ± .005*
MOS min AP (m)‡	*.011 ± .009*	*.011 ± .009*	*.009 ± .012*	*.009 ± .006*
WBAM range ML, †, ††**	*.055 ± .018*	*.054 ± .013*	*.049 ± .015*	*.048 ± .013*
WBAM range AP*, **, †, ††, ‡	*.109 ± .019*	*.102 ± .014*	*.107 ± .014*	*.101 ± .014*

Alpha level at p < .05
** - Significant effect of leg*
† - Significant effect of Step width
‡ - Significant effect of Stance Time
*** - Significant effect of Sex*
†† - Significant effect of Walking speed

Discussion: We examined the effects of a 12-week individualized exercise intervention on the dynamic stability of cancer survivors during curb negotiation. However, the results showed no significant effects of the exercise intervention on the outcome variables. These results were puzzling as we did expect to see a difference across curb and ground steps post intervention. Therefore, we investigated further and found very conflicting results within and between participants.

Significance: With no dynamic stability improvement among this group of cancer survivors, this research result is puzzling. ***This finding calls for exercise and balance measurement optimization, but how?***

References

[1]Rock *et al.*(2022) *Cancer J. Clin.*, 72(3) [2]AminiAghdam *et al.*,(2019) *Gait Posture*, 71: 38–43 [3]Shokouhi *et al,* (2024) *Sci. Rep.*, 14(1) [4]Yamagata *et al.*,(2024). *R. Soc. Open Sci.*, 11(1) [5]Brown *et al.*,(2019) *Transl. J. Am. Coll. Sport. Med.*, 4(7)

ESTIMATING REAL-TIME CENTER OF PRESSURE MOTION DURING PERTURBED STANDING IN PEOPLE WITH CHRONIC STROKE

Isabelle Museck[1*] and Jesse Dean[1,2]
[1]Medical University of South Carolina, [2]Ralph H. Johnson VA Health System
*museck@musc.edu

Introduction: Many people with chronic stroke (PwCS) exhibit standing balance deficits [1], which are associated with a decreased quality of life [2], poorer functional mobility [3], and an increased risk of falls [4]. Those with chronic stroke are particularly vulnerable to mediolateral losses of balance [5], as evidenced by the high proportion of sideways falls in this population [6]. While training reactive responses to lateral losses of balance would likely be of value [7], an additional approach is to prevent these losses of balance from occurring. Foundational experiments have shown that non-invasive stimulation can be used to generate artificial somatosensory feedback that elicits predictable balance responses. However, this type of sensory augmentation often involves real-time measurement of the user's center of pressure (CoP), which would not be available in either a typical rehabilitation or real-world setting. Wearable sensors such as inertial measurement units (IMUs) may allow this barrier to be addressed, as these devices offer a low-cost, portable way to measure real-time biomechanics [8]. However, it is presently unclear whether a single IMU would be sufficient to estimate CoP motion, or if simple processing methods can overcome IMU placement variability.

Methods: 10 PwCS completed a single session, in which they wore 7 IMU sensors (sacrum, bilateral thigh, shank, and foot) and stood on a force plate that translated mediolaterally in varying, unpredictable patterns. This perturbation required participants to adjust their CoP to avoid losses of balance. Multiple 30-second trials were conducted as the challenge of the balance task was increased by scaling the platform translation velocity. Our present analyses focused on the final trial, in which CoP rms velocity exceeded 20 mm/s, an indicator of an increased risk of falls. Mediolateral CoP motion was compared with IMU accelerometer, magnetometer, and gyroscope data to quantify potential linear relationships. Principal component analysis (PCA) was performed using data from all accelerometers to determine whether the principal components revealed a stronger correlation with CoP motion than raw accelerometer data, as this method can identify signal commonalities despite potential misalignment between the IMU and user reference frames. Identification of the correlations between IMU inputs and corresponding differences in CoP will open the door for the next steps that involve going beyond simple linear correlations to determine whether machine learning methods can make more accurate predictions.

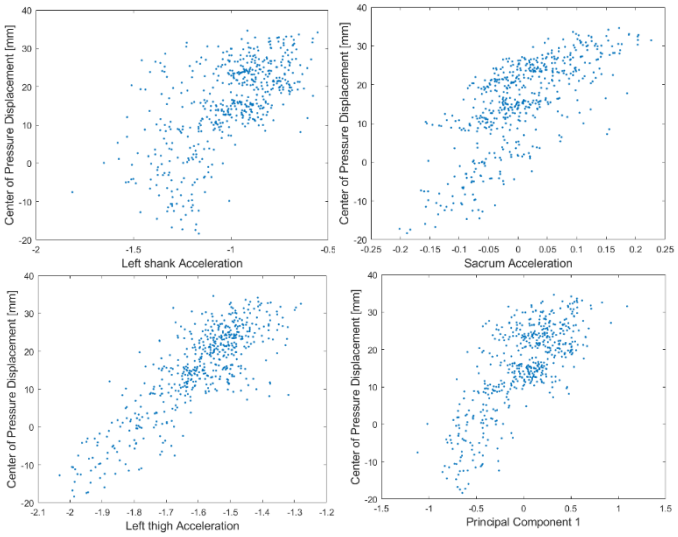

Figure 1. Sample comparison of CoP displacement correlations with raw ML Acceleration Measurements versus top principal component.

Results and Discussion: From the raw IMU data, mediolateral (ML) acceleration was most strongly correlated with CoP motion. Across participants, ML acceleration of the trunk, left thigh, and right thigh yielded high average correlation coefficients of 0.70±0.20, 0.67±0.29, and 0.77±0.15 (mean±s.d.), respectively. These results are consistent with a recent study demonstrating that a single IMU placed on the sacrum can estimate CoP displacement with reasonable accuracy during walking [9]. Moreover, ML acceleration of the left and right shanks demonstrated moderate correlations, with average coefficients of 0.45±0.30 and 0.58±0.22, respectively. Foot accelerations had very weak correlations, which is to be expected as the feet tend to not sway very much during data collection. Our PCA analyses revealed a top component average correlation of 0.78±0.16 with CoP motion, indicating only a minimally better performance than the raw accelerometer data as demonstrated in **Figure 1.** The ML right thigh (90%) left thigh (70%), and right shank (30%) accelerometers were the largest contributors to the top principal components. The presence of moderate to strong correlations between IMU and CoP measurements shows that IMUs placed on the trunk, shanks, and/or thighs have the potential to provide real-time information that can be used to estimate CoP displacement. However, these correlation values vary across patients and trials, likely limiting the effectiveness of a sensory augmentation device that relies on these simple estimates. Additionally, a simple PCA approach was not sufficient to substantially improve estimates of CoP motion. Future work will apply machine learning to personalize CoP estimations from IMU data and integrate this into a system that can provide portable therapeutic stimulation when patient instability is detected.

Significance: These results demonstrate the initial feasibility of using a portable device to roughly estimate CoP motion in a clinical population with balance deficits, an early step toward translating existing sensory augmentation approaches out of the laboratory. Ongoing work will integrate machine learning methods toward optimizing the delivered real-time sensory stimulation.

References: [1] Geurts, et al (2005),*Gait Post.* 22, 267–281; [2] Schmid, et al (2013), *Stroke Rehabil.* 20,340–346; [3] Wesselhoff, et al (2018), *Stroke Rehabil.* 25, 224–238; [4] Hyndman, et al (2003), *Disabil. Rehabil.* 25, 817–822; [5] Gray, et al (2017), *JNPT* 41, 222–228; [6] Hyndman, et al (2002), *Arch. Phys. Med. Rehabil.* 83, 165–170; [7] Gray, et al (2020), *Phys. Ther.* 100, 1557–1567; [8] Ghislieri, et al (2019), *Sensors* 19(19):4075; [9] Lee, et al (2020) *Sensors*, *20*, 6277.

THE USE OF ROBOTIC LEG PROSTHESES ON RAMPS AND STAIRS CAN OFFLOAD THE POSITIVE AND NEGATIVE BIOLOGICAL JOINT WORK OF WEARERS WITH ABOVE-KNEE AMPUTATION

Sixu Zhou*[1,2], Sujay Kestur[3], Jairo Maldonado[1,2], Kinsey Herrin[1,2], Nicholas Fey[4] and Aaron Young[1,2]
[1]Institute of Robotics and Intelligent Machines, Georgia Institute of Technology
[2]George W. Woodruff School of Mechanical Engineering, Georgia Institute of Technology
[3]Parker H. Petit Institute for Bioengineering and Bioscience, Georgia Institute of Technology
[4]Walker Department of Mechanical Engineering, The University of Texas at Austin

Introduction: Powered and passive prostheses can restore mobility for individuals with transfemoral amputation (TFA). Passive devices can render both passive stiffness and resistance and are cost-effective and lightweight. With improved future access to prostheses with powered (i.e., robotic) joints, a comprehensive understanding of their respective biomechanical effects on an individual with TFA is critical. Biological joint work, or the sum of the sound side lower limb joints and the amputated intact hip joint work, aid scientists and clinicians in understanding joint degradation and its long-term impacts on prosthesis users. The overuse of biological joints to compensate for the energy loss from the amputated joints can lead to higher incidences of long-term joint diseases such as osteoarthritis or lower back pain [1]. Thus, we comprehensively quantified the effect of powered knee-and-ankle prostheses on the biological joint work (or energy), with the goal of reducing compensatory increases in energy of the biological joints. With this motivation, we studied the locomotion of ramp ascent/descent and stair ascent/descent to compare the biomechanics of TFA using a passive knee-and-foot prosthesis, Rheo (Össur; Iceland) inclusive of the user's clinically prescribed prosthetic foot, and the powered knee-and-ankle prosthesis, the Open Source Leg (OSL) [2]. We tested the hypotheses that 1) the powered prosthesis would reduce positive biological joint work in ramp and stair ascending tasks, and 2) the powered prosthesis would reduce negative biological joint work in ramp and stair descending tasks.

Methods: Nine participants with TFA consented to an IRB approved protocol and were fit and trained on both passive and powered prostheses after tuning by the research team and a certified prosthetist. Following acclimation, motion capture (Vicon; CO) and force plates (Bertec; OH), data were collected as the participants completed the ramp and stair ascent and descent walking tasks for ten trials at a fixed terrain context (5.2° for the ramp slope angle and 127mm for the stair height) at their self-selected walking speed for each device. The biomechanical results were generated using OpenSim (Stanford; CA) and the joint power is computed as the product of joint velocity and joint torque. The joint work is determined by the trapezium integration of the joint power with respect to time in separation of positive and negative work.

Results & Discussion: As shown in Fig 1A and 1C, the non-amputated sound side hip showed significant reduction in ramp and stairs ascent positive stance work ($p < 0.05$), therefore allowing us to accept Hypothesis 1. As shown in Fig 1B and 1D, all biological joints showed no significant differences in ramp and stair descent negative stance work ($p > 0.05$), therefore allowing us to reject Hypothesis 2. In ramp ascent, the powered prosthetic knee yielded an active pre-flexion before the heel contact. This kinematic change assisted the user with a more natural foot placement and allowed the device to provide active extension at the early stance phase, resulting in a greater positive stance energy from the prosthetic knee and reduced the sound side hip work. With such assistance from the powered prosthesis, the user also yielded lower non-amputated intact hip work in the stair ascent. In the descending ambulation tasks, the powered prosthetic ankle absorbed more negative energy by allowing it acting as a virtual rotational damper instead of a spring system like the passive prosthesis. This allowed the prosthesis to consistently offer resistance by rolling over the prosthetic ankle without experiencing energy return.

Significance: The powered prosthesis demonstrated multiple advantages in reducing the biological joint work for both energy generation and absorption during ramp ascent and descent, as well as during stair ascent (but not stair descent).

Acknowledgements: This work is funded through a grant from the DoD CDMRP Award Number W81XWH-21-1-0686.

References: [1] Struyf et al., *Archives of Physical Medicine and Rehabilitation*; [2] Azocar et al., *Nature Biomedical Engineering*

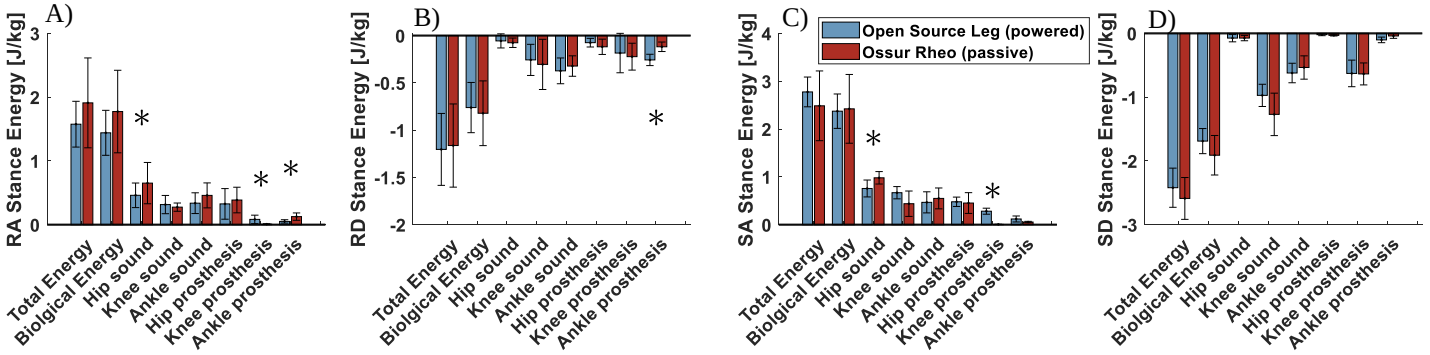

Fig 1: A) Ramp ascent, B) ramp descent, C) stair ascent and D) stair descent stance phase energy comparison between the powered and passive prosthesis

Postural response to optokinetic stimulation in a computer assisted rehabilitation environment (CAREN)

Celeste M. Delap[1]*, William C. Denton[2], Liana C. Johnson[1], Nicole P. Bautista[1], Kaitlyn P. Keyes-Rhames[1], Gabriel D. Mork[1], Charlotte A. Bolch[3] and Tian Zhou[3]
[1]Midwestern University, Physical Therapy Program
[2]Midwestern University, Therapy Institute
[3]Midwestern University, Research and Sponsored Programs
*Corresponding author's email: cdelap@midwestern.edu

Introduction: Human balance is a complex process that requires the integration of visual, vestibular, and somatosensory information. Dysfunction in these systems can lead to dizziness, vertigo, imbalance, and decreased quality of life [1]. Optokinetic stimulation (OKS) has been used to provide mismatched visual information to our other balance systems, which can cause impairments as shown through several center of pressure (COP) balance measures [1-4]. Virtual reality (VR) is now being used in diagnosing and treating vestibular disorders. It has shown promise as an effective and safe method for improving vestibular dysfunction, particularly when there is a conflict between sensory inputs, such as visual stimuli, leading to reduced postural control [5]. The purpose of this study was to compare the effects of eight different OKS conditions on postural control of healthy adults, as measured from COP movement. Due to the strong link between our vision and balance, we expected increased COP movement from the baseline to each OKS condition. Further, we expected the increased COP movement to be greatest parallel to the OKS movement direction. For example, if the tunnel in Figure 1 was moving from in the screen to out of the screen, the increased COP movement would primarily be seen in the anterior-posterior (AP) direction compared to the medial-lateral (ML) direction.

Figure 1: Participant on the CAREN during optokinetic stimulation.

Methods: Postural control of 100 healthy, able-bodied adults (35 male, 65 female; mean age: 40.1±13.2 years; age range: 21-68 years) was investigated for an eyes open baseline, eyes closed baseline, followed by eight, randomized, experimental conditions shown in Table 1. Mean Distance, RMS Distance, Total Excursions, Mean Velocity, and Mean Frequency [4] were calculated from force plate measurements of COP (CAREN, Houten, Netherlands). Paired t-tests were used to compare the eyes open baseline to the eight experimental OKS conditions. The Holm method was used to adjust the p-values to account for type I errors.

Results & Discussion: Results for the comparison between eyes open baseline and each OKS condition are shown in Table 1. The measures generally showed worse postural control during the OKS conditions, supporting our first hypothesis. Three measures for all conditions and five conditions for all measures showed worse postural control in both the combined (comb.) and AP COP measures: Total Excursions, Mean Velocity, and Mean Frequency, and Bottom-to-Top, Top-to-Bottom, Out-to-In, Clockwise Roll, and Counter-clockwise Roll (Mean Distance and RMS Distance included). The second hypothesis was not supported, as most conditions showed increased AP movement, regardless of the OKS direction and the ML measures were generally not different. Mean Distance and RMS Distance were not different for Left-to-Right and Right-to-Left in comb., AP, or ML COP. Nor was Mean Distance for In-to-Out, perhaps because this is generally the direction that we traverse our environment.

Table 1. COP-based measures of postural control of healthy adults during OKS. Significant differences ($p<0.05$) are denoted with an asterisk (*).

	Dir.	Total Excursions	Mean Velocity	Mean Frequency
Eyes Open Baseline	comb.	306.87±110.31	10.23±3.71	0.37±0.13
	AP	256.54±90.53	8.55±3.02	0.40±0.15
Left-to-Right	comb.	381.03±166.53 *	12.69±5.55 *	0.46±0.16 *
	AP	331.95±152.66 *	11.06±5.09 *	0.51±0.20 *
Right-to-Left	comb.	368.66±143.44 *	12.28±4.78 *	0.46±0.16 *
	AP	318.93±131.34 *	10.62±4.38 *	0.52±0.20 *
Bottom-to-Top	comb.	406.87±210.99 *	13.55±7.03 *	0.44±0.17 *
	AP	358.66±202.72 *	11.94±6.75 *	0.49±0.21 *
Top-to-Bottom	comb.	437.83±244.00 *	14.57±8.12 *	0.46±0.18 *
	AP	385.27±229.53 *	12.82±7.64 *	0.51±0.22 *
Out-to-In	comb.	476.99±203.91 *	15.89±6.79 *	0.47±0.16 *
	AP	428.04±194.21 *	14.26±6.47 *	0.53±0.19 *
In-to-Out	comb.	465.48±200.79 *	15.50±6.69 *	0.51±0.18 *
	AP	415.33±193.81 *	13.83±6.46 *	0.58±0.22 *
Clockwise	comb.	580.76±385.35 *	19.34±12.84 *	0.45±0.15 *
	AP	432.07±241.09 *	14.39±8.03 *	0.56±0.20 *
Counter-clockwise	comb.	583.51±429.60 *	19.42±14.31 *	0.43±0.15 *
	AP	441.67±286.92 *	14.70±9.56 *	0.54±0.21 *

Significance: This study shows that postural control is affected by different types of OKS in healthy adults and provides normative data for comparison to clinical populations with a wide array of balance and dizziness disorders.

References: [1] Rosiak, O. et al. (2022). *Sensors (Basel, Switzerland)*, *22*(20). [2] Luo, H. et al. (2018). *Frontiers in neurology*, *9*, 48. [3] Choi, et al. (2021). *Scientific reports*, *11*(1). [4] Prieto et al. (1996) IEEE Transactions on Biomedical Engineering, 43 (9). [5] Hazzaa, et al. (2023). *Head and Neck Surgery*, *280*(7).

GAIT ENTRAINMENT OF YOUNG ADULTS TO DISCRETE MEDIOLATERAL PERTURBATIONS

Lindsey Lee[1*], Kayley Romero[1*] and Helen J. Huang[1]
[1]Department of Mechanical and Aerospace Engineering, University of Central Florida, Orlando, FL 32816, USA
*email: li016205@ucf.edu ka837824@ucf.edu

Introduction: Biological entrainment occurs when a biological process synchronizes with an external stimulus. Entrainment has proven to be impactful in the rehabilitation field as auditory stimulus has been used to entrain the gait of post-stroke patients to faster walking speeds [1]. Visuomotor entrainment has been shown through changes in gait kinematics when a visual scene was continuously shifted at different frequencies as participants walked on a fixed speed treadmill [2]. Previously, we found subjects increase their walking speed in response to discrete mediolateral mechanical perturbations. We believed it would be insightful to apply disruptions of different frequencies to see if walking speed increases and if entrainment occurs to this type of external stimulus. The purpose of this study is to investigate to what extent healthy young adults will entrain to discrete mediolateral surface perturbations delivered with a fixed frequency like a metronome. We hypothesize that young adults will entrain to the perturbations, similar to the metronome phenomenon. We also hypothesized that young adults will walk faster with perturbations based on our previous findings.

Methods: One young adult walked in self-paced mode while experiencing discrete mediolateral perturbations of different frequencies on an instrumented treadmill (M-Gait, Motek Medical). We recorded a baseline which consisted of five-minutes of self-paced walking. Following this there were five perturbation conditions where the perturbation of 3cm magnitude varied in onset frequency; 1) 15, 2) 30, 3) 45, 4) 60 and 5) 75 bpm. Each condition consisted of 2 minutes of self-paced walking (PRE), followed by 5-minutes of the specified onset frequency (PERT), and ended with 2-minutes of self-paced walking (POST). Throughout conditions we recorded lower limb movements (Optitrack) and energy expenditure (Qubit). We quantified entrainment as the probability of the perturbation occurring within specific phases in the gait cycle. The data collection is ongoing, and we plan to collect up to twenty young adults before the conference.

Results & Discussion: The young adult did not demonstrate any clear entrainment for the conditions, except for 60bpm (Fig. 1a, b). For the 60bpm condition the subject showed a trend of experiencing the perturbation right before right heel strike (RHS) during late swing (LSw). Although no explicit entrainment was found, throughout the 30bpm and 45bpm conditions the perturbations were often experienced during mid and terminal stance of the gait cycle. The young adult analyzed generally walked faster in PERT compared to PRE and walked even faster in POST (Fig. 1c). For the 75bpm condition the subject had a faster walking speed for all phases of the condition compared to other conditions. Our results so far show that when given the opportunity to change their walking speed young adults walk faster when perturbations are applied and retain these faster walking speeds when the perturbations are removed, which directly aligns with our previous study, further supporting perturbations of this type can tune ones walking speed. Analyzing metabolic data during the PERT phase, 45bpm had the lowest cost of transport while 75bpm had the highest cost of transport (Fig. 1d). Our results show that the highest frequency of perturbations resulted in highest cost in energy.

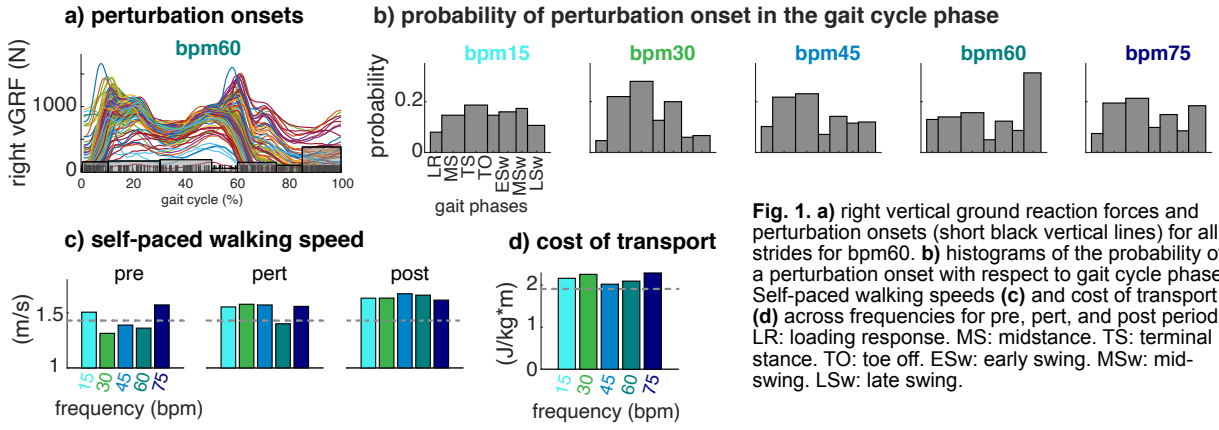

Fig. 1. a) right vertical ground reaction forces and perturbation onsets (short black vertical lines) for all strides for bpm60. **b)** histograms of the probability of a perturbation onset with respect to gait cycle phases. Self-paced walking speeds **(c)** and cost of transport **(d)** across frequencies for pre, pert, and post periods. LR: loading response. MS: midstance. TS: terminal stance. TO: toe off. ESw: early swing. MSw: mid-swing. LSw: late swing.

Significance: Faster walking speeds are critical to maintain mobility for populations such as older adults, stroke patients or patients recovering from injury. If mechanical perturbations of different frequencies cause subject to entrain, resulting in increased walking speeds, these perturbations can be used as a tool to tune one's gait.

References:

[1] Awad, et al., 2024, Nat. Commun., **15**(1), p. 1081.
[2] Thompson, et al., 2017, Hum. Mov. Sci., **54**, pp. 34–40.

LIGHTEN THE LOAD: HARNESSING MACHINE LEARNING AND WEARABLE SENSORS TO ESTIMATE JOINT LOADING DURING INDUSTRY-RELEVANT TASKS

Felicia R. Davenport*[1], Aaron J. Young[1], Gregory S. Sawicki[1]
[1]George W. Woodruff School of Mechanical Engineering, Georgia Institute of Technology, Atlanta, GA, USA
*Corresponding author's email: fdavenport6@gatech.edu

Introduction:
Lower-limb joint injuries remain prevalent in manual labor tasks on construction sites and warehouses where tasks involve moving heavy loads with awkward postures. Modifications to workers' kinematic patterns have not yet resolved the problem, so companies have sought out wearable devices to assist users and offload daily bodily wear and tear. However, such equipment can be costly to distribute to an entire company's workforce; therefore, there is a need to find inexpensive, portable, and reliable wearable sensing systems to provide 'real-time' monitoring of joint loads in the work environment. For this, we can look to IMUs and pressure insoles to measure segment positioning and ground reaction forces, respectively [1]. Wearable sensors have shown promise for estimating risk of injury [2], joint moments [3] and joint contact forces (JCFs) [4], but the minimal sensor inputs needed to build a reliable biological joint loading estimation tool are unknown. We hypothesized that combining IMU and insole data as input to a deep learning model would provide the best performance ($R^2 > 0.7$) at estimating both biological joint moments and JCFs at the knee and back during industrial lifting tasks.

Methods: In this study, we assessed the performance (R^2) of a temporal convolutional network (TCN) trained for estimation of participant-dependent biological joint moments and internal joint contact forces using simulated wearable sensors: IMUs and insoles (Fig. 1A). Our N=9 'ground truth' dataset consisted of moments and contact forces at the L5/S1 and knee joint (Fig 1A). Each participant performed 24 combinations of lifting conditions, with varying lifting turn symmetries (0°, 90°, 180°) and start-end heights (knee-to-waist (KW), waist-to-knee (WK), shoulder-to-waist (SW), waist-to-shoulder (WS), and waist-to-waist (WW)). On this dataset, we utilized the TCN to estimate L5/S1 and knee joint contact forces and biological moments with variation in wearable sensing inputs 1) IMUs and insoles, 2) IMUs *only*, and 3) insoles *only*. IMU data were simulated from inverse kinematics and transformed into the reference frame of sensor-segment locations and insole data were transformed from force plates. Joint moments and contact forces were computed using OpenSim 4. The machine learning models were executed via Python scripts and their R^2 values were evaluated with MATLAB scripts using the *fitlm* function.

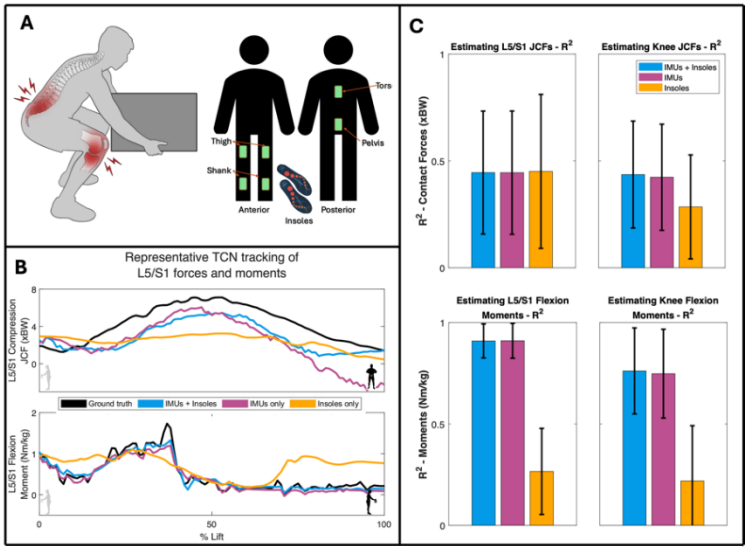

Figure 1: (A) We targeted our estimates of 'ground truth' biomechanical outputs at the L5/S1 and knee joint (left) using simulated IMUs (green) and insoles as inputs (right). (B) A representative time series of L5/S1 compression joint contact force (JCF) and biological L5/S1 flexion moment estimates compared to ground truth (black) using IMUs + insoles (blue), IMUs *only*, (pink), and insoles *only* (gold) during asymmetric lifting. (C) Group averages of each model's performance in estimating contact forces and biological moments at the L5/S1 and knee across all lifting tasks.

Results & Discussion: We found that utilizing IMUs *only* as input to a TCN model had comparable performance to utilizing both IMUs + insoles in estimating joint contact forces (Fig. 1C, top). This contradicted the notion that ground reaction forces would provide useful additional information when added to motion data – especially for internal states like joint contact forces (JCFs). Overall, the TCN estimated joint moments (average $R^2 = 0.64$) better than JCFs (average $R^2 = 0.42$). For JCFs, L5/S1 compression estimates using IMUs + insoles, IMUs *only*, and insoles *only* ($R^2 = 0.45, 0.45, 0.45$) showed negligible differences - whereas estimates of knee compression forces using IMUs + insoles ($R^2 = 0.44$), and IMUs *only* ($R^2 = 0.42$) showed an improvement of 53% and 49%, respectively, compared to using insoles *only*. Estimates of L5/S1 flexion moments using IMUs + insoles ($R^2 = 0.91$), and IMUs *only* ($R^2 = 0.91$) provided a 242.0% and 242.4% improvement versus insoles *only* ($R^2 = 0.27$). Similarly, knee flexion moment estimation using IMUs + insoles ($R^2 = 0.76$), and IMUs *only* ($R^2 = 0.75$) provided a 248% and 242% improvement compared to insoles *only* ($R^2 = 0.22$). Overall, using IMUs as the lone input to a TCN-based joint kinetic estimator may be effective for monitoring external states (e.g. joint moments), but falls short of providing accurate estimates for more indirect states like joint contact forces (JCFs) – even when insole data are incorporated. Because JCFs depend primarily on forces from muscles surrounding the joint – it may be necessary to incorporate sensors that indicate muscle force/activation (e.g., EMG, or bioimpedance).

Significance: Our findings highlight the potential to employ a consolidated set of wearable sensors and machine learning tools for estimating joint kinetic variables related to injury risk 'in the field'. More work is needed to find the optimal set of sensor types and locations to improve estimates further. Long-term, we hope to realize lean, wearable technology capable of warning people doing demanding physical work when they are using hazardous postures – so they can modify their behaviours and reduce injury risk.

Acknowledgments: Supported by the U.S. Department of Energy's Office of Environmental Management and Sandia National Labs.

References: [1] Manupibul et al., 2023. [2] Nurse et al., 2023. [3] Molinaro et al., 2022. [4] Giarmatzis et al., 2020.

ASSESSING MAGNITUDE AND LOCATION OF MINIMUM FOOT CLEARANCE ACROSS INTERVENTIONS IN MULTIPLE SCLEROSIS WITH FOOT DROP

Jennifer Bartloff[1*], Katherine Heidi Fehr[1], Yisen Wang[1], Scott J. Hetzel[2], Katherine Konieczka[1], Julia Mastej[1], Peter G. Adamczyk[1]
University of Wisconsin-Madison Departments of Mechanical Engineering[1] and Department of Biostatistics and Medical Informatics [2]
*bartloff@wisc.edu

Introduction: Persons with multiple sclerosis (PwMS) commonly exhibit footdrop (FD) and fatigability during gait.[1] Fatigability can worsen FD, increasing fall risk.[2] This study's purpose was to compare minimum foot clearance (minimum height of any part of the foot during swing, mFC) and fatigability during gait, among three conditions: no intervention for FD (NI), a carbon fiber ankle-foot orthosis (cfAFO), and a peroneal nerve functional electrical stimulator (FES). A secondary purpose of this study was to demonstrate minimum foot clearance (mFC) measurement using a novel method of pairing IMU trajectories with 3D shoe geometry. **We hypothesized:** 1. Due to the prevalent trait of fatigability in MS, foot drop severity would increase across a 6-minute walk test, observed as a shift in the location on the foot of late-swing minimum clearance toward the Forefoot region (and away from the Hindfoot region), in all interventions. 2. Due to the ankle posture support provided by cfAFO, subjects would exhibit a lower percentage of mFC points in the Forefoot region in this intervention vs. NI and FES. 3. Due to differences in degree of frontal plane ankle control provided in each condition, there would be significantly different quantities of minimum point percentages in the Medial region across conditions.

Methods: 11 PwMS exhibiting FD (age 32–65 years; Self-EDSS range 2–6) participated. We secured one IMU sensor (APDM Opal) on each shoe, then 3D-scanned participants' feet/shoes (Occipital Structure Sensor). Participants first performed a 6–minute walk test (6MWT) with no FD intervention (NI). They received the cfAFO and FES for two consecutive take-home device familiarization periods of at least one week, each followed by a 6MWT test with the device. Fatigability was quantified by the Distance Walked Index (DWI): percent change in distance walked in the 6th vs. 1st minute of the 6MWT. Similarly, mFC change (mFCΔ) was the change in average mFC from the first to the last minute of the 6MWT. For mFC location analysis, the sole of the shoe was divided into 4 quadrants distinguishing Medial/Lateral and Forefoot/Rearfoot regions. A heat map showing the smoothed distribution of mFC locations across all forward swing phases in a bout of walking was approximated using Gaussian kernel functions around observed mFC points (Fig. 1). Linear mixed effects models (LME) were used to determine statistical differences among interventions in DWI, mFC, and Forefoot/Medial mFC location. At study's end, participants indicated their preference: NI, cfAFO, or FES.

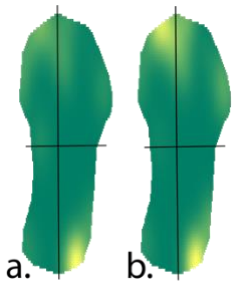

Fig 1. Example division of shoe into regions, with heat map representing probability of lowest point by location. (a) minute 1, (b) minute 6 from same participant

Results & Discussion: The table below shows results for DWI, mFCΔ, and percentage of mFC locations in the Forefoot and Medial regions. On average, the study observed fatigability across all conditions, as indicated by DWI. The LME fits showed no significant intervention effect on DWI or mFCΔ, but both interventions increased mFC relative to NI ($p < 0.001$). The first-minute percentage of mFC in the Forefoot region varied across treatments ($p<0.05$), with NI having the highest rate; however, in each condition the percentage of measurements in the Forefoot increased by minute 6. In minute 1, the percentage of Medial mFC location was higher in NI than either intervention ($p < 0.001$), and not different between FES and cfAFO. By minute 6, the percentage of mFC locations in the Medial region showed differences among FES and cfAFO treatments also. Participant preferences leaned towards devices offering the best within-participant DWI (6 out of 11), and/or the best mFCΔ (also 6 of 11). 10 of 11 participants preferred a device over NI.

Inter-vention	DWI	mFCΔ	Forefoot mFC, Min 1	Forefoot mFC, Min 6	Medial mFC, Min 1	Medial mFC, Min 6
	mean (95%CI) (%)	*mean (s.d.) (mm)*	*mean (95%CI) (%)*	*Mean (95%CI) (%)*	*mean (95%CI) (%)*	*mean (95%CI) (%)*
NI	-8.05 (-19.1 - 3.05)	-1.4 (7.6)	72.6 (68.7-76.2)	77.6% (74.0-80.7)	56.2% (49.9-62.3)	51.2 (44.8-57.5)
cfAFO	-3.15 (-13.2 - 3.05)	+0.27 (3.6)	65.6 (61.1-69.7)	67.8% (63.4-71.8)	50.7% (44.4-57.1)	58.9 (52.6-64.9)
FES	-10.3 (-20 - -0.6)	-2.5 (3.3)	71.7 (67.6-75.4)	74.1% (70.2-77.6)	50.5% (44.1-56.8)	54.3 (47.9-60.6)

Significance: Average mFC was greater in both intervention conditions vs. NI. User preference did not correlate well with objective outcomes, indicating factors beyond DWI and mFC affect preference. Regional analysis was consistent with a fatigue-driven worsening of foot-drop over time in the 6MWT for all conditions, indicated by an increased percentage of lowest points in Forefoot. Such analyses may be useful to clinical testing of orthotic devices to compare relative risk of trips and foot scuffs.[3] Further exploration of frontal-plane regional differences among interventions will likely enhance that utility. Limitations of in-clinic testing, the positive relationship between patient satisfaction and access to objective data for decision-making, and the need for evidence to support clinical recommendations all warrant deeper investigation into objective outcomes about how interventions influence FD. Ongoing work includes analysis of real-world data from the acclimation periods to better understand performance of FD interventions in everyday life. Further exploration of mFCΔ and mFC regions as outcome measures in people with FD is warranted.

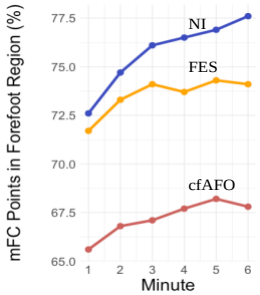

Fig 2. Of all late-swing mFC points, the % that fall in Forefoot. This increases over time in all interventions. Whole-group averages represented.

Acknowledgments: Supported by award W81XWH-19-2-0024. Views do not reflect official policy of nor implied endorsement by the DoD or US Government.

References: [1] Leone et al. (2016) *NeurorRehab & Neuro Rep,* 30(4); [2] Van Der Linden et al. (2014), *PLoS ONE* 9(8*)*; [3] Peebles et al. (2017), *J Biomech* 63(158-163).

A COMPARISON OF TWO SENSOR-BASED APPROACHES FOR CALCULATING THE REAL-WORLD WALKING SPEED OF OLDER ADULTS WITH AND WITHOUT KNEE OSTEOARTHRITIS

Spencer N. Miller[1*], Julien A. Mihy[2], Mayumi Wagatsuma[2], Jocelyn F. Hafer[2], Stephen M. Cain[1]
[1]West Virginia University, Morgantown, WV, and [2]University of Delaware, Newark, DE
[*]Corresponding author's email: sm00170@mix.wvu.edu

Introduction: Knee osteoarthritis (OA) is a degenerative joint condition that affects nearly 365 million people worldwide with symptoms that are affected by gait biomechanics [1]. Currently, gait mechanics are studied and modified in controlled lab or clinic settings while walking at constant speeds. Gait mechanics in the lab are not likely to represent gait mechanics in the real world due to the high variability of walking speed and the amount of starts and stops during walking bouts in real-world gait. Various wearable sensor-based algorithms exist for calculating walking speed in the real world, including zero-velocity update (ZUPT) [2] and inverted pendulum algorithms [3]. The ZUPT algorithm uses data from a foot-mounted inertial measurement unit (IMU) to calculate foot displacement via double integration of linear acceleration and makes no assumptions about walking mechanics. A commonly used inverted pendulum algorithm [4] uses data from a sacrum-mounted IMU to calculate the vertical displacement of the sacrum and uses the assumption that walking is represented well by the inverted pendulum model to estimate step length. While the inverted pendulum method has been shown to work well for gait data collected in a lab [3], we hypothesized that when applied to real-world gait data it would provide stride speed estimates that differ from stride speeds calculated using a ZUPT algorithm.

Methods: Using data from our IRB-approved study, we analyzed data from four participants—two with symptoms matching ACR clinical criteria for medial compartment knee OA and two healthy controls. Participants wore a total of five IMUs (APDM Opal; linear acceleration ±160m/s^2, angular velocity ±2000deg/s, sampling frequency 240Hz) for three consecutive days: one each on the sacrum, dominant or affected thigh, dominant or affected shank, right foot, and left foot of the subject. From raw IMU data, we identified walking bouts using the correlation of oscillations of the thigh and foot sensors [5]. Foot trajectories were calculated using a ZUPT algorithm [2]. Gait events were identified using a continuous wavelet transform approach. Stride length using ZUPT was defined by the linear displacement between heel strikes of the same foot, while stride time was defined as the time between heel strikes of the same foot. We followed the inverted pendulum algorithm of [4] to estimate stride speed from sacrum-IMU data. In this approach, linear acceleration measured at the sacrum was resolved into an inertial frame and gravity was subtracted. A double integral of the vertical acceleration data was taken between right and left heel strikes to obtain the change in the vertical position of the IMU during each step. The change in vertical position and the leg length of each subject were used to estimate right and left step lengths, which were then added together to obtain stride length [6]. We divided stride lengths by stride times to obtain stride speeds. Stride speeds from the two methods were compared for all strides that occurred in bout lengths of 10 minutes or longer. We calculated the limits of agreement (LOA) to quantify the agreement between the two algorithms.

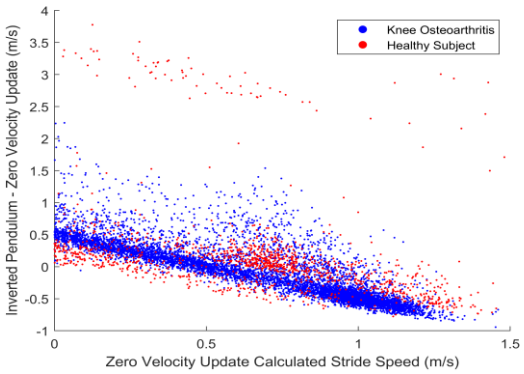

Figure 1. Difference between stride speeds calculated using ZUPT and inverted pendulum algorithms. The difference follows a linear trend with speed, suggesting that the inverted pendulum approach does not provide accurate estimates of stride speed for real-world gait.

Results & Discussion: Figure 1 illustrates the difference between the ZUPT and inverted pendulum calculated stride speeds. The difference between the stride speeds calculated via each method follows a somewhat linear trend for all participants. We found that when the ZUPT algorithm estimated slower stride speeds (< 0.6m/s), the inverted pendulum estimates were about 0.5m/s faster on average. Similarly, when stride speeds calculated by the ZUPT algorithm are faster (> 0.6m/s), the corresponding stride speeds calculated by the inverted pendulum algorithm are up to 0.5m/s slower. The 95% LOA were -0.93m/s to 0.75m/s for subjects with knee OA and -1.26m/s to 1.64m/s for healthy subjects. Our results suggest that the inverted pendulum algorithm does not provide accurate estimates of walking speed for real-world gait. Real-world gait is often not steady-state and may not be modeled well by an inverted pendulum, especially for individuals with musculoskeletal conditions or diseases with altered gait mechanics.

Significance: We found that a commonly used inverted pendulum algorithm, which assumes inverted pendulum-like gait dynamics, provides stride speed calculations that are much different from those calculated via a ZUPT algorithm, which makes no assumptions about gait dynamics. Stride speeds estimated by an inverted pendulum approach must be used and interpreted with caution.

Acknowledgments: This work was supported by a grant from the National Institute on Aging (R21AG076989) from NIH.

References: [1] Long H. et al. (2022). *Arthritis & Rheumatology*. [2] Rebula JR et al. (2013). *Gait & Posture* [3] del Din S. et al. (2016). *Journal of NeuroEngineering and Rehabilitation*. [4] Zijlstra, A., Hof AL (2003). *Gait & Posture.* (2013). *Gait & Posture*. [5] Baroudi L et al. (2022) *Gait & Posture.* [6] Zijlstra, A., & Zijlstra, W. (2013). *Gait & Posture*

INVESTIGATING KINEMATIC ASYMMETRY IN SIT/STAND TRANSITIONS WITH A POWERED KNEE-ANKLE PROSTHESIS CONTROLLER

Kellen Waters[1*], Benson Zou[2], Emily Macqueene[2], Cara Gonzalez Welker[1-2]
[1]Biomedical and [2]Mechanical Engineering, University of Colorado Boulder, Boulder, CO 80309
*kellen.waters@colorado.edu

Introduction: The lack of ability to stand up from a seated position predisposes those with lower-limb amputation to a sedentary lifestyle, where more than 61% are classified as "not sufficiently active" and 30% are classified as sedentary [1]. The average healthy adult transitions from sitting to standing over 60 times daily [2]. Asymmetry during sit/stand transitions is used as a clinical metric due to increased asymmetry being linked to higher rates of osteoarthritis [3]. These trends are commonly seen in wearers of conventional passive and semi-active prostheses due to their inability to supply net positive energy like biological joints [4].

One solution that has seen progress towards improving these clinical outcomes is the design of lower-limb powered prostheses that assist in sit/stand transitions. Welker et al. have designed a powered knee-ankle prosthesis controller that can assist sit/stand =transitions at variable seat height positions while reducing ground reaction force (GRF) asymmetry [4]. The purpose of this study is to determine how this controller affects user kinematics compared to a passive prosthesis. We hypothesize that while using the powered prosthesis, users will experience reduced kinematic asymmetry during sit/stand transitions compared to the passive device.

Methods: Experimental data was collected by Welker *et al.* from three individuals with transfemoral amputation performing sit/stand transitions with both a passive and powered prosthesis [4]. Participants wore 28 optical motion capture markers on their lower extremities captured with a VICON system. Participants were given 15 minutes of training wearing each prosthesis and then completed trials of sitting and standing 5x each at two different speed conditions (fast and slow) for three different stool heights (53.5 cm, 51.0 cm, and 48.5 cm). Each condition (height and speed) was repeated three times with a one-minute break between each trial, for a total of 15 sit/stand repetitions per condition.

To analyze kinematic differences, a custom model was scaled for each subject and prosthesis type using OpenSim [5]. Inverse kinematics was performed to observe the joint angle differences between the passive and powered devices across all subjects. As in previous work [6], the index of kinematic asymmetry was calculated by taking the difference between the normalized joint angle of the biological side and the normalized joint angle of the prosthesis side over the percent completion of the motion. The maximum kinematic asymmetry was calculated for each sit/stand repetition from the index of kinematic asymmetry.

Using the maximum asymmetry found for each sit/stand repetition as an individual datapoint, we fit a linear mixed-effects model to determine the effect of prosthesis type, chair height, and subject on maximum kinematic asymmetry for both the slow and fast conditions at the hip and the knee. Significance values were corrected for multiple comparisons using the Holm-Bonferroni method.

Results & Discussion: While wearing the passive prosthesis during stand-to-sit, participants consistently had greater knee and hip extension on the prosthetic side compared to the biological side. When wearing the powered prosthesis during stand-to-sit movements, participants saw significant reductions in maximum kinematic asymmetry ($p < 0.05$), with the overall changes varying between 10.1% and 56.4% across conditions (Figure 1). This reduction in kinematic asymmetry is consistent with the reduction in GRF asymmetry found in Welker *et al.*, wearing the same controller [4].

The same results were not found in sit-to-stand trials, with no significant differences based on prosthesis type and overall changes in kinematic asymmetry from -5.8% to 17.0% across conditions. Similarly, previous work found increased kinematic asymmetry with increasing magnitude of knee torque provided by powered prostheses during sit-to-stand [6]. No significant effects were found based on chair height.

Significance: Previously, Welker *et al.* demonstrated reduced GRF asymmetry in individuals with above-knee amputation using their novel sit/stand powered prosthesis controller [4]. We have found reductions in kinematic asymmetry in stand-to-sit across chair heights and speeds with the same controller. This further motivates that this controller could benefit populations with lower-limb amputation by reducing secondary conditions like osteoarthritis that are correlated with lower-limb asymmetries.

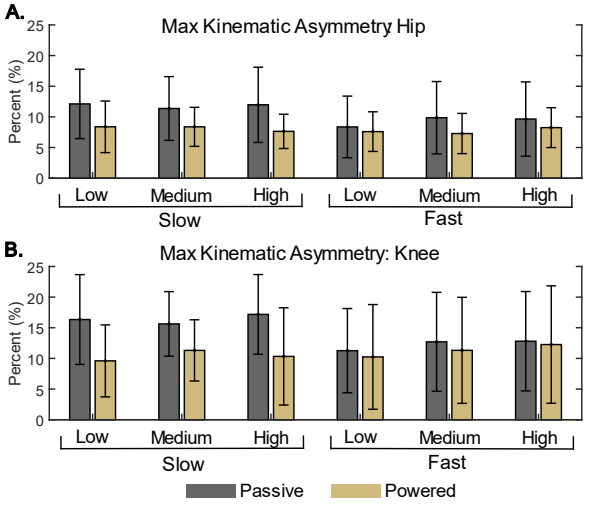

Figure 1. Maximum kinematic asymmetries for both the powered and passive prosthesis are shown for the hip (A) and knee (B) for varying chair heights and speeds during stand-to-sit transitions. Error bars indicate standard deviation across all trials within a condition. The average of the maximum kinematic asymmetry was reduced with the powered prosthesis compared to participants' passive prosthesis for all stand-to-sit conditions.

Acknowledgments: The authors thank the University of Michigan Locomotor Systems Lab for their assistance in data collection.

References : [1] Langford J *et al.* Disabil Rehabil. 2017. **[2]** Dall P. M. and Kerr A, Appl. Ergon. 2010. **[3]** Gailey R *et al.* J Rehabil Res Dev. 2008 **[4]** Welker CG *et al.* IEEE Trans Neural Syst Rehabil Eng. 2023 **[5]** Seth A, Hicks JL, Uchida TK, Habib A, Dembia CL, *et al.* PLOS Comput Biol. 2018 **[6]** Hunt *et al.* Trans Neural Syst Rehabil Eng. 2023.

Medial and lateral knee joint contact forces during load carriage and vGRF feedback

Blake W. Jones[1], John D. Willson[2], Paul DeVita[3], Ryan D. Wedge[2]
[1]Wake Forest University School of Medicine, [2]Department of Physical Therapy, East Carolina University,
[3]Department of Kinesiology, East Carolina University
*Corresponding author's email: blwjones@wakehealth.edu

Introduction: Prolonged load carriage has been associated with lower extremity injuries possibly due to elevated peak vertical ground reaction forces (vGRF) [1-5]. vGRF increase proportionately to the magnitude of carried load [1], while peak total, medial (mTFJ), and lateral tibiofemoral joint contact (lTFJ) forces and impulses increase disproportionately with load carriage [6,7]. A previous study using vGRF biofeedback reported that participants could raise their impact peak vGRF when cued with a visual increase in vGRF but decreased vGRF targets did not reduce vGRF impact peak during gait [8]. However, decreased targets did decrease internal knee abduction moment (KAM) and vGRF during early and midstance [8]. It remains unknown if visual vGRF biofeedback during load carriage can reduce peak vGRF and decrease mTFJ and lTFJ contact forces impulses.

The first aim of this study was to investigate if individuals can decrease peak vGRF when given real-time vGRF biofeedback while carrying vest-borne loads. The second aim of this study was to examine if gait adaptations induced by the peak vGRF biofeedback decrease mTFJ or lTFJ contact force impulse. We hypothesized that vGRF would be decreased with biofeedback during the loading conditions and that mTFJ and lTFJ impulse would decrease.

Methods: Twenty-four young adults (Age 18-30, BMI 18-25 $kg \cdot m^{-2}$) participated in the study. An unloaded weighted vest was fitted to the participant, followed by the marker placement on bony landmarks and vest. Marker data (200 Hz) and force data (2000 Hz) were sampled on an instrumented split belt treadmill as participants walked at 1.4 $m \cdot s^{-1}$ for 10 minutes in 3 loading conditions (0%, 15%, and 30% body mass). In each condition, participants walked without feedback for the first 5 minutes and then with peak vGRF biofeedback for the second 5 minutes. vGRF biofeedback was displayed on a monitor in front of the participant with a target determined from 10 strides during the no feedback phase. Participants were instructed to lower vGRF peaks as low as able by exploring different walking patterns. Once the participant had a consistent pattern that lowered peak vGRF based on the tester's visual observation, 10 seconds of motion capture data were collected. Five right stance phases were analyzed with an inverse-dynamics kinematics informed TFJ model that parsed forces to the medial and lateral compartments [9-11]. The dependent variables were peak vGRF and vGRF impulse along with mTFJ and lTFJ contact force impulses. Comparisons between load and feedback conditions were made using 3x2 repeated measures ANOVAs with post-hoc paired T-tests (Feedback v. No Feedback) and one-way repeated measures ANOVAs (Load) (α=0.05).

Results & Discussion: There were no significant interactions for peak vGRF or vGRF impulse, but both variables increased with load ($p<.001$) (Table 1). There was no significant difference in peak vGRF between the feedback and no feedback conditions. Surprisingly, the feedback condition induced a decrease in vGRF impulse ($p<.001$) compared with the no feedback load counterparts.

There was an interaction for lTFJ impulse ($p=.027$). Probing the conditions revealed that lTFJ impulse during feedback significantly greater than no feedback at each level of load ($p=.006$, $p<.001$, $p<.001$) and that load significantly increased lTFJ impulse in both feedback and no feedback conditions ($p<.001$, $p<.001$). The 0% load, 15% load, and 30% load feedback conditions induced a 21%, 31% and 35% increase in lTFJ respectively, which was contrary to the hypothesis. mTFJ impulse did not demonstrate and interaction and there was no significant difference between the feedback and no feedback conditions contrary to our hypothesis. However, mTFJ impulse did increase with load as expected ($p<.001$) [6,7].

Despite feedback decreasing vGRF impulse, lTFJ contact force increased, potentially due to crouched gait characteristics participants adopted in attempt reduce peak vGRF. Crouching requires greater quadriceps recruitment which increases TFJ contact forces. The lack of difference in mTFJ may be due to decreased knee adduction moment, consistent with previous results [8]. The participants received feedback about right and left limb vGRF peaks, but this analysis was only of the right limb, possibly explaining why there was not a difference in peak vGRF between conditions with this analysis.

Table 1. Mean for No Feedback vs Feedback Across Load

Variable		0%	15%	30%
Peak vGRF (BW)	NF	1.24	1.43	1.60
	F	1.29	1.44	1.61
vGRF Impulse (BW·s)	NF	0.55	0.62	0.69
	F	0.51	0.57	0.63
mTFJ Impulse (BW·s)	NF	0.86	0.98	1.11
	F	0.91	1.08	1.25
lTFJ Impulse (BW·s)	NF	0.43	0.50	0.60
	F	0.53	0.68	0.86

Means for first peak and impulse of vGRF, and impulses of medial and lateral TFJ contact forces; 0% load, 15% load, and 30% load; BW: Body Weights; s: seconds; NF = no feedback; F = feedback

Significance: These data demonstrate that peak vGRF feedback may decrease vGRF impulse but may not decrease peak vGRF or medial and lateral TFJ contact force impulses during load carriage. Using direct TFJ contact force or KAM feedback may be more effective in decreasing TFJ contact forces.

Acknowledgments: Graduate research assistants, Alex Clark and Brian McGill, for assistance with this project.

References: [1]Birrell SA et al. *Gait Posture*. 2007; [2]D. Fox B et al. *J Orthop Orthop Surg*. 2020; [3]Knapik JJ et al. *Mil Med*. 2004; [4]Molloy JM et al. *Mil Med*. 2020; [5]Schuh-Renner A et a. *J Sci Med Sport*. 2017; [6]Jones BW et al. *J Appl Biomech*. 2023; [7]Willy RW et al. *Mil Med*. 2019; [8]Evans-Pickett A et al. *Clin Biomech*. 2020; [9]Willy RW et al. *J Sports Sci*. 2016; [10]DeVita P & Hortobágyi T. *J Appl Biomech*. 2001; [11]Messier S et al. *Osteoarthritis Cartilage*. 2011;

OLDER ADULTS AND INDIVIDUALS WITH PARKINSON'S DISEASE CONTROL POSTURE ALONG SUBORTHOGONAL DIRECTIONS THAT DEVIATE FROM THE TRADITIONAL ANTEROPOSTERIOR AND MEDIOLATERAL DIRECTIONS

Madhur Mangalam[1], Damian G. Kelty-Stephen[2], & Nick Stergiou[1,3]
[1]Department of Biomechanics, University of Nebraska at Omaha, Omaha, NE 68182, USA
[2]Department of Psychology, State University of New York at New Paltz, New Paltz, NY 12561, USA
[3]Department of Department of Physical Education, & Sport Science, Aristotle University, Thessaloniki 570 01, Greece
email: mmangalam@unomaha.edu

Introduction. Individuals with Parkinson's disease commonly face posture-related challenges, particularly in orientation and stabilization against external forces, leading to postural instability and an increased risk of falls. In this study, the optimal movement variability hypothesis served as the theoretical foundation, proposing that a healthy postural control system exhibit organized yet complex temporal structures in sway variability. It is also proposed that aging and neurological diseases compromise this system, leading to stiff and predictable postural sway. Hence, individuals with Parkinson's disease might demonstrate highly predictable temporal structure of postural sway due to the loss of long-range correlations, indicating reduced flexibility. The present study employed oriented fractal scaling component analysis (OFSCA) to explore this hypothesis by examining the directional characteristics of postural sway beyond traditional anteroposterior (AP) and mediolateral (ML) axes.

Methods. We employed the OFSCA [1] to assess angle-dependent scaling properties within postural center of posture (CoP) trajectories. In the context of 2D planar postural CoP trajectories, our traditional model of postural control along the anatomical AP and ML axes assumes two distinct sample paths of fractional Brownian motion (fBm) and fractional Gaussian noise (fGn). We posit perpetual orthogonality between these components, with their scaling characteristics remaining steadfast. It's essential to note that this assumption of isotropy may be less common, as planar postural sway trajectories may not consistently demonstrate isotropic behavior. In essence, fluctuations exhibit a spatial distribution of temporal correlations, with the directions showcasing the most robust correlations influencing posture control directions, with the angle between the two indicated by $\Delta\theta$.

Results & Discussion. Examining group-level effects (Fig. 1, the eyes closed condition led to a reduction in $\Delta\theta$ by 3.762±1.650º (t = –2.280, p = 0.023), while the unstable postural condition resulted in a reduction by 6.449± 1.698º (t = –3.779, p = 1.512×10^{-4}). In comparison to healthy young adults, older adults exhibited a decrease in $\Delta\theta$ by 6.308±3.025º (t = –2.085, p = 0.038), and individuals with Parkinson's disease demonstrated a threefold greater reduction in $\Delta\theta$ than older adults, specifically by 20.776±2.756º (t = –7.537, p = 1.180×10^{-12}). This threefold excess of $\Delta\theta$ in the Parkinson's disease group, beyond what was observed in the healthy older adult group, indicates altered and suborthogonal axes of postural control in Parkinson's disease that surpass the effects of healthy aging. It's noteworthy that the increase in $\Delta\theta$ in Parkinson's patients is almost five standard errors greater than in healthy older adults. Importantly, levodopa medication did not contribute to restoring healthy postural control in individuals with Parkinson's disease, as they exhibited comparable distortion in postural control compared to healthy young adults: 18.652±2.773º (t = –6.727, p = 1.390×10^{-10}). The increase in long-range correlations in sway along the two axes of postural control was associated with an increase and reduction in $\Delta\theta$, respectively (t = 2.702, p =0.007; t = –3.997, p =6.780×10^{-5}).

We found that healthy young adults control posture along traditional anatomical axes, while older adults and those with Parkinson's disease exhibit deviations from these axes. Additionally, changes in the temporal structure of postural sway variability predict alterations in directional characteristics, suggesting a close link between Parkinsonism and the temporal structure of sway variability that is important for postural control beyond age-related effects.

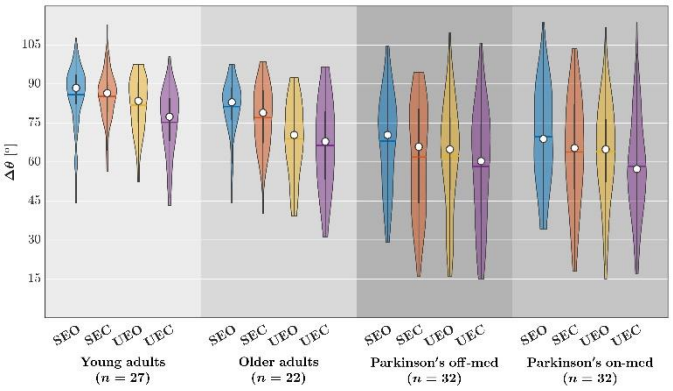

Figure 1: The relative orientation of the two axes of postural control, $\Delta\theta = \theta_1 \sim \theta_2$. Horizontal bars indicate group *mean*, and white circles indicate group *median*. SEC: Stable, eyes closed; UEO: Unstable, eyes open; UEC: Unstable, eyes closed.

Significance. This research holds crucial significance as it unveils the intricate temporal dynamics of postural control in individuals with Parkinson's disease. The innovative use of oriented fractal scaling component analysis not only offers a novel method for dissecting postural sway but also reveals a distinctive pattern in older adults and those with Parkinson's disease, emphasizing the broader implications of altered temporal structure beyond the effects of natural aging. These findings pave the way for a deeper comprehension of Parkinsonism-related postural deficits and potentially open avenues for targeted interventions.

Acknowledgments. This work was supported by the NIH award P20GM10909.

References. [1] Seleznov et al. (2020), *Scientific Data* 10, 21892.

REDUCING KNEE LOADING WITH AN EXOSKELETON FOR PEOPLE WITH KNEE OSTEOARTHRITIS

Dominic Locurto[1*], Patrick Slade[1]
[1]School of Engineering and Applied Sciences, Harvard University, Boston, MA
*Corresponding author's email: dlocurto@fas.harvard.edu

Introduction: 14 million US adults have knee osteoarthritis and suffer from knee pain due to knee loading during walking [1]. Knee osteoarthritis is defined as the wear of cartilage in the knee joint, exposing the ends of the femur and tibia to bone-on-bone contact. Patients with knee osteoarthritis experience knee pain that is well correlated to compressive knee loading [2]. Knee osteoarthritis worsens over time, causing functional decline as patients get older.

There is an unmet clinical need for knee osteoarthritis treatment because existing solutions do not adequately reduce knee loading to provide long-term pain relief. Knee replacement surgery is the only effective long-term solution but is invasive, expensive, and has a long recovery time. There is a 12-year treatment gap between diagnosis and surgery, meaning that patients must endure knee pain and functional decline during that period [3]. One solution for pain reduction is steroid injections, but the relief is only temporary and requires repeated visits. Offloading knee braces shift loading in the knee but provide limited reductions in knee load [4]. Powered exoskeletons aim to reduce knee loading by augmenting movement but only provide moderate reductions [5]. There remains a gap in developing more effective exoskeletons to reduce knee joint loading.

Methods: We propose an exoskeleton that dramatically reduces knee loading compared to existing solutions by using a design that is unique in reducing both muscle and intersegmental forces at the knee. Musculoskeletal simulations found the most effective method of assisting knee loading during stance is by assisting the force along a vector between the foot and the hip. Both the muscle and intersegmental forces are compressive forces at the knee, so providing a percentage of the opposite force may be more effective than assisting joint torques. We designed an exoskeleton that provides a lifting force to the person through a strap on their upper thigh with an equal and opposite force applied to the ground through their shoe (Fig. 1A) in the direction of the leg. This exoskeleton uses offboard motors to explore many potential assistance conditions without the constraints of a portable device. A Bowdoin cable transmits power from the motors to the linear actuation mechanism attached to the thigh strap (Fig. 1B).

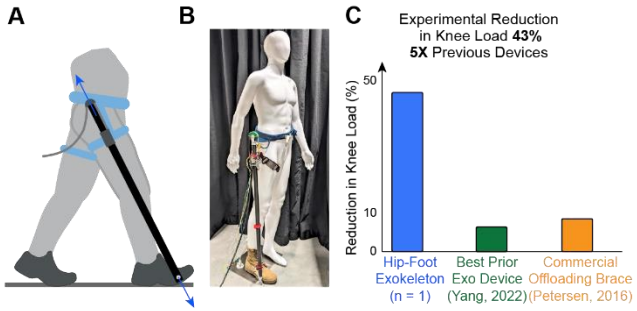

Figure 1: **A**, The exoskeleton applies a force to the upper thigh and an equal and opposite force at the bottom of the foot. **B**, The exoskeleton applies this force using Bowdoin cables attached to offboard motors. **C**, The exoskeleton provided 43% reduction in knee loading for a pilot subject.

We are performing experiments with healthy subjects to validate this device's effectiveness and systematically determine the optimal assistance level. For each subject, we collect kinematic data using a motion capture system (Vicon Motion Systems), electromyography of relevant muscles around the knee (Delsys Inc.), and ground reaction force measurements on an instrumented treadmill (Bertec Corporation). The experimental conditions include a no exoskeleton condition and 3 assistance conditions providing the user with 15%, 25%, and 35% of their normal ground reaction force. To process the data and estimate knee loading we use the inverse kinematics, inverse dynamics, and static optimization tools provided in the OpenSim API.

Results & Discussion: Our exoskeleton dramatically reduced knee loading during pilot experiments. The pilot subject reduced knee loading by 43% when provided with an assistive force of 35% of their normal ground reaction force. This is nearly five times the reduction found by existing devices. Both muscle forces and intersegmental forces decreased during the stance phase, which likely contributed to the large knee loading reduction. Knee loading decreased proportionally to the level of assistance. We would like to find the relationship between knee loading and perceived pain level after more data is gathered. A long-term goal is to find how assisting both components of the total knee joint loading force affects cartilage health.

The knee loading reduction provided by our design has the potential to solve problems in current exoskeleton and knee osteoarthritis research**.** This device could impact tens of millions of people with knee osteoarthritis. This drastic reduction in knee loading may help address the 12-year treatment gap between diagnosis and surgery and potentially eliminate some of the knee pain people experience. The trend between assistance level and knee contact force shows that there is a potential to further reduce knee loading. This requires more testing in the lab with a larger population to better understand this relationship. We can expand upon this research by reducing knee loading over longer amounts of time with a portable version of this device. At-home patient tests allow us to understand more about how well these devices work out in the real world.

Significance: The significant reduction in knee joint loading proves that this linear force assistance performs better than that of devices that target joint torque assistance. Further experimentation will allow us to find relationships between knee joint loading, cartilage health, and perceived pain level over longer time scales than in-lab tests allow.

References: [1] Deshpande et al. (2016), *Arthritis care* 68(12); [2] Felson (2004), *J Rheumatol Supp* 70; [3] Desmeules et al. (2009) *DMC Musculoskeletal Disorders* 10; [4] Petersen et al. (2016) *Arch Orthop Trauma Surg* 136; [5] Yang et al. (2022) *IEEE RA-L* 7(3)

Adaptive split-belt treadmill to encourage single-limb propulsion: a preliminary validation study

Rucha Kulkarni[1*], Jill Higginson[1,2]
[1]Dept. of Biomedical Engineering, University of Delaware
[2]Dept. of Mechanical Engineering, University of Delaware
*Corresponding author's email: rnk@udel.edu

Introduction: Propulsive (push-off) forces are an important aspect of walking. Neurological conditions like stroke can lead to lower propulsion, and thus lower walking speeds and higher gait asymmetries [1]. Treadmills can be used to train walking speed and gait symmetry. However, typical treadmill training uses fixed speeds, preventing instantaneous changes to gait. Adaptive treadmills that modify speed based on propulsive impulse and step length have been shown to improve walking speed, propulsion, etc. [2]. We developed a user-driven split-belt treadmill that can be preferentially weighted to encourage increased propulsive forces on one or both sides to maintain a comfortable walking speed. The purpose of this study was to validate the modified split-belt treadmill against an existing tied-belt user-driven treadmill by Pariser et al. [2] and determine the effect of changing the propulsive feedback gain of one belt on propulsion and walking speed in healthy young adults. We hypothesized that propulsion and walking speed for the split-belt without preferential weighting between belts would be equivalent to the tied-belt treadmill. We further hypothesized that there would be differences in propulsion between limbs when propulsion was preferentially weighted for one belt on the split-belt user-driven treadmill.

Methods: For this preliminary study, a single neurologically healthy, young participant performed a series of trials on the split and tied adaptive treadmills. The tied adaptive treadmill changes the speed of both belts based on propulsive impulse, step length, and the participant's position on the treadmill. The split adaptive treadmill is modified such that the speed of each belt changes based on the ipsilateral propulsive impulse with the participant's position on the treadmill as a safety factor. The speed of each belt is defined by: $v_{i+1} = v_i + \gamma(v_{PI}) - \gamma(v_i) \pm \beta\left(COM_{pos}{}^2\right)$ where $\gamma = 1 - e^{-\frac{dt}{\tau_\gamma}}, \beta = 0.5, \tau_\gamma = 150$, dt is stride time, v_i is current velocity, v_{PI} is velocity due to propulsion, and COM_{pos} is the position on the treadmill. The participant performed 5 trials of 1.5 minutes each with different modes of the adaptive treadmill: Tied Normal ($\tau_{\gamma,tied} = 1.5$), Tied Hard ($\gamma_{hard} = 1.5\gamma_{tied}$), Split Normal ($\gamma_{R,L} = \gamma$), Split Hard ($\gamma_{R,L,hard} = 10\gamma$), Split Preferential ($\gamma_R = 10\gamma_L = 10\gamma$). To ensure that the belt speeds did not diverge for healthy levels (5%) of anterior ground reaction force (AGRF) asymmetry for the Split Original and Hard trials, an extra term $-sign\left(AGRF_{Asymm}\right) * 0.05 * \gamma\left(v_{PI,Avg}\right)$ was added to the velocity calculation [3,4]. Each trial started with the velocity of both belts at 1 m/s. The participant was encouraged to walk at their preferred walking speed. For each condition, practice trials of 2 min each were performed. The outcome measures were propulsive impulse and walking speed.

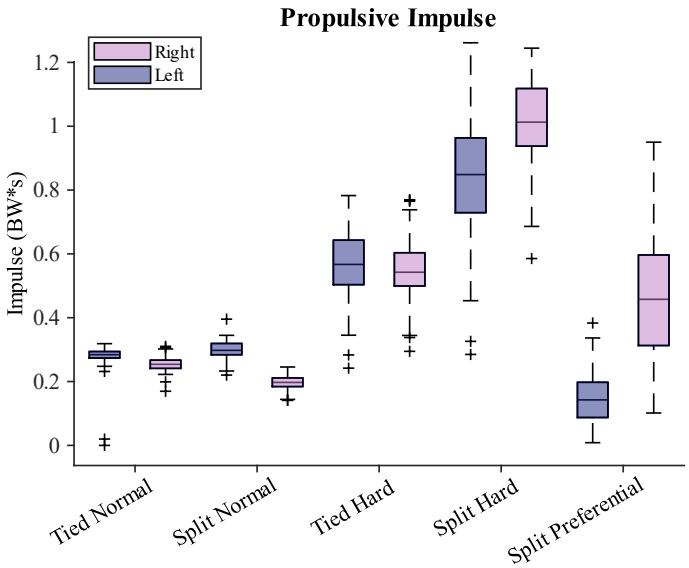

Fig 1. Propulsive impulse for all conditions. Each pair of box plots contains the propulsive impulse from the right and left leg.

Results & Discussion: Propulsive impulse and walking speed were compared between all trials (Fig 1). There were no differences in walking speed or propulsive impulse in the Tied and Split Normal trials. Propulsive impulse was higher in both Hard trials than both Normal trials. Propulsive impulse was higher in the Split Hard than the Tied Hard trials. However, walking speed in the Tied Hard trial was slightly higher than the Split Hard trial. The ratio of γ_{normal} to γ_{hard} was higher for the Split treadmill, thus higher propulsion would be required to increase the speed compared to Tied Hard. For the Preferential trial, the speed and propulsive impulse of the right belt was higher than the left belt. The findings partially support our hypotheses – the Tied and Split adaptive treadmills are equivalent in the Normal trials, and the Split treadmill can be modified to encourage higher propulsion on one side. This suggests that a split-belt adaptive treadmill that uses only propulsive impulse as an input can be used to modulate and control walking speed on both belts by the user. Future work would involve changing the ratio of γ_{normal} to γ_{hard} to ensure propulsion is equivalent in the Tied and Split treadmills, as well as the preferential weighting of γ between belts to observe the effects on neurologically healthy and post-stroke participants.

Significance: Stroke is a highly prevalent cause of disability, and can lead to impaired walking and lower community ambulation. Specifically, the paretic (affected) leg generates lower propulsive forces at push-off, leading to lower walking speed and higher gait asymmetries. An adaptive treadmill with preferential weighting on the paretic side could encourage higher paretic propulsion and reduce gait asymmetries. This could improve therapeutic and rehabilitation techniques for gait training interventions by providing more specific training targets.

References: [1] Awad et. al.(2020), *J NeuroEngineering Rehabil* 17(139); [2] Pariser et. al.(2022), *J Biomech* 133(110971); [3] Herzog et. al (1989), *Med Sci Sports Exec* 21(1); [4] Lauzière et al. (2014), *Int J Phys Med Rehabil* 2(3)

AUTOMATIC STEP TIME DETECTION IN OLDER AUDLTS DURING PERTURBED WALKING

Shuaijie Wang[1], Omar, Kazi Shahrukh[2], Fabio Miranda[2], Tanvi Bhatt[1*]
[1]Department of Physical Therapy, University of Illinois Chicago
[2]Department of Computer Science, University of Illinois Chicago
*Corresponding author's email: tbhatt6@uic.edu

Introduction: Gait event detection is crucial for gait analysis of regular and perturbated walking to assess various gait characteristics necessary for evaluating gait disorders and the effectiveness of interventions. This process, especially for perturbed walking, is time-consuming, highlighting the need for automatic detection methods. The standard method involves using force plates to identify foot touchdowns and liftoffs based on ground reaction forces (GRF). However, issues like incomplete data from older adults and the lack of force plates in many clinics have led to the development of kinematic-based gait event detection algorithms using motion capture systems or wearable sensors.

Studies have demonstrated high accuracy of automatic gait events detection algorithms based on marker position or marker velocity for regular walking in healthy adults, and a few studies also developed automatic algorithms to detect gait events in pathological gait patterns, with absolute errors under 30ms [1]. However, to our acknowledge, no such algorithms exist for gait events detection in a walking following slip or trip perturbation, which is critical to assess balance control and fall risk. One reason for this is the inherent challenge in gait event detection during perturbed walking, slip perturbation could result in various recovery strategies, including recovery steps with toe-contact first, recovery steps with heel-contact first, and aborted steps without clear toe liftoff. Similarly, the trip perturbation could result in lowering, elevating, and crossing strategies [2]. This variability complicates accurate gait event detection. Our study introduces three deep learning algorithms for detecting gait events in older adults during perturbed walking, using ground reaction forces, marker data, and angular data. Lastly, we compare the accuracy of gait detection among the three algorithms.

Methods: 307 healthy old participants (70 ± 6.3 years; 58% female) from our NIH project (R01-AG050672) were included in this study, all participants experienced at least 10 regular walking, 1 slip, and 1 trip perturbation trials on a 7-meter walkway. The first 2 slips (if available), first 2 trips, and 3 random regular walking trials were selected. The dataset consists of 927 regular walking, 399 trip, and 529 slip trials. Slip and trip perturbations were induced using a movable slider and a fixed obstacle, respectively. Kinematic data were captured using a motion capture system and synchronized with force plate data. The study utilized GRF, marker trajectories (heel, toe, knee, hip for both limbs), and segment angles (foot, shank, thigh for both limbs) as inputs, with touchdown (TD) and liftoff (LO) events manually identified as outputs.

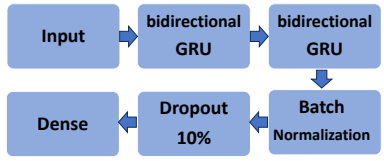

Figure 1: multi-layer neural network architecture

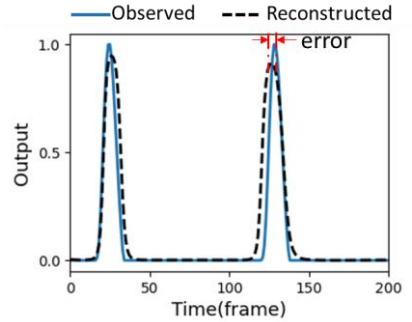

Figure 2: a sample of observed 1D time series output and reconstructed output, each peak represents an TD event.

To mapping the multivariate time series input data to the 1-dimentional (1D) time series output data, we constructed and trained deep learning models containing bidirectional GRU (Fig. 1), as they are efficient for sequential modelling [3]. To map the multivariate time series input data to the 1D time series output data, we pre-processed the input data using 4th order low-pass filters, applied an impulse-response function (HRF) to the 1D output data, and split our dataset into training (64%), validation (16%), and test (20%) sets for model training and evaluation. Lastly, we employed a peak detection algorithm (find_peaks) to identify gait events from the output, and the errors between detected outputs and observed outputs were calculated and compared across different models.

Results & Discussion: All models detected TD and LO events with a mean error of <30ms and accurately detected over 88% of TD and over 93% of LO events with errors <50ms. One-way ANOVA showed significant differences in TD detection errors (F=6.83, p=0.001), with marker data-based models showing the highest error, but no significant differences for LO detection. The angle-based model had the best overall detection rates, 91.2% for TD and 96.6% for LO.

Despite the GRF-based method being the standard, its model performed worse in detection rates for both TD and LO due to cross-landing issues. All models had a large standard deviation in errors (>48ms) mainly because of extra peaks detected in the estimated 1D output data, causing errors ranging from 200 to 600ms. Excluding these, mean errors were about 10ms with a standard deviation of about 20ms for kinematic-based models.

Model	Mean error(ms)	SD of error(ms)	% of error <50ms	% of error <30ms
GRF-TD	23.6	83.01	88.2%	82.6%
Angle-TD	22.06	50.95	91.2%	81.7%
Marker-TD	29.16	106.05	90.9%	83.0%
GRF-LO	20.59	96.27	93.3%	87.9%
Angle-LO	16.76	84.52	96.6%	93.2%
Marker-LO	14.54	48.88	96.8%	92.9%

Table 1: the accuracy of models for TD and LO detection

Significance: Our study pioneers the use of deep learning for automatic gait event detection in perturbed walking, which is essential for studying balance control and fall prevention strategies. Angle-based models, particularly when combined with wearable sensors, hold promise for real-time gait monitoring in everyday settings.

References: [1] Bruening, D. A., & Ridge, S. T. (2014), *Gait & posture*, 39(1), 472-477; [2] Wang, Y. et al. (2020), Aging clinical and experimental research, 32, 893-905. [3] Singh, B. et al. (2021). CENTCON (Vol. 1, pp. 27-32). IEEE

FIREFIGHTER HELMET INERTIAL PROPERTIES AND CERVICAL SPINE: AN OPENSIM-BASED BIOMECHANICAL STUDY

Gustavo M. Paulon[1], S. Sudeesh[1], Suman K. Chowdhury[1*]
[1]Department of Industrial, Manufacturing and Systems Engineering, Texas Tech University, Lubbock, Texas, USA
*Corresponding author's email: suman.chowdhury@ttu.edu

Introduction: Neck pain is the fourth most prevalent musculoskeletal health issue in the world, affecting 222.7 million people world-wide [1]. In the occupational settings, the prevalence of neck pain is mainly found in occupations that require wearing a heavyweight helmet for prolonged duration. Firefighting is such an occupation, where firefighters are required to wear heavyweight helmet in awkward head-neck positions for prolonged duration. A previous study on U.S. and Chinese firefighters reported that the majority of the firefighters view their helmets as an undesirable ill-fitting personal protection equipment [2]. This was mainly due to the heavyweight (with the addition of accessories, such as face shield, lighting, and other accessories) and imbalanced center of mass (COM) of the helmet that can lead to increased compressive forces at individual cervical spinal joints. However, our systematic literature review showed that the influence of heavyweight, imbalanced firefighter helmets on individual cervical intervertebral joint reaction forces (JRFs) have remained hitherto unknown. Therefore, the objective of this study was to investigate the influence of the inertial properties of two different firefighter helmet designs—traditional US-style helmet and European-style helmet—on the cervical JRFs.

Methods: We recruited a total of 36 firefighters to perform various full-range of head-neck static and dynamic exertions (IRB # 2020-708). Briefly, firefighters performed a self-paced, controlled full flexion-extension (FE) and lateral bending (LB) dynamic head movements. All participants performed each task in three different helmet conditions: no helmet (baseline condition), US-style helmet (Bullard UM6WH), European-style helmet (Cairns XF1) in a random order. Motion capture (10-camera *Krestel* 1300 motion capture system; Motion Analysis Corporation, Rohnert Park, California, USA) and ground reaction force data (*Bertec* force plates; Bertec, Columbus, Ohio, USA) were collected during the tasks. The data were processed using *Cortex-9* software (Motion Analysis Corporation) and then used as input in OpenSim musculoskeletal platform [5] to create anthropometric-specific models by scaling the MASI model [6] and to calculate JRFs with the Static Optimization and Joint Reaction Analysis tools. In this preliminary study, we analysed data collected from a total of five male (weight: 93.3 kg ± 19.2 kg; height: 179 cm ± 36.8 cm; BMI: 29.1 kg/m^2 ± 6.37 kg/m^2) and five female (weight: 71.1 kg ± 9.58 kg; height: 169 cm ± 57.8 cm; BMI: 24.7 kg/m^2 ± 3.14 kg/m^2) firefighters. We employed a randomized complete block design (RCBD) test to understand the effects of various helmet inertial properties. The RCBD test was performed with 95% confidence level ($\alpha = 0.05$) and by considering compressive forces of eight cervical joints (C0-C1, C1-C2, C2-C3, C3-C4, C4-C5, C5-C6, C6-C7, and C7-T1) as dependent, *helmet type* and *sex* as independent, and *subject* as randomized block variables.

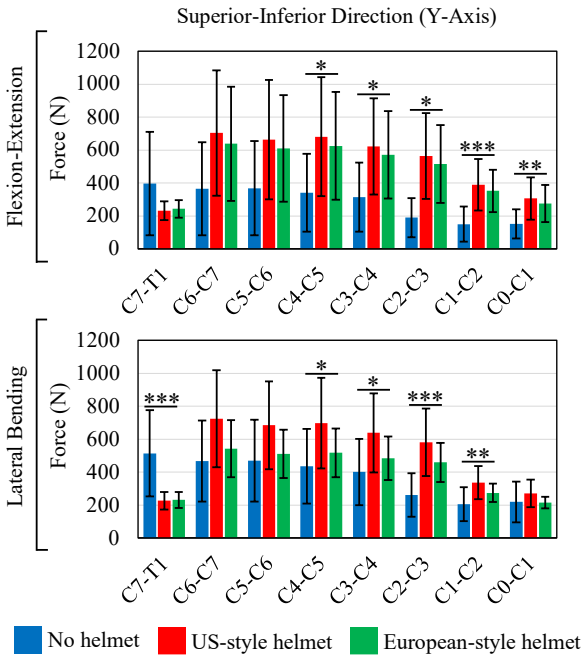

Fig. 01: Compressive reaction forces at each cervical intervertebral joint during flexion-extension and lateral bending dynamic tasks for each helmet condition (*: p<0.05; **: p<0.01; ***: p< 0.001).

Results & Discussion: Helmet usage was a significant factor for C4-C0 JRFs and for C5-C1 JRFs for FE and LB tasks, respectively (**Fig. 01**). Helmet usage presented an increase in the compressive force at the cervical joints when compared to the baseline no-helmet condition (US-style helmet: 196% (FE) and 122% (LB) at C2-C3; European-style helmet: 171% (FE) and 75% (LB) at C2-C3), except for C7-T1 JRF. Furthermore, this study revealed that the biological difference between males and females is a significant factor (FE: p<0.0433) in the neck compressive forces with females having comparatively lower JRFs than males. Overall, the usage of the US-style helmet resulted in a higher compressive force, despite being lighter than the European-style helmet (12.4%; 250 g). The US-style helmet has a more superior COM than the European-style helmet (38.2%; 5.8 cm), which increased the effective moment of inertia of the head by 10% with respect to C0-C1. Additionally, the more superior COM resulted in a higher moment arm for the gravitational loads to the neck, leading to a higher force when compared to the European-style helmet.

Significance: Our study revealed that current firefighter helmet designs adversely affect the neck reaction forces that could potentially lead to neck pain and injury. These findings can help practitioners and researchers to develop ergonomically realistic helmet design by locating the COM closer to the C0-C1 joint, i.e., by designing a low-profile helmet that would cause less neck pain in the long run.

Acknowledgments: We acknowledge the Department of Homeland Security (70RSAT21CB0000023) to support this study.

References: [1] Global Burden of Disease Study Results (2019); [2] Wang et al. (2021), International Journal of Occupational Safety and ergonomics 27(3); [3] Campbell et al. (2022), National Fire Protection Association; [4] Mathys and Fergunson (2012), Journal of Biomechanics 45(14); [5] Delp et al. (2007), IEEE transactions on biomedical engineering 54(11); [6] Cazzola et al. (2017), PloS one 12(1); [7] Vasavada et al. (2008), Journal of Biomechanics 41(1)

EFFECT OF THROWING APPROACH ON SHOULDER AND ELBOW KINETICS

Diego Ferreira and Jeff Barfield*
Lander University, Greenwood, SC
*Corresponding author's email: jbarfield@lander.edu

Introduction

Baseball pitchers have a high injury occurrence given the forceful and repetitive movements performed throughout the season [1,2]. With the increasing prevalence of an injury to the elbow [2] or shoulder [1,2] among baseball pitchers that has been reported across the years, every aspect of the rehabilitation protocol should be specified to best serve the injured athlete's specific demands. The throwing motion has long been considered a sequential action that demands proximal stability for distal mobility, ensuring optimum energy flow throughout the entire kinetic chain. [3,4] However, the approach to the throwing motion has seldom been examined past the standard crow-hop.

Therefore, the purpose of this study aimed to investigate the effects of throwing approach on elbow varus and shoulder internal rotation among collegiate baseball players. We hypothesized that a difference of elbow varus torque and shoulder internal rotation torque would be found between throwing approaches, with the step-behind throwing approach being the most favourable.

Methods

Seven participants (20.41±1.89 years; 1.86±0.02 m; 88.72±7.64 kg) performed three trials each of three different throwing approaches: step behind approach (Figure 1a), step together approach (Figure 1b), and step in-front approach (Figure 1c) on a level surface in a randomized order. Kinematic data were collected at 240 Hz using an electromagnetic tracking system. Maximum elbow varus torque and shoulder internal rotation torque occurring during the throwing motion were calculated using inverse dynamics in the MotionMonitor software (Innovative Sports Training). Only the second trial of each approach was analysed to account for the Hawthorne effect. A series of 1-way (3 throwing approaches) ANOVA with repeated measures were conducted with a significance level set at $\alpha = 0.05$.

Figure 1a. Step behind approach foot work.

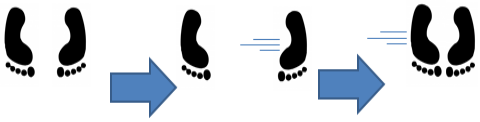

Figure 1b. Step together approach foot work.

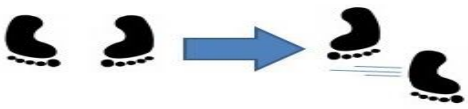

Figure 1c. Step in-front approach foot work.

Results & Discussion:

Our results indicate that the throwing approach does not elicit a statistically significant difference in elbow varus torque ($F(2) = 0.40$, $p = 0.678$) or shoulder internal rotation torque ($F(2) = 0.35$, $p = 0.713$). Means and standard deviation of elbow varus torque and shoulder internal rotation torque are found in Figure 2 and 3. This preliminary study indicates that the footwork taken in the throwing approach does not influence the kinetics acting on the shoulder and elbow during the throwing motion. Any differences observed in throwing arm kinetics due to the footwork used in the throwing approach could be mitigated by altered pelvic and trunk kinematics. When considering the kinematic chain through the baseball throwing motion, other factors such as pelvic and trunk position, angular velocity, and timing between peak angular velocity should be considered to fully understand the impact that the approach to throw has on the throwing motion.

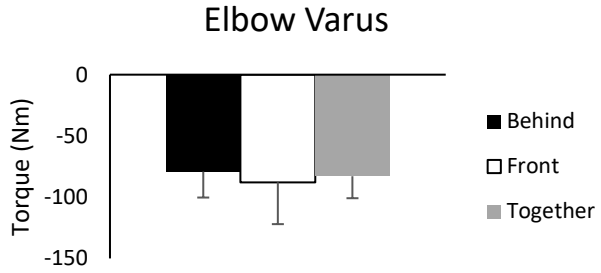

Figure 2. Elbow varus torque during baseball throwing.

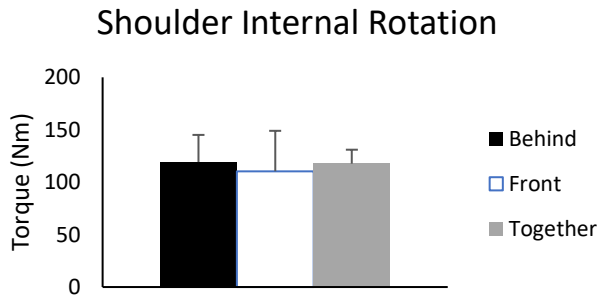

Figure 3. Shoulder internal rotation torque during baseball throwing.

Significance: Clinicians setting and monitoring a rehabilitative throwing program for an athlete coming off shoulder or elbow injury should be concerned with throwing intensity more than the athlete's approach to throwing.

Acknowledgments
No financial support was received for this project.

References:

[1] Dowling B, et al., *International Journal of Sports Physical Therapy*, 19(2), 176-188, 2024.
[2] Lightsey H.M., et al., *Orthopaedic Journal of Sports Medicine*, 7(3), 2019.
[3] Wasserberger, K.W., et al., *Sports Biomechanics*, 1-16. 2021.
[4] Kibler, W. B., et al., *Sports medicine*, *36*, 189-198. 2006.

A PROPOSED SOLUTION TO HEADGEAR-SENSOR INTERACTION DURING A HEAD PERTURBATION EXPERIMENT

Hogene Kim[1], James A. Ashton-Miller[1,2], James T. Eckner[2*]
[1]Dept. of Mechanical Engineering, College of Engineering, University of Michigan, Ann Arbor, MI
[2]Dept of Physical Medicine & Rehabilitation, University of Michigan Hospital, Ann Arbor, MI
*Corresponding author's email: jeckner@med.umich.edu

Introduction: Head perturbation experiment is commonly done for understanding head concussion biomechanics research. There is no universally accepted head injury metrics. We believe the area under the curve of head acceleration (AUC) is better metric than peak acceleration because it accounts for both magnitude and duration of impulse. However, complex head gear sensor interaction may confound these measurements as we shall see below.

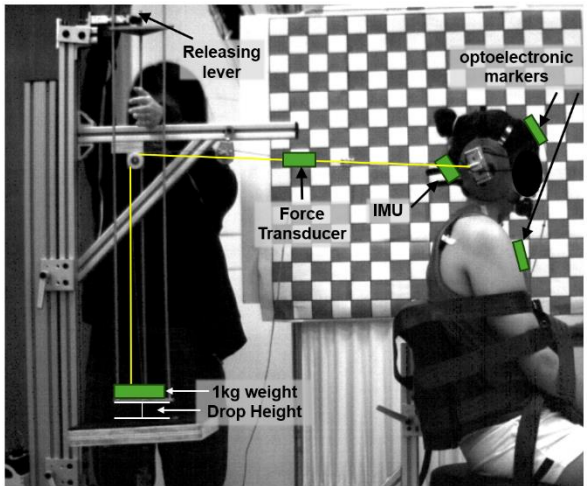

Figure 1 Tug machine Configuration with test administrator (left) and participant(right)

Methods: The 'Tug machine' was designed and implemented to provide given head perturbation by dropping a weight [1,2]. As shown in Figure 1, a participant was seated at the Tug machine wearing head gear with chin guard and ear caps. The subject experienced a direct head perturbation while torso and arms were fastened firmly with three straps. The 1kg weight drop delivers the direct head perturbation force released at random time (1~5sec) by an administrator, with the drop height determined proportional to participant's weight (2~4.5 cm). A stranded light metal cable was directly attached to the ear cap in head gear and a uniaxial force transducer (AMTI, Watertown, MA), then attached to the 1kg weight. In the head gear, an Inertial Measurement Unit (IMU, APDM Wearable Technologies, Portland, Oregon) was placed to the back side of head gear. Two optoelectrical marker triads were placed at mid-chest and forehead to measure head kinematics relative to chest during trials. A high-speed camera (AOS Technologies AG, Baden, Switzerland) and all the other sensor measurements were synchronized and recorded commonly at 500Hz. In testing 22 high school students (15.3±1.3 yrs, M:15, F:7), we quantified magnitude of the AUC before the head movement onset (preAUC), to determine how much including it had on the value of total AUC (AUC100).

Results & Discussion: Figure 2 shows that the force profile (1st row) was peaked at 13.2±7.7ms after the force activation onset and that the linear and angular accelerations (2nd and 4th rows) and displacements (3rd and 5th rows) were measured by IMU and optoelectronic markers respectively. The linear and angular acceleration onsets happened at 3.3±1.8ms and 2.4±2.1ms respectively and the linear and angular movement onsets were significantly delayed than acceleration onsets; 13.5±5.2ms ($p<0.001$) and 11.1±4.3ms ($p<0.001$) respectively. High-speed camera showed that there exists significant time delay between force onset and actual head movements due to various kinematic reasons, e.g. head gear interaction. As recorded in high-speed video clips, IMU detected head acceleration before head movements, which were highly related to the head gear movements. Thus, when considering head acceleration AUC as a parameter, head movement onset is an important indicator to exclusively consider head-movement-related AUC that may reduce effects of head gear interaction after the onset movement in this experiment. The percents of the magnitude of the preAUC over AUC100 are 19.6±18.0% (linear) and 14.4±16.1% (angular).

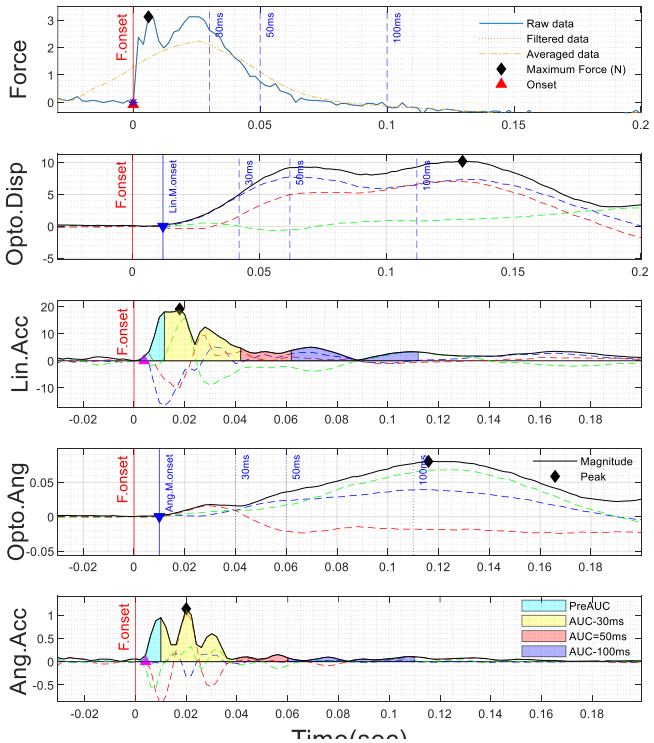

Figure 2 Time profiles of Force (1st row), linear and angular displacements (2nd & 4th) and accelerations & AUC (3rd & 5th)

Significance: We conclude that AUC measurement of the net head acceleration vector should only begin after the onset of the head movement in order to avoid artifact from head gear movements. Failing to do so would mean overestimating the AUC approximately 17.0%.

Acknowledgements: This study is supported by NIH R01 grant (grant #)

References: [1] Tierney, R.T., Sitler, M.R., Swanik, C.B., Swanik, K.A., Higgins, M., Torg, J., 2005. Med. Sci. Sports Exerc. 37 (2), 272–279
[2] Mansell, J., Tierney, R.T., Sitler, M.R., Swanik, K.A., Stearne, D., 2005. J. Athlet. Train. 40 (4), 310–319.

DESIGN OF A MODULAR INSTRUMENTED PEDIATRIC HARNESS FOR BODY-WEIGHT SUPPORTED TRAINING

Tristan McCarty[1], Sophia Sevic[1], Jiexin Li[1], Nolan Do[1], Tina Conley[1], Ernest Joseph Romero[1], Madie Barrett[2], Jackie Gardner-Hoag[2], Rhonda Nelson[2], Elena Kokkoni[1]*,
[1]Dept. of Bioengineering, University of California, Riverside, Riverside, CA 92521, USA.
[2]The WonderLab Clinic, Redlands, CA 92374, USA
*Corresponding author's email: elena.kokkoni@email.ucr.edu

Introduction: Motor training through the use of assistive technology, such as body weight support (BWS) devices, has been shown to positively impact motor skill acquisition and development in pediatric populations with motor delays [1]. These devices provide safe, effective, and controlled amounts of unweighting in the vertical plane, allowing pediatric users to train a variety of locomotor and postural actions. At the interface of the BWS system and the user is the wearable harness; current harness designs primarily provide support to the body through the armpits or groin of the user, and may be insufficient for controlling movement in other areas of the body, such as the trunk or pelvis. This results in low comfort and lack of stabilizing force where it is most needed, which may lead to user dropout or reduced training efficacy [2]. Furthermore, current designs lack the sensing capabilities necessary to provide feedback to clinicians regarding training effectiveness, while coming at a significant monetary cost. To address these shortcomings, a novel, low-cost, modular instrumented unweighting harness (UH) was developed for pediatric users through interdisciplinary efforts from engineers and clinicians.

Methods: Our UH was designed for use by children within the range of 5-9 years of age. It is constructed using nylon fabric due to its durability and flexibility, polyester fabric, polyester thread for high tensile strength, 1" and 2" straps and buckles, and polyester fiber for padding. For the sensing components, the sensors are encased in a rubber sheet within the polyester lining, which snaps closed using fasteners to secure the circuits within the UH and ensure user safety. Stress-strain analyses were conducted on the different fabric and strap connections to assess strength under normal usage conditions and identify potential failure points. Each sample was 2.8" by 2". The completed UH can be seen in (Fig. 1 E-H) This analysis was conducted using a TestResources Force Transducer SM-500-294 running the WinCom data collection system. All data analysis was conducted using Matlab R2023b, and curve fitted with 95% confidence bounds.

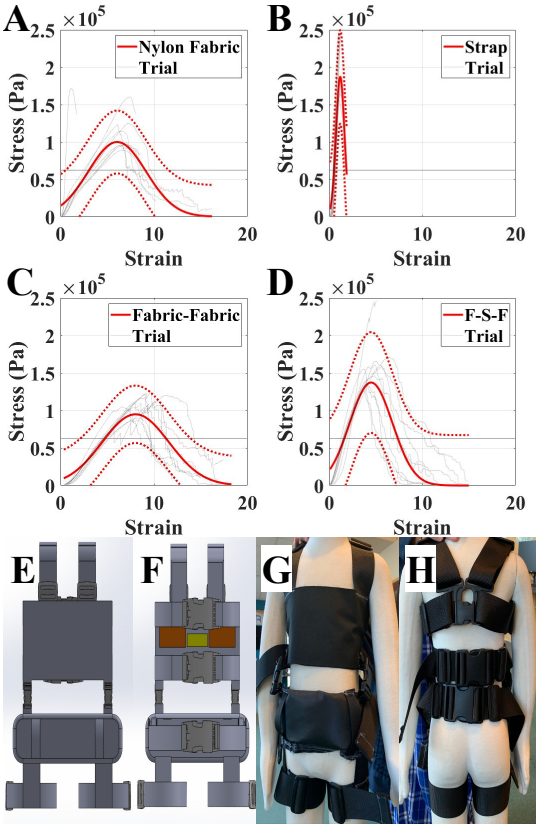

Figure 1: Stress strain relationship for the **(A)** nylon fabric, **(B)** harness straps, **(C)** fabric to fabric connections, **(D)** fabric to strap to fabric connections used to construct the UH. 95% confidence bounds shown as dotted lines. **(E)** Computer aided design of the front and **(F)** back view of the UH system. **(G)** Front and **(H)** Back view of the UH.

Results & Discussion: The system consists of two primary elements: (1) An upper-body chest harness and (2) Lower-body pelvic harness, which can each be used independently or in conjunction with each other. This serves two purposes: to have the option of removing one portion of the harness to focus the support in either the trunk or pelvic region, and to collect sensor information for specific tasks as needed, allowing clinicians to tailor the harness training around training requirements. We found that the UH failure points withstood forces in excess of 100lbs, as shown in (Fig. 1 A-D), which significantly exceeded the 95th percentile of weight for 9 year old males [3]. The general design of the trunk element utilizes shoulder straps and a multi-directional buckle to secure the harness to the user. The lower element consists of a cushioned belt which sits under the hips to provide pelvic support, relieving the pressure exerted on the groin by the leg cuffs. The UH records and transmits physiological and kinematic data from users undergoing BWS training as well as pressure exerted on the user by the harness. Information collected: (1) Pressure applied by the UH on the user via pressure sensors in the groin and trunk elements, (2) step count and (3) stride length via an inertial measurement unit located in the leg cuff, and (4) heart rate as measured through electrocardiogram leads. These measures are collected through the use of low-cost SparkFun components and an Arduino Uno micro controller, which promotes customization and open-source availability to clinicians and researchers. These components are connected to a Bluetooth transceiver, which sends the information to clinicians in real time to inform rehabilitative and motor training decisions.

Significance: Current UHs have difficulties providing targeted unweighting forces to the trunk and pelvis of their users, while providing little to no feedback to the researchers and clinicians who rely on these devices to make meaningful changes in the lives of pediatric populations. Modular UHs incorporating sensing mechanisms have the potential to provide valuable feedback to users regarding the efficacy of their BWS training, while also providing a repertoire of training options dependent on rehabilitative requirements. This harness system uses low-cost, open access materials and sensing systems while retaining the durability required for use in dynamic BWS motor training, allowing for customization and widespread adoption in pediatric rehabilitation environments.

References: [1] Damiano & DeJong (2009), *J Neurol Phys Ther* 33:27-44; [2] Lobo et al. *Phys. Ther. Rehabil. J.* 99:647–657; [3] Centers for Disease Control and Prevention (2000).

THE Y-BALANCE TEST AS A MEASURE OF DYNAMIC STABILITY AMONG COLLIEGIATE AMERICAN FOOTBALL PLAYERS

Aaron Griffith[1*], Sally Barfield[1], Von Homer[2], R. Christopher Mason[2], Melissa Harrington[2], Harish Chander[1], Adam Knight[1]
[1]Mississippi State University
[2]Delaware State University
*Corresponding author's email: ag2843@msstate.edu

Introduction: An estimated 23,000 ankle sprains occur every day in the United States, which amounts to approximately 1 in every 10,000 people [1]. In many sports, ankle sprains are the most common injury, partly because an athlete who incurs a first ankle sprain is at increased risk of another. The risk of reinjury is highest in the year immediately following the initial sprain [2]. Foot & ankle instability is a primary contributor to ankle sprains and furthermore leads to chronic ankle instability (CAI). The Y-Balance Test (YBT) is a dynamic balance tool widely utilized in lower extremity injury rehabilitation. Previous research suggests that decreased reach distances in the YBT may heighten the risk of lower extremity injuries [3]. This study aimed to assess reach distances in collegiate American football players at preseason and midseason intervals, examining potential differences between healthy players and those sustaining lower extremity injuries.

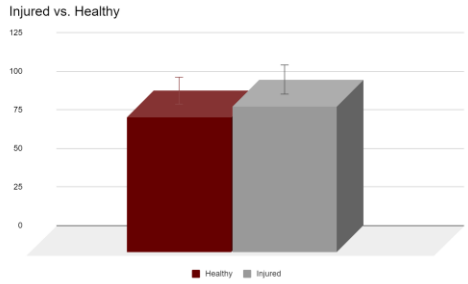

Figure 1: Displays the difference between health and injured groups amongst the sample size.

Methods: Ten Division One football players were recruited for this study. Participants reported to the laboratory for testing on two separate occasions, once in the preseason in late July and again at the midseason in early November. Prior to the YBT assessment, all participants completed a questionnaire and underwent the subtalar neutral joint manual foot and ankle test. Anthropometric measurements including height, weight, foot evaluation, leg length, and foot type (rigid or flexible) were recorded for each participant. Testing involved participants balancing on their right leg and reaching out with their left leg on a sliding block as far as possible, then returning to the starting position. This was completed for all three reach directions. Composite scores from the test were generated by first normalizing the reach distances to an individual's leg length, then by adding the three reach directions together, dividing the result by three times the leg length, and then multiplying the outcome by 100. Participants self-reported any lower extremity injuries that occurred while playing football between the two testing sessions.

Results & Discussion: A repeated measures ANOVA revealed no significant interaction between group (injured vs. healthy) (refer to fig.1) and time (pre- vs. midseason) ($F = 2.126$, $P = .179$). Neither time ($F = 2.839$, $P = .126$) nor group ($F = 1.882$, $P = .203$) demonstrated significant main effects. Despite the lack of significance, ongoing monitoring, and targeted interventions to enhance lower extremity stability in collegiate football players remain crucial during the season. Future studies should consider larger sample sizes.

Despite the lack of statistical significance, it is important to note the implications of these findings. The absence of significant interaction suggests that the change in Y-Balance Test (YBT) scores from preseason to midseason did not differ significantly between healthy players and those who sustained lower extremity injuries. Similarly, the nonsignificant main effects for time and group indicate that overall, there were no significant differences in YBT scores between preseason and midseason assessments, nor between healthy and injured players.

Significance: This study contributes to understanding the dynamics of lower extremity stability in collegiate football players over a competitive season. However, it is crucial to recognize the limitations of this study, including the small sample size. Despite nonsignificant findings, the importance of ongoing monitoring and targeted interventions to enhance lower extremity stability in collegiate football players during the season cannot be understated. Although statistical significance was not achieved, the findings underscore the importance of continual monitoring and interventions to optimize athlete performance and minimize injury risk. Future research should aim to address these limitations by including larger sample sizes to improve statistical power and enhance the generalizability of findings.

References:

1. Wukich, D.K. and D.A. Tuason, *Diagnosis and treatment of chronic ankle pain.* Instr Course Lect, 2011. **60**: p. 335-50.
2. Hayman, J., S. Prasad, and D. Stulberg, *Help patients prevent repeat ankle injury.* J Fam Pract, 2010. **59**(1): p. 32-4.
3. Butler, R.J., et al., *Dynamic Balance Performance and Noncontact Lower Extremity Injury in College Football Players.* Sports Health: A Multidisciplinary Approach, 2013. **5**(5): p. 417-422.

ARHTROKINEMATICS AND COMPOSITIONAL MEASUREMENTS WITH QMRI 1-2 YEARS FOLLOWING ACL RECONSTRUCTION WITH MENISCAL SURGERY

Sadegh Khodabandeloo[1*], John Ramsdell, Bruce Beynnon, Mathew Failla, Mathew Geeslin, Jiming Zhang, Mickey Krug, Michael DeSarno, Niccolo Fiorentino[1]
[1]Departmnet of Mechanical Engineering, University of Vermont, USA
email: sadegh.khodabandeloo@uvm.edu

Introduction: Risk of post-traumatic osteoarthritis (PTOA) following anterior cruciate ligament reconstruction (ACLR) is increased when ACLR is combined with a meniscus lesion (ACLR+M), affecting 50% of patients 10-20 years after the surgery [1]. Traumatic injury and ACLR create the potential for abnormal joint arthrokinematics—relative movement of the articulating surfaces—during in vivo motion and altered structural properties of the articular cartilage due to changes in loading patterns [2]. The increased likelihood of PTOA in patients who have undergone ACLR+M makes them a valuable population for studying how mechanical and biological factors interact shortly after surgery, possibly leading to the onset and early progression of knee OA. Therefore, the purposes of this study were to: 1) quantify the effect of ACLR+M on the joint arthrokinematics 1-2 years post-surgery with dual-fluoroscopy and model-based tracking (MBT) and 2) measure the effects of ACLR+M on cartilage composition with quantitative magnetic resonance imaging (qMRI) at the same timepoint.

Methods: Twelve patients were recruited 1-2 years after ACL reconstruction with either a concomitant meniscal repair or partial meniscectomy. All patients reported having an uninjured, normal contralateral limb. Uninjured status was confirmed by a Musculoskeletal Radiologist read of the contralateral knee's MRI. For arthrokinematics measurements, each participant performed two dynamic activities, walking and jogging, three times for both injured and uninjured knees. These tasks were chosen for determining the three-dimensional arthrokinematics of common daily activities. Patient-specific tissue models from MRI, and a validated MBT method [5], were used to measure the side-to-side (reconstructed vs contralateral) differences of the overlapping area of tibial and femur cartilage (contact overlap) and of the point of contact as determined by the weighted centroid of contact area between the cartilage surfaces (**Figure 1A**). Results were reported at 6 and 3 percent of the gait cycle for walk and jog, respectively, because these were the portion of the gait cycle at which the highest number of trials were included across all the subjects. For qMRI, T1rho relaxion times were measured at the regions of tibial and femoral cartilage that were in contact in the medial and lateral compartments (**Figure 1B**). All values reported as reconstructed minus uninjured.

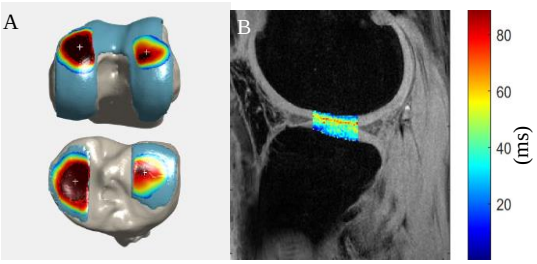

Figure 1: (**A**) An example of the contact overlap (dark red area) and the weighted centroid of contact area (white markers) between two cartilage surfaces. (**B**) An example of $T_{1\rho}$ relaxion times on the region of articular cartilage-cartilage contact.

Results & Discussion: On average, there was significant increased anterior transition of the tibia relative to the femur in the reconstructed joint, compared to the healthy joint, with values of 2.7mm (P=0.01) and 1.9mm (P=0.01), during walking and jogging, respectively**.** Reconstructed knees demonstrated a significant 1.8mm (P<0.005) posterior shift of the contact point in the medial compartment of the tibia and 0.96mm (P<0.005) in the lateral compartment during the walking activity. The point of contact was not different between the reconstructed and contralateral healthy limbs during jogging. The contact overlap areas in the medial compartment were 15% more (P<0.005) and 10% more (P<0.005) for the reconstructed knee's cartilage surfaces for walking and jogging, respectively. A trend towards a significant decrease in $T_{1\rho}$ relaxation times was observed for the tibial cartilage in the lateral compartment (P=0.062), while femoral cartilage demonstrated higher values in the injured knees in the lateral compartment (P=0.045), and a trend toward significant increase in the medial compartment (P=0.053). The results demonstrate that articular cartilage has greater contact overlap with increased anterior tibial translation in the ACL+M knee compared to the normal knee, which is consistent with previous studies of ACLR patients [6]. The qMRI results suggest that water content and/or proteoglycan concentrations also differ 1-2 year after the index trauma and reconstruction. The correlation between the side-to-side arthrokinematics differences and qMRI differences will be accomplished in the future statistical analysis. In addition, future work at 2-3 years after surgery (one year after the timepoint reported herein) will assess the predictive value of side-to-side differences in arthrokinematics and compositional values on longitudinal changes in these values.

Significance: Given that not everyone develops osteoarthritis after ACLR+M, discovering the initiation in the early stages for those who are at highest risk may prove crucial as it holds significant importance for potential future clinical interventions. Arthrokinematics changes exist 1-2 years after ACLR+M in people that are otherwise functioning "normally." The side-to-side differences in qMRI also means that cartilage experiences compositional changes after the surgery. Understanding the relationship between arthrokinematics and qMRI will provide insights into the link between mechanics and biology in the development of post-traumatic osteoarthritis in patients who have undergone ACLR and meniscal surgery.

Acknowledgments: Rebecca Choquette for coordination of the study, and Amanda Haddad for helping with data processing.
References: [1] Lohmander et al. (2007), *J Sports Med* 35(10); [2] Chaudhari et al. (2008), *MSSE 40(2).* [3] Li et al. (2012) *J Biomech 45(15);* [4] Atkinson et al. (2019) *BMC Musculoskelet Disord 20(182*). [5] Ramsdell et al. (2023*), Med Eng Phys 114.* [6] Amano et al. (2016) *Orthop J Sports Med.*

EFFECTS OF VELOCITY INTENT ON JOINT KINETICS AND IMPULSE DURING SUBMAXIMAL BACK SQUATS

Paige M. Agnew[1], Hunter J. Bennett[1], Zachary A. Sievert [1,2]
[1]Old Dominion University, [2] University of Cincinnati
*Corresponding author's email: pagne002@odu.edu

Introduction: Research has shown that verbal encouragement and direction, including velocity-based cues, has improved performance for athletes across a myriad of sports [1-3]. Velocity based training (VBT) has been widely studied regarding improvements in sports performance in conjunction with using the typical percentage-based approach [4]. Back squatting is an essential movement in strength and conditioning utilized to improve strength, athletic performance, and in rehabilitation settings. In recent years, velocity-based training techniques and new technology have become prevalent to enhance neuromuscular adaptations during strength training. With the integration of velocity-based training techniques many athletes have altered training methods from percentage based to velocity based instead [4-5]. Recent research has found that peak hip moments increase with the instruction to squat faster [5]. However, joint moment impulses, which detail the cumulative loads at the joints across time, are arguably more important from a training perspective considering time under tension is generally of import. In addition, an understanding of the load placed on individual muscles can provide insights beyond the net moment approach. Therefore, the purpose of this investigation was to quantify neuromuscular activity and joint moment impulse across 70% and 80% loads while cueing participants to squat with the intent to increase velocity during the concentric (ascent) phase.

Methods: 15 male participants, ages 18–30 years old with a mean training age of 7 years, participated in this study. Inclusion criteria were at least one-year of resistance training experience and currently engaging in resistance training three times per week with one lower body focused training day per week. Participants were appropriately prepped for electromyography (EMG) and 3-D motion capture using standardized procedures. EMG were placed on the right leg quadriceps, hamstrings, and gluteal muscles. Full-body motion capture and force dynamometry were collected for each trial. Participants were given a ten-minute self-selected warm-up period prior to completing a 1 repetition maximum (1RM) back squat. Following the 1RM participants performed two sets of 3 reps at 70% and 80% of their measured 1RM. The first set was completed at a self-selected pace and the second set verbal and visual instructions were given to squat as fast as possible. A velocity-based training system was enabled throughout the session to provide real-time feedback during lifts. The first two repetitions, parallel to fully upright, were extracted from each trial in Visual 3D. Linear envelopes for each muscle were calculated and normalized to the 1RM attempt. Kinematic and kinetic data were low pass filtered at 5Hz. Integrated EMG (iEMG) and sagittal plane hip and knee moment impulses were calculated in MATLAB (MathWorks). Dependent T-Tests were run for 70% and 80% RM to compare quadriceps, hamstrings, and gluteal iEMG and hip and knee moment impulses between velocity conditions.

Results & Discussion: Speed was 27% and 22% greater during purposeful compared to self-selected conditions across both 70% and 80% RM, respectively. Significant differences were found for the quadriceps (p=0.035; p=0.012) and gluteal (p=0.003 & p=0.002) muscles during the ascent for both 70% and 80% RM, respectively. No significant differences were observed in the biceps femoris muscle (p>0.05) for either 70% or 80% RM. Hip and knee moment impulse were reduced at 70% RM (p=0.001 & p=0.002) with increased velocity; however, no significant differences were found for 80% RM (p=0.078 & p=0.156; Figure). These data indicate that an increase in velocity is achieved generally by an emphasis on both hip and knee extensor musculature; however, increases in velocity are achieved via load specific mechanics. Increased gluteal iEMG, decreased hip moment impulse, and increased peak hip moments [5] with increased velocity at 70% RM indicate a greater load generated over a significantly shorter period for the hips (i.e., hip dominance). However, when reaching the top end of submaximal loads, differences in time under tension are less pronounced, resulting in equivocal reductions in time as the increases in hip joint moments [5]. However, the presence of increased hip and knee muscle iEMG suggest back squatting with intent is a superior exercise regimen.

Figure. Joint Moment Impulses

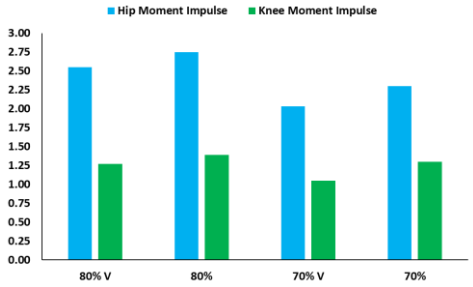

Table. iEMG for knee and hip musculature and joint impulse averages

	iEMG					
	VM	**RF**	**VL**	**GMax**	**GMin**	**BF**
80%V	61.53	55.68	48.06	50.36	42.90	69.54
80%	54.81	51.56	42.06	43.45	34.30	52.02
70%V	61.63	55.68	48.06	48.48	39.71	46.67
70%	54.68	51.55	42.15	37.81	31.51	42.70

Significance: Velocity based training techniques are growing in popularity as another method to incorporate for improving training adaptations and should be highly considered to induce higher muscular effort for the hip musculature during squatting. Future research considerations should assess the neuromuscular effort and mechanical changes closer to near maximal squatting efforts (i.e, >90% 1RM). Lastly, this present data set indicates that there is mechanical advantage to back squatting faster at higher submaximal percentages.

References:

[1] Blazevich & Jenkins (2002) *J Sport Sci*, 20(12), 981-990; [2] McNair et al (1996) *Br J Sports Med* 30: 243–245; [3] Weakley et al. (2020) *J Strength Cond Res*, 34(11), 3157- 3163; [4] Weakley et al. (2021). *Strength Cond J*, 43(2), 31-49; [5] Parrish et al (2023) *Old Dominion University*

APPLICATION OF DEEP LEARNING IN SOLEUS MUSCLE ACTIVATION PREDICTION DURING WALKING

Jobelle B. Hernandez[1], Oliver Gu, Aymen Elassa, Mariam Sharobim, Samira Santana, Jongsang Son[1*]
[1]Department of Biomedical Engineering, New Jersey Institute of Technology, Newark, NJ, USA
*Corresponding author's email: jongsang.son@njit.edu

Introduction: Although the superior combination of qualitative clinical judgment and quantitative movement analysis of electromyogram (EMG) data provides helpful information on musculoskeletal or cardiovascular issues, it has its limitations. The lack of objectiveness in physician observations has led to limitations in the qualitative diagnosis of gait differences. Despite its objectiveness, quantitative analysis has its limitations due to time-consuming steps in its collection and analysis of data such as EMG [1]. This issue demonstrates the need for more convenient and simplified quantitative data collection and analysis approaches. Thus, this proof-of-concept study seeks to demonstrate the feasibility of a deep learning model application in predicting soleus muscle activation patterns (MAPs) from lower limb joint angles during normal walking.

Methods: The long short-term memory (LSTM)-based neural network model was trained using data from a dataset published by Lencioni et al. [2]. The chosen data comprises of computed joint angle and EMG data from the normal walking trials of healthy adult-aged individuals with no self-declared locomotor disorders [2]. Each subject walked at varying speeds in multiple trials. To train the model for the soleus MAP prediction from joint angles, the 12 joint angles (i.e., flexion, adduction, and rotation angles of the pelvis, hip, knee, and ankle) were used as input. The soleus EMG data were processed into MAP data through resampling, rectification, smoothing, and normalization steps. During development, the data were randomly split into 3 sets: 80% of the subjects were assigned for training, 10% for validation, and 10% for testing. Data augmentation was used to expand the dataset by adding random noise. The metrics, root-mean-square error (RMSE) and coefficient of determination (R^2) between the predicted and measured MAP, are used to assess the model performance. The model training and performance analysis explained in this section are performed in MATLAB (The MathWorks, Inc., Natick, MA).

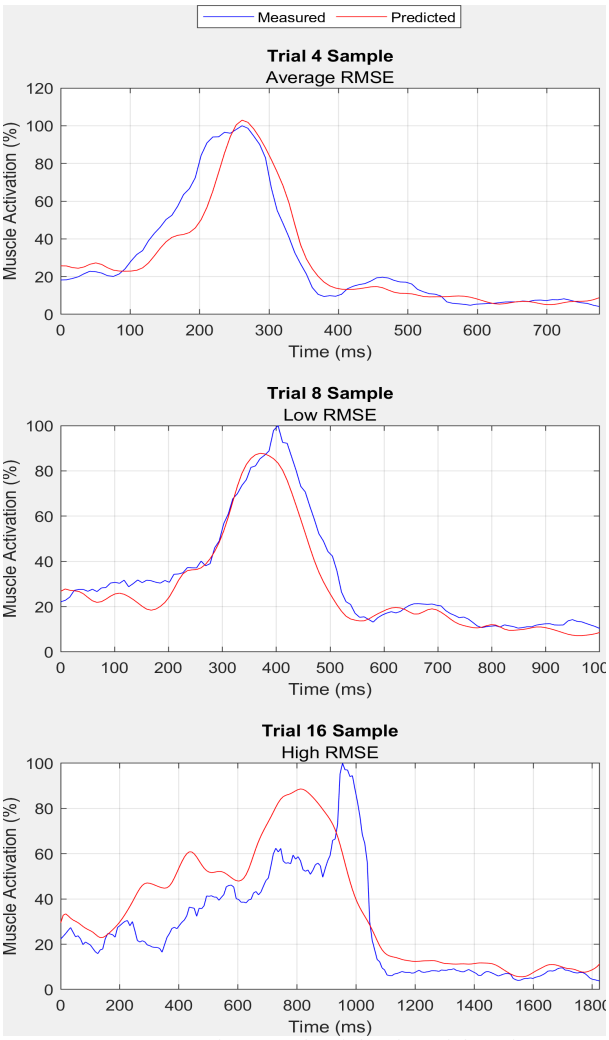

Figure 1: Representative sample trials of Model Performance

Results & Discussion: The proposed model was tested on 31 trials, and yielded an average RMSE of ~0.10 and R^2 of 0.85. Figure 1 displays a sample of model performance in three trials with the measured and predicted MAPs. The trial in the middle plot has a low RMSE of 0.07. The trial in the top plot has an RMSE of 0.10, the overall model average. The bottom trial has a high RMSE of ~0.17 (1 of 4 outliers). The RMSE range (excluding outliers) is 0.06 to 0.13, with a median value of 0.09 that is close to the average value. The average performance, range, and median RMSE show the application feasibility of a deep learning model to predict soleus MAP from lower-limb joint angles during walking. However, the outliers demonstrate the need for further model generalization in the future. Further studies are required to optimize the model performance.

Significance: This study demonstrated the feasibility of using a deep learning model to predict muscle activation patterns from the joint angles during walking. Considering that some promising portable and/or wearable sensor technologies become available to quantitatively collect and analyze joint kinematics, our models will ultimately provide a promising tool that allows researchers and clinicians to study human movements in a more practical manner.

References: [1] Simon, Sheldon R. "Quantification of human motion: gait analysis-benefits and limitations to its application to clinical problems." Journal of biomechanics, (vol. 37,12 (2004): 1869-80. doi:10.1016/j.jbiomech.2004.02.047
[2] T. Lencioni, I. et al, "Human kinematic, kinetic and EMG data during different walking and stair ascending and descending tasks," Scientific Data, 2019 (Vol. 6 Issue 1)

ASSISTIVE SHOES CAN IMPROVE THE VERTICAL GROUND REACTION FORCES IN PATIENTS WITH PERIPHERAL ARTERY DISEASE

Zahra Salamifar[1*], Farahnaz Fallahtafti[1], Iraklis I. Pipinos[2,3], Jason M. Johanning[2,3], Hafizur Rahman[1,2], Sara Myers[1,2]
[1]Department of Biomechanics, University of Nebraska at Omaha, Omaha, NE US
[2] Research and Surgery Service, Omaha Veterans Affairs Medical Center, Omaha, NE USA.
[3] Department of Surgery, University of Nebraska Medical Center, Omaha, NE USA
*Corresponding author's email: ssalamifar@unomaha.edu

Introduction: Blockages of arteries in the legs cause peripheral artery disease (PAD), which reduces blood flow, muscle oxygenation, and muscle strength in calf muscles [1]. A common symptom in patients with PAD is intermittent claudication, which causes pain during walking and limits walking capacity [1]. Previous gait analysis showed reduced peak vertical ground reaction forces (V_{GRF}) in patients with PAD compared to healthy individuals [2,3,4]. The V_{GRF} curve also fluctuates less in patients with PAD compared to healthy people. Assistive devices such as ankle-foot orthoses have been shown to improve the V_{GRF} in patients with PAD by absorbing energy during heel contact and releasing it during push-off [2,3,4]. However, limitations of ankle-foot orthoses, such as physical discomfort and lack of natural ankle motion, decrease adherence to this assistive device. Assistive shoes, such as spring-loaded (SL) and carbon-fiber (CF), can potentially improve push-off like other assistive devices, by absorbing energy at heel contact and releasing it during push-off. Yet, the impact of assistive shoes on the V_{GRF} of patients with PAD has remained unclear. This study examined the impact of assistive shoes on V_{GRF} during baseline visits and following a three-month intervention, aiming to evaluate the effects of assistive shoes in both short-term and long-term contexts.

Methods: Ten individuals with PAD (with an average age of 70.0±8.0 years, height of 177.1±6.6 cm, and body mass of 78.1±8.4 kg) performed a progressive treadmill test using a pressure-instrumented treadmill. At the end of the baseline visit, participants selected their preferred assistive shoe based on comfort and ease of walking, and were asked to wear them for three months in their daily activities. We calculated the average peak V_{GRF} during loading response (F_z1), mid stance ($F_z$min), and push-off (F_z2) during walking both with and without pain (Figure 1). We performed independent, paired sample t-tests to compare the effect of SL versus CF on V_{GRF} discrete points during pain free and pain induced conditions from the baseline session. We also assessed the impact of a three-month intervention with assistive shoes on V_{GRF} of patients with PAD.

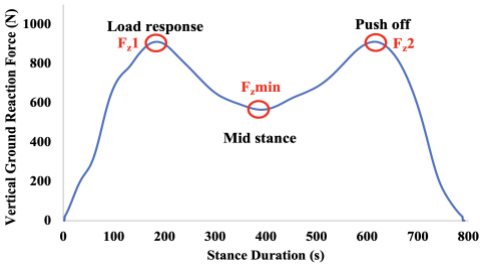

Figure 1: Vertical ground reaction force (V_{GRF}) during walking. **F_z1:** The first V_{GRF} peak during the loading repones phase of the gait. **$F_z$min:** The local minimum between two peaks during the mid-stance phase of the gait. **F_z2:** The second V_{GRF} peak during push-off phase of the gait.

Results & Discussion: No significant differences were observed at the baseline visit for the V_{GRF} between walking with SL and CF shoes in either the pain free or pain induced conditions. However, patients with PAD exhibited a 9% greater F_z1, 3.0% greater average $F_z$min, and 2.7% greater F_z2 in the pain-free condition when walking with CF compared to SL. Also at baseline, patients with PAD displayed 4.6% greater F_z1, 3.7% greater $F_z$min, and 3.6% greater F_z2 during the pain condition with CF compared to SL. Overall there was increased V_{GRF} fluctuation when walking with CF compared to SL in both pain-free and pain conditions at baseline. This means gait patterns' of patients with PAD closer to healthy individuals when wearing CF shoes [3]. Although a three-month intervention with assistive shoe did not significantly change the V_{GRF} during walking in either condition, after three months of intervention, the patients exhibited an increase in F_z1 by 9.4%, an increase in average $F_z$min by 7.7%, and an increase in F_z2 by 6.7% in the pain-free condition. Additionally, a three-month intervention with the assistive shoe increased the F_z1 by 14.5%, $F_z$min by 9.7%, and F_z2 by 9.0 in the pain condition. A flatter V_{GRF} curve during walking in patients with PAD is an indication of less center of mass fluctuation and an increase in double support time compared to healthy people [4,5,6]. A notable improvement in the peaks of V_{GRF} after a three-month intervention with a preferred assistive shoe led the gait pattern to become closer to healthy individuals [4,5,6].

Significance: The CF shoes caused a greater V_{GRF} fluctuation improvement compared to the SL shoes in one session. In addition, a three-month intervention with a preferred assistive shoe enhances the overall V_{GRF} in both pain-free and pain conditions. This indicates enhanced support and potentially improved gait dynamics. As a result of the greater V_{GRF} improvement when experiencing pain, the assistive shoe seemed to decrease the impact of pain during walking. To reach significant differences, more subjects need to be studied.

Acknowledgments: This study is supported by a SPiRE VA grant (I01RX003266).

References: [1] Fallahtafti F, et al. (2022), *Entropy.* 24(10); [2] Bapat, et al.(2023), *Vasc. Med.* 28(1); [3] Evans, et al. (2024). *RCAF Omaha, Nebraska, abstract*; [4] Salamifar, et al. (2022), *RCAF. Omaha, Nebraska, abstract*; [5] Scott-Pandorf, et al. (2007) *Vasc. Med.* 6(3). [6] Evangelopoulou, et al. (2021) *Clin Biomech.* 83(105309).

ADAPTATION-AWARE OPTIMIZATION PREDICTS LOCOMOTOR PERFORMANCE WITH ASSISTANCE

Inseung Kang[1] and Nidhi Seethapathi[1*]
[1] Department of Brain and Cognitive Sciences, Massachusetts Institute of Technology, Cambridge, MA USA
*Corresponding author's email: nidhise@mit.edu

Introduction: Humans naturally adapt their movement when exposed to a novel device, such as an assistive robotic exoskeleton [1]. Although assistive devices are designed to enhance biomechanical performance, the individual's natural adaptation response can fall short of the intended performance level. Indeed, researchers typically conduct a sweep of either the assistance profiles or the exposure times to identify the ideal assistance strategy [2]. Optimization-based computer simulations of human locomotion could anticipate the effect of a planned assistance strategy on biomechanical performance, thereby accelerating the search process. However, we lack evidence establishing the ability of computer simulations to reliably predict locomotor performance with assistance. Here, by combining experimental and simulation approaches from biomechanics [3, 4] and motor learning [5, 6], we compare adaptation-aware optimization and traditional trajectory optimization models in their ability to predict locomotor performance with assistance.

Our contributions in this work include: (i) a comprehensive experimental characterization of locomotor performance as a function of assistance magnitude and exposure time, and (ii) a simulation study comparing state-of-the-art computational models in their ability to predict locomotor performance with assistance. While existing experimental studies separately vary assistance magnitude and exposure time, in this study, we find that varying both aspects of assistance simultaneously impacts locomotor performance in a qualitatively different way. By comparing computational models in their ability to predict this dual impact of assistance magnitude and exposure time, we find that "adaptation-aware" optimization i.e. the optimization model that takes motor learning principles into consideration in addition to biomechanics, outperforms the trajectory optimization-based biomechanical model. Our findings highlight the importance of understanding the interplay between motor learning and biomechanics for the development of effective assistive strategies.

Methods: Our study included both experimental and simulation methods. In our experiments, 27 healthy individuals (22.5 ± 3.4 years), without prior experience walked on a split-belt treadmill with randomly assigned assistance magnitudes and a long exposure time of 45 minutes. The protocol began with tied-belt walking at 1 m/s, followed by randomly selected assistance magnitude with the belt speed difference as 0.4, 0.7, or 1.0 m/s, while average belt speed was 1 m/s. Locomotor performance i.e. energy and symmetry were measured as a function of assistance using indirect calorimetry and standard motion capture respectively. In our simulations, we modified an existing trajectory optimization-based biomechanical model [3] and a locomotor adaptation-based optimization model [6] to incorporate our experimental paradigm. We then compared the two models in their ability to predict energy and symmetry with assistance.

Results & Discussion: Our experimental findings reveal how assistance magnitude and exposure time, which are studied separately in existing work, can interact with each other to impact locomotor performance. Existing work suggests that increasing the exposure time for a given assistance magnitude can lead the individual to further decrease their energy cost [5]. Contrary to this, we find here that longer exposure need not further decrease the energy cost, even if the assistance magnitude is high (Fig. 1A). Other existing work found that locomotor asymmetry becomes more negative with increasing assistance for a fixed short exposure time [4]. Contrary to this, we find here that with longer exposure time the locomotor asymmetry tends to positive values for increasing assistance magnitudes (Fig. 1B). Taken together, our experiments varying both assistance magnitude and exposure time reveal the multifaceted non-intuitive impact that assistance can have on performance, necessitating predictive simulations.

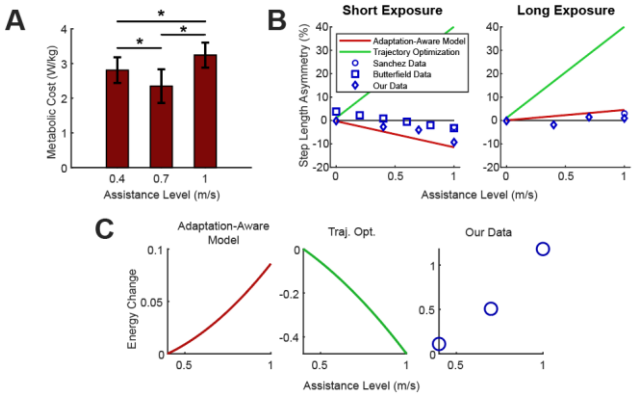

Figure 1: Insights into locomotor performance with assistance from experiments and simulation. (A) Locomotor energetic cost after long exposure to an assistance profile depends on the assistance magnitude. (B) Locomotor symmetry performance varies with both assistance magnitude and exposure time. The adaptation-aware model captures the experimentally observed symmetry trends. (C) The adaptation-aware model qualitatively captures the change in energy cost relative to baseline with increasing assistance magnitude.

Our simulation findings compare optimization-based models in their ability to capture the observed locomotor performance with assistance. For the energetic performance, we find that the adaptation-aware optimization captures our experimental finding i.e. that the energy change will increase with assistance (Fig. 1C). On the other hand, the trajectory optimization-based biomechanical model predicts the opposite trend. The adaptation-aware model also predicts how locomotor symmetry will change with exposure and assistance magnitude, whereas the trajectory optimization model only captures the qualitative trend for long exposure (Fig 1B). Taken together, our simulation results suggest that a combination of biomechanical and motor learning principles, as exhibited by the adaptation-aware model [6], are needed to predict locomotor performance with assistance.

Significance: We put forth a comprehensive analysis combining experiments and simulation to understand how locomotor performance is impacted by assistance magnitude and exposure time. Compared to existing work, our experiments provide a more complete picture of how assistance strategies (i.e. magnitude and time) interact and influence locomotor performance. Our simulation work highlights the importance of modeling interactions between motor learning and biomechanics to successfully capture these multifaceted non-intuitive effects of assistance on locomotor performance. Future research can build on our work to benchmark and improve simulations of locomotor performance, and to enable model-guided design of effective assistance strategies.

References: [1] Selinger et al. (2015), *Curr. Biol.*; [2] Poggensee et al. (2021), *Sci. Rob.*; [3] Price et al. (2023), *J. Neurophy.*; [4] Butterfield and Collins. (2022), *J. Biomech.*; [5] Sanchez et al. (2021), *J. Neurophy.*; [6] Seethapathi et al. (2021), *bioRxiv*.

ADAPTIVE ANKLE-FOOT ORTHOSES STIFFNESS POWERED USING ARTIFICIAL MUSCLES

George S. Elias[1, 2*], Braeden C. Harrell[2], Marissa McFadden[2], Kirsten M. Anderson[3],
Jason M. Wilken[2], Caterina Lamuta[1], & Deema Totah[1]
[1] Department of Mechanical Engineering, [2] Department of Biomedical Engineering, [3] Department of Physical Therapy and Rehabilitation Science, University of Iowa, Iowa City, IA
*Corresponding author's email: george-elias@uiowa.edu

Introduction: Ankle-foot orthoses (AFOs) are assistive braces that can provide support, reduce pain, and/or improve gait mechanics to the ankle joint and lower limb. Understanding the biomechanics and mechanical properties of these devices is essential for optimizing AFO functionality based on user needs to assist mobility and improve quality of life. Currently, passive AFOs, characterized by their static mechanical elements such as springs and dampers, are commonly prescribed but provide limited functional assistance to users and lack the ability to dynamically optimize AFO stiffness. AFO stiffness is the resistance to rotation in the sagittal plane about the ankle joint and is often defined by the slope of the ankle torque-angle curve [1]. Optimal AFO stiffness varies between patients due to different muscle strengths, weights, and walking speeds. Optimizing AFO stiffness based on user needs has been experimentally shown to improve biomechanics, walking speed, and reduce walking energy cost [2]. While active AFOs offer the advantage of tunable assistive torque and variable stiffness, this often comes at the expense of increased weight and high-power requirements, introducing a trade-off between power and weight [3]. Striking the right balance between these two parameters remains a critical challenge in the pursuit of effective active AFO designs. We propose a novel variable-stiffness, powered AFO design that harnesses the potential of artificial muscles. This innovative approach presents a transformative opportunity for lightweight actuation with low power requirements.

Methods: The AFO (Fig. 1) consists of a carbon fiber shell for lightweight durability, and a dual-action ankle joint with spring modules (Nexgear Tango Ankle Joint, Ottobock). The device's innovation lies in the incorporation of Twisted and Coiled Artificial Muscles (TCAMs) into a posterior actuation module. The TCAMs' contraction is driven by joule heating of coated and twisted fibers, which induces radial expansion, leading to controlled contraction. TCAMs require only a small input power (0.025 W cm^{-1}) to move 12,600 times their weight [4]. The design incorporates 32 TCAMs (four rows of eight) that can deliver 800 N of force with a 1.4 cm contraction [5]. During contraction they can reach up to 200 °C. Thus, the actuation module was enclosed within an origami-style folding insulator sleeve to protect the user from the high heat without interfering with ankle joint motion.

Figure 1: Powered AFO

To create a *variable stiffness* powered AFO, we used closed-loop PID control of the TCAM actuation level to match chosen reference torque-angle stiffness profiles. An in-line loadcell (FUTEK LCM300) measures force, which is converted to torque with a simple moment arm multiplication. A hall-effect sensor (ams-OSRAM AS5048B) placed at the ankle joint measures its flexion angle. To determine actuation timing, a gait-phase detection algorithm uses real-time ankle angle, foot inclination from a gyroscope (MPU6050), and ground contact detection from three footswitches. Safety features include a break-away cable within the actuation module and hard stops in the dual-action joint to prevent overextension. Saturation thresholds and soft limit-switches are also implemented in software to ensure safe movement throughout the gait cycle. Benchtop validation of the powered AFO is currently underway. The TCAMs' actuation and reference stiffness tracking abilities will be tested using an existing robotic leg that can flex the AFO in both plantar and dorsiflexion while measuring the stiffness. The real-time gait phase detection was tested at different walking speeds and elevations on a treadmill.

Results & Discussion: The combination of artificial muscles (TCAMs) with minimal sensors and carbon-fiber shell provides a lightweight, portable, capable, and efficient powered AFO design with non-invasive sensing capabilities that can grant users active damping upon heel strike and a powered push-off assist. This artificial-muscle powered, variable-stiffness AFO can be used as a portable version of tethered emulator platforms like [6] to test the effect of AFO stiffness on users while walking in the real world, outside a lab environment. The current design is limited to unidirectional actuation aiding plantarflexion (the TCAMs only apply force in contraction, but allow passive extension) and has a bulky actuation module that protrudes posteriorly. However, the flexible nature of the TCAMs lends itself to cable-driven actuation that is extremely versatile, opening up the low-profile device design space. Future lower-profile iterations can be used as variable-stiffness assistive devices to compensate for both plantarflexor and/or dorsiflexor weakness.

Significance: With the ability to vary stiffness, clinicians can tailor therapy to better match user needs, improving quality of life. This portable powered AFO will also allow for real-world testing leading to a more complete understanding of AFO stiffness effects on biomechanics, thus enabling better AFO manufacturing for greater user satisfaction and performance.

Acknowledgment: Supported by start-up funds from the University of Iowa. Thank you to Jeffrey Palmer, CPO for AFO manufacturing.
References: [1] Totah et al., Gait & Pos, 2019; [2] Waterval et al., BMJ Open, 2017, [3] Esposito et al., J Neuoreng Rehabil, 2018, [4] Lamuta et al., Smart Mater, 2018, [5] Kotak et al., J Biomech Eng, 2021, [6] Zhang et al., Science, 2017.

A NUMERICAL MODEL TO PREDICT PROSTHETIC LEG SWING PHASE BEHAVIOR IN TRANSFEMORAL PROSTHETIC GAIT: A PLATFORM FOR PRESCRIPTION GUIDELINES AND PROSTHESIS DESIGN

Miguel Vaca[1,2]*, Steven A. Gard[1,2], Matthew J. Major[1,2]
[1]Northwestern University, Chicago, IL; [2]Jesse Brown VA Medical Center, Chicago IL
*Corresponding author's email: miguelvm@u.northwestern.edu

Introduction: Careful management of prosthesis ground clearance and knee extension timing during prosthetic limb swing are important requirements for gait safety when using a transfemoral prosthesis as they help avoid stumbles due to ground collision and prepare the limb for heel contact to transition into stance [1-2]. Management of those gait objectives is partially dependent on the combined function of the prosthetic knee and foot, which affects the hip-toe distance [3] and swing phase timing [1]. Here we present a numerical simulation of transfemoral gait swing phase that predicts foot clearance and terminal knee extension timing as a function of prosthetic knee and ankle-foot mechanics, namely knee rotation damping, thigh-to-shank changes of geometry, and foot dorsiflexion-plantarflexion angle. The purpose of the simulation is to develop a platform for predicting user outcomes relevant to gait safety in transfemoral prosthetic gait as a function prosthetic knee and ankle-foot mechanical properties to: 1) inform prescription guidelines of existing prosthetic components, and 2) offer a systematic method for identifying solution spaces to optimize prosthetic leg design with the goal of maximizing gait safety.

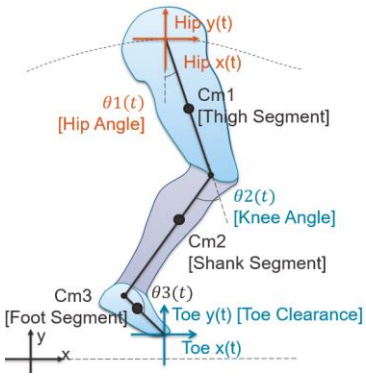

Figure 1: Numerical model diagram, consisting of: three solid segments (thigh, shank and foot), thigh position and angle as inputs (orange) and knee angle and toe clearance as outputs (blue).

Methods: A numerical model (see Figure 1 for definitions) was developed in Simscape Multibody (Simulink-MATLAB) to simulate sagittal plane prosthetic leg behavior during swing phase. The model was designed such that hip joint kinematics (hip joint center motion and hip flexion-extension angle) served as the 'driver' for swing motion given that these dynamics are volitionally controlled by a transfemoral prosthesis user (TFPU). The independent input variables, apart from hip kinematics, were prosthetic knee flexion-extension damping coefficient and a constant prosthetic foot dorsiflexion. The model consists of three solid segments (thigh, shank and foot) connected through rotational joints. The output variables were instantaneous knee joint angle and vertical and horizontal toe position. While the simulation was designed to allow systematic adjustments of time-varying knee resistive torque (damping), thigh-to-shank geometry changes (due to polycentric knees), and foot angular position, here we present results on modifying knee damping (coefficient B=0.0-1.4Nm/(rad/s)) only with initial conditions and hip kinematics defined from previous human subject experimental data with a participant walking with a single-axis knee joint (B=.56 Nm/(rad/s)) and rigid dynamic foot [1], using instantaneous knee angle and toe position results from that previous experiment for quantitative validation as evaluated through root mean square error (RMSE).

Results & Discussion: Instantaneous prosthetic limb knee angle and toe clearance (position with respect to level ground) at constant values of B ranging from 0.0 to 1.4 as generated by the simulation are presented in Figure 2 superimposed on human subject data from the previous study. Simulation results with B=0.56Nm/(rad/s) closely match that of the experimental data in terms of instantaneous profile with an RMSE of 4.9° and 1.1 cm for knee angle and toe clearance, respectively. Differences appear to partially result from a mismatch in inertial properties between the experimental and simulated prosthesis. The simulated results suggest that systematic increases to damping generates a decrease in knee angle range-of-motion, including less peak knee flexion and inability to return to full extension in terminal swing. Increased damping also reduces toe clearance through swing. Importantly, the simulated results suggest an inverse relationship between toe clearance and knee full extension in terminal swing, suggesting a tradeoff between these two critical elements of transfemoral prosthetic gait safety, aligning with results from our previous human subject results [1]. These tradeoffs should be considered when optimizing the prosthesis through clinical tuning or design. A limitation of the present simulation is that results reflect differences assuming no changes in hip kinematics (i.e., not considering alterations in compensatory motions for a given prosthesis).

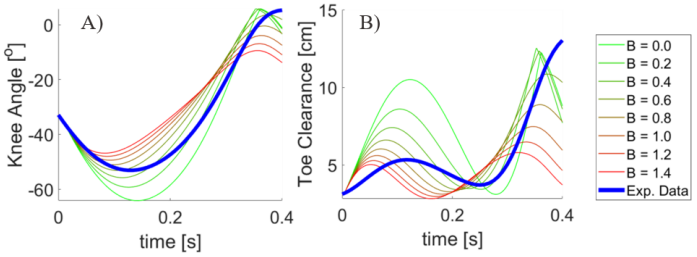

Figure 2: Experimental (blue line) and simulated (green/red lines) results for instantaneous A) knee flexion (negative) angle and B) toe clearance, from toe off until knee arrives to full extension (~0.4 s).

Significance: Here we present a valuable and novel means to systematically assess the effects of both prosthetic knee and ankle-foot design parameters on key factors of gait safety of TFPUs. This numerical platform can help inform evidence-based practice when clinically prescribing and tuning prostheses as well as identify appropriate solution spaces for prosthesis design to maximize gait safety.

Acknowledgments: This study was supported by the Department of Defense (W81XWH1910447). We thank Marcus Cisco for his assistance with data analysis.

References: [1] Kent et al. (2021), *IEEE Transactions on Neural Systems and Rehabilitation Engineering* 29; [2] Sensinger et al. (2013) *IEEE Transactions on Neural Systems and Rehabilitation Engineering* 21.; [3] Moosabhoy & Gard (2006), *Gait & Posture* 24.

ADAPTING A HIGH-FIDELITY SIMULATION OF HUMAN SKIN FOR COMPARATIVE TOUCH SENSING

Andrew K. Schulz[1,*], Gokhan Serhat[1,2], Katherine J. Kuchenbecker[1]
[1]Haptic Intelligence Department, Max Planck Institute for Intelligent Systems, Stuttgart, Germany
[2]Department of Mechanical Engineering, KU Leuven, Bruges, Belgium
*Corresponding author's email: aschulz@is.mpg.de

Introduction: Skin is a complex biological composite consisting of layers with distinct mechanical properties, morphologies, and mechanoreceptors (**Fig. 1A**) [1]. Skin's complexities directly relate to the function of the skin site: for example, human plantar skin has a thick stratum corneum (SC) for protection and a dermis organized with collagen perpendicular to the exterior to allow for axial load bearing [2]. This form-function relationship extends to non-human specimens like elephants: the skin throughout the elephant trunk has a dermis of entangled collagen fibers along with thick epidermal armor [3] to blend flexibility and rigidity [4]. In this work, we looked to the extensive literature on human tissue mechanics to create a comparative model that elucidates the form-function relationship across selected morphological properties. We hypothesize that *the elephant trunk's thick protective dorsal skin significantly dulls its tactile sensing ability*. To facilitate safe and dexterous motion, *the distributed dorsal whiskers might serve as pre-touch antennae*, transmitting an amplified version of impending contact to the mechanoreceptors in the dermis (**Fig. 1A**).

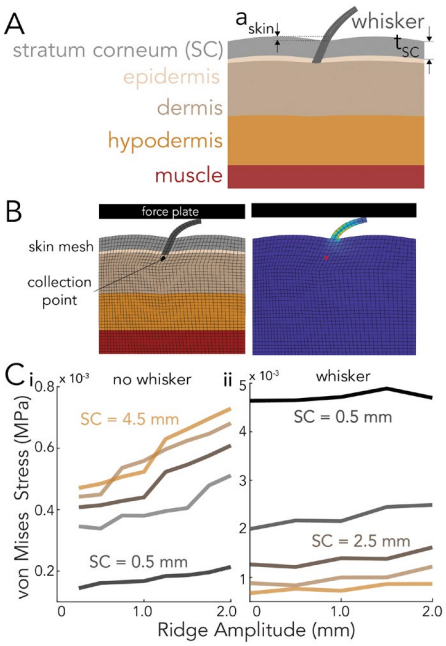

Figure 1: A) The adapted high-fidelity model including one whisker and four laminated skin layers connecting to the muscle. B) Parametric model of skin showing overlay of FE mesh and force plate to deform the model followed by screenshot of the simulated stress distribution in the skin. C) von Mises stress at the marked point in the dermis layer for (i) no whisker and (ii) whisker conditions showing effects of wrinkle ridge amplitude and SC thickness.

Methods: We tested these hypotheses by simulating soft-tissue deformation through high-fidelity linear 2D finite element (FE) modeling based on a previously published human finger-pad model [5]. This model was re-configured with different material properties, different layer thicknesses, a wrinkled surface, and an optional curved whisker embedded between two wrinkles. Our investigation mainly examined variations in SC layer thickness and wrinkle amplitude (**Fig. 1A**). These morphological parameters are selected based on African elephant trunk (*Loxodonta africana*) preserved specimens examined with microCT and microscopy images of histochemical staining. We tested three primary parameter shifts in the model: SC layer thickness, wrinkle ridge amplitude, and presence of whiskers embedded in the skin (**Fig. 1B).** The material properties of each layer and the whisker were taken from published data on each layer's effective modulus. Simulations involved pressing a rigid plate into the skin with a gentle force that was constant across trials and examining the von Mises (VM) stress at a single fixed-depth point in the dermis below the optional whisker (**Fig. 1B**). In examining the impact of layer thickness, we shifted the SC from a thickness of 0.5 mm to 4.5 mm in steps of 0.5 mm, which is consistent with the thickness increase from the distal tip to the proximal base of an adult African elephant trunk [3]. To examine wrinkling, we shifted the wrinkle ridge amplitude from 0.25 mm to 2.0 mm, which is consistent with the wrinkles along the distal tip of an adult African elephant trunk [6].

Results & Discussion: We ran the high-fidelity model at each combination of model parameters. We found that thicker SC increases the stress communicated to the studied point at a fixed depth in the dermis of non-whiskered elephant skin (**Fig. 1Ci)**. This increase in VM stress for increased SC thickness could occur because the very stiff SC transmits the effects of the localized surface contact deeper as it becomes thicker [7]. In examining the impact of a wrinkle amplitude, we see a minimal impact of ridge amplitude for the lowest thickness of SC; however, as we increase the thickness of the SC from 0.5 mm to 4.5 mm, the increasing ridge amplitude amplifies the simulated stress by 75% (**Fig. 1Ci)**, likely due to the notch effect. Examining the whisker condition, we see that a thicker SC has an effect opposite that found in the no-whisker condition: the thicker the SC, the smaller the von Mises stress. The whisker condition also shows little effect of ridge amplitude on the von Mises stress. When we compare the whisker to the non-whisker condition, we see an order of magnitude difference in the stress. Specifically, adding a whisker to the model amplifies the stress at the studied point by a factor of more than 15 (**Fig. 1Cii)**. These interesting findings highlight the complexity of skin and whisker contact mechanics. This study is limited by the assumptions made, as we model isotropic skin layers without transversely anisotropic material properties; adding the anisotropy known to occur in biological tissues such as collagen, keratin, and elastin could bring the model even closer to biological relevance. It also may be necessary to expand this 2D model to include the differing third dimension of the whisker and skin.

Significance: This work seeks to expand the comparative biomechanics field to include tissue engineering, analyzing a comparative skin model by redesigning a previously published human finger-pad model [5] with morphological parameters measured from an elephant trunk. We hope this work will motivate further investigations into the impact that different morphological parameters can have on skin mechanics including SC thickness and wrinkling. Finally, this work serves as a potential inspiration to create future models that allow the user to adjust morphological and mechanical parameters, such as skin wrinkling and material properties, as a means to understand sensory impacts across mammalian skin structures using the ample literature of human biomechanics and tactile sensitivity.

References: [1] Eder et al. (2018) *Science*; [2] Boyle et al. (2018) *Sci. Adv.*; [3] Schulz et al (2023*) bioRXiV*; [4] Schulz et al. (2022) *PNAS*; [5] Serhat et al. (2022) *PLOS ONE*; [6] Schulz et al. (2023) *Bioinsp. & Biomim.*; [7] Leyva-Mendivil et al. (2015) *JMBBM.*

USING ULTRASOUND TO QUANTIFY MUSCLE INTEGRITY IN LATE ONSET TAY SACHS DISEASE

Euan Forrest, BS[1]; Frances T. Sheehan, PhD[1]*; Cynthia Tifft, MD, PhD[2];
Camillo Toro, MD[2]; Derek Day, MD[3]; Jared A. Stowers, MD[3]; Abdullah AlQahtani, MD, MPH[3]; Katherine E. Alter, MD[1]
[1]Rehabilitation Medicine and [2]National Human Genome Research Institute, NIH, Bethesda, MD;
[3] MedStar National Rehabilitation Hospital, Washington, DC; [4]The Johns Hopkins University, Baltimore, MD
*Corresponding author's email: gavellif@cc.nih.gov

Introduction: Late Onset Tay Sachs Disease (LOTS) is a rare, genetic, lysosomal storage disorder caused by a mutation in the *HEXA* gene, resulting in the absence of enzyme β-hexosaminidase A. This absence fosters abnormal ganglioside accumulation in the central nervous system, resulting in progressive, neurogenic muscle weakness, dysphagia, tremors, etc. With promising emerging therapies, it becomes imperative to develop accurate tools that directly quantify changes in muscle integrity. something currently lacking in the LOTS literature. Although magnetic resonance imaging can provide measures of muscle integrity, it is costly and often patients with LOTS cannot endure the required scan times. Thus, the objective of this study is to determine if ultrasound (US), which is clinically more accessible and less expensive, can provide such quantitative measures. Specifically, we set out to determine if measures of muscle quality, thickness, and stiffness can be used as biomarkers for muscle integrity by comparing these measures between patients with LOTS and healthy controls.

Methods: From an ongoing, prospective, longitudinal study, muscle integrity was measured in a cohort of 23 patients with LOTS. For the current study, only patients with matched controls were included (n=10). Patients (4/6 M/F; age=42.0±12.1 years; BMI=26.3±4.2) were matched to controls (4/6 M/F; age=42.2±12.1 years; BMI=26.6±4.2) by gender, age, and BMI (age Δ=2.81±1.45 years; BMI %Δ=3.83±2.61%).

Using a Siemens Accuson 2000US with a 9L4 linear probe, greyscale US images were captured for the biceps, triceps, rectus femoris and semimembranosus in both the long and short axes. In addition, shear-wave elastography measures were captured in the long axes for each of these muscles. Heckmatt scores were visually determined by a qualified clinician (author KEA). Three measures of muscle thickness were acquired in the long axis images of the muscles and averaged for final thickness measure. Three to six measures of stiffness were acquired within the belly of the muscle and average for a final stiffness measure.

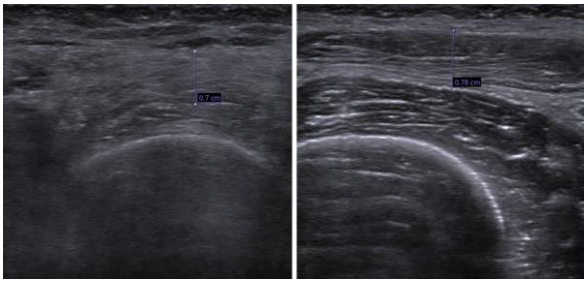

Figure 1: Comparison of Rectus Femoris (RF)

(Left) US image of the rectus femoris of an individual with LOTS (M; 58.1 y/o; BMI = 23.9; Heckmatt = 3).
(Right) US image of the rectus femoris of a healthy control (M; 58.7 y/o; BMI =24.5; Heckmatt = 1).

Results & Discussion: Patients had higher Heckmatt scores for all muscles (Δ =1.5±0.5, =0.7±0.5, =2.0±0.5, =1.6±0.7, $p<0.001$; for the triceps, biceps, rectus femoris, and semimembranosus). The rectus femoris was atrophied (thickness Δ=-0.78±0.18 cm, $p<0.001$) and stiffer (stiffness =1.26±1.40 m/s, $p=0.01$) in the patients with LOTS. Cross-cohort differences in thickness and stiffness were not found for triceps, biceps, or semimembranosus. Differences in extensor-flexor thickness (Δ=-0.15±.09, $p<.001$) and stiffness (Δ=0.62±0.74, $p=0.048$) ratios were found in the patients' lower limb, but not upper.

US measures of muscle integrity serve as key biomarkers reflective of muscle involvement in LOTS. The significant differences in lower, but not upper limb muscles, for all but the Heckmatt scores likely arises from earlier involvement of the lower limbs in LOTS and the progression variability within our patients, indicating ultrasound's ability to nuance fine differences in disease progression. Once the ongoing data collection for matched healthy controls is complete, the full dataset will be analyzed and compared to functional markers (e.g., muscle strength, gait parameters, etc) to determine the relationship between the US measures and function.

Significance: With new therapies coming into the clinical trials stage for numerous musculoskeletal genetic disorders, such as LOTS, it is imperative that we have accurate clinically accessible measuring tools to evaluate their effectiveness in slowing or reversing the loss of muscle integrity. In this preliminary study, standard US measures and US elastography measures demonstrated their ability to detect alterations in muscle that is associated with LOTS.

Acknowledgments: This work was funded by the Intramural Research Program of the NIH Clinical Center and the National Human Genome Research Institute at the National Institutes of Health, Bethesda, MD, USA.

MUSCLE SYNERGY COMPLEXITY IS ASSOCIATED WITH ALTERED POST-STROKE GAIT DYNAMICS

Benjamin C. Fargnoli*, Taniel S. Winner, Trisha M. Kesar, Gordon J. Berman, Lena H. Ting, Michael C. Rosenberg
W.H. Coulter Dept. Biomedical Engineering, Emory University and Georgia Tech, Atlanta, Georgia, United States of America
*Corresponding author's email: benjamin.fargnoli@emory.edu

Introduction: Understanding how post-stroke impairments alter the complex neural and biomechanical processes governing gait (*i.e.*, gait dynamics) could inform rehabilitation personalization. We recently showed that a recurrent neural network (RNN) gait dynamics model revealed individual differences in post-stroke gait dynamics, termed *gait signatures*, that differ from able-bodied (AB) adults [1]. Compared to faster walkers, slower-walking stroke survivors' gait signatures were less similar to AB adults. However, how neural or biomechanical impairments impact post-stroke gait signatures remains unclear [2].

Muscle coordination constraints, as described by muscle synergies [3], may underlie individual differences in gait signatures. Stroke survivors whose muscle activity can be described by fewer muscle synergies (*i.e.*, lower synergy complexity) tend to walk slower. Further, muscle coactivation patterns (*i.e.*, synergy structures) are altered post-stroke [3].

Here we characterized the relationship between post-stroke muscle synergies and gait signatures. We predicted that (1) lower muscle synergy complexity would be associated with lower gait signature similarity to AB, and (2) people with more similar synergy structures would have more similar gait signatures.

Methods: We used an existing dataset of 20 AB adults and 55 adults with post-stroke hemiparesis during 30 seconds of treadmill walking at their self-selected speed [3]. Muscle activity was recorded from 8 muscles bilaterally using electromyography (EMG). Sagittal plane joint kinematics were estimated using optical motion capture.

We computed individual-specific gait signatures by training an RNN to predict the time evolution of joint kinematics [1]. For each participant, we defined gait signatures as the first 6 principal components of the RNN latent states (Fig 1A; right). To quantify the inter-individual similarity of gait signatures, we computed the Euclidean distance between all pairs of gait signatures and between each participant's gait signature and the average AB gait signature.

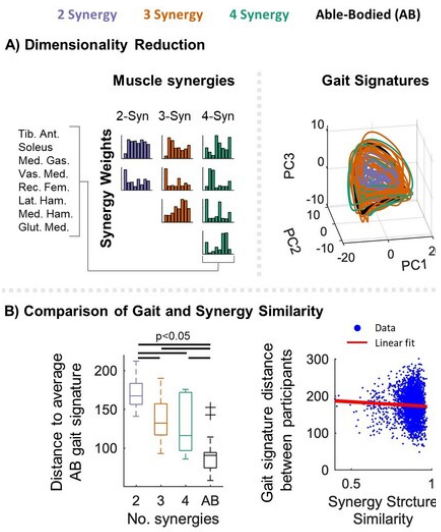

Figure 1: Comparison of muscle synergies and gait signatures. A) Stroke group-average synergy weights (left) and individual-specific gait signatures (right; average AB signature is shown in black). B) Comparison of complexity-based group gait signature distances to the average AB signature (left) and regression of synergy structure similarity versus gait signature similarity (right).

To quantify muscle coordination, we computed participant- and leg-specific paretic/left-leg muscle synergies using non-negative matrix factorization (Fig 1A; left) [3]. We defined synergy complexity as the number of synergies needed to describe 90% of the variance in EMG data [3]. We defined synergy structure similarity as the variance in one participant's EMG data that was explained by another participant's synergy structures [4].

To determine if lower post-stroke synergy complexity is associated with increased deviations from AB gait signatures, we compared the similarity of gait signatures to the AB average signature between groups with two, three, and four synergies (one-way ANOVA with Tukey-Kramer post-hoc tests; $\alpha = 0.05$). To determine if people with more similar muscle synergy structures have more similar gait signatures, we regressed the similarity of gait signatures against the similarity of synergy structures for all participants.

Results & Discussion: Supporting our first prediction, the 2-, 3-, and 4-synergy groups' gait signatures differed from AB, with the 3- and 4-synergy groups' gait signatures being more similar to the average AB signature than those of the 2-synergy group ($p < 0.005$, Cohen's $d > 1.32$; Fig 1B; left). Consistent with the relationship between less-complex synergy control and walking speed, more-severe muscle coordination constraints post-stroke correspond to a reduced ability to walk with AB gait dynamics [1, 3]. Contrary to our second prediction, synergy structure similarity was not associated with gait signature similarity ($r^2 = 0.01$; Fig 1B; right). Synergy similarity, therefore, does not uniquely determine the inter-individual similarity of gait dynamics. Individual differences in biomechanical or sensorimotor impairments may also influence the inter-individual similarity of post-stroke gait dynamics [5].

Significance: This study advances our understanding of how muscle coordination impacts post-stroke walking function by identifying the impacts of synergy complexity on the dynamics governing locomotion.

Acknowledgments: This work was supported by a Petit-Lanier Scholarship, the NIH (F32HD108927, F31HD107968, R01HD095975), the NSF (CMMI 1762211/1761679), the Simons Foundation (707102). We thank Bryant Seamon, Steven Kautz, Richard Neptune, and David Clark for sharing the data for this study.

References: [1] Winner TS, *et al*. *PLOS Comp Bio*. 2023. 19(10); [2] Ting LH, *et al. Neuron.* 2013. 86(1); [3] Clark DJ, *et al. J Neurophysiol*. 2010. 103(2); [4] Cheung VC, *et al*. *J Neurophysiol*. 2024. 131(2); [5] Beyaert C *et al. Clin Neurophysiol*. 2015. 45.

HUMAN MULTI-JOINT COORDINATION IN STANDING AND SUPINE INVERTED-PENDULUM BALANCING

Kreg G. Gruben*, Jennifer Bartloff
Departments of Kinesiology and Mechanical Engineering, University of Wisconsin-Madison, Madison, WI
*Corresponding author's email: kreg.gruben@wisc.edu

Introduction: The human neural coordination strategy of quiet standing remains unknown. Brain imaging could provide insight, if humans performed a supine task in a scanner that requires motor control similar to standing. Functional Magnetic Resonance Imaging (fMRI) has been employed to quantify central nervous system activity and connectivity during a supine inverted-pendulum balancing (SIPB) task [1], however SIPB similarity to standing was quantified only with center-of-pressure (CP) metrics which cannot demonstrate multi-joint coordination equivalence. The purpose of this pilot study was to demonstrate similarity of multi-joint coordination in standing and SIPB to validate a dynamic task that can be used in an MRI scanner to elucidate brain regions and connectivity that contribute to human standing.

To quantify multi-joint coordination recent studies have demonstrated that humans stand by producing a distinct pattern of foot-ground force (F) wherein the anterior-posterior CP varies linearly with the sagittal-plane orientation of F (θ) within narrow frequency bands of those two signals [2]. That linear covariation can be geometrically represented by the F lines-of-action passing near a fixed point in space (intersection point, IP). The height of the IP (zIP) varies across frequency; being above the CM for frequencies below about 1.75 Hz and below the CM above that frequency. The zIP is systematically altered for various conditions such as muscle co-contraction [3], sloped-surfaces [4], and stroke [5]. The zIP characterizes the relative contributions of hip and ankle torque [5] and optimal control of a double inverted pendulum model can replicate the zIP versus frequency function observed in non-disabled adults [6]. This pilot study measured F during a supine task in which ankle torque drove the movement of a single inverted pendulum interfaced with the human via foot sole pressure.

Methods: The SIPB device consisted of dual side-by-side force plates (AMTI AccuGait) mounted to a horizontal low-friction bearing axis coincident with the ankle joints (~0.13 m from the plate surface). The plates rotated about this axis ±10° from vertical. The rotating mass consisted of the force plates, mounting frame, and added mass to position the CM about one m directly above the bearing axis when the plates were vertical to provide a toppling torque analogous to a standing human. The participant lay on a horizontal padded surface wearing a wide belt around the upper pelvis. The belt was attached with adjustable length cables to the support frame near the bearing axis with length adjusted to enable approximately 400-500 N force perpendicular to the plates surface with the legs extended. The participant's feet pressed on the force plate and by altering CP location produced a torque about the bearing axis to stabilize the rotating mass as an inverted pendulum.

The participants (n=3) practiced stabilizing the inverted pendulum for ~2 minutes and then F data were recorded for 30 s at 100 Hz. To evaluate the coordination of CP and θ in a non-balancing task the plates were locked in a vertical position and the participant was provided with visual feedback of the anterior-posterior location of their combined-feet CP. The participants attempted to modulate the CP location to match a target which was the bandpass filtered CP location of a standing human. The bandpass filters were set to 0.25 Hz width and centered at 0.3, 0.8, 1.3, and 2.55 Hz. The amplitude was set to ± 0.03 m for all frequencies and participants were selected to prioritize matching frequency and not minimize instantaneous error. Thirty seconds of data at 100 Hz were acquired.

zIP was extracted from all F recordings [2] by first bandpass filtering CP and θ signals (0.25 Hz bandwidth for center frequencies at 0.3, 0.55, 0.8, …, 6.05 Hz). For each frequency band the zIP was the slope of the CP vs θ plot (orientation of the first principal component). For the CP targeting task only the zIP for the frequency band of the target signal is reported.

Results & Discussion: The SIPB task produced zIP vs frequency curves similar to that of vertical standing (Fig. 1) with low frequency zIP above the CM and higher frequency zIP below the CM, however the values appeared closer to the CM than vertical standing. The non-balancing CP tracking task zIP values were all lower than the CM and trended lower for higher frequencies (Fig. 1). These results suggest that humans do employ multi-joint coordination in a supine balancing task that is qualitatively similar to that of vertical standing. The somewhat flatter curve is similar to that observed for standing on sloped surfaces [4] and so do indicate some control discrepancy from vertical standing on a horizontal firm surface. The non-balancing task demonstrates that simply activating leg muscles does not elicit control similar to standing.

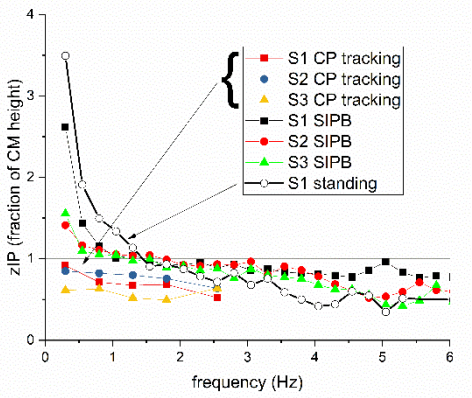

Figure 1: zIP for supine inverted-pendulum balancing (SIPB) task was similar to that of vertical standing. Modulating CP without a balancing task also modulated force orientation to give an IP however the zIP was consistently below the CM.

Significance: These results provide initial validation that this SIPB task may be useful in eliciting multi-joint control similar to standing and is thus justified for use as a functional task in a supine brain imaging scanner.

Acknowledgments: Marsh Fund, University of Wisconsin - Madison

References:

[1] E. P. Pasman *et al.*, "Brain connectivity during simulated balance in older adults with and without Parkinson's disease," *NeuroImage: Clinical*, vol. 30, p. 102676, Jan. 2021, doi: 10.1016/j.nicl.2021.102676.

[2] W. L. Boehm, K. M. Nichols, and K. G. Gruben, "Frequency-dependent contributions of sagittal-plane foot force to upright human standing," *J Biomech*, vol. 83, pp. 305–309, Jan. 2019, doi: 10.1016/j.jbiomech.2018.11.039.

[3] M. Yamagata, K. Gruben, A. Falaki, W. L. Ochs, and M. L. Latash, "Biomechanics of Vertical Posture and Control with Referent Joint Configurations," *Journal of Motor Behavior*, vol. 53, no. 1, Art. no. 1, Jan. 2021, doi: 10.1080/00222895.2020.1723483.

[4] A. Dutt-Mazumder and K. G. Gruben, "Modulation of sagittal-plane center of pressure and force vector direction in human standing on sloped surfaces," *Journal of Biomechanics*, vol. 119, p. 110288, Apr. 2021, doi: 10.1016/j.jbiomech.2021.110288.

[5] J. N. Bartloff, W. L. Ochs, K. M. Nichols, and K. G. Gruben, "Frequency-dependent behavior of paretic and non-paretic leg force during standing post stroke," *Journal of Biomechanics*, p. 111953, Jan. 2024, doi: 10.1016/j.jbiomech.2024.111953.

[6] K. Shiozawa, J. Lee, M. Russo, D. Sternad, and N. Hogan, "Frequency-dependent force direction elucidates neural control of balance," *J NeuroEngineering Rehabil*, vol. 18, no. 1, Art. no. 1, Dec. 2021, doi: 10.1186/s12984-021-00907-2.

A METHOD FOR UNDERSTANDING LOAD CHARACTERISTICS OF RUNNING SPECIFIC PROTHETICS *IN SITU*

Paige M. Agnew[1], Stacie I. Ringleb[1], Hunter J. Bennett[1]
[1]Old Dominion University
*Corresponding author's email: pagne002@odu.edu

Introduction: Running specific prosthetics (RSP) have paved the way for athletes with a lower extremity amputation to engage in sprinting, jumping, and running recreationally and competitively. Since the development of RSPs, research has been focused on understanding and quantifying the mechanical properties of RSPs, especially as it relates to athletic performance on the competitive stage (i.e., the Paralympic and Olympic games) [1-3]. RSPs were primarily tested with commercial materials testing systems or custom drop tests of the prosthetic devices to quantify the force-displacement relationship across a range of loads to simulate those experienced during running [1], which does not consider the variations in stiffness that occurs at different loading rates. Few studies have investigated methods to quantify the stiffness properties *in situ* to better understand the nature of the prosthetic under dynamic load without using machine stiffness values [4]. Despite the fact that the RSP stiffness varies across different speeds, manufacturers recommendations are guided on the user's weight instead of their running speed. Therefore, the purpose of this investigation is to develop a method for quantifying load characteristics of RSPs while *in situ* (during running) and at different speeds. We expected to find similar stiffness decreases as running speeds increase as seen in previous research; however, we expected to find the *in situ* model more accurately depicts the dynamic nature of the RSP during running than previous materials testing research.

Figure 1. Marker placement for running prosthetic.

Methods: One female competitive multi-sport athlete with a left limb below-knee amputation (55yr, 1.67m, 59kg, K-4) volunteered for this study. She completed the running trials using an Ossur Cheetah Xceed prosthetic fitted by a board-certified prosthetist. Six running trials were recorded and analysed for this investigation. Three trials were at a self-selected jogging pace and three at a self-selected running pace. Full body motion capture (collected at 200Hz) included bilateral marker placements on the acromion, medial/lateral epicondyles of the elbow, styloid process, ulnar process, medial/lateral condyles of the knee, greater trochanters, anterior/posterior iliac spine, and iliac crest. Unilaterally, markers were placed on the right foot 2nd toe, 1st and 5th metatarsal head, medial/lateral epicondyle of the ankle, heel and on the prosthetic blade (fig. 1). Two Bertec Force plates were used to collect ground reaction force data, sampled at 2000Hz. Data were time normalized with a custom MATLAB (MathWorks) program. The load-displacement curves were fit with a third order polynomial to determine stiffness. A single subject design was utilized; therefore, results are reported as a percentage relative to self-selected running pace averaged trials.

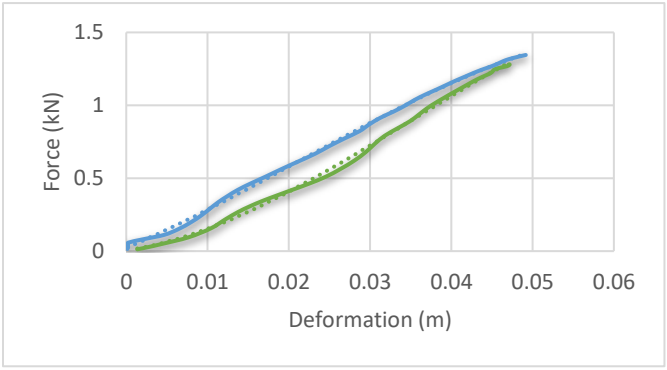

Figure 2. Force deformation during loading response for self-selected (blue) and fast (green) trials fitted with a 3rd order polynomial.

Results & Discussion: The fast run condition was performed 29% faster than self-selected running (3.29m/s vs. 2.54m/s, respectively). Stiffness for fast run was 27.2kN/m, while stiffness at self-selected reached 25.9kN/m. Albeit small, the 4% increase in stiffness conflicts with previous reports, conducted via mechanical testing of prosthetics, indicating that stiffness decreases as speed increases [1-3]. A similar 5% increase in loading rate (peak force / time to peak) was found at faster speeds compared to the self-selected speeds (14.4kN/s vs. 13.68kN/s). Force-deformation during the loading response of stance indicated a curvilinear (3rd order polynomial) displacement as force increases (Fig. 2) for both speeds; however, at slower speeds, it took longer for peak force to occur compared to faster speeds which impacted the loading rate and allows for higher peak force to be achieve. Despite running 29% faster, peak resultant ground reaction forces were only 5% smaller in the fast condition (1.28kN) compared to self-selected (1.35kN) running. This increase in force as the participant runs at slower speeds indicates a biomechanical change possibly due to an increase in confidence or stability on the prosthetic side at slower speeds [5]. These results also indicate that the spring-mass model typically used to explain the behaviour of prosthetic devices should be modified to include the viscoelastic properties. Furthermore, *in situ* biomechanical considerations like utilizing participant-specific analyses are necessary when quantifying prosthetic properties. Machine testing does not consider the dynamic loading, rotational movement, or participant-specific loading characteristics due to perceived stability; therefore, *in situ* stiffness quantification is necessary.

Significance: The significance of this methodology indicates that an alternative model for representing the viscoelastic nature of RSPs is necessary to assess the mechanical properties *in situ.* Additionally, this methodology signifies the importance of calculating stiffness for each participant rather than using a global data set as previous research has indicated [2].

References: [1] Beck et al (2017) *PLOS One*, [2] McGowan et al (2012) *J R Soc Interface*, [3] Hobara et al (2013) *J Biomech*, [4] Barnett et al. (2022) *Gait Posture*, [5] Keller et al. (1996) *Clin Biomech*

ADAPTATIONS OF LOCOMOTOR STABILITY ACROSS EXPOSURE TO ANXIETY-INDUCING VIRTUAL REALITY SETTINGS

Kelly Poretti[1*], Nicole Stark[2], Francesca Wade[3], Peter C. Fino[4], Tiphanie E Raffegeau[1,4]
[1]School of Kinesiology, College of Education and Human Development, George Mason University, Manassas, VA
*Corresponding author's email: kporetti@gmu.edu

Introduction: Experiencing a fear of falling during gait, referred to as mobility-related anxiety, can be induced in a high elevation virtual reality (VR) environment to investigate how anxiety impairs walking performance [1, 2]. Current evidence shows that individuals standing on a high-elevation surface exhibit a stiffening response, reflected in decreased sway variability and increased sway frequency [1]. The changes mediolateral stability, represented by center of pressure (COP), during quiet standing often align with the stiffening hypothesis [1], but during dynamic locomotor tasks like gait, stiffening might be maladaptive. When healthy participants walk in high elevation VR settings, they slow their gait speed and take shorter steps [1,3,4]. However, the reason for these strategies is unclear, as the mechanisms underlying threat-related changes to mediolateral gait stability over time require further investigation. Portable in-shoe load sensors provide a validated measure of the distribution of loads during gait in a way that corresponds to COP measures from force platforms [5]. The difference between medial and lateral plantar loads is an approach to quantify 'the ankle strategy' for controlling mediolateral locomotor balance during gait [6,7], and changes over time may reveal stability-related adaptations to anxiety-inducing settings. The purpose of this study was to explore if compensatory changes to locomotor balance due to state mobility-related anxiety, elicited through anxiety-inducing VR settings, decrease with increasing exposure. Specifically, we sought to investigate adaptations in the distribution of medial and lateral plantar loads across time.

Methods: Participants walked on a walkway (0.4m wide x 5.2m long) at a self-selected pace in VR low and high elevation settings for one minute while wearing a head-mounted display (HTC Vive Pro Eye) and in-shoe load sensors recording medial, lateral, and rear plantar loads (novel Loadsol Pro) as part of a larger study [8]. Balance control during walking was estimated by extracting straight steps from in-shoe sensors using a visualization interface [9], modified for the three-compartment signal in MATLAB (v2022b). Ground reaction force (GRF) was normalized to participants' body weight and 0-100% of stance. Statistical parametric mapping revealed significantly greater asymmetry in the distribution of medial and lateral loads between 33-35.5% of stance due to mobility-related anxiety [7]. Medial and lateral plantar load distributions were examined by calculating the difference between the medial and lateral loads at 34% of stance. After removing gait initiation and termination (4 steps), the first five steady state steps (T1) and the last five steady state steps (T2) were extracted for each participant [10]. Linear mixed-effect regression (LMER) compared the distribution of medial and lateral plantar loads due to mobility-related anxiety (2 levels: Low (reference), High) and across time (2 levels: T1 (reference), T2). Cohen's *d* effect sizes adjusted for small sample sizes (Hedge's *G*) were calculated to interpret (0.2 = small, 0.5 = medium, and 0.8 = large) effect sizes.

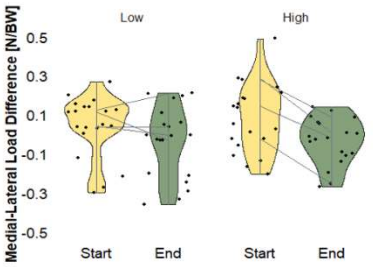

Figure 1: Individuals walk with more evenly distributed medial and lateral plantar loads at the end of one-minute of walking in high VR settings (Hedge's $G = 0.86$). Minimal changes occur over time in low VR settings (Hedge's $G = 0.45$).

Results & Discussion: Four healthy young adults, (1 woman, mean (SD): age[years] = 27.6(4.3), mass[kg] = 68.7(10.6), height[cm] = 169.7(6.5), were included in this analysis. The LMER revealed no interaction effects or main effects of time ($p = .397$, Hedge's $G = -0.05$) or height ($p = .227$, Hedge's $G = 0.66$), despite a visual representation of an interaction (Figure 1). Exploratory follow-up analysis suggested that in high VR environments, participants walked with a more lateral load distribution at the beginning of a trial (T1), shifting to a more even load distribution at the end of a trial (T2). In high elevation this shift had a large effect size (Hedge's $G = 0.86$) as compared to moderate changes between T1 and T2 at low elevation (Hedge's $G = 0.45$). At low height, there was a small change in load distribution, suggesting there is no need to adapt without a postural threat. At low VR environments, there is no need to adapt stability as there is no presence of postural threat, therefore it makes sense to observe less change over time at low VR elevations. However, at high VR heights, the shifting plantar load distribution from lateral to medial across time suggests that stability adapts with exposure in anxiety-inducing settings, with individuals adopting more typical loading patterns over time. Lateral loading at the start of the trial suggests that young adults exhibit exploratory gait patterns, attempting to determine their boundaries in the VR environment and postural threat. Future analyses will include additional data collections to assess true interaction effects.

Significance: Adaptations in the distribution of medial and lateral plantar loads, reflecting stability, were observed over time only when exposed to postural threat experienced through VR-induced mobility-related anxiety. The results represent the first step towards demonstrating the utility of the VR setting as an intervention to reduce mobility-related anxiety and subsequently reduce fall-risk in older adults.

Acknowledgements: Novel electronics inc. (St. Paul, MN) via the 2019 National Biomechanics Day Contest. This work was supported by Mason@4VA and the College of Education and Human Development at George Mason.

References: [1] Brown et al. (2002), *Exp Brain Res*, 145(3); [2] Adkin et al. (2018), *Gait & Posture*, 9; [3] Lindenberger et al. (2000), *Psychology and Aging*, 15(3); [4] Schaefer et al. (2015), *Exp Brain Res* 233(1); [5] Brindle et al. (2022), *Wearable Technologie*s 3; [6] Fettrow et al. (2019), *PLoS One,* 14(12); [7] Poretti et al. (2024), *Under Review*. [8] Raffegeau et al. (2023), *bioRxiv*, Pre-Print; [9] Luftglass et al. (2021), *Clin Biomech* 88; [10] Muir et al. (2014), *Gait & Posture* 39(1)

SUPER-SHOE FOAM COMPRESSION ACROSS RUNNING SPEEDS

Camille L. Nguyen[1], Kyle Coleman[1], Luke VanKeersbilck[1], Iain Hunter[1]*
[1]Brigham Young University, Provo, UT
*Corresponding author's email: iain_hunter@byu.edu

Introduction: The "super shoe", also referred to as Advanced Footwear Technology (AFT), was created with a carbon fiber plate in the midsole and an innovative high energy return foam leading to improvements in running economy of 3-4% [1,2]. It is understood that the carbon fiber plate found in these shoes, embedded between two separate pieces of highly responsive and lightweight foam, aids in increasing the lever arm between the lower extremity musculature and both the talocrural and metacarpophalangeal joints which can reduce the energetic cost of running by ~1% [1, 3]. While characterization of the longitudinal bending stiffness of AFTs between different populations and conditions has assisted in the understanding of the shoe's interaction with the athlete, studies aiming to characterize the compression of the foam at specific points of the shoe under different circumstances is lacking. Hoogkamer found similar metabolic benefits for a range of running speeds from 14-18 km/hr, however, Joubert found slower running speeds received an attenuated metabolic benefit [1, 4]. Greater foam compression was expected due to greater ground reaction forces experienced with faster running. The timing of maximal compression will likely change since the stiffness of the foam is fixed, but the loading will be greater and at a higher rate during faster running speeds. Thus, the purpose of this study was to characterize the magnitude and timing of AFT foam underneath the midfoot and heel during different running speeds.

Methods: Thirty-three runners (twenty heel strike and thirteen midfoot strike) participated in the study by running two trials for 30 s– once at 3.35 m/s (8:00/mi pace) and again at 4.46 m/s (6:00/mi pace)– wearing shoes instrumented with a Hall effect sensor below the midsole and magnets under the insole. The hall effect sensor measured magnetic field strength and output a voltage that was matched with the distance to the magnets. These devices were placed under the heel and midfoot providing shoe midsole compression throughout foot contacts during a 10 s sample. Data were recorded at 960 Hz.

Peak midsole compression under the midfoot and heel along with the percentage of time during compression that the peak compressions occurred were recorded and averaged through each trial. Differences between these variables across the two running speeds were determined using paired t-tests with alpha adjusted to 0.0125 due to multiple comparisons.

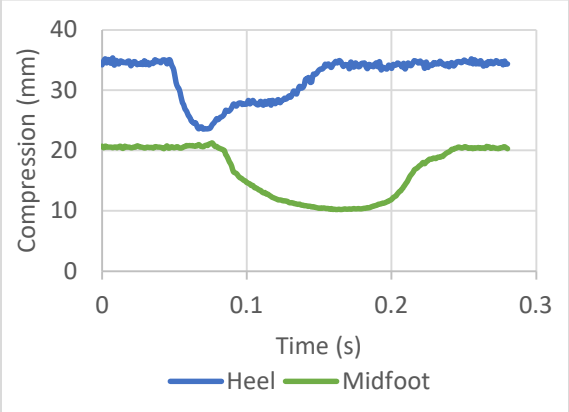

Figure 1. Heel and midfoot foam compression curve Examples.

Results & Discussion: Foam compression observed under the heel and midfoot significantly increased as speed changed from 3.35 m/s to 4.46 m/s (Table 1). Similar metabolic benefits exist across a wide range of speeds when using AFT [1]. However, at slower speeds than Hoogkamer investigated, a smaller benefit was found [4]. Our results show the difference in foam compression between two very different running speeds. When minimal compression is performed due to slower running, there may not be enough energy returned to the runner to provide running economy benefits.

The timing of peak compression throughout the duration of heel compression was shorter when running faster while there were no significant differences for the midfoot location between speeds (Table 1). The compression curves under the heel were dramatically different from the symmetrical shape under the midfoot (Fig. 1). It is not yet understood which curve is more desirable for optimizing the amount and timing of energy returned to the runner.

	Heel Comp (mm)	Midfoot Comp (mm)	Heel Percent to Peak	Midfoot Percent to Peak
3.35 m/s	8.17 ± 4.58	8.76 ± 1.77	26 ± 8%	55 ± 5%
4.46 m/s	9.78 ± 4.84	9.08 ± 2.04	27 ± 7%	54 ± 7%
p-value	0.006*	0.006*	0.009*	0.983

Table 1. Heel and midfoot foam compression and the percent of time to peak compression observed during different speeds.

Significance: The projected end goal for this line of research is to determine which foam properties are more effective for specific running patterns. This study demonstrated the need for different foam properties dependent on running speed. Other considerations should include foot strike type, runner height and mass, and other running mechanics. The next step will be to determine compression timing patterns of various runners compared to observed metabolic benefit.

Acknowledgments: Our lab would like to thank Saucony (Boston, MA) for providing the shoes for this research.

References: [1] Hoogkamer et al., 2018. *Sports Medicine* 48(4); [2] Hunter et al., 2019. *J Sports Sci.* 37; [3] Jean-Pierre and Darren, 2006. *Medicine and Science in Sports and Exercise*. 38(3); [4] Joubert et al., 2023. *International Journal of Sports Physiology and Performance*. 18(2).

SPATIOTEMPORAL GAIT METRICS AND THEIR RELATION TO MEDIAL KNEE JOINT CONTACT FORCES IN ADULTS WITH KNEE OSTEOARTHRITIS.

Sharf M. Daradkeh[1*], Samantha K. Price[1], Kaila A. Fennell[1], John Willson[2], Joshua J. Stefanik[3], Patrick Corrigan[1]
[1]Saint Louis University, [2]East Carolina University, [3]Northeastern University
sharf.daradkeh@slu.edu

Introduction: Medial tibiofemoral joint loading during walking is associated with knee pain and osteoarthritis (OA) progression [1]. Thus, the ability to assess and monitor medial tibiofemoral joint loading could provide valuable insights for treatments that reduce pain, slow OA progression, and maximize physical function. Unfortunately, joint- and compartment-specific forces are not feasibly assessed in clinical settings. With advancements in wearable technologies, spatiotemporal gait metrics are readily accessible to clinicians, but the extent of their relationship to medial knee joint loading is unclear. In this study, we aimed to characterize the relation of common spatiotemporal gait metrics to medial tibiofemoral joint contact forces during walking in adults with knee OA. We hypothesized that increased stance time and step length and decreased cadence would be associated with greater medial tibiofemoral contact forces during walking in adults with knee OA.

Methods: 15 adults (9 Female; age=60 (9) years; height=170 (10) cm; body mass=82.7 (20.5) kg) with clinically defined unilateral symptomatic knee OA based on the National Institute for Heath and Care Excellence (NICE) criteria (≥ 45 years old, knee pain lasting > 3 months, knee pain ≥ 3/10 with walking, and knee stiffness lasting < 30 minutes) were included. Average (SD) knee pain with walking, on a 0-10 scale, was 1.4 (1.3) for the painful limb and 0 (0) for the nonpainful limb. Participants walked for two minutes at a self-selected speed (0.91(0.11) m/s) on a force-instrumented treadmill (Bertec Inc., Columbus, OH, USA). A three-dimensional motion capture system tracked markers affixed to the legs and trunk (Qualisys AB; Gotenburg, Sweden). Marker trajectories and ground reaction forces were sampled at 180 and 2160 Hz, respectively, during the second minute and then reduced to 10 gait cycles. Average stance time, cadence, and step length were determined. Additionally, medial tibiofemoral contact forces were determined for each step using a validated inverse dynamics-informed musculoskeletal model that includes quadriceps, hamstrings, and gastrocnemius muscle forces. After scaling the medial tibiofemoral force waveform to bodyweight (BW), we determined average loading rate during weight acceptance, peak force during the first half of stance, and impulse throughout stance. Generalized linear models were used to determine relationships between spatiotemporal gait metrics and medial tibiofemoral contact forces. Both limbs were included in the models as stratified analyses showed similar associations in painful and nonpainful limbs. Generalized estimating equations were used to account for the correlation between limbs. Each model was also adjusted for gait speed.

Results & Discussion: Mean (SD) stance time, cadence, and step length were 0.81 (0.08) s, 99 (9) steps/min, and 0.50 (0.06) m, respectively. Mean (SD) peak force, average loading rate, and impulse of the medial tibiofemoral compartment were 1.37 (0.35) BW, 8.96 (4.67) BW/s, and 0.73 (0.19) BW*s, respectively. There were no significant relationships between spatiotemporal gait metrics and medial tibiofemoral contact forces (Figure 1). Our findings indicate that these specific spatiotemporal gait metrics may not relate to medial tibiofemoral contact forces during walking in adults with knee OA. While these preliminary data show nonsignificant relationships, an increased number of participants may impact the results.

Significance:
In clinical settings, spatiotemporal gait metrics may not be a valuable predictor of medial tibiofemoral contact forces during walking in adults with knee OA.

Acknowledgments: Funding for the study was provided by the Rheumatology Research Foundation and Academy of Orthopaedic Physical Therapy.

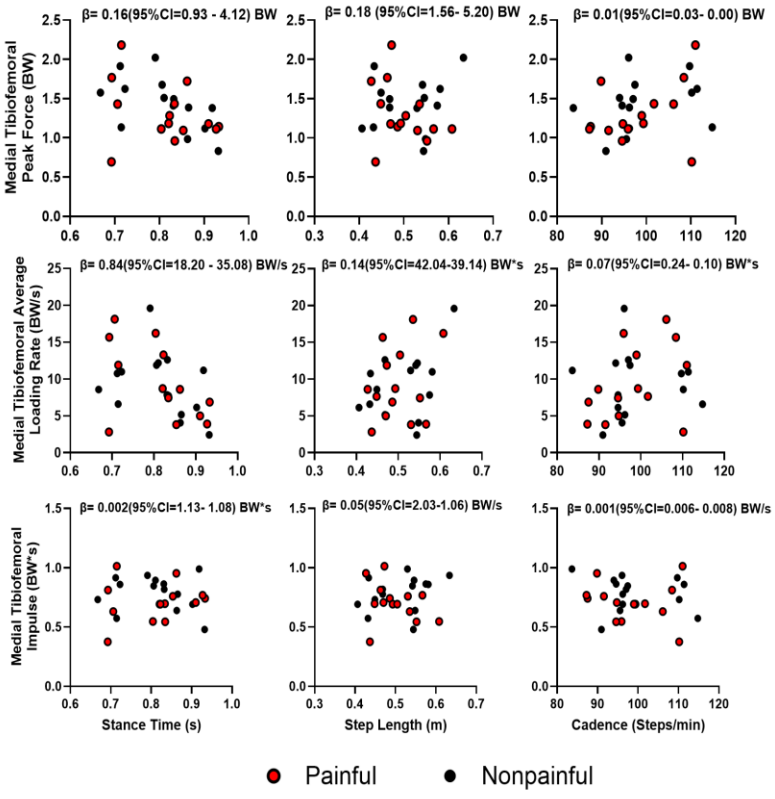

Figure 1: The relationship between spatiotemporal metrics and medial tibiofemoral contact forces. Effect estimates are reported for 0.1 s, 0.1 m, and 1 step/min increase in stance time, step length, and cadence, respectively.

References: [1] Yamagata et al. (2021)

FALL RISK IN PEOPLE EXPERIENCING HOMELESSNESS – A PRELIMINARY META-ANALYSIS

Claire Kim[1] and Feng Yang[2*]
[1]The Westminster Schools, [2]Georgia State University
*Corresponding author's email: fyang@gsu.edu

Introduction: Falls are a serious health concern with severe adverse consequences in general older adults [1]. Limited work has been conducted to examine the fall risk among people experiencing homelessness. It was reported that the fall prevalence is higher among homeless adults than general older adults. However, there is a lack of consensus about the fall risk among this population. This is a non-trivial issue given that over half a million Americans experience homelessness each night, the portion of single homeless adults aged over 50 is growing [2], and the fall risk heightens with the aging process. To develop effective fall prevention treatments for the homeless population, it is essential to understand the magnitude of falls for this population. The main purpose of this preliminary meta-analysis was to summarize the published articles concerning the fall prevalence or number of falls among homeless adults.

Methods: A literature search was conducted in the common databases by using "homeless," "falls," "fall risk," and "fall prevention" as the search terms. Only studies that reported the annual or semi-annual fall prevalence and the number of falls were included. Non-English and non-peer-reviewed articles were excluded to ensure the rigor of the analysis. After removing the duplicates, and examining the title and abstract, the full text of the remaining articles were read to assess their eligibility. The publication characteristics (author(s), publication year, region), sample characteristics (sample size, age), and study characteristics (fall prevalence, the number of fallers, number of falls, and fall tracking duration) were extracted. For each study, the fall prevalence was calculated as the ratio of the number of fallers to the sample size within each study throughout a 12-month period (for the annual fall prevalence) or 6 months (for the semi-annual fall prevalence). A faller was defined as a person who experienced at least one fall during the respective period. The average number of falls was the total number of falls over the corresponding fall tracking period divided by the sample size within each study. The number of fallers, number of falls, sample size, and standard error values were extracted to calculate the pooled fall prevalence and average number of falls over a 12-month or 6-month fall tracking duration. Extracted data were entered into Review Manager (RevMan) 5.3 software (Nordic Cochrane Centre, Denmark) and meta-analyzed using a random-effects model with the inverse variance weight. The 95% confidence intervals (CI) were estimated for the outcome measures. The results were presented using forest plots.

Results & Discussion: Five studies satisfied the inclusion criteria [3-7]. Among the included studies, two reported the fall prevalence over 12 months [4, 5] while the other three documented the fall prevalence in 6 months. Two studies also reported the number of falls over 6 months [3, 6] while one study provided the number of falls in 12 months [5]. The meta-analyses were conducted for the annual and semi-annual fall prevalence and the semi-annual number of falls. No meta-analysis was performed for the annual number of falls. The five included studies enrolled 911 adults experiencing homelessness. The age of homeless adults ranged from 45 [7] to 60.7 [5] years. The majority of the individuals were males (60% [5] - 80.8% [4]). The studies were conducted in the U.S. [3-6] and Ireland [7]. The composite annual fall prevalence was 76.29% (95% CI: [30.43% 122.15%]) (Fig. 1a). The meta-analysis derived a semi-annual fall prevalence of 47.80% (95% CI: [30.70% 64.90%]) (Fig. 1b). The annual average number of falls based on one study was 1.50 falls/person (95% CI: [1.08 1.92]). The average number of falls over 6 months was about 0.98 falls/person (95% CI: [0.83 1.13]) (Fig. 1c). Due to the small sample size of studies, the heterogeneity of the meta-analyses was high. In addition, the prevalence of recurrent fallers, the proportion of injured falls, and the fall risk factors were not considered in the current meta-analyses. More studies with larger sample size are needed to examine the fall risk for homeless people.

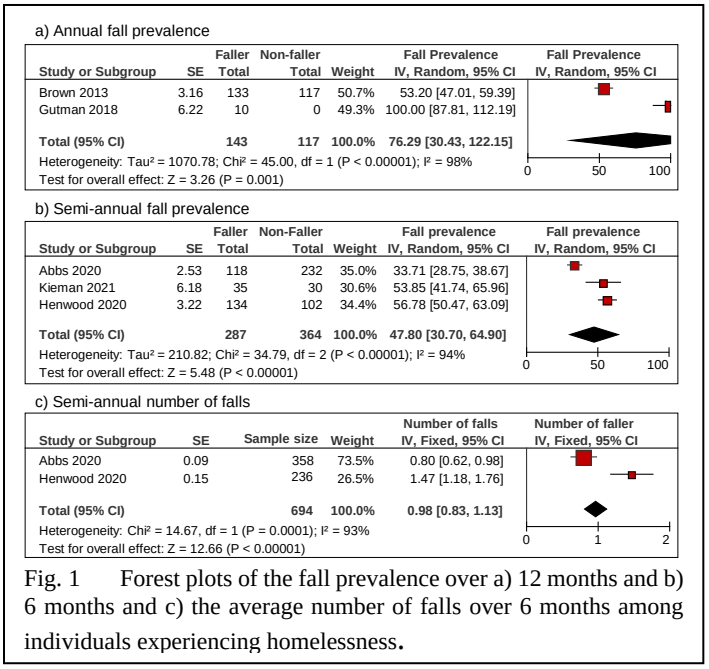

Fig. 1 Forest plots of the fall prevalence over a) 12 months and b) 6 months and c) the average number of falls over 6 months among individuals experiencing homelessness.

Significance: This preliminary meta-analysis extended our understanding of the fall risk among people experiencing homelessness. The results indicated that the fall risk among homeless adults is much higher than that for general older adults (number of falls: 0.21 falls/person/year and annual fall prevalence: 26.5% [1]). The results could provide preliminary results for future studies to further investigate the fall risk among homeless people, for the stakeholders to allocate healthcare resources for preventing falls targeting this population, and for researchers and clinicians to develop effective fall prevention paradigms for people experiencing homelessness.

References: [1] Salari. Journal of Orthopaedic Surgery and Research, 2022. [2] Henry. The 2017 Annual Homeless Assessment Report (AHAR) to Congress, 2018. [3] Abbs. Journal of General Internal Medicine, 2020. [4] Brown. Journal of Health Care for the Poor and Underserved, 2013. [5] Gutman. Annals of International Occupational Therapy, 2018. [6] Henwood. Health and Social Care in the Community, 2019. [7] Kiernan. Scientific Reports, 2021.

EFFECTS OF A 6-WEEK IMMERSIVE, VIRTUAL REALITY PROGRAM FRUIT NINJA VR+ ON STATIC AND DYNAMIC BALANCE FOR YOUNG ADULTS WITH INTELLECTUAL AND DEVELOPMENTAL DISABILITIES

Alana J. Turner[1*], Kaitlyn Wojciechowski[1], Isabelle Farm[1], Emma Wilkinson[1], Matthew Wade[1], Aaron A. Griffith[2], Harish Chander[2], & Adam C. Knight[2]
[1]Coastal Carolina University, Conway, SC 29528
[2]Mississippi State University, Mississippi State, MS 39762
*Corresponding author's email: aturner4@coastal.edu

Introduction: For the general population, 1-3% of individuals have an intellectual and developmental disability (IDD). IDD is characterized by "limitations in intellectual and adaptive functioning [1]." Due to these limitations, individuals with IDD present a greater risk for health concerns including complications with motor development and fundamental movement skills [1]. For example, previous literature demonstrates young adults with IDD tend to have decreases in balance performance and overall postural control when compared to their typically developing peers. Balance deficits are concerns for young adults with IDD because this increases their prevalence of falls [2]. Over thirty percent of adults with IDD fall each year where fifteen percent of these fall result in serious injury and hospitalizations [1]. Efforts to create or find interactive balance interventions to delay or limit these deficits are essential for individuals with IDD to improve movement skills and quality of life. Immersive virtual reality (VR) is defined as "the use of interactive simulation created by a computer to provide users with environments [3]." Immersive VR is currently used as a training tool for young adults with IDD for improvement in social behaviors and interactions [3]. However, there is limited research on the effects of VR training on balance for young adults with IDD. The purpose of this research was to examine static and dynamic postural control/balance in young adults with IDD before and after a commercially available, immersive VR program (Fruit Ninja VR+™). Due to the immersive environment and requirements of the gaming program movements which is like therapeutic balance training exercises (i.e., anterior-posterior weight shifts, unilateral stances, and squats), the researchers expected to see improvements in static and dynamic balance for young adults with IDD after 6 weeks.

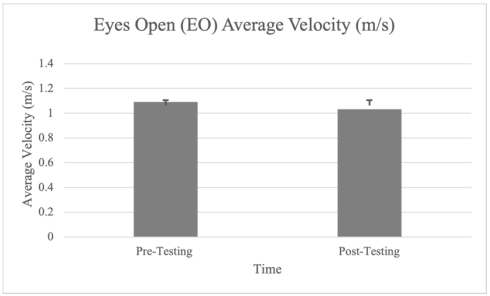

Figure 1: EO average velocity (m/s) from pre-testing to post-testing. Standard deviation bars displayed.

Methods: 12 participants (70.84 ± 16.6 kg; 163.48 ± 9.37 cm; 20.42 ± 1.44 years of age; 4 females and 8 males) participated in a 6-week immersive virtual reality intervention, Fruit Ninja VR+™. Participants completed two 30-minute sessions twice a week for 6 weeks (12 VR sessions with 360 total minutes of VR exposure). The study followed a repeated measures design (pre-and-post) one week before and after the intervention. Static balance measurements included bilateral stance during eyes open (EO) (20s) and eyes closed (EC) (20s), and unilateral stance on the dominant leg (1LEO) (10s) on a BTrackS™ (San Diego, CA) balance platform. Dynamic balance measurements included a Timed Up & Go (TUG) (s) movement test. Static balance center of pressure (COP) sway measurements included: average anterior/posterior (A/P) displacement (cm), average medial/lateral (M/L) displacement (cm), average 95% ellipsoid area (EA) (cm^2), average velocity (AV) (m/s), and path length (PL) (cm). Dynamic balance measurements included movement time (s). A within-subjects one-way repeated measures multivariate analysis of variance (RM-MANOVA) utilized the Wilks' lambda values if significant main effects were identified at an alpha level of ($p < 0.05$) with IBM SPSS™ (Version 29.0.0) (Chicago, IL).

Results & Discussion: No significant main effects or interactions were reported for static balance for A/P displacement, M/L displacement, EA, AV, or PL during the EO, EC, and 1LEO conditions (Fig. 1). Also, no significant main effects or interactions were reported for dynamic balance for movement time. Previous literature reported non-immersive VR could improve muscular endurance , cardiovascular fitness, dynamic balance (TUG), agility, and muscular strength for individuals with IDD [4-8]. However, very few immersive VR studies have reported improvements in static and dynamic balance within a duration of 6 weeks. For example, Lee et al. (2016) reported improvements in static balance, gait, and functional balance in adolescents with intellectual disabilities after an 8-week intervention [9]. Therefore, the researchers concluded the duration of the study (6 weeks) as a possible indication of why postural mechanisms were not improved. Previous studies observed improvements in static and dynamic balance after a minimum of 8 weeks [10]. In addition, the selection of the VR video game (Fruit Ninja VR+™), may not be as versatile or dynamic in its movements as a traditional balance training program. Overall, the commercially available, immersive VR intervention did not improve postural control mechanisms for this population; however, the participants did maintain their current balance measurements across 6 weeks and did not report decrements in balance performance. Future studies should investigate the effects of immersive virtual reality across a longer duration of time with a control group.

Significance: To reduce the prevalence of falls for this population, there is a need to create or investigate a fall prevention program to reduce the risk of falls. Because of the popularity and interest of VR and video gaming amongst the IDD population, this type of program could motivate those with IDD to not only improve or maintain postural control mechanisms but to become physically active. Overall, immersive VR could be an alternate balance training program for young adults with IDD to delay the onset of balance decrements through postural control maintenance.

References: [1] Maulik et al. (2011), *Res Dev Disabil* 32(2); [2] Blomqvist et al. (2013), *Res Dev Disabil* 34(198); [4] Weiss et al. (2006), *Med Neuro Rehab;* [5] McMahon et al. (2020) *J Spec Educ* 35(2); [6] Lotan et al. (2011) *J Phys the Educ* 25(1); [7] Lotan et al. (2015) *Palaestra*, 29(4); [8] Toffalini et al. (2018) *J Intellect Disabil Res* 62(1); [9] Lin et al. (2012) *Res Dev Disabil* 33(6); [10] Lee et al. (2016) *Disabil. Health J*. 9(3).

TOWARD A NON-INVASIVE METRIC OF MICRODAMAGE IN TENDON FASCICLES

Shreya Kotha[1*], Samantha M. Kahr[1], Jonathon L Blank[2], Alex J. Reiter[3], Darryl G Thelen[1,4]
[1]Department of Biomedical Engineering, University of Wisconsin-Madison, Madison, WI, USA
[2]McKay Orthopaedic Research Laboratory, University of Pennsylvania, Philadelphia, PA, USA
[3]Department of Biomedical Engineering, Saint Louis University, St. Louis, MO, USA
[4]Department of Mechanical Engineering, University of Wisconsin-Madison, Madison, WI, USA
srkotha@wisc.edu

Introduction: Shear wave tensiometry is a noninvasive method to gauge axial stress in tendons. Tensiometry is premised on a tensioned beam model [1], which predicts that shear wave speed varies in proportion to the square root of axial stress. Tendon stress is borne by axial stretch of the collagen fibers and adhesion between structures at both the fibrillar and fascicle levels [2]. Fatigue loading is known to induce localized fibrillar damage [3] such that stress in intact fibers may be elevated. This in turn could affect wave propagation along the tissue. The objective of this study is to investigate how wave speed changes in response to fatigue loading in isolated tendon fascicles. We hypothesized that the repetitive loading would result in elevated wave speeds due to accumulated microdamage.

Methods: Rat tail fascicles (F344/BN) from two 9-month-old rats (n=9) were dissected and tested. Fascicle cross-sectional profiles and areas (CSA) were measured at three cross-sections (5 mm apart) using a laser micrometer (Keyence LS-7010) that rotated about the structure. Fascicles were immersed in a PBS bath and secured in a custom benchtop loading system (Aerotech PRO165LM) that used an in-line load cell (Futek LSB210) to measure tensile force. Fascicles were preconditioned by cyclically stretching them to 5% strain at 1 Hz for 10 seconds followed by a cyclic loading (0.5 Hz, 5% peak strain) protocol until failure. Transient shear waves were induced by impulsive lateral taps (50 Hz, 0.3 ms pulse) and wave propagation was measured every 60 seconds (30 cycles) using two laser Doppler vibrometers (Polytec PDV 100). Wave travel time between vibrometer points was used to compute wave speed [4]. Engineering axial stress was determined as the axial force divided by the initial cross-sectional area [5]. For each tap, we used least squares fitting to determine the effective density and unloaded shear modulus that resulted in the best fit of a tensioned beam model to measure stress and wave speed. We determined the stiffness of the linear region of the loading portion of the force-displacement profile using an iterative fitting procedure [6]. Wave speeds at engineering stresses below 5 MPa were excluded in the fitting due to misalignment of the laser and fascicle under low-load and slack conditions. We performed a one-factor analysis of variance (ANOVA) to determine the effect of fatigue life on shear wave speed^2-stress slope and axial stiffness (α=0.05).

Results & Discussion: Fascicles survived an average of 797 ± 317 (mean ± SD) cycles prior to failure. The average effective density computed at initial fatigue life was 2483 ± 320 kg/m^3. At a given stress level, we observed a mild increase in shear wave speeds for a given axial stress with increasing fatigue cycles, though the magnitude of the effect was variable across specimens (Fig. 1a). The estimated effective density decreased significantly ($p < 0.01$) decreased with repetitive loading (Fig.1b). As observed in prior fatigue studies [7], fascicle stiffness also decreased (Fig.1c) with repetitive loading ($p < 0.01$). The decrease in stiffness thought to be the result of localized microdamage which can consist of ruptured and buckled fibers. Such damage may have also contributed to the elevated wave speeds if the intact fibers borne higher stress. Further testing is needed to fully understand how wave speeds change with fatigue, while imaging is also required to confirm the presence of microdamage.

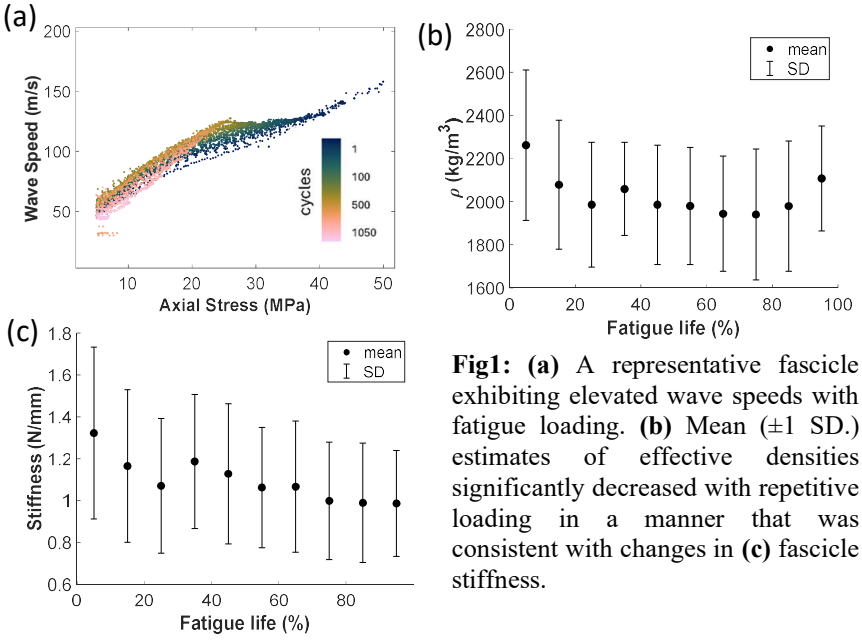

Fig1: (a) A representative fascicle exhibiting elevated wave speeds with fatigue loading. **(b)** Mean (±1 SD.) estimates of effective densities significantly decreased with repetitive loading in a manner that was consistent with changes in **(c)** fascicle stiffness.

Significance: This study provides some initial evidence tensiometry based measurements of fascicle wave speed are altered with repetitive loading, and hence could serve as a noninvasive surrogate measure of microdamage.

Acknowledgments: Funding from NSF (DGE-177503) and DOD (129866603).

References: [1] Martin JA et al., Nat. Commun., 9:2–10, 2018.[2] Shepherd JH et al., Int J Exp Pathol., 4: 260–270,2013.[3] Szczesny SE et al., J. Biomech., 71:251-256,2018 [4] Schmitz DG et al., Sensors, 22:2283– 2298, 2022. [5] Zitnay JL et al., Science Adv., 6,2020.[6] Tanaka ML et al., J. Biomech., 133:074-502, 2011. [7] Keuler EM et al., Sci. Rep., 9:13419, 2019. [8]. Shephard CF et al., Nat. Commun., 11:5444,2020 [9] Blank JL et al., J. Mech. Behav. Biomed. Mater., 125, 2022.[10] Blank JL et al., Ann. Biomed. Eng., 50:751-768, 2022.

SENSORY CONTRIBUTION TO STANDING BALANCE IN PEOPLE WITH DIABETES

Kai Cheng[1,2], Carl Luchies[3], John Miles[4], Chun-Kai Huang[1,2*]
[1]Department of Physical Therapy, Rehabilitation Science, and Athletic Training; [2]KU Mobility Consortium; [3]Department of Mechanical Engineering, University of Kansas, Lawrence, KS, USA; [4]Department of Endocrinology, Diabetes and Clinical Pharmacology; University of Kansas Medical Center, Kansas City, KS, USA
*Corresponding author's email: chuang7@kumc.edu

Introduction: Balance and postural control require the coordination between the sensory systems such as vision, somatosensory, and vestibular. Diabetes mellitus (DM)-induced complications that negatively impact sensory systems may lead to future falls [1]. The annual fall incidence in older DM patients is up to 39%, which is two times higher than healthy older adults [2]. Measuring center of pressure (COP) is one of the most common methods to quantify balance, but COP fails to characterize the impact of individual sensory system contributes to postural control. Decomposing COP through Rambling and trembling (RM-TR) approaches may compliment traditional COP analysis by providing additional insights. For example, RM describes the migration of reference point at which body's equilibrium is maintained, while TR describes the COP migration around the moving reference point [4]. It is speculated that RM may reflect the information processing of central nervous system while TM reflects the peripheral mechanism of postural control [5]. The objective of this study is to investigate the contribution of sensory system to standing balance in patients with DM using RM-TR analysis. Because of DM's comprehensive impact on sensory systems [6,7], we hypothesized that the significant COP changes in DM's vision, somatosensory, and vestibular system will be presented using RM-TR approaches.

Methods: Ten participants with Type 2 DM and ten healthy age-matched adults (HC) were recruited. A virtual-reality-based sensory organization test [8] was applied to examine individual sensory system that contributes to postural control. Participants were instructed to stand on the AMTI force plate (Watertown, MA) for 20 seconds and wore a VR head mounted display (HTC Vive, New Taipei City, Taiwan) with the Solo Step harness system (Sioux city, SD). RM-TR time series were decomposed from COP data using the custom MATLAB® code [9] and the root-mean-square values (RMS) in anteroposterior (AP) and mediolateral (ML) directions were calculated. Difference in RMS between baseline and sensory system examination trials were calculated. Two-way (sensory system x group) repeated-measures analysis of variance with Bonferroni as the post hoc was performed. The alpha level was set as 0.05.

Results & Discussion: Table 1 summarizes the changes of RM-TR displacement when examining different sensory systems between DM and HC. When examining individual sensory systems, increased RM-TR displacement in both AP and ML directions can be observed in both groups. Compared to HC, greater change of both RM and TR displacement was observed in DM group when examining three different sensory systems. Especially in the vestibular system, DM shows significant increase as compared to HC group in ΔRMS of Rambling in AP direction and Trembling in ML direction, which suggests the impaired vestibular system in DM [5].

Our results present the contribution of sensory system to balance in DM population. Compared to healthy adults, greater change of postural control can be observed in people with DM when sensory systems are challenged, especially when vestibular system dominates.

Significance: The findings of this study applying RM-TR approach to COP are important to further our understanding of postural control mechanisms with respect to sensory systems in DM population. The significant findings can promote the application of RM-TR analysis regarding fall risk assessment in people with sensory deficit. More sample sizes are warranted to consolidate this statement.

References:

[1] Ahmad I, et al (2020), *J Musculoskelet Neuronal Interact* 20(2):234-248.
[2] Tilling LM, et al (2006), *Journal of Diabetes and its Complications* 20(3):158-162.
[4] Zatsiorsky VM, et al (2000), *Motor control* 4(2):185-200.
[5] Shin S, et al (2019), *PLOS ONE* 14(10):e0223850.
[6] Li J et al (2019), *Audiology and Neurotology* 24(3):154-160.
[7] HUZMELI I, et al (2017), *GEOSPORT* 53.
[8] Moon S, et al (2021), *Front Bioeng Biotechnol* 9:678006.
[9] Gerber ED, et al (2022), *Gait & Posture* 91:276-283.

Table 1. Changes of Rambling and Trembling in Different Dominant System

ΔRMS (cm)		Rambling (AP)	Rambling (ML)	Trembling (AP)	Trembling (ML)
Somatosensation	DM	0.01	0.04	0.01	0.04
	HC	-0.06	-0.01	0.00	0.04
p-value		0.22	0.59	0.64	0.98
Vision	DM	0.52	0.43	0.26	0.53
	HC	0.36	0.41	0.19	0.36
p-value		0.17	0.88	0.37	0.34
Vestibular	DM	0.63	0.61	0.19	0.68
	HC	0.39	0.40	0.19	0.34
p-value		**0.02**	0.11	0.93	**0.02**

UNDERWATER TREADMILL IMPROVES POSTURAL CONTROL IN CHILDREN WITH CEREBRAL PALSY

Oluwaseye P. Odanye[1*], Joseph W. Harrington[1], Joel H. Sommerfeld[1,2], Aaron D. Likens[1,2], David C. Kingston[1], Brian A. Knarr[1].
[1]Department of Biomechanics, University of Nebraska at Omaha, NE.
[2]Nonlinear Analysis Core, Centre for Human Movement Variability, Omaha, NE.
*Corresponding author's email: oodanye@unomaha.edu

Introduction: Cerebral palsy (CP) refers to a group of lifelong neuromuscular disabilities with postural and movement-based functional limitations. Balance deficits are a common problem for people with CP due to poor trunk control, which may be seen as asymmetry in the movement of the pelvis [1]. Balance issues can lead to falls, making rehabilitation interventions like treadmill training essential to improving their overall function and quality of life [2]. Conventional treadmill training is effective at improving balance in persons with CP [2], [3], and growing evidence indicates that treadmill variants offering some bodyweight support are more effective [1], [4], [5]. A treadmill variant is an aquatic treadmill, which leverages viscosity (hydrodynamic drag) and buoyancy to allow for a support-rehabilitation environment. Hydrodynamic drag offers a resistance force relative to speed, while buoyancy decreases the gravitational effect, reducing joint loading and risk of falls [1], [6]. Although, an aquatic environment is effective for rehabilitating persons with CP [1], [6], it is not clear how aquatic treadmill affects dynamic balance. This study used sample entropy (SE), a measure of movement variability, to investigate how aquatic treadmill walking impacts postural control in typically developing (TD) children and children with CP. SE aided comparison of pelvis dynamics (prediction of the randomness of pelvic motion in all planes) on a dry treadmill and aquatic treadmill in speed-modulated conditions. We hypothesized that there would be less pelvic SE for the CP group compared to the TD at a slow-walking aquatic treadmill condition compared to other conditions because the aquatic exercises have been shown to improve the balance of persons with CP compared to dry exercise conditions [1].

Methods: Fifteen TD children (7:8 M:F, age = 11.3 ± 4.1 years, 1.46 ± 0.18 m, and 44.2 ± 16.8 kg) and 8 CP children (4:4 M:F, age = 12.4 ± 3.6 years, 1.31 ± 13.96m, 45.56 ± 21.47 kg) participated in this study. The participants performed DRY treadmill walking trials followed by aquatic (WET) treadmill walking trials in a block-randomized design. Walking trials were 3 minutes each at 75 %, 100 %, and 125 % of their self-selected speed (Slow, Normal, and Fast respectively) for each environment, totaling 18-min of walking. Segmental pelvic angles were collected with waterproof inertial measurements unit (IMU) sensors (WaveTrack Cometa, Milan, Italy). Data were analyzed in MATLAB (2021a, The Mathworks, Natick, MA, USA), and statistical analysis was done in R/R-studio (R Core Team, 2021; RStudio Inc., Boston, MA, USA) using a multilevel model to determine the effect of walking speed, treadmill environment, and population on the SE of pelvic angles in the sagittal (X), frontal (Y), and transverse planes (Z) at $\alpha = 0.05$.

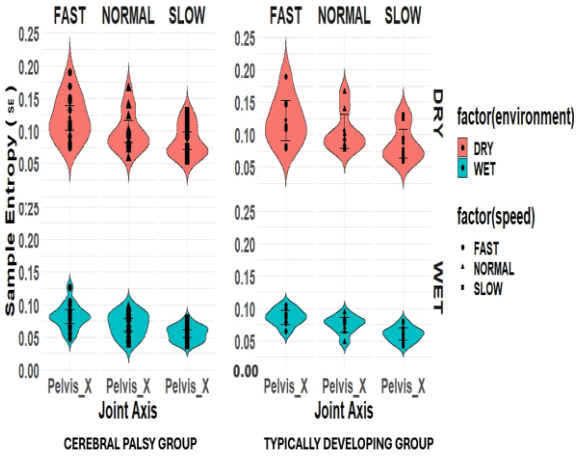

Figure 1: The figure shows the plot of the cerebral palsy group and the typically developing group, with the dry condition above and the wet condition below, and the speed factors represented by shapes for the pelvis X axis.

Results & Discussion: The model for sagittal plane pelvis SE values that included speed only, and the model that included speed and environment were significant ($p > 0.05$). Models including the group factor were not significant. We selected the 2nd model ($X^2(1, N = 23) = 92.76$; $p < 0.0001$) due to improved AIC, and a pairwise comparison on the model result showed that SE at the WET condition was significantly lower than at the DRY condition ($t = 11.63$, $p < 0.0001$). Differences in SE for each speed-condition pairs were also significant, with the lowest SE seen at the slow speed for both the TD and CP groups (figure 1). Both groups had improved mediolateral control of their pelvis at the slow speed and WET treadmill condition compared to the other walking trials, inferring improved mediolateral control of their pelvis at the slow speed and WET treadmill condition compared to the other walking trials, inferring improved postural control for the participants in the sagittal plane of motion. Similar findings occurred for pelvis motion in the transverse plane. There was a significant interaction effect of the environment, speed, and population on the anteroposterior pelvis motion SE ($X^2(7, N = 23) = 15.46$; $p = 0.03058$), with a significantly lower entropy value at the WET condition compared to the DRY condition and the slow speed compared to the other speed trials. Lower SE was found for the CP group than the TD group, inferring that the aquatic environment/slow speed condition may have aided anteroposterior pelvis control more in the CP group than the TD group. This finding for the pelvis-Y axis was in line with our hypothesis, while the group factor (CP and TD) did not impact results for the pelvis X and Z axis.

Significance: This innovative study showed that an aquatic treadmill environment has the potential to improve postural control in children with CP, a condition that is characterized by poor postural control. A longitudinal study will show the tendency to retain and translate this intervention following a therapeutic program.

References: [1] Badawy (2019), *Med. J. Cairo Univ.* 84(1); [2] Elnaggar et al. (2023), *Physical & Occu Therapy In Pediatrics* 43(6); [3]Grecco et al. (2013), *Clin Rehabil* 27(8); [4]Emara et al (2016), *European Journal of Physical and Rehabilitation Medicine* 52(3); [5] Rasooli et al (2017), *International Conference on Rehabilitation Robotics (ICORR)* 101–105; [6]Becker (2020), *PM&R* 12(12).

DEVELOPING A TACTILE AUGMENTING EXOSKELETON ASSISTANCE SYSTEM FOR GAIT REHABILITATION

Christopher P. Engsberg[1], Phillippe Malcolm[1], Nathaniel H. Hunt[1], & Mukul Mukherjee[1]
[1] Department of Biomechanics, University of Nebraska at Omaha, Omaha, NE USA
email: cengsberg@unomaha.edu

Introduction: Asymmetric walking in stroke survivors leads to an increased risk of injury [1], and importantly, reduced balance control [2]. Ankle exoskeletons (EXO) have been shown to improve gait symmetry by assisting the push-off phase of the more paretic limb during walking [3]. However, rarely does this improvement persist after the EXO is removed [4]. Sensory augmentation through tactile stimulation (TS) may aid in the preservation of symmetry by providing additional feedback about their asymmetric walking patterns. TS on its own has been shown to reduce asymmetry [5], however, the functional deficits at the ankle may limit the ability to adjust hemiparetic gait from stimulation alone. Thus, combining the use of an EXO with tactile sensory augmentation would allow stroke survivors to sense their movement errors as well as give them the means to correct them. We aim to investigate if the combined use of an ankle EXO and TS would lead to greater improvements in gait symmetry and balance control than EXO or TS on their own. This abstract describes the development of a real-time adaptive symmetric assistance for both an ankle EXO and a plantar TS device.

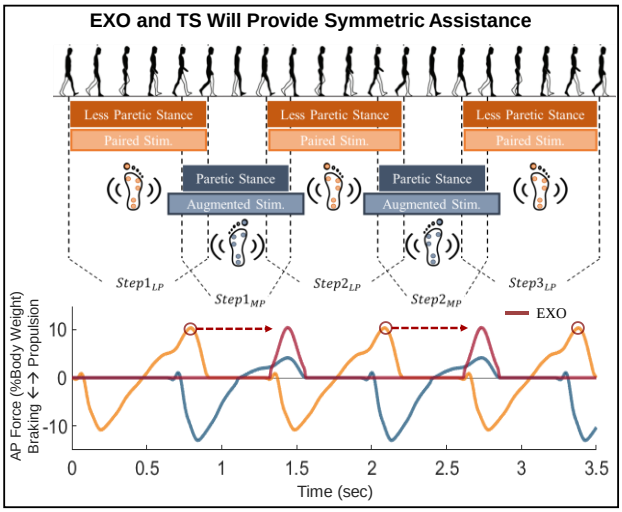

Figure 1: (**Top**) TS provides stimulation to the more paretic foot as a directive for increasing the stance time of the paretic side. The duration of the stimulation is equivalent to the stance time of the less paretic side plus the asymmetry. (**Bottom**) The overall EXO propulsion assistance applied to the more paretic side will match the propulsive power of the less paretic side.

Methods: EXO: The EXO (HuMoTech) provides plantarflexion torque in parallel to the biological plantarflexors (Fig. 2C). Force timing is determined by estimating the current gait percentage from changes in the vertical ground reaction forces (GRF), and force magnitude is monitored using real-time signals from a load cell attached to the EXO. We tested the system in a pilot test (Fig. 2B).

TS: The TS system was already tested on a stroke survivor (M, 65yrs, 172cm, 90.7kg) after providing informed consent (Fig. 2A). TS was applied to the plantar surfaces with custom-made insoles, each with six C-2 tactors (EAI) that provide suprathreshold mechanical vibrations at 250Hz. The duration of these vibrations reinforced walking with symmetrical stance times by instructing the subject to have keep their paretic foot on the ground as long as the tactors on it were vibrating (Fig. 1).

Results & Discussion: Our preliminary results demonstrate the adaptive control of our EXO and TS systems (Fig. 2). The stroke survivor experienced vibrations on the more paretic side for 0.186±0.05sec longer than the actual paretic stance time on average, while the less paretic side received vibrations that were only 0.002±0.01sec longer than the actual stance time. The stroke survivor had an average baseline asymmetry of 10.35%, that reduced while walking with the TS to 8.9% (a Δ of -13.8%).

Pilot testing with the EXO device shows adaptive control that provided peak plantarflexion assistance with the actual force and AP GRF differences as 41.5±13.1N and a time delay of the peaks at only 0.038±0.21sec. With our devices working appropriately, we hope to begin testing the combination of these devices together in more subjects.

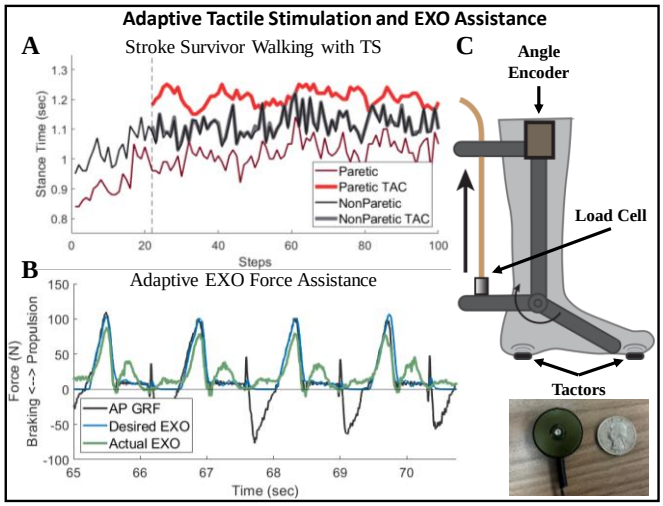

Figure 2: (**A**) Subject stance and ON times of TS. Dashed vertical line indicates tactors starting. (**B**) EXO force profiles adapted to the timings and magnitude of the actual AP GRFs while walking. (**C**) Depiction of EXO and TS set up together.

Significance: With these adaptive functional and sensory assistive devices, more detailed questions can be performed to better understand how the motor and sensory deficits of stroke negatively impact their gait patterns. Future work with these devices is anticipated to show that the combination of motor and sensory augmentation allows for greater retention of therapeutic interventions.

Acknowledgments: This work is supported by AHA awards (24PRE1196160 and 18AIREA33960251, #959486), an NIH P20 award (P20GM109090). In addition, intramural GRACA and NU collaborative NRI grants also provided support.

References: [1] Norvell D. et al. Arch Phys Med Rehabil. (2005); 86: 487-93; [2] Hendrickson J. et al. Gait Posture (2014); 39: 177-81.; [3] Miguel-Fernandez, J. et al. IEEE RAL (2022); 7: 7574-80. [4] Wutzke C. et al. Top Stroke Rehabil. (2013); 20: 233-40. [5] Afzal M. et al. Biomed Res Int. (2015); 2015.

COMPARING REAL VS. SIMULATED LINEAR ACCELERATION IMU DATA DURING STEADY-STATE WALKING

Taryn A. Harvey[1*], Jennifer K. Leestma[1,2], Gregory S. Sawicki[1,2] Aaron J. Young[1,2]
[1]Woodruff School of Mechanical Engineering, [2]Institute for Robotics and Intelligent Machines, Georgia Institute of Technology
*Corresponding author's email: taryn.harvey@me.gatech.edu

Introduction: Inertial measurement units (IMUs) provide valuable information about human kinematics and provide a portable method for data acquisition in comparison to typical motion capture software. The portable and wearable nature of these sensors has made them invaluable in wearable robotics, specifically in data-driven applications that require real-time biomechanical information about the user. Previous work has replicated physical IMUs that would be placed on the body (RealIMU) using post-hoc analyses on motion capture data to create simulated IMUs (SimIMU), where IMU data is generated as though the sensor was attached to a specific body segment. Therefore, SimIMU data is often considered *ideal*, exhibiting less noise from soft tissue artifact than RealIMU data because it is perfectly coupled to the skeleton. SimIMU data has been used to successfully train data-driven models to predict factors such as biological joint angles and moments for use in gait analysis [1] and robotic control applications [2]. They have advantages over RealIMUs because researchers can simulate any combination of locations and choose optimal placement for a given wearable design. While predictions from data-driven models have shown promise, errors between the raw RealIMU and SimIMU data are rarely shown in detail to determine if foot impact-induced soft tissue noise impacts the accuracy of SimIMU estimates throughout specific gait cycle regions. In this work, we sought to investigate the relationship between RealIMU and SimIMU data throughout different regions of the gait cycle in the anteroposterior direction (AP) during steady-state walking. We hypothesized that error would be highest for all sensors at ipsilateral heel contact, due to high impact forces and resultant soft tissue noise, and relatively minimal throughout the rest of the gait cycle.

Methods: We collected motion capture at 100 Hz (Vicon Motion Systems, UK) and IMU data at 200 Hz (Microstrain by HBK, USA) from one participant walking at 1.25 m/s on a CAREN treadmill (Motek Medical, The Netherlands). We placed full-body motion capture markers on the subject, who also wore a pair of pants with five IMUs integrated into the fabric and one IMU on the sternum. We placed markers on each IMU to measure their locations on each segment. We collected steady-state walking data from 150 gait cycles of a protocol approved by the Georgia Institute of Technology Institutional Review Board. We calculated the body kinematics of each segment using OpenSim and simulated IMU signals at each marker location that marked a physical IMU [3]. We identified gait events using a kinematic method, used these events to define single and double stance regions, and resampled all data to 0-100% of double and single stance phases [4]. We evaluated the mean absolute error (MAE) between SimIMU data and RealIMU data over each single and double stance phase with respect to the right leg.

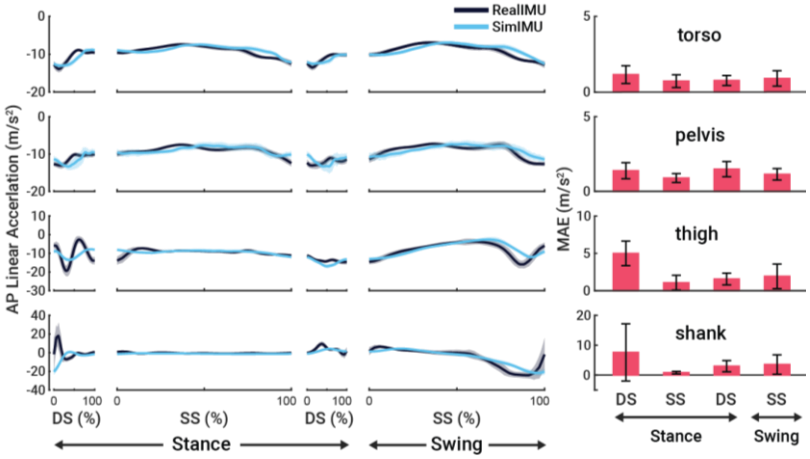

Figure 1: (Left) RealIMU and SimIMU linear acceleration in the anteroposterior (AP) direction during steady-state walking for the torso, pelvis, right thigh, and right shank across right stance/swing as percent double-support (DS) and single-support (SS). (Right) Corresponding RealIMU and SimIMU mean absolute error (MAE).

Results & Discussion: MAE between RealIMU and SimIMU is relatively low (<10 m/s) for the torso, pelvis, and thigh segments throughout all gait cycle regions. However, MAE increases during the transition from swing to stance phase – a period of ~10ms. The shank MAE exhibits high variability (7.57 ± 9.57 m/s^2) and reaches a peak of 33.34 m/s^2 at 7% of stance limb DS (Fig. 1). Overall SimIMUs appear smoothed, resulting in lower peak accelerations than RealIMUs at heel contact. These results partially support our hypothesis, showing higher error around heel contact and minimal error throughout the rest of the gait cycle for only the sensor on the shank. Proximal sensors produce lower errors during heel contact, rejecting our hypothesis and suggesting that high-acceleration signals are dissipated once they reach the upper thigh. This analysis proves that RealIMU data is vital to capturing distal lower-limb movement with high-fidelity, especially at heel contact. However, it is unclear if this disparity is due to soft tissue noise and sensor-user decoupling in RealIMUs or due to position-derived and filtered SimIMUs that are failing to capture transient, high-acceleration signals.

Significance: This analysis demonstrates that SimIMUs possess value as inputs to a data-driven model for proximal sensors. Researchers can take advantage of existing motion capture data, incorporate SimIMUs, and further extract compelling information about human physiological states *offline*, ranging from spatiotemporal gait parameters to ML-driven exoskeleton control. However, the translation of SimIMU to *real-time* monitoring is not perfect for distal segments. RealIMU is invaluable for capturing high-acceleration signals at distal locations – an important observation for those studying high-speed maneuvers such as perturbations.

Acknowledgments: This work was funded by the NSF GRFP Award #1324585 and NIH Award DP2-HD111709.

References: [1] Mundt et al. (2020), *Front. Bioeng. Biotechnol*. [2] Camargo et al. (2022), *J Biomech*. [3] Rajagopal et al. (2016), *IEEE TBME* [4] Zeni & Higginson (2008), *Gait Posture*

EFFECTS OF NON-TREADMILL TRIP TRAINING ON LAB-INDUCED TRIPS AMONG COMMUNITY-DWELLING OLDER ADULTS

Youngjae Lee[1], Neil B. Alexander[2], Christopher T. Franck[3], Michael L. Madigan[1*]
[1]Grado Department of Industrial and Systems Engineering, Virginia Tech, Blacksburg, VA, United States
[2]Department of Internal Medicine, University of Michigan, Ann Arbor, MI, United States
[3]Department of Statistics, Virginia Tech, Blacksburg, VA, United States
*Corresponding author's email: mlm@vt.edu

Introduction: Trip-induced falls are a major source of injuries among older adults aged 65 years or older [1]. Reactive balance training using specialized treadmills has emerged as a promising exercise intervention to reduce the risk of trip-induced falls [2]. However, the need for a specialized treadmill presents a large financial barrier that may hinder its wider adoption. We have proposed a so-called trip training protocol that targets key kinematic requisites of balance recovery after tripping [3] yet does not require a specialized treadmill [4]. The purpose of this study was to investigate the effects of this non-treadmill training (NT) on kinematic responses to lab-induced trips among community-dwelling older adults. We hypothesized (1) NT and treadmill training (TT) would improve reactive balance in response to lab-induced trips compared to a control intervention, and (2) TT would improve reactive balance more than NT because TT involves responses to more sudden trip-like perturbations. These hypotheses were based on prior step training and treadmill training studies eliciting improvements in reactive balance [5].

Methods: Thirty community-dwelling older adults (18F and 12M; mean ± SD age = 71.8 ± 4.4 years; height = 1.68 ± 0.10 m; mass = 77.1 ± 16.8 kg; unipedal stance time = 17.6 ± 12.3 sec) were recruited from the local community. NT (n=10) and TT (n=10) participants attended two 45-minute training sessions per week for three weeks, and CG (n=10) participants received no training. After training, all participants were exposed to two lab-induced trips while walking on a walkway. Each trip was classified as either a fall, recovery, harness-assist, or miss (i.e., improper triggering of trip obstacle) based on the force applied to the fall-protection harness and video review. Key trip recovery kinematic measures were determined using optical motion capture and two critical temporal events (i.e., trip onset and touchdown of the first recovery step). Fisher's exact test and a mixed-model ANOVA with *a priori* contrasts were used to investigate differences between groups with a significance level of 0.05.

Results & Discussion: 60 trips resulted in 22 falls and 27 recoveries (11 trials were harness-assisted or missed trips and excluded from further analysis) (Table 1). Unexpectedly, TT exhibited a higher fall rate than NT, but neither NT nor TT exhibited a fall rate that differed from CG. Despite this, NT and TT showed improved recovery kinematics compared to CG. NT showed a longer recovery step length and a faster recovery step speed compared to CG, while TT showed a smaller trunk angle at touchdown compared to CG and NT. Results suggest different beneficial effects between NT and TT in that NT might be more beneficial in improving recovery step kinematics, while TT might be more beneficial in improving trunk kinematics. These results partially supported our hypotheses, and support NT as eliciting improvements in some aspects of reactive balance after lab-induced trips.

Table 1. Percentage/count or least squares means (95% confidence intervals) and *p*-value for each outcome measure and *a priori* contrast. Positive trunk angle means flexion movement. Max value was from trip onset to one second after touchdown. Bold means statistically significant. AP = Anterior-posterior.

	NT	TT	CG	NT vs. CG	TT vs. CG	NT vs. TT
Fall rate	24% of 17 trips	63% of 16 trips	50% of 16 trips	0.157	0.722	**0.037**
Stepping strategy (elevating / lowering) [6]	5 / 12	4 / 12	3 / 13	0.688	0.999	0.999
Trunk angle at touchdown (deg)	29.8 (26.1, 33.5)	24.5 (21.0, 28.1)	30.0 (26.4, 33.6)	0.921	**0.027**	**0.039**
Recovery step length (% body height)	49.3 (45.6, 52.7)	45.4 (41.6, 48.9)	40.8 (36.4, 44.8)	**0.002**	0.080	0.112
Recovery step speed (m/s)	1.80 (1.68, 1.91)	1.73 (1.60, 1.84)	1.59 (1.43, 1.73)	**0.022**	0.134	0.358
AP distance between mid-hips and step at touchdown (% body height)	-14.6 (-19.5, -8.6)	-12.4 (-17.4, -6.3)	-8.9 (-14.8, -2.0)	0.150	0.386	0.543
Max sacrum drop (% sacrum height)	19.3 (15.5, 23.1)	18.1 (14.5, 21.6)	15.8 (12.1, 19.5)	0.154	0.339	0.610

Significance: Our results provided support for beneficial effects of NT, yet different beneficial effects compared to more commonly used TT in improving reactive balance kinematics. Additional research may be able to improve the benefits of NT. Future studies are needed to investigate the effects of NT on real-world reactive balance and falls.

Acknowledgments: Research reported in this publication was supported by the National Institute on Aging of the National Institutes of Health under Award Number R21AG075430. The content is solely the responsibility of the authors and does not necessarily represent the official views of the National Institutes of Health. The authors also thank Michelle Morris for her contributions to data acquisition.

References: [1] Berg et al. (2016), *MMWR* 65(37); [2] Gerards et al. (2017), *Geria & Geron Int* 17(12); [3] Pavol et al. (2001), *J Geron* 56(7); [4] Lee et al. (2022), *Front Spo Act Liv 4*; [5] Okubo et al. (2017), *BJSM* 51(7); [6] Eng et al. (1994), *Exp Brain Res* 102.

Assessment of Wearable Hip Exoskeleton Impedance Control on Human Lower-Limb Kinematics, kinetics, and Muscle Contractility During Walking

Qiang Zhang[1*], Sahar Ostadrahimi[1], Hao Su[2]

[1]Department of Mechanical Engineering, the University of Alabama, Tuscaloosa, AL 35401 USA [2]Department of Mechanical and Aerospace Engineering, NC State University, Raleigh, NC 37695 USA. *Corresponding author email: qiang.zhang@ua.edu

Introduction: Hip exoskeletons have attracted much attention from the exoskeleton research community in recent years. Compared to the more distal ankle and knee exoskeletons, the proximal placement of motors and electronics near the waist could add less moment inertia during walking. In addition, the manipulation of the hip joints by using powered devices could directly and effectively affect gait parameters, such as step length, step width, and walking cadence [1-4]. Furthermore, according to Frank et al. [5], hip-only and ankle-only robotic assistance could separately reduce the metabolic cost during walking by 26% and 30%, respectively, relative to walking with a full unassisted lower-limb exoskeleton. Those results suggest that both hip and ankle joint assistance are essential and comparable to each other for improving the energetics of human walking. However, the research studies on how hip joint assistance affects the distal lower-limb biomechanics during walking were very limited [6]. Therefore, this study aims to assess the hip exoskeleton's assistance to lower-limb kinematics, kinetics, and muscle contractility during walking.

Methods: The wearable bilateral hip exoskeleton developed by Dr. Hao Su's lab at NCSU was used in the current study. The overall experimental study design is shown in Fig. 1. To provide multiple assistive levels, the finite-state-machine impedance control (FSM-IC) was applied as a middle-level controller for both stance and swing phases during walking, where the assistance can be calculated as

$$\tau_{ext} = K_{ext}(q - q_{ee}), \tau_{ext} = K_{flex}(q - q_{ef}).$$

Six groups of impedance control parameters were selected manually to generate the assistance profiles (Fig. 1 (a)). The lower-level closed-loop torque control was designed based on an L1 adaptive controller. During the walking experiments, the treadmill speed was set at 1.0 m/s, and each assistance level was applied to both hip joints, representing one walking condition. Under each walking condition of 3 minutes, both onboard sensing signals and plantarflexor muscles' ultrasound imaging signals from plantarflexor muscles, were collected synchronously by using a trigger system in Matlab. The muscle contractility was determined by ultrasound images in Matlab. To enhance the effect of six controlled conditions on hip exoskeleton adjustments, we selected the last 10 gait cycles of each condition. Images from each gait cycle were converted from RGB to 2D gray and compared to the initial frame using Pearson's correlation coefficient as a distance metric. Then, we found the mean correlation of 10 cycles in each condition. The treadmill walking protocol was approved by the IRB of the University of Alabama (# 23-09-6911). Six participants (mass: 74.9 ± 8.1 kg, height: 170.1 ± 3.7 cm, age: 27.6 ± 5.6 years) without any neurological disorders were recruited.

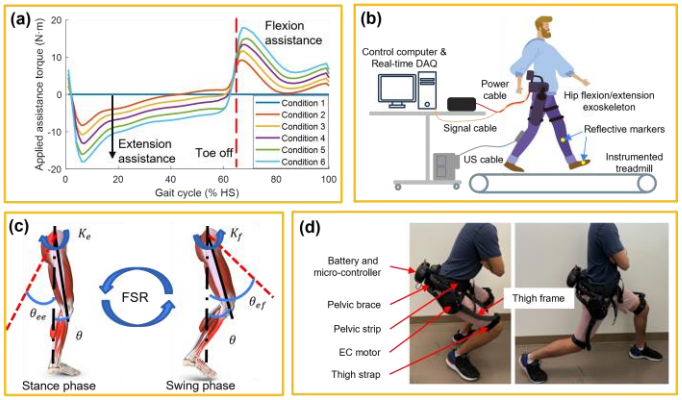

Figure 1: (a) Assistance torque profiles as a percentage of the gait cycle (b) Schematic diagrams of the experimental study design (c) Demonstration of the finite-state-machine impedance control (FSM-IC) (d) The components of the wearable bilateral hip exoskeleton.

Results & Discussion: The hip joint range of motion (ROM) was increased through 6 conditions compared to baseline zero assistive torque from 40 to 50 degrees as shown in Fig. 2 (a). The RMS of assistive torque increased from 1.4 Nm to 5.6 Nm compared to baseline (Fig. 2 (b)). Under each waking condition, the muscle contractility was determined according to the 2-D image correlation between frames of heel strike and peak deformation. Across walking conditions, the muscle contractility was compared by using Pearson's correlation coefficient matrix. It showed that the correlation decreased from 1 to 0.88 compared to baseline and the highest muscle contractility variation occurred in condition 5 (Fig. 2 (c)). Although results showed that individual subjects had a different correlation matrix, demonstrating human-to-human variability of muscle contractility (Fig. 2 (c)), the overall results across six participants implied that muscle activity corresponds to energy cost, and the correlations matrix of ultrasound imaging could be used as an indicator of muscle energy when designing muscle-in-the-loop optimal control approaches.

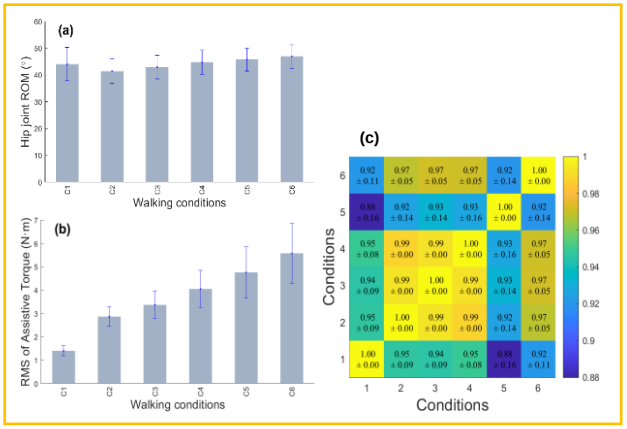

Figure 2: Hip joint kinematics (a), kinetics (b), and plantarflexor muscle contractility levels (c) during treadmill walking under six assistance conditions of all subjects.

Significance: We proposed the first attempt in the field of human-assistive robotics to evaluate lower-limb muscle contractility with ultrasound imaging when adding external hip joint assistance from a wearable bilateral hip exoskeleton. The muscle deformation is related to the applied hip joint assistive torque conditions. The ultrasound imaging shows deeply real-time muscle morphology information compared to the sEMG muscle changes indicator method. As a significant clinical outcome, these outcomes from the current study will facilitate the development of muscle-in-the-loop control algorithms.

Acknowledgments: This work was supported by the ROH fund from the University of Alabama with FOAP of #13009-214271-200.

References: [1] Pan et al. (2023), *Annals Biomed. Eng.* 51(410); [2] Lim et al. (2019), *IEEE Trans. Robot.* 35(4); [3] Zhang et al. (2017), *Science* 356(6344); [4] Ding et al. (2018), *Sci. Robot.* 3(15); [5] Franks et al. (2021), *Wear. Technol.* 2; [6] Tu et al. (2021), *ICRA*.

PERSONALIZED SOUND BIOFEEDBACK FOR OLDER ADULT BALANCE TRAINING: A THEMATIC ANALYSIS

Zahava Hirsch[1*], Samantha Villanueva[1], Jake Stahl[1], Daivarsi Malik[1], Matias Vilaplana Stark, Luke Dahl, Antonia Zaferiou[1]
[1]Stevens Institute of Technology, Department of Biomedical Engineering, Hoboken, NJ USA
*Corresponding author's email: zhirsch@stevens.edu

Introduction: Sonified biofeedback uses auditory signals to convey biomechanical measures. Sonified biofeedback movement training is a growing research field that has shown positive effects in rehabilitation [1,2]. We developed a sonified biofeedback gait training system to help older adults improve their balance towards future fall prevention. Given music's ability to improve motivation and engagement, there is a benefit in incorporating music into balance training [3]. However, music preferences are highly individualized. Therefore, we conducted a thematic analysis on two balance metric sound designs – a center of mass to base of support distance, "Lateral Distance", using a drum beat tempo change, and whole-body frontal plane angular momentum using a pitch change. As part of the user-centered design process, we thematically analyzed the transcripts of "think-out-loud" experiential sessions in which older adults shared their impressions, thoughts, feelings, and preferences while becoming familiar with two sonified biofeedback prototypes.

Methods: This study included nine healthy older adults (7 f; age 71 ± 5.6 years; mass 73.7 ± 15.4 kg; height 1.65 ± 0.06 m) who provided written informed consent to participate**.** A 13-segment whole body kinematic model [4] was built using optical motion capture data (250 fps; OptiTrack, USA). Real-Time balance metrics were calculated: lateral distance (LD) – the horizontal distance between the body's center of mass and the lateral edge of the base of support, and whole-body frontal plane angular momentum (Hf) - which can convey mediolateral balance regulation information. These balance metrics were mapped to electronic musical instruments, creating two sonified biofeedback prototypes. Changes in LD measurements were mapped to a drum tempo change – as LD became smaller or negative (the center of mass is lateral to the base of support), the drum tempo increased (example video). Changes in Hf measurements were mapped to a pitch change – as Hf increased, the pitch increased (example video). Each participant interacted with both prototypes in a randomized order. Each balance metric was explained to them using a script, and then they were shown a video of someone changing the sound heard by changing their movements (i.e., walking with wider steps to increase their LD and slow down the drum tempo). To demonstrate understanding, the participant was then asked to purposefully change the sound using simple movements. They were then instructed by a physical therapist to move around the lab. They were provided some minor guidance about movements to try to interact with the sound, before doing so freely (example video). The participants were encouraged to ask questions at any time and were offered options to personalize the sound, including different brightness filters and instrument tones (e.g., adding chords, changing from string instruments to brass). Following each prototype interaction, participants were asked about what they liked, what they did not like, what surprised them, and whether the sound changed their movements in any way. These sessions were transcribed and coded separately by three researchers. Each researcher found codes, and then all three discussed their codes to form common themes and sub-themes [5].

Results & Discussion: The codes formed five themes that related to overall experience: 1) Clarity of the balance metric, 2) ability to perceive sound-movement associations, 3) engagement with the sonification system, 4) perception of the sound design, and 5) the impact of sound and movement on one another (**Fig. 1**). A pattern became apparent within these themes that initial confusion or frustration while interacting with the system stemmed from a lack of understanding of the balance metric or a lack of enjoyment of the sound. Once the balance metric was re-explained and demonstrated, or the sound parameters were re-adjusted, the participant began to share correct sound-movement interaction observations - a majority of participants were able to notice how the balance metric measurements changed during walking turns (LD becomes smaller, Hf becomes larger) - and began to enjoy interacting with the system. Of those who indicated a prototype preference, three preferred the LD drum design because it was more intuitive and easier to understand; four preferred the Hf pitch design because it was more musical and easier to perceive changes. Although we expected the LD drum design to have more of an effect on movement (i.e., entraining to rhythmic sounds), what we found was that some participants found their gait being affected by the LD drum design while others found their gait to be more affected by the Hf pitch design. We suspect that some confusion resulted from the open-ended interaction instead of a training session with explicit instructions. This was done so that we could incorporate design improvements before our next steps, which include evaluating the *use* of these prototypes in balance training.

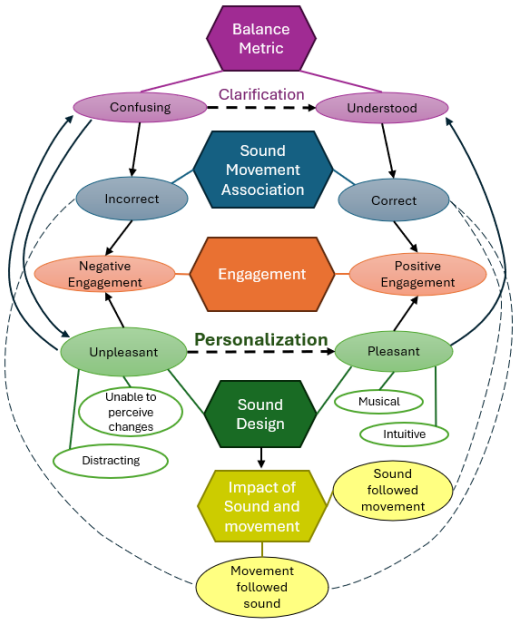

Figure 1: Five themes and how they relate to engagement. Left side of the graph is more negative, right side is more positive. Clarification and personalization span sides.

Significance: These findings highlight the importance of personalized design in sonification systems to optimize understanding and engagement. Furthermore, while complex biomechanical measurements such as LD and Hf are valuable for analysing older adult balance and fall-risk, simpler metrics may be more effective for sonification training systems to reduce the burden of understanding the design.

Acknowledgments: National Science Foundation Award #1944207. Thank you to Evan Papageorge for transcribing.

References: **[1]** Gorgas et al. (2017) *J Biosytems, and Biorobotics*; **[2]** Friedman et al. (2014) *J. NeuroEngineering Rehabil.* 11(1); **[3]** Newbold et al. (2020) *J Multimodal User Interfaces.* 14(2); **[4]** de Leva (1996). *J Biomech.* 29; **[5]** Kiger et al. (2020) *Medical Teacher*

Markerless motion capture can assess symmetry of knee range of motion during rehabilitation for ACL reconstruction

Morgan A. Lamarre[1*], E.L. King[1,2], G. Gibson[1], S.A. Acuña[1,2], S. Sikdar[1,2], P.V. Chitnis[1,2]
[1]Department of Bioengineering, George Mason University, Fairfax, VA, USA
[2]Center for Adaptive Systems of Brain-Body Interactions, George Mason University, Fairfax, VA, USA
*Corresponding author's email: mlamarre@gmu.edu

Introduction: Rupture of the anterior cruciate ligament (ACL) is a prevalent injury, particularly among athletes engaged in high-impact sports. Surgical ACL reconstruction (ACLR) is a common choice for active individuals, with postoperative rehabilitation crucial for restoring function [1]. During postoperative rehabilitation, main goals include returning to preinjury range of motion (ROM) with emphasis on ROM symmetry between knee joints [2]. ROM symmetry is important in reducing the prevalence of reinjury, which ranges from 1.5% to 37.5%, and improving return to sport, as only 65% of patients return to preinjury levels of activity [3,4]. Physical therapists measure patient ROM at each visit either by visual estimation or goniometer, both of which are highly examiner-dependent [5]. A quantitative approach to understanding ROM is by using motion capture systems, which can provide more consistent and accurate ROM values, but require lengthy calibration and set-up time. Markerless motion capture systems offer a quick, contactless alternative to goniometers and traditional systems. The purpose of this study was to explore the feasibility of markerless motion capture technology to track changes in knee joint ROM symmetry during recovery from ACLR surgery.

Methods: Participants (4 control, 1 with right ACLR) performed rehabilitation exercises while joint kinematics were recorded using a markerless motion capture system (Kinotek, Portland, ME, USA). Controls were tested on four separate days within a two-week timeframe and performed 3 trials of 3 bilateral, bodyweight squats at each session. The ACLR participant was tested every two weeks for five months (10 sessions) beginning eight weeks after ACLR surgery. Rehabilitation tasks were gradually added to correspond with the participant's rehabilitation plan. Tasks were added in the following order: step-ups, anterior step-downs, lunges, bodyweight squats. The ACLR participant performed 3 trials of 3 repetitions for each task using each leg. The maximum knee flexion ROM values for each exercise were used to calculate the limb symmetry index, LSI (LSI = 1 indicates perfectly symmetric) [6]. The participant self-reported their physical function using a modified Short Musculoskeletal Function Assessment (SMFA) for each visit, with a high score indicating poor function and a lower score indicating improved function (best score = 17, worst score = 85) [7]. We used the coefficient of variation (COV) to quantify the variability of LSI over multiple days in controls. A Pearson's correlation compared LSI to SMFA across tasks.

Results & Discussion: Average LSI for controls' bodyweight squats was 0.96±0.05, with a corresponding COV of 5.4% indicating good measurement consistency. The average LSI for the ACLR participant's bodyweight squats was comparable to that of the healthy controls (0.97±0.02) (**Fig. 1**). Average LSI for the additional tasks throughout rehabilitation was also within the normal range, with values greater than 0.85 [6]. The ACLR participant's average LSI percent change from the first to last session during step-ups, step-downs, lunges, and squats was a 2.5% increase, 7.1% decrease, 1.7% decrease, and 2.8% increase, respectively. As expected, the ACLR participant's SMFA scores decreased over time (indicating improvement), with scores changing from 44 to 28 over the 5 months of rehabilitation. LSI for the four tasks was not significantly correlated with SMFA (p-values ≥ 0.067). Given that the ACLR participant's average LSI remained within the healthy range for each task throughout rehabilitation, the markerless motion capture system was able to track a lack of significant change in knee joint ROM symmetry during recovery.

Significance: The significance of these results lies in their implications for the effectiveness and reliability of markerless motion capture technology in tracking rehabilitation progress following ACL reconstruction surgery. Markerless motion capture was shown to be a valid tool for this purpose but may need to be supplemented with time-variant data to gain more specific insights into function over time, given the lack of correlation found between limb range of motion symmetry and functional assessment scores.

Acknowledgments: Efforts are sponsored by the Government under Other Transactions Number MTEC-MPAI W81XWH-15-9-0001 and NIH HEAL 1R61AT012286.

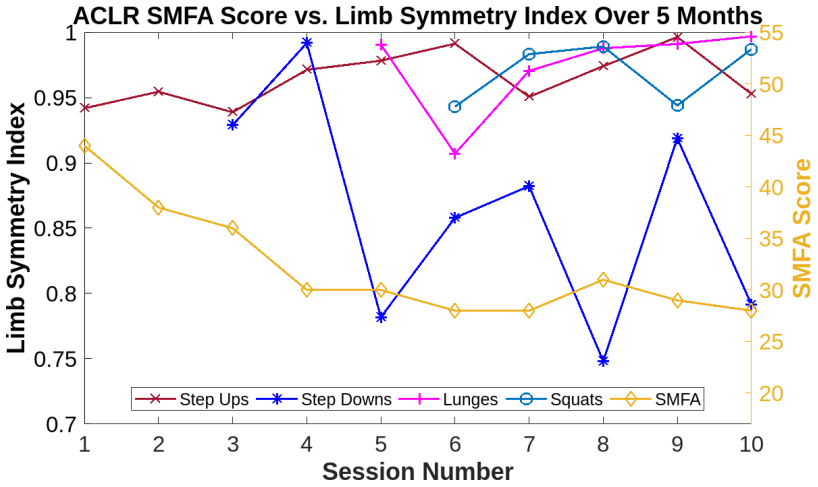

Figure 1: Comparison of ACLR SMFA scores vs. LSI of rehabilitation tasks over 10 sessions during a 5-month rehabilitation period for a single ACLR participant.

References: [1] Jenkins et al. (2022) *Curr. Rev. Musculoskelet. Med.* [2] Shelbourne et al. (2022) *Orthop. J. Sports Med.* [3] Rodriguez-Merchan, Valentino (2022) *Arch. Bone Jt. Surg.* [4] Waldron, et al. (2022) *Arthrosc. Sports Med. Rehabil.* [5] Hancock et al. (2018) *J. Exp. Orthop.* [6] Parkinson et al. (2021) *J. Sports Sci. Med.* [7] Obermeier et al. (2018) *Sports Health*

A MACHINE LEARNING APPROACH TO TASK CLASSIFICATION OF MILITARY-RELEVANT MANEUVERS

Aaron D. Likens[1*], Courtney A. Haynes[2]
[1]Department of Biomechanics, University of Nebraska at Omaha
[2]US Army DEVCOM Army Research Laboratory, Humans in Complex Systems Division, Aberdeen Proving Ground, MD
*Corresponding author's email: alikens@unomaha.edu

Introduction: Modern physical augmentation systems are often designed to detect a user's activity or state and apply mechanical actuation with a magnitude and timing complementary to the user's action. This control approach has shown to be effective in the design of walk-assist devices which leverage the well-characterized and cyclical mechanics of gait to identify the critical phases for actuation. This control paradigm becomes increasingly difficult, however, when attempting to design a system which can accommodate multiple physical tasks. Doing so would require better understanding of the movement profiles which define these additional tasks and also designing the system to accommodate the movement variability present within these tasks. Towards these goals, we quantified movement kinematics as subjects completed a series of physical maneuvers relevant to military operations. With this data set, we aim to identify characteristic movement patterns for a variety of physical tasks and quantify the variability of task execution. To address that aim, we used a combination of feature engineering and supervised machine learning models to classify the tasks Soldiers performed based on the frequency spectrum obtained from a single thigh worn inertial measurement unit (IMU). To preview, this approach was largely successful, with several models generating accuracies up to 93%.

Methods: Seventeen young, active subjects (8 civilian/9 military, 15M/2F, 177.4±7.1 cm, 89.4±16.1 kg, 32.2±8.4 years) completed a series of physical tasks including walking, running, stair climbing, stepping over a 45.7-cm (18 in) obstacle, climbing over a 1.22 m (4 ft) wall, and passing through a 76.2 cm x 76.2 cm (30 in x 30 in) window. All subjects were instrumented with 14 IMUs (Noraxon Inc., Scottsdale, AZ) on the pelvis, upper thoracic region, and bilaterally on the upper arms, forearms, hands, thighs, shanks, and feet. Five trials were completed for each of the tasks while full-body kinematics were recorded. Civilian subjects completed the tasks wearing only athletic clothing (unloaded) while military subjects completed the tasks for both unloaded and loaded conditions. The loaded configuration included a body armor vest with ballistic plates, helmet, loaded assault pack, mock grenades and ammunition magazines, and a dummy weapon resulting in a carried mass of approximately 60 kg. Data only from unloaded trials were split into training and test sets using a 70/30 split, taking care not to include the same participants in both sets to avoid bias from repeated measures. Then, we performed a discrete Fourier transform (DFT) on a single (frontal) axis of the thigh acceleration data. DFT frequencies were treated as features, with corresponding amplitudes serving as the feature measure. Those features were subsequently used to train several models: C5.0, k-nearest neighbors (KNN), linear discriminant analysis, multinomial logistic regression (MLR), naïve Bayes (NB), random forests (RF), and support vector machines (SVM) [1-3] to classify the tasks being performed. Models were evaluated on the 30% holdout data. Models were summarized with confusion matrices.

Results and Discussion: Accuracy data for each model are presented in the table below. Most models performed reasonably well, with 7 out of 8 models producing accuracies > 70%. The exception was the MLR method with only 30% accuracy. The results suggest that machine learning models can effectively identify physical tasks based on thigh acceleration data obtained from IMUs. The highest accuracies were achieved by NB, RF, and SVM, which were all 93%. These findings demonstrate the potential of using IMU data for task recognition which could be useful in the design of physical augmentation systems that accommodate multiple tasks. Moreover, these results highlight the importance of feature engineering and machine learning models in analyzing complex kinematic data. The use of a discrete Fourier transform (DFT) to extract features from thigh accelerations successfully captured characteristic movement patterns for the various tasks. This approach could be extended to other body regions or task types, giving insight into the profiles of different physical activities.

Table 1. Classification Accuracy as a Function of Machine Learning Method.

MLR	SVM	RF	LDA	GBM	KNN	NB	C5.0
0.30	0.93	0.93	0.70	0.87	0.70	0.93	0.73

Significance: Overall, this study advances our understanding of using IMU data for task recognition, paving the way for the development of more versatile and intelligent physical augmentation systems. Future research directions include expanding the dataset with more diverse tasks and subjects, investigating additional sensors (e.g., electromyography, pressure sensors), and exploring real-time implementations for potential applications in assistive technologies and wearable devices.

Acknowledgements: The authors would like to acknowledge Mr. Mike Kozinski, Mr. David Kuhn, and the ARL wood shop for the design and construction of the physical obstacles used in this study. Thanks also to Dr. Philip Crowell and Mr. Paul Shorter for their assistance with data collection and processing.

References: [1] Duda, R. O., Hart, P. E. & Stork, D. G. Pattern Classification. (Wiley, New York, 2001),[2] Hastie, T., Tibshirani, R. & Friedman, J. H. The Elements of Statistical Learning: Data Mining, Inference, and Prediction. (Springer, New York, NY, 2017). [3]James, G., Witten, D., Hastie, T. & Tibshirani, R. An introduction to statistical learning. Vol. 112, 18 (Springer, New York, 2013).

COMPARISON OF KNEE JOINT MOMENTS AND WORK BETWEEN THE NORDIC HAMSTRING EXERCISE AND MULTI-SPEED RUNNING

Kristen Steudel[1*], Nicos Haralabidis[2], Reed Gurchiek[3], Jennifer Hicks[2], Scott Delp[1,2]
[1]Department of Mechanical Engineering, Stanford University, USA.
[2]Department of Bioengineering, Stanford University, USA.
[3]Department of Bioengineering, Clemson University, USA.
*Corresponding author's email: steudelk@stanford.edu

Introduction: Hamstring strain injuries (HSI) are the most prevalent injury in field-based sports [1]. They are believed to occur in the late swing phase of running when the muscle-tendon unit is lengthening and performing negative work [2]. Prior studies have found the Nordic hamstring exercises may reduce injury risk [3], potentially by promoting beneficial muscle adaptations (e.g., longer fascicles, increased strength) [4]. However, Nordic exercises are not always adopted in elite sporting settings [5]; thus, researchers and practitioners have sought alternative exercises to reduce HSI risk, such as high-speed running. Comparisons of the efficacy between Nordics and sprinting for reducing injury risk have yielded inconclusive results, potentially due to differences in the biomechanical loads between these activities [6]. Controlling for the load is difficult because no studies have directly compared the biomechanical loads between the two training modalities. Therefore, the purpose of this study was to compare the joint-level knee loads (knee flexion peak moment and negative work) incurred during the Nordic hamstring exercise and the flight phase of high-speed running, across a range of running speeds.

Methods: Five trained athletes (3 males and 2 females; age: 26 ± 2 years; mass: 76.1 ± 12.0 kg; height: 1.75 ± 0.06 m) volunteered to run at a range of speeds (4, 5, 6, and 7 m/s) and complete 5 Nordic repetitions as slowly and with the greatest range as possible. Marker trajectories were measured (200 Hz) during the runs and Nordics using a motion capture system (Motion Analysis, CA, USA). Ground reaction forces were synchronously collected (2000 Hz) using an instrumented treadmill (Bertec, OH, USA) during the runs. The Nordics were performed on a pair of custom devices that supported each lower-limb independently on top of separate force plates (Bertec, OH, USA; 2000 Hz) with ankles held in place using straps instrumented with uniaxial load cells (HT Sensor Technology, Shaanxi, China; 2000 Hz). We used AddBiomechanics [7] to scale a generic musculoskeletal model [8] to match each subject and perform an inverse kinematics analysis based on the marker trajectories recorded during all trials of a participant. We analyzed three flight phases per running speed and the second, third, and fourth repetitions of the Nordics. The flight phase was chosen as prior work has shown that the hamstring muscles produce the most negative work during this phase [9]. Inverse dynamics was performed using OpenSim to compute knee flexion moment and knee flexion work for both the Nordics and sprinting; we report the results for the left limb.

Results & Discussion: For four of the five participants, peak knee flexion moments for running were similar to or larger than moments for the Nordic repetitions at speeds of 6 m/s and above (Figure 1A). For sprinting, the peak moments were found to occur around the instant of peak knee extension. The average peak moment at 6 m/s was 1.77 Nm/kg, compared to 1.59 Nm/kg for the Nordics. For one participant, they achieved higher than average peak moments in the Nordic, but peak moments in running slightly below the group average, highlighting that loads can be variable. For all of the participants, the negative knee flexion work for running was similar to or larger than the work for the Nordic repetitions (0.80 ± 0.33 J/kg) at speeds of 5 m/s and above (1.22 ± 0.19 J/kg; Figure 1B). A prior study has reported slightly larger peak knee flexion moments for the Nordics (1.88 ± 0.34 Nm/kg for a single leg) [4], suggesting the loads we observed during the Nordics might increase with a rigorous training program. The negative knee flexion work for the fastest running speed (2.02 ± 0.42 J/kg) compared favorably with the cumulative negative hamstrings muscle work at 95% of maximum speed in a prior study (2.23 ± 0.97 J/kg) [9], supporting our joint work measure as an appropriate surrogate for muscle work. Together, the peak moments and negative work we observed during high-speed sprinting (6 m/s or higher) could be a potent stimulus for hamstring training. Further work should compare the eccentric work of the hamstrings muscles for the Nordic exercise and sprinting.

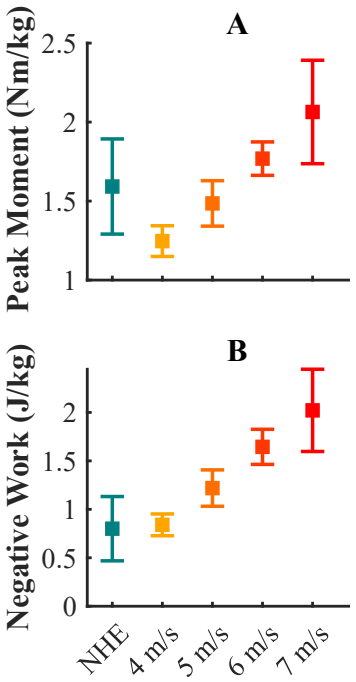

Figure 1: Mean (± 1 SD) knee flexion peak moment (A) and negative work (B) for the Nordic hamstring exercise (NHE) and running speeds.

Significance: The results of this study provide an important step towards developing recommendations for coaches to prescribe the necessary dosages and intensities of high-speed running to achieve the sought-after adaptations from Nordics training.

Acknowledgments: This work was supported by the National Science Foundation and the Joe and Clara Tsai Foundation through the Wu Tsai Human Performance Alliance.

References:[1] Hägglund et al. (2009), *Scand J Med Sci Sports* 19; [2] Kenneally-Dabrowski et al. (2019), *Scand J Med Sci Sports* 29; [3] van Dyk et al. (2019), *Br J Sports Med* 53; [4] Pincheira et al. (2022), *J Sport Health Sci* 11; [5] Bahr et al. (2015), *Br J Sports Med* 49; [6] Ripley et al. (2023), *PLoS ONE* 18; [7] Werling et al. (2023), *PLoS ONE* 18; [8] Lai et al. (2017), *Annals Biomed Eng* 45; [9] Chumanov et al. (2007), *JoB* 40.

SAGITTAL PLANE COMPENSATIONS OF THE TRUNK AND LOWER EXTREMITY DURING RUNNING ON ARTIFICIAL TURF AND NATURAL GRASS SURFACES

Brandi E. Decoux[1*], Christopher M. Wilburn[2], Wendi H. Weimar[2]
[1] Southeastern Louisiana University, Hammond, LA
[2] Auburn University, Auburn, AL
*Corresponding author's email: brandi.decoux@selu.edu

Introduction: The surface upon which running takes place can significantly influence biomechanical factors such as joint kinematics, stride characteristics, and energy expenditure. Recreational athletes often run on various surface types, including natural grass and different artificial turf systems. Each surface possesses unique properties that may affect the way the body moves and the demands placed upon it during running. This study compared the biomechanical effects of running on three distinct artificial turf (AT) surfaces and a natural grass (NG) surface in healthy recreational athletes. The AT surfaces varied in design and construction, while the NG surface represented a traditional natural grass playing surface. By examining variables such as trunk, hip, knee, and ankle kinematics, as well as stride frequency and running velocity, this research aimed to investigate the impact of these four surface conditions on the lower extremity biomechanics during short bouts of submaximal running.

Methods: Seventeen healthy male recreational athletes (age: 23.1 ± 2.9 yrs; height: 1.81 ± 0. 06 m; mass: 77.8 ± 9.9 kg) were recruited from the surrounding community to participate in this study. All participants indicated their voluntary involvement by signing an informed consent document approved by the Institutional Review Board prior to participation. An inertial motion capture system and accompanying software (MTw, MVN Analyze v2019.0, Xsens Technologies B.V., Enschede, the Netherlands) were used to obtain kinematic data at 100 Hz during three 35m submaximal running trials on each of the four surfaces tested. The collected data were then imported in Visual3D (C-Motion, Germantown, Maryland, USA) for reduction. Mean trunk flexion angle, peak hip flexion, peak knee flexion, and peak ankle dorsiflexion values during the middle four stance phases of the dominant foot for each running trial were extracted for analysis. For each variable of interest, the mean of all trials in each condition for each participant were included in the statistical analyses conducted in SPSS (Version 29.0, SPSS Inc, Chicago, IL, USA). Differences between the four surfaces were analyzed using repeated measures Friedman ANOVA by Ranks tests ($\alpha = .05$). Post-hoc Wilcoxon Signed Ranks Tests with Bonferroni correction were carried out when necessary to determine where specific differences lie.

Table 1. Mean and standard deviation of all variables of interest on each surface tested.

	AT1	AT2	AT3	NG
Mean trunk flexion angle (°)	11.44 ± 4.68	11.60 ± 3.70	13.89 ± 4.19	11.08 ± 4.23
Peak hip flexion angle (°)	23.74 ± 8.64	23.78 ± 8.56	24.71 ± 9.11	22.58 ± 8.05
Peak knee flexion angle (°)	38.00 ± 6.05	38.02 ± 5.66	37.61 ± 5.58	37.82 ± 5.49
Peak ankle dorsiflexion angle (°)	22.96 ±4.19	23.03 ± 3.86	23.30 ± 3.64	20.78 ± 3.82
Running velocity (m/s)	3.79 ± 0.61	3.85 ± 0.65	3.80 ± 0.73	3.64 ± 0.70
Stride Frequency (strides/s)	1.34 ± 0.09	1.35 ± 0.10	1.37 ± 0.11	1.34 ± 0.11

Results & Discussion: Descriptive statistics for all variables of interest are summarized in Table 1. A significant effect of surface was observed for mean trunk flexion angle ($\chi^2(3) = 12.539$, $p = .006$, $W = .246$), peak ankle dorsiflexion angle ($\chi^2(3) = 19.800$, $p < .001$, $W = .388$), and stride frequency ($\chi^2(3) = 10.765$, $p = .013$, $W = .211$). Mean trunk flexion angle was significantly greater on AT3 compared to AT1 ($Z = 3.053$, $p = .012$), AT2 ($Z = 3.101$, $p = .012$), and NG ($Z = 3.621$, $p = .003$). Peak ankle dorsiflexion angle was less on NG compared to AT1 ($Z = 2.769$, $p = .036$), AT2 ($Z = 2.817$, $p = .03$), and AT3 ($Z = 3.621$, $p = .002$). Stride frequency was significantly greater on AT3 compared to NG ($Z = 3.053$, $p = .012$). Higher mean trunk flexion angle on AT3 compared to the other surfaces suggests an altered joint contribution strategy, potentially redirecting energetic demand from the knee and to the hip [1, 2]. Additionally, the presence of greater peak ankle dorsiflexion angles on all surfaces compared to NG may be the related to the vertical deformation of NG during stance which is considered a force reduction characteristic [3]. However, this may also imply that more ankle contribution is needed during propulsion if the forces absorbed by the natural surface are not effectively returned to the body. Increased stride frequency on AT3 compared to NG with no effect of surface on running velocity suggests that a shorter stride length may be adopted on AT3, which may result in greater locomotor cost [2, 4].

Significance: Understanding how different running surfaces influence joint kinematics, stride patterns, and movement dynamics can provide valuable insights for enhancing performance, mitigating injury risk, and optimizing surface selection, design, and maintenance. With most research on artificial and natural playing surfaces focusing on maximal effort performance outcomes, studies such this one that shed light on the biomechanics of an important submaximal movement offer new information for athletes, coaches, researchers, and manufacturers to consider.

References: [1] Teng & Powers (2015), *Med Sci Sports Exerc* 47(3). [2] Warrener et al. (2021), *Hum Mov Sci* 78. [3] Fleming (2011), *Proc Inst Mech Eng Part P-J Sport Eng Technol* 225. [4] Lieberman et al. (2015), *J Exp Biol* 218(21).

ARE RUNNING BIOMECHANICS DIFFERENT BETWEEN RUNNERS WHO PREFER MAXIMAL SHOES AND RUNNERS WHO PREFER TRADITIONAL SHOES?

J.J. Hannigan[1*], Andrew Traut[2], Lily Bartel[1], Bethany Burr[1], Christine Pollard[1]
[1]College of Health, Oregon State University – Cascades, Bend, OR USA
[2]Department of Biological Sciences, Montana Technological University, Butte, MT USA
*Corresponding author's email: jj.hannigan@osucascades.edu

Introduction: Despite advances in running footwear over the past 50 years, running injuries are still common, with recent incidence estimates around 40% [1]. Over the past decade, one footwear option gaining traction is maximal running shoes, loosely defined as shoes with greater midsole stack height than traditional running shoes. Research on maximal shoes is growing, with several studies investigating the effect of maximal shoes on biomechanical risk factors for injury. To date, literature is mixed, with some studies suggesting maximal shoes may affect ankle eversion kinematics [2,3] and loading rates [2,4], potentially increasing the risk of injury.

Despite this potential increased injury risk, maximal shoes are becoming increasingly popular amongst runners. Limited current evidence suggests that comfort and cushioning may be the two most important factors that runners consider when choosing their footwear [5]. However, it is currently unknown why certain runners may choose or prefer maximal shoes, and whether their biomechanics may play a role in their maximal shoe preference.

Therefore, the purpose of this study was to compare running biomechanics between runners who prefer maximal shoes, and runners who prefer traditional shoes, with a primary focus on ankle kinematics and loading rates. Based on previous research on maximal shoes [2-4], it was hypothesized that runners who prefer maximal shoes would display significantly higher inversion at toe-off and significantly lower loading rates compared to runners who prefer traditional shoes.

Methods: Forty healthy runners participated in this study, 20 who preferred and currently trained in maximal shoes (MSPref: 10 female, 10 male), and 20 who preferred and currently trained in traditional shoes (TSPref: 11 female, 9 male). Maximal shoes were defined as having an average stack height >30mm. All participants ran overground in the laboratory wearing a maximal shoe (Hoka Bondi v7) and traditional shoe (New Balance 880 v11) while three-dimensional kinematics and kinetics were collected using a 10-camera motion capture system sampling at 200 Hz (Qualisys) and 3 embedded force plates sampling at 2000 Hz (AMTI). Each trial was approximately 20-meters, with 5 successful trials per shoe collected. Kinematic data were further processed using Visual3D. Variables of interest included ankle kinematics (sagittal and frontal plane angles at initial contact, peak angles, angular excursion, and angle at toe-off) and the average vertical loading rate (AVLR). A 2x2 repeated measures ANCOVA compared data between shoe preference groups and shoes ($\alpha = .05$). Due to differences in foot strike pattern between groups, foot strike was entered as a covariate.

Results & Discussion: Foot strike pattern was notably different between groups, with 12 out of 20 MSPref runners displaying a forefoot strike, and 4 out of 20 TSPref runners displaying a forefoot strike. With foot strike entered as a covariate, no interaction effects, nor main effects of group or shoe, were noted for any measure of dorsiflexion, eversion, or loading rate ($p > .05$), largely refuting our hypotheses.

For eversion, while no differences between groups were noted for inversion at initial contact ($p = .974$), peak eversion ($p = .574$), and eversion excursion ($p = .667$), inversion at toe-off was trending toward significance with a moderate effect size (MSpref: 7.87°, TSPref: 5.29°, $p = .095$, $\eta^2 = .073$, Figure 1), suggesting that some runners who prefer maximal shoes may display slight differences in eversion mechanics during terminal stance. Re-inverting the foot prior to toe-off locks the transverse tarsal joint and creates a rigid lever for push-off, but maximal shoes have been noted to impair this function [3]. More research is needed to determine if this trend holds for additional runners and whether this contributes to shoe preference.

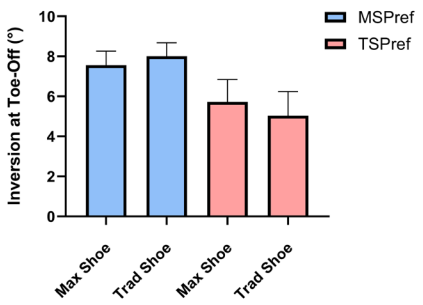

Figure 1: Inversion angle at toe-off across shoe preference groups and shoe conditions.

After accounting for foot strike pattern, no main effect of group was noted in dorsiflexion at initial contact ($p = .711$), peak dorsiflexion ($p = .529$) or dorsiflexion excursion ($p = .960$). It is important to note that significant differences were identified in dorsiflexion at initial contact and dorsiflexion excursion before accounting for foot strike pattern, but these differences appear to be driven by the disparity in the number of forefoot strike runners between groups.

No differences were noted in AVLR between groups ($p = .299$). Similar to dorsiflexion mechanics, significantly lower AVLRs were identified in the maximal shoe preferred group before accounting for foot strike pattern, but it appears these differences were also driven by the disparity in foot strike pattern between groups.

Significance: A notably high percentage of MSPref runners displayed a forefoot strike pattern. Otherwise, outside of a trending difference in inversion at toe-off, maximal shoe preference does not appear to be strongly influenced by ankle kinematics or loading rates during running. It is likely that other factors not studied in this investigation may be affecting maximal shoe preference.

Acknowledgments: The authors would like to acknowledge Rami Shehadeh and Mo Elwefati for their assistance with data collection.

References: [1] Kakouris et al. (2021), *J Sport Health Sci* 10(5); [2] Hannigan & Pollard (2019), *Am J Sport Med* 47(4); [3] Barrons et al. (2023), *Foot Sci* 15(3); [4] Kulmala et al. (2018), *Sci Rep* 8(1); [5] Fife et al. (2023), *Foot Sci* 15(2).

ASSISTIVE SHOES AFFECT THE GAIT OF PATIENTS WITH PERIPHERAL ARTERY DISEASE

Jania Williams[1], Farahnaz Fallahtafti[1], Zahra Salamifar[1], Iraklis Pipinos[2], Sara A. Myers[1,2]
[1]Department of Biomechanics, University of Nebraska at Omaha, Omaha, NE USA
[2]Department of Surgery and Research Service, Omaha Veterans' Affairs Medical Center, Omaha, NE USA
Email: janiawilliams@unomaha.edu
Presentation Preference: Podium

Introduction: Intermittent claudication is a common symptom observed in peripheral artery disease (PAD) that causes pain during walking [1]. Previous research in patients with PAD wearing unloading shoes supports the concept of reducing claudication pain by reducing ankle power generation and calf muscle load [2,3]. Two examples of unloading shoes are spring loaded and carbon fiber. Spring-loaded shoes provide shock absorbance and energy return while carbon fiber shoes increase mechanical storage and return. This study evaluated spatiotemporal parameters of gait in patients with PAD when walking with regular, carbon fiber, and spring-loaded shoes. Our hypothesis posits that the use of carbon fiber and spring-loaded shoes will enhance gait characteristics by absorbing energy during weight acceptance and returning it during push-off, thus supplementing for effort of the calf muscles.

Methods: Ten patients with PAD participated in a progressive treadmill test, walking at a speed of 2 mph. During the baseline condition, patients wore regular, carbon fiber, and spring-loaded shoes in randomized order. Mean and standard deviation values for step width, stride length, stride time, cadence, and velocity, were recorded. Following the progressive treadmill test, participants were provided with their preferred shoes and instructed to wear them daily for three months. After three months of using assistive shoes, the participants returned for a post-intervention visit, similar to the baseline. A one-way repeated measure analysis of variance (ANOVA) was performed to investigate the effect of footwear on gait outcomes within three conditions. The mean percentage difference (% difference) was assessed to compare alterations in outcome values between the spring-loaded and carbon fiber conditions relative to the regular shoe condition. Paired sample t-tests were conducted to assess the statistical differences in outcome measures before and after the intervention. Moreover, the percentage change in mean values of spatiotemporal outcomes from baseline to post three-month intervention, while walking with the preferred shoes is reported.

Results & Discussion: No significant differences were observed in the spatiotemporal parameters across any of the conditions during the baseline visit, as well as no change observed between baseline and post intervention. **The effect of SL and CF on gait parameters compared to the regular condition:** In the spring-loaded condition compared to regular shoe, stride length increased by 14%, step width decreased by 11.4%, and no relevant differences were observed in stride time or velocity. In the carbon fiber condition, there was an increase of 8.3% for stride length, a decrease of 3.6% for stride time, and a decrease of 10% for cadence, with no detectable changes observed in step width or velocity. Although statistical analysis showed no significant differences, noticeable percentage variances were observed between the spring-loaded and carbon fiber conditions. The spring-loaded condition outperformed the carbon fiber condition, increasing stride length and inducing a faster gait compared to the regular condition. While both assistive shoes increased step length, the spring-loaded shoe resulted in further improvements by decreasing step width and increasing cadence, indicating more efficient walking patterns **The effect of an intervention with an assistive shoe on the gait parameters:** After wearing the assistive shoes for three months, the baseline-to-post percentage change in stride length, step width, and stride time during walking was assessed. There was a decrease of 4.6% in stride length, 9.09% in step width, and 2.45% in stride time after intervention (Figure 1). Quicker and narrower steps bring the walking pattern of PAD patients closer to that of healthy individuals.

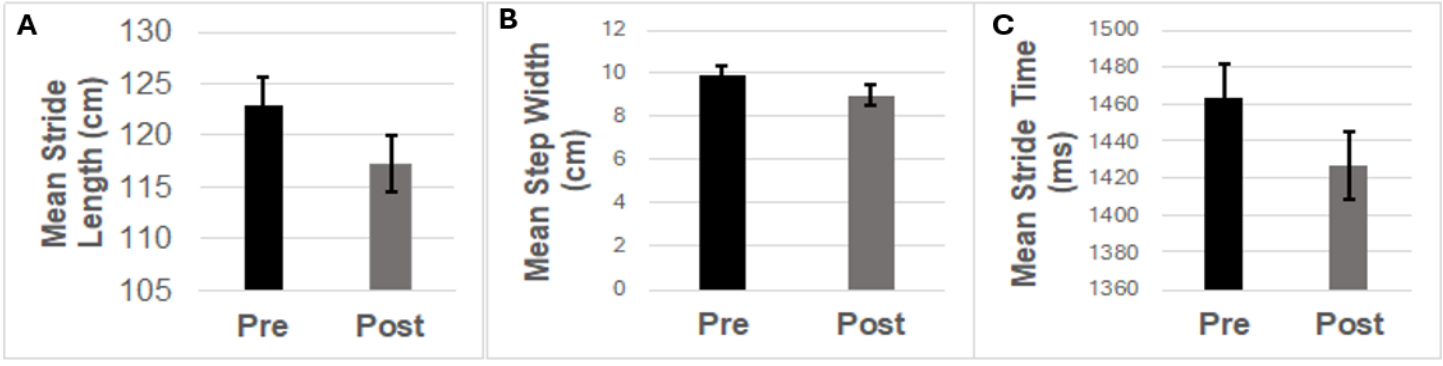

Figure 1. The mean values of the subject's preferred shoe, worn for three months, from pre to post. (A) Stride length, the anterior posterior distance from one heel strike to the next, decreased by 4.6% from baseline to post, indicating that subjects are taking shorter steps. (B) Step width, the mediolateral distance between the heels of the foot when both feet are on the ground, decreased by 9.09% baseline to post. The decrease in step width indicates values closer to healthy individuals. (C) Stride time, the duration between two consecutive contacts of the same heel, decreased by 2.45% baseline to post. A reduction in stride time suggests quicker steps.

Conclusion: Our study suggests potential enhancements in gait for PAD patients following a period of adaptation to assistive shoes.

REFERENCES

1. Cassar K. *Intermittent claudication*. *BMJ*. **333**,2006, 2. Tew et al. *BMC Cardiovasc Disord*, **17**, 76 2017, 3. Jordan, A. *Gait & Posture*, **67**, 31–36, 2019

ACKNOWLEDGEMENTS: This study is supported by a SPiRE VA grant (I01RX003266).

Expanded Validation of loadsol® Sensors Over Various Running Conditions

Shannon Hugard[1*], Seth Donahue[2], Aida Chebbi[1], Rachel Robinson[1], Michael E. Hahn[1]
[1]University of Oregon, Bowerman Sports Science Center; [2]Northwestern University, Prosthetics and Orthotics Rehabilitation Technology Assessment Laboratory (PORTAL)
*Corresponding author's email: hugard@oregon.edu

Introduction: loadsol® sensors (Novel Electronics, St. Paul, MN) offer a relatively inexpensive and versatile alternative to instrumented treadmills for gait parameter assessment. Previous work has found good to excellent agreement between loadsol® sensors and instrumented treadmills at 1.39m/s, 2.78m/s, 3.0m/s and 3.5 m/s over -10°, 0°, and 10° grades [1, 2]. The purpose of the current post-hoc analysis is to examine whether these findings are consistent across a wider range of velocities and grades. Unlike instrumented treadmills, loadsol® sensors are compatible with most footwear and ground surfaces. Expanded validation of loadsol® sensors could give researchers the ability to collect high-quality ground reaction force data in a wider variety of experimental conditions.

Methods: This study examines data collected as part of a larger study [3]. Fourteen participants completed a series of one-minute running trials based on each participant's self-reported 5k pace. Each participant ran four to five progressively faster trials at -7°, 0°, and 7° grades, for a total of 13 trials. Although all participants did not run at the same set of prescribed velocities, 16 of the 32 velocity/grade conditions had n>=5. Vertical ground reaction forces and foot-shoe normal forces were collected simultaneously using a Bertec instrumented treadmill and loadsol® sensors respectively. Bertec data were collected at 1000 Hz and downsampled to 100 Hz, while loadsol data were collected at 100 Hz. Impulse, peak force, and loading rate were calculated for each step and then averaged for each trial in MATLAB. Bland-Altman plots were generated for all gait parameters in each velocity/grade condition. Bland-Altman plots were also generated to illustrate average gait parameter values for all trials. Two-way mixed effects intraclass correlation coefficients (ICC3,k) with 95% confidence intervals were calculated for all conditions with n >= 5. ICC values were categorized as excellent (0.75-1.0), good (0.6-0.74), fair (0.4 - 0.59), or poor (<0.4) [4].

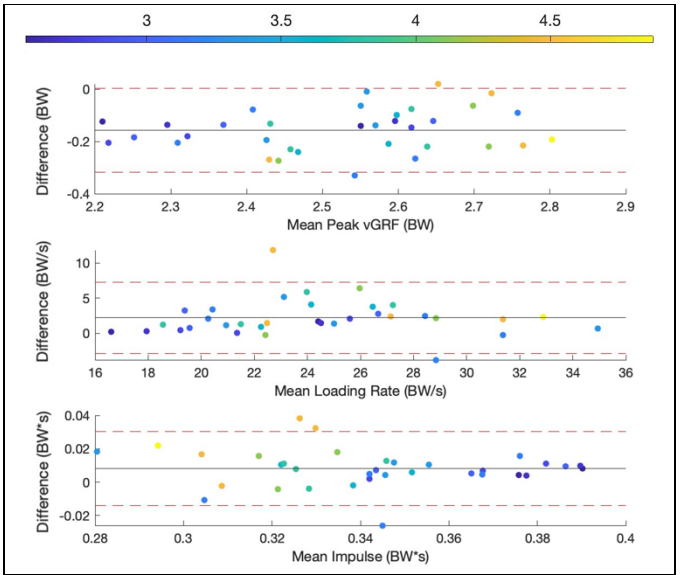

Figure 1: Bland-Altman plots for average peak force, loading rate and impulse at 0° grade. Marker color indicates trial velocity (m/s), as indicated by the colorbar. Difference was calculated by subtracting average loadsol® from average Bertec-generated values.

Results & Discussion: ICC values calculated for impulse indicated high agreement between loadsol® and Bertec measures across most conditions (12/16 excellent, 1/16 good, 1/16 poor). Loading rate ICC values similarly indicated high accuracy across most conditions (12/16 excellent, 1/16 good, 2/16 fair, 1/16 poor). Peak force values displayed greater discrepancies (5/16 excellent, 5/16 good, 3/16 fair, 3/16 poor). However, Bland-Altman plotting for conditions with poor ICC values show that few trials fall outside of the 95% confidence interval boundaries. As ICC3,k measures are the ratio of variance between trials to variance between measurement systems, poor ICC values could be due to low variability between trials. Low variance between trials may be a result of the relatively small sample sizes evaluated in this study; further work is needed to confirm this possibility. Additional analysis is also required to investigate correlation between condition velocity and loadsol® accuracy.

Significance: Instrumented treadmills are the current gold-standard for measuring ground reaction forces for controlled pace running conditions. However, these devices are costly, limited to in-lab operation, and can only be used for walking and running tasks. Previous work has validated loadsol® sensors to have good to excellent agreement with instrumented treadmills at 1.39m/s, 2.78m/s, 3.0m/s and 3.5 m/s over -10°, 0°, and 10° grades [1, 2]. The current study expands this comparison by evaluating accuracy between loadsol® and Bertec over 32 velocity and grade conditions, with 16 conditions having sample sizes n>=5. The relative portability and affordability of loadsol® sensors creates opportunities for athletic and clinical gait parameter testing that cannot be completed on an instrumented treadmill. Expanded validation of loadsol® insoles has the potential to increase researcher confidence in the sensors as an acceptable alternative to instrumented treadmills for calculating gait parameters.

Acknowledgments: This work was supported by the Wu Tsai Human Performance Alliance and the Joe and Clara Tsai Foundation.

References: [1] Burns et al. J. Sports Sci. 2018. [2] Renner KE et al. Sensors (Basel). 2019 [3] Donahue et al. Sci Rep 2023 [4] Cicchetti, et al. Psychol. Assess. 1994.

EFFECTS OF COMPOSITE OUTSOLE FOOTWEAR ON GAIT IN INDOOR AND OUTDOOR SETTINGS

Kelly Poretti[1], Ahmadreza Souri [1], Sabrina Islam [2], Nelson Glover [3], Shaghayegh Bagheri [2], Quentin Sanders [2,3], Tiphanie E. Raffegeau [1]
[1]School of Kinesiology, George Mason University, Manassas, VA
[2] Department of Mechanical Engineering, [3] Department of Bioengineering, George Mason University, Fairfax, VA
*Corresponding author's email: kporetti@gmu.edu

Introduction: Fall-related injuries are one of the leading causes of workplace fatalities in both indoor and outdoor environments [1]. A critical factor influencing the likelihood of a fall is the friction between footwear outsoles and the underlying surface friction characteristics [2]. Anti-slip footwear featuring composite materials in their outsoles increase friction with microscopic fibers that dig into ice substrates [3] demonstrate promise in reducing slips, specifically in icy outdoor conditions [4]. However, further research is needed to understand the utility of composite materials in preventing slips on different surface types (i.e. tile versus asphalt). The purpose of this study is to investigate the effects of composite-footwear on gait performance while walking on different surfaces and at different speeds to determine if composite outsoles might reduce real-world fall-risk.

Methods: Healthy adult men (fitting a men's size 9.5 shoe) wore two types of footwear with similar designs, 1) a shoe with a non-composite outsole (Keen, Circadia Mid Polar), and 2) a shoe with a composite outsole (Keen, Revel IV Mid Polar, Fig 1). Participants were fitted with XSENS Awinda inertial measurement unit (IMU) sensors (Movella, Inc.) on the chest, pelvis, thigh and shank of both legs and each foot. Footwear type was randomized and counterbalanced, and in a fixed order, participants completed 10 trials of walking at a self-selected, followed by a fast pace in two blocks. In block one, participants walked in a traditional indoor setting (~15 meters on laboratory flooring) at both speeds and in block two, participants walked in an outdoor setting (~15 meters on flat sidewalk) at both speeds. To examine the influence of composite outsoles on indoor gait kinetics, participants walked over four floor-embedded force plates (Bertec, Columbus, OH). Peak braking and propulsion forces were extracted and normalized by bodyweight using a custom MATLAB code (v2.2 Natick, MA). Linear mixed effect regression (LMER) models compared gait speed, step length, and step width in an Environment (2 levels: Indoor (ref), Outdoor) by Footwear (2 levels: Non-composite (ref), Composite) by Speed (2 levels: self-selected, fast) model. A similar LMER model compared indoor peak braking and propulsion in a Footwear (2 levels: Non-composite (ref), Composite) by Speed (2 levels: self-selected, fast) model. Significant effects (p <.05) were explored with post-hoc comparisons.

Figure 1: Keen footwear worn in this study. Non-Composite outsoles (Top) and Composite outsoles (Bottom).

Results & Discussion: Six adult men (mean (SD) age= 31.2 (4.6 years), mass = 77.2 (10.6 kg), height = 171.9 (1.8 cm), leg length = 88.1 (2.0 cm) were included in this study. A three-way interaction for gait speed (p=.007) showed that in composite shoes, people walk with faster gait speeds outdoors than indoors (B = 0.09, t = 6.9, p<.001), but no effect was revealed for non-composite shoes. A three-way interaction for step width (p<.001) showed walking at self-selected speeds in composite outsoles led to narrower steps outdoors compared to indoors (B = -0.05, t = -2.9, p=.004), but in non-composite shoes, individuals walk with wider steps outdoors than indoors (B = 0.11, t = 2.4, p=.018). At fast speeds, only composite shoes led to narrower steps outdoors (B = -0.03, t = -2.8, p=.005). A faster and narrower step in outdoor settings implies that wearing composite outsoles enabled participants to walk faster with a smaller base of support, leveraging increased momentum to walk with decreased mechanical stability. Indoors, propulsive forces revealed no significant interaction between Speed and Footwear (p=.064), and no effect of footwear was detected (p =.559), however, an interaction in braking forces (B= 0.02, t=2.4, p =.016) showed that at fast walking speed, braking forces were larger in composite footwear (B= 0.02, t=3.3, p = .001) but at self-selected speed, there were no differences in braking due to footwear (p = .818). Kinetics showed composite footwear effectively decelerates each step, supporting that composite footwear may reduce slip-risk indoors by decreasing the required surface coefficient of friction for steps at fast speeds.

Significance: Footwear with composite outsoles enhanced gait parameters outdoors, demonstrated by participants achieving faster gait speeds with narrower steps while walking outdoors in composite footwear. Indoors, composite footwear may reduce slip risk at fast walking speeds by enhancing braking capabilities and may increase friction on slippery surfaces, highlighting the potential utility of composite outsoles to enhance gait for workers on indoor surfaces with a range of friction characteristics (e.g. ice, oil, etc.).

Acknowledgments: Dr. Bagheri is supported by the National Institute of Occupational Health and Safety (NIOSH # U54OH007542-20-01). Dr. Raffegeau is supported by the College of Education and Human Development.

References: [1] Mekkodathil et al. (2020), *BMC Public Health*. 20; [2] Anwer et al. (2017), *Adv. Mater. Interfaces* 4(6); [3] Bagheri et al. (2018), *Wear* 418-419; [4] Bagheri et al. (2021), *Appl Ergon*. 90

FUNCTIONAL OUTCOMES FOLLOWING SINGLE LEVEL FOCAL SELECTIVE DORSAL RHIZOTOMY

Cara M. Masterson[1*], Amy Barbuto[1], Jeffrey S. Shilt[1,2], Nisha Gadgil[1,3], Eric L. Dugan[1,2]
[1]Texas Children's Hospital, TX, USA
[2]Department of Orthopaedic Surgery, Baylor College of Medicine, TX, USA
[3]Department of Neurosurgery, Baylor College of Medicine, TX, USA
*Corresponding author's email: cmmaster@texaschildrens.org

Introduction: Cerebral palsy (CP) is a prevalent (about 1 in 350), heterogeneous, and debilitating condition characterized by motor deficits such as spasticity, stemming from atypical early brain development or damage. Spasticity arises due to abnormally increased muscle stretch reflex responses. As children with spastic CP age, their functional mobility typically declines. Selective dorsal rhizotomy (SDR) is a neurosurgical intervention aimed at reducing spasticity and potentially enhancing gait mechanics, particularly when paired with rehabilitative physical therapy. The purpose of this study is to quantify the effects of a combined single-level focal S1 selective dorsal rhizotomy and gastrocsoleus complex lengthening procedure (S1 SDR+gastroc) on the ankle dynamics of patients with CP. It was hypothesized that S1 SDR+gastroc would result in improved ankle dynamic function when compared to pre-surgical measures.

Methods: This was a retrospective analysis of 17 patients with CP who were classified as Gross Motor Function Classification System I or II and presented with primary impairment at the ankle joint. All patients underwent 3D gait analysis in our lab before S1 SDR+gastroc intervention and a follow-up 3D gait analysis an average (SD) of 408 (184) days post-surgery. A standard six-degree-of-freedom model with a multi-segment foot model [1] was used. A total of 23 limbs were analyzed, corresponding to the patients' surgically treated limbs. The cohort consisted of 10 males and 7 females, with mean (SD) ages of 6.6 (2.0) years pre-surgery and 8.8 (2.0) years post-surgery. The sagittal plane (dorsiflexion) joint angle between the calcaneus segment and the shank segment was analysed (ShaCal), as well as the Ankle Deviation Index (ADI) [2] score of the ShaCal, the passive range of motion measurement of ankle dorsiflexion with knee extended (AnkleROM), and the gastrocsoleus complex modified modified Ashworth Scale (MMAS) spasticity score. The ADI score is a subset of the Gait Deviation Index [3] using only the ankle dorsiflexion data.

Paired t-tests were used to compare pre and post ADI and AnkleROM values, while a Wilcoxon signed-rank test was used to compare pre and post intervention gastrocsoleus spasticity scores. A statistical parametric mapping (SPM) paired-sample t-test (SPM{t}) was used to compare ShaCal dorsiflexion curves pre and post intervention. Significance for all tests was a priori set at $p < 0.05$.

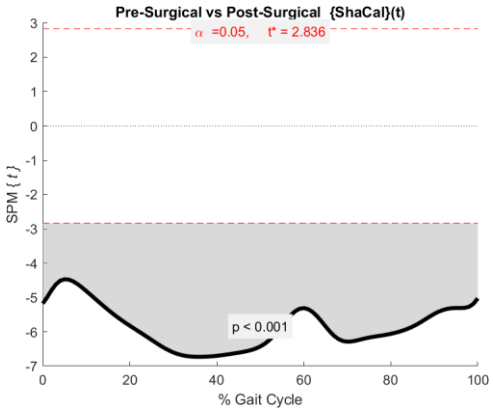

Figure 1: Paired SPM paired t-test (SPM{t}) showed significant difference between pre-surgical and post-surgical ShaCal sagittal plane data throughout gait cycle.

Results & Discussion: Statistical analyses revealed statistically significant improvements following S1 SDR + gastroc. Specifically, ADI values increased from 55.26 (SD = 18.56) pre-surgery to 76.35 (SD = 15.21) post-surgery ($p < 0.001$). Similarly, AnkleROM improved from a mean of -22 degrees (SD = 12) pre-surgery to 4 degrees (SD = 7) post-surgery ($p < 0.001$). The Wilcoxon signed-rank test indicated a significant post-intervention reduction in gastrocsoleus spasticity, with median values decreasing from 2.3 (SD = 0.6) to 0.2 (SD = 0.4) ($p < 0.001$). There were also significant changes in ShaCal dorsiflexion throughout the entire gait cycle (Figure 1) with the post intervention data being in less equinus than pre-intervention data (Figure 2).

These results collectively suggest that the S1 SDR+gastroc intervention effectively increased ADI values, improved dynamic ankle function and AnkleROM, while significantly reducing gastrocsoleus spasticity. The results of this focal intervention on ankle function are consistent with results from previous studies that have reported reductions in equinus foot patterns [4, 5] in patients that underwent full SDR.

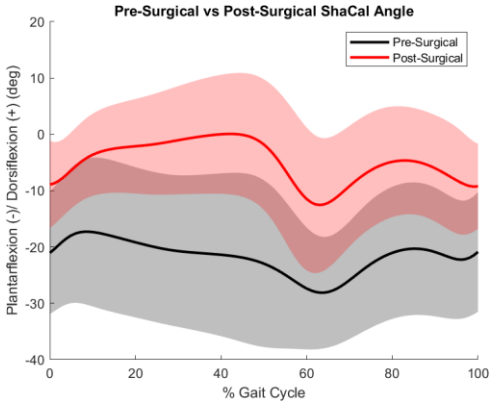

Figure 2: Pre-surgical and post-surgical sagittal

Significance: The results from this study highlight the changes that occur at the ankle following S1 SDR+gastroc in ambulatory children with CP. Our results demonstrate that the significant improvements in ankle spasticity and passive ankle dorsiflexion range of motion noted on clinical exam result in clinically meaningful improvements in dynamic ankle function during gait as quantified by changes in ADI and dorsiflexion time series analysis.

References: [1] Portinaro et al. (2014) *Journal of Foot and Ankle Research* 7(57); [2] Rajagopal et al. (2020) *PLoS ONE* 15(6); [3] Schwarts et al. (2008), *Gait & Posture* 28(351); [4] Schwartz et al. (2008) *Developmental Medicine & Child Neurology* 50(765); [5] Carraro et al. (2014) *European Journal of Paediatric Neurology* 18(6);

DOES SEQUENTIAL IMPLEMENTATION OF BIOMECHANICAL CONSTRAINTS IMPROVE COMPUTER VISION SOLUTIONS FOR MARKERLESS MOTION TRACKING?

Zhixiong (Jack) Li[1*], Soyong Shin[1], Vu Phan[1], Evy Meinders[1], Eni Halilaj[1]
[1]Department of Mechanical Engineering, Carnegie Mellon University, Pittsburgh, PA, USA
*Corresponding author's email: zhixionl@andrew.cmu.edu

Introduction: Markerless motion tracking is an emerging tool for biomechanical analysis, but given the wide range of methods available, we currently lack understanding of the advantages and disadvantages of each. Many of these methods are primarily developed by the computer vision community. While there are opportunities for biomechanists to contribute and improve the accuracy of such methods, it remains unclear whether sequential implementation of biomechanical constraints leads to practical improvements in kinematics-estimation accuracy. Accordingly, the goal of this work was two-fold. First, we aimed to provide clarity on how state-of-the-art methods, single- and multi-view, open-source and commercial, compare to marker-based motion capture and to one another. Second, we aimed to determine if sequential incorporation of biomechanical constraints after applying deep learning tools provides practical improvements in accuracy. Our hypothesis was that biomechanical constraints improve the accuracy of computer vision algorithms.

Methods: We selected five single-view computer vision algorithms and two multi-view methods based on their popularity in computer vision and biomechanics, respectively. The single-view methods were VIBE [1], HMR2 [2], CLIFF [3], REFIT [4], and WHAM [5], while the multi-view methods included OpenCap (2 cameras) [6] and Theia3D (10 cameras) [7]. After receiving approval from Carnegie Mellon University's Institutional Review Board, we collected data from 10 subjects (5F, 5M; age: 32.8 ± 7.7 years), with both marker-based and markerless motion capture systems (OptiTrack, Corvallis, OR; Fig. 1A). Each subject performed eight physical therapy exercises with three repetitions in the following order: 1) Lateral step down; 2) Step up and down; 3) Drop jump; 4) Countermovement jump; 5) Squat; 6) Step and hold; 7) Single leg squat; 8) Sit to stand. After first comparing all the algorithms using the Friedman test and post-hoc Wilcoxon signed rank test, we selected the best-performing single-view one to address the second question. Virtual markers were extracted from the human-body mesh and inverse kinematics were carried out in OpenSim (Fig. 1B). The Wilcoxon signed-rank test was used to test the second hypothesis. Results are reported as Median and 95% Confidence Interval.

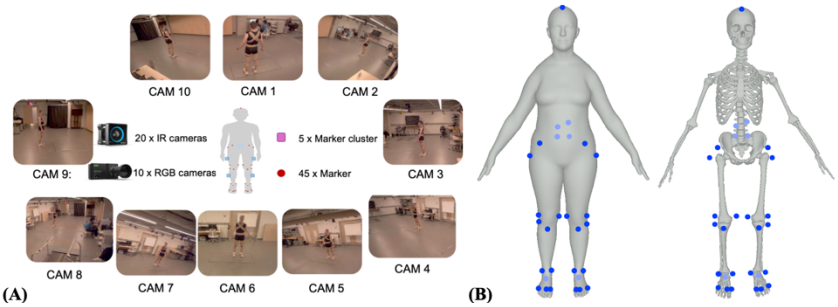

Figure 1: Experimental Setup. (A) Motion capture lab equipped with both marker-based and vision-based systems (20 IR and 10 RGB cameras, respectively). **(B)** Virtual markers enabled integration of biomechanical modeling with computer vision outputs.

Results & Discussion: The best-performing single-view method (WHAM:7.0° [6.5, 7.5]) underperformed compared to OpenCap (5.0° [4.7, 5.3]) and Theia3D (4.4° [4.1, 4.7]; p<0.0001; Fig. 2A). Theia3D performed better than OpenCap in sagittal-plane kinematics (ankle: 1.7° [0.8, 2.5], knee: 1.6° [0.8, 2.3], hip: 2.0° [0.9, 3.2]; p<0.0001), while OpenCap performed better in hip ab/adduction (0.9° [0.2, 1.7]; p=0.001) and hip rotation (2.0° [0.6, 3.4]; p=0.009).

Biomechanical modeling lowered the total RMSE by 0.7° [-0.2, 1.6] (p<0.0001; Fig. 2B). Specifically, it improved hip int/external rotation by 0.9° [-0.1, 1.9] and hip ab/adduction by 0.8° [-1.4, 3.0] (p<0.0001). However, it did not improve hip and knee flexion/extension. We therefore conclude that sequential implementation of biomechanical constraints currently provides limited advantage over the use of off-the-shelf computer vision approaches. The two- or three-degree improvement that OpenCap and Theia3D provide are likely due to factors such as the integration of multi-camera information, or better training data, rather than implementation of sequential biomechanical constraints.

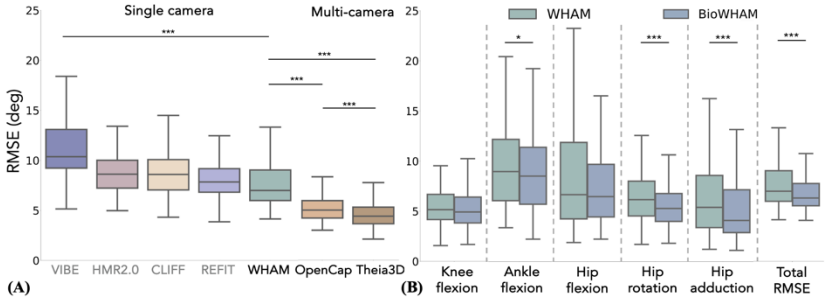

Figure 2: Model Performance. (A) WHAM achieved the highest accuracy for single-view methods, with an RMSE difference of 2-3°compared to multi-view methods. **(B)** Biomechanical modeling provided limited advantage. (*: $p < 0.05$; ***: $p < 0.001$)

Significance: This work has implications for both researchers who apply and those who seek to improve markerless motion tracking. With a plenitude of techniques emerging and both commercial and open-source options available, it is important to know that open-source single-view algorithms that do not require calibration or spatial constraints are only 2.6° less accurate than commercial multi-camera systems. For those seeking to improve these open-source algorithms, sequential application of biomechanical constraints does not seem to be yielding notable improvements. Instead, the biomechanics community should seek to leverage other domain knowledge.

Acknowledgements: This work was funded by the National Science Foundation, under Award # CBET 2145473.

References: [1] Kocabas, *et al.*, 2020, *CVPR.*; [2] Goel, *et al.*, 2023, *ICCV.* ; [3] Li, *et al.*, 2022, *ECCV.* ; [4] Wang, *et al.*, 2023, *ICCV.* ; [5] Shin, *et al.*, 2024, *CVPR.* ; [6] Uhlrich, *et al.*, 2023, *PLoS computational biology (19.10).* ; [7] Theia Markerless Inc., Kingston, ON

BIOMECHANICAL AND METABOLIC RESPONSES TO WALKING IN ADVANCED FOOTWEAR TECHNOLOGY

Luke VanKeersbilck[1], Jared Steele[1], Iain Hunter[1], Dustin Bruening[1*]
[1]Brigham Young University Provo, Utah
*Corresponding author's email: dabruening@byu.edu

Introduction: In recent years, there has been a revolution in running shoe technology because of the introduction of the super shoe or Advanced Footwear Technology (AFT). This technology has been shown to reduce metabolic expenditure of running by an average of 4% [1], but is reduced at slower running speeds [2]. This prompts the question: can this technology be used to reduce the metabolic expenditure of walking? The aim of this study was to examine whether AFT can effectively decrease metabolic energy expenditure during walking and to explore the mechanisms underlying this potential reduction in energy expenditure.

Figure 1: The two test shoes. The grey shoe in front is the control shoe and the white shoe in the back is the AFT shoe.

Methods: Three college age subjects (1 male, 2 female) participated. Participants alternated between wearing control shoes (CON) and AFT shoes. Shoe order was randomized. At the beginning of testing each participant performed a 5-minute familiarization in each shoe. They then completed two sets of 5-minute trials in a BAAB order. All trials were completed on the treadmill at 1.4 m/s. As they walked, subjects' metabolic expenditure was recorded and was averaged for the last 2 minutes of each trial. Then the metabolic equipment was removed, and markers were placed on the legs and shoes. Subjects performed a minimum of 3 successful trials of overground walking in each shoe. The speed of these trials was measured using timing gates and was matched to the treadmill speed with a range of +/- 0.05 m/s. Marker trajectories and ground reaction forces were recorded and used to calculate ankle joint and distal-to-hindfoot power.

Results & Discussion: All three participants saw a decrease in their $\dot{V}O_2$ when wearing the AFT by 3.2, 3.2 and 3.8% respectively. This is similar to metabolic savings observed during running. This change in metabolic coincided with mechanical changes in ankle joint and distal-to-hindfoot power. The peak positive ankle joint power *(figure 2*) in late stance was lower when walking in the AFT for all three subjects (18.1%, 9.8%, and 11.0%). This will result in a decrease in the positive work that is required from the ankle in late stance. There was also an increase in the distal-to-hindfoot power in early midstance (51.6%, 90.7, 40.3%). This likely represents the foam rebound following heel compression. The highly resilient foam gives back more energy in the AFT than the EVA foam of the CON shoe. This may also be related to the reduced power requirements for the ankle as this time coincides with the opposite foot late stance. There are also other factors that may be related to the metabolic savings when walking in AFT. Future work will investigate the knee and hip joint powers to help determine if they may be part of the metabolic benefits. These investigations will also differentiate the sources of power distal to the hindfoot to help further determine how ATF affects foot mechanics when walking.

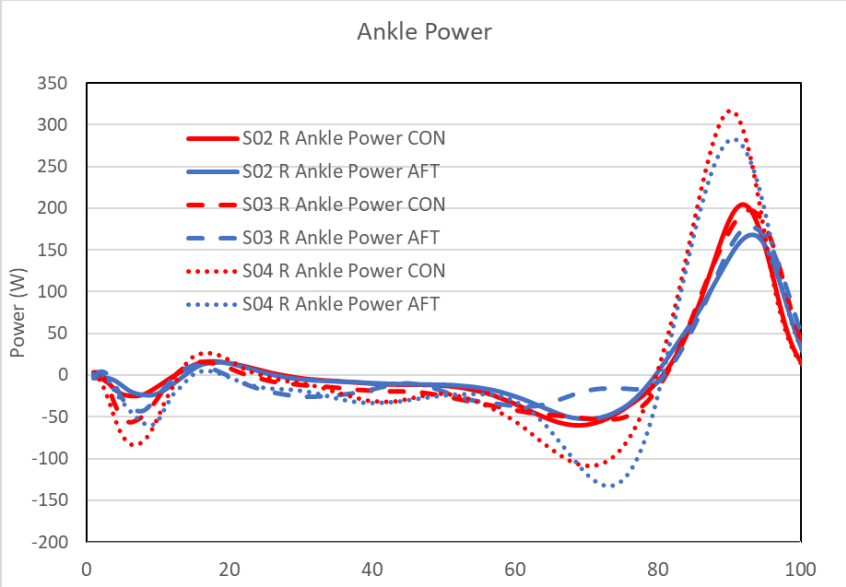

Figure 2: Ankle joint power for the three participants. Red lines represent the CON shoe and blue lines represent AFT

Significance: If similar trends in $\dot{V}O_2$ continue, AFT holds promise in aiding individuals with diminished cardiovascular function to regain functionality. Annually, approximately 805,000 people in the United States suffer from heart attacks (3), experiencing significantly impaired walking speed and capacity compared to healthy counterparts (4). The implementation of this technology offers potential for enhancing functional abilities and improving overall quality of life for these individuals.

References: [1] Hoogkamer et al. (2019), *Sports Med.* 48(4); [2] Joubert et al. (2023), *Int J of Sports Phys and Perf* 18(2); [3] Tsao et al. (2023), *Circulation* 147(8); [4] Bona et al. (2017), *Eur J Prev Cardiol.* 24(5)

GRF PREDICTIONS FROM MARKERLESS MOTION DATA DURING ATHLETIC CUTTING MOVEMENTS

Hailey L. Wrona[1*], Caroline E. Nealon[1], Shawn D. Russell[1,2]
[1]Departmant of Mechanical and Aerospace Engineering, University of Virginia, USA
[2] Department of Orthopaedic Surgery, University of Virginia, USA
*Corresponding author's email: hlw6br@virginia.edu

Introduction: As motion capture technology continues to develop and evolve beyond the need for marker placement with markerless motion capture, new opportunities arise for the capture of more diverse human movement in a range of different environments. Although markerless motion capture has great potential, moving the data collection process outside the conventional laboratory setting also comes with the loss of auxiliary equipment, such as embedded force plates. Force plates provide information about the ground reaction force (GRF) magnitude and center of pressure (COP) location that provide information for inverse dynamics and joint moments. Video analysis has been used to characterize sagittal-plane motion [1,2], but there is a current gap in research in the investigation of video-based GRF and COP estimation for dynamic athletic motion. The use of video-based COP estimation has great applicability to supplement markerless motion capture in athletics due to the high volume of broadcast video readily available. With 58.7% of lower extremity injuries in the NFL occurring during gameplay [3], the use of an accurate video-based GRF estimation would allow for a better characterization of the external loads experienced to cause lower extremity injuries. The purpose of this study was to determine a novel way of estimating GRF magnitude and COP position during athletic cutting movements to be applied to markerless video.

Methods: Fourteen subjects performed a series of American football agility drills, one 90° cut on the inside foot (3-cone) and one 90° cut on the outside foot (v-cut). In both movements, the subject is in single contact, reflecting many other expected athletic movements. All trial motion data was collected with a three-dimensional motion analysis camera system, and ground reaction force data was recorded at the feet using two in-ground force plates. OpenSim was used to calculate joint center trajectories similar to those found via markerless capture and calculate center of mass (CoM) acceleration, for GRF magnitude calculations, from filtered marker data and scaled models. Trends in the anterior-posterior (AP) and mediolateral (ML) COP relative to the sagittal global foot angle were identified and applied with curve fits. The estimated COP locations and GRF magnitude predictions for each trial were used in OpenSim Inverse Dynamics to compute joint moments. For validation, direct comparisons were performed between the GRF predictions and marker-based motion capture, the gold standard. Root mean square error (RMSE) was calculated as the main metric to evaluate the accuracy of the predicted data.

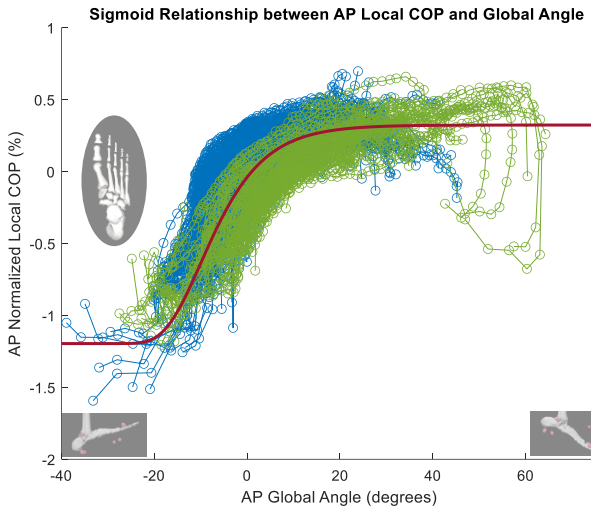

Figure 1: Calculated Gompertz Sigmoid fit between the global foot angle and the AP normalized local COP. Blue represents v-cut data and green represents 3-cone data.

Results & Discussion: A Gompertz Sigmoid function was the best fit ($r^2 = 0.776$) between the AP global foot angle and the measured local AP COP location (Fig.1). Quadratic functions were the best fit for the v-cut ($r^2 = 0.468$) and 3-cone ($r^2 = 0.526$) between the AP global foot angle and the measured local ML COP location. The estimated COP location had an average RMSE of 17.4% and 8.36% of the foot length in the AP and ML direction. The estimated GRF magnitudes had an average RMSE of 7.16%, 13.3%, and 6.91% of the maximum magnitude for the AP, vertical and ML force, respectively. Table 1 lists the resulting joint moment RMSE values.

Significance: The findings of the current study show that GRF magnitude and COP location values can be estimated from dynamic single-support motion. Accurately estimating external loads from video allows a better understanding of lower extremity gameplay injuries.

Movement	Joint Moment	RMSE Error (Nm/kg)
3CONE	Hip Adduction	1.944
	Hip Flexion	2.158
	Hip Rotation	0.455
	Knee Flexion	1.255
	Ankle Dorsiflexion	0.627
	Ankle Inversion	0.327
VCUT	Hip Adduction	1.807
	Hip Flexion	2.147
	Hip Rotation	0.671
	Knee Flexion	1.714
	Ankle Dorsiflexion	0.844
	Ankle Inversion	0.415

Table 1: RMS error of the joint moments between estimated COP and GRF and measured COP and GRF values.

References: [1] Straub et al. (2021), *Gait Posture* 90; [2] Martinez et al. (2022), *Int J Sports Phys Ther* 17(4); [3] Mack et al. (2020), *Am J Sports Med* 48(9).

SPATIAL VARIABILITY OF FRACTAL TEMPORAL CORRELATIONS SUPPORTS CENTER OF MASS (COM) AND CENTER OF PRESSURE (COP) COUPLING IN HEALTHY YOUNG AND COLD ADULTS

Brian Schlattmann[1], Mahsa Barfi[1], and Madhur Mangalam[1]
[1]Department of Biomechanics, University of Nebraska at Omaha, Omaha, NE 68182, USA
email: bschlattmann@unomaha.edu

Introduction. The prevailing connection between statistical evidence of fractal temporal structure in postural sway variability and theoretical mechanisms while providing heuristic value has faced criticism for its conceptual hollowness. This critique is part of a broader skepticism towards dynamical systems approaches. To overcome such criticisms, we take a novel approach in the present study by modeling endogenous fractal temporal relationships across the 2D support surface, derived from postural control strategies that generate fractal scaling intermittently. Specifically, we propose that the Hurst exponent *H* encoding fractal temporal relationships may not be the simple incidental product of inverted pendulum control models but might serve as a control parameter.

Methods. Ground reaction forces and kinematic data was collected on healthy young (N = 27) and older adults (N = 22) in four different postural conditions: (I) rigid surface, eyes open; (II) rigid surface, eyes closed; (III) foam surface, eyes open; (IV) foam surface, eyes closed [1]. We employed the oriented fractal scaling component analysis (OFSCA) [2] to decompose the CoP trajectory along the 2D support surface and quantify the minimum and maximum values of the Hurst exponent, *H*, quantifying the strength of fractal temporal correlations in CoP fluctuations (H_1 and H_2, respectively), and the standard deviation of *H* along the 2D support surface (SD_H; **Fig. 1**).

Results & Discussion. Our results supported the hypothesis that spatial variability in the fractal temporal structure of CoP could elucidate the CoP-CoM distance between the two groups. The interaction effects revealed that the impact of angular variance in the endogenous fractal properties of CoP fluctuations (H_1, H_2, and SD_H) on the standard deviation of CoP-CoM distance was contingent upon age. Specifically, older adults with higher values of the minimum Hurst exponent and greater standard deviation of Hurst exponents across the 2D support surface exhibited an increased standard deviation of CoP-CoM distance. This result suggests that the fractal temporal structure played a much greater role in maintaining proximity between CoP and CoM in older adults than in their healthy young counterparts. Notably, this result challenges the conventional notion of associating aging with the loss of fractal temporal structure. Instead, as hypothesized, we observed systematic variations in postural CoP beyond the standard anatomical axes, wherein the fractal temporal structure of CoP fluctuations potentially acts as the "control variable," regulating CoP response to instantaneous changes in CoM. This mechanism ultimately serves to narrow the gap between CoP and CoM. This line of thinking aligns with the growing body of evidence that uses fractal and "multifractal" estimates of movement variations as causal predictors of adaptive behavior.

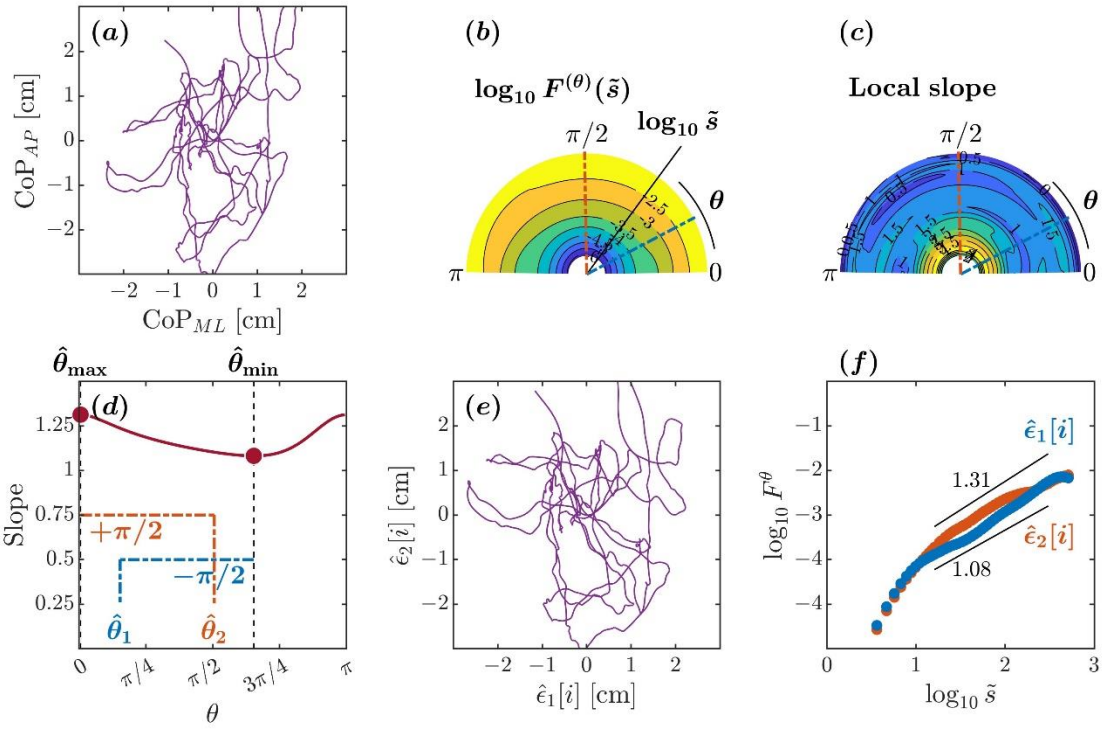

Figure 1. Orientation decomposition of the CoP planar trajectory of a representative older adult maintaining an upright balance on an unstable surface with closed eyes.

Significance. The present work provides novel avenues to integrate postural studies into the etiology of various movement disorders; an additional dimension regarding the causality of movement variability degradation with age can be considered, in addition to the established notions of diminished mechanical and neural control. This approach will yield unambiguous insights into the mechanics underlying observed postural deficits and enable the identification of effective rehabilitative strategies.

Acknowledgments. This work was supported by the NIH award P20GM10909.

References. [1] dos Santos et al. (2017), *PeerJ* 5, e3626. [2] Mangalam et al. (2024), *Scientific Reports* 14, 4117.

COMPARISON OF JUDGING AND BIOMECHANICAL ANALYSIS OF COMMON HIP - HOP DANCE MOVES

Joshua A. Vicente[1*], Belle P. Ponce de Leon[1], Jacob Hinkel-Lipsker, Ph.D.[1]
[1] California State University, Northridge (CSUN)
*Corresponding author's email: joshua.vicente@csun.edu

Introduction: Hip - hop dance has branched out from the genesis of breakdancing into several different types of styles with their own identifiable characteristics (e.g. - Krumping, Popping, Locking). The characteristics used to assess them rely on subjective interpretation of their movement as they are commonly performed in settings meant to appeal to their audience [1]. The criteria being used to assess hip - hop dancers are not always consistent, allowing physical appearance to hold as much weight as technique or execution during a performance, further skewing a score. With breakdancing making its Olympic debut, there are some concerns on how these competitions will be judged, who is qualified to judge similar competitions, and how to address any potential bias judges may have. When examining this issue with biomechanical analysis tools, the literature is limited on methodology suited to capture this unique kind of movement data. This led to my research question, is there a biomechanical predictor between how a professional judge will score you and the performance of common dance moves across different dancers? From this, we hypothesized that hip - hop dancers should display similar biomechanical predictors that judges are using to assess mastery during their performance. To start, we looked at two unique upper and lower body dance movements: The Arm Wave and "Happy Feet" (AKA Footwork). We operationally defined the arm wave as the sequential movement of upper extremity joints from one side to the other. For Footwork, we defined this as oppositional heel and toe movement between both feet. Since dance experience would vary between potential participants, we were focused on key biomechanical measurements like joint displacement, propagation velocity, and shape deviation during the arm wave while examining force distributions, center of pressure measurements, and timing differences of both feet for the footwork. Due to limited previous literature, we expected dancers with higher scores to examine a higher amount of joint displacement, faster propagation velocity, and a smaller shape deviation to be correlated with higher scores. As for footwork, we expected participants to have higher scores to have a bigger force distribution, similar center of pressure measurements, and smaller timing differences between both feet.

Methods: Using the operational definitions above for "The Arm Wave" and "Footwork", a choreographed dance routine was made integrating the two moves of interest. Potential participants were recruited via flyers and screened to ensure that they met the following inclusion criteria: (1) Be between 18 - 65 years old, (2) Must have at least 2+ years of hip - hop experience, and (3) must have at least one formal performance within the last seven years. As judges were also going to be utilized during this study, they had their own criteria for selection and would serve as confederates of the research team. Judges must have: (1) 5+ years of teaching and coaching award-winning hip - hop competition teams, and (2) must have familiarity with the auditioning/scoring process. After recruiting participants, they scheduled a meeting time to go over all informed consent documents, collect movement data, and were sent an online choreography video to learn before their appointment. All movement data was captured on a 12-camera motion capture system (240 Hz) set up with two integrated force plates (sampling rate of 1200 Hz) and a reflective marker setup [2, 3]. Participants then came in during their scheduled meeting time, confirmed all paperwork, and performed the dance routine underneath the motion capture system. These performance attempts of participants were recorded and sent to three judges to be scored. These scores were collected for each participant and averaged. From here, all biomechanical data was exported for analysis via a custom MATLAB script. All this data was analyzed via multiple stepwise linear regressions via JASP to determine any significance between biomechanical measurements and judges' scores.

Variable	P-value ***(p< .05)**	Adj. R2
Displacement (R3P)	<.001**	.650*
Propogation Velocity (L Forearm)	.010**	.748*
Propogation Velocity (R Forearm)	.037**	.805*
Timing Difference (Footwork)	.022**	.242

Table 1: Table with significant returned values from multiple stepwise regressions for arm wave and footwork.

***Same Regression**

Results & Discussion:
Our results (Table 1) showcased that the Stepwise Linear Regression for "The Arm Wave" had propagation velocity of the left and right forearm, and displacement of the right 3rd phalange to be significant predictors of judges scores. All of these results seemed to showcase an inverse relationship where judges' scores were higher with lower displacement and propagation velocity values. As for the dancers' performance, they may have showcased mastery by minimal movement and slower progression through the arm wave. For "Footwork", the only significant predictor was the timing difference between the maximal forces of both feet. As this move does require rapid and alternating foot coordination, this factor is key to its successful interpretation.

Significance:
With hip - hop dance becoming more and more prevalent in today's global culture, I strongly believe this to be a perfect melding of biomechanical analysis, and analyzing common dance moves would be key to allowing applicability across the various sub-styles of hip - hop dance and its frequency in academic literature.

References: [1] Miura A, et al. JDMS, 2019. ; [2] Sato, N., et al. J. Appl. Biomech 31, 2015.; [3] Sato, N., et al. J. Appl. Biomech 30, 2014.

A METHODOLOGY ADVANCEMENT TO QUANTIFY HABITUAL MOTION PATH DEVIATIONS WHEN RUNNING

Jennifer Sumner[1*], Evan M. Day[1], Katherine Wagner[1], Jessica Thompson[1], Steffen Willwacher[2], Matthieu B. Trudeau[1]
[1]Brooks Sports, Inc., Seattle, WA USA
[2]Offenburg University of Applied Sciences, Offenburg, Germany
*Corresponding author's email: evan.day@brooksrunning.com

Introduction: Every individual has a unique habitual motion path (HMP) defined by their bone structure, ligament laxity, muscular strength, and injury history [1]. It is postulated that deviating away from one's HMP, defined as one's joints moving differently when running compared to habitual daily movements, may raise an increased injury risk as joint loading will occur on less-adapted areas of soft tissues when a deviation occurs. It may be advantageous to decrease deviation from one's HMP as this is associated with decreased soft tissue loading [2]. One tool for reducing HMP deviations is footwear. Trudeau et al. (2019) developed a novel method to quantify one's HMP and deviation [1]. The primary limitations of this method were using a single movement to establish one's HMP, and using a single time point during stance phase to quantify deviation when running. This abstract describes an advancement in this methodology and application to using this biomechanical insight for footwear creation.

Methods: Three-dimensional kinematic data of lower limb segments (rearfoot, shank, thigh) from 185 participants were used for method development and analysis. The three joint angles of interest analysed for all movements were ankle eversion-inversion, knee internal-external rotation, and knee ab-adduction. For all habitual movements and running, participants wore a sock shoe (5.5mm sock liner with rubber on bottom and affixed running sock on top) to eliminate any potential effects of footwear geometries on gait. To more holistically quantify an individual's HMP, three new movements were added: lunge, walk, and stair descent; in addition to the squat. These movements were chosen because they cover a greater range of motion at the ankle and knee joint than during running and represent common daily tasks such as sitting down in a chair. To quantify an individual's HMP deviation when running, kernel density plots (KDP) were created using time-normalized joint angle data from the stance phase of movements to represent habitual movement and running kinematics (Fig 1). The kernel density plots were equally divided into 51 segments to which a weighting factor was applied using the vertical ground reaction force magnitude, normalized to body weight. Weighting was used to apply more meaning to kinematics that are occurring under higher external loading. To quantify one's deviation, the weighted area of each KDP was quantified. The area of the run KDP *not* overlapping with the habitual movement KDP was quantified to represent the deviation when running (Fig 1). This analysis was performed on all three joint angles using all participants' data to update thresholds for quantifying someone as a Low or High deviator, described as being above or below the population median (Fig 2).

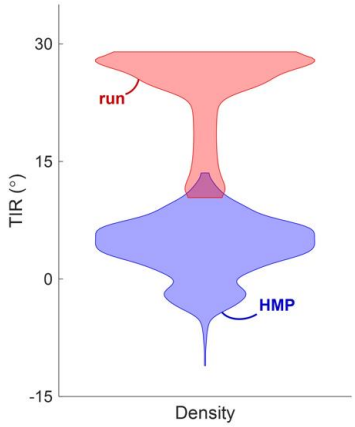

Figure 1: Exemplar kernel density plots for running (red) and habitual motion path (blue). TIR = knee internal rotation

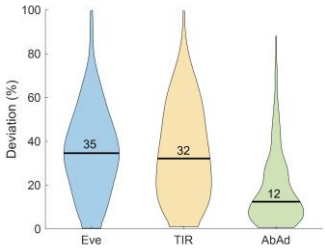

Figure 2: Population distributions (n=185) for three joint angles. Eve = ankle eversion; TIR = knee internal rotation; AbAd = knee ab-adduction

Results & Discussion: This new methodology advances the ability to quantify HMP deviations by utilizing more habitual movements and using the entire stance phase when running. These advancements allow us to better understand an individual's unique HMP and kinematics when running by also providing information regarding the joint's range of motion, where that motion is occurring (joint angle magnitudes), and where the joint is most commonly oriented (mode of the KDP). This advances our classification of runners from exhibiting high or low to deviation (Fig 2) to also understanding more robustly *how* they are moving, and what HMP pattern that individual needs guided back to via proper footwear (Fig 1). Further research investigating creation of functional groups of various HMP patterns will inform what or how many products are required to help guide all runners back to or keep them close to their HMP when running. Furthermore, utilizing the entire stance phase to quantify deviations creates the ability for sub-phase analysis. This will allow us to further investigate functional groups of runners based on *when* during stance phase they deviate, which will inform where in a shoe support technologies are needed.

Significance: This new method advances our ability to understand the runner and their unique HMP and deviation when running. By robustly understanding how a runner uniquely moves, we can better create footwear that helps guide a runner back to or keep them close to their HMP when running. This new method paves the way for moving beyond a 'neutral' or 'support' framework for footwear creation when solving for minimization of an individual's HMP deviation; as well as more targeted footwear construction recommendations.

Acknowledgments: Thank you to all Brooks' Run Research Team members who assisted with data collection and processing.

References: [1] Trudeau et al. (2019), *Footwear Sci* (3) 135-145; [2] Willwacher et al. (2020), *Sci Reports* 10(1363).

PRECISION AND ACCURACY OF 3D FREEHAND ULTRASOUND CALIBRATION USING A CROSSWIRE PHANTOM

Hidetaka Hayashi[1*], Michael Hahn[1]
[1]Department of Human Physiology, University of Oregon, Eugene, USA
*Corresponding author's email: hhayash7@uoregon.edu

Introduction: While the Achilles tendon is the largest and strongest tendon in the human body, it is susceptible to developing tendinopathy due to its relatively long and compliant nature, and that it is subject to loads as high as 10 times bodyweight during activities such as running. Structurally, Achilles tendinopathy is accompanied by an increase in cross-sectional area as well as decreased elastic modulus [1]. Previously, it has been demonstrated that a "sweet-spot" of about 5-6% strain of the free Achilles tendon promotes positive adaptations such as increased stiffness and increased expression of type 3 collagen fibers [2]. Yet, common approaches to quantify Achilles tendon strain, such as 2D B-mode ultrasonography, often include the proximal aponeurosis-like portion of the tendon, which likely underestimates strain. Thus, the quantification of the free Achilles tendon strain is important to better inform rehabilitative practices.

One approach to quantify free Achilles tendon strain is 3D freehand ultrasound (3DfUS). The use of ultrasonography provides a more cost effective alternative to other imaging modalities such as MRI. This technique involves obtaining a stack of ultrasound images whilst simultaneously tracking the position and orientation of the ultrasound probe. The images are then mapped into 3D space, and the structure of interested segmented to obtain a 3D reconstructed volume. To obtain accurate reconstructions, the precision and accuracy of the calibration step is crucial. Therefore, the purpose of this study was to assess the precision and accuracy of spatial calibration performed using the crosswire phantom.

Methods: A crosswire phantom composing of a pair of intersecting wires within an acrylic box submersed filled with water was constructed. A cluster of 4 retroreflective markers attached rigidly to the ultrasound probe were used to define the probe coordinate system and were tracked using a 5 camera motion captures system at 120 Hz. (Motion Analysis Corp., USA). The homogenous transformation matrix was then calculated by imaging the crosswire at several different angles and positions of the ultrasound probe (fig. 1) [3]. This was performed 3 times on separate days to test the repeatability of spatial calibration.

The quality of spatial calibration was assessed by reconstruction precision and accuracy. To test calibration precision, 10-15 ultrasound images of the crosswire were obtained, and the position coordinates of the crosswire in the ultrasound image were mapped onto the 3D global coordinate space. This created a cloud of points in 3D space, and the average distance between each pair of points was calculated. This corresponds to the average of 45-105 calculations, depending on the number of ultrasound images obtained. To assess calibration accuracy, the same images of the crosswire from the precision test were used. The distance between the known location of the crosswire in 3D space and the reconstructed position of the crosswire from the ultrasound images were calculated according to the following equation:

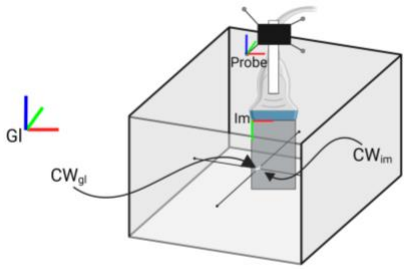

Figure 1. Illustration of the crosswire phantom imaged with the ultrasound probe, and the coordinate systems involved. Made with biorender.com

$$accuracy = CW_{gl} - T_{pr\to gl} * T_{im\to pr} * CW_{im} \quad (1)$$

where CW_{gl} indicates the known position of the crosswire in the global coordinate system, and $T_{pr\to gl} * T_{im\to pr} * CW_{im}$ indicates the transformation of the crosswire in the image onto the global coordinate system.

Results & Discussion: Across the three trials, the average calibration precision was 0.90 ± 0.55 mm, and the average calibration accuracy was 0.63 ± 0.37 mm. These results are consistent with previous studies [4] and indicate good calibration quality.

To obtain accurate volume reconstructions of anatomical structures using 3DfUS, accurate special calibration of the system is a crucial step. Our results suggest that calibration using a crosswire phantom design produces high quality calibration in both precision (how close the reconstructed points are to each other), and accuracy (how close the reconstructed points are to its known location). Further work to assess the quality of calibration in terms of volume reconstruction accuracy is needed and is the next phase of this work.

Significance: The high precision and accuracy of 3DfUS calibration indicates that 3DfUS offers an alternative to obtain 3D reconstructed volumes of the free Achilles tendon that is more cost effective compared to other imaging modalities. Given that 3DfUS can measure subject specific tendon morphology and quantify tendon deformation under load, this method may inform individualized rehabilitation protocols to promote tendon healing in patients with Achilles tendinopathy.

Acknowledgments: This work was supported by the Wu Tsai Human Performance Alliance and the Joe and Clara Tsai Foundation.

References: [1] Arya & Kulig (2010) *J App Physiol* 108(3); [2] Pizzolato et al. (2019), *Br J Sports Med* 53(1); [3] Weide et al. (2017) *J Vis Exp* 129; [4] Prager et al. (1998) *Ultrasound Med Biol* 24(6).

CHANGES TO NEUROMECHANICAL COORDINATION OF ENERGY ABSORPTION IN THE LEGS AFTER NEUROMUSCULAR FATIGUE

Melody S. Modarressi[1*], Joelle Dick[1], Gregory S. Sawicki[1,2], Young-Hui Chang[1]
[1]School of Biological Sciences, [2]School of Mechanical Engineering, Georgia Institute of Technology, Atlanta, GA, USA
*Corresponding author's email: mmodarressi3@gatech.edu

Introduction: Neuromuscular fatigue has been shown to alter physiological and neuromechanical characteristics of joints and soft tissues like muscle and has profound implications for understanding mechanisms of injury and recovery [1]. The sensorimotor system is able to leverage motor redundancies to compensate for such changes within these components, in order to continue task performance despite fatigue-induced deficiencies [2]. During single-legged jumps (SLJs), highly controlled coordination is necessary to generate sufficient force to propel the body upward while also stabilizing landing to minimize impact forces, requiring a delicate balance between positive and negative mechanical energy generation and absorption [3]. The efficient dissipation of mechanical energy is especially essential when landing from a jump, where failure to absorb power generated during the lift-off and aerial phases can result in instability and injury [4]. Our previous analyses highlight the use of an inter-joint strategy of compensation in the lift-off phase of SLJs following fatigue; the diminished mechanical work contribution of joints experiencing greater fatigue was offset by increased contributions of their less fatigued counterparts. The work presented here expands upon that dataset by identifying and quantifying the degree of redistribution in joint-level mechanical work during the power absorption phase of SLJs with the progression of fatigue. We **hypothesized** that, similar to positive mechanical work during lift-off, joints of the lower limb would experience varying degrees of fatigue when landing from a SLJ after strenuous exertion, resulting in shifts in the joint contributions to meet the negative mechanical work demands of power absorption. We **predicted** that the ankle would play a larger role in power absorption with the onset of fatigue, in order to compensate for diminished contributions at the knee and hip joints.

Methods: We collected data on nine healthy participants (25.2 ± 2.3 years; 71.85 ± 18.8 kg; 177.27 ± 14.47 cm; 4 male and 5 female) with the goal of inducing neuromuscular fatigue across major muscles of the lower limbs; participants provided informed consent prior to participating in this IRB-approved protocol. Following a brief warm-up, participants performed three maximal SLJs on their dominant leg. The maximum vertical displacement of these "pre-fatigue" jumps was recorded and used to calculate the target height for subsequent SLJs (75% of maximum displacement). Next, participants underwent the fatigue protocol in which they squatted repeatedly to a knee flexion angle of 90 degrees. Squatting occurred at a pace of 50 bpm and continued until one of two possible criteria was met: the participant squatted for four consecutive minutes or failed to complete three successive squat cycles to the target knee flexion angle to the given tempo. Once failure was reached, the participant repeated the three maximal SLJs. If the vertical displacement target was reached in any of these jumps, the fatigue protocol was repeated until all three SLJs failed to reach the target height, or until a maximum of five blocks of squatting occurred. Sagittal plane joint kinetics and kinematics were calculated and compared between the pre-protocol and the progression through the fatiguing protocol for the seven participants who completed all five squatting blocks and subsequent SLJs.

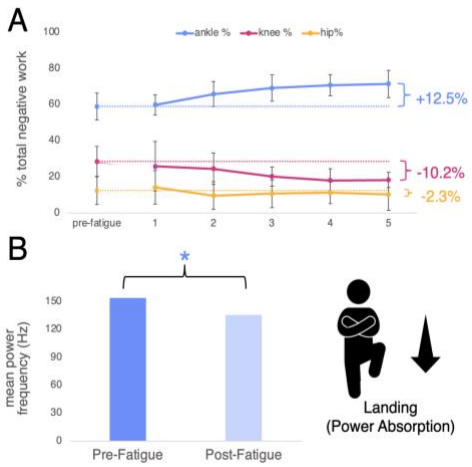

Figure 1: *A)* Mean ± SD of mechanical work contribution of ankle, knee, and hip during landing (n=7). Dashed lines indicate pre-fatigue baseline for each joint. *B)* Average mean power frequency of soleus muscle EMG during landing phase of SLJ across participants prior to and following the fatigue protocol. Asterisk indicates statistical significance (paired t-test, $p < 0.05$) and confirms presence of fatigue in key muscles.

Results & Discussion: We observed notable redistributions of joint contributions to total mechanical work across participants during landing (Fig. 1A). Our results show that the ankle joint compensated for diminished contributions by the hip and knee joints during power absorption (ankle: +12.5%; knee: -10.2%; hip: -2.3%). We used mean power frequency to confirm that fatigue was present in the soleus muscle following the protocol (Fig. 1B). From our data, we propose that reduced knee joint relative contributions to total mechanical negative power post-fatigue suggest that the knee joint experienced a greater degree of fatigue relative to the other joints, but this needs to be confirmed with a MPF analysis on knee muscles. In sum, shifting to greater ankle contributions during power absorption may suggest a strategy that spares injury about more proximal joints such as the knee and hip following fatigue.

Significance: The objective of this study is to pinpoint underlying changes in coordination strategies when the body experiences fatigue-induced deficiencies. We speculate that fatigued participants begin to prefer an ankle-based strategy in their landings, possibly as a protective mechanism over more fragile joints like the knee, which could have downstream implications for overall CoM dynamics. By quantifying and comparing shifts in joint-level power contributions during SLJ landings, we hope to further understand mechanisms of dynamic neuromuscular control in the context of jumping as well as other functionally relevant movements.

Acknowledgements: This work is supported through the Department of Education GAANN Fellowship (DSP200A210046).

References: [1] Padua et al. (2006), *J Athl Train* 41(3); [2] Bonnard et al. (1994), *Neurosci Lett* 166; [3] Augustsson et al. (2006), *Scand J Med Sci Sports* 16(2); [4] *Tamura et al. (2016), Orthop. J. Sports Med.* 4(1).

THE EXAMINATION OF INERTIAL MEASUREMENT DEVICES FOR GAIT ANALYSIS IN AUTISTIC PERSONS

Lauren A. Luginsland[1,2*], Kiara B. Barrett[2], Hunter J. Bennett[2]
[1]Morsani College of Medicine, University of South Florida
[2] Neuromechanics Lab, Old Dominion University
*Corresponding author's email: llugi001@odu.edu

Introduction: Inertial measurement units (IMU's) offer a practical solution for collecting movement data in autistic persons, a population that typically has hypersensitivities and difficulty tolerating equipment. Given the unique intra- and inter gait variability reported in autistic persons, the purpose of this study was to investigate the use of IMU's to calculate sagittal plane segmental angles of the foot, shank, and thigh during gait compared to MoCap. Due to the unique walking characteristics of the population (e.g. variability), we hypothesize differences in the sagittal plane waveform data between IMU's and MoCap.

Methods: Eleven participants with a confirmed autism diagnosis (Females: 2, 24±13yrs., 1.73±0.13m, 76.82±33.34kg) were recruited for this study. IMU data was collected at 200Hz with Delsys Trigno Avanti wireless sensors (triaxial accelerometer range and bandwidth: ±16G and 24–473Hz; triaxial gyroscope range and bandwidth: ±200°/s and 24-360Hz) and the Delsys Trigno base system and trigger module (Delsys, Inc.). IMU data was simultaneously collected with the VICON MoCap system (Vantage, VICON Motion Systems Ltd) sampled at 200 Hz and three in-line Bertec force plates at 2000 Hz. Calibration of the IMUs were completed to address sources of errors including axis misalignment and bias for both the accelerometer and gyroscope [1]. IMU sensors were placed on the foot (dorsum of shoes), shank (halfway between the lateral malleoli and lateral femoral epicondyle), and thigh (5cm above the base of the patella). A static standing trial was conducted to define the vertical axis of each IMU. Functional tasks, including sit-to-stand, seated ankle raises and seated leg extensions were implemented to define the mediolateral axis and the cross-product of the axes were used to determine the anteroposterior axis. Participants walked overground at their self-selected speed across an 18-meter walkway 10 times. Data collection of ten steps for each participant was analyzed. Raw marker trajectory and ground reaction force data was imported into Visual 3D (Version 6, C-Motion, Inc.). The Cartesian coordinate system and the right-hand rule were followed for 3D rotations. Prior to distinguishing rotation matrices and orientation, the raw IMU data was debiased and axes were corrected according to Stančin (2014) [1]. The IMU-segment coordinate system transformation matrices were derived using the unit vectors of the mean accelerometer recordings from the static trial (vertical axis), the root mean square of the gyroscope recordings from the functional trials (mediolateral axis), and their cross products (anteroposterior axis). Orientation for each IMU were determined via MATLAB's imufilter function, which implements an indirect Kalman Filter. Rotation matrices obtained via the IMU filter were pre-multiplied with the respective segment transformation matrices. IMU gait events were determined by peak foot acceleration during windows established by sagittal plane foot angles (SIacc/APacc; [2]) and MoCap events were determined by a 10N vertical ground reaction force cut-off. Statistical parametric mapping (SPM; v.M01.1, www.spm1d.org [3]) analyses [4] were utilized in MATLAB (R2023a, The Mathworks, Inc.). The SPM-equivalent of a paired-samples t-test was conducted to compare the IMU and motion capture sagittal plane waveforms for each segment (alpha < 0.017).

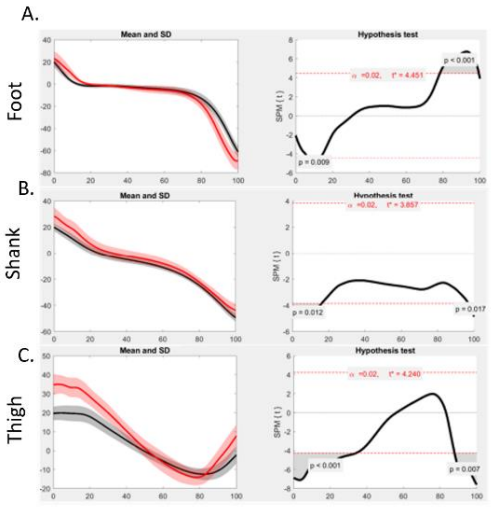

Fig 1. The graphs represent the mean sagittal angles across the stance phase (Red - IMU angle, Black - MoCap). The graphs on the right shows the SPM {t}-statistic as a function of the stance phase. The shaded regions indicate when the critical threshold was exceeded and represents the statistically significant differences between the waveforms. Segmental angles of the foot (A, top), shank (B, middle), and thigh (C, bottom)

Results & Discussion: There were supra-threshold clusters for the sagittal plane angles of the foot (7-14% and 79-100%) (Fig 1a), shank (1-17% and 98-101%; Fig 1b) and the thigh (1-35% and 89-101%; Fig 1c). Our results for the foot sagittal angle were in accordance with the range in the literature (our sagittal plane RMSE=7.47° & r=0.99; Kobsar (2020) RMSE=4.0-7.8° & r=0.80) and slightly outside the limits outlined in the current literature for the shank and thigh (our shank sagittal RMSE=5.91° & r=1.00; Kobsar (2020) RMSE=0.7-4.6° & r=0.98; our thigh sagittal plane RMSE=9.38° & r=0.98; Kobsar (2020) RMSE=2.7-6.3° & r=0.97) [5]. Our IMU sensor location placement aligned with the current literature recommendations [6]. The results are consistent with existing literature, indicating similar findings in the sagittal plane between IMU and MoCap. This is supported by the relative agreement in root mean square values compared to populations without autism.

Significance: These findings come with precautions and recommendations including the consideration of the unique attributes of autistic participants (e.g. stimming, sensitivities). Sagittal plane segmental angles may provide similar findings between IMU and MoCap, however, one must consider the participant's performance of functional tasks to define IMU axes. Given the range of MoCap and IMUs methodologies, it remains challenging to compare angles across technologies and within the existing literature, particularly findings across populations with different movement patterns.

References: [1] Stančin, S., & Tomažič, S. (2014). *Sensors*, *14*(8), 14885–14915. [2] Jasiewicz, J. M. et al. (2006). *Gait & Posture*, *24*(4), 502–509. [3] Pataky TC (2010). *Journal of Biomechanics* 43**,** 1976-1982. [4] Friston, K.J. et al. (2007). Statistical Parametric Mapping: The Analysis of Functional Brain Images. Elsevier, London. [5] Kobsar, D. et al. (2020). *Journal of NeuroEngineering and Rehabilitation,* 17,62. [6] Laudanski, A. et al. (2013). *Journal of Healthcare Engineering*, *4, 555-576.*

PREFERRED MOVEMENT DURATION SHIFTS TO INCREASE POWER FROM AN ASSISTIVE SHOULDER EXOSUIT

Kaleb Burch[1*], Jill Higginson[1,2]
[1]Mechanical Engineering, University of Delaware, Newark, DE, USA
[2]Biomedical Engineering, University of Delaware, Newark, DE, USA
email: kburch@udel.edu

Introduction: Shoulder exosuits are a promising technology for assisting individuals with neuromuscular disabilities and workers in demanding occupational settings. Exosuits have been shown to reduce muscle activity across various tasks [1], however, it is not understood how assistance affects spatial and temporal movement features or what mechanism would drive such changes. One possible goal that may drive adaptation to exosuit-assisted motion is energy or effort minimization. Prior studies have shown that individuals alter movement kinematics to reduce effort when introduced to unfamiliar forces such as robot-imposed force fields [2], resistive knee exoskeletons [3], or split belt treadmills [4]. We conducted an experiment with an assistive shoulder exosuit that operated in closed-loop speed control which presented a force-velocity trade-off. After completing the study, we observed that assistance altered subject's preferred reaching movement duration. We hypothesized that subjects interacted with the exosuit to converge on durations that minimized effort or maximized exosuit power.

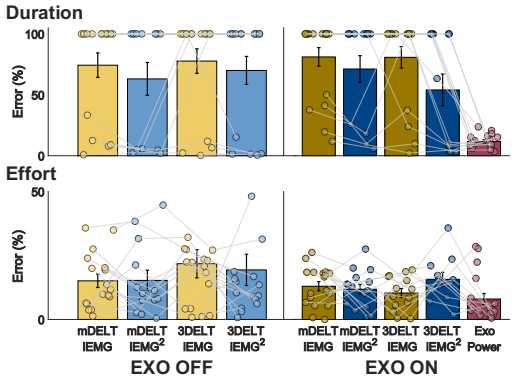

Figure 1: Model errors for EXO OFF and EXO ON conditions. Top: Duration errors. Bottom: Effort errors. Bars depict group average and dots depict individual subjects. Error bars indicate standard error of the mean. The mDELT model is depicted in yellow and the 3DELT model is depicted in blue. Light colors indicate EXO OFF and dark colors indicate EXO ON. Exo Power is depicted in red. Effort errors from one subject were substantially larger than other subjects for 3DELT in EXO OFF and not depicted visually but were included in group averages.

Methods: We collected data from 18 healthy adults wearing a cable-driven shoulder exosuit; subjects performed 40 unassisted reaches (EXO OFF) followed by 120 assisted reaches (EXO ON). Upper limb kinematics and exosuit cable motion were recorded with motion capture, muscle activity of the anterior, middle, and posterior deltoids were recorded with electromyograms (EMG), and exosuit cable force was recorded with a load cell.

We tested 5 models of effort to capture how individuals may have adapted duration. Two models quantified effort using the middle deltoid (mDELT), one based on integrated muscle activity (iEMG) and one based on integrated squared muscle activity (iEMG^2). Another two models used the same parameters but using the sum of all 3 deltoid muscles (3DELT). Finally, we tested a model that considered only average exosuit power (Exo Power). All muscle activity models were defined by fitting 2nd order polynomials of the form $E = c_2 d^2 - c_1 d + c_0$ (EMG models: $c_2, c_1, c_0 > 0$; Power model: $c_2, c_1, c_0 < 0$) where E represents the metric of interest and d represents duration. Optimal movement durations and optimal efforts were identified for each subject at the global minima of the 4 EMG model polynomials and at the global maxima of the power model polynomials. Assuming that the average duration and effort in the last 20 EXO ON trials indicated the true optima, we quantified model errors relative to these values.

Results: The four EMG models exhibited large errors in optimal movement duration for both the EXO OFF and EXO ON condition (Figure 1). The mDELT iEMG^2 model performed the best on the EXO OFF condition at 63.1 $\pm$ 48.6% (mean $\pm$ standard deviation) error and the 3DELT iEMG^2 model performed the best on the EXO ON condition at 54.0 $\pm$ 46.9% error. The Exo Power model exhibited much lower duration errors with optimal durations within 11.7 $\pm$ 5.7% of the true durations. The models exhibited lesser error in optimal effort, with the four EMG models ranging from 15.1-21.8% or EXO OFF and 10.3-15.7% across models for EXO ON. Exo Power model optimal powers were within 8.0 $\pm$ 9.2 % of the true powers.

Discussion: This study did not identify a relationship between duration of exosuit-assisted reaching movements and muscle activity-related effort metrics. However, movement duration was captured by optimal exosuit power. Increased assistive power could allow individuals to perform tasks more quickly with less effort, and so individuals may be sensitive to the benefit of increased power. As a post-hoc analysis, this study was not designed to probe how exosuit power or muscle activity varied with duration, and so subjects explored a relatively narrow range of durations. Future work could expand on this study by testing a wider range of movement durations to better characterize how muscle activity and power relate to duration. Furthermore, a better effort metric could be used by recording muscle activity from more muscles or by estimating energy expenditure or fatigue with a musculoskeletal model. Likewise, exosuit power could be predicted by modelling the dynamics and control of the exosuit.

Significance: Individuals might be sensitive to the power delivered by an exosuit as a means to reduce effort, and they might adapt movement duration to obtain increased exosuit power.

Acknowledgments: UNIDEL Foundation, Inc.

References: [1] Moeller et al. (2022), *Front. Rob. AI*; [2] Huang et al. (2012), *J Neuro* 32(6); [3] Sánchez et al. (2019), *J Physiol* 597(15):4053-4068; [4] Selinger et al. (2015), *Curr Biol* 2:2452-2456;

THE INFLUENCE OF GOLF SHOE DESIGN ON SWING PERFORMANCE AND JOINT LOADING

Colin R. Smith[1]*, Austin Carcia[1], Kristen Seballos[1],
Thos A. Evans[1,2], Marc J. Philippon[1,2], Sonny S. Gill[1,2], Scott Tashman[1], Steve Atherton[1]
[1]Steadman Philippon Research Institute, [2]Steadman Clinic, Vail, CO, USA
*Corresponding author's email: csmith@sprivail.org

Introduction: There are over 55 million people who play golf worldwide, and thus experience the associated benefits and detriments to their physical and mental health. In competitive golfers, the explosive rotational motion and high axial loads lead to a high prevalence of hip labral tears and femoral acetabulum impingement [1]. Elderly golfers commonly suffer from low back pain, which reduces their overall rates of physical activity [2]. Thus, understanding how the joints are loaded throughout the golf swing, and how interventions alter swing biomechanics and joint function is important to reduce injuries and maximize performance.
Over time, golf shoe designs have evolved from hard metal spikes, to soft plastic spikes, to spikeless soles, each providing differing amounts of traction between the foot and the ground. This study aimed to investigate how golfers altered their golf swing performance and joint biomechanics when wearing golf shoes compared to athletic shoes.

Methods: We recruited 10 healthy male golfers (mean age: 36.5 years, mean handicap 8.5, mean driver carry distance 270 yards) to hit golf shots wearing soft spike golf shoes (Callaway Coronado V2) and athletic shoes (Nike Air Monarch 4). Each participant performed three swings with a 7 iron and driver in each shoe. Ground reaction forces (Bertec) and fullbody kinematics (55 markers, 18 Camera Qualisys Oqus 7) were measured. A launch monitor (Foresight GCQUAD) was used to measure club speed, ball speed, and carry distance for each shot. Artificial turf was adhered to force plates to replicate real-world traction. We developed a custom musculoskeletal model that can realistically capture the high rotations of the golf swing by modifying the joint kinematic constraints of a full body musculoskeletal model [3]. Inverse kinematics and dynamics was performed in OpenSim and the resulting joint angles and torques were analysed at 10 swing positions (P1-P10) as well as at their peak values. All statistics are reported as mean ± standard deviation.

Results & Discussion: Golfers achieved longer shot distances, but also experienced higher joint loads when wearing golf shoes compared to athletic shoes. Ground reaction forces, joint kinematics, and joint torque patterns demonstrated substantial variability between golfers, demonstrating the uniqueness of each participants swing biomechanics. Generally, the driver swings showed the same trends as the iron swings, with larger differences. Driver carry distance was on average 7.8 yards longer in golf shoes. The improved traction of the golf shoes enabled participants to coil/uncoil into their trail leg during the backswing resulting in a more explosive weight shift into the lead leg prior to impact. The peak vertical ground reaction torque on the trail foot, which occurred at the top of the backswing, increased by 11.5±19 %. The vertical ground reaction force on the lead foot, which peaked nearly at impact, increased by 5±17%. The pushoff torque generated by the trail ankle peaked during the downswing, and increased by 8±12% in golf shoes. Just prior to impact, the golf shoes lead to increases in the peak subtalar (7 ±11 %), knee adduction (7 ±10 %), knee rotation (11±21%), hip adduction (12.6 ± 22%) and hip rotation (8±18.5%) torques in the lead leg.

Significance: Wearing golf shoes compared to athletic shoes increased shot distance, but also increased joint loading and thus potential injury risk. Accordingly, golfers who experience joint pain may benefit from wearing spikeless or athletic shoes. Our findings of distinct loading patterns in the lead and trail legs suggests that an asymmetric golf shoe design that provides traction on the backswing to increase shot distance and cushion at impact to reduce joint loading could optimize the benefits of both shoe designs that we studied.

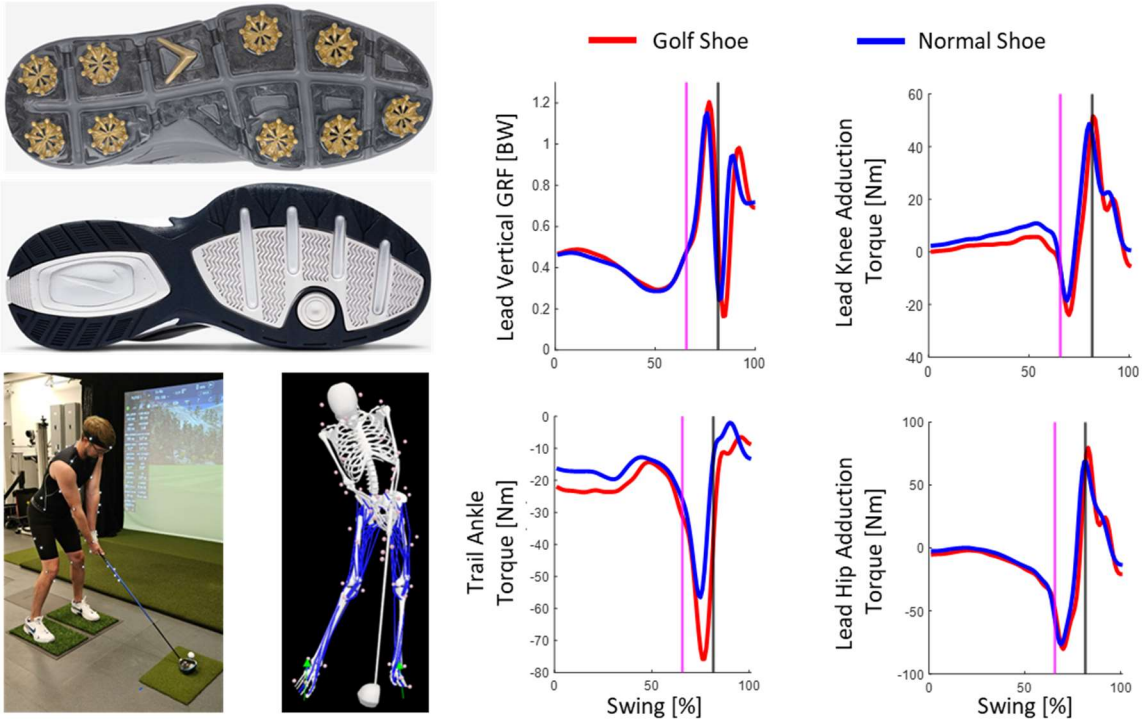

Figure 1- Inverse dynamics analysis revealed that golf shoes increased loading in the trail leg prior to impact and the lead leg after impact. The average of three driver swings with golf and normal shoes are plotted for a representative subject. Vertical lines represent the top of the back swing (P4) and impact (P7) positions.

References: [1] Philippon. (2005), *Oper Tech Orthop 15(261)*; [2] Edwards. (2020), *Sports Med Health Sci* 2(1). [3] Rajagopal. (2016), *IEEE Trans Biomed Eng* 63(10).

COMPARISON OF SEX-BASED BIOMECHANICAL MODELS TO A DEFAULT MODEL

Abigail R. Brittain[1] and Tyler N. Brown[2]
[1]Biomedical Engineering PhD Program, [2]Boise State University, Boise, Idaho
email: abbybrittain@boisestate.edu

Introduction: Joint kinetic analysis is dependent on the accuracy of link-segment models, which, rely upon segment anthropometric parameters, including segment center of mass, moments of inertia, and geometry. Visual 3D is a biomechanics software commonly used for kinetic analysis that uses segment anthropometric parameters that do not account for sex variation in their link-segment model, potentially producing inaccurate kinetic analyses. It is unknown if using models that include sex-specific segment properties alters joint kinetic output. We hypothesized that a sex-based biomechanical model would produce significant alterations in knee joint kinetics compared to a default Visual 3D model for both male and females, but larger alterations would be observed for females.

Methods: 14 female and 17 male had 3D lower-limb biomechanics quantified while running (4 m/s ± 5%) with 4 body borne loads (20, 25, 30, and 35 kg).

Three (default, male, and female) lower limb link-segment models consisting of 7 segments and 24 DOFs were created in Visual 3D. The default model was built as described in [1]. Each sex-specific model had segment mass, mass moment of inertia, center of mass, and geometry modified using male and female anthropometrics published in [2]. Kinematic and GRF data recorded during each run trial were filtered (fourth-order, low-pass Butterworth filter at 12 Hz), and processed in Visual 3D using standard inverse dynamics analysis to obtain dominant limb stance phase (heel strike to toe off) knee joint kinetics with each model. Knee joint kinetics were normalized to participant mass.

Peak knee flexion, abduction, and internal rotation joint moments, and anterior knee joint reaction force were submitted to a two-way (load*model) repeated measures ANOVA, and the corresponding waveforms were submitted to a statistical parametric mapping (SPM) two-way repeated measures ANOVA. Males and females were analysed separately, and alpha was $p < 0.05$.

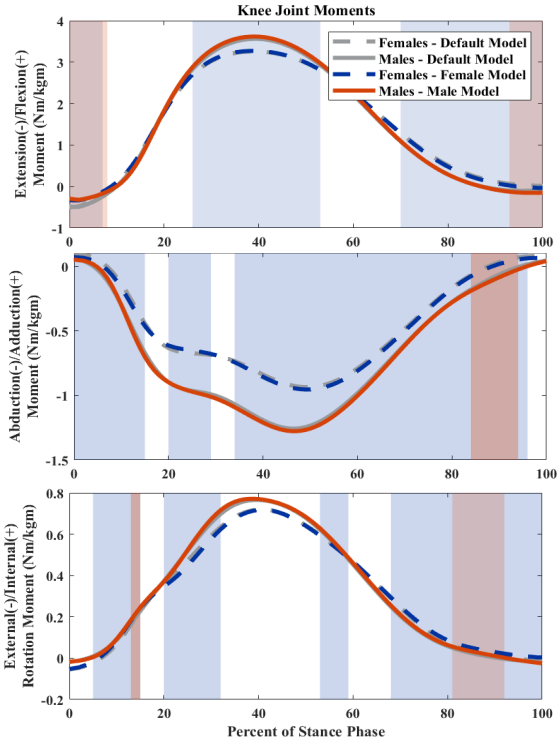

Figure 1: Knee Joint Moments Compared Between Model Significant differences identified by SPM analysis are shaded in blue (females) and orange (males).

Results & Discussion: In agreement with our hypothesis, both male and female sex-based models produced significant alterations in peak and waveform knee joint kinetics compared to the default Visual 3D model.

For females, there were significant load by model interaction for peak anterior (p=0.038) knee joint reaction force. Significant main effects of model were only seen for females. The current default model may underestimate female knee joint kinetics, as both peak knee flexion (p<0.001) and abduction (p<0.001) moments were greater for the female-based model than the default model.

Unexpectedly, adding body borne load only increased peak knee abduction moment (males: p=0.016, females: p=0.01) and anterior knee joint reaction force (both: p=0.003). Females exhibited greater peak knee abduction moment with 25kg and 30kg than 20kg load (p=0.002; p=0.011), while males exhibited greater knee abduction moment with the 35kg compared to 30kg (p=0.009) and 20kg (p=0.006) loads. Both sexes exhibited greater anterior knee joint reaction force with the 35kg than the 20kg (p=0.015; p=0.003) and 25kg (p=0.007; p=0.002) loads, but the males also exhibited greater reaction force with the 30kg than the 20kg (p=0.003) load.

Both the male and female-based model impacted each knee joint kinetic waveform (Fig. 1). For knee flexion moment, the female-based model significantly differed from default between 0-7%, 26-53%, and 70-100% of stance (p<0.033), and the male-based model differed between 0-8% and 93-100% of stance (p<0.029). For knee abduction moment, the female-based model significantly differed from default between 0-15%, 20-29%, and 34-96% of stance (p<0.024), while the male-based model differed between 84-94% (p=0.015) of stance. For knee internal rotation moments, the female-based model significantly differed from default between 5-15%, 20-32%. 53-59%, and 68-100% (p<0.034), of stance, and the male-based model differed between 13-15% and 81-92% (p<0.048) of stance.

Significance: The current findings support the need for sex-based biomechanical models in research. Updating the link-segment model with sex-specific anthropometric measures lead to significant alterations in knee joint kinetics for both male and female participants. Surprisingly, more model effects were found significant than load effects.

Acknowledgments: Battelle Energy Alliance/Idaho National Laboratory, Natick Soldier Systems Center and NIH NIGMS (#P20GM148321) supported this work.

References: [1] Brown et al. (2018), *J Biomech* 69; [2] Dumas et al., (2007), *J Biomech* 40; [3] https://spm1d.org/

JOINT LOADS DURING GAIT WITH A UNILATERAL TRANSTIBIAL PROSTHESIS: OPENSIM SIMULATIONS OF LEVEL AND DOWNSLOPE WALKING

Yuzhen Yan[1*], Edward D. Lemaire[2,3], Thomas K. Uchida[1]
[1]Department of Mechanical Engineering, University of Ottawa, Ottawa, Canada
[2]The Ottawa Hospital Rehabilitation Centre, Ottawa Hospital Research Institute, Ottawa, Canada
[3]Faculty of Medicine, University of Ottawa, Ottawa, Canada
*Corresponding author's email: yyan103@uottawa.ca

Introduction: Individuals with unilateral transtibial amputation are at greater risk of developing osteoarthritis in the knee and hip of the intact limb compared to the general population [1]. Gait kinetics change when walking on different surfaces. For example, the first peak knee adduction moment in the intact limb is greater during downslope walking than during level walking [2]. Considering the first peak contact force in the hip and knee for able-bodied individuals, Giarmatzis et al. [3] reported 4.2 ± 0.7 bodyweights (BW; mean ± standard deviation) for the hip during level walking at 3 km/h. During downslope walking, Yamin et al. [4] reported a first peak force of 7.5 ± 1.7 BW at the hip and 8.5 ± 1.8 BW at the knee for a 7.5° slope. Alexander and Schwameder [5] found that downslope walking increased hip joint compression forces significantly compared to level walking. These forces have not been extensively studied in individuals with unilateral transtibial amputation. Estimation of joint reaction forces during level and downslope walking will provide deeper understanding of joint loads in individuals with transtibial amputation.

Methods: Kinematics and ground reaction forces were collected in a previous study from seven participants who used a unilateral transtibial prosthesis during level and downslope (7° decline) treadmill walking [2]. The musculoskeletal model of Willson et al. [6] was calibrated to match each participant's anthropometry in OpenSim [7, 8] using the Scale Tool. This model was based on the model of Rajagopal et al. [9] where the left limb was modified to include a transtibial prosthesis. Inverse Kinematics, Residual Reduction Analysis, and Computed Muscle Control were then used to estimate skeletal kinematics and muscle forces during three gait cycles for each participant during both level and downslope walking. Finally, Joint Reaction Analysis was used to estimate contact force magnitudes in the hip and knee of the intact limb. For comparison to able-bodied individuals, the Joint Reaction Analysis was used to estimate contact force magnitudes during level walking in seven individuals, three gait cycles each, using data from Dembia et al. [10]. These data had been generated using the original model from Rajagopal et al. [9]. For each contact force curve, the first peak was identified and the mean of the first peak was computed over three gait cycles for each individual and condition.

Results & Discussion: For able-bodied individuals, the first peak contact force was 4.30 ± 0.39 BW in the hip (mean ± standard deviation) and 3.76 ± 0.43 BW in the knee during level walking. During level walking with a unilateral transtibial prosthesis, the first peak contact force in the intact limb was 5.22 ± 1.76 BW in the hip and 5.37 ± 1.17 BW in the knee. During downslope walking with a unilateral transtibial prosthesis, the first peak contact force in the intact limb was 6.84 ± 1.95 BW in the hip and 9.11 ± 0.76 BW in the knee. The hip and knee contact forces for a representative participant walking with a unilateral prosthesis are shown in Fig. 1. During level walking, the first peak knee contact force for prosthesis users was greater than that for able-bodied individuals ($p < 0.01$, t-test). For prosthesis users, the first peak in intact-limb knee contact force was greater during downslope walking than during level walking ($p < 0.01$, t-test), with an average difference of 74% and a range of 31% to 100%.

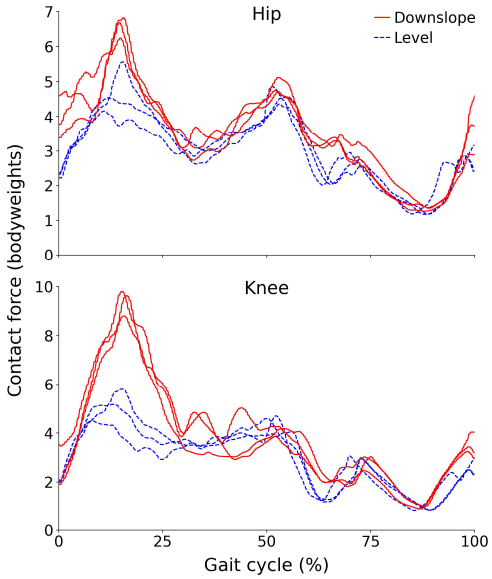

Figure 1: Contact force in the hip (top) and knee (bottom) of the intact limb for one representative participant while walking with a unilateral transtibial prosthesis. Three gait cycles are shown during downslope (red solid lines) and level walking (blue dashed lines). The first peak of the contact force was greater during downslope walking than during level walking.

Significance: For unilateral transtibial prosthesis users, the first peak in intact-limb knee contact force was 74% greater, on average, during downslope walking than during level walking. This result highlights the importance of studying gait on surfaces that are encountered in daily life when evaluating prosthesis designs and when studying joint health in unilateral transtibial prosthesis users. This study motivates research on prostheses that can adapt to different walking surfaces, thereby potentially reducing these limb loading differences.

Acknowledgments: The authors thank Emily Sinitski for helping to process the experimental data. The authors also acknowledge the support of the Natural Sciences and Engineering Research Council of Canada (NSERC).

References: [1] Struyf et al. (2009), *Arch Phys Med Rehabil* 90:440; [2] Doyle et al. (2019), *J Neuroeng Rehabil* 16:37; [3] Giarmatzis et al. (2015), *J Bone Miner Res* 30:1431; [4] Yamin et al. (2022), *Acta Bioeng Biomech* 24:67; [5] Alexander & Schwameder (2016), *Gait Posture* 45:137; [6] Willson et al. (2023), *Comput Methods Biomech Biomed Eng* 26:412; [7] Delp et al. (2007), *IEEE Trans Biomed Eng* 54:1940; [8] Seth et al. (2018), *PLoS Comput Biol* 14:e1006223; [9] Rajagopal et al. (2016), *IEEE Trans Biomed Eng* 63:2068; [10] Dembia et al. (2017), *PLoS One* 12:e0180320.

HEAD SUPPORTED MASS LOAD CONFIGURATION MODERATES NECK MUSCLE COORDINATION

Seung Kyeom Kim[1*], Kolby J. Brink[1], Marina G. Carboni[2], Theresa D. Hardin[2] & Aaron D. Likens[1]
[1]Division of Biomechanics and Research Development, Department of Biomechanics, and Center of Research in Human Movement Variability, University of Nebraska at Omaha, Omaha, Nebraska, USA
[2]DEVCOM Soldier Center, Natick, Massachusetts
*Corresponding author's email: seungkyeomkim@unomaha.edu

Introduction: The number of equipment items attached to Soldier's helmets has increased with technological advancements. The side effect of wearing weighted helmets for a prolonged period of time is that it can cause fatigue on the neck musculature [1]. Neck muscle fatigue may result in the loss of neck muscle coordination, which can negatively affect static and dynamic balance. Eventually, the effect of neck muscle fatigue can cascade down around the whole body, impairing Soldiers' gait dynamics and task performance [2]. Therefore, understanding how head supported mass (HSM) loads and configurations influence neck muscle coordination is important for injury prevention and preserving task performance. The study aim was to examine how the impact of neck muscle fatigue on neck muscle coordination would be influenced by HSM load configuration. We hypothesized that the HSM load configuration that exerts greater inertial force will lead to greater change in neck muscle coordination due to fatigue.

Methods: To investigate how HSM load and configuration impacts the alteration of neck muscle coordination due to fatigue, 14 male Soldiers, walked on a treadmill for 60 min at 60% of Froude speed while equipped with five different HSM conditions. The 5 different load configurations were: 1) LMRO, low-mass (1.5kg) rear-offset (-2cm), 2) MMFO, mid-mass (2.5kg) forward-offset (3.5cm), 3) MMM, mid-mass (2.5kg) midline (0cm), 4) HMM, high-mass (3kg) midline (0cm), and 5) HMFO, high-mass (3kg) forward-offset (3cm). Offsets were relative to the subject's tragion notch. Surface electromyography (EMG) data were collected from the sternocleidomastoid (SCM) and trapezius (TRAP) muscles at 5, 18, 25, 35, 45, and 57 min. Intensity analyses were performed on EMGs to obtain the power of each signal in time resolved across frequencies (6.90, 19.29, 37.71, 62.09, 92.36, 128.48, 170.39, 218.08, 271.50, 330.63, 395.46Hz) [3]. To quantify neck muscle coordination, correlations among signal power time series were computed within each frequency. Multilevel models were used to evaluate the joint effects of time, frequency, and HSM configuration.

Results & Discussion: Compared to LMRO, all other conditions produced greater neck muscle coordination, with HMFO producing the highest correlation (LMRO: 0.0448 [0.0018 0.0877]; MMFO: 0.0615 [0.01851 0.1045]; MMM: 0.0753 [0.0324 0.1182]; MHH: 0.0586 [0.0157 0.1016]; HMFO: 0.0867 [0.0437 0.12297]); however, those differences seem to depend on time. That is, all conditions other than HMFO, showed a statistically significant interaction between time and condition (MMFO: 0.0371±0.0151, p = .0141; MMM: 0.0440±0.0148, p = .0029; HMM: 0.0575±0.0150, p =. 0001). While the interaction involving HMFO did not reach statistical significance despite producing a similar trend, this may be a limitation of sample size. For all conditions except LMRO, muscle coordination tended to increase over time. The key take-away from these results is that increasing mass, regardless of position, tends to increase SCM and TRAP neck muscle coordination. The change in correlation over time implies that Soldiers may be adopting compensatory strategies to accommodate mass-based fatigue.

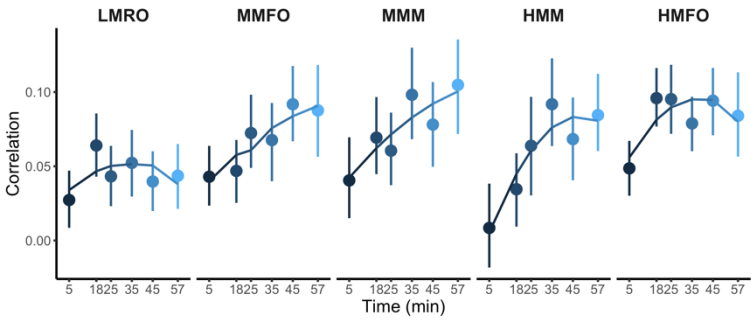

Figure 1. Correlation between SCM and TRAP signal power time series. Dots indicate the correlation averaged across frequencies at each time. Vertical lines indicate the 95% confidence limit. Curved lines represent the multilevel model for each HSM load configuration. Color change reflects time change.

Significance: To determine the impact of extended HSM wear during a walking task, neck muscle coordination of the SCM and TRAP was assessed with 5 different HSM load configurations The results revealed that the effect of HSM and wear time depended on the inertial properties of each HSM load configuration. This can provide insights when establishing guidelines of Soldier head-borne equipment (e.g. helmets, night vision devices) for total mass and distribution of that mass. Such insight can be crucial in minimizing muscle fatigue and potentially in preventing alteration of static and dynamic balance.

Acknowledgments: US Army DEVCOM Soldier Center under the Measuring and Advancing Soldier Tactical Readiness and Effectiveness (MASTR-E) Program, National Strategic Research Institute and the Department of Defense (U2-20-F0101)

References:

[1] Branch, B. (2008).
[2] Manoogian, S. J., et al. (2006), *Aviation, space, and environmental medicine*, 77(5).
[3] Von Tscharner, V. (2000). *Journal of Electromyography and Kinesiology*, 10(6).

TRAUMATIC TRANSTIBIAL PROSTHESIS USERS EXPERIENCE MEDIAL-LATERAL, NOT ANTERIOR-POSTERIOR, POSTURAL INSTABILITY COMPARED TO UNIMPAIRED AGE- AND SEX-MATCHED ADULTS

Moaz Tobaigy[1,2], Julie Ferrell-Olson[1], Andrew Sawers[1]
[1] Department of Kinesiology, University of Illinois Chicago, [2]Faculty of Medical Rehabilitation Science, King Abdulaziz University
*Corresponding author's email: asawers@uic.edu

Introduction: Upright balance during quiet standing represents the basic unit of postural control. The ability to maintain stability while standing is a necessary prerequisite to perform many activities of daily living, including locomotion, without falling [1]. As such, studying postural stability in quiet stance can provide important insight into functional impairments [2]. Deficits in postural stability among transtibial prosthesis users, however, remain poorly characterized relative to unimpaired adults. This gap can largely be attributed to the lack of systematic control for age and gender, as well as level and cause of amputation in prior studies [2]. In the absence of understanding how transtibial amputation effects postural stability during quiet stance, designing or prescribing prosthetic technologies and rehabilitation strategies to mediate balance impairments remains challenging. Therefore, the objective of this study was to identify the direction and magnitude of transtibial prosthesis users' postural stability deficits relative to unimpaired age- and sex-matched adults. Due to the reduction in prosthetic ankle motion [3, 4] we hypothesized that traumatic unilateral transtibial prosthesis users would exhibit greater postural instability in the anterior-posterior and medial-lateral directions compared to unimpaired age- and sex-matched adults [4, 5, 6].

Methods: Twelve unilateral traumatic transtibial prosthesis users and 12 unimpaired age- and sex-matched adults (i.e., matched controls) participated in the study. Each group consisted of 9 men and 3 women, mean age was 52 and 53 years, and time since amputation for the transtibial prosthesis users ranged from 4 to 57 years. Participants performed three 70 second trials of a quiet stance task with their eyes open. Stance width was standardized to pelvic width, and arms were crossed over their chest. Ground reaction forces were collected at 1200Hz from AMTI force platforms, and low-pass filtered at 10Hz (Butterworth filter 4th order). Processed ground reaction force data from the middle 60 seconds of each trial was used to calculate the net anterior-posterior (AP) and medial-lateral (ML) center-of-pressure (COP) trajectories. Postural stability was quantified by calculating the mean velocity of the net AP and ML COP trajectories. A Hotelling's multivariate T^2 test was run to test for differences in net AP and net ML COP mean velocity between transtibial prosthesis users and matched controls.

Results & Discussion: Hotelling's T^2 test revealed a statistically significant difference in net COP mean velocity between the transtibial prosthesis users and matched controls during quite stance, $F\,(2, 21) = 5.78$, $p= 0.01$. In partial support of our hypothesis, post hoc tests with a Bonferroni correction ($\alpha=0.025$) revealed that net ML but not net AP COP mean velocity was significantly greater in the transtibial prosthesis users than matched controls (ML: $F\,(1, 22) = 10.85$, $p= 0.003$; AP: $F\,(1, 22) = 3.42$, $p= 0.078$) (Table 1). Evidence suggests traumatic transtibial amputation induces postural instability predominantly in the frontal rather than sagittal plane. Increased ML postural instability may be due in part to the design of prosthetic feet which lack ML ankle motion essential for the control of stability in the frontal plane [8]. Additionally, compensations for the loss of direct control over ML motion at the amputated ankle are limited to the ipsilateral hip, whereas AP compensations may occur at both the ipsilateral hip and knee.

Table 1. Net COP mean velocity for transtibial prosthesis users (n=12) and unimpaired age-and sex-matched adults (n=12) during quiet stance. Data are reported as mean (95% confidence interval lower limit, upper limit).

	Transtibial prosthesis users	Unimpaired adults
Anterior-posterior (mm/s)	7.48 (5.89, 9.07)	5.88 (4.99, 6.77)
Medial-lateral (mm/s)	1.72 (1.39, 2.04)	1.23 (1.01,1.44)

Significance: The findings from this study offer valuable insight into the directional specificity of traumatic unilateral transtibial prosthesis users' postural instability. The results of this study emphasize the need to develop and evaluate prosthetic technologies and rehabilitation strategies that focus on frontal plane balance for traumatic transtibial prosthesis users. Further research examining limb-specific contributions to ML deficits, and the impact of proximal levels and dysvascular causes of amputation is required.

References: [1] Horak, (2006), *Age and Ageing*, 35 (2); [2] Ku et al., (2014), *Gait & Posture 39*(2); [3] Vittas et al., (1986), *Prosthet Orthot Int (?);* [4] Hermodsson et al., (1994). *Prosthet Orthot Int*, *18*(3); [5] Toumi et al., (2021), *J Bodw Mov Ther (*27); [6] Buckley et al (2002). *Am J Phys Med Rehabil*, 81(1); [8] Allard et al., (1995*), Med Biol Eng Comput* 33.

EFFECTS OF EXOSKELETON BOOTS WITH NOVEL ANKLE BRACING ON STATIC POSTURAL CONTROL AND AGILITY

Corbin M. Rasmussen[1,3*], Joe Malloy[1], Yassine Mahamane Iro[1], Keith Eriks[2], Thomas Cotton[2], Mark C. Roser[1,2,3], Sara A. Myers[1,3]
[1]Department of Biomechanics, University of Nebraska at Omaha, Omaha, NE USA
[2]Results Group, LLC dba Motive Labs, Glastonbury, CT USA
[3]Omaha Veterans' Affairs Medical Center, Omaha, NE USA
*Corresponding author's email: cmrasmussen@unomaha.edu

Introduction: Lateral ankle sprains are a major source of restricted duty days and chronic musculoskeletal injury in the U.S. military, negatively impacting force readiness [1,2]. Ankle bracing is the standard-of-care for these injuries, however service member adherence to traditional braces is poor due to lack of comfort, restricted propulsion, and social factors [3]. To address these limitations, the FlyBand® ExoBoot™ was developed with an integrated exoskeleton and hidden, exchangeable cartridges in the boot upper to provide concurrent propulsion assistance and ankle stabilization. This project determined the effect of the FlyBand exoskeleton and lateral bracing system on wearers' static balance, assessed by a single-leg stance test, and their agility, assessed by a three-cone shuttle drill. Our hypotheses were that, compared to standard-issue boots (i.e., Conventional) with ankle braces, FlyBand ExoBoots and bracing cartridges would perform similarly in static balance in terms of center of pressure (CoP) areas, but provide improved agility as illustrated by faster shuttle drill times.

Methods: Five healthy adult males (mean±SD age: 25.80±2.59 years, height: 1.72±0.04 m, mass: 64.34±14.23 kg, all right dominant) were fitted with a compression singlet, lower-body marker set, and one of six possible combinations of two boot types (Conventional, FlyBand) and three lateral ankle bracing levels (Low, Mid, High). Bracing was provided by commercially available ankle braces when wearing the Conventional boots but by integrated bracing inserts when wearing the FlyBand exoskeleton boots. While wearing each boot/brace combination, participants were instructed to stand on a force platform (AMTI; Watertown, MA) on their right leg. Trials ended after 30 seconds or if participants stepped or contacted their stance leg with their offloaded leg to regain balance. This test was repeated twice per condition. Ground reaction force data were collected throughout all trials at 1000 Hz, from which areas of 95% confidence ellipses encompassing CoP locations were derived. Ellipse areas were normalized by foot area, which was estimated as a rectangle fit to the first metatarsal head, second toe, fifth metatarsal head, and heel markers [4]. Participants also ran through a modified three-cone shuttle drill twice while wearing each boot/brace condition as completion time was recorded. All outcome measures were compared between boots and bracing levels using linear mixed effects models.

Results & Discussion: All participants were able to remain in single-leg stance for 30 seconds without losing their balance in all trials. Neither boot type ($t(52)=-1.297$, $p=0.201$; Fig. 1) nor bracing level (Mid: $t(52)=1.847$, $p=0.070$; High: $t(52)=1.339$, $p=0.186$; Fig. 1) had significant effects on CoP areas. On the shuttle drill, increased ankle bracing caused significantly longer course completion times in general (High: $t(52)=2.098$, $p=0.041$; Fig. 1), but the FlyBand bracing system had significantly less impact on agility illustrated by faster times ($t(52)=-4.390$, $p<0.001$; Fig. 1). Our hypothesis of no boot- or brace-related differences in static balance was supported. All study participants here were healthy and without history of ankle sprain, therefore it is possible that their CoP excursions in any direction rarely reached positions able to be aided by bracing, particularly during the task of one-leg stance. Our results may differ in individuals with acute or chronic ankle instability who are known to exhibit static balance deficits that benefit from ankle bracing [5,6]. While concurrently providing equivalent levels of support illustrated by consistent CoP areas, FlyBand ExoBoots posed less resistance to wearer agility, which is essential in combat scenarios.

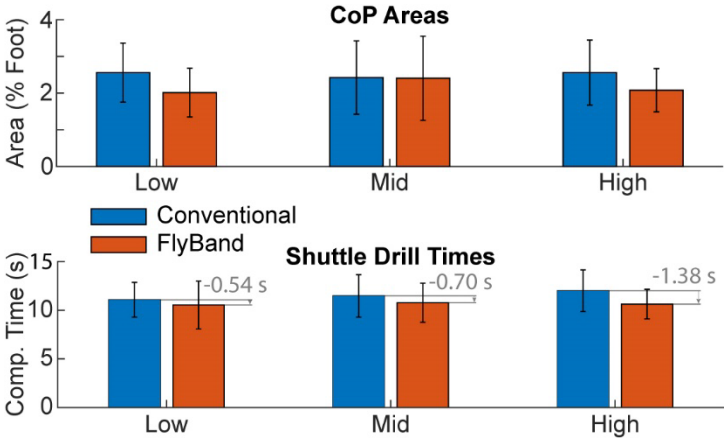

Figure 1: Means and standard deviations of CoP areas and shuttle drill times for each boot (Conventional, FlyBand) and brace (Low, Mid, High). Mean differences between boots at each bracing level are in gray.

Significance: Integrated boot exoskeletons and exchangeable bracing cartridges have the potential to optimize service member capabilities and provide customizable ankle stability for preventative or rehabilitative use. Additional comparisons between Conventional and FlyBand boots during more dynamic activities that stress lateral ankle stability are ongoing to fully characterize their function. Future work will also evaluate FlyBand exoskeleton boots in women with female-specific boot shapes and sizing, which are not currently available in Conventional military boots.

Acknowledgments: This research was supported by an SBIR Phase II award from the Defense Health Agency (DHA224D003).

References: [1] Teyhen et al. (2018), *J Orthop Sports Phys Ther* 48; [2] Molloy et al. (2020), *Mil Med* 185; [3] Dubuc et al. (2022), *Expert Rev Med Devices* 19; [4] van Wegen et al. (2001), *Mot Control* 3; [5] Hertel et al. (2007), *Gait Posture* 25; [6] Reyburn et al. (2021), *J Sport Rehabil* 30.

CLUSTERING OF CLINCAL AND PATIENT REPORTED VARIABLES FOR SECOND ACL INJURY PREDICTION

Nathaniel A. Bates,[1] Nathan D. Schilaty,[3] Gregory D. Myer,[2] Kim Barber Foss,[2] April McPherson,[1,2] Aaron J. Krych[4]
[1]The Ohio State University Wexner Medical Center, Columbus, OH, USA; [2]Emory University, Flowery Brach, GA, USA; [3]University of South Florida, Tampa, FL, USA; [4]Mayo Clinic, Rochester, MN, USA
*Corresponding author's email: Nathaniel.Bates@osumc.edu

Introduction: 15-30% of ACL reconstruction (ACLR) patients who return to sport suffer second ACL injury within 2 years.[1,2] This is a devastating problem that can lead to loss of scholarship, functional disability, and expedite osteoarthritis onset. Accordingly, research investments have been targeted to enhance rehabilitation and identify risk factors for second injury. This study utilized clinical evaluation metrics and patient reported outcomes (PROs) in a primary ACL injury population to determine whether statistical clustering of these pertinent variables can predict relative risk of second ACL injuries.

Methods: 144 subjects who suffered primary ACL injury and underwent ACLR were recruited across four academic medical centers. Surgical selection and clinical rehabilitation were left to discretion of each patient and their medical team. Following clinical clearance for return to sport, subjects were recruited into the study. Clinical metrics were collected in a biomechanics laboratory setting where subjects performed single, triple, and triple crossover hopping for distance, 6-meter hopping for time, isokinetic knee flexion/extension strength at 180° and 300° per second, isometric hip strength at 20° hip flexion, and limb symmetry index for each. PROs included Marx, Tegner, IKDC, KOOS, SKE, and KOS questionnaires. After data collection, subjects were longitudinally tracked for additional ACL injuries once a month for 6 months, then once a year for up to 4 years. All subjects had reached at least one year of follow-up at time of analysis. Follow-up identified 17 unique secondary ACL ruptures across 15 unique subjects. K-means clustering was used to separate the dataset into three distinctive clusters. Clustering was completed independently based on (1) clinical metrics, (2) PROs, and (3) clinical metrics + PROs. Fisher's exact test was used to assess distribution of secondary ACL injuries across clusters. ROC analysis was used to assess sensitivity and specificity of cluster classification to predict secondary injury outcomes.

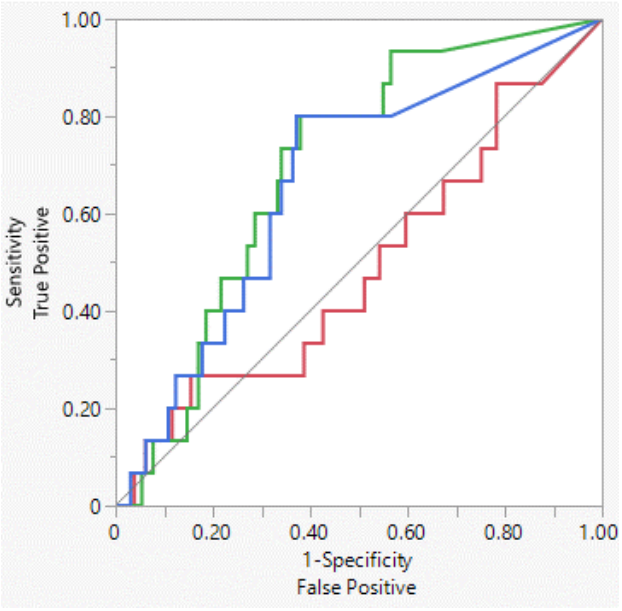

Figure 1: ROC analysis for each of the three clustering models (clinical measures = RED; PROs = GREEN; clinical measures + PROs = BLUE). PROs offered the best predictive clustering of the three models evaluated, while clinical metrics clustering did not

Results & Discussion: Clinical measures clustering organized 128 subjects into three distinct clusters that were not well-parsed (n = 19, 105, 2). Clinical measures clusters did not predict secondary ACL injury well as Fisher's exact showed proportionally even distribution of secondary injures across clusters (P=1.00) with ROC sens = 27%, spec = 84%, and area under the curve (AOC) = 0.486. PRO clustering organized 100 subjects into three distinct clusters (n = 4, 71, 25). PRO clusters offered moderate predictive value of secondary ACL as Fisher's did not show proportionally different distribution of secondary injury across clusters (P=0.31) with ROC sens = 80%, spec = 62%, and AUC = 0.694. Combining clinical measures with PROs did not improve the predictive model as 86 subjects were clustered into three distinct clusters (n = 1, 79, 6). Clinical measures + PROs also offered moderate predictive value of secondary ACL as Fisher's did not show proportionally different distribution of secondary injury across clusters (P=1.00) with ROC sens = 63%, spec = 80%, and AUC = 0.663. It should be noted that combining clinical measures with PROs failed to influence the predictive potential of the PRO model. Thus, not only did clinical performance metrics fail to predict secondary injury better than chance, but they added no value to the PRO model. Debate continues over which clinical metrics are most relevant to return to sport clearance as only ~34% of patients actually achieve metric standards at time of return to sport.[3] Per the current dataset, measures of strength and hopping performance do not contribute to identification of secondary injury risk, whereas PROs may offer utility. Further work should be done to parse out individual PRO contributions to the overall predictive model; analysis of this dataset is ongoing. K-means clustering is disrupted by missing data points due to subjects declining participation in selective activities. In addition, analysis should consider the implications of imputing the dataset on cluster analysis.

Significance: Among commonly assessed clinical metrics and PROs at time of return to sport clearance, PROs offer superior predictive potential for identifying relative risk for secondary ACL injuries. Thus, clinical metrics of strength and hopping ability may offer clinical utility for functional performance and return to sport readiness assessments, but should not be considered contributors to parsing out relative risk for secondary ACL injury in ACLR patient populations.

Acknowledgments: NIH R01-AR055563; Florida Department of State Center for Neuromusculoskeletal Research

References: [1] Paterno et al. (2014), *Am J Sports Med* 42(7):1567-73; [2] Webster et al. (2016) *Am J Sports Med* 44(11):2827-32; [3] Hurley et al. (2022) *Knee* 34:134-40.

2D UNCALIBRATED VIDEO TRACKING OF HEAD IMPACT SPEEDS USING MODEL-BASED IMAGE MAPPING

Nicole E.-P. Stark[1*], Ethan S. Henley, Brianna A[1]. Reilly, Gabrielle M. Ferro[1], Michael L. Madigan[1], Damon Kuehl[1,2], Steve Rowson[1]
[1]Virginia Tech Blacksburg, VA [2]Carilion Clinic Roanoke, VA
*Corresponding author's email: nestark@vt.edu

Introduction: Studying concussive and non-concussive head impacts is crucial for comprehending injury mechanisms and devising effective prevention strategies. A current challenge is that most recordings of non-helmeted head impacts are in 2D. Although extracting head impact speeds from 2D footage is feasible, it typically requires a calibrated environment and multiple camera views [1-7], limiting the analysis of many real-world incidents captured by single-view cameras in uncalibrated spaces. Model-based image mapping (MBIM) could allow for tracking head impacts from single-view camera footage without environmental calibration by projecting a scaled 3D model onto a 2D video frame. This study aims to assess the accuracy of a novel MBIM program in tracking head impact velocities using a single-camera view. We are testing this program to determine whether it can accurately track head impact speeds in controlled drop tests and participant fall simulations. In addition, we are evaluating the effectiveness of capturing vertical impact speed based on changes in camera angle and distance. The successful implementation of MBIM could significantly improve our understanding of head impact kinematics, which could help develop more effective prevention strategies.

Methods: We used two validation data sets to evaluate the MBIM software's accuracy. The first comprised 36 video-recordings (30 fps) of twin-guided drop tests using a NOCSAE headform, conducted at three heights (1, 1.4, 2.8 m), three distances (3, 6.1, 9.1 m), from different camera angles (90, 75, 65, 55 degrees), and two impact speed (2, 4.0 m/s) where vertical impacts speed measured with a speed gate. The second set consisted of nine video-recordings of ladder falls in which participants, equipped with helmets marked with four retroreflective markers, performed backward and side falls. These falls were captured with a 12-camera motion capture system (Qualisys North America, Inc.) at 128 Hz and a GoPro at 30 fps. Marker data was filtered at 14 Hz (fourth-order zero-phase-lag Butterworth), and we calculated vertical and horizontal impact speeds based on the center of mass determined from the four markers, taken 7 ms before impact.

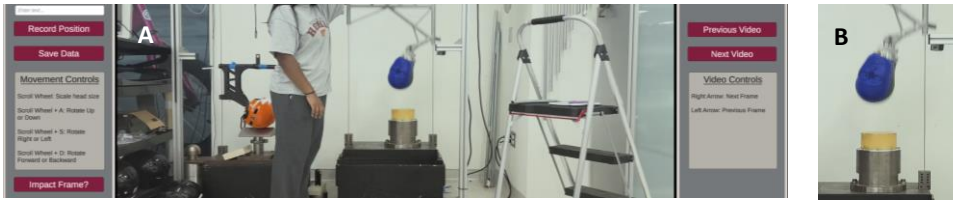

Figure 1: (A) MBIM tracking software interface where the imported 3D NOCSAE headform was matched to the video frame-by-frame to track the vertical and horizontal head impact speeds. (B) The 3D NOCSAE headform matched to a frame in the NOCSAE drop video.

Each video was tracked frame-by-frame in a novel MBIM software developed in Unity (version 2022.3.8f1). This software virtually posed a to-scale 3D model of a NOCSAE headform onto the video frame (Figure 1). The headform was then manually matched to the 2D video fame, and the vertical and horizontal speed was calculated based on two frames and the frame before impact. Each video was tracked until the standard error of the tracked speed was under 0.25 m/s. We evaluated the accuracy of the MBIM system by comparing observed and the MBIM-tracked speeds by calculating the mean difference and standard deviation (SD), calculating Root Mean Square Error (RMSE), and performing a Bland-Altman analysis to determine the 95% limits of agreement [8]. We also used a linear model to evaluate the influence of camera placement on the accuracy of tracked vertical impact speed.

Results & Discussion: The average impact speed recorded for the NOCSAE headform drops using the twin-guided tower was 4.0 m/s and 1.95 m/s. Comparing ideal camera views at 90 degrees and a height of 1 or 1.4 m, the MBIM-tracked vertical speeds were 0.400.25 m/s slower (mean difference ± SD) than the true speed (95% limits of agreement [-0.88,0.09] m/s; RMSE 0.46 m/s). Across all 36 NOCSAE headform drop videos, MBIM vertical speeds were 0.51±0.33 m/s slower than the true speed ([-1.15,0.14] m/s; RMSE 0.60 m/s). The analysis revealed that accuracy in tracking vertical speed decreased as the height increased (p=.26), indicating less precision at 2.8 m compared to 1 m. The accuracy of tracking vertical speed also decreased as the camera angle decreased (p=.28), which is aligned with expectations. This is because as the camera angle decreases, there is more out-of-plane motion, which affects the accuracy of tracking vertical speed. Conversely, the distance of the video capture did not affect the accuracy of the tracked vertical speed (p=.91).

The MBIM software exhibited similar accuracy for both vertical and horizontal speed when tracking the participant ladder fall videos. MBIM tracked vertical speed was 0.39±0.36 m/s slower ([-1.11, 0.32] m/s, RMSE 0.52), and tangential speed was 0.38±0.44 m/s slower ([-1.25, 0.49] m/s, RMSE 0.56 m/s) compared to observed speeds. This novel MBIM software performed within the range accuracy of other options in the literature (RMSE 0.24-1.29 m/s) [1-7]. However, on average, this tracking system was slightly worse at tracking impact speed compared to other systems, but this only required a monocular view, and the only calibration was the model match.

Significance: The ability to track 2D monocular videos in an uncalibrated space with reasonable accuracy, compared to other methods that require calibration or multiple views, offers a vast opportunity to capture head impact kinematics. Tracking head impact kinematics captured on video will facilitate the development of effective prevention strategies.

References: [1] Hendrick (2012) *J Sports Sci.* 12(30); [2] Shishov (2021), *Plos One* 10(16); [3] Krosshaug and Bahr (2005), *J Biomech* 5(38); [4] Tierney (2018), *Sports BioMech.* 1(17); [5] Choi (2015), *J Biomech* 6(48); [6] Jadischke (2020), *Sports & Exc. Med.* (6); [7] Bailey (2020), *Sports BioMech* 5(19); [8] Giavarina (2015) *Biochem Med* 25(2)

CHANGES IN GAIT SIGNATURES WITH REVERSIBLE ELECTRICAL NERVE BLOCK: IMPLICATIONS FOR MOTOR LEARNING

Nathan J. Kirkpatrick[1,3*], Robert J. Butera[1,2], Young-Hui Chang[1,3]
[1]Coulter Department of Biomedical Engineering, Georgia Institute of Technology & Emory University, Atlanta, GA, USA
[2]School of Electrical and Computer Engineering, Georgia Institute of Technology, Atlanta, GA, USA
[3]Comparative Neuromechanics Lab, School of Biological Sciences, Georgia Institute of Technology, Atlanta, GA, USA
*Corresponding author's email: nk@gatech.edu

Introduction: In response to nerve injury, redundant degrees of freedom are leveraged to continue moving. Traditionally, transection has been used to study this adaptation process. However, this technique is temporally imprecise. The animal begins acclimating to the impairment immediately upon recovery from anesthesia, preventing accurate kinematics observations of this early adaptation period. To overcome these obstacles, we applied Kilohertz Electrical Stimulation (KES) [1] to temporarily inhibit action potential transmission in the tibial nerve, which innervates several major ankle extensors muscles. Acute experiments have shown KES to be a repeatable and reversible technique, but the process of transitioning to studies with chronically implanted electrodes is poorly understood [2]. It has been shown that surgically nerve-transected animals eventually conserve whole-limb parameters such as limb length rather than individual joint angles [3], but it is not known if other distinct performance targets are attempted and discarded beforehand. Here, we applied a gait signatures framework [4] to reveal and distinguish joint coordination patterns in use throughout the adaptation process.

Methods: 1 male Lewis rat was implanted with a tri-polar Pt-Ir block cuff electrode around the right tibial nerve in accordance with a protocol approved by Georgia Tech's IACUC. Block thresholds, the minimum amplitude for a 20kHz sine wave to inhibit conduction of e-stim pulses, were identified. High speed biplanar x-ray video of treadmill locomotion was acquired on days 11, 14, 17 & 21 post-implantation. Gait data were collected before, during and after KES was administered for four sessions of 10 minutes of continuous nerve block (S1, S2, S3, S4).

To identify distinct movement strategies during block, gait signatures were generated. A 512-node recurrent neural network was trained on bilateral sagittal plane hindlimb joint angles and projected segment lengths. Principal components analysis was performed on the extracted internal states of the model. By feeding a subset of the resulting principal components (PCs) into the trained model, kinematic reconstructions were generated to reveal what each PC encodes. The root mean square error between reconstructions for a given session were computed to quantify how distinct a movement pattern is with and without block during a session.

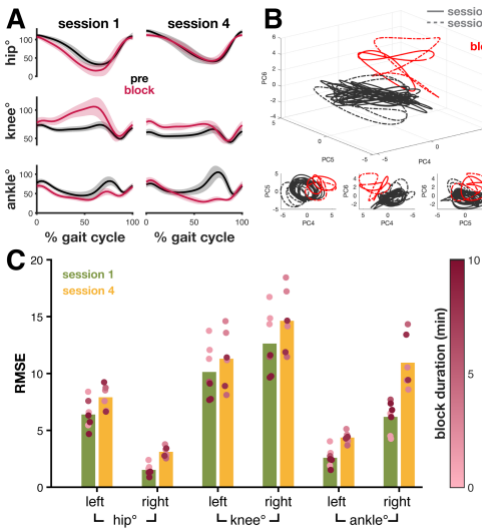

Figure 1: Movement patterns identified while adapting to temporary nerve block. **A:** raw sagittal plane joint angles of the right hindlimb. Shaded regions are mean ± S.D. **B:** 3D gait signatures of principal components 4, 5 and 6 distinguish blocked gait cycles (red). **C:** Error between blocked and unblocked gait cycles reconstructed using PCs 4, 5 and 6. Individual error values color-coded by elapsed time since block onset.

Results & Discussion: Different nerve block-induced movement changes were present on sessions S1 and S4 (Fig. 1A). The first session was marked by more knee extension relative to same session unblocked cycles. Blocked gait on S4 had smaller ankle angles. However, large differences between unblocked cycles were also present, highlighting the difficulty in deriving explanatory meaning from looking at raw data traces alone.

PCs 4, 5 and 6 of the gait signatures indicate a difference between blocked and unblocked gait cycles (Fig. 1B). In all, the first 6 PCs explain 71% of the variance, but the last three of these components capture the spatiotemporal movement patterns that set blocked gait apart even with the changes in baseline gait between sessions.

Reconstructed kinematics derived from PCs 4, 5 and 6 reveal the varying influence of these components on different types of gait cycles. If a PC encoded for a specific movement pattern that was present in both the unblocked and blocked groups of a given session, then the root mean square error (RMSE) between these reconstructions would be 0. However, large error is present in all but the ipsilateral hip and contralateral ankle (Fig. 1C). Distinct movement strategies are revealed by comparing the error magnitudes between days. Although the overall RMSE of the right limb angles was greater for S1 than S4 in the raw data shown in Fig. 1A, (S1:20.7° v S4:18.8°), S4's reconstruction had the dominant error as shown in Fig 1C (S1:6.8° v S4:9.6°), suggesting these three movement patterns were more present later in adaptation after longer exposure to nerve block.

Significance: Combining new temporary nerve block and model-driven analysis techniques, our understanding of locomotor adaptation can be expanded. Further, by refining KES, we can use it to better understand nerves with more complex functions like those in the autonomic and enteric nervous systems.

Acknowledgments: We would like to thank members of the Comparative Neuromechanics Laboratory for their help and support. NIH R01AR080154

References: [1] Patel & Butera (2014), *J Neurophys* 113(10); [2] Roldan et al. (2019), *J Neuro Meth* 315(2019); [3] Bauman & Chang (2013), *Bio. Let* 9(5); [4] Winner et al. (2023), *PLoS Comp Bio* 19(10);

JOINT MECHANICS DURING UNDERFOOT PERTURBATIONS WITH VARYING PHYSICAL CERTAINTY

Paula Kramer[1*], Nicholas Kreter[2], Christina Giesler[1], Zachary Barker[1], Francisca Moreira[1] ,Peter Fino[1]
[1]University of Utah [2]University of Oregon
*Corresponding author's email: paula.kramer@utah.edu

Introduction: When walking across complex terrain, humans flexibly use four different strategies to maintain balance and stay upright: (1) foot placement, (2) ankle torque, (3) hip torque, and (4) impulse / push-off control [1,2]. While foot placement is the dominant strategy for frontal-plane balance control, all strategies are used in concert, especially when there are external perturbations. Our previous work explored the control of foot placement and stability when presented with perturbations of varying physical certainty (i.e., the participants did or did not know the physical nature of the upcoming perturbation) [3]. When individuals could predict the physical nature of the perturbation, they recovered normal stepping kinematics faster than when disturbances were uncertain. However, participants did not pre-emptively change foot placement to mitigate the effects of the known perturbation [3]. As the prior work only examined foot placement, this study aimed to compare joint-level mechanics at the ankle, knee, and hip between these physically certain and uncertain underfoot perturbations. We hypothesized that, when certain about the physical features of the perturbations, individuals would have different frontal-plane torques during the perturbed stance that facilitated the faster kinematic recovery.

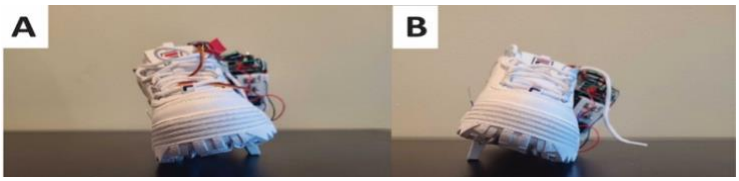

Figure 1. Mechanized shoe eliciting an eversion (A) and eversion (B) underfoot perturbation for the left foot

Methods: Nine Participants (Female = 5, Male = 4)[mean (SD) 26.8 (5.6) yrs.]; provided informed written consent and completed three five-minute walking trials wearing a mechanized shoe (Fig. 1) as part of a larger IRB-approved protocol. During the three trials, participants randomly experienced an underfoot perturbation to their left foot every 5-9 strides. The physical effect of the perturbations differed by rolling the ankle outward (eversion, Fig. 1A) or inward (inversion, Fig. 1B)[3.4]. Physically certain conditions included two blocks: eversion and inversion. The uncertain condition consisted of one block with a mixture of eversion and inversion perturbations interleaved together[4]. Kinetic and kinematic data were collected using an instrumented treadmill with an embedded force plate (Bertec Fit) and a motion capture system (Vicon) with 34 retro-reflective markers for the lower body. Kinetic and kinematic data were low-pass filtered at 15 Hz and 6 Hz, respectively. Joint moments were calculated for each step via inverse dynamics using Visual 3D. Mean joint moment was calculated for each perturbed stance, as well as for 'normal' stance. Normal stance was defined as non-perturbed steps that occurred between two steps after and before a perturbation. The mean joint torque was calculated across the gait cycle for each condition. Statistical analysis was run using a one-way repeated measures ANOVA via statistical parametric mapping (SPM) for the mean joint torques of each subject [5,6]. A Bonferroni post-hoc test followed by a two-tailed paired t-test was then performed to compare the certain and uncertain conditions using spm1d package(α=0.05) (version M.0.4.10).

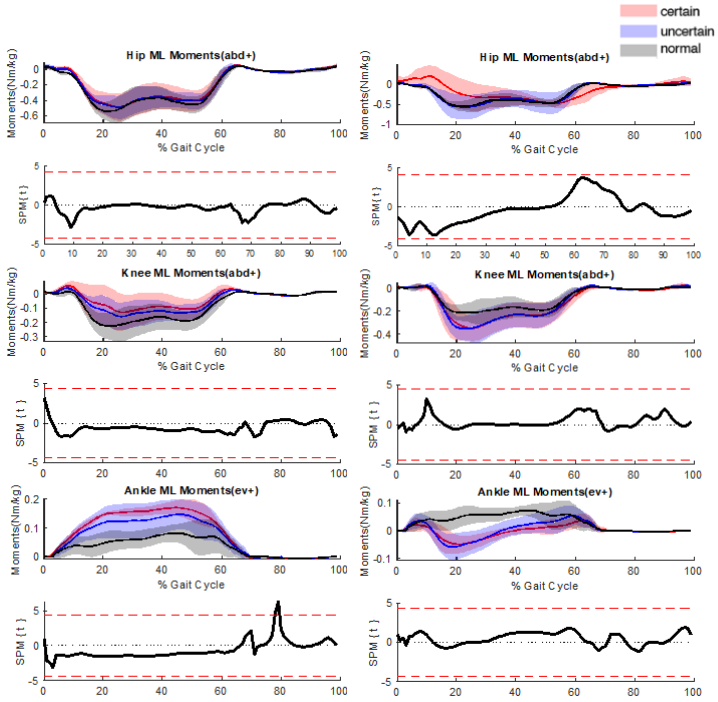

Figure 2. Ensemble curves of the mean and standard deviation (shaded) frontal plane joint torques for the hip, knee, and ankle during certain (red) uncertain (blue) and unperturbed (gray) steps (Right side = eversion, Left = inversion). Below each ensemble curve plot is the SPM{t}plot comparing joint moments between the certain and uncertain

Results & Discussion: Individuals did not exhibit any differences between certain and uncertain conditions in joint moments at the hip, knee, or ankle during the stance phase of the perturbation (Fig. 2). Although not statistically significant, there was a notable trend at the hip; whereby a greater hip abduction moment was evident in early stance (~10%) when the physical features of the perturbation were known in advance. In conclusion, faster recovery of normal gait kinematics does not appear to be facilitated by different joint torques during the perturbed stance. Larger sample sizes and further analyses of the joint mechanics during steps preceding and following the perturbation are needed.

Significance: This study adds to our knowledge of how individuals control locomotion in uneven terrain and supports prior work that healthy individuals do not exhibit pro-active, anticipatory strategies before perturbations [4,7]**.**

References: [1] Bruijn 2018, *J. of The R Societ. Interf.[*2] Reimann 2018, *Frontiers* [3] Kreter 2023, *J. of Exp. Biology* [4] Kreter 2021, *Clin. Biomech.* [5] Pataky 2013, *J. of Biomech.* [6] Pataky 2017, ISB [7] Eichenlaub 2023, *Hum.Mov. Sc.*

DIFFERENCES IN TURNING PERFORMANCE DURING SINGLE-TASK AND DUAL-TASK TIMED UP AND GO

Mackenzie Barrowman*[1], Patrick King[1], Kelly Poretti[1], Tiphanie Raffegeau[1]
[1]School of Kinesiology, George Mason University, Manassas VA
*Corresponding author's email: mbarrowm@gmu.edu

Introduction: Everyday activities often require managing concurrent motor and cognitive demands (i.e. a dual-task) [1] and over 40% of daily steps involve turning [2]. Compared to steady state gait, turning increases the motor demands of maintaining balance [3] and increases the risk [4] of older adult falls since turning steps require added motoric coordination (decelerating forward motion, rotating the body, and stepping out in a different direction) [5]. In healthy older adults, cognitive interference due to a verbal fluency task (i.e. naming animals) negatively affects straight walking (i.e., decreased gait speed) during the Timed Up and Go (TUG) [6], a well-validated physical function assessment of both turning and straight steps [7]. However, it remains unclear how cognitive demands affect turning steps during the TUG. The purpose of this analysis was to determine how healthy adults manage verbal fluency cognitive demands during the turning portion of the TUG, indicated by the proportion of turning time, peak turning velocity, and TUG duration in the dual-task TUG test.

Methods: Participants wore inertial sensors (APDM Inc, Portland, OR) on the lumbar spine, trunk, both feet, and wrists recording data at 128 Hz. Participants completed three trials of the TUG in two conditions in a fixed order: single-task followed by dual-task. For single-task trials, participants stood up from a chair with their arms crossed over their chest, walked straight three meters at a 'comfortable pace' around a cone, and returned to their seat, as per established clinical guidelines [8]. For dual-task trials, participants were instructed to name as many different animals as they could without repeating, and no instructions were given regarding prioritization. Turn duration (duration of 180º turn; developed by Salarian et al. [9]) and total TUG duration (the total time of the TUG test) were extracted using Moveo Explorer (APDM Inc, Portland, OR). A custom MATLAB code extracted peak angular velocity of the lumbar sensor. A one-way ANOVA examined differences across conditions. A p-value < .05 was deemed significant. Cohen's d effect sizes adjusted for small samples (Hedge's G) were calculated to compare conditions, defined as small (G > 0.2), medium (G> 0.5), and large (G > 0.8) effects.

Table 1. Comparison of Peak Turn Velocity, Total TUG Time, and Turn Proportion during Single- and Dual-Task TUG

Outcome Variables	Single-Task Mean (SD)	Dual-Task Mean (SD)	*p*-Value	Hedge's *G*
Peak Turn Velocity (deg/s)	233.0 (48.7)	203.0 (40.6)	.006*	-0.62
Total TUG Duration (s)	9.3 (1.5)	11.1 (2.9)	.004*	0.76
Turn Proportion of TUG (%)	22.3 (3.1)	21.2 (4.4)	.238	-0.30

Notes: deg = degrees, s = seconds, % = percent of total TUG. *Indicates significance, p < .05.

Results & Discussion: Ten adults, (n = 7 women, mean (SD): age = 22.9 (3.3) years, mass = 73.8 (11.4) kg, height = 167.8 (9.6) cm, leg length = 88.2(15.2) cm) were included in this analysis using data from a larger study. Participants had significantly slower peak turning velocity during dual-task (p = .006) TUG trials versus single-task TUG trials (Table 1). Turn proportion of the TUG test during single-task compared to dual-task revealed no significant difference (p = .238). However, consistent with current literature [9], there was a significant increase in the total TUG duration (p = .004) during dual-task versus single-task trials, suggesting individuals allowed motor costs to occur under cognitive demands of the verbal fluency test. Decreased in peak turn velocity during dual-task TUG indicates motor costs due to the cognitive demand of the verbal fluency test. Turn proportion of the TUG did not change from single- to dual-task, indicating under cognitive demand, healthy adults may have taken faster steps at the end of the turn to compensate for decreased velocity during the turn, which could potentially lead to loss of balance. Future analyses should focus on incorporating performance outcomes of the cognitive task to determine tradeoffs between cognitive and motor demands.

Significance: Healthy adults adopted compensatory strategies to complete the turn portion of the TUG due to the cognitive demands of the dual-task. In impaired populations, adoption of this compensatory strategy could lead to increased fall-risk, compelling further study.

Acknowledgments: This work was supported by Mason @4VA and the College of Education and Human Development.

References: [1] Floriano et al. (2015), *Fisioter. mov.* 23; [2] Glaister et al. (2007), *Gait & Posture.* 25(2); [3] Xu et al. (2004), *J. Mot. Behav.* 36(3); [4] Yamaguchi et al. (2012), *J. Biomech.* 45(15); [5] Hase et al. (1999), *J. Neurophysiol.* 81(6); [6] Cedervall et at. (2020), *Int. J. Environ. Res. Public Health.* 17(5); [7] Podsiadlo & Richardson (1991), *J. Am Geriatr Soc.* 39(2); [8] CDC- STEADI (2017), *TUG Assessment*;); [9] Salarian et al. (2010), *IEEE Trans. Neural. Syst. Rehabil. Eng.* 18(3); [10] Åberg et al. (2023), *J Aging Phys Act.* 31(5).

DOES ACCOUNTING FOR FAT INFILTRATION IN MUSCLE VOLUME CALCULATIONS IMPROVE JOINT TORQUE PREDICTIONS IN HEALTHY SUBJECTS?

Mario E. Garcia[1*], Emily M. McCain[1], Allen Luk[1], Xiao Hu[1], Shawn D. Russell[1], Silvia S. Blemker[1]
[1]University of Virginia, Charlottesville, VA, USA
*Corresponding author's email: nfq3bd@virginia.edu

Introduction: While summed muscle volumes across functional groups correlate with measured maximal isometric torques, they do not account for all measured variability across individuals. Variations in muscle quality, characterized by fat infiltration, may impact these relationships; studies have accounted for fat infiltration by excluding fat from muscle volumes [1]. However, minimal prior research has examined the extent to which fat infiltration influences torque generation in healthy individuals. **This study compares relationships between whole muscle volume and muscle volume adjusted for fat fraction to torque, in male and female subjects.**

Methods: 43 healthy, active adults (22 female, 21 male) between 20-49 (26.98±7.79 years) within five height (1.70±0.09 m) and mass (70.10±15.39 kg) categories based on a recent population study [2] were recruited. Dynamometry: Following a gait trial, subjects completed two repetitions of a three-second maximum voluntary isometric contraction (MVIC) for ankle plantar/dorsiflexion (PF/DF), knee extension/flexion (KE/KF), hip extension/flexion (HE/HF), and hip abduction/adduction (HAb/HAd) for the right limb using a Biodex System 4 dynamometer (Biodex Medical Systems Inc.). For each joint, direction and angle were randomized to reduce order bias. During hip trials, a Donjoy T-ROM brace and custom-built rigid frame were used to stabilize the knee and torso. Muscle volumes: Subjects laid supine during a two-point Dixon sequence with field of view: 280 mm x 450 mm, slice thickness: 5 mm, and in plane spatial resolution: 1.1 mm x 1.1 mm, 3T MRI scanner (Trio, Siemens, Munich Germany) to identify bone and muscle boundaries. This scan allowed for volume calculations of muscle and non-contractile tissue through a deep convolution neural network-based segmentation method [3], and manual vetting (Springbok Analytics, Charlottesville, VA). Analysis: Peak torques were extracted from dynamometry data using custom MATLAB (MathWorks) functions that corrected for gravitational contributions. The joint angle analyzed corresponded to maximum MVIC. Full muscle group volume was assigned based on functional groupings [4] and lean muscle group volumes were calculated by uniform removal of fat infiltration. Linear regressions were compared using Fishers z-Transformation ($\alpha<0.05$) [5].

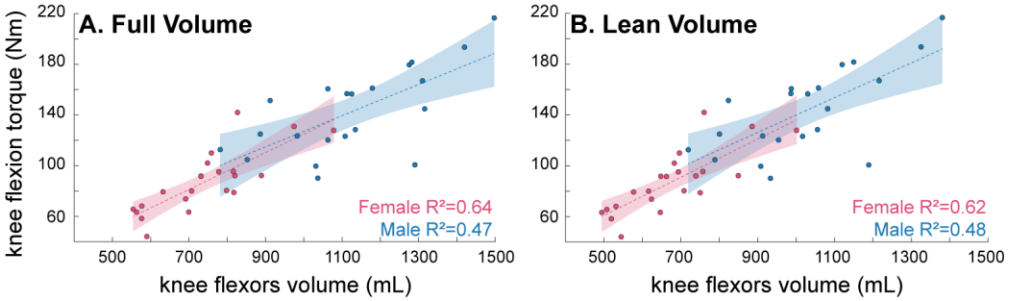

C	Full Female R^2	Lean Female R^2	Female p-value	Full Male R^2	Lean Male R^2	Male p-value
DF 15°	0.6546	0.6445	0.22	0.6986	0.6978	0.49
PF 0°	0.0759	0.0816	0.44	0.1916	0.1726	0.35
HAb 0°	0.4592	0.4654	0.43	0.3091	0.2488	0.21
HAd 20°	0.3374	0.3294	0.39	0.2441	0.2806	0.20
HE 0°	0.1410	0.1125	0.32	0.0002	0.0045	0.48
HF 30°	0.3466	0.3403	0.39	0.2098	0.2035	0.44
KE 90°	0.3490	0.3456	0.45	0.3150	0.3407	0.16
KF 15°	0.6414	0.6204	0.22	0.4679	0.4780	0.43

Figure 1: A) Joint torque and full volume linear regression at 15° knee flexion, **B)** joint torque and lean volume linear regression at 15° knee flexion, **C)** R^2 and p-values for all MVIC comparisons

Results & Discussion: There were no significant differences in correlations between volume and maximum isometric joint torque, when using full vs. lean muscle group volume regardless of sex. In female subjects, full muscle volume linear regressions were moderate in DF, and KF ($R^2>0.64$), low in HAb, HAd, HF, and KE ($0.30<R^2<0.46$) and did not have a significant correlation in PF and HE. In males, full muscle volumes were highly correlated in DF ($R^2=0.70$), low in HAb, HAd, HF, KE, KF ($0.20<R^2<0.47$), and were not well correlated in PF and HE. While no differences in correlations were significant, it is worth noting lean muscle volume in females resulted in lower correlations, with the exception of PF and HAb. In male subjects, lean muscle volume resulted in higher correlations in the hip and knee, with the exception of HF and HAb, and lower in the ankle. Further work regarding fat distribution associated within muscles is required.

Significance: Preliminary data suggests there is no significant difference in torque prediction using lean muscle volume with uniform volume correction based on fat infiltration. Future studies will examine how fat distribution impacts muscle force and torque production.

Acknowledgments: Research funded by NIH Award T32GM145443 and NIH Grant #R01AR078396.

References: [1] Davison et al. (2017), *Clin Biomech* [2] Fryar et al. (2016), *Vital Health Stat* [3] Ni et al. (2019), *J Med Imaging* [4] Delp et al. (2007), *TBME* [5] Meng et al. (1992), *Psychol. Bull*

WHICH MUSCLE DIMENSIONS BEST RELATE TO MAXIMUM ISOMETRIC PLANTAR FLEXOR TORQUE?

Mario E. Garcia[1*], Emily M. McCain[1], Allen Luk[1], Xiao Hu[1], Shawn D. Russell[1], Silvia S. Blemker[1]
[1]University of Virginia, Charlottesville, VA, USA
*Corresponding author's email: nfq3bd@virginia.edu

Introduction: Ankle plantar flexors are major contributors of the power needed to walk [1]. Interestingly, determinants of ankle plantar flexor muscle strength remain elusive, likely due to unique and complex architectures of the triceps surae. While muscle volume, cross-sectional area (CSA), and thickness are correlated with joint torque in most muscle groups, these relationships are weak in the plantar flexors [2]. Advancements in imaging allow for *in vivo* measurements of triceps surae muscle architecture, enabling better understanding of the interaction between these metrics and torque production. **In this study, we aim to characterize the relationship between joint torque at the ankle to cross sectional area (measured in different planes), length, maximum feret diameter and thickness.**

Methods: 43 healthy, active adults (22 female, 21 male) between 20-49 (26.98±7.79 years) within five height (1.70±0.09 m) and mass (70.10±15.39 kg) categories [3] were recruited for this study. Dynamometry: Following a gait trail, subjects completed two repetitions of a three-second unilateral maximum voluntary isometric contraction (MVIC) using a Biodex System 4 dynamometer (Biodex Medical Systems Inc.), for multiple angles at the ankle and knee. The joint and angle were randomized to reduce order bias. Muscle volumes: Subjects laid supine during a two-point Dixon sequence with field of view: 280 mm x 450 mm, slice thickness: 5 mm, and in plane spatial resolution: 1.1 mm x 1.1 mm, 3T MRI scanner (Trio, Siemens, Munich Germany) to identify bone and muscle boundaries. Lower limb muscle volumes were quantified using a deep convolution neural network-based segmentation method [5] and manual vetting (Springbok Analytics, Charlottesville, VA). Analysis: Peak torques were extracted from dynamometry data at 0° plantar flexion (PF) and 65° knee flexion (KF) and corrected for gravitational contributions using MATLAB (MathWorks). KF was selected as a comparison to ankle PF due to differences in structure, such as pennation angle and thickness. Based on the muscle segmentations (**Fig 1A**), we calculated muscle length, maximum feret diameter (MFD), and maximum perpendicular thickness to MFD (**Fig 1B**) using custom MATLAB functions. Muscle length values were within the range of cadaveric measurements [4]. MFD and thickness were found for the slice with the maximum CSA (**Fig 1A**). Muscle length was calculated based on the segmentation's superior-inferior axis. We used these dimensions to estimate anatomical axial CSA (CSA_{axial}: MFD*thickness) as well coronal CSA ($CSA_{coronal}$: MFD*length). Correlated between each dimension and joint torque were determined, and Pearson correlation ($\alpha<0.05$) was used to establish significance. Comparisons between correlations were analyzed using Fishers z-Transformation ($\alpha<0.05$) [6].

Results & Discussion: Across the plantar flexor dimensions (**Fig 1C-F**), $CSA_{coronal}$ had the highest (and most significant) correlation ($R^2= 0.27$) with joint torque. Summed lengths ($R^2= 0.21$) and summed MFD ($R^2= 0.20$) were also significantly correlated with PF torque; however, the correlations were not significantly different from each other. Summed thickness ($R^2= 0.03$) and CSA_{axial} ($R^2= 0.09$) had no correlation. By contrast, across the knee flexor dimensions, CSA_{axial} had the highest (and most significant) correlation ($R^2= 0.71$) with KF torque. KF torque was also highly correlated with summed MFD ($R^2= 0.69$) and summed thickness ($R^2= 0.59$); all were significant correlations though not significantly different from each other. Summed length resulted in a low, but significant, correlation ($R^2= 0.23$). The summed length correlation in KF was statistically significantly lower than summed MFD and summed thickness correlations. Correlations using $CSA_{coronal}$ ($R^2= 0.64$) and CSA_{axial} ($R^2= 0.71$) were high, had significant Pearson correlations ($r>0.80$) and were significantly higher than summed length. In PF, thickness had no correlation when summed or used to create CSA_{axial}, compared to KF where thickness was highly correlated in both metrics.

Significance: CSA in the coronal plane was a better indicator of strength of the plantar flexors (as compared to axial CSA), likely due to their highly pennated architecture, a result that was not the case for the more parallel fibered knee flexors. Future work will incorporate more architecture parameters to explore variation in strength across the population.

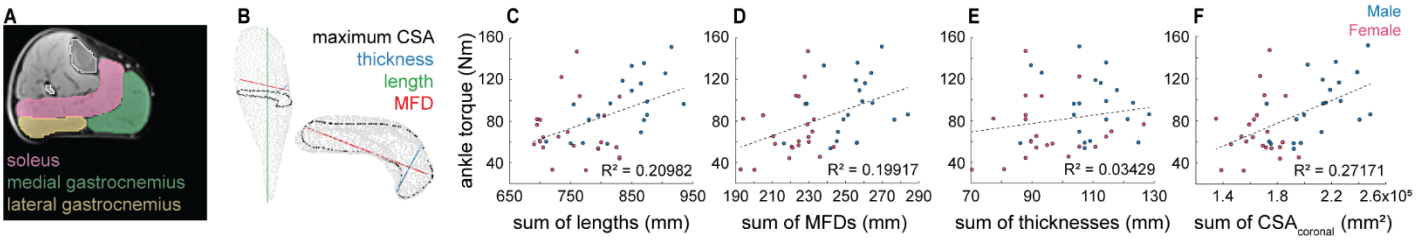

Figure 1: A) Segmentations of soleus, medial and lateral gastrocnemius from MRI **B)** Muscle characteristics of the soleus **C)** Sum of muscle lengths, **D)** Sum of MFDs, **E)** Sum muscle's thickness **F)** Linear regressions using sum of characteristic CSA

Acknowledgments: Research funded by NIH Award T32GM145443 and NIH Grant #R01AR078396.

References: [1] Sawicki et al. (2009), *J Exp. Biol* [2] Piazza et al. (2014), *J Appl. Psychol* [3] Fryar et al. (2016), *Vital Health Stat* [4] Andjelkov et al. (2016), *JPRAS* [5] Ni et al. (2019), *J Med Imaging* [6] Meng et al. (1992), *Psychol. Bull*

TAPING TECHNIQUES AND THEIR EFFECTS ON MUSCLE ACTIVATION AND ENERGY EXPENDITURE

Andrew Craig-Jones[1*], Amador Landaverde[1]
[1]Department of Kinesiology, Augusta University, Augusta, GA
*Corresponding author's email: acraigjones@augusta.edu

Introduction:
Joint instability is a major concern for many athletes; however, this concern can be addressed by reinforcing the joints with either a brace or Athletic trainer's tape (AT tape)[1]. More recently, Kinesiotape Tape (KT tape) has been developed and is an elastic version of traditional training tape. There is limited research completed on the effects of KT-Tape compared to its predecessor, but a few studies have found that KT tape can alter joint mechanics when compared to the less flexible AT tape [2,3]. Both tape materials have been found to reduce joint pain and alter lower extremity realignment [4,5]. Based on its adhesive and elastic properties, KT tape may have the ability to affect muscle activation and energy expenditure if applied differently than traditional techniques. With KT tape pulling its attachments towards the center of the tape, it may be possible it could serve as a supplemental pseudo-muscle around a joint. Therefore, we aimed to explore whether the type of knee taping technique influences muscle activity and oxygen consumption during running at steady state. Our secondary aim is to investigate if Kinesiotape applied to the knee in a spring like fashion can reduce energy expenditure during running. Due to clear evidence that altering an individual's gait characteristics influences energy expenditure, we believe that taping technique will change in muscle activity and oxygen consumption. For our second question, although there is no current literature on passive spring assistance during running, we believe that due to the natural H:Q ratio, assisting the hamstrings during running will reduce the hamstring's muscle activity as well as overall energy expenditure.

Methods: Self-identified recreational runners (7F7M, ht:1.65±.08m, wt:73.31±17.20kg, age:22.79±4.79yrs) were recruited for the study. All participants signed consent forms and biometric data was obtained. Following a brief self-selected warmup, participants' preferred speed was obtained, and all conditions were run at the participant's preferred speed. The four tape applications used for the study are no tape (CON), Athletic Trainers tape (AT, Figure 1), Kinesiology Tape (KT, Figure 2), and lastly a novel spring method using Kinesiology Tape and Athletic Trainers Tape (Spring, Figure 3). Conditions were counterbalanced prior to negate fatigue bias.

Participants then ran on a treadmill at their preferred speed for 6 minutes per condition. Each condition was separated by a period of rest while a new taping technique was applied. During running, HR, stride frequency (SF), Muscle activity (EMG), and Oxygen consumption ($\dot{V}O_2$) were collected. For data reduction, DC bias was removed from the EMG data and a full-wave rectification applied. Average EMG was calculated from 5 complete strides during the last minute of each condition. $\dot{V}O_2$ were averaged across 3 minutes of steady state running. Accelerometer data were used to identify SF from 5 complete strides. All values were averaged and used per condition to evaluate differences. A repeated measures ANOVA was used to assess differences in conditions for each variable. Alpha level was set at 0.05.

Fig. 1. AT taping technique.

Fig. 2. KT taping technique.

Fig. 3. Spring taping technique.

Results & Discussion: For $\dot{V}O_2$, the control was not different from any condition ($p>0.05$). The average oxygen consumption of each condition was 31.77±4.34ml/kg/min, for AT was 32.09±3.58ml/kg/min, for KT was 31.61±3.88ml/kg/min, and for spring was 32.17±3.92ml/kg/min. These results indicate that although using traditional taping techniques (AT and KT) did not enhance efficiency while running, they also did not have a negative impact on the overall energy expenditure of the participants. The same can be said of the novel spring technique. These data do not support our hypothesis that oxygen consumption would be changed by traditional tape and improved by spring tape. To our knowledge, there were no previous studies investigating the effect of taping techniques on oxygen consumption and these results will need further investigation to further verify their validity. It was also determined that SF as well as muscle activity of the rectus femoris and biceps femoris were not different between conditions ($p>0.05$). These findings contradict our hypothesis that muscle activity would be altered depending on taping technique. This determination was surprising and disagreed with the rationale previously drawn from the available data. If gait characteristics are altered using tape, then muscle activity should also be altered during these conditions. Once again, it is important to illustrate that there is no additional cost to muscle activity when using tape, but more research is needed to fully understand the relationship between tape application and its effect on running mechanics.

Significance: These results are meaningful and significant to the field of athletics as they shed light on a product that is widely used but has little research exploring its effects. Athletes and coaches should use these data to understand that there is no increase in energy expenditure while using tape. Additionally, we were unsuccessful in using KT tape as a passive spring exoskeleton of the knee. It is possible that the KT tape did not aid the hamstrings as intended and a new design creating a greater pull is needed. If it is possible to increase a runner's efficiency using a spring model behind the knee, this could lead to a novel ergogenic aid for running. More research is needed around this concept that explores the manipulation of the H:Q ratio for athletic gain.

References: [1] Karlsson, J. et al. (1993), *Sports Med, 16.* [2] Cochrane, M. E., et. al. (2023). *South African Journal for Research in Sport, Physical Education and Recreation Social Sciences*, *45*(1). [3] Alrawaili, S. M. (2019). *Clinics*, *74*. [4] Wild, C. Y., et. al. (2016). *American Journal of Sports Medicine*, *44*(8). [5] Watcharakhueankhan, P et. al. (2022). *Gait & Posture*, *91*.

MEASURING THE ANKLE PLANTAR-FLEXION STRENGTH CURVE

Axelle M Wasiak*, Samuel Marsh, John H Challis
Biomechanics Laboratory, The Pennsylvania State University, University Park, PA 16802, USA
*Corresponding author's email: avw5667@psu.edu

Introduction: A strength curve is the net moment caused at a joint by the muscles crossing that joint, for a given degree of freedom for that joint, across the complete range of motion of that joint, and under isometric conditions. Strength curves have many useful applications, such as analyzing movements for the elderly to acquire a deeper understanding of the strength challenges for tasks of everyday living. For example, strength curves for the knee extensors for elderly subjects indicated some used around 97% of their knee extensor maximum isometric strength to rise from an average height chair [1]. Quantifying strength curves can be useful in the designing of exercise interventions for a variety of populations. A common method to determine a strength curve is to measure the maximum isometric moment for a range of joint angles. However, such an approach for determining a strength curve has limitations including fatigue effects and the time required for testing. These limitations can be exasperated if a joint is crossed by any multi-articular muscles, therefore requiring testing with another joint's orientation varied.

During walking and running, positive power generated at the ankle constitutes the majority of the mechanical power generated by the lower limb during stance [2, 3], therefore the focus of this study was to determine the strength curve of the plantar-flexors. The study had two components: simulation, and experimental. The simulations used a model to determine how to map from angle-moment curves from low angular velocity isokinetic trials to isometric angle-moment curves for ankle plantar-flexion. For the experimental component, the strength curves for subjects were measured under both isokinetic and isometric conditions and compared.

Methods: A Hill-type muscle model was developed of the gastrocnemius and soleus. The model included activation dynamics, force-length properties, force-velocity properties, and an elastic tendon in series with the muscle fibers. Using model parameters based on Out et al. [4], simulations were used to determine ankle plantar-flexor strength curves with the knee fully extended, and flexed to 90°. Further simulations were performed for slow isokinetic plantar-flexions (5°/s, and 10°/s).

Experimentally, nine subjects (74.3 kg ± 9.9; height 1.77 m ± 0.07; age 22.8 years ± 3.2) provided informed consent for participation in this study, which was approved by the Institutional Review Board. Data were collected from the subjects, using a Biodex, which mirrored those simulated using the model. Once the isokinetic portion of testing was completed, the isometric testing consisted of four fixed ankle angles (110°, 100°, 90°, and 85°), and two knee angles (fully extended, and flexed to 90°). Three maximal trials were performed under each angle configuration. The order of presentation of angle configurations was varied randomly between subjects.

Results & Discussion: The results of simulations indicated that at an angular velocity of 5°/s the curves obtained for the angle-moment curve were similar in shape to the isometric curves (Figure 1). These two curves could be closely aligned if the difference between the curves at an ankle angle of 100° was used to adjust the offset.

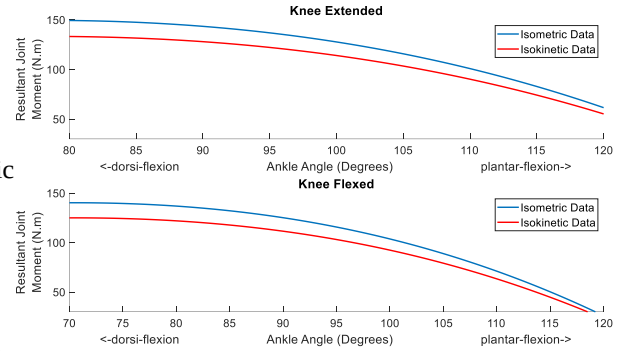

Figure 1: Simulations of isometric and isokinetic ankle plantar-flexion strength curves.

For the experimental data, to compare maximal isokinetic and isometric data, two one-sided tests (TOST [6]) were completed for the moments from each of the ankle joint angles where there were nine pairs of data that corresponded to each participant; the 100° ankle joint angle moment data were not compared because this was the reference angle. As with classical point-null hypothesis testing, TOST is subject to multiplicity concerns as more comparisons are made, therefore the p values were adjusted using the Holm method [7]. The percent root mean squared difference between the isometric and isokinetic data was in excess of 23%, once these values were adjusted (offset value at 100°) there was no statistically significant difference between the isometric and isokinetic moment curves.

These results mean, at least for ankle plantar-flexion, that a strength curve can be determined with one isometric effort and one isokinetic effort. One of the major plantar-flexors is bi-articular, the gastrocnemius, which means that the strength curve for the ankle plantar-flexors is really a surface not a single curve. Such surfaces can be obtained using this new method for determining strength curves. It would be useful to establish if this result holds for other joints.

Significance: For many analyses strength curves can be useful, including identifying the impact of strength curves on the performance of activities of daily living in subjects experiencing muscular weakness (e.g., the elderly), and as a means of evaluating the veracity of musculo-skeletal models. The new method provides a relatively quick way for determining strength curves.

References:

[1] Hughes et al. (1996) *Journal of Biomechanics*, 29(12), 1509-1513.
[2] Farris & Sawicki (2012) *Journal of The Royal Society Interface*, 9(66), 110-118.
[3] Zelik et al. (2015) *The Journal of Experimental Biology*, 218(6), 876-886.
[4] Out et al. (1996) *Journal of Biomechanical Engineering*, 118(1), 17-25.
[5] Lakens (2017) *Social Psychological and Personality Science*, 8(4), 355-362.
[6] Holm (1979) *Scandinavian Journal of Statistics*, 6(2), 65-70.

EFFECTS OF ASYMMETRIC STIFFNESS WALKING ON WEIGHT BEARING SYMMETRY

Jenna Chiasson[1*], Leah Metsker[2], Elena Schell[1], Jonaz Moreno Jaramillo[1], Meghan E. Huber[3], Mark Price[1,3], Wouter Hoogkamer[1]
[1] Department of Kinesiology, University of Massachusetts Amherst
[2]Department of Biomedical Engineering, University of Massachusetts Amherst
[3]Department of Mechanical and Industrial Engineering, University of Massachusetts Amherst
*Corresponding author's email: jmchiasson@umass.edu

Introduction: Stroke, a leading cause of long-term disability, leaves about 80% of survivors with gait impairments and an estimated 55% of chronic stroke survivors exhibit gait asymmetries [1,2]. Recent research shows improvements in spatiotemporal aspects of gait in post-stroke individuals using asymmetric speed on a dual belt treadmill [3]; however, this intervention does not improve weight bearing symmetry during walking [2,4]. Prior work has shown that walking on an asymmetric stiffness dual-belt treadmill can evoke interlimb coordination pathways leading to aftereffects in vertical ground reaction forces (vGRFs) [5]. was to explore the effects of a single bout of asymmetric foot-ground stiffness walking on weight bearing symmetry. We expected that participants would adapt towardanceo the low stiffness (perturbed) , and would require greater push-off on that side to initiate swing. These expectations led to the following hypotheses: vGRF during weight acceptance (first vGRF peak) and mid-stance (minimum vGRF between the peaks) would be larger for the leg that walked on the high stiffness side than the low stiffness side (H1 and H2, respectively), but vGRF during push-off (second vGRF peak) would be larger for the low stiffness side than the high stiffness side (H3) immediately after the perturbation compared to baseline. We also anticipated an increase in stance time for the leg that walked on the high stiffness side compared to the low stiffness side after the perturbation relative to baseline (H4).

Methods: Five healthy individuals (age: 18-42; mass: 67.6 ± 11.6 kg) with no musculoskeletal or neurological injuries participated in this study. Participants completed 3 bouts of walking in a single session: two bouts on a regular instrumented dual-belt treadmill (Bertec, Columbus, OH, USA) and one bout on a dual-belt adjustable stiffness treadmill. For all trials both belts of each treadmill were going at the same speed (1.25 m/s). First, participants completed a 5-minute walking trial at 1.25m/s on the instrumented treadmill ("Baseline"). Then, each participant performed a 12-minute walking trial on the dual-belt adjustable stiffness treadmill with one foot on each belt. The first 2-minutes were used for acclimatization to the new treadmill with both sides set to high stiffness, after which stiffness under the left foot was adjusted to 30 kN/m while the participant was walking, within a single step. Participants walked for 10-minutes with asymmetric stiffness before being transferred to a wheelchair and moved to the instrumented treadmill to ensure that they did not reacclimate to normal walking before measuring their response. Aftereffects in walking kinetics were assessed during a 5-minute walking trial on the instrumented dual-belt treadmill ("Post"). We evaluated changes between sides by calculating the asymmetry ratio for each measure, defined as the difference between measures recorded for the perturbed and unperturbed limb and their sum: $(M_P - M_U)/(M_P + M_U) \times 100\%$. We calculated the average of this ratio over 20-stride windows at the end of the Baseline condition, and the start and end of the Post condition (Post-Early and Post-Late). We performed a repeated measures ANOVA to evaluate the effect of stiffness condition (Baseline, Post-Early, Post-Late) on vGRF during weight acceptance, push-off, and mid-stance, and stance time asymmetry. Planned comparisons in the form of paired t-tests on were used to evaluate our hypotheses for all asymmetry measures (Baseline vs. Post-Early).

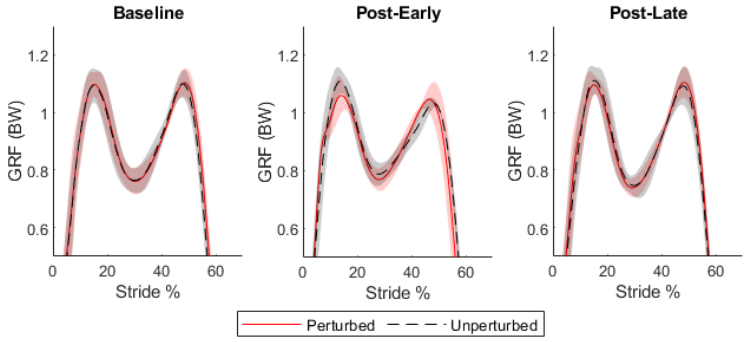

Figure 1: Vertical ground reaction force profiles averaged across all participants before, immediately after, and 5 minutes after the asymmetric stiffness perturbation. Shaded lines represent mean ± 1 SD.

Results: The ANOVA revealed a significant effect of condition on weight acceptance vGRF ($p = .006$) and stance time asymmetry ($p = .009$), but not push-off or mid-stance vGRF asymmetry ($p > .1$). In support of H1 and H4, weight acceptance vGRF shifted toward the unperturbed side (Mean difference = -2.95%; $p = .008$) and stance time increased on the unperturbed side relative to the perturbed side (Mean difference = -2.36%; $p = .018$) from Baseline to Post-Early. Group mean vGRF over stride percentage is illustrated in Figure 1. As predicted, weight acceptance shifted to the unperturbed leg during early post adaptation compared to baseline, suggesting an evocation of the interlimb coordination pathways. Contrary to our hypotheses H2 and H3, there was no significant change in vGRF during push-off or mid-stance.

Significance: These results show that changing foot-ground stiffness during walking can elicit changes in weight bearing strategy after the perturbation, suggesting that neuromotor adaptation has occurred. The observed aftereffect in weight-bearing symmetry during walking is promising for the potential of this intervention and warrants further study investigating if these changes occur in people after stroke, and if they persist with repeated training.

References: [1] Duncan, et al. (2005). *Stroke*, *36*(9); [2] Hendrickson et al. (2014). *Gait & posture*, *39*(1); [3] Reisman et al. (2013). *Neurorehabilitation and neural repair*, *27*(5); [4] Hoogkamer (2017). *Exercise and sport sciences reviews*, *45*(1); [5] Chambers & Artemiadis. (2023) *Frontiers in robotics and AI*, *9*(3).

CURVE ANALYSIS OF WALKING GAIT KINEMATICS IN YOUNG AND MIDDLE-AGED ADULTS

Zahra Mollaei[1*], Mikel Joachim[2], Emily Gerstle[1], Bryan Heiderscheit[2], Kristian O'Connor[1], Stephen C. Cobb[1]
[1]Foot & Ankle Biomechanics Laboratory, Zilber College of Public Health, University of Wisconsin-Milwaukee, Milwaukee, WI, USA
[2]Department of Orthopedics and Rehabilitation, University of Wisconsin-Madison, Madison, WI, USA
*Corresponding author's email: zmollaei@uwm.edu

Introduction: Walking gait impairments, which increase with advancing age, can lead to increased fall risk, reduced physical activity, and other health comorbidities that adversely impact an individual's independence and quality of life [1]. A meta-analysis of gait mechanics in aging concluded that when walking at matched speeds, older adults (OA) exhibit significant ankle, knee, and hip sagittal plane differences at discrete gait cycle events compared to young adults (YA) [2]. While previous studies have improved the understanding of the effect of age on gait, analyzing discrete events fails to characterize the continuous sequence of movements associated with walking. Approaches such as statistical parametric mapping (SPM) that assess the entire time-normalized gait waveform may improve the identification of aging-related kinematic changes [3]. Further, most studies investigating the effect of age on walking have compared OA to YA. Few studies have evaluated age-related changes between YA and middle-aged adults (MA). This may be important because age-related kinematic changes can start in the 40s [4,5]. Thus, the purpose of this study was to utilize SPM to examine differences in lower extremity joint angles between YA and MA during walking. It was hypothesized that MA would walk with a more flexed hip and knee posture [2].

Methods: 92 healthy adult participants were recruited for the study. Participants were placed in a YA (18 - 44 y) or MA (45 - 64 y) group (Table 1). 3D lower extremity kinematics were captured using Moiré phase tracking markers (Metria Innovation Inc.) applied with Velcro to neoprene bands affixed to each participant's pelvis, thigh, shank, and shoe [6]. Following a standing calibration trial to identify additional pelvis, thigh, and shank anatomical landmarks, participants performed treadmill walking trials (1.34 m/s) in their own footwear. A MATLAB program was then used to low-pass filter (20 Hz) the data and calculate left lower extremity gait cycle joint angles. The spm1d package for 1D SPM (spm1d.stats.ttest2) was used to perform independent t-tests of the hip, knee, and ankle time series.

Table 1: Participants Demographics (mean ± 1SD)

Group	Sex (F/M)	Age (yr)	Height (m)	BMI (kg/m^2)
YA	36/33	29.6 ± 7.5	1.73 ± 0.1	23.3 ± 3.5
MA	9/14	52.9 ± 7.2	1.73 ± 0.1	23.9 ± 3.0

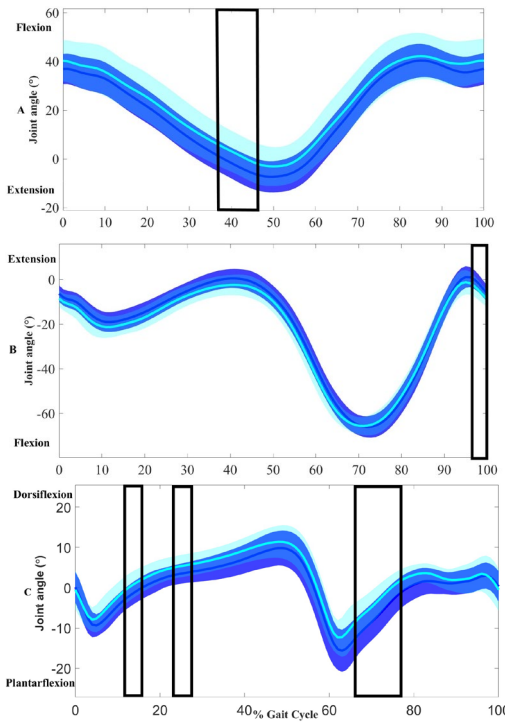

Figure 1: Hip (A), knee (B), ankle (C) sagittal plane gait cycle joint angles. Light blue: middle-aged adult (mean ± 1 SD); Dark blue: young adult (mean ± 1 SD). Boxes indicate areas of significant group differences.

Results & Discussion: As hypothesized, MA demonstrated a more flexed lower extremity posture during the gait cycle compared to YA. At the hip, MA were in significantly less hip extension from 38 - 46% (mean diff = 4.76°, p = 0.041) of the gait cycle. At the knee, MA were in significantly greater knee flexion from 99 - 100% (mean diff. = 2.64°, p = 0.04) of the gait cycle. At the ankle, MA were in less ankle plantarflexion from 12 - 14% (mean diff. = 2.18°, p = 0.04), greater dorsiflexion from 22% - 24% (mean diff. = 1.88°, p = 0.03), and less plantarflexion from 66 -79% (mean diff. = 3.48°, p = 0.001) of the gait cycle (Fig. 1). The decreased hip extension (increased hip flexion) in the MA versus the YA was consistent with the increased hip flexion in OA from previous studies [2]. The increased knee flexion in the MA versus YA at the end of terminal swing, just prior to initial contact, is also consistent with the decreased extension (increased flexion) at initial contact in previous OA [2] and MA [3] studies. The decreased ankle plantarflexion position in early midstance and increased dorsiflexion position near the middle of midstance in MA versus YA was not consistent with previous studies that have reported decreased dorsiflexion at initial contact in OA [2]. However, the decreased plantar flexion in MA versus YA during initial swing and early mid swing is consistent with the decreased plantar flexion at toe-off in OA [2].

Significance: The results of this study suggest the more flexed lower extremity posture that occurs in OA [2] is also present in MA. The more flexed posture, which is associated with increased metabolic cost [7], could contribute to the development of compensatory movement patterns, which may lead to increased fall risk, reduced physical activity, and other health comorbidities that adversely impact an individual's independence and quality of life. If this is the case, it may be important to identify and address the causes of the kinematic gait changes during an individual's middle-age years versus during older age.

Acknowledgments: National Institute on Aging of the National Institutes of Health (Award number R44AG052199).

References: [1] Rowe et al. (2021), *Gait Posture* 88; [2] Boyer et al. (2017), *Exp Gerontol* 95; [3] Kowalski et al.(2022), *Gait Posture* 95; [4] Jin et al. (2018), *Hum Mov Sci* 58; [5] Chien et al. (2015), *J Phys Act Nutr Rehabil* ;[6] Weinhandl et al. (2010) , *J Biomech* 43; [7] Carey et al.(2005), *J Hum Evol* 48.

HEALTHY AGING ACCENTUATES THE COLLECTIVE DYNAMICS OF POSTURAL CONTROL

Mahsa Barfi[1], Brian Schlattmann[1], Aaron D. Likens[1], and Madhur Mangalam[1]
[1]Department of Biomechanics, University of Nebraska at Omaha, Omaha, NE 68182, USA
email: mbarfi@unomaha.edu

Introduction. While convenient conclusions have been drawn regarding loss of the fractal temporal structure due to aging and various pathophysiologies, a perturbed healthy posture may occasionally resemble a systematically diseased posture. On the other hand, a so-called "disease" postural control system may reflect adaptations. The fractal temporal structure of postural sway variability is known to be influenced by task-related factors, such as static vs. dynamic stances, and the attentional state. However, it is imperative not to mix postural responses that may be entirely adaptive in the short term with enduring group differences. To address this concern, we analyzed the causal relationship between postural center of pressure (CoP) and center of mass (CoM) in healthy young and older adults beyond the currently dominant "less is bad, good is more" perspective concerning the fractal temporal correlations observed in CoP fluctuations.

Methods. Ground reaction forces and kinematic data was collected on healthy young (N = 27) and older adults (N = 22) in four different postural conditions: (I) rigid surface, eyes open; (II) rigid surface, eyes closed; (III) foam surface, eyes open; (IV) foam surface, eyes closed [1]. We employed the multiscale regression analysis [2] to identify the causal influence of CoP on CoM and CoM on CoP across multiple timescales of activity, ranging from 100 to 1000 milliseconds.

Results & Discussion. We found a notable absence of causal influence from the CoP and CoM (**Fig. 1**). Instead, we consistently observed a significant influence of CoM on CoP in both young and older adults. This unexpected result challenges previous assumptions about the directionality of influence between these two key variables in postural control. It suggests a primary role of the CoM in driving postural adjustments, with the CoP responding to these movements rather than exerting a causal influence itself. Older adults exhibited a stronger causal influence of the CoM on the CoP than their younger, healthier counterparts. This influence was particularly evident within shorter to medium timescales of activity, indicating a heightened sensitivity to postural control dynamics among the elderly. Our findings have also revealed that this relationship between CoP and CoM becomes significantly amplified in challenging task conditions characterized by the absence of vision or destabilizing perturbations. The impact of these task constraints was more pronounced among older adults than their younger counterparts, highlighting an adaptation mechanism in the aging population not captured by simply quantifying the strength of fractal temporal correlations in CoP or CoM fluctuations by evident in the causal coupling (i.e., the collective dynamics) of postural control.

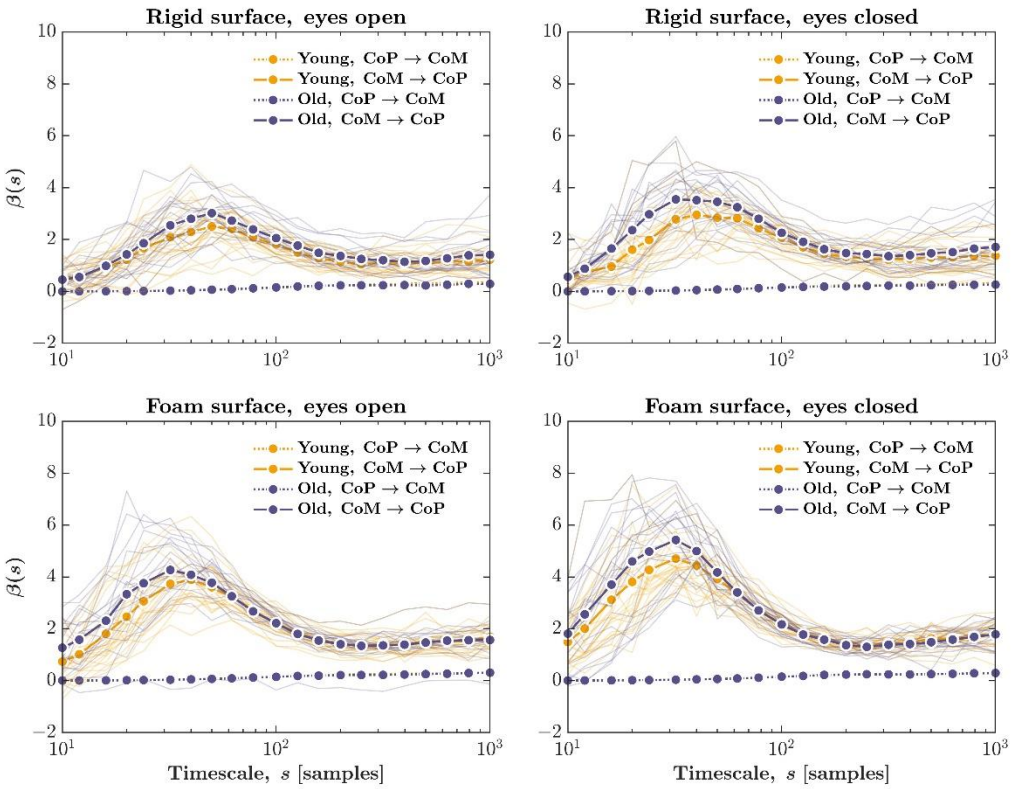

Figure 1. Multiscale regression analysis revealed strong causal influence of CoM on CoP—and an absence of causal influence of CoP on CoM—across short to medium timescales (i.e., < 100 samples or < 1 second) in both healthy young and old adults which accentuated with postural task demands. Dashed and solid lines represent the causal relationship from CoP to CoM and CoM to CoP, respectively. Circles indicate group means (young: N = 27; old: N = 22), while thin traces indicate individual participants.

Significance. The present findings highlight the pivotal role of the CoM in driving postural adjustments, with the CoP responsive to these movements rather than exerting a causal influence itself. These findings offer crucial insights into the nuanced dynamics of postural control across age groups and emphasize the necessity of considering task constraints in assessing and managing balance and mobility, notably in older adults.

Acknowledgments. This work was supported by the NIH award P20GM10909.

References. [1] dos Santos et al. (2017), *PeerJ* 5, e3626. [2] Likens et al. (2019), *Physica A* 532, 121580.

High-Density Surface Electromyography to Monitor Neuromuscular Activity Across Joints Affected by Common Musculoskeletal Pathologies

Maggie M. Wagner[1*], Flavia Vitale[1], and Josh R. Baxter[2]
[1]Department of Bioengineering, University of Pennsylvania, Philadelphia, PA, US
[2]Department of Orthopaedic Surgery, University of Pennsylvania, PA, US
*Email: magwag@seas.upenn.edu

Introduction: Muscle neuromechanics govern the complex network of motor units that control everyday movements. These complex control mechanisms are often compromised following injury, immobilization, and treatment – complicating return to sport and activity [1]. Researchers and clinicians use traditional surface electromyography (sEMG) to quantify muscle activity during functional tasks. However, sEMG only provides a localized approximation of neuromechanics. Our group is addressing this unmet clinical need by designing and fabricating customizable high-density surface electromyography (HDsEMG) using a carbon-based nanomaterial, $Ti_3C_2T_x$ MXene – which we call "MXtrodes." Our earlier validation work found that MXtrodes have comparable or better electrical properties to traditional metal electrodes, including a higher signal-to-noise ratio without conductive gels [2]. In this study, we implement MXtrodes across two muscle groups affected by common musculoskeletal injuries: 1) the plantar flexors that are impacted by Achilles tendon pathology and 2) the shoulder muscles that are impacted by rotator cuff injuries. We integrated MXtrodes into our custom-developed data acquisition tool that uses a wireless EMG processor to facilitate unimpeded movement from subjects.

Methods: We fabricated sets of four MXtrodes, consisting of two 20-electrode and two 12-electrode arrays, for a total of 64 electrodes per set (Fig. 1A). We fabricated these MXtrodes by saturating a laser-patterned absorbent substrate with conductive MXene ink and then insulated the resultant electrodes in a silicone polymer. We studied the plantar flexors and shoulder muscles to demonstrate MXtrode utility across two commonly studied joints. Plantar flexors. We measured bilateral plantar flexor function using pairs of 20-electrode arrays on each gastrocnemius and pairs of 12-electrode arrays on each soleus in two healthy controls. These subjects performed maximum voluntary isometric contractions on a dynamometer (Biodex, System 4) and a series of heel raises with their toes pointed inward, outward, and neutral. Shoulder. We measured bilateral infraspinatus function using 20-electrode arrays and deltoid function using 12-electrode arrays in one healthy control and three individuals with rotator cuff pathology. These subjects completed a series of functional exercises, including loaded and unloaded reaching exercises. We recorded their muscle activation using a wireless EMG processor (Ripple Neuromed, Explorer Summit) that permitted free movement and synchronized recordings from the dynamometer and MXtrodes using our custom data acquisition tool. We filtered the collected EMG data using a 20-450 Hz bandpass 2nd order Butterworth filter, calculated the root-mean-square potential for each electrode, and visualized the HDsEMG signals using color heat maps (Fig. 1B).

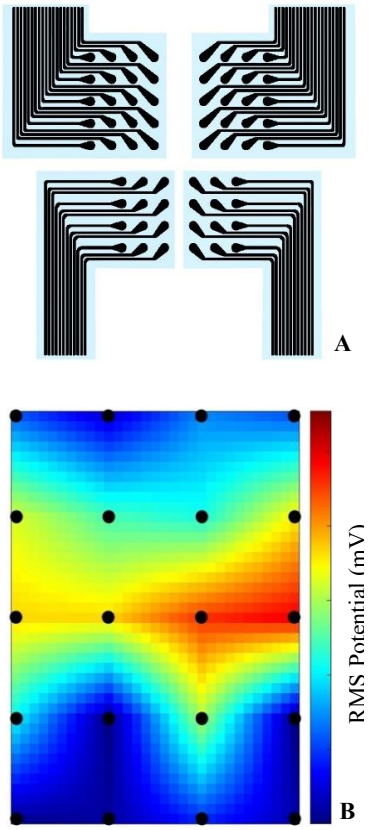

Figure 1. HDsEMG array design (A) and example muscle activation heat map (B). Each black dot on the heat map represents an electrode, with the recorded potential interpolated between the dots.

Results and Discussion: Plantar flexor and shoulder muscle activation differed depending on activity. Plantar flexors. We found that gastrocnemius muscle activity increased during neutral heel raises, which involves an extended knee that increases gastrocnemius engagement. Shoulder. We found that infraspinatus muscle activity decreased and shifted towards the trapezius in participants with shoulder cuff pathology. These findings demonstrate the utility of HDsEMG because detecting regional changes in muscle activity is less likely with a single EMG sensor or a low-density electrode grid. Our HDsEMG system incorporates high-density electrode arrays that we custom design and fabricate based on the muscle, a wireless data logging system to facilitate unencumbered movement, and a custom-written data acquisition interface that provides real-time access to HDsEMG signals and other lab equipment, including dynamometers and constant current stimulators, to control experimental conditions. Our ongoing work is identifying activation patterns during rehabilitation exercises to develop personalized strategies to rehabilitate specific muscles in orthopaedic populations. By controlling for changes in muscle activation through HDsEMG during rehabilitation, we expect to mitigate suboptimal outcomes associated with altered muscle neuromechanics.

Significance: Through our MXtrode data acquisition platform, we aim to identify patterns of muscle activity during rehabilitative exercises and changes in muscle activation throughout healing from musculoskeletal pathologies. By better understanding the underlying mechanisms that affect patients' functional outcomes, we could better inform and guide rehabilitation and potentially improve their functional outcomes following rehabilitation.

Acknowledgements: Supported by NIH (R01AR081062, P50AR080581) and NSF Graduate Research Fellowship (DGE-2236662)

References: [1] J. T. Hopkins and C. D. Ingersoll, *J. Sport Rehabil.*, 9(2):135, 2000; [2] R. Garg et al., *Small Methods*, 2201318, 2022

Sharpening balance assessments to detect reduced balance capacities.

Christopher P Hurt[1*], Emily Jenkins[2], Karina Martinez-Vargas[2], Seth Shelton[2], Alyson Moll[1]
[1] Rehabilitation Science [2] Physical Therapy, University of Alabama at Birmingham
*Corresponding author's email: cphurt@uab.edu

Introduction: Parkinson's disease (PD) is a neurodegenerative disorder of the basal ganglia resulting in a loss of dopamine producing neurons in the brain. By the time individuals with Parkinsons begin to experience motor symptoms, 60% of dopamine producing neurons in the brain are lost [1] and a continued neuronal loss will eventually manifest in gait and postural instability, about 5-10 years after diagnosis [2]. This directly impacts individuals' ability to regain balance following postural disturbances [3]. Early intervention is important however traditionally individuals with PD will seek out physical therapy after a significant amount of function is already lost or they have fallen multiple times [4]. Further, traditional clinical tests require a significant loss in function before triggering the need for a physical therapist. For example, using the MiniBest Test, a commonly used test of balance and gait function in PD, a 43% reduction from the maximum score relates to increased fall risk [5]. Thus, there is a critical gap to identify a test that can differentiate the balance capacity of individuals prior to their development of balance dysfunction. The purpose of our study is to determine if a scaled static balance task can differentiate between individuals with PD compared to an age similar control group.

Methods: We recruited 10 healthy controls over the age of 65 and 9 individuals with PD ranging from 63-79 years old who came to the lab in their optimally medicated state for this institutionally approved study. We collected the following tests of mobility: 1) 10m walk test to assess overground comfortable (CWS) and maximum walking speed (MWS), 2) 10m backward walk speed test (BWS), 3) Timed up and go, as well as the TUG dual task which asks individuals to perform the test while completing a cognitive task (counting backwards by threes) [6]. Individuals also completed the Mini Balance Evaluation Systems Test (mini-BESTest) [6]. Fall history in the past year was also obtained. In addition to mobility tests, participants performed four static feet-in-place tasks of graded difficulty:1) standing with-feet at hip width with eyes open; 2) standing with feet together eyes open; 3) standing semi-tandem with eyes open and 4) standing tandem stance eyes open. All tasks were performed standing barefoot on a force plate flush with the laboratory floor. For all tasks, individuals stood quietly while fixating their gaze to a spot on the wall directly in front of them. Standardized feet positions were used for each task over all trials. Task failure was a step taken prior to the trial's completion (i.e., 60 seconds) for any given trial of the task. Task success task completion on all trials without a step. For these balance tasks, we quantified sway area, which defines an area that includes 95% of all the center of pressure data. We assessed data by group, by fall status and by success in completing all the balance conditions. Two-sample t-tests were used to compare each group's data. Statistical significance was p-value <0.05.

Results & Discussion: No statistically significant differences were detected between groups (e.g., PD and controls) for the quiet stance sway area, feet together sway area, and semi-tandem sway area. (p value >0.05 for all comparisons). Next, we dichotomized groups based on whether individuals reported a single fall in the past year. Within the sample, 8 individuals identified as fallers while 11 were non-fallers. Data differentiated by fall status also did not reveal group differences for the quiet stance sway area, feet together sway area, and semi-tandem sway area ($p>0.05$ for all comparisons). Finally, we divided groups based on their ability to hold the most challenging static posture position, tandem (completers n=10, and non-completers n=9). When dichotomizing groups based on tandem task completion, we begin to see significant differences between groups. Sway area increased, for those not able to hold tandem stance, for feet together ($p=0.01$) and semi tandem postures ($p=0.04$) but not for quiet stance $p=0.28$. We then compared the other assessments of gait and balance function (comfortable walk speed (CWS) max walk speed (MWS), backward walking speed (BWS), TUG and Dual TUG, Mini Best Test) to see if tandem stance performance could be indicative of gait function and balance loss. MWS and Mini Best scores both showed statistically significant differences between groups. Completers' average MWS was 1.65 m/s (SD= 0.2) while non-Completers averaged 1.32 (SD= 0.28) and a p-value = 0.01. For the Mini Best, completers averaged 24.5 (SD=1.43) while non-completers averaged 21.13 (SD= 4.09) and the p-value was 0.03. Our data suggests that disease classification and fall status did not differentiate groups. This may be a surprise however because balance dysfunction is complex and the effect of PD on balance is variable. Previous studies looking at falls show that falls are difficult to predict and using this as a post hoc method to differentiate groups may not be as useful to predict the onset of balance dysfunction [6]. Tandem stance was the most challenging within our battery of tests so it is reasonable that individuals who may be developing balance dysfunction would fail at task completion but be able to perform the other tasks because the nervous system is able to compensate to complete the simpler tasks.

Significance: These results suggest that detecting balance dysfunction benefits from using challenging tasks that elicit a "maximal" performance where task failure is a possible outcome. We only observed differences in functional ability and balance when dichotomizing data based on the successful completion or incompletion of a very challenging balance task. Prospective collections are an important follow-up.

References: [1] Fearnley JM, Lees AJ. (1991) *Brain* 114 [1] Fasano et al. (2015), *Nat Review Neurology* 11(2); [2] Yaksi E et al. (2013), *Arq Neuropsiquiatr 80*(9).[3] King LA, Horak FB. (2009) *Phy Ther* 89(4); [4] Leddy et al. (2011) *J Neuro Phys Ther* 35 (2); [5] King LA et al. (2012) *Parkinsons Dis* 2012:375419 [6] Rosenblatt et al. (2013) *JAGS* 61(9).

CALCULATING THE CONTINUOUS RELATIVE PHASE OF ROCK CLIMBERS CONTRALATERAL MOVEMENTS

Jeromy D. Miramontes*, Steven Leigh, Suzanne Konz, and Robert Powell
Biomechanics, School of Kinesiology, Marshall University, Huntington, WV, USA
*Corresponding author's email: miramontes1@marshall.edu

Introduction: Continuous Relative Phase (CRP) is a higher-order measure of coordination used to display the phase plane dynamics of two connected segments or joints, and their relationship between limb synergy using joint or limb angles [1]. CRP is preferred over Discrete Relative Phase and Relative Fourier Phase, because of the ability to define a specific start and end point for a motion that is cyclical in nature [1]. Rock-climbing is a quadrupedal movement that is cyclical in nature [2], but provides the freedom of the individual to contemplate a route [3], imply a coordinative stylistic approach [4], and adapt the selected approach to unrealized constraints of the movement workspace [5]. MATLAB® is a commonly used program in the field of biomechanics with capabilities to compute complex kinematic and kinetic variables. The purpose of this study was to create MATLAB® code to calculate and compare relative joint angles as participants ascended a rock-climbing route. CRP angles were compared among subjects to investigate how climbers vary coordination strategies to complete a bouldering move.

Methods: Nineteen experienced climbers' data were used in this study (29 ± 7 years old, 7 ± 7 years of experience, 1.76m ± 0.08 m). Following a two-minute viewing period, the participants climbed a boulder problem that increased in difficulty as many times as they could in four minutes. One standardized move within the problem was selected as the climbing movement of interest and the start and end of that move was identified. Inertial measurement units (IMUs) (Ultium, Noraxon, Scottsdale, AZ) were placed on the participants' trunk, right arm, and left leg to record joint kinematics throughout the climbing movement of interest. We wrote MATLAB® code to calculate CRP of contralateral joint angles in three dimensions. We filtered raw data using a low pass Butterworth filter to reduce noise. We calculated angular kinematics for each joint as the relative difference between the IMUs on the limb segments proximal and distal to the joint. These joint kinematics defined a phase space relative to human movement (Kugler et al., 1980). We normalized phase angles to the ranges of angular velocities and angular positions and resampled the phase angles to a percentage of the full movement. We calculated the interlimb relative phase angle coordination by subtracting the contralateral normalized phase angle joints (Fig. 1). The averaged root mean square (RMS) CRP of the right shoulder to left hip and RMS CRP of the right elbow to left knee were calculated and compared among three emergent climbing styles.

Figure 1: CRP Angle between the shoulder and hip for a rock-climbing movement.

Results & Discussion: The mean RMS CRP of the right shoulder to left hip was 29.3° ± 11.3° with a range of 11.0° to 48.9°. Mean RMS CRP of the right elbow to left knee was 37.9° ± 15.1° with a range of 12.7° to 58.0°. Movements of the right shoulder to left hip being mostly in-phase is an indication of joints working together to provide a more stable pivot point when compared to movements of the right elbow to left knee shoulder and hip joints may be for larger, more deliberate angular positioning, while elbow and knee being mostly in-phase are adjusted throughout the entire movement, possibly in response to other variables during movement. Floria et al. (2018) found no significant differences between trained and non-trained runners for any intralimb coupling pairs at their preferred running speeds. CRP increased as more distal segments were involved for both non-runners and runners. Rock climbing CRP values were greater than for running overall, and the distal CRP values were greater than proximal but did not show the same magnitude of change. Of the total 128 completed primary move attempts, 42 (32.81%) attempts were performed as planned (Style 1) extending off the left foot reaching with the right hand to the next hold with their right foot not in contact with the wall. Style 2 was performed 62 (48.44%) times and seemed to be the most practical using the right foot to push off of the "planned" hold allowing the hips to stay closer to the wall. Style 3 was completed 22 (17.19%) times and was similar to Style 1 but had the left foot go to a high hold instead of the low "planned" hold. Style 4 was completed 2 (1.56%) times and only by 1 participant who had the anthropometrics to reach a lower left foot hold with the right foot on the "planned" foot hold.

Significance: Our study shows that IMUs can be used with MATLAB® code to quantify human coordinative movement in a rock-climbing setting. To our knowledge there is no opensource code that can calculate CRP from inertial measurement units to understand joint coordination. Our research is the first to identify how limbs work together while in transition between two holds during a boulder attempt.

References:

[1] Van Emmerik et al. (1999), *Arch. Phys. Med. Rehabil.* 80.
[2] Zampagni et al. (2011), *Scand. J. Med. Sci. Sports. 21*(5).
[3] Sanchez et al. (2012), *Scand. J. Med. Sci. Sports. 22*(1).
[4] Fanchini et al. (2013). *J. Strength and Cond. Res. 27*(2).
[5] Seifert et al. (2013). *Sports Med. 43*(3).
[6] Kugler et al. (1980). *Adv. Psychol. 1*.

KNEE JOINT LOADING IS ASSOCIATED WITH INCREASED ARTICULAR CARTILAGE STRAIN AFTER ACLR

Timothy Lowe[1*], Emily Y. Miller[2], Danielle Dresdner[2], Hongtian Zhu[1], James Kelly[2], Corey P. Neu[1,2]
[1]University of Colorado Boulder Mechanical Engineering Department
[2]University of Colorado Boulder Biomedical Engineering Program
*Corresponding author's email: timothy.lowe@colorado.edu

Introduction: The risk of knee osteoarthritis (OA) dramatically increases after anterior cruciate ligament (ACL) reconstruction (ACLR). The initial development and progression of OA after ACL injury can be difficult to predict and detect without the use of routine imaging. Evidence of altered biomechanics has been demonstrated early after ACL injury and ACLR, and abnormal joint loading is a key mechanism that may contribute to the early development of OA. Identifying a link between joint loading and OA is a critical step in better understanding and possibly preventing early-onset knee joint OA. Cartilage remodels according to the loading environment and altered loading during gait is believed to contribute to the development of OA. Higher knee moments have been associated with the presence and severity of idiopathic knee OA in older populations. However, external knee adduction moments (KAM) have been reported to be lower in the limb at risk for OA after ACLR. KAM is widely used as an indicator of knee joint loading of the medial tibiofemoral compartment. However, reports of changes in KAM have varied with studies finding increases, decreases or no change in KAM. Therefore, knee joint medial contact forces (MCF) may provide a more comprehensive understanding of the knee's loading environment after ACL injury than do joint moments alone. DENSE MRI sequences may be used to calculate displacement and strain maps of cartilage [1], providing insight into mechanical property changes in articular cartilage. The purpose of this study was to examine associations between knee loading and strain in individuals 12 months post-ACLR.

Methods: Ten individuals with unilateral ACLR (time since surgery 12±2 months) underwent gait analysis and MRI. Kinematics were estimated from video using deep learning models and inverse kinematics in OpenSim, and dynamics were estimated using a physics-based musculoskeletal simulation approach (Figure 1A) [2]. Peak KAM and MCF were calculated during the loading phase. The knee imaging protocol consisted of 3D double echo steady state (DESS) acquisition to visualize morphology, and DENSE MRI acquisition during cyclic varus loading on the knee joint [3-5]. All DENSE images were acquired while the knee underwent a cyclic load mimicking the walking cycle provided by an exogenous loading device (Figure 1B). The articular cartilage was segmented via a semi-automatic segmentation algorithm into tibial and femoral regions of interest (ROI). Displacements were extracted and processed to derive in-plane Green Lagrange strains (Figure 1C) [1]. The spatial average (SA) of the strains within each ROI was then calculated. To provide a single measure that incorporates all three finite strains, Von Mises strains (VMS) were calculated. Individuals were classified as having clinically relevant knee symptoms if Quality of Life score <87.5, and two or more of pain <86.1, symptoms <825.7, ADL <86.8, or sports/rec <85.8 [6]. Differences were compared between symptomatic and asymptomatic individuals. Pearson correlation coefficients assessed associations between knee loading and strains.

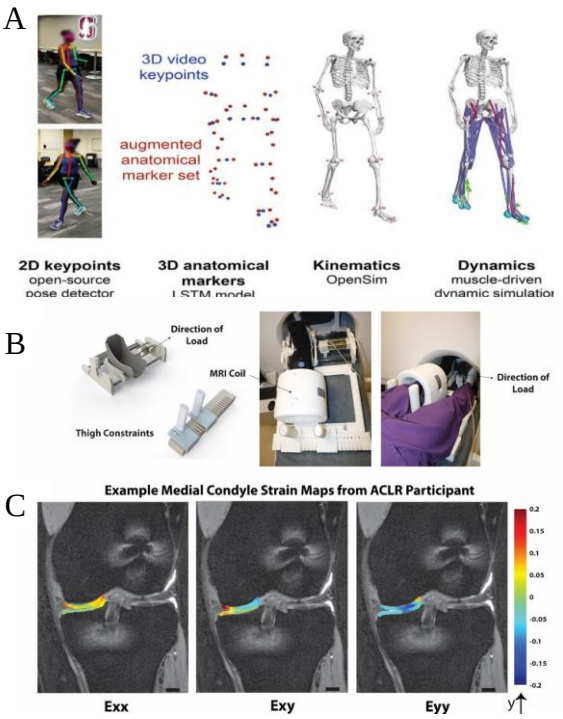

Figure 1A: OpenCap video-based motion analysis. **B.** MRI compatible loading device**. C.** Example strain maps.

Results & Discussion: Symptomatic individuals demonstrated smaller peak KAM (0.025±0.003 vs 0.04±0.004 Bw*ht, P = 0.006) and MCF (2.02±0.28 vs 3.03±0.21, P = 0.01) than the asymptomatic individuals. This suggests that symptomatic individual's underload the medial compartment during gait. Significant positive correlations were observed between MCF and femoral cartilage Exx (R=0.72, P=0.001), Eyy (R=0.57, P<0.001), and Exy (R=0.5, P=0.001), indicating that as MCF increased, transverse, axial and shear strains increased. VMS provided an efficient method to combine the transverse, axial, and shear strains into a single measure and a positive association was observe between MCF and VMS (R=0.57, P<0.001). Positive correlations were observed between KAM and femoral cartilage Eyy (R=0.44, P<0.001) and VMS (R=0.73, P=0.011). There were also significant positive correlations between MCF and tibial cartilage Exx (R=0.66, P<0.001), Eyy (R=0.8, P<0.001), and Exy (R0.85, P<0.001), indicating that as MCF increased transverse, axial and shear strains increased in the tibial cartilage as well. MCF also had a positive correlation with tibial VMS (R=0.78, P<0.001). There were no correlations between KAM and any tibial cartilage strains. Finally, similar to previous reports, we observed a strong positive correlation between KAM and MCF (R=0.97, P=0.001). Therefore, it may be possible to modulate MCF through altering KAM.

Significance: Early unloading of the knee may cause cartilage softening which results in increased knee loading later. Interventions targeted at increased knee loading early, such as gait retraining, in symptomatic individuals may help reduce cartilage degeneration.

Acknowledgments: This work was supported by NIH grant 2 R01 AR063712.

References: [1]. Chan D. et al., Sci. Rep. 2016. [2] Uhlrich et al., PLoS Comput Biol. 2023 [3] Lee W. et al., MRM, 2023. [4] Lee W. et al., MRM, 2023. [5]. Zhu H. et al., SSRN 4569548 [6] Englund et al., Arthritis Rheum, 2003.

MUSCULOSKELETAL MODEL OF CHANGES IN BALANCE STRATEGY WITH INCREASES IN AGE-RELATED DELAY OF CENTER OF MASS FEEDBACK

Rachel F. Jones[1], Neethan Ratnakumar[1], Kübra Akbaş[1], Xianlian Zhou[1*]
[1]Departmant of Bioengineering, New Jersey Institute of Technology, Newark, NJ, USA
*Corresponding author's email: alexzhou@njit.edu

Introduction: One of the leading causes of non-disease death and injury in the elderly is falls [1]. The elderly are more prone to falls due to the delayed sensory neural feedback, which is essential for balance [2]. Directly measuring or manipulating this delay can be difficult to accomplish, thereby making neuromusculoskeletal modeling the ideal way to explore the relationship between sensory neural feedback delay and balance control. To prevent falls, the nervous and musculoskeletal systems constantly communicate to dynamically fine tune the body's posture and keep the center of mass (COM) within the base of support. In the lower limbs, balance is maintained by flexing joints to shift the COM back towards the center of the base of support, and the specific joints involved will determine the balance strategy used. Thus, incorporating these feedback mechanisms into the framework of the neuromusculoskeletal model is imperative for accurately simulating human balance dynamics. In this study, we focus on examining how variations in the length of sensory neural feedback for COM influence the choice of balance strategy utilized.

Methods: This study used an adapted 2D musculoskeletal model available in OpenSim with 9 DOFs and 18 Millard-type muscles, all with actuation only on the sagittal plane [3]. A moving platform that translated in the anterior-posterior direction was added to model, and the contact between the feet and the platform were modeled as Hunt-Crossley contact forces [4]. To simulate the neuro-muscular feedback relationship, the model's balance was controlled by a three-way feedback control approach, using the following feedback controllers: muscle length, muscle force, and COM (Fig. 1). The COM feedback controller was adjustable for three delay lengths: 100 ms (fast/healthy), 150 ms (slow/aging/slightly delayed), and 200 ms (slowest/severely delayed). The platform moved at a frequency of 1 Hz at 10 magnitudes: 0, 2, 4, 6, 8, 10, 20, 40, 60, 80 mm. A 10-second simulation was conducted at each COM feedback delay length (100, 150, and 200 ms). All simulations were performed in SCONE, which uses Covariance Matrix Adaptation Evolution Strategy to optimize model parameters [5]. The balance strategy was calculated by finding the Pearson's Correlation Coefficient of the moments of adjacent joints at each time step of the simulation, and the sign of the coefficients determine which strategy is used [6].

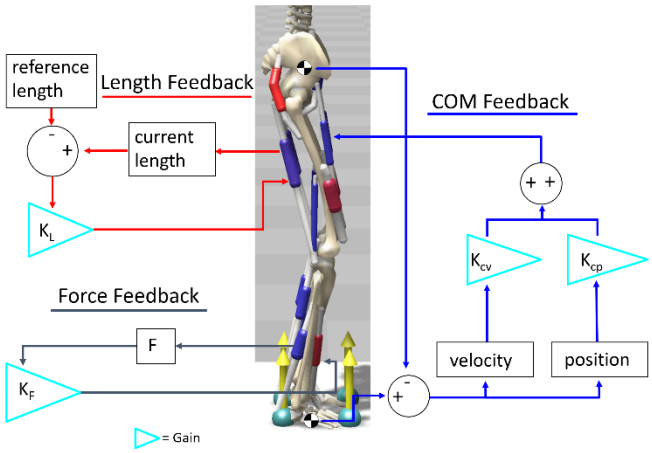

Figure 1: The three-way feedback control approach used to balance the model. Length and force feedback mimic sensory feedback in the muscles, while COM feedback reacts to the position and velocity of the body and foot COM.

Results & Discussion: The human body employs the intricate coordination of the hip, knee, and ankle joints to shift body weight, thereby regulating the COM position. Often, the moments and angles of these joints are analyzed and how they relate to each other to determine balance strategy. To maintain balance, ankle strategy is typically used for fine adjustments in response to mild perturbations, whereas more severe perturbations necessitate the engagement of the knee to hip strategy for larger corrective actions. This pattern is reflected in our results, where the ankle strategy was used in the overwhelming majority (94%) of simulations below 20 mm perturbation; however, a different pattern emerges when considering the balance strategy by delay condition. Results of the balance strategy analysis showed that the ankle strategy was used most (53%), but not by an overwhelming amount with knee and hip being used 22% and 14% of the time respectively. When comparing the healthy delay with slower delays, the ankle strategy was used more in both slow conditions – 47% versus 51% and 61%. This finding reflects observations in literature, where elderly subjects were found to use ankle strategy more than young subjects [7]. In future research, factors such as speed, direction, and the anticipation of perturbations should also be explored to comprehensively understand the interplay of these elements in shaping balance strategy.

Significance: Longer COM feedback delays led to noticeable shifts in balance strategies used in perturbed standing. The heavier reliance on ankle strategy for slower delays – which model the elderly population – are concerning as ankle strategy may not be enough to stabilize an individual in response to larger perturbances. This knowledge of potential inclination toward ankle strategy can inform balance training for elderly individuals. Further, the modeled feedback delay used in this study could be used in future studies to further research on aging and balance through accurate, simple models that reflect human experimental data. The controllers developed in this study will be useful for future experimentation with balance models by providing an in-silico framework for COM feedback. Furthermore, this controller has been shown to work well alongside length feedback and reflex feedback controllers developed in previous studies, allowing the COM feedback controller to be used in combinations with other controllers.

References: [1] Rubenstein. (2006), *Ageing* 35(Suppl 2); [2] Hsu et al. (2013), *Age* 35; [3] Delp et al. (2007), *IEEE Trans Biomed* 54; [4] Hunt et al (1975), *J Appl Biomech* 42; [5] Geijtenbeek (2019), *J Open Source Softw* 4; [6] Blenkinsop et al (2017), *R Soc Open Sci* 4; [7] Gurses et al (2011), *Biomed Signal Process Control* 6.

VALIDITY AND RELIABILITY OF ESTIMATION OF ORBITAL STABILITY OF HUMAN GAIT

Jeongin Moon[1], Jooeun Ahn[1, 2] *
[1]Department of Physical Education, Seoul National University, Seoul, Republic of Korea
[2]Institute of Sport Science, Seoul National University, Seoul, Republic of Korea
*Corresponding author's email: ahnjooeun@snu.ac.kr

Introduction: Assessing the stability of human gait is important in numerous fields including rehabilitation, biomechanics and neuroscience. One popular metric of the gait stability is Floquet multiplier (FM), which quantifies how rapidly a perturbed gait converges to a limit cycle [1]. However, given the diversity in human gait strategies and the inherent noise in data, the estimation of FM is likely to be biased, heavily influenced by the specific conditions under which data are collected. Despite the critical role of data sampling condition in minimizing bias and variance in FM estimates, a standard protocol or guideline on data collection is absent. Prior research highlights the effects of data length on mitigating noise-related bias [2] and the importance of multiple measurements in enhancing consistency in FM estimation [3]. However, the optimal data sampling criteria for FM estimation still remain undefined. We aim to address this gap by assessing the validity and reliability of FM estimation under a broad range of sampling conditions.

Methods: The state was defined by a vector consisting of 14 joint angles (6 hip, 2 knee, 6 ankle) at the heel strike of the left leg. The error of each kinematic state was defined as the deviation from the mean kinematic state. The least squares method was utilized to define the Jacobian matrix that estimates linear tendency of error dissipation between successive strides. Among the eigenvalues of the Jacobian matrix, the one with the maximum magnitude (max FM) serves as a measure of orbital stability.

Twenty young and healthy adults participated in the study. All participants walked for 10 minutes at 1.2 m/s on a treadmill five times. The participants' gait kinematics were recorded using a motion capture system (Qualysis) with lower-body marker sets (Rizzoli), and then joint angles were calculated using an inverse kinematics tool (Visual 3D).

Twenty representative Jacobian matrices were extracted from the experimental data (one from each individual). The representative Jacobian matrix for each individual was determined as the one whose max FM was closest to the personal average of five trials. For mathematical simulation, we used a Gaussian linear model; we created 1000 discrete time series of 500 data points for each participant. From the data with artificially added noise, FM was re-estimated for each participant with various data lengths (≤500) and numbers of measurements (≤10). Under each condition, the estimation was repeated 100 times and averaged for regularization. We performed a repeated measures two-way ANOVA to assess the effects of the data length and number of measurements. The validity and reliability of FM estimation for each data collection condition were additionally evaluated by the correlation analysis and the intraclass correlation (ICC2), respectively.

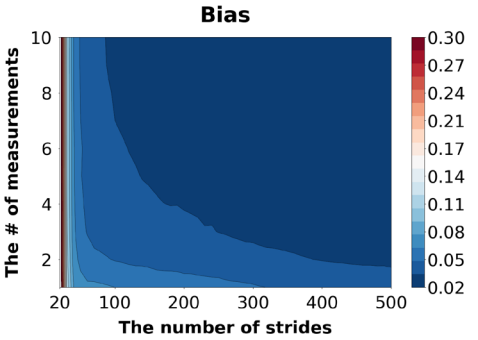

Figure 1: The mean discrepancy between true and estimated FM for 20 participants was evaluated for various sampling conditions.

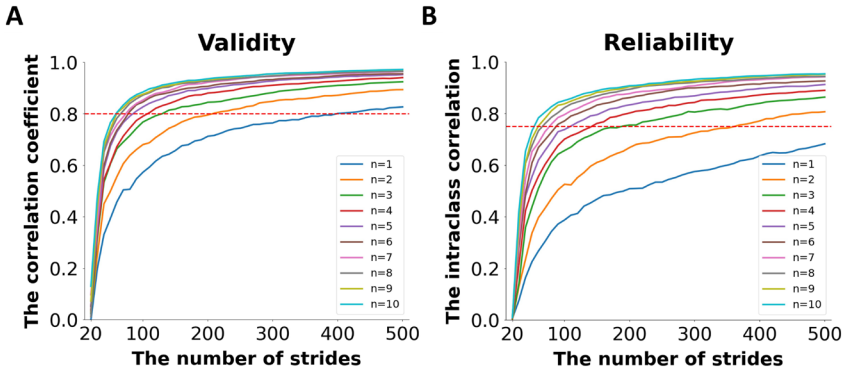

Figure 2: The average correlation coefficients between true and estimated FM (A) and intraclass correlations (B) for 20 participants were calculated in accordance with the specified data sampling condition (n=number of measurements). The thresholds for very strong and excellent agreement are shown by red dotted lines, respectively.

Results & Discussion: Both the length of time series and the number of measurements affected FM estimation with significant interaction ($F[6.791, 129.024]=13.009$, $p<0.001$, Figure 1). The required number of strides for the correlation coefficient to be over 0.8 was 400, 190, 140, 110, and 90 strides when the number of measurements was 1, 2, 3, 4 and 5, respectively (Figure 2 A). The minimum number of strides required for the intraclass correlation of each trial condition to be greater than 0.75 was 370, 190, 150, and 110 strides when the number of measurements was 2, 3, 4, and 5, respectively (Figure 2 B).

Significance: We evaluated the validity and reliability of FM estimation depending on data sampling conditions. The discovered effects of the data length and number of repetitions on FM estimation and their interaction underscore the importance of selecting appropriate sampling conditions. These findings will contribute to establishing proper experimental guidelines for assessing human gait stability.

Acknowledgments: This work was supported in part by the Korea Health Technology R&D Project through the Korea Health Industry Development Institute (KHIDI) funded by the Ministry of Health & Welfare (No. HK23C0071), Industrial Strategic Technology (No. 20018157) and Industrial Technology Innovation Program (No. 20007058, Development of safe and comfortable human augmentation hybrid robot suit) funded by the Ministry of Trade, Industry & Energy (MOTIE, Korea), and the National Research Foundation of Korea (NRF) grants funded by the Korean Government (MSIT) (No. RS-2023-00208052).

References: [1] Hurmuzlu et al. (1994), J Biomech Eng; [2] Ahn et al. (2016), *PLoS One*; [3] Lee et al. (2020), *J NeuroEngineering Rehabil*.

EXPLORING THE RELATIONSHIP BETWEEN PAIN AND BIOMECHANICAL ADAPTATIONS IN INDIVIDUALS EXPERIENCING PATELLOFEMORAL PAIN SYNDROME

Ross J. Brancati[1*], Katherine A. Boyer[1]
[1]Department of Kinesiology, University of Massachusetts, Amherst, MA
*Corresponding author's email: rbrancati@umass.edu

Introduction: Patellofemoral pain (PFP) is one of the most common injuries experienced by individuals who participate in running related activities with an estimated prevalence of ~23% in adults [1, 2]. Elevated patellofemoral joint stress, the mechanism of PFP, is associated with several biomechanical factors including altered kinematics and kinetics at the hip, knee, and ankle joints [3]. Yet, there is a lack of consensus in cross-sectional studies investigating biomechanical alterations displayed by those experiencing PFP compared to healthy controls, suggesting potential subgroups within the PFP population [4, 5]. Recent research has successfully identified such subgroups while considering biomechanical variables in a rested state [6-8]. However, a unique characteristic of the PFP population is that many individuals report little to mild pain at the beginning of activity and tend to report increased pain during and after activity [9].

Exploring biomechanical features that predict onset of pain or that change over a prolonged run designed to elicit pain may be useful for identifying and characterizing subgroups. Therefore, the goal of this study was first to quantify the differences in biomechanical outcomes previously highlighted in the literature between PFP and healthy active adults, and then to determine the impact of a prolonged run on those kinematic and kinetic variables. It was hypothesized that such key biomechanical factors would differ between PFP and healthy controls before the run. Additionally, it was hypothesized that these same variables would change after a prolonged running bout within the PFP group, indicating a relationship with pain.

Methods: Seven individuals with symptomatic for PFP (4F, 28.8±7.5 yrs, 1.7±0.1 m, 73.5±11.4 kg, baseline pain: 1.0±1.5) and ten healthy individuals (5F, 24.3±6.5 yrs, 1.7±0.7 m, 69.9±8.34 kg) were recruited for this study. All participants performed overground running trials at their self-selected running pace while 10 motion capture cameras (Qualisys, Sweeden) recorded marker trajectories and a force plate (AMTI, MA, USA) recorded ground reaction forces. Following the overground running trials, the PFP group completed a 21-minute treadmill run (TMR), and verbally self-reported their symptomatic limb knee pain on a scale of zero to ten where zero was descried as *no pain at all* and ten was described as *the worst pain imaginable*. Immediately following the treadmill run, this group repeated the same overground running trials.

Joint kinematics and internal joint moments were calculated in Visual 3D (C-Motion, MD, USA). Kinematic variables including peak hip adduction, hip internal rotation, rear foot eversion, knee adduction, knee flexion, and knee internal rotation angles, and kinetic variables including peak hip extension, knee extension, knee abduction, and ankle plantarflexion moments were computed using python (Python Software Foundation). T-tests were used to test for differences between the healthy and PFP groups before the TMR. Paired sample t-tests were used to test for differences from before to after the TMR within the PFP group. Additionally, percent changes and Cohen's *d* effect sizes (ES) were calculated in the PFP group from before to after the TMR.

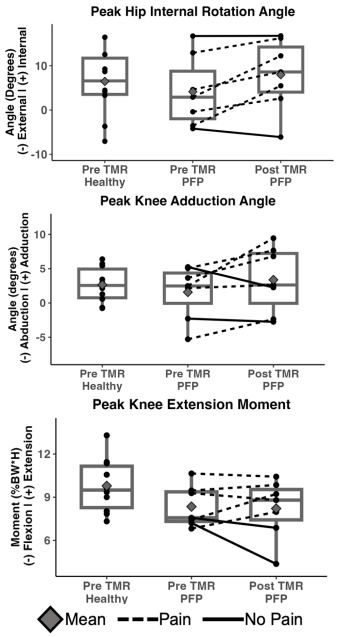

Figure 1: Distributions of peak hip rotation and knee adduction angles and peak knee extension moment. Dotted and solid lines represent changes with the TMR in the PFP group for those that did and did not report pain, respectively.

Results & Discussion: Five of the seven PFP participants reported a change in pain over the TMR, while two reported no pain (baseline pain: 1.0±1.5, pain following run: 3.3±3.1). There were no significant differences in kinematics or kinetics between the healthy and PFP group before the treadmill run. A significant increase in peak hip internal rotation angle was found with the TMR (Fig 1. p=0.05, ES: 0.43). Although not statistically significant, there was also a 114% increase in peak knee adduction angle with the TMR (Fig 1. p=0.18, ES: 0.36). Greater hip internal rotation and knee adduction angles have been identified as risk factors for PFP, and in agreement with prior work, these results suggest a link between movement patterns and pain symptoms. Although other kinematic and kinetic variables showed less than a 10% change from before to after the TMR and were not statistically significant, this may be due to a variable pain response to the TMR. The peak internal knee extension moment increased in those reporting pain, but tended to decrease in those who did not report pain, suggesting that biomechanical adaptations may be driven by or drive pain response.

Significance: Investigating biomechanical factors that predict onset of pain or change following a prolonged run could be important for identifying subgroups within the PFP population. Biomechanical variables that are sensitive to pain flares were identified with the TMR, potentially improving understanding of patient specific pain mechanisms, and contributing to targeted treatment plans in PFP.

References: [1] Willy et al. (2019), *J Ortho Sports PT* 49(9); [2] Smith et al. (2018), *PLoS ONE* 12(1); [3] Powers et al. (2017), *Br J Sports Med* 51(24); [4] Witvrouw et al. (2013), *Br J Sports Med* 48(6); [5] Bazett-Jones et al. (2022), *Sports Med*; [6] Selfe et al. (2016), *Br J Sports Med* 50(14); [7] Drew et al. (2019), *J Ortho Sports PT* 49(7); [8] Watari et al. (2018), *BMC Msk Disord* 19(1); [9] Bazett-Jones et al. (2013), *Med Sci Sport Exerc* 45(7);

Validation of a Wireless Device-Driven Method of Estimating Caloric Expenditure during Running

Matthew Moriarty[1], Austin Cronen[2], Kristen Renner[2]
[1]Department of Physiology, University of Arizona, Tucson, AZ, USA
[2]University of Arizona College of Medicine – Phoenix, Phoenix, AZ, USA
*Corresponding author's email: kristenrenner@arizona.edu

Introduction: Measuring caloric expenditure during activities such as running has applications in both the athletic and clinical spaces. Breath-by-breath respirometry is the most commonly used method to measure caloric expenditure. This study uses the COSMED and VO2 Master, each of which have their own set of limitations. The COSMED Quark CPET has a setup cost exceeding $30,000, is not portable, and uses a mask that can be uncomfortable due to the physical connection between the runner's mask and the CPET. The VO2 Master addresses some of these limitations with a setup cost of only $6,000 and the ability to datalog onto the face mask with improved portability. But the setup is still uncomfortable for many athletes and financially out of reach for many groups. Consumer available wearable smartwatches often provide an estimate of caloric expenditure, but they have been shown to have an error rate ranging from 27 to 93% depending on brand and athlete [1].

In 2021, researchers developed a novel Wearable System that estimates metabolic energy expenditure and has a cumulative error of 13% across common activities [1]. This is a substantial improvement compared to even the lower end of the error rate range of consumer wearable devices. The setup is comprised of a microcontroller worn on a belt as well as two IMUs placed on the thigh and shank of one leg. Unlike some alternatives, it does not necessitate a mask, yet it is somewhat bulky and includes external wires that may impact performance during specific activities. The Wearable System requires self-assembly, some coding knowledge and costs approximately $140. The battery offers a run time exceeding 7 hours on a single charge, showing significant enhancements over prior systems. However, there is a need to develop a wireless, lightweight system that has the capacity to store data locally for longer sessions. Therefore, the purpose of this study is validate a new device-driven system that is wireless, lightweight and capable of data logging.

Methods: Six healthy, adult male participants were recruited for the study. Participants had to be injury free and able to run for 15 minutes with no pain and complete at least 150 minutes of physical activity per week. Participants were fitted with either a COSMED (n=3) or VO2 Master (n=3) system to provide the "true" value for energy expenditure. The VO2 Master was validated against the COSMED [2]. Both systems were calibrated according to manufacturer guidelines. All participants were then outfitted with the device-driven system. Two IMUs (MMS) were placed laterally on the left shank and thigh mid-segment. The IMUs collected continuous triaxial accelerometry (200 Hz ±16Gs) and gyroscope (200 Hz, 2000 º/s) data. All data was logged to the devices and then downloaded via Bluetooth.

Simultaneous data was collected for the IMUs and respirometry system during a submaximal exercise protocol completed on an indoor treadmill. Demarle1: The initial treadmill speed will be set at the average running speed the participant maintains over 1.5 miles (as reported by the participant). The participant will run at the specified speed for 3 minutes. Every 3 minutes the speed of the treadmill will be increased by 1 km/h (0.62 mph) until exhaustion as indicated by the participant signals that they want to stop, saying stop, hit the stop button on the treadmill or the VO2 graph shows a plateau in oxygen consumption [3]. Data processing was performed in Matlab following Slade's regression algorithm [1].

Results & Discussion: The device-driven system had an average error rate of 8.68% ranging from 6.14% to 11.58% and an average RMSE of 2.11 W/kg ranging from 0.24 to 4.13 W/kg. There was an increased difference between the device-driven and gold standard systems for the first 180 seconds of each participant's trial. We hypothesize that this is largely due to the progressive physiological changes that occur as the body acclimates to exercise and the impact that it has on breath-by-breath respirometry. The device-driven model is not for an end-user that is interested in the early phases of exercise (< 5 minutes or so), because the system does not incorporate physiological data.

However, this personalized system does not require a mask, contains no wires, and requires no calibration. The ease of use makes it convenient for large-scale use, but it does require some programming skills to process the data. While this validation does have a small sample size, it is an incremental change from a previously validated system with a robust validation process.

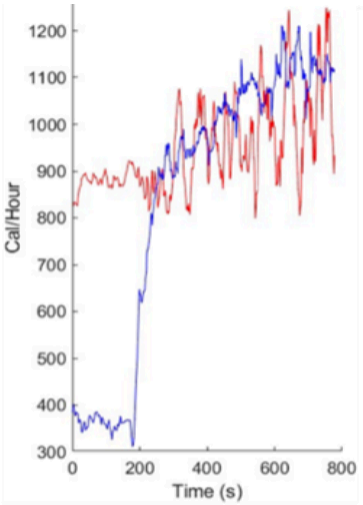

Figure 1: Device-driven model caloric estimate (red) and respirometry (blue) caloric estimate expressed in kilocal/hour.

Significance: This system has the potential to expand accessibility to an accurate measure of caloric expenditure to consumers, medical groups and research groups. This cost-effective system also has the capacity to record data for upwards of 30 hours. Future studies can expand on the system by incorporating methods of biofeedback and automatic report generation. This system may have additional applications to tactical athletes including military personnel to decrease injury risk.

Acknowledgments: We thank the University of Arizona's Sensor Lab Seed Grant for partially funding this research.
References: [1] Slade et al. (2021) Nat Communication, 12(1). [2] Montoye et al. (2020), *Int J of Ex Sci*, 13(4). [3] Demarle et al. (2001), *J Appl Physiol*, *90*(3).

QUANTIFYING PERSONALIZED INTERNAL REWARDS DURING EXOSKELETON-ASSISTED WALKING USING INVERSE REINFORCEMENT LEARNING

Keya Ghonasgi[1*], Aaron Young[1,2]
[1]George W. Woodruff School of Mechanical Engineering and [2]Institute for Robotics and Intelligent Machines,
Georgia Institute of Technology, Atlanta, GA, USA
*Corresponding author's email: keya.ghonasgi@me.gatech.edu

Introduction: Robotic exoskeletons offer a novel and unique approach for assisting movements, such as walking, in individuals who have suffered from motor impairment [1]. Efficient robotic interaction design requires knowledge of the wearer's goals which are difficult to quantify explicitly. These goals are typically estimated by observing changes in performance metrics as the interaction between the robot and the wearer changes. However, it remains unclear how these changes relate to each individual's internal reward and intent, and how these rewards differ across individuals. We propose a novel method to investigate the relationship between observed performance metrics and internal reward by leveraging recent advances in the field of inverse reinforcement learning (IRL).

Methods: We present results from a case study where one chronic stroke participant walked on a treadmill while wearing a lightweight bilateral hip exoskeleton (Gait Enhancing and Motivating System, Samsung Electronics, South Korea). We observed the participant's response to the exoskeleton under 16 interaction conditions, with four levels of exoskeleton assistance (from no assistance or 0, to maximum assistance or 3) on each leg (paretic - P, and non-paretic - N, see Figure 1a) [2]. The timing of the assistance was tuned for the participant and remained unchanged across the different conditions. Spatiotemporal, symmetry-related, and joint-effort-related metrics are extracted for each step under these different conditions. To generate sufficient data for training of the proof-of-concept IRL model, the data from each condition is used to identify the mean and standard deviation for each metric, and new data is randomly sampled from this distribution.

Our goal in this case study is to better understand how an individual's internal reward can be quantified in terms of their observed performance under certain interventions. An IRL-based approach has previously been used to verify the effect of visual biofeedback training on an individual's internal reward [3]. Our approach, however, is more general and explores implicit responses of the individual to different interaction modes without explicit training. The IRL model is built upon the AVRIL framework [4]. As seen in Figure 1b, this framework uses an encoder model that takes in the gait performance features to build a reward probability distribution ($R(s,a)$). This reward is then used to decode the discrete exoskeleton interaction mode as the interaction policy ($\pi(s) = a$). We define a linear regression model for the encoder which takes in gait performance features and translates these into the learned reward distribution as $R(s,a) = w_1\phi_1(s,a) + w_2\phi_2(s,a) + \cdots + w_k\phi_k(s,a) = w^T\phi(s,a)$. Each feature is represented as $\phi_i(s,a)$ and the encoder learns the weights of the linear regression to generate the corresponding reward.

Results and Discussion: After training the IRL model, the learned policy is validated against true data that was left out during training. We achieve over 60% accuracy of classifying the interaction condition. Although this accuracy is much higher than the nominal (random chance) accuracy of 6.25%, it is relatively low due to similarity of responses in different interaction modes (which are only differentiated by 2Nm of peak assistive torque). We use 9 gait features as the states (ϕ_i): step length asymmetry, step time asymmetry, non-paretic hip peak angle, non-paretic hip range of motion, non-paretic peak hip power, non-paretic total energy, stride length, and non-paretic stance time. Their relative weights in the learned reward (Figure 1c) suggest that as the exoskeleton's interaction was modulated, the participant's internal reward was most correlated with changes in step time asymmetry, step length asymmetry, and non-paretic stance time compared to the other observed metrics. This correlation suggests that the participant was more likely to change their gait symmetry and temporal when responding to exoskeleton assistance compared to the other metrics.

Significance: This study explores an IRL framework to design personalized reward functions from observed performance metrics during exoskeleton interaction. Preliminary results suggest we could characterize an individual's response, such as a more pronounced response in specific temporal performance metrics compared to spatial or effort-related metrics. Building such task-agnostic personalized reward models could further inform personalized assistance control for individuals with varying mobility needs post injuries like stroke.

Acknowledgments: National Institutes of Health Grant No. 1DP2HD111709-01

References: [1] Herrin, K., et al. (2023), [2] Pan, Y.-T et al. (2023), [3] Liu W. et al (2022), [4] Chan, A.J., et al. (2021)

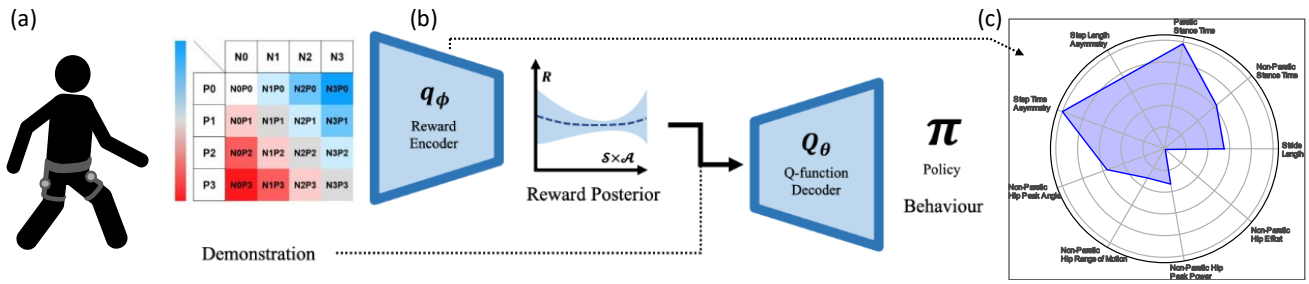

Figure 1. Learning personalized internal rewards during walking. (a) 16 Experimental conditions (P – paretic, NP – non-paretic). (b) IRL framework that learns a reward encoder and a policy decoder. (c) Results from an example model trained using 9 performance features.

THE RISK OF FALLING: COMPENSATORY CHANGES TO LOCOMOTION BASED ON THREATS

Nooshin Seddighi[1*], Nicholas J. Woo[1], Nicholas Kreter[2], Mindie Clark[3], A. Mark Williams[4], Tiphanie E. Raffegeau[5], Peter C. Fino[1]
[1]University of Utah, [2]University of Oregon, [3]Rocky Mountain College, [4] Florida Institute of Human and Machine Cognition, [5]George Mason University; *Corresponding author's email: nooshin.seddighi@utah.edu

Introduction: Previous research has applied risk-based frameworks to understand human motor control [1]. Classical definitions of risk stem from the maximum expected utility hypothesis, whereby the expected utility or risk of action a, $E[U|a]$ is the product of the probability of some event x given action a, $P(x|a)$, and the utility or cost of that event, $U(x)$; $E[U|a] = \sum_x P(x|a)\,U(x)$. Similar frameworks may describe compensatory locomotor changes when faced with threats related to falling [2, 3]. For example, humans may adopt locomotor patterns that reduce the probability of falling in environments that increase the expected cost of a fall (i.e., the likelihood of a severe fall-related injury)- such efforts may intend to maintain a constant expected value of risk. The purpose of this study was to directly examine how individuals may modify the Probability of Falling (PoF) in the presence of different perceived costs of a fall.

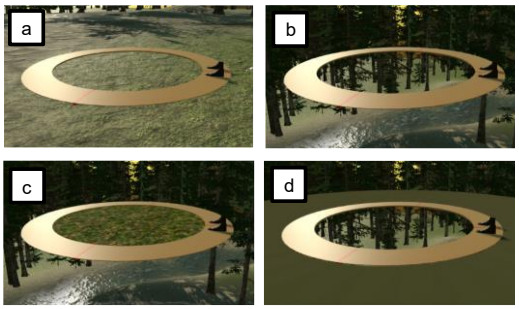

Figure 1: Environments: (a) ground, (b) bilateral threats, (c) outer threat, and (d) inner threat conditions.

Methods: Fifteen healthy young adults (8 female; mean (SD) age = 25.5 (1.9) years) provided written consent in this study approved by the University of Utah's Institutional Review Board. Participants completed four walking trials around a circular walkway (1.2 m inner radius, 1.6 m outer radius) (Figure 1). Participants wore a head-mounted display that presented an immersive virtual reality (VR) environment with four conditions: a ground condition and high elevations with inner, outer, and bilateral (i.e., both inner and outer) threats present conditions (Figure 1). Gait speed was controlled using a metronome paced to ¼ of the average, self-selected lap time. Feet and approximate center of mass (CoM) kinematics were recorded by two VR trackers placed around the lateral ankle joint, proximal to the lateral malleolus, and two VR hand controllers placed in a waistbelt located over the navel and approximate L2-L3 vertebrae, respectively. The primary outcome was PoF, defined using the distributions of the position of the extrapolated CoM relative to the nearest edge of the walkway[4]. Additional outcomes included the ML velocity of the CoM and radial foot placement. Linear mixed models evaluated the effect of condition on each outcome. Posthoc contrasts focused on comparing the ground level vs. both threats (effect of increased cost of falling) and the inner vs. outer threat comparison (directional effect).

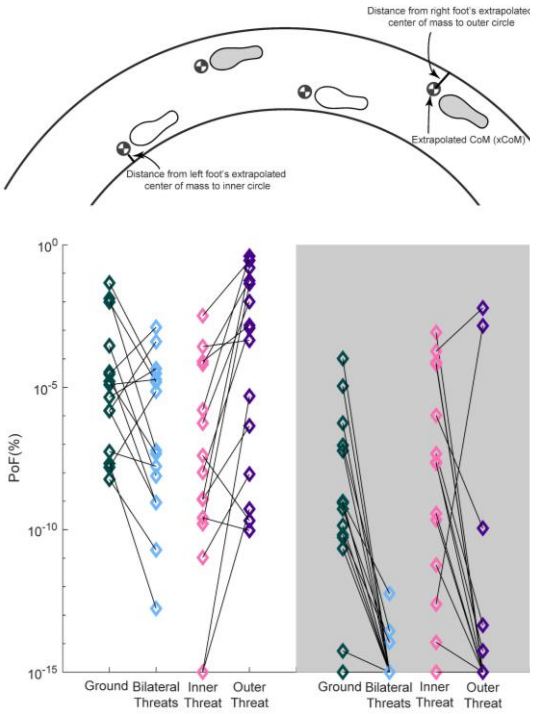

Figure 2: Images of the probability of Falling (PoF) across conditions, with the inner limb depicted on white (left side) and the outer limb depicted on gray background (right side).

Results & Discussion: Participants' responses to threats varied depending on the direction of the threat. When presented with a bilateral threat compared to the ground level with no threat, participants decreased the PoF in both directions (Figure 2). This change in the PoF was accomplished by narrowing the base of support and restricting the mediolateral CoM velocity ($p = 0.040$). When presented with a unilateral threat, participants decreased the PoF in the direction of the threat ($p = .0218$ and $p = .003$), and increased the PoF in the direction opposite the threat (Figure 2). This change in the PoF was driven by changing position on the walkway; participants walked closer to the inner edge when outer threats were present, and vice versa ($p<.0001$). The study reveals that height-based postural threats significantly impact both the likelihood of falling and gait characteristics. Participants display adaptive locomotor responses by actively avoiding the perceived threat, thereby reducing fall risk. Notably, individuals adjust their proximity to the threat when they are able, and resort to compensatory changes in postural control when unable (i.e., bilateral threats).

Significance: This study elucidates how height-based postural threats prompt adaptive locomotor responses – including trajectory and postural control changes. Participants actively adjust their probability of falling when presented with increased cost to falling, supporting the risk-based framework of locomotor behavior.

Acknowledgments: This work was supported by the Eunice Kennedy Shiver National Institute of Child Health and Human Development of the National Institutes of Health (award no. K12HD073945 to P.C.F.). Opinions, interpretations, and conclusions are those of the author and are not necessarily endorsed by the funders.

References: [1] Braun, D.A. et al., (2011) Front. Hum. Neurosci., 5:1. [2] O'Brien, M.K. & Ahmed, A.A., J. (2013) Neurophysiol., 109(7). [3] O'Brien, M. & Ahmed, A. (2015), Front. Behav. Neurosci., 9:150. [4] Kazanski, M.E. et al. (2023), bioRxiv.

FALL RISK IN SPINE PATIENTS – HOW PATIENT'S CONE OF ECONOMY CHANGES IN A SIMULATED UNSTABLE ENVIRONMENT

Ram Haddas, PhD; Justin Jablonski, MS; Emmanuel Menga, MD; Robert Molinari, MD; Addisu Mesfin, MD; Clarke I. Cady-McCrea, MD; Paul Rubery, MD; Varun Puvanesarajah, MD; Ashely Rogerson, MD
University of Rochester Medical Center
Ram_Haddas@URMC.Rochester.edu

Introduction: Falls remain a common cause of death and disability in elderly patients, with related injuries imposing costs of over $20 billion annually.[1] Sway and the resulting larger Cone of Economy (CoE) increases the risk for falls.[2] CoE dimensions are typically measured with a Romberg test in a controlled environment. However, this may not accurately represent a patient's balance and fall risk. Recently, an alternative test was introduced using Computer Dynamic Posturography (CDP) to determine the etiology of balance disorder in stable and experimental unstable environments that trigger fall.[3] While balance is maintained through vestibular, visual, and proprioceptive/somatosensory inputs, broader health metrics including reflex mechanisms, muscle tone, strength, range of motion, and motor skills, are also known to aid in the prevention of falls as well.[4] Unfortunately, these systems degenerate with natural aging and thus must be monitored in the elderly.[4] Therefore, the purpose of this study was to determine risk factors for falls in spine patients using CoE measurements in a simulated unstable environment.

Methods: Fifteen Lumbar Degenerative surgical candidates (LD) and 10 healthy controls were protected by a safety harness and performed a series of Romberg Tests in a Computerized Dynamic Posturograph (CDP, Bertec, Columbus, Ohio, USA) system. The CDP system influences the vestibular, visual, and proprioceptive systems using controlled motion of the floor and surroundings. All patients and control subjects performed six sensory organization tests: normal and perturbed stability, both with and without visual cues. Each subtest, Eyes Open with Fixed Support (EOFS), Eyes Closed with Fixed Support (ECFS), Eyes Open Sway Surround with Fixed Support (EOSAFS), Eyes Open with Sway Support (EOSS), Eyes Closed with Sway Support (ECSS), and Eyes Open Sway Surround with Sway Support (EOSASS) was performed for 20 seconds (Figure 1). PROMIS data was collected before the test. Repeated-measure ANOVA was used to compare between conditions.

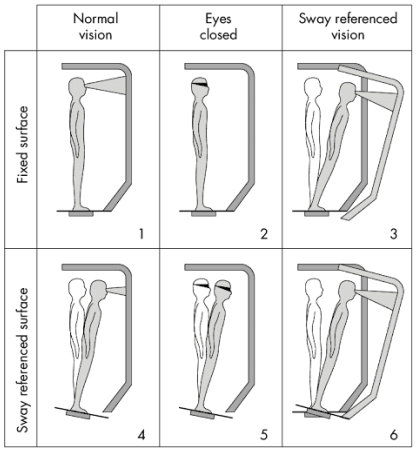

Figure 1: Computerized Dynamic Posturography six sensory organization tests.

Results & Discussion: Cone of Economy dimensions were found to be larger in LD patients compare to controls. Significant differences were seen in the EOSS (Total Sway: LD: 126.5±35.7 vs H: 61.4±5.7 cm, p=0.05; Range of Sway sagittal: LD: 67.6±26.1 vs H: 28.5±1.7 cm, p=0.02) and EOSASS conditions (Total Sway: LD: 78.0±30.3 vs H: 36.1±4.5 cm, p=0.05; Range of Sway coronal: LD: 37.5±7.0 vs H: 17.2±1.6 cm, $p < 0.01$). Total sway was significantly higher with perturbed stability and without visual cues in LD patients (EOFS: 15.6±6.5, ECFS: 27.2±15.5, EOSAFS: 28.8±21.0, EOSS: 52.7±23.8, ECSS: 61.0±21.6, EOSASS: 60.7±24.8 cm) and were significantly higher compared to H (EOFS: 11.6±3.1, ECFS: 14.7±5.1, EOSAFS: 14.1±5.9, EOSS: 26.5±9.1, ECSS: 37.7±7.7, EOSASS: 46.9±23.5 cm, $p < 0.05$; Figure 2). Positive moderate correlation was found between CoE measurements, CoP and PROMIS scores in LD patients ($r=0.4$-0.7, $p < 0.01$). Falls are the leading cause of morbidity and mortality for spine patients aged 65 years and older, affecting more than two million people annually. Here we demonstrate the feasibility of generating CoE dimensions of spine patients in simulated unstable environments using CDP. We also find that patients CoE dimensions and total sway were significantly larger when the sway surround and sway support conditions were introduced. The ability to quantify balance capacity and drivers of balance disorders in spine patients is vital.

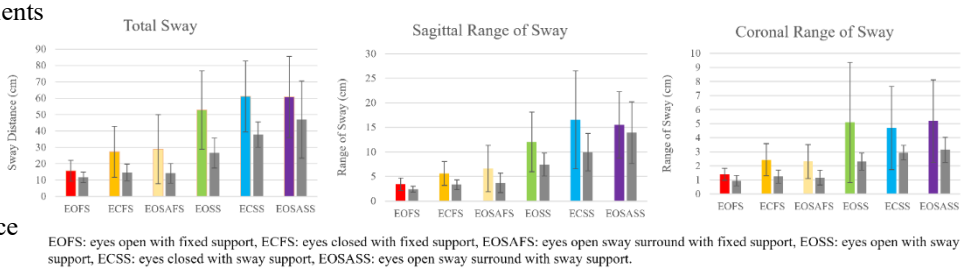

EOFS: eyes open with fixed support, ECFS: eyes closed with fixed support, EOSAFS: eyes open sway surround with fixed support, EOSS: eyes open with sway support, ECSS: eyes closed with sway support, EOSASS: eyes open sway surround with sway support.

Figure 2: Cone of Economy result during the sensory organization tests for lumbar degenerative patients (colors) and control (gray) in the Computerized Dynamic Posturography machine.

Significance: By allowing patients to replicate the motions that may result in a fall within a safe environment, clinicians and scientists can better understand the cause of balance disorders and provide patients with better treatment options.

References: [1] Burns et al. (2016), J *Safety Res.*58(1); [2] Haddas et al. (2021), *European Spine Journal* 30(8); [3] Rojas et al. (2022), *Sensors* 22(23); [4] Wiesmeier et al. (2017), *Front Aging Neurosci* 9.

IN SUPPORT OF NURSES AND PATIENTS - IDENTIFYING CHANGES IN MEAN AND PEAK PRESSURES WITH THE USE OF A NEW POSITIONING SYSTEM TO PREVENT TISSUE INJURY

Somlata Dev Sharma[1*], Justin Scott[1], Tamara Reid Bush[1]
[1]Department of Mechanical Engineering, Michigan State University
*Corresponding author's email: sharm242@msu.edu, reidtama@msu.edu

Introduction: Pressure injuries (PIs) have a profound impact on wheelchair users, being both painful and costly to treat. The healing process can take over 5 months, significantly diminishing an individual's quality of life [1]. On average, treating a PI costs over **$**30**,**000 per incident, and in some cases, treatment costs exceed **$**100**,**000 [2], [3]. PIs are the second most common medical complication among wheelchair users, and more than half of wheelchairs users will develop at least one PI during their lifetime [4]. Research on PI prevention strategies has considered the mean and peak pressures on the buttocks as metrics for the effectiveness of these strategies. Two commonly used strategies for preventing PIs are seated repositioning and the use of specialized cushions. The seated repositioning strategies include back recline and tilt-in-space [5]. Meanwhile, people also use specialized cushions such as ROHO cushions to more evenly distribute pressure on the buttocks. However, there is limited research that has examined how cushion choice affects the relationships between mean pressure and peak pressure in different seated positions. This work is needed to determine whether the benefits from multiple PI prevention strategies are additive. The goal of this work was to investigate the relationships between mean and peak pressure in multiple seated positions with a foam cushion and a ROHO cushion, and we hypothesized that the magnitudes of the linear regression relationships would be different for the two cushions.

Methods: An articulating chair with independent rotations of the chair back and seat pan, allowing for separate adjustments of back recline and seat pan tilt, was created for this study (Fig. 1). A 42x48 sensor pressure mat was attached to and aligned with the front of the seat pan of the chair. Pressure data were collected on the seat pan for combinations of 3 levels of back recline (6°, 10°, 20° from vertical) and seat pan tilt (0°, 15°, 30° from horizontal). Pressure data were collected from 9 participants (5 females, 4 males) sitting on a foam cushion and a subset of 7 of those participants (4 females, 3 males) sitting on a ROHO cushion. The data were split into the front half and back half of the seat pan, of which the back half was called the buttocks. Mean and peak pressures from the buttocks were calculated in every position for the two cushions. Peak pressures were determined by taking the average magnitude over the 3x3 sensor area with the highest average pressure. A multiple linear regression was used to describe the relationships between mean and peak pressures in each position for each cushion.

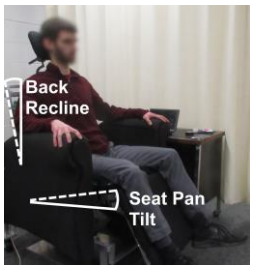

Figure 1: The articulating recliner and angles of the chair back and seat pan

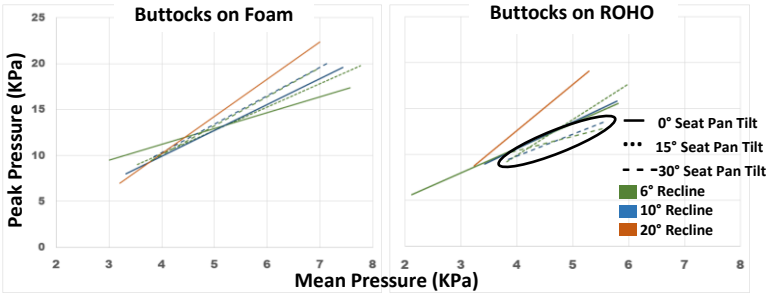

Figure 2: Linear relationships of mean and peak pressures on the buttocks seated on foam and ROHO cushions, respectively, for all positions tested. The ratios of peak to mean pressure were lower for increased seat pan tilt on the ROHO cushion (circled), showing the potential of using the strategies together.

Results & Discussion: The multiple linear regressions describing the relationships between the mean and peak pressures in buttocks with the foam and ROHO cushions in all the positions are given in Figure 2. There was a positive relationship between mean and peak pressures in all positions. On average, the slope of the linear relationship for the buttocks on the ROHO cushion (m = 3.03) was larger than for buttocks on foam (m = 2.64), which was not statistically significant (P = 0.422). This was, in part, because the average pressure values on the buttocks with the ROHO cushion were smaller than with the foam cushion, as can be seen in the regressions in Figure 2. The relationships between mean and peak pressure on both cushions were similar in all levels of back recline. However, the relationships between mean and peak pressures for both cushions at various levels of seat pan tilts were different. For greater seat pan inclinations, the ratios of peak to mean pressure were larger for the foam cushion than that for the ROHO cushion. This means that the ROHO cushion had decreased mean pressures on the buttocks relative to the foam cushion and that increased seat pan tilt was able to reduce the peak pressure relative to mean pressure on the buttocks even more using the ROHO cushion. Previous work has shown that increasing seat pan tilt is a strategy to reduce pressures on regions prone to PI formation on the buttocks, so these data indicate that a pressure relieving cushion like the ROHO cushion may be used to augment that repositioning strategy [6].

Significance: Limited research has addressed how different cushions affects the relationships between average and peak pressures on the body in various seated positions. As these are two of the most prominent PI prevention strategies, the potential of them being used together is a topic of interest to populations at risk of developing PIs. The results demonstrate that the benefits of the two strategies may potentially be additive. The presented data can be used for computational biomechanics studies that investigate PI formation in the future, thus contributing to both clinical and computational biomechanics.

Acknowledgments: The authors would like to thank the Michigan State University ADVANCE Grant Program for funding this work.

References: [1] Brewer et al. (2010), *J Wound Care*; [2] Brem et al. (2010), *Am J Surg*; [3] Chan et al. (2017), *J Wound Care* 26; [4] Donovan et al. (1984), *Paraplegia*; [5] Ding et al. (2008), *JRRD*; [6] Scott and Bush (2021), *J Biomech Eng*.

Monitoring Limb Symmetry After ACL Injury Using Instrumented Insoles

Gabriel E. Gibson[1]*, E.L. King[1,2], M.A. Lamarre[1], S. A. Acuña[1,2], S. Sikdar[1,2], P.V. Chitnis[1,2]
[1] Department of Bioengineering, George Mason University, Fairfax, VA, USA
[2] Center for Adaptive Systems of Brain-Body Interactions, George Mason University, Fairfax, VA, USA
*Corresponding author's email: ggibson8@gmu.edu

Introduction: Patients who experience an anterior cruciate ligament injury (ACL) face a higher risk of damaging their contralateral ACL [1] [2]. To reduce this risk and design safer rehabilitation protocols, it is important to monitor how ground reaction forces are distributed across limbs and prevent excessive loading within the healthy leg, for example during a squat exercise. Clinicians can visually assess limb symmetry during rehabilitation but have limited ways of quantifying force imbalances. One popular method is using force plates to assess bilateral differences in ground reaction forces, but force plates are not portable and may not be accessible to every clinical setting. An alternative technology is to use instrumented insoles for monitoring the normal plantar force inside the shoes during rehabilitation tasks and can easily be implemented in real-world settings. The purpose of this study was to explore the feasibility of instrumented shoe insoles to monitor force imbalances in ACL-injured participants during a squat.

Methods: Participants (4 controls, 1 with a left ACL-III deficiency) performed 6 trials of 3 bilateral bodyweight squats over multiple days. Instrumented insoles (Loadsol, Novel, Pittsburgh, PA) were placed in the participants' shoes to track changes in normal plantar force between the foot and the shoe within three sections: the medial forefoot, the lateral forefoot, and the heel. We recorded plantar forces during squats for controls on three different days with 24 hours between tests. We recorded plantar forces for the ACL subject during squats weekly over 4 weeks, during which they also completed 4 weeks of clinical rehabilitation. At each testing session, the ACL subject completed a modified clinical qualitative functional assessment survey (scores: 17 to 85 = best to worst) to indicate functional ability. Limb imbalance for each foot section was quantified using a bilateral symmetry index (BSI) with a BSI of 1 equating perfect symmetry. BSI was computed by subtracting the dominant (or non-injured) limb from the nondominant (or injured) limb dividing by the mean of both limbs squaring the results and the subtracting from 1. Coefficient of variation (COV) was used with control data to determine the stability of measures over time.

Results & Discussion: The bilateral symmetry of foot forces showed high variability for individual sections but was less variable when considering the total foot force output. For controls, the BSI of the total force, heel force, lateral force, and medial force was 0.86 ± 0.06, 0.51 ± 0.14, 0.27 ± 0.08, 0.55 ± 0.09 respectively (Fig. 1A). COV for controls was 7.2%, 27%, 30%, 16.6% for total, heel, lateral, and medial respectively. For ACL-III subject force distribution changed in total, heel, lateral, and medial by 0.218, -0.47, -0.076, 0.112 respectively from week 1 to week 4 (Fig. 1B). The ACL subject's functional assessment scores decreased from 70 to 45 indicating improved function throughout rehabilitation. This corresponds to the positive changes in BSI scores from the total and medial force distributions. Overall variations in total and medial force output were stable unlike for heel and lateral sections. Heel and lateral also decreased in symmetry in the ACL subject from week 1 to week 4. These variations may be due to compensatory movements made during the squat task. Time series analysis may need to be conducted to fully understand these asymmetries.

Significance: Evaluation of force distribution between limbs after ACL injury is important to understand where and how patients are compensating. Tracking abnormal compensatory movements can inform patient recovery and help clinicians personalize care decreasing the risk of re-injury.

Acknowledgments: Efforts supported by the Government under Other Transactions Number MTEC-MPAI W81XWH-15-9-0001.

A.

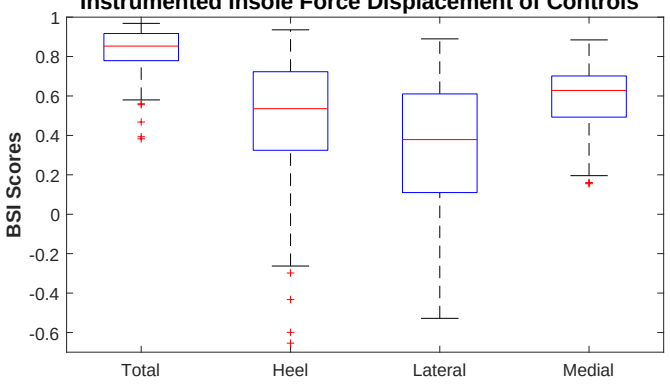

B.

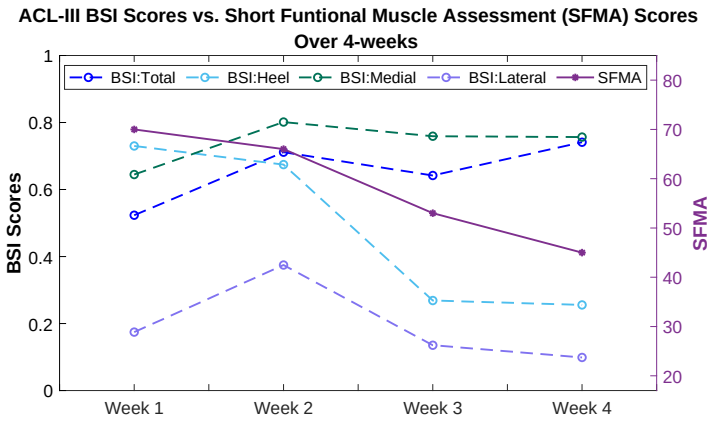

Figure 1. A). Average force displacement of controls over three days for total foot, heel, lateral, and medial compartments. B). BSI Scores of force displacement and SFMA scores over a week period in ACL-III deficient subject.

References: [1] King E, et al. *Am J Sports Med*. 2021
[2] Swärd P et al., *Knee Surg Sports Traumatol Arthrosc*. 2010 [3] Chinn L, et al., *Clin Sports Med.* 2010

METABOLIC COST MODEL FOR TIME-VARYING ISOMETRIC CONTRACTIONS: COST TO REDUCE FORCE IS MORE THAN INCREASING

Sriram Sekaripuram Muralidhar[1*], Kristen Heitman[2], Ross Baldwin[1], Sam Walcott[3], Manoj Srinivasan[1]
[1]Mechanical and Aerospace Engineering, The Ohio State University, Columbus OH 43201
[2]School of Health and Rehabilitation Sciences, The Ohio State University, Columbus OH 43201
[3]Mathematical Sciences, and Bioinformatics and Computational Biology, Worcester Polytechnic Institute, Worcester MA01609
*muralidhar.19@osu.edu

Introduction: Muscles utilize metabolic energy (ATP) to generate force and enable movement. Previous literature underscores the significance of minimizing metabolic energy expenditure in determining healthy human behavior across various dynamic tasks [1,2]. Consequently, there is a growing interest in estimating metabolic energy consumption during various tasks. However, the current popular indirect calorimetry-based techniques are time-consuming and lack the capacity to estimate instantaneous costs [3]. A mathematical model for metabolic energy would be instrumental in overcoming these experimental limitations and would also facilitate simulation-based studies. In this study, we developed a metabolic energy cost model for time-varying isometric tasks based on human experiments. We model metabolic cost as a power law function of external force and force rate, which can be extended to joint torque and torque rate. Additionally, utilizing a mathematical framework, we illustrate the metabolic cost model's power law dependence on muscle force and force rate. Our focus on isometric tasks is motivated by the fact that either previous energy cost models derived from isolated muscle experiments have not been validated against isometric human experiments [4], and those developed from human experiments either predict zero cost for isometric tasks, fail to consider changes in force magnitude and frequency together, or conducted fewer trials and explicitly did not seek a simultaneous relation with force and force rate [5-8].

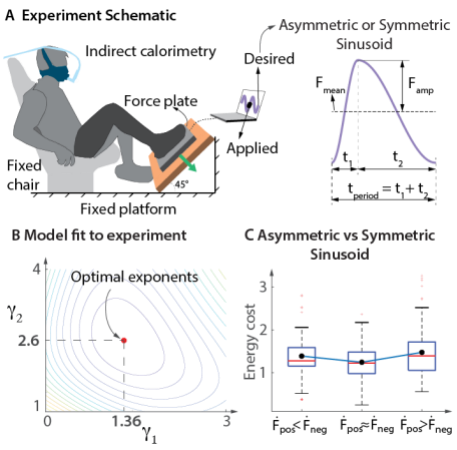

Figure 1: (A) Participants maintain a seated position while applying normal force to the platform using their right leg to track sinusoids of varying means (3), amplitudes (2), and time periods t1, t2 (16), with energy cost assessed through breath analysis. (B) Mean squared error fit to the data for different exponent values. (C) Boxplot comparing energy costs across all subjects with identical or different up and down slopes.

Methods: We performed human experiments measuring the metabolic cost of producing sinusoidal forces with the right leg using visual feedback. We used indirect calorimetry to measure energy cost and force plates to measure real-time applied force. Subjects (N = 11) tracked piecewise sinusoidal forces with different means, amplitudes, time periods, upward and downward slopes with no repetition of trials resulting in a rich dataset consisting of 297 unique metabolic cost trials ($\dot{E}_{task}$) lasting 6 mins each (Figure 1A). Further, we fit the metabolic cost model: $\dot{E}_{model} = a_0 + a_1 F^{\gamma 1} + a_2 \dot{F}_{pos}^{\gamma 2} + a_3 \dot{F}_{neg}^{\gamma 2}$ to each trial data with subject specific a_0 and other coefficients common to all subjects. The model parameters-force, positive and negative force rates are estimated by averaging 2nd half of force-time series data.

Results & Discussion: Our analysis revealed that the optimal model cost scales with exponents of 1.36 for force and 2.6 for force rate, achieving a R-squared value of 79.4% (Figure 1B). This force cost scaling aligns with our prior research [2]. Our model indicates a scaling of force rate cost faster than the quadratic scaling implicitly hypothesized by Van der Zee and Kuo [8], although their data does also suggest a faster-than-quadratic scaling. Crucially, our model's high goodness of fit suggests that the force and force rate terms can be de-coupled as hypothesized in tasks that simultaneously change force and force rate. The metabolic cost of tracking asymmetric sinusoids, where the positive and negative force rates are not equal, is higher compared to symmetric sinusoids (Figure 1C, t-test p = 3e-9). Notably, we found that the coefficient for negative force rate exceeds that of positive force rate by approximately fourfold ($a_3 \sim 4 * a_2$). This difference implies that reducing force incurs greater metabolic cost than increasing force within the same force range. At the molecular level, the expenditure involved in pumping calcium ions back to the sarcoplasmic reticulum, leading to force reduction, likely contributes to force rate cost and the higher cost for negative force rates.

Significance: Our model was obtained from a rich and large dataset that involved simultaneous change of force and force rates, and thus has the potential to be generally applicable to model isometric tasks with arbitrary force changes. We have distinguished between the metabolic costs associated with force, positive and negative force rates during cyclic force production, allowing correlation with corresponding molecular cost mechanisms, as well as fill a critical gap in current metabolic models for cyclic force production (as argued in [8]). Our model is both straightforward and versatile, enabling real-time estimation of costs for various types of time-varying forces in experimental setups and simulations.

Acknowledgments: This work was supported by NIH-R01GM135923 and NSF SCH grant 2014506.

References: [1] Srinivasan M. (2009), Chaos; [2] S. S. Muralidhar et al, preprint. (2023) (https://doi.org/10.1101/2023.12.24.573267); [3] Selinger and Donelan. (2014), J applied Phy; [4] Umberger et al. (2003), Comp methods Biomech and Biomed; [5] Hawkins and Mole. (1997), Annal Biomed Engg; [6] Doke and Kuo. (2005), J Expt Bio; [7] Dean and Kuo. (2011), J applied Phy; [8] Van der Zee and Kuo. (2021), J Expt Bio.

USER-CENTRIC DESIGN AND BIOMECHANICAL ANALYSIS OF A WEARABLE ASSIST DEVICE TO PROVIDE SOLDIERS RELIEF FROM BODY ARMOR WEIGHT

Paul R. Slaughter*, Chad C. Ice, Shimra J. Fine, Karl E. Zelik
Center for Rehabilitation Engineering and Assistive Technology, Vanderbilt University, Nashville, TN
*Corresponding author's email: paul.r.slaughter@vanderbilt.edu

Introduction: Soldiers who wear body armor vests have been repeatedly linked to the development of back and shoulder pain in epidemiological studies [1], biomechanical studies [2], and in our own interviews with soldiers [3]. The weight of these vests is supported by the soldier's shoulders, which subsequently increases the compressive loading throughout the shoulders and back. Redistributing body armor weight directly to the waist can offload the shoulders and back which may reduce shoulder discomfort [4], spine compression force [5], and back injury risk. However, the problem is that previous devices that sought to address this problem can be uncomfortable, offload only part of the weight, or restrict the user from performing critical tasks. This project's objective was to develop a wearable device to offload the weight of body armor from the back and shoulders while being comfortable and usable by soldiers in the field, without interfering with other tasks.

Methods: Our design goal was to fully offload a body armor vest from the back and shoulders while also meeting usability constraints informed by interviews with soldiers. This offloading must be effective during common tasks like standing, walking, and sitting to reduce spine and shoulder loading. This device must integrate into a soldier's existing body armor and offload at least 40 lbs. off the shoulders, which represents the typical weight of the vest and additional gear that soldiers need to attach to it. Many of the largest design challenges involve the usability of the device. The device must not restrict a user's range of motion or interfere during other important tasks they perform, including highly dynamic motions like running or crawling.

Results & Discussion: We created a novel, low-profile prototype with the ability to offload body armor weight and to quickly retract out of the way so as not to interfere with other tasks. Our design uses two adjustable scissor arms and a waist belt to redistribute trunk-worn weight off the shoulders and back, and instead onto the waist. The scissor arms (*A*) can integrate into U.S. Army body armor (e.g., Improved Outer Tactical Vest Gen III) by attaching to the inside of the vest's left and right side panels (*B*). The ends of these scissor arms attach via a small rope to a padded belt that is worn around the user's waist (*C*). Overall, this device modifies the biomechanical load path of the body armor to travel through the vest's side panels, the scissor arms, the belt, and finally onto the user's waist and lower body – bypassing their shoulders and back. The prototype weighs 2.1 pounds and contains no motors or batteries. The degree of trunk offloading can be controlled manually via two rotary ratchet-pawl mechanisms (*D*), both of which control the extension of one of the scissor arms. The more the user twists the ratchet, the more the scissor arms extend and lift the vest off the shoulders and back. When trunk offloading is not desired, the device can be disengaged by manually releasing the ratchet mechanism via a lever switch. In this disengaged configuration, the scissor arms are automatically retracted into the vest's side panels by a spring. This disengaged configuration is key to allowing the user to perform other key job tasks without impeding movement or needing to doff the device.

Initial benchtop testing demonstrated that our prototype was able to support a 40-pound vest. The scissor arms were also able to be extended in under 5 seconds and retracted in under 2 seconds. Human subject testing is forthcoming to evaluate biomechanics and usability. We are currently investigating different biomechanical modeling and measurement tools to quantify how this device impacts kinematics, spine loading and musculoskeletal injury risk. The trunk is a challenging body segment to estimate forces within, and the vest and belt occlude most of the trunk and pelvis bony landmarks traditionally used in motion analysis studies. However, in early pilot testing users have reported less back and shoulder discomfort when wearing the device and we have not observed increases in trunk muscle activity compared to when wearing only the vest. Further design and testing updates will be presented at the conference.

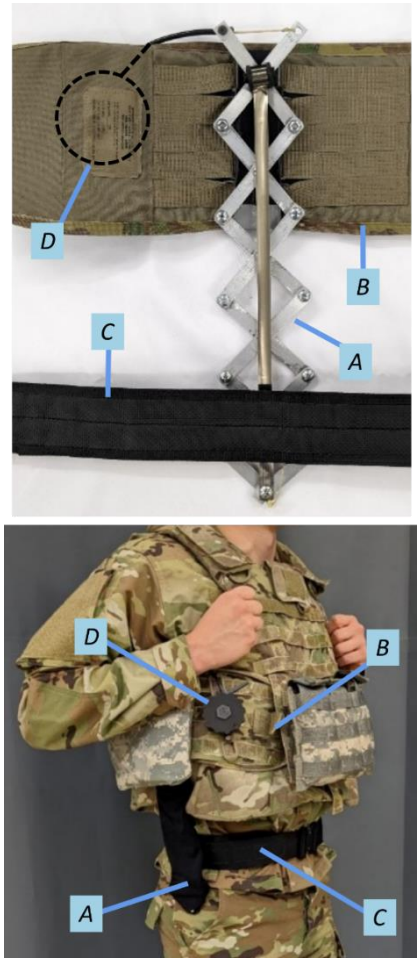

Figure 1: The inside (top) and outside (bottom) view of the device with the scissor arms extended calling out the scissor arms (*A*), IOTV side panel (*B*), waist belt (*C*) and ratchet mechanism (*D*). This set of components are on the left and right side of the vest.

Significance: We present a new type of wearable weight distribution device that has the potential to provide practical and effective relief from body armor. Reducing back and shoulder loading on soldiers has the potential to alleviate one of the largest causes of musculoskeletal injury, limited duty days, and medical discharge within the Army.

Acknowledgments: NSF Fellowship and the Vanderbilt Scaling Success Grant

References: [1] Roy et. al., 2013, SPINE 38(15) [2] Sessoms et. al., 2020, Ergonomics 63(2). [3] Slaughter et. al., 2023, Wearable Technologies 4 [4] Lenton et. al., 2018, Ergonomics 61(4) [5] Sturdy et. al., 2021 ASB Poster

PROGRESSIVE ADAPTATION OF GAIT BIOMECHANICS TO MINIMALIST FOOTWEAR: A LONGITUDINAL STUDY

Bahman Adlou[1*], Ava Davis[1], John Grace[1], Jerad Kosek[1], Grace Tortorice[1], Matt Gilbert[1], Christopher Wilburn[1], Wendi Weimar[1]
Auburn University
*Corresponding author's email: bza0058@auburn.edu

Introduction: The biomechanics of human gait and its response to external factors like footwear have been extensively researched. While barefoot walking is considered the most natural and evolutionarily optimal state, modern footwear designs often prioritize protective features at the expense of preserving inherent foot biomechanics. Minimalist footwear aims to bridge this divide by providing essential protection while allowing the foot to function more similarly to barefoot conditions. This study investigated whether prolonged use of minimalist footwear would progressively shape gait patterns to more closely resemble barefoot walking mechanics.

Methods: Eleven healthy, minimalist footwear-naive participants (4 females; mean(SD) age: 27.3 (4.5) years) completed walking trials across three visits (Day 0, 28, 56) in barefoot (bf), typical cushioned shoe (ts), and minimalist footwear (vivo: Vivobarefoot Primus Lite III) conditions. Each visit included three trials per condition on an instrumented walkway. Compliance monitoring ensured participants wore vivo >5 days/week, >5 hours/day. Linear mixed effects models assessed differences between bf and other conditions at each visit, with participants as random effects. Bf condition was set as the refence in the analysis.

Results & Discussion: Stride length, step length, velocity, and cadence were significantly different between bf and footwear conditions across visits ($p<0.001$). At Visit 1, vivo stride length (137.4±10.5 cm) and step length (68.4±5.4 cm) were intermediate between bf (138.4±18.4 cm, 69.0±9.2 cm) and ts (128.2±18.4 cm, 64.3±9.2 cm). Cadence in vivo (109.1±6.9 steps/min) was reduced versus bf (110.8±8.3 steps/min) but higher than ts (108.5±8.3 steps/min). Increased stride/step lengths with footwear suggest compensatory mechanisms to maintain velocities similar to bf (130.0±24.0 cm/s vivo, 130.2±24.7 cm/s ts, 130.0±24.0 cm/s bf) despite reduced cadence. Smaller deviations from bf in stride length, step length and cadence for vivo versus ts align with previous findings that minimalist footwear more closely replicates natural barefoot gait patterns[1]. Gradual reductions in stride/step length differences between vivo and bf from Visit 1 to 3 suggest participants progressively adapted their minimalist footwear gait toward barefoot mechanics over time.

Significance: These findings demonstrate the potential of minimalist footwear designs to promote gait biomechanics that more closely resemble barefoot walking patterns, considered optimal for musculoskeletal health. Even over this 8-week period of intermittent minimalist use, spatiotemporal gait parameters like stride length and cadence significantly adapted toward barefoot values, suggesting the foot was able to regain some inherent function despite the presence of footwear. With longer adaptation periods or more focused interventions, it is plausible that further progression toward natural barefoot mechanics could occur, allowing minimalist footwear to provide essential protection while facilitating the proposed benefits of barefoot gait for foot strength and musculoskeletal loading.

Acknowledgments: Thank you to all Sport Biomechanics Lab assistants for assisting in data collections. Special thanks to VivoHealth for their collaboration on this project.

References: [1] Murínová, L., Janura, M., Klein, T. (2023), Gait & Posture 106(S1); doi: 10.1016/j.gaitpost.2023.07.166.

AN AMBULATORY SEARCHING TASK FOR REHABILITATION RESEARCH: RELIABILITY AND VALIDITY ASSESSMENT

Katie M. Bricarell[1*], Janet S. Dufek[2], Jenny A. Kent[1]
[1]Department of Physical Therapy, University of Nevada, Las Vegas
[2]Department of Kinesiology and Nutrition Sciences, University of Nevada, Las Vegas
*Corresponding author's email: katherine.bricarell@unlv.edu

Introduction: Somatosensation is important in maintaining postural stability [1]. Individuals use proprioceptive and cutaneous inputs to safely accomplish tasks of daily living [2]. As task difficulty and complexity increase, individuals integrate information from multiple sensory systems to maintain postural stability [3]. As individuals age, impairments in sensation, strength, reaction time, vestibular function, and vision are believed to collectively contribute to declines in postural stability and increased risk of falls [4,5]. While multiple tests have been proposed to assess somatosensory acuity and locomotor function in isolation, practical assessments that tie somatosensation to function are lacking. The novel ambulatory searching task (AST) described by Christie et al. [6] may be a candidate test for exploring the role of somatosensation in human movement. The goal of this task is to assess an individual's ability to locate and step on a narrow walking surface using somatosensation alone. Participants are timed while traversing a horizontal ladder with unequally spaced rungs, wearing a blindfold to eliminate visual feedback. The purpose of this research was to determine whether the AST is a viable measure to be used in clinical and rehabilitation research. As a first step, we evaluated interrater reliability, and examined the learning trajectory across several AST trials. To explore known groups validity we compared performance across cohorts of young adults (YA) and older adults (OA). We expected that OA would show increased trial completion time compared to YA.

Methods: Eleven YA (28.0 ± 7.9 years, 1.8 ± .13 m, 83.4 ± 17.8 kg) and seven OA (71.9 ± 3.8 years, 1.7 ± .12 m, 78.1 ± 21.5 kg) attended two laboratory sessions. The AST involves a ladder placed horizontally on the ground with unequal and modifiable inter-rung spacing; at 19, 28.5, 38, or 47.5 cm apart. Participants were timed while traversing across the rungs, using bilateral handrails. Between trials, the rung spacing was changed to minimize potential learning effects. Participants completed 10 trials during each session, for a total of 20 trials. Two assessors measured the completion time for each trial using handheld stopwatches

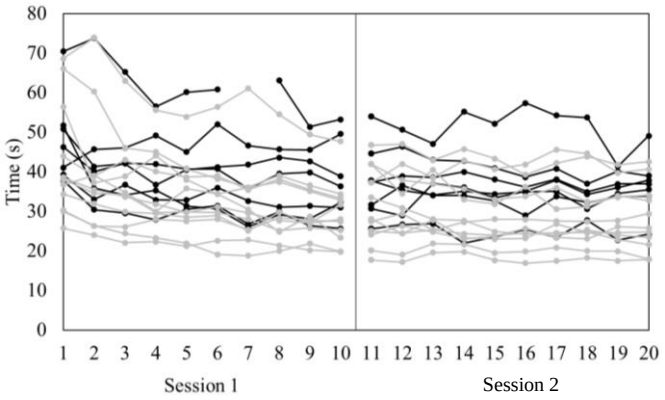

Figure 1: Trial completion time. OA – black; YA – gray.

Results & Discussion: Excellent interrater reliability was observed (ICC = .995). A learning curve was evident (Fig. 1). A greater traverse time in OA compared to YA approached but did not reach significance (p = .066, Fig 2). Preliminary results indicate that this test may be viable, however a greater number of participants are needed for further validation and refinement. The test is simple to administer with adequate space but appears to require the time to adjust to the learning curve. Differences between OA and YA may be masked by the differences in individual task completion strategies. It is also possible that individualistic motivations and beliefs play a role in the performance of this task that are outside the scope of control of the researchers, such as participant self-efficacy.

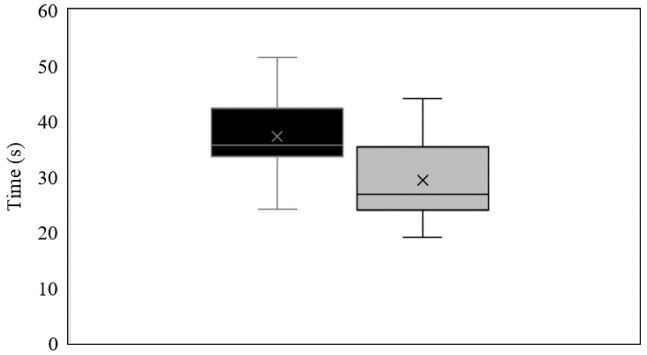

Figure 2: Trial completion time. Average of Session 2 trials 3-5. OA – black; YA – gray.

Significance: Many populations including older adults, people with amputation, and individuals with other neurological deficits experience declines or disruptions to their somatosensation. There is a need for more robust functional assessments that explore the integration of sensory information during locomotion. The findings of this study suggest that this novel ambulatory searching task may have utility in the investigation of the role of somatosensation in human locomotion.

Acknowledgements: We would like to thank Rosario Martinez, Melissa Samaniego, and Jade Burbank for their assistance in data collection for this project. This work was supported by a Faculty Opportunity Award and a TTDGRA Award from the University of Nevada, Las Vegas.

References:

[1] Lord et al. (1991), *J Gerontology*, *46*(3); [2] Shaffer et al. (2007), *Physical Therapy*, *87*(2); [3] Bacsi et al. (2005). *Exp Brain Res*, *160*; [4] Lord et al. (1994), *Age and ageing*, *23*(6); [5] Lord et al. (1999), *J American Ger Soc*, *47*(9); [6] Christie et al. (2020), *Scientific reports*, *10*(1)

LOGISTIC REGRESSION MODEL TO PREDICT FALLERS OR NON-FALLERS USING CLINICAL MEASURES AND FALL RISK ASSESSMENT OF OLDER ADULTS

Junwoo Park[1], Jongwon Choi[1], Kitaek Lim[1], Seyoung Lee[1], Woochol Joseph Choi[1*]
[1] Injury Prevention and Biomechanics Laboratory, Dept. of Physical Therapy, Yonsei University
*Corresponding author's email: wcjchoi@yonsei.ac.kr

Introduction: Identifying potential fallers in older adults is important in the prevention of fall-related injuries (i.e., hip fractures, concussion). We conducted logistic regression analyses with various clinical measures and fall risk assessments, in order to provide a predicting model of fallers in the older population.

Methods: 62 community-dwelling older adults (13 males and 49 females) with a mean age of 78.6 were recruited. We acquired demographic information including age, body height, body weight, body mass index (BMI), gender, education level, whether they use assistive devices for gait (i.e., walker, cane) and vision (i.e., multifocal lens), whether they live alone, and whether they drink and/or smoke. We also acquired clinical measures including whole body muscle mass using a body composition analyser (Inbody H20N, InBody, Seoul, Korea), bilateral hand grip strength (HGS) using a portable handgrip dynamometer, fear of fall (FOF), and Korean fall efficacy scale-International (KFES-I). The FOF was determined using a 5-point Likert scale. The KFES-I is a Korean version of valid and reliable questionnaire for FOF that consists of 16 questions. Furthermore, we also assessed individuals' risk of falls using short form-physiological profile assessment (PPA), Berg balance scale (BBS), and timed up and go test (TUG). Fallers were defined if they experienced a fall within a year, resulting in 17 fallers (2 males and 15 females) and 45 non-fallers (11 males and 34 females).

Binary logistic regression analyses (faller = 1, non-faller = 0) were performed with all independent variables mentioned above (primary analysis), and with variables belonging to the fall risk assessment category (secondary analysis). All analyses were conducted with SPSS (version 25.0, IBM Co., Armonk, NY, USA).

Results & Discussion: The logistic regression model of the primary analysis suggested that several demographic factors (age, sex, smoking) were associated in predicting fallers or non-fallers in older adults (Cox-Snell's R-squared = 0.37, accuracy = 82.3%, sensitivity = 58.8%, specificity = 91.1%) (Table 1). The probability of being a faller increased about 1.2-fold and 71-fold when the age increased and when they were female, respectively. The probability also increased with smoking behaviour. These results agree well with previous findings [1,2,3].

Our secondary analysis suggested that PPA, BBS, and TUG were not associated in predicting fallers or non-fallers, even in simple logistic regression (p = 0.23, p = 0.85, p = 0.33, respectively) (Figure 1).

	B	p value	Exp(B)
Age	0.213	.041*	1.238
Sex	4.263	.046*	71.053
Smoking	-6.131	.016*	0.002

Table 1: Logistic regression model to predict fallers and non-fallers in older adults.

Significance: We have shown a decent-performing logistic regression model to predict fallers and non-fallers using demographic information of older adults. We have also shown that three common fall risk assessment tools are ineffective in predicting fallers or non-fallers in older adults. These results should inform the enhancement of fall and injury prevention strategies in older adults.

Acknowledgments: This work was supported, in part, by the "Brain Korea 21 FOUR Project", and by the "Regional Innovation Strategy (RIS)" through the National Research Foundation of Korea (NRF) funded by the Ministry of Education (MOE) (2022RIS-005).

References: [1] Lee et al., 2019, Topics in stroke rehabilitation; [2] Wang et al., 2021, Journal of Advanced Nursing; [3] Kim et al., 2017, PloS one.

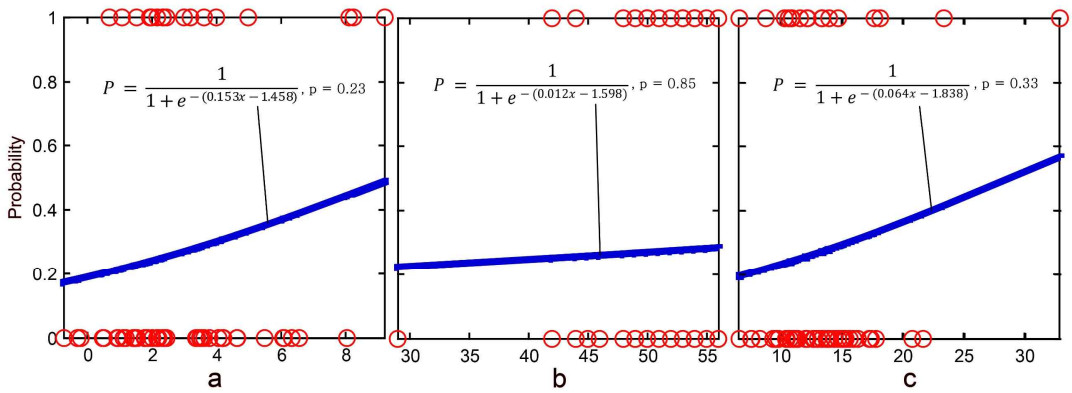

Figure 1: Simple logistic regression models to predict fallers or non-fallers in older adults with (a) PPA, (b) BBS, and (c) TUG. None of fall risk assessments were predictors.

RE-EVALUATION OF LOAD RATE PATTERNS WITH RUNNING-RELATED INJURIES USING COMPREHENSIVE LOAD-RELATED METRICS

Ryan M. Nixon[1,2*], Melanie Beceiro[1], Michelle McGrath[1], Aiden Villasuso[1], Kevin R. Vincent[1,2] and Heather K. Vincent[1,2]
[1]Department of Physical Medicine and Rehabilitation, [2]UF Health Sports Performance Center
*Corresponding author's email: ozswinem@ufl.edu

Introduction: Despite the growth in running medicine and biomechanics research, definitive relationships between running-related injuries (RRI) and impact loading rates (LRs) are lacking (Milner et al., 2023; Senevirathna et al., 2023). Methodological considerations, such as pre-processing filtering and smoothing, and the focus on positive LR to a specific region of interest or peak point or within the ground reaction force waveform (see Figure 1A) are likely contributors to this lack of agreement. Moreover, soft tissue vibrations, ground reaction force, and LR oscillations following a foot strike are nearly always overlooked during clinical gait analysis. As such, our clinical interpretation of LR on RRI has been limited to summary statistics and is incomplete. This study provides a re-evaluation of LR with RRI using a comprehensive collection of LR metrics during the entire stance.

Methods: Runners (N=534; 52% female; 61% with RRI [69 % of which were soft tissue and 31% were bone injuries]) ran at a self-selected speed on an instrumented treadmill. Ground reaction forces were collected at 1200 Hz and kinematic data were collected with 3D motion capture. Runners were grouped by a recent history of RRI and foot strike (rearfoot [RF] or non-rearfoot [non-RF]). Net ground reaction forces were processed with a 4th-degree Butterworth low-pass filter across cutoff frequencies 600, 100, 60, and 10 Hz across the entire stance. Positive and negative LR patterns were investigated for the full stance through backward subtraction numerical differentiation. LR metric asymmetry was measured as the percent difference between the left and right sides compared to the average.

Results & Discussion: Varying pre-processing cutoff frequencies influenced whole-stance ground reaction forces and LR values, with lower frequencies (60&10Hz) smoothing LR values and reducing instantaneous LR in early (1-7%) and late (96-100%) stance ($p<0.05$). See Figure 1. Higher filtering cutoffs (≥100 Hz) maintained better signal integrity and captured oscillations after foot strike. Raw normalized data showed that 40% of maximal positive LRs and all negative LRs are excluded from the conventionally published gait metrics and region of interest. The region of interest was modified by lowpass filtering. In the first 5% of the stance, 49% of all runners produced peak positive LR, and 32% produced peak negative LR within the first 20% of the stance.

Rearfoot strikers exhibited 8% higher positive LR and 18% higher when injured ($p<.003$). Injured non-rearfoot strikers demonstrated 17% earlier peak negative LR than uninjured non-rearfoot strikers, with 18% less time in between peaks ($p<.001$). For the overall population, early peak negative LR occurred in 50% of rearfoot strikers compared to 12.2% of non-RF strikers. Large LR oscillations early in stance indicate low-impact attenuation and maximal negative LR at this time indicates pronounced impact features during braking. RRI subsets like lower extremity tendinopathies show 35% greater negative LR that occurs 29% earlier in the stance phase ($p<.05$), and recently-healed lower extremity stress fractures were associated with greater limb LR asymmetries versus non-injured runners ($p<.05$).

Significance: Filtering affects the accuracy of LR in regions necessary to find differences among RRI subgroups. The conventional region of interest for LR excludes many features associated with injury and foot strikes. Positive and negative LR should be further investigated over the entire stance to help characterize differences among various RRI types. The implementation of alternative preprocessing approaches holds promise for enhancing the discriminative capacity of LR in predicting RRI occurrence.

Acknowledgments: This work was supported by the UF Health Sports Performance Center and the UF Strategic Funding Initiative, Sports Collaborative.

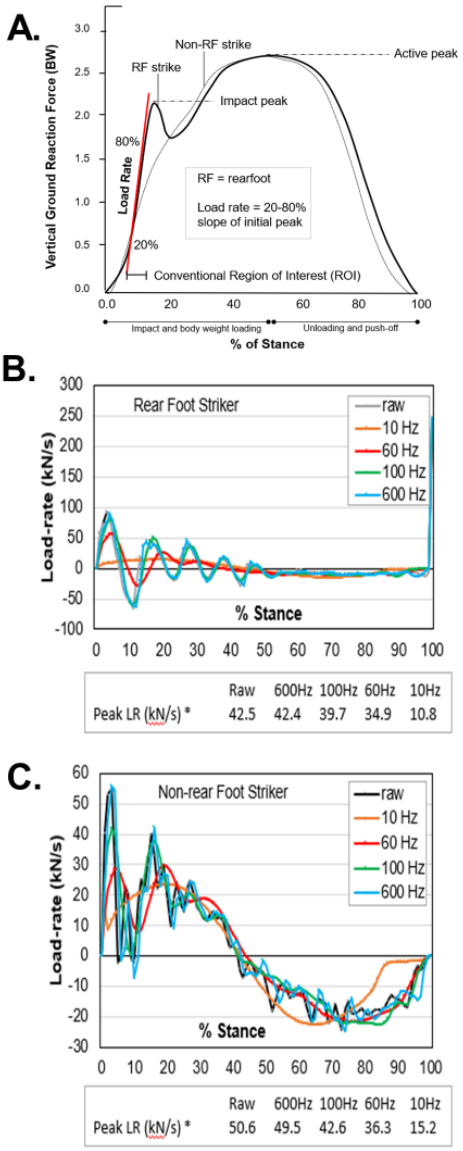

Figure 1: A. Conventional LR measures for running gait. Effect of different filtering cutoffs on LR during stance for: **B.** rearfoot strikers, and **C**. non-rearfoot strikers. Values are presented as a percent of stance.

References: Milner, C.E., Foch, E., Gonzales, J.M., Petersen, D., 2023. Biomechanics associated with tibial stress fracture in runners: A systematic review and meta-analysis. J. Sport Health Sci. 12, 333–342. https://doi.org/10.1016/j.jshs.2022.12.002

Senevirathna, A.M., Pohl, A.J., Jordan, M.J., Edwards, W.B., Ferber, R., 2023. Differences in kinetic variables between injured and uninjured rearfoot runners: A hierarchical cluster analysis. Scand. J. Med. Sci. Sports 33, 160–168. https://doi.org/10.1111/sms.14249

LOWER EXTREMITY BIOMECHANICS AFTER INTEGRA ANKLE REPLACEMENT OVER 3 AMBULATORY EXERCISES

Caroline Nealon[1], Sana Farrukh [2], Evan Dooley [3], Shawn D. Russell Ph.D.[1,2,3]
University of Virginia, Depts of [1]Biomedical Eng., [2]Mechanical Eng., and [3]Orthopaedic Surgery, Charlottesville, VA, USA
Email : cen6gxh@virginia.edu

Introduction: Over the last two decades, total ankle arthroplasty (TAA), also known as replacement, has become the increasingly popular surgical treatment of end-stage ankle joint arthritis compared to ankle arthrodesis (AA), also known as fusion. Despite reports of TAA having improved patient outcomes [1, 2], little has been done to examine how TAA affects the motion of adjacent joints within the foot. Ankle replacements aim to return patients to full function, though we know that they reduce the range of motion (ROM) attained at the ankle joint. Previous studies have found little change in joint angles when looking at level walking, so to elicit difference we added a laterally tilted surface. The study utilizes the seven segment (pelvis, left and right femur, left and right tibia, left and right feet) Vicon Nexus Plug-in Gait model to examine the differences in the lower limb kinematics and spatiotemporal parameters in patients before and after TAA. We expected the step length, velocity, and ROM at the ankle joint to increase.

Figure 1. Full-body marker set with extra foot markers was used for collecting data

Methods: Full-body experimental motion capture data (Fig. 1) has been collected for 10 ankle replacement candidates over multiple visits: pre-surgery baseline, 6 months post-surgery, and 12 months post-surgery. Subjects performed three activities: (1) Walking at self-selected speed over level ground (15m); (2) Walking over a 15-degree laterally-inclined surface with injured side uphill; and (3) Walking over the same inclined surface with injured side downhill. Lower extremity kinematics and spatiotemporal parameters were determined by implementing the Vicon Nexus Plug-in Gait model to calculate the ankle, knee, hip, and pelvis angles in the three anatomical planes, in addition to stride length and velocity.

Results & Discussion: Stride length and velocity increased for all activities after ankle replacement (Tab. 1). This result of longer steps and faster walking compared to pre-surgery is statistically significant ($p<0.05$) at 12 months after surgery when walking on a tilt when the injured leg is both uphill and downhill. For walking on flat ground, the result was that subjects take longer steps and walk faster compared to baseline as seen in the tilted walking, however it is not statistically significant.

Kinematic results revealed that a greater ROM was achieved for sagittal and transverse planes compared to before the ankle replacement. Statistically significant change was observed at every activity for hip internal rotation angle at 6 months. For flat walking at 6 months, the ankle internal rotation excursions resulted in statistically significant increase in ROM in the joints transverse plane. At 12 months, statistically significant change in ROM was exhibited during tilted walking with the injury downhill for hip internal rotation.

		Baseline		Month 6		Month 12	
		Mean	SD	Mean	SD	Mean	SD
Walk	Stride Length	0.98	0.22	1.06	0.18	1.07	0.15
	Velocity	0.80	0.22	0.90	0.19	0.92	0.15
	Hip Flexion	35.30	6.77	37.32	4.75	37.18	1.69
	Hip Adduction	8.82	2.75	9.43	2.98	9.49	2.76
	Hip Int. Rot.	21.08	6.87	25.82*	6.29	24.09	7.29
	Knee Flexion	49.59	7.37	51.82	9.00	49.82	8.85
	Ankle Flexion	19.74	7.19	22.02	6.66	20.55	6.52
	Ankle Inversion	5.58	2.44	5.87	1.97	7.23	4.02
	Ankle Int. Rot	21.05	7.47	23.96*	7.28	21.26	6.28
Tilt (Injury Up)	Stride Length	0.77	0.20	0.85	0.14	0.94*	0.19
	Velocity	0.59	0.20	0.68	0.13	0.76*	0.14
	Hip Flexion	29.77	10.74	31.06	4.71	35.25	8.74
	Hip Adduction	10.46	3.45	9.55	2.78	9.33	1.88
	Hip Int. Rot.	18.12	5.82	24.67*	5.47	22.03	6.66
	Knee Flexion	42.74	7.94	46.25	8.53	47.98	7.86
	Ankle Flexion	17.75	7.25	18.62	6.98	19.92	8.71
	Ankle Inversion	4.45	1.74	4.81	2.04	6.47	3.19
	Ankle Int. Rot	16.64	7.26	19.15	6.61	18.31	5.44
Tilt (Injury Down)	Stride Length	0.76	0.21	0.89	0.13	0.95*	0.15
	Velocity	0.57	0.19	0.72	0.12	0.76*	0.11
	Hip Flexion	30.66	6.23	33.83	4.91	35.94	6.20
	Hip Adduction	7.83	3.58	8.55	2.53	8.05	1.81
	Hip Int. Rot.	20.45	8.13	24.85*	6.73	25.20*	6.37
	Knee Flexion	41.84	7.46	44.78	7.55	46.07	7.69
	Ankle Flexion	17.70	7.52	18.99	7.04	17.76	5.67
	Ankle Inversion	4.96	1.74	4.90	1.99	6.42*	2.25
	Ankle Int. Rot	19.17	6.02	20.29	7.16	20.25	5.33

Table 1. Kinematics and spaciotemporal parameters for baseline, month 6, and month 12 data. P-values show paired t-test results and * indicate statistical significance ($p<0.05$)

Significance: We expected the motion of the ankle to change with TAA, so this method was developed to analyze this change and ultimately design better ankle replacement mechanisms. Only evaluating the gait of a patient walking on a flat surface is not sufficient in determining whether the replacement was successful. Having candidates perform more strenuous exercises is an improved method to identify differences in gait mechanics before and after surgery.

A marked difference observed following surgery with the TAA candidates would allow for conclusion that TAA is a highly effective means for treating ankle joint arthritis. The trends of increased stride length, velocity, and ROM suggest that the replacements are effective and successful, however the lack of statistical significance makes us unable to conclude this for certain at this time. Since paired t-tests were used to determine significance, this points to a power issue which could be solved by increasing the number of subjects. This would allow for higher confidence and potentially more statistically significant outcomes of the t-tests.

In addition, the multisegmented model provides a view of how each segment functions in relation to one another as well as how the lower extremities work during ambulatory exercises making it best suited to evaluate the progress of TAA candidates and highlights the model's overall importance in understanding internal foot motion.

Acknowledgments: UVA MAMP Lab and Integra Life Sciences

References: [1] Philippe (2008) F&A Int. [2] Norvell (2019) JB&JS.

DEEP LEARNING AUTOMATIC VIDEO HAND ACTIVITY LEVEL ESTIMATION

Ting-Hung Lin[1*], Yu Hen Hu[1], Robert Radwin[1]
[1]University of Wisconsin-Madison
[*]tlin89@wisc.edu

Introduction: The assessment of ACGIH Hand Activity Level (HAL) is vital for managing hand injuries in workers performing repetitive tasks, associated with risks like carpal tunnel syndrome [1]. Traditionally, HAL measurement relies on manual observation, leading to time-consuming and inconsistent evaluations, while recent computer vision advancements offer the potential for automation [2][3]. This study introduces an end-to-end approach for direct HAL estimation from video data, leveraging deep learning techniques to regress HAL values associated with observed tasks. Contrary to previous methods requiring manual intervention, our approach automates HAL estimation from video data, providing a more efficient and scalable solution for HAL analysis. Our approach achieves a mean absolute error of 0.27 HAL and 93% accuracy within ±1 HAL of ground truth values. The adoption of data-driven machine learning techniques not only streamlines HAL assessment but also enables broader-scale studies in workplace safety analysis.

Methods: This section details the proposed HAL estimation methodology, which consists of the following steps:

1. Pose Estimation: For each video, utilize a deep learning algorithm Mask-R-CNN to estimate the locations of 17 body joints, including the wrists and shoulders of the subject, in each video frame.
2. Feature extraction: The trajectory of hand motion is estimated as the relative locations of the wrist to the shoulder over the entire video. The motion trajectory then will be partitioned into segments of 150 point (5 seconds of video) with 15 points overlapping between successive segments. All segments belonging to the same video will have the same HAL value label.
3. Data partitioning: The above steps will be performed for each video in the dataset. Hand motion segments corresponding to each video then will be assigned to a training dataset or a testing dataset, such that the HAL value distributions at each of them are approximately the same.
4. Regression model development: Using segments of hand motion as input to train an LSTM (Long Short-Term Memory) deep learning model, whose output will predict the HAL value corresponding to the hand motion in the input segment. The model will be trained on a training dataset and its performance will be evaluated using the testing dataset.
5. HAL value prediction: Since the hand motion trajectory of a video may be partitioned into multiple segments, during testing, the LSTM model will predict a HAL value for each segment. These predicted HAL values may not be identical. If the number of segments of a testing video exceeds a minimum threshold, a robust estimate of the HAL value of the video can be obtained by first removing the maximum and the minimum estimates of the HAL values and averaging the remaining HAL estimates.

Results & Discussion: Through extensive experimentation and validation, our model demonstrated good performance, including a mean absolute error (MAE) of 0.27 and a R^2 score of 0.84. Evaluating the testing dataset, 93% was within the tolerance value ±1 of the ground truth HAL values. This study highlights the robustness and effectiveness of the proposed methodology for estimating HAL. Yet, it is important to acknowledge some limitations inherent in our dataset and experimental design:

- The dataset used in this study contains only five distinct HAL values, posing limitations on capturing the full spectrum of HAL variability and potentially hindering the model's generalizability.
- The dataset used in our study primarily focused on tasks with uniform characteristics with a duty cycle of around 50%. While this controlled setup ensures consistency and reproducibility, it may not fully reflect the complexity and variability of real-world scenarios.

Despite these limitations, the study represents a significant step forward in the field of automatic HAL estimation, demonstrating the feasibility and effectiveness of deep learning techniques in this domain. By acknowledging and addressing these limitations in future research endeavors, we can further enhance the applicability and robustness of HAL estimation models in real-world settings.

Significance: The machine learning technique we've developed for determining HAL from video recordings has demonstrated encouraging outcomes, with a mean absolute error in predictions of 0.27. This method significantly reduces reliance on manual labeling in the evaluation of HAL and represents a substantial advancement in the precision of HAL predictions. It highlights the effectiveness of deep learning methods in this field and their broader implications for improving safety measures in the workplace.

Acknowledgments: This work was supported, in part, by grants from the National Institute of Occupational Safety and Health and industry contracts.

References:

[1] Palmer, K. T., Harris, E. C., Coggon, D., & Cooper, C. (2012). Carpal tunnel syndrome and its relation to occupation: a systematic literature review. Occupational Medicine, 57(1), 57–66
[2] Yen, T. Y., & Radwin, R. G. (1995). A video-based system for acquiring biomechanical data synchronized with arbitrary events and activities. IEEE Transactions on Biomedical Engineering, 42(9), 944–948.
[3] Chen, C.-H., et al. (2015, June). The accuracy of conventional 2D video for quantifying upper limb kinematics in repetitive motion occupational tasks. Ergonomics, 58(12), 2057–2066.

THE USE OF THE OPENCAP FRAMEWORK TO ESTIMATE BILATERAL VERTICAL GROUND REACTION FORCES DURING JUMPING

Briana M. Robinson[1], Alan R. Needle[1,2], Herman van Werkhoven[1*]
[1]Department of Public Health and Exercise Science, Appalachian State University, Boone, NC, USA
[2]Department of Rehabilitation Sciences, Appalachian State University, Boone, NC, USA
*Corresponding author's email: vanwerkhovenh@appstate.edu

Introduction: Current gold standard methods of human movement analysis (i.e., marker-based motion capture and force plates) present several limitations related to excessive cost, marker placement, and procedure duration. A new open-source, web-based framework, called OpenCap, has proposed the use of smartphones to estimate three-dimensional kinematics and associated kinetics [1]. This study investigated the validity of the OpenCap framework with associated OpenSim modelling software in its ability to estimate ground reaction forces (GRF) when compared to force plates. It was hypothesized that there would be good agreement between OpenCap/OpenSim generated bilateral vertical GRF estimates and bilateral GRF measured using force plates.

Methods: Twenty participants performed three trials each of single leg (left and right) countermovement jumps (SLCMJ), and single leg (left and right) drop jumps (SLDJ). The OpenCap framework was employed to record video at 240 Hz from two smartphones and GRF force data were collected at 1000 Hz using two force plates. Resultant kinematic data from Opencap were used to estimate GRF using two methods: 1) center-of-mass method (GRF_{COM}), where COM acceleration was computed with OpenSim and used to derive ground reaction forces ($\Sigma F = ma$), 2) a torque-driven simulation (GRF_{TORQUE}) using OpenSim to predict ground reaction forces. Continuous force measures were analysed for 0.5 s prior to toe-off for the SLCMJs and from foot-contact to toe-off for the SLDJs. Root mean square error (RMSE) and mean absolute error (MAE) were used to quantify errors between the gold-standard (GRF_{FP}), GRF_{COM}, and GRF_{TORQUE} methods. Differences in the error measures (RMSE and MAE) of the two methods (GRF_{COM} and GRF_{TORQUE}) across jump types (SLCMJ and SLDJ) were analysed using a 2x2 ANOVA (two within-subject factors: Method, Jump Type)

Results & Discussion: Results indicate that average RMSE values varied between 32% BW and 47% BW and MAE between 23% BW and 36% BW depending on the method (GRF_{COM} or GRF_{TORQUE}) and the type of jump (SLCMJ or SLDJ) (Table 1). ANOVA results for RMSE indicated no interaction effect, but a significant main effect for both Method ($F(1, 19) = 7.057$, $p = .016$) and Jump Type ($F(1, 19) = 20.736$, $p < .001$). Similar results were obtained comparing MAE. Pairwise comparisons indicated that the GRF_{COM} method was more accurate than the GRF_{TORQUE} method and analysing SLCMJ results were more accurate than SLDJ results. Example GRF results shows that the accuracy varied across different trials as the estimated GRF curves were comparable in some trials but not others, possibly due to errors in kinematic tracking using OpenCap (Fig. 1). RMSE and MAE results from this study are similar to those from the original OpenCap validation study which used muscle driven simulations [1]. The GRF_{COM} method used here does not require the complex simulations associated with muscle or torque driven modelling and gave more accurate results. However, this method is not able to differentiate between legs during double leg movements, which the GRF_{TORQUE} method is able to do.

Table 1: Error measure (RMSE, MAE) results averaged across all participants and all trials.

Jump Task	$RMSE_{AVE}$ GRF_{COM}	$RMSE_{AVE}$ GRF_{TORQUE}	MAE_{AVE} GRF_{COM}	MAE_{AVE} GRF_{TORQUE}
SLCMJ	32%	36%	23%	26%
SLDJ	40%	47%	29%	36%

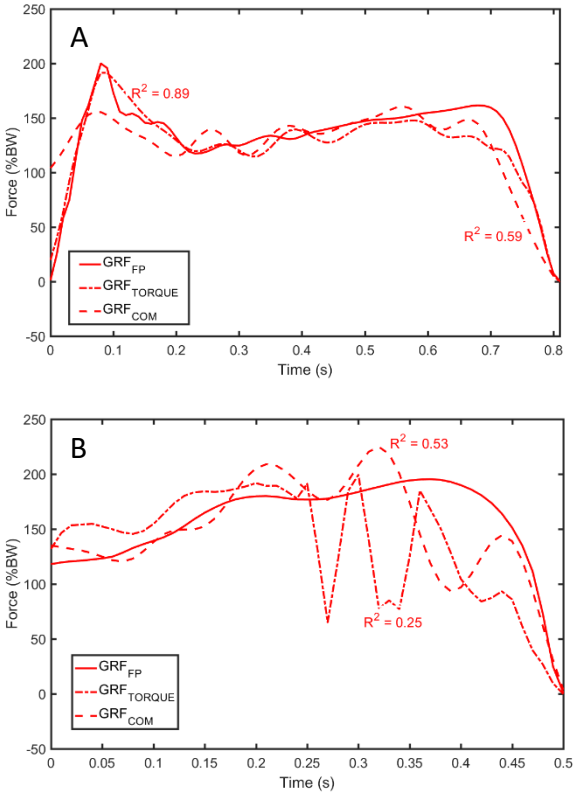

Figure 1: Two examples comparing results from GRF_{FP} to estimates from GRF_{COM} and GRF_{TORQUE}. A) Example of good comparison where curves match well during a SLDJ with GRF_{COM} and GRF_{TORQUE} showing similar trends B) Example of a trial where curves do not match well during a SLCMJ.

Significance: Our findings highlight the potential use of OpenCap for estimating GRF during jump tasks. Continuous updates to OpenCap can potentially improve the accuracy of both methods used here. The use of a more task specific torque-driven model, or perhaps a more advanced muscle-driven model could also improve results compared to the torque-driven simulation method used here (based on a running model). Improvements might reduce the need for marker-based systems and associated force plates in the future.

References: [1] Uhlrich et al. (2023). *PLoS Computational Biology 19(10)*: e1011462. https://doi.org/10.1371/journal.pcbi.1011462

LOAD SYMMETRY DURING DIFFERENT CHILD CARRYING CONDITIONS IN POSTPARTUM WOMEN

Alison Henry[1*], Robin M. Queen[1], Sara L. Arena[1]
[1]Kevin Granata Biomechanics Lab, Biomedical Engineering & Mechanics, Virginia Tech, Blacksburg, VA
*Corresponding author's email: alisonh19@vt.edu

Introduction: In 2021, over 3.5 million mothers entered the postpartum period in the United States [1]. During pregnancy, 45% of women experience lumbopelvic or pelvic pain and 25% continue to experience this pain 6 to 8 weeks post-delivery into the postpartum period [2]. In other populations limb loading asymmetries have been linked to self-identified pain in the lower back, pelvis, and hips [3,4]. Specifically in postpartum women, the added weight of a child is a risk factor for developing musculoskeletal pain or injury [5] and may increase the degree of asymmetric loading present in lower extremities [6]. Postpartum health has been largely overlooked with women only receiving one check in with their medical provider at 6 weeks postpartum. The aim of this study was to examine the effects of child-care relevant carrying on limb loading symmetry in postpartum women during level walking. We hypothesize a greater limb loading asymmetry when the external load was carried on the preferred hip compared to in a midline carrier and to no additional load condition.

Methods: Fourteen women between six and twelve months postpartum were recruited for this study approved by the Virginia Tech Institutional Review Board (IRB #24-159). To be included in the study, the most recent birth had to have been a vaginal delivery, participants had to wear a women's size 5.5 to 9.5 shoe, have no prior serious lower extremity injury or surgery, not be currently pregnant, and be between the ages of 18 and 40. Testing was completed using a lab provided neutral cushioned running shoe (Nike Zoom Pegasus: Nike, Inc., Beaverton, OR, USA) to standardize footwear between participants. The loadsol® sensors (Novel Electronics, Pittsburgh, PA, USA) were placed bilaterally inside the lab-provided shoes and data was captured at 100 Hz.

Figure 1: Baby carrying conditions during level walking

The carrying load consisted of an infant mannequin weighing 8.55 kg to simulate a 50th percentile, 9-month infant. Participants were asked to walk 14-meters at a self-selected walking speed under three loading conditions: no additional load, baby carrying on the preferred hip, and baby carrying in a midline carrier (**Figure 1**). Three trials were completed in each of the carrying conditions. All participants completed the no load carrying condition first, and the order of the other carrying conditions was randomly assigned to minimize order effects. For statistical analysis, a mixed effects model was used to determine if there was a difference in the peak impact force (PIF) or average load rate (ALR) Normalized Symmetry Index (NSI) between the three baby carrying conditions with an alpha level of 0.05 [7]. With NSI, a value of 0 represents perfect symmetry and 100 represents perfect asymmetry between limbs [7].

Results & Discussion: For PIF NSI there was no difference between the carrying conditions during level walking (p = 0.432). There was also no difference between carrying conditions for the ALR NSI during the level walking (p = 0.283) (**Figure 2**). Participants were an average of 166 cm, 72.3 kg, and 8.75 months postpartum While no statistically significant differences were found across these baby carrying conditions, the baby on hip condition tended to have the lowest asymmetry values, suggesting postpartum women may be more habituated to the carrying on the hip condition. Another potential study limitation was the lack of an adjustment period to a new baby carrier, which could have an influence on the loading patterns during this condition. In addition, the difference between carrying a weighted mannequin and a (moving) baby could alter loading patterns. Future work could include a never pregnant cohort for comparison as well as increasing the sample size given that a post-hoc power analysis indicates the need to collect 66 participants for the study to be powered to detect a difference between carrying conditions.

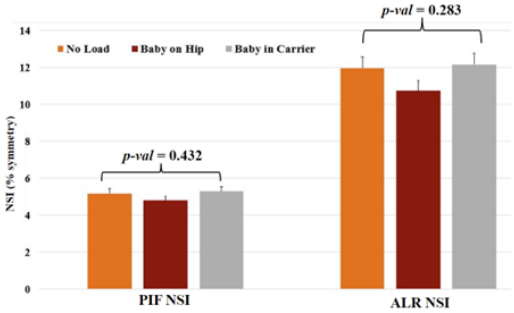

Figure 2: Symmetry differences between baby carrying conditions.

Significance: Our investigation of differences in load symmetry during child-care related carry conditions highlights the need to examine potential asymmetries during level walking while carrying a child on the preferred hip or in a carrier. Asymmetries in loading of the lower limbs may increase postpartum women's risk of a musculoskeletal injury, experiencing prolonged pain, or prevent women from fully recovering post-delivery [8]. While this was a pilot study, these results indicate the need to continue to examine different tasks and carrying conditions in postpartum women to better understand potential risk factors for musculoskeletal pain and injury and to provide evidence-based recommendations for postpartum activity progression.

References: [1] DeVita et al. (1991), *J Biomech* 24(12); [2] MulHolland et al. (2005), *PubMed* 14(1); [3] Sorensen et al. (2016), *Hum Mov Sci* 50(38-46); [4] Zagrodny et al. (2021), *Appl Bionics Biomech* (Volume 2021); [5] Vincent et al. (2013), *Physiother Res Int.* 18(2); [6] Liu et al. (2023), [7] Queen et al. (2020), J Biomech 23(99), [8]Solomonow et al. (2009), *J Bodywork and Movement* 13(2)

COMPARATIVE ANALYSIS OF DEEP LEARNING-BASED GAIT PHASE ESTIMATION ALGORITHMS USING MINIMAL KINEMATIC INFORMATION UNDER VARIOUS WALKING CONDITIONS

Tran Ngoc Bao Huynh[1], Vishnu Pisharam[1], and Hyunglae Lee[1,*]
[1]Neuromuscular Control and Human Robotics Laboratory, Arizona State University, Tempe, USA
*Corresponding author's email: hyunglae.lee@asu.edu

Introduction: Accurately estimating the gait phase–a continuous variable denoting the timing as a percentage of the gait cycle–is crucial for a variety of applications. These applications include controlling wearable robotic devices such as lower extremity exoskeleton robots and prostheses, assessing abnormal gait patterns clinically, and facilitating rehabilitation and physical therapy. Although multiple strategies have been developed to tackle this problem, deep learning (DL)-based algorithms have recently gained popularity over traditional methods. However, most studies to date face one or more of the following limitations: estimation under highly constrained walking conditions, the need for multiple sensors, and the development of algorithms that do not easily generalize to new subjects. To overcome these challenges, this study aims to test recent popular DL algorithms for estimating the gait phase under a variety of walking conditions using minimal joint kinematic information and to evaluate each algorithm's ability to generalize to new subjects.

Methods: Twelve healthy young adults (8 males, 4 females; Mean age: 24.5 years; Mean height: 1.70 m; Mean mass: 69.2 kg) participated in this study which was approved by the Institutional Review Board of Arizona State University (STUDY00014244). Each participant walked for 5 minutes on an instrumented treadmill (Bertec, OH), five times, but at different inclination angles (0–5 degrees). During the walks, the treadmill speed randomly changed from 0.8 to 1.5 m/s every 30 seconds. Hip kinematic data were captured at 200 Hz using a 3D motion capture system (VICON, UK). The data were segmented by gait cycle, determined from the initial contact of the foot with the ground to the next time the same foot contacts the ground. Hip phase angle, defined as polar angle in the phase plane that consists of hip angle and hip angular velocity, was used as sole joint information for gait phase estimation. The gait phase percentage and hip phase angle were converted to Cartesian coordinates (i.e., pair of sine and cosine values) to ensure continuity and avoid boundary condition issues at 0 (or 100) % of the gait cycle for gait phase and 0 (or 360) degrees for hip phase angle.

Five different DL models were implemented for performance comparison: Convolutional Neural Network (CNN), Long Short-Term Memory network (LSTM), CNN–LSTM, Auto-Encoder (AE)–LSTM, and Variational Auto-Encoder (VAE)–LSTM. The hip phase angle, leg length, step length (approximated by the hip angle and leg length), and weight were consistently used as input to the models, while the gait phase was used as output from the models. The CNN–LSTM, AE–LSTM, and VAE–LSTM models used self-attention mechanisms to weigh the importance of different input components differently. Only single-leg (left leg) information was used in this study to test the algorithm with minimal kinematic information. To perform a subject-independent evaluation, the models were trained using data from 11 subjects and tested on the twelfth subject, repeating this process for all subjects. The mean root-mean-square error (RMSE) was calculated to compare the performance of the DL models.

Results & Discussion: The performance of VAE–LSTM outperformed the other DL models in predicting gait phase under various walking conditions, as can be seen from the bar graphs in Figure 1. The mean and standard deviation for the RMSE of CNN, LSTM, CNN–LSTM, AE–LSTM, and VAE–LSTM were 6.2 ± 4.6%, 6.0 ± 4.1%, 3.4 ± 1.7%, 4.4 ± 2.2%, and 2.7 ± 0.7%, respectively. Pairwise comparisons between VAE–LSTM and the other 4 models using Wilcoxon signed rank test showed statistical significance: $p = 0.00048$ with CNN and LSTM, and $p = 0.0068$ with CNN–LSTM and AE–LSTM. Furthermore, VAE–LSTM was more robust in predicting the gait phase for unseen subjects, as evidenced by the low maximum RMSE values: 16.2%, 16.7%, 6.8%, 9.0%, and 4.1% for CNN, LSTM, CNN–LSTM, AE–LSTM, and VAE–LSTM, respectively. The robust performance of the VAE–LSTM for subject-independent analysis may be because its probabilistic approach of modeling the latent space as a distribution provides a more smooth and structured way to capture and learn the variability across subjects.

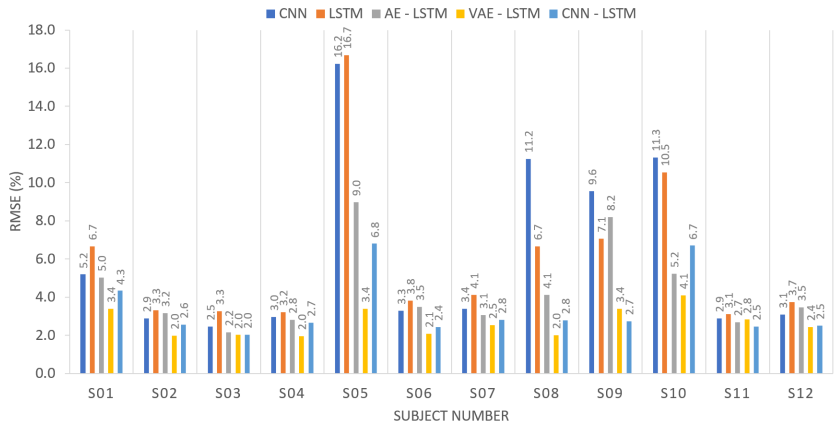

Figure 1: Performance comparison of the 5 different DL models. The RMSE (%) was presented at the top of each bar.

Significance: Accurate estimation of the continuous gait phase through advanced DL algorithms has substantial potential to overcome the limitations of traditional approaches and contribute to gait studies in various applications, including clinical biomechanics, wearable robotics, and rehabilitation. By training and testing DL models with cross-subject data under a wide range of walking conditions such as different walking speeds and terrains, we can significantly improve the robustness and precision of gait phase estimation. Furthermore, by relying on minimal kinematic information (such as hip kinematics, as demonstrated in this study) for robust prediction, we can streamline real-time applications, reducing the need for numerous sensors and simplifying the technology without compromising performance.

References: [1] Kang, I et al. (2019), *IEEE Transactions on Medical Robotics and Bionics*; [2] Park, H et al. (2023), *Frontiers in Human Neuroscience*

Simulating faster walking speed to encourage greater knee kinetics and kinematics

Kyle Southall[1], Stephenie Fowler[1], Colby Kunkel[1], Christopher Hurt[1,2]*
[1]Rehabilitation Science, [2]Physical Therapy, University of Alabama at Birmingham
*Corresponding author's email: cphurt@uab.edu

Introduction: After anterior cruciate ligament reconstruction, gait maladaptations resulting in changes to knee motion and muscular activity may increase risk of early onset osteoarthritis [1]. Larger knee range of motion and muscular activation can be encouraged by walking at faster speeds or with increased treadmill slope however, each method has limitations for patients. We have previously shown that walking on a treadmill at a constant speed against a progressively increasing posteriorly directed resistive force applied at an individual's COM can result in similar physiologic outcomes as the Bruce Protocol in which individuals often end the test running uphill [2]. This suggests that backward directed resistive forces are a valid way to increase mechanical work. Thus, slower walk speeds against resistive forces may also result in similar amounts of EMG and gait kinematics compared to faster walking speeds. The purpose of this study is to compare knee kinematics and muscle activation of young healthy individuals at two different speeds against progressive backward directed resistance.

Methods: We recruited healthy individuals for this institutionally approved study (n=10, H= 1.71 m, SD= 0.11 m, mass= 77 kg, SD= 21.8 kg). Inclusion criteria were individuals between the ages of 18-35 without any known musculoskeletal impairments. All participants were active at least 3 days each week in an effort to reflect a similar population to those who experience ACL tears that require reconstructive surgery. Participants were asked to walk on ResistX, an innovative treadmill interface that allows for a constant applied force at the center of mass while individuals ambulate. Participants walked for twelve trials against forces between 0-25% of their bodyweight (incremented by 5% bodyweight per trial) at 0.5 m/s and 1.0 m/s. The order of the trials was random, and each participant walked for one minute during each trial. The motion of passive reflective markers was tracked with an 8-camera motion capture system (Vicon), at 100 Hz. Marker position was processed and tracked in Vicon Nexus Software processed in Visual 3D. Bilateral knee joint angular data was processed and filtered at 6 Hz with a low pass Butterworth filter. In order to determine the relationship between resistive forces and joint kinematics, maximum and minimum knee joint flexion during stance, knee angle at heel strike, and total knee range of motion were quantified. A wireless electromyography (EMG) data acquisition system was used to collect EMG data during each trial (Delysis). EMG data was collected from the vastus lateralis, vastus medialis, and biceps femoris. The data was zeroed, rectified, and filtered using a low pass Butterworth filter at 25 Hz. A linear envelope was created, and the data integrated between heelstrike and toeoff to quantify EMG during the stance phase of gait. Our statistical analysis consisted of a two-factor repeated-measures ANOVA for the kinematic and EMG data respectively. The two factors were speed (0.5 m/s and 1 m/s) and resistive force (0%, 5%, 10%, 15%, 20%, and 25% of body weight). For significant main effects we performed a post-hoc comparisons with a Bonferroni correction. Significance level was set to $p < 0.05$.

Results & Discussion: For maximum knee flexion during stance, we observed no significant interaction between speed and force ($p=0.181$), a main effect of speed ($p=0.422$), and a main effect of force ($p<0.01$). Posthoc analysis showed that at least 15% added force was required to see a difference compared to 0 force ($p=0.01$). For total knee range of motion, we observed no significant interaction between speed and force ($p=0.60$), a main effect of speed ($p=0.491$), and a main effect of force ($p<0.01$). Posthoc analysis showed that at least 15% added force was required to see a difference compared to 0 force ($p=0.01$). Regarding the EMG data, for the vastus medialis we observed no significant interaction between walking speed and force trials ($p=0.455$), a main effect of walking speed ($p=0.022$) and a main effect of force ($p<0.01$). Posthoc analysis showed that at least 15% added force was required to see a difference compared to 0 force ($p<0.01$). For the vastus lateralis we observed no significant interaction between walking speed and force trials ($p=0.119$), a main effect of speed ($p=0.600$), and a main effect of force ($p<0.01$). Posthoc analysis showed that 10% was required to achieve a difference compared to 0 force ($p=0.041$). For the biceps femoris we observed no significant interaction between walking speed and force trials ($p=0.283$), a main effect of speed ($p=0.283$), and a main effect of force ($p<0.01$). Posthoc analysis showed that at least 15% added force was required to see a difference compared to 0 force ($p<0.04$). We have previously used backward resistive forces to create exercise testing paradigms that limit the extent that individuals have to walk faster or encounter increased treadmill slope [2]. Some individuals are limited to slower walk speed or may become unstable with greater treadmill slope. For these individuals, using resistive forces at the center of mass could be beneficial as a therapeutic intervention early in a rehabilitative protocol to accentuate range of motion and muscular activation while performing a functionally relevant task (i.e., walking).

Significance: We report a pilot study consisting of healthy active individuals and these results can be used to design a study for individuals who are in the recovery phase from an ACL injury. Resistive treadmill walking at a slow speed and with backward resistive forces equaling at least 15% body weight could be utilized as a potential intervention for targeting the impairments of knee joint stiffness and decreased quadriceps activation.

References: [1] Lewek et al. (2006), *Gait & Posture* 23(4); [2] Hurt et al. (2020), *Strength & Cond 34*(12).

LOCOMOTION MODE CLASSIFICATION USING MOTION CAPTURE DATA

Jayden Oh[1*]
[1]Phillips Exeter Academy
*Corresponding author's email: jayden.oh.08@gmail.com

Introduction: The integration of motion capture technology into the study of human locomotion has not only opened new avenues for enhancing assistive device technologies, such as robotic exoskeletons but also holds significant potential for advancing human health monitoring. Unlike traditional methods that rely heavily on invasive and user-specific sensors, motion capture offers a non-invasive, highly accurate alternative for analyzing human movement. This research aims to leverage motion capture data to develop a subject-independent classification system for locomotion mode classification, which is crucial for the adaptive functionality of robotic exoskeletons. Additionally, this technology can be applied to monitor vital health metrics and detect anomalies in movement patterns, potentially indicating underlying health issues. Such a system promises to significantly improve the autonomy and usability of assistive devices by enabling them to adjust to the user's locomotion, without the need for extensive personal calibration, while also providing valuable insights into the user's health and physical condition. Our study explores the potential of motion capture technology to redefine the interaction between exoskeletons and their users, aiming to make these devices more intuitive and accessible to a broader population, and to extend the application of this technology to comprehensive health monitoring, thereby offering a dual benefit of enhanced mobility assistance and health oversight.

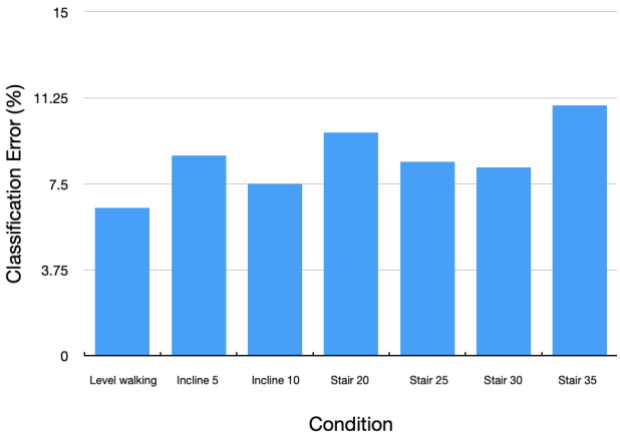

Figure 1: Results showed classification error for each condition.

Methods: This study utilizes previously published motion capture data to collect detailed kinematic data from participants performing a variety of locomotion tasks, including different levels of incline walking, and ascending stairs. Participants were outfitted with reflective markers placed at key anatomical locations to ensure comprehensive motion tracking. The motion capture data were then processed to extract relevant features, such as joint angles and velocities, which are critical for distinguishing between different modes of locomotion. A CNN model was trained with these features to classify the locomotion modes in a subject-independent manner. The model's performance was assessed through cross-validation techniques to ensure its accuracy and generalizability across different individuals. Our approach emphasizes the fusion of high-fidelity motion capture data with advanced computational methods to achieve precise and user-independent locomotion mode classification.

Results & Discussion: The implementation of motion capture data in locomotion mode classification demonstrated exceptional accuracy, outperforming traditional sensor-based methods in terms of both precision and adaptability. The model achieved a high classification success rate across all tested locomotion modes, highlighting the effectiveness of motion capture technology in capturing nuanced human movements. Notably, the system's subject-independent performance underscores its potential for widespread application in robotic exoskeletons, eliminating the need for user-specific calibration.

The discussion focuses on the transformative impact of integrating motion capture data into the development of assistive technologies. The precision of motion capture allows for a more nuanced understanding of human locomotion, enabling the creation of exoskeletons that can more naturally complement the user's movements. Furthermore, our findings reveal the feasibility of real-time locomotion mode classification using motion capture data, a critical requirement for the seamless operation of adaptive exoskeletons in everyday environments. Challenges such as the processing speed of motion capture data and the need for marker placement optimization are addressed, with suggestions for future research to enhance system efficiency and user experience.

Significance: Utilizing motion capture data for continuous locomotion mode classification represents a significant leap forward in the field of assistive robotics. Our research not only demonstrates the feasibility of a subject-independent, adaptive control system for robotic hip exoskeletons but also paves the way for more natural and intuitive human-device interactions. By reducing the barrier to effective exoskeleton use, motion capture technology has the potential to dramatically improve the mobility and quality of life for individuals with locomotion impairments, marking a pivotal step towards the realization of fully adaptive, user-friendly assistive devices.

References: [1] Emma et al. (2021), *Scientific Data* 8(1)

IN VIVO SEGMENTAL CONTRIBUTIONS TO PLANAR MOTION: IMPLICATIONS FOR THOSE WITH CHRONIC NECK PAIN

Craig C. Kage, Rebecca E. Abbott, Matthew MacEwen, Alain Nishimwe, Jonathan Sembrano, Nathaniel Helwig, Arin M. Ellingson
University of Minnesota – Twin Cities
*Corresponding author's email: ellin224@umn.edu

Introduction: Neck pain (NP) remains a globally prevalent and disabling musculoskeletal condition. Clinically, range of motion (ROM) is a valuable component for pathology screening and documentation [1-3] but is imprecise and unable to capture subtle underlying movement abnormalities or dynamic motion at an individual vertebral level. Kinematic differences have been identified between those with and without NP at the global kinematic level (head-relative-to-torso) [4,5] and video-fluoroscopy (single plane) has been utilized to investigate kinematic differences in those with neck pain, but only for flexion and extension motions. [6,7] The limitation of examination techniques has resulted in challenges in specific diagnosis for those with NP and appropriate associated treatment. The purpose of this work was to measure cervical spine kinematics across 3 trials of each cardinal plane ROM (flexion/extension, lateral bending, and axial rotation) between healthy controls and those with chronic NP. Head-to-torso and intersegmental kinematics of the cervical spine (C4-C7) were investigated to identify any group differences based on segmental ROM and contribution to total ROM.

Methods: After IRB approval and informed consent, 13 individuals with chronic mechanical NP (>12 weeks) and 10 age/sex matched healthy adults were enrolled. Global (head-to-torso) kinematics were captured using optical motion capture (Vicon) and segmental kinematics (C4, C5, C6, C7) via biplane videoradiography using a CT-based digitally reconstructed radiograph (DRR) optimization approach. Global (head-to-torso) and segmental (head-C4, C4-C5, C6-C7, and C7-torso) ROM were measured from each dynamic trial. The percent contribution to global ROM was further calculated for each level (head-C4, C4-C5, C5-C6, C6-C7, and C7-torso). Differences between groups were elucidated using non-parametric permutation tests [8] across each distinct trial and the average of the three trials for both ROM and %ROM.

Results & Discussion: Table 1 displays the summary statistics across level and trial, with statistically significant differences between groups denoted. Although chronic NP is a very heterogeneous group, these data showed a statistically significant reduction in axial rotation ROM at the C5-C6 level. Further analysis is underway to determine trial and level difference between groups, along with exploration into the individual pathways of motion across individuals.

Significance: To the authors' knowledge, this is the first study to examine individuals with chronic neck pain using biplane videoradiography for all cardinal plane motions.

Table 1. Summary Statistics across level and trial.
**indicates significant difference ($p<0.05$) and † ($p<0.1$) between groups for that trial.*

			Trial 1		Trial 2		Trial 3		Average	
			Neck Pain	Control	Neck Pain	Control	Neck Pain	Control	Neck Pain	Control
Range of Motion (degrees)	AR	Head-Torso	139.7±10.6	147.3±12.9	139.1±12.6	148.7±11.9	141.1±10.6	148.8±11.9	140±10.8	148.3±11.9
		Head-C4	98.3±7.5	97.3±8.5	98.1±7.7	98±9.2	98.4±7.3	96.6±8.5	98.3±7.3	97.3±8.6
		C4-C5	10.8±2.8	11.6±2	10.5±2.5	11.7±2.1	10.7±2.8	12±2.2	10.7±2.6	11.8±2.1
		C5-C6	8.3±1.7	10.3±2.2	**8.1±1.6***	**10.8±1.8***	**8.4±1.5***	**10.5±1.7***	**8.3±1.5***	**10.5±1.8***
		C6-C7	5.1±1.4	5.9±1.7	5.2±1.5	6.1±1.4	5.6±1.4	6.2±1.9	5.3±1.3	6.1±1.6
		C7-Torso	7.7±2.9	10.2±3.6	7.4±4.1	10.1±3.9	7.7±3.8	10.3±3.7	7.6±3.4	10.2±3.5
	LB	Head-Torso	91.7±12.3	91.7±9.5	91.4±12.3	90.7±10.4	91.8±12.7	90.2±12.1	91.6±12.3	90.9±10.4
		Head-C4	39.9±7.5	41.5±7	40.3±7.4	41.9±6.8	40.1±7.2	41.5±6.3	40.1±7.3	41.6±6.5
		C4-C5	13.2±2.3	13.5±2.3	12.9±2.4	13.1±3.1	13.4±2.3	12.9±2.7	13.1±2.2	13.2±2.6
		C5-C6	13.6±2.9	13.4±2.9	13.4±3.2	13.8±2.5	13.5±3.1	13.7±3.5	13.5±3	13.6±2.9
		C6-C7	14.4±3.1	15±2.3	14.4±3	15.2±2.4	14.5±3.6	15±2.6	14.4±3.1	15.1±2.4
		C7-Torso	14.3±5.3	13.3±4.6	14.3±4.7	12.2±3.7	13.9±4.5	12.3±5.4	14.2±4.7	12.6±4.2
	FE	Head-Torso	114.8±13.5	128.2±12.8	114.3±12.8	127.6±13.3	117±15.1	128.5±12.5	115.4±13.5	128.1±12.6
		Head-C4	**57.5±11.5†**	**68.2±7.6†**	59.6±13.7	67.4±6.8	59.8±12.8	67.3±7.4	59±12.6	67.6±7.1
		C4-C5	19.2±3.7	19.1±2.9	19.4±3.4	19.6±2.2	19.8±3.4	19.2±2.6	19.5±3.4	19.3±2.5
		C5-C6	18.3±3.8	20.6±2.5	**17.3±4.3†**	**20.8±1.6†**	17.9±3.7	20.5±2.2	17.8±3.7	20.6±2
		C6-C7	15.5±3.7	16.3±3.7	14.7±3.9	16.4±4	14.8±3.9	16±4.1	15±3.7	16.2±3.9
		C7-Torso	12.3±4.9	12.7±5.1	12.1±5.1	12.5±5.8	13±4	13.1±6.5	12.5±4.5	12.7±5.6
Percent Contribution (% head-torso ROM)	AR	Head-C4	70.4±4.7	66.2±5.4	70.7±5.6	65.9±4.4	69.9±5	65±4.7	70.3±5	65.7±4.6
		C4-C5	7.6±1.6	7.9±1.2	7.5±1.6	7.9±1.2	7.5±1.7	8.1±1.3	7.6±1.6	7.9±1.2
		C5-C6	5.9±0.9	7±1.3	**5.8±0.9***	**7.3±1.1***	5.9±0.9	7±1.1	**5.9±0.9***	**7.1±1.1***
		C6-C7	3.6±0.8	3.9±0.9	3.7±0.9	4.1±0.9	3.9±0.8	4.1±1.1	3.7±0.7	4.1±0.9
		C7-Torso	5.5±2.1	6.8±2.1	5.2±2.6	6.7±2.1	5.4±2.5	6.8±2	5.4±2.3	6.8±1.9
	LB	Head-C4	43.5±6.3	45.3±6.2	44.2±6.1	46.1±5.6	43.8±5.8	46.1±4.9	43.8±5.9	45.8±5.5
		C4-C5	14.4±2.1	14.8±2.2	14.2±2.5	14.5±2.9	14.7±2.5	14.5±3	14.4±2.2	14.6±2.5
		C5-C6	14.8±2.4	14.6±2.8	14.5±2.5	15.2±2.4	14.7±2.8	15.1±2.8	14.7±2.5	14.9±2.6
		C6-C7	15.7±2.5	16.4±2.1	15.7±2.4	16.9±2.4	15.6±2.8	16.7±2.6	15.7±2.4	16.7±2.2
		C7-Torso	15.5±4.9	14.4±4.5	15.5±4.2	13.3±3.5	15.1±4.1	13.4±4.7	15.3±4.3	13.7±3.8
	FE	Head-C4	50.1±8.7	53.3±5.1	51.8±9.3	53.3±6.6	51±8.2	52.6±5.8	51±8.6	53.1±5.8
		C4-C5	16.7±2.3	14.9±1.7	17±2.4	15.4±1.6	17±2.4	14.9±1.5	16.9±2.3	15.1±1.5
		C5-C6	16±3.6	16±1.2	15.3±4.3	16.4±0.8	15.4±3.3	15.9±0.8	15.6±3.6	16.1±0.7
		C6-C7	13.4±2.6	12.8±2.6	12.9±3.1	12.8±2.6	12.6±2.7	12.4±2.8	13±2.7	12.6±2.6
		C7-Torso	10.8±4.6	9.7±3.5	10.7±4.5	9.5±4	11.1±3.4	10±4.4	10.9±4	9.7±3.9

Acknowledgments: Funding was provided by the following NIH awards: R03HD09771 and F32AR082276.

References: [1] Stiell et al. JAMA, 2001. [2] Treleaven et al. Man Ther, 2016. [3] Wibault et al. Eur Spine J, 2014. [4] Moghaddas et al. Physiotherapy, 2019. [5] Salehi et al. Musculoskelet Sci Pract, 2021. [6] Branney and Breen, Chiropr Man Therap, 2014. [7] Qu et al. Clin Biomech, 2020. [8] Helwig. Computational Statistics, 2019.

RESTORING ASSYMETRY IN KNEE FUNCTION AFTER ANTERIOR CRUCIATE LIGAMENT RECONSTRUCTION: A DYNAMIC STEREO XRAY IMAGING AND NEUROMUSCULAR SIMULATION STUDY

Colin R. Smith[1*], Austin Carcia[1], Kristen Seballos[1], Armando Vidal[1,2], Jonathan Godin[1,2], Thomas Hackett[1,2], Matthew T. Provencher[1,2], Peter J. Millett[1,2], Johnny Huard[1], Scott Tashman[1]
[1]Steadman Philippon Research Institute, [2]Steadman Clinic, Vail, CO, USA
*Corresponding author's email: csmith@sprivail.org

Introduction: While modern anterior cruciate ligament reconstruction (ACLR) surgeries are largely successful at restoring knee stability, high rates of long term post-traumatic osteoarthritis are still prevalent. Dynamic Stereo Xray (DSX) and quantitative MRI have demonstrated that altered cartilage contact patterns during functional movements are correlated with degeneration [1]. However, while modern surgical techniques aim to anatomically reconstruct the ACL and rehabilitation protocols aim to restore neuromuscular function before return to sport, asymmetries in joint function continue to persist in today's patients.

We developed a next-generation musculoskeletal simulation framework, OpenSim-JAM (Joint and Articular Mechanics), to predict the influence of surgical and neuromuscular factors on post-operative cartilage loading patterns [2]. This investigation aims to 1) validate simulation predictions of knee joint kinematics, cartilage contact, and ACL elongation against *in vivo* DSX measurements and 2) investigate whether altered muscle strength and neuromuscular coordination are the cause of abnormal cartilage loading after ACLR.

Methods: Seventeen patients (11 Female, Age = 32.8±3.1 years) who underwent unilateral, anatomical bone-patellar tendon-bone ACLR were included in this study. These patients represent a subset of a larger group participating in an IRB-approved, ongoing clinical trial investigating the use of platelet-rich plasma and bone marrow concentrate to accelerate healing (IRB# 2019-13, NCT04205656). The participants underwent a CT scan, MRI, muscle strength test, and dynamic stereo x-ray (DSX) assessment of knee joint function at 6 and 12 months after surgery. DSX imaging was collected using 1ms pulsed exposures (90 kVp and 120mA) at 120 frames/s during downhill running (10-degree decline, 2.5 m/s) on an instrumented, dual-belt treadmill, with acquisitions triggered just before foot-strike. The CT scans were segmented and registered to the biplanar x-ray images to assess knee kinematics. ISB standard coordinate systems were used to calculate the asymmetry between the intact and ACLR knee. Isokinetic muscle strength tests were performed over the knee flexion/extension range of motion and were summarized by the asymmetry in the peak torque and total work.

A personalized full body musculoskeletal model was constructed for a single patient. Measured ground reaction forces and motion capture kinematics of a single cycle of downhill running at 12 months post-op were used as inputs to OpenSim-JAM simulations to predict the internal knee mechanics. A detailed knee model including 5 tibiofemoral, 6 patellofemoral, and 12 tibiomeniscal degrees of freedom was integrated into the musculoskeletal model based on MRI segmentations of the tibia, femur, patella and meniscus geometries from the ACLR knee. Contact between cartilage and meniscus articular contact was represented using an elastic foundation model. A sensitivity study was performed where the muscle redundancy optimization cost function was altered to encourage medial and lateral hamstrings co-activation and the predicted joint kinematics were compared against the synchronized DSX measurements.

Results & Discussion: Knee extensor (6 month: 41.3%, 12mo: 26.2%) and flexor (6 month: 11.1%, 12mo: 6.4%) muscle strength weakness was measured in nearly all ACLR knees. Similar to previous DSX studies, patient-to-patient variability was observed in the anterior translation asymmetry where both increased and decreased anterior translation was present among the ACLR knees. However, in nearly every patient, the ACLR knee was externally rotated compared to the healthy contralateral.

The musculoskeletal simulations demonstrated better agreement with the DSX measurements in anterior translation compared to internal rotation. This is consistent with our previous sensitivity studies of ACLR pretension and muscle coordination, which demonstrated the largest uncertainty in predictions of internal rotation. Preferentially activating the medial vs lateral hamstrings modulated the predicted internal rotation suggesting that restoring neuromuscular function may be key to achieving healthy cartilage loading patterns.

Significance: For several decades it has been known that ACL reconstructed knees exhibit altered knee kinematics during dynamic activities. However, after achieving anatomic ACL reconstruction, it remains unknown how to improve clinical treatments to restore symmetric knee function. This investigation is the first *in vivo* validation of OpenSim-JAM predictions of knee mechanics in ACLR knees during highly dynamic activities and suggests that persistent asymmetries in neuromuscular function may be the key factor driving abnormal cartilage loading in ACLR knees.

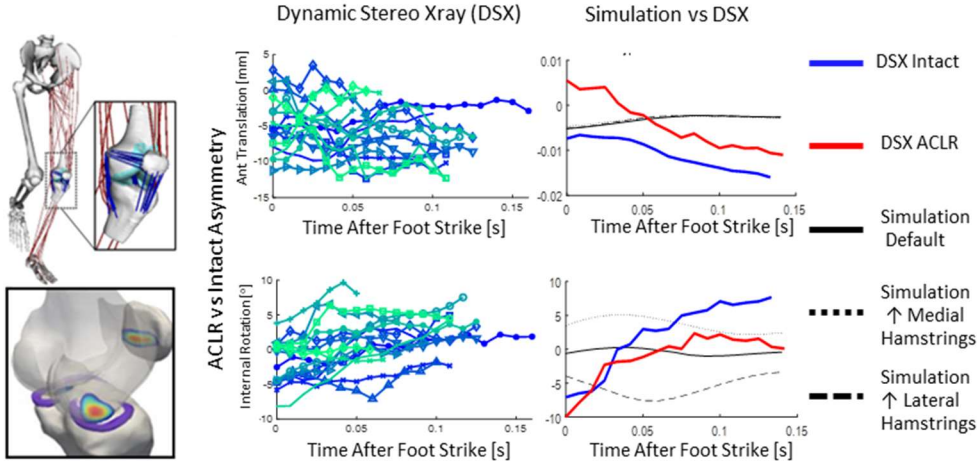

Figure 1 (left) Personalized simulation prediction of ACLR knee joint mechanics. (middle) DSX measured asymmetries in ACLR kinematics. (right) Simulation validation and sensitivity study.

Acknowledgments: Department of Defence, Office of Naval Research, Contract # N00014-19-C-2052

References:

[1] Tashman. (2021), *KSSTA*, 29:2676-83;
[2]https://simtk.org/projects/opensim-jam

The Impact of Cushioned Flooring on Metatarsophalangeal Joint Loads During Single Leg Landings

Ankur Padhye[1*], Stacey Meardon[1], and John Willson[1]
[1]Department of Physical Therapy, East Carolina University, Greenville. NC
*Email: padhyea20@students.ecu.edu

Introduction: Single leg landing maneuvers are integral to high-intensity sports[1] and there has been an increase in such high-intensity sports participation on cushioned artificial surfaces designed to moderate musculoskeletal forces during landing. However, there is conflicting evidence about the impact of flooring surface on injury risk[2,3] and little analysis of foot injury risk factors including metatarsophalangeal (MTP) joint contact forces (JCF). Thus, the purpose of this study was to compare MTP JCF during a single-leg landing task with and without a cushioned artificial sports-court flooring surface.

Methods: Time synchronized left foot 3D marker data (200 Hz), ground reaction forces (2000 Hz), and in-shoe plantar pressure data (200 Hz) were recorded from 14 individuals (9F, 5M, 1.69 m, 69.54 kg) during single leg landings from 80% max vertical jump height with (Mat) and without (NoMat) sports-court flooring with ASTM F2772 Class 4 shock absorption properties, in random order. Plantar pressure data used regression equations to define areas (masks) of the foot[4] which were used to assign GRF to metatarsal and toe regions for MTP joint moment and joint reaction force inverse dynamics calculations at each MTP joint. Toe flexor muscle force contributions to MTP JCF were estimated using subject-specific moment arms from scaling factors derived using CT informed individual metatarsal radii. The resultant JCF (RJCF) at each MTP joint were calculated and peak RJCF and RJCF impulse averaging over 5 trials were compared between Mat and NoMat conditions using paired t-tests (α=.05).

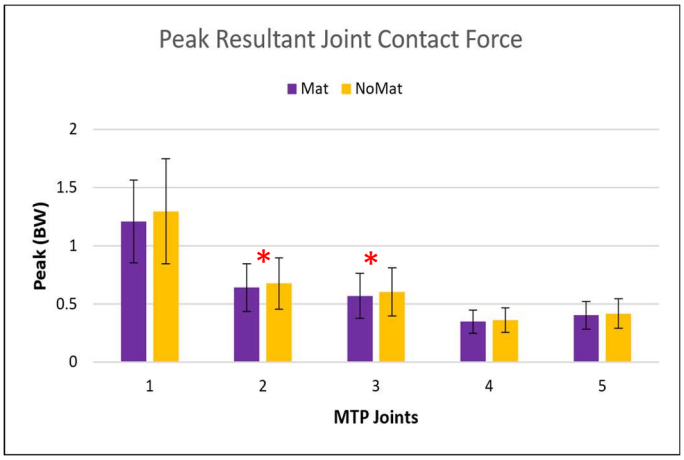

Figure 1: Body weight normalized peak RJCF for all 5 MTP joints. Error bars represent standard deviation. *p < 0.05.

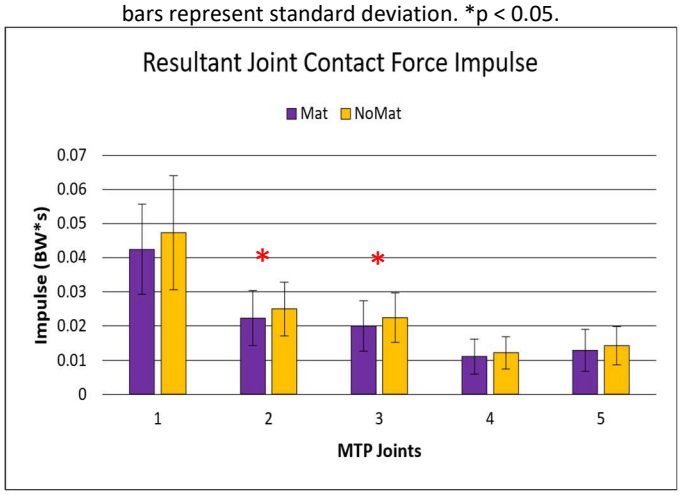

Figure 2: Body weight normalized RJCF impulse for all 5 MTP joints. Error bars represent standard deviation. *p < 0.05.

Results and Discussion: Sports-court flooring reduced peak RJCF at the 2nd and 3rd MTP joints by 5% (p=.03) and 6% (p=.02), respectively (Figure 1). The RJCF impulse was 12% lower during the Mat condition at the 2nd (p=.049) and 3rd (p=.045) MTP joints compared to the NoMat condition (Figure 2). This is consistent with previous literature [5] where the metatarsal strain lowered with use of cushioned footwear compared to barefoot. Further, a 12% reduction in the RJCF impulse suggests that flooring affects both the amplitude and duration of 2nd and 3rd MTP joints kinetics. As the 2nd and 3rd metatarsals are most prone to bone stress injury, lower peak JCFs and JCF impulse may therefore reduce metatarsal injury risk for jumping athletes. Moreover, transitions between facilities with and without cushioned surfaces may impose novel MTP joint loads that contribute to injury risk.

Significance: Decreased MTP JCF were observed in response to cushioned sports-court flooring during a high-intensity, sports specific landing task. The results of this study may contribute to a better understanding of modifiable environmental factors that affect metatarsal bone and MTP joint injury risk in athletes. For instance, the substantial decrease in peak RJCF and RJCF impulse at the 2nd and 3rd MTP joint over a sports court flooring could encourage performance of sports activity with cushioned flooring. Conversely, these results also highlight that athletes accustomed to training on cushioned flooring may experience greater MTP loads, during the same activities, when performing without cushioned flooring, possibly increasing their foot injury risk.

References: [1] Maniar et.al. (2022), Sci Rep 12, 11486. [2] Pine et.al. (1991), Physician Sportsmed. 19;125-128. [3] Dufek et.al. (1991), Sports Med 12(5), 326-337. [4] Parham et.al. (1991). [5] Milgrom et.al. (2002), Foot & Ankle international, 23(3); 230-235. [6] Nagel et.al. (2008), Gait & Posture 27, 152-155.

PREDICTING LOSS OF BALANCE DURING WALKING FROM BASELINE GAIT DATA

Trevor Evans[1], Ajit Chaudhari[1], Dan Merfeld[1], Mark Shelhamer[2]
[1]The Ohio State University
[2]Johns Hopkins University
Corresponding author: evans.2374@osu.edu

Introduction: Falls are a major health concern with high financial and social costs, and reducing them remains a priority. One common research approach focuses on inducing slips and trips, then creating algorithms to distinguish those who fall from those who recover [1,2]. This approach is promising, but it is limited to detecting falls or training recovery and not preventing them from happening altogether. Additionally, the movement patterns of simulated falls likely differ from real-world falls, however there is a lack of research investigating more natural losses of balance during walking [3]. To bridge this gap, we proposed a novel method of generating more natural losses of balance (LOB) such as trips and stumbles during sensory-perturbed walking, and we used this improved dataset to identify baseline gait characteristics of those who later experienced LOB versus those who did not. We hypothesized that in the group who did go on to experience a LOB during perturbed gait demonstrate significantly higher movement variability during initial baseline gait than the group that did not trip.

Methods: 43 healthy participants walked on a split-belt, custom self-paced walking treadmill with a reflective marker cluster placed over the sacrum to approximate the center of mass (COM). After an acclimation period, five minutes of baseline walking data were collected. Following the baseline trials, participants walked while experiencing combinations of three different perturbations: blurry vision, backwards counting, and brown noise played through noise-cancelling headphones. Each condition lasted five minutes followed by a two-minute washout period.
During perturbed walking, several participants temporarily lost their balance and tripped while walking, which was noted as an LOB at the instant it occurred. Participants were then split into one of two groups: those who experienced an LOB (n=10), and those who did not (n=33). The parameters of interest were COM anterior-posterior (A-P) and medio-lateral (M-L) movement variability. Two-sample t-tests were utilized to compare average variability between the LOB and no-LOB participant groups at the level $\alpha = 0.05$.

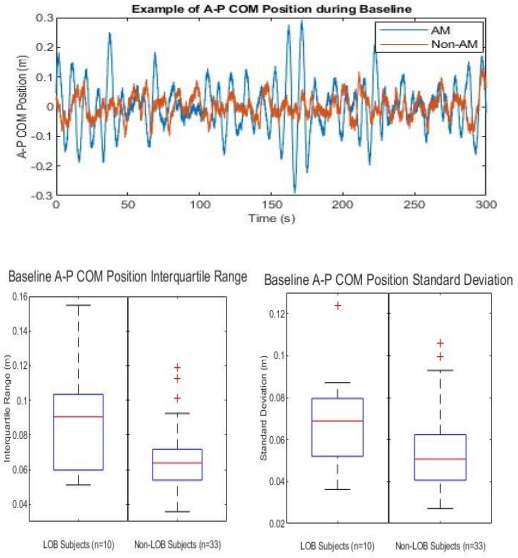

Figure 1: (top) Comparison A-P COM position during baseline walking of one typical non-LOB (orange) and one LOB (blue) participant; (bottom) Comparisons of interquartile range and standard deviation variability between LOB and non-LOB groups.

Results & Discussion: The interquartile range (IQR) for COM A-P variability was larger in the LOB group compared to the non-LOB group ($p = 0.01$), with a mean difference of 0.023 (±0.01) m/s. The standard deviation for COM A-P variability was larger in the LOB group compared to the non-LOB group ($p = 0.04$), with a mean difference of 0.015 (±.013) m/s (Figure 1). Although we also saw increases in M-L variability from some non-LOB participants relative to the LOB group, these differences were not significantly different for the groups as a whole ($p=0.24$). There were no significant differences in overall average gait speed or gait speed variability.

This study examined how baseline COM movement variability differs between participants who later tripped during sensory-perturbed walking and those who did not. We found significant increases in A-P movement variability from the LOB group compared to the non-LOB group, confirmed by two variability metrics (IQR and standard deviation). This means that participants who later tripped during perturbed walking had more positional variability in their unperturbed, baseline walking trials. This suggests that the LOB group may have a lesser ability to maintain a steady-state speed. Future work will examine if the increased position variability remains true during the actual trials where the trips occurred, and whether the results can be explained by the LOB group just needing more time to acclimate to the novel self-pacing treadmill.

Significance: Gait variability has long been a topic associated with fall risk [4,5], and this study suggests that positional variability may be a useful metric to identify individual risk, particularly on a treadmill. By being able to observe natural trips and other losses of balance in a controlled setting, this novel approach potentially can support development of a prediction model of future elevated risk of LOB.

Acknowledgments: This study was funded through MURI #12731926.

References: [1] (Tong, 2013), *IEEE Sensors Journal* [2] (Begg, 2005), *IEEE Biomedical Engineering* [3] (Bargiotas, 2023), *Journal of Neurology* [4] (Verghese, 2009), *Journal of Gerontology* [5] (Hausdorff, 2001), *Archives of PM&R*

GENERALIZING SPINAL NEURAL CIRCUITRY TO COMPLEX MUSCULOSKELETAL MODELS

Chun Kwang, Tan[1*], Seungmoon, Song[1]
[1]Mechanical and Industrial Engineering, Northeastern University, Boston, MA, USA
*Corresponding author's email: chu.tan@northeastern.edu

Introduction: Neuromechanical simulation, which combines musculoskeletal models, motor control models, and physics simulations, is gaining traction as an effective tool in understanding and predicting human gait dynamics. Although there has been notable progress in modeling the complex biomechanics of most muscles relevant to human movement, the integration of physiologically grounded control models into these simulations remains a challenge. This gap primarily arises from the control models being hand-crafted for a small set of muscles hindering their application to models that more accurately reflect the complexity of biological muscle arrangements. For example, our previously proposed reflex-based control model was capable of generating human-like diverse locomotion behaviors [1], reacting to perturbations in ways comparable to humans [2], and elucidating gait modifications due to aging [3]; however, it was designed for a musculoskeletal model comprising only 9 to 11 muscles per leg. Here, we propose general approaches for extending control models from a small set of muscles to a wide array of muscle configurations. We apply these approaches to our previously proposed reflex-based control model [1] for a musculoskeletal model with 80 leg muscles and simulate walking at various speeds and slopes in MyoSuite [4].

Methods: We implemented in MyoSuite [2], the original reflex-based controller with 22 leg muscles [1], as well as two methods of extending the controller to 80 leg muscles (Fig. 1). The original 22 leg muscles represent all monoarticular and biarticular muscles that span the hip, knee, and ankle joints and consist of 47 control parameters that can be tuned to produce different behaviors. In the extensions for 80 muscles, we simply copy the circuits of the 22 muscles to their corresponding muscle groups in the 80 muscle-model that span the same or functionally similar joints. The two extension methods differ in the way how the control parameters of these circuits are set:

- The unified control method sets the same values for the control parameters of the copied circuits. As a result, it has a total of 50 parameters, where the additional three parameters are for the added toe muscles. This approach allows the controller to function with a smaller control space, as compared to the individual control approach, which reduces control complexity.
- The individual control method allows independent adjustment of control parameters in all the individual muscle circuits, adding up to 104 parameters. Theoretically, this expanded control space enables the controller to generate more behaviors.

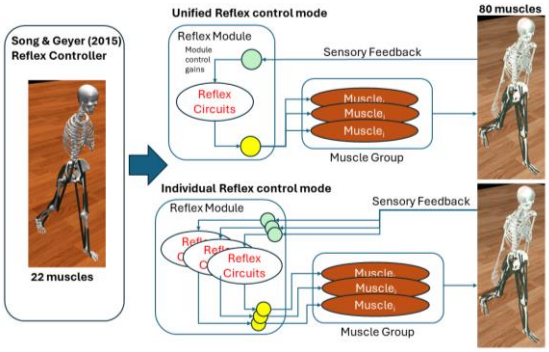

Figure 1: Extension of a reflex controller [3] to musckuloskeletal models with 80 leg muscles

We use covariance matrix adaptation evolution strategy to find the parameters that can produce steady walking at various speeds and slopes. Starting at 1.2 m/s at zero slope, we swept speeds and slopes by 0.2 m/s and 5-degree increments/decrements, respectively. We report on the speed and slope combinations where these models can successfully walk at.

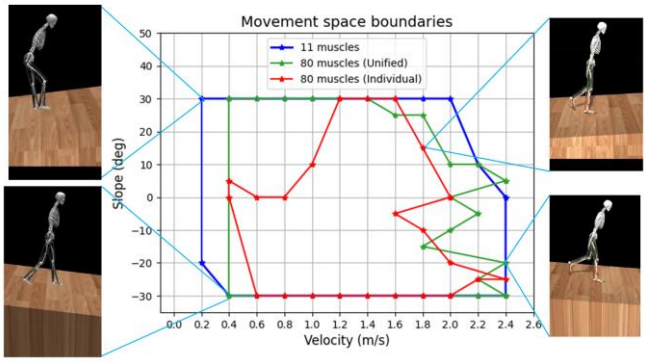

Figure 2: Ranges of achievable terrain and velocities**.** This figure depicts bounded areas of the velocities and the slopes where the reflex controllers can achieve locomotion.

Results & Discussion: Both extension methods were successfully implemented, and the range of walking speeds and slopes they can produce were evaluated (Fig. 2). Intriguingly, as the number of muscles and control parameters increased, the models became less adept at producing more speeds and slopes. This phenomenon could be attributed to computational limitations involved in identifying the optimal control parameters in the highly non-linear and discontinuous cost landscape.

We plan to further explore the speed and slopes ranges of the individual control method by bootstrapping its optimization processes with the parameters identified in the unified method. Additionally, we plan to further explore the distinctions between the two extension strategies by conducting muscle synergy analysis.

Significance: While there are considerable challenges in working with complex models, the benefits of being able to test controllers on more detailed musculoskeletal models brings research closer to real-world conditions. Additionally, the use of complex models also helps to clarify the limitations of simple models, which ultimately leads to the design of better controllers, and understanding of human gait.

Acknowledgments: The work was funded by the National Institutes of Health (R00AG065524)

References: [1] Song, S. & Geyer, H. (2015) J Physiol 593.16 [2] Song, S. & Geyer, H. (2017), Front. Comput. Neurosci. 11 [3] Song, S. & Geyer, H. (2018) J Physiol 596.7 [4] Caggiano et al (2022), Conf. Learning Dyn. Ctrl

A SELF-ALIGNING PASSIVE ANKLE EXOSKELETON TO REDUCE TRICEPS SURAE LOAD IN WALKING

Patrick J. Buban[1*], Dylan G. Schmitz[2], Darryl G. Thelen[1,2]
[1]Department of Biomedical Engineering, University of Wisconsin-Madison
[2]Department of Mechanical Engineering, University of Wisconsin-Madison
*Corresponding author's email: pbuban@wisc.edu

Introduction: The triceps surae generate significant force during the push-off phase of walking. Passive ankle exoskeletons and ankle-foot orthoses have been introduced that can offload the triceps surae by storing energy during mid-stance and releasing that energy during push-off. For example, Collins et al. showed that a clutched passive exoskeleton that utilizes a spring acting in parallel with the triceps surae can reduce the metabolic cost of human walking [1]. One challenge with a parallel spring approach is that it requires a calf interface for proximal spring attachment which must be secure enough to prevent slip during walking. This can be achieved using a carbon fiber shank frame [1] or a tightfitting calf wrap [2]. However, the rigid frame approach can require a customized fit to an individual, and a calf wrap can be uncomfortable given the high shear forces at the skin-interface that are needed to prevent slipping due to the longitudinal spring force. These challenges can be potentially mitigated by changing the direction that the force acts on the shank attachment and using a self-aligning mechanism. Sarkisian et al. [3] introduced such a self-aligning interface to improve performance and comfort in active hip exoskeletons. With a redesigned ankle exoskeleton that creates forces normal to the shank instead of axially, slipping of the calf interface can be prevented and discomfort can be reduced. As a result, the objective of this research was to design and test a self-aligning passive ankle exoskeleton that has capacity to offload the triceps surae during steady-state walking.

Methods: The passive exoskeleton uses a carbon fiber bar to store and release energy during gait (Fig. 1a). The bar pivots about a hinge point that rigidly extends from the shoe and is positioned posterior to the ankle. Translation of the distal end of the bar is constrained posteriorly by an adjustable backstop on a heel attachment to the shoe. The proximal end of the bar is constrained to flex posteriorly against a roller at the calf interface while being free to translate vertically along it. As a result, the bar undergoes flexural bending during dorsiflexion and thus generates a plantarflexion torque about the ankle. To evaluate how the exoskeleton altered triceps surae loading, a shear wave tensiometer [4] was secured over the right Achilles tendon of two subjects. Tendon wave speeds were recorded for 10 seconds when walking with and without the exoskeleton engaged at speeds ranging from 0.9 to 1.8 m/s on a treadmill.

(a)

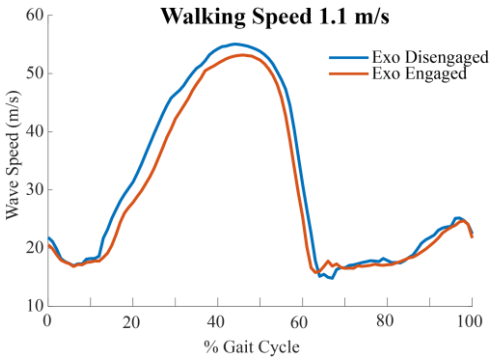

(b)

Figure 1: a) Self-aligning passive ankle exoskeleton. b) Representative walking trial in which the Achilles tendon wave speed is diminished during stance when the exoskeleton is engaged, reflecting a reduction in tendon loading.

Results & Discussion: When compared to the no exoskeleton condition, Achilles tendon wave speeds were diminished during the mid- and early terminal stance phases of walking, particularly at the slower walking speeds (Fig. 1b). As a result, integrated squared wave speeds over the gait cycle were substantially lower (reduced by 11-23 %) in the engaged exoskeleton condition, when compared to the unengaged condition at slow (0.9-1.1 m/s) walking speeds. Exoskeleton effects on integrated wave speeds at higher walking speeds (1.3-1.8 m/s) were modest and less consistent (reduced by 0-14%). These results suggest it may be feasible to use a self-aligning ankle exoskeleton to offload the triceps surae during the stance phase of walking. To accomplish this, the device seems to generate a sufficient amount of force to aid in heel-off and provide some amount of propulsion during steady-state walking. Further study is needed to ascertain why the current exoskeleton was less effective at reducing triceps surae loading at higher walking speeds. The challenge may arise from the walking pattern used while wearing the device, and/or over-engagement of the triceps surae muscles by the user at high speeds. Future enhancements will incorporate a clutch in the shoe backstop to enable engagement in stance while allowing for unencumbered motion in swing.

Significance: This study introduces a simple, self-aligning passive exoskeleton that has the potential to reduce triceps surae loading during human walking and be more comfortable than other ankle exoskeletons that rely on transmitting assistive forces in parallel with the triceps surae.

Acknowledgments: NSF CBET-2019621

References: [1] Collins+, *Nature* vol. 522,7555, 2015; [2] Schmitz+, ASB 2023; [3] Sarkisian+, *IEEE* vol. 29, pp. 629-640, 2021; [4] Martin+, *Nat. Commun*. vol. 9, 1592, 2018.

APPARATUS FOR INVESTIGATION OF ISOLATED PLANTARFLEXOR FUNCTION WITH CONTROLLED GEAR RATIO

Lauren Hickox, Logan Faux-Dugan[1], Stephen J. Piazza[1*]
[1]Dept. of Kinesiology, The Pennsylvania State University, University Park, PA, USA.
*Corresponding author's email: piazza@psu.edu

Introduction: The "gear ratio" of the output lever arm of the ground reaction force about the ankle joint to the input lever arm of the Achilles tendon is understood to play a critical role in determining the function of the plantarflexor muscles. This ratio determines not only the tendon force required to be produced for a given ground reaction force, but also sets the plantarflexor shortening velocity for a given rate of ankle plantarflexor rotation. While the influence of the gear ratio on plantarflexor function has been investigated by considering the variation in gear ratio that occurs as the center of pressure translates anteriorly during the stance phase [1], or by the application of insoles of varying stiffness that influence the location of the center of pressure [2], precise control of the gear ratio is difficult to achieve experimentally. Here, we describe the design of a customized experimental apparatus that permits specification of the gear ratio in order to examine the influence of the gear ratio on the demands placed on the triceps surae.

Methods: This device, called the Ergometer with Leverage MOdulation (ELMO) allows the user to raise and lower a weight cyclically via the application of force with the toes and repeated plantarflexions (Fig. 1). An aluminum frame fitted with parallel rails permits a box on linear bearings containing variable weights to be translated along the rails. The foot of the user is affixed to a foot plate that is attached to the weight box via a ball joint and a 6-DOF load cell. The position of the foot plate relative to the ball joint may be adjusted to modulate the output lever arm. Coupled with assessment of the input lever arm of the Achilles tendon [3], setting of the output lever arm effectively sets the gear ratio. The entire frame is mounted upon an examination table upon which the subject lies supine, with the thigh supported in a manner such that the knee is fixed, ensuring that the box is moved by the actions of ankle muscles and not knee or hip muscles.

As the weight box moves along the rails, its position is tracked using a cable displacement encoder and this signal is used to provide real-time feedback to the subject to facilitate cyclic motion of the weight with a desired amplitude and frequency. The subject sees the actual and target positions of the weight on a LED bar graph display and receives auditory indication of the desired movement frequency, all of which is implemented using an Arduino microcontroller.

During testing, electromyography is employed to monitor the activity of the ankle muscles, and three-dimensional motion analysis may be used to track the motion of the weight box and to verify that the motion of the thigh is minimized. Measurements made using the 6-DOF load cell permit verification that the force applied to the load is along the direction of travel and not perpendicular to it. Shaft collars placed on the rails prevent excessive motion of the box as a safety mechanism.

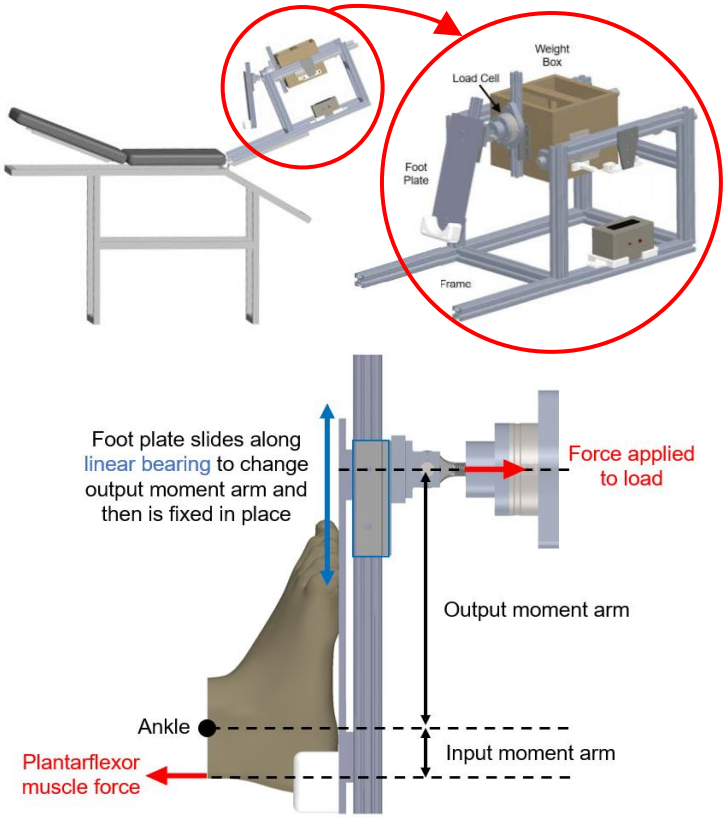

Figure 1: Views of the ELMO device with detail of the mechanism for modulation of the output moment arm and therefore the gear ratio.

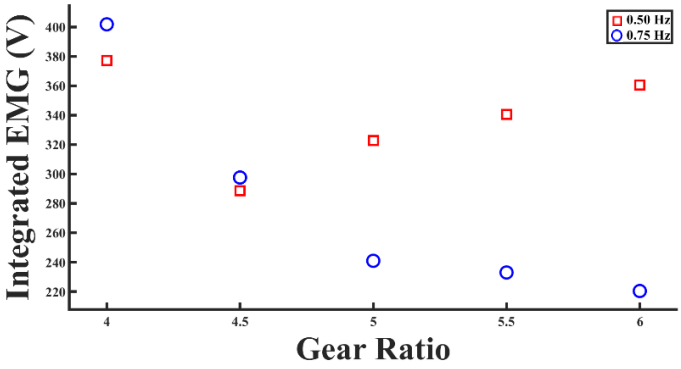

Figure 2: Pilot data collected using ELMO, showing the integrated EMG collected from lateral gastrocnemius during plantarflexions performed with varied gear ratio at two movement frequencies.

Results & Discussion: Preliminary testing has been performed in which the gear ratio has been varied along with the cycling frequency. Data for a single subject are shown (Fig. 2), illustrating the capacity of ELMO for investigation of the effects of gear ratio and movement speed on muscle activation.

Significance: Presented is a novel device which allows for manipulation of gear ratio and movement speed for the purpose of studying isolated plantarflexor function during a submaximal task working against an inertial load.

References: [1] Carrier et al. (1994), *Science* 265(5172); [2] Takahashi et al. (2016), *Sci Rep* 6: 29870; [3] Wade et al. (2019) *J Biomech* 90.

TOWARDS A TASK-AGNOSTIC EXOSKELETON ARM ASSISTANT USING DEEP REINFORCEMENT LEARNING AND NEUROMECHANICAL SIMULATION

Chinmayi Goyal[1], Chun Kwang Tan[2], Seungmoon Song[2*]
[1] Yorktown High School, Yorktown Heights, New York
[2]Mechanical & Industrial Engineering, Northeastern University, Boston, Massachusetts
*Corresponding author's email: s.song@northeastern.edu

Introduction: Movement disorders affect nearly one in seven adults [1], transforming routine tasks into a formidable challenge. Recent research has shown promise in robotic interventions for assisting and restoring movement. Accurate and efficient computer simulations of human-robot interaction can facilitate the development of optimal robotic technologies entirely in silico [1]. However, traditional physics-based musculoskeletal engines are computationally expensive and lack support for contact-rich interactions [2]. In contrast, forward neuromechanical simulations, like MyoSuite, can be leveraged to investigate and modulate physical interactions between the neuromusculoskeletal system and wearable robotic devices [2]. Furthermore, advancements in machine learning [3], particularly the strides made in deep reinforcement learning (RL) have paved the way for conducting large-scale neuromechanical simulations involving complex musculoskeletal models. Here, we introduce Deep RL as a control methodology for exoskeletons to produce user-driven assistance, based on muscle activations.

Methods: We explored the potential of training elbow exoskeleton controls using deep RL to augment human arm movements by responding to the arm's state without knowledge of the intended movements (Fig 1). Our study utilizes a musculoskeletal arm model in MyoSuite [2], adapted from OpenSim, featuring a single-degree-of-freedom elbow joint actuated by six Hill-type muscles. We used two model variants: one for a healthy condition and another for sarcopenia, characterized by a 50% reduction in muscle strength. For each of these musculoskeletal models, we trained an elbow control policy that represents human motor control. These deep RL policies processed inputs such as joint angle, angular velocity, muscle activation, and target angle, and output muscle stimulations to achieve the target angles. Then, for the sarcopenia model, we integrated an elbow exoskeleton capable of providing assistive torque and trained a deep RL policy for it. This exoskeleton policy could measure joint angle, velocity, and muscle activation but remained uninformed of the target angle.

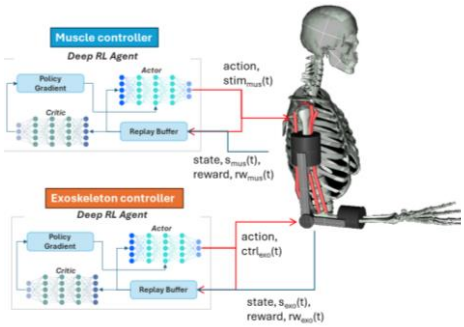

Figure 1: Deep RL for muscle and exoskeleton control. Overview of control policies for simulated muscles and exoskeleton.

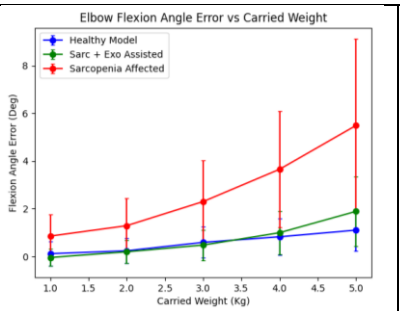

Figure 2a: Deviation from target angles. Exoskeleton policy supports sarcopenia muscles to achieve desired target angles

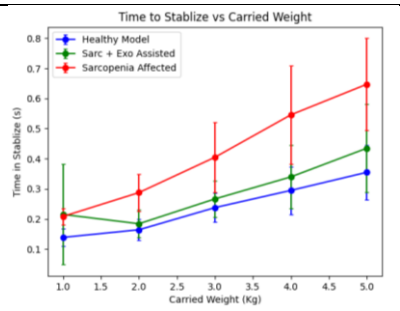

Figure 2b: Time to stabilize arm at target. Exoskeleton policy stabilizes arm at a similar rate as the healthy policy

Results & Discussion: We assessed the potential efficacy of the target-agnostic exoskeleton policy based on the precision and speed with which an arm holding a weight could achieve specified target angles (Fig. 2). This evaluation involved 1000 tests of the trained policies under varying conditions of weight, initial angles, and target angles. The healthy model consistently succeeded in reaching the target angles, even with added weight, whereas the sarcopenia model displayed a maximum deviation of approximately 5 degrees from the target angle and 0.3 seconds slower than the healthy model for the highest weight of 5 kg. The condition with the elbow exoskeleton demonstrated its capability to reduce the sarcopenia effect and reduce the error and time to target (approximately 1 degree deviation to target angles, 0.4 sec stabilization time), highlighting the potential of the target-agnostic control policies.

Significance: This study has shown how Deep RL can be utilized to estimate intended movements from muscle activations. The results demonstrate that such an approach can be effective for user-driven exoskeleton control, and it opens research avenues for integrating simulation-to-real world methods into exoskeleton control. Simulations are considerably cheaper, in the sense where does not require subject-intensive experiments for data collection. Future work can investigate generalizing this approach for task-agnostic assistance in exoskeletons.

Acknowledgements: Compute resources and support by the Yorktown High School and the Northeastern University.

References: [1] Cashaback, J.G.A. et al (2021), *JNeuroEngineering Rehabil 21, 23* [2] Wang, H. et. al. (2022), *IEEE ICRA*, [3] Song, S. et. al. (2021), *JNeuroEngineering Rehabil 18, 126*; [4] Delp, S. L. et al. (2007), Proc *IEEE Trans. Biomedical Engineering*, vol. 54, no. 11

THE EFFECTS OF AN EXTEMPORANEOUS SPEECH DUAL-TASK ON GAIT STABILITY IN OLDER ADULTS

Ahmadreza Souri[1], Mandana Sanandaji[1], Rahul Bashyal[1], Shane Caswell[1], Abigail Schmitt[2], Tiphanie Raffegeau[1]
[1]School of Kinesiology, George Mason University, Manassas, VA, [2]University of Arkansas, Fayetteville, Arkansas, USA
*Corresponding author's email: asouri@gmu.edu

Introduction: Previous studies have shown older adults (OA) must take slower, shorter and wider steps to complete a dual-task (DT) walk, suggesting they are attempting to gain mechanical stability in their gait so they can dedicate attentional resources to a concurrent cognitive task without losing their balance [1], but the underlying stability-related mechanisms remain unclear. Foot placement and lateral ankle mechanisms are two ways to control locomotor stability. The lateral ankle mechanism pertains to ankle torques generated by inversion and eversion of the stance leg that guide the center of pressure (CoP) trajectory towards the direction of fall of the swing limb. Foot placement control refers to the placement of the swing leg relative to the body to maintain stability and forward progression [2]. Although OA demonstrate decreased ability to adjust their steps during DT [3], studies often use unrealistic tasks and participants may devote added attention because the task is unfamiliar or causes sensory interference [4]. We expand on current methods with a continuous extemporaneous speech dual-task that mimics the cognitive demands and implicit goals of conversational speech [5]. The purpose of our study was to investigate how extemporaneous speech would change balance control in OA by examining gait kinematics, CoP displacement, and CoP velocity, during DT walking. We hypothesized that because OA take slower, shorter, and wider steps to complete a DT walk, participants would show an increase in medial-lateral (ML) and a decrease in anterior-posterior (AP) CoP displacement and velocity.

Methods: OA walked in their comfortable footwear at self-selected speeds 10 times on a 10-meter path across floor-embedded force plates (Bertec, Columbus, OH) recording forces at a frequency of 1000Hz. Position data were recorded using motion capture technology wearing 39 reflective markers, following the Plug-in-Gait model (Vicon, Nexus). Participants walked in two conditions: the single task (ST), focusing only on walking at self-selected speeds, and the DT, walking while performing a simultaneous extemporaneous speech task, talking continuously about an assigned topic (e.g. first job, favorite sport, pets) for one minute (~8-10 passes on the walkway). Trajectory data from the pelvis, heel, and toe markers were used to calculate horizontal position, extracting toe-offs and heel strikes to determine single stance phase [6]. Step length, velocity, width, single stance time, CoP displacement and velocity in ML and AP directions for each single stance phase in both left and right legs were found using a custom MATLAB code. CoP variables were compared between ST (reference condition) and DT conditions using linear mixed-effect regression (LMER) models and included a random effect of participant and participant within step number and condition.

Results and Discussion: Nine OA (6 females, 3 males; mean ± SD: age = 71 ± 4 years, height = 1.68 ± 0.1 meters, mass = 69.1 ± 7.65 kg) were included. 95 left and 96 right steps were analysed. LMER showed a decrease from ST to DT in AP CoP displacement in the left ($p < .001$) and right leg ($p = .02$, Table 1). AP CoP mean velocity declined from ST to DT in the left leg ($p < .001$) and the right leg ($p = .002$). There was no difference between conditions in ML CoP displacement in either left ($p = .76$) or right leg ($p = .15$). ML CoP velocity did not show differences between conditions in the left ($p = .2$) or right leg ($p = .5$). Step length and step velocity decreased ($p < .001$) and single stance time increased from ST to DT walking ($p = .004$), step width did not change ($p = .75$).

Table 1. Comparisons of CoP and stepping outcome measures between DT and ST

Variables	ST(Mean(SD)	DT(Mean(SD)	*B*	*t*	*p*
L AP CoP D (cm)	11.33 (1.26)	10.05 (1.27)	-1.17	-4.13	< 0.001
L AP CoP V (cm/s)	30.31 (4.11)	25.86 (4.61)	-4.64	-6.71	< 0.001
L ML CoP D (cm)	-0.97 (1.37)	-1.01 (0.92)	0.04	0.31	0.76
L ML CoP V (cm/s)	-2.72 (3.51)	-2.55 (2.30)	0.48	1.30	0.2
R AP CoP D (cm)	11.62 (1.64)	10.50 (1.78)	-1.01	-2.28	0.02
R AP CoP V (cm/s)	31.28 (5.37)	26.75 (6.63)	-4.30	-3.17	0.002
R ML CoP D (cm)	0.88 (1.14)	1.31 (0.93)	0.2	1.44	0.15
R ML CoP V (cm/s)	2.32 (3.03)	3.21 (2.22)	0.30	0.69	0.5
Step length (m)	0.69 (0.05)	0.63 (0.04)	-0.06	-5.6	< 0.001
Step velocity (m/s)	1.27 (0.17)	1.08 (0.16)	-0.20	-6.76	< 0.001
Step width (m)	0.10 (0.03)	0.10 (0.03)	0.001	0.32	0.75
Single support (s)	0.36 (0.08)	0.41 (0.13)	0.04	2.92	0.004

Notes: ST = Single task, DT = dual-task, SD = standard deviation, D = displacement, V = velocity, cm = centimeter, s = second, m = meter

Significance: Increases in single support time during DT walking supports that OA experience cognitive-motor interference during a well-practiced extemporaneous speech task. No differences from ST to DT in ML CoP displacement and velocity or step widths suggest that OA can perform extemporaneous speech without interfering with mediolateral balance control during overground gait, perhaps due to an inflexibility of mediolateral balance mechanisms. Instead, step length, velocity, and AP CoP displacement and velocity decreased during a DT, suggesting OA flexibly control AP balance to perform the conversational speech task while walking. OA may prefer to adjust AP placement of the foot of the swing leg relative to the body to regulate gait stability. Future studies should determine how AP versus ML balance control influences the flexibility of cognitive-motor systems across different types of gait tasks.

References: [1] Plummer-D' Amato et al. (2011), *Gait & Posture* 33(2):233-237 [2] Fettrow et al.(2019), *PLOS ONE* 14(12)[3] Mazaheri et al.(2015), *Exp Brain Res* 233;3467-474 [4] Patel et al. (2014), *Neuroscience* 260:140-148. [5] Raffegeau et al., (2018) *Gait & Posture*. 2018;64:59-62. [6] Zeni et al. (2008), *Gait & Posture* 27(4):710-714

Gait variables between the injured and uninjured sides of people with plantar fasciitis

Halime Gulle[1*], Torstein E. Dæhlin[1], Ronaldo H. Cruvinel Júnior[1,2], Irene S. Davis, FACSM[1]
[1]School of Physical Therapy and Rehabilitation Science, University of South Florida, FL, USA
[2]Department of Physical Therapy, Speech, and Occupational Therapy, School of Medicine, University of São Paulo, SP, Brazil

Introduction: Plantar fasciitis (PF) is one of the most common painful foot conditions which can result in gait deviations. A key feature of PF is the pain that is associated with weight-bearing activities such as gait. To mitigate this pain, individuals with PF can develop compensatory strategies, such as reducing their loading during stance of the injured side. Additionally, with the fascial connections between the Achilles tendon and the plantar fascia, adjusting the ankle dorsiflexion position influence the tension in the plantar fascia. Specifically, decreasing the dorsiflexion angle at initial contact (IC) and during stance will reduce the tension. An individual might also shift weight towards the outer edge of the foot in response to pain, reducing the inversion angle at IC, and reducing peak eversion during stance. The current studies investigating these variables in PF primarily focus on a comparison between people with PF and healthy controls. However, there is limited evidence regarding compensatory gait patterns in individuals with unilateral PF. Therefore, the aim of this study is to examine kinetic and kinematic differences between limbs in individuals with unilateral PF. We hypothesized that all variables of interest would be lower on the injured side with the exception of inversion at IC, which we expected to be greater.

Methods: To date, data from 14 individuals (50.5 ± 5.8 yrs., 12 F and 2 M) with unilateral PF, are included in this ongoing randomized controlled trial. The average daily pain (out of 10) of this group was rated as 5.02±1.8 with a range of 3 to 7. Participants completed 5 walking trials along a 75-foot walkway, while being recorded with a motion capture (MOCAP) system. Simultaneously ground reaction forces were recorded with 2 force platforms embedded in the center of the walkway. Visual 3D was used to compute kinetic and kinematic variables. Variables of interest included the propulsive impulse of the ground reaction force, stance duration, ankle dorsiflexion and inversion at initial contact (IC) and peak dorsiflexion and eversion during stance phase. The outcomes of interest were extracted from each individual trial and then averaged across each condition. Due to the current low subject numbers, data were analyzed descriptively. The mean (±sd) was calculated, as well as the effect size (ES) using the following criteria: small ES=0.20, medium ES=0.50 and large ES>0.80 (Cohen's d.)

Results & Discussion: The results (Table 1) suggest that individuals with PF exhibit a mild compensatory gait on the injured side. As expected, dorsiflexion angles (IC and peak) were lower on the injured side. This adjustment might help to reduce the tensile load on the plantar fascia. In the frontal plane, with a lower inversion angle at IC and similar peak eversion, the injured side likely went through lower eversion excursion. This may also serve to alleviate strain on the plantar fascia, potentially leading to pain reduction. The plantar fascia is most elongated during the push-off phase of gait. People with PF alter their gait by reducing their push-off force, thereby decreasing the propulsive impulse. With stance duration similar between sides, it is likely a reduction in the magnitude of their propulsive force that resulted in the lower impulses.

Significance: The results of this ongoing study suggest that people with unilateral PF may develop compensatory strategies to mitigate the pain. These strategies include reducing IC and peak ankle dorsiflexion, the propulsive impulse, and redistributing weight toward the foot's outer edge. The average magnitude of these differences was small. However, examination of the relationship between the magnitude of these variables and the average daily pain is ongoing and may lend further insight into these compensatory strategies.

References:

1. Phillips, A., & McClinton, S. (2017). Gait deviations associated with plantar heel pain: a systematic review. Clinical Biomechanics, 42, 55-64.

Acknowledgments: Research reported in this abstract was supported by the National Institute for Aging of the National Institutes of Health under award number R01AG071646.

Table 1: Comparison of (mean ± standard deviations) of kinetic and kinematic variable between uninjured and injured limb

	Uninjured (Mean ± SD)	**Injured** (Mean ± SD)	**Effect size**
Propulsive Impulse (BW*s^{-1})	3.23±0.36	3.11±0.35	**0.32**
Dorsiflexion angle at IC (°)	2.34±2.85	1.34±3.52	**0.31**
Peak dorsiflexion angle at IC (°)	4.22±2.25	3.11±3.60	**0.36**
Inversion Angle at IC (°)	3.82±2.37	2.74±2.56	**0.43**
Peak Eversion angle (°)	-9.59±-5.78	-9.36±-4.19	0.04
Stance phase duration (s)	-0.62±-0.04	-0.61±-0.05	0.16

Key: BW: Body Mass, IC: Initial contact, Vgrf: Vertical ground reaction forces, °:degree, s^{-1}: second

Intrinsic muscle properties of intact vs reinnervated guinea fowl LG

Rubi M Tapia Rayo, M. Janneke Schwaner, Monica A. Daley
University of California Irvine - School of Biological Sciences – Department of Ecology and Evolutionary Biology

Email: Rubitapia0@gmail.com

Introduction:

Surgical self-reinnervation can be a useful manipulation for investigating neuromechanical control mechanisms in locomotion [1]. We have found several changes in gait kinematics, motor control and in vivo muscle function following self-reinnervation of the lateral gastrocnemius (LG) in guinea fowl. However, the mechanisms underlying these changes remain unclear [2]. Our lab is investigating mechanisms that may help explain the observed changes in in-vivo neuromechanical control of locomotion. A shift in fiber type distribution (slow-twitch vs fast-twitch) is one hypothesized mechanism that could help explain observed differences in the rate of in vivo force development and shortening velocity. Here we aim to compare the force frequency relationship between reinnervated and intact guinea fowl and its variation among individuals, as an indicator of shifts in motor unit and fiber type distribution in the LG muscle. We address the question of whether there is a shift in force-frequency characteristics or activation kinetics between reinnervated (R) vs intact (I) LG muscle in guinea fowl [3].

Figure 1) 'strut-like' function in birds with proprioceptive deficit [1]

Methods: We used 9 guinea fowl (n=5 reinnervated) with average body mass of 1.83±0.16 kg and average lateral gastrocnemius (LG) mass of 8.73±1.32g. Five birds underwent a reinnervation surgery under surgical anaesthesia (isoflurane 1.5-3%, mask delivery) [4], at the age of 7-12 weeks. The surgery involved making a lateral incision posterior-distal to the knee to access the nerve branch to the LG muscle, transecting and immediately repairing this nerve. After full recovery from this nerve injury, we collected in vivo data followed by in-situ data at 7-9 months after reinnervation. In the in-situ experiments, birds were maintained under deep surgical anesthesia throughout the experiment (induction at 2.5-3% isoflurane, maintenance at 1.5 – 2%, mask delivery). A ~25 mm incision was made posterior to the thigh muscles to access the sciatic nerve which was isolated and instrumented with a custom-built nerve cuff [5]. The LG muscle was instrumented with sonomicrometry transducers (1.0 mm, Sonometrics Inc, London, Canada), positioned mid-belly along the fascicle to measure fascicle length, and force was measured using an Aurora Instruments muscle lever.

Results & Discussion:

Force data was collected for contractions at multiple stimulus frequencies (5, 10, 12.5, 20, 25, 40, 50, 80, 100, 150 Hz). Force vs time plots were created for each bird and data were normalized relative to each bird's maximum isometric tetanic force (F_{max}). We fit a sigmoidal curve to the measured peak force as a function of stimulus frequency. Between 8-10 points were used for each individual's curve fit (**Figure 2A**). Average Fmax at the maximum frequency and average F_{max} was 116.87±23.09N (mean±SD across all birds and was found to be similar for reinnervated and intact individuals: 111.7±27.35N (reinnervated), 123.33±18.01N (intact). Half activation time plots also show similar patterns across reinnervated and intact individuals (**Figure 2B**). Peak half-activation time was: 99.11±13.48ms averaged across all birds (mean±SD) 97.2±16.18ms for reinnervated and 101.50±11.03ms for intact. These findings suggest that recovery from reinnervation did not lead to significant shifts in activation or force-frequency dynamics in the guinea fowl LG.

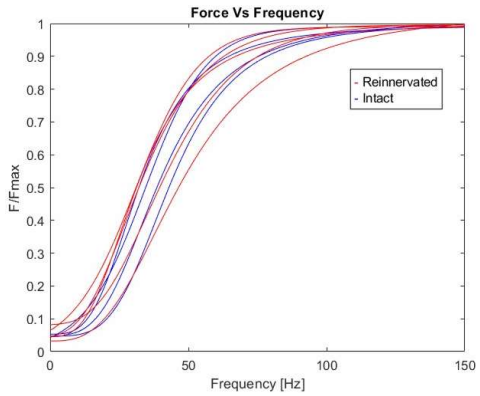

Figure 2A) Force-frequency relationship for the 9 individual guinea fowl, reinnervated in red, intact in blue.

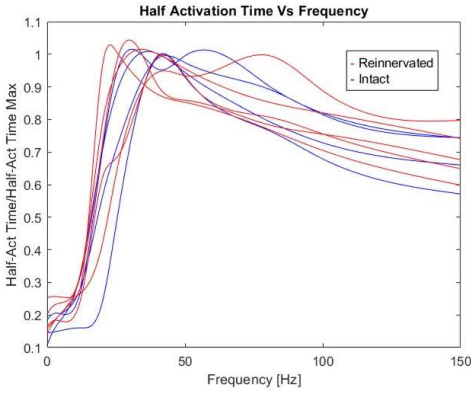

Figure 2B) Half-activation time against frequency for the same individuals.

Significance: While there is currently a substantial body of literature on in vivo muscle function, biomechanics, and energetics of locomotion in guinea fowl, there is little published data on muscle contractile properties including force-frequency characteristics. These data can help inform muscle modelling efforts and help provide integrative understanding from tissue to organismal scales of biomechanical function.

Acknowledgments: This work is funded by the National Science Foundation (NSF), grant number: 2016049 (to M.A.D). A special thank you to Dr. Azizi for introducing me to Dr. Daley's Neuromechanics Lab.

References: [1] Schwaner et al. (2023), *J Exp Biol* 226(12), [2] Kernell et al. (1983), *Exp Brain Res* 50(2-3), [3] Colecraft (2021). In *Ion Channels*, [4] Schwaner et al. (2023), *BioRxiv*, [5] Naples et al. (1988) *IEEE TBME* 35(11)

PREDICTING WALKING SPEED USING A CONVOLUTIONAL NEURAL NETWORK (CNN) MODEL ON A BIOMECHANICS DATASET

Daejin Jung[1*]
[1]Salisbury school
*Corresponding author's email: eowlsdl17@gmail.com

Introduction: Walking speed is a quintessential marker of human health and functional mobility, correlating with an individual's capability to perform daily activities and predicting long-term health outcomes. However, accurately predicting walking speed necessitates a nuanced understanding of the intricate biomechanical factors at play, a complexity often oversimplified by conventional models. The advent of deep learning, and specifically CNNs, offers a promising pathway to unravel these complexities. By harnessing the analytical capabilities of CNNs applied to a detailed biomechanics dataset, this study aims to not only predict walking speed with unprecedented accuracy but also to deepen our biomechanical understanding of human locomotion, thereby informing more effective rehabilitation techniques and the development of personalized assistive devices.

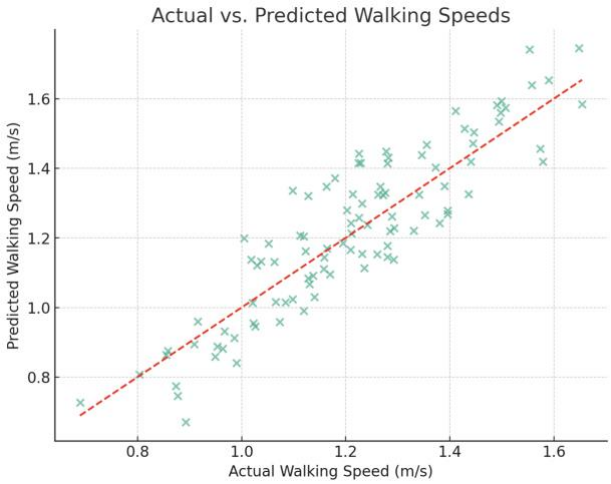

Figure 1: Results show the relationship between actual and predicted walking speeds, with the red dashed line indicating perfect prediction for reference. This visualization helps to illustrate the predictive accuracy of the CNN model, despite the inherent challenges in modeling complex human gait dynamics.

Methods: An elaborate biomechanics dataset, capturing the kinematics and kinetics of healthy adult gait across a spectrum of conditions, serves as the foundation of this study. Parameters including but not limited to ground reaction forces, joint angles, and muscle activation patterns, were collected, providing a holistic view of the biomechanical aspects of walking. A tailored CNN model was constructed, featuring an architecture designed to adeptly navigate the dataset's complexity through multiple convolutional layers for feature extraction, culminating in a regression analysis layer tasked with predicting walking speeds. Following a split of the dataset into 80% for training and 20% for testing, the model's efficacy was quantitatively assessed using mean squared error (MSE) and R-squared (R^2) metrics.

Results & Discussion: The CNN model exhibited an MSE of 0.055 m/s^2 and an R^2 of 0.82, showcasing its robust predictive accuracy and a strong correlation with actual walking speeds. These outcomes signify a significant leap over traditional biomechanical models, underscoring the CNN's prowess in deciphering the complex web of biomechanical data to predict gait parameters accurately. The model's analysis highlighted the pre-eminence of ground reaction forces and joint angles as critical determinants of walking speed, echoing biomechanical theories that posit these factors as central to understanding gait mechanics. However, the model's current iteration, based predominantly on data from healthy subjects, signals a need for future research to adapt and validate its application for clinical populations with distinct gait patterns, thereby broadening its clinical and rehabilitative applications.

Significance: This study marks a significant milestone in the confluence of machine learning and biomechanical gait analysis, heralding a new era where CNNs unlock previously unattainable insights into human locomotion. The implications are vast, spanning enhanced diagnostic tools in rehabilitation medicine, refined strategies for gait improvement, and the innovative design of gait-assisting devices. The methodology delineated herein provides a robust framework for future explorations into the biomechanics of human movement, promising not only to advance scientific understanding but also to foster the development of interventions that improve the quality of life for individuals worldwide.

References: [1] Yang et al. (2012), *Sensors* 12(5)

Enhancing Prosthetic Control with Ultrasound Imaging: A Convolutional Neural Network Approach for Real-Time Hand Gesture Recognition

Yun Chen[1] and Qiang Zhang[1*]
[1]Department of Mechanical Engineering, The University of Alabama, Tuscaloosa, AL 35487, USA.
*Corresponding author email: qiang.zhang@ua.edu

Introduction: Globally, millions are affected by the challenges of living with amputations resulting from accidents or illnesses, with transradial amputation being notably prevalent. Traditionally, electromyography (EMG) has been employed to non-invasively capture and interpret forearm muscle movements [1], offering insights into the intricate coordination of muscle activities and thus, an individual's intended motions. Recent research has leveraged machine learning techniques, such as the support vector machine (SVM), for gesture recognition by analyzing EMG signals [2]. Yet, surface EMG (sEMG) faces notable challenges, including a low signal-to-noise ratio and sensitivity to skin conditions and electrode placement, which can hinder its effectiveness [3]. To handle these limitations, ultrasound (US) imaging emerges as a compelling alternative. This method provides views of the muscle's morphological anatomy, alongside the capability to monitor muscle contractions and relaxations in real-time, presenting a clearer picture of muscular dynamics [4]. Despite the potential of US imaging, traditional machine learning approaches like SVM and principal component analysis (PCA) fall short when it comes to processing and classifying image data. In this study, we apply convolutional neural networks (CNN) and develop a classifier based on brightness mode (B-mode) ultrasound images. For the first time, we implement this classifier for quasi-real-time classification, marking a significant advancement in the field of prosthetic control and movement disorder rehabilitation.

Methods: We designed 8 gestures and corresponding ultrasound B-mode images were collected to train a CNN classifier. During the experiment, we placed the ultrasound probe at an angle of 30 degrees with the radius and fixed it on the subjects' forearm with a strap. Subjects were requested to perform each gesture consecutively, holding their hand gesture for ten seconds and resting for 5 seconds between gestures. For offline performance evaluation, six subjects participated in the experiment to constitute a dataset, which was divided into a training set and a validation set. To validate the real-time performance, we conducted the preliminary study with a quasi-real-time situation, where data from 5 trials was collected from a single subject. Among those data, 4 random trials were used for training and validation during the model-building procedure and the remaining trial was used for pure validation. Before being incorporated into the dataset, all images underwent pre-processing steps, where pixel values below 15 were converted to 0. At the same time, we applied data augmentation, so that the images were cropped, translated, and rotated to expand our dataset. The structure of the applied CNN is depicted in Fig. 1.

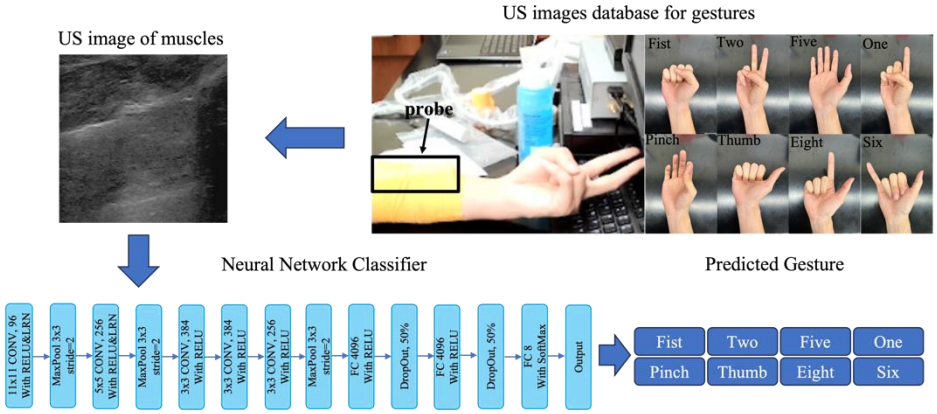

Figure 1: Experimental setup for data collection and the structure of applied CNN.

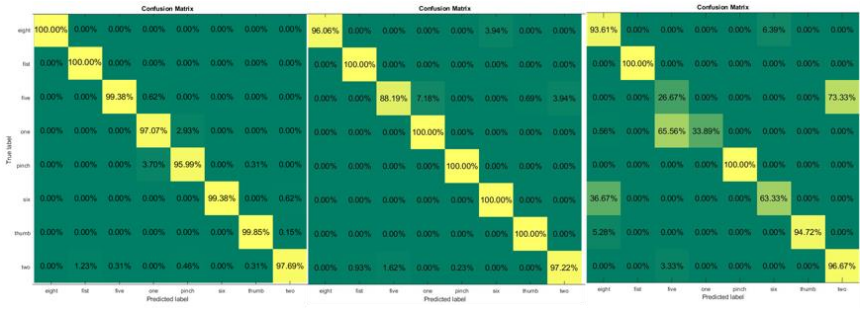

Figure 2: Confusion matrix of different cases. (a) Offline classification of 6 subjects. (b) Quasi-real-time classification on the validation set. (c) Quasi-real-time classification on a trial which is not included in training.

Results & Discussion: All confusion matrices are shown in Fig. 2. The offline classifier trained by using the dataset from multiple subjects achieved an average prediction accuracy of 98.67%. For the preliminary quasi-real-time validation on the representative subject, when offline training the classifier, the accuracy on the validation set reached 97.69%. When applying the classifier to the new dataset from the fifth trial that was not included in the classifier modeling, the average accuracy of the validation was 76.11%. Since the dataset used for pure validation was collected independently from the training dataset, this can be considered as a quasi-real-time condition. Additionally, several gestures that have very similar muscle structure configurations performed well in the classifier model training procedure but exhibited worse classification accuracy when used in the remaining trial.

Significance: This method proved to efficiently and effectively identify gestures in a quasi-real-time manner. We streamlined the data collection process using just one ultrasound probe, a significant simplification compared to the traditional surface electromyography (sEMG) method, which typically requires multiple sensors attached around the forearm. B-mode ultrasound imaging not only eases the experimental setup but also enhances data quality. To ensure the CNN model doesn't overfit, we utilized data augmentation techniques. Remarkably, our classifier achieved a high accuracy after about 10 minutes of training. Considering the wide variation in muscle structure from person to person, this quick training process allows for easy customization of the gesture prediction model for individual users, making it a practical solution for personalized assistive device development.

Acknowledgment: This work was supported by the ROH funding at the University of Alabama #13009-214271-200.
References: [1] Khushaba, et al. Expert Syst. Appl. 61 (2016): 154-161. [2] Tavakoli, et al. Biomed. Signal Process. Control 46 (2018): 121-130. [3] Li, Kexiang, et al. Biomed. Signal Process. Control 62 (2020): 102074. [4] McIntosh, et al. CHI. (2017).

MYOSUITE: A UNIFIED NEUROMECHANICAL SIMULATION PLATFORM FOR HUMAN MOVEMENT RESEARCH

Chun Kwang Tan[1*], Guillaume Durandau[2], Massimo Sartori[3], Vikash Kumar[4,5], Vittorio Caggiano[4], Seungmoon Song[1]
[1]Mechanical and Industrial Engineering, Northeastern University, Boston, MA, USA
[2]Department of Mechanical Engineering, McGill University, Canada
[3]Department of Biomechanical Engineering. University of Twente, Netherlands
[4]MyoLab Inc, Pittsburgh, PA, USA
[5]Robotics Institute, CMU, Pittsburgh, PA, USA
*Corresponding author's email: chu.tan@northeastern.edu

Introduction: The interdisciplinary challenge of modeling human motor control and biomechanics spans musculoskeletal biomechanics, motor control, physics simulation, and computation. Despite its significance, research efforts remain fragmented, with critical domains working in isolation. This fragmentation limits cohesive advancement and integration, underscoring the need for a unified simulation platform to foster multidisciplinary collaboration and innovation.

Methods: We introduce MyoSuite [1,2] as the solution to this challenge, an open-source and open science ecosystem designed to simulate human movement comprehensively. MyoSuite comprises an extensive collection of musculoskeletal environments and tasks, powered by the MuJoCo physics engine and integrated within the OpenAI Gym API, making it highly conducive to reinforcement learning applications. By seamlessly bridging the gap between precise musculoskeletal models and sophisticated deep reinforcement learning techniques, MyoSuite propels research in human motor control into new territories. It strives to ensure physiological plausibility, physical accuracy, computational efficiency, and provides a rich assortment of challenging and diverse motor tasks.

Results & Discussion (Current Status): Since its launch in May 2022, the MyoSuite team has been dedicated to the platform's development and the cultivation of a community-focused open-source and open science ecosystem (Fig.). As of March 2024, MyoSuite's milestones include:

- **MyoSuite Software:** The software is available on GitHub, over 30,000 downloads on PyPI, including 5 musculoskeletal models and 9 task family environments (with x2 difficulty levels x 3 reset conditions x 8 (or 4) non-stationary variations), alongside four baseline controllers for manipulation and locomotion tasks. These range from basic strategies to advanced deep reinforcement learning agents/policies [3,4,5], as well as a reflex-based control model [6].
- **MyoChallenge:** We hosted the MyoChallenge [7] at the NeurIPS conference for two consecutive years, with the latest competition in 2023 featuring two separate tracks for manipulation and locomotion and attracted 60+ teams from 15+ countries.
- **MyoWeb:** The introduction of a web portal enables users to experiment with MyoSuite's features without needing software installation, providing access to musculoskeletal models, changing muscle stimulation, and real-time movement visualizations.
- **Online tutorials:** A series of 10 tutorials is available to help new users get started with MyoSuite. These tutorials cover the basics of MyoSuite environments and examples of training reinforcement learning policies within these environments. Additionally, the community has contributed tutorials covering a range of topics, including inverse dynamics, reinforcement learning with muscle synergies [4], reinforcement learning on dynamic movement primitives [5] and a reflex-based controller [6].
- **Other activities:** We have organized, and are planning to continue, workshops on a variety of topics related to human movement simulation, deep reinforcement learning, and assistive robots. These workshops are being held at several prestigious conferences, including NeurIPS, ICRA, and BioRob.

Significance (to the ASB community): We invite the biomechanics community to explore MyoSuite as a comprehensive platform for research and education in human movement. By fostering multidisciplinary collaboration, MyoSuite is dedicated to advancing the study of human motor control and biomechanics. We are actively seeking contributors to this open-source platform, especially from within the fields of biomechanics and assistive robotics, to help further enhance and develop its capabilities.

References: [1] Caggiano, V. et al (2022), Conf. Learning Dyn. Ctrl, L4DC [2] https://sites.google.com/view/myosuite; [3] Caggiano, V. et al (2023), ICML [4] Berg, C. (2023), RSS [5] Schumacher, P. et al (2023), ICLR [6] Song, S. & Geyer, H. (2015) J Physiol 593.16 [7] Caggiano, V. et al (2022), PMLR.

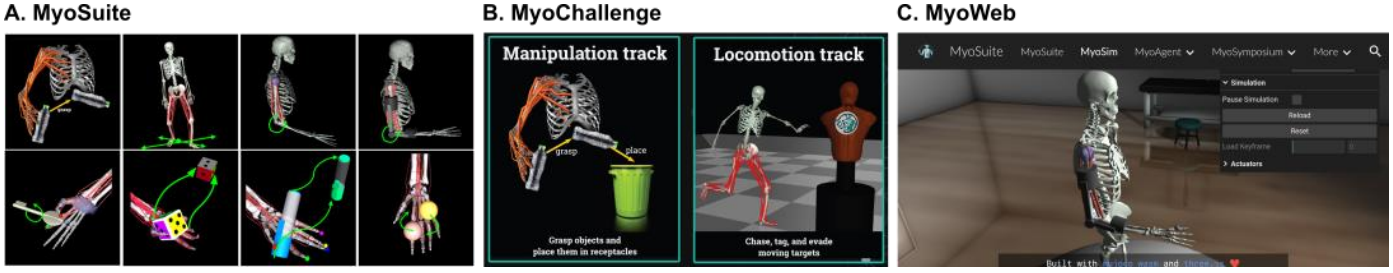

Figure: MyoSuite ecosystem.

EFFECT OF TAI CHI ON ALPHA-RANGE LOWER LIMB CORTICOMUSCULAR COHERENCE IN OLDER ADULTS

Yang Hu[1], Manuel E. Hernandez[2*]
[1]Department of Kinesiology, San Jose State University
[2]Department of Biomedical and Translational Sciences, Cale Illinois College of Medicine, University of Illinois Urbana-Champaign
*Corresponding author's email: mhernand@illinois.edu

Introduction: Falls in older adults are a prevalent and significant problem. Tai Chi practice (TCP) has been widely used as an evidence-based approach to improve balance and help prevent falls in older adults [1]. However, the neural mechanisms underlying the benefits of TCP are difficult to evaluate during traditional balance assessments due to limitations in duration or ceiling effects in performance. Coherence between electroencephalography (EEG) and electromyography (EMG) is thought to reflect corticospinal coupling between the cortex and muscle motor units [2], measurable through corticomuscular coherence (CMC). Prior work has found significantly higher alpha (8-12 Hz) wave amplitude in TCP experts, in comparison to novices [3], while increases in alpha band CMC have been observed in older adults during dual task conditions, in comparison to younger adults [4]. Considering the few observations of the effects of aging on CMC and the neuromuscular basis of TCP benefits on postural control, the purpose of this study was to evaluate the effects of TCP and healthy aging on cortical and neuromuscular function, as evaluated by CMC, while standing in realistic and challenging environments. This study investigated the connection between cortical activation, lower limb muscle activities, and underlying postural control in novel standing balance conditions to achieve this goal. We hypothesized a significant cohort x condition interaction in alpha CMC, given prior observations [3-4], and expected adaptations in cortical control with TCP.

Methods: Ten healthy young adults (18-30), ten healthy older adults (65+), and ten healthy older adults (65+) with TCP experience were recruited for this study. This study consisted of a single session cross-sectional experimental design. To incorporate sensory and mechanical perturbations, virtual reality (VR) was used to provide a simulation of virtual height changes (3, 6, or 9 m), which introduced sensory perturbations and integrated an actuator to provide mechanical perturbations using a SMART EquiTest-Clinical Research System. Participants were asked to stand as still as possible without taking steps while EEG, EMG, and center of pressure (COP) data were recorded. All data processing was performed with customized MATLAB scripts (MathWorks, Natick, MA, USA). For each condition (30 seconds), the power spectral density of cleaned EEG (after filtering and removal of artifacts using Independent Component Analysis) and rectified EMG were computed using Welch's method with 500s non-overlapping Hanning windows. Magnitude square coherence (MSC) was computed to quantify cortical muscular coherence for each EEG channel/EMG channel paired. All the statistical analyses were performed using R (R 4.0.3, RStudio 1.2.1335). Outliers were detected and removed using an Interquartile Range (IQR) method with a 1.5 IQR cut-off. To achieve residual normality, a positive square-root transformation was used. Linear mixed effect models (LMMs) were used to identify the cohort differences for cortical activities, using subject as a random factor, and cohort (young adult, older adult, and TCP groups), condition (ground, height, ground with perturbation, and height with perturbation), cortical region (frontal, central, parietal, and occipital), and muscle (TA=Tibialis Anterior, GAM=Medial Gastrocnemius, GAL=Lateral Gastrocnemius, and S=Soleus) as fixed effects. Model significance was evaluated using the likelihood ratio test.

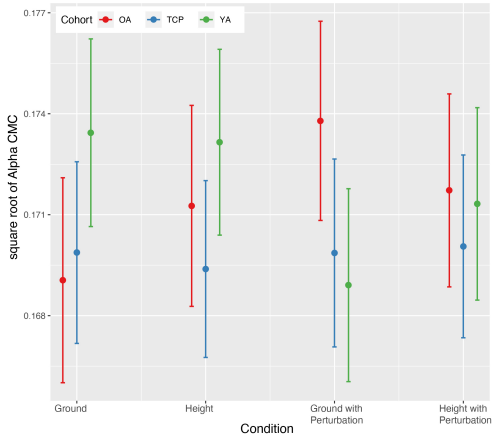

Figure 1: Predicted square root of alpha-band corticomuscular coherence (CMC), using magnitude square coherence across conditions and cohorts (OA = healthy older adults; TCP = OA with Tai Chi Practice experience; YA = young adults).

Results & Discussion: A statistically significant muscle effect ($p < 0.01$), cohort-condition interaction effect ($p < 0.01$), and condition-muscle interaction effect ($p < 0.01$) was observed on MSC (**Fig. 1**). Compared to TA, GA ($p $<$ 0.05$) and S ($p < 0.01$) demonstrated statistically significant higher MSC. For the cohort-condition interaction effect, compared to ground condition, ground with perturbation condition demonstrated statistically significant higher MSC in older adults ($p < 0.05$) and statistically significant lower MSC in YA ($p < 0.05$). For condition-muscle interaction effect, statistically significant higher TA MSC was found in height condition ($p < 0.01$) and ground with perturbation condition ($p < 0.01$) in comparison to ground condition. The findings revealed aging affects corticomuscular coherence during standing postural control and the corresponding adaptations due to Tai Chi practice in older adults.

Significance: To our knowledge, this is the first study investigating the effects of aging and Tai Chi on corticomuscular coherence during standing postural challenges in a novel virtual reality height control task and point at a potential marker of the benefits of TCP in older adults that merits further exploration.

Acknowledgments: We thank participants for their participation and members of the Mobility and Fall Prevention Lab for assistance with data collection and recruitment.

References: [1] Liu et al. (2019), *JAMA Network Open* 2; [2] Mima and Hallett (1999), *Journal of Clinical Neurophysiology* 16; [3] Liu et al. (2003), *Journal of Physiological Anthropology and Applied Human Science* 22; [4] Johnson and Shinohara (2012), *Journal of Applied Physiology* 112;

ANGLES AT PEAK ISOKINETIC TRANSVERSE HIP TORQUE IN YOUNG HEALTHY WOMEN AND MEN

Vered Arbel*, Maeve Gobeyn, Feras Atassi, Steven A. Garcia, Kharma C. Foucher
Department of Kinesiology and Nutrition, University of Illinois Chicago
*Corresponding author's email: varbel2@uic.edu

Introduction: Transverse plane hip function is important during activities of daily living such as walking or getting in and out of a car, as well as higher level recreational activities like golf, dance, or figure skating. Each of these activities requires the hip musculature to produce rotational force at different ranges of hip flexion. It is well known that the transverse plane moment arm, and thus the moment generating capacity and function, of the hip rotators changes with hip flexion. For this reason, we previously developed a protocol for evaluating internal and external hip strength in a supine position [1], which allows assessment at a more functional, near neutral, hip flexion angle. However, different activities also require different amounts of rotational force at different points in the transverse plane ranges of motion (ROMs). The specific angle at which peak torque occurs likely varies based on the specific functional demands of an individual as well as factors such as sex and available range of motion in internal and external rotation. Finally transverse strength symmetry between limbs could vary for similar reasons. Having more information about what constitutes normal ranges of angle at peak torque in internal and external rotation, and the factors that determine these angles, would enable more accurate evaluation and better individualization of training or corrective exercise programming. Therefore, this study investigated the angle of peak torque (APT) for hip internal and external rotators, characterize APT asymmetry, and identify associations between transverse plane APT and ROM in young healthy men and women. After evaluating bilateral APT for hip internal and external rotators, we tested the hypotheses that (i) APT is higher in women than in men and (ii) higher ROM is associated with higher APT in internal and external rotation.

Methods: Fourteen adults with no history of lower extremities injuries (9 men, 22.4 ± 2.2 years; 76 ±6 kg, 171 ±1 6 cm, and 5 women, 21.8 ± 2.2 years; 54 ± 9 kg, 157 ± 7 cm) participated in a previous study [1]. Isokinetic torque was measured at 60º/s in internal rotation and in external rotation on an isokinetic dynamometer [Biodex System 4 Pro, Medical Systems, Inc., Shirley, NY] according to a previously described protocol [1]. Notably, participants were positioned in supine, with hips and knees in neutral. During testing, the range of motion (ROM) in each direction was recorded and the angle at which the peak torque was measured (APT) was identified using manufacturer provided software. For this analysis we used the highest APT and ROM recorded in internal rotation and in external rotation for each leg from all trials. Statistical analysis was conducted using SPSS software version 29 (SPSS Inc, Chicago, IL). We used two-way ANOVAs to evaluate side-to-side differences in men and women and Pearson correlations to evaluate associations between APT and ROM for men and women in internal and external rotation.

Results and Discussion: Maximum internal rotation torque occurred at 32.5° ± 11.1° of internal rotation, but this angle ranged from 13.7° to 50.0°. There were no significant interaction or main effects of sex or side ($p \geq 0.344$). Maximum external rotation torque occurred at 26.8° ± 12.9° of external rotation (range 4.3° to 49°). There was a significant sex by side interaction ($p = 0.005$), where external rotation torque peaked at a higher angle of external rotation for women than men, and at a higher angle on the right hip for men only (Figure 1). For right hips, there was a significant correlation between APT and ROM in internal rotation ($r = 0.578$, $p = 0.030$) but this association seemed to be driven by the relationship in men (Figure 2). There were no other significant associations between APT and ROM for left hips in internal rotation or for either hip in external rotation ($p \geq 0.111$). To our knowledge, this is the first report of potential sex differences and asymmetry in the angle of peak transverse plane torque production. Interpretation of these results is limited by our not having collected data on specific sports and recreational activities that may influence APT variability. Future work will investigate the implications of transverse plane APT on function.

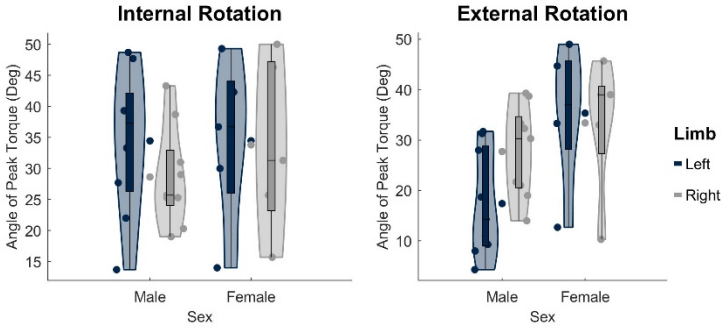

Figure 1. Violin plots depicting APT values for hip internal (IR) and external rotation (ER) between limbs and sexes. Circles plotted in between violins indicate mean IR and ER APT for each limb.

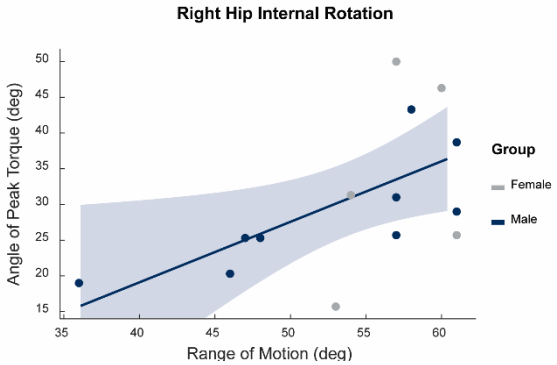

Figure 2. Scatter plots depicting significant associations between ROM and APT values stratified by sex (Pearsons $r = 0.578$, $p = 0.03$).

Significance: Understanding how peak torque angle of the hip rotators contribute to joint control can be applied during clinical and sports-related evaluation and further to develop sex-specific interventions and corrective exercise programming.

References: [1] Arbel et al., American Society of Biomechanics Annual Meeting 2023.

IMPACT OF TESTING ENVIRONMENT ON SYMMETRY DURING SIT-TO-STAND ASSESSMENT

Samantha Weiss[1*], Sara L Arena[1], Robin M. Queen[1]
[1]Kevin Granata Biomechanics Lab, Biomedical Engineering and Mechanics, Virginia Tech, Blacksburg, VA
*Corresponding author's email: samweiss24@vt.edu

Introduction: Utilizing and adapting the technology from controlled lab settings to clinics, sport fields and other non-lab environments has always been a goal within the biomechanics community. The ability to capture data within natural and familiar environments outside of a lab has allowed for improved understanding of how individuals complete activities more naturally. However, there has been a limited focus on movement and loading patterns when completing tasks in these different environments. Independent of the technology or movement completed, a direct comparison of performance differences based on task and location are needed to understand the effects of the testing environment on study outcomes. Load symmetry is a common measure associated with performance and injury [1,2]. With this metric, it is possible to assess differences in symmetry in and out of a controlled lab setting using a highly repeatable task. Comparing load symmetry using a common, everyday movement such as sit-to-stand (STS) in these different environments will allow us to determine potential performance differences based on the testing environment. Differences in outcomes based on testing location could impact interpretation of results and the ability to compare results from data collected in different environments. The purpose of this study was to compare peak force symmetry between two datasets, one collected in a controlled lab environment and the other at the Biomedical Engineering Society (BMES) conference, using the sit-to-stand (STS) task. We hypothesized that when comparing the testing environment, there would be a small, but not significant difference in the peak force symmetry.

Methods: 116 healthy adults between the ages of 18-53 were included in this institutional review board approved study (45 M (22.6 ± 4.7 yrs), 71 F (24.7 ± 7.2 yrs), 72 in lab environment (22.3 ± 2.97), and 44 in conference environment (26.6 ± 9.1)). Peak force symmetry was collected bilaterally at 200Hz using the loadsol® (Novel Electronics, Pittsburgh, PA), a flat and flexible sensor that covers the bottom of the foot and measures the resultant force between the foot and shoe. Testing was completed using a lab provided neutral cushioned running shoe (Nike Zoom Pegasus: Nike, Inc., Beaverton, OR, USA) to standardize footwear between participants. During the STS task, participants began seated in a folding chair with their arms folded across their chest. They then stood up to a fully upright position and returned to a seated position transferring their weight fully back onto the chair. All participants completed 2 sets of 5 repetitions at the BMES conference and 2 sets of 7 repetitions in the lab setting. Force symmetry was calculated using the normalized symmetry index (NSI) with an opensource MATLAB code [3,4]. The controlled lab environment included the research participant as well as the researcher with a maximum of 3 individuals in the room, while data that was collected within the conference environment included more distractions as the data was collected within the exhibitor space with conference attendees walking past, visiting the booths, and having discussions nearby. While the participants performed the tasks in an area where other attendees could not directly interact with the participant, the presence of 100s of people in the exhibit hall resulted in constant noise and people moving around creating distractions. A linear mixed effects model (α=0.05) was used to determine differences in peak force symmetry during the STS task between the controlled lab and conference environment using JMP software (SAS Institute Inc., Cary, NC).

Results & Discussion: Sex and age were not significant factors in the differences in peak force symmetry between the two data collection locations. Significant results were found in peak force symmetry ($p = 0.003$) between individuals when performing the STS in a controlled lab (NSI= 8.66 ± 6.98) versus a conference environment (NSI= 12.29 ± 10.59). With the differences in performance between these two settings, the need to develop and implement testing with portable technology becomes even greater. While this is only one task directly compared between a lab and a conference environment, STS is an activity of daily living and therefore highly repeatable. Despite there being little prior research examining possible outcome differences based on the environment in which the data is collected, these results indicate the need to consider the impact of environment when interpreting data and comparing outcomes across studies. One limitation of this work is that different individuals completed the task in the lab environment and the conference environment, potentially allowing for between group differences to result in differences between environments. Therefore, future work should include a single set of participants who complete the same tasks in two different environments, one a quiet, controlled lab environment and the other a simulated conference environment with distractions that could better replicate natural environments. Future work should expand to determine the impact of environment on additional tasks and outcome measures.

Significance: This study provides new insights on the importance of considering the testing environment and potential environmental distractions when interpreting study results. Specifically, it could be important to understand possible differences in outcomes when comparing results obtained in more distracting environments versus a more controlled lab environment.

Acknowledgments: We would like to thank all members of the study team and attendees of the BMES 2023 Meeting who participated in our study amidst all the conference events, and the study team and participants who completed data collection at the Kevin P. Granata Biomechanics Lab at Virginia Tech.

References:

[1] Patterson, KK. et al. (2010), *Gait and Posture*; [2] Drillis, R. et al. *Ann NY Acad Sci* (1958); [3] Queen, R. et al. (2020), *J Biomech*; [4] Luftglass, AR. et al. (2021) *Clin Biomech;*

ENABLING DEVICE-AGNOSTIC PHYSIOLOGICAL STATE ESTIMATION FOR EXOSKELETONS THROUGH BODY-MOUNTED SENSOR SUITES

Dongho Park[1*], Taryn A. Harvey[1], Yash Mhaskar[1], Keya Gosnagi[1], Ryan Casey[1], Kinsey R. Herrin[1], Aaron J. Young[1]
[1]George W. Woodruff School of Mechanical Engineering, Georgia Institute of Technology, Atlanta, GA, 30332-0405 USA
*Corresponding author's email: dpark@gatech.edu

Introduction: The quest for refining assistive exoskeleton technologies necessitates precise physiological state estimation to facilitate user movement in a natural and supportive manner [1]. Traditional exoskeleton control has relied on sensors attached to the device, which must be calibrated in torque mode due to mechanical influences affecting sensor readings. To mitigate this, we introduce the Second Skin (SS) technology, an array of inertial measurement units (IMUs) designed to be worn directly on the body. Our premise is that body-mounted sensors will be less influenced by device mechanics and can be trained to be agnostic to the exoskeleton's torque assistance. We hypothesize that SS technology will independently estimate physiological states, specifically hip moment estimation, with high accuracy, regardless of exoskeleton interaction. We conducted experiments comparing the root mean square error (RMSE) of hip moment estimates from the SS-only model against those of the SS combined with active exoskeleton torque (SS+Exo). This comparison aimed to evaluate the SS's ability to function independently from the exoskeleton's torque.

Methods: To evaluate the precision of IMU-based Second Skin in hip joint moment prediction, we conducted experiments with three able-bodied participants. Each individual performed gait tasks in two distinct setups: wearing the Second Skin system alone (SS only) and in conjunction with a hip exoskeleton providing active torque assistance (SS+Exo). The exoskeleton's assistance was intended to emulate real-world use, where its torque can affect movement patterns and potentially introduce noise into sensor data.

We collected kinematic data through Second Skin's IMUs on the shank, thigh, pelvis, and trunk. Additionally, we utilized motion capture and ground reaction force (GRF) measurements to perform inverse dynamics calculations, establishing the ground truth for hip joint moments. In this study, we employed a temporal convolutional network (TCN) to predict the hip flexion and extension moments for individuals using an SS [2]. The architecture of the TCN was designed with a singular output node, tasked with the estimation of the hip flexion or extension moments, scaled by the mass of the user. The input to the TCN comprised a sequence of data points from six-axis IMUs that were mounted on the trunk, pelvis, thigh, and shank.

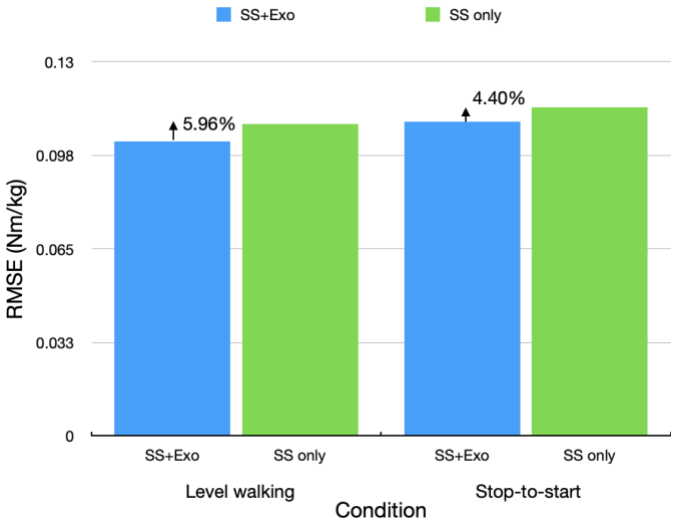

Figure 1: The RMSE for hip joint moment estimation using the Second Skin with and without a hip exoskeleton providing assistive torque. The comparison is made for two different movements: level walking and stop-to-start transitions. The bars represent the accuracy of the predictions in each scenario.

The control strategy implemented in the exoskeleton involved a sequence of operations on the estimated hip moments, including scaling, buffering with a specific delay, and lowpass filtering. These processed torque commands were then delivered to the exoskeleton's actuators, aiming to synchronize the assistance with the user's natural gait pattern effectively.

By comparing the RMSE of the SS-only model against the SS+Exo, we aimed to assess whether SS technology could independently predict hip joint moments with comparable accuracy to when combined with exoskeletal assistance.

Results & Discussion: In level walking, the SS+Exo model showed an RMSE of 0.1023 Nm/kg, while the SS-only model reported a slightly higher RMSE of 0.1084 Nm/kg, a nominal increase of 6%. During stop-to-start transitions, the RMSEs were 0.1092 Nm/kg for SS+Exo and 0.1140 Nm/kg for SS-only. These closely matched values, detailed in Fig. 1, suggest that SS technology can accurately estimate hip joint moments without exoskeletal torque assistance. The data supports our hypothesis, indicating the feasibility of a device-agnostic physiological state estimation system.

Significance: This study presents substantial evidence for the benefits of implementing SS technology in exoskeleton control. Our findings suggest that the SS can lead to the development of universal, device-agnostic control systems for exoskeletons, simplifying the technology and reducing its invasiveness while maintaining a high standard of user assistance and motion augmentation. Such a system has the potential to standardize physiological state estimations across various hardware platforms, enhancing the modularity and adaptability of exoskeletal applications.

Acknowledgments: This work was supported by the NSF FRR Award #2233164 and NIH Award DP2-HD111709.

References:

[1] Molinaro et al. (2022), *IEEE Transactions on Medical Robotics and Bionics* 4 (1). [2] Shaojie et al. (2018), *arXiv preprint arXiv*: 1803.01271. [3] Molinaro et al. (2024), *Science Robotics*.

DOES BIOMECHANICAL MODELING IMPROVE IMU-BASED ESTIMATION OF LOWER-LIMB KINEMATICS?

Vu Phan*, Zhixiong Li, Evy Meinders, and Eni Halilaj
Mechanical Engineering Department, Carnegie Mellon University, Pittsburgh, PA USA
*Corresponding author's email: vuphan@andrew.cmu.edu

Introduction: While promising for motion capture in the wild, estimation of kinematics with inertial measurement units (IMUs) is still challenging in the context of human movement, where skin motion results in difficult-to-extract noise that is not characteristic of robotic systems, where IMUs are widely adopted. To improve accuracy, biomechanical models are starting to be sequentially integrated with state-estimation filters [1]. The value that biomechanical constraints add has not been explicitly investigated, however. Accordingly, the primary aim of this work was to assess if biomechanical constraints applied sequentially after state-estimation filters improve estimation of lower-limb kinematics. We also investigated if this relationship is modulated by movement speed, magnetic disturbance, and filter type or different depending on the degree of freedom.

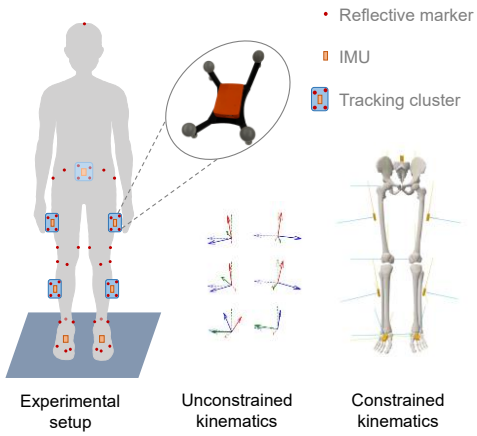

Figure 1: Experimental Setup. IMU and optical motion capture data were collected simultaneously.

Methods: After obtaining approval by the Institutional Review Board of Carnegie Mellon University, 11 subjects (6 M, 5F; age: 32.3 ± 7.2 *years*; weight: 70.0 ± 12.6 *kg*; height: 174.1 ± 9.7 *cm*) were recruited to perform 2 locomotion tasks and 8 physical-therapy exercises. Lower extremity motion was captured with 7 IMUs (MTw Awinda, Movella, USA) and compared to ground truth obtained from a 20-camera optical motion capture system (OptiTrack, NaturalPoint, USA) (Fig. 1).

Madgwick [2], Mahony [3], EKF [4], VQF [5], and built-in Xsens filters with 9 axes were used for state estimation, termed here the unconstrained method. For the constrained method, a biomechanical model was applied to constrain solutions into physiological plausibility using the open-source framework OpenSense [1]. Data from static, walking, and jumping tasks were used for sensor-to-segment calibration. The filters were tuned with data from two subjects, which were not included in the evaluation. We used a generalized linear model to determine the effects of biomechanical modelling and its interaction with degree of freedom, filter type, speed, and magnetic disturbance. Wilcoxon signed-rank tests were used for post-hoc analyses.

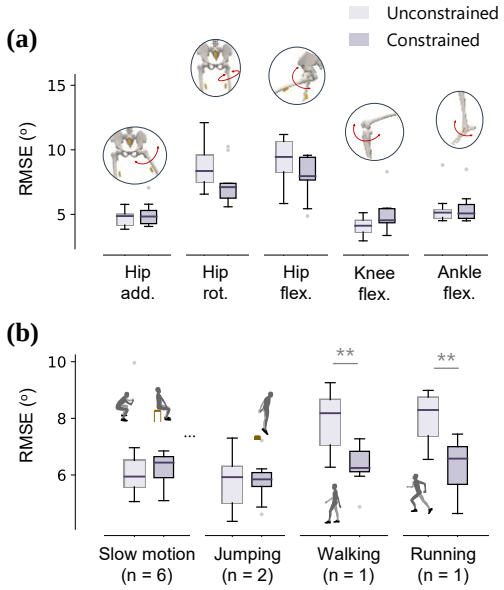

Figure 2: Impact of Biomechanical Modeling. The model (a) did not help across degrees of freedom, but (b) it did at higher speeds. ** p < 0.01

Results & Discussion: Integrating a biomechanical model sequentially after state-estimation filters did not overarchingly improve estimation of lower-limb kinematics (Fig 2a; $p = 0.72$). The use of a biomechanical model did not interact with degrees of freedom, filter type, and magnetic-disturbance level, but it interacted with speed (Fig 2b; $p < 0.001$). Due to the high variability of accelerations [6] and soft-tissue motion, the accuracy of lower-limb kinematics during walking and running was lower than during squatting or jumping. Applying biomechanical modeling improved the accuracy of high-speed kinematics ($p < 0.001$). For example, applying the biomechanical model to the Xsens filter reduced the mean RMSEs from 7.92° ± 4.51° to 6.31° ± 2.30° for walking and from 8.00° ± 3.58° to 6.31° ± 2.00° for running (Fig. 2b). While biomechanical modelling could not mitigate the impact of other factors, future work may consider alternative computational approaches. For example, magnetic disturbance negatively impacted accuracy ($p < 0.01$), but a biomechanical model did not mitigate such effects (p=0.23). Given that modern state-estimation filters already minimize the weight of unreliable magnetometer data (e.g., VQF), it is reasonable that the cases under which the solutions they propose would be non-physiological, and therefore relevant for correction by biomechanical constraints, are sparse. It is worth noting that the longest trial tested here was 1 min. It therefore remains to be determined if biomechanical modelling offers more value as drift accumulates over a longer period.

Significance: This study informs the selection of existing and development of new methods for estimation of lower-limb kinematics using IMUs. Given the lack of practically meaningful improvements resulting from sequential integration of biomechanical constraints following the application of state-estimation filters, we conclude that future efforts should be channelled toward other innovative approaches that combine different computational approaches in new creative ways, along with testing of long-duration trials.

Acknowledgments: This work was funded by the National Science Foundation (CBET 2145473).

References: [1] Al Borno et al. (2022), *JNER* 19(1); [2] Madgwick (2010), *Report x-io & Uni of Bristol* (25); [3] Mahony (2008), *IEEE TAC* 53(5); [4] Sabatini (2011), *Sensors* 11; [5] Laidig and Seel (2023), *Inf Fusion* 91; [6] Shen et al. (2018), *MobiCom*.

HOW DOES FOOT-GROUND CONTACT MODEL PERSONALIZATION AFFECT DYNAMICALLY CONSISTENT TRACKING SIMULATIONS OF WALKING?

Spencer T. Williams*, Claire V. Hammond, Kayla M. Pariser, and Benjamin J. Fregly
Department of Mechanical Engineering, Rice University, Houston, TX, United States
*Email: stw6@rice.edu

Introduction: The ability to design optimal personalized treatments for patients with movement impairments is a critical goal of musculoskeletal modeling research [1, 2]. Researchers typically combine neuromusculoskeletal (NMS) models with direct collocation optimal control to generate dynamically consistent pre-treatment walking simulations that can be used as a starting point for predicting post-treatment walking function [3]. To achieve dynamic consistency for the predicted walking motion, the optimal control solver must utilize an NMS model that includes foot-ground contact (FGC) models for estimating new ground reaction forces (GRFs) and moments (GRMs). Although the goal of developing personalized treatments implies a need for personalized models, optimal control simulations using personalized FGC models are rare [1]. Personalizing FGC models has historically required significant time and effort. However, the new Neuromusculoskeletal Modeling (NMSM) Pipeline software [4] developed by the authors includes a Ground Contact Personalization (GCP) tool that can automatically personalize parameter values in FGC models [5]. This study investigates how the extent of FGC model personalization affects prediction accuracy and computational speed of dynamically consistent walking simulations generated using the NMSM Pipeline's Tracking Optimization (TO) tool.

Methods: This study used experimental kinematic and ground reaction gait data collected from a single subject post-stroke walking at a self-selected speed of 0.5 m/s [6]. Three models, each utilizing a two-segment foot model, were created for the subject. The first (Model 1) was a generic FGC model using a sparse non-uniform grid of nonlinear springs [7] commonly used with OpenSim Moco [8]. The second (Model 2) was generated by manually adjusting the height of the generic spherical contact elements by a common value to account for the subject's shoe height. The third (Model 3), was generated using GCP with a dense uniform grid of linear springs. GCP adjusted model parameter values (individual stiffness coefficients, friction coefficients, and a common resting spring length) while adjusting foot kinematics to reproduce experimental GRFs and GRMs, with the cost function additionally penalizing kinematic changes and discontinuities in stiffness profile. GCP calibrated both feet simultaneously using symmetric properties. All models were used within the NMSM Pipeline TO tool to produce dynamically consistent torque-controlled walking simulations. Solutions possessed root segment residual forces ≤1 N and residual moments ≤0.1 Nm while minimizing changes in tracked joint motions and moments, GRFs, and GRMs.

Results & Discussion: All TO simulations satisfied residual load constraints with similar small errors in tracked quantities (Table 1). However, RMS errors for the subtalar angle were significantly greater without using GCP (5.113° for Model 1 and 5.148° for Model 2 compared to 0.733° for Model 3). The CPU time for TO convergence decreased as the level of FGC model personalization increased. Simply adjusting the height of the generic contact elements made TO take about 32% less time, while the GCP personalized model took less than half the time of Model 1. Application of GCP results to Model 1 helps explain this finding: the generic model could not reproduce experimental ground reactions without kinematic changes too large for the GCP cost function to allow. The generic contact model made large kinematic changes to the untracked vertical translation coordinate during TO not needed by personalized models.

These results indicate that generic FGC models can produce dynamically consistent simulations, in agreement with past findings [9], but model personalization may improve performance. Subtalar angle matching suggests more thorough model personalization may be appropriate for researchers specifically studying foot kinematics. Model 3's process may also be useful for foot models possessing more than two segments or for predicting foot pressure distributions, though such predictions have not yet been evaluated.

Table 1: RMS errors for matching tracked quantities in TO and GCP optimizations with CPU time for TO. For Models 1 and 2, GCP did not modify any model parameter values but attempted to reproduce experimental ground reactions only by minimizing kinematic changes.

	Tracking Optimization (TO)					**Ground Contact Personalization (GCP)**			
Model	Joint angles (°)	Joint moments (Nm)	GRFs (N)	GRMs (Nm)	CPU Time (hours)	Rotation (°)	Translation (mm)	GRFs (N)	GRMs (Nm)
Model 1	1.754	2.066	17.280	2.134	26.5	0.574	6.496	194.451	8.055
Model 2	1.753	2.090	17.493	2.129	18.0	0.522	3.805	10.645	7.425
Model 3	1.243	2.791	20.810	2.221	12.5	1.449	4.392	4.152	1.829

Significance: This study provides useful guidelines for how researchers developing dynamically consistent walking simulations should personalize FGC models. Improving the efficiency of gait simulations makes the use of this technology more feasible for clinicians to personalize their patients' therapies to treat movement impairments. These results indicate that even matching only a subject's shoe height can greatly improve performance. Source code and tutorials for the NMSM Pipeline are available on SimTK.org.

Acknowledgments: This research was supported by a National Science Foundation Graduate Research Fellowship under Grant No. 1842494 and by the National Institutes of Health under grant R01 EB030520.

References: [1] Meyer, A et al., Front Bioeng Biotech, 4, 2016.; [2] Seth, A et al., PLoS Comput Biol, 14(7), 2018.; [3] van den Bogert, A J et al., Procedia IUTAM, 2: 297-316, 2011.; [4] Fregly, B J et al., Int Sym Comput Sim Biomech, 2023.; [5] Williams, S T et al., Int Sym Comput Sim Biomech, 2023.; [6] Meyer A et al., Front Bioeng Biotech, 4, 2016.; [7] Serrancolí, G et al., IEEE Trans Neural A Rehab Eng, 27(8), 2019.; [8] Bianco, N et al., PLoS Comput Biol, 19(8), 2023.; [9] Lin, Y C et al., J of Biomech, 59, 2017.

ANALYSIS OF EMG SIGNALS AND ELECTROMECHANICAL DELAY FOR EXOSKELETON CONTROL

Sierra J. Eady[1*], Michael E. Zabala[1]
[1]Auburn University, Auburn, AL, USA
*Corresponding author's email: sje0011@auburn.edu

Introduction: Exoskeletons are wearable assistive devices that augment human motion. They have been reported to be uncomfortable for the operator [1]. One of the reasons for this is a delay between the operator's motion and the actuation of the exoskeleton. Research has been done to mitigate this delay by using predictive machine learning algorithms [2-5]. Some of these algorithms have attempted to utilize electromyography (EMG) with minimal success. Additionally, research has shown that electromechanical delay (EMD) - the time between a muscle receiving an electrical signal and the initiation of force output – should be accounted for when designing exoskeletons [6], but few incorporate EMD into their design. Therefore, the objective of this study was to identify characteristics of EMG and EMD that could improve the use of EMG sensors to assist in the synchronization of an exoskeleton and its operator. It was hypothesized that (1) the average EMD would be shorter for higher contraction levels, (2) the average EMD during a fatigued state would be longer than that of non-fatigued trials of any contraction level, (3) the average EMG amplitude and frequency would be increased for higher contraction levels, and (4) the average EMG amplitude and frequency would be decreased compared to non-fatigued trials of any contraction level.

Methods: This study evaluated the antagonistic muscle pair at the ankle – the gastrocnemius (GM) and the tibialis anterior (TA) – during fatigue and two levels of contraction. The test population consisted of two men and one woman (height: 1.74 ± 0.07 m; weight: 73.9 ± 22.7 kg) between the ages of 18 and 30 (IRB no. 23-619 MR 2312). One Delsys surface EMG sensor was placed on each muscle, a surface EMG sensor was placed on the left rib cage to monitor the subject's heart rate, and a force sensitive resistor (FSR) array was placed on the proximal phalanges of the foot. Participants performed isometric dorsiflexions and plantarflexions while seated and with an inelastic strap placed around the proximal phalanges opposing the direction of the contraction force. Each participant performed maximum voluntary contractions (MVC) followed by alternating isometric contractions at 60% MVC and 20% MVC three times for five seconds each. After a rest period, each participant performed MVCs again to mitigate any possible muscle fatigue from the previous part of the study. A fatigue protocol was then performed where the EMG signal magnitude was sustained at 60% MVC until the participant could no longer achieve that percentage for three consecutive seconds. Each participant's EMG signal was normalized to their MVC. The average values were calculated by averaging each participant's three repetitions of a trial and then averaging those across participants. The p-values were calculated by one-tail paired t-tests, and a p-value below 0.05 was considered significant. The mean difference and p-value for each comparison are provided in Table 1.

Results & Discussion: The hypothesis that the average EMD would be shorter for higher contraction levels was accepted for the GM ($p<0.05$). The p-value for this hypothesis for the TA is trending toward being statistically significant ($p=0.054$) and may become significant as more subjects are tested. The hypothesis that the average EMG amplitude would be higher for higher contraction levels was accepted for both muscles ($p<0.01$). All other hypotheses were rejected.

The accepted hypotheses suggest that exoskeleton synchronization with the operator could be improved by EMG data. Machine learning algorithms could track changes in average EMG amplitude and EMD and use them to identify the speed at which the exoskeleton should move. This would allow the exoskeleton to adapt to the operator over time as their needs change.

In the future, this study will be expanded to include at least 12 participants and will also analyze the effects of stress on EMG signals and EMD. Additionally, this study will analyze how the EMG signals change over time rather than only evaluating the averages of the trials.

Table 1. A paired t-test was used to find p-values based on the means of the trials. P-values highlighted in green are significant ($p<0.05$).

	TA		GM	
	Mean Difference	P-value	Mean Difference	P-value
EMD (s)				
60% MVC - 20% MVC	-0.044	0.054	-0.042	0.010
Fatigue - 20% MVC	-0.002	0.522	-0.075	0.838
Fatigue - 60% MVC	0.042	0.177	-0.033	0.706
Average Amplitude (V)				
60% MVC - 20% MVC	0.121	0.006	0.076	0.007
Fatigue - 20% MVC	0.245	0.983	0.148	0.997
Fatigue - 60% MVC	0.124	0.916	0.071	0.975
Average Frequency (Hz)				
60% MVC - 20% MVC	-5.079	0.579	-6.074	0.587
Fatigue - 20% MVC	9.236	0.659	37.309	0.908
Fatigue - 60% MVC	14.316	0.950	43.382	0.902

Significance: Utilizing changes in EMG signal characteristics and/or EMD could improve the efficacy of EMG for exoskeleton control. This could result in positive impacts to clinical populations in need of rehabilitation, soldier augmentation, and improved occupational safety.

References: [1] Sun et al. (2022), *Annual Reviews in Control* 53; [2] Hollinger et al. (2023), *IEEE Transactions on Medical Robotics and Bionics* 5(2); [3] Coker et al. (2021), *Sensors* 21(11); [4] Gui et al. (2019), *IEEE/ASME Transactions on* Mechatronics 24(2); [5] He et al. (2007), *6th International Special Topic Conference on Information Technology Applications in Biomedicine* (292-295); [6] Vette et al. (2008), *Biomed Tech* 53.

GAUSSIAN MIXTURE MODEL CLUSTERING GAIT BIOMECHANICS OF TOTAL KNEE ARTHROPLASTY PATIENTS 6-MONTHS AFTER SURGERY

Jingyu Hu[1]*, Bret Freemyer[2], Christopher Stickley[3]
[1]University of Hawaii at Mānoa, Kinesiology and Rehabilitation Science
*Corresponding author's email: hujingyu@hawaii.edu

Introduction: Total knee arthroplasty (TKA) is the well-established surgical intervention for end stage knee osteoarthritis (OA) [1] Postoperatively patients improve function, have less pain, and may have more normal gait. However, previous research indicates that some TKA patients never regain normal gait patterns, particularly in frontal plane loading.[2] Thus, improved understanding of loading characteristics for TKA patients is important during the postoperative phase.[3] Machine learning algorithms may help identify gait data clusters to obtain specific subgroups with similar loading features to better identify how to best treat patients. The main advantage of Gaussian mixture model approach is that it can compare different mixture models and automatically identify the best cluster algorithm. [4] Therefore, the purpose of this study was to categorize knee loading patterns 6-months following TKA by using the gaussian mixture method.

Methods: 35 TKA patients a minimum of 6 months postoperative participated in this study. Gait biomechanics were collected at the University of Hawaii at Manoa utilizing a Vicon Nexus motion caption system (Nexus 2.5.0 Vicon Motion Systems, Vicon LA, Culver City, CA USA). Participants were asked to walk barefoot at a self-selected velocity. Kinetic data were collected by a force plate (Advanced Mechanical Technology, Inc., Massachusetts, MA, USA) embedded in the ground. The kinematic and kinetic gait variables for the knee were processed with Visual 3D (C-Motion, Inc., Germantown, MD). Principal component analysis (PCA) was used to reduce the dimensions of the biomechanics knee gait variables. Following PCA, the principal components (PCs) that accounted for 95% of explained variance criterium were selected as the new dataset for the gaussian mixture model (GMM) to assign the participants to individual clusters with similar gait characteristics (Python Version 3.10.12). Finally, a one-way ANOVA (SPSS Version 26.0, with an alpha level of $p < 0.05$) and subsequent Tukey post hoc tests were used to analyze the differences in knee gait variables among the clusters.

Results & Discussion: The explained variance of the first 13 PCs was over 95%, thus, the first 13 PCs were used for the Gaussian mixture model training for clustering. After GMM, there were 4 clusters for the TKA participants (Cluster 1, n=2; Cluster 2: n=11; Cluster 3: n=8; Cluster 4: n=11). Cluster 1 was removed from further analyses due to the sample size of 2. Thus, the ANOVA and the post hoc only compared clusters 2 to 4. The optimal group appears to be cluster 3, based on higher knee moments in the frontal and sagittal planes relative to their knee adduction angles. Typical gait restoration following TKA is identified by increased walking velocity and increasing loading as indicated by increased flexion and adduction external moments. Table 1 shows that cluster 2 and 4 both demonstrate increased knee loading characteristics compared to cluster 3. The primary difference between clusters 2 and 4 is the amount of peak knee adduction angles, with decreased amounts of knee adduction in cluster 4. Cluster 4 appears demonstrated the lowest magnitude of knee flexion and adduction moments and indicate patients that could benefit from further therapeutic interventions, such as additional therapy or gait retraining.

Table 1. Tukey post hoc comparisons for knee gait variables between Gaussian clusters

Knee Variables	Cluster 2	Cluster 3	Cluster 4	2 vs 3		2 vs 4		3 vs 4	
	Mean (SD)	Mean (SD)	Mean (SD)	MD	P value	MD	P value	MD	P value
PEAK KAM RATE (Nm/Kg/s)	2.18(1.15)	3.87(1.36)	2.13(0.62)	-1.69	0.007*	0.05	0.999	1.74	0.005*
PEAK KAM (Nm/Kg)	0.33(0.10)	0.48(0.17)	0.30(0.06)	-0.16	0.021*	0.03	0.919	0.19	0.005*
PEAK KFM RATE (Nm/Kg/s)	4.85(1.55)	7.90(2.16)	4.29(1.08)	-3.05	0.001*	0.55	0.833	3.61	<.001*
PEAK KFM (Nm/Kg)	0.66(0.10)	0.88(0.23)	0.54(0.18)	-0.22	0.045*	0.12	0.376	0.34	0.001*
KAM IMPULSE (Ns)	0.16(0.04)	0.19(0.05)	0.11(0.03)	-0.03	0.442	0.051	0.028*	0.08	0.001*
PEAK KNEE ADD ANGLE (degrees)	1.71(2.65)	3.73(3.48)	-2.43(0.70)	-2.02	0.409	4.41	0.006*	6.18	<.001*
MD: Mean Difference; *: $p < 0.05$; KAM: knee adduction moment; KFM: knee flexion moment; ADD: adduction.									

Significance: The current study provides a new method to interpret the postoperative gait data in TKA patients. A better understanding of the similarities within clusters and differences between clusters may provide improved identification of patients with abnormal loading patterns.

References: [1] Farquhar, S. J. et al. (2008), *Physical therapy* 88(5). [2] Noble et al. (2005). [3] Elbaz, A. et. al (2014) *Journal of orthopaedics*, 11(2). [4] Dolatabadi et al. (2016), *IEEE* 21(5).

SCLERAL COLLAGEN REMODELING AND REPAIR ASSESSED IN INTACT EYES THORUGH SECOND HARMONIC GENERATION

Aldo Tecse[1, 2*], Kaitlin Wozniak[2], James Germann[2], Alex J. Mcmullen[1], Mark Buckley[1, 2], Robert Baratta[3], Eric Schlumpf[3], Brian J. Del Buono[3], Michael Telias[2], Susana Marcos[2]

[1] Department of Biomedical Engineering, University of Rochester School of Arts and Sciences, Rochester, NY, United States

[2] Center for Visual Science, Rochester, NY, United States

[3] Stuart Therapeutics, Inc, Florida, United States

*Corresponding author's email: atecse@ur.rochester.edu

Introduction: Myopia affects more than 20% of the population and is projected to affect 50% by 2050. Therefore, investigating the onset and progression of this disease is crucial [1]. Myopia is characterized by residual defocus, where the power of the cornea and lens does not match the retinal plane. This mismatch is believed to trigger a cascade of events that results in posterior scleral remodeling and axial elongation [2]. During myopia development, matrix metalloproteases (MMPs) have been reported to cause thinning of the collagenous framework and remodeling of the extracellular matrix composition [3, 4]. Studies have shown alterations in the glycosaminoglycans and collagen fibers, which are believed to underlie changes in the mechanical properties of the tissue.

Additionally, the collagen network in the sclera is affected by the intraocular pressure (IOP) and its interaction with various tissues, including the cornea, eye muscles, optic nerve, and choroid, resulting in regional variations [5]. The mechanical properties of the sclera are highly dependent on the density, orientation, and crimping of the collagen network [6], due to its non-linear nature. Recently, we also identified reparative capabilities of collagen-mimetic peptides (CMPs) within collagen structures in excised sclera. In this study, we used Second Harmonic Generation (SHG) Microscopy to investigate the structural changes of the scleral collagen network induced by MMP-1 digestion in intact eyes.

Methods: A custom-built two-photon SHG microscope was used to measure the direct backward scattering signal of collagen bundles in the posterior sclera. This system was coupled with a compressive fixture (3mm-height) enabling *ex vivo* intact eye imaging of male C57BL/6J mice, postnatal age 34-43 days (n = 10 eyes). Stacks of images were captured along the optical axis (1-µm intervals) in two field of view configurations (FoV): 200µmx200µm (0.7 µm/px) and 500µmx500µm (1.7 µm/px). Sample eyes were imaged at three timepoints: Immediately after enucleation (virgin) and MMP-1 treatments (TDzyme; 10µL drop, 200 µg/mL, 30 min), and CMP treatment "ST-103" (Stuart Therapeutics; 10µL drop, 250µg/mL, 30 min). Custom processing algorithms were used to assess anisotropy (FoV1; order coefficient: OC) and collagen density (FoV2; normalized Irradiance: NI). The OC measures the alignment of collagen bundles, so that a highly interweaved collagen network has a low alignment coefficient.

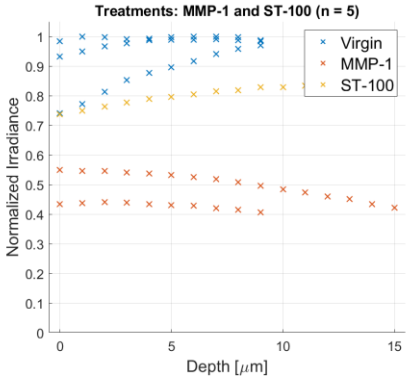

Figure 1: Matrix metalloproteases decrease collagen network density and interweaving between collagen bundles. In contrast, collagen mimetic peptides partially restore virgin conditions.

Results & Discussion: Control experiments in contralateral eyes did not show any differences in collagen organization between untreated eyes and sham controls along time (n = 5). Collagen structure was observed to a depth of at least 9 µm in virgin and CMP-treated eyes and 15 µm in MMP-treated eyes. Virgin sclerae exhibited a high degree of collagen interweaving and density throughout the entire depth (n = 5: OC=0.26±0.02 and NI=0.96±0.06, respectively). MMP-1 produced a reduction of collagen interweaving (OC=0.32±0.04) and density (NI=0.46±.07). In contrast, CMP was able to restore collagen anisotropy (OC=0.24±0.02) and density (NI=0.79±0.04, respectively) to levels similar to those of the virgin state. Although we only considered the effect of MMP-1, multiple MMPs have been reported during myopia, such as MMP-2 and MT1-MMP [3]. However, our focus is not on validating the treatment, but on quantifying alterations to the collagen network.

Significance: Many of the current studies use animal models to study the global change of mechanical properties during myopia progression because the assessment of mechanical properties requires enucleation and tissue dissection [7]. However, it is not known if the growth patterns in myopia, including direction and magnitude, are homogeneous due to regional variances in scleral mechanical properties. This study characterized local alterations in the scleral collagen network in intact murine eyes, eliminating the need for tissue excision. Additionally, this method enables the evaluation of the efficacy of future therapeutic treatments for myopia.

References:

[1] Holden, B.A., et al. (2016). *Ophthalmology*. **123**(5): p. 1036-1042.
[2] Baird, P.N., et al. (2020). *Nature Reviews Disease Primers*. **6**(1): p. 99.
[3] Summers Rada, J.A., S. Shelton, and T.T. Norton (2006). *Experimental Eye Research*. **82**(2): p. 185-200.
[4] Zhao, F., et al. (2018). *The American Journal of Pathology*. **188**(8): p. 1754-1767.
[5] Boote, C., et al. (2020). *Progress in Retinal and Eye Research*. **74**: p. 100773.
[6] Ehret, A.E., et al. (2017). *Nature communications*. **8**(1): p. 1002.
[7] Brown, D.M., et al. (2023). *Investigative Ophthalmology & Visual Science*. **64**(5): p. 22-22.

Ground Reaction Forces and Batting Velocity in Relationship to Different Hitting Locations in a Baseball Swing.

Adam Zeidan*[1], Samuel R Zeff, Scott Ducharme, Will Wu

[1]Department of Kinesiology, California State University, Long Beach.

*Corresponding author's email: Adam.Zeidan01@student.csulb.edu

Introduction: Hitting a baseball is a dynamic motion in which all parts of the body must generate and transfer energy to create a fast swing [1]. Swinging a baseball bat is dependent upon the propulsive forces applied from the back leg (i.e. pivot), which are transferred to braking forces at the front (lead) leg to generate energy that leads to a successful swing of the bat. Propulsive and braking forces coincide with the anterior-posterior ground reaction force (GRF). Considering which factors that affect the velocity of a baseball bat, researchers have noted that hitting locations have a strong influence on bat speeds. Previous studies have investigated how hitting locations affect batting velocity, reporting that the inside hitting conditions (innermost part of the plate) have higher bat speeds than the outside hitting locations [3]. Previous studies have also explored how GRFs contribute to bat speeds. One study reported that peak GRF values in the stride (i.e., front) foot correlated with increased bat speed [2]. Hashimoto et al., 2023, also reported a similar relationship and found that peak vertical GRF was a predictor of bat speeds as well [1]. Overall, earlier research observing the impact of batting locations on GRF variables is limited. Therefore, the purpose of this study was to investigate the relationship between GRFs and different hitting locations, specifically examining both the lead/front-foot propulsive forces and the pivot/back-foot breaking GRFs. Based on previous research [2], we hypothesized that inside-hitting conditions would produce the highest of peak forces, resulting in faster batting speeds at the point of contact.

Methods: Eight recreationally active university students (Age range: 21-29) participated in hitting a baseball positioned on a tee in two different locations. Inside-high-hitting (IH) conditions were standardized for each subject by placing an anatomical marker at 75% of the distance between the greater trochanter and acromioclavicular joint with the ball placed on the most inside part of the plate, and outside-low-hitting (OL) conditions were standardized by placing the ball at patella level at the most lateral part of the plate. Participants swung a bat while standing on two force plates, one for the lead/front foot and one for the pivot/back foot, while a Blast Motion device was placed on the end of the bat handle to measure bat velocity at ball contact. The forces being measured included the vertical forces (front and back foot), braking forces in the front foot, and propulsive forces in the back foot when hitting a baseball at inside and outside hitting conditions. Participants were instructed to swing the bat as fast as they could to hit the baseball five times for each hitting condition. Analyses of variance (ANOVAs) with repeated measures were used to assess the main effects of hitting location on bat velocity, with the CI set at 95% to mark statistical significance at a P-value of $\leq .05$. Peak vertical GRF in both feet, braking in the front foot, and propulsive forces in the back foot were recorded and averaged. Furthermore, the bat velocity at the point of contact was recorded and averaged.

Results & Discussion: No significant differences were observed for the peak vertical GRFs for both the pivot (IH: 862.55±137.98; OL: 826.15±75.68; $p = 0.429$) and lead limbs (IH: 945.6±224.9; OL: 1024.73±266.73; $p = 0.336$). We observed significantly reduced peak propulsive forces during IH compared to OL hitting locations (IH:152.87±28.24 N; OL 171.28±36.19N; $p = 0.009$). Similarly, peak braking forces were also significantly reduced in the IH compared to OL location (IH -255.03; ±93.3; OL: -320.53±89.57; $p = 0.045$). Lastly, batting velocity was reduced in the IH hitting condition (IH: 48.35±5; OL: 57.76±9.88; $p=.003$). This finding contradicts previous research that found that IH locations have higher batting velocities than outside-hitting locations [3]. This may be due to the fact that this study used a recreationally active population, while the previous study included Division 1 collegiate baseball players.

Significance: In a recreationally active population, results of the study demonstrated significant changes in GRFs and batting velocity at different hitting locations. These findings provide a more detailed understanding of how hitting location constraints influence force profiles and bat speeds during a swing. Further studies should examine how hitting locations affect hitting performance across athletes with a broader range of training experience.

References: [1] Hashimoto, J. et al., 2023.ISBS *Proceedings Archive*, *41*(1), 45.;[2] Horiuchi, G., & Nakashima, H. (2023). *Sports Biomechanics*, 1–12.;[3] Williams, C. C et al., (2020). *International Journal of Kinesiology and Sports Science* 8.2 (2020): 1-6.

FASCIAL GLIDING ASSESSMENT FOR MYOFASCIAL PAIN SYNDROME YIELDS CONSISTENT UPPER TRAPEZIUS ACTIVATION

Kirubel B. Tadesse[1*], Siddhartha Sikdar[1,2], Samuel Acuña[1,2]
[1]Department of Bioengineering, George Mason University, Fairfax, VA, USA
[2]Center for Adaptive Systems of Brain-Body Interactions, George Mason University, Fairfax, VA, USA
*Corresponding author's email: ktadess@gmu.edu

Introduction: Myofascial Pain Syndrome (MPS) is a highly prevalent form of chronic soft tissue pain that is often present in the neck and shoulder muscles. Although the ultimate underlying cause of the chronic pain is multifactorial, MPS is characterized by discrete palpable sensitive areas within muscle tissue known as myofascial trigger points (MTrPs). There are several potential treatments for MPS and the MTrPs, including dry needling, acupuncture, and pharmacology, but choosing a targeted treatment is limited by a lack of quantitative diagnostic measures to distinguish the precise tissue-level mechanisms driving myofascial dysfunction [1]. Therefore, there is a strong need to identify specific biomarkers of impaired myofascial tissue.

It has been hypothesized that abnormal changes in the dynamic viscoelastic properties of the fascia (the connective tissue network surrounding muscles and fascicle bundles and is critical for force transmission) plays a role in the pathogenesis and pathophysiology of MPS [2]. These abnormal changes can impede the gliding of muscle compartments, impeding force transmission as well as proprioception. The assessment of fascial gliding can therefore be one promising method to extract a tissue-level biomarker [2]. However, there are several technical challenges that need to be overcome to develop a reproducible assessment protocol.

Due to the high prevalence of MPS in the neck and shoulder muscles, our interest is in assessment of fascial gliding between the trapezius and rhomboid muscles. Our pilot testing indicated that trapezius–rhomboid gliding can be observed for participants doing an isometric shoulder shrug while prone. However, there are many ways to execute a shoulder shrug, and not all of them can produce observable gliding. Thus, a participant needs to focus on contracting their upper trapezius in a specific way, which requires they follow visual feedback from the ultrasound imaging. However, ultrasound imaging can only capture tissue deformation, and it is still unclear if the observed gliding represents passive motion through connected tissue or an activated upper trapezius. Thus, the purpose of this study was to investigate the reliability of upper trapezius activation during observed trapezius–rhomboid gliding.

Methods: We instructed 17 participants to lie prone on an exam table such that they could observe a display of the acquired ultrasound imaging (Aixplorer, SuperSonic Imagine, France). The ultrasound probe was placed medial to the scapula to observe the fascial gliding (**Fig 1A**). Participants grasped the handle of a cable instrumented with a load cell (SM-250, Interface Inc., Scottsdale, AZ) such that they could pull on the handle to perform an isometric shoulder shrug. We placed an electromyographic (EMG) sensor (Trigno Galileo, Delsys Inc, Natick, MA) over the upper trapezius in the direction of the muscle fibers. We asked the participants to perform an isometric shoulder shrug to produce trapezius-rhomboid gliding using ultrasound imaging as visual feedback (**Fig 1B**). A metronome playing at 25 bpm provides an audio cue to signal the cycling of contractions and relaxations. Load cell data was filtered at 10 Hz and periods of contraction were identified when force exceeded half the RMS. EMG was bandpass filtered (5-500 Hz), rectified, and low pass filtered (5 Hz) to create linear envelopes of muscle activation, amplitude normalized to maximum value. The reliability of activation was quantified as the coefficient of variation over the ensemble average [3].

Results & Discussion: We observed 102 shoulder shrugs across all participants and found consistent upper trapezius activation (**Fig 1C**). The coefficient of variation was 0.45, which is consistent with EMG activation over other cyclic tasks such as treadmill walking [3]. Future studies will examine the EMG signals themselves to examine possible biomarkers in the frequency content of the activations.

Significance: We are determining quantitative biomarkers to characterize MPS, which must be sensitive and specific to the tissue-level mechanisms that contribute to MTrPs. Our findings confirm that a specific isometric shoulder shrug can produce observable trapezius–rhomboid gliding due to a consistent and reliable activation of the upper trapezius. Impairments in the observed fascial gliding may inform clinical diagnoses of MPS and identify subgroups of patients that may better respond to targeted treatments.

Acknowledgments: Funded by NIH HEAL 1R61AT012286. A. Aher , M. Jirsaraei, M. Lamarre for assistance with data collection.

References: [1] Duarte (2021), *Cur Rheum Rep*; [2] Sikdar (2023), *Front Pain Res* 4(1237820). [3] Acuña et al. (2018), *Gait & Pos*.

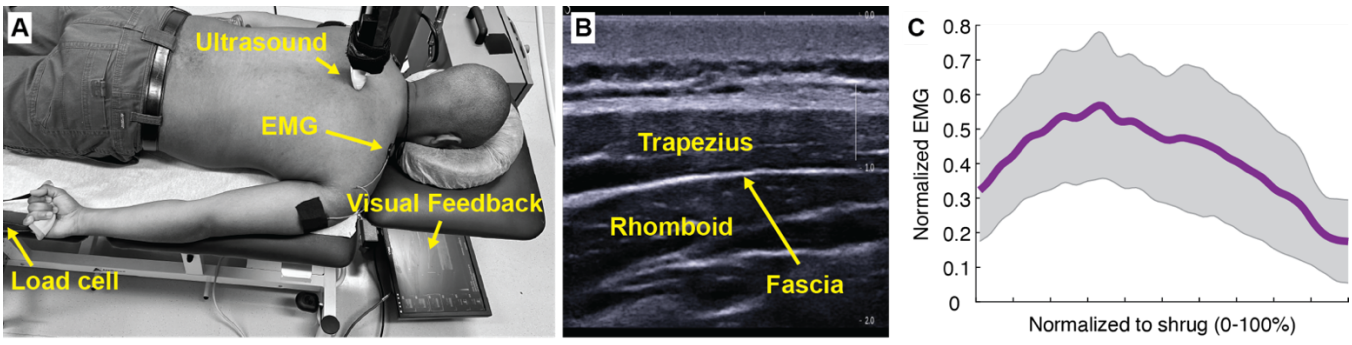

Figure 1. A) Experimental setup. B) Ultrasound image of fascial gliding. C) Ensemble averaged EMG over a shoulder shrug

PROSTHETIC ANKLE-FOOT STIFFNESS MAY INFLUENCE RESIDUUM SOCKET INTERFACE PRESSURE AND USER PERCEIVED COMFORT IN TRANSTIBIAL PROSTHESIS USERS

Michael Jacobson[1], Kiley Armstrong[2], Ashutosh Tiwari[1], Sebastian Pantoja[1], Matthew J. Major[2], Myunghee Kim[1*]
[1]Department of Mechanical & Industrial Engineering, University of Illinois at Chicago, Chicago, IL, USA
[2]Northwestern University Department of Physical Medicine & Rehabilitation, Jesse Brown VA Medical Center, Chicago, IL, USA
*Corresponding author's email: myheekim@uic.edu

Introduction: For individuals with transtibial amputation, comfort and fit of the prosthesis are critical to mobility and quality of life, and to a large extent depend on the coupling and dynamics of the prosthetic socket. Evidence suggests that adjusting the alignment of the ankle-foot prosthesis, which effectively changes its stiffness profile during use, has the potential to modulate the socket-residuum interface pressure, which would impact force transmission and possible socket comfort. However, the direct effect of ankle-foot prosthesis stiffness on socket pressure and comfort has not been systematically investigated. The purpose of this study was to evaluate the effect of ankle-foot prosthesis (AFP) stiffness on the residuum-socket interface pressure and user perceived socket comfort in unilateral transtibial prosthesis users. In this study, we further constructed an objective function based on socket interface pressure ('Pressure Objective') to better reflect the pressure dynamics at the residuum-socket interface over time during gait.

Methods: Three persons with unilateral transtibial amputation (2 M, 1 F, 47.7 ± 8.9 yrs, 80.5 ± 17.7 kg) participated in this study. Pressure sensors (model 9811E, Tekscan, US) were fixed to the lateral and anterior walls of the socket, which commonly reflect pressure intolerant zones and can provide information on user discomfort[1]. Each subject walked at a self-selected comfortable pace on a treadmill while wearing a robotic AFP that permits rapid adjustments in ankle-foot stiffness. Participants experienced walking for two minutes with five discrete AFP (keel) stiffness values of increasing stiffness spanning a range of commercial stiffness values. After each 2 min of walking, the subjects were asked about their socket comfort and level of exertion using the Socket Comfort score[2] and Rate of Perceived Exertion (RPE)[3], respectively. In post-processing, the measured residuum-socket interface pressures were used to calculate the 'Pressure Objective', defined as the sum of the pressure over the entire trial divided by the peak pressure. To evaluate the relationship of the 'Pressure Objective' against comfort and effort, we estimated the Pearson's Correlation coefficient between each variable set.

Results & Discussion: Fig. 1 displays the Pressure Objective data versus comfort and log-transformed RPE, as well as the linear best fit line and Pearson's Correlation coefficient for both the ln(RPE) (r=-0.67) and comfort (r=0.75) against the 'Pressure Objective'. These preliminary results suggest that a decrease in residuum-socket interface is associated with increased socket comfort and reduced walking effort. In other words, a reduction in socket pressure may be directly linked to a transtibial prosthesis user's experience of how comfortable their socket is to walk with and the perceived amount of exertion needed to ambulate. These findings have important clinical implications as small changes in prosthetic ankle-foot stiffness could impact user perceptions that influence their mobility and quality of life, as well as offer set objectives for 'smart' prostheses to achieve for maintaining high levels of prosthesis user experience.

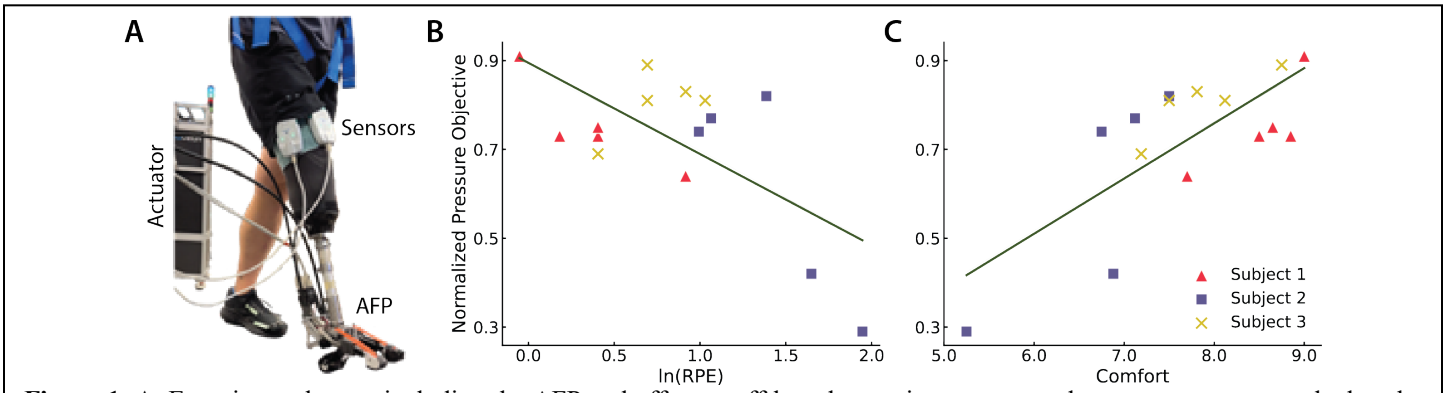

Figure 1. **A**. Experimental setup including the AFP end-effector, off-board actuation system, and pressure sensors attached to the residual limb. **B**. Log-transformed RPE vs. Normalized Pressure Objective graph. **C**. Comfort vs. Normalized Pressure Objective graph. Each graph incorporates data from three subjects, distinguished by varying shapes and colors.

Significance: Our findings contribute to understanding the relationship between residuum socket-interface pressures and the perceived comfort and exertion of transtibial prosthesis users. Knowledge gained from systematic studies of this type can also offer a paradigm shift towards patient-centered and data-driven wearable robot assistance. Importantly, this objective function can be used to personalize AFP stiffness through the human-in-the-loop optimization framework[4-5]. Overall, our study's outcomes have the potential to help inform prescription guidelines of AFP stiffness if the clinical aim is to maximize user comfort during walking.

Acknowledgments: This work was partially supported by the US Dept of Veterans Affairs (#I21RX004077, granted to MJ Major). Contents do not reflect opinions of the US Department of Veterans Affairs or the US Government.

References: [1] Armitage et al. (2020) *Prosthetics and Orthotics International*. [2] Hanspal et al. (2003), *Disability and rehabilitation*; [3] Borg (1998) *Human kinetics*, [4] Jacobson et al. (2022), *Scientific Reports*; [5] Wen et al. (2020), *IROS*.

THE INFLUENCE OF FOOT ARCH STIFFNESS ON RUNNING ECONOMY

Hui Tang * & Owen N. Beck
Department of Kinesiology and Health Education, University of Texas at Austin
*Corresponding author's email: hui.tang@utexas.edu

Introduction: Human runners bounce along the ground using spring-like mechanics [1]. During a running step, the stance leg lowers and decelerates the center of mass from initial ground contact until midstance. Much of the center of mass's decreased mechanical energy during initial stance is converted and stored as potential energy in elastic leg structures (e.g., tendons & foot arch). Then, the elastic potential energy is converted to kinetic energy and assists active leg muscles to accelerate the body into the ensuing aerial phase. Recycling mechanical energy via elastic structures is thought to elicit economical running by reducing the mechanical work required by energy consuming leg muscles. The longitudinal foot arch possesses spring-like qualities [2], and its ability to store and return mechanical energy depends on stiffness. And because foot arch hysteresis is sizeable (~22%), stiffer feet store and dissipate less energy per unit force. Here, we tested whether stiffer feet decrease user's metabolic energy expenditure during running. Because stiffer feet dissipate less mechanical energy per step than compliant feet, they likely reduce net muscle work & metabolism during running [3]. Thus, we hypothesized that artificially stiffening participant feet would reduce metabolic energy expenditure during running.

Methods: Thirteen runners (Avg ± SD; age: 25 ± 6 yrs; height: 1.74 ± 0.09 m; mass: 68.8 ± 8.3 kg) participated. We stiffened each participant's transverse and longitudinal arch by tightly wrapping the distal transverse arch using an elastic wrap [4]. Participants performed foot arch stiffness testing [4]. Then, participants performed a shod treadmill running trial, followed by 4 treadmill running trials involving bare or wrapped feet. All trials lasted 5 min and were at 3.5 m/s. We counterbalanced the trial order of bare and wrapped foot conditions (ABBA or BAAB). We collected ground reaction forces (GRFs), motion capture data, electromyography (EMG), and $\dot{V}o_2$ & $\dot{V}co_2$ during each trial. We computed net aerobic power using a standard equation [5] and normalized to mass.

Results & Discussion: By wrapping the distal transverse arch, we stiffened participant feet 36.4 ± 27.7% (Fig. 1ab). Running with stiffer feet decreased net aerobic power for 10 of 13 participants by an average ± SD of 0.80 ± 1.44% across all participants (Fig. 1d). Biomechanically, running with wrapped vs. bare feet elicited less longitudinal arch compression (Fig. 1c) despite the corresponding longer strides, and greater center of mass work rate (Table 1). Until our inverse dynamics are complete (to be presented at ASB), we surmise that wrapped feet yielded more net mechanical work than bare feet. In turn, wrapping the foot may have reduced leg muscle net mechanical work, which is supported by our muscle activation data (Fig. 2). Numerically, running with wrapped vs. bare feet reduced tibialis anterior, medial gastrocnemius, and soleus muscle activity by 28%, 9%, and 5%, respectively. Overall, stiffening the foot may reduce participant net aerobic power during running by modifying the mechanical energy profile of the foot, thereby enabling participants to run using longer strides and less leg muscle activity.

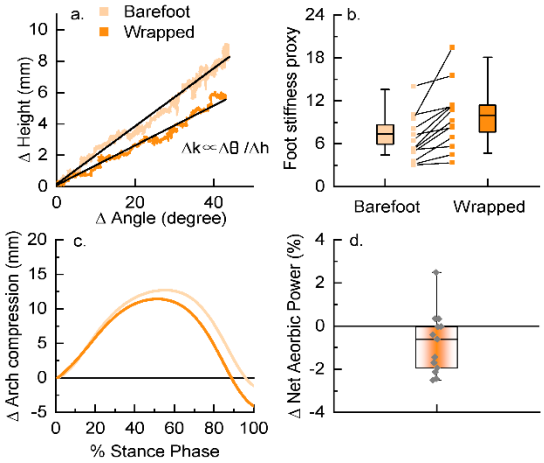

Figure 1. (a) Representative longitudinal arch stiffness approximation, (b) box & whisker plot and individual estimated longitudinal arch stiffness, (c) longitudinal arch compression during stance, and (d) box & whisker plot of the change of net aerobic power during wrapped vs. barefoot running.

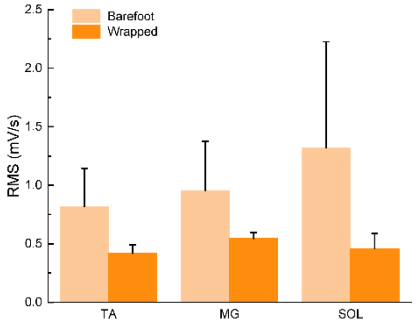

Figure 2. Avg (± SE) root mean squared (RMS) EMG signals of tibialis anterior (TA), medial gastrocnemius (MG), soleus (SOL) of bare and wrapped feet during running.

Table 1. Avg ± SD spatiotemporal and kinetic variables

Variable	Barefoot	Wrapped
Stride frequency (Hz)	1.47 ± 0.11	1.44 ± 0.12
Contact time (s)	0.21 ± 0.02	0.20 ± 0.02
Duty factor	0.30 ± 0.04	0.29 ± 0.04
Positive CoM work rate (J/kg/s)	2.23 ± 0.51	2.29± 0.45

Significance: Mere seconds often separate runners who make the podium from those who fail to medal. Based on our preliminary findings, wrapping the distal transverse arches of runner feet may elicit more economical running. Such improved economy likely translates to improved running performance. Thus, for distance runners hoping to win a medal in the upcoming Paris Olympics, perhaps wrapping their feet will improve their odds of making the Olympic podium. Moreover, this foot-stiffening strategy may inform the development of future wearable clothing that can tune the mechanical properties of the user's feet to enhance their running performance.

References: [1] Blickhan R. (1989), J Biomech 22(11-12); [2] Ker et al. (1987), Nature 325 (7000);[3] Margaria et al. (1963), J Appl Physiol 18(3); [4] Yawar A (2022), Yale University; [5] Péronnet, F. & Massicotte, D. (1991), Can. J. Sport Sci. 16(1).

USING PROJECTED VIRTUAL STEPPING STONES TO EVALUATE VISUALLY COMPLEX GAIT PERFORMANCE

Adam Grimmitt[1], Adam Knight[1], Jonaz Moreno Jaramillo[1], Paul McDonnell[2], Douglas Martini[2], Wouter Hoogkamer[1]
[1]Integrative Locomotion Laboratory, University of Massachusetts Amherst
[2]Movement Neuroscience Laboratory, University of Massachusetts Amherst
*Corresponding author's email: agrimmitt@umass.edu

Introduction: Many older adults show gait deficits, particularly during complex walking tasks (1,2). It has been shown that unsuccessful body weight shifts, including missteps, accounts for over 40% of the falls that older adults experience. Challenging environments can increase the risk of falling by limiting optimal step responses and impacting step accuracy (3). Corrective step adjustments demand additional cognitive resources (4). Previous work has found that older adults are less accurate when responding to external perturbations while dual tasking (1). To further identify the roles of cortical control in visually complex gait performance, we developed an experimental setup that projects virtual stepping stones onto a treadmill. Size, spacing and progression speed of the stepping stones can all be adjusted based on the participant's shoe size and habitual gait parameters. Further, approaching stepping stones can be shifted to a different location once they come within a specified distance from the participant. Here we demonstrate the utility of our setup by comparing stepping accuracy between two conditions: stepping stones projected at the participant's habitual step length and width vs. stepping stones that included shifts.

Methods: We evaluated 6 young (2F; 23.8 ± 3.6years; 65.8 ± 9.9kg, 171.1 ± 8.6cm) and 5 older (4F; 67.0 ± 1.6years; 79.2 ± 16.0kg, 165.1 ± 7.7cm) healthy adults walking on a dual belt treadmill at their habitual speed, while using a GUI (*Pygame* library) to project virtual stepping stones, across two conditions of steady and perturbed walking. Retroreflective markers were placed on the sacrum, as well as the toe, 5th metatarsal, and heel of each foot. The foot was defined as the line between the heel and toe, with the center of the foot set at 50% of this line (1). If required, a toe marker was reconstructed using markers on the 5th metatarsal and heel. The treadmill and virtual stepping stone speeds were determined from overground gait. The size of each stone was adjusted to foot size, while the distance between stepping stones (Figure 1; purple) was initially always equal to participants' habitual step length and width calculated during treadmill walking using a custom MATLAB script and optical motion capture (sampled at 100Hz; Qualisys, Gothenburg, Sweden). Participants were instructed to aim for the center of each stone with the center of their foot, hitting each stone only once. In the first, steady condition, all stones steadily approached the participant at consistent spacing. In the perturbed condition, random lateral (20% of step length), anterior, and posterior (both 40% of step length) shifts in target position were triggered every 5-7 stones, when the approaching stepping stone was 130% of step length away from a sacral marker (Figure 1; red). Foot placement accuracy was defined as the absolute distance between the center of the stepping stone and the center of the foot at midstance. Comparisons between conditions were conducted using a paired sample t-test.

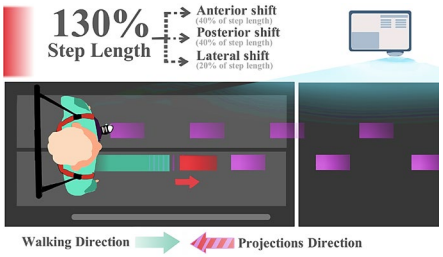

Figure 1. Top-down visual of the experimental setup. Purple and red rectangles are steady and shifted stones, respectively. At 130% of step length (green), a color change as well as an anterior, posterior, or lateral shift was randomly applied to a steady stone.

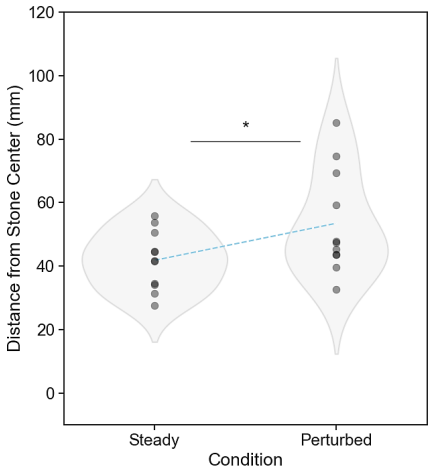

Figure 2. Lower accuracy was observed in perturbed walking. Each datapoint represents an average distance of the foot from the closest target for each subject over the course of a trial. * p = 0.002

Results & Discussion: Distance from stone center was significantly higher (*t (11) = -3.9; p = 0.002*) in the perturbed condition (Figure 2, +11.7 mm; +27.9% increase). This indicates that task difficulty impacts step accuracy while walking, as performance was worse between conditions, and is demonstrated in the literature for older adults (1).

Significance: Overall, these data show that increased visual complexity of a walking task increases the incidence of inaccurate steps in adults. This is important as it demonstrates that our experimental setup is both functional and sensitive enough to impact step accuracy. In future work we will leverage this setup to compare key gait metrics and activity in the posterior parietal and prefrontal cortex of healthy young, old, and older adult fallers during increasingly complex gait tasks, while elucidating the potential effects that posterior parietal and prefrontal cortex activity have on the relationship between gait and fall predictors in older adult fallers and non-fallers.

Acknowledgments: This work was supported by the National Institute of Health (R21AG075489). We thank Zachary Barrons, PhD for his role in data analysis.

References: **1.** Mazaheri, M. et al. (2015) *Experimental brain research, 233, 3467-3474.* **2.** *Boyer, K. A. (2023) Experimental Gerontology, 173, 112102.* **3.** Chapman, G. J. et al (2007) *Gait & Posture, 26(1), 59–67* **4.** Pelicioni PHS et al. (2021) *Front Medicine: Sec. Geriatric Medicine 8 - 2021.*

ANTERIOR GLENOHUMERAL RELEASE AND CORACOIDECTOMY FOR RESTORATION OF EXTERNAL ROTATION IN OLDER CHILDREN WITH BRACHIAL PLEXUS BIRTH INJURY

Lauren N Lottier, MS[1], Stephanie A Russo, MD, PhD[2], Natalie Williams, BS[3], Kyrillos Akhnoukh, BS[3], Spencer Warshauer, MS[3], Scott H Kozin, MD[4]

[1]Cleveland State University, Cleveland, OH, USA; [2]Dept of Orthopedic Surgery, Akron Children's Hospital, Akron, OH, USA; [3]Research Dept, Shriners Children's, Philadelphia, PA, USA; [4]Dept of Orthopedic Surgery, Shriners Children's, Philadelphia, PA, USA

Email: llottier@akronchildrens.org

Introduction: Children with brachial plexus birth injuries (BPBI) often exhibit impaired external rotation of the shoulder [1]. External rotation has substantial importance in BPBI individuals' activities of daily living (ADL), with even a small improvement in external rotation leading to a decrease in disability [2]. Numerous treatment options exist to improve external rotation in children with BPBI. Anterior glenohumeral joint release is traditionally reserved for children under age four years [3]; however, we hypothesized that anterior glenohumeral joint capsular release (ACR) and coracoidectomy would successfully restore external rotation in older children with BPBI.

Methods: A retrospective review of all children with internal rotation contractures age ≥4 years who underwent open ACR with subscapularis fractional lengthening and coracoidectomy as well as pre- and postoperative motion capture assessment was performed. Eleven children ages 4-13 years (average 9.6 years) had preoperative magnetic resonance imaging confirming concentric glenohumeral alignment and minimal fat atrophy of the infraspinatus. Scapulothoracic, glenohumeral, and humerothoracic joint angles were measured with three-dimensional motion capture in a neutral, resting position and each of the modified Mallet positions (Figure 1). Scapular markers were re-palpated in each static posture. Helical angles were utilized for the scapulothoracic joint, and a modified globe method was used for the glenohumeral and humerothoracic joints [3]. External rotation and elevation joint angles before and after surgery were compared using multivariate analyses of variance with repeated measures and univariate post hoc tests.

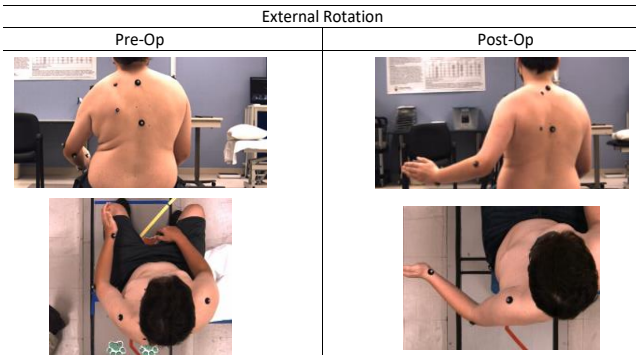

Figure 1: A representative subject in the external rotation position before and after surgery.

Results: There were significant ($p<0.05$) increases in glenohumeral and humerothoracic external rotation across all positions (Table 1). Scapulothoracic internal rotation was significantly increased in the neutral and internal rotation positions. Glenohumeral and humerothoracic elevation were significantly decreased in the external rotation and internal rotation positions. Glenohumeral elevation was also significantly decreased in the hand to neck (nape) position. Scapulothoracic upward rotation was significantly increased in the nape position. Glenohumeral and humerothoracic internal rotation in the internal rotation position were decreased in all but one and two patients, respectively. Increased scapulothoracic internal rotation was noted in the internal rotation position to help compensate for decreased glenohumeral internal rotation. Loss of midline function was noted in one patient.

Table 1: Significant differences for all positions measured. Elevation angles in the positions not included in this table were not significantly different.

Position	Joint Angle	Pre-Op (Mean +/- SD)	Post-Op (Mean +/- SD)	MANOVA	Univariate
Elevation	ST IR	47.0 +/- 5.5	52.3 +/- 10.7	0.016	0.159
	GH ER	0.3 +/- 14.9	44.6 +/- 25.9		0.002
	HT ER	-48.9 +/- 24.3	-3.3 +/- 38.0		0.007
External Rotation	ST Dwn Rot	-4.7 +/- 7.7	-5.9 +/- 11.3	0.013	0.767
	GH Elev	46.0 +/- 12.4	25.1 +/- 8.3		<0.001
	HT Elev	47.4 +/- 13.3	25.8 +/- 9.0		0.002
	ST IR	37.8 +/- 11.7	38.7 +/- 12.3	<0.001	0.782
	GH ER	-8.5 +/- 15.7	55.8 +/- 17.2		<0.001
	HT ER	-45.6 +/- 17.5	17.6 +/- 14.4		<0.001
Internal Rotation	ST Dwn Rot	-4.7 +/- 5.6	1.5 +/- 11.2	0.007	0.128
	GH Elev	43.9 +/- 16.4	29.4 +/- 14.9		0.002
	HT Elev	44.7 +/- 14.8	24.7 +/- 8.7		<0.001
	ST IR	43.5 +/- 6.4	53.9 +/- 8.3	0.002	0.004
	GH ER	-15.5 +/- 13.2	20.8 +/- 19.6		<0.001
	HT ER	-59.0 +/- 13.0	-32.9 +/- 17.9		0.004
Mouth	ST IR	52.7 +/- 8.7	64.1 +/- 12.1	0.014	0.073
	GH ER	-0.03 +/- 9.0	32.7 +/- 20.4		0.002
	HT ER	-48.8 +/- 13.0	-25.9 +/- 16.8		0.018
Nape	ST Dwn Rot	-47.3 +/- 12.2	-58.4 +/- 6.6	0.017	0.038
	GH Elev	57.0 +/- 17.1	41.8 +/- 15.7		0.009
	HT Elev	99.6 +/- 20.8	93.3 +/- 16.6		0.459
	ST IR	45.1 +/- 6.4	47.3 +/- 8.7	0.010	0.505
	GH ER	8.4 +/- 20.5	-33.0 +/- 27.1		<0.001
	HT ER	-33.0 +/- 27.1	16.8 +/- 28.8		0.005
Neutral	ST IR	46.7+/- 5.3	52.8 +/- 7.1	0.005	0.014
	GH ER	-8.1 +/- 17.4	30.2 +/- 15.1		<0.001
	HT ER	-55.2 +/- 15.2	-23.3 +/- 10.3		<0.001
Spine	ST IR	42.4 +/- 9.3	47.7 +/- 8.6	0.008	0.166
	GH ER	-48.6 +/- 16.4	-4.2 +/- 41.5		<0.001
	HT ER	-94.8 +/- 18.1	-54.8 +/- 40.0		0.001

Discussion: Although this proof-of-concept cohort is small, glenohumeral and humerothoracic external rotation were improved in all patients as objectively measured with three-dimensional motion capture. Interpretation of the results shows that open ACR with subscapularis fractional lengthening and coracoidectomy successfully improved glenohumeral and humerothoracic external rotation in children over age 3 with concentric glenohumeral joint alignment.

Significance: Findings from this study refute the prior claims that concomitant tendon transfer or salvage procedures (i.e. humeral osteotomy) must be utilized in children with BPBI over 3 years of age. This study demonstrated objective data that will impact surgical planning for children with BPBI to improve external rotation and overall shoulder function.

References:

[1] Frade F, et al. (2019) *J Clin Med*. 8(7):980.
[2] Langer, et al. (2012). *J Hand Surg*. 37(7): 1430-1436
[3] Pearl et.al., (1992). J Shoulder Elbow Surg. 1(2):113-8.

A TURN BOUNDING TASK PROVIDES UNIQUE INFORMATION COMPARED TO A LATERAL BOUND

Alexis N. Henderson[1], Kristen E. Renner[2*]
[1]Department of Biomedical Engineering, University of Arizona, Tucson, AZ, USA
[2]University of Arizona College of Medicine – Phoenix, Phoenix, AZ, USA
*Corresponding author's email: kristenrenner@arizona.edu

Introduction: Many biomechanics studies focus on motions that primarily occur in the sagittal plane. The vertical drop jump task is widely used as an injury risk assessment tool especially with regard to knee kinematics and kinetics in anterior cruciate ligament (ACL) research [1]. Due to frequency of single- and double-leg stop jump motions in sports that commonly include ACL injuries, the stop jump task has become more commonly used in biomechanics studies as well [2]. These tasks have been used to determine injury predictors through impact forces, knee loading, and mechanics that are observed in the sagittal plane [1,3]. Despite the prevalence of their use, these tasks do not accurately represent motions that occur in the frontal and transverse planes. Understanding how an uninjured individual accomplished complex bounding tasks may provide unique information when considering injury and reinjury prevention as common mechanisms of injury for ACL tears occur in the frontal plane such as cutting, landing, and pivoting [4]. The mechanics of both a lateral bound and 90 degree turn bound tasks are not well studied in current literature [4]. The purpose of this study was to determine if a 90 degree turn bounding task provides unique information compared to a lateral bounding task.

Methods: 20 healthy individuals (10 male, 10 female) between the ages of 18 and 25 years old were recruited for this study. Participants were excluded if they were pregnant, could not complete study tasks without pain, had lower extremity surgery in the past year, had a lower extremity injury in the past 6 months that had kept them from participating in normal activities for three or more days. Each participant wore their own shoes, and tight-fitting, comfortable athletic clothing during testing.

Kinematics were collected at 240 Hz using a 9-camera Vicon motion capture system (Vicon, Oxford, United Kingdom) and 43 retroreflective markers in a modified Helen Hayes marker set. Ground reaction forces were collected at 1000 Hz using one tri-axial embedded force plate (AMTI, Watertown, Massachusetts). Each participant completed five repetitions of lateral bound (LB) and seven repetitions of a ninety degree turn bound (TB) on each foot. Motion capture data was processed using Vicon Nexus where a maximum gap of 20 frames were reconstructed using a rigid body fill and spline fill for gaps of ≤5 frames. The resulting data was processed with custom Visual 3D (C-Motion Inc., Germantown, MD) and MATLAB (Mathworks, Natik, MA) pipelines using a 4th order recursive Butterworth filter with a force plate cutoff of 15 Hz and marker cutoff of 7 Hz. For this analysis, the joint angles, moments, and powers at initial contact, takeoff, and the peak angles, moments, and powers for the hip and knee flexion, knee abduction, and ankle dorsiflexion were calculated for the dominant and non-dominant legs. Trunk flexion and pelvic tilt angles at initial contact, takeoff, and peak angles were also calculated. Leg dominance was determined by the leg that would be used to kick a soccer ball [5].

Results & Discussion: Paired t-tests were completed between the LB and TB tasks regarding joint angles, moments, and powers at initial contact (IC), takeoff (TO), and peak values on both dominant (D) and non-dominant (ND) legs. Significance was defined as a p-value < 0.05. It was found that trunk and pelvis joint angles were significantly different between TB and LB at all events (IC, TO, and peak angles). Significant differences observed between the TB and LB landing mechanics for knee flexion, knee abduction, hip flexion, and ankle dorsiflexion are included in **Table 1**. Previous literature has demonstrated that restricted dorsiflexion range of motion is not only indicative of chronic ankle stability, but also is a factor of increased ACL injury risk [6,7]. By providing unique ankle mechanics and peak ankle dorsiflexion angles these tasks may provide unique information on ankle stability that correlates with this literature. Additionally, while the peak ground reaction forces of the LB and TB were significantly different in the anterior/posterior direction and the medial/lateral direction, this was not true in the vertical direction. Interestingly, the LB task resulted in larger AP and ML ground reaction force peaks compared to the turn bound, contradicting that our hypothesis that greater values in TB would indicate it was more challenging for participants. While this study had a relatively small sample size and included healthy individuals, the results indicate that including the ninety degrees turn in the bounding task results in unique lower leg landing mechanics.

Table 1: Joints that displayed significant differences across variables and events.

Joint Variable	Event	Joint
Angle	IC	Knee flexion (ND) Knee Abduction
	Peak	Ankle dorsiflexion
	TO	Knee Abduction
Moment	Peak	Ankle dorsiflexion (D) Knee flexion (D) Knee Abduction
	TO	Ankle dorsiflexion (D)
Power	Peak	Ankle dorsiflexion Hip flexion
	TO	Ankle dorsiflexion (D)

Significance: The results of this study indicate that clinical populations may benefit from the use of the lateral and 90 degree turn bounding tasks to determine ankle stability in dynamic motions. Additionally, patients returning to sport after an injury that resulted in instability or decreased proprioception may benefit from these tasks, but these populations would need to be investigated in future studies to provide relevant clinical values.

Acknowledgments: This research was supported in part by the University of Arizona's Undergraduate Biology Research Program.

References: [1] Mok et al. (2016), *G&P* 46. [2] Wang L. I. (2011), *JSSM* 10(1). [3] Yu et al. (2006), *Clin biomech* 21(3). [4] Waldhelm et al. (2022) *IJSPT* 17(3). [5] Peebles et al. (2020), *J_Biomech* 105. [6] Drewes et al. (2009) *J Sci and Med Sport* 12(6). [7] Hamilton and Velasquez (2011), *IJATT* 16(6).

ADVANCED FOOTWEAR TECHNOLOGY FOAM COMPRESSION BETWEEN FOOTSTRIKES

Kyle Coleman[1]*, Camille L Nguyen[1], Luke VanKeersbilck[1], Iain Hunter[1]
[1]Brigham Young University, Provo, UT
*Corresponding author's email: kyle.coleman5501@gmail.com

Introduction: Since the 2017 release of the Nike Vaporfly 4, many other brands have developed similar shoe types, commonly referred to as "Advanced Footwear Technology", that have led to improved performance time in road racing. These shoes contain a curved carbon fiber plate embedded in the midsole, thick responsive foam, overall light weight, and often an altered midsole shape. AFT often leads to lower peak vertical ground reaction forces, more time on the ground, and a longer stride [1,2,3]. These shoes reduce the metabolic costs of running by an average of around 3-4% [1,2,3]. However, biomechanical variability between runners may explain why energy savings are not the same for every runner. Since 2017, studies have attempted to understand the reason for these metabolic savings but have proven the need for further research [4,5]. This study aims to characterize midsole foam compression between heel strike (HS) and non-heel strike (NHS) runners. Results may grant a better understanding of the reason behind the AFT's effectiveness. Due to the differing landing patterns of heel and midfoot strikers, we hypothesized a significant difference between the magnitudes and timing of foam compression between foot strike types.

Methods: Eighteen men and 16 women wore Saucony Endorphin Pro 3s while running at 3.35 m/s (8:00/mi pace) and 4.47 m/s (6:00/mi pace) for 30 s each. The shoes were fitted with hall effect sensors to measure magnetic fields and were connected to a custom-made Raspberry PI device for power and output reading through analog input channels sampling at 960 Hz. A collection of five neodymium magnets were placed under the midfoot and heel. Calibration of volts per mm between the magnets and hall sensors was completed with measured distances prior to data collections. A 10-s sample was taken while running at each speed (Fig. 1). Data were processed using a custom Matlab program which detected the beginning and end of compression for each foot contact along with the peak compression magnitude and the percent of time where the peak occurred within each compression. Heel and midfoot compression magnitudes and percent times to peak compression were averaged for each trial. T-tests checked for differences in the four listed variables between foot strike types. Alpha was adjusted to 0.0125 to account for multiple comparisons.

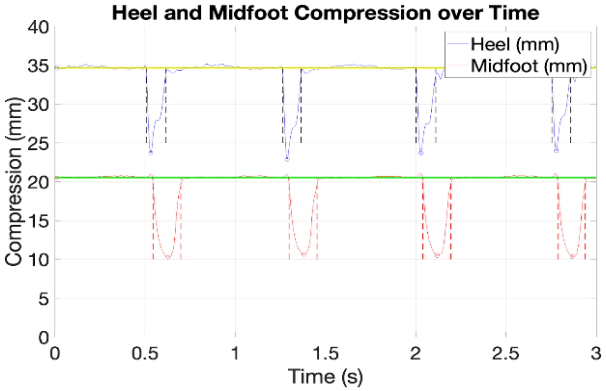

Fig 1: Example data of compression under the heel and midfoot for four steps.

Results & Discussion: Heel strikers compress the heel foam an average of 11.3mm ± 4.18 while the NHS runners compress an average of 5.2mm ± 2.78. These measurements are consistent with our hypotheses about magnitudes of compression as expected. Most of the NHS runners in our sample still compressed the heel after initial contact with the ground. Even though midfoot compression was statistically different between foot strike groups, the difference was less than 1mm (7.5%) (Table 1). Over the duration of a race like a marathon, these small differences may produce a large impact. The timing of heel and midfoot compressions were similar between groups. This could partly explain why previous research finds no difference in metabolic savings between foot strike groups [1,3]. With the magnitudes of foam compression being different between groups, the NHS runners may be optimizing other aspects of the AFT such as the plate and shape to help provide equal metabolic benefits between HS and NHS runners.

	Heel Compression (mm)	Heel Percent to Peak	Midfoot Compression (mm)	Midfoot Percent to Peak
Heel strike	11.3mm ± 4.18	23.5% ± 3.4	8.67mm ± 1.84	53.9% ± 5.2
Midfoot strike	5.2mm ± 2.78	31.3% ± 9.34	9.32mm ± 1.97	56.0% ± 6.8
p-value	<0.001*	0.181	<0.001*	0.151

Table 1. Foam compression values and percent of time to peak compression during heel and midfoot compression.

Significance:
Understanding the foam responsiveness in AFT between foot strike groups allows a better understanding of why AFT is more beneficial for running than traditional footwear. Future models can be crafted to better accommodate different foot strikes and these specific modifications can allow for enhanced performance in competition.

Acknowledgments: Shoes were provided by Saucony (Boston, MA).

References: [1] Hunter et al, 2019. *J Sports Sci.* 37: 2367-2373; [2] Barnes & Kilding, 2019. *Sports Med.* 49: 331-342; [3] Hoogkamer et al, 2018. *Sports Med.* 48: 1009-1019; [4] Healey & Hoogkamer, 2022. *JSHS*. 2(3). 285-292; [5] Patoz et. al, 2022. *Footwear Sci.* 14(3): 147-150.

BILATERAL SYMMETRY AND SEX DIFFERENCES IN HIP JOINT HELICAL AXES OF MOTION DURING GAIT

Edward Godbold*, Connor Luck, Camille Johnson, Ashley Disantis, Craig Mauro, Michael McClincy, William Anderst
Department of Orthopaedic Surgery, University of Pittsburgh, Pittsburgh, PA, USA
*Corresponding author's email: edg54@pitt.edu

Introduction: Evaluation of hip kinematics has previously focused on 6-degree-of-freedom kinematics and various predictive or functional approaches to identify the hip joint center of rotation[1,2]. The helical axis of motion (HAM) is an alternative kinematics measure that describes motion based upon the center of rotation and the axis of rotation. The HAM has been proposed as a biomarker for joint stability in the knee[3], spine[4,5], and shoulder[6], but the HAM has not been reported for the hip during physiological loading. Bilateral symmetry in hip joint HAM in healthy adults, and differences in hip joint HAM between men and women, have not been investigated. The aim of this analysis was to quantify the HAM in healthy hips during gait and to quantify side-to-side differences (SSD) and sex differences in hip HAM during gait so that "abnormal" symmetry can be identified in future studies of individuals with pathology.

Methods: 24 healthy adults (13F, 11M; age 21.9±2.2 years; BMI 21.5±5.0 kg/m^2) consented to be included in this IRB-approved study. Synchronized biplane radiographs were collected at 50 images/sec for 1 second (80 kV, 320mA, 4 ms exposure, 3 trials per hip) during treadmill walking at a self-selected speed. Subject-specific bone models were created by segmenting computed tomography (CT) scans of each participant's femur and pelvis. Bone motion was determined by a validated volumetric model-based tracking technique that matched digitally reconstructed radiographs created from the bones to the radiographs with submillimeter accuracy during each trial (bias: 0.2˚, 0.2 mm; precision: 0.8˚, 0.3 mm)[7]. Anatomic coordinate systems were established in each femur and hemi-pelvis[8], mirrored to the contralateral side, and co-registered to produce identical coordinate systems for each hip. The HAM was calculated at the femoroacetabular joint using methods described by Spoor et al.[9] and freely available MATLAB code[10]. Starting with the maximum flexion angle (beginning of active extension), the HAM was calculated for every three-degree interval of extension to maximum extension. The process was repeated for the active flexion phase (maximum extension to maximum flexion). The femoroacetabular HAM was described by the orientation of the HAM relative to the sagittal, transverse and coronal planes of the pelvis (Fig. 1) and by the intersection point of the HAM with the pelvic sagittal plane. Results were interpolated to 1% instants of gait cycle and averaged across all 3 trials per hip. SSD and sex differences in HAM orientation were assessed using statistical parametric mapping (SPM) unpaired Student's t-tests (α=0.05).

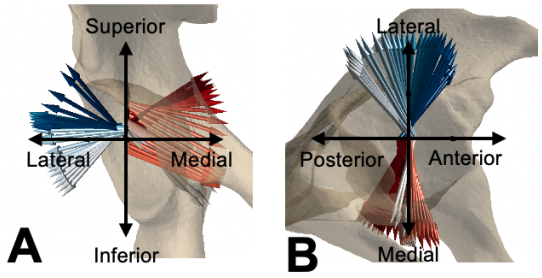

Figure 1: 3D view of the HAM on a typical right pelvis. Colored arrows describe the HAM during extension (red to white) and flexion (white to blue). **A** An anterior to posterior view. A HAM arrow oriented superiorly indicates coupled internal rotation; inferiorly indicates coupled external rotation. **B** Inferior to superior view. A HAM arrow oriented anteriorly indicates coupled adduction; posteriorly indicates coupled abduction.

Results & Discussion: 109 walking trials were included in the analysis. No significant SSD or sex differences (Fig. 2) in the orientation of the HAM were identified (all SSD under 8.6±6.7°; all sex differences under 13.7±9.3°). The intersection point of the HAM with the sagittal plane varied in the anterior-posterior direction by an average of 7.3±5.4mm for a given subject, and in the inferior-superior direction by 14.5±7.8mm.

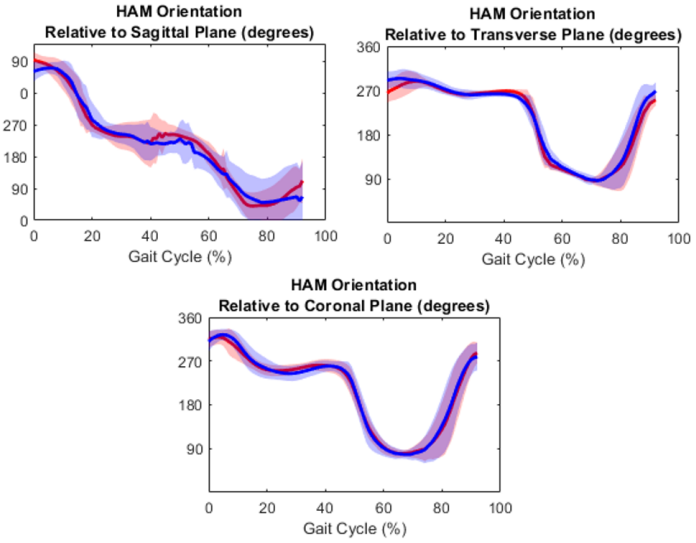

Figure 2. Average HAM orientation relative to sagittal, transverse, and coronal planes for male (red) and female (blue) during walking (shaded areas indicate standard deviation, 0% is foot strike).

Significance: Knowledge of hip kinematics under physiologic load is important for identifying, properly treating, and evaluating outcomes for patients with symptomatic hip pathology. Our results provide baseline values for the HAM and SSD in healthy individuals that can be used evaluate hip stability in surgical patients. Motion of the intersection point of the HAM with the sagittal plane indicates a moving center of rotation in healthy hips. This contradicts the assumption that the hip rotates about a fixed center of rotation.

References: [1] Johnson et al. (2022), *J Biomech* 143. [2] Kainz et al. (2015), *Clin Biomech* 30(4). [3] Grip et a., (2015), *J. Biomech*. 48(10). [4] Ellingson et al., (2015), *J. Biomech*. 48(2). [5] Ellingson et al., (2013), *Clin. Biomech*. 28(7). [6] Temoriti et al. (2019), *J. Biomech*. 88. [7] Martin et al. (2011), *J Arthroplasty* 26(1). [8] Wu et al. (2002), *J Biomech* 35(4). [9] Spoor et al, *J Biomech* (1980). [10] Reinschmidt, Kinemat (1994).

IMPACT OF LOWER-LIMB ADJUSTABLE-VOLUME PROSTHETIC SOCKETS ON PATIENT MOBILITY

Martin P. Kilbane[1], Jeffrey Wensman[1], Anthony R. Gutierrez[2], Noah J. Rosenblatt[3], and Deanna H. Gates[1]
[1]University of Michigan, [2]Bionic Prosthetics and Orthotics, [3]Rosalind Franklin University of Medicine and Science
*Corresponding author's email: mkilbane@umich.edu

Introduction: Discomfort in the prosthetic socket is the most common symptom referred to in a prosthetic clinic [1]. For a traditional socket, prosthesis users accommodate for changes in limb volume throughout the day by adding or removing prosthetic socks. Adjustable-volume sockets allow users to modify socket volume for individual fit and comfort [2]. Our objective was to determine the impact of lower-limb prosthetic sockets on patient mobility by comparing new, commercially available, adjustable prosthetic sockets, to conventional, laminated sockets.

Methods: This study was a non-blinded randomized cross-over intervention across two sites. All participants had unilateral transfemoral amputation and at least six-months of independent ambulation. 29 people (4 female) enrolled in the study. Participants self-reported their race and ethnicity with the option to select more than one. Twenty-three identified as white, 6 were black, 2 American Indian or Alaska Native, 1 Hispanic or Latino, and 1 Native Hawaiian or Other Pacific Islander. Two participants dropped out after completing testing in their baseline socket and were not fit with any adjustable socket. The remaining 27 participants had an average age, height and weight of 48 (13) years, 1.77 (0.09) m and 95.4 (22.3) kg. Participants completed testing with a laminated socket and each of three styles of commercially available adjustable-volume sockets: Infinite Socket (LIM Innovations, San Francisco, CA, USA), CJ Sail (CJ Socket Technologies, Inc., Beverly, MA, USA), and Quatro (Quorum, Windsor, CO, USA). Participants acclimated to each socket for a minimum of four weeks before testing.

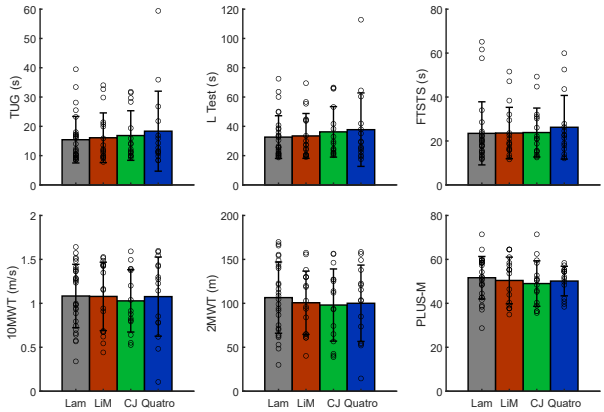

Figure 1: Functional mobility measures and self-reported mobility. Lower values indicate improved performance for the TUG, L Test, and FTSTS (less time to complete). Higher values indicate improved performance for the 10MWT (longer distance), 2MWT (faster speed), and PLUS-M (greater mobility). The PLUS-M provides T-scores that range from 21.8 to 71.4, where higher values indicate greater mobility [3].

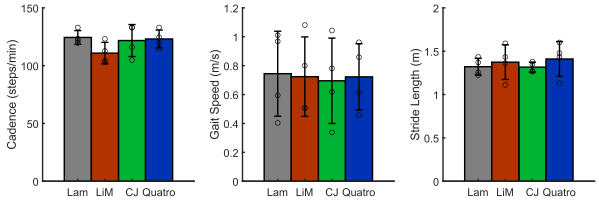

Figure 2: Free movement parameters for a subset of all 2-minute walk test trials. Gait metrics of cadence, gait speed, and stride length are reported as a subset of the full dataset.

Mobility was assessed using several validated functional assessments: 10-m walk test (10MWT), 2-minute walk test (2MWT), timed-up-and-go (TUG), the L Test, and five times sit-to-stand (FTSTS). Participants wore a lower-limb set of five APDM Opal inertial measurement units (IMUs), with one on the lumber, one on each thigh, and one on each shank. Free movement IMU data was analyzed in Moveo Explorer to determine gait metrics, reported for a subset of the full dataset. We also measured prosthetic users' mobility with the Prosthetic Limb Users Survey of Mobility (PLUS-M) 12-Item Short Form. The PLUS-M provides T-scores that range from 21.8 to 71.4, where higher values indicate greater mobility [3]. A linear mixed model with subjects as a random variable, and socket type as a repeated, fixed factor was used for functional mobility measures and PLUS-M T-scores. Significant effects of socket type were explored using post-hoc testing with LSD corrections. 2MWT cadence, gait speed, and stride length for the subset analyzed were summarized with means and standard deviations.

Results & Discussion: Participants who were fit with a traditional laminated socket (26/26) were able to successfully wear it to complete all testing. In contrast, 61% (14/23), 73% (16/22), and 74% (14/19) of participants were able to successfully wear the CJ Sail, LiM, and Quatro sockets to complete all testing, respectively. This suggests that commercially available adjustable sockets have a lower success rate than standard-of-care laminated prosthetic sockets. Functional mobility measures and self-reported mobility (Fig. 1) were not statistically significant ($p > .29$), suggesting that users experienced similar mobility regardless of socket design. Seven participants were able to successfully complete testing in all four socket types. 2MWT gait metrics for a subset of four of these seven participants (Fig. 2) were 120 (9.9) steps/min cadence, 0.72 (0.24) m/s gait speed, and 1.36 (0.14) m stride length. Our future work will determine if there are specific patient characteristics that affect mobility with a particular socket design.

Significance: Mobility, as measured by the 10MWT, 2MWT, TUG, L Test, FTSTS, and PLUS-M were similar when wearing adjustable sockets compared to conventional, laminated sockets. Therefore, adjustable-volume sockets can provide users the ability to modify socket volume for individual fit and comfort without compromising mobility.

Acknowledgments: Funded by the Department of Defense under award number W81XWH-18-1-0656. MK was supported by a National Science Foundation Graduate Research Fellowship.

References: [1] Seaman (2010), *J Prosth Orthot*, 22(4); [2] McLean et al. (2019), *Clin Biomech*, 63; [3] Hafner et al. (2017), *Arch Phys Med Rehabil*, 98(2).

INVESTIGATION OF AGE-RELATED CHANGES IN WAVE PROPAGATION IN TENDON FASCICLES

Samantha Kahr[1*], Shreya Kotha[1], Jonathon L. Blank[2], Alex J. Reiter[3], Darryl G. Thelen[1,4]
[1]Department of Biomedical Engineering, University of Wisconsin-Madison, Madison, WI, USA, [2]McKay Orthopaedic Research Laboratory, University of Pennsylvania, Philadelphia, PA, USA, [3]Department of Biomedical Engineering, Saint Louis University, St. Louis, MO, USA, [4]Department of Mechanical Engineering, University of Wisconsin-Madison, Madison, WI, USA
*kahr2@wisc.edu

Introduction: Aging is associated with changes in tendon structural and mechanical properties at multiple scales. Two notable structural changes are a reduction in tendon collagen turnover and an accumulation of microdamage which can compromise the non-collagenous matrix [1,2]. Structural changes likely are reflected in macroscale mechanical properties. For example, aging human tendon exhibited a decreased elastic modulus and strength relative to younger adult tendons [3,4,5]. However, it is not understood how structural changes may alter wave propagation in tendon, which is important to consider when using wave propagation to assess loading [6] or evaluate tissue stiffness. A prior study found that Achilles tendon wave speeds are significantly lower (-22%) in old relative to young adults during walking [7] which in large part was due to a reduction in triceps loading during walking. However, there may also be a fundamental change in wave propagation within the tissue due to the structural changes. The objective of this study was to investigate the influence of aging on wave speed in isolated fascicles undergoing axial loading. The results are important to consider shear wave speed to evaluate tissue stiffness or loading [6].

Methods: Rat tail tendon fascicles were extracted from two 9-month-old rats (F344/BN) and one 32-month-old rat to create a sample size (n=5) for each age group. The fascicles were clamped into a custom benchtop loading device (Fig.1) and immersed in PBS solution, then preloaded to 0.1 N and subjected to 10 cycles (1 Hz) of preconditioning between 0 and 5% strain. After 300s of rest, the fascicles were cyclically loaded from 0 to 5% strain at 0.4 Hz. Two 10s trials at each frequency were collected with 60s of rest between each trial. Impulsive lateral taps (50Hz, 0.3 ms pulse) were used to induce shear waves, and wave propagation was measured with two laser Doppler vibrometers placed 30mm apart and 16mm from the tapper. Laser vibrometer, load cell, and stage displacement data were synchronously recorded using an 8-channel AD board (NI USB-6251). Shear wave speed was calculated with a Kalman filtering routine to correlate vibrometer signals [8]. A rotary micrometer was utilized to collect CSA measurements.

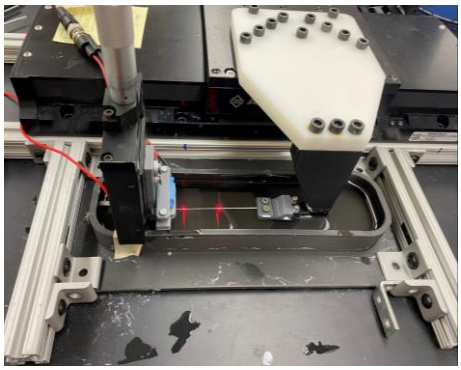

Figure 1: Custom benchtop loading device. Fascicle is loaded in a PBS bath with load cell on the right and linear stage arm on the left. Lateral taps induced on the load-cell end of the fascicle and laser measurements collected from the middle.

Results & Discussion: Older fascicles tended to have a lower absolute stiffness than young fascicles (Fig.2a), which would be consistent with observations on human tendons [7] and prior studies on fascicles [9]. The wave speed-force relationship (Fig.2b) for both young and old fascicles exhibited a square root relationship, which is the relationship predicted by a tensioned beam model [6]. Wave speeds were slightly lower in old fascicles than in young fascicles at a given stress level. These initial results are consistent with the lower wave speeds observed in humans [7], suggesting a potential structural effect that is independent of loading. Further exploration with a larger sample size and microstructural imaging is required to assess if the mechanical changes observed are due to identifiable structural effects.

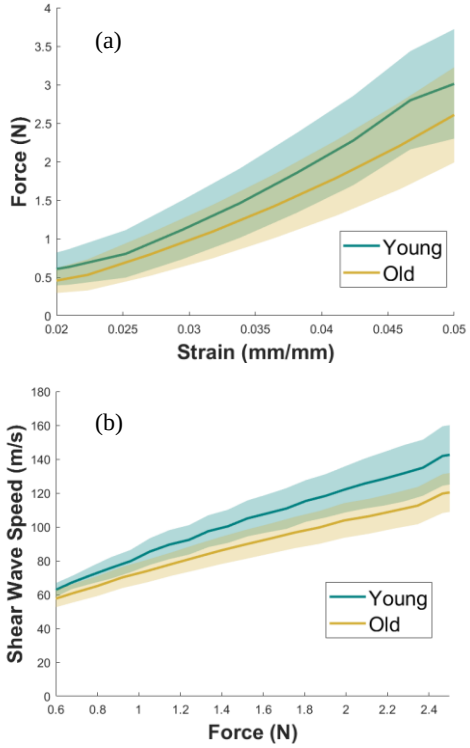

Figure 2: Mean and standard deviation of force vs. strain **(a)** and wave speed vs. force **(b)** plots for compounded measurements of old and young fascicles.

Significance: This study demonstrates the use of a benchtop system to investigate wave propagation in isolated young and old tendon fascicles subjected to axial loading. The system can be used to probe fundamental relationships between wave speed, loading, stiffness, and structure, which is relevant when using wave propagation measures to noninvasively assess tendon mechanics and tissue health.

Acknowledgments: Funding from NSF GRFP DGE-177503, DOD CDMRP (129866603)

References: [1] Heinemeier KM et al., FASEB J., 27:2074-2079, 2013. [2] Svensson RB et al., J. Appl. Physiol., 121:1353-1362, 2016. [3] Kubo K et al., Acta Physiol. Scand., 178:25-32, 2003. [4] Onambele GL et al., J. Appl. Physiol., 100:2048-2056, 2006. [5] Stenroth L et al., J. Appl. Physiol., 113:1537-1544, 2012. [6] Martin JA et al,. Nat. Commun., 9:2-10, 2018. [7] Ebrahimi A et al., Exp. Gerontol., 137:110966, 2020. [8] Schmitz DG et al., Sensors., 22:2283-2298, 2022. [9] Muench JR et al., Biomech. Model Mechan., 19:841-849, 2020.

Effects of post-traumatic osteoarthritis on joint kinematics following medial meniscal transection in rats

Seyed Mohammadali Rahmati[1*], Marin Plemmons[1*], Rachel Watermeier[1], Liang-Ching Tsai[2], Jarred Kaiser[3,4], Young-Hui Chang[1]
[1] Comparative Neuromechanics Lab, School of Biological Sciences, Georgia Institute of Technology, Atlanta, GA, USA
[2]Department of Physical Therapy, Georgia State University, Atlanta, GA, USA
[3]School of Medicine, Emory University, Decatur, GA, USA, [4]Atlanta VA Medical Center, Decatur, GA, USA
*Co-corresponding authors' emails: mplemmons6@gatech.edu, srahmati3@gatech.edu

Introduction: Traumatic knee injuries not only disrupt connective tissue integrity but also increase the risk of developing knee osteoarthritis (OA) tenfold [1,2]. Post-traumatic osteoarthritis (PTOA) may appear 10-20 years sooner than aging-associated OA [3]. Active individuals are particularly at risk, including those susceptible to meniscal tears, which can severely impact their ability to participate in sports or perform physically demanding jobs once early PTOA symptoms emerge [2,3]. This study seeks to investigate how PTOA progression alters knee joint kinematics during locomotion in rats by comparing pre-surgical and post-surgical data. We hypothesized that knee PTOA progression would disrupt 3D joint kinematics across the entire limb during stance phase post-surgery compared to the pre-surgical control baseline. To assess these hypotheses, we developed a novel three-dimensional (3D) modeling technique to obtain accurate, high-throughput joint angles during locomotion in the rat.

Methods: In preliminary results, eight male Lewis rats underwent medial meniscal transection (MMT) on their left hindlimbs in a GaTech IACUC approved protocol. Rats engaged in controlled dose wheel running activity before and after injury. Prior to surgery and six weeks after, when mild/moderate PTOA is expected in this well-established model [2], 3D locomotor movements during treadmill running were captured using biplanar X-ray videography [4]. These data were processed with DeepLabCut to track joint movements, and XMALab to reconstruct 3D positions of bone landmarks. Singular value decomposition (SVD) was used to accurately map key points on a bone mesh to corresponding landmarks. Bone axes were established to calculate Euler angles, allowing for the modelling of 3D joint angles—internal-external rotation (I-E Rot), abduction-adduction (Abd-Add), and flexion-extension (Flex-Ext)—across all cardinal planes (Figure 1).

Results & Discussion: In the hindlimbs affected by PTOA, we observed significant changes in specific joint angles and the total range of motion (ROM) from pre-surgery to 6 weeks post-surgery. Notably, the knee abduction angle at the onset of swing significantly decreased from 9±1.5° pre-surgery to 6±2° post-surgery ($p=0.004$). During the onset of the stance phase, marked changes were seen in hip flexion (decreasing from 33±2° to 28.7±3°, $p=0.004$), and in ankle adduction (decreasing from 16.2±4° to 6±3.3°, $p<<0.001$). Furthermore, analyses of total ROM highlighted significant reductions in hip Flex-Ext (from 59.7±5.1° to 55.2±2.2°, $p=0.02$) and ankle I-E Rot (from 23±2.4° to 17.2±2°, $p<0.001$) throughout the gait cycle. In contrast, duty factor, reflecting the duration of the stance phase relative to the total gait cycle, did not show a significant difference between the pre-surgery and PTOA conditions in the PTOA-affected limb. Taken together, our findings suggest that the overall temporal pattern of gait might be preserved, whereas the observed changes in joint angles and ROM indicate a post-surgical change in the spatial control of limb movements.

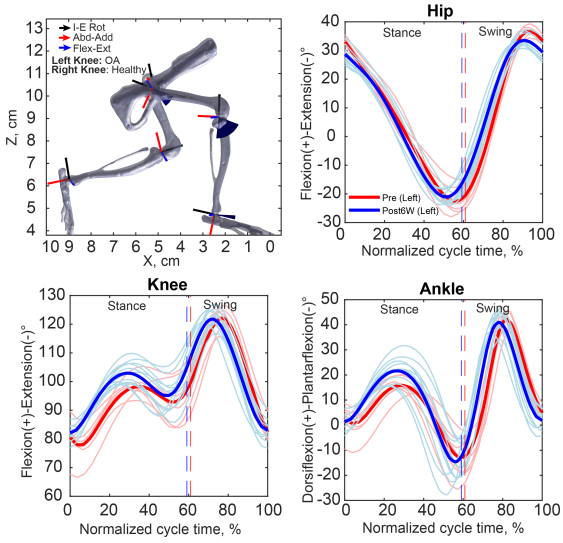

Figure 1. Top left panel shows hind limb skeletal model of an PTOA rat (6 weeks post-surgery) with computed joint coordinate axes and angles at the time of right paw contact. The left leg is the affected (PTOA) knee. Anatomical axes are indicated by color-coded arrows (blue: Flex-Ext, red: Abd-Add, black: I-E Rot). Blue patches represent hip, knee, and ankle Flex-Ext angles. The top right, bottom left, and bottom right panels display joint angles for the hip, knee, and ankle in flexion-extension over 10 gait cycles, illustrating changes after surgery throughout the gait cycle.

Significance: Given the high incidence of knee injuries [6] and subsequent early onset of PTOA, understanding kinematic abnormalities arising secondary to injury is critical to understanding the progression of cartilage degeneration, prophylaxis, and refining rehabilitation strategies. In this study, we demonstrated that PTOA progression results in a wide range of joint kinematics deviations across multiple planes of motion and across the entire gait cycle, with a reduction in functional range of motion in the affected limb. Leveraging rats and computational modelling serves to increase applicability and efficiency of biomechanical research by studying the most used biomedical model, and by streamlining high-throughput analysis to enhance insight to pre-clinical biomechanics [7].

Acknowledgments: Supported by NIH R01AR080154.

References: [1] Anderson et al. (2011), *J Orthop Res* 29(802); [2] Tsai, L.-C et al. (2019) *Osteoarthritis and Cartilage* 27, no. 12 [3] Meunier et al. (2007), *Scan J Med Sci* 17(230); [4] Raj and Bubnis (2017), *StatPearls Publishing*; [5] Kirkpatrick, Nathan J., et al. (2022), *J Exp Biol* 225(16); [6] Long et al. (2022), *Arthritis and Rheumatology* 74(1172); [7] Bauman and Chang (2010) *J Neurosci Methods* 186(1).

HANG IN THERE: A TIME-TO-FALL PENDULUM MODEL TO PREDICT LIMB FREQUENCIES OF BOUNDING GAITS IN MAMMALIAN CLIMBING

Cassie Shriver[1*], Dylan Scott[2], Jennifer Elgart[3], Joseph Mendelson III[1,3], David L. Hu[1,2], Young-Hui Chang[1]
Georgia Institute of Technology, Schools of Biological Sciences[1] and Mechanical Engineering[2], Atlanta, GA; Zoo Atlanta[3], GA.
*Email: cshriver7@gatech.edu

Introduction: During terrestrial locomotion, gravity acts as a restoring force to bring an individual's mass back into contact with the substrate. During climbing, however, gravity directly resists the direction of travel, and restoring forces must be provided by muscles. The consequences of gravity are exacerbated by size scaling, with larger mammals exhibiting postural changes in terrestrial locomotion to reduce muscle force generation and locomotor stress [1], yet little work has been done to evaluate how larger climbing mammals overcome this challenge. Non-primate mammals exhibit two main types of climbing gaits: 1) a (more common) bounding gait characterized by synchronous movement in the forelimbs and hindlimbs to 'inchworm' upwards, displaying pendular motion perpendicular to the climbing surface, and 2) a lateral sequence gait characterized by synchronous movement of diagonal limbs, comparable to a human climbing a ladder [2]. If we assume that pendular dynamics are beneficial for reducing the muscular energy cost of climbing, we developed a pendular time scale model for climbing mammals to determine how body morphology influences gait step frequency, particularly for the bounding gait. We then determined experimental time scale values in mammalian climbers and compared these to our model. We hypothesized that there is a cut-off time, determined by body morphology and limb posture, at or below which mammals will need to regain contact between their forelimbs and the climbing surface before they swing too far away from a hindfoot pivot point, which would increase fall risk. Specifically, we predicted that larger mammals would have greater delays between forelimb contacts because longer effective pendulum lengths created by their hindlimbs will increase the time to swing away from the surface.

Methods: We modeled sagittal plane dynamics of climbing mammals as pendulums with the pivot point where the hindlimbs contact the climbing surface (Fig 1, A). The effective pendulum length, a, is defined as the distance between the pivot point and the animal's center of mass (COM). Assuming the mammal lets go with its forelimbs while maintaining contact with its hindlimbs, the time scale to fall through a pendular arc away from the surface is:

$$\tau = \sqrt{\frac{a^2}{hg}} = \sqrt{\frac{\frac{L^2}{4} + h^2}{hg}} \qquad (1)$$

We approximated the horizontal distance, h, between the COM of the animal and the climbing surface as the length of the hindlimbs. Theoretical time scale values were then determined for a range of body lengths, L, up to 2 meters with respective hindlimb lengths approximated as $h = L^b$, where b represents power-law scaling relationships between 0.25 and 0.5 for mammals [3, 4].

We obtained videos of seven representative animals climbing both in collaboration with Zoo Atlanta (Georgia Tech IACUC protocol A100628) and from online media sources. Using dltdv8 software [5], we determined limb contact event times. Experimental time scale values were calculated as the time between forelimb lift-off and when the forelimbs would contact the climbing surface again. Body and hindlimb lengths were determined from veterinary measurements at Zoo Atlanta or approximated using values from literature.

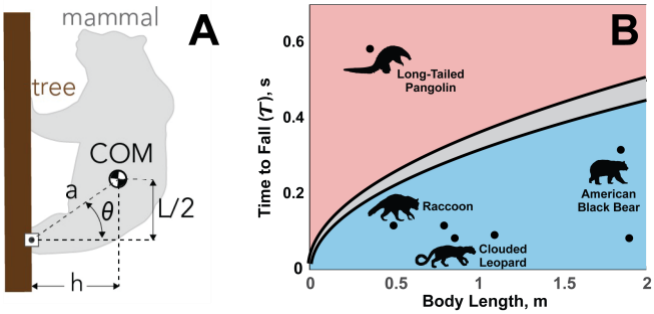

Figure 1: Time-to-fall pendulum model for mammalian climbing. **A**: Free-body diagram defining the effect pendulum length, a, as the distance between the hindfoot pivot and the center of mass of the mammal. **B**: Theoretical and experimental results for the pendular time scale, τ, describing the characteristic time to fall some constant angular amount after forelimb lift-off. The gray shaded region describes this theoretical cut-off, determined by calculating τ using a range of h values for different body lengths as described in Equation (1). Below this cut-off, an animal will be able to grab the surface again before falling (blue shaded region) and above this cut-off, the animal would theoretically fall (red shaded region). Experimental results are plotted for bounding gaits (black dots).

Results & Discussion: We determined a theoretical time-to-fall cut-off range for mammalian climbing based on body length (Fig 1, B). The gray shaded region shows the range of this cut-off, with the variability resulting from different possible h values for respective body lengths. All but one of the experimental time scales fall within or below this cut-off range, aligning with the theoretical model to suggest that there exists a maximum time scale within which climbing mammals must recontact the surface to prevent falling. Rather than exploiting the dynamics of pendular motion to dictate its stride cycle, the long-tailed pangolin, as the exception, appears to depend entirely on muscular action to slowly extends its body upwards with each stride cycle.

Significance: Larger mammals present intriguing scaling challenges, particularly with how climbing biomechanics scale with size. We developed a novel pendular time scale model in climbing mammals and compared the theoretical limitations with observed climbing. Understanding mammalian climbing principles is critical for behavioral insights and can inform habitat protection in the wild and design in zoological settings. This work also has great potential for rapid bio-inspired climbing robotics capable of carrying larger payloads.

Acknowledgments: We thank the Zoo Atlanta keepers, curators, and research team for their assistance in collecting data on their animals. C. Shriver is supported by a National Science Foundation Graduate Research Fellowship and the ARCS foundation.

References: [1] Biewener, A.A. (1989) *Science*. Vol 245. [2] Shriver, C. et al, in prep (2024). [3] Kilbourne, B.M. and Hoffman, L.C. (2013). *PLoS One*, 8(11). [4] Silva, M. (1998). *J. Mammalogy* Vol 79(1). [5] Hedrick, T.L. (2008) *Bioinspir. Biomim.* 3.

CHANGES IN LOWER-LIMB MUSCLE FORCE WHEN WEARING A BACK-SUPPORT EXOSKELETON DURING SINGLE-STEP BALANCE RECOVERY FOLLOWING A FORWARD LOSS OF BALANCE

Ananya Nagabhushana Rao, Jangho Park*, Divya Srinivasan
Department of Industrial Engineering, Clemson University, Clemson, SC 29634, USA
email: janghop@clemson.edu, web: www.cecas.clemson.edu/ergo

Introduction: Back-support exoskeletons (BSEs) are wearable devices designed to provide external torques assisting trunk/hip extensions. While extensive studies have shown the benefits of BSE use (e.g., decreased lumbar muscle activity and torque during repetitive and/or heavy lifting), the importance of identifying potential adverse impacts of BSE use (e.g., increased risk of falls) has also been emphasized for the safe adoption of BSEs in the workplace [1]. In earlier studies, we investigated the effects of wearing a BSE on single-step balance recovery following a forward loss of balance (i.e., simulated trips) using a tether-release protocol. We found that BSE use impaired reactive stepping (e.g., decreased hip flexion angle and step length) [2] by decreasing the stepping limb kinetic energy for forward propulsion [3]. However, there is still limited understanding of how BSE use alters muscle coordination strategies or co-contractions during balance recovery. Hence, the objective of this study was to quantify the effects of BSE use on muscle force produced by the hip, knee, ankle flexors and extensors. Based on our previous studies showing that BSE use impeded hip flexion, we focused on the swing phase (i.e., toe-off to heel-strike of the stepping foot) of balance recovery in this study.

Methods: Sixteen (8M, 8F) young, healthy participants were released from static forward-leaning postures and attempted to recover their balance with a single-step while wearing a BSE (backX™ with high supportive torque) and in a control condition (NoBSE) (Figure 1). Whole body kinematics were sampled at 120 Hz and ground reaction forces (GRFs) were sampled at 1200 Hz during balance recovery trials. Data processing was performed using OpenSim software (version 4.4; Figure 3). First, the gait2354_simbody model was scaled to participants' anthropometry. Next, inverse kinematics and dynamics were calculated using measured kinematics and GRFs. For the BSE condition, calculated hip torques ($T_{HIP\text{-}TOTAL}$) included the sum of the torque generated by participant and BSE. Hence, hip torque generated by the participant only ($T_{HIP\text{-}HUMAN}$) was calculated by subtracting the torque generated by the device ($T_{HIP\text{-}BSE}$; Figure 2) from $T_{HIP\text{-}TOTAL}$. Finally, lower-limb muscle forces were estimated using the Computed Muscle Control (CMC) tool. Outcome measures included peak muscle force (N) produced by rectus femoris, biceps femoris, tibialis anterior, and gastrocnemius. The time (% swing phase) at which the peak force occurred was also quantified.

Results & Discussion: In NoBSE control condition, mean (SD) of peak muscle force produced by rectus femoris, biceps femoris, tibialis anterior, and gastrocnemius were 591 (458), 1462 (828), 745 (426), and 978 (577) N, respectively. Mean (SD) of the time at which these peak forces occurred were 60 (22), 93 (25), 96 (7), and 56 (30) % swing phase, respectively. Results from repeated measures analysis of variance (ANOVA) models indicated that wearing the backX had minimal effects on both the peak muscle forces and their timing (p-values > 0.05), suggesting that participants did not exhibit different muscle coordination strategies in the BSE condition. Thus, for example, net hip flexion torque exerted by the participant plus BSE decreased due to the external hip extension torques generated by BSE, leading to reduced kinetic energy for forward propulsion, which aligns with our previous findings [2-3]. However, our results also revealed significant interaction effects of *BSE* condition and gender on all peak muscle forces. While BSE use led to increased peak muscle forces by 92-217 % only among males (p-values < 0.01), females did not present such changes (e.g., Figure 4). Given that lower limb strengths are generally lower among females compare to males [4], females may not have been capable of producing compensatory adjustments when wearing the BSE. Further studies need to elucidate the underlying reasons for these sex differences in BSE effects.

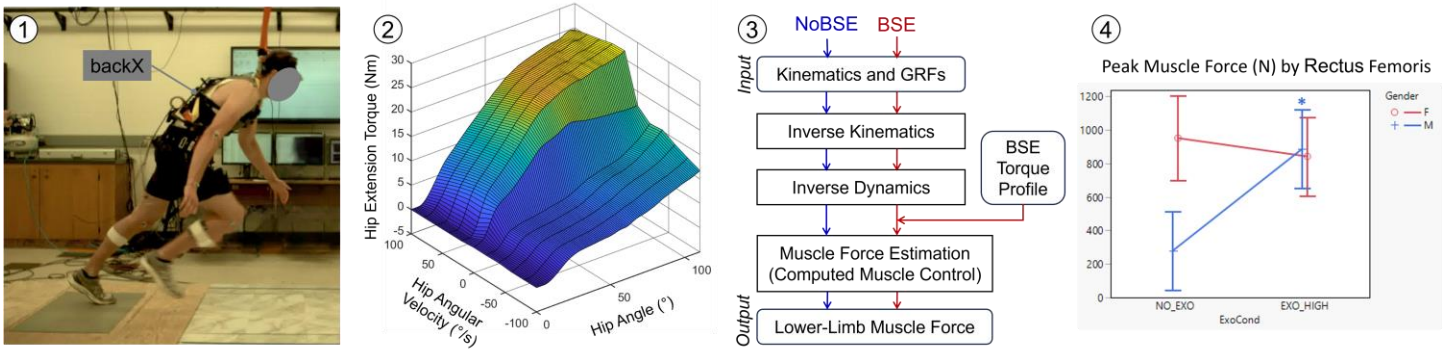

Figure 1: An individual performing single-step balance recovery while wearing the backX; **Figure 2:** The backX torque profile applied on each hip [5]; **Figure 3:** Schematic flow of data processing; and **Figure 4:** Peak muscle force produced by rectus femoris.

Significance: The findings of this study elucidate why wearing a BSE can adversely impact single-step balance recovery after a forward loss of balance. Moreover, the observed sex differences in peak muscle forces underscore the importance of incorporating considerations of female anthropometry and strength into future BSE design.

References: [1] Nussbaum et al. (2019), *IISE Trans Occup Ergon Hum Factors* 7(3-4); [2] Park et al. (2022), *J Biomech* 144; [3] Park et al. (under review), *J Biomech*; [4] Harbo et al. (2012), *Eur J Appl Physiol* 112; and [5] Madinei et al. (2022), *J Biomech* 145.

Demonstrating feasibility of optomyography for active prosthetics

Nicholas Volpe[1], Luis Paulino[2], Oluwaseun Abiona[3], Dr. Jongsang Son[4]
[1]New Jersey Institute of Technology
[2,3,4]New Jersey Institute of Technology
ncv8@njit.edu

Introduction: Current solutions for muscular sensing in active prosthetics (e.g., electromyography and mechanomyography) have proven to be expensive and unreliable for daily use. According to the World Health Organization, 9 out of 10 people who need active prosthetics do not have access due to the technology being too expensive [1]. In addition to cost, current technologies are prone to interference; in particular, electromyography (EMG) is sensitive to hair, sweat, and electromagnetic interference, while Mechanomyography (MMG) is sensitive to vibrations that are caused by muscles not related to the hand movement. Optomyography (OMG), which relies on reflective optical sensors, avoids these issues due to its dependence on distance, which should only change during muscle movement. Therefore, this project seeks to implement an optomyography based armband with the purpose of training a bidirectional long short-term memory (Bi-LSTM)-based network for hand gesture recognition. The hope is to develop an accurate, efficient, and affordable device meant for active prosthetic control, among other things.

Methods: An armband-like device, consisting of multiple optical sensors placed around a circumference, was developed to collect data. To verify our results, our device needed to be tested by collecting data on hand gestures and analyzing them in real time to check the reliability and accuracy of the solution. Therefore, testing methods were developed for this purpose.
Hand gesture data was collected from 3 participants using a prototype of the optomyography-based armband. which was used to train a Bi-LSTM-based network for hand gesture recognition. A graphical user interface application was developed to predict hand gestures from the trained model using new optomyography data in real time.

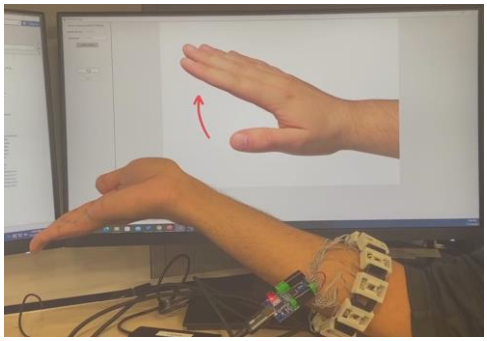

Figure 1: An example of using the Optoband and a graphical user interface application developed for hand gesture recognition.

Results & Discussion: The prototype was able to reliably recognize some gestures, although not very complex ones, while being a fraction of the cost of the average EMG or MMG device. Therefore, we believe the design was successful to demonstrate the feasibility of using optomyography for a cost-effective active prosthetic. This is not without some current caveats.
With only 3 test subjects, our model cannot feasibly be fully realized. With an approved IRB request, the number of test subjects can be ethically expanded, and a more reliable model can be trained. Furthermore, our BiLSTM-based model only works for specific hand gestures. Pivoting to a sequence-to-sequence model, along with developing a proper dataset collecting environment, will allow for the next generation of this method to fully go under way. Implementing the model weights into a phone app would enable the sensor array to be fully portable assuming the user has a smart phone.

Significance: Using OMG to sense muscle movement instead of MMG and EMG can help deal with some of the issues present in current muscle sensing technologies, like interference, while being affordable and efficient due to the reliance on optical sensors, which are usually low-cost. Such device can improve the affordability and performance of muscle movement-based applications, like active prosthetics.

References: [1] WHO standards for prosthetics and orthoics. Geneva: World Health Organization; 2017. Licence: CC BY-NC-SA 3.0 IGO. [2] H.H. Muhhammed et al. IBIOMED; 2016, 6(26):972-1018.

EFFECTS OF WALKING SPEED ON LOWER LIMB TRAJECTORY ERROR ESTIMATED FROM A SINGLE INERTIAL MEASUREMENT UNIT DURING STEADY-STATE GAIT

Zach N. Hoegberg[1*], Seth R. Donahue[1,2], Matthew J. Major[1,2]
[1] Dept. of Physical Medicine & Rehabilitation, Northwestern University, Chicago IL, USA
[2]Jesse Brown VA Medical Center, Chicago IL US
*Corresponding author's email: zacharyhoegberg2024@u.northwestern.edu

Introduction: As a diagnostic and therapeutic tool for gait assessment, Inertial Measurement Units (IMUs) offer several advantages over typical motion capture methods: they are low-cost, can be used for real-time analysis, and can track individuals across real-world locomotion contexts. Despite their potential benefits in rehabilitation protocols, IMUs have not been widely adopted as a clinical tool. Limited adoption is partially due to commercial systems requiring proprietary software and large sensor suites to provide meaningful data, and the assessment of the robustness of wearable sensor measures [1]. This study aimed to address these two limitations by demonstrating the use of a single IMU system with open-source code, capable of measuring shank kinematics to calculate Lower Limb Trajectory Error (LLTE) and assess the effects of walking speed on the LLTE when using a commercial IMU. The LLTE is a scalar metric that consolidates time-normalized kinematics of the shank during stance phase and compares it against a reference trajectory and is defined as the root mean squared error between the measured and target trajectory incorporating the vertical and anterior-posterior knee position and shank angle with respect to vertical (Figure 1). The LLTE was previously used as a design criterion for personalized prosthetic feet to encourage close-to-able-bodied prosthetic leg kinematics [2]. The LLTE is a promising candidate for clinical quantification of deviations in gait patterns as it can be calculated from a single IMU sensor. This study developed an algorithm to calculate LLTE from a single IMU sensor and assessed effects of walking speed on this IMU estimate to evaluate its robustness.

$$LLTE = \frac{1}{N}\sum_{i=1}^{N}\left[\left(\frac{x_i-\hat{x}_i}{L_{ll}}\right)^2 + \left(\frac{y_i-\hat{y}_i}{L_{ll}}\right)^2 + \left(\frac{\theta_i-\hat{\theta}_i}{\text{atan}\left(\frac{L_{ll}}{L_f}\right)}\right)^2\right]^{1/2}$$

Figure 1. LLTE equation. x_i, y_i, and θ_i are shank IMU anterior-posterior position, vertical position, and shank orientation, respectively, for each instant *i* during stance. $\hat{x}_i$, $\hat{y}_i$, and $\hat{\theta}_i$ denotes the target motion at the same time instants. L_{ll} and L_f are the lower leg length and foot length.

Methods: Eight able-bodied persons participated (4m/4f, age: 27.22 yrs, ht: 1.69 m, wt: 67.04 kg). As this analysis is part of a larger protocol, participants were fit with 8 wireless IMUs (Xsens MTw, USA), attached with Velcro wraps at the sternum, sacrum, and each leg segment. Data from only the dominant limb shank IMU was used for analysis. IMUs were aligned with segment anatomical coordinate systems with a function calibration prior to data collections, with repeated toe touches and 10 seconds of walking [3]. Participants walked for one minute on a treadmill (Cosmed T170, Italy) at 0.80, 1.00, 1.25, and 1.50 ms^{-1}. Data collection and processing were performed using a custom Python script. Gait events were detected using a shank angular velocity method [4]. For this study, the LLTE target trajectory was derived from a reference IMU kinematic set from one individual walking at 0.8 ms^{-1}. A one-way repeated measures ANOVA assessed the main effect of walking speed on LLTE value (α=0.05).

Table 1. Average LLTE values for each walking speed.

Velocity (ms^{-1})	0.80	1.00	1.25	1.25
LLTE (mean ± std)	0.42 ± 0.13	0.42 ± 0.15	0.44 ± 0.23	0.43 ± 0.28

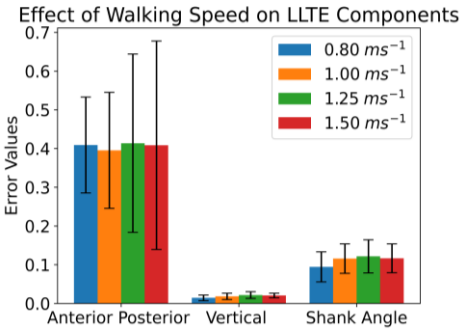

Figure 2. Mean error value of each LLTE constituent variable at tested walking speeds that contribute to the overall LLTE value. Error bars denote one std. dev.

Results & Discussion: Results suggest that errors for each component of the LLTE are generally insensitive to walking speed (Figure 1), and this is reflected in the non-significant effect of walking speed on LLTE (p=0.97, Table 1). These results were expected given the time-normalization of this metric but also emphasizes the robustness of the LLTE as a scalar variable that consolidates leg kinematics as calculated from a single IMU sensor. The majority of error contributing to LLTE was the anterior-posterior position of the shank. Here we demonstrate use of a scalar kinematic variable integrating multiple components of leg dynamics that quantifies error compared to a target trajectory and can be estimated from a single IMU. Such a technique could be used clinically to estimate divergence of kinematics from an expected trajectory in gait-impaired populations and as feedback for gait training if the aim is to encourage a defined leg kinematic pattern. Future work involves building a reference set of IMU estimated reference trajectories, and quantifying LLTE for patient groups with this approach, and the development of a biofeedback tool for gait retraining.

Significance: This study highlights the use of a scalar metric that reflects an individual's divergence from a given target leg kinematic trajectory, can be estimated from a single wireless IMU, is generally robust to walking speed, and therefore has important clinical applicability given its need for minimal resources and constraints while producing relevant information on gait quality.

Acknowledgments: Funded by ACL NIDILLR Switzer Fellowship, Award # 90SFGE0048-01-00.

References: [1] Vargas-Valencia, L.S. Sensors 16, 2090, 2016. [2] Prost, V. J Biomech Eng 145, 041002, 2023. [3] Cain, S.M. Gait & Posture 43, 65-69, 2016. [4] Meng-Jung, C. Gait & Posture 31(1), 131-135, 2010.

VALIDATING A NEW TUNING APPROACH FOR POWERED KNEE : THE EFFECT OF STIFFNESS ADJUSTMENTS

Woolim Hong[1*], He (Helen) Huang[1]
[1]Joint Department of Biomedical Engineering, NC State University, Raleigh, NC & University of North Carolina, Chapel Hill, NC
*Corresponding author's email: whong3@ncsu.edu

Introduction: Lower limb amputation significantly affects a person's ability to move and maintain balance, increasing their risk of falling and sustaining injuries [1]. Over the years, powered prostheses (i.e., robotic prostheses) have been designed and researched to replicate the natural gait of non-amputees as closely as possible. Despite these advancements, there remains a notable gap in providing personalized controls for individuals with amputations [2], and many of the existing studies require extensive adjustments for each user and walking situation to achieve satisfactory gait performance [3]. In our previous work, we introduced an innovative method for adjusting the continuous impedance control framework used in powered prostheses [4]. This method involves modifying the weights assigned to the principal components (PCs) of continuous stiffness, damping, and the equilibrium angle throughout the gait cycle. We demonstrated the potential to create a range of impedance functions by adjusting the stiffness, damping, and equilibrium PCs' weights. Yet, this technique has not been tested experimentally with a powered prosthesis. The main objective of this study is to examine the alterations in the human knee profile with different tuning parameters and to validate the effectiveness of our tuning strategy with a powered knee prosthesis.

Methods: In our proposed tuning approach, we introduce six tuning parameters, including the weights of two PCs each for stiffness, damping, and equilibrium angle [4]. This study focuses on adjusting the weight of the first stiffness PC (Kw1) from 0.1 to 1.0 in increments of 0.1 to explore its impact on knee kinematics during walking with a powered knee prosthesis. We maintained invariance in the other tuning parameters, such as damping and equilibrium angles, based on an initial tuning set derived from offline optimization using a dataset from human subjects [5]. A healthy young male subject (34 years, 1.7 m, 70 kg) participated in walking on an instrumented treadmill (Bertec, Columbus, OH, USA) at his preferred speed of 0.60 m/s, using a custom-built powered knee prosthesis [6]. The prosthesis was controlled using the continuous impedance control framework based on a time-based linear phase variable. Safety measures included handrails on both sides of the treadmill. In each stiffness scenario, the subject walked for one minute, completing approximately 30 gait cycles.

Results & Discussion: Figure 1 depicts the knee stiffness and knee angle profiles measured from the powered knee prosthesis. It demonstrates that knee stiffness linearly increases as the weight of the first stiffness PC (Kw1) adjusts from 0.1 to 1.0 in increments of 0.1. Notably, the powered prosthesis exhibits varied knee motions in response to different levels of knee stiffness. Specifically, the knee profile undergoes significant and consistent changes between Kw1 values of 0.2 and 0.7. This is attributed to the fact that as Kw1 increases, so does the knee stiffness during the swing phase, resulting in better tracking of the targeted equilibrium angle profile, which includes up to 62 degrees of maximum knee flexion. Consequently, higher Kw1 values lead to increased knee flexion.

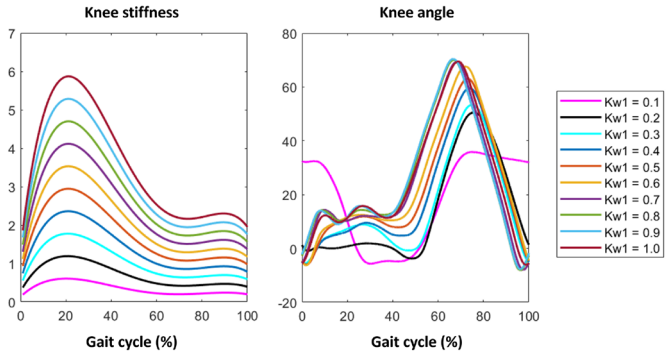

Figure 1: Variations in the weight of the first stiffness PC (ranging from 0.1 to 1.0) and the corresponding profiles for knee stiffness and knee angle in a powered prosthesis.

On the other hand, beyond a Kw1 value of 0.7, the knee profile shows negligible differences at higher values and exhibits oscillatory movements during the stance phase. This may be due to excessively high stiffness at these Kw1 values during the stance phase. With the lowest Kw1 values, the knee profile deviates significantly from a typical human physiological knee profile because of insufficient knee stiffness in the swing phase, leading to a loss of tracking to the desired human-like knee equilibrium profile. These observations provide valuable insights into the optimal tuning range for Kw1, highlighting the importance of avoiding values below 0.2 and above 0.7 to ensure user safety while tuning the Kw1 for control of the powered knee prosthesis.

Significance: Although the continuous impedance control framework for powered lower-limb prostheses has recently attracted attention, its controller tuning has yet to be explored. In this study, we conduct empirical validation of our proposed tuning scheme for the continuous impedance controller by adjusting the stiffness tuning parameters. This work aims to establish a more efficient tuning process for the continuous impedance control of powered lower-limb prostheses.

Acknowledgments: This work was supported in part by the National Institute on Disability, Independent Living, and Rehabilitation Research (NIDILRR; #90ARHF0004 and #90SFGE0050), and in part by National Science Foundation (NSF; #2211739).

References: [1] Miller et al. (2001), Arch Phys Med Rehab 82(9); [2] Best et al. (2023), IEEE Trans Robotics; [3] Li et al. (2021), IEEE Trans Robotics 38(1); [4] Hong et al. (2023), ICORR, pp. 1-6; [5] Camargo et al. (2021), J Biomech; [6] Wen et al. (2016), EMBC, pp. 5071-5074.

A NOVEL ADAPTIVE PURSUIT ROTOR TASK FOR TRIAL-TO-TRIAL PERFORMANCE NORMALIZATION

Adam M. Fullenkamp[1*], Zoe Kriegel[2], Jason A. Whitfield[3]
[1]School of Applied Human Development/Exercise Science Program, Bowling Green State University, Bowling Green, OH
[2]Division of Communication Disorders, University of Wyoming, Laramie, WY
[3]Department of Communication Sciences and Disorders, Bowling Green State University, Bowling Green, OH
*Corresponding author's email: fullena@bgsu.edu

Introduction: Continuous pursuit tasks are a staple of motor behavior assessment [1-3]. Such tasks offer insight into the influence of both intrinsic (e.g. neuropathy, attention, etc.) and extrinsic (e.g., environment, end effector, etc.) factors upon human motor control [4]. A popular variation of the pursuit paradigm is the pursuit rotor task (PRT). A PRT generally involves the manual tracking of a target around a circular path with a stylus, mouse, or mechanical rotor handle. The difficulty of a PRT is most commonly mediated by either a) adjusting the size of the target, or b) adjusting the speed of target movement around the circle. For a PRT to offer valid between-subjects comparison, individual performance must be normalized to a goal % time-on-target (TOT). For example, because some individuals will demonstrate natural aptitude for tracking performance compared to others, the difficulty of the task (i.e. target speed or size) must be adapted to each test participant to achieve an approximate goal difficulty/performance. PRT difficulty normalization faces two challenges. First, the identification of PRT target characteristics needed to achieve a goal performance can involve an exhaustive number of normalization trials [5]. In the traditional normalization process, an individual will often repeat multiple PRT trials, sometimes lasting minutes, for a range of target velocities to identify the target velocity. This process raises concerns of within-session fatigue and transient practice-based performance improvements. Often, to address the concerns associated with prolonged normalization, experimenters will separate the normalization and testing protocols into different sessions [5]. The obvious concern with this control method is that intrinsic and extrinsic conditions may differ from session-to-session. Second, even if PRT target characteristics are normalized in a prior session, and an individual begins the test session at the calibrated tracking performance, there is still the likelihood that participants will demonstrate within-session performance improvements over the course of testing. Therefore, we propose an adaptive, trial-to-trial PRT paradigm to address these limitations.

We have developed, and conducted preliminary assessment of, an adaptive PRT tool that conducts dynamic performance normalization prior to each PRT trial. It was hypothesized that participant performance during the adaptive PRT would not differ significantly from the goal performance criterion. Additionally, it was hypothesized that performance would not change across multiple trials, but that target speed would increase across trials as participants experienced transient practice effects.

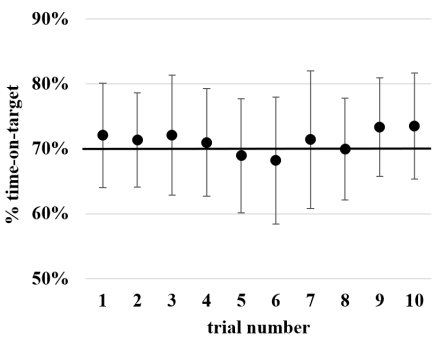

Figure 1: Mean (SD) % time-on-target results from ten consecutive trials of adaptive pursuit rotor performance (n = 25). Goal % time-on-target was 70% in each trial.

Methods: A custom, adaptive PRT was developed and assessed with 25 college-aged participants (23F, 2M). All participants provided informed consent as approved by the local IRB. Each participant performed 10 PRT trials which involved a 60-second dynamic adaptation phase, followed by a 20 second tracking phase. The goal performance for all trials was 70% TOT. The dynamic adaptation phase involved an acceleration and deceleration of the moving target to identify the ideal trial target speed to achieve 70% TOT. Target speed was controlled in terms of ms delay from one target position to the next. All participants began adaptation with a target delay of 45ms (i.e. 44.4°/s). TOT was evaluated throughout the adaptation phase and target delay was adjusted to achieve 70% TOT. The target delay at the end of adaptation was applied to the 20-second PRT trial. Paired-samples and one-sample t-tests were performed to evaluated tracking performance (α = 0.05).

Results & Discussion: Percent TOT for all participants across all trials was 71% +/- 4% [mean (SD)]. This grand mean was not significantly different from the goal TOT of 70% (p = 0.13). Figure 1 depicts the mean (SD) of tracking performance for each trial. None of the trial-specific means were found to be different from 70%, and there was no statistical difference in mean performance between trials 1 and 10 (p = 0.30). Further, there was a significant reduction in mean target delay (i.e. increase in target velocity) across the ten trials (trial 1 = 40.6ms vs. trial 10 = 33.3ms; $p < 0.001$). These findings suggest that a) the adaptive PRT accurately determined the target velocity that ensured goal tracking performance, and b) the adaptive PRT accounted for within-session performance adaptation. Future assessment of the adaptive PRT model should emphasize testing with a range of %TOT performance goals, and the evaluation of varying adaption and tracking phase durations.

Significance: The PRT is a standard visuomotor assessment tool in the broader field of motor behavior. For PRT testing to offer valid between-subjects pooling and comparison, a PRT tool must offer valid performance normalization and resistance to within-session adaptation. Preliminary assessment of the novel adaptive PRT presented here demonstrates the potential to resolve prior limitations with trial-to-trail normalization. The approach may ultimately offer more valid and reliable visuomotor results.

References: [1] Humphreys (1937), *J Psych* 3(2); [2] Archer & Namikas (1958), *J Exp Psych* 56(4); [3] Kemper et al. (2009), *J Age Neuropsych Cog* 16(3); [4] Whitfield et al. (2021), *JSLHR* 64(6S); [5] Whitfield & Goberman (2017), *JSLHR* 60(6S).

WE WORK WITH THE ZOO, AND YOU CAN, TOO!
ZOO-ACADEMIA GUIDELINES FOR RESEARCH COLLABORATIONS AND OUTREACH

Cassie Shriver[1*], Andrew K. Schulz[2], Emily G. Weigel[1], Staci Wiech[3], Joseph R. Mendelson III[1,3], David L. Hu[1,4], Young-Hui Chang[1]
Georgia Institute of Technology, Schools of Biological Sciences[1] and Mechanical Engineering[4], Atlanta, GA;
Max Planck Institute for Intelligent Systems[2], Haptic Intelligence Department, Stuttgart, Germany; Zoo Atlanta[3], Atlanta, GA
*Email: cshriver7@gatech.edu

Introduction: For biomechanics research and outreach, collaborating with zoos provides opportunities to greatly expand both the diversity of species being studied and the number of people being reached [1]. Despite such excellent opportunities, long-term collaborations between zoos and academic institutions are rare, potentially due to little normalized guidance on how to start or maintain these collaborations. The authors have decades of combined experience in zoo-academia partnerships. Here, we discuss our framework for establishing and maintaining successful research collaborations [2] and highlight how we leveraged these collaborations for a significant biomechanics outreach event [3]. While zoos have inherent interest in research output for their animals [4], we hypothesize that key factors for academics interested in collaborating with zoos are prioritizing animal safety, deferring to the zoo for reasonable timelines and media policies, and communicating clearly to make the research process as easy as possible for the zoo.

Methods: To determine how academics can best establish research collaborations, we created a survey for zoo associates using the Qualtrics software platform. The survey comprised three sections: 1) acknowledgement of consent to participate in the research study, 2) background information including job title, zoo affiliation, and experience in academic collaborations, and 3) opinions on the importance of different aspects of academic collaborations regarding establishing novel and maintaining existing partnerships. We distributed the survey using our contacts at zoos in the United States, through professional lists, and with online zoo forums.

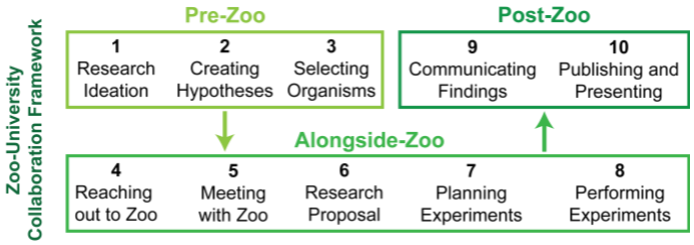

Figure 1: Schematic of the zoo-university research collaboration process. We identify ten distinct steps academics should take to engage in successful research collaborations with zoos. These steps are divided into three phases, with three steps occurring before reaching out to the zoo, five steps occurring while actively working with the zoo, and two steps occurring after experiments have concluded at the zoo.

Results & Discussion: We received a total of 168 responses to our survey, 97 of which were completed in full by affiliates of zoological institutions and were used in our analyses [2]. These 97 responses represented 59 different zoos, with 85% from AZA-accredited zoos and the other 15% from either international zoos or zoos accredited by other national organizations (e.g., the Zoological Association of America). Using the opinions from responders on the importance of various aspects of zoo-academia collaborations, we developed a ten-step guideline for a single research partnership (Fig. 1). In this guideline, researchers are not actually performing any experiments until step eight, highlighting the extensive amount of preparation and communication required with a zoological institution. Overall, zoo staff valued consistent and clear communication, awareness that keepers must volunteer their time for experiments, and compromising on methods to prioritize the health and safety of their animals. Because of Georgia Tech's extensive research collaborations with Zoo Atlanta, we proposed establishing an annual biomechanics outreach event called "Biomechanics Day: Animals in Motion" (Fig 2). In its second year, we hosted over forty researchers from five different universities and Vicon Motion Systems to setup stations throughout Zoo Atlanta to share their biomechanics research and techniques with the public, many of which showcased active research collaborations between the universities and Zoo Atlanta. In two years, we have reached a combined attendance of 11,677, as determined by ticket sales to Zoo Atlanta on those days.

Figure 2: Zoo Biomechanics Day 2024 outreach event logo. Participants from the University of Akron, Belmont University, Clemson University, Emory University, the Georgia Institute of Technology, and Vicon Motion Systems hosted stations throughout Zoo Atlanta to share ongoing biomechanics research and techniques with the public.

Significance: Collaborating with zoological institutions benefits the field of biomechanics by increasing both the diversity of species able to be studied and the size of potential outreach populations. We have created a comprehensive guideline for academics interested in establishing their own research collaborations with zoos, which can directly assist in expanding the comparative biomechanics field. We also exemplify how are utilizing our existing collaborations to create a biomechanics outreach event with nearly 12,000 attendees total in two years, demonstrating the benefits of partnering with non-academic institutions to achieve growing outreach goals.

Acknowledgments: The authors would like to acknowledge R. Moore, who assisted with survey edits, and the zoo survey participants for their time. We thank the academic research volunteers and the Zoo Atlanta education staff for their assistance during Zoo Biomechanics Day. C. Shriver is supported by a National Science Foundation Graduate Research Fellowship and the ARCS foundation.

References: [1] Light, D. and Cerrone, M. (2018). *Visitor Studies*, Vol 21(2). [2] Schulz et al. (2022), *Integ. and Comp. Biol*, 62(5). [3] Shriver, C. et al. (2024). *SICB Nat. Conf.* [4] Escribano, N. et al. (2021). *Cons. Biol.* Vol 35(6).

GROWTH-PERIOD TREADMILL TRAINING EFFECTS ON CENTER OF MASS MECHANICS IN GUINEA FOWL

Jessica Murawski[1], Derek Jurestovsky[1], Stephen J. Piazza[1*], and Jonas Rubenson[1]
Dept. of Kinesiology, The Pennsylvania State University, University Park, PA, USA.
Corresponding author's email: piazza@psu.edu

Introduction: A quarter of the global population does not meet the recommended levels of physical activity and around 80% of adolescents are insufficiently physically active [1], a major contributing factor to increased risk of mortality and metabolic and cardiovascular disease [2]. Exercise during childhood and adolescence has the potential to not only establish activity as a habit, but also to reduce physical barriers to exercise in adulthood by making it less effortful. As part of an ongoing study of the effects of growth-period exercise on locomotor function and energetics using a guinea fowl animal model, we examined the mechanical work performed on the center of mass during treadmill locomotion. We hypothesized that animals that underwent extensive treadmill training during growth would perform less positive work on the center of mass (COM) than is performed by untrained control animals, indicating that training leads to a more economical gait pattern that reduces the effort associated with locomotion.

Methods: A total of 60 guinea fowl (*Numida meleagris*) were acquired from a hatchery as two-days old keets and were raised in a brooding pen. When the keets reached 2 weeks old, they were separated into an exercise group (EXE; n=30) and a control group (CON; n=30) and were transferred into cages. The exercise group ran on treadmills with a 6-degree incline for 5 days a week at a speed of 1.34 ms^{-1}. The control group remained in their cages during the training period, with no exercise outside of the cages except for occasional treadmill accommodation runs. After one year of training, a subsample of 8 EXE and 13 CON animals were tested on a treadmill equipped with a custom AMTI force plate and treadmill chassis to measure forces while the guinea fowl moved at speeds of 0.45 ms^{-1} (walking) and 1.34 ms^{-1} (running) at a 6-degree incline. Ground reaction force sampled at 2000 Hz using the force plate were subsequently low-pass filtered with a cut-off frequency of 15 Hz.

Ground reaction force was used to compute acceleration of the COM, and integration of these accelerations produced the COM velocity. A final integration yielded the displacement of the COM. Displacement and velocity values were used to compute the mechanical energy (gravitational potential energy and kinetic energy) associated with the COM. Change in the total mechanical energy was computed to find the positive work done on the COM during a single stride. Five strides at each speed were analyzed for each animal using custom-written Matlab routines.

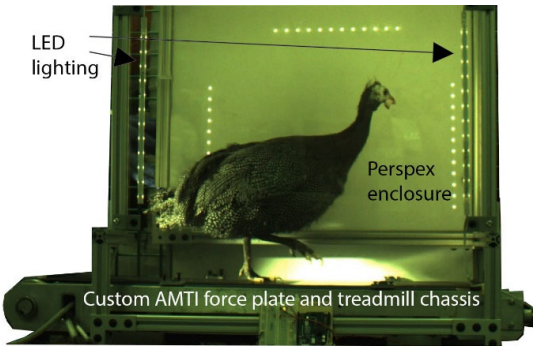

Figure 1. Guinea fowl running on the avian force treadmill fitted with a force platform.

Results & Discussion: The hypothesis was not supported by the results: During running at 1.34 ms^{-1}, positive work per stride was not significantly different between groups ($p = 0.565$; 1.24 ± 0.29 J for EXE and 1.18 ± 0.19 J for CON). Similarly during walking at 0.45 ms^{-1}, positive work per stride was not significantly different ($p = 0.613$; 0.82 ± 0.36 J for EXE and 0.77 ± 0.14 J for CON). As expected, the positive work per stride was significantly greater for running as compared to walking ($p < 0.001$).

Significance: The finding of no significant difference in positive work between groups suggests that growth-period training does not substantially affect locomotor kinematics and kinetics in guinea fowl. Separate tests of locomotor energetics using respirometry indicated significant differences in metabolic energy used to run at 1.34 ms^{-1}, with EXE animals moving more efficiently, using less energy. The present study suggests that the mechanisms underlying the enhanced efficiency are not rooted in altered movement patterns.

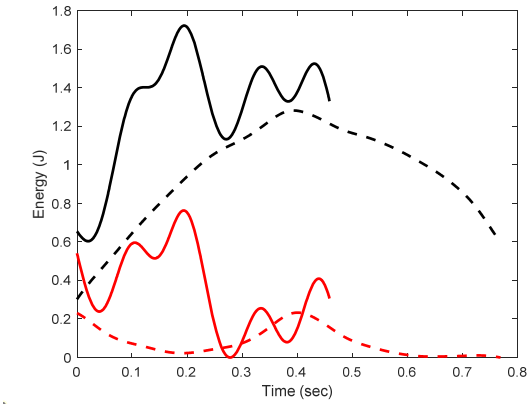

Figure 2. Mechanical energies during representative trials for running uphill at 1.34 ms^{-1} (solid curves) and walking uphill at 0.45 ms^{-1} (dashed curves). Total energy (*black*) and kinetic energy (*red*) are shown. Total positive work is calculated as the sum of the positive changes in the total energy throughout the stride.

Acknowledgments: We would like to thank the Animal Care Staff and lab technicians. Supported by NIH Grant R01AR080711.

References: [1] World Health Organization. Physical activity fact sheet. (2021). [2] Haileamlak A *Ethiop J Health Sci.* 2019.

INFLUENCE OF ANTEROPOSTERIOR AND MEDIOLATERAL VIBROTACTILE FEEDBACK ON AMPUTEE POSTURAL CONTROL

Brendan Driscoll[1*], Joshua Tacca[1], Helen Huang[1]
[1]North Carolina State University, Raleigh, NC, USA
*Corresponding author's email: bhdrisco@ncsu.edu

Introduction: Lower limb amputees are at a high risk of falls due to postural instability [1]. This instability is partially attributed to the impaired sensory motor loop, where amputees have limited ability to sense how their prosthetic limb interacts with the environment. Because of this they rely heavily on their non-amputated (NA) limb for balance. This is reflected in the center of pressure (CoP) profiles of both feet, where the NA side has a much lower sample entropy (SampEn) than the amputated (A) side. SampEn is a measure of randomness, and the high entropy in the A side signifies a lack of active control while they focus on the NA side [2]. One promising approach to restore the sensory motor loop for amputees is sensory substitution, in which biofeedback signals are delivered to the amputee, often using a haptic feedback interface, to compensate for sensory deficits [3]. While most sensory substitution studies focused on lower limb amputees only give feedback on anteroposterior (AP) CoP [4], amputees experience instability in both the AP and mediolateral (ML) directions. One way to provide feedback in both the AP & ML directions is with high-density haptic interfaces. Such interfaces include haptic vests embedded with high-density haptic grids on both the front and back. Using one such interface, our study investigates the effects of providing 1D and 2D CoP feedback on the postural stability of amputees by observing its effects on SampEn to gauge the participants control over their amputated (A) side, and postural stability performance metrics, such as CoP path length (PL) [5]. We hypothesize that providing 2D feedback will reduce amputees' overreliance on their intact limb and enhance postural stability in both the AP and ML directions. In doing so our study aims to contribute to the understanding of sensory substitution mechanisms and offer insights into how haptic feedback interfaces can best be used for improving postural control in lower limb amputee populations.

Methods: Two transtibial amputees were recruited for this study. Haptic feedback was delivered with a Tactsuit x40 (bHaptics, Daejeon, South Korea), while CoP was recorded at 1000Hz using forceplates in a Bertec treadmill (Bertec, Columbus, Ohio). The Tactsuit used a 4x5 grid of vibrotactile motors on both the front and back to deliver feedback. AP feedback was provided by modulating the amplitude of the bottom row of motors on the front and back of the vest based on whether the CoP had drifted forward or backwards from the neutral position. ML feedback was delivered by shifting the location of the stimulus to the left or right accordingly, this was done with the phantom actuator encoding method [6]. Each quiet standing trial was 50 seconds, with 3 trials per condition: no feedback (NF), AP feedback (1D), and AP & ML feedback (2D) for both the eyes open (EO) and eyes closed (EC) conditions. Each trial was split into five 10-second segments. For each segment PL and SampEn were calculated. Our SampEn calculation used an embedded dimension of 3 and r = 0.05. Statistical comparisons were done using ANOVA to assess differences between feedback conditions, with $\alpha = 0.05$.

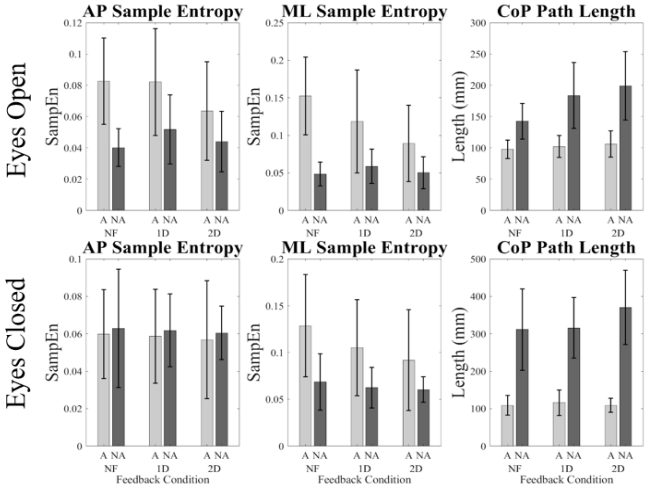

Figure 1. Mean values and standard deviations of SampEn in the AP and ML directions and CoP path length across different conditions. Amputated (A) side is displayed in light grey while the non-amputated (NA) is displayed in dark grey.

Results & Discussion: Experimental results in Fig 1. show that under the EO condition there was a significant difference in entropy between the amputated (A) and NA limbs (AP, $p < 0.01$) (ML, $p < 0.01$) with higher SampEn observed in the A side. This aligns with expectations, as amputees would be less stable on that side leading to more random movement of the CoP. The exception to this seems to be the EC condition, where no significant differences in AP SampEn was found ($p = 0.95$), this is in part due to the 2 participants responding differently to the EC condition. For both EO and EC conditions, 1D feedback significantly reduced ML SampEn on the A side, with further reduction seen when 2D feedback was provided ($p < 0.05$), this signifies that with feedback amputees were able to move more deliberately and reduce the amount of random CoP drift on their prosthetic side. The results for path length suggest that in order to achieve this reduced random movement on the A side, participants compensated with their NA side as shown by the increased path length for both the 1D and 2D EO conditions ($p < 0.01$) and the 2D EC condition ($p < 0.05$).

Significance: This study's findings suggest that TT amputees can interpret and respond to haptic feedback providing AP and ML CoP information during quiet standing, although to act on the feedback they must use compensatory strategies with their NA limb. Participants used passive prosthetic devices that they could not directly control, they had no way of modulating their A side without compensating with their NA side. As a potential solution to get amputees to rely less on the NA side, our future research will focus on implementing sensory substitution with volitionally controlled prosthetic devices, which could better implement a functional sensory motor control loop.

References: [1] Miller et al. (2001), *Arch Phys Med Rehabil* 82(8); [2] Hlavackova et al. (2011) *PLoS One* 6(5) [3] Kaczmarek et al. (1991) *IEEE TBME* 38(1); [4] Huang & Yao (2022) *Mater. Today Phys.* 22; [5] Richmond et al. (2021) *J. Biomech*;[6] Driscoll & Liu (2023) *WHC*;

MODIFYING THE INPUT SPACE FOR DIRECT MYOELECTRIC CONTROL OF ROBOTIC PROSTHESES

Joshua R. Tacca[1*], Brendan Driscoll[1], Austin Mituniewicz[1], and He (Helen) Huang[1]
[1]North Carolina State University, Raleigh, NC, USA
*Corresponding author's email: jrtacca@ncsu.edu

Introduction: Surface electromyography (EMG) from residual muscles of people with transtibial amputation (TTA) can be used to directly control powered ankle prostheses. Direct EMG control enables people with TTA to improve balance by allowing them to make anticipatory adjustments to perturbations and enhance postural control by restoring neural control pathways [1]. However, the ability of people with TTA to activate and co-activate their residual muscles to control a powered prosthesis can vary [2]. For example, some people with TTA struggle to separate activation between their residual tibialis anterior (TA) and gastrocnemius (GAS) muscles and have natural co-activation when they are trying to activate only one muscle [2]. Co-activation or EMG cross-talk can pose a challenge to direct EMG control by signalling a prosthetic ankle to stiffen when the participant is trying to plantarflex or dorsiflex the prosthesis, which limits the potential control space and can impede the prosthesis range of motion. Therefore, we hypothesize that controlling a powered prosthesis based on EMG signals transformed so that they are relative to natural co-activation may improve people with TTA's ability to control a powered prosthesis and allow them to increase their ankle range of motion compared to use of non-transformed EMG signals.

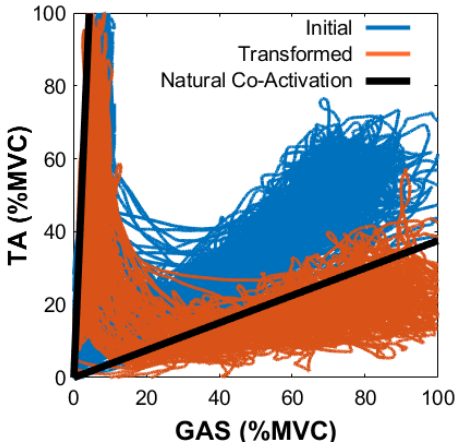

Figure 1: Residual gastrocnemius (GAS) and tibialis anterior (TA) electromyography (EMG) during the initial control task (blue). Natural co-activation lines for the GAS and TA during the initial control task (black). These lines were used to define the transformation matrix. Residual GAS and TA EMG during the second control task (orange) when the EMG was transformed based on the natural co-activation lines. EMG is normalized to peak EMG during a maximum voluntary contraction (MVC).

Methods: 1 person (M, 56 years) with a unilateral TTA activated residual TA and GAS muscles to move a cursor on a computer screen through a grid [2]. The TA controlled y-axis movement and the GAS x-axis movement. As the cursor moved to different squares in the grid, the squares changed colour. The participant was instructed to change the colour of as many squares as possible in several 1-minute trials followed by 3-minute rest until the participant was no longer able to reach new squares. We determined natural co-activation of the TA and GAS as two lines bounding the area filled by the participant in the control space. The co-activation lines were used as a new basis of the control space. The transformed x- and y-axis coordinates of the control space were the TA and GAS activity relative to the co-activation lines. The participant repeated the task in the transformed coordinate system. Then, the participant controlled an experimental prosthesis with artificial pneumatic muscles [3]. EMG from the TA and GAS were filtered and rectified in a controller board (dSPACE, Inc, Wixom, MI) to generate control signals that adjusted the air pressure and contracted artificial pneumatic muscles. The participant maximally dorsiflexed and plantarflexed the prosthesis four times while we measured prosthetic ankle angle in the sagittal plane from motion capture markers placed on the shank, ankle, and foot. The participant repeated the task with the transformed control coordinate system.

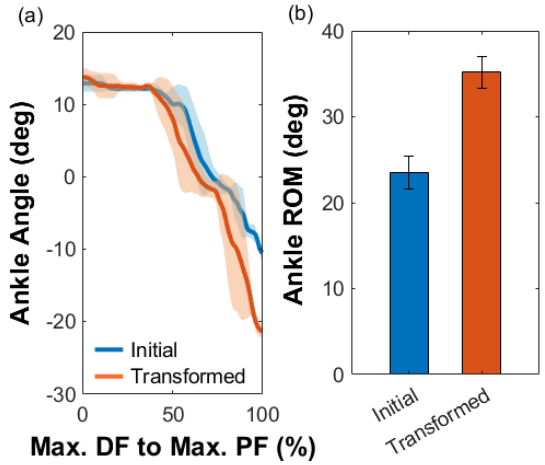

Figure 2. (a) Average prosthetic ankle angle (deg) in the sagittal plane from maximum (max.) dorsiflexion (DF) to max. plantarflexion (PF) for the initial (blue) and transformed (orange) control input conditions. Shaded areas are ± standard deviation (STD). DF is positive and PF is negative. (b) Average prosthetic ankle range of motion (ROM; deg) for the initial (blue) and transformed (orange) input conditions. Error bars are ± STD.

Results & Discussion: The participant was able to move the cursor along the y-axis and activate their TA independent of their GAS during the initial task (Figure 1). However, they struggled to activate their GAS independent of their TA (Figure 1). After transforming the coordinate system, the participant was able better able to activate the GAS independent of the TA and move the cursor along the x-axis (Figure 1). When using the initial control inputs, the participant was able to dorsiflex the prosthesis 13.0 degrees and plantarflex the prosthesis 10.5 degrees for an average range of motion of 23.5 degrees (Figure 2). When using the transformed control inputs, the participant was able to increase the maximum plantarflexion to 21.3 degrees and range of motion to 35.2 degrees (Figure 2). The increase in the ability to plantarflex the prosthesis may be beneficial for tasks such as walking where a biological ankle plantarflexes up to 19 degrees at natural and fast speeds [4].

Significance: Direct EMG control of powered prostheses can be improved by using control inputs based on EMG signals in a coordinate system relative to natural co-activation of antagonistic muscles. Participants may be able to better volitionally control powered prostheses which could help them with tasks related to walking, balance, or postural control. We plan to examine this method with additional participants and to test the effect on different balance and postural control tasks.

References: [1] Fleming et al. (2023) *Sci. Robot.* **8**, eadf5758 [2] Huang and Huang (2019) *IEEE TNSRE.* **27:** 85-95 [3] Huang et al. (2014) *J. Med. Devices.* **8:** 024501 [4] Winter (1983) *J. Mot. Behav.* **15:** 302-330

Relationships between bilateral squat symmetry 3 months post-anterior cruciate ligament reconstruction and countermovement jump symmetry at time of return to sport in collegiate athletes

Daniel G. Cobian[1,2,3*], Keith A. Knurr[1,2,3], Mikel R. Joachim[1,2]
[1]Department of Orthopedics and Rehabilitation, University of Wisconsin-Madison, Madison, WI
[2]Badger Athletic Performance Program, University of Wisconsin-Madison, Madison, WI
[3]Doctor of Physical Therapy Program, University of Wisconsin-Madison, Madison, WI
*cobian@ortho.wisc.edu

Introduction: Asymmetrical lower extremity biomechanics are commonly observed during running [1], jumping [2], and other athletic movements [3] after anterior cruciate ligament reconstruction (ACLR). These abnormal movement strategies may impair on-field performance [4], contribute to increased re-injury risk [5], and contribute to the development and/or progression of post-traumatic osteoarthritis [6]. As such, restoring movement symmetry remains a goal of rehabilitation efforts post-ACLR. A growing volume of evidence suggests "early" (e.g. 1-4 months post-ACLR) post-operative outcomes may have predictive value in determining outcomes at the time of return to sport [7,8,9]. Thus, the purpose of this study was to investigate the relationships between bilateral squat symmetry assessed at 12 weeks post-surgery and countermovement jump symmetry at the time of return to sport in Division I collegiate athletes.

Methods: Bilateral squatting performance was assessed at 12.0 ± 2.0 weeks (3-months) post-ACLR in 36 Division I athletes (17 females) who underwent unilateral ACLR. Athletes were instructed to perform a bilateral squatting movement with hands on hips to a depth of 90° of knee flexion while following visual cues to promote a movement tempo of 1 second down and 1 second up across 5 consecutive trials. A dual force plate system was utilized for the assessment of between-limb symmetry (Leonardo Mechanograph GRFP, Novotec Medical, Pforzheim, Germany). Ground reaction force (GRF) signals were sampled at 800 Hz and peak eccentric phase force symmetry ($Squat_{ECC}$) and peak concentric phase force symmetry ($Squat_{CON}$) were computed. At 8.1 ± 1.4 months (8-months) post-ACLR, athletes performed countermovement jumps (CMJ) while 3D kinematics and ground reaction forces were recorded. Peak GRF symmetry during the eccentric ($CMJ_{ECC\text{-}PF}$), concentric ($CMJ_{CON\text{-}PF}$), and landing ($CMJ_{LAND\text{-}PF}$) phases were computed, along with between-limb symmetry of knee positive ($CMJ_{CON\text{-}KPW}$) and negative work ($CMJ_{ECC\text{-}KNW}$ and $CMJ_{LAND\text{-}KNW}$). Limb Symmetry Indices (LSI) were calculated for all variables. All between-limb symmetry calculations utilized the formula: *[1 - (Nonsurgical Limb – Surgical Limb)/(Nonsurgical Limb + Surgical Limb)] x 100* [10]. Multivariable regression models were constructed using 3-month $Squat_{ECC}$ and $Squat_{CON}$ symmetry as predictors of 8-month GRF, knee positive work, and knee negative work symmetry. R^2 results with associated p-values are reported.

Results: Descriptive statistics for all variables and between-limb symmetry calculations are reported in Table 1. 3-month $Squat_{ECC}$ and $Squat_{CON}$ LSIs were significantly associated with 8-month $CMJ_{LAND\text{-}PF}$ LSI (R^2=0.32, p<0.01) and 8-month $CMJ_{LAND\text{-}KNW}$ LSI (R^2=0.22, p=0.02). 3-month squatting symmetry explained approximately 30% of the variance in 8-month peak GRF symmetry and 20% of the variance in 8-month knee kinetic symmetry during the landing phase of the CMJ. No other significant associations were detected.

Discussion: Weak-to-moderate associations were observed between 3-month squatting symmetry and 8-month CMJ landing symmetry in Division I collegiate athletes post-ACLR. Athletes with more pronounced squatting asymmetries early post-ACLR may struggle to achieve desired between-limb symmetries during more dynamic tasks near the time of return-to-sport, as demonstrated by the associations we observed between 3-month squatting performance and 8-month CMJ landing symmetry. As altered knee biomechanics during jump landing tasks may increase knee injury risk [5], maximizing bilateral squatting symmetry early post-surgery may contribute to improved jump symmetry later in rehabilitation, potentially reducing re-injury risk.

Significance: Earlier resolution of bilateral squatting symmetry post-ACLR may improve jump landing symmetry near the time of return to sport in competitive athletes. Following ACLR, rehabilitation interventions should aim to maximize bilateral squat symmetry within 3 months post-surgery.

Time Period	Variable	Nonsurgical	Surgical	LSI (%)
3-month	Squat Eccentric Peak Force (N/kg)	3.2 (0.9)	2.8 (0.7)	94.7 (9.1)
3-month	Squat Concentric Peak Force (N/kg)	4.2 (1.0)	3.5 (0.9)	90.6 (8.2)
8-month	CMJ Eccentric Peak Force (N/kg)	9.9 (1.3)	9.2 (1.4)	95.7 (6.0)
8-month	CMJ Concentric Peak Force (N/kg)	11.6 (1.3)	10.4 (1.4)	94.5 (4.1)
8-month	CMJ Landing Peak Force (N/kg)	18.7 (4.6)	16.3 (4.1)	93.1 (10.1)
8-month	CMJ Eccentric Knee Negative Work (J/kg)	0.39 (0.13)	0.26 (0.09)	81.1 (17.6)
8-month	CMJ Concentric Knee Positive Work (J/kg)	1.16 (0.23)	0.81 (0.21)	81.6 (10.3)
8-month	CMJ Landing Knee Negative Work (J/kg)	1.19 (0.36)	0.78 (0.28)	78.3 (17.1)

Table 1. Descriptive statistics and limb symmetry indices for all 3-month and 8-month post-ACLR variables of interest. Means and associated standard deviations are reported.

References: [1] Knurr et al. (2021), *AJSM* 49(10); [2] Kotsifaki et al. (2023), *BJSM* 57(20); [3] King et al. (2019), *AJSM* 47(5); [4] Wise (2019), *OJSM* 18;7(4); [5] Paterno et al. (2010), *AJSM* 38(10); [6] Chaudhari et al. (2008), *MSSE* 40(2); [7] Beischer et al. (2019), *BMJ Open* 26;5(1); [8] Pua et al. (2017), *JOSPT* 47(11); [9] Pietrosimone et al. (2018), *JOR* 36(11); [10] Bishop et al. (2018), *S&C Journal* 40(4)

THE EFFECTS OF STABILIZED ADDRESS POSTURE ON THE HAND AND WRIST MOVEMENT CONSISTENCY IN GOLF PUTTING: PRELIMINARY RESULT

Sung Eun Kim[1], Hannah Heigold[2], Amy L. Ladd[1*]
[1]Department of Orthopaedic Surgery, Stanford University / Stanford, CA, USA.
[2]Department of Bioengineering, Stanford University / Stanford, CA, USA.
*Corresponding author's email: alad@stanford.edu

Introduction: Measuring performance, rather than using technology as a training tool has been the current focus, with intention to improve performance as the purpose [1]. Identifying a biomarker that is associated with performance is needed in order to develop such a training tool. A previous study found that external stabilization reduces the metabolic cost and variability in step width during walking [2]. However, the association between the stability and movement consistency of the upper-limb distal segment has yet to be investigated. In golf, putting contributes to almost half of the overall performance outcome (score), and the consistency of hand and wrist movements plays an important role.

Therefore, this research aims to confirm the impact of stability on the consistency of hand and wrist movements in golf putting as a pilot study before collecting a large dataset. For an intervention to improve address posture stability, participants were asked to perform address posture on an unstable surface. The specific aim was to assess the consistency of hand and wrist movement before and after that intervention. We hypothesize that the intervention lowers the center of mass (COM) and increases lower-limb joint angles, indicating a more stable address posture. Furthermore, we hypothesized that the more stabilized address posture will result in improved consistency of hand and wrist movements during golf putting.

Figure 1: The intervention

Methods: Recreational golfers (n = 4) participated in this study. OpenCap, which only needs phone cameras to capture 3D human dynamics [3], was equipped on the actual putting green (3 iPhones, 120 Hz) and one inertial measurement unit (IMU) was placed on the lead wrist (Vicon Blue Trident, 1125 Hz). Ten trials of 4 m putting per condition (the pre- and post- intervention) were captured. For the intervention, participants were asked addressing on the balance plate (BOSU®) for 2 minutes, with guidance from a golf expert (Fig 1).

For the data analysis, the COM and lower-limb angles from OpenCap and the acceleration data from IMU were filtered using a Butterworth low-pass filter with a cut-off frequency of 4 Hz. The acceleration data from the IMU were used to calculate wrist consistency: the variabilities of peak resultant linear accelerations during backswing and downswing and the variability of timing between those peaks. The variability of timing was the first time used in a golf putting study and was chosen because the tempo is critical in golf putting (coaches often use the piano metronome to train golfers). The acceleration data was only calculated when we clearly saw the swing events of backswing and downswing, as the 4 m putt requires the short length of the swing path, and some trials had difficulty distinguishing the swing events. For the future, we will add one more IMU to help determine the swing events. For instance, give the other IMU up and down by the researcher just before the golfer's putting stroke starts.

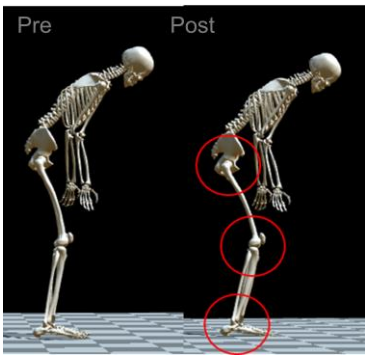

Figure 2: Lower-limb angles between pre- and post- intervention

Results & Discussion: As we hypothesized, the intervention lowered the COM by 1-2 cm with increased lower-limb (hip, knee, ankle) flexion angles by 3-10° for all participants (10 trials) (Fig 2). As partially we hypothesized, out of three variables for wrist consistency, one participant improved for all three, another for two, and two others for one by 27-65% (5-7 trials) (Fig 3).

This pilot study shows the feasibility that stabilization at the address posture could be the biomarker associated with golf putting performance, and it is worth investigating further with a larger dataset. This finding is consistent with a previous study that found external stabilization during walking can reduce metabolic costs and variability in step width [2].

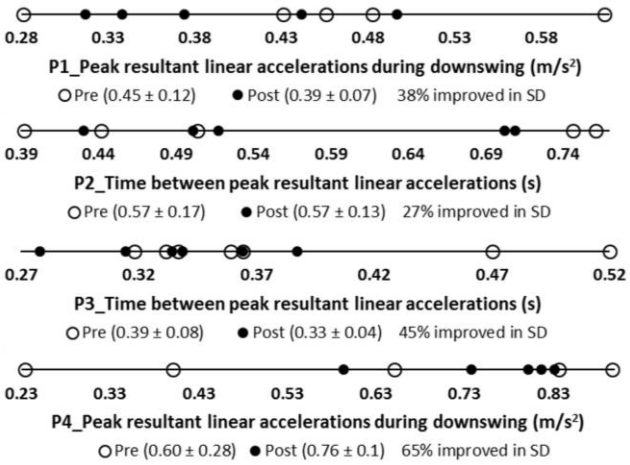

Figure 3: Each participant's representative wrist consistency

Significance: This finding implies that postural changes can have an immediate impact on performance, unlike muscle strengthening. It can also be utilized in digital sports coaching to provide meaningful information beyond motion measurement.

Acknowledgments: We truly thank the Human Performance Lab, Stanford University, and Stanford Golf Course for supports on the use of their resources.

References: [1] Smith A et al. (2012), *9th Conf Int Sports Eng Assoc* 34, 224-229; [2] Donelan JM et al. (2004), *J Biomech* 37, 827-835; [3] Uhlrich SD et al. (2023), *Plos Comput Biol* 19(10).

PERFORMANCE EVALUATION OF HANDS-FREE LEAN-TO-STEER CONTROL OF A BALLBOT WHEELCHAIR

Seung Yun Song[1], Nadja Marin[1], Chenzhang Xiao[1], Mahshid Mansouri[1], Yu Chen[1],
João Ramos[1], W. Robert Norris[2], Elizabeth T. Hsiao-Wecksler[1]*
[1] Mechanical Science & Engineering, [2] Industrial & Enterprise Systems Engineering, University of Illinois at Urbana-Champaign
*Corresponding author's email: ethw@illinois.edu

Introduction: PURE is a novel ballbot wheelchair controlled with torso motions to provide a Personal Unique Rolling Experience for manual wheelchair users (mWCUs) (Fig. 1a). It features a unique ballbot drivetrain to provide dynamic stability and omnidirectional movement ability [1]. To accommodate limited torso range of motion of some mWCUs, a Torso-dynamics Estimation System (TES), based on an IMU and custom force plate, is integrated into the seat [2]. A control interface with tunable sensitivity was developed to convert TES torso motions into omnidirectional translation commands (steer, slide, spin) for hands-free (HF) control (Fig. 1b-d). Braking is achieved by leaning backward. The performances of HF and baseline joystick (JS) control of PURE during indoor navigation tests and HF braking performance tests were compared between mWCUs and able-bodied users (ABUs). We hypothesized no significant difference in the performance of HF and JS control in the navigation tests and HF braking between mWCUs and ABUs.

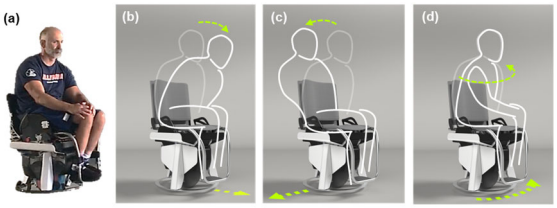

Figure 1. (a) PURE, a ballbot based wheelchair that uses (b-d) torso based hands-free control.

Methods: Twenty young adults, ABUs (5M:5F, 24.6±3.2 yrs, 62.0±11.3 kg) and mWCUs (5M:5F, 26.0±5.3 yrs, 53.8±11.4 kg), provided informed consent to participate in this IRB-approved study. Before the test, the seat on PURE was individually adjusted for each rider to ensure comfort and safety. Subsequently, the participant underwent training on riding PURE with HF and JS control in a training course with delineated boundaries and obstacles. During the training, the sensitivity parameters for the HF control scheme were customized during this process, aiming for the completion of the courses without collisions. The test course consisted of four laps with different layouts and difficulties based on six sections: 1) straight, 2) turn left/right, 3) bathroom, 4) lateral slide, 5) static obstacle, and/or 6) moving obstacle (Fig. 2). Sections 1 - 2 were repeated for wide, medium, narrow, and extremely narrow widths (244, 183, 122, and 61 cm). For each section, number of collisions (N_C) and successful completion time (T_{SC}) were recorded (averaged for sections with various width). Following completing the test, each participant filled out a NASA Task Load indeX (TLX) [3] survey to measure subjective mental and physical workload. The following metrics were utilized for assessment of effectiveness, efficiency, comfort, and robustness, respectively: N_C, T_{SC}, six NASA TLX scores, and two indexes of performance (IOPs) for straight and turn sections (derived from Accot-Zhai Steering Law [4]). Two repeated-measures MANOVA tests were performed to assess the performance difference between 1) control: HF and JS, and 2) group: mWCUs and ABUs. They include a three-way MANOVA {control × group × section} with two dependent variables (N_C, T_{SC}) and a two-way MANOVA {control × group} with eight dependent variables (six NASA TLX scores + two IOP). Follow-up univariate ANOVAs were performed for significant dependent variables. A braking test was performed to assess HF braking performance when driving PURE at a walking speed of 1.4 m/s. Braking time (T_b), braking distance (L_b) and normalized maximum torso torque (τ_{norm}) and ROM (ϕ_{norm}) were obtained. Normalization based on subject-specific maximum value for same metric during a seated ROM test. A MANOVA test was conducted on these four metrics.

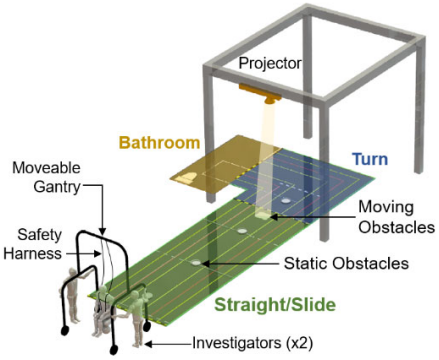

Figure 2. Test courses was divided into sections replicating real-life indoor environments. For safety, the divisions, widths, and obstacles were made using tape, flat objects, or projected images.

Results & Discussion: ABUs and mWCUs had comparable performance across all tests. The MANOVA tests found no statistically significant differences ($p > 0.05$) between the HF and JS control for all selected performance metrics, except for physical demand score from NASA TLX survey, where HF was reported to be more physically demanding ($p < 0.001$ for ANOVA). The tests also suggested no statistically significant differences between the navigation performance of mWCUs and ABUs. In the braking test (TABLE I), both groups were able to brake within 3m. The MANOVA test found no statistically significant difference for ABUs and mWCUs during braking ($p = 0.4$), although mWCUs had trends of lower braking performance (T_b, L_b) and higher effort (τ_{norm}, ϕ_{norm}). Hence, HF control of PURE is as effective, efficient, comfortable, and robust as the baseline JS control for mWCUs and ABUs, with comparable braking for both groups.

TABLE I. BENCHMARK RESUTLS FOR BRAKING TEST

	T_b (sec)	L_b (m)	τ_{norm} (%)	ϕ_{norm}(%)
mWCUs	2.7±0.3	2.7±0.4	77.6±57.0	139.5±106.4
ABUs	2.3±0.6	2.4±0.4	35.0±9.4	85.3±28.0
Diff.	14.3%	10.0%	121.7%	63.5%

Significance: PURE's lean-to-steer hands-free control can afford mWCUs the opportunity to use their hands for other life experiences such as holding hands with a loved one during a stroll and reduced upper extremity overuse injury from wheelchair propulsion.

Acknowledgements: NSF NRI #2024905. Thanks to Coach Adam Bleakney, Dr. Jeannette Elliot, Prof. Deana McDonagh, Dr. Patricia Malik, Yixiang Guo, Chentai Yuan, Eddie Kwon, Patric Li, and Yintao Zhou.

References: [1] C. Xiao et al. *IROS*, 2023. [2] S.Y. Song et al. *IEEE ROMAN*, 2023. [3] S.G. Hart and L.E. Staveland, *Human Mental Workload*, pp.139–183, 1988. [4] S. Zhai and R. Woltjer, *IEEE Virtual Reality*, pp. 149–156, 2003.

THE INFLUENCE OF CONCURRENT SPEECH AND PURSUIT ROTOR TRACKING ON MANUAL KINEMATIC VARIABILITY

Adam M. Fullenkamp[1*], Jason A. Whitfield[2], Zoe Kriegel[3]
[1]School of Applied Human Development/Exercise Science Program, Bowling Green State University, Bowling Green, OH
[2]Department of Communication Sciences and Disorders, Bowling Green State University, Bowling Green, OH
[3]Division of Communication Disorders, University of Wyoming, Laramie, WY
*Corresponding author's email: fullena@bgsu.edu

Introduction: Manual pursuit rotor tasks (PRT) have been used to study the influence of dual-task conditions on speech performance [1,2]. Specifically, Whitfield et al. [2] observed that concurrent speaking and PRT performance resulted in a reduction in speech intensity (i.e. loudness) and lip aperture range compared to speaking alone. Further, the authors observed that there was no change in PRT tracking performance (as indicated by % time-on-target) between single-task (PRT tracking-only) and dual-task conditions. The findings emphasized the influence of concurrent manual tracking on speech, but did not observe a bi-directional effect of speech on manual tracking based upon PRT tracking performance alone. Although tracking performance was not changed under the dual-task condition, it is possible that other elements of manual kinematic performance were affected. For example, imagine two different individuals walking a tightrope. Both may successfully complete the task of walking to the other side, but one may demonstrate significantly more stability in completing the task. Likewise, other aspects of manual kinematic performance, aside from success in meeting higher-order task goals, may be affected by concurrent speaking and PRT tracking. In this study, we proposed the evaluation of manual kinematic variability during single- (tracking only) and dual-task (tracking and speaking) conditions. A significant challenge associated with evaluating movement variability during a PRT is that smaller kinematic aberrations are transposed over top of larger, goal-directed oscillations. Regular, sinusoidal movement in both the anterior-posterior and medial-lateral directions are expected as a participant follows the target around a circular path. Accordingly, the goal of kinematic analyses is to ignore the larger amplitude rotary movements and to compare smaller, transient movements about the tracking path. Here we present a method of analysis intended to achieve isolated kinematic variability assessment. It was hypothesized that the removal of large amplitude rotary oscillation from manual kinematic data would allow for the observation of smaller amplitude variability differences associated with dual-task performance.

Methods: Eighteen, college-aged female participants were recruited for this study. All participants provided informed consent as approved by the local IRB. Each participant performed 10 PRT trials under both single-task (PRT tracking-only; ST) and dual-task (tracking and speaking; DT) conditions. The goal performance for all PRT trials was 70% time-on-target (TOT). The speech condition involved repeating the phrase, "Buy Bobby a puppy." This utterance reflects a bilabial speech pattern commonly employed in clinical practice. Manual kinematic performance was evaluated by analyzing the x- and y-direction movement of a computer mouse controlled by participants during the PRT. Both x- and y-direction movement variability was assessed to ensure that findings were not unidimensional. Composite kinematic variability was determined by calculating the standard deviation of raw mouse movement during each trial (SD_C). Determination of isolated kinematic variability was accomplished by first filtering the rotary oscillations from the raw kinematic waveform. In every case, rotary oscillations represented the lowest movement frequency as well as the movement frequency of greatest power amplitude. Accordingly, linear power spectral density analyses were conducted to identify the frequency of rotary oscillation (F_{peak}). Next, a 4th order, high-pass filter was applied to the kinematic waveform with a cut-off of F_{peak} + 0.1Hz. Finally, isolated kinematic variability was determined by calculating the standard deviation from the filtered waveform (SD_I). Kinematic variability was compared using paired-samples t-tests at an alpha level of 0.05.

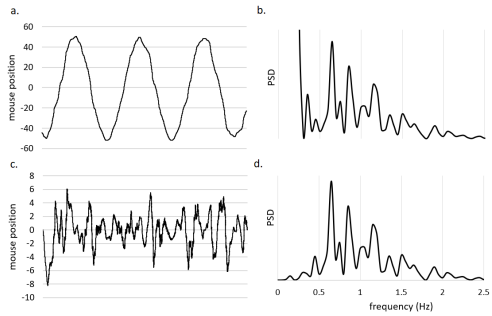

Figure 1: Example of a composite kinematic waveform (a) and its associated power spectral density (b). Example of the isolated waveform (c) and the associated power spectral density (d).

Results & Discussion: Figure 1 depicts a representative composite kinematic waveform and the associated power spectral density profile (a & b) as well as the processed, isolated version of the same kinematic data (c & d). A comparison of ST and DT composite variability revealed no significant difference in either the x- or y-direction ($p = 0.22$ and $p = 0.06$, respectively). However, comparison of ST and DT isolated variability metrics demonstrated a clear effect of DT on manual motor performance. Specifically, the DT condition resulted in increased isolated kinematic variability compared to ST in both the x- and y-direction ($SD_I = 2.56$ vs. 2.37, respectively for x, $SD_I = 2.25$ vs. 2.09, respectively for y; $p < 0.001$). The results demonstrate that the isolation of manual kinematics not associated with the pursuit rotor task-specific oscillations allowed for observation of DT effects. Essentially, although participants achieved similar task-level success in both DT and ST conditions, the kinematic variability associated with smaller, localized movements throughout each trial were clearly affected by DT interference.

Significance: The interpretation of DT influences on motor performance relies on the ability to detect subtle changes in kinematics. The method described in this abstract offers an assessment with improved sensitivity to kinematic variability in a manual PRT.

References: [1] Whitfield & Goberman (2017), *JSLHR* 60(6S); [2] Whitfield et al. (2021), *JSLHR* 64(6S).

MEDIOLATERAL FOOT PLACEMENT CONTROL IN HUMAN WALKING EXHIBITS ADAPTIVE ADJUSTMENTS

Seongwoo Mun[1], Corbin M. Rasmussen[1], Nathaniel H. Hunt[1*]
[1]Department of Biomechanics, University of Nebraska at Omaha, Omaha, NE, USA
email: nhunt@unomaha.edu

Introduction: Achieving stable gait necessitates the precise control of the body's center of mass (CoM) in relation to the base of support, which can be established through appropriate foot placement. Previous studies have established a linear relationship between deviations in CoM trajectory and subsequent foot placement adjustments [1]. However, it remains unclear whether adaptive adjustments occur in this relationship. In this study, we sought to elucidate the adaptive nature of foot placement control by exposing participants to repetitive and systematic perturbations.

Methods: Nine young, healthy participants engaged in walking sessions conducted within the Computer Assisted Rehabilitation Environment (CAREN, Motek Medical B.V., Amsterdam, Netherlands), comprising a treadmill mounted on a movable platform with a 180° cylindrical screen projecting a virtual environment. Kinematic data from 15 reflective markers (five on the pelvis, four on each foot, and one on each shank) were captured using a 10-camera motion capture system (Vicon, Oxford Metrics, Oxford, UK). Participants underwent five continuous periods, walking for a total of 40 minutes. Two 5-minute perturbation periods, involving Lateral Perturbations (LP) and Medial Perturbations (MP), were interspersed with three 10-minute periods of normal walking. On every step, the perturbations translated the stance foot 5 cm during single stance phase in either the lateral direction during LP or in the medial direction during MP. Intermittent catch steps, left unperturbed, were randomly introduced once every 20 steps to observe potential gradual motor adaptation. The position of the CoM was estimated as the pelvis position. An equation relating CoM position at midstance to the subsequent mediolateral step placement was derived during unperturbed walking. Subsequently, modeled step width was computed using CoM position in the following periods, and actual widths were compared with the modeled step width using paired t-tests.

Results & Discussion: Given that repetitive MP translated the stance foot in the medial direction, we anticipated a compensatory widening of step width. Consequently, we hypothesized a gradual widening in step width compared to the modeled step width over the 5-minute MP period. However, significant deviations were found as early as the initial 30 seconds of the MP period (Fig. 1A, 1B), indicating rapid coordination adjustments between the body's CoM and foot placement in response to balance perturbations. In contrast, we expected a gradual narrowing in step width during adaptation to LP. However, unlike MP, LP did not significantly alter step width compared to the modeled step width, underscoring the greater sensitivity of balance control adjustments to medial rather than lateral foot placement perturbations. Moreover, only MP induced an aftereffect of widened step width compared to the modeled step width post-perturbation. The gradual decay of this aftereffect over approximately 60 seconds suggests that error-based motor adaptation is involved in dynamic balance control using mediolateral foot placement in response to body's CoM.

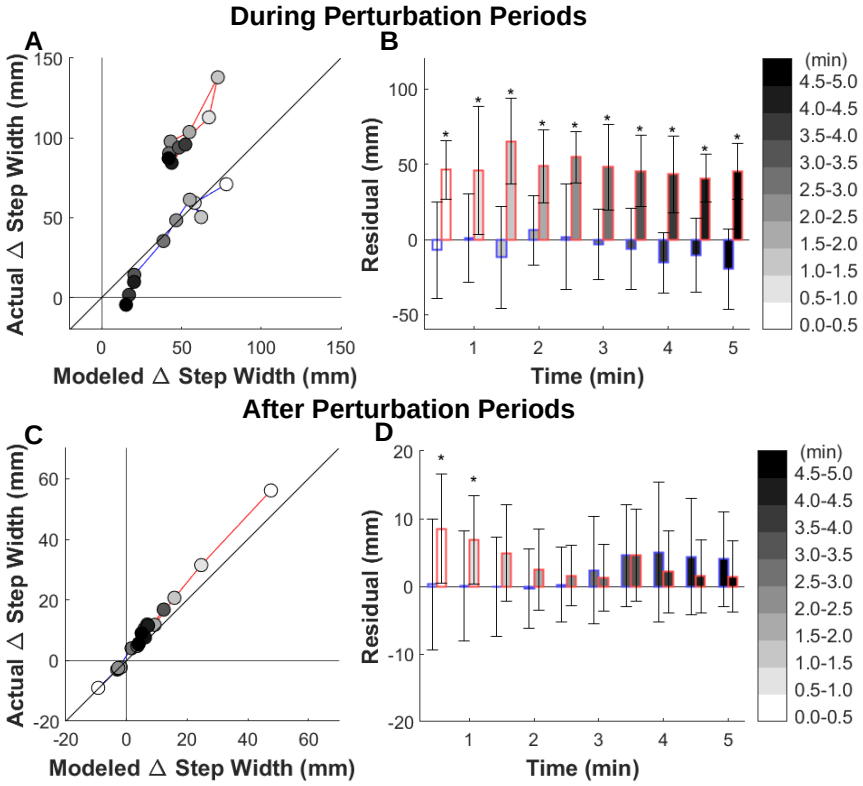

Figure 1: Changes in step width control during (A, B) and after (C, D) perturbation periods. Each data point represents the average value across each 30 second section. Data with red lines represent MP, and with blue lines represent LP. (A, C): Modeled Δ Step width was calculated using pelvis position at midstance. (B, D): Residual was calculated as the distance from actual Δ step width to modeled Δ step width. Error bars indicate standard deviation, and asterisks (*) indicate significant differences between conditions at an alpha level of 0.05.

Significance: Understanding the adaptability of balance control based on healthy adults' foot placement can serve as a foundation for research aimed at improving gait in seniors at high risk of falls or individuals with walking difficulties. Additionally, it can provide valuable groundwork for the development of learning algorithms for bipedal robots to walk in diverse environments.

Acknowledgments: This study is funded by Graduate Research and Creative Activity

References: [1] Wang (2014), *Biol. Lett.*, 10(9)

Changes in step down kinematics after foot strike run retraining in individuals with patellofemoral pain

Adam C. Bunn[1,2], Scot Morrison[3], Richard Willy[4], Marisa Pontillo[1,2]
[1]1Extremity Trauma and Amputation Center of Excellence, San Diego, CA
[2]Department of Physical and Occupational Therapy, Chiropractic Services, and Sports Medicine, Naval Medical Center San Diego, San Diego, CA, USA
[3] Miami Marlins
[4]University of Montana
*Corresponding author's email: adam.c.bunn.civ@health.mil

Introduction: Foot strike run retraining has been reported beneficial to individuals with patellofemoral pain to reduce running pain secondary to changes in run kinematics and kinetics.[1-5] Specifically, altering foot strike pattern from rearfoot to non-rearfoot has been shown to decrease pain and increase function in patients with patellofemoral pain (PFP) by decreasing ground reaction forces, and subsequently, loading of the knee joint. However, it is unknown if the favorable changes seen in running mechanics post training could carry over to related changes in other functional, weightbearing activities. The purpose of this study is to investigate if kinematic changes are also evident in a step-down task after foot strike run retraining in individuals with patellofemoral pain.

Methods: Nine military Service members with unilateral patellofemoral pain participated in this study: 4 males; age: 26.11±8.10 years; BMI:24.23±4.02. Participants were diagnosed with patellofemoral pain via clinical examination and were deemed appropriate for foot strike retraining as they had self-selected bilateral rearfoot strike pattern during running, and running increased their knee symptoms. Participants underwent 7.8±0.3 foot strike retraining sessions over an average of 14.0±4.3 days. Running speed was self-selected and could be adjusted during sessions. Participants received real-time, faded visual feedback on bilateral foot inclination angles, targeting a non-rearfoot strike pattern.[5,6] During treatment sessions, real-time visual feedback was provided on a television screen positioned in front of the treadmill displaying bilateral foot inclination angles[5] as a line graph (Figure 1). Joint angles for real-time feedback were provided by a series of 8 inertial measurement units affixed to the trunk and lower extremities (Movella, Enschede, Netherlands). A running analysis was completed at pre-training and post-training, including 3D kinematics and kinetics measured using a 14-camera, passive-optical motion capture system at 120 Hz with simultaneous digital camera video (Motion Analysis, Rohnert Park, CA). Ground reaction forces were collected via an instrumented treadmill (AMTI, Watertown, MA) sampling at 1200Hz. In the same sessions, participants completed one set of 5 consecutive anterior step-downs on the painful limb on a 4- or 6-inch box with their hands on their hips. Kinematic data was reduced for the step-down task, and peak angles and moments were calculated for the involved limb at the x, y, and z axes for the hip, knee, and ankle. Effect sizes (Cohen's d) were calculated to compare pre- and post- values and interpreted as 0.2=small, 0.5=medium, 0.8=large.

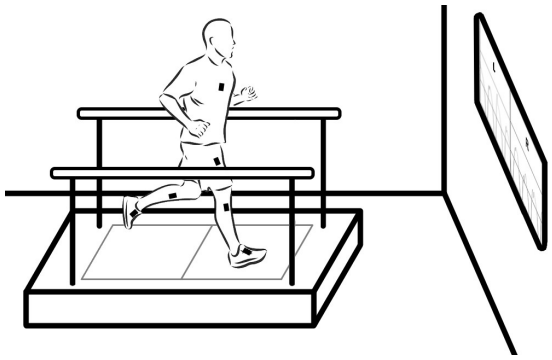

Figure 1: Real time feedback setup

Results & Discussion: For involved limb, pre- to post-training changes in peak hip angle (and effect sizes) were x=4.68°, *d*=0.38; y=0.80°, *d*=0.32; and z=3.16°, *d*=1.96, respectively. Changes in peak knee angle were x=2.99°, *d*=0.16; y=0.04°, *d*=0.04; and z=2.14°, *d*=4.70, respectively. Changes in peak ankle angles were x=-1.84°, *d*=-0.23; y=2.89°, *d*=1.90; and z=-3.79°, *d*=2.22, respectively.

Changes in peak hip moments were x=0.17, *d*=1.25; y=0.08, *d*=2.45; and z=0.02, *d*=1.59, respectively. Changes in peak knee moments were x=0.10, *d*=0.22; y=0.10, *d*=7.00; and z=-0.01, *d*=0.90, respectively. Changes in peak ankle moments were x=-0.02, *d*=-0.26; y=0.02, *d*=0.47; and z=-0.01, *d*=0.53, respectively.

Significance: Although the participants in this study received movement retraining only for running and not other weightbearing activities, these results show subtle changes were apparent post-training in step-down joint angles and joint moments in the involved lower extremity. Future work should elucidate if these preliminary changes in peak joint angle(s) and moment(s) could be indicative of long-term, favorable alteration in movement patterns and a concurrent reduction in knee pain and improved knee function.

Acknowledgments: The views expressed herein are those of the author(s) and do not reflect the official policy or position of the Naval Medical Center San Diego, the Defense Health Agency, the Department of Defense, or any agencies under the U.S. Government.

References: [1] Davis et al (2020), *Curr Rev Musculoskelet Med* 13(1). [2] Vannatta et al (2015), *Med Sci Sports Exerc* 47(5). [3] Bowersock et al (2017), *J Sports Sci* 35(20). [4] Cheung et al (2011), *J Orthop Sport Phys Ther* 41(12). [5]Yoder et al (2019), *Prosthet Orthot Int* 43(4). [6] Willy et al (2017), *Scand J Med Sci Sports*v 27(5).

Sensitivity of Prosthetic Socket Moments to Ground Incline and Two-Axis Ankle Angle

Rebecca A. Roembke[1*], Sofya Akhetova[1], Peter G. Adamczyk[1]
[1]University of Wisconsin-Madison Mechanical Engineering Dept.
*Corresponding author's email: rroembke@wisc.edu

Introduction: Walking with a misaligned prosthesis can cause rubbing and discomfort on the user's socket [1]. Prostheses are aligned to flat normal walking, but this alignment is inappropriate for walking up or down a hill, on a side slope, or with different step widths. Most prosthesis can't adapt for situations like these, leading to potential instability and discomfort. The Two Axis aDaptable Ankle (TADA) is a prosthetic ankle with the ability to plantarflex (PF), dorsiflex (DF), invert (IV), and evert (EV) up to ten degrees in each direction [2]. In this study, we explore the relationship among ground slope, ankle angle setting, and the resulting pylon moment and discomfort level. Our hypothesis is that socket moments will be linearly related to ankle angle changes in the same plane, and that users will prefer the angle setting that matches the ground slope.

Fig 1: TADA ankle-foot prosthesis with a load cell pylon adapter

Methods: The TADA ankle (Figure 1) is a semi-active system with two degrees of freedom actuated by nonbackdriveable internal cams and digital servo motors. The mechanism moves during unloaded swing phases and passively locks during stance phases to hold its current angle in support of body weight loads. For this experiment, one healthy active adult with transtibial amputation (female, 67 yrs, right amputation) walked on a treadmill with various sagittal and frontal-plane surface slopes and several settings of the TADA in each slope condition. The treadmill was inclined to 3 and 6 degrees upward, 3 degrees downward, 3 degrees leftward and 3 degrees rightward using the incline mechanism and/or elevating blocks. On 3 degree slopes, the TADA was set to ankle angles of 0, 2, 3, 5, 7, 9 degrees in the assistive direction (e.g. dorsiflexion for inclines, eversion for right-inclined surface, etc.), and for the 6 degree incline, to 0, 2, 4, 6, 8, and 10 degrees dorsiflexion. A wireless pylon load cell was mounted above the prosthetic ankle to measure pylon moments during walking. The subject was instrumented with full body a XSENS motion capture suit and data were recorded during trials to measure body kinematics. At least 25 steps were taken in each condition; 10 steps were allowed to acclimate to the condition, and 10 clean strides thereafter were analyzed. We measured the peak moments in the sagittal and frontal planes. We analyzed frontal plane moment in conditions where frontal plane angles were manipulated (IV/EV) and sagittal plane moments in conditions where sagittal plane angles were manipulated (PF/DF). We evaluated the sensitivity of moment to in-plane angle changes using statistical significance of the coefficient of a linear fit (α=0.05). The subject rated each condition using a discomfort scale of 0-10.

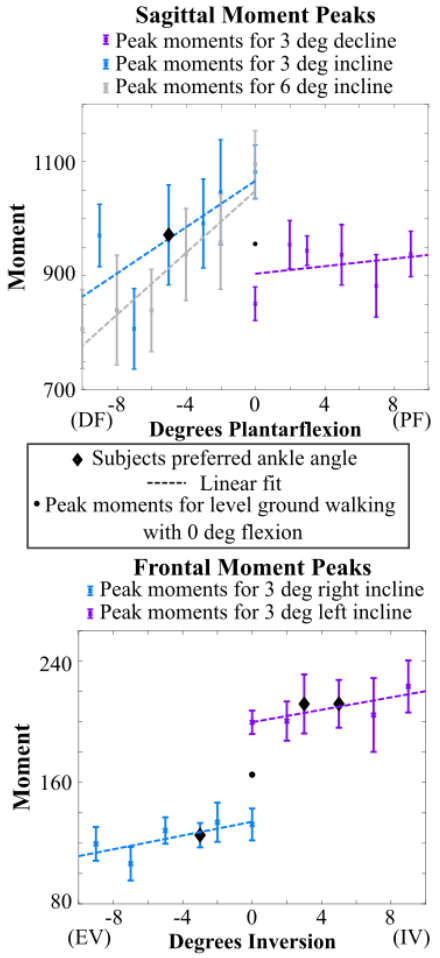

Fig 2: Peak moments for different slopes and TADA angles, with linear fits.

Results & Discussion: For a side ground slope of 3 degrees, an increase in IV tended toward an increase in peak frontal moments and an increase in EV tended toward a decrease in peak frontal moment, though variability rendered these effects statistically marginal (see Table). Despite this positive sensitivity of frontal moment to IV, the subject rated 3 and 5 degree IV and 3 degrees EV as the least uncomfortable. For inclines, the sagittal moment peaks tended to be larger in conditions with increasing PF, with substantial variability; for the 6 degree incline, the trend was statistically significant. The decline (downhill) condition did not show a clear trend. For a 3 degree incline the subject's preferred alignment was 5 degree DF, but preferences for 3 degree decline and 6 degree incline were unclear. The extreme PF conditions in downhill walking led to some toe scuffing and the participant strongly disliked walking with 7 and 9 degree PF.

Table 1: Linear slope fits and statistics

Slope Condition	Linear Fit Slope	P-value
3 degree right incline	2.27	0.0898
3 degree left incline	2.05	0.0783
3 degree decline	3.29	0.611
3 degree incline	20.28	0.113
6 degree incline	27.12	0.00488*

Significance: This study explores the relationship between prosthetic ankle angle and ground incline in both the sagittal and frontal planes. The pylon moments and patient feedback show that a neutral ankle is not always the preferred nor the most comfortable ankle angle for slopes despite it being the configuration users are typically stuck with. These results show a need for foot angle adjustability in cases such as hills or sloped sidewalks. The TADA and other adaptable systems may give persons with amputation the freedom to do activities they may have been previously uncomfortable with, such as hiking. Testing with additional participants will further cement and clarify the observed effects.

Acknowledgments: Supported by DOD W81XWH-20-1-0884 and NSF GRFP through DGE-1747503. Views do not reflect official policy of nor implied endorsement by the DoD, NSF, nor US Government.

References: [1] Kobayashi et al. (2014), *J Biomech* 47(6); [2] Adamczyk, Chapter 9 in Dallali+ ed. (2020), *Acad. Press*.

Assessing CO_2 levels exhibited in nose deformation

Giada A. Brandes[1*], Holly L.Overa[2], Andrew Bossert[3], and Erin M. Mannen, PhD[4]
Boise Applied Biomechanics of Infants Lab, Boise State University, Boise, ID
*email: giadabrandes@u.boisestate.edu

Introduction: The nose is a primary system for respiration, acting as airway filtration and thermal regulation. Obstructed breathing during sleep (OBS) creates a challenge for nasal respiration during the night, affecting nearly 24% of the population between ages 30 to 60 years old. OBS derives from infectious, genetic, and physiological factors, affecting an individual's nasal resistance. Nasal resistance is calculated using the radius of the nose's entrance near the nasal valve, which is the narrowest part of the nose and divides the nasal cavities with a thin cartilage. Dilator muscles within the nose are able to manipulate the size and shape of the nasal valve, allowing more or less air to pass through. Because airflow depends on the radius of the nasal entrance, physiological features such as soft, deformable cartilage or even abnormal tissue such as cysts, can alter breathing patterns throughout each individual [1]. The ultimate goal of this research is to apply the mechanics of adult nasal breathing and deformation to infant physiology. Neonates and infants have underdeveloped nasal cavities which cause higher nasal resistance caused by the radially smaller middle cavity and the lack of an inferior meatus, resulting in less airflow [2].

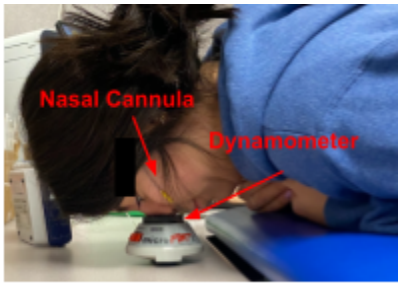

Figure 1: Participant performing "tip-down" nasal orientation on the dynamometer with a nasal cannula.

Methods: Six young, healthy adults (21.3∓1.7, 3M/3F) were asked to lay prone on a bench and rest their noses on a MicroFet dynamometer. Afterwards, the peak force was recorded in Newtons using the device. Participants' noses were in contact with the plate with inserted nasal cannulas that were connected to a Capnostream 35 Portable Respiratory Monitor. To simulate face-down positioning on a pillow, four explicit nose deformations were defined as right ala closed, left ala closed, the tip of the nose pushed upwards, and the tip of the nose pressed downwards which is shown in Figure 1. Participants completed five trials for each nose deformation, totaling 21 trials per participant which includes the control trial containing nasal respiration under no deformation (baseline reading). After an eight second duration, participants slowly lifted their head from the plate while the dynamometer read the maximum force that was exerted during the trial.

Results & Discussion: A total of 120 trials were conducted throughout the study. Overall CO_2 levels decreased from the baseline trials as shown in Figure 2, averaging 38 mm Hg across all participants. Tip-down orientation was found to have significant correlation to breathing patterns ($p = 0.01$) as all participants experienced lower CO_2 levels during this stage. Because over-breathing causes excessive loss of carbon dioxide from the blood, leading to reduced tissue oxygenation [3], this indicates that less air is being exhaled from the body. Tip-down orientation also had the largest average force reading (22.23 N) compared to the other stages. The average weight of a human head is roughly 5 kg (49.05 N), denoting that approximately 45% of the head weight is being exerted on the nose in this position. The remaining stages did not show enough significance in correlation to respiration patterns, with the left ala closed being the least significant and had the smallest force reading of 20.3 N.

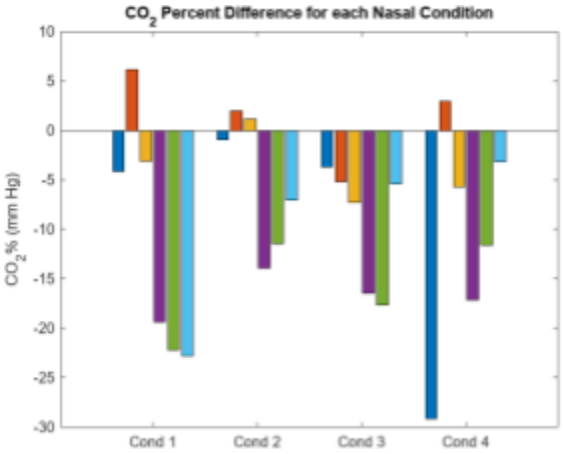

Figure 2: Graph of CO_2 percent differences for each nasal condition. Each color represents a participant (n = 6). Percentages were derived from calculating the difference between participants' baseline trials and their average CO_2 level for that specific trial. Cond 1: right ala closed, Cond 2: left ala closed, Cond 3: tip-down, Cond 4: tip-up.

Significance: Considering nasal characteristics and obstructed breathing can help mitigate effects of breathing problems, such as over-breathing, snoring, or hypercapnia. This study also demonstrates the basis of future research and development of synthetic nasal breathing devices and infant nasal respiration.

Acknowledgements: We acknowledge support from the Institutional Development Awards (IDeA) from the National Institute of General Medical Sciences of the National Institutes of Health under Grant #P20GM148321

References: [1] Mirza, Natasha "The Nasal Airway and Obstructed Breathing during Sleep". [2] Corda, John "Nasal airflow comparison in neonates, infant and adult nasal cavities using computational fluid dynamics". [3] Ruth, Allen "The health benefits of nose breathing".

ASSESSING NEUROMUSCULAR CHARACTERISTICS OF STATIC POSTURAL CONTROL IN AUTISM USING ELECTROMYOGRAPHY AND POSTUROGRAPHY

Isabel Munoz Orozco[1†], Stacey B. Hirsch[1†], Tylan N. Templin[2], Nicholas E. Fears[1,3], Haylie L. Miller[1*]
[1]School of Kinesiology, University of Michigan
[2]Southwest Research Institute
[3]School of Kinesiology, Louisiana State University
[†] Co-first authors
*Corresponding author's email: millerhl@umich.edu

Introduction: Autism is a complex neurodevelopmental condition characterized by social-communication and commonly observed motor differences including atypical gait, clumsiness, and difficulty with postural control [1, 2]. Although postural control differences are seen across the autistic lifespan, their underlying sensorimotor mechanisms are not well-characterized [2]. Existing literature demonstrates that autistic people exhibit differences in sensory reweighting ability when visual or proprioceptive information is manipulated, manifesting in greater postural sway, greater sway variability in the medial-lateral directions, and an increase in center or pressure (CoP) variability compared to neurotypical people [2-5]. However, few studies have quantified the relation between patterns of muscle activation, coactivation/synergies across muscle groups, and sway variability in autism especially during quiet standing [6]. To understand the neuromuscular mechanisms underlying autistic postural control problems, we aimed to quantify differences in muscle activation patterns between autistic and neurotypical people: (1) in relation to CoP sway area, and (2) under different surface (e.g., firm, foam) and visual (e.g., eyes open, eyes open with directed fixation point, eyes closed) conditions.

Due to known differences in vision, proprioception, and sensory reweighting ability, we expected that autistic participants would have larger sway area and longer sway path length than neurotypical participants in conditions with less reliable visual or proprioceptive input, but not in the optimal condition of eyes open with a directed fixation point on a firm surface. Based on earlier work in other neurological conditions showing differences in the timing and magnitude of coactivation [6, 7], we expected that autistic people would have high, consistent coactivation of agonist-antagonist pairs (e.g., tibialis anterior and gastrocnemius), whereas neurotypical participants would have lower, more variable coactivation. This pattern of results would suggest that quiet standing is more effortful for autistic people, as opposed to a relatively automatic, low-complexity task for neurotypical people [7]. Prior studies using clinical measures such as the Mini-BEST or PANESS report autistic people's tendency to fall during quiet standing with eyes closed or on foam. We expect to observe this same tendency reflected in greater maximum excursions outside of the base of support followed by higher-amplitude spikes in activation of the tibialis anterior and gastrocnemius during recovery from loss of balance compared to neurotypical.

Methods: We used integrated motion capture (Motion Analysis Corp.), immersive virtual reality with embedded force plates (CAREN; Motek Forcelink), and electromyography (EMG; Delsys Trigno) to assess 11 autistic (Male=8, Female=3) and 13 neurotypical (Male=7, Female=6) participants. Participants were instructed to stand as still as possible without moving their feet while either on a firm or foam surface with their eyes open without a target, eyes open with a directed fixation point, or eyes closed for 30 sec per trial. Six surface electrodes were placed on the lower limbs and trunk at the approximate center of muscle bodies of interest. Reflective markers were placed on anatomical landmarks of the trunk, legs, and feet and recorded by infrared cameras at 120 Hz.

Results & Discussion: Preliminary results suggest differences in postural control between autistic and neurotypical participants in some, but not all, visual and surface conditions. We compared the path length and sway area of autistic and neurotypical participants within each condition. Autistic individuals had longer path lengths than their neurotypical counterparts in the foam surface condition with eyes closed. These results suggest that autistic individuals may have greater difficulty or variability in postural control under more challenging visual and proprioceptive conditions (e.g., eyes-closed, foam surface), in line with our hypotheses. Planned integrated analyses of multi-modal EMG, force plate, and motion-capture data will provide more insight into the specific neuromotor mechanisms underlying differences in postural control task performance.

Significance: This study is relevant to the autistic community. Results can help to shed light on the specific conditions under which postural control is challenged in autism compared to neurotypicality. This can, in turn, be used to inform refinement of neurorehabilitation approaches targeting balance and mobility to meet the specific needs of autistic individuals. Tailored interventions for autistic postural control differences are needed to support physical activity participation, reduce fall risk, and improve quality of life and health outcomes.

Acknowledgments: This research was supported in part by the National Institutes of Health (K01-MH107774).

References: [1] American Psychiatric Association (2013), *DSM-5*; [2] Lim et al. (2017), *J Autism Dev Disord* 47(7); [3] Morris et al. (2015), *Neuroscience* 307; [4] Fears et al. (2022), *J Autism Dev Disord*, 16, [5] Memari et al. (2013), *Res in Autism Spectr Disord* 7(2); [6] Mohd et al. (2016), *IEEE Symp on Comp App and Industr Electr;* [7] Latash (2018), *J Neurophys* 120(1).

TIRING TASKS: A SYSTEMATIC REVIEW OF MULTIDIMENSIONAL FATIGUE ON MOVEMENT MECHANICS

Cabel J. McCandless[1*], Christopher A. Aiken[1]
[1]New Mexico State University, Department of Kinesiology
*Corresponding author's email: cmccand1@nmsu.edu

Introduction: Fatigue, a well-documented [1,2,3] phenomenon in sports and exercise, encompasses physical fatigue (PF) from prolonged or intense physical activity, and mental fatigue (MF) from cognitive exertion. Although distinct, both often coexist in performers of all types [4]. Understanding how these types of fatigue, alone or combined (CF), influence movement biomechanics is crucial for optimizing performance and minimizing injury risk. While previous studies have documented the impact of fatigue on movement, such as decreases in sprint times, muscular force production, and overall lower-limb muscle function [5], there remains a need for a systematic review to assess existing research and provide recommendations for future work. Therefore, this study aims to comprehensively evaluate existing research on the impact of physical and mental fatigue, both independently and concurrently, on movement mechanics.

Methods: This systematic review followed the "Preferred Reporting Items for Systematic Review and Meta-analyses (PRISMA)" guidelines. A comprehensive search strategy was employed across five electronic databases (Google Scholar, PubMed, Web of Science, PsycInfo, and ProQuest) from 1990 to 2023. The population, interest, and context framework (PICO) was applied to identify relevant articles focusing on healthy adults engaged in sports and exercise, subjected to physical, mental, or concurrent fatigue, and the effects on movement mechanics. Following initial screening, abstracts, conference reports, duplicates, and articles not aligned with the research objective were excluded. Subsequent full-text evaluation determined inclusion eligibility based on specific criteria: peer-reviewed articles published in English, involved healthy adults, induced fatigue (PF, MF, CF), and explored movement mechanics (kinematics or kinetics). Exclusion criteria encompassed studies solely investigating physiological responses (e.g., EEG, ECG), biochemical parameters (e.g., lactate, cortisol), or psychological effects on mental health. Data extraction included critical details such as author(s), publication year, study design, sample size, demographics, fatigue type and protocol, and key findings to ascertain the impact of fatigue on movement mechanics.

Results: The systematic review encompassed 1,112 journal articles, with 28 selected after multiple screenings. The majority of papers used a pre-post-test design (N=25), and only six in total included a control group (No fatigue). Among all the studies, half (N=14) investigated female participants, either alongside or separate from the male participants. Sample sizes ranged from medium to large, with eight studies employing sample sizes larger than 30 participants. The most common fatigue protocol was physical (N=22), typically through a running exercise (N=11). Mental and concurrent fatigue were less common in the current body of literature (N=6). Physical fatigue studies focusing on kinematics saw increases in step frequency, contact time, duty factor, movement time, sway velocity, and upper extremity joint range of motion while having decreases in aerial time, step length, limb stiffness, and joint center velocities (N=15). Physical fatigue studies with kinetic data revealed reduced muscle activations and ground reaction forces during landing and jumping tasks (N=6). In contrast, mental fatigue's impact on movement kinematics varied, showing inconsistencies in response to cognitive tasks like the Stroop test (N=4). Limited research explored mental fatigue's effect on kinetic variables, yielding conflicting findings (N=3). When examining concurrent (N=3) fatigue movement complexity decreased (slower joint kinematics, decreases in step rate and stride length), but only niche sporting populations were examined (rowers and orienteers) and all used different protocols for physical and mental fatigue.

Discussion: Despite extensive research on fatigue's impact on human movement in sports and exercise science, significant gaps persist in the literature. Physical fatigue consistently led to reduced muscle activations and ground reaction forces, underlining its critical role in performance and injury risk. However, findings on mental fatigue's influence on movement kinematics were diverse. Concurrent fatigue studies revealed decreased movement complexity in specific sports, suggesting performance implications. The absence of temporal data collection beyond pre- and post-fatigue sessions limits our understanding of fatigue's longitudinal effects. Moreover, the lack of a control (no fatigue) group in most studies hinders comprehensive comparisons. Gender disparities in research participation were also noted. Addressing these limitations through controlled experimental designs, standardized protocols, and longitudinal assessments is crucial for a nuanced understanding of fatigue's effects across diverse populations and activities, ultimately optimizing training regimens and performance outcomes.

Significance: Building structured protocols that encompass various dimensions of fatigue, including no fatigue, physical, mental, and concurrent states, is essential in kinesiology, particularly within sports and exercise research. This comprehensive review offers valuable insights into the effects of fatigue on movement mechanics, serving as a foundational resource for enhancing athlete performance. Furthermore, the findings may inform coaches and practitioners in designing targeted interventions to support performers, optimize training regimens, and minimize injury risk.

References: [1] Apte et al. (2021), Front Physiol 12; [2] Aquino et al. (2022), Biomechanics 2(4), Article 4; [3] Van Cutsem et al. (2017), Sports Med 47(8); [4] Knicker et al. (2011), Sports Med 41(4); [5] Silva et al. (2018), Sports Med 48(3).

Is there an ideal heel-toe drop for economical running?

Kaleigh Renninger[1]* & Owen N. Beck[2]
[1]Walker Department of Mechanical Engineering, The University of Texas at Austin, TX
[2]Department of Kinesiology and Health Education, The University of Texas at Austin, TX
*email: kaleigh.renninger@utexas.edu

Introduction: An athlete's distance-running performance is influenced by their rate of metabolic energy expenditure (running economy) [1]. Athletes can enhance their running economy, and in turn their running performance, by improving their running mechanics. Recent advancements in running shoe technology have improved user running mechanics, and in turn their running economy and performance. With the 2024 Olympic Games looming, it is an optimal time to further enhance athletic performance by tuning footwear properties to improve user running mechanics and economy.

One key component of running shoes is heel-toe drop. Heel-toe drop affects the sagittal plane angle of the user's ankle during stance. During running, higher heel-toe drops likely decrease the required plantar flexion muscle force by improving the ankle's effective mechanical advantage. However, higher heel-toe drops also shorten the length of the triceps surae muscle-tendon, thereby decreasing calf muscle operating lengths. Because decreasing both active muscle force production and muscle operating length have contrasting effects on the volume of activated muscle required to run [2], they also have contrasting effects on metabolic energy expenditure. Accordingly, it remains uncertain how (or if) heel-toe drop affects running economy. Based on the high-heel walking literature and the notable influence of muscle length on metabolic energy expenditure [3], we hypothesized that higher heel-toe drops would increase metabolic energy expenditure during running (decrease running economy).

Methods: Two runners participated after providing informed written consent in accordance with the University of Texas at Austin IRB. Participants performed a standing trial followed by a treadmill familiarization running trial at 3.5 m/s in their own shoes. They subsequently performed four 5-min running trials at 3.5 m/s in four footwear conditions distinguished by varying heel-toe drop heights: 0, 10, 20, & 30 mm (Fig. 1). The shoes had EVA midsole foam and Nike Pegasus upper mesh. We mass-matched all shoes by screwing small weights to the back of the shoes. We measured the runner's expired gas ($\dot{V}o_2$ uptake and $\dot{V}co_2$ production), ground reaction forces, and leg muscle activity during each trial. To calculate metabolic power, we used the $\dot{V}o_2$ and $\dot{V}co_2$ over the last 2 min of each trial and a standard equation [4]. We then subtracted the runner's standing metabolic power from each running trial and divided it by body mass to achieve mass-normalized net metabolic power (W/kg).

Table 1: Ground reaction force (GRF) and stride kinematics during running for both runners across footwear conditions (AVG ± SD).

Biomechanical Variables	0 mm	10 mm	20 mm	30 mm
Peak vGRF (BW)	2.56 ± 0.27	2.53 ± 0.3	2.53 ± 0.23	2.54 ± 0.25
Peak Braking GRF (BW)	-0.33±0.01	-0.31 ± 0.02	-0.33 ± 0.01	-0.32 ± 0.01
Peak Propulsive GRF (BW)	0.33 ± 0.08	0.32 ± 0.06	0.33 ± 0.07	0.33 ± 0.07
Duty Factor	0.33 ± 0.03	0.34 ± 0.03	0.33 ± 0.01	0.34 ± 0.02
Step Frequency (Hz)	2.81 ± 0.04	2.84 ± 0.03	2.81 ± 0.03	2.82 ± 0.02

Results & Discussion: Shoe heel-toe drop affected net metabolic power during running for P1 and P2. Compared to the 0 mm heel-toe-drop condition, P1's net metabolic power decreased 3.0 and 2.9% when running in the 10-mm and 20-mm heel-toe-drop, respectively. P2's net metabolic power decreased 4.5% when running in the 30 mm heel-toe-drop relative to the 10 mm shoe condition (Fig. 1). Biomechanically, there was no apparent relationship between heel-toe drop and ground reaction force (GRF) or kinematic variables between P1 and P2 (Table 1). Further, we combined anatomical data with measured soleus and lateral gastrocnemius muscle activity to estimate active muscle volume of calf muscles during running. Overall, P2's active calf muscle volume increased with shoe heel-toe drop, whereas P1 had no apparent trend (Fig. 1).

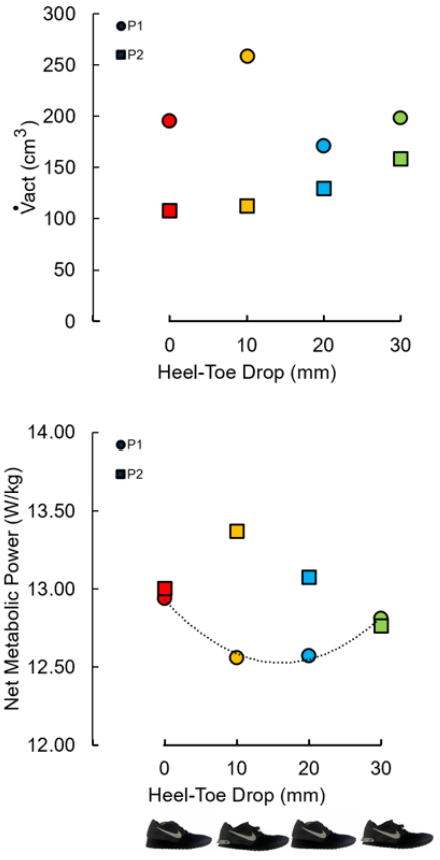

Figure 1. (Top) Estimated active muscle volume ($\dot{V}act$) of the participants' (P1 & P2) soleus & lateral gastrocnemius during running vs. shoe heel-toe drop. (Bottom) Net metabolic power vs. shoe heel-toe drops for both participants. A best fit line for P1 predicts the lowest metabolic power occurred between heel-toe drop of 10 and 20 mm.

Significance: Preliminarily, the ideal heel-toe drop for economical running either varies per athlete or does not exist. Accordingly, athletes looking to gain a competitive edge and outrun their competition may want to consider heel-toe drop when buying running shoes.

Acknowledgements: We would like to thank Dr. Rodger Kram for donating the running shoes used in this study.

References: [1] Daniels, 1985. *Med Sci Sports Exerc.* [2] Beck et al., 2019 *Exerc Sport Sci Rev.* [3] Beck et al., 2022. *J Appl Physiol.* [4] Peronnet & Massicotte, 1991. *Can. J. Sports Sci.*

Impacts of asymmetric crankarm lengths on knee biomechanics during cycling

Songning Zhang and Sean A. Brown
Kinesiology, Recreation, and Sport Studies, University of Tennessee, Knoxville, TN, USA
*Corresponding author's email: szhang@utk.edu

Introduction: Cycling is commonly employed in rehabilitation exercises for people with total knee arthroplasty (TKA) and osteoarthritis (OA). Past research has shown that patients with TKA had reduced internal knee extension moment in both cycling [1] and gait [2-4] conditions. Patients with TKA faced challenges from being fully engaged in and benefitted from this mode of exercise during the early stages of their rehabilitation [5]. Crankarm length can be adjusted and effects of symmetrical (bilateral) adjustments have been examined [6]. However, the effects of asymmetrical adjustments on knee biomechanics have not been fully explored. Such information may provide initial evidence for using differential crankarm lengths in early rehabilitation for patients with TKA. Therefore, the purpose of this study was to examine effects of adjusting crankarm lengths on one limb, while maintaining a constant crankarm length on the contralateral limb, on knee joint kinematics and kinetics in healthy participants. We hypothesized that the knee range of motion (ROM) and peak knee extension velocity would decrease with reduced crankarm lengths while the peak knee extension moment and power would not change.

Methods: Eleven recreationally active and healthy young adults (5 females, Age: 25.3±4.4 years, BMI: 24.5±3.0 kg/m^2) participated in the study. They cycled on an electrically braked cycle ergometer (Excalibur Sport, Lode) at seven different crankarm length conditions on the right limb: from 130 – 190 mm at 10 mm increments using customized adjustable crankarms. The left crankarm length was fixed at the standard 170 mm. The participants started with the 170 mm crankarm lengths on both sides while the right crankarm length was randomly adjusted in the six other conditions. The participants cycled at a fixed workrate of 100 Watts and cadence of 80 revolutions per minute. A 13-camera motion capture system (240 Hz, Vicon Motion Analysis Inc) collected 3-dimensional kinematic data and a pair of customized instrumented pedals (1200 Hz, Kistler) collected pedal reaction force data. A 2 (limb) x 7 (crankarm length) mixed model analysis of variance was performed to detect differences of selected knee kinematic and kinetic variables ($\alpha = 0.05$).

Results & Discussion: Both knee extension ROM and peak knee extension velocity saw a significant interaction ($p<0.001$). Post hoc comparisons showed that each reduction in crankarm length is associated with decreased knee ROM and peak extension velocity (all $p<0.05$, Table 1). Although there was no significant interaction for peak knee moment, it showed a trend ($p=0.072$). The post hoc comparisons showed that the crankarm lengths of 170 - 190mm decreased peak knee moment compared to 130mm, while the 190mm reduced the peak moment compared to all other crankarm lengths (Table 1). However, peak knee extension power generation showed no significant interactions or main effects of crankarm length and limb. Our hypotheses about the knee sagittal-plane ROM and peak velocity were supported by our results. With each incremental reduction of 10 mm of crankarm length, both knee extension ROM and peak extension velocity were reduced. Our hypothesis on peak knee joint moment and power were partially rejected as the peak knee joint moments were significantly reduced at crankarm lengths greater than and equal to 170 mm compared to 130 mm. These results suggest that an asymmetrical reduction of crankarm length is feasible in a healthy population, and may be beneficial to patients with TKA with stiff knee with reduced ROM. Knee joint moment results seem to also suggest that the reduced crankarm length at 130 mm requires greater knee extensor efforts compared to the normal crankarm length (170 mm) or longer (up to 190mm), and yet are not as clear as the results of the knee kinematics. In addition, increases in knee extension velocity and reductions in knee joint moment renders non-significant changes in peak knee joint power.

Significance: These results provided some of the initial evidence that small reductions in crankarm length in stationary cycling may accommodate the reduced knee ROM while still maintaining knee muscular demands for patients with TKA during their earlier rehabilitation, potentially enhancing the recovery process for patients with TKA by aligning exercise intensity with their biomechanical capabilities.

References: [1] Hummer et al. (2019), *J Biomech* 115 (110111); [2] Mandeville et l. (2007), Clin Biomech 22 (7); [3] Standifird et al. (2016), *J Arthroplasty* 31 (1); Wen et al. (2019), *J Biomech* 89 (40-47); [5] Liebs et al. (2010), *J Bone Joint Surg Am* 92 (4); [6] Barratt et al. (2016), *Med Sci Sports Exerc* 48 (4).

Table 1: Knee ROM (Deg), and peak knee velocity (Deg/s), moments (Nm) and power (Watts): Mean ± STD.

		130mm	140mm	150mm	160mm	170mm	180mm	190mm
Extension ROM	Left	77.1±8.1	77.7±8.5	77.6±8.1	77.4±7.8	77.4±8.9	77.6±8.6	77.5±8.0
	Right	58.4±7.4	63.1±8.2 [a]	67.9±7.8 [a,b]	72.2±8.9 [a,b,c]	76.6±9.3 [a,b,c,d]	81.4±8.8 [a,b,c,d,e]	85.7±8.7 [a,b,c,d,e,f]
Extension Velocity	Left	335.7±34.2	332.9±33.7	335.6±34.3	338.7±35.0	334.8±37.9	338.7±36.5	335.5±32.3
	Right	252.7±32.5	270.0±35.3 [a]	290.8±34.3 [a,b]	313.5±45.5 [a,b,c]	326.8±46.0 [a,b,c,d]	347.0±41.0 [a,b,c,d,e]	360.0±37.6 [a,b,c,d,e,f]
Extension Moment	Left	33.9±7.6	33.2±7.3	35.8±7.9	33.9±7.3	31.9±7.2	33.2±6.1	32.7±6.8
	Right	34.9±4.1	34.0±6.0	33.6±6.0	31.9±4.9	30.0±4.6 [a]	29.9±6.3 [a,b]	25.7±5.7 [a,b,c,d,e,f]
Power	Left	195.1±36.3	186.5±30.3	204.7±34.5	195.8±33.6	185.4±46.7	192.6±29.3	187.8±36.7
	Right	152.0±21.6	156.7±21.6	169.9±30.2	170.3±20.2	166.8±39.1	175.8±31.9 [a]	154.0±30.5

Note: Significantly different compared to [a]130mm, [b]140mm, [c]150mm, [d]160mm, [e]170mm, [f]180mm.

Thank you to our Sponsors

AMTI
FORCE AND MOTION

Grainger Institute for Engineering
UNIVERSITY OF WISCONSIN–MADISON

destination madison

novel

QUALISYS

OptiTrack

THEIA
Markerless

Department of Mechanical Engineering
UNIVERSITY OF WISCONSIN–MADISON

COLLEGE OF ENGINEERING
BIOMEDICAL ENGINEERING AND MECHANICS
VIRGINIA TECH

XSENSOR
Intelligent Dynamic Sensing